

The Chemistry of Organic Silicon Compounds, Volume 3
Edited by Zvi Rappoport and Yitzhak Apeloig
Copyright © 2001 John Wiley & Sons, Ltd.
ISBN: 0-471-62384-9

The chemistry of
organic silicon compounds
Volume 3

THE CHEMISTRY OF FUNCTIONAL GROUPS

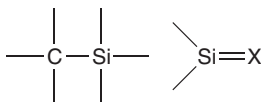
A series of advanced treatises founded by Professor Saul Patai and under the general editorship of Professor Zvi Rappoport

- The chemistry of alkenes (2 volumes)
- The chemistry of the carbonyl group (2 volumes)
 - The chemistry of the ether linkage
 - The chemistry of the amino group
- The chemistry of the nitro and nitroso groups (2 parts)
 - The chemistry of carboxylic acids and esters
 - The chemistry of the carbon–nitrogen double bond
 - The chemistry of amides
 - The chemistry of the cyano group
 - The chemistry of the hydroxyl group (2 parts)
 - The chemistry of the azido group
 - The chemistry of acyl halides
 - The chemistry of the carbon–halogen bond (2 parts)
- The chemistry of the quinonoid compounds (2 volumes, 4 parts)
 - The chemistry of the thiol group (2 parts)
- The chemistry of the hydrazo, azo and azoxy groups (2 volumes, 3 parts)
 - The chemistry of amidines and imidates (2 volumes)
 - The chemistry of cyanates and their thio derivatives (2 parts)
 - The chemistry of diazonium and diazo groups (2 parts)
 - The chemistry of the carbon–carbon triple bond (2 parts)
- The chemistry of ketenes, allenes and related compounds (2 parts)
 - The chemistry of the sulphonium group (2 parts)
- Supplement A: The chemistry of double-bonded functional groups (3 volumes, 6 parts)
- Supplement B: The chemistry of acid derivatives (2 volumes, 4 parts)
- Supplement C: The chemistry of triple-bonded functional groups (2 volumes, 3 parts)
- Supplement D: The chemistry of halides, pseudo-halides and azides (2 volumes, 4 parts)
- Supplement E: The chemistry of ethers, crown ethers, hydroxyl groups and their sulphur analogues (2 volumes, 3 parts)
- Supplement F: The chemistry of amino, nitroso and nitro compounds and their derivatives (2 volumes, 4 parts)
 - The chemistry of the metal–carbon bond (5 volumes)
 - The chemistry of peroxides
 - The chemistry of organic selenium and tellurium compounds (2 volumes)
 - The chemistry of the cyclopropyl group (2 volumes, 3 parts)
 - The chemistry of sulphones and sulphoxides
 - The chemistry of organic silicon compounds (3 volumes, 6 parts)
 - The chemistry of enones (2 parts)
 - The chemistry of sulphinic acids, esters and their derivatives
 - The chemistry of sulphenic acids and their derivatives
 - The chemistry of enols
 - The chemistry of organophosphorus compounds (4 volumes)
 - The chemistry of sulphonic acids, esters and their derivatives
 - The chemistry of alkanes and cycloalkanes
 - Supplement S: The chemistry of sulphur-containing functional groups
 - The chemistry of organic arsenic, antimony and bismuth compounds
 - The chemistry of enamines (2 parts)
 - The chemistry of organic germanium, tin and lead compounds
 - The chemistry of dienes and polyenes (2 volumes)
 - The chemistry of organic derivatives of gold and silver

UPDATES

- The chemistry of α -haloketones, α -haloaldehydes and α -haloimines
 - Nitrones, nitronates and nitroxides
 - Crown ethers and analogs
 - Cyclopropane derived reactive intermediates
- Synthesis of carboxylic acids, esters and their derivatives
 - The silicon–heteroatom bond
 - Synthesis of lactones and lactams
- Syntheses of sulphones, sulphoxides and cyclic sulphides

Patai's 1992 guide to the chemistry of functional groups—*Saul Patai*



The chemistry of organic silicon compounds

Volume 3

Edited by

ZVI RAPPOPORT

The Hebrew University, Jerusalem

and

YITZHAK APELOIG

Israel Institute of Technology, Haifa

2001

JOHN WILEY & SONS, LTD

CHICHESTER-NEW YORK-WEINHEIM-BRISBANE-SINGAPORE-TORONTO

An Interscience® Publication

Copyright © 2001 John Wiley & Sons, Ltd,
Baffins Lane, Chichester,
West Sussex PO19 1UD, England
National 01243 779777
International (+44) 1243 779777
e-mail (for orders and customer service enquiries): cs-books@wiley.co.uk
Visit our Home Page on <http://www.wiley.co.uk>
or <http://www.wiley.com>

All Rights Reserved. No part of this publication may be reproduced, stored in a retrieval system, or transmitted, in any form or by any means, electronic, mechanical, photocopying, recording, scanning or otherwise, except under the terms of the Copyright, Designs and Patents Act 1988 or under the terms of a licence issued by the Copyright Licensing Agency Ltd, 90 Tottenham Court Road, London W1P 0LP, UK, without the permission in writing of the Publisher.

Other Wiley Editorial Offices

John Wiley & Sons, Inc., 605 Third Avenue,
New York, NY 10158-0012, USA

Wiley-VCH Verlag GmbH
Pappelallee 3, D-69469 Weinheim, Germany

John Wiley & Sons Australia, Ltd
33 Park Road, Milton, Queensland 4064, Australia

John Wiley & Sons (Asia) Pte Ltd, 2 Clementi Loop #02-01,
Jin Xing Distripark, Singapore 129809

John Wiley & Sons (Canada) Ltd, 22 Worcester Road,
Rexdale, Ontario, M9W 1L1, Canada

Library of Congress Cataloging-in-Publication Data

The chemistry of organic silicon compounds / edited by Zvi Rappoport, Yitzhak Apeloig.
p. cm. — (The chemistry of functional groups. Supplement; Si)
Includes bibliographical references and index.
ISBN 0-471-62384-9 (alk. paper)
1. Organosilicon compounds. I. Rappoport, Zvi. II. Apeloig, Yitzhak. III. Series.
QD305.S54 C48 2001
547'.08—dc21 00-043917

British Library Cataloguing in Publication Data

A catalogue record for this book is available from the British Library

ISBN 0 471 62384 9

Typeset in 9/10pt Times by Laser Words, Madras, India.
Printed and bound in Great Britain by Biddles Ltd, Guildford, Surrey.
This book is printed on acid-free paper responsibly manufactured from sustainable forestry,
in which at least two trees are planted for each one used for paper production.

To
Noa, Nimrod
and
Naama

Contributing authors

Yitzhak Apeloig	Department of Chemistry, and the Ise Meitner Minerva Center for Computational Quantum Chemistry, Technion-Israel Institute of Technology, Haifa 32000, Israel
H. Bock	Institute of Inorganic Chemistry, Johann Wolfgang Goethe University, Marie-Curie Street 11, D-60439 Frankfurt am Main, Germany
Bruno Boury	Laboratoire de Chimie Moléculaire et Organisation du Solide, UMR 5637, Université de Montpellier II, CC007, Place E. Bataillon, 34095 Montpellier cedex, France
C. Chatgililoglu	I.Co.C.E.A., Consiglio Nazionale delle Ricerche, Via P. Gobetti 101, 40129 Bologna, Italy
Cheol Ho Choi	Department of Chemistry, Iowa State University, Ames, Iowa 50011, USA
Robert J. P. Corriu	Laboratoire de Chimie Moléculaire et Organisation du Solide, UMR 5637, Université de Montpellier II, CC007, Place E. Bataillon, 34095 Montpellier cedex, France
Simonetta Fornarini	Dipartimento di Studi di Chimica e Tecnologia delle Sostanze Biologicamente Attive, Università di Roma 'La Sapienza', P.le A. Moro 5, I-00185 Roma, Italy
Mark S. Gordon	Department of Chemistry, Iowa State University, Ames, Iowa 50011, USA
U. Herzog	Institute of Inorganic Chemistry, Freiberg University of Mining and Technology, Leipziger Strasse 29, D-09596, Freiberg, Germany
Takeaki Iwamoto	Department of Chemistry, Graduate School of Science, Tohoku University, Aoba-ku, Sendai 980-8578, Japan
Bettina Jaschke	Institute of Inorganic Chemistry, University of Goettingen, Tammannstrasse 4, D-37077 Goettingen, Germany
Jürgen Kapp	Computer Chemistry Center of the Institute of Organic Chemistry, The University of Erlangen-Nürnberg, Henkestrasse 42, 91054 Erlangen, Germany
Miriam Karni	Department of Chemistry, and the Ise Meitner Minerva Center for Computational Quantum Chemistry, Technion-Israel Institute of Technology, Haifa 32000, Israel

Mitsuo Kira	Department of Chemistry, Graduate School of Science, Tohoku University, Aoba-ku, Sendai 980-8578, Japan
Uwe Klingebiel	Institute of Inorganic Chemistry, University of Goettingen, Tammannstrasse 4, D-37077 Goettingen, Germany
William J. Leigh	Department of Chemistry, McMaster University, 1280 Main Street West, Hamilton, Ontario, L8S 4M1, Canada
Paul D. Lickiss	Department of Chemistry, Imperial College of Science, Technology and Medicine, London SW7 2AY, UK
Tracy L. Morkin	Department of Chemistry, McMaster University, 1280 Main Street West, Hamilton, Ontario, L8S 4M1, Canada
Daniel E. Morse	Marine Biotechnology Center and Department of Molecular, Cellular and Developmental Biology, University of California, Santa Barbara, California 93106, USA
Peter Neugebauer	Institute of Inorganic Chemistry, University of Goettingen, Tammannstrasse 4, D-37077 Goettingen, Germany
Thomas R. Owens	Department of Chemistry, McMaster University, 1280 Main Street West, Hamilton, Ontario, L8S 4M1, Canada
C. H. Scheisser	School of Chemistry, University of Melbourne, Victoria 3010, Australia
Paul von Ragué Schleyer	Centre for Computational Quantum Chemistry, University of Georgia, Athens, GA 30602-2525, USA
Jan Schraml	Institute of Chemical Process Fundamentals, Academy of Sciences of the Czech Republic, 165 02 Prague, Czech Republic
B. Solouki	Institute of Inorganic Chemistry, Johann Wolfgang Goethe University, Marie-Curie Street 11, D-60439 Frankfurt am Main, Germany
David Y. Son	Department of Chemistry, P.O. Box 750314, Southern Methodist University, Dallas, Texas 75275-0314, USA
Kohei Tamao	Institute for Chemical Research, Kyoto University, Uji, Kyoto 611-0011, Japan
Kozo Toyota	Department of Chemistry, Graduate School of Science, Tohoku University, Aoba-ku, Sendai 980-8578, Japan
Manfred Weidenbruch	Fachbereich Chemie, Universität Oldenburg, D-26111 Oldenburg, Germany
Robert West	Organosilicon Research Center, Department of Chemistry, University of Wisconsin, Madison, WI 53706, USA
Shigehiro Yamaguchi	Institute for Chemical Research, Kyoto University, Uji, Kyoto 611-0011, Japan
Masaaki Yoshifuji	Department of Chemistry, Graduate School of Science, Tohoku University, Aoba-ku, Sendai 980-8578, Japan

Foreword

The preceding volume on *The chemistry of organic silicon compounds* (Vol. 2) in 'The Chemistry of Functional Groups' series (Z. Rappoport and Y. Apeloig, Eds.) appeared in 1998. It followed an earlier volume with the same title (S. Patai and Z. Rappoport, Eds.) published in 1989 (now referred to as Vol. 1) and an update volume *The silicon-heteroatom bond* in 1991. The appearance of the present volume only three years after the three parts of Vol. 2 reflects the continuing rapid growth of many sub-fields of organosilicon compounds and their chemistry.

The volume covers three types of chapters. First, the majority are new chapters, including those which were planned but did not appear in Vol. 2 which we promised then to include in a future volume. These include a comparison of the chemistry of organosilicon compounds with that of their heavier group congeners, photoelectron spectroscopy (which was covered in Vol. 1), silyl migrations, polysilanes, polysilanol, polysiloles, organosilicon halides, nanostructured hybrid organic-inorganic solids, chemistry on silicon surfaces, silicon based dendrimers and star compounds, synthesis of multiply-bonded silicon-phosphorus compounds and a chapter on a biotechnological approach to polysilsesquioxanes.

Second, chapters on topics which were covered incompletely or partially in Vol. 2 were extended here by including new sub-topics related to the same themes. These include ^{29}Si NMR, ion-molecule reactions of silicon ions and the reactivity of multiply-bonded silicon compounds.

Finally, the rapid developments in recent years led to chapters which are updates of those in Vol. 2. These include recent developments in the chemistry of silyl radicals, of silicon-silicon multiple bonds and of silicon-nitrogen bonds.

The literature coverage in the book is mostly up to mid- or late-2000.

Two originally planned chapters, on the interplay between theory and experiments on silicon and on silsesquioxanes, did not materialize, although these topics are covered partially in other chapters. We hope to include these chapters in a future volume.

The chapters in this volume were written by authors from nine countries, thus reflecting the international research activity in the chemistry of organosilicon compounds. We are grateful to the authors for their contributions and we hope that this volume together with its predecessor will serve as a major reference to the chemistry of organosilicon compounds in the last decades.

We will be grateful to readers who draw our attention to mistakes in the present volume and to those who mention new topics which deserve to be included in a future volume on organosilicon compounds.

Jerusalem and Haifa
March 2001

ZVI RAPPOPORT
YITZHAK APELOIG

The Chemistry of Functional Groups

Preface to the series

The series 'The Chemistry of Functional Groups' was originally planned to cover in each volume all aspects of the chemistry of one of the important functional groups in organic chemistry. The emphasis is laid on the preparation, properties and reactions of the functional group treated and on the effects which it exerts both in the immediate vicinity of the group in question and in the whole molecule.

A voluntary restriction on the treatment of the various functional groups in these volumes is that material included in easily and generally available secondary or tertiary sources, such as Chemical Reviews, Quarterly Reviews, Organic Reactions, various 'Advances' and 'Progress' series and in textbooks (i.e. in books which are usually found in the chemical libraries of most universities and research institutes), should not, as a rule, be repeated in detail, unless it is necessary for the balanced treatment of the topic. Therefore each of the authors is asked not to give an encyclopaedic coverage of his subject, but to concentrate on the most important recent developments and mainly on material that has not been adequately covered by reviews or other secondary sources by the time of writing of the chapter, and to address himself to a reader who is assumed to be at a fairly advanced postgraduate level.

It is realized that no plan can be devised for a volume that would give a complete coverage of the field with no overlap between chapters, while at the same time preserving the readability of the text. The Editors set themselves the goal of attaining reasonable coverage with moderate overlap, with a minimum of cross-references between the chapters. In this manner, sufficient freedom is given to the authors to produce readable quasi-monographic chapters.

The general plan of each volume includes the following main sections:

- (a) An introductory chapter deals with the general and theoretical aspects of the group.
- (b) Chapters discuss the characterization and characteristics of the functional groups, i.e. qualitative and quantitative methods of determination including chemical and physical methods, MS, UV, IR, NMR, ESR and PES — as well as activating and directive effects exerted by the group, and its basicity, acidity and complex-forming ability.
- (c) One or more chapters deal with the formation of the functional group in question, either from other groups already present in the molecule or by introducing the new group directly or indirectly. This is usually followed by a description of the synthetic uses of the group, including its reactions, transformations and rearrangements.
- (d) Additional chapters deal with special topics such as electrochemistry, photochemistry, radiation chemistry, thermochemistry, syntheses and uses of isotopically labelled compounds, as well as with biochemistry, pharmacology and toxicology. Whenever applicable, unique chapters relevant only to single functional groups are also included (e.g. 'Polyethers', 'Tetraaminoethylenes' or 'Siloxanes').

This plan entails that the breadth, depth and thought-provoking nature of each chapter will differ with the views and inclinations of the authors and the presentation will necessarily be somewhat uneven. Moreover, a serious problem is caused by authors who deliver their manuscript late or not at all. In order to overcome this problem at least to some extent, some volumes may be published without giving consideration to the originally planned logical order of the chapters.

Since the beginning of the Series in 1964, two main developments have occurred. The first of these is the publication of supplementary volumes which contain material relating to several kindred functional groups (Supplements A, B, C, D, E, F and S). The second ramification is the publication of a series of 'Updates', which contain in each volume selected and related chapters, reprinted in the original form in which they were published, together with an extensive updating of the subjects, if possible, by the authors of the original chapters. A complete list of all above mentioned volumes published to date will be found on the page opposite the inner title page of this book. Unfortunately, the publication of the 'Updates' has been discontinued for economic reasons.

Advice or criticism regarding the plan and execution of this series will be welcomed by the Editors.

The publication of this series would never have been started, let alone continued, without the support of many persons in Israel and overseas, including colleagues, friends and family. The efficient and patient co-operation of staff-members of the publisher also rendered us invaluable aid. Our sincere thanks are due to all of them.

The Hebrew University
Jerusalem, Israel

SAUL PATAI
ZVI RAPPOPORT

Sadly, Saul Patai who founded 'The Chemistry of Functional Groups' series died in 1998, just after we started to work on the 100th volume of the series. As a long-term collaborator and co-editor of many volumes of the series, I undertook the editorship and this is the third volume to be edited since Saul Patai passed away. I plan to continue editing the series along the same lines that served for the first hundred volumes and I hope that the continuing series will be a living memorial to its founder.

The Hebrew University
Jerusalem, Israel
May 2000

ZVI RAPPOPORT

Contents

1	Theoretical aspects of compounds containing Si, Ge, Sn and Pb Mirian Karni, Jürgen Kapp, Paul von Ragué Schleyer and Yitzhak Apeloig	1
2	(Helium I)-photoelectron spectra of silicon compounds: History and achievements concerning their molecular states H. Bock and B. Solouki	165
3	²⁹ Si NMR experiments in solutions of organosilicon compounds Jan Schraml	223
4	Silyl radicals C. Chatgililoglu and C. H. Schiesser	341
5	Recent advances in the chemistry of silicon–silicon multiple bonds Manfred Weidenbruch	391
6	Recent developments in the chemistry of compounds with silicon–nitrogen bonds Peter Neugebauer, Bettina Jaschke and Uwe Klingebiel	429
7	Organosilicon halides — synthesis and properties Uwe Herzog	469
8	Synthesis of multiply bonded phosphorus compounds using silylphosphines and silylphosphides Masaaki Yoshifuji and Koze Toyota	491
9	Polysilanes: Conformations, chromotropism and conductivity Robert West	541
10	Nanostructured hybrid organic–inorganic solids. From molecules to materials Bruno Boury and Robert J. P. Corriu	565
11	Polysiloles and related silole-containing polymers Shigehiro Yamaguchi and Kohei Tamao	641
12	Polysilanols Paul D. Lickiss	695

13	Silicon-based dendrimers and hyperbranched polymers David Y. Son	745
14	Biotechnology reveals new routes to synthesis and structural control of silica and polysilsesquioxanes Daniel E. Morse	805
15	Chemistry on silicon surfaces Cheol Ho Choi and Mark S. Gordon	821
16	Silyl migrations Mitsuo Kira and Takeaki Iwamoto	853
17	Kinetic studies of the reactions of Si=C and Si=Si bonds Tracy L. Morkin, Thomas R. Owens and William J. Leigh	949
18	Ion-molecule reactions of silicon cations Simonetta Fornarini	1027
	Author index	1059
	Subject index	1127
	Contents of Volume 1	
	Contents of Volume 2	

List of abbreviations used

Ac	acetyl (MeCO)
acac	acetylacetone
Ad	adamantyl
AIBN	azoisobutyronitrile
Alk	alkyl
All	allyl
An	anisyl
Ar	aryl
Bn	benzyl
Bz	benzoyl (C ₆ H ₅ CO)
Bu	butyl (also <i>t</i> -Bu or Bu ^t)
CD	circular dichroism
CI	chemical ionization
CIDNP	chemically induced dynamic nuclear polarization
CNDO	complete neglect of differential overlap
Cp	η^5 -cyclopentadienyl
Cp*	η^5 -pentamethylcyclopentadienyl
DABCO	1,4-diazabicyclo[2.2.2]octane
DBN	1,5-diazabicyclo[4.3.0]non-5-ene
DBU	1,8-diazabicyclo[5.4.0]undec-7-ene
DIBAH	diisobutylaluminium hydride
DME	1,2-dimethoxyethane
DMF	<i>N,N</i> -dimethylformamide
DMSO	dimethyl sulphoxide
ee	enantiomeric excess
EI	electron impact
ESCA	electron spectroscopy for chemical analysis
ESR	electron spin resonance
Et	ethyl
eV	electron volt

Fc	ferrocenyl
FD	field desorption
FI	field ionization
FT	Fourier transform
Fu	furyl(OC ₄ H ₃)
GLC	gas liquid chromatography
Hex	hexyl(C ₆ H ₁₃)
<i>c</i> -Hex	cyclohexyl(C ₆ H ₁₁)
HMPA	hexamethylphosphortriamide
HOMO	highest occupied molecular orbital
HPLC	high performance liquid chromatography
<i>i</i> -	iso
Ip	ionization potential
IR	infrared
ICR	ion cyclotron resonance
LAH	lithium aluminium hydride
LCAO	linear combination of atomic orbitals
LDA	lithium diisopropylamide
LUMO	lowest unoccupied molecular orbital
M	metal
<i>M</i>	parent molecule
MCPBA	<i>m</i> -chloroperbenzoic acid
Me	methyl
MNDO	modified neglect of diatomic overlap
MS	mass spectrum
<i>n</i>	normal
Naph	naphthyl
NBS	<i>N</i> -bromosuccinimide
NCS	<i>N</i> -chlorosuccinimide
NMR	nuclear magnetic resonance
Pc	phthalocyanine
Pen	pentyl(C ₅ H ₁₁)
Pip	piperidyl(C ₅ H ₁₀ N)
Ph	phenyl
ppm	parts per million
Pr	propyl (also <i>i</i> -Pr or Pr ^{<i>i</i>})
PTC	phase transfer catalysis or phase transfer conditions
Pyr	pyridyl (C ₅ H ₄ N)

R	any radical
RT	room temperature
<i>s</i> -	secondary
SET	single electron transfer
SOMO	singly occupied molecular orbital
<i>t</i> -	tertiary
TCNE	tetracyanoethylene
TFA	trifluoroacetic acid
THF	tetrahydrofuran
Thi	thienyl(SC ₄ H ₃)
TLC	thin layer chromatography
TMEDA	tetramethylethylene diamine
TMS	trimethylsilyl or tetramethylsilane
Tol	tolyl(MeC ₆ H ₄)
Tos or Ts	tosyl(<i>p</i> -toluenesulphonyl)
Trityl	triphenylmethyl(Ph ₃ C)
Xyl	xylyl(Me ₂ C ₆ H ₃)

In addition, entries in the 'List of Radical Names' in *IUPAC Nomenclature of Organic Chemistry*, 1979 Edition, Pergamon Press, Oxford, 1979, p. 305–322, will also be used in their unabbreviated forms, both in the text and in formulae instead of explicitly drawn structures.

CHAPTER 1

Theoretical aspects of compounds containing Si, Ge, Sn and Pb

MIRIAM KARNI and YITZHAK APELOIG

Department of Chemistry, and the Lise Meitner Minerva Center for Computational Quantum Chemistry, Technion-Israel Institute of Technology, Haifa 32000, Israel
Fax: 972-4-8294601; email: chrmiri@techunix.technion.ac.il and chrapel@techunix.technion.ac.il

and

JÜRGEN KAPP and PAUL VON R. SCHLEYER^a

Computer Chemistry Center of the Institute of Organic Chemistry, The University of Erlangen-Nürnberg, Henkestrasse 42, 91054 Erlangen, Germany

^a*Current address: Center for Computational Quantum Chemistry, University of Georgia, Athens, GA 30602-2525, USA*
Fax: 706 542-7514; email: schleyer@chem.uga.edu

I. LIST OF ABBREVIATIONS	3
II. INTRODUCTION	5
III. PERIODIC TRENDS IN THE PROPERTIES OF GROUP 14 ELEMENTS	7
A. Radial Orbital Extensions	8
B. Relativistic Effects	9
C. Hybridization	10
D. Electronegativity and Bonding	11
E. Spin-Orbit Coupling	11
F. The Role of d Orbitals	11
IV. THEORETICAL METHODS	12
A. Nonrelativistic Theoretical Methods	12
B. Relativistic Methods	13
C. Effective Core Potential Basis Sets	13
D. Methods for Analysis of the Electronic Structure	14

V. SINGLY BONDED COMPOUNDS	14
A. MH ₄ (metallanes)	14
1. Geometries, ionization potentials and nuclear spin–spin couplings	14
2. Bond energies	16
3. The stability of MH ₄ relative to MH ₂ + H ₂	17
4. Charged MH ₄ species: MH ₄ ⁺ and MH ₄ ²⁺	19
B. Mono-substituted Singly-bonded MH ₃ R Metallanes	20
1. General trends in the M–R bond dissociation energies	21
2. MH ₃ R, R = halogen	23
a. Geometries	23
b. M–R bond dissociation energies	23
3. Ethane analogs	24
a. Geometries and rotational barriers	24
b. Bond dissociation energies	26
c. Nonclassical bridged structures of ethane analogs	27
4. Classical linear M _n H _{2n+2} chains	27
C. Multiply-substituted Singly-bonded Compounds	28
1. M(CH ₃) ₄ and MX ₄ , X = halogen	28
2. (CH ₃) _n MX _{4–n}	31
3. Relative stabilities of M ^{IV} and M ^{II} compounds	32
4. Oxides and sulfides	35
5. MLi ₄	35
D. Hypercoordinated Systems	36
1. MH ₅	36
2. MX ₅ , X = alkali metals	37
3. MX ₆ , MX ₇ and MX ₈ , X = alkali metals	38
E. Cyclic Metallanes: Rings, Polycyclic and Polyhedral Compounds	38
1. Saturated ring compounds	39
a. <i>c</i> -M ₃ H ₆ and <i>c</i> -M ₄ H ₈	39
i. Structures	39
ii. Strain	41
iii. Stability towards cleavage	43
iv. Other structures of 3-MRs	44
b. Metalloles	46
c. Heterocyclic 3- and 4-membered rings	48
i. 3-MRs, <i>c</i> -(R ₂ M) ₂ X	48
ii. 1,3-Dioxa-2,4-dimetalanes, <i>c</i> -(MH ₂) ₂ O ₂	50
2. Polycyclic and polyhedral metallanes	52
a. Bicyclic compounds	52
b. Propellanes	54
c. Polyhedral cage compounds: tetrahedrane, prismane, cubane and larger M _n H _n systems	58
d. Polyhedral metallaboranes	62
VI. MULTIPLY-BONDED SYSTEMS	63
A. Historical Overview	63
B. M=M' Doubly-bonded Compounds (Metallenes)	64
1. Structures	64
2. The double-bond strength	69
3. Stability relative to isomeric structures	74

1. Theoretical aspects of compounds containing Si, Ge, Sn and Pb	3
a. Relative to the corresponding metallylenes	74
b. Relative to bridged isomers	75
i. Hydrogen bridged isomers	75
ii. π -Donor bridged isomers	77
C. $R_2M=X$ Compounds	79
1. Structures and bond energies	79
2. Isomerization to metallylenes	80
D. Increasing the Number of Double Bonds	82
1. Heavier analogs of 1,3-butadiene	82
2. Heavier analogs of allene	87
E. Triply-bonded Metallenes, $RM\equiv M'R'$	91
1. Structures and bond nature	91
2. Potential energy surfaces	94
a. $HC\equiv MH$, $M = Si, Ge$	94
b. $HM\equiv MH$ and $HM\equiv M'H$	96
F. Aromatic compounds	101
1. The congeners of benzene and their isomers	101
2. Metallacyclopropenium cations	105
3. Metallacyclopentadienyl anion and dianion	106
4. Metallocenes	108
VII. REACTIVE INTERMEDIATES	110
A. Divalent Compounds (Metallylenes)	110
1. MH_2 and MX_2 ($X = \text{halogen}$)	110
2. Stable metallylenes	113
3. Reactions	116
a. 1,2-Hydrogen shifts	116
b. Insertion and addition reactions	118
i. Insertion into H_2	118
ii. Insertion into $M-H$ bonds	119
iii. Insertion into $X-H$ σ -bonds	120
iv. Addition to double bonds	124
v. Addition to acetylene	126
B. Tricoordinated Compounds	128
1. Tricoordinated cations	128
a. Structures	128
b. Thermodynamic and kinetic stability of MR_3^+ cations	132
2. Tricoordinated radicals	138
3. Tricoordinated anions	138
C. Pentacoordinated Compounds	141
1. Pentacoordinated cations	141
2. Pentacoordinated radicals	142
3. Pentacoordinated anions	144
VIII. CONCLUSIONS AND OUTLOOK	146
IX. ACKNOWLEDGMENTS	147
X. REFERENCES	147

I. LIST OF ABBREVIATIONS

ARPP	averaged relativistic pseudopotential
ASE	aromatic stabilization energy

B3LYP	Becke's 3-parameter hybrid with Lee, Young and Parr's correlation functional
BLYP	B88 exchange functional with Lee, Young and Parr's correlation functional
CASSCF	complete active space SCF
CCSD(T)	coupled cluster with single and double excitations (followed by a perturbation treatment of triple excitations)
CEP	compact effective potential
CI	configuration interaction
CIDVD	configuration interaction calculation including single and double substitutions with the contribution of quadruple excitations estimated with Davidson's formula
CISD	configuration interaction calculations including single and double substitutions
Dep	2,6-diethylphenyl
DFT	density functional theory
DHF	Dirac Hartree-Fock
Dip	2,6-diisopropylphenyl
Dmp	2,6-dimethylphenyl
DSSE	divalent state stabilization energy
DZ+d	double-zeta quality basis set augmented with polarization functions on non-hydrogen atoms
DZP	double-zeta quality basis set augmented with polarization functions on all atoms
ECP	effective core potential
LANL1DZ	Los Alamos ECP + double-zeta quality basis set
LDA	local density approximation
LSDA	local spin density approximation
Mes	mesityl (2,4,6-trimethylphenyl)
MNDO	modified neglect of diatomic overlap
MP n	Møller-Plesset perturbation method of the n th order
MRSDCI	multireference singles + doubles configuration interaction
MRSOCI	multireference second order configuration interaction
NAO	natural atomic orbital
NBO	natural bond orbital analysis
NICS	nucleus independent chemical shift
NLMO	natural localized molecular orbital
NPA	natural population analysis
NRT	natural resonance theory
PM3	modified neglect of diatomic overlap-parametric method number 3
PSP	pseudopotential
PT	perturbation theory
QCISD	quadratic configuration interaction calculations including single and double substitutions
QCISD(T)	quadratic configuration interaction calculations including single and double substitutions with the addition of triples contribution to the energy
RCEP	relativistic compact effective potential
RECP	relativistic effective core potential
SCF	self-consistent field
SDD	the Stuttgart/Dresden double-zeta effective core potential
SOC	spin-orbit coupling
SOCI	second order configuration interaction
Tbt	2,4,6-tris[bis(trimethylsilyl)methyl]phenyl

TCSCF	two-configuration self-consistent field
Tip	2,4,6-tris(isopropyl)phenyl
TMS	trimethylsilyl
VDZ	valence double-zeta quality basis set
VQZ	valence quadruple-zeta quality basis set

II. INTRODUCTION

It is difficult to select ‘the most important group of the Periodic Table of the Elements’—but if such a choice has to be made group 14, consisting of carbon, silicon, germanium, tin and lead, would have a good chance of being chosen. Carbon is of major importance to life, silicon is the most abundant element in the earth’s crust and, jointly with germanium, drives the computer revolution, while the metals, tin and lead, known since antiquity, still continue to play an important role in science and technology. Numerous review articles deal with the different chemical and physical properties of carbon and its congeners^{1–7}. It is now well accepted that the chemical behavior of the heavier main group elements (not only those of group 14) should be described as ‘normal’, while that of the first row, including the elements Li to Ne, is exceptional⁶. A large gap in physical properties and in chemical behavior is evident between carbon, the non-metal, and silicon the (semi-)metal, and this point has been discussed extensively in the literature^{3,6,7}. However, it is a gross oversimplification to assume that the chemistry of the heavier group 14 elements Ge, Sn and Pb resembles the chemistry of silicon. The known chemistry of silicon, germanium, tin and lead refute this assumption⁸. Striking and surprising changes down the group are observed, when compounds of the heavier congeners with common functional groups are compared¹. Examples are double bonds and small strained rings composed of group 14 metals. The review and analysis of the similarities and differences which occur when silicon is substituted by its heavier congeners is the focus of this chapter. The review focuses on the contributions of theoretical studies, but important experimental developments are also discussed briefly and the reader is directed to the original references for further reading.

The experimental progress of the chemistry of compounds containing silicon and its congeners during the last two decades has been spectacular^{1,9–24}. These developments were paralleled by the extension of computational methods to the heavier elements²⁵. Quantum mechanical calculations were extremely helpful in explaining the differences between carbon and silicon chemistry and in directing some of the pioneering experimental work in silicon chemistry. The theoretical studies on silicon compounds were reviewed extensively by Apeloig in 1989⁷. Reviews on the theoretical aspects of the chemistry of specific groups of silicon compounds are also available, e.g. multiply-bonded and divalent silicon compounds^{26,27}, aromatic and antiaromatic silicon compounds^{28a} and others^{4,28b–d,29}. However, considerably fewer theoretical studies dealt with compounds of germanium and the heavier group 14 metals. This is not surprising, as reliable calculations of heavier elements required larger basis sets and more sophisticated theoretical treatments, e.g. the inclusion of relativistic effects³⁰, and therefore much larger computer capabilities. Consequently, most of the earlier theoretical surveys on group 14 compounds included only compounds of carbon and silicon^{4,7,26–29}, and occasionally also germanium compounds. Nevertheless, calculations on small molecules like MH₄ and MO with all group 14 elements (M = C to Pb) date back to the early 1970s³¹. The results of the calculations on small molecules³², for which sufficient experimental information (geometries, dipole moments etc.) was available for calibration³³, were used as benchmarks to

check the performance of new computational procedures, such as relativistic Dirac–Fock calculations³².

Larger systems can be calculated with more reasonable computer resources and time requirements than required for all-electron basis sets, by employing effective core potentials (ECPs)³⁴. ECPs, which were refined mostly during the 1980s, replace the explicit treatment of the core electrons (i.e. nonvalence electrons) by a suitable function. This reduces dramatically the computer time required for a particular calculation. In addition, most ECPs were fit to include also relativistic procedures³⁴ and they thus introduce relativistic effects into formally nonrelativistic calculations. This is the reason why most theoretical calculations on compounds of heavier group 14 elements are currently carried out using ECPs. ECPs are, of course, an approximation and many effects, e.g. core polarization and correlation between core and valence electrons, are ignored. Errors can therefore be expected to be larger than in full theoretical treatments. Nevertheless, the advantages of ECPs override their disadvantages, making them very popular and widely used. A more detailed discussion of the theoretical methods is given in Section IV. In any event, the goal of most investigations on compounds of heavy group 14 elements is not necessarily to achieve the highest possible accuracy but to gain insights, e.g., on the variation of the structures and bonding when moving down the Periodic Table. *Such insight is indeed the major purpose of this chapter.*

Unfortunately, experimental investigations can contribute relatively little to the calibration and testing of the theoretical calculations for the heavier group 14 elements, in contrast to the very close theoretical–experimental calibration which is possible in carbon chemistry. Many basic systems, which can be calculated with a variety of theoretical methods including very sophisticated ones, are in many cases unknown experimentally. In addition, many of the group 14 compounds with unusual structures or properties, synthesized in the last decade, are stabilized by large bulky substituents^{1,2,9–24}. Therefore, their experimental properties (structure, spectroscopy, reactivity) are often dominated by substituent effects and they do not necessarily represent the characteristic inherent behavior of the parent compounds. Furthermore, many of these sterically crowded systems are too large to be computed adequately, and hence, in many cases, the theoretical calculations are performed for model systems and not for the actual experimental systems, making a theoretical–experimental comparison difficult and sometimes even speculative as various assumptions have to be made.

The main objective of this chapter is to compare compounds of silicon with compounds of its heavier congeners, germanium, tin and lead. Therefore, we review mostly studies which provide a comparison between at least silicon and one of the heavier congeners. For completeness of the picture we mention in many cases also the behavior of the corresponding carbon compounds.

We will discuss first the general trends that lead to the differences in behavior of group 14 elements. Next, we discuss singly-bonded compounds of group 14 metals and then multiply bonded systems, e.g. doubly-bonded analogs of ethylene and triply-bonded analogs of acetylene. We continue with a discussion of aromatic systems, e.g. benzene analogs, and complete the chapter with a discussion of reactive intermediates, mainly the divalent carbene-like MR_2 systems, charged species and radicals. We will also present a short overview of the major different theoretical methods which were applied to calculate group 14 element compounds, so that experimentalists who are unfamiliar with the theoretical methods, terms and jargon will be able to follow the discussion.

The amount of theoretical work done in this field in the last 15 years has been overwhelming. As the main purpose of this review is to provide insight and guidelines to the similarities and differences between the compounds of group 14 elements, this review

is not comprehensive. We have concentrated on the systems from which we believe the most important lessons can be learned.

III. PERIODIC TRENDS IN THE PROPERTIES OF GROUP 14 ELEMENTS

An understanding of the properties of the elements is the key to understanding the properties of their compounds.

Some important physical properties of group 14 elements are given in Table 1^{35–44}. A detailed comparison of the atomic properties of C and Si was given by Apeloig⁷ and by Corey³. A comparison of the important physical properties of all group 14 elements was given by Basch and Hoz⁴⁵. Much of the discussion below is based on the landmark review of Kutzelnigg which was published in 1984⁶.

TABLE 1. Physical properties of group 14 elements

	C	Si	Ge	Sn	Pb
Electronegativity					
Allred–Rochow ^a	2.50	1.74	2.02	1.72	1.55
Pauling ^b	2.55	1.90	2.01	1.96	2.33
Allen ^c	2.54	1.92	1.99	1.82	—
Atomic and ionic radii (pm) ^d					
neutral	77	118	121	140	175 ^e
2+			73	93	118–120
4+	16	40–42	53	69–71	78–84
Valence orbital energy (eV) ^f					
s	–19.39	–14.84	–15.52	–13.88	–15.41
p ^g	–11.07	–7.57	–7.29	–6.71	–6.48
Difference	8.32	7.27	8.23	7.17	8.93
$\Delta r = (r_p - r_s)$ (pm) ^h	–0.2	20.3	24.9	28.5	35.8
Atomic spin–orbit coupling (kcal mol ^{–1}) ⁱ	0.05	0.2	1.6	4.8	22.4
Ionization energy (eV) ^j					
ns ^k	16.60	13.64	14.43	13.49	16.04
np ^l	11.26	8.15	7.90	7.39	7.53
Electron affinity (eV) ^m	1.26	1.76	1.81	1.68	1.91
Hybridization of M in MH ₄ ⁿ	sp ^{3.17}	sp ^{2.08}	sp ^{2.05}	sp ^{1.79}	sp ^{1.75}

^aFrom Reference 35a.

^bFrom Reference 35b.

^cFrom Reference 36.

^dFrom References 37–39.

^eMetallic distance.

^fFrom Reference 40.

^gSpin–orbit averaged.

^hDifference of the orbital radii of maximal electron density between the valence p and s orbitals; from Reference 40.

ⁱ³P₀ → ³P₁ energy difference, see text; from Reference 41.

^jSpin–orbit averaged; from Reference 42.

^kFor the process: $ns^2np^2(^3P) \rightarrow ns^1np^2(^4P)$.

^lFor the process: $ns^2np^2(^3P) \rightarrow ns^2np^1(^2P)$.

^mFrom Reference 43.

ⁿAccording to NBO analysis, at B3LYP/TZ+P; from Reference 44.

A. Radial Orbital Extensions

The changes of the radii (r) of the ns and np atomic orbitals of group 14 elements as a function of the element are shown in Figure 1. It could have been expected that the radii of the ns and the np orbitals would increase monotonically down the group because the principal quantum number n increases. However, a zig-zag behavior, with an irregular behavior for Ge and Pb, is actually found (Figure 1). This behavior is common to the third- and fifth-row atoms of the Periodic Table. Thus, in C, the $2s$ orbital is relatively extended, as a result of the repulsion of the $2s$ electrons by the $1s^2$ core electrons, while the $2p$ orbitals which are not shielded by other p electrons are relatively contracted. In silicon the radii of both the $3s$ and the $3p$ orbitals increase (due to the presence of $2s$ and $2p$ electrons), but the latter expand more than the former because now the $2p$ electrons repel the $3p$ shell. Ge exhibits a break in the trend due to the imperfect screening by the $3d^{10}$ shell which increases the effective nuclear charge for the $4s$ and $4p$ electrons. This causes the $4s$ orbital to contract and, to a limited extent, the $4p$ orbital as well (the so-called d-block contraction³⁰). In Sn, the $5s$ and $5p$ orbitals increase in size. This is followed by a drop in the size of the $6s$ orbital of Pb and less so for the $6p$ orbitals due to the ‘lanthanide and relativistic contraction’³⁰ (see below).

Of great importance is the radial orbital extension difference, $\Delta r = r_p - r_s$, (Table 1 and Figure 1). Due to the orbital behavior described above, Δr for carbon is only -0.2 pm. However, Δr increases successively in a zig-zag fashion (caused by the d-block

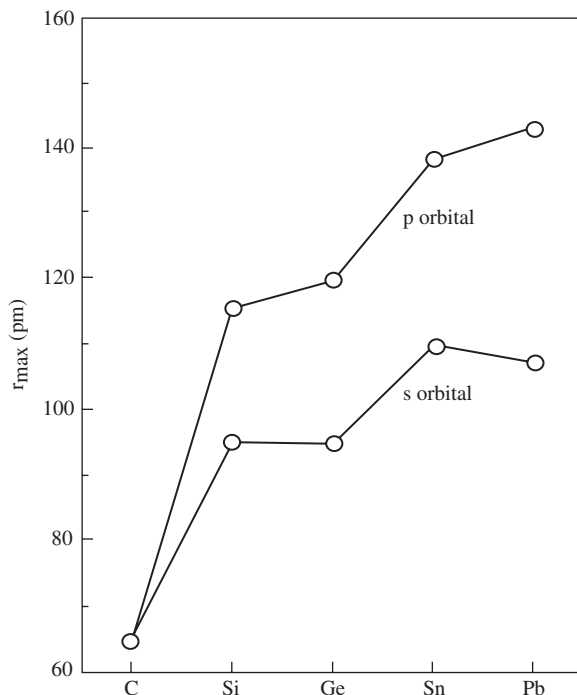


FIGURE 1. The calculated sizes of the valence ns and np orbitals of group 14 elements. Adapted from Reference 5

contraction and relativistic effects) on moving down the Periodic Table. The largest Δr is found for Pb and this contributes to the unique structures of Pb containing molecules (Section V.C.2).

B. Relativistic Effects

As the nuclei become heavier, the strong attraction of the electrons by the very large nuclear charge causes the electrons to move very rapidly and behave relativistically, i.e. their relative mass (m) increases according to equation 1, and the effective Bohr radius (a_0) for inner electrons with large average speeds decreases according to equation 2³⁰.

$$m = m_0/(1 - v/c)^{1/2} \quad (1)$$

In equation 1, m_0 is the rest mass of the electron, v is the average electron speed and c is the speed of light (137 au); $(1 - v/c)^{1/2}$ is the relativistic correction. The average speed for a 1s electron at the nonrelativistic limit is Z au, where Z is the atomic number³⁰.

$$a_0 = (4\pi\epsilon_0)(h^2/me^2) \quad (2)$$

In equation 2, ϵ_0 is the permittivity of free space and e is the charge on the electron.

According to equations 1 and 2 the relativistic 1s contractions of Ge, Sn and Pb are 3%, 8% and 20%, respectively^{30b}. Because the higher shells have to be orthogonal to the lower ones, the higher ns -orbitals will suffer similar contractions^{30a}. The effect of relativity on the np orbitals is smaller than for the ns orbitals, since the angular momentum keeps p electrons away from the nucleus. The relativistic contraction of ns orbitals for the heavy elements stabilizes them as shown in Figure 2, having the largest effect for Pb, where the s - p energy difference of 8.93 eV is the largest in the series (Table 1).

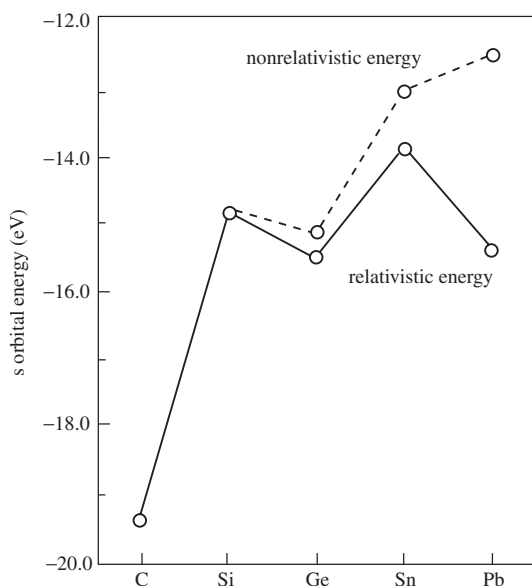


FIGURE 2. Stabilization of the valence ns orbital due to the relativistic effect. Reproduced by permission of Gordon and Breach Science Publishers from Reference 5

Wang and Schwarz have pointed out recently⁴⁶ that although the direct influence of the relativistic effect is in the vicinity of the nucleus, and thus is most important for the core electrons, the orbitals of the valence s electrons and to a lesser extent also those of the outer p electrons have ‘inner tails’ that penetrate the core. For this reason the valence electrons also experience a direct relativistic effect. Thus, although the probability of a valence electron to be close to the nucleus is small, the relativistic effects propagate to the outer valence shell and change also the energies of the valence orbitals. The d and f orbitals are not core-penetrating and they experience indirect relativistic destabilization, due to a more effective shielding by the contracted s and p shells, particularly those with the same quantum number as the d and f orbitals^{30,46–50}. The effects of relativity on orbital energies and on their radial extension affects the excitation energies, ionization potentials, electron affinities, electronegativity and atom polarizability, and through these properties influence the chemical bonding and reactivity of heavier group 14 elements.

The effect of relativity on various properties (e.g. ionization energies, electron affinity etc.) of the ‘eka-lead’ element 114 in comparison to the other group 14 elements was studied recently by Schwerdtfeger and coworkers^{48b}.

C. Hybridization

The major reason for the different structural behavior of compounds of the second period of the Periodic Table (i.e. Li to F) and those of higher periods is the relative radial extension of the valence s and p orbitals. For carbon, the radial extension of the 2s and 2p orbitals is almost the same (Figure 1). Thus hybridization, which requires the promotion of an electron from 2s to 2p, is very effective. In contrast, the 3p, 4p and higher period atomic orbitals are significantly ‘larger’ than the corresponding 3s, 4s and higher period orbitals, and consequently $\Delta r = r_p - r_s$ increases when moving down group 14 (Table 1). Hybridization is thus more difficult for the heavier elements of the group. This simple trend explains many striking phenomena in group 14 chemistry, such as, the ‘inert s-pair effect’, which states that the pair of s electrons is ‘inert’ and only the p electrons are employed in the bonding^{44,51}, and hence the preference of Pb (which has the largest Δr) to form divalent PbR_2 compounds rather than tetravalent PbR_4 compounds (see Section V.C.3).

Let us consider the two common oxidation states (II and IV) of group 14 elements. In divalent compounds (oxidation state II), the valence s orbitals of the heavy elements, the ‘inert pair’, are lone pairs with minor p contributions; the chemical bonds are formed primarily by p orbitals (one p orbital remains empty). In tetravalent compounds of heavier group 14 elements (Si \rightarrow Pb), the s-orbitals of the metal do contribute to the bonding⁵³. However, as hybridization is less effective for these elements than for C⁵², these elements have less tendency to form sp_n hybrids and they tend to keep the atomic s^2p^2 valence hybridization. However, as there are 4 bonds to be made, the s orbitals of the tetravalent group 14 metals (Si \rightarrow Pb) do contribute to the bonding⁵³. When localized molecular orbitals are used, the sp^n hybridizations of M in MH_4 show a strong decrease in n along the series: C > Si > Sn > Pb (Table 1), far from the values expected geometrically; e.g. the Pb–H bonds in PbH_4 adopt $sp^{1.8}$ hybridization although the geometry is tetrahedral⁴⁴. This causes poor spatial orbital overlap and deviations from the ‘ideal’ geometries, a phenomenon called ‘hybridization defect’⁶. Nevertheless, the s orbital contributions to the bonds are energetically more favorable than contributions from the larger and more diffuse p orbitals. By using a high contribution of the s orbital in the hybridization of tetravalent compounds, the heavy elements also keep electron density close to the nucleus as much as possible. Due to these large differences in the hybridization of

C and other group 14 elements, Kutzelnigg pointed out⁶ that the heavier main-group elements Si to Pb, actually exhibit ‘normal’ chemical behavior, while the behavior of the first-row elements Li to Ne is actually ‘exceptional’. According to this view, carbon should be considered as the ‘unusual’ member of group 14 elements rather than the prototype.

D. Electronegativity and Bonding

The decrease of electronegativity between carbon (2.5) and the other group 14 elements, whose electronegativities range between 2.02 and 1.55 (see Table 1)^{35a}, is of primary importance in affecting the different behavior of carbon and the other group 14 elements. The relative energies of the M–R σ bonds (M = C to Pb) are influenced by the relative electronegativity of M and R. As all M atoms are less electronegative than C, the M–R bonds are usually more ionic than the corresponding C–R bonds^{54,55}. For instance, electronegative R groups (such as OH, F) form stronger σ bonds to silicon and other group 14 elements than to carbon, due to the larger ionic contributions of the type $M^{+\delta}-R^{-\delta}$, in the metal compounds⁵⁶.

According to exchange equation 3 (see the discussion in Section V.B.1), for both electronegative and electropositive R the $\sigma(\text{Si}-\text{R})$ bond is stronger than the $\sigma(\text{C}-\text{R})$ bond⁵⁴. As M becomes heavier, the M–R bond strength decreases and the following M–R bond strength order was computed: $\text{C} \ll \text{Si} > \text{Ge} > \text{Sn} > \text{Pb}$ ^{45,55,57}. The ionic $M^{+\delta}-R^{-\delta}$ contributions to the M–R bonding do not change significantly down group 14, while the covalent bond strength decreases due to a smoothly reduced orbital overlap in the $\sigma(\text{M}-\text{R})$ bond⁵⁷.



E. Spin–Orbit Coupling

Another important factor in heavy element chemistry is spin–orbit coupling (SOC), i.e. the interaction between the electron spin and the orbital angular momentum. SOC is expected to be small for closed-shell species near their equilibrium geometries, and can therefore be neglected in thermochemical calculations for reactions that involve closed-shell molecules^{44,53}. However, as the atomic SOC increases with increasing atomic weight (Table 1), it must be taken into account in atomization and radical reactions, especially for Sn and Pb. SOC cannot be calculated with most *ab initio* programs and experimental values⁴¹ must be employed. In the case of group 14 atoms, the ^3P state splits into $^3\text{P}_0$, $^3\text{P}_1$ and $^3\text{P}_2$. To obtain the exact thermochemistry of reactions involving atomic species, e.g. atomization energies, the $^3\text{P}_0 \rightarrow ^3\text{P}_1$ energy difference must be added to the calculated atomic energies^{44,53}. These values are negligible for C and Si, but become important when tin and particularly lead are involved, reaching a value of 22.4 kcal mol^{−1} for Pb (Table 1).

F. The Role of d Orbitals

There is now a general consensus among theoreticians that d orbitals do not contribute significantly to bonding to silicon, and even less so to bonding to the heavier congeners^{58–60}. For example, the hybridization of SiF_6^{2-} is $\text{sp}^{2.62}\text{d}^{0.044}$.

IV. THEORETICAL METHODS

Below, we review briefly the methods used most commonly for calculating molecules of heavy group 14 elements. More details about the methods can be found in Reference 25, which give an overall view of the field, and in the more specific references given in the discussion below.

A. Nonrelativistic Theoretical Methods

The standard computational packages available today allow one to calculate, using a variety of theoretical methods (reviewed below), a large number of molecular properties such as structures, total energies, charge distribution, NMR chemical shifts, infrared and Raman frequencies and intensities, zero-point vibrational energies and more²⁵. These computer programs also make it possible to determine the nature of stationary points on the potential energy surface of a particular molecular system (from the number of imaginary frequencies) as being minima, transition states or higher saddle points.

The standard theoretical procedure for *ab initio* computations starts at the (nonrelativistic) Hartree–Fock (HF) level, and then adds electron correlation in subsequent calculations. The most frequently used approaches for including electron correlation are perturbation theory i.e. Møller–Plesset of *n*th order (MP*n*)^{25,61–64}, configuration interaction (CI) and coupled-cluster (CC) methods^{25,65–69}. These methods are systematic and at the high levels are highly reliable, reproducing geometries to within 0.5 pm in bond lengths, 0.5° in bond angles and energies to within 1 kcal mol⁻¹. The major drawback of all these treatments is that they require very large computer resources, and therefore the size of the system which can be studied by these methods is limited.

Density Functional Theory (DFT)^{70,71}, which includes electron correlation indirectly, requires only little more computer time than HF calculations and therefore these methods allow one to study quite reliably larger molecules. The B3LYP hybrid is the most popular DFT functionals to be used in recent years^{70,72}. The DFT-B3LYP method usually yields geometries and relative energies which are as good as those calculated by sophisticated correlated *ab initio* methods^{70,73}. The major disadvantage of the DFT methods is that they do not offer the rigor of the *ab initio* methods and do not allow systematic improvement of the theoretical method. DFT methods should therefore be applied with caution and should be tested against known experimental data for molecules similar to those being studied.

Ab initio and DFT calculations require basis sets to describe the wave functions of the molecule of interest. For compounds of carbon and silicon, the calculations usually employ all-electron basis sets. The most widely used are Pople’s basis sets, e.g. 6-31G(d) and 6-311G(d,p), but many other basis sets are available^{25,74–77}. The quality of a basis set mainly depends on the description of the valence region. The widely used 6-31G(d) basis set is of double- ζ quality (i.e. the valence region is split twice), while the 6-311G(d) basis set is of triple- ζ quality. Both basis sets include also sets of polarization functions on the heavy atoms and, in 6-311G(d,p), also on the hydrogens. In recent years several very good and reliable basis sets (i.e. of triple- ζ quality) have been developed for all elements through bromine⁷⁶.

To describe the computational procedure employed in a particular calculation, we will use the convenient designation introduced by Pople’s group^{25c}. In general, the computational procedure is designated as follows: [level 1/basis set 1]//[level 2/basis set 2]. Level 2 and basis set 2 are those that were used for optimizing the structure and level 1 and basis set 1 are those used to obtain the final total energy of the molecule. For example, a single point energy calculation using the MP4 method with a 6-311G(d,p) basis set which

uses the geometry obtained by geometry optimization that use the MP2 method with a 6-31G(d) basis set is designated MP4/6-311G(d,p)/MP2/6-31G(d).

Very large systems which cannot be studied even by DFT methods can be studied with semiempirical methods. MNDO and PM3 parameters are also available for all heavier group 14 elements: Si⁷⁸, Ge⁷⁹, Sn⁸⁰ and Pb⁸¹. However, as these parameters are based on experimental geometries, such calculations can be expected to give reasonably good results only for limited types of structures upon which the parametrization was based. As many group 14 elements adopt unusual structures, the reliability of semiempirical methods is limited; studying new types of structures using these methods may be highly risky.

B. Relativistic Methods

Relativistic methods are crucial for calculating accurately the properties of compounds of heavy elements and are therefore of special importance for Sn and Pb, although they are relevant also for Ge and in some cases even for Si compounds (Section III.B). A number of methods have been developed for incorporating relativistic effects in molecular electronic structure calculations^{30a,c,50b}. In principle, the Dirac equation^{30a} should be used to include relativity in a rigorous manner. However, a solution of the Dirac equation imposes much greater demands on the computing resources than the corresponding nonrelativistic treatment, and calculations on large molecules are prohibitively expensive. Nevertheless, efficient Dirac–Hartree–Fock (DHF) codes have been developed and results of systematic DHF calculations on small molecules are available^{30a,c,32,82}. Although these DHF calculations neglect electron correlation, they provide a standard for other calculations. An excellent overview on Dirac-based methods was published by Pyykkö^{30a}. Perturbation theory (PT) provides another approach for including relativistic effects^{83,84}.

C. Effective Core Potential Basis Sets

There are two basic problems with accurate calculation of compounds that contain elements from the third or higher rows of the Periodic Table: (a) Such systems have a large number of core electrons which in general are chemically inactive. However, in order to describe properly the chemically active valence electrons, it is necessary to use a large number of basis functions to describe also the inactive core electrons. This makes the computation highly CPU-time consuming and expensive. (b) In the lower part of the Periodic Table, relativistic effects must also be considered (see above), which makes a full-electron calculation prohibitive. The most convenient and most popular method for solving simultaneously both problems and making the computation of compounds with heavy elements feasible and relatively accurate is by employing effective core potentials (ECPs)^{34,85,86}. The basic strategy of the ECP method is to model the chemically inactive core electrons by an effective core potential and to treat only the valence electrons explicitly with high quality basis sets. The ECPs are optimized so that the solution of the Schrödinger or Dirac equations, using ECPs, will produce valence orbitals that match the orbitals calculated using all-electron basis sets. There are two different types of ECPs: (a) the model potential methods, which are fit to node-showing valence orbitals that are approximations to the all-electron valence orbitals⁸⁷; (b) the pseudopotential (PSP) methods which rely on the pseudo-orbital transformation (i.e. using nodeless valence orbitals)^{88–92}.

Relativistic effects are implemented in many ECPs and these are denoted RECPs. RECPs can be generated by several techniques^{34,86,93}, e.g. *ab initio* ECPs can be derived from the relativistic all-electron Dirac–Fock solution of the atom. Thus, the RECPs implicitly include the indirect relativistic effects of the core electrons on the radial distribution of the valence electrons⁹⁴. The use of RECPs therefore enables one to carry out

calculations within traditional nonrelativistic schemes, yet incorporating relativistic effects. A comparison of calculations performed with relativistic and nonrelativistic pseudopotentials allow one to evaluate the magnitude and the importance of relativistic effects^{44,53}.

In general, for heavier elements, ECPs enable a better description of the valence space than the smaller basis sets typically used in all-electron treatments, since no basis functions are needed to describe the core region and high quality basis sets can be applied for the valence electrons. However, ECPs do not describe properly the polarization of the core electrons and the valence–core correlation. This problem can be avoided by using ECPs in which some of the core electrons are included in the valence space, i.e. including the $(n - 1)$ d subshell in the valence space^{87–89}, but this trick increases the number of electrons calculated explicitly and reduces the advantages of the ECP method. Thus, for compounds of germanium (as well as compounds of other elements of the third row, i.e. K to Br), it is better to use high quality all-electron basis sets than to use ECPs. For heavier elements the use of ECPs becomes a practical necessity, except for very small molecules.

D. Methods for Analysis of the Electronic Structure

Important information about the molecules of interest can be deduced from an analysis of the wave function, the electron distribution, hybridizations at the various atoms etc. The traditional Mulliken atomic charges are still often used, but as these charges are not very reliable⁹⁵ most of the more recent studies use two newer methods: the atoms-in-molecules procedure ('Bader analysis')^{96–99} and the natural population analysis (NPA), based on a Löwdin transformation of the canonical molecular orbitals [i.e. the natural bond orbital (NBO) analysis]^{100,101}. Beside being a useful tool in evaluating charge distributions, the NBO analysis has a much broader use for analyzing the nature of the bonding in the molecule. This analysis is used to evaluate a variety of electronic characteristics such as NPA, atomic hybridization, energetic consequences of conjugation, bond orders and the various Lewis structures (i.e. resonance structures) that form the total molecular structure [using the natural resonance theory (NRT)]¹⁰².

V. SINGLY BONDED COMPOUNDS

A. MH₄ (metallanes)

1. Geometries, ionization potentials and nuclear spin–spin couplings

Table 2 presents the M–H bond lengths in MH₄ as calculated using a wide variety of theoretical levels, allowing one to compare their performance and reliability. The tetrahedral MH₄ molecules were first computed in 1974 within the relatively crude spherically symmetric one-center Hartree–Fock approximation by Desclaux and Pyykkö³¹, who found that relativistic effects shorten the M–H bond lengths by 0.6%, 2.3% and 5.6% for GeH₄, SnH₄ and PbH₄, respectively. Despite the crudeness of the 'spherical approximation', the experimental M–H bond lengths of GeH₄ and SnH₄ were reproduced quite well (Table 2). Unfortunately, the experimental geometry of plumbane, the most interesting compound in the series, was and remains unknown.

Almlöf and Faegri computed the MH₄ [and M(CH₃)₄] series¹⁰⁴ at the Hartree–Fock level with very large all-electron basis sets and relativistic first-order perturbation theory. In general they obtained very good agreement between the calculated and experimental M–R (R = H, Me) distances for M = C to Sn (Table 2). They also found relativistic bond shortening [of up to 10 pm (*ca* 6%) in PbH₄] and obtained a Pb–H bond

TABLE 2. Calculated M–H bond lengths (in pm) in MH₄ at various levels of theory, basis sets or ECPs

M	Dyall and coworkers ^a							AREP ^b		AIMP ^c		CPP ^l	DHF2 ^m	
	exp. ^d	D&P ^e	A&F ^f	NR ^g	DHF ^h	PT ⁱ	HW ^j	CC ^k	ECP1	ECP2	MP1			MP2
C	108.6	109.9	108.3	108.2	108.2	108.2							108.6	
Si	147.5	157.2	148.2	147.8	147.7	147.7	146.0				147.7		148.0	148.7
Ge	152.0	158.6	152.1	153.2	152.5	152.4	153.2	153.4	151.6	161.6	152.8	152.6	152.9	155.7
Sn	170.0	176.2	170.5	172.7	170.6	170.6	169.9	170.8	168.9	170.4	170.9	171.2	170.3	173.3
Pb	175.4 ⁿ	179.7	170.3	181.5	174.2	174.1	171.7	173.2	173.9	176.4	173.6	174.4	174.4	173.5

^aFrom Reference 32.

^bHF calculations with averaged relativistic core potentials (AREP). ECP1: only the *ns* and *np* electrons are included in the valence space (i.e. 4-valence electrons); ECP2: the (*n* – 1)*d* subshell is also included in the valence space (i.e. 14-valence electrons); from References 88 and 89.

^c*Ab initio* core model potential (AIMP) calculations (SCF). MP1: 4-valence electrons; MP2: the (*n* – 1)*d* subshell is also included in the valence space (i.e. 14-valence electrons); from Reference 103.

^dExperimental equilibrium distances *r*_e, estimated from experimental *r*₀ values; from Reference 32.

^eSpherical approximation (Desclaux and Pyykkö, Reference 31).

^fFirst-order perturbation theory (Almlöf and Faegri, Reference 104).

^gNonrelativistic HF; from Reference 32.

^hRelativistic Dirac–Hartree–Fock; from Reference 32.

ⁱPerturbation theory, including relativistic effects without the contribution of spin–orbit coupling; from Reference 32.

^jHF calculations with Hay and Wadt pseudopotentials; from Reference 90.

^kCCSD(T) calculations with Hay and Wadt pseudopotentials; from Reference 105.

^lCore polarization pseudopotentials, by Stoll and coworkers (4-valence electrons); from Reference 106.

^mDirac–Hartree–Fock calculations by Visser and coworkers; From Reference 82.

ⁿEstimated using the equation $r_e(\text{PbH}_4) = r_e(\text{PbH}) \times r_e(\text{SnH}_4)/r_e(\text{SnH})$; From Reference 31.

length of 170.3 pm. In the early 1990s, all-electron Dirac–Hartree–Fock (DHF) computer programs were developed and applied to the MH₄ series^{32,82}, showing excellent agreement with the experimental M–H bond lengths. At DHF the Pb–H bond length in PbH₄ is 174.2 pm, by 3.9 pm longer than the value calculated by first-order perturbation theory¹⁰⁴. According to the DHF calculations, the relativistic contractions of the Pb–H and Sn–H bonds are 7.3 pm and 2.1 pm, respectively (Table 2). Schwerdtfeger and coworkers analyzed in more detail the effect of relativity and spin–orbit coupling on the orbital energies and on the bond length contraction in lead compounds¹⁰⁷. They concluded that the relativistic bond contraction in PbH_{*n*} systems is dependent on the degree of the Pb 6*s*-orbital participation in the M–H bond, i.e. the relativistic contractions in *r*_e(Pb–H) are 4 pm for PbH⁺, PbH and PbH₂ and 7 pm for PbH₄ (which has the highest contribution of the 6*s* orbital in the Pb–H bonds). The molecular spin–orbit coupling contributions in the PbH_{*n*} series were calculated to be only 10–20% of the atomic corrections, and to have practically no influence on molecular geometries¹⁰⁷. However, as the contribution of the experimental atomic spin–orbit coupling to the energy of lead is quite large, 22.4 kcal mol^{–1} (Table 1)⁴¹, this effect should be included when thermodynamic stabilities of Pb–H compounds are calculated (see below).

The ionization energies of the ‘relativistic’ Pb 6*s* electrons were found to be much higher than those calculated using nonrelativistic pseudopotentials, e.g. the ionization energy increases by 4.7 eV (Pb³⁺) and 3.7 eV (Pb²⁺), due to relativity¹⁰⁷. This results from the relativistic contraction of the 6*s* orbital which is about 12% for the neutral Pb atom¹⁰⁷.

Relativistic effects have also a strong effect on the nuclear spin–spin coupling constants in the NMR spectra of MH₄ and Pb(CH₃)₃H. The relativistic effect on the spin–spin

coupling is significant both for coupling with the heavy atom itself [$J(M,H)$] and also for the two-bond [$J(H,H)$] couplings through the heavy atom. Even in GeH_4 the relativistic increase in the coupling constants is 12%, and for PbH_4 it amounts to as much as 156% for a one-bond coupling¹⁰⁸.

2. Bond energies

The stepwise dissociations of the MH_n series received significant attention^{109–113} due to their importance in the semiconductor industry. The available information is listed in Table 3. Several experimental and theoretical investigations have addressed the stepwise dissociation of neutral GeH_n species, and the various Ge–H bond energies are now known with reliable accuracy^{114–117} (Table 3). These bond energies are similar to those of the corresponding SiH_n series^{118–120}, but are remarkably different from those of CH_n ^{72b,121–123}. Direct calculations or experimental measurements of the stepwise dissociation energies of SnH_4 and PbH_4 are still not available, but the individual Sn–H bond energies have been estimated from the Si and Ge values^{116,124a}.

Moving down the period for a particular MH_n series, the M–H bond energy decreases; e.g. for MH_4 (kcal mol^{-1} , Table 3), 104 (C) > 90 (Si) > 85 (Ge) > 72 (Sn).

The bond energies of neutral and cationic GeH_n and SiH_n species exhibit a ‘zig-zag’ pattern as a function of n ¹¹⁴ (Table 3). For example, the Ge–H bond energy decreases

TABLE 3. Stepwise bond dissociation energies (BDE, kcal mol^{-1}) for MH_n

	MH_4	MH_3	MH_2	MH
		C		
exp. ^a	103.2	109.0	100.2	80.0
calc. ^b	104.1	110.6 ^c	98.0 ^c	80.6
		Si		
exp. ^d	88.8 ± 1.6	69.6 ± 2.1^e 72.5 ± 2.1^e	72.6 ± 1.4^e 75.6 ± 1.4^e	68.7 ± 0.7
calc. ^f	90.1	71.0	74.1	67.4
		Ge		
exp. ^g	$<82 \pm 2$	>59	<66	>63
calc. ^h	84.8	58.0	68.5	63.8
calc. ⁱ	85.2	56.9	69.2	63.2
		Sn		
est. ^j	71.6	51.5	58	55 ^k

^aFrom Reference 121. For additional experimental values see References 122 and 123. The stepwise BDEs (kcal mol^{-1}) of CH_4^+ , CH_3^+ , CH_2^+ and CH^+ are 128.8, 196.2, 175.8 and 148.2, respectively.

^bAt G2(MP3); from Reference 123b.

^cFor triplet CH_2 .

^dPhotoionization study; from Reference 120.

^eThe two alternative values are based on two different adiabatic IPs of SiH_2 (1A_1); from Reference 120.

^fAt MP4/6-31G*/HF/6-31G*; from Reference 119.

^gPhotoionization study; from Reference 116, see also Reference 117.

^hAt MP4/HF, using a Dunning all-electron basis set + d-polarization function; from Reference 115.

ⁱAt CASSCF/SOCI/MRSDCI. The stepwise BDEs (kcal mol^{-1}) of GeH_4^+ , GeH_3^+ , GeH_2^+ and GeH^+ are: 15.2, 82.2, 37.9 and 68.0, respectively; from Reference 114.

^jEstimated from SiH_n and GeH_n bond energies; from Reference 116.

^k53 kcal mol^{-1} using a relativistic ECP¹²⁴.

from GeH_2 to GeH_3 , while it increases from GeH to GeH_2 and from GeH_3 to GeH_4 . Similar alterations occur for the GeH_n^+ cations, but in the opposite direction; i.e. the Ge–H bond energies follow the order: $\text{GeH}_4^+ < \text{GeH}_3^+ > \text{GeH}_2^+ < \text{GeH}^+$ (Table 3). These trends have been understood as follows: MH_4 , MH_2 , MH_3^+ and MH^+ have closed-shell ground states; therefore, the M–H bonds are more difficult to break. The second dissociation energy of MH_4 (or any MR_4) is always smaller than the first one, since the stable MH_2 (or MR_2) species are formed. This difference between the first and second dissociation energies was defined by Walsh as the ‘Divalent State Stabilization Energy’ (DSSE, equation 4)¹²⁵ (see also Sections V.E.1.a, VI.B.3 and VII.A.3).

$$\text{DSSE}(\text{MR}_2) = D(\text{R}_3\text{M-R}) - D(\text{R}_2\text{M-R}) \quad (4)$$

3. The stability of MH_4 relative to $\text{MH}_2 + \text{H}_2$

Systematic studies of reaction energies for the abstraction of H_2 from MH_4 (equation 5) for $\text{M} = \text{Si, Ge, Sn and Pb}$ were reported by Dyal who also compared the results of the DHF calculations with those of other methods (ECP, PT)¹²⁶, by Schwerdtfeger and coworkers^{48b} who included also the ‘eka-lead’ element 114 and by Thiel and coworkers¹⁰⁵ who studied also the activation barriers for this reaction. More recent computations concentrated on the evaluation of the quality of the various theoretical approaches^{103,106}. The results of the calculations are collected in Table 4 and are shown graphically in Figure 3a.



The DHF results¹²⁶, as well as the CCSD(T)/DZ+d (with inclusion of relativistic effects for Ge, Sn and Pb) results¹⁰⁵, indicate that the stability of the tetrahydrides with respect to the corresponding dihydrides and H_2 (equation 5) decreases significantly down group 14 and the reaction becomes exothermic for PbH_4 (Table 4 and Figure 3a); i.e. ΔE (equation 5, at CCSD(T)/DZ+d, kcal mol^{-1}) = 57.7 (Si), 36.1 (Ge), 15.6 (Sn) and

TABLE 4. Calculated reaction energies (ΔE) and activation energies (E_a) for equation 5 at various levels of theory^a

	ΔE^b							E_a	
	NR ^c	PT ^d	DHF ^e	HW ^f	ECP1 ^g	ECP2 ^h	AIMP ⁱ	CCSD(T) ^j	CCSD(T) ^j
Si	56.7	56.4	56.1					57.7	62.7 (55.9 ^k)
Ge	39.9	36.9	36.8	41.5	39.0	40.9	41.7	36.1	56.4 (54.3 ^k)
Sn	27.0	22.6	19.2	23.2	23.8	20.3	21.6	15.6	53.3
Pb	18.0	3.3	−9.8	−1.8	−4.5	−11.1	−2.2	−7.7	45.3

^aAll energies are in kcal mol^{-1} and they include corrections for ZPEs.

^bFrom Reference 126, unless stated otherwise.

^cnonrelativistic Hartree–Fock (NR).

^dPerturbation theory (PT).

^eDirac–Hartree–Fock (DHF).

^fPseudopotentials by Hay and Wadt⁹⁰.

^gECP1: 4-valence electrons^{88,89}.

^hECP2: ($n - 1$)d subshells are included in the valence space, i.e. 14-valence electrons^{88,89}.

ⁱQuasi-relativistic *ab initio* core model potential calculations (SCF level): the ($n - 1$)d subshell is included in the valence space (i.e. 14-valence electrons). The reaction energies do not include ZPE; from Reference 103.

^jUsing Hay and Wadt pseudopotentials; from Reference 105.

^k Experimental; from Reference 127.

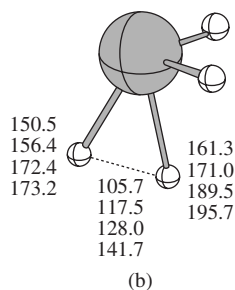
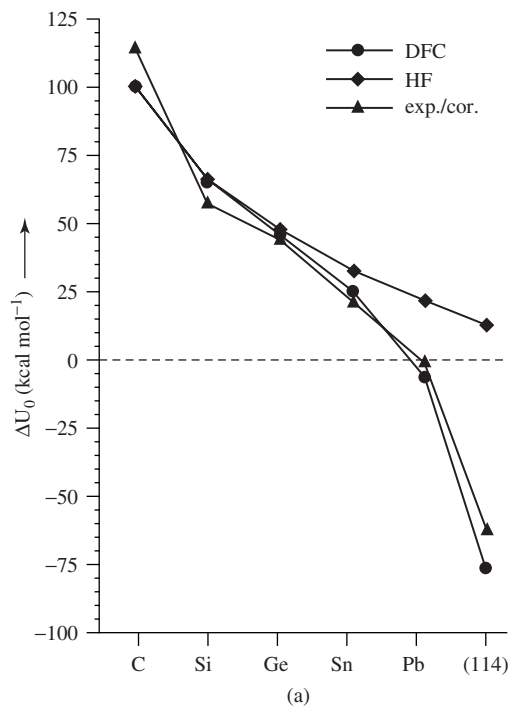


FIGURE 3. (a) Calculated decomposition energies, ΔU_0 (in kcal mol⁻¹) for equation 5. DFC: relativistic Dirac–Fock calculations; HF: nonrelativistic HF calculations; exp./cor.: the values for C and Si are experimental, for Ge and Sn they are MP2/ECP values and for Pb, QCISD(T)/ECP values. (114) is element 114 ('eka-lead'). Adapted from Reference 48b. (b) Calculated geometries of the transition state for the dissociation reaction: $MH_4 \rightarrow MH_2 + H_2$. Bond lengths (pm) are given in the order M = Si, Ge, Sn and Pb¹⁰⁵

-7.7 (Pb)¹⁰⁵ (similar values were obtained by the DHF method¹²⁶, see Table 4). For all heavier group 14 elements, the reaction energies are dramatically lower than for CH₄ (117 kcal mol⁻¹¹²⁸). The relativistic stabilization of the s orbitals of M = Pb and Sn is more pronounced in MH₂, which have a higher s occupation, than in the corresponding MH₄, causing a significant relativistic decrease in the energy of equation 5, of 27.8

and 7.8 kcal mol⁻¹ for M = Pb and Sn, respectively¹²⁶. Furthermore, the contribution of molecular spin-orbit coupling to the dissociation energy of PbH₄ is -7 kcal mol⁻¹^{107,126} relative to only -1 kcal mol⁻¹ for SnH₄¹²⁶. The inclusion of relativistic effects and spin-orbit coupling reduces the energy of equation 5 by 28.1 kcal mol⁻¹ for M = Pb¹⁰⁷.

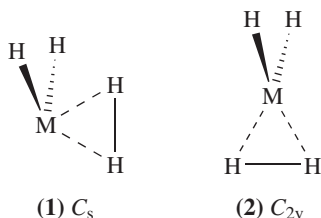
The activation barriers for the dissociation of MH₄ (E_a , equation 5) also decrease in the order Si (62.7) > Ge (56.4) > Sn (53.3) > Pb (45.3) (kcal mol⁻¹)¹⁰⁵. The optimized transition structures for reaction 5 are shown in Figure 3b¹⁰⁵. The barrier for the decomposition of PbH₄, of 45.3 kcal mol⁻¹, is sufficiently large to allow its observation despite the fact that the dissociation reaction is exothermic. To support the search for plumbane (and methylplumbane), their IR vibrational spectra along with the spectra of their lower congeners were computed¹⁰⁵. The IR spectrum of PbH₄ in the gas phase was indeed recently reported¹²⁹.

Reaction 6, the elimination of MH₂ from H₃MCH₃, exhibits a similar trend in the reaction energies and activation barriers. The reaction energy decreases with increasing the atomic number of M, but the endothermicity is smaller than for MH₄, i.e. ΔE (equation 6, in kcal mol⁻¹): 54.0 (Si); 30.3 (Ge); 9.3 (Sn) and -15.3 (Pb)¹⁰⁵. Consequently, the reverse reaction, i.e. the insertion of MH₂ into a C-H bond, is less exothermic and less facile than the insertion of MH₂ into an H-H bond^{105,130,131}. A detailed discussion of the mechanism of the insertion reactions of MR₂ is given in Section VII.A.3.b.

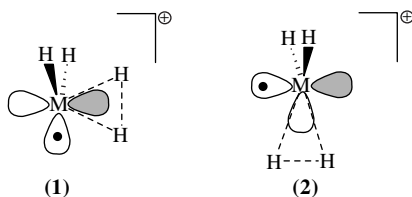


4. Charged MH₄ species: MH₄⁺ and MH₄²⁺

Unlike the tetrahedral MH₄, the MH₄⁺ cations have Jahn-Teller distorted structures. At MP2/DZP a H₂M⁺ ··· H₂ (M = Si to Pb) ‘side-on’ C_s complex (**1**) was located as the global minimum. At this level the C_{2v} ‘head-on’ structure (**2**) is by 10, 14, 20 and 24 kcal mol⁻¹ less stable than the ‘side-on’ C_s structure^{132,133} for M = Si, Ge, Sn and Pb, respectively.



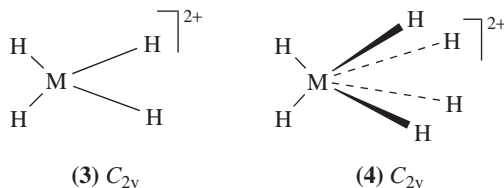
The C_{2v} and C_s structures can be regarded as arising from electron transfer from H₂ to the electron-deficient MH₂⁺ unit. MH₂⁺ is a good acceptor using its empty p orbital in the ‘side-on’ C_s structure (**1**) as shown in Figure 4. In order to form the C_{2v} ‘head-on’ structure (**2**), an electron has to be promoted from the singly-occupied s orbital of MH₂⁺ to its empty p orbital, exciting the MH₂⁺ from the ²A₁ state to the ²B₁ state (Figure 4). This is why **1** is more stable than **2**. As M becomes heavier, the energy difference between **1** and **2** increases following the increase in the ²A₁ → ²B₁ excitation energies as M becomes heavier¹³³. However, this analysis might be premature as it was later found to be dependent on the computational method. Geometry optimization of GeH₄⁺ at MRS-DCI/CASSCF reveals that **1**, M = Ge collapsed without a barrier to **2**, M = Ge¹¹⁴. The

FIGURE 4. $\text{H}_2\text{M}^+ \cdots \text{H}_2$ complexes: 'Side-on' C_s (1) and 'head-on' C_{2v} (2)

strong dependence of the structure on the computational method indicates that $\text{H}_2\text{Ge}^+ \cdots \text{H}_2$ is a loose complex with a flat potential energy surface. The flatness of the PES was also demonstrated by the nearly barrierless rotation of the H_2 ligand in SnH_4^+ and PbH_4^+ , giving rise to two C_s structures of type **1**, which have essentially the same stability¹³³.

The dissociation energy of MH_4^+ into MH_2^+ and H_2 decreases down group 14^{132,133}, requiring 14 (SiH_4^+), 8 (GeH_4^+), 5 (SnH_4^+) and 3.6 (PbH_4^+) kcal mol⁻¹, and it occurs without an activation barrier for all M ^{132,133}. The dissociation of GeH_4^+ to form GeH_3^+ and H is much more endothermic (25.5 kcal mol⁻¹)¹¹⁴. MR_4^+ cations with $\text{R} =$ alkyl rather than hydrogen were observed for $\text{M} = \text{Sn}$ and Pb ¹³⁴.

The MH_4^{2+} dications are planar (C_{2v} -symmetry, **3**) with two short and two long $\text{M}-\text{H}$ bonds; the latter represent 3-center-2-electron bonding between H_2 and MH_2^{2+} . CH_4^{2+} is strongly bound with $r(\text{MH}_2 \cdots \text{H}_2)^{2+} = 112.9$ pm, while significantly longer distances of 184.6 pm and 197.2 pm were calculated for $\text{M} = \text{Si}$ and Ge , respectively, which is consistent with their considerably smaller binding energies. The calculated dissociation energies of the MH_4^{2+} series into H_2 and MH_2^{2+} are 103.7 (CH_4^{2+}), 32.0 (SiH_4^{2+}) and 28.3 (GeH_4^{2+}) kcal mol⁻¹ [B3LYP/6-311++G(2df,2pd)]¹³⁵, considerably higher than the corresponding dissociation energies of MH_4^+ . The much weaker complexation energies of H_2 to MH_2^{2+} for $\text{M} = \text{Si}$ and Ge than for $\text{M} = \text{C}$ are explained by their superior ability to accommodate a positive charge, due to their lower electronegativities and higher polarizabilities, relative to $\text{M} = \text{C}$. A similar trend of the dissociation energies was calculated for the dissociation of MH_6^{2+} (**4**, $\text{M} = \text{C}, \text{Si}, \text{Ge}$) to $\text{MH}_4^{2+} + \text{H}_2$ ¹³⁵.



B. Mono-substituted Singly-bonded MH_3R Metallanes

Two important comprehensive studies of mono-substituted singly-bonded group 14 compounds of type MH_3R were carried out by Basch and Hoz^{45,136}. Their extensive CCSD(T), B3LYP and MP4//MP2 computations encompassed a very large set of H_3MR molecules ($\text{M} = \text{C}$ to Pb), where R spans over 50 different substituents (e.g. CH_3 , SiH_3 , GeH_3 , SnH_3 , PbH_3 , OH , SH , halogens, pseudohalogens, CHO , COOH , CN , NH_2 , NO_2 etc.). These authors have also summarized the available experimental data and previous theoretical publications on similar group 14 compounds. $\text{M}-\text{R}$ bond distances⁴⁵, $\text{M}-\text{R}$

bond dissociation energies^{45,136}, Mulliken charges and other molecular properties⁴⁵ were discussed in great detail. Thus, these extensive studies can be regarded as an *ab initio* database, which compares various levels of theory and, when available, also experimental data, for simple group 14 compounds. The discussion below is based to a large extent on these two studies and the reader is referred to the original papers for additional data and discussion^{45,136}. Of the wide variety of MH₃R molecules that were studied by Basch and Hoz, we will discuss briefly mainly MH₃R compounds with R = halogen and R = M'H₃ (M' = group 14 element).

1. General trends in the M–R bond dissociation energies

The M–R bond dissociation energies (BDEs) are defined in equation 7. Several factors cause imbalance in the theoretical description of the two sides of the equation and thus affect the reliability of the calculated BDEs. One factor is the purity of the calculated spin states of the radicals, MH₃ and R. The closer the method is to a full configuration interaction description, the less important is the initial extent of spin contamination at the UHF level. In DFT methods, spin contamination is generally found to be less important. When the spin contamination is small ($\langle S^2 \rangle$ value close to 0.75), the CCSD(T) method has little advantage over the MPn methods. However, when the calculated UHF spin contamination is large (e.g. in radicals containing double bonds), the CCSD(T) results show considerable improvement over the MPn values. The CCSD(T) values usually underestimate the BDEs. The DFT-B3LYP methods [either with all-electron basis sets or with core effective potentials (CEPs)] give binding energies that are even lower than the CCSD(T) values¹³⁶. A second potential theoretical imbalance in equation 7 is the number and type of multiple bonds on both sides of the equation.



The trends in the M–R BDEs in going down group 14 were divided into three groupings⁴⁵: (1) R substituents, referred to as 'covalent'-type, for which the BDEs decrease steadily from M = C to M = Pb, e.g. R = H, M'H₃ (these compounds will be discussed in the subsequent section), BH₂, AlH₂, PH₂; (2) R substituents, referred to as 'ionic'-type, which reveal a significant increase in the BDEs between C and Si and then steadily decrease from Si to Pb, e.g. R = halogens, NH₂, OH, SH (the calculated and the available experimental BDEs for this group of substituents are given in Table 5); (3) substituents which obey the trends in (1) or (2) above but reveal an increase (or no change) in the BDEs on going from Sn to Pb, e.g. R = CHO, NO₂. The following M–R BDEs (kcal mol⁻¹) were calculated at

TABLE 5. Calculated^a and experimental^b (in parentheses) M–R bond dissociation energies (kcal mol⁻¹) in H₃MR

M	R					
	F	Cl	Br	NH ₂	OH	SH
C	103.2 (112.8)	76.5 (83.5)	66.5 (70.6)	78.3 (84.7)	85.9 (92.5)	69.2 (74.6)
Si	142.7 (160; 153)	99.2 (108; 110)	84.8 (92; 90)	95.6 (100.0)	116.2	81.1
Ge	122.7	89.4	77.3	79.9	97.2	72.5
Sn	117.7	87.6	76.3	72.4	90.6	69.1
Pb	111.3	86.2	75.3	68.8	85.2	67.9

^aAt CCSD(T)/CEP-TZDP+//MP2/CEP-TZDP, a set of diffuse sp functions was added to all atoms except hydrogen (denoted by the ++ sign); from Reference 136.

^bExperimental values are from Reference 45 and Chapter 4 by R. Becerra and R. Walsh in Reference 9.

CCSD(T)//MP2 (using a TZP basis set for the valence electrons and CEPs and relativistic CEP for the core electrons of Sn and Pb; experimental values are given in parentheses) for these substituents: R = CHO: 79.5 (83.4) (C); 65.1 (Si); 57.5 (Ge); 49.5 (Sn); 48.7 (Pb); R = NO₂: 57.3 (60.6) (C); 61.2 (Si); 52.0 (Ge); 47.6 (Sn); 48.6 (Pb).

The bond dissociation energies correlate very well with the electronegativity difference between M and R. For a given M the bond dissociation energies decrease with a decrease in the electronegativity of R, while for a given R the BDE increases from C to Si and then decreases steadily on moving down group 14 (Table 5). A similar relationship is found between the heats of the exchange reaction between H₃MR (M = Si to Pb) and H₃C-R (equation 3, Section III.D) and the Allred-Rochow electronegativity of R, as shown in Figure 5. Figure 5a, which compares the Si-R BDEs to those of C-R, reveals

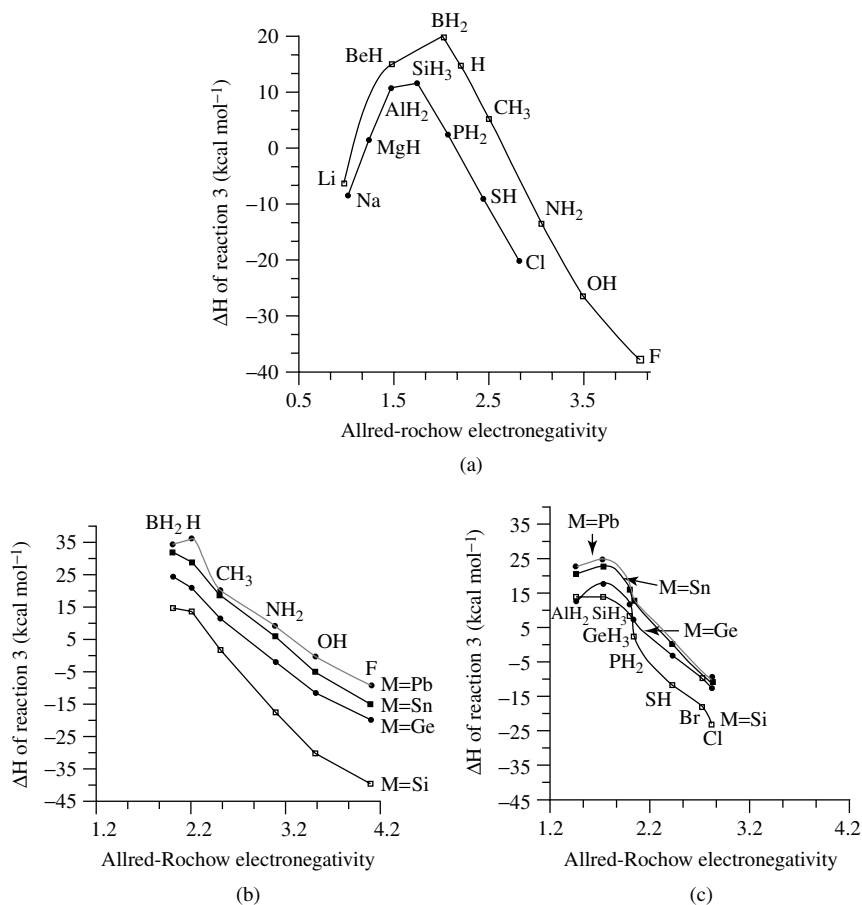


FIGURE 5. Calculated energies for the exchange reaction of equation 3, plotted vs. the electronegativity of R. (a) For M = Si, R = H, Li to Cl [at MP4/6-31G(d)//HF/3-21G(d)]. (b) For M = Si to Pb, R = H, B to F (at MP4/TZDP+//MP2/TZDP). (c) For M = Si to Pb, R = Al to Cl, GeH₃ and Br (at MP4/TZDP+//MP2/TZDP). (a) is adapted from Reference 54. (b) and (c) are plotted by us from the data given in Reference 45

two inverted V-shaped curves⁵⁴, one for the first-row and the other for the second-row substituents R. All the Si–R bonds that are below the zero-energy line in Figure 5a are stronger than the corresponding C–R bonds, and vice versa (this is also valid in Figures 5b and 5c). Particularly remarkable are the much stronger Si–R bonds compared to C–R bonds for R = F, Cl and OH, i.e. by 38, 20 and 27 kcal mol⁻¹, respectively⁵⁴. Figures 5b and 5c show the relative M–R and C–R bond energies for all M atoms over the entire range of the standard first- and second-row substituents. For R substituents of both the first- and second-row atoms the Si–R bonds are stronger than all other M–R bonds. The relative M–R bond strength decreases as M becomes heavier. For example, the Si–OH bond is stronger by *ca* 28 kcal mol⁻¹ than the C–OH bond in H₃COH; in contrast, the Pb–O bond in H₃PbOH is by *ca* 2 kcal mol⁻¹ weaker. The larger the difference in the electronegativity between M and R, the stronger is the M–R bond, due to a larger contribution from ionic structures (see also below).

2. MH₃R, R = halogen

a. Geometries. The calculated and experimental M–R (R = F, Cl, Br, I) bond lengths are given in Table 6. Experimental structures in the gas phase are known for the entire set of compounds, except for H₃SnF and the plumbyl halides. As seen in Table 6, the calculated bond lengths, using effective core potentials at both the HF and MP2 levels, are in good agreement with experimental gas-phase values. The HF/ECP calculations are of similar quality to the all-electron HF calculations of molecules with first-row atoms¹³⁷, giving confidence in the effective core potentials that were used.

b. M–R bond dissociation energies. The M–R, R = halogen, bond dissociation energies are given in Table 5. The trends in their bond dissociation energies were discussed

TABLE 6. Calculated and experimental (in parentheses) M–R (R = F, Cl, Br, I) bond lengths (pm) in MH₃R^a

H ₃ M	R			
	F	Cl	Br	I
H ₃ C	136.5 ^b	177.7 ^b	195.7 ^b	215.0 ^b
	140.0 ^c (138.2)	179.6 ^c (177.8)	194.4 ^c (193.3)	213.2 (213.2)
H ₃ Si	157.7 ^b	204.2 ^b	222.9 ^b	244.6 ^b
	161.9 ^c (159.3)	207.0 ^c (204.9)	223.4 ^c (221.0)	243.7 (243.7)
H ₃ Ge	169.7 ^b	215.5 ^b	233.3 ^b	254.1 ^b
	173.8 ^c (173.5)	217.1 ^c (215.0)	232.1 ^c (229.9)	250.9 (250.9)
H ₃ Sn	184.0 ^b	233.6 ^b	250.3 ^b	270.8 ^b
	191.0 ^c	235.0 ^c (232.8)	249.6 ^c (246.9)	267.5 (267.5)
H ₃ Pb	202.0 ^b	246.6 ^d		
	202.6 ^c	241.4 ^c	254.9 ^c	

^aExperimental values are from Reference 137.

^bHF/ECP; from Reference 137.

^cMP2/CEP-TZDP (for the valence electrons) for M = C, Si and R = F and MP2/RCEP (TZDP for the valence electrons) for all heavier elements; from Reference 45.

^dHF/ECP; from Reference 44.

above along with other R substituents. Here we discuss in more detail the nature of the M–Cl bonds in H_3MCl , which were the focus of two recent papers^{55,57}. Both studies show, in agreement with earlier investigations^{45,136}, that the BDE of M–Cl follows the trend: $\text{C} \ll \text{Si} > \text{Ge} > \text{Sn} > \text{Pb}$ (i.e. group 2 above, Table 5). Bickelhaupt and coworkers⁵⁷ analyzed the M–Cl bonding mechanisms by the extended transition state method¹³⁸ which uses density functional component analysis. Their analysis shows that the sharp increase in the BDEs from $\text{M} = \text{C}$ to $\text{M} = \text{Si}$ results from the increase in the electronegativity difference between Si and Cl. They associated the monotonic decrease from $\text{M} = \text{Si}$ to $\text{M} = \text{Pb}$ to a balance between an orbital interaction term and a steric repulsion term (Pauli repulsion), i.e. to a decrease in the bond overlap between the singly occupied orbitals of the MH_3 and Cl fragments in combination with the decrease in the Pauli repulsion⁵⁷. A different approach, which uses VB theory to analyze the M–Cl bond strength, was provided by Shaik and coworkers⁵⁵. These authors defined a new class of chemical bonds, ‘charge-shift’ bonds, where all or most of the bond energy is provided by the resonance between the covalent and ionic structures. ‘Charge-shift’ bonds are not necessarily associated with bond polarity and exist among homonuclear as well as heteronuclear bonds. The VB analysis of Shaik and coworkers shows that the contribution of the covalent bonding to the total bond energy is relatively small for all M atoms and becomes smaller monotonically on going from Si to Pb, i.e. the appropriate M–Cl covalent contribution to the bonding is 39.9, 33.9, 26.6 and 17.4 kcal mol⁻¹ for Si, Ge, Sn and Pb, respectively. According to this analysis the covalent bond energy is a balance between the interaction energy due to spin exchange and a nonbonded repulsive interaction between the M–Cl and M–H bonding electrons and the lone-pair electrons on the Cl atoms (very similar to the conclusion of Bickelhaupt and coworkers⁵⁷). The low covalent bond energies mean that the much higher M–Cl BDEs of 80.1 (M = C), 102.1 (M = Si), 88.6 (M = Ge), 84.6 (M = Sn) and 76.3 (M = Pb) kcal mol⁻¹ arise from resonance between the covalent $\text{H}_3\text{M}-\text{Cl}$ and ionic $\text{H}_3\text{M}^+\text{Cl}^-$ VB structures. This resonance energy is largest when the gap between the energy minima of the ionic and covalent structures is smallest, i.e. for the most stable charged structure. The positive charge localization in MH_3^+ appears to be a key factor leading to ‘charge-shift’ bonds with strong bonding energies. The charge localization property exhibits a ‘saw-tooth’ behavior: it is small for C, rising to a maximum for Si and then alternating down and up from Ge to Pb. The origin of this alternating behavior is associated with the transition metal contraction due to imperfect screening of the $3d^{10}$ shell in Ge and the lanthanide and relativistic contractions in Pb (see also Sections III.A and III.B and Figures 1 and 2). These two effects cause a zig-zag variation in the electronegativities of M (Table 1) and in the charge localization on MH_3^+ . Thus, H_3Si^+ is the cation with the highest charge localization, leading to the strongest Si–Cl bond, and CH_3^+ with the highest charge delocalization leads to the second weakest M–Cl bond. ‘Charge-shift’ bonding is manifested also in the tendency of Si and Sn (and less so of Ge and Pb) to form hypercoordinate compounds⁵⁵.

3. Ethane analogs

a. Geometries and rotational barriers. Calculated M–M’ bond lengths, where both M and M’ are group 14 elements, at various levels of theory are given in Table 7. Earlier computations of the geometries and rotational barriers of all possible $\text{H}_3\text{MM}'\text{H}_3$ systems, at the Hartree–Fock level¹³⁹ using only moderate basis sets and including relativistic effective core potentials only for Pb, prompted criticism by experimentalists who pointed out discrepancies between the calculated and measured bond distances for some germanium compounds (e.g. Ge_2H_6 , H_3SiGeH_3)¹⁴⁰. These methods gave M–M’ bond lengths which

TABLE 7. Calculated^a and experimental^b M–M' bond lengths (pm) in H₃MM'H₃

H ₃ M	M'H ₃				
	CH ₃	SiH ₃	GeH ₃	SnH ₃	PbH ₃
H ₃ C	154.2 ^c	188.3 ^c	199.0 ^c	218.8 ^c	227.5 ^c
	152.6 ^d	188.3 ^d	199.6 ^d	217.8 ^d	224.2 ^d
	153.3 ^e	187.9 ^e	195.5 ^e	214.0 ^e	218.1 ^e
exp. ^b	153.1	186.4	194.5	214.0	
H ₃ Si	188.3 ^c	234.2 ^{c,f}	240.9 ^c	261.0 ^c	269.5 ^c
	188.3 ^d	235.5 ^d	242.5 ^d	261.0 ^d	264.0 ^d
	187.9 ^e	234.7 ^e	238.9 ^e	257.9 ^e	258.4 ^e
exp. ^b		233.3 ^g	237.2 ^g		
	186.4	232.7	235.7		
H ₃ Ge	199.0 ^c	240.9 ^c	249.9 ^{c,f}	266.2 ^c	274.1 ^c
	199.6 ^d	235.5 ^d	249.9 ^d	266.9 ^d	270.5 ^d
	195.5 ^e	238.9 ^e	242.7 ^e	261.0 ^e	262.1 ^e
exp. ^b		237.2 ^g	241.6 ^g		
	194.5	235.7	240.3		
H ₃ Sn	218.8 ^c	261.0 ^c	266.2 ^c	285.0 ^{c,f}	292.8 ^c
	217.8 ^d	261.0 ^d	266.9 ^d	284.3 ^d	286.9 ^d
	214.0 ^e	257.9 ^e	261.0 ^e	278.5 ^e	279.7 ^e
exp. ^b	214.0			277.6	
H ₃ Pb	227.5 ^c	269.5 ^c	274.1 ^c	292.8 ^c	301.2 ^{c,f}
	224.2 ^d	264.0 ^d	270.5 ^d	286.9 ^d	289.7 ^d
	218.1 ^e	258.4 ^e	262.1 ^e	279.7 ^e	281.2 ^e
exp. ^b				285.1	

^aFor calculations at other computational levels see Sections V.B and V.B.3.c.

^bThe experimental values are for substituted compounds, and are taken from References 139–142.

^cAll-electron nonrelativistic, at HF/DZP; from Reference 139.

^dAt HF/ECP (DZP basis set for the valence electrons); from Reference 139.

^eAt MP2/ECP (TZ basis set augmented with a double set of polarization functions for the valence electrons); from Reference 45.

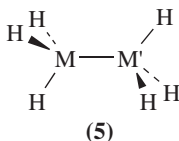
^fThe M–M' bond distances calculated at CCSD with a core polarization pseudopotential which takes care of the core-valence correlation effects are (in pm): 233.3 (M = Si); 242.9 (M = Ge); 278.0 (M = Sn) and 285.1 (M = Pb); from Reference 141.

^gAll-electron nonrelativistic calculation, at CISD/TZP(f,d); from Reference 142.

were somewhat too long, leading to an underestimation of the rotation barriers around the M–M' bonds. More recent theoretical studies using better computational methods for geometry optimizations, e.g. methods that include the effects of electron correlation such as MP2, CISD, CCSD(T) etc., with TZ basis sets or basis sets which include f-functions, showed that the geometries of the H₃MM'H₃ compounds can be reproduced very accurately (Table 7)^{45,139,141,142}. In most cases the M–M' bonds obtained from all-electron calculations agree well with the ECP results. With lead compounds, the quasi-relativistic ECP calculations gave Pb–M distances which are substantially shorter than the all-electron results¹³⁹, in correlation with the well-known relativistic bond contractions for Pb^{30a,104}. Inclusion of core-valence correlation, by using core polarization pseudopotentials, becomes increasingly important as the nuclear charge is increased. It contracts the M–M bond length by 7 pm for M = Ge and M = Sn and by 16 pm for M = Pb, relative to values that were calculated at CCSD with a relativistic ECP. The vibrational

frequencies calculated at MP2 and B3LYP agree well with experiment after inclusion of scaling factors of 0.945 and 0.98, respectively¹⁴³.

For all H₃MM'H₃ the staggered *D*_{3d} conformation, **5**, is more stable than the eclipsed one^{139,143}. This preference was attributed to a stabilizing vicinal $\sigma(\text{MH}) \rightarrow \sigma^*(\text{M}'\text{H})$ delocalization¹³⁹. A quantitative agreement of the calculated rotational barriers with experiment requires the use of large basis sets and high level electron correlation treatments (CISD, CCSD). The B3LYP rotational barriers are somewhat too low. The CCSD/TZ(2d,2p) rotational barriers (kcal mol⁻¹, experimental values in parentheses) are 3.08 (2.9); 1.38 (1.22); 0.79 and 0.70, for C₂H₆, Si₂H₆, H₃SiGeH₃ and Ge₂H₆, respectively. The rotational barriers for Sn₂H₆ and Pb₂H₆ are even smaller, being 0.4 and 0.2 kcal mol⁻¹, respectively^{139,141}. The drop in rotational barriers down group 14 is attributed to smaller overlap between the $\sigma(\text{MH})$ and $\sigma^*(\text{M}'\text{H})$ orbitals due to the longer M–M' bond¹⁴³.



b. Bond dissociation energies. The M–M' bond dissociation energies of H₃MM'H₃ decrease monotonically as M and M' become heavier and they range between *ca* 90 kcal mol⁻¹ for C–C to 50 kcal mol⁻¹ for Pb–Pb, as shown in Table 8. The general discussion in Section V.B.1 regarding the calculations of BDEs and the pitfalls that may cause errors are valid also here. As expected, the strongest bond is the C–C bond and the weakest is the Pb–Pb bond. For each M atom the M–M' bond energy decreases as M' becomes heavier.

The fluorinated distannanes¹⁴⁴ present an especially interesting subgroup of compounds with M–M bonds. For H₃SnSnFH₂, H₂FSnSnFH₂, F₃SnSnH₃, HF₂SnSnF₂H and F₃SnSnF₃ there is no correlation between the Sn–Sn bond lengths and the bond dissociation energies; e.g. the Sn–Sn bond lengths in H₂FSn–SnFH₂ and F₃Sn–SnF₃ are 276.5 and 275.8 pm, respectively, while their bond dissociation energies are 58.0 and 49.5 kcal mol⁻¹ (CCSD/ECP), respectively¹⁴⁴. What is the reason for the shorter but yet weaker bonds in fluorinated distannanes? Fluorine substitution removes electronic charge

TABLE 8. Calculated^a and experimental^b (in parentheses) M–M' bond dissociation energies (in kcal mol⁻¹) in H₃MM'H₃ (M, M' = C to Pb)

M'	M				
	C	Si	Ge	Sn	Pb
C	85.5 (89.8)	83.9 (88.2)	74.3	66.7	64.1
Si	83.9 (88.2)	70.5 (73.8)	66.7	61.5	59.3
Ge	74.3	66.7	63.1	58.8	56.8
Sn	66.7	61.5	58.8	55.3	53.1
Pb	65.3	59.3	56.8	53.1	50.8

^aAt CCSD(T)/CEP-TZDP+//MP2/CEP-TZDP, a set of diffused s and p functions was added to all atoms except hydrogen (denoted by the ++ sign); from Reference 136.

^bFrom References cited in Reference 45.

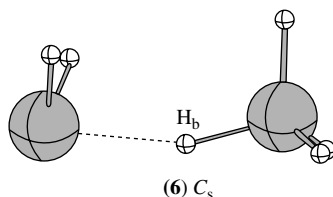
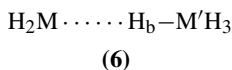


FIGURE 6. The C_s bridged structure (6) of M_2H_6

from the central Sn atom thereby causing contraction of its effective size. As a result, the difference in the radial orbital extension of the s and p orbitals of the tin atoms increases, making hybridization even more difficult than for the parent distannane (see Section III.C). This ‘hybridization defect’ causes a sharp decrease in the ratio between the s and p orbitals forming the Sn–Sn bond as the number of fluorines increases, i.e. from $p/s = 2$ for H_3SnSnH_3 to $p/s = ca\ 1$ for F_3SnSnF_3 . The less effective sp hybridization for Sn (which have a higher charge) results in increased s and decreased p character thereby making it weaker. However, the weaker bonds do not become longer, as the effect is compensated by the reduced size and the related larger net s character of the Sn atoms¹⁴⁴.

c. Nonclassical bridged structures of ethane analogs. In addition to the classical ethane-like D_{3d} structures, $H_3MM'H_3$ compounds of heavier group 14 elements exhibit also nonclassical structures, such as **6**, which can be described as bridged complexes of $M'H_4$ and MH_2 ¹⁴⁵. The structure of **6** is shown in Figure 6. Important geometric parameters of **6** as well as of the corresponding **5** are shown in Table 9. The energy difference between the $MH_4 \cdots MH_2$ complex and the D_{3d} H_3MMH_3 structure decreases down group 14, i.e. from 48 kcal mol⁻¹ for Si_2H_6 to only 9 kcal mol⁻¹ for Pb_2H_6 (Table 9). The energy barrier required for the insertion reaction which converts $MH_4 \cdots MH_2$ (**6**) to H_3MMH_3 increases from nearly zero for $M = C$ and Si to 20 kcal mol⁻¹ for $M = Pb$ (a detailed discussion on the insertion reaction of MH_2 into MH_4 is given in Section VII.A.b.ii). This implies that the nonclassical structures **6** of Pb_2H_6 and Sn_2H_6 should be accessible experimentally¹⁴⁵. On the other hand, the dissociation energies of the $MH_4 \cdots MH_2$ complexes to $MH_2 + MH_4$ are quite small (2–5 kcal mol⁻¹), making the experimental detection of these species very challenging.



4. Classical linear M_nH_{2n+2} chains

In contrast to linear alkanes, the heavier $H_3M(MH_2)_nMH_3$ species have properties which resemble somewhat unsaturated conjugated polyenes^{146–148}. For example, $H_3M(MH_2)_nMH_3$ chains show intense low-energy absorption maxima, which are red-shifted with increasing chain length. This is ascribed to the ‘ σ -delocalization’ and results in the fact that electronic excitations from the energetically high-lying orbitals of $H_3M(MH_2)_nMH_3$ are much easier than in alkanes. Hence, novel optical/electronic properties are found for these polymetallane systems¹⁴⁷, and several new synthetic approaches to these compounds have been developed in recent years¹⁴⁸. The experimental

TABLE 9. Important geometric parameters of isomers of M_2H_6 and their dissociation energies^a

		$D_{3d}(5)$	mono-bridged $C_s(6)$
C_2H_6	ΔE	110.9 (93.5) ^b	1.1 ^c
	d(M–M)	152.6	357.2
	d(M–H)	109.3	109.2; 283.8 ^d
	$\angle MH_bM$		124.4
Si_2H_6	ΔE	53.3 (69.6) ^b	4.8 ^c
	d(M–M)	234.7	354.7
	d(M–H)	144.7	149.0; 213.2 ^d
	$\angle MH_bM$		156.4
Ge_2H_6	ΔE	41.4 (64.2) ^b	5.1 ^c
	d(M–M)	249.7	361.5
	d(M–H)	154.9	156.9; 222.2 ^d
	$\angle MH_bM$		144.4
Sn_2H_6	ΔE	33.6 (58.5) ^b	9.8 ^c
	d(M–M)	279.7	352.9
	d(M–H)	171.4	175.6; 211.9 ^d
	$\angle MH_bM$		131.0
Pb_2H_6	ΔE	17.9 (50.8) ^b	9.1 ^c
	d(M–M)	283.6	373.1
	d(M–H)	174.6	178.4; 233.7 ^d
	$\angle MH_bM$		129.3

^aAt MP4/HF/ECP (for all nonhydrogen atoms). Bond lengths (d) in pm, bond angles (\angle) in deg and ΔE in kcal mol⁻¹; from Reference 145.

^bDissociation energy to two H_3M fragments.

^cDissociation to $MH_4 + MH_2$.

^dThe $H_3M \cdots H_b$ and $H_b \cdots MH_2$ distances, respectively; see Figure 6.

efforts in this field were accompanied by some theoretical investigations of the electronic structures, energy gaps and optical transitions of silicon^{149–151}, germanium^{150,151} and tin¹⁵¹ homopolymers as well as of alternating Si–Ge copolymers¹⁵⁰. These compounds were studied both in the *trans*-planar and in the *gauche*-helix skeleton conformations. Using the local density functional method it was found that for both the *trans*-planar and *gauche*-helix conformations the band-gap energies (i.e. the energy difference between the highest occupied valence band and lowest unoccupied conduction band) decrease on going from Si to Sn, and they are considerably higher for the *gauche*-helix conformation. The calculated band-gap energies are 3.89 (Si), 3.31 (Ge) and 2.80 (Sn) (eV)^{150,151}. Increasing the M–M–M bond angles causes a decrease in the band gaps. For a Sn–Sn–Sn bond angle of 150° the valence band and conduction bands were found to overlap, introducing the possibility of making ‘molecular metals’ if some effect (e.g. pressure) could be found to balance the required distortion energy¹⁵¹.

C. Multiply-substituted Singly-bonded Compounds

1. $M(CH_3)_4$ and MX_4 , $X = \text{halogen}$

The geometries of $M(CH_3)_4$ and MX_4 where X = halogen were calculated using a variety of all-electron and ECP methods^{152,153}. The M–C and M–X bond lengths in $M(CH_3)_4$ and MX_4 compounds, calculated using HF/ECP¹⁵² and various DFT/ECP¹⁵³ methods, are in good agreement with available experimental results and are comparable

(and in some cases even superior) to all-electron calculations^{152,153} (Table 10). This finding provides confidence in the reliability of ECPs and DFT methods for calculating the geometries of compounds with heavy elements. Among the various DFT methods used were for example Local Spin Density Approximation (LSDA), BLYP and B3LYP; the LSDA method provides the best geometrical parameters, but the hybrid B3LYP functional also gives good agreement with experiment.

Escalante and coworkers have studied in detail the contribution of relativistic effects to the geometries of MX_4 molecules. The changes in M–X bond distances (ΔR) caused by relativistic effects are presented graphically in Figure 7a. It was found that for the bromides and iodides, relativity causes M–X bond contraction which increases (excluding the tin compounds) as one descends group 14 (Figures 7a). For fluorides and chlorides,

TABLE 10. Calculated and experimental^a M–C and M–X bond lengths (pm) in $\text{M}(\text{CH}_3)_4$ and MX_4

X =	CH_3	F	Cl	Br	I
CX ₄	154.0 ^b	131.6 ^c	177.0 ^c	198.2 ^c	223.1 ^c
	153.5 ^e	131.9 ^f	178 ^d 178.2 ^f 176.7 ^e	194.5 ^f	218.7 ^f
exp.	153.9	131.9 ^g	177	194.2 ^g	210 ^g
SiX ₄	190.2 ^b	158.4 ^c	203.2 ^c	224.7 ^c	250.6 ^c
	187.9 ^e	155.2 ^h 157.6 ^f	204.0 ^d 204.6 ^f 201.5 ^e	221.5 ^f	246.6 ^f
exp.	188.8	155.2 ^g	202	218.3 ^g	—
GeX ₄	197.2 ^e	172.9 ^c	214.8 ^c	235.4 ^c	260.7 ^c
		172.7 ^f	213 ^d 216.1 ^f 211.4 ^e	232.0 ^f	256.0 ^f
exp.	194.5	171 ^g	211	227.2 ^g	250.7 ^g
SnX ₄	215.0 ^b	187.0 ^c	228.1 ^c	248.6 ^c	273.1 ^c
	215.0 ^e	190.5 ^f	232 ^d 234.0 ^f 228.6 ^e	248.8 ^f	271.8 ^f
exp.	214.4	188 ^g	228	244 ^g	264 ^g
PbX ₄	224.7 ^b	197.0 ^c	241.8 ^c	262.4 ^c	286.6 ^c
	219.8 ^e	198.1 ^f	240 ^d 243.8 ^f 233.6 ^e	258.4 ^f	280.0 ^f
exp.	229	192.4 ⁱ	238.1 ⁱ 243		

^aExperimental values are from References 137, 139, 142, 152, unless stated otherwise.

^bFirst-order perturbation theory all-electron calculation; from Reference 104.

^cAt LSDA, with nonrelativistic ECPs for inner-shell electrons, except for M = C; from Reference 153.

^dRelativistic DFT all-electron calculation; from Reference 46.

^eAt HF/ECP; from Reference 152.

^fAt LSDA, with quasi-relativistic ECPs for inner-shell electrons; from Reference 153.

^gSee references cited in Reference 153.

^hAt CCSD(T)/VQZ+1, all-electron calculation; from Reference 154.

ⁱAt HF/ECP; from Reference 44.

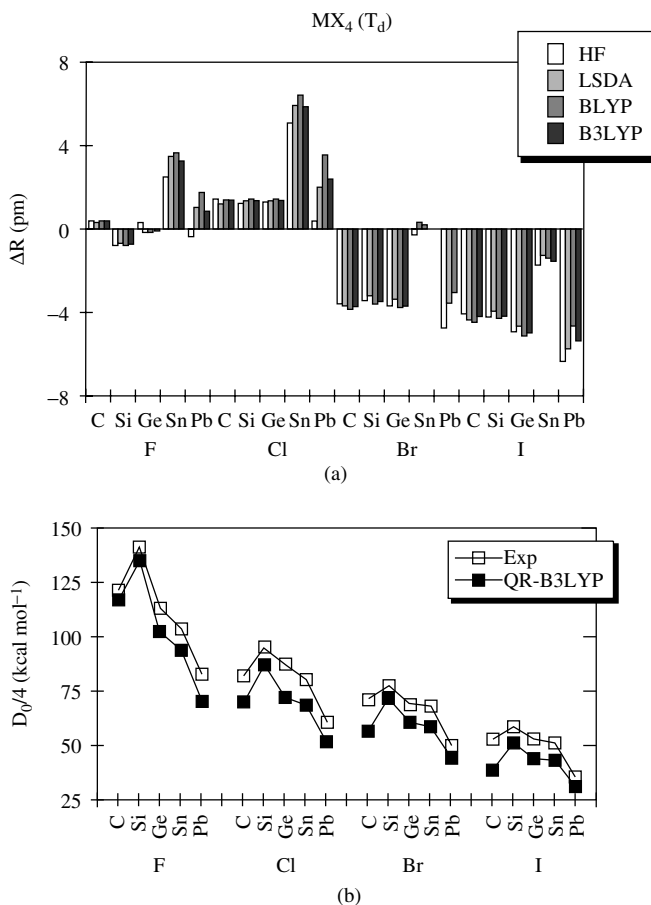


FIGURE 7. (a) Relativistic effects on the M–X bond distances (in pm) of group 14 tetrahalides; $\Delta R = R(\text{relativistic}) - R(\text{nonrelativistic})$. (b) Mean bond dissociation energies ($D_0/4$, in kcal mol^{-1}) for group 14 tetrahalides (T_d), calculated according to equation 8, with a quasi-relativistic (QR) effective core potential and using the B3LYP exchange-correlation energy functional. Adapted from Reference 153

the addition of relativistic effects induces bond elongation, being the largest in the tin halides¹⁵³.

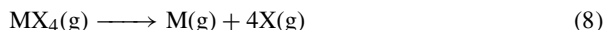
The total bond dissociation energies [$D_0 = \Delta E(\text{equation 8})$] and the mean bond energies ($D_0/4$), for all halides, follow the trend: C << Si > Ge > Sn > Pb (Table 11 and Figure 7b)^{153,155}. The LSDA functional overestimates the experimental mean dissociation energy while BLYP and B3LYP give results which are close to the experimental values¹⁵³. However, the stepwise dissociation energies of $MX_n \rightarrow MX_{n-1} + X$ ($n = 4$ to 1, for M = C and Si) vary in a zig-zag fashion according to n , i.e. $MX_3-X > MX_2-X < MX-X > M-X$, similar to the behavior of the MH_n series (Section V.A.2). The experimental individual BDEs for CX_n , X = F and Cl, respectively, are CX_3-X (129.6, 70.9) > CX_2-X (87.9, 67.0) < $CX-X$ (123.5, 92.0) > C–X (129.1, 80.3) kcal mol^{-1} ; and for

TABLE 11. Calculated mean M–X bond dissociation energies^a (kcal mol⁻¹) in MX₄^b (experimental values are given in parentheses^c)

M	X			
	F	Cl	Br	I
C	111.9 (116.0)	67.1 (78.4)	53.2 (61.3)	37.0 (51.0)
Si	128.8 (135.1)	83.4 (91.1)	68.7 (74.1)	49.1 (55.9)
Ge	98.1 (108.2)	69.3 (83.5)	58.2 (66.1)	42.2 (50.7)
Sn	89.8 (99.0)	65.8 (77.3)	56.3 (65.3)	41.5 (49.0)
Pb	67.3 (79.2)	49.5 (58.1)	41.8 (48.1)	29.8 (34.0)

^aD₀/4 [D₀ = ΔE(equation 8)].^bAt B3LYP, including ZPE and atomic spin-orbit corrections; from Reference 153.^cFrom Reference 155.

SiX_n, X = F, Cl, Br, I, respectively, they are SiX₃–X (145.6, 94.1, 77.8, 60.3) > SiX₂–X (137.9, 82.0, 62.4, 39.2) < SiX–X (154.7, 116.7, 95.4, 78.4) > Si–X (131.8, 89.6, 78.5, 58.5) kcal mol⁻¹¹⁵⁶. The smallest BDEs are found for the dissociation of MX₃ to MX₂ + X, reflecting the high stability of MX₂. Unfortunately, experimental information for the heavier congeners is unavailable. Escalante and coworkers have shown that, although inclusion of atomic spin-orbit corrections do not change the trends in BDEs, this inclusion is essential for achieving better agreement between the calculated and experimental dissociation energies¹⁵³.



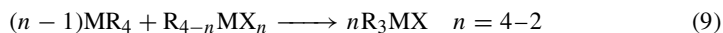
2. (CH₃)_nMX_{4-n}

Large deviations from idealized tetrahedral geometries were found in unsymmetrically substituted tetravalent tin and lead compounds of the type R_nMX_{4-n} (R = H, CH₃, SiH₃; X = F, Cl)^{44,157}. For example, the F–Pb–F angle in (CH₃)₂PbF₂ is 101.4°, while the C–Pb–C angle is 134.8°. The bond angle distortions are even larger when the substituents differ more in electronegativity, i.e. in (SiH₃)₂PbF₂ the F–Pb–F angle is 101.0°, and the Si–Pb–Si angle is very large, 141.3°. Similarly, the PbC₃ moiety in (CH₃)₃PbF approaches planarity. Similar structures were calculated for (CH₃)₂SnCl₂ and (CH₃)₃SnCl, although their deviation from a tetrahedral structure is slightly smaller⁴⁴. In contrast, the methylated mixed hydrides, H_nPb(CH₃)_{4-n}, do not deviate significantly from tetrahedral geometry. This is consistent with the rather similar electronegativities of H and CH₃⁴⁴. The significant distortions in the geometry of R_nMX_{4-n} were attributed to electronic effects⁴⁴. The computed structures of monomeric R₂MX₂ and R₃MX compounds (X = F, Cl) exhibit the structural features found experimentally for oligo- and polymeric tin and lead compounds which have substituents with different electronegativities^{44,158–160}. It was also noticed that the Pb–R and Pb–X bonds in the R_nPbX_{4-n} series are shorter when more electronegative groups X are present⁴⁴, despite the destabilization of the Pb^{IV} compounds upon successive substitution by halogens. This was attributed to the depletion of the high-lying p orbitals and the larger contribution of the 6s orbitals to the bonding⁴⁴ (see below).

The geometries of all (CH₃)_nMCl_{4-n} (M = C to Pb)¹⁵² were optimized using all-electron 3-21G(d), 6-31G(d) and ECP basis sets in order to evaluate the performance

of ECPs vs. all-electron calculations. The major conclusion was that the Hay and Wadt effective core potentials give geometries that are comparable and even superior to those calculated with all-electron basis sets with similar valence shell descriptions. The paper reports the geometries of these compounds, but the changes in the geometries caused by changing M or by successive substitution of methyl groups by Cl atoms was not discussed¹⁵². Inspection of the reported results reveal that for all metals the M–C and M–Cl bonds become shorter as the number of Cl atoms increases, in agreement with the results discussed above for M = Sn and Pb⁴⁴. The CIMC bond angle in (CH₃)₃MCl decreases as M becomes heavier, i.e. it is 107.3°, 107.2°, 106.0°, 105.2° and 103.7° for M = C, Si, Ge, Sn and Pb¹⁵², respectively, pointing to increased deviation from a tetrahedral structure on going from M = C to M = Pb.

The effect of electronegative substituents on the stability of (CH₃)_nMCl_{4–n} compounds was evaluated by the isodesmic equation 9^{44,152}. The results, presented in Table 12, show that molecules with mixed methyl and halogen ligands are more stable than the corresponding molecules where these are in different molecules, e.g. four molecules of (CH₃)₃MCl are more stable than 3(CH₃)₄M + MCl₄, for every M (equation 9, n = 4), and the relative stability of (CH₃)₃MCl increases in the order: Si < Ge < Sn < C < Pb. The carbon molecules are the exception to the common trend which shows that reaction 9 is more exothermic as M becomes heavier¹⁵². In addition, reaction 9 becomes more exothermic for larger n^{44,152} (Table 12).



3. Relative stabilities of M^{IV} and M^{II} compounds

A question of interest is the stability of tetravalent MR₄ compounds relative to the corresponding divalent MR₂ compound and R₂. This question was studied for the entire series of MF₄ and MCl₄ by Schwerdtfeger and coworkers^{48b}. They found that the stability of MX₄ relative to MX₂ + X₂ decreases in the already familiar ‘zig-zag’ fashion, i.e. for MF₄ the reaction energies are 178.1 (CF₄), 244.4 (SiF₄), 160.0 (GeF₄), 163.5 (SnF₄), 95.9 (PbF₄) and –6.7 [(‘eka-lead’ 114)F₄] kcal mol^{–1}^{48b}.

Another interesting question is the effect of the substituent R on these dissociation reactions. For carbon compounds it is well known that CR₄, R = alkyl or halogen, are significantly more stable than the corresponding CR₂ + R₂. Of the other group 14 MR₄

TABLE 12. Relative stabilities of (CH₃)_nMX_{4–n}^a

Equation	ΔE (kcal mol ^{–1})
3(CH ₃) ₄ C + CCl ₄ → 4(CH ₃) ₃ CCl	–46.5 ^b
3(CH ₃) ₄ Si + SiCl ₄ → 4(CH ₃) ₃ SiCl	–28.1 ^c
3(CH ₃) ₄ Ge + GeCl ₄ → 4(CH ₃) ₃ GeCl	–34.4 ^c
3(CH ₃) ₄ Sn + SnCl ₄ → 4(CH ₃) ₃ SnCl	–43.4 ^c
3(CH ₃) ₄ Pb + PbCl ₄ → 4(CH ₃) ₃ PbCl	–54.1 ^c
3(CH ₃) ₄ Pb + PbF ₄ → 4(CH ₃) ₃ PbF	–60.9 ^d
(CH ₃) ₄ Pb + (CH ₃) ₂ PbF ₂ → 2(CH ₃) ₃ PbF	–5.5 ^d
2(CH ₃) ₄ Pb + CH ₃ PbF ₃ → 3(CH ₃) ₃ PbF	–24.5 ^d

^a According to equation 9.

^b At HF/6-31G(d); from Reference 152.

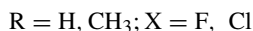
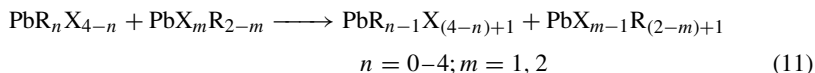
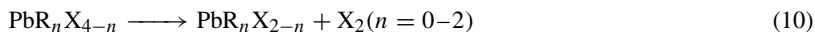
^c At HF/ECP; from Reference 152.

^d At MP4SDQ with quasi-relativistic ECP for Pb; from Reference 44.

compounds, this question was studied in detail mostly for $M = \text{Pb}$ (the stability of MH_4 relative to MH_2 and H_2 was discussed in Section V.A.3). The experimental facts which these studies tried to explain were: Why is PbEt_4 a relatively stable compound and PbEt_2 is unknown^{44,157}, while PbCl_4 decomposes even at room temperature and PbCl_2 is perfectly stable^{44,157}? Are thermodynamic or kinetic reasons responsible for these apparently contradictory observations?

Schwerdtfeger and coworkers addressed this question and suggested that PbR_4 , $R =$ alkyl compounds, although being thermodynamically unstable, are kinetically stable due to a barrier for their decomposition to PbR_2 and R_2 . They suggested that the barrier is caused by steric problems in the transition state and by distortions in the organic groups R necessary to form R_2 ¹⁰⁷. Such factors are not present in PbCl_4 and the dissociation into MCl_2 and Cl_2 is therefore more facile.

Kaupp and Schleyer evaluated the relative stabilities of various $\text{PbR}_n\text{X}_{4-n}$ ($n = 0-4$) and $\text{PbR}_m\text{X}_{2-m}$ ($m = 0-2$) where $R = \text{H}, \text{CH}_3$; $X = \text{F}, \text{Cl}$, from the heats of reactions 10 and 11, using nonrelativistic and quasi-relativistic pseudopotentials⁴⁴. Note, however, that decomposition reactions such as equation 10 are not ideal measures of the 'stability' of the M^{IV} vs. M^{II} oxidation states. For example, the σ -bond energy of F_2 is quite small⁶, and therefore a 1,1-elimination of F_2 from TlF_3 , PbF_4 and BiF_5 is unfavorable. Group exchange reactions such as equation 11 provide a better assessment of stability^{44,157}.



The isodesmic group exchange reaction (equation 11) and the elimination reactions (equation 10) reveal strong destabilizations of Pb^{IV} compounds upon successive substitution by electronegative substituents (Table 13). For example, the dissociation of PbH_3F to PbH_2 and HF is exothermic by only $1.6 \text{ kcal mol}^{-1}$, while the loss of HF from PbHF_3 is exothermic by 51 kcal mol^{-1} . The exchange of methyl groups by hydrogen atoms has no significant effect⁴⁴.

The Pb-X and Pb-R bonds in tetravalent lead compounds are both weakened by successive substitution with $X = \text{F}$ and Cl (although the M-R and M-X bonds are both shortened, see above). Consequently, the Pb-X bonds in PbX_4 are weaker than those in PbX_2 , in contrast to the Pb-R bonds in PbR_4 which are stronger than those in PbR_2 . This is in agreement with findings that the average Pb-F BDE in PbF_4 is only *ca* 80% of that in PbF_2 while the average Pb-H BDE in PbH_4 is larger than in PbH_2 ⁵³.

Kaupp and Schleyer explained these observations⁴⁴ in terms of 'hybridization defects'⁶ in Pb^{IV} species. The relative p-orbital contributions to covalent bonding in compounds of heavier main-group elements are generally smaller than expected from symmetry considerations and the resulting tetrahedral hybrids have smaller p/s ratios (Section III.C). Furthermore, with increasing number of electronegative substituents the positive charge at the lead atom increases, depleting the 6p orbitals much more than the 6s orbitals^{44,46}. The remaining 6s-electron density is strongly attracted by the nuclear charge, and is contracted more strongly than the p electrons, causing an even larger difference in the radial extension of the 6s and 6p electrons, which makes the hybridizations even less effective. The calculated hybridizations of several lead halogenides are given in Table 14. The calculated hybridization in PbH_4 is $\text{sp}^{1.80}$ while in PbF_4 it is $\text{sp}^{0.91}$. As depletion of the 6s orbital is unfavorable, the bonds to the less electronegative ligands adopt higher

TABLE 13. Relative stabilities of substituted Pb^{IV} and Pb^{II} compounds calculated using equations 10 and 11^a

Equation	ΔE (kcal mol ⁻¹)
<i>equation 10</i>	
PbH ₂ F ₂ → PbH ₂ + F ₂	134.7
PbF ₄ → PbF ₂ + F ₂	67.0
PbH ₂ Cl ₂ → PbH ₂ + Cl ₂	74.7
PbCl ₄ → PbCl ₂ + Cl ₂	25.3
PbH ₃ F → PbH ₂ + HF	-1.6
PbH ₂ F ₂ → PbHF + HF	-20.2
PbHF ₃ → PbF ₂ + HF	-51.4
(CH ₃) ₂ PbF ₂ → (CH ₃) ₂ Pb + F ₂	144.0
CH ₃ PbF ₃ → CH ₃ PbF + F ₂	114.0
(CH ₃) ₄ Pb → (CH ₃) ₂ Pb + H ₃ CCH ₃	-17.9
(CH ₃) ₃ PbF → CH ₃ PbF + H ₃ CCH ₃	-27.7
(CH ₃) ₂ PbF ₂ → PbF ₂ + H ₃ CCH ₃	-44.1
<i>equation 11</i>	
(CH ₃) ₂ PbF ₂ + PbF ₂ → PbF ₄ + (CH ₃) ₂ Pb	77.3
(CH ₃) ₃ PbF + PbF ₂ → (CH ₃) ₂ PbF ₂ + CH ₃ PbF	46.3
(CH ₃) ₄ Pb + PbF ₂ → (CH ₃) ₂ PbF ₂ + (CH ₃) ₂ Pb	26.4
(CH ₃) ₄ Pb + PbF ₂ → (CH ₃) ₃ PbF + CH ₃ PbF	10.3

^aAt MP4SDQ with a quasi-relativistic pseudopotential for Pb; from Reference 44.TABLE 14. Hybridization and atomic charges of lead halogenides and hydrides^a

	Charge at Pb	Orbital population		Pb orbital hybridization, sp ⁿ ^b	
		Pb(6s)	Pb(6p)	Pb-H	Pb-X
PbH ₄	0.88	1.11	2.01	1.80	
PbH ₃ F	1.52	1.06	1.41	1.24	2.54
PbH ₂ F ₂	2.04	0.98	0.98	0.80	1.90
PbHF ₃	2.48	0.79	0.72	0.55	1.29
PbF ₄	2.88	0.54	0.57		0.92
PbH ₃ Cl	1.25	1.12	1.63	1.31	2.60
PbH ₂ Cl ₂	1.53	1.11	1.36	0.93	1.91
PbHCl ₃	1.74	1.06	1.20	0.67	1.33
PbCl ₄	1.92	0.99	1.09		0.91

^aThe SCF wave function was analyzed using the NBO procedure, ECP was used for Pb and a DZP type basis set was used for the other elements; from Reference 44.^b Only *n* is given.

s character, while those to the more electronegative ligands reveal higher 6p contributions (Table 14)⁴⁴. Thus, lead (and tin) compounds obey Bent's rule¹⁶¹, which states that 'more electronegative substituents "prefer" hybrid orbitals having less s-character, and more electropositive substituents "prefer" hybrid orbitals having more s-character'. The very large 'hybridization defects'⁶ in Pb^{IV} compounds reduce efficient directional bonding, resulting in geometry distortions and leading to weakening of the covalent bonds when electronegative ligands are present⁴⁴. Thus, the preference of inorganic lead compounds to occur as Pb^{II} species (e.g. PbCl₂) is due to the 'hybridization defects' in Pb^{IV} species.

In general, relativistic effects have been found to destabilize bonds to lead, and the effect is larger in compounds which have larger 6s contributions to the bonds. Therefore,

relativistic factors affect significantly the stability of PbX_4 compounds (e.g. PbF_4) while divalent compounds show almost no change⁴⁴, shifting the stability balance in favor of the divalent lead compounds.

The destabilization of tetravalent lead compounds by multiple substitution with electronegative ligands stands in sharp contrast to the opposite behavior of analogous carbon and silicon compounds, where the stabilization of the multiply-substituted tetravalent compounds was explained by a dominant stabilizing $n(\text{F}) \rightarrow \sigma^*(\text{M}-\text{F}$ or $\text{M}-\text{H})$, negative hyperconjugation^{59f,162}. However, for fluoroplumbanes, geminal $\sigma(\text{Pb}-\text{H}) \rightarrow \sigma^*(\text{Pb}-\text{F}$ or $\text{Pb}-\text{H})$ hyperconjugation is more important and, as a result, geminal fluoro substitution destabilizes lead^{IV} fluorohydrides⁴⁴.

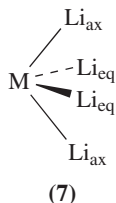
A comprehensive study which considers the kinetic stability (i.e. the barriers to dissociation to lead^{II} and X_2) of various lead^{IV} compounds is not yet available and is highly desirable.

4. Oxides and sulfides

In an early study, a model series of group 14 oxides and sulfides $\text{M}(\text{OH})_4$, $\text{M}(\text{SH})_4$, $(\text{MH}_3)_2\text{O}$ and $(\text{MH}_3)_2\text{S}$ ($\text{M} = \text{C}$ to Sn) was computed in order to understand the geometric variations in silicates and germanates¹⁶³. Although performed only at the HF/3-21G(d) level of theory, the calculations reproduced quite well the crystal structures. It was concluded that the forces governing the variations in the bond lengths and angles in the isolated small model molecules resemble those in a wide class of chemically similar oxide crystals¹⁶³.

5. MLi_4

CLi_4 has a tetrahedral ground state. In contrast, SiLi_4 , GeLi_4 and SnLi_4 have a C_{2v} ground state structure (7)¹⁶⁴. The $C_{2v}-T_d$ energy differences (at RHF, in parentheses at MP2) are 3.5 (7.0) (SiLi_4), 4.8 (7.0) (GeLi_4) and 4.7 (SnLi_4) kcal mol^{-1} . Figure 8 shows the calculated geometries of 7, $\text{M} = \text{Si}$, Ge and Sn .



The MLi_4 compounds are highly ionic; in T_d CLi_4 , each Li carries a positive charge of +0.78 and in C_{2v} SiLi_4 , the charges are +0.74 and +0.44 at each of the axial and equatorial lithium atoms, respectively. The acute bond angles: $\text{Li}_{\text{ax}}-\text{Si}-\text{Li}_{\text{eq}}$ (83.5°), $\text{Li}_{\text{eq}}\text{SiLi}_{\text{eq}}$ (84.1°) and $\text{Li}_{\text{ax}}\text{SiLi}_{\text{ax}}$ (162.3°) and the relatively short $\text{Li}_{\text{ax}}-\text{Li}_{\text{eq}}$, $\text{Li}_{\text{eq}}-\text{Li}_{\text{eq}}$ distances (319.8 pm and 324.6 pm, respectively), suggest the presence of attractive Li-Li interactions. An NBO analysis found that the bonding in C_{2v} SiLi_4 is best described as composed of two $\sigma(\text{Si}-\text{Li}_{\text{eq}})$ bonds, one $\text{Li}_{\text{ax}}\text{SiLi}_{\text{ax}}$ 2-electron-3-center (2e-3c) bond and a lone pair on Si (n_{Si}). The $\sigma(\text{Si}-\text{Li}_{\text{eq}})$ bonds are polarized toward Si and are composed from hybrids of 96% p character on Si and 98% s character on Li. The 2e-3c bond has a nearly pure p character on Si and a pure s character on both lithiums, and the n_{Si} is essentially a pure Si 3s orbital. Three major factors are responsible for this C_{2v} -bonding pattern:

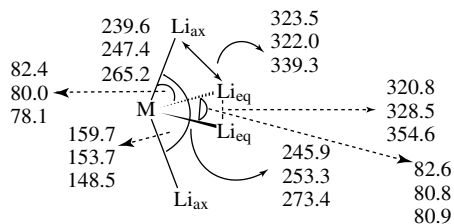


FIGURE 8. Optimized geometry of C_{2v} MLi_4 ($M = \text{Si, Ge, Sn}$, given in this order from top to bottom), calculated at MP2/6-31G* ($M = \text{Si, Ge}$) and RHF ($M = \text{Sn}$)¹⁶⁴; bond lengths in pm, bond angles in deg

(a) The high ionicity of the Si–Li bond, which enhances the lone-pair character on Si. (b) The tendency of second-row elements to concentrate s character in lone-pair hybrids and p character in bonding hybrids, thus employing two 3p orbitals in the two Si–Li_{eq} bonds and the third 3p orbital in the 3-center Li_{ax}–Si–Li_{ax} bond. This picture explains the nearly 90° Li_{eq}SiLi_{eq} and Li_{ax}SiLi_{eq} bond angles and the nearly linear Li_{ax}–Si–Li_{ax} bond. (c) Covalent Li–Li bonding which results from delocalization of electrons from the $\sigma(\text{Si–Li}_{\text{eq}})$ and $\sigma(\text{Li}_{\text{ax}}\text{–Si–Li}_{\text{ax}})$ bonding orbitals into the 2s and 2p orbitals of the other lithium atoms. In accord with a significant correlation-induced increase in the Li–Li bonding character, a decrease of up to 20 pm in the ‘nonbonded’ Li–Li distances was found for SiLi₄ in the MCSCF, MP2 and CISD optimization levels relative to the RHF calculations. Similar results, but with longer Li–Li distances (Figure 8), are found for GeLi₄ and SnLi₄¹⁶⁴. In CLi₄, factor (b) is missing, and a tetrahedral structure is preferred and is the only minimum on the PES. In MH₄, factors (a) and (c) are missing, and the molecules adopt the regular tetrahedral geometry.

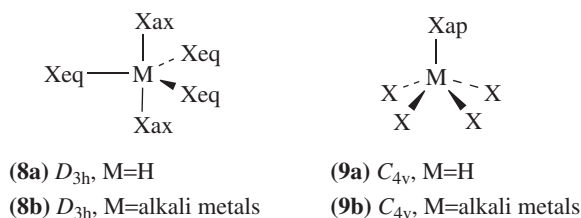
C_{2v} geometries were also calculated (at HF/DZ) for SiNa₄, GeNa₄, GeK₄, SnNa₄ and SnK₄¹⁶⁵. The total binding energies of MX₄ (i.e. $\text{MX}_4 \rightarrow \text{M} + 4\text{X}$) decrease when either M or X becomes heavier, being [at QCISD(T)/DZP//HF/DZ] 108.6 (SiNa₄), 104.5 (GeNa₄), 100.6 (SnNa₄), 87.8 (GeK₄) and 83.7 (SnK₄) kcal mol⁻¹¹⁶⁵. A similar trend is found for MX₅ and MX₆ (see below).

D. Hypercoordinated Systems

In contrast to carbon, silicon and its higher congeners form penta- and hexa-coordinated compounds. These compounds are of current theoretical and experimental interest due to their unusual geometries and electronic structures. The most recent developments in the chemistry of hypervalent silicon chemistry were reviewed by Kost and Kalikhman¹⁶⁶. Structural aspects of hypervalent compounds containing Ge, Sn and Pb were reviewed previously by Mackay¹⁶⁷. Theoretical aspects of penta-coordinated silicon compounds were reviewed by Apeloig⁷. The general consensus among theoreticians is that the bonding in these compounds includes the formation of 3-center–4-electron bonds and that the d orbitals of the metal do not play a significant valence role; rather the d orbitals serve as polarization functions^{58,60} compensating for the limitations of the molecular wave function when it is restricted to only s and p functions centered on the metal nuclei.

1. MH₅

No minimum on the PES was located for MH₅ radicals. The trigonal-bipyramidal D_{3h} structures¹⁶⁸, **8a**, are transition states for the hydrogen exchange reaction $\text{H} + \text{MH}_4 \rightarrow$



$\text{H}^+\text{MH}_3 + \text{H}^{169-171}$ (see also Section VII.C.2). The calculated geometries of **8a** are given in Figure 9. A square-pyramidal C_{4v} isomer, **9a**, was located for $\text{M} = \text{Si}^{169a}$ and Ge^{169b} , being by *ca* 2 kcal mol⁻¹ less stable than **8a**, but this isomer is not a minimum as well. The dissociation of MH_5^* to MH_4 and a hydrogen atom is highly exothermic for $\text{M} = \text{C}$ (61 kcal mol⁻¹), but the exothermicity decreases to only 36–38 kcal mol⁻¹ for $\text{M} = \text{Si}$ to Sn (using ROHF with a DZ diffused and polarized type basis set¹⁷⁰ and only 17.4 kcal mol⁻¹ for SiH_5^* using CI^{171}). Thus, the barrier for the H-exchange reaction via **8a** is high even for the heavier congeners of carbon. Dissociation of MH_5 to MH_3 and H_2 is even more exothermic, e.g. 55 kcal mol⁻¹ for $\text{M} = \text{Ge}^{169b}$. ESR evidence for the existence of SiH_5^* and GeH_5^* was presented by Nakamura and coworkers, but the authors point also to different interpretations of the observed ESR spectra^{172,173}.

2. MX_5 , $\text{X} = \text{alkali metals}$

As M and X become heavier, MX_5 prefers the square-pyramidal structure **9b** over the trigonal-bipyramidal structure, **8b**. Thus, **9b** is preferred over **8b**, by 0.2, 1.5, 1.5, 8.7, 5.8 and 5.3 kcal mol⁻¹ for SiNa_5 , GeNa_5 , SnNa_5 , GeK_5 , SnK_5 and PbNa_5 , respectively¹⁶⁵. An imaginary degenerate pair of vibrational frequencies was calculated for PbNa_5 . The total binding energies of SiNa_5 , GeNa_5 , SnNa_5 and SnK_5 are [at QCISD(T)/DZP] 131.7, 126.0, 119.6 and 100 kcal mol⁻¹, respectively. The incremental energy (i.e. the energy required to remove one X atom from MX_5) is 23.2 (SiNa_5), 21.5 (GeNa_5), 18.9 (SnNa_5), and 16.7 (SnK_5) kcal mol⁻¹. Thus, both the total binding energies and incremental binding energies decrease as both M and X become heavier¹⁶⁵.

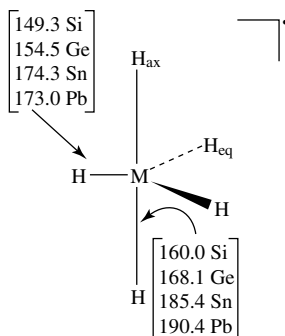
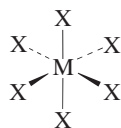


FIGURE 9. Optimized structures of D_{3h} MH_5 , $\text{M} = \text{Si, Ge, Sn}$ and Pb (at QCISD/TZP for $\text{M} = \text{Si}$ to Ge and QCISD/RECP for $\text{M} = \text{Pb}$); from Reference 168

3. MX_6 , MX_7 and MX_8 , $X = \text{alkali metals}$

The existence of CLi_6 was first predicted by *ab initio* computations¹⁷⁴ and later detected experimentally¹⁷⁵. The stability of this amazing molecule is due to strong ionic interactions between the positively charged alkali metals and the highly negatively charged carbon atom and significant $Li \cdots \cdots Li$ interactions¹⁶⁰. The experimental observation of $PbNa_6$ ¹⁷⁶ prompted theoretical investigations of the complete set of MX_6 compounds ($M = C$ to Pb , $X = Li$ to Cs)^{165,177,178} and the main results are collected in Table 15.

All MX_6 clusters are stable toward dissociation and adopt the octahedral structure (10). The dissociation energies according to equation 12, as well as the atomization energies, decrease steadily as M and X become heavier, i.e. $CX_6 > SiX_6 \approx GeX_6 > SnX_6 \approx PbX_6$ (Table 15), and $MLi_6 > MNa_6 > MK_6$. All MX_6 clusters are more stable than an M atom and three X_2 molecules (Table 15)^{165,177}. The incremental bond dissociation energies of MX_6 , i.e. to $MX_5 + X$ are [at QCISD(T)/DZP] 32.0 ($SiNa_6$), 31.6 ($GeNa_6$), 25.6 ($SnNa_6$), 27.7 (SnK_6) and 24.9 ($PbNa_6$) kcal mol^{-1} , being higher than for the corresponding MX_5 clusters¹⁶⁵. The average binding energies per cluster atom for MX_6 and MX_4 systems are similar¹⁶⁵. Hence, according to the calculations the complete set of MX_6 clusters should be accessible experimentally^{165,177}.



(10)



Although the electronegativities of all alkali metals are similar, the negative charge at M decreases significantly from $X = Li$ to $X = K$. On the other hand, the variation of the charges at M for a given alkali metal is relatively small (Table 15). Therefore, the size of the partially positively charged alkali metal determines the electron density distribution; the small Li can stabilize a much larger negative charge at the central atoms than Na or K ligands. The trend in the Wiberg $M-X$ bond indices (WBIs) is: $Li < Na < K$, indicating the reduced ionic contribution as the alkali metal becomes heavier¹⁷⁷. Ligand–ligand bonding is found in all MX_6 clusters, with WBIs of *ca* 0.11.

The large lead atom might also be hepta- or octa-coordinated, but computations indicate that $PbNa_7$ and $PbNa_8$ clusters are only weakly bound, with dissociation energies to $MX_{n-1} + X$ of only 7.9 and 6.7 kcal mol^{-1} , respectively (26.3 kcal mol^{-1} in $PbNa_6$)¹⁶⁵.

E. Cyclic Metallanes: Rings, Polycyclic and Polyhedral Compounds

In this section we will review theoretical studies of 3- and 4-membered rings (3-MRs and 4-MRs) of silicon and its heavier congeners (systematic theoretical studies that investigate larger singly bonded rings of the heavier congeners of silicon are not available), of cage systems which are composed of 3- and 4-MRs and of larger polycyclic systems, e.g. propellanes with a variety of ring sizes. The general interest of chemists in the nature of chemical bonds in highly strained organic ring systems¹⁷⁹, applies also to similar systems which contain higher homologues of carbon. In recent years, many types of new cyclic, polycyclic and cage compounds of heavier group 14 elements have been synthesized

TABLE 15. Calculated properties of octahedral group 14 MX_6 ($X =$ alkali metal) clusters

X	Parameter	C	Si	Ge	Sn	Pb
Li^a	d(M–X) (pm)	198.9	240.6	242.4	261.1	263.2
	Diss. ^b	217.9	156.2	153.8	125.1	123.8
	Charge ^c	–3.25	–3.44	–3.46	–3.27	–3.27
	Bond order ^d	0.22	0.18	0.17	0.23	0.22
Na^a	d(M–X) (pm)	240.9	277.7	279.6	296.6	298.9
	Diss. ^b	132.9	109.0	108.9	91.1	91.5
	Charge ^c	–2.30	–2.93	–3.00	–2.63	–2.63
	Bond order ^d	0.41	0.30	0.28	0.36	0.36
K^a	d(M–X) (pm)	290.9	326.2	327.9	343.5	346.0
	Diss. ^b	98.0	99.5	99.7	90.1	89.7
	Charge ^c	–1.89	–2.57	–2.67	–2.31	–2.32
	Bond order ^d	0.46	0.37	0.35	0.41	0.41
Rb^e	d(M–X) (pm)	329.3/348.7 ^f	366.0	371.5	385.3	388.1
Cs^e	d(M–X) (pm)	—	390.5	396.4	410.7	414.3

^aAt B3LYP/ECP; from Reference 177.

^bDissociation energy (kcal mol^{-1}), according to equation 12. It was suggested that the cited energies should be reduced by 1.6, 4.8 and $22.4 \text{ kcal mol}^{-1}$ for Ge, Sn and Pb, respectively, due to contributions from atomic spin–orbit coupling⁴¹. When these contributions are included, the PbX_6 clusters are computed to be the least stable in the whole set.

^cNatural atomic charge at M (from NBO analysis).

^dWiberg’s bond index for M–X.

^eAt HF/ECP; from Reference 165.

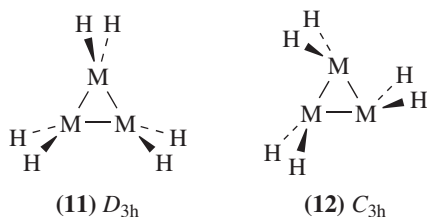
^f CRb_6 distorts to a structure with D_{4h} symmetry.

and in many cases their detailed geometries were determined by X-ray analysis^{21,180}. However, many of their most interesting properties, such as their strain energies, relative energies, quantitative substituent effects and the nature of their chemical bonds, are still available only from high level computational studies. These are discussed below.

1. Saturated ring compounds

a. c-M₃H₆ and c-M₄H₈. i. Structures. The only systematic study of the geometry of both $c\text{-M}_3\text{H}_6$ and $c\text{-M}_4\text{H}_8$ for $M = \text{Si}$ to Sn was presented by Rubio and Illas¹⁸¹. They used double-zeta (DZ) and double-zeta + polarization (DZ+d) basis sets, with a nonempirical pseudopotential for the core electrons of Si and Ge and a relativistic pseudopotential for the core of Sn. Electron correlation was not included. For $c\text{-Si}_3\text{H}_6$ and $c\text{-Si}_4\text{H}_4$, it was shown earlier that polarization functions must be included in the basis-set, since with nonpolarized dz basis sets the calculated Si–Si bonds are too long¹⁸².

The cyclic M_3H_6 having D_{3h} symmetry, **11**, are minima on the PES for $M = \text{C}$, Si, Ge and Sn ^{181,183}, while for $M = \text{Pb}$ this structure is a transition state leading to a C_{3h} skewed-type structure, **12**, which is 10 kcal mol^{-1} more stable than **11**, $M = \text{Pb}$ ^{5,184}. The calculated geometry of **12**, $M = \text{Pb}$ is shown in Figure 10a; **12** can be described as a donor–acceptor complex of three singlet H_2Pb : units, as shown in Figure 10b. The donor is the lone-pair orbital on Pb, and the acceptor is the empty np orbital on Pb. It was commented that such skewed-type structures are also favored in the lighter analogs ($c\text{-M}_3\text{H}_6$, $M = \text{Si}$, Ge and Sn) when the hydrogens are replaced by electronegative substituents such as fluorine atoms, because the singlet states of the divalent species become much more stable than the triplet states (however, explicit data were not presented)¹⁸⁴ (see



also Sections VI.B.1. and VI.B.3.b). For $M = \text{Sn}$ and Pb , H-bridged structures become the global minima¹⁸³ (Section V.E.1.a.iv).

For $c\text{-C}_4\text{H}_8$ and $c\text{-Si}_4\text{H}_8$ the planar D_{4h} structure (13) is not a minimum; rather, it is a transition state connecting two equivalent D_{2d} puckered structures (14) which are minima on the PES. The planarization barrier for $c\text{-C}_4\text{H}_8$ is $0.9\text{--}2.5 \text{ kcal mol}^{-1}$ (at MP2 and B3LYP, respectively; $1.5 \text{ kcal mol}^{-1}$, experimental¹⁸⁵) and for $c\text{-Si}_4\text{H}_8$ it is $1.5\text{--}1.75 \text{ kcal mol}^{-1}$ (at various levels)^{182,186}. The MMMM torsional angle is 21° for $c\text{-C}_4\text{H}_8$ ¹⁸⁵ and 31.2° for $c\text{-Si}_4\text{H}_8$ ¹⁸². For $c\text{-Ge}_4\text{H}_8$ ^{181,187} and $c\text{-Pb}_4\text{H}_8$ ¹⁸⁴ planar structures were located as minima, while the puckered D_{2d} structures are not minima. For $c\text{-Pb}_4\text{H}_8$, a C_{4h} -symmetry structure with the hydrogens skewed around the 4-MR (15) was also located as a minimum on the PES, being by $0.7 \text{ kcal mol}^{-1}$ more stable than the planar D_{4h} structure¹⁸⁴. As mentioned above, even a stronger tendency for a skewed structure was found for $c\text{-Pb}_3\text{H}_6$ (12). These skewed structures reflect the low energy of the ‘inert-pair’ of Pb ¹⁸⁴. For $c\text{-Sn}_4\text{H}_8$, the planar D_{4h} structure is the preferred structure at HF/ECP¹⁸¹. However, at this level of theory, $c\text{-Si}_4\text{H}_8$ was also calculated to be square planar¹⁸¹ and therefore this conclusion may change at higher levels of theory.

The experimentally known 4-MRs, all carrying substituents other than hydrogen, exhibit both planar and puckered configurations. For example, $c\text{-(Me}_2\text{Si)}_4$ and $c\text{-[(Me}_3\text{Si)}_2\text{Si]}_4$ are planar^{188a}, while $c\text{-}[(t\text{-BuCH}_2)_2\text{Si}]_4$ and $c\text{-}[(i\text{-Pr}_2\text{Si}]_4$ are highly folded with out-of-plane angles, θ , of 38.8° and 37.1° respectively^{188b}. $c\text{-Ge}_4\text{Ph}_8$ is nearly planar ($\theta = 3.9^\circ$), while $c\text{-}(t\text{-BuClGe)}_4$ is strongly puckered ($\theta = 21^\circ$). $c\text{-}(t\text{-Bu}_2\text{Sn)}_4$ has a planar Sn_4 ring, while in $c\text{-}(t\text{-Am}_2\text{Sn)}_4$ ($t\text{-Am} = t\text{-Amyl}$) the Sn_4 ring is puckered by 20° . The degree of puckering reflects the balance between the $\text{M}\text{--}\text{M}$ distance and the steric requirements of the substituents¹⁶⁷. A systematic computational study of the effect of substituents, both electronic and steric, on the degree of puckering of 4-MRs is desired.

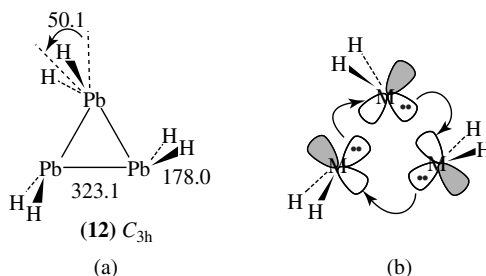
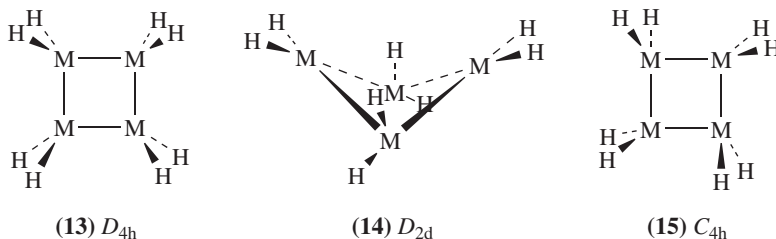


FIGURE 10. Skewed $c\text{-Pb}_3\text{H}_6$ (12). (a) Optimized geometry at HF/DZ¹⁸⁴ (bond lengths in pm, bond angles in deg); (b) orbital interaction leading to 12



The M–M bond lengths in $c\text{-M}_3\text{H}_6$ and $c\text{-M}_4\text{H}_8$ are collected in Table 16^{189,190}. Some experimental values are also presented, although a direct comparison between the calculated and known experimental bond lengths is hampered by the very bulky substituents in the synthesized compounds^{1,2a,11f} which certainly affect the geometries.

The bonds in the cyclic compounds are all longer than those of the corresponding H_3MMH_3 , reflecting the weakening of the bonds in the rings. The M–M bond lengths in $c\text{-M}_3\text{H}_6$ are generally shorter than in $c\text{-M}_4\text{H}_8$, despite the fact that the former are more strained (see below). Nagase explained this trend by the need of the M atoms in the 3-MRs to form bonds as effective as possible in order to compensate (even in part) for the energy loss caused by the unfavorable hybridization required to maintain a 3-membered ring skeleton⁵.

ii. Strain. In an important series of papers on polyhedral compounds of the heavier group 14 elements Nagase and coworkers^{190–196} employed homodesmotic equations 13 to evaluate the strain of ring systems (see below).



Their findings (based on MPn//HF calculations), shown in Table 17, are surprising. While the strain in four-membered rings decreases drastically from C (26.7 kcal mol⁻¹)

TABLE 16. Calculated M–M bond lengths (pm) in $c\text{-M}_3\text{H}_6$ (D_{3h}), $c\text{-M}_4\text{H}_8$ (planar, D_{4h}) and H_3MMH_3

M	$c\text{-M}_3\text{H}_6$ (11) ^a	$c\text{-M}_4\text{H}_8$ (13)	H_3MMH_3 ^b
C	150.2 ^c	155.0 ^d ; 154.5 ^{d,e}	153.3
Si	238.1 ^f ; 233.0 ^g	237.7 ^f ; 237.6 ^g ; 237.3 ^h	234.7
Ge	249.5 ^{f,i}	252.4 ^{f,i}	242.7
Sn	280.0 ^f	280.8 ^f	278.5
Pb	293.4 ^j ; 323.1 ^k	290.8 ^l ; 300.3 ^m	281.2

^aSee Sections V.E.1.a.iv and V.E.1.c.i for values at other theoretical levels.

^bAt MP2/ECP; from Reference 45. For values at other theoretical levels see Table 7.

^cAt CCSD(T)/cc-pVQZ; from Reference 189.

^dAt MP2/6-31G(d); from Reference 185.

^ePuckerd, D_{2d} symmetry.

^fAt HF/DZ+P, (HF/ECP + relativistic core for Sn); from Reference 181.

^gHF/DZ+d; from Reference 182.

^hPuckerd, D_{2d} symmetry; from Reference 190.

ⁱ244.8 pm for $c\text{-M}_3\text{H}_6$ (D_{3h}) and 246.2 pm for $c\text{-M}_4\text{H}_8$ (D_{4h}), at HF/3-21G(d)¹⁸⁷.

^j D_{3h} symmetry; from Reference 184.

^kFor **12**; from Reference 184.

^l D_{4h} structure; from Reference 184.

^mFor **15**; from Reference 184.

TABLE 17. Calculated strain energies^a (kcal mol⁻¹) in *c*-M₃H₆ (**11**, *D*_{3h}) and *c*-M₄H₈ (**13**, *D*_{4h})

M	<i>c</i> -M ₃ H ₆	<i>c</i> -M ₄ H ₈
C	28.7 ^b	26.7 ^b
R = Me ^c	35.5	—
R = SiH ₃ ^c	34.8	—
Si	39.2 ^d	16.7 ^b
R = Me ^c	37.6	—
R = SiH ₃ ^c	28.1	—
Ge ^d	39.4	15.2
Sn ^d	36.6	12.2
Pb ^d	33.7 ^e	10.1 ^e

^aAccording to equation 13.^bAt HF/6-31G(d); from References 190.^cFor *c*-M₃R₆, at HF/6-31G(d); from References 191 and 192.^dAt HF/DZ+d; from Reference 193.^eThe skewed structures of *c*-M₃H₆ (**12**, *C*_{3h}) and *c*-M₄H₈ (**15**, *C*_{4h}) are by 9.8 and 0.7 kcal mol⁻¹, respectively, more stable¹⁸⁴.

to Pb (10.1 kcal mol⁻¹), as might be expected because the bonds get longer, the three-membered rings of heavier group 14 metals are significantly more strained than cyclopropane. Thus, while the strain in *c*-C₃Me₆ is 35.5 kcal mol⁻¹, the strain in *c*-Si₃Me₆ is 37.6, and even *c*-Pb₃H₆ is more strained (33.7 kcal mol⁻¹) than cyclopropane (28.7 kcal mol⁻¹). Furthermore, while the strain of *c*-C₃H₆ and *c*-C₄H₈ is almost the same, i.e. 28.7 and 26.7 kcal mol⁻¹, respectively, for Si, Ge, Sn and Pb the calculated strain in the 3-MRs is significantly greater than in the corresponding 4-MRs (Table 17). Within the *c*-M₃H₆ series the strain behaves ‘normally’, decreasing monotonically from Si to Pb¹⁹¹ (Table 17).

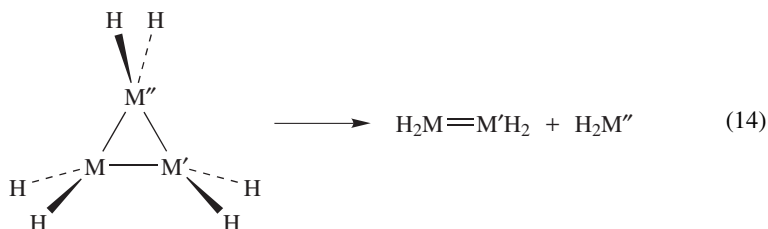
A critical examination of the data in Table 17 shows that among all 3-MRs of group 14 elements the behavior of cyclopropane is unusual. Furthermore, cyclopropane is less strained than expected from the strain energy progression involving six-, five- and four-membered carbon rings; i.e. for M = C the strain energy follows the order: 3-MR ~ 4-MR > 5-MR > 6-MR. In contrast, the three-membered metaliranes (**11**, M = Si to Pb) fit well into the regular strain energy progression as a function of the ring size, i.e. the ring strain increases with decreasing ring size^{195,196}. This exceptional behavior of cyclopropane has been the subject of many theoretical studies^{182,197–201}, which attributed this behavior to σ -electron delocalization (σ -aromaticity)^{197–199}, to angle deformation and torsional strain (i.e. M–H bond eclipsing)^{182,201} and to hybridization considerations²⁰¹. Another explanation for the reduced strain in cyclopropane relative to trisilacyclopropane uses the concept of bent bonds²⁰². According to ‘Atoms in Molecules’ calculations, the angle between the pathways of maximum electron density (MED) in cyclopropane is 78.8°^{52,198,199}, considerably larger than the 60° angle between the internuclear axes, thus, decreasing the angular strain. The bending of the MED path in *c*-Si₃H₆ was calculated to be 81.7°, larger than in *c*-C₃H₆, and the MED of the Si–Si bonds resides at a larger distance from the internuclear axes than required by optimal bent bonds, thus reducing their stability⁵². While the C–C bonds of cyclopropane are formed by orbitals with *ca* sp⁵

hybridization²⁰³, allowing the formation of flexible bent bond orbitals, orbitals with such high p character are not possible in three-membered rings of the heavier group 14 metals for which rehybridization is much less favorable energetically. As a result, bending of the MED path for the heavier M–M bond becomes larger than for carbon and the path deviates strongly from optimal bending. Consequently, the M–M bonds of the heavier metaliranes are weaker and considerably more strained than the analogous C–C bonds (Table 17)⁵². In four-membered rings, the larger bond angle reduces significantly the hybridization problem. The M atoms maintain the regular $ns^2n p^2$ electronic configuration which favors 90° bond angles and thus provide low-strain 4-membered rings¹⁹⁵ (Table 17).

The strain in mixed 3-MRs which are composed of combinations of C, Si and Ge, e.g. *c*-SiC₂H₆, *c*-GeC₂H₆, *c*-GeSi₂H₆ etc., is almost constant, *ca* 37–42 kcal mol⁻¹. The most strained ring is *c*-CGe₂H₆ (39.2 kcal mol⁻¹, CCSD/DZ+d//DZ+d)²⁰⁴.

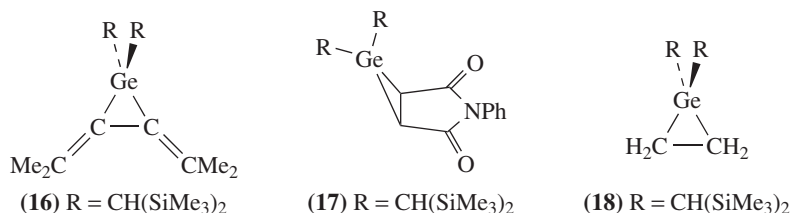
The effects of substituents on the ring strain is expected to be similar to their effects on the stability of double bonds (see Sections VI.B.1 and VI.B.2): electropositive substituents (e.g. SiH₃) reduce the ring strain^{191,192} because they decrease the MR₂ singlet–triplet energy gap and thus the ability to form σ -bonds with high p character increases. Indeed, the calculated strain of *c*-Si₃R₆ is 37.6 kcal mol⁻¹ for R = Me and only 28.1 kcal mol⁻¹ for R = SiH₃ (Table 17). As SiH₃ increases the strain in cyclopropane to 34.8 kcal mol⁻¹, *c*-Si₃(SiH₃)₆ becomes less strained than *c*-C₃(SiH₃)₆, making the former a suitable building block in forming polycyclic compounds (see below)^{191,192}. On the other hand, electronegative substituents which increase the singlet–triplet energy gap are expected to increase the ring strain^{182,205a}; e.g. the ring strain of hexafluorocyclopropane is 75–80 kcal mol⁻¹^{205b}. A systematic study of the electronic and steric effect of substituents on the strain of *c*-M₃R₆ is unavailable and is a worthwhile project for future theoretical studies.

iii. *Stability towards cleavage.* *c*-MH₂M'H₂M''H₂ (M, M', M'' are group 14 elements) serve as precursors in the photolytic and in some cases thermolytic synthesis of H₂M=M'H₂ and of carbene-like species, M''R₂ (equation 14)^{10,11f,13,14,206}, and knowledge of their stability towards fragmentation is therefore of practical importance.



The dissociation of *c*-M₃H₆ (equation 14, M=M'=M'') is calculated (at CCSD/DZ+d//HF/DZ+d) to be highly endothermic for M = C and the endothermicity decreases in the order 98.6 (M = C) > 62.3 (M = Si) > 47.1 (M = Ge) kcal mol⁻¹²⁰⁴. Data are not available for M = Sn and Pb. Among the 10 possible *c*-MH₂M'H₂M''H₂ (M, M', M'' = C, Si, Ge) the highest fragmentation energy is calculated for the reaction: *c*-CSi₂H₆ → CH₂ + Si₂H₄ (120.3 kcal mol⁻¹). However, *c*-CSi₂H₆ has also a less demanding fragmentation route, i.e. *c*-CSi₂H₆ → SiH₂ + H₂C=SiH₂, requiring only 64.7 kcal mol⁻¹. The least stable member among these 3-MRs is the germirane *c*-GeC₂H₆, whose fragmentation to C₂H₄ + GeH₂ requires only 18.3 kcal mol⁻¹. This low fragmentation energy may be one of the reasons for the many failures to synthesize germiranes²⁰⁴. Electronegative substituents reduce this fragmentation energy further (see below), and the fragmentation

of $c\text{-F}_2\text{GeC}_2\text{H}_4$ to $\text{GeF}_2 + \text{H}_2\text{C}=\text{CH}_2$ is actually exothermic by 27 kcal mol^{-1} with an energy barrier of only $16.1 \text{ kcal mol}^{-1}$ [at MP4/6-31G(d,p) with RECP for Ge]²⁰⁷. The first germiranes (**16** and **17**) were synthesized only recently and they are stabilized by substituents on the carbons which destabilize the olefinic fragmentation product^{208a}, i.e. **16** when fragmented will produce the relatively high energy $\text{Me}_2\text{C}=\text{C}=\text{CMe}_2$. The stability of **17** was attributed to the electron-poor maleimide group and the weakened C–C π -bond in free *N*-methylmaleimide^{208a}. The first germirane with hydrogens on the ring carbon atoms, **18**, was detected recently by ^1H NMR in the reaction mixture of GeR_2 [$\text{R} = (\text{Me}_3\text{Si})_2\text{CH}$] with ethylene^{208b}, but it was not yet isolated.



$c\text{-H}_2\text{SnC}_2\text{H}_4$ is predicted to be unstable, as according to the calculations it fragments to SnH_2 and ethylene by a slightly exothermic reaction of $2.8 \text{ kcal mol}^{-1}$ with a very small activation barrier of only $1.1 \text{ kcal mol}^{-1}$ ²⁰⁷.

Beside a direct calculation, the dissociation enthalpy of equation 14 can be predicted (quite reliably) from the contributions of the single bond dissociation energies (D), strain enthalpy of the ring, π -bond enthalpy (D_π) and the divalent stabilization energy (DSSE), according to equation 15²⁰⁴. Equation 15 provides a tool to analyze the various factors that affect the fragmentation of the 3-MRs. Thus, substituent effects on equation 14 can be estimated from the known substituent effects on the above-mentioned components. For example, F increases the DSSE and therefore reduces considerably the stability of a fluorine-substituted three-membered ring (e.g. the energy of equation 14 is reduced from *ca* 40 kcal mol^{-1} for $c\text{-H}_2\text{SiC}_2\text{H}_4$ to *ca* 15 kcal mol^{-1} for $c\text{-F}_2\text{SiC}_2\text{H}_4$ ²⁰⁷), while SiH_3 groups are expected to have the opposite effect. From known energy values (e.g. σ bond strength, DSSE)²⁶, it can be predicted that any cycloplumbirane, PbC_2R_6 , is expected to be unstable thermodynamically with respect to dissociation into PbR_2 and C_2R_4 .

$$\Delta H(\text{equation 14}) \cong D(\text{H}_3\text{M}-\text{M}'\text{H}_3) + D(\text{H}_3\text{M}'-\text{M}''\text{H}_3) + \text{strain enthalpy} \\ - D_\pi(\text{H}_2\text{M}=\text{M}'\text{H}_2) - \text{DSSE}(\text{H}_2\text{M}'') \quad (15)$$

The reverse reactions of equation 14, i.e. the addition of metallylenes MR_2 to doubly-bonded species, is discussed in detail in Section VII.A.3.b.iv.

iv. Other structures of 3-MRs. The classical cyclic M_3H_6 structures with D_{3h} symmetry are minima for all group 14 elements, with the exception of lead which adopts the skewed structure, **12**^{5,184}. For silicon and tin, two additional minima, **19** and **20**, were located (at the MP2/6-31G* and MP2/LANL1DZ levels of theory)¹⁸³. In **19**, 3 of the 6 hydrogens are bridging (Figure 11a) and, in **20**, all the 6 hydrogens are bridging (Figure 11b). For Ge and Pb the singly H-bridged structure, **19**, is a minimum while the doubly H-bridged structure, **20**, is not a stationary structure. In all cases, the singly H-bridged conformer is somewhat lower in energy than the doubly H-bridged structure. The calculated relative energies of the classical D_{3h} structure, **11**, and the bridged structures **19** and **20** for all group 14 M_3H_6 molecules are collected in Table 18.

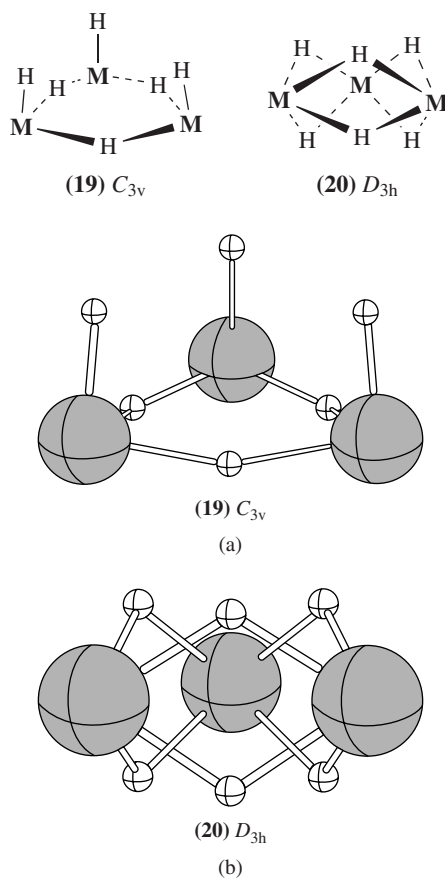


FIGURE 11. H-bridged structures of $c\text{-M}_3\text{H}_6$: (a) monobridged, C_{3v} (**19**) and (b) dibridged, D_{3h} (**20**)

For cyclopropane only the classical D_{3h} structure (**11**) is a minimum. For $c\text{-Si}_3\text{H}_6$ the classical D_{3h} structure is also strongly preferred (i.e. by 84–92 kcal mol⁻¹) but it becomes less stable as one proceeds down group 14. Sn_3H_6 and Pb_3H_6 prefer the H-bridged isomers **19**, which are the global minima and are favored by 1.7 and 45.4 kcal mol⁻¹, respectively, over the cyclopropane-like isomers¹⁸³. Similar behavior was found also for the heavier congeners of the cyclopropenyl cation, $c\text{-M}_3\text{H}_3^+$ ($M = \text{Ge}$ to Pb), which prefers an H-bridged global minima of C_{3v} symmetry^{209a}, although the classical cyclopropenyl-type structure is strongly stabilized by aromaticity (see Section VI.F.2).

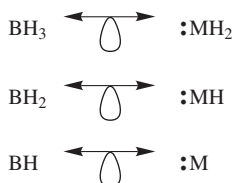
The chemical bonding in **19** and **20** is best understood by using an isolobal analogy to boron chemistry. Thus, the electronic configuration of MH_2 with a σ lone pair and an empty p orbital is isolobal to that of a trivalent BH_3 unit, where one of the B–H bonds is equated to the lone pair at M (Scheme 1)^{209b}. The well-known ‘diagonal relationship’ in the Periodic Table^{35a} also supports this relationship. Following the isolobal analogies in Scheme 1, novel compounds can be proposed. For example, the C_{3v} structure of $c\text{-M}_3\text{H}_6$

TABLE 18. Relative energies (ΔE , kcal mol⁻¹) and geometries (pm, deg) of three-membered rings and their nonclassical H-bridged isomers^a

M		Classical D_{3h} (11)	Singly bridged C_{3v} (19)	Dibridged D_{3h} (20)
C	ΔE	0.0	197.0 ^b	297.0 ^b
	d(M–M) ^c	150.4	161.9	<i>d</i>
	d(M–H(b)) ^e	—	126.6	<i>d</i>
Si	ΔE	0.0	84.0	92.2
	d(M–M) ^c	233.2	308.0	<i>d</i>
	d(M–H(b)) ^e	—	166.1	<i>d</i>
Ge	ΔE	0.0	36.0	76.1
	d(M–M) ^c	249.6	341.7	<i>d</i>
	d(M–H(b)) ^e	—	177.7	<i>d</i>
Sn	ΔE	0.0	–1.7	22.3
	d(M–M) ^c	286.0	378.3	<i>d</i>
	d(M–H(b)) ^e	—	194.9	<i>d</i>
Pb	ΔE	0.0 ^f	–45.4	–25.3
	d(M–M) ^c	295.4	388.9	<i>d</i>
	d(M–H(b)) ^e	—	200.7	<i>d</i>

^aAt MP2/ECP; from Reference 183.^bNot a minimum.^cd(M–M) values at other computational levels are given in Table 16. See for comparison the M–M bond lengths in H₃MMH₃, given in Tables 7 and 16.^dNot available.^eThe bond distance from M to the bridging hydrogen [H(b)].^fNot a minimum. **12** is by 10.6 kcal mol⁻¹ lower in energy than the D_{3h} structure¹⁸⁴.

(**19**) was found by applying the isolobal analogy between BH₃ and MH₂^{209b}. Extensions of this analogy allow one to predict from the structures of boranes new and unexpected structures for group 14 compounds.

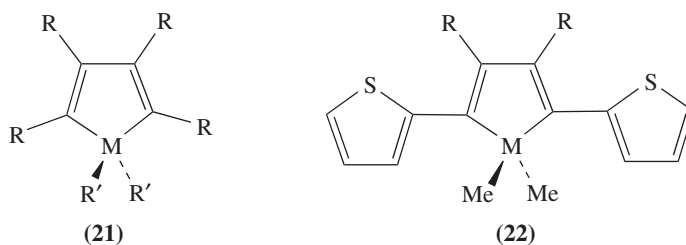


SCHEME 1

b. Metalloles. Metalloles (**21**) and especially siloles (**21**, M = Si) have received much attention as new building units for the preparation of π -conjugated polymers with very small band gaps that potentially can exhibit conductivity and semiconductivity, as well as thermochromism and nonlinear optical properties^{210,211}. Germoles (**21**, M = Ge) and stannoles (**21**, M = Sn) have received so far much less attention as building blocks in π -conjugated polymers. Despite the remarkable recent developments in the synthesis

of metalloles, there are only few theoretical studies of their properties, most of which concentrate on siloles²¹².

The structures, magnetic susceptibilities χ and magnetic exaltations Λ of **21**, $M = C$ to Pb , $R=R'=H$, were computed by Goldfuss and Schleyer using the B3LYP/6-31+G(d) level of theory²¹³. The structure of the C_4H_4 fragment of **21**, $R=R'=H$ remains unchanged for all group 14 elements; the $C-M-C$ angle decreases gradually from 103.2° for **21**, $M = C$ to 82.6° for **21**, $M = Pb$ as the $M-C$ bond distances increase. The magnetic properties are almost constant for **21** with all group 14 elements²¹³. Despite the great importance of metalloles in optics and electronics, there is no systematic theoretical study which deals with the characteristic electrochemical and photophysical properties of metalloles and with the effect of M on these properties. The only available theoretical studies deal with a specific behavior of particular metalloles, i.e. **21**, $M = Si, Ge$ and Sn , $R = Ph$, $R' = Me$ and $R = R' = Ph$ ²¹⁴ and **22**, $M = C$ to Sn , $R = H$ ²¹⁵. These theoretical studies accompanied the experimental studies of these specific systems and were aimed to explain the experimental findings.



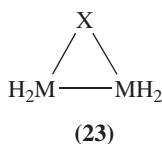
A notable property of silole is its high electron-accepting ability due to the low-lying LUMO, which is ascribed to the orbital interaction between the σ^* orbitals of the two exocyclic $Si-R'$ σ bonds with the π^* orbital of the butadiene moiety^{212,215,216}. The dependence of the LUMO energy on M has not yet been studied.

In an earlier study, Tamao and coworkers found that silole-containing π -conjugated compounds show unique photophysical properties, e.g. λ_{max} of the UV-vis absorption spectra of 2,5-dithienylsilole, **22**, is at 416 nm, by about 60 nm longer than for the thiophene trimer²¹⁶. This finding increased their interest in the properties of π -conjugated systems containing heavier group 14 metalloles, and particularly in the effects of the central group 14 elements on their electronic structures. To study these effects, a series of metalloles **22**, $M = C, Si, Ge$ and Sn were synthesized, and their photophysical properties and electrochemical behavior were studied. The experimental studies were accompanied by theoretical studies using the B3LYP method. The theoretical calculations have shown that for the heavier group 14 elements, the energy of the LUMO orbital of **22** is almost invariant with respect to the identity of M , but there is a significant difference between the cyclopentadiene derivative, **22**, $M = C$ and the silole derivative, **22**, $M = Si$. The energy of the LUMO orbital is reduced from 1.22 eV for **22**, $M = C$ to 0.93, 0.97 and 0.93 eV for **22**, $M = Si, Ge$ and Sn , respectively, indicating a similar $\sigma^*-\pi^*$ conjugation for the last three metals, and thus implying a similar UV-vis absorption spectra. Indeed, **22**, $M = Si, Ge$ and Sn have comparable UV-vis spectra, the maxima of which are shifted by *ca* 50 nm relative to **22**, $M = C$ ²¹⁵.

Experimental studies of **21**, $R = Ph$, $R' = Me$ show strong dependence of the emission maxima on the identity of M . Thus, **21**, $M = Si$, emits at longer wavelengths than **21**, $M = Ge$, while **21**, $M = Sn$ does not emit at all. On the other hand, the emission maxima of **21**, $R = R' = Ph$ are invariant to the change in M . It was proposed, based

on the semiempirical AM1 calculations of the electron density, that the increased electron density at Sn deactivates the emissive state²¹⁴. The presence of the phenyl group on **21**, M = Sn, R = R' = Ph serves to stabilize the emissive state and luminescence is observed²¹⁴.

c. Heterocyclic 3- and 4-membered rings. i. 3-MRs, c-(R₂M)₂X. Computational studies on *c*-(R₂M)₂X (**23**) are available only for M = C, and Si^{52,217,218}, but the models that were used to explain their peculiar structures can explain also the known experimental structures of **23** with M = Ge and Sn, which exhibit a similar behavior^{19,22}. When one MH₂ group of the (H₂M)₃ ring is replaced by another element or group X (e.g. CH₂, O, NH, S, PH), the bond distance between the remaining two M metals decreases and the H₂M–MH₂ moiety becomes more planarized as the electronegativity of X increases^{19,22,52,217,218}. A variety of calculated and experimental structures of compounds of type **23** are presented in Table 19. The Si–Si bond lengths in **23**, M = Si, X = CH₂, S, O, NH, PH are significantly shorter than a normal Si–Si single bond length, e.g. for M = Si, X = O, the Si–Si distance is 220 pm, (235 pm, for X = SiH₂, Table 19), which is actually very close to that of a Si=Si double bond length (214 pm)²¹⁸. Experimental evidence agrees well with the calculated geometries (Table 19^{19,22,167,217–220}), and also for **23**, M = Ge and Sn the experimentally measured M–M bond lengths are shorter when X is electronegative^{19,22}(Table 19).



Two models were used to explain the unusual geometries of these cyclic compounds. Grev and Schaefer²¹⁸ adopted the well known Dewar–Chatt–Duncanson²²¹ model for transition metal–olefin complexes. According to this model (shown schematically in Figure 12), the H₂M=MH₂ double bond acts as a π donor into an appropriate orbital on X, and X back-donates electron density from its lone pairs (or filled π orbitals) into the π* orbital of the M=M unit. According to this model a spectrum of interactions, from normal three-membered rings to complexes with T-shaped electron density distribution, are possible, depending on the donor/acceptor ability of X and the M=M bond. In terms of this model the unusual geometries of **23** for electronegative X groups are a direct result of decreased back-donation from X into the π* orbital of the M=M bond. Steric effects also might be partially responsible for the M–M bond length shortening as most electronegative groups (e.g. oxygen) are smaller than MH₂²¹⁷, and much smaller than the large MR₂ groups used experimentally.

Boatz and Gordon explained²¹⁷ the unusual geometries of **23**, M = Si, using the bent bond formalism (see Section V.E.1.a). They concluded that the short Si–Si internuclear distances in **23** are a consequence of severe bond bending, rather than the result of a significant π character in the Si–Si bond as suggested by Grev and Schaefer²¹⁸. According to Boatz and Gordon the calculated Si–Si bond paths (MED path) are in the range of 231–238 pm, suggesting that these bonds are still really single bonds. The Si–Si bond paths also decrease with increase in the electronegativity of X⁵². As the relative electronegativity of X increases and back-donation decreases, the M–X bonds will become more concave (inwardly curved) reaching a π-complex of T-structure (i.e. the two concave M–X bonds coincide, and X acts only as an acceptor)⁵². However, although the

TABLE 19. Calculated^a and representative experimental^b (in parentheses) M–M bond lengths (pm) in *c*-(R₂M)₂X (**23**)

M	X	R ^c	d(M–M)
C ^d	CH ₂	H	149.7 (151.3)
	NH	H	147.1 (148.0)
	O	H	145.3 (147.2)
	SiH ₂	<i>e</i>	155.3 (158.6)
	PH	H	149.2 (150.2)
	S	H	147.3 (149.2)
Si ^f	SiH ₂	Dmp ^g	235.0 (240.7)
	CH ₂	Dmp ^h	225.8 (227.2)
	NH	Mes ^h	223.8 (223.0 ⁱ)
	O	Mes ^h	220.0 (222.7)
	PH		228.2
	S	Mes ^h	226.0 (228.9)
Ge	GeH ₂	Dep ^j	249.5 ^k (259.0)
	CH ₂	Dep ^h	237.3 ^l (237.9)
	NPh	Dep ^h	(237.9)
	SiH ₂	Mes ^h	246.0 ^t (250.8)
	S	Dep ^h	(238.7)
Sn	SnH ₂	Dep ^h	280.0 ^k (285.5)
	NR	Mes ^m	(270.9)

^aAll reported calculated values are for R = H.

^bSubstituted by bulky R substituents as indicated.

^cDmp = 2, 6-dimethylphenyl; Mes = 2,4,6-trimethylphenyl; Dep = 2,6-diethylphenyl.

^dCalculated at HF/6-31G(d); from Reference 217 which includes also references to the experimental values.

^eFor *c*-[(MeHC)₂Si(2,4,6-triisopropylphenyl)₂]; from Reference 219.

^fAt HF/6-31G(d) from References 52 and 217. Similar values were obtained at HF/DZ+d²¹⁸.

^gFor *c*-(Dmp₂Si)₃; from Reference 220.

^hReferences cited in Reference 19.

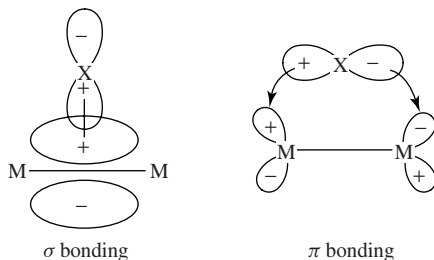
ⁱX = N-TMS.

^jFrom Reference 167.

^kAt HF/DZ+d; from Reference 181.

^lAt HF/DZ+d; from Reference 204.

^mFrom Reference 22.

FIGURE 12. The Dewar–Chatt–Duncanson orbital model for three-membered XM₂H₄ rings

π -complex character increases along the series: $X = S > PH > SiH_2 > CH_2 > NH > O$, neither of these compounds possesses a concave Si–X bond, and they are therefore considered to be true 3-membered rings⁵².

Freinking calculated the electron density of azadistanniridine, $c-(H_2Sn)_2NH$, and concluded that it can be viewed as a cyclic N-donor–Sn₂-acceptor compound with a concavely bent Sn–Sn bond. This description is different from the Dewar–Chatt–Duncanson formalism that describes the $c-(H_2Sn)_2NH$ as a complex where HN is the acceptor and $H_2Sn=SnH_2$ is the donor (private communication from Freinking reported in Reference 22). The calculated electron density distribution, shown in Figure 13a, shows that $c-(H_2Sn)_2NH$ has an inwardly bent concave Sn–Sn bond²², contrary to the convex (outwardly curved) Si–Si bond calculated for $c-(H_2Si)_2NH$ ⁵² (see Figure 13b, as an example for the effect of an electronegative substituent on the electron density distribution).

The strain energies of $c-(H_2Si)_2X$ are larger than those of their carbon analogs^{52,217,222}, similar to the trend found for $c-M_3H_6$, $M = C$ vs. $M = Si$. The strain energy of **23** generally decreases as the electronegativity of X increases (for X within the same period), except for **23**, $M = Si$, $X = CH_2$, NH and O, where the strain increases as the electronegativity of X increases⁵². The MP2/6-31G* strain energies (in kcal mol⁻¹) of **23**, X = CH₂, NH, O, SiH₂, PH, S are (a) for M = C: 27.3, 23.2, 19.9, 40.9, 20.0, 15.5, respectively, and (b) for M = Si: 42.6, 44.5, 50.8, 35.6, 28.4, 26.7, respectively²¹⁷. The most strained compound is $c-(H_2Si)_2O$. No information is available on the strain energies of **23**, M = Ge, Sn and Pb.

ii. 1,3-Dioxa-2,4-dimetaletanes, $c-(MH_2)_2O_2$ The 1,3-dioxa-2,4-dimetaletanes (**24**, R = H) might be regarded as complexes of $H_2M=MH_2$ with two oxygen atoms^{223,224}. These complexes can be derived either by (a) an addition of dioxygen to $H_2M=MH_2$ (equation 16), or by (b) the head-to-tail dimerization of $H_2M=O$ (equation 17)²²⁴. Both reactions are highly exothermic for M = Si to Pb, and the exothermicity increases as

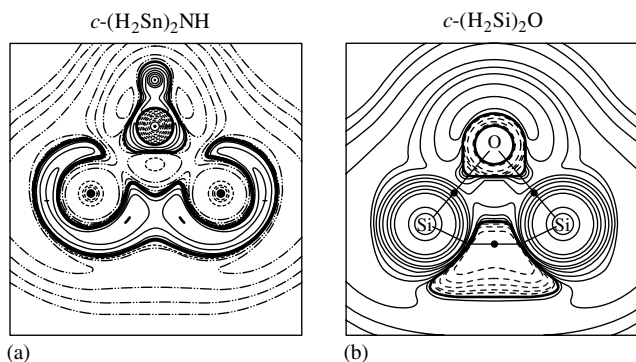
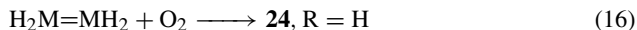
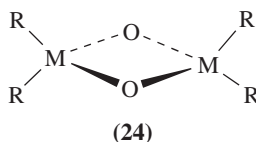


FIGURE 13. Contour line diagrams of the Laplace charge concentration $-\nabla^2\rho(r)$, showing the M–M bond curvature for (a) $c-(H_2Sn)_2NH$ (**23**, M = Sn, X = NH)²². Solid lines show higher charge density; dashed lines show lower charge density. Reproduced by permission of Wiley-VCH from Reference 22. (b) $c-(H_2Si)_2O$ (**23**, M = Si, X = O); a similar curvature was calculated for **23**, M = Si, X = NH⁵². Dashed contour lines are in regions with negative charge concentration [$-\nabla^2\rho(r) < 0$], solid lines are in regions where negative charge is depleted [$-\nabla^2\rho(r) > 0$]. Reproduced by permission of Elsevier Science Publishers. Copyright (1988) from Reference 52

M becomes heavier, reflecting the high stability of these dioxo-cyclic 4-MRs and the low stability of the precursors. The calculated reaction energies (at B3LYP/RECP with a DZ+P basis set for the valence electrons) for reaction 16 are -50.6 , -193.3 , -117.0 , -101.0 and -104.7 (-38.8 including relativistic effects) kcal mol^{-1} for $M = \text{C}$, Si , Ge , Sn and Pb , respectively. The corresponding energies for reaction 17 are 11.8 , -96.9 , -81.7 , -95.5 and -104.1 (-75.5 including relativistic effects) kcal mol^{-1} . The highest exothermicities are found for $M = \text{Si}$, due to the very strong $\text{Si}-\text{O}$ σ bonds²²⁴. The high exothermicities of reactions 16 and 17 relatively to the lower reaction energies for $M = \text{C}$ are attributed to the smaller strain in **24** as one goes down group 14 and the smaller stability of $\text{H}_2\text{M}=\text{MH}_2$ and $\text{H}_2\text{M}=\text{O}$ relative to $\text{H}_2\text{C}=\text{CH}_2$ and $\text{H}_2\text{C}=\text{O}$ ²²⁴. The large relativistic corrections for $M = \text{Pb}$ in reactions 16 and 17 are attributed²²⁴ to the unfavorable formation of two Pb^{IV} centers bonded to two electronegative ligands (i.e. $\text{O}-\text{Pb}-\text{O}$ fragments)⁴⁴.



Grev and Schaefer described compounds **24** as an ‘extended’ Dewar–Chatt–Duncanson dibridged π complex²¹⁸. For $M = \text{Si}$, the geometry of **24**, $\text{R} = \text{H}$ is quite unusual: the nonbonding $\text{Si}\cdots\text{Si}$ distance of 241.5 pm (exp. 235 – 240 pm for **24**, with various R substituents^{225a}) is comparable to that of a single $\text{Si}-\text{Si}$ bond (235.4 pm, at B3LYP/ECP/DZ+P²²⁴). However, the small $^{29}\text{Si}-^{29}\text{Si}$ coupling constants in the NMR spectrum of unsymmetrically substituted 1,3-dioxo-2,4-disilaetanes indicate that the Si atoms are not connected by a σ bond^{225b}. The unusually short $\text{Si}\cdots\text{Si}$ bond and the small $\text{Si}\cdots\text{Si}$ NMR coupling constant brought Grev and Schaefer to suggest that the two silicon atoms are connected by a π bond, unsupported by a σ bond²¹⁸. In contrast, Schleyer and coworkers found according to NBO analysis that there is no covalent interaction between the Si atoms and that the Wiberg bond index is 0.03 , the same as for **24**, $M = \text{C}$ ²²⁴. These authors have therefore suggested that the short $\text{Si}\cdots\text{Si}$ distance results from the inflexible $\text{Si}-\text{O}$ bonds and the electrostatic repulsion between the oxygen atoms. Any increase in the $\text{Si}\cdots\text{Si}$ bond distance would decrease the $\text{O}\cdots\text{O}$ distance and consequently would decrease the undesirable electrostatic repulsion between the oxygen atoms²²⁴. As M becomes heavier (and the ring larger), the $\text{O}\cdots\text{O}$ repulsion becomes smaller and the $\text{M}-\text{O}-\text{M}$ angle increases, enabling $\text{M}\cdots\text{M}$ distances (calculated values for $\text{R} = \text{H}$) of 255.7 (exp. 261.7 pm, for **24**, $\text{R} = 2,6$ -diethylphenyl¹⁶), 273.2 [exp. 294 pm, for **24**, $\text{R} = (\text{Me}_3\text{Si})_2\text{CH}$] and 282.6 pm for $M = \text{Ge}$, Sn and Pb , respectively, to be somewhat longer than those in $\text{H}_3\text{M}-\text{MH}_3$ (Table 7), but they are still relatively short. As for **24**, $M = \text{Si}$, also for $M = \text{Ge}$ to Pb the Wiberg $\text{M}\cdots\text{M}$ bond indices are very small (0.02), indicating that there is no direct $\text{M}-\text{M}$ bond in the heavier 1,3-dioxo-2,4-dimetaletanes²²⁴.

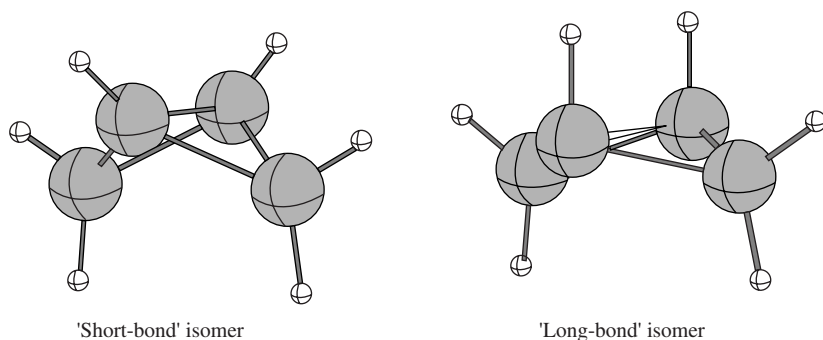
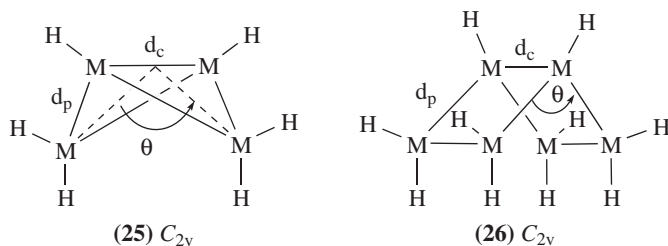


FIGURE 14. 'Bond-stretch' isomers of [1.1.0]metallabicyclobutanes

2. Polycyclic and polyhedral metallanes

a. Bicyclic compounds. Polycyclic compounds composed of highly strained three-membered rings of group 14 elements are found to have 'bond-stretch' isomers. The heavier group 14 analogs of bicyclo[1.1.0]butane (**25**) with $M = \text{Si}$ and Ge have two distinctly different structures (both of which are minima on the PES) with either a 'short' or a 'long' central $M-M$ bridge distance^{187,226,227} (see Figure 14 and Table 20). For $M = \text{Sn}$ and Pb only 'long-bond' isomers were located at the GVB/ECP level^{184,227}. The 'bond-stretch' phenomenon is due to the fact that the heavier group 14 elements prefer to be part of a 4-membered rather than of a 3-membered ring, due to their reluctance to form hybrid orbitals²²⁷. The 'short' $M-M$ bonds are similar in length to those in the corresponding 3-membered rings and have interflap angles, θ (see **25**), of *ca* 120° for $M = \text{Si}$ and Ge . The 'long-bond' isomers have significantly longer $M-M$ separations and larger interflap angles, which increase from $\theta = 140.0^\circ$ for $M = \text{Si}$ to $\theta = 151.6^\circ$ for $M = \text{Pb}$ (at GVB/ECP)²²⁷. These 'bond-stretched' isomers can be viewed as 4-membered monocyclic rings with reduced strain and a weak transannular bond, exhibiting some singlet biradical character. For Si_4H_6 and Ge_4H_6 the 'short-bond' isomer is less stable than the 'long-bond' isomer by 12.3 [at GVB/6-31G(d)] and 22.3 kcal mol^{-1} [at GVB/ECP with a DZ(d) basis-set for the valence electrons], respectively.



Ionization of an electron from the $M-M$ bond of the 'long' M_4H_6 isomers leads to the ${}^2A_1 M_4H_6^+$ cation radicals which have significantly shorter central $M-M$ bonds than in the neutral 'long-bond' isomer (Table 20), contrary to the tentative expectation that this bond will be longer in the cation radicals. The extent of $M-M$ bond shortening upon ionization increases from $M = \text{Si}$ to $M = \text{Pb}$ (Table 20). Ionization from the 'short-bond'

TABLE 20. Structures of group 14 analogs of bicyclo[1.1.0]butanes, of their cation radicals and of metallabicyclo[2.2.0]hexanes (pm, deg)

M		M ₄ H ₆ (25) ^a		M ₄ H ₆ ^{+b} (25 ⁺)	M ₆ H ₁₀ (26) ^c
		'short'	'long'	'long'	
C	d_c^d	146.7		169.5	155.9 ^e
	d_p^f	148.8		149.0	154.5 ^e
	θ	120.9		133.8	115.0 ^e
Si	d_c^d	241.2	294.2 (277.5)	277.7	238.9
	d_p^f	231.0	234.2 (232.3)	234.9	236.5
	θ	121.7	140.0 (142.0)	140.7	112.6
Ge	d_c^d	260.3	317.1 (309.3)	301.2	252.7
	d_p^f	244.8	248.3 (248.0)	249.3	250.6
	θ	121.5	140.8 (142.8)	142.3	113.1
Sn	d_c^d	<i>g</i>	371.3 (365.9)	352.9	288.3
	d_p^f		285.7 (286.6)	286.6	286.5
	θ		144.0 (146.8)	146.2	113.6
Pb	d_c^d	<i>g</i>	390.1 (393.1)	365.3	293.4 ^h (295.3) ⁱ
	d_p^f		296.8 (300.0)	295.8	291.9 ^h (296.6) ⁱ
	θ		151.6 (156.4)		114.7 ^h (111.3) ⁱ

^aAt HF/6-31G(d) for M = C, at GVB/6-31G(d) for M = Si, and at GVB/ECP with DZ+d for the valence electrons for M = Ge, Sn and Pb. The values in parentheses are at the HF level with the corresponding basis sets; from Reference 227.

^bAt HF/6-31G(d) for M = C and Si and HF/ECP (DZ+d) for M = Ge, Sn and Pb; from Reference 227.

^cAt HF/DZ+d, in C_{2v} symmetry; from Reference 194.

^dThe central M...M distance (cf. **25** and **26**). The following are average calculated M–M and M=M bond lengths (in pm, Sections V.B.3 and VI.B.1): 151 (C–C), 234 (Si–Si), 242 (Ge–Ge), 278 (Sn–Sn), 284 (Pb–Pb); 133 (C=C), 213 (Si=Si), 224 (Ge=Ge), 250–254 (Sn=Sn), 257–270 ('Pb=Pb').

^eAt HF/6-31G(d); from Reference 194.

^fBetween the central M atoms to the peripheral MH₂ ligands (cf. **25** and **26**).

^gNot a minimum at the GVB/ECP level of theory²²⁷.

^hThe C_{2v} structure is not a minimum on the PES¹⁹⁴.

ⁱUsing relativistic ECPs. In parentheses, the minimum C₂ structure¹⁹⁴.

isomer, gives the same ²A₁ state. No stationary point resembling the 'short-bond' structure was located on the ²A₁ PES. Thus, unlike the neutral M₄H₆, the corresponding cation radicals do not exhibit bond stretch isomerism on the same PES²²⁷. When the M–M bond lengths were fixed at several distances *R*, and all other geometrical parameters were optimized, a high-energy ²A₂ state which resembles the 'short-bond' neutral isomer was located for M = Si to Sn²²⁷. The ²A₂ state of Si₄H₆⁺ has a shorter central Si–Si bond length than in the 'short-bond' neutral isomer. For Pb₄H₆⁺ at HF/ECP (with DZ basis set for the valence electrons), both the ²A₂ and ²A₁ states of Pb₄H₆⁺ are not minima, but correspond to a transition structure that leads to a single structure of C₂ symmetry in the ²A state. The latter has a very weak central Pb–Pb bond and skewed hydrogens around the Pb₄ skeleton resembling the C_{4h} structure of Pb₄H₈ (**15**). The ²A and ²A₂ states, despite their considerable different geometries, have almost the same energy (i.e. within 0.5 kcal mol⁻¹) reflecting the very flat PES of Pb₄H₆⁺²²⁷. The vertical and adiabatic ionization potentials of M₄H₆, M = Si to Pb are in the range of 7.2–7.7 eV, decreasing only slightly from Si₄H₆ to Pb₄H₆, but all are considerably smaller than for C₄H₆, being 8.2 (adiabatic) and 9.0 eV (vertical)²²⁷.

TABLE 21. Strain energies (kcal mol⁻¹) of metallabicyclo[2.2.0]hexane (**26**), metallabicyclo[1.1.0]butane (**25**) and *c*-M₄H₈ (**13**)

M	Bicyclo[2.2.0]hexane (26) ^a	Bicyclo[1.1.0]butane (25) ^b	<i>c</i> -M ₄ H ₈ (13) ^c
C	53.8	68.9	26.7 ^d
Si	33.9	65.2	16.7 ^d
Ge	29.2	<i>e</i>	15.2 ^f
Sn	23.4	<i>e</i>	12.2 ^f
Pb	19.1 ^g	<i>e</i>	10.1 ^f

^aAccording to equation 18, at HF/DZ+d; from Reference 194.

^bAccording to the following equation: **25** + 5M₂H₆ → 2(MH₃)₃MH + 2(MH₃)₂MH₂, calculated at HF/6-31G(d); from Reference 226a.

^cAccording to equation 13.

^dAt HF/6-31G(d); from References 190.

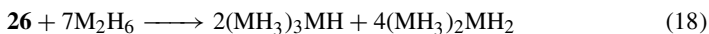
^eNot available.

^fAt HF/DZ + d; from Reference 193.

^gThe C₂ structure is by 0.2 kcal mol⁻¹ more stable than the C_{2v} **26**¹⁹⁴.

All heavier analogs of bicyclo[2.2.0]hexane, **26**, have a C_{2v} structure^{187,194,226b} except for bicyclo[2.2.0]hexaplumbane, **26**, M = Pb for which a deformed C₂ structure was located as a minimum¹⁹⁴. In the C₂ structure the 4-membered rings are slightly puckered (with a PbPbPbPb dihedral angle of 3.6°) and the central Pb–H groups are highly skewed, i.e. the HPbPbH dihedral angle is 46.7°. However, the C_{2v} isomer is by only 0.2 kcal mol⁻¹ less stable (0.03 kcal mol⁻¹ at MP2/DZ+d). No ‘bond-stretch’ isomers were found for **26**, and *d_c* is only slightly longer than *d_p* (Table 20)¹⁹⁴.

Metallabicyclo[2.2.0]hexanes **26** are considerably less strained than **25**. The strain in M₆H₁₀, calculated by the homodesmotic equation 18, decreases in the order: M = C > Si > Ge > Sn > Pb from *ca* 54 kcal mol⁻¹ for M = C to 19 kcal mol⁻¹ for M = Pb, very similar to the trend in the monocyclic M₄H₈ series (Table 21). Nagase and Kudo observed that the strain energy in polycyclic and polyhedral compounds (see below) is additive, e.g. it is twice as large in **26** than in the monocyclic M₄H₈¹⁹⁴.



b. Propellanes. The parent [1.1.1]propellane, **27**, M = C, was investigated extensively due to the inverted tetrahedral configurations at the bridgehead carbon atoms²²⁸. The silicon analogs have also received considerable attention^{229,230}. The general shape of the [1.1.1]metallapropellanes, **27**, is shown in Figure 15. As in the [1.1.0]bicyclobutanes M₄H₆ (**25**)^{184,227}, the central bond between the bridgehead metal atoms of M₅H₆ (**27**) is significantly elongated^{184,231–233}, e.g. in **27**, M = Sn, the central Sn_b–Sn_b bond distance (*d_c*) is 347 pm compared to 286 pm of the Sn_b–Sn_p bonds (*d_p*) (Table 22^{184,231–234}). These theoretical results are nicely supported by the experimental X-ray results for a pentastanna[1.1.1]propellane^{234,235}. In contrast, for M = C, *d_c* is 162.5 pm, only slightly longer than *d_p* (152.3 pm) and significantly shorter than *d_c* (188.3 pm) in the bicyclic **28**, M = C²³¹. For the heavier congeners the differences between the M_b···M_b distances in **27** and those in the corresponding **28** are much smaller than for M = C (26 pm) and they decrease down group 14, i.e. the differences are 13.2, 6.0 and 3.1 pm for M = Si, Ge and Sn, respectively²³¹.

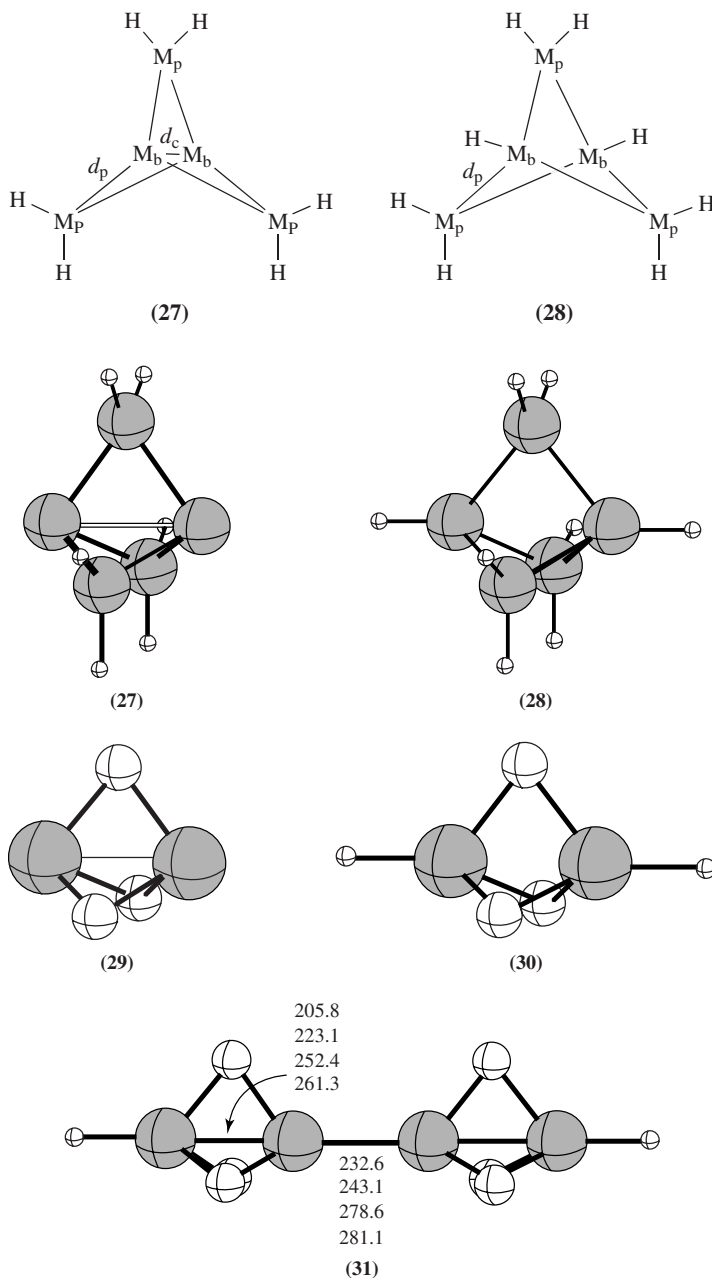


FIGURE 15. Group 14 [1.1.1]propellanes (27), bicyclopentanes (28), trioxa[1.1.1]propellanes M_2O_3 (29), $M_2O_3H_2$ (30) and its dimer (31). For 31, bond lengths (pm) are given in the order $M = Si, Ge, Sn$ and Pb ¹⁸⁴. The larger gray circles denote the M elements and the white circles denote oxygens

TABLE 22. Structures of group 14 metallapropellanes and their analogs (pm, deg)

		M ₅ H ₆ ^a (27)	M ₅ H ₈ ^a (28)	M ₂ O ₃ ^b (29, X = O)	H ₂ M ₂ O ₃ ^b (30, X = O)	H ₂ M ₄ O ₆ ^c (31, X=O)
C	d_c^d	162.5 ^e	188.3	151.1	162.2	
	d_p^f	152.3	155.5	140.8	142.7	
	θ					
Si	d_c^d	279.3 ^e	292.5	207.6	206.0 (206.9)	205.8
	d_p^f	235.8	236.8	170.7	170.0 (170)	
	θ					
Ge	d_c^d	299.3 ^e	305.3	225.0	222.5 (223.5)	223.1
	d_p^f	250.0	247.7	180.6	179.5 (179.9)	
	θ					
Sn	d_c^d	346.9 ^{e,g}	350.0	257.7	254.6 (252.5)	252.4
	d_p^f	285.7 ^g	284.0	198.5	197.1 (195.1)	
	θ					
Pb	d_c^d	370.3 ^{e,h}			(261.4)	261.3
	d_p^f	298.4 ^h			(199.6)	
	θ					

^aAt GVB/ECP; from Reference 231.

^bAt GVB/ECP; from Reference 232. Values in parentheses are at HF/ECP; from Reference 184.

^cAt HF/ECP; from Reference 184.

^dThe central M...M distance. The following are average calculated M–M and M=M bond lengths (in pm, Sections V.B.3 and IV.B.1): 151 (C–C), 234 (Si–Si), 242 (Ge–Ge), 278 (Sn–Sn), 284 (Pb–Pb); 133 (C=C), 213 (Si=Si), 224 (Ge=Ge), 250–254 (Sn=Sn), 257–270 ('Pb=Pb').

^eThe corresponding distances d_c in the M₅H₆⁺ radical cations are 154.1 (C), 253.5 (Si), 274.4 (Ge), 320.7 (Sn), 337.1 (Pb) pm²³³.

^fThe distance between the central M atoms and the peripheral MH₂ or O ligands.

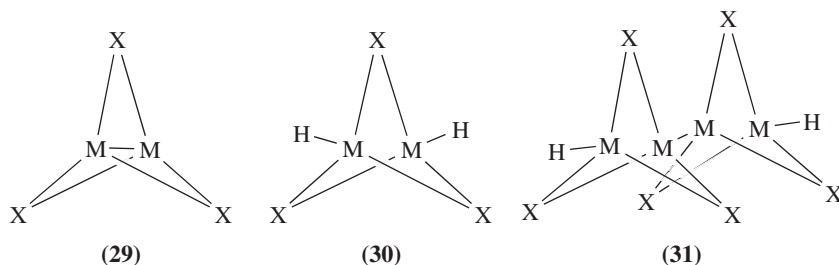
^gExperimental distances (pm): 336.8 (d_c) and 287.1 (d_p)²³⁴.

^hFrom Reference 233.

Is there a chemical bond between the bridgehead atoms of the metallapropellanes, **27**? This question has been debated and a consensus has not been reached. Nagase has presented evidence which supports the existence of such a bond; first, the overlap between the orbitals forming the central M–M bonds in **27**, M = Si, Ge and Sn is comparable to that for the C–C bond in [1.1.1]propellane; second, the diradical character of the Sn–Sn bond in **27**, M = Sn is very small and is comparable to that of **27**, M = C¹⁸⁴. On the other hand, Gordon and coworkers^{231,232} pointed out that the similarity of the M_b...M_b distances in **27** and **28** for M = Ge and Sn (see above) puts in doubt the existence of a M–M bridgehead bond in **27**, M ≠ C^{231,232}. They also found that the M_b...M_b interactions are weaker than the M–M interactions in M₂H₆ even for M = Si, and that these bonding interactions decrease on descending group 14, so for M = Sn there is little difference in the M_b...M_b bonding interactions in **27** and in **28**. Other evidence against significant M_b...M_b bonding includes: (a) the similarity of the M_b–M_b distances in the singlet and triplet states of M₅H₆; (b) a detailed electron distribution study using Bader's AIM topological analysis⁹⁹ and (c) localized orbital density analysis^{231,232}.

Substitution of the MH₂ groups in **27** by suitable X groups, as in **29**, was predicted to stabilize the central bond and to shorten it^{184,231,232}. Nagase and Kudo²³⁶ and Gordon and coworkers²³² have indeed found that when X are electronegative groups the central M...M distance for both M₂X₃, **29** and for M₂X₃H₂, **30**, shortens significantly (Table 22). For X = O the M–M distances in **29** and **30** are very similar for M = Si to Sn

(Table 22). The M–M distances in 2,4,5-trioxa-1,3-dimetallabicyclo[1.1.1]pentanes, **30**, X = O are much shorter than the single bond distances in the corresponding H₃MMH₃ (Table 19)^{184,236}. In **30**, M = Si, X = O, the M–M distance is very short (206 pm), approaching the calculated triple bond distance in $D_{\infty h}$ HSi≡SiH, and for M = Ge and Sn this bond is of similar length to that in the corresponding H₂M=MH₂ and is unprecedentedly short for M = Pb (261 pm). Such short M–M distances are also found in dimers and oligomers of **30**, e.g. **31** (Figure 15 and Table 22). From a geometric point of view, the metalla skeleton of the H₂(M₂O₃)_n polymers may be regarded as being a ‘polymetallene’. However, this reflects only their enforced bond distances, but it does not reflect their electronic structure¹⁸⁴.



The [1.1.1]metallapropellanes (**25**) and their hetero-substituted derivatives, **29**, can formally be described as donor–acceptor complexes between a central M₂ unit and three surrounding X groups (MH₂, O etc.)^{184,237}. When the peripheral X groups are MH₂, M₂ acts as an acceptor, carrying a negative charge (i.e. –0.16e for M = Ge²³⁶ and –0.12e for M = Sn¹⁸⁴), while the peripheral MH₂ units act as the donors. The dominant electron donation into the π^* orbital of the original M₂ unit is responsible for the stretching of the central M–M bond^{184,236}. When the peripheral ligands are more electronegative, e.g. CH₂ or O, the bridgehead atoms become the donors and maintain a positive charge. Consequently, the central bond is shortened^{184,236}. Analogies include the doubly bridged structure of Si₂H₂ (Section VI.E.2.b.) and 1,3-disubstituted four-membered rings, e.g. **22** (Section V.E.1.c.ii)²¹⁸. Nagase suggested that a π complex between M₂ and three X (e.g. oxygen) groups results in three 3-center–2-electron bonds. The electron density distribution of the bond paths adopts a T-shaped structure¹⁸⁴. In contrast, Gordon and coworkers found no support for the T-shaped bonding description²³². In their view, the short M–M distances in the trioxa[1.1.1]propellanes (**29**, X = O) and in the bicyclopentane analogs (**30**, X = O) could result simply from geometrical constraints, as was proposed previously for the 1,3-disubstituted four-membered rings M₂X₂H₄, **24**. Furthermore, Gordon and coworkers concluded, based on TCSCF calculations and total density plots, that the unusually short bridgehead distances in both M₂O₃ and H₂M₂O₃ do not result in significant bonding interaction and, despite the short bridgehead distances, these compounds (with M = Si, Ge, Sn) possess a considerable degree of diradical character²³². The general conclusion from the above discussion is that shorter M···M distances do not necessarily correspond to bonding interactions and likewise bonding interactions can occur between atoms separated by long internuclear distances, as in [1.1.1] metallapropellanes, **27**²³².

Like in metallabicyclo[1.1.0]butanes (**25**), the metallapropellanes, **27**, show a significant shortening of the central M···M distances (by 20–30 pm) upon ionization to the corresponding radical cations²³³.

c. Polyhedral cage compounds: tetrahedrane, prismane, cubane and larger M_nH_n systems. Polyhedral M_nH_n clusters have long been a subject for scientific curiosity because of their unique properties and high symmetry esthetic appeal. Prismane (C_6H_6), cubane (C_8H_8) and pentaprismane ($C_{10}H_{10}$) have been synthesized and fully characterized. Simple derivatives of tetrahedrane (C_4H_4) are also known. A limited number of polyhedral clusters of heavier group 14 elements, all substituted by bulky R substituents, have been synthesized: For $M = Si$: $(RSi)_4$, **32**, $R = t\text{-Bu}_3Si$ ²³⁸; $(RSi)_6$, **33**, $R = \text{Dip} = 2, 6\text{-diisopropylphenyl}$ ^{239a}; $(RSi)_8$ ^{180,240}, **34**, $R = t\text{-BuMe}_2Si$ ^{239b}, $t\text{-Bu}$ ^{239c,d}, 1,1,2-trimethylpropyl^{239e} and $\text{Dep} = 2,6\text{-diethylphenyl}$ ^{239f}; for $M = Ge$: $(RGe)_4$, **32**, $R = t\text{-Bu}_3Si$ ^{239g}; $(RGe)_6$, **33**, $R = (\text{Me}_3Si)_2\text{CH}$ ^{239h} and Dip ^{239a}; $(RGe)_8$, **34**, $R = \text{Dep}$ ^{239f}; for $M = Sn$: $(RSn)_6$, **33**, $R = t\text{-Bu}_3Si$ ²³⁹ⁱ; $(RSn)_8$, **34**, $R = \text{Dep}$ ^{239j} and $(RSn)_{10}$, **35**, $R = \text{Dep}$ ^{239k}. For a general review on the experimental studies of cage systems of heavier group 14 elements, see Reference 180.

A large series of polyhedral M_nH_n clusters ($M = C, Si, Ge, Sn, Pb$) were studied systematically using *ab initio* methods in a series of papers by Nagase and coworkers^{184,190,191,193,195,196} and more recently also by Early²⁴¹. These included group 14 analogs of tetrahedrane (**32**, $R = H$), prismane (**33**, $R = H$), cubane (**34**, $R = H$), $M_{10}H_{10}$ (**35**, $m = 5$), $M_{12}H_{12}$ (**35**, $m = 6$), $M_{16}H_{16}$ (**35**, $m = 8$), $M_{20}H_{20}$ (**35**, $m = 10$), pagodane, **36**, dodecahedrane, **37** and $M_{24}H_{24}$ (**35**, $m = 12$). Examination of the calculated $M-M$ bond lengths (Table 23^{193,196,241,242}), which are in reasonable agreement with known experimental values (taking into account that the experimental compounds carry very bulky substituents), reveal the following features. The shortest $M-M$ bonds are found in the cage compounds which consist only of 3-membered rings. In the prismanes,

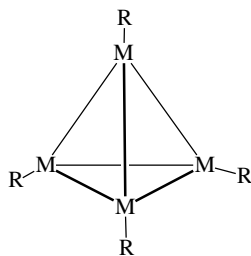
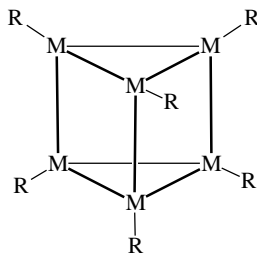
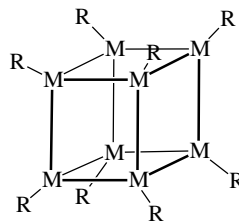
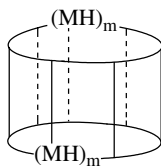
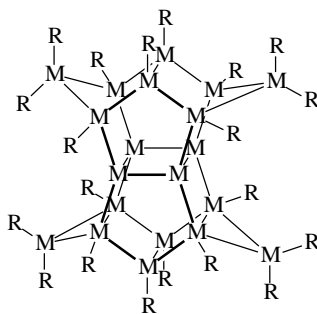
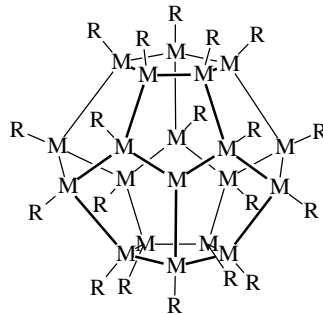
(32) T_d (33) D_{3h} (34) O_h (35) D_{mh} (36) D_{2h} (37) I_h

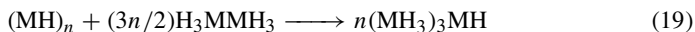
TABLE 23. Calculated bond distances (pm) in M_nH_n cage compounds^a

M_nH_n	HF/6-31G(d)		Effective core potentials ^b		
	C	Si	Si	Ge	Sn
M_4H_4 (32)	146.3	232.0	232.2	245.9	283.8 ^c
M_6H_6 (33)					
3-MR	150.7	236.6	236.5	249.3	286.7
4-MR	154.9	238.2	238.2	248.9	285.0
M_8H_8 (34)	155.9	240.2	240.0	250.5	286.7
	155.9 ^d	—	238.2 ^d	252.7 ^d	288.7 ^d
$M_{10}H_{10}$ (35 , $m = 5$)					
4-MR	155.8	240.0	239.9	250.3	286.6
5-MR	155.2	239.8	239.8	249.7	285.8
$M_{12}H_{12}$ (35 , $m = 6$)					
4-MR	155.4	239.8	239.7	250.2	286.5
6-MR	155.1	239.7	239.8	249.8	285.8
$M_{20}H_{20}$ (37), 5-MR	154.8	239.1	239.2	248.2	284.1
				250.3 ^e	286.2 ^e

^aFrom Reference 241.^bCEP-31G(d)²⁴².^cThis structure has 3 negative eigenvalues.^dAt HF/DZ+d; from Reference 193.^eAt HF/DZ+d; from Reference 197.

the M–M bond lengths in the 3-MRs are slightly shorter than those in the 4-MRs for M = C and Si, while for M = Ge and Sn, the opposite trend is observed.

The strain energies of some M_nH_n polyhedral cage compounds, calculated according to equation 19, are given in Table 24 and are also shown graphically as a function of n in Figure 16. The strain energies of the polyhedra can be estimated from the sum of the strain energies of the individual rings that build them^{184,241}, e.g. the strain energy of the metallacubanes, M_8H_8 , is about 6 times larger than that of the corresponding 4-membered M_4H_4 rings (Tables 17 and 24)^{184,190,193}. Early²⁴¹ suggested a formula for estimating the strain of cage systems which is based on the number of the atoms in the rings composing the cage.



In general, the M_nH_n polyhedra, especially those that are composed of 3-MRs and 4-MRs, are highly strained. For M = C the total strain energy decreases in the order **34** > **33** > **32**. This order is reversed with the heavier congeners, i.e. the strain decreases as follows: **32** > **33** > **34** and when descending group 14. Thus, Sn_8H_8 (**34**, M = Sn) is significantly less strained than C_8H_8 or Si_8H_8 (70.1 vs. 158.6 and 99.1 kcal mol⁻¹, respectively). This is similar to the trends found in the single 3- and 4-membered metalla rings (see Section V.E.1.a.ii and Table 17). However, while the ring strain is smaller for the heavier M elements, the M–M bonds are also weaker, destabilizing the cage systems. Thus, for M_4H_4 (M = Sn and Pb) the ring strain, although smaller than for M = Si or Ge, is still sufficiently large to overcome the relatively weak M–M bonds, and alternate structures, e.g. H-bridged structures²⁴³, are preferred over the cage structures²⁴¹ (see discussion below).

The most strained cages for all M elements are the tetrahedranes (except for M = C) which contain four 3-MRs. As a result of their high strain and relatively weak M–M bonds, the heavier tetrahedranes are subject to ‘bond-stretch’ or ‘bond-break’ isomerism, as well as to hydrogen bridging²⁴³. The preference for alternative structures increases strongly when descending group 14, as is clearly evident from Table 25 which gives

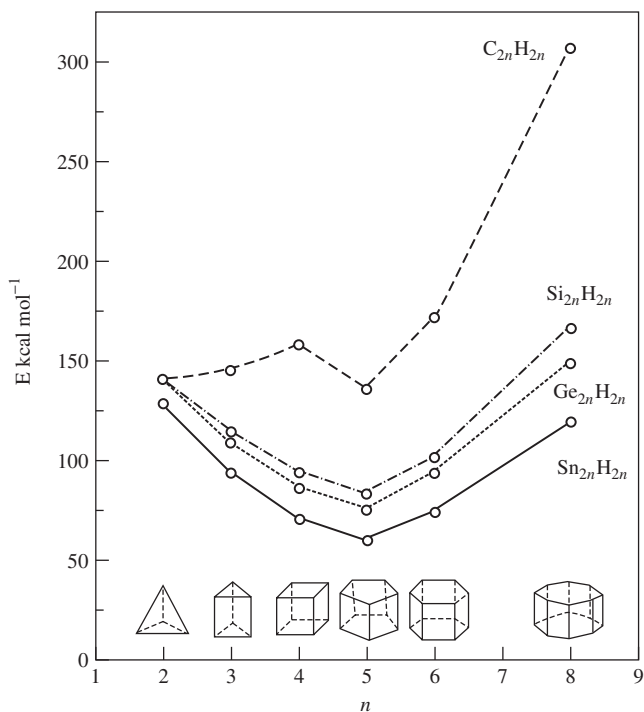


FIGURE 16. Strain energies (E) of group 14 metallatetrahedranes and $[n]$ -prismanes ($M_{2n}H_{2n}$), calculated at HF/6-31G(d) for $M = C$ and Si and at HF/DZ+d for $M = Ge$ and Sn . Reprinted with permission from Reference 195. Copyright (1995) American Chemical Society

TABLE 24. Strain energies (kcal mol^{-1}) in M_nH_n cage compounds^a

M	Tetrahedrane (32) ^b	Prismane (33) ^b	Cubane (34) ^b	$M_{20}H_{20}$ (35, $m = 10$) ^c	$M_{20}H_{20}$ (36) ^c	$M_{20}H_{20}$ (37) ^c
C	141.4	145.3	158.6	492.1		43.6; 43.7 ^d
Si	140.3	118.2	99.1	252.1		32.3; 40.0 ^e
R = Me ^f	134.6	105.6	88.9			
R = SiH ₃ ^f	114.5	95.7	77.9			
Ge	140.3	109.4	86.0	223.6	51.3	29.3; 32.2 ^e
Sn	128.2	93.8	70.1 ^g	180.1	40.1	21.0; 19.5 ^e
Pb	119.3	65.2	59.6			

^a According to equation 19.

^b At HF/6-31G(d); from References 190 and 193; strain energies calculated at CEP-31G(d) are given in Reference 241.

^c At HF/DZ+d; from References 196 and 197.

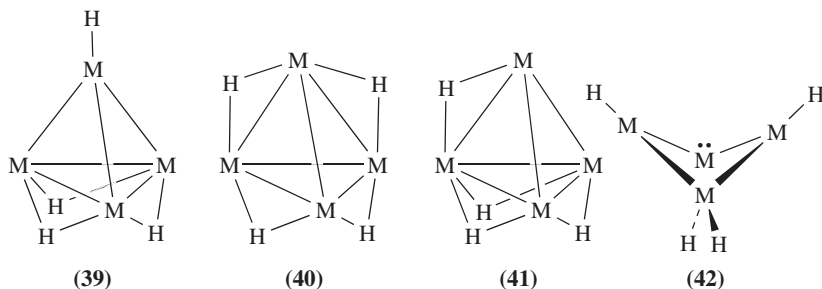
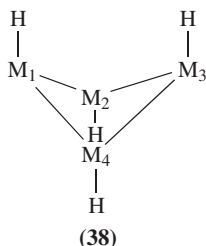
^d At HF/6-31G(d); from Reference 241.

^e At CEP-31G(d); from Reference 241.

^f For M_nR_n , at HF/6-31G(d); from References 191,192 and 196.

^g At HF/DZ. The strain energies of substituted octastannacubanes (Sn_8R_8) are 77.0, 75.7, 65.0, 62.0 and 58.4 kcal mol^{-1} , for R = H, CH₃, SiH₃, GeH₃ and SnH₃, respectively¹⁹¹.

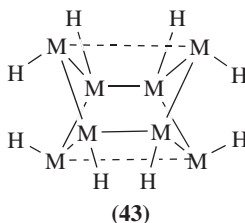
the relative energies of various M_nH_n isomers. Thus **32**, $M = \text{Si}$, isomerizes without a significant barrier, by breaking two Si–Si bonds, to form the 4-membered ring isomer **38**, $M = \text{Si}^{244}$ with four equal Si–Si bonds of 230.1 pm (similar to that in **32**, Table 23) and a $\text{Si}_1\text{–Si}_3$ distance of 302.3 pm. **38** ($M = \text{Si}$) is by 28.3 kcal mol⁻¹ (CIDVD/DZP//HF/DZP) more stable than **32**, $M = \text{Si}^{244a}$. Srinivas and Jemmis found that H-bridged structures are favored over the classical tetrahedrane structure for all metatetrahedranes, **32**, $R = \text{H}$, and for $M = \text{Sn}$ and Pb the preference is as large as 69 and 120 kcal mol⁻¹, respectively (Table 25). Thus, at the MP2 and B3LYP levels, when $M = \text{Si}$, Ge and Sn , triply H-bridged structures (**39**) are preferred over **32**, and for $M = \text{Pb}$ the four-H-bridged C_s structure (**40**) is preferred. When using quasi-relativistic methods structure **41** is the most stable for $M = \text{Ge}$, Sn and Pb^{243} . For Si and Ge the most stable M_4H_4 isomer is the rearranged 4-membered ring metallylene, **42**^{243,244c} (Table 25). However, due to the high bridging tendency of hydrogen, it is not clear if the bridged structures will be preferred also for alkyl, aryl or silyl substituted tetrahedranes. The experimentally synthesized tetrasilatetrahedrane, **32**, $M = \text{Si}$, $R = t\text{-Bu}_3\text{Si}^{238}$ with substituents other than hydrogen indeed possesses the classical tetrahedrane structure.

TABLE 25. Relative energies of M_4H_4 isomers^a

M	32	39	40	41	42
Si	0.0	-20.7	-2.9	<i>b</i>	-49.4
Ge	0.0	-55.6	-46.8	<i>b</i>	-68.3
Sn	0.0	-69.3	-66.0	-66.1	-66.0
Pb	0.0	-111.4	-119.8	-121.7	-93.4

^aAt MP2/6-31G(d); from Reference 243.^bCollapses to **39**.

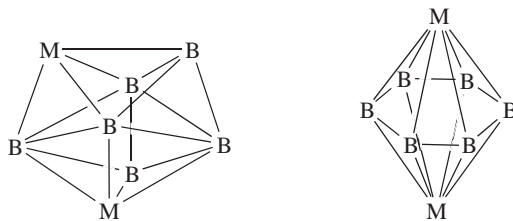
'Bond-stretch' isomerism was found in plumbaprismane, **33**, $M = \text{Pb}$, which collapses to a six-membered monocycle, and in plumbacubane **34**, $M = \text{Pb}$, where two bonds are stretched to form two six-membered rings as shown in **43**¹⁹⁵. Activation energies for all the isomerizations described above are not available.



As in the case of monocyclic 3- and 4-MRs (see Section V.E.1.a.ii), electropositive substituents stabilize also M_nH_n cage systems which include such rings, e.g. tetrahedranes, prismanes and cubanes (Table 24)^{191,192,195}. The only isolated tetrasilatetrahedrane indeed carries the electropositive $\text{Si}(\text{Bu}-t)_3$ groups as substituents²³⁸. Nevertheless, the steric protection afforded by the bulky silyl ligands is probably the most important factor allowing the isolation of the tetrasilatetrahedrane^{179,195}.

The least strained $[n]$ -prismane is $M_{10}H_{10}$ (**35**, $m = 5$), which is built from two 5-MRs and five 4-MRs. The strain in this particular $[n]$ -prismane is reduced because the angle in the 5-MR approaches the normal tetrahedral angle and the number of the 4-MRs increases. The strain increases as the number of the polygon sides increase and their angles deviate significantly from the tetrahedral value. For $M_{20}H_{20}$ (**35**, $m = 10$), where the MMM angle of the top polygon is 144° , the strain is extremely large, i.e. $492 \text{ kcal mol}^{-1}$ for $M = \text{C}$ and smaller but still very large for the heavier congeners, e.g. $180 \text{ kcal mol}^{-1}$ for $M = \text{Sn}$ (Table 24). The high strain gives rise to two alternative isomers which are dramatically lower in energy: dodecahedrane **37**, which contains only 5-MRs and is the more stable isomer, and pagodane **36**, which is slightly more strained (Table 24)^{195,196,241}.

d. Polyhedral metallaboranes. The isolobal analogy between $M:$ and BH fragments (see Scheme 1) can be observed also in the structures of the heavier congeners of the well investigated carbaboranes²⁴⁵. However, only a few theoretical studies deal with metallaboranes^{246,247}. For all $M_2B_6H_6$ ($M = \text{SiH}$, GeH , SnH , and PbH) it was found that the same bisdisphenoid structure (**44**) is the global minimum²⁴⁷. However, the energy difference between **44** and its octahedral isomer **45** (D_{6h}) is reduced in a zig-zag fashion from (in kcal mol^{-1}) 193.6 for $M = \text{CH}$ to 21.9 for $M = \text{SiH}$, 32.2 for $M = \text{GeH}$, 28.0 for $M = \text{SnH}$ and 50.4 for $M = \text{PbH}$. As the size of the boracyclic ring increases (as



(44) $M = \text{SiH}$, GeH , SnH , PbH (45) $M = \text{SiH}$, GeH , SnH , PbH

in **45**), a larger capping group with more diffuse p orbitals is needed to stabilize the ring–cap interactions through increased overlap. Thus carbon, which is small in size and possesses contracted p orbitals, is expected to prefer a smaller boracyclic ring and should be unfavorable as a cap for a larger ring. On the other hand, Si, Ge and Sn, which are larger in size and possess more diffuse p orbitals, enable a better overlap with the molecular orbitals of the six-membered boron ring and thereby stabilize the hexagonal bipyramid, **45**. The stability of **45** decreases again for $M = \text{PbH}$, probably because of relativistic effects²⁴⁷.

VI. MULTIPLY-BONDED SYSTEMS

A. Historical Overview

For many years the synthesis of stable compounds containing multiple bonds to silicon and its heavier congeners was one of the major challenges in main-group chemistry. The many early failures to synthesize such compounds^{11a–c,14,16,248} attracted the attention of theoreticians who tried to understand the reasons for the dramatically different behavior of carbon and silicon and its heavier congeners in forming multiple bonds^{3,6,7,249}. The theoretical studies and the experimental failures lead to the formulation of the ‘double bond rule’, which stated that elements having principal quantum numbers greater than 2 do not form π bonds among themselves or with other elements²⁵⁰. However, in the 1970s, considerable evidence pointing to the existence of compounds with multiple bonds to silicon as reactive intermediates was accumulated^{2,9–11}. The great breakthroughs occurred in 1981 with the syntheses of the first stable compounds containing C=Si and Si=Si bonds by Brook¹² and by West²⁵¹ and their coworkers, respectively. Much progress has been made since then in the synthesis and characterization of doubly-bonded group 14 compounds. This includes the synthesis of stable compounds with double bonds between silicon and heteroatoms, i.e. Si=N, Si=P, Si=As, Si=S^{2,9–11}, as well as compounds with Ge=C, Sn=C and Ge=Si double bonds^{24a}. $\text{R}_2\text{Sn}=\text{SnR}_2$ and $\text{R}_2\text{Ge}=\text{GeR}_2$ [$\text{R} = (\text{Me}_3\text{Si})_2\text{CH}$] were isolated and characterized by Lappert and coworkers already in 1973 and 1976²⁵², but these compounds were stable only in the solid state and they dissociated to the corresponding stannylenes and germlylenes in solution or in the gas phase^{253–255}. More recently $\text{R}_2\text{Sn}=\text{SnR}_2$ and $\text{R}_2\text{Ge}=\text{GeR}_2$, which are stable also in solution, were isolated^{24a,d}. Several diplumbenes, $\text{RR}'\text{Pb}=\text{PbRR}'$, were isolated recently^{24a}, for example with $\text{R} = \text{R}' = \text{Tip} = 2,4,6(i\text{-Pr})_3\text{C}_6\text{H}_2$ ^{256a} and $\text{R} = \text{Tip}$, $\text{R}' = \text{Si}(\text{SiMe}_3)_3$ ^{256b}. However, as the Pb=Pb distances of 305.1 pm and 299 pm, respectively, in these compounds are even longer than that of a Pb–Pb single-bond in the corresponding R_3PbPbR_3 compounds (Table 7), the bonding in these compounds was described by donor–acceptor interactions between the doubly occupied 6s orbitals and the empty 6p orbitals of the two singlet plumblylene fragments (see below)²⁵⁶. The syntheses and isolation of compounds with double bonds of the types Ge=N, Ge=P, Ge=O, Ge=S, Ge=Se, Ge=Te and Sn=P, Sn=S and Sn=Se were also reported^{24b,c}. The remarkable progress regarding multiply-bonded group 14 compounds was extensively reviewed in the last decade^{11f,16,20,24} and the interested reader is referred to these reviews for more information. One general observation is that the known number of stable doubly-bonded compounds and the ease of their synthesis decreases drastically on going down group 14, and that in solution most of the reported tin and lead doubly-bonded compounds dissociate to their corresponding divalent MR_2 fragments or slowly dimerize.

Stable triply-bonded compounds with group 14 elements are still unknown. Several formally triply-bonded silicon compounds were detected and characterized in matrix and

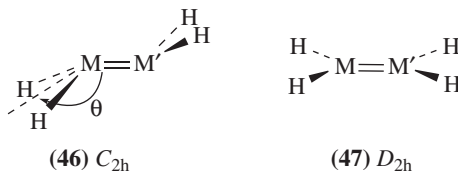
in the gas phase, i.e. $\text{HSi}\equiv\text{N}^{257\text{a}}$, $\text{HN}\equiv\text{Si}^{257\text{b}}$, $\text{C}_6\text{H}_5\text{N}\equiv\text{Si}^{257\text{c}}$ (by matrix isolation spectroscopy), $\text{C}_6\text{H}_5\text{N}\equiv\text{Si}^{257\text{d}}$ (by photoelectron spectroscopy) and $\text{HC}\equiv\text{SiX}$, $\text{X}=\text{Cl}$, F^{258} (by neutralization-reionization mass spectrometry). Most recently, evidence for the existence of $\text{RGe}\equiv\text{CSiMe}_3$ [$\text{R} = 2,6\text{-}(i\text{-Pr}_2\text{NCH}_2)_2\text{C}_6\text{H}_3$] as a reactive intermediate was reported by Couret and coworkers²⁵⁹ while Power and coworkers reported the synthesis, isolation and characterization by X-ray crystallography of RPbPbR ($\text{R} = 2,6\text{-Tip}_2\text{C}_6\text{H}_3$)²⁶⁰. However, the latter compound is highly bent ($\angle\text{RPbPb} = 94.3^\circ$) and the $\text{Pb}\text{--}\text{Pb}$ bond length is 318.8 pm, considerably longer than the typical $\text{Pb}\text{--}\text{Pb}$ single bond length of 284.4 pm in $\text{Ph}_3\text{PbPbPh}_3$. These structural features imply that the electronic structure of the $\text{Pb}\text{--}\text{Pb}$ bond in this formal analog of acetylene is that of a single $\text{Pb}\text{--}\text{Pb}$ bond with a lone pair that resides on each of the Pb atoms, rather than that of a triply-bonded compound²⁶⁰. Recent attempts to synthesize triply-bonded RMMR ($\text{M} = \text{Ge}$, Sn) compounds have led so far to the isolation of their reduced salts such as $\text{Na}_2(\text{RGeGeR})$ and $\text{K}_2(\text{RSnSnR})$ ($\text{R} = \text{C}_6\text{H}_3\text{-}2,6\text{-Tip}_2$)^{261\text{a}}. Stable germylene–transition metal complexes with formal GeM triple bonds were also reported^{261\text{b,c}}. The new theoretical and experimental studies of triply-bonded systems were highlighted recently by Jutzi²⁶².}}

Theoretical studies accompanied and complemented the experimental developments and provided detailed insights into this fascinating area of chemistry^{7,26}. Much of what we know about these compounds comes from theory. In the section below we review the relevant theoretical knowledge with emphasis on the understanding that was gained concerning the nature of these bonds and the differences in their structures and stability on moving down group 14 from C to Pb.

B. $\text{M}=\text{M}'$ Doubly-bonded Compounds (Metallenes)

1. Structures

Basic structural and energetic data about $\text{M}=\text{M}'$ bonds of group 14 elements are collected in Table 26. The most striking difference between ethylene and its heavier analogs is that, unlike ethylene which has a D_{2h} -planar ground state structure, the heavier group 14 analogs are calculated to be *trans*-bent with C_{2h} symmetry (**46**), while the D_{2h} -planar structure (**47**) is generally not a minimum on the PES^{7,19,26,263–269}. For disilene ($\text{H}_2\text{Si}=\text{SiH}_2$) the potential energy surface along the $D_{2h} \rightarrow C_{2h}$ coordinate is very flat and subtle changes in the theoretical method used for geometry optimization can have a dramatic effect on the out-of-plane distortion angle θ ; e.g. $\theta = 0.0^\circ$ at HF/DZP²⁷⁰ and 38.5° at HF/TZP²⁷¹. Correlated methods invariably find $\text{H}_2\text{Si}=\text{SiH}_2$ to be *trans*-bent with *trans*-bending angles that range from 17° to 36° , depending on the method used^{19,224,268}, but the planar **47** is only *ca* 1 kcal mol⁻¹ higher in energy (Table 26).



Many of the experimentally known disilenes are planar, and the largest out-of-plane bending angle for carbon substituted disilenes is 18° , measured for $\text{Mes}_2\text{Si}=\text{SiMes}_2$ ^{24\text{a}} ($\text{Mes} = \text{mesityl}$). A significantly larger bending angle of *ca* 33° was measured for a}

TABLE 26. Geometrical and energetic parameters and bonding analysis of $H_2M=M'H_2$ (46)^d

M, M'	$H_2M=M'H_2$			Dissociation energies ^b		Double bond analysis ^c				
	d(M=M) ^c	θ^d	ΔE^c	d(M-M') (in $H_3M-M'H_3$)	M=M'	M-M'	$\sigma_{M=M'}$	$\pi_{M=M'}$	σ/π^f	
C, C										
JZ ^g	132.3	0.0		151.1	176.8	86.8	209.3 ^f ; 88.4 ^h	75.4 ^f ; 65–70 ^h		2.78
KRS ⁱ	133.5	0.0		153.3	160.2					
Exp. ^j	133.9	0.0		153.7	152 ⁱ	88 ⁱ				
C, Si										
JZ ^g	168.7	0.0		184.7	110.5	81.6	138.3 ^f ; 82.6 ^h	54.5 ^f ; 35–43 ^h		2.56
exp. ^j	170.2			186.9						
Si, Si										
JZ ^g	215.0 (212.7)	36.1	1.7	232.2	59.8	70.1	89.2 ^f ; 70.5 ^h	37.8 ^f ; 22–24 ^h		2.36
KRS ⁱ	218.4 (214.1)	34.1	1.2	235.4	53.4					
exp. ^j	214–225 ^k	0–18 ^k		232.7 ⁱ	63.4±1 ^j	74 ⁱ				
C, Ge										
JZ ^g	177.0	0.0		192.4	85.4	68.2	125.4 ^f	45.5 ^f		2.76
WG ^m	181.4			196.6				32.2		
exp. ^j	180–183			194.3				43		
Si, Ge										
WG ^m	228.4 (222.2)	38.7	3.5	237.4				25.7		
exp. ^j				235.7						
Ge, Ge										
JZ ^g	224.5 (220.5)	47.3	5.5	241.3	43.1	61.5	84.9 ^f	37.8 ^f (33.0)		2.09
KRS ⁱ	236.2 (225.8)	46.3	6.5	247.9	32.7			25.4		
WG ^m	227.0(227.0)	42.4	5.3	241.5				22.2		
exp. ^j	221–245 ^k	0–47 ^k		240.3						
C, Sn										
JZ ^g	194.5	0.0		212.7	67.0	57.1	107.2 ^f	39.0 ^f		2.75
WG ^m	206.3 (204.1)	26.8	0.6	217.8				20.9		
exp. ^j	202.5			214.3				45		
Si, Sn										
WG ^m	251.1 (242.8)	42.2	5.6	258.5				21.5		

(continued overleaf)

TABLE 26. (continued)

M, M'	H ₂ M=M'H ₂		Dissociation energies ^b		Double bond analysis ^c			
	d(M=M') ^c	θ ^d	ΔE ^e	M=M'	M-M'	σ _{M=M'}	π _{M=M'}	σ/π ^f
Ge, Sn WG ^m	255.5 (246.6)	43.7	6.9				21.6	
Sn, Sn JZ ^g	256.9 (250.1)	51.0	7.4	28.9	52.6	67.2 ^f	32.1 ^f (28.2) ^f	2.10
KRS ⁱ	274.8 (258.3)	50.4	10.1	22.5				
WG ^m	276.9 (266.2)	47.1	8.7				19.7	
exp. ^j	277–364 ^k	21–46 ^k		12.9 ^l				
C, Pb JZ ^g	204.5			45.7	52.9	95.5 ^f	32.3 ^f	2.96
Pb, Pb JZ ^g	281.9 (269.3)	53.6	23.2					
KRS ⁱ	292.6 ⁿ ; 293.2 ^o	53.1 ⁿ ; 48.1 ^o	7.2 ⁿ ; 23 ^o	10.0	44.3	59.8 ^f	42.3 ^f (20.6) ^f	1.41
exp. ^j	(264.0 ⁿ ; 278.4 ^o) 299–413 ^k	34–51 ^k		10.5 ⁿ ; 24.5 ^o			13.1 ⁿ ; 26.2 ^o (20.3 ⁿ ; 15.5 ^o)	

^aBond lengths in pm, bond angles in deg and energies in kcal mol⁻¹. Data taken from References 268 (JZ), 224 (KRS) and 272 (WG). See also Reference 273. Other studies on the title compounds focused on selected M or were performed at lower levels of theory.

^bFor the reaction: H₂MM'H_n → MH_n + M'H_n (n = 2 or 3).

^cData for the non-minimum planar H₂M=M'H₂ structures are given in parentheses.

^dOut-of-plane bending angle, see structure 46 for definition.

^eEnergy difference between *trans*-bent [C_{2h} (M = M') or C_s (M ≠ M')] and planar (D_{2d} or C_{2v}, respectively) H₂M=M'H₂.

^fThe intrinsic σ and π M=M bond energies and the corresponding σ/π ratios were calculated by JZ²⁶⁸ at LDA/TZ+P. These bond energies should not to be compared to bond energies calculated using other methods (indicated by footnote *h*). JZ²⁶⁸ do not comment on the reasons for the very large difference in their estimation of the σ component and the estimation obtained by other methods (e.g. compare with values marked by footnote *h*).

^gCalculated at LDA/TZ+P. JZ = Jacobsen and Ziegler; from Reference 268.

^hNot an intrinsic bond energy. At MP4SDTQ/6-31G**/6-31G(d); from Reference 56.

ⁱCalculated at B3LYP/DZ+P. The core electrons of all group 14 elements were replaced by quasi-relativistic pseudopotentials. KRS = Kapp, Remko and Schleyer; from Reference 224.

^jFrom References 268 and 272, unless stated otherwise. The experimental values are probably affected significantly by the bulky substituents.

^kSee Reference 24a. The wide range of bond lengths and *trans*-bending angles is caused by the bulky substituents on the double bonds.

^lFrom Reference 224.

^mCalculated at MCSCF/3-21G(d). WG = Windus and Gordon; from Reference 272.

ⁿComputed with nonrelativistic Pb pseudopotentials.

^oComputed with relativistic Pb pseudopotentials.

Z-diaminodisilyldisilene²⁷⁴. The differences between the theoretical predictions and the experimental structures were attributed to the presence of bulky substituents in the experimentally studied molecules²⁶⁸.

$H_2M=MH_2$ with $M = Ge, Sn$ and Pb are also calculated (at all levels of theory) to favor *trans*-bent structures^{19,224,253–255,268,275–276}, in agreement with the experimental evidence²⁴. The bending angles θ and the barriers for planarization increase down group 14, reaching for $H_2Pb=PbH_2$ a θ of 53° and a barrier to planarity of 23 kcal mol^{-1} (Table 26)^{224,268}. In contrast to the dimetallene $H_2M=M'H_2$ (where M and M' are Si to Pb), the metallenes $H_2C=MH_2$, with $M = Si, Ge, Sn$ and Pb , are planar [HF/DZP^{269,277}; HF/3-21G(d)^{272,278a}; LDA/TZP²⁶⁸; MP2/3-21G(d) and MCSCF/3-21G(d)²⁷², Table 26]. Experimentally, substituted germenes and stannens exhibit both planar and pyramidal Ge and Sn centers²⁰. In a recent study the heavier analogs of triafulvene were calculated to be non planar; while the corresponding pentafulvenes are planar. The question of the aromaticity of these compounds is discussed^{278b}.

The $M=M$ bonds in the planar $H_2M=MH_2$ become longer as M becomes heavier, but they are all considerably shorter than the corresponding $M-M$ single bond in H_3MMH_3 . Bending at M results in a considerable elongation of the $M=M$ bonds, so that in the strongly bent $H_2Sn=SnH_2$ and $H_2Pb=PbH_2$ the $M=M$ distance approaches that of a single $M-M$ bond (Table 26)^{224,268,272}.

Why are the heavier $R_2M=M'R_2$ systems bent? This peculiar geometric preference was rationalized by two different MO models²⁶. According to one model, planar double bonds are formed by the interaction of two MR_2 units in their triplet state, as shown schematically in Figure 17a. Because the heavier MR_2 fragments have a singlet ground state (in contrast to methylene, which has a triplet ground state), they need first to be excited to the triplet state, requiring one to pay the energetic cost of the singlet–triplet energy gap (ΔE_{ST} , see also below). Instead, they prefer to interact via two donor–acceptor interactions in which the filled lone pair of one MR_2 unit donates electron density into the empty p orbital of the second MR_2 unit and consequently *trans*-bent $R_2M=MR_2$

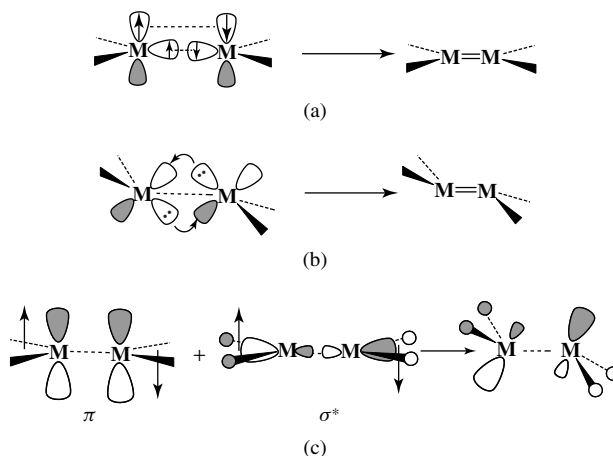
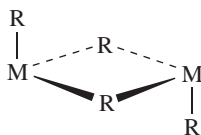


FIGURE 17. (a) Construction of D_{2h} - M_2H_4 (**47**) from two triplet MH_2 fragments; (b) construction of C_{2h} - M_2H_4 (**46**) from two singlet MH_2 fragments; (c) a schematic description of the π – σ^* mixing upon *trans*-bending

molecules are formed (Figure 17b)^{265,279,280}. An alternative explanation is that the *trans*-bent geometries are stabilized relative to the planar ones by mixing of the M=M π and σ^* orbitals (i.e. a second-order Jahn–Teller effect), as shown in Figure 17c^{254,265,280}. Upon bending at the M atoms, the π (b_{2u}) orbital and the σ^* (b_{3u}) orbital acquire the same symmetry (b_u) and mixing can occur (Figure 17c). The degree of mixing increases as the π – σ^* energy difference decreases. The magnitude of the π – σ^* orbital gap in D_{2h} $H_2M=MH_2$ decreases on going down group 14, being (in kcal mol⁻¹): 168.3 for M = C, 103.8 for M = Si, 92.2 for M = Ge, 78.4 for M = Sn and 27.7 for M = Pb²⁶⁸. This leads to a larger π – σ^* stabilizing interaction, and consequently to larger bending angles at M as M becomes heavier, in agreement with the observation^{265–268,280}. A detailed NBO analysis shows that the energy stabilization due to the interaction between the M=M π and σ^* orbitals increases from only 6.3 kcal mol⁻¹ for M = Si to 53.5 kcal mol⁻¹ for M = Pb²²⁴. Considerably smaller contributions were calculated for the alternative σ – π^* interaction²²⁴.

In a series of important papers, Trinquier, Malrieu and coworkers explored the M_2H_4 potential energy surfaces^{265,269,280}. Based on these studies, Trinquier presented simple rules to predict the occurrence of *trans*-bent M=M double bonds and their degree of bending, as well as of other M_2H_4 structural isomers such as dibridged **48**, R = H. These rules are based on the relative magnitudes of the singlet–triplet energy gap of the MR_2 fragments (ΔE_{ST}) and the overall bond energy of the M=M bond, $E_{\sigma+\pi}$ ²⁶⁹. For a homopolar M_2H_4 species, a *trans*-bent doubly-bonded molecule (**46**) is predicted to be more stable than the planar **47** or than the isomeric dibridged (**48**) structures, when ΔE_{ST} is in the range given in equation 20.

(48) C_{2h}

$$\frac{1}{4}E_{\sigma+\pi} \leq \Delta E_{ST} \leq \frac{1}{2}E_{\sigma+\pi} \quad (20)$$

When the singlet–triplet splitting of the MH_2 fragment is smaller than one quarter of the bond energy, the M=M double bond is planar, while when ΔE_{ST} is larger than one half of the M=M bond energy, a direct M–M link is less favored, and the bridged isomer, **48**, is the most stable (see also Section VI.B.3.b). For example, for all MF_2 (except CF_2), ΔE_{ST} is larger than $\frac{1}{2}E_{\sigma+\pi}$ and bridged structures (**48**, R = F) are favored for M = Si to Pb, while the *trans*-bent structures are not minima on the PES²⁸¹. The π – σ^* energy gap is related to ΔE_{ST} of the MR_2 fragments and it decreases as ΔE_{ST} increases^{265,280}. Thus, moving down group 14 both ΔE_{ST} and the π – σ^* orbital interaction increase, stabilizing the *trans*-bent structures and inducing larger bending angles at M.

The effect of the electronegativity of substituents on the degree of *trans*-bending of heavier group 14 ethylene analogs (for M = Si to Sn) was studied by Liang and Allen²⁶⁷ using the HF/3-21G computational level (a very small basis set by today's standards). The effects of the electronegativity of the substituents was studied by a perturbation approach, in which the nuclear charge of the hydrogens was increased or decreased stepwise to mimic a change in the substituent electronegativity. Based on this analysis they suggested that the geometries of double bonds are determined by both their intrinsic π – σ^* separation and

the electronegativity of the substituents. The calculated optimized geometries show that changing the nuclear charge of the hydrogens has a small effect on the M=M bond lengths, but it has a significant effect on the degree of the *trans*-bending. The degree of *trans*-bending increases for electron-withdrawing substituents (which increase the π - σ^* orbital mixing) and decreases for electropositive substituents. Explicit geometry optimization of $(\text{H}_3\text{Si})_2\text{M}=\text{M}(\text{SiH}_3)_2$ has indeed shown that these compounds are planar for M = Si, Ge and Sn (M = Pb was not studied). For ethylene, the π - σ^* gap is so large that no substituent can increase the π - σ^* orbital mixing sufficiently to cause *trans*-bending at the C=C bond (e.g. $\text{F}_2\text{C}=\text{CF}_2$ is planar)²⁶⁷.

Karni and Apeloig²⁶³ found, in agreement with the semiquantitative rules of Trinquier, a linear correlation between ΔE_{ST} of RHSi (R = Li, BeH, BH_2 , SiH_3 , F, OH and NH_2) and the *trans*-bending angle of the corresponding substituted disilenes, $\text{H}_2\text{Si}=\text{SiHR}$ and $\text{RHSi}=\text{SiHR}$. A similar correlation was found between ΔE_{ST} and the Si=Si bond length. Electronegative substituents (F, OH and NH_2), which increase ΔE_{ST} (see Section VII.A.1), cause strongly bent disilenes, while electropositive substituents which reduce ΔE_{ST} cause smaller bending angles²⁶³, e.g. $(\text{H}_3\text{Si})\text{HSi}=\text{SiH}_2$ is planar. The theoretically predicted planarizing effect of the electropositive R_3Si substituent is manifested in experimental structures. Thus, $[(i\text{-Pr})_3\text{Si}]_2\text{Ge}=\text{Ge}[\text{Si}(\text{Pr-}i)_3]_2$ is planar and the *trans*-bending angle of $[(\text{Me}_3\text{Si})_3\text{Si}]\text{Sn}=\text{Sn}[\text{Si}(\text{SiMe}_3)_3]$ is only 28° relative to *ca* 40° for aryl substituted distannenes^{24a}. Following the study of Karni and Apeloig²⁶³, a similar linear correlation between ΔE_{ST} of GeR_2 or SiR_2 and the *trans*-bending angles in $\text{R}_2\text{Ge}=\text{GeH}_2$, $\text{R}_2\text{Ge}=\text{SiH}_2$ and $\text{H}_2\text{Ge}=\text{SiR}_2$ (R = H, CH_3 , NH_2 , OH, F, Cl) was reported recently by Chen and coworkers²⁸². The energy differences between the planar and *trans*-bent structures of these substituted germenes are also linearly correlated with ΔE_{ST} of the MR_2 fragment, reaching 26 kcal mol^{-1} for $\text{F}_2\text{Ge}=\text{GeH}_2$ ²⁸².

2. The double-bond strength

The dissociation energy of $\text{H}_2\text{M}=\text{MH}_2$ to two units of MH_2 [$D(\text{H}_2\text{M}=\text{MH}_2)$] is a measure of the total double-bond strength. As shown in Table 26 there is a dramatic decrease in $D(\text{H}_2\text{M}=\text{MH}_2)$ as M becomes heavier, being only 10 kcal mol^{-1} for M = Pb²⁶⁸. Thus, if entropy is taken into account, $\text{H}_2\text{Pb}=\text{PbH}_2$ does not exist at room temperature. The same trend was found for the dissociation energy of singly-bonded H_3MMH_3 to two MH_3 radicals [$D(\text{H}_3\text{M}-\text{MH}_3)$], but the decrease in $D(\text{H}_3\text{M}-\text{MH}_3)$ as a function of M is much smaller than in $D(\text{H}_2\text{M}=\text{MH}_2)$. For M = C, $D(\text{H}_2\text{M}=\text{MH}_2)$ amounts to twice the dissociation energy of a M-M single bond, but for every heavier M, the dissociation energy of a M=M double bond is smaller than that of the corresponding single bond (Table 26); e.g. $D(\text{H}_2\text{Ge}=\text{GeH}_2) = 33\text{--}43 \text{ kcal mol}^{-1}$ while $D(\text{H}_3\text{Ge}-\text{GeH}_3) = 61.5 \text{ kcal mol}^{-1}$. This curious fact, first recognized by Gordon and coworkers²⁸³, was attributed by Grev²⁶ to the increasing stability of the MH_2 fragment when moving down group 14 (Table 3) which is manifested by the increase in their divalent state stabilization energies (DSSEs, see equation 4), i.e. the DSSEs of CH_2 , SiH_2 and GeH_2 are -5.6 , 19.3 and $25.8 \text{ kcal mol}^{-1}$ ²⁶, respectively. A similar conclusion was reached by the bond analysis of Jacobsen and Ziegler (vide infra)²⁶⁸. According to Grev, $D(\text{H}_2\text{M}=\text{MH}_2)$ can be estimated by equation 21, where $D_\pi = \pi$ -bond energy, which demonstrates the dominant effect of the DSSE on the total BDE of $\text{H}_2\text{M}=\text{MH}_2$.

$$D(\text{H}_2\text{M}=\text{MH}_2) \cong D(\text{H}_3\text{M}-\text{MH}_3) - 2\text{DSSE}(\text{MH}_2) + D_\pi \quad (21)$$

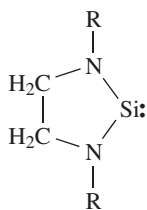
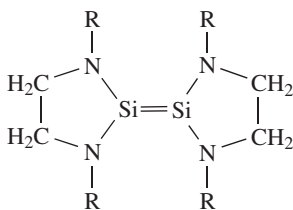
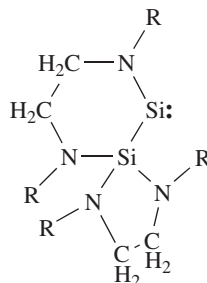
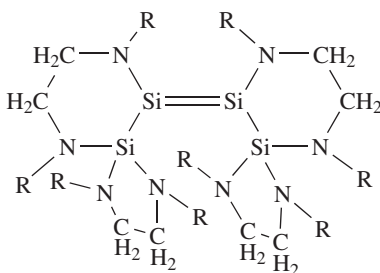
Using equation 21, it was predicted that when H is replaced by electronegative or π -donor substituents R (e.g. R = NH_2 , OH, SH, halogen), the M=M double bond

is weakened due to the greater DSSEs of the MR_2 fragments, while electropositive substituents were predicted to strengthen the $\text{M}=\text{M}$ bond²⁶. In agreement with these qualitative predictions, a quantitative linear correlation was found by Karni and Apeloig between $\Delta E_{\text{ST}}(\text{RR}'\text{Si})$ and $D(\text{RR}'\text{Si}=\text{SiRR}')^{263}$. For example, the BDE of $(\text{H}_3\text{Si})\text{HSi}=\text{SiH}(\text{SiH}_3)$ to two $(\text{H}_3\text{Si})\text{HSi}$ fragments is 64 kcal mol^{-1} while the dissociation energy of $(\text{HO})\text{HSi}=\text{SiH}(\text{OH})$ is only 30 kcal mol^{-1} . It was also predicted that when $\Sigma\Delta E_{\text{ST}} \geq 120 \text{ kcal mol}^{-1}$, the corresponding substituted disilene will dissociate spontaneously to two silylenes even at 0 K^{263} . An example is $\text{F}_2\text{Si}=\text{SiF}_2$ ($\Sigma\Delta E_{\text{ST}} = 147.6 \text{ kcal mol}^{-1}$), which indeed is not a minimum on the Si_2F_4 potential energy surface (at the HF level^{264,265a}, at the B3LYP level a very weak *trans*-bent complex with a very long Si–Si bond of 265.3 pm was located^{284a}). Similarly, a *trans*-bent structure could not be located for F_4Ge_2 as it dissociated spontaneously to two GeF_2 units^{284b}. A linear correlation was recently reported also between the BDEs of $\text{R}_2\text{Ge}=\text{GeH}_2$ and ΔE_{ST} of the corresponding GeR_2 ²⁸².

The connection between $\Delta E_{\text{ST}}(\text{RR}'\text{Si})$ and the existence or nonexistence of the corresponding disilene was recently demonstrated by Apeloig, Kira and coworkers in a joint experimental–theoretical study of the dimerization of $(\text{R}_2\text{N})_2\text{Si}^{285a}$. When $\text{R} = \text{H}$ the diaminosilylene is planar and ΔE_{ST} is large ($79.3 \text{ kcal mol}^{-1}$), and the calculations show that $(\text{H}_2\text{N})_2\text{Si}=\text{Si}(\text{NH}_2)_2$ is not a minimum on the PES and, if formed, it dissociates spontaneously. An N-bridged isomer **48**, $\text{R} = \text{NH}_2$ is a minimum on the PES (see also below) and it is by $16.3 \text{ kcal mol}^{-1}$ [CCSD(T)/6-311G(d,p)] more stable than two $(\text{H}_2\text{N})_2\text{Si}$ units. As the steric bulk of the R substituents at the nitrogens increases, the amino groups are twisted out of planarity and conjugation with the empty $3p(\text{Si})$ orbital, and consequently ΔE_{ST} decreases to $66.9 \text{ kcal mol}^{-1}$ for $\text{R} = \text{Me}$ and to $54.3 \text{ kcal mol}^{-1}$ for $\text{R} = i\text{-Pr}$. Consequently, $(\text{R}_2\text{N})_2\text{Si}=\text{Si}(\text{NR}_2)_2$, $\text{R} = \text{Me}, i\text{-Pr}$, become minima on the PES, which are more stable than two isolated $(\text{R}_2\text{N})_2\text{Si}$ units. The results of the calculations are in agreement with the experimental observation that at low temperature an equilibrium exists between $(\text{R}_2\text{N})_2\text{Si}$ and $(\text{R}_2\text{N})_2\text{Si}=\text{Si}(\text{NR}_2)_2$ ($\text{R} = i\text{-Pr}$)^{285b,c}. The relatively high ΔE_{ST} of $(i\text{-Pr})_2\text{NSi}$ results, however, in a highly unusual structure of $((i\text{-Pr})_2\text{N})_2\text{Si}=\text{Si}(\text{N}(\text{Pr}-i)_2)_2$, which exhibits a very long Si–Si bond of 247.2 pm , a large *trans*-bending angle of 42.6° and a large twisting angle around the Si–Si axis. This structure is not consistent with the presence of a Si=Si double bond and the bonding between the silicon centers is better described as a very weak double donor–acceptor bond^{285a} (Figure 17b), as was also suggested for related stannylenes^{254,286}.

Additional support for the theoretical prediction that diaminosilylenes avoid dimerization to tetraaminodisilenes is the recent finding by West, Apeloig and coworkers²⁷⁴ that the stable cyclic diaminosilylene **49a**, $\text{R} = t\text{-Bu}$, does not dimerize to the corresponding tetraaminodisilene, **49b**, $\text{R} = t\text{-Bu}$, but instead undergoes an insertion reaction leading to silylene **49c**, which dimerizes to a stable *Z*-diaminodisilyldisilene, **49d**, $\text{R} = t\text{-Bu}$. In full agreement with the experimental findings, the calculations [at B3LYP/6-31G(d)] predict that **49d**, $\text{R} = \text{Me}$ with only two amino groups attached to the Si=Si bond is a minimum on the PES, while the tetraaminodisilene **49b**, $\text{R} = \text{Me}$, is not²⁷⁴. Furthermore, **49d** is substituted by two silyl groups which stabilize the Si=Si double bond, i.e. the Si=Si double bond in $\text{H}_3\text{Si}(\text{H})\text{Si}=\text{Si}(\text{H})\text{SiH}_3$ is stronger by 8 kcal mol^{-1} (relative to the corresponding silylenes) than in the parent disilene²⁶³. The stabilization of the doubly-bonded system by the silyl groups is consistent with the calculated ΔE_{ST} for $(\text{H}_3\text{Si})(\text{Me}_2\text{N})\text{Si}$ of $45.2 \text{ kcal mol}^{-1}$, which is considerably smaller than that of $(\text{Me}_2\text{N})_2\text{Si}$: ($66.9 \text{ kcal mol}^{-1}$). The calculated structure of **49d**, $\text{R} = \text{Me}$ is in very good agreement with the X-ray structure of **49d**, $\text{R} = t\text{-Bu}$, including the very long Si–Si distance (of 228.9 pm , exp.;

228.5 pm, calculated) and the large twisting and bending angles around the formal Si=Si double bond²⁷⁴.

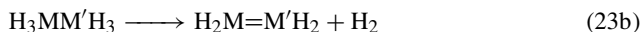
(49a) R = *t*-Bu, Me(49b) R = *t*-Bu, Me(49c) R = *t*-Bu, Me(49d) R = *t*-Bu, Me

The π -bond strengths (D_π) of hypothetical planar $M=M'$ molecules received considerable attention. Dobbs and Hehre used two different methods to estimate the $M=C$ bond energies^{278a}: (a) from the energy difference between the planar π -bonded and the perpendicular biradical structures (i.e. the rotational barrier around the $M=M$ bond) and (b) using Benson's thermochemical method²⁸⁷ based on the hydrogenation energy of the double bond (equations 22 and 23a,b). Both methods gave very similar π -bond energies for $H_2C=MH_2$. Windus and Gordon also obtained good agreement for the π -bond energies of $H_2M=M'H_2$ using either the rotational barrier method or Benson's thermochemical method (employing a mixture of experimental $M-H$ bond energies and theoretically calculated hydrogenation energies, Table 26)²⁷². Using these methods it was concluded that the ability to form π bonds decreases in the order $C > Si \sim Ge > Sn$, and that all *trans*-bent $H_2M=M'H_2$ species ($M, M' = Si$ to Sn) are stable toward dissociation ($M = Pb$ was not studied). It was predicted from these calculations that the $Si=Sn$ and $Ge=Sn$ systems, which have not yet been synthesized, should be accessible experimentally if appropriate substituents are present to provide kinetic stability²⁷².



$$D_\pi = D(M-H) + D(M'-H) - D(H-H) - \Delta H^\circ (0 K) \quad (23a)$$

In equation 23a, $\Delta H^\circ (0 K)$ is the heat of reaction 23b.



However, the methods used above for estimating the double-bond strengths (and the values in Table 26 under the column ‘dissociation energies’) do not give the ‘clean’ π -bond strengths. Thus, when using the rotational barrier method, in addition to breaking the π bond, geometric changes (e.g. lengthening of the σ bond, changes in the M–H bond lengths, pyramidalization at the M centers) accompany the rotation and thus affect the π -bond strength calculated by this method. In addition, upon rotation, hyperconjugation between the p orbital of M and the σ and σ^* orbitals of the adjacent M–R bonds, may stabilize the transition state for rotation, and thus cause an underestimation in the π -bond strength; i.e. the rotational barrier is the minimal estimate for the π -bond energy. For example, the measured rotation barrier for $(R_3Si)_2Si=Si(SiR_3)_2$ is only 15 kcal mol⁻¹, by about 10 kcal mol⁻¹ smaller than the *E,Z*-isomerization energies of known stable disilenes with alkyl and aryl substituents²⁸⁸, or than the calculated π -bond strength of $H_2Si=SiH_2$ (ca 22–24 kcal mol⁻¹)⁵⁶. The methods using thermochemical cycles suffer from similar problems of geometric changes between the two sides of the equations and include also other approximations. To circumvent these disadvantages, Shaik and coworkers developed recently a Valence Bond (VB) method which unpairs the π -bond electrons while keeping all other geometry parameters constant. According to this method the ‘clean’ π -bond strengths of $H_2C=SiH_2$ and planar $H_2Si=SiH_2$ are 47.1 and 35.1 kcal mol⁻¹, respectively²⁸⁹, compared to 38 and 25 kcal mol⁻¹ calculated using Benson’s thermochemical cycle²⁹⁰.

Jacobsen and Ziegler (JZ) published a detailed analysis of the bonding in $H_2M=MH_2$ based on DFT calculations which included also relativistic effects²⁶⁸. The results of their analysis are included in Table 26 under the ‘double bond analysis’ columns. According to their energy analysis, the total bond energy of a $H_2M=MH_2$ molecule is composed of the so-called ‘snapping energy’ minus the so-called ‘preparation energy’. The ‘snapping energy’ is the interaction energy of two MH_2 fragments in their triplet (3B_1) state to form $H_2M=MH_2$ (Figure 17a), when the unpaired electrons of one fragment possess α -spin and the electrons on the other fragment are of β -spin. The ‘preparation energy’ is the energy needed to prepare the H_2M fragment for the interaction, i.e. the energy required to deform the geometry of the fragment to its final geometry in the dimer and to transform the 1A_1 ground state to the 3B_1 state (which is the familiar ΔE_{ST}). The ‘snapping energy’ was further broken down to the following terms: (1) the attractive orbital interactions of singly occupied orbitals of the two 3B_1 MH_2 moieties (‘intrinsic bond energy’, E_{int}); (2) the electrostatic attraction of the nuclear charge of one fragment to the electron density of the other; and (3) exchange (or Pauli repulsion) between the doubly occupied orbitals of the two fragments, which is usually destabilizing. Due to the larger size of the orbitals of the heavier group 14 metals (compared with carbon), the Pauli repulsion is very large even at large M–M distances. Consequently, the MH_2 fragments cannot approach each other closely (e.g. the M–M and M=M bond distances differ only by 8–12%, while the C–C vs. C=C bond distances differ by 25%, Table 26)²⁶ and consequently the M=M bond energy is small. This weakening of the M=M bond is compensated by the π - σ^* interaction, which strengthens the π bond (Figure 17c) and which is stronger for the heavier M elements. Therefore, the ‘intrinsic bond strengths’ of the π bonds (since the HOMO of the *trans*-bent structures has b_u symmetry its classification as a π bond is not strictly valid) do not decrease sharply down group 14 (Table 26). The ranking of π -bond strengths in the *trans*-bent $H_2M=MH_2$ (in kcal mol⁻¹) is: C=C (75.4) >> **Pb=Pb**(42.3) > Si=Si (37.8) ~ Ge=Ge (37.8) > Sn=Sn (32.1)²⁶⁸. The position of the Pb=Pb bond in this series is unusual. The Pb=Pb bond, despite having a large intrinsic π -bond energy, has the smallest overall bond energy of 10–24 kcal mol⁻¹ (Table 26). This is due to the fact that the overall bond strength is dictated by the Pauli

repulsion and the MH_2 singlet–triplet splitting. Hence the large 1A_1 – 3B_1 promotion energy of PbH_2 is mainly responsible for the very small total bond energy of $\text{Pb}=\text{Pb}$ ²⁶⁸. In the planar M_2H_4 series, the π -bond energy decreases gradually down group 14 (Table 26). As expected, the calculated intrinsic π -bond energies in $\text{H}_2\text{M}=\text{MH}_2$ ²⁶⁸ are higher than the π -bond energies based on the 90° rotation barriers (see above)^{272,278a}.

The σ -bond energies also decrease on going down group 14 due to a less efficient orbital overlap. As a result, the ratio of the σ and π components of the intrinsic bond energy of the $\text{M}=\text{M}$ bond, (i.e. σ/π) decreases down the group from 2.8 for D_{2h} C_2H_4 to 1.4 for C_{2h} Pb_2H_4 (Table 26). According to this analysis the *trans*-bent structures possess even higher π -bond character than ethene itself.

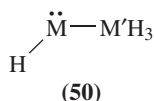
The result obtained by JZ, that the intrinsic π -bond energy of *trans*-bent diplumbene of $42.3 \text{ kcal mol}^{-1}$ is much larger than that of the corresponding planar $\text{H}_2\text{Pb}=\text{PbH}_2$ of $20.6 \text{ kcal mol}^{-1}$ ²⁶⁸ (Table 26), was questioned by Schleyer and coworkers²²⁴. They have calculated for *trans*-bent diplumbene a rotation barrier ($C_{2h} \rightarrow C_2$) of only $13.1 \text{ kcal mol}^{-1}$, significantly smaller than the rotation barrier ($D_{2h} \rightarrow D_{2d}$) of $20.3 \text{ kcal mol}^{-1}$ for the planar structure. The latter value is very similar to the intrinsic π -bond energy of $20.6 \text{ kcal mol}^{-1}$ calculated by JZ²⁶⁸. The similarity of these two π -bond energies indicate that hyperconjugation is not important energetically in the rotated $\text{H}_2\text{Pb}^\bullet-\bullet\text{PbH}_2$ structure. Thus, hyperconjugation cannot explain the large discrepancy between the π -bond energies calculated for the *trans*-bent isomers by the two groups^{224,268}. The small rotation barrier of only $13.1 \text{ kcal mol}^{-1}$ lead Schleyer and coworkers to conclude that in the *trans*-bent $\text{H}_2\text{Pb}=\text{PbH}_2$ the π overlap is small²²⁴.

The surprising fact that dissociation of some $\text{M}-\text{M}$ single bonds requires more energy than dissociation of the corresponding double bonds (Table 26) was attributed by JZ²⁶⁸ mainly to the high ‘preparation energy’ of the MH_2 fragments, in contrast to the very small ‘preparation energy’ of MH_3 radicals. In other words, $\text{H}_2\text{M}=\text{MH}_2$ dissociates to the favorable singlet closed-shell ground state MH_2 fragments, while the MH_3 radicals formed from H_3MMH_3 are not as favorable (see Section V.A.2 and Table 3). Hence, the dissociation of $\text{H}_2\text{M}=\text{MH}_2$ may be easier than that of H_3MMH_3 , although the intrinsic bond energy of the double bonds is always higher than that of the $\text{M}-\text{M}$ single bonds. This, and the theoretical evidence that the π bond makes an important contribution to the overall $\text{M}=\text{M}$ bond strength underlines the fact that the heavier $\text{H}_2\text{M}=\text{MH}_2$ have real double bonds²⁶⁸. This conclusion is supported by calculated $\text{M}=\text{M}$ bond orders, which are larger than 1 for all $\text{M}=\text{M}$ bonds except $\text{M} = \text{Pb}$, i.e. the calculated Wiberg bond indices are 1.88, 1.65, 1.49 and 1.09 for $\text{M} = \text{Si, Ge, Sn and Pb}$, respectively²²⁴ (similar results were obtained by Lendvay²⁹¹ using a different bond order method). $\text{H}_2\text{Pb}=\text{PbH}_2$, for which the Wiberg bond index is only 1.09 and the rotation barrier is $13.1 \text{ kcal mol}^{-1}$ ²²⁴, is an exception and is best described as a $\text{H}_2\text{Pb}^\bullet-\bullet\text{PbH}_2$ singlet biradical with modest interactions between the singly-occupied orbitals rather than as a doubly-bonded species²²⁴.

The character of $\text{M}=\text{M}$ ($\text{M} = \text{Si to Pb}$) double bond was also addressed in a recent analysis using electron localization functions (ELF). In a very simplistic way, ELF represents the probability of finding two electrons with the same spin α (or β) in a given space. In regions where this probability is small, electrons are localized. ELF divides the valence electron density into regions of bonding and nonbonding electron pairs. Based on the similarities in the topographical ELF representations of ‘classical’ planar double bonds and *trans*-bent $\text{M}=\text{M}$ double bonds, it was concluded that all heavy element $\text{M}=\text{M}$ bonds, even in strongly bent molecules, can be described as real double bonds²⁹².

3. Stability relative to isomeric structures

a. *Relative to the corresponding metallyenes.* Grev formulated simple guidelines, according to equation 24²⁶, for estimating the thermodynamic stability of $\text{H}_2\text{M}=\text{M}'\text{H}_2$ species relative to the corresponding metallylenes, $\text{HMM}'\text{H}_3$ (50) (equation 25). In equation 24, $D(\text{H}_3\text{M}-\text{H})$ is the M–H bond dissociation energy, D_π is the π bond energy of $\text{H}_2\text{M}=\text{M}'\text{H}_2$ and DSSE (MH_2) is the divalent state stabilization energy of MH_2 (see equation 4, Section V.A.2). Equation 24 uses typical values of σ and π bond energies and DSSE values which are available either from theory or from experiment^{293,294}.



$$\Delta H(\text{equation 25}) = D(\text{H}_3\text{M}-\text{H}) - D(\text{H}_3\text{M}'-\text{H}) + D_\pi - \text{DSSE}(\text{MH}_2) \quad (24)$$



For example, based on equation 24, it can be concluded that the isomerization reaction of $\text{H}_2\text{M}=\text{CH}_2$ to HMCH_3 becomes more exothermic as M becomes heavier, due to the decrease in the M–H bond dissociation energy (Table 3) and in D_π , and the increase in the DSSE of the MH_2 fragments. This conclusion is supported by *ab initio* calculations. For example, equation 24 leads to predicted isomerization energies of $\text{H}_2\text{M}=\text{CH}_2$, M=Si and Ge of 5.8 and $-15.3 \text{ kcal mol}^{-1}$, respectively, in good agreement with the *ab initio* calculated values of 4²⁹⁵ and -15 ²⁹⁶ kcal mol^{-1} , respectively.

The calculated isomerization energies of $\text{H}_2\text{M}=\text{M}'\text{H}_2$ to $\text{HMM}'\text{H}_3$ and the activation barriers for this isomerization are collected in Table 27^{7,269,295,296–301}. One of the major conclusions from Table 27 is that doubly bonded molecules involving elements heavier than silicon are unstable thermodynamically toward isomerization to the corresponding metallylenes. However, the barriers for the isomerization are significant for all heavier group 14 elements, thus stabilizing kinetically the doubly-bonded isomers toward isomerization and suggesting that both $\text{H}_2\text{M}=\text{M}'\text{H}_2$ and $\text{HMM}'\text{H}_3$ should in principle be

TABLE 27. Reaction energies (ΔE) and activation barriers (E_a) for the isomerization of $\text{H}_2\text{M}=\text{M}'\text{H}_2$ to $\text{HMM}'\text{H}_3$ (equation 25)^a

M	Si		Ge		Sn	Pb
	ΔE	E_a	ΔE	E_a	ΔE	ΔE
$\text{H}_2\text{M}=\text{MH}_2 \rightarrow \text{HMMH}_3$	7.9 ^b	17.3 ^c	2.3 to -2.0 ^d ; 2.4 ^e	12 – 14 ^d	-2.1 ^e	-6.4 ^e
$\text{H}_2\text{M}=\text{CH}_2 \rightarrow \text{HMCH}_3$	4.7 to -2.1 ^f	42.2 ^f	-11.4 to -15.9 ^d	13.0–15.0 ^d	—	—
$\text{H}_2\text{M}=\text{SiH}_2 \rightarrow \text{HMSiH}_3$	7.9 ^{b,g}	17.3 ^c	-3.2 ^h	13.0 ^h	—	—

^aIn kcal mol^{-1} . A negative sign indicates that the isomerization is exothermic.

^bAt the G1 level; from Reference 298. For older (usually lower level) values, see Reference 7.

^cAt $\text{MP}_3/6-31\text{G}(\text{d,p})/\text{HF}/6-31\text{G}(\text{d})$; from Reference 299.

^dAt various CISD and CCSD levels; from Reference 296.

^eAt CI/ECP; from Reference 269.

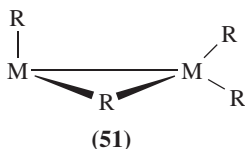
^fAt various correlated computational methods; from References 295 and 300.

^g ΔE for $\text{H}_2\text{Si}=\text{SiH}_2^- \rightarrow \text{HSiSiH}_3^-$ is $-3.0 \text{ kcal mol}^{-1}$ ²⁹⁷.

^hCCSD(T) all-electron calculation; from Reference 301.

observable molecules^{275–277,296,301}. When substituents other than hydrogen are present, the DSSE of MR_2 increases with the electronegativity of R^{26} and ΔH of equation 25 becomes more exothermic.

b. Relative to bridged isomers. i. Hydrogen bridged isomers. Hydrogen bridging is common in electron deficient molecules such as boranes and other group 13 compounds²⁴⁵. Hydrogen bridged structures are preferred also for strained heavier group 14 molecules such as 3-MRs and metallatetrahedranes (see Sections V.E.1.a.iv and V.E.2.c). Trinquier predicted, based on equation 20, that when $\Delta E_{ST}(MH_2) > \frac{1}{2}E_{\sigma+\pi}(H_2M=MH_2)$ ^{269,302}, the M_2H_4 systems prefer to have doubly- (**48**) or singly- (**51**, $R = H$) hydrogen-bridged structures over the *trans*-bent (or planar) $H_2M=MH_2$ structures. Actual calculations support this prediction, but there are exceptions as discussed below. The doubly hydrogen-bridged structures, **48**, have two 3-center–2-electron MHM bonds with no formal M–M bond, while the singly hydrogenbridged isomers **51**, $R = H$ have a 3-center–2-electron hydrogen bridge between the metal atoms and a dative bond from one metal to the other^{273,302}.



At the SCF/DZP level, the doubly-bonded $H_2Si=SiH_2$ (D_{2h}) and $H_2Ge=GeH_2$ (C_{2h}) isomers are the most stable species on the Si_2H_4 and Ge_2H_4 PESs, respectively. Doubly-bridged isomers were also located as minima, but they are higher in energy (Table 28^{269,281,284,302}). The singly hydrogen-bridged isomers do not exist for $M = Si$ and Ge ²⁶⁹. For Sn_2H_4 and Pb_2H_4 the dibridged **48**, $R = H$ are the most stable, and the stability order of the other isomers follows the order: *trans*-dihydrogen bridged (**48**, $R = H$) (the *cis*-isomers are by a few kcal mol⁻¹ less stable) > singly hydrogen bridged (**51**, $R = H$) > $HMMH_3$ (**50**) > *trans*-bent $H_2M=MH_2$ (**46**). Thus, the conventional doubly-bonded isomer **46** is the least stable isomer for Sn_2H_4 and for Pb_2H_4 . For Pb_2H_4 , the *trans*-bent isomer is actually not even a minimum on the PES³⁰². The finding that a doubly-bonded structure does not exist for diplumbene is consistent with equation 20, as ΔE_{ST} of PbH_2 of 34.8 kcal mol⁻¹ > $\frac{1}{2}E_{\sigma+\pi}(H_2Pb=PbH_2)$ of ca 25–30 kcal mol⁻¹. We note, however, that equation 20 fails to predict the existence and high stability of the dibridged isomer of Sn_2H_4 , as ΔE_{ST} of SnH_2 of 23 kcal mol⁻¹ is smaller than $\frac{1}{2}E_{\sigma+\pi}$ of $H_2Sn=SnH_2$ of ca 30–35 kcal mol⁻¹²⁶⁹. ΔE_{ST} of SiH_2 and GeH_2 of 18–21 and 22 kcal mol⁻¹, respectively, are smaller than $\frac{1}{2}E_{\sigma+\pi}$ of $H_2Si=SiH_2$ (35–38 kcal mol⁻¹) and $H_2Ge=GeH_2$ (30–35 kcal mol⁻¹), consistent with the fact that the doubly-bonded isomers are lower in energy than the hydrogen-bridged isomers. Interestingly, for all heavier group 14 elements the binding energy of the doubly-hydrogen bridged isomers (**48**, $R = H$) relative to two isolated MH_2 fragments is 30 ± 3 kcal mol⁻¹²⁶⁹.

The first experimental example of a doubly-hydrogen bridged structure, i.e. *trans*-[$RSn(\mu-H)_2$] ($R = 2,6\text{-Tip}_2C_6H_3$, $Tip = 2,4,6\text{-triisopropylphenyl}$), was reported recently³⁰³. This compound is stable in the solid state at room temperature, but in hydrocarbon solvents (e.g. hexane, benzene, toluene) and diethyl ether it dissociates to $RHSn$ monomers.

TABLE 28. Geometries and relative energies (ΔE) of various isomers of M_2H_4 and M_2F_4 and their dissociation energies ($\Delta E'$)^a

M_2R_4		$R_2M=MR_2$ 47 ^b	R_2M-MR_2 distorted ^c	$RMMR_3$ 50	$RM(R)_2MR$ 48 ^d	$RMRMR_2$ 51 ^e
C_2H_4	ΔE	0.0		80.1	164.7 ^f	
	$\Delta E'/g$	-192.0	—	-111.9	-27.3 ^f	
	d(M-M)	132.2		148.7	—	—
	d(M-R-M) $\angle RMR$				128.2 ^f 83.0 ^f	
C_2F_4	ΔE	0.0	44.0	38.9	118.8 ^f	
	$\Delta E'/g$	-56.3	-12.3	-17.4	62.5 ^f	
	d(M-M)	130.2	149.4	153.5	—	—
	d(M-R-M) $\angle RMR$				169.7 ^f 78.4 ^f	
Si_2H_4	ΔE	0.0	-1.2 ^h	9.8	22.5	
	$\Delta E'/g$	-53.7	-53.4 ^h	-43.9	-31.2	
	d(M-M)	211.7	218.4 ^h	239.9	—	—
	d(M-R-M) $\angle RMR$				165.4 77.2	
Si_2F_4 ⁱ	ΔE	0.0 (0.0)	-11.7 (-41.0 ^j)	-50.5 (-47.1)	-46.8 (-40.3)	
	$\Delta E'/g$	44.2 (39.1)	32.5 (-1.9 ^j)	-6.3 (-8.0)	-2.6 (-1.2)	
	d(M-M)	204.8 (208.6)	233.0 (265.3 ^j)	241.0 (248.3)	—	—
	d(M-R-M) $\angle RMR$				190.6 (191.3) 72.2 (74.7)	
Ge_2H_4	ΔE	0.0	-3.2	-0.8	5.8	
	$\Delta E'/g$	-32.7	-35.9	-33.5	-26.9	
	d(M-M)	224.5	231.5	257.4	—	—
	d(M-R-M) $\angle RMR$				177.5 75.9	
Ge_2F_4 ^k	ΔE	0.0 (0.0)	-22.7	-65.2 (-72.0)	-97.3 (-100.4)	
	$\Delta E'/g$	73.5 (80.9)	50.8	8.3 (8.9)	-23.8 (-19.5)	
	d(M-M)	217.4	250.8	262.2 (263.6)	—	—
	d(M-R-M) $\angle RMR$				199.8 (201.9) 71.6 (74.6)	
Sn_2H_4	ΔE	0.0	-9.4	-11.5	-18.5	-10.6
	$\Delta E'/g$	-14.7	-24.1	-26.2	-33.2	-25.3
	d(M-M)	253.7	271.2	288.6	—	274.4
	d(M-R-M) $\angle RMR$				193.3 73.9	204.4/191.5 87.7 ^l
Sn_2F_4	ΔE	0.0	-31.3	-73.1	-133.1	
	$\Delta E'/g$	82.2	51.5	9.1	-50.9	
	d(M-M)	247.0	282.6	294.3	—	
	d(M-R-M) $\angle RMR$				211.3 69.6	
Pb_2H_4	ΔE	0.0	-19.8 ^m	-26.2	-43.7	-28.4
	$\Delta E'/g$	15.0	-4.8	-11.2	-28.7	-13.4
	d(M-M)	257.2	299.9	295.9	—	293.6
	d(M-R-M) $\angle RMR$				203.8 74.1	202.0/213.3 89.9 ^l

TABLE 28. (continued)

M ₂ R ₄		R ₂ M=MR ₂ 47^b	R ₂ M–MR ₂ distorted ^c	RMMR ₃ 50	RM(R) ₂ MR 48^d	RMRMR ₂ 51^e
Pb ₂ F ₄	ΔE	0.0	–77.8	–123.5	–212.2	
	ΔE' ^g	149.9	72.1	26.4	–62.3	
	d(M–M)	249.9	294.3	307.7	—	
	d(M–R–M)				220.1	
	∠RMR				70.9	

^aCI//HF/DZ calculations using ECPs for all non-hydrogen atoms with inclusion of relativistic effects for Sn and Pb. Energies in kcal mol^{–1}, bond lengths in pm and bond angles in degs. The data for M₂H₄ are from References 269 and 302, and for M₂F₄ from Reference 281.

^bFor the planar D_{2h} geometry. This geometry is not a minimum on the PES, except for H₂C=CH₂, F₂C=CF₂ and H₂Si=SiH₂ (D_{2h} H₂Si=SiH₂ is also not a minimum when optimized at correlated levels of theory).

^cFor M₂H₄ the given data are for the *trans*-bent C_{2h} dimetallenes (**46**); for M₂F₄ the data are for the twisted triplet (³B) M₂F₄ in C₂ symmetry. *Trans*-bent C_{2h} M₂F₄ are not minima for all M.

^dData for the *trans*-isomer (**48**). The *cis*-isomers are 2–3 kcal mol^{–1} less stable and their structural parameters are almost identical to those of the *trans*-isomers.

^eThe singly-bridged isomer was located as a minimum only for Sn₂H₄ and Pb₂H₄.

^fConstrained to C_{2h} symmetry. Not a minimum on the PES.

^gEnergy relative to two MR₂ units in the ¹A₁ state.

^hData at B3LYP/DZ+P²²⁴ (a *trans*-bent C_{2h} structure could not be located at HF/DZP²⁶⁹). See Table 26 for values at other levels of theory.

ⁱValues in parentheses are at B3LYP/DZP++; from Reference 284a.

^jFor **46**, M = Si, R = F, which is a minimum at B3LYP although with a very weak Si=Si bond^{284a}.

^kValues in parentheses are at B3LYP/DZP++; from Reference 284b.

^lThe MHM angle.

^mNot a minimum on the PES³⁰².

ii. π-Donor bridged isomers. Halogen substituents often increase the singlet–triplet splitting of MX₂ (X = halogen) beyond the critical value of $\frac{1}{2}E_{\sigma+\pi}$ required (according to equation 20) to favor stable bridged structures. This implies that in dimers of MX₂, a direct M···M link is less favored and bridged arrangements, e.g. **48**, R = X, become the most stable.

Trinquier and Barthelat computed all group 14 M₂F₄ species using Hartree–Fock geometry optimizations and CI relative energies²⁸¹ and their results are presented in Table 28. The planar F₂M=MF₂ (D_{2h}) structures are not minima on the PESs for all group 14 elements (except C) and they are unstable toward dissociation to two MF₂ units. However, the detailed features of the potential energy surfaces change significantly down group 14. The global minima of M₂F₄ are: F₂C=CF₂ (D_{2h}) for M = C, the silylene FSi–SiF₃ (C_s) for M = Si and the fluorine dibridged structures (**48**, R = F) for Ge, Sn and Pb²⁸¹ (Table 28). The latter prediction is in agreement with the experimental structures of several M₂X₄ and M₂X₂R₂, R = alkyl, aryl compounds of Ge, Sn and Pb^{304,305}. The binding energies of the fluorine dibridged M₂F₄ structures relative to two MF₂ units increase in the order (values in kcal mol^{–1}): 2.6 (Si) < 23.8(Ge) < 50.9(Sn) < 62(Pb)²⁸¹. This order contrasts the almost constant binding energy of *ca* 30 kcal mol^{–1} of HM(μ-H)₂MH compounds²⁶⁹ (Table 28). For M = Ge, Sn and Pb the F₃MMF metallylenes are by 32.1, 60.0 and 88.7 kcal mol^{–1}, respectively, less stable than the fluorine dibridged isomers (**48**, R = F).

The *trans*-bent HFSi=SiHF is the most stable H₂Si₂X₂ isomer, but the fluorine bridged HSi(μ-F)₂SiH and the hydrogen bridged FSi(μ-H)₂SiF isomers are by only 9.5 and 6.1 kcal mol^{–1} [at MP3/6-31G(d)//HF/6-31G(d)] higher in energy, and they

are substantially more stable than the corresponding silylenes³⁰⁶. The small energy difference between $\text{HSi}(\mu\text{-F})_2\text{SiH}$ and $\text{HFSi}=\text{SiHF}$ lead Maxka and Apeloig³⁰⁶ to suggest that the species which was observed by low-temperature NMR and claimed to be $c\text{-C}_5\text{H}_5\text{FSi}=\text{SiF}(\text{C}_5\text{H}_5\text{-}c)$ ³⁰⁷ is actually the difluoro-bridged $c\text{-C}_5\text{H}_5\text{Si}(\mu\text{-F})_2\text{Si}(\text{C}_5\text{H}_5\text{-}c)$.

Attempts to determine the structure of Ge_2Br_4 by gas-phase electron diffraction were not successful, probably due to the interference from bridged dimers³⁰⁸. A subsequent *ab initio* investigation (at HF/DZ+d) found Ge_2Cl_4 and Ge_2Br_4 to be the *cis*-dibridged complexes, but these dimers are only weakly bound (by less than 10 kcal mol^{-1}), explaining the experimental difficulties³⁰⁹. Dimerization of RCIM (R = 2,6-Mes₂C₆H₃) lead for M = Ge to the isolation of $\text{RCIGe}-\text{GeRCl}$ with a weak Ge-Ge interaction [$d(\text{Ge}-\text{Ge}) = 244.3\text{ pm}$], while for M = Sn an asymmetric dichloro-bridged dimer, $\text{RSn}(\mu\text{-Cl})_2\text{SnR}$, was isolated with Sn-Cl bond lengths of 260 and 268.5 pm³¹⁰. Both compounds are stable at room temperature in both the solid state and solution, and they were characterized by X-ray crystallography³¹⁰. The fact that $\text{R}_2\text{Sn}_2\text{Cl}_2$ is bridged while $\text{R}_2\text{Ge}_2\text{Cl}_2$ is not, is consistent with the stability order calculated for M_2F_4 (Table 28). Calculations for M_2X_4 , X = Cl, Br are not yet available.

The dibridged structures (**48**, M = Si) are substantially stabilized also by amino and hydroxy bridging groups, i.e. $\text{HSi}(\mu\text{-NH}_2)_2\text{SiH}$ is by 10 kcal mol^{-1} more stable and $\text{HSi}(\mu\text{-OH})_2\text{SiH}$ is by only 3.2 kcal mol^{-1} less stable than the corresponding $\text{RHSi}=\text{SiRH}$ disilenes³¹¹.

The dimerization of $(\text{R}_2\text{N})_2\text{Si}$ is a particularly interesting example of the interplay between $\text{Si}\cdots\text{Si}$ bonded structures and dibridged structures (see also Section VI.B.2). Scrambling experiments of the dimerization of $(i\text{-Pr}_2\text{N})_2\text{Si}$ (produced by reduction of the corresponding chlorosilane with K in boiling benzene) at 75°C were interpreted to be consistent with the intermediacy of the N-bridged dimer, **48**, R = $(i\text{-Pr})_2\text{N}$, although a more complex sequence of reactions involving $(i\text{-Pr}_2\text{N})_2\text{Si}=\text{Si}(\text{N}(\text{Pr-}i)_2)_2$, could not be excluded^{285c}. This interpretation was consistent with earlier theoretical predictions by Apeloig and Müller^{311a}. In contrast, $(i\text{-Pr}_2\text{N})_2\text{Si}$ (produced photolytically at 77 K) dimerizes to the disilene $(i\text{-Pr}_2\text{N})_2\text{Si}=\text{Si}(\text{N}(\text{Pr-}i)_2)_2$ ^{285b}. To gain more insight into this puzzle, Takahashi and coworkers studied computationally the dimerization of $(\text{R}_2\text{N})_2\text{Si}$, R = Me and $i\text{-Pr}$ ^{285a}. The computations show that the tetraaminodisilenes and the N-dibridged dimers are both minima on the PES for both R = Me and $i\text{-Pr}$. However, the dibridged $(\text{Me}_2\text{N})\text{Si}[\mu\text{-}(\text{NMe}_2)]_2\text{Si}(\text{NMe}_2)$ dimer is by $12.5\text{ kcal mol}^{-1}$ [at MP2/6-311G(d,p)//MP2/6-311G(d,p)] more stable than the corresponding disilene, but **48**, R = $(i\text{-Pr})_2\text{N}$ is by $16.0\text{ kcal mol}^{-1}$ [at MP2/6-31G(d)//B3LYP/6-31G(d)] higher in energy than $(i\text{-Pr}_2\text{N})_2\text{Si}=\text{Si}(\text{N}(\text{Pr-}i)_2)_2$. The very large change in the relative stabilities between R = Me and R = $i\text{-Pr}$ of the N-bridged isomers relative to the corresponding disilene isomers results [in addition to the change in ΔE_{ST} of the corresponding silylenes (see Section VI.B.2)] from the severe steric interactions between the bulky $i\text{-Pr}$ groups in the dibridged isomer. These interactions are significantly smaller when R = Me than when R = $i\text{-Pr}$ ^{285a}. The calculations thus imply that for R = $i\text{-Pr}$ both isomers may exist, and the higher energy of the bridged species suggests that it should be formed at higher temperatures while the disilene should be favored at lower temperatures. The computational study was accompanied by two new experiments in which the $(i\text{-Pr}_2\text{N})_2\text{Si}$ monomer was produced photolytically under the same conditions but at different temperatures. In agreement with the theoretical predictions, scrambling, pointing clearly to the intermediacy of the N-bridged dimer **48**, R = $\text{N}(\text{Pr-}i)_2$, occurred only above room temperature, while the disilene isomer was formed only at low temperatures^{285a}. The calculations and experiments are now in harmony.

C. R₂M=X Compounds

For many years, the existence of the heavier element congeners of ketones, R₂C=O ('heavy ketones'), imines, R₂C=NR' or phosphenes, R₂C=PR' which include heavier group 14, 15 and 16 elements was doubted. However, in the last two decades stable R₂M=X compounds have been prepared by taking advantage of the kinetic stabilization gained by using very bulky R substituents^{24a-c,312,313}. Recent successful syntheses of stable 'heavy ketones' include: RR'Si=S^{313a}, RR'Ge=X (X=S^{313b}, Se^{313b} and Te^{313c}) and RR'Sn=X (X=S and Se)^{24a,313d,e} where R and/or R' are, e.g. 2,4,6-tris[bis(trimethylsilyl)methyl]phenyl (denoted as Tbt) or 2,4,6-triisopropylphenyl (Tip). Stable compounds R₂M=O are still not available, but H₂Si=O was detected and identified spectroscopically in the gas phase^{314a-c} and in matrix^{314d-f}, and (CH₃)₂Si=O and Ph₂Si=O were detected in a matrix and studied by IR spectroscopy^{314g}. Evidence for the existence of H₂Ge=O^{315a} and Me₂Ge=O^{315b} in a matrix was obtained from IR Spectra. The assignment of the vibrational spectral bands of Me₂Ge=O was done in comparison with the calculated frequencies and IR intensities^{315b}. Similarly, stable R₂M=NR', M=Si, Ge, Sn and R₂M=PR', M=Si, Ge and Sn, were recently synthesized^{24a,c}.

1. Structures and bond energies

A theoretical investigation of the M=X bond lengths and the relative σ - and π -bond energies of H₂M=X (for all group 14 M and group 16 X)^{313a} accompanied efforts to synthesize stable R₂M=X compounds³¹³, and these results and those of related studies are presented in Table 29^{56,224,316}.

The calculated M=X bond lengths are shorter by 8–10% than the corresponding single M–X bond lengths irrespective of the identity of M or X. This bond length contraction is slightly smaller than in H₂C=X, being 15% for X=O and 10% for X=Te (Table 29). The σ - and π -bond energies were calculated using the procedure suggested by Schleyer and Kost⁵⁶, according to which the difference in energy between two M–X single bonds and a M=X double bond is calculated by means of isodesmic equations. The M=X π -bond energy is then calculated by subtraction of this energy difference from the dissociation energies of the corresponding singly-bonded systems. The latter dissociation energies are also taken as the σ -bond energy component of the total M=X bond energy⁵⁶.

Nearly equal σ - and π -bond energies are found only for H₂C=O, which also has the strongest π bond in the series. The strongest σ bond in the series is that of Si=O. The σ - and π -bond energies decrease as M or X become heavier (Table 29). For a given X, the σ/π ratios for H₂Sn=X and H₂Pb=X are significantly higher than for H₂Si=X and H₂Ge=X (which are yet larger than for H₂C=X). The σ/π ratios are also significantly higher for H₂M=O than for the corresponding heavier H₂M=X congeners, except for M=C where the trend is opposite (Table 29). The high σ/π ratios for all M elements explains the high reactivity of these M=X doubly-bonded compounds in addition reactions, because the formation of two new σ bonds to M and X with a concurrent cleavage of the π bond results in a substantial overall energy gain, which increases for the heavier M congeners^{313a}.

The M=O double bonds are highly polarized; the metals are highly positively charged (+1.5e to +1.7e) and the charge increases in a 'zig-zag' pattern from M=Si to M=Pb. The oxygen has a charge of ca -1. The π - and σ -electron densities are both polarized toward the oxygen. H₂C=O is significantly less polarized; the charge on the carbon is +0.3e and on oxygen -0.5e. The M=O bond orders in H₂M=O, M=Si to Pb are in the range of 0.8–0.9 compared to 1.4 for M=C, reflecting the higher ionic character of the M=O bonds in the heavier analogs of formaldehyde³¹⁶.

TABLE 29. M=X bond lengths (pm) and bond energies (kcal mol⁻¹) in H₂M=X (X = O, S, Se and Te)^a

H ₂ M=X	Parameter	X			
		O	S	Se	Te
H ₂ C=X	d(M=X)	120.0	161.7	175.8	194.9
	d(M-X) ^b	142.1	183.5	197.9	216.5
	σ	93.6	73.0	65.1	57.5
	π	95.3	54.6	43.2	32.0
	σ + π	188.9	127.6	108.3	89.5
H ₂ Si=X	σ/π	0.98	1.34	1.51	1.80
	d(M=X)	151.4	194.5	208.2	228.8
	d(M-X) ^b	164.9	214.8	229.4	250.8
	σ	119.7	81.6	73.7	63.2
	π	58.5	47.0	40.7	32.9
H ₂ Ge=X	σ + π	178.2	128.6	114.4	96.1
	σ/π	2.05	1.74	1.81	1.92
	d(M=X)	163.4	204.2	217.4	237.3
	d(M-X) ^b	178.8	225.6	239.3	259.6
	σ	101.5	74.1	67.8	59.1
H ₂ Sn=X	π	45.9	41.1	36.3	30.3
	σ + π	147.4	115.2	104.1	89.4
	σ/π	2.21	1.80	1.87	1.95
	d(M=X)	180.2	222.2	234.6	254.3
	d(M-X) ^b	195.0	243.8	256.5	276.8
H ₂ Pb=X	σ	94.8	69.3	64.3	56.4
	π	32.8	33.5	30.6	26.3
	σ + π	127.6	102.8	94.9	82.7
	σ/π	2.89	2.07	2.10	2.14
	d(M=X)	185.3 ^c	227.3	239.4	259.0
	d(M-X) ^b	202.5 ^c	250.2	262.8	281.9
	σ	80.9	60.9	57.0	50.3
	π	29.0	30.0	27.8	24.4
	σ + π	109.9	90.9	84.8	74.7
	σ/π	2.79	2.03	2.05	2.06

^aAt B3LYP/TZ(d,p)//B3LYP/TZ(d,p); σ- and π-bond energies were calculated according to the procedure proposed in Reference 56 from Reference 313a. For calculations of H₂M=O at other computational levels, see References 224 and 316.

^bIn H₃MXH.

^cAt B3LYP with quasi-relativistic ECPs, the Pb=O and Pb-O bond lengths are 192.7 pm and 211.4 pm, respectively (194.3 pm and 208.7 pm with nonrelativistic ECPs)³¹⁶.

The π-bond strengths of H₂M=XH where X is a heavy group 15 element, i.e. X = P, As, Sb and Bi (as calculated from rotational barriers), decreases with increasing atomic numbers of M and X. It is 47 kcal mol⁻¹ for H₂C=PH and it decreases to ca 32, 29 and 22 kcal mol⁻¹ for H₂Si=PH, H₂Ge=PH and H₂Sn=PH. The π-bond energies decrease further for heavier X elements, i.e. they are 28, 23 and 21 kcal mol⁻¹ for H₂Si=X, X = As, Sb and Bi, respectively³¹⁷.

2. Isomerization to metallylenes

Calculated reaction energies and activation barriers for the isomerization of RR'M=X to the corresponding metallylenes RMXR' are given in Table 30. Except for M = C (where

$\text{H}_2\text{C}=\text{O}$ is more stable than HCOH by *ca* 52 kcal mol⁻¹), the divalent metallylenes, HMxH , are more stable than the corresponding $\text{H}_2\text{M}=\text{X}$, and the isomerization becomes more exothermic for heavier M; e.g. silanone and hydroxysilylene have nearly the same energy, but germanone is by *ca* 24–31 kcal mol⁻¹ less stable than hydroxygermylene and HPbOH is more stable than $\text{H}_2\text{Pb}=\text{O}$ by 69.5 kcal mol⁻¹³¹⁶ (Table 30^{296,316,318–324}). However, very high barriers separate the doubly-bonded compounds from their divalent isomers (this was calculated only for M = Si and Ge), so that both isomers are relatively stable kinetically toward this isomerization reaction.

A very significant substituent effect was found for the $\text{RR}'\text{M}=\text{O} \rightarrow \text{RMOR}'$ rearrangement (Table 30). In general, the isomerization reaction becomes less exothermic (or more endothermic) when hydrogen is substituted by other groups and the activation barrier for the rearrangement increases. For example, the isomerization reactions of $\text{Me}_2\text{Si}=\text{O}$ and $\text{Me}_2\text{Ge}=\text{O}$ are less exothermic by *ca* 20 kcal mol⁻¹ (for $\text{Me}_2\text{Si}=\text{O}$ it is endothermic by 21.1 kcal mol⁻¹) than for the corresponding $\text{H}_2\text{M}=\text{O}$ and the rearrangement barriers increase by 18 and 12 kcal mol⁻¹ to 75.0 and 61.8 kcal mol⁻¹, respectively^{316,319}. These large barriers ensure that both isomers will survive if produced, as was demonstrated

TABLE 30. Reaction energies (ΔE) and activation barriers (E_a) for the isomerization of $\text{RR}'\text{M}=\text{XH}_n$ to $\text{RMXH}_n\text{R}'^a$
s(l)

M	Si		Ge		Sn	Pb
	ΔE	E_a	ΔE	E_a	ΔE	ΔE
$\text{H}_2\text{M}=\text{O} \rightarrow \text{HMOH}$	-1.8 ^b ; -0.2 ^c	57.0 ^c	-30.7 ^b ; -23.8 ^d	47.9 ^d	-49.0 ^b	-69.5 ^{b,e}
$\text{Me}_2\text{M}=\text{O} \rightarrow \text{MeMOMe}$	21.1 ^b ; 20.7 ^f	75.0 ^f	-11.5 ^b ; -6.6 ^{d,f}	61.8 ^{d,f}	-31.5 ^b	-55.3 ^{b,e}
$\text{HFM}=\text{O} \rightarrow \text{FMOH}^g$			-35.7	45.7		
$\text{F}_2\text{M}=\text{O} \rightarrow \text{FMOF}^h$			61.4	109.8		
$\text{H}(\text{M}=\text{O})\text{OH} \rightarrow \text{M}(\text{OH})_2^i$	-7.9		-30.0		-50.4	-73.6
$\text{H}(\text{M}=\text{O})\text{OH} \rightarrow \text{HMOOH}^i$	104.7		75.8		56.3	26.9
$\text{H}_2\text{M}=\text{NH} \rightarrow \text{HMNH}_2^j$	-14.2	54.6	-32.6	45.2		
$\text{H}_2\text{N}(\text{H})\text{M}=\text{NH} \rightarrow \text{M}(\text{NH}_2)_2^j$	-19.2	50.8	-40.7	40.6		
$\text{H}_2\text{P}(\text{H})\text{M}=\text{PH} \rightarrow \text{M}(\text{PH}_2)_2^k$	18.2	47.4	2.1	42.5	-14.8 ^l	-32.4 ^m

^aIn kcal mol⁻¹. A negative sign indicates that the isomerization is exothermic. Only recent high level calculations are included.

^bAt B3LYP/ECP; from Reference 316, see also Reference 296. For $\text{H}_2\text{C}=\text{O}$ the isomerization is endothermic by 52.2 kcal mol⁻¹³¹⁶.

^cAt G2//MP2/6-31G(d); from Reference 318.

^dAt B3LYP/6-311G(d); from Reference 319a.

^eIncluding the contribution of relativistic effects.

^fAt B3LYP/6-311G(d); from Reference 320.

^gAt CCSD(T)/6-311G(d)//B3LYP/6-311G(d); ΔE for R = Cl and Br is -33.0 and -32.1 kcal mol⁻¹, respectively; E_a for R = Cl and Br is 42.3 and 42.9 kcal mol⁻¹, respectively; ΔE and E_a for the reaction $\text{HFGe}=\text{O} \rightarrow \text{HGeOF}$ are 81.2 and 114.7 kcal mol⁻¹, respectively; from Reference 319b.

^hAt CCSD(T)/6-311++G(d,p)//B3LYP/6-311G(d); ΔE for R = Cl and Br is 35.4 and 28.1 kcal mol⁻¹, respectively; E_a is 62.8 and 54.0 kcal mol⁻¹, respectively; from Reference 319a.

ⁱAt CCSD(T)/ECP(TZ2P)//BLYP/ECP(TZ2P); from Reference 321a. For M = C the isomerization is endothermic by 41.8 kcal mol⁻¹^{321a}.

^jAt CCSD(T)/ECP; from Reference 322, see also Reference 323.

^kAt MP2/LANL1DZ+P; from Reference 324.

^lThe activation barrier is 39.8 kcal mol⁻¹³²⁴.

^mThe activation barrier is 38.2 kcal mol⁻¹³²⁴.

recently by the observation of the IR spectrum of a mixture of MeSiOMe and Me₂Si=O produced in a matrix at low temperature in the photo-irradiation of a co-condensate of Si and MeOMe.³²⁰

For HR'M=O, two isomerization reactions are possible: (a) HR'M=O → R'MOH and (b) HR'M=O → HMOR'. In general, for R' = F, Cl, Br reaction (a) is expected to be preferred over reaction (b) due to the stronger OH bond relative to OR' and also to be more exothermic than for H₂M=O due to the increased stability of R'MOH, as a result of electron donation from the halogen lone-pair to the empty p orbital on M in R'MOH. Indeed for M = Ge the rearrangement energy of FHM=O to FMOH is more exothermic and the rearrangement barrier is lower relative to that of the parent system (Table 30). On the other hand, reaction (b) is highly endothermic for M = Ge, R' = F, Cl, Br and the barrier for rearrangement increases dramatically; e.g. for R' = F, ΔE = 81.2 kcal mol⁻¹ and E_a = 114.7 kcal mol⁻¹ [at CCSD(T)/6-311G(d)//B3LYP/6-311G(d)]^{319b}. This large substituent effect was attributed to the much stronger Ge–F bond relative to the O–F bond [e.g. the corresponding bond dissociation energies are (kcal mol⁻¹): Ge–F = 116, O–F = 53]^{319b}. Similarly, high energies and reaction barriers were calculated for R₂Ge=O (R = F, Cl, Br, Table 30)^{319a}. A similar trend, with even stronger halogen substitution effects, was calculated for silanones, i.e. ΔE (HFSi=O → HSiOF) = 126.5 kcal mol⁻¹ vs. -5.4 kcal mol⁻¹ for H₂Si=O [MP3/6-31G(d,p)//3-21G]³²⁵.

Formic acid is the most stable H₂CO₂ isomer. In contrast, for all heavier group 14 elements the divalent dihydroxycarbene analogs, M(OH)₂, are more stable than the corresponding H(M=O)OH acids (Table 30), and the former becomes relatively more stable as M becomes heavier; i.e. ΔE (H(M=O)OH → M(OH)₂) (in kcal mol⁻¹) is: Si(-7.9) < Ge(-30.0) < Sn(-50.4) < Pb(-73.6). These results show again that divalency is increasingly preferred over tetravalency on moving down group 14 (see also Sections V.A.3 and V.C.3). However, for all M, the tetravalent formic acid congeners are more stable than the corresponding hydroperoxy divalent congeners, HMOOH, though the stability of the latter relative to the acid increases on going from M = Si to M = Pb (Table 30)³²¹.

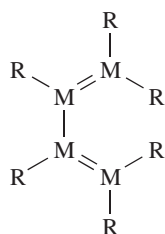
The isomerization reactions of H₂M=NH to HMNH₂ and of H₂N(H)M=NH to M(NH₂)₂ are exothermic but the barriers for these reactions are high (Table 30). The exothermicity of these rearrangements increases from -14.2 kcal mol⁻¹ for the isomerization of H₂Si=NH to -32.6 kcal mol⁻¹ for H₂Ge=NH and from -19.2 kcal mol⁻¹ to -40.7 kcal mol⁻¹ for the isomerization of H₂N(H)M=NH, M = Si and Ge, respectively. In contrast to H₂Si=NH, the isomerization of H₂Si=PH to HSiPH₂ is endothermic by 14.3 kcal mol⁻¹ [at G2//MP2/6-31G(d)]^{326a}, 15.0 kcal mol⁻¹ at MP3/6-31G(d)//HF/3-21G(d)]^{326b} and the barrier to this 1,2-H shift is 40 kcal mol⁻¹^{326b}. Calculations for this isomerization for the heavier M congeners are not available. The isomerization of H₂P(H)Si=PH to Si(PH₂)₂ is endothermic by 18.2 kcal mol⁻¹ and it becomes less endothermic down group 14, becoming exothermic by -32.4 kcal mol⁻¹ for M = Pb (Table 30)³²⁴. These trends reflect the higher stability of the heavier group 14 metallylenes.

D. Increasing the Number of Double Bonds

1. Heavier analogs of 1,3-butadiene

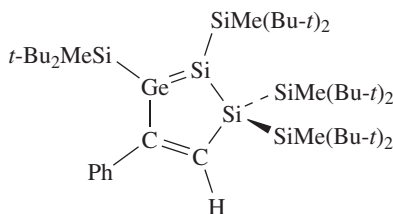
Two recent remarkable experimental achievements in this field are the syntheses by Weidenbruch and coworkers of the first stable tetrasil- and tetragermabutadienes, **52a**^{327a} and **52b**^{327b}, respectively. In the crystal, the 1,2-Si=Si and 1,2-Ge=Ge bond lengths are 217.5 pm and 235.7 pm, respectively, being longer than the Si=Si and the Ge=Ge

double bonds in aryl-substituted disilenes and digermenes of, e.g., 214 pm and 221 pm, respectively. The 2,3-Si-Si and 2,3-Ge-Ge bond lengths are 232.1 pm and 245.8 pm, respectively. Both compounds adopt a twisted *s-cis* conformation of C_2 symmetry, with Si_4 and Ge_4 dihedral angles of 51° and 22° , respectively. The tetrasilabutadiene has planar Si centers, while the $Ge=Ge$ double bonds in **52b** display a considerable *trans*-bending of the substituents of *ca* $31-35^\circ$. The observed red shifts in the UV spectra of both compounds relative to the characteristic $\pi-\pi^*$ transitions in disilenes and digermenes and the structural features indicate the existence of π -conjugation in both metallabutadienes^{327,328}. Sekiguchi and coworkers reported more recently the synthesis and X-ray characterization of a silole-type metalladiene (**53**); however, the structural parameters and the UV/vis spectrum show no indication for a significant π -conjugation in the silole ring³²⁹. Noncyclic stable heterodienes with one or two group 14 metals have not yet been isolated, although several such silicon and germanium compounds were suggested as intermediates^{20,330,331}



(52a) M = Si, R = Tip

(52b) M = Ge, R = Tip

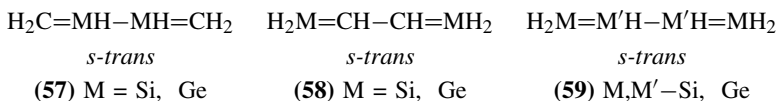


(53)

Theoretical studies of butadiene analogs which contain one or more group 14 heavy atoms are limited to silabutadienes^{328,332-334} and germabutadienes³³⁵⁻³³⁷. A systematic theoretical study of the heavier analogs of butadiene is not yet available.

2-Silabutadiene, $H_2C=SiH-CH=CH_2$ (**54**), is the most stable SiC_3H_6 isomer, but 1-silabutadiene, $H_2Si=CH-CH=CH_2$ (**55**), and methylvinylsilylidene, $H_3CSiCH=CH_2$ (**56**), are by only *ca* 5 kcal mol^{-1} less stable³³².

Two possible isomers were studied for dimetallabutadienes: 2,3-dimetallabutadiene, **57**, $M = Si$ ^{328b} and $M = Ge$ ³³⁷ and 1,4-dimetallabutadiene, **58**, $M = Si$ ^{328b,333,334} and $M = Ge$ ³³⁵.



57, $M = Ge$ is predicted to be more stable than **58**, $M = Ge$ by *ca* 4 kcal mol^{-1} ³³⁷ (the energy difference between **57** and **58** was not reported for $M = Si$). Substitution of carbon by germanium (or silicon) at positions 2 and 3 has two major effects: (1) The π conjugation is significantly reduced and is estimated to be about half of the conjugation energy in 1,3-butadiene (Table 31). (2) The relatively long $M-M$ central bond reduces the steric hindrance that causes the *s-cis* isomer of 1,3-butadiene to distort into a nonplanar *gauche* conformation. Consequently, **57**, $M = Ge$ has two stable planar conformers, *s-trans* and *s-cis*, the latter being less stable by only $0.4 \text{ kcal mol}^{-1}$ and the barrier for rotation from the *s-trans* to the *s-cis* conformation is $1.6 \text{ kcal mol}^{-1}$ [at MP4/ECP(DZ+p)]³³⁷ and

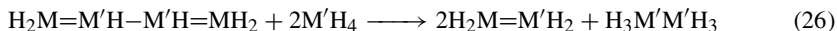
TABLE 31. Bond lengths (pm), rotation barriers around the central M'–M' bond, ΔE_{rot} (kcal mol⁻¹), and bond separation energies ΔE (kcal mol⁻¹), in H₂M=M'H–M'H=MH₂^a

M	M'	d(M'=M) ^b	d(M'–M') ^b	ΔE_{rot}^c	ΔE^d
H ₂ C=M'H–M'H=CH ₂					
C	C	132.8 ^e	145.6 ^f ; 147.0 ^e	6.7 ^f ; 5.8 ^g , 7.6 ^h	13.2 ^f ; 12.5 ^g
C	Si	<i>i</i>	<i>i</i>	2.6 ^f	6.0 ^f
C	Ge	179.1 ^e	245.1 ^e	1.6 ^g	5.0 ^g
H ₂ M=CH–CH=MH ₂					
Si	C	174.1 ^j	142.7 ^f	10.1 ^f ; 11.4 ^h	13.2 ^f
Ge	C	181.7 ^k	143.2 ^e	9.5 ^{k,l}	16.0 ^k
H ₂ M=M'H–M'H=MH ₂					
Si	Si	<i>i</i>	227.4 ^f	3.8 ^f	11.0 ^f
Ge	Ge	233.7 ^m	248.4 ^m	2.9 ⁿ	11.7 ⁿ

^aData for the *s-trans* conformer (**59**).^bd(M'=M) in H₂M'=MH₂ are: 132.2^e (M = M' = C); 178.4^e (M' = C, M = Ge); 232.7^l (M = M' = Ge); d(M'–M') in H₃M'–M'H₃ are: 153.1^f; 152.7^e (M' = C); 235.4^f (M' = Si); 250.1^e (M = Ge).^cBarrier for rotation around the central M'–M' bond.^dAccording to equation 26.^eAt HF/DZ+P (ECP for Ge); from Reference 337.^fAt B3LYP/6-311+G(d,p); from Reference 328b.^gAt MP4/DZ+P (ECP for Ge); from Reference 337.^hAt B3LYP/6-31G(d,p); from Reference 333.ⁱNot given.^jFor the *gauche* rotamer, at B3LYP/6-31G(d); from Reference 333.^kAt MP4/DZ+P (ECP for Ge); from Reference 335.^lThe rotation barrier around the C=Ge bond is less than 5 kcal mol⁻¹ 335^mAt HF/DZ+P (ECP for Ge); from Reference 336.ⁿAt MP4/DZ+P (ECP for Ge); from Reference 336.

2.6 kcal mol⁻¹ in **57**, M = Si at B3LYP/6-311G(d,p)^{328b}]. The PES of **57**, M = Ge is significantly different from that of 1,3-butadiene for which the *s-trans* rotamer is more stable than the *gauche* rotamer by 2.8 kcal mol⁻¹ and the rotamers are separated by a rotation barrier of 5.8 kcal mol⁻¹, while the planar *s-cis* rotamer is a transition structure connecting the two equivalent *gauche* enantiomers (Figure 18a).

In contrast to the reduced conjugation in **57**, π conjugation across the central C–C bond in 1,4-disilabutadiene (**58**, M = Si) is similar to that in 1,3-butadiene and in 1,4-digerabutadiene (**58**, M = Ge); it is *ca* 1.3 times larger than that in 1,3-butadiene, i.e. ΔE (equation 26) is 13.2^{328b} and 16³³⁵ kcal mol⁻¹ for **58**, M = Si and Ge, respectively, compared to 12.5³³⁷–13.2^{328b} kcal mol⁻¹ for 1,3-butadiene (Table 31). The significant π conjugation in **58**, M = Ge is also reflected in a shorter C–C bond of 143.2 pm compared to 147.0 pm in 1,3-butadiene³³⁵, the higher rotation energies around the central C–C bond and the lower rotation barriers around the C=Ge bonds (see below).



The PES for rotation around the C–C bond of **58**, M=Si, Ge (Figure 18) shows two minima: the *s-trans* and the *gauche*, while the *s-cis* structure is a saddle point that connects two *gauche* enantiomers. The *gauche* rotamer is by *ca* 4³³³ and 3 kcal mol⁻¹ 335 for **58**, M = Si, Ge, respectively, less stable than the *s-trans* rotamer, an energy difference very similar to that in 1,3-butadiene. However, the rotation barrier about the central C–C bond in **58**, M = Si and Ge, of *ca* 10–11 and 9.5 kcal mol⁻¹, respectively, is

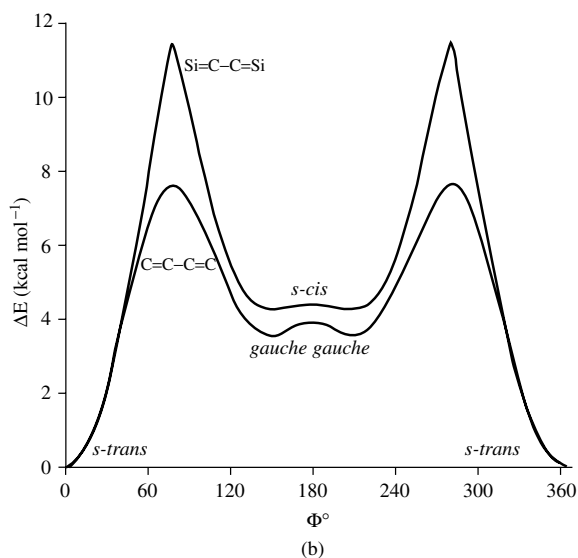
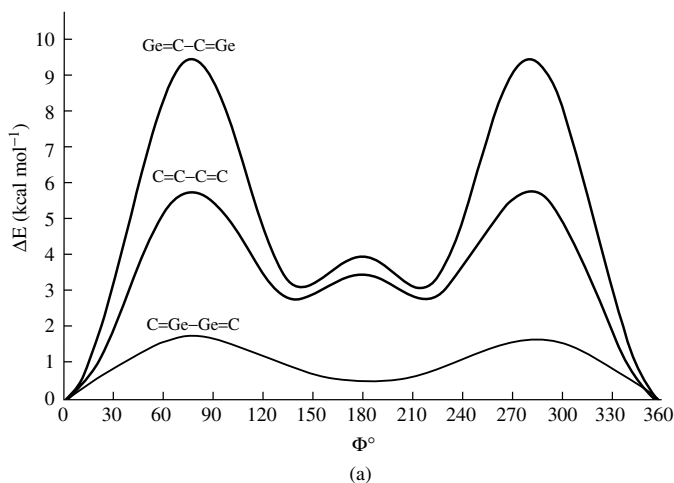


FIGURE 18. Schematic PES for rotation about the central 2–3 bond in (a) 1,3-butadiene³³⁷, 2,3-digermabutadiene [at MP4/ECP(DZ+p)]³³⁷ and 1,4-digermabutadiene [at MP4/ECP(DZ+p)]³³⁵; (b) 1,4-disilabutadiene and 1,3-butadiene [at B3LYP/6-31G(d,p)]³³³ (Φ is the rotation angle, where Φ for *s-trans* is defined as zero and *c-cis* is defined as 180°). (a) is adapted from References 335 and 337, (b) is adapted from Reference 333

higher than the 5.8 kcal mol⁻¹ barrier in 1,3-butadiene (Figure 18 and Table 31). On the other hand, the rotation barrier around the terminal C=Ge double bonds is very small, only *ca* 5 kcal mol⁻¹ vs. 60 kcal mol⁻¹ in 1,3-butadiene. This peculiar property of 1,4-digermabutadiene, which undergoes an easier rotation about its formal Ge=C double bond than about its formal C–C single bond is a consequence of the efficient conjugation across

In the parent tetrasil- and tetragermabutadiene (**59**, $M = M' = \text{Si, Ge}$) the calculated 1,2- $M=M$ and 2,3- $M-M$ ($M = \text{Si, Ge}$) bond lengths are 218.7 pm and 230.2 pm, respectively, for $M = \text{Si}$ ^{328b} and 233.9 pm and 248.8 pm, respectively, for $M = \text{Ge}$ ³³⁶, in good agreement with the experimental values (see above)³²⁷. The Si and Ge centers in **59**, $M = M' = \text{Si, Ge}$ are calculated to be pyramidal^{328b,336}, similarly to the M centers in $\text{H}_2\text{M}=\text{MH}_2$. The X-ray structure of tetragermabutadiene^{327b} reveals significant *trans*-bending in agreement with the calculations, but the experimental structure of tetrasilabutadiene reveals a planar arrangement around the silicons^{327a}. The degree of conjugation in both molecules, based on equation 26, is high, *ca* 90% of the conjugation energy in 1,3-butadiene³³⁶ (Table 31). However, unlike in 1,3-butadiene, the *s*-orbital in **59** plays a significant role in the conjugation which occurs via a b_u-a_g orbital mixing in the *trans*-bent $M=M$ doubly-bonded units³³⁶.

Tetrametallabutadienes (**59**) are kinetically very unstable. Rotation around the $M'-M'$ bond in the *s-trans* conformer to the *gauche* is very facile and the latter cyclizes in a highly exothermic reaction to metallacyclobutene (**60b**) with a reaction barrier of only 2.5^{328b} and 2.0 kcal mol⁻¹³³⁶ for $M = \text{Si}$ and Ge , respectively (Table 32). The high reactivity of **58** and of **59**, $M = \text{Si, Ge}$ towards cyclization is one of the major obstacles in the synthesis of stable metallabutadienes. Bulky substituents, which increase substantially the barrier for cyclization, are required for the synthesis of stable heavy group 14 analogs of 1,3-butadiene, as was demonstrated recently by the successful isolation of **52a** and **52b**³²⁷.

The Si_4H_6 and Ge_4H_6 PESs (Figures 19a and b, respectively) include a large number of isomers, most of them being more stable than the tetrametallabutadienes. The two most stable $M_4\text{H}_6$ ($M = \text{Si}$ or Ge) isomers are the metallabicyclobutanes (**25**) and the metallacyclobutene (**60b**), which are by *ca* 30–40 kcal mol⁻¹ more stable than the *s-trans*, **59** ($M = M' = \text{Si}$ or Ge)^{328b,336}. For Ge_4H_6 , the hydrogen-dibridged structures are the least stable on the Ge_4H_6 PES³³⁶ (Figure 19b). The relative energies of the analogous hydrogen-bridged isomers on the Si_4H_6 PES are not available. The PES of C_4H_6 is, as expected, dramatically different: the *s-trans* 1,3-butadiene is the global minimum, and cyclobutene and bicyclobutane are less stable by 14.8 and 31.1 kcal mol⁻¹, respectively^{328b} (Figure 19a). The PESs of Sn_4H_6 and Pb_4H_6 have not yet been studied.

The increasing complexity of the PESs of $M_4\text{H}_6$ as M becomes heavier was summarized beautifully by Trinquier: 'The thirteen isomers studied in this work (for Ge_4H_6) are far from being the only possibilities for such an $M_4\text{H}_6$ system. The two unsaturations in Ge_4H_6 can be accommodated by any combination of the following permitted forms of unsaturation in germanium compounds: triple bond, double bond, three membered ring, germylene divalent form, and double hydrogen bridge... this allows some thirty feasible structures. For heavier systems involving tin or lead atoms, one should add the single hydrogen bridge as a further possible form of unsaturation, expanding the structure diversity to some sixty conceivable minima, whereas carbon, with its propensity to give fewer minima, would largely favor multiple bonded arrangements, such as butadiene and butyne forms'³³⁶. However, as we have noted above for other parent systems, the number of possible isomers will be reduced significantly when the hydrogen atoms are replaced by alkyl (or aryl) groups.

2. Heavier analogs of allene

The first stable 1-silaallenes ($\text{R}_2\text{Si}=\text{C}=\text{CR}'_2$) and 1-germaallenes ($\text{R}_2\text{Ge}=\text{C}=\text{CR}'_2$) were synthesized recently by West and coworkers^{338a-d}. Stable 2-metallaallenes, $\text{R}_2\text{C}=\text{M}=\text{CR}_2$, are not yet known. In contrast to allene (**61**), which has a

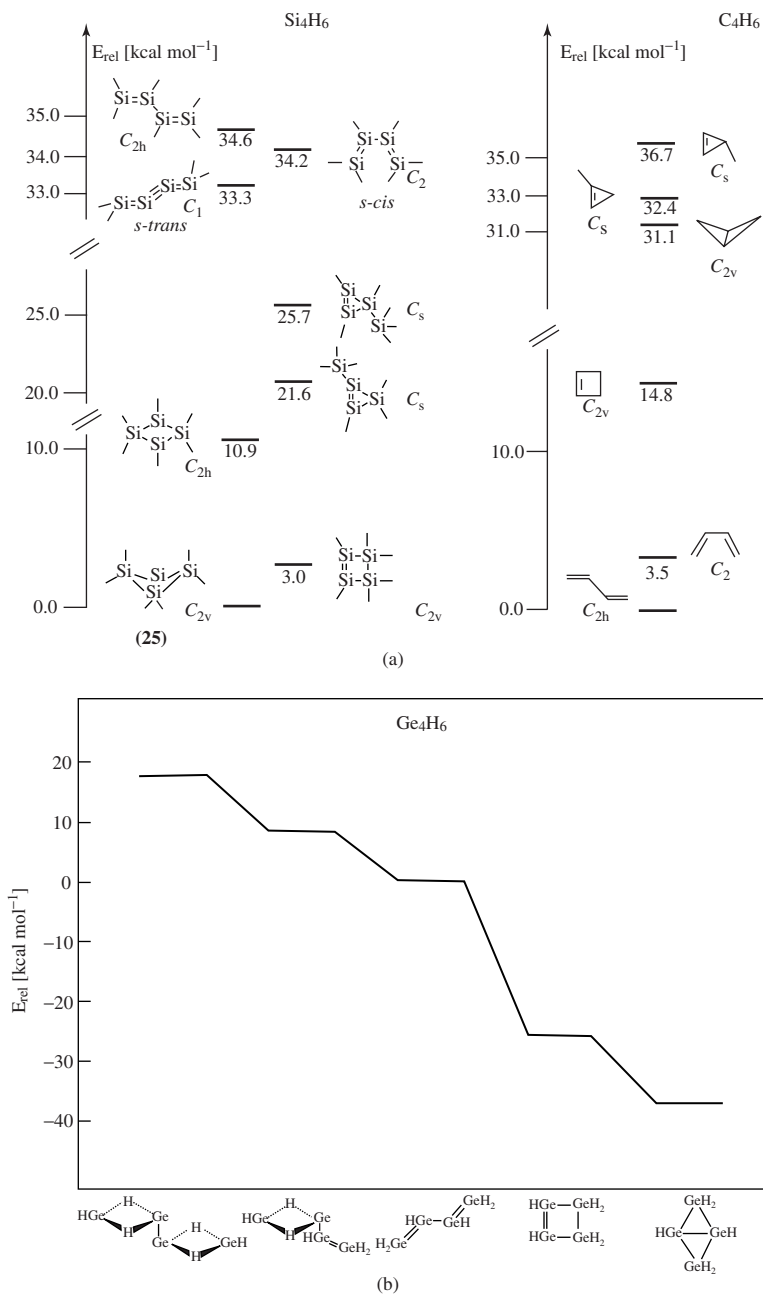


FIGURE 19. (a) Relative energies of Si₄H₆ and C₄H₆ isomers [at B3LYP/6-311+G(d,p)//B3LYP/6-311+G(d,p) + ZPE]; hydrogens are not shown; adapted from Reference 328b. (b) Relative energies of Ge₄H₆ isomers [at MP4/ECP(DZ+p)]; adapted from Reference 336

TABLE 33. Selected properties of $R_2M=C=CH_2$ and $H_2C=M=CH_2^a$

Metallaallene	Bending angle, α	Pyramidity $\Sigma\theta$	ΔE_{lin}^b	ΔE^c
$R_2M=C=CH_2$				
M = Si, R = H	180.0	360.0	—	-1.1
R = Me	180.0	360.0	—	—
R = H ₃ Si	180.0	360.0	—	—
R = F	147.1	332.5	5.9	—
M = Ge, R = H	162.3	342.7	0.9	-1.4
R = Me	159.6	346.7	1.1	—
R = H ₃ Si	165.9	346.1	0.55	—
R = F	140.0	317.0	20.6	—
M = Sn, R = H	157.2	327.2	4.2	3.0
R = Me	154.5	330.0	4.4	—
R = H ₃ Si	161.0	327.4	3.2	—
R = F	141.1	308.5	29.4	—
M = Pb, R = H	153.4	316.1	11.1	8.7
R = Me	150.3	321.9	12.1	—
R = H ₃ Si	159.4	311.3	9.1	—
R = F	<i>d</i>	<i>d</i>	<i>d</i>	<i>d</i>
$H_2C=M=CH_2$				
M = Si	180.0	360.0	—	-9.2
M = Ge	179.9	360.0	0.01	-7.7
M = Sn	135.3	352.0	2.44	-7.6
M = Pb	122.0	349.4	4.73	-1.6

^aAngles in deg, energies in kcal mol⁻¹. The definitions of α and $\Sigma\theta$ are given in Figure 20. Calculated at B3LYP/SDD//B3LYP/SDD (SDD denotes the Stuttgart/Dresden double zeta ECP); at this level results are available for all species^{339a}. For some of these systems, calculations at higher levels are also reported in Reference 339a.

^b $\Delta E_{lin} = E(\text{linear}, D_{2h}) - E(\text{bent})$.

^cStabilization energies calculated by the bond separation in equations 27a and 27b.

^dNot a minimum on the PES.

linear C=C=C skeleton, the X-ray structures of $\text{Tip}_2\text{Si}=\text{C}=\text{C}(\text{Bu}-t)_2$ ^{338a,b} and $\text{Tip}_2\text{Ge}=\text{C}=\text{C}(\text{Bu}-t)_2$ ^{338c-e}, exhibit a nonlinear M=C=C skeleton, bent at the central C atom with the MCC bond angle, α , being significantly smaller for M = Ge (159.2°) than for M = Si (172.0°). The Ge and Si atoms are not planar, and the Ge atom is more strongly pyramidalized than the Si atom (the sum of the bond angles, $\Sigma\theta$, around M is 348.4° for Ge and 357.2° for Si). Is the M=C=C (M = Si, Ge) skeleton inherently nonlinear as found experimentally, or do the observed bent structures reflect substituent effects, crystal packing forces etc.? A computational study by Sigal and Apeloig of $R_2M=C=CH_2$ (**62**) and of $H_2C=M=CH_2$ (**63**) (M = Si, Ge, Sn and Pb; R = H, Me, H₃Si and F) addressed these and other questions related to these interesting metallaallenes^{339a}. The main results of the calculations, mostly at the B3LYP/SDD//B3LYP/SDD level (which could be applied to all systems), are presented in Table 33. A schematic drawing of the general structures of 1- and 2- metallaallenes as well as the definitions of the main geometrical parameters are given in Figure 20.

The calculations show that 1- and 2-silaallenes have a linear SiCC skeleton (and are planar at Si in **62**, M = Si) and the nonlinearity found in the X-ray structure of $\text{Tip}_2\text{Si}=\text{C}=\text{C}(\text{Bu}-t)_2$ is therefore probably *not* an inherent property of the silaallene skeleton, but is caused by the steric effects of the bulky substituents or by crystal packing forces. This is reasonable in view of the very flat calculated PES where only 1 kcal mol⁻¹ is

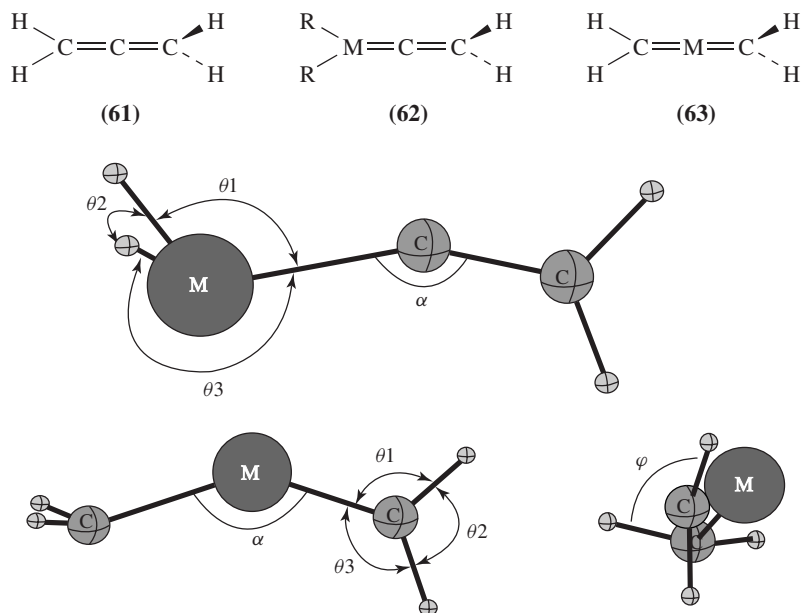


FIGURE 20. Definitions of geometric parameters of 1-metallallenes and 2-metallallenes. $\Sigma\theta = \theta_1 + \theta_2 + \theta_3$. Adapted from Reference 339a

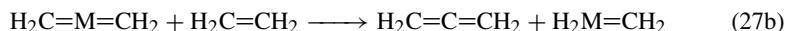
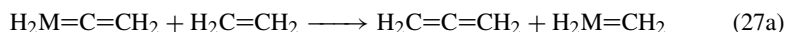
required to bend **62**, $\text{M} = \text{Si}$, $\text{R} = \text{H}$, by 20° at the central carbon. In contrast to the linear $\text{H}_2\text{Si}=\text{C}=\text{CH}_2$, $\text{H}_2\text{Ge}=\text{C}=\text{CH}_2$ is calculated to be bent and pyramidal at Ge, in agreement with the X-ray structure of $\text{Tip}_2\text{Ge}=\text{C}=\text{C}(\text{Bu}-t)_2$. The degree of bending at the central atom in **62** and **63** and the degree of pyramidalization at M in **62** and at the C atoms in **63** increase as M becomes heavier. This is accompanied by an increase in the energy required for linearization (ΔE_{lin}) of the MCC (or CMC) skeleton, i.e. ΔE_{lin} increases from $0.9 \text{ kcal mol}^{-1}$ for **62**, $\text{M} = \text{Ge}$, $\text{R} = \text{H}$ to $11.1 \text{ kcal mol}^{-1}$ for **62**, $\text{M} = \text{Pb}$, $\text{R} = \text{H}$. The 2-metallaallenes **63** exhibit a similar trend (Table 33).

NBO analysis shows that in both **62**, $\text{R} = \text{H}$ and **63** the relative contribution of the s orbital to the metal-carbon bonds decreases and the contribution of the p orbital increases in the order: $\text{M} = \text{Si}$ [sp^2 (**62**); sp (**63**)] $>$ $\text{M} = \text{Ge}$ [$\text{sp}^{2.29}$ (**62**); sp (**63**)] $>$ $\text{M} = \text{Sn}$ [$\text{sp}^{2.57}$ (**62**); $\text{sp}^{1.2}$ (**63**)] $>$ $\text{M} = \text{Pb}$ [$\text{sp}^{2.79}$ (**62**); $\text{sp}^{1.44}$ (**63**)]. This trend is a result of the increasing reluctance of heavier group 14 elements to hybridize (see Section III.C) and it explains the increasing pyramidalization and nonlinearity of **62** and **63** as M becomes heavier.

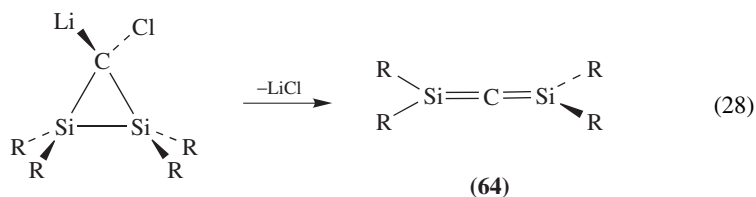
Substituents have a major effect on the geometry of metallallenes (Table 33). H_3Si (an electropositive substituent) decreases the degree of bending of the MCC skeleton, while F (an electronegative π -donor substituent) induces much smaller MCC angles and a stronger pyramidalization at M than hydrogen. This behavior is reminiscent of the *trans*-bending behavior of substituted $\text{R}_2\text{M}=\text{MR}_2$ (Section VI.B.1). The combination of heavy M atoms and fluorine substituents can lead to highly distorted structures: e.g. in $\text{F}_2\text{Sn}=\text{C}=\text{CH}_2$ the bending angle α is 141° and M is strongly pyramidalized ($\Sigma\theta = 308.5^\circ$) and $\text{F}_2\text{Pb}=\text{C}=\text{CH}_2$ is not a minimum on the PES^{339a}.

The parent 1-metallaallenes **62**, $\text{R} = \text{H}$ are more stable than the parent 2-metallaallenes **63** for all M, but the energy difference between them remains almost constant at

8.1–10.6 kcal mol⁻¹ (at B3LYP/SDD) for all M^{339a}. The stability of the parent **62** and **63** relative to the corresponding H₂M=CH₂ as calculated by equations 27a and 27b, respectively (ΔE values in Table 33), increases from M = Si to M = Pb (Table 33). For **62**, R = H equation 27a is slightly exothermic for M = Si and Ge but it is endothermic for M = Sn and Pb. **63**, M = Si, Ge, Sn and Pb are less stable than the corresponding H₂M=CH₂ (negative ΔE values for equation 27b), but their relative stability increases as M becomes heavier (Table 33).



1,3-Disilaallenes (**64**) (and its higher congeners) are as yet unknown experimentally. A recent theoretical study^{339b} suggests that ring opening of α -halolithiodisilirane can provide a possible route for the synthesis of 1,3-disilaallenes (equation 28). The calculations predict that the activation energy for reaction 28 (for R = H) is only 6.5 kcal mol⁻¹, suggesting that this reaction is a feasible method for the synthesis of 1,3-disilaallenes. The analogous reaction for lithiochlorocyclopropane to give allene has a much higher barrier of 45.3 kcal mol⁻¹, yet this reaction is commonly used for the synthesis of allenes.



E. Triply-bonded Metallynes, $\text{RM}\equiv\text{M}'\text{R}'$

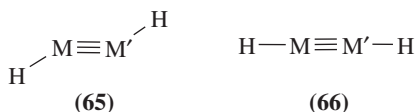
The elusiveness of stable compounds with a triple bond between two group 14 elements (see Section VI.A) makes their synthesis, isolation and characterization one of the 'holy grails' of main-group chemistry. In view of the many experimental failures to produce such compounds, even as short-lived intermediates (except for a few successes, see Section VI.A), theory remains the only reliable source of information. Furthermore, the calculations can be used to develop and test ideas of how to stabilize this group of compounds, hopefully directing experimentalists to their synthesis and isolation.

According to theoretical studies, the major obstacles preventing the synthesis and observation of triply-bonded compounds of heavier group 14 elements are: (1) the existence of more stable isomers; (2) small energy barriers for isomerization; and (3) high reactivity. Some ideas of how to overcome these problems were suggested by theoretical studies^{340–343}. The theoretical predictions³⁴⁰ have already lead to experiments which provided the first unequivocal proof for the existence of transient silynes ($\text{HC}\equiv\text{SiF}$ and $\text{HC}\equiv\text{SiCl}$) in the gas phase²⁵⁸. Other theoretical predictions which suggest the use of bulky substituents to stabilize kinetically, e.g. toward dimerization, silynes and disilynes^{341–343} (see below) are awaiting experimental testing.

1. Structure and bond nature

A common feature of all group 14 heavy element triply-bonded compounds is their *trans*-bent structure, **65**^{7,26,258,262,340–356}, in contrast to the linear $D_{\infty h}$ structure (**66**)

of acetylene ($M = M' = H$). The linear structures, **66**, are not minima on the PES for all combinations of heavy group 14 atoms. The instability of the linear dimetallynes was explained by the reluctance of the heavier group 14 elements to form *sp* hybrids due to the different spatial distribution of their *ns* and *np* orbitals (Figure 1)^{5,6}. As a result, the MH fragments prefer the doublet ground state, with 2 electrons paired in the *ns* orbital of M, over the quartet state which is required for forming the linear structure (as shown in Figure 21a). When the MH fragment is in the doublet state, the linear structure of $HM \equiv M'H$ suffers from exchange repulsion between the lone pairs on M as shown in Figure 21b. This repulsion is relieved by increasing the M–M distance and by forming *trans*-bent structures where the $M \cdots M$ bonding consists of two donor–acceptor dative bonds (Figure 21b). Another possibility which relieves the exchange repulsion is to form monobridged and dibridged structures (as shown in Figures 21c and 21d, respectively), which are the lowest energy isomers on all M_2H_2 PESs^{262,343,357}. The $M \equiv M'$ bond lengths in the (hypothetical) linear **66** are shorter than the corresponding $M=M'$ double bonds for all M and M' combinations. Upon bending, the $M \equiv M'$ bonds become longer, but also in **65** they remain shorter than the double bonds in the corresponding $H_2M=M'H_2$ [both in the *trans*-bent and in the planar (non minimum) geometries (see Tables 34 and 26)].



Trinquier and Malrieu²⁸⁰ suggested that the occurrence and extent of such distortions is related to the energy difference $\Delta E(^4\Sigma^- - ^2\Pi)$ between the doublet $^2\Pi$ ground state and the quartet $^4\Sigma^-$ first excited state of the MH fragments that form the triple bond. This suggestion, however, was based on $\Delta E(^4\Sigma^- - ^2\Pi)$ values for HC and HSi. Thus, the stability of the bent structure (**65**) relative to the linear structure **66** [$\Delta E(\mathbf{66}-\mathbf{65})$ in Table 34] follows the order: $\text{HSi} \equiv \text{CH}$ ($9.1 \text{ kcal mol}^{-1}$ ³⁵⁰) < $\text{HGe} \equiv \text{CH}$ < $\text{HSi} \equiv \text{SiH} \approx \text{HGe} \equiv \text{GeH}$ < $\text{HSn} \equiv \text{SnH} \ll \text{HPb} \equiv \text{PbH}$ ($55.3 \text{ kcal mol}^{-1}$ ^{343a}). This order does not follow the trend in $\Delta E(^4\Sigma^- - ^2\Pi)$ for GeH to PbH, for which $\Delta E(^4\Sigma^- - ^2\Pi)$ is nearly constant. The experimental values of $\Delta E(^4\Sigma^- - ^2\Pi)$ (in kcal mol^{-1}) are 17^{280} , 37^{280} , 45^{361a} , $40-43^{124a,361b}$ and 45^{361c} for CH, SiH, GeH, SnH and PbH, respectively. The bending angles in $\text{HSi} \equiv \text{SiH}$, $\text{HGe} \equiv \text{GeH}$, $\text{HSi} \equiv \text{GeH}$ and $\text{MeSn} \equiv \text{SnMe}$ are almost the same, *ca* 125° (the structure of **65**, $M = \text{Pb}$ has not yet been reported), which is also not consistent with the suggestion of Trinquier and Malrieu²⁸⁰. The X-ray structure of $\text{RPb}-\text{PbR}$ ($R = 2,6\text{-Tip}_2\text{C}_6\text{H}_3$) has been determined recently²⁶⁰ and it has a CPbPb angle of 94.5° and a CPbPbC dihedral angle of 180° , but the long Pb–Pb distance in this compound implies that the Pb–Pb bond is a single bond rather than a triple bond (Section VI.A)²⁶⁰.

The Trinquier–Malrieu model²⁸⁰ works well, however, for a particular M. Thus, for SiR, $R = \text{SiH}_3$, $\Delta E(^4\Sigma^- - ^2\Pi)$ is smaller by $16.6 \text{ kcal mol}^{-1}$ than for SiH, and consequently the linearization energy of $\text{H}_3\text{SiSi} \equiv \text{SiSiH}_3$ of $10.1 \text{ kcal mol}^{-1}$ is smaller by 10 kcal mol^{-1} than that of $\text{HSi} \equiv \text{SiH}$, and the bending angle increases (i.e. approaches linearity) by 5° ^{342,343a}. On the other hand, electronegative π -donor substituents increase $\Delta E(^4\Sigma^- - ^2\Pi)$, and consequently the linearization energy, to 63 kcal mol^{-1} for $\text{FSi} \equiv \text{SiF}$. However, the FSiSi bending angle decreases by only 4° relative to $\text{HSi} \equiv \text{SiH}$ [MP4/6-31G(d,p)/MP2/6-31G(d,p)]³⁶².

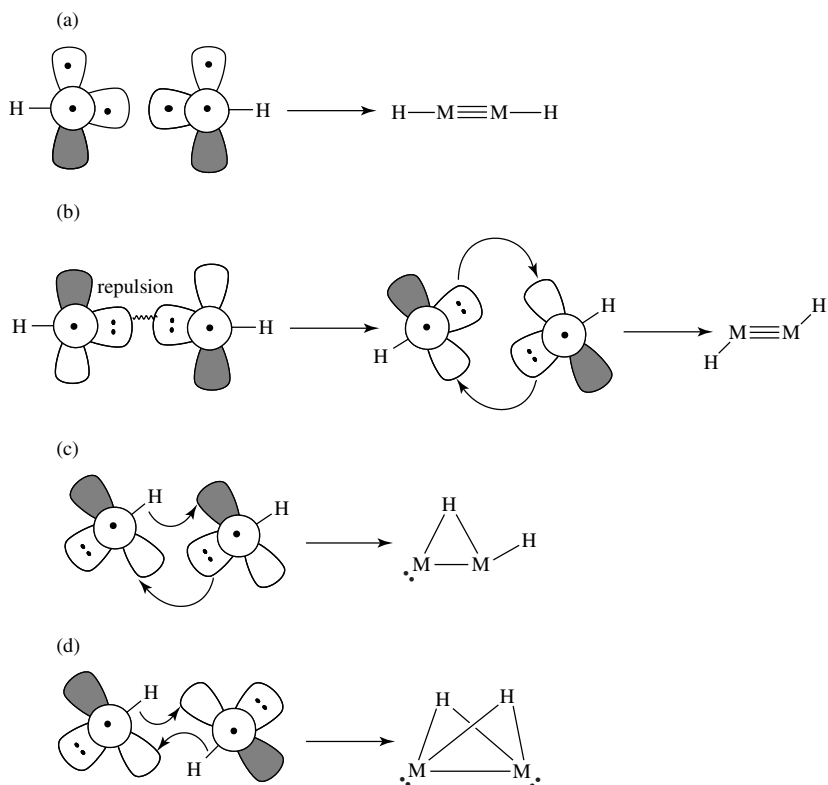


FIGURE 21. Schematic drawing of orbital interactions which lead to (a) linear M_2H_2 , (b) *trans*-bent M_2H_2 , (c) monobridged M_2H_2 and (d) dibridged M_2H_2 . Based on References 262 and 343a

The fact that all heavy element $HM\equiv M'H$ are *trans*-bent raises the question as to whether these compounds are truly triply bonded and what is the energetic benefit of nonlinearity? Similar questions, regarding the nature of the $M-M$ bonds in *trans*-bent formally triply-bonded compounds of group 13 (e.g. $M = Ga^{24a,c,292,363}$), have initiated a vigorous debate which is not yet resolved. Shaik, Apeloig and coworkers³⁶⁴ have recently investigated these issues in detail for $HC\equiv SiH$ and $HSi\equiv SiH$, using a new VB technique which allows the total energy to be dissected into the contributions of the σ and π bonds, with simultaneous computation of the energies of the two π bonds. This analysis, which was also supported by spin-coupled valence bond calculations as well as by NBO analysis, shows that *ca* 2.5 bonds connect the Si and C atoms in silyne and the two Si atoms in disilyne. The VB analysis shows that the σ bonds of $HSi\equiv CH$, $HSi\equiv SiH$ (and of $HC\equiv CH$) are stabilized by *trans*-bending, while the in-plane π bond is weakened. In acetylene, π bonding overrides the σ bonding and establishes a linear molecule. In contrast, in silyne and disilyne the stabilization of the σ bonds dominates due to bending and lead to *trans*-bent structures. Thus $HSi\equiv CH$ and $HSi\equiv SiH$ have 2.5 bonds, but these bonds are stronger than the three bonds present in the corresponding linear structures.

Calculations for $MeMMMMe$, $M = Ge, Sn$ led to the conclusion that the $M-M$ bond in these molecules is a double bond rather than a triple bond. Thus, the Pauling bond

TABLE 34. Geometrical parameters and linearization energies $\Delta E(\mathbf{65}-\mathbf{66})$ of *trans*-bent $\text{HM}\equiv\text{M}'\text{H}$ ($\mathbf{65}$)^a

M, M'	d(M≡M') (65)	d(M≡M') (66)	∠HMM'	∠HM'M	ΔE(65 - 66)	Method	Reference
M = Si; M' = C	166.5	160.4	123.9	149.5	9.1	CCSD(T)/TZ2P	350 ^b
M = Ge, M' = C	172.7	165.8	127.9	145.2	9.6	CCSD(T)/TZ(2df,2pd)	354 ^c
	169.8	166.8	148.7	139.9	3.8	MP2/TZV(2df,2p)	355
M = M' = Si	210.3	197.0	125.8	125.8	20.5 ^d	QCISD/TZ2P	344 ^e
M = M' = Ge	218.8	206.7	125.5	125.5	24.7 ^f	MP2/TZV(2df,2p)	355 ^g
M = Ge, M' = Si	216.8	203	128.2	120.5	25.1	CCSD(T)/DZP	358 ^h
	214.4	202.8	127.6	123.3	22.5	MP2/TZV(2df,2p)	355
M = M' = Sn ⁱ	267.3	243.2	125.0	125.0	33.7	HF/3-21G	359
M = M' = Pb	<i>j</i>	<i>j</i>	<i>j</i>	<i>j</i>	55.3	MP2/6-311G(2d,2p) ^k	343a

^a Bond lengths in pm, bond angles in deg and energies in kcal mol⁻¹.

^bFor values at other computational levels, see References 7, 340, 349, 350 and references cited therein.

^cSee also Reference 356.

^d19.0 kcal mol⁻¹ at MP2/6-311G(2d,2p)^{343a}.

^eSee also References 7, 342, 346, 351, 353.

^f25.8 kcal mol⁻¹ at MP2/6-311G(2d,2p)^{343a}.

^gSee also Reference 347.

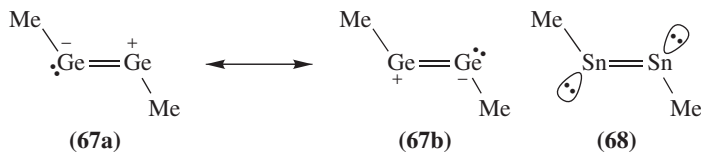
^hSee also Reference 360.

ⁱData for MeSnSnMe.

^jThe geometries were not reported.

^kUsing relativistic ECPs.

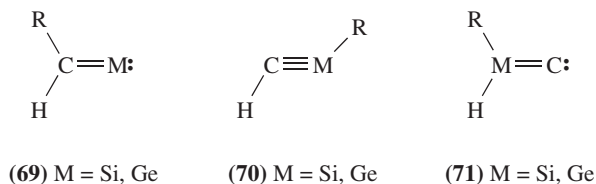
order in *trans*-bent MeGeGeMe is 2.0 and the Ge–Ge bond length of 219.7 pm is similar to that in planar *trans*-HMeGe=GeHMe (221.8 pm). This lead to the conclusion that the Ge–Ge bond in *trans*-bent MeGeGeMe is best described as a resonance hybrid of **67a** and **67b**³⁶⁵. The Sn–Sn bond in *trans*-bent MeSnSnMe has even a smaller Pauling bond order of 1.46 and the authors suggest that MeSnSnMe is best described as having a single bond between the two Sn atoms with a lone pair residing on each of the Sn atoms as shown in **68**³⁵⁹. A similar electronic structure was suggested for the experimentally isolated ArPbPbAr, based on its structure and in particular the long Pb–Pb bond²⁶⁰. A more detailed analysis is, however, required to substantiate these conclusions.



2. Potential energy surfaces

a. HC≡MH, M = Si, Ge. The PESs of only HC≡SiH and HC≡GeH have been studied so far. Three minima, **69**–**71**, connected by two transition states, were located on the PESs of H₂CSi and H₂CGe. The most stable isomer is the metallylidene H₂C=M (**69**, R = H), which is more stable than the *trans*-bent triply-bonded species, **70**, R = H, by 34–37 kcal mol⁻¹ for M = Si^{7,340,349,350} and by 50–58 kcal mol⁻¹ for M = Ge^{354,356}. Significantly higher in energy lies the metallavinylidene carbene **71**, R = H. The energy barriers that connect **70**, R = H with **69**, R = H are relatively small, only 3–7 kcal mol⁻¹

for both $M = \text{Si}^{7,340,349,350}$ and $M = \text{Ge}^{354,356}$. Thus, the calculations imply low kinetic and thermodynamic stability for $\text{HC}\equiv\text{MH}$ in unimolecular reactions, and indeed only $\text{H}_2\text{C}=\text{Si}^{366}$ and $\text{H}_2\text{C}=\text{Ge}^{367}$ have been detected so far in attempts to produce $\text{HC}\equiv\text{MH}$ in the gas phase.



Electronegative substituents ($R = \text{F, Cl}$ and OH) attached to the Si stabilize **70** relative to **69** and increase substantially the barrier for their interconversion, as shown in Figure 22^{258,340}. For example, $\text{HC}\equiv\text{SiF}$ is more stable than $\text{HFC}=\text{Si}$ by $10.4 \text{ kcal mol}^{-1}$ and the energy barrier separating the two isomers is $24.9 \text{ kcal mol}^{-1}$ ^{258,340}. Based on these calculations Karni and coworkers devised a sophisticated neutralization–reionization experiment, which led to the first unequivocal detection of $\text{HC}\equiv\text{SiR}$, $R = \text{F, Cl}$ in the gas phase²⁵⁸. The substituent effects are smaller for $M = \text{Ge}$ than for $M = \text{Si}$. Thus, $\text{HC}\equiv\text{GeF}$ is still by $16.6 \text{ kcal mol}^{-1}$ less stable than $\text{HFC}=\text{Ge}$ and the barrier for its rearrangement is only $10.3 \text{ kcal mol}^{-1}$ ³⁵⁶ (Figure 22). Based on these results it is clear that the generation of $\text{HC}\equiv\text{GeR}$, $R = \text{F, Cl}$ using similar neutralization–reionization²⁵⁸ methods will be more difficult.

Bulky substituents can also stabilize $\text{RC}\equiv\text{SiR}'$ relative to $\text{RR}'\text{C}=\text{Si}$ and simultaneously can also stabilize the triply-bonded species toward dimerization to 1,3-disilacyclobutadiene, a process which is highly exothermic [e.g. by $91.3 \text{ kcal mol}^{-1}$, at QCISD(T)/6-31G(d,p) for **70**, $M = \text{Si}$, $R = \text{H}$]. The effect of several substituents on the $\text{RC}\equiv\text{SiR}'$ vs. $\text{RR}'\text{C}=\text{Si}$ energy difference and on the dimerization energy of $\text{RC}\equiv\text{SiR}'$ to the corresponding 1,3-disilacyclobutadiene was recently studied by Karni and Apeloig

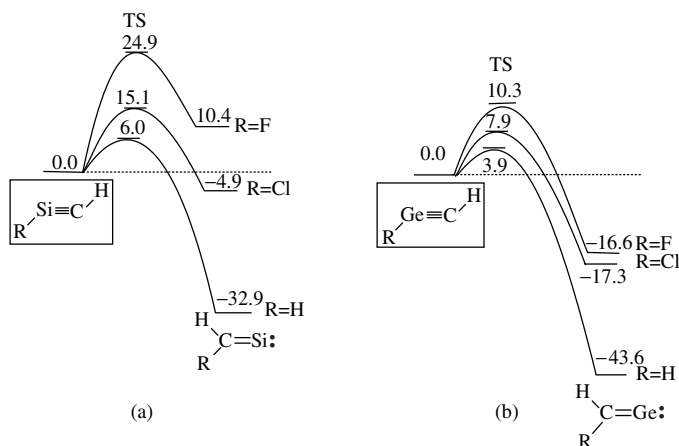


FIGURE 22. Potential energy surfaces for the isomerization of HMCH to $\text{H}_2\text{C}=\text{M}$ (energies in kcal mol^{-1}): (a) $M = \text{Si}$, calculated at QCISD(T)/6-31G(d,p)^{258,340}; (b) $M = \text{Ge}$, calculated at QCISD/6-311G(d)³⁵⁶

using DFT and ONIOM³⁶⁸ methods³⁴¹. They found that *t*-Bu₃SiSi≡CTbt is more stable than (*t*-Bu₃Si)TbtC=Si and that it is stable also toward dimerization, making it an attractive synthetic target³⁴¹.

b. HM≡MH and HM≡M'H. The PESs of M₂H₂ systems (M ≠ C) are more complex than those of CMH₂. Four possible minima, **72–75**, were located on these PESs for M = Si to Pb. In all these cases the linear acetylene analog (**76**) is not a minimum on the PES. This stands in a sharp contrast to the PES of C₂H₂, where in addition to the linear HC≡CH which is the global minimum, only H₂C=C^{369a} is a minimum on the PES. The important geometric parameters of **72–76**, M = Si and Ge (the geometric parameters for M = Sn and Pb were not reported) are shown in Figure 23. Of particular interest are the relatively short M–M bonds in the dibridged (**72**) and especially in the monobridged (**73**) isomers.

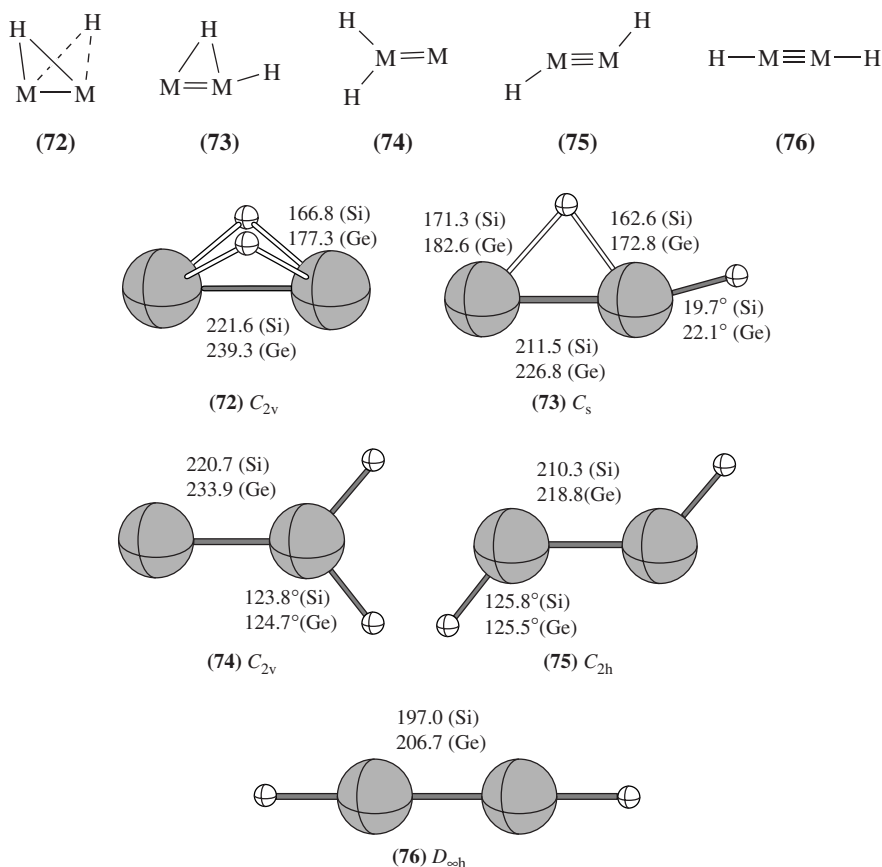


FIGURE 23. Optimized geometries of M₂H₂, M = Si, Ge isomers, **72–76**. Bond lengths in pm, bond angles in deg. For M = Si, at CISD/TZ2P³⁴⁴; for M = Ge: **72–74** at CCSD/DZP³⁶⁰ and **75** and **76** at MP2/TZV(2df,2p)³⁵⁵

The elucidation of the Si_2H_2 potential energy surface is an outstanding example of fruitful interplay between theory and experiment. The most surprising outcome of the theoretical studies was the location of the dibridged isomer, **72**, $M = \text{Si}$ as the global minimum on the Si_2H_2 PES^{357,369}. Inspired by these theoretical predictions, this species was later indeed detected and characterized experimentally both in the gas phase³⁷⁰ and in a matrix³⁷¹. A reinvestigation of the Si_2H_2 PES using very high level coupled-cluster methods revealed the presence of a new low-lying isomer, the monobridged **73**, $M = \text{Si}$ ^{344–346} which lies by $10.2 \text{ kcal mol}^{-1}$ above **72**. This theoretical discovery encouraged new experiments, which indeed lead to the detection of the monobridged isomer³⁷². Additional minima on the Si_2H_2 PES are the familiar silylidene: $\text{H}_2\text{Si}=\text{Si}$ which lies by $12.2 \text{ kcal mol}^{-1}$ above **72** and the *trans*-bent $\text{HSi}\equiv\text{SiH}$ located $17.3 \text{ kcal mol}^{-1}$ above **72** [all the above results are at CCSD(T)/TZ2df]³⁴⁵. More recent studies which used the quadratic complete basis set method^{351a} and various DFT methods predict a similar PES with the stability of $\text{H}_2\text{Si}=\text{Si}$ slightly overestimated at the DFT level^{351b}.

Addition of an electron to Si_2H_2 changes qualitatively the PES. The disilavinylidene anion H_2SiSi^- (**74**⁻, $M = \text{Si}$) is the global minimum and is predicted to lie 24 kcal mol^{-1} below the dibridged anion (**71**⁻, $M = \text{Si}$) and by $12.6 \text{ kcal mol}^{-1}$ below the monobridged anion (**73**⁻, $M = \text{Si}$). A planar *trans*-bent structure (**75**⁻, $M = \text{Si}$) was not located on this PES, but instead a twisted C_2 structure with a HSiSiH dihedral angle of 41.5° was located $11.9 \text{ kcal mol}^{-1}$ above **74**⁻, $M = \text{Si}$. The electron affinity of **74**, $M = \text{Si}$ is computed (at B3LYP/DZP) to be 1.87 eV and that of **72**, $M = \text{Si}$ is 0.45 eV ²⁹⁷.

The PESs of the heavier group 14 M_2H_2 are similar to that of Si_2H_2 , as shown schematically in Figure 24^{343a,347,360}. The PES of Ge_2H_2 closely resembles that of Si_2H_2 . For $M = \text{Sn}$ and Pb the dibridged isomer **72** becomes more stable, both thermodynamically and kinetically (higher barriers) relative to all other isomers^{343a} (Figure 24). The triply-bonded *trans*-bent $\text{HM}\equiv\text{MH}$ (**75**) is the highest energy isomer on the H_2M_2 PES for all M atoms and its energy relative to the dibridged isomer (**72**) increases as M becomes heavier [at MP2/6-311G(2d,p), in kcal mol^{-1}]: 18.7 (Si), 20.2 (Ge), 27.6 (Sn) and 36.1

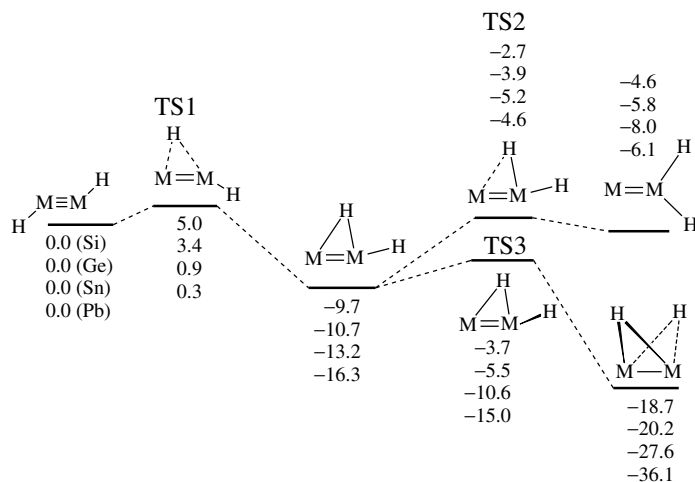
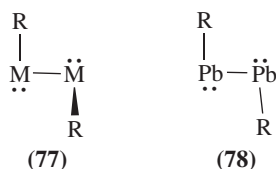


FIGURE 24. Potential energy surfaces of M_2H_2 , $M = \text{Si, Ge, Sn and Pb}$, calculated at MP2/6-311G(2d,p); energies are given in kcal mol^{-1} . Adapted from Reference 343a

(Pb). The barriers that connect *trans*-bent $\text{HM}\equiv\text{MH}$ with the other isomers (i.e. TS1 in Figure 24) decrease down group 14^{343a}, making it kinetically less stable. Thus, according to the calculations the prospects of detecting $\text{HPb}\equiv\text{PbH}$ or $\text{HSn}\equiv\text{SnH}$, for which the barriers for rearrangement are less than 1 kcal mol⁻¹, are not encouraging.

A similar PES with five minima within a narrow energy interval of 15–20 kcal mol⁻¹ was calculated for H_2SiGe ^{355,358}. The relative energy of the isomers are [at CCSD(T)/DZP in kcal mol⁻¹]: dibridged (0.0) < $\text{H}_2\text{Si}=\text{Ge}$ (3.1) < monobridged(1) $\text{Ge}(\text{H})\text{SiH}$ (4.6) < monobridged(2) $\text{Si}(\text{H})\text{GeH}$ (10.0) < *trans*-bent $\text{HSi}\equiv\text{GeH}$ (13.0) < $\text{H}_2\text{Ge}=\text{Si}$ (14.1) < < linear $\text{HSi}\equiv\text{GeH}$ (38.1, not a minimum)³⁵⁸.

Substituents have a significant effect on the M_2R_2 PES. For Si_2R_2 , $\text{R} = \text{CH}_3$ ³⁷³ and SiH_3 ^{342,362} the bridged isomers are no longer minima on the PES, and the remaining isomers are $\text{RSi}\equiv\text{SiR}$, the silylidene ($\text{R}_2\text{Si}=\text{Si}$) and a new nonplanar, ‘twisted’ isomer, **77**, $\text{M} = \text{Si}$. The latter isomer has a RSiSiR dihedral angle of *ca* 90° and a relatively long Si–Si bond of 238 pm (for $\text{R} = \text{Me}$, at HF/DZPP)^{373a} and 227 pm [for $\text{R} = \text{SiH}_3$, at HF/6-31G(d)]³⁶². $\text{R}_2\text{Si}=\text{Si}$ is the only isomer that is more stable (by 7.8 and 5.6 kcal mol⁻¹ for $\text{R} = \text{CH}_3$ and SiH_3 , respectively³⁴²) than the *trans*-bent triply-bonded isomer. $\text{MeSi}\equiv\text{SiMe}$ was suggested as an intermediate in a thermolysis experiment³⁷⁴, but conclusive evidence for its existence was not presented. With bulky R substituents, such as $\text{Si}(\text{Bu-}t)_3$ ³⁴², SiDep_3 ³⁴² ($\text{Dep} = 2,6\text{-Et}_2\text{C}_6\text{H}_3$) and Tbt ^{343a}, the *trans*-bent structures are more stable than $\text{R}_2\text{Si}=\text{Si}$ by 9.7, 12.0 and 23.0 kcal mol⁻¹, respectively [at B3LYP/3-21G(d)]. Such disilynes are, however, calculated to be very reactive, and the dimerization of RSiSiR , $\text{R} = \text{SiDep}_3$ is highly exothermic, by 80 kcal mol⁻¹. However, with the very bulky Tbt group the dimerization of $\text{TbtSi}\equiv\text{SiTbt}$ is endothermic by 58 kcal mol⁻¹^{343b}, making $\text{TbtSi}\equiv\text{SiTbt}$ a good candidates for synthesis^{342,343}. The use of bulky substituents has enabled the recent synthesis of a stable RPbPbR ($\text{R} = 2,6\text{-Tip}_2\text{C}_6\text{H}_3$)²⁶⁰. However, as discussed above (Section VI.A) this compound adopts the singly-bonded planar skeleton **78** (the CPbPbC dihedral angle is 180°) with a long $\text{Pb}–\text{Pb}$ distance of 318.8 pm.



The PESs of M_2F_2 ($\text{M} = \text{Si}$ and Ge) are significantly different from those of the corresponding parent systems or of $\text{RSi}\equiv\text{SiR}$, $\text{R} = \text{Me}$, SiH_3 . The geometries and the relative energies of the Si_2F_2 and Ge_2F_2 isomers are shown in Figures 25 and 26, respectively. The most significant difference between these PESs and those of the parent systems is the existence of low-lying triplet states. The global minimum of Si_2F_2 is the triplet (3A_2) difluorosilylidene ($\text{F}_2\text{Si}=\text{Si}$) isomer which is by 8.1 kcal mol⁻¹ more stable than the corresponding singlet state. The triplet (3A_u) *trans*-bent difluorodisilyne isomer is only 1.8 kcal mol⁻¹ higher in energy and it is by 15.5 kcal mol⁻¹ more stable than the singlet (1A_g) *trans*-bent isomer (Figure 25)^{284a}. These results are in contrast with those for the parent H_2Si_2 system where the triplet (3A_u) *trans*-bent $\text{HSi}\equiv\text{SiH}$ isomer is by 16.1 kcal mol⁻¹ less stable than the singlet *trans*-bent isomer³⁶². The most stable isomer on the singlet PES is $\text{F}_2\text{Si}=\text{Si}$, but it lies 6.7 kcal mol⁻¹ above the 3A_2 triplet. The singlet dibridged C_{2v} isomer lies 12.8 kcal mol⁻¹ above the global minimum (Figure 25)³⁶⁰.

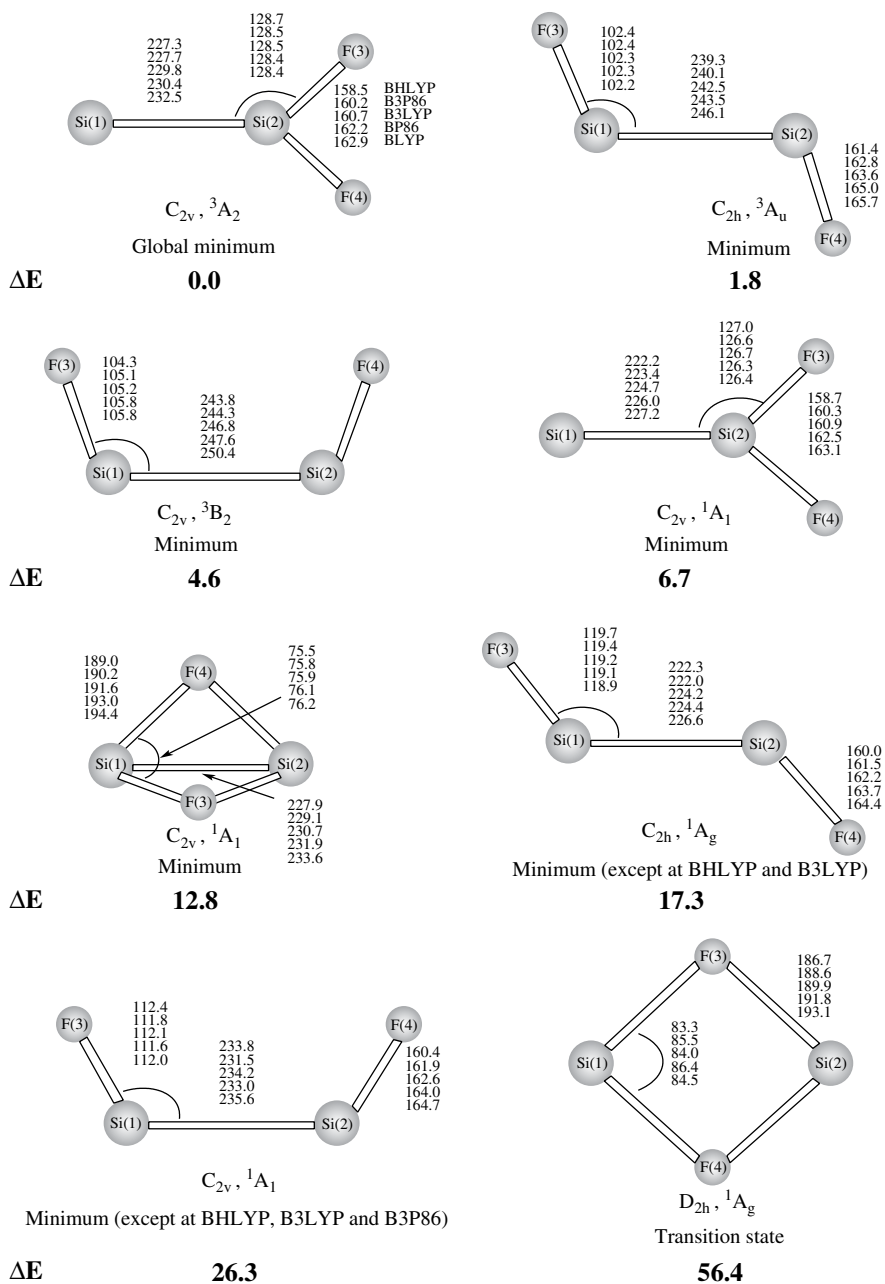


FIGURE 25. Optimized structures of stationary points on the Si_2F_2 PES and their relative energies (ΔE , in kcal mol^{-1}), calculated at B3LYP/DZP++; bond lengths in pm and bond angles in deg. Adapted from Reference 284a

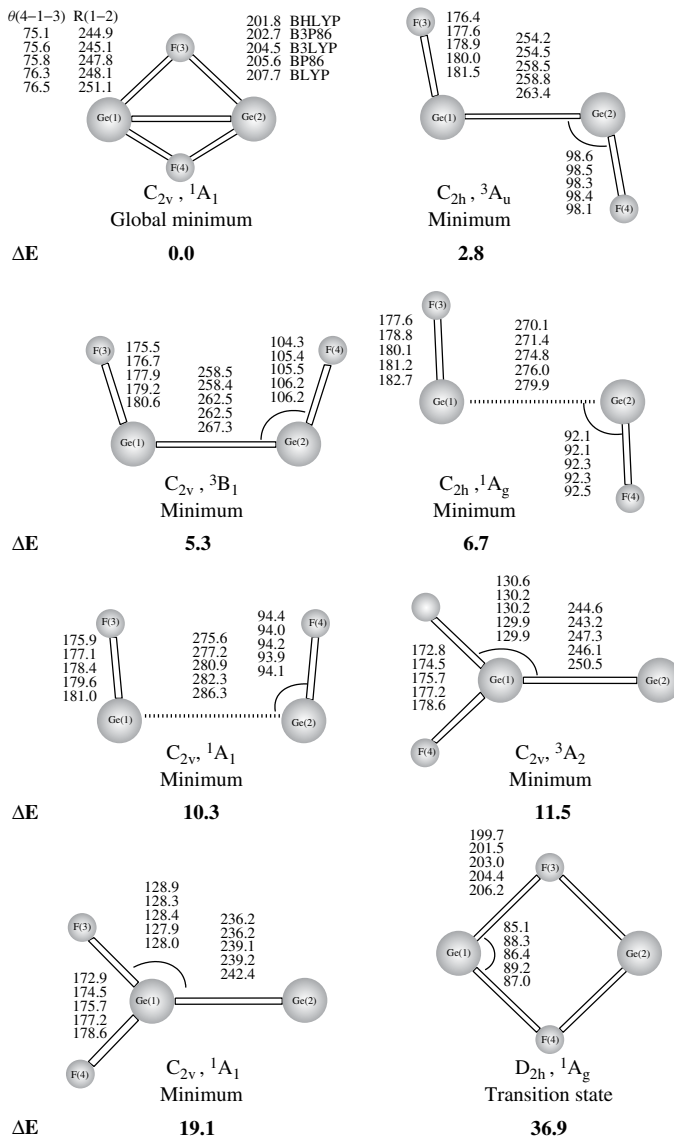


FIGURE 26. Optimized structures of stationary points on the Ge_2F_2 PES and their relative energies (ΔE , in kcal mol^{-1}), calculated at B3LYP/DZP++; bond lengths in pm and bond angles in deg. Adapted from Reference 284b

On the Ge_2F_2 PES, seven minima are located within an energy range of only 19 kcal mol^{-1} (Figure 26)^{284b}. The global minimum is the singlet dibridged isomer and the least stable isomer is the singlet $\text{F}_2\text{Ge}=\text{Ge}$. The singlet *trans*-bent difluorodigermyne is by $6.7 \text{ kcal mol}^{-1}$ less stable than the dibridged Ge_2F_2 and by $3.9 \text{ kcal mol}^{-1}$ less

stable than the triplet (3A_u) *trans*-bent isomer. However, the singlet FGeGeF isomer has a very long Ge–Ge bond of 270–280 pm²⁸⁴, indicating that this species does not possess a multiple Ge–Ge bond and it is best described as a weak complex between two GeF fragments. The linear FMMF structures are not minima on the PESs for both Si₂F₂ and Ge₂F₂.

The global minima on the PESs of the corresponding anions are F₂Si=Si^{-284a} (as are the global minima of C₂F₂⁻ and Si₂H₂⁻) and the *trans*-bent FGeGeF^{-284b}. The dibridged structures are not minima on the PESs for both anionic systems²⁸⁴.

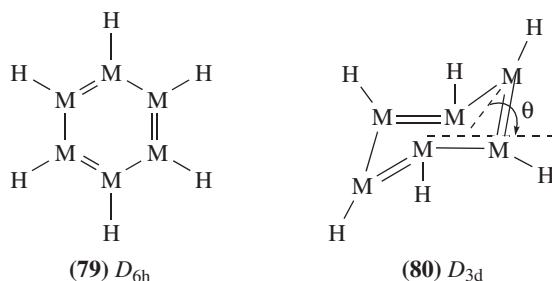
As shown above, the PESs of group 14 M₂R₂ derivatives with R ≠ H are very different from those of the parent M₂H₂. A detailed computational study of the PES of M₂R₂ systems for M = Ge–Pb with various R substituents may lead to new interesting findings as well as to clues for the experimentalists seeking to synthesize these highly interesting and challenging molecules.

F. Aromatic Compounds

Theoretical and experimental studies of compounds which include silicon or its heavier congeners as part of the aromatic ring have been reviewed recently by Apeloig and Karni^{28a} and by Sekiguchi and coworkers³⁷⁵. In view of these recent comprehensive reviews we discuss this topic only briefly, emphasizing the effect of the heavier congeners of silicon on the structure and degree of aromaticity in metalla-aromatic compounds.

1. The congeners of benzene and their isomers

The most striking feature of the heavier congeners of benzene, M₆H₆, is that the planar D_{6h} structure, **79**, is not a minimum on the PES, except for benzene itself. The planar D_{6h} structures are transition states or even higher order saddle points on the M₆H₆ PESs and, upon energy optimization, they distort to puckered D_{3d} structures (**80**) which are minima on the PESs. The preference for the puckered structures, with pyramidal M atoms, increases down group 14^{184,376a} (Tables 35). The bending angle θ (defined in **80**) increases significantly from Si ($\theta = 12.7^\circ$) to Pb ($\theta = 58^\circ$) and this is accompanied by a considerable lengthening of the M–M bonds, which for M = Sn and Pb are comparable to those of a single M–M bond (Table 36). Electropositive substituents (e.g. SiH₃) decrease the bending angle θ (similar to their effect on *trans*-bending in disilenes, Section VI.B.1) and increase the degree of aromaticity (see below). Electronegative substituents, such as fluorine, have the opposite effect¹⁹².



In a recent comprehensive theoretical study of all the possible combinations of silabenzenes, C_nSi_{6-n}H₆ ($n = 1-6$), Baldrige, Uzan and Martin³⁸⁰ found (using basis sets of

TABLE 35. Relative energies (kcal mol⁻¹) of M₆H₆ isomers^a

M	<i>D</i> _{6h} M ₆ H ₆ (79) ^b	<i>D</i> _{3d} M ₆ H ₆ (80) ^c	Metallaprismane 81	Metalla-Dewar- benzene (82)	Metalla- benzvalene (83)
C	<u>0.0</u>	—	117.5 ^d	81.0 ^d	74.8 ^d
Si	0.0	-1.0; -2.3 ^e	<u>-11.9^{d,f}</u>	-1.4 ^d	-6.0 ^{d,g}
Ge	0.0	-9.1; -14.5 ^e	<u>-13.5^{f,h}</u>	-1.8 ^h	-1.2 ^h
Sn	0.0	-23.1	<u>-31.3^h</u>	-6.5 ^h	-11.0 ^h
Pb	0.0	-63.3	<u>-67.0^{h,i}</u>	-10.6 ^h	—

^aThe most stable isomer for each M is underlined.

^bExcept for C₆H₆, all other **79** are not minima on the PES and, when optimized, they distort to **80**.

^cAt MP2/DZ+d//HF/DZ+d; from Reference 184. Additional data for M = Si and Ge are given in Reference 376a.

^dAt MP2/6-31G(d,p)//MP2/6-31G(d,p); from Reference 377a. See also Reference 377b for M = C and Reference 378 for M=Si.

^eAt B3LYP/6-311+G(d,p); from Reference 379.

^fSee also Reference 376a.

^gNot a minimum at the MP2/6-31G(d,p) level, but a minimum at the HF level^{377a}.

^hAt MP2/DZ+d//HF/DZ+d; from Reference 196.

ⁱNot a minimum on the PES¹⁹⁶.

TABLE 36. Structural parameters^a of metallabenzenes M₆H₆ and their aromatic stabilization energies (ASE)^b

M	79 ^{c-e} d(M-M)	80 ^{c,d} d(M-M)	80 θ ^c	ASE (for 79)
C	139.1 ^f	—	—	24.7 ^g ; 34.1 ^h
Si	222.0	223.1; 223.3 ⁱ	12.7; 29.4 ⁱ	11.8 ^g ; 15.6 ^{h,j}
Ge	231.4	236.5	38.0	10 ^k ; 15.3 ^h
Sn	265.7	277.8	50.8	10 ^k
Pb	269.6	295.5	58.0	10 ^k

^aBond lengths in pm and the puckering angle θ (see **80** for definition) in deg.

^bAccording to equation 29, in kcal mol⁻¹.

^cAt HF/DZ(d) [for M = Si at HF/6-31G(d)]; from Reference 184.

^dCompare with *d*(M=M) and *d*(M-M) in H₂M=MH₂ and H₃MMH₃, respectively (Table 26).

^eExcept for C₆H₆, all other **79** are not minima on the PES and when optimized, they distort to **80**.

^fAt B3LYP/cc-pVTZ; from Reference 380.

^gAt HF/6-31G(d); from References 378 (for C) and 192 (for Si).

^hAt B3LYP/6-311+G(d,p)//B3LYP/6-311+G(d,p); from Reference 379; 15.1 kcal mol⁻¹ at MP2/6-31G(d,p)//MP2/6-31G(d,p)^{377a}.

ⁱAt B3LYP/cc-pVTZ (with addition of high exponent polarization d function on Si); from Reference 380.

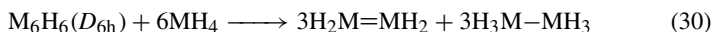
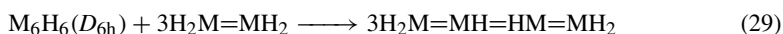
^j15.2 kcal mol⁻¹ relative to 22.8 kcal mol⁻¹ for C₆H₆, at CCSD(T)/cc-pVTZ +ZPE³⁸⁰.

^kAt MP2/DZ+d//HF/DZ+d; from Reference 196.

spdf quality and many-body perturbation theory, hybrid density functional theory and coupled cluster methods) that in contrast to the M₆H₆ molecules which distort to a *D*_{3d} geometry, all silabenzenes with three or less silicon atoms in the ring are planar. Distortion from planarity occurs in C_{*n*}Si_{6-*n*}H₆ molecules with four or more silicon atoms, except for 1,2,4,5-tetrasilabenzene which is planar³⁸⁰. 1,3,5-C₃Ge₃H₆ also has a planar *D*_{3h} structure^{376b}.

Although the planar D_{6h} M_6H_6 are not minima on the PESs, their study is important in order to understand how the degree of aromaticity of these molecules changes as a function of M . These hypothetical molecules were therefore studied extensively by theory^{28a}. The most popular criteria used to evaluate the degree of aromaticity are: (a) structural—bond length equalization due to cyclic electron delocalization; (b) energetic—using isodesmic or homodesmotic reactions to evaluate aromatic stabilization energies (ASE); (c) magnetic—e.g. nucleus independent chemical shift (NICS) values and exalted magnetic susceptibilities (Λ). A detailed description of these criteria and their application to evaluate aromaticity can be found in our previous review^{28a} and in Reference 381.

The M – M bond lengths of the D_{6h} M_6H_6 (**79**) molecules (Table 36) are intermediate between regular single and double M – M bond lengths (Table 26), indicating some degree of electron delocalization. The aromatic stabilization energies (ASEs) of all D_{6h} M_6H_6 , except for $M = C$, calculated according to equation 29, are in the range of 10–16 kcal mol⁻¹, while for benzene it is 25–34 kcal mol⁻¹³⁷⁸ (Table 36), implying a degree of aromaticity when $M \neq C$ that is about 35–50% of that of benzene. When equation 30 was used to calculate the ASE, the estimated degree of aromaticity in the heavier metallabenzene relative to benzene was higher, i.e. $\Delta E(\text{equation 30}) = 58\text{--}60$ kcal mol⁻¹ for Si_6H_6 , Ge_6H_6 and $1,3,5\text{-}Si_3Ge_3H_6$, relative to 75 kcal mol⁻¹ for C_6H_6 (at MP2/ECP), pointing to a degree of aromaticity of about 80% of that of benzene^{376b}. The degree of aromaticity of hexasilabenzene and hexagermabenzene as evaluated from their magnetic properties varies from *ca* 80% of that of benzene (according to the calculated NICS values) to about 36% of that of benzene (according to the calculated ring-size adjusted exalted magnetic susceptibilities Λ , estimated from the difference between the diamagnetic susceptibility of M_6H_6 and that of reference systems without cyclic delocalization³⁷⁹). The large difference between the estimations of the degree of aromaticity based on Λ and on the NICS values was not discussed (see also References 28a and 381 for a critical evaluation of these methods as measures of aromaticity).



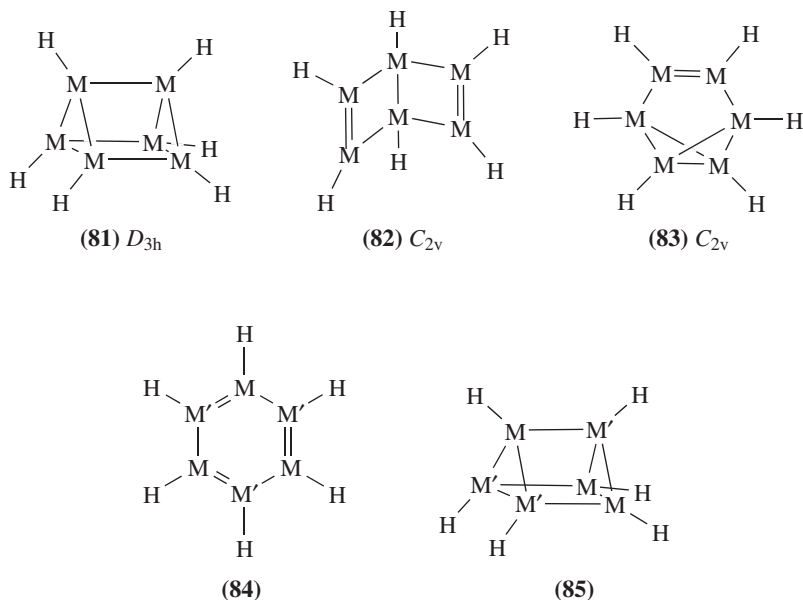
In the nonplanar D_{3d} metallabenzene (**80**) the metal atoms have some degree of radical character with localized ' π ' electrons, causing a decrease in the degree of aromaticity. This is manifested in the decrease (in absolute values) of the exalted magnetic susceptibilities and the NICS values of **80** relative to **79** for $M = Si$ and $M = Ge$ ³⁷⁹. However, the ASEs of **80**, $M = Si, Ge$, of 17.9 and 29.8 kcal mol⁻¹, respectively [equation 29, at B3LYP/6-311+G(d,p)], which are even larger than for the planar D_{6h} conformers, seem to point to an opposite conclusion than implied by the magnetic criteria. However, this apparent conflict is not directly related to aromaticity. Rather, it reflects the increased stability of **80** relative to **79** caused by the reduced strain in the puckered metallabenzene. Thus in this case the energetic criterion measures also effects other than 'aromaticity'³⁷⁹.

The degree of aromaticity of $C_nSi_{6-n}H_6$ ($n = 1\text{--}6$) was derived from their structures, molecular orbitals, isodesmic and homodesmotic bond separation energies and a variety of magnetic criteria. The energetic criteria (i.e. homodesmotic and isodesmic reaction energies similar to equations 29 and 30) suggest that 1,3,5-trisilabenzene and to a lesser extent 1,3-disilabenzene and 1,2,3,5-tetrasilabenzene have very high stabilities relative to benzene, e.g. 1,3,5-trisilabenzene possesses *ca* 80% of the ASE of benzene. However, by the magnetic criteria, the latter three silabenzene are among the least aromatic of

the $C_nSi_{6-n}H_6$ ($n = 1-6$) family while the most aromatic are 1,2-disilabenzene, 1,2,3-trisilabenzene and 1,2,3,4-tetrasilabenzene. Analysis of the electron population and the calculated bond orders reveals that the former three systems derive part of their stability from ionic contributions to the bonding, showing again that the energetic criterion should be used carefully to evaluate aromaticity as it measures, in addition to aromaticity, also other effects. The degree of aromaticity as derived from the magnetic properties decreases with increasing number of Si atoms, hexasilabenzene being the least aromatic³⁸⁰.

In analogy to Ge_6H_6 , the germanium analogs of naphthalene, $Ge_{10}H_8$, and of higher linear acenes $Ge_{4n+2}H_{2n+4}$ ($n = 2, 3, \dots$) are also less stable in their planar D_{2h} geometries than in the corresponding puckered C_{2h} structures, and it was therefore concluded that the germanium analog of graphite is not planar¹⁹⁶.

Another striking feature of the heavier M_6H_6 compounds is the fact that, unlike in C_6H_6 where benzene is by far the most stable isomer, other isomers, **81–83** (Table 35), are more stable than the D_{6h} M_6H_6 and even than the lower energy puckered D_{3d} M_6H_6 ^{196,376a,377a,378}. The metallaprismanes (**81**), despite having two strained three-membered rings, are the most stable M_6H_6 ($M \neq C$) isomers because they have no $M=M$ double bonds; an exception is the hexaleadprismane **81**, $M = Pb$ which is not a minimum in D_{3h} symmetry, and the minimum is calculated to be a highly distorted structure¹⁹⁶. The second most stable isomers are usually the puckered **80** followed by the metallabenzvalenes (**83**) and the metalla-Dewar-benzenes (**82**). For $M_3M'_3H_6$ systems having different M and M' atoms, the stability of the metallaprismanes, **85** ($M \neq M'$) relative to their benzene analogs, **84** ($M \neq M'$), follows the order (in kcal mol^{-1}): $Si_3Ge_3H_6$ (-6.4 (-1.6 relative to the puckered conformer, which is the minimum on the PES)) $>$ $C_3Ge_3H_6$ (27.2) $>$ $C_3Si_3H_6$ (35.5)^{376a}. Thus, for $Si_3Ge_3H_6$, **85** is more stable than both the puckered and the D_{6h} metallabenzene isomers. When carbon atoms replace three of the heavier congeners, the stability order is reversed



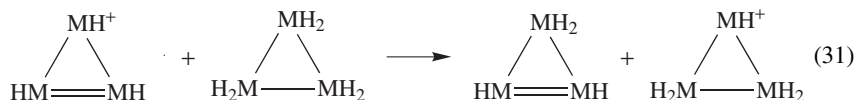
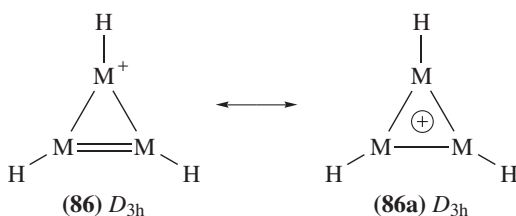
and, for $C_3Ge_3H_6$ and $C_3Si_3H_6$, **85** is less stable than **84** by 27.2 and 35.5 kcal mol⁻¹, respectively [all values are at MP2/6-311G(d,p)//HF/ECP(d)]. Heavier compounds of the type $M_3M'_3H_6$ have not yet been studied, but based on experience with related systems it seems safe to predict that all these systems will prefer structure **85** over D_{3h} **84**.

It is interesting to note that the energy of the metalla-Dewar-benzene (**82**) and the metallabenzvalene (**83**) relative to **79** changes relatively little as a function of M and they are only moderately (by up to 11 kcal mol⁻¹) more stable than **79** ¹⁹⁶.

The fact that many metallaprismanes^{24,240,382} and metalla-Dewar-benzenes²⁴⁰ have been synthesized, but that not even a single M_6R_6 metalla-analog of benzene has been isolated, is consistent with theoretical predictions regarding their relative stabilities.

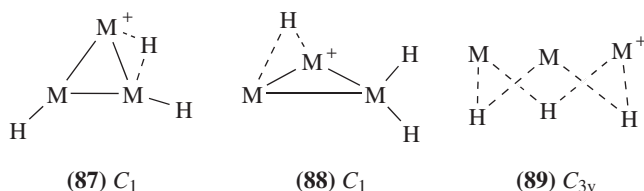
2. Metallacyclopropenium cations

The cyclopropenium cation (**86**, M = C) is a well established aromatic system, with a high aromatic stabilization energy (equation 31) of 58.7 kcal mol⁻¹ [at B3LYP/6-311++G(2d,2p)]^{209a}, as represented by resonance structure **86a**, M = C.



The D_{3h} metallacyclopropenium cations, **86**, M = C, Si, Ge are the global minima on the $M_3H_3^+$ PESs. However, **86** is a transition structure for M = Sn and a third-order saddle point for M = Pb. The aromatic stabilization energy (equation 31) of **86**, M = Si, is 35.6 kcal mol⁻¹ [B3LYP/6-311++G(2d,2p)]^{209a}, being about 60% of that of the cyclopropenium cation. On going down group 14 the aromatic stabilization of **86** is reduced, i.e. ΔE (equation 31) = 31.9, 26.4 and 24.1 kcal mol⁻¹ for M = Ge, Sn and Pb^{209a}. However, the ASE is significant even for D_{3h} $Pb_3H_3^+$ (which, as pointed out above, is not a minimum on the PES). The calculated M–M bond lengths in **86** are (in pm): 135.9 (M = C), 220.3 (M = Si), 236.1 (M = Ge), 274.6 (M = Sn) and 294.6 (M = Pb). For M = C, Si, Ge and Sn^{209a} these values are intermediate between those of single and double M–M bond distances (see Tables 7 and 26 for comparison), consistent with a delocalized aromatic description (**86a**). In **86**, M = Pb the Pb–Pb bond length is very similar to that of a single bond distance. The M–M Wiberg bond indices in **86** are: 1.4, 1.4, 1.3, 1.3 and 1.1 for M = C, Si, Ge, Sn and Pb, respectively^{209a}, consistent with the calculated M–M bond distances. The overall conclusion is that the trimetallacyclopropenium cations with M = C to Sn have significant aromatic character and they are thus better represented by resonance structure **86a** than by the localized description **86**.

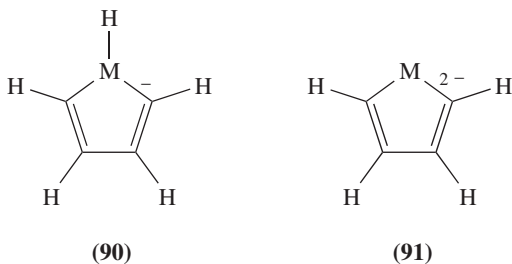
For Si_3H_3^+ , three hydrogen-bridged isomers, **87**, **88** and **89**, which are by *ca* 20–25 kcal mol⁻¹ less stable than **86**, were also located as minima^{209a,383}. However, for heavier M atoms the classic D_{3h} structures are not the global minimum on the PES. For M = Ge, Sn and Pb the C_{3v} triply hydrogen-bridged isomer, **89**, is the most stable M_3H_3^+ isomer, and it becomes increasingly more stable as M becomes heavier; i.e. $\Delta E(\mathbf{89}-\mathbf{86})$ at B3LYP/6-311++G(2d,2p) is: 23.7, -17.4 (+3.8 at G2³⁸⁴), -32.4 and -63.3 kcal mol⁻¹ for M = Si, Ge, Sn and Pb, respectively^{209a}. This trend was attributed to the increased stability of divalent structures on moving down group 14^{209a}. However, we speculate that the D_{3h} structure may again become the global minimum when the hydrogens are replaced by other substituents, e.g. methyl, aryl, silyl, etc. (such systems have not yet been studied theoretically).

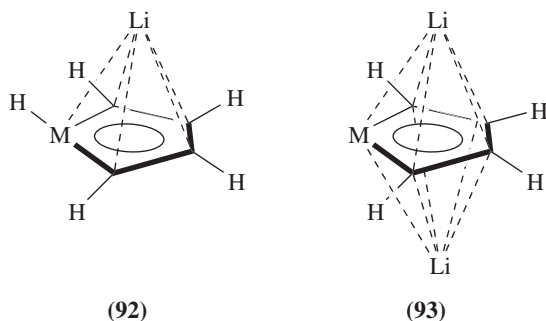


The first free trigermacyclopropenium cation $[(t\text{-Bu}_3\text{SiGe})_3^+ \text{BPh}_4^-]$, which was recently synthesized and characterized by X-ray crystallography, indeed has the classic D_{3h} structure **86**³⁸⁵. The three germanium atoms form an equilateral triangle with Ge–Ge distances of 232.1–233.3 pm, in good agreement with the calculated value of 236.1 pm for Ge_3H_3^+ ^{209a}. The experimental Ge–Ge distances are intermediate between the Ge–Ge double-bond and single-bond distances in the cyclotrigermene precursor of 223.9 pm and 252.2 pm, respectively, reflecting a delocalized 2π -electron system^{375,385}, as predicted by theory.

3. Metallacyclopentadienyl anion and dianion

How is the aromaticity of the cyclopentadienyl anion (**90**, M = C) and dianion (**91**, M = C) affected by substitution by heavier group 14 atoms? In a comprehensive study Goldfuss and Schleyer²¹³ evaluated for all group 14 elements the degree of aromaticity of mono- and dianions of group 14 metalloles **90** and **91** and their lithium salts, **92** and **93**. They used a variety of criteria: structural, energetic (ASE) and magnetic, i.e. diamagnetic susceptibility exaltations (Λ) and nucleus independent chemical shift (NICS). Their main conclusions are:



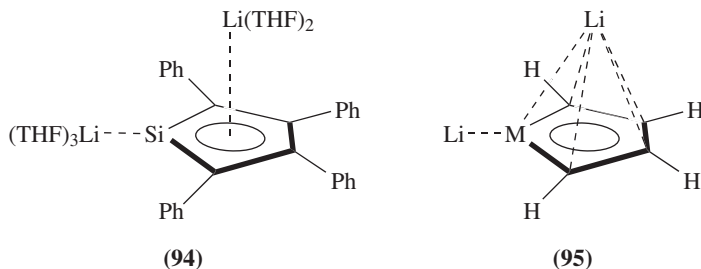


(a) The aromaticity of the metallolyl monoanions **90** decreases in the order: C (most aromatic) > Si > Ge > Sn > Pb (least aromatic). This is manifested in an increased bond alternation, stronger pyramidality at M, higher inversion barriers at M and decreased ASE, along the C to Pb series. Similarly, the diamagnetic susceptibility exaltations (Λ) and the NICS values become less negative in going down group 14, also indicating a decrease in aromaticity.

(b) The aromaticity of the lithium metallolides **92** decreases along the C \rightarrow Pb series similarly to the $c\text{-C}_4\text{H}_4\text{MH}^-$ free anion series. However, $\text{Li} \cdots \text{H}$ interactions between the η^5 -coordinated Li atom and the M–H hydrogen stabilize significantly the heavier lithium metallolides with M = Sn and Pb relative to their lower congeners.

(c) In contrast to the $c\text{-C}_4\text{H}_4\text{MH}^-$ (**90**) and $[c\text{-C}_4\text{H}_4\text{MH}]\text{Li}$ (**92**) systems, the degree of aromaticity of the metallole dianions **91** and of their dilithium complexes (**93**) is remarkably constant for all group 14 elements.

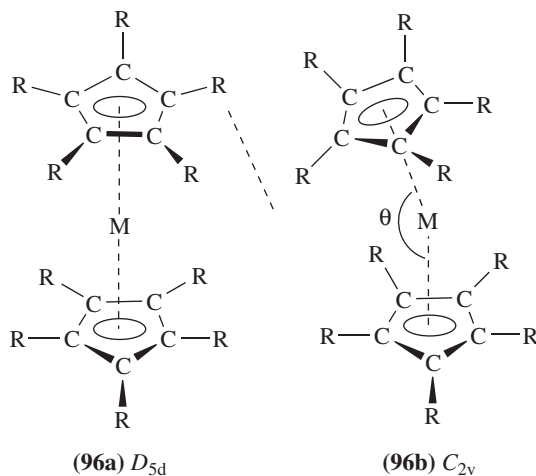
West, Apeloig and coworkers recently reported an X-ray structure of an η^1, η^5 -dilithium silole (**94**) in which one Li atom (with its associated two THF solvating molecules) is η^5 -bonded to the silole ring and the second Li is η^1 -bonded to the Si (and to three THF molecules)^{386a}. According to the calculations **93**, M = Si is by 21 kcal mol⁻¹ more stable than the corresponding η^1, η^5 -dilithium silole **95**, M = Si [at MP2/6-31+G(d) //MP2/6-31+G(d)] and the authors suggest that solvation by THF probably reverses this stability order leading to the isolation of **94**^{386a}. More recently, the analogous germoles were crystallized from dioxane in two distinct structures: one with η^1, η^5 -coordination of the two Li⁺ cations as in **95**, M = Ge (the η^5 -bonded Li is coordinated also to two dioxane molecules and the η^1 -bonded Li is associated also with three dioxane molecules) and the other having a η^5, η^5 -coordination as in **93**, M = Ge (each Li atom is also coordinated to two dioxane molecules). As in the silicon case, also for germanium the



calculations (MP2/LANL2DZ) find the η^5 , η^5 -[*c*-C₄H₄Ge]Li₂ (**93**, M = Ge) isomer to be by 25 kcal mol⁻¹ more stable than the η^1 , η^5 -[*c*-C₄H₄Ge]Li₂ (**95**, M = Ge) isomer^{386b}.

4. Metallocenes

Metallocenes have potential ‘three dimensional aromaticity’^{28a,381a,387}. Ferrocene has a symmetric *D*_{5d} structure (**96a**, M = Fe)³⁸⁸, while the majority of the analogous group 14 sandwich compounds, (C₅R₅)₂M, M = Si, Ge, Sn and Pb, have bent *C*_{2v} structures (**96b**) or *C*_s structures³⁸⁹. Several structures, however, possess parallel cyclopentadienyl rings: i.e. (C₅Me₅)₂Si^{390a}, (C₅Ph₅)₂Sn^{390b}, (C₅(CHMe₂)₅)₂Sn^{390c}, (C₅(CHMe₂)₃H₂)₂Pb^{390d} and (C₅Me₄(SiMe₂Bu-*t*))₂M, M = Ge, Sn and Pb³⁹¹ [when the *t*-Bu groups were replaced by Me groups, i.e. in (C₅Me₄(SiMe₃))₂M, bent structures were observed for M = Sn and Pb³⁹¹, indicating that the tilting energy is small].



The calculations for Cp₂M (Cp = *c*-C₅H₅) for all group 14 elements show that the bent structures, either in *C*_{2v}, *C*_s or *C*₂ symmetry (which are all very close in energy), are more stable than the *D*_{5d} structures. However, the energy lowering due to bending at M is small, i.e. (in kcal mol⁻¹) 4.4 for M = Si [at CCSD(T)/6-31G(d)//B3LYP/6-31G(d)]³⁹², 6.4 for M = Ge, 4.0 for M = Sn and 0.7 for M = Pb (at HF/LANL1DZ)³⁹³. Only for M = C is the bending energy significantly larger, i.e. 49.4 kcal mol⁻¹³⁹².

The X-ray and/or electron diffraction structures for **96**, R = H, M = Ge, Sn and Pb show tilt angles θ of 152°, 144°–147° and 117°–135°, respectively^{389,391} [carbocene (**96**, M = C) is not known experimentally]. The corresponding calculated bending angles are 125.3° and 137.9° (HF/LANL1DZ)³⁹³ for Cp₂Sn and Cp₂Pb, respectively. For M = Si, the closest experimentally known compound for comparison with the calculations is **96** (M = Si, R = Me) whose structure analysis indicates the presence of two structures, **96a**, and **96b**, in a ratio of 1 : 2, respectively. In **96b**, R = Me the rings form a tilt angle θ of 167.4° in the crystal and 169.6° in the gas phase³⁸⁹ compared to the calculated θ in Cp₂Si of 152.4° (at HF/DZP)³⁹⁴.

The driving force for bending is thought to be the stabilization upon bending of the HOMO-1 orbital (2*a*_{1g} symmetry), shown schematically in **97**, due to mixing with the

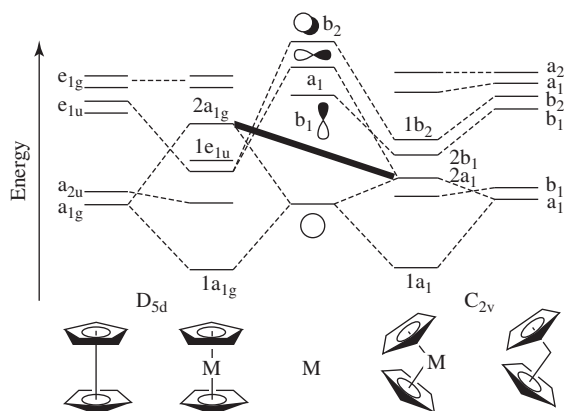
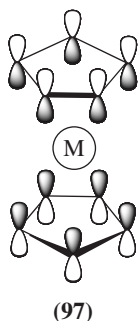


FIGURE 27. General molecular orbital diagrams showing the construction of the orbitals of 14 electron Cp_2M metallocenes, in parallel (D_{5d}) and bent (C_{2v}) conformations, from the orbitals of the Cp_2 and M fragments (only the occupied orbitals are shown). Adapted from Reference 389

p orbital of M of a_1 symmetry. The stabilization of the $2a_{1g}$ orbital upon bending is shown (by the heavy line) in the molecular orbital diagram in Figure 27^{389,393}. The tilting of the Cp rings stabilizes the $2a_{1g}$ orbital by $9.2 \text{ kcal mol}^{-1}$ for $\text{M} = \text{Sn}$, but by only $2.5 \text{ kcal mol}^{-1}$ for $\text{M} = \text{Pb}$ [calculated using HF/LANL1DZ for the tin and lead atoms and HF/6-311G(d,p) for all other atoms]³⁹³. Bending produces a lone pair at M and the contribution of the a_1 p-orbital to this lone pair decreases in the order (the electron occupancy of the p-orbital is given in parentheses): $\text{Ge} (0.61e) > \text{Sn} (0.51e) \gg \text{Pb} (0.39e)$, in correlation with the decrease in the hybridization propensity of these elements (see Sections III.A and III.C) and with the degree of the calculated bending of the rings which is smaller in Cp_2Pb than in Cp_2Sn ³⁹³ (note, however, that experimentally the degree of bending in Cp_2Pb is larger than in Cp_2Sn ^{389,391}). These trends correlate with the decrease in the tilting energies on going from Ge to Pb³⁹³. In the D_{5d} conformers of Cp_2Pb and $(\text{C}_5\text{Me}_4(\text{SiMe}_2\text{Bu}-t))_2\text{Pb}$, the calculated $2a_{1g}$ orbital is by 23 kcal mol^{-1} ³⁹³ and 15 kcal mol^{-1} ³⁹¹, respectively, more stable than in the corresponding tin metallocenes. This enhanced stability of the $2a_{1g}$ orbital of Cp_2Pb was attributed to relativistic effects³⁹¹.

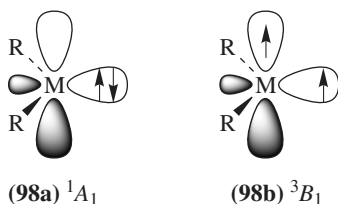


VII. REACTIVE INTERMEDIATES

A. Divalent Compounds (Metallylenes)

1. MH_2 and MX_2 ($X = \text{halogen}$)

The determination of the fundamental properties of carbene, CH_2 , such as its structure, its electronic state and its singlet–triplet energy difference, was a challenge for a long time, and agreement between theory and experiment was achieved only after many years of intensive debate³⁹⁵. It is of similar importance to determine these properties for the heavier metallylenes (metalladiyls). Silylene, SiH_2 , has been studied extensively, employing a variety of theoretical methods^{7,396,397}, whereas germylene (GeH_2) was less thoroughly investigated^{398–401}. Reliable calculation of the properties of the heavier carbene analogs, SnH_2 and PbH_2 , require the consideration of relativistic and spin–orbit coupling (SOC) effects^{400,401}, particularly for the determination of the singlet (1A_1)–triplet (3B_1) energy gap (ΔE_{ST}). The electronic configurations of the 1A_1 and 3B_1 states of a metallylene, MR_2 , are shown schematically in **98a** and **98b**, respectively.



The most elaborate systematic study of the structures and of the 1A_1 – 3B_1 splitting of the heavier carbene analogs was carried out by Balasubramanian⁴⁰⁰. He carried out extensive multiconfiguration calculations (CASSCF) followed by configuration interaction calculations, using basis sets that included f-polarization functions, and the results of these calculations are collected in Table 37.

CH_2 has a triplet ground state (**98b**) which is 9 kcal mol⁻¹ lower in energy than the singlet state (**98a**)^{395,403,404}. In contrast, all the heavier group 14 MH_2 have singlet ground states. The calculated singlet–triplet energy splitting (ΔE_{ST}) (experimental values are available only for SiH_2 , Table 37) increases from 19.6 kcal mol⁻¹ for SiH_2 , (21.0 kcal mol⁻¹, experimental) to 23.1 kcal mol⁻¹ for GeH_2 and 23.8 kcal mol⁻¹ for SnH_2 . For PbH_2 , ΔE_{ST} is much larger (41.0 kcal mol⁻¹), mainly due to the relativistic contraction of the 6s orbital and SOC (the SOC contribute 4 kcal mol⁻¹ to ΔE_{ST})⁴⁰⁰.

The M–H bond lengths in the 1A_1 singlet states are longer than those in the 3B_1 states, and they become longer as M becomes heavier, in both the singlet and triplet states. The HMH bond angles are always wider in the triplet state than in the singlet state. However, while in the 1A_1 states the HMH bond angle is almost constant (90.5°–92.7°) for M = Si to M = Pb, in the 3B_1 state HMH becomes narrower moving down group 14 [with the exception of GeH_2 for which the HGeH bond angle (119.8°) is slightly wider than for SiH_2 (118.5°); see Table 37].

Group 14 MX_2 ($X = \text{halogen}$) are intermediates in the chemical processes associated with chemical deposition and halogen etching reactions of semiconductors. In view of their technical importance they have been subjected to numerous experimental⁴⁰⁹ as well as to high-level calculations using the MRSDCI (multi-reference, single and double configuration interaction calculations)^{405,407,408} and DFT^{153,402} methods. The calculated

TABLE 37. Calculated and experimental (in parentheses) geometries and singlet–triplet energy splittings (ΔE_{ST}) of MH_2 and MX_2 ($X = \text{halogens}$) metallylenes^a

MX_2	Singlet		Triplet		ΔE_{ST}
	$d(M-X)^b$	$X-M-X^b$	$d(M-X)$	$\angle X-M-X$	
CH_2^c	110.9 (111) ^d	102.1 (102.4) ^d	107.8	131.5	-9.0 (-9.0) ^d
SiH_2^e	152.0 (151.6) ^f	92.7 (92.8) ^f	148.4	118.5	19.6(21.0) ^f
GeH_2^g	158.7	91.5	153.4	119.8	23.1
SnH_2^g	178.5	91.1	173.0	114.9	23.8
PbH_2^g	189.6	90.5	186.5	109.8	41.0
CF_2^c	131.5; 130.4 (130.0)	104.2; 104.1 (104.8)	132.9	119.8	57.6(56.7) ^d
SiF_2^h	159.8; 161.5 (159.1)	99.5; 100.2 (100.8)	159.6	114.0	71.0(75.2) ⁱ
GeF_2^j	172.3; 177.7 (173.2)	97.1; 97.8 (97.2)	171.5	113.1	81.6(86.7) ⁱ
SnF_2^j	186.5; 194.8	92.0; 96.0	185.8	112.9	78.4
PbF_2^j	213.9; 201.8 (203.3)	98.5; 95.8 (97.8)	213.1	126.2	94.1
CCl_2^c	171.8; 175.3 (171.6)	109.9; 109.1 (109.2)	167.9	127.6	20.5
$SiCl_2^k$	210.8; 211.4 (206.3)	101.9; 102.0 (101.5)	207.6	119.0	53.5(52.8)
$GeCl_2^l$	219.1; 223.6 (216.9)	100.5; 100.9 (99.9)	204.0	118.6	60.3(63.8)
$SnCl_2^m$	254.2; 241.7 (234.7)	98.4; 98.9 (99)	233.6	116.0	60.0
$PbCl_2^m$	254.2; 250.5 (246)	100.8; 99.8 (96)	259.9	139.9	69.7
CBr_2^c	189.3; 191.7 (174)	111.0; 110.2 (114)	184.0	129.9	16.5
$SiBr_2^k$	228.8; 228.5 (224)	102.8; 103.0 (103)	225.7	120.8	43.7
$GeBr_2^l$	237.3; 239.2 (233.7)	101.8; 102.3 (101.2)	234.8	120.8	55.5
$SnBr_2^m$	253.5; 256.7 (250.4)	99.7; 100.0 (98.9)	251.1	119.8	55.5
$PbBr_2^m$	268.4; 264.9 (260)	101.5; 100.8 (98.8)	272.0	132.4	65.0
CI_2^c	210.5; 214.9	112.6; 111.9	203.4	132.3	11.2
SiI_2^k	252.4; 253.2	104.2; 104.6	249.1	121.8	41.0
GeI_2^l	257.4; 262.4 (254)	102.8; 104.4 (102.1)	255.6	122.3	42.4

(continued overleaf)

TABLE 37. (continued)

MX ₂	Singlet		Triplet		ΔE_{ST}
	d(M–X)	X–M–X ^b	d(M–X)	\angle X–M–X	
SnI ₂ ^m	273.8; 279.6 (269.9)	100.9; 102.3 (103.5)	271.8	121.4	47.1
PbI ₂ ^m	287.8; 286.6 (279)	103.6; 103.0 (99.7)	293.8	132.6	53.8

^aBond lengths in pm, bond angles in deg, energies in kcal mol⁻¹. Experimental values are taken from references cited in References 138 and 153. See Reference 401 for other computational results on MH₂.

^bd(M–X) denotes bond length, \angle X–M–X denotes bond angle. For each MX₂ the second bond length and bond angle given are at B3LYP with quasi-relativistic ECPs; from Reference 153. Calculated values using other DFT functionals, correlated *ab initio* methods and experimental values can be found in references cited in References 153 and 402.

^cAt MP4/6-311G(2df)//MP2/6-31G(d); from Reference 403.

^dFrom Reference 404; the experimental values are cited in Reference 403.

^eAt MRSOCI; from Reference 396.

^fFrom references cited in Reference 396.

^gAt CASCF using relativistic CI ECPs (RCI) with inclusion of spin-orbit coupling effects; from Reference 400.

^hAt CI/DZ2d; from Reference 281.

ⁱFrom Reference 402.

^jAt CASSCF/MRSDCI (ECP); from Reference 405.

^kAt B3LYP/6-311++G(2d), unpublished results⁴⁰⁶.

^lAt CASSCF/MRSDCI (ECP); from Reference 407.

^mAt CASSCF/MRSDCI (ECP); from Reference 408.

(and available experimental) geometries and the ¹A₁–³B₁ energy splittings (ΔE_{ST}) of all possible MX₂ (M = C to Pb, X = F to I) metallylenes are gathered in Table 37. Other properties, such as dipole moments, ionization potentials and electron affinities, were also calculated and they are discussed in References 153, 402, 405, 407 and 408. In general, ΔE_{ST} increases for all halogen substitutions relative to that in the corresponding MH₂. For a given halogen ΔE_{ST} increases from Si to Pb, with a sharp increase between tin and lead (similar to the behavior of the corresponding MH₂). On the other hand, for a given metal M, ΔE_{ST} decreases as the halogen substituent becomes heavier and less electronegative; e.g. ΔE_{ST} (kcal mol⁻¹) = 53.5 for SiCl₂, 43.7 for SiBr₂ and 41.0 for SiI₂ (Table 37).

Examination of the calculated geometries of MX₂ reveals that in all cases the triplet states exhibit shorter bond lengths and larger bond angles than in the singlet states, as was also observed for MH₂. In general, the MX bond lengths increase in both the ¹A₁ and ³B₁ states as the central atom and the halogen become heavier (Table 37). For a given halogen, the XMX bond angle decreases sharply from M = C to M = Si (for both the singlet and triplet states), and it decreases monotonically further for the higher congeners (Table 37, Figure 28). This decrease in the XMX bond angles as M becomes heavier was attributed to the larger contribution of the s orbital to the lone pair on the heavier M, which in turn is due to the increasing reluctance of M to hybridize when it becomes heavier²². The smallest XMX bond angles were calculated for M = Sn, and for all PbX₂ compounds the quasi-relativistic ECP calculations predict a small increase of 2–3°¹⁵³ (Figure 28). For a given group 14 element the XMX bond angle is slightly widened when the halogen becomes heavier, probably as a result of the stronger repulsion between the larger halogens.

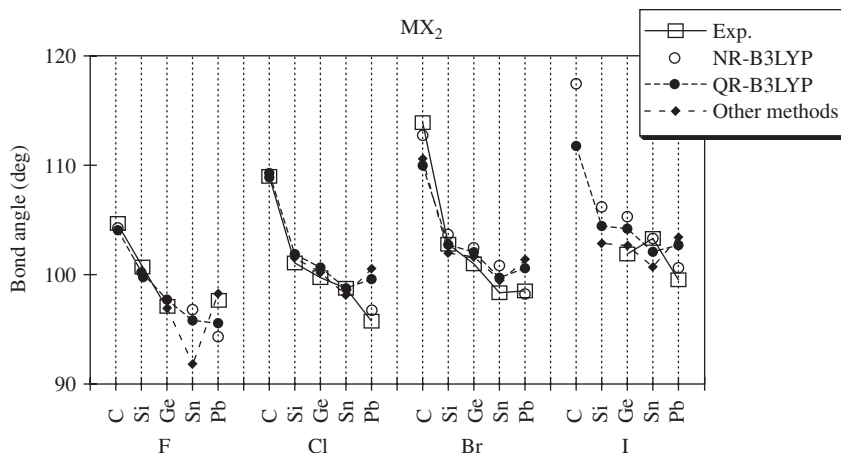
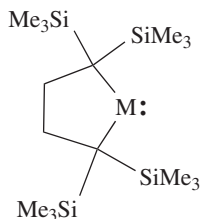


FIGURE 28. The MX_2 bond angles (deg) in MX_2 , calculated with nonrelativistic (NR) and quasi-relativistic (QR) effective core potentials using the B3LYP functional. Reprinted with permission from Reference 153. Copyright (1999) American Chemical Society

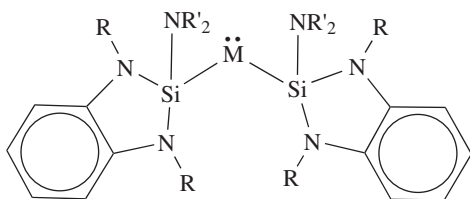
2. Stable metallylenes

The divalent state of group 14 metallylenes becomes increasingly favorable with heavier M atoms⁴¹⁰. Thus, while carbenes and silylenes are highly reactive, the inorganic chemistry of lead is dominated by oxidation state II (see Section V.C.3). A large variety of stable MR_2 (M = Ge, Sn, Pb) compounds where R = π -donor ligand (such as NR'_2 ²², PR'_2 ^{324, 411}, AsR'_2 ³²⁴, hypersilyl $(Si(SiMe_3)_3)$ ²⁸⁶, diaryl or dialkyl, have been synthesized and isolated in recent years^{22, 23, 24f, 412}. All these stable metallylenes are substituted with very bulky substituents that protect them from further bimolecular reactions. Some specific examples of stable silyl and alkyl substituted metallylenes which have recently been synthesized are: $M[CH(SiMe_3)_2]_2$ (M = Ge, Sn, Pb), which are stable in solution but dimerize upon crystallization^{413a}, and $(Me_3Si)_3CGeCH(SiMe_3)_2$, which is monomeric even in the solid state^{413b, c}. The dialkylsilylene (**99**, M = Si) is storable at 0° in the solid state, but it isomerizes slowly to the corresponding silene apparently by a 1,2-migration of a trimethylsilyl group^{414a}. The analogous germylene (**99**, M = Ge)^{414b} and stannylene (**99**, M = Sn)^{414c} are more stable and show no such isomerization even at 100°. $Pb(Si(SiMe_3)_3)_2$ is monomeric both in the solid state (it decomposes only at

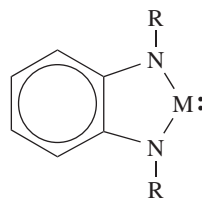


(**99**) M = Si, Ge, Sn

152 °C) and in solution, while $\text{Sn}(\text{Si}(\text{SiMe}_3)_3)_2$ is monomeric in solution but dimerizes to the corresponding distannene in the solid²⁸⁶. The stable bis(silyl)tin (**100**, $\text{M} = \text{Sn}$) and bis(silyl)lead (**100**, $\text{M} = \text{Pb}$) were recently isolated from an insertion reaction of **101** ($\text{M} = \text{Si}$) into the $\text{M}-\text{N}$ bond of $\text{M}[\text{N}(\text{SiMe}_3)_2]_2$ ($\text{M} = \text{Sn}$ and Pb)⁴¹⁵. $\text{Ge}(2,4,6\text{-}t\text{-Bu}_3\text{C}_6\text{H}_2)_2$ is stable both in solution and in the solid below 20 °C^{416a,b}, and $\text{Sn}(2,4,6\text{-}t\text{-Bu}_3\text{C}_6\text{H}_2)_2$ is stable under inert conditions even at room temperature^{416c}.

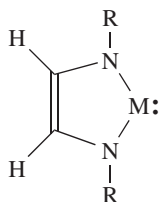


(**100**) $\text{M} = \text{Sn}, \text{Pb}$; $\text{R} = \text{CH}_2\text{Bu-}t$, $\text{R}' = \text{SiMe}_3$



(**101**) $\text{M} = \text{C}, \text{Si}, \text{Ge}, \text{Pb}$; $\text{R} = \text{CH}_2\text{Bu-}t$

The remarkable syntheses of the stable diamino carbenes⁴¹⁷, **102a**^{418a,b} and **103a**^{418c} (and later also **101**, $\text{M} = \text{C}$ ⁴¹⁹), was followed by the synthesis of the analogous stable silylenes^{23b}, **102b**^{420a-c}, **103b**^{420b-d} and **101** ($\text{M} = \text{Si}$)⁴²¹. These achievements as well as the very recent synthesis of **99**, $\text{M} = \text{Si}$ demonstrated that also the lighter group 14 elements can exist in oxidation state II as stable 'bottleable' molecules. Taking advantage of similar strategies, the corresponding germynes, **102c**⁴²² and **103c**⁴²² and **101**, $\text{M} = \text{Ge}$ ⁴²³, Sn ⁴²⁴ and Pb ⁴²³, were also synthesized, isolated and characterized.

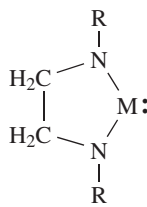


(**102a**) $\text{M} = \text{C}$, $\text{R} = t\text{-Bu}, 1\text{-Ad}$,
 $\text{Ar} = \text{Mes}, 4\text{-MeC}_6\text{H}_4$

(**102b**) $\text{M} = \text{Si}$, $\text{R} = t\text{-Bu}$

(**102c**) $\text{M} = \text{Ge}$, $\text{R} = t\text{-Bu}$

(**102d**) $\text{M} = \text{C}, \text{Si}, \text{Ge}$, $\text{R} = \text{H}$



(**103a**) $\text{M} = \text{C}$, $\text{R} = \text{Ar}$

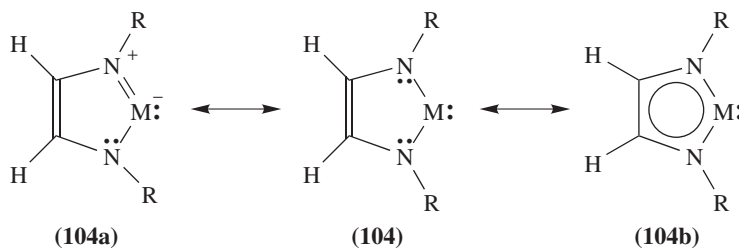
(**103b**) $\text{M} = \text{Si}$, $\text{R} = t\text{-Bu}$

(**103c**) $\text{M} = \text{Ge}$, $\text{R} = t\text{-Bu}$

Why are these metallylenes stable? Is the stabilization due to the presence of the two α -nitrogen atoms? Are these compounds aromatic? These questions have been studied extensively^{322,323,425,426} and reviewed recently by Apeloig and Karni^{28a}.

The conclusion from these studies is that the stability of the imidazol-2-ylidene-type systems, **102**, results mainly from the presence of the two α -nitrogen atoms which stabilize the metallylene by electron donation from the nitrogen lone-pair to the empty p orbital on M , as shown in resonance structure **104a**. The calculations predict a stabilizing

effect [estimated from the barrier for the rotation of both amino substituents in $M(\text{NH}_2)_2$ from the planar ground state geometry to the perpendicular geometry] of $66.8 \text{ kcal mol}^{-1}$ for $M = \text{C}^{425}$, $35.8 \text{ kcal mol}^{-1}$ for $M = \text{Si}^{425}$ and $31.9 \text{ kcal mol}^{-1}$ for $M = \text{Ge}^{322}$. The major discussion and debate regarding **102** and **103** centered around the contribution of 6π -electron delocalization, i.e. ‘aromaticity’, as shown in resonance structure **104b**. The question was studied by a variety of structural, energetic and magnetic criteria, as well as by analysis of the charge distribution and the low-energy ionization processes ^{28a,322,323,425,426}. All these criteria point to the existence of π -electron delocalization and thus to some degree of aromaticity in the unsaturated metallylenes of type **102**. However, the degree of conjugation and aromaticity depends on the criteria which were used to evaluate these effects. The degree of aromaticity in **102** is quite small according to the ‘Atoms-in-Molecules’ topological charge analysis⁴²⁵, but it is more significant according to NBO charge analysis³²³ or according to the structural, energetic and magnetic properties^{323,425}. However, regardless of the criteria used, π -electron delocalization is generally found to be less extensive in the unsaturated silylenes and germylenes of type **102** compared to their carbene analogs, and it is much smaller than in prototype aromatic systems such as benzene or imidazolium cations^{323,425}. In agreement with this theoretical conclusion, the saturated compounds, **103**, where ‘ π -aromaticity’ is absent, are more reactive than the ‘aromatic’ **102**. For example, **102b** is stable indefinitely, while **103b** dimerizes slowly with a half-life of *ca.* 6 days at room temperature^{420b-d}. However, saturated silylenes^{420b-d} and germylenes⁴²² of type **103** still have unusual stability and they can be isolated and stored, pointing to the strong stabilization effect of the two α -nitrogen atoms. Steric protection of the divalent M center by the bulky alkyl or aryl groups on N also contributes to the unusual kinetic stability of **102a-c** and **103a-c** metallylenes.



Interesting trends in the structures and ΔE_{ST} values of the **102d** series, as a function of M, were calculated [B3LYP/6-31G(d)]⁴²⁷. Thus, for **102d**, $M = \text{C}$, the C–N distance shortens and the NCN angle widens on going from the singlet to the triplet state. In contrast, for $M = \text{Si}$ and Ge the M–N bond is longer and the NMN angle smaller in the triplet state than in the singlet state. ΔE_{ST} decreases in the order (in kcal mol^{-1}): $\text{C}(82) > \text{Si}(60) > \text{Ge}(50)$. This behavior contrasts with the general behavior of noncyclic MR_2 metallylenes for which the M–R bonds are shorter and the RMR angle is wider in the triplet state than in the singlet state, and ΔE_{ST} follows the order (in kcal mol^{-1}): $\text{C}(\text{NH}_2)_2(51) < \text{Si}(\text{NH}_2)_2(55) \approx \text{Ge}(\text{NH}_2)_2(56)$ (see also the trends for MH_2 and MX_2 , X = halogen in Table 37). The opposite trends found for $M(\text{NH}_2)_2$ and for **102d** were attributed⁴²⁷ to the change in the order of the molecular orbitals of **102**, when C is replaced by Si or Ge, as shown in Figure 29^{22,427,428}. In the carbene the HOMO is mainly a lone pair of electrons on carbon [$\sigma(\text{C})$], while in the silylene and the germylene the HOMO is a π orbital of the imidazole ring which is composed from the out-of-phase combination of the $\pi(\text{C}=\text{C})$ orbital with the p orbitals on the nitrogens and on M.

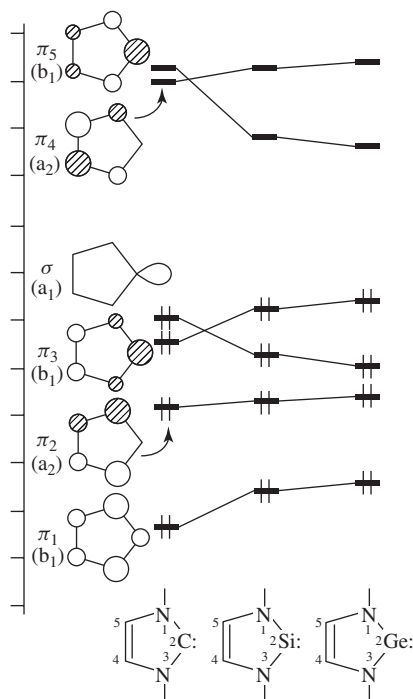


FIGURE 29. A schematic representation of the relative energies of the frontier orbitals of **102d**, M=C, Si and Ge. Reprinted with permission from Reference 427. Copyright (1999) American Chemical Society

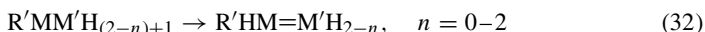
Accordingly, the PE spectra (assigned on the basis of DFT calculations) show that the ionization energy (eV) from the $\sigma(M)$ orbital increases in the order: 7.68 (**102a**, M = C) < 8.21 (**102b**, M = Si) < 8.60 (**102c**, M = Ge)⁴²⁸. In contrast, the ionization energy from the π_3 orbital (see Figure 29) decreases with increasing atomic number of M. In addition, the electron density distribution in the π_3 orbital changes between the three compounds. In the carbene the electron density is concentrated on the C=C double bond, but for Si and Ge the $\pi(C=C)$ contribution decreases and more electron density is localized on the divalent M center⁴²⁸. Imidazol-2-ylidene-type systems (**102**) or their saturated analogs (**103**) with M = Sn or Pb have not yet been studied either by theory or by experiment and their study is desirable.

3. Reactions

In this section we review trends in the reactivity of group 14 metallylenes in a variety of reactions which were studied computationally.

a. 1,2-Hydrogen shifts. 1,2-Hydrogen shifts of carbenes to the corresponding ethylenes (equation 32, M = M' = C) are highly exothermic; e.g. the energy for the rearrangement of H₃CCH (¹A) to H₂C=CH₂ was calculated to be 77.4 kcal mol⁻¹ (66.7 kcal mol⁻¹ for the rearrangement of the ground state triplet carbene)²⁹³ and the reaction barrier was only

0.5–1.5 kcal mol⁻¹^{429a,b}. In agreement with the calculations, singlet methylcarbene has a very short life-time of 500 ps and the activation barrier for its isomerization to ethylene was estimated experimentally to be less than 2.3 kcal mol⁻¹^{429c}. The activation barrier for the 1,2-hydrogen shift was calculated to correlate linearly with the σ_R° substituent constants of the substituent at carbon; e.g. the activation energies are 11.5 kcal mol⁻¹ for CH₃CCl and 27.2 kcal mol⁻¹ for CH₃COMe^{429b}. The heavier metallylenes are much more stable thermodynamically than the corresponding carbenes with respect to 1,2-hydrogen rearrangement, i.e. the isomerization reaction in equation 32 becomes less exothermic (or more endothermic) as M becomes heavier. The barriers for the rearrangement depend both on M and on the substituent M'; e.g. the reaction energies and activation barriers for the rearrangement of HMCH₃ to H₂M=CH₂ are (in kcal mol⁻¹): 2.1 and 44.3, respectively, for HSiCH₃ and 15.9 and 28.9, respectively, for HGeCH₃ (see Table 27 and references cited therein).



Similarly, the reaction energies and the activation barriers for the isomerization of HMOH to H₂M=O (in kcal mol⁻¹) are: 0.2 and 57.2, respectively, for M = Si and 23.8 and 71.7, respectively, for M = Ge (Table 30). Thus, HMOH becomes increasingly more stable relative to H₂M=O, both thermodynamically and kinetically, as M becomes heavier. For further discussion we refer the reader to Sections VI.B.3.a and VI.C.2 (and Tables 27 and 30) where the reverse reaction of equation 32, i.e. the isomerization of M=M' doubly-bonded species to the corresponding metallylenes (equation 25), is discussed.

The reaction energies and the activation barriers for the 1,2-hydrogen shift isomerization of amino- and diamino-metallylenes are gathered in Table 38 (see Table 30 for the reverse reaction). According to the calculations the carbene **102d**, M = C is by 26 kcal mol⁻¹ less stable than the corresponding imidazole (**105**, M = C), and the barrier for this isomerization is high, 46.8 kcal mol⁻¹ which makes **102d**, M = C kinetically stable⁴²⁵. The isomerization energy becomes endothermic, 31.8 and 37.4 kcal mol⁻¹ for **102d**, M = Si and Ge, respectively, and the barriers for the isomerization for both M = Si and M = Ge are above 50 kcal mol⁻¹, making **102d**, M = Si, Ge highly stable both thermodynamically and kinetically. These calculations are consistent with the fact that in the cyclic metallylenes of type **102** and **103** a 1,2-hydrogen rearrangement to the corresponding silaimines or germaimines has not been observed^{23a,b,323,425}. The noncyclic amino metallylenes, **106** and **107**, show a similar behavior to the cyclic metallylene, **102**. The noncyclic aminocarbene (**106**, M = C) and diaminocarbene (**107**, M = C) are by 35.6 and 22.6 kcal mol⁻¹ less stable than the corresponding imines (**108**, M = C and **109**, M = C, respectively) and the barriers for the isomerizations of **106**, M = C to **108**, M = C and **107**, M = C to **109**, M = C are high, 52.6 and 52.1 kcal mol⁻¹, respectively⁴²⁵. In contrast, the aminosilylenes and aminogermaylenes (**106** and **107**, M = Si and Ge) are more stable than their tetravalent imine isomers (**108** and **109**, M = Si, Ge)³²² and their stability increases significantly on changing M from Si to Ge (Table 38). Furthermore, the barriers for the

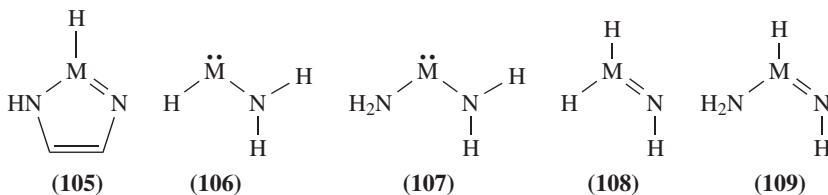


TABLE 38. Reaction energies (ΔE) and activation barriers (E_a) (in kcal mol⁻¹) for the 1,2-hydrogen shift isomerization of amino- and diamino-metallylenes

Reaction	M = C ^a		M = Si ^b		M = Ge ^b	
	ΔE	E_a	ΔE	E_a	ΔE	E_a
102d \longrightarrow 105	-26.0 ^c	46.8 ^c	31.8	54.4	37.4 ^d	54.3 ^d
106 \longrightarrow 108	-35.6	52.6	14.2	68.8	32.6	77.8
107 \longrightarrow 109	-22.6	52.1	19.2	70.0	40.7	81.3

^aAt CISD+Q/TZ2P//HF/TZ2P; from Reference 425.

^bAt CCSD(T)/6-31G(d,p) (ECP for Ge and Si)//HF/6-31G(d,p) (ECP for Ge and Si); from Reference 322.

^c $\Delta E = -27.0$ kcal mol⁻¹, $E_a = 44.1$ kcal mol⁻¹, at MP4/6-311G(d,p)//MP2/6-31G(d); from Reference 323.

^dThe data given are for a non-planar 2-germainidazole (a planar **105**, M = Ge could not be located as a minimum)³²².

1,2-hydrogen rearrangement, E_a , are very high, being 68.8 and 77.8 kcal mol⁻¹ for the rearrangement of **106**, M = Si and Ge to **108**, M = Si and Ge, respectively and 70.0 and 81.3 kcal mol⁻¹ for the rearrangement of **107**, M = Si and Ge to **109**, M = Si and Ge, respectively (at CCSD(T)DZP, Table 38)³²².

b. Insertion and addition reactions. i. Insertion into H₂. The insertion of MH₂ into H₂ (equation 33) is the reverse of the reaction for H₂ elimination from MH₄ (equation 5), which was discussed in detail in Section V.A.3. The reaction energies and the activation barriers for reaction 5 are given in Table 4 and they are used here to calculate the energetic data for equation 33. The insertion of SiH₂ into the H-H bond is highly exothermic, by *ca* 57 kcal mol⁻¹ (Table 4). However, the exothermicity of the insertion reaction decreases as M becomes heavier and for M = Pb it is endothermic by *ca* 10 kcal mol⁻¹. The activation barrier for the insertion of MH₂ into H₂ increases with the mass of M, from a barrierless reaction for CH₂^{128b} through a small barrier of 5 kcal mol⁻¹ for SiH₂, to higher barriers of 20.3, 37.7 and 53 kcal mol⁻¹ [at CCSD(T)/ECP] for the insertion into H₂ of GeH₂, SnH₂ and PbH₂¹⁰⁵, respectively, reflecting the higher stability of the divalent species as M becomes heavier.



The geometries of the transition structures for the insertion reaction are given in Figure 3b. Calculations for the insertion of SiH₂ and GeH₂ into H₂ show that the first reaction step involves the formation of a loose intermediate complex, **110**, and this step is followed by a hydrogen shift via an unsymmetrical transition state (Figure 3b). This mechanism, which is shown schematically by the PES in Figure 30, is supported by recent gas-phase experiments of the insertion of GeH₂ into H₂⁴³⁰ and was also suggested by previous calculations for M = Si^{111,130a,431,432}. The intermediate complex (**110**) is only half as strongly bound for GeH₂ ($\Delta E_c = -2.1$ kcal mol⁻¹) than for SiH₂ ($\Delta E_c = -3.8$ kcal mol⁻¹). The calculated activation energies are 3 kcal mol⁻¹ (1.7 kcal mol⁻¹¹¹¹) and 13.9 kcal mol⁻¹ for SiH₂ and GeH₂, respectively, in good agreement with the experimentally determined values of 1.7 kcal mol⁻¹⁴³³ and 15–20 kcal mol⁻¹⁴³⁰, respectively. The calculated reaction energies, ΔH_r , are -54.0 and -38.3 kcal mol⁻¹ for SiH₂ and GeH₂, respectively [all the above-quoted values are calculated at QCISD(T)/6-311G++(3df,2pd)//QCISD/6-311G(d,p)]⁴³⁰.

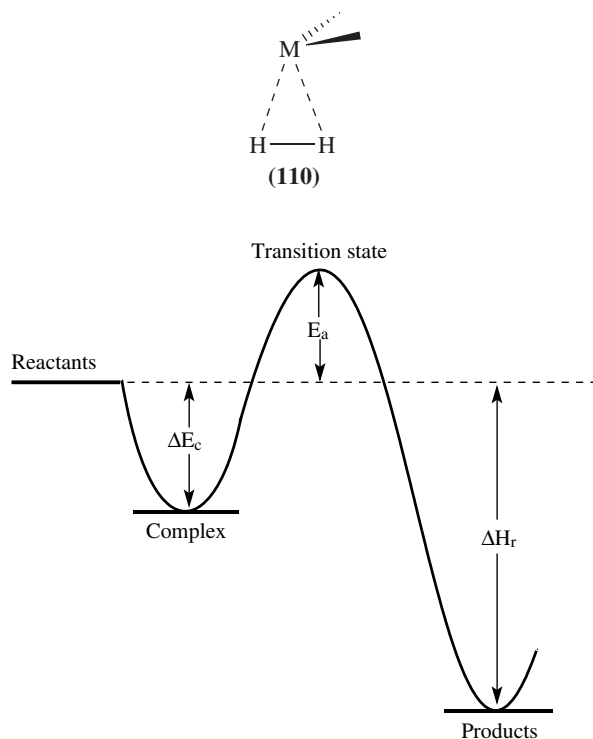
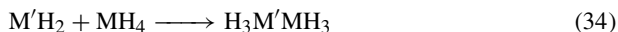
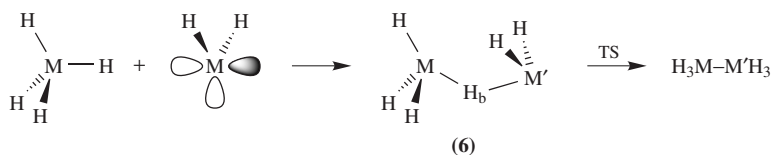


FIGURE 30. A schematic drawing of the energy profile for insertion and addition reactions of metallylenes

The high stability of the cyclic metallylenes **102d**, $M = \text{Si}$ and Ge is reflected in their low heats of hydrogenation which are $-9.8 \text{ kcal mol}^{-1}$ (exothermic) for **102d**, $M = \text{Si}$ and $23.2 \text{ kcal mol}^{-1}$ (endothermic) for **102d**, $M = \text{Ge}$, compared to the highly exothermic energies of -61.2 and $-32.5 \text{ kcal mol}^{-1}$ for the hydrogenation of SiH_2 and GeH_2 , respectively [MP4/6-311G(d,p)//MP2/6-31G(d)]³²³.

ii. Insertion into M–H bonds. The insertion of $M'H_2$ into $M-H$ bonds, where M and M' are both group 14 elements (equation 34), occurs via the initial formation of a $\text{H}_2M' \cdots \text{H}-\text{MH}_3$ complex (**6**) which rearranges to $\text{H}_3M'\text{MH}_3$, as shown in Scheme 3. This mechanism was supported by both experiments and calculations^{145,434–438}. A detailed discussion on the structure and energy of **6** relative to $\text{H}_3\text{MM}'\text{H}_3$, for the cases where $M = M'$, can be found in Section V.B.3.c, Table 9 and Figure 6. Structure **6** is a bound complex for all M , but it is very weakly bound for $M = M' = \text{C}$ [$1.1 \text{ kcal mol}^{-1}$ at MP4/DZP//HF/DZP¹⁴⁵, $2.1 \text{ kcal mol}^{-1}$ at QCISD(T)/6-311+G(2df,p)//QCISD(T)/6-31G(d)⁴³⁸]. However, the stability of **6** increases as M becomes heavier, because the increasing polarity of the $M-H_b$ bond in the direction $M^+-H_b^-$, makes the complexation of $M'H_2$ stronger, reaching $9.1 \text{ kcal mol}^{-1}$ for $M = M' = \text{Pb}$ ¹⁴⁵.





SCHEME 3

The energy profiles for the insertion of MH_2 into MH_4 are shown schematically in Figure 31. The binding energies of **6** relative to $MH_4 + M'H_2$ ($M = M'$) (not shown in Figure 31) are from 5 kcal mol^{-1} (for Si and Ge) to 9.8 and $9.1 \text{ kcal mol}^{-1}$ (for Sn and Pb, respectively) (at MP4/DZP//HF/DZP). The second step of the insertion reaction, the rearrangement of **6** to $H_3MM'H_3$ ($M = M'$), becomes less exothermic as M becomes heavier, and it changes from $-110 \text{ kcal mol}^{-1}$ for C to $-48 \text{ kcal mol}^{-1}$ for Si and to only -9 kcal mol^{-1} for Pb¹⁴⁵. The lower exothermicity of the insertion reaction of the heavier group 14 elements is accompanied by an increase in the reaction activation barrier. Thus, the insertion of CH_2 and SiH_2 into methane and silane, respectively, are essentially barrierless^{145,436,437} (for the insertion of the more stable $SiMe_2$ into silane, a barrier of $7.8 \text{ kcal mol}^{-1}$ is calculated⁴³⁷). The activation barriers for the insertion of GeH_2 into GeH_4 and of SnH_2 into SnH_4 are also very small, 1.0 [$-4.0 \text{ kcal mol}^{-1}$ at G2//MP2/6-311G(d,p)⁴³⁵, i.e. the minus sign indicates a negative activation energy relative to the reactants] and $2.6 \text{ kcal mol}^{-1}$, respectively. The small negative activation barrier for the insertion of H_2Ge into H_4Ge is consistent with the decrease in the measured rate constant upon increasing the reaction temperature⁴³⁵. However, the activation barrier increases to $11.0 \text{ kcal mol}^{-1}$ for the insertion of PbH_2 into PbH_4 (at MP4/DZP//HF/DZP)¹⁴⁵.

Insertion of SiH_2 and GeH_2 into a C–H bond of CH_4 also proceeds via the formation of an initial complex **6**, $M = C$, $M' = Si, Ge$ and the activation barrier is relatively large, i.e. 22.1 ⁴³⁹ and 33.2 ¹³¹ kcal mol^{-1} (relative to the reactants), respectively. The activation barrier for the insertion of Me_2Ge into CH_4 is $39.1 \text{ kcal mol}^{-1}$, by 6 kcal mol^{-1} higher than for GeH_2 ¹³¹. The activation energy for the insertion of $GeMe_2$ into SiH_4 is much smaller, $15.7 \text{ kcal mol}^{-1}$ ⁴⁴⁰ (Table 39).

In agreement with the qualitative configuration mixing model, described in subsection iii below, Su and Chu found a relatively good linear correlation connecting ΔE_{ST} of the metallylene with the activation barriers and the reaction energies for the insertion into CH_4 of various substituted germynes, $GeRR'$, $R = H$, $R' = CH_3, F, Cl, Br$ and $R = R' = CH_3, F, Cl, Br$ as well as for germylidene $H_2C=Ge$ ⁴⁴¹. Substituents which decrease the ΔE_{ST} of $GeRR'$, such as π -acceptors or electropositive substituents, cause a lower activation energy and a larger exothermicity for the insertion of $GeRR'$ into C–H bonds. The opposite trend is expected according to this correlation for π -donors or electronegative substituents which increase ΔE_{ST} . Steric effects also contribute to the insertion activation barrier, but it was concluded that the electronic factors, rather than steric factors, play the decisive role in determining the chemical reactivity of germynes⁴⁴¹.

The insertion reactivity of cyclic metallylenes **102d** toward CH_4 also decreases in the order $M = C > M = Si > M = Ge$, i.e. E_a and ΔH_r (kcal mol^{-1}), respectively, are: 56.4 ; -8.7 for **102d**, $M = C$; 77.8 ; -1.0 for **102d**, $M = Si$ and 86.5 ; 19.4 for **102d**, $M = Ge$ ⁴²⁷. These very high barriers and low reaction exothermicities (and even endothermicity for $M = Ge$) are in agreement with the high stability of these cyclic metallylenes.

iii. *Insertion into X–H σ -bonds.* The insertion of metallylenes into X–H bonds ($X = N, O, F, P, S, Cl$, equation 35) follows in general the mechanism shown in Figure 30^{7,440,442}.

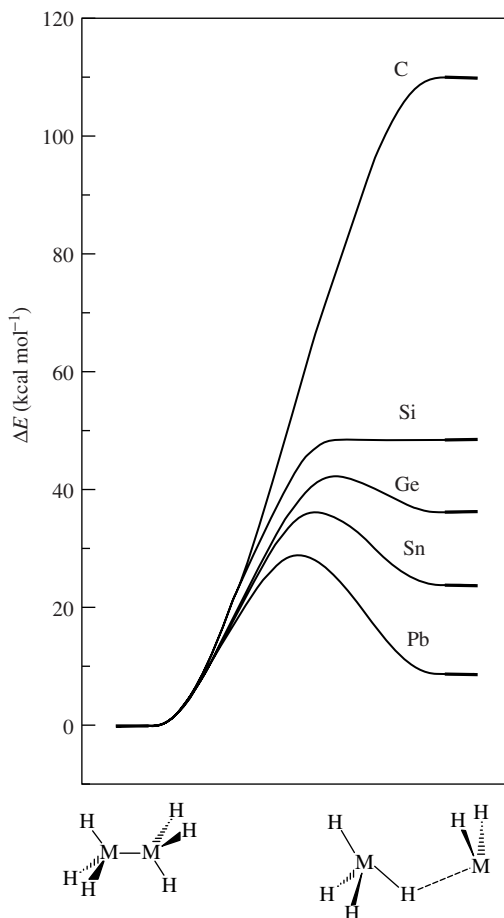


FIGURE 31. Energy profiles for the rearrangement of the intermediate complex $\text{H}_2\text{M}\cdots\text{H}_b\text{-MH}_3$ (**6**) in the insertion reaction of MH_2 into MH_4 to produce H_3MMH_3 (calculated at MP4/DZP//HF/DZP). Adapted from Reference 145

The reaction energies for the insertion of H_2Si and Me_2Ge into various X-H bonds are given in Table 39. It would have been desirable to compare the insertion reactions of SiH_2 with those of GeH_2 , but unfortunately such data are not available. GeMe_2 is expected to be less reactive than GeH_2 (i.e. to have higher E_a and less exothermic ΔH_f), and this fact should be kept in mind when comparing the data in Table 39 for SiH_2 and GeMe_2 . Unfortunately, calculations for the addition of SnH_2 and PbH_2 are also not available for comparison.



The first step in the reaction of MH_2 with the X-H bond is the formation of a complex (Figure 30) as was the case in the reaction with an M-H bond. However, as X possesses a lone pair of electrons, complexation occurs with the lone pair as shown in **111** [rather

TABLE 39. Relative energies (kcal mol⁻¹) for equation 34 and equation 35^a

H–MH ₃ or H–XH _{n-1}	H ₂ Si ^b			Me ₂ Ge ^c		
	ΔE_c	E_a	ΔH_r	ΔE_c	E_a	ΔH_r
CH ₄	—	22.1 ^d [17–19] ^d	-49.8 ^d	-0.02 ^e (-1.1)	39.1 ^e (35.6)	-25.1 ^e (-32.6)
SiH ₄	-7.4 ^{f,g} -1.6 ^h	-6.9 ^{f,g} 7.8 ^h	-56.4 ^{f,g} -51.8 ^h	-0.6 (-2.2)	15.7 (11.4)	-33.8 (-41.3)
NH ₃	-25.1	13.2	-60.0	-20.8 (-25.0)	25.1 (22.7)	-33.3 (-40.4)
H ₂ O	-13.3	8.7	-70.2	-13.9 (-16.9)	14.8 (15.1)	-45.1 (-50.2)
HF	-7.0	2.7	-84.3	-7.2 (-7.1)	4.7 (9.6)	-59.1 (-61.2)
PH ₃	-17.5	2.2	-53.1	-9.0 (-14.1)	11.7 (8.1)	-37.4 (-46.1)
H ₂ S	-8.6	4.8	-60.2	-6.1 (-9.7)	6.0 (3.9)	-45.8 (54.9)
HCl	-1.8	5.9	-68.8	-1.6 (-3.7)	1.2 (2.5)	-56.4 (-64.2)

^a See Figure 30 for definitions. The reactants are placed at 0.0 kcal mol⁻¹

^b At MP4SDTQ/6-31G(d,p)//HF/6-31G(d); from Reference 442.

^c At B3LYP/6-311G(d) [MP2/6-311G(d,p) values are given in round brackets]; from Reference 440.

^d At MP4SDTQ/6-311G(d,p)//MP2/6-31G(d)+ZPE; from Reference 439; experimental value (from Reference 130b) is given in square brackets.

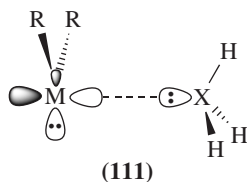
^e The corresponding values for the insertion of GeH₂ into CH₄ are [in kcal mol⁻¹, at B3LYP/6-311G(d)]: $\Delta E_c = -0.94$, $E_a = 33.2$, $\Delta H_r = -28.0$ ³¹. See also Reference 105.

^f At MP4/6-31G(d,p)//MP2/6-31G(d,p); from Reference 437.

^g At MP2/6-311G(d,p), $\Delta E_c = -12.3$, $E_a = -11.6$, $\Delta H_r = -56.4$, in kcal mol⁻¹; from Reference 436.

^h For the insertion of SiMe₂, at MP4/6-31G(d,p)//MP2/6-31G(d,p); from Reference 437.

than with the $\sigma(M-H)$ electrons in **6**], and the resulting complex, **111**, is therefore more strongly bound than with MH₄. The intermediate complex, **111**, can be described as a donor (lone pair on X)–acceptor (empty p orbital of MR₂) complex. The depth of the well in which **111** resides (ΔE_c) is affected by the energy difference between the donor's HOMO and the acceptor's LUMO and the overlap between them which is determined largely by steric effects⁴⁴⁰.



The following trends can be extracted from the data in Table 39: (a) The binding energy (in kcal mol⁻¹) of the complex ($-\Delta E_c$) for M = Si and Ge, respectively, decreases in the order: M–N (21 to 25) > M–O > M–F (ca 7); M–P(9 to 17) > M–S > M–Cl (1.8 to 1.6), and it is smaller when X is a second-row element than when it is a first-row element. (b) The activation barrier for the insertion step, E_a , ranges between 25.1 kcal mol⁻¹ for

$\text{Me}_2\text{Ge} + \text{NH}_3$ to only 1.2 kcal mol⁻¹ for $\text{Me}_2\text{Ge} + \text{HCl}$. E_a decreases as a function of X, in the order $\text{NH}_3 > \text{H}_2\text{O} > \text{HF}$ and it is significantly smaller when X is a second-row element, e.g. $E_a(\text{NH}_3) > E_a(\text{PH}_3)$. (c) All activation barriers calculated for the insertion of GeMe_2 (except for the reaction with HCl) are larger than those calculated for SiH_2 ^{440,442}.

The trends in the activation barriers were explained^{440,442} using the valence bond configuration mixing model^{443,444}, as shown schematically in Figure 32a. According to this

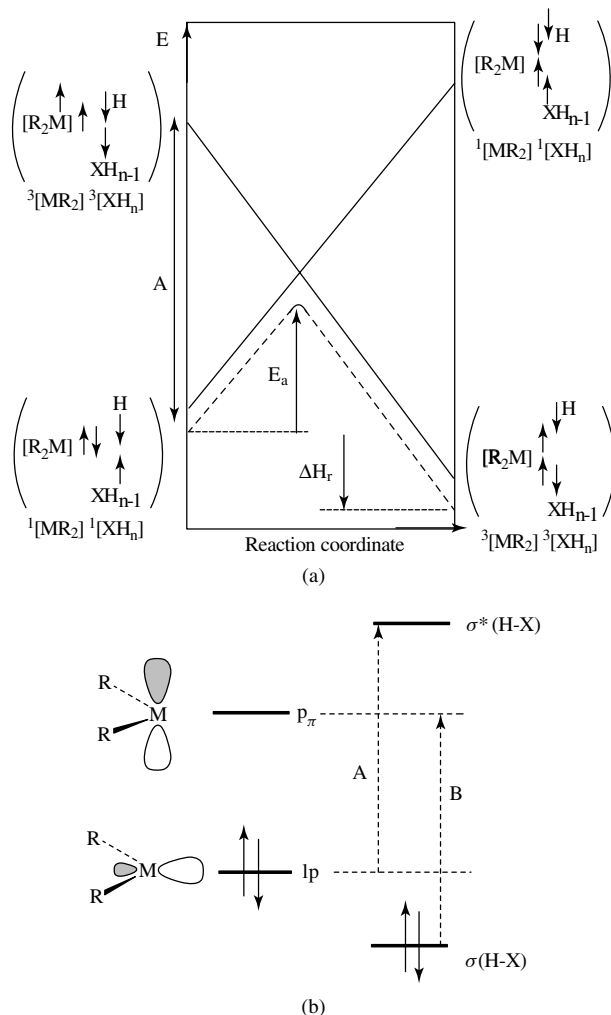
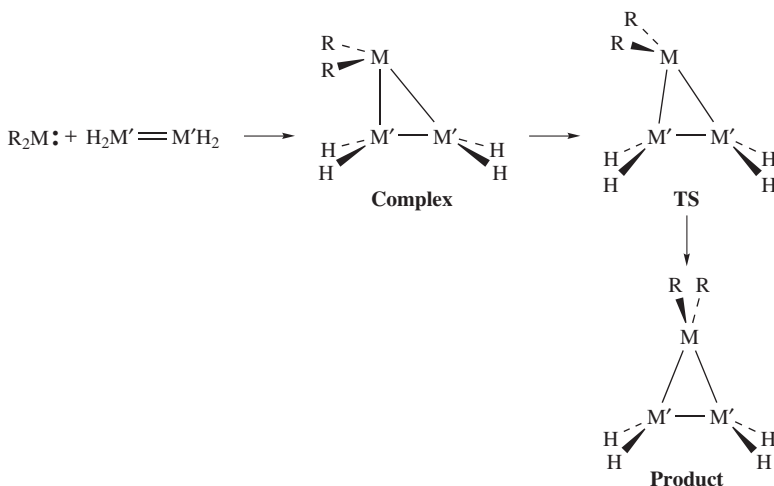


FIGURE 32. (a) A schematic configuration mixing diagram for the insertion of MR_2 into XH_n . A is the energy gap between the singlet and triplet configurations of the reactants. Adapted from Reference 440. (b) Dominant orbital interactions in the transition state of the insertion reactions of MR_2 into a X–H bond. Based on the discussion in Reference 431

model the reaction barrier (E_a) and the heat of reaction (ΔH_r) are proportional to the excitation energy of an electron in the $\sigma(X-H)$ orbital of XH_n (singlet configuration) to the triplet $\sigma^*(X-H)$ configuration + the ΔE_{ST} of the metallylene. Thus, if ΔE_{ST} is a constant and the $\sigma(X-H) \rightarrow \sigma^*(X-H)$ excitation energy is reduced, then the curve crossing occurs at a lower energy, leading to a lower activation barrier and to a higher reaction exothermicity. On the other hand, if ΔE_{ST} of MR_2 is increased, either by changing M or by changing the substituents R, the barrier is expected to become higher and the exothermicity is expected to decrease^{440,441} (and vice versa). The observed trends can also be explained by a simple perturbation molecular orbital model as shown schematically in Figure 32b. According to this model, the dominant interactions in the transition state are: (a) a two-electron stabilizing interaction between the lone pair (lp) of the metallylene and the $\sigma^*(X-H)$ orbital (interaction A in Figure 32b) and (b) a two-electron stabilizing interaction between the empty p orbital of the metallylene and the $\sigma(X-H)$ orbital (interaction B in Figure 32b). According to this model, increasing either the lp-p energy difference (i.e. ΔE_{ST}) or the $\sigma-\sigma^*$ splitting (e.g. by changing X from a first-row to a second-row element) will reduce the stability of the transition state and increase the insertion barrier⁴³¹.

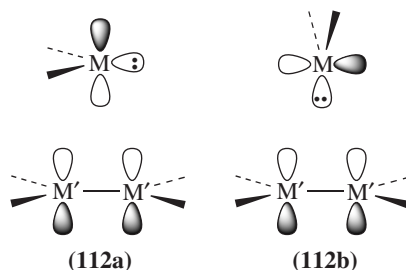
iv. Addition to double bonds. The addition of the heavier MR_2 analogs to double bonds proceeds in general according to the mechanism described in Scheme 4 and Figure 30. The thermochemistry of the reverse reaction, i.e. the elimination of $M''H_2$ from $c-H_2MH_2M'H_2M''$ (M, M' and M'' are group 14 elements), was discussed in Section V.E.1.a.iii.



SCHEME 4

The initial step of the addition reaction proceeds along the non-least-motion C_s path (cf. **112a**) in which the empty p orbital of MR_2 interacts initially with the filled π orbital of the $M'=M'$ bond ('electrophilic phase'). This step is followed by a 'nucleophilic phase' in which the lone pair on MR_2 interacts with the π^* orbital of the $M'=M'$ bond^{207,445-447}. The more symmetric C_{2v} least-motion ' σ -approach' (**112b**) is forbidden according to orbital symmetry rules⁴⁴⁸ and indeed is not followed by any of the MR_2 metallylenes. The calculated structures^{207,445} of the intermediate complexes and transition states support

this description. In Figure 33, we bring for demonstration the structures of the complex, transition state and product of the addition of GeH_2 to C_2H_4 ⁴⁴⁵. The relevant geometries of the complexes and transition states in the reactions of other MR_2 metallylenes with ethylene can be found in References 207 and 445.



The energies of the stationary points on the PES for the addition reactions of metallylenes to ethylene (Scheme 4 $M' = \text{C}$) are given in Table 40 (no data are available for $M = \text{Pb}$).

The addition of singlet carbene to ethylene is highly exothermic i.e. $\Delta H = -103.9 \text{ kcal mol}^{-1}$ [at $\text{MP2/6-31G(d,p)} + \text{ZPE}$ ²⁰⁷; $-98.6 \text{ kcal mol}^{-1}$ ²⁰⁴ at $\text{CCSD/DZ+d/DZ+d} + \text{ZPE}$, exp. $-99.4 \text{ kcal mol}^{-1}$ ⁴⁴⁹]. As M becomes heavier, the exothermicity is reduced considerably, and for H_2Sn the reaction is endothermic by $4.7 \text{ kcal mol}^{-1}$ ²⁰⁷. Electronegative substituents on the metallylene reduce considerably the reaction energy and for most such substituted metallylenes the reaction is highly endothermic^{207,445,450} (Table 40); e.g. ΔH_r values for the addition of GeR_2 to ethylene are [at B3LYP/6-31G(d) , in kcal mol^{-1}]: -27.4 ; $+8.7$; $+11.4$; $+13.8$; $+8.6$ and $+5.5$ for $R = \text{H}$, NH_2 , OH , F , Cl , Br , respectively⁴⁴⁵. ΔH_r for the addition of SnF_2 to ethylene is as high as $+45.3 \text{ kcal mol}^{-1}$ (Table 40)²⁰⁷. ΔH_r for the addition of substituted germylenes to ethylene correlate linearly with the ΔE_{ST} of the germylenes⁴⁴⁵ and the trends in ΔH_r as M becomes heavier can be understood in terms of the DSSE of the metallylene (see equation 15 in Section V.E.1.a.ii)²⁰⁴.

The addition of singlet carbene and silylene to ethylene is calculated^{207,446,450,451} to proceed without the intermediacy of an initial complex and is barrierless, in agreement with experiment^{447,452}. For the heavier M , an intermediate complex is formed and the PES has the general form shown in Figure 30. In general, the barrier required to pass from the complex to the products increases as M becomes heavier. Electronegative substituents at M

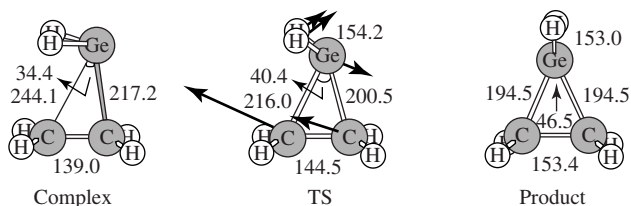


FIGURE 33. Optimized geometries (at B3LYP/6-31G(d)) of stationary points on the PES for the addition of GeH_2 to $\text{H}_2\text{C}=\text{CH}_2$. Bond lengths in pm, angles in deg. The heavy arrows indicate the main atomic motions in the transition state eigenvector. Adapted from Reference 445

TABLE 40. Relative energies and Gibbs free energies (ΔG) (in kcal mol⁻¹) for stationary points on the PES for the addition of metallylenes to ethylene (Scheme 4)^a

MR ₂	ΔH_c	ΔG_c	E_a	ΔG_a	ΔH_r	ΔG_r
CH ₂	<i>b</i>	<i>b</i>	<i>b</i>	<i>b</i>	-103.9	-92.3
SiH ₂	<i>b</i>	<i>b</i>	<i>b</i>	<i>b</i>	-40.1	-28.6
GeH ₂	-10.5; (-23.5 ^c)	-0.4	-7.9; (-21.5 ^c)	3.2	-12.4; (-27.4 ^c)	-1.0
SnH ₂	-7.4	1.4	5.5	16.5	4.7	15.8
CF ₂	-1.3	3.6	14.3	25.0	-44.9	-32.2
SiF ₂	-3.2	3.1	22.4	33.9	-13.1	-1.0
GeF ₂	-2.6; (-8.2 ^c)	3.4	45.5; (27.9 ^c)	57.2	30.5; (13.8 ^c)	42.4
SnF ₂	-3.8	3.9	51.0	62.6	45.3	56.7

^aAt MP4/6-31G(d,p)//MP2/6-31G(d,p)+ZPE; from Reference 207. The given energies are relative to the reactants. ΔG is given at 298.15 K. ΔH_c and ΔG_c are complexation energies, E_a and ΔG_a are activation barriers, ΔH_r and ΔG_r are reaction energies (see Figure 30).

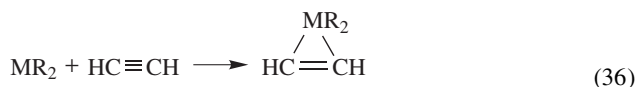
^bThe addition reaction is concerted and barrierless.

^cAt B3LYP/6-31G(d)//B3LYP/6-31G(d); from Reference 445.

reduce the depth of the complex well and increase the activation energy (Table 40)^{207,445}, making the addition reaction slower. Sakai concluded, based on a CAS/LMO/CI analysis, that most of the activation energy is controlled by the energy difference between the singlet ground state and the first excited singlet of the metallylene, $\Delta E(^1A_1 - ^1B_1)$ ²⁰⁷. A linear correlation was found between the ΔE_{ST} of GeR₂ (R = CH₃, NH₂, OH, F, Cl, Br) and both the activation energy and the heat of the reaction for the addition of these germlylenes to ethylene⁴⁴⁵. The correlation was explained⁴⁴⁵ using a configuration mixing model along the lines shown in Figure 32a. This correlation is in line with Sakai's conclusion²⁰⁷, as the $^1A_1 - ^1B_1$ energy difference of the metallylene is very similar to its ΔE_{ST} .

Changing the substrate from ethylene to disilene (Scheme 4, M' = Si) or digermene (Scheme 4, M' = Ge) increases the exothermicity of the reaction (Table 41). For each H₂M, M = C, Si, Ge the addition to H₂Si=SiH₂ is more exothermic than the addition to H₂Ge=GeH₂ (Table 41)²⁰⁴. In these reactions the complexes and transition states were not studied.

v. *Addition to acetylene.* The reaction enthalpies and activation barriers for the addition of MR₂ (M = C, Si, Ge, Sn; R = H, F) to acetylene (equation 36)⁴⁵³ are given in Table 42

TABLE 41. Relative reaction energies (kcal mol⁻¹) for the addition of MH₂ to H₂M'=M'H₂ (Scheme 4)^a

MH ₂	H ₂ C=CH ₂	H ₂ Si=SiH ₂	H ₂ Ge=GeH ₂
CH ₂	-98.6	-120.3	-100.1
SiH ₂	-43.2	-62.3	-57.3
GeH ₂	-18.3	-52.5	-47.1

^aEnergies given are relative to the energy of the reactants. Calculated at CCSD/DZ+d//HF/DZ+d; from Reference 204.

TABLE 42. Reaction enthalpies and activation energies (in kcal mol⁻¹) for the addition of MR₂ to acetylene (equation 36)^{a,b}

MR ₂	ΔH_r	E_a
CH ₂	-101.5 (-95.6)	-2.8 (-2.3)
SiH ₂	-56.8 (-50.4)	-18.2 (-15.1)
GeH ₂	-20.0	-20.0
SnH ₂	-12.5	-7.3
CF ₂	-47.2 (-44.9)	14.1 (13.0)
SiF ₂	-40.9 (-27.3) ^c	14.3 (17.8) ^c
GeF ₂	14.4	38.4
SnF ₂	16.5	27.5

^aAll values are relative to the energy of the reactants; from Reference 453.

^bAt MP2/3-21G(d)//3-21G(d), the numbers in parentheses are at MP4SDTQ/6-31G(d,p)//HF/3-21G(d). All values are corrected to 298 K.

^c ΔH_r and E_a at CCSD(T)/6-31+G(d)//MP2/6-31G(d) are: -22 and 23.9 kcal mol⁻¹, respectively⁴⁵⁶.

Two major trends are observed: (a) the reaction exothermicity decreases steadily as one proceeds from C to Sn for both MH₂ and MF₂ (for GeF₂ and SnF₂ the reaction is endothermic). (b) The exothermicity of the addition reaction is always lower for MF₂ than for the corresponding MH₂. The major contributors to these trends are: (a) a parallel increase in the stability of MH₂ and a decrease in the stability of the product ring compound (due to weakening in the M–C bonds) as M becomes heavier, and (b) increase in the stability of MR₂ upon fluorine substitution (this effect dominates over the strengthening of the M–C bonds in the product caused by fluorine substitution)⁴⁵³.

The transition states for the addition of MH₂ (M = Si, Ge and Sn) to acetylene to form the corresponding metallacyclopropenes are all lower in energy than the energies of the reactants (Table 42). This was attributed to the existence of long-range acetylene...MH₂ van der Waals complexes, although such species were not located computationally⁴⁵³. It was concluded that for MH₂ reaction 36 proceeds spontaneously and without a barrier, in agreement with experimental findings for the addition of SiH₂⁴⁵⁴ and GeH₂⁴⁵⁵ to acetylene. In contrast, the addition reactions of all fluorinated metallylenes, MF₂, to acetylene are predicted to have substantial barriers which change in the order M = C (14.1 kcal mol⁻¹) ~ Si < Ge (38.4 kcal mol⁻¹) > Sn (Table 42)⁴⁵³.

Comparing the data for the addition of MR₂ to ethylene (Table 40) with that for the addition of MR₂ to acetylene (Table 42) shows that: (a) The trends in the reactivity of both MH₂ and MF₂ in the two reactions are similar; e.g. the addition of all MH₂ to both ethylene and acetylene is barrierless (or has a negative E_a) and the activation energy of the addition of MF₂ increases in both reactions as M becomes heavier. ΔH_r for both reactions becomes less exothermic (or more endothermic) as the mass of M increases. (b) In general the activation barriers are smaller for the addition of MR₂ to acetylene than to ethylene, and the former reactions are also more exothermic (or less endothermic) than the corresponding additions to ethylene.

In conclusion, for both the insertion and addition reactions of MH₂, the reaction enthalpy and the reaction activation barrier correlate with the metallylene's ΔE_{ST} , pointing to a decrease in the metallylene reactivity as M becomes heavier and when the metallylene is substituted by electronegative substituents which increase ΔE_{ST} (Table 37). According to these trends, plumblylenes and especially plumblylenes substituted with electronegative

substituents are expected to be quite inert and significantly more so than their lighter analogs. This explains why HPbOH does not undergo insertion or addition reactions, comparable to those of its lighter HMOH congeners (including Sn), which add hydrogen (i.e. insert into the H–H bond), trimerize to form $(\text{H}_2\text{MO})_3$ or polymerize³¹⁶.

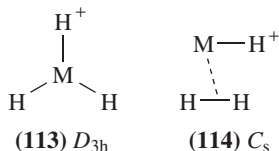
B. Tricoordinated Compounds

In this section we will review mainly the theoretical studies of tricoordinated MR_3 cations, anions and radicals of group 14 elements. Relevant experimental data will be mentioned briefly to supplement and complete the theoretical discussion.

1. Tricoordinated cations

Silylium (or silicinium) cations, SiR_3^+ have been the subject of many theoretical and experimental studies over the last few decades. These studies were reviewed extensively by Apeloig⁷, Maerker and Schleyer^{4,28b}, Lickiss^{28c}, Reed^{28d}, Houk⁴⁵⁷ and Lambert and coworkers⁴⁵⁸. Much effort throughout about half a century were made to synthesize ‘free’ tricoordinate silyl cations in the condensed phase (or in the solid), i.e. cations which do not have strong interactions with the solvent and the counterions^{28b–d,457,458}. Only recently were these experiments successful⁴⁵⁹. The synthetic efforts are now being extended to cations of heavier congeners of silicon. However, the number of such studies is still limited and those are reviewed by Zharov and Michl⁴⁶⁰.

a. Structures. The planar D_{3h} structure, **113**, is a minimum on the PES of MH_3^+ cations for all group 14 elements^{57,114,461,462}. However, a C_s side-on complex $\text{HM}^+ \cdots \text{H}_2$, **114**, was also located on the MH_3^+ PESs⁴⁶¹, except for CH_3^+ where **114** does not exist and only a weakly bound van der Waals $^+\text{C}-\text{H} \cdots \text{H}_2$ complex was located. The calculated structures and relative energies of MH_3^+ cations are presented in Table 43. **114** is a high-lying local minima for $\text{M} = \text{Si}$ and Ge , but it is the most stable structure for SnH_3^+ and PbH_3^+ , i.e. $\text{HPb}^+ \cdots \text{H}_2$ (**114**, $\text{M} = \text{Pb}$) is more stable than PbH_3^+ (**113**, $\text{M} = \text{Pb}$) by $23.3 \text{ kcal mol}^{-1}$ (Table 43)⁴⁶¹. The large preference of the side-on complex for $\text{M} = \text{Pb}$ is due to relativistic effects which stabilize the 6s lone pair on $\text{H}-\text{Pb}^+$. The side-on complexes, **114**, can be described as donor–acceptor complexes in which the LUMO of the HM^+ cationic fragment is populated whereas the HOMO of dihydrogen is depopulated⁴⁶².



The dissociation energy, ΔE , of MH_3^+ (D_{3h}) to MH^+ and H_2 decreases down group 14 and the reaction becomes exothermic for $\text{M} = \text{Sn}$ and Pb (Table 43). However, as this dissociation proceeds through the side-on complex intermediate, **114**, it has to overcome a high activation barrier (E_a) of *ca* 50 kcal mol^{-1} ⁴⁶¹. The planar MH_3^+ (D_{3h}) cations are thus kinetically stable even for $\text{M} = \text{Sn}$ and Pb and are therefore predicted to be observable. The side-on complexes are less stable than the D_{3h} isomer toward expulsion

TABLE 43. Relative energies (kcal mol⁻¹) and geometries (pm, deg) of MH₃⁺ isomers^a

MH ₃ ⁺	Isomer	Relative energy	d(M–H)	d(H–H) ^b	d(M···H ₂) ^c
CH ₃ ⁺	113	0.0	109.1		
	CH···H ₂ ^{+d}	128.8	114.5	74.9	307.4 ^e
	ΔE^f	130.7			
SiH ₃ ⁺	113	0.0	146.8		
	114	27.1	151.4	78.2	198.3
	ΔE^f	34.7			
	E_a^g	57.8			
GeH ₃ ⁺	113	0.0	152.4		
	114	10.0	159.1	77.3	212.1
	ΔE^f	16.3			
	E_a^g	51.3			
SnH ₃ ⁺	113	0.0	168.9		
	114	-5.2	176.5	75.9	248.6
	ΔE^f	-2.3			
	E_a^g	52.9			
PbH ₃ ⁺	113	0.0	171.9		
	114	-23.3	181.7	75.6	261.9
	ΔE^f	-22.2			
	E_a^g	44.7			

^aAt B3LYP/6-311++G(2d,2p) (quasi-relativistic ECP for Sn and Pb); from Reference 461.

^bd(H–H) in free H₂ is 74.3 pm.

^cThe distance between the H₂ midpoint and M.

^dA side-on complex (**114**) does not exist. Only a weakly bound C_{2v} van der Waals C–H···H₂⁺ complex was located.

^eThe C–H···H₂ distance is 192.9 pm.

^fThe relative energy of the MH⁺ + H₂ fragments.

^gThe activation barrier for the isomerization of **113** to **114**.

of H₂, having dissociation energies (in kcal mol⁻¹) of: 7.6 (**114**, M = Si), 6.3 (**114**, M = Ge), 2.9 (**114**, M = Sn) and 1.1 (**114**, M = Pb). Thus, the HSi⁺···H₂ and HGe⁺···H₂ complexes are the most promising targets for experimental observation⁴⁶¹. As expected, the stronger the interaction between MH⁺ and H₂, the higher the observed elongation of the H–H bond (Table 43).

Trinquier investigated the PESs of the H₃MMH₂⁺ cations for all group 14 elements^{145,463} and they are shown schematically in Figure 34. The carbon-containing system has a single deep minimum on the PES, while the heavier analogs have several local minima. In addition to the classical localized H₃M–MH₂⁺ C_s structure (**115**) and the C_{2v}-bridged structure (**116**), two new minima were located for all heavier group 14 M₂H₅⁺ cations: the doubly hydrogen-bridged (**117**) and the singly hydrogen-bridged (**118**) structures (H_b is the bridging hydrogen). The geometries and relative energies of **115**–**118** are given in Table 44 and their three-dimensional structures are shown schematically in Figure 35. The bridged structures **117** and **118** can be described as complexes of MH₄ units interacting with a MH⁺ fragment via one (i.e. **118**) or two (i.e. **117**) M–H bonds⁴⁶³. The bridged C_{2v} **116** is the global minimum for M = C, being by 7.6 kcal mol⁻¹ more stable than the classical structure **115**. For M = Si, isomers **115** and **116** are nearly degenerate and are the lowest in energy on the PES, with a

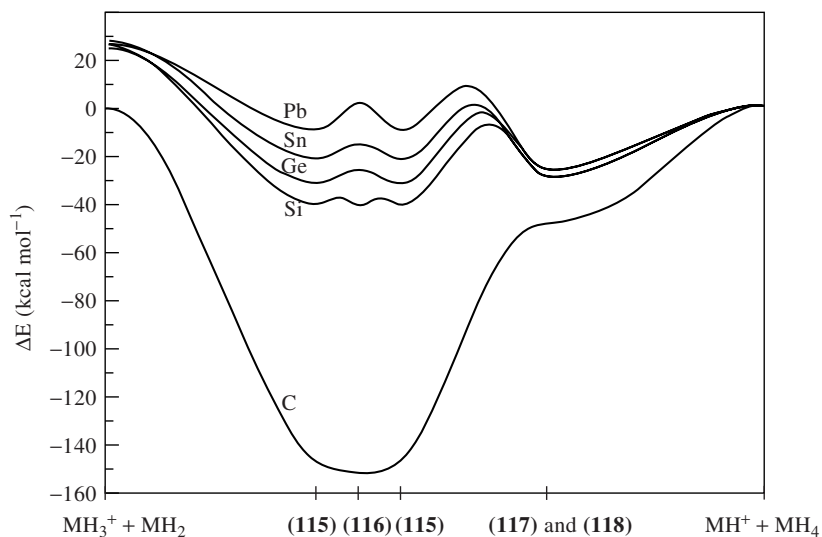
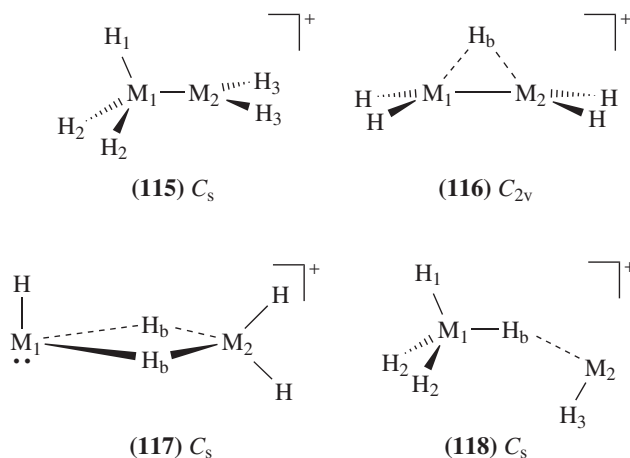


FIGURE 34. A schematic drawing of the $M_2H_5^+$ PESs calculated at MP4/DZP. Adapted from Reference 463



small activation barrier of $2.8 \text{ kcal mol}^{-1}$ that separates between them (MP4/DZP). **115** is the global minimum for $M = \text{Ge}$, while the bridged structures **117** and **118** are favored for tin and lead (Table 44, Figure 34). This trend was rationalized by the increasing propensity of the heavier elements of group 14 for lower oxidation states (e.g. MH^+ has oxidation state II). The doubly hydrogen-bridged $M_2H_5^+$ species (**117**) are in all cases more stable than the singly bridged (**118**) isomers, but only by $2\text{--}4 \text{ kcal mol}^{-1}$ (Table 44). The activation barriers that connect **115** with **117** are in the range of $29\text{--}34 \text{ kcal mol}^{-1}$ for $M = \text{Si}$ to $M = \text{Pb}$. The dissociation energies of **117** and **118** isomers into MH_4 and MH^+ are almost constant for $M = \text{Si}$ to Pb , at $25\text{--}30 \text{ kcal mol}^{-1}$ ⁴⁶³ — a value close

TABLE 44. Geometries and relative energies on the $M_2H_5^+$ potential energy surface^a

$M_2H_5^+$	(115) C_s	(116) C_{2v}	(117) C_s (dibridged)	(118) C_s (monobridged)	$MH_3^+ + MH_2$	$MH_4 + MH^+$
$C_2H_5^+$	ΔE^b 0.0 ^c d(M–M) 141.8 d(M–H) 113.6; 108.9 ^e $\angle MH_bM$	<u>–7.6</u> <u>137.5</u> 131.7 ^f 62.9	95.3 ^d 163.8 119.7; 134.5 ^g 79.6	117.2 ^d — 128.7; 126.9 ^h 173.0	143.1 108.9; 110.6 ⁱ	143.7 109.2; 111.7 ^j
$Si_2H_5^+$	ΔE^b 0.0 d(M–M) 238.8 d(M–H) 146.5; 146.2 ^e $\angle MH_bM$	<u>–0.1</u> <u>218.0</u> 169.6 ^f 80.0	11.9 260.2 153.2; 186.0 ^g 99.8	16.6 — 160.0; 174 174.8	65.30 145.2; 150.8 ⁱ	41.3 147.3; 148.4 ^j
$Ge_2H_5^+$	ΔE^b <u>0.0</u> d(M–M) 256.6 d(M–H) 153.4; 153.7 ^e $\angle MH_bM$	<u>5.3</u> ^d <u>232.9</u> 181.5 ^f 79.8	5.5 286.1 161.0; 208.8 ^g 100.6 ^o	7.8 — 168.3; 185.1 ^h 163.4	55.3 152.2; 159.7 ⁱ	32.3 154.7; 157.8 ^j
$Sn_2H_5^+$	ΔE^b 0.0 d(M–M) 288.2 d(M–H) 169.5; 170.2 ^e $\angle MH_bM$	<u>5.9</u> ^d <u>262.9</u> 197.6 ^f 79.0	<u>–7.3</u> <u>310.5</u> 178.2; 218.3 ^g 102.6	–3.6 — 183.7; 199.0 ^h 157.0	48.2 168.6; 176.8 ⁱ	22.4 171.0; 175.0 ^j
$Pb_2H_5^+$	ΔE^b 0.0 d(M–M) 298.1 d(M–H) 171.8; 174.5 ^e $\angle MH_bM$	<u>10.9</u> ^d <u>269.6</u> 207.2 ^f 81.2	<u>–15.6</u> <u>328.9</u> 181.8; 238.4 ^g 102.2	–14.1 — 190.1; 209.7 ^h 153.1	35.0 171.1; 183.2 ⁱ	10.5 174.0; 180.7 ^j

^aAt MP4/DZP//HF/DZP (using ECPs for all nonhydrogen atoms). The global minima are underlined; energies in kcal mol^{–1}, bond lengths in pm and bond angles in deg. H_b is the bridging hydrogen, see structures **115**–**118**, from Reference 463.

^bEnergy relative to **115**.

^cThe eclipsed conformation.

^dNot a minimum.

^ed(M₁–H₁) and d(M₂–H₃), respectively.

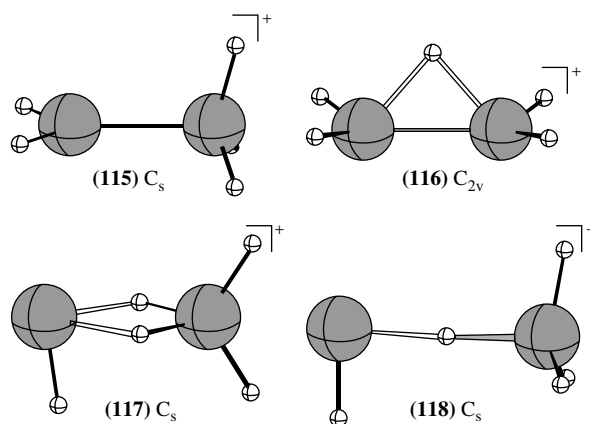
^fd(M–H_b).

^gd(M₂–H_b) and d(M₁–H_b), respectively.

^hd(M₁–H_b) and d(M₂–H_b), respectively.

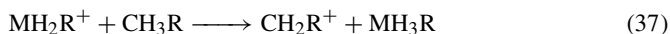
ⁱM–H bond distances in MH₃⁺ and MH₂, respectively.

^jM–H bond distances in MH₄ and MH⁺, respectively.

FIGURE 35. Schematic drawing of the structures of $M_2H_5^+$ isomers

to the dissociation energies of the M_2H_4 doubly bridged isomers into two molecules of MH_2 (Section VI.B.3.b.i and Table 28)²⁶⁹. Bridged structures were also located as global minima on the PES of cyclic $M_3H_3^+$ cations^{209a} (see Section VI.F.2).

b. Thermodynamic and kinetic stability of MR_3^+ cations. The elusiveness of ‘free’ silyl cations in the condensed phase stands in remarkable contrast to the behavior of the isoelectronic carbocations^{4,464} which were characterized as ‘free’ species by their X-ray structures^{4,465}. Furthermore, the lower electronegativity of silicon compared to carbon should favor the generation of silylium over carbenium ions. This is indeed the situation in the gas phase where silyl cations are well-characterized experimentally⁴⁶⁶. The calculations support this stability order; SiH_3^+ is calculated to be more stable than CH_3^+ by 58.9 kcal mol⁻¹ (according to the isodesmic equation 37 for $M = Si$, $R = H$)^{7,467}.



Although the stability of silylium ions is higher than that of carbenium ions, observation of silyl cations in the condensed phase proved to be extremely difficult^{28b-d,457,458}. The experimental efforts to isolate a ‘free’ silyl cation and the significant recent success by Lambert^{458,468} and Reed⁴⁶⁹ and their coworkers in generating such ions having various degrees of coordination and in solving their X-ray structures, arouse a lively debate about how ‘free’ are these ‘silyl cations’^{4,28b-d}? This discussion, which was accompanied by computational studies^{4,28b,470}, lead to the conclusion that the observed cationic species are not truly ‘free’ silyl cations, but are coordinated even with weakly nucleophilic solvents such as toluene and with non-nucleophilic counterions^{4,28b-d}. For example, *ab initio* calculations demonstrated that in $Et_3Si^+ B[C_6F_5]_4^-$ the Et_3Si^+ cation (**119**), claimed by Lambert and coworkers^{458,468} to be the first free silylium ion, is actually a σ -complex between Et_3Si^+ and a toluene solvent molecule having a relatively short Si–C contact distance of 214 pm (in the calculated $[Me_3Si-toluene]^+$ complex; 218 pm in Lambert’s $Et_3Si^+ B[C_6F_5]_4^-$ salt) and is bound by 28–34 kcal mol⁻¹, more strongly than by just a weak van der Waals interaction^{4,28b,470,471}. The calculated geometry [at HF/6-31G(d)] of the $[Me_3Si-toluene]^+$ complex with the corresponding experimental values from the X-ray data of $Et_3Si^+ B[C_6F_5]_4^-$ are shown in Figure 36.

Several reasons were given for the difficulties in producing ‘free’ silylium ions in the condensed phase: (a) stabilization by substituents is less effective for silylium ions than for carbenium ions, due to the longer M–R bonds and the lower tendency of silicon to conjugate; (b) the high ‘appetite’ of silyl cations for nucleophiles, including leaving groups, counterions and solvent molecules; calculations have shown that silyl cations can complex even with rare gases⁴; (c) the possibility for hypervalent coordination^{4,28b-d}. These difficulties were recently overcome by Lambert and coworkers who reported the formation of the trimesitylsilylium ion (**120**)^{459a}, which is the first **free** silylium ion prepared in the condensed phase⁴⁵⁹ and lacking any coordination to the solvent or counterion. This was achieved by a very clever design of the generation of **120**, which was formed by the elimination of an allyl group from $Mes_3SiCH_2CH=CH_2$ (equation 38)^{459a}. Although an X-ray structure of **120** is not available, the free nature of **120** was concluded from the following evidence: (a) close agreement between the calculated $\delta^{29}Si$ NMR chemical shift values of 226–228 ppm^{459c,d} with the measured value of 225.5 ppm^{459a}; (b) the calculated low coordination energy of **120** to benzene of only 1.8 kcal mol⁻¹^{459d} and

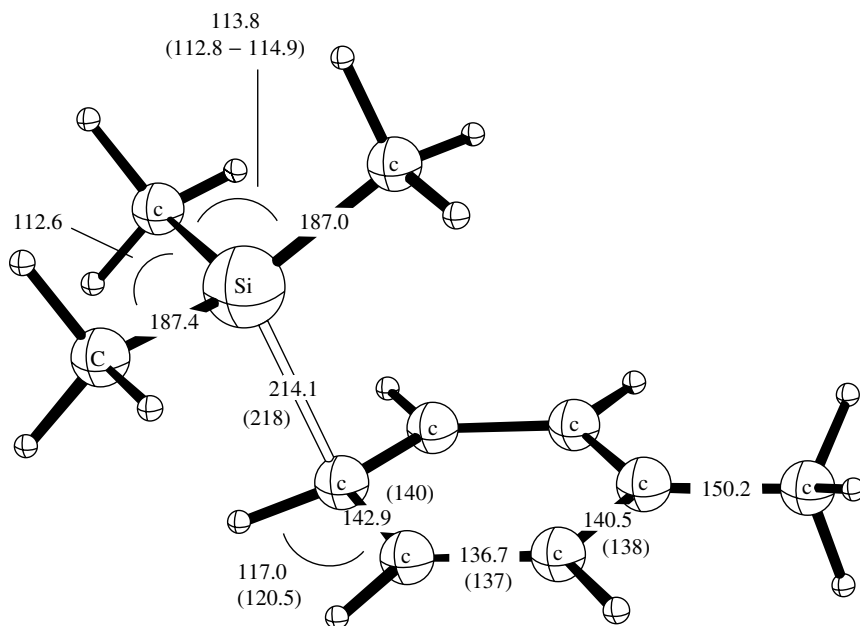
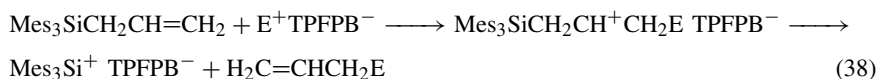
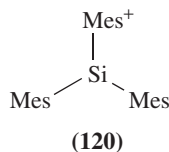
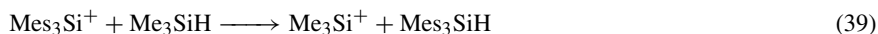


FIGURE 36. Calculated geometry [at HF/6-31G(d)] of the $[\text{Si}(\text{CH}_3)_3\text{—toluene}]^+$ complex; experimental values are given in parentheses, bond lengths in pm, bond angles in deg. Adapted from Reference 470a

(c) the calculated long Si–C(benzene) contact distance of 587 pm^{459d} [compared to the relatively short Si–C(toluene) contact distance of 218 pm in **119**^{468,470}]. **120** is stabilized thermodynamically by π -conjugation with the three mesityl substituents, which amounts to 24.3 kcal mol⁻¹ (calculated by isodesmic equation 39) being 60% of the stabilization energy calculated for the trityl cation (calculated relative to Me_3C^+)^{459c}, thus reducing its nucleophilicity. The mesityl substituents also protect the silylium ion sterically from nucleophilic attack by the solvent^{459c,d}.



E = electrophile; TPFPB⁻ = tetrakis(pentafluorophenyl)borate $[\text{B}(\text{C}_6\text{F}_5)_4]^-$



How does the stability of MR_3^+ ions change on going down group 14 from Si to Pb? How large are the effects of R substituents on their thermodynamic stability? How is the energy of coordination to H_2O and toluene affected by changing M and R (for R = halogens and vinyl)? These questions were tackled by Frenking and coworkers^{467,472,473} and Basch⁴⁷¹ and their results are collected in Tables 45 and 46.

The stability of MH_3^+ (M = Si to Pb) relative to CH_3^+ increases gradually from M = Si to M = Pb. While SiH_3^+ is more stable than CH_3^+ by $58.9 \text{ kcal mol}^{-1}$, this value is $97.9 \text{ kcal mol}^{-1}$ for PbH_3^+ (according to equations 37 and 40, at MP2/VDZ+P with quasi-relativistic ECPs for Si to Pb, Table 45)⁴⁷⁴.

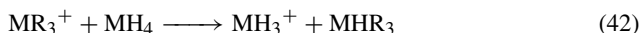
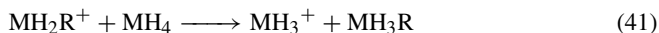
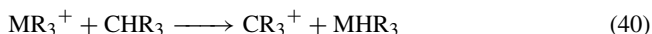


TABLE 45. Stabilization energies (ΔE , kcal mol^{-1}) of $\text{MH}_n\text{R}_{3-n}^+$, calculated according to isodesmic equations 37 and 40–42^a

M =	Equation	ΔE , R =						
		H	CH ₃	F	Cl	Br	I	H ₂ C=CH ^b
		MH_2R^+						
C ^c	41	0.0	40.6	25.1	24.8	29.8	33.5	60.0
	37	0.0	—	0.0	0.0	0.0	0.0	0.0
Si ^c	41	0.0	31.8	-1.2	1.1	5.7	10.3	27.5
	37	58.9	15.1	35.0	33.0	33.4	33.8	—
Ge	41	0.0	—	-6.3	-4.6	0.4	5.4	23.2
	37	70.7	—	42.4	40.3	41.0	41.7	—
Sn	41	0.0	—	-8.6	-8.2	-3.6	1.2	15.7
	37	87.5	—	56.6	52.8	53.0	53.3	—
Pb	41	0.0	—	-9.2	-11.0	-6.5	-1.6	14.3
	37	97.9	—	66.3	60.9	61.1	61.4	—
		MR_3^+						
C ^c	42	0.0	74.8	18.8	42.9	54.7	63.1	—
	40	0.0	—	0.0	0.0	0.0	0.0	—
Si ^c	42	0.0	38.4	-34.9	-3.6	11.5	25.5	—
	40	58.9	21.0	9.1	9.7	13.8	18.4	—
Ge	42	0.0	—	-50.8	-17.8	-0.7	15.4	—
	40	70.7	—	6.1	9.6	15.7	22.4	—
Sn	42	0.0	—	-50.5	-27.1	-10.8	5.1	—
	40	87.5	—	20.8	15.8	21.1	27.4	—
Pb	42	0.0	—	-58.5	-35.2	-17.6	-0.4	—
	40	97.9	—	22.1	19.2	25.9	33.6	—

^aThe energies of equations 41 and 42 are from Reference 467; the energies of reactions 37 and 40 were calculated by us, based on the total energies that are given in the supporting material of Reference 467. All energies are calculated at MP2/VDZ+P; quasi-relativistic pseudopotentials were used for Si, Ge, Sn and Pb and for Cl, Br and I.

^bAt MP2/VDZ+P, quasi-relativistic pseudopotentials were used for Si to Pb; from Reference 473.

^cAt MP2/6-31G(d); from Reference 4.

TABLE 46. M–L bond dissociation energies (BDE, kcal mol⁻¹) in [R₃M—L]⁺ complexes

M/R	L = H ₂ O ^a					L = toluene ^b		
	H	F	Cl	Br	I	H	CH ₃	Cl
C	71.3	43.7	10.9	4.9	-0.6	85.1	17.8	32.6
Si	54.7	72.4	46.8	39.2	31.3	53.9	28.9	49.0
Ge	44.5	62.7	40.4	33.6	26.6	47.6	26.2	48.3
Sn	38.9	56.7	40.8	35.0	28.9	40.3	25.7	47.7
Pb	31.4	46.4	33.2	28.6	23.8	44.2	30.5	56.1

^aAt MP2/VTZ+D+P, quasi-relativistic pseudopotentials were used for Si, Ge, Sn and Pb and for Cl, Br and I; from Reference 467.

^bAt MP2/CEP (RCEP). Compact effective potentials (CEPs) were used for C, Si and Cl, and their relativistic analogs (RCEP) were used for Ge, Sn and Pb. The contribution of basis set superposition errors (BSSE) is included; from Reference 471.

All halogens stabilize the carbenium ions CH₂R⁺ and CR₃⁺ relative to CH₃⁺ [equations 41 and 42 (M = C), Table 45] and the stabilizing effect of the halogen increases from F to I (equation 42). Moving down group 14, the stabilizing effect of the halogens is weakened and becomes destabilizing for the more electronegative halogens and more electropositive M. Thus, F and Cl destabilize SiR₃⁺ while Br and I stabilize the silylium ion. Iodine has a stabilizing effect on GeI₃⁺ and SnI₃⁺ while all other halogens destabilize GeR₃⁺ and SnR₃⁺ (equation 42, Table 45). All halogens destabilize PbR₃⁺ (equation 42). For a given halogen, there is a constant decrease in their stabilizing effect (or increase in their destabilizing effect) as M becomes heavier (equations 41 and 42), e.g. Δ*E* (equation 42, R = Br, in kcal mol⁻¹) = 11.5, -0.7, -10.8, -17.6 for M = Si, Ge, Sn and Pb, respectively⁴⁶⁷.

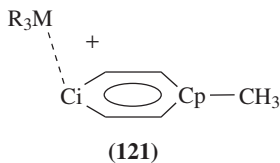
The metallaallyl cations H₂C=CHMH₂⁺ are planar and are stabilized by π-conjugation. The stabilization energies (according to equation 41, R = CH=CH₂) decrease as M becomes heavier (Table 45). As in other cases, there is a large drop in the stabilization between M = C (60 kcal mol⁻¹) and Si (27.5 kcal mol⁻¹) and a gradual decrease as M becomes heavier, to only 14.3 kcal mol⁻¹ for M = Pb. This trend is also reflected in the barrier for the rotation about the C–MH₂ bond in H₂C=CHMH₂⁺, which decreases in the order (in kcal mol⁻¹): 37.8 (M = C) > 14.1 (M = Si) > 12.0 (M = Ge) > 7.2 (M = Sn) > 6.2 (M = Pb)⁴⁷³.

The greater stabilization of the MR₃⁺ (R = halogen) cations by the heavier halogens is also reflected in the trend of the calculated bond dissociation energies of R₃M⁺–OH₂ complexes which decrease in the order: R = F > R = Cl > R = Br > R = I (Table 46). For example, the binding energy of water to PbR₃⁺ changes from 46.4 kcal mol⁻¹ for PbF₃⁺ to 23.8 kcal mol⁻¹ for PbI₃⁺⁴⁶⁷. For a given substituent the binding energy of MR₃⁺ decreases from M = C to M = Pb, e.g. the binding energies of MH₃⁺ to water (in kcal mol⁻¹) are: 71.3 for M = C, 54.7 for M = Si, 44.5 for M = Ge, 38.9 for M = Sn and 31.4 for M = Pb. A similar trend was measured by high pressure mass spectrometry for the binding energies of MR₃⁺ (M = Si, Ge and Sn; R = Me, Et, *n*-Pr and *n*-Bu) to water⁴⁷⁵.

The cation–ligand bond dissociation energies in [R₃M—L]⁺ complexes (M = C and Si; R = H, CH₃ and F and L = NH₃, H₂O, HCN, H₂CO, MeCN, Me₂O, Me₂CO, FCN, F₂O, F₂CO and NF₃) is larger for CH₃⁺ than for SiH₃⁺, but the opposite trend was predicted when R = CH₃ or F. Thus, the binding energy of SiR₃⁺ to the above

ligands is larger than the binding energy of these ligands to CR_3^+ ; e.g. for $\text{L} = \text{NH}_3$, the binding energies are 113.3 and 79.6 kcal mol^{-1} for CH_3^+ and SiH_3^+ , respectively, while they are 43.7 and 54.4 kcal mol^{-1} for $\text{C}(\text{CH}_3)_3^+$ and $\text{Si}(\text{CH}_3)_3^+$, respectively. This opposite trend in the complexation energies upon substitution at M reflects a smaller conjugative interaction in SiR_3^+ relative to CR_3^+ ⁴⁷⁶. The complexation effectiveness of the above-mentioned ligands, e.g. to SiMe_3^+ , follows the order (binding energy in kcal mol^{-1}): $\text{NH}_3(54.4) > \text{MeCN}(49.6) \sim \text{Me}_2\text{C}=\text{O} > \text{Me}_2\text{O}(44.0) > \text{H}_2\text{O} \sim \text{HCN} \sim \text{H}_2\text{C}=\text{O}(ca\ 38-40) > \text{FCN}(35.7) > \text{F}_2\text{CO}(23.2) > \text{F}_3\text{N}(13.8) > \text{F}_2\text{O}(7.8)$ ⁴⁷⁶.

The complexation of MR_3^+ cations with toluene is of special interest because of the above-mentioned experiments of Lambert and coworkers^{458,459a,468}. Basch computed the geometric and electronic structure of complexes of MH_3^+ , $\text{M}(\text{CH}_3)_3^+$ and MCl_3^+ with toluene (**121**) for all group 14 elements⁴⁷¹. Going down group 14, the nature of the complex changes gradually from a strongly bound σ -bonded carbenium or silylium ion complex to a π complex with an almost planar toluene unit for $\text{M} = \text{Pb}$. The plumblyum ion is located directly above the *ipso*-carbon (Ci) of the ring, making an angle of 90° with the plane of the benzene ring. Important geometric parameters of $[\text{MR}_3\text{—toluene}]^+$ complexes as well as charge distributions are given in Table 47. The binding energies of the $[\text{MR}_3\text{—toluene}]^+$ complexes decrease from CH_3^+ to SiH_3^+ , but increase on going from $\text{M} = \text{C}$ to $\text{M} = \text{Si}$ for $\text{M}(\text{CH}_3)_3^+$ and MCl_3^+ (Table 46). For all M, the binding energy of MR_3^+ to toluene decreases from $\text{R} = \text{H}$ to $\text{R} = \text{CH}_3$, and then increases for $\text{R} = \text{Cl}$, i.e. the binding energies of GeR_3^+ to toluene are (in kcal mol^{-1}): 47.6 ($\text{R} = \text{H}$) $>$ 26.2 ($\text{R} = \text{CH}_3$) $<$ 48.3 ($\text{R} = \text{Cl}$). The calculated Mulliken charges (Table 47) show delocalization of the positive charge from MR_3^+ to the complexed toluene. The charge delocalization is largest for MCl_3^+ . Among M, the largest charge transfer is found for $\text{M} = \text{C}$ and it is reduced as M becomes heavier. Based on the short M–toluene distances (M–Ci values in Table 47) and the large complexation energies (Table 46), it was concluded that none of the studied group 14 metal cations is truly ‘free’^{471,477}.



Since even an inert solvent like toluene can be strongly coordinated, it was concluded that the synthesis of a free MR_3^+ cation is extremely difficult, as was manifested by several attempts to form ‘free’ trivalent tin cations^{460,478–480}. Substitution with bulky substituents, e.g. $\text{R} = \text{mesityl}$, resulted in the formation of the first free silylium cation (**120**)⁴⁵⁹ (see above). However, utilizing the same method to form free germeryl and stannyl cations⁴⁸¹ produced trimesitylgermyl and trimesitylstannyl cations, which are concluded to be less than ‘fully cationic’. The measured ^{119}Sn chemical shift of the trimesitylstannyl cation is 806 ppm. Cremer and coworkers calculated (IGLO/DZ+P) a $\delta(^{119}\text{Sn})$ of 774 ppm for the free SnH_3^+ cation and estimated (from methyl group increments) a $\delta(^{119}\text{Sn})$ of 1075 ppm for the free $(\text{CH}_3)_3\text{Sn}^+$ cation. Coordination of these cations with a water molecule shifts $\delta(^{119}\text{Sn})$ of SnH_3^+ to 54 ppm and that of

TABLE 47. Geometries and charges in $[\text{MR}_3\text{—toluene}]^+$ complexes (R = H, Me, Cl)^a

MR_3^+	Parameter	C	Si	Ge	Sn	Pb
H_3MCH_3	$d(\text{M—C})^b$	153.3	187.9	195.5	214.0	218.1
R = H	$d(\text{M—Ci})^c$	158.0	206.4	218.7	241.1	242.4
	$\angle\text{MCiCp}^d$	133.5	104.1	101.1	97.6	91.8
	Charge ^e	0.11	0.33	0.33	0.44	0.39
R = CH_3	$d(\text{M—Ci})^c$	165.5	214.8	228.6	249.3	250.2
	$\angle\text{MCiCp}^d$	129.4	105.3	101.3	96.8	91.3
	Charge ^e	0.24	0.39	0.43	0.52	0.50
R = Cl	$d(\text{M—Ci})^c$	157.2	200.9	211.4	232.8	235.3
	$\angle\text{MCiCp}^d$	137.3	114.2	108.3	100.9	92.7
	Charge ^e	0.00	0.21	0.14	0.23	0.15

^aAt MP2/CEP (RCEP). Compact effective potentials (CEPs) were used for C, Si and Cl, and their relativistic analogs (RCEP) were used for Ge, Sn and Pb. The contribution of basis set superposition errors is included. See **121** for structure definitions; bond lengths in pm, bond angles in deg; from Reference 471.

^bAt MP2/ECP (TZ basis set augmented with a double set of polarization functions for the valence electrons); from Reference 45.

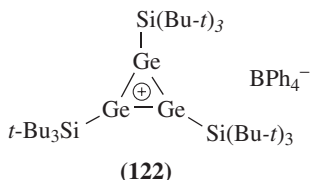
^cDistance between M and the coordinated carbon atom (Ci) of toluene.

^dAngle between M and the plane of toluene ring.

^eMulliken charge on the MR_3^+ group.

$(\text{CH}_3)_3\text{Sn}^+$ to 352 ppm (estimated value)⁴⁷⁷. Calculations of the ^{119}Sn chemical shift of a stannyl–toluene complex are not available. An empirical linear correlation was found between measured ^{29}Si and ^{119}Sn chemical shifts of silanes and stannanes having various degrees of charge localization on Si and Sn⁴⁷⁸. According to this correlation, $\delta(^{29}\text{Si})$ of 225 ppm [which is the chemical shift measured for the free $\text{Si}(\text{Mes})_3^+$ cation] translates to $\delta(^{119}\text{Sn})$ of ca 1000–1100 ppm. This empirical estimation is in good agreement with the above mentioned calculations by Cremer and coworkers. Using this supporting information it was concluded that Mes_3Sn^+ has more than three quarters of the chemical shift expected for a free stannylum ion, having the highest cationic character known to date for any stannyl cations⁴⁸¹. The measured ^{119}Sn chemical shifts previously reported for tributylstannyl cation in benzene and dichloromethane are 360 ppm^{479a} and 356 ppm^{479b} respectively, comparable to the values calculated for water-coordinated stannyl cations⁴⁷⁷, implying that these stannyl cations are more tightly coordinated than Mes_3Sn^+ .

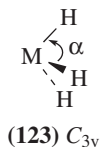
The cationic character of the trimesitylgermyl cation could not be evaluated from the chemical shifts of ^{73}Ge because of its very low sensitivity, but the analysis of the aryl ^{13}C chemical shifts is consistent with charge development on Ge which is comparable to that on the corresponding silicon and tin analogs⁴⁸¹. Enclosure of the cations in a cage may be a possible strategy for forming free cations of Si to Sn^{28b}. Recently, Sekiguchi and coworkers synthesized the first free germylium cation, $(t\text{-Bu}_3\text{SiGe})_3^+$ (**122**) (as its BPh_4^- salt) which does not show any significant interaction with the counterion^{375,385} (see Section VI.F.2). A systematic theoretical study of the NMR chemical shifts of MR_3^+ cations with various substituents and in a variety of solvents is needed in order to be able to establish the cationic character of newly formed group 14 MR_3^+ cations.



2. Tricoordinated radicals

Theoretical aspects of silyl radicals R_3Si^\bullet were reviewed earlier by Apeloig⁷. Recent developments in the chemistry of silyl radicals are reviewed in a chapter by Chatgililoglu and Schiesser in this book²⁹. Experimental studies of tricoordinate MR_3 radicals of heavier group 14 elements ($M = Ge, Sn$ and Pb) are reviewed by Mochida⁴⁸².

In contrast to the MH_3^+ cations (and CH_3^+) which are planar, the MH_3^\bullet radicals ($M = Si-Sn$) favor pyramidal C_{3v} structures (123)⁵⁷. While the bending angles (α) are $110 \pm 1^\circ$ for SiH_3^\bullet , GeH_3^\bullet and SnH_3^\bullet radicals (Table 48)⁴⁸³, the inversion barrier of SiH_3^\bullet and of GeH_3^\bullet are very similar (3.7 and 3.8 kcal mol⁻¹, respectively), but they are almost twice as large (7.0 kcal mol⁻¹) for SnH_3 . This behavior can be explained using MO terms, through the operation of the second-order Jahn–Teller effect^{26,57}, as shown in Figure 37. The mixing between the p_z SOMO orbital ($1a_2''$) and the M–H anti-bonding LUMO orbital ($2a_1'$) stabilizes the pyramidal MH_3^\bullet . As M becomes heavier, the SOMO–LUMO gap decreases due to the higher energy of the SOMO (more electropositive and more diffuse M), and the lower M–H LUMO which becomes less antibonding as M becomes heavier. Thus the tendency to pyramidalize increases down group 14. The Jahn–Teller effect is opposed by the rising energy of the $1e_1'$ orbital due to a decrease in the M–H bonding overlap upon pyramidalization. CH_3^\bullet is planar because the Jahn–Teller effect cannot outweigh the destabilization of the $1e_1'$ orbitals. Steric repulsion between the hydrogen ligands is also responsible for the planar structure of the small CH_3^\bullet radical⁵⁷.



3. Tricoordinated anions

Experimental studies of tricoordinated anions of heavier group 14 elements ($M = Ge, Sn$ and Pb) were reviewed by Riviere and coworkers⁴⁸⁴.

All MH_3^- anions have a C_{3v} pyramidal structure. The degree of pyramidity is larger than that of the corresponding radicals, as is reflected in the smaller HMH bond angles, α , which are in the range of $92^\circ-96^\circ$ ¹⁶⁸; only CH_3^- is nearly planar with $\alpha = 109.1^\circ$ ^{483a} (Table 48). The higher degree of pyramidity in the anions relative to the radicals can be attributed to a stronger Jahn–Teller effect in the anions due to the occupation of the p_z HOMO by two electrons (Figure 37).

The electron affinity (EA) of the MH_3^\bullet radicals increases significantly from CH_3^\bullet to SiH_3^\bullet while SiH_3^\bullet and GeH_3^\bullet have similar EAs; i.e. the calculated electron affinities

TABLE 48. Calculated geometries of MH_3^+ , MH_3^\bullet and MH_3^- ^a

M	$\text{MH}_4(T_d)^b$	$\text{MH}_3^+(D_{3h})^c$	$\text{MH}_3^\bullet(C_{3v})^c$		$\text{MH}_3^-(C_{3v})^d$	
	d(M–H)	d(M–H)	d(M–H)	$\angle\text{HMH}$	d(M–H)	$\angle\text{HMH}$
C	108.6	110.6	108.9 ^e	120.0 ^e	110.2 ^f	109.1 ^f
Si	148.0	146.3	148.8	111.2	153.9	95.8
Ge	152.9	148.5	151.6	111.7	161.2	94.0
Sn	170.3	172.1	173.8	110.2	180.5	93.6
Pb	174.4	171.9 ^g	—	—	186.0	92.2

^aBond length in pm, bond angles in deg.

^bCore polarization pseudopotentials (4-valence electrons); from Reference 106. See Table 2 for values at other computational levels.

^cAt LDA/TZ2P; from Reference 57. See also the values in Table 43.

^dAt QCISD/TZP including diffused functions. A relativistic ECP was used for Pb; from Reference 168.

^eFor the planar D_{3h} minimum.

^fAt CCSD(T)/aug-cc-pVQZ; from Reference 483a.

^gAt B3LYP using quasi-relativistic ECPs; from Reference 461.

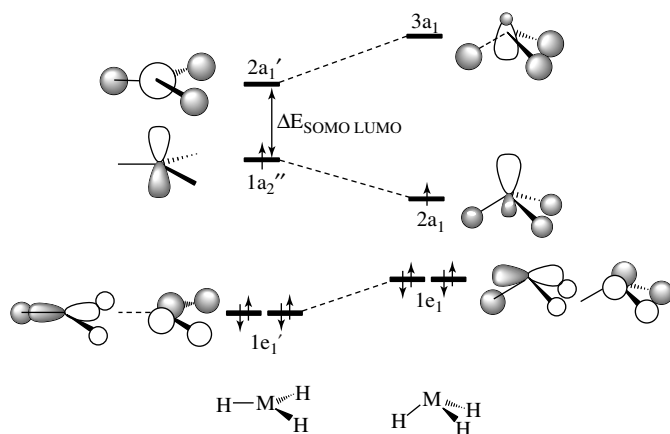


FIGURE 37. A molecular orbital diagram which explains the operation of a second-order Jahn–Teller effect in the pyramidalization of MH_3^\bullet . Reprinted with permission from Reference 57. Copyright (1996) American Chemical Society

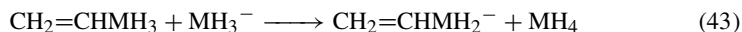
using the G2 method (experimental values are given in parentheses) are (in kcal mol^{-1}): 0.9⁴⁸⁵ (1.8)^{486a} for CH_3^\bullet ^{483a–c}; 32.7⁴⁸⁵ (≤ 33.2)^{486b} for SiH_3^\bullet ^{483b}; 36.9^{486c} (≤ 40.1)^{486b} for GeH_3^\bullet ^{483d}. A significantly higher electron affinity in the range of 80–85 kcal mol^{-1} was calculated for GeF_3^\bullet using different density functionals and *ab initio* methods^{483d}. The high electron affinities of SiH_3^\bullet and GeH_3^\bullet can be attributed to the character of the orbital which accommodates the two lone-pair electrons in the anions. Thus, the small HMH bond angles in SiH_3^- and GeH_3^- relative to that of CH_3^- (Table 48) imply that the orbital in which the lone pair resides in SiH_3^- and GeH_3^- has a significant s-character, as opposed to CH_3^- for which the orbital is predominantly p in character, thereby increasing the energy required to remove the electron from SiH_3^- and GeH_3^- ^{486c}.

The calculated vertical ionization potentials of MR_3^- are (in kcal mol⁻¹): 11.8 for CH_3^- , 41.3 for SiH_3^- and 43.4 for GeH_3^- ; the corresponding adiabatic IPs are 4.4, 30.2 and 32.0 kcal mol⁻¹, respectively⁴⁸⁷, in good agreement with photoelectron spectroscopy measurements^{486a,b,488}. The proton affinity of the MH_3^- anions decreases slightly from SiH_3^- to GeH_3^- , but is significantly larger for CH_3^- , i.e. the proton affinities (in kcal mol⁻¹ at G2) are: 416.9 for CH_3^- ⁴⁸⁵, 372.3 for SiH_3^- ⁴⁸⁵ and 361.7 for GeH_3^- ^{483d,486c}. The trends in the EAs of the MH_3 radicals, and the proton affinities and ionization potentials of the corresponding anions, imply that the ability to accommodate a negative charge increases as the central atom becomes heavier and as the substituents are more electronegative (see below). Unfortunately, calculations of these properties for the heavier SnH_3^- and PbH_3^- are still not available.

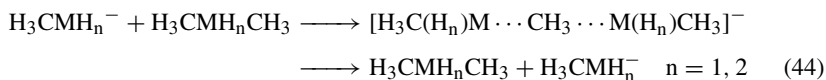
The effect of various substituents on the stability of MR_3^- anions was studied only for the silyl anion and these studies were reviewed by Apeloig⁷. Silyl anions substituted by first-row substituents (BH_2 to F) are all pyramidal, except for $H_2SiBH_2^-$ which is planar⁴⁸⁹. The α -substituents have also a strong effect on the inversion barriers of the $RSiH_2^-$ anions, which at HF/DZ were calculated to be (in kcal mol⁻¹): 34.3 for SiH_3^- , 40.4 for $CH_3SiH_2^-$, 42.8 for $H_2NSiH_2^-$, 50.7 for $HOSiH_2^-$ and 57.3 for $FSiH_2^-$ ^{489a}.

The calculated acidities of substituted silanes relative to that of SiH_4 [at HF/6-31+G(d), a positive value indicates a higher acidity] are: 13.4 (H_2BSiH_3), -6.8 (CH_3SiH_3), -5.9 (H_2NSiH_3), -2.1 ($HOSiH_3$) and 5.8 ($FSiH_3$); thus, π -donor substituents (NH_2 , OH) were calculated to decrease the acidity of $RSiH_3$ relative to that of SiH_4 , while σ (e.g. F) and π acceptors (e.g. H_2B) increase their acidity^{489b}. The calculated (using DFT methods) proton affinity of $MeGeH_2^-$ is 365.6 kcal mol⁻¹ (exp. 367 kcal mol⁻¹), larger than that of GeH_3^- (of 361.7 kcal mol⁻¹), indicating that methyl substitution decreases the gas-phase acidity of germanes. On the other hand, the calculated proton affinities of $Ge(OH)_3^-$ and GeF_3^- are 342 and 316.1 kcal mol⁻¹, respectively, significantly smaller than that of GeH_3^- , indicating an increase in the gas-phase acidity of hydroxy- and fluorogermanes relative to GeH_4 ^{483d}. Similar substituent effects, although quantitatively different, are expected also for the heavier metalla anions, but, as mentioned above, such studies are not yet available.

The metallaallyl anions, $CH_2=CHMH_2^-$, have strongly pyramidal MH_2 groups which can rotate around the M-C bond with little or no barrier. The reaction energies of equation 43 are very small for M = Si to Pb [1.7–4.1 kcal mol⁻¹ at MP2/6-31G(d); ECPs for Si–Pb] and suggest that these $CH_2=CHMH_2^-$ anions gain very little stabilization by π conjugation, in contrast to the corresponding allyl anion for which the energy of equation 43 is 29.8 kcal mol⁻¹. The calculated charge distribution, which shows that the negative charge is localized mainly on the terminal MH_2 group and the central CH group while the terminal CH_2 group carries only a small negative charge, also indicates that π conjugation is small. The electronic structure of the molecules was also studied using the Laplacian of the electron density distribution, which shows the formation of a lone pair of electrons on M ⁴⁷³.



Hoz and coworkers have recently studied the intrinsic barriers in identity S_N2 reactions (equation 44)⁴⁹⁰.



The calculated barriers [at the G2(+) level] for reaction 44 are (in kcal mol⁻¹): 44.7 for M = C, 45.8 for M = Si, 38.1 for M = Ge and 30.6 for M = Sn. These barriers are significantly higher than for M = N, P, As and Sb⁴⁹⁰.

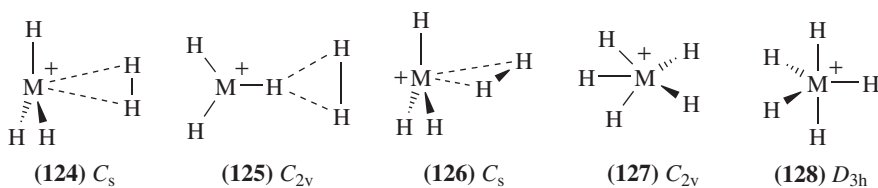
The interesting aromatic metalolyl anions *c*-(C₄H₄)MH⁻ (**90**) and *c*-(C₄H₄)M²⁻ (**91**) are discussed in Section VI.F.3.

C. Pentacoordinated Compounds

A general introduction to hypercoordinated systems and a discussion on MH₅, MX₅, MX₆, MX₇ and MX₈ are given in Sections V.D.1, V.D.2, V.D.3

1. Pentacoordinated cations

There are countless publications concerning CH₅⁺⁴⁹¹⁻⁴⁹³. The methonium ion has no discrete structure as hydrogen scrambling is essentially barrierless⁴⁹¹⁻⁴⁹³. In contrast, for SiH₅⁺ and GeH₅^{+462,494-497}, the global minimum can be described as a side-on complex between an almost planar MH₃⁺ cation and a dihydrogen molecule (**124**). For M = Ge, **125** was also located as a minimum but it is by *ca* 10 kcal mol⁻¹ less stable than **124**. All other structures that were studied (some examples are **126-128**) are not minima on the PES for both SiH₅⁺ and GeH₅^{+494,495,497}. The energy of **126**, which is a transition structure for the rotation of the hydrogen molecule, is almost equal to that of **124**, implying free rotation of the hydrogen molecule in both SiH₅⁺ and GeH₅⁺.



The calculated geometries of SiH₅⁺ and GeH₅⁺ (**124**) are given in Figure 38. The structures shown exhibit very small perturbations relative to the isolated MH₃⁺ and H₂ fragments. The three equal Ge–H and Si–H bonds are by only 0.2 and 0.1 pm shorter than those in the corresponding free MH₃⁺, respectively, and the H–H bond is by *ca* 3 pm longer than that in the isolated H₂^{494,497}. The proton affinity of SiH₄ of 153.2 kcal mol⁻¹ and of GeH₄ of 156.4 kcal mol⁻¹ are similar, as are the dissociation energies of MH₅⁺ to MH₃⁺ + H₂ of 10.3 kcal mol⁻¹ for M = Si and 10.0 kcal mol⁻¹ for M = Ge. This similarity is somewhat surprising, as one would have expected that the dissociation energy of GeH₅⁺ would be smaller than for SiH₅⁺ due to the smaller charge on germanium in GeH₃⁺ (+0.84) compared to that on silicon in SiH₃⁺ (1.01). However, the binding between the MH₃⁺ cation and H₂ is due mostly to an interaction between the vacant p orbital (LUMO) on the MH₃⁺ part and the σ orbital (HOMO) of H₂. The smaller HOMO–LUMO gap for GeH₃⁺ and H₂ than for SiH₃⁺ and H₂ dictates a more stable GeH₅⁺ than expected from its electronegativity^{494,497}. The proton affinity of germane is slightly higher than that of silane and considerably higher than that of methane (130.5 kcal mol⁻¹). Consequently, germane is able to abstract hydrogen from both CH₅⁺ and SiH₅⁺⁴⁹⁴. No studies are yet available for SnH₅⁺ and PbH₅⁺.

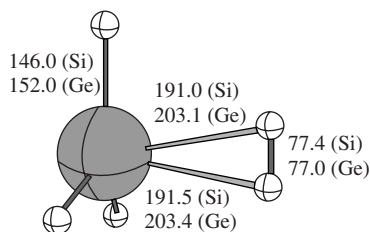
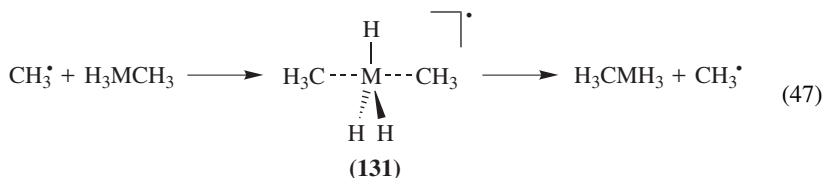
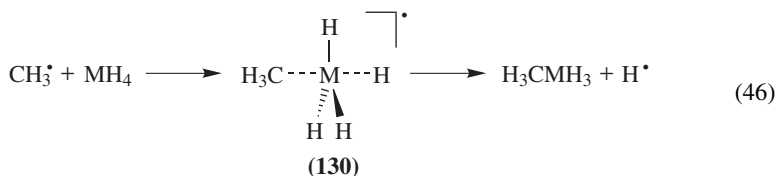
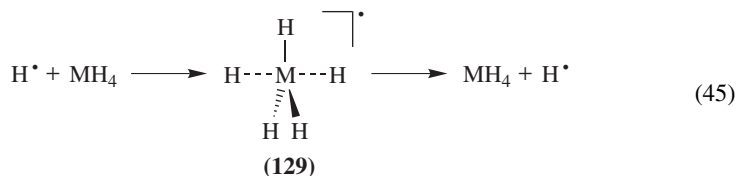


FIGURE 38. Calculated geometries (at CCSD/TZ2P for $M = \text{Si}^{497}$ and CCSD/TZP+f for $M = \text{Ge}^{494}$) of the side-on complex of MH_5^+ (**124**). Bond lengths in pm

2. Pentacoordinated radicals

A detailed discussion on the properties of MH_5^\bullet is given in Section V.D.1 and its calculated structure is shown in Figure 9. In this section we will discuss the role of pentacoordinated MR_5^\bullet in free-radical homolytic substitution reactions.

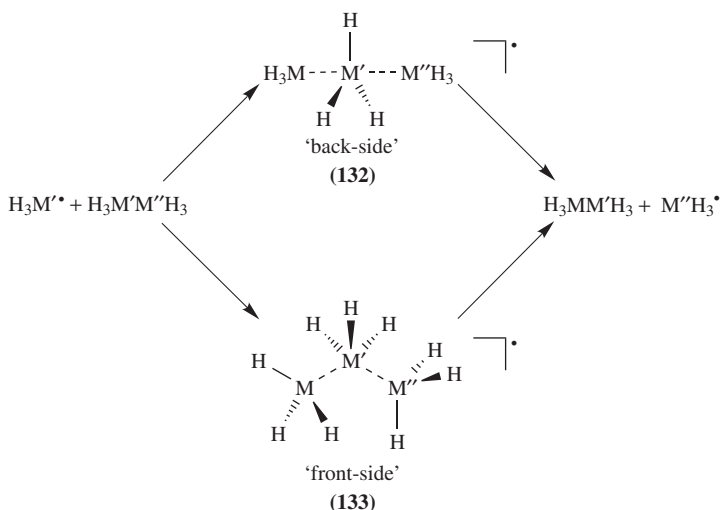
The potential energy surfaces for the attack of a hydrogen atom and of a methyl radical at the heteroatom in MH_4 and H_3CMH_3 ($M = \text{Si}, \text{Ge}$ and Sn) (equations 45, 46 and 47)^{498a} and the attack of MH_3 on $\text{H}_3\text{M}'\text{M}''\text{H}_3$ (M, M' and M'' are Si, Ge and Sn) (equation 48)^{498b} were studied in order to provide a better understanding of the parameters which affect and control the mechanism of such radical substitution reactions. Calculations for substitutions at lead are not available.



All the results presented below were calculated using QCISD/DZP//MP2/DZP with ECPs for Si, Ge and Sn. Reactions 45 and 46 pass through pentacoordinated transition structures (**129**, **130**), while **131** is a minimum on the PES (see below). The activation barriers for the homolytic degenerate hydrogen substitution in MH_4 (equation 45) are (in kcal mol^{-1}): 17.1, 18.2 and 16.6 for $M = \text{Si}, \text{Ge}$ and Sn , respectively; the activation

barriers for the nondegenerate substitution of hydrogen by a methyl group are higher, being (in kcal mol⁻¹): 24.2, 25.5 and 22.8 for M = Si, Ge and Sn, respectively. However, the activation barriers for the reverse reaction, an attack by an hydrogen radical on H₃CMH₃ and the expulsion of a methyl radical, are considerably lower, i.e. 16.5, 16.2 and 13.5 kcal mol⁻¹, showing that the methyl radical is a better leaving group than the hydrogen radical and that the latter is a better attacking group. The degenerate methyl substitution (equation 47) passes through a C_{3v}-symmetry transition state which leads to a weakly bound, intermediate structures **131** of D_{3h} symmetry. The activation energies for the decomposition of **131** to the corresponding products are only 0.3–0.5 kcal mol⁻¹. However, when ZPEs are included **131** is less stable than the C_{3v}-transition state by *ca* 1.5–3.0 kcal mol⁻¹. The calculated activation barriers for equation 47 are (in kcal mol⁻¹) 28.1, 26.6 and 22.8 for M = Si, Ge and Sn, respectively. These relatively high activation barriers suggest that homolytic substitution is most likely not a viable mechanism for reactions involving silyl, germyl or stannyl group transfers between methyl groups^{498a}. Addition of alkyl groups on M (e.g. the use of Me₄Si instead of MeSiH₃) or better leaving radicals than the methyl radical may reduce the activation barriers.

Reactions 48 (M, M' and M'' are Si, Ge and Sn) were investigated for both degenerate and nondegenerate situations. 'Back-side' (**132**) and 'front-side' (**133**) approaches of MH₃[•] were considered. Both approaches involve pentacoordinate transition states (Scheme 5). The optimized structures of **132** and **133**, M = M' = M'' = Si are shown in Figure 39a.

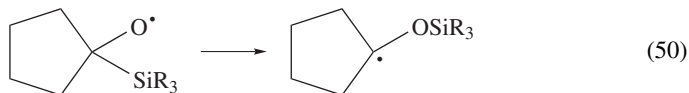
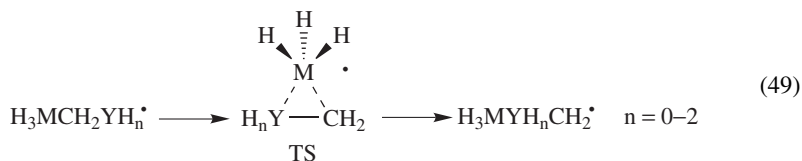


SCHEME 5

The calculations predict that the degenerate homolytic substitution by silyl radical at the silicon atom of disilane proceeds by mechanisms that involve either a 'back-side' or a 'front-side' attack, having similar activation barriers of 12.6 and 13.9 kcal mol⁻¹, respectively. Similar conclusions were obtained for the degenerate homolytic substitution reactions involving GeH₃[•] and SnH₃[•], with barriers of 15.6 kcal mol⁻¹ ('back-side') and

18.3 kcal mol⁻¹ ('front-side') for germyl radical attack at digermene, and 14.0 kcal mol⁻¹ ('back-side') and 14.1 kcal mol⁻¹ ('front-side') for stannyl radical attack at distannane [calculated at CCSD(T)/aug-cc-pVDZ//MP2/DZP]^{498b}. Calculations of the analogous non-degenerate reactions of disilane, digermene and distannane as well as reactions involving silylgermane, silylstannane and germylstannane find that, while homolytic substitution at silicon and germanium favors the 'back-side' mechanism, reactions involving free radical attacks at Sn are predicted to be less discriminate; the activation barriers for both approaches are very similar, e.g. the barriers for the attack of SiH₃[•] on H₃SnSnH₃ are 9.9 kcal mol⁻¹ and 9.4 kcal mol⁻¹ for the 'back-side' and 'front-side' approaches, respectively^{498b}.

An *ab initio* study⁴⁹⁹ of homolytic 1,2-migration reactions (equation 49) of SiH₃, GeH₃ and SnH₃ groups between two carbon centers (Y = C), between carbon and nitrogen centers (Y = N) and between carbon and oxygen centers (Y = O) predict that these reactions proceed via homolytic substitution mechanisms involving 'front-side' attack at the group 14 element (equation 49). In such a mechanism, chiral groups involving group 14 elements are expected to migrate with retention of configuration. The intramolecular migrations between carbons (equation 49, Y = C) were predicted to be unlikely, with calculated (at QCISD/DZP//MP2/DZP) activation barriers of 24.6, 24.7 and 17.8 kcal mol⁻¹ for M = Si, Ge and Sn, respectively. 1,2-Migrations from carbon to nitrogen and carbon to oxygen were predicted to be more facile, with activation barriers of 15.1, 16.5 and 9.3 kcal mol⁻¹ for M = Si, Ge and Sn, respectively (equation 49, Y = N) and 8.2 and 9.2 kcal mol⁻¹ for the 1,2-migration of silyl and germyl radicals in silylmethoxyl and germylmethoxyl, respectively (equation 49, Y = O). MP2/DZP calculations predict that H₃SnCH₂O[•] rearranges to H₃SnOCH₂[•] without a barrier. The H₃SiCH₂O[•] to H₃SiOCH₂[•] isomerization is the prototype for the radical Brook-type rearrangement (e.g. equation 50). The 'front-side' pentacoordinated transition structures of reaction 49, Y = N and O are shown in Figures 39b and 39c, respectively. All the above mentioned 1,2-migrations that involve a migration of a GeH₃ group have larger barriers than the analogous silicon or tin rearrangements, in agreement with the experimental results of Kim and coworkers⁵⁰⁰ who found that 1,6-migrations involving trialkylgermanium substituents proceed less readily than their Si or Sn analogs.



3. Pentacoordinated anions

The calculated structures (at the QCISD level with triple- ζ basis sets which include diffuse and polarization functions for Si, Ge and Sn, and ECPs for Pb)¹⁶⁸ of D_{3h} MH₅⁻ group 14 anions, which are all minima on the PES, are given in Figure 40. The M—H

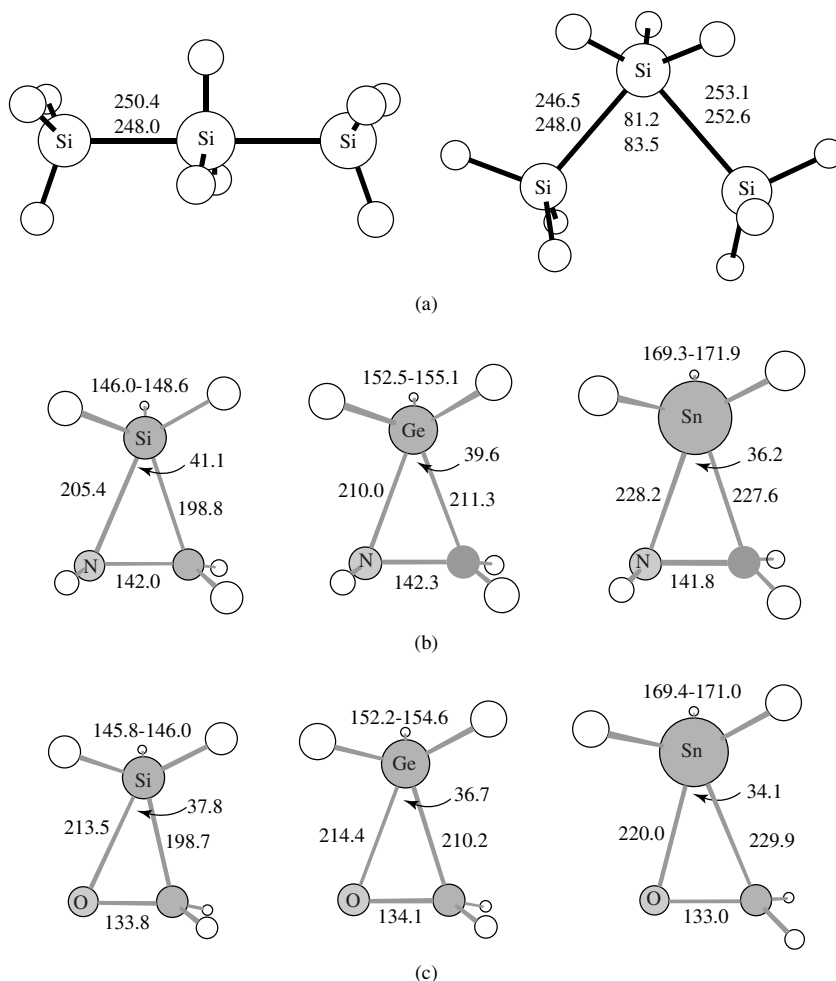


FIGURE 39. (a) Calculated geometric parameters [at MP2/6-311G(d,p) and B3LYP/DZP, given one below the other] of the transition state structures **132** and **133** for the degenerate ‘back-side’ and ‘front-side’ reactions of a SiH_3^\bullet radical with H_3SiSiH_3 . Adapted from Reference 498b. (b) Optimized transition state structures (at MP2/DZP) for the 1,2-migration reactions 49, $\text{M} = \text{Si, Ge and Sn}$; $\text{YH}_n = \text{NH}$. (c) Optimized transition state structures (at MP2/DZP for Si and Ge and HF/DZP for Sn) for the 1,2-migration reactions 49, $\text{M} = \text{Si, Ge and Sn}$; $\text{Y} = \text{O}$ ($n = 0$). Bond lengths in pm, bond angles in deg. (b) and (c) are adapted from Reference 499

bond lengths, especially the equatorial bonds, are longer than those in the corresponding radicals (Figure 9). Difference density maps reveal that, upon anion formation, the incoming electron density accumulates preferentially in nonbonded regions of the axial and, to a lesser extent, equatorial hydrogens¹⁷⁰.

The electron binding energies in MH_5^- are in the range of 41–55 kcal mol⁻¹^{168,170}. The dissociation of MH_5^- to $\text{MH}_3^- + \text{H}_2$ is exothermic by 6.0, 25.4, 22.5 and 46.9 kcal mol⁻¹

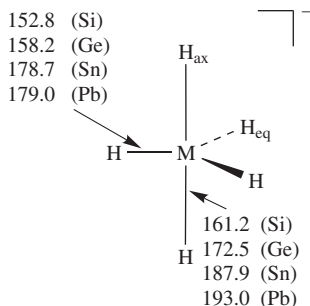


FIGURE 40. Optimized geometries of D_{3h} MH_5^- anions calculated at QCISD/6-311++G(d,p) for $M = Si$, QCISD/TZ2P with two sets of diffuse s and p functions for $M = Ge$ and Sn and QCISD/RECP for $M = Pb$. Bond lengths in pm; data from Reference 168

for $M = Si, Ge, Sn$ and Pb , but it occurs via a two-step mechanism. The first step, the dissociation of MH_5^- to $MH_4 + H^-$, is endothermic for $M = Si$ to Pb and its energy changes irregularly with M , i.e. the dissociation energy is 20.2, 16.4, 33.0 and 23.0 kcal mol⁻¹ for $M = Si, Ge, Sn$ and Pb , respectively. The second step, i.e. the proton transfer step, $MH_4 + H^- \rightarrow MH_3^- + H_2$, has been calculated to be barrierless and exothermic for all M ¹⁶⁸. The energy decomposition analysis of Morokuma was used to clarify the calculated trends in these dissociation reactions¹⁶⁸.

VIII. CONCLUSIONS AND OUTLOOK

The developments during the last two decades in the chemistry of organic compounds of germanium, tin and lead, both experimental and theoretical, have been spectacular. The experimental achievements are, no doubt, extremely impressive, with the syntheses of numerous new types of molecules, many of which were previously believed to be 'non-existent'. However, in our opinion the big leap forward in this field, and essentially in its systematization and deeper understanding, has been theoretical. Fifteen years ago only very small molecules of group 14 elements could be calculated with reasonable accuracy and reliability and the role of theory in this field of chemistry was small. Due to intense effort over the last 15 years, new theoretical methods have been developed allowing reliable calculations of relatively large molecules containing heavy group 14 elements.

This impressive progress in theoretical methodology resulted in intensive computational work, which is summarized in this review and in its nearly 650 references, and in a much deeper understanding of the periodic trends, major as well as subtle, expected as one moves down along the group from carbon through silicon and germanium to tin and lead.

However, although much has been learned, the field of the organic chemistry of germanium, tin and lead is still in its infancy and many interesting territories remain to be explored and discovered. We have no doubt that computational methods will continue to play a major role in the study of Ge-, Sn- and Pb-containing compounds, and that this is the most powerful tool currently available to the chemist with which to study systematically these compounds in order to understand trends within the compounds of group 14 elements. What is already clear is that the chemistry of germanium, tin and lead is *not* a simple extension of the chemistry of silicon. Striking and surprising differences are found when compounds of the heavier congeners are compared with those of the lighter congeners.

The relatively short experience in this field has taught us that the future lies in the close collaboration and joint research of theoreticians and experimentalists. The models that can

be generated by calculations have become indispensable in understanding and evaluating experimental results and interpretations, and in suggesting synthetic targets which may have useful and interesting properties. Without doubt this strategy would lead to many interesting new developments which will maintain group 14 chemistry as a fruitful, active field of research for many years to come.

IX. ACKNOWLEDGMENTS

M. Karni and Y. Apeloig thank the German Federal Ministry of Science, Research Technology and Education, the Minerva Foundation and the US–Israel Binational Science Foundation (BSF) for financial support.

X. REFERENCES

- (a) S. Patai (Ed.), *The Chemistry of Organic Germanium, Tin and Lead Compounds*, Wiley, Chichester, 1995.
(b) Z. Rappoport and Y. Apeloig (Eds.), *The Chemistry of Organic Germanium, Tin and Lead Compounds*, Vol. 2, Wiley, Chichester, in press.
- S. Patai and Z. Rappoport (Eds.), *The Chemistry of Organic Silicon Compounds*, Wiley, Chichester, 1989.
- J. Y. Corey, Chap. 1 in *The Chemistry of Organic Silicon Compounds*, (Eds. S. Patai and Z. Rappoport), Wiley, Chichester, 1989, pp. 1–56.
- C. Maerker, J. Kapp and P. v. R. Schleyer, in *Organosilicon Chemistry II. From Molecules to Materials* (Eds. N. Auner and J. Weis), VCH, Weinheim, 1996, pp. 329–359 and references cited therein.
- S. Nagase, Chap. 8 in *The Transition State* (Ed. T. Fueno), Gordon and Breach, London, 1999, pp. 147–161.
- W. Kutzelnigg, *Angew. Chem., Int. Ed. Engl.*, **23**, 272 (1984).
- Y. Apeloig, Chap. 2 in *The Chemistry of Organic Silicon Compounds* (Eds. S. Patai and Z. Rappoport), Wiley, Chichester, 1989, pp. 57–226.
- C. Elschenbroich and A. Salzer, *Organometallics—A Concise Introduction*, VCH, Weinheim, 1989, pp. 95–146.
- Z. Rappoport and Y. Apeloig (Eds.), *The Chemistry of Organic Silicon Compounds*, Vol. 2, Wiley, Chichester, 1998.
- M. A. Brook, *Silicon in Organic, Organometallic and Polymer Chemistry*, Wiley, Chichester, 1999.
- (a) A. G. Brook and K. M. Baines, *Adv. Organomet. Chem.*, **25**, 1–44 (1986).
(b) A. G. Brook and M. A. Brook, *Adv. Organomet. Chem.*, **39**, 71–158 (1996).
(c) R. Okazaki and R. West, *Adv. Organomet. Chem.*, **39**, 232–274 (1996).
(d) I. Hemme and U. Klingebiel, *Adv. Organomet. Chem.*, **39**, 159–192 (1996).
(e) M. Driess, *Adv. Organomet. Chem.*, **39**, 193–231 (1996).
(f) K. M. Baines and W. G. Stibbs, *Adv. Organomet. Chem.*, **39**, 275–324 (1996).
- (a) A. G. Brook, F. Abdesaken, B. Gutekunst, G. Gutekunst and R. K. Kallury, *J. Chem. Soc., Chem. Commun.*, 191 (1981).
(b) A. G. Brook, J. W. Harris, J. Lernnon and M. El Sheikh, *J. Am. Chem. Soc.* **101**, 183 (1979).
(c) A. G. Brook, S. C. Nyburg, W. F. Reynolds, Y. C. Poon, Y.-M. Chang, J.-S. Lee and J. P. Picard, *J. Am. Chem. Soc.*, **101**, 6750 (1979).
- R. West, *Angew. Chem., Int. Ed. Engl.*, **26**, 1201 (1987).
- G. Raabe and J. Michl, *Chem. Rev.*, **85**, 419 (1985).
- N. Wiberg, *J. Organomet. Chem.*, **273**, 141 (1984).
- J. Barrau, J. Escudié and J. Satgé, *Chem. Rev.*, **90**, 283 (1990).
- A. H. Cowley and N. C. Norman, *Prog. Inorg. Chem.*, **34**, 1 (1986).
- S. Masamune, in *Silicon Chemistry* (Ed. J. Y. Corey), Wiley, New York, 1988, p. 257.
- T. Tsumuraya, S. A. Batcheller and S. Masamune, *Angew. Chem., Int. Ed. Engl.*, **30**, 902 (1991).
- J. Escudié, C. Couret, H. Ranaivonjatovo and J. Satgé, *Coord. Chem. Rev.*, **130**, 427 (1994).

21. A. Sekiguchi and H. Sakurai, *Adv. Organomet. Chem.*, **37**, 1 (1995).
22. M. Driess and H. Grützmacher, *Angew. Chem., Int. Ed. Engl.*, **35**, 828 (1996).
23. For reviews see:
 - (a) Divalent compounds of germanium, tin and lead: M. F. Lappert, *Main Group Metal Chem.*, **17**, 183 (1994).
 - (b) Stable silylenes: M. Haaf, T. A. Schmedake and R. West, *Acc. Chem. Res.*, **33**, 704 (2000); N. Tokitoh and R. Okazaki, *Coord. Chem. Rev.*, **210**, 251 (2000).
24.
 - (a) P. P. Power, *Chem. Rev.*, **99**, 3463 (1999).
 - (b) N. Tokitoh, *Pure Appl. Chem.*, **71**, 495 (1999).
 - (c) P. P. Power, *J. Chem. Soc., Dalton Trans.*, 2939 (1998).
 - (d) J. Escudié, C. Couret and H. Ranaivonjatovo, *Coord. Chem. Rev.* **178–180**, 565 (1998).
 - (e) M. A. Chaubon, H. Ranaivonjatovo, J. Escudié and J. Stagé, *Main Group Metal Chem.*, **19**, 145 (1996).
 - (f) M. Weidenbruch, *Eur. J. Inorg. Chem.*, 373 (1999).
25.
 - (a) *Encyclopedia of Computational Chemistry* (P. v. R. Schleyer, N. L. Allinger, T. Clark, J. Gasteiger, P. A. Kollman, H. F. Schaefer III and P. R. Schreiner (Eds.), Wiley, New York, 1998).
 - (b) F. Jensen, *Introduction to Computational Chemistry*, Wiley, Chichester, 1999.
 - (c) W. J. Hehre, L. Radom, P. v. R. Schleyer and J. A. Pople, *Ab Initio Molecular Orbital Theory*, Wiley, New York, 1986.
 - (d) D. C. Young, *Computational Chemistry*, Wiley, New York, (2001).
26. R. S. Grev, *Adv. Organomet. Chem.*, **33**, 125 (1991).
27.
 - (a) M. S. Gordon, Chap. 6 in *Modern Electronic Structure Theory* (Ed. D. R. Yarkony), Part I, World Scientific, Singapore, 1995, p. 311.
 - (b) T. Veszprémi, *Advances in Molecular Structure Research*, Vol. 6, JAI Press, London, 2000, p. 267.
 - (c) K. K. Baldridge, J. A. Boatz, S. Koseki and M. S. Gordon, *Annu. Rev. Phys. Chem.*, **38**, 211 (1987).
 - (d) M. S. Gordon, J. S. Francisco and H. B. Schlegel, in *Advances in Silicon Chemistry*, Vol. 2, JAI Press, London, 1993, p. 137.
28.
 - (a) Y. Apeloig and M. Karni, Chap. 1 in Reference 9, pp. 1–101.
 - (b) C. Maerker, and P. v. R. Schleyer, Chap. 10 in Reference 9, p. 513.
 - (c) P. D. Lickiss, Chap. 11 in Reference 9, p. 557.
 - (d) C. A. Reed, *Acc. Chem. Res.*, **31**, 325 (1998).
29. C. Chatgililoglu and C. H. Schiesser, Chap. 4 in *The Chemistry of Organic Silicon Compounds*, Vol. 3 (Eds. Z. Rappoport and Y. Apeloig), Wiley, Chichester, 2001.
30.
 - (a) P. Pyykkö, *Chem. Rev.*, **88**, 563 (1988).
 - (b) A. Schultz and T. M. Klapötke, in Reference 1, pp. 585–601.
 - (c) K. Balasubramanian, *Relativistic Effects in Chemistry*, Wiley, New York, (1997).
31. J. P. Desclaux and P. Pyykkö, *Chem. Phys. Lett.*, **29**, 534 (1974).
32. K. G. Dyall, P. Taylor, K. Faegri, Jr. and H. Partridge, *J. Chem. Phys.*, **95**, 2583 (1991).
33. K. P. Huber and G. Herzberg, *Molecular Structure and Molecular Spectra IV. Constants of Diatomic Molecules*, Van Nostrand Reinhold, New York, 1979.
34. W. J. Stevens, M. Krauss, H. Basch and P. G. Jasien, *Can. J. Chem.*, **70**, 612 (1992).
35.
 - (a) A. L. Allred and E. J. Rochow, *J. Inorg. Nucl. Chem.*, **5**, 264 (1958).
 - (b) A. L. Allred, *J. Inorg. Nucl. Chem.*, **17**, 215 (1961).
36. L. C. Allen, *J. Am. Chem. Soc.*, **111**, 9003 (1989).
37. L. Pauling, in *The Nature of the Chemical Bond*, 3rd Edn., Cornell University Press, Ithaca, 1960.
38. L. E. Sutton, *Tables of Interatomic Distances and Configurations in Molecules and Ions*, in *Chemical Society Special Publications*, Vols. 11 and 18, London, 1958 and 1965.
39.
 - (a) R. D. Shannon and C. T. Prewitt, *Acta. Crystallogr.*, **B25**, 925 (1969).
 - (b) R. D. Shannon and C. T. Prewitt, *Acta. Crystallogr.*, **B26**, 1056 (1970).
40. J. P. Desclaux, *At. Data Nucl. Data Tables*, **12**, 311 (1973).
41. C. E. Moore, *Atomic Energy Levels, Nat. Bur. Stand. Circular 467*, Vols. II & III, Washington, 1971.
42.
 - (a) C. E. Moore, *Atomic Energy Levels, NSRDS-NBS 35/V.I*, U.S. Government Printing Office, Washington, D.C., 1971.

- (b) C. E. Moore, *Atomic Energy Levels, NSRDS-NBS 35/V.II*, U.S. Government Printing Office, Washington, D.C., 1971.
- (c) C. E. Moore, *Atomic Energy Levels, NSRDS-NBS 35/V.III*, U.S. Government Printing Office, Washington, D.C., 1971.
43. (a) H. Hotop and W. C. Lineberger, *J. Phys. Chem. Ref. Data*, **14**, 731 (1985).
(b) T. M. Miller, A. E. S. Miller and W. C. Lineberger, *Phys. Rev. A*, **33**, 3558 (1986).
44. M. Kaupp and P. v. R. Schleyer, *J. Am. Chem. Soc.*, **115**, 1061 (1993).
45. H. Basch and T. Hoz, Chap. 1 in Reference 1, pp. 1–96.
46. S. G. Wang and W. H. E. Schwarz, *J. Mol. Struct.*, **338**, 347 (1995).
47. A. Rose, I. P. Grant and N. C. Pyper, *J. Phys. B*, **11**, 1171 (1978).
48. (a) E. J. Baerends, W. H. E. Schwarz, P. Schwerdtfeger and J. G. Snijders, *J. Phys. B*, **23**, 3225 (1990).
(b) M. Seth, K. Faegri and P. Schwerdtfeger, *Angew. Chem., Int. Ed. Engl.*, **37**, 2493 (1998).
49. W. H. E. Schwarz, E. M. van Wezenbeek, E. J. Baerends and J. G. Snijders, *J. Phys. B*, **22**, 1515 (1989).
50. (a) B. A. Hess, *Phys. Rev. A*, **33**, 3742 (1986).
(b) B. A. Hess, in Reference 25a, pp. 2499–2508.
51. J. E. Huheey, *Inorganic Chemistry, Principle of Structure and Reactivity*, 3rd Edn., Harper and Row, New York, 1983.
52. D. Cremer, J. Gauss and E. Cremer, *J. Mol. Struct.*, **169**, 531 (1988).
53. P. Schwerdtfeger, G. A. Heath, M. Dolg and M. A. Bennett, *J. Am. Chem. Soc.*, **114**, 7518 (1992).
54. B. T. Luke, J. A. Pople, M.-B. Krogh-Jespersen, Y. Apeloig, J. Chandrasekhar and P. v. R. Schleyer, *J. Am. Chem. Soc.*, **108**, 260 (1986).
55. A. Shurki, P. C. Hiberty and S. Shaik, *J. Am. Chem. Soc.*, **121**, 822 (1999).
56. P. v. R. Schleyer and D. Kost, *J. Am. Chem. Soc.*, **110**, 2105 (1988).
57. F. M. Bickelhaupt, T. Ziegler and P. v. R. Schleyer, *Organometallics*, **15**, 1477 (1996).
58. A. E. Reed and P. v. R. Schleyer, *J. Am. Chem. Soc.*, **112**, 1434 (1990).
59. (a) Y. Mo, Y. Zhang and J. Gao, *J. Am. Chem. Soc.*, **121**, 5737 (1999).
(b) N. W. Mitzel and H. Oberhammer, *Inorg. Chem.*, **37**, 3593 (1998).
(c) E. Magnusson, *J. Am. Chem. Soc.*, **115**, 1051 (1993).
(d) E. Magnusson, *J. Am. Chem. Soc.*, **112**, 7940 (1990).
(e) A. E. Reed and P. v. R. Schleyer, *Inorg. Chem.*, **27**, 3969 (1988).
(f) A. E. Reed, C. Schade, P. v. R. Schleyer, P. Vishnu Kamath and J. Chandrasekhar, *J. Chem. Soc., Chem. Commun.*, 67 (1988).
(g) P. v. R. Schleyer, T. Clark, A. J. Kos, G. W. Spitznagel, C. Rohde, D. Arad, K. N. Houk and N. G. Rondan, *J. Am. Chem. Soc.*, **106**, 6467 (1984).
60. D. L. Cooper, T. P. Cunningham, J. Gerratt, P. B. Karadakov and M. Raimondi, *J. Am. Chem. Soc.*, **116**, 4414 (1994).
61. M. Head-Gordon, J. A. Pople and M. J. Frisch, *Chem. Phys. Lett.*, **153**, 503 (1988).
62. M. J. Frisch, M. Head-Gordon and J. A. Pople, *Chem. Phys. Lett.*, **166**, 275 (1990).
63. M. J. Frisch, M. Head-Gordon and J. A. Pople, *Chem. Phys. Lett.*, **166**, 281 (1990).
64. R. Krishnan and J. A. Pople, *Int. J. Quantum Chem.*, **14**, 91 (1978).
65. J. A. Pople, R. Krishnan, H. B. Schlegel and J. S. Binkley, *Int. J. Quantum Chem.*, **14**, 545 (1978).
66. G. D. Purvis and R. J. Bartlett, *J. Chem. Phys.*, **76**, 1910 (1982).
67. G. E. Scuseria, C. L. Jansen and H. F. Schaefer III, *J. Chem. Phys.*, **89**, 7382 (1988).
68. G. E. Scuseria and H. F. Schaefer III, *J. Chem. Phys.*, **90**, 3700 (1989).
69. J. A. Pople, M. Head-Gordon and K. Raghavachari, *J. Chem. Phys.*, **87**, 5968 (1987).
70. (a) J. K. Labanowski and J. W. Andzelm, *Density-Functionals in Chemistry*, Springer-Verlag, Berlin, 1991.
(b) R. G. Parr and W. Young, *Density-Functional Theory of Atoms and Molecules*, Clarendon Press, Oxford, 1989.
(c) W. Koch and M. C. Holthausen, *A Chemist's Guide to Density Functional Theory*, Wiley-VCH, Weinheim, 2000.
71. T. Ziegler, *Chem. Rev.*, **91**, 651 (1991).
72. (a) A. D. Becke, *Phys. Rev. A*, **38**, 3098 (1988).
(b) A. D. Becke, *J. Chem. Phys.*, **98**, 5648 (1993).

73. P. M. W. Gill, B. G. Johnson, J. A. Pople and M. J. Frisch, *Chem. Phys. Lett.*, **197**, 499 (1992).
74. (a) A. D. McLean and G. S. Chandler, *J. Chem. Phys.*, **72**, 5639 (1980).
(b) R. Krishnan, J. S. Binkley, R. Seeger and J. A. Pople, *J. Chem. Phys.*, **72**, 650 (1980).
75. M. J. Frisch, J. A. Pople and J. S. Binkley, *J. Chem. Phys.*, **80**, 3265 (1984).
76. A. Schäfer, H. Horn and R. Ahlrichs, *J. Phys. Chem.*, **97**, 2571 (1992).
77. S. Huzinaga, J. Andzelm, M. Kloubutowski, E. Radzio-Andzelm, Y. Saka and H. Tatewaki, in *Gaussian Basis Sets for Molecular Calculations* (Ed. S. Huzinaga), Elsevier, Amsterdam, 1984.
78. (a) M. J. S. Dewar, J. Friedheim, G. Gardy, E. F. Healy and J. P. Stewart, *Organometallics*, **5**, 375 (1986).
(b) J. P. Stewart, *J. Comput. Chem.*, **10**, 209 (1989).
(c) W. Thiel and A. A. Voityuk, *Theochem*, **119**, 141 (1994).
(d) W. Thiel and A. A. Voityuk, *J. Phys. Chem.*, **100**, 616 (1996).
79. M. J. S. Dewar, G. L. Grady and E. F. Healy, *Organometallics*, **6**, 186 (1987).
80. M. J. S. Dewar, G. L. Grady, D. R. Kuhn and K. M. Merz, *J. Am. Chem. Soc.*, **106**, 6773 (1984).
81. M. J. S. Dewar, M. K. Holloway, K. L. Grady and J. P. Stewart, *Organometallics*, **4**, 1973 (1985).
82. O. Visser, L. Visscher, P. J. C. Aerts and W. C. Nieuwpoort, *Theor. Chim. Acta*, **81**, 405 (1992).
83. (a) R. D. Cowan and D. C. Griffin, *J. Opt. Soc. Am.*, **66**, 1010 (1976).
(b) R. L. Martin, *J. Phys. Chem.*, **87**, 730 (1983).
84. T. Ziegler, J. G. Snijders and E. J. Baerends, *J. Chem. Phys.*, **74**, 1271 (1981).
85. O. Gropen, in *Methods in Computational Chemistry*, Vol. 2 (Ed. S. Wilson), Plenum Press, New York, 1988, p. 109.
86. K. Balasubramanian, in Reference 25a, p. 2471 and references cited therein.
87. (a) Z. Baradírán, L. Seijo and S. Huzinaga, *J. Chem. Phys.*, **93**, 5843 (1990).
(b) Z. Baradírán and L. Seijo, *Can. J. Chem.*, **70**, 409 (1992).
88. (a) L. F. Pacios and P. A. Christiansen, *J. Chem. Phys.*, **82**, 2664 (1985).
(b) M. M. Hurley, L. F. Pacios, P. A. Christiansen, R. B. Ross and W. C. Ermler, *J. Chem. Phys.*, **84**, 6840 (1986).
89. (a) L. A. LaJohn, P. A. Christiansen, R. B. Ross, T. Atashroo and W. C. Ermler, *J. Chem. Phys.*, **87**, 2812 (1987).
(b) R. B. Ross, J. M. Powers, T. Atashroo, W. C. Ermler and P. A. Christiansen, *J. Chem. Phys.*, **93**, 6654 (1990).
90. (a) P. J. Hay and W. R. Wadt, *J. Chem. Phys.*, **82**, 270 (1985).
(b) P. J. Hay and W. R. Wadt, *J. Chem. Phys.*, **82**, 284 (1985).
(c) P. J. Hay and W. R. Wadt, *J. Chem. Phys.*, **82**, 299 (1985).
91. M. Dolg, U. Wedig, H. Stoll and H. Preuss, *J. Chem. Phys.*, **86**, 866 (1986).
92. (a) A. Bergner, M. Dolg, W. Küchle, H. Stoll and H. Preuss, *Mol. Phys.*, **80**, 1431 (1993).
(b) W. Küchle, M. Dolg, H. Stoll and H. Preuss, *Mol. Phys.*, **74**, 1245 (1991).
93. For reviews see:
(a) K. Balasubramanian, *Chem. Rev.*, **89**, 1801 (1989).
(b) K. Balasubramanian, *Chem. Rev.*, **90**, 93 (1990).
94. K. G. Dyall, *J. Chem. Phys.*, **93**, 2191 (1993) and references cited therein.
95. K. B. Wiberg and P. R. Rablen, *J. Comput. Chem.*, **14**, 1504 (1993).
96. (a) R. F. W. Bader, *Atoms in Molecules: A Quantum Theory*, Clarendon Press, Oxford, 1990.
(b) P. Popelier, *Atoms in Molecules, An Introduction*, Pearson Education, Essex, 2000.
97. (a) R. F. W. Bader, T. T. Nguyen-Dang and Y. Tal, *Rep. Prog. Phys.*, **44**, 893 (1981).
(b) R. F. W. Bader and T. T. Nguyen-Dang, *Adv. Quantum Chem.*, **14**, 63 (1981).
98. R. F. W. Bader, *Acc. Chem. Res.*, **18**, 9 (1985).
99. R. F. W. Bader, P. L. A. Popelier and T. A. Keith, *Angew. Chem., Int. Ed. Eng.*, **33**, 620 (1994).
100. (a) A. E. Reed, R. B. Weinstock and F. Weinhold, *J. Chem. Phys.*, **83**, 735 (1985).
(b) A. E. Reed and F. Weinhold, *J. Chem. Phys.*, **83**, 1736 (1985).
101. A. E. Reed, L. A. Curtis and F. Weinhold, *Chem. Rev.*, **88**, 899 (1988).

102. (a) E. D. Glendening and F. Weinhold, *J. Comput. Chem.*, **19**, 593 (1998).
(b) E. D. Glendening and F. Weinhold, *J. Comput. Chem.*, **19**, 628 (1998).
103. Z. Barandiarán and L. Seijo, *J. Chem. Phys.*, **101**, 4049 (1994).
104. J. Almlöf and K. Faegri, Jr., *Theor. Chim. Acta*, **69**, 437 (1986).
105. T. A. Hein, W. Thiel and T. J. Lee, *J. Phys. Chem.*, **97**, 4381 (1993).
106. U. Steinbrenner, A. Bergner, M. Dolg and H. Stoll, *Mol. Phys.*, **82**, 3 (1994).
107. P. Schwerdtfeger, H. Silberbach and B. Miehlich, *J. Chem. Phys.*, **90**, 762 (1989).
108. T. Enevoldsen, L. Vissler, T. Saue, H. J. A. Jensen and J. Oddershede, *J. Chem. Phys.*, **112**, 3493 (2000).
109. D. J. Lucas, L. A. Curtiss and J. A. Pople, *J. Chem. Phys.*, **99**, 6697 (1993) and references cited therein.
110. (a) K. Raghavachari, *J. Chem. Phys.*, **95**, 7373 (1991).
(b) K. Raghavachari, *J. Chem. Phys.*, **96**, 4440 (1992).
111. M. S. Gordon, D. R. Gano, J. S. Binkley and M. J. Frisch, *J. Am. Chem. Soc.*, **108**, 2191 (1986).
112. M.-D. Su and H. B. Schlegel, *J. Phys. Chem.*, **97**, 9981 (1993).
113. P. Nachtigall, K. D. Jordan, A. Smith and H. Jónsson, *J. Chem. Phys.*, **104**, 148 (1996).
114. K. K. Das and K. Balasubramanian, *J. Chem. Phys.*, **93**, 5883 (1990).
115. R. C. Binning, Jr. and L. A. Curtiss, *J. Chem. Phys.*, **92**, 1860 (1990).
116. R. Ruscic, M. Schwarz and J. Berkowitz, *J. Chem. Phys.*, **92**, 1865 (1990).
117. M. J. Almond, A. D. Doncaster, P. N. Noble and R. Walsh, *J. Am. Chem. Soc.*, **104**, 4717 (1982).
118. J. A. Pople and L. A. Curtiss, *J. Phys. Chem.*, **91**, 155 (1987).
119. J. A. Pople, B. T. Luke, M. J. Frisch and J. S. Binkley, *J. Phys. Chem.*, **89**, 2198 (1985).
120. J. Berkowitz, J. P. Greene, H. Cho and B. Ruscic, *J. Chem. Phys.*, **86**, 1235 (1987).
121. S. G. Lias, J. E. Bartmess, J. F. Liebman, J. L. Holmes, R. D. Levin and W. G. Mallard, *J. Phys. Chem. Ref. Data*, **15**, Suppl. 1, 1988.
122. A. Becke, *J. Chem. Phys.*, **98**, 1372 (1993).
123. (a) B. G. Johnson, P. M. W. Gill and J. A. Pople, *J. Chem. Phys.*, **98**, 5612 (1993).
(b) L. A. Curtiss, K. Raghavachari and J. A. Pople, *J. Chem. Phys.*, **98**, 1293 (1993).
124. (a) K. Balasubramanian and K. S. Pitzer, *J. Mol. Spectrosc.*, **103**, 105 (1984).
(b) P. A. Christiansen, K. Balasubramanian and K. S. Pitzer, *J. Chem. Phys.*, **76**, 5087 (1982).
125. R. Walsh, *Acc. Chem. Res.*, **14**, 246 (1981).
126. K. G. Dyall, *J. Chem. Phys.*, **96**, 1210 (1992).
127. Experimental Values: Si: H. K. Moffat, K. F. Jensen and R. W. Carr, *J. Phys. Chem.*, **96**, 7695 (1992); Ge: C. G. Newman, J. Dzarnoski, M. A. Ring and H. E. O'Neal, *J. Chem. Kinet.*, **12**, 661 (1980).
128. (a) M. Sironi, D. L. Cooper, J. Garrat and M. Raimondi, *J. Am. Chem. Soc.*, **112**, 5054 (1990);
(b) C. W. Bauschlicher, Jr., K. Habber, H. F. Schaefer III and C. F. Bender, *J. Am. Chem. Soc.*, **99**, 3610 (1977).
129. V. M. Krivtsov, Y. A. Kuritsin and E. P. Snegirev, *Opt. Spektrosk.*, **86**, 771 (1999); *Chem. Abst.*, **131**, 278506 (1999).
130. (a) R. S. Grev and H. F. Schaefer III, *J. Chem. Soc., Chem. Commun.*, 785 (1983).
(b) I. M. T. Davidson, F. T. Lawrence and N. A. Ostah, *J. Chem. Soc., Chem. Commun.*, 659, (1980).
131. M.-D. Su and S.-Y. Chu, *Tetrahedron Lett.*, **40**, 4371 (1999).
132. T. Kudo and S. Nagase, *Chem. Phys. Lett.*, **148**, 73 (1988).
133. T. Kudo and S. Nagase, *Chem. Phys. Lett.*, **156**, 289 (1989).
134. B. W. Walther, F. Williams, W. Lau and J. K. Kochi, *Organometallics*, **2**, 688 (1983).
135. P. Babinec and J. Leszczynski, *Int. J. Quantum Chem.*, **72**, 319 (1999).
136. H. Basch, *Inorg. Chim. Acta*, **252**, 265 (1996).
137. W. Schneider and W. Thiel, *J. Chem. Phys.*, **86**, 923 (1986).
138. T. Ziegler and A. Rauk, *Inorg. Chem.*, **18**, 1558 (1979).
139. P. v. R. Schleyer, M. Kaupp, F. Hampel, M. Bremer and K. Mislow, *J. Am. Chem. Soc.*, **114**, 6791 (1992).
140. H. Oberhammer, T. Lobreyer and W. Sundermeyer, *J. Mol. Struct.*, **323**, 125 (1994).
141. A. Nicklass and H. Stoll, *Mol. Phys.*, **86**, 317 (1995).

- 152 Miriam Karni, Yitzhak Apeloig, Jürgen Kapp and Paul von R. Schleyer
142. J. Leszczynski, J. O. Huang, P. R. Schreiner, G. Vacek, J. Kapp, P. v. R. Schleyer and H. F. Schaefer, III, *Chem. Phys. Lett.*, **244**, 252 (1995).
143. J. Urban, P. R. Schreiner, G. Vacek, P. v. R. Schleyer, J. Q. Huang and J. Leszczynski, *Chem. Phys. Lett.*, **264**, 441 (1997).
144. M. Kaup, B. Metz and H. Stoll, *Angew. Chem., Int. Ed.*, **39**, 4607 (2000) and references cited therein.
145. G. Trinquier, *J. Chem. Soc., Faraday Trans.*, **89**, 775 (1993).
146. L. R. Sita, *Acc. Chem. Res.*, **27**, 191 (1994).
147. L. R. Sita, *Adv. Organomet. Chem.*, **38**, 189 (1995).
148. L. R. Sita, K. W. Terry and K. Shibata, *J. Am. Chem. Soc.*, **117**, 8049 (1995).
149. R. W. Bigelow, *Chem. Phys. Lett.*, **126**, 63 (1986).
150. K. Takeda, K. Shiraishi and N. Matsumoto, *J. Am. Chem. Soc.*, **112**, 5043 (1990).
151. K. Takeda and K. Shiraishi, *Chem. Phys. Lett.*, **195**, 121 (1992).
152. V. Jonas, G. Frenking and M. T. Reetz, *J. Comput. Chem.*, **13**, 935 (1992).
153. S. Escalante, R. Vargas and A. Vela, *J. Phys. Chem. A*, **103**, 5590 (1999).
154. J. Breidung, J. Demaison, L. Margulès and W. Theil, *Chem. Phys. Lett.*, **313**, 713 (1999).
155. J. E. Huheey, E. A. Keiter and R. L. Keiter, *Inorganic Chemistry*, 4th Edn., Harper Collins, New York, 1990.
156. Calculated from gas-phase heat of formations: M. W. Chase, Jr., NIST-JANAF Thermochemical Tables, Fourth Edition, *J. Phys. Chem. Ref. Data, Monograph 9*, 1–1951 (1998).
157. M. Kaupp and P. v. R. Schleyer, *Angew. Chem., Int. Ed. Engl.*, **31**, 1224 (1992).
158. (a) P. G. Harrison, T. J. King, J. A. Richard and R. C. Philip, *J. Organomet. Chem.*, **116**, 307 (1976).
(b) J. L. Baxter, E. M. Holt and J. Zuckerman, *Organometallics*, **4**, 255 (1985).
159. B. Beagly, K. McAloon and J. M. Friedman, *Acta Crystallogr., Sect. B*, **30**, 444 (1974).
160. P. G. Harrison, in *Comprehensive Coordination Chemistry*, Vol. 3 (Ed. G. Wilkinson), Pergamon Press, Oxford, 1987, pp. 183–235.
161. H. A. Bent, *Chem. Rev.*, **61**, 275 (1961).
162. A. E. Reed and P. v. R. Schleyer, *J. Am. Chem. Soc.*, **109**, 7362 (1987).
163. G. V. Gibbs, P. D'Arco and M. B. Boisen, Jr., *J. Phys. Chem.*, **91**, 5347 (1987).
164. A. E. Reed, P. v. R. Schleyer and R. Janoschek, *J. Am. Chem. Soc.*, **113**, 1885 (1991).
165. C. Marsden, *Chem. Phys. Lett.*, **245**, 475 (1995).
166. D. Kost and I. Kalikhman, Chap. 23 in Reference 9, p. 1339.
167. K. M. Mackay, Chap. 2, in Reference 1, p. 97.
168. J. Moc, *J. Mol. Struct.*, **461–462**, 249 (1999).
169. (a) J. Moc, J. M. Rudzinski and H. Ratajczak, *J. Mol. Struct. (Theochem)*, **228**, 131 (1991).
(b) J. Moc, J. M. Rudzinski and H. Ratajczak, *Chem. Phys. Lett.*, **173**, 557 (1990).
170. M. T. Carroll, M. S. Gordon and T. L. Windus, *Inorg. Chem.*, **31**, 825 (1992).
171. F. Voltaron, P. Mañre and M. Pélissier, *Chem. Phys. Lett.*, **166**, 49 (1990).
172. K. Nakamura, N. Masaki, S. Sato and K. Shimokoshi, *J. Chem. Phys.*, **83**, 4504 (1985).
173. K. Nakamura, N. Masaki, M. Okamoto, S. Sato and K. Shimokoshi, *J. Chem. Phys.*, **86**, 4949 (1987).
174. (a) P. v. R. Schleyer, in *New Horizons of Quantum Chemistry* (Eds. F.-O. Lödwin and B. Pullman), Reidel, Dordrecht, 1983, p. 95.
(b) P. v. R. Schleyer, E. V. Wuerthwein, E. Kaufmann, T. Clark and J. A. Pople, *J. Am. Chem. Soc.*, **105**, 5930 (1983).
(c) E. E. Bolton, H. F. Schaefer, III, W. D. Laidig and P. v. R. Schleyer, *J. Am. Chem. Soc.*, **116**, 9602 (1994).
(d) Z. Wang, X. Zheng and A. Tang, *Theochem*, **453**, 225 (1998).
175. H. Kudo, *Nature*, **355**, 432 (1992).
176. C. Yeretizian, U. Röthlisberger and E. Schumacher, *Chem. Phys. Lett.*, **237**, 334 (1995).
177. P. v. R. Schleyer and J. Kapp, *Chem. Phys. Lett.*, **255**, 363 (1996).
178. J. Chang, M. J. Scott and J. A. Alonso, *J. Chem. Phys.*, **104**, 8043 (1996).
179. For example: L. Paquette, *Chem. Rev.*, **89**, 1051 (1989).
180. A. Sekiguchi and V. Y. Lee, in *The Chemistry of Organic Germanium, Tin and Lead Compounds*, Vol. 2, (Eds. Z. Rappoport and Y. Apeloig), Wiley, Chichester, in press.
181. J. Rubio and F. Illas, *J. Mol. Struct.*, **110**, 131 (1984).
182. R. S. Grev and H. F. Schaefer III, *J. Am. Chem. Soc.*, **109**, 6569 (1987).

183. G. Naga Srinivas, B. Kiran and E. D. Jemmis, *J. Mol. Struct.*, **361**, 205 (1996).
184. S. Nagase, *Polyhedron*, **10**, 1299 (1991).
185. D. Hensler and G. Hohlneicher, *J. Phys. Chem.*, **102**, 10828 (1998).
186. A. F. Sax, *Chem. Phys. Lett.*, **127**, 163 (1986).
187. S. Nagase and M. Nakano, *J. Chem. Soc., Chem. Commun.*, 1077 (1988).
188. (a) C. Kratky, H.-G. Schuster and E. Hengge, *J. Organomet. Chem.*, **247**, 253 (1983).
(b) H. Matsumoto, M. Minemura, K. Takatsuna, Y. Nagi and M. Goto, *Chem. Lett.*, 1005 (1985).
189. J. Gauss, D. Cremer and J. F. Stanton, *J. Phys. Chem. A*, **104**, 1319 (2000).
190. S. Nagase, M. Nakano and T. Kudo, *J. Chem. Soc., Chem. Commun.*, 60 (1987).
191. S. Nagase, K. Kobayashi and M. Nagashima, *J. Chem. Soc., Chem. Commun.*, 1302 (1992).
192. S. Nagase, *Pure and Appl. Chem.*, **65**, 675 (1993).
193. S. Nagase, *Angew. Chem., Int. Ed. Engl.*, **28**, 329 (1989).
194. S. Nagase and T. Kudo, *J. Chem. Soc., Chem. Commun.*, 630 (1990).
195. S. Nagase, *Acc. Chem. Res.*, **28**, 469 (1995).
196. S. Nagase, K. Kobayashi and T. Kudo, *Main Group Metal Chem.*, **17**, 171 (1994).
197. M. J. S. Dewar, *J. Am. Chem. Soc.*, **106**, 699 (1984).
198. D. Cremer and E. Kraka, *J. Am. Chem. Soc.*, **107**, 3800 (1985).
199. D. Cremer and E. Kraka, *J. Am. Chem. Soc.*, **107**, 3811 (1985).
200. D. Cremer and J. Gauss, *J. Am. Chem. Soc.*, **108**, 7467 (1986).
201. P. v. R. Schleyer, in *Substituent Effects in Radical Chemistry* (Eds. H. G. Viehe, R. Janoschek and R. Merenyi), Reidel, Dordrecht, 1986, p. 69.
202. R. F. W. Bader, T. S. Slee, D. Cremer and E. Kraka, *J. Am. Chem. Soc.*, **105**, 5061 (1983) and references cited therein.
203. M. Radnic and Z. B. Maksic, *Theor. Chim. Acta*, **3**, 59 (1965).
204. D. A. Horner, R. S. Grev and H. F. Schaefer III, *J. Am. Chem. Soc.*, **114**, 2093 (1992).
205. (a) J. D. Dill, A. Greenberg and J. F. Liebman, *J. Am. Chem. Soc.*, **101**, 6814 (1979).
(b) A. Greenberg, J. F. Liebman and W. R. Dolbier, K. S. Medinger and A. Skancke, *Tetrahedron*, **39**, 1533 (1983).
206. M. Weidenbruch, *Main Group Metal Chem.*, **17**, 9 (1994).
207. S. Sakai, *Int. J. Quantum Chem.*, **70**, 291 (1998).
208. (a) W. Ando, H. Ohgaki and Y. Kabe, *Angew. Chem., Int. Ed. Engl.*, **33**, 659 (1994).
(b) H. Ohgaki, Y. Kabe and W. Ando, *Organometallics*, **14**, 2139 (1995).
209. (a) E. D. Jemmis, G. N. Srinivas, J. Leszczyński, J. Kapp, A. A. Korkin and P. v. R. Schleyer, *J. Am. Chem. Soc.*, **117**, 11361 (1995).
(b) E. D. Jemmis, B. V. Prasad, S. Tsuzuki and K. Tanabe, *J. Phys. Chem.*, **94**, 5530 (1990).
210. (a) J. Dubac, A. Laporterie and G. Manuel, *Chem. Rev.*, **90**, 215 (1990).
(b) J. Dubac, C. Guérin and P. Meunier, Chapter 34 in Reference 9, pp. 1961.
211. (a) K. Tameo, S. Yamaguchi, M. Uchida, T. Izumizawa and K. Furukawa, in *Organosilicon Chemistry IV. From Molecules to Materials* (Eds. N. Auner and J. Weis), VCH, Weinheim, 2000, p. 245.
(b) K. Tamao, Chap. 11 in *The Chemistry of Organic Silicon Compounds, Vol. 3* (Eds. Z. Rapoport and Y. Apeloig), Wiley, Chichester, 2001.
212. (a) K. Tamao and S. Yamaguchi, *Pure Appl. Chem.*, **68**, 139 (1996).
(b) Y. Yamaguchi and J. Shioya, *Mol. Eng.*, **2**, 339 (1993).
(c) V. N. Khabashesku, V. Balaji, S. E. Boganov, O. M. Nefedov and J. Michl, *J. Am. Chem. Soc.*, **116**, 320 (1994).
213. B. Goldfuss and P. v. R. Schleyer, *Organometallics*, **16**, 1543 (1997).
214. J. Ferman, J. P. Kakareka, W. T. Klooster, J. L. Mullin, J. Quattrucci, J. Ricci, H. J. Tracy, W. J. Vining and S. Wallace, *Inorg. Chem.*, **38**, 2464 (1998).
215. S. Yamaguchi, Y. Itami and K. Tamao, *Organometallics*, **17**, 4910 (1998).
216. K. Tamao, S. Yamaguchi, M. Shiozaki, Y. Nakagawa and Y. Ito, *J. Am. Chem. Soc.*, **114**, 5867 (1992).
217. J. A. Boatz and M. S. Gordon, *J. Phys. Chem.*, **93**, 3025 (1989).
218. R. S. Grev and H. F. Schaefer III, *J. Am. Chem. Soc.*, **109**, 6577 (1987).
219. W. Ando, M. Fujita, H. Toshida and A. Sekiguchi, *J. Am. Chem. Soc.*, **110**, 3310 (1988).
220. S. Masamune, Y. Hanzawa, S. Murakami, T. Bally and J. F. Blount, *J. Am. Chem. Soc.*, **104**, 1150 (1982).

221. (a) M. J. S. Dewar, *Bull. Soc. Chim. Fr.*, **18**, C71 (1951).
(b) J. Chatt and L. A. Duncanson, *J. Chem. Soc.*, 2939 (1953).
222. J. F. Liebman and P. N. Skancke, *Int. J. Quantum Chem.*, **58**, 707 (1996).
223. For a detailed review on heterocyclic 4-MRs for M = Si, see Reference 7.
224. J. Kapp, M. Remko and P. v. R. Schleyer, *Inorg. Chem.*, **36**, 4241 (1997).
225. (a) H. Sohn, R. P. Tan, D. R. Powell and R. West, *Organometallics*, **13**, 1390 (1994).
(b) H. B. Yokelson, A. J. Millevolte, B. R. Adams and R. West, *J. Am. Chem. Soc.*, **109**, 4116 (1987).
226. (a) P. v. R. Schleyer, A. F. Sax, J. Kalcher and R. Janoschek, *Angew. Chem., Int. Ed. Engl.*, **26**, 364 (1987).
(b) S. Nagase and T. Kudo, *J. Chem. Soc., Chem. Commun.*, 54 (1988).
227. T. Kudo and S. Nagase, *J. Phys. Chem.*, **96**, 9189 (1992).
228. (a) D. Ginsburg, *Propellane: Structure and Reactions*, Technion—I.I.T., Dept. of Chemistry, Haifa, 1981.
(b) K. B. Wiberg, *Chem. Rev.*, **89**, 975 (1989).
229. (a) P. v. R. Schleyer and R. Janoschek, *Angew. Chem., Int. Ed. Engl.*, **26**, 1267 (1987).
(b) S. Nagase and T. Kudo, *Organometallics*, **6**, 2456 (1987).
(c) W. W. Schoeller, T. Dabisch and T. Thilo, *Inorg. Chem.*, **26**, 4383 (1987).
230. Y. Kabe, T. Kawase, K. Okada, O. Yamashita, M. Goto and S. Masamune, *Angew. Chem., Int. Ed. Engl.*, **29**, 794 (1990).
231. M. S. Gordon, K. A. Nguyen and M. T. Carroll, *Polyhedron*, **10**, 1247 (1991).
232. K. A. Nguyen, M. T. Carroll and M. S. Gordon, *J. Am. Chem. Soc.*, **113**, 7924 (1991).
233. T. Kudo and S. Nagase, *Rev. Heteroatom Chem.*, **8**, 122 (1993).
234. L. R. Sita and R. D. Bickerstaff, *J. Am. Chem. Soc.*, **111**, 6454 (1989).
235. (a) L. R. Sita and I. Kinoshita, *J. Am. Chem. Soc.*, **112**, 8839 (1990).
(b) L. R. Sita and I. Kinoshita, *J. Am. Chem. Soc.*, **113**, 5070 (1991).
236. S. Nagase and T. Kudo, *Organometallics*, **7**, 2534 (1988).
237. (a) N. Gallego-Planas and M. A. Whitehead, *J. Mol. Struct.*, **260**, 419 (1992).
(b) N. Gallego-Planas and M. A. Whitehead, *Theochem*, **391**, 51 (1997).
238. N. Wiberg, C. M. M. Finger and K. Polborn, *Angew. Chem., Int. Ed. Engl.*, **32**, 1054 (1993).
239. (a) A. Sekiguchi, T. Yatabe, C. Kabuto and H. Sakurai, *J. Am. Chem. Soc.*, **115**, 5853 (1993).
(b) H. Matsumoto, K. Higuchi, Y. Hoshino, Y. Naoi and Y. Nagai, *J. Chem. Soc., Chem. Commun.*, 1083 (1988).
(c) K. Furukawa, M. Fujino and M. Matsumoto, *J. Organomet. Chem.*, **515**, 37 (1996).
(d) K. Furukawa, M. Fujino and M. Matsumoto, *Appl. Phys. Lett.*, **60**, 2744 (1992).
(e) M. Matsumoto, K. Higuchi, K. Kyushin and S. Goto, *Angew. Chem., Int. Ed. Engl.*, **31**, 1354 (1992).
(f) A. Sekiguchi, T. Yatabe, H. Kamatani, C. Kabuto and H. Sakurai, *J. Am. Chem. Soc.*, **114**, 6260 (1992).
(g) N. Wiberg, W. Hochmuth, H. Nöth, A. Appel and M. Schmidt-Amelunxen, *Angew. Chem., Int. Ed. Engl.*, **35**, 1333 (1996).
(h) A. Sekiguchi, C. Kabuto and H. Sakurai, *Angew. Chem., Int. Ed. Engl.*, **28**, 55 (1989).
(i) N. Wiberg, H.-W. Lerner, H. Nöth and W. Ponikwar, *Angew. Chem., Int. Ed.*, **38**, 1103 (1999).
(j) L. R. Sita and I. Kinoshita, *Organometallics*, **9**, 2865 (1990).
(k) L. R. Sita and I. Kinoshita, *J. Am. Chem. Soc.*, **113**, 1856 (1991).
240. A. Sekiguchi and S. Nagase, Chap. 3 in Reference 9.
241. C. W. Early, *J. Phys. Chem. A*, **104**, 6622 (2000).
242. W. J. Stevens, H. Basch and M. Krauss, *J. Chem. Phys.*, **81**, 6026 (1984).
243. G. N. Srinivas and E. D. Jemmis, *J. Am. Chem. Soc.*, **119**, 12968 (1997).
244. (a) B. F. Yates, D. A. Clabo Jr. and H. F. Schaefer III, *Chem. Phys. Lett.*, **143**, 421 (1988).
(b) S. Nagase and M. Nakano, *Angew. Chem., Int. Ed. Engl.*, **27**, 1081 (1988).
(c) B. F. Yates and H. F. Schaefer III, *Chem. Phys. Lett.*, **155**, 563 (1989).
245. M. Bühl and P. v. R. Schleyer, *J. Am. Chem. Soc.*, **114**, 477 (1992).
246. (a) G. J. Mains, C. W. Bock and M. Trachtman, *J. Phys. Chem.*, **93**, 1745 (1989).
(b) C. W. Bock, M. Trachtman, P. D. Maker, H. Niki and G. J. Mains, *J. Phys. Chem.*, **90**, 5669 (1986).
247. E. D. Jemmis, G. Subramanian and M. L. McKee, *J. Phys. Chem.*, **100**, 7014 (1996).

248. (a) F. S. Kipping, *Proc. Chem. Soc.*, **27**, 143 (1911).
(b) F. S. Kipping, *J. Chem. Soc.*, **123**, 2590 (1923).
(c) F. S. Kipping, *J. Chem. Soc.*, **125**, 2291 (1924).
(d) F. S. Kipping, *Proc. R. Soc. London*, **159**, 139 (1937).
249. (a) K. S. Pitzer, *J. Am. Chem. Soc.*, **70**, 2140 (1948).
(b) R. S. Mulliken, *J. Am. Chem. Soc.*, **72**, 4493 (1950).
250. P. Jutzi, *Angew. Chem., Int. Ed. Engl.*, **14**, 232 (1975).
251. R. West, J. Fink and J. Michl, *Science*, **214**, 1343 (1981).
252. (a) J. Davidson and M. F. Lappert, *J. Chem. Soc., Chem. Commun.*, 317 (1973).
(b) D. E. Goldberg, D. H. Harris, M. F. Lappert and K. M. Thomas, *J. Chem. Soc., Chem. Commun.*, 261 (1976).
(c) P. J. Davidson, D. H. Harris and M. F. Lappert, *J. Chem. Soc., Dalton Trans.*, 2268 (1976).
253. T. Fjeldberg, A. Haaland, M. F. Lappert, B. E. R. Schilling, R. Seip and A. J. Thorne, *J. Chem. Soc., Chem. Commun.*, 1407 (1982).
254. D. E. Goldberg, P. B. Hitchcock, M. F. Lappert, K. M. Thomas, A. J. Thorne, T. Fjeldberg, A. Haaland and B. E. R. Schilling, *J. Chem. Soc., Dalton Trans.*, 2387 (1986).
255. T. Fjeldberg, A. Haaland, B. E. R. Schilling, M. F. Lappert and A. J. Thorne, *J. Organomet. Chem.*, **276**, C1 (1984).
256. (a) M. Strümann, W. Saak, H. Marsmann and M. Weidenbruch, *Angew. Chem., Int. Ed.*, **38**, 187 (1999).
(b) M. Strümann, W. Saak, H. Marsmann, M. Weidenbruch and K. W. Klinkhammer, *Eur. J. Inorg. Chem.*, 579 (1999).
257. (a) G. Maier and J. Glatthaar, *Angew. Chem., Int. Ed. Engl.*, **33**, 473 (1994).
(b) J. F. Ogilvie and S. Craddock, *J. Chem. Soc., Chem. Commun.*, 364 (1966).
(c) J. G. Radziszewski, D. Littmann, V. Balaji, L. Fabry, G. Gross and J. Michl, *Organometallics*, **12**, 4816 (1993).
(d) H. Bock, and R. Dammel, *Angew. Chem., Int. Ed. Engl.*, **24**, 111 (1985).
258. M. Karni, Y. Apeloig, D. Schröder, W. Zummack, R. Rabazzana and H. Schwarz, *Angew. Chem., Int. Ed.*, **38**, 332 (1999).
259. C. Bibal, S. Mazières, H. Gornitzka and C. Couret, *Angew. Chem., Int. Ed.*, **40**, 952 (2001).
260. L. Pu, B. Twamley and P. P. Power, *J. Am. Chem. Soc.*, **122**, 3524 (2000).
261. (a) L. Pu, M. O. Senge, M. M. Olmstead and P. P. Power, *J. Am. Chem. Soc.*, **120**, 12682 (1998).
(b) L. Pu, B. Twamley, S. T. Haubrich, M. M. Olmstead, R. V. Mork, R. S. Simons and P. P. Power, *J. Am. Chem. Soc.*, **122**, 650 (2000).
(c) A. C. Filippou, A. I. Philippopoulos, P. Portius and D. U. Neumann, *Angew. Chem., Int. Ed.*, **39**, 2778 (2000).
262. P. Jutzi, *Angew. Chem., Int. Ed.*, **39**, 3797 (2000).
263. M. Karni and Y. Apeloig, *J. Am. Chem. Soc.*, **112**, 8589 (1990).
264. K. Krogh-Jespersen, *J. Am. Chem. Soc.*, **107**, 537 (1985).
265. (a) J.-P. Malrieu and G. Trinquier, *J. Am. Chem. Soc.*, **111**, 5916 (1989).
(b) G. Trinquier and J.-P. Malrieu, *J. Phys. Chem.*, **94**, 6184 (1990).
266. G. Trinquier and J.-P. Malrieu in *The Chemistry of Double-Bonded Functional Groups*, (Ed. S. Patai), Wiley, Chichester, 1989, pp. 1–52.
267. C. Liang and L. C. Allen, *J. Am. Chem. Soc.*, **112**, 1039 (1990).
268. H. Jacobsen and T. Ziegler, *J. Am. Chem. Soc.*, **116**, 3667 (1994).
269. G. Trinquier, *J. Am. Chem. Soc.*, **112**, 2130 (1990).
270. (a) H. Lischka and H.-J. Kohler, *Chem. Phys. Lett.*, **85**, 467 (1982).
(b) H.-J. Kohler and H. Lischka, *Chem. Phys. Lett.*, **98**, 454 (1983).
271. G. Olbrich, *Chem. Phys. Lett.*, **130**, 115 (1986).
272. T. L. Windus and M. S. Gordon, *J. Am. Chem. Soc.*, **114**, 9559 (1992).
273. K. W. Klinkhammer, T. F. Fässler and H. Grützmacher, *Angew. Chem., Int. Ed.*, **37**, 124 (1998).
274. T. A. Schmedake, M. Haaf, Y. Apeloig, T. Müller, S. Bulkalov and R. West, *J. Am. Chem. Soc.*, **121**, 9479 (1999).
275. T. Kudo and S. Nagase, *Chem. Phys. Lett.*, **84**, 375 (1981).
276. S. Nagase and T. Kudo, *Organometallics*, **3**, 324 (1984).
277. G. Trinquier, J.-C. Barthelat and J. Satgé, *J. Am. Chem. Soc.*, **104**, 5931 (1982).

278. (a) K. D. Dobbs and W. J. Hehre, *Organometallics*, **5**, 2057 (1986).
(b) S. Saebø, S. Stroble, W. Collier, E. Ethridge, Z. Wilson, M. Tahai and C. U Pittman, Jr., *J. Org. Chem.*, **64** 1311 (1999).
279. G. Trinquier, J.-P. Malrieu and P. Rivière, *J. Am. Chem. Soc.*, **104**, 4529 (1982).
280. G. Trinquier and J.-P. Malrieu, *J. Am. Chem. Soc.*, **109**, 5303 (1987).
281. G. Trinquier and J.-C. Barthelat, *J. Am. Chem. Soc.*, **112**, 9121 (1990).
282. W.-C. Chen, M.-D. Su and S.-Y. Chu, *Organometallics*, **20**, 564 (2001).
283. M. S. Gordon, T. N. Truong and E. K. Bonderson, *J. Am. Chem. Soc.*, **108**, 1421 (1986).
284. (a) G. Li, Q. Li, W. Xu, Y. Xie and H. F. Schaefer III, *Mol. Phys.*, in press.
(b) G. Li, Q. Li, W. Xu, Y. Xie and H. F. Schaefer III, *J. Am. Chem. Soc.*, submitted.
285. (a) M. Takahashi, S. Tsutsui, K. Sakamoto, M. Kira, T. Müller and Y. Apeloig, *J. Am. Chem. Soc.*, **123**, 978 (2001).
(b) S. Tsutsui, K. Sakamoto and M. Kira, *J. Am. Chem. Soc.*, **120**, 9955 (1998).
(c) K. Sakamoto, S. Tsutsui, H. Sakurai and M. Kira, *Bull. Chem. Soc. Jpn.*, **70**, 253 (1997).
286. K. W. Klinkhammer and W. Schwarz, *Angew. Chem., Int. Ed. Engl.*, **34**, 1334 (1995).
287. S. W. Benson, *Thermochemical Kinetics*, Wiley, New York, 1976, pp. 63–65.
288. M. Kira, S. Ohya, T. Iwamoto, M. Ichinohe and C. Kabuto, *Organometallics*, **19**, 1817 (2000).
289. J. M. Galbraith, E. Blank, S. Shaik and P. Hiberty, *Chem. Eur. J.*, **6**, 2425 (2000).
290. M. W. Schmidt, P. N. Truong and M. S. Gordon, *J. Am. Chem. Soc.*, **109**, 5217 (1987).
291. G. Lendvay, *Chem. Phys. Lett.*, **181**, 88 (1991).
292. H. Grützmacher and T. F. Fässler, *Chem. Eur. J.*, **6**, 2317 (2000).
293. B. T. Luke, J. A. Pople, M.-B. Krogh-Jespersen, Y. Apeloig, M. Karni, J. Chandrasekhar and P. v. R. Schleyer, *J. Am. Chem. Soc.*, **108**, 270 (1986).
294. M. B. Coolidge and W. T. Borden, *J. Am. Chem. Soc.*, **110**, 2298 (1988).
295. R. S. Grev, G. E. Scuseria, A. C. Scheiner, H. F. Schaefer III and M. S. Gordon, *J. Am. Chem. Soc.*, **110**, 7337 (1988).
296. R. S. Grev and H. F. Schaefer III, *Organometallics*, **11**, 3489 (1992).
297. C. Pak, J. C. Rienstra-Kiracofe and H. F. Schaefer III, *J. Phys. Chem.*, **104**, 11232 (2000).
298. J. A. Boaz and M. S. Gordon, *J. Phys. Chem.*, **94**, 7331 (1990).
299. K. Krogh-Jespersen, *Chem. Phys. Lett.*, **93**, 327 (1982).
300. H. F. Schaefer III, *Acc. Chem. Res.*, **15**, 283 (1982).
301. R. S. Grev, H. F. Schaefer, III and K. M. Baines, *J. Am. Chem. Soc.*, **112**, 9458 (1990).
302. G. Trinquier, *J. Am. Chem. Soc.*, **113**, 144 (1991).
303. B. E. Eichler and P. P. Power, *J. Am. Chem. Soc.*, **122**, 8785 (2000).
304. A. F. Wells, *Structural Inorganic Chemistry*, 5th Edn., Clarendon Press, Oxford, 1984.
305. M. Hargittai, *Coord. Chem. Rev.*, **91**, 35 (1988).
306. J. Maxka and Y. Apeloig, *J. Chem. Soc., Chem. Commun.*, 737 (1990).
307. P. Jutzi, U. Holtman, H. Bogge and A. Muller, *J. Chem. Soc., Chem. Commun.*, 305 (1988).
308. G. Schultz, J. Tremmel, I. Hargittai, N. D. Kagramanov, A. K. Maltsev, J. H. Miller and L. Andrews, *J. Mol. Struct.*, **82**, 107 (1982).
309. J. M. Coffin, T. P. Hamilton, P. Pulay and I. Hargittai, *Inorg. Chem.*, **28**, 4092 (1989).
310. R. S. Simons, L. Pu, M. M. Olmstead and P. P. Power, *Organometallics*, **16**, 1920 (1997).
311. (a) Y. Apeloig and T. Müller, *J. Am. Chem. Soc.*, **117**, 5363 (1995).
(b) Y. Apeloig, M. Karni and T. Müller, in *Organosilicon Chemistry II. From Molecules to Materials* (Eds. N. Auner and J. Weis), VCH, Weinheim, 1996, p. 263.
312. R. Okazaki and N. Tokitoh, *Acc. Chem. Res.*, **33**, 625 (2000).
313. (a) H. Suzuki, N. Tokitoh, R. Okazaki, S. Nagase and M. Goto, *J. Am. Chem. Soc.*, **120**, 11096 (1998).
(b) T. Matsumoto, N. Tokitoh and R. Okazaki, *J. Am. Chem. Soc.*, **121**, 8811 (1999).
(c) N. Tokitoh, Y. Natsuhara, K. Shibata, T. Matsumoto, H. Suzuki, M. Saito, K. Manmaru and R. Okazaki, *Main Group Metal Chem.*, **17**, 55 (1994).
(d) N. Tokitoh, M. Saito and R. Okazaki, *J. Am. Chem. Soc.*, **115**, 2065 (1993).
(e) M. Saito, N. Tokitoh and R. Okazaki, *J. Am. Chem. Soc.*, **119**, 11124 (1997).
314. (a) S. Bailleaux, M. Bogey, C. Demuyne, J. Destombes and A. Walters, *J. Chem. Phys.*, **101**, 2729 (1994).
(b) M. Bogey, B. Delcroix, A. Walters and J.-C. Guillemin, *J. Mol. Spectrosc.*, **175**, 421 (1996).
(c) R. Srinivas, D. K. Bohme, D. Stülzle and H. Schwarz, *J. Phys. Chem.*, **95**, 9837 (1991).

- (d) R. J. Glinski, J. L. Gole and D. A. Dixon, *J. Am. Chem. Soc.*, **107**, 5891 (1985).
(e) R. Withnall and L. Andrews, *J. Phys. Chem.*, **89**, 3261 (1985).
(f) R. Withnall and L. Andrews, *J. Am. Chem. Soc.*, **107**, 2567 (1985).
(g) V. N. Khabashesku, Z. A. Kerzina, K. N. Kudin and O. M. Nefedov, *J. Organomet. Chem.*, **45**, 556 (1998).
315. (a) R. Withnall and L. Andrews, *J. Phys. Chem.*, **94**, 2351 (1990) and references cited therein.
(b) V. N. Khabashesku, S. Boganov, K. N. Kudin, T. L. Hargreave and O. M. Nefedov, *Organometallics*, **17**, 5041 (1998).
316. J. Kapp, M. Remko and P. v. R. Schleyer, *J. Am. Chem. Soc.*, **118**, 5745 (1996).
317. W. W. Schoeller, C. Begemann, U. Tubbesing and J. Strutwolf, *J. Chem. Soc., Faraday Trans.*, **93**, 2957 (1997).
318. D. J. Lucas, L. A. Curtiss and J. A. Pople, *J. Chem. Phys.*, **99**, 6697 (1993).
319. (a) C.-L. Lin, M.-D. Su and S.-Y. Chu, *Chem. Commun.*, 2383 (1999).
(b) C.-L. Lin, M.-D. Su and S.-Y. Chu, *Chem. Phys.*, **249**, 145 (1999).
320. V. N. Khabashesku, S. E. Boganov, K. N. Kudin, J. L. Margrave, J. Michl and O. M. Nefedov, *Russian Chem. Bull.*, **48**, 2003 (1999).
321. (a) N. A. Richardson, J. C. Reinstra-Kiracofe and H. F. Schaefer III, *Inorg. Chem.*, **38**, 6271 (1999).
(b) N. A. Richardson, J. C. Reinstra-Kiracofe and H. F. Schaefer III, *J. Am. Chem. Soc.*, **121**, 10813 (1999).
322. C. Heinemann, W. A. Herrmann and W. Thiel, *J. Organomet. Chem.*, **475**, 73 (1994).
323. C. Boehme and G. Frenking, *J. Am. Chem. Soc.*, **118**, 2039 (1996).
324. M. Driess, R. Janoschek, H. Pritzkow, S. Rell and U. Winkler, *Angew. Chem., Int. Ed. Engl.*, **34**, 1614 (1995).
325. T. Kudo and S. Nagase, *J. Organomet. Chem.*, **253**, C23 (1983).
326. (a) A. G. Baboul and H. B. Schlegel, *J. Am. Chem. Soc.*, **118**, 8444 (1996).
(b) K. J. Dykema, T. Truong and M. S. Gordon, *J. Am. Chem. Soc.*, **107**, 4535 (1985).
327. (a) M. Weidenbruch, S. Willms, W. Saak and G. Henkel, *Angew. Chem., Int. Ed.*, **36**, 2503 (1997).
(b) H. Schäfer, W. Saak and M. Weidenbruch, *Angew. Chem., Int. Ed.*, **39**, 3703 (2000).
328. (a) T. Müller, *Angew. Chem., Int. Ed.*, **37**, 68 (1998).
(b) T. Müller, in *Organosilicon Chemistry IV. From Molecules to Materials*. (Eds. N. Auner and J. Weis), VCH, Weinheim, 2000, pp. 110–116.
329. V. Y. Lee, M. Ichinohe and A. Sekiguchi, *J. Am. Chem. Soc.*, **122**, 12604 (2000).
330. (a) M. Ishikawa, K. Watanabe, H. Sakamoto and A. Kunai, *J. Organomet. Chem.*, **435**, 249 (1992).
(b) B. R. Yoo, M. E. Lee and I. N. Jung, *Organometallics*, **11**, 1626 (1992).
331. C. Kerst, M. Byloos and W. J. Leigh, *Can. J. Chem.*, **75**, 975 (1997).
332. G. Trinquier and J.-P. Malrieu, *J. Am. Chem. Soc.*, **103**, 6313 (1981).
333. K. Yoshizawa, S.-Y. Kang, T. Yamabe, A. Naka and M. Ishikawa, *Organometallics*, **18**, 4637 (1999).
334. S. Sakai, *J. Mol. Struct. (Theochem)*, **461–462**, 283 (1999).
335. C. Jouany and G. Trinquier, *Organometallics*, **16**, 3148 (1997).
336. G. Trinquier and C. Jouany, *J. Phys. Chem. A*, **103**, 4723 (1999).
337. C. Jouany, S. Mathieu, M.-A. Chaubon-Deredempt and G. Trinquier, *J. Am. Chem. Soc.*, **116**, 3973 (1994).
338. (a) G. E. Miracle, J. L. Ball, D. R. Powell and R. West, *J. Am. Chem. Soc.*, **115**, 11598 (1993).
(b) G. E. Miracle, B. E. Eichler, D. R. Powell and R. West, *Organometallics*, **16**, 5737 (1997).
(c) B. E. Eichler, D. R. Powell and R. West, *Organometallics*, **17**, 2147 (1998).
(d) B. E. Eichler, D. R. Powell and R. West, *Organometallics*, **18**, 540 (1999).
(e) N. Tokitoh, K. Kishikawa and R. Okazaki, *Chem. Lett.*, 811 (1998).
339. (a) N. Sigal and Y. Apeloig, *Organometallics*, submitted (2001).
(b) N. Sigal and Y. Apeloig, *J. Organomet. Chem.*, in press (2001).
340. Y. Apeloig and M. Karni, *Organometallics*, **16**, 310 (1997).
341. M. Karni and Y. Apeloig, *Silicon Chemistry*, submitted (2001).
342. K. Kobayashi and S. Nagase, *Organometallics*, **16**, 2489 (1997).
343. (a) S. Nagase, K. Kobayashi and N. Takagi, *J. Organomet. Chem.*, **611**, 264 (2000).
(b) K. Kobayashi, N. Takagi and S. Nagase, *Organometallics*, **20**, 234 (2001).

344. B. T. Colegrove and H. F. Schaefer III, *J. Phys. Chem.*, **94**, 5593 (1990).
345. R. S. Grev and H. F. Schaefer III, *J. Chem. Phys.*, **97**, 7990 (1992).
346. Y. Yamaguchi, B. J. DeLeeuw, C. A. Richards, Jr., H. F. Schaefer III and G. Frenking, *J. Am. Chem. Soc.*, **116**, 11922 (1994).
347. R. S. Grev, B. J. DeLeeuw and H. F. Schaefer III, *Chem. Phys. Lett.*, **165**, 257 (1990).
348. W. W. Schoeller and J. Strutwolf, *J. Mol. Struct.*, **305**, 127 (1994).
349. M. T. Nguyen, D. Sengupta and L. G. Vanquickenborne, *Chem. Phys. Lett.*, **244**, 83 (1995).
350. R. Stegmann, and G. Frenking, *J. Comput. Chem.*, **17**, 781 (1996).
351. (a) B. S. Jursic, *J. Mol. Struct.*, **459**, 221 (1999).
(b) B. S. Jursic, *J. Mol. Struct.*, **491**, 1 (1999).
352. J. M. Galbraith and H. F. Schaefer III, *J. Mol. Struct.*, **424**, 7 (1998).
353. B. J. DeLeeuw, R. S. Grev and H. F. Schaefer III, *J. Chem. Educ.*, **69**, 441 (1992).
354. S. M. Stogner and R. S. Grev, *J. Chem. Phys.*, **108**, 5458 (1998).
355. A. J. Boone, D. H. Magers and J. Leszczyński, *Int. J. Quantum Chem.*, **70**, 925 (1998).
356. H.-Y. Liao, M.-D. Su and S.-Y. Chu, *Inorg. Chem.*, **39**, 3522 (2000).
357. J. S. Binkley, *J. Am. Chem. Soc.*, **106**, 603 (1984).
358. P. O'leary, J. R. Thomas, H. F. Schaefer III, B. J. Duke and B. O'leary, *Int. J. Quantum Chem. Quantum Chem. Symp.*, **29**, 593 (1995).
359. M. M. Olmstead, R. S. Simons and P. P. Power, *J. Am. Chem. Soc.*, **119**, 11705 (1997).
360. Z. Palágyi, H. F. Schaefer III and E. Kapuy, *J. Am. Chem. Soc.*, **115**, 6901 (1993).
361. (a) J. J. BelBruno, *J. Chem. Soc., Faraday Trans.*, **94**, 1555 (1998).
(b) A. B. Alexseyev, H.-P. Lieberman, R. J. Buenker and H. Hirsch, *Mol. Phys.*, **88**, 591 (1996).
(c) K. Balasubramanian and K. Pitzer, *J. Phys. Chem.*, **88**, 1146 (1984).
362. Y. Apeloig and M. Karni, unpublished results.
363. (a) G. H. Robinson, *Acc. Chem. Res.*, **32**, 773 (1999).
(b) G. H. Robinson, *Chem. Commun.*, 2175 (2000).
(c) F. A. Cotton, A. H. Cowley and X. Feng, *J. Am. Chem. Soc.*, **119**, 1795 (1998).
(d) K. W. Klinkhammer, *Angew. Chem., Int. Ed. Engl.*, **36**, 2320 (1997).
(e) Y. Xie, R. S. Grev, J. Gu, H. F. Schaefer III, P. v. R. Schleyer, J. Su, X.-W. Li and G. H. Robinson, *J. Am. Chem. Soc.*, **120**, 3773 (1998).
(f) Y. Xie, H. F. Schaefer III and G. H. Robinson, *Chem. Phys. Lett.*, **317**, 174 (2000).
(g) N. Takagi, M. W. Schmidt and S. Nagase, *Organometallics*, in press (2001).
(h) I. Bytheway and Z. Lin, *J. Am. Chem. Soc.*, **120**, 12133 (1998).
(i) J. Grunenberg and N. Goldberg, *J. Am. Chem. Soc.*, **122**, 6045 (2000).
364. D. Danovich, F. Ogliaro, M. Karni, Y. Apeloig, D. L. Cooper and S. Shaik, *Angew. Chem. Int. Ed.*, in press (2001).
365. T. L. Allen, W. H. Fink and P. P. Power, *J. Chem. Soc., Dalton Trans.*, 407 (2000).
366. (a) R. Damrauer, C. H. DePuy, S. E. Barlow and S. Gronert, *J. Am. Chem. Soc.*, **110**, 2005 (1988).
(b) R. Srinivas, D. Sülzle and H. Schwarz, *J. Am. Chem. Soc.*, **113**, 52 (1991).
(c) D. Sherril and H. F. Schaefer III, *J. Phys. Chem.*, **99**, 1949 (1995).
(d) M. Izuha, S. Yamamoto and S. Saito, *J. Chem. Phys.*, **105**, 4923 (1996).
(e) W. W. Harper, K. W. Waddell and D. J. Clouthier, *J. Chem. Phys.*, **107**, 8829 (1997).
367. D. A. Hostutler, T. C. Smith, H. Li and D. J. Clouthier, *J. Chem. Phys.*, **111**, 950 (1999).
368. S. Daprich, I. Komáromi, K. S. Byun, K. Morokuma and M. J. Frisch, *J. Mol. Struct.*, **461-462**, 1 (1999).
369. (a) N.-Y. Chang, M.-Y. Shen and C.-H. Yu, *J. Chem. Phys.*, **106**, 3237 (1997).
(b) H. Lischka and H. Köhler, *J. Am. Chem. Soc.*, **105**, 6646 (1983).
370. (a) M. Bogey, H. Bolvin, C. Demuynck and J.-L. Destombes, *Phys. Rev. Lett.*, **66**, 413 (1991).
(b) M. Bogey, H. Bolvin, M. Cordonnier, C. Demuynck, J.-L. Destombes and A. G. Csaszar, *J. Chem. Phys.*, **100**, 8614 (1994).
371. G. Maier, H. Reisenauer, A. Meudt and H. Egenolf, *Chem. Ber.*, **130**, 1043 (1997).
372. M. Cordonnier, M. Bogey, C. Demuynck and J.-L. Destombes, *J. Chem. Phys.*, **97**, 7984 (1992).
373. (a) B. S. Thies, R. S. Grev and H. F. Schaefer, III, *Chem. Phys. Lett.*, **140**, 355 (1987).
(b) B. T. Colegrove and H. F. Schaefer III, *J. Am. Chem. Soc.*, **113**, 1557 (1991).
374. A. Sekiguchi, S. Zigler and R. West, *J. Am. Chem. Soc.*, **108**, 4241 (1986).

375. V. Y. Lee, A. Sekiguchi, M. Ichinohe and N. Fukaya, *J. Organomet. Chem.*, **611**, 228 (2000).
376. (a) N. Matsunaga and M. S. Gordon, *J. Am. Chem. Soc.*, **116**, 11407 (1994).
(b) N. Matsunaga, T. R. Cundari, M. W. Schmidt and M. S. Gordon, *Theor. Chim. Acta*, **83**, 57 (1992).
377. (a) M. Zhao and B. M. Gimarc, *Inorg. Chem.*, **35**, 5378 (1996).
(b) A. F. Sax and R. Janoschek, *Angew. Chem., Int. Ed. Engl.*, **25**, 651 (1986).
378. S. Nagase, T. Kudo and M. Aoki, *J. Chem. Soc., Chem. Commun.*, 1121 (1985).
379. P. v. R. Schleyer, H. Jiao, N. v. E. Hommes, V. G. Malkin and O. Malkina, *J. Am. Chem. Soc.*, **119**, 12669 (1997).
380. K. K. Baldrige, O. Uzan and J. M. L. Martin, *Organometallics*, **19**, 1477 (2000).
381. (a) I. V. Minkin, M. N. Glukhovtsev and B. Ya. Simkin, *Aromaticity and Antiaromaticity*, John Wiley, New York, 1994.
(b) P. v. R. Schleyer and H. Jiao, *Pure Appl. Chem.*, **68**, 209 (1996).
382. (a) W. Ando, Y. Kabe and C. Nami, *Main Group Metal Chem.*, **17**, 209 (1994).
(b) A. Sekiguchi and V. Y. Lee, in *The Chemistry of Organic Germanium, Tin and Lead compounds* Vol. 2 (Eds. Z. Rappoport and Y. Apeloig), Wiley, Chichester, in press.
383. A. Korkin, M. Glukhovtsev and P. v. R. Schleyer, *Int. J. Quantum Chem.*, **46**, 137 (1993).
384. S. P. So, *Chem. Phys. Lett.*, **313**, 587 (1999).
385. (a) A. Sekiguchi, H. Yamazaki, C. Kabuto, H. Sakurai and S. Nagase, *J. Am. Chem. Soc.*, **117**, 8025 (1995).
(b) A. Sekiguchi, M. Tsukamoto and M. Ichinohe, *Science*, **275**, 60 (1997).
(c) A. Sekiguchi, N. Fukaya, M. Ichinohe and Y. Ishida, *Eur. J. Inorg. Chem.*, 1155 (2000).
386. (a) R. West, H. Sohn, U. Bankwitz, J. Calabrese, Y. Apeloig and T. Müller, *J. Am. Chem. Soc.*, **117**, 11608 (1995).
(b) R. West, H. Sohn, D. R. Powell, T. Müller and Y. Apeloig, *Angew. Chem., Int. Ed. Engl.*, **35**, 1002 (1996).
387. E. D. Jemmis and P. v. R. Schleyer, *J. Am. Chem. Soc.*, **104**, 4781 (1982).
388. T. A. Albright, J. K. Burdett and M.-H. Whangbo, *Orbital Interactions in Chemistry*, Wiley, New York, 1984.
389. P. Jutzi and N. D. Burford, *Chem. Rev.*, **99**, 969 (1999) and references cited therein.
390. (a) P. Jutzi, D. Kanne and C. J. Krüger, *Angew. Chem., Int. Ed. Engl.*, **24**, 773 (1985).
(b) M. J. Heeg, C. Janiak and J. J. Zuckerman, *J. Am. Chem. Soc.*, **106**, 4259 (1984).
(c) H. Sitzmann, R. Boese and P. Stellberg, *Z. Anorg. Allg. Chem.*, **622**, 751 (1996).
(d) M. L. Hays and T. P. Hanusa, *Adv. Organomet. Chem.*, **40**, 117 (1996).
391. S. P. Constantine, H. Cox, P. B. Hitchcock and G. A. Lawless, *Organometallics*, **19**, 317 (2000).
392. W. W. Shoeller, O. Friedrich, A. Sundermann and A. Rozhenko, *Organometallics*, **18**, 2099 (1999).
393. D. R. Armstrong, M. J. Duer, M. G. Davidson, D. Moncrieff, C. A. Russel, C. Stourton, A. Steiner, D. Stalke and D. S. Wright, *Organometallics*, **16**, 3340 (1997).
394. T. J. Lee and J. E. Rice, *J. Am. Chem. Soc.*, **111**, 2011 (1989).
395. (a) I. Shavitt, *Tetrahedron*, **41**, 1531 (1985).
(b) H. F. Schaefer III, *Science*, **231**, 1100 (1986).
396. K. Balasubramanian and A. D. McLean, *J. Chem. Phys.*, **85**, 5117 (1986).
397. W. D. Allen and H. F. Schaefer III, *Chem. Phys.*, **108**, 243 (1986).
398. J.-C. Barthelat, B. Saint Roch, G. Trinquier and J. Satgé, *J. Am. Chem. Soc.*, **102**, 3080 (1980).
399. A. Selmani and D. R. Salahub, *J. Chem. Phys.*, **89**, 1529 (1988).
400. K. Balasubramanian, *J. Chem. Phys.*, **89**, 5731 (1988).
401. N. Matsunaga, S. Koseki and M. S. Gordon, *J. Chem. Phys.*, **104**, 7988 (1996).
402. E. Sicilia, M. Toscano, T. Mineva and N. Russo, *Int. J. Quantum Chem.*, **61**, 571 (1997).
403. A. Gobbi and G. Frenking, *J. Chem. Soc., Chem. Commun.*, 1162 (1993).
404. See for example: (a) A. R. W. McKellar, P. R. Bunker, T. J. Sears, K. M. Evanson, R. J. Saykally and S. R. Langhoff, *J. Chem. Phys.*, **79**, 5251 (1983).
(b) P. Jensen and P. R. Bunker, *J. Chem. Phys.*, **89**, 1327 (1988).
405. D. Dai, M. M. Al-Zahrani and K. Balasubramanian, *J. Phys. Chem.*, **98**, 9233 (1994).
406. P. v. R. Schleyer and J. Kapp, unpublished results.
407. M. Benavides-Garcia and K. Balasubramanian, *J. Chem. Phys.*, **97**, 7537 (1992).
408. M. Benavides-Garcia and K. Balasubramanian, *J. Chem. Phys.*, **100**, 2821 (1994).

409. For example: M. S. Tyagi, *Introduction to Semiconductor Materials and Devices*, Wiley, New York, 1991. See also references cited in References 153, 405, 407 and 408.
410. F. A. Cotton and G. Wilkinson, *Advanced Inorganic Chemistry*, 6th Edn., Wiley, New York, 1999.
411. (a) W.-W. du Mont and H.-J. Kroth, *Angew. Chem., Int. Ed. Engl.*, **16**, 792 (1977).
(b) S. C. Goel, M. Y. Chiang, D. J. Rauscher and W. E. Buhro, *J. Am. Chem. Soc.*, **115**, 160 (1993).
(c) M. Westerhausen, M. M. Enzelberger and W. Schwarz, *J. Organomet. Chem.*, **485**, 185 (1995).
412. M. F. Lappert, *J. Organomet. Chem.*, **600**, 144 (2000).
413. (a) T. Fjeldberg, A. Haaland, B. E. R. Schilling, M. F. Lappert and A. J. Thorne, *J. Chem. Soc., Dalton Trans.*, 1551 (1986).
(b) P. Jutzi, A. Becker, H. G. Stammer and B. Neumann, *Organometallics*, **10**, 1647 (1991).
(c) P. Jutzi, A. Becker, C. Leue, H. G. Stammer and B. Neumann, *Organometallics*, **10**, 3838 (1991).
414. (a) M. Kira, S. Ishida, T. Iwamoto and C. Kabuto, *J. Am. Chem. Soc.*, **121**, 9722 (1999).
(b) M. Kira, S. Ishida, T. Iwamoto, M. Ichinohe, C. Kabuto, L. Ignatovich and H. Sakurai, *Chem. Lett.*, 263 (1999).
(c) M. Kira, R. Yauchibara, R. Hirano, C. Kabuto and H. Sakurai, *J. Am. Chem. Soc.*, **113**, 7785 (1991).
415. (a) B. Gehrhus, P. B. Hitchcock and M. F. Lappert, *Angew. Chem., Int. Ed. Engl.*, **36**, 2514 (1997).
(b) B. Gehrhus, P. B. Hitchcock and M. F. Lappert, in *Organosilicon Chemistry IV. From Molecules to Materials* (Eds. N. Auner and J. Weis), VCH, Weinheim, 2000, pp. 84–87.
416. (a) P. Jutzi, H. Schmidt, B. Neumann and H. G. Stammer, *Organometallics*, **15**, 741 (1996).
(b) L. Lange, B. Meyer and W.-W. du Mont, *J. Organomet. Chem.*, **329**, C17 (1987).
(c) M. Weidenbruch, J. Schlaefke, A. Schäfer, K. Peters, H. G. von Schnering and H. Marsmann, *Angew. Chem., Int. Ed. Engl.*, **33**, 1846 (1994).
417. W. A. Herrmann and C. Köcher, *Angew. Chem., Int. Ed. Engl.*, **36**, 2162 (1997).
418. (a) A. J. Arduengo III, R. L. Harlow and M. Kline, *J. Am. Chem. Soc.*, **113**, 361 (1991).
(b) A. J. Arduengo III, H. V. Rasika Dias, R. L. Harlow and M. Kline, *J. Am. Chem. Soc.*, **114**, 5530 (1992).
(c) A. J. Arduengo III, J. R. Goerlich and W. J. Marshall, *J. Am. Chem. Soc.*, **117**, 11027 (1995).
419. F. E. Hahn, L. Wittenbecher, R. Boese and D. Bläser, *Chem. Eur. J.*, **5**, 1931 (1999).
420. (a) M. Denk, R. Lennon, R. Hayashi, R. West, A. V. Belyakov, H. P. Verne, A. Haaland, M. Wagner and N. Metzler, *J. Am. Chem. Soc.*, **116**, 2691 (1994).
(b) R. West and M. Denk, *Pure Appl. Chem.*, **68**, 785 (1996).
(c) M. Denk, R. West, R. K. Hayashi, Y. Apeloig, R. Paunz and M. Karni, in *Organosilicon Chemistry II, From Molecules to Materials* (Eds. N. Auner and J. Weis), VCH, Weinheim, 1996, p. 251.
(d) M. Denk, J. C. Green, N. Metzler and M. Wagner, *J. Chem. Soc., Dalton Trans.*, 2405 (1994).
421. (a) B. Gehrhus, M. F. Lappert, J. Heinicke, R. Boese and D. Bläser, *J. Chem. Soc., Chem. Commun.*, 1931 (1995).
(b) B. Gehrhus, P. B. Hitchcock, M. Lappert, J. Heinicke, R. Boese and D. Bläser, *J. Organomet. Chem.*, **521**, 211 (1996).
(c) P. Blakeman, B. Gehrhus, J. C. Green, J. Heinicke, M. Lappert, M. Kindermann and T. Veszprèmi, *J. Chem. Soc., Dalton Trans.*, 1475 (1996).
422. W. A. Herrmann, M. Denk, J. Behm, W. Scherer, F.-R. Klingan, H. Bock, B. Solouki and M. Wagner, *Angew. Chem., Int. Ed. Engl.*, **31**, 1485 (1992).
423. B. Gehrhus, P. B. Hitchcock and M. F. Lappert, *J. Chem. Soc., Dalton Trans.*, 3094 (2000).
424. H. Braunschweig, B. Gehrhus, P. B. Hitchcock and M. F. Lappert, *Z. Anorg. Allg. Chem.*, **621**, 1922 (1995).
425. C. Heinemann, T. Müller, Y. Apeloig and H. Schwarz, *J. Am. Chem. Soc.*, **118**, 2023 (1996).
426. C. Heinemann and W. Thiel, *Chem. Phys. Lett.*, **217**, 11 (1994).
427. M.-D. Su and S.-Y. Chu, *Inorg. Chem.*, **38**, 4819 (1999).

428. A. J. Arduengo III, H. Bock, H. Chen, M. Denk, D. A. Dixon, J. C. Green, W. A. Herrmann, N. L. Jones, M. Wagner and R. West, *J. Am. Chem. Soc.*, **116**, 6641 (1994).
429. (a) B. Ma and H. F. Schaefer III, *J. Am. Chem. Soc.*, **116**, 3539 (1994).
(b) J. D. Evanseck and K. N. Houk, *J. Phys. Chem.*, **94**, 5518 (1990).
(c) D. A. Modarelli and M. S. Platz, *J. Am. Chem. Soc.*, **115**, 470 (1993).
430. R. Becerra, S. E. Boganov, M. P. Egorov, V. I. Faustov, O. M. Nefedov and R. Walsh, *Can. J. Chem.*, **78**, 1428 (2000).
431. C. Sosa and B. H. Schlegel, *J. Am. Chem. Soc.*, **106**, 5847 (1984).
432. (a) M. S. Gordon, *J. Chem. Soc., Chem. Commun.*, 890 (1981).
(b) A. Sax and G. Olbrich, *J. Am. Chem. Soc.*, **107**, 4868 (1985).
433. J. M. Jasinski and J. O. Chu, *J. Chem. Phys.*, **88**, 1678 (1988).
434. (a) J. E. Baggott, M. A. Blitz, H. M. Frey and R. Walsh, *J. Am. Chem. Soc.*, **112**, 8337 (1990).
(b) R. Becerra, H. M. Frey, B. P. Mason, R. Walsh and M. S. Gordon, *J. Am. Chem. Soc.*, **114**, 2751 (1992).
(c) R. Becerra, H. M. Frey, B. P. Mason and R. Walsh, *J. Chem. Soc., Faraday Trans.*, **89**, 411 (1993).
435. R. Becerra, S. E. Boganov, M. P. Egorov, V. I. Faustov, O. M. Nefedov and R. Walsh, *J. Am. Chem. Soc.*, **120**, 12657 (1998).
436. R. Becerra, H. M. Frey, B. P. Mason, R. Walsh and M. S. Gordon, *J. Chem. Soc., Faraday Trans.*, **91**, 2723 (1995).
437. S. Sakai and M. Nakamura, *J. Phys. Chem.*, **97**, 4960 (1993).
438. R. D. Bach, M.-D. Su, E. Aldabbagh, J. L. Andrés and H. B. Schlegel, *J. Am. Chem. Soc.*, **115**, 10237 (1993).
439. M. S. Gordon and T. N. Troung, *Chem. Phys. Lett.*, **142**, 110 (1987).
440. M.-D. Su and S.-Y. Chu, *J. Phys. Chem. A*, **103**, 11011 (1999).
441. M.-D. Su and S.-Y. Chu, *J. Am. Chem. Soc.*, **121**, 4229 (1999).
442. K. Raghavachari, J. Chandrasekhar, M. S. Gordon and K. J. Dykema, *J. Am. Chem. Soc.*, **106**, 5853 (1984).
443. S. Shaik, H. B. Schlegel and S. Wolfe, *Theoretical Aspects of Physical Organic Chemistry*, Wiley, New York, 1992.
444. (a) A. Pross, *Theoretical and Physical Principles of Organic Reactivity*, Wiley, New York, 1995.
(b) A. Pross and R. A. Moss, *Tetrahedron Lett.*, **31**, 4553 (1990).
445. M.-D. Su and S.-Y. Chu, *J. Am. Chem. Soc.*, **121**, 11478 (1999).
446. F. Anwari and M. S. Gordon, *Isr. J. Chem.*, **23**, 129 (1983).
447. N. Al-Rubaiey and R. Walsh, *J. Phys. Chem.*, **98**, 5303 (1994).
448. (a) R. B. Woodward and R. Hoffmann, *The Conservation of Orbital Symmetry*, Verlag Chemie, Academic Press, Weinheim, 1971.
(b) R. Hoffmann, *J. Am. Chem. Soc.*, **90**, 1475 (1968).
449. S. G. Lias, J. E. Bartmess, J. F. Liebman, J. L. Holmes, R. D. Levin and W. G. Mallard, *J. Phys. Chem. Ref. Data*, **17**, Suppl. 1 (1988).
450. M. S. Gordon and W. Nelson, *Organometallics*, **14**, 1067 (1995).
451. D. Sengupta and M. T. Nguyen, *Mol. Phys.*, **89**, 1567 (1996).
452. (a) N. Al-Rubaiey, I. W. Carpenter, R. Walsh, R. Becerra and M. S. Gordon, *J. Phys. Chem. A*, **102**, 8564 (1998).
(b) N. Al-Rubaiey, H. M. Frey, B. P. Mason, C. McMahon and R. Walsh, *Chem. Phys. Lett.*, **204**, 301 (1993).
453. J. A. Boatz, M. S. Gordon and L. R. Sita, *J. Phys. Chem.*, **94**, 5488 (1990).
454. (a) R. Becerra, H. M. Frey, B. P. Mason and R. Walsh, *J. Chem. Soc., Chem. Commun.*, 1050 (1993).
(b) R. Becerra and R. Walsh, *J. Chem. Kinet.*, **26**, 45 (1994).
455. (a) R. Becerra, S. E. Boganov, M. P. Egorov, O. M. Nefedov and R. Walsh, *Chem. Phys. Lett.*, **260**, 433 (1996).
(b) U. N. Alexander, K. D. King and W. D. Lawrance, *Chem. Phys. Lett.*, **319**, 529 (2000).
456. G. Chung and M. S. Gordon, *Organometallics*, **18**, 4881 (1999).
457. K. N. Houk, *Chemtracts Org. Chem.*, **6**, 360 (1993).
458. J. B. Lambert, L. Kania and S. Zhang, *Chem. Rev.*, **95**, 1191 (1995).

459. (a) J. B. Lambert and Y. Zhao, *Angew. Chem., Int. Ed. Engl.*, **36**, 400 (1997).
(b) P. v. R. Schleyer, *Science*, **275**, 39 (1997).
(c) T. Müller, Y. Zhao and J. B. Lambert, *Organometallics*, **17**, 278 (1998).
(d) E. Kraka, C. P. Sosa, J. Gräfenstein and D. Cremer, *Chem. Phys. Lett.*, **279**, 9 (1997).
460. I. Zharov and J. Michl, a chapter in *The Chemistry of Organic Germanium, Tin and Lead Compounds*, Vol. **2** (Eds. Z. Rappoport and Y. Apeloig), Wiley, Chichester, in press.
461. J. Kapp, P. R. Schreiner and P. v. R. Schleyer, *J. Am. Chem. Soc.*, **118**, 12154 (1996).
462. E. del Río, M. I. Menandez, R. Lopez and T. L. Sordo, *Chem. Commun.*, 1779 (1997).
463. G. Trinquier, *J. Am. Chem. Soc.*, **114**, 6807 (1992).
464. (a) G. A. Olah, *Angew. Chem., Int. Ed. Engl.*, **32**, 767 (1993).
(b) M. Saunders and H. A. Jimenez-Vazquez, *Chem. Rev.*, **91**, 375 (1991) and references cited therein.
465. (a) P. v. R. Schleyer and C. Maerker, *Pure Appl. Chem.*, **67**, 755 (1995) and references cited therein.
(b) T. Laube and C. Lohse, *J. Am. Chem. Soc.*, **116**, 9001 (1994) and references cited therein.
466. N. Goldberg and H. Schwarz, Chap. 18 in *The Chemistry of Organic Silicon Compounds*, Vol. 2 (Eds. Z. Rappoport and Y. Apeloig), Wiley, Chichester, 1998.
467. G. Frenking, S. Fau, C. M. Marchand and H. Grützmacher, *J. Am. Chem. Soc.*, **119**, 6648 (1997).
468. (a) J. B. Lambert, S. Zhang, C. L. Stern and J. C. Huffman, *Science*, **260**, 1917 (1993).
(b) J. B. Lambert, S. Zhang and S. M. Ciro, *Organometallics*, **13**, 2430 (1994).
469. Z. Xie, J. Manning, R. W. Reed, R. Mathur, P. D. W. Boyd, A. Benesi and C. A. Reed, *J. Am. Chem. Soc.*, **118**, 2922 (1996).
470. (a) P. v. R. Schleyer, P. Buzek, T. Müller, Y. Apeloig and H.-U. Siehl, *Angew. Chem., Int. Ed. Engl.*, **32**, 1471 (1993).
(b) L. Olsson and D. Cremer, *Chem. Phys. Lett.*, **215**, 433 (1993).
471. H. Basch, *Inorg. Chim. Acta*, **242**, 191 (1996).
472. A. Gobbi and G. Frenking, *J. Am. Chem. Soc.*, **116**, 9275 (1994).
473. A. Gobbi and G. Frenking, *J. Am. Chem. Soc.*, **116**, 9287 (1994).
474. Based on the total energies given in the supporting material of Reference 467.
475. J. A. Stone and W. J. Wytenburg, *Can. J. Chem.*, **65**, 2146 (1987).
476. H. Basch, T. Hoz and S. Hoz, *J. Phys. Chem. A*, **103**, 6458 (1999).
477. D. Cremer, L. Olsson, F. Reichel and E. Kraka, *Isr. J. Chem.*, **33**, 369 (1993).
478. M. Arshadi, D. Johnels and U. Edlund, *J. Chem. Soc., Chem. Commun.*, 1279 (1996).
479. (a) J. B. Lambert and B. Kuhlmann, *J. Chem. Soc., Chem. Commun.*, 931 (1992).
(b) M. Kira, T. Oyamada and H. Sakurai, *J. Organomet. Chem.*, **471**, C4 (1994).
480. I. Zharov, B. T. King, Z. Havlas, A. Pardi and J. Michl, *J. Am. Chem. Soc.*, **122**, 10253 (2000).
481. J. B. Lambert, Y. Zhao, H. Wu, W. C. Tse and B. Kuhlmann, *J. Am. Chem. Soc.*, **121**, 5001 (1999).
482. K. Mochida, in *The Chemistry of Organic Germanium, Tin and Lead Compounds*, Vol. **2** (Eds. Z. Rappoport and Y. Apeloig), Wiley, Chichester, in press.
483. For calculations at other computational levels see, for example:
(a) D. A. Dixon, D. Feller and K. A. Peterson, *J. Phys. Chem. A*, **101**, 9405 (1997).
(b) U. Salzner and P. v. R. Schleyer, *Chem. Phys. Lett.*, **199**, 267 (1992).
(c) L. A. Curtiss, P. C. Redfern, K. Raghavachari, V. Rassolov and J. A. Pople, *J. Chem. Phys.*, **110**, 4703 (1999).
(d) N. H. Morgon and J. M. Riveros, *J. Phys. Chem. A*, **102**, 10399 (1998).
484. P. Riviere, A. Kastel and M. Riviere-Baudet, in *The Chemistry of Organic Germanium, Tin and Lead Compounds*, Vol. **2** (Eds. Z. Rappoport and Y. Apeloig), Wiley, Chichester, 2002.
485. L. A. Curtiss, K. Raghavachari, G. W. Trucks and J. A. Pople, *J. Chem. Phys.*, **94**, 7221 (1991).
486. (a) G. B. Ellis, P. C. Engleking and W. C. Lineberger, *J. Am. Chem. Soc.*, **100**, 2556 (1978).
(b) K. J. Reed and J. I. Brauman, *J. Chem. Phys.*, **61**, 4830 (1974).
(c) P. M. Mayer, J.-F. Gal and L. Radom, *Int. J. Mass Spectrom. Ion Processes*, **167/168**, 689 (1997).
487. J. V. Ortiz, *J. Am. Chem. Soc.*, **109**, 5072 (1987).

488. M. R. Nimlos and G. B. Ellison, *J. Am. Chem. Soc.*, **108**, 6522 (1986).
489. (a) A. C. Hopkinson and M. H. Lien, *Tetrahedron*, **37**, 1105 (1981).
(b) E. Magnusson, *Tetrahedron*, **41**, 2945 (1985).
490. S. Hoz, H. Basch, J. L. Wolk, T. Hoz and E. Rosental, *J. Am. Chem., Soc.*, **121**, 7724 (1999).
491. P. v. R. Schleyer and J. W. de M. Carneiro, *J. Comput. Chem.*, **13**, 997 (1992).
492. P. R. Schreiner, H. F. Schaefer III and P. v. R. Schleyer, in *Advances in Gas Phase Ion Chemistry*, Vol. 2 (Eds. N. Adams and L. M. Babcock), JAI Press Inc., London, 1996.
493. P. R. Schreiner, S.-J. Kim, H. F. Schaefer III and P. v. R. Schleyer, *J. Chem. Phys.*, **99**, 3716 (1993).
494. P. R. Schreiner, H. F. Schaefer III and P. v. R. Schleyer, *J. Chem. Phys.*, **101**, 2141 (1994).
495. E. F. Archibong and J. Leszczyński, *J. Phys. Chem.*, **98**, 10084 (1994).
496. P. v. R. Schleyer, Y. Apeloig, D. Arad, B. T. Luke and J. A. Pople, *Chem. Phys. Lett.*, **95**, 477 (1983).
497. C.-H. Hu, M. Shen and H. F. Schaefer III, *Chem. Phys. Lett.*, **190**, 543 (1992).
498. (a) C. H. Schiesser, M. L. Styles and L. M. Wild, *J. Chem. Soc., Perkin Trans. 2*, 2257 (1996).
(b) S. M. Horvat, C. H. Schiesser and L. M. Wild, *Organometallics*, **19**, 1239 (2000).
499. C. H. Schiesser and M. L. Styles, *J. Chem. Soc., Perkin Trans. 2*, 2335 (1997).
500. S. Kim, J. Y. Do and K. M. Lim, *Chem. Lett.*, 669 (1996).

CHAPTER 2

(Helium I)-photoelectron spectra of silicon compounds: History and achievements concerning their molecular states

H. BOCK AND B. SOLOUKI

Institute of Inorganic Chemistry, Johann Wolfgang Goethe University, Marie-Curie Street 11, D-60439 Frankfurt am Main, Germany
Fax: 0049-69-798-29188; e-mail: solouki@chemie.uni-frankfurt.de

I. INTRODUCTORY REMARKS: PHOTOELECTRON SPECTROSCOPY TODAY AND THE SCOPE OF THIS REVIEW	166
II. REAL-TIME GAS ANALYSIS USING PHOTOELECTRON SPECTROSCOPIC VERTICAL IONIZATION FINGERPRINTS	167
A. Principle of PES Measurement and Some Experimental Details	167
B. The Molecular State Approach to Silicon Compounds	169
III. INTRODUCTORY 'CLASSIC' EXAMPLES OF PHOTOELECTRON SPECTROSCOPIC INFORMATION ON PROPERTIES OF AND BONDING IN SILICON-CONTAINING MOLECULES	172
A. The Tremendous Difference in Effective Nuclear Potentials of Carbon and Silicon	172
B. Charge Delocalization in Polysilane Radical Cations	174
C. Silicon-Substituted Carbon- π -Systems: First and Second Order Perturbation	178
D. One-Electron Ionization and One-Electron Oxidation of Organosilicon Compounds	180
E. Sterically Overcrowded Organosilicon Molecules	186
F. Kinetically Unstable Silicon Intermediates: Detection in Unimolecular Flow Systems by their PE-spectroscopic Ionization Fingerprints	191
G. Interim Summary	192

IV. (He I)-PHOTOELECTRON SPECTROSCOPIC RESULTS	
1990–2000	195
A. Organosilicon Compounds Containing Main Group 13 Elements	195
B. Organosilicon Molecules (Main Group 14 Elements)	197
1. Silicocene	197
2. Cation charge delocalization in the Si ₆ skeleton of hexakis(trimethylsilyl)disilane	199
3. Organosilicon cations in solvents and their matrix isolation	199
4. Further PE spectroscopic investigations of organosilicon compounds with group 14 elements	201
C. Organosilicon Molecules Containing Main Group 15 Elements	202
1. (He I) PE spectrum of stable ‘imidazole’-silylene	202
2. Sterically overcrowded trimethylsilyl- <i>p</i> -phenylenediamines	203
3. Thermal generation of trimethyl silanimine in the gas phase	206
4. Further PE spectroscopic investigations of organosilicon compounds with group 15 elements	207
D. Organosilicon Molecules Containing Main Group 16 Elements	208
1. Oxygen lone pair ionization energies of siloxanes	208
2. Sulfur lone pair ionization energies of silthianes	210
3. Further PE spectroscopic investigations of organosilicon compounds with group 16 elements	213
E. Silicon Molecules Containing Main Group 17 Elements	214
1. The PE spectrum of SiI ₂ — A novel triatomic molecule with a relativistic touch	214
2. PE spectroscopic investigations of organosilicon compounds with group 17 elements	216
V. RETROSPECTIVE AND PERSPECTIVES	216
VI. REFERENCES AND NOTES	217

I. INTRODUCTORY REMARKS: PHOTOELECTRON SPECTROSCOPY TODAY AND THE SCOPE OF THIS REVIEW¹

The period of the early tempestuous years of (helium I) photoelectron (PE) spectroscopy between 1970 and 1980, during which the method had been developed and thousands of ionization patterns of a large variety of volatile molecules were recorded^{2–9}, and which was superseded between 1980 and 1990 by a period of practical applications such as the prediction of radical cation generation in solution¹⁰ or the advantageous gas analysis in flow systems^{11,12}, has now passed. Still, however, results of one or another investigation using information from the powerful and relatively easy to handle radical cation state analysis method are published, but the emphasis has shifted in the meantime to other measurement techniques from the arsenal of physics: The Nobel prize honored Electron Spectroscopy for Chemical Analysis (ESCA)¹³ still provides valuable information on surface phenomena of novel materials including heterogeneous catalysts, or the more recently developed high-resolution Zero Kinetic Energy (ZEKE)¹⁴ spectroscopy opens new doors for the observation of molecular ions as well as other species in the gas phase.

Why then write another review on the (helium I) photoelectron spectroscopy of silicon compounds? At a time of rapidly increasing computer application to various aspects of preparative chemistry, it seems worthwhile to summarize historic and more recent achievements in the rapidly progressing knowledge of silicon-containing molecules, and their molecular state properties, which are via Koopmans' theorem intimately connected to quantum chemical calculations. Above all, some selected cases are well-suited to illustrate

what has and still can be learned concerning more general rules of bonding in main group element compounds containing centers of low effective molecular charge, such as silicon¹⁵.

This review will therefore attempt to summarize aspects of the advantageous molecular state approach to volatile silicon compounds based on selected (helium I) photoelectron spectra including their quantum chemical assignment¹⁶, and will cover some of the applications to investigations in solution as well as to the structures determined in crystals¹⁷.

II. REAL-TIME GAS ANALYSIS USING PHOTOELECTRON SPECTROSCOPIC VERTICAL IONIZATION FINGERPRINTS

Despite the nowadays fading use of (helium I) photoelectron spectroscopy, its principles^{3,4}, facets of the instrumentation^{2,11} and a brief introduction to the molecular state approach for rationalization of the vertical ionization fingerprints recorded¹⁵ has to be given, because otherwise many arguments concerning ionization patterns of silicon compounds might remain difficult to comprehend.

A. Principle of PES Measurement and Some Experimental Details

Photoelectron spectroscopy uses the photoionization of a neutral molecule M to its radical cation $M^{\bullet\oplus}$,



to determine the n vertical ionization potentials IE_n^V of M ,

$$IE_n^V(M) = h\nu + E_{\text{kin}}(e^{\ominus}) \quad (2)$$

from the difference of the photon energy $h\nu$ and the kinetic energy E_{kin} of the ejected electron. If the usual helium(I) discharge lamp is chosen as a source of monochromatic photons with $h\nu = 21.21$ eV, all ionization potentials up to 21.21 eV can be measured by counting the emitted electrons of specific kinetic energy²⁻⁴, separated when leaving the ionization chamber (Figure 1a: H) by passing a cylindrical (Figure 1a: I) or spherical analyzer (Figure 1b) of continuously varying voltage.

For the recording of (helium I) spectra of volatile molecules or for gas-phase reactions monitored by PE spectroscopic real-time analysis in a flow system, the parts of a variable building block apparatus are assembled and directly connected to the spectrometer, which generates the compound stream by its respective vacuum pump system (Figure 1a and b). Out of numerous possible combinations¹¹, only a few applications shall be pointed out (cf. Figure 1).

Thermal decomposition of molecules. Compound A is pumped through the heating zone C via bypass E into the spectrometer. Additional options are: after optimization of the decomposition temperature, the pyrolysis product can be isolated in trap E (cf. e.g. References 11 and 12) or by-products like HCl removed by injecting the stoichiometric amount of, e.g., NH_3 from F, depositing NH_4Cl on the inner wall of the mixing bulb G to record the PE spectrum of the pure pyrolysis product (cf. e.g. References 11 and 16).

Optimization of heterogeneously catalyzed reactions. Compound A, which can be mixed in B with other components, runs over the catalyst heated in C to the optimum temperature determined by continuously recording the PE spectra of the gas mixture (cf. e.g. References 11, 18 and 19). Using capillary D, the reaction may be carried out at atmospheric pressure, side-tracking a negligible amount at 10^{-2} mbar pressure for analysis into the PE spectrometer. The reaction products are either analyzed PE spectroscopically

via bypass E or trapped for additional gas-chromatographic determination by switching the stopcocks E (cf. e.g. References 12 and 20).

The advantages of the above procedures are: millimole amounts of the precursor—in the case of heterogeneously catalyzed reactions, therefore, only a few cubic centimeters of the (precious) catalyst—and a couple of hours allow one to optimize temperature and flow conditions in the heated reaction zone (Figure 1a) with the gas stream being transported by the vacuum pump system of the PE spectrometer. The spectra can be registered on-line, displaying on a screen continuously the band pattern of the resulting reaction mixture^{21,22}, and for analysis of gas components, their digitally preregistered PE spectra can be computer-subtracted from the flow mixture.

Detection of short-lived (partly interstellar) molecules. For their identification, the distance^{11,16} between heating zone and target chamber has to be as short as possible. Advantageously, a short-path pyrolysis oven (Figure 1b) can be built into the PE spectrometer. The molybdenum tube of the latter is heated resistively and, in addition, also

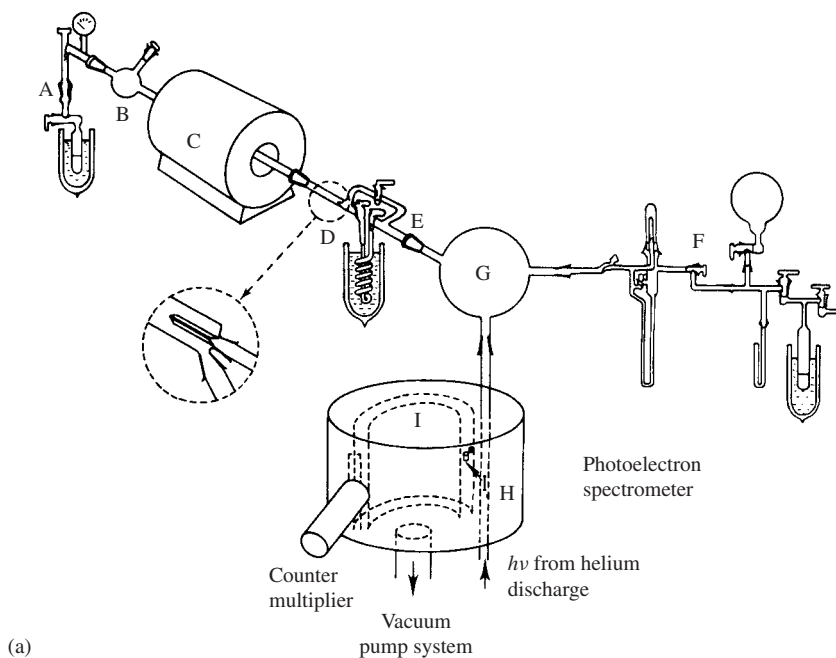


FIGURE 1. (a) Photoelectron spectroscopic measurement principle and assembly kit^{11,16} possibilities for gas-phase reaction monitored by real-time PES gas analysis. A: Compound inlet system with manometer; B (as well as G): optional mixing bulb for adding another gas; C: temperature-controlled oven with quartz tube filled with quartz wool or catalyst; D: optional capillary for branching off a side-stream of reduced pressure to the PE spectrometer while running the gas-phase reaction at atmospheric pressure; E: cooling trap for isolation of compounds after the reaction has been optimized via the bypass; F: gas storage and inlet system to add stoichiometric amounts of other gases, e.g. to deposit gas components as salts at the inner wall of G. The respective building block apparatus is directly connected to the PE spectrometer containing the ionization chamber H and the analyzer I. (b) Outline of the short-path pyrolysis apparatus integrated into the PE spectrometer Leybold Heraeus UPG 200¹¹: U₁ resistive heating, U₂ electron impact heating

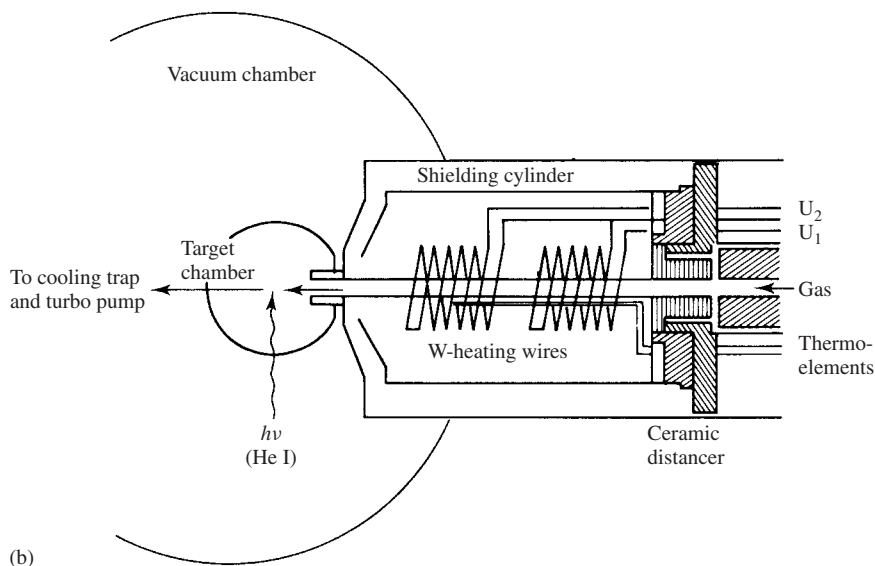


FIGURE 1. (continued)

by electron impact (Figure 1b: U_1 , U_2); the distance between the end of the oven zone and the PES ionization chamber amounts to only 3 cm. Use of this short-path pyrolysis technique permits the detection of thermal decomposition products with lifetimes in the millisecond range^{11,12,23}.

B. The Molecular State Approach to Silicon Compounds

At a time when at least one chemical publication appears in every one of the 525,600 minutes of a 365-day year, the planning and evaluation of experiments assisted by computer calculation are a necessity. In addition, the real building blocks of a chemist are no longer the over 10^7 molecules now known, but—as convincingly documented, for example, by photochemical synthesis steps or by multielectron-transfer redox reactions—increasingly their numerous molecular and molecular-ion states^{9,10,15,16} accessible via various routes of energy transfer (Figure 2a). These states are revealed by spectroscopic band or signal patterns, by which the respective compounds may be identified as well as characterized, and can be ordered with respect to both energy^{10,15,24} (Figure 2a) or time scales^{10,24} (Figure 2c). In addition to this analytical ‘ear-marking’, such measurements afford as a rule valuable, but often unused, information about the compound investigated, including the energies and symmetries of its various states, as well as the energy-dependent electron distribution over its effective nuclear potentials (Figure 2b).

For closer elaboration of the numerous radical cation states of molecules on energy and time scales (Figure 2a and c), photoelectron (PES)^{3,5,16} and electron spin resonance (ESR/ENDOR)^{10,25} spectroscopic techniques have complementary time ranges: ‘Vertical’ ionization energy patterns are measured with a time resolution of less than 10^{-15} s (Figure 2c) without any vibrational structural changes on electron ejection and can therefore be correlated to the eigenvalues calculated for the neutral molecule by

applying Koopmans' theorem, $IE_n^v = -\varepsilon_j^{\text{SCF}3,5}$. In contrast, ESR/ENDOR signal patterns are recorded 'adiabatically' with a considerably smaller time resolution of $>10^{-8}$ s, that is, long after the activation of molecular dynamics at about 10^{-13} s. The spin populations ρ_μ detected for the individual radical ion centers μ can be rationalized according to the McConnell relation, $\rho_\mu \propto c_{j\mu}^2$, by comparison with the calculated squared orbital

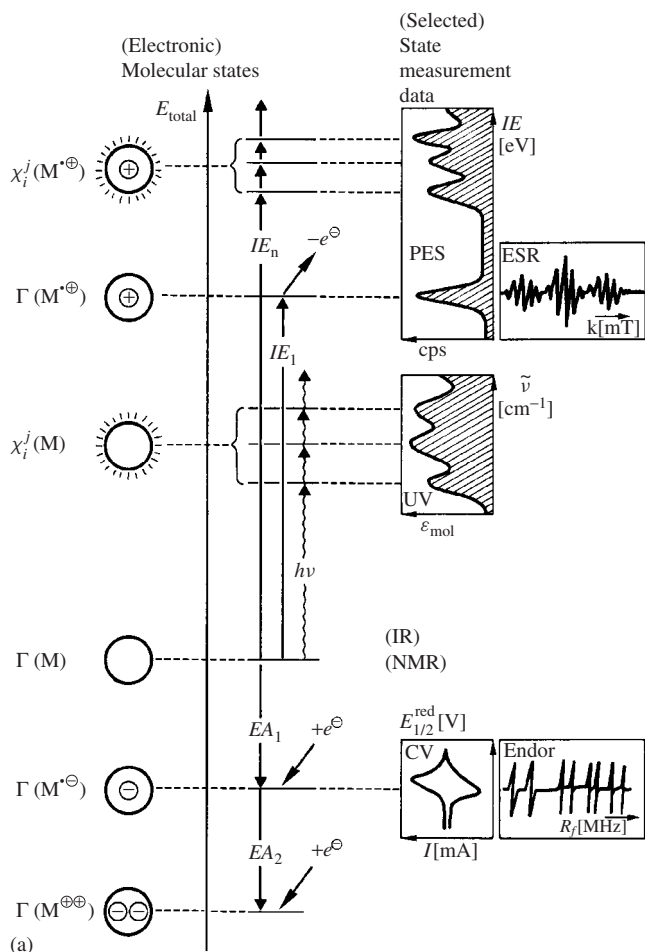


FIGURE 2. (a) Schematic energy scale for electronic ground (Γ) and excited (χ_i^j) states of a neutral molecule M, its radical cation $M^{\bullet\oplus}$ generated by ionization or oxidation and its radical anion $M^{\bullet\ominus}$ and dianion $M^{\ominus\ominus}$ resulting from electron insertion. Representative measurement methods used in many investigations are NMR, IR, UV, PE, ESR and ENDOR spectroscopy as well as cyclic voltammetry (CV). (b) Qualitative molecular-state model. (c) Schematic time scale for molecular states and their changes (in seconds, the time unit intermediate between the duration of a human heart-beat and the transmission of stimuli by the eye)¹⁰: \square Radiation frequencies and \boxplus measurement methods and information obtained

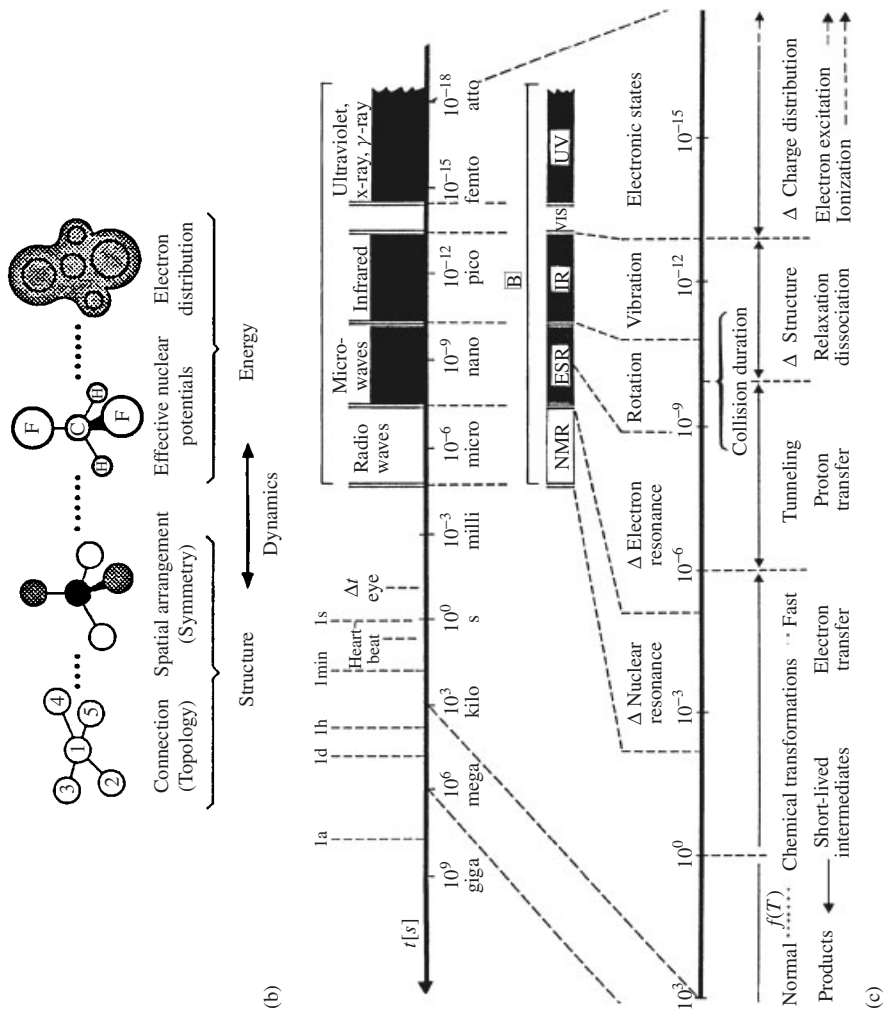


FIGURE 2. (continued)

coefficients $(c_{j\mu}^2)^{10,25}$. The data obtained from the two measurement techniques complement each other because of their different time resolution and allow, in combination with approximate energy hypersurface calculations⁹, reliable estimates of structural changes in molecules M on adiabatic one-electron oxidation $M \rightarrow M^{\bullet\oplus} + e^{\ominus}$ including the inherent molecular dynamics within the complexity of the $3N - 6$ degrees of freedom⁹.

In conclusion, the general point of view is put forward that molecules act as ‘self-dedicated computers’, ‘printing out’ measurement data which provide complete, self-consistent and completely correlated solutions of the Schrödinger equation^{10,11}. The follow-up Shakespearean question, whether to measure or to calculate, which arises from the rapid development of both the measurement techniques as well as of numerical quantum mechanics, is best answered with reference to how successful and stimulating the combination of the two proves to be.

III. INTRODUCTORY ‘CLASSIC’ EXAMPLES OF PHOTOELECTRON SPECTROSCOPIC INFORMATION ON PROPERTIES OF AND BONDING IN SILICON-CONTAINING MOLECULES

The decreasing number of PE spectroscopic investigations since 1994, which will be examined in Section IV under various specified aspects, should be preceded by some selected topics^{10,15,16} to provide the basis needed for comparison and rationalization. With their landmark character, the cases presented will in addition introduce historical aspects of achievements and their benefit to silicon chemistry.

A. The Tremendous Difference in Effective Nuclear Potentials of Carbon and Silicon

One most informative ionization fingerprint comparison is that of the iso(valence)electronic molecules ethane and disilane (Figure 3).

The ethane radical cation state sequence, $\tilde{X}(^2E_g) < \tilde{A}(^2A_g) < \tilde{B}(^2E_u) < \tilde{C}(^2A_u)$, is well established from its repeatedly recorded PE spectrum³⁻⁵ (Figure 3). Both $\sigma_{CH}(e) M^{\bullet\oplus}$ states exhibit considerable Jahn/Teller distortions of 0.7 eV and 0.8 eV, respectively, and the ionization into the predominantly σ_{CC} -bonding $M^{\bullet\oplus}$ state $\tilde{A}(^2A_g)$ is located at about 13.4 eV in between them.

Comparison with the PE spectrum of the iso(valence)electronic disilane²⁶ (Figure 3) reveals surprisingly large differences: Judging from the intensities 1 : 2 : 2 of the three low-energy PES bands, the σ_{SiSi} ionization has been lowered by 3 eV or about 271 kJ mol⁻¹ (!) relative to the σ_{CC} value. The silane radical cation ground state is shifted out of the $\sigma(\text{SiH}_2)$ ionization hill and becomes the well-separated first vertical ionization peak of the disilane PE spectrum (Figure 3). As concerns the σ_{SiH} ionizations, both the e_g/e_u split as well as the $D_{3d} \rightarrow C_{2h}$ Jahn/Teller distortions are smaller than in ethane, reflecting the considerably longer σ bond length $d_{SiSi} = 235$ pm vs. $d_{CC} = 153$ pm. It is pointed out that also the $3s_{Si}$ dominated $M^{\bullet\oplus}$ state is lowered relative to the analogous $2s_C$ one in energy by 3.6 eV! Altogether, the center of gravity of six ionizations within the He(I) measurement region is shifted from $\overline{14.9}$ eV for H_3CCH_3 ⁵ by 2.1 eV(!) to $\overline{12.8}$ eV for H_3SiSiH_3 ²⁶.

The tremendous lowering of the effective nuclear charge of silicon relative to carbon can be substantiated by the difference in their average atomic ionization energies for all n valence electrons,

$$\overline{IE}_{\text{valence}}^{\text{Atom}} = [IE_1(A) + IE_1(A^+) + IE_1(A^{++}) \dots + IE_1(A^{+(n-1)})]/n \quad (3)$$

The values of $\overline{\text{IE}}_{\text{valence}}^{\text{Atom}}$, 25.8 eV for Si and, 11 eV(!) higher, 37.0 eV for C are reflected by a 'united atom' comparison of valence electron ionization energies for third-row iso-electronic species AH_n ²⁷ containing 18 electrons, in which one proton after the other with nuclear charge $Z = 1$ is drawn out of the nucleus of the preceding central element on its left⁹, and also incorporating the iso(valence)electronic 10-electron molecule CH_4 (Figure 3a). In the respective PE spectroscopic vertical ionization patterns (Figure 3b), two regions are easily recognized: the energetically higher AH_n^{\oplus} states with 3s holes of a_1 symmetry and the band of partly degenerate 3p-type ones, which are assigned to the ionization of electron pairs n_A or the symmetry-adapted bond combinations σ_{AH} . The 3s electrons in the proximity of the nucleus become more readily ionizable with decreasing effective nuclear charge, as demonstrated by the 3s and 2s vertical ionization energies (Figure 3b). The 3p electrons, which are on average farther away from the nucleus, expectedly prove less susceptible to the influence of the core potential and split for the AH_n molecules into their characteristic M^{\oplus} levels (Figure 3b). For SiH_4 ^{26,27}

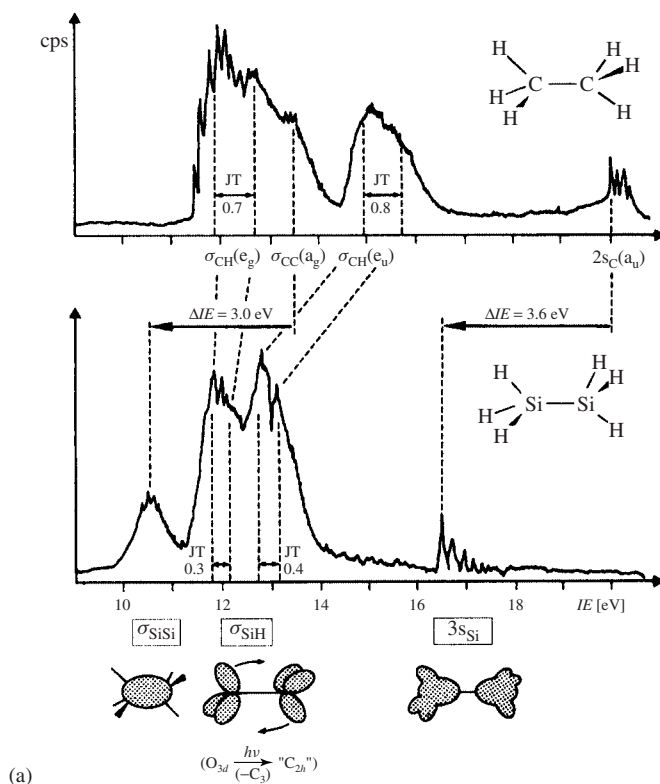


FIGURE 3. (a) Comparison of the He(I) PE spectra of the D_{3d} -symmetric molecules ethane and disilane, which exhibit Jahn/Teller splitting (J/T) of their M^{\oplus} (e) states with dominant contributions (\square) to positive hole delocalization, based on their quantitative radical cation state assignment (see text). (b) 'United Atom' correlation for the iso-electronic 18-electron species from Ar to SiH_4 including the iso(valence)electronic 10-electron molecule CH_4 with average atomic ionization energies $\overline{\text{IE}}_{\text{valence}}^{\text{Atom}}$ and their vertical ionization patterns (see text)

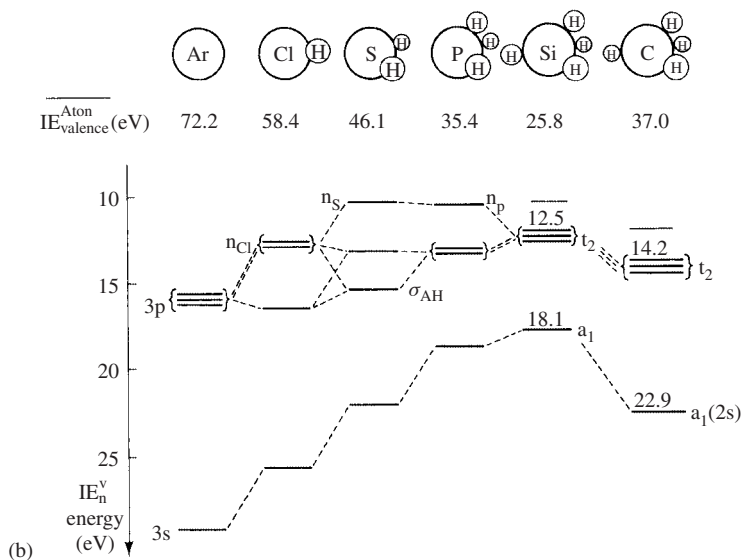


FIGURE 3. (continued)

relative to CH₄^{5,27}, the center of gravity of the four valence ionization energies is shifted by 2.5 eV (!) in close correspondence to the average shift for six of the seven valence electron ionizations for Si₂H₆ and C₂H₆ by 2.1 eV (Figure 3a).

The experimental quantity $\overline{IE_{\text{valence}}^{\text{Atom}}}$ also serves for estimating Slater potentials⁹ and is much more reliable than the ambiguously definable and far too imprecise parameter ‘electronegativity’²⁸.

B. Charge Delocalization in Polysilane Radical Cations

The (He I) PE spectra of the open-chain silanes Si_nH_{2n+2} provide essential information for silicon polymer chemistry, and therefore their daring recording due to potential violent explosion if ignited in mixtures with air has been well worth the effort²⁶ (Figure 4a). Additional facets are recognized in ionization patterns of lipophilically shifted, harmless permethyl-substituted linear and cyclic derivatives²⁹ (Figure 4b). Above all, they yield a linear correlation with topological eigenvalues^{1,10,15,16} (Figure 4c), which proves the delocalization of positive charge in polysilane radical cations³⁰ and thus allow one to rationalize as well as help to design new silicon conducting materials¹⁵ (Figure 5).

Starting from the PE spectrum of disilane (Figures 3 and 4a) with its rather low first vertical ionization σ_{SiSi} at 10.53 eV, the Si_nH_{2n+2}^{•+} state sequences are straightforwardly assigned. Of special interest is the ionization range between 9 and 11 eV, from which by analysis of the Gaussian-shaped PES bands, an asymmetric splitting pattern caused by additional interaction with adjacent symmetry-equivalent (SiH)^{•+} states of higher energy becomes either clearly visible or can be deduced by band deconvolution²⁶ (Figure 4a). The observed split into $n - 1$ (σ_{SiSi})^{•+} states convincingly demonstrates the electron hole delocalization along the Si molecular backbone^{1,10,15,16} (Figure 4a).

The (He I) photoelectron spectra^{29,30} of permethylated polysilanes also exhibit characteristic contours of partly overlapping bands in the low-energy region up to 10 eV (Figure 4b), assigned analogously to radical cation states with predominant SiSi framework contributions^{1,10,15,16}. For rationalization, a linear combination of bond orbitals (LCBO) provides a fully occupied molecular orbital (MO) scheme (Figure 4c) with topological eigenvalues, $\varepsilon_J^{\text{HMO}} = \alpha_{\text{SiSi}} + x_J^{\text{HMO}} \beta_{\text{SiSi/SiSi}}$, which on correlation with the PE spectroscopic vertical ionization energies IE_n (eV) yield a satisfactory linear regression. It passes through $\text{IE}_1^{\text{v}}(\text{R}_3\text{Si} - \text{SiR}_3) = 8.69$ eV, defined as Coulomb integral parameter $\alpha_{\text{SiSi}}^{\text{R}}$, and its slope yields the resonance integral interaction parameter $\beta_{\text{SiSi/SiSi}}^{\text{R}} \sim 0.5$ eV^{8,9} (Figure 4c). For all alternate^{9,31} $\sigma_{\text{SiSi}}^{\text{R}}$ systems such as $\text{R}(\text{SiR}_2)_{3,4}\text{R}$ or $(\text{SiR}_2)_6$, the $\sigma_{\text{SiSi/SiSi}}^{\oplus}$ splitting observed is expectedly³¹ almost equidistant from the center $\alpha_{\text{SiSi}}^{\text{R}}$, and for the five- and six-membered rings two degenerate ionization band pairs as well as one identical ionization at $\varepsilon_J^{\text{HMO}} = \alpha_{\text{SiSi}}^{\text{R}} + 2\beta_{\text{SiSi/SiSi}}$ are predicted and found, further substantiating the application of the rather simple topological HMO model³¹ for the saturated σ_{SiSi} systems^{1,8,9,15,16,35}.

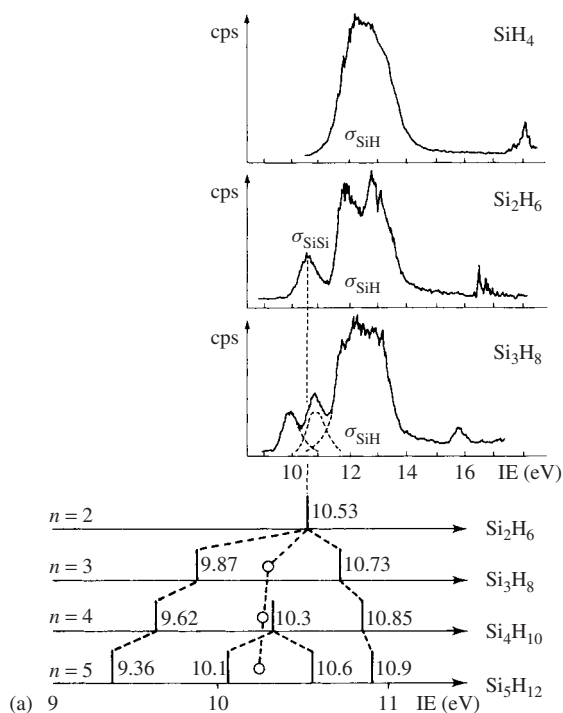


FIGURE 4. (He I) Photoelectron spectra of silanes: (a) Linear parent compounds $\text{Si}_n\text{H}_{2n+2}$ with assignments σ_{SiSi} or (SiH) and low energy σ_{SiSi} ionization band splitting scheme (cf. text), (b) linear or cyclic permethyl-substituted silanes, $\text{Si}_n(\text{CH}_3)_{2n+2}$ or $\text{Si}_n(\text{CH}_3)_{2n}$, with indicated band analysis (---) and (c) σ_{SiSi} vertical ionization patterns of permethylated polysilanes, their correlation with topological eigenvalues χ_J^{OMO} as well as spectroscopic evaluation of Coulomb parameter α_{SiSi} and interaction parameter $\beta_{\text{SiSi/SiSi}}$ (cf. Text)

The assigned ionization patterns of the polysilanes^{26,29} (Figure 4) not only provide interesting information about charge delocalization along their σ_{SiSi} backbones, but also prove to be useful for the parametrization of respective band-structure calculations aimed at the development of novel photoconducting materials with low ionization thresholds and narrow valence bands³². The band structures of the polymers $\text{R}(\text{SiR}_2)_\infty\text{R}$ of infinite chain length and different alkyl groups R were calculated by *ab initio* methods using Bloch functions³³, which had been calibrated with vertical PES ionization energies of silanes (Figure 5).

In the band structure calculations, the wave vector k runs from $\Gamma(k = 0)$ to $X(k = \pi/a)$ (a is the lattice constant)³³. The resulting state 'dispersion' (Figure 5: DIS) shows a '3p_{Si}'

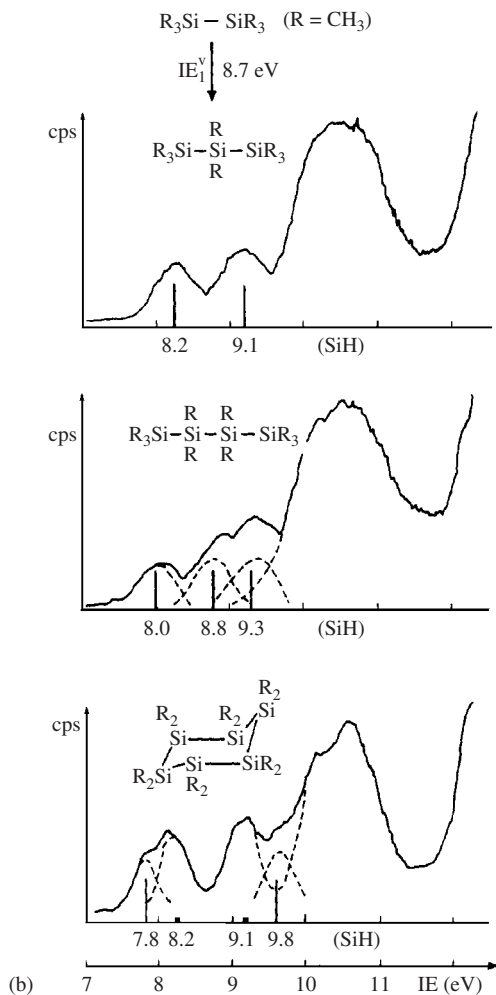


FIGURE 4. (continued)

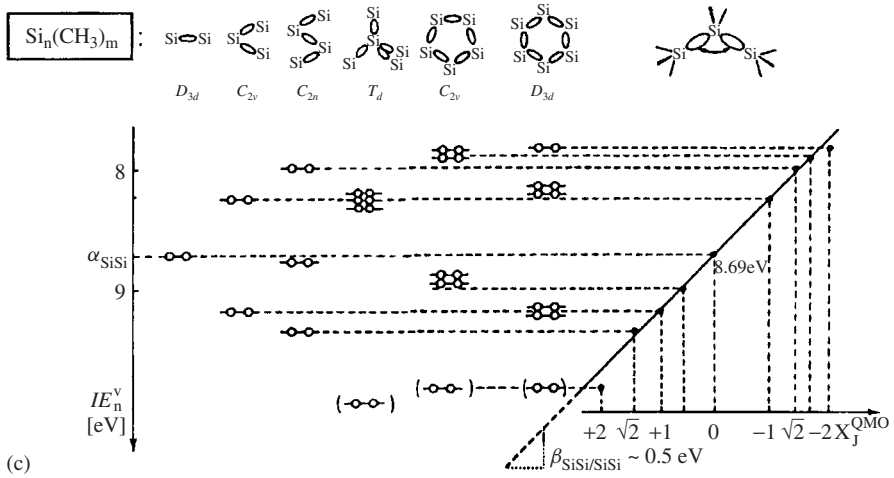


FIGURE 4. (continued)

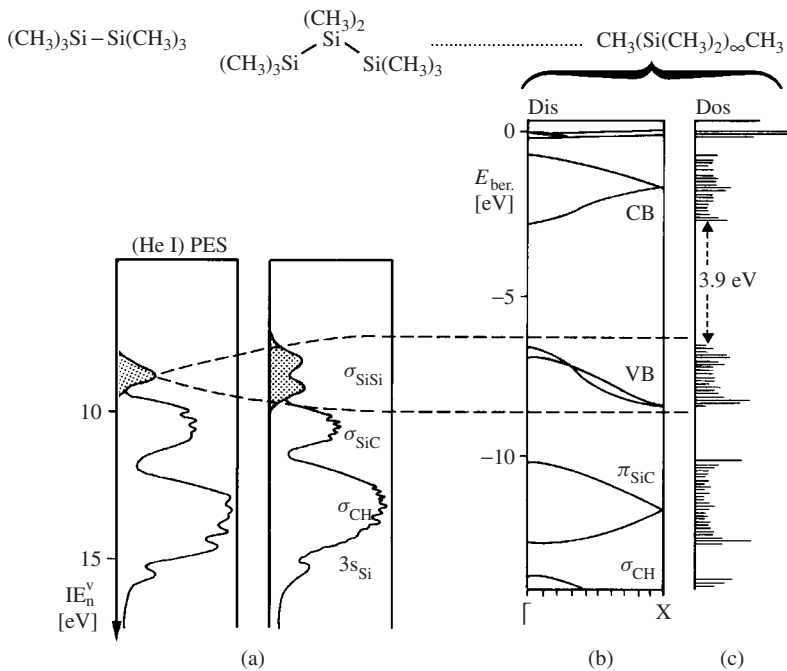


FIGURE 5. Band structure correlation for linear peralkylated polysilanes: (a) (He I) PE spectra of hexamethyldisilane and octamethyltrisilane, (b) *ab initio* calculated band-structure dispersion (DIS) and (c) state density (DOS) for poly-dimethylsilane $R(SiR_2)_\infty R^{32}$

valence band (VB) about 2 eV wide and an ionization threshold of 5.9 eV³². The calculations reveal an unfilled 4s_{Si} conduction band (CB) some 3.9 eV above the valence band and π_{SiC} , σ_{CH} and 3s_{Si} bands below it³². The analogously scale-adjusted state-density diagram (Figure 5: DOS) agrees satisfactorily with X-PES-determined ionization energies (cf. e.g. Figure 3b). The close correspondence between experimental and calculated values, vice versa, supports the predicted low ionization threshold and the narrow valence band width³⁴.

In closing, it should be emphasized that the M^{•⊕}-state assignment of methylsilanes (Figure 4) still serves today, some 30 years later, as a most valuable source of information and greatly enhances our understanding of the intriguing molecular state properties of polysilanes^{1,10,15,16,35}.

C. Silicon-Substituted Carbon- π -Systems: First and Second Order Perturbation

Every chemist will try to disentangle the multitude of his compounds and sort their molecular-state data in the optimum way possible. There are countless different possibilities for selecting chemically related molecules within each area of research. Subdivision lines may be drawn, for instance, according to topological features such as coordination numbers¹⁵ or the connection of individual building blocks and their spatial arrangement (Figure 2b). For heteroconjugate systems, the different potentials within the molecular framework and the respective number of valence electrons prove to be useful as selection criteria (Figure 2b). Especially, the widespread and extremely useful separation of large molecules into parent systems and substituents and the comparison of their molecular state measurement data (Figure 2a) based on first- and second-order perturbation arguments^{9,31} has proved to be tremendously valuable for organosilicon compounds as well¹⁵. For illustration, one example each will be given: the straightforward prediction of the three vertical π ionizations of silabenzene^{15,35,36}, which helped to identify the then still unknown molecule in its high-temperature gas phase generation³⁷ (Figure 6a) and the transparent π interaction in air-explosive silylacetylene as gathered from a photoelectron spectroscopic comparison with silane and acetylene³⁸ (Figure 6b).

Looking at organosilicon compounds with a 'molecular state-sensitive' eye (Figure 2) reveals numerous molecular properties, which are dominated by specific potential changes at certain centers and can therefore be rationalized by first-order perturbation arguments^{15,31}. A classical example is the 6 π -electron system of benzene (Figure 6a), for which substitution and the accompanying symmetry lowering lifts the degeneracy of its $\pi(e_{1g})$ states and which, owing to its π -nodal planes (i.e. those of zero electron density), possesses unperturbed 'standard states' for certain substitution patterns. As concerns the π ionization energies of hetero-substituted benzenes, a correlation (Figure 6a) between the PE-spectroscopically determined vertical π ionization energies of benzene and its monohetero derivatives (HC)₅ER (ER = CH, N, P, As, Sb, Bi) and the ionization energies (⁴S_{3/2} → ³P₀) of the perturbing atoms E has been reported³⁶, in which the gradients of the resulting regression lines reflect the squared coefficients, $c_{\pi\mu}^2$ of the perturbed center μ . Inserting the silicon-atom ionization energy of 8.15 eV allowed one to predict the vertical π ionization energies of silabenzene, which could be experimentally measured only two years later after the development of a short-path pyrolysis apparatus (Figure 1) for generating kinetically unstable molecules under 'unimolecular' conditions¹⁰. Especially, the correctly predicted first vertical π ionization band at 8.11 eV helped considerably in optimizing the reaction conditions by PE-spectroscopic real-time gas analysis^{10,15,37}.

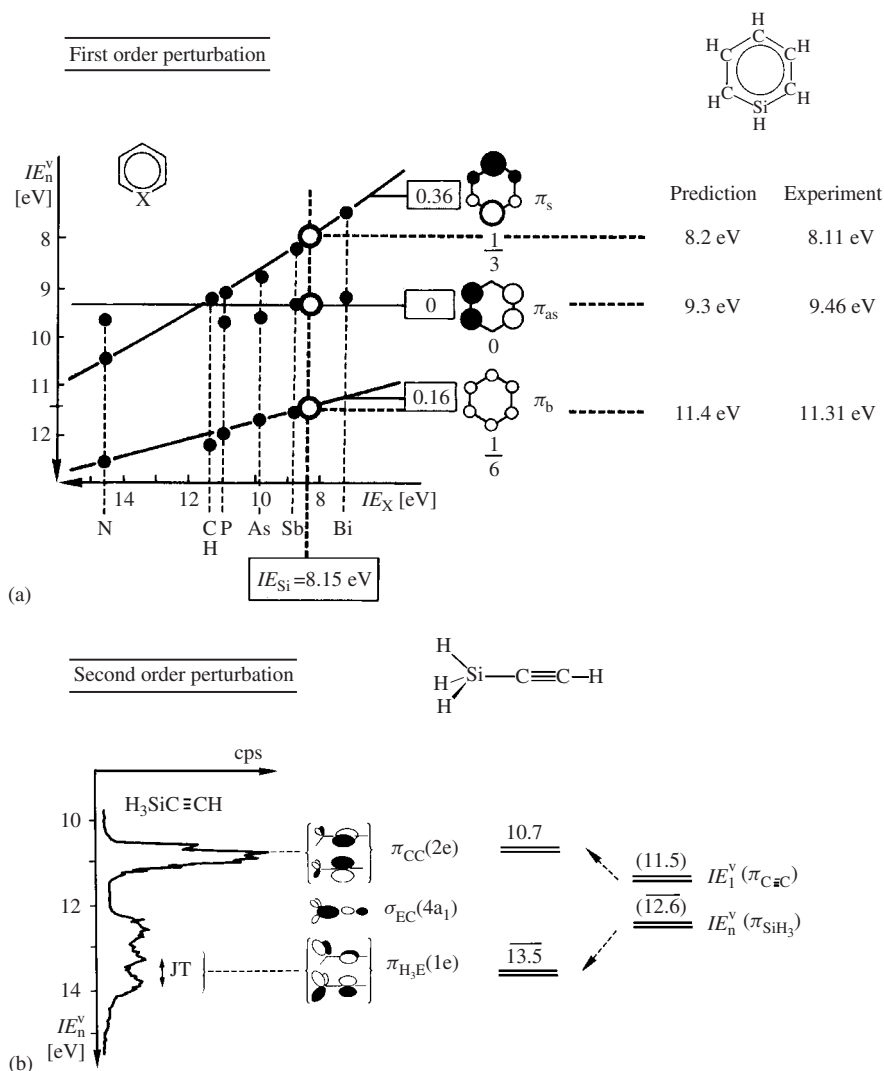


FIGURE 6. Examples for comparison of molecular state data based on first and second order perturbation: (a) Correlation of the vertical π -ionization energies of heterobenzenes $C_5H_5X^{36}$ with atomic ionization energies of elements X allowing a correct prediction for silabenzene^{15,37} and (b) second order perturbation in silylacetylene as visualized by its (helium I) photoelectron spectrum

Second-order perturbations are characterized by the necessary expansion of the wave function, and within simplifying fictitious MO models interaction between symmetry-equivalent orbitals will cause a split into an antibonding and a bonding linear combination. This orbital mixing increases both with the square of the interaction parameter, β_π^2 , and with decreasing energy difference $\Delta\alpha$. For radical cation states of a molecule, in which the

corresponding stabilization and destabilization become particularly apparent, this implies a different delocalization of the positive charge generated by ionization. The simplest example of such a second-order perturbation in organosilicon compounds is the fictitious π_{CC}/σ_{SiH_3} hyperconjugation in silylacetylene³⁸, which forms explosive mixtures with air. The molecule $H_3Si-C\equiv CH$ can be formally subdivided into a cylindrical electron cloud around the CC triple bond and the C_{3v} -symmetric ‘three-blade H_3Si propeller’ (Figure 6b). The interaction between the two 2E radical cation states of identical symmetry can be determined by inserting the ionization energies IE_1^v of $HC\equiv CH$ and the mean value $\overline{IE}_n^v(SiH_3)$ of H_3SiSiH_3 (Figure 3)^{15,16} into the second-order interaction determinant³¹:

$$\begin{aligned}\beta_{CC/SiH_3}^\pi &= \sqrt{(\alpha_{CC} - \varepsilon)(\alpha_{SiH_3} - \varepsilon)} \\ &= \sqrt{(IE_1^v(HC\equiv CH) - IE_1^v)(\overline{IE}_n^v(SiH_3) - IE_1^v)} = -1.2 \text{ eV}\end{aligned}\quad (4)$$

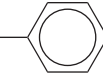
Comparison with the analogous methylacetylene interaction parameter $\beta_{CC/SiH_3}^\pi = -2.1$ eV demonstrates that the π_{CC}/σ_{CH_3} hyperconjugation is more effective—as expected from the shorter distance H_3C-C ³⁸. Altogether, π -type interaction models such as the one presented for silylacetylene prove to be useful in assigning the PES ionization patterns of numerous silicon-containing molecules such as $H_3Si-C\equiv C-SiH_3$ ³⁸ or the likewise C_{3v} -symmetric silicon halides H_3SiHal ¹⁵.

Summarizing, first- and second-order perturbation approaches^{8,9,31} allow one to rationalize molecular state properties of silicon-containing molecules^{15,16} (cf. Figure 6) based on the wealth of measurement data already available and often provide not only reliable insight into a specific problem, but also suggestions for its solution. In addition, perturbation arguments are extremely valuable in the context of quantum chemical calculations and, above all, in the proper design of experiments. Therefore, frequent application of first- and second-order perturbation wherever appropriate is highly recommended to the organosilicon chemist^{15,16,31}.

D. One-Electron Ionization and One-Electron Oxidation of Organosilicon Compounds

The extreme donor effect of β -trimethylsilyl substituents $-CH_2Si(CH_3)_3$ in molecules containing π systems or n_E lone pairs¹⁵, which were discovered 30 years ago^{39,40} and stabilizes the positive charge in radical cations by its considerable delocalization, is most elegantly revealed by the low first ionization energies of the respective molecules (Table 1). The perturbation sequence of the substituents, $SiH_3 < CH_3 \sim Si(CH_3)_3 < CH_2Si(CH_3)_3$ ^{15,16,40} (Table 1), clearly demonstrates that the first vertical ionization energies of

TABLE 1. First ionization energies of silicon-containing molecules

IE_1^v (MX)	X = H	SiH ₃	CH ₃	Si(CH ₃) ₃	CH ₂ Si(CH ₃) ₃	ΔIE_1^v (H)
H ₂ C=CH-X	10.51	10.37	10.03	9.86	→9.10	1.41
X-  -X	9.25	(9.11)	8.44	8.70	→7.86	1.39
NX ₃	10.85	9.70	8.44	8.60	→7.66	3.19

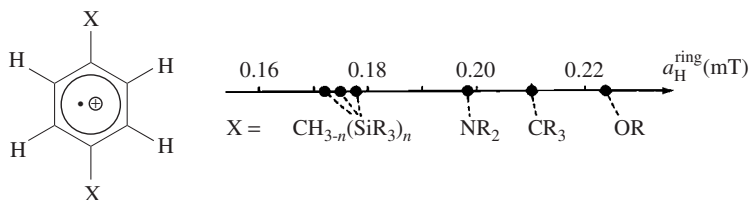
the parent molecules MH are always lowered most (cf. $\Delta IE_1^Y(\text{H})$) by trimethylsilylmethyl groups.

The small effective nuclear charge of silicon (Section IIIA, Figure 3) and the powerful delocalization of positive charges by β -trimethylsilyl groups (Table 1) can lower the PE-spectroscopically determined first vertical (*ca* 10^{-15} second) ionization energies of organosilicon compounds to an extent that also a far slower adiabatic ($<10^{-10}$ second) one-electron oxidation to the respective radical cation in solvents of low polarity seemed to be feasible^{9,41} (Section II.B, Figure 2b). This is indeed the case (Figure 7)^{25,41-43}.

The structure of the tetrachloroaluminate salt of an organosilicon radical cation crystallized from the aprotic one-electron oxidation solution⁴² (Figure 7a) provides, together with the gas chromatographically identified reaction product $\text{ClH}_2\text{C}-\text{CH}_2\text{Cl}$, some clues how the 'Bock one-electron oxidation reagent', discovered by chance in 1978^{41,43,44}, might accomplish the selective single electron transfer by AlCl_3 in water-free H_2CCl_2 : It is most likely due to a chlorocarbenium ion, $\text{H}_2\text{CCl}^\oplus$, produced by Cl^\ominus abstraction from the solvent H_2CCl_2 , as substantiated by formation of the structurally characterized AlCl_4^\ominus anion (Figure 7a). The cyclovoltammetrically determined unexpectedly high oxidation potential for the $\text{AlCl}_3/\text{H}_2\text{CCl}_2$ system of +1.8 V (!)⁴¹ could indicate that a single electron uptake by $\text{H}_2\text{CCl}^\oplus$ forms a $\text{H}_2\text{CCl}^\bullet$ radical intermediate, which most likely dimerizes to 1,2-dichloroethane detected by gas chromatography in the oxidation solution⁴² (Figure 7a). A correlation of the (often irreversible) oxidation potentials of organosilicon molecules with their first ionization energies, $E^{\text{ox}}[\text{V}] = -4.58 + 0.78 \text{ IE}_1$ (eV)⁴¹, provides an enormously useful and widely applicable⁴³ prediction: All molecules with first ionization energies below 8 eV—as determined by either PE spectroscopy or easily accessible⁴⁴ UV/VIS spectroscopy of a suitable donor–acceptor complex—will be oxidized selectively to their radical cation by the water-free $\text{AlCl}_3/\text{H}_2\text{CCl}_2$ redox system^{15,25}.

The advantageous one-electron oxidation system $\text{AlCl}_3/\text{H}_2\text{CCl}_2$ ^{15,25,43} (Figure 7a)—powerful, predictable and water-free—opened the door to the study of numerous novel organosilicon radical cations (Figure 7b) in detail^{15,16,25} as exemplified by selected results each for spin distribution (Scheme 1 and Table 2), structural changes (Scheme 2) or dynamic phenomena (Scheme 3).

ESR and ²⁹Si ENDOR⁴⁵ signal patterns recorded prove an effective π -spin delocalization by substituents $\text{CH}_{3-n}(\text{SiR}_3)_n$ exceeding that by 'prototype' donors such as OR or NR_2 (Scheme 1), which increase the ring hydrogen coupling $a_{\text{H}}^{\text{ring}}$.



SCHEME 1

The coupling constants $a_{29\text{Si}}$ and $a_{\text{H}}^{\text{Si}(\text{CH}_3)_2}$ of various radical ions of planar tetrasilabicyclo[3.3.0]octane derivatives allow one to 'read off' how large the π -spin density in the β (H_3C)₂Si substituted $\text{CC}^\bullet\oplus$ radical cations actually is—especially in contrast to the

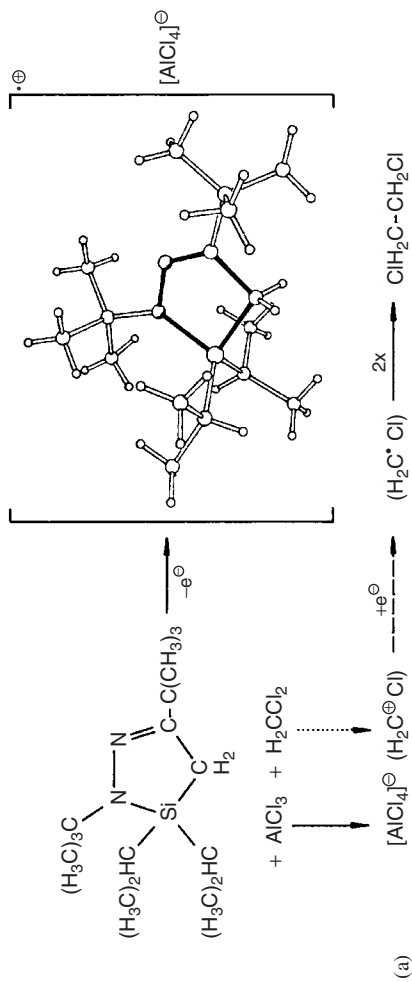


FIGURE 7. (a) Organosilicon radical cation tetrachloroaluminate salt, with structure determined for the crystal grown from H_2CCl_2 solution⁴², and the proposed electron transfer pathway for the selective one-electron oxidation by $\text{AlCl}_3/\text{H}_2\text{CCl}_2$ (see text). (b) Representative examples of organosilicon compounds ($\text{R}=\text{CH}_2$) with first vertical ionization energies $\text{IE}_1^v < 8 \text{ eV}$ (known values in parentheses), which could be selectively oxidized to their radical cations by using the 'Bock oxidation' reagent $\text{AlCl}_3/\text{H}_2\text{CCl}_2$.^{41,43}

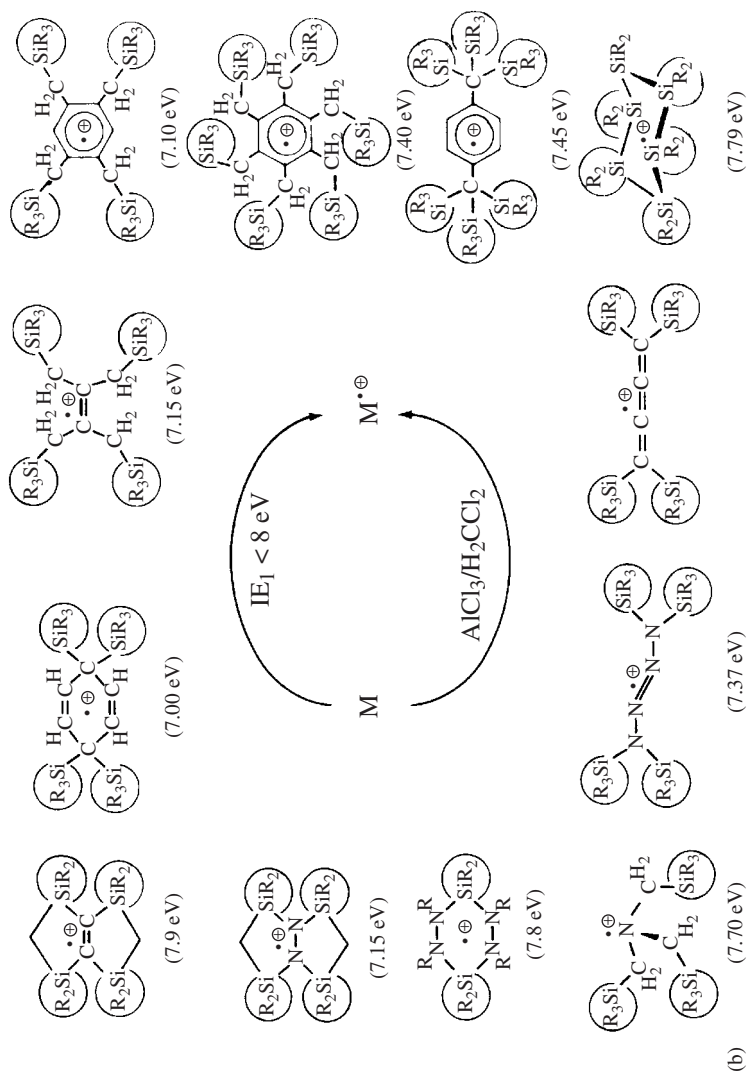


FIGURE 7. (continued)

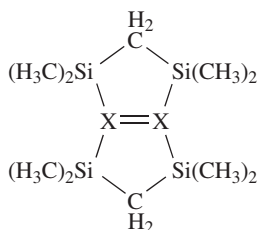
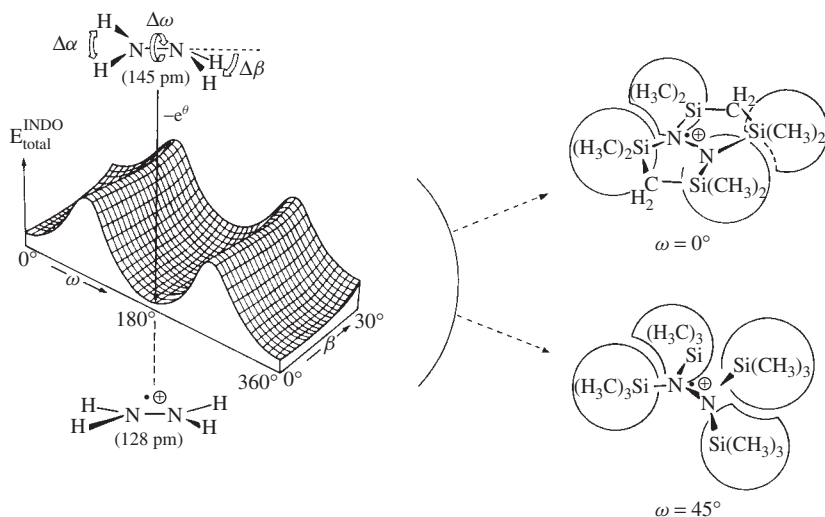


TABLE 2. Coupling constants of radical ions of tetrasilabicyclo[3.3.0]octane derivatives

X=X	C \cdot^{\ominus} C	C \cdot^{\ominus} C	N \cdot^{\oplus} N	
$a_{29\text{Si}}$	2.271	0.685	0.500	(mT)
a_{H}	0.062	0.048	0.030	(mT)

pair of valence-isoelectronic CC^{\ominus} and NN^{\oplus} species, in which the unpaired electron is preferentially localized in the region of the central bond (Table 2).

The changes in energy and electron distribution on vertical transition from the ground state of a neutral molecule to that of its radical cation (Figure 2a) will indispensably lead to structural changes via molecular dynamics outside the femtosecond region (Figure 2b), which can be determined from the M^{\oplus} ESR signal patterns and reproduced by quantum chemical open-shell energy hypersurface calculations^{15,16,25}. For hydrazine and its $(\text{H}_3\text{C})_n\text{Si}$ derivatives, an INDO open-shell hypersurface (Scheme 2) calculated for the six-atom parent radical cation $\text{N}_2\text{H}_4^{\oplus}$ with its $3n - 6 = 12$ degrees of freedom covered by the three angular coordinates $\alpha(\text{HNH})$, $\beta(\text{NNH}_2)$, and $\omega(\text{H}_2\text{N}-\text{NH}_2)$ predicts that the neutral C_2 molecule flattens on electron removal to a planar D_{2h} radical cation. For the resulting three-electron two-center π bond, a shortening of the NN bond length from 145 pm by $\Delta d_{\text{NN}} \approx 17$ pm (!) to 128 pm has been precalculated and structurally confirmed¹⁵ (Scheme 2).

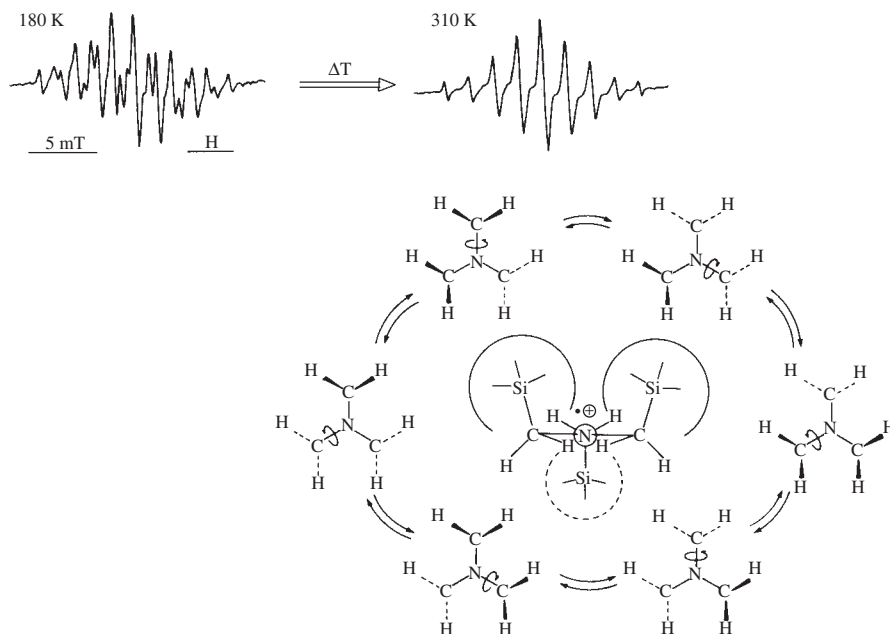


SCHEME 2

For $(\text{H}_3\text{C})_n\text{Si}$ -substituted hydrazine derivatives (Table 2 and Scheme 2) the following structural changes are detected from the ESR signal patterns or other molecular state data and confirmed by the hypersurface calculations (Scheme 2): The bicyclic hydrazine

derivative shows an enormous PES splitting $\Delta IE_{1,2}^v$ (n_N/n_N) = 1.8 eV¹⁵ and therefore must be an almost planar molecule, which will not change its structure significantly on one-electron oxidation (Scheme 2): $\omega = 0^\circ$. In contrast, the open-chain derivative with the rather small PES splitting $\Delta IE_{1,2}$ (n_N/n_N) of only 0.2 eV should contain two almost perpendicular molecular halves, with their dihedral angle predicted to be reduced in the radical cation to a sterically enforced minimum value of about 45° (Scheme 2), in good agreement with the observed ESR coupling constants^{15,25}.

The tris(trimethylsilyl)methylamine radical cation and its 'cog wheel' dynamics will conclude the ESR/ENDOR information on radical cation state properties. Many organosilicon radical cations with several β -trimethylsilyl groups are sterically overcrowded and therefore rigid with respect to substituent rotations. One interesting exception is the planar radical cation $[(H_3C)_3SiH_2C]_3N^{\bullet\oplus}$ with angles $\angle NCN = 120^\circ$, which shows a characteristic ESR line broadening with increasing temperature: Its 25 signals at 180 K are reduced to 9 at 310 K (Scheme 3)⁴⁶.



SCHEME 3

The temperature-dependent ESR signal pattern change is due to rotations of the $(H_3C)_3SiH_2C$ substituents on the opposite side of the NC_3 molecular plane within the ESR time scale of 10^{-6} to 10^{-8} second: Because each side of the NC_3 plane offers room for only two of the bulky $(H_3C)_3Si$ groups, a 'cog wheel'-like coupled dynamic process (Scheme 3) results and the CH_2 hydrogens become equivalent on the ESR time scale^{15,46}.

To summarize this essential introductory subchapter, an advantageous, powerful and most elegant single-electron oxidation procedure has been established: all organosilicon compounds with first vertical ionization energies below 8 eV can be oxidized by $AlCl_3/H_2CCl_2$ selectively to their radical cations^{15,16,25} (Figure 6). The ESR/ENDOR

signal patterns registered provide important information on the influence of Si substitution on the spin distribution (Scheme 1 and Table 2), changes in structure (Scheme 2) and molecular dynamics (Scheme 3) within the ESR time range: The temperature-dependent ESR signal patterns reveal another molecular-state property: the storage of internal energy in the $3n - 6$ degrees of freedom of n -atomic three-dimensional molecules^{9,15}.

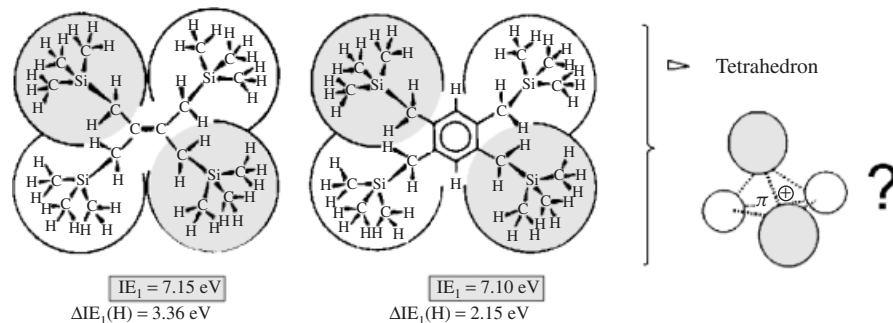
E. Sterically Overcrowded Organosilicon Molecules

Unshielded, air-stable molecules are rather rarities in the organosilicon collection: most of them are lipophilically wrapped by bulky substituent groups in fascinating spatial arrangements giving rise to often intriguing static and dynamic properties (cf. e.g. Figure 7 or Table 2 and Schemes 2 and 3). This central point of main group chemistry is predominantly based on structures from crystals⁴⁷, which contain molecules in general in their ground state close to the global minimum of the total energy and with largely ‘frozen’ molecular dynamics²⁴, and which are therefore a suitable starting point for the discussion of essential molecular properties⁴⁸ as well as for their quantum chemical calculation (Section II.B). In addition, structural differences due to steric congestion in molecules and/or due to charge perturbation of molecules become visible in crystals²⁴ and, last but not least, valuable information on molecular recognition and self-organization⁴⁹ is provided.

The following facets of sterical overcrowding in organosilicon compounds are forwarded as introductory questions:

Will Charges in Fourfold Trimethylsilylmethyl-substituted π -Systems Delocalize Tetrahedrally?

The 4-fold $(\text{H}_3\text{C})_3\text{SiCH}_2$ -substituted ethene and benzene derivatives, $\text{C}_{18}\text{H}_{44}\text{Si}_4$ and $\text{C}_{22}\text{H}_{46}\text{Si}_4$, exhibit almost identical first vertical ionization energies of about 7.1 eV due to tremendous substituent perturbations of the parent hydrocarbons amounting to $10.51 - 3.36 = 7.15$ eV or $9.25 - 2.15 = 7.10$ eV, respectively (Scheme 4).



SCHEME 4

The π subunits, ethene and benzene, differing in both size as well as topology, but containing the same tetra-substitution pattern, seem to approach identity^{15,16}. ESR spin delocalization data of their organosilicon radical cations as well as additional information from own structures of sterically overcrowded molecules and many more registered in the Cambridge Structural Database stimulate speculation that both tetra-substituted molecules

and especially their radical cations (Scheme 4) are tetrahedrally shaped with each two R_3SiCH_2 groups above and below the central π skeletal plane.

How to Measure Steric Overcrowdedness and its Consequences?

Comparing structural data of chemically related molecules and especially their rotational angles often allows a correlation with the differing van der Waals contours of the respective substituent groups^{24,47,48}. One of the most transparent examples concerns organosilicon compounds, in which two substituent half-shells are separated along their central C_3 axes by spacers of different lengths (Figure 8).

The structural comparison of the C_3 -symmetric skeletons of the organosilicon (half-shell \cdots (spacer) \cdots half-shell) molecules (Figure 8a) provides a rational criterion for steric overcrowdedness: Obviously, at distances $Y \cdots Y$ below 333 pm different dihedral angles $\omega(X_3Y \cdots YX_3)$ between the half-shell substituents are observed, whereas above 414 pm they are identical. The accompanying torsion $D_{3d} \rightarrow D_3$ within the molecular skeleton is therefore a criterion for steric overcrowding⁴⁸.

The structure of hexakis(trimethylsilyl)silane, for which unexpectedly a molecular skeleton $Si_3Si-SiSi_3$ of D_3 symmetry (Figure 8b) with different dihedral angles of 43° and 77° is determined^{50,53}, exhibits a drastic cogwheel meshing of the methyl groups between the two molecular halves leading to some extremely short non-bonded $C \cdots C$ distances (Figure 8b): The shortest ones between the two molecular halves are 352 pm long and thus are about 12% shorter than the sum of the van der Waals radii of two methyl groups $C(H_3) \cdots (H_3)C$ generally assumed to be about 400 pm^{24,48}.

The structural discussion of the disilane derivative $(R_3Si)_3Si-Si(SiR_3)_3$, lipophilically wrapped by 18 methyl groups, raises the question about how supersilyl substituents will modify especially the ground states of the respective molecular ions. A comparison with first vertical ionization energies of disilane and its hexamethyl derivative (Figures 3, 4 and 7c) proves a lowering on methylation of disilane by 1.8 eV and on trimethylsilylation by 2.8 eV down to 7.7 eV, i.e. even below dodecamethylcyclohexasilane $Si_6(CH_3)_{12}$ exhibiting 7.8 eV (Figure 4c): Apparently, the delocalization of the positive charge into the half-shells $Si(SiR_3)_3$ is energetically favorable and these half-shells are therefore excellent donor substituents.

There are numerous consequences of sterical overcrowding as a general phenomenon of many, although each weak, attractive van der Waals interactions between organosilicon molecules with their Si centers of low effective nuclear charge (Figures 2b and 3). The following three examples will document other unexpectedly strong effects due to Si \rightarrow C exchange, π interaction or charge delocalization^{48,50}.

(i) *Intramolecular van der Waals Bonding.* Correlation of SiSi bond lengths in disilane derivatives $X_3Si-SiX_3$ with substituents $X=CH_3$, $C(CH_3)_3$ and $Si(CH_3)_3$ ^{48,51} together with those of sterically overcrowded cyclic and linear trisilane derivatives versus their Pauling bond orders $\lg(PBO) = [d(1) - d(x)]/60$ ^{51,52} (11: PBO values), expectedly produces linear regression (Scheme 5)⁴⁸.

The distance-dependent Pauling bond orders range from 1.00 in hexamethyldisilane with a SiSi bond of 235 pm length to 0.26 for hexakis(*tert*-butyl)disilane (Scheme 5) with an extremely elongated spacer distance of 270 pm between its bulky $Si(C(CH_3)_3)_3$ half-shells⁵¹ (Figure 8a): The C-C bond lengths are approximately 40 pm shorter than the C-Si ones and thus the tri(*tert*-butyl)silyl half-shell 'umbrellas' compress their size and increase their congestion. Despite its considerably weakened central SiSi bond (Scheme 5) the sterically overcrowded hexakis(*tert*-butyl)disilane, according to ESR experiments, does not dissociate into two radicals even at elevated temperature, which further supports the

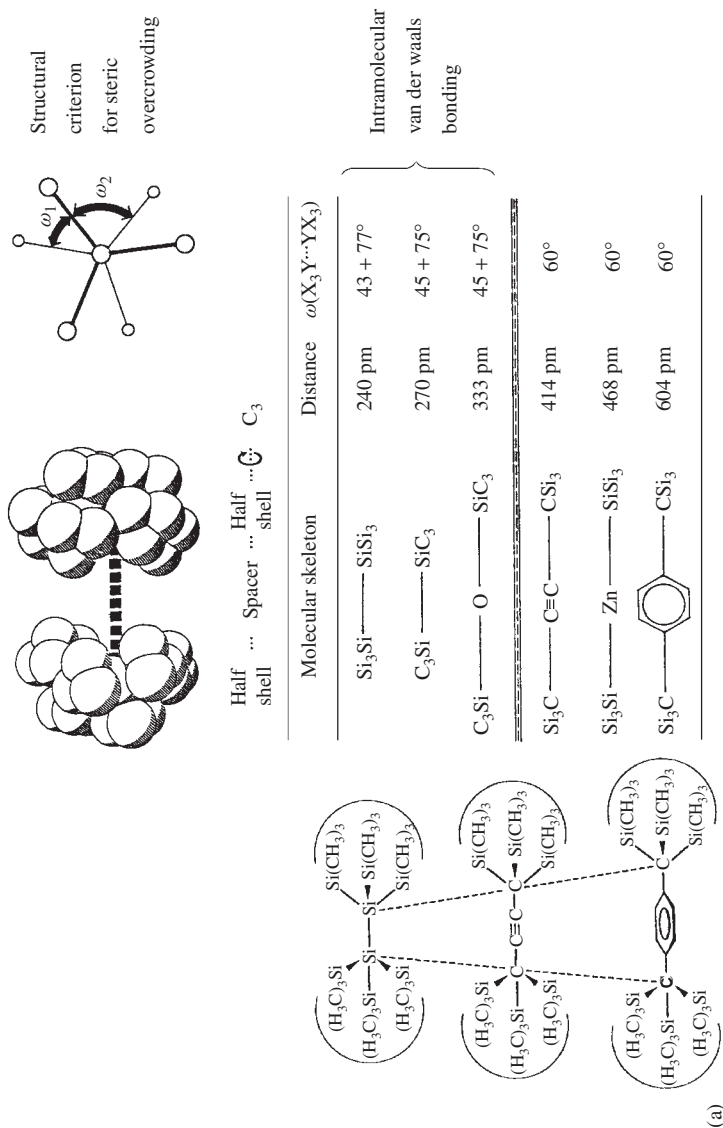


FIGURE 8. (a) Half-shell structure model for organosilicon compounds with different spacers along the C_3 symmetric substituent axis and dihedral angles $\omega(X_3Y-YX_3)$ determined for the molecular skeletons as a most transparent overcrowdedness criterion; (b) single crystal structure of $(H_3C)_3Si)_3Si-Si(CH_2)_3$; (SV) side view with essential bond lengths and angles as well as the shortest non-bonding $C \cdots C$ distances and (AV) axial view (50% thermal ellipsoids) with different dihedral angles $\omega(Si_3Si-SiSi_3)$; (c) first vertical ionization energies of various hexa-substituted disilanes

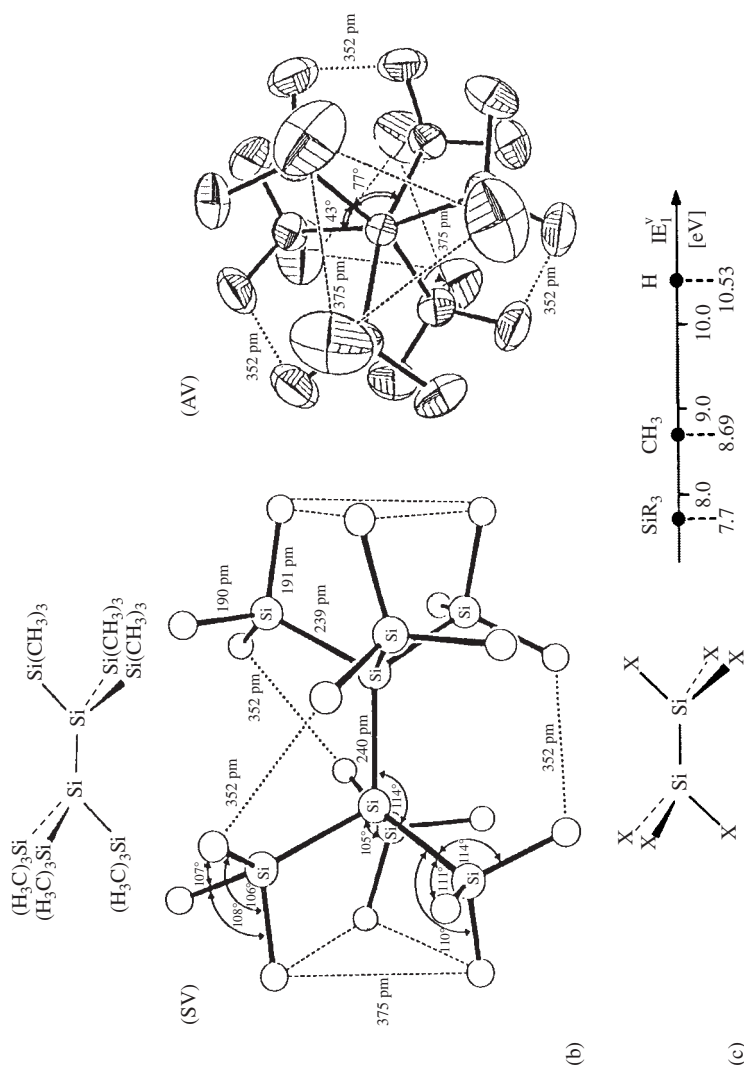
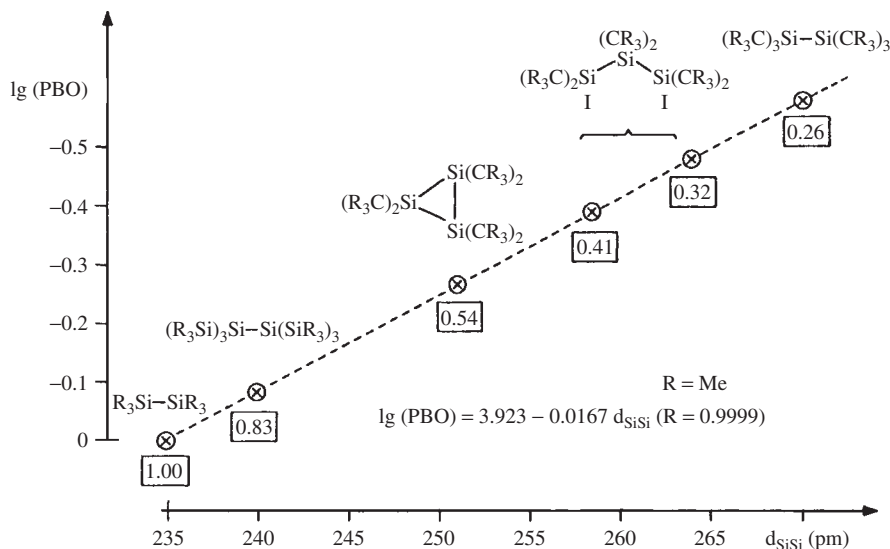


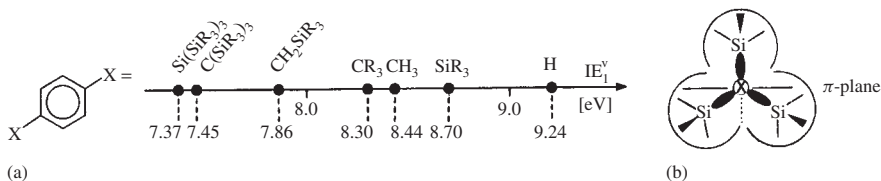
FIGURE 8. (continued)



SCHEME 5

proposed additional attractive van der Waals interactions within the hydrocarbon wrapping of organosilicon molecules^{48,50,51}. This assumption is also in accord with the structure of hexakis(trimethylsilyl)disilane (Figure 8b), which exhibits extremely short non-bonded $C(H_3) \cdots (H_3)C$ distances of only 352 pm — in full agreement with the considerable polarization $Si^{\delta\oplus}-C^{\delta\ominus}-H^{\delta\oplus}$ predicted quantum chemically.

(ii) π Interactions of Half-Shell Supersilyl Substituents. β -Trimethylsilyl substituents $(H_3C)_3SiCH_2-$ are well established as powerful electron donors to π -systems, lowering ionization potentials to $IE_1^V < 8$ eV and oxidation potentials to $E_{1/2}^{OX} < +1.8$ V (Figure 7b). As concerns three trimethylsilyl groups at one C or Si center, these often-called 'supersilyl groups', $((H_3C)_3Si)_3C-$ and $((H_3C)_3Si)_3Si-$, are expectedly not three times as powerful but still among the most potent substituents known. According to their vertical first ionizations, the Si_3Si- one is slightly more effective than the Si_3C- iso(valence)electronic one^{10,48,50,53,54} as demonstrated for the 1,4-disubstituted benzenes (Scheme 6).

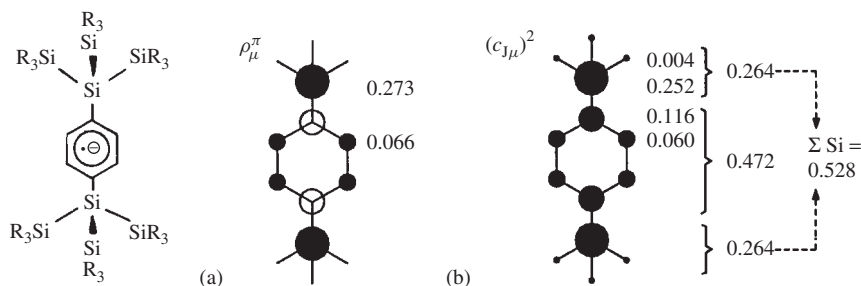


SCHEME 6

The substituent perturbations can be fully parametrized: For $(R_3Si)_nCH_{3-n}$ -substituted radical cations, coupling constants are rationalized and predicted by the angularly

dependent Heller/McConnell equation, $a_x = (B_o + B_2 \cos^2 \Theta_{CX}) \rho_\mu^\pi$ ²⁵. Using the same angular increments $\cos^2 \Theta_{CX}$, vertical first ionization energies (Scheme 6b $\rightarrow 1 \cos^2 0^\circ + 2 \cos^2 60^\circ$ and $IE_1^v = \sum d_{CX} < \cos^2 \Theta >$ with $d_{CH} = 0.27$ eV or $d_{CSi} = 0.68$ eV) can be satisfactorily predicted^{10,25}.

Supersilyl substituents are also well-suited to stabilize negative charges leading to ‘Guinness Book of Records’ results:



SCHEME 7

The ESR/ENDOR π -spin populations ρ_μ^π in the radical anion of 1,4-di[tris(trimethylsilyl)silyl]benzene (Scheme 7a) and the corresponding squared HMO coefficients $(c_{J\mu})^2$, which allow one to augment the ‘blind centers’ without a CH bond (Scheme 7b), prove that more than half of the π -spin population ρ_μ^π is located in the $[(\text{H}_3\text{C})_3\text{Si}]_3\text{Si}$ half-shell ‘supersilyl’ substituents.

(iii) *Perspectives of Supramolecular Organosilicon Chemistry.* Sterically overcrowded organosilicon molecules are of interest in numerous aspects: Often, spatially enforced structural changes or hindered molecular dynamics will be observed⁴⁸ and the charge delocalization in their molecular ions, which are in general kinetically stabilized by lipophilical wrapping, can be studied by various measurement methods. Little is known so far, however, about molecular recognition⁴⁹ and self-assembly of organosilicon ensembles, which should be strongly supported by the considerably polarized linkages $\text{Si}^{\delta\oplus} - \text{C}^{\delta\ominus} - \text{H}^{\delta\oplus}$ calculated for the formation of intramolecular clusters with Si coordination numbers 7 and 8⁴⁹.

F. Kinetically Unstable Silicon Intermediates: Detection in Unimolecular Flow Systems by their PE-spectroscopic Ionization Fingerprints

Based on the photoelectron-spectroscopic experience gathered^{9,16}, reactions of flowing gases can be advantageously and ‘visually’ optimized by the temperature-dependent changes in the continuously recorded real-time PES ionization patterns^{11,16,55} (cf. Section II.A): The ‘molecular ionization fingerprints’ of the reactants give way to those of the products. This technique proved to be especially valuable for the generation and unequivocal identification of numerous reactive intermediates⁵⁵. With millimole quantities of a suitable precursor and within half a day, the optimum temperature and flow parameters can be determined to prepare the respective short-lived molecule under nearly unimolecular conditions, which due to the low gas-phase concentrations present cannot cause any thermal chain-reaction explosion. The existence of the respective reactive

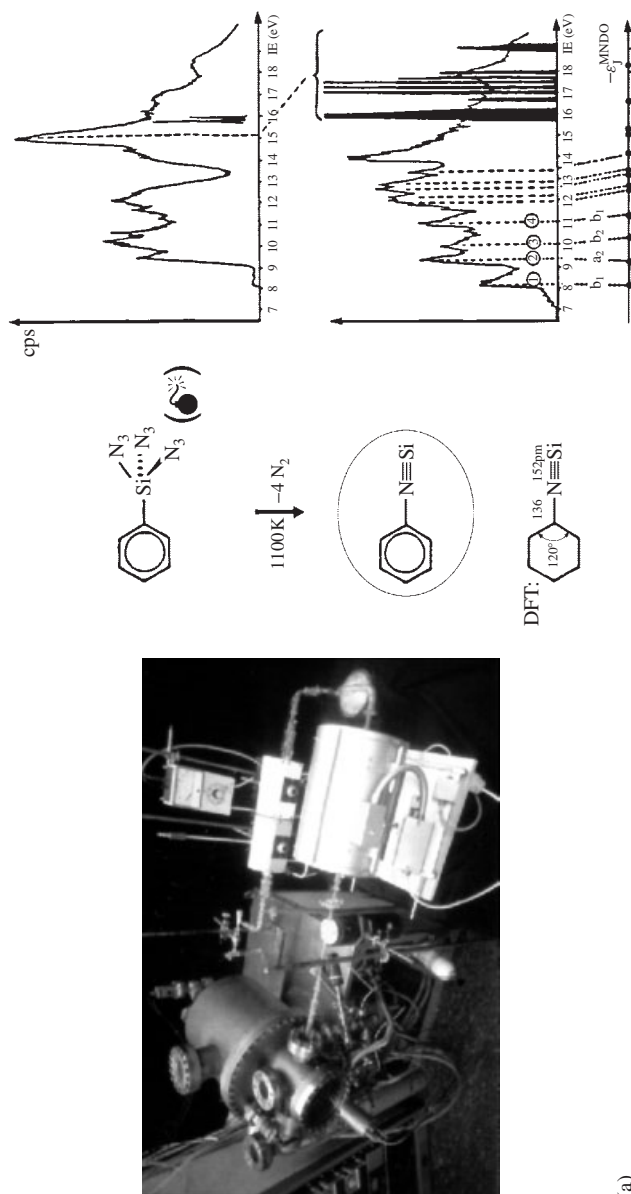
species is readily established by comparing its recorded radical cation state sequence with those of chemically related, preferably iso(valence)electronic compounds or with a precalculated one. Often, the optimized conditions did stimulate to trap the molecule at low temperatures, e.g. in a matrix experiment, and to further characterize it by other spectroscopic techniques. This procedure (Figure 9a) allowed one to discover numerous kinetically unstable compounds containing silicon centers of coordination numbers 3, 2 or 1 — from silabenzene via silylenes to phenyl silaisocyanide (Figure 9b).

Starting from literature reports⁵⁶ that $\text{H}-\text{N}^{\delta\oplus}\equiv\text{Si}^{\delta\ominus}$ is generated on photolysis of H_3SiN_3 in a 4 K argon matrix, the total energy, the structure, and the ionization pattern of the more stable phenyl derivative have been calculated⁵⁷. Small-scale azide exchange of phenyltrichlorosilane yields triazido(phenyl)silane, the controlled explosion of which in a flash pyrolysis apparatus (Figure 1b) under approximately unimolecular conditions ($p \approx 10^{-3}$ Pa, $c \approx 10^{-3}$ mM) can be carried out without danger. Real-time PE-spectroscopic analysis of the band intensities¹¹ revealed that the optimum reaction conditions require a temperature of 1100 K (i.e. red heat) for the complete elimination of four molecules of N_2 (Figure 9a: blackened ionization bands). The identification of the first organosilicon compound with a partly ionic triple bond $\text{R}-\text{N}^{\delta\oplus}\equiv\text{Si}^{\delta\ominus}$ and a silicon coordination number of 1 was accomplished by Koopmans' correlation of all nine resolved low-energy ionization bands (Figure 9a) with calculated MNDO eigenvalues. The formation of the valence isomer $\text{H}_5\text{C}_6-\text{Si}^{\delta\oplus}\equiv\text{N}^{\delta\ominus}$, which is predicted to be 400 kJ mol^{-1} less stable, can be excluded, for example, by comparison of the radical cation state sequence with that of the valence-isoelectronic carbon species $\text{H}_5\text{C}_6-\text{N}^{\delta\oplus}\equiv\text{C}^{\delta\ominus}$. In the meantime, the PE-spectroscopic results have been confirmed by matrix isolation of $\text{H}_5\text{C}_6-\text{N}^{\delta\oplus}\equiv\text{Si}^{\delta\ominus}$ ^{58,59}.

After the development of the PE-spectroscopic ionization fingerprint gas analysis in flow systems (Section II.A)¹¹, numerous kinetically unstable small main group element molecules have been generated under unimolecular conditions and unequivocally identified by each of their unique radical cation state ionization patterns⁵⁵. To begin with, the then elusive silabenzene, for which by first order molecular state perturbation the low π energies had been predicted¹⁵ (Figure 6a), were thermally prepared both by energetically favorable propene elimination as well as by H_2 split-off²³ (Figure 9b: 1979) and, by using the PES-optimized thermolysis conditions, matrix-isolated²³. An analogous procedure allowed one to produce and matrix-isolate the rather short-lived silaethene (Figure 9b: 1980). Following the early reports on SiF_2 gas-phase preparation⁶⁰, also SiCl_2 and SiBr_2 ^{16,40} and, finally, even SiI_2 with 90% iodine content and therefore relativistically dominated (Section IV.E.1), have been PE-spectroscopically assigned⁶¹. The most elegant way to thermally synthesize dichlorosilylene is the naphthalene elimination from 3,3-dichloro-3*H*-3-benzosilepin²¹ (Figure 9b: 1984). As a subproject within the thermal N_2 elimination from numerous azides¹² as well as other suitable precursors⁵⁵, five-membered rings of tetrazole derivatives were opened at 800 K (i.e. red heat) to the corresponding nitrilimines⁶². Following these prototype gas-phase thermolysis preparations of organosilicon intermediates 20 years ago¹⁶, several groups worldwide added numerous interesting results. Novel compounds were generated, PE-spectroscopically identified and their radical cation state sequences were calculated quantum chemically.

G. Interim Summary

Faced with the 'torrent' of novel silicon compounds and the 'sea' of their molecular states, any review article can illustrate at best only some aspects of selected examples.



(a)

FIGURE 9. (a) Generation of phenyl silaisocyanide, the first organosilicon molecule reported to contain a multiply bonded, singly coordinated silicon center, by controlled explosion of triazido(phenyl)silane in a double-oven pyrolysis set-up connected to a PE spectrometer and its PE-spectroscopic identification together with the ionization fingerprints of N₂ (black), a most advantageous leaving molecule; and (b) some of the short-lived silicon intermediates prepared by the Frankfurt Group between 1979 and 1987⁵⁵

It should, however, be kept in mind that each chemical species will—depending on its energy—change its structure, exhibit different dynamics and hence possess molecular state-dependent properties. Such a general statement will be of help to the preparative chemist, who would like to classify the multiplicity of his compounds by chemical intuition only, especially if he gets used to advantageously compare equivalent states of chemically related molecules based on their measurement data, that is, to stay as close to experiment as possible and to support experiment by quantum chemically-based models. Other methods such as force-field approximations offer alternative approaches. This also applies to the emphasized measurement techniques of PE and ESR/ENDOR spectroscopy, which cover different time domains, are quite sensitive to molecular or molecular ion perturbations and whose energy differences or spin populations measured can be correlated—for example, via Koopmans' theorem or the McConnell relation (Section II.B)—with results from approximate calculations, even for larger molecules.

Following the general introductory remarks on photoelectron spectroscopy today (Section I), the principle of PES measurements (Section II.A) and the molecular state approach to silicon compounds (Section II.B), the following essential facets of silicon-containing molecules have been demonstrated and illustrated (Section III.A to F): the effective nuclear potentials of Si and C, the charge delocalization in polysilane chains and rings, silicon perturbations of molecules, one-electron oxidation to organosilicon radical cations, sterical overcrowdedness in lipophilically wrapped organosilicon molecules and kinetically unstable silicon intermediates.

All of these facets are connected to the photoelectron spectroscopy of organosilicon molecules. Given the fact that 40 years ago hardly any gas chromatographs, NMR instruments or computers were available, astonishing progress has been accomplished, including our knowledge about molecular states, which has been improved considerably by measurement techniques such as photoelectron spectroscopy and the quantum chemical interpretation of the molecular ionization fingerprints registered.

IV. (HE I)-PHOTOELECTRON SPECTROSCOPIC RESULTS 1990–2000

It has been emphasized (Section I–III) how much the silicon chemist had learned concerning the σ and π states of his molecules and their often breathtaking properties, from photoelectron spectroscopy, the right method available at the right time. The activity in this once very prosperous research area, however, has ceased considerably, as is obvious especially from the results summarized in 1995¹⁰ and their rather small number published since then. In the following, the last PE spectroscopic (100-page and 252-citation) overview¹⁶ up to 1989 is taken as a starting point for the upgrading, subdivided in subsections dealing with main group element centers in the respective organosilicon compounds assorted according to the periodic table classification from main group 13 to main group 17 elements. An outlook will try to assess present activities and future prospects.

A. Organosilicon Compounds Containing Main Group 13 Elements

The PE spectrum of 1,2-dimethyl-1,2-disila-*closo*-dodecaborane(12) ($(\text{H}_3\text{CSi})_2\text{B}_{10}\text{H}_{10}$), a 30-center disiladecaborane cluster with two Si of coordination number 6, can be recorded at 10^{-5} mbar pressure using a heated inlet system^{10,63} (Figure 10a).

For the parent *closo*-dodecaborane(12) $(\text{H}_2\text{C})_2\text{B}_{10}\text{H}_{10}$ framework, 13 cluster as well as 10 BH ionizations are assigned in the literature⁶³ and, for the two H_3CSi subunits, an additional 14 are expected. An estimate based on the relative (HeI) photoelectron spectroscopic band intensities (Figure 10) suggests about 25 ionizations with predominant $2s/p_{\text{B}}$, $1s_{\text{H}}$, $3p_{\text{Si}}$ and $2p_{\text{C}}$ contributions within the He I measurement region. A geometry-optimized MNDO calculation predicts the ionizations of lowest energy to be grouped

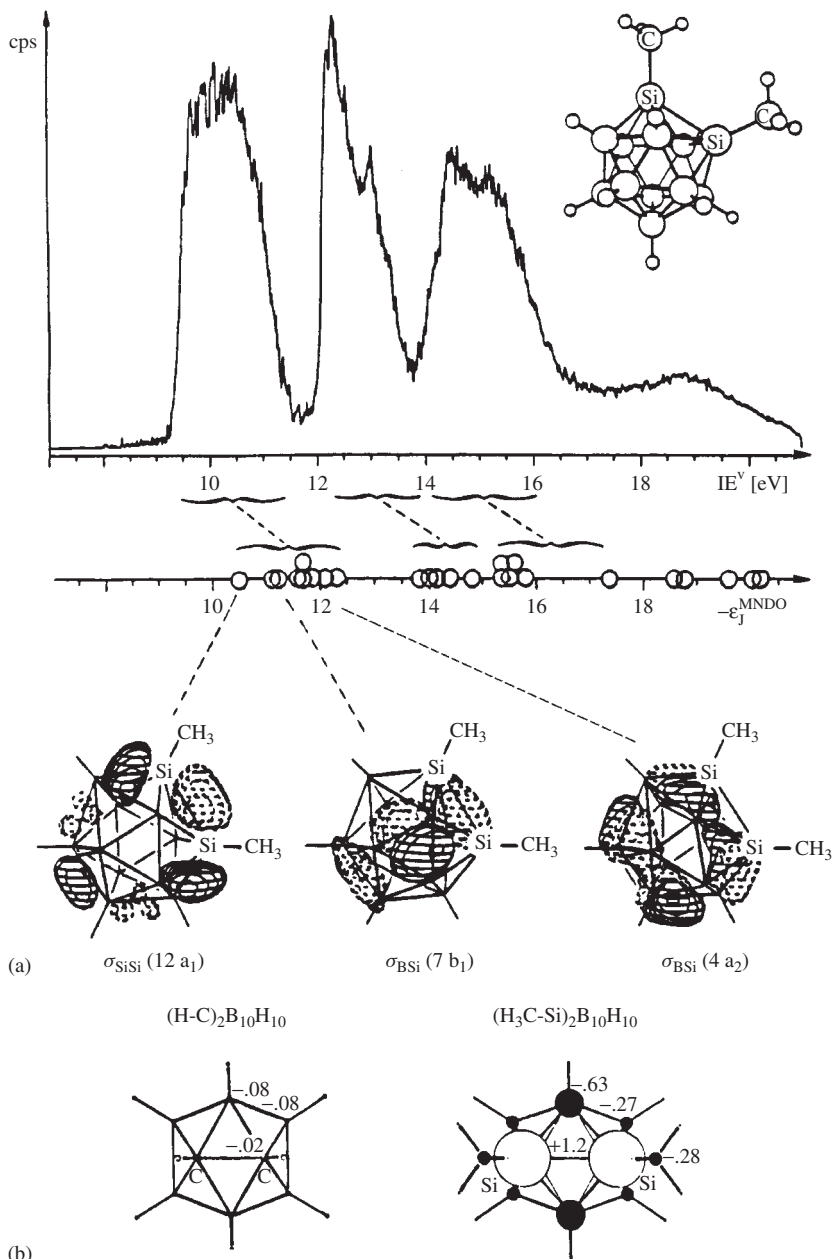


FIGURE 10. (a) (He I) PE spectrum of 1,2-dimethyl-1,2-disila-*closo*-dodecaborane(12) ($(\text{H}_3\text{CSi})_2\text{B}_{10}\text{H}_{10}$) with Koopmans' assignment by MNDO eigenvalues as well as cluster orbital diagrams for the three radical cation states of lowest energy; (b) comparison of MNDO charge distributions for both 1,2-carborane as well as 1,2-bis(silamethyl)-*closo*-dodecaborane(12)

into nine cluster-type and ten additional transitions within the band hill between 9.5 and 10.5 eV, five of BH and SiC character within the bands overlapping between 12 and 13.5 eV, and another five of predominant BH and CH contributions within the double band region between 14 and 16 eV (Figure 10a). The overall PES band pattern is satisfactorily reproduced by Koopmans' correlation, $IE_n^v = \varepsilon_j^{\text{MNDO}}$, although Koopmans' defects, $\Delta = \varepsilon_j^{\text{MNDO}} - IE_n^v$, up to *ca* 1.5 eV, are calculated, indicating that the proposed sequence of radical cation states assigned has to be viewed with some caution.

A comparison with the respective ionizations of the parent 1,2-carborane⁶³ demonstrates that upon replacement of the cluster CH subunits by SiCH₃, all three ionization regions are shifted to lower energies by at least 1.5 eV⁶³. This PE spectroscopic observation can be traced again to the considerable decrease in effective nuclear charge from carbon to silicon centers (Section III.A and Figure 3). Accordingly, silicon cluster subunits SiCH₃ are expected to act as electron donors even to the surrounding B(H) centers. This assumption is substantiated by the calculated MNDO charge distributions for both 1,2-carborane and 1,2-bis-(silamethyl)-*closo*-dodecaborane(12) (Figure 10b), which suggest that the (H₃C)SiSi(CH₃) subunit considerably increases the electron density within the (BH)₁₀ cluster framework and thus provides a plausible explanation for the remarkable 1.5 eV shift of the three separated low energy bands to even lower energy⁶³ (Figure 10).

Summarizing, 1,2-bis(silamethyl)-*closo*-dodecaborane(12), which exhibits in its PE spectrum (Figure 10a) the lowest ionization onset of only 9.5 eV observed so far in analogous compounds⁶³, is therefore presently the most electron-rich cluster, XYB₁₀H₁₀, with two adjacent main group element centers XY each of coordination number six.

B. Organosilicon Molecules (Main Group 14 Elements)

In this section, the selected topics of photoelectron spectroscopic investigations on silicocene (Section IV.B.1), the charge delocalization in (R₃Si)₃Si–Si(SiR₃)₃^{•⊕} (Section IVB.2) and matrix isolation of organosilicon radical cations (Section IVB.3) are presented. Table 3 will provide data on all other organosilicon molecules investigated by their ionization patterns.

1. Silicocene

This section opens with a discussion of the silicocene radical cation states⁶⁴, which have only been mentioned in the preceding report from 1989¹⁶ based on a personal communication. The bis(η^5 -pentamethylcyclopentadienyl)silicon sandwich exhibits the highest Si coordination number of 10 observed so far¹⁵. The rather unusual organosilicon compound is synthesized by reacting bis(pentamethylcyclopentadienyl)silicon dichloride (R₅C₅)₂SiCl₂ with sodium naphthalide, and the crystal structure proves two conformers with rings either coparallel (*D*_{5d}) or bent (*C*_{2v}) with an interplanar angle of 25°. Electron diffraction in the gas phase yields an average (large amplitude motion) value of 23°⁶⁴. The novel compound can be evaporated and its PE spectrum recorded (Figure 11).

The twisted conformer of *C*_s symmetry is predicted to represent the global minimum⁶⁴ by SCF calculations on the probably insufficient STO-3G level, with the two *C*_{2v} conformers higher in energy by only 5–6 kJ mol⁻¹ (Figure 11a). The lowest five vertical ionizations of *D*_{5d} symmetric silicocene are straightforwardly assigned to the sequence $\pi(3e_{1g}) < 3s_{Si}(+\pi) < \pi(3e_{1u})$ in orbital notation by Koopmans' correlation with the SCF eigenvalues, by the 2 : 1 : 2 intensity ratio of the different steep–broad–steep band contours (Figure 11b) and by the M^{•⊕} state comparison with the Ge and Sn derivatives

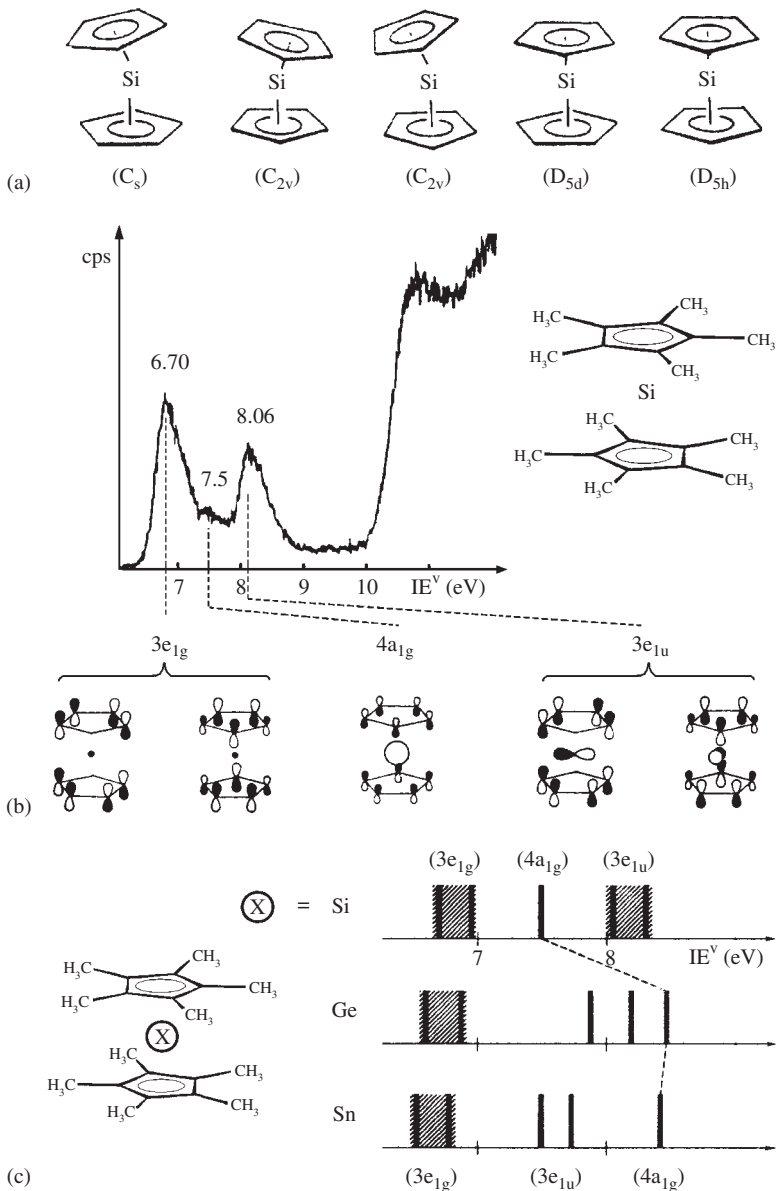


FIGURE 11. (a) Possible silicocene conformers and their symmetry notation, (b) (HeI) PE spectrum (6–10 eV) of bis(η^5 -pentamethylcyclopentadienyl)silicon with Koopmans' assignment, $IE_n^v = \epsilon_j^{\text{MNDO}}$, for the most likely D_{5d} conformer and (c) comparison of radical cation states with analogous Ge and Sn pentamethylcyclopentadienyl sandwiches

(Figure 11c). The doublet radical cation ground state $\tilde{X}(^2E_{1g})$, by symmetry arguments, must have its positive charge exclusively delocalized within the π system of the pentamethylcyclopentadienyl ligand.

2. Cation charge delocalization in the Si_8 skeleton of hexakis(trimethylsilyl)disilane

The low-energy region (7–9.5 eV) in the (He I)PE spectrum of the sterically overcrowded (Figure 8b) D_{3d} -symmetric molecule $[(H_3C)_3Si]_3Si-Si(Si(Si(CH_3)_3)_3)$ exhibits a high-resolution ionization structure⁵⁰, which can be reasonably deconvoluted into 6 overlapping Gaussian-shape bands (Figure 12a).

The parameter set $\alpha_{SiSi} = 8.7$ eV and $\beta_{SiSi/SiSi} = 0.5$ eV of the well-tested topological σ_{SiSi} bond model (Section III.B and Figure 4b) has to be enlarged by an additional Coulomb value $\alpha_{(SiSi)Si6} = 9.05$ eV for the central SiSi disilane bond to cover the seven σ_{SiSi} skeleton ionizations including the one at about 10.6 eV, hidden in a broad ionization hill⁵⁰. With the exception of the Jahn/Teller splitting not accounted for, the values of the deconvoluted band maxima correlate satisfactorily with the topological eigenvalues — x_j (eV) calculated⁵⁰ (Figure 12b).

Within this context, it is noted that $Si(Si(CH_3)_3)_4$ (Figure 4b) has been remeasured^{15,16,26} using various photon energies⁶⁵ and the previous assignment¹¹ confirmed by $X\alpha$ calculations⁶⁵.

3. Organosilicon cations in solvents and their matrix isolation

First vertical ionization energies of organosilicon molecules below 8 eV frequently stimulated the generation of their radical cations in solution^{15,16,25} (Figure 7) by using the selective, oxygen-free and powerful redox reagents $AlCl_3/H_2CCl_2$ ⁴¹ or $SbCl_5/H_2CCl_2$ (Section III.D): The correlation with $IE_1^v < 8$ eV for a successful one-electron transfer hardly ever failed to yield persistent paramagnetic species²⁵, which in the resulting methylene dichloride solutions could be characterized by ESR and ENDOR spectroscopy²⁵. In addition, matrix isolation techniques¹⁰ have proven valuable for investigations of rather reactive radical cation intermediates.

The application of matrix techniques to investigate organosilicon compounds—for instance, the matrix photolysis of phenyltriaidosilane ($H_5C_6Si(N_3)_3$) to phenylsilaisocyanide ($H_5C_6-N\equiv Si$)⁵⁷ (Section III.F)—will be exemplified here by presenting the ESR spectra of three different radical cations, e.g. of σ -type- $Si(CH_3)_4^{\bullet\oplus}$, of π -type $((H_3C)_3Si)_2C=CH_2^{\bullet\oplus}$ and of the parent silylene $H_2Si^{\bullet\oplus}$ (Figure 13a–c).

The photoelectron spectrum of tetramethylsilane (Section III.B) has been assigned assuming a Jahn/Teller distortion from T_d symmetry⁶⁹, which is supported by the ESR spectrum of its matrix generated radical cation (Figure 13a) exhibiting a septet of septets due to two pairs of equivalent, freely rotating methyl groups⁶⁶. The most likely structural change on one-electron expulsion, $T_d \rightarrow C_{2v}$, can be rationalized by the quantum chemically predicted orbital splitting, $1t_1 \rightarrow 2a_1(\uparrow) > 1b_2(\uparrow\downarrow) > 1b_1(\uparrow\downarrow)$ ⁷⁰.

For silyl-substituted ethylene radical cations, quantum chemical calculations predict⁷¹ the two molecular halves to be twisted around the central C=C bond by about 30°, lowering the total energy by about 5 kJ mol⁻¹. The recorded ESR multiplet (Figure 13b) with g values between 2.0031 and 2.0038 fulfills the expectation. For the CH_2 hydrogens, a triplet with $a_H = 4.42$ mT results, and the rather large ethylene hydrogen coupling recorded, reproduced by open-shell INDO hypersurface calculations, further confirms the expected twisting.

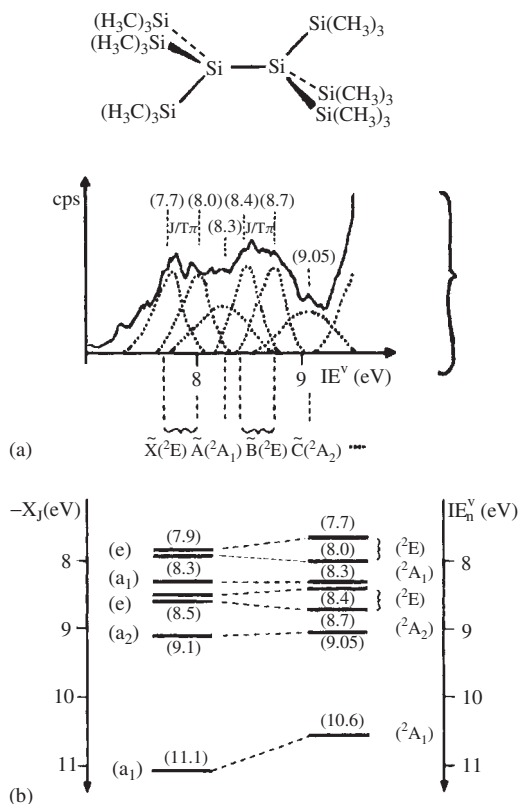


FIGURE 12. Low-energy region of the (He I)PE spectrum of hexakis(trimethylsilyl)disilane: (a) Gaussian-shape band deconvolution between 7.5 and 9.5 eV and (b) topological SiSi bond interaction model with radical cation state assignment

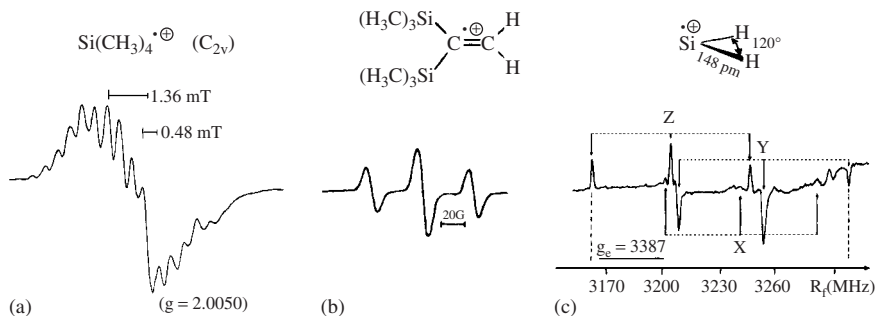
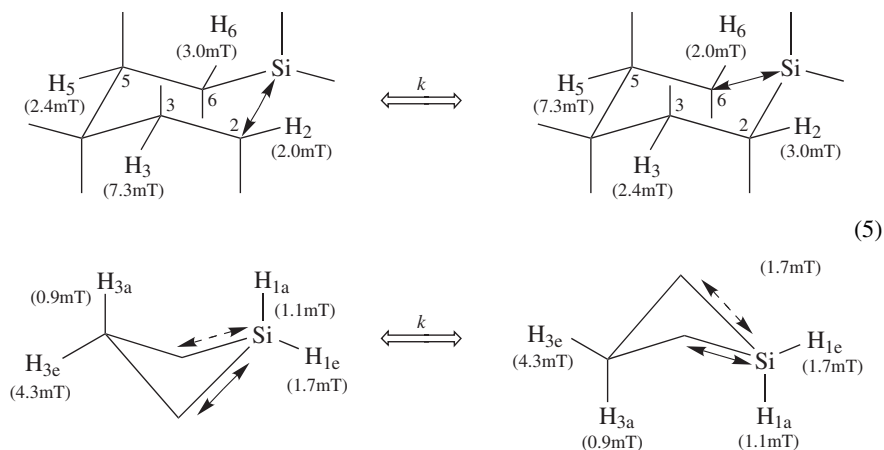


FIGURE 13. Examples of matrix-trapped silicon radical cations: (a) tetramethylsilane radical cation in 8% mol solid solution in trichlorofluoromethane at 90 K, generated by γ -irradiation (dose, 1 Mrad, C_{2v} : septet of septets⁶⁶), (b) 1,1-bis(trimethylsilyl)ethylene radical cation generated in trichlorofluoromethane matrix at 77 K by ^{60}Co γ -irradiation (triplet with $a_{\text{H}} = 4.42 \text{ mT}$ ⁶⁷) and (c) silylene radical cation, generated by SiH_4 photolysis in a 4 K neon matrix [^{29}Si ($I = \frac{1}{2}$) ESR doublet hyperfine coupling in $\Theta = 90^\circ$ position⁶⁸]

A literature search for organosilylene radical cations ($R_2Si^{\bullet\oplus}$) located only that of the parent molecule ($H_2Si^{\bullet\oplus}$), which has been generated in a neon matrix at 4 K by photoionization of SiH_4 and characterized by its solid state ESR pattern proving an $\tilde{X}(^2A_1)$ ground state (Figure 13c). The A tensor assignment was facilitated by the preferential orientation of $SiH_2^{\bullet\oplus}$ in the neon lattice, which allowed one to resolve all the X, Y, Z components as confirmed by the spectrum simulation⁶⁸. Correlated wave function calculations at the MP4 level confirm the selective generation of $SiH_2^{\bullet\oplus}$ and exclude $SiH_4^{\bullet\oplus}$ or $SiH^{\bullet\oplus} \cdots H_2$. As concerns the $SiH_2^{\bullet\oplus}$ structure, an angle $\angle HSiH = 120^\circ$ and a bond length $d_{SiH} = 148$ pm are predicted.

The three exemplary matrix investigations of prototype organosilicon radical cations (Figure 13) have been chosen to demonstrate the interesting structural information, which can be gathered concerning their respective gas-phase photoelectron spectra. Many more alkylsilane radical cations have been studied¹⁰ such as those of 1-methylsilacyclohexane and of silacyclobutane, generated in C_7F_{16} matrices at 77 K by γ -irradiation. The molecular dynamics involved as indicated by the temperature-dependent ESR data can be rationalized by two-site jump models: Either a distorted bond oscillates between two equivalent positions or a ring-puckering motion is activated (equations 5: coupling constants in parentheses)⁷²:



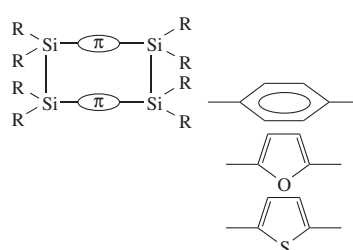
Here again, the vertical ionization time domain of 10^{-15} s is crossed into the adiabatic one below 10^{-13} s (Figure 2c), in which molecular motions are activated.

4. Further PE spectroscopic investigations of organosilicon compounds with group 14 elements

The literature search for 1990–2000 yielded many isolated PE-spectroscopic results, which will not fill an independent topic and are therefore summarized with their first vertical ionization (Table 3).

The molecules and their first vertical ionization energies listed (Table 3) supplement those already presented as examples. The parent silylene has been generated by the $SiH_4 + 2F^\bullet \rightarrow SiH_2 + 2HF$ reaction and investigated by photoionization mass spectroscopy, which yields the adiabatic onset value quoted⁷³. Silyl derivatives such as $C(SiH_3)_4$ have been thermally decomposed to detect new routes to amorphous,

TABLE 3. Survey of additional photoelectron spectra recorded for organosilicon molecules with group 14 elements between 1988–2000 with their first vertical ionizations and $M^{\bullet\oplus}$ ground state symmetry

Compound (R = CH ₃)	Reference (year)	IE ₁ ^v (eV)	$M^{\bullet\oplus}(\chi_{\mu})$
SiH ₂	73 (1989)	(8.2)	$\tilde{X}(^2A_1)$, onset
C(SiH ₃) ₂ HR	74 (1992)	10.30	$\tilde{X}(^2A'')$
C(SiH ₃) ₃ H		10.58	$\tilde{X}(^2E)$
C(SiH ₃) ₄		10.75	$\tilde{X}(^2T_2)$
SiR ₄	65a (1994)	10.35	$\tilde{X}(^2T_2)$
Si ₂ R ₆		8.45	$\tilde{X}(^2A_1)$
Si(SiR ₃) ₄		8.26	$\tilde{X}(^2T_2)$
Ge(SiR ₃) ₄		8.13	$\tilde{X}(^2A_2)$
(SiR ₂) ₆		7.89	$\tilde{X}(^2A_{1u})$
<i>c</i> -[(R ₂ Si) ₄ (CH ₂) ₁]	65b (1997)	7.90	$\tilde{X}(\sigma_{SiSi})$
<i>c</i> -[(R ₂ Si) ₄ (CH ₂) _{<i>n</i>}] <i>n</i> = 2–4		8.00	$\tilde{X}(\sigma_{SiSi})$
	76 (1988)	7.80 7.40 7.40	$\tilde{X}(^2B_{3u})$ $\tilde{X}(^2A_u)$ $\tilde{X}(^2A_u)$

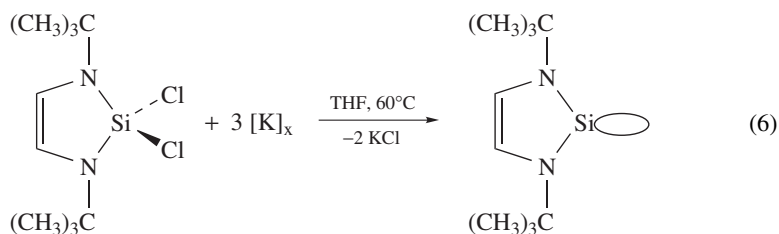
hydrogen-containing silicon, a promising new material⁷⁵. The methylsilane ionizations have been redetermined more precisely using synchrotron radiation⁷⁴. The ionization patterns of the paracyclophane derivatives⁷⁶ provide another example of π -perturbation (Section III.C). Altogether, the years of publication quoted as references (Table 1) support the introductory statements (Section I) that the ‘early tempestuous years of helium (I) photoelectron spectroscopy are ... long over’, but results of one or another investigation are still published.

C. Organosilicon Molecules Containing Main Group 15 Elements

The selected topics comprise the surprisingly stable ‘imidazole’-silylenes (Section IV.C.1), the sterically overcrowded trimethylsilyl-*p*-phenylenediamines (Section IV.C.2) and the thermal gas-phase generation of trimethyl silanimine (Section IV.C.3).

1. (He I) PE spectrum of stable ‘imidazole’-silylene

In addition to the novel triatomic molecule SiI₂⁶¹, dominant relativistic due to its 90% iodine composition (Section IV.E.1), another unexpected and breathtaking PE spectroscopic silylene story was published in 1994⁷⁷: Following the surprising discovery of the first ‘bottlable’ carbenes by Arduengo and collaborators⁷⁸ as well as of the subsequent analogous germanium derivatives⁷⁹, the first isoelectronic silylene has been synthesized (equation 6), crystallized and its structure determined⁸⁰:



Its photoelectron spectrum⁷⁷ (Figure 14a) is best discussed by a radical cation state comparison with the isosteric C and Ge derivatives and based on the results of density functional calculations with a triple- ξ basis set (e.g. Si, 73111/6111/1).

The radical cation state comparison of the three isosteric unsaturated molecules $(\text{HC})_2(\text{NC}(\text{CH}_3)_3)_2\text{X}$ with $\text{X}=\text{C}$, Si or Ge (Figure 14a) reveals that the ground state of the carbene $\tilde{\text{X}}(^2\text{A}_1)$ is dominated by a n_{C} lone pair contribution, whereas both the silylene and the germylene exhibit π -type states, $\tilde{\text{X}}(^2\text{B}_1)$. According to the density functional calculations, the crossover $n_{\text{C}}/\pi_1 \rightarrow \pi_1/n_{\text{Si}}$ (Figure 14) between 7.68 – 8.21 eV and 8.22 – 6.96 eV can be readily rationalized by the calculated densities, viewed both in the molecular plane (Figure 14b: MP) and the one bisecting the $\text{C}=\text{C}$ double bond as well as the two-coordinate main group element C or Si (Figure 14b: SV): The electron density shape of the lone pairs varies from ellipsoidal n_{C} to circular n_{Si} ⁷⁰.

The electron densities calculated by Density Functional Theory (DFT) for both the carbene and silylene derivatives (Figure 14b) confirm the experimentally determined electron distribution in 1,3,4,5-tetramethylimidazol-2-ylidene- d_{12} ⁷⁷ by an ellipsoidally distorted n_{C} lone pair density around the divalent C center, and predict the distributions at both the Si and Ge centers⁷⁷ to be essentially spherical. These DFT results allow one to rationalize the differing radical cation state sequences observed PE spectroscopically (Figure 14a, $n_{\text{C}} < \pi_1$ versus $\pi_1 < n_{\text{Si,Ge}}$): With the decreasing effective nuclear charge $\text{C} \ll \text{Si} < \text{Ge}$ both π ionizations are lowered by 9.22 – 6.65 = 1.6 eV and 9.24 – 8.80 = 0.4 eV (Figure 14b). The lone pair ionization energies, however, increase in the opposite direction, $n_{\text{C}} - n_{\text{Si}}$ by 7.68 – 8.21 = (-)0.5 eV, and can be traced to the varying electron density shape of the lone pairs from ellipsoidal n_{C} to circular n_{Si} ⁷⁰.

2. Sterically overcrowded trimethylsilyl-*p*-phenylenediamines

The *N,N'*-bis- and *N,N,N',N'*-tetrakis(trimethylsilyl)-*p*-phenylenediamines⁸¹ provide an interesting example of steric overcrowding with their single crystal structures determined by X-ray diffraction and their gas-phase conformations investigated by photoelectron spectroscopy⁸¹ (Figure 15).

The starting point is the ‘Wurster’s Blue’ radical cation, discovered in 1879 and thoroughly investigated since then: The twofold N pyramidal *N,N,N',N'*-tetraalkyl-*p*-phenylenediamine precursors are completely flattened on two-electron oxidation as proven by crystal structure analyses of the resulting redox salts (Scheme 8a).

In contrast, surprisingly, the tetrakis(trimethylsilyl)-substituted *p*-phenylenediamine can be reduced in ether solution containing [2,2,2] cryptand by a potassium metal mirror to a ‘Wurster’s Blue’ radical anion (Scheme 8b)⁸¹, identified by its ESR spectrum showing the quintet of the four benzene ring hydrogens together with ²⁹Si silicon satellites. The missing N coupling indicates twisting of the bulky $\text{N}(\text{Si}(\text{CH}_3)_3)_2$ substituents due to van der Waals overlap with the adjacent *ortho* ring hydrogens as confirmed by a

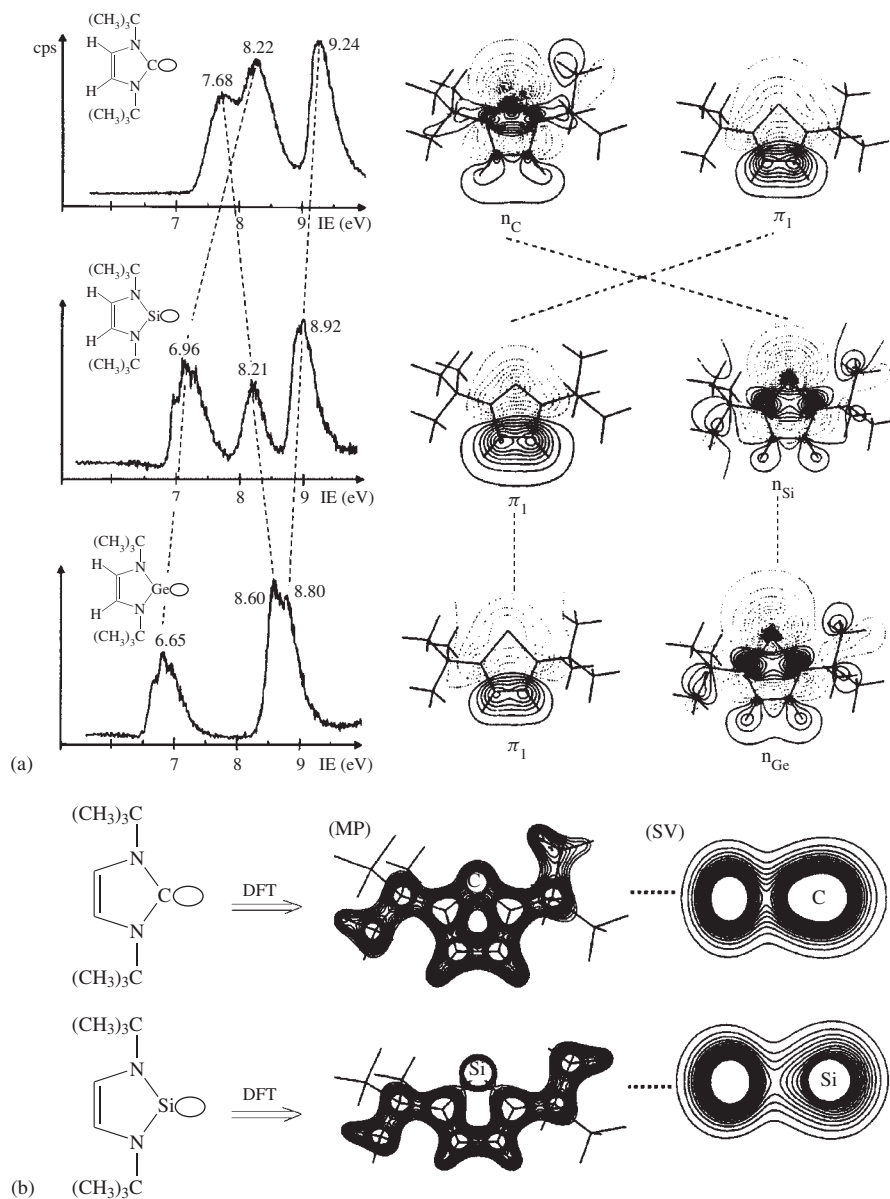


FIGURE 14. (a) High-resolution photoelectron spectra (6–10 eV) of the carbene (1,3-di-*tert*-butylimidazol-2-ylidene), the iso(valence)electronic silylene (1,3-di-*tert*-butyl-1,3,2-diazasilol-2-ylidene) and germylene (1,3-di-*tert*-butyl-1,3,2-diazagermol-2-ylidene), with assignment of the first two M^{\oplus} states by density functional molecular orbitals n_X and π_1 ; (b) electron density contour lines viewed in the molecular plane (MP) as well as side view (SV) on the plane bisecting the C=C double bond and the twofold coordinate main group center

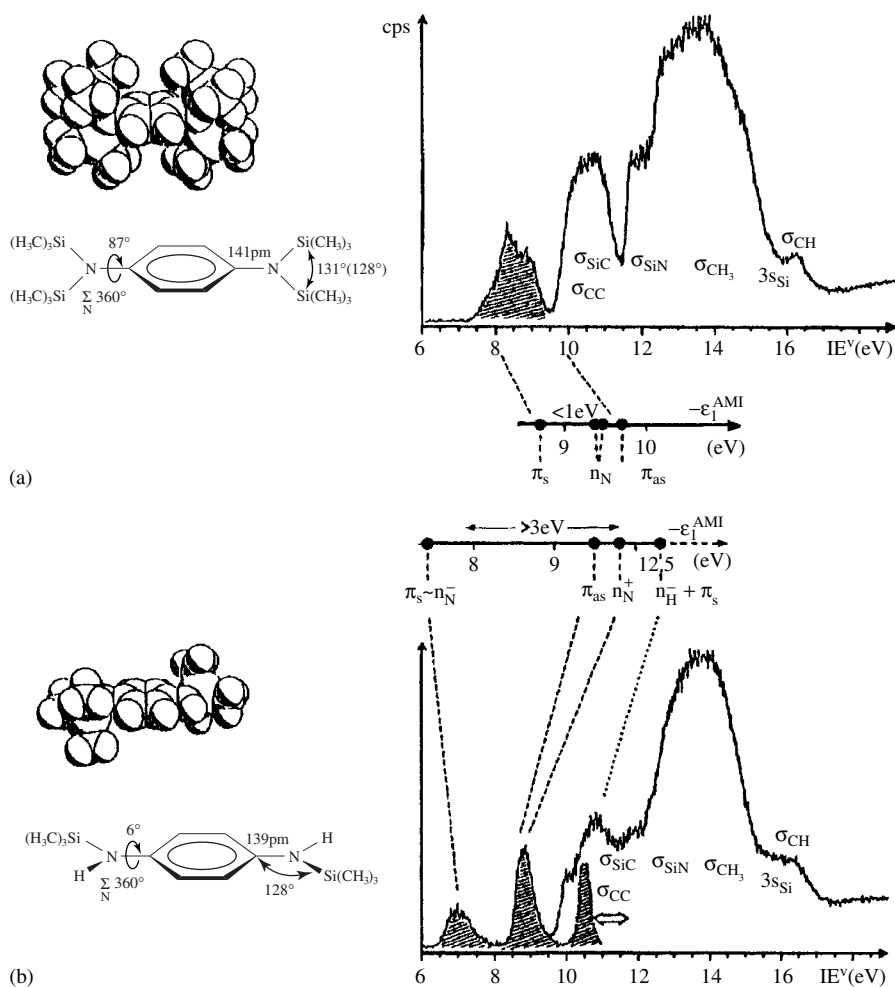
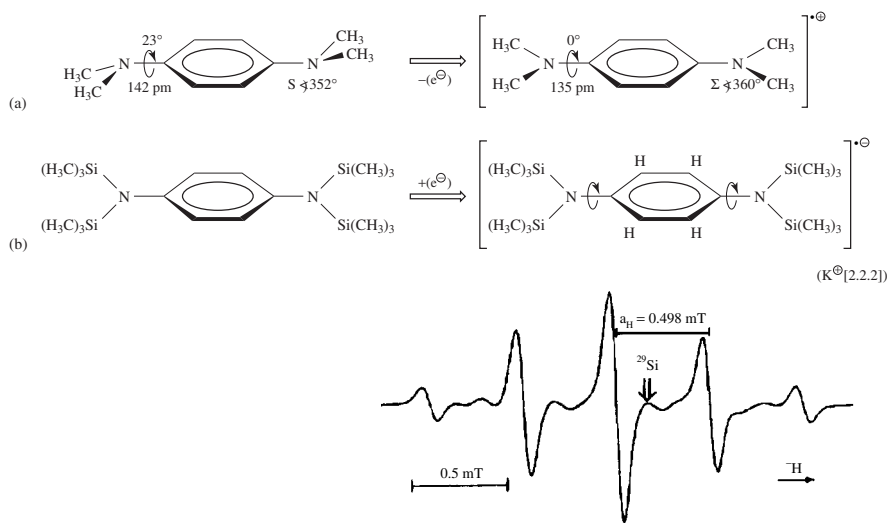


FIGURE 15. He I photoelectron spectra (6–18 eV) of (a) *N,N,N',N'*-tetrakis(trimethylsilyl)- and (b) *N,N'*-bis(trimethylsilyl)-*p*-phenylenediamines with Koopmans' assignment based on the eigenvalues $-\epsilon_j^{\text{AM1}}$ of geometry-optimized AM1 calculations with structural data for the space-filling representations of the crystal molecular structures

subsequent crystal structure of the neutral molecule containing an 83° dihedral angle $\omega(\text{CC}-\text{NSi})$ ⁸¹. This substituent group twisting explains why the already electron-rich tetrasilyl-*p*-phenylenediamine can accept an additional electron: the electron-donating n_{N}/π delocalization is replaced by a $\text{Si} \rightarrow \text{N}$ electron withdrawal due to the huge difference in the effective nuclear charges, $Z_{\text{eff}}(\text{Si}) \ll Z_{\text{eff}}(\text{N})$, of the adjacent centers (Section III.A). In 1994 the conformation of tetrakis(trimethylsilyl)-*p*-phenylenediamine could be determined both by crystal structure analysis⁸¹ as well as for the gas phase by quantum chemical analysis of the photoelectron spectroscopic ionization pattern⁸¹



SCHEME 8

(Figure 15). The optimized gas-phase conformation most likely also represents the solution structure (Scheme 8b) in aprotic solvents.

Both the space-filling representations of the crystal structures⁸¹ as well as AM1-geometry-optimized conformations clearly demonstrate the structure-determining influence of the trimethylsilyl substituents on *p*-phenylenediamine (Figure 15). In the 1,2-disubstituted one, the n_N lone pairs of the planar $(R_3Si)HN$ subunits interact with the six-membered ring π cloud and the photoelectron spectrum exhibits a tremendously large n_N/π ionization band splitting of well over 3 eV (Figure 15b, shaded). In the tetra-substituted derivative (Figure 15a), the p-type N electron pairs of the planar $(R_3Si)_2N$ substituent groups are twisted into the benzene molecular plane due to the spatial overlap of the bulky $(H_3C)_3Si$ units with the *ortho*-ring hydrogens. The lack of n_N/π delocalization lengthens the NC bond from 141 to 144 pm and keeps the splitting of the low energy ionization bands smaller than 1 eV (Figure 15a).

Altogether, the AM1 geometry-optimized gas-phase structures not only allow a satisfying assignment of the 40 and 52 center (!) molecules, but in addition provide a rationale for the preparative feasibility to generate a radical anion. The sterically congested tetrakis(trimethylsilyl)-*p*-phenylenediamine will most likely be twisted also in solution. Both the zero n_N/π donation and the considerable σ -acceptor perturbation of the benzene ring due to the high effective nuclear charge of the adjacent N centers support the electron insertion to the ‘Wurster’s Blue Radical Anion’ (Scheme 8b)⁸¹.

3. Thermal generation of trimethyl silanimine in the gas phase

The Pau-PE group keeps on generating interesting kinetically unstable nitrogen-^{82a}, phosphorous-^{82b} and sulfur-containing organosilicon intermediates under unimolecular conditions in the gas phase (see Tables 4 and 6). For illustration, the thermal monomerization of hexamethylcyclodisilazane to trimethylsilanimine^{82a} (Figure 16) is selected.

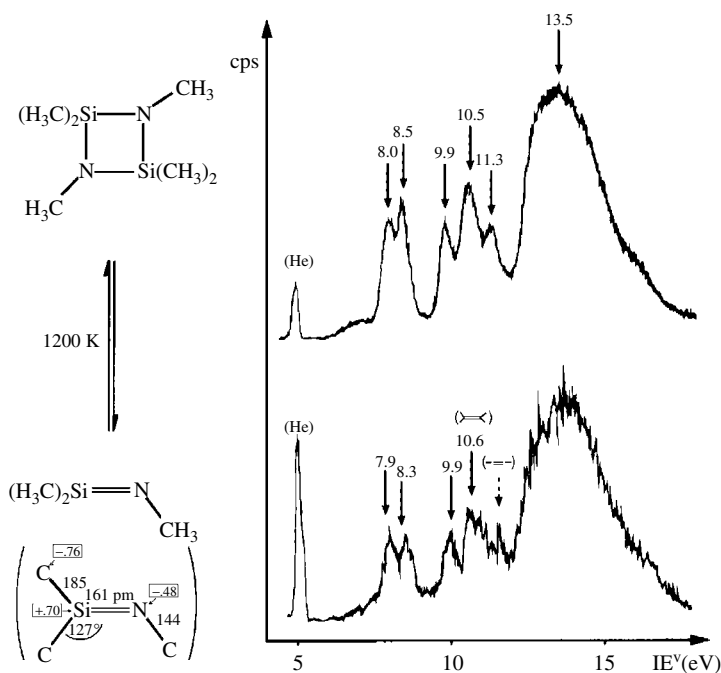


FIGURE 16. (He I) PE spectra of hexamethylcyclodisilazane at room temperature and of trimethylsilylanimine at 1200 K (after subtraction of precursor PE bands; spectra are calibrated by the He autoionization band at 4.98 eV; in parentheses, MP2 geometry-optimized structure data and total atomic charges)^{82a}

Surprisingly, the ionization pattern changes only slightly with temperature (Figure 16). However, the thermal results are not only supported by calculations at the MP2 level but also by the thermolysis results for isopropyl- and *tert*-butyl-substituted cyclodisilazane derivatives^{82a}. The MP2 calculations provide the interesting geometry-optimized structural data and total atomic charges (Figure 16, in parentheses). As expected, the bond $\text{Si}^{+0.70} - \text{N}^{-0.48}$ is strongly polarized and should be 161 pm long.

4. Further PE spectroscopic investigations of organosilicon compounds with group 15 elements

The literature search of 1990–2000 produced additional PE spectroscopic publications not fitting into the selected topics, so they are listed compound-wise with their first vertical ionizations (Table 4).

The group IV diphenyl(trimethylsilyl) derivatives $[(\text{H}_3\text{C}_6)_2\text{XSiR}_3]$ expectedly show a constant second vertical ionization energy, which is assigned to the benzene- π_{as} radical cation state⁸³ and is therefore well-suited for internal calibration. The N-phenyl derivatives⁸⁴ support the conformer discussion of the *p*-phenylenediamines $p\text{-(R}_3\text{Si)}_n\text{H}_{2-n}\text{NC}_6\text{H}_4\text{NH}_{2-n}\text{(SiR}_3)_n$ (Figure 15). Lower ionization energies for isothiocyanates relative to the corresponding cyanates have been reported before and amount to $\Delta\text{IE}_1^{\text{v}} = 1.56$ eV for the parent molecules H_3SiNCX and to 1 eV for the

TABLE 4. Survey of photoelectron spectra recorded for organosilicon molecules with additional group 15 elements (1988–2000) containing first vertical ionization energies and $M^{\bullet\oplus}$ ground state symmetries

Compound (R = CH ₃)	Reference (year)	IE ₁ ^v (eV)	$M^{\bullet\oplus}$ (X_{μ})
(C ₆ H ₅) ₂ XSiR ₃			
X=N	83 (1988)	7.44	(n _N)
X=P		7.74	(n _P)
X=As		7.72	(n _{As})
X=Sb		7.66	(n _{Sb})
C ₆ H ₅ NHSiR ₃	84 (1991)	7.70	(n _N)
(C ₆ H ₅) ₂ NSi(C ₆ H ₅) ₃		7.32	(n _N)
(C ₆ H ₅) ₂ NSi(C ₆ F ₅) ₃		8.07	(n _N)
C ₆ H ₅ Si(NCO) ₃	85 (1992)	9.73	$\tilde{X}(^2E_{1g})$
(PSiCR ₃) ₄	86 (1990)	7.60	$\tilde{X}(^2E) + \tilde{A}(^2B_2)$
XSi(OCH ₂ CH ₂) ₃ N	87 (1988)		
X=CH ₃		8.50	(σ_{SiN})
X=CH ₂ Cl		9.20	(σ_{SiN})
X=HC=CH ₂		8.50	(σ_{SiN})
X=Cl		9.60	(σ_{SiN})
X=F		9.70	(σ_{SiN})

larger methyl derivatives R₃SiNCX⁸⁵. Tetraphosphatetrasilicubane, [PSiC(CH₃)₃]₄, is synthesized from (H₃C)₃CSiCl₃ and Li[⊕][AlPH₂]₄[⊖] and its first vertical ionization energy exceeds that of its carbon analogue, [PCC(CH₃)₃]₄, by only 0.25 eV⁸⁶. The publication reporting on the silatranes⁸⁷ with a silicon center of coordination number 5 contains data for 17 derivatives with partly substituted alkyl chains or groups. Altogether organosilicon nitrogen compounds attracted some attention at the beginning of the decade (Section IV.C.1–4).

D. Organosilicon Molecules Containing Main Group 16 Elements

Another PE spectroscopic general topic of the decade 1990–2000 has been the attempt to complete a list of first and second order organosilicon substituent perturbation increments (Section III.C) for both σ and π parent molecules. Quite often, as has been demonstrated over and over in the preceding chapters, they prove to be useful to the silicon chemist in the proper planning of his experiments.

1. Oxygen lone pair ionization energies of siloxanes

The lone pair n_X vertical ionization of a saturated molecule with heteroatom centers often generates the radical cation in the ground state (Figure 2A) and is therefore well-suited to probe substituent effects^{15,16}. Within the period 1989–1995, organosilicon oxygen⁸⁸ and sulfur^{89–92} derivatives have been investigated PE spectroscopically with special emphasis on the sometimes tremendous donor properties of β -silyl groups CH_{3–n}(SiR₃)_n^{10,40}.

The β -silyl perturbation of n_O lone pairs is one of the largest substituent effects ever detected by PE spectroscopy^{15,16,88} and caused by the tremendous difference in effective nuclear charges, $Z_{\text{eff}}(\text{Si}) \ll Z_{\text{eff}}(\text{O})$ ¹⁵ (Section III.A). The vertical first ionization energies of oxygen compounds range from 12.62 eV for H₂O to 7.97 eV for H₃COSi(Si(CH₃)₃)₃ (Figure 17), i.e. a difference of more than 4.7 eV (!).

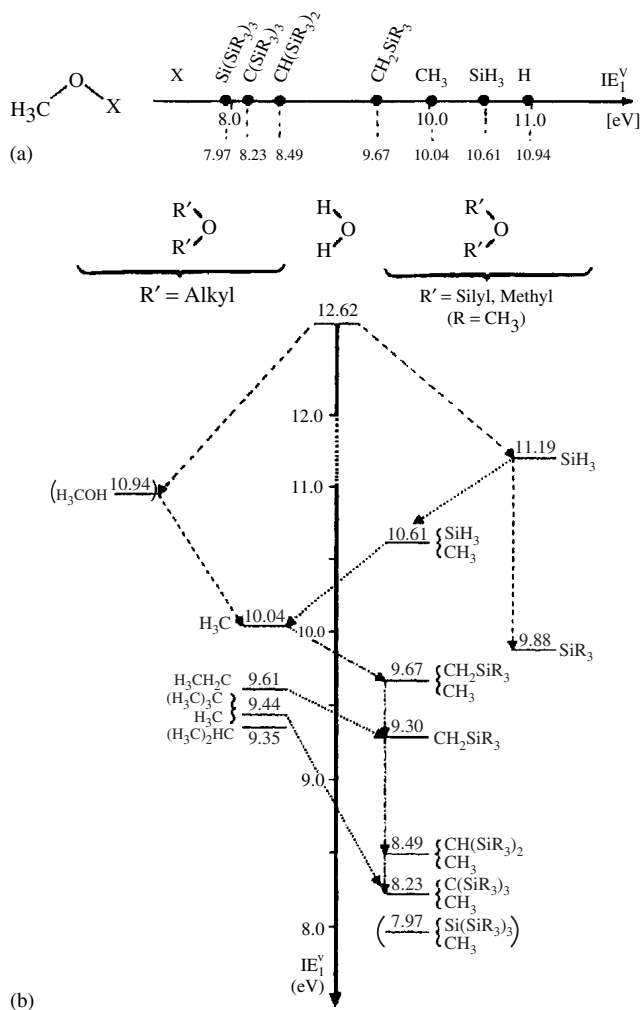
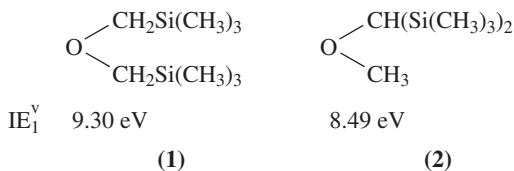


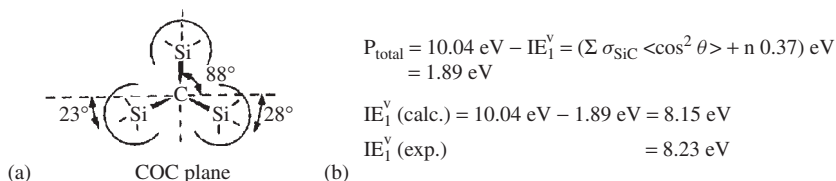
FIGURE 17. First vertical ionization energies IE_1^v (n_{O}): (a) Methoxy derivatives $\text{H}_3\text{C}-\text{O}-\text{X}$ and (b) derivatives of H_2O with alkyl, silyl, trimethylsilyl and (trimethylsilyl)methyl substituents (—: identical mono- and disubstitution, ···: alkyl/silyl comparison, and - - -: β -silyl substituent effects)

Starting with the organosilicon methoxy derivatives (Figure 17a), the first vertical ' π -type n_{O}^{π} lone pair' ionizations of the molecules ranging from the parent pentaatomic H_3COH through saturated methyl ethers with alkyl and silyl substituents span a wide range of 3 eV down to $((\text{H}_3\text{C})_3\text{Si})_3\text{SiOCH}_3$, with its 'Guinness Book of Records' low $\text{IE}_1^v = 7.97$ eV⁸⁸. The substituent effects, which increase in the order $\text{H} < \text{SiH}_3 < \text{Si}(\text{CH}_3)_3 \sim \text{CH}_3 < \text{CH}_2\text{Si}(\text{CH}_3)_3 < \text{C}(\text{Si}(\text{CH}_3)_3)_3$, are mostly nonadditive, as is convincingly demonstrated by the ionization energies IE_1^v for isomers such as **1** and **2**⁸⁸, which show no specific increments for their two β -silyl groups.



The methoxy organosilicon series (Figure 17a) can be enlarged to comprehend additional substituents (Figure 17b), which show the following effects: Methylation of methyl groups to ethyl and isopropyl ones (Figure 17b, left hand side) lowers IE_1^{v} only slightly and nonadditively. Exchange of CH_3 by SiH_3 substituents increases IE_1^{v} (n_{O}^{π}) from 10.04 to 11.19 eV (Figure 17b) and even the bulkier $\text{Si}(\text{CH}_3)_3$ one decreases it only by 0.06 eV to 9.88 eV. The largest ionization energy difference is observed upon introduction of β -trimethylsilylmethyl groups, which on twofold substitution, $\text{H}_3\text{COCH}_3 \rightarrow \text{R}_3\text{SiCH}_2\text{OCH}_2\text{SiR}_3$, lower IE_1^{v} (n_{O}^{π}) by 0.64 eV and on triple replacement at one-center $\text{H}_3\text{COCH}_3 \rightarrow \text{H}_3\text{COC}(\text{SiR}_3)_3$ by 1.81 eV (Figure 17b). The largest decrease from H_2O recorded is by 4.65 eV (!) to $\text{H}_3\text{COC}(\text{SiR}_3)_3$ (Figure 17b, bottom).

Organosilicon oxygen derivatives are often sterically overcrowded because the van der Waals interactions between the bulky alkylsilyl substituent groups are increased by the relatively short CO bonds. For lowering the n_{O}^{π} ionization energies, angle-dependent models have to be applied^{10,15,25}. The procedure is illustrated in Scheme 9 for methyltris(trimethylsilyl)methyl ether $\text{H}_3\text{COC}(\text{Si}(\text{CH}_3)_3)_3$ by rationalizing or predicting its low first ionization energy of 8.2 eV starting from its semiempirically optimized structure and from $\text{IE}_1^{\text{v}} = 10.04$ eV for the reference compound H_3COCH_3 (Figure 17). The product sum of each CSi bond parameter δ_{CSi} and the dihedral angle component $\langle \cos^2 \theta \rangle$ together with the angle-independent increment 0.37 eV for each SiR_3 group⁵⁰ yields the total perturbation $P = 1.89$ eV and a first ionization energy lowered to $\text{IE}_1^{\text{v}} = 8.15$ eV⁵⁰.



SCHEME 9

Using the calculated values, the first vertical ionization energy of the 39-center siloxane molecule $\text{H}_3\text{COC}(\text{Si}(\text{CH}_3)_3)_3$ is reproduced satisfactorily.

2. Sulfur lone pair ionization energies of silthianes

The organosilicon sulfide derivatives (Figure 18) show additional features. To begin with, the lone pair n_{S}^{π} perturbation in sulfides by β -trimethylsilyl groups⁸⁹ is considerably smaller than that of oxygen lone pair n_{O}^{π} in ethers⁸⁸ (Figures 17 and 20), as convincingly demonstrated by iso(valence)electronic ethylene oxide and sulfide derivatives⁹⁰ (Table 5).

TABLE 5. IE_1^v values for ethylene oxide and ethylene sulfide derivatives

Compound	R=H	Si(CH ₃) ₃	ΔIE_1^v (eV)
X=O	10.57	9.07	1.50
S	9.03	8.19	0.84

For rationalization, the large difference in effective nuclear charges, $Z_{\text{eff}}(\text{O}) \gg Z_{\text{eff}}(\text{S})$, as well as the considerably shorter bond lengths of *ca* 142 pm for CO vs. *ca* 182 pm for CS are dominant factors. The first vertical ionization energies of H₂O and H₂S differ by 12.62 – 10.47 = 2.15 eV (!) (cf. Reference 9) and even those of H₃COH and H₃CSH differ by 10.94 – 9.46 = 1.48 eV (Figure 18a).

The organosilicon sulfide derivatives exhibit first vertical sulfur n_S^π lone pair ionizations of standard molecules ranging from the parent triatomic H₂S through saturated sulfides with alkyl and silyl substituents^{89–92}, which span a wide range of 2.8 eV, down to ((H₃C)₃Si)₃CSCH₃, with its ‘Guinness Book of Records’ low $IE_1^v = 7.66$ eV⁸⁹ next to phosphorus ylide ionizations⁹³. The mostly nonadditive substituent effects increase in the order H < SiH₃ < Si(CH₃)₃ ~ CH₃ < CH₂Si(CH₃)₃ < C(Si(CH₃)₃)₃, in close analogy to the organosilicon oxygen derivatives (Figure 18 and 17). For instance, within the series of β -(trimethylsilyl)methyl derivatives H₂S → HSCH₂SiR₃ → S(CH₂SiR₃)₂, the differences ΔIE_1^v are 1.51 eV and 0.93 eV (Figure 18b).

For rationalization of the observed organosilicon substituent effects on the n_S^π ionization in the rather large molecules of low symmetry (Figure 18b), any discussion by orbital perturbation models is not promising. In an attempt to further characterize the equivalent n_S^π radical cation ground states of the chemically related organosulfide molecules, generated by vertical electron expulsion, $M \rightarrow M^{\bullet+} + e^-$, within 10⁻¹⁵ s with a ‘frozen core’ geometry (Section II.B), the charge distributions around the sulfur centers in the neutral sulfides have been calculated and correlated with the respective first vertical ionization energies⁸⁸ (Figure 19). Obviously, this approach, which neglects all other aspects of the complex ionization process and does not account specifically for the change

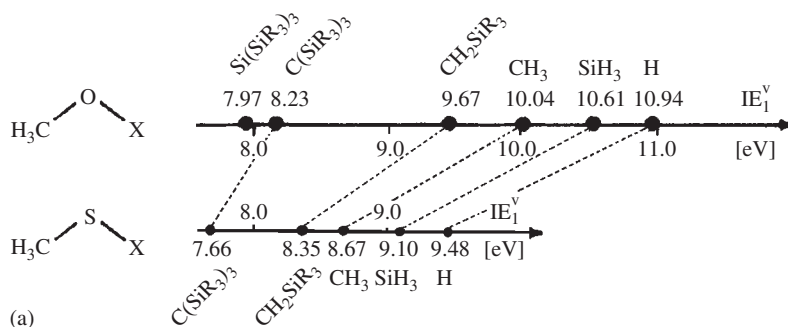
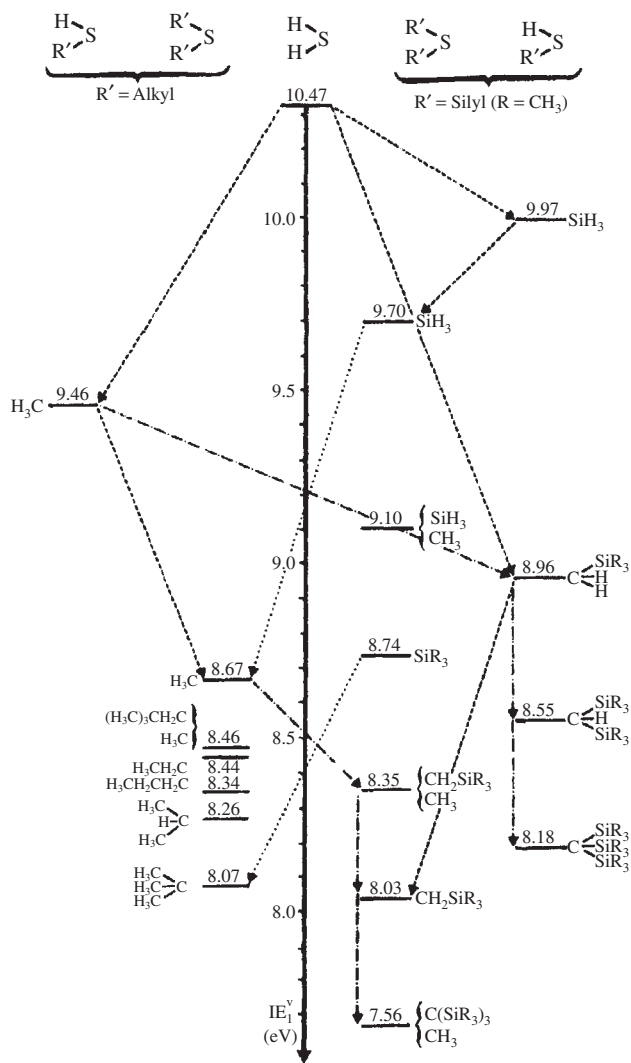


FIGURE 18. First vertical ionization energies IE_1^v (nS) (eV): (a) Comparison between thiomethyl and methoxy derivatives and (b) derivatives of H₂S and its alkyl, silyl, trimethylsilyl and (trimethylsilyl)methyl derivatives (—: identical mono- and di-substitution, ...: alkyl/silyl comparison, ---: β -silyl substituent effects)



(b)

FIGURE 18. (continued)

in correlation energies between M and $M^{\bullet\oplus}$, nevertheless yields a satisfactory linear regression between experimental ionization energy and calculated charge⁸⁸ (Figure 19).

The linear regression in Figure 19 resulting from the rather crude correlation approach indicates that the charge delocalization in the radical cations generated vertically in the 'frozen' structure of the neutral molecules, due to their electronic relaxation before the onset of vibration, should be an essential feature in the ionization process of organosilicon sulfides^{10,89}, a point of view not covered by orbital models¹⁵.

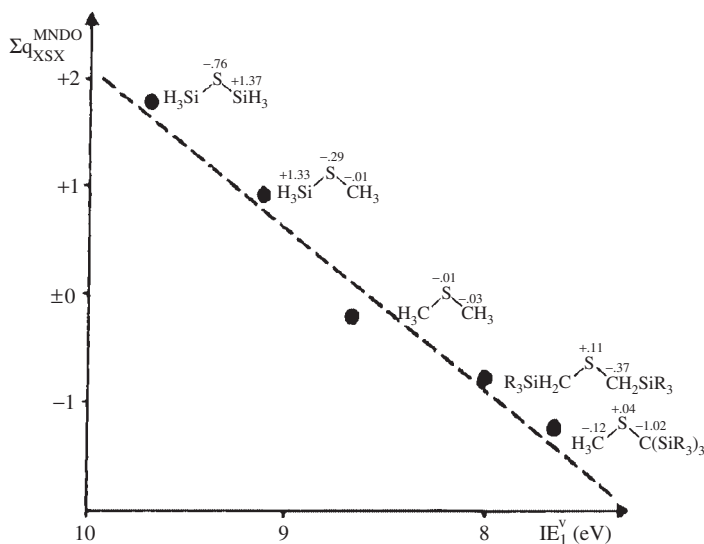


FIGURE 19. A Linear regression between calculated charge and the experimental ionization energy

3. Further PE spectroscopic investigations of organosilicon compounds with group 16 elements

Additional PE spectroscopic publications in 1988–2000 found in the literature search will be listed compound-wise with their first vertical ionization energies (Table 6).

The silatrane molecules with their intramolecular Si ← N Lewis acid/base bond have already been listed together with other nitrogen compounds (Table 4). For 1,4-bis(trimethylsiloxy)benzene, a crystal structure analysis proves a 60° dihedral angle for the conrotatory twist of the R₃SiO substituents around the OC₆H₄O axis, reducing the n_{O}^{π}/π interaction to 9.24 – 7.96 = 1.28 eV (cf. Figure 15).

TABLE 6. Additional photoelectron spectra recorded in 1988–2000 for organosilicon compounds containing group 16 elements

Compound (R = CH ₃)	Reference (year)	IE ₁ ^V (eV)	M ^{•⊕} (X _μ)
R ₃ SiOH	94 (1988)	10.00	$\tilde{X}(^2A)$
R ₃ SiOSO ₂ CF ₃		(10.0)	
R ₃ SiOCOFCF ₃		(10.9)	
R ₃ SiOCOCH ₃		(10.2)	
XSi(OCH ₂ CH ₂) ₃ N	87 (1988)		
X=CH ₃		8.5	$\tilde{X}(\sigma_{\text{SiN}})$
X=CH ₂ Cl		9.2	(σ_{SiN})
X=HC=CH ₂		8.5	(σ_{SiN})
X=Cl		9.6	(σ_{SiN})
X=F		9.7	(σ_{SiN})
<i>p</i> -R ₃ SiOC ₆ H ₄ OSiR ₃	95 (1994)	7.96	$\tilde{X}(\pi_{\text{S}} + n_{\text{O}}^{\pi})$

E. Silicon Molecules Containing Main Group 17 Elements

The literature on PE spectra of halogen compounds including those of silicon has been covered up to 1983 in a special review within this series⁹⁶; the few, most recently investigated organosilicon halides are listed with their first vertical ionization energies in Table 7. The example selected is silicon diiodide or diiodosilylene containing 90% iodine and twofold coordinated silicon, which shall conclude this review as a radical cation with dominant relativistic properties.

1. The PE spectrum of SiI_2 – A novel triatomic molecule with a relativistic touch

Combination of the 13 most important main group elements (H, B, C, Si, N, P, O, S, F, Cl, Br, I, Xe) allows the construction of 1638 triatomic molecules, of which 1183 are linear and 455 are cyclic. With rather few exceptions such as SiI_2 , most of them are already known⁶¹. The novel triatomic molecule can be prepared in analogy to other dihalosilylenes^{10,16} by the reaction of especially purified, white crystalline SiI_4 with elemental silicon (Figure 20).

For the assignment of the complex relativistic radical cation state sequence of $\text{SiI}_2^{\bullet\oplus}$, it is advantageous to begin with that of $\text{SiBr}_2^{\bullet\oplus}$ (Figure 20c), for which relativistic effects might be neglected in a qualitative approximation. By a useful rule of thumb⁹, six radical cation states of low energy are expected for the altogether twelve $3p_{\text{Si}}$ and $4p_{\text{Br}}$ valence electrons, with all higher ones including increasing $3s_{\text{Si}}$ contributions^{10,61}. The MNDO diagrams (Figure 20c) illustrate a plausible assignment: the $\text{M}^{\bullet\oplus}$ ground state $\tilde{\text{X}}(^2\text{A}_1)$ is generated by electron expulsion from the divalent silicon electron pair (Figure 20c: $4a_1$) followed by four n_{Br} bromine electron-pair (Figure 20c: $3b_2$, $1a_2$, $1b_1$ and $3a_1$) and two σ_{SiBr} ionizations (Figure 20c: $2b_2$ and $2a_1$) with a dominant $3s_{\text{Si}}$ contribution^{10,61}. On PE spectroscopic comparison of SiF_2 , SiCl_2 and SiBr_2 ¹⁰, the lowering of the halogen electron-pair ionizations $n_{\text{F}} > n_{\text{Cl}} > n_{\text{Br}}$ is especially striking, reflecting the tremendous influence of the decreasing effective nuclear charge of the halogen substituents⁹⁶ and their increasingly smaller difference from that of the silylene Si center^{10,61}.

On comparison of the radical cation state-patterns of SiI_2 and SiBr_2 (Figure 20b and c), two effects are recognized: a significant shift of only the $3s_{\text{Si}}$ ionization to lower energies and a distinct spread to largely isolated bands, which are separated by 0.4–0.7 eV. For the assignment of the vertical ionization energies IE_n^{v} of SiI_2 via Koopmans' correlation, $\text{IE}_n^{\text{v}} = -\varepsilon_j^{\text{SCF}}$, the relativistic effects due to the two heavy-atom substituents, responsible for the experimentally observed hyperfine structure splitting of the ($5s^2$, $5p^5$) states of the iodine atom, $2P_{3/2}$ and $2P_{1/2}$, of 0.94 eV⁹⁶, have been taken into account by using a quasi-relativistic two-component pseudopotential SCF method with a double-zeta (DZ) polarization function (p) basis set. The calculated data for SiI_2 correlate well with the experimental values and the maximum Koopmans' defect for the PES band maxima between 9.70 – 12.18 eV (Figure 20) amounts to only 0.33 eV (!). The spin/orbit coupling within the C_{2v} molecular symmetry of less than 0.07 eV is unexpectedly small, e.g. in contrast to the analogous GeI_2 with a no longer negligible 0.3 eV split⁶¹. The SiI_2 structural parameters from the geometry-optimized DZP-SCF calculation are supported by the satisfactory agreement between the experimental and calculated values of other dihalosilylenes^{10,16}. The population analysis for SiI_2 based on the optimized structure yields for the Si center a positive charge of +0.54 and, correspondingly, for each of the I centers a negative one of –0.27. Comparison with the values obtained for the Si centers of the other dihalosilylenes (SiF_2 : +0.91; SiCl_2 : +0.78 and SiBr_2 : +0.66)⁶¹ demonstrates

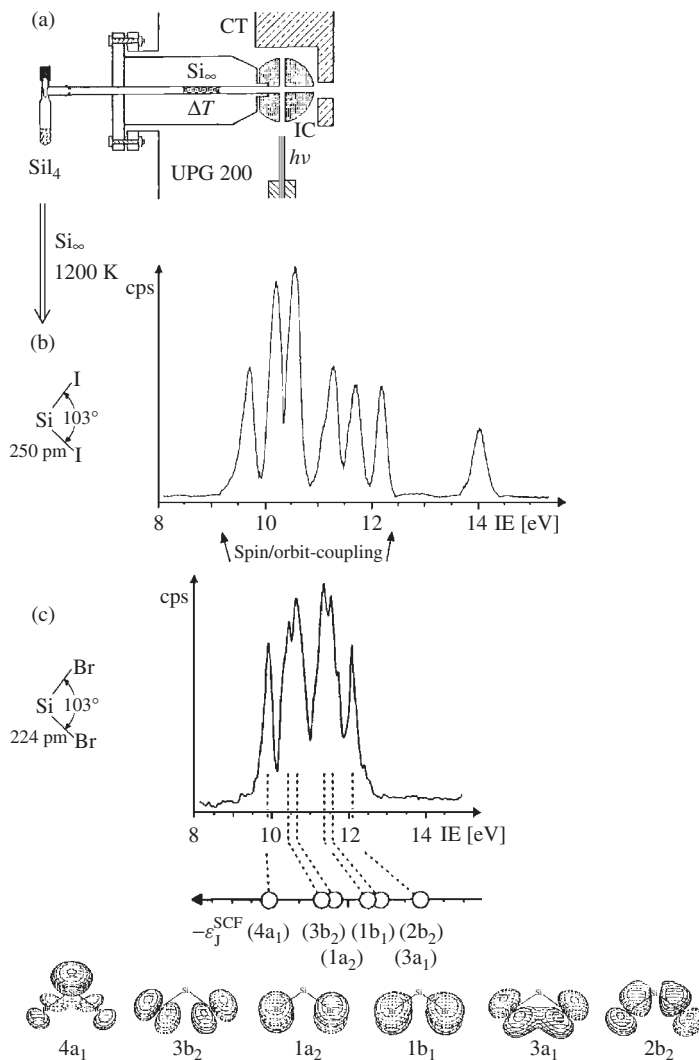


FIGURE 20. (a) Short-path apparatus for the gas-phase preparation of SiI_2 in the electron-bombardment oven of the Leybold Heraeus UPG 200 PE spectrometer ($h\nu$ He(I) lamp; IC: ionization Chamber; CT cooling trap) and He(I) PE spectra as well as SCF-optimized structures of (b) SiI_2 and (c) SiBr_2 with SCF orbitals for Koopmans' assignment of the spin/orbit-coupled radical states (see text)

again the tremendous influence of the effective nuclear charges of halogen decreasing from F to I (cf. Section III.A).

In closing, it is pointed out again that the charm of SiI_2 consists not only in being relativistic, but also in being one of the few still unknown triatomic main-group element molecules.

TABLE 7. Additional photoelectron spectra recorded in 1988–2000 for organosilicon compounds containing group 17 elements

Compound (R=CH ₃)	Reference	IE ₁ ^v (eV)	M ^{•⊕} (<i>X</i> _μ)
SiF ₂ Cl ₂	75	12.66	$\tilde{X}(^2B_1)$
SiFCl ₃		12.21	$\tilde{X}(^2A_2)$
<i>c</i> -(SiCl ₂) ₄	97	8.85	$\tilde{X}(^2B_{2g})$
<i>c</i> -(SiCl ₂) ₅		9.50	$\tilde{X}(^2A)$
<i>c</i> -(SiCl ₂) ₆		9.00	$\tilde{X}(^2A_{1u})$
R ₃ SiF	94	11.00	$\tilde{X}(^2E)$

2. PE spectroscopic investigations of organosilicon compounds with group 17 elements

Halogen derivatives in general are valuable synthetic building blocks, in contrast to their often less attractive redox or acid/base molecular properties, a fact reflected also by the comparatively few PE spectroscopic investigations^{10,15,16,96} published recently (Table 7).

Both chlorofluorosilanes have been prepared by reacting Na₂SiF₆ with (AlCl₃)₂⁷⁵. The ionization energy differences of cyclic perchlorosilanes [(SiCl₂)_{4–6}] are rationalized by calculation of geometry-optimized structures of *D*_{4h}, *C*₁ or *D*_{3d} symmetry⁹⁷.

V. RETROSPECTIVE AND PERSPECTIVES

Organosilicon radical cations generated in the gas phase by vertical ionization within 10⁻¹⁵ s, in solution by adiabatic redox electron transfer within ≤10⁻⁷ s or in matrix by irradiation provide interesting and essential information concerning both the molecules before and the radical cations after electron expulsion (Section II.B). Among the numerous methods suited for their investigation, photoelectron spectroscopy in the gas phase (Section II.A) and ESR/ENDOR measurements in solution (cf. Section III.D) complement each other both as eigenvalue-determined (via Koopmans' theorem) as well as eigenfunction squared correlated (e.g. via the McConnell relation; Section II.B) and also by their different 10⁻¹⁵ and 10⁻⁷ s time scales. Quantum chemical calculations at various levels of sophistication—from topological eigenvalues (Section III.B) to pseudorelativistic eigenfunctions (Section IV.E.1)—considerably help to assign spectra, to assess spin and charge distributions and, above all, to interpret and rationalize the fascinating molecular or radical cation properties, including their dynamics^{10,15,16}.

Prominent features, resulting from over 30 years of investigation by many groups worldwide, are, for instance:

(i) The low effective nuclear charge of silicon centers in organic molecules causes internal polarization Si^{δ⊕}–C^{δ⊖} and, depending on the respective substituent perturbation pattern (Section III.C), will reduce first vertical ionization potentials in the gas phase as well as oxidation potentials in solution to often surprisingly low values.

(ii) Within main group element chemistry, striking substituent effects of partly bulky and kinetically shielding trialkylsilyl groups on π-systems and electron-rich lone pair centers have been discovered, many of which are nowadays used in organic synthesis.

(iii) Numerous thermodynamically stable but kinetically short-lived organosilicon intermediates have been generated in gas-flow systems or low temperature matrices by using the PES or ESR molecular state fingerprints for reaction optimization (Section III.F). The coordination numbers of the Si centers, ranging from one as in H₅C₆N^{δ⊕}≡Si^{δ⊖} (Figure 9)

to ten as in the silicocene sandwich π -complex $(R_5C_5)_2Si$ (Figure 11), demonstrate the breathtaking bonding span of Si centers.

Returning to the Review subtitle 'History and Achievements', (HeI) photoelectron spectroscopy as a gas-phase probe for radical cations exemplified here for organosilicon compounds has opened new insights into bonding in and properties of molecular states, supported and promoted by the also rapidly developing quantum chemical calculations. The tremendous progress has opened numerous areas for future research from new materials based on polysilane band structures (Figure 5) or Rydberg states in photochemical reactions of organosilicon compounds¹⁵, to dynamics of Si-containing molecules (Scheme 3) including calculated energy hypersurfaces etc., etc., not forgetting the increasing impact of both the constantly improved and newly developed techniques of physical measurement such as ZE(ro) K(inetic) E(nergy) spectroscopy^{14,98} or femtosecond laser technology⁹⁹. In addition, there is an avalanche of quantum chemical, ever faster and more number crunching calculations for larger molecules of increasing importance. Therefore, an 'intellectual tunneling' is necessary between the only seemingly different viewpoints of preparative and theoretical chemistry, which both meet in the reality of molecular states.

In closing, Galileo Galilei may be quoted also with reference to organosilicon radical cations¹⁰⁰: 'Measure everything and the unmeasurable make measurable'.

VI. REFERENCES AND NOTES

1. Part 160 of *Photoelectron Spectra and Molecular Properties*; also Part 93 of *Gasphase Reactions and Essay 35 on Molecular States and Models*; for preceding parts see H. Bock, *Fascinating Silicon Chemistry-Retrospection and Perspectives in Organosilicon Chemistry IV* (Eds. N. Auner and J. Weis), Wiley—VCH, Weinheim, 2000, as well as Essay 34, H. Bock, *99 Semesters of Chemistry—A Personal Retrospective on the Molecular State Approach by Preparative Chemists, Coll. Czech. Chem. Commun.* **62**, 1–41 (1997).
2. D. W. Turner, C. Baker, A. D. Baker and C. R. Brundle, *Molecular Photoelectron Spectroscopy*, Wiley-Interscience, London, 1970, contains a summary, illustrated with hundreds of He(I) photoelectron spectra of prototype molecules.
3. The five volumes of the handbook: A. D. Baker and C. R. Brundle (Eds.), *Electron Spectroscopy: Theory, Techniques and Applications*, Academic Press, London, 1977–84, contain a comprehensive view of the topic, including X-ray photoelectron spectroscopy, in individual contributions written by experts.
4. J. W. Rabalais, *Principles of Ultraviolet Photoelectron Spectroscopy*, Wiley, New York, 1977, is mentioned among the numerous monographs because of its literature review and the lucid presentation of difficult topics, such as photoionization cross-sections.
5. K. Kimura, S. Katsumata, Y. Achiba, T. Yamazaki and S. Iwata, *Handbook of Hel Photoelectron Spectra of Fundamental Organic Molecules*, Halstead Press, New York, 1981, is the standard compendium containing several hundred PE spectra assigned by *ab initio* calculations and many references.
6. In Special Reports on *Electron Structure and Magnetism of Inorganic Compounds* (Ed. P. Day), Chemical Society, London, comprehensive literature reviews on technical details of the instrumentation as well as on the PE spectra of small molecules are provided by A. F. Orchard, S. Evans and A. Hammett in Vols. **1** (1970) to **3** (1972), and by R. G. Edgell and A. W. Potts in Vols. **6** (1980) and **7** (1982).
7. E. Heilbronner has made fundamental contributions to the assignment of photoelectron spectra of organic compounds. Summaries are found in: (a) *Pure Appl. Chem.*, **7**, 9 (1971); (b) R. Daudel and B. Pullmann (Eds), *The World of Quantum Chemistry*, D. Reidel, Dordrecht, 1974, p. 211; (c) *Helv. Chim. Acta*, **60**, 2248 (1977) and (d) *Phys. Scr.*, **16**, 202 (1977) G. Bieri, E. Heilbronner, T. B. Jones, E. Kloster-Jensen and J. P. Maier.
8. H. Bock and B. G. Ramsey, *Angew. Chem.*, **85**, 773 (1973); *Angew. Chem., Int. Ed. Engl.*, **12**, 734 (1973), report on the interpretation of the PE spectra of main group element compounds by comparison of equivalent radical cation states of chemically related molecules, based on MO perturbation arguments.

9. H. Bock, *Angew. Chem.*, **89**, 631 (1977); *Angew. Chem., Int. Ed. Engl.*, **16**, 613 (1977), discusses advantages and limits of the rationalization of molecular states by molecular orbital models, including numerous examples of radical cation states from photoelectron spectra.
10. H. Bock and B. Solouki, *Chem. Rev.*, **95**, 1161–1190 (1995), summarize generation and properties of *Organosilicon Radical Cations* including the PE spectroscopic prediction of their possible generation in solution.
11. H. Bock and B. Solouki, *Angew. Chem.*, **93**, 425 (1981); *Angew. Chem., Int. Ed. Engl.*, **20**, 427 (1981), report on application of PE spectroscopy to determine thermal decomposition routes to detect unstable intermediates and to optimize heterogeneously catalyzed reactions (142 references).
12. H. Bock and R. Dammel, *Angew. Chem.*, **99**, 518 (1987); *Angew. Chem., Int. Ed. Engl.*, **26**, 487 (1987), demonstrate the usefulness of PE spectroscopy in studies of gas-phase pyrolysis of azides and report on information obtained concerning the pathways of thermal fragmentation.
13. K. Siegbahn, G. Johansson, J. Hedman, P. F. Heden, K. Hamrin, U. Gelius, T. Bergmark, L. O. Werme, R. Manne and Y. Bear, *ESCA Applied to Free Molecules*, North-Holland, Amsterdam, 1969.
14. E. W. Schlag, *ZEKE Spectroscopy*, Cambridge University Press, 1988.
15. H. Bock, *Angew. Chem.*, **101**, 1659–1682 (1989), *Angew. Chem., Int. Ed. Engl.* **28**, 1627–1650 (1989), correlates in *Fundamentals of Silicon Chemistry: Molecular States of Silicon-containing Compounds* PES and ESR/ENDOR measurement data with first and second order MO perturbation models.
16. H. Bock and B. Solouki, review the literature on *Photoelectron Spectra of Silicon Compounds* until 1989 in *The Chemistry of Organic Silicon Compounds* (Eds. S. Patai and Z. Rappoport), Wiley, Chichester, 1989 (252 references).
17. H. Bock, *Sterically Overcrowded Organosilicon Compounds and their Properties in Organosilicon Chemistry* (Eds. N. Auner and J. Weis), VCH, Weinheim, 1994.
18. H. Bock, B. Solouki, J. Wittmann and H.-J. Arpe, *Angew. Chem.*, **90**, 933 (1978); *Angew. Chem., Int. Ed. Engl.*, **17**, 986 (1978); cf. also *Chem. Ber.*, **115**, 2346 (1982).
19. H. Bock, J. Mintzer, J. Wittmann and J. Russow, *Angew. Chem.*, **92**, 136 (1980); *Angew. Chem., Int. Ed. Engl.*, **19**, 147 (1980); cf. also *Chem. Ber.*, **115**, 2346 (1982).
20. H. Bock and M. Bankmann, *Angew. Chem.*, **98**, 288 (1986); *Angew. Chem., Int. Ed. Engl.*, **25**, 265 (1986).
21. H. Bock, B. Solouki and G. Maier, *Angew. Chem.*, **97**, 205 (1985); *Angew. Chem., Int. Ed. Engl.*, **24**, 205 (1985).
22. M. Binnewies, B. Solouki, H. Bock, R. Becherer and R. Ahlrichs, *Angew. Chem.*, **96**, 704 (1984); *Angew. Chem., Int. Ed. Engl.*, **23**, 731 (1984).
23. P. Rosmus, H. Bock, B. Solouki, G. Maier and G. Mihm, *Angew. Chem.*, **93**, 616 (1981); *Angew. Chem., Int. Ed. Engl.*, **20**, 598 (1981). For the matrix isolation of silaethene see G. Maier, G. Mihm and H. P. Reisenauer, *Angew. Chem.*, **93**, 615 (1981); *Angew. Chem., Int. Ed. Engl.*, **20**, 597 (1981).
24. H. Bock, K. Ruppert, C. Näther, Z. Havlas, H.-F. Herrmann, C. Arad, I. Göbel, A. John, J. Meuret, S. Nick, A. Rauschenbach, W. Seitz, T. Vaupel and B. Solouki, *Angew. Chem.*, **104**, 564–595 (1992); *Angew. Chem., Int. Ed. Engl.*, **31**, 550–581 (1992).
25. H. Bock and W. Kaim, *Acc. Chem. Res.*, **15**, 9 (1982).
26. H. Bock, W. Enßlin, F. Feher and R. Freund, *J. Am. Chem. Soc.*, **98**, 668 (1976).
27. A. W. Potts and W. C. Price, *Proc. R. Soc. London, Ser. A*, **326**, 165, 181 (1972); cf. also H. J. Lempka, T. R. Passmore and W. C. Price, *Proc. R. Soc. London, Ser. A*, **304**, 53 (1968).
28. The electronegativity is defined by Pauling and Mulliken as an energy, and by others as a force or as a dimensionless ratio. Cf. numerous textbooks, e.g. Holleman-Wiberg, *Lehrbuch der Anorganischen Chemie*, Editions 91–100, de Gruyter, Berlin, 1985, p. 152. The entire range of chemistry is embraced by the ridiculously small difference of only 3.54 units (Fr 0.86 to Ne 4.40) and the variation of the central atom in various substituent groups like C in CH₃, CN or CF₃ is not accounted for at all; cf. e.g. J. Hintze, *Fortschr. Chem. Forsch.*, **9**, 448 (1968).
29. H. Bock and W. Enßlin, *Angew. Chem.*, **83**, 435 (1971); *Angew. Chem., Int. Ed. Engl.*, **10**, 404 (1971).
30. H. Bock, W. Kaim, M. Kira and R. West, *J. Am. Chem. Soc.*, **101**, 7767 (1979); cf. also B. Hierholzer, Ph.D. Thesis, University of Frankfurt, 1988.

31. Cf. e.g. E. Heilbronner and H. Bock, *The HMO Model and its Application*, Vols. 1–3, Wiley-Interscience, London, 1975.
32. K. Takeda, H. Teramae and H. Matsumoto, *J. Am. Chem. Soc.*, **102**, 8186 (1980); H. Teramae and K. Takeda, *J. Am. Chem. Soc.*, **111**, 1281 (1989) and references cited therein.
33. Cf. the introduction to band-structure calculations with Bloch functions $\psi_k = \sum_n e^{ikna} \chi_n$ by R. Hoffmann, *Angew. Chem.*, **99**, 871 (1987); *Angew. Chem., Int. Ed. Engl.*, **26**, 846 (1987) and references cited therein.
34. Cf. Lecture Abstracts 'Advances in Silicon-Based Polymer Science', Makaha, Hawaii, 1987, *ACS Symp. Ser.* **224** (1989).
35. Not cited, however, by R. West in his review on *Polysilanes in The Chemistry of Organic Silicon Compounds* (Eds. S. Patai and Z. Rappoport), Wiley, Chichester, 1989, pp. 1208–1240.
36. C. Batick, E. Heilbronner, V. Hornung, A. J. Ashe III, D. T. Clark, U. T. Colbey, D. Kilcast and I. Scanlan, *J. Am. Chem. Soc.*, **95**, 928 (1973). For C_5BiH_6 cf. J. Bastide, E. Heilbronner, J. P. Maier and A. J. Ashe III, *Tetrahedron Lett.*, 411 (1976).
37. H. Bock, P. Rosmus, B. Solouki and G. Maier, *J. Organomet. Chem.*, **271**, 145 (1984).
38. W. Enßlin, H. Bock and G. Becker, *J. Am. Chem. Soc.*, **96**, 2757 (1974) and references cited therein.
39. Cf. the Chemistry Award Lecture of the Academy of Science in Göttingen 1969 by H. Bock, 'The Perturbation of π Systems as a Molecular Probe of Substituent Effects', *Jahrb. Akad. Wiss. Göttingen*, 1969, pp. 13–25. For a summary of silicon compounds investigated see Ref. 40.
40. H. Bock, B. Solouki, P. Rosmus, R. Dammel, P. Hänel, B. Hierholzer, U. Lechner-Knoblauch and H. P. Wolf, 'Recent Investigations on Short-lived Organosilicon Molecules and Molecular Ions' in H. Sakurai (Ed.), *Organosilicon and Bioorganosilicon Chemistry*, Ellis Horwood, Chichester, 1985, pp. 45–73, and references cited therein such as H. Bock and H. Seidl, *J. Am. Chem. Soc.*, **90**, 5694 (1968); *J. Chem. Soc. B*, 1158 (1968); H. Bock and H. Alt, *J. Am. Chem. Soc.*, **91**, 355 (1969); *J. Organomet. Chem.*, **13**, 103 (1968); H. Bock, H. Alt and H. Seidl, *J. Am. Chem. Soc.*, **91**, 355 (1969).
41. H. Bock and U. Lechner-Knoblauch, *J. Organomet. Chem.*, **294**, 295 (1985) and references cited therein.
42. O. Graalmann, M. Hesse, U. Klingebiel, W. Clegg, M. Haase and G. M. Sheldrick, *Angew. Chem.*, **95**, 630 (1983); *Angew. Chem., Int. Ed. Engl.*, **22**, 621 (1983); *Angew. Chem. Suppl.* 874 (1983).
43. The selective 'Bock Oxidation' using $AlCl_3/CH_2Cl_2$ in the meantime has formed widespread application for main group element compounds; the prediction of one-electron oxidizability based on first ionization energies $IE_1^y < 8$ eV is valid also for numerous other classes of compounds. For examples of ESR/ENDOR-detected radical cations or their rearrangement products, see: BN heterocycles: H. Nöth, W. Winterstein, W. Kaim and H. Bock, *Chem. Ber.*, **112**, 2494 (1979); tetra-*tert*-butyltetrahedrane: H. Bock, R. Roth and G. Maier, *Chem. Ber.*, **117**, 172 (1984); tetrakis(dimethylamino)-*p*-benzoquinone: H. Bock, P. Hänel and U. Lechner-Knoblauch, *Tetrahedron Lett.*, **26**, 5155 (1985); 1,2-dithiolane: H. Bock, B. I. Chenards, P. Rittmeyer and U. Stein, *Z. Naturforsch. B*, **43**, 177 (1988), and references cited therein.
44. H. Bock and W. Kaim, *Chem. Ber.*, **111**, 3552 (1978) as well as **111**, 3573 (1978).
45. H. Bock, B. Hierholzer, H. Kurreck and W. Lubitz, *Angew. Chem.*, **95**, 817 (1983); *Angew. Chem., Int. Ed. Engl.*, **22**, 787 (1983); *Angew. Chem. Suppl.* 1088–1105 (1983).
46. H. Bock, W. Kaim, M. Kira, H. Osawa and H. Sakurai, *J. Organomet. Chem.*, **164**, 295 (1979).
47. For a review on Structural Chemistry of Organic Silicon Compounds cf. W. S. Sheldrick, in *The Chemistry of Organic Silicon Compounds*, Part 1 (Eds. S. Patai and Z. Rappoport), Wiley, Chichester, 1989, p. 227–304 (425 references).
48. Cf. the lecture review *Sterically Overcrowded Organosilicon Compounds and their Properties*, H. Bock, J. Meuret, C. Näther, K. Ruppertin *Organosilicon Chemistry* (Eds. N. Auner and J. Weis), VCH, Weinheim, 1994, pp. 11–19.
49. Cf. e.g. H. Bock, Z. Havlas and V. Krenzel, *Angew. Chem.*, **110**, 3305 (1998); *Angew. Chem., Int. Ed. Engl.*, **37**, 3163 (1998) and references cited therein.
50. H. Bock, J. Meuret and K. Ruppert, *Angew. Chem.*, **105**, 413 (1993); *Angew. Chem., Int. Ed. Engl.*, **32**, 414 (1993) and *J. Organomet. Chem.*, **445**, 19 (1993).

51. (a) N. Wiberg, H. Schuster, A. Simon and K. Peters, *Angew. Chem.*, **98**, 100 (1986); *Angew. Chem., Int. Ed. Engl.*, **25**, 79 (1986).
(b) N. Wiberg, E. Kühnel, K. Schurz, H. Borrmann and A. Simon, *Z. Naturforsch. B*, **43**, 1075 (1988).
52. (a) A. Schäfer, M. Weidenbruch, K. Peters and H. G. v. Schnering, *Angew. Chem.*, **96**, 311 (1984); *Angew. Chem., Int. Ed. Engl.*, **23**, 302 (1984).
(b) M. Weidenbruch, B. Flintjer, K. Peters and H. G. v. Schnering, *Angew. Chem.*, **98**, 1090 (1986); *Angew. Chem., Int. Ed. Engl.*, **25**, 1129 (1986).
53. Cf. also H. Bock, J. Meuret, K. Ruppert and R. Baur, *J. Organomet. Chem.*, **445**, 19 (1993); **446**, 113 (1993); **462**, 31 (1993).
54. Cf. also H. Bock, J. Meuret, H. Schödel and K. Ruppert, *Chem. Ber.*, **126**, 2227,2237 (1993).
55. Cf. the review: H. Bock, B. Solouki, S. Aygen, M. Bankmann, O. Breuer, R. Dammel, J. Dörr, T. Hirabayashi, D. Jaculi, J. Mintzer, S. Mohmand, H. Müller, P. Rosmus, B. Roth, J. Wittmann and H.-P. Wolf, *Optimization of Gas phase Reactions Using Real-Time PES Analysis: Short-Lived Molecules and Heterogeneously Catalyzed Processes*, *J. Mol. Struct.*, **173**, 31–49 (1988).
56. J. F. Ogilvie and S. Cradock, *J. Chem. Soc., Chem. Commun.*, **364** (1966); cf. additional calculations: J. N. Murrel, H. W. Kroto and M. F. Guest, *J. Chem. Soc., Chem. Commun.*, **619** (1977); R. Preuss, R. J. Buenker and S. D. Peyerimhoff, *J. Mol. Struct.*, **49**, 171 (1978).
57. H. Bock and R. Dammel, *Angew. Chem.*, **97**, 128 (1985); *Angew. Chem., Int. Ed. Engl.*, **24**, 111 (1985).
58. J. G. Radziszewski, D. Littmann, V. Balaji, L. Fabry, G. Gross and J. Michl, *Organometallics*, **12**, 4186 (1993); cf. also Y. Apeloig and K. Albrecht, *J. Am. Chem. Soc.*, **117**, 7263 (1995).
59. Not cited in M. Karni, Y. Apeloig, D. Schröder, W. Zunnack, R. Rabbezzana and H. Schwarz, *Angew. Chem.*, **111**, 344 (1999); *Angew. Chem., Int. Ed. Engl.*, **38**, 332 (1999).
60. T. P. Fehlner and D. W. Turner, *Inorg. Chem.*, **13**, 754 (1974), as well as N. P. C. Westwood, *Chem. Phys. Lett.*, **25**, 588 (1974).
61. H. Bock, M. Kremer, M. Dolg and H.-W. Preuss, *Angew. Chem.*, **103**, 1200 (1991); *Angew. Chem., Int. Ed. Engl.*, **30**, 1186 (1991).
62. H. Bock, R. Dammel, F. Fischer and C. Wentrup, *Tetrahedron Lett.*, **28**, 617 (1987).
63. D. Seyfert, K. D. Büchner, W. S. Rees, L. Wesemann, W. M. Davis, S. S. Bukalov, L. A. Leites, H. Bock and B. Solouki, *J. Am. Chem. Soc.*, **115**, 5386 (1993).
64. P. Jutzi, U. Hoffmann, D. Kanne, C. Krüger, R. Blom, R. Gleiter and I. Hyla-Krispin, *Chem. Ber.*, **122**, 16229 (1989).
65. (a) D. G. J. Sutherland, J. Z. Xiong, Z. Liu, T. K. Sham, G. M. Bancroft, K. M. Baines and K. H. Tan, *Organometallics*, **13**, 3671 (1994),
(b) R. Imhof, D. Antic, D. E. David and J. Michl, *J. Phys. Chem. A*, **101**, 4579 (1997).
66. L. Bonazzola, J. P. Michaut and J. Roncin, *New J. Chem.*, **16**, 489 (1992).
67. O. Takahashi, K. Morihashi and O. Kiruchi, *Bull. Chem. Soc. Jpn.*, **64**, 1178 (1991).
68. L. B. Knight, M. Winiski, P. Kudelko and C. A. Arrington, *J. Chem. Phys.*, **91**, 3368 (1989).
69. R. D. Frey and E. R. Davidson, *J. Chem. Phys.*, **89**, 4227 (1988).
70. See for example: B. W. Walther and D. Williams, *J. Chem. Soc., Chem. Commun.*, **270** (1982) and references cited therein.
71. See for example: M. Kira, H. Nakazawa and H. Sakurai, *J. Am. Chem. Soc.*, **105**, 6983 (1983), as well as *Chem. Lett.*, 1845 (1985).
72. M. Shiotani, K. Komaguchi, J. Oshita, M. Ishikawa, L. Sjöqvist and K. Sasaki, *Chem. Phys. Lett.*, **188**, 93 (1992) or K. Komaguchi, M. Shiotani, M. Ishikawa and K. Sasaki, *Chem. Phys. Lett.*, **200**, 580 (1992).
73. J. Berkowitz, *Acc. Chem. Res.*, **22**, 413 (1989).
74. H. Bock, M. Kremer and H. Schmidbaur, *J. Organomet. Chem.*, **429**, 1 (1992).
75. O. Grabandt, C. A. de Lange, R. Mooyman and P. Vernooijs, *Chem. Phys. Lett.*, **184**, 221 (1991).
76. R. Gleiter, W. M. Schäfer, G. Krennrich and H. Sakurai, *J. Am. Chem. Soc.*, **110**, 4117 (1988).
77. A. J., III Arduengo, H. Bock, H. Chen, K. M. Denk, D. A. Dixon, J. C. C. Green, W. A. Herrmann, M. Wagner and R. West, *J. Am. Chem. Soc.*, **116**, 6641 (1994) and references cited therein. See also M. Denk, J. C. Green, N. Metzler and M. Wagner, *J. Chem. Soc., Dalton Trans.*, 2405 (1994).

78. A. J., III Arduengo, R. L. Harlow and M. Kline, *J. Am. Chem. Soc.*, **113**, 361 (1991) and A. J., III Arduengo, H. V. R. Dias, R. L. Harlow and M. Kline, *J. Am. Chem. Soc.*, **114**, 5530 (1992). See also: A. J., III Arduengo, D. A. Dixon, K. K. Kumashiro, C. Lee, W. P. Power and K. W. Zilm, *J. Am. Chem. Soc.*, **116**, 6361 (1994) or A. J., III Arduengo, H. V. R. Dias, D. A. Dixon, R. L. Harlow, W. T. Kloster, T. F. Koetzle, *J. Am. Chem. Soc.*, **116**, 6812 (1994).
79. W. A. Herrmann, M. Denk, J. Behn, W. Scherer, F.-H. Klingan, H. Bock, B. Solouki and M. Wagner, *Angew. Chem.*, **104**, 1489 (1992); *Angew. Chem., Int. Ed. Engl.*, **31**, 1485 (1992).
80. M. Denk, R. Lennon, R. Hayashi, R. West, A. V. Belyakow, H. P. Verne, A. Haaland, M. Wagner and N. Metzler, *J. Am. Chem. Soc.*, **116**, 2691 (1994).
81. H. Bock, J. Meuret, C. Näther and U. Krynitz, *Chem. Ber.*, **127**, 55 (1994), as well as *Tetrahedron Lett.*, **34**, 7553 (1993) and all the literature cited on alkyl derivatives. See also F. Gerson, U. Krynitz and H. Bock, *Angew. Chem.*, **81**, 786 (1969); *Angew. Chem., Int. Ed. Engl.*, **8**, 767 (1969).
82. (a) V. Métail, S. Joanteguy, A. Chrostowska-Senio, G. Pfister-Guillouzo, A. Systemans and J. L. Ripoll, *Inorg. Chem.*, **36**, 1482 (1997).
(b) V. Lefèvre, J. L. Ripoll, Y. Dat, S. Joanteguy, V. Métail, A. Chrostowska-Senio and G. Pfister-Guillouzo, *Organometallics*, **16**, 1635 (1997).
83. G. Distefano, L. Zanathy, L. Szepes and H. J. Breunig, *J. Organomet. Chem.*, **338**, 181 (1988).
84. A. Nagy, J. C. Green, L. Szepes, and L. Zanathy, *J. Organomet. Chem.*, **419**, 27 (1991).
85. T. Veszpremi, T. Pasinszki, L. Nyulaszi, G. Csonka and I. Barta, *J. Mol. Struct.*, **175**, 411 (1988). See also T. Pasinszki, J. Reffy and T. Veszpremi, *Monatsh. Chem.*, **123**, 949 (1992).
86. R. Gleiter, K.-H. Pfeifer, M. Baudler, G. Scholz, T. Wettling and M. Regitz, *Chem. Ber.*, **123**, 757 (1990).
87. J. B. Peel and W. Dianxun, *J. Chem. Soc., Dalton Trans.*, 1963 (1988). See also V. F. Sidorkin and G. K. Balakhchi, *Struct. Chem.*, **5**, 189 (1994).
88. H. Bock and J. Meuret, *J. Organomet. Chem.*, **459**, 43 (1993).
89. H. Bock, J. Meuret and U. Stein, *J. Organomet. Chem.*, **398**, 65 (1990).
90. E. Block, A. J. Yench, M. Aslam, V. Eswarakrishnan, J. Luo and A. Sano, *J. Am. Chem. Soc.*, **110**, 4748 (1988).
91. M. Y. Maroshina, N. N. Vlasova and M. G. Voronkov, *J. Organomet. Chem.*, **406**, 279 (1991).
92. L. Nynlaszi, T. Veszpremi and J. Reffy, *J. Organomet. Chem.*, **445**, 29 (1993).
93. H. Bock, *Phosphorus, Sulfur and Silicon*, **49/50**, 3–53 (1990).
94. N. H. Werstiuk, M. A. Brook and P. Hülser, *Can. J. Chem.*, **66**, 1430 (1988).
95. H. Bock, J. Meuret, J. W. Bats and Z. Havlas, *Z. Naturforsch. B*, **49**, 288 (1994).
96. K. Wittel and H. Bock, *Photoelectron Spectra of Halogen Compounds*, in *The Chemistry of Functional Groups, Supplement D* (Ed. S. Patai and Z. Rappoport), Wiley, Chichester, 1983.
97. H. Stüger and R. Janoscheck, *Phosphorus, Sulfur, Silicon Relat. Elem.*, **68**, 129 (1992).
98. For Electron Detachment of Si_n^{\ominus} Ions see, e.g., C. C. Arnold and D. M. Neumark, *J. Chem. Phys.*, **100**, 1797 (1994).
99. E. W.-G. Diau, J. L. Herek, Z. H. Kim and A. H. Zewail, *Science*, **279**, 847 (1998).
100. Cf. e.g. H. Bock, in *Organosilicon Chemistry IV: From Molecules to Materials* (Eds. N. Auner and J. Weis), Wiley VCH, Weinheim, 2000, pp. 37–58.

CHAPTER 3

^{29}Si NMR experiments in solutions of organosilicon compounds

JAN SCHRAML

Institute of Chemical Process Fundamentals, Academy of Sciences of the Czech Republic, 165 02 Prague, Czech Republic
Fax: 4202 20 92 0661; e-mail: schraml@icpf.cas.cz

I. INTRODUCTION	224
II. BASIC FACTS	225
III. REFERENCING	226
IV. SOLVENT EFFECTS	230
V. SENSITIVITY ENHANCEMENTS	240
A. Selective Polarization Transfer (SPT)	241
B. Non-selective Polarization Transfers (INEPT, DEPT, PENDANT, PASSADENA and Their Variants)	245
C. <i>J</i> Cross-polarization (JCP)	255
VI. LINE ASSIGNMENTS AND CONNECTIVITY	257
A. Correlations	258
1. ^{29}Si detected heteronuclear correlations	258
2. Indirectly detected heteronuclear correlations	261
3. INADEQUATE	273
4. DQF COSY	282
5. ^{29}Si – ^{29}Si couplings, $^nJ(^{29}\text{Si}$ – $^{29}\text{Si})$	283
B. Triple Resonance	296
1. 1D experiments	296
2. 2D experiments	298
3. 3D experiments	300
C. Selective Experiments	303
1. Selective excitation	304
2. Selective detection	306
VII. DETERMINATION OF COUPLING CONSTANTS	311

VIII. RELAXATIONS	314
IX. NUCLEAR OVERHAUSER EFFECT (NOE)	316
X. MISCELLANEOUS	319
A. Isotopic Enrichment and Substitution	319
B. DOSY (<i>Diffusion Ordered Spectroscopy</i>)	321
C. Quantitative Measurements	323
D. Ultrahigh Resolution	325
E. Shift and Relaxation Reagents	325
XI. COMMON MISTAKES AND PITFALLS—COMMENTS AND WARNINGS	326
XII. ACKNOWLEDGEMENTS	329
XIII. REFERENCES	330

I. INTRODUCTION

Advances in ^{29}Si NMR spectroscopy have been enormous during the last few decades, both in technical means and in achievements. This progress, as in many other fields of science and technology, has been reflected in an exponential growth of the number of publications. Our database currently comprises over 6000 papers containing ^{29}Si NMR data, and we cannot claim that it is complete. Just for comparison, the NMR bible of the seventies¹, in its attempt to cover most of the published work on structural applications of NMR at that time, contained 496 references to ^1H NMR papers. Since that time, however, no one has attempted to cover all aspects of ^1H NMR spectroscopy.

Nowadays, valuable ^{29}Si NMR data (e.g. ^{29}Si – ^{74}W couplings, etc.) are often 'hidden' in footnotes of 'synthetic' papers, while not long ago the same data warranted independent publication. It would be most desirable if a reviewer could extract such data and collate them into generalized trends. Unfortunately, this is not realistic, as original data were obtained under considerably varied experimental conditions (solvents, temperature and reference) and are often presented without an adequate description that would indicate their precision and reliability.

Workers in a field usually know the values of relevant parameters in the classes of compounds they study, and, if not, they can use abstracting/indexing services to localize the source of the data for the compound of interest. The traditional sources of such information (Chemical Abstracts, Beilstein Data) have been supplemented by sources dedicated to ^{29}Si NMR data collection².

The previous ^{29}Si NMR review in this series³ has stressed the recent trend in combining NMR spectroscopy with other methods, mainly X-ray diffraction, a marriage that has enabled well-equipped laboratories to determine by X-ray the structure of any compound that can be crystallized. Solution NMR data then serve only two minor purposes: confirming the same structure in solution and allowing fast identification of the compound. It is this latter purpose that further emphasizes the importance of correct measurements and presentation of NMR data; this is of even more importance in the case of ^{29}Si NMR spectra, which (in contrast to ^1H or ^{13}C NMR spectra) usually contain only a few lines, and thus the structure of the spectrum or internal shifts are of little use with identification resting on precise values of chemical shifts and coupling constants.

On current spectrometers, spectral line frequencies can be determined with a precision of ± 0.1 Hz or better and a difference in frequencies better than ± 0.2 Hz. The same reproducibility can be achieved for repeated measurements of a sample without need for excessive care when the measurement is run with temperature control and stable lock.

Apparently, such precision is routinely achieved, as ^{29}Si coupling constant values are presented with that precision in the overwhelming majority of synthetic papers. The ± 0.2 Hz in frequency translates into a precision of the ^{29}Si chemical shift of ± 0.005 ppm on a 200 MHz spectrometer operating at 39 MHz for ^{29}Si NMR (and accordingly to a higher precision on a higher field spectrometer). The most frequently implied accuracy of ^{29}Si chemical shifts published in synthetic papers is much lower, around ± 0.2 ppm (as the shifts are presented to one decimal place). The lower accuracy reflects uncertainty in exact experimental conditions (sample and solvent purity, temperature, concentration, referencing, short acquisition time etc.) and their reproducibility. In some cases the uncertainty is recognized by the authors, in others it is an outcome of journal brevity rules as imposed by the editors. A synthetic chemist who is busy making new interesting compounds has no time to study NMR textbooks; he takes full advantage of user-friendly software of current NMR spectrometers to run sophisticated experiments. It is then no wonder that many synthetic papers contain many errors in data presentation that often make even the measurement suspect. Errors frequently encountered in such papers are briefly described in the last section of the present review.

Therefore, this review will draw only from those papers that already contain some discussion of ^{29}Si NMR experiments. It will concentrate on experimental aspects of ^{29}Si NMR in organosilicon liquids. This area will be covered irrespective of earlier excellent reviews³⁻⁹ in order to enable independent reading without continued need for recourse to other treatises.

The overwhelming majority of pulse sequences in use in ^{29}Si NMR have been developed for ^{13}C nuclei and then adapted for ^{29}Si . Perhaps with the exception of adjustment for the negative gyromagnetic ratio (changing the polarity of magnetic field gradients and replacing continuous proton decoupling with gated decoupling) the adaptation is trivial; the adjustments for different coupling values or longer relaxation times do not differ from those needed to optimize the experiment for a ^{13}C NMR experiment on a different class of organic compounds. Of the plethora of NMR experiments (pulse sequences) described in the literature, practically all can be adapted for use in ^{29}Si NMR spectroscopy even though some are not likely to find such a use (e.g. TOCSY and its variants). This review will concentrate only on those experiments that have a record of proven usefulness for organosilicon chemistry, although it might be only a matter of time until these other experiments are tried on organosilicon compounds.

To save space and yet enable limited discussion, the pulse sequences are given here in very condensed form in the body of the text; for phase cycling, etc. the reader is referred to the source literature.

II. BASIC FACTS

Parameters of the ^{29}Si nucleus have been given in all previous reviews of ^{29}Si NMR, and detailed comparison with other nuclei can be found in reviews of Harris and coauthors^{6,10} and Brevard and Granger¹¹, which also give clear definitions of the terms (e.g. relative receptivity) used in the discussion.

Some experimental difficulties in measuring ^{29}Si NMR spectra come, as in ^{15}N NMR, from the negative gyromagnetic ratio γ , but the natural abundance (4.70%) makes ^{29}Si receptivity twice as high as that of ^{13}C ($D_{\text{Si}}^{\text{C}} = 2.09^{10}$). This is especially welcome in experiments like INADEQUATE, which are easier to perform in ^{29}Si NMR than in ^{13}C NMR spectroscopy, despite the lower resonance frequency. On the other hand, ^{29}Si isotopic enrichment has remained prohibitively expensive (with the possible exception of

TABLE 1. ^{29}Si NMR resonance frequencies and relative sensitivities in different magnetic fields^a

^1H NMR ^b	^{29}Si NMR frequency ^c	Relative sensitivity ^d
100	19.87	0.4
200	39.73	1.0
250	49.66	1.4
300	59.60	1.8
400	79.46	2.8
500	99.33	4.0
600	119.19	5.2
760	150.97	7.4
800	158.92	8.0

^aThe magnetic field is expressed as the ^1H NMR resonating frequency.

^b ^1H NMR frequency in MHz; the spectrometer frequency is usually a part of the spectrometer model name (e.g. UNITY 400 or AVANCE 400).

^c ^{29}Si NMR frequency in MHz.

^dVery approximate relative sensitivity (signal-to-noise) of ^{29}Si NMR at the given resonance frequency relative to that at 39.73 MHz (i.e. in the lowest field superconductive magnet); the figures reflect magnetic field changes only ($S/N \propto B_0^{1.5}$)¹².

silicates, see Section X.A) while the cost of ^{13}C enrichment has decreased considerably in recent years. The never-ending drive for higher magnetic fields brings with it a higher sensitivity and a higher spectral resolution (Table 1). In a laboratory, a significant increase in sensitivity can be achieved by replacing the old probe (and preamplifier) by their latest counterparts and/or by use of techniques with a higher sensitivity (e.g. inverse detection). With the (negative) gyromagnetic ratio of the ^{29}Si nucleus being of the opposite sign compared to the gyromagnetic ratios of the more common and abundant nuclei (e.g. ^1H , ^{19}F or ^{31}P) some care is necessary in preparing ^{29}Si NMR experiments. A negative Overhauser effect (when nuclei with positive gyromagnetic ratios are saturated) can reduce or even null the signal, and under the influence of magnetic field gradients ^{29}Si magnetization rotates in an opposite direction than magnetizations of other nuclei.

In practice, problems might come from slow relaxation of ^{29}Si nuclei in some species. Although long spin–spin relaxation T_2 is beneficial, as it leads to narrow lines in the spectrum, long spin–lattice relaxation T_1 is troublesome as it requires slow pulse repetition, thus making ^{29}Si NMR experiments time-demanding. The use of relaxation reagents can shorten this time but it contaminates the sample and can also broaden the lines (see Sections IV and X.E).

III. REFERENCING

We shall spend time and space on the trivial matter of referencing for a simple reason—referencing is vital for the accuracy of the reported chemical shifts. While current spectrometers measure line positions easily with a precision of ± 0.02 ppm, referencing errors can cause and do cause systematic errors of 1–3 ppm.

It has been very fortunate that the δ scale and the universal primary reference, tetramethylsilane (TMS), were widely accepted rather early in ^{29}Si NMR history. (For other suggested references, their relative merits and conversion factors, see earlier reviews⁹.) Not only does TMS have a relatively short relaxation time $T_1^{13,14}$, but it also has 12 protons that can be utilized for polarization transfer. Thus TMS can be used as a reference at low

concentrations (*ca* 1–3%) independently of the measuring technique employed. Since NOE of TMS depends on temperature¹⁴, the intensity of its signal might change with the temperature. With modern stable superconducting spectrometers, the fact that the TMS resonance lies in the middle of common ^{29}Si chemical shifts¹⁵ is no longer an argument against its use unless coupled spectra are to be recorded.

The δ scale (with ppm units) is defined by equation 1

$$\delta = \frac{\nu - \nu_{\text{TMS}}}{\nu_{\text{TMS}}} \times 10^6 \quad (1)$$

where ν and ν_{TMS} are the resonance frequencies (in Hz units) of the signal in question and the TMS reference in a given solvent. This definition is satisfactory for most practical purposes, but for studies of solvent effect and the highest achievable precision and reproducibility, infinite dilution in an inert reference solvent should be used (at a chosen temperature). (For discussion of reference requirements in solvent effect studies, see the next Section and References 16–19.) The definition implicitly assumes that the reference is fully inert and so a change of solvent or temperature affects the reference frequency only through the change in bulk magnetic susceptibility. As this assumption is not valid for TMS in a number of solvents^{18,19}, it is unlikely to be met by secondary references in use.

The use of a secondary reference and/or employment of external referencing is a result of some practical considerations. Aspects considered range from principal factors like sample solubility, boiling point or signal overlap to trivial matters of convenience such as routine or tradition in a laboratory. In practice, the chemical shift δ' , measured relative to a secondary reference as an internal reference, is converted into the δ scale according to the equation 2

$$\delta = \delta' + \delta_{\text{S}} = \left(\frac{\nu - \nu_{\text{S}}}{\nu_{\text{S}}} + \frac{\nu_{\text{S}} - \nu_{\text{TMS}}}{\nu_{\text{TMS}}} \right) \times 10^6 \quad (2)$$

where δ_{S} and ν_{S} are the chemical shift and resonance frequency, respectively, of the secondary reference. Obviously, the numerical error due to the replacement of ν_{TMS} by ν_{S} in the denominator of the first term is negligible, but substantial errors can occur because of differences in physical and chemical properties of the primary and secondary references. Since neither the solvent nor the secondary references used are fully inert, the chemical shift of the secondary reference, δ_{S} , varies with the solvent (for some examples, see Table 2). Clearly, for a correct conversion of δ' values to the δ scale according to equation 2, one single value of δ_{S} for each secondary reference is not sufficient; the δ_{S} value must be determined in the same solvent and temperature as used in the measurements. Unfortunately, the most widely used secondary references are methylsiloxanes (HMDSO, OMTS, hexamethylcyclotrisiloxane), which are proton acceptors, and their ^{29}Si chemical shifts are influenced by the hydrogen bonds both with the measured substrate and also with protic solvents as exemplified in Figure 1 (note the large solvent effects on the ^{29}Si chemical shift of hexamethyldisiloxane, HMDSO, the most common secondary reference). Solvent effects are usually smaller in the case of secondary references not containing oxygen or other heteroatoms like HMDSS or TTSM [tetrakis(trimethylsilyl)methane], the latter being especially convenient for high-temperature work (m.p. = 307 °C, δ_{S} = 2.74–3.12²⁰).

Reproducible chemical shifts of a secondary reference and substrate as well can be obtained at sufficient dilution even in a protic donor solvent²¹. This dilution procedure is not always practical for sensitivity reasons, but when a polarization transfer provides

TABLE 2. Chemical shifts δ_S of some secondary references in different solvents measured at 302 K^a

Solvent	HMDSS ^b	HMDSO ^c	OMTS ^d
<i>c</i> -C ₆ H ₁₂	-19.779	6.847	-19.690
C ₆ D ₆	-19.557	7.606	-18.584
CCl ₄	-19.791	6.951	-19.530
CDCl ₃	-19.779	7.314	-19.087
THF	-19.806	7.154	-19.293
C ₅ H ₅ N	-19.527	7.919	-18.224
CD ₃ COCD ₃	-19.729	7.329	-19.004
CH ₃ CN	-19.680	7.802	-18.424
DMSO-d ₆	-19.874	7.713	-18.476

^aMeasured as dilute solutions ($1.5 \pm 0.4\%$ w/w) of an equimolar mixture of the secondary references and TMS in the solvents indicated, acquisition time 4 s, spectral width 4 kHz, 32 K complex data points.

^bHexamethyldisilane, (Me₃Si)₂; we prefer this abbreviation as it eliminates possible ambiguity (HMDS sometimes used for this reference is also used to denote HMDSO).

^cHexamethyldisiloxane, (Me₃Si)₂O; Marsmann's review⁸ lists a number of chemical shift values in the range 4.0–7.2.

^dOctamethylcyclotetrasiloxane, (Me₂SiO)₄.

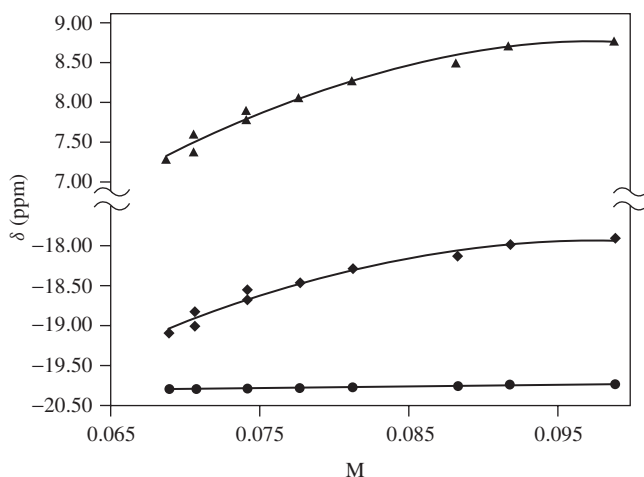


FIGURE 1. ²⁹Si chemical shift dependencies of common references on phenol concentration M [HMDSS (●), OMTS (◆) and HMDSO (▲)]

increased ²⁹Si NMR sensitivity, this is the best route to accurate and precise chemical shift values.

Depending upon whether or not the reference compound is present in the same solution as the measured substance, the method of referencing is denoted as internal or external. *Internal referencing*, when the reference is in the same solution as the measured substrate, eliminates the effect of magnetic susceptibility, χ_V ; both reference and substrate are in the same magnetic field. It does not eliminate, however, any of the many possible specific

interactions between solution components that can affect ^{29}Si chemical shifts of both substrate and reference. Irrespective of this influence, the internally referenced shifts are reproducible (and are therefore useful for compound identification and for other purposes) if relevant experimental conditions are provided. It is a pity to see valuable chemical shifts without indicated solution composition, temperature and method of referencing, which reduces the possible uses of the data.

With superconducting magnets and almost universal use of the deuterium signal of the solvent for the spectrometer lock, two different methods of *external referencing* are in use. Both solve the problem of different solubility of the sample and reference and both eliminate the need to contaminate the sample with the reference compound. The older of the two methods ('true external referencing') measures simultaneously the signals of the reference and substrate, but they are placed in physically separate parts of the sample tube (most often, the reference is contained in a glass capillary inside the sample). The second method, the *substitution method*, measures the sample and the reference in separate experiments with precautions being taken that the magnetic field and other experimental conditions do not change.

Magnetic susceptibility correction should be applied to the values obtained by either of the external referencing methods if the susceptibilities of the two solutions involved are different. In the case of true external referencing, care must be taken to use the proper correction formula; it depends not only on the geometry of the sample container (capillary or sphere)²² but also on the geometry of the receiver coil of the spectrometer²³. For a cylindrical capillary (currently the most frequently used) in an NMR tube in a superconducting magnet with the magnetic field parallel to the axis of the tube, the corrected chemical shift is given by equation 3

$$\delta_{\text{corr}} = \delta_{\text{obs}} - \frac{4\pi}{3} (\chi_{\text{V}}^{\text{ref}} - \chi_{\text{V}}^{\text{sample}}) \quad (3)$$

where symbols χ_{V} denote dimensionless volume susceptibilities of the reference and the sample.

The substitution method is usually preferred as it does not reduce the effective sample volume (a loss in sensitivity) and does not affect adversely the achievable dynamic range by adding another signal. Also, it is easier and simple to implement. If the same deuteriated solvent and low sample and reference concentrations are used, the difference in the susceptibility might be negligible (as easily verified by a comparison of lock conditions).

When solubility dictates use of different deuteriated solvents for reference and measured samples, the chemical shift δ_{corr} measured against the external reference and corrected for susceptibility difference must be also corrected for the difference in the chemical shifts of the lock signals, Δ . With a deuterium lock this difference is just the difference in ^2H NMR chemical shifts of the two deuteriated solvents, which equals the difference in ^1H shifts of their protic isotopomers (equation 4):

$$\delta = \delta_{\text{corr}} + \Delta = \delta_{\text{corr}} + (\delta_{\text{lock}}^{\text{sample}} - \delta_{\text{lock}}^{\text{reference}}) \quad (4)$$

A different method of referencing is used in the Ξ -scale of chemical shifts, sometimes referred to as 'universal referencing'. (We shall reserve the term 'absolute scale', which is also used in this context²⁴, for a different concept; see below.) In this scale the chemical shift is given as the absolute frequency of the signal that would be observed in a magnetic field in which the ^1H NMR signal of TMS appears exactly at 100 MHz. Thus

$$\Xi = (100.000000/\nu_{\text{TMS}}) \cdot \nu \quad (5)$$

the Ξ value of a signal (equation 5, in Hz units), is determined from its resonance frequency, ν , and TMS frequency, ν_{TMS} , in the ^1H NMR spectrum measured under the same conditions (i.e. it includes the temperature dependence of the ^1H NMR chemical shift of TMS)^{25–27}. Different but equivalent definitions and a detailed description of how to arrive at the Ξ values can be found in the literature^{28,29} together with Ξ values of reference compounds for other nuclei^{10,30}. This scale has not gained much popularity in the area of ^{29}Si NMR; apparently the large number of significant digits (many of them redundant for our purposes as they do no more than define the ^{29}Si nucleus) required to express the chemical shifts in this scale (and hence the large probability of typing errors), combined with some initial reluctance of spectrometer manufacturers to incorporate it into the spectrometer software, worked against its wider acceptance.

Measurements in water and in other highly polar solvents require a short comment. Since the primary reference is insoluble in these media, secondary references are used with their δ_{S} values determined through external referencing. However, use of a TMS emulsion might overcome the need for susceptibility correction as the dispersed reference might form perfect spheres³¹ although it might lessen the resolution. The common ^1H NMR secondary references, DSS or TSPSA [sodium 4,4-dimethyl-4-silapentane-1-sulfonate or the Na^+ salt of 3-(trimethylsilyl)propane sulfonic acid] and DSC or TSPA [4,4-dimethyl-4-silapentane sodium carboxylate or the Na^+ salt of 3-(trimethylsilyl)propionic acid] are most frequently used for ^{29}Si referencing as well. Their ^{29}Si referencing properties have not been systematically investigated but care should be exercised, as it is known from ^1H studies that the chemical shift of DSS is affected by interactions with other solutes^{32,33}; it forms micelles in concentrated solutions containing paramagnetic ions³⁴, and some unexpected reactions of DSS were reported³⁵.

Absolute scale (or absolute shielding) is another scale used in shielding theory. It gives shifts in ppm units relative to the bare nucleus with positive values indicating less shielding (higher frequency). Jameson and Jameson³⁶ calculated ^{29}Si absolute shielding in SiH_4 (475.3 ± 10 ppm), SiF_4 (482 ± 10 ppm) and in TMS (368.5 ± 10 ppm), which are important constants that allow comparison of chemical shifts obtained by molecular calculations.

IV. SOLVENT EFFECTS

Various solvents have been used in ^{29}Si NMR studies and applications. It appears that the choice of solvent and concentration has been dictated more by the tradition in the particular field of organosilicon chemistry or laboratory than by the more general consideration of obtaining comparable and reproducible results. The solvents used include chloroform, benzene, tetrahydrofuran, pyridine, dioxane, dimethyl sulfoxide etc., usually in their fully deuteriated isotopomers; the effects of these solvents on common secondary references were summarized earlier in Table 2.

The ever-increasing sensitivity of NMR spectrometers (higher magnetic field combined with a better circuitry) together with introduction of polarization transfer schemes for ^{29}Si NMR have now removed for virtually all classes of organosilicon compounds the need to measure samples in high concentrations or as neat liquids (with its requirement for 1 g or more of the compound), as was the case in the sixties.

Although observations are scattered throughout the literature, solvent effects on ^{29}Si NMR parameters have been studied systematically only to a slight extent. Attention has been focussed mainly on effects on chemical shifts despite the fact that all parameters are affected by solvent, concentration and temperature.

As mentioned above in Section III, satisfactory definition of chemical shifts for solvent effect studies is a problem that can be important, especially when the effects are small. In their studies of solvent effects on the ^{29}Si chemical shift of TMS, Bacon and Maciel and their coworkers^{18,19,37} adopted the following definitions that are closely related to the method of measurement they used: in a CW spectrometer they kept the ^1H resonance of TMS at a fixed frequency (irrespective of the solvent) and measured the ^{29}Si chemical shift in the magnetic field thus defined. These shifts reflect the solvent effects on the shifts of both ^1H and ^{29}Si nuclei. The values (named apparent shifts and denoted $\Delta\sigma_{\text{Si}}^{\text{a}}$) were given relative to the value obtained in the same manner for pure TMS. In order to eliminate the solvent effect on the ^1H chemical shift, the authors determined 'intrinsic' ^1H solvent shifts $\Delta\sigma_{\text{H}}$ in separate measurements. (The $\Delta\sigma_{\text{H}}$ shifts were measured relative to an external reference, and the susceptibility effect was eliminated by measuring with the cylindrical axis of the sample tube both parallel and perpendicular to the magnetic field.) The corrected or intrinsic ^{29}Si solvent shift is $\Delta\sigma_{\text{Si}} = \Delta\sigma_{\text{Si}}^{\text{a}} + \Delta\sigma_{\text{H}}$. Factor analysis of the data revealed that there are just two significant factors influencing the solvent shifts, but their relationship to current models of solvent effect has remained unclear. Since ^1H and ^{29}Si chemical shifts vary similarly with the solvent, the range of ^{29}Si intrinsic shifts $\Delta\sigma_{\text{Si}}$ spans 0.65 ppm, while the range of ^{29}Si apparent shifts $\Delta\sigma_{\text{Si}}^{\text{a}}$ is only 0.22 ppm in 15 solvents (20 vol% solutions in mostly halobenzenes and halocyclohexanes), which is certainly of not much concern in practical applications.

The early CW direct measurements of ^{29}Si chemical shifts, which established the major trends (and large substituent effects), were not particularly concerned with solvent effects. The measured samples usually had high concentrations or were neat liquids and the shifts were referenced externally. It was believed that the small error introduced by the failure to apply a bulk susceptibility correction was bound to be preferable to the possibility of larger errors introduced by solvent effects¹³. It was also generally held that ^{29}Si shifts (in contrast to ^{119}Sn but similar to ^{13}C shifts) are little affected by solvents, concentration and temperature. Certainly, the solvent effects observed then were small (<0.5 ppm) compared to effects arising from structural changes and experimental inaccuracy. This view was supported by the above-mentioned small solvent effects on the shift of TMS and by other isolated observations. For example, in their double resonance study of *ca* 30% samples in CCl_4 , McFarlane and Seaby³⁸ noted that the ^{29}Si shifts of methylsilyl carboxylates were not appreciably affected by the presence of hydrolysis products (free acid and hexamethyldisiloxane); additions of pyridine or triethylamine affected the shieldings by less than 0.3 ppm. The shifts were independent of concentration in inert solvents except for $\text{ClCH}_2\text{COOSiMe}_3$, the shift of which was decreased by 0.5 ppm by an addition of CH_2Cl_2 . (Incidentally, the opposite effect of the same solvent on the shifts of polysiloxanes was reported by Harris and Kimber³⁹.) However, Williams and coworkers^{40,41} realized that the strong interaction of acidic silanols with basic solvents should be reflected in ^{29}Si chemical shifts. Experiments confirmed this hypothesis. They found linear correlations between the ^{29}Si chemical shifts of silanols (and other compounds with acidic protons) measured in different solvents and 'donor numbers' of the solvents (DN); see Figure 2. DN, a measure of basicity of the solvent, was introduced by Gutmann^{42,43}. Compounds without an acidic proton [e.g. Ph_3SiCl , $(\text{MeO})_3\text{SiH}$] showed small solvent shifts (<0.5 ppm), while in other compounds the effects were larger but without a linear relationship to DN [e.g. $(\text{Me}_2\text{CHNHSiMe}_2)_2\text{O}$, $(\text{Me}_2\text{HSi})_2\text{NH}$ and $(\text{EtNH})_2\text{SiMe}_2$]. To explain this relationship with the solvent donicity, it was suggested that in silanols the electron pair donor (EPD) solvents increase the O–H distance with subsequent decrease of the Si–O distance⁴³. This type of linear correlation was confirmed for trimethylsilanol

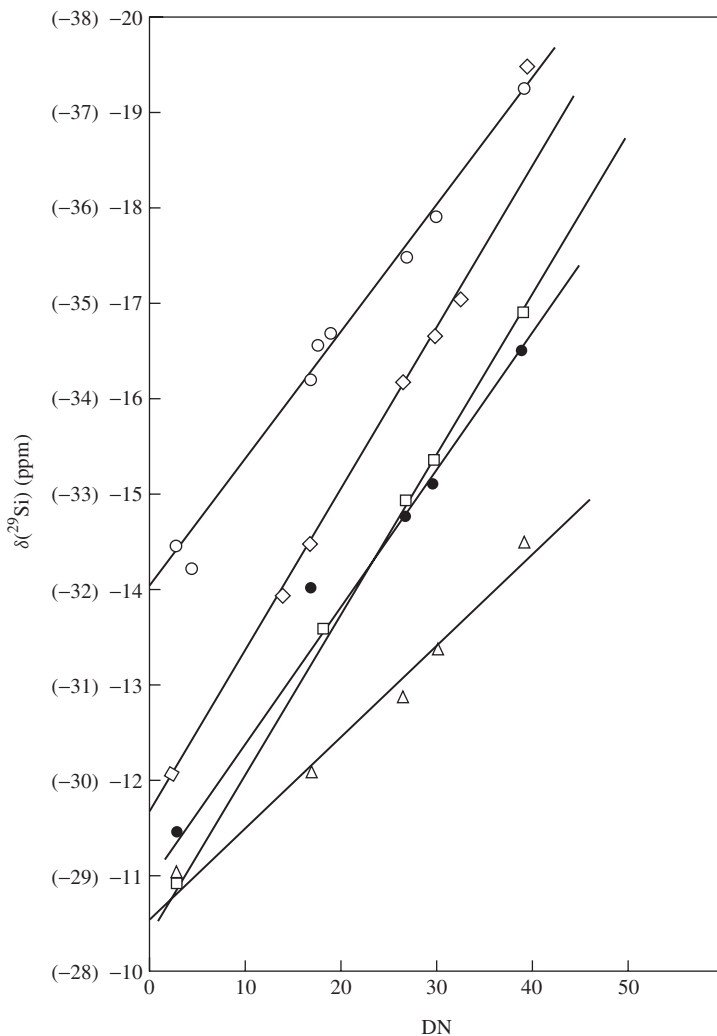


FIGURE 2. ^{29}Si chemical shifts vs solvent donor numbers, DN: ○— Ph_3SiOH ; ◇— $\text{Ph}_2\text{Si(OH)}_2$; □— $(\text{HOSiMe}_2)_2\text{O}$; ●— $\text{HO}(\text{Me}_2\text{SiO})_6\text{H}$; △— $(\text{PhNH})_2\text{SiMe}_2$. The scale in parentheses corresponds to $\text{Ph}_2\text{Si(OH)}_2$. Donor numbers of solvents (DN) were taken from Reference 42. Reprinted from Reference 41, Copyright 1976, with permission from Elsevier Science

in 18 solvents (Figure 3; $r = 0.99$;) and so it could be used for the determination of DN values of several syndone compounds⁴⁴. In view of these dependencies, it is surprising that solvents such as C_6D_6 , CDCl_3 , DMSO-d_6 and THF-d_8 have very little or no effect on the chemical shifts of silanetriols⁴⁵.

The effect of hydrogen bonding propagates (though it is attenuated) through the siloxane chain; even the shifts of inner D units of **1** exhibit good linear correlation with donicity

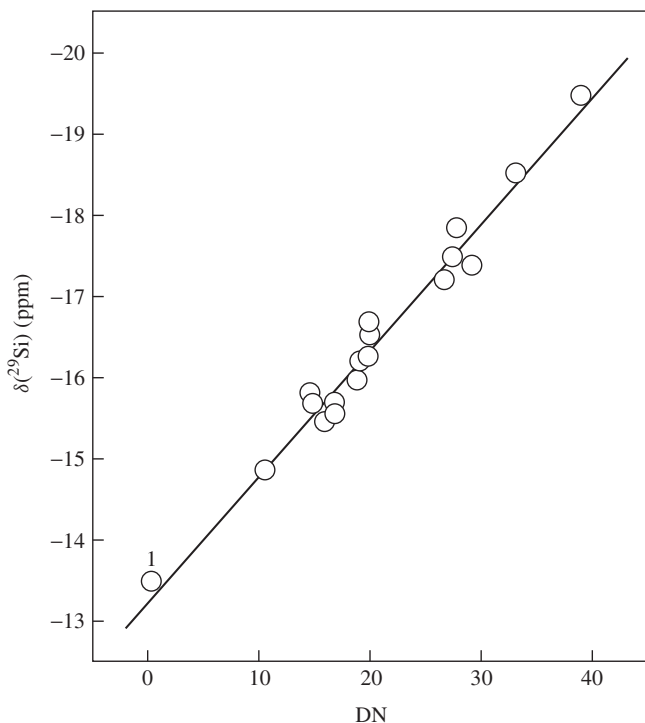
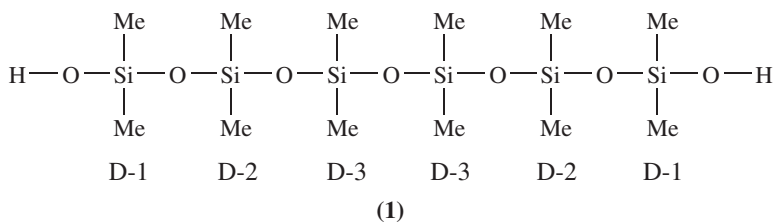


FIGURE 3. ^{29}Si chemical shifts of trimethylsilanol vs. solvent donor numbers, DN. Reproduced by permission of The Chemical Society of Japan from Reference 44

and, as the D-3 units are less sensitive than the D-2 units, the two units alter their order in the spectra in solvents with high DN. Starting from a neat sample **1**, addition of DMSO produces the titration curves shown in Figure 4. The curves indicate preferential hydrogen bonding to DMSO⁴¹.



A completely opposite situation is encountered in siloxanes, alkoxy silanes and other compounds that can act as proton acceptors in hydrogen bonding. In these cases hydrogen bonding shifts the signals to higher frequency (Figures 5 and 6) and titration curves have the same shape as in the previous case (except for the inverse sign of the change)⁴⁶. Proton donor solvents can also change the order of the shifts within one compound⁴⁷.

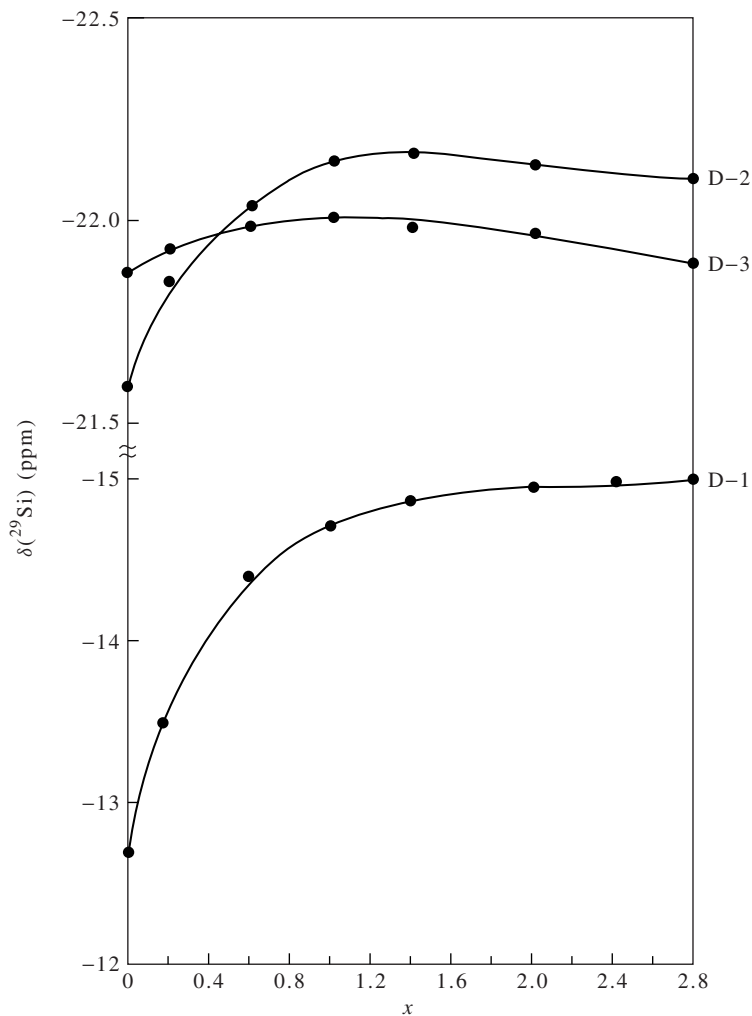


FIGURE 4. ^{29}Si chemical shifts vs mole fraction x of DMSO for the three different silicon atoms in **1**. Reprinted from Reference 41, Copyright 1976, with permission from Elsevier Science

The sensitivity of silicon is different in different steric arrangements; as exemplified in Figure 5, the shifts in 'infinitely dilute solution' in chloroform have a clear relationship to the stereochemistry of the compound⁴⁸ (Figure 7). It is obvious that this steric effect is mediated through the solvent effect. The shift to high frequency is larger as the hydrogen bonding gets stronger, and it gets stronger with increasing basicity and increasing solvent accessible surface of the siloxane oxygen. In view of the gross simplifications involved (constant basicity, molecular geometry), the theoretical dependence of the observed chemical shift on the calculated oxygen accessible

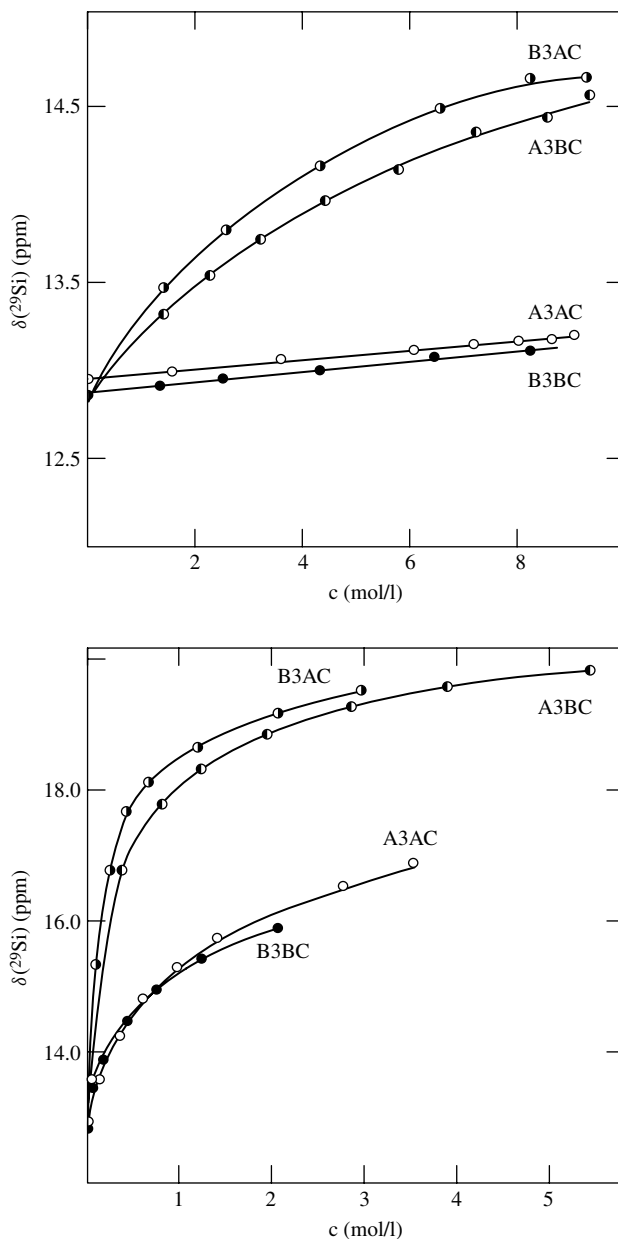


FIGURE 5. ^{29}Si chemical shifts in trimethylsilylated steroids vs. concentration (c) of proton donors: chloroform (top) and phenol (bottom): A3AC — 3α -trimethylsiloxy- 5α -cholestane; A3BC — 3α -trimethylsiloxy- 5β -cholestane; B3AC — 3β -trimethylsiloxy- 5α -cholestane; B3BC — 3β -trimethylsiloxy- 5β -cholestane (for the structures see Figure 7). Reproduced by permission of The Royal Society of Chemistry from Reference 46

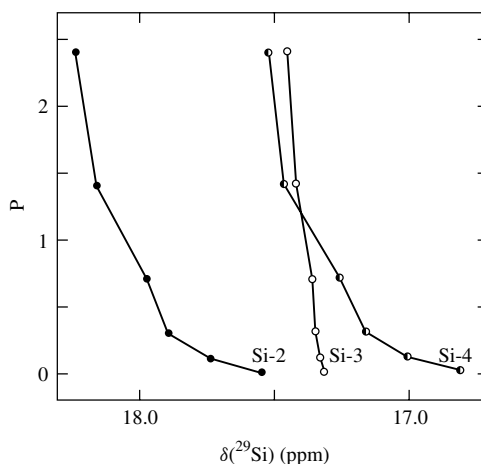
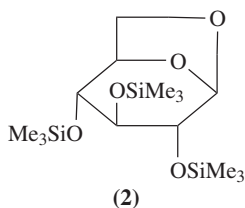


FIGURE 6. ^{29}Si chemical shifts in 2,3,4-tri(*O*-trimethylsilyl)-1,6-anhydro- β -D-glucopyranose (**2**) vs. molar concentration of chloroform in a ternary mixture with C_6D_6 . (*P* is the molar ratio of chloroform to the C_6D_6). Reproduced with permission of Collection of Czechoslovak Chemical Communications from Reference 47



surface predicts the trend correctly⁴⁹ (Figure 8). Chloroform-induced shifts in mono- and bis(trimethylsilyloxy)adamantanes also agree with predictions based on oxygen basicity and accessibility⁵⁰.

Comparison of the chemical shifts shown in Figure 7 with those measured earlier⁵¹, and which could not be satisfactorily interpreted in stereochemical terms, suggests that with a correct choice of solvent some factors contributing to the observed shifts can be made more visible and helpful in structural analysis. Comparison of Hammett-type dependencies of the ^{29}Si chemical shifts in $\text{YC}_6\text{H}_4\text{OSiMe}_3$ measured in neat liquids and in chloroform shows how chloroform suppresses the sensitivity of the ^{29}Si shifts to the substituent effect. Apparently, substituents that increase the shielding of silicon also increase the basicity of oxygen. In chloroform solutions this means a stronger hydrogen bond, which decreases the shielding of the silicon as described above⁵².

Obviously, the solvent effects are not only a nuisance with adverse effects on the reproducibility of measurements, but they can be utilized in a number of ways. Measurement of the chemical shifts of the reaction mixtures of *N*-trimethylsilylimidazole with Me_3SiX ($\text{X} = \text{Cl}, \text{Br}, \text{I}, \text{OCIO}_3, \text{OSO}_2\text{CF}_3$) in three solvents (in which the chemical shifts of the product changed very little with the solvent and counterion, while that of Me_3SiX changed more) proved that the product has a bis-silylimidazolium ion **3** structure and is probably the active silylating species in silylations promoted by *N*-trimethylsilylimidazole⁵³.

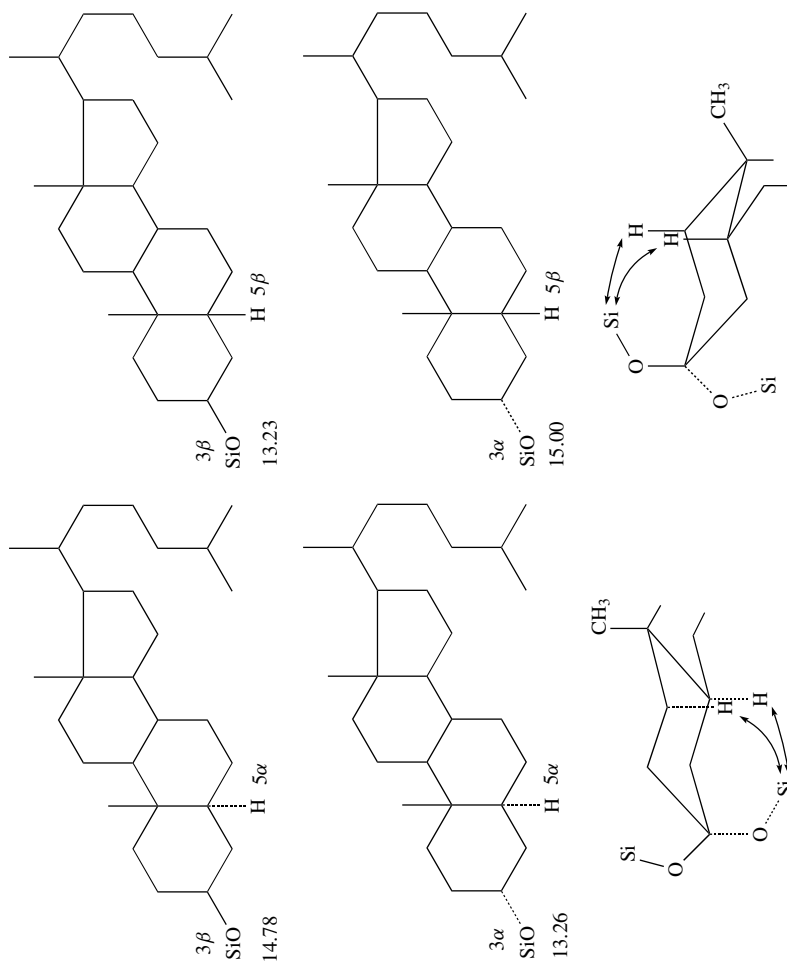


FIGURE 7. Stereochemical arrangement around the silicon in four isomeric trimethylsilylated cholestanols. Si in the Figure stands for the Me₃Si group

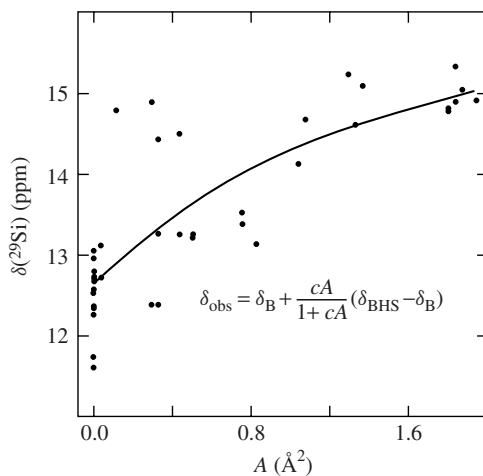
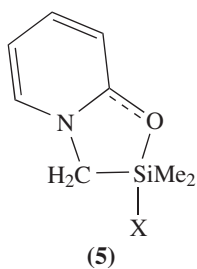
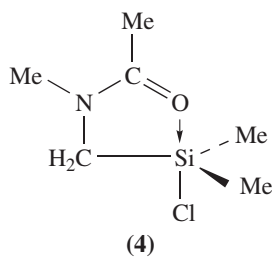
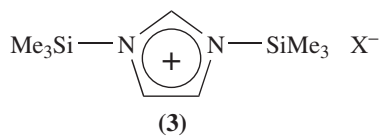


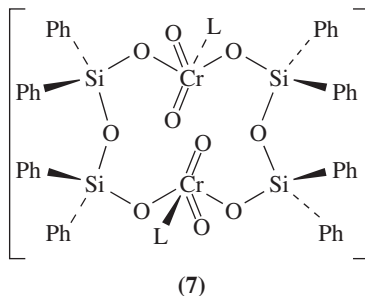
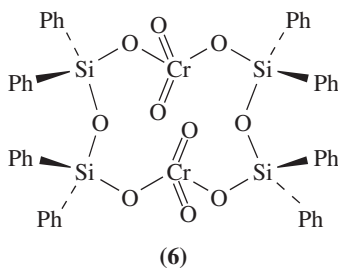
FIGURE 8. The dependence of ^{29}Si chemical shifts on the solvent accessible surface of oxygen (A) in steroids. Reproduced by permission of John Wiley & Sons, Ltd from Reference 49



Solvent, concentration and temperature effects also help in elucidation of a bonding situation. For example, in *N*-methyl-*N*-(dimethylchlorosilylmethyl)acetamide **4** or in its *N*-phenyl analog, the ^{29}Si resonance shifts to low frequency (by 3.2 ppm) when going from dichloromethane to acetone solution or to a lower temperature in these solvents and in methanol (20 ppm when changing from 20 to -90°C). The shift characterizes the compound as the one with the weakest coordinative component of hypervalent O–Si–Cl fragment⁵⁴ according to the criteria established by Voronkov and coworkers^{55,56}. Closely related compounds **5** (with X = Cl, Br) were studied in great detail by Kummer and Halim⁵⁷. They described ^{29}Si chemical shift changes (in the range $\delta = 4$ to -39) with solvent, temperature and concentration, and the changes correlate with changes in the ^{13}C chemical shifts. In these compounds the shifts change as a consequence of changing ionization, dissociation and aggregation equilibria with the solvent. The results were taken as evidence for a reversible transition from $\text{O}\rightarrow\text{SiCl}$ to $\text{OSi}\leftarrow\text{Cl}$ coordination via a true pentacoordinated state with a maximum of the ^{29}Si low frequency shift.

Pestunovich and coworkers⁵⁸ observed that while the chemical shift of methyltrimethoxysilane does not change with the solvent (± 1 ppm), the shift of methylsilatrane varies in the range of 12 ppm with the solvent (and while the shielding of ^{29}Si increases, the shielding of ^{15}N decreases).

A different situation occurs when the 'solvent' reacts with the solute or forms adducts, etc. A nice example is provided by the $[\text{Cr}(=\text{O})_2\{(\text{OSiPh}_2)_2\text{O}\}]_2$ complex (**6**) which has $\delta = -31.91$ in dichloromethane solution, but upon addition of pyridine or tetrahydrofuran it shifts to -40.36 or -39.61 ppm, respectively. This change is caused by formation of an adduct **7** where L is pyridine or tetrahydrofuran⁵⁹.



Measurements in different solvents (and different temperatures) are sometimes used to model reaction or bonding conditions⁶⁰ or to replace internal coordination by coordination of the solvent⁶¹. A frequently used silylating reagent, hexamethyldisilazane, HMDSN, was measured in a few solvents and at two temperatures. In contrast to its ¹H and ¹³C shifts, the ²⁹Si shift depends on both the solvent and temperature, although the overall range is small ($\delta = 1.9 - 2.5$)⁶².

The effects of various halomethanes and halosilanes as solvents on the ¹J(²⁹Si–¹⁹F) coupling in SiF₄ reported by Coyle and coworkers^{63–65} were analysed by Raynes⁶⁶. They found that seventeen of the observed couplings (ranging from 169.97 Hz in liquid SiF₄ to 176.83 Hz in CCl₄) can be calculated (with a mean positive deviation of calculated from observed coupling of only 0.12 Hz) using an additive scheme in which each C–X or Si–X bond in the solvent is described by an additive parameter that bears a relationship to the polarizabilities of the atoms. The same coupling is also concentration-dependent⁶³, e.g. in TMS it changes from 174.68 Hz to 173.78 Hz when going from 15 to 50% solution.

Going from C₆D₆ to THF solution increases spin–lattice relaxation time T_1 by 25–30% in the *cis*-isomer but leaves almost unchanged relaxation in the *trans*-isomer of 2,4,6-trimethyl-2,4,6-triphenylcyclotrisiloxane⁶⁷.

The spin–lattice relaxation time, T_1 , of ²⁹Si is shortened in viscous solvents much more than the spin–spin relaxation time, T_2 . Hence, measurement of the spectra can be hastened in viscous solvents (glycerol, toluene/polystyrene mixtures) without significant broadening of the ²⁹Si lines⁶⁸. This approach to increase ²⁹Si NMR performance could not be accepted in organosilicon chemistry for a number of obvious chemical reasons.

As has been shown, several solvents produce specific effects on chemical shifts, and care should be taken when assigning lines or structures on the basis of comparison of chemical shifts obtained in different solvents or when using literature data with no experimental details given.

V. SENSITIVITY ENHANCEMENTS

In general, pulsed Fourier transform NMR spectroscopy techniques (FT NMR) have brought a large improvement in time performance, i.e. a reduction in the time required to obtain spectra, compared to the older CW measurements (for details of CW techniques see elsewhere^{13,69}). In the case of ²⁹Si nuclei, FT NMR measurements are hampered as mentioned above (Section II) by slow relaxation and a negative NOE that further reduce the sensitivity below that already present from the natural abundance and low γ value. Although both adverse effects can be eliminated by means of addition of a relaxation reagent (Section X.E), other means are often preferable. Conventional FT NMR measurements of proton-decoupled ²⁹Si NMR spectra employ so-called inverse gated decoupling (IGD) to minimize NOE. IGD uses proton (or any other γ -positive nucleus) decoupling only during FID data acquisition and leaves a long relaxation delay without decoupling (this gating of the decoupler is just the opposite or inverse of that used for measurement of coupled spectra with NOE enhancement, e.g. in ¹³C NMR spectroscopy). The method is based on the different time dependence of decoupling and NOE buildup^{70,71}; its application is a trivial matter.

Other available enhancement schemes are based on scalar J spin–spin couplings of silicon-29 with nuclei of higher γ and higher abundance, most commonly with protons. The J -coupling based schemes achieve a potentially greater enhancement, and the measurements proceed faster since the repetition rate is governed by the proton relaxation rate, which is usually faster than that of silicon. The mechanism for the larger enhancement is polarization transfer. Nuclei with higher γ have a larger difference between NMR

energy level populations, i.e. a larger polarization. The polarization transfer experiment transfers the large population difference to the low γ (NMR insensitive) nuclei, so that the difference of their (non-equilibrium) populations is increased.

The experiments to be described can be classified either as population transfer (PT) or as cross-polarization (CP) experiments. The former is also termed ‘spin-order transfer by radio frequency (rf) pulses’ as it employs either selective rf pulses (SPT experiments) or a series of properly timed pulses (INEPT, DEPT) to transfer the population in a non-selective manner. The latter is based on subjecting protons and silicon nuclei to their resonant rf fields simultaneously for time τ (cross-polarization time). If the two fields satisfy the so-called Hartmann–Hahn condition, protons periodically exchange their magnetization with the silicon nuclei. These experiments are therefore sometimes also referred to as ‘spin-lock PT’^{30,72} or ‘spin-order transfer under an average Hamiltonian’⁷³ when multiple-pulse sequences are invoked to satisfy the Hartmann–Hahn condition for wider chemical shift ranges. Although the picture might change, CP experiments have thus far found limited use in ^{29}Si NMR of liquids (of course, Hartmann–Hahn cross-polarization⁷⁴ utilizing dipolar couplings is used extensively in solid-state ^{29}Si NMR⁷⁵). We shall discuss several experiments of this type (JCP, RJCP, ACP, ADRF) in Section V.C, while other PT experiments will be treated in Sections V.A and V.B in more detail as they have been used extensively in ^{29}Si NMR of organosilicon liquids.

All these experiments require, however, some *a priori* knowledge or estimate of the coupling constant to be employed in the enhancement. They yield proton coupled or decoupled ^{29}Si NMR spectra and can often be modified for line assignment purposes.

An SPT experiment requires identification of at least one ^{29}Si satellite in the ^1H NMR spectrum; non-selective experiments (INEPT, DEPT) and JCP require for optimum performance an estimate of the coupling constant, and the correct estimate of the number of coupled protons improves the performance of INEPT and DEPT experiments. While an SPT experiment achieves enhancement through one selective irradiation, the other methods use series of pulses. The group of experiments that are referred to here as ‘non-selective’ use a series of properly timed pulses, and JCP, which is also non-selective, differs from them in that it uses a train of pulses known as a spin-lock.

All of these methods increase the ^{29}Si signal intensity in one transient. Additional improvement in time performance is obtained by the increased pulse repetition rate, as it is now governed by the faster proton relaxation. Proton relaxation can be further accelerated by the SNARE (Sensitive-Nucleus Accelerated Relaxation for Enhancement) method⁷⁶, though its usefulness for ^{29}Si NMR remains to be seen.

A. Selective Polarization Transfer (SPT)

The physics behind SPI (Selective Polarization Inversion)⁷⁷ or SPT (Selective Polarization Transfer)^{78,79} experiments is described and explained in every current NMR textbook, since it provides a nice introduction to understanding some of the more common current experiments (e.g. INEPT or 2D homo- and heteronuclear correlation experiments). The two names, SPI and SPT, are used indiscriminately for the same experiment, although in general SPI might be considered a special case of an SPT experiment with maximum polarization transfer achieved by inversion⁷⁸.

The experiment is very simple—one line of a multiplet is selectively inverted (by a selective 180° pulse of duration τ) immediately before the usual non-selective read pulse is applied and the FID sampled. The Fourier transform then yields the whole spectrum with altered line intensities. Populations of the energy levels connected by the selectively irradiated line are changed (inverted) by the selective pulse, and this leads to changes in

Applications of SPT experiments (recently more or less monopolized by French research groups) are usually aimed not only at ^{29}Si signal enhancement but also at their assignment (through correlation with an assigned ^1H NMR spectrum) and at determination of the number of coupling constants and their relative signs^{86–89}.

The relative signs of coupling constants can be determined by SPT experiments as demonstrated in Figure 9 on the $^3J(^1\text{H}-^1\text{H})$ and $^1J(^{29}\text{Si}-^1\text{H})$ couplings in $[(\text{CH}_3)_2\text{HSi}]_2\text{O}$ ⁸⁰. In this case each line of the satellite doublet of CH_3 protons (separated by $|^2J(^{29}\text{Si}-^1\text{H})| = 7.12$ Hz) is further split into a doublet by $|^3J(^1\text{H}-^1\text{H})| = 2.8$ Hz in the proton spectrum. Inversion of the ^1H line with the lowest frequency gives rise to the SPT spectrum shown (a septet of doublets at low frequency within the large $|^1J(^{29}\text{Si}-^1\text{H})| = 205.4$ Hz doublet in the ^{29}Si spectrum). The same effect is seen in the high frequency part of the $^1J(^{29}\text{Si}-^1\text{H})$ doublet when the selective pulse is applied at 2.8 Hz [$^3J(^1\text{H}-^1\text{H})$] higher frequency. Therefore $^3K(^1\text{H}-^1\text{H}) \cdot ^1K(^{29}\text{Si}-^1\text{H}) > 0$ (where the reduced coupling is defined as $K_{ij} = 4\pi^2 J_{ij} / h\gamma_i\gamma_j$), and the two reduced couplings have the same sign. Considering the negative γ_{Si} , the coupling constants have opposite signs.

The coupling constant values and sometimes also their relative signs can be obtained by a detailed analysis of the SPT spectra using simulation programs^{90,91}. The procedure as well as the basis of the SPT experiment is described by Grignon–Dubois and Laguerre⁹⁰ very lucidly, especially for a non-specialist; the self-explanatory Figure 10 is reproduced from that source.

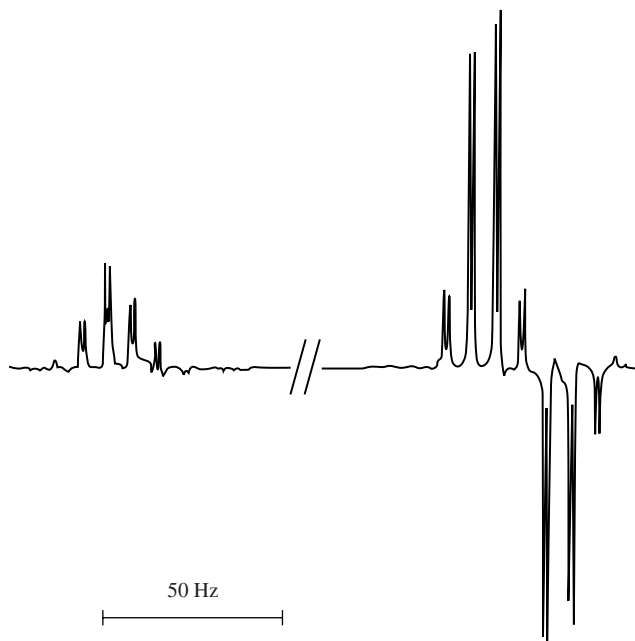


FIGURE 9. ^{29}Si SPT NMR spectrum of $[(\text{CH}_3)_2\text{HSi}]_2\text{O}$: determination of relative signs of coupling constants (acquisition time 4 s). Reprinted with permission from Reference 80. Copyright 1975 American Chemical Society

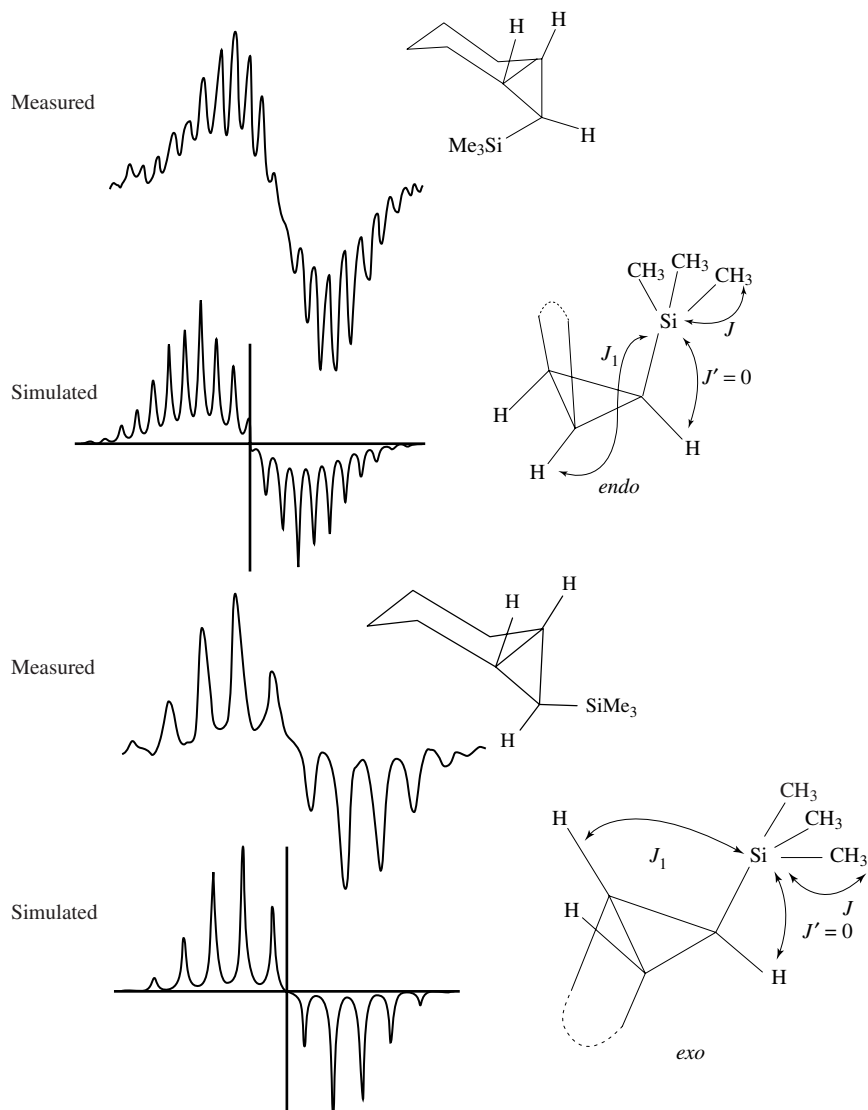


FIGURE 10. ^{29}Si SPT NMR spectra (measured and simulated) of cyclopropane derivatives. Reproduced with permission of M. Grignon-Dubois from Reference 90

When the SPT spectra become too complicated, they can be simplified by selective proton decoupling during the acquisition^{92,93}; of course, the splittings in these spectra are the so-called residual splittings⁹⁴, J_R . In order to get the true values of the coupling constants, the residual splittings must be corrected for the effect of the decoupling field⁹⁵ as in any other off-resonance decoupling experiment.

Two types of doubly selective polarization transfer (DSPT) experiments were suggested. Harris and coworkers⁹⁶ proposed an experiment in which selective inversion of a ^{29}Si satellite is followed by inversion of a ^{29}Si line. The experiment could save some time in measurements of spin–lattice relaxation time but it has been overcome by INEPT variants. The second experiment selectively inverts X and Y satellites of rare nuclei in ^1H NMR spectrum and then the NMR signal from one of the two nuclei is recorded⁹⁷. The spectrum contains the satellites of the other rare nucleus with enhanced intensity, thus allowing measurements of coupling constants between rare nuclei.

One could imagine a number of improvements or modifications of the SPT experiment, but since Morris and Freeman introduced the INEPT experiment in 1979⁹⁸, authors have directed their efforts into modifying and improving the INEPT experiment since it had certain advantages over SPT. (Later, some of these developments were also incorporated into the SPT experiments; refocusing and decoupling during the acquisition yielded selectively enhanced lines of a single nucleus⁸¹.) The advantages of the INEPT experiment (no need to measure the ^1H spectrum and create the selective pulse) that were very important in the past, lost some of their importance with the construction of multinuclear probes and waveform generators being available. However, the lack of generality remains; to achieve polarization transfer for all non-equivalent nuclei in the sample, the SPT experiment must be performed repeatedly for each and every one of them. The INEPT does it simultaneously for all ^{29}Si resonances in a single one-step experiment, which is why the INEPT experiment has been so popular since 1980.

B. Non-selective Polarization Transfers (INEPT, DEPT, PENDANT, PASSADENA and Their Variants)

Non-selective methods of polarization transfer enhance the signal of silicon as do SPT experiments, but in contrast do not require the exact position of the ^{29}Si satellite—an approximate estimate of the coupling constant(s) is enough to get all silicon nuclei with similar couplings enhanced in one experiment. Hence it is no surprise that since its invention by Morris and Freeman⁹⁸ in 1979, INEPT has quickly become not only one of the indispensable methods of the NMR arsenal on its own (with several modifications), but it has also been used as a building block in a number of other useful pulse sequences. INEPT (*Insensitive Nuclei Enhanced by Polarization Transfer*) was soon followed by the discovery of DEPT (*Distortionless Enhancement by Polarization Transfer*)⁹⁹ which produces coupled spectra with ordinary splitting patterns. The tremendous potential of these methods for ^{29}Si (and ^{15}N) NMR was obvious to the authors of both schemes¹⁰⁰, as well as the possibility of also employing long-range Si–H couplings for the polarization transfer¹⁰¹. This was demonstrated convincingly by Helmer and West¹⁰² who obtained significant enhancements, close to theoretical values, even when the couplings were as small as 3.7 Hz [$^3J(^{29}\text{Si}-^1\text{H})$ in $(\text{MeO})_4\text{Si}$]. The possibility of using INEPT as a routine method for measurement of ^{29}Si NMR spectra of trimethylsilyl derivatives [in which $^2J(^{29}\text{Si}-^1\text{H})$ varies only slightly around 6.7 Hz] was stressed by Schraml¹⁰³. Figure 11 illustrates the tremendous gain in sensitivity in a routine INEPT application to a compound with an unknown exact value of the coupling constant. It was shown analytically that INEPT spectra of these derivatives that were set up for $J(^{29}\text{Si}-^1\text{H}) = 6.7$ Hz have better signal-to-noise ratio than IGD spectra unless the true J is either smaller than 2 Hz or larger than 12 Hz, which is far beyond the range of found values¹⁰³.

A refocused INEPT experiment^{100,104}, also referred to as INEPTR¹⁰⁵, which allows proton broad-band decoupling during acquisition, is performed as the following

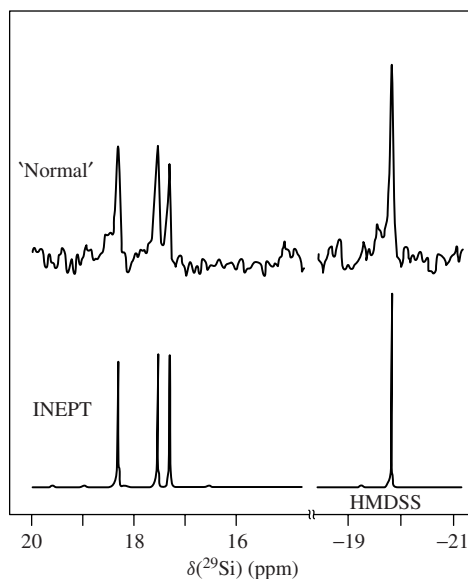


FIGURE 11. Routine INEPT (bottom) and 'normal' ^{29}Si NMR spectra of 0.1 M solution of 2,3,4-tri(*O*-methylsilyl)-1,6-anhydro- β -D-glucopyranose (**2**) with 1% of HMDSS measured at 39 MHz; the two spectra were acquired in the same measuring time. Reproduced with permission of Collection of Czechoslovak Chemical Communications from Reference 103

pulse sequence:

$$\begin{array}{l}
 {}^1\text{H} : 90_x^\circ - \tau - 180_x^\circ - \tau - 90_y^\circ - \Delta/2 - 180_x^\circ - \Delta/2 - (\text{decouple}) \\
 {}^{29}\text{Si} : \quad 180_x^\circ \quad 90_x^\circ \quad 180_x^\circ \quad \text{acquire}
 \end{array}$$

and DEPT^{99,106}

$$\begin{array}{l}
 {}^1\text{H} : 90_y^\circ - 2\tau - 180_x^\circ - 2\tau - \theta_x^\circ - 2\tau - (\text{decouple}) \\
 {}^{29}\text{Si} : \quad 90_x^\circ \quad 180_x^\circ \quad \text{acquire}
 \end{array}$$

These sequences produce enhanced proton decoupled ^{29}Si NMR spectra. Coupled spectra can be measured by the same sequences as described below. For the simple case of one silicon coupled to n equivalent protons, the optimum settings of delays τ and Δ and pulse θ° is^{99,106,107}:

$$\tau = 1/(4J)$$

$$\Delta = \arcsin(n)^{-1/2}/(\pi J)$$

$$\theta^\circ = 180^\circ \cdot \arcsin(n)^{-1/2}/\pi$$

With optimum settings the achievable enhancement for decoupled experiments is

$$E_{d,\text{opt}} = (\gamma_{\text{H}}/\gamma_{\text{Si}})n^{1/2}(1 - 1/n)^{(n-1)/2}$$

for both INEPT^{101,106,107} and DEPT¹⁰⁸. Obviously, the enhancement which increases with n is larger than that provided by NOE ($\gamma_{\text{H}}/2\gamma_{\text{Si}}$), even for $n = 1, 2$ [$E_{d,\text{opt}} =$

($\gamma_{\text{H}}/\gamma_{\text{Si}}$). For example, it reaches 9.4 for the nine protons of a trimethylsilyl group or 15.9 for the 27 protons coupled to the central silicon of the hypersilyl group, $\text{Si}(\text{SiMe}_3)_3$. Note also that the refocusing delay, Δ , gets shorter with larger n , thus reducing the adverse effect of relaxation. Similarly, as in SPT experiments, additional gain of the order of $(T_{1\text{Si}}/T_{1\text{H}})^{1/2}$ is achieved by the faster pulse repetition rate allowed by the (usually) shorter spin–lattice relaxation time T_1 of proton ($T_{1\text{H}}$) than silicon ($T_{1\text{Si}}$).

These simple formulas get considerably involved when all of the n protons coupled to silicon are not equivalent, have different couplings with silicon, $J(\text{SiH}^p)$, and exhibit homonuclear ^1H – ^1H couplings, $J(\text{H}^p\text{H}^q)$. Formulas describing the enhancement were derived numerically by Schenker and von Philipsborn¹⁰⁸ and analytically by Blechta and Schraml¹⁰⁹. Repeated analysis confirmed the formulas¹¹⁰. The derived formulas for the decoupled variants are:

$$E_{\text{INEPT,dec}} = \frac{\gamma_{\text{H}}}{\gamma_{\text{Si}}} \sum_p \sin[\pi\tau J(\text{SiH}^p)] \sin[\pi\Delta J(\text{SiH}^p)] \\ \times \prod_q \cos[\pi\tau J(\text{H}^p\text{H}^q)] \cos[\pi\Delta J(\text{SiH}^q)]$$

and

$$E_{\text{DEPT,dec}} = \frac{\gamma_{\text{H}}}{2\gamma_{\text{Si}}} \sum_p \sin^2[\pi\tau J(\text{SiH}^p)] \sin\theta \prod_q \cos[\pi\tau J(\text{H}^p\text{H}^q)] \{\cos^2[\pi\tau J(\text{SiH}^q)] \\ + \cos\theta \sin^2[\pi\tau J(\text{SiH}^p)]\}$$

Obviously, optimization of the sequences is more difficult, but both sequences provide good enhancement even for non-optimum settings. Although homonuclear ^1H – ^1H couplings can be obtained from ^1H NMR spectra, the values of different ^{29}Si – ^1H couplings can usually be only estimated. It should be noted, however, that in these cases it is the INEPT experiment that is less prone to perturbation by additional homo- and heteronuclear couplings¹⁰⁸. (These formulas also explain why the suggested performance test for spectrometers based on INEPT and DEPT spectra of hexamethyldisiloxane¹¹¹ could not be accepted.) Optimization for siloxanes was discussed at great detail^{110,112}.

Proton coupled ^{29}Si NMR spectra are obtained simply by eliminating decoupling during the acquisition period in the above given pulse sequences. The apparent inequality in the enhancement of the two parts of the INEPT multiplets is, as in SPT spectra, due to the initial equilibrium population of silicon states; it can be eliminated by a 90° pulse on ^{29}Si prior to the start of the sequence¹⁰⁴. Phase and multiplet anomalies that may be present in coupled refocused INEPT spectra are easily eliminated by introducing a 90° purging proton pulse immediately before data acquisition (INEPT⁺)¹¹³. Similar elimination of artifacts from coupled DEPT spectra requires considerable extension of the sequence (DEPT⁺⁺)¹¹³. When spin–spin relaxation is fast, coupled INEPT spectra can be obtained by also eliminating the entire refocusing period ($\Delta/2 - 180 - \Delta/2$) from the above INEPT sequence. This reduced sequence is the basic INEPT sequence⁹⁸, which produces spectra with multiplets due to the coupling employed in the polarization transfer in antiphase (while other splittings remain in phase), as in SPT spectra.

The undesirable off-resonance effects become important in high field spectrometers. Schenker and von Philipsborn¹¹⁴ analysed them and found that they can be partly diminished by phase cycling and composite pulses, but a better solution would be increased rf intensities to shorten the pulses in both observing and decoupling channels.

To compensate for a broad range of coupling constants encountered within one sample, Wimperis and Bodenhausen¹¹⁵ developed Broadband-INEPT which includes six more pulses and four more delays, but the need for broadband-INEPT has apparently not yet been sufficiently felt in ²⁹Si NMR just as better refocusing of INEPT CR¹¹⁶ went unnoticed in the organosilicon community.

The use of the basic INEPT and DEPT sequences in the field of ²⁹Si NMR of organosilicon compounds (especially polysilanes and siloxanes) was tested by Blinka and colleagues¹¹⁷, although they also listed some modifications available at that time. Their findings can be summarized as follows: (i) for small couplings ($J < 10$ Hz) or fast spin-spin relaxation (short T_2 due, e.g., to the presence of quadrupolar nuclei such as ¹⁵N or ³⁵Cl), the INEPT sequence, the shorter of the two, is superior to DEPT (despite the larger number of pulses), and (ii) coupled DEPT spectra that have a 'normal' splitting pattern tend to be better resolved than the corresponding INEPT spectra. Another observation (iii) that DEPT is less sensitive to variation in J values (because θ° is independent of J), is obviously (see formulas for enhancements) an oversimplification.

In view of the subsequent developments¹¹⁸, the recommendations for a potential user would be: for decoupled spectra when only enhancement is required—use INEPT (it is shortest); for spectral editing—use DEPT (less cross talk); for coupled spectra use INEPT⁺ or, if antiphase multiples can be tolerated, use INEPT. To enhance the uniformity of excitation over larger J ranges, experiments measured with different τ values can be added.

Non-refocused INEPT spectra can be used to determine both ²⁹Si–¹H and ¹H–¹H couplings (but not their signs) in a manner similar to that described earlier for SPT spectra. The INEPT spectra are measured with several τ values chosen almost arbitrarily and then a simulation program¹¹⁹ is used to determine the exact values of the coupling constants^{120,121}.

In ¹³C NMR spectroscopy the dependence of INEPT and DEPT on n (number of equivalent protons) is utilized for spectral editing—separating the spectra of carbons with different numbers of equivalent protons directly attached ($n = 1, 2, 3$; multiplicity editing)¹²². This simple method has only limited use in ²⁹Si NMR and thus is seldom used for obvious chemical reasons (for an example of its use see Reference 123). The structure of organosilicon compounds requires a more complex approach as n is usually larger (than 3) and involves non-equivalent protons. Two techniques worth mentioning in this context are DEPT editing of the spectra of alkoxyalkylsilanes¹²⁴ and identification of ²⁹Si signals of trimethylsilyl groups in silylated sugars according to the ¹H–¹H couplings in the sugar backbone¹²⁵. On the basis of the above formula for $E_{\text{DEPT,dec}}$, the former method selects suitable combinations of θ and τ that lead to different enhancements in the different groups present and thus allows their differentiation as illustrated in Figure 12. Using the analogous formula for INEPT enhancement, $E_{\text{INEPT,dec}}$, involving homonuclear couplings, the latter method chooses a range of Δ values ('geometrical imprint domain') such that a few INEPT experiments with Δ from the domain will allow one to assign the ²⁹Si signals according to the spatial environment around these silicon atoms. The method does not require assigned ¹H NMR spectra but an estimate of ²⁹Si–¹H couplings as well as the usual values of geminal and vicinal ¹H–¹H couplings (axial–axial, axial–equatorial etc.). The method is illustrated in Figure 13 on an example of methyl 2,3,4,6-tetra(*O*-trimethylsilyl)- β -D-galactopyranoside (**8**).

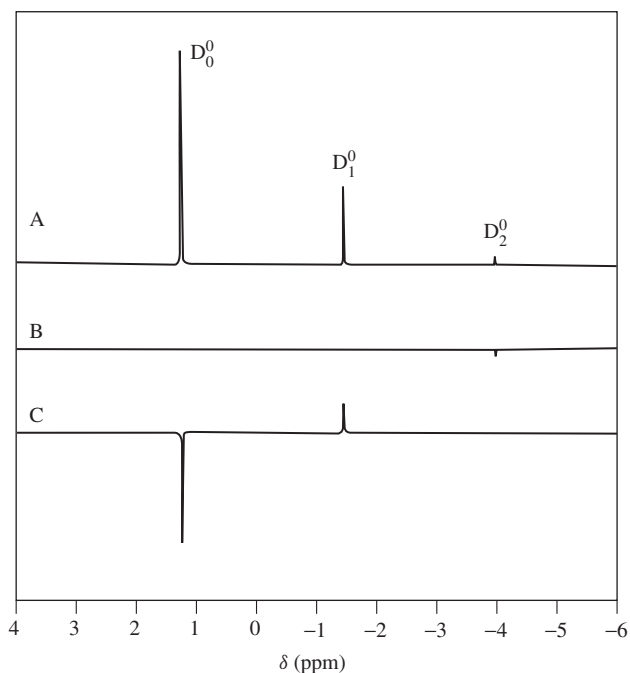


FIGURE 12. ^{29}Si NMR spectra of 2.24 M dimethyldimethoxysilane (D_0^0) hydrolysis leading to dimethylmethoxysilanol (D_1^0) and dimethylsilanediol (D_2^0). DEPT pulse sequence with the following parameters: (A) $\tau = 70$ ms, $\theta = 20^\circ$; (B) $\tau = 70$ ms, $\theta = 160^\circ$; (C) $\tau = 140$ ms, $\theta = 150^\circ$. The three species are identified unambiguously by these spectra. Reprinted from Reference 124, Copyright 1997, with permission from Elsevier Science

Recently a new pulse sequence PENDANT (*Polarization Enhancement Nurtured During Attached Nucleus Testing*) was suggested^{126–128}:

$$\begin{array}{l}
 {}^1\text{H} : 90_x^\circ - \tau - 180_x^\circ - \tau - 90_{-y}^\circ - \Delta/2 - 180_x^\circ - \Delta/2 - (\text{decouple}) \\
 {}^{29}\text{Si} : 90_x^\circ \quad 180_x^\circ \quad 90_{-y}^\circ \quad 180_x^\circ \quad \text{acquire}
 \end{array}$$

where the delay $\Delta = 5/(4J)$ and τ has the same value as in INEPT. This sequence yields decoupled spectra that show alternating phases of quaternary, CH, CH_2 and CH_3 carbon resonances (and similarly for silicon analogues), but it also enables the simultaneous detection of all these resonances with enhancements comparable to those of INEPT. The sequence must be modified in order to obtain also undistorted coupled spectra¹²⁷. Application of the basic sequence to the measurement of decoupled ^{29}Si spectrum of tetramethylsilane has demonstrated the importance of the lengths of the final delay for achieved signal intensity¹²⁷.

Tremendous gains in sensitivity can be obtained in hydrogenation studies when parahydrogen labeling can be employed. The PASADENA (*Parahydrogen And Synthesis Allow Dramatically Enhanced Nuclear Alignment*) effect originates from the breakdown of parahydrogen symmetry when the two protons are found in non-equivalent positions after hydrogenation. (For the theory behind the experiments, see References 129 and 130.) Two

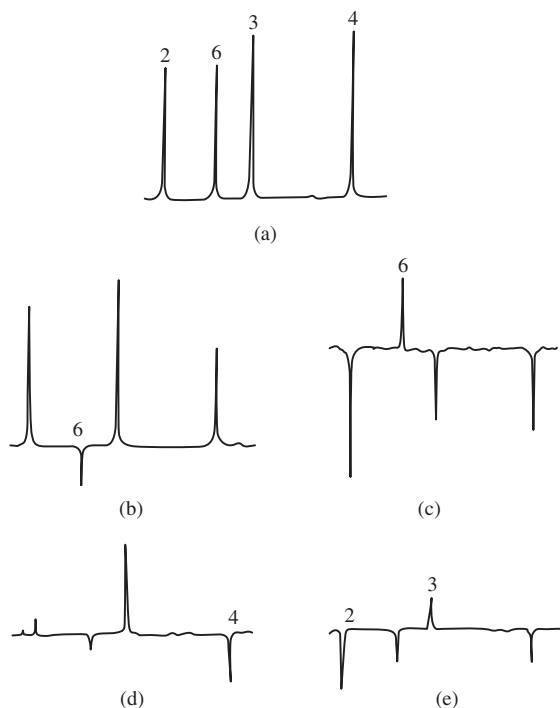
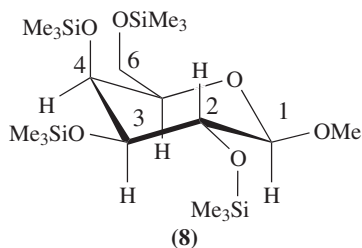
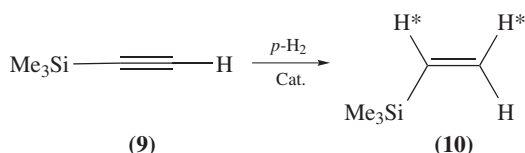


FIGURE 13. Edited refocused and decoupled INEPT spectra of methyl 2,3,4,6-tetra(*O*-trimethylsilyl)- β -D-galactopyranoside (**8**): (a) $\tau = 35.7$ ms, $\Delta = 20$ ms, optimal enhancement; (b) $\tau = 35.7$ ms, $\Delta = 289.6$ ms, edited according to even/odd number of active couplings; (c) $\tau = 35.7$ ms, $\Delta = 320.0$ ms, edited according to even/odd number of active couplings; (d) $\tau = 35.7$ ms, $\Delta = 160.0$ ms, edited according to homo- and heteronuclear couplings—geometrical imprint domain; (e) $\tau = 60$ ms, $\Delta = 145.0$ ms, edited according to homo- and heteronuclear couplings—geometrical imprint domain. Reproduced by permission of John Wiley & Sons, Ltd from Reference 125



types of experiments must be distinguished. When hydrogenation is carried out outside the spectrometer and the sample is subsequently transported for detection into the spectrometer, the experiment is referred to as an ALTADENA (*A*diabatic *L*ongitudinal *T*ransport *A*fter *D*issociation *E*ngenders *N*et *A*lignment) experiment, while when hydrogenation and NMR detection are carried out inside the NMR spectrometer the experiment is also termed

PASADENA. The use of parahydrogen calls for modifications of INEPT. Three modifications have been proposed: (1) PH-INEPT (*Para Hydrogen INEPT*) replaces the first 90° proton pulse of the basic (coupled and not refocused INEPT) by a 45° pulse; it yields signals stemming solely from the parahydrogen product; (2) PH-INEPT⁺ adds a refocusing period to PH-INEPT, and (3) PH-INEPT($+\pi/4$) is just the basic (coupled and not refocused INEPT) in which a 45° pulse is inserted between the last proton pulse and the beginning of data acquisition. The PH-INEPT depends critically on homonuclear ^1H – ^1H couplings; in their absence the sequence cannot be used and PH-INEPT($+\pi/4$) should be used. (For more details see Reference 131 and references cited therein.) The application to hydrogenation of trimethylsilylthyne (**9**), which yields trimethylvinylsilane (**10**) (in which H* denotes hydrogen atoms coming from *para*-hydrogen $P\text{-H}_2$), is shown in Figure 14.



A number of authors have utilized the non-selectivity of INEPT and DEPT in combination with selective decoupling for assignment purposes; usually, the imagination of the authors is limited only by the available hardware. The simplest is decoupling of the protons used as a vehicle in polarization transfer; this INEPT variant (dubbed as SPINEPTR) of the method used earlier by the Harris group¹³² without polarization enhancement requires only different power levels in the decoupler channel during pulses and acquisition¹³³. It does not require either shaped decoupling pulses or changes in frequency offsets and produces ^{29}Si NMR spectra that show residual splittings due to couplings with protons not decoupled (Figure 15). (A more reliable sequence for the same experiment was published¹³⁴ under the name of BINEPTR²¹; it uses slightly modified refocusing and phase cycling.) The hardware of current spectrometers (namely a waveform generator in a decoupler channel and the possibility to program decoupling during acquisition) allows one to combine INEPT with any selective (narrow, band selective or broad band) decoupling method; the aspects to consider were discussed recently by Kupče and Wrackmeyer¹³⁵. As in any experiment where decoupling is performed during acquisition, one should be aware that the splittings seen in the spectra are residual splittings and the proton chemical shifts are altered by Bloch–Siegert shifts. However, as Figure 16 illustrates, use of this combination for ^{29}Si line assignment is straightforward and the shortest basic INEPT pulse sequence (without refocusing) can be used for such a purpose^{136–138}.

Of course, these polarization schemes are not limited to $^1\text{H} \rightarrow ^{29}\text{Si}$ polarization transfer. If needed, another abundant nucleus with gyromagnetic ratios larger than silicon can be used (e.g. ^{31}P or ^{19}F , providing the required hardware is available)¹³⁹. Similarly, such nuclei can be decoupled in order to simplify the spectra measured with polarization transfer from protons and vice versa, e.g. ^{29}Si – ^1H (^{31}P) INEPT or (^{29}Si) INEPT(^1H , ^{31}P) (i.e. INEPT that used ^1H polarization transfer and ^{31}P decoupling) was used to prove the structure of a ruthenium bis(silane) complex¹⁴⁰ or for determination of $J(^{29}\text{Si}$ – $^{195}\text{Pt})$ couplings¹⁴¹. There is no consent how should such experiments be denoted. While $\{^{31}\text{P}\}$ -INEPT stands for INEPT which utilized polarization transfer from ^{31}P nuclei¹³⁹, this notation become unclear when decoupling of (3^{rd}) another nucleus is involved as described here. Obviously, these experiments fall into the triple resonance category (Section VI.B).

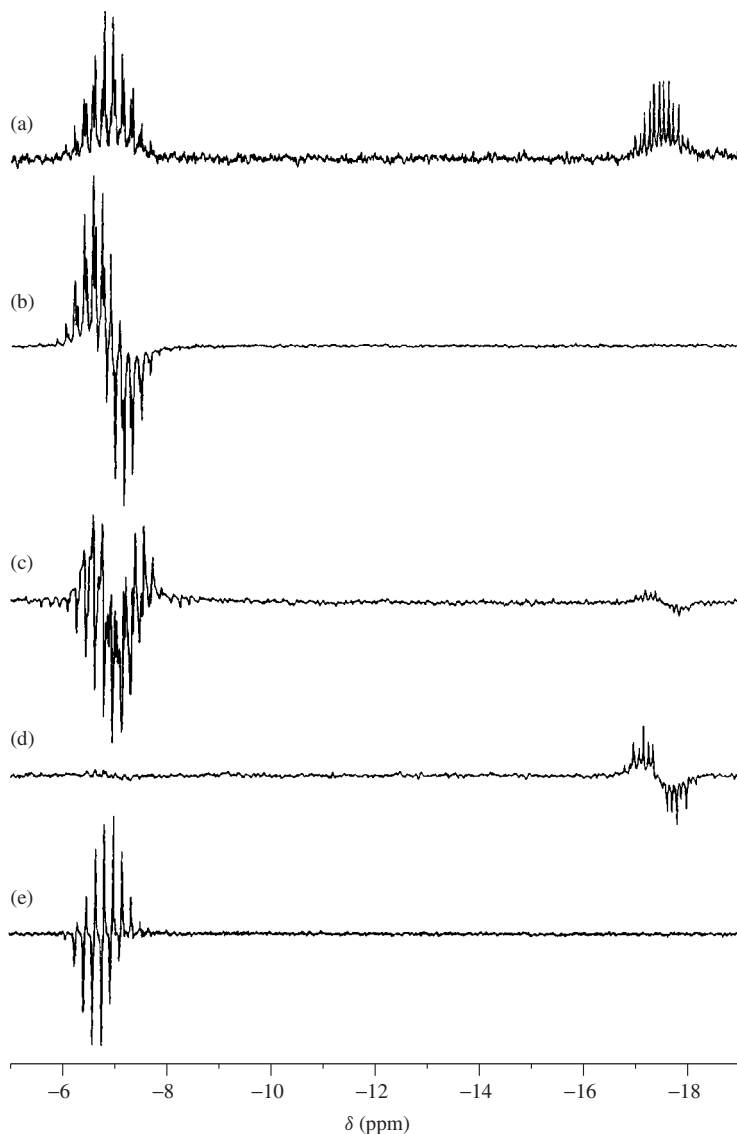


FIGURE 14. ^{29}Si spectra (at 39 MHz) of **9** ($\delta = -17.5$) and **10** ($\delta = -6.5$): (a) **9** and **10** at thermal equilibrium; (b) ^{29}Si PH-INEPT spectrum (8 scans; $2\tau = 0.032$ s) of **10** after a total of 1 min hydrogenation (0.6 mg of the product) under PASADENA conditions (note the complete absence of any signal belonging to **9**); (c) ^{29}Si INEPT($+\pi/4$) spectrum (8 scans, $2\tau = 0.036$ s) of **10** after a total of 1 min hydrogenation under PASADENA conditions (the signal of **9** is slightly visible); (d) ^{29}Si INEPT spectrum (16 scans, $2\tau = 0.070$ s) after 8 min hydrogenation time (5 mg of **10** formed) and after the system has returned to thermal equilibrium; (e) ^{29}Si spectrum after the ALTADENA experiment using a $\pi/2$ Si pulse, single scan, spinning sample. Reprinted with permission from Reference 131. Copyright 1996 American Chemical Society

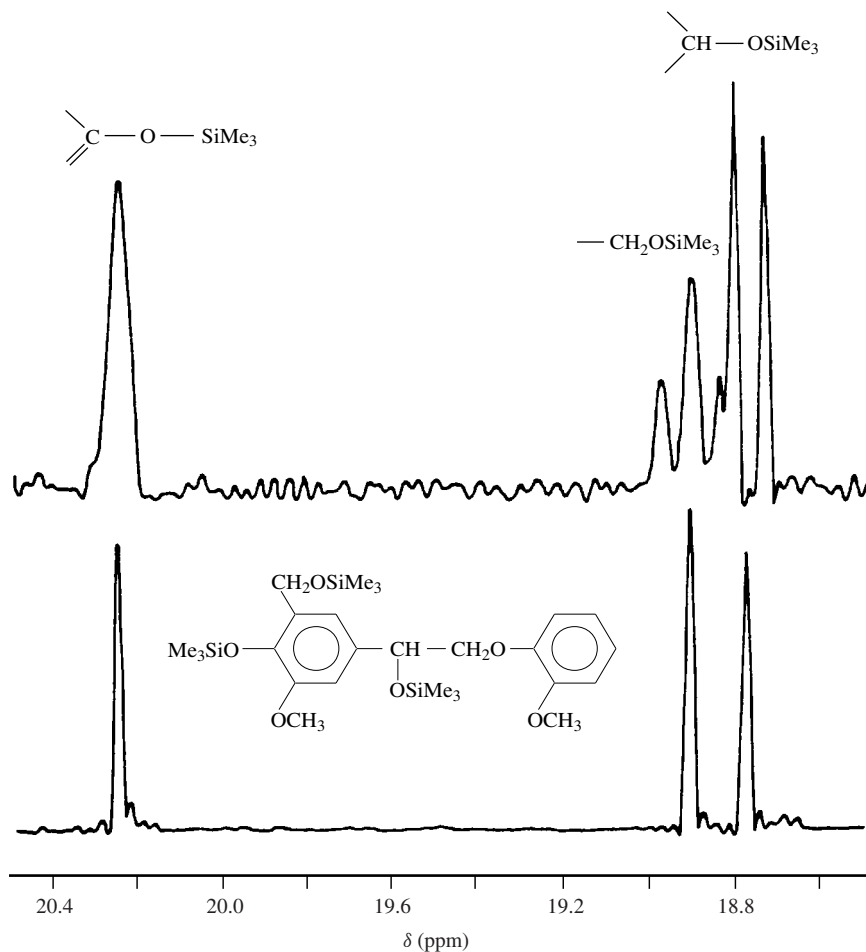


FIGURE 15. 'Normal' INEPT (bottom) and SPINEPTR (top) ^{29}Si NMR spectra and the resulting assignment for the compound shown in the inset. Reprinted from Reference 21, Copyright 1990, with permission from Elsevier Science

For selectively deuterated compounds, an interesting opportunity is offered by polarization transfer from ^2H as demonstrated for ^{13}C INEPT and DEPT¹⁴²; among the advantages of the method is that all probes have the needed deuterium lock coil. Of course, the last-mentioned experiment can enhance the silicon signal only due to rapid deuterium relaxation but can be useful for line assignment through selective deuteration.

Simplified INEPT (with the first 180° pulses in both channels omitted) or INEPT combined with a 'jump and return' pulse can be also used for determination of signs of spin-spin couplings between rare nuclei as described in detail by Kupče and Wrackmeyer¹⁴³.

It is impossible to cover here all experiments that contain an INEPT or DEPT building module in the sequence. We shall cover those experiments that employ INEPT or

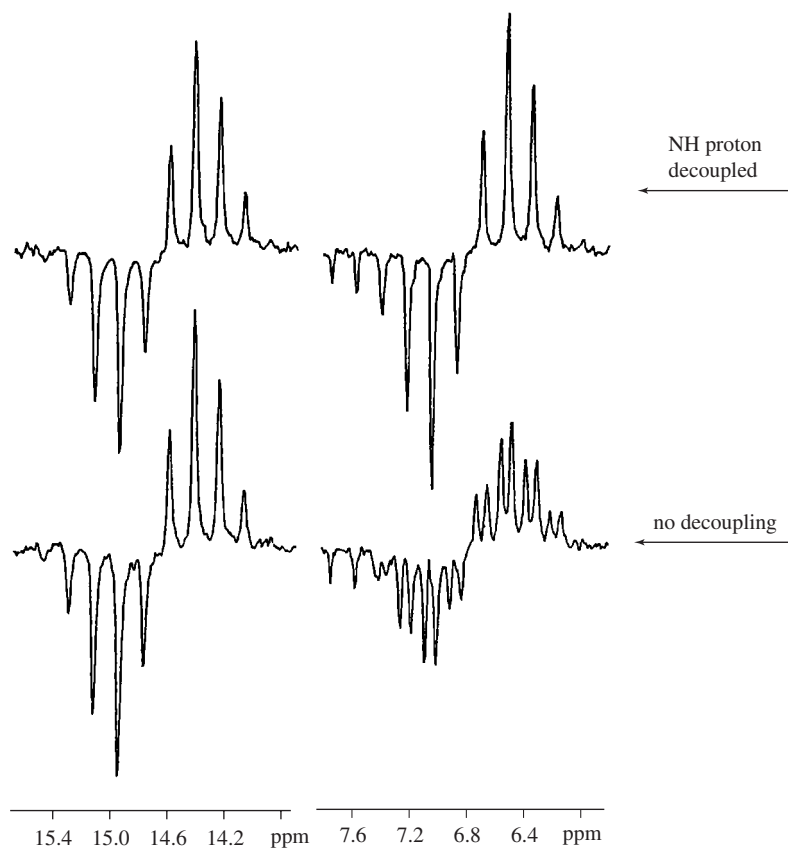
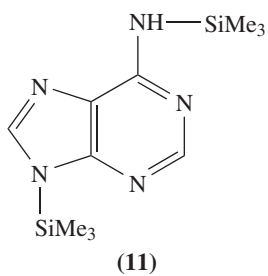


FIGURE 16. ^{29}Si INEPT spectra (not refocused) of bis(trimethylsilyl)adenine **11** measured without decoupling (bottom) and with selective decoupling of NH proton (top) during acquisition. The selective decoupling identifies the silicon with chemical shift $\delta = 6.88$ as Si–NH while that at $\delta = 14.77$ is Si–N< silicon. Reproduced by permission of John Wiley & Sons, Ltd from Reference 138



DEPT to enhance the signal of some other experiment in the sections devoted to those experiments (e.g. heteronuclear correlations, INADEQUATE, DQF COSY, J -resolved spectra). Similarly, an INEPT experiment can be made selective in a number of ways; some are discussed in Section VI.C.1 on selective experiments.

Since the general polarization transfer schemes discussed have become common for signal enhancement, a comment on their use for quantitative estimates is appropriate here (for more details see Section X.C). The topic has been seriously discussed only in connection with INEPT and PENDANT experiments. Undoubtedly, both increase reproducibility of signal integration as they improve signal-to-noise ratio and baseline (as compared to IGD experiments). The reproducible integrals can, however, be subject to considerable systematic errors. In comparison with carefully prepared quantitative IGD experiments, INEPT and PENDANT introduce two additional sources of systematic errors inherent to polarization transfer. With the given timing of the pulse sequence, the observed signal intensities depend on the actual couplings of each silicon which differs for different silicon atoms (see the formula for $E_{\text{INEPT,dec}}$). The second source of systematic errors is the relaxation during the pulse sequence, which also affects various ^{29}Si signals to a different extent. The importance of the second factor decreases with the increasing coupling used for polarization transfer and can be estimated from the linewidth of the ^1H NMR line of the employed proton (a broader ^1H NMR line means faster T_2 relaxation of the proton and a larger loss of the ^{29}Si signal). For compounds with known structure, the accuracy can be increased up to that of conventional measurements by a calibration with a suitably chosen mixture of compounds; neither of the sequences should be used indiscriminately without due attention to the specifics of compounds under study^{127,144}.

C. J Cross-polarization (JCP)

Cross-polarization is a well-known method for enhancement of low- γ nuclei signals in solids (CP MAS experiments)¹⁴⁵. The theory and first cross-polarization experiment in liquid were presented by Hartmann and Hahn in the same paper that laid the foundation of the famous CP experiments in solids in 1962⁷⁴. It took almost two decades until CP experiments in liquids were investigated in more detail by Ernst and coworkers¹⁴⁶ and Bertrand and coworkers¹⁴⁷.

In comparison with solids, a CP application to liquids involves an important change in mechanism. Instead of dipolar coupling (which is averaged to zero in liquids), it is J or spin-spin scalar coupling that is responsible for the exchange of polarization in liquids; hence, we have the abbreviation JCP for this J cross-polarization experiment. In liquids, only those silicon lines that belong to a silicon with some non-zero J coupling to a proton (or another abundant high γ nuclei) can be enhanced by JCP. The other main features, however, remain: polarization transfer is coherent (in contrast to NOE enhancement); pulse repetition rates are governed by proton longitudinal relaxation times T_1 rather than those of silicon (the relaxation rates of protons can be further shortened by a relaxation reagent); signal enhancement is given by the ratio $\gamma_{\text{H}}/\gamma_{\text{Si}}$ and the protons and silicon nuclei exchange polarizations periodically during the experiment as described below.

The pulse sequence for JCP experiments appears simple: a 90° proton pulse is followed immediately by a spin lock radio-frequency (rf) field of strength B_1^{H} that is phase shifted by 90° relative to the first pulse. By a spin-lock field is meant a strong rf field B_1 that is on resonance with the given nucleus; it keeps magnetization in a 'spin-locked' orientation parallel to the B_1 direction where the decay of magnetization is governed by $T_{1\rho}$. At present the strong continuous B_1 field is replaced by multipulse sequences that are well known from other spin-lock experiments such as TOCSY, ROESY etc. Simultaneously,

rf field B_1^{Si} is applied near the resonance of the ^{29}Si line. When the two fields satisfy the Hartmann–Hahn (HaHa) condition ($\gamma_{\text{H}}B_1^{\text{H}} = \gamma_{\text{Si}}B_1^{\text{Si}}$)⁷⁴ for cross-polarization time τ , the intensity of proton decoupled silicon magnetization varies as

$$M_{\text{Si}} = M_{\text{H0}} \sum A_k \sin^2(\pi\tau J/k)$$

while the proton magnetization varies according to the complementary dependence

$$M_{\text{H}} = M_{\text{H0}} \sum A_k \cos^2(\pi\tau J/k)$$

The sum of M_{Si} and M_{H} remain constant. In the above expressions M_{H0} is the initial magnetization of the protons, the values of k and A_k and the exact number of summation terms depend on the number of J coupled protons (for SiH systems $k = 2$, $A_k = 1$ and only one term remains; for SiH₂ systems $k = 2^{1/2}$, $A_k = 1$ and only one term remains; but for SiH₃ three terms with $k = 2$, $2/3^{1/2}$ and 1 and with $A_k = 1/2$, $1/2$ and $1/4$, respectively, remain in the sum)^{147,148}. Obviously, selection of optimum cross-polarization time for an optimum enhancement is not a simple task. It was suggested¹⁴⁷ that a series of preliminary experiments for selected τ values be performed first, after the rf fields had been calibrated to match the HaHa condition, and from the periodicity of the observed signal the optimum time τ be determined. The first ^{29}Si JCP experiments¹⁴⁹ measured the entire τ dependence of the signal and then used a fitting procedure to derive the values of coupling constants, $J(^{29}\text{Si}-^1\text{H})$, from the dependence. An alternative procedure is to use the Fourier transform of the cross-polarization intensity as a function of τ ¹⁴⁷. A faster method giving even more reliable estimates of unknown J values is provided by another modification of the JCP sequence, PCJCP (*Phase Corrected JCP*)¹⁵⁰. In this sequence the spin-lock irradiation of one of the nuclei is prolonged for the duration of the corresponding 90° pulse τ_{90} ($\gamma_{\text{H}}B_1^{\text{H}}\tau_{90} = \pi/2$) and the FID registered without proton decoupling. The value of $J(^{29}\text{Si}-^1\text{H})$ coupling is obtained after Fourier transform directly from the coupled spectrum and the experiment can be optimized¹⁵⁰.

In addition to the difficulty of finding the optimal τ , the JCP experiment also suffers from extreme sensitivity to the HaHa match. Moreover, the original experiment required both rf fields (Si and H) to be highly homogenous, preferably created by the same transmitter coil, to keep the same ratio of the two fields within the whole active volume of the sample¹⁴⁷. To reduce the sensitivity of the enhancement to the HaHa condition and cross-relaxation time, a modified, refocused JCP experiment (RJCP) was suggested¹⁵¹. In this experiment the spin-lock field on the silicon resonance is interrupted at $\tau = \frac{1}{2}J$ for a duration corresponding to a conventional 90° pulse, and later ($\tau = \frac{3}{2}J$) the spin-lock field on protons is similarly interrupted; both fields then remain on until $\tau = 2/J$.

The problem of matching the rf fields is eliminated in modifications that utilize an adiabatic increase or decrease of the spin locking field. (Adiabatic means a sufficiently slow change of effective magnetic field direction so that the magnetization can follow it.) Adiabatic J Cross-Polarization (AJCP)¹⁵² uses an adiabatically decreasing spin-locking field for protons and an increasing field for silicon; an ADRF experiment (Adiabatic Demagnetization in the Rotating Frame), in which the spin lock field on protons decreases while no spin lock is applied to silicon, can be immediately followed by an ARRF (Adiabatic Remagnetization in the Rotating Frame) stage during which the spin-lock field on silicon adiabatically increases from zero to its full value¹⁵³. Since these experiments have not found general use, the reader is referred to the source literature for more details and comparison.

Despite the above-mentioned modifications that reduce some of the severe requirements of JCP, the technique as performed in the quoted papers suffers from limitations: the ^1H and ^{29}Si pulses must be on resonance, and the HaHa condition must be established for full enhancement and polarization time should be optimized. These conditions are not trivial to obtain, and the difficulty in establishing them has prohibited routine applications of the JCP method to ^{29}Si NMR spectroscopy.

All the JCP experiments described employ a strong rf continuous (CW) field for spin-lock. Increasing the rf field strength would solve the limitations mentioned, but the power required might not be tolerated by the probe. With the development of multipulse sequences that enable spin-locking within large spectral offsets without the need for excessively strong rf field (and hence excessive power dissipated in the NMR probe), the situation has changed. The possibilities offered by several of these multipulse sequences to heteronuclear experiments were analysed⁷³. The pulse sequences considered are well known from heteronuclear decoupling and homonuclear spin-lock applications (WALTZ-16¹⁵⁴, WALTZ-17¹⁵⁵, DIPSI-2¹⁵⁶, MLEV-16¹⁵⁷, MLEV-17¹⁵⁸). The theoretical analysis, confirmed by experiments, has shown that when either the WALTZ-16 or DIPSI-2 sequence is used for spin-lock of both nuclei, the JCP experiment is competitive with INEPT or DEPT and might even outperform INEPT when small long-range couplings are the only vehicle for polarization transfer with a competitive leak of polarization through homonuclear couplings. The optimized polarization time is the same as in an optimized INEPT experiment.

These results were confirmed by Wagner and Berger⁷² from measurements of JCP ^{29}Si NMR spectra of a few methylsiloxanes; unfortunately, none of the tested compounds exhibited homonuclear ^1H – ^1H couplings. Detailed instructions on how to perform the CP experiment (on TMS) using a WALTZ-16 sequence in both channels and rf fields satisfying the HaHa condition are available³⁰. It is claimed that the JCP experiment in this version requires more calibrations in advance (pulse strengths, power for spin-lock and phase difference between the hard pulse and the attenuated spin-locking pulses), but once set, the experimental parameters can be used for other samples. The duration of the spin-lock, however, should be adjusted approximately to $1/J(\text{Si-H})$ independent of the number of coupled protons. Naturally, the spin-lock field must cover the whole chemical shift range.

VI. LINE ASSIGNMENTS AND CONNECTIVITY

Unless it is a one-line spectrum of a model compound with a known structure, it is necessary to assign the line(s) in a ^{29}Si NMR spectrum to silicon atoms in the molecular structure. The choice of methods is almost unlimited, and the topic is covered in NMR textbooks and dedicated volumes^{23,30,159,160}.

An optimum assignment strategy depends on the chemical problem at hand; the first problem is whether or not the structure of the compound (or compounds) is known. A full line assignment requires the determination of the entire structure, and that is seldom determined by ^{29}Si NMR measurements only. Often, a number of additional experiments are required.

Four aspects are of primary concern: (i) the complexity of the sample and its ^{29}Si NMR spectrum, (ii) how detailed an assignment is needed, (iii) the time factor and (iv) the amount of the sample available (and, perhaps, disposable).

Conventional methods for mixture analysis have been supplemented by DOSY (see Section X.B), which could be useful when the components differ in molecular size. While

simple multiplicity determination (through measurement of edited spectra or coupled spectra) might suffice in one case, another might demand a sophisticated triple resonance experiment.

In this review we shall discuss only those methods that have been found useful in organosilicon studies; ‘chemical’ approaches (isotopic substitution and use of a shift reagent) are mentioned in Section X. We are concerned here with ‘spectroscopic’ experiments that are loosely and arbitrarily divided into three categories: correlations, triple resonance and selective experiments.

Under ‘Correlations’ and ‘Selective Experiments’ we shall discuss 2 and 1D NMR measurements that use resonance of one additional nucleus (most often protons) besides silicon-29; achievements accomplished by experiments involving resonance of three nuclei will be covered under ‘Triple Resonance’ (Section VI.B).

A. Correlations

Most of the common heteronuclear correlations of ^{29}Si signals serve to determine correlations with ^1H signals either through one-bond couplings or through long-range couplings. (Correlations with other nuclei fall into triple resonance experiments, as they are usually measured with proton decoupling, see Section VI.B). Heteronuclear correlations can be measured by acquiring either ^{29}Si NMR signals (Section VI.A.1) or by so-called inverse detection by recording ^1H signals (Section VI.A.2), the latter being more sensitive but with limited precision of chemical shift determinations. Homonuclear Si–Si correlations can be measured by variants of the famous INADEQUATE experiment (Section VI.A.3) or by a COSY experiment that can be improved by introduction of double quantum filtration (DQF COSY, Section VI.A.4). The relative sensitivity of the two approaches is difficult to compare. While DQF COSY does not require any *a priori* estimate of the value of $J(^{29}\text{Si}–^{29}\text{Si})$ coupling, performance of the INADEQUATE experiment depends on the closeness of the estimate to the true value of the coupling. The better the estimate, the lower the signal losses and the better the signal-to-noise ratio. For that reason, a short survey of available values of these couplings is included (Section VI.A.5).

1. ^{29}Si detected heteronuclear correlations

Soon after the groundbreaking book of Bax¹⁶¹ became available, with its clear introduction to the field and practical instructions, several laboratories started independently to apply 2D heteronuclear correlation spectroscopy to the problem of line assignment in ^{29}Si NMR spectra of trimethylsilylated saccharides and their mixtures^{162–165}. Assignment of these lines was at that time the recognized obstacle to a wider application of the ^{29}Si NMR tagging technique suggested^{51,132,166,167} for identification of various organic functional groups (for a review see elsewhere²¹). All of these measurements utilized $^3J(^{29}\text{Si}–\text{O}–\text{C}–^1\text{H})$ couplings (about 3 Hz) of silicon with the nearest skeletal proton(s). Another early application included assignment of ^1H and ^{29}Si lines in a mixture of four $(\text{MeClSiO})_4$ stereoisomers¹⁶⁸ that utilized $^2J(^{29}\text{Si}–\text{C}–^1\text{H})$ couplings of silicon with methyl group protons. All of these experiments employed the simplest pulse sequence of the time with the direct ^{29}Si detection (as dictated by available hardware)¹⁶¹:

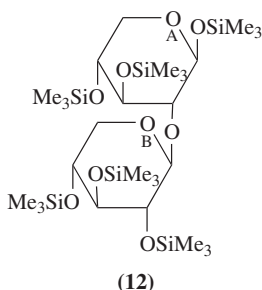
$$\begin{array}{l} ^1\text{H} : \quad 90_x^\circ - t_1/2 - \quad \quad - t_1/2 - \Delta_1 - 90_x^\circ - \Delta_2 - \text{decouple} \\ ^{29}\text{Si} : \quad \quad \quad \quad \quad 180_x^\circ \quad \quad \quad \quad \quad 90_x^\circ \quad \quad \quad \text{acquire} \end{array}$$

where the polarization delay is $\Delta_1 = 1/(2J)$ and the optimum refocusing delay Δ_2 should be $1/(2J)$ for Si–H, $1/(4J)$ for Si–H₂ correlations etc. [in general, $\Delta_2 = \arcsin(n)^{-1/2}/(\pi J)$, where n is the number of equivalent protons].

This is the simple heteronuclear ^1H -X COSY (or HETCOR) pulse sequence adapted to long-range correlations simply by adjustment of the Δ_1 and Δ_2 delays. Small coupling constants rule out the use of broad-band proton decoupling during evolution time t_1 by BIRD, and thus the correlation cross-peaks display the structure of proton multiplets, which reduces further the sensitivity of the experiment.

In many organosilicon compounds the silicon atom bears methyl groups. Their ^1H or ^{13}C chemical shifts are usually not structurally sensitive and so are of little use for ^{29}Si line assignments; however, their strong signals often cause some difficulty in ^{29}Si detected correlations, a notable exception being compounds with no other protons except SiMe protons suitable for structure elucidation^{168–172}. Careful positioning of the ^1H carrier and selection of the spectral width is usually necessary to avoid folding this strong signal into the interesting part of the 2D spectrum where it could be mistaken for the correlation sought. (Because of negative NOE, elimination of these signals by presaturation of methyl protons is not advisable.) On the other hand, in phenylmethylpolysilanes, where $^2J(^{29}\text{Si}-\text{C}-^1\text{H})$ couplings are of comparable magnitude to $^3J(^{29}\text{Si}-\text{Si}-\text{C}-^1\text{H})$ couplings, silicon–silicon connectivity can be determined indirectly from 2D $^{29}\text{Si}-^1\text{H}$ correlation spectra, which show¹⁷⁰ at the same time correlations through both 2J and 3J .

Practice has shown that if the ^1H lines must also be assigned experimentally, it is advantageous to perform all 2D experiments ($^1\text{H}-^1\text{H}$ COSY, $^1\text{H}-^{13}\text{C}$ COSY and $^1\text{H}-^{29}\text{Si}$ COSY) with the same resolution along the F1 axis (^1H axis). The homonuclear and heteronuclear contour plots can be juxtapositioned as shown in Figure 17 for compound 12. Interpretation of the spectra arranged in this manner is straightforward; establishing the connectivity is facilitated by the comparisons.



The results of systematic studies of related series have shown how unreliable were the empirical assignment rules that had been suggested earlier¹⁷³. The results were very convincing that 2D $^{29}\text{Si}-^1\text{H}$ correlation spectroscopy is the method for ^{29}Si line assignment whenever the proton spectra can be assigned^{174,175}. Since that time use of selective deuteration, shift reagents and selective decoupling experiments were more or less abandoned for line assignment. 2D experiments kept improving as new ideas were advanced and pulse schemes were better understood (thanks mainly to the development of product operator formalism¹⁷⁶ that could be adapted to large spin systems¹⁰⁹ such as the SiH₃ system of $-\text{SiMe}_3$).

Besides their use for line assignments^{93,177}, $^{29}\text{Si}-^1\text{H}$ 2D correlations can also be used to determine coupling constants [$^nJ(^{29}\text{Si}-\text{X})$ and $^nJ(^1\text{H}-\text{X})$] involving another isotope

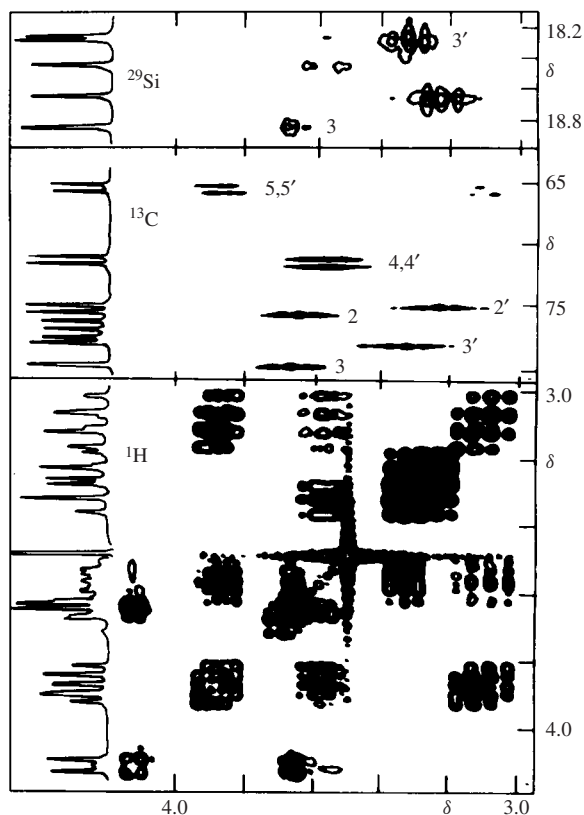


FIGURE 17. Relevant parts of ^1H , ^{13}C and ^{29}Si NMR spectra of **12**, their correlations and assignments. A and B are the different rings of **12**. The numbers denote carbon atoms in monosaccharide units, and the primes distinguish carbons in unit B from those in unit A. (200 MHz spectrometer Varian XL-200; 0.2 M solution in CDCl_3 , HMDSS internal reference, 64 transients for each of 100 increments in ^{29}Si correlation.) Reprinted from Reference 165 by courtesy of Marcel Dekker Inc.

X present in the molecule (nucleus X is passive in the correlation). Moreover, from the tilt of the line connecting the satellite cross-peaks involving this passive nucleus, the relative signs of the couplings can be determined. When a sufficient signal-to-noise ratio can be reached so that satellites due to isotope X become visible, the method can also be applied to less abundant isotopes X. The method with its variants has often been used by Wrackmeyer and coworkers for a variety of nuclei X^{178–180}. The low sensitivity of these experiments allows application to isotopes like ^{207}Pb or ^{77}Se ; their relatively high natural abundances of 22.7 and 7.6%, respectively, make this determination less demanding^{179,181–183}. For rare isotopes, more sensitive types of correlation experiments have to be used and/or the HEED filter incorporated, as will be described later. (Of course, ^{29}Si couplings can be obtained from heteronuclear correlations of other nuclei in an analogous manner using ^{29}Si as a passive nucleus¹⁸⁴. In some of these experiments it is necessary to employ a z -filter¹⁸⁵ to suppress the centre line against closely spaced satellites¹⁷⁹.)

A number of polarization transfer sequences can be modified to yield heteronuclear correlations¹⁸⁶; some were especially designed for long-range correlations (e.g. those based on DEPT¹⁸⁷ or COLOC¹⁸⁸) but only a few were applied to organosilicon compounds (e.g. COLOC to arylsilanes⁸⁹).

Though a novice might be surprised by the good signal-to-noise ratio of these experiments (due to the involved polarization transfer) the experiments require a large amount of the compound to keep the measuring time within reasonable limits, especially when high resolution along the F1 axis is required. The sensitivity of ^{29}Si detected experiments can be immensely increased through isotopic enrichment (see Section X.A), but this approach is impractical for organosilicon compounds. The sensitivity of heteronuclear correlations is increased when detection of a weak ^{29}Si signal is replaced by detection of ^1H NMR signal. Though not all methods of signal enhancement in the reversed detection can be applied to ^{29}Si - ^1H experiments (e.g. saturation of protons in the preparatory period, which would lead through negative NOE to a loss of signal), a number of methods have been adopted for this measurement; they are discussed in the next Section.

2. Indirectly detected heteronuclear correlations

Since the problems of line assignment and sensitivity are very acute for ^{29}Si NMR spectra of silylated natural products and other compounds, experiments for increasing the sensitivity of assignments are quite understandably being sought. In accord with the general trends in NMR spectroscopy of the early 1980s, the solution was to use indirect (or inverse or reversed) detection. In such an arrangement, the strong signals of the protons (or other NMR strong nuclei) coupled to silicon are detected instead of a weak ^{29}Si NMR signal, and the ^{29}Si chemical shift (and/or coupling constants) are determined indirectly from changes in the strong signals. The experiments can be carried out in two different ways: as selective decoupling experiments (e.g., ^1H - $\{^{29}\text{Si}\}$, ^{19}F - $\{^{29}\text{Si}\}$ or ^{31}P - $\{^{29}\text{Si}\}$) or as 2D experiments. The former experiments were used in the era of CW spectrometers for determination of ^{29}Si chemical shifts (e.g. $\{^{29}\text{Si}\}$ - ^1H INDOR¹⁸⁹ or $\{^{29}\text{Si}\}$ - ^{19}F INDOR¹⁹⁰) as well as for their assignment¹⁹¹. For complicated ^1H spectra, the decoupling experiments are tedious and require careful preparation. In contrast, as is well known, 2D NMR experiments can be carried out automatically in a systematic manner. The slow start of 2D ID ^{29}Si - ^1H experiments was caused by the absence of now common hardware (that provides, e.g., phase coherence between the proton decoupler and receiver¹⁹², and high-quality filters for the lock channel to reject ^{29}Si frequencies). Less than optimum performance was obtained when an ordinary broad-band probe was used instead of the so-called reversed configuration probe. This probe, often referred to as an ID (*Indirect Detection*) probe, has the ^1H coil as the inner coil with the higher filling factor and better homogeneity. Even with current ID probes, care must be taken not to burn them when recording spectra with ^{29}Si broad-band decoupling during acquisition. The difficulty in setting up ID experiments for low-abundance nuclei such as ^{29}Si stems from the need to suppress or to reject the parent signals that come from more abundant isotopomers; in the case of ^{29}Si it means that we must suppress a signal that is 20 times stronger than the ^{29}Si satellites.

The first modern ^{29}Si ID experiments merely employed the early primitive procedures described for ^{13}C - ^1H experiments — signal winnowing¹⁹³ to determine the relevant spectral width in the ^1H spectrum and the corresponding $J(^{29}\text{Si}$ - $^1\text{H})$ couplings and HMQC 2D sequence^{194,195}. In the applications to $>\text{CH}-\text{O}-\text{SiMe}_3$ moieties, $^3J(^{29}\text{Si}-\text{O}-^1\text{H})$

couplings (about 3 Hz) can be used and the complexity of ^1H NMR spectra depends on the number of protons coupled to the CH proton¹⁹⁶.

The signal winnowing sequence used may be written as¹⁹³:

$$\begin{array}{l} ^1\text{H} : 90_x^\circ - \tau - 180_x^\circ - \tau - \text{acquire}(\pm) \\ ^{29}\text{Si} : 180^\circ/0^\circ \quad (\text{decouple broad-band}) \end{array}$$

where delay time τ is chosen to equal $1/(2J)$. Subtraction of the signals acquired in the scans without the 180° silicon pulse from those acquired after the 180° pulse suppresses the signals from parent lines and leaves only the signals from ^{29}Si satellites for constructive averaging by accumulation. This simple sequence works satisfactorily for samples with no vicinal protons as demonstrated in Figure 18; in complex systems with vicinal and other coupled protons, the spectra provided by this sequence show the relevant regions for 2D

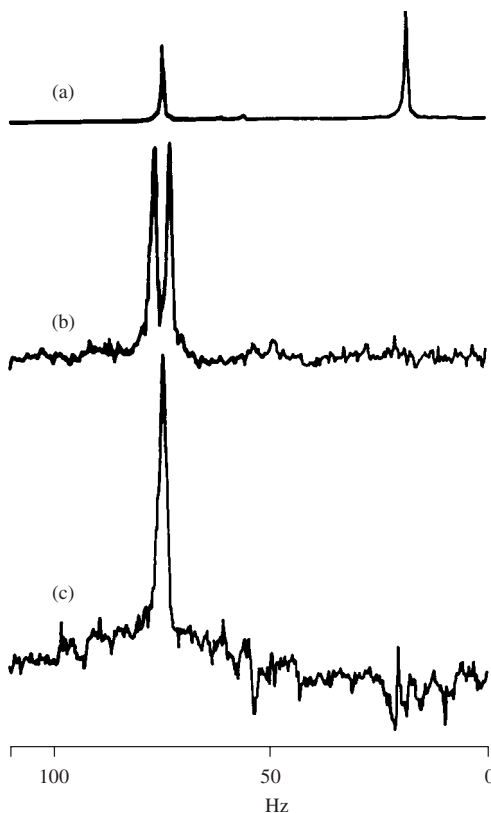


FIGURE 18. The CH part of the ^1H NMR spectrum of a mixture of $(\text{Me}_3\text{C})_2\text{CHOSiMe}_3$ and $(\text{Me}_3\text{C})_2\text{CHOH}$ (no protons vicinal to CH group). (a) Ordinary ^1H NMR spectrum measured with a one-pulse sequence, 4 transients. (b) Winnowed ^1H NMR spectrum, 32 transients, $\tau = 0.143$ s; other conditions as in (a). (c) Winnowed ^1H NMR spectrum measured with $\{^{29}\text{Si}\}$ decoupling, other conditions as in (b). Reproduced by permission of the Society for Applied Spectroscopy from Reference 196

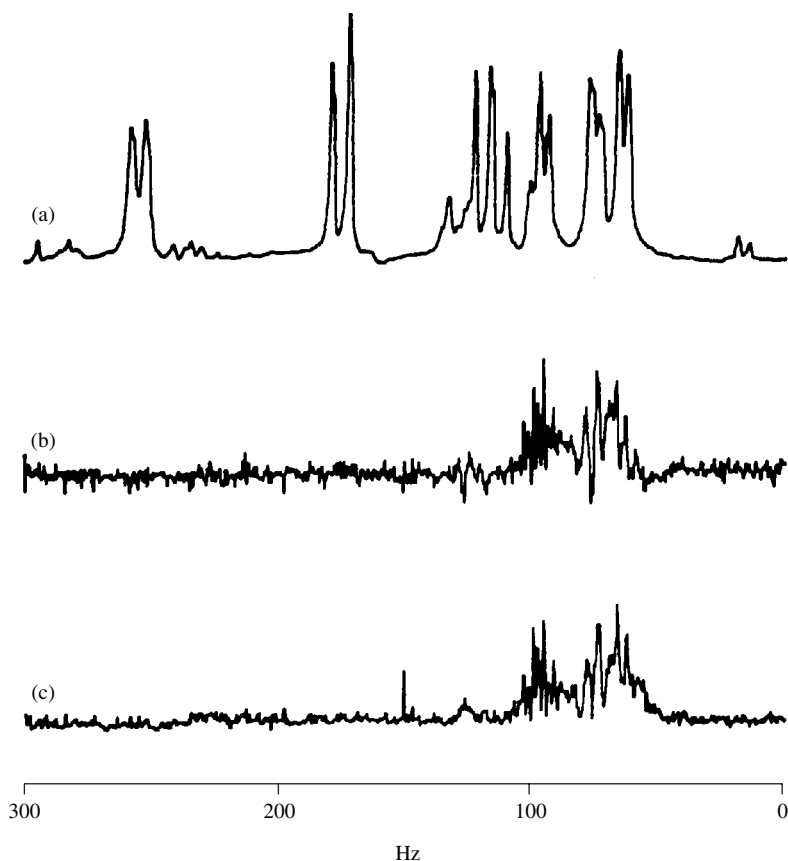


FIGURE 19. Partial ^1H NMR spectra of 2,3,4-tri(*O*-trimethylsilyl)-1,6-anhydro- β -D-glucopyranose (2). (a) Ordinary ^1H NMR spectrum measured with one-pulse sequence, 4 transients. (b) Winnowed ^1H NMR spectrum, phase-sensitive presentation, 256 transients, $\tau = 0.143$ s; other conditions as in (a). (c) Winnowed as in (b) but absolute value presentation. Reproduced by permission of the Society for Applied Spectroscopy from Reference 196

chemical shift correlations (see Figure 19); all other parts of the ^1H NMR spectrum can be eliminated by analog or digital filtration. This further improves the signal-to-noise ratio and the economy of the experiment.

The first variant of HMQC employed for ^{29}Si followed the basic sequence^{194,195}:

$$\begin{array}{l}
 ^1\text{H} : 90_x^\circ - \tau - \quad - t_1/2 - 180_x^\circ - t_1/2 - \quad - (\tau) - \text{acquire} \\
 ^{29}\text{Si} : \quad \quad 90_\phi^\circ \quad \quad \quad \quad \quad \quad 90_x^\circ \quad \quad \quad (\text{decouple broad-band})
 \end{array}$$

which is described and analysed in every 2D NMR textbook. The phase cycling of pulses and a receiver that ensures that only signals evolved during the t_1 period as double (or zero) quantum coherences are added constructively is in the source literature. The quality of the central line suppression is well apparent from Figure 20, and an example of

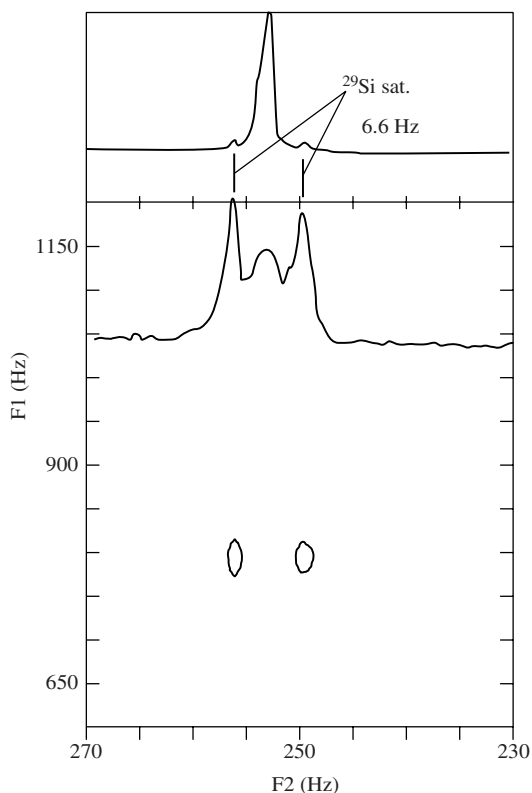


FIGURE 20. ^{29}Si – ^1H NMR spectra of $(\text{Me}_3\text{Si})_2\text{O}$ in CDCl_3 . Top—ordinary ^1H NMR spectrum; middle—HMQC filtered 1D spectrum; bottom— ^{29}Si – ^1H HMQC correlation without decoupling during acquisition

correlation measured by this sequence is shown in Figure 21. The theoretical sensitivity gain $(\gamma_{\text{H}}/\gamma_{\text{Si}})^{1.5} \approx 11.3$ in indirect detection relative to direct detection represents a limit that might be achieved for an optimized experiment, probe etc. It would allow a 100-fold reduction in measurement time. There are, however, additional benefits of using ID besides higher sensitivity: faster pulse repetition and the possibility of filtering out ^1H signals that are outside the relevant region in the ^1H NMR spectrum. The faster pulse repetition that is allowed by the faster proton relaxation has been mentioned in relation to other experiments similarly controlled by ^1H relaxation. The ^1H signals of trimethylsilyl or similar groups with a strong singlet of ^1H signals of protons coupled to the silicon are usually of no use for assignment purposes [an exception being compounds containing no other protons, such as oligo(yne)s^{171,172}]. Due to their distinct position in the ^1H spectrum, these signals can be easily filtered out during the signal acquisition; a similar filtration by analog filters is not possible in ^{29}Si detected correlations as it would require digital filtration along the F1 axis.

1D spectra measured by the HMQC pulse sequence in which the evolution period was replaced by a fixed short delay (without the refocusing pulse) and recorded without ^{29}Si

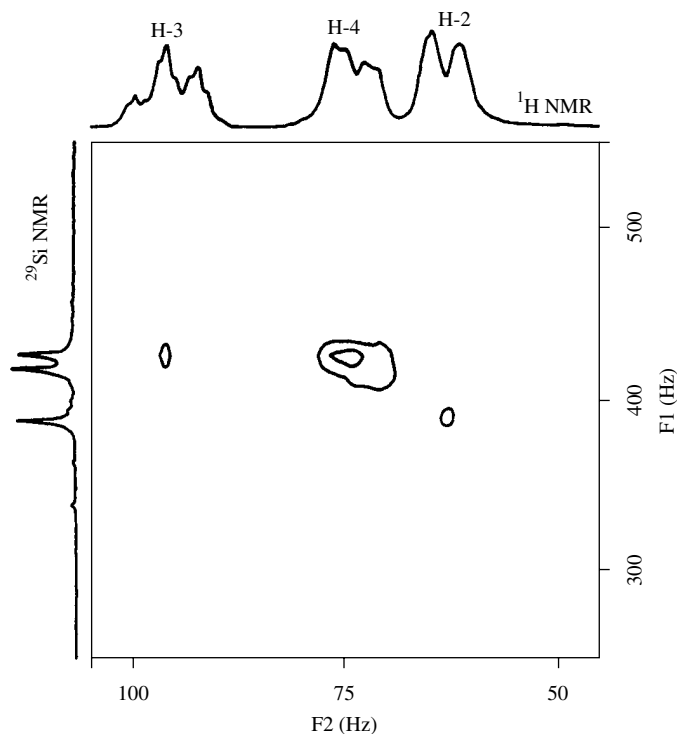


FIGURE 21. ^{29}Si - ^1H HMQC correlation 2D NMR spectrum and ^{29}Si and ^1H 1D NMR spectra of 2,3,4-tri(*O*-trimethylsilyl)-1,6-anhydro- β -D-glucopyranose, (**2**) (CDCl_3 solution). Acquisition time 3.41 s, relaxation delay 2 s, 64 transients, 64 increments; ^{29}Si WALTZ-16 decoupling during acquisition. Reproduced by permission of the Society for Applied Spectroscopy from Reference 196

decoupling are convenient for determination of ^1H - ^{29}Si couplings¹⁹⁷ and identification of silyl groups¹⁹⁸.

The ID experiments were gradually improved as new ideas (BIRD) emerged and new technical means became available (pulsed field gradients). Placing the BIRD cluster¹⁹⁹ in front of the above HMQC sequence with a properly adjusted delay d between BIRD and the HMQC parts of the BIRD-HMQC combination greatly improves the suppression of the central lines²⁰⁰. The BIRD sandwich is the following cluster of pulses:

$$\begin{array}{l} ^1\text{H} : 90_x^\circ - \tau - 180_x^\circ - \tau - 90_{-x}^\circ \\ ^{29}\text{Si} : \quad \quad \quad 180^\circ \end{array}$$

where $\tau = 1/(2J)$ ¹⁹⁹. When combined with HMQC it gives the BIRD-HMQC sequence²⁰⁰:

$$\begin{array}{l} ^1\text{H} : 90_x^\circ - \tau - 180_x^\circ - \tau - 90_{-x}^\circ - d - 90_x^\circ - \tau - \quad - t_1/2 - 180_x^\circ - t_1/2 - \quad - (\tau) - \text{acquire} \\ ^{29}\text{Si} : \quad \quad \quad 180^\circ \quad \quad \quad \quad \quad 90_\phi^\circ \quad \quad \quad \quad 90_x^\circ \quad \quad \quad (\text{decouple b.b.}) \end{array}$$

where decouple b.b. denotes some kind of broad-band decoupling.

While the BIRD sequence leaves the magnetizations of the ^{29}Si satellites in the original position, it inverts the magnetizations of the centre lines. The inverted line relaxes through delay d back to its equilibrium position. In preliminary trial experiments one selects delay d when the inverted central line changes from negative to positive. By selecting delay τ in BIRD and in HMQC one selects the satellites (one-bond, two-bond etc.), and ^{29}Si pulses ensure that the selected satellites are the ^{29}Si satellites. A different situation is encountered when this BIRD pulse is replaced by Ψ -BIRD²⁰¹:

$${}^1\text{H} : 90_x^\circ - \tau_2 - 90_x^\circ$$

(no ^{29}Si pulses). In this variant, the 180° pulses of BIRD are replaced by putting the ${}^1\text{H}$ frequency of the two 90° pulses on the parent line. This Ψ -BIRD leaves all signals separated by the frequency difference $n/(2\tau_2)$ (where $n = 1, 2, 3, \dots$) from the parent line virtually unperturbed while the parent line is inverted as in the BIRD sandwich. The delay d is optimized similarly to the above description for BIRD; with an optimum d value the centre line is suppressed and only selected signals with a given frequency separation from the parent line are retained. In this case the selection is based entirely on the satellite separation; no other nucleus besides the proton is affected by the Ψ -BIRD. By appropriate delay τ_2 one can select satellites due to coupling with another nucleus (Y), e.g. one-bond ^{13}C satellites, the choice of the other τ delay for the HMQC part being independent. This enables reduction of triple resonance experiments (e.g. ${}^1\text{H}\{^{13}\text{C}, {}^{29}\text{Si}\}$) to essentially double resonance ${}^1\text{H}\{^{29}\text{Si}\}$ (with ^{13}C as a passive nucleus in this example). Such pseudo-triple resonance does not, of course, require a triple resonance probe or an additional channel on the spectrometer. The same effect as is produced by Ψ -BIRD, i.e. suppression of the central line and selective excitation of the satellites, can be also achieved by bi-selective (BIS) pulses. If such a pulse replaces the first 90° pulse of an HMQC sequence, we get a BIS HMQC sequence. The details and possibilities of how to construct such pulses were discussed and demonstrated by Kupče and coworkers²⁰².

The Ψ -BIRD HMQC sequence was used by Wrackmeyer and coworkers in a number of studies to determine coupling constants and their relative signs^{179,180}; important data have been also obtained from analogous pseudo-triple resonance experiments in which the ^{29}Si nucleus played the role of the passive spin. For example, in a ^{13}C - ${}^1\text{H}$ HMQC correlation after Ψ -BIRD has selected the ^{29}Si satellites [${}^1J(^{29}\text{Si}-{}^1\text{H}) = 199$ Hz] of the HSi proton in Ph_3SiH , it was possible to determine ${}^1J(^{29}\text{Si}-^{13}\text{C}) = -68.5$ Hz, ${}^2J(^{29}\text{Si}-^{13}\text{C}) = -4.7$ Hz and also ${}^2J(^{13}\text{C}-{}^1\text{H}) = 6.4$ Hz and ${}^3J(^{13}\text{C}-{}^1\text{H}) = 3.1$ Hz couplings to α and *ortho* carbons²⁰³. The procedure is analogous to that to be shown later for HSQC sequence.

In general, the cleanest 2D HMQC spectra are obtained by the PFG HMQC sequences that utilize pulsed field gradients; a selection of such sequences can be found in the review of Keeler and coworkers²⁰⁴ or in recent textbooks (such as that of Claridge¹⁵⁹), but applications to ^{29}Si have been scarce up to now. Of course, it requires an ID probe tunable to the ^{29}Si frequency with PFG coil(s). An example of a nice application of the PFG HMQC sequence to a difficult long-range ${}^1\text{H}$ - ^{29}Si correlation was presented by Rinaldi's group in their 3D study of 1-phenyl-silabutane polymer tacticity²⁰⁵, to be shown later in Section VI.B (Figure 42). The sequence they used was described as using PFG along three different axes to eliminate gradient echoes from the strong water signals²⁰⁶. In other solvents one z -gradient would apparently suffice. The typical gradient enhanced

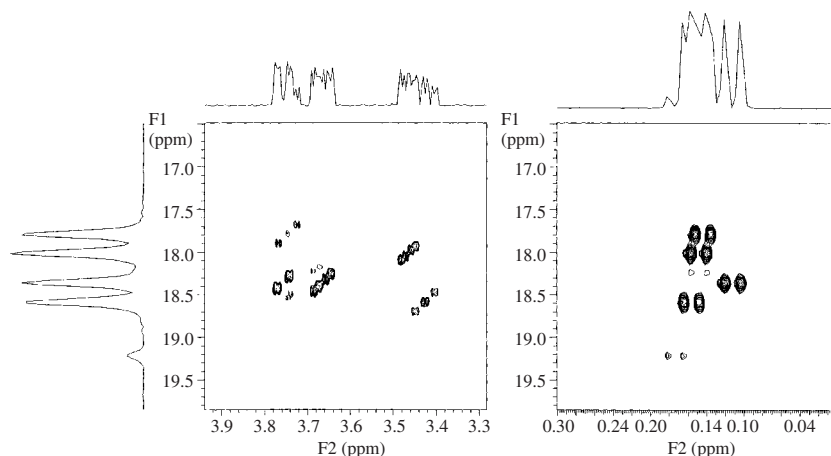
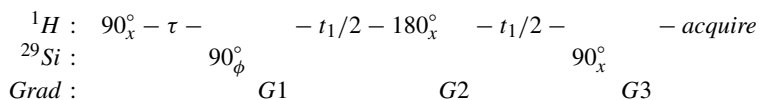
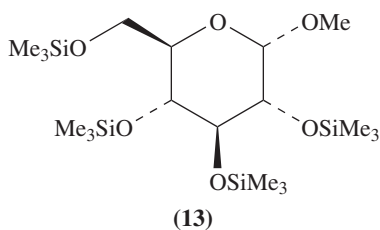


FIGURE 22. ge-HMOC ^1H – ^{29}Si correlation in methyl 2,3,4,6-tetra(*O*-trimethylsilyl)- α -D-glucopyranoside **13**; expansions of the sugar proton region (left) and methyl proton region (right). (^1H at 399.94 MHz, ^{29}Si at 79.46 MHz, 5 mm ID PFG probe, 0.03 M solution in CDCl_3 , internal TMS as a reference, spectral widths 3500 and 2000 Hz for ^1H and ^{29}Si respectively, optimized for $J = 3$ Hz, 512 increments each 16 scans, zero filled to 4096×2048 data points). Reproduced by permission of John Wiley & Sons, Ltd from Reference 207

HMOC sequence (dubbed ge-HNMOC)



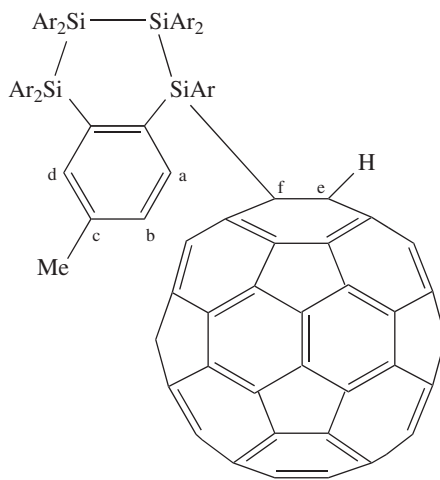
(with a gradient ratio G1 : G2 : G3 of 5 : 5 : –2) was used for line assignment in trimethylsilylated saccharides by Provera and coworkers²⁰⁷. Details from the typical correlation spectrum of compound **13** are shown in Figure 22 demonstrating the high resolution achievable.



In ^{29}Si NMR spectroscopy HMOC spectra are often not distinguished from HMB (Heteronuclear Multiple Bond Correlation) spectra; the two names are used indiscriminately as both experiments employ the same pulse sequence. Both are based on heteronuclear double quantum coherence and differ only in the value of the coupling used for setting up delay τ . HMB uses small values of coupling through (multiple) several bonds while HMOC is intended for large one-bond couplings. The resulting longer τ

delays in the HMBC experiments do have, however, some consequences: homonuclear ^1H – ^1H couplings also evolve during the long delays and cause phase distortions and lower the sensitivity. For this reason (and sensitivity losses through relaxation) the final refocusing delay is usually omitted, and hence the spectra can be recorded only without ^{29}Si decoupling. An absolute value presentation masks phase distortions. Obviously, when there are no homonuclear ^1H – ^1H couplings (as in the above examples of trimethylsilyl derivatives), the difference between HMQC and HMBC is immaterial.

A nice example of a true ‘multiple-bond’ correlation was presented by Kusakawa, Kabe and Ando²⁰⁸ who used a ^1H – ^{29}Si HMBC correlation to assign ^{29}Si lines in the product **14** (with Ar = 4-MeC₆H₄) derived by addition of cyclo[(4-MeC₆H₄)₂Si]₄ to C₆₀. Their 2D spectrum is shown in Figure 23. Although each of the four silicon lines has a cross-peak with two protons, it is only the line at –12.66 ppm that has a cross-peak with the H^a proton, thus identifying silicon signal at $\delta = 12.66$.



(14)

Despite the very different mechanism, the HSQC sequence (*H*eteronuclear *S*ingle *Q*uantum *C*orrelation) yields results equivalent to an HMQC sequence except that HSQC offers an additional benefit—the cross-peaks do not exhibit homonuclear ^1H – ^1H couplings along the F1 axis. These splittings reduce sensitivity and resolution along this axis in HMQC spectra. On the other hand, the HSQC sequence contains more pulses and is more sensitive to errors in calibrations etc. The sequence is²⁰⁹:

$$\begin{array}{l}
 ^1\text{H} : \quad 90_x^\circ - \tau - 180_x^\circ - \tau - 90_\phi^\circ - \quad \quad \quad 180_x^\circ \quad \quad - 90_e^\circ - \Delta - 180_x^\circ - \Delta - \text{acquire} \\
 ^{29}\text{Si} : \quad \quad \quad 180_x^\circ \quad \quad 90_\phi^\circ - t_1/2 - \quad \quad - t_1/2 - 90_x^\circ \quad \quad 180_x^\circ \quad \quad (\text{decouple } b.b.)
 \end{array}$$

where the symbols have their usual meanings. The sequence is easy to understand: first, INEPT transfers polarization of protons to silicon, silicon magnetization evolves during time t_1 with heteronuclear couplings refocused and then polarization is transferred back to protons by reversed INEPT to be detected with possible decoupling of silicon. For this mechanism the sequence is sometimes referred to as ‘double INEPT’¹⁹² although some understand this name to apply to a slightly different sequence (more suitable for

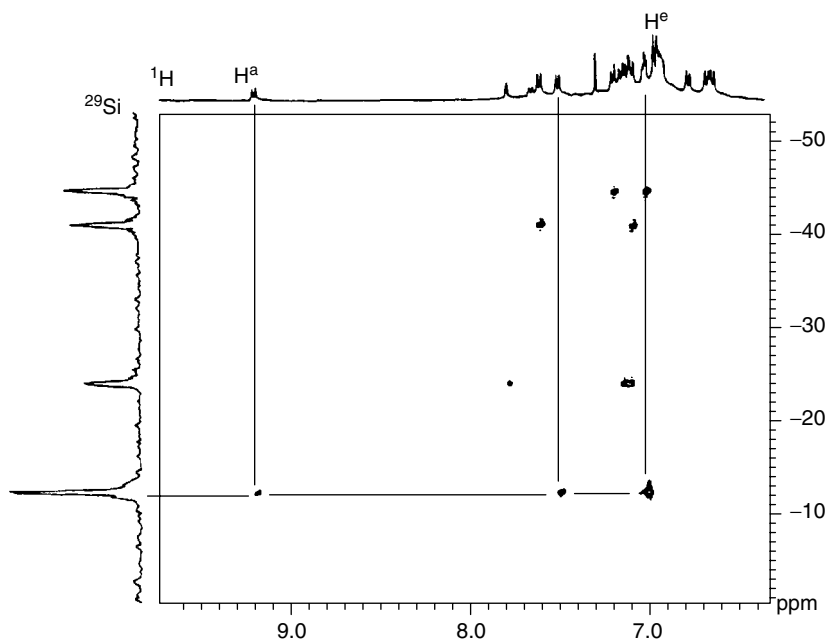
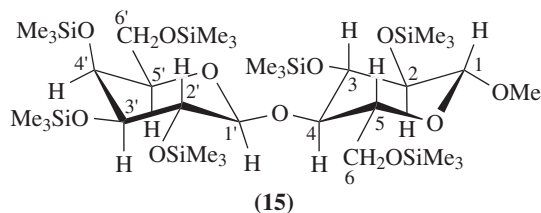


FIGURE 23. ^1H - ^{29}Si HMBS spectrum of compound **14** in 1 : 1 CDCl_3 - CS_2 mixture. [Value of $^3J(^{29}\text{Si}-^1\text{H})$ used for setting up correlation experiment not given.] Reprinted with permission from Reference 208. Copyright 1995 American Chemical Society

macromolecules)²¹⁰; the sequence is also known under the name the Overbodenhausen experiment²¹¹. Uhrín and coworkers²¹² developed a double-INEPT constant-time phase-sensitive sequence especially suited for trimethylsilylated products:

$$\begin{array}{l}
 ^1\text{H} : (\cap 90_x^\circ - T -) 90_x^\circ - \tau - 180_x^\circ - \tau - 90_y^\circ - \quad \quad \quad - \cap - x/2 - 180_x^\circ \quad \quad \quad - 90_x^\circ \Pi_y^{\text{SL}} - \text{acquire} \\
 ^{29}\text{Si} : \quad \quad \quad 180_x^\circ \quad \quad 90_\phi^\circ - (\Delta - x + t_1)/2 - \quad \quad \quad - 180_x^\circ - (\Delta - t_1)/2 - 90_x^\circ
 \end{array}$$

in which \cap stands for a selective 180° pulse on methyl protons, Π^{SL} for spin-lock and $(\cap 90_x^\circ - T -)$ is an optional T_1 filter (for phase cycling and independent optimization of all the delays; see the source reference). A comparison of 2D correlations obtained by HMBC and by this sequence on the same sample of **15** shown in Figure 24 is quite convincing as to the advantages of the latter.



(keeping the symbols introduced earlier, although they differ from those in the source literature). The use of the sequence is similar to that discussed above for the same variant of HMQC^{201,213}. The mentioned narrow cross-peaks along the F1 axis are useful for measurements of small ^{29}Si -X couplings (couplings as small as 0.45 Hz were measured); the procedure is demonstrated in Figure 25 for $X = ^{13}\text{C}$. In this example, $^2J(^{29}\text{Si}-^{13}\text{C}) = +1.2$ Hz is well resolved in F1 and the tilt of the satellites indicates that the reduced couplings $^1K(^{13}\text{C}-^1\text{H})$ and $^2K(^{29}\text{Si}-^{13}\text{C})$ have opposite signs.

^1H - ^{29}Si HSQC spectra are used routinely for line assignment in complex silane mixtures²¹⁴, for silylated products such as humic substances²¹⁵ and possibly others.

As in many other sequences PFG greatly improves the quality of HSQC spectra²⁰⁶; undoubtedly they will find use also in ^{29}Si NMR.

Indirect detection is also used in the XYI sequence (XY coupling by *Inverse spectroscopy*)²¹⁶. This complicated sequence can be used for measurement of spin-spin couplings between rare spin nuclei X and Y [$J(\text{XY})$] at their natural abundance. The authors believe that the sequence can be applied routinely for characterization of novel compounds available in small amounts. The sensitivity of this approach is apparent from Figure 26, which shows the determination of $^1J(^{29}\text{Si}-^{13}\text{C})$ (and other) couplings from the XYI spectrum of **16** measured in 5% v/v solution.

For obvious reasons it is becoming increasingly popular to use indirect methods as a replacement of direct ^{29}Si measurement of ^{29}Si chemical shifts (see, e.g., Reference 217). One should be aware, however, that indirect detection inherently implies certain editing,

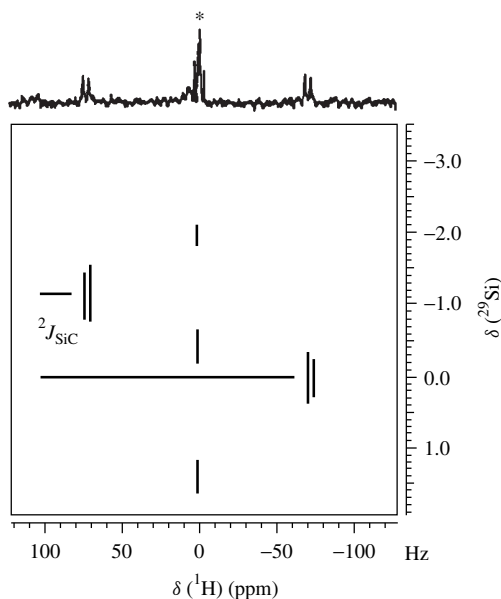


FIGURE 25. ^1H - ^{29}Si Ψ -BIRD HSQC phase-sensitive refocused and not decoupled spectrum of $\text{Si}(\text{OMe})_4$ (500 MHz, 5 mm ID probe, 2 mg in 450 mg of C_6D_6 , $d = 2$ s, $\tau_2 = 7.0$ ms, $\tau = 68.3$ ms, 16 increments of 32 transients each, spectral width 10 Hz in F1). The residual parent signal is marked with an asterisk. Reproduced by permission of John Wiley & Sons, Ltd from Reference 203

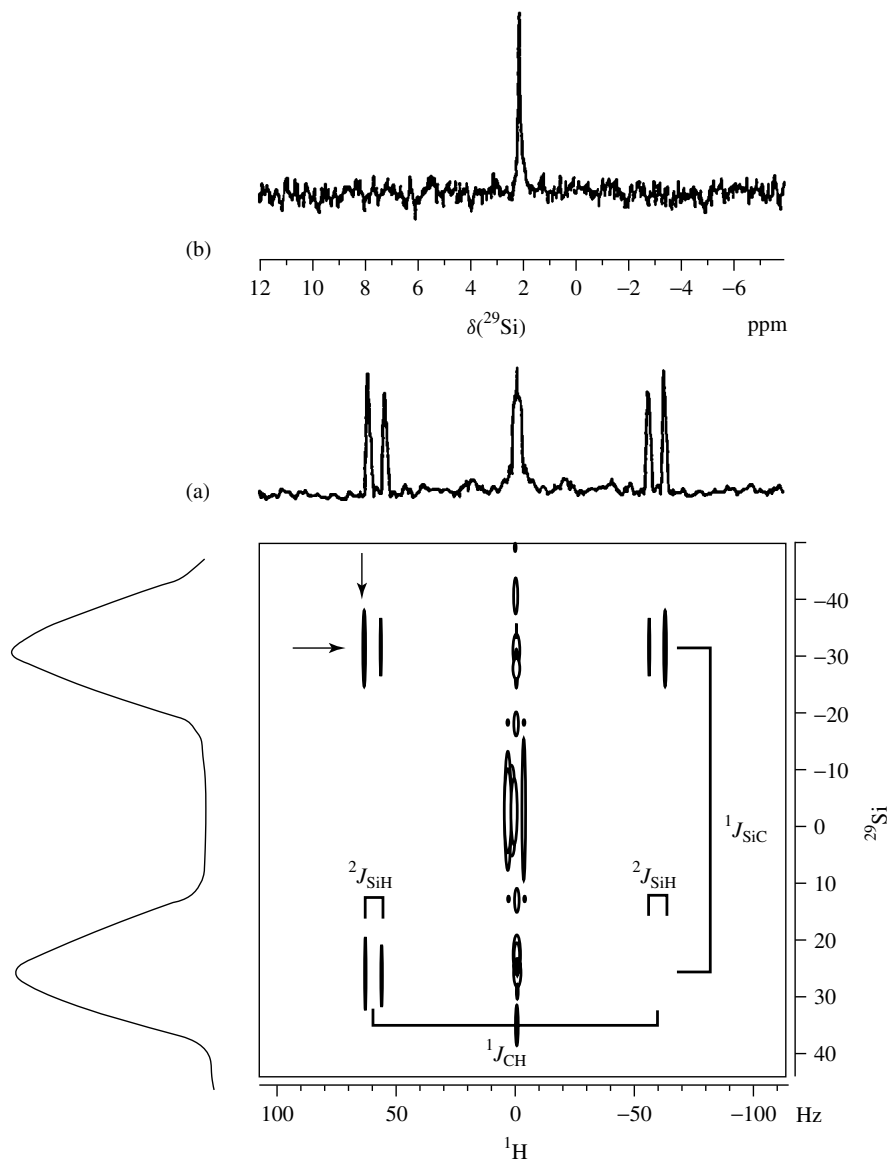
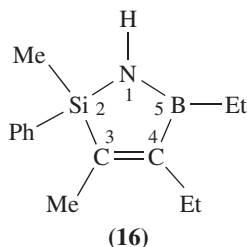


FIGURE 26. (a) Inverse 2D ^1H - ^{29}Si -correlated XYI spectrum of **16** (approx. 5%, v/v in CDCl_3 , 16 increments of 1 K data points each zero filled to 4 K, LB = -2 Hz, GB = 0.3 Hz, symmetrization applied along both axes; ^1H at 300 MHz, ^{29}Si at 59.63 MHz, no decoupling of ^{29}Si ; slices indicated by arrows are shown along F1 and F2 axes). (b) ^{29}Si NMR spectrum measured by refocused and decoupled INEPT. Reproduced by permission of Academic Press from Reference 216



as some value of $^{29}\text{Si}-^1\text{H}$ coupling must be assumed for the delay calculation. Also, if a precision of chemical shifts comparable to that of direct measurement is to be achieved (along the F1 axis), the experiment might be time-consuming when the spectral width of ^{29}Si signals is large.

3. INADEQUATE

INADEQUATE experiments aim at observing selectively the weak satellites of normal signals of rare nuclei, which arise from the low abundance of molecules containing two spin-spin coupled rare nuclei. Homonuclear ($^{29}\text{Si}-^{29}\text{Si}$) INADEQUATE experiments seem to enjoy some popularity among organosilicon chemists as a method for elucidation of polysilane skeletons^{218,219}.

INADEQUATE uses a so-called double-quantum filter to suppress strong singlet signals of isolated ^{29}Si nuclei and thus make visible the weak satellite lines due to $^{29}\text{Si}-^{29}\text{Si}$ coupling [i.e. the ^{29}Si satellites of ^{29}Si lines separated by $J(^{29}\text{Si}-^{29}\text{Si})$ couplings] that are retained in the spectrum; see schematic Figure 27. In its original pulse sequence the double-quantum filter uses different phase properties of the desired signal and eliminates undesirable signals through phase cycles. With some advantages the same filtering can be accomplished through pulsed magnetic field gradients, which eliminate the undesirable signal in each transient by properly chosen gradients, and thus higher spectrometer gain can be used.

In its first 1D form an INADEQUATE experiment²²⁰

$$^{29}\text{Si} : 90_x^\circ - \tau - 180_{\pm y}^\circ - \tau - 90_x^\circ - \Delta - 90_\phi^\circ - \text{acquire}(\psi)$$

yields values of $^{29}\text{Si}-^{29}\text{Si}$ coupling constants. If Si-Si connectivity is sought, it can be found by careful comparison of the values of coupling constants providing that the differences in the couplings are significant. When connectivity is the main goal, the 2D variant²²¹ is more convenient.

$$^{29}\text{Si} : 90_x^\circ - \tau - 180_{\pm y}^\circ - \tau - 90_x^\circ - t_1 - 90_\phi^\circ - \text{acquire}(\psi)$$

In this form the sequence does not differentiate the sign of double quantum coherence (i.e. the sign of the sum of the two chemical shifts of the two coupled ^{29}Si nuclei) and thus the efficiency of such an experiment is not optimal. This disadvantage is removed in a modified 2D experiment in which the last 90° pulse is replaced with a pulse having an arbitrary flip angle²²² α :

$$^{29}\text{Si} : 90_x^\circ - \tau - 180_{\pm y}^\circ - \tau - 90_x^\circ - t_1 - \alpha_x^\circ - \text{acquire}(\psi)$$

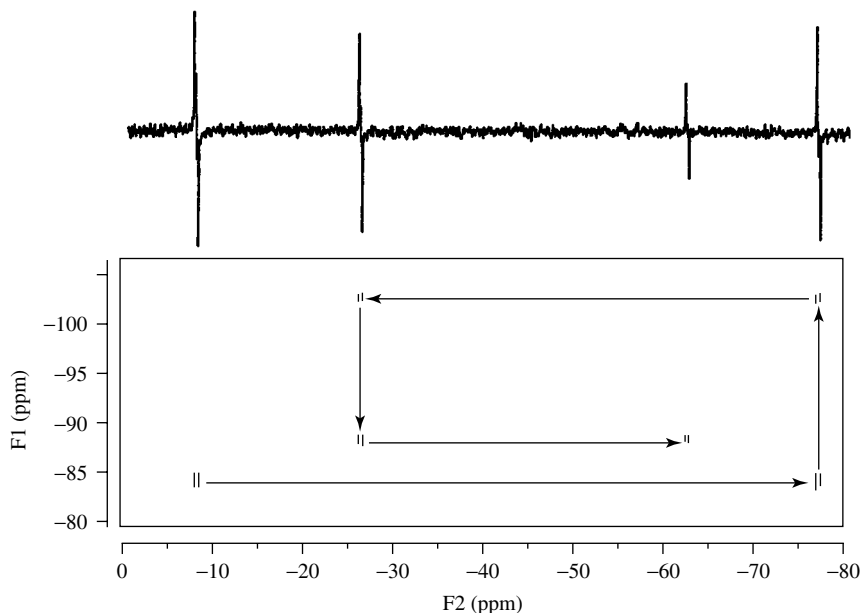


FIGURE 28. ^{29}Si – ^{29}Si INADEQUATE spectra of $[\text{Me}_3\text{Si}]_2\text{SiMeSiMe}_2]_3\text{SiMe}$. Top: 1D spectrum ($\tau = 4.1$ ms, $\Delta = 3$ μs); bottom: 2D spectrum ($\tau = 4.1$ ms). Reprinted from Reference 223. Copyright 1998, with permission from Elsevier Science

Overlooked thus far by ^{29}Si NMR users is J -resolved INADEQUATE²²⁹

$$^{29}\text{Si} : 90_x^\circ - t_1/2 - 180_{\pm y}^\circ - t_1/2 - 90_x^\circ - \Delta - 90_\phi^\circ - \text{acquire}(\psi)$$

in which the fixed delay τ is replaced by the evolution time t_1 . One such J -resolved experiment yields all $J(^{29}\text{Si}$ – $^{29}\text{Si})$ coupling values (i.e. one-bond and long-range) for each silicon atom and the values can be determined with high precision, thanks to the refocusing 180° pulse in the middle of the evolution period.

However, ^{29}Si – ^{29}Si INADEQUATE suffers, as do other ^{29}Si NMR techniques, from negative NOE and long relaxation times²¹⁸. As in other experiments, relaxation can be shortened and continuous decoupling replaced by gated decoupling that decouples protons during the acquisition time only (to minimize NOE). When shortening the relaxation time one must exercise care as some of the INADEQUATE pulse sequences are long and the signal might decay before the beginning of acquisition. At the same time, resolution also degrades with the relaxation reagent added (thus reducing the signal-to-noise ratio). Similar concerns apply also to increasing the sample concentration. Gated decoupling can lead to line broadening along the F1 axis and signal loss due to ^1H – ^{29}Si coupling (which is not refocused at the end of time t_1 in the above sequences). A simple remedy is to insert a 180° pulse (^1H) in the middle of the evolution period²¹⁸. INADEQUATE experiment without proton broad-band decoupling during acquisition is a useful tool for measuring $J(\text{Si}$ – $\text{Si})$ couplings between chemically equivalent silicon nuclei, e.g. in symmetrical disilanes²³⁰. Of course, absence of proton decoupling severely degrades the sensitivity of the experiment.

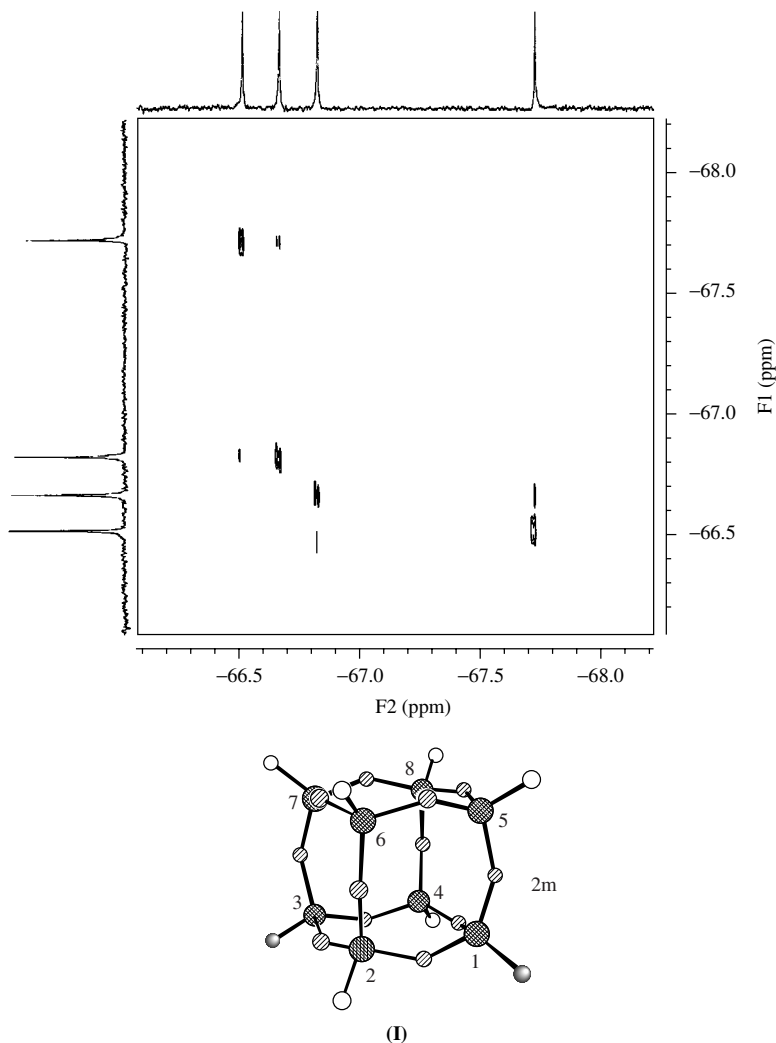


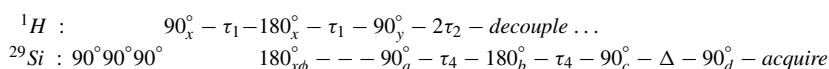
FIGURE 29. ^{29}Si – ^{29}Si 2D INADEQUATE spectrum of $(\text{Si}_8\text{O}_{12})(n\text{-C}_3\text{H}_7)_6(3\text{-ClC}_3\text{H}_6)_2$, **I** (●, Si; ⊗, O; ○, *n*-Pr; ●, 3-ClC₃H₆), in CDCl₃ solution (59.60 MHz, delays optimized for $J = 0.7$ Hz, relaxation delay 20 s). Reprinted from Reference 226. Copyright 1994, with permission from Elsevier Science

Considering the low sensitivity of (^{29}Si – ^{29}Si) INADEQUATE, it is no surprise to see that practically all methods of INADEQUATE sensitivity improvement were soon implemented into ^{29}Si applications, although the sensitivity problem is not as acute as in ^{13}C NMR of natural products (with 1.1% natural abundance of ^{13}C isotope and usually only a limited amount of compound), and thus there has been no report of special data

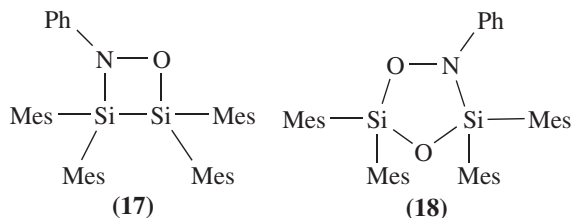
processing applied to ^{29}Si – ^{29}Si INADEQUATE to find the signal buried in the noise (e.g. as in ^{13}C NMR^{231,232}).

The signal-to-noise ratio of INADEQUATE can be increased by transferring proton polarization to the ^{29}Si spin system just prior to the INADEQUATE experiment itself. Thus, INEPT–INADEQUATE (Sørensen and coworkers²³³) or DEPT–INADEQUATE (in the original version²³⁴ or modified²³⁵) combinations achieve sensitivity increase through excitation enhancement by application of non-selective polarization transfer from protons, thus bringing the advantages of these polarization transfer schemes (signal intensity increase and faster pulse repetition); both are applicable to 1D and 2D versions of INADEQUATE. Often expressed objection to such enhanced experiments, that they fail to enhance the signal from nuclei not coupled to protons, was proved incorrect²³⁴. With a proper phasing, polarization is transferred alternatively to silicon coupled to protons and to silicon remotely coupled to protons²³⁴.

The INEPT–INADEQUATE²³³ sequence is:



In the field of ^{29}Si NMR, the INEPT–INADEQUATE combination was used for the first time by West's group²³⁶ as a 1D method to determine $J(\text{Si}–\text{Si})$ in unsymmetrical disilenes (${}^1J = 155–158$ Hz) and 1,3-cyclodisiloxanes (${}^2J = 3.8–4.0$ Hz). (Perhaps a warning from the field of ^{13}C NMR is appropriate here; in some cyclobutenone derivatives ${}^2J(^{13}\text{C}–^{13}\text{C})$ couplings were found in some cases to be larger than their one-bond counterparts²³⁷.) When the signal of isolated ^{29}Si nuclei is not completely filtered out, the INADEQUATE spectra can still be used for coupling constant determination (see the spectrum of 17 in the top part of Figure 30) unless the remnants of the central line distort the satellites (which is very likely in the case of small couplings²³⁸, such as shown in the bottom part of Figure 30 for compound 18). For the 2D version of the experiment the last delay Δ , has to be replaced by evolution time t_1 ; detailed description of such experiments for establishing Si–Si connectivity are available^{169,239}.



Mes = Mesityl

Kuroda and coworkers²⁴⁰ used a 2D INEPT–INADEQUATE sequence with a symmetrization similar to the simple INADEQUATE used by Henge and Schrank²¹⁸ as mentioned above. Their pulse sequence

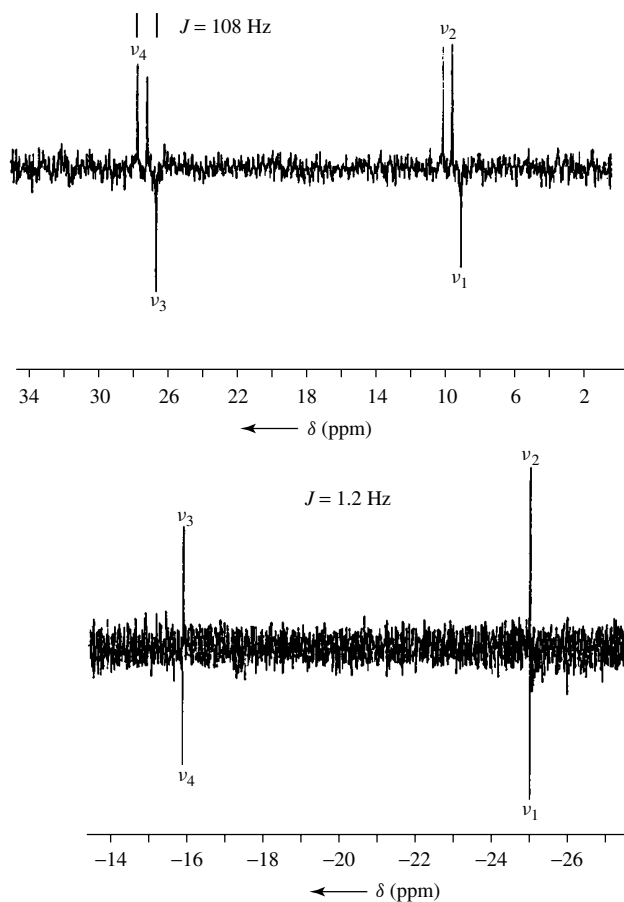
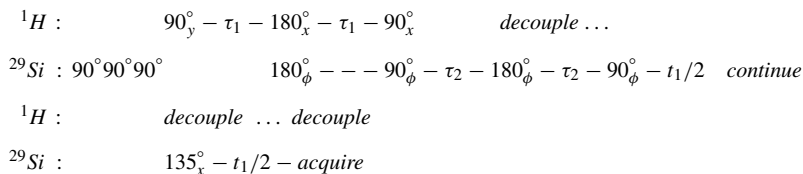


FIGURE 30. ^{29}Si – ^{29}Si 1D INEPT–INADEQUATE spectra; top: spectrum for **17**, $J = 108$ Hz; bottom: spectrum for **18**, $J = 1.2$ Hz (no experimental details given). Reproduced by permission of Wiley-VCH from Reference 238



yields 2D INADEQUATE spectra with a different symmetry as illustrated for compound **18** in Figure 31.

^1H detected INADEQUATE, dubbed INSIPID (*INadequate Sensitivity Improvement by Proton Detection*)²⁴¹, has not been applied to (^{29}Si – ^{29}Si) INADEQUATE, but its combination with INEPT excitation might be useful when sensitivity is the most important

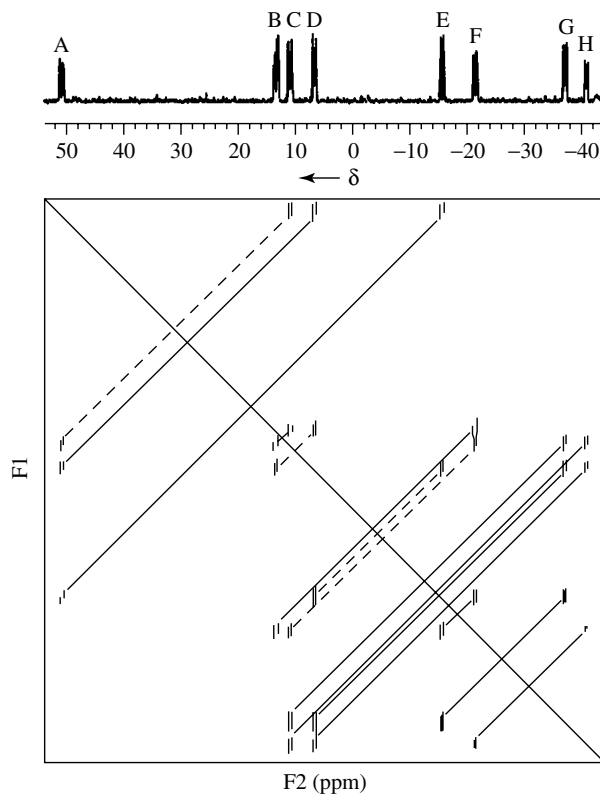
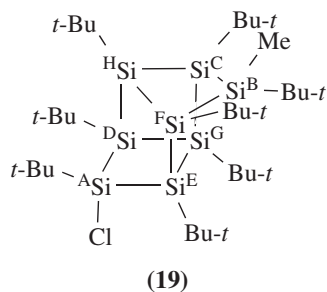


FIGURE 31. ^{29}Si – ^{29}Si 2D INEPT–INADEQUATE spectrum of the tetracycle **19** in C_6D_6 measured at 53.7 MHz (timing not given). The trace at the top is a projection on the F2 axis. Signals connected by solid lines correspond to one-bond interactions, those connected by dashed line denote long-range couplings (note the smaller separation of the satellites in the latter case). Reproduced by permission of Wiley-VCH from Reference 240



consideration—it offers the highest sensitivity of the described methods. However, connectivities of silicon atoms without one- or two-bond couplings to protons could be missed.

The version described by Weigelt and Otting²⁴² utilizes pulsed field gradients to suppress the ^1H signal from protons not coupled to ^{29}Si :

$$\begin{array}{r} ^1\text{H} : 90_y^\circ - \tau_1 - 180_x^\circ - \tau_1 - 90_x^\circ \qquad \qquad \qquad 180_x^\circ \\ ^{29}\text{Si} : \qquad \qquad \qquad 180_\phi^\circ - \dots - 90_\phi^\circ - \tau_2 - 180_\phi^\circ - \tau_2 - 90_\phi^\circ - t_1/2 - \dots \\ G_z : \end{array}$$

continue:

$$\begin{array}{r} ^1\text{H} : \qquad \qquad \qquad \qquad \qquad \qquad \qquad \qquad \qquad 90_x^\circ \qquad \qquad 180_x^\circ \qquad \textit{acquire} \\ ^{29}\text{Si} : \quad t_1/2 - \Delta - 180_x^\circ - \Delta - 90_x^\circ - \tau_2 - 180_x^\circ - \tau_2 - 90_x^\circ - \tau_1 - 180_x^\circ - \tau_1 - \textit{decouple} \\ G_z : \qquad \qquad \pm g \qquad \qquad \mp g \qquad \qquad \qquad \qquad \qquad \qquad \qquad \qquad \qquad g \end{array}$$

In this arrangement the typical easy-to-analyse INADEQUATE appearance is lost. The 2D plot would contain ^{29}Si double-quantum frequencies (i.e. sum of the chemical shifts of the two coupled silicon nuclei) along axis F1 and ^1H frequencies along the F2 axis. A pair of cross-peaks at the same ^{29}Si double-quantum frequency would indicate a Si–Si fragment; two cross-peaks with the same ^1H frequency indicate a Si–Si ··· H fragment.

INADEQUATE CR (Composite Refocusing), the latest among the methods for sensitivity enhancement of INADEQUATE experiments²²⁸, was first applied to ^{29}Si – ^{29}Si couplings by Lambert and Wu²⁴³ (Figure 32).

INADEQUATE CR

$$\begin{array}{r} ^{29}\text{Si} : 90_x^\circ - \tau/2 - 180_x^\circ - \tau/2 - 90_x^\circ - t_1 - \delta/2 - 180_x^\circ - \delta/2 - 90_{-x}^\circ - \tau/2 - \textit{continue} \\ G_z : \qquad \qquad \qquad \qquad \qquad \qquad \qquad \qquad \qquad \pm g \qquad \qquad \mp g \end{array}$$

$$\begin{array}{r} ^{29}\text{Si} : 180_y^\circ - \tau/2 - 45_\psi^\circ 45_\psi^\circ - \tau/2 - 180_y^\circ - \tau/2 - 90_y^\circ - \delta/2 - 180_x^\circ - \delta/2 - \textit{acquire} \\ G_z : \qquad \qquad \qquad \qquad \qquad \qquad \qquad \qquad \qquad \qquad \qquad \qquad -2g \qquad \qquad +2g \end{array}$$

(Note the different meaning of τ delay in this sequence.) This modification utilizes pulsed field gradients and, through a series of properly chosen pulses, combines the intensities of ^{29}Si doublets into a single line. Depending on the choice of phase cycles, the intensities of the two satellites are combined either into the ‘left’ or into the ‘right’ satellite line (and the two can be merged) with obvious gain in sensitivity. Of course, both echo and anti-echo signals must be recorded. Echo requires the first two gradients with + and – polarity and $\varphi = y$, $\psi = -x$ for the left satellite line or $\varphi = -y$, $\psi = x$ for the right line; anti-echo needs – and + polarity of the two gradients and $\varphi = -y$, $\psi = -x$ for the left and $\varphi = y$, $\psi = x$ for the right line. The 2D spectrum loses the typical INADEQUATE appearance of doublets symmetrically disposed around the ‘double quantum diagonal’ ($\omega_1 = 2\omega_2$) but that is a small price to pay for doubled sensitivity. The retained single lines of the satellite doublets (i.e. one for each of the two coupled ^{29}Si nuclei) differ in their distance (along ω_2) from the double quantum diagonal by $J(^{29}\text{Si}$ – $^{29}\text{Si})$, so tracing out the skeleton remains easy as in the original INADEQUATE and the magnitude of the coupling can be read as this difference.

The performance of all INADEQUATE experiments (except J -resolved) depends on the estimate of the value of $J(^{29}\text{Si}$ – $^{29}\text{Si})$ coupling prior to the experiment and on the spread of its value in the sample under study. In the generic experiment for the weakly coupled ^{29}Si nuclei, the sensitivity varies with $\sin(2\pi\tau J)$, where $J = J(^{29}\text{Si}$ – $^{29}\text{Si})$, and

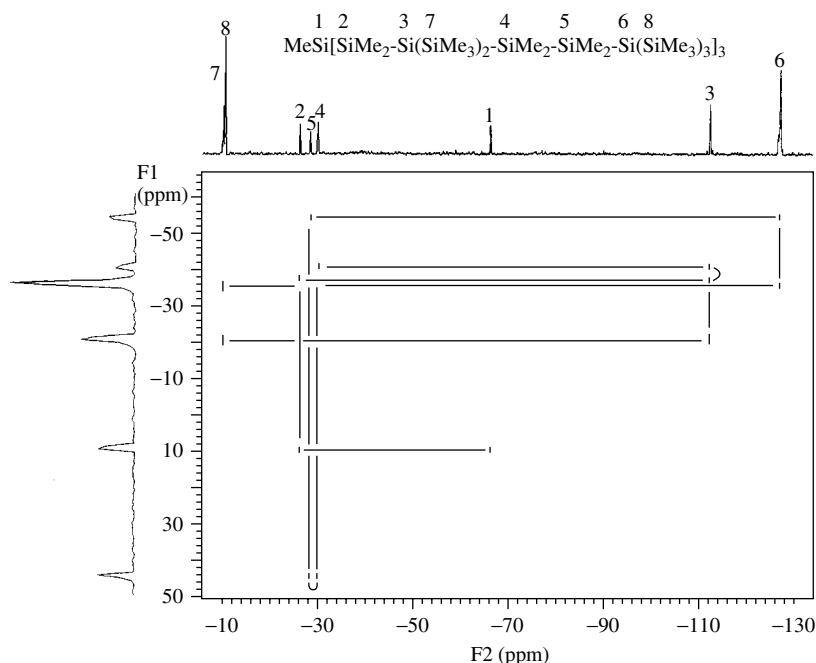


FIGURE 32. ^{29}Si – ^{29}Si 2D INADEQUATE CR spectrum of the dendritic polysilane tris[2,2,5,5-tetrakis(trimethylsilyl)hexasily]methylsilane measured at 99.300 MHz (70 mg of the sample in CDCl_3 ; 256 transients in 75 h, acquisition time 0.203 s, delays τ and δ not given). Reproduced by permission of John Wiley & Sons, Ltd from Reference 243

2τ is the time delay between the first two ^{29}Si $\pi/2$ pulses that create the double-quantum coherence between the two coupled ^{29}Si atoms. The optimum value²²⁰ of the delay is $\tau = (2n + 1)/[4J(^{29}\text{Si} - ^{29}\text{Si})]$. Since the sine dependence on J changes slowly around its maximum, variations of 10% in J around the estimated J value are not detrimental to the success of the experiment. On the other hand, with a different value of n the optimum condition set for one-bond coupling might be satisfied by another coupling as well. Then, long-range couplings can be observed simultaneously with one-bond couplings in 1D INADEQUATE; in the 2D variants, when establishing the silicon backbone, one should watch for the separation of ^{29}Si satellites in the 2D spectrum and differentiate those originating from long-range couplings that accidentally satisfy the above condition. On the other hand, it is possible to run J -resolved INADEQUATE first and then set the τ delay according to the J values found. Naturally, enhancement achieved by combination with polarization transfer schemes depends also on the estimates of the relevant coupling constants, $J(^{29}\text{Si} - ^1\text{H})$, utilized in the transfer.

In contrast to sensitivity enhancements, other modifications of INADEQUATE received little attention among organosilicon chemists although they can be quite useful. Thus, the use of composite pulses might be important for covering full spectral width and ensuring artifact-free performance of the INADEQUATE experiment^{244–246}. Other modifications allow a uniform excitation of double-quantum coherences even in the case of non-uniform coupling constants^{247,248}.

claimed higher sensitivity of a DQF COSY experiment than of an INADEQUATE experiment. The spectra enable direct and unambiguous assignments of the various units present in alkoxysilane polymers and yield values of $^2J(^{29}\text{Si}-\text{O}-^{29}\text{Si})$ couplings.

5. ^{29}Si – ^{29}Si couplings, $^nJ(^{29}\text{Si}-^{29}\text{Si})$

While silicon couplings to more abundant nuclei were routinely determined in the era of CW spectrometers (as the separation of 4.7% ^{29}Si satellites in ^1H , ^{19}F and ^{31}P NMR spectra), common measurement of ^{29}Si – ^{29}Si couplings has awaited the increase in sensitivity (per time) as provided by FT spectrometers. The satellites can be clearly seen on the ^{29}Si NMR lines of central silicon atoms in compounds of the type $(\text{R}_3\text{Si})_4\text{Si}^{28,259}$ or in the more general class of compounds $(\text{R}_3\text{Si})_3\text{Si}-\text{X}$ (Table 3) or in hypersilyl groups, $(\text{Me}_3\text{Si})_3\text{Si}-$ (Table 4). However, couplings were also determined in compounds without the benefit of equivalent silicon atoms²⁵⁹. Of course, measurements became routine and much less time-consuming after introduction of the INADEQUATE experiment (and its sensitivity-enhanced forms, see Section VI.A.3). Progress in spectrometer hardware must also be mentioned in this connection. To begin with, new probes have much higher sensitivity, pulsed field gradients permit one to use a higher gain and with fewer artifacts in the spectra, and the performance of multi-pulse programs has greatly improved giving almost artifact-free subtraction of signals during phase cycling of the INADEQUATE pulse sequence. These improvements allow determination of the couplings in compounds with non-equivalent silicon atoms. The currently achieved sensitivity might even permit determination of coupling between equivalent atoms (by measuring the ^{29}Si – ^{29}Si couplings in, e.g. ^{13}C satellite spectra in which the ^{13}C atom removes equivalence of the two

TABLE 3. Coupling constants $J(^{29}\text{Si}^{\text{A}}-^{29}\text{Si}^{\text{B}})$ in compounds of the type $(\text{R}_3\text{Si}^{\text{A}})_3\text{Si}^{\text{B}}\text{X}^{a260}$

R	X	$^1J(^{29}\text{Si}^{\text{A}}-^{29}\text{Si}^{\text{B}})$
CH ₃	F	64.7
	OCH ₃	66.2
	Cl	60.3
	Br	57.7
	I	55.1
	CH ₃	62.0
	H	60.3
	Si(CH ₃) ₃	52.6
		52.5
CH ₃ O	OCH ₃	144.1
	Cl	144.3
	Br	141.9
	I	139.7
	H	132.4
	Si(OCH ₃) ₃	122.2
	Si ₄ (OCH ₃) ₉	126.3
Cl	Cl	133.1
	Br	130.2
	I	125.0
	H	121.0
	SiCl ₃	109.3

^aAbsolute values of coupling constants in Hz.

TABLE 4. Coupling constants $J(^{29}\text{Si}-^{29}\text{Si})$ in compounds with $(\text{Me}_3\text{Si})_3\text{Si}$ Groups^{a,261}

Compound	$^1J(\text{Si}^{\text{A}}-\text{Si}^{\text{B}})$
$(\text{Me}_3\text{Si})_3\text{SiCO}\text{CMe}_3$	56.7
$(\text{Me}_3\text{Si})_3\text{SiCO}\text{CEt}_3$	55.8
$(\text{Me}_3\text{Si})_3\text{SiCO}(1\text{-methyl-1-cyclohexyl})$	56.1
$(\text{Me}_3\text{Si})_3\text{SiCO}[1\text{-bicyclo}[2.2.2]\text{octyl}]$	56.1
$(\text{Me}_3\text{Si})_3\text{SiCO}(1\text{-adamantyl})$	56.2
$(\text{Me}_3\text{Si})_3\text{SiCOPh}$	57.0
$(\text{Me}_3\text{Si})_3\text{SiCOC}_6\text{H}_4\text{OMe-}p$	56.2
$(\text{Me}_3\text{Si})_3\text{SiCOC}_6\text{H}_4\text{OMe-}o$	56.6
$(\text{Me}_3\text{Si})_3\text{SiCOOH}$	55.7
$(\text{Me}_3\text{Si})_3\text{SiCOOSiPh}_3$	58.0
$(\text{Me}_3\text{Si})_3\text{SiSiMe}_3$	52.5
$(\text{Me}_3\text{Si}^{\text{A}})_3\text{Si}^{\text{B}}\text{Si}^{\text{C}}(\text{Si}^{\text{D}}\text{Me}_3)_2\text{CMe}_2\text{SiMe}_3^b$	47.6

^aCoupling constants J in Hz, C_6D_6 solution.

^bData from Reference 262.

$^1J(\text{Si}^{\text{B}}-\text{Si}^{\text{C}}) = 30.6$ Hz, $^1J(\text{Si}^{\text{C}}-\text{Si}^{\text{D}}) = 56.7$ Hz.

silicon nuclei by way of the different ^{13}C isotopic effects on their ^{29}Si chemical shifts). On the other hand, detailed analysis of satellites in ^1H NMR spectra of symmetrical silanes with Si–H bonds can yield $^{29}\text{Si}-^{29}\text{Si}$ couplings as demonstrated by Pfisterer and Dreeskamp²⁶³ on $^2J(^{29}\text{Si}-\text{O}-^{29}\text{Si})$ coupling in $\text{O}(\text{SiH}_3)_2$ ($J = \pm 1.0 \pm 0.2$ Hz) in 1969. This approach is now facilitated by utilizing information provided by INADEQUATE spectra measured without proton decoupling as verified on a number of symmetrical disilanes²³⁰. The procedure is illustrated here in Figure 33. The power of the method to determine otherwise inaccessible couplings between chemically equivalent nuclei should be apparent from Table 5.

TABLE 5. Coupling constants (in Hz) in symmetrical disilane derivatives²³⁰

Compound	$^1J(^{29}\text{Si}-^1\text{H})$	$^2J(^{29}\text{Si}-\text{Si}-^1\text{H})$	$^3J(^1\text{H}-^1\text{H})$	$^1J(^{29}\text{Si}-^{29}\text{Si})$
$(\text{H}_3\text{Si})_2$				77.2 ± 0.6^a
$(\text{HPh}_2\text{Si})_2$	–188.6	–8.4	2.3	78.4 ± 1
$(\text{HBr}_2\text{Si})_2$	–283.6	–33.3	3.9	137.2 ± 0.5
$(\text{HI}_2\text{Si})_2$	–271.0	–26.9	3.9	106.9 ± 0.5
$(\text{HTf}_2\text{Si})_2$	–316.5	–25.3	3.5	137.0 ± 2
$(\text{H}(t\text{-Bu})_2\text{Si})_2$	–158.2	–6.0	0.9	62.6 ± 0.5
$(\text{HMe}_2\text{Si})_2$	–163.3	–8.9	1.3	82.6 ± 0.5
$(\text{H}_2\text{ISi})_2$	–235.6	–13.7	3.1	92.4 ± 0.5
$(\text{H}_2\text{PhSi})_2$	–193.1	–6.6	2.9	71.7 ± 1
$(\text{H}_2\text{TfSi})_2$	–267.3	–15.1	2.6	106.5 ± 1

^aData from Reference 264.

With this progress it is no surprise to see that the number of available $J(^{29}\text{Si}-^{29}\text{Si})$ values has greatly increased since the time of the exhaustive review of Marsmann⁸. Most of the new data come from the polysilane area, with much less on two-bond couplings, $^2J(^{29}\text{Si}-\text{O}-^{29}\text{Si})$, in siloxanes, which are still rather scarce. Interesting

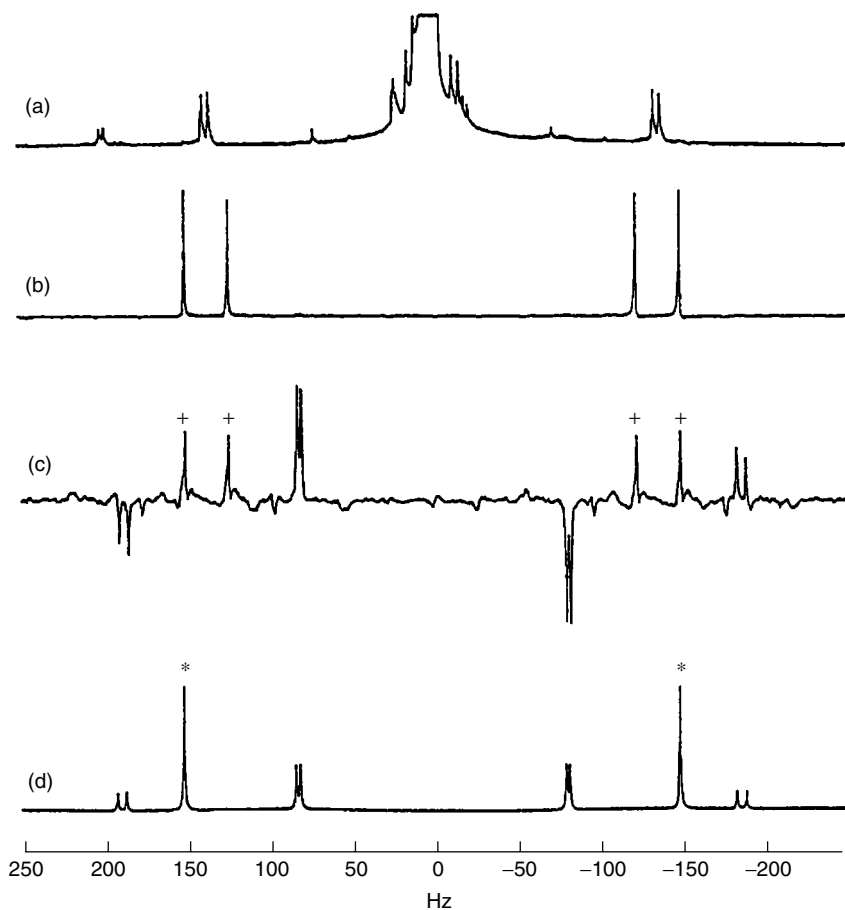


FIGURE 33. ^1H and ^{29}Si NMR spectra of 1,1,2,2-tetraiododisilane, $(\text{HI}_2\text{Si})_2$: (a) ^1H NMR spectrum for determination of $^3J(^1\text{H}-^1\text{H})$ couplings (300 MHz); (b) ^{29}Si NMR coupled spectrum with both $J(^{29}\text{Si}-^1\text{H})$ couplings visible (59.63 MHz); (c) INADEQUATE spectrum, lines due to ^{29}Si ^{28}Si isotopomer are marked by + sign (59.63 MHz, 600 increments, spectral width 2 kHz, relaxation delay 60 s); (d) simulated AA'XX' spectrum (the A_2 transition marked by asterisks does not show in the INADEQUATE spectrum). All spectra measured in *ca* 50% C_6D_6 solution at 22 °C. Reprinted from Reference 230, Copyright 1991, with permission from Elsevier Science

data²¹⁸, including long-range $^{29}\text{Si}-^{29}\text{Si}$ couplings in polysilanes with a more complex structure²⁴⁰, were already reproduced in this series³. Some selected data are presented in Tables 3–13.

The major trends or correlations governing one-bond couplings in disilanes have been known since the pioneering work of Sharp and coworkers²⁵⁹, who showed a linear correlation between $^1J(^{29}\text{Si}-^{29}\text{Si})$ and the sum of the electronegativities of the six substituents X on the two coupled silicon atoms ($\Sigma\chi_X$) (Figure 34) and also suggested

TABLE 6. Coupling constants $^1J(^{29}\text{Si}-^{29}\text{Si})$ in disilanes^a

Compound	Solvent	$^1J(^{29}\text{Si}-^{29}\text{Si})$	Reference
$\text{Me}_3\text{Si}^{\text{A}}\text{Si}^{\text{B}}\text{Me}_2\text{H}$	$(\text{CD}_3)_2\text{CO}$	84.6	259
$\text{Me}_3\text{Si}^{\text{A}}\text{Si}^{\text{B}}\text{Me}_2\text{Ph}$	$(\text{CD}_3)_2\text{CO}$	86.1	259
$\text{Me}_3\text{Si}^{\text{A}}\text{Si}^{\text{B}}\text{Ph}_3$	CDCl_3	86.5	259
$\text{Me}_3\text{Si}^{\text{A}}\text{Si}^{\text{B}}\text{Me}_2\text{Cl}$	CDCl_3	94.0	259
$\text{Me}_3\text{Si}^{\text{A}}\text{Si}^{\text{B}}\text{Cl}_3$	CDCl_3	115.7	265
$(\text{Me}_3\text{Si}^{\text{A}}\text{Si}^{\text{B}}\text{Me}_2)_2\text{NH}$	CDCl_3	96.0	259
$\text{Me}_3\text{Si}^{\text{A}}\text{Si}^{\text{B}}\text{Me}_2\text{F}$	CDCl_3	98.7	259
$(\text{Me}_3\text{Si}^{\text{A}}\text{Si}^{\text{B}}\text{Me}_2)_2\text{O}$	CDCl_3	103.4	259
$\text{Me}_3\text{Si}^{\text{A}}\text{Si}^{\text{B}}\text{Me}_2\text{Br}$	<i>b</i>	92.2	266
$\text{Me}_3\text{Si}^{\text{A}}\text{Si}^{\text{B}}\text{MeBr}_2$	<i>b</i>	103	265
$\text{Cl}_3\text{Si}^{\text{A}}\text{Si}^{\text{B}}\text{ClMe}_2$	<i>b</i>	150.6	265
$(\text{MeO})_3\text{Si}^{\text{A}}\text{Si}^{\text{B}}\text{Ph}_3$	<i>b</i>	160.0	259
$\text{Cl}_3\text{Si}^{\text{A}}\text{Si}^{\text{B}}\text{Cl}_2\text{Me}$	<i>b</i>	245.6	265
$\text{Br}_3\text{Si}^{\text{A}}\text{Si}^{\text{B}}\text{BrMe}_2$	<i>b</i>	127	265
$\text{MeH}_2\text{Si}^{\text{A}}\text{Si}^{\text{B}}\text{HBrMe}$	<i>b</i>	77.0	266

^a Absolute values of coupling constants in Hz, ± 0.5 Hz, assumed to be positive.^b No solvent was given.TABLE 7. Coupling constants $^1J(^{29}\text{Si}-^{29}\text{Si})$ in halodisilanes^a

Structure	X = Cl ^b	X = Br ^c	X = I ^c
$\text{XH}_3\text{SiSiH}_3$	88.3	86.6	83.4
$\text{X}_2\text{HSiSiH}_3$	105.0	98.6	
$\text{X}_2\text{HSiSiH}_2\text{X}$	128.0 ^d	113.6	97.8
X_3SiSiH_3	131.3	117.7	97.8
$\text{X}_3\text{SiSiH}_2\text{X}$	158.5	138.8	107.5
$\text{X}_3\text{SiSiHX}_2$	221.0	171.6	119.2

^a Absolute values of coupling constants in Hz.^b Data of Reference 267, error ± 0.5 Hz.^c Data of Reference 268, C_6D_6 solutions.^d Error ± 6.0 Hz.TABLE 8. Coupling constants $J(^{29}\text{Si}-^{29}\text{Si})$ in trisilanes^a

Compound	Solvent	$^1J(\text{Si}^{\text{A}}-\text{Si}^{\text{B}})$	$^1J(\text{Si}^{\text{B}}-\text{Si}^{\text{C}})$	$^2J(\text{Si}^{\text{A}}-\text{Si}^{\text{C}})$	Reference
$(\text{Me}_3\text{Si}^{\text{A}})_2\text{Si}^{\text{B}}\text{Me}_2$	CDCl_3	73.2			259
$(\text{Cl}_3\text{Si}^{\text{A}})_2\text{Si}^{\text{B}}\text{Cl}_2$	C_6H_6	186			259
$\text{Cl}_2\text{Si}^{\text{A}}(\text{Si}^{\text{B}}\text{Me}_3)_2$	<i>b</i>	76			265
$\text{H}_2\text{Si}^{\text{A}}(\text{Si}^{\text{B}}\text{Me}_3)_2$	<i>b</i>	69			265
$\text{Cl}_2\text{Si}^{\text{A}}(\text{Si}^{\text{B}}\text{ClMe}_2)_2$	<i>b</i>	98			265
$\text{Br}_2\text{Si}^{\text{A}}(\text{Si}^{\text{B}}\text{BrMe}_2)_2$	<i>b</i>	90			265
$\text{H}_2\text{Si}^{\text{A}}(\text{Si}^{\text{B}}\text{HMe}_2)_2$	<i>b</i>	68			265
$\text{Me}_2\text{Si}^{\text{A}}(\text{Si}^{\text{B}}\text{BrMe}_2)_2$	$\text{C}_6\text{H}_5\text{CH}_3$	79			266
$\text{Me}_2\text{Si}^{\text{A}}(\text{Si}^{\text{B}}\text{HMe}_2)_2$	$\text{C}_6\text{H}_5\text{CH}_3$	72			266
$\text{BrMeSi}^{\text{A}}(\text{Si}^{\text{B}}\text{BrMe}_2)_2$	$\text{C}_6\text{H}_5\text{CH}_3$	84			266

continued overleaf

TABLE 8. (continued)

Compound	Solvent	$^1J(\text{Si}^{\text{A}}-\text{Si}^{\text{B}})$	$^1J(\text{Si}^{\text{B}}-\text{Si}^{\text{C}})$	$^2J(\text{Si}^{\text{A}}-\text{Si}^{\text{C}})$	Reference
$\text{HMeSi}^{\text{A}}(\text{Si}^{\text{B}}\text{HMe}_2)_2$	$\text{C}_6\text{H}_5\text{CH}_3$	70			266
$\text{H}_2\text{MeSi}^{\text{A}}\text{Si}^{\text{B}}\text{Me}_2\text{Si}^{\text{C}}\text{Me}_3$	<i>b</i>	68.3	75.3	7.9	269
$\text{F}_2\text{MeSi}^{\text{A}}\text{Si}^{\text{B}}\text{Me}_2\text{Si}^{\text{C}}\text{Me}_3$	<i>b</i>	99.4	75.1	9.4	269
$\text{Cl}_2\text{MeSi}^{\text{A}}\text{Si}^{\text{B}}\text{Me}_2\text{Si}^{\text{C}}\text{Me}_3$	<i>b</i>	83.1	75.6	11.2	269
$\text{Br}_2\text{MeSi}^{\text{A}}\text{Si}^{\text{B}}\text{Me}_2\text{Si}^{\text{C}}\text{Me}_3$	<i>b</i>	74.6	75.4	11.8	269
$\text{I}_2\text{MeSi}^{\text{A}}\text{Si}^{\text{B}}\text{Me}_2\text{Si}^{\text{C}}\text{Me}_3$	<i>b</i>	64.4	74.7	12.2	269
$(\text{MeO})_2\text{MeSi}^{\text{A}}\text{Si}^{\text{B}}\text{Me}_2\text{Si}^{\text{C}}\text{Me}_3$	<i>b</i>	106.0	74.2	5.9	269
$\text{Ph}_2\text{MeSi}^{\text{A}}\text{Si}^{\text{B}}\text{Me}_2\text{Si}^{\text{C}}\text{Me}_3$	<i>b</i>	73.5	72.7	7.6	269
$(\text{HMe}_2\text{Si})_2\text{SiMeH}$	<i>b</i>	70.4			269
$(\text{FMe}_2\text{Si})_2\text{SiMeF}$	<i>b</i>	96.8			269
$(\text{ClMe}_2\text{Si})_2\text{SiMeCl}$	<i>b</i>	89.3			269
$(\text{BrMe}_2\text{Si})_2\text{SiMeBr}$	<i>b</i>	84.4			269
$(\text{IMe}_2\text{Si})_2\text{SiMeI}$	<i>b</i>	76.8			269
$(\text{MeOMe}_2\text{Si})_2\text{SiMeOMe}$	<i>b</i>	94.9			269
$(\text{PhMe}_2\text{Si})_2\text{SiMePh}$	<i>b</i>	72.1			269
$(\text{Cl}_3\text{Si})_2\text{SiMe}_2$	<i>b</i>	121.1			269
$(\text{Br}_3\text{Si})_2\text{SiMe}_2$	<i>b</i>	105.7			269
$(\text{I}_3\text{Si})_2\text{SiMe}_2$	<i>b</i>	82.2			269
$((\text{MeO})_3\text{Si})_2\text{SiMe}_2$	<i>b</i>	143.7			269
$(\text{Ph}_3\text{Si})_2\text{SiMe}_2$	<i>b</i>	74.4			269
$(\text{HMe}_2\text{Si})_2\text{SiMe}_2$	C_6D_6 , <i>c</i>	72.3			270
$(\text{FMe}_2\text{Si})_2\text{SiMe}_2$	C_6D_6 , <i>c</i>	85.9			270
$(\text{ClMe}_2\text{Si})_2\text{SiMe}_2$	C_6D_6 , <i>c</i>	81.5			270
$(\text{BrMe}_2\text{Si})_2\text{SiMe}_2$	C_6D_6 , <i>c</i>	78.7			270
$(\text{IMe}_2\text{Si})_2\text{SiMe}_2$	C_6D_6 , <i>c</i>	74.6			270
$(\text{MeOMe}_2\text{Si})_2\text{SiMe}_2$	C_6D_6 , <i>c</i>	85.1			270
$(\text{PhMe}_2\text{Si})_2\text{SiMe}_2$	C_6D_6 , <i>c</i>	72.7			270
$(\text{HMe}_2\text{Si})_2\text{SiMeH}$	C_6D_6 , <i>c</i>	70.4			270
$(\text{FMe}_2\text{Si})_2\text{SiMeF}$	C_6D_6 , <i>c</i>	96.8			270
$(\text{ClMe}_2\text{Si})_2\text{SiMeCl}$	C_6D_6 , <i>c</i>	89.3			270
$(\text{BrMe}_2\text{Si})_2\text{SiMeBr}$	C_6D_6 , <i>c</i>	84.4			270
$(\text{IMe}_2\text{Si})_2\text{SiMeI}$	C_6D_6 , <i>c</i>	76.8			270
$(\text{MeOMe}_2\text{Si})_2\text{SiMeOMe}$	C_6D_6 , <i>c</i>	94.9			270
$(\text{PhMe}_2\text{Si})_2\text{SiMePh}$	C_6D_6 , <i>c</i>	72.1			270
$(\text{Et}_2\text{N})_2\text{Si}^{\text{A}}(\text{Si}^{\text{B}}\text{Me}_3)_2$	CDCl_3	92.0			271
$\text{Et}_2\text{NSi}^{\text{A}}(\text{Si}^{\text{B}}\text{Me}_3)_3$	CDCl_3	65.8			271
$(\text{Me}_3\text{Si}^{\text{A}})_2\text{Si}^{\text{B}}\text{Cl}_2$	CDCl_3	75.9			271
$(\text{Me}_3\text{Si}^{\text{A}})_2\text{Si}^{\text{B}}\text{Br}_2$	CDCl_3	69.4			271
$(\text{Me}_3\text{Si}^{\text{A}})_2\text{Si}^{\text{B}}\text{I}_2$	CDCl_3	62.4			271
$\text{Et}_2\text{NClSi}^{\text{A}}(\text{Si}^{\text{B}}\text{Me}_3)_2$	CDCl_3	89.0			271
$(\text{IH}_2\text{Si}^{\text{A}})_2\text{Si}^{\text{B}}\text{H}_2$	C_6D_6	76.1			272
$(\text{IH}_2\text{Si}^{\text{A}})_2\text{Si}^{\text{B}}\text{HI}$	C_6D_6	78.6			272
$(\text{I}_3\text{Si}^{\text{A}})_2\text{Si}^{\text{B}}\text{I}_2\text{Si}^{\text{C}}\text{H}_3$	C_6D_6	89.6	75.9	18.1	272

^a Absolute values of coupling constants in Hz, 1J assumed to be positive, assumed accuracy ± 0.5 Hz.

^b No experimental conditions given.

^c 50% solution at 22 °C.

TABLE 9. Coupling constants $^1J(^{29}\text{Si}-^{29}\text{Si})$ in tetra- and oligosilanes^a

Compound	Solvent	$^1J(\text{Si}^{\text{A}}-\text{Si}^{\text{B}})$	Reference
$(\text{Me}_3\text{Si}^{\text{A}})_4\text{Si}^{\text{B}}$	CDCl_3	52.5	259
$(\text{Cl}_3\text{Si}^{\text{A}})_4\text{Si}^{\text{B}}$	CDCl_3	110.5	259
$\text{Si}^{\text{A}}\text{Me}(\text{Si}^{\text{B}}\text{ClMe}_2)(\text{Si}^{\text{C}}\text{Me}_3)_2$	<i>b</i>	63	273
$\text{Si}^{\text{A}}\text{Me}(\text{Si}^{\text{B}}\text{ClMe}_2)_2(\text{Si}^{\text{C}}\text{Me}_3)$	<i>b</i>	63	273
$\text{Si}^{\text{A}}\text{Me}(\text{Si}^{\text{B}}\text{HMe}_2)_2(\text{Si}^{\text{C}}\text{Me}_3)$	<i>b</i>	61	273
$\text{Si}^{\text{A}}\text{Me}(\text{Si}^{\text{B}}\text{ClMe}_2)_3$	<i>b</i>	70	273
$\text{Si}^{\text{A}}\text{Me}(\text{Si}^{\text{B}}\text{ClMe}_2)_2(\text{Si}^{\text{C}}\text{HMe}_2)$	<i>b</i>	69	273
$\text{Si}^{\text{A}}\text{Me}(\text{Si}^{\text{B}}\text{HMe}_2)_3$	<i>b</i>	62	273
$\text{Si}^{\text{A}}\text{Me}(\text{Si}^{\text{B}}\text{Cl}_2\text{Me})_3$	<i>b</i>	86.4	273
$\text{Si}^{\text{A}}\text{Me}(\text{Si}^{\text{B}}\text{Cl}_2\text{Me})_2(\text{Si}^{\text{C}}\text{H}_2\text{Me})$	<i>b</i>	82.2	273
$\text{Si}^{\text{A}}\text{Me}(\text{Si}^{\text{B}}\text{Cl}_2\text{Me})(\text{Si}^{\text{C}}\text{H}_2\text{Me})_2$	<i>b</i>	61.8	273
$\text{Si}^{\text{A}}\text{Me}(\text{Si}^{\text{B}}\text{H}_2\text{Me})_3$	<i>b</i>	61.8	273
$\text{MeSi}^{\text{A}}(\text{Si}^{\text{B}}\text{Me}_3)_3$	<i>b</i>	62.0	274
$\text{MeSi}^{\text{A}}(\text{Si}^{\text{B}}\text{Me}_2\text{H})_3$	<i>b</i>	61.8	274
$\text{MeSi}^{\text{A}}(\text{Si}^{\text{B}}\text{Me}_2\text{F})_3$	<i>b</i>	73.6 ^c	274
$\text{MeSi}^{\text{A}}(\text{Si}^{\text{B}}\text{Me}_2\text{Cl})_3$	<i>b</i>	70.1	274
$\text{MeSi}^{\text{A}}(\text{Si}^{\text{B}}\text{Me}_2\text{Br})_3$	<i>b</i>	67.6	274
$\text{MeSi}^{\text{A}}(\text{Si}^{\text{B}}\text{Me}_2\text{I})_3$	<i>b</i>	63.8	274
$[(\text{Me}_3\text{Si}^{\text{B}})_2\text{MeSi}^{\text{A}}]_2$	<i>b</i>	61.9	274
$[(\text{Me}_2\text{HSi}^{\text{B}})_2\text{MeSi}^{\text{A}}]_2$	<i>b</i>	61.6	274
$[(\text{Me}_2\text{FSi}^{\text{B}})_2\text{MeSi}^{\text{A}}]_2$	<i>b</i>	73.4	274
$[(\text{Me}_2\text{ClSi}^{\text{B}})_2\text{MeSi}^{\text{A}}]_2$	<i>b</i>	69.0	274
$[(\text{Me}_2\text{BrSi}^{\text{B}})_2\text{MeSi}^{\text{A}}]_2$	<i>b</i>	66.2	274
$[(\text{Me}_2\text{ISi}^{\text{B}})_2\text{MeSi}^{\text{A}}]_2$	<i>b</i>	62.1	274
$\text{Si}^{\text{A}}\text{Me}(\text{Si}^{\text{B}}\text{HMe}_2)_2(\text{Si}^{\text{C}}\text{Me}_3)$	$\text{C}_6\text{H}_5\text{CH}_3$	61	266
$\text{Si}^{\text{A}}\text{Me}(\text{Si}^{\text{B}}\text{BrMe}_2)_3$	$\text{C}_6\text{H}_5\text{CH}_3$	68	266
$\text{Si}^{\text{A}}\text{Me}(\text{Si}^{\text{B}}\text{HMe}_2)_3$	$\text{C}_6\text{H}_5\text{CH}_3$	62	266
$\text{Si}^{\text{A}}\text{Me}(\text{Si}^{\text{B}}\text{Br}_2\text{Me})_3$	$\text{C}_6\text{H}_5\text{CH}_3$	79.5	266
$\text{Si}^{\text{A}}\text{Me}(\text{Si}^{\text{B}}\text{H}_2\text{Me})(\text{Si}^{\text{C}}\text{Br}_2\text{Me})_2$	$\text{C}_6\text{H}_5\text{CH}_3$	74.8	266
$\text{Si}^{\text{A}}\text{Me}(\text{Si}^{\text{B}}\text{H}_2\text{Me})_2(\text{Si}^{\text{C}}\text{Br}_2\text{Me})$	$\text{C}_6\text{H}_5\text{CH}_3$	65	266
$\text{Si}^{\text{A}}\text{Me}(\text{Si}^{\text{B}}\text{H}_2\text{Me})_3$	$\text{C}_6\text{H}_5\text{CH}_3$	61.8	266
$\text{Si}^{\text{A}}(\text{Si}^{\text{B}}\text{BrMe}_2)_4$	$\text{C}_6\text{H}_5\text{CH}_3$	57	266
$\text{Si}^{\text{A}}\text{Me}(\text{Si}^{\text{B}}\text{BrMe}_2)_2(\text{Si}^{\text{C}}\text{Me}_3)$	$\text{C}_6\text{H}_5\text{CH}_3$	64.5	266
$\text{P}(\text{Si}^{\text{A}}\text{Me}_2\text{Si}^{\text{B}}\text{Me}_2)_3\text{Si}^{\text{C}}\text{Me}$	<i>b</i>	66.7 ^d	276
$(\text{PhMe}_2\text{Si}^{\text{A}}\text{Si}^{\text{B}}\text{Me}_2)_3\text{Si}^{\text{C}}\text{Me}$	<i>b</i>	71.9 ^e	276
$(\text{TfMe}_2\text{Si}^{\text{A}}\text{Si}^{\text{B}}\text{Me}_2)_3\text{Si}^{\text{C}}\text{Me}$	<i>b</i>	77.4 ^f	276
$(\text{ClMe}_2\text{Si}^{\text{A}}\text{Si}^{\text{B}}\text{Me}_2)_3\text{Si}^{\text{C}}\text{Me}$	<i>b</i>	78.5 ^g	276
$[(\text{Ph}_2\text{MeSi}^{\text{A}})_2\text{Si}^{\text{B}}\text{Me}]_2$	<i>b</i>	61.0	277
$[(\text{PhMe}_2\text{Si}^{\text{A}})_2\text{Si}^{\text{B}}\text{Me}]_2$	<i>b</i>	61.0	277
$(\text{Ph}_3\text{Si}^{\text{A}})_3\text{Si}^{\text{B}}\text{Me}$	<i>b</i>	61.0	277

continued overleaf

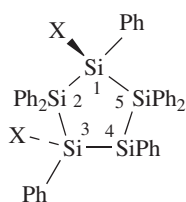
TABLE 12. Coupling constants $J(^{29}\text{Si}-^{29}\text{Si})$ in selected compounds^{a,b}

Compound	$^1J(^{29}\text{Si}-^{29}\text{Si})$	$^nJ(^{29}\text{Si}-^{29}\text{Si})$ ($n \geq 2$)
22	68.4 (C-D)	4.9 (B-D)
	65.4 (A-B)	2.9 (A-C)
	57.6 (B-C)	2.9 (A-D)
23	62.1 (C-D or C'-D)	9.4 (B-D or B'-D)
	57.4 (A-B or A-B')	8.2 (A-C or A-C')
	^c (B-C, B'-C')	
24	57.6 (A-B or A-B')	9.8 (A-C or A-C')
	^c (B-C, B'-C')	9.8 (B-C', C-B')
25	46.9 (A-B or A-B')	27.3 (A-C)
	46.9 (B-C or B'-C')	
26	24.1 (A-B or A-B')	

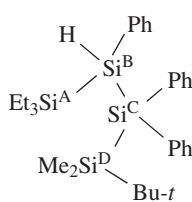
^aData of Reference 240; absolute values of coupling constants in Hz, measured in C_6D_6 solutions at 25 °C at 53.7 MHz.

^bThe letters in parentheses refer to the silicon atom labeling shown in the structures.

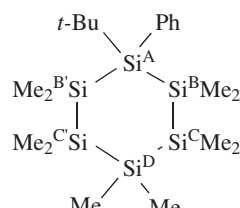
^cThe chemical shifts of these ^{29}Si nuclei were too close to permit accurate measurement of the coupling constant between them.



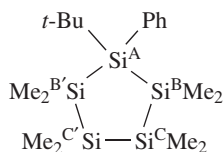
(21)



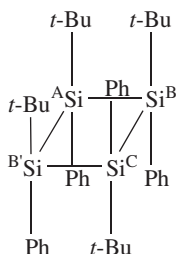
(22)



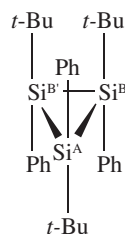
(23)



(24)



(25)



(26)

TABLE 13. Coupling constants in selected silaethylenes, **27**^a

R	$^1J(\text{Si}^{\text{A}}-\text{Si}^{\text{B}})$
CMe ₃	70.8
CEt ₃	73.2
1-(1-Methylcyclohexyl)	72.1
1-Adamantyl	72.0

^aAbsolute values of coupling constants in Hz, measured in C_6D_6 ; data taken from Reference 261.

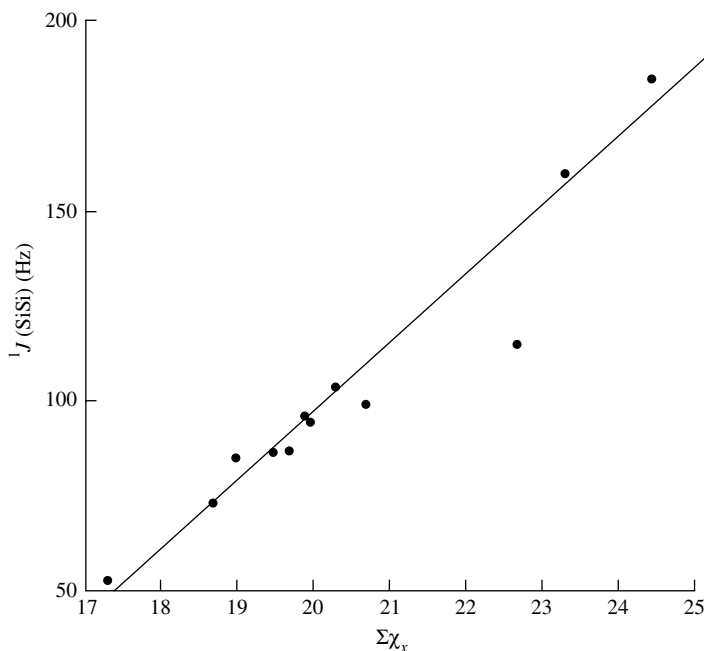
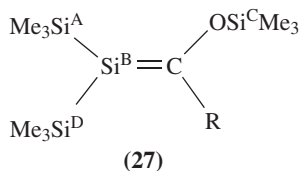


FIGURE 34. Correlation of $|^1J(^{29}\text{Si}-^{29}\text{Si})|$ ($^1J(\text{SiSi})$) coupling constants vs the sum of the substituent electronegativities ($\Sigma\chi_x$) in substituted disilanes. Reprinted with permission from Reference 259. Copyright 1976 American Chemical Society

some parallels between the trends in these couplings and trends in $^1J(^{29}\text{Si}-^{13}\text{C})$ and $^1J(^{13}\text{C}-^{13}\text{C})$ couplings, including their relationships with the s -character of the carbon nuclear involved in $^1J(^{29}\text{Si}-^{13}\text{C})$. Correlations with chemical shifts were poor. Extrapolation of the correlation with electronegativity led to the prediction of $^1J(^{29}\text{Si}-^{29}\text{Si}) = 40-45$ Hz in disilane, Si_2H_6 . Theoretical calculations yielded the values of 10.3 Hz²⁷⁸ and 95.03 Hz²⁷⁹ while the experimentally found value is 77.2 Hz in $(\text{SiH}_2\text{D})_2$ ²⁶⁴. In a series of chlorohydrogen disilanes, $\text{Si}_2\text{Cl}_n\text{H}_{6-n}$, the $J(^{29}\text{Si}-^{29}\text{Si})$ coupling increases with n , but the dependence is not linear (Table 6) and no relation to $^1J(^{29}\text{Si}-^1\text{H})$ or $^2J(^{29}\text{Si}-^1\text{H})$ could be found²⁶⁷.

Comparison with $^1J(^{29}\text{Si}-^{13}\text{C})$ and $^1J(^{13}\text{C}-^{13}\text{C})$ couplings and the fact that there are no coupling values close to zero lead to the suggestion that $^1J(^{29}\text{Si}-^{29}\text{Si})$ as well as the reduced coupling $^1K(^{29}\text{Si}-^{29}\text{Si})$ are positive²⁵⁹. Small couplings were not found

even in silanes with sterically demanding substituents that have a long Si–Si bond and a small force constant²³⁰; the positive sign is generally accepted. The positive sign of $^1J(^{29}\text{Si}-^{29}\text{Si})$ coupling in $\text{Si}(\text{SiMe}_3)_4$ was confirmed by heteronuclear correlation experiment²⁸⁰. To the best of our knowledge, experiments like SLAP^{281–283} have not been applied to organosilicon compounds to determine experimentally the relative signs of the $J(^{29}\text{Si}-^{29}\text{Si})$ couplings.

In an extensive study of tetrasilanes of the type $(\text{R}_3\text{Si})_3\text{Si}-\text{X}$, Marsmann and coworkers²⁶⁰ found that the coupling increases with the electronegativities of both R and X, the effect of R being dominant, but the dependence on the electronegativity is not so clear in a series with a fixed substituent R (Table 3). Similarly, correlation between $^1J(^{29}\text{Si}-^{29}\text{Si})$ and $^1J(^{29}\text{Si}-^{13}\text{C})$ (in compounds with $\text{R} = \text{CH}_3$) has the shape of a parabola. These observations could be understood in terms of the role of substituent electronegativity on rehybridization of the silicon atom. The role of silicon hybridization was stressed by Brook and coworkers²⁶¹, who noted that the one-bond coupling between two sp^3 hybridized silicon atoms is about 56 Hz and that between one sp^3 and one sp^2 hybridized silicon is about 72 Hz (Table 4).

Subsequent studies used different electronegativity scales^{230,284}, introduced a quadratic term^{284,285} ($\Sigma\chi_\chi$) and extended the correlation with electronegativity holding for disilanes to higher silanes^{270,271}. Attempts to correlate these couplings with other polarity descriptors did not improve the fit, and an attempt to correlate them with bond length failed²³⁰. Interesting correlations with Si–Si valence force constants^{230,269,286} and heteronuclear $^1J(^{29}\text{Si}-^1\text{H})$ couplings²³⁰ were advanced (Figures 35 and 36). While the values of $^1J(^{29}\text{Si}-^{29}\text{Si})$ couplings increase with the substituent electronegativity according to the above-mentioned correlation, $^2J(^{29}\text{Si}-^{29}\text{Si})$ couplings appear to decrease in oligosilanes²⁷⁴.

Not in line with these correlations, the $^1J(^{29}\text{Si}-^{29}\text{Si})$ coupling in **28** is slightly larger (89 Hz) than that in **29** (84 Hz). In the latter compound, one of the silicon atoms is bonded to a sp^2 centre²⁸⁷. (At the same time the values found in **29** are close to those in disilanes, which suggests that little or no π -bonding is present²⁸⁸.)

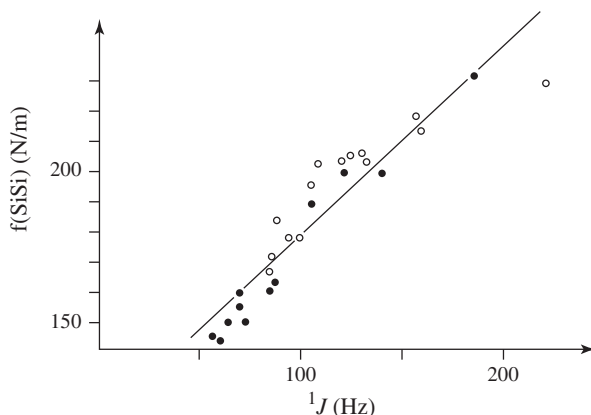


FIGURE 35. Correlation between $^1J(^{29}\text{Si}-^{29}\text{Si})$ coupling constants and Si–Si valence force constants $f(\text{SiSi})$ (N/m) in oligosilanes. Reprinted from Reference 269. Copyright 1995, with permission from Elsevier Science

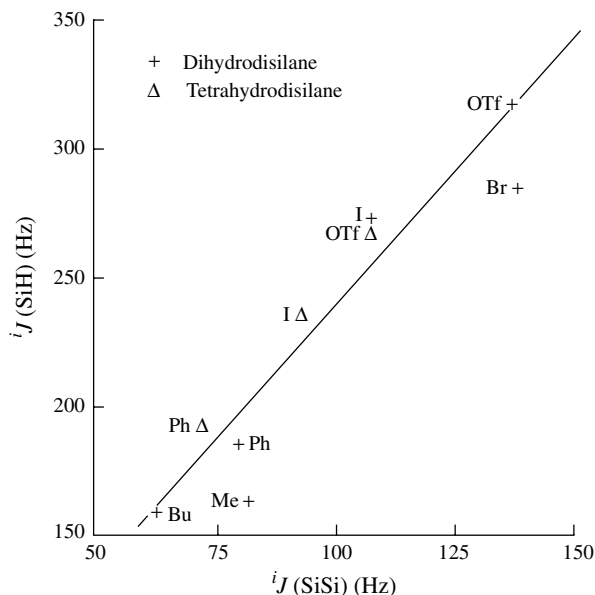
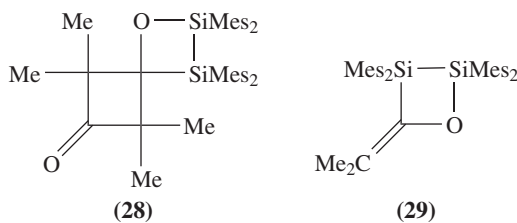


FIGURE 36. Correlation between $^1J(^{29}\text{Si}-^{29}\text{Si})$ and $^1J(^{29}\text{Si}-^1\text{H})$ coupling constants in symmetrical dihydrodisilanes $\text{X}_2\text{HSiSiHX}_2$ and tetrahydrodisilanes $\text{XH}_2\text{SiSiH}_2\text{X}$, $\text{X} = \text{Ph}, \text{C}, \text{Br}, \text{IMe}, t\text{-Bu}, \text{OTf}$ (OSO_2CF_3). Reprinted from Reference 230, Copyright 1991, with permission from Elsevier Science



Mes = Mesityl

In oligosilyl anions, $^{29}\text{Si}-^{29}\text{Si}$ couplings provide a good measure of the negative charge on the metallated silicon while the chemical shifts do not appear reliable in this respect²⁸⁹.

Data on long-range couplings $^nJ(^{29}\text{Si}-^{29}\text{Si})$ through other than a Si-Si pathway are scarce. An example of $^3J(^{29}\text{Si}-\text{C}-\text{C}-^{29}\text{Si})$ coupling (8.9 Hz)²⁹⁰ is given in Figure 37. Two-bond Si-O-Si couplings in the range 1.2–2.5 Hz enable double-quantum filtration of COSY spectra (DQF COSY) of siloxanes that are so useful for assignment and determination of their structure^{256–258}. Two-bond Si-N-Si couplings are of similar magnitude (1.0–3.1 Hz)²⁹¹.

The limited data available on polysilanes (Table 12) allowed Kuroda and coworkers²⁴⁰ to draw some obvious conclusions: two- and three-bond couplings are an order of magnitude smaller than one-bond couplings. While the one-bond couplings increase with ring size, the two-bond couplings decrease and the changes are more pronounced in strained

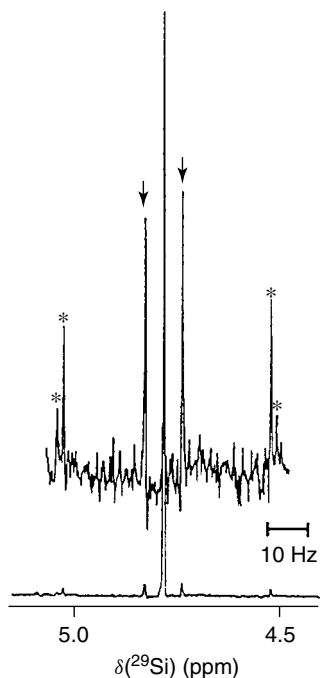
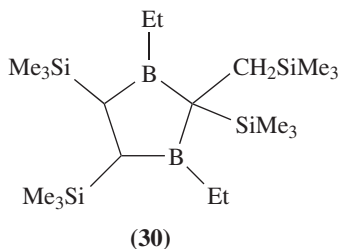


FIGURE 37. Me_3SiCH_2 part of refocused INEPT ^{29}Si NMR spectrum of **30**. Arrows mark ^{29}Si satellites due to $^3J(^{29}\text{Si}-\text{C}-\text{C}-^{29}\text{Si})$ coupling while asterisks denote ^{13}C satellites [99.3 MHz, toluene- d_8 solution, $^3J(^{29}\text{Si}-\text{C}-\text{C}-^{29}\text{Si}) = 8.9$ Hz]. Reproduced by permission of Wiley-VCH from Reference 290

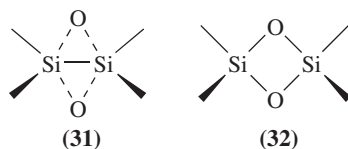


systems. The trend found for one-bond couplings is consistent with the correlation of 1J with the amount of *s*-character of the silicon atom orbitals participating in the Si–Si bond.

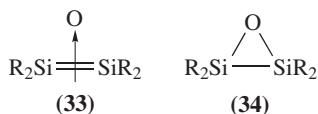
In phenylated cyclopentasilanes, $\text{Si}_5\text{Ph}_9\text{X}$ (Tables 10 and 11), the $^1J(^{29}\text{Si}-^{29}\text{Si})$ values for the substituted silicon atom increase and the $^2J(^{29}\text{Si}-^{29}\text{Si})$ values decrease with the increasing electronegativity of the halogen substituent²¹⁹. In related methyl derivatives $\text{Si}_5\text{Me}_9\text{X}$, $\text{Si}_5\text{Me}_9\text{SiMe}_2\text{X}$ and $\text{Si}_6\text{Me}_{11}\text{X}$ such correlations with electronegativity hold only for $^1J(\text{Si1}-\text{Si2})$ couplings²⁹².

Two areas of applications of ^{29}Si – ^{29}Si coupling are already established: (i) in oligo- and polysilanes the coupling constant values are needed to set correctly 2D INADEQUATE experiments for establishing Si–Si connectivity [similarly, $^2J(^{29}\text{Si}$ – O – $^{29}\text{Si})$ couplings could be used in siloxanes] and (ii) in elucidating the bonding in some compounds through the relation with σ^* orbital contribution or s -character in the Si–Si bond. Let us look into some illustrative examples of the latter.

Comparison of the coupling constant $^1J(^{29}\text{Si}$ – $^{29}\text{Si})$ in unsymmetrical aryldisilenes [$^1J(^{29}\text{Si}$ – $^{29}\text{Si}) = 155$ – 160 Hz] with those in aryldisilanes (around 85 Hz) indicated much greater s character in the $\sigma_{\text{Si}-\text{Si}}$ bond in disilenes than in disilanes, consistent with approximate sp^2 hybridization of the Si atoms in the disilenes²⁹³. A similar comparison of the $J(^{29}\text{Si}$ – $^{29}\text{Si})$ coupling found in 1,3-cyclodisiloxanes (3.8–4.0 Hz) with the $^1J(^{29}\text{Si}$ – $^{29}\text{Si})$ couplings typical for organodisilanes (80–90 Hz) and $^2J(^{29}\text{Si}$ – O – $^{29}\text{Si})$ couplings in siloxanes (1–4 Hz) led to the rejection of the hypothesis that there is a σ bond between the silicon atoms in 1,3-disiloxanes²³⁶. The σ bond between the silicon atoms (structure **31**) would lead to a much larger $J(^{29}\text{Si}$ – $^{29}\text{Si})$ than in structure **32**. The values found indicate that there is little if any s orbital contribution to the bonding between the silicon atoms in 1,3-cyclodisiloxanes.



Analogous lines of thought provided support for the model of the bonding in disilaoxiranes²⁹⁴. According to this model a significant amount of double bond character of the disilene is retained in the oxirane. Accordingly, the $^1J(^{29}\text{Si}$ – $^{29}\text{Si})$ coupling of 99 Hz in an unsymmetrical aryldisilaoxirane is intermediate between the couplings in aryldisilanes and aryldisilenes (the ranges given above). Thus, the disilaoxiranes have some of the character of **33** as well as oxiranes **34**.



The 1D INADEQUATE spectrum of **17** shown in Figure 27 indicates $^1J(^{29}\text{Si}$ – $^{29}\text{Si}) = 108$ Hz, the value attesting to a larger s character in the Si–Si bond than in disilanes (with smaller coupling constants). The value is close to that found in 1,2-dioxadisiletane (96–98 Hz), which indicates similarity of the unusual bonding in these isoelectronic ring systems²³⁸.

The unusually small value of the coupling constant, $^1J(^{29}\text{Si}$ – $^{29}\text{Si}) = 19.1$ Hz, in (pentamethyldisilanyl)lithium, $(\text{Me}_3\text{SiSiMe}_2)\text{Li}$, supports the suggestion that the negative charge is localized on the silicon atom attached to the lithium. This small value was found in THF- d_8 solution at 180 K where the compound is monomeric; in toluene or benzene solutions the coupling was much larger, $^1J(^{29}\text{Si}$ – $^{29}\text{Si}) = 43.2$ Hz, due to aggregation with lesser ionic and more covalent character of the compound in these solvents²⁹⁵.

B. Triple Resonance

Triple resonance experiments are used when double resonance experiments (either 1D or 2D) fail to provide the needed answer, whether it be assignment of ^{29}Si lines, their resolution, or separation of NMR parameters. A number of determinations, however, can be carried out using pseudo-triple resonance that is less demanding on the spectrometer hardware as described in Sections V.B, VI.A, and VI.C.2.

Triple resonance does not necessarily mean 3D spectroscopy, a point that is often misunderstood. A 3D experiment (i.e. experiment that depends on three varied time parameters, is usually subject to three Fourier transforms and requires presentation as a 4-dimensional result) might use only resonance of one nucleus or two nuclei. Triple resonance requires spectrometer hardware capable of irradiating three different isotopes in the sample in one experiment (in addition to locking). Until recently, such hardware was not commercially available and so the experiments could be done only in laboratories with sufficient technical expertise and resources to carry out the necessary modifications. Usually, the resulting spectra were 1D spectra, as exemplified by assignment techniques based on $^{29}\text{Si}-\text{O}-^{13}\text{C}$ couplings^{47,253,254}. At present, all leading manufacturers offer multichannel spectrometers (allowing a much higher number of nuclei to be irradiated), but the standard probe offering usually does not include ^{29}Si multinuclear probes. Certainly, this picture will change with growing demand and with progress in probe design. The demand will certainly come, as triple resonance is the only choice for assigning ^{29}Si resonances experimentally in a number of heteronuclear moieties, and also as a consequence of the elegant 3D triple-resonance ($^1\text{H}-^{13}\text{C}-^{29}\text{Si}$) experiments of Rinaldi's group which demonstrated the power of the method to solve significant chemical problems.

1. 1D experiments

The simplest triple resonance experiments to perform are $^1\text{H}-^{29}\text{Si}$ INEPT experiments employing decoupling of another nucleus, usually ^{31}P . These experiments are described in Section V.B.

Experiments involving decoupling of less abundant nuclei are somewhat more sophisticated. In selective decoupling experiments used for ^{29}Si signal assignment in cases where other methods cannot be applied, e.g. in fragments containing $\text{Si}-\text{X}-\text{C}\equiv$ ($\text{X} = \text{O}$, N , quaternary C etc.), one can use either $^{13}\text{C}-\{^{29}\text{Si}\}$ or $^{29}\text{Si}-\{^{13}\text{C}\}$ experiment (both combined with proton decoupling). The $^1\text{H}-^{13}\text{C}-^{29}\text{Si}$ triple resonance is a demanding experiment, as it detects only the 0.05% of the molecules in the sample that contain such an isotopomer.

Of the two possibilities, one has to choose that which gives satellites easier to distinguish from other signals in the spectrum. The two ^{29}Si satellites in the ^{13}C spectrum each amount to 2.4% of the centre line (i.e. in the $^{13}\text{C}-\{^{29}\text{Si}\}$ experiment) while those of ^{13}C only amount to 0.6% of the central ^{29}Si line (in the $^{29}\text{Si}-\{^{13}\text{C}\}$ experiment). Experiments of the former type had already been performed in 1985⁴⁷ in the very simple and not sophisticated manner offered by the then current spectrometers. The ^{13}C NMR spectra were recorded with proton broad-band decoupling and with selective continuous ^{29}Si decoupling. The decoupling frequency alternated between two values in two consecutive scans and the FIDs were summed with opposite signs. If both decoupler frequencies were far away from the silicon resonance frequency, the subtracted FIDs completely cancel. When the two frequencies are near the ^{29}Si resonance, the coupling is reduced, the centre

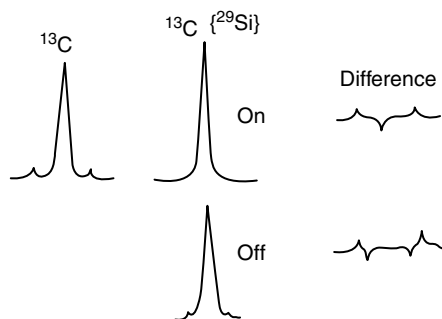


FIGURE 38. Scheme of resultant ^{13}C NMR spectrum formation from two subtracted spectra with different selective decoupling ^{29}Si frequencies. Reproduced with permission of Collection of Czechoslovak Chemical Communications from Reference 47

line is suppressed, and two pairs of satellites with residual splittings and opposite phases appear in the spectrum (Figure 38). When one of the frequencies is on the ^{29}Si resonance, the corresponding satellites collapse and the spectrum has the appearance shown in the figure. The method is generally applicable to other cases, for example cases of unresolved ^1H spectra. It requires, however, that the ^{29}Si lines be well separated. If that is not the case, perhaps the reverse experiment of the type $^{29}\text{Si}-\{^{13}\text{C}\}$ could be employed in spite of the lower relative intensity of the satellites.

Another 1D experiment that can be and has been utilized for ^{29}Si line assignment in even more difficult situations [with $J(^{29}\text{Si}-^{13}\text{C}) \approx 1-2$ Hz] is selective heteronuclear INADEQUATE^{253,254}. 1D heteronuclear INADEQUATE with ^{13}C detection is a simple two-step pulse sequence in which the pulses are applied simultaneously to both nuclei:

$$\begin{aligned}
 ^1\text{H} &: \text{decouple broad-band} \\
 ^{29}\text{Si} &: 90_x^\circ - \tau - 180_{\pm y}^\circ - \tau - 90_x^\circ - \Delta - 90_\phi^\circ \\
 ^{13}\text{C} &: 90_x^\circ - \tau - 180_{\pm y}^\circ - \tau - 90_x^\circ - \Delta - 90_\phi^\circ - \text{acquire}(\psi)
 \end{aligned}$$

(With current understanding of multiple quantum coherences, the sequence could be simplified.)

When more than one long-range coupling affects some carbon nuclei, the satellite spectra can be quite complicated. For that reason the selective version is advantageous. At present, a number of selective pulses to achieve this goal are available, but in 1985 the authors could achieve the selectivity by weak long pulses on the frequency of the ^{29}Si NMR line, which leaves only the ^{29}Si satellites of the carbons coupled to that silicon in the INADEQUATE spectrum. A typical example of such spectra is shown in Figure 39 for three selective experiments performed on the Si-1, Si-2 and Si-3 lines in the spectrum of 2,3,4-tris(*O*-trimethylsilyl)-1,6-anhydro- β -D-glucopyranose (**2**). The ^{13}C lines were assigned to the carbon atoms as indicated on the top of the figure by standard 2D NMR techniques. Obviously, when the ^{29}Si frequency is set on the Si-2 frequency, satellites of C-2 and C-3 are apparent in the INADEQUATE spectrum since the two- and three-bond couplings $J(^{29}\text{Si}-^{13}\text{C})$ are of similar magnitude. Application of this method requires careful calibration of the rf field strength. The method works well even if the coupling constants are small.

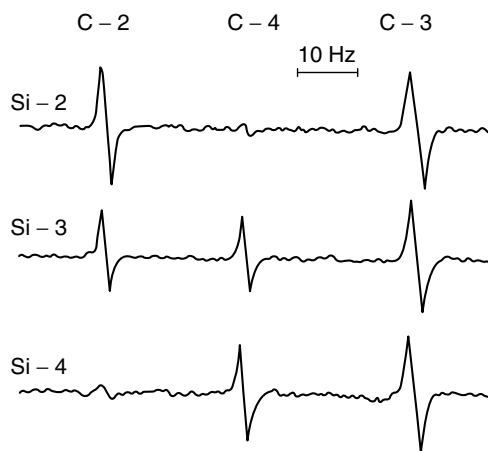


FIGURE 39. The ^{29}Si satellites in the ^{13}C NMR spectra of **2** at 90.6 MHz measured with the selective heteronuclear INADEQUATE (the ^{29}Si line selectively irradiated is indicated on the left for each trace, ^{13}C assignment is given on the top). Total experimental time 15 min. Reproduced by permission of John Wiley & Sons, Ltd from Reference 253

2. 2D experiments

The requirements of general X–Y heteronuclear²⁹⁶ and especially X– ^{13}C ¹⁹² two-dimensional correlations have recently been reviewed by Berger and coworkers; the reviews included examples of X = ^{29}Si but did not cover pulsed field gradient variants of the methods. They viewed Y–X heteronuclear correlations as a simple alteration of the better known H–X correlations (double resonance) in which proton pulses are replaced by Y pulses while protons are continuously broad-band decoupled. In such a case there are three classes of methods: (1) HETCOR in which nucleus Y is first permitted to develop during evolution time t_1 (according to its chemical shift with or without the coupling) and then polarization is transferred to nucleus X, which is detected; (2) HMQC (or HMBC) in which heteronuclear double-quantum correlation is created first, and after its evolution under the influence of the chemical shift of nucleus Y it is converted back to magnetization of X, which is detected; (3) HSQC in which INEPT first transfers polarization from X to Y and after evolution is brought back to X, which is detected. In shorthand these sequences are:

HETCOR:

^1H : *decouple broad-band*
 X : 180_x° 180_{-x}° 90_x° 180_x° *acquire(x)*
 Y : $90_x^\circ - t_1/2 -$ $- t_1/2 - \Delta -$ $180_x^\circ - \Delta -$ $90_{\pm y}^\circ - \Delta -$ $180_{-x}^\circ - \Delta -$ (*decouple*)

HMQC:

^1H : *decouple broad-band*
 X : 90_x° 180_x° *acquire(x)*
 Y : $- 2\Delta - 90_x^\circ - t_1/2 -$ $- t_1/2 - 90_x^\circ - 2\Delta -$ (*decouple*)

HSQC:

$$\begin{array}{l}
 {}^1\text{H} : \text{decouple broad-band} \\
 \text{X} : 90_x^\circ - \Delta - 180_x^\circ - \Delta - 90_y^\circ \qquad 180_x^\circ \qquad 90_y^\circ \qquad 180_x^\circ \qquad \text{acquire}(x) \\
 \text{Y} : \qquad 180_x^\circ \qquad 90_x^\circ - t_1/2 - \qquad - t_1/2 - 90_x^\circ - \Delta - 180_x^\circ - \Delta - (\text{decouple})
 \end{array}$$

where Δ is the usual delay $\{1/[4 \cdot J(\text{XY})]$, assuming no X or Y equivalent nuclei}. In the case of ^{29}Si correlations ${}^1\text{H}$ broad-band decoupling should be applied only during acquisition (NOE); to eliminate effects of proton couplings during the sequence, the 180° pulses in X and Y channels should be accompanied by simultaneous refocusing proton pulses.

The optional decoupling of nuclei X or Y further enhances the signal-to-noise ratio but might limit the length of acquisition (i.e. resolution along the F2 axis), as otherwise the dissipated heat might damage the probe. If decoupling is not needed and if the antiphase appearance of the signals can be tolerated, the final refocusing delay Δ can be dropped from the sequences.

As in all correlation experiments, the experiments require measurable coupling between nuclei X and Y and sufficiently slow relaxation so that non-equilibrium magnetizations survive for the duration of the sequence.

HMQC and HSQC are about equally sensitive, the sensitivity being proportional to $(\gamma_X)^{5/2}$, but as the HSQC pulse sequence uses more than twice as many pulses as HMQC, the latter is preferred (especially on older spectrometers). Both use two polarization transfer steps while HETCOR uses only one transfer. If the coupling constants vary within the sample, HETCOR might be a better choice for lower losses in polarization transfers. Since the sensitivity of HETCOR is proportional to $(\gamma_X)^{3/2}(\gamma_Y)$, the choice of nucleus for detection is not trivial.

One should realize that in all three methods one needs not only high sensitivity but also good suppression of signals coming from the other isotopomers. For example, when ^{29}Si is used for detection in an ^{29}Si – ^{19}F correlation experiment, each line is split by $J(^{29}\text{Si}$ – $^{19}\text{F})$ couplings, but if ^{19}F detection is used instead, only 4.7% of the satellites are of interest and the central line (95.3%) must be suppressed.

Another important consideration is the linewidth and lineshape. The detected nucleus should have narrow lines, as narrow lines indicate the long T_2 relaxation times that are needed for the magnetization to survive for the duration of the sequence. The linewidth and lineshape are especially important if closely spaced lines are expected in a spectrum of large width. In 2D experiments one can use a sufficiently long acquisition time (t_2) to resolve close lines without prolonging the total measuring time excessively, so it is advantageous when the most sensitive coil also has the narrowest lines. Resolving such closely spaced lines along the F1 axis with a large spectral width would require a very large number of increments and lead to a very long experimental time. Fortunately, ^{29}Si lines are usually narrow. Long T_1 relaxation of ^{29}Si is a disadvantage, as it calls for slow repetition in ^{29}Si detected HSQC and HMQC experiments and ^{29}Si indirectly detected HETCOR triple resonance experiments.

In practice, one must also consider the properties of the available probe (additional channels in the commercial spectrometers are usually broad-band). Complete freedom for the experimentalist would be provided if the probe had a ${}^1\text{H}$ coil on the outside (as broad-band probes do) and the inner coil(s) for X and Y tunable and with equal sensitivity for X and Y. Such probes are not offered, and if they were, their performance would probably be poor (sensitivity, handling, pulse length etc.) as the price to pay for the flexibility. The second choice would be a ${}^1\text{H}$ – ^{29}Si –X probe; such probes are available, but more common are ${}^1\text{H}$ – ^{13}C –X probes (with inverse configuration, i.e. with a ${}^1\text{H}$

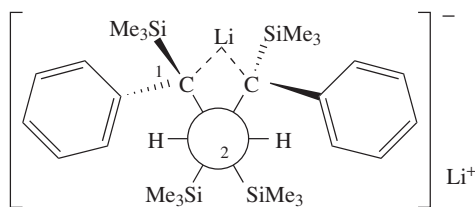
inner coil designed for maximum sensitivity). Of course, the latter probes limit the choice of heteronuclear correlations to ^{29}Si – ^{13}C correlations. Of the two heteronuclei available on a given probe, the one that offers the highest sensitivity should be used for detection (in place of nucleus X in the above pulse sequences) unless the sample is enriched in the other isotope. A good estimate of sensitivity is the pulse length as given in the probe specification divided by the resonance frequency; a shorter 90° pulse means better coupling between the coil and the sample (values of S/N usually given in the probe specification refer to a standard solution that is different for each nucleus, and thus the value might be misleading). A short duration of 90° and especially 180° pulses disposes of the need to use composite pulses to cover the whole spectral range in high field spectrometers.

The sensitivity of these experiments can be increased by employing INEPT polarization transfer to nucleus Y in HETCOR or to nucleus X in HMQC or HSQC in place of the first 90° pulse (as in a number of 3D experiments). The INEPT–HMQC combination:

$$\begin{array}{l}
 {}^1\text{H} : 90_x^\circ - \Delta - 180_x^\circ - \Delta - 90_y^\circ \quad \text{decouple broad-band} \dots \\
 {}^{29}\text{Si} : \quad \quad \quad 180_x^\circ \quad \quad 90_x^\circ - d - \quad \quad \quad 180_x^\circ \quad \quad \text{acquire}(x) \\
 {}^{13}\text{C} : \quad \quad \quad \quad \quad \quad \quad \quad 90_x^\circ - t_1/2 - \quad \quad \quad - t_1/2 - 90_x^\circ
 \end{array}$$

with $\Delta = 1/[4J(^{29}\text{Si}$ – $^1\text{H})]$ and $d = 1/[2J(^{29}\text{Si}$ – $^{13}\text{C})]$ was used for ^{29}Si – ^{13}C correlation by Berger²⁹⁷. In this sequence, delay d represents some compromise value between the requirements of optimum start of proton decoupling and polarization transfer $^{29}\text{Si} \rightarrow ^{13}\text{C}$. The power of the method is apparent from Figure 40, where the region of ^{29}Si NMR signals of siloxane oil D units is resolved (note that no ^{13}C decoupling is used in the sequence and so ^{29}Si – ^{13}C couplings also spread the signals along the F1 axis).

An interesting and instructive example was provided by Böhler and Günther²⁹⁸, who successfully ran a ^6Li – ^{29}Si HMQC experiment (with ^6Li detection in a sample enriched above 98% in ^6Li) on 1,4-diphenyl-1,2,3,4-tetrakis(trimethylsilyl)butane-1,4-diyl dilithium (**35**). Using the above INEPT–HMQC sequence without decoupling and refocusing, they saw (Figure 41) cross-peaks due to $^2J(^{29}\text{Si}$ – $^6\text{Li}) = 0.3$ Hz and $^3J(^{29}\text{Si}$ – $^6\text{Li}) = 0.7$ Hz couplings. The problem of the probe was overcome by running the experiment without lock and tuning the lock coil to ^6Li resonance.



(35)

Pulsed field gradient variants of the above sequences have been described; HMQC and HSQC have in their gradient versions a higher sensitivity as they allow the use of higher spectrometer gain and usually lead to ‘cleaner’ spectra with fewer artifacts. For a review see Reference 299.

3. 3D experiments

In addition to the above-mentioned challenges of all triple resonance experiments, pulse sequences for 3D experiments are demanding to develop and test as well as to run

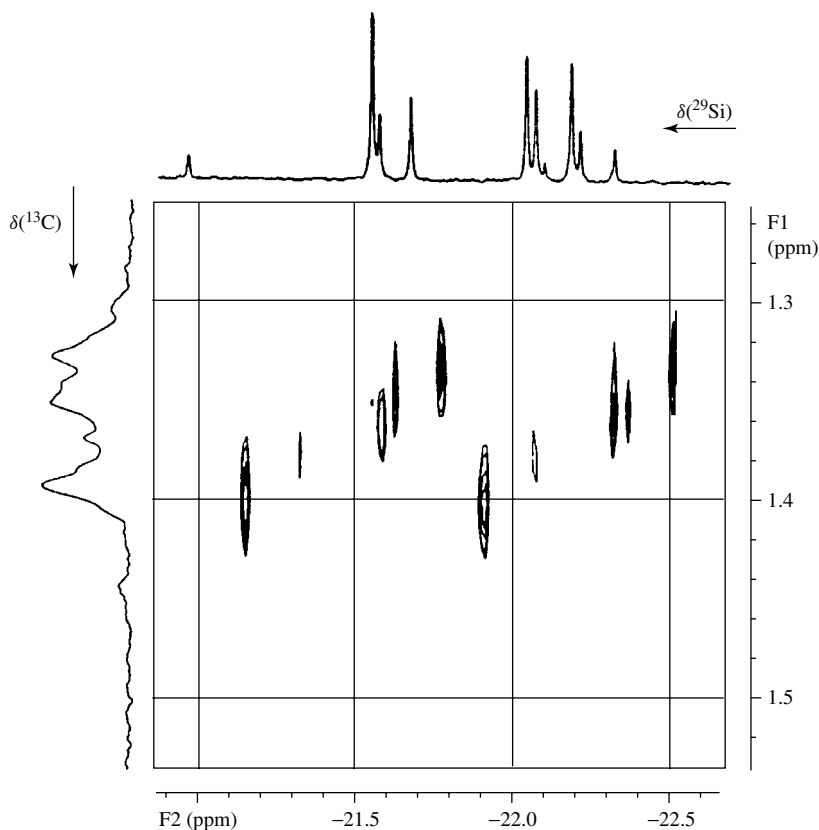


FIGURE 40. ^{29}Si detected ^{29}Si – ^{13}C correlated 2D spectrum enhanced by ^1H – ^{29}Si INEPT (50% solution of polymer silicon oil in CD_3COCD_3 ; triple resonance probe with ^1H inner coil double tuned to ^{13}C frequency, 64 increments with 128 scans each, 1024 data points in F2 relaxation delay 3 s, $d = 7$ ms and $\Delta = 30$ ms). Reproduced by permission of Academic Press from Reference 297

routinely. For example, the sequences used for 3D correlations (the pulse sequences with phase cycling are given in the references or in the references cited therein) contain more than 30 pulses (some 90° , some 180° pulses in ^1H , ^{13}C and ^{29}Si channels) with 2 to 3 gradient pulses and a number of delays between them, all of which must be calibrated or optimized. (And, of course, heteronuclear decoupling of ^{13}C and ^{29}Si nuclei during acquisition if ^1H detection is used.) However, the experimentalist is rewarded with results that are unlikely to be obtained in any other way.

In their study of poly(1-phenyl-1-silabutane) (**36**) tacticity²⁰⁵ Rinaldi and coworkers used a sequence of INEPT transfers $^1\text{H} \rightarrow ^{13}\text{C}$; $^{13}\text{C} \rightarrow ^{29}\text{Si}$; $^{29}\text{Si} \rightarrow ^{13}\text{C}$; and $^{13}\text{C} \rightarrow ^1\text{H}$ based on $^1J(^{13}\text{C}-^1\text{H})$ and $^2J(^{29}\text{Si}-^{13}\text{C})$ couplings with two gradient pulses to ensure that only ^1H signals from the ^1H – ^{13}C – ^{29}Si isotopomer are detected. The $^2J(^{29}\text{Si}-^{13}\text{C})$ coupling was chosen instead of $^1J(^{29}\text{Si}-^{13}\text{C})$ couplings, as correlation with the β methylene ^1H and ^{13}C resonances provides more useful information about the structure of the

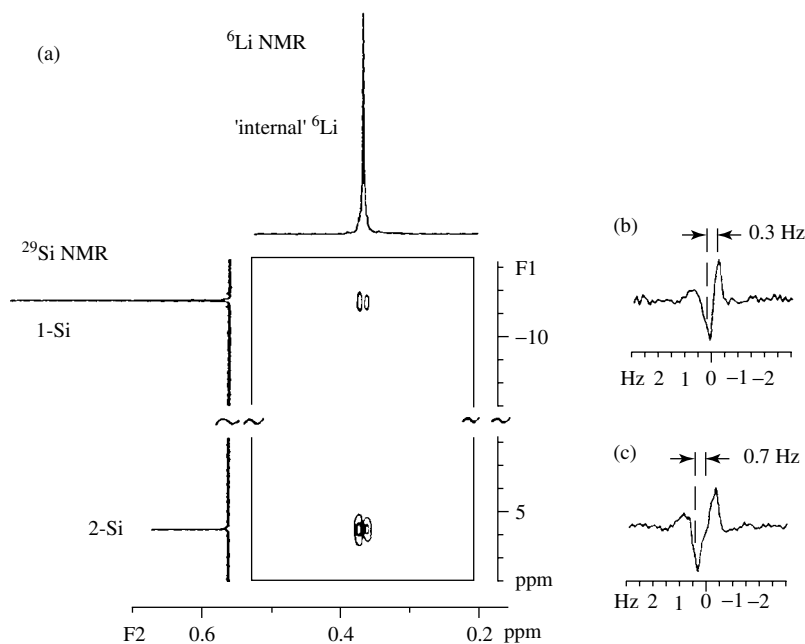
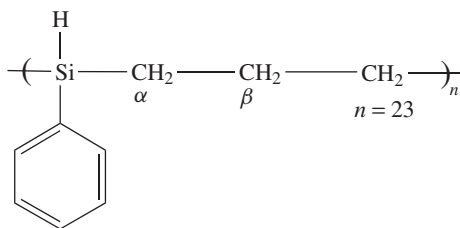


FIGURE 41. Part (a) is a ${}^6\text{Li}$ - ${}^{29}\text{Si}$ HMQC correlation for **35** (0.7 M in THF-d_8) measured at 294 K [sweep width F1 (${}^{29}\text{Si}$) 27.46 ppm at 79.5 MHz, ref. TMS; sweep width F2 (${}^6\text{Li}$) 3.05 ppm at 58.6 MHz, 64 increments, acquisition time 5.71 s; evolution time determined by ${}^6\text{Li}$ relaxation]. The ${}^6\text{Li}$ signal at -1.20 ppm is not shown as it yields no cross-peaks—it is assigned to the solvent-separated 'external' ${}^6\text{Li}$ cation. Parts (b) and (c) are traces through the cross-peaks. Reprinted from Reference 298. Copyright 1996, with permission from Elsevier Science



(36)

polymer. 2D ${}^1\text{H}$ - ${}^{29}\text{Si}$ long-range correlation (Figure 42, part a) revealed three additional cross-peaks (D-F) not seen in the 1D spectra due to limited chemical shift dispersion and assigned to penultimate silicon atoms. The three F2F3 slices from the 3D spectrum (Figure 42, parts b-d) are taken at the three different ${}^{29}\text{Si}$ chemical shifts of the main-chain repeating units. Depending on whether or not the silicon has equivalent methylene carbons two bonds away, the slice contains one or two cross-peaks along the ${}^{13}\text{C}$ axis. Along the ${}^1\text{H}$ axis we see also one or two cross-peaks depending whether the two

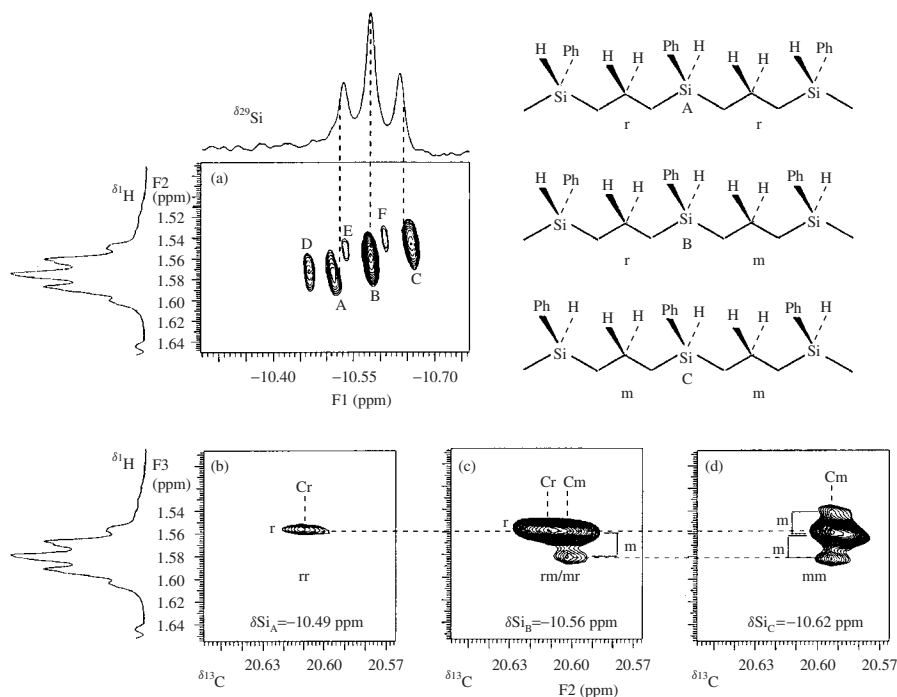


FIGURE 42. NMR spectra of poly(1-phenyl-1-silabutane). (a) Long-range ^1H – ^{29}Si HMQC 2D-NMR spectrum [$^3J(^{29}\text{Si}$ – $^1\text{H}) = 9$ Hz] showing ^1H and ^{29}Si 1D spectra along F2 and F1 axes; (b) F2F3 slice from $^1\text{H}/^{13}\text{C}/^{29}\text{Si}$ correlation 3D spectrum at $\delta(^{29}\text{Si}) = -10.49$; (c) F2F3 slice from $^1\text{H}/^{13}\text{C}/^{29}\text{Si}$ correlation 3D spectrum at $\delta(^{29}\text{Si}) = -10.56$; (d) F2F3 slice from $^1\text{H}/^{13}\text{C}/^{29}\text{Si}$ correlation 3D spectrum at $\delta(^{29}\text{Si}) = -10.62$. The 3D spectrum was obtained with delays corresponding to $^2J(^{29}\text{Si}$ – $^{13}\text{C}) = 5$ Hz, $^1J(^{13}\text{C}$ – $^1\text{H}) = 140$ Hz; total experiment time was 14 h. Reprinted with permission from Reference 205. Copyright 1997 American Chemical Society

methylene protons are equivalent (racemic diads, r) or not (meso diads, m). Using this reasoning, the ^{29}Si lines could be assigned to different triads and the polymer structure elucidated without isotopic labeling or stereoselective synthesis. Similarly, with a slightly different pulse sequence the same group managed to assign completely the spectra of two carbosilane dendrimers {first generation, $\text{Si}(\text{CH}_2\text{CH}_2\text{SiHMe}_2)_4$, and second generation, $\text{Si}[\text{CH}_2\text{CH}_2\text{SiMe}(\text{CH}_2\text{CH}_2\text{SiHMe}_2)_2]_4$ }, and provide definitive proof of the structure³⁰⁰.

C. Selective Experiments

Selective excitation and selective detection have been recently reviewed by the recognized leaders in this field¹³⁵ who viewed ^{29}Si NMR applications from a broader perspective. In this review we focus on those selective experiments that have found wider use in studies of organosilicon compounds, selective INEPT and HEED as representatives of the two classes (excitation and detection) of selective experiments. Some other selective experiments are mentioned in other sections (e.g. SPT, selective decoupling, SPINEPTR, ψ -BIRD HMQC, DQF COSY).

1. Selective excitation

Why would one like to have a selective version of non-selective polarization transfer when the advantages of non-selective transfer over SPT are so obvious? The answer is simple: in many cases selective INEPT (or DEPT) is easier to perform and offers different control over the selectivity. In selective INEPT one selects the ^1H multiplet (together with its ^{29}Si satellites) and by the choice of delay(s) τ (and Δ) selects the coupling (one-, two-bond etc.) active in the polarization transfer. In contrast, in the SPT experiment one must locate the ^{29}Si satellites of the selected multiplet in the ^1H NMR spectrum and invert it selectively; this is often difficult, particularly in the case of long-range couplings when low-intensity ^{29}Si satellites are likely to be buried in other signals. Hence, selective INEPT is more convenient to use than SPT, especially in the case of unresolved resonances and complex coupling systems. In contrast to general INEPT or DEPT experiments, the selective version yields assignment of ^{29}Si signals, providing that the assignment of the ^1H multiplet is clear.

The selectivity of INEPT can be achieved in the most straightforward way, as suggested by Bax and coworkers^{301,302}, by replacing all the ‘hard’ non-selective proton pulses of INEPT with selective (‘soft’) pulses (this pulse sequence is sometimes denoted as SPINEPT). To retain full sensitivity, the selective pulses must cover the selected multiplet and its ^{29}Si satellites, i.e. the excitation band should be approximately equal to the width of the multiplet plus the value of $J(^{29}\text{Si}-^1\text{H})$ to be used for polarization transfer. For the choice of suitable selective pulses, see Reference 135.

Selective INEPT can be run without decoupling and refocusing, and it can be further combined with selective decoupling as described for ^{13}C and ^{15}N NMR by Uhrin and Liptaj³⁰³.

This all-proton-pulses-selective variant eliminates the undesirable influences of homonuclear (during τ delay) and heteronuclear (during Δ delay) couplings. As Blechta and Schraml³⁰⁴ had noted, the same can be achieved if all 90° proton pulses are retained as ‘hard’ pulses and only the refocusing 180° pulses are made selective. This was a useful simplification when DANTE pulse train had to be used to create selective pulses. Moreover, since the selective INEPT should yield enhancement of only one ^{29}Si line (which is easy to phase), there is no need for the final refocusing and thus the final refocusing pulses can also be omitted. The simplified pulse sequence for the selective INEPT is:

$$\begin{array}{l} ^1\text{H} : \quad 90_x^\circ - \tau - \cap_x^{180} - \tau - 90_y^\circ - \Delta - \text{decouple} \\ ^{29}\text{Si} : \quad \quad \quad 180_x^\circ \quad \quad 90_x^\circ \quad \quad \text{acquire} \end{array}$$

where \cap_x^{180} denotes selective refocusing pulse. The delay Δ might require optimization in the case of passive couplings of silicon to other protons. An example of an application of selective INEPT is shown in Figure 43. In this example two ^{29}Si lines are assigned to the silicon atoms in a bis(trimethylsiloxy) derivative of a steroid **37**; the picture is self-explanatory.

When a high selectivity is needed because of multiplet overlap in the ^1H NMR spectrum, the selective pulse can step through the proton multiplet and maximum ^{29}Si signal sought. The procedure is illustrated in Figure 44, where it is shown that the low-frequency ^{29}Si line (at $\delta = 19.8$) is due to the silicon from the Si–O–CH moiety (maximum signal when ^1H multiplet around $\delta = 3.86$ is selected); the Si–O–CH₂ silicon has the strongest signal when the selective pulse is at $\delta = 3.56$.

To excite only a satellite of a selected singlet line in the ^1H NMR spectrum for the measurements of heteronuclear couplings and/or isotopic shifts, INEPT can be combined

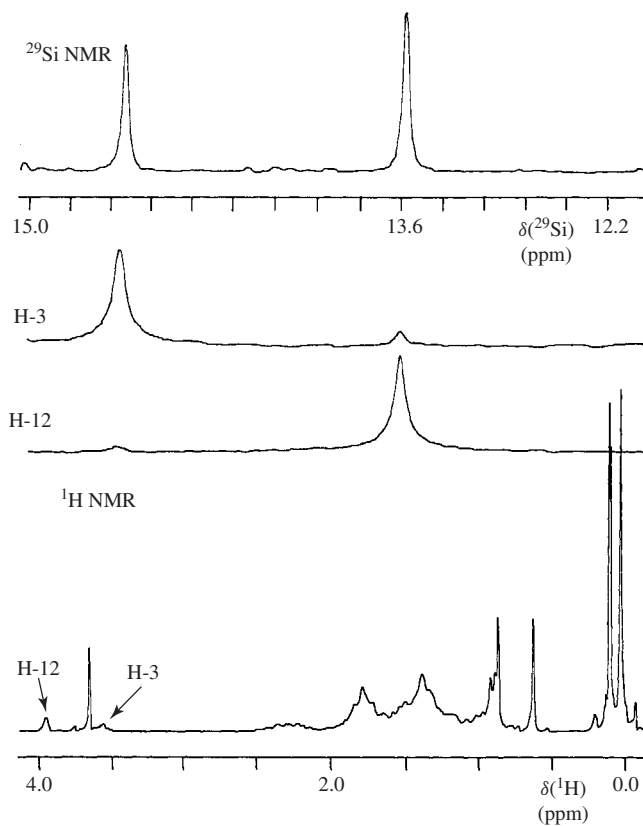
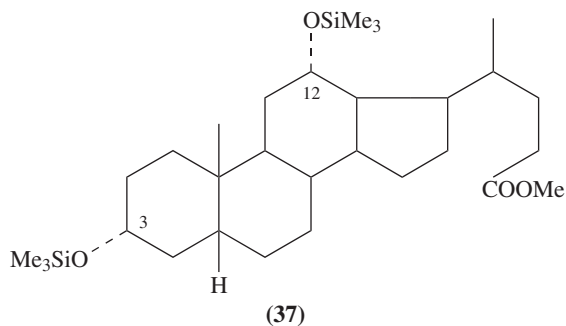


FIGURE 43. Assignment of the two lines in the ^{29}Si NMR spectrum of methyl $3\alpha,12\alpha$ -bis(trimethylsilyloxy)- 5β -cholenate, **37**, by selective INEPT. Top trace: ^{29}Si INEPT spectrum; two middle traces: selective INEPT spectra measured with selective excitation of ^1H lines indicated by arrows in the bottom trace with partially assigned ^1H NMR spectrum (25 mg of the sample in 0.7 ml of CDCl_3 , ^1H frequency 200 MHz, ^{29}Si frequency 39.7 MHz, 5 mm broad-band probe, selective pulse by DANTE train, $\tau = 70$ ms, $\Delta = 149$ ms). Reproduced with permission of Collection of Czechoslovak Chemical Communications from Reference 304



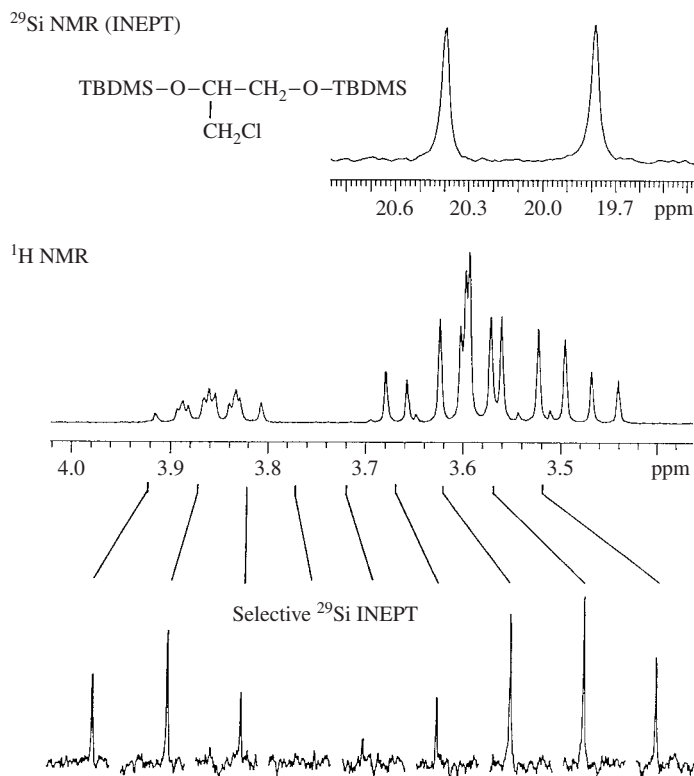


FIGURE 44. Assignment of the two lines in the ^{29}Si NMR spectrum of the compound shown in the inset by selective INEPT. (TBDMS = Z-Bu Me₂Si) Top trace: ^{29}Si NMR spectrum; middle trace: CH-CH₂ part of ^1H NMR spectrum; bottom traces: selective INEPT spectra measured with selective pulses placed at the indicated positions in the ^1H NMR spectrum (40 mg of the sample in 0.7 ml of CDCl₃, ^1H frequency 200 MHz, ^{29}Si frequency 39.7 MHz, 5 mm broad-band probe, all ^1H pulses soft pulses with $\text{pw}_{90} = 8$ ms, $\tau = 75$ ms, $\Delta = 150$ ms). Reproduced from Reference 136

with the 'jump and return' (JR) pulse¹⁴³. The JR pulse pair ($90_x^\circ - \delta - 90_{-x}^\circ$)³⁰⁵ replaces the first 90° proton pulse in INEPT. Since the JR-INEPT combination requires placing the ^1H carrier at one of the satellites in the ^1H NMR spectrum, the method has the drawbacks of SPT experiments. The JR pulse pair has also been combined with the XYZ sequence²¹⁶ (Section VI.A.2).

As in other 1D assignment methods, the advantages of selective excitation over 2D measurements include sensitivity, high resolution and time savings when the number of ^{29}Si lines to assign is low.

2. Selective detection

Various NMR pulse sequences contain certain building blocks like BIRD, INEPT, refocusing delay etc., that perform some specific functions. A building block that serves

as a filter to eliminate broad lines from the resulting spectrum, i.e. a T_2 filter¹³⁵, was dubbed HEED (*Hahn spin-Echo Extended*)³⁰⁶ after it was used³⁰⁷ in a combination with INEPT under the name INEPT+HE. HEED utilizes the large difference between spin-spin relaxation times of narrow and broad lines in the NMR spectrum by delaying the start of FID acquisition until the FID signal from the broad line is sufficiently weak. Possible phase distortions of the desired signals are eliminated by a refocusing 180° pulse in the middle of the delay; this experiment is performed by the pulse sequence known since 1950 as a Hahn echo (HE)³⁰⁸:

$$\begin{array}{l} {}^1\text{H} : \quad \text{decouple broad-band} \\ {}^{29}\text{Si} : \quad 90^\circ - T - 180^\circ - T - \text{acquire} \end{array}$$

(HE was used, e.g., in ^{29}Si NMR to eliminate the broad signal coming from the glass of the NMR tube and the probe insert.) The delayed acquisition leads, of course, to a loss in sensitivity; the loss is determined by the difference in relaxation times T_2 of the desired and unwanted signals. The delay $2T$ can be adjusted experimentally according to the linewidth of the broad line and the desired suppression of the unwanted broad line. HEED takes the $T-180^\circ-T$ building block and inserts it into other pulse sequences between the last (reading) pulse and acquisition (or, in other words, the 90° pulse of HE is replaced in HEED combinations by another pulse sequence). So we have HEED-INEPT, HEED-DEPT, HEED-HETCOR and possibly others. The combinations just mentioned are discussed in great detail by the authors of the method³⁰⁶ who have exploited them extensively in numerous studies on a variety of compounds^{213,309-314} mainly for determining $^{29}\text{Si}-^{15}\text{N}$ couplings (and their signs) and measurements of isotope effects, $\Delta^{15/14}\text{N}(^{29}\text{Si})$, on silicon chemical shifts^{213,315}.

The $^{29}\text{Si}-^{15}\text{N}$ couplings, which are a valuable source of information, can be measured directly from satellites in either ^{15}N or ^{29}Si NMR spectra. The relative intensities of the satellites suggest using measurements of ^{29}Si satellites in the ^{15}N NMR spectra (each of the two ^{29}Si satellites in ^{15}N NMR spectrum has an intensity of 2.35% of the central line; the ^{15}N satellite in ^{29}Si spectrum has a relative intensity of only 0.18%); the measurements of ^{29}Si spectra are 8 times more sensitive than the measurement of ^{15}N NMR spectra (at natural abundance). Since the centre line in the ^{29}Si NMR spectrum is due to an ^{14}N isotopomer, it is usually broadened because of scalar relaxation, which depends on $J(^{29}\text{Si}-^{14}\text{N})$ coupling and the relaxation rate of ^{14}N nuclei³⁰⁷. Hence, HE can effectively suppress the centre line and make the variant of measuring ^{15}N satellites in ^{29}Si spectra more favorable. The sensitivity of these measurements can be enhanced by HEED-INEPT, thus obviating the need for isotopic enrichment or triple resonance ($^{29}\text{Si}-^{15}\text{N}-^1\text{H}$) experiments. Measurement by HEED-INEPT does not require irradiation of ^{15}N nuclei and thus the more common double resonance equipment is sufficient.

The original HEED-INEPT sequence^{306,307} that enhances narrow lines is:

$$\begin{array}{l} {}^1\text{H} : \quad 90_x^\circ - \tau - 180_x^\circ - \tau - 90_x^\circ - \Delta/2 - 180_x^\circ - \Delta/2 - \text{decouple broad-band} \\ {}^{29}\text{Si} : \quad \quad \quad 180_x^\circ \quad \quad 90_x^\circ \quad \quad 180_x^\circ \quad \quad T - 180_x^\circ - T - \text{acquire} \end{array}$$

where delays τ and Δ have their usual meaning in an INEPT pulse sequence. The spectra of $\text{HN}(\text{SiMe}_3)_2$ measured by simple INEPT and INEPT-HEED are compared in Figure 45.

The sequence can be simplified along the lines suggested by Blechta and Schraml³¹⁶:

$$\begin{array}{l} {}^1\text{H} : \quad 90_x^\circ - \tau - 180_x^\circ - \tau - 90_x^\circ - \Delta - \text{decouple broad-band} \\ {}^{29}\text{Si} : \quad \quad \quad 180_x^\circ \quad \quad 90_x^\circ \quad \quad T - 180_x^\circ - T - \Delta - \text{acquire} \end{array}$$

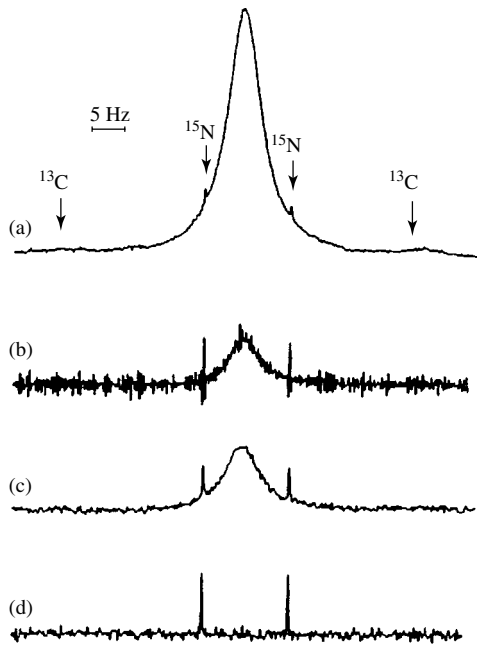


FIGURE 45. ^{29}Si spectra of $\text{HN}(\text{SiMe}_3)_2$ (at 71.55 MHz, 80% in C_6D_6 , 10 mm sample tube, 2 K data points zero-filled to 8 K) acquired (a) with INEPT (16 transients); (b) the same as (a) after Gaussian multiplication ($\text{LB} = -1$ Hz, $\text{GB} = 0.7$); (c) with DEPT (16 transients)—note the effect of the longer sequence; (d) with HEED-INEPT (64 transients, $\tau = 35.7$ ms, $\Delta = 19.06$ ms, $T = 0.3$ s). Reproduced by permission of Academic Press from Reference 307

with two 180° pulses omitted and a seemingly prolonged pre-acquisition delay of Δ . The overall duration of the delay ($\Delta + 2T$) can be reduced by a corresponding adjustment of the T delay¹³⁸.

Magnetic field shimming and elimination of temperature gradients or paramagnetic impurities is important in carrying out these experiments. Otherwise, the line broadening might reduce the difference between the effective relaxation times T_2^* of the two nitrogen isotopomers and detection of ^{15}N satellites would be difficult. This is also the case with chemical exchange broadened lines or the presence of other fast relaxing quadrupolar nuclei. The authors²¹³ prefer to perform these experiments on spectrometers with a lower magnetic field B_0 .

As mentioned above, HEED can be also added to 2D heteronuclear correlations. Thus we get basic HEED-HETCOR^{306,317}:

$$\begin{array}{l}
 {}^1\text{H} : 90_x^\circ - t_1/2 - \quad \quad - t_1/2 - 2\Delta_1 - 90_y^\circ - 2\Delta_2 - \text{decouple broad-band} \\
 {}^{29}\text{Si} : \quad \quad \quad 180_x^\circ \quad \quad \quad 90_\phi^\circ \quad \quad T - 180_\phi^\circ - T - \text{acquire}
 \end{array}$$

or ${}^1\text{H}$ - ${}^1\text{H}$ decoupled HEED-HETCOR³⁰⁶:

$$\begin{array}{l}
 {}^1\text{H} : 90_x^\circ - t_1/2 - 90_y^\circ - 2\Delta_1 - 180_x^\circ - 2\Delta_1 - 90_y^\circ - t_1/2 - 2\Delta_1 - 90_y^\circ - 2\Delta_2 - \text{decouple broad-band} \\
 {}^{29}\text{Si} : \quad \quad \quad 180_x^\circ \quad \quad \quad 90_\phi^\circ \quad \quad T - 180_x^\circ - T - \text{acquire}
 \end{array}$$

and INEPT based phase-sensitive HETCOR³⁰⁶:

$$\begin{array}{l}
 {}^1\text{H} : 90_x^\circ - t_1/2 - \quad -t_1/2 - \Delta_1 - 180_x^\circ - \Delta_1 - 90_y^\circ - \Delta_2 - 180_x^\circ - \Delta_2 - \text{decouple broad-band} \\
 {}^{29}\text{Si} : \quad \quad \quad 180_x^\circ \quad \quad \quad 180_x^\circ \quad \quad \quad 90_\phi^\circ \quad \quad \quad 180_x^\circ \quad \quad \quad T - 180_x^\circ - T - \text{acquire}
 \end{array}$$

An example showing the relative advantages of 2D correlations measured by HEED-HETCOR and phase-sensitive HEED-HETCOR is given in Figure 46.

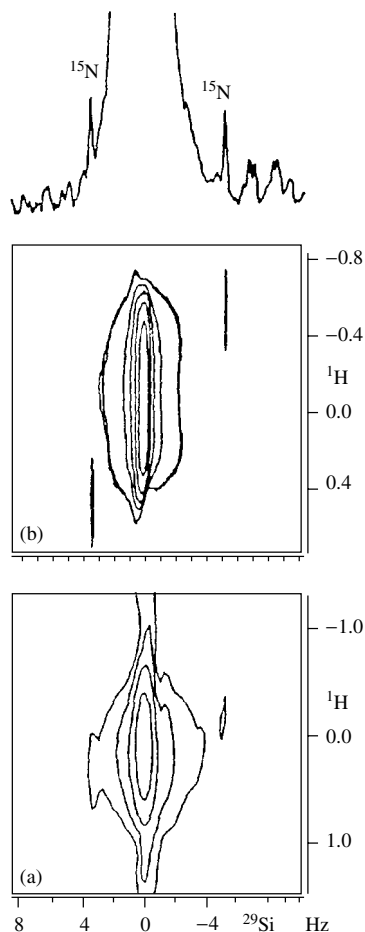


FIGURE 46. 2D ^{29}Si -H correlation spectra (59.63 MHz) of Si-N silicon of $\text{Me}_3\text{SiN}=\text{C}=\text{C}$ (SiMe_3)₂ measured by (a) HEED-HETCOR pulse sequence (magnitude mode, 16 increments, 128 transients and 1 K data points each zero-filled to 4 K, spectral width 120 Hz in F2 and 2 Hz in F1 zero-filled to 64 W, Gaussian multiplication in both dimensions). Because of a sharp parent line, a compromise delay $T = 0.8$ s has been used, giving rise to a rather intensive residual parent peak. (b) The same spectrum measured by the phase-sensitive HEED-HETCOR based on INEPT and shorter delay $T = 0.28$ s, which leads to an even stronger residual peak. Nevertheless, improved resolution of the satellites was obtained in considerably shorter time: 32 transients per increment were sufficient. Reproduced by permission of Academic Press from Reference 306

In addition to determining the absolute value of $J(^{29}\text{Si}-^{15}\text{N})$ coupling, the 2D correlations often yield the relative signs of the couplings (see Figure 47) from the tilt of the satellite cross-peaks.

In long-range correlations or in polarization transfers based on small long-range coupling constants, some of the delays might be so long as to provide a built-in T_2 filter without the need to extend the sequence by HEED (e.g. DEPT or HMQC experiments). Owing to fast T_2 relaxation of ^{14}N nuclei, signals coming from the otherwise broad lines of ^{14}N containing isotopomers might become unobservable in such experiments (Figure 47)¹³⁵.

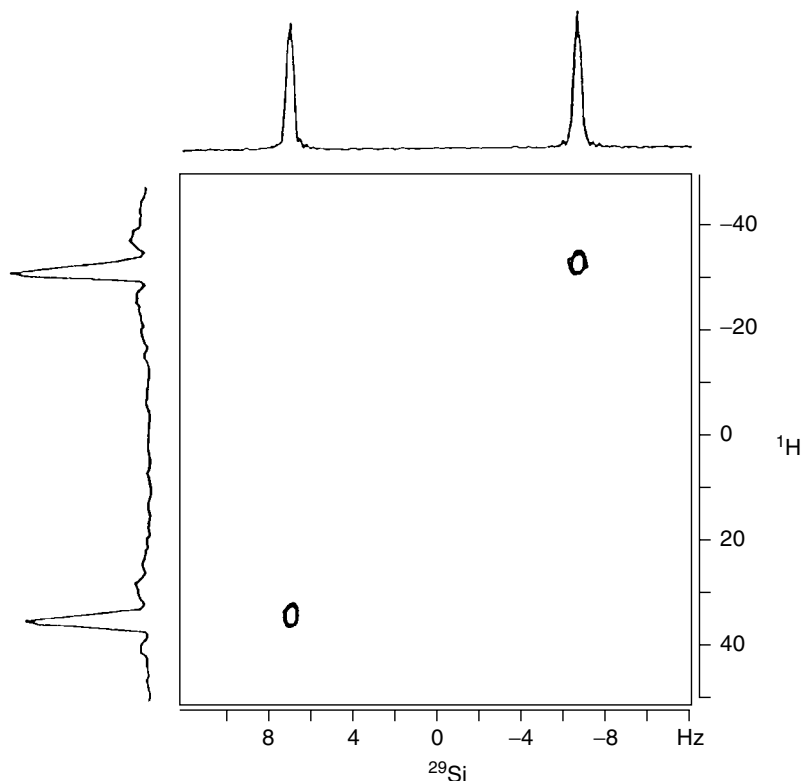


FIGURE 47. 2D ^{29}Si - ^1H correlation spectrum of $\text{HN}(\text{SiMe}_3)_2$ measured by a standard HETCOR pulse sequence with delay based on $^2J(^{29}\text{Si}-\text{N}-\text{H}) = 3.4$ Hz (at 59.63 MHz, 128 increments, 24 transients and 1 K data points each zero-filled to 4 K, spectral width 300 Mz in F2 and 100 Hz in F1 zero-filled to 256 W, Gaussian multiplication in both dimensions). The spectrum shows only ^{15}N satellites as the parent line from the ^{14}N isotopomer has been completely suppressed in the F1 dimension due to long Δ delay (0.144 s) and broad ^1H line (about 20 Hz). The tilt shows that reduced couplings $^1K(^{29}\text{Si}^{15}\text{N})$ and $^1K(^{15}\text{N}^1\text{H})$ have the same sign. Reproduced by permission of Academic Press from Reference 306

When there is more than one nitrogen atom attached to silicon, it might be advantageous to use z -filtered INEPT or combine z -filtered INEPT with HEED³¹⁸.

VII. DETERMINATION OF COUPLING CONSTANTS

The current literature is abundant with values of coupling constants between silicon and nuclei that were only recently considered rather obscure, e.g. ^{195}Pt , ^{183}W , ^{103}Rh and many others. As demonstrated by the large number of silicon coupling constants already available in 1976⁹, measurements of the couplings from ^{29}Si satellites in the spectra of other nuclei is not too demanding an experiment. Measurements of ^{29}Si couplings with nuclei like ^{13}C or ^{15}N from the satellites in INEPT or DEPT enhanced spectra and from correlation 2D spectra (pseudo-triple resonance experiments) were mentioned in Sections V.B and VI.A. Double selective population transfer⁹⁷ for similar measurements was described in Section V.A. For the sake of completeness we shall cover in this section J -resolved spectroscopy, although it is seldom needed in the realm of ^{29}Si .

Homonuclear ^{29}Si – ^{29}Si J -resolved spectra can be measured by J -resolved INADEQUATE in natural abundance as mentioned in the section on INADEQUATE experiments; in enriched samples standard methods for homonuclear J -resolved spectra can be applied³¹⁹ without problems. Heteronuclear J -resolved experiments are well described in all current NMR textbooks and manuals. When setting up a heteronuclear X– ^{29}Si J -resolved experiment, one must first decide which nucleus to detect. The consideration involves (besides availability of hardware, see Section VI.B) isotopic abundance, receptivity, spectral dispersion and eventually the ability to suppress the centre line. With X-detection the low intensity of ^{29}Si satellites might be a problem, especially when small couplings have to be determined. In such a case it might be more productive to use some correlation experiment as described in Section VI. Unless sensitivity dictates otherwise, ^{29}Si detection would be advantageous for nuclei X with high abundance. When using ^{29}Si detection one should employ decoupling (of ^1H , ^{19}F or ^{31}P nuclei) only during acquisition in order to prevent build-up of negative NOE (i.e. use spin flip instead of the gated decoupling method). The problem of low sensitivity might be lessened by employing polarization transfer (selective or non-selective), which brings with it both signal enhancement and increased repetition rate as discussed already in several places. Both INEPT and DEPT can be modified in several ways to produce J -resolved spectra; a detailed comparison can be found, e.g. in Reference 186. Despite the many possibilities, it is only INEPT that has been used for determination of ^{29}Si couplings. A simple example of INEPT with polarization delay turned into evolution delay and refocusing delay held constant is shown in Figure 48.

Many well-known pulse sequences can be modified to produce a J -resolved type of spectra but only a few were applied to organosilicon compounds. One such example is a modified³²⁰ long-range correlation experiment COLOC¹⁸⁸. A combined utilization of the 2D INEPT spin-flip J -resolved technique (i.e. INEPT with refocusing delay turned into evolution period¹⁸⁶) for J determination and ^{29}Si line assignment was described³²¹. Traces along the F1 axis depend not only on ^{29}Si – ^1H coupling but also on homonuclear ^1H – ^1H couplings as explained in Section VI.A.2 and shown in Figure 49. The cross-sections are analysed to yield all the couplings involved^{121,322}. A similar method (Geometrical Imprint Domain)¹²⁵ was discussed and illustrated in Section V.B.

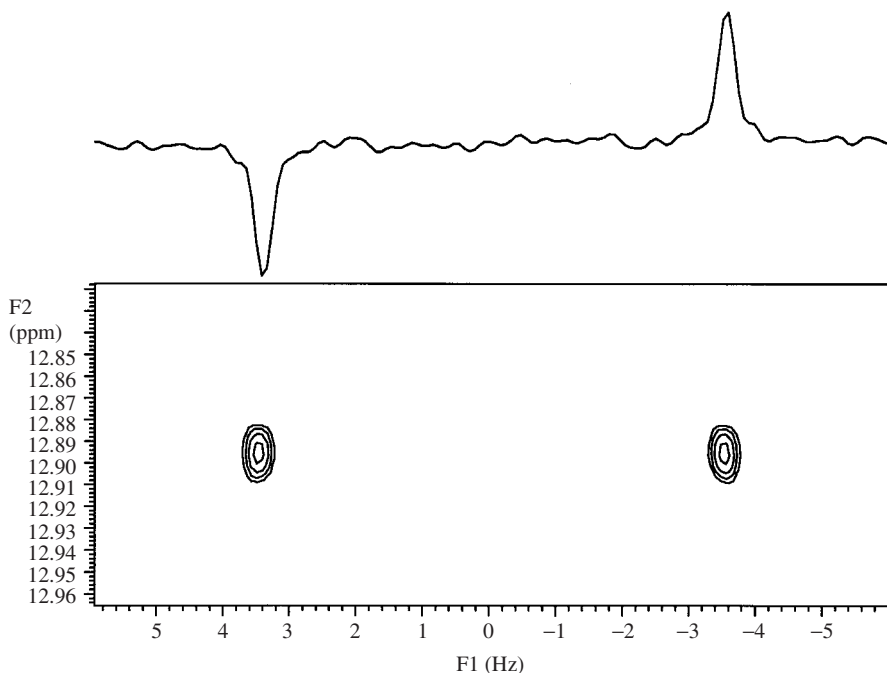


FIGURE 48. J -resolved ^{29}Si - ^1H spectrum of *tert*-butyldimethylchlorosilane measured by INEPT [polarization period used for t_1 evolution, refocusing delay 16 ms, dilute CDCl_3 solution, 39.743 MHz (^{29}Si), 60 increments 4 transients each, spectral width 200 and 20 Hz along F2 and F1 axes, respectively, zero-filled to 512 (t_1) and 2 K (t_2), no data weighting]. Under these conditions, couplings to *ortho* protons of phenyl groups and their homonuclear couplings are not visible

A variant for measurement of heteronuclear J -resolved spectra with ^1H detection was proposed under the name ACT (Active Coupling-pattern Tilting)^{323,324}. The ACT pulse sequence is:

$$\begin{array}{l}
 ^1\text{H} : 90_{x/y}^\circ - t_1/2 - \quad - t_1/2 - \Delta/2 - \cap_x - \Delta/2 \quad \text{acquire} \\
 ^{29}\text{Si} : \quad \quad \quad 180_x^\circ \quad \quad \quad 180_x^\circ \quad \quad 90_x^\circ 180_y^\circ 90_x^\circ - t_1 - 90_x^\circ 180_{-y}^\circ 90_x^\circ
 \end{array}$$

where \cap_x is a multiplet-selective 180° pulse, optimum $\Delta = 1/[2J(^{29}\text{Si}-^1\text{H})]$ (for details of phase cycles, see the source references). The claimed advantages of this sequence are shown in Figure 50 for **38**; they include pure phases, tilted cross-peak patterns with active coupling in antiphase and homonuclear ($^1\text{H}-^1\text{H}$) decoupling along the F1 axis. However, the pulse sequence is quite long, and so the achievable resolution along F1 is likely to be limited by proton T_2^* relaxation. Certainly, determination of the stereochemistry of substituted vinylsilanes through the determination of $^3J(^{29}\text{Si}-\text{C}=\text{C}-^1\text{H})$ couplings (3–12 and 9–21 Hz in *cis* and *trans* disposition of Si and H atoms, respectively) is often the only possibility, but such determinations were accomplished previously by much simpler tools^{93,325–327}.

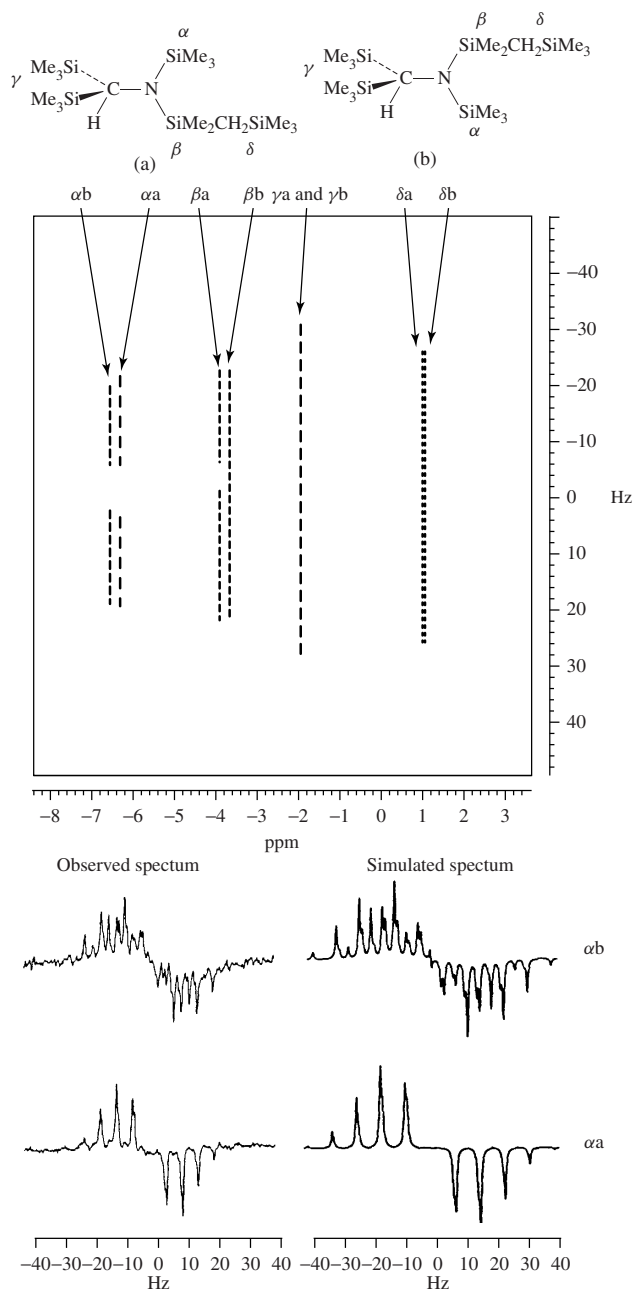


FIGURE 49. J -resolved ^{29}Si NMR spectrum of a mixture of compounds shown in the inset and the observed and simulated traces along the F1 axis. Reprinted with permission from Reference 121. Copyright 1993 American Chemical Society

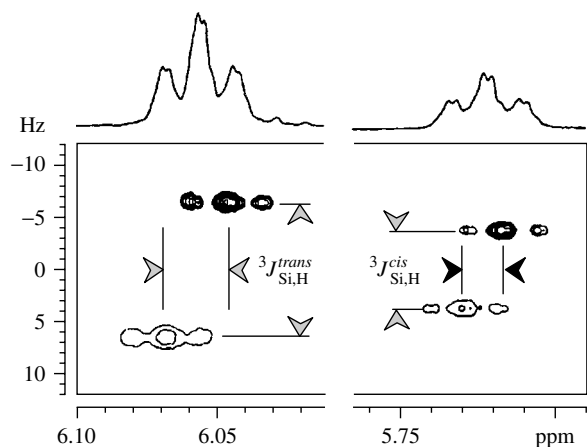
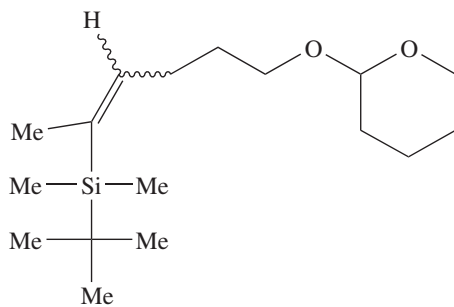


FIGURE 50. Part of ^{29}Si - ^1H ACT- J -spectrum of E/Z mixture of **38** (0.12 M CDCl_3 solution, E/Z ratio approx. 3/2; 600 MHz spectrometer, 5 mm ID broad-band probe, spectral widths 25 and 1200 Hz along F1 and F2 axis, respectively, 16 increments 32 transients each, total measuring time 1 h). Proton chemical shifts along F2, only heteronuclear couplings along F1 axis. Only two levels are plotted for negative peaks. Reproduced by permission of Academic Press from Reference 323



(38)

VIII. RELAXATIONS

In contrast to the tremendous advancement in other NMR techniques (as exemplified by the closely related NOE measuring techniques), measurements of relaxation times rely essentially on techniques developed several decades ago¹²; inversion recovery, progressive saturation or saturation recovery (for spin-lattice relaxation time T_1) and linewidth measurement or the Carr-Purcell-Meiboom-Gill (CPMG) train (for spin-spin relaxation T_2) remain with their variants and modifications the most commonly used methods. The development of other techniques, however, have made it possible to measure the corresponding quantities that govern relaxation of multiple quantum (MQ) coherences or relaxation in the rotating frame ($T_{1\rho}$). In several instances these quantities were studied on organosilicon compounds as suitable models. Interest in these quantities stems from the fact that MQ relaxation rates can contain information about cross-correlation spectral densities that cannot be obtained by other means.

To measure relaxation of (^1H - ^{29}Si) zero-quantum (ZQ) and double-quantum (DQ) coherences in SiHCl_3 , Kowalewski and Larsson³²⁸ used the 2D pulse sequence now known as the HMQC sequence with refocusing and decoupling (see Section VI.A.2). Depending on phase cycling, this sequence can yield both ZQ and DQ in one spectrum or only one of them as selected. It was estimated from linewidths in the 2D spectra along the F1 axis that relaxation rates were $T_2^{-1}(\text{ZQ}) = 23 \text{ s}^{-1}$ and $T_2^{-1}(\text{DQ}) = 56 \text{ s}^{-1}$. Measurement of T_1 and T_2 (by conventional methods) of ^1H , ^{29}Si and ^{35}Cl nuclei in the same sample allowed estimates of $J(^{29}\text{Si}-^{35}\text{Cl})$ and $J(^1\text{H}-^{35}\text{Cl})$ (44 and 9.1 Hz, respectively), which led to a cross-correlation spectral density of $\pm 7.1 \text{ s}^{-1}$, which corresponds to line broadening of about 4.5 Hz for either ZQ or DQ and narrowing by the same amount for the other. A subsequent study of temperature dependence of ^{29}Si , ^{35}Cl and ^{13}C relaxation in SiHCl_3 , MeSiHCl_2 and Me_2SiHCl measured by conventional methods utilized ^{29}Si as a dual probe of molecular motion; it allowed determination of both reorientational and angular momentum correlation times³²⁹.

The same compound, SiHCl_3 , and also SiCl_4 had been studied previously^{330,331} and yielded ^{29}Si relaxations of $T_1 \approx 100 \text{ s}$ and $T_2 \approx 0.5 \text{ s}$ at room temperature. The linewidths determined can also be analysed in terms of scalar coupling mechanism of the second kind to yield the coupling constant $J(^{29}\text{Si}-^{35}\text{Cl})$ ³³². Measurement of $T_{1\rho}$ relaxation (of protons) led to the spin-lattice relaxation time of ^{35}Cl (again in SiHCl_3)³³⁰; through $T_{1\rho}$ values, various types of molecular motions could be detected and characterized in polysiloxanes³³³.

Numerous studies of relaxation and molecular motion that measured T_1 (and sometimes also T_2) by conventional methods^{14,28,334-341} evaluated the contribution of the dipole-dipole relaxation mechanism from NOE measurements (Section IX); measurement of dynamic NOE (DNOE)⁷¹ yields both T_1 and NOE factors in a single experiment³⁴²⁻³⁴⁴. DNOE appears to be the only conventional possibility to measure T_1 in the cases when NOE nulls the signals [as in $\text{MeSi}(\text{OEt})_3$]^{335,345}.

Interpretation of measured ^1H , ^2H , ^{13}C and ^{29}Si relaxation values T_1 can be supported by NMR measurements of self-diffusion (see Section X.B) as shown by the example of hexamethyldisilane³⁴⁶.

In setting up conventional measurements of T_1 by inversion recovery (in any of its variants) one should be aware of possible effects of proton (or other nuclei) decoupling. As elaborated by Levy and coworkers³⁴⁷, the results of ^{29}Si relaxation measurements should not be affected by the presence or absence of a decoupling field due to the much faster T_1 relaxation of protons compared to silicon. Therefore, measurements are performed with decoupling in order to speed up the measurements. However, Marsmann and Meyer³⁴³ noticed a shortening of T_1 when it was measured under proton decoupling conditions. Of course, a build-up of NOE should be prevented and thus gated decoupling is used. Since the measurements are time-consuming, various sources of errors and instability may substantially affect the accuracy of the measurements. The measurements should utilize block averaging of the data with interleaving of variable time t to compensate for changes in experimental conditions. A pulse sequence that incorporates such a compensation was suggested by Levy and coworkers³⁴⁷:

$$\begin{array}{l} ^1\text{H} : \quad \quad \quad - \text{decouple b.b.} - \quad \quad \quad - \text{decouple b.b.} \\ ^{29}\text{Si} : \quad - T - 90_x^\circ - \text{acquire}_\infty - T - 180_x^\circ - t - 90_x^\circ - \text{acquire} \end{array}$$

where the time t is varied and the relaxation delay T should be set greater than 3–4 times the longest T_1 to be measured (usually 300 s ³⁴⁸). The signal acquired after the second

90° pulse, S_t (i.e. the signal after inversion), is subtracted from the signal acquired after the first 90° pulse, S_∞ (which is the 'equilibrium' signal). A plot of $\log(S_\infty - S_t)$ against time t then yields T_1 . (A simple and obvious modification of the sequence ensures the subtraction of the two signals directly in the measurement.)

Other methods that have found use in measurement of T_1 relaxation of organosilicon compounds are FIRFT (*Fast Inversion Recovery* combined with *Fourier Transform*)^{344,349–352} and saturation recovery³⁵³. Each of these sequences produces some dependence of the signal on a time parameter. In order to get the relaxation time, the dependence must be analysed; often, a non-linear three-parameter analysis is used³⁵⁴.

Additional insights into molecular motion can also be obtained by studying solvent effects on relaxation times and their temperature and magnetic field dependencies as demonstrated on siloxanes by Kosfeld and coworkers⁶⁷.

Reproducibility of the results depends strongly on the signal-to-noise ratio achieved. Therefore, whenever polarization transfer can give some sensitivity enhancement, use of INEPT (or other scheme) for T_1 measurement would increase the precision and save experimental time. It is also possible to measure the relaxation times indirectly through measurements of ^{29}Si satellites in ^1H NMR spectra³⁵⁵, but application of the INEPT variant of such measurements is much more straightforward.

Besides measurements of proton relaxation in crowded ^1H NMR spectra indirectly through measurements of the much less crowded ^{13}C or ^{29}Si spectra³⁵⁶, INEPT can be used to speed up the direct measurements of ^{29}Si spin–lattice relaxation³⁵⁷. The pulse sequence used for INEPT-enhanced measurement of spin–lattice relaxation times is just a minor modification of decoupled refocused INEPT (Section V.B):

$$\begin{array}{l}
 {}^1\text{H} : \quad 90_x^\circ - \tau - 180_x^\circ - \tau - 90_y^\circ - \Delta/2 - 180_x^\circ - \Delta/2 - \text{decouple} \dots \\
 {}^{29}\text{Si} : \quad \quad \quad 180_x^\circ \quad \quad 90_x^\circ \quad \quad 180_x^\circ \quad \quad 90_{\pm y}^\circ - T - 90_x^\circ \text{ acquire}
 \end{array}$$

The first 90° proton pulse is, of course, preceded by an equilibration delay. The added part turns the enhanced magnetization of silicon to the $\pm z$ -axis, where it relaxes during time T toward its Overhauser-enhanced equilibrium value. Depending on the phase of the penultimate 90° silicon pulse, the experiment measures enhanced inversion-recovery ($+y$) or enhanced dynamic NOE ($-y$). The former is a good choice when dipole–dipole relaxation does not dominate (NOE enhancement $\eta > -1$), and the latter when this relaxation mechanism dominates silicon relaxation (NOE enhancement $\eta < -1$). Considerable time savings result from the improved signal-to-noise ratio for small values of relaxation delay T and from the much shorter equilibration delay ($2T_{1\text{H}}$ as opposed to $5T_{1\text{Si}}$ in the conventional inversion-recovery measurement). An example is given in Figure 51.

While the methods mentioned allow determination of relaxation times of all ^{29}Si signals in one experiment, it is sometimes useful to employ selective versions of the experiments, e.g., to differentiate possible relaxation mechanisms^{358,359}.

IX. NUCLEAR OVERHAUSER EFFECT (NOE)

The nuclear Overhauser effect is well known as a unique source of spatial information about molecules in solution. The NOE is defined as the change in line intensity of one nucleus (I) when the line (S) of another nucleus is perturbed (it is assumed that the two lines are not connected through spin–spin scalar coupling; otherwise, we would get a variant of the SPT experiment). The NOE from nucleus S (Source) to nucleus I (nucleus

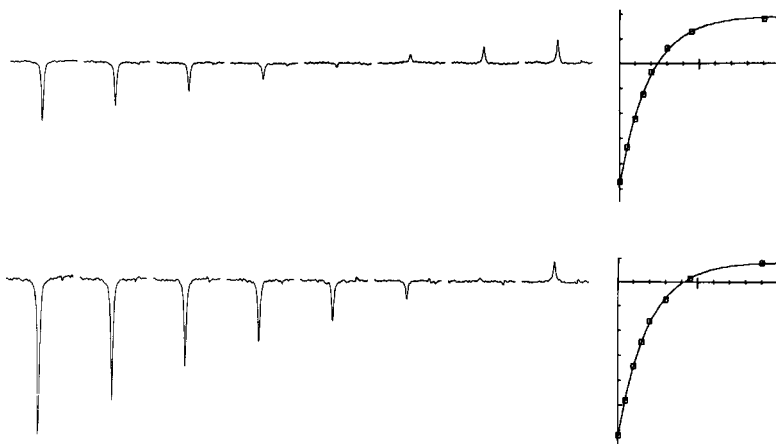


FIGURE 51. Measurement of ^{29}Si spin-lattice relaxation time in 1,1,3,3-tetramethyldisilazane using conventional inversion-recovery (top, measuring time 6.5 h, $T_1 = 37.6 \pm 1.4$ s) and INEPT enhanced version (bottom, measuring time 45 min, $T_1 = 38.1 \pm 0.9$ s) with the phase of penultimate proton pulse $+y$. Reproduced by permission of Academic Press from Reference 357

of Interest) is measured as

$$f_I \{S\} = \frac{I - I_0}{I_0} \times 100(\%)$$

where I_0 is the equilibrium intensity and I is the intensity when S is perturbed (some books use the symbol η for this quantity, while Neuhaus and Williamson³⁶⁰ reserve this symbol for the theoretical maximum observable NOE in a given case).

When we talk about perturbing line S , we mean perturbation of populations of the two energy levels connected by line (transition) S . Obviously, the populations can be perturbed in different ways, thus producing different NOEs. When line S is continuously irradiated by a weak rf field, the line is saturated and a steady state of the populations is reached, thereby producing steady-state NOE. When line S is affected only temporarily (e.g. by a selective 90° or 180° pulse), the changes in the populations are transient and the observed NOE is called transient NOE (with NOESY and its heteronuclear equivalent, HOESY, being the best known examples). Experimentally, the values of observed NOEs depend on the extent of perturbation (e.g. on the flip angle of the selective pulse used to irradiate line S) and on the time, t_{mix} : the perturbation is allowed to propagate through the system before the intensity I is measured.

Although homonuclear measurements may be useful for structural determination of organosilicon compounds, in the realm of ^{29}Si NMR we are more concerned with heteronuclear NOE, mostly $^{29}\text{Si}\{^1\text{H}\}$ NOE. There, the relationship between maximum observable NOE and molecular tumbling rate (characterized by the correlation time τ_c , the time an average molecule needs to rotate one radian) follows the dependence depicted in Figure 52. Using the approximation that $\tau_c = 10^{-12} \cdot M$ (where M is the molecular mass), the dependence indicates that the achievable maximum NOE is (-251%) for molecules with molecular mass <2000 in a spectrometer with ^{29}Si resonating frequency of 39 MHz ($\omega = 2\pi \cdot 39 \cdot 10^6$). For molecules with molecular mass larger than 4000, the maximum observable NOE is less (in absolute value). With increasing magnetic field, the borderlines shift accordingly to lower molecular mass values.

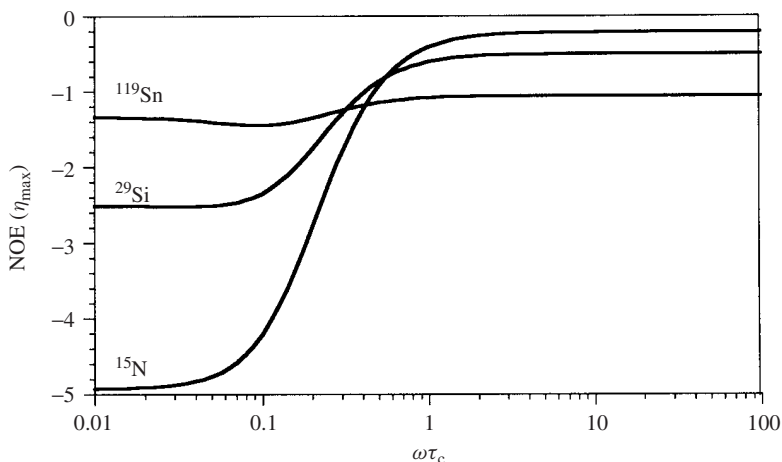


FIGURE 52. Dependence of maximum theoretical NOE enhancement on $\omega\tau_c$ for $X\{^1\text{H}\}$ NOE experiments; $X = ^{119}\text{Sn}$, ^{29}Si , and ^{15}N . Reproduced by permission of John Wiley & Sons Inc from Reference 360

An overwhelming majority of ^{29}Si NMR papers have utilized NOE measurements not for structural determination but for separating the contribution of the dipole–dipole relaxation mechanism from the overall relaxation. Such separation allows assessment of contributions due to other mechanisms and the role of various types of motion with the corresponding correlation times. Illustrative examples of studies of such series of compounds can be found in the papers of Harris and coworkers^{28,335–338,361}, Levy and coworkers^{14,334,347}, Kowalewski and coworkers^{344,350–352}, Engelhardt and coworkers^{362,363} and others^{343,364,365}.

Experimentally, all of these studies measured steady-state NOE or its buildup rates with broad-band perturbation of all ^1H NMR lines; to the best of our knowledge, no proton-selective heteronuclear $\{^1\text{H}\}$ - ^{29}Si NOE has been measured. NOE was measured directly as defined above. The studies employed some kind of broad-band proton decoupling to get the perturbed intensities of ^{29}Si lines (I) and obtained unperturbed intensity (I_0) from the inverse gated proton decoupling experiments (also termed ‘pulse-modulated’) or from coupled spectra. Some authors measured dynamic NOE^{342,344,352}, which is especially valuable when NOE nulls the signal³³⁵.

The direct measurement of heteronuclear NOEs is straightforward. Care must be taken to ensure sufficiently long relaxation delays, and acquisition time should be a compromise between sensitivity and resolution since it is the signal-to-noise ratio in the final spectrum that affects substantially the precision of NOEs; the usual precision of NOE factors is about 10%. Samples for NOE (and relaxation) measurements should be degassed to remove paramagnetic oxygen; usually, repeated freeze–pump–thaw cycles or bubbling nitrogen through the sample are used for this purpose. The absence of other paramagnetic impurities (which includes traces of chromic acid remaining from tube washing) is a must. The measurement should be conducted under temperature control as the NOEs are temperature-dependent¹⁴. Protonated solvents should be avoided as they increase the rate

of intermolecular relaxation. An adaptation of dynamic NOE measurements³⁴² of ^{29}Si involved proton irradiation for long ($>5 \cdot T_1$) and short (10 ms) periods before the read pulse³⁵¹.

Exceptionally, NOE has been measured on other (mostly ^1H) nuclei in organosilicon compounds for their structural determination. Examples include NOE on eight-membered organosilicon rings³⁶⁶, on hexacoordinated silicon complexes^{367,368}, difference NOE measured on phenylmethylpolysilanes¹⁷⁰ and ROESY applied for determination of species present in a mixture of $(\text{HSiCl}_2)_2\text{NH}$ and 3-picoline²¹⁴.

The choice of a homonuclear ^1H - ^1H NOE experiment is dictated by the rates at which the molecules tumble in solution. Considering typical organic molecules in non-viscous solvents, steady-state (or equilibrium) NOE is suitable only for small molecules ($M < 1000$) for which NOEs are positive. Transient NOE measurements are the domain of large molecules ($M > 2000$) with large negative NOEs but they can be also used for small molecules. Mid-sized molecules cause problems, as their NOEs tend to be very small; for these molecules measurements in the rotating frame, ROESY, may be a better choice. The ROESY experiment (*Rotating frame Overhauser Effect Spectroscopy*, sometimes also called CAMELSPIN experiments, Cross-relaxation Appropriate for *Mini*-molecules *EmuLated* by *SPIN*-locking) measures the transient NOE during irradiation (spin-lock field). Under these conditions, different molecular tumbling rates are relevant and so ROEs are positive even for medium-sized molecules. The above-mentioned NOE difference experiment is designed so that it measures directly the difference $I - I_0$ without measuring I_0 ; thus, it reveals lines with NOEs but does not yield enhancement factors.

It is rather frustrating for organometallic chemists to see that a three-dimensional structure of relatively large biomolecules (>20 kD) in solution can be reasonably well estimated from NOEs and coupling constants (measured in water!), while the same methods seldom yield the structure of much smaller organometallic compounds. There are several reasons for this: (i) larger molecules have larger, though negative NOE; (ii) the number of measurable NOEs is larger, and so the larger number of distance constraints enables better calculation of the most probable structure; (iii) the large number of hydrogen bonds fixes the most stable conformations; (iv) it is often difficult to find NOE between two nuclei that can be used for 'distance calibration' (in biomolecules, NOEs between non-equivalent geminal protons are customarily used for this purpose). In addition, (v) the number of different molecular fragments and substituents is much more limited in biomolecules and thus the dependencies of the coupling constants can be studied in greater detail (e.g. Karplus-type dependencies of vicinal coupling constants), and (vi) coupling pathways are not interrupted by heteroatom gaps as frequently as in some organometallic compounds.

X. MISCELLANEOUS

A. Isotopic Enrichment and Substitution

The traditional aid in measurements and assignments of NMR spectra, i.e. selective isotopic substitution, has also been used in ^{29}Si NMR spectroscopy. In the case of the ^{29}Si isotope it has been mainly total ^{29}Si substitution while selective isotopic enrichment in other isotopes (e.g. ^2H) has been used to facilitate some types of measurements such as assignments.

^{29}Si NMR from enriched material began in 1954 when Williams, McCall and Gutowsky³⁶⁹ used ^{29}Si -enriched (70%) SiF_4 to determine the spin and estimate the

gyromagnetic ratio of silicon-29 from ^{29}Si – ^{19}F coupling constants. The next application appeared 26 years later when Harris and coworkers^{370,371} used enriched SiO_2 in studies of silicate solutions, and a series of applications to silicates then followed. The strong signal from enriched samples was also used to study complexation with tropolone (2-hydroxy-2,4,6-cycloheptatrien-1-one)³⁷².

High non-selective enrichment of ^{29}Si offers the possibility of using the homonuclear methods that are well known from ^1H NMR. Of course, the ^{29}Si NMR spectra of such samples have a complicated appearance due to homonuclear ^{29}Si – ^{29}Si and heteronuclear ^1H – ^{29}Si couplings that often require second-order analysis^{373,374}. The first method employed was homonuclear $^{29}\text{Si}\{^{29}\text{Si}\}$ decoupling. Harris and coworkers^{371,373,374} used enriched samples in a high-field spectrometer (operating at *ca* 100 MHz for ^{29}Si) to assign splittings and to determine the structure of several problematic species in the spectrum of potassium silicate. The double resonance technique, however, required a number of separate experiments, had low resolution, and Si–Si couplings complicated the spectra. It was soon replaced by 2D techniques: homonuclear *J*-resolved spectroscopy³¹⁹ and Si,Si-COSY of various silicates^{319,375} (even in glasses³⁷⁶) and germanosilicate^{377–379}, and enrichment enabled the application of EXSY spectroscopy to potassium silicate solutions^{380,381}. ^{29}Si isotopic enrichment leads to small isotope effects on ^{29}Si chemical shifts. In silicates the isotope shift, $\Delta^{29}\text{Si}(^{29}\text{Si})$, varies with temperature; it can amount to 0.22 ppm (to lower frequency) but is usually smaller³⁸².

^{29}Si enrichment also permitted the study of the process of hydration of Ca_3SiO_5 (in the solid state); without enrichment, the time dependence could not be followed as the measurement of a single point would have taken too long³⁸³. An interesting method, called selective isotopic enrichment, was used to study species formed in this process. Enriched SiO_2 was mixed with normal tricalcium silicate and the time dependence of ^{29}Si spectra (MAS) measured. Since only silicon from SiO_2 was enriched (labeled), its fate during the reaction could be followed. Enrichment in both ^{29}Si and ^{117}Sn allowed measurements of ^{29}Si – ^{117}Sn heteronuclear 2D NMR correlated spectra (Figure 53) that identified Si–Sn connectivities in stannosilicate anions³⁸⁴.

It is not clear whether enrichment will find use in organosilicon studies even if isotopic enrichments become feasible for polysilanes or siloxanes.

Organosilicon compounds have been enriched in other isotopes. Thus, ^{15}N enrichment allowed measurement of $J(^{29}\text{Si}$ – $^{15}\text{N})$ coupling in trisilylamine [$(\text{H}_3\text{Si})_3\text{N}$, $^1J = +6$ Hz]³⁸⁵ in 1973. Recently, a sample highly enriched (98%) in ^6Li was used in a triple resonance ^6Li – ^{29}Si correlation experiment²⁹⁸ discussed in Section VI.B. The coupling constants $^1J(^{29}\text{Si}$ – $^{13}\text{C})$ of a SiCN unit were determined from the ^{29}Si spectra of ^{13}C -labelled silylene-isocyanide adducts³⁸⁶.

Selective deuteration has been used for ^{29}Si line assignment as in other fields of NMR spectroscopy. The application has been limited to assignment of the lines in per-trimethylsilylated sugars^{132,166,167} as exemplified in methyl 2,3,4,6-tetra-*O*-trimethylsilyl- α -D-glucopyranoside **39** in Figure 54. The isotope effect of ^2H on the ^{29}Si chemical shifts in silicates amounts to up to 0.15 ppm (to higher frequency)³⁸². The ease and in-expense of deuteration can be combined with INEPT or DEPT polarization transfer from ^2H ^{142,387,388}. It seems that with the advent of 2D NMR spectroscopy selective deuteration techniques are used for other than assignment purposes. For example, Jutzi and

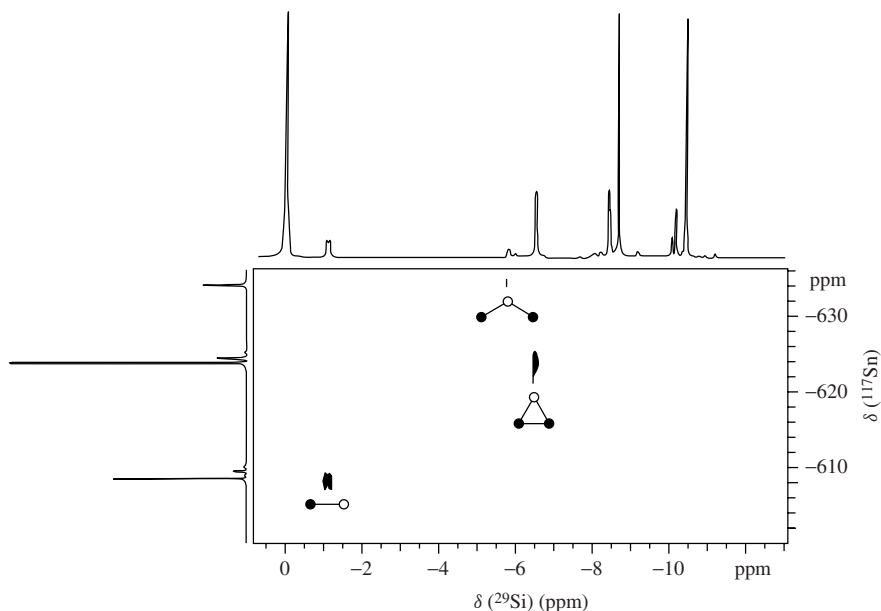
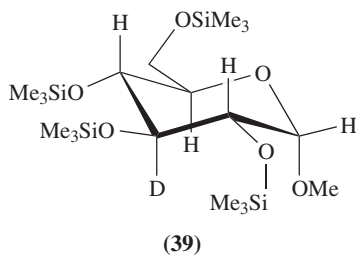


FIGURE 53. Expanded part of ^{29}Si – ^{117}Sn NMR heteronuclear 2D spectrum of stannosilicate solution (enriched in both ^{29}Si and ^{117}Sn). The circles represent octahedral stannate centres, filled circles represent tetrahedral silicate centres and lines represent shared oxygen links. Reprinted with permission from Reference 384. Copyright 1996 American Chemical Society

Bunte prepared deuterated cation $[(\pi\text{-Me}_5\text{C}_5)_2\text{SiD}]^+$ and measured its ^2H and ^{29}Si NMR spectra to confirm the structure of the cation³⁸⁹.



B. DOSY (Diffusion Ordered Spectroscopy)

The NMR technique for measuring self-diffusion in liquids was first reported in 1965³⁹⁰, and its variant for multicomponent mixtures became available with the introduction of the Fourier transform. Wider use had to wait until pulsed field gradients became generally

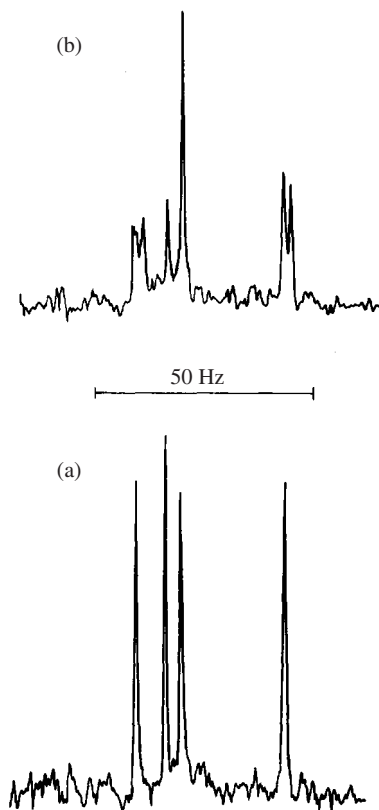


FIGURE 54. ^{29}Si NMR spectra (IGD) of the 3-deuterio derivative **39** under conditions of proton noise decoupling (a) and with selective proton decoupling of $(\text{CH}_3)_3\text{Si}$ protons (b). The line due to silicon from the $^2\text{HC}(3)\text{-O-Si}$ fragment is the line that does not exhibit any splitting in spectrum b. Reproduced by permission of John Wiley & Sons, Ltd from Reference 167

available and software for routine data processing developed. There is no question that the fancy name also contributed to its current popularity. All of the numerous experimental methods available (for a review see Reference 391) are based on a diminution of the NMR spin-echo signal by diffusion. The exponential decrease of the signal with diffusion time is analysed to yield the coefficient of self-diffusion (D) for each signal in the spectrum. DOSY allows recognition of the resolved signals that belong to the same molecule (and have the same value of D) and differentiates them from signals coming from other molecules with different diffusion (molecular size). Self-diffusion coefficients of hexamethyldisilane were determined from ^1H and ^{13}C NMR measurements³⁴⁶; applicability to ^{29}Si NMR was demonstrated by Harris's group on enriched sodium silicate in concentrated solutions³⁸¹. DOSY holds great promise for organosilicon polymers, dendrimers and persilylated mixtures of organic compounds. Since hydrogen bonding affects the diffusion³⁹², DOSY order is not always the order of molecular sizes; trimethylsilylation should lead to DOSY spectra ordered according to the molecular size of mixture

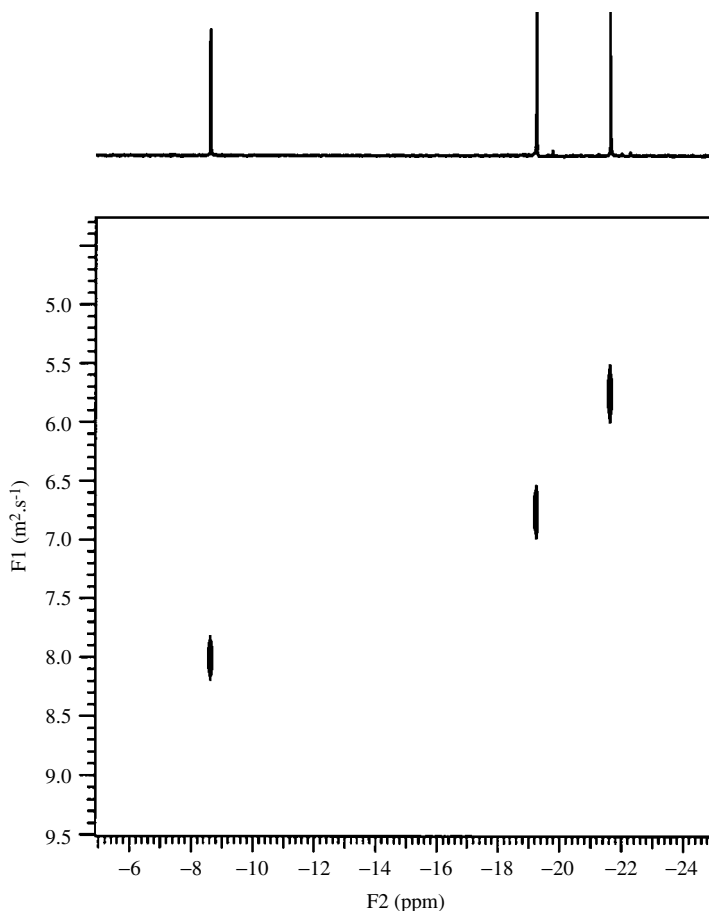


FIGURE 55. DOSY-INEPT spectrum of a mixture of cyclodimethylsiloxanes $(\text{OSiMe}_2)_n$ ($n = 3, 4$ and 5; CDCl_3 solution, 23°C , diffusion coefficients not calibrated, pulse sequence INEPT-DOSY³⁹¹, 32 transients, 10 increments of gradient strength). Diffusion order agrees with the molecular size and the known chemical shifts of the siloxanes

components. Sensitivity to the molecular size is demonstrated in Figure 55 on an artificial mixture of cyclodimethylsiloxanes, $(\text{OSiMe}_2)_n$. An application to mixtures of trimethylsilylated sugars has been reported³⁹³.

C. Quantitative Measurements

Quantitative NMR measurements always require a number of precautions¹⁵⁹. The well-known unfavourable properties of silicon nuclei are a further aggravation. Quantitative measurements of ^{29}Si NMR require the use of IGD to eliminate NOE, long delays between scans (5–10 times the longest T_1 in the sample) and/or addition of a relaxation reagent [e.g. chromium or iron triacetylacetonate, $\text{Cr}(\text{acac})_3$ or $\text{Fe}(\text{acac})_3$], to enhance relaxation

and thus effectively level T_1 values and suppress NOE. When reliable quantitative data are needed and the chemistry permits, the methods are combined: a relaxation reagent is added and an IGD with long relaxation delays is used³⁹⁴. Repeated independent determinations are averaged³⁹⁵, as is common in other analytical methods but is a bit unusual in NMR practice.

When a relaxation reagent is used to reduce all the relaxation times T_1 to approximately the same value, a compromise concentration must be found so that the lines are not broadened more than can be tolerated (signal overlap). The shortest acquisition time compatible with the required resolution (or achievable resolution in the presence of a relaxation reagent) should be used to have a good signal-to-noise ratio (though mathematical line deconvolution has been successfully used to reveal triad proportions in polysilylenes³⁹⁶). A relaxation delay should be at least five times the longest T_1 ^{29}Si relaxation time in the sample, but with a relaxation reagent this might not be so critical when all the relaxation times become equal. If an estimate of the relaxation time is available, it would be useful to set the pulse flip angle to the Ernst angle. Such precautions are needed when the molecular mass or an average degree of polymerization is to be determined for a polymer or similar compounds (see, e.g., Reference 397). In these conventional measurements employing IGD and relaxation reagents, pulse flip angles around 45° and a pulse repetition of 6–10 s are typically used to ensure quantitative results. These considerations apply to quantification of signals within one sample; a much more complex problem is encountered when quantitative comparison of different samples (or absolute intensity) is needed and the samples cannot be mixed together. In such cases, some quantitative standard is required³⁷². A particularly difficult case of silicates containing colloidal particles was analysed by Harris's group³⁹⁸. In applications of TMS tagging to mixture analysis, an internal quantitative (or integral) standard can be added in an exact amount to the mixture prior to silylation. The standard (e.g. benzoic acid^{399–401} or *N*-benzoyl-*N*-phenylhydroxylamine⁴⁰²) is also trimethylsilylated and thus provides an intensity reference that compensates (at least partially) for some possible errors in the sample preparation.

It has been demonstrated on a number of polysiloxanes that recycled-flow NMR is superior to the use of relaxation reagents⁴⁰³. It levels spin–lattice relaxation, minimizes NOE, shortens the experiment time by a factor of 3–5 and gives spectra with improved resolution. However, as the flow method requires some additional equipment, it is unlikely to be used for isolated cases when quantitative ^{29}Si NMR is needed. On the other hand, when such spectra are run often, it is certainly worth consideration, especially when flow cells (probes) for LC NMR are available.

A good signal-to-noise ratio is of key importance for getting precise intensity ratios and reproducible results. Time economy dictates that one of the non-selective polarization transfer schemes be used for such purposes. It is true that these experiments give strong signals and a good base line, but they can also introduce systematic errors and inaccuracies. Let us consider INEPT, for example. As shown in Section V.B, the INEPT signal intensity depends on the number of coupled protons, on the values of their ^{29}Si – ^1H coupling constants and also on their homonuclear couplings with other protons. INEPT would yield accurate intensities (i.e. intensities proportional to the concentrations) only if all these parameters were the same for all the measured signals, and moreover all relaxation times should be the same so that losses through the duration of the pulse sequence would be the same. Obviously, these conditions cannot be met, but it has been estimated that for related trimethylsilyl derivatives with comparable linewidths of ^{29}Si signals, the errors are unlikely to exceed 30%. For compounds of known structure, however, a suitable reference

can be chosen, the systematic error would not exceed that in conventional measurements and reproducibility would be high¹⁴⁴.

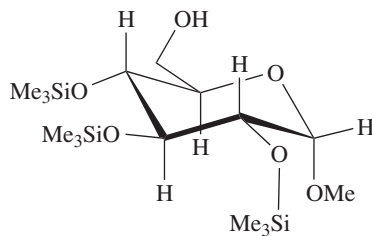
D. Ultrahigh Resolution

The wave of ultrahigh resolution (UHR) experiments⁴⁰⁴ (see Reference 405 for the leading reference) has also hit ^{29}Si NMR, which is particularly suited for this technique because of its narrow lines and long relaxation times. Technical requirements and procedures for UHR ^{29}Si NMR were examined by Kupče and Lukevics^{405–407}, who also showed promising results for a few simple organosilicon compounds and employed INEPT and INEPT + HE methods. The UHR ^1H NMR spectrum of tetramethylsilane⁴⁰⁸ revealed a very small two-bond $^{29}\text{Si}/^{28}\text{Si}$ isotopic effect on the ^1H chemical shift (30 mHz at 500 MHz, i.e. 0.06 ppb). The current techniques of gradient shimming and volume selective excitation should make UHR resolution less tedious⁴⁰⁹ but the topic seems to have been abandoned at present, except for a few studies of Wrackneyer and coworkers^{410,411}.

E. Shift and Relaxation Reagents

Chemical shift reagents (lanthanide shift reagents, LSR) are used to remove undesirable overlap of signals, help in line assignment and/or determine the geometry of the molecule by a comparison of the induced shifts (for a review see Reference 412). It is perhaps due to the large spectral dispersion of ^{29}Si chemical shifts and progress of other assignment techniques that the need for the use of chiral reagents has been very limited. On the other hand, relaxation agents have been used so often that only some applications can be mentioned here.

The effect of association of $\text{Pr}(\text{fod})_3$ (fod = 1,1,1,2,2,3,3-heptafluoro-7,7-dimethyloctane-4,6-dione) on the ^{29}Si chemical shift of $(\text{EtO})_2\text{Me}_2\text{Si}$ [in a 0.01 M solution of $\text{Cr}(\text{acac})_3$ in CDCl_3] is quite large⁴¹³. The lanthanide induced shift (LIS) to lower frequency can amount up to 70 ppm (at a reagent/substrate molar ratio of 2 : 2), and it is assumed that the dialkoxysilane acts through its two oxygen atoms as a bidentate ligand towards LSR. The application of LSR to ^{29}Si line assignments requires the molecule under study to have one clearly preferred site of complexation with the LSR, and this condition is seldom met. A rare example of a compound satisfying this condition is **40** with the one hydroxyl group remaining unsilylated becoming the preferred complexation site. The LSR $[\text{Pr}(\text{dpm})_3, \text{praseodymium(III) dipivaloylmethanato}]$ -affected ^{29}Si chemical shifts were correlated with ^1H chemical shifts of SiMe_3 groups through selective ^1H decoupling experiments, and selective deuteration confirmed that among the SiMe_3 resonances the one most affected by the LSR is that on the C-4 carbon¹⁶⁷.



(40)

Relaxation reagents. When polarization transfer schemes cannot be used to speed up the measurements, time can be saved by increasing the relaxation rates of ^{29}Si nuclei. The time savings achieved can be substantial, as it often happens that the ^{29}Si nucleus to which polarization cannot be transferred is the slowest relaxing nucleus in the sample. Although saturation of the sample with oxygen gas (paramagnetic)^{334,347} and use of viscous solutions⁶⁸ were also tried, addition of relaxation reagents is the common practice although it contaminates the sample. As discussed in Section X.C, the added bonus of these reagents is that they also eliminate nuclear Overhauser effects, thus enabling quantitative applications of ^{29}Si NMR.

The use of relaxation reagents, most often $\text{Fe}(\text{acac})_3$ or $\text{Cr}(\text{acac})_3$, if mentioned in the experimental part at all, is often accompanied by the adjectival phrase ‘shiftless relaxation reagent’ and yet this ‘shiftlessness’ has been confirmed only in a very few cases⁴¹³. Addition of $\text{Fe}(\text{acac})_3$ or $\text{Cr}(\text{acac})_3$ in concentrations up to $5 \cdot 10^{-2}$ M does not affect the relative shifts of $(\text{EtO})_4\text{Si}$, TMS and HMDSO (within 0.1 ppm)¹⁵. In the overwhelming majority of ^{29}Si NMR applications, i.e. in quantitative determinations of component ratios, in line assignment experiments etc., it is immaterial. It is not important even for compound identification—if the concentration of the reagent in the measured solution is given, the chemical shift values are reproducible irrespective of the shifts it might induce. Concentrations of 0.02—0.04 M of $\text{Cr}(\text{acac})_3$ are usually sufficient^{39,334}. (For concentration dependencies see Reference 347) The reagent could, however, affect some trends and correlations with other molecular properties. $\text{Cr}(\text{acac})_3$ has been observed to cause low-frequency shifts (5 Hz at 19.87 MHz) in siloxanes³⁹, and decomposition of some perhalosilanes⁸⁶ occurred.

XI. COMMON MISTAKES AND PITFALLS — COMMENTS AND WARNINGS

When processing original ^{29}Si NMR data into our database, we note many errors or misunderstandings. Some of them would be humorous (e.g. magnetic field $B_0 = 5$ Torr) if they were not misleading. If native English-speaking authors write about ‘NMR images’ when they did not in fact measure images but spectra, to which they also refer as ‘NMR spectroscopy curves’, the whole study becomes suspect. A spectrum that shows large FID truncation or FID clipping artifacts in the figure would have a similar effect on the reader.

The present review can do nothing to help eliminate these types of errors (except to advise reading some basic NMR textbooks), but it attempts to help eliminate errors related to the NMR experiment itself, errors that often have their origin in the ease and widespread use of advanced NMR techniques by non-specialists. Some of these errors or misconceptions are frequent as they have a tendency to propagate, when experimental parts are apparently copied from a previously published paper into a new manuscript, thus reducing the usefulness of the newly presented data. In this Section we shall comment on errors related to spectroscopic details (without literature references); the need to give details about the measured solutions and referencing was stressed already in several instances in this review.

Measuring frequency seems to be a problem when concise data presentation in the format ^{29}Si -NMR (XXX MHz, CDCl_3 , TMS int.) is required by the journal. Some authors correctly interpret XXX as the ^{29}Si NMR measuring frequency, i.e. the resonance frequency of ^{29}Si nuclei, (39.73, 59.63 and 99.32 MHz); others assume it to be the spectrometer frequency, i.e. the ^1H NMR measuring frequency (200, 300 and 500 MHz, respectively). The use of the spectrometer frequency then leads to the occurrence of

expressions like '²⁹Si-NMR (250 MHz) and ¹⁵N-NMR (250 MHz)' in one line. At the present time, statements like '²⁹Si NMR spectra were obtained ... the resonance frequency was 600 MHz' are obviously in error, but the error might not be so obvious when spectrometers with a proton frequency of 3 GHz become available.

Acquisition parameters. Acquisition time (i.e. time during which FID data are collected) and spectral width (i.e. the frequency with which the FID data are sampled and collected during the acquisition time) affect the precision of the spectral line frequencies in a decisive way. A small spectral width can bring signal folding, thus producing a systematic error; the acquisition time determines the observed line width (the longer the acquisition, the higher the resolution—providing acquisition is shorter than T_2^*). Simply put, two lines can be resolved only if their frequency difference is larger than the reciprocal of acquisition time. In general, ²⁹Si NMR lines are narrow (observable line width $1/\pi T_2^*$, where T_2^* is the effective spin–spin relaxation time) but data collection after $3T_2^*$ is of little value as the signal has decreased to 5% of its maximum value and hence prolonged data acquisition decreases S/N. (Note that the textbooks of the seventies considered the effects of acquisition time and spectral width from the point of view of very limited computer memory of fixed size.)

Names of experiments and pulse sequences. The rule here is clear, though often difficult to comply with. A name without reference to the published full description of the experiment/sequence is of very limited value; many well-known and widely used sequences have several modifications that sometimes substantially affect the performance of the parent sequence. Thus the name used might cover an entire class of similar experiments instead of one well-defined experiment (e.g. 'saturation transfer experiment'). Often, the name given to a sequence in the software does not resemble the name in the source literature. (Who besides Jeol users could recognize that 'SGNNE' is an inverse gated experiment?) Recently, a manufacturer has gone a long way to help the user in this respect and assembled this information on a CD⁴¹⁴.

Parameters of pulse sequences. In contrast to acquisition parameters, which are always important for assessing the precision of presented data, the importance of the other parameters of a pulse sequence must be judged from case to case. For example, if INEPT or DEPT is used just to determine the chemical shifts in one compound, the delays are not relevant for the reported values as they affect only the sensitivity of the measurements, i.e. the time it takes. However, if the same sequence were used as evidence that some product is absent from the sample, almost all parameters of the sequence become relevant (any incorrectly set delay or erroneous estimate of the expected couplings in the sequence can null the signal and thus provide misleading evidence). When the parameter is relevant, it must be clear to the reader which parameter of the pulse sequence the author had in mind, so the parameters should be either defined or the same name used as in the source literature for the pulse sequence instead of the name the programmer gave it in the software. Also, although in such a case one individual's terminology might well be understood by colleagues having the same software, it might appear cryptic to those who have some other product (e.g. while Varian users would recognize parameters like *tof*, others would have difficulty realizing that this is *O1* or *o1* on their Bruker spectrometer or *x_* *offset* on a Jeol and vice versa; for translation of these dialects see Reference 30).

Data processing affects considerably the appearance of both 1D and 2D spectra. Among other things, processing can make spectral lines broader or narrower with concomitant

increase or decrease in signal-to-noise ratio, respectively. In 2D spectra, an improper choice of processing and threshold can make some important cross-peak disappear from the contour plot. Despite this, processing details seldom accompany 2D plots presented in journals even in cases when the plot is used as evidence of a missing peak. In contrast, authors often give the value of digital resolution, which deserves a separate comment.

Digital resolution (e.g. 0.2 Hz/point) is valuable information in some special cases, e.g. when the spectra are reproduced in the paper. But when it is the only experimental detail given, it is meaningless. It tells us only how well the spectrum could be drawn in order to please the eye, i.e. how well cosmetics were applied to the raw data. High digital resolution can be achieved simply just by extensive zero-filling of the raw FID data. Zero-filling above doubling the number of FID data points prior to Fourier transform does not improve spectral resolution (i.e. it does not make the lines narrower); it only improves interpolation between data points when the spectrum is drawn (perhaps making shoulders or inflexes more apparent)^{415,416}. Of course, when digital resolution (e.g. 1.4 Hz/point) is much lower than the assumed accuracy of the presented data (e.g. coupling constants reported to 0.1 Hz), something is wrong.

Referencing, as explained (Section III), significantly affects the accuracy of the reported chemical shifts; it can introduce a systematic error. If any secondary reference is employed, the relationship used for the conversion should be given, including the numerical value (δ_S). Statements like 'chemical shifts measured relative to external hexamethyldisiloxane and internal octamethylcyclotetrasiloxane were scaled to TMS δ -scale' leave the δ values with a large additional uncertainty, perhaps 1–2 ppm.

Accuracy and precision. Overly optimistic and overly pessimistic precision estimates for shifts and coupling constants occur with equal frequency. On the one hand, when authors give the chemical shift to 0.001 ppm it is most probably not realistic (not only in the case of CP MAS chemical shifts but also in a solution measured at 39.7 MHz with internal TMS referencing). On the other hand, when the internally referenced shift is given to 1 ppm, it implies a conservative estimate including possible inaccuracy due to the secondary reference employed, uncertainty in exact solution composition etc. With some precautions, chemical shifts can be reproducible to ± 0.02 – 0.03 ppm on a current spectrometer. Precision of coupling constant values is easier to evaluate as it does not require any referencing; usually, without excessive care, the coupling can be determined to 0.1 Hz.

Overly optimistic estimates probably have their origin in the line positions as given by the spectrometers. The excessive number of 'significant' digits in such listings reflects only that the software provided does not round the calculated positions according to the resolution achieved. The fact that these digits appear reproducible is due to a robust algorithm of the calculation. (To illustrate—if you calculate a coupling constant J as one-third of the separation of the outer lines of a quartet, and this separation is 10.0 Hz, $J = 10.0/3 = 3.333333\dots$ the division by 3 is very reproducible on any hand-held calculator, but this certainly does not reflect the precision of the J -value determination. Similarly, the line positions that come out from the same FID using the same data processing are identical.)

It is not uncommon to see the values of one-bond couplings [e.g. $J(\text{Si}-\text{Si})$ or $J(\text{Si}-\text{H})$] reported with a precision of 1 Hz and two-bond and longer-range couplings with a precision of 0.1 Hz, although all of these couplings were determined from the same experiment. This leaves the reader asking if the decimal places in the former were left out by mistake or was the high precision of the latter in error? (The reader's doubts are not put at ease

when the proton–proton couplings are reported to 0.01 Hz in the same paper and almost no experimental detail is given.)

In 2D experiments, the precision of the measured values is determined by the precision with which peak positions can be determined in a 2D spectrum. The precision of the values measured along the F2 axis is determined by the acquisition time (as in 1D spectra), but the precision of the values measured along the F1 axis (i.e. indirectly detected) is determined by the maximum evolution time used in the experiment (assuming it is shorter than the T_2^* relaxation time of the signal). Hence, if a heteronuclear coupling [e.g. $^2J(\text{Si}-\text{H})$] has to be determined with a precision of 0.1 Hz, it would require a maximum evolution time of the order of 10 s, that is, some 40,000 increments if the spectral width along F1 were 4 kHz (in a correlation experiment), which is not very realistic. On the other hand, chemical shifts can be easily determined with the needed precision of 1 Hz along F1.

When NMR of different nuclei is used to determine their heteronuclear coupling, the values must be the same within experimental error [when ^{29}Si NMR yields $J(\text{Si}-\text{H}) = 200$ Hz and ^1H yields for the same coupling the value of 209 Hz, which of the two is a typo?].

Use of non-standard abbreviations might let the paper go unnoticed, as the abbreviation in the title or in the text might not be recognized by automatic indexing services (e.g. MASS NMR instead of the common MAS NMR or MASNMR; similarly, SSNMR for Solid-State NMR could mean high-resolution or broad-line NMR).

Though the recommendations expressed in the preceding paragraphs are definitely trivial, experience shows that very often they are violated, especially in synthetic papers presented in general or synthetically oriented chemistry journals that stress brevity and in which the referees cannot be experts in all fields considered in the paper. In dedicated NMR journals the situation is the opposite—those journals adhere to IUPAC^{417,418} and ASTM⁴¹⁷ recommendations on NMR data presentation, give ample space for experimental detail, and the referee is always asked one question: ‘Does the Experimental section give enough detail?’

The request of brevity imposed by some journals makes some authors put the journal to a test and they inject some certainly irrelevant information into otherwise innocent experimental detail (e.g. ‘spectra were recorded in London at 7.05 T’).

Recommendations for authors publishing in brevity-conscious journals that do not specialize in NMR and do not allow the author to follow exceedingly detailed IUPAC recommendations can be summarized as follows: Omit spectrometer manufacturer and model identification as well as software version but insist on full description of the measured solution, temperature and referencing, and indicate the measuring frequency. State in the text the estimate of precision of values given. If the data were obtained by any method other than an inverse gated pulse experiment, give the pertinent experimental and processing details, perhaps in the form of supplementary information or in a figure legend.

XII. ACKNOWLEDGEMENTS

The author expresses his gratitude to Prof. Alan Bassindale for invaluable advice on how to start writing this review and to Prof. Jon Michael Bellama for careful conversion of the review from Czech English into American English. Special thanks should go to the coworkers in the Institute who have maintained the database: Ing. M. Bártlová, Mrs. J. Karasová, Ing. E. Macháčková, Ing. L. Soukupová and Mrs. E. Vilimovská. Numerous colleagues throughout the world were kind enough to send reprints and preprints of their work related to the topic and originals of their artwork; their help was very valuable but the list is too long to be published here. The database was created and maintained thanks

to grant no. 203/99/0132 provided by the Granting Agency of the Czech Republic. This project was supplied with subvention by The Ministry of Education of the Czech Republic (Project LB98233).

XIII. REFERENCES

1. J. W. Emsley, J. Feeney and L. H. Sutcliffe, *High Resolution Nuclear Magnetic Resonance Spectroscopy*, Pergamon Press, Oxford, 1965.
2. F. Uhlig, U. Herrmann and H. Marsmann, ²⁹Si NMR Database System, http://oc30.uni-paderbon.de/~chemie/fachgebiete/ac/ak_marsmann or <http://platon.chemie.uni-dortmund.de/acii/fuhlig>, 2000.
3. Y. Takeuchi and T. Takayma, in *The Chemistry of Organic Silicon Compounds*, Vol. 2/Part 1 (Eds. Z. Rappoport and Y. Apeloig), John Wiley & Sons, Chichester, 1998, pp. 267–354.
4. H. C. Marsmann, in *Encyclopedia of Spectroscopy and Spectrometry* (Eds. J. C. Lindon, G. E. Tranter and J. L. Holmes), Academic Press, New York, 1999, pp. 2031–2042.
5. E. A. Williams, in *The Chemistry of Organic Silicon Compounds*, Vol. 1 (Eds. S. Patai and Z. Rappoport), John Wiley & Sons, Chichester, 1989, pp. 511–554.
6. R. K. Harris, J. D. Kennedy and W. McFarlane, in *NMR and the Periodic Table* (Eds. R. K. Harris and B. E. Mann), Chap. 10, Academic Press, London, 1978, pp. 309–378.
7. R. K. Harris, in *The Multinuclear Approach to NMR Spectroscopy* (Eds. J. B. Lambert and F. G. Riddell), Chap. 16, D. Reidel Publishing Company, Dordrecht, 1988, pp. 343–359.
8. H. Marsmann, in *NMR Basic Principles and Progress*, Vol. 17 (Eds. P. Diehl, E. Fluck and R. Kosfeld), Springer-Verlag, Berlin, 1981, pp. 65–235.
9. J. Schraml and J. M. Bellama, in *Determination of Organic Structures by Physical Methods*, Vol. 6 (Eds. F. Nachod, J. J. Zuckerman and E. W. Randall), Academic Press, New York, 1976, pp. 203–269.
10. R. K. Harris, in *NMR and the Periodic Table* (Eds. R. K. Harris and B. E. Mann), Chap. 1, Academic Press, London, 1978, pp. 1–19.
11. C. Brevard and P. Granger, *Handbook of High Resolution Multinuclear NMR*, John Wiley & Sons, New York, 1981.
12. D. Shaw, *Fourier Transform N.M.R. Spectroscopy*, Elsevier Scientific Publ. Co., Amsterdam, 1976.
13. B. K. Hunter and L. W. Reeves, *Can. J. Chem.*, **46**, 1399 (1968).
14. G. C. Levy, *J. Am. Chem. Soc.*, **94**, 4793 (1972).
15. G. C. Levy, J. D. Cargioli, G. E. Maciel, J. J. Natterstad, E. B. Whipple and M. Ruta, *J. Magn. Reson.*, **11**, 352 (1973).
16. P. Laszlo, *Prog. NMR Spectrosc.*, **3**, 231 (1967).
17. P. Laszlo, A. Speert, R. Ottinger and J. Reisse, *J. Chem. Phys.*, **48**, 1732 (1968).
18. M. Bacon, G. E. Maciel, W. K. Musker and R. Scholl, *J. Am. Chem. Soc.*, **93**, 2537 (1971).
19. M. R. Bacon and G. E. Maciel, *J. Am. Chem. Soc.*, **95**, 2413 (1973).
20. N. N. Zemlyanskij and O. K. Sokolikova, *Zh. Anal. Khim.*, **36**, 1990 (1981); *Chem. Abstr.*, **96**, 78788q (1982).
21. J. Schraml, *Prog. NMR Spectrosc.*, **22**, 289 (1990).
22. J. A. Pople, W. G. Schneider and H. J. Bernstein, *High-resolution Nuclear Magnetic Resonance*, McGraw-Hill, New York, 1959.
23. H. Günther, *NMR Spectroscopy*, John Wiley & Sons, Chichester, 1995.
24. P. Granger, *ESN-European Spectroscopy News.*, **72**, 22 (1987).
25. C. J. Jameson, A. K. Jameson and S. M. Cohen, *J. Magn. Reson.*, **19**, 385 (1975).
26. A. K. Jameson and C. J. Jameson, *J. Am. Chem. Soc.*, **95**, 8559 (1973).
27. F. G. Morin, M. S. Solum, J. D. Withers, D. M. Grant and D. K. Dalling, *J. Magn. Reson.*, **48**, 138 (1982).
28. R. K. Harris and B. J. Kimber, *J. Magn. Reson.*, **17**, 174 (1975).
29. S. Brownstein and J. Bornais, *J. Magn. Reson.*, **38**, 131 (1980).
30. S. Braun, H.-O. Kalinowski and S. Berger, *150 and More Basic NMR Experiments*, Wiley-VCH, Weinheim, 1999.
31. J. Homer, *J. Magn. Reson.*, **54**, 1 (1983).
32. D. H. Live and S. I. Chan, *Org. Magn. Reson.*, **5**, 275 (1973).

33. B. L. Sagan and J. A. Walmsley, *Magn. Reson. Chem.*, **25**, 219 (1987).
34. B. R. Donaldson and J. C. P. Schwarz, *J. Chem. Soc.(B)*, 395 (1968).
35. R. E. DeSimone, *J. Chem. Soc., Chem. Commun.*, 780 (1972).
36. C. J. Jameson and A. K. Jameson, *Chem. Phys. Lett.*, **149**, 300 (1988).
37. R. L. Scholl, G. E. Maciel and W. K. Musker, *J. Am. Chem. Soc.*, **94**, 6376 (1972).
38. W. McFarlane and J. M. Seaby, *J. Chem. Soc., Perkin Trans. 2*, 1561 (1972).
39. R. K. Harris and B. J. Kimber, *J. Organomet. Chem.*, **70**, 43 (1974).
40. J. D. Cargioli, E. A. Williams and R. W. LaRochelle, *Solvent Effects in ^{29}Si NMR in IXth Organosilicon Award Symposium*, Case Western Reserve University, Cleveland, Ohio, 1975, Abstracts, p. 19.
41. E. A. Williams, J. D. Cargioli and R. W. LaRochelle, *J. Organomet. Chem.*, **108**, 153 (1976).
42. V. Gutmann, *Chem. Ind.*, 102 (1971).
43. V. Gutmann, *Electrochim. Acta*, **21**, 661 (1976).
44. M. Handa, M. Kataoka, M. Wakaumi and Y. Sasaki, *Bull. Chem. Soc. Jpn.*, **70**, 315 (1997).
45. A. Voigt, R. Murugavel, U. Ritter and H. W. Roesky, *J. Organomet. Chem.*, **521**, 279 (1996).
46. J. Schraml, M. Jakoubková, M. Kvičalová and A. Kasal, *J. Chem. Soc., Perkin Trans. 2*, 1 (1994).
47. J. Past, J. Puskar, J. Schraml and E. Lippmaa, *Collect. Czech. Chem. Commun.*, **50**, 2060 (1985).
48. J. Schraml, J. Čermák, V. Chvalovský, A. Kasal, C. Bliefert and E. Krahé, *J. Organomet. Chem.*, **341**, C6 (1988).
49. A. Kasal, J. Schraml and J. Čermák, *Magn. Reson. Chem.*, **32**, 394 (1994).
50. J. Schraml and J. Čermák, *Collect. Czech. Chem. Commun.*, **55**, 452 (1990).
51. J. Schraml, J. Pola, H. Jancke, G. Engelhardt, M. Černý and V. Chvalovský, *Collect. Czech. Chem. Commun.*, **41**, 360 (1976).
52. J. Schraml, J. Hetflejš, V. Blechta, S. Šabata and L. Soukupová, unpublished results.
53. A. R. Bassindale and T. Stout, *J. Chem. Soc., Perkin Trans.*, **2**, 221 (1986).
54. V. V. Negrebetsky, V. V. Negrebetsky, A. G. Shipov, E. P. Kramarova and Yu. I. Baukov, *J. Organomet. Chem.*, **496**, 103 (1995).
55. M. G. Voronkov, V. A. Pestunovich and Yu. I. Baukov, *Organomet. Chem. USSR*, **4**, 593 (1991).
56. M. G. Voronkov, V. A. Pestunovich and Yu. I. Baukov, *Metalorg. Khim.*, **4**, 1210 (1991); *Chem. Abstr.*, **116**, 41503y (1991).
57. D. Kummer and S. H. A. Halim, *Z. anorg. allg. Chem.*, **622**, 57 (1996).
58. V. A. Pestunovich, S. N. Tandura, B. Z. Shterenberg, V. P. Baryshok and M. G. Voronkov, *Izv. Akad. Nauk SSSR, Ser. Khim.*, 2653 (1978); *Chem. Abstr.*, **96**, 86545z (1979).
59. H. C. L. Abbenhuis, M. L. W. Vorstenbosch, R. A. van Santen, W. J. J. Smeets and A. L. Spek, *Inorg. Chem.*, **36**, 6431 (1997).
60. S. Bruzaud, A.-F. Mingotaud and A. Soum, *J. Organomet. Chem.*, **561**, 77 (1998).
61. C. Eaborn, P. B. Hitchcock, J. D. Smith and S. E. Sözerli, *Organometallics*, **16**, 5653 (1997).
62. A. W. K. Khanzada, M. A. R. Abid and G. H. Kazi, *Pak. J. Sci. Ind. Res.*, **32**, 805 (1989).
63. T. D. Coyle, R. B. Johannesen, F. E. Brinckman and T. C. Farrar, *J. Phys. Chem.*, **70**, 1682 (1988).
64. R. B. Johannesen, F. E. Brinckman and T. D. Coyle, *J. Phys. Chem.*, **72**, 660 (1968).
65. T. D. Coyle, R. B. Johannesen, F. E. Brinckman and T. C. Farrar, *J. Chem. Phys.*, **70**, 1682 (1966).
66. W. T. Raynes, *Mol. Phys.*, **15**, 435 (1968).
67. R. Kosfeld, C. Kreuzburg and R. Krause, *Makromol. Chem.*, **189**, 2077 (1988).
68. B. P. Bammel and R. F. Evilia, *Anal. Chem.*, **54**, 1318 (1982).
69. P. C. Lauterbur, in *Determination of Organic Structures by Physical Methods*, Vol. 2 (Eds. F. C. Nachod and W. D. Phillips), Academic Press, New York, 1962, pp. 511–515.
70. R. Freeman and H. D. W. Hill, *J. Magn. Reson.*, **5**, 278 (1971).
71. K. F. Kuhlmann and D. M. Grant, *J. Chem. Phys.*, **55**, 2998 (1971).
72. R. Wagner and S. Berger, *Phosphorus, Sulfur, and Silicon*, **91**, 213 (1994).
73. M. Ernst, C. Griesinger, R. R. Ernst and W. Bermel, *Mol. Phys.*, **74**, 219 (1991).
74. S. R. Hartmann and E. L. Hahn, *Phys. Rev.*, **128**, 2042 (1962).
75. A. Pines, M. G. Gibby and J. S. Waugh, *J. Chem. Phys.*, **59**, 569 (1973).

76. J. Homer, M. C. Perry and S. A. Palfreyman, *J. Magn. Reson.*, **125**, 20 (1997).
77. K. G. R. Pachler and P. L. Wessels, *J. Magn. Reson.*, **12**, 337 (1973).
78. S. Sørensen, R. S. Hansen and H. J. Jakobsen, *J. Magn. Reson.*, **14**, 243 (1974).
79. H. J. Jakobsen, S. Aa. Linde and S. Sørensen, *J. Magn. Reson.*, **15**, 385 (1974).
80. S. Aa. Linde, H. J. Jakobsen and B. J. Kimber, *J. Am. Chem. Soc.*, **97**, 3219 (1975).
81. S. K. Sarkar and A. Bax, *J. Magn. Reson.*, **62**, 109 (1985).
82. T. Bundgaard and H. J. Jakobsen, *J. Magn. Reson.*, **18**, 209 (1975).
83. S. Aa. Linde and H. J. Jakobsen, *J. Am. Chem. Soc.*, **98**, 1041 (1976).
84. K. G. R. Pachler and P. L. Wessels, *J. Magn. Reson.*, **28**, 53 (1977).
85. K. G. R. Pachler and P. L. Wessels, *Org. Magn. Reson.*, **9**, 557 (1977).
86. S. Li, D. L. Johnson, J. A. Gladysz and K. L. Servis, *J. Organomet. Chem.*, **166**, 317 (1979).
87. G. Deleris, M. Birot, J. Dunogues, B. Barbe, M. Petraud and M. Lefort, *J. Organomet. Chem.*, **266**, 1 (1984).
88. B. Bennetau, M. Birot, G. Deleris, J. Dunogues, J.-P. Pillot, B. Barbe and M. Petraud, *Reviews of Silicon, Germanium, Tin and Lead Compounds*, **8**, 327 (1985).
89. M. Grignon-Dubois, M. Petraud, M. Laguerre and I. Pianet, *Spectrochim. Acta*, **50A**, 2059 (1994).
90. M. Grignon-Dubois and M. Laguerre, *Actual. Chim.*, 21 (1983).
91. M. Grignon-Dubois and M. Laguerre, *Comput. Chem.*, **9**, 279 (1985).
92. H. J. Jakobsen, P. J. Kanyha and W. S. Brey, *J. Magn. Reson.*, **54**, 134 (1983).
93. V. Baudrillard, D. Davoust and G. Ple, *Magn. Reson. Chem.*, **32**, 40 (1994).
94. R. R. Ernst, *J. Chem. Phys.*, **45**, 3845 (1966).
95. K. G. R. Pachler, *J. Magn. Reson.*, **7**, 442 (1972).
96. R. A. Craig, R. K. Harris and R. J. Morrow, *Org. Magn. Reson.*, **13**, 229 (1980).
97. O. W. Sørensen, H. Bildsøe and H. J. Jakobsen, *J. Magn. Reson.*, **45**, 325 (1981).
98. G. A. Morris and R. Freeman, *J. Am. Chem. Soc.*, **101**, 760 (1979).
99. D. T. Pegg, D. M. Doddrell and M. R. Bendall, *J. Chem. Phys.*, **77**, 2745 (1982).
100. G. A. Morris, *J. Am. Chem. Soc.*, **102**, 428 (1980).
101. D. M. Doddrell, D. T. Pegg, W. Brooks and M. R. Bendall, *J. Am. Chem. Soc.*, **103**, 727 (1981).
102. B. J. Helmer and R. West, *Organometallics*, **1**, 877 (1982).
103. J. Schraml, *Collect. Czech. Chem. Commun.*, **48**, 3402 (1983).
104. D. P. Burum and R. R. Ernst, *J. Magn. Reson.*, **39**, 163 (1980).
105. P. H. Bolton, *J. Magn. Reson.*, **41**, 287 (1980).
106. D. M. Doddrell, D. T. Pegg and M. R. Bendall, *J. Magn. Reson.*, **48**, 323 (1982).
107. D. T. Pegg, D. M. Doddrell, W. M. Brooks and M. R. Bendall, *J. Magn. Reson.*, **44**, 32 (1981).
108. K. V. Schenker and W. von Philipsborn, *J. Magn. Reson.*, **61**, 294 (1985).
109. V. Blechta and J. Schraml, *J. Magn. Reson.*, **69**, 293 (1986).
110. P. Lux, F. Brunet, J. Virlet and B. Cabane, *Magn. Reson. Chem.*, **34**, 100 (1996).
111. B. Parbhoo, *J. Magn. Reson.*, **87**, 372 (1990).
112. F. Brunet, P. Lux and J. Virlet, *New J. Chem.*, **18**, 1059 (1994).
113. O. W. Sørensen and R. R. Ernst, *J. Magn. Reson.*, **51**, 477 (1983).
114. K. V. Schenker and W. von Philipsborn, *J. Magn. Reson.*, **66**, 219 (1986).
115. S. Wimperis and G. Bodenhausen, *J. Magn. Reson.*, **69**, 264 (1986).
116. O. W. Sørensen, J. C. Madsen, N. C. Nielsen, H. Bildsøe and H. J. Jakobsen, *J. Magn. Reson.*, **77**, 170 (1988).
117. T. A. Blinka, B. J. Helmer and R. West, *Adv. Organomet. Chem.*, **23**, 193 (1984).
118. O. W. Sørensen and H. J. Jakobsen, in *Pulse Methods in 1D and 2D Liquid-Phase NMR* (Ed. W. S. Brey), Chap. 3, Academic Press, San Diego, 1988, pp. 149–258.
119. V. Gouron, B. Jousseume, M. Ratier, J.-C. Lartigue and M. Petraud, *Magn. Reson. Chem.*, **28**, 755 (1990).
120. J.-B. Verlhac, H. Kwon and M. Pereyre, *J. Organomet. Chem.*, **437**, C13 (1992).
121. J.-P. Picard, S. Grelier, T. Constantieux, J. Donogues, J. M. Aizpurua, C. Palomo, M. Pétraud, B. Barbe, L. Lunazzi and J. -M. Léger, *Organometallics*, **12**, 1378 (1993).
122. G. A. Morris, in *Topics in Carbon-13 NMR Spectroscopy*, Vol. 4 (Ed. G. C. Levy), John Wiley & Sons, New York, 1984, pp. 179–196.
123. F. Brunet and B. Cabane, *J. Non-Cryst. Solids*, **163**, 211 (1993).

124. T. M. Alam, *Spectrochim. Acta*, **53**, A, 545 (1997).
125. L. Pouységu, M. Harket, B. De Jéso, J. C. Lartigue, M. Pétraud and M. Ratier, *Magn. Reson. Chem.*, **35**, 735 (1997).
126. J. Homer and M. C. Perry, *J. Chem. Soc., Chem. Commun.*, 373 (1994).
127. J. Homer and M. C. Perry, *J. Chem. Soc., Perkin Trans. 2*, 533 (1995).
128. J. Homer, M. C. Perry and S. A. Palfreyman, *J. Magn. Reson.* **125**, 20 (1997).
129. A. H. Cowley, W. D. White and S. L. Manatt, *J. Am. Chem. Soc.*, **89**, 6433 (1967).
130. T. C. Eischenschmid, R. U. Kirss, P. P. Deutsch, S. I. Hommeltoft, R. Eisenberg, J. Bargon, R. G. Lawler and A. L. Balch, *J. Am. Chem. Soc.*, **109**, 8089 (1987).
131. M. Haake, J. Natterer and J. Bargon, *J. Am. Chem. Soc.*, **118**, 8688 (1996).
132. D. J. Gale, A. H. Haines and R. K. Harris, *Org. Magn. Reson.*, **7**, 635 (1975).
133. J. Schraml, *J. Magn. Reson.*, **59**, 515 (1984).
134. V. Blechta and J. Schraml, *J. Magn. Reson. A*, **101**, 47 (1993).
135. É. Kupče and B. Wrackmeyer, in *Advanced Applications of NMR to Organometallic Chemistry* (Eds. M. Gielen, R. Willem and B. Wrackmeyer), Chap. 1, John Wiley & Sons, Chichester, 1996, pp. 1–28.
136. V. Blechta, J. Čermák, M. Kvíčalová and J. Schraml, in *16th International Conference, Organometallic Chemistry*, University of Sussex, Brighton, England, 1994, P189.
137. J. Schraml, M. Kvíčalová, V. Blechta, J. Čermák, and P. Herdewijn, in *XIth International Symposium on Organosilicon Chemistry*, Université Montpellier, Montpellier, France, 1996, PC93.
138. J. Schraml, M. Kvíčalová, V. Blechta, Ř. Reřicha, J. Rozenski and P. Herdewijn, *Magn. Reson. Chem.*, **36**, 55 (1998).
139. C. Brevard and R. Schimpf, *J. Magn. Reson.*, **47**, 528 (1982).
140. F. Delpech, S. Sabo-Etienne, B. Chaudret and J.-C. Daran, *J. Am. Chem. Soc.*, **119**, 3167 (1997).
141. B. Wrackmeyer, K. Horchler von Locquenghien, É. Kupče and A. Sebald, *Magn. Reson. Chem.*, **31**, 45 (1993).
142. P. L. Rinaldi and N. J. Baldwin, *J. Am. Chem. Soc.*, **105**, 7523 (1983).
143. É. Kupče and B. Wrackmeyer, *J. Magn. Reson.*, **101**, 324 (1993).
144. J. Schraml, V. Blechta, M. Kvíčalová, L. Nondek and V. Chvalovský, *Anal. Chem.*, **58**, 1892 (1986).
145. C. A. Fyfe, *Solid State NMR for Chemists*, C.F.C. Press, Guelph, Ontario, Canada, 1983.
146. A. A. Maudsley, L. Müller and R. R. Ernst, *J. Magn. Reson.*, **28**, 463 (1977).
147. R. D. Bertrand, W. B. Moniz, A. N. Garroway and G. C. Chingas, *J. Am. Chem. Soc.*, **100**, 5227 (1978).
148. R. D. Bertrand, W. B. Moniz, A. N. Garroway and G. C. Chingas, *J. Magn. Reson.*, **32**, 465 (1978).
149. P. D. Murphy, T. Taki, T. Sogabe, R. Metzler, T. G. Squires and B. C. Gerstein, *J. Am. Chem. Soc.*, **101**, 4055 (1979).
150. G. C. Chingas, R. D. Bertrand, A. N. Garroway and W. B. Moniz, *J. Am. Chem. Soc.*, **101**, 4058 (1979).
151. G. C. Chingas, A. N. Garroway, R. D. Bertrand and W. B. Moniz, *J. Magn. Reson.*, **35**, 283 (1979).
152. G. C. Chingas, A. N. Garroway, W. B. Moniz and R. D. Bertrand, *J. Am. Chem. Soc.*, **102**, 2526 (1980).
153. A. N. Garroway and G. C. Chingas, *J. Magn. Reson.*, **38**, 179 (1980).
154. A. J. Shaka, J. Keeler, T. Frenkiel and R. Freeman, *J. Magn. Reson.*, **52**, 335 (1983).
155. M. Rance, *J. Magn. Reson.*, **74**, 557 (1987).
156. A. J. Shaka, C. J. Lee and A. Pines, *J. Magn. Reson.*, **77**, 274 (1988).
157. M. H. Levitt, R. Freeman and T. Frenkiel, *J. Magn. Reson.*, **47**, 328 (1982).
158. A. Bax and D. G. Davis, *J. Magn. Reson.*, **65**, 355 (1985).
159. T. D. W. Claridge, *High-Resolution NMR Techniques in Organic Chemistry*, Pergamon, Amsterdam, 1999.
160. G. E. Martin and A. S. Zektzer, *Two-Dimensional NMR Methods for Establishing Molecular Connectivity. A Chemist's Guide to Experiments Selection, Performance, and Interpretation*, VCH, Weinheim, 1988.

161. A. Bax, *Two-Dimensional Nuclear Magnetic Resonance in Liquids*, Delft University Press, Delft, Holland, 1982.
162. J. Schraml, ²⁹Si-NMR Analytical Tool for Organic Chemistry, in *3rd International Symposium on NMR Spectroscopy*, Tabor, Czech Republic 1982, P49.
163. E. Liepinš, I. Sekacis and E. Lukevics, *Magn. Reson. Chem.*, **23**, 10 (1985).
164. R. Nardin and M. Vincendon, *J. Magn. Reson.*, **61**, 338 (1985).
165. J. Schraml, E. Petráková, J. Pelnař, M. Kvíčalová and V. Chvalovský, *J. Carbohydr. Chem.*, **4**, 393 (1985).
166. D. J. Gale and N. A. Evans, *Org. Magn. Reson.*, **21**, 567 (1983).
167. A. H. Haines, R. K. Harris and R. C. Rao, *Org. Magn. Reson.*, **9**, 432 (1977).
168. H. Jancke and A. Porzel, *Z. Chem.*, **25**, 251 (1985).
169. J. Maxka, L.-M. Huang and R. West, *Organometallics*, **10**, 656 (1991).
170. J. Maxka, F. K. Mitter, D. R. Powell and R. West, *Organometallics*, **10**, 660 (1991).
171. B. Wrackmeyer, G. Kehr, J. Süß and E. Molla, *J. Organomet. Chem.*, **562**, 207 (1998).
172. B. Wrackmeyer, G. Kehr, J. Süß and E. Molla, *J. Organomet. Chem.*, **577**, 82 (1999).
173. J. Schraml, E. Petráková and J. Hirsch, *Magn. Reson. Chem.*, **25**, 75 (1987).
174. H. B. Yokelson, D. A. Siegel, A. J. Millevolte, J. Maxka and R. West, *Organometallics*, **9**, 1005 (1990).
175. A. D. Fanta, D. J. DeYoung, J. Belzner and R. West, *Organometallics*, **10**, 3466 (1991).
176. O. W. Sørensen, G. V. Eich, M. H. Levitt, G. Bodenhausen and R. R. Ernst, *Prog. NMR Spectrosc.*, **16**, 163 (1983).
177. Y. H. Mariam and P. Abrahams, *Polym. Prepr., Am. Chem. Soc., Div. Polym. Chem.*, **29**, 364 (1988).
178. B. Wrackmeyer, K. Horchler and H. Zhou, *Spectrochim. Acta*, **46A**, 809 (1990).
179. B. Wrackmeyer, R. Köster and G. Seidel, *Magn. Reson. Chem.*, **33**, 493 (1995).
180. B. Wrackmeyer, G. Kehr, R. Köster and G. Seidel, *Magn. Reson. Chem.*, **34**, 625 (1996).
181. B. Wrackmeyer and K. Horchler, *Magn. Reson. Chem.*, **28**, 56 (1990).
182. B. Wrackmeyer, G. Kehr, D. Wettinger and W. Milius, *Main Group Metal Chem.*, **16**, 445 (1993).
183. M. Herberhold, V. Tröbs and B. Wrackmeyer, *J. Organomet. Chem.*, **541**, 391 (1997).
184. B. Wrackmeyer and U. Klaus, *J. Organomet. Chem.*, **520**, 211 (1996).
185. E. Kupče and B. Wrackmeyer, *J. Magn. Reson.*, **99**, 338 (1992).
186. W. E. Hull, in *Two-Dimensional NMR Spectroscopy, Applications for Chemists and Biochemists*, (Eds. W. R. Croasmun and R. M. K. Carlson), Chap. 2, VCH Publishers, New York, 1994, pp. 67–456.
187. K. E. Kóvér and Gy. Batta, *Magn. Reson. Chem.*, **27**, 68 (1989).
188. H. Kessler, C. Griesinger, J. Zarbock and H. R. Loosli, *J. Magn. Reson.*, **57**, 331 (1984).
189. E. B. Baker, *J. Chem. Phys.*, **37**, 911 (1962).
190. R. B. Johannesen and T. D. Coyle, *Endeavour*, **31**, 10 (1972).
191. J. Schraml, M. F. Larin and V. A. Pestunovich, *Collect. Czech. Chem. Commun.*, **50**, 343 (1985).
192. T. Fäcke, R. Wagner and S. Berger, *Concepts Magn. Reson.*, **6**, 293 (1994).
193. R. Freeman, T. H. Mareci and G. A. Morris, *J. Magn. Reson.*, **42**, 341 (1981).
194. A. Bax, R. H. Griffey and B. L. Hawkins, *J. Magn. Reson.*, **55**, 301 (1983).
195. A. Bax, R. H. Griffey and B. L. Hawkins, *J. Am. Chem. Soc.*, **105**, 7188 (1983).
196. J. Pelnař, V. Blechta and J. Schraml, *Appl. Spectrosc.*, **44**, 396 (1990).
197. E. Liepinš, I. Birgele, P. Tomsons and E. Lukevics, *Magn. Reson. Chem.*, **23**, 485 (1985).
198. G. Aagaard, N. R. Andersen and K. Schaumburg, *Magn. Reson. Chem.*, **34**, 945 (1996).
199. J. R. Garbow, D. P. Weitekamp and A. Pines, *Chem. Phys. Lett.*, **93**, 504 (1982).
200. M. F. Summers, L. G. Marzilli and A. Bax, *J. Am. Chem. Soc.*, **108**, 4285 (1986).
201. É. Kupče and B. Wrackmeyer, *J. Magn. Reson.*, **99**, 343 (1992).
202. É. Kupče, E. Lukevics and B. Wrackmeyer, *Magn. Reson. Chem.*, **32**, 326 (1994).
203. É. Kupče and B. Wrackmeyer, *Magn. Reson. Chem.*, **30**, 950 (1992).
204. J. Keeler, R. T. Clowes, A. L. Davis and E. D. Laue, *Methods in Enzymology*, **239**, 145 (1994).
205. M. Chai, T. Saito, Z. Pi, C. Tessier and P. L. Rinaldi, *Macromolecules*, **30**, 1240 (1997).

206. G. W. Vuister, R. Boelens, R. Kaptein, R. E. Hurd, B. John and P. C. M. Van Zijl, *J. Am. Chem. Soc.*, **113**, 9688 (1991).
207. S. Provera, S. Davalli, G. H. Raza, S. Contini and C. Marchioro, *Magn. Reson. Chem.*, in press (2000).
208. T. Kusakawa, Y. Kabe and W. Ando, *Organometallics*, **14**, 2142 (1995).
209. G. Bodenhausen and D. J. Ruben, *Chem. Phys. Lett.*, **69**, 185 (1980).
210. C. Griesinger, H. Schwalbe, J. Schleucher and M. Sattler, in *Two-Dimensional NMR Spectroscopy, Applications for Chemists and Biochemists* (Eds. W. R. Croasmun and R. M. K. Carlson), Chap. 3, VCH Publishers, New York, 1994, pp. 457–580.
211. A. Bax, M. Ikura, L. E. Kay, D. A. Torchia and R. Tschudin, *J. Magn. Reson.*, **86**, 304 (1990).
212. D. Uhrín, S. Uhrínová, E. Eichler and J.-R. Brisson, *J. Magn. Reson.*, **115**, 119 (1995).
213. B. Wrackmeyer, É. Kupče, R. Köster and G. Seidel, *Magn. Reson. Chem.*, **33**, 812 (1995).
214. H. Fleischer, K. Hensen and T. Stumpf, *Chem. Ber.*, **129**, 765 (1996).
215. N. Hertkorn, A. Günzl, E. M. Perdue, D. Freitag, F. Jäkle, and A. Kettrup, in *4. Iglar NMR Tage, Perspectives in NMR Spectroscopy*, University of Innsbruck, Innsbruck, 2000, Abstract, P4.
216. É. Kupče, B. Wrackmeyer and P. Granger, *J. Magn. Reson.*, **100**, 401 (1992).
217. C. Kerst, C. W. Rogers, R. Ruffolo and W. J. Leigh, *J. Am. Chem. Soc.*, **119**, 466 (1997).
218. E. Hengge and F. Schrank, *J. Organomet. Chem.*, **362**, 11 (1989).
219. U. Pöschl, H. Siegl and K. Hassler, *J. Organomet. Chem.*, **506**, 93 (1996).
220. A. Bax, R. Freeman and S. P. Kempell, *J. Am. Chem. Soc.*, **102**, 4849 (1980).
221. A. Bax, R. Freeman and T. A. Frenkiel, *J. Am. Chem. Soc.*, **103**, 2102 (1981).
222. T. H. Mareci and R. Freeman, *J. Magn. Reson.*, **48**, 158 (1982).
223. J. B. Lambert, E. Basso, N. Qing, S. H. Lim and J. L. Pflug, *J. Organomet. Chem.*, **554**, 113 (1998).
224. D. L. Turner, *J. Magn. Reson.*, **49**, 175 (1982).
225. A. Bax and T. H. Mareci, *J. Magn. Reson.*, **53**, 360 (1983).
226. B. J. Hendan and H. C. Marsmann, *J. Organomet. Chem.*, **483**, 33 (1994).
227. A. Bax, R. Freeman, T. Frenkiel and M. H. Levitt, *J. Magn. Reson.*, **43**, 478 (1981).
228. N. C. Nielsen, H. Thogersen and O. W. Sørensen, *J. Am. Chem. Soc.*, **117**, 11365 (1995).
229. A. Bax, R. Freeman and S. P. Kempell, *J. Magn. Reson.*, **41**, 349 (1980).
230. K. Hassler, E. Hengge, F. Schrank and M. Weidenbruch, *Spectrochim. Acta*, **47A**, 57 (1991).
231. R. Dunkel, C. L. Mayne, R. J. Pugmire and D. M. Grant, *Anal. Chem.*, **64**, 3133 (1992).
232. R. Dunkel, C. L. Mayne, M. P. Foster, C. M. Ireland, D. Li, N. L. Owen, R. J. Pugmire and D. M. Grant, *Anal. Chem.*, **64**, 3150 (1992).
233. O. W. Sørensen, R. Freeman, T. Frenkiel, T. H. Mareci and R. Schuck, *J. Magn. Reson.*, **46**, 180 (1982).
234. S. W. Sparks and P. D. Ellis, *J. Magn. Reson.*, **62**, 1 (1985).
235. I. S. Podkorytov, *J. Magn. Reson.*, **89**, 129 (1990).
236. H. B. Yokelson, A. J. Millevolte, B. R. Adams and R. West, *J. Am. Chem. Soc.*, **109**, 4116 (1987).
237. H. Bauer, J. Buddrus, W. Heyde and W. Kimpenhaus, *Angew. Chem.*, **97**, 860 (1985).
238. G. R. Gillette, J. Maxka and R. West, *Angew. Chem., Int. Ed. Engl.*, **28**, 54 (1989).
239. J. Maxka, B. R. Adams and R. West, *J. Am. Chem. Soc.*, **111**, 3447 (1989).
240. M. Kuroda, Y. Kabe, M. Hashimoto and S. Masamune, *Angew. Chem., Int. Ed. Engl.*, **27**, 1727 (1988).
241. P. J. Keller and K. E. Voge, *J. Magn. Reson.*, **68**, 389 (1986).
242. J. Weigelt and G. Otting, *J. Magn. Reson. A*, **113**, 128 (1995).
243. J. B. Lambert and H. Wu, *Magn. Reson. Chem.*, **38**, 388 (2000).
244. M. H. Levitt and R. R. Ernst, *Mol. Phys.*, **50**, 1109 (1983).
245. M. H. Levitt, *Prog. NMR Spectrosc.*, **18**, 61 (1986).
246. A. M. Torres, T. T. Nakashima and R. E. D. McClung, *J. Magn. Reson.*, **99**, 99 (1992).
247. O. W. Sørensen, M. H. Levitt and R. R. Ernst, *J. Magn. Reson.*, **55**, 104 (1983).
248. A. M. Torres, T. T. Nakashima, R. E. D. McClung and D. R. Muhandiram, *J. Magn. Reson.*, **99**, 99 (1992).
249. N. C. Nielsen, H. Bildsøe, H. J. Jakobsen and O. W. Sørensen, *J. Magn. Reson.*, **78**, 223 (1988).
250. O. W. Sørensen, U. B. Sørensen and H. J. Jakobsen, *J. Magn. Reson.*, **59**, 332 (1984).

251. R. Benn, *J. Magn. Reson.*, **55**, 460 (2000).
252. M. Köck, B. Reif, W. Fenical and C. Griesinger, *Tetrahedron Lett.*, **37**, 363 (1996).
253. J. Past, J. Puskar, M. Alla, E. Lippmaa and J. Schraml, *Magn. Reson. Chem.*, **23**, 1076 (1985).
254. J. Schraml, J. Past, J. Puskar, T. Pehk, E. Lippmaa and R. Brežný, *Collect. Czech. Chem. Commun.*, **52**, 1985 (1987).
255. U. Piantini, O. W. Sørensen and R. R. Ernst, *J. Am. Chem. Soc.*, **104**, 6800 (1982).
256. P. Lux, F. Brunet, H. Desvaux and J. Virlet, *Magn. Reson. Chem.*, **31**, 623 (1993).
257. P. Lux, F. Brunet, H. Desvaux and J. Virlet, *J. Chim. Phys.*, **91**, 409 (1994).
258. P. Lux, F. Brunet, J. Virlet and B. Cabane, *Magn. Reson. Chem.*, **34**, 173 (1996).
259. K. G. Sharp, P. A. Sutor, E. A. Williams, J. D. Cargioli, T. C. Farrar and K. Ishibitsu, *J. Am. Chem. Soc.*, **98**, 1977 (1976).
260. H. C. Marsmann, W. Raml and E. Hengge, *Z. Naturforsch.*, **35B**, 1541 (1980).
261. A. G. Brook, F. Abdesaken, G. Gutenkunst and N. Plavac, *Organometallics*, **1**, 994 (1982).
262. H. Oehme, R. Wustrack, A. Heine, G. M. Sheldrick and D. Stalke, *J. Organomet. Chem.*, **452**, 33 (1993).
263. G. Pfisterer and H. Dreeskamp, *Ber. Bunsenges. Phys. Chem.*, **73**, 654 (1969).
264. K. Hassler and F. Schrank, *Spectrochim. Acta*, **A47**, 57 (1991).
265. U. Herzog and G. Roewer, *J. Organomet. Chem.*, **544**, 217 (1997).
266. U. Herzog and G. Roewer, *J. Organomet. Chem.*, **527**, 117 (1997).
267. H. Söllradl and E. Hengge, *J. Organomet. Chem.*, **243**, 257 (1983).
268. K. Hassler and G. Bauer, *J. Organomet. Chem.*, **460**, 149 (1993).
269. K. Schenzel and K. Hassler, *J. Mol. Struct.*, **349**, 161 (1995).
270. K. Schenzel and K. Hassler, *Spectrochim. Acta*, **50A**, 127 (1994).
271. J. Heinicke, S. Mantey, A. Oprea, M. Kindermann and P. G. Jones, *Heteroatom Chem.*, **10**, 605 (1999).
272. K. Hassler and U. Katzenbeisser, *J. Organomet. Chem.*, **480**, 173 (1994).
273. U. Herzog, E. Brendler and G. Roewer, *J. Organomet. Chem.*, **511**, 85 (1996).
274. G. Kollegger and K. Hassler, *J. Organomet. Chem.*, **485**, 233 (1995).
275. K. Hassler, *Monatsh. Chem.*, **117**, 613 (1986).
276. K. Hassler, G. M. Kolleger, H. Siegl and G. Klintschar, *J. Organomet. Chem.*, **533**, 51 (1997).
277. C. Notheis, E. Brendler and B. Thomas, *GIT Labor-Fachzeitschrift*, 824 (1997).
278. A. H. Cowley and W. D. White, *J. Am. Chem. Soc.*, **91**, 1917 (1969).
279. G. Fronzoni and V. Galasso, *Chem. Phys.*, **103**, 29 (1986).
280. B. Wrackmeyer and H. Zhou, *Spectrochim. Acta*, **47A**, 849 (1991).
281. O. W. Sørensen and R. R. Ernst, *J. Magn. Reson.*, **54**, 122 (1983).
282. O. W. Sørensen and R. R. Ernst, *J. Magn. Reson.*, **63**, 219 (1985).
283. J. Lambert, K. Wilhelm and M. Klessinger, *J. Magn. Reson.*, **63**, 189 (1985).
284. K. Hassler, W. Köll and M. Ernst, *Spectrochim. Acta*, **53**, 213 (1997).
285. U. Katzenbeisser and K. Hassler, in *Organosilicon Chemistry From Molecules to Materials* (Eds. N. Auner and J. Weis), VCH, Weinheim, 1994, pp. 37–38.
286. K. Hassler, *Spectrochim. Acta*, **41A**, 729 (1985).
287. A. D. Fanta, J. Belzner, D. R. Powell and R. West, *Organometallics*, **12**, 2177 (1993).
288. A. D. Fanta, D. J. DeYoung, J. Belzner and R. West, *Organometallics*, **10**, 3466 (1991).
289. C. Grogger, C. Kayser, and C. Marschner, in *4. Iglar NMR Tage, Perspectives in NMR Spectroscopy*, University of Innsbruck, Innsbruck, 2000, Abstract, P3.
290. R. Köster, G. Seidel, F. Lutz, C. Krüger, G. Kehr and B. Wrackmeyer, *Chem. Ber.*, **127**, 813 (1994).
291. É. Kupče, E. Liepiņš, E. Lukevics and B. Astapov, *J. Chem. Soc., Dalton Trans.*, 1593 (1987).
292. P. K. Jenkner, A. Spielberger, M. Eibl and E. Hengge, *Spectrochim. Acta*, **49A**, 161 (1993).
293. R. Okazaki and R. West, *Adv. Organomet. Chem.*, **39**, 231 (1996).
294. H. B. Yokelson, A. J. Millevolte, G. R. Gillette and R. West, *J. Am. Chem. Soc.*, **109**, 6865 (1987).
295. A. Sekiguchi, M. Nanjo, C. Kabuto and H. Sakurai, *Organometallics*, **14**, 2630 (1995).
296. S. Berger, T. Fäcke and R. Wagner, *Magn. Reson. Chem.*, **34**, 4 (1996).
297. S. Berger, *J. Magn. Reson. A*, **101**, 329 (1993).
298. B. Böhler and H. Günther, *Tetrahedron Lett.*, **37**, 8723 (1996).
299. T. Parella, *Magn. Reson. Chem.*, **36**, 467 (1998).
300. M. Chai, Z. Pi, C. Tessier and P. L. Rinaldi, *J. Am. Chem. Soc.*, **121**, 273 (1999).

301. A. Bax, C.-H. Niu and D. Live, *J. Am. Chem. Soc.*, **106**, 1150 (1984).
302. A. Bax, *J. Magn. Reson.*, **57**, 314 (1984).
303. D. Uhrin and T. Liptaj, *J. Magn. Reson.*, **81**, 82 (1989).
304. V. Blechta and J. Schraml, *Collect. Czech. Chem. Commun.*, **56**, 258 (1991).
305. P. Plateau and M. Guéron, *J. Am. Chem. Soc.*, **104**, 7310 (1982).
306. É. Kupče and B. Wrackmeyer, *J. Magn. Reson.*, **97**, 568 (1992).
307. É. Kupče and E. Lukevics, *J. Magn. Reson.*, **76**, 63 (1988).
308. E. L. Hahn, *Phys. Rev.*, **80**, 580 (1950).
309. B. Wrackmeyer, H. E. Maisel and H. Zhou, *Main Group Metal Chem.*, **16**, 475 (1993).
310. M. Herberhold, S. Gerstmann, W. Milius and B. Wrackmeyer, *Z. Naturforsch.*, **48b**, 1041 (1993).
311. B. Wrackmeyer, B. Schwarze and W. Milius, *J. Organomet. Chem.*, **489**, 201 (1995).
312. B. Wrackmeyer and B. Schwarze, *Z. anorg. allg. Chem.*, **622**, 2048 (1996).
313. B. Wrackmeyer, I. Ordnung and B. Schwarze, *J. Organomet. Chem.*, **532**, 71 (1997).
314. B. Wrackmeyer, G. Kehr, H. E. Maisel and H. Zhou, *Magn. Reson. Chem.*, **36**, 39 (1998).
315. B. Wrackmeyer, G. Kehr, H. Zhou and S. Ali, *Magn. Reson. Chem.*, **34**, 921 (1996).
316. V. Blechta and J. Schraml, *J. Magn. Reson.*, **O 101**, 47 (1992).
317. É. Kupče and B. Wrackmeyer, *Magn. Reson. Chem.*, **29**, 351 (1991).
318. É. Kupče and B. Wrackmeyer, *J. Magn. Reson.*, **99**, 338 (1992).
319. R. K. Harris, M. J. O'Connor, E. H. Curzon and O. W. Howarth, *J. Magn. Reson.*, **57**, 115 (1984).
320. M. Ratier, B. Jousseume, N. Noiret, N. Petit, J.-C. Lartigue and M. Pétraud, *Magn. Reson. Chem.*, **31**, 176 (1993).
321. M. Harket, B. De Jeso, J.-C. Lartigue, M. Pétraud and M. Ratier, *Carbohydr. Res.*, **263**, 155 (1994).
322. J.-P. Picard, personal communication.
323. W. Kozmiński, S. Bienz, S. Bratovanov and D. Nanz, *J. Magn. Reson.*, **125**, 193 (1997).
324. S. Bratovanov, W. Koźmiński, J. Fässler, Z. Molnar, D. Nanz and S. Bienz, *Organometallics*, **16**, 3128 (1997).
325. M. Grignon-Dubois and M. Laguerre, *Organometallics*, **7**, 1443 (1988).
326. R. Rossi, A. Carpita, F. Bellina and M. De Santis, *Gazz. Chim. Ital.*, **121**, 261 (1991).
327. U. Behrens, C. Wolff and D. Hoppe, *Synthesis*, 644 (1991).
328. J. Kowalewski and K. M. Larsson, *Chem. Phys. Lett.*, **119**, 157 (1985).
329. K. M. Larsson, J. Kowalewski and U. Henriksson, *J. Magn. Reson.*, **62**, 260 (1985).
330. A. Briguët, J.-C. Duplan, D. Graveron-Demilly and J. Delmau, *Mol. Phys.*, **28**, 1777 (1974).
331. J. Puskar, T. Saluvere, and E. Lippmaa, in *18th Ampere Congress*, Nottingham, 1974, Abstracts, pp. 519–520.
332. A. Briguët, J. C. Duplan and J. Delmau, *J. Magn. Reson.*, **42**, 141 (1981).
333. G. Hempel, M. Wobst, G. Israel and H. Schneider, *Makromol. Chem., Macromol. Symp.*, **72**, 161 (1993).
334. G. C. Levy, J. D. Cargioli, P. C. Juliano and T. D. Mitchell, *J. Magn. Reson.*, **8**, 399 (1972).
335. R. K. Harris and B. J. Kimber, *Org. Magn. Reson.*, **7**, 460 (1975).
336. R. K. Harris and B. J. Kimber, *Adv. Mol. Relax. Proc.*, **8**, 23 (1975).
337. R. K. Harris and B. Lemairé, *J. Magn. Reson.*, **23**, 371 (1976).
338. R. K. Harris and B. J. Kimber, *Adv. Mol. Relax. Proc.*, **8**, 15 (1976).
339. W. Storek, *Chem. Phys. Lett.*, **98**, 267 (1983).
340. R. A. Newmark and B. C. Copley, *Macromolecules*, **17**, 1973 (1984).
341. R. Kosfeld, R. Krause and M. Hess, in *Integration of Fundamental Polymer Science and Technology*, Vol. 2 (Eds. P. J. Lemstra and L. A. Kleintjens), Elsevier Applied Science, London, 1988, pp. 169–172.
342. J. Kowalewski, A. Ericsson and R. Vestin, *J. Magn. Reson.*, **31**, 165 (1978).
343. H. C. Marsmann and E. Meyer, *Makromol. Chem.*, **188**, 887 (1987).
344. L. Mäler, L. D. Bari and J. Kowalewski, *J. Phys. Chem.*, **98**, 6244 (1994).
345. B. J. Kimber and R. K. Harris, *J. Magn. Reson.*, **16**, 354 (1974).
346. D. W. Aksnes and L. Kimtys, *Acta Chem. Scand.*, **49**, 722 (1995).
347. G. C. Levy, J. D. Cargioli, P. C. Juliano and T. D. Mitchell, *J. Am. Chem. Soc.*, **95**, 3445 (1973).

348. Y.-M. Pai, W. P. Weber and K. L. Servis, *J. Organomet. Chem.*, **288**, 269 (1985).
349. D. Canet, G. C. Levy and I. R. Peat, *J. Magn. Reson.*, **18**, 199 (1975).
350. J. Kowalewski and E. Berggren, *Magn. Reson. Chem.*, **27**, 386 (1989).
351. J. Kowalewski and Z. Ali, *Acta Chem. Scand.*, **49**, 734 (1995).
352. J. Kowalewski, T. Nilsson and K. W. Törnroos, *J. Chem. Soc., Dalton Trans.*, 1597 (1996).
353. R. A. Assink, R. Deshpande and D. M. Smith, *J. Magn. Reson.*, **105**, 19 (1993).
354. J. Kowalewski, G. C. Levy, L. F. Johnson and L. Palmer, *J. Magn. Reson.*, **26**, 533 (1978).
355. A. Briguet and A. Erbeia, *J. Phys. C*, **5**, L58 (1972).
356. G. A. Morris, *J. Magn. Reson.*, **41**, 185 (1980).
357. J. Kowalewski and G. A. Morris, *J. Magn. Reson.*, **47**, 331 (1982).
358. C. T. G. Knight and R. K. Harris, *Magn. Reson. Chem.*, **24**, 872 (1986).
359. A. V. McCormick, A. T. Bell and C. J. Radke, *J. Phys. Chem.*, **93**, 1737 (1989).
360. D. Neuhaus and M. P. Williamson, *The Nuclear Overhauser Effect in Structural and Conformational Analysis*, Wiley-VCH, Weinheim, 2000.
361. R. K. Harris and B. J. Kimber, *J. Chem. Soc., Chem. Commun.*, 255 (1973).
362. H. Jancke, G. Engelhardt, M. Mägi and E. Lippmaa, *Z. Chem.*, **43**, 435 (1973).
363. G. Engelhardt and H. Jancke, *Z. Chem.*, **14**, 206 (1974).
364. K. H. Pannell, A. R. Bassindale and J. W. Fitch, *J. Organomet. Chem.*, **209**, C65 (1981).
365. K. H. Pannell and A. R. Bassindale, *J. Organomet. Chem.*, **229**, 1 (1982).
366. L. P. Burke, A. D. DeBellis, H. Fuhrer, H. Meier, S. D. Pastor, G. Rihs, G. Rist, R. K. Rodebaugh and S. P. Shum, *J. Am. Chem. Soc.*, **119**, 8313 (1997).
367. D. Kost, I. Kalikhman and M. Raban, *J. Am. Chem. Soc.*, **117**, 11512 (1995).
368. D. Kost, I. Kalikhman, S. Krivonos, D. Stalke and T. Kottke, *J. Am. Chem. Soc.*, **120**, 4209 (1998).
369. G. A. Williams, D. W. McCall and H. S. Gutowsky, *Phys. Rev.*, **93**, 1428 (1954).
370. R. K. Harris, J. Jones, C. T. G. Knight and D. Pawson, *J. Mol. Struct.*, **69**, 95 (1980).
371. R. K. Harris, C. T. G. Knight and W. E. Hull, *J. Am. Chem. Soc.*, **103**, 1577 (1981).
372. S. Sjöberg, N. Ingri, A.-M. Nenner and L.-O. Öhman, *J. Inorg. Biochem.*, **24**, 267 (1985).
373. R. K. Harris and C. T. G. Knight, *J. Chem. Soc., Faraday Trans. 2*, **79**, 1525 (1983).
374. R. K. Harris and C. T. G. Knight, *J. Chem. Soc., Faraday Trans. 2*, **79**, 1539 (1983).
375. C. T. G. Knight, *J. Chem. Soc., Dalton Trans.*, 1457 (1988).
376. C. T. G. Knight, R. J. Kirkpatrick and E. Oldfield, *J. Non-Cryst. Solids*, **116**, 140 (1990).
377. C. T. G. Knight, R. J. Kirkpatrick and E. Oldfield, *J. Am. Chem. Soc.*, **108**, 30 (1986).
378. C. T. G. Knight, R. J. Kirkpatrick and E. Oldfield, *J. Am. Chem. Soc.*, **109**, 1632 (1987).
379. R. K. Harris, J. Parkinson and A. Samadi-Maybodi, *J. Chem. Soc., Dalton Trans.*, 2533 (1997).
380. C. T. G. Knight, R. J. Kirkpatrick and E. Oldfield, *J. Magn. Reson.*, **78**, 31 (1988).
381. E. K. F. Bahlmann, R. K. Harris, K. Metcalfe, J. W. Rockliffe and E. G. Smith, *J. Chem. Soc., Faraday Trans.*, **93**, 93 (1997).
382. S. D. Kinrade and T. W. Swaddle, *Inorg. Chem.*, **27**, 4253 (1988).
383. A. R. Brough, C. M. Dobson, I. G. Richardson and G. W. Groves, *J. Mater. Sci.*, **29**, 3926 (1994).
384. S. D. Kinrade, R. T. Syvitski, K. Marat and C. T. G. Knight, *J. Am. Chem. Soc.*, **118**, 4196 (1996).
385. D. W. W. Anderson, J. E. Bentham and D. W. H. Rankin, *J. Chem. Soc., Dalton Trans.*, 1215 (1973).
386. N. Takeda, H. Suzuki, N. Tokitoh, R. Okazaki and S. Nagase, *J. Am. Chem. Soc.*, **119**, 1456 (1997).
387. T. T. Nakashima, R. E. D. McClung and B. K. John, *J. Magn. Reson.*, **58**, 27 (1984).
388. J. R. Wesener and H. Günther, *Org. Magn. Reson.*, **21**, 433 (1983).
389. P. Jutzi and E.-A. Bunte, *Angew. Chem., Int. Ed. Engl.*, **31**, 1605 (1992).
390. E. O. Stejskal and J. E. Tanner, *J. Chem. Phys.*, **42**, 288 (1965).
391. C. S. Johnson, Jr., *Prog. NMR Spectrosc.*, **34**, 203 (1999).
392. G. S. Kapur, E. J. Cabrita and S. Berger, in *Proceedings of the 15th European Experimental NMR Conference*, University of Leipzig, Leipzig, 2000, Abstracts, pp. 32–32.
393. J. Schraml, V. Blechta, L. Soukuporá and E. Petráková, *J. Carbohydr. Chem.*, in press (2001).
394. I. R. Herbert and A. D. H. Clague, *Macromolecules*, **22**, 3267 (1989).
395. R. K. Harris, E. K. F. Bahlmann, K. Metcalfe and E. G. Smith, *Magn. Reson. Chem.*, **31**, 743 (1993).

396. R. G. Jones, R. E. Benfield, P. J. Evans, S. J. Holder and J. A. M. Locke, *J. Organomet. Chem.*, **521**, 171 (1996).
397. R. W. LaRochelle, J. D. Cargioli and E. A. Williams, *Macromolecules*, **9**, 85 (1976).
398. E. K. F. Bahlmann, R. K. Harris and B. J. Say, *Magn. Reson. Chem.*, **31**, 266 (1993).
399. J.-M. Dereppe and B. Parbhoo, *Anal. Chem.*, **58**, 2641 (1986).
400. J.-M. Dereppe and B. Parbhoo, *Anal. Chem.*, **56**, 2740 (1984).
401. K. S. Seshadri, D. C. Young and D. C. Cronauer, *FUEL*, **64**, 22 (1985).
402. M. O. J. Nieminen, E. Pulkkinen and E. Rahkamaa, *Holzforschung*, **43**, 303 (1989).
403. D. A. Jr. Laude and C. L. Wilkins, *Macromolecules*, **19**, 2295 (1986).
404. S. R. Maple and A. Allerhand, *J. Magn. Reson.*, **80**, 394 (1988).
405. É. Kupče and E. Lukevics, *J. Magn. Reson.*, **80**, 359 (1988).
406. E. L. Kupče and E. Lukevic, *Izv. Akad. Nauk. Latv. SSR, Ser. Khim.*, 633 (1987); *Chem. Abstr.*, **107**, 248756t (1987).
407. É. Kupče, E. Liepinš, I. Zicmane and E. Lukevics, *J. Chem. Soc., Chem. Commun.*, 818 (1989).
408. F. A. L. Anet and M. Kopelevich, *J. Am. Chem. Soc.*, **109**, 5870 (1987).
409. É. Kupče, personal communication.
410. B. Wrackmeyer and É. Kupče, *Z. Naturforsch.*, **536**, 411 (1998).
411. B. Wrackmeyer, G. Seidel and R. Köster, *Magn. Reson. Chem.*, **38**, 520 (2000).
412. O. Hofer, *Top. Stereochem.*, **10**, 287 (1976).
413. M. Hirayama and J. Arai, *Chem. Lett.*, 1401 (1987).
414. J. Rohonczy and T. Parella, *NMR Guide and Encyclopedia*, Bruker, Karlsruhe, 1999.
415. E. Bartholdi and R. R. Ernst, *J. Magn. Reson.*, **11**, 9 (1973).
416. J. C. Lindon and A. G. Ferrige, *Prog. NMR Spectrosc.*, **14**, 27 (1982).
417. R. K. Harris, J. Kowalewski and S. C. De Menezes, *Pure Appl. Chem.*, **69**, 2489 (1997).
418. R. K. Harris, J. Kowalewski and S. C. De Menezes, *Magn. Reson. Chem.*, **36**, 145 (1998).
419. American Society for Testing and Materials, E386-90(99)e1 Standard Practice for Data Presentation Relating to High-Resolution Nuclear Magnetic Resonance (NMR) Spectroscopy, American Society for Testing and Materials, Philadelphia, PA 19103, 1999.

CHAPTER 4

Silyl radicals

C. CHATGILIALOGLU AND C. H. SCHIESSER

*I.Co.C.E.A., Consiglio Nazionale delle Ricerche, Via P. Gobetti 101,
40129 Bologna, Italy
email: chrys@area.bo.cnr.it*

and

C. H. SCHIESSER

School of Chemistry, The University of Melbourne, Victoria, Australia, 3010

I. INTRODUCTION	341
II. ORGANOSILYL RADICAL STRUCTURE, REACTIONS AND MECHANISMS	342
A. Structural Investigations	342
B. Chemical Properties of Silyl Radicals	345
1. Experimental studies	345
2. Theoretical studies	354
III. ORGANOSILANES AS REAGENTS IN RADICAL CHAIN REACTIONS	362
A. General Aspects	362
B. Tris(trimethylsilyl)silane	364
1. Reductions	364
2. Consecutive radical reactions	369
C. Other Silicon Hydrides	381
D. Allylations	384
IV. REFERENCES	387

I. INTRODUCTION

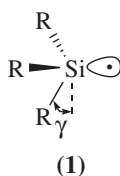
The chemistry of silyl radicals in the last decade has expanded considerably. Silyl radicals play an important role in diverse areas such as organic synthesis, material science and polymer chemistry. Since the early works have already been reviewed by one of the authors¹, the purpose of this chapter is to bring together all the recent developments. Furthermore,

specific accounts on tris(trimethylsilyl)silane in organic synthesis^{2,3} and the reaction kinetics of silicon, germanium and tin hydrides have recently appeared⁴. Therefore, a few words about the organization of this chapter will be useful. Structural and chemical properties of silyl radicals since 1995 are dealt with in Section II. Both theoretical and experimental work will be considered. In Section III, the radical chain reactions involving silyl radicals are examined. In particular, the chemistry of tris(trimethylsilyl)silane will be reviewed starting from 1997^{2,3}. For a detailed discussion of the most important elementary steps involving silyl radicals, i.e. the reaction of radicals with silicon hydrides, the reader is referred to a recent review⁴. However, some salient features of earlier works will be included when relevant to the discussion.

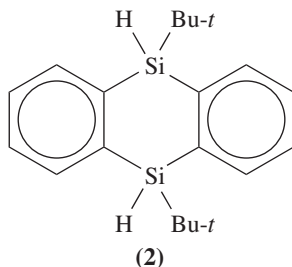
II. ORGANOSILYL RADICAL STRUCTURE, REACTIONS AND MECHANISMS

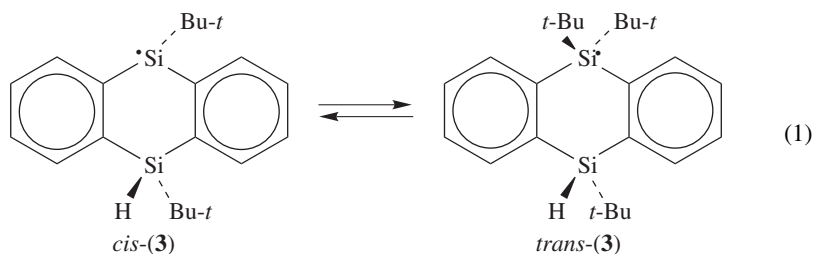
A. Structural Investigations

Silyl radicals (**1**) are generally tetrahedral species. Deviation angles (γ) have been calculated (UHF/DZP; the DZP basis set is a double-zeta basis set with polarization functions) by Guerra to range from 13.4°[(H₃Si)₃Si•] to 22.7°[(PH₂)₃Si•]⁵.

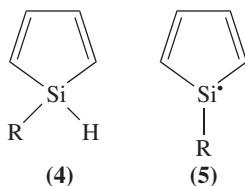


Since 1995¹, to the best of our knowledge, there have appeared few papers detailing structural investigations of silyl radicals. Of those few, Matsumoto and coworkers investigated the isomerization of silyl radicals derived from 9,10-di-*tert*-butyl-9,10-dihydro-9,10-disilanthracenes (**2**)⁶. Irradiation of a di-*tert*-butyl peroxide (DTBP)/pentane solution of either *cis*-**2** or *trans*-**2** affords the same 81% *cis*/19% *trans* mixture of **2**. In the absence of DTBP and irradiation, solution NMR studies indicate that each isomer of **2** is unchanged in the -85 to 20 °C temperature range. The authors propose that the radicals **3** derived from **2** isomerize to each other via inversion of the radical centre (equation 1) followed by hydrogen abstraction from the parent compound **2** (an identity reaction).





The question of aromatic stability on the structure of radicals derived from silacyclopentadienes (**4**) has also been investigated computationally^{7a}. MP2/6-311G** calculations indicate that silanes (**4**) react with methyl radical with energy barriers of 41.5, 42.2 and 35.0 kJ mol⁻¹ for R = H, Me and SiH₃, respectively. In comparison, trimethylsilane is calculated to react with a barrier of 54.4 kJ mol⁻¹ at a similar level of theory⁸, suggesting that radicals **5** derive some stability from the delocalization of spin in a similar fashion to phenyl substituted silyl radicals¹. Indeed, radicals (**5**) are still calculated to have average deviation angles in the range of 15–20°^{7b}.

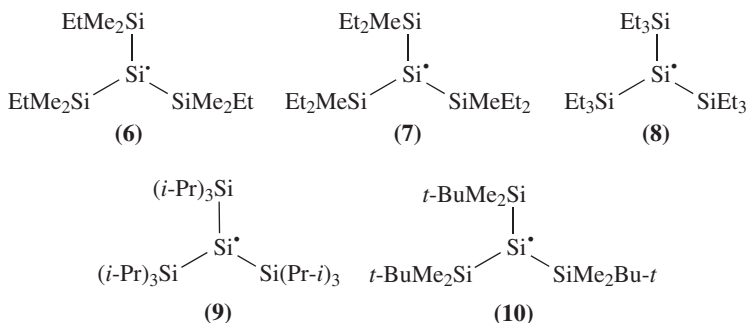


Bickelhaupt and coworkers investigated the fundamental origin of the pyramidalization of $\cdot\text{SiH}_3$ and related radicals by high-level *ab initio* calculations⁹ and concluded that $\cdot\text{CH}_3$ is planar because of steric repulsions between the hydrogen ligands. This repulsion is much weaker for the other $\cdot\text{XH}_3$ radicals in which the ligands are further removed from each other. Electron-pair bonding stabilizes the pyramidal configuration around the central heteroatom, with additional stabilization derived from the X- np_z unpaired electron. This results in an increase in the degree of stabilization along the series $\cdot\text{SiH}_3$, $\cdot\text{GeH}_3$ and $\cdot\text{SnH}_3$ ⁹.

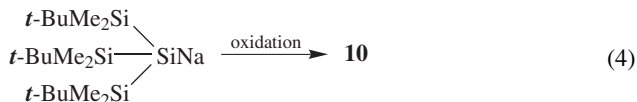
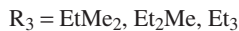
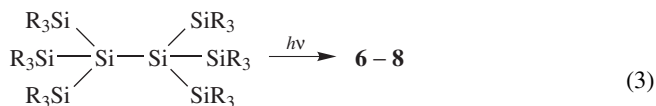
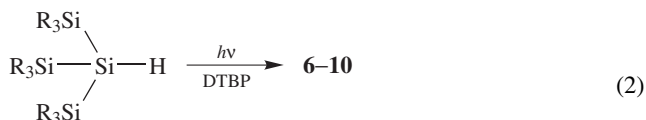
The vibrational and photoelectron spectra of a number of free radicals have been determined by computational techniques^{10a}. Included among the species investigated was $\cdot\text{SiH}_3$, which was optimized using the CEPA-1 method^{10b}. The silyl radical was calculated with a basis set containing 82 Gaussian-type orbitals to have equilibrium Si–H separations of 1.4793 Å and H–Si–H angles of 111.22°. These values are calculated to be 1.4743 Å and 111.24° with a basis set containing 125 Gaussian-type orbitals. The vibrational spectrum of $\cdot\text{SiH}_3$ is predicted to have absorptions at 2276, 2247, 951 and 780 cm⁻¹ using the larger basis set, in excellent agreement with available experimental data, while the photoelectron spectrum of $\cdot\text{SiH}_3$ is also calculated to agree well with experimental data.

Most silyl radical studies to date provide electron paramagnetic parameters with *g*-values in the range 2.0003–2.0053, depending on substitution, and ²⁹Si hyperfine splitting (hfs) constants $a(\alpha\text{-}^{29}\text{Si})$ in the range 6.4–49.8 mT¹. These values correlate well with the

percentage of 3s character in the singly-occupied molecular orbital (SOMO) on silicon, which in turn is dependent on the geometry of the radical centre.



Very recently, Matsumoto and coworkers have been interested in the generation of persistent silyl radicals where the substituents on the silicon centre enforce highly planar architectures¹¹. A series of silylated silyl radicals (**6–10**) were generated by photolysis of the corresponding silane or disilane, or by oxidation of the silylsodium precursor, and their EPR spectra recorded (equations 2–4).



Values of $a(\alpha\text{-}^{29}\text{Si})$ for radicals **6–10** fall in the range 5.56–6.28 mT (Table 1) and are consistent with these radicals being the most planar silyl radicals reported to date. In addition, the steric and electronic properties of the substituents on silicon in structures **6–10** provide for highly persistent silyl radicals. Half-lives of 3 h, 1 day, 1.5 months, 5 days and 1 day at 15 °C have been measured for **6–10**, respectively¹¹.

Recently, Guerra investigated the structures and hyperfine interactions in a series of silyl radicals by computational techniques¹². UMP2/DZP and UMP2/DZP//TZP calculations appear to reproduce the isotropic splitting constants [$a(\alpha\text{-}^{29}\text{Si})$] for a series of substituted silyl radicals. The data presented in Table 2 indicate a large variation in hyperfine splitting data which was found to be due to the electronic influence of the α -substituent rather than to the structural changes of the radicals in question, which are found to remain essentially tetrahedral across the series. Guerra suggests caution in the use of the

TABLE 1. EPR data for radicals **6–10**^a

Silyl radical	<i>T</i> (°C)	<i>g</i>	<i>a</i> (α - ²⁹ Si) ^c	<i>a</i> (β - ²⁹ Si) ^c
Me ₃ Si ^{•b}	—	2.0031	18.1	—
(Me ₃ Si) ₃ Si ^{•b}	−25	2.0053	6.4	0.71
6	15	2.0060	6.28	0.71
7	15	2.0060	6.03	0.73
8	15	2.0063	5.72	0.79
9	15	2.0061	5.56	0.81
10	15	2.0055	5.71	0.81

^aFrom Reference 11.^bFrom Reference 1.^cmT.TABLE 2. Calculated (UMP2/DZP//TZP) and experimental splitting constants (mT) for some substituted silyl radicals^a

Radical	<i>a</i> (²⁹ Si) (theory)	<i>a</i> (²⁹ Si) (exp.)	<i>a</i> (α - ¹ H) (theory)	<i>a</i> (α - ¹ H) (exp.)
H ₃ Si [•]	−18.32	18.9	0.21	0.796
MeH ₂ Si [•]	−18.42	18.1	0.60	1.182
Me ₂ HSi [•]	−18.55	18.3	1.03	1.699
Me ₃ Si [•]	−18.75	18.1	—	—
Me ₂ ClSi [•]	−23.23	22.9	—	—
MeCl ₂ Si [•]	−30.19	29.5	—	—
Cl ₃ Si [•]	−41.23	41.6	—	—
Me ₂ (Me ₃ Si)Si [•]	−14.79	13.7	—	—
Me(Me ₃ Si) ₂ Si [•]	−10.78	9.0	—	—
(Me ₃ Si) ₃ Si [•]	−7.32	6.4	—	—

^aFrom Reference 12.

linear relationship found between the Si-3s contribution to the SOMO in silyl radicals and the analogous contribution to the σ (Si–H) bonding molecular orbital of the parent silanes, which appears to provide unreliable structural information. These calculations appear to perform more poorly in their ability to reproduce proton [*a*(α -¹H)] splitting constants.

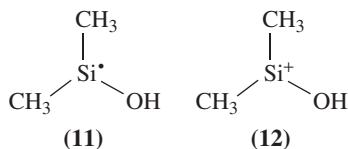
Karna recently reported an *ab initio* study of linear electric field effects on the *g*-tensor and on the hyperfine splitting constant (the Bloembergen effect) of the silyl radical ([•]SiH₃)¹³. TDUHF calculations predict an increase in hyperfine splitting in [•]SiH₃ due to the Bloembergen effect, predictions which have yet to be verified experimentally.

B. Chemical Properties of Silyl Radicals

1. Experimental studies

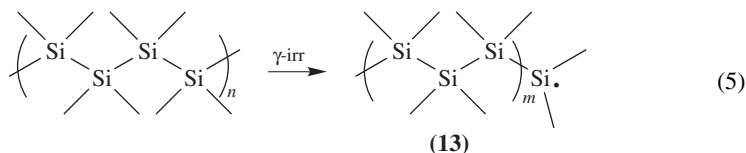
Silyl radicals have been observed during femtosecond reduction of the corresponding cations in the gas phase and the dissociations of these excited radicals have been monitored. In neutralization–reionization mass spectrometric experiments, the fragmentation of the dimethylhydroxysilyl radical (**11**), and related deuterium labelled species, generated through the collisional neutralization of the corresponding cation (**12**) was examined¹⁴. Extensive dissociation of the carbon–silicon bond in **11** was observed, with the degree of fragmentation dependent on the internal energy of the precursor cation. Radicals (**11**),

when generated in this manner, are calculated at the MP4(SDTQ)/6-31 + G(d) level of theory, to be affected strongly by large Frank–Condon effects; the vertical reduction of **12** is predicted to dump 229 kJ mol⁻¹ into the radical formed¹⁴. These experiments also allow the determination of the dissociation energies of the O–H and C–Si bonds in **11**, which are found to be 166 and 195 kJ mol⁻¹, respectively.

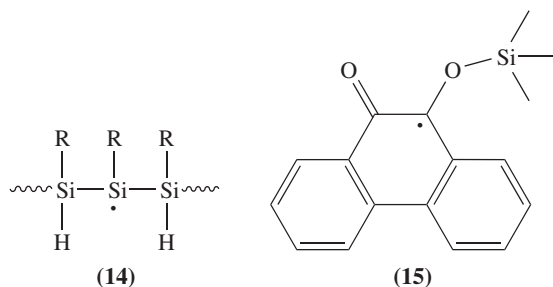


Measurements of rate constants for the reaction of radicals with a variety of silanes have continued to be an active area⁴. Rate constants for the reactions of peroxy¹⁵ and aminyl¹⁶ radicals with silanes have been reported for the first time. In particular, the reaction of cumylperoxy radicals with *t*-BuMe₂SiH, Ph₃SiH, PhMe₂SiH, Ph₂SiH₂, Ph₂MeSiH and PhSiH₃ are in the range 0.1–0.9 M⁻¹ s⁻¹ whereas for (TMS)₃SiH [TMS = (CH₃)₃Si] the value is 2–3 orders of magnitude higher¹⁵. On the other hand, rate constants and activation parameters have been measured for the hydrogen transfer reaction from Et₃SiH, Ph₃SiH, Ph₂SiH₂, PhSiH₃, (TMS)₂SiHMe and (TMS)₃SiH to the hindered aminyl radical 2,2,6,6-tetramethylpiperidiny¹⁶. The rate constants for hydrogen or deuterium transfer from *t*-BuMe₂SiH(D) and Me₃SiSiMe₂H(D) to RCF₂CF₂[•] radicals along with measurements of side-chain H transfer from the deuteriated silanes have also been determined¹⁷. Rate constants of primary alkyl radicals with a variety of silicon hydrides are briefly discussed in Section III.A (see Table 4).

Silyl radicals have also been observed during γ -irradiation of solid polysilanes. Tagawa and coworkers examined the EPR spectrum observed upon irradiation of solid poly(dimethylsilane) and concluded that the spectrum corresponded to silyl radicals generated by homolysis of the silicon skeleton in the polysilane (equation 5)¹⁸. Indeed, the EPR spectrum of the poly(dimethylsilane) radical (**13**), with hyperfine splitting constants $a(\beta\text{-}^1\text{H})$ and $a(\gamma\text{-}^1\text{H})$ of 0.813 and 0.046 mT respectively, corresponded remarkably well to that published for the dimethyl(trimethylsilyl)silyl radical [$a(\beta\text{-}^1\text{H}) = 0.821$ mT; $a(\gamma\text{-}^1\text{H}) = 0.047$ mT]¹. Radical (**13**) appears to be very stable in solid poly(dimethylsilane), since the EPR signal was strong and clearly observable at room temperature.

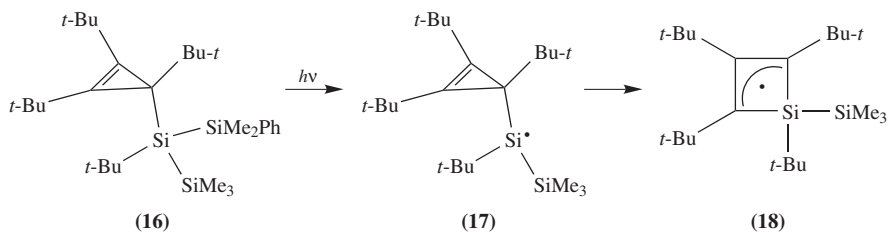


EPR studies provided information on the structural characteristics of silyl radicals generated from poly(hydrosilane)s by hydrogen abstraction¹⁹. Radical **14** (R = *n*-hexyl) has been identified as the transient species. Furthermore, the chemical reactivity of radicals **14** (R = *n*-hexyl or phenyl) in the addition to multiple bonds has been monitored by EPR spectroscopy and the corresponding adducts have been recorded. For example, the addition of silyl radicals to 9,10-phenanthroquinone gave rise to the adduct **15** characterized by the equivalence of the two aromatic rings, which means that the intramolecular migration of the silyl radical between the two oxygens is fast on the EPR timescale.

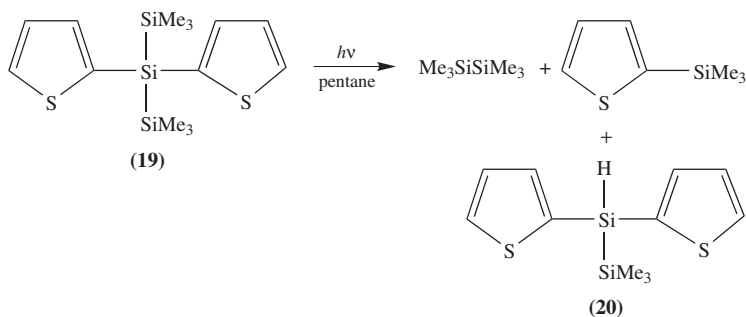


The photochemistry of poly(di-*n*-hexylsilane) (PDHS) has been investigated by excimer laser flash photolysis²⁰. Transient absorptions were found to be strongly dependent on the solvent employed and the near-UV absorptions at 385 and 360 nm observed in cyclohexane and tetrahydrofuran, respectively, were ascribed to polysilylated silyl radicals, while that at 345 nm observed in dichloromethane was attributed to the radical cations of PDHS formed during the electron photoejection process.

The photochemistry of trisilanes **16** and **19** has been investigated in some detail (Schemes 1 and 2)²¹. Upon irradiation of compound **16** only the Si–SiMe₂Ph bond is broken and the initially formed silyl radical **17** undergoes a rearrangement to the more stable silacyclobutenyl radical **18** whose EPR spectrum has been recorded (Scheme 1)^{21a}. Irradiation of trisilane **19** with a medium pressure mercury lamp resulted in the formation of hexamethyldisilane, 2-(trimethylsilyl)thiophene and **20**, with **20** dominating (Scheme 2)^{21b}. In the presence of carbon tetrachloride, a significant yield (19.2%) of the

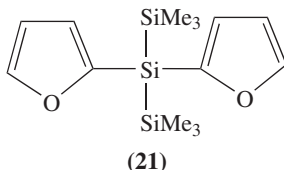


SCHEME 1

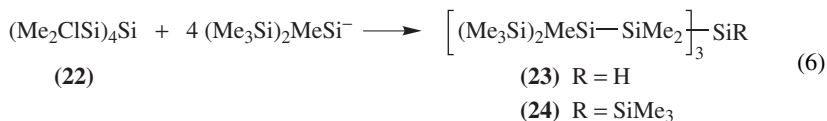


SCHEME 2

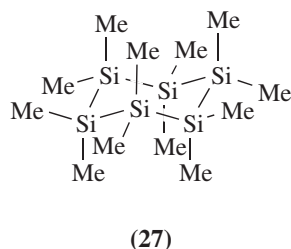
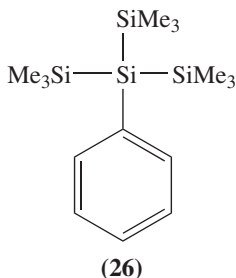
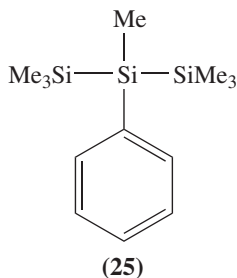
analogue of **20** with a Si–Cl instead of a Si–H bond was obtained, strongly suggesting the intermediacy of silyl radicals generated by Si–Si bond homolysis. The intermediacy of silyl radicals was also confirmed by EPR experiments by using a trapping technique. It is interesting to note that the authors observed remarkable differences between the photochemical reactions of **19** and of di(α -furyl)hexamethyltrisilane (**21**) where silylene intermediates play an important role. These observed differences have been explained in terms of the possible greater silyl radical stabilizing effect of the sulphur-containing thiophene ring^{21b}.

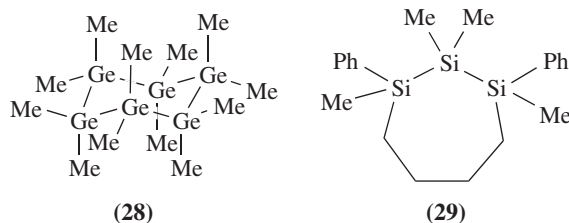


Lambert and coworkers have recently investigated anionic and radical processes involved in the fragmentation of dendritic polysilanes²². Reaction of tetrakis(chlorodimethylsilyl)silane (**22**) with methylbis(trimethylsilyl)silyl lithium afforded the two dendritic polysilanes **23** and **24** in 90 and 5% yield, respectively (equation 6). The authors propose that the initial reaction affords, in the first instance, a dendrimer with a four-fold core which undergoes a Si–Si bond cleavage facilitated by steric compression. This would appear to represent the first report of the formation of a dendritic polysilane containing a four-fold core, and further, a rare example of the formation of silyl radicals through Si–Si bond scission facilitated by steric congestion.

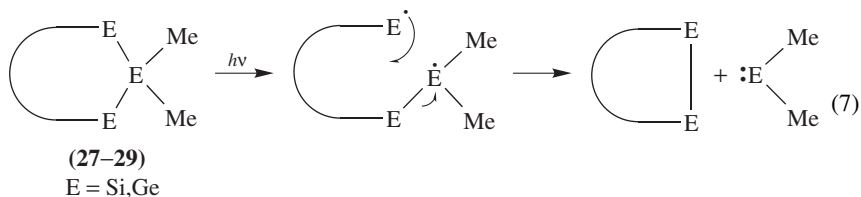


The generation of di- and trimethylsilyl radicals by the reactions of hydrogen atoms with di- and trimethylsilane and their subsequent reactions have been described²³. Three main products were observed in these reactions: 1,1,2,2-tetramethyldisilane, pentamethyldisilane and hexamethyldisilane which are formed by both radical coupling and disproportionation processes. The authors describe a detailed kinetic analysis of the various reactions of interest but have difficulty in providing a mechanistic description that fully fits their observed data²³.

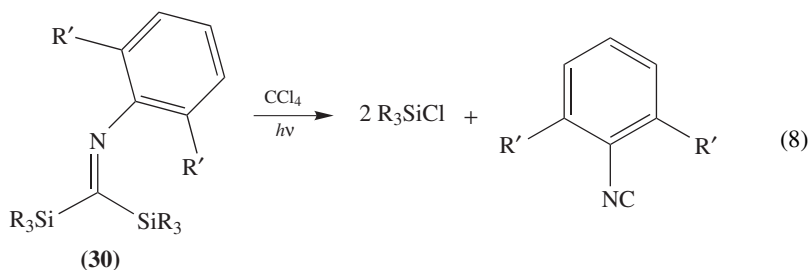




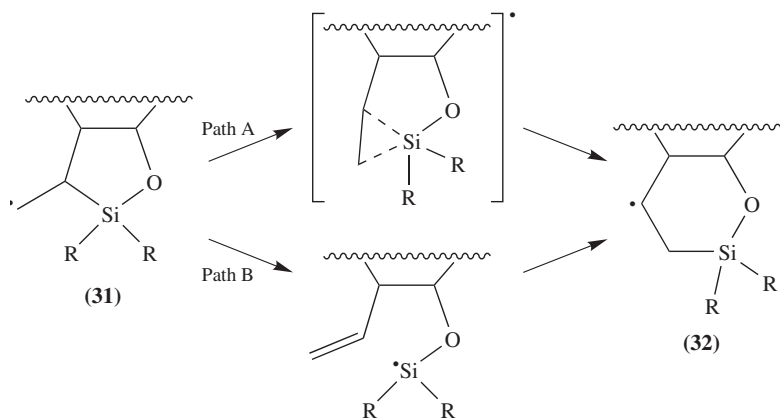
Sulkes, Fink and their associates recently investigated the molecular beam photochemistry of oligosilanes and related germanes²⁴. In particular, photolysis of compounds **25–29** in the nozzle region of a supersonic jet by a 193 nm laser and subsequent analysis by 118 nm photoionization followed by time-of-flight mass spectrometry revealed the formation of several products. Dimethylsilylene ($\text{Me}_2\text{Si}:$) was observed as a direct photoproduct from the cyclic precursors (**27**, **29**), while the analogous germylene was observed from the cyclic polygermane (**28**). Photolysis of the non-cyclic precursors **25** and **26** gave products derived from silyl radicals which are formed by a direct Si–Si bond homolysis, with little evidence of silylene formation. The authors propose a mechanism to explain the different observations for cyclic and non-cyclic systems (equation 7).



The photolysis of bis(organosilyl)imines **30** in CCl_4 afforded the corresponding silyl chlorides and isocyanides as the products (equation 8). Evidence that the reaction proceeds via a homolytic process involving silyl radicals is provided²⁵.

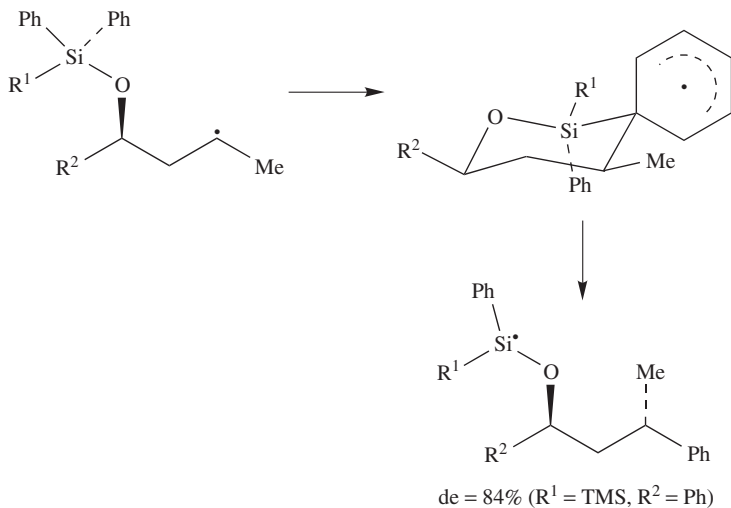


The mechanism of the ring expansion of primary alkyl radicals **31** to radical **32** (Scheme 3) is postulated²⁶ either to involve a 1,2-silyl group migration (path A: homolytic substitution at silicon), of which there are numerous examples in the literature²⁷, although this would appear to be the first example involving a bicyclic transition state, or alternatively to follow a mechanism involving β -scission to afford a silyl radical, followed by 6-*endo* addition to provide the ring-expanded product (Path B).

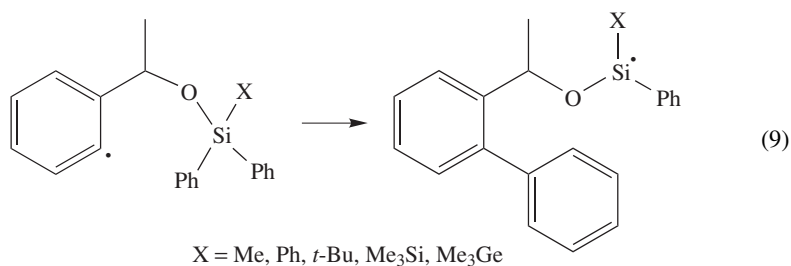


SCHEME 3

Recent interest in aryl group transfer from silicon to carbon has resulted in some impressive stereoselective outcomes. Examples from the group of Studer are shown in Scheme 4. 1,5-Phenyl group migration was shown to be more effective than the analogous 1,4 process, with diastereomeric ratios exceeding 6 : 1²⁸. When the substituent on silicon was trimethylstannyl, ring closure by intramolecular homolytic substitution at silicon was observed to compete with phenyl group transfer^{29a}. The same group have also recently demonstrated that biaryls are conveniently prepared by intramolecular aryl group migration from silicon to carbon (equation 9)^{29b}.

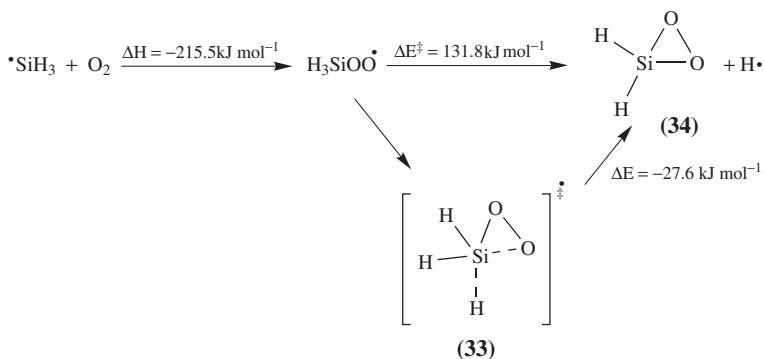


SCHEME 4



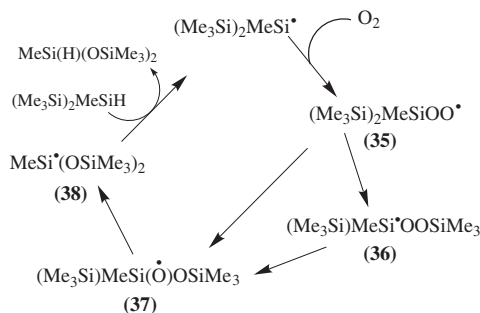
The generation of silyl radicals through electron transfer reactions has been known for some time now. The reader's attention is drawn to a recent review on this topic³⁰. It would appear, however, that new papers detailing the involvement of silyl radicals have not appeared in the time period covered by this chapter.

The reaction of $\cdot\text{SiH}_3$ radicals with molecular oxygen and the mechanism of SiO formation during the laser photolysis of $\text{SiH}_4/\text{O}_2/\text{CCl}_4$ mixtures have been reported³¹. The bimolecular rate constant for the production of SiO was determined to be $6.8 \times 10^9 \text{ M}^{-1} \text{ s}^{-1}$. *Ab initio* calculations at G2(MP2)//MP2(full)/6-31G(d) level indicate that silyl radical and oxygen react to form $\text{H}_3\text{SiOO}\cdot$, which irreversibly decomposes to various excited products. During this investigation, a new transition state (**33**) for the formation of siladioxirane **34** was found (Scheme 5). Interestingly, the proposed pathway to **34** involves a rare example of homolytic substitution at silicon by an oxygen-centred radical via a frontside attack³¹. The authors also discuss the various possible decomposition channels leading to SiO.



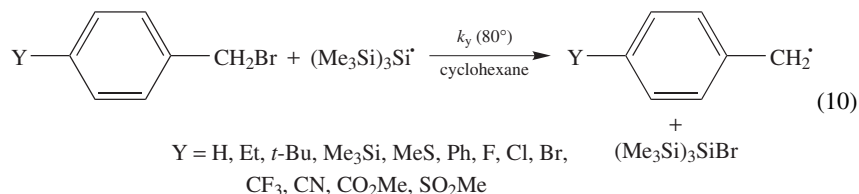
SCHEME 5

Poly(hydrosilanes), $\text{H}(\text{RSiH})_n\text{H}$, are found to be air sensitive³². Oxidizability values of 1.2×10^{-2} and $1.8 \times 10^{-2} \text{ M}^{-1/2} \text{ s}^{-1/2}$ were found for $\text{R} = n$ -hexyl and phenyl, respectively. The oxidation of $(\text{Me}_3\text{Si})_2\text{Si}(\text{H})\text{Me}$ performed as a model reaction has been shown by labelling experiments to proceed via the radical chain reaction reported in Scheme 6, which involves two or three consecutive unimolecular steps³². The peroxy radical **35** rearranges to **37** either by means of an unusual 1,3-shift of the Me_3Si group to give **36** followed by a homolytic internal substitution or by the direct rearrangement of **35** to **37**. The latter could rearrange to **38** by a 1,2-shift of the Me_3Si group.

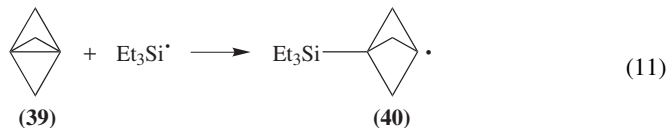


SCHEME 6

The nucleophilicities of silyl radicals have been determined through a dual-parameter correlation analysis of the relative rates of bromine atom abstraction reactions³³. This work demonstrated that the relative rates (k_Y) of bromine abstraction reactions involving thirteen *para*-substituted benzyl bromides by $(\text{Me}_3\text{Si})_3\text{Si}^\bullet$ radicals in cyclohexane at 80° fit a dual-parameter equation [$\log(k_Y/k_H) = \rho^X\sigma^X + \rho^\bullet\sigma^\bullet$], showing that the $(\text{Me}_3\text{Si})_3\text{Si}^\bullet$ radical is distinctly nucleophilic (equation 10). The transition states in these abstraction reactions are strongly affected by both the polar and spin-delocalization effects of the *para*-substituent Y.



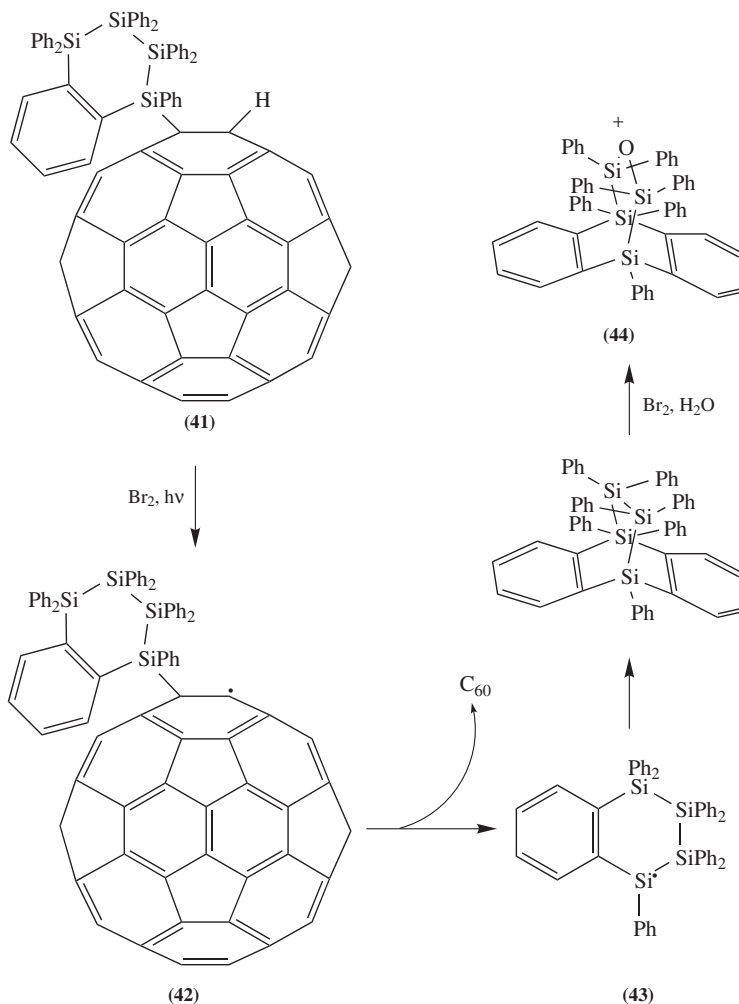
Scaiano has recently published the absolute kinetic data for the addition (homolytic substitution at carbon²⁷) of a variety of free radicals to [1.1.1]propellane (**39**) as determined by laser flash photolysis³⁴. Included among the reactions investigated was the addition of triethylsilyl radical, a reaction which had earlier been reported by Wiberg and coworkers³⁵. $\text{Et}_3\text{Si}^\bullet$ was found to react with **39** to afford **40** (equation 11) with a rate constant of $6.0 \times 10^8 \text{ M}^{-1} \text{ s}^{-1}$ at 19 °C. This value is to be compared with that for triethylsilyl radical addition to styrene ($2 \times 10^8 \text{ M}^{-1} \text{ s}^{-1}$) and 1-hexene ($5 \times 10^6 \text{ M}^{-1} \text{ s}^{-1}$)¹. Thus, it would appear that [1.1.1]propellane is slightly more reactive toward attack by triethylsilyl radicals than is styrene, and significantly more reactive than 1-hexene.



Several reports of the reactions of either silyl radicals with C_{60} (buckminsterfullerene), or of C_{60} -substituted systems to generate silyl radicals have recently appeared in the literature^{36–39}.

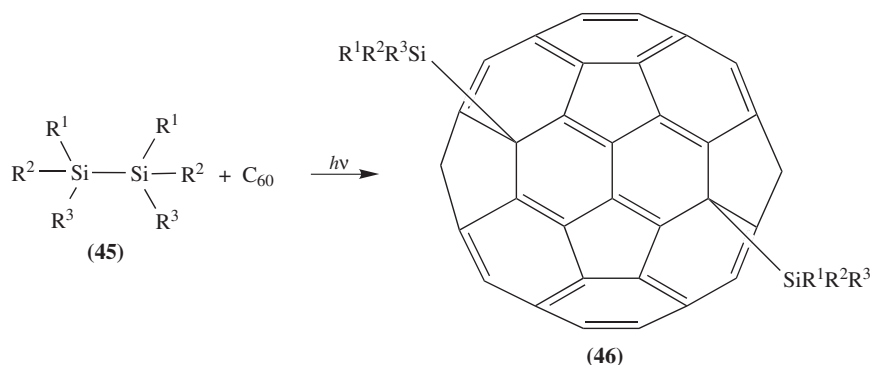
In the earliest such report, Ando and his research team reacted a C_{60} -substituted benzo-tetrasilacyclohexene (**41**) with bromine under irradiation (Scheme 7)³⁶. Hydrogen atom

abstraction to give radical **42** is followed by β -scission to generate C_{60} (the thermodynamic sink) and an intermediate silyl radical **43**, which rearranges by intramolecular addition to a pendant phenyl moiety. Elimination of H-atom and further reaction with Br_2-H_2O ultimately provides **44** in 45% isolated yield.



SCHEME 7

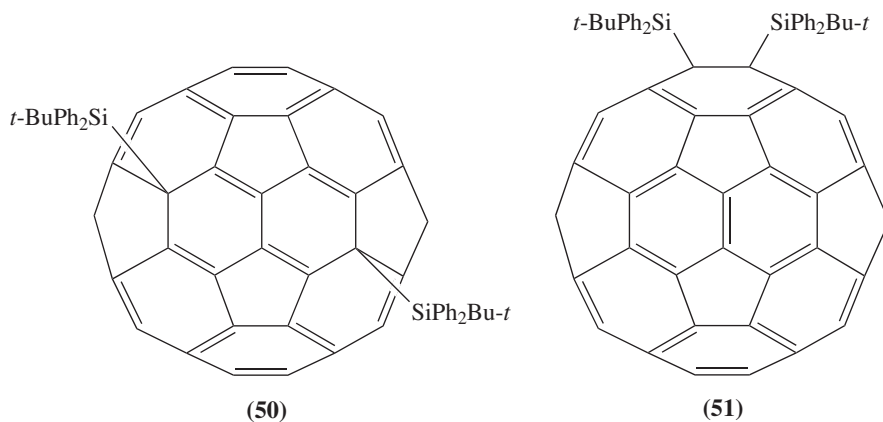
Ando demonstrated that the photolysis of partially *tert*-butyl-substituted disilanes **45** in the presence of C_{60} results in the formation of 1,16-adducts **46** in 54–62% yield (Scheme 8)^{37,38}. Interestingly, unusual adducts similar to **49** were obtained as by-products with disilanes having trimethylsilyl substituents (Scheme 9). The authors explain these observations by a mechanism involving the intermediacy of silyl radicals which are generated photochemically by Si–Si bond homolysis. Initial free-radical addition of silyl



SCHEME 8

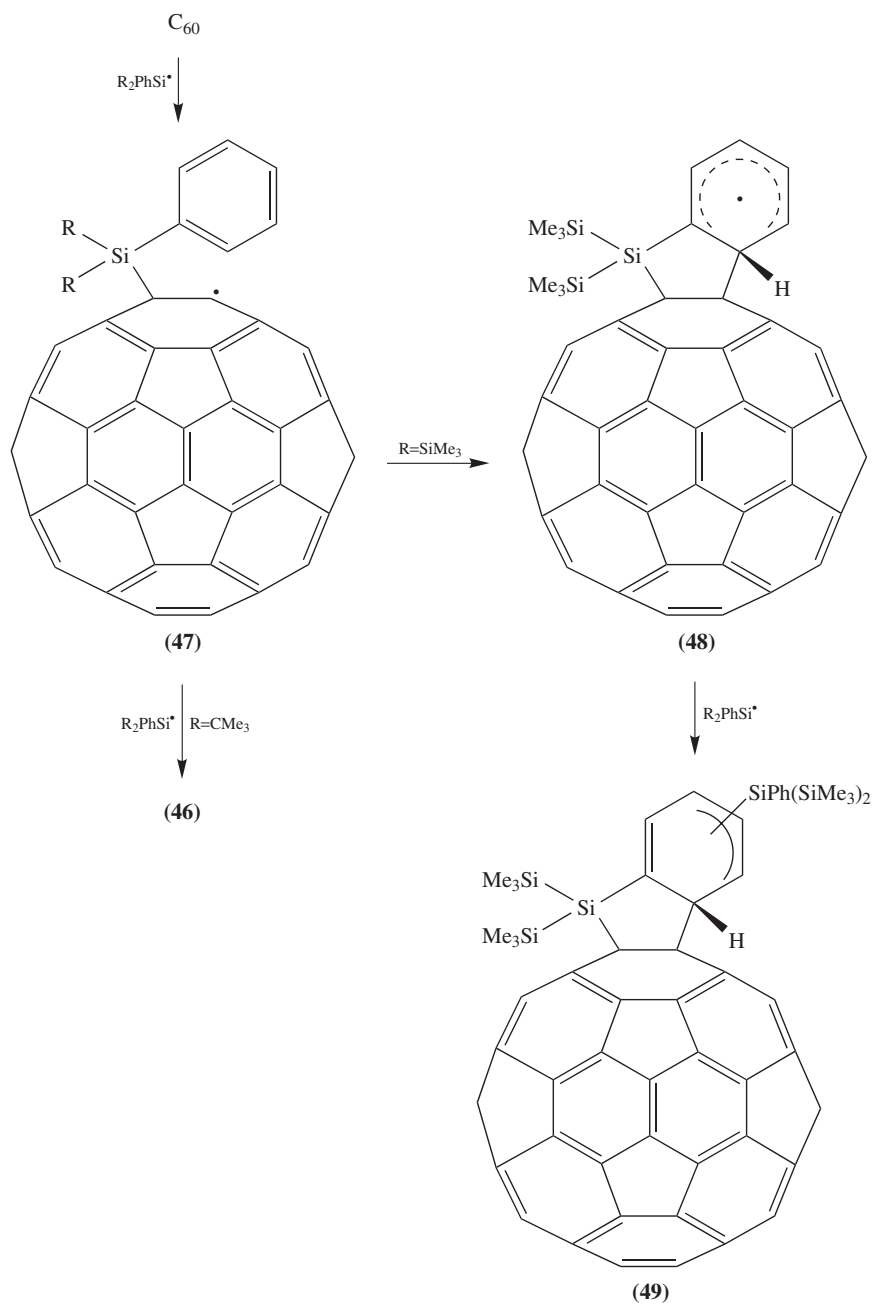
radicals to C_{60} affords the delocalized adduct radical **47** which, depending on substitution, either couples with another silyl radical to form **46**, or adds to an aromatic ring to give **48**. Subsequent radical coupling provides the unusual adducts like **49** (Scheme 9).

The photochemical bis-silylation of C_{60} with disilanes has also been reported by Akasaka and coworkers³⁹. Reactions of buckminsterfullerene with 1,1,2,2-tetraphenyl-1,2-di-*tert*-butyl-1,2-disilane, hexaphenyldisilane and 1,2-diphenyl-1,2-disilane afford the 1,16-bissilylated adducts (Scheme 8). The assignment of the structures is supported by NMR, IR and UV-vis spectroscopies and is also supported by AM1 calculations. For example, the 1,16-adduct **50** was calculated by AM1 to be 150 kJ mol^{-1} more stable than the isomeric 1,2-adduct **51**, the next most stable calculated reaction product.



2. Theoretical studies

One of us, as well as Bottoni, recently investigated homolytic substitution reactions of silyl radicals at the halogen atom of halomethanes (CH_3X , $X = Cl, Br, I$), and the chalcogen atom in methanechalcogenols (CH_3EH , $E = S, Se, Te$) and alkyltellurols, with expulsion of alkyl radical (equations 12 and 13)^{40–43}.



SCHEME 9



In the earlier studies, the parent silyl radicals were calculated (QCISD/DZP//MP2/DZP) to react with chloromethane, bromomethane and iodomethane with energy barriers of 73.7, 44.3 and 21.8 kJ mol⁻¹, respectively, while analogous reactions involving methanethiol, methaneselenol and methanetellurol have associated barriers of 60.3, 35.5 and 9.6 kJ mol⁻¹^{40,41}. In the work of Bottoni, reactions of both [•]SiH₃ and [•]SiCl₃ with chloromethane, dichloromethane and chloroform were modelled at several levels of theory⁴². Some limited studies involving fluoromethane and bromomethane are also reported⁴². In the recent work of Schiesser and Skidmore, reactions of silyl (H₃Si[•]) and trisilylsilyl radicals [(H₃Si)₃Si[•]] with a series of alkyl tellurols (R₃TeH) with expulsion of the alkyl radical as a leaving group were modelled by *ab initio* techniques⁴³. Selected energy barriers calculated by both research groups are displayed in Table 3.

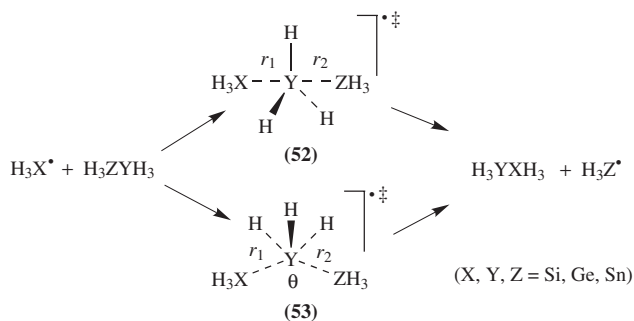
In all cases, the transition states (TS) involved in intermolecular homolytic substitution by silyl radicals at halogen are predicted to prefer collinear arrangements of attacking and leaving radicals, with typical Si–Cl_{TS}, Si–Br_{TS} and Si–I_{TS} distances of around 2.5, 2.6 and 2.8 Å, respectively, depending on the level of theory^{40–42}. The analogous transition states involving chalcogen are predicted to deviate slightly from collinearity, with typical

TABLE 3. Some calculated energy barriers (ΔE^\ddagger in kJ mol⁻¹) for homolytic substitution by some silyl radicals at the halogen atom in some alkyl halides (RX), and the chalcogen atom in some alkylchalcogenols (REH) (equations 12 and 13)

Silyl radical	RX	Level of theory	ΔE^\ddagger	Reference
H ₃ Si [•]	CH ₃ F	B3LYP/6-31G*	74.1	42
H ₃ Si [•]	CH ₃ Cl	QCISD/DZP//MP2/DZP	73.7	40
		MP4/6-311G**//MP2/6-311G**	62.0	42
		B3LYP/6-311G**	36.2	42
H ₃ Si [•]	CH ₂ Cl ₂	MP4/6-311G**//MP2/6-311G**	51.3	42
		B3LYP/6-311G**	28.2	42
H ₃ Si [•]	CHCl ₃	MP2/6-31G*	41.3	42
		B3LYP/6-31G*	15.6	42
H ₃ Si [•]	CH ₃ Br	B3LYP/6-31G*	4.2	42
		QCISD/DZP//MP2/DZP	44.3	40
H ₃ Si [•]	CH ₃ I	QCISD/DZP//MP2/DZP	21.8	40
Cl ₃ Si [•]	CH ₃ Cl	MP2/6-31G*	45.1	42
Cl ₃ Si [•]	CH ₃ Cl	B3LYP/6-31G*	30.7	42
Cl ₃ Si [•]	CH ₂ Cl ₂	MP2/6-31G*	39.2	42
		B3LYP/6-31G*	25.9	42
Cl ₃ Si [•]	CHCl ₃	MP2/6-31G*	30.9	41
		B3LYP/6-31G*	20.1	41
H ₃ Si [•]	CH ₃ SH	QCISD/DZP//MP2/DZP	60.3	41
H ₃ Si [•]	CH ₃ SeH	QCISD/DZP//MP2/DZP	35.5	41
H ₃ Si [•]	CH ₃ TeH	QCISD/DZP//MP2/DZP	9.6	41
H ₃ Si [•]	EtTeH	QCISD/DZP//MP2/DZP	9.4	43
H ₃ Si [•]	<i>i</i> -PrTeH	QCISD/DZP//MP2/DZP	8.6	43
(H ₃ Si) ₃ Si [•]	CH ₃ TeH	QCISD/DZP//MP2/DZP	16.6	43

Si-S_{TS}, Si-Se_{TS} and Si-Te_{TS} separations of around 2.4, 2.5 and 2.6 Å, respectively, depending on the level of theory⁴¹.

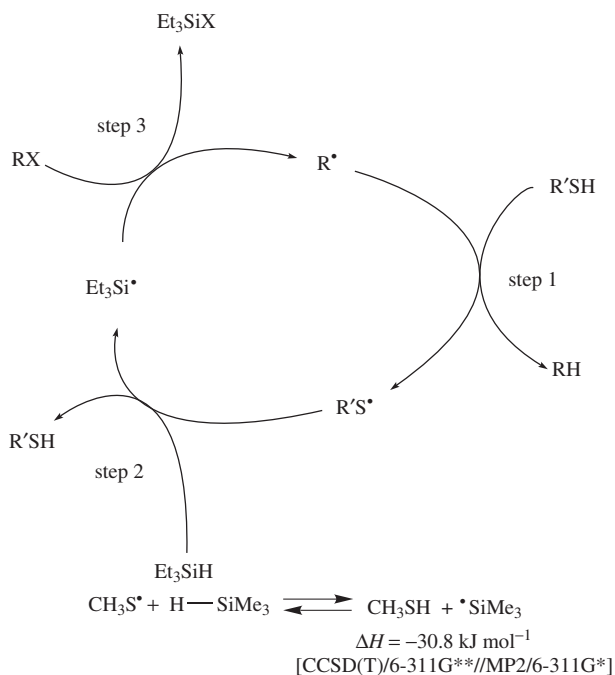
Very recently, the mechanism of homolytic substitution by silyl, germyl and stannyl radicals at group 14 higher heteroatoms was investigated by *ab initio* calculations (Scheme 10). Not only were mechanisms involving both frontside and backside attack found to be mechanistically feasible, the energy barriers for both pathways are approximately equal⁴⁴. Not unexpectedly, the transition states (52) for backside attack prefer to adopt collinear arrangements of attacking and leaving radicals, while the transition states (53) for frontside attack resemble those located in an earlier study involving 1,2-silyl, germyl and stannyl group migrations between carbon centres, or between carbon and either nitrogen or oxygen⁴⁵. Values of r_1 (Scheme 10) for reactions involving attack of silyl radical (X = Si) lie between approximately 2.5 Å (Y = Si) and 2.8 Å (Y = Sn), while CCSD(T)/DZP//MP2/DZP calculated energy barriers for reactions involving silyl radical lie in the range 40–65 kJ mol⁻¹ and depend on the nature of the leaving radical and the heteroatom undergoing attack.



SCHEME 10

Recent interest in hydrogen abstraction reactions⁴ have prompted several theoretical investigations. Zavitsas reported a non-parametric model for the estimation of the reactivity of various classes of hydride toward hydrogen abstraction by several classes of alkyl radical⁴⁶. Included among the species investigated was Me₃SiH, which reacts to give Me₃Si• radical (identity reaction). The E* (ee-star) method⁴⁶ provides good agreement with experiment. For example, E* provides an activation energy of 73.2 kJ mol⁻¹ for the reaction of Me₃SiH with ethyl radical⁴⁶. This value is in a very good agreement with available experimental data (*viz.* 66.5 kJ mol⁻¹)¹. It is interesting to note that Roberts and Steel had reported earlier an extended form of the Evans–Polanyi equation for predicting activation energies for a large cross section of hydrogen transfer reactions to within ±2.0 kJ mol⁻¹ with a correlation coefficient of 0.988⁴⁷.

In a series of papers, Roberts and coworkers demonstrated that trialkylsilanes, in the presence of a catalytic amount of a thiol, are capable of reducing alkyl halides and other precursors (*vide infra*)^{48,49}. On the basis of relative Si–H and S–H bond strengths, Roberts argued that the electrophilic thiyl radical (RS•) is capable of abstracting the hydrogen atom from a silane (step 2, Scheme 11) and that this reaction ‘could be thermoneutral or even slightly endothermic’; this reaction might also benefit from favourable polar effects⁴⁸. Dubbed *Polarity Reversal Catalysis*^{48,49}, the (apparent) application of



SCHEME 11

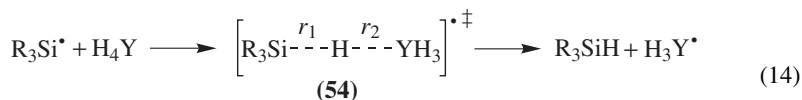
Scheme 11 has led to the development of an alternative method for conducting radical chain reactions with inexpensive reagents such as triethylsilane and alkylthiols.

The role of polar effects operating in the transition states in question was also described quantitatively by Roberts and Steel⁴⁷, although their interpretation has been questioned by Zavitsas and is somewhat controversial⁴⁶. In particular, Zavitsas questions the explanation put forth by Roberts for the catalytic activity of thiols in 'polarity reversal catalysis' and suggest that structures such as $\text{H}_3\text{Si}^+ \cdots \text{H}^* \cdots \text{CH}_3$ are reasonable, based on electronegativity differences together with the intense C–Si stretching in the IR. 'The qualitative polar effect approach would lead to the expectation that H-abstraction by methyl radicals from silane would be subject to greater polar effects and lower E_a . The opposite is observed⁴⁶. X–Y antibonding terms in addition to enthalpy terms would appear to be important for estimating energy barriers to hydrogen abstraction reactions⁴⁶.

In a follow-up paper, Roberts describes the application of the 'Evans–Polyani algorithm' and addresses some of the issues raised by Zavitsas⁵⁰. Specific to criticisms raised, the identity reaction between H_3Si^* and H_4Si was examined as a test case. The value of 37.6 kJ mol^{-1} for the activation energy calculated by Roberts is to be compared with 71.5 kJ mol^{-1} calculated by E^* , 53.6 kJ mol^{-1} calculated at the QCISD/DZP//MP2/DZP level of theory⁵¹ and 46.2 kJ mol^{-1} calculated at the MP4(full)/6-311++G**//MP2(fc)/6-31G** level of theory⁵⁰. The experimental value for the activation energy for this degenerate reaction has been determined⁵² to be at least 60 kJ mol^{-1} . Zavitsas describes more fully the importance of the 'triplet repulsion term' of his *a priori* method described above in a further publication⁵³.

Of direct relevance to the debate described above, Skidmore examined extensively the mechanism of *polarity reversal catalysis* described in Scheme 11 and concluded that the key step (step 2, Scheme 11) in the proposed mechanism, namely the transfer of hydrogen atom from a trialkylsilane to a thiyl radical, is severely endothermic^{54,55}.

At the highest level of theory used in this study [CCSD(T)/6-311G**//MP2/6-311G**], the reaction of Me₃SiH with methylthiyl radical (MeS[•]) was calculated to be endothermic by 30.8 kJ mol⁻¹ and to have an associated energy barrier of 41.9 kJ mol⁻¹, leading to an approximate equilibrium constant of 1.3 × 10⁻⁴ at 80 °C, in all likelihood too small to sustain the radical chain⁵⁵. By way of comparison, the analogous reaction involving silane (SiH₄) is calculated at the CCSD(T)/aug-cc-pVDZ//MP2/aug-cc-pVDZ + ΔZPE level of theory to be endothermic by 19.4 kJ mol⁻¹ and to have an associated energy barrier of 28.1 kJ mol⁻¹, leading to an approximate equilibrium constant of 1.4 × 10⁻³ at 80 °C, a value which verges on chain sustainability⁵⁴. It is interesting to note that the data provided by the quantum methods employed provide little evidence for the existence of polar transition states operating in these reactions. These computational data have distinct significance and may require that the synthetically useful chemistry developed by Roberts be mechanistically re-examined.



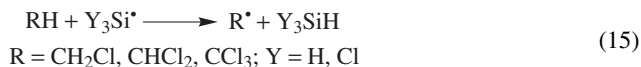
Y = Si, Ge, Sn

Recently, Schiesser and his colleagues examined the hydrogen atom transfer reactions between silyl, germyl and stannyl radicals and their hydrides (equation 14) by using *ab initio* computational techniques⁵¹. Transition states **54** for silyl and trimethylsilyl radical attack at the hydrogen atom in SiH₄, GeH₄ and SnH₄ are calculated to adopt staggered, collinear arrangements of attacking and leaving species. The transition state attack distance r_1 is calculated at the MP2/DZP level of theory to be 1.757 and 1.828 Å for H₃Si[•] and Me₃Si[•] attack, respectively, at the hydrogen atom in SiH₄, with values of 1.757 and 1.714 Å, respectively, for r_2 . The analogous distances (r_1 , r_2) in transition state **54** involved in the analogous reactions with GeH₄ and SnH₄ are: 1.848, 1.747 Å (H₃Si[•] with GeH₄); 1.798, 1.799 Å (Me₃Si[•] with GeH₄); 1.999, 1.849 Å (H₃Si[•] with SnH₄); 2.092, 1.831 Å (Me₃Si[•] with SnH₄)⁵¹. QCISD/DZP//MP2/DZP calculated values of ΔE[‡] for the reaction depicted in equation 14 lie in the range 61–97 kJ mol⁻¹. Consistent with expectation¹, transition states **54** involving trimethylsilyl radical are calculated to be later than those involving H₃Si[•] at all levels of theory.

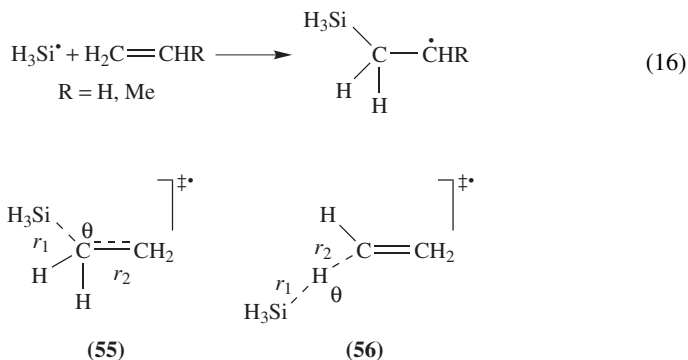
Dakternieks, Henry and Schiesser recently investigated hydrogen abstraction reactions by hydrogen atom, as well as by alkyl radicals from silane, methylsilane, dimethylsilane, trimethylsilane and trisilylsilane with the formation of the corresponding silyl radical⁸. Once again, transition states in these reactions were found to prefer a collinear arrangement of groups at the hydrogen atom undergoing transfer, with all silanes predicted to react with MP2/DZP energy barriers of 50–54 kJ mol⁻¹ for reactions with methyl radical. In agreement with experimental observation^{1–4}, these barriers are calculated to decrease on moving to primary, secondary and tertiary radicals, with MP2/DZP calculated barriers of about 50, 45 and 38 kJ mol⁻¹, respectively. Interestingly, trisilylsilane [(H₃Si)₃SiH] is predicted to react with significantly lower barriers than the other silanes in this study; MP2/DZP values of 28–35 kJ mol⁻¹ calculated for methyl and ethyl radical reactions are

more similar to those calculated for stannanes at the same level of theory⁸ and are consistent with reports of $(\text{TMS})_3\text{SiH}$ behaving more like a stannane than a silane (*vide infra*).

Bottoni also reported the results of computational studies into the abstraction of hydrogen atom by silyl and trichlorosilyl radicals from chloromethane, dichloromethane and chloroform (equation 15)⁴², and concluded that hydrogen abstraction does not effectively compete with halogen abstraction in the systems investigated. B3LYP/6-31G* calculated energy barriers for these reactions fall in the approximate range of 46–72 kJ mol⁻¹.

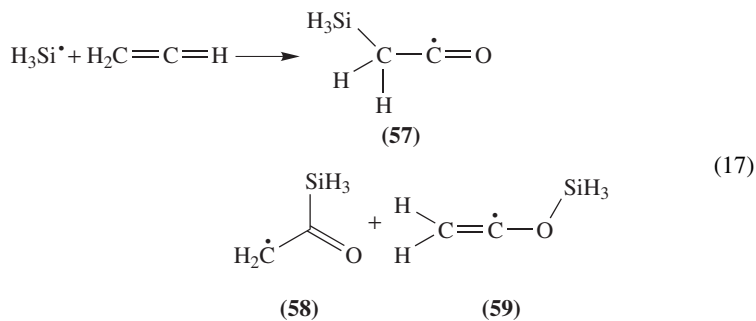


Bottoni investigated reactions of the silyl radical with ethylene and propylene (equation 16) by *ab initio* molecular orbital techniques⁵⁶. Transition states (**55**, **56**) for homolytic addition to, and hydrogen abstraction from, ethylene, respectively, were calculated at the PMP2/6-31G* level to lie 21.8 and 126.0 kJ mol⁻¹, respectively, above the energy of the reactants. At the CCSD(T)/6-311G**//PMP2/6-31G* level, these energy barriers are calculated to be 27.0 and 114.5 kJ mol⁻¹. Clearly then, homolytic addition to ethylene by silyl radical is predicted to be favoured over hydrogen abstraction. Transition state distances (r_1 , r_2) are calculated at the MP2/6-31G* level of theory to be 2.577 and 1.344 Å in **55**, and 1.603 and 1.577 Å in **56**. The attack angles (θ) are predicted to be 97.6 and 172.2°, respectively, at the same level.



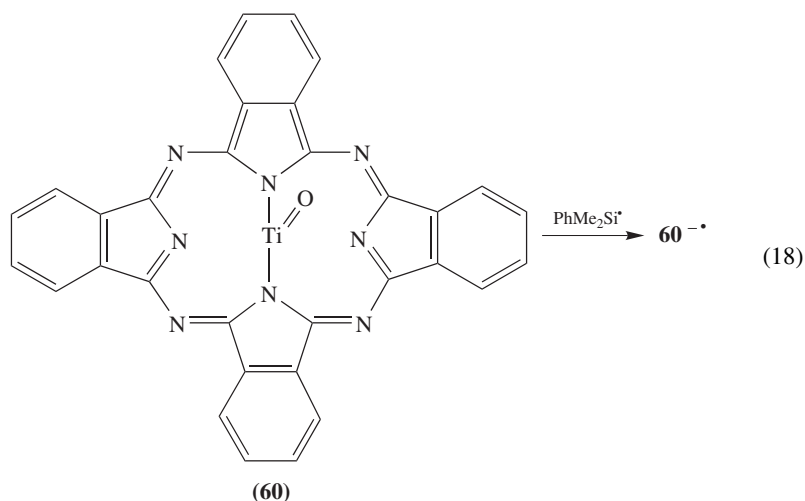
Similar data are presented for the analogous reactions involving propylene. Addition to the terminus of the olefinic residue of propylene ($\Delta E^\ddagger = 23.0$ kJ mol⁻¹) is favoured over addition to the central position ($\Delta E^\ddagger = 30.0$ kJ mol⁻¹), which in turn is favoured over abstraction of the methyl ($\Delta E^\ddagger = 77.7$ kJ mol⁻¹) and olefinic hydrogen atoms ($\Delta E^\ddagger = 115.4, 128.9$ kJ mol⁻¹), respectively⁵⁶.

Calculations for the addition of trimethylsilyl and dimethyl(trimethylsilyl)silyl radicals to olefinic monomers using AM1 and PM3 semiempirical techniques have been reported⁵⁷. The enthalpy of reaction (ΔH_f) values of Me_3Si^* with acrylonitrile, butyl vinyl ether and styrene were calculated using the AM1 technique to be -96.2, -100.4 and 115.9 kJ mol⁻¹, respectively. AM1 values of ΔH_f for the analogous reactions involving $(\text{Me}_3\text{Si})\text{Me}_2\text{Si}^*$ were calculated to be -94.6, -70.3 and -106.7 kJ mol⁻¹, respectively. Transition states for $(\text{Me}_3\text{Si})\text{Me}_2\text{Si}^*$ attack at the terminus of acrylonitrile and butyl vinyl ether were calculated to have attack distances of 3.096 and 3.008 Å, respectively.



Sung and Tidwell reported the results of an *ab initio* study of the reactivity of ketene with several free radicals⁵⁸. Included in the series was $\text{H}_3\text{Si}^\bullet$ (equation 17). All levels of theory used in this study predict that silyl radical prefers to add to the carbon terminus of the ketene leading to **57**; B3LYP/6-31G* calculations provide an energy barrier of 13.8 kJ mol^{-1} for this process. This number is to be compared with values of 26.4 and 46.9 kJ mol^{-1} for the reactions leading to **58** and **59**, respectively, at the same level of theory⁵⁸.

Denisov provided an analysis of the reactivity of free-radical reactions in terms of the parabolic model of the transition states involved in these reactions⁵⁹. Sixteen groups of reactions of silanes and silyl radicals were used to establish the required parameters for the parabolic model. Subsequently, these parameters were used to calculate the activation energies of 112 free-radical reactions and to estimate the dissociation energies of the Si–H bond in 21 compounds and the C–Cl bond in some substituted benzyl chlorides. Good correlation between calculated and experimental activation energies is reported. For example, activation energies of 21.7 , 33.8 , 39.4 and 7.0 kJ mol^{-1} were calculated for the reactions of methyl and ethyl radicals with SiH_4 , trichloromethyl radical with Et_3SiH and $\text{Me}_3\text{CO}^\bullet$ with $(\text{MeS})_3\text{SiH}$, respectively⁵⁹. These numbers are to be compared with 28.8 , 31.6 , 36.2 and 7.8 kJ mol^{-1} , determined experimentally¹.



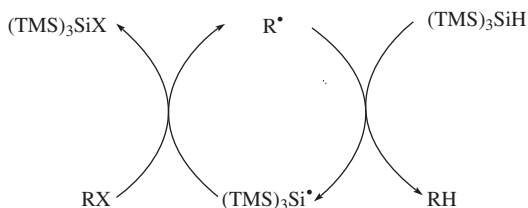
Yokoyama and coworkers investigated the discolouration of titanylphthalocyanine **60**, and related porphyrins by silyl radicals derived from methylphenylpolysilane by molecular orbital methods⁶⁰. Calculated values of ΔN , the index derived from the 'hard and soft acids and bases' concept was determined from HF/3-21G^(*) calculated ionization potentials, electron affinities, and HOMO and LUMO orbital energies of the systems of interest. These studies predict that $\text{PhMe}_2\text{Si}^\bullet$ should donate an electron readily to **60** to form $\text{60}^{-\bullet}$ (equation 18). This prediction is of direct relevance to observations that irradiation of titanylphthalocyanine-coated methylphenylpolysilane films leads to discolouration of the film⁶⁰.

III. ORGANOSILANES AS REAGENTS IN RADICAL CHAIN REACTIONS

A. General Aspects

The synthetic application of free radical reactions has increased dramatically within the last decade. Nowadays, radical reactions can often be found driving the key steps of multi-step chemical syntheses oriented towards the construction of complex natural products⁶¹. The majority of radical reactions of interest to synthetic chemists are chain processes. Tributyltin hydride is the most commonly used reagent for the reduction of functional groups and formation of C—C bonds either inter- or intramolecularly (cyclization)^{62–66} although there are several problems associated with organotin compounds². The main drawback consists of the incomplete removal of highly toxic tin by-products from the final material. Some years ago, one of us introduced tris(trimethylsilyl)silane, $(\text{TMS})_3\text{SiH}$, as an alternative approach^{2,3}. $(\text{TMS})_3\text{SiH}$ has proven to be a valid alternative to tin hydride for the majority of its radical chain reactions, although in some cases the two reagents can complement each other. Indeed, there is an increasing number of cases where the two reagents behave differently⁶⁷.

Scheme 12 shows the two propagation steps of a chain process for the simple reduction of an organic halide by $(\text{TMS})_3\text{SiH}$. The chain reactions are terminated by radical combination or disproportionation. In order to have an efficient chain process, the rate of chain-transfer steps must be higher than that of chain-termination steps. The following observations: (i) the termination rate constants in liquid phase are controlled by diffusion (i.e. $10^{10} \text{ M}^{-1} \text{ s}^{-1}$), (ii) radical concentrations in chain reactions are about 10^{-7} – 10^{-8} M (depending on the reaction conditions) and (iii) the concentration of reagents is generally between 0.05–0.5 M, indicate that the rate constants for the chain transfer steps must be much higher than $10^3 \text{ M}^{-1} \text{ s}^{-1}$.



SCHEME 12

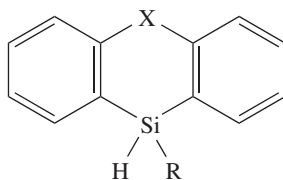
The reaction of radicals with silicon hydrides is the key step for the majority of reactions forming silyl radicals (equation 19). All available rate constants and activation parameters for reaction 19 have been recently collected and discussed together with those

TABLE 4. Rate constants for the reaction of primary alkyl radicals with a variety of silicon hydrides^a

Silane	$k(\text{M}^{-1} \text{s}^{-1})$ at 80 °C
Et ₃ SiH	5.2×10^3
Ph ₂ Si(H)Me	8.0×10^3
Me ₃ SiSi(H)Me ₂	2.3×10^4
PhSiH ₃	2.9×10^{4b}
Ph ₂ SiH ₂	5.6×10^{4b}
Ph ₃ SiH	4.6×10^{4b}
61	4.5×10^4
62	8.7×10^4
(Me ₃ Si) ₂ Si(H)Me	1.5×10^5
(MeS) ₃ SiH	3.9×10^5
(Me ₃ Si) ₃ SiH	1.2×10^6
63	2.1×10^6

^aFrom Reference 4.^bAt 110 °C.

for germanium and tin hydrides⁴. In order to help readers who are not familiar with these data, we report in Table 4 the rate constants of primary alkyl radicals with a variety of silicon hydrides for direct comparison.

**(61)** X = SiMe₂, R = Me**(62)** X = S, R = Me**(63)** X = SiH₂, R = H

The trends in reactivity for reaction 19 are the following: (i) For a primary alkyl radical, the rate constants increase along the series Et₃SiH < Ph₃SiH < (MeS)₃SiH < (TMS)₃SiH with the expected intermediate values for silanes having mixed substituents. Similar behaviour is found with other carbon-centered radicals⁴. Phenyl substitution, whether single or multiple, has only a small effect on the rate constant in contrast with that on the carbon analogues. The lack of resonance stabilization by phenyl groups on the silicon centred radical has been attributed to the larger size of silicon (compared to carbon) and to the pyramidal nature of the radical centre. The silanthrene derivatives **61** and **63** are more reactive than the corresponding diphenylsilanes (Table 4). For example, 5,10-dihydrosilanthrene (**63**) is an order of magnitude more reactive than Ph₂SiH₂ towards primary alkyl radicals (taking into account the statistical number of hydrogen abstracted). The enhancement of the reactivity is probably due to the stabilization of the silyl radical

induced either by a transannular interaction of the vicinal Si substituent or by the *quasi*-planar arrangement of the radical centre. Table 4 shows that for a particular radical, the rate constant increases substantially with successive substitution of alkyl or phenyl by thiol or silyl groups at the Si–H function. In particular, for primary alkyl radicals, by replacing a methyl with a Me₃Si group, the rate increases by an order of magnitude, this effect being cumulative (Table 4). These results are in good agreement with the thermodynamic data for these silanes^{4,68}, which show the weakening of the Si–H bond strength by replacing the alkyl substituent with thiol or silyl groups. The rate constants for the reaction of primary, secondary and tertiary alkyl radicals with (TMS)₃SiH are very similar in the range of temperatures that are useful for chemical transformation in the liquid phase⁴.

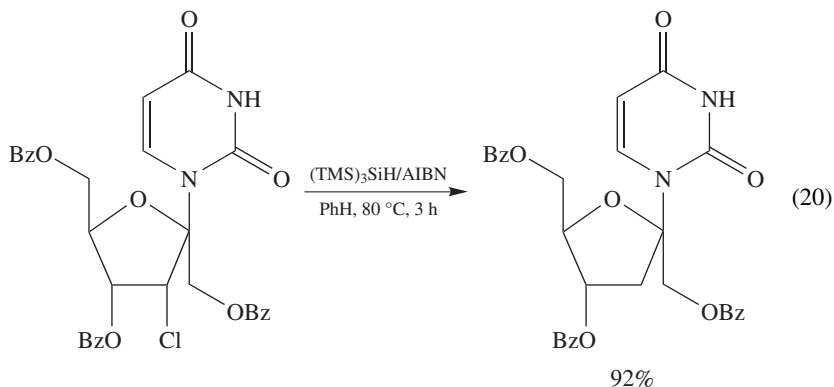
B. Tris(trimethylsilyl)silane

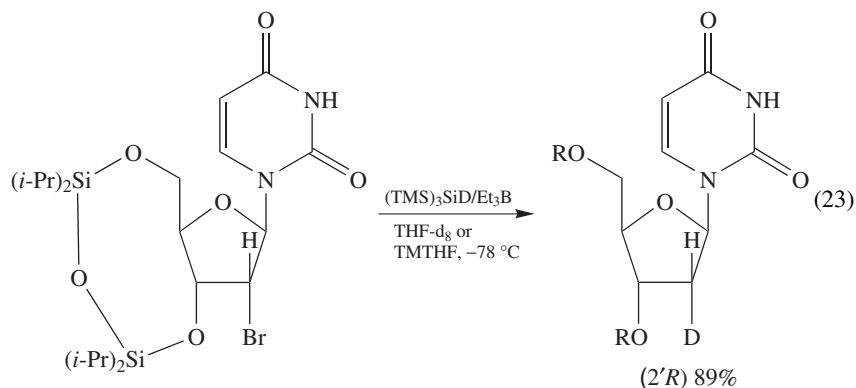
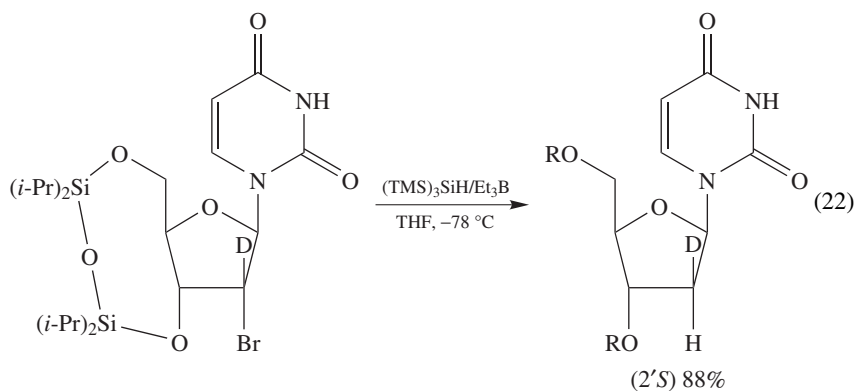
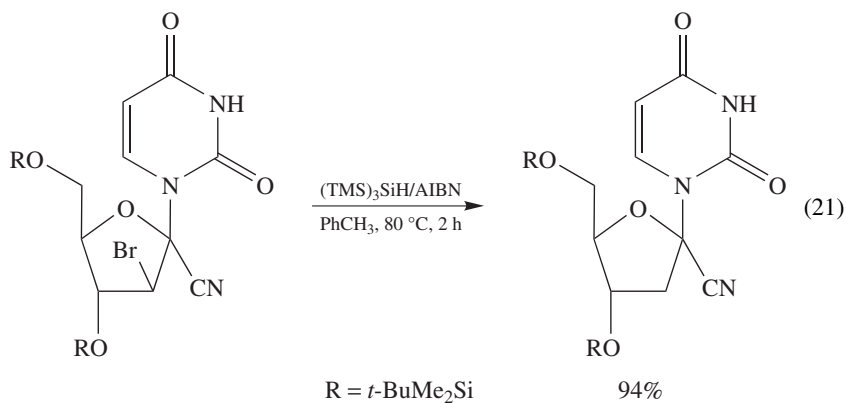
In this section, our purpose is not to review the entire chemistry of (TMS)₃SiH but to deal mainly with the literature from 1997 to the beginning of 2000 on the application of (TMS)₃SiH in organic synthesis. For early reviews on this subject see References 2 and 3.

1. Reductions

Tris(trimethylsilyl)silane is found to be an efficient reducing agent for a variety of functional groups. In particular, the reductions of halides, chalcogen groups, thiono esters (i.e. deoxygenation of secondary alcohols) and isocyanides (i.e. deamination of primary amines) are the most commonly described applications. The efficiency of these reactions is also supported by available kinetic data.

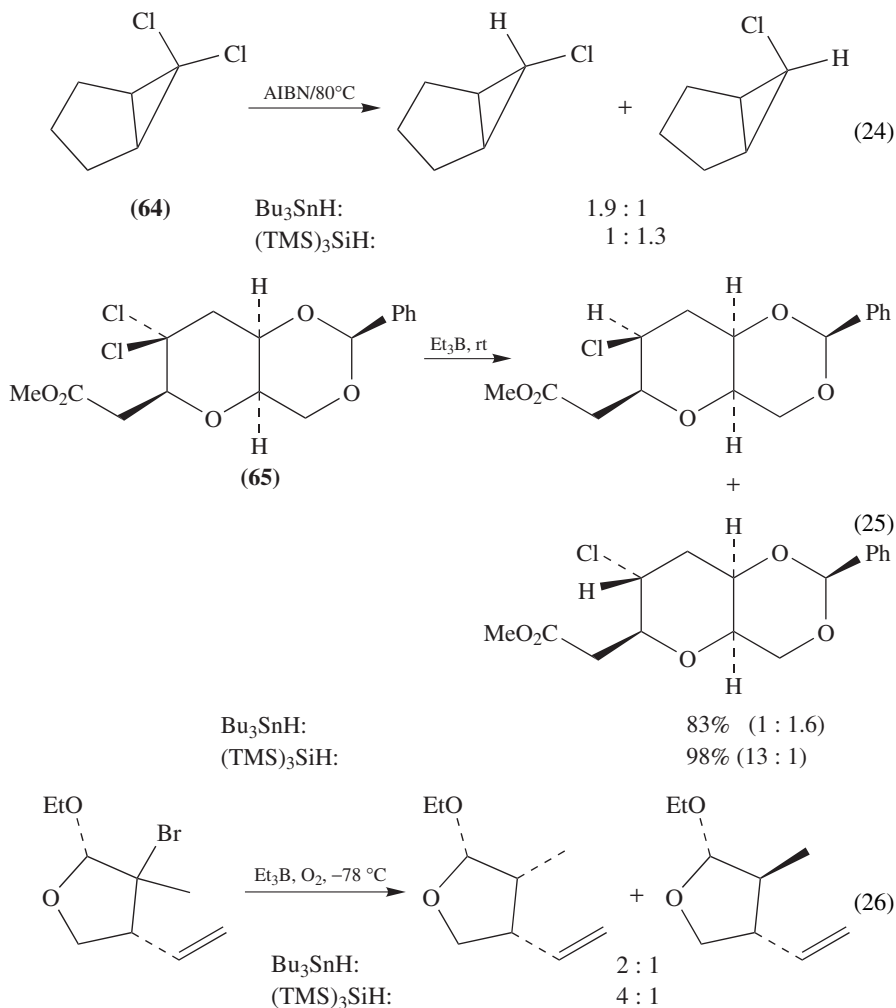
To illustrate the efficiency of dehalogenation reactions, a few examples are chosen from the area of nucleoside chemistry. Equations 20 and 21 show the chlorine and bromine atom removal from the 2'-positions of nucleoside sugar moieties under mild conditions and in very good yield^{69,70}. Ishido and coworkers have developed a highly diastereoselective and efficient method for the synthesis of (2'*S*)- and (2'*R*)-2'-deoxy [2'-²H]ribonucleoside derivatives starting from the corresponding bromide or thionocarbonate at the 2'-position⁷¹. Equations 22 and 23 show the flexibility of this methodology to obtain a single diastereoisomer, (2'*S*) and (2'*R*), respectively. The high stereoselectivity in these reactions is due to the transfer of hydrogen or deuterium atoms from the less hindered side of the ring. It is worth mentioning that the solvent employed in equation 23 was either THF-d₈ or 2,2,5,5-tetramethyltetrahydrofuran (TMTHF), in order to eliminate a small percentage of hydrogen donation from the reaction medium.



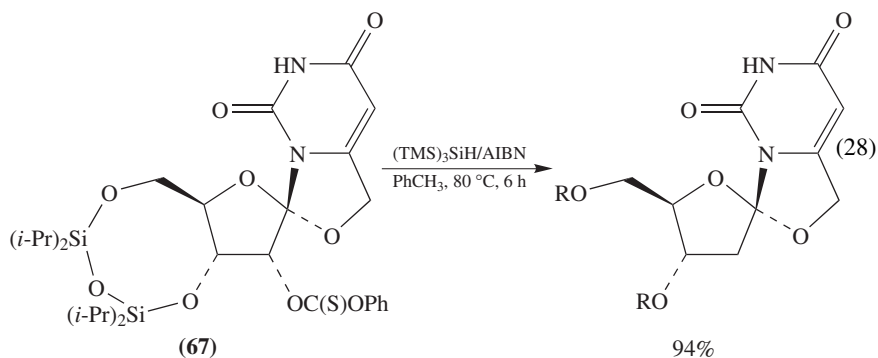
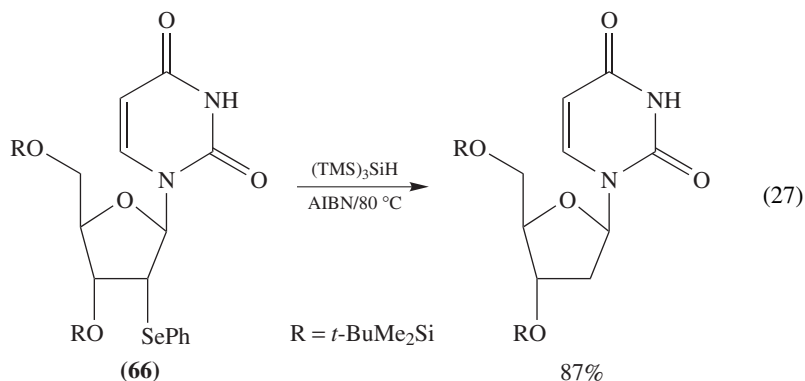


The complementarity of $(\text{TMS})_3\text{SiH}$ and Bu_3SnH in dehalogenation reactions can be appreciated from some recent works depicted in equations 24–26. In the reduction of *gem*-dichloride **64** by $(\text{TMS})_3\text{SiH}$ and Bu_3SnH (equation 24), it was shown that the silane has a stronger preference than tin to deliver a hydrogen atom from the less hindered side of the ring due to the different spatial shapes of the two reagents⁷². The

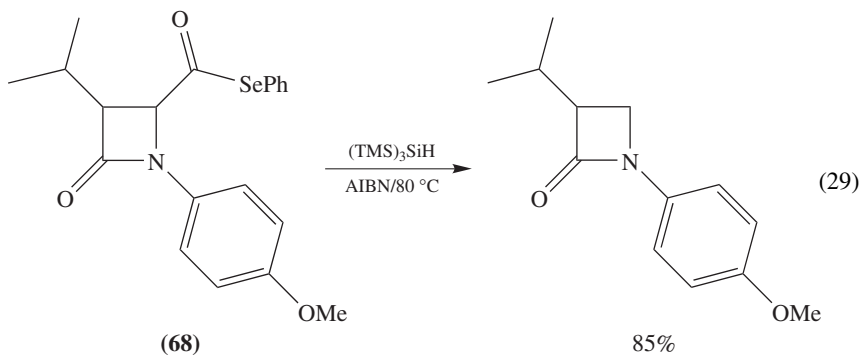
reduction of the dichloride **65** by $(\text{TMS})_3\text{SiH}$ at room temperature (equation 25) afforded the desired monochloride in high yield and stereoselectively whereas the stannane gave the other epimer as the major product⁷³. Following this concept, the better stereocontrol obtained with $(\text{TMS})_3\text{SiH}$ in equation 26 is attributed to the bulkier reducing agent which approaches the radical intermediate from the less hindered face *anti* to the two vicinal substituents⁷⁴.

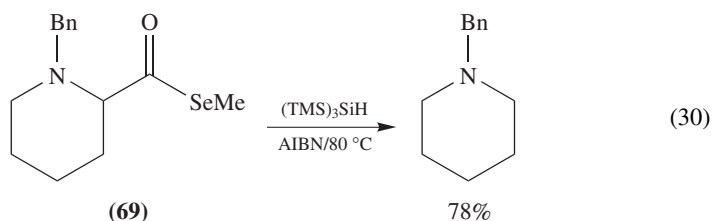


Equation 27 shows the phenylseleno removal from the 2'-position of **66**⁷⁵ whereas in equation 28 the removal of 2'-hydroxy group has been accomplished via the phenoxythio-carbonyl derivative **67** under normal free-radical conditions to produce the protected spironucleoside in good yield⁷⁶.

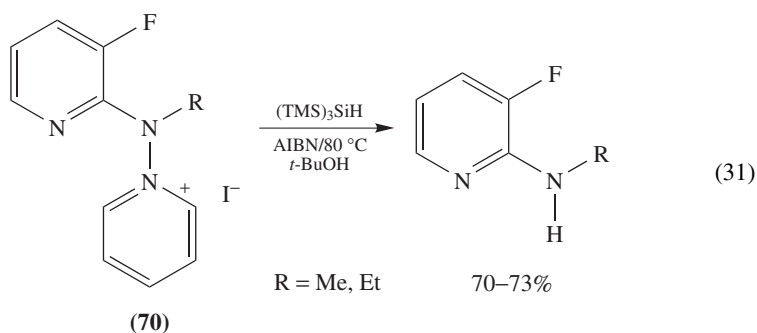


Phenyl selenoesters have been reported to undergo reduction to the corresponding aldehydes and/or alkanes in the presence of $(\text{TMS})_3\text{SiH}$ under free-radical conditions⁷⁷. The decrease of aldehyde formation through the primary, secondary and tertiary substituted series, under the same conditions, indicated that a decarbonylation of acyl radicals takes place. An example is shown in equation 29 in which the phenylseleno ester **68** reacts with $(\text{TMS})_3\text{SiH}$ to give the decarbonylated β -lactam in good yield⁷⁸. Equation 30 shows that the methylseleno ester **69** when treated under similar conditions gave the reduction product in 78% yield⁷⁹.



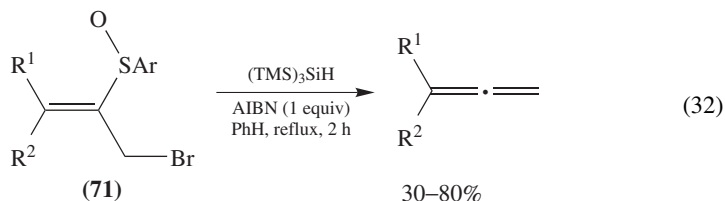


An unusual replacement of a pyridinium moiety in **70** by hydrogen has also been successful with $(\text{TMS})_3\text{SiH}$ under normal radical conditions. In fact, the two substrates in equation 31 afforded 3-fluoro-2-aminopyridine derivatives in good yields⁸⁰.

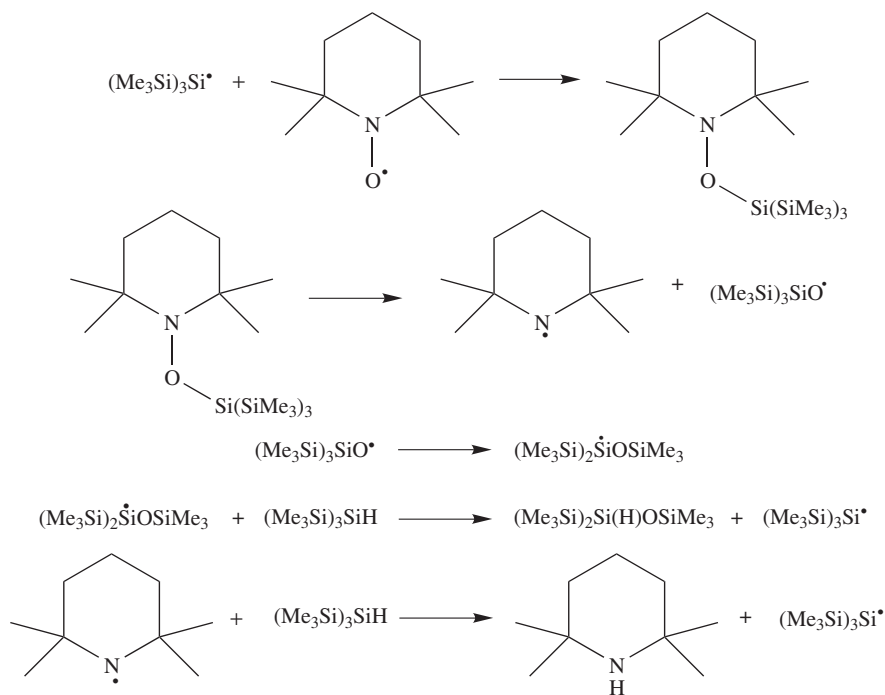


Another unusual reaction is the deoxygenation of nitroxides by $(\text{TMS})_3\text{SiH}$ ¹⁶. In fact, this silane reacts with TEMPO in the presence of thermal or photochemical radical initiators, to afford the corresponding amine in quantitative yield. The reaction mechanism for this transformation is shown in Scheme 13. The driving force of this reaction appears to be the formation of a strong oxygen–silicon bond.

Malacria's group recently developed a new method for the synthesis of allenes based on the radical reduction of bromides **71**⁸¹. Equation 32 shows the general reaction for the terminally substituted allenes. Eight examples were reported with yields in the range of 30–80%. As pointed out by the authors, the use of large excesses of initiator suggests that these transformations do not involve straightforward chain reactions.



The addition of $(\text{TMS})_3\text{SiH}$ across carbon–carbon multiple bonds under free-radical conditions is well documented⁸². Although no recent reports of such hydrosilylation processes are reported, the addition of $(\text{TMS})_3\text{Si}^\bullet$ radical to multiple bonds, followed by other radical reactions, were investigated (*vide infra*). The hydrosilylation of ketones and aldehydes is also well known⁸³. In this respect Brook and coworkers have recently shown that the $(\text{TMS})_3\text{Si}$ group can be used for the protection of primary and secondary alcohols⁸⁴.



SCHEME 13

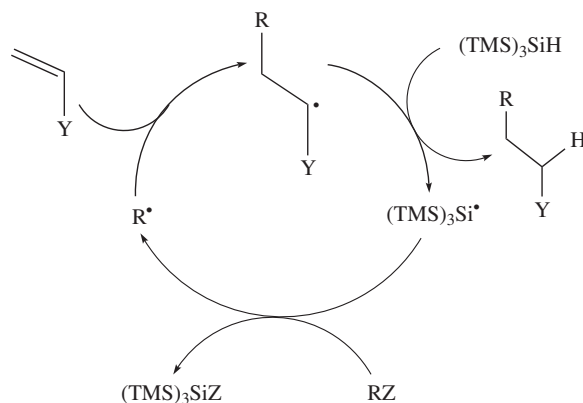
The corresponding silyl ethers are stable under the usual conditions employed in organic synthesis for the deprotection of silyl groups and were deprotected using photolysis at 254 nm in yields ranging from 62–95%. Therefore, the hydrosilylation of ketones and aldehydes followed by this deprotection procedure is formally equivalent to the reduction of carbonyl moieties to the corresponding alcohols.

2. Consecutive radical reactions

The formation of an alkyl radical resulting from the initial atom (or group) abstraction by $(\text{TMS})_3\text{Si}^\bullet$ radical or by addition of $(\text{TMS})_3\text{Si}^\bullet$ to unsaturated bonds is often designed so that this intermediate can undergo a number of consecutive reactions.

The free-radical construction of C–C bonds either inter- or intramolecularly using a hydride as mediator is a widely employed methodology in chemical synthesis. The propagation steps for the intermolecular version are shown in Scheme 14. For a successful outcome, it is important that (i) the $(\text{TMS})_3\text{Si}^\bullet$ radical reacts faster with RZ (the precursor of radical R $^\bullet$) than with the alkene and (ii) the alkyl radical reacts faster with alkene (to form the adduct radical) than with the silane. Therefore, in a synthetic plan one is faced with the task of considering kinetic data or substituent influence on the selectivity of radicals.

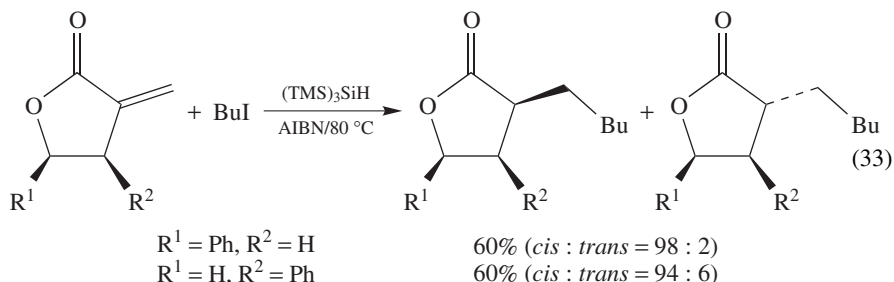
Care must be taken in order to ensure that the effective rates of the consecutive radical reactions are higher than the rate of hydrogen abstraction from $(\text{TMS})_3\text{SiH}$. Apart from the standard synthetic planning based on known rate constants, this is usually effected either by controlling the concentration of the reducing agent in the reaction medium



SCHEME 14

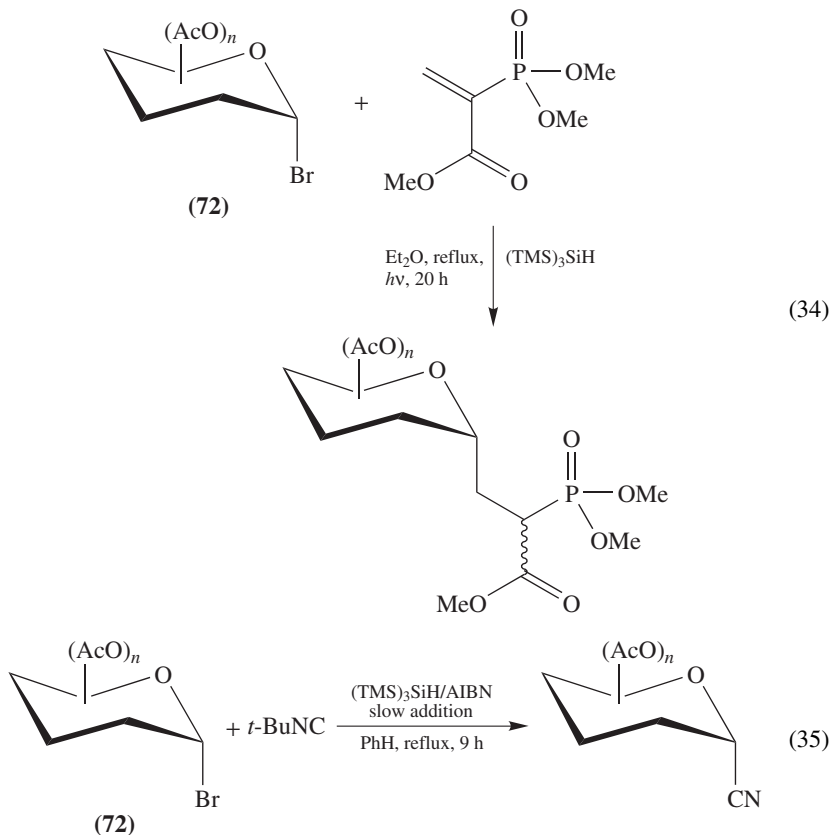
(slow addition by syringe pump) or, in the case of intermolecular addition reactions, by adding a large excess of the radical acceptor. It is worth mentioning that $(\text{TMS})_3\text{SiH}$ is advantageous when compared with Bu_3SnH due to its lower hydrogen donation ability, which provides the intermediate radical species with time to undergo the desired sequential reactions prior to reduction. In fact, in many cases the direct addition of $(\text{TMS})_3\text{SiH}$ gives results comparable to the syringe-pump addition of Bu_3SnH .

The reactions of β - or γ -phenyl substituted α -methylenebutyrolactones with BuI in the presence of $(\text{TMS})_3\text{SiH}$ afforded α,β - or α,γ -disubstituted lactones in good yield and with high diastereoselectivity (equation 33)⁸⁵. With β - or γ -alkyl substituted substrates the same reaction was found to be less selective.

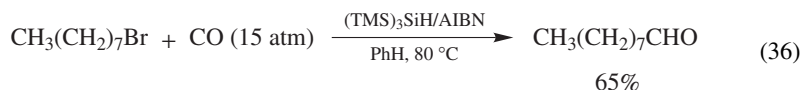


The intermolecular C–C bond formation mediated by $(\text{TMS})_3\text{SiH}$ has been applied to sugar derivatives. Diastereoselective syntheses of α -substituted C–glycosyl phosphonates were obtained by reaction of bromide **72** with α -phosphonoacrylate (equation 34)⁸⁶. Yields depend on the sugar configuration, i.e. D-galacto (80%), D-manno (47%), D-gluco (30%) and L-fuco (62%). In all cases a α : β ratio of 98 : 2 was obtained. The C–C bond formation at the anomeric position of carbohydrates has also been extended to synthesis of α -cyanoglycosides through glycosyl radical cyanation mediated by $(\text{TMS})_3\text{SiH}$ (equation 35)⁸⁷. Also, in these experiments yields depend on the configuration of sugar: D-galacto (73%), D-manno (40%), D-gluco (71%) and L-fuco (25%). The α -cyano anomers

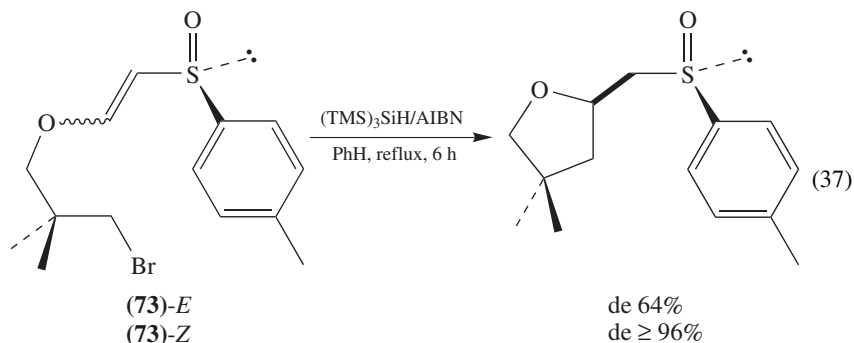
were exclusively formed. The key propagation steps for these transformations are the addition of glycosyl radical to isocyanide, followed by a fragmentation yielding a *tert*-butyl radical and the desired glycosyl cyanide.



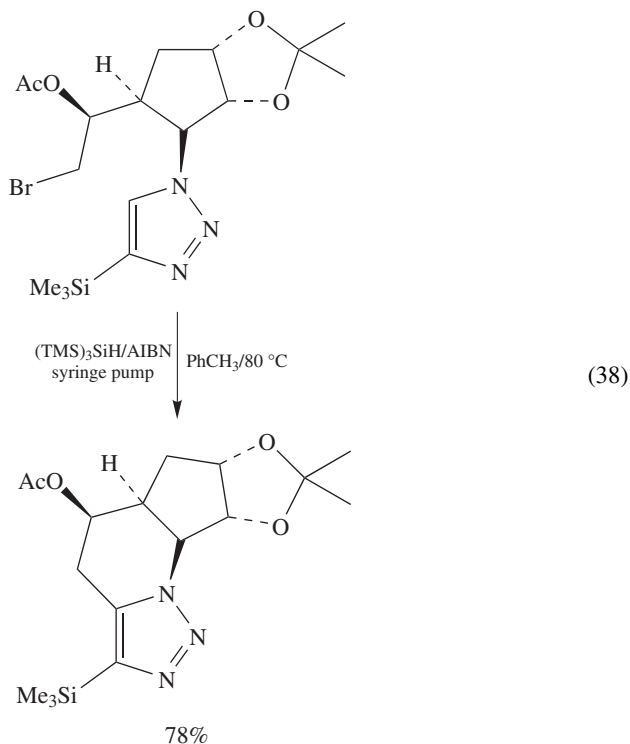
Alkyl halides could be carbonylated under moderate pressure of CO (15–30 atm) in benzene at $80^\circ C$ in the presence of $(TMS)_3SiH$ and AIBN⁸⁸. Equation 36 shows an example starting from a primary alkyl bromide.

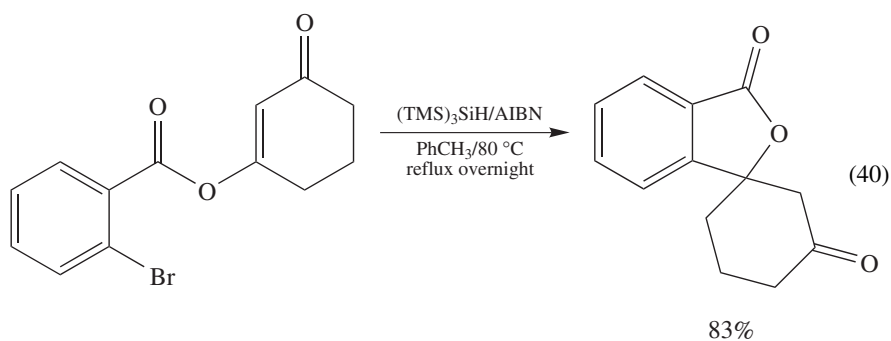
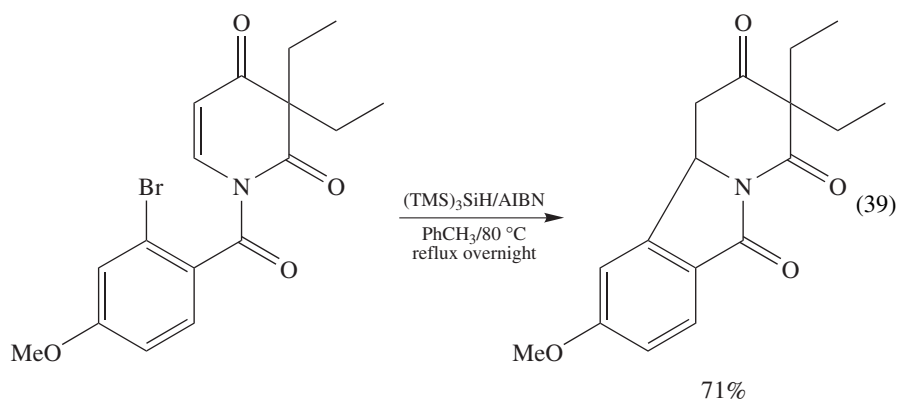


The intramolecular C–C bond formation (or cyclization) mediated by $(TMS)_3SiH$ has been the subject of numerous publications in the last few years. For example, radical cyclization of bromides **73** was found to be totally regioselective following 5-*exo* mode ring closure and afforded tetrahydrofuran derivatives (equation 37)⁸⁹. Furthermore, the chiral auxiliary together with the configuration of the double bond allow for complete diastereocontrol.

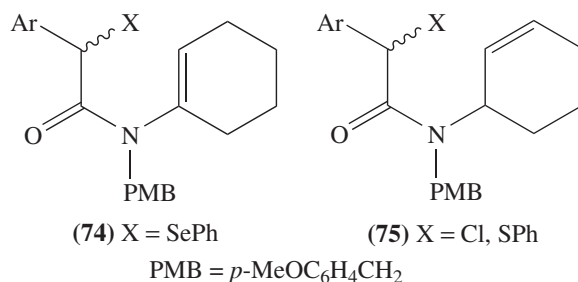


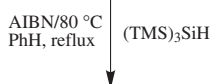
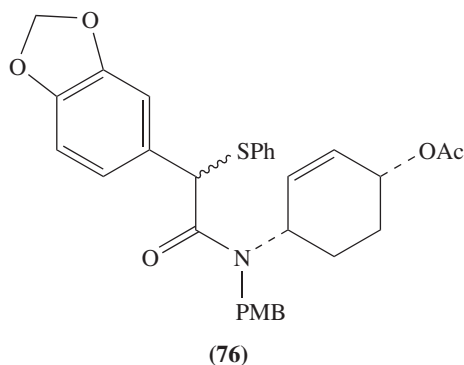
Equation 38 presents an example starting from a bromide, the key step being a 6-*endo*-trig cyclization on a functionalized 1,2,3-triazole⁹⁰. For the synthesis of tricyclic isoindolinones the 5-*exo*-trig cyclization of aryl radicals has been applied⁹¹. An example is shown in equation 39 in which the tricyclic system was obtained in 71% yield. The 5-*exo*-trig cyclization of aryl radicals has also been successfully applied to the synthesis of spiro derivatives⁹². Thus, keto spiro- γ -lactones, keto spiro- γ -lactams, spirodilactones, spiro lactone-lactams and spiro lactone-thiolactones have been prepared. An example is given in equation 40⁹².



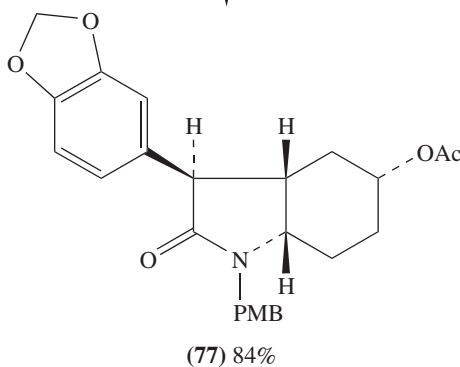


Ikeda and coworkers have studied the stereoselectivity of 5-*endo*-trig cyclization in compound **74** and 5-*exo*-trig cyclization in **75** using $(\text{TMS})_3\text{SiH}$ or Bu_3SnH as radical mediators⁹³. In system **74** a mixture of *cis*-fused and *trans*-fused rings is obtained, whereas in system **75** the reaction proceeds in a stereoselective manner to give only the *cis*-fused product. It is noteworthy that in all cases the silane gave slightly better yield and facilitated the workup of the reaction. $(\text{TMS})_3\text{SiH}$ was further applied to the synthesis of derivative **77**, as the key intermediate for the preparation of alkaloid (\pm)-pancracine⁹³. In fact, the reaction of **76** under normal conditions gave **77** in 84% yield as a single stereoisomer (equation 41).





(41)

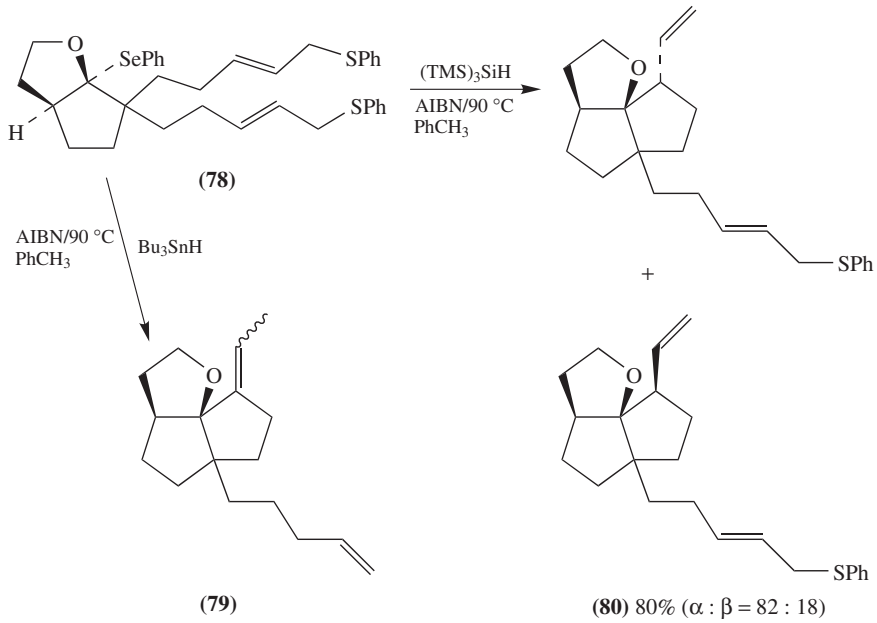


(TMS)₃SiH-mediated 7-*endo*-trig cyclization of bromides was employed as the key step for the construction of the azepinoindole tricyclic core of the *Stemona* alkaloid⁹⁴.

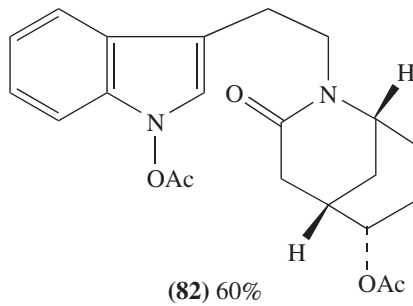
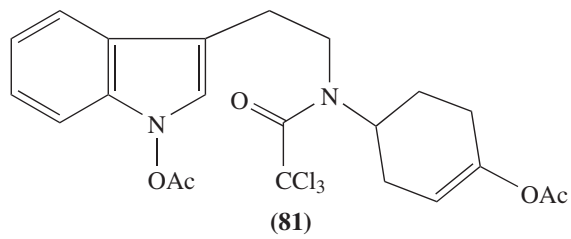
Exploring different methods for the intramolecular radical cyclization of **78** (Scheme 15)⁹⁵, Usui and Paquette observed that (TMS)₃SiH under normal conditions affords the expected functionalized diquinane **79** in 80% yield and in a $\alpha : \beta$ ratio of 82 : 18. MM2 calculations suggest it is the result of a kinetic controlled process. It is worth mentioning that the endothermic reaction 42 is expected to be one of the propagation steps in this chain process (*vide infra*). By replacing the silane with tin hydride under similar experimental conditions, the unexpected product **80** was obtained in a 77% yield.



The reduction of the trichloroacetamide derivative **81** with (TMS)₃SiH affords **82** in a 60% yield (equation 43)⁹⁶. It should be noted that the final product is the result of cyclization and further removal of two chlorine atoms. In fact, 3.5 equiv of silane and 1.1 equiv of AIBN are used.

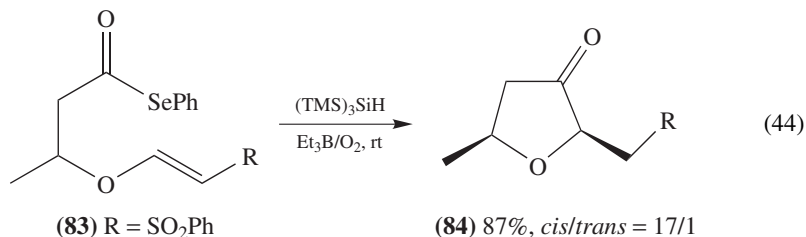


SCHEME 15

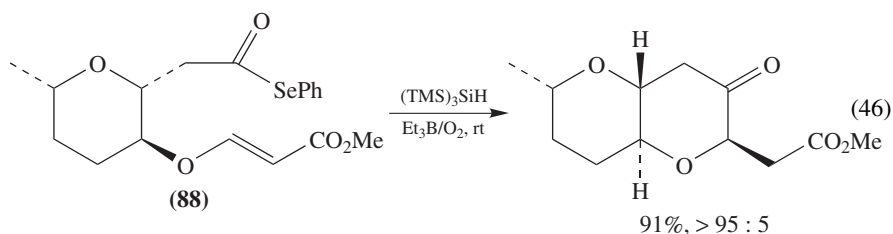
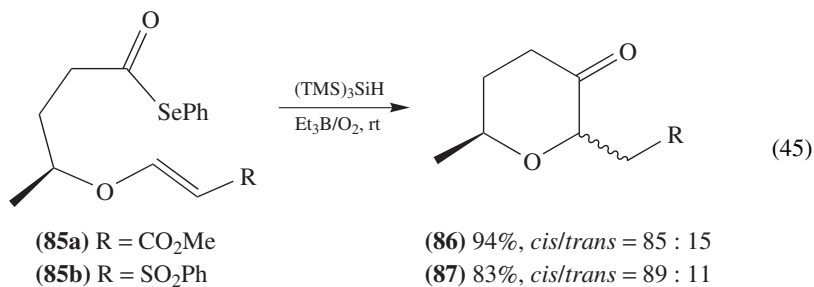


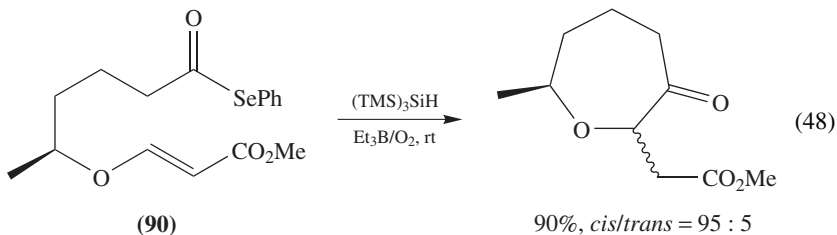
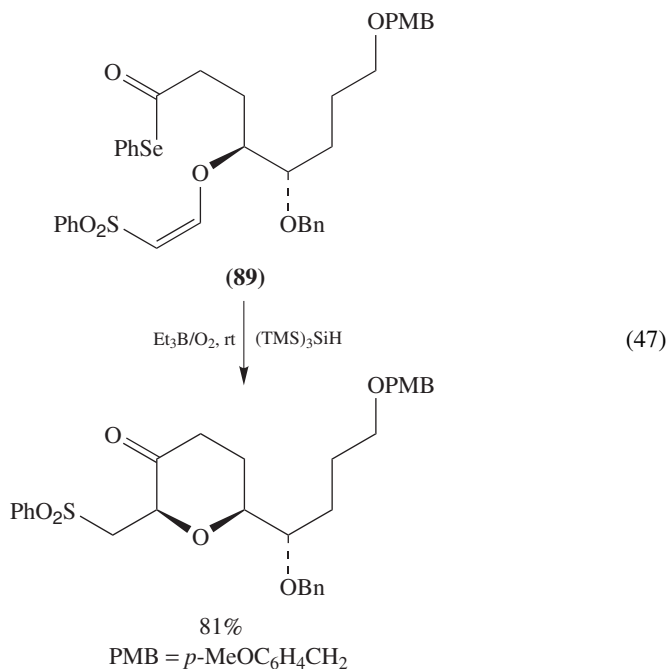
(43)

(TMS)₃SiH-mediated acyl radical reactions of phenylseleno esters have been utilized for the diastereoselective synthesis of cyclic ethers by Evans's group. Equation 44 shows that the acyl selenide **83** affords the *cis*-disubstituted tetrahydrofuran **84** in good yield on exposure at room temperature to (TMS)₃SiH and the Et₃B/O₂ combination as the initiator via a 5-*exo*-trig cyclization^{97,98}.



A number of very highly diastereoselective 6-heptenoyl radical cyclizations have been described by the same group. Some examples are given in equations 45–48. All the substrates are derived from vinyl ethers, and in each case the *cis*-disubstituted product is preferentially formed as the result of the regioselective *exo* cyclization as shown by conversion of **85a** and **85b** to **86** and **87** (equation 45). Attention is drawn to the improved selectivity obtained with the fused ring systems **88** (equation 46) which is thought to arise from the increased rigidity imposed on the transition state by the pre-existing ring^{99a}. The higher selectivity observed with the *cis* alkene **89**^{99b} (equation 47) as compared, for example, to **85b**⁹⁸ (equation 45) is thought to arise from stronger 1,3-diaxial interactions in the chair-like transition state for the formation of the minor isomer. Synthetically more demanding 2,7-disubstituted oxepan-3-ones are also available by the same cyclization strategy starting from the acyl selenide **90** (equation 48)⁹⁸.

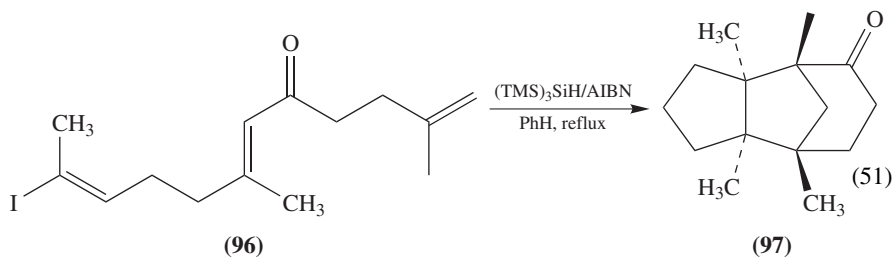
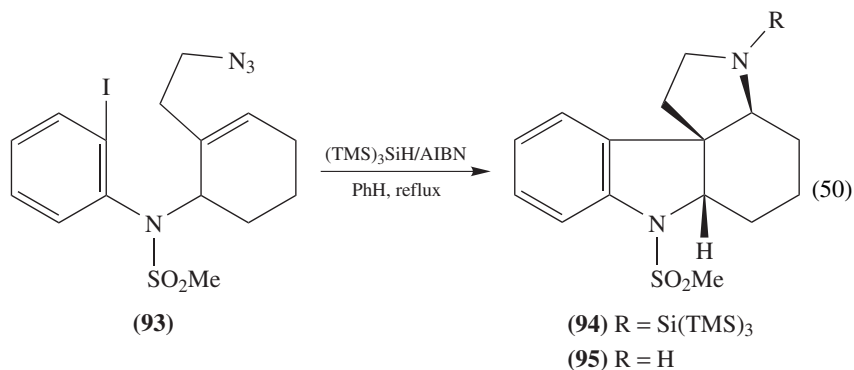
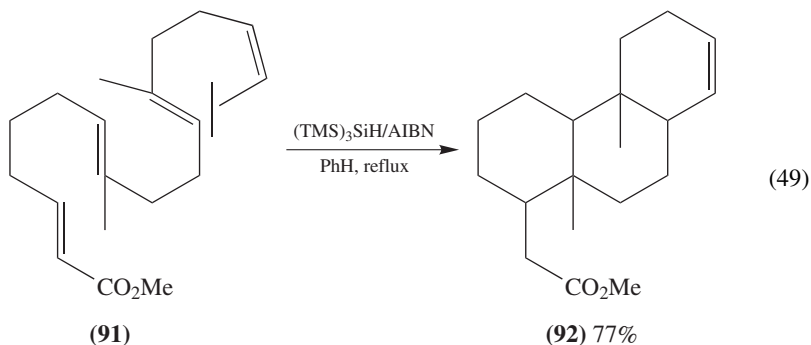




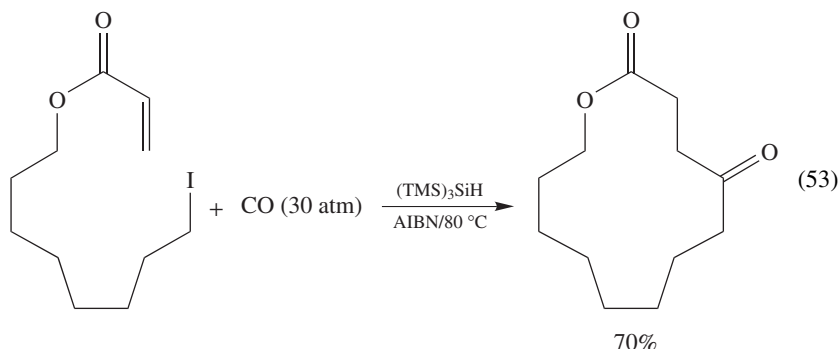
(TMS)₃SiH has also been applied for kinetic studies of one-carbon ring expansion in the cyclopentanone series for both primary and secondary alkyl radicals¹⁰⁰.

The increasing popularity of radical reactions is certainly due to the so-called 'reaction cascade', i.e. the ability of forming and breaking several bonds in a one-pot procedure. Treatment of the iodo derivative **91** with (TMS)₃SiH starts a cascade of 6-*endo*, 6-*endo* and 6-*exo* cyclizations to afford exclusively **92** in 77% yield (equation 49)¹⁰¹. Reaction of the iodo derivative **93** with (TMS)₃SiH under normal conditions afforded, after workup, the tetracyclic **95** as a single diastereoisomer in a 83% yield (equation 50)¹⁰². It is noteworthy that the crude reaction mixture appeared to contain the (TMS)₃Si-protected alkaloid **94** [formed by reaction of amine **95** with the byproduct (TMS)₃SiI] which is hydrolysed during the workup. Haney and Curran reported a radical cascade reaction of 5-*exo*, 6-*endo* and 5-*endo* cyclizations in which the last radical cyclization occurs at the same carbon atom where the initial radical was generated¹⁰³. Equation 51 shows the starting material **96** of this sequence; the product of interest (**97**) was obtained in 17% yield. Three other products resulting from incomplete cyclization were also observed.

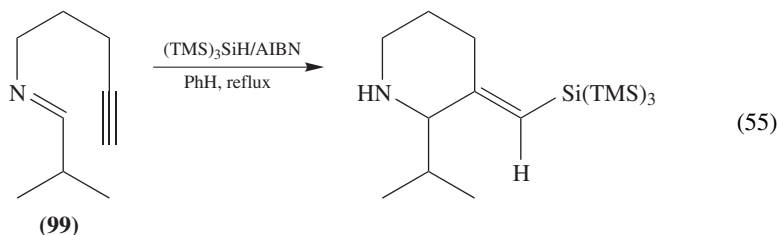
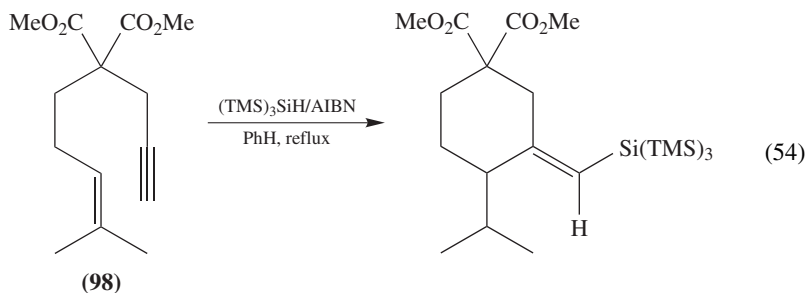
Preparation of an oestrone analogue has been made by treatment of a polyene iodide with $(\text{TMS})_3\text{SiH}$ via a radical cascade involving a 13-*endo* macrocyclization followed by successive opening of a cyclopropane ring and a 6-*exo*/5-*exo* transannular cyclization (equation 52)¹⁰⁴.



Macrocyclization reactions resulting from an $(n + 1)$ -type radical annulation were further investigated¹⁰⁵. An example of 13-membered ring formation is shown in equation 53. It is worth mentioning that these reactions need high dilution conditions.

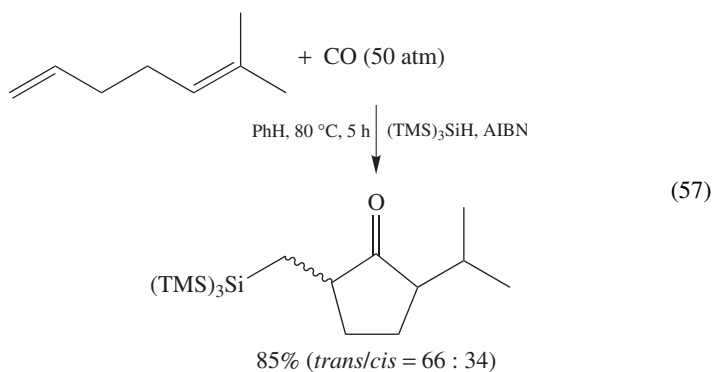
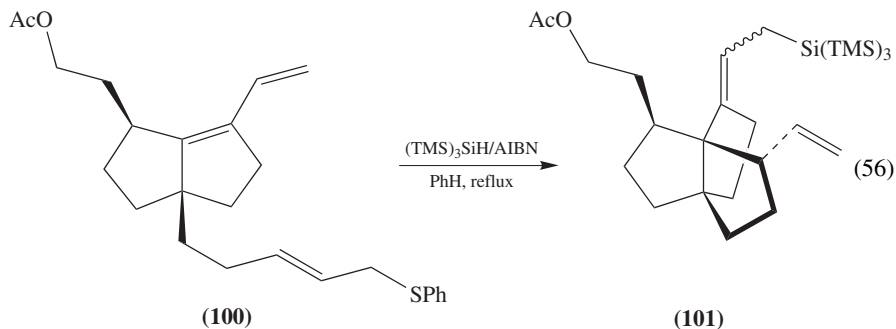


Radical reaction cascades can be initiated by $(\text{TMS})_3\text{Si}^{\bullet}$ radical addition to unsaturated bonds. Two recent examples are illustrated in equations 54 and 55. The reaction of $(\text{TMS})_3\text{SiH}$ with the 1,6-enyne derivative **98** afforded the 6-membered cyclic compound having exclusively the exocyclic double bond in *E* configuration via a 6-*exo* mode¹⁰⁶. On the other hand, hydrosilylation of **99** afforded the 6-membered ring via a 6-*endo* cyclization of the vinyl radical onto the C=N bond¹⁰⁷.

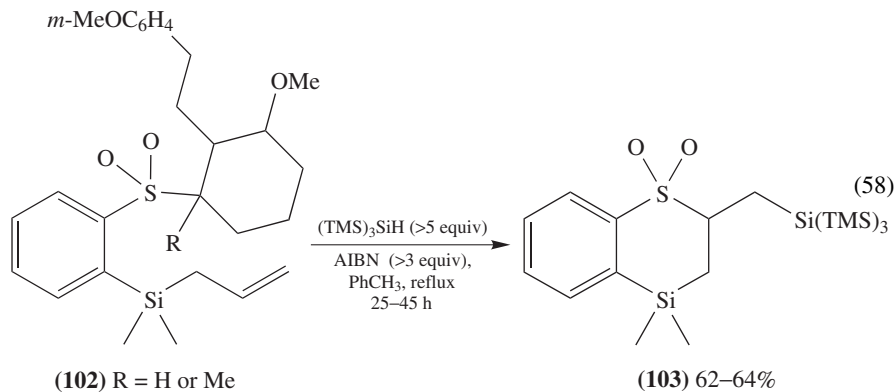


The addition of silyl radicals to conjugated dienes to form allylic-type radicals and their subsequent intramolecular addition to C=C double bonds has been investigated^{108,109}. Paquette and Usui provided a convenient route to triquinane **101** by exposure of **100** to $(\text{TMS})_3\text{SiH}$ and AIBN in refluxing toluene (equation 56). An unoptimized 51% yield was obtained¹⁰⁸. The addition of $(\text{TMS})_3\text{SiH}$ to substituted 1,5-dienes in the presence of CO has been studied by Ryu and coworkers¹¹⁰. An example is shown in equation 57. From

a mechanistic point of view, the initial addition of silyl radicals to the least substituted terminus is followed by carbonylation and acyl radical cyclization prior to hydrogen abstraction.



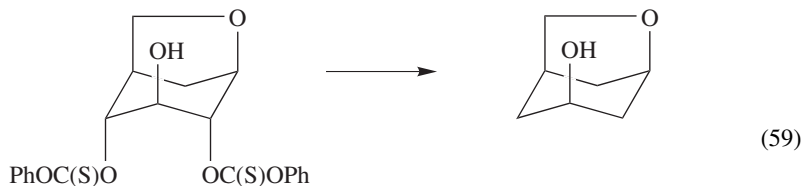
It has been reported that the reaction of **102** with $(\text{TMS})_3\text{SiH}$ affords the cyclic sulphone **103** (equation 58)¹¹¹. The authors have proposed an unusual mechanistic scheme for this reaction, equivalent to a reductive desulphonylation process. However, a simple chain reaction process cannot account for the large amount of $(\text{TMS})_3\text{SiH}$ and AIBN used and the prolonged reaction time (>20 h) required.



C. Other Silicon Hydrides

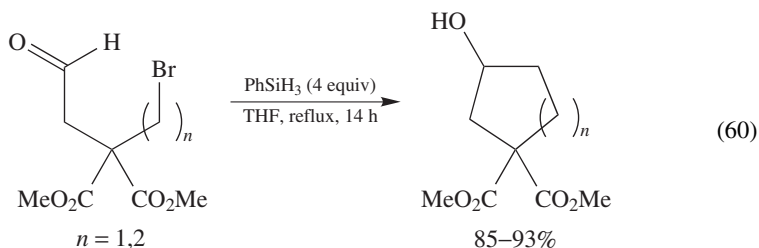
Following the success of $(\text{TMS})_3\text{SiH}$, other organosilanes capable of sustaining analogous radical chain reactions have been introduced¹¹². In Table 4 the reactivities of a variety of organosilanes towards primary alkyl radicals are reported. The rate constants cover a range of several orders of magnitude and therefore the hydrogen-donating abilities of organosilanes can be modulated by substituents.

Trialkylsilanes are unable to donate hydrogen atoms at a sufficient rate to propagate the chain. The forced reduction of thionoesters by Et_3SiH is not a common chain process^{113,114}. In fact, the attack of primary alkyl radicals on Et_3SiH occurs in about 60% of the cases at the SiH moiety and 40% at the ethyl groups at 130°C ¹¹⁴. Similar reactivities have been observed with other alkyl and/or phenyl substituted organosilanes having low hydrogen-donating abilities. Therefore, these organosilanes do not support chain reactions unless they are used at elevated temperatures and in the presence of large quantities of initiator¹¹⁵. A comparative example between Ph_2SiH_2 and $(\text{TMS})_3\text{SiH}$ is given in equation 59 for the dideoxygenation of 1,6-anhydro-D-glucose¹¹⁶.



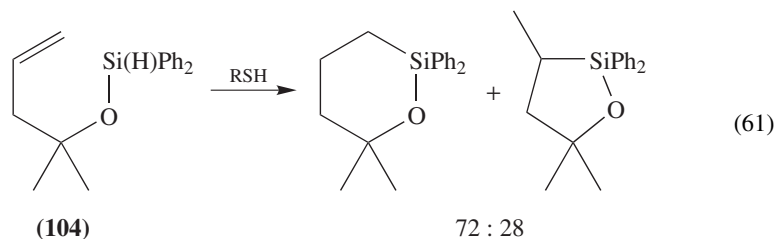
Ph_2SiH_2 (4 equiv), AIBN (100%), reflux, toluene, 100 min, yield 46%
 $(\text{TMS})_3\text{SiH}$ (2.2 equiv), AIBN (5%), reflux, toluene, 30 min, yield 87%

Batey and MacKay have taken advantage of the high reactivity of alkoxy radicals towards organosilanes which is 2–3 orders of magnitude higher than that of primary alkyl radicals, and achieved the cyclization of halocarbonyl compounds¹¹⁷. Two examples are shown in equation 60 using PhSiH_3 as mediator.

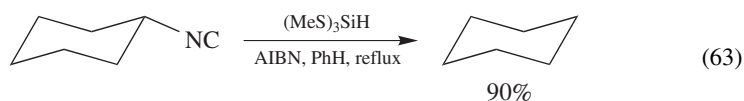
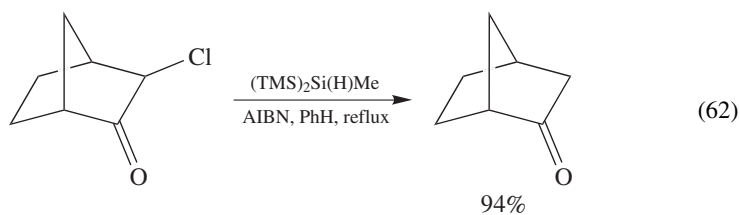


Roberts had reported that the low reactivity of alkyl and/or phenyl substituted organosilanes in the reduction processes can be ameliorated in the presence of a catalytic amount of alkanethiols (*vide supra*)⁴⁹. The general reaction mechanism (Scheme 11) shows that alkyl radicals abstract hydrogen atom from thiols and the resulting thiyl radicals abstract hydrogen from the silane. This procedure has been applied in dehalogenation, deoxygenation and desulfurization reactions. This approach has also been extended by the same

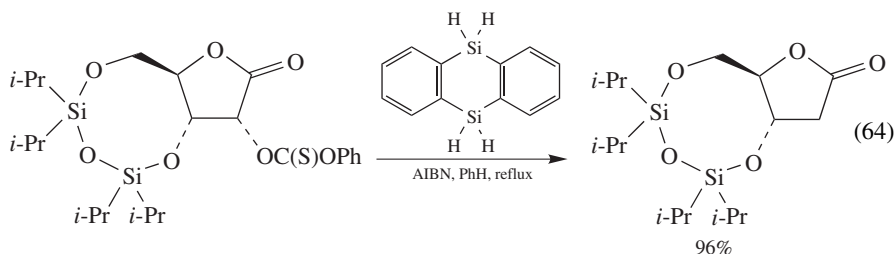
research group to hydrosilylation reactions. An intramolecular radical-chain hydrosilylation of homoallyloxysilane **104** afforded the expected cyclic products in a 72 : 28 mixture as the result of competitive 6-*endo* and 5-*exo* cyclizations (equation 61)¹¹⁸.

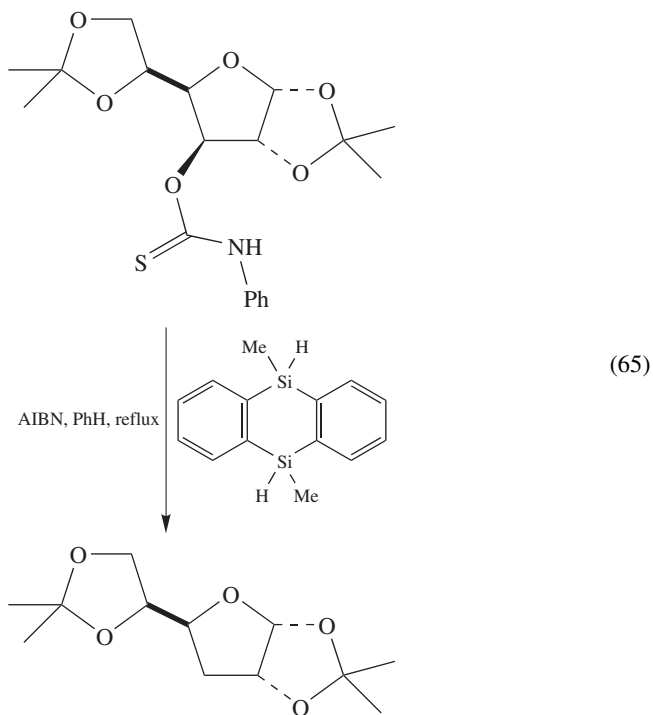


The reductions of organic halides, phenyl selenides, isocyanides and thionocarbonates with $(\text{TMS})_2\text{Si}(\text{H})\text{Me}$ ¹¹⁹ and $(\text{RS})_3\text{SiH}$ ¹²⁰ are achieved under normal conditions. Two examples are shown in equations 62 and 63. $(\text{TMS})_2\text{Si}(\text{H})\text{Me}$ is an effective reducing agent which allows the formation of the desired product to be favoured due to a slower hydrogen transfer (Table 4).

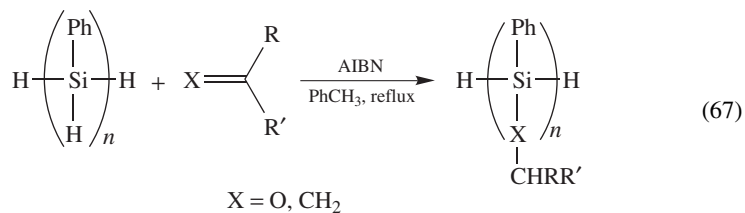
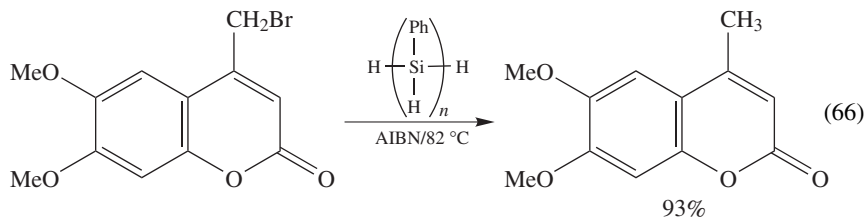


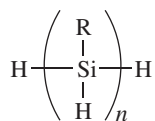
The introduction of silanthzenes as the alternative silanes for the reduction of halides and thionocarbonates has been proposed^{121,122}. Two examples are given in equations 64 and 65. The rate constants for hydrogen abstraction from these substrates depend on the number of available hydrogens and can reach values as high as those for $(\text{TMS})_3\text{SiH}$ (Table 4).





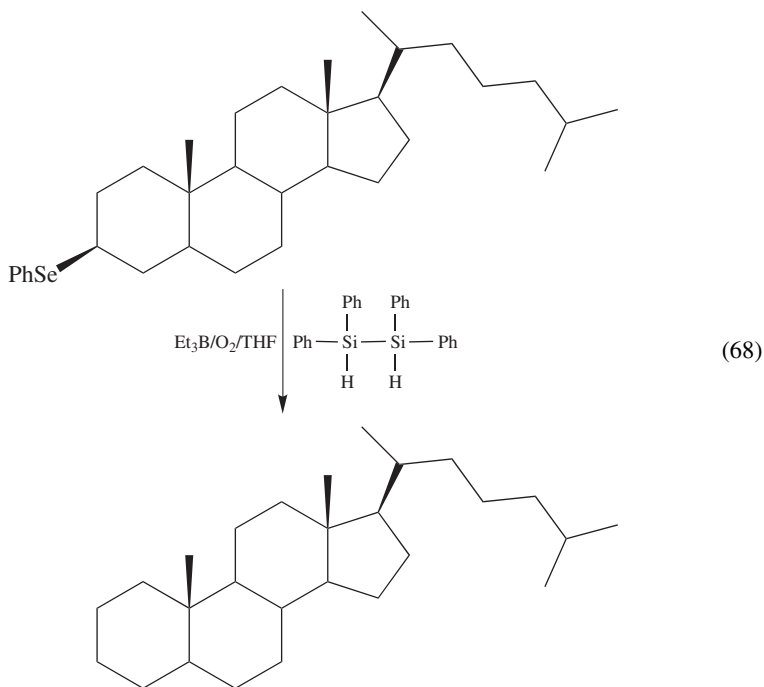
Polysilanes of type **105** have been used as radical-based reducing agents for organic halides¹⁹. The reduction of a bromide is given as an example in equation 66. The hydrosilylation of these polysilanes with unsaturated compounds allows the synthesis of functional polysilanes¹²³. Equation 67 depicts the general reaction with suitable substrates including terminal alkenes, ketones and aldehydes. The efficiency of the Si–H bond replacement varies from 70 to 90%.





(105) R = alkyl or phenyl

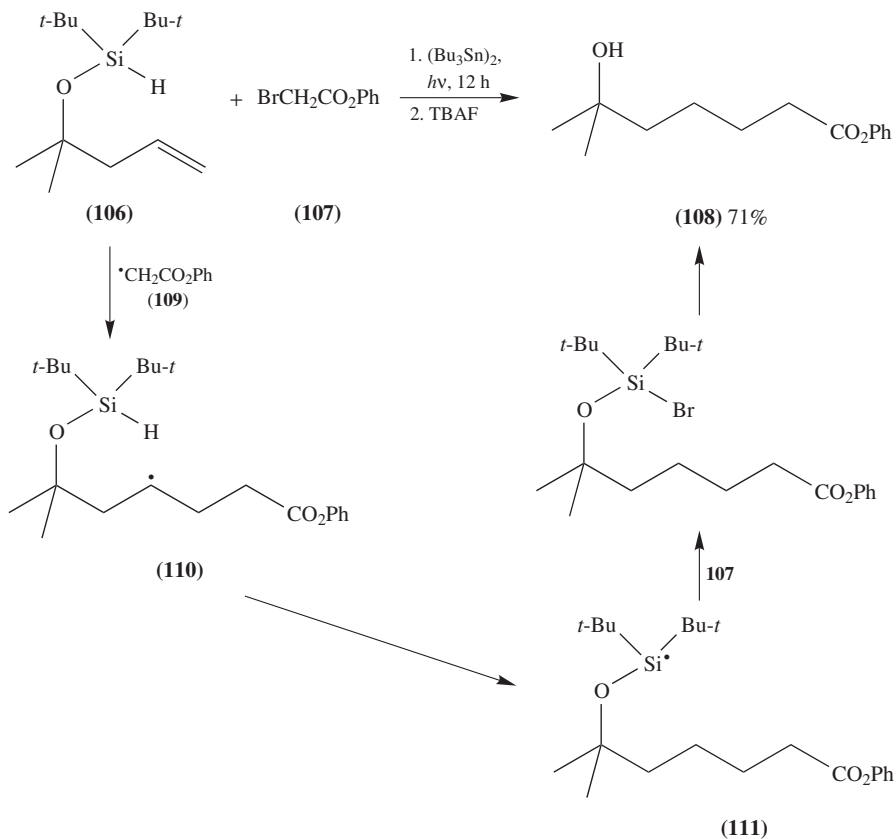
1,1,2-Tetraphenyldisilane has also been introduced as a diversified radical reagent for the reduction of alkyl bromides and phenyl chalcogenides¹²⁴. An example with 3-cholestanyl phenyl selenide is given in equation 68.



Intramolecular hydrogen abstraction by alkyl radicals from the Si–H moiety has been reported as a key step in several unimolecular chain transfer reactions¹²⁵. An example is given in Scheme 16, where the reaction of silane **106** with bromide **107** affords the hydroxy ester **108** in 71% yield. In particular, the initially generated radical **109** adds to silane **106**, providing radical **110** which undergoes an intramolecular hydrogen transfer reaction to give the silyl radical **111**. Bromine abstraction from **107** completes the cycle of radical chain reactions and the desilylation step affords the final product **108**.

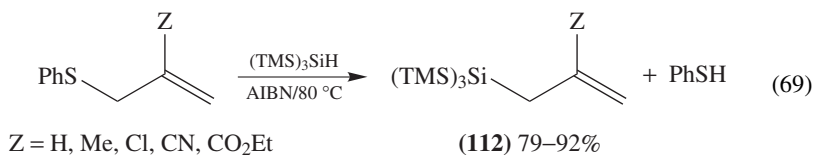
D. Allylations

Reactions of unsubstituted and 2-substituted allyl phenyl sulphides with (TMS)₃SiH provided the corresponding allyl tris(trimethylsilyl)silanes (**112**) in high yields



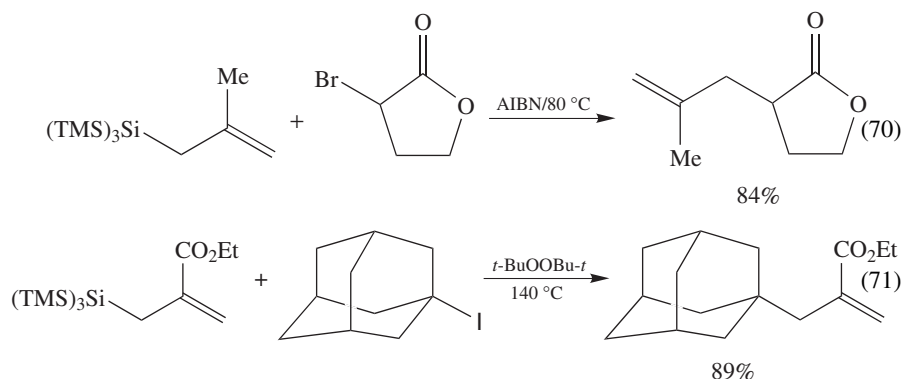
SCHEME 16

(equation 69)¹²⁶. That is, $(\text{TMS})_3\text{Si}^\bullet$ radical adds to the double bond giving rise to a radical intermediate that undergoes β -scission with the ejection of a thiyl radical. Hydrogen abstraction from the silane completes the cycle of these chain reactions. The same silanes **112** can be obtained from the analogous allyl phenyl sulphones in yields of 45–82%¹²⁶.

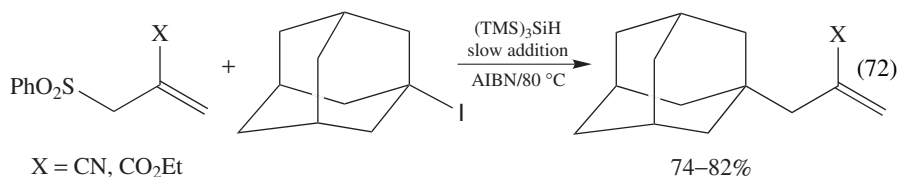


Radical allylations with allylsilanes **112** occur under mild conditions in good to excellent yields, provided that the radical precursor and the silane have the appropriate electronic pairing¹²⁷. The two examples in equations 70 and 71 show the reactivity

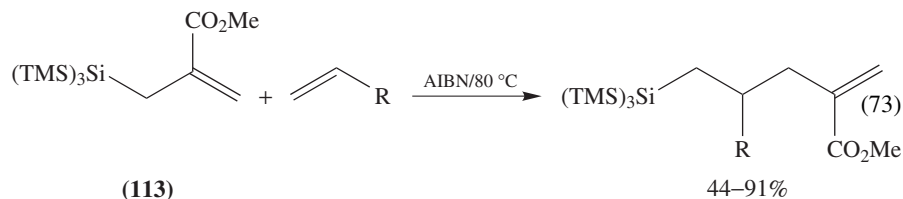
matching of the allylating agent with the radical. These reactions offer tin-free alternatives for the transformations that are currently carried out by allyl stannanes.

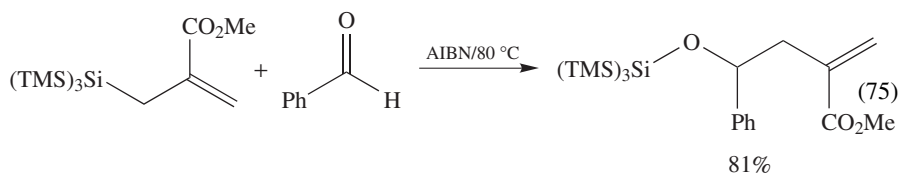
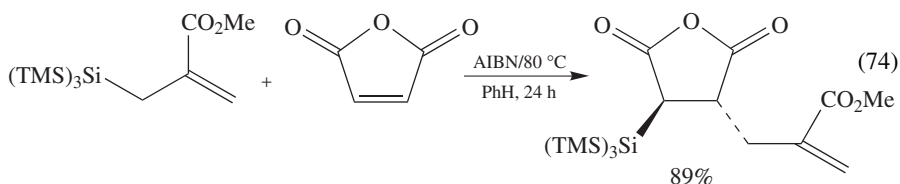


Radical allylation with 2-functionalized allyl phenyl sulphones have been performed using $(\text{TMS})_3\text{SiH}$ as the radical mediator¹²⁸. Yields varied from moderate to good depending on the nature of the starting materials. Two examples are given in equation 72. The reaction proceeds via addition of the adamantyl radical to the double bond, giving rise to an intermediate that undergoes β -scission to form PhSO_2^\bullet radical which abstracts hydrogen from the silane to regenerate the $(\text{TMS})_3\text{Si}^\bullet$ radical.



Hosomi and coworkers have successfully applied allylsilanes in allylsilylation procedures of carbon–carbon and carbon–oxygen double bonds under free radical conditions¹²⁹. For example, the reaction of **113** with a variety of monosubstituted alkenes (R = CN, CO_2Me , Ph, $n\text{-C}_8\text{H}_{17}$, OBU, SPh) gives the corresponding allylsilylated products in moderate to very good yields (equation 73). These reactions were found to be highly regioselective. Examples of high stereoselectivity have also been observed with dimethyl maleate and maleic anhydride (equation 74). Similar experiments were performed by replacing the alkene by alkynes with the formation of bisallylic derivatives¹²⁹. This allylsilylation methodology is also applicable to carbonyl derivatives, as shown in equation 75¹²⁹.





IV. REFERENCES

1. C. Chatgililoglu, *Chem. Rev.*, **95**, 1229 (1995).
2. C. Chatgililoglu, *Acc. Chem. Res.*, **25**, 188 (1992).
3. C. Chatgililoglu, C. Ferreri and T. Gimisis, in *The Chemistry of Organic Silicon Compounds*, Vol. 2 (Eds. Z. Rappoport and Y. Apeloig), Wiley, Chichester, 1997, pp. 1539–1579.
4. C. Chatgililoglu and M. Newcomb, *Adv. Organomet. Chem.*, **44**, 67 (1999).
5. M. Guerra, *J. Am. Chem. Soc.*, **115**, 11926 (1993).
6. S. Kyushin, T. Shinnai, T. Kubota and H. Matsumoto, *Organometallics*, **16**, 3800 (1997).
7. (a) C. H. Schiesser and S. Zahirovic, *J. Chem. Soc., Perkin Trans. 2*, 933 (1999).
(b) C. H. Schiesser and S. Zahirovic, personal communication.
8. (a) D. Dakternieks, D. J. Henry and C. H. Schiesser, *J. Chem. Soc., Perkin Trans. 2*, 591 (1998).
(b) D. Dakternieks, D. J. Henry and C. H. Schiesser, *J. Chem. Soc., Perkin Trans. 2*, 1665 (1997).
9. F. M. Bickelhaupt, T. Ziegler and P. v. R. Schleyer, *Organometallics*, **15**, 1477 (1996).
10. (a) M. Horn, M. Oswald, R. Oswald and P. Botschwina, *Ber. Bunsenges. Phys. Chem.*, **99**, 323 (1995).
(b) For further details, see: P. Botschwina and M. Oswald, *J. Chem. Phys.*, **96**, 4044 (1992).
11. (a) S. Kyushin, H. Sakurai, T. Betsuyaku and H. Matsumoto, *Organometallics*, **16**, 5386 (1997).
(b) S. Kyushin, H. Sakurai and H. Matsumoto, *Chem. Lett.*, 107 (1998).
(c) M. Kira, T. Obata, I. Kon, H. Hashimoto, M. Ichinohe, H. Sakurai, S. Kyushin and H. Matsumoto, *Chem. Lett.*, 1097 (1998).
12. (a) M. Guerra, *J. Chem. Soc., Perkin Trans. 2*, 1817 (1995).
(b) M. Guerra, *Pure Appl. Chem.*, **67**, 797 (1995).
(c) M. Guerra, *Chem. Phys. Lett.*, **246**, 251 (1995).
13. S. P. Karna, *J. Comput. Chem.*, **20**, 1274 (1999). For further information on the Bloembergen effect, see: S. P. Karna, *J. Quantum Chem.*, **70**, 771 (1998).
14. V. Q. Nguyen, S. A. Shaffer, F. Turecek and C. E. C. A. Hop, *J. Phys. Chem.*, **99**, 15454 (1995).
15. C. Chatgililoglu, V. I. Timokhin, A. B. Zaborovskiy, D. S. Lutsyl and R. E. Prystansky, *J. Chem. Soc., Perkin Trans 2*, 577 (2000); C. Chatgililoglu, V. I. Timokhin, A. B. Zaborovskiy, D. S. Lutsyl and R. E. Prystansky, *Chem. Commun.*, 405 (1999).
16. M. Lucarini, E. Marchesi, G. F. Pedulli and C. Chatgililoglu, *J. Org. Chem.*, **63**, 1687 (1998).
17. A. B. Shtarev, W. R. Dolbier, Jr. and B. E. Smart, *J. Am. Chem. Soc.*, **121**, 2110 (1999).
18. S. Seki, S. Tagawa, K. Ishigure, K. R. Cromack and A. D. Trifunac, *Radiat. Phys. Chem.*, **47**, 217 (1996).
19. C. Chatgililoglu, C. Ferreri, D. Vecchi, M. Lucarini and G. F. Pedulli, *J. Organomet. Chem.*, **545/546**, 455 (1997).
20. S. Seki, S. Tsuji, K. Nishida, Y. Matsui, Y. Yoshida and S. Tagawa, *Chem. Lett.*, 1187 (1998).

21. (a) G. Maier, A. Kratt, A. Schick, H. P. Reisenauer, F. Barbosa and G. Gescheidt, *Eur. J. Org. Chem.*, 1107 (2000).
(b) S. Wu, Y. Luo, F. Liu and S. Chen, *J. Heteroatom Chem.*, **7**, 45 (1996).
22. J. B. Lambert, X. Liu, H. Wu and J. L. Pflug, *J. Chem. Soc., Perkin Trans. 2*, 2747 (1999).
23. I. Lein, C. Kerst, N. L. Arthur and P. Potzinger, *J. Chem. Soc., Faraday Trans.*, **94**, 2315 (1998).
24. I. Borthwick, L. C. Baldwin, M. Sulkes and M. J. Fink, *Organometallics*, **19**, 139 (2000).
25. A. Matsumoto and Y. Ito, *J. Org. Chem.*, **65**, 624 (2000).
26. S. Shuto, I. Sugimoto, H. Abe and A. Matsuda, *J. Am. Chem. Soc.*, **122**, 1343 (2000).
27. C. H. Schiesser and L. M. Wild, *Tetrahedron*, **52**, 13265 (1996).
28. A. Studer, M. Bossart and H. Steen, *Tetrahedron Lett.*, **39**, 8829 (1998).
29. (a) A. Studer and H. Steen, *Chem. Eur. J.*, **5**, 759 (1999).
(b) A. Studer, M. Bossart and T. Vasella, *Org. Lett.*, **2**, 985 (2000).
30. M. Kako and Y. Nakadaira, *Coord. Chem. Rev.*, **176**, 87 (1998).
31. Y. Murakami, M. Koshi, H. Matsui, K. Kamiya and H. Umeyama, *J. Phys. Chem.*, **100**, 17501 (1996).
32. C. Chatgililoglu, A. Guerrini, M. Lucarini, G. F. Pedulli, P. Carrozza, G. Da Roit, V. Borzatta and V. Lucchini, *Organometallics*, **17**, 2169 (1998).
33. X.-K. Jiang, W. F.-X. Ding and Y.-H. Zhang, *Tetrahedron*, **53**, 8479 (1997).
34. P. F. McGarry and J. C. Scaiano, *Can. J. Chem.*, **76**, 1474 (1998).
35. K. B. Wiberg, S. T. Wadell and R. E. Rosenberg, *J. Am. Chem. Soc.*, **112**, 2184 (1990).
36. T. Kusukawa, K. Ohkubo and W. Ando, *Organometallics*, **16**, 2746 (1997).
37. T. Kusukawa and W. Ando, *Organometallics*, **16**, 4027 (1997).
38. K. Kusukawa and W. Ando, *J. Organomet. Chem.*, **559**, 11 (1998).
39. T. Akasaka, T. Suzuki, Y. Maeda, M. Ara, T. Wakahara, K. Kobayashi, S. Nagase, M. Kako, Y. Nakadaira, M. Fujitsuka and O. Ito, *J. Org. Chem.*, **64**, 566 (1999).
40. C. H. Schiesser, B. A. Smart and T.-A. Tran, *Tetrahedron*, **51**, 3327 (1995).
41. C. H. Schiesser and B. A. Smart, *Tetrahedron*, **51**, 6051 (1995).
42. A. Bottoni, *J. Phys. Chem., A*, **102**, 10142 (1998).
43. C. H. Schiesser and M. A. Skidmore, *J. Organomet. Chem.*, **552**, 145 (1998).
44. S. M. Horvat and C. H. Schiesser, *Organometallics*, **19**, 1239 (2000).
45. C. H. Schiesser and M. L. Styles, *J. Chem. Soc., Perkin Trans. 2*, 2335 (1997).
46. A. A. Zavitsas and C. Chatgililoglu, *J. Am. Chem. Soc.*, **117**, 10645 (1995); A. A. Zavitsas, *J. Chem. Soc., Perkin Trans. 2*, 391 (1996).
47. B. P. Roberts and A. J. Steel, *J. Chem. Soc., Perkin Trans. 2*, 2155 (1994).
48. S. J. Cole, J. N. Kirwan, B. P. Roberts and C. R. Willis, *J. Chem. Soc., Perkin Trans. 2*, 103 (1991).
49. B. P. Roberts, *Chem. Soc., Rev.*, **28**, 25 (1999) and references cited therein.
50. B. P. Roberts, *J. Chem. Soc., Perkin Trans. 2*, 2719 (1996).
51. D. Dakternieks, D. J. Henry and C. H. Schiesser, *Organometallics*, **17**, 1079 (1998).
52. M. A. Ring, M. J. Puentes and H. E. O'Neal, *J. Am. Chem. Soc.*, **92**, 4845 (1970).
53. A. A. Zavitsas, *J. Chem. Soc., Perkin Trans. 2*, 499 (1998).
54. C. H. Schiesser and M. A. Skidmore, *J. Chem. Soc., Perkin Trans. 2*, 2329 (1998).
55. M. A. Skidmore, PhD thesis, The University of Melbourne (2000).
56. A. Bottoni, *J. Phys. Chem., A*, **101**, 4402 (1997).
57. A. E. Lozano, A. Alonso, F. Catalina and C. Peinado, *Macromol. Theory Simul.*, **8**, 93 (1999).
58. K. Sung and T. T. Tidwell, *J. Org. Chem.*, **63**, 9690 (1998).
59. E. T. Denisov, *Russ. Chem. Bull.*, **47**, 1274 (1998).
60. Y. Sakurai, H. Shiozaki and M. Yokoyama, *Chem. Lett.*, 883 (1999).
61. For examples, see: (a) M. Malacria, *Chem. Rev.*, **96**, 289 (1996).
(b) I. Ryu, N. Sonoda and D. P. Curran, *Chem. Rev.*, **96**, 177 (1996).
62. B. Giese, *Radicals in Organic Synthesis: Formation of Carbon-Carbon Bonds*, Pergamon Press, Oxford, 1986.
63. W. B. Motherwell and D. Crich, *Free Radical Chain Reactions in Organic Synthesis*, Academic Press, London, 1992.
64. D. P. Curran, N. A. Porter and B. Giese, *Stereochemistry of Radical Reactions*, VCH, Weinheim, 1995.
65. D. P. Curran, *Synthesis*, 417 and 489 (1988).

66. D. P. Curran, in *Comprehensive Organic Synthesis* (Eds. B. M. Trost and I. Fleming), Vol. 4, Pergamon Press, Oxford, 1991, pp. 715–831.
67. For examples, see: C. Chatgililoglu and P. Renaud, in *General Aspects of the Chemistry of Radicals* (Ed. Z. B. Alfassi), Wiley, Chichester, 1999, pp. 501–538.
68. L. J. J. Laarhoven, P. Mulder and D. D. M. Wayner, *Acc. Chem. Res.*, **32**, 342 (1999).
69. C. Chatgililoglu, C. Costantino, C. Ferreri, T. Gimisis, A. Romagnoli and R. Romeo, *Nucleosides Nucleotides*, **18**, 637 (1999).
70. C. Chatgililoglu and T. Gimisis, *Chem. Commun.*, 1249 (1998).
71. E. Kawashima, S. Uchida, M. Miyahara and Y. Ishido, *Tetrahedron Lett.*, **38**, 7369 (1997).
72. Y. Apeloig and M. Nakash, *J. Am. Chem. Soc.*, **116**, 10781 (1994).
73. E. Lee, C. M. Park and J. S. Yun, *J. Am. Chem. Soc.*, **117**, 8017 (1995).
74. F. Villar, O. Andrey and P. Renaud, *Tetrahedron Lett.*, **40**, 3375 (1999).
75. T. Gimisis, G. Ialongo, M. Zamboni and C. Chatgililoglu, *Tetrahedron Lett.*, **36**, 6781 (1995).
76. C. Chatgililoglu, T. Gimisis and G. P. Spada, *Chem. Eur. J.*, **5**, 2866 (1999).
77. C. Chatgililoglu, C. Ferreri, M. Lucarini, P. Pedrielli and G. F. Pedulli, *Organometallics*, **14**, 2672 (1995).
78. B. Alcaide, A. Rodriguez-Vicente and M. A. Sierra, *Tetrahedron Lett.*, **39**, 163 (1998).
79. J. Quirante, C. Escolano and J. Bonjock, *Synlett*, 179 (1997).
80. A. García de Viedma, V. Martínez-Barrasa, C. Burgos, M. Luisa Izquierdo and J. Alvarez-Builla, *J. Org. Chem.*, **64**, 1007 (1999).
81. B. Delouvrié, E. Lacôte, L. Fensterbank and M. Malacria, *Tetrahedron Lett.*, **40**, 3565 (1999).
82. B. Kopping, C. Chatgililoglu, M. Zehnder and B. Giese, *J. Org. Chem.*, **57**, 3994 (1992).
83. (a) K. J. Kulicic and B. Giese, *Synlett*, 91 (1990).
(b) A. Alberti and C. Chatgililoglu, *Tetrahedron*, **46**, 3963 (1990).
84. (a) M. A. Brook, C. Gottardo, S. Balduzzi and M. Mohamed, *Tetrahedron Lett.*, **38**, 6997 (1997).
(b) M. A. Brook, S. Balduzzi, M. Mohamed and C. Gottardo, *Tetrahedron*, **55**, 10027 (1999).
85. H. Urabe, K. Kobayashi and F. Sato, *J. Chem. Soc., Chem. Commun.*, 1043 (1995).
86. (a) H.-D. Junker, N. Phung and W.-D. Fessner, *Tetrahedron Lett.*, **40**, 7063 (1999).
(b) H.-D. Junker and W.-D. Fessner, *Tetrahedron Lett.*, **39**, 269 (1998).
87. J. Martin, L. M. Jaramillo and P. G. Wang, *Tetrahedron Lett.*, **39**, 5927 (1998).
88. I. Ryu, M. Hasegawa, A. Kurihara, A. Ogawa, S. Tsunoi and N. Sonoda, *Synlett*, 143 (1993).
89. M. Zahouily, M. Journet and M. Malacria, *Synlett*, 366 (1994).
90. J. Marco-Contelles and M. Rodríguez-Fernández, *Tetrahedron Lett.*, **41**, 381 (2000).
91. W. Zhang and G. Pugh, *Tetrahedron Lett.*, **40**, 7591 (1999).
92. (a) W. Zhang and G. Pugh, *Tetrahedron Lett.*, **40**, 7595 (1999).
(b) W. Zhang, *Tetrahedron Lett.*, **41**, 2523 (2000).
93. (a) M. Ikeda, M. Hamada, T. Yamashita, K. Matsui, T. Sato and H. Ishibashi, *J. Chem. Soc., Perkin Trans. 1*, 1949 (1999).
(b) M. Ikeda, M. Hamada, T. Yamashita, F. Ikegami, T. Sato and H. Ishibashi, *Synlett*, 1246 (1998).
94. J. H. Rigby, S. Laurent, A. Cavezza and M. J. Heeg, *J. Org. Chem.*, **63**, 5587 (1998).
95. S. Usui and L. A. Paquette, *Tetrahedron Lett.*, **40**, 3495 (1999).
96. J. Quirante, C. Escolano, F. Diaba and J. Bonjoch, *J. Chem. Soc., Perkin Trans. 1*, 1157 (1999).
97. P. A. Evans and T. Manangan, *Tetrahedron Lett.*, **38**, 8165 (1997).
98. P. A. Evans and J. D. Roseman, *J. Org. Chem.*, **61**, 2252 (1996).
99. (a) P. A. Evans, J. D. Roseman and L. T. Garber, *J. Org. Chem.*, **61**, 4880 (1996).
(b) P. A. Evans and J. D. Roseman, *Tetrahedron Lett.*, **38**, 5249 (1997).
100. C. Chatgililoglu, C. Ferreri, M. Lucarini, A. Venturini and A. A. Zavitsas, *Chem. Eur. J.*, **3**, 376 (1997); C. Chatgililoglu, V. I. Timokhin and M. Ballestri, *J. Org. Chem.*, **63**, 1327 (1998).
101. K. Takasu, J. Kuroyanagi, A. Katsumata and M. Ihara, *Tetrahedron Lett.*, **40**, 6277 (1999).
102. M. Kizil, B. Patro, O. Callaghan, J. A. Murphy, M. B. Hursthouse and D. Hibbs, *J. Org. Chem.*, **64**, 7856 (1999).
103. B. P. Haney and D. P. Curran, *J. Org. Chem.*, **65**, 2007 (2000).
104. G. Pattenden and P. Wiedenau, *Tetrahedron Lett.*, **38**, 3647 (1997).

105. K. Nagahara, I. Ryu, H. Yamazaki, N. Kambe, M. Komatsu, N. Sonoda and A. Bada, *Tetrahedron*, **53**, 14615 (1997).
106. R. Moreno-Fuquen, L. M. Jaramillo-Gómez and J. Martín-Franco, *Acta Crystallogr.*, **C55**, 630 (1999).
107. I. Ryu, S. Ogura, S. Minakata and M. Komatsu, *Tetrahedron Lett.*, **40**, 1515 (1999).
108. L. A. Paquette and S. Usui, *Tetrahedron Lett.*, **40**, 3499 (1999).
109. N. E. Restrepo-Sánchez, F. J. Gómez, L. M. Jaramillo-Gómez and T. Hudlicky, *Synth. Commun.*, **29**, 2795 (1999).
110. I. Ryu, K. Nagahara, A. Kurihara, M. Komatsu and N. Sonoda, *J. Organomet. Chem.*, **548**, 105 (1997).
111. P. C. van Dort and P. L. Fuchs, *J. Org. Chem.*, **62**, 7142 (1997).
112. P. A. Baguley and J. C. Walton, *Angew. Chem., Int. Ed. Engl.*, **37**, 3072 (1998).
113. D. H. R. Barton, D. O. Jang and J. Cs. Jaszberenyi, *Tetrahedron Lett.*, **32**, 7187 (1991).
114. C. Chatgililoglu, C. Ferreri and M. Lucarini, *J. Org. Chem.*, **58**, 249 (1993).
115. For example, see: C. Chatgililoglu and C. Ferreri, *Res. Chem. Intermed.*, **19**, 755 (1993).
116. P. Bouquet, C. Loustau Cazalet, Y. Chapleur, S. Samreth and F. Bellamy, *Tetrahedron Lett.*, **33**, 1997 (1992).
117. R. A. Batey and D. B. MacKay, *Tetrahedron Lett.*, **39**, 7267 (1998).
118. Y. Cai and B. P. Roberts, *J. Chem. Soc., Perkin Trans. 1*, 467 (1998).
119. C. Chatgililoglu, A. Guerrini and M. Lucarini, *J. Org. Chem.*, **57**, 3405 (1992).
120. C. Chatgililoglu, M. Guerra, A. Guerrini, G. Seconi, K. B. Clark, D. Griller, J. Kanabus-Kaminska and J. A. Martinho-Simoes, *J. Org. Chem.*, **57**, 2427 (1992).
121. (a) T. Gimisis, M. Ballestri, C. Ferreri, C. Chatgililoglu, R. Boukherroub and G. Manuel, *Tetrahedron Lett.*, **36**, 3897 (1995).
(b) C. Chatgililoglu, V. I. Timokhin and M. Ballestri, *J. Org. Chem.*, **63**, 1327 (1998).
122. (a) M. Oba and K. Nishiyama, *Chem. Commun.*, 1703 (1994).
(b) M. Oba, Y. Kawahara, R. Yamada, H. Mizuta and K. Nishiyama, *J. Chem. Soc., Perkin Trans. 2*, 1843 (1996).
123. Y.-L. Hsiao and R. Waymouth, *J. Am. Chem. Soc.*, **116**, 9779 (1994).
124. O. Yamazaki, H. Togo, S. Matsubayashi and M. Yokoyama, *Tetrahedron Lett.*, **39**, 1921 (1998); O. Yamazaki, H. Togo and M. Yokoyama, *J. Chem. Soc., Perkin Trans. 1*, 2891 (1999).
125. D. P. Curran, J. Xu and E. Lazzarini, *J. Chem. Soc., Perkin Trans. 1*, 3049 (1995); D. P. Curran, J. Xu and E. Lazzarini, *J. Am. Chem. Soc.*, **117**, 6603 (1995).
126. C. Chatgililoglu, M. Ballestri, D. Vecchi and D. P. Curran, *Tetrahedron Lett.*, **37**, 6383 (1996).
127. C. Chatgililoglu, C. Ferreri, M. Ballestri and D. P. Curran, *Tetrahedron Lett.*, **37**, 6387 (1996).
128. C. Chatgililoglu, A. Alberti, M. Ballestri, D. Macciantelli and D. P. Curran, *Tetrahedron Lett.*, **37**, 6391 (1996).
129. K. Miura, H. Saito, T. Nakagawa, T. Hondo, J. Tateiwa, M. Sonoda and A. Hosomi, *J. Org. Chem.*, **63**, 5740 (1998).

CHAPTER 5

Recent advances in the chemistry of silicon–silicon multiple bonds

MANFRED WEIDENBRUCH

Fachbereich Chemie, Universität Oldenburg, D-26111 Oldenburg, Germany
Fax: 49(0)441-7983352; e-mail: Manfred.Weidenbruch@Uni-Oldenburg.de

I. ABBREVIATIONS	391
II. INTRODUCTION	392
III. ACYCLIC DISILENES	392
A. Preparation	392
B. Molecular Structures	396
C. Spectroscopy	399
D. Reactions	400
1. Addition reactions	401
2. Formation of disiliranes	402
3. Other cycloadditions	405
4. Oxidation reactions	411
IV. TETRASILABUTA-1,3-DIENE	414
V. CYCLIC DISILENES	417
A. Preparation	417
B. Molecular Structures and Spectroscopy	419
C. Reactions	420
VI. DISILYNES	421
VII. CONCLUSION	423
VIII. ACKNOWLEDGMENTS	423
IX. REFERENCES	424

I. ABBREVIATIONS

Ad = 1-adamantyl
Dep = 2,6-diethylphenyl
Dis = bis(trimethylsilyl)methyl
Dmt = 4-*tert*-butyl-2,6-dimethylphenyl
m-CPBA = *meta*-chloroperbenzoic acid

Mes = 2,4,6-trimethylphenyl (mesityl)

Tbt = 2,4,6-tris[bis(trimethylsilyl)methyl]phenyl

Xyl = 2,6-dimethylphenyl (o-xylyl)

II. INTRODUCTION

Since the isolation of the first, thermally stable molecular compound containing a silicon–silicon double bond in 1981¹, the chemistry of the disilenes has experienced an explosive development as reflected in the many review articles published in the meantime^{2–6}. Several novel classes of compounds that are only accessible with difficulty by other routes have become readily available with the use of disilenes as starting materials.

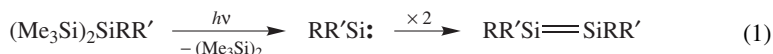
The rapid expansion of our knowledge in this field is illustrated exemplarily by the ever increasing number of known and structurally characterized disilenes. Up to 1987 only three such molecules were known^{2,3}, while up to 1995 this number had increased to eleven⁶. Since then the number has doubled again due to the synthesis of a tetrasilabutadiene and the first compounds with endocyclic Si=Si double bonds. Okazaki and West⁶ concluded the most recent and most comprehensive review article on this topic, published in 1996, with the comment: ‘At this time, although details remain to be elucidated, it seems that most of the main modes of reaction of disilenes have been discovered.’ In harmony with this opinion the only review on the reactivity of disilenes in Volume 2 of *The Chemistry of Organic Silicon Compounds* published in 1998 is principally concerned with a detailed investigation of the addition reactions of alcohols and phenols to Si=Si double bonds⁷. On the other hand, the syntheses of molecules containing endocyclic Si=Si double bonds as well as of a tetrasilabutadiene realized, successfully for the first time in the past few years, have revealed that the formation of fundamentally new classes of compounds, the chemistry of which has mostly not yet been fully uncovered, is still possible.

Accordingly, emphasis in this chapter is placed mainly on the more recent developments. Even so, for completeness the numerous pioneering studies in this field have not been neglected but rather are discussed briefly, even though they have already been summarized in numerous review articles. The literature up to the end of 1999 has been covered although no claim for completeness is made, especially with regard to the older publications.

III. ACYCLIC DISILENES

A. Preparation

Photolysis of acyclic trisilanes leads in a first step to the extrusion of a silylene which, in the presence of sufficient shielding by its substituents, undergoes dimerization to furnish a thermally stable disilene (equation 1). This strategy led not only to the first isolated disilene¹, but is still the most frequently used method to prepare compounds of this type.

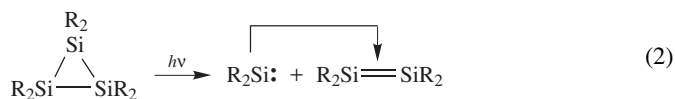


A prerequisite for the success of this reaction, however, is that one of the substituents R or R' is an aryl group. Although the photolytic generation of silylenes from 2-aryltrisilanes has been known for a long time^{8–10} and has been discussed in several reviews^{11–16}, the actual course of the reaction was the subject of controversy for some time. By means of photophysical and photochemical studies on 2,2-diphenylhexamethyltrisilane as an example, Kira and coworkers demonstrated that, among the competing processes of Si–Si bond homolysis, 1,3-silyl shift, and silylene extrusion, the latter process proceeds through

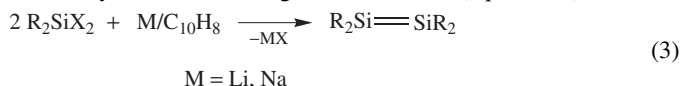
the 1L_a state of the trisilane. Since the 1L_a state involves the contribution of the $\sigma\sigma^*$ state of the Si–Si σ system due to hyperconjugation between the σ and σ^* orbitals and the aromatic π orbitals, the low-lying doubly excited state, which is responsible for the silylene extrusion, may be produced adiabatically¹⁷.

The photolysis of trisilanes makes possible the formation of homo- and heteroleptic tetraaryldisilenes as well as 1,2-diaryldisilenes that may have alkyl, silyl or even amino groups as substituents. The heteroleptic disilenes formed in this way are usually obtained as mixtures of the *E*- and *Z*-isomers which can be isolated as pure compounds after fractional crystallization and/or can be converted thermally or photochemically to the other isomer.

An alternative method for the preparation of disilenes involves the photolysis of cyclo-trisilanes¹⁸ in which a disilene and a silylene are formed simultaneously through cleavage of two Si–Si bonds. The latter species undergoes dimerization to furnish the corresponding disilene (equation 2).

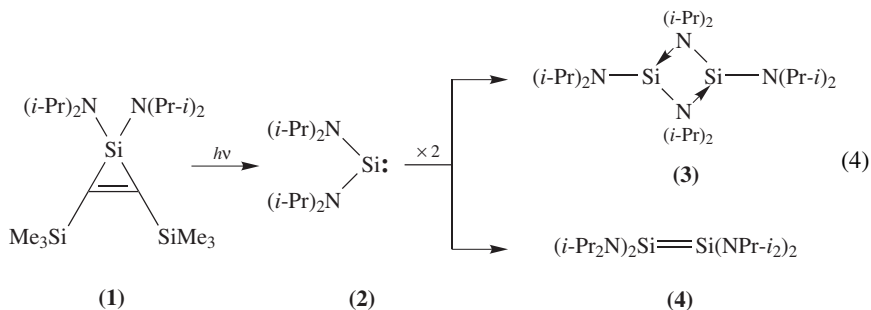


The first cyclotrisilane was prepared by Masamune and coworkers in 1982 by reductive dehalogenation of a diaryldichlorosilane and it was then transformed photochemically to the corresponding disilene¹⁹. Although aryl-, alkyl- and even silyl-substituted disilenes are accessible by this method, its use is subject to restrictions since larger rings are formed with smaller organic groups as substituents whereas in the presence of very large groups the disilenes are formed directly from the dehalogenation reaction (equation 3)^{4,18}.



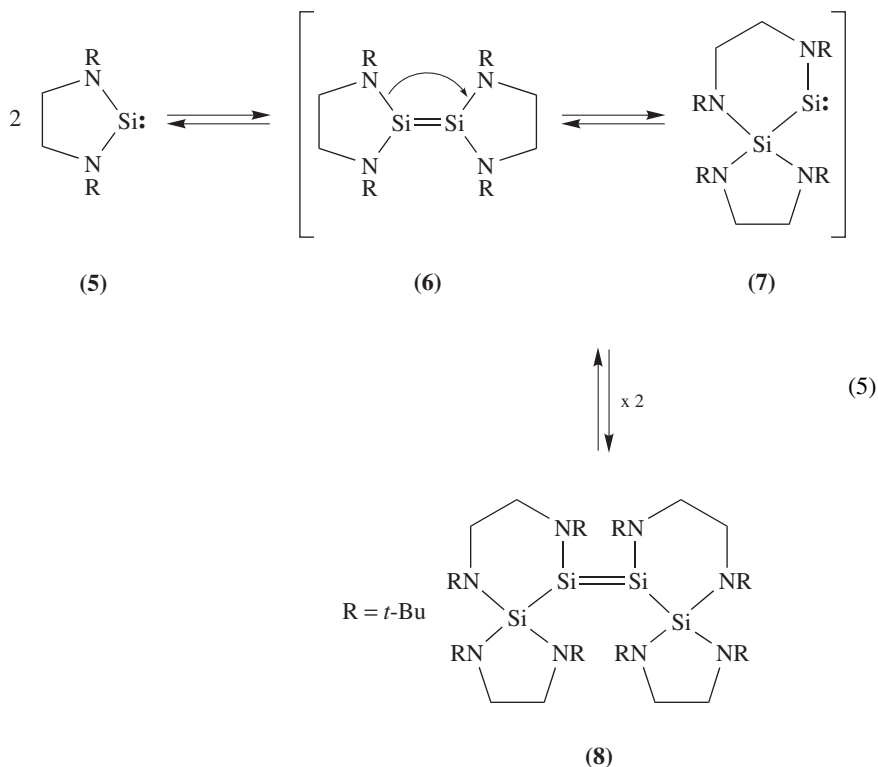
The as yet only known tetraalkyldisilene $\text{R}_2\text{Si}=\text{SiR}_2$, R = CH(SiMe₃)₂, was also prepared by this method²⁰. The elimination of halogen from 1,2-dichlorosilanes offers a potential alternative to the dehalogenation of dichlorosilanes, but this method has only been successful for the syntheses of $\text{Tip}_2\text{Si}=\text{SiTip}_2$ (Tip = 2,4,6-*i*-Pr₃C₆H₂)²¹ and the unsymmetrically substituted disilene $\text{Tip}_2\text{Si}=\text{SiMes}_2$ (Mes = 2,4,6-Me₃C₆H₂)²².

Of the more specialized methods for the formation of acyclic disilenes, two new methods deserve mention. Kira and coworkers reported that photolysis of the silirene **1** afforded the diaminosilylene **2**²³. In contrast to theoretical predictions^{24–27}, the silylene **2** apparently does not undergo dimerization to afford the bridged dimer **3** as is usually preferred in the presence of electronegative substituents but rather, according to the results of variable-temperature electronic spectroscopy, furnishes the disilene **4** (equation 4)²³.



More recent theoretical calculations show that **4** is a viable molecule but that it is better described not as a Si=Si doubly bonded species but as a weak adduct between two silylene species with a very long Si–Si distance of 2.472 Å²⁷.

A loose adduct of the type **6** of two marginally stable diaminosilylenes **5** could possibly be a precursor of the aminosilylsilylene **7** which, in the solid state, is obtained in the form of red crystals of the disilene **8** (equation 5)²⁸. In this case also, theoretical calculations for **5**, R = H, Me, predict that a nitrogen-bridged dimer of the type **3** should be more stable than the putative intermediate **6**, which is predicted not to exist²⁶. Actually, that **6** is not observed but **8** is, is fully consistent with the theoretical expectations, as **8** has only two amino substituents attached to the Si=Si bond. Actually, the theoretically calculated geometry of **8** is in excellent agreement with the experimental structure²⁸.



Surprisingly, a dynamic equilibrium exists between the silylene **5** and the disilene **8** as has been demonstrated by ²⁹Si NMR spectroscopy and trapping reactions with methanol. An analogous reaction of **5** with a germylene possessing the same substitution pattern also gave in the case of R = *t*-Bu a *Z*-diaminodisilyldigermene analogous to the disilene **8** which exhibits a very long Ge=Ge double bond and a very large *trans*-bent angle^{29–31}.

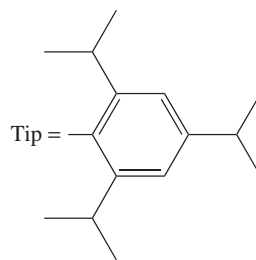
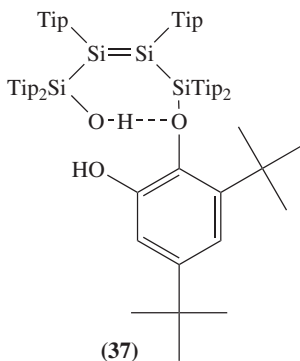
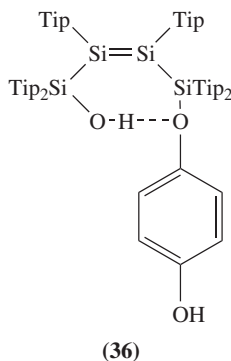
Table 1 summarizes the currently known, thermally stable acyclic disilenes.

Compound **8**²⁸ and two other disilenes **36** and **37**, formed by the reaction of the tetrasilabutadiene (see later) with quinones in the presence of water^{43,47}, also belong to this group.

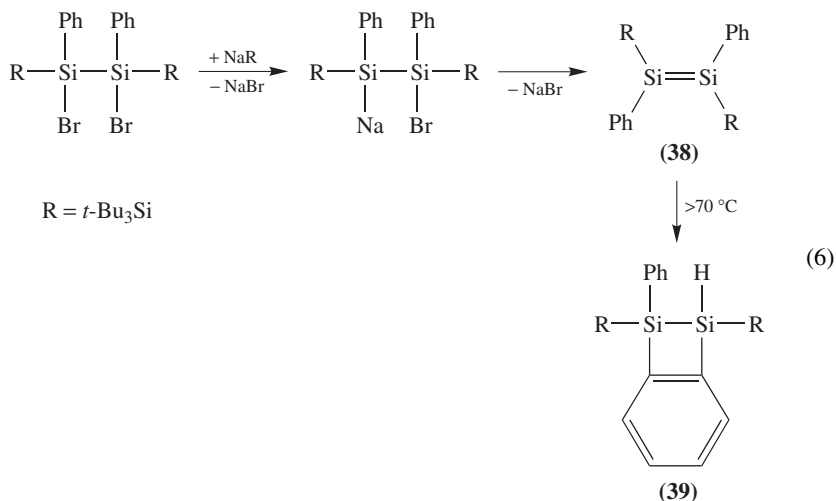
TABLE 1. Thermally stable acyclic disilenes $R^1R^2Si=SiR^3R^4$

Compound	R^1	R^2	R^3	R^4	References
9	Mes	Mes	Mes	Mes	1, 32
10	2,6-Me ₂ C ₆ H ₃	2,6-Me ₂ C ₆ H ₃	2,6-Me ₂ C ₆ H ₃	2,6-Me ₂ C ₆ H ₃	19
11	2,6-Et ₂ C ₆ H ₃	2,6-Et ₂ C ₆ H ₃	2,6-Et ₂ C ₆ H ₃	2,6-Et ₂ C ₆ H ₃	33, 34
12	2,4,6-Et ₃ C ₆ H ₂	2,4,6-Et ₃ C ₆ H ₂	2,4,6-Et ₃ C ₆ H ₂	2,4,6-Et ₃ C ₆ H ₂	35
13	Tip	Tip	Tip	Tip	21, 36, 37
14	Dmt	Dmt	Dmt	Dmt	38
15	Dis	Dis	Dis	Dis	20
16	<i>t</i> -BuMe ₂ Si	<i>t</i> -BuMe ₂ Si	<i>t</i> -BuMe ₂ Si	<i>t</i> -BuMe ₂ Si	39
17	<i>i</i> -Pr ₂ MeSi	<i>i</i> -Pr ₂ MeSi	<i>i</i> -Pr ₂ MeSi	<i>i</i> -Pr ₂ MeSi	39
18	<i>i</i> -Pr ₃ Si	<i>i</i> -Pr ₃ Si	<i>i</i> -Pr ₃ Si	<i>i</i> -Pr ₃ Si	39
<i>E</i> - 19	<i>t</i> -Bu	Mes	<i>t</i> -Bu	Mes	32
<i>Z</i> - 19	<i>t</i> -Bu	Mes	Mes	<i>t</i> -Bu	40
<i>E</i> - 20	Ad	Mes	Mes	Ad	41
<i>Z</i> - 20	Ad	Mes	Ad	Mes	41
<i>E</i> - 21	Mes	2,6-Me ₂ C ₆ H ₃	2,6-Me ₂ C ₆ H ₃	Mes	38
<i>Z</i> - 21	Mes	2,6-Me ₂ C ₆ H ₃	Mes	2,6-Me ₂ C ₆ H ₃	38
<i>E</i> - 22	Mes	Dmt	Dmt	Mes	38
<i>Z</i> - 22	Mes	Dmt	Mes	Dmt	38
<i>E</i> - 23	Mes	N(SiMe ₃) ₂	N(SiMe ₃) ₂	Mes	40
<i>Z</i> - 23	Mes	N(SiMe ₃) ₂	Mes	N(SiMe ₃) ₂	40
<i>E</i> - 24	Mes	Tip	Tip	Mes	37
<i>Z</i> - 24	Mes	Tip	Mes	Tip	37
<i>E</i> - 25	Tip	SiMe ₃	SiMe ₃	Tip	42
<i>Z</i> - 25	Tip	SiMe ₃	Tip	SiMe ₃	42
<i>E</i> - 26	Tip	<i>t</i> -Bu	<i>t</i> -Bu	Tip	42
<i>Z</i> - 26	Tip	<i>t</i> -Bu	Tip	<i>t</i> -Bu	42
27	Mes	Mes	2,6-Me ₂ C ₆ H ₃	2,6-Me ₂ C ₆ H ₃	38
28	Mes	Mes	Dmt	Dmt	38
29	Mes	Mes	Tip	Tip	22, 37
30	Mes	Mes	2,6-Me ₂ C ₆ H ₃	Mes	38
31	2,6-Me ₂ C ₆ H ₃	2,6-Me ₂ C ₆ H ₃	Dmt	2,6-Me ₂ C ₆ H ₃	38
32	2,6-Me ₂ C ₆ H ₃	2,6-Me ₂ C ₆ H ₃	Dmt	Dmt	38
<i>E</i> - 33	2,6-Et ₂ C ₆ H ₃	Mes	Mes	2,6-Et ₂ C ₆ H ₃	44
<i>Z</i> - 33	2,6-Et ₂ C ₆ H ₃	Mes	2,6-Et ₂ C ₆ H ₃	Mes	44
<i>E</i> - 34	2,6- <i>i</i> -Pr ₂ C ₆ H ₃	Mes	Mes	2,6- <i>i</i> -Pr ₂ C ₆ H ₃	44
<i>Z</i> - 34	2,6- <i>i</i> -Pr ₂ C ₆ H ₃	Mes	2,6- <i>i</i> -Pr ₂ C ₆ H ₃	Mes	44
<i>E</i> - 35	Mes	Tbt	Tbt	Mes	45, 46
<i>Z</i> - 35	Mes	Tbt	Mes	Tbt	45, 46

^a Ad = 1-adamantyl; Dis = bis(trimethylsilyl)methyl; Dmt = 4-*tert*-butyl-2,6-dimethylphenyl; Mes = 2,4,6-trimethylphenyl; Tbt = 2,4,6-tris[bis(trimethylsilyl)methyl]phenyl; Tip = 2,4,6-triisopropylphenyl

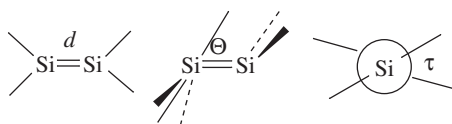


An additional arylsilyldisilene, **38**, which is stable up to 70 °C, is obtained from a 1, 2-dihalodisilane by metallation and subsequent elimination of NaBr. At higher temperatures it undergoes isomerization to the isomeric disilacyclobutene derivative **39** (equation 6)⁴⁸.



B. Molecular Structures

The molecular structures of eleven acyclic disilenes are described in detail in two recent review articles covering the literature up to about the middle of 1995^{6,49a}. The number of known compounds has doubled in the subsequent few years^{49b}. These new, structurally characterized disilenes include not only a tetrasilabutadiene and the first molecules with an endocyclic Si=Si double bond, described in separate sections, but also some acyclic disilenes and, in particular, the unusual compound **8**. Thus, another brief survey of all the known molecular structures of disilenes reported through the end of 1999 seems to be justified.



Characteristic features of the structures of disilenes are the lengths of the Si=Si double bond d , the *trans*-bent angle Θ and the twist angle τ . In contrast to the C=C double bonds of sterically crowded alkenes in which variations of the bond lengths are small, the Si=Si bond lengths of disilenes vary between 2.14 Å and 2.29 Å (Table 2). The percent bond shortening is markedly less than that found on going from ethane (1.54 Å) to ethene (1.33 Å) but is more pronounced than in homonuclear multiple bonds between the heavier elements of group 14. In the case of lead, the formal double bond may even be longer than the corresponding single bonds^{52,53}.

A further peculiarity of the disilenes, not observed in the alkenes, is the possibility for *trans*-bending of the substituents, which is described by the *trans*-bent angle Θ between the R₂Si planes and the Si-Si vector. This effect which, especially for double bonds

TABLE 2. Bond lengths and angles in acyclic disilenes

Compound	$d(\text{Si}=\text{Si})$ (Å) ^a	Θ (deg) ^a	τ (deg) ^a	References
8	2.289(1)	32.3, 33.8	25.1	28
9	2.143	13	3	49
9 •toluene	2.160(1)	18	12	32
9 •THF	2.146	0	13	50
11	2.140(3)	0.8	9.7	33
12	2.143(1)	6.8, 13.6	10.9	35
13	2.144	0	3	36
16	2.202(1)	0.1	8.9	39
17	2.228(2)	5.4	0	39
18	2.251(1)	10.2	0	39
<i>E</i> - 19	2.143(1)	0	0	32
<i>E</i> - 20	2.138(2)	2.8	0	41
<i>E</i> - 25	2.152(3)	0	0	42
<i>E</i> - 26	2.157(2)	0	0	42
<i>E</i> - 35 •C ₁₀ H ₈	2.228(2)	9.4, 14.6	8.7	45, 46
<i>Z</i> - 35	2.195(4)	7.6, 9.8	14	46
36	2.220(1)	2.2, 2.7	17.7	43
37	2.220(1)	0.9	15.1	47
38	2.182(2)	4.5	0	48

^a d = Si=Si double bond length; Θ = *trans*-bent angle; τ = twist angle

between the heavier elements of group 14, can lead to *trans*-bent angles of up to 50°, can be rationalized as follows. Carbenes have either a triplet ground state (*T*) or a singlet ground state (*S*) with relatively low *S* → *T* transition energies. The familiar picture of a C=C double bond results from the approach of two triplet carbenes, as shown schematically in Figure 1a.

In contrast to carbenes, all silylenes, germylenes, stannylenes and plumblyenes characterized to date have exclusively singlet ground states, with the *S* → *T* energy gap increasing towards the heavier elements⁵⁴. Very recently, it was calculated that the goal of generating a triplet silylene might be achieved if both the electronic effect of electropositive groups R and the steric widening of the R–Si–R angle could be combined. It was predicted that (*t*-Bu₃Si)₂Si: has a triplet ground state multiplicity⁵⁵. However, it was found that the bulky substituted silylenes with *tert*-butyl, mesityl or 1-adamantyl groups were ground state singlets. Despite the theoretical predications of a triplet ground state for [(*i*-Pr₃Si)₂Si:]^{55a}, stereospecific addition of this molecule to *cis*- and *trans*-but-2-ene was observed^{55b}. Approach of two such singlet species should result in repulsion rather than in bond formation (Figure 1b). However, if the two electron sextet molecules are rotated with respect to one another (Figure 1c), interactions between the doubly-occupied s-type orbitals and the vacant p orbitals can also lead to the creation of a double bond which, in contrast to that in alkenes, arises by way of a double donor–acceptor adduct formation. This is accompanied by a *trans*-bending of the substituents about the E=E vector^{56–60}. While the *trans*-bending angle Θ increases appreciably on going to the heavier elements, most disilenes have a slightly *trans*-bent structure because of a flat potential energy surface for bending. Once again compound **8** is an exception and exhibits the largest *trans*-bent angle of approximately 33° observed so far in a disilene.

In addition to the *trans*-bending, a mutual twisting of the two SiR₂ planes can also occur, as reflected by the twist angle τ . As a result of this type of distortion, which has also been observed in alkenes with bulky substituents, close contacts between the usually voluminous groups are avoided.

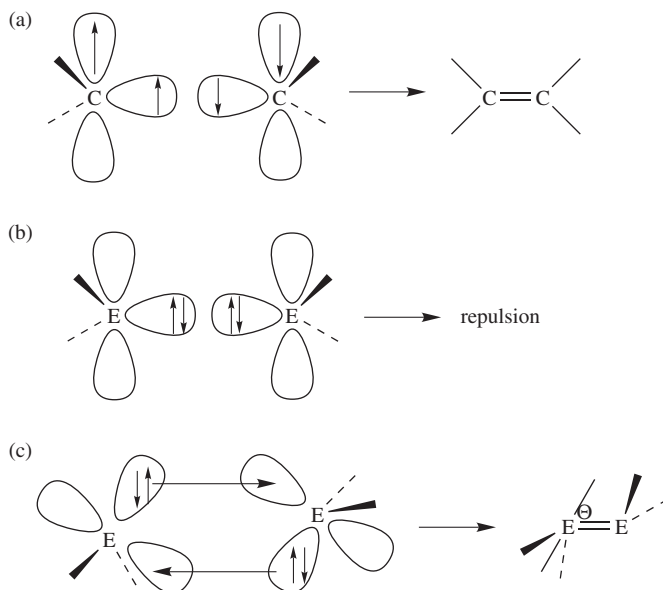


FIGURE 1. Double bond formation from two carbenes and their homologues

Three structurally characterized forms of the very first disilene, compound **9**, are known. In addition to the orange-colored, unsolvated crystals of **9**, a yellow toluene solvate and also a yellow THF solvate have been isolated⁵⁰. Although the separations between the centers of the Si=Si bond and the solvent molecules are too large for a coordinating interaction, all three forms exhibit different structures that manifest themselves less in the Si=Si double bond lengths and more in the markedly differing *trans*-bent and twist angles. Although, with the exception of the sterically overcrowded compounds *E*-**35** and *Z*-**35**, tetraaryldisilenes exhibit Si=Si double bond lengths between 2.14 and 2.16 Å, the corresponding bond lengths in the tetrasilyldisilenes **16**, **17** and **18** are on average 0.1 Å longer. On the other hand, calculations have predicted that the introduction of silyl groups in disilenes would result in a planar environment at the Si=Si double bond, as is observed in some cases, but would have hardly any effect on the bond length^{24a,61}. Another unusual feature is that the sterically more crowded *Z*-form of **35** has a shorter Si=Si double bond length than the *E*-form. In view of the flat energy potential surface of the disilenes, these variations are not really surprising and the most favorable conformation for the molecules is apparently the result of an interplay between bond lengths and the two angles Θ and τ .

The diaminodisilyldisilene **8** has a most unusual structure: it not only exhibits the longest Si=Si formal double bond length observed to date but also the largest *trans*-bent and twist angles. These structural parameters are probably attributable to the substitution patterns in **8**. Although the Si-Si bond in the intermediate **7** promotes the formation of an Si=Si double bond, the Si-N bond also present hinders electronically Si-Si contacts, with the overall result that the structural parameters described above represent a compromise between these opposing effects²⁸. It is important to note that theoretical calculations fully reproduce the experimentally determined structure of **8**²⁷.

C. Spectroscopy

Electron and ^{29}Si NMR spectroscopy, in particular, have provided valuable information for the description of the bonding in disilenes. In this section, only a few general principles and new developments are mentioned. The interested reader is referred to the comprehensive review published by Okazaki and West in 1996 for detailed information about the earlier work⁶.

The color of the stable disilenes in the solid state ranges from pale yellow to red and, in solution, it corresponds to absorptions at the longest wavelengths between 390 and 480 nm in the UV/VIS spectra. These absorptions are assigned in most cases to $3\pi-3\pi^*$ transitions. The variety of colors and the low transition energies clearly reveal that the energies are only about half as large as the corresponding energies for $2\pi-2\pi^*$ transitions of alkenes².

The longest wavelength absorptions of the tetraaryldisilenes occur in the region of 400–430 nm. The three tetrasilyldisilenes **16–18** also exhibit absorption bands between 412 and 425 nm that are attributed to $\pi \rightarrow \pi^*$ transitions. Disilene **18**, the sterically most heavily overcrowded compound, exhibits an additional absorption band at 480 nm. The surprising color change from yellow in the solid state to deep red in solution suggests that **18** adopts a twisted form in solution in order to reduce the steric strain³⁹.

The *Z*- and *E*-isomers of the diaminodiaryldisilenes **23** exhibit large bathochromic shifts with the absorption bands at the longest wavelength being in the region of 480 nm, similar to the *Z*-1,2-diamino-1,2-disilyldisilene **8**^{28,40}. This red shift is probably due to an interaction between the free electron pair at nitrogen and the Si=Si π -HOMO, with the latter being pushed to a higher energy⁶.

The thermochromic behavior, first observed for the classical disilene **9**, has also been found for other disilenes. Thus, the *Z*- and *E*-forms of **25** exhibit a darkening of their colors with increasing temperature. In the case of some of the tetrasilyldisilenes, this even occurs in solution at room temperature³⁹.

The ^{29}Si NMR chemical shifts, like the electron spectra, are characteristic for the disilenes and occur in the low field region between 50 and 155 ppm as a result of the coordination number 3. While the ^{29}Si NMR signals of the tetraaryldisilenes appear at about 60 ppm, those of the 1,2-diaryldisilyldisilenes are found at *ca* 100 ppm and those of the tetrasilyldisilenes at a low field of approximately 150 ppm.

According to theoretical calculations as well as the results of solid state ^{29}Si NMR spectroscopy (see below), this is mainly due to the lengthening of the Si=Si bond which, in turn, leads to a smaller overlap of not only the σ - but also the π -orbitals. This increases the energy of the Si–Si σ -orbital while lowering that of the Si–Si π^* -orbital.

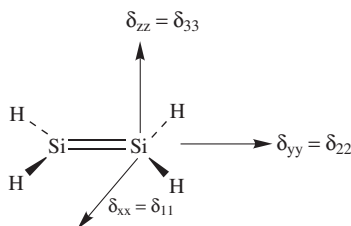
Some selected solution and solid state ^{29}Si NMR data of disilenes are presented in Table 3.

The ^{29}Si NMR chemical shift tensors accessible from solid state NMR spectra also provide important insights into the nature of the chemical bonds in disilenes. After the disilene **9**⁶² and some other disilenes⁶³ had been investigated by this method in earlier studies, West and coworkers recently reported the solid state NMR spectra of seven disilenes with widely differing substitution patterns as well as of two solvates of compound **9** (Table 3). These results in combination with MO calculations on model substances support a classical π -bonding model for the Si=Si bonds⁶⁴.

The orientations of the various tensors in the parent disilene are shown in Figure 2. Since the calculations show that *trans*-bending or twisting has only a small effect on the values of the tensors⁶⁴, the parent compound $\text{H}_2\text{Si}=\text{SiH}_2$ is shown for simplicity in the planar form.

TABLE 3. Solution and solid state ^{29}Si NMR spectral data of some disilenes⁶⁴

Compound	δ_{iso}		δ_{11}	δ_{22}	δ_{33}	$\Delta\delta$
	solution	solid state				
9	63.3	63.2	181	31	-22	203
9 •toluene	63.3	65.0	185	34	-22	207
9 •THF	63.0	59.6	165	40	-25	190
13	53.4	50.8(53.2)	155	30	-31	186
15	90.4	86.1	182	55	21	161
17	144.5	143	414	114	-100	514
18	154.5	164	412	149	-69	481
<i>E</i> - 19	90.3	86.1	178	77	3	175
<i>E</i> - 25	94.4	94.5	296	46	-59	355

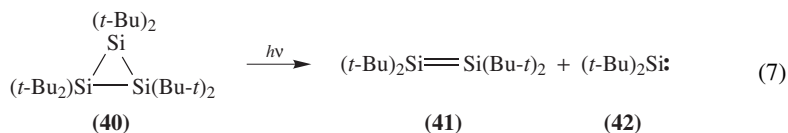
FIGURE 2. Orientation of the principal tensor components in the parent compound $\text{H}_2\text{Si}=\text{SiH}_2$

All disilenes investigated to date show a strong deshielding along the δ_{11} axis with extremely large values being attained by the tetrasilyldisilenes **17** and **18**. Together with the stronger shielding in the δ_{33} direction this gives rise to chemical shift anisotropy $\Delta\delta$ values ($\Delta\delta = \delta_{11} - \delta_{33}$) that are about a factor of two larger than all other values measured for ^{29}Si nuclei to date. These $\Delta\delta$ values thus show a trend similar to that seen when going from a C–C single bond to a C=C double bond. According to calculations the lengthening of the Si=Si bond is mainly responsible for the observed chemical shielding tensors while the twisting or pyramidalization has practically no influence⁶⁴. Thus, we may await with interest the determination of the chemical shielding tensors in the disilene **8** with its extremely long Si=Si bond.

The high anisotropy, $\Delta\delta$, of the chemical shielding tensors favors a description of the bonding in terms of a classical π -bond between two sp^2 -hybridized silicon atoms, that are only slightly influenced by the relatively small twisting or *trans*-bending of the substituents. These results are supported by the $^1J_{\text{Si},\text{Si}}$ coupling constants for unsymmetrically substituted tetraaryldisilenes of 155–160 Hz which are almost twice as large as those found for analogously substituted disilanes and thus also reflect the high s character of the Si=Si double bond²².

D. Reactions

The reactions of the tetraaryldisilene **9** and those of the marginally stable tetra-*tert*-butyldisilene **41** are the most thoroughly investigated. The latter compound, together with di-*tert*-butylsilylene **42**, is obtained most simply by photolysis of the cyclotrisilane **40**⁶⁵ (equation 7)⁶⁶.

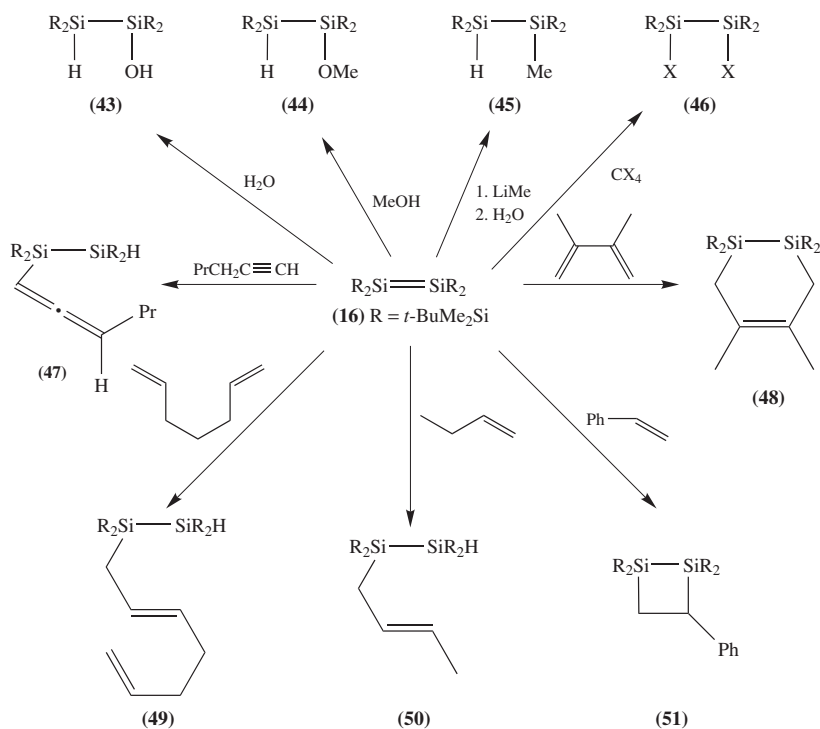


Many reactions of disilenes have already been described in the above-mentioned review articles^{2–6}. However, in order to present a relatively complete survey of current knowledge on the chemistry of disilenes, the older works will also be mentioned briefly while emphasis is placed on the more recently discovered modes of reaction.

1. Addition reactions

1,2-Additions of smaller molecules such as halogens or hydrogen halides to the Si=Si bond in **9** were among the first reactions of disilenes to be studied⁶⁷. Similarly, compounds with active hydrogen atoms such as alcohols and even water also react smoothly with this double bond system. Addition occurs with tributyltin hydride while lithium aluminum hydride effects hydrogenation of the Si=Si double bond⁶⁸. The course of the addition reaction of alcohols has been reviewed comprehensively elsewhere in this series⁷.

Kira and coworkers recently reported their extensive investigations on addition and cycloaddition reactions of the tetrasilyl disilene **16** and described not only expected reactions but also some surprising results⁶⁹. These reactions are summarized in Scheme 1.



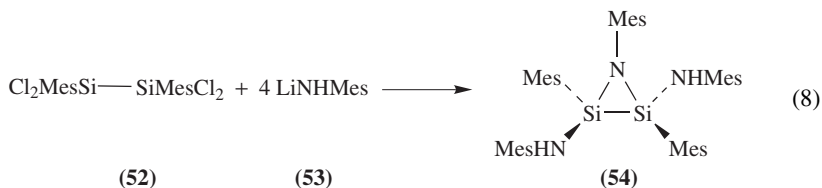
SCHEME 1. Some addition and cycloaddition reactions of disilene **16**

Although the reactions with water and methanol yield the expected 1,2-addition products **43** and **44**, the addition of methyl lithium to the Si=Si bond, which is expected to give the disilane **45** after subsequent hydrolysis, has not yet been observed. Haloalkanes react to furnish compounds **46** (X = Cl, Br). In contrast, those haloalkanes in which halide abstraction is impaired react to form the disilanes R₂R'Si–SiR₂X preferentially; this is also observed in the reactions of **9** with benzyl chloride and 2-chloro-2-methylpropane⁷⁰.

Ene addition products have been isolated from reactions with various alkenes containing allylic hydrogen atoms; compounds **49** and **50** are shown here as examples. Analogously, the reaction with a 1-alkyne furnishes the adduct **47** while styrene, in contrast, reacts to afford the [2 + 2] cycloaddition product **51**. The latter mode of reaction, however, is no longer considered to be unusual since the tetraalkyldisilene **41** also forms [2 + 2] cycloadducts with various C=C double bond systems^{71–73}. On the other hand, until very recently [2 + 2] cycloadditions of the tetraaryldisilene **9** were unknown. It has now been shown that **9**⁷⁰, as well as **41**⁷¹, can undergo cycloadditions with the C=C double bonds of styrene and 2-methylstyrene. [4 + 2] Cycloaddition reactions of disilenes with 1,3-dienes are still very rare. A first example of the latter process is the reaction of **41** with cyclopentadiene to yield the structurally characterized Diels–Alder product, albeit in low yield⁷⁴. The more strongly electrophilic disilene **16** reacts quantitatively with 1,3-dimethylbutadiene to afford the corresponding [4 + 2] adduct **48**⁶⁹.

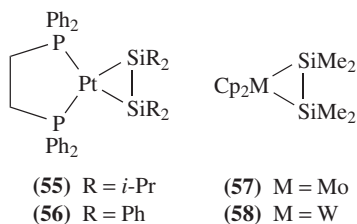
2. Formation of disiliranes

One of the most fascinating reaction modes of disilenes is the ready formation of disiliranes, three-membered ring systems containing two silicon atoms and one heteroatom in the ring, which are hardly accessible by other routes. They are mostly formed by [2 + 1] cycloadditions of atoms or molecular fragments to the Si=Si double bond. One of the few examples of other accesses to this ring system is the reaction of *N*-lithio-2,4,6-trimethylanilide **53** with the disilane **52**, which affords the azadisilacyclopropane **54** in modest yield (equation 8)⁷⁵.

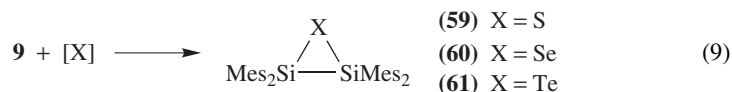


Similar to other disiliranes with electronegative atoms in the ring, the Si–Si bond length in **54** is short [2.288(1) Å] and the environments about the two silicon atoms with the exocyclic substituents and the other silicon are almost planar having angular sums of 359.4^{o75}.

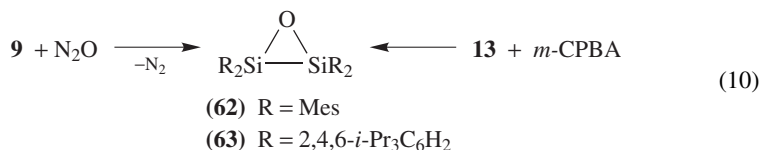
The transition metal derivatives **55–58** were also obtained by other methods and the structure of compound **58** has been determined by X-ray crystallography^{76,77}.



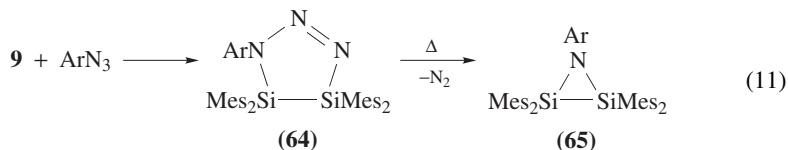
On the other hand, typical [2 + 1] cycloaddition reactions occur on treatment of disilene **9** with the heavier chalcogens^{78,79} or, in the case of sulfur, also with thiiranes^{80,81} (equation 9).



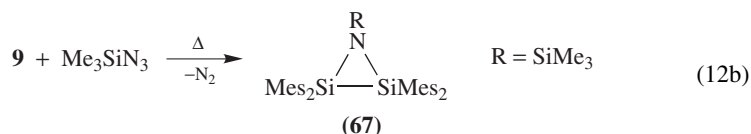
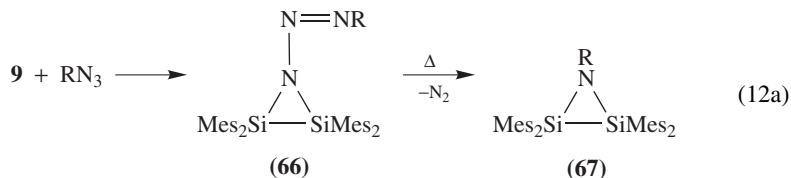
The disilaoxiranes **62**^{82,83} and **63**⁸⁴ are readily accessible from the disilenes **9** and **13** respectively, by reaction with N₂O or *meta*-chloroperbenzoic acid (*m*-CPBA). The absence of a reaction between N₂O and the highly shielded disilene **13** suggests that the formation of **62** probably involves a [2 + 3] addition of N₂O to the Si=Si bond with subsequent elimination of nitrogen (equation 10).



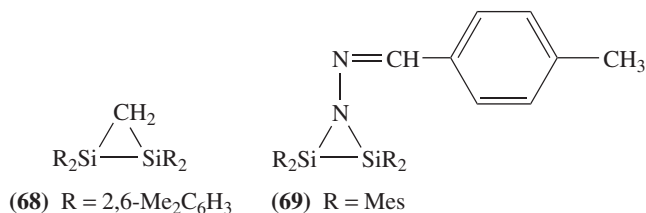
In the reactions of **9** with aromatic azides, the primarily occurring [2 + 3] cycloaddition to afford the disilatriazolines **64** has been confirmed; on heating, nitrogen is eliminated from **64** to afford the azadisilacyclopropanes **65** (equation 11)⁸⁵.



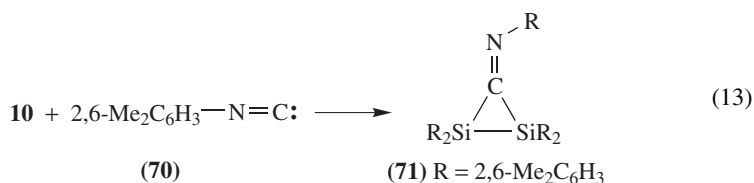
In contrast, aliphatic azides (R = PhCH₂, Me₃SiCH₂) seem to participate in an initial [2 + 1] cycloaddition to give **66**, from which nitrogen is subsequently eliminated to leave the three-membered ring system **67** (equation 12a). The reaction of **9** with trimethylsilyl azide furnishes an azadisilacyclopropane of the type **67** as the only isolated product (equation 12b)⁸⁵.



The reactions of disilenes with diazomethane derivatives are similarly inhomogeneous. While the reaction of diazomethane with the disilene **10** provides the disilirane **68**⁸⁶, that between *p*-tolyl diazomethane and **9** yields the compound **69**⁸⁷.



The reaction of 2,6-dimethylphenyl isocyanide **70** with the disilene **10** gives the disilacyclopropane imine **71**⁸⁸, the unusually bright red color of which was the subject of an intensive theoretical investigation (equation 13)⁸⁹.



As mentioned above, the structures of the disilranes (listed in Table 4), especially those containing heteroatoms that are both strongly electronegative and relatively small, exhibit some conspicuous features.

In spite of the presence of usually bulky substituents at the silicon atoms, the Si–Si bond lengths are dramatically shortened and approach those of disilenes. This bond shortening is accompanied by a planar or almost planar arrangement of the substituents R¹, R² and the other silicon atom about each silicon atom. Such a geometrical arrangement resembles the bonding situation in transition metal-olefin complexes which, according to the model

TABLE 4. Selected structural parameters for disilranes (R¹R²Si)₂X

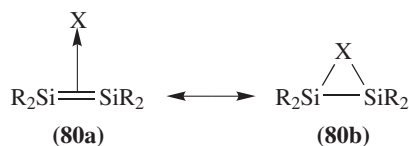
Compound	R ¹	R ²	X	d(Si–Si) (Å)	∑ ∠ ^a (deg)	Reference
68	2,6-Me ₂ C ₆ H ₃	2,6-Me ₂ C ₆ H ₃	CH ₂	2.272	357.5	86
72	Mes	Mes	C=C<	2.327		90
71	2,6-Me ₂ C ₆ H ₃	2,6-Me ₂ C ₆ H ₃	C=NR	2.328		88
73	Me ₃ Si	Me ₃ Si	Ge(SiMe ₃) ₂	2.377		91
74	Mes	Mes	NSiMe ₃	2.232	358	85
75	Mes	Mes	As–As<	2.315		92
62	Mes	Mes	O	2.227	360	82
63	Tip	Tip	O	2.254	359.7	84
79	2,6-Et ₂ C ₆ H ₃	c	O	2.214	359.8	93
76	<i>t</i> -Bu	<i>t</i> -Bu	S	2.305	358.7	74
59	Mes	Mes	S	2.289	357.4	78
<i>trans</i> - 77	<i>t</i> -Bu	Mes	S	2.270	357.1	81
<i>cis</i> - 78	<i>t</i> -Bu	Tip	S	2.318	359 ^b	81
<i>trans</i> - 78	<i>t</i> -Bu	Tip	S	2.294	354.4	81
60	Mes	Mes	Se	2.303	355.8 ^b	79
61	Mes	Mes	Te	2.337	355.5 ^b	79

^a ∑ ∠ = ∠R¹–Si–R² + ∠R¹–Si–Si + ∠R²–Si–Si.

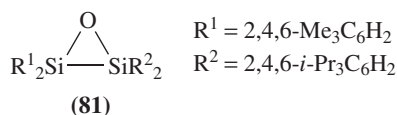
^b Average value.

^c R² = 2,6-Et₂-4-*t*-BuC₆H₂; Mes = 2,4,6-trimethylphenyl, Tip = 2,4,6-triisopropylphenyl

of Dewar, Chatt and Duncanson^{94,95} exist in a continuum between three-membered rings and π -complexes. In harmony with this model, short Si–Si bond lengths and an almost planar environment of the silicon atoms should reflect the bonding situation presented in **80a** while longer Si–Si bonds and a pyramidalization of the substituents suggest a major contribution of the classical three-membered ring structure **80b**.



Indirect evidence for the validity of this assumption is provided by the structure [$d(\text{Si}-\text{Si})=2.229(1) \text{ \AA}$, $\sum \angle 359.9^\circ$], and especially the $^1J_{\text{Si},\text{Si}}$ coupling constant of the disilaoxirane **81** derived from the unsymmetrically substituted disilene **29**⁹⁶. With a $^1J_{\text{Si},\text{Si}}$ value of 123 Hz, this coupling constant is appreciably larger than those observed for other disilanes with a similar substitution pattern (85 Hz) and approaches the value of 160 Hz for the disilene **29**.



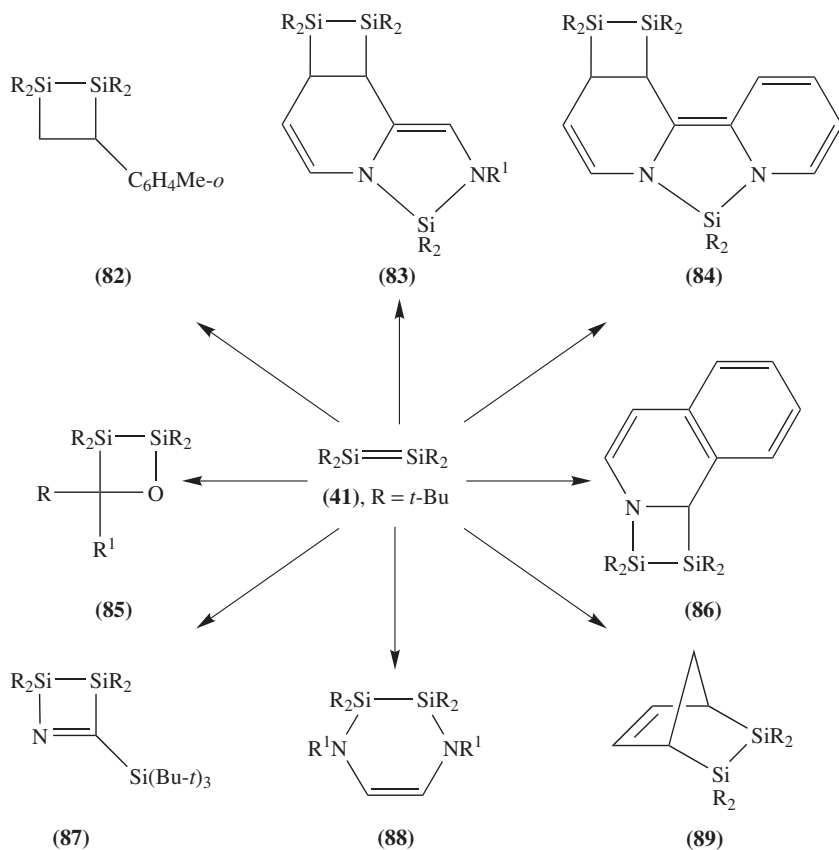
The bonding of transition metal fragments to a silicon surface can also be described with the Dewar–Chatt–Duncanson model. There is a striking similarity between the reactivity of the Si(100) surface and that of disilene (Si_2H_4)⁹⁷.

Irrespective of whether the bonding situation in the disiliranes is best represented by a partial π -character^{98,99}, as indicated in **80a**, or rather by an extremely arched Si=Si bond¹⁰⁰, the disiliranes—mostly derived from disilenes—constitute an interesting class of compounds with unusual properties.

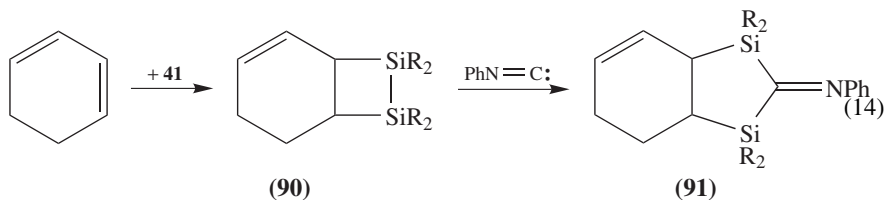
3. Other cycloadditions

Disilenes react with numerous unsaturated compounds to afford [2 + 2] cycloadducts. These reaction partners include homo- and heteronuclear double bond systems as well as the triple bonds of cyanides or unsymmetrically substituted acetylenes. Cycloadditions also occur with cumulated multiple bond systems but are often accompanied by subsequent reactions. Although confirmed [2 + 3] cycloadditions are still rather rare, a larger number of the corresponding [2 + 4] cycloaddition products are known. Since disilenes often behave similarly to highly strained, electron-rich olefins; they preferentially undergo Diels–Alder reactions with inverse electron demand¹⁰¹. Suitable reaction partners include, for example, 1,2-diketones, α -ketoimines, *o*-quinones⁹⁶ or 1,4-diazabutadienes. On the other hand, there have been very few reports on reactions with 1,3-dienes. Although a cycloadduct was obtained in low yield from **41** and 2,3-dimethylbutadiene in 1983¹⁰², structurally characterized compounds of this type were isolated for the first time just recently. Some cycloaddition reactions of disilene **41** are summarized in Scheme 2.

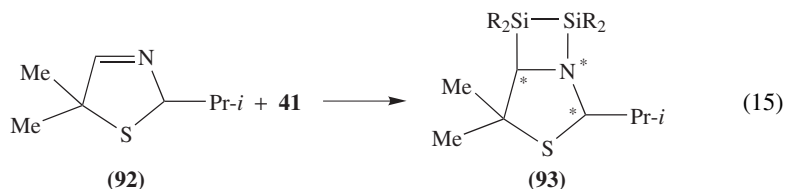
Disilene **41** reacts with the C=C double bonds of *ortho*-methylstyrene, a pyridine-2-alimine, and an *N,N'*-bipyridylsilane to give compounds **82–84**^{71,103,104}. The

SCHEME 2. Some cycloaddition reactions of disilene **41**

preference for [2 + 2] over the competing [2 + 4] cycloaddition is also manifested in the reaction with cyclohexa-1,3-diene to furnish the adduct **90**¹⁰⁵; the constitution of this product was confirmed by an X-ray crystallographic analysis of the isocyanide insertion product **91** (equation 14)¹⁰⁶.

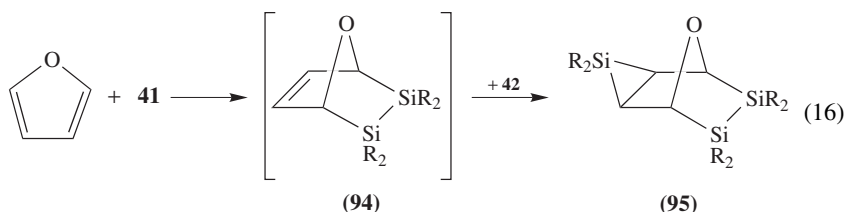


Additions to the C=O double bonds of various ketones⁶⁶ as well as to a C=N multiple bond of isoquinoline¹⁰⁷ afford the compounds **85** and **86**, respectively. The reaction of **41** with the racemic 3-thiazoline **92** is diastereoselective and yields the azadisilacyclobutane **93** (equation 15)⁷².

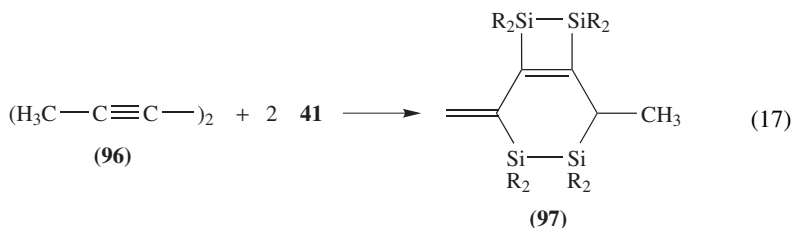


When the substituents at nitrogen are not too bulky, reactions with 1,4-diazabutadienes furnish the the highly strained [2 + 4] cycloadducts **88** but not the also feasible, strain-free five-membered product from a competing reaction of the silylene **42**¹⁰⁸.

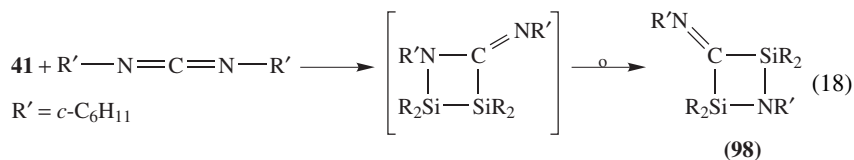
The first structurally confirmed [2 + 4] adduct of a disilene and a 1,3-diene was compound **89**, obtained from cyclopentadiene and **41**⁷⁴. The formation of the tricyclic compound **95** from furan and the cyclotrisilane **40** is probably initiated by a [2 + 4] cycloaddition of **41** to the five-membered ring to afford **94**, which then undergoes a [2 + 1] addition at the newly formed double bond with the silylene **42** formed concomitantly in the photolysis of **40** (equation 16)⁷⁴.

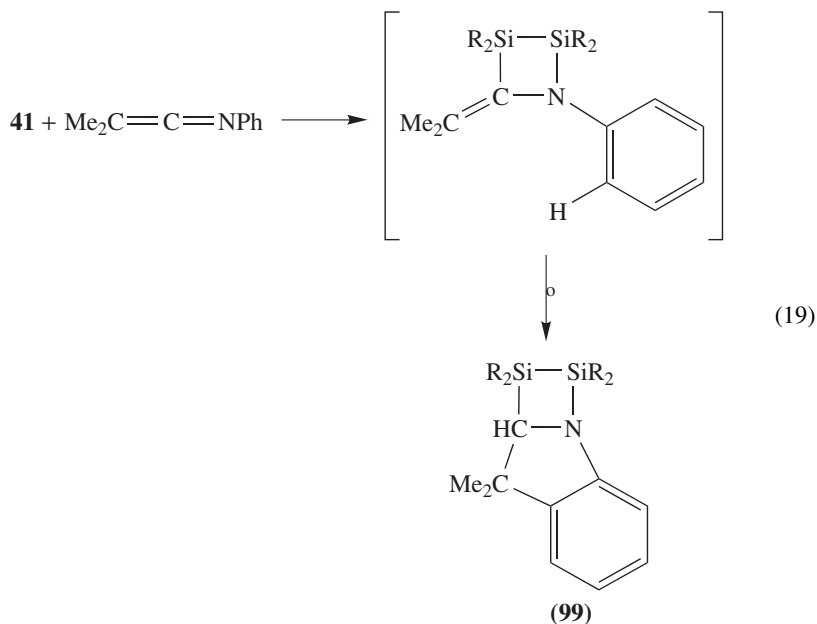


Disilene **41** also reacts smoothly with the triple bonds of phenylacetylene and tri-*tert*-butylsilyl cyanide to form the corresponding 1,2-disilacyclobutene⁶⁶ and compound **87**¹⁰⁹, respectively. The reaction of **41** with the 1,3-diyne **96** follows an unusual course to afford the bicyclic species **97** isolated in high yield (equation 17)¹¹⁰. The reaction sequence may be initiated by the addition of two molecules of **41** to the two triple bonds of **96**; this would then be followed by a thermally-allowed 1,5-hydrogen shift together with ring opening and ring closure reactions.



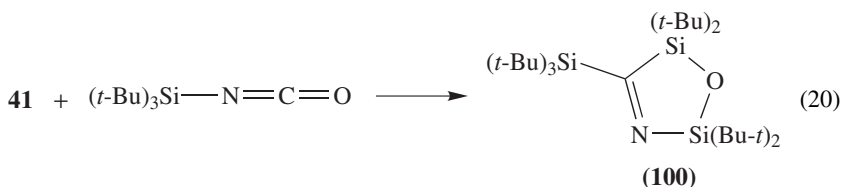
Like the reaction with the diyne **96**, reactions of **41** with cumulenes also follow an unexpected course. Thus, the reactions of **41** with a carbodiimide and a ketene imine afford the products **98**¹⁰⁷ and **99**¹⁰⁸ (equations 18 and 19, respectively).





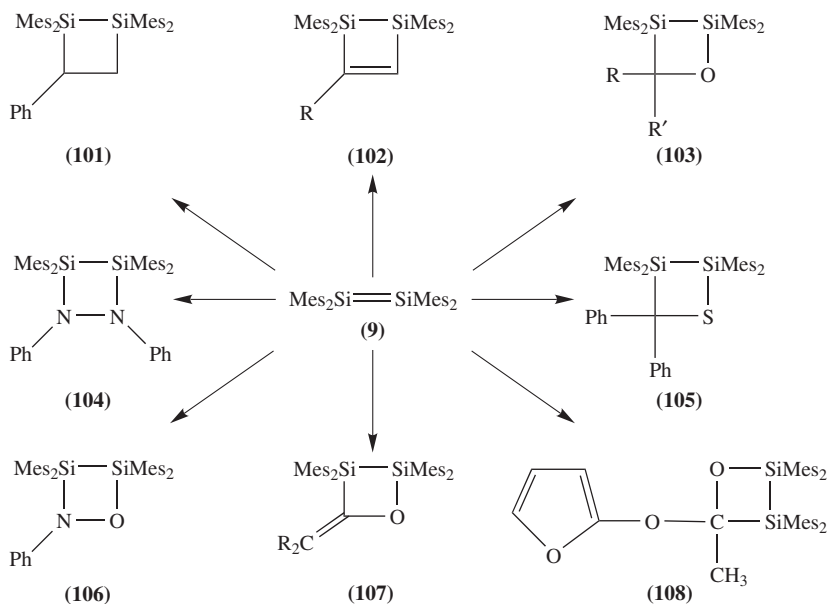
It is possible in both cases that the reaction sequences begin with [2 + 2] cycloadditions of the disilene to the C=N multiple bonds. For the formation of **98** this is followed by a formal NR' insertion whereas a 1,4-hydrogen shift with subsequent ring closure would be necessary for the formation of **99**.

The reaction between **41** and *tri-tert*-butylsilyl isocyanate with its bulky substituent leads to the five-membered heterocyclic system **100**¹⁰⁹. The formation of this ring requires cleavage of the Si=Si multiple bond, but nothing is as yet known about the reaction mechanism (equation 20).



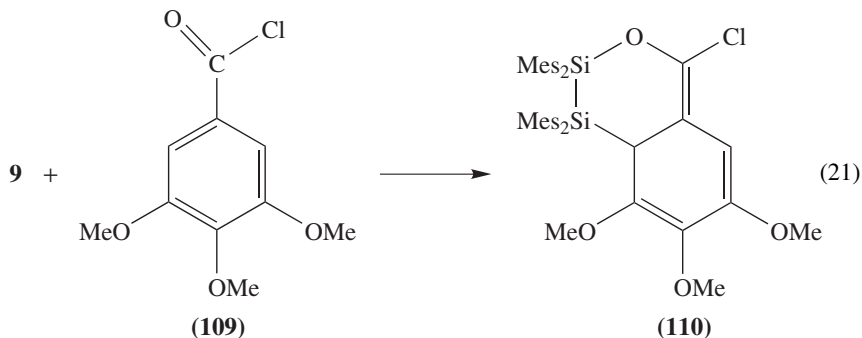
The tetraaryldisilenes participate in a similar variety of cycloaddition reactions as the tetraalkyldisilene **41**. The reactions of the classical tetramesityldisilene **9** have been most thoroughly investigated and some of them are summarized in Scheme 3.

Treatment of **9** with styrene furnished the disilacyclobutane **101** as the first example of a successful [2 + 2] cycloaddition of **9** to a C=C double bond⁷⁰. In the meantime it has been shown that acrylonitrile can form [2 + 2] cycloadducts, although in low yield, not only with **9** but also with the germsilene $\text{Me}_2\text{Si}=\text{GeMe}_2$ ¹¹¹. The reactions of **9** with unsymmetrically substituted acetylenes furnishing compounds **102** have been known for a long time^{67,112}. The addition reactions of **9** to various aldehydes and ketones have also been investigated in detail and give rise to products of the type **103**^{67,113}. Reaction with

SCHEME 3. Some cycloaddition reactions of disilene **9**

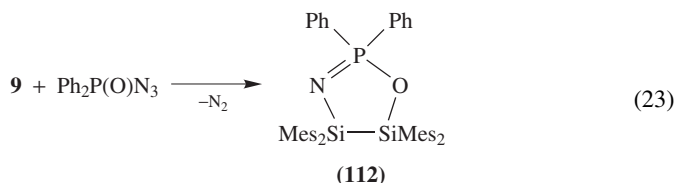
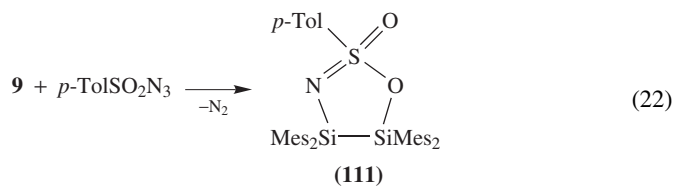
thiobenzophenone yields the adduct **105**, which undergoes cycloreversion under photochemical conditions to a silanethione that can be trapped with ethanol¹¹⁴. Disilene **9** reacts with the N=N and N=O double bonds in azobenzene and nitrosobenzene, respectively, to furnish the adducts **104**¹¹⁵ and **106**¹¹⁶, while its reactions with ketenes and esters afford the products **107**¹¹⁷ and **108**, respectively¹¹³.

Of particular interest is the reaction of **9** with the acid chloride **109** from which the [2 + 4] cycloaddition product **110** is isolated. In this compound the aromatic ring supplies two of the 4 π -electrons of the formal heterodiene system (equation 21)¹¹⁷.

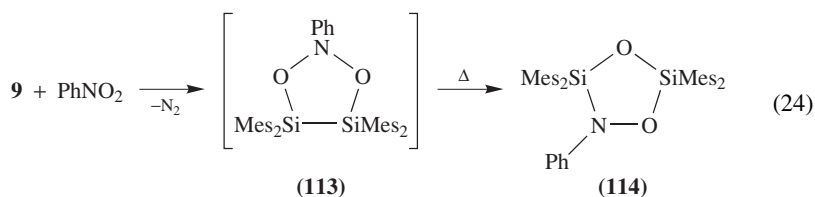


Unambiguous [2 + 3] cycloadducts are much less common than the products of [2 + 4] and especially [2 + 2] cycloadditions. These include the disilatriazolines **64** and the spectroscopically detected products **111** and **112** of the reactions of **9** with the sulfuryl and

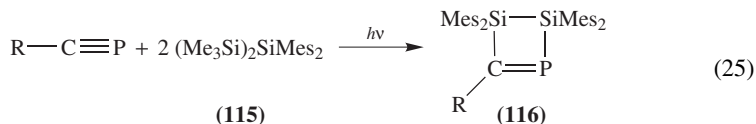
phosphoryl azides (equations 22 and 23, respectively)⁸⁵.



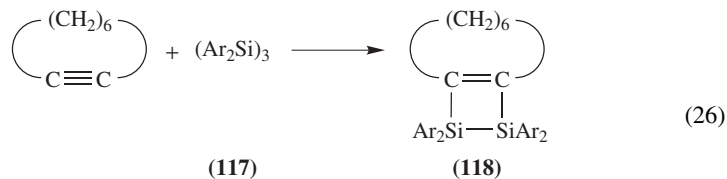
The reaction of **9** with nitrobenzene is probably initiated by a [2 + 3] cycloaddition to give the adduct **113**, which can be identified at low temperature by NMR spectroscopy. On increasing the temperature, the Si–Si bond is cleaved to afford the rearranged five-membered ring product **114** (equation 24).¹¹⁶ The similarity to the formation of the ring system **100** is noteworthy.



Not all cycloadducts with Si–Si bonds are formed by addition of a disilene to multiple bonds. Thus, reactions of phosphalkynes with the trisilane **115**, usually used for the generation of the disilene **9**, are assumed to proceed via addition and insertion of two silylene molecules, $\text{Mes}_2\text{Si}:$, to yield the formal [2 + 2] adducts **116** (equation 25)¹¹⁸.



The same process also holds for the reactions of various alkynes with the cyclotrisilane **117**, which also involves a sequence of addition and insertion steps to furnish disilacyclobutenes, such as **118** (equation 26)¹¹⁹.

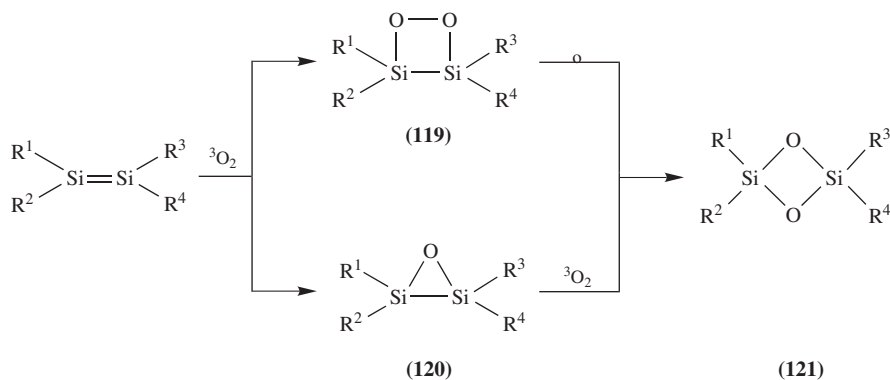


4. Oxidation reactions

As a consequence of the low electronegativity of silicon, many of the reactions described in the preceding sections can be formally classified as oxidations. Thus, this section is intended to provide a short survey of the extensive investigations on the air oxidation of disilenes as well as on the reactions of epoxides and P₄ and As₄ molecules with the Si=Si double bond.

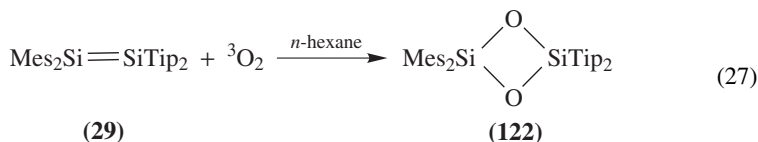
In the solid state disilenes react at varying rates, depending on the steric demands of their substituents, to furnish the 1,3-cyclodisiloxanes (1,3-dioxo-2,4-disilolanes) **121** as the respective main products^{67,120}. Although cyclooligosiloxanes are important intermediate products in the silicone industry and are produced in large amounts, compounds **121** were the first four-membered ring compounds to contain this structural unit which was previously only known in six-membered and larger rings.

At lower temperature in solution, the aerial oxidation of disilenes initially furnishes the 3,4-disiladioxetanes **119** together with small amounts of the disilaoxiranes **120**, both of which react further in the solid state and in solution to give the cyclodisiloxanes **121** (Scheme 4).



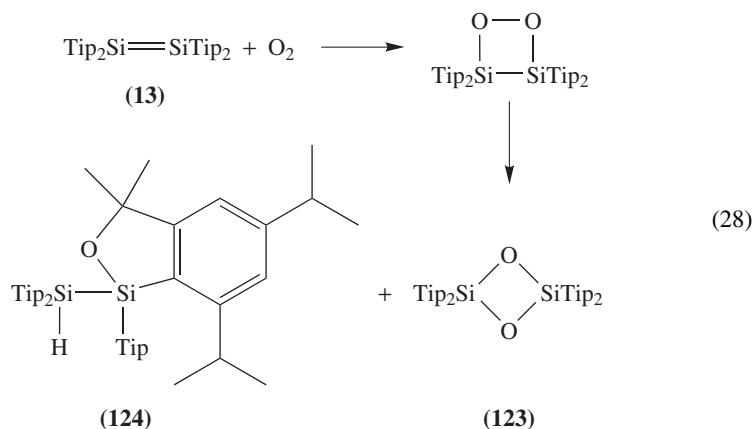
SCHEME 4. Air oxidation of disilenes

Using *E*- and *Z*-**19**, R¹ = R³ = Mes, R² = R⁴ = *t*-Bu, West and coworkers demonstrated that all steps of the reaction proceed with retention of configuration. Furthermore, ¹⁸O-labelling experiments have shown that the rearrangement is strictly intramolecular in the solid state and in solution¹²¹. Most other disilenes undergo analogous reactions with atmospheric oxygen, as illustrated by the transformation of the unsymmetrically substituted disilene **29** to **122** (equation 27)⁹⁶.



Oxidation of the disilene **13** follows a somewhat different course; although a 3,4-disiladioxetane is formed in a first step, the subsequent products are the cyclodisiloxane

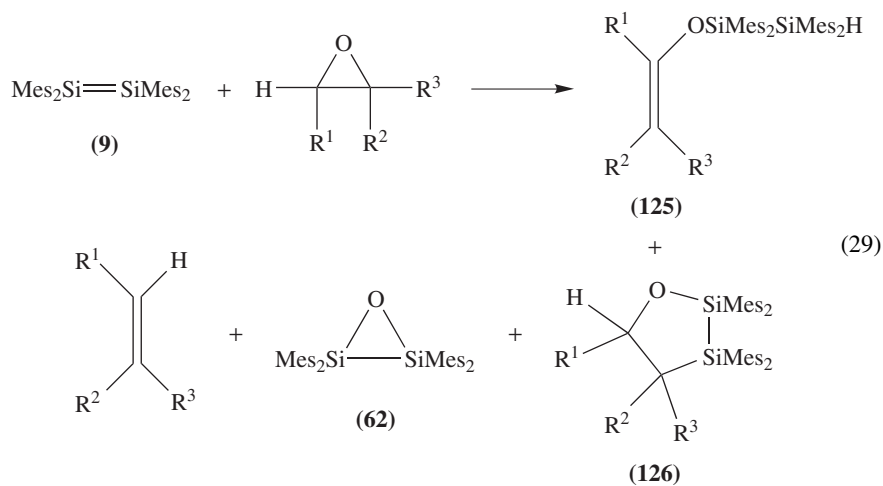
123 together with **124**, the product of hydrogen transfer (equation 28)^{36,84}.



The *E*- and *Z*-isomeric disilenes **35** are remarkably stable towards oxygen: at 50 °C, 10 h are needed before the oxidation is completed. These reactions are also stereoselective and afford the *E*- and *Z*-cyclodisiloxanes⁴⁶.

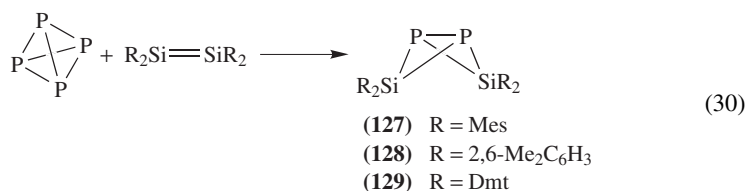
The cyclodisiloxanes **121** have unusual structures with short transannular Si···Si separations ranging from 235 to 243 pm^{46,96,122,123}. These values are thus of the same magnitude as that of Si–Si single bonds having the same substitution pattern. Although the question of possible Si···Si interactions has not been completely resolved⁶, it can be assumed that the geometry of the ring and the repulsive interactions of the two ring oxygen atoms are the main reasons for these small separations.

In a series of papers West and coworkers described the reactions of disilene **9** with several epoxides to give the disilyl enol ethers **125**, the five-membered ring compounds **126**—the formal insertion products, as well as the products of epoxide deoxygenation, namely alkenes and the disilaoxirane **62** (equation 29)^{80,83,124,125}.

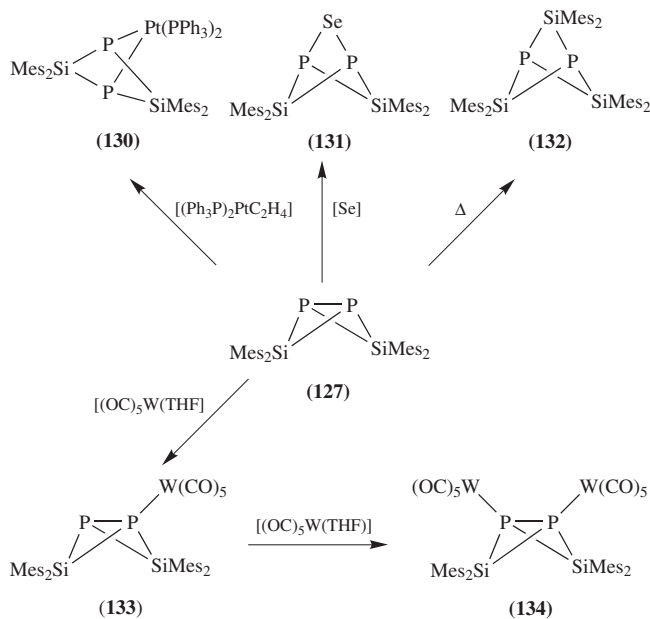


The products **125** and **126** are formed with complete regioselectivity, suggesting involvement of an epoxide ring-opened intermediate. Product ratios vary systematically, depending on the steric properties of the epoxides. As the size of the epoxide substituents increases, the amount of the five-membered ring compounds **126** in the reaction mixture decreases appreciably¹²⁵.

The Si=Si π -bond is cleaved in practically all reactions of disilenes while the σ -bond remains intact. Even the action of the very reactive oxygen on the Si=Si bond initially results in the formation of the 3,4-disiladioxetanes **119** which, however, rapidly rearrange to give the cyclodisiloxanes **121**. The reactions of the disilenes **9**, **10** and **14** [R = Mes, 2,6-Me₂C₆H₃, 4-*t*-Bu-2,6-Me₂C₆H₂ (Dmt)] with white phosphorus follow a different course and proceed with cleavage of both Si=Si bonds to furnish the bicyclo[1.1.0]butane derivatives **127–129** (equation 30)^{126,127}.

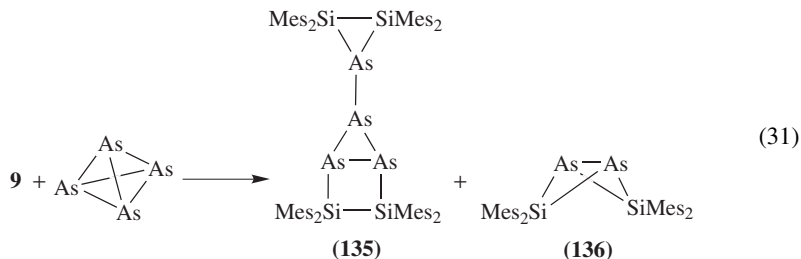


The P–P bond still present in **127** readily undergoes insertion reactions with various reagents, e.g., to afford the products **130–132** (Scheme 5)¹²⁸. In addition, the phosphorus atoms can also serve as ligands in transition metal complexes. The complexes **133** and **134** with one or two W(CO)₅ fragments are two typical examples¹²⁶ (Scheme 5).



SCHEME 5. Insertion and complex-forming reactions of **127**

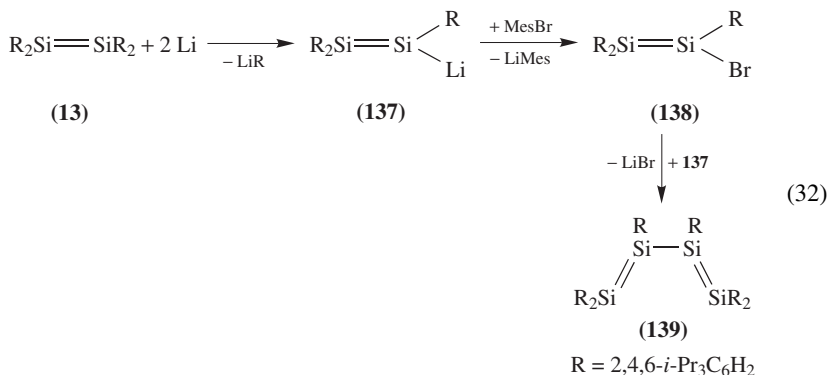
Even more unusual is the reaction of **9** with the metastable yellow arsenic, from which compounds **135** and **136** are isolated. On longer heating at 95 °C compound **135** rearranges to afford the butterfly-type molecule **136** (equation 31)¹²⁸.



The results described above clearly reflect the diversity of the possible reactions of acyclic disilenes. The 1,2-aryl migrations in tetraaryldisilenes have not been mentioned as they have already been reviewed in depth⁶. The same is true for the thermally induced decomposition of the disilene **35** to furnish the silylene molecule $\text{Tbt}(\text{Mes})\text{Si}:$, the unusual chemistry of which is reviewed elsewhere in this series¹²⁹.

IV. TETRASILABUTA-1,3-DIENE

The first and as yet only molecule with conjugated Si=Si double bonds is the tetrasilabuta-1,3-diene (tetrasil-1,3-diene) **139**, which was prepared as follows. The disilene **13** is treated with excess lithium to give the putative disilynyllithium species **137**. In the second step of the sequence mesityl bromide was added in the expectation that the bulk of the aryl group and the poor solubility of mesityllithium would favor halogenation over the competing transarylation. Indeed, the bromodisilene **138** does appear to be formed smoothly but, like **137**, it has not yet been positively identified. Intermolecular cleavage of lithium bromide from the two intermediates then furnishes the tetrasilabuta-1,3-diene **139** in 60% yield (equation 32)¹³⁰.



The brown-red crystals of **139** are thermally very stable but extremely sensitive to air. In the solid state, and presumably also in solution, **139** exists in the *s-cis*-form with a dihedral angle of 51° between the planes defined by the atoms Si1–Si2–Si2a and Si1a–Si2a–Si2 (Figure 3). Similar to the situation in other molecules with conjugated double bonds, the Si=Si double bonds are slightly lengthened [2.175(2) Å] while the central Si–Si single bond length of 2.321(2) Å is remarkably short in view of its bulky substituents¹³⁰.

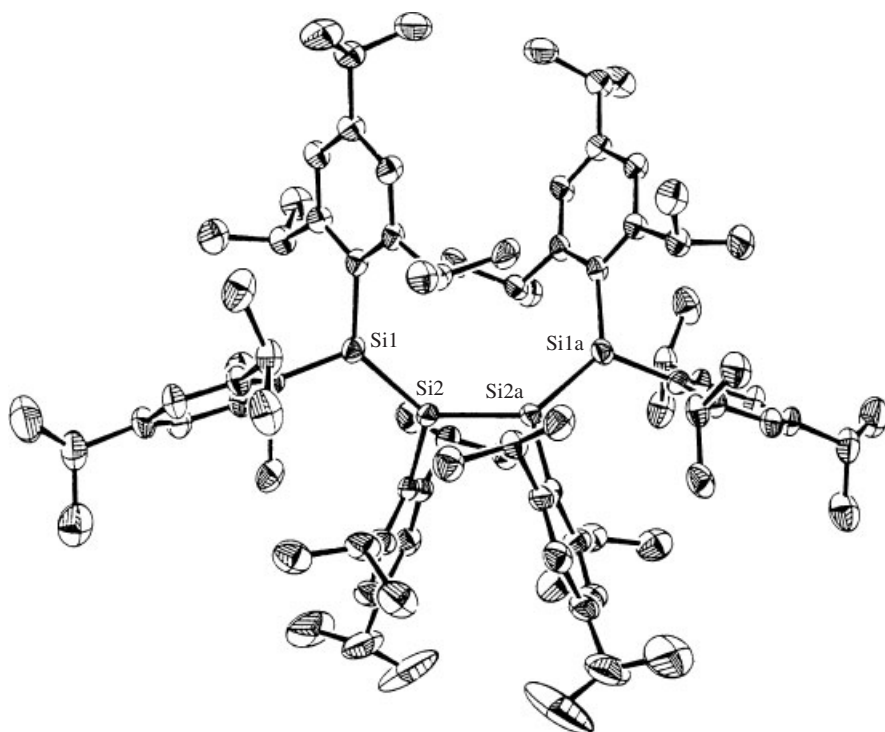
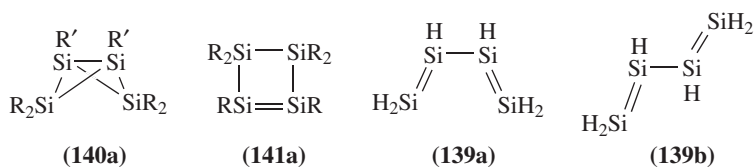


FIGURE 3. Molecular structure of **139** in the crystal

The electronic spectrum of **139** clearly reveals that the conjugation between the two halves of the molecule remains intact in solution. The longest wavelength absorption at 518 nm ($\epsilon = 25\,700$) is bathochromically shifted by *ca* 100 nm in comparison to those of other disilenes with similar substitution patterns and thus exhibits a similar red shift to that observed between ethenes and buta-1,3-dienes¹³¹.

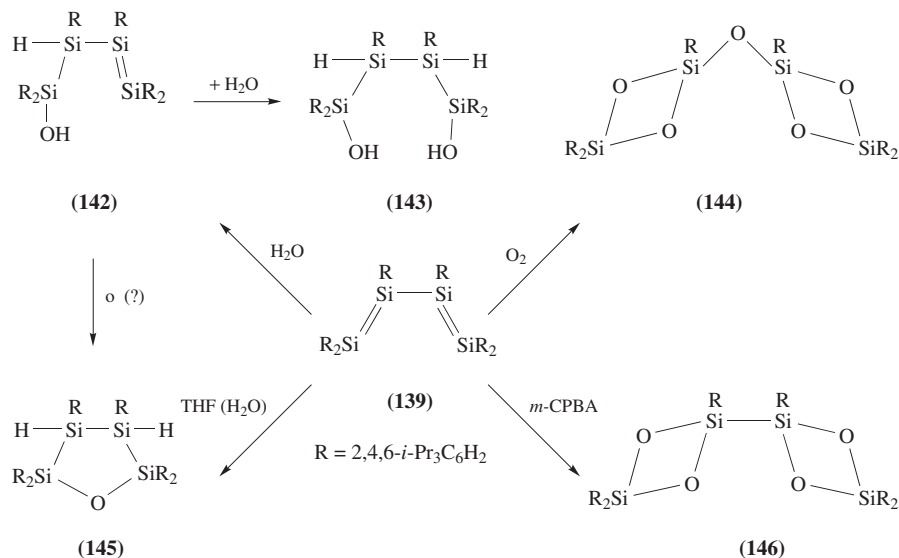
The synthesis of **139** has added another representative to the group of compounds with the composition Si_4R_6 . Although the tetrasilabicyclo[1.1.0]butane **140a** has been known for some time^{132,133}, the tetrasilacyclobutenes **141a** were described for the first time only recently (see next section). *Ab initio* calculations on the parent compounds Si_4H_6 show an energy minimum for compound **140a** with the bicyclo[1.1.0]butane skeleton and that the energy of the cyclobutene derivative of type **141a** is only slightly higher. On the other hand, the tetrasilabutadienes **139**, $\text{R} = \text{H}$, have energy maxima with the *s-trans* form **139b** being slightly favored over the *s-cis* form **139a**¹³⁴.



In view of the large energy difference between **140a**, R = H, and **141a**, R = H, on the one hand and **139**, R = H, on the other, we have examined whether **139** could be converted into one of these ring systems by thermal or photochemical means. Although irradiation of **139** did not lead to any detectable change, heating at 300 °C does cause conversion to a colorless solid which has, as yet, not been identified¹³⁵.

In view of the preference of the tetrasilabuta-1,3-diene **139** for the *s-cis* form, it seemed worthwhile to examine its behavior in [4 + 2] cycloadditions of the Diels–Alder type. Since **139**, like many disilenes, should behave as an electron-rich diene, we attempted to react it with various electron-poor and also with some electron-rich olefins. No reaction was detected in any case. Only in the presence of water did **139** react with quinones to furnish the unsymmetrically substituted disilenes **36** and **37** (see Section III.A). The effective shielding of the double bonds by the bulky aryl groups and, above all, the 1, 4-separation of the terminal silicon atoms of about 5.40 Å appear to be responsible for these failures. Thus, it was surprising that treatment of **139** with the heavier chalcogens afforded five-membered ring compounds in a formal [4 + 1] cycloaddition (see below).

As opposed to the attempted [4 + 2] cycloadditions, reactions of **139** with small molecules, as summarized in Scheme 6, were more successful. Treatment of **139** with water finally led via the monoaddition product **142** to the tetrasilane-1,4-diol **143**, which showed no tendency to eliminate water with formation of **145**. However, the oxatetrasilacyclopentane **145**, an analogue of tetrahydrofuran, is smoothly obtained upon heating **139** in THF containing water. The unusual oxidation product **144** is formed on exposure of **139** to atmospheric oxygen. In addition to the presence of two cyclodisiloxane units, this conversion is of particular interest due to the insertion of oxygen into the sterically protected Si–Si single bond which proceeds at room temperature with formation of a disiloxane group. In contrast, the Si–Si single bond is not attacked by *m*-CPBA; instead compound **146**, which contains two Si–Si linked cyclodisiloxane rings, is formed. The structures of **144**, **145** and **146** have been confirmed by X-ray crystallography¹³⁵.



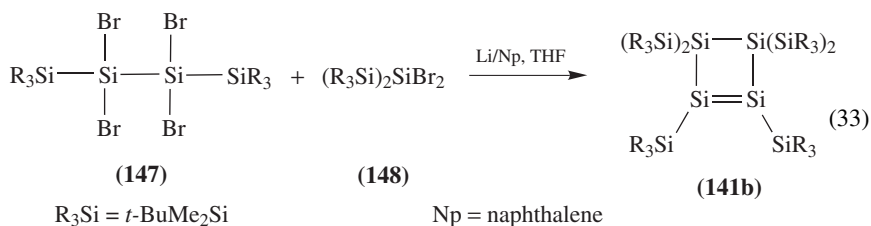
SCHEME 6. Reactions of **139** with oxygen and water

V. CYCLIC DISILENES

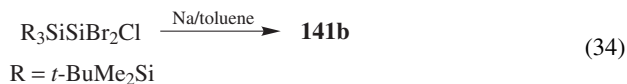
Molecules with endocyclic Si=Si double bonds, like the tetrasilabutadiene **139**, have also only recently become accessible and their chemistry has not yet been reviewed. In the less than four years since 1996 two three-membered, two four-membered and three five-membered ring compounds containing an Si=Si double bond have been prepared and, in most cases, their structures have been characterized by X-ray crystallography. Although two synthetic routes dominate in the synthesis of acyclic disilenes, the cyclic disilenes have mostly been prepared by the special methods summarized below.

A. Preparation

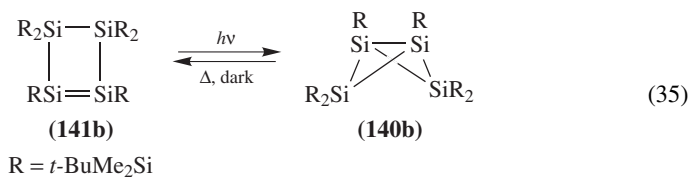
The first disilene with an endocyclic double bond, the tetrasilacyclobutene **141b**, was prepared by Kira and coworkers through reductive coupling and debromination of the oligosilanes **147** and **148**; however, the yield of the pure, isolated product was merely 1.5% (equation 33)¹³⁶.



A marked improvement of the yield of **141b** (to 64%) was achieved by the dehalogenation of an oligosilane with sodium in toluene at room temperature; however, the mechanism of this reaction has not yet been elucidated (equation 34)¹³⁷.

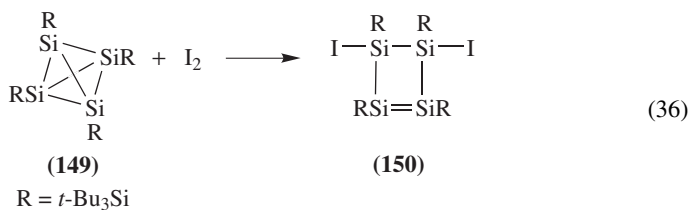


Under photochemical conditions the cyclotetrasilene **141b** undergoes ready rearrangement to the tetrasilabicyclo[1.1.0]butane derivative **140b** which, in turn, undergoes reversion to **141c** upon heating. Experiments with deuterium-labelled compounds **141b** and **140b** demonstrate that both isomerizations proceed through 1,2-silyl migrations (equation 35)¹³⁸.

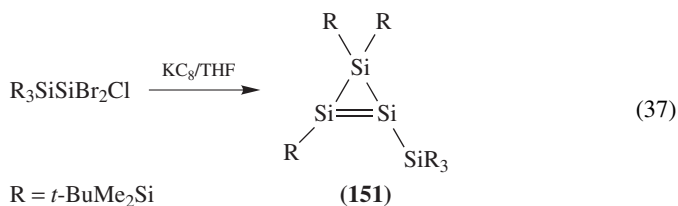


Wiberg and coworkers followed a different route for the preparation of a further cyclo-tetrasilene. The action of iodine on the *tetrahedro*-tetrasilane **149**¹³⁹ furnished the disilene

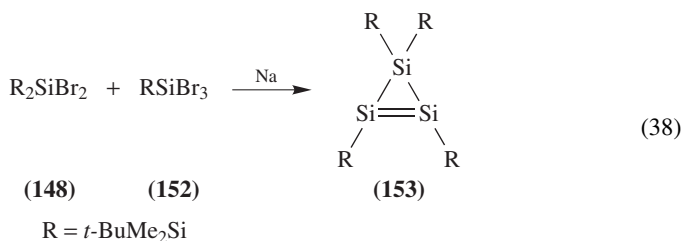
150 in almost quantitative yield (equation 36)¹⁴⁰.



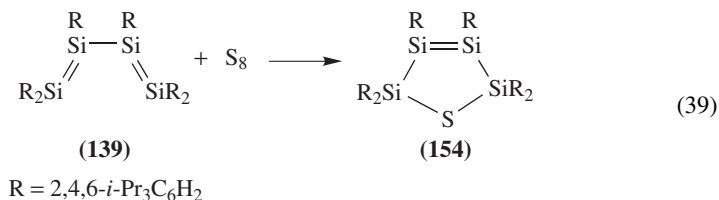
The size of the ring formed in each case is strongly dependent on the reaction conditions. When KC_8 is used instead of sodium for the dehalogenation of the oligosilane $\text{R}_3\text{SiSiBr}_2\text{Cl}$, the unsymmetrically substituted disilene **151** is obtained. **151** is the first synthesized cyclotrisilene (equation 37)¹³⁷. The mechanism of formation of **151** is also still a matter of speculation.



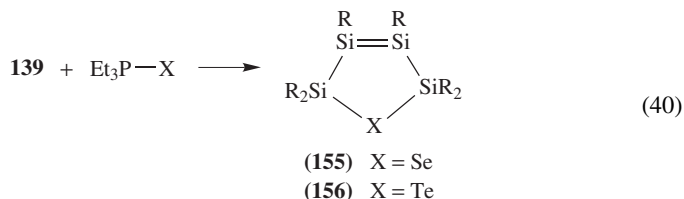
A second cyclotrisilene, compound **153**, was isolated after reductive dehalogenation of a mixture of the oligosilanes **148** and **152** (equation 38)¹⁴¹.



Three additional rings systems containing endocyclic $\text{Si}=\text{Si}$ double bonds were obtained from the tetrasilabutadiene **139**. Since Diels–Alder products of this compound have as yet not been synthesized, probably because of the steric overcrowding and the large 1, 4-separation of the terminal silicon atoms, it was surprising to find that the action of sulfur on **139** resulted in a formal [4 + 1] cycloaddition to furnish the thiatetrasilacyclopentene **154** in high yield (equation 39)¹⁴².



Treatment of **139** with selenium and tellurium did not lead to any reaction. However, upon addition of a small amount of a triethylphosphane, the corresponding five-membered heterocyclic compounds **155** and **156** were isolated in high yield (equation 40)¹⁴².



In analogy to the reactions of acyclic disilenes with the heavier chalcogens^{78,79} it can be assumed that an initial [2 + 1] cycloaddition of the respective chalcogen to one of the Si=Si double bonds of **139** takes place, followed by a rearrangement of the resultant three-membered ring to a less strained five-membered ring.

B. Molecular Structures and Spectroscopy

X-ray crystallographic analyses have been carried out for six of the currently known disilenes with endocyclic double bonds. The Si=Si bond lengths, the ²⁹Si NMR chemical shifts of the double bonded silicon atoms and the longest wavelength absorptions in the electronic spectra are summarized in Table 5.

The Si=Si double bond lengths are in the range 2.14 to 2.26 Å and thus of similar lengths as those observed for acyclic disilenes. Also, like the tetrasilyldisilenes³⁹, the bond lengths in the four-membered ring compounds **141b** and **150** increase with increasing steric requirements of the substituents. The cyclotrisilene **153**, however, is an exception; its Si=Si bond length (2.138 Å) is extremely short in relation to its substitution pattern. The cyclopropenes exhibit a similar trend and also have markedly shortened C=C double bonds in comparison to analogous acyclic olefins¹⁴³. In the cyclopentenes **154** to **156** the Si=Si separations are slightly larger than that in the comparably substituted acyclic disilene **25**⁴² and they increase somewhat with increasing size of the ring heteroatom.

The four-membered ring in disilene **141b** is nonplanar with an average folding angle of 37°. In addition, it exhibits a slight *trans*-bending and torsion about the double bond with angles of 13.2° and 12.3°. The *trans*-bent angles in **150** are appreciably smaller, 2.2° and 2.9°, while the torsion angle is considerably larger, 30.8°. The five-membered rings are nearly planar (sum of angles 539.5°) with a slight deviation from planarity towards the twist form.

TABLE 5. Selected structural and spectroscopic data of cyclic disilenes

Compound	$d(\text{Si}=\text{Si})$ (Å)	$\delta(^{29}\text{Si})(>\text{Si}=\text{Si})^a$	λ_{max} (nm) (ϵ)	Reference
141b	2.174(4)	160.4	465(6810), 359(1060)	136
151	n. d. ^b	81.9, 99.8	482(2640), 401(1340)	137
153	2.138(2)	97.7	466(440)	141
150	2.257(2)	164.4	n. d. ^b	140
154	2.170(1)	86.0	423(16240)	142
155	2.181(1)	90.3	431(10140)	142
156	2.198(2)	97.8	459(11440)	142

^a ²⁹Si NMR in C₆D₆.

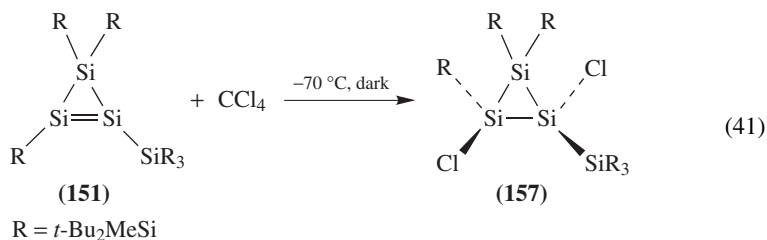
^b n. d. = not determined.

Like acyclic disilenes, all the disilenes having endocyclic double bonds are colored with the spectrum of colors extending from yellow to dark red. This is also reflected in the electronic spectra (Table 5) in which the absorptions at longest wavelength exhibit pronounced red shifts with decreasing ring size and hence with increasing ring strain.

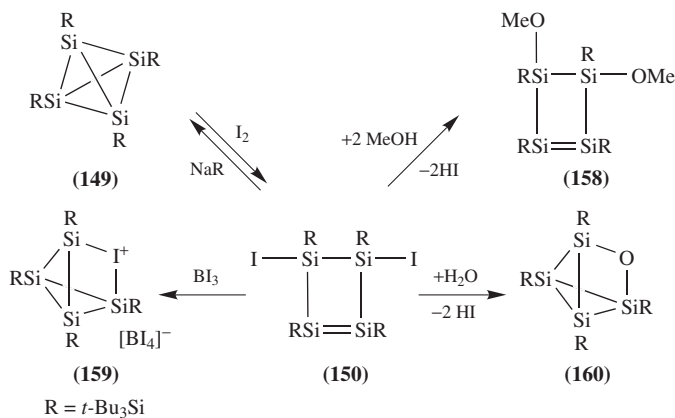
The ^{29}Si NMR chemical shifts of the doubly bonded silicon atoms in the cyclopentenes **154–156** are of a similar magnitude to those of the acyclic 1,2-diaryl-1,2-disilyldisilenes⁴². The Si=Si bonds in the four-membered ring compounds **141b** and **150** experience a strong deshielding and their chemical shifts even exceed those of the tetrasilyldisilenes **16–18** (142–155 ppm). The corresponding atoms in the three-membered ring compounds **151** and **153** are more highly shielded and thus follow the trends also observed for siliranes or cyclotrisilanes¹⁸.

C. Reactions

In contrast to the acyclic disilenes, very little is yet known about the reactivity of the cyclic members of this class of compounds. The photochemically induced isomerization of the cyclotetrasilene **141c** to the bicyclo[1.1.0]butane derivative **140b** (Section V.A) has already been mentioned. Similarly to the tetrasilyldisilenes⁶⁹ the cyclotrisilene **151** also reacts spontaneously with tetrachloromethane even at -70°C to furnish the *trans*-1,2-dichlorocyclotrisilane **157** (equation 41)¹³⁷.



The available information about the reactions of the cyclotetrasilene **150** is summarized in Scheme 7.



SCHEME 7. Reactions of the cyclotetrasilene **150**

Remarkably, most reactions do not take place at the unsaturated part of the molecule, presumably because of the steric shielding of the Si=Si double bond by the bulky *t*-Bu₃Si groups, but rather proceed through substitution of the iodine atoms. The reaction of **150** with water affords the product **160**, whereas that with methanol furnishes compound **158** with retention of the tetrasilacyclobutene skeleton. On treatment of **150** with NaR the *tetrahedro*-tetrasilane **149** — the starting material for the preparation of **150** — is reformed. Finally, the reaction with BI₃ proceeds with abstraction of an iodide ion to form the ionic compound **159**¹⁴⁰.

The Si=Si double bonds of the five-membered ring compounds **154**–**156** also exhibit a similar low reactivity and, for example, are not attacked by atmospheric oxygen. However, the tellurium compound **156** is photochemically labile and decomposes on exposure to daylight with deposition of tellurium¹⁴².

VI. DISILYNES

Stable molecules containing a silicon-silicon triple bond are still unknown. Lischka and Köhler¹⁴⁴ were the first to predict that the parent compound, Si₂H₂, would not possess an Si≡Si triple bond like its group homologue acetylene, C₂H₂, but should rather exist in a di-bridged disilyne, Si(H)₂Si, form in its lowest energy minimum. In fact, Bogey and coworkers¹⁴⁵ were able to experimentally demonstrate the existence of the di-bridged molecule **161** by submillimeter spectroscopy of a silane plasma cooled to –196 °C. The disilyne **161** possesses C_{2v} symmetry with an Si–Si separation of 2.2079 Å, Si–H bond lengths of 1.6839 Å and a dihedral angle $\tau = 103.2^\circ$ (Figure 4). The mono-bridged disilyne **162** has also been observed experimentally and found, in excellent agreement with theoretical calculations^{146,147}, to exist as a local minimum exhibiting the following, albeit provisional, structural parameters¹⁴⁸: Si1–Si2 = 2.113 Å, Si2–H1 = 1.629 Å, Si2–H2 = 1.474 Å, Si1–Si2–H2 = 157.5° (Figure 4).

An additional isomer, the disilavinylidene, SiSiH₂, has not yet been detected; it should certainly have a higher energy than the forms **161** and **162**¹⁴⁷. The least stable H₂Si₂ isomer is the acetylene analogue H–Si≡Si–H with D_{∞h} symmetry, which readily distorts to a *trans*-bent form. This molecule with C_{2h} symmetry is also too unstable for a possible detection^{146,149}.

This opens the interesting question of whether upon replacing the hydrogen atoms with suitable substituents it would be possible to realize a linear disilyne with an Si≡Si triple bond. As early as 1986 West and coworkers^{150,151} reported the preparation of a synthon of dimethyldisilyne, bis(7-silanorbornadiene) **163** which, at very high temperature, sets the desired molecule free, as demonstrated, for example, by trapping reactions with anthracene or 3,4-dimethylbutadiene to give the products **164** and **165**, respectively (equation 42)¹⁵².

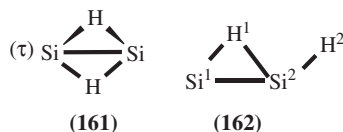
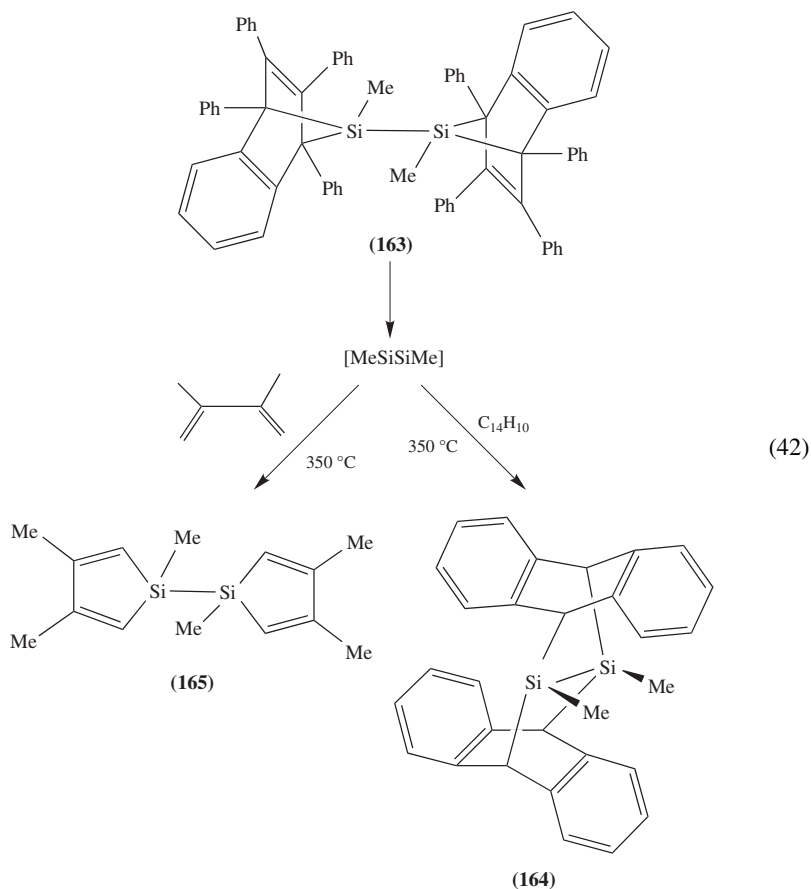


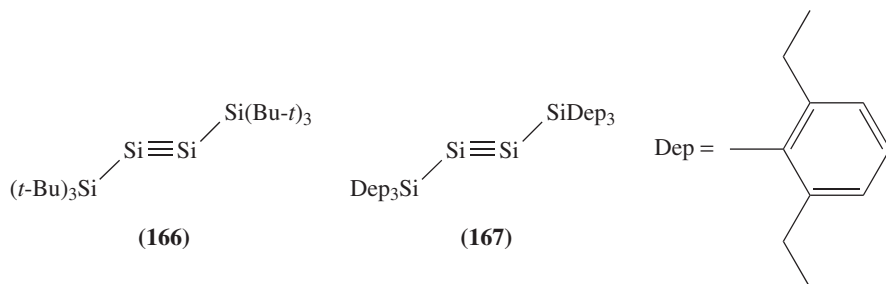
FIGURE 4. Experimental structures of the double-bridged, **161**, and mono-bridged, **162**, isomers of disilyne Si₂H₂. τ is the HSiSiH dihedral angle



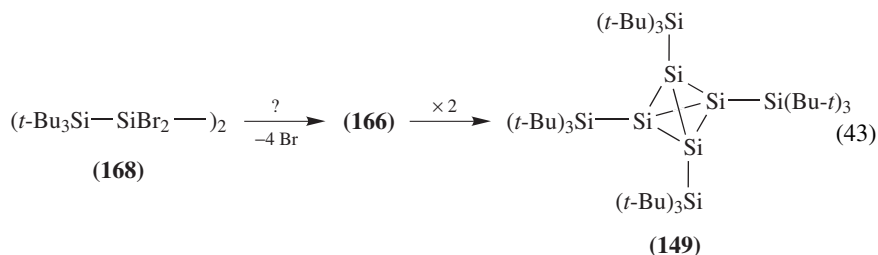
The assumption that dimethyldisilyne participates as an intermediate in these reactions is supported by calculations on the system Si_2Me_2 . Although the silylene-like molecule SiSiMe_2 is found to be the lowest minimum on the potential energy surface, the isomeric *trans*-dimethyldisilyne, however, is only about 12 kcal mol^{-1} higher in energy and is, furthermore, protected against this isomerization by the high activation for the 1,2-methyl shift from one silicon atom to the other¹⁵³.

However, the methyl groups are much too small to shield a possible $\text{Si}\equiv\text{Si}$ triple bond from subsequent reactions. Kobayashi and Nagase reported on the results of density functional theory calculations under the title ‘Silicon–Silicon Triple Bonds: Do Substituents Make Disilynes Synthetically Accessible’¹⁵⁴. According to these calculations, electropositive silyl groups SiR_3 with very voluminous R groups should be promising candidates to achieve this objective. The molecules **166** and **167** may be mentioned here as examples; they should be relatively stable both against attack by reactive species as well as against dimerization.

However, it will probably be very difficult to achieve this objective. Accordingly, Wiberg and coworkers investigated the dehalogenation of the tetrasilane **168**, which would presumably involve the disilyne **166** as an intermediate but this intermediate, in analogy



to the formation of perpendicular acetylene complexes¹⁵⁵, spontaneously reacts further to afford the *tetrahedro*-tetrasilane **149** (equation 43)^{139,156}.



Thus, the synthesis of molecules with an Si≡Si triple bond remains a challenge for preparative chemistry.

VII. CONCLUSION

The chemistry of the Si=Si double bond has experienced dramatic developments in the past two decades and has progressed from an esoteric topic to an important field of chemical research. It would appear that the most important modes of reaction of the disilenes have been discovered so that future research will be concerned with the elucidation of the often not very well understood reaction mechanisms.

The situation is different for the molecules containing endocyclic Si=Si double bonds which just recently became accessible and for the as yet sole known tetrasilabutadiene, the chemistry of which still remains mostly unknown. Not only are further representatives of these classes of compounds to be expected but also novel modes of reactions that have as yet not been observed for the acyclic disilenes. Another interesting question is whether it will be possible to prepare molecules with an extended system of conjugated double bonds.

Silicon–silicon multiple bonds with a bond order greater than two are still unknown. According to theoretical calculations, voluminous and concomitantly electropositive substituents are the most promising candidates with the potential to stabilize disilynes having a formal Si≡Si triple bond. When and by what synthetic route this challenge for experimental chemistry will be realized is a question that only time can answer.

VIII. ACKNOWLEDGMENTS

Financial support of our work from the Deutsche Forschungsgemeinschaft and the Fonds der Chemischen Industrie is gratefully acknowledged. The author is deeply indebted to

all collaborators and coworkers whose names are given in the references and also to Petra Rösner for the preparation of the manuscript.

IX. REFERENCES

1. R. West, M. J. Fink and J. Michl, *Science*, **214**, 1343 (1981).
2. R. West, *Angew. Chem.*, **99**, 1231 (1987); *Angew. Chem., Int. Ed. Engl.*, **26**, 1201 (1987).
3. G. Raabe and J. Michl, in *The Chemistry of Organic Silicon Compounds* (Eds. S. Patai and Z. Rappoport), Chap. 17, Wiley, Chichester, 1989, p. 1015.
4. T. Tsumuraya, S. A. Batcheller and S. Masamune, *Angew. Chem.*, **103**, 916 (1991); *Angew. Chem., Int. Ed. Engl.*, **30**, 902 (1991).
5. M. Weidenbruch, *Coord. Chem. Rev.*, **130**, 275 (1994).
6. R. Okazaki and R. West, *Adv. Organomet. Chem.*, **39**, 231 (1996).
7. H. Sakurai, in *The Chemistry of Organic Silicon Compounds*, Volume 2 (Eds. Z. Rappoport and Y. Apeloig), Chap. 15, Wiley, Chichester, 1998, p. 827. For recent papers on phenol additions to the Si=Si double bond of disilenes see: Y. Apeloig and M. Nakash, *Organometallics*, **17**, 1260 (1998); Y. Apeloig and M. Nakash, *Organometallics*, **17**, 2307 (1998).
8. M. Ishikawa and M. Kumada, *J. Organomet. Chem.*, **81**, C3 (1974).
9. M. Ishikawa, K. Nakagawa, M. Ishiguro, F. Ohi and M. Kumada, *J. Organomet. Chem.*, **152**, 155 (1978).
10. M. Ishikawa, K. Nakagawa, M. Ishiguro, F. Ohi and M. Kumada, *J. Organomet. Chem.*, **201**, 151 (1980).
11. H. Sakurai, *J. Organomet. Chem.*, **200**, 261 (1980).
12. M. Ishikawa and M. Kumada, *Adv. Organomet. Chem.*, **19**, 51 (1981).
13. M. G. Steinmetz, *Chem. Rev.*, **95**, 1527 (1995).
14. A. G. Brook, in *The Chemistry of Organic Silicon Compounds* (Eds. S. Patai and Z. Rappoport), Chap. 15, Wiley, Chichester, 1989, p. 965.
15. A. G. Brook, in *The Chemistry of Organic Silicon Compounds*, Volume 2 (Eds. Z. Rappoport and Y. Apeloig), Chap. 21, Wiley, Chichester, 1998, p. 1233.
16. M. Kira and T. Miyazawa, in *The Chemistry of Organic Silicon Compounds*, Volume 2 (Eds. Z. Rappoport and Y. Apeloig), Chap. 22, Wiley, Chichester, 1998, p. 1311.
17. T. Miyazawa, S. Koshihara, C. Liu, H. Sakurai and M. Kira, *J. Am. Chem. Soc.*, **121**, 3651 (1999).
18. M. Weidenbruch, *Chem. Rev.*, **95**, 1479 (1995).
19. S. Masamune, Y. Hanzawa, S. Murakami, T. Bally and J. F. Blount, *J. Am. Chem. Soc.*, **104**, 1150 (1982).
20. S. Masamune, Y. Eriyama and T. Kawase, *Angew. Chem.*, **99**, 601 (1987); *Angew. Chem., Int. Ed. Engl.*, **26**, 584 (1987).
21. H. Watanabe, K. Takeuchi, K. Nakajima, Y. Nagai and M. Goto, *Chem. Lett.*, 1342 (1988).
22. (a) M. Weidenbruch, A. Pellmann, Y. Pan, S. Pohl, W. Saak and H. Marsmann, *J. Organomet. Chem.*, **450**, 67 (1993).
(b) H. B. Yokelson, A. J. Millevolte, D. R. Adams and R. West, *J. Am. Chem. Soc.*, **109**, 4116 (1987).
23. S. Tsutsui, K. Sakamoto and M. Kira, *J. Am. Chem. Soc.*, **120**, 9955 (1998).
24. (a) M. Karni and Y. Apeloig, *J. Am. Chem. Soc.*, **112**, 8589 (1990).
(b) M. Maxka and Y. Apeloig, *J. Chem. Soc., Chem. Commun.*, 737 (1990).
25. R. S. Grev, *Adv. Organomet. Chem.*, **33**, 125 (1991).
26. Y. Apeloig and T. Müller, *J. Am. Chem. Soc.*, **117**, 5363 (1995).
27. Y. Apeloig, T. Müller, M. Takahashi and M. Kira, *J. Am. Chem. Soc.*, **123**, 347 (2001).
28. T. A. Schmedake, M. Haaf, Y. Apeloig, T. Müller, S. Bukalov and R. West, *J. Am. Chem. Soc.*, **121**, 9479 (1999).
29. A. Schäfer, W. Saak and M. Weidenbruch, *Chem. Ber./Recueil*, **130**, 1733 (1997).
30. A. Schäfer, W. Saak and M. Weidenbruch, *Z. Anorg. Allg. Chem.*, **624**, 1405 (1998).
31. M. Weidenbruch, *Eur. J. Inorg. Chem.*, 373 (1999).
32. M. J. Fink, M. J. Michalczuk, K. J. Haller, R. West and J. Michl, *Organometallics*, **3**, 793 (1984).

33. S. Masamune, S. Murakami, J. T. Snow, H. Tobita and D. J. Williams, *Organometallics*, **3**, 333 (1984).
34. S. Murakami, S. Collin and S. Masamune, *Tetrahedron Lett.*, **25**, 2131 (1984).
35. A. Grybat and M. Weidenbruch, unpublished results.
36. H. Watanabe, K. Takeuchi, N. Fukava, M. Kato, M. Goto and Y. Nagai, *Chem. Lett.*, 1341 (1987).
37. R. S. Archibald, Y. van den Winkel, D. R. Powell and R. West, *J. Organomet. Chem.*, **446**, 67 (1993).
38. H. B. Yokelson, D. A. Siegel, A. J. Millevolte, J. Maxka and R. West, *Organometallics*, **9**, 1005 (1990).
39. (a) M. Kira, T. Maruyama, C. Kabuto, K. Ebata and H. Sakurai, *Angew. Chem.*, **106**, 1575 (1994); *Angew. Chem., Int. Ed. Engl.*, **33**, 1489 (1994).
(b) A. Sekiguchi, M. Ichinohe and S. Yamaguchi, *J. Am. Chem. Soc.*, **121**, 10231 (1999).
40. M. J. Michalczyk, R. West and J. Michl, *Organometallics*, **4**, 826 (1985).
41. B. D. Shephard, D. R. Powell and R. West, *Organometallics*, **8**, 2664 (1989).
42. R. S. Archibald, Y. van den Winkel, A. J. Millevolte, J. M. Desper and R. West, *Organometallics*, **11**, 3276 (1992).
43. A. Grybat, W. Saak and M. Weidenbruch, unpublished results.
44. S. A. Batcheller, T. Tsumuraya, O. Tempkin, W. M. Davis and S. Masamune, *J. Am. Chem. Soc.*, **112**, 9394 (1990).
45. N. Tokitoh, H. Suzuki, R. Okazaki and K. Ogawa, *J. Am. Chem. Soc.*, **115**, 10428 (1993).
46. H. Suzuki, N. Tokitoh, R. Okazaki, J. Harada, K. Ogawa, S. Tomoda and M. Goto, *Organometallics*, **14**, 1016 (1995).
47. A. Grybat, S. Willms and M. Weidenbruch, unpublished results.
48. N. Wiberg, W. Niedermayer and K. Polborn, unpublished results; cited in: N. Wiberg, *Coord. Chem. Rev.*, **163**, 217 (1997).
49. (a) M. Kaftory, M. Kapon and M. Botoshansky, in *The Chemistry of Organic Silicon Compounds*, Volume 2 (Eds. Z. Rappoport and Y. Apeloig), Chap. 5, Wiley, Chichester, 1998, p. 181.
(b) P. P. Power, *Chem. Rev.*, **99**, 3463 (1999).
50. B. D. Shephard, C. F. Campana and R. West, *Heteroatom Chem.*, **1**, 1 (1990).
51. M. Wind, D. R. Powell and R. West, *Organometallics*, **15**, 5772 (1996).
52. M. Stürmann, W. Saak, H. Marsmann and M. Weidenbruch, *Angew. Chem.*, **111**, 145 (1999); *Angew. Chem., Int. Ed.*, **38**, 187 (1999).
53. M. Stürmann, W. Saak, M. Weidenbruch and K. W. Klinkhammer, *Eur. J. Inorg. Chem.*, 579 (1999).
54. Y. Apeloig, in *The Chemistry of Organic Silicon Compounds* (Eds. S. Patai and Z. Rappoport), Chap. 2, Wiley, Chichester, 1989, p. 57.
55. (a) M. C. Holthausen, W. Koch and Y. Apeloig, *J. Am. Chem. Soc.*, **121**, 2623 (1999).
(b) P. P. Gaspar, A. M. Beatty, T. Chen, T. Haile, D. Lei, W. R. Winchester, J. Braddock-Wilking, N. P. Rath, W. T. Klooster, T. F. Koetzle, S. A. Mason and A. Albinat, *Organometallics*, **18**, 3921 (1999).
56. D. E. Goldberg, P. B. Hitchcock, M. F. Lappert, K. M. Thomas, A. J. Thorne, T. Fjeldberg, A. Haaland and B. E. R. Schilling, *J. Chem. Soc., Dalton Trans.*, 2387 (1986).
57. G. Trinquier and J. P. Malrieu, *J. Am. Chem. Soc.*, **109**, 5303 (1987).
58. G. Trinquier, *J. Am. Chem. Soc.*, **112**, 2130 (1990).
59. T. L. Windus and M. S. Gordon, *J. Am. Chem. Soc.*, **114**, 9559 (1992).
60. H. Jacobsen and T. Ziegler, *J. Am. Chem. Soc.*, **116**, 3667 (1994) and references cited therein.
61. C. Liang and L. C. Allen, *J. Am. Chem. Soc.*, **112**, 1039 (1990).
62. K. W. Zilm, D. M. Grant, J. Michl, M. J. Fink and R. West, *Organometallics*, **2**, 193 (1983).
63. J. D. Cavalieri, R. West, J. C. Duchamp and K. W. Zilm, *Phosphorus, Sulfur, Silicon, Relat. Elem.*, **93–94**, 213 (1995).
64. R. West, J. D. Cavalieri, J. J. Buffy, C. Fry, K. W. Zilm, J. C. Duchamp, M. Kira, T. Iwamoto, T. Müller and Y. Apeloig, *J. Am. Chem. Soc.*, **119**, 4972 (1997).
65. A. Schäfer, M. Weidenbruch, K. Peters and H. G. von Schnering, *Angew. Chem.*, **96**, 311 (1984); *Angew. Chem., Int. Ed. Engl.*, **23**, 302 (1984).
66. A. Schäfer, M. Weidenbruch and S. Pohl, *J. Organomet. Chem.*, **282**, 305 (1985).
67. M. J. Fink, D. J. DeYoung, R. West and J. Michl, *J. Am. Chem. Soc.*, **105**, 1070 (1983).

68. D. J. DeYoung, M. J. Fink, R. West and J. Michl, *Main Group Met. Chem.*, **10**, 19 (1987).
69. T. Iwamoto, H. Sakurai and M. Kira, *Bull. Chem. Soc. Jpn.*, **71**, 2741 (1998).
70. C. E. Dixon, H. W. Liu, C. M. Van der Kant and K. M. Baines, *Organometallics*, **15**, 5701 (1996).
71. M. Weidenbruch, E. Kroke, H. Marsmann, S. Pohl and W. Saak, *J. Chem. Soc., Chem. Commun.*, 1233 (1994).
72. M. Weidenbruch, B. Flintjer, S. Pohl, D. Haase and J. Martens, *J. Organomet. Chem.*, **328**, C1 (1988).
73. M. Weidenbruch, A. Lesch, K. Peters and H. G. von Schnering, *J. Organomet. Chem.*, **423**, 429 (1992).
74. E. Kroke, M. Weidenbruch, W. Saak, S. Pohl and H. Marsmann, *Organometallics*, **14**, 5695 (1995).
75. J. L. Shibley, R. West, C. A. Tessier and R. K. Hayashi, *Organometallics*, **12**, 3480 (1993).
76. E. K. Pham and R. West, *J. Am. Chem. Soc.*, **111**, 7667 (1989).
77. D. H. Berry, J. H. Chey, H. S. Zipin and P. J. Carroll, *J. Am. Chem. Soc.*, **112**, 452 (1990).
78. R. West, D. J. DeYoung and K. J. Haller, *J. Am. Chem. Soc.*, **107**, 4942 (1985).
79. R. P. Tan, G. R. Gillette, D. R. Powell and R. West, *Organometallics*, **10**, 546 (1991).
80. J. E. Mangette, D. R. Powell and R. West, *J. Chem. Soc., Chem. Commun.*, 1348 (1993).
81. J. E. Mangette, D. R. Powell and R. West, *Organometallics*, **14**, 3551 (1995).
82. H. B. Yokelson, A. J. Millevolte, G. R. Gillette and R. West, *J. Am. Chem. Soc.*, **109**, 6865 (1987).
83. J. E. Mangette, D. R. Powell and R. West, *Organometallics*, **13**, 4097 (1994).
84. A. J. Millevolte, D. R. Powell, S. G. Johnson and R. West, *Organometallics*, **11**, 1091 (1992).
85. G. R. Gillette and R. West, *J. Organomet. Chem.*, **394**, 45 (1990).
86. S. Masamune, S. Murakami, H. Tobita and D. J. Williams, *J. Am. Chem. Soc.*, **105**, 7776 (1983).
87. H. Piana and U. Schubert, *J. Organomet. Chem.*, **348**, C49 (1988).
88. H. B. Yokelson, A. J. Millevolte, K. J. Haller and R. West, *J. Chem. Soc., Chem. Commun.*, 1605 (1987).
89. R. S. Grev and H. F. Schaefer, III, *J. Am. Chem. Soc.*, **111**, 6137 (1989).
90. M. Ishikawa, H. Sugisawa, M. Kumada, T. Higuchi, K. Matsui, K. Hirotsu and J. Iyoda, *Organometallics*, **2**, 174 (1983).
91. A. Heine and D. Stalke, *Angew. Chem.*, **106**, 121 (1994); *Angew. Chem., Int. Ed. Engl.*, **33**, 113 (1994).
92. R. P. Tan, N. M. Comerlato, D. R. Powell and R. West, *Angew. Chem.*, **104**, 1251 (1992); *Angew. Chem., Int. Ed. Engl.*, **31**, 1217 (1992).
93. W. Ando, M. Kako, T. Akasaka and S. Nagase, *Organometallics*, **12**, 1514 (1993).
94. M. J. S. Dewar, *Bull. Soc. Chim. Fr.*, **18**, C17 (1951).
95. J. Chatt and L. A. Duncanson, *J. Chem. Soc.*, 2939 (1953).
96. M. Weidenbruch, A. Pellmann, S. Pohl, W. Saak and H. Marsmann, *Chem. Ber.*, **128**, 935 (1995).
97. R. Konecny and R. Hoffmann, *J. Am. Chem. Soc.*, **121**, 7918 (1999).
98. R. S. Grev and H. F. Schaefer III, *J. Am. Chem. Soc.*, **109**, 6577 (1987).
99. D. Cremer, J. Gauss, and E. Cremer, *J. Mol. Struct. (THEOCHEM)*, **163**, 531 (1988).
100. J. A. Boatz and M. S. Gordon, *J. Phys. Chem.*, **93**, 3025 (1989).
101. D. L. Boger and S. M. Weinreb, *Hetero Diels–Alder Methodology*, Academic Press, San Diego, 1987.
102. S. Masamune, S. Murakami and H. Tobita, *Organometallics*, **2**, 1464 (1983).
103. M. Weidenbruch, A. Schäfer and H. Marsmann, *J. Organomet. Chem.*, **354**, C12 (1988).
104. M. Weidenbruch, H. Piel, A. Lesch, K. Peters and H. G. von Schnering, *J. Organomet. Chem.*, **454**, 35 (1993).
105. M. Weidenbruch, A. Schäfer and K. L. Thom, *Z. Naturforsch.*, **38B**, 1695 (1983).
106. M. Weidenbruch, E. Kroke, K. Peters and H. G. von Schnering, *J. Organomet. Chem.*, **461**, 35 (1993).
107. M. Weidenbruch, A. Lesch, K. Peters and H. G. von Schnering, *Chem. Ber.*, **123**, 1795 (1990).
108. M. Weidenbruch, A. Lesch and K. Peters, *J. Organomet. Chem.*, **407**, 31 (1991).
109. M. Weidenbruch, B. Flintjer, S. Pohl and W. Saak, *Angew. Chem., Int. Ed. Engl.*, **28**, 95 (1989).

110. L. Kirmaier, M. Weidenbruch, H. Marsmann, K. Peters and H. G. von Schnering, *Organometallics*, **17**, 1237 (1998).
111. C. E. Dixon, J. E. Cooke and K. M. Baines, *Organometallics*, **16**, 5437 (1997).
112. D. J. DeYoung and R. West, *Chem. Lett.*, 883 (1986).
113. A. D. Fanta, D. J. DeYoung, J. Belzner and R. West, *Organometallics*, **10**, 3466 (1991).
114. K. Kabeta, D. R. Powell, J. Hanson and R. West, *Organometallics*, **10**, 827 (1991).
115. A. Sakakibara, Y. Kabe, T. Shimizu and W. Ando, *J. Chem. Soc., Chem. Commun.*, 43 (1991).
116. G. R. Gillette, J. Maxka and R. West, *Angew. Chem.*, **101**, 90 (1989); *Angew. Chem., Int. Ed. Engl.*, **28**, 54 (1989).
117. A. D. Fanta, J. Belzner, D. R. Powell and R. West, *Organometallics*, **12**, 2177 (1993).
118. M. Weidenbruch, S. Olthoff, K. Peters and H. G. von Schnering, *Chem. Commun.*, 1433 (1997).
119. J. Belzner, H. Ihmels, B. O. Kneisel and R. Herbst-Irmer, *J. Chem. Soc., Chem. Commun.*, 1989 (1994).
120. M. J. Fink, K. J. Haller, R. West and J. Michl, *J. Am. Chem. Soc.*, **106**, 822 (1984).
121. K. L. McKillop, G. R. Gillette, D. R. Powell and R. West, *J. Am. Chem. Soc.*, **114**, 5203 (1992).
122. H. Son, R. P. Tan, D. R. Powell and R. West, *Organometallics*, **13**, 1390 (1994).
123. M. J. Michalczyk, M. J. Fink, K. J. Haller, R. West and J. Michl, *Organometallics*, **5**, 531 (1986).
124. J. E. Mangette, D. R. Powell, J. C. Calabrese and R. West, *Organometallics*, **14**, 4064 (1995).
125. J. E. Mangette, D. R. Powell, T. K. Firman and R. West, *J. Organomet. Chem.*, **521**, 363 (1996).
126. M. Driess, A. D. Fanta, D. R. Powell and R. West, *Angew. Chem.*, **101**, 1087 (1989); *Angew. Chem., Int. Ed. Engl.*, **28**, 1038 (1989).
127. A. D. Fanta, R. P. Tan, N. M. Comerlato, M. Driess, D. R. Powell and R. West, *Inorg. Chim. Acta*, **198–200**, 733 (1992).
128. R. P. Tan, N. M. Comerlato, D. R. Powell and R. West, *Angew. Chem.*, **104**, 1251 (1992); *Angew. Chem., Int. Ed. Engl.*, **31**, 1217 (1992).
129. P. P. Gaspar and R. West, in *The Chemistry of Organic Silicon Compounds*, Volume 2 (Eds. Z. Rappoport and Y. Apeloig), Chap. 23, Wiley, Chichester, 1998, p. 2643. See also: R. Okazaki, *Pure Appl. Chem.*, **68**, 895 (1996).
130. M. Weidenbruch, S. Willms, W. Saak and G. Henkel, *Angew. Chem.*, **109**, 2612 (1997); *Angew. Chem., Int. Ed. Engl.*, **36**, 2503 (1997).
131. J. March, *Advanced Organic Chemistry*, 4th ed., Wiley, New York, 1992, p. 294.
132. S. Masamune, Y. Kabe, S. Collins, D. J. Williams and R. Jones, *J. Am. Chem. Soc.*, **107**, 5552 (1985).
133. R. Jones, D. J. Williams, Y. Kabe and S. Masamune, *Angew. Chem.*, **98**, 176 (1986); *Angew. Chem., Int. Ed. Engl.*, **25**, 173 (1986).
134. T. Müller, in *Organosilicon Chemistry IV* (Eds. N. Auner and J. Weis), Wiley-VCH, Weinheim, 2000, p. 110.
135. S. Willms, A. Grybat, W. Saak, M. Weidenbruch and H. Marsmann, *Z. Anorg. Allg. Chem.*, **626**, 1148 (2000). See also: S. Willms and M. Weidenbruch, in *Organosilicon Chemistry IV* (Eds. N. Auner and J. Weis), Wiley-VCH, Weinheim, 2000, p. 117.
136. M. Kira, T. Iwamoto and C. Kabuto, *J. Am. Chem. Soc.*, **118**, 10303 (1996).
137. T. Iwamoto, C. Kabuto and M. Kira, *J. Am. Chem. Soc.*, **121**, 886 (1999).
138. T. Iwamoto and M. Kira, *Chem. Lett.*, 227 (1998).
139. N. Wiberg, C. M. M. Finger and K. Polborn, *Angew. Chem.*, **105**, 1140 (1993); *Angew. Chem., Int. Ed. Engl.*, **32**, 923 (1993).
140. N. Wiberg, H. Auer, H. Nöth, J. Knizek and K. Polborn, *Angew. Chem.*, **110**, 3030 (1998); *Angew. Chem., Int. Ed. Engl.*, **37**, 2869 (1998).
141. M. Ichinohe, T. Matsuno and A. Sekiguchi, *Angew. Chem.*, **111**, 2331 (1999); *Angew. Chem., Int. Ed. Engl.*, **38**, 2194 (1999).
142. A. Grybat, S. Boomgaarden, W. Saak, H. Marsmann and M. Weidenbruch, *Angew. Chem.*, **111**, 2161 (1999); *Angew. Chem., Int. Ed. Engl.*, **38**, 2010 (1999).
143. K. B. Wiberg, G. B. Ellison, J. J. Wendolowski, W. E. Pratt and M. D. Harmony, *J. Am. Chem. Soc.*, **100**, 7837 (1978).
144. H. Lischka and H. Köhler, *J. Am. Chem. Soc.*, **105**, 6646 (1983).

145. M. Bogey, H. Bolvin, C. Demuynck and J. L. Destombes, *Phys. Rev. Lett.*, **66**, 413 (1991).
146. B. T. Colegrove and H. F. Schaefer III, *J. Phys. Chem.*, **94**, 5593 (1990).
147. R. S. Grev and H. F. Schaefer III, *J. Chem. Phys.*, **97**, 7990 (1992).
148. M. Cordonnier, M. Bogey, C. Demuynck and J. L. Destombes, *J. Chem. Phys.*, **97**, 7984 (1992).
149. R. S. Grev, *Adv. Organomet. Chem.*, **33**, 161 (1991).
150. A. Sekiguchi, S. S. Zigler, R. West and J. Michl, *J. Am. Chem. Soc.*, **108**, 4241 (1986).
151. A. Sekiguchi, G. R. Gillette and R. West, *Organometallics*, **7**, 1226 (1988).
152. A. Sekiguchi, S. S. Zigler, K. J. Haller and R. West, *Recl. Trav. Chim. Pays-Bas*, **107**, 197 (1988).
153. B. T. Colegrove and H. F. Schaefer III, *J. Am. Chem. Soc.*, **113**, 1557 (1991).
154. K. Kobayashi and S. Nagase, *Organometallics*, **16**, 2489 (1997).
155. D. M. Hoffman, R. Hoffmann and C. R. Fisel, *J. Am. Chem. Soc.*, **104**, 3858 (1982).
156. N. Wiberg, *Coord. Chem. Rev.*, **163**, 217 (1997).

CHAPTER 6

Recent developments in the chemistry of compounds with silicon–nitrogen bonds

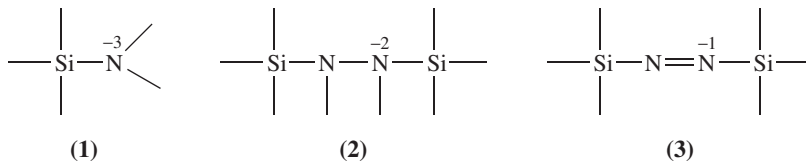
PETER NEUGEBAUER, BETTINA JASCHKE and UWE KLINGEBIEL

*Institute of Inorganic Chemistry, University of Goettingen, Tammannstr. 4, D-37077
Goettingen, Germany*
Fax: 49-551-393373; e-mail: uklinge@gwdg.de

I. INTRODUCTION	430
II. PREPARATION AND PROPERTIES OF THE Si–N BOND	430
III. AMINOSILANES	431
IV. LITHIUM DERIVATIVES OF SILYLAMINES	434
V. LITHIUM DERIVATIVES OF HYDRAZINES	439
VI. IMINOSILANES	440
VII. CYCLIC SILICON–NITROGEN COMPOUNDS	442
A. Synthesis	442
B. Interconversions	444
VIII. CYCLODISILAZANES	445
A. Synthesis	445
B. Calculated and Measured Parameters of Cyclodisilazanes	445
C. Reactions of Cyclodisilazanes	447
IX. CYCLOTETRASILAZANES	449
A. Synthesis	449
B. Reactions of Cyclotrisilazanes	450
C. Interconversions of Anionic Cyclotri- and Cyclodisilazanes	453
X. CYCLOTETRASILAZANES	458
A. Synthesis	458
B. Reactions of Cyclotetrasilazanes	458
C. Interconversion Reactions	460
D. Cage Cyclosilazanes	463
XI. APPLICATION OF CYCLOSILAZANES AS PRECURSORS FOR SILICON-BASED CERAMICS	464
XII. REFERENCES	465

I. INTRODUCTION

The versatility of nitrogen in its compounds depends in large measure on the existence of a range of oxidation states between -3 and $+5$. In its combination with silicon, systems are known in which N has an oxidation state of -3 as in the derivatives of silylamines (**1**), of -2 as in the derivatives of silylhydrazines (**2**), and of -1 as in the derivatives of silylazenes (**3**). Whereas in these compounds silicon is tetrahedral, nitrogen has a changing coordination geometry: in silylamines it is planar but in silylazenes it is linear.

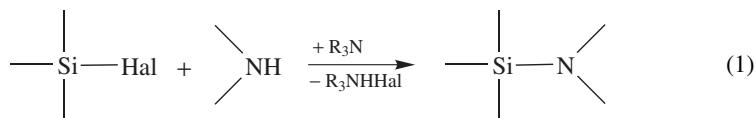


This chapter reviews Si–N compounds, their preparation, properties and reactions. Other reviews on Si–N compounds have appeared elsewhere^{1–10}. However, as the chemistry of Si–N compounds has developed very rapidly in the past years, it seems appropriate to write a review dealing with recent developments.

II. PREPARATION AND PROPERTIES OF THE Si–N BOND

Two main methods of Si–N bond preparation were developed.

(a) *Treatment of an amine with halosilane.* The silylamines are formed by intermolecular loss of a hydrogen halide (equation 1). This is the most common method for preparation of chloro-, bromo-, or iodosilanes¹. Often, auxiliary bases such as triethylamine (as in equation 1) or pyridine are added. However, when an amine is treated with fluorosilanes or silanes, no condensation is observed because of the reduced reactivity. Fluorosilanes only form adducts with amines. Due to the extremely strong Si–F bond, no cleavage of HF or condensation with amine is observed¹. In this case another preparation method must be chosen.

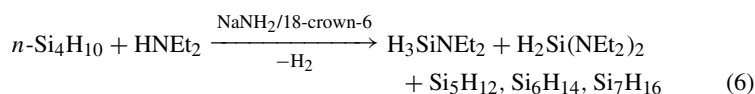
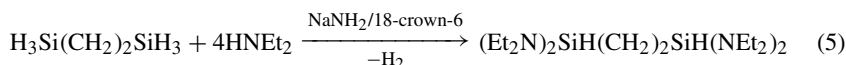
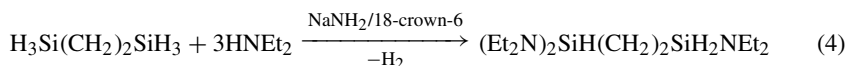
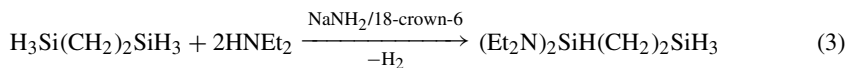


(b) *Treatment of lithiated amines with halosilanes, especially fluorosilanes, with elimination of lithium halide* (equation 2). Elimination of lithium hydride is also possible. The formation of the silylamines depends on the reactivity and the bulk of the halosilane. The yield of the condensation product increases with increasing number of hydrogen atoms on the silicon.



A preparation of silylamines involving H₂ elimination is also possible. 1,4-Disilabutane reacts with the appropriate number of equivalents of diethylamine in an alkane solvent

and in the presence of the two-phase catalyst $\text{NaNH}_2/18\text{-crown-6}$ to give silylamines under H_2 elimination (equations 3–5), whereas $n\text{-Si}_4\text{H}_{10}$ undergoes a cleavage reaction under similar conditions to yield H_3SiNEt_2 , $\text{H}_2\text{Si}(\text{NEt}_2)_2$ and a mixture of polysilanes $\text{Si}_n\text{H}_{2n+2}$ (equation 6)¹¹. Treatment of $n\text{-Si}_4\text{H}_{10}$ with pyrrole (pyrr) leads to the formation of trisilane accompanied by pyrrosilanes $\text{pyrr}_2\text{SiH}_2$, pyrr_3SiH and pyrr_4Si ¹¹.



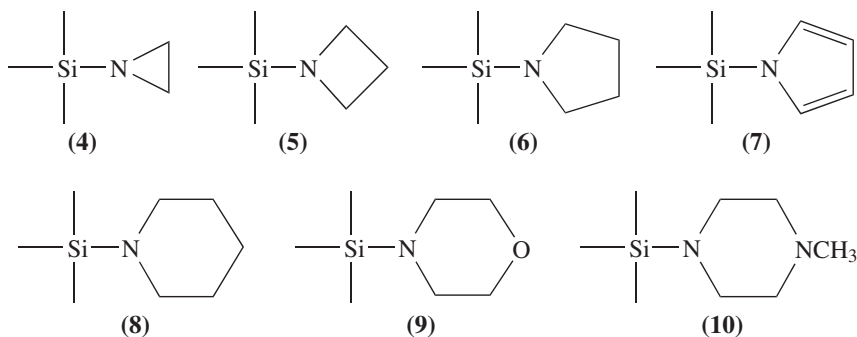
III. AMINOSILANES

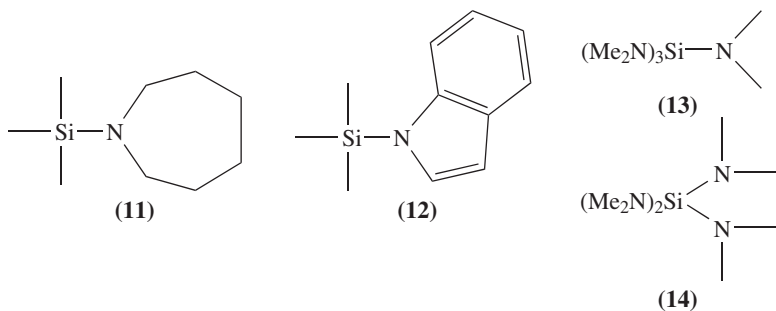
The products formed in equation 1 or 2 depend not only on the number of substituents on nitrogen, but also on their bulk, and on the bulk of the substituents at silicon. Since secondary aminosilanes have the tendency to deaminate, particularly in the presence of an acid catalyst, several products are often the result of amination of chlorosilanes.

Secondary amines give the aminosilane, with the more hindered amines requiring heating under pressure. With primary amines, the aminosilane is formed initially, but the size of the substituents at nitrogen and silicon determines whether deamination subsequently occurs. Prolonged heating under reflux in the presence of ammonium sulfate, or the precipitated amine hydrochloride as acid catalyst yields the disilazane in good yield.

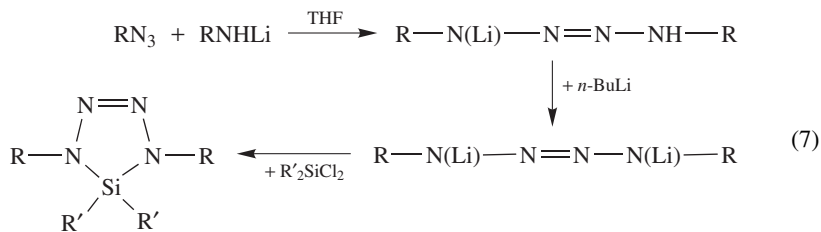
Chlorosilane and chloromethylsilane both give the tris(silyl)amine with ammonia, while the disilazane is the only silicon–nitrogen product formed from chlorotrimethylsilane. Increasing the size of the silicon substituents impedes deamination, so both aminosilane and disilazane result and the amount of the latter increases on prolonged heating.

In the past years new mono-, bis-, tris- and tetrakis-aminosilanes **4–14** with a variety of Si–N units have been synthesized^[12–16].

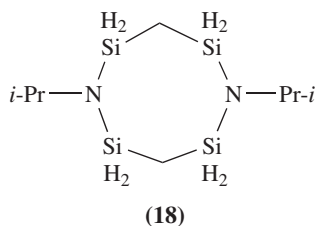
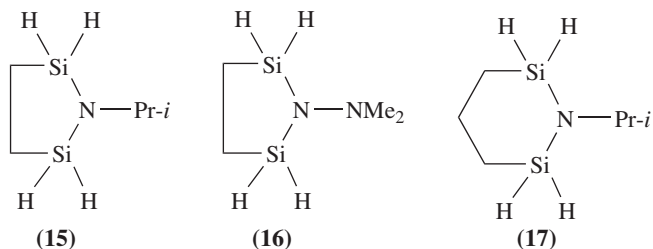




The reaction between aryl azides and lithiated aryl amines leads to tetrazenes, which give cyclic silatetrazenes with halosilanes (equation 7)¹⁷. Also, the new mono-, bis- and tris-silylamines **15–28** were obtained^{18–22}. The hydrazine **16** was analyzed by electron and X-ray diffraction¹⁸.



R = Ph, Mes, *p*-Tol ; R' = H, Me, Cl, Br





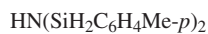
(19)



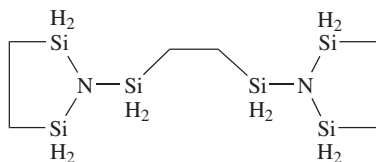
(21)



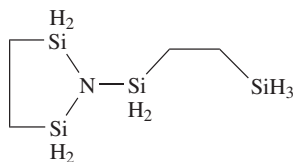
(20)



(22)



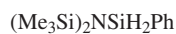
(23)



(24)



(25)



(26)

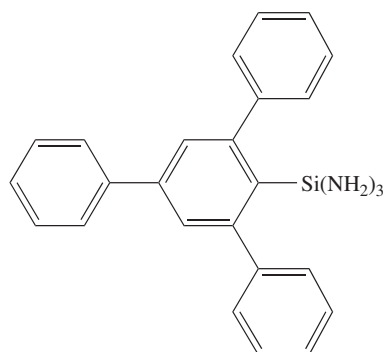


(27)

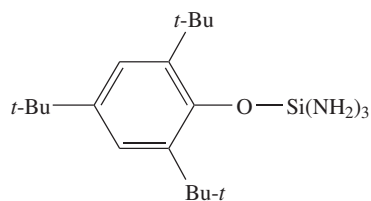


(28)

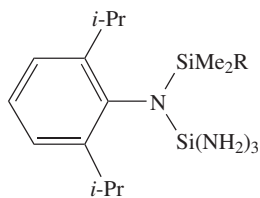
Diaminosilane $\text{R}_2\text{Si}(\text{NH}_2)_2$ can be isolated if at least one substituent is bulky^{23,24}. The isolation of triaminosilanes is possible with very bulky substituents at silicon^{25,26}. Examples are shown in compounds **29–32**.



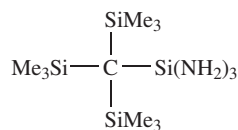
(29)



(30)

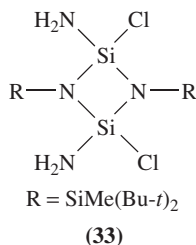
R = Me, *i*-Pr

(31)



(32)

The nitrogen atom in SiNH_2 derivatives is normally pyramidal, but compound **33** with a trigonal planar environment is also known. The exocyclic Si–N bond is extremely short, being 167.1 pm^{27} . In the reaction of methyltrichlorosilane with ammonia a silsesquiazane was obtained²⁸.



IV. LITHIUM DERIVATIVES OF SILYLAMINES

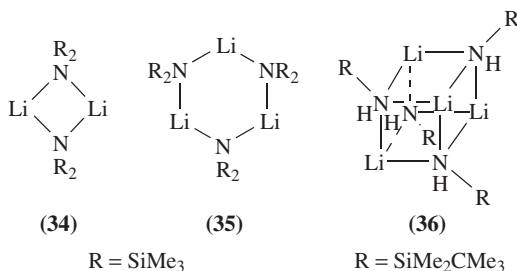
Silylamido groups are used throughout the periodic table to stabilize unusual types of bonding, coordination numbers and oxidation states. Lithium silylamides, generally prepared by reaction of the silylamine with alkyl- or aryllithium derivatives, play an important role in the synthesis of such molecules.

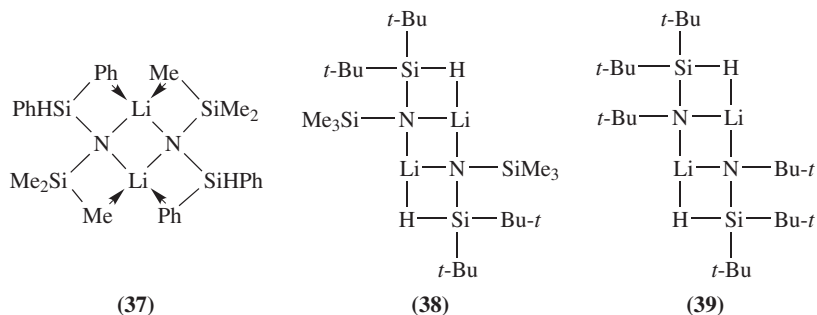
Lithium amides have been the subject of recent reviews, in which the principles underlying their structure were also discussed^{8,29–35}.

Lithium silylamides are solids with definite melting points and they may often be distilled in vacuo without decomposition. They are stable in air, but are sensitive against moisture. They decompose explosively when heated with oxygen or treated with concentrated nitric acid. Further reactions of silylamides can be found in reviews^{1,2,8}.

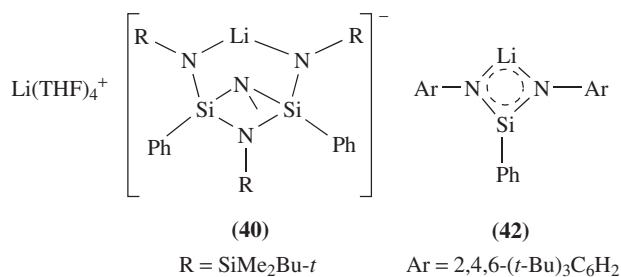
In polar solvents lithium silylamides dissolve as coordinated monomers, but by using 12-crown-4 a separation of the lithium cation and the nitrogen-substituted anion can be obtained. In nonpolar solvents the lithium silylamides dissolve as dimers, trimers or oligomers.

The first structure published of a compound of this group was the trimeric $\text{Li}[\text{N}(\text{SiMe}_3)_2]$ ^{36,37}. Since then a large number of lithium silylamides with ring- (e.g. **34** and **(35)**), lattice- or cage- (**(36)**)³⁸ structures have been analyzed^{8,29–31}. The lithium atoms are not only coordinated by nitrogen atoms, but also by carbon, fluorine or hydrogen atoms of ligands bonded to nitrogen or silicon, or by donor solvent molecules^{39–41}. Examples are compounds **37–39**. These latter lithium derivatives are stable in boiling *m*-xylene. The Si–H stretching vibrations and the ²⁹Si–¹H coupling constants indicate a high hydride character for the H of the Si–H groups⁴².

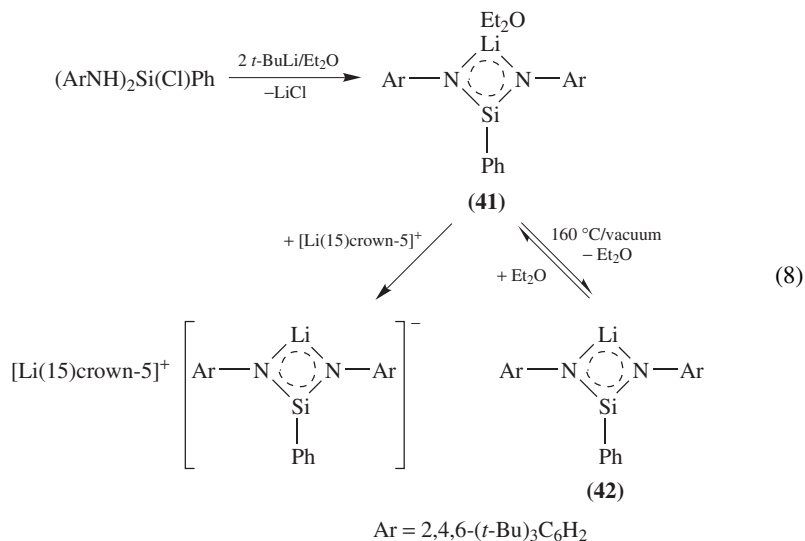




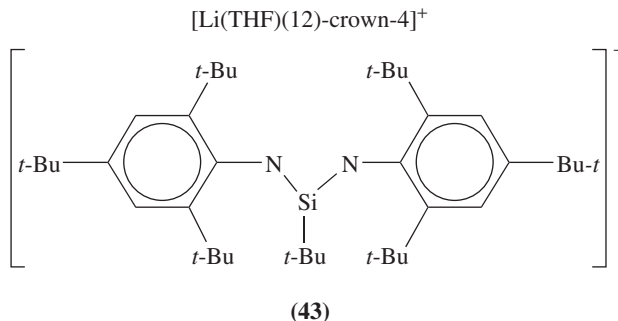
The isolation and characterization of silaamidide ions **40** and **42** as salts have been described in 1991³⁹, 1995 and 1996^{9,40} respectively. Depending on the basicity of the solvent they crystallize as contact ion pairs and free ions.



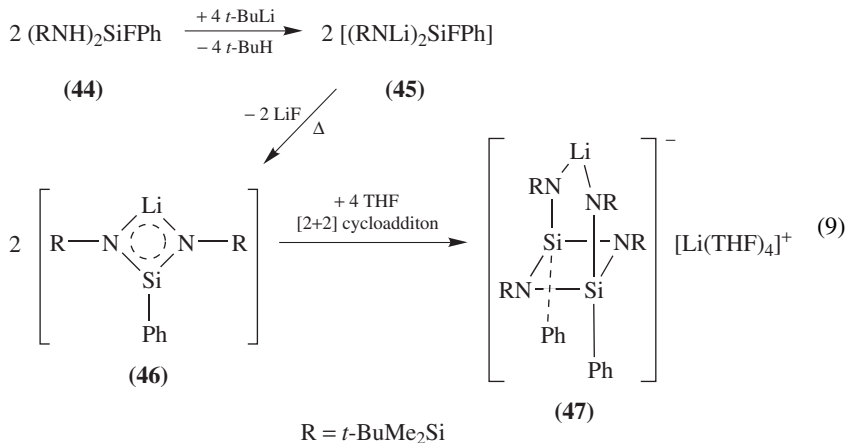
The preparation of the lithium-*N,N'*-bis(2,4,6-tri-*tert*-butylphenyl)phenylsilaamidide **42** via its ether adduct **41** is presented as an example for the preparation of the silaamidides in equation 8. All the silaamidides are moisture-sensitive, but they are thermally stable.



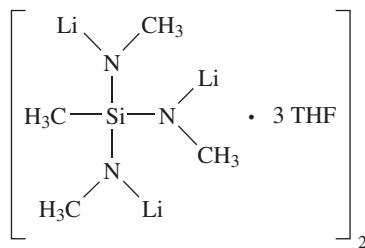
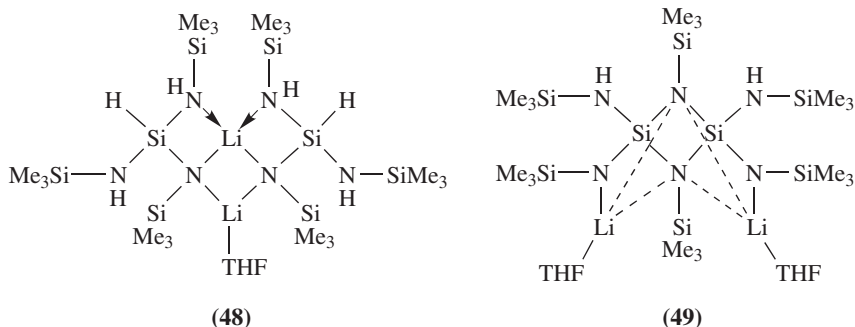
Some of them lose ether when they are heated above 100 °C under vacuum to give the unsolvated salts. The lithium-*N,N'*-bis(2,4,6-tri-*tert*-butylphenyl)-*tert*-butylsilaamidide (THF)(12-crown-4) etherate **43** has been isolated as single crystals and studied by X-ray crystallography. The structure of this silaamidide salt consists of well-separated noninteracting lithium cations [Li(12-crown-4)THF]⁺ and *N,N'*-bis(2,4,6-tri-*tert*-butylphenyl)-*tert*-butylsilaamidide anions. In the anion, the silicon is tricoordinated to a carbon atom of the *tert*-butyl group and to two nitrogen atoms. The silicon–nitrogen bond distances in this molecule are 159.4 pm and 162.6 pm.



In 1995 the first dimeric silaamidides was described^{9,40}. It is formed in a [2 + 2] cycloaddition only if the substituents are not bulky enough to stabilize the monomeric compound. Bis(*tert*-butyldimethylsilylamino)fluorophenylsilane **44** reacts with *t*-BuLi in a 1 : 2 molar ratio to give a dilithium derivative, PhSiF(NLiR)₂ (**45**). LiF elimination in the presence of THF leads to the formation of a silaamidide **46**, which is isolated as a four-membered cyclosilazane anion, (PhSi-NR)₂Li(NR)₂⁻, and Li(THF)₄⁺ cation **47** (equation 9). The endocyclic Si–N bonds are much longer (174.9 and 176.7 pm) than the exocyclic ones (165.0 and 165.6 pm). The (Si–N)₂ ring is not planar and the sum of angles at the nitrogen atoms differs from 360°, being 356.4° and 352.4°⁴⁰. Hydrolysis of dimeric silaamidides is the only, but facile, synthesis of cyclodisilazanes in a *cis*-conformation⁴¹.

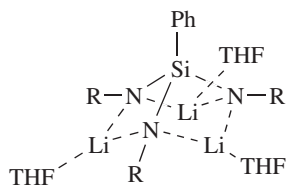


Lithiation of $(\text{Me}_3\text{SiNH})_3\text{SiH}$ in nonpolar solvents leads to an equilibrium of a mono-, di- and triamide. Dissolution in THF gives a dimeric monolithiated amide (**48**) with two different coordinated Li atoms. Reaction of the diamide with chlorotrimethylsilane in boiling THF yields the *cis*-isomer (**49**) of the cyclic diamide. Both lithium atoms coordinate one oxygen atom, one nitrogen atom and the two nitrogen atoms of the cyclodisilazane ring⁴³. An X-ray study of a mixture of the diamide and the triamide was obtained showing alternating cages⁴³. Another cage structure is that of the triamide **50**, which crystallizes as a dimer. The cluster is a cage structure grouped around a crystallographic center of inversion. The silicon and lithium atoms are tetrahedrally tetracoordinated, but the nitrogen atoms are pentacoordinated and have a square pyramidal environment of one carbon, one silicon and three lithium atoms⁴⁴.



(50)

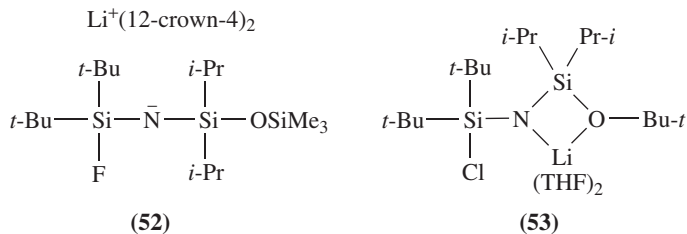
A monomeric structure of a trillithium amide is **51**, which contains three planar (LiNSiN) rings⁴⁵.



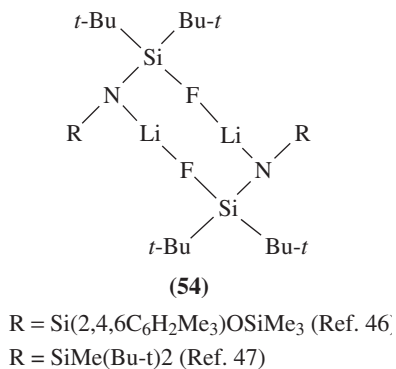
(51)



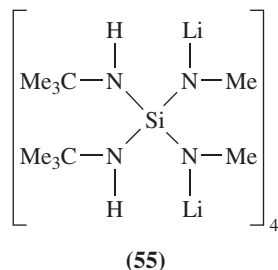
Separation of lithium and the anion is possible with 12-crown-4 as shown in structure **52**. Other donor molecules result in the cyclic structure **53**⁴⁶.



Without a donor solvent an eight-membered ring can be obtained. The coordination sphere in **54** is saturated by carbon atoms of the aromatic substituent⁴⁶. Depending on the basicity of the nitrogen atoms, the eight-membered ring is formed as a Li–N or a Li–F dimer^{8,46,47}.

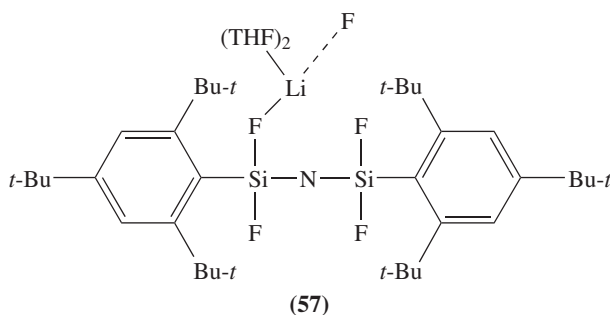
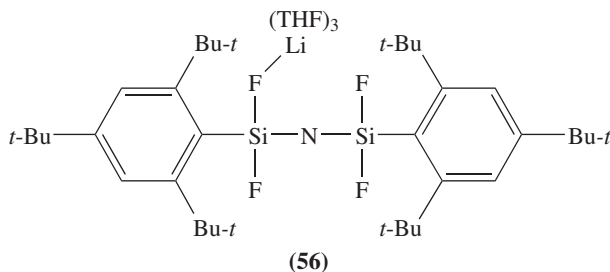


The dilithium derivative of di(*tert*-butylamino)di(methylamino)silane **55** crystallizes in the absence of donor solvents as a tetramer. The lithium is coordinated in three different ways. In the crystal structure two eight-membered (NLiNSi)₂ rings are connected by two lithium atoms⁴⁸.



Another derivative, the Me₂Si(NLiSiMe₃)₂, was prepared by Zimmer and Veith⁴⁹. In the two lithium derivatives **56** and **57** the lithium has no contact to nitrogen. Whereas

compound **57** crystallizes as a polymer via F–LiF bridges compound **56** is a monomeric derivative⁵⁰.

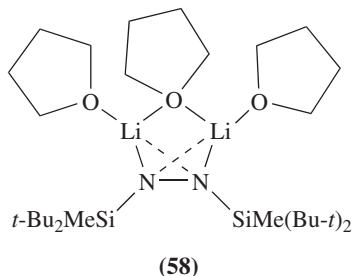


V. LITHIUM DERIVATIVES OF HYDRAZINES

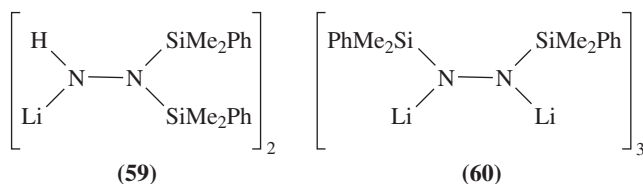
The synthesis of the first silylhydrazines was described in the 1950s^{51,52}. In spite of the successful use of lithium hydrazides in preparative chemistry, the first structure analyses were carried out over 30 years later^{53,54}. Nowadays dimeric, trimeric, tetrameric and hexameric hydrazides have been described^{53–58}.

The lithium ions in these oligomers are differently ‘side-on’ and ‘end-on’ coordinated to the N–N unit. The degree of oligomerization decreases with increasing bulk of the silyl substituents. The chemistry of silylhydrazines and their lithium derivatives has been reviewed⁵³.

The new lithium derivatives **58–60** have been synthesized in the past few years^{59,60}. Dilithiated hydrazine reacts with two equivalents of chlorodimethylphenylsilane to give

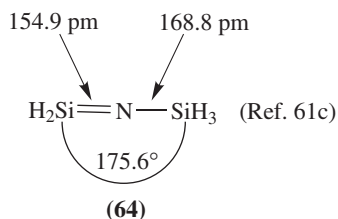
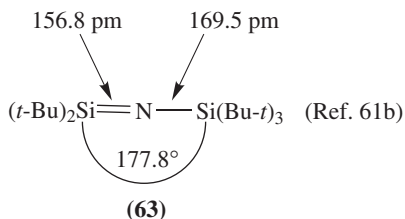
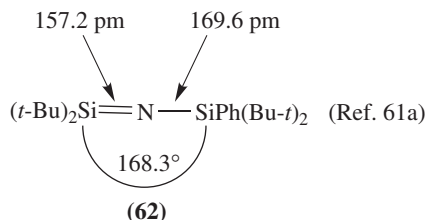
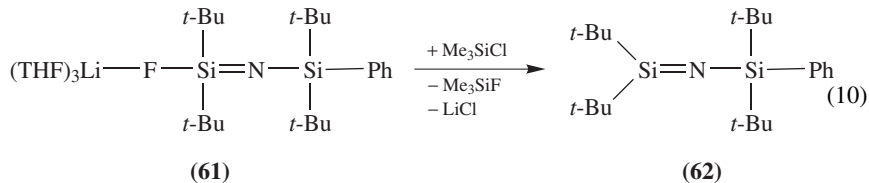


isomeric bis(silyl)hydrazines, such as **58**. Further reaction with one equivalent of *n*-butyllithium leads to the dimeric lithium derivative (**59**) with the lithium coordinated only 'end-on'⁶⁰. Reaction with two equivalents of *n*-butyllithium leads to the trimeric lithium derivative (**60**), containing a Li₆N₆ cluster with equivalent lithium atoms in the crystal structure. This compound is also stable in the gas phase⁶⁰.



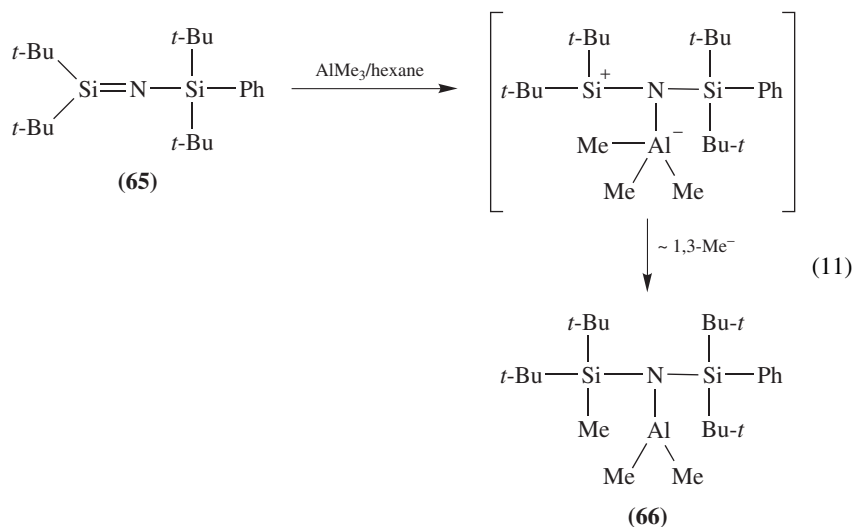
VI. IMINOSILANES

The uncoordinated and thermally stable iminosilane R₂Si=NR' (**62**) is formed in a quantitative yield in the reaction between a lithiated fluorosilylamine **61** and SiClMe₃. The reaction (equation 10) is based on a fluorine/chlorine exchange with a subsequent thermal LiCl elimination. The crystal structure of **62** shows a trigonal arrangement of the C₂Si=N unit. In the solid state the iminosilane is monomeric and the Si=N–Si skeleton is nearly linear with an angle of 168.3°. The Si–N bond lengths are drastically different. The Si–N single bond is 169.6 pm and the Si=N double bond is 157.2 pm. The results are consistent with Wiberg's experimental and Schleyer's calculated results on compounds **63** and **64**^{8,9,61}.

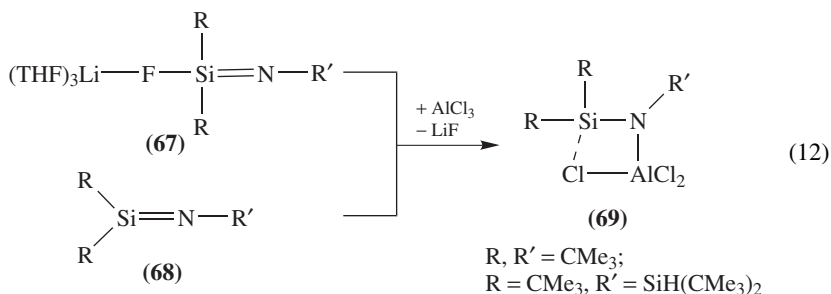


Iminosilanes react with Lewis bases such as ethers or tertiary amines with formation of adducts. The adducts are often thermally stable and can be distilled without decomposition^{8,9}.

Di-*tert*-butyl(di-*tert*-butylphenylsilyl)iminosilane (**65**) reacts with trimethylalane, AlMe₃, to give the monomeric aminoalane (**66**)⁶¹. For the first time a Me⁻ ion migration is observed from the aluminum to the silicon (equation 11). The structure consists of well-separated Me₂AlN(R')R monomers. The Al–N bond length is 186.9 pm. The geometry of the Al atom is nearly planar (sum of angles = 357.8°). The C–Al–C angle is 108.0°. The geometry of the nitrogen center is also planar (sum of angles = 360° with the widest angle of 133.9° (**66**) between the silyl groups)⁶¹.

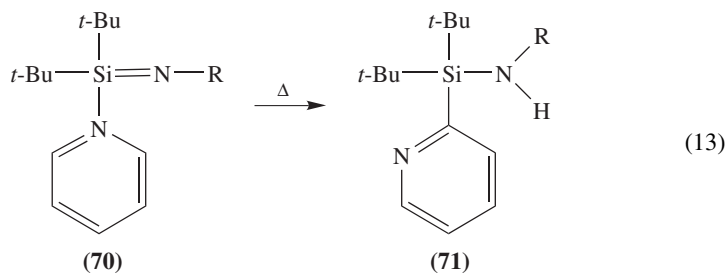


LiF adducts of iminosilanes and uncoordinated iminosilanes (**68**) react with AlCl₃ to give amino silicenium trichloroaluminates (**69**) containing a SiNAlCl four-membered rings (equation 12)^{62,63}.



Iminosilanes form stable adducts with Lewis bases, e.g. THF, NEt₃, Py, etc⁶⁴. The pyridine adduct of the iminosilanes **70** [R = Si(*t*-Bu)₂Ph, Si(*i*-Pr)₂Bu-*t*] isomerizes

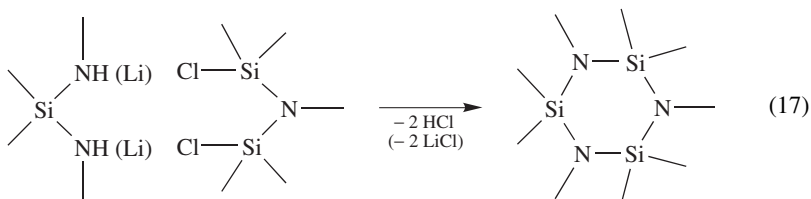
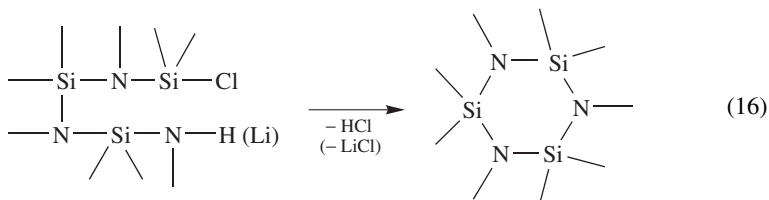
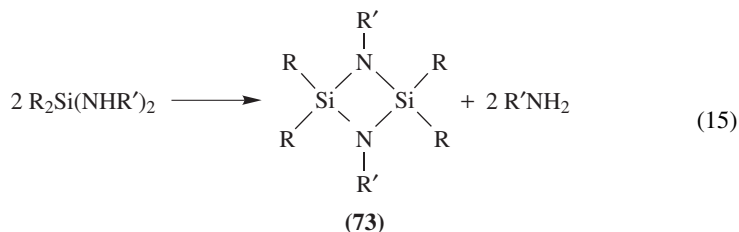
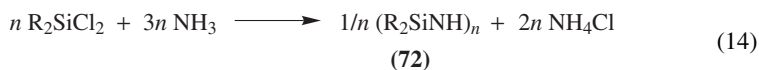
under Stevens migration to **71** (equation 13)⁶⁴.



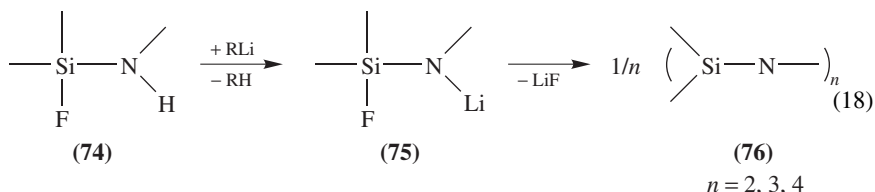
VII. CYCLIC SILICON-NITROGEN COMPOUNDS

A. Synthesis

The ammonolysis of dichlorosilanes leads to the formation of cyclotri- and cyclotetrasilazanes **72**, $n = 3, 4$ (equation 14)⁶⁵⁻⁶⁷. Other classical preparation methods of four- (**73**) to eight-membered cyclosilazanes are the condensation of difunctional building units (equations 15 and 16) and the reaction of amino-functional compounds with halosilyl-functional compounds (equation 17)⁶⁶⁻⁶⁸.



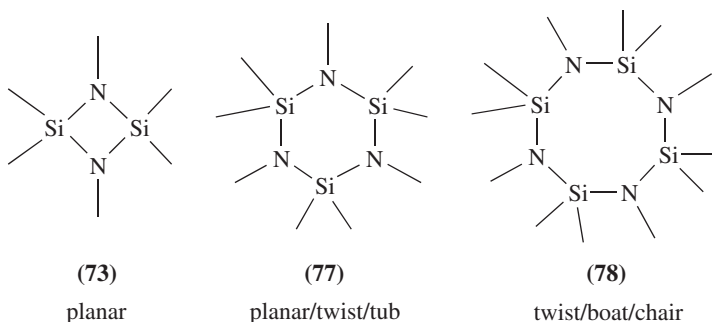
The reaction of equation 14 probably occurs stepwise, and it is a complex process involving substitution reactions and/or homo- and heterofunctional condensations. Numerous cyclodi-, tri- and tetrasilazanes (**76**) are obtained in the reactions of aminofluorosilanes (**74**) with lithium organyls via thermal LiF elimination of lithium aminofluorosilane derivatives (**75**) (equation 18)^{69–75}. The primary products of such condensations in the reaction of fluorosilanes with lithium amide have been synthesized in order to study the mechanisms of their formation. An ($R_2SiFNLiH$) compound was characterized by X-ray diffraction^{8,76,77}.



In contrast to the ammonolysis of chlorosilanes, the four-membered ring was formed along with the six- and eight-membered rings by heating the lithium salts. Four-membered rings of the type (R_2SiNH)₂ had been hitherto unknown. However, the rings can also be synthesized stepwise via acyclic compounds^{76,77}.

The isolation of the 1-fluoro-5-aminohexa-*tert*-butyltrisilazane⁷⁸ shows the last compound in the stepwise synthesis of the bulkiest cyclotrisilazane so far known, the hexa-*tert*-butylcyclotrisilazane, a planar six-membered ring⁷⁹. The bulkiest known cyclotetrasilazane is the octa-*tert*-butyl-substituted ring⁷⁸. Symmetrically substituted six-membered rings are often planar. The octa-*tert*-butylcyclotetrasilazane is the most planar eight-membered ring prepared so far.

Four- and six-membered cyclosilazanes **76** are also obtained in the reaction of dihalosilanes and lithiated silylamines (equation 19)⁴. X-ray determinations show that four-membered (Si–N) rings (**73**) are mostly planar, that the six-membered rings **77** are planar, twisted or have a tub conformation, and that the eight-membered rings (**78**) have twist, boat or chair conformations.



B. Interconversions

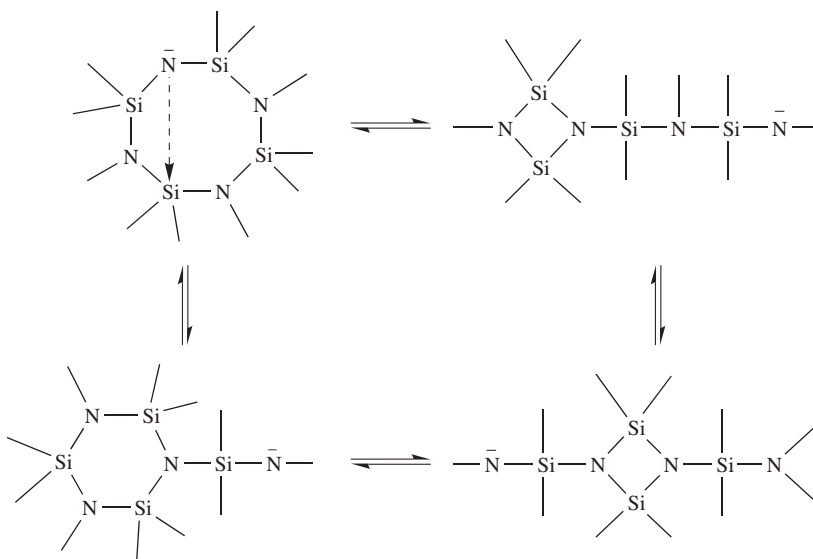
The anions of the eight-, six-, and four-membered cyclosilazanes are in an equilibrium (Schemes 1 and 2). The position of the equilibrium depends very strongly on the temperature, the electronic and steric effects of the ligands and the nucleophilic or electrophilic properties of the attacking ligand according to the following generalizations^{80–84}.

1. Higher temperatures lead to a better N–Si contact across the ring, so isomerization is possible.

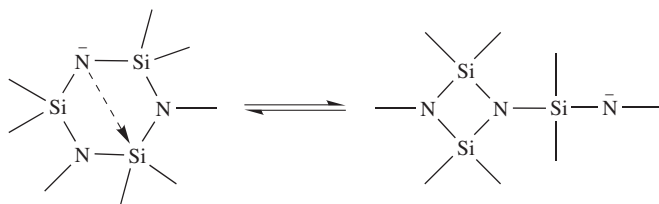
2. $-I$ and $-M$ ligands decrease the basic character of the anion and therefore reduce the tendency for ring contraction. Substituents with $+I$ or $+M$ effect increase the basic character of the ring and raise the tendency for ring contraction.

3. Bulky substituents increase the tendency for ring contraction, because they are better bonded at small rings.

4. If the attacking ligand is a Lewis acid, the basic character of the nitrogen is decreased and the ring size is retained.



SCHEME 1

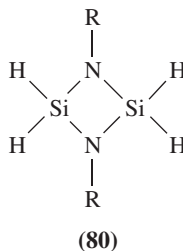
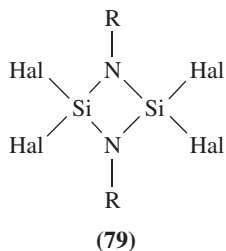


SCHEME 2

VIII. CYCLODISILAZANES

A. Synthesis

Cyclodisilazanes are synthesized according to equations 15, 18 and 19^{85–87}. The cyclodisilazanes **79–84** have been prepared in the last few years.



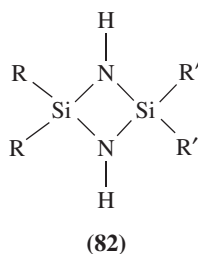
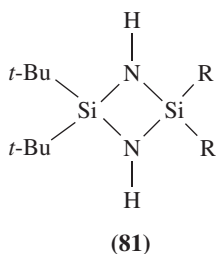
R = Si(*t*-Bu)₂Me, Hal = F (Ref. 85)

Hal = Cl (Ref. 88)

R = Si(*t*-Bu)₂Ph, Hal = F (Ref. 88)

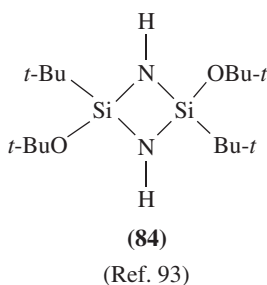
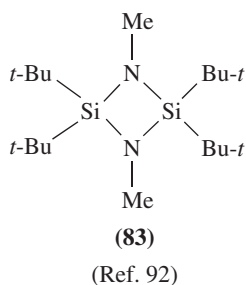
R = *t*-Bu Hal = F, Cl (Ref. 87)

R = Si(*t*-Bu)₂Me (Ref. 89)



R = Me (Ref. 90); R = *i*-Pr (Ref. 91)

R = *t*-Bu, R' = F, R'' = N(SiMe₃)₂ (Ref. 92)



B. Calculated and Measured Parameters of Cyclodisilazanes

Compared with cyclosilazanes bearing organic substituents, only very few Si–N ring systems in which some or all of the substituents are inorganic are known. The former

compounds have the following common structural properties: (1) The endocyclic Si–N–Si angles are larger while the N–Si–N angles are smaller than 90° ; (2) the endocyclic Si–N bonds are longer than the exocyclic Si–N bonds as a result of ring strain.

Cyclosilazanes bearing silyl groups at the nitrogen and fluorine or chlorine substituents at the silicon atoms⁸⁸ display opposite structural features to their organic-substituted counterparts, i.e. the Si–N–Si angles are smaller while the N–Si–N angles are larger than 90° , and the observed endocyclic Si–N bonds are shorter than the exocyclic bonds. Theoretical calculations for model compounds⁸⁸ demonstrate that fluorination of the parent compound, i.e. $(\text{H}_2\text{Si}-\text{NH})_2 \rightarrow (\text{F}_2\text{Si}-\text{NH})_2$, leads to shortening of the endocyclic Si–N bonds from 173 to 170 pm and thus to stabilization of the ring system. Furthermore, silylation at the nitrogen atoms, i.e. $(\text{F}_2\text{Si}-\text{NH})_2 \rightarrow (\text{F}_2\text{Si}-\text{NSiH}_3)_2$, leads to decrease in the endocyclic Si–N–Si angles from 92 to 88° . The combined effect of four fluorine atoms at silicon and of two silyl groups at the nitrogen atoms leads to an overall shortening of the transannular Si...Si distance. The shortest Si...Si contact (242 pm) has been predicted for $(\text{F}_2\text{Si}-\text{NSiH}_3)_2$. The data for several compounds are summarized in Table 1.

The bulk of the exocyclic silyl groups of the measured compounds explains the discrepancy of about 5 pm in the endocyclic Si...Si distance found experimentally. The $(\text{F}_2\text{Si}-\text{N}-\text{Si}(\text{Bu}-t)_2\text{Ph})_2$ is the smallest (Si–X)₂ four-membered ring known so far (X = C, N, O, S)⁸⁷.

The compounds in Table 2 have been structurally analyzed by gas-phase electron diffraction or by X-ray crystal structure analysis and confirm the calculated effects of the substituents^{85,87,88}.

TABLE 1. Calculated and measured geometrical parameters of cyclodisilazanes^{88,89}

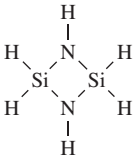
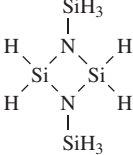
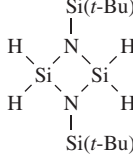
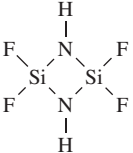
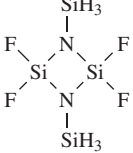
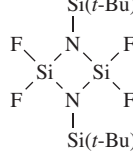
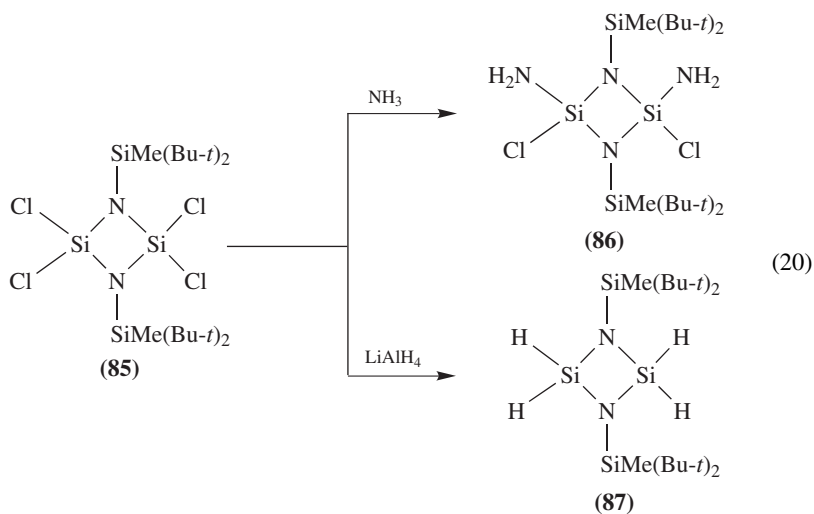
			
	Calc.	Calc.	Measured
Si...Si	254.2 pm	249.7 pm	244.7 pm
Si–N(<i>endo</i>)	173.5 pm	174.6 pm	173.4 pm
N–Si(<i>exo</i>)	—	172.4 pm	173.3 pm
Si–N–Si(<i>ring</i>)	94.2°	91.3°	89.0°
			
	Calc.	Calc.	Measured
Si...Si	247.6 pm	242.5 pm	237.6 pm
Si–N(<i>endo</i>)	171.1 pm	171.8 pm	170.1 pm
N–Si(<i>exo</i>)	—	174.5 pm	178.3 pm
Si–F	157.5 pm	157.4 pm	156.7 pm
Si–N–Si(<i>ring</i>)	92.7°	89.8°	88.4°

TABLE 2. Measured geometrical parameters of (*t*-BuN-SiF₂)₂ and (*t*-BuN-SiCl₂)₂

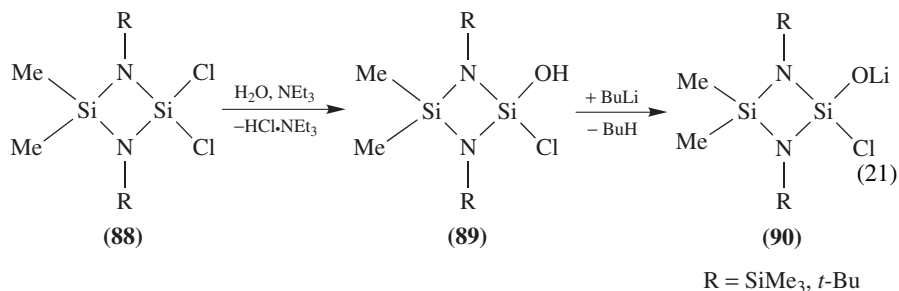
	Gas-phase structure	X-ray structure
Si ... Si	241.3 pm	244.9 pm
Si–N	170.6 pm	171.1 pm
Si–Hal	156.7 pm	203.1 pm
Si–N–Si	90.0°	91.5°

C. Reactions of Cyclodisilazanes

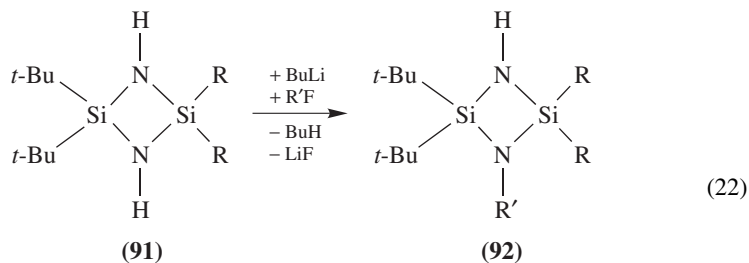
The reaction of the di-*tert*-butylmethylsilyl substituted tetrachlorocyclodisilazane (**85**) with ammonia leads only to the *cis*-(diaminodichloro)cyclodisilazane (**86**), which is not planar. The N–Si₂–N angle is found to be 7.1°²⁷. The first tetrahydridocyclodisilazane (**87**) was obtained in the reaction with LiAlH₄ (equation 20)⁸⁹.



The controlled hydrolysis of dichlorocyclodisilazanes (**88**) in the presence of triethylamine leads to the novel chloro(hydroxy)cyclodisilazanes **89** (equation 21). They are colorless solids which sublime without decomposition, despite the fact that they have both a Cl and an OH function at the same silicon atom. In the crystalline phase the compounds form tetramers by oxygen hydrogen bridges. On treatment with BuLi the lithium salts (**90**) are formed, which crystallize as tetramers in a cubane like oxygen/lithium cages, in which the lithium atoms are coordinated by three oxygen and one chlorine atom. The lithium compounds can be recrystallized from hot nonpolar solvents without elimination of LiCl. Boiling in THF for 50 hours leads to the elimination of LiCl and the formation of amino-functionalized cyclotrisiloxanes⁹⁰.



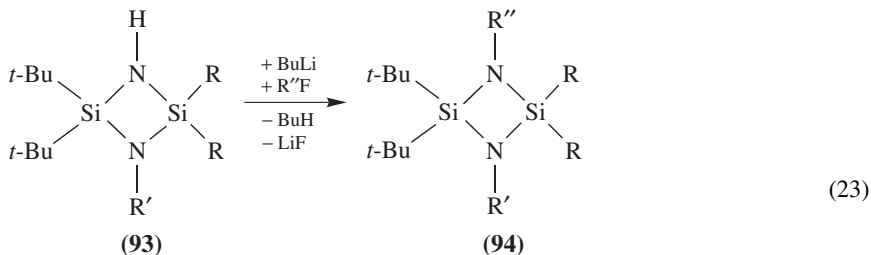
Lithiation of NH-functional cyclodisilazanes **91** and **93** allows a stepwise substitution with silyl groups and ring coupling via silyl groups to give **92** and **94** (equations 22 and 23)^{91–93}. The cyclodisilazane **94**, R' = SiF₂Bu-*t*, R'' = SiF₂Ph forms monoclinic crystals, space group C2/c. The angles between the atoms N–N–Si are 166.5° and 176.4°. The N atoms have a pyramidal environment, a very rare example in case of nitrogen atoms bonded to three silicon atoms. The exocyclic silyl groups are in a *cis* relationship. The electron-withdrawing effect of the fluorine atoms leads to a shortening of the exocyclic Si–N bonds⁹¹.



R = Me, R' = SiFMe₂ (Ref. 90)

R = *i*-Pr, R' = SiF₃, SiF₂Bu-*t*, SiHFMe (Ref. 91)

R = *t*-Bu, R' = SiF₂Bu-*t* (Ref. 91)

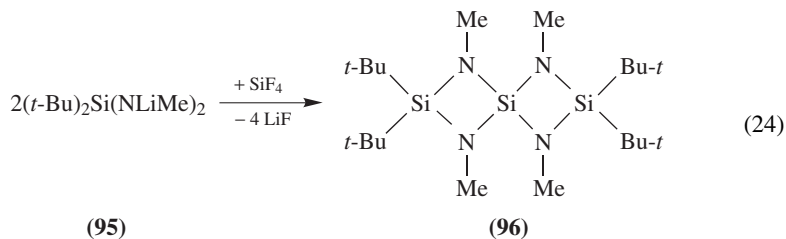


R = Me, R' = R'' = SiFMe₂ (Ref. 90)

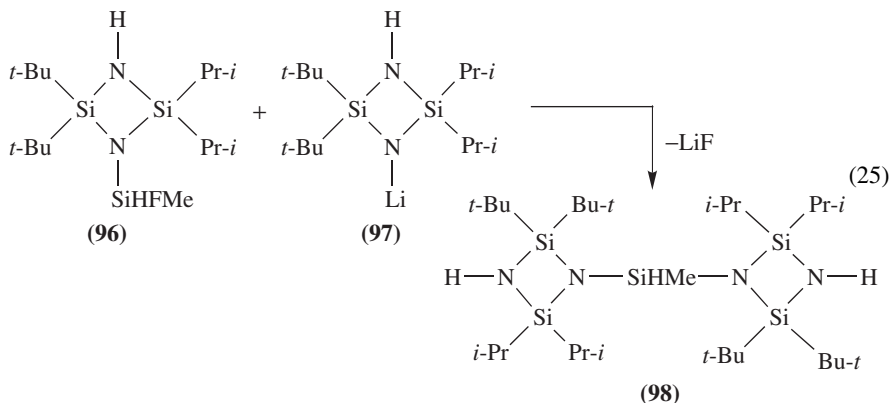
R = *i*-Pr, R' = R'' = SiF₃, SiF₂Bu-*t*, SiHFMe, R' = SiF₂Bu-*t*, R'' = SiF₂Ph (Ref. 91)

R = *t*-Bu, R' = R'' = SiF₂Bu-*t* (Ref. 91)

In the reaction of the dilithium derivative **95** with SiF₄, the spirocyclo **96** rather than the substituted compound was isolated (equation 24)⁹⁴.



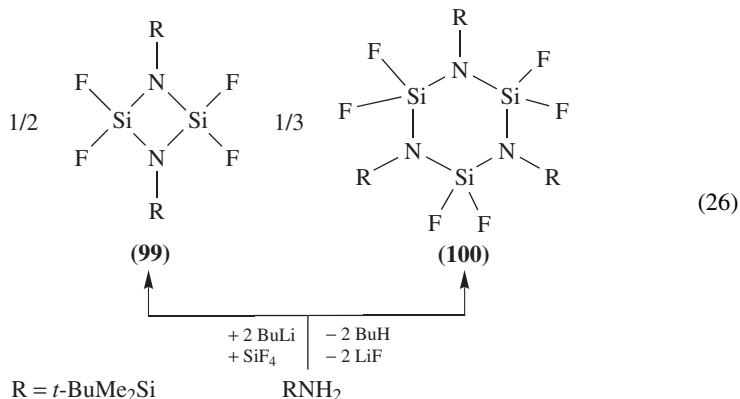
Ring coupling of **96** and **97** via a silyl group to give **98** is described in equation 25⁹².



IX. CYCLOTRISILAZANES

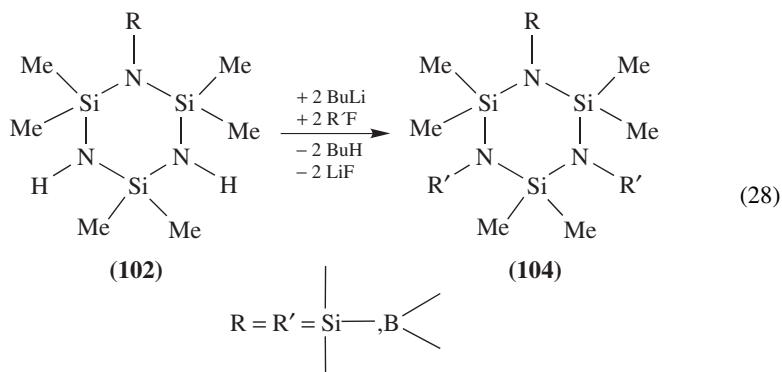
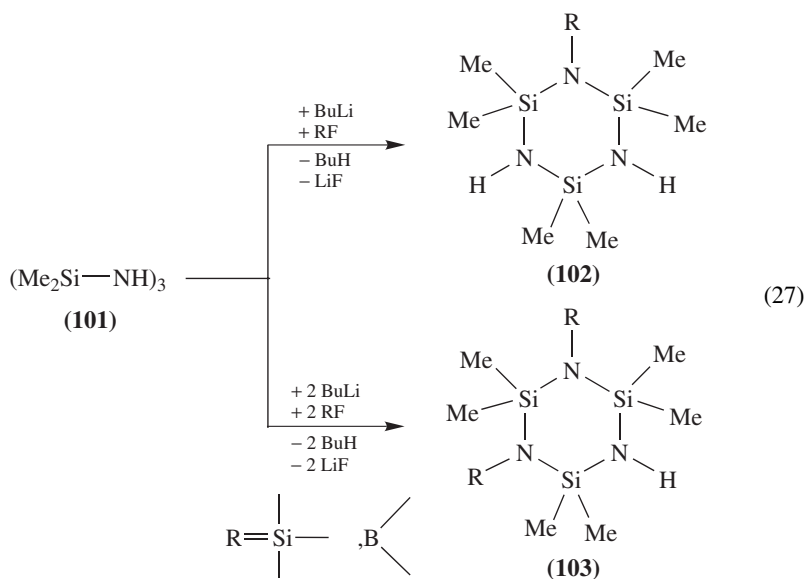
A. Synthesis

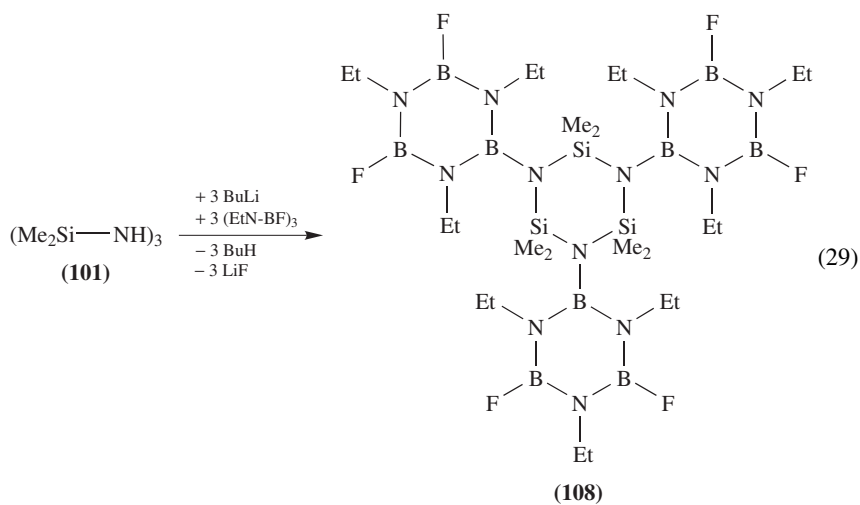
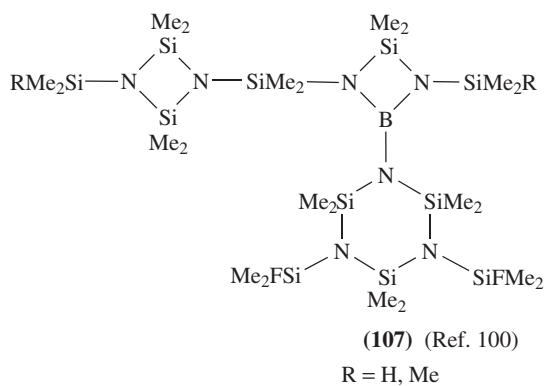
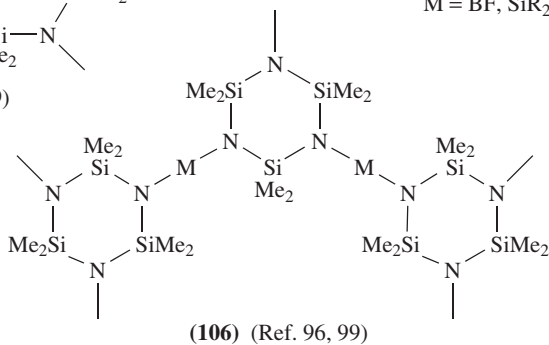
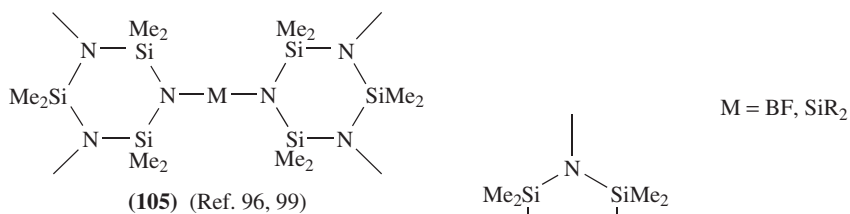
Cyclotrisilazanes are obtained in the ammonolysis of dichlorosilanes (equation 14), LiF elimination from lithiated amino fluorosilanes (equation 18) and Me_3SiHal elimination from trimethylsilylamino halosilanes (equation 19). In the reaction of the dilithiated *tert*-butyldimethylsilylamine and SiF_4 the only known hexafluorocyclotrisilazane (**100**) was isolated beside a four-membered ring **99** (equation 26). The cyclotrisilazane is the first Si–N six-membered ring which crystallizes in a twist conformation.



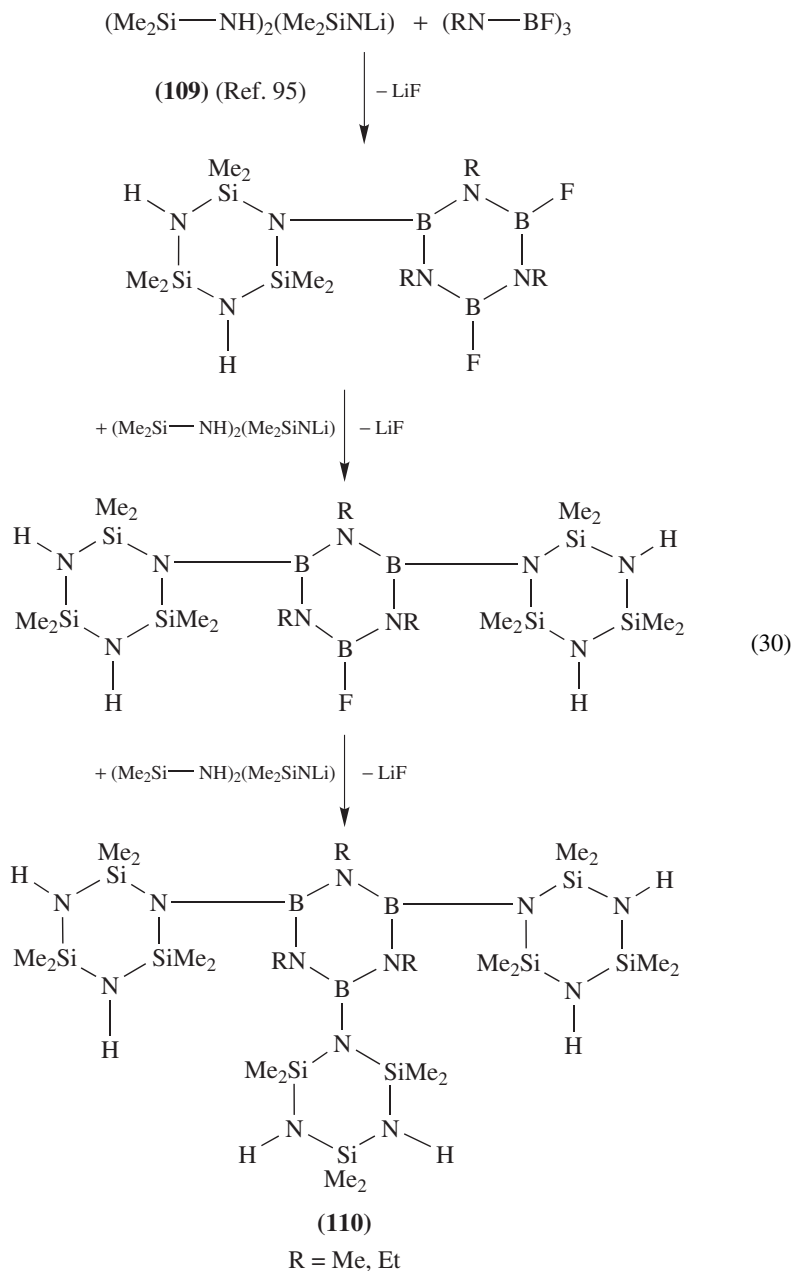
B. Reactions of Cyclotrisilazanes

Hexamethylcyclotrisilazane (**101**) and hexamethyl-trimethylsilylcyclotrisilazane (**102**) form with BuLi lithium derivatives, which crystallize as dimers⁹⁵. Mono- (**102**), di- (**103**), and trisubstitution (**104**) of cyclotrisilazanes with silyl and boryl groups are described (equation 27 and 28)^{95–99}. The silyl groups are alkyl, aryl, fluorine, pyrrole, indole and amino substituted^{95–98}. The boryl groups are fluorine and silylamino-substituted^{99,100}. One six-membered ring is bonded to a PF₂ group¹⁰¹. Cyclotrisilazanes could be coupled via silyl⁹⁶ and boryl groups to give **105** and **106**^{96,99}, and with 1,3-diaza-2-bora-4-silacyclobutanes to give **107**¹⁰⁰. Hexamethylcyclotrisilazane (**101**) was substituted with one, two and three borazine rings¹⁰². Formation of a tri-substituted system (**108**) is described in equation 29.



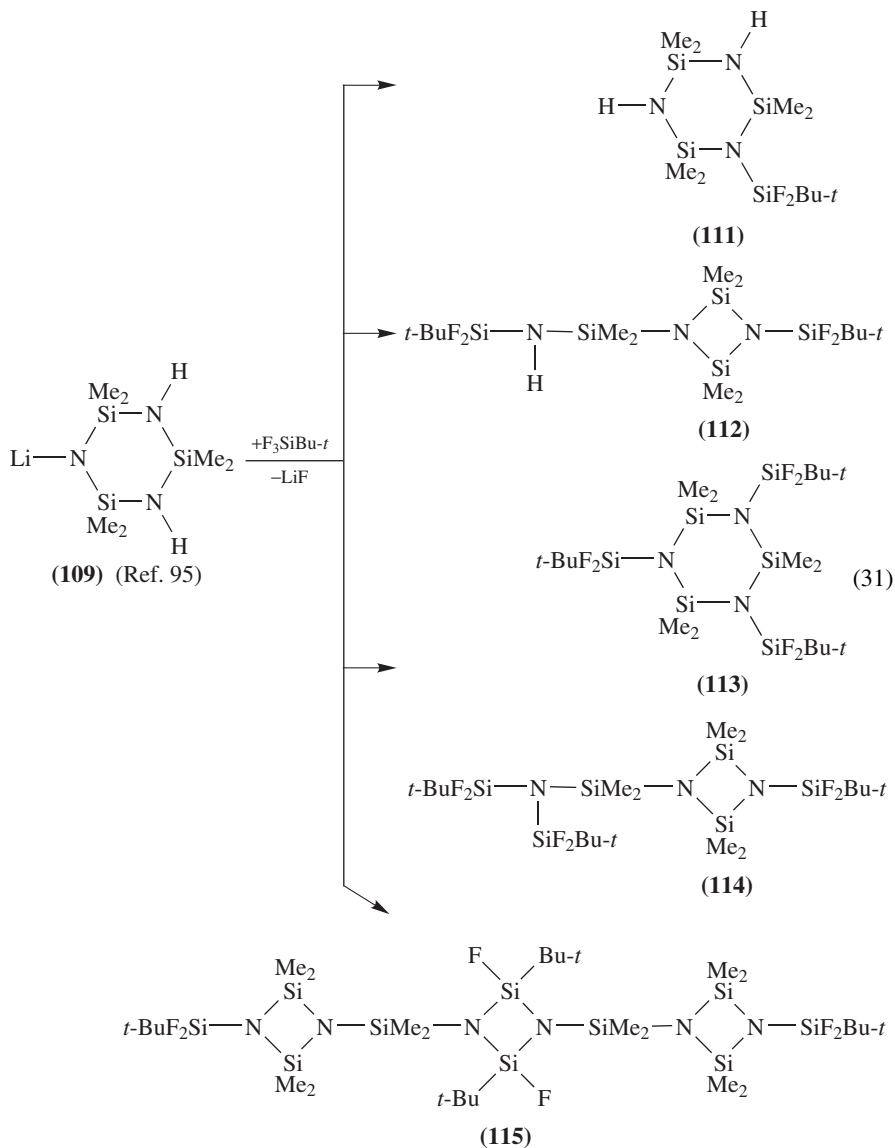


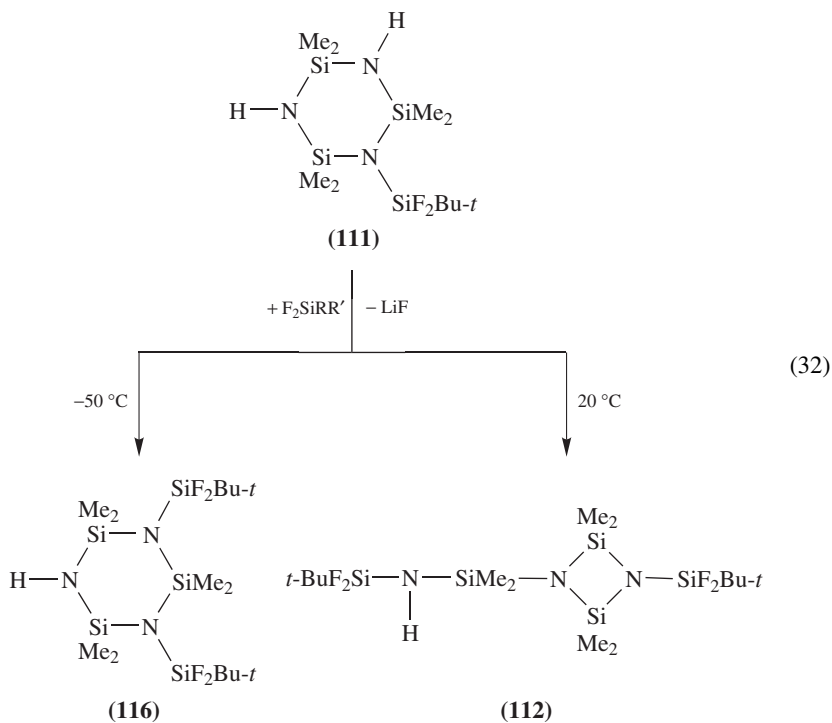
Compounds that are totally symmetric and free of halogen atoms such as **110**, can be formed in a stepwise synthesis of cyclotrisilazanes from **109** and borazines (equation 30)¹⁰².



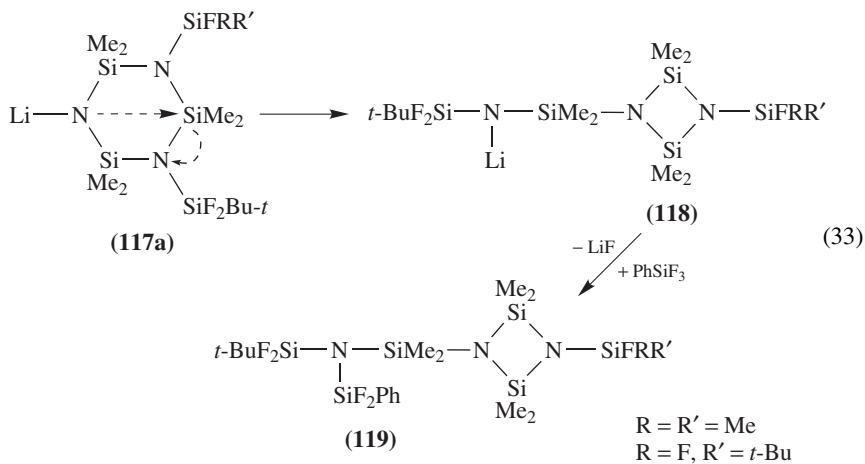
C. Interconversions of Anionic Cyclotri- and Cyclodisilazanes

According to Scheme 2 an equilibrium exists between the anions of cyclotri- and cyclodisilazanes. Based on that equilibrium many isomeric ring compounds, silyl coupled four-membered rings and bicyclic Si–N compounds **111–115** are prepared (equation 31)^{96,97}. The equilibrium of the lithium derivatives depends very strongly on the reaction conditions, for example on the temperature of the reaction: **112** and **116** are formed at different temperatures (equation 32).

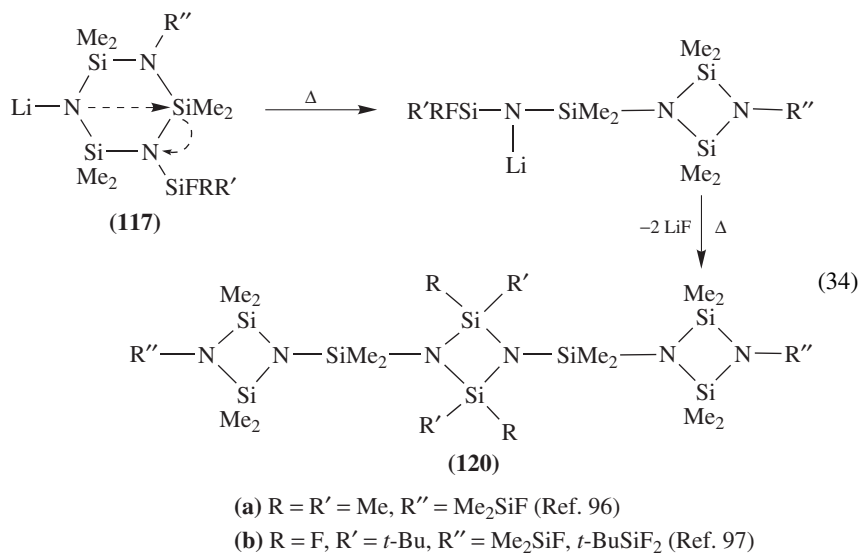




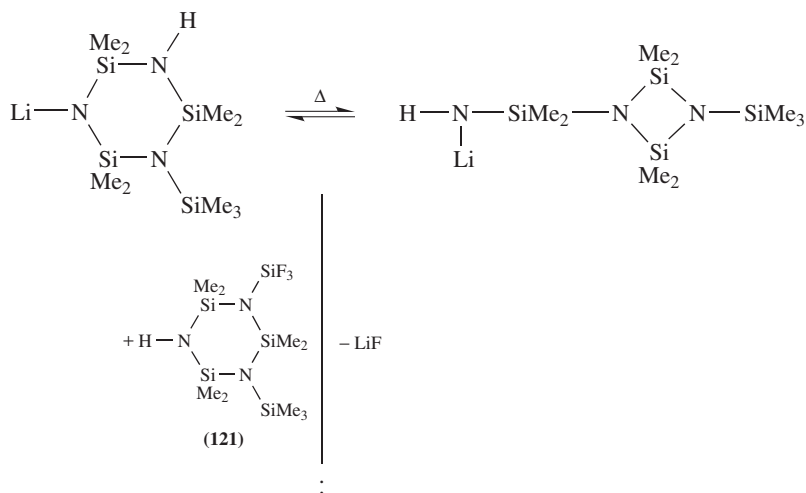
The ring contraction occurs with cleavage of one Si–N bond. It is always the bond with the most electron-withdrawing substituent bonded to the N atom, e.g. the SiF₂ group instead of the SiF group (equation 33). The lithium derivative of the 1-*tert*-butyldifluorosilyl-3-fluorodimethylsilylhexamethylcyclotrisilazane (**117**) was studied by X-ray crystallography⁹⁷. It crystallizes as isomeric cyclodisilazane (**118**) (equation 33).

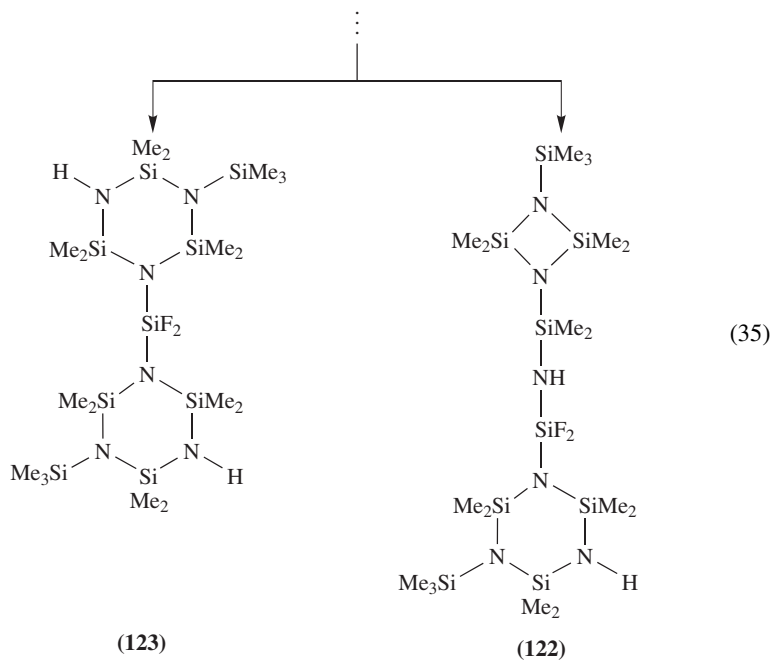


The lithium compound has a polymeric lattice structure in the crystal, formed via $\text{Li} \cdots \text{F}$ contacts. The LiNSiF part of the compound forms an eight-membered ring. The lithium is three-coordinated (sum of the angles = 359.3°)^{96,97}. In the reactions of the lithium derivative with fluorosilanes, exocyclic substitution occurs, e.g., to give **119** (equation 33). The lithium compounds are stable up to about 100°C . At higher temperatures $\text{Li}-\text{F}$ elimination occurs and silyl coupled cyclodisilazanes (**120**) are obtained (equation 34)^{96,97}.

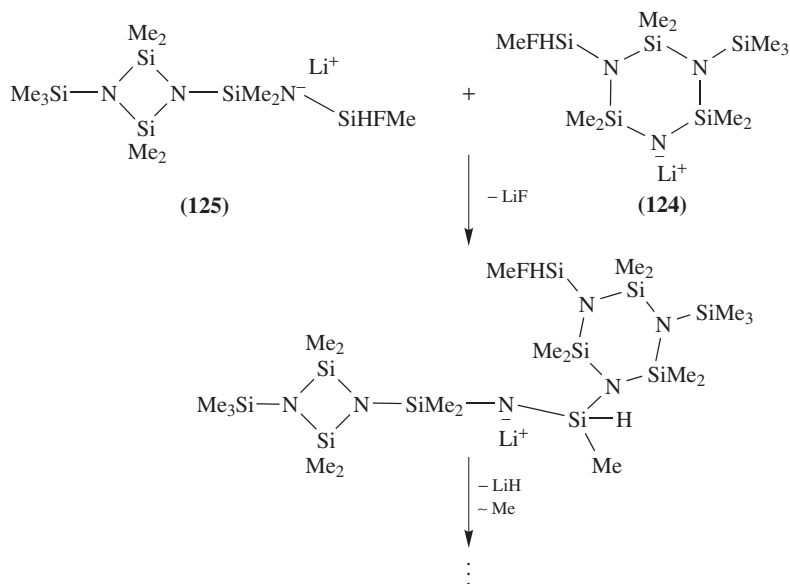


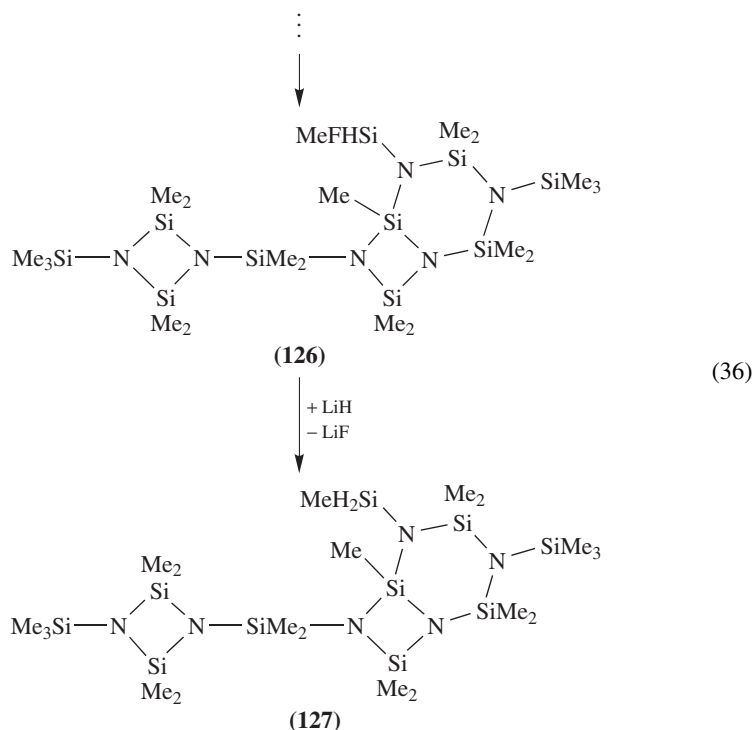
Lithiated isomeric cyclodi- and cyclotrisilazanes can be coupled with fluorosilyl substituted rings such as **121** to give derivatives **122** and **123** (equation 35)⁹⁶.



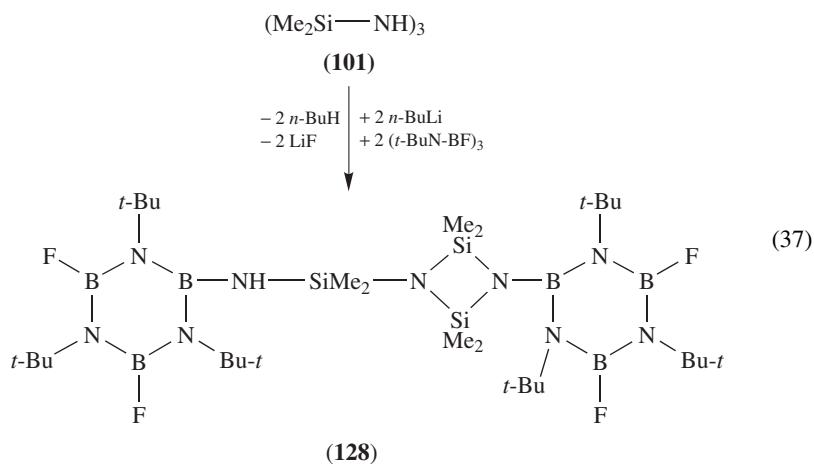


Lithium derivatives having SiF and SiH functional coupled rings, such as **124** and **125**, react under Li–F elimination connected with a Me[−] ion migration to give bicyclic systems **126** and **127** (equation 36)⁹⁶.





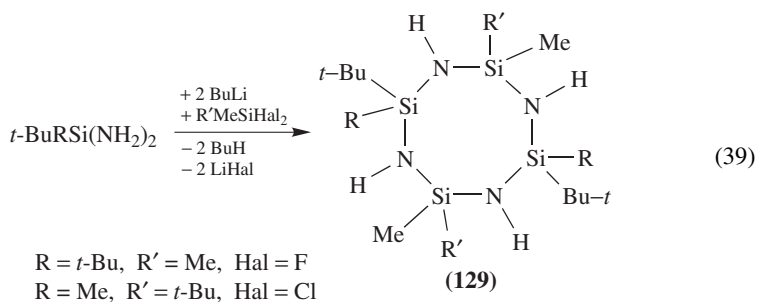
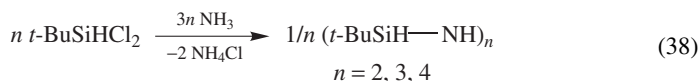
An anionic rearrangement can be observed in the coupling of two bulky fluoroborazines with hexamethylcyclotrisilazanes **101** which gives **128** (equation 37)¹⁰². Compound **128** contains nonplanar N atoms; e.g. the sum of the angles of the cyclodisilazane-nitrogen Si₂N–B is found to be 352.2°.



X. CYCLOTETRASILAZANES

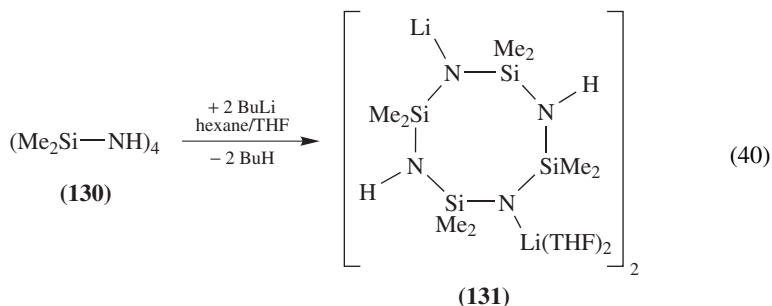
A. Synthesis

Cyclotetrasilazanes are synthesized according to equations 14 and 18, as shown in equation 38. Recently the *tert*-butylcyclodi-, tri- and tetrasilazanes were prepared¹⁰². Another route to NH-functional cyclotetrasilazanes (**129**) starts with the dilithiated diaminosilanes and their reaction with dihalosilanes (equation 39)⁹⁰. The (*t*-Bu₂Si-NH-SiMe₂-NH)₂ ring was characterized by X-ray determination. The ring forms triclinic crystals, space group P $\bar{1}$ and has a saddle conformation with the Si atoms approximately coplanar and the N atoms alternately above and below this plane⁹⁰.

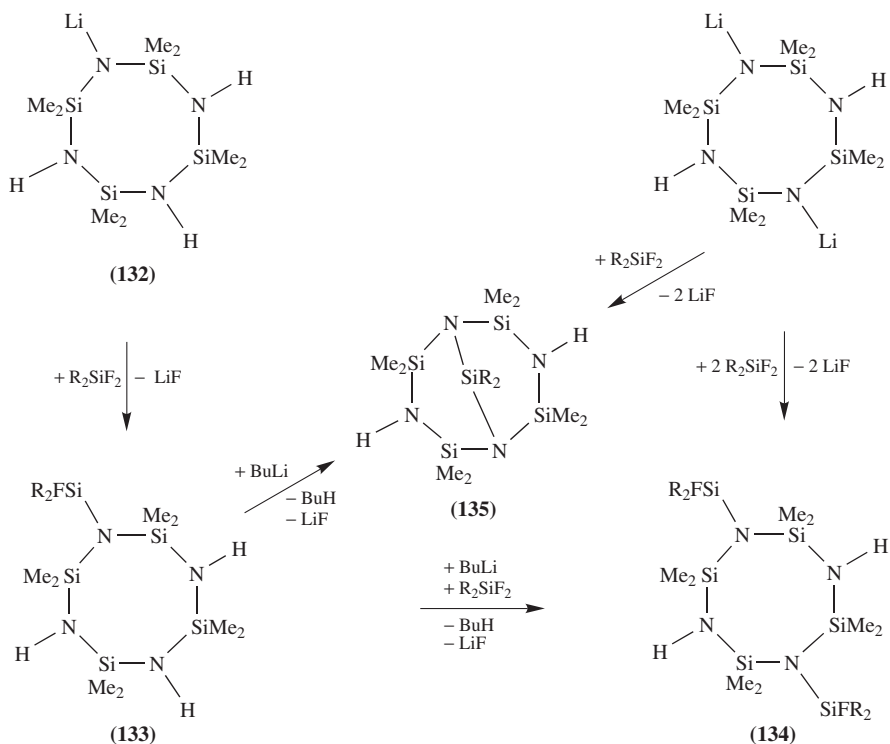


B. Reactions of Cyclotetrasilazanes

Octamethylcyclotetrasilazane (**130**) reacts with *n*-butyllithium or alkaline metals to give the alkali salts, which crystallize as dimeric THF adducts (equation 40). In the dimers, two eight-membered rings are connected by a planar alkali metal–nitrogen four-membered ring. Lithium is tricoordinated, sodium tetracoordinated and potassium penta- and hexacoordinated. The coordinatively bonded THF in the lithium compound (**131**) can be exchanged with the Lewis base TMEDA¹⁰³.



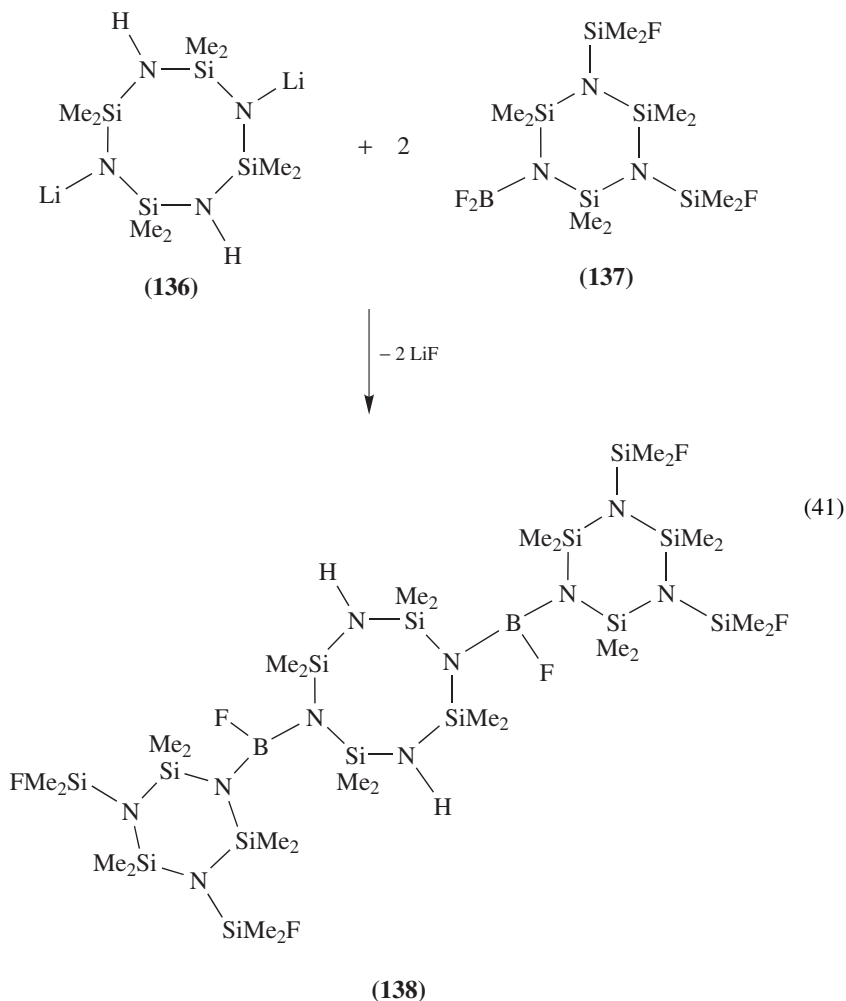
The lithium derivatives (**132**) react with fluorosilanes in a molar ratio 1 : 1 or 1 : 2 to give mono- (**133**) and disubstituted (**134**) 'monomeric' products containing eight-membered rings (Scheme 3)⁸⁴. The monofluorosilyl-substituted eight-membered rings crystallize in a boat conformation. The molecules form chains via H–F bridges in the crystals. The ring of **134**, R = Me crystallizes in a chair conformation. The molecule contains three-dimensional H–F bridges. The rings are perpendicular to each other^{84,104}.



SCHEME 3

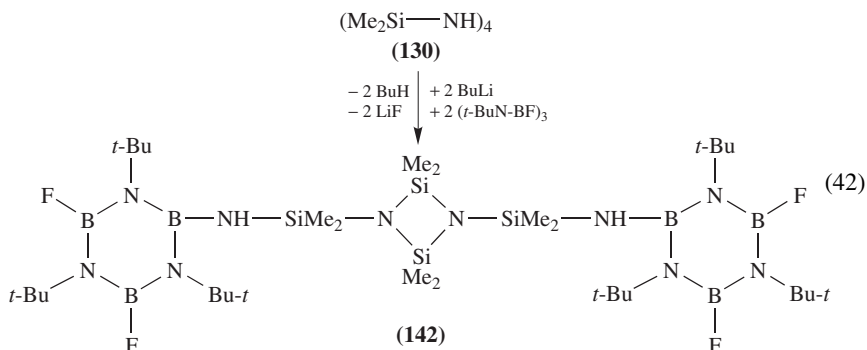
Besides silyl groups the eight-membered ring was disubstituted with BFN(SiMe₃)₂, PF₂ groups and borazines^{101,102,104}. In the reaction of the dilithiated ring (**136**) with F₃SiPh and F₃SiBu-*t* in equivalent amounts, bicyclic compounds (**135**) are obtained (Scheme 3)¹⁰⁴. The X-ray structure of the FSiPh-bridged compound indicates that the nitrogen of the Si₃N units has a pyramidal environment.

Dilithiated octamethylcyclotetrasilazane (**136**) reacts with a difluoroboryl substituted cyclotrisilazane (**137**) to give the BF coupled 6-8-6-membered cyclosilazane **138** (equation 41)¹⁰⁰. The eight-membered ring has a chair conformation.

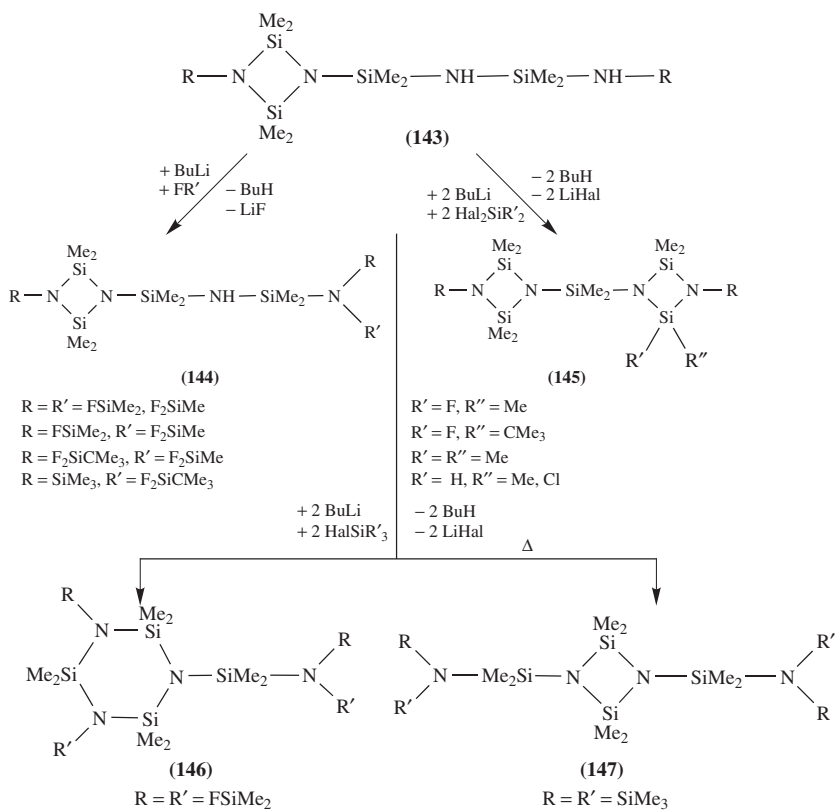


C. Interconversion Reactions

According to Scheme 1 an equilibrium exists between the anions of the eight-, six- and four-membered rings, which depends very strongly on the substituents and the attacking reagents. The mono anion of the eight-membered ring contracts and forms a six-membered ring (cf **139**), according to route (I) in Scheme 4. This six-membered ring can be substituted or contracts with formation of a symmetrically disubstituted four-membered ring **140** (Scheme 4)⁸⁴. A symmetrically substituted isomeric cyclodisilazane (**142**) was obtained in the reaction of the dilithiated eight-membered ring with borazines (equation 42)¹⁰². The dilithiated eight-membered ring contracts according to route (II) in Scheme 4 with formation of the unsymmetrically disubstituted four-membered ring^{84,105–109}.



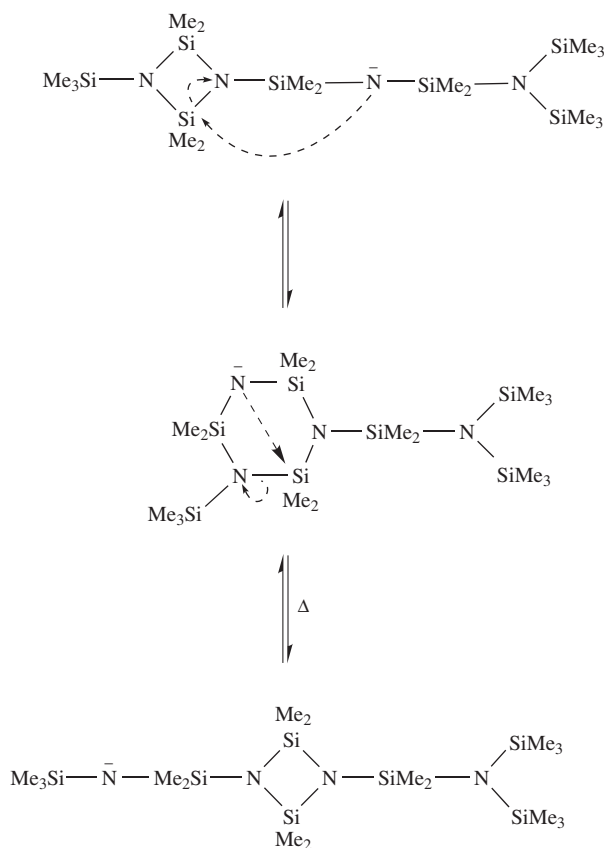
Till now, no tris(silyl)-substituted cyclotetrasilazane is known. Starting with the isomeric unsymmetrically substituted cyclodisilazane (**143**), the substituent R' is bonded exocyclically at the four-membered ring of **144** (Scheme 5)^{103,105}. Difunctional halides react with the dilithium derivatives spontaneously and quantitatively, forming a second



SCHEME 5

four-membered ring (**145**). Ring closure is also observed with boron halides, tin chloride or germanium dichloride. Hydroxy or amino groups are also stabilized in this position. They do not condense with formation of bis(silyl)amines or siloxanes^{105–109}.

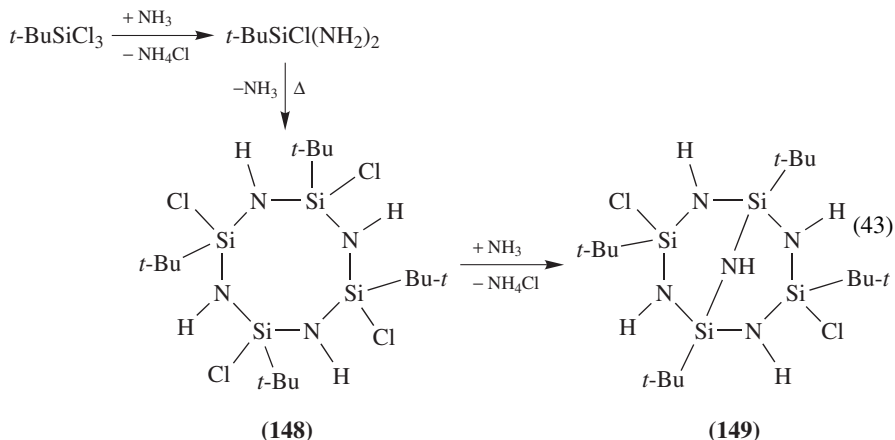
Ring expansion occurs with the fourth substituent to give a six-membered ring (**146**). Also formed is the symmetrically substituted four-membered ring of **147**. This means that the tris(silyl)-substituted unsymmetrical four-membered ring **143** forms in an interconversion reaction the tetrakis(silyl)-substituted symmetrical four-membered ring **147**. The formation of **147** can be ascribed to an isomerization of the anion of the (silyl)-substituted ring, as described in Scheme 6.



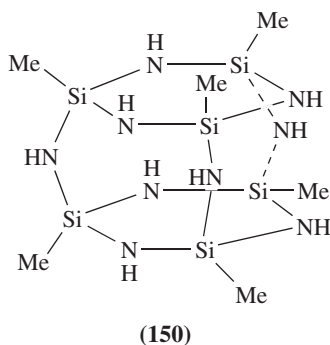
SCHEME 6

D. Cage Cyclosilazanes

The reaction of *tert*-butyltrichlorosilane with an excess of ammonia leads to the formation of a tetrasilabicyclo[3.3.1]nonane (**149**), an NH-bridged cyclotetrasilazane, presumably via **148** (equation 43)¹¹⁰. The bicyclic system contains two six-membered rings in boat conformations. The *t*-Bu groups of the ClSiN₂ unit are in *cis*-position¹¹⁰.

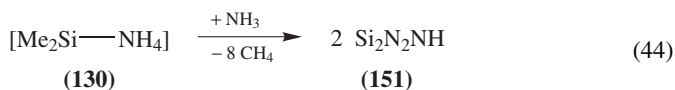


In the comparable reaction of Me_3SiCl with sodium and NH_3 , the cage compound $(\text{MeSi})_6(\text{NH})_9$ was obtained²⁸. The N atoms are coordinated in a nearly planar arrangement as shown in **150**.



XI. APPLICATION OF CYCLOSILAZANES AS PRECURSORS FOR SILICON-BASED CERAMICS

$\alpha\text{-Si}_3\text{N}_4$ (**152**) is synthesized by an ammonia thermal synthesis using the cyclic silazane, $[\text{Me}_2\text{Si}-\text{NH}]_4$ (**130**), as the starting material. **130** reacts in the presence of ammonia at high temperatures and high pressure to give silicon nitride/imide, **151** (equation 44). Subsequently, **151** is converted into **152** by thermal decomposition above 1000°C with the simultaneous loss of NH_3 (equation 45)¹¹¹. **151** is considered to be an intermediate compound in the ammonolysis of SiCl_4 . In the X-ray diagram of the product heat-treated at 1200°C , reflex peaks of **152** appear next to those of **151**. After annealing at 1500°C a 94% yield of **152** is obtained, which can be determined from the X-ray results¹¹¹.



33. M. Westerhausen and W. Schwarz, *Z. Anorg. Allg. Chem.*, **619**, 1053 (1993).
34. R. E. Mulvey, *Chem. Soc. Rev.*, **20**, 167 (1991).
35. M. F. Lappert, P. P. Power, A. R. Sanger and R. C. Srivastava, *Metal and Metalloid Amides*, Ellis Horwood, Chichester, 1980.
36. D. Mootz, A. Zinnius and B. Böttcher, *Angew. Chem.*, **109**, 6509 (1969).
37. R. D. Rogers, J. L. Atwood and R. J. Grüning, *J. Organomet. Chem.*, **157**, 229 (1978).
38. L. Ruwisch, U. Klingebiel, S. Rudolph, R. Herbst-Irmer and M. Noltemeyer, *Chem. Ber.*, **129**, 823 (1996).
39. G. E. Underiner, R. P. Tan, D. R. Powell and R. West, *J. Am. Chem. Soc.*, **113**, 8437 (1991).
40. I. Hemme, M. Schäfer, R. Herbst-Irmer and U. Klingebiel, *J. Organomet. Chem.*, **223**, 493 (1995).
41. U. Klingebiel, P. Tecklenburg, N. Noltemeyer, D. Schmidt-Bäse, R. Herbst-Irmer, *Z. Naturforsch.*, **53b**, 335 (1998).
42. K. Junge, E. Popowski, R. Kempe and W. Baumann, *Z. Anorg. Allg. Chem.*, **624**, 1369 (1998).
43. P. Kosse, E. Popowski, V. Huch and M. Veith, *Chem. Ber.*, **127**, 2103 (1994).
44. G. Huber, A. Jockisch and H. Schmidbauer, *Z. Naturforsch.*, **54b**, 8 (1999).
45. I. Hemme, U. Klingebiel, S. Freitag and D. Stalke, *Z. anorg. allg. Chem.*, **621**, 2093 (1995).
46. K. Dippel, U. Klingebiel, D. Schmidt-Bäse, *Z. Anorg. Allg. Chem.*, **619**, 836 (1993).
47. D. Grosskopf, L. Marcus, U. Klingebiel and M. Noltemeyer, *Phosphorus, Sulfur, Silicon*, **97**, 113 (1994).
48. H.-J. Rakebrandt, U. Klingebiel and M. Noltemeyer, *Z. Anorg. Allg. Chem.*, **623**, 288 (1997).
49. M. Veith and M. Zimmer, *Chem. Ber.*, **127**, 2099 (1994).
50. R. Herbst-Irmer, U. Klingebiel and M. Noltemeyer, *Z. Naturforsch.*, **54b**, 314 (1999).
51. B. J. Aylett, *J. Inorg. Chem.*, **2**, 325 (1956).
52. U. Wannagat and W. Liehr, *Angew. Chem.*, **69**, 783 (1957).
53. K. Bode and U. Klingebiel, *Adv. Organomet. Chem.*, **40**, 1 (1996).
54. S. Dielkus, C. Drost, R. Herbst-Irmer and U. Klingebiel, *Angew. Chem.*, **105**, 1689 (1993); *Angew. Chem., Int. Ed. Engl.*, **32**, 1625 (1993).
55. N. Metzler, H. Nöth and H. Sachdev, *Angew. Chem.*, **106**, 1837 (1994); *Angew. Chem., Int. Ed. Engl.*, **33**, 1746 (1994).
56. H. Nöth, H. Sachdev, M. Schmidt and H. Schwenk, *Chem. Ber.*, **128**, 105 (1995).
57. K. Bode, U. Klingebiel, H. Witte-Abel, M. Gluth, M. Noltemeyer, R. Herbst-Irmer, M. Schäfer and W. Shomaly, *Phosphorus, Sulfur, Silicon*, **108**, 121 (1996).
58. K. Bode, C. Drost, C. Jäger, U. Klingebiel, M. Noltemeyer and Z. Zak, *J. Organomet. Chem.*, **482**, 285 (1994).
59. H. Witte-Abel, U. Klingebiel and M. Noltemeyer, *Chem. Commun.*, 771 (1997).
60. H. Witte-Abel, U. Klingebiel and M. Schäfer, *Z. Anorg. Allg. Chem.*, **624**, 271 (1998).
61. (a) J. Niesmann, U. Klingebiel, M. Noltemeyer and R. Boese, *Chem. Commun.*, 365 (1997); (b) N. Wiberg, K. Schurz, G. Reber and G. Müller, *Chem. Commun.*, 365 (1997); (c) P. v. R. Schleyer and P.O. Staut, *Chem. Commun.*, 1373 (1986).
62. U. Klingebiel, M. Noltemeyer, H.-G. Schmidt and D. Schmidt-Bäse, *Chem. Ber.*, **130**, 753 (1997).
63. J. Niesmann, U. Klingebiel, C. Röpken, M. Noltemeyer and R. Herbst-Irmer, *Main Group Chem.*, **2**, 297 (1998).
64. J. Niesmann, U. Klingebiel, M. Schäfer and R. Boese, *Organometallics*, **17**, 947 (1998).
65. S. D. Brewer and C. P. Haber, *J. Am. Chem. Soc.*, **70**, 3888 (1948).
66. W. Fink, *Angew. Chem.*, **78**, 803 (1966); *Angew. Chem., Int. Ed. Engl.*, **5**, 760 (1966).
67. I. Haiduc, *The Chemistry of Inorganic Ring Systems*, Wiley-Interscience, London, 1970.
68. U. Wannagat, *Chem. Ztg.*, **97**, 105 (1997).
69. U. Klingebiel and A. Meller, *Chem. Ber.*, **109**, 2430 (1976).
70. U. Klingebiel and A. Meller, *Z. Naturforsch.*, **32b**, 537 (1977).
71. U. Klingebiel and A. Meller, *Z. Anorg. Allg. Chem.*, **428**, 27 (1977).
72. U. Klingebiel, H. Hluchy and A. Meller, *Chem. Ber.*, **111**, 906 (1978).
73. W. Clegg, U. Klingebiel, G. M. Sheldrick and N. Vater, *Z. Anorg. Allg. Chem.*, **428**, 88 (1981).
74. W. Clegg, U. Klingebiel, C. Krampe and G. M. Sheldrick, *Z. Naturforsch.*, **35b**, 275 (1980).
75. W. Clegg, U. Klingebiel and G. M. Sheldrick, *Z. Naturforsch.*, **37b**, 423 (1982).
76. U. Klingebiel and N. Vater, *Chem. Ber.*, **116**, 3277 (1983); U. Klingebiel and N. Vater, *Angew. Chem.*, **94**, 870 (1982); *Angew. Chem., Int. Ed. Engl.*, **21**, 857 (1982).

77. U. Kliebisch, U. Klingebiel and N. Vater, *Chem. Ber.*, **118**, 4561 (1985).
78. T. Kottke, U. Klingebiel, M. Noltemeyer, U. Pieper, S. Walter and D. Stalke, *Chem. Ber.*, **124**, 1941 (1991).
79. W. Clegg, G. M. Shelbrick and D. Stalke, *Acta Crystallogr.*, **C40**, 433 (1984).
80. W. Fink, *Helv. Chim. Acta*, **52**, 2261 (1969).
81. L. W. Breed, *Inorg. Chem.*, **7**, 1940 (1968).
82. U. Klingebiel, *Inorg. React. Methods*, **17**, 116 (1990).
83. U. Klingebiel, M. Noltemeyer and H.-J. Rakebrandt, *Z. Anorg. Allg. Chem.*, **623**, 281 (1997).
84. K. Dippel, E. Werner and U. Klingebiel, *Phosphorus, Sulfur, Silicon*, **64**, 15 (1992).
85. B. Tecklenburg, U. Klingebiel, M. Noltemeyer and D. Schmidt-Bäse, *Z. Naturforsch.*, **47b**, 855 (1992).
86. S. Bartholmei, U. Klingebiel, G. M. Shelbrick and D. Stalke, *Z. Anorg. Allg. Chem.*, **129**, 556 (1988).
87. C. Brönnecke, R. Herbst-Irmer, U. Klingebiel, P. Neugebauer, M. Schäfer and H. Oberhammer, *Chem. Ber./Recueil*, **130**, 835 (1997).
88. T. Müller, Y. Apeloig, I. Hemme, U. Klingebiel and M. Noltemeyer, *J. Organomet. Chem.*, **494**, 133 (1995).
89. B. Jaschke, R. Herbst-Irmer, U. Klingebiel, P. Neugebauer and T. Pape, *J. Chem. Soc., Dalton Trans.*, 2953 (1998).
90. M. Veith and A. Rammo, *Phosphorus, Sulfur, Silicon*, **123**, 75 (1997).
91. H.-J. Rakebrandt, U. Klingebiel, M. Noltemeyer, U. Wenzel and D. Mootz, *J. Organomet. Chem.*, **524**, 237 (1996).
92. D. Großkopf and U. Klingebiel, *Z. Anorg. Allg. Chem.*, **619**, 1857 (1993).
93. S. Dielkus, D. Großkopf, R. Herbst-Irmer and U. Klingebiel, *Z. Naturforsch.*, **50b**, 844 (1995).
94. H.-J. Rakebrandt and U. Klingebiel, *Z. Anorg. Allg. Chem.*, **623**, 1264 (1997).
95. E. Egert, U. Kliebisch, U. Klingebiel and D. Schmidt, *Z. Anorg. Allg. Chem.*, **548**, 89 (1987).
96. E. Werner and U. Klingebiel, *Phosphorus, Sulfur, Silicon*, **83**, 9 (1993).
97. U. Klingebiel, M. Noltemeyer and H.-J. Rakebrandt, *Z. Anorg. Allg. Chem.*, **623**, 281 (1997).
98. A. Frenzel, R. Herbst-Irmer, U. Klingebiel and M. Schäfer, *Phosphorus, Sulfur, Silicon*, **112**, 155 (1996).
99. S. Schaible, R. Riedel, R. Boese, E. Werner and U. Klingebiel, *Appl. Organomet. Chem.*, **8**, 491 (1994).
100. E. Werner, U. Klingebiel, S. Dielkus and R. Herbst-Irmer, *Z. Anorg. Allg. Chem.*, **620**, 1093 (1994).
101. U. Klingebiel, M. Noltemeyer and H.-J. Rakebrandt, *Z. Naturforsch.*, **52b**, 775 (1997).
102. B. Jaschke, U. Klingebiel and M. Noltemeyer, in preparation; B. Jaschke, Dissertation Göttingen, 2000.
103. K. Dippel, U. Klingebiel, T. Kottke, F. Pauer, G. M. Shelbrick and D. Stalke, *Chem. Ber.*, **123**, 237 (1990).
104. K. Dippel, U. Klingebiel, T. Kottke, F. Pauer, G. M. Shelbrick and D. Stalke, *Z. Anorg. Allg. Chem.*, **584**, 87 (1990).
105. K. Dippel, U. Klingebiel, T. Kottke, F. Pauer, G. M. Shelbrick and D. Stalke, *Chem. Ber.*, **123**, 779 (1990).
106. K. Dippel and U. Klingebiel, *Chem. Ber.*, **123**, 1817 (1990).
107. E. Werner and U. Klingebiel, *J. Organomet. Chem.*, **470**, 35 (1994).
108. K. Dippel and U. Klingebiel, *Z. Naturforsch.*, **45b**, 1147 (1990).
109. K. Dippel, U. Klingebiel, L. Marcus and D. Schmidt-Bäse, *Z. Anorg. Allg. Chem.*, **612**, 130 (1992).
110. H.-J. Rakebrandt, U. Klingebiel, M. Noltemeyer and Z. Zak, *Z. Naturforsch.*, **51b**, 498 (1996).
111. S. Schaible, R. Riedel, E. Werner and U. Klingebiel, *Appl. Organomet. Chem.*, **7**, 53 (1993).

CHAPTER 7

Organosilicon halides – synthesis and properties

UWE HERZOG

*Institute of Inorganic Chemistry, Freiberg University of Mining and Technology,
Leipziger Str. 29, D-09596 Freiberg, Germany.
Fax: 49-3731-394058; e-mail: herzog@merkur.hrz.tu-freiberg.de*

I. INTRODUCTION	469
II. SYNTHETIC ROUTES TOWARD ORGANOSILICON HALIDES	470
A. Chloro-substituted Silanes	470
B. Fluorosilanes	479
C. Bromo- and Iodosilanes	480
III. LEWIS-BASE ADDUCTS OF SILICON HALIDES	482
IV. REFERENCES	486

I. INTRODUCTION

Organosilicon halides are one of the most important groups of functional organosilanes. A vast variety of their substitution reactions leads to many different organosilicon derivatives. The chemistry of perhalogenosilanes and halogenohydrogensilanes is strongly correlated with that of organo-substituted halogenosilanes, therefore these compounds will also be included in this chapter.

The silicon–halogen bonds are relatively strong compared to the Si–C bond in SiMe_4 ($94.2 \text{ kcal mol}^{-1}$), the Si–H bond in SiH_4 ($91.8 \text{ kcal mol}^{-1}$) or the Si–Si bond in Me_6Si_2 ($79.3 \text{ kcal mol}^{-1}$). However, the bond dissociation energies decrease dramatically from fluorine (the Si–F bond in SiF_4 is the strongest single bond known) to iodine, and only the Si–F bond has a higher dissociation energy than typical Si–O bonds ($136 \text{ kcal mol}^{-1}$ in $\text{Me}_3\text{SiOSiMe}_3$) (Table 1).

Among the silicon halides, the chlorosilanes have attracted by far the greatest attention. Silicon tetrachloride, trichlorosilane and the methylchlorosilanes are produced on an industrial scale and are used, for instance, in the production of pure silicon or silicones.

TABLE 1. Silicon-halogen bond dissociation energies (in kcal mol⁻¹)¹

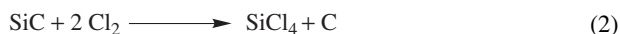
Compound	<i>D</i> (Si-X)	Compound	<i>D</i> (Si-X)	Compound	<i>D</i> (Si-X)	Compound	<i>D</i> (Si-X)
H ₃ Si-F	152	H ₃ Si-Cl	109	H ₃ Si-Br	90	H ₃ Si-I	71
Me ₃ Si-F	158	Me ₃ Si-Cl	117	Me ₃ Si-Br	102	Me ₃ Si-I	82
F ₃ Si-F	167	Cl ₃ Si-Cl	110	Br ₃ Si-Br	90	I ₃ Si-I	68

Due to the high affinity of silicon to oxygen, the silicon halides (except fluorides) are usually easily hydrolyzed by water or alcohols.

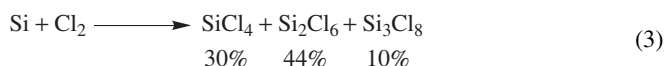
II. SYNTHETIC ROUTES TOWARD ORGANOSILICON HALIDES

A. Chloro-substituted Silanes

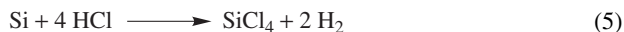
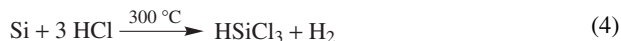
The direct reaction of elemental silicon or ferrosilicon with chlorine yields silicon tetrachloride. The reductive chlorination of SiO₂ with chlorine (equation 1) or the chlorination of silicon carbide (equation 2) can also be applied, but are less important.



Under controlled reaction conditions, the chlorination of ferrosilicon yields besides SiCl₄ also remarkable amounts of hexachlorodisilane and octachlorotrisilane² (equation 3).



Trichlorosilane, SiHCl₃, is synthesized on an industrial scale by treatment of silicon with hydrogen chloride at ~300 °C³ (equation 4). With increasing temperature the yield of the thermodynamically preferred product, i.e. silicon tetrachloride, is raised^{4,5} (equation 5).



The addition of 0.5% Cu decreases the reaction temperature to 280 °C and the selectivity of HSiCl₃ exceeds 95%. Reaction of pure Si containing 0.5% copper also produces up to 15% H₂SiCl₂ at temperatures below 280 °C⁶.

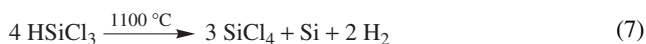
Usually, the selectivity of HSiCl₃ in the industrial operation of this reaction is lower, and this is attributed to a contamination with phosphorus which increases the formation of SiCl₄.

Addition of aluminum can restore to some degree the trichlorosilane selectivity decreased by phosphorus. The action of P and Al could be interpreted in terms of a change in the electronic state (p or n dotation) of the reacting silicon⁷.

Trichlorosilane is used in the production of semiconductor grade silicon. By repeated distillation the content of boron or phosphorus impurities can be reduced to <0.1 ppb. Elemental silicon is obtained by reduction with hydrogen at high temperatures according to the idealized equation 6.



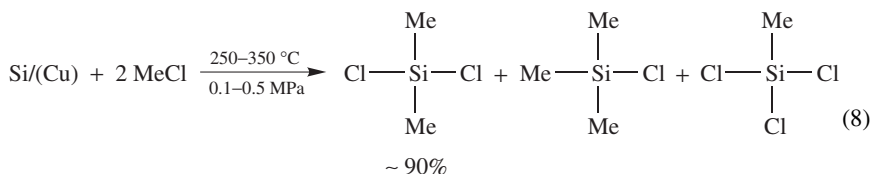
In fact, the reaction proceeds rather according to equation 7



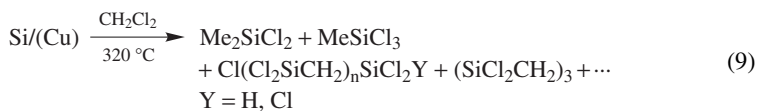
yielding large amounts of highly pure silicon tetrachloride as by-product.

Trichlorosilane can be dismutated in the presence of basic catalysts into SiCl_4 and SiH_2Cl_2 , SiH_3Cl and SiH_4 . This is the basis of the Union Carbide process to produce pure silicon via SiH_4 .

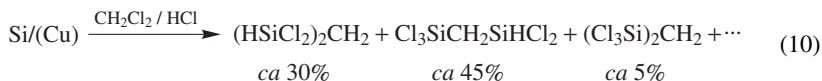
The simplest possible organochlorosilanes, the series of methylchlorosilanes, $\text{Me}_x\text{SiCl}_{4-x}$, is produced on an industrial scale (*ca* 10^6 t per year) by the direct process⁸⁻¹⁰ (equation 8).



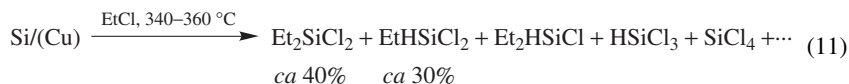
Besides the main product dimethyldichlorosilane (DDS) approximately 40 by-products are formed, including methyltrichlorosilane (MTS) and trimethylchlorosilane (TMCS), the hydrogen-substituted silanes methylchlorosilane and dimethylchlorosilane, tetramethylsilane, silicon tetrachloride, methylchlorodisilanes ($\text{Me}_x\text{Si}_2\text{Cl}_{6-x}$)¹¹ and disilylmethanes ($\text{Me}_x\text{Cl}_{3-x}\text{SiCH}_2\text{SiCl}_{3-y}\text{Me}_y$)¹². Very careful distillation is needed in order to separate the methylchlorosilanes due to their very similar boiling points. If the reaction is carried out in the presence of butadiene as a silylene trapping agent, 1-silacyclopent-3-enes are formed together with methylchlorosilanes, suggesting the presence of silylene species as intermediates of this heterogeneous reaction¹³. Disilylmethanes and higher carbosilanes can be obtained in better yield by a direct reaction of methylene chloride with elemental silicon¹⁴ (equation 9).



The amount of bis(chlorosilyl)methanes can be increased by using a $\text{CH}_2\text{Cl}_2/\text{HCl}$ mixture (1 : 4) at temperatures between 260 and 340 °C¹⁵ (equation 10).



The direct process can also be applied to produce further organochlorosilanes; e.g. the reaction with ethyl chloride yields ethylchlorosilanes¹⁶ but with lower selectivity toward the dialkyldichlorosilane (equation 11).

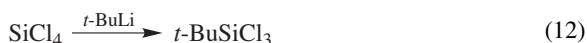


The reaction of chlorobenzene with silicon yields phenyltrichlorosilane and diphenyldichlorosilane^{17,18} and analogously $\text{H}_2\text{C}=\text{CHSiCl}_3$ and $(\text{H}_2\text{C}=\text{CH})_2\text{SiCl}_2$ are made in significant commercial quantities from vinyl chloride and silicon.

Ethylchlorosilane can also be obtained in 47% selectivity from Si, C₂H₄ and HCl and H₂C=CHSiHCl₂ in 39% from Si, C₂H₂ and HCl at 240 °C¹⁹.

Physical data and ²⁹Si NMR chemical shifts of the most important chlorosilanes are given in Table 2.

The stepwise substitution of silicon tetrachloride by Grignard reagents or organolithium compounds is another facile process to obtain organochlorosilanes with the exception of methylchlorosilanes. The latter compounds cannot be conveniently prepared by this method because there is a high degree of randomization in the substitution reaction and all four chloro components boil within 13 °C of each other. A stepwise substitution is easier with the more hindered Grignard and organolithium reagents like phenyl or *tert*-butyl²³ (equations 12 and 13).

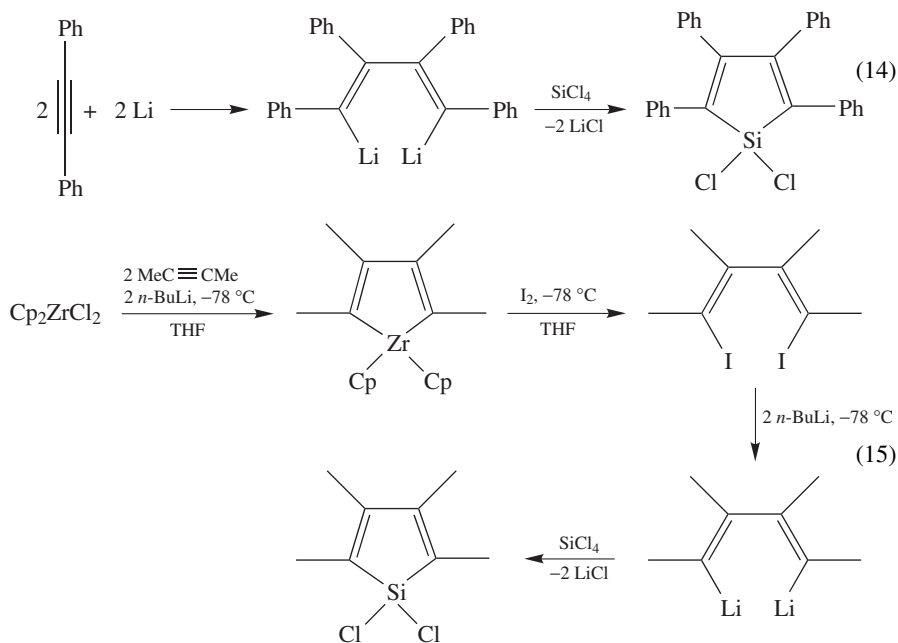


t-Butyldimethylchlorosilane has been extensively used in organic synthesis to protect alcohols²⁴.

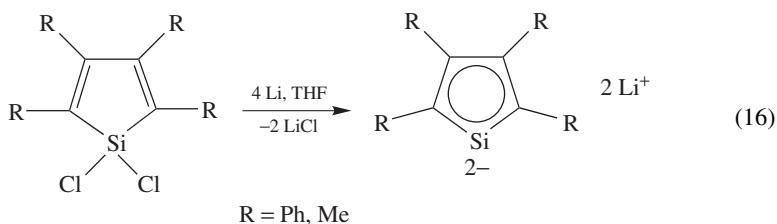
1,1-Dichloro-2,3,4,5-tetraphenyl-1-silacyclopentadiene is prepared from diphenylacetylene, lithium and SiCl₄²⁵ (equation 14). The tetramethyl analog could be obtained via 1,4-diiodo-1,2,3,4-tetramethylbutadiene²⁶ (equation 15).

TABLE 2. Melting points, boiling points, densities, refractive indices and ²⁹Si NMR chemical shifts of the most important chlorosilanes^{20–22}

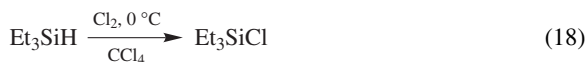
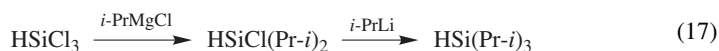
Compound	mp (°C)	bp (°C)	D ₄ ²⁰ (g cm ⁻³)	n _D ²⁰	δ _{Si} (ppm)
SiCl ₄	-70	57.6	1.481	1.4153	-18.5
HSiCl ₃	-128	31.9	1.3417	1.4020	-9.8
H ₂ SiCl ₂	-122	8.3	1.22		-11.0
			(at 7 °C)		
H ₃ SiCl	-118	-30.4	1.145		-36.1
			(At -113 °C)		
Si ₂ Cl ₆	2.5	145	1.562	1.4750	-6.1
Si ₃ Cl ₈	-76	216			-3.7
					(SiCl ₃)
					-7.4
					(SiCl ₂)
Me ₃ SiCl	-57.7	57.6	0.8580	1.3885	29.9
Me ₂ SiCl ₂	-76	70.0	1.0637	1.4055	32.2
MeSiCl ₃	-78	66.4	1.275	1.4110	12.2
MeHSiCl ₂	-93	41.5	1.1047	1.4222	9.7
PhMeSiCl ₂	-53	205	1.187	1.5180	17.9
Ph ₃ SiCl	91	368			1.5
Ph ₂ SiCl ₂	-22	305	1.2216	1.5819	6.3
PhSiCl ₃	-33	201	1.324	1.5247	-0.8
H ₂ C=CHSiCl ₃	-95	93	1.2426	1.4295	-3.2
Cl ₂ MeSiSiMeCl ₂	9	153			18.1



Both compounds react with four equivalents of lithium to give a dilithio derivative having some aromatic character of the C_4Si ring²⁷ (equation 16). The dilithio derivative of tetraphenylsilole reveals in its crystal structure a $\eta^1\eta^5$ -coordination of the two lithium ions²⁸.



Starting from trichlorosilane, a triorganosilane can be prepared by treatment with three equivalents of relatively unhindered Grignard reagents. In the case of triisopropylsilane the introduction of the third isopropyl substituent affords the more active isopropyllithium reagent (equation 17). The triorganosilanes formed in this way can be easily converted into triorganochlorosilanes by reaction with chlorine (equation 18).



The substitution occurs with retention of configuration at silicon. In contrast to the normal nucleophilic attack at silicon, it is relatively unaffected by steric hindrance and makes sterically crowded triorganochlorosilanes like tri-*t*-butylchlorosilane accessible²⁹.

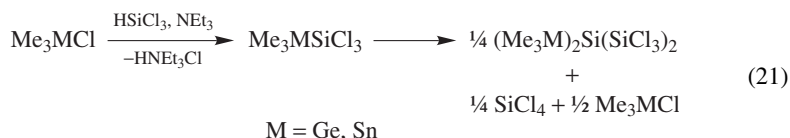
Alkyl or acyl halides can be transformed into trichlorosilanes by treatment with HSiCl_3 and NEt_3 (Benkeser reaction)^{30,31} (equation 19).



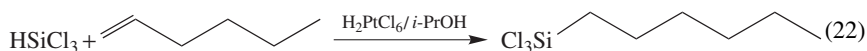
This type of reaction has also been applied in the synthesis of trichlorosilylphosphanes^{32,33} (equation 20)



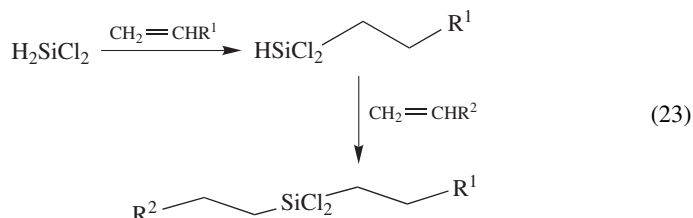
and germyl- and stannylsilanes. In this case the initially formed trimethylgermyl- and trimethylstannyltrichlorosilanes are unstable and disproportionate³⁴ (equation 21).



Hydrosilylation is another convenient approach to organochlorosilanes: e.g. hexyltrichlorosilane is formed by the reaction of trichlorosilane with 1-hexene (equation 22).



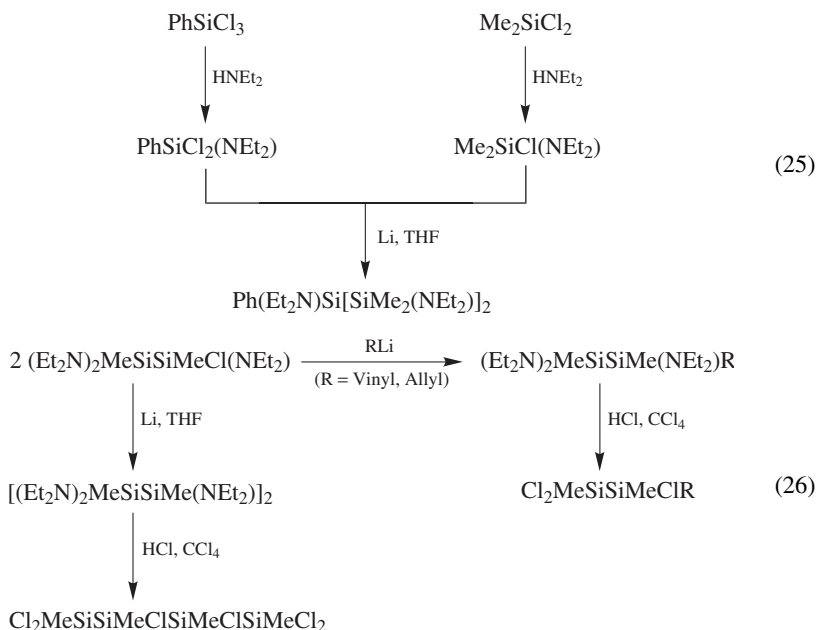
Starting from dichlorosilane, two different organyl substituents can be introduced successively, e.g. with $\text{R}^1 = \text{Pr}, \text{Bu}, \text{Pent}$ and $\text{R}^2 = \text{CH}_2\text{OPh}$ ³⁵ (equation 23).



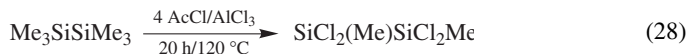
Many functionally substituted silanes can be converted back to the chlorides by using BCl_3 , PCl_3 , TiCl_4 , SOCl_2 , benzoyl or acetyl chloride ($\text{X} = \text{OR}, \text{NR}_2, \text{SR}, \text{SeR}$) (equation 24).



Especially, dialkylamino groups are frequently used as protecting groups to mask chloro functions³⁶⁻⁴⁰ (equation 25). The resulting amino-substituted oligosilanes are converted back into the chloro derivatives by HCl ^{41,42} (equation 26).



Organo substituents can also be replaced by chlorine if HCl ^{43,44} or acetyl chloride is used in the presence of a Lewis acid catalyst like AlCl_3 . Unsaturated substituents (vinyl, allyl, phenyl) are selectively substituted at first⁴⁵ (equation 27) whereas methyl groups need more drastic reaction conditions¹¹ (equation 28).



Whereas all phenyl substituents in Si_2Ph_6 can be replaced by HCl , a substitution of more than four methyl groups in Si_2Me_6 is not possible^{46,47}. In hexamethyldisilylmethane the central SiCH_2Si unit remains intact, and only the terminal methyl groups are substituted⁴⁷ (equation 29).

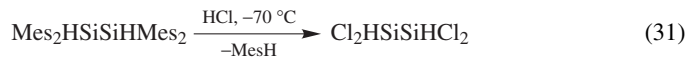


The perphenylated cyclosilanes $(\text{SiPh}_2)_{4,5,6}$ can be converted into the perchlorocyclosilanes $(\text{SiCl}_2)_{4,5,6}$ by treatment with HCl in the presence of AlCl_3 ^{48–50}. When the yellow $(\text{SiCl}_2)_4$ ⁵¹ is sublimed at -10°C , colorless crystals of $(\text{SiCl}_2)_n$ are formed. The molecular structure of $(\text{SiCl}_2)_n$ reveals infinite parallel-aligned all-*trans* chains of SiCl_2 repeating units⁵².

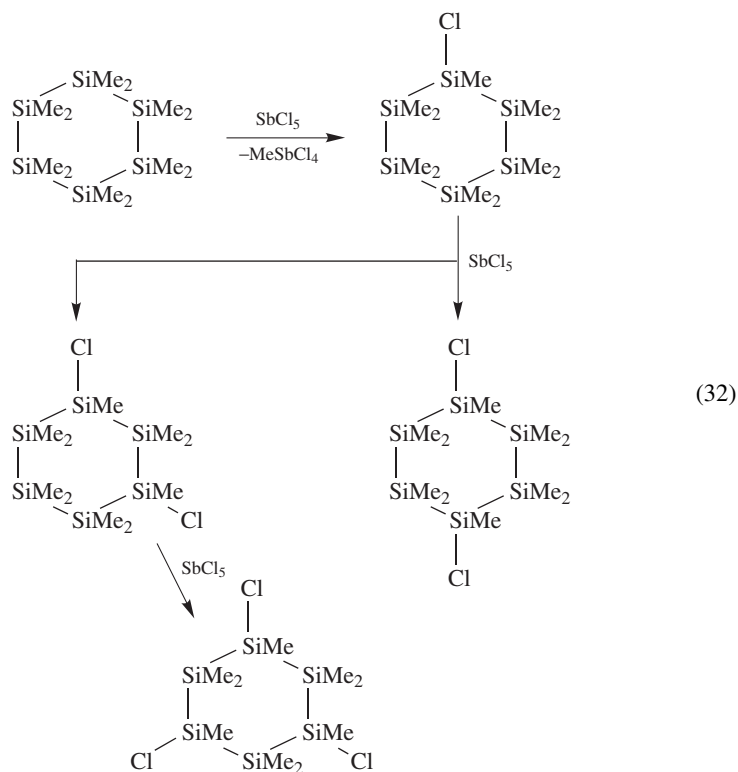
If liquid HCl in an autoclave is applied, phenyl substituents are also substituted in the absence of a Lewis acid catalyst, but in oligosilanes bearing SiPh_3 terminal units one phenyl substituent still remains⁵³ (equation 30).



The synthesis of chlorohydrogendisilanes by reaction of phenylhydrogendisilanes with HCl in benzene has been complicated by equilibration reactions in the cases of mono- and dichlorodisilanes and by the formation of azeotropic mixtures of the chlorodisilanes with the solvent and the by-product benzene⁵⁴. This could be overcome by the use of the larger mesityl (Mes) substituent⁵⁵ (equation 31).



If *all-trans*-(PhMeSi)₆ is reacted with HCl and AlCl₃, an isomeric mixture of all possible (SiClMe)₆ isomers results, which means that the chlorination is accompanied by racemization⁵⁶. In the course of the chlorination of the permethylated six-membered ring (SiMe₂)₆, the second substitution occurs only in the 3 and 4 position⁵⁷ (equation 32). The formed 1,3- and 1,4-dichlorodecamethylcyclohexasilanes can be separated via their hydrolysis products, 1,3-dihydroxydecamethylcyclohexasilane and decamethyl-7-oxahexasilanorbornane⁵⁸. 1,2-Dichlorodecamethylcyclohexasilane is accessible via a stepwise synthesis of the cyclohexasilane skeleton⁵⁹.

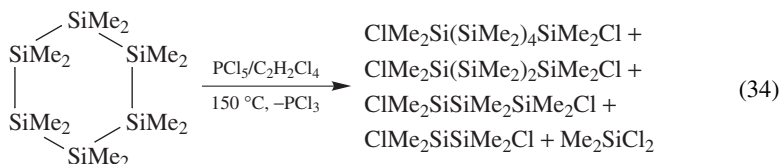


The introduction of chlorine substituents can also be achieved by an aluminum chloride catalyzed equilibration with trimethylchlorosilane⁶⁰ (equation 33).

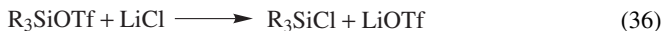


Continuous removal of the low-boiling Me_4Si by-product drives this reaction to completion.

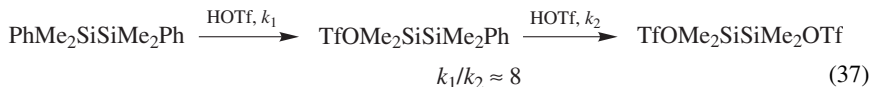
The stepwise cleavage of Si—Si bonds in dodecamethylcyclohexasilane yields mixtures of α, ω -dichloropermethyloligosilanes⁶¹ (equation 34). The Si—Si bond cleavage occurs preferentially between silicon atoms which do not bear chlorine substituents. Thus the pentasilane is not formed in this reaction.



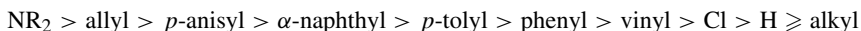
More recently, trifluoromethanesulfonic acid (triflic acid, TfOH) has been used to functionalize silanes by electrophilic substitution of aryl substituents^{62,63} (equation 35). The silyl triflates formed in this reaction are useful building blocks for a wide variety of products. Chlorosilanes can be obtained by treatment with lithium chloride (equation 36).



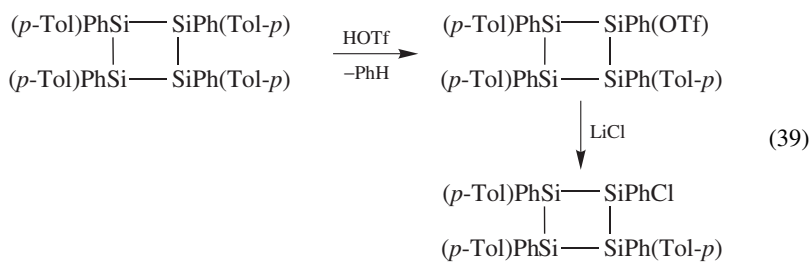
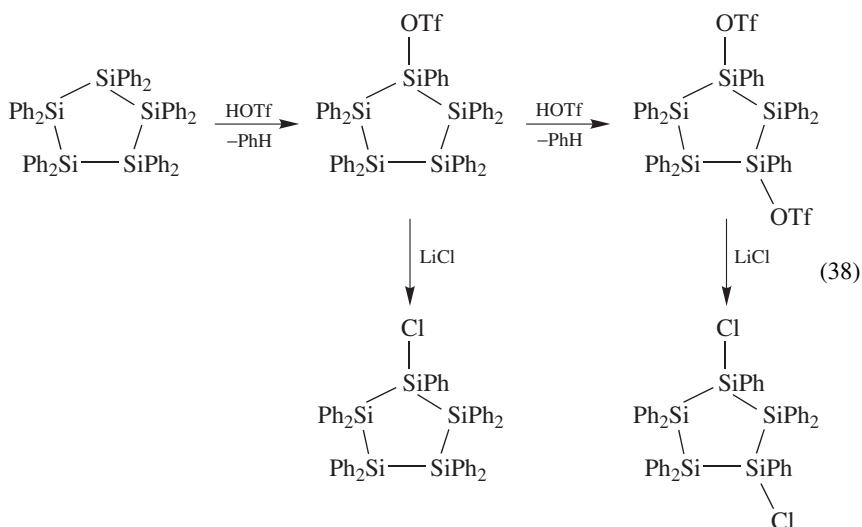
If several aryl substituents are present, a stepwise substitution and further functionalization can be achieved even if the aryl substituents are at different silicon atoms⁶⁴ (equation 37).



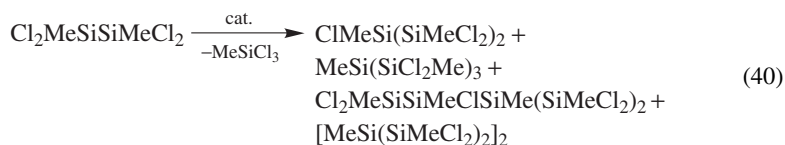
The reactivity of the substituents at silicon in the protodesilylation reaction with triflic acid decreases in the order⁶⁵:



Whereas cyclic $\text{Si}_5\text{Ph}_{10}$ can be selectively mono- and difunctionalized by triflic acid⁶⁶ (equation 38), the reaction of Si_4Ph_8 always yields mixtures of mono- and polyfunctionalized products⁶⁷. The introduction of the more reactive *p*-tolyl substituents in $[\text{SiPh}(p\text{-Tol})_4]_4$ (four stereoisomers possible) results in a selective monofunctionalization but the products consist of all six possible stereoisomers⁶⁸ (equation 39).

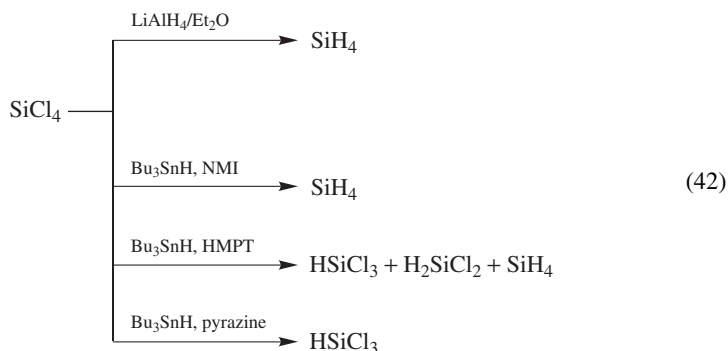


The catalytic disproportionation of methylchlorosilanes, especially 1,1,2,2-tetrachlorodimethyldisilane, offers convenient access to highly chlorine functionalized oligosilanes (equation 40). Useful catalysts are HMPT or *N*-heterocycles, especially *N*-methylimidazole (NMI)⁶⁹. The reaction is thought to proceed via a Lewis-base coordinated silylene SiClMe , which inserts into a SiCl bond of another disilane under formation of the trisilane. Computational investigations have confirmed this reaction pathway via Lewis-base coordinated silylene species, while a homolytic cleavage of $\text{SiCl}_2\text{Me-SiCl}_2\text{Me}$ into two SiCl_2Me fragments is unfavorable⁷⁰. The exclusive formation of the branched tetrasilane shows that the insertion of a second silylene takes place exclusively into the silicon-chlorine bond at the middle silicon atom of the trisilane⁷¹. The very reactive catalyst *N*-methylimidazole, which catalyzes the disproportionation of 1,1,2,2-tetrachlorodimethyldisilane even at room temperature, also catalyzes the disproportionation of 1,2-dichlorotetramethyldisilane into Me_2SiCl_2 and α, ω -dichloropermethylogosilanes with up to 5 silicon atoms⁷¹ (equation 41).





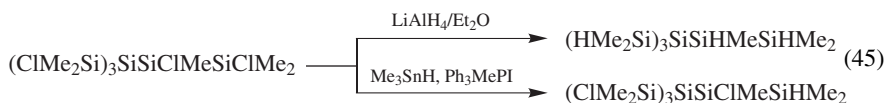
While the hydrogenation of chlorosilanes by LiAlH_4 in diethyl ether always leads to the complete hydrogenation of all chloro-functions, a partial hydrogenation can be achieved by the Lewis base assisted hydrogenation with triorganostannanes, $\text{R}_3\text{SnH}^{72}$ (equation 42). The product spectrum depends significantly on the Lewis basicity of the applied catalyst⁷³. Organochlorosilanes ($\text{Me}_x\text{SiCl}_{4-x}$) can also be hydrogenated by Bu_3SnH , but relatively strong bases like N-methylimidazole have to be used in these cases to catalyze these reactions.



More reactive are methylchlorooligosilanes, e.g. $\text{MeCl}_2\text{SiSiCl}_2\text{Me}$ can be hydrogenated with two equivalents of R_3SnH to either $\text{H}_2\text{MeSiSiCl}_2\text{Me}$ or to a mixture of all possible partial hydrogenated species $\text{Cl}_x\text{H}_{2-x}\text{MeSiSiCl}_y\text{H}_{2-y}\text{Me}$ by a variety of Lewis catalysts⁷⁴. In higher oligosilanes, SiCl bonds at middle silicon atoms are hydrogenated selectively at first (examples are given in equations 43 and 44^{75,76})



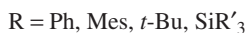
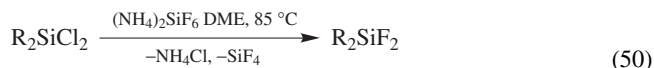
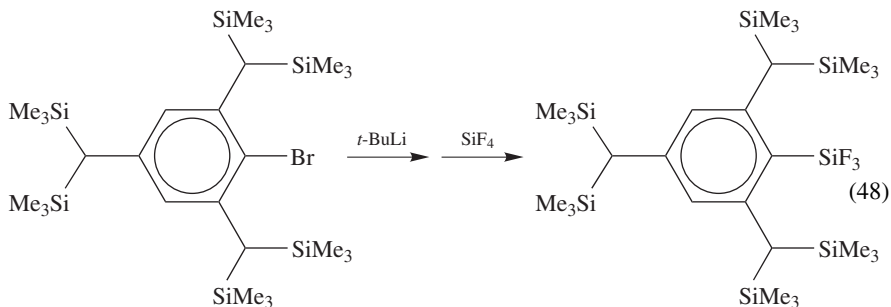
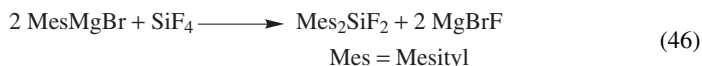
whereas SiCl bonds in the vicinity of quaternary silicon atoms are not hydrogenated by stannanes⁷⁷ (equation 45).



B. Fluorosilanes

Organofluorosilanes are accessible by reaction of Grignard compounds with SiF_4 , especially if sterically crowded silanes are formed⁷⁸ (equations 46–48), but in most cases a halogen exchange reaction with chloro- or bromosilanes is applied to form organofluorosilanes. Fluorinating agents include KF^{79} , ZnF_2^{80} (equation 49), SbF_3^{81} or $(\text{NH}_4)_2\text{SiF}_6^{82}$

(equation 50). The fluorination with $(\text{NH}_4)_2\text{SiF}_6$ can be accelerated by ultrasound⁸³.



Starting from silyl triflates, fluorosilanes are obtained by reaction with LiF in ether^{84,85} (equation 51).

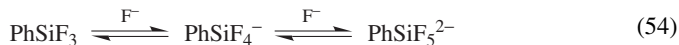


This method fails in the preparation of oligosilanes bearing SiF_3 units.

Alkoxysilanes can be converted into fluorosilanes by treatment with concentrated (40%) hydrofluoric acid^{86,87} (equation 52).



Difluoro- and trifluorosilanes tend to coordinate fluoride anions under formation of five- and six-coordinate fluorosilicates^{88,89} (equations 53 and 54).



Physical data and NMR parameters for the most important fluorosilanes are given in Table 3.

C. Bromo- and Iodosilanes

Bromo- and even more iodo-substituted silanes are by far more sensitive to moisture than chlorosilanes, especially polyhalogenated species. Elemental bromine or iodine, respectively, is formed in air after a short time.

TABLE 3. Melting points, boiling points, densities, refractive indices, ^{29}Si NMR chemical shifts and $^1J_{\text{SiF}}$ coupling constants of the most important fluorosilanes^{20–22}

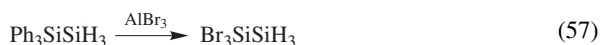
Compound	mp (°C)	bp (°C)	D_4^{20} (g cm ⁻³)	n_D^{20}	δ_{Si} (ppm)	$^1J_{\text{SiF}}$ (Hz)
SiF ₄	-90	-86	1.66 (At -95 °C)		-113.0	170
HSiF ₃	-131	-97.5			-77.8	276
H ₂ SiF ₂	-122	-76			-28.5	297
H ₃ SiF		-98.6			-17.4	279
Me ₃ SiF	-74	17	0.793		31.0	275
Me ₂ SiF ₂	-88	2			4.4	288
MeSiF ₃	-73	-30			-56.2	267
Ph ₃ SiF	62	208 ₁₂	1.212		-4.7	
Ph ₂ SiF ₂		156 ₅₀	1.145	1.5221	-29.1	303
			(At 17 °C)	(At 25 °C)		
PhSiF ₃	-19	101	1.2169	1.4110	-73.2	268
FMe ₂ SiSiMe ₂ F		93			28.0	304
F ₂ MeSiSiMeF ₂		57			-2.8	335
Si ₂ F ₆	-19	-19			-77.9	322
Si ₃ F ₈	-1.2	42			SiF ₃ : -79.9 SiF ₂ : -17.7	344 357

Tribromosilane, HSiBr₃, is obtained together with silicon tetrabromide by the reaction of crystalline silicon with hydrogen bromide. As in the reaction with HCl, the amount of SiBr₄ increases when the temperature is raised (31% at 360 °C, 55% at 470 °C and 80% at 700 °C)⁹⁰.

Methylbromosilanes can be obtained by the direct synthesis from MeBr and silicon, but are normally obtained on a small scale by exchange reactions. Siloxanes can be converted into bromosilanes by reaction with phosphorus tribromide⁹¹ (equation 55).



Like chlorosilanes, bromosilanes and iodosilanes are synthesized by cleavage of aryl substituents by acetyl bromide^{92,93} or hydrogen bromide⁹⁴ or iodide in the presence of a Lewis acid like AlBr₃ or AlI₃ (equations 56 and 57). If liquid hydrogen halide is used in an autoclave, the aluminum halide is not necessary. Under carefully controlled conditions SiH bonds remain intact.



Iodotrimethylsilane is conveniently prepared from hexamethyldisiloxane with anhydrous aluminum iodide⁹⁵ (equation 58).



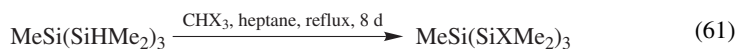
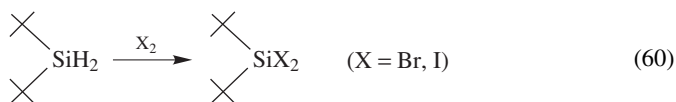
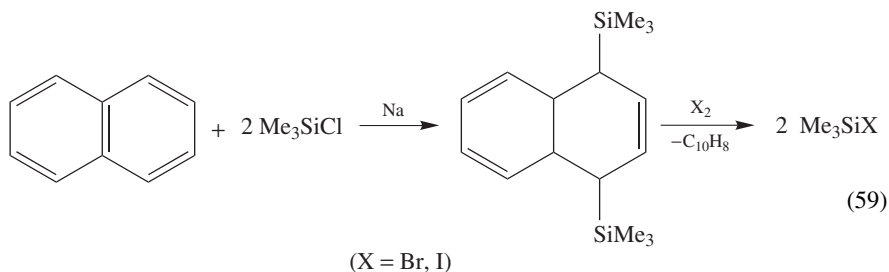
It is a useful reagent in organic synthesis for cleavage of ethers or for conversion of ketals or acetals into diiodides^{96,97}. In most cases iodotrimethylsilane is generated *in situ* using Me₃SiCl/NaI in acetonitrile, which is as effective as the iodosilane itself^{98,99}.

Both bromotrimethylsilane and iodotrimethylsilane are also accessible via 1,4-bis(trimethylsilyl)dihydronaphthalene¹⁰⁰ (X = Br, I) (equation 59). Starting from

TABLE 4. Melting points, boiling points, densities, refractive indices and ^{29}Si NMR chemical shifts of the most important bromo- and iodosilanes^{20–22}

Compound	mp ($^{\circ}\text{C}$)	bp ($^{\circ}\text{C}$)	D_4^{20} (g cm^{-3})	n_D^{20}	δ_{Si} (ppm)
SiBr_4	5	154	2.772 (At 25°C)	1.5627	-93
HSiBr_3	-73	112.2			-43.3
H_2SiBr_2	-70.1	66			-30.4
H_3SiBr	-94	1.9			-48.5
Me_3SiBr	-44	79.5	1.1725	1.422	26.2
Me_2SiBr_2	-58.5	112.3	1.727	1.470	19.8
MeSiBr_3	-28.4	133.5	2.253	1.515	-18.5
Ph_2SiBr_2	3.8	192.2	1.587 (At 25°C)	1.618	
PhSiBr_3	-21	178.3	2.023 (At 25°C)	1.597	
$\text{Br}_2\text{MeSiSiMeBr}_2$	96.5				3.6
Si_2Br_6	95	240			-35.6
SiI_4	120	287	4.198		-352
HSiI_3	8	220 (dec.)			-178
H_2SiI_2	-1	57	2.834		-99.6
H_3SiI	-57	45.6			-83.3
Me_3SiI		107	1.470	1.4742	8.6
Me_2SiI_2		170	2.203		-33.7
MeSiI_3		229	2.946		-144

hydrosilanes, bromo- and iodosilanes are obtained by treatment with elemental halogen¹⁰¹ (equation 60). If CBr_4 or CHX_3 ($\text{X} = \text{Br}, \text{I}$) are applied^{102–104}, SiSi bonds are not cleaved (equation 61).

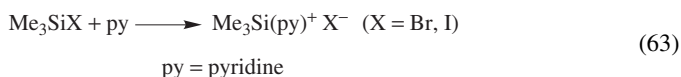
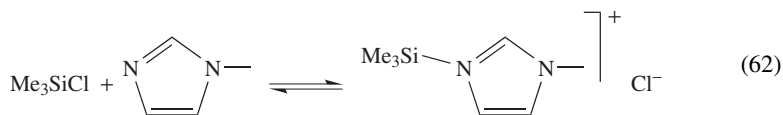


Physical data and chemical shifts for the important bromo- and iodosilanes are given in Table 4.

III. LEWIS-BASE ADDUCTS OF SILICON HALIDES

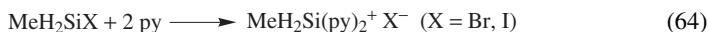
Tetravalent silicon compounds are able to form adducts with Lewis bases, depending on the acceptor strength of the silicon atom. Tetraorganosilanes show only very little

tendency to form hypercoordinated species¹⁰⁵; however, the characterization of the species SiPh_5^- ¹⁰⁶ and $(\text{CF}_3)_2\text{Me}_3\text{Si}^-$ ¹⁰⁷ has been reported. Several adducts of triorganomonosilanes R_3SiX with Lewis bases are in fact substitution products^{108,109} (equations 62 and 63).



Such ionic species could also be detected in solution by ²⁹Si NMR spectroscopy. Nucleophiles like *N*-methylimidazole, *p*-*N,N*-dimethylaminopyridine and HMPA showed the strongest coordinating effects¹¹⁰. Mixtures of electrophilic trimethylsilyl compounds and nucleophiles(L), such as amines and amides, are common silylation agents¹¹¹ and salts $\text{Me}_3\text{SiL}^+\text{X}^-$ have been discussed as the active silylation species¹¹².

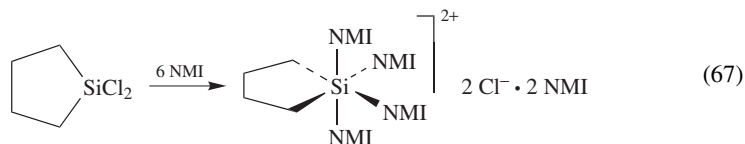
If one or more organo-substituents are replaced by the smaller hydrogen atom, ionic pentacoordinate adducts are formed^{108,113,114} (equations 64 and 65).



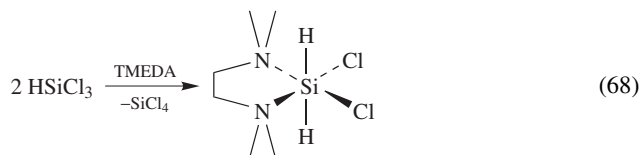
Me_2SiCl_2 forms with *N*-methylimidazole (NMI) a 1 : 2 adduct, but after sublimation crystals of a 1 : 4 adduct were obtained. The crystal structure analysis of the 1 : 4 adduct revealed a pentacoordinated silicon atom¹⁰⁸ (equation 66).



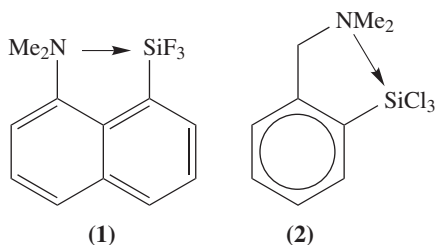
1,1-Dichloro-1-silacyclopentane forms an octahedral complex with NMI¹¹⁵ (equation 67). On the other hand, trichlorosilanes and SiCl_4 form stable octahedral 1 : 2 adducts with many Lewis bases including phosphanes¹¹⁶, tertiary amines¹¹⁷ and *N*-heterocycles like pyridine¹¹⁸, bipyridyl¹¹⁹ or *N*-methylimidazole⁷¹.



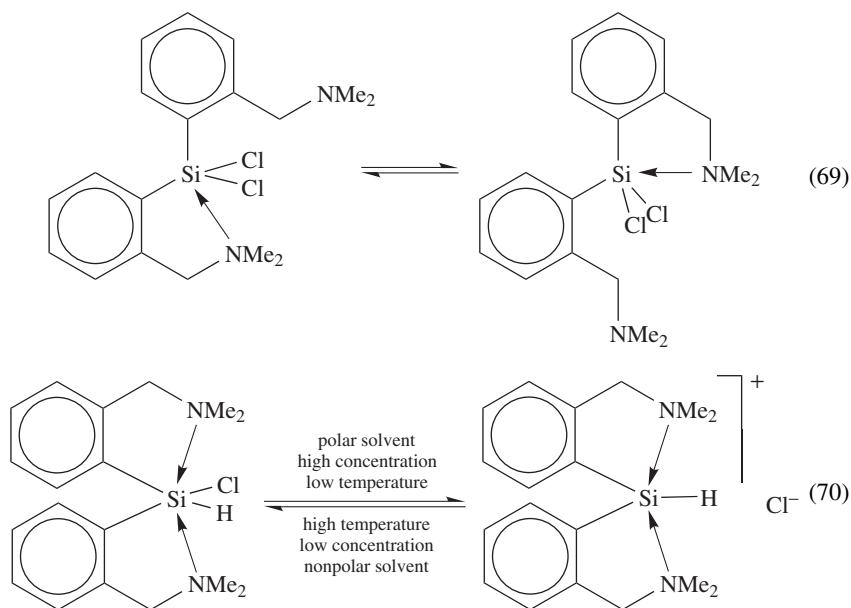
The formation of an adduct between HSiCl_3 and TMEDA or TEEDA (tetraethylethyl, endiamine) is accompanied by an unexpected redistribution of the trichlorosilane¹²⁰ (equation 68).



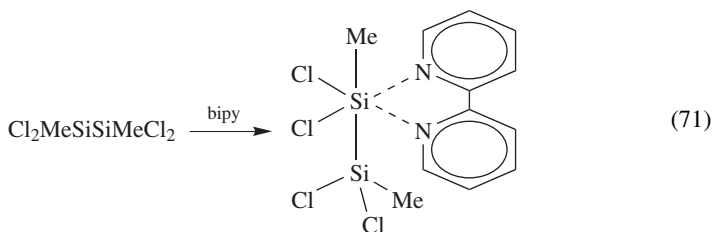
The hypercoordination of silicon can be forced by intramolecular coordination, as shown in structures **1** and **2**¹²¹.



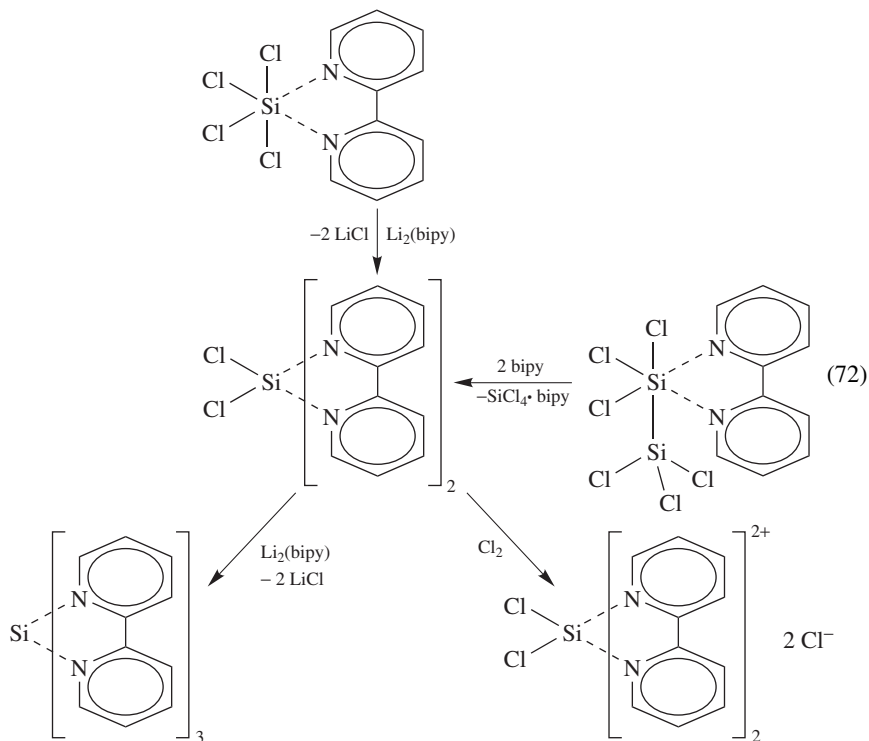
Bis(*o*-dimethylaminomethylphenyl)dichlorosilane reveals in solution an intramolecular dynamic coordination of one dimethylaminomethyl group to silicon with pentacoordination^{122,123} (equation 69). The corresponding monochloro derivative shows in solution an equilibrium between a neutral hexacoordinated modification (which is also observed in the solid state) and an ionic pentacoordinated modification¹²⁴ (equation 70).



In contrast to the numerous adducts of monosilanes, only few stable base adducts of halogenated oligosilanes are known. If NMe_3 is added to a solution of Si_2Cl_6 at -78°C , adducts $\text{Si}_2\text{Cl}_6 \cdot 1-2\text{NMe}_3$ are formed in solution but, at higher temperature, they dissociate and the disilane disproportionates^{125,126}. Similar behavior has been found in the reactions of Si_2Cl_6 and $\text{Cl}_2\text{MeSiSiMeCl}_2$ with pyridine¹²⁷. Only with bipyridyl (bipy) and 1,10-phenanthroline (phen) do several halogenated disilanes, including Si_2X_6 , $\text{X}_2\text{MeSiSiMeX}_2$ ($\text{X} = \text{F}, \text{Cl}, \text{Br}$) and $\text{Me}_3\text{SiSiCl}_3$ and the trisilane Si_3Cl_8 form stable 1 : 1 adducts¹²⁷. The bidentate ligand coordinates to one silicon atom; the other remains tetracoordinated (equation 71).



The molecular structure of $\text{Cl}_2\text{MeSiSiMeCl}_2 \cdot \text{bipy}$ ¹²⁸ reveals very expanded and unequal silicon–chlorine bonds at the octahedral coordinated silicon atom. In donor solvent solutions the bipy adducts of SiCl_4 or $\text{Cl}_2\text{MeSiSiMeCl}_2$ decompose rapidly¹²⁹, in the first case with formation of $\text{SiCl}_4 \cdot \text{bipy}$ (colorless) and $\text{SiCl}_2 \cdot 2 \text{ bipy}$ (green)¹³⁰, which can be regarded as a base stabilized silylene. Oxidation with chlorine leads to the remarkable stable cation $\text{cis-}[\text{SiCl}_2(\text{bipy})_2]^{2+}$ ¹³¹. $\text{SiCl}_4 \cdot \text{bipy}$, on the other hand, can be reduced by $\text{Li}_2(\text{bipy})$ to $\text{SiCl}_2 \cdot 2 \text{ bipy}$ and $\text{Si}(\text{bipy})_3$ ¹³² (equation 72).

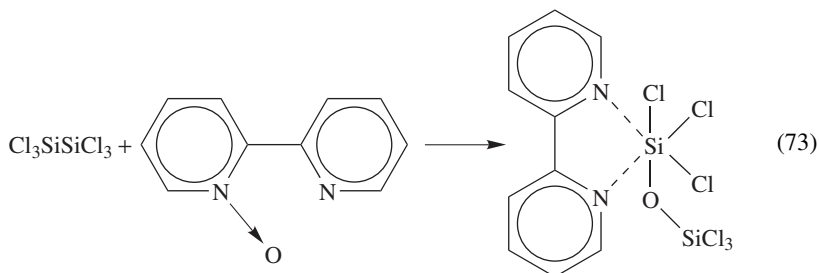


In $\text{Si}_3\text{Cl}_8 \cdot \text{phen}$ ¹³³ the phenanthroline ligand is coordinated at the middle silicon atom, suggesting that the acceptor strength of the middle silicon atom with two chlorine substituents is even higher than those of the terminal silicon atoms bearing three chlorine substituents. This means that despite their lower electronegativity, silyl groups also increase the acceptor strength like chlorine substituents. A comparison of the stability

of several bipy and phen adducts results in the graduation:



While silicon tetrahalides also form adducts with amine N-oxides (Me_3NO , pyO or bipyO)¹³⁴, the reaction of Si_2Cl_6 with bipyO results in a redox reaction under cleavage of the Si–Si bond¹³⁵ (equation 73).



A similar redox reaction can also be observed between Ph_3PO and $\text{Cl}_2\text{MeSiSiMeCl}_2$ ¹³⁶ (equation 74).



IV. REFERENCES

1. R. Walsh, *Bond dissociation energies in organosilicon compounds*, in *ABCR Catalogue*; Gelest Inc., Tully town, Pa, (USA), 2000, p. 92.
2. H. Ikeda, M. Tsunashima and A. Mieda, EP 283905 1988; *Chem. Abstr.*, **110**, 138155a (1988).
3. W. C. Breneman, in *Catalyzed Direct Reactions of Silicon* (Eds. K. M. Lewis and D. G. Rethwisch), Elsevier, Amsterdam, 1993, p. 441.
4. O. Ruff and K. Albert, *Ber.*, **38**, 2222 (1905).
5. A. Stock and L. Zeidler, *Ber.*, **56B**, 986 (1923).
6. H. Ehrlich, T. Lobreyer, K. Hesse and H. Lieske, in *Silicon for the Chemical Industry IV*, (Eds. H. A. Oye, H. M. Rong, L. Nygaard, G. Schüssler and J. Kr. Tuset), Geiranger (Norway), 1998, p. 113.
7. S. Wakamatsu, K. Hirota and K. Sakata, in *Silicon for the Chemical Industry IV*, (Eds. H. A. Oye, H. M. Rong, L. Nygaard, G. Schüssler and J. Kr. Tuset), Geiranger (Norway), 1998, p. 123.
8. A. D. Petrov, B. F. Mironov, V. A. Ponomarenko and E. A. Chernyshev, *Synthesis of Organosilicon Monomers*, Heywood & Co. Ltd., London, 1964.
9. R. J. H. Vorhoeve, *Organohalosilanes: Precursors to Silicenes*, Elsevier, Amsterdam, 1967.
10. M. P. Clarke, *J. Organomet. Chem.*, **376**, 165 (1989).
11. R. Lehnert, M. Höppner and H. Kelling, *Z. Anorg. Allg. Chem.*, **591**, 209 (1990).
12. G. Déléris, M. Birot and J. Dunoguès, *J. Organomet. Chem.*, **266**, 1 (1984).
13. M. Okamoto, S. Onodera, T. Okano, E. Suzuki and Y. Ono, *J. Organomet. Chem.*, **531**, 67 (1997).
14. G. Fritz and E. Matern, *Carbosilanes: Synthesis and Reactions*, Springer, New York, 1986, p. 46.
15. S. H. Yeon, I. S. Han, B. R. Yoo and I. N. Jung, *J. Organomet. Chem.*, **516**, 91 (1996).
16. R. Decker and H. Holz, British Patent 681387 1952; *Chem. Abstr.*, **47**, 4129 (1953).
17. S. Nitzsche, US-patent 2666776 (1954); *Chem. Abstr.*, **48**, 5552f (1954).
18. E. G. Rochow and W. F. Gilliam, *J. Am. Chem. Soc.*, **67**, 1772 (1945).
19. M. Okamoto, S. Onodera, Y. Yamamoto, E. Suzuki and Y. Ono, *Chem. Commun.*, 1275 (1998).

20. E. G. Rochow, in *Comprehensive Inorganic Chemistry*, Vol. 1 (Eds. J. C. Bailar, H. J. Emeléus, R. Nyholm and A. F. Trotman-Dickenson), Pergamon Press, Oxford, New York, 1973, p. 1323.
21. H. Marsmann, in *NMR 17 Basic Principles and Progress* (Eds. P. Diehl, E. Fluck and R. Kosfeld), Springer, Heidelberg, 1981; p. 65 and references cited therein.
22. *ABCR Catalogue*, Gelest Inc., Tullytown, Pa. (USA), 2000.
23. L. H. Sommer and L. J. Tyler, *J. Am. Chem. Soc.*, **76**, 1030 (1954).
24. E. J. Corey and A. Venkateswarlu, *J. Am. Chem. Soc.*, **94**, 6190 (1972).
25. P. Jutzi and A. Karl, *J. Organomet. Chem.*, **214**, 289 (1981).
26. U. Bankwitz, H. Sohn, D. R. Powell and R. West, *J. Organomet. Chem.*, **499**, C7 (1995).
27. T. Müller, Y. Apeloig, H. Sohn and R. West, in *Organosilicon Chemistry III* (Eds. N. Auner and J. Weis), Wiley-VCH, Weinheim, 1998; p. 144.
28. R. West, H. Sohn, U. Bankwitz, J. Calabrese, Y. Apeloig and T. Müller, *J. Am. Chem. Soc.*, **117**, 11608 (1995).
29. M. P. Doyle and C. T. West, *J. Am. Chem. Soc.*, **97**, 3777 (1975).
30. R. A. Benkeser, K. M. Foley, J. B. Grutzner and W. E. Smith, *J. Am. Chem. Soc.*, **92**, 697 (1970).
31. R. A. Benkeser, *Acc. Chem. Res.*, **4**, 94 (1971).
32. L. P. Müller, W.-W. du Mont, J. Jeske and P. G. Jones, *Chem. Ber.*, **128**, 615 (1995).
33. W.-W. du Mont, L. P. Müller, L. Müller, S. Vollbrecht and A. Zanim, *J. Organomet. Chem.*, **521**, 417 (1996).
34. L. Müller, W.-W. du Mont, F. Ruthe, P. G. Jones and H. C. Marsmann, *J. Organomet. Chem.*, **579**, 156 (1999).
35. U. Herzog and R. West, *J. Prakt. Chem.*, **342**, 27 (2000).
36. K. Tamao, A. Kawachi and Y. Ito, *Organometallics*, **12**, 580 (1993).
37. K. Tamao, E. Nakajo and Y. Ito, *Tetrahedron*, **44**, 3997 (1988).
38. K. Tamao, A. Kawachi, Y. Nakagawa and Y. Ito, *J. Organomet. Chem.*, **473**, 29 (1994).
39. S. Mantey and J. Heinicke, in *Organosilicon Chemistry III* (Eds. N. Auner and J. Weis), Wiley-VCH, Weinheim, 1998; p. 254.
40. K. Trommer, G. Roewer and E. Brendler, *J. Prakt. Chem.*, **339**, 82 (1997).
41. K. Trommer, U. Herzog and G. Roewer, *J. Prakt. Chem.*, **339**, 637 (1997).
42. K. Trommer, U. Herzog and G. Roewer, *J. Organomet. Chem.*, **540**, 119 (1997).
43. K. Schenzel and K. Hassler, *Spectrochim. Acta*, **50A**, 127 (1994).
44. B. Reiter and K. Hassler, *J. Organomet. Chem.*, **467**, 21 (1994).
45. M. Ishikawa, T. Fuchkami and M. Kumada, *J. Organomet. Chem.*, **118**, 139 (1976).
46. H. Sakurai, T. Watanabe and M. Kumada, *J. Organomet. Chem.*, **7**, P15, (1967).
47. H. Sakurai, K. Tominaga and T. Watanabe, *Tetrahedron Lett.*, 5493 (1966).
48. E. Hengge and D. Kovar, *Z. Anorg. Allg. Chem.*, **458**, 163 (1979).
49. E. Hengge and H. Schuster, *J. Organomet. Chem.*, **186**, C45 (1980).
50. E. Hengge and D. Kovar, *Angew. Chem.*, **89**, 417 (1977).
51. J. R. Koe, D. R. Powell, J. J. Buffy and R. West, *Polyhedron*, **17**, 1791 (1998).
52. J. R. Koe, D. R. Powell, J. J. Buffy, S. Hayase and R. West, *Angew. Chem., Int. Ed. Engl.*, **37**, 1441 (1998).
53. K. Hassler, U. Katzenbeisser and B. Reiter, *J. Organomet. Chem.*, **479**, 193 (1994).
54. H. Söllradl and E. Hengge, *J. Organomet. Chem.*, **243**, 257 (1983).
55. K. Hassler and W. Köll, *J. Organomet. Chem.*, **487**, 223 (1995).
56. E. Hengge, W. Kalchauer and F. Schrank, *Monatsh. Chem.*, **117**, 1399 (1986).
57. M. Eibl, U. Katzenbeisser and E. Hengge, *J. Organomet. Chem.*, **444**, 29 (1993).
58. A. Spielberger, P. Gspaltl, H. Siegl, E. Hengge and K. Gruber, *J. Organomet. Chem.*, **499**, 241 (1995).
59. W. Uhlig, *J. Organomet. Chem.*, **452**, C6 (1993).
60. K. Hassler, *Monatsh. Chem.*, **117**, 613 (1986).
61. H. Gilman and S. Inoue, *J. Org. Chem.*, **29**, 3418 (1964).
62. W. Uhlig and A. Tzschach, *J. Organomet. Chem.*, **378**, C1 (1989).
63. W. Uhlig and C. Tretner, *J. Organomet. Chem.*, **436**, C1 (1992).
64. K. Matyjaszewski and Y. L. Chen, *J. Organomet. Chem.*, **340**, 7 (1988).
65. W. Uhlig and C. Tretner, *J. Organomet. Chem.*, **467**, 31 (1994).
66. U. Pöschl, H. Siegl and K. Hassler, *J. Organomet. Chem.*, **506**, 93 (1996).

67. J. Chrusciel, M. Cypriak, E. Fossum and K. Matyjaszewski, *Organometallics*, **11**, 3257 (1992).
68. U. Pöschl and K. Hassler, *Organometallics*, **14**, 4948 (1995).
69. R. Richter, G. Roewer, U. Böhme, K. Busch, F. Babonneau, H.-P. Martin and E. Müller, *Appl. Organomet. Chem.*, **11**, 7 (1997).
70. H. Hildebrandt and B. Engels, *Z. Anorg. Allg. Chem.*, **626**, 400 (2000).
71. U. Herzog, R. Richter, E. Brendler and G. Roewer, *J. Organomet. Chem.*, **507**, 221 (1996).
72. J. J. D'Errico and K. G. Sharp, *Inorg. Chem.*, **28**, 2177 (1989).
73. U. Pätzold, G. Roewer and U. Herzog, *J. Organomet. Chem.*, **508**, 147 (1996).
74. U. Herzog, G. Roewer and U. Pätzold, *J. Organomet. Chem.*, **494**, 143 (1995).
75. U. Herzog, E. Brendler and G. Roewer, *J. Organomet. Chem.*, **511**, 85 (1996).
76. U. Herzog and G. Roewer, *J. Organomet. Chem.*, **544**, 217 (1997).
77. U. Herzog and G. Roewer in *Organosilicon Chemistry III* (Eds. N. Auner and J. Weis), Wiley-VCH, Weinheim, 1998, p. 312.
78. H. Suzuki, N. Tokitoh and R. Okazaki, *Organometallics*, **14**, 1016 (1995).
79. K. Tamao, T. Kakui and M. Kumada, *J. Am. Chem. Soc.*, **100**, 2268 (1978).
80. G. Kollegger and K. Hassler, *J. Organomet. Chem.*, **485**, 233 (1995).
81. H. Bürger, W. Kilian and K. Burczyk, *J. Organomet. Chem.*, **21**, 291 (1970).
82. R. Damrauer, R. A. Simon and B. Kanner, *Organometallics*, **7**, 1161 (1988).
83. P. D. Lickiss and R. Lucas, *J. Organomet. Chem.*, **510**, 167 (1996).
84. U. Baumeister, K. Schenzel and K. Hassler, *J. Organomet. Chem.*, **503**, 93 (1995).
85. P. K. Marat and A. F. Hengge, *J. Organomet. Chem.*, **430**, 259 (1992).
86. M. S. Maraus, L. H. Sommer and F. C. Whitmore, *J. Am. Chem. Soc.*, **73**, 5127 (1951).
87. E. Hengge and S. Waldhör, *Monatsh. Chem.*, **105**, 671 (1974).
88. R. Müller and C. Dathe, *Z. Anorg. Allg. Chem.*, **343**, 150 (1966).
89. R. K. Marat and A. F. Janzen, *J. Chem. Soc., Chem. Commun.*, 671 (1977).
90. W. C. Schumb and R. C. Young, *J. Am. Chem. Soc.*, **52**, 1464 (1930).
91. M. R. Detty, *Tetrahedron Lett.*, 4189 (1979); M. R. Detty, *J. Org. Chem.*, **45**, 924 (1980).
92. W. Malisch, *J. Organomet. Chem.*, **82**, 185 (1974).
93. U. Herzog and G. Roewer, *J. Organomet. Chem.*, **544**, 217 (1997).
94. H. Schmölzer and E. Hengge, *Monatsh. Chem.*, **115**, 1125 (1984).
95. J. E. Drake, B. M. Glavinicevski, R. T. Hemmings and H. E. Henderson, *Inorg. Synth.*, **19**, 268 (1979).
96. T. Morita, S. Yoshida, Y. Okamoto and H. Sakurai, *Synthesis*, 379, (1979).
97. M. E. Jung, A. B. Mossman and M. A. Lyster, *J. Org. Chem.*, **43**, 3698 (1978).
98. D. E. Seitz and L. Ferreira, *Synth. Commun.*, **9**, 931 (1979).
99. M. E. Jung and T. A. Blumenkopf, *Tetrahedron Lett.*, 3657 (1978).
100. L. Birkhofer and E. Krämer, *Chem. Ber.*, **100**, 2776 (1967).
101. M. Weidenbruch, A. Schäfer and R. Rankers, *J. Organomet. Chem.*, **195**, 171 (1980).
102. K. Hassler and U. Katzenbeisser, *J. Organomet. Chem.*, **421**, 151 (1991).
103. P. Boudjouk and R. Sooriyakumaran, *J. Chem. Soc., Chem. Commun.*, 777 (1984).
104. U. Herzog and G. Roewer, *J. Organomet. Chem.*, **527**, 117 (1997).
105. A. H. J. F. de Keijzer, F. J. J. de Kanter, M. Schakel, V. P. Osinga and G. W. Klumpp, *J. Organomet. Chem.*, **548**, 29 (1997).
106. A. H. J. F. de Keijzer, F. J. J. de Kanter, M. Schakel, R. F. Schmitz and G. W. Klumpp, *Angew. Chem.*, **108**, 1183 (1996).
107. A. Kolomeitsev, G. Bissky, E. Lork, V. Movchun, E. Rusanov, P. Kirsch and G.-V. Röschen-thaler, *Chem. Commun.*, 1107 (1999).
108. K. Hensen, T. Zengerly, T. Müller and P. Pickel, *Z. Anorg. Allg. Chem.*, **558**, 21 (1988).
109. K. Hensen, T. Zengerly, P. Pickel and G. Klebe, *Angew. Chem.*, **95**, 739 (1983).
110. A. R. Bassindale and T. Stout, *Tetrahedron Lett.*, **26**, 3403 (1985).
111. W. P. Weber, *Silicon Reagents for Organic Synthesis*, Springer-Verlag, Berlin, 1983.
112. G. A. Olah and S. C. Narang, *Tetrahedron*, **38**, 2225 (1982).
113. A. R. Bassindale and T. Stout, *J. Chem. Soc., Chem. Commun.*, 1387 (1984).
114. H. J. Campbell-Ferguson and E. A. V. Ebsworth, *J. Chem. Soc., A*, 705 (1967).
115. K. Hensen, F. Gebhardt and M. Bolte, *Z. Anorg. Allg. Chem.*, **623**, 633 (1997).
116. H. E. Blyden and M. Webster, *Inorg. Nucl. Lett.*, **6**, 703 (1970).
117. I. R. Beatie and G. A. Ozin, *J. Chem. Soc., A*, 2267 (1969).
118. K. Hensen and R. Busch, *Z. Naturforsch.*, **37B**, 1174 (1982).

119. D. Kummer, S. C. Chaudhry, T. Debaerdemaeker and U. Thewalt, *Chem. Ber.*, **123**, 945 (1990).
120. P. Boudjouk, S. D. Kloos, B.-K. Kim, M. Page and D. T. Weatt, *J. Chem. Soc., Dalton Trans.*, 877 (1998).
121. R. J. P. Corriu, M. Mazhar, M. Poirier and G. Royo, *J. Organomet. Chem.*, **306**, C5 (1986).
122. H. Handwerker, C. Leis, R. Probst, P. Bissinger, A. Grohmann, P. Kiprof, E. Herdtweck, J. Blümel, N. Auner and C. Zybilla, *Organometallics*, **12**, 2162 (1993).
123. J. Belzner, U. Dehnert, H. Ihmels, M. Hübner, P. Müller and I. Usón, *Chem. Eur. J.*, **4**, 852 (1998).
124. D. Schär and J. Belzner, in *Organosilicon Chemistry III* (Eds. N. Auner and J. Weis), Wiley-VCH, Weinheim, 1998, p. 429.
125. G. Urry, *J. Inorg. Nucl. Chem.*, **26**, 409 (1964).
126. A. Kaczmarczyk and G. Urry, *J. Inorg. Nucl. Chem.*, **26**, 415 (1964).
127. D. Kummer, A. Balkir and H. Köster, *J. Organomet. Chem.*, **178**, 29 (1979).
128. G. Sawitzki and H.-G. v. Schnering, *Chem. Ber.*, **109**, 3728 (1976).
129. D. Kummer, H. Köster and M. Speck, *Angew. Chem.*, **81**, 574 (1969).
130. D. Kummer and H. Köster, *Angew. Chem.*, **81**, 897 (1969).
131. D. Kummer and T. Seshadri, *Z. Anorg. Allg. Chem.*, **428**, 129 (1977).
132. S. Herzog and F. Krebs, *Naturwissenschaften*, **50**, 330 (1963).
133. D. Kummer, S. C. Chaudhry, W. Depmeier and G. Mattern, *Chem. Ber.*, **123**, 2241 (1990).
134. K. Issleib and H. Rheinhold, *Z. Anorg. Allg. Chem.*, **314**, 113 (1962).
135. D. Kummer and T. Seshadri, *Z. Anorg. Allg. Chem.*, **425**, 236 (1976).
136. Z. Qu, B. Chen, B. Kuang and Q. Zhang, *Zhongguo Yiyao Gongye Zazhi*, **22**, 179 (1991); *Chem. Abstr.*, **115**, 159270c (1991).

CHAPTER 8

Synthesis of multiply bonded phosphorus compounds using silylphosphines and silylphosphides

MASAAKI YOSHIFUJI AND KOZO TOYOTA

Department of Chemistry, Graduate School of Science, Tohoku University, Aoba-ku, Sendai 980-8578, Japan

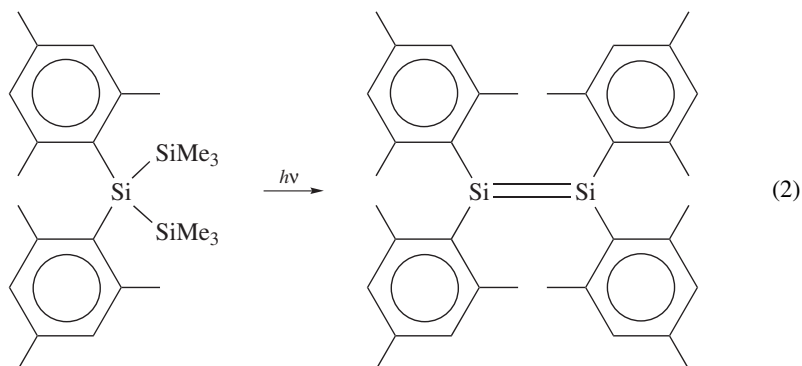
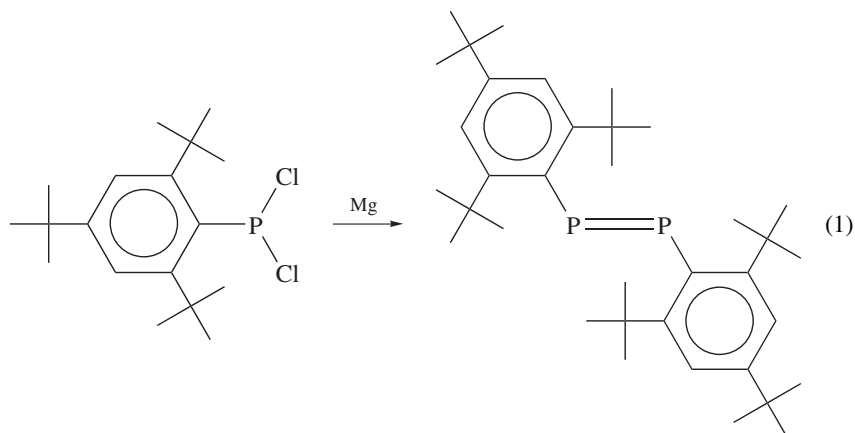
Fax: +81-22-217-6562; e-mail: yoshifj@mail.cc.tohoku.ac.jp

I. INTRODUCTION	491
II. SURVEY OF SILYLPHOSPHINES AND ALKALI METAL SILYL-PHOSPHIDES	494
A. Trisilylphosphines	494
B. Disilylphosphines and Alkali Metal Disilylphosphides	496
C. Monosilylphosphines and Alkali Metal Monosilylphosphides	510
D. Monosilylphosphaethenes	514
III. DISILYL(2,4,6-TRI- <i>t</i> -BUTYLPHENYL)PHOSPHINES	519
IV. MONOSILYL(2,4,6-TRI- <i>t</i> -BUTYLPHENYL)PHOSPHINES	522
V. ALKALI METAL MONOSILYL(2,4,6-TRI- <i>t</i> -BUTYLPHENYL)PHOSPHIDES	523
A. Preparation of Phosphaethenes	523
B. Preparation of Phosphaallenes	528
C. Other Synthetic Applications of Silylphosphides	530
VI. PHOSPHASILENES	534
VII. REFERENCES	536

I. INTRODUCTION

The successful development of 'kinetic stabilization' with bulky substituents (so-called steric protection) was established in the early 1980s. By introducing extremely bulky substituents such as the 2,4,6-tri-*t*-butylphenyl group (hereafter abbreviated to Mes*) into

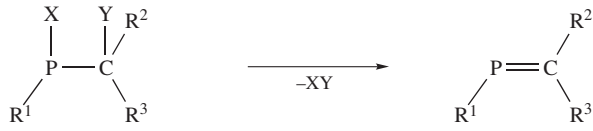
molecules, compounds containing multiply bonded heavier main group elements, such as diphosphenes (equation 1)¹ and disilenes (equation 2)², have been isolated. Soon after this finding, it turned out that a combination^{3,4} of the steric protection methodology^{1,2,5} and synthetic methodology utilizing silyl groups⁶ offers fertile preparative tools for various types of *multiply bonded phosphorus compounds*⁷.



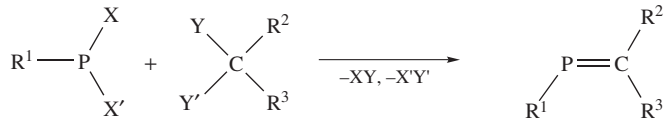
The efficiency of the combined method has been well demonstrated, particularly in the preparations of phosphathenes ($R^1P=CR^2R^3$). The synthetic routes to phosphathenes can be classified into three major categories, i.e. the '1,2-elimination method', the 'condensation method', and the '1,3-silyl migration method' (Scheme 1)⁸. Among variations of the 'condensation method' is included the 'addition-elimination method' using, for example, bis(trialkylsilyl)phosphines and carbonyl compounds (Scheme 2).

The 'silyl migration method' involves intramolecular 1,3-silyl migration which is useful for introducing phosphorus multiple bonds. Variations of this 1,3-silyl migration have been classified as the 'condensation-silatropy method' and the 'addition-silatropy method' (Scheme 3)⁸. Becker reported a reaction involving rearrangement of silyl-substituted acylphosphine for the first time in 1976 (equation 3)⁹.

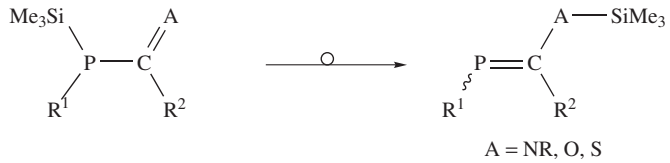
1,2-elimination



condensation

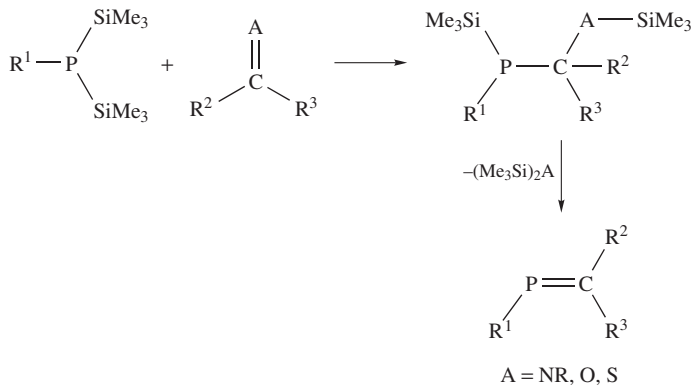


1,3-silyl migration

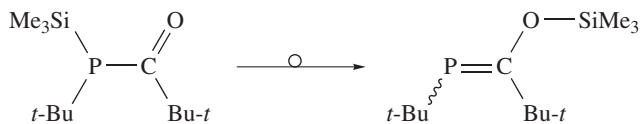


SCHEME 1

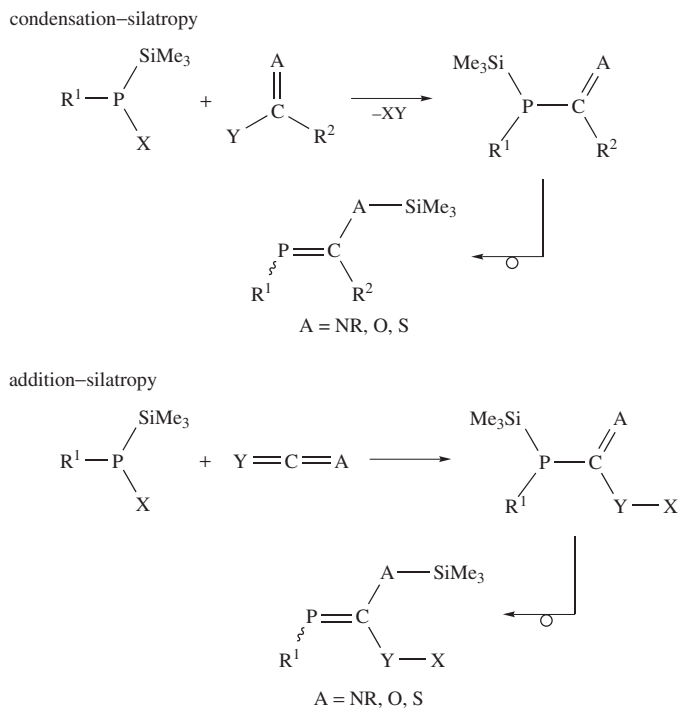
addition-elimination



SCHEME 2



(3)



SCHEME 3

These silatropy methods utilize compounds having phosphorus-silicon bond(s) as starting materials. Preparation and properties of such compounds, i.e. organosilicon derivatives of phosphorus, have been reviewed by Armitage in *The Chemistry of Functional Groups* series in 1989¹⁰, and more recently by Fritz and Scheer¹¹. Thus, the present chapter mainly describes, in Sections III-V, synthetic applications of the Mes*-substituted phosphorus compounds containing phosphorus-silicon bond(s) to kinetically stabilized, multiply bonded phosphorus compounds^{7,12} such as diphosphenes, phosphathenes, phosphapolyenes, phosphacumulenes and phosphathynes, while in Section II, silylphosphines *without* the very bulky Mes* substituent are reviewed in order to evaluate the substituent effect of the Mes* group.

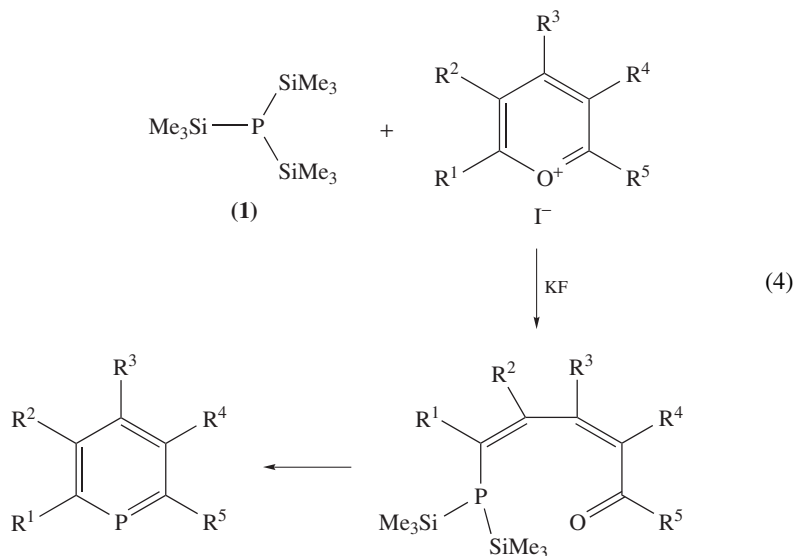
It should be mentioned that some of the Mes*-substituted reagents such as Mes*PCl₂, Mes*P=C=O and Mes*P=C=NR appear in Section II. In such cases, the substituent effect should be evaluated carefully because the Mes* group plays an important role in the stabilization of the products.

II. SURVEY OF SILYLPHOSPHINES AND ALKALI METAL SILYLPHOSPHIDES

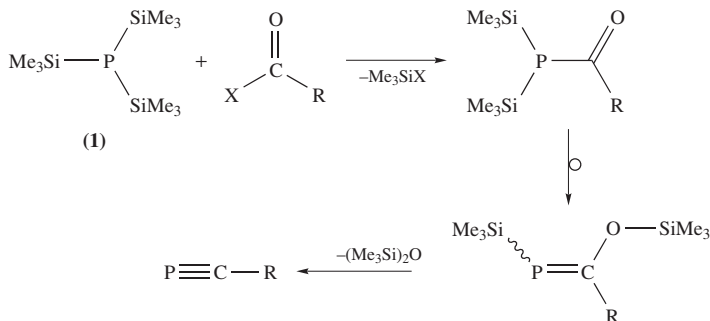
A. Trisilylphosphines

Tris(trimethylsilyl)phosphine **1**¹³ reacted with pyrylium salts in the presence of potassium fluoride to give thermodynamically stabilized phosphabenzene derivatives (λ^3 -phosphinines) (equation 4)¹⁴. In addition, various heterophosphabenzene and

heterophospholes, such as azaphosphabenzenes¹⁵ and azaphospholes¹⁶, were prepared by using **1**¹⁷.

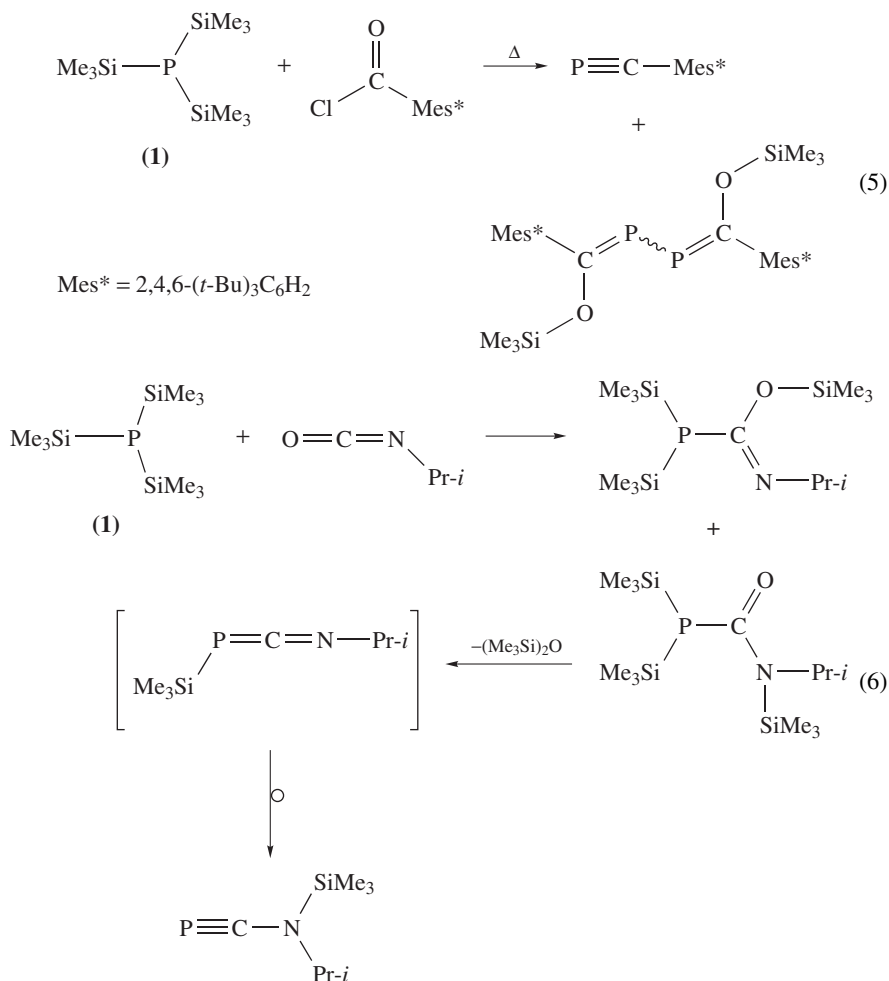


Compound **1** was also used in the preparation of various 1-trimethylsilyl-2-trimethylsilyloxy-1-phosphetenes and phosphaethyne by the 'condensation-silatropy method'¹⁸ and 'condensation-silatropy-elimination method', respectively (Scheme 4)¹⁹.



SCHEME 4

Reaction of **1** with 2,4,6-tri-*t*-butylbenzoyl chloride formed a 2,3-diphosphabuta-1,3-diene as well as a phosphaethyne (equation 5)²⁰. An amino-substituted phosphaethyne was prepared starting from **1** and isopropyl isocyanate by an addition-elimination-silatropy reaction (equation 6)²¹. Addition of **1** to kinetically stabilized phosphaketene (see Section III) gave a 1 : 1 adduct²² or a 1 : 2 adduct²³; the former was converted to 1,3-diphosphabuta-1,3-dienes by treatment with acyl chlorides (equation 7)²². Both adducts could be converted to the same 1,2,4-triphosphabuta-1,3-diene^{23,24}.



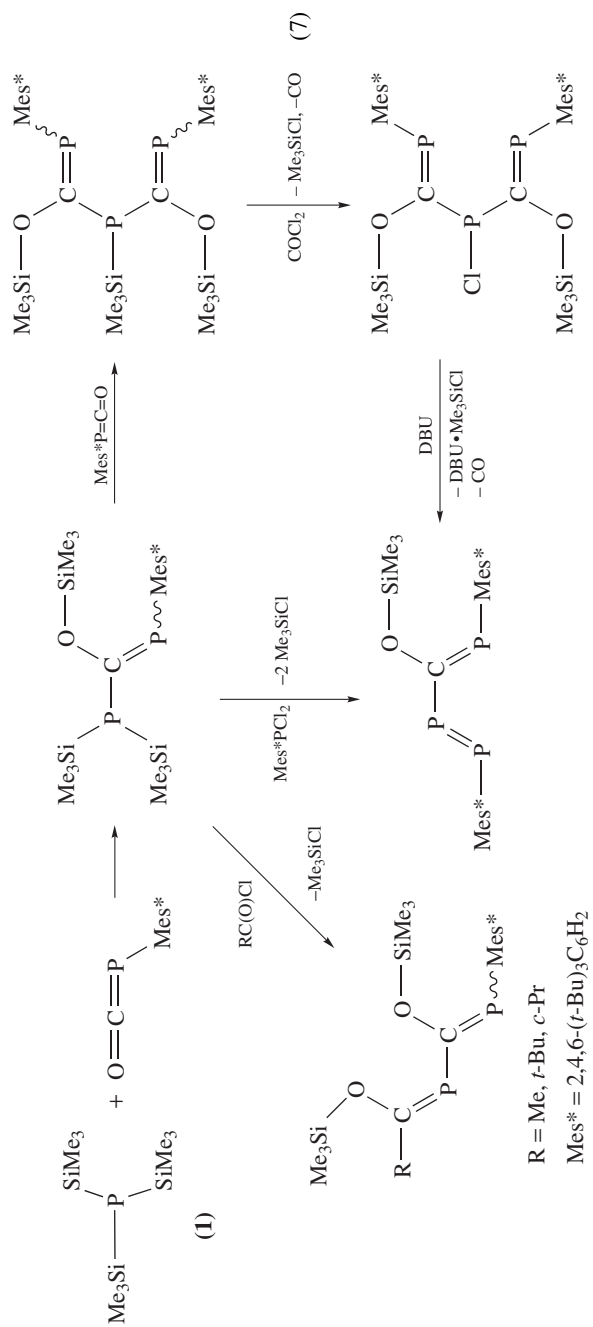
2-Phosphaallyl cation was formed from **1** and tetramethylchloroformamidinium chloride²⁵. When **1** was treated with sterically hindered (2,4,6-tri-*t*-butylphenyl)phosphonous dichloride (Mes*PCl₂), signals due to a symmetrical Mes*P=PMes* and an unsymmetrical diphosphene (probably Mes*P=PSiMe₃) were observed by ³¹P NMR spectroscopy²⁶.

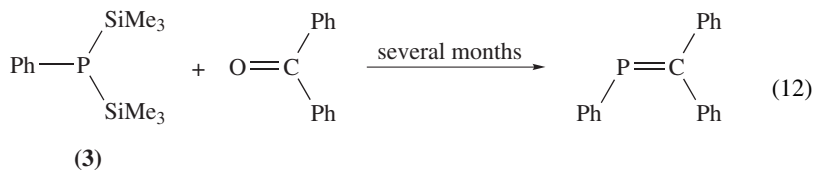
The structure of bis(trimethylsilyl)(triphenylsilyl)phosphine (Ph₃Si)(Me₃Si)₂P was determined by X-ray crystallography²⁷.

B. Disilylphosphines and Alkali Metal Disilylphosphides

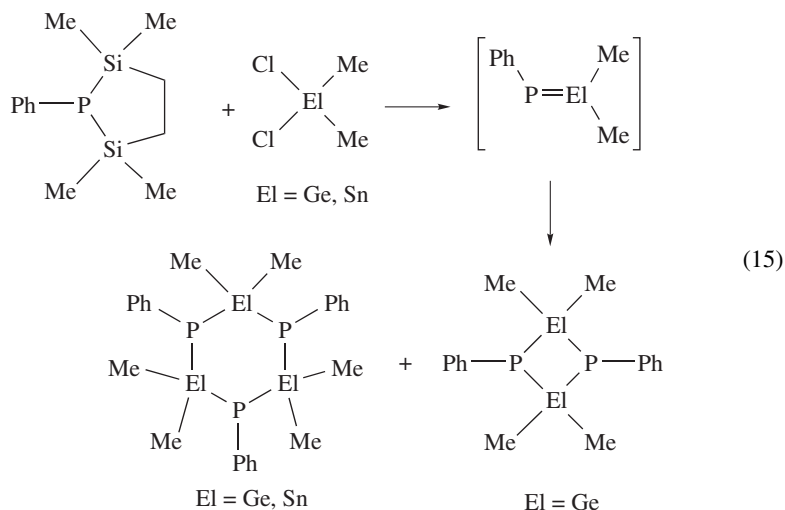
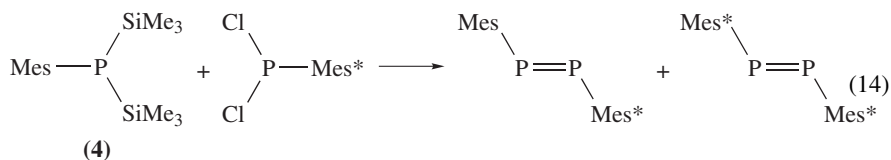
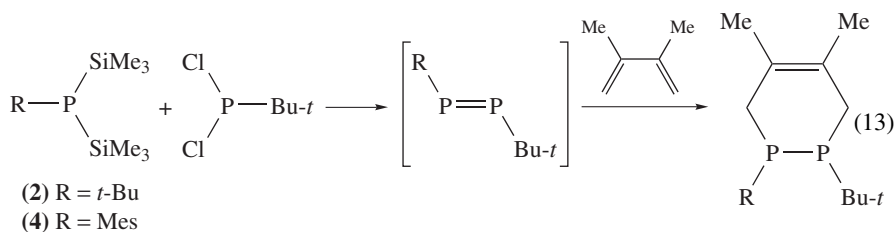
1. Bis(trialkylsilyl)phosphines

Preparations and reactions of some bis(trialkylsilyl)phosphines derived from tris(trialkylsilyl)phosphines were described briefly in Section II.A (see, e.g., Scheme 4).

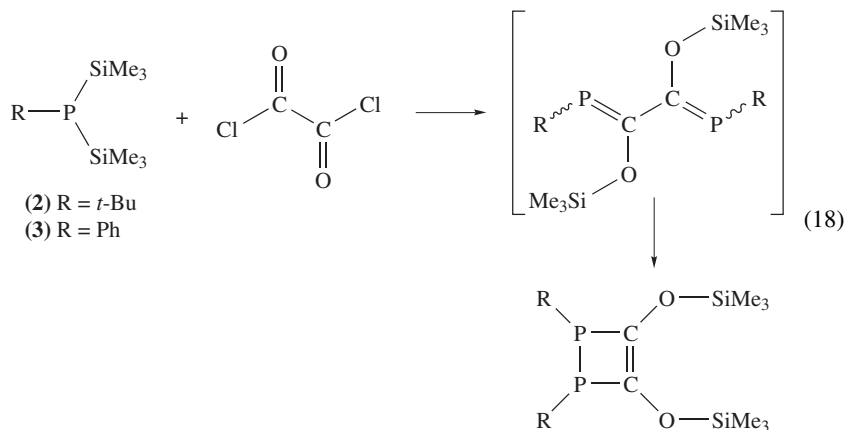
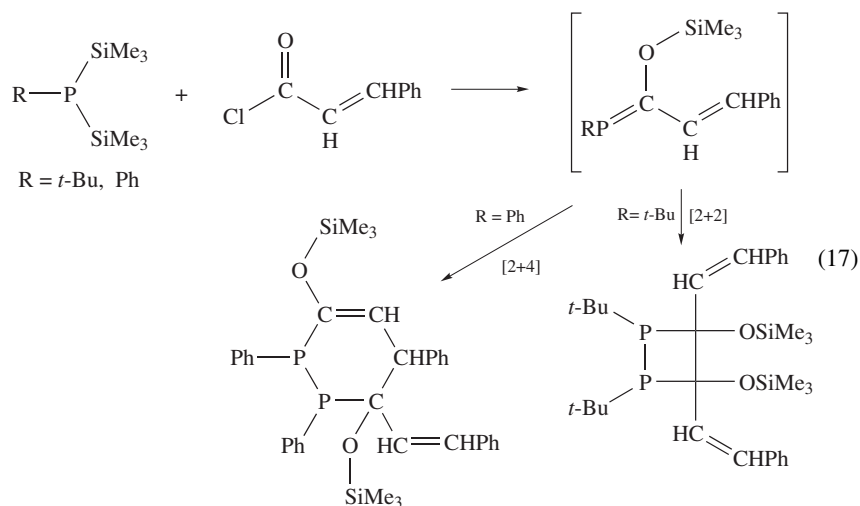
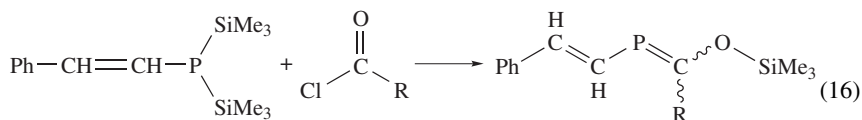


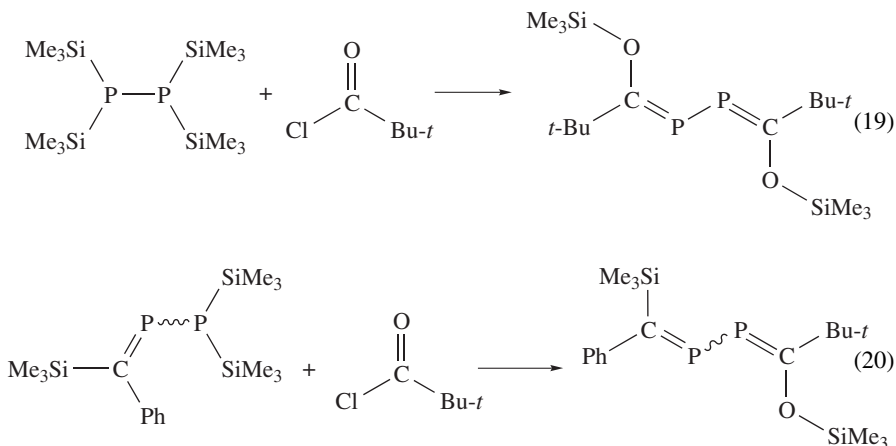


Reactions of *t*-BuP(SiMe₃)₂ (**2**) or mesityl[bis(trimethylsilyl)]phosphine (**4**) with *t*-BuPCl₂ seem to generate diphosphenes, which were trapped by 2,3-dimethylbuta-1,3-diene (equation 13)³². When **4** was allowed to react with a bulky Mes*PCl₂, an unsymmetrical 1-mesityl-2-(2,4,6-tri-*t*-butylphenyl)diphosphene³³ as well as a symmetrical 1,2-bis(2,4,6-tri-*t*-butylphenyl)diphosphene was formed (equation 14)²⁶. Generations of phosphagermene or phosphastannene by the reaction of cyclic (disilyl)(phenyl)phosphine with dichlorodimethylgermane or stannane, respectively, have been assumed on the basis of the formed dimers and trimers (equation 15)^{34,35}.

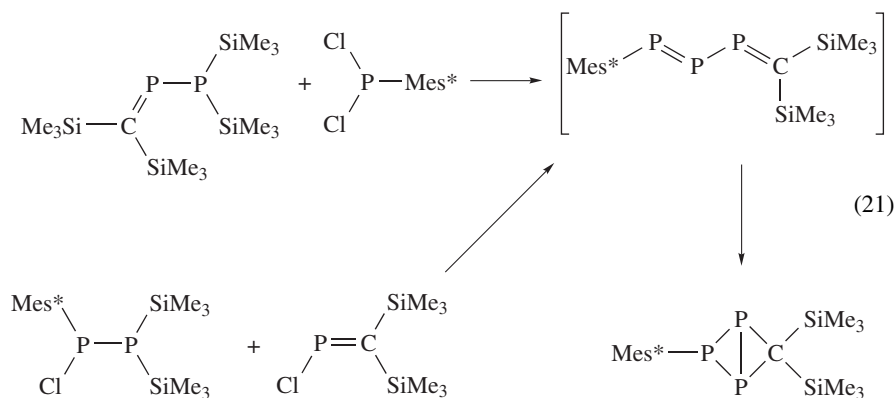


Bis(trialkylsilyl)phosphines were also applied to the preparation or generation of various phosphabuta-1,3-dienes. 2-Phosphabuta-1,3-dienes were formed from styryl[bis(trimethylsilyl)]phosphine and acyl chlorides (equation 16)³⁶. 1-Phosphabuta-1,3-dienes were generated as reactive intermediates in the reactions of bis(trimethylsilyl)phosphines and α,β -unsaturated acyl chlorides (equation 17)³⁶. Reaction of **2** or **3** with oxalyl chloride gave 3,4-diphosphacyclobutene, probably via 1,4-diphosphabuta-1,3-butadiene (equation 18)³⁷. 2,3-Diphosphabuta-1,3-dienes were prepared from reaction of *t*-BuCOCl with $(\text{Me}_3\text{Si})_2\text{PP}(\text{SiMe}_3)_2$ (equation 19)³⁷ or $\text{Ph}(\text{Me}_3\text{Si})\text{C}=\text{P}-\text{P}(\text{SiMe}_3)_2$ (equation 20)³⁸.

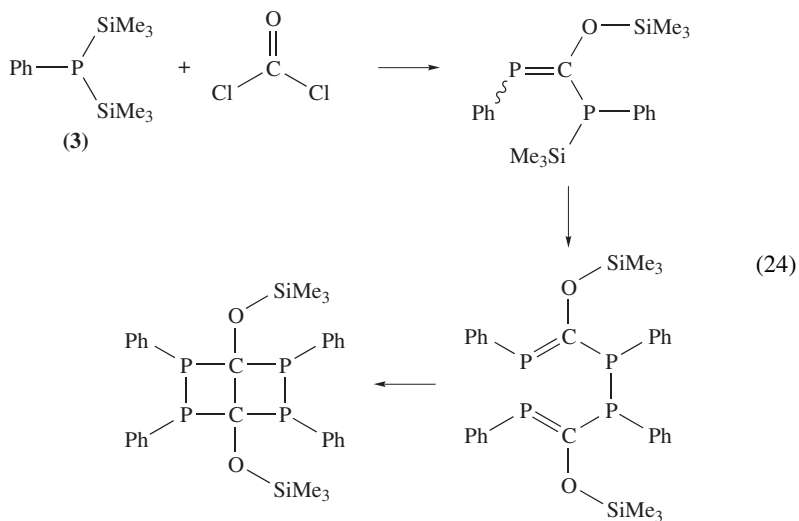
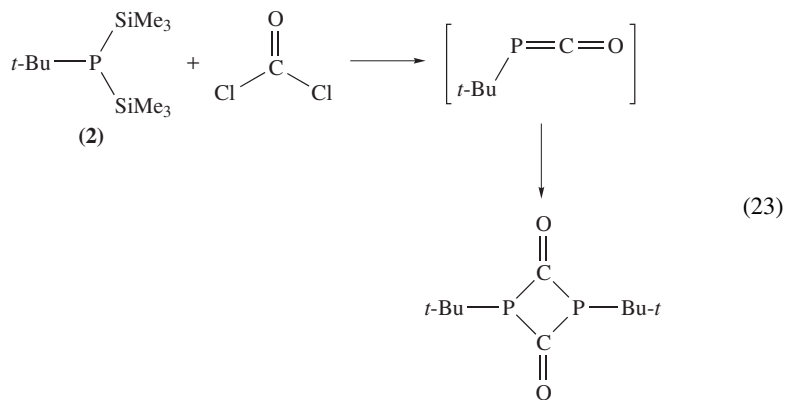
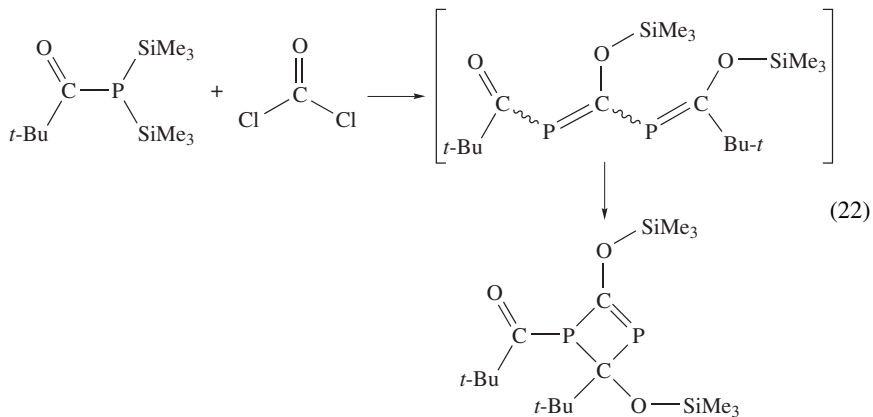


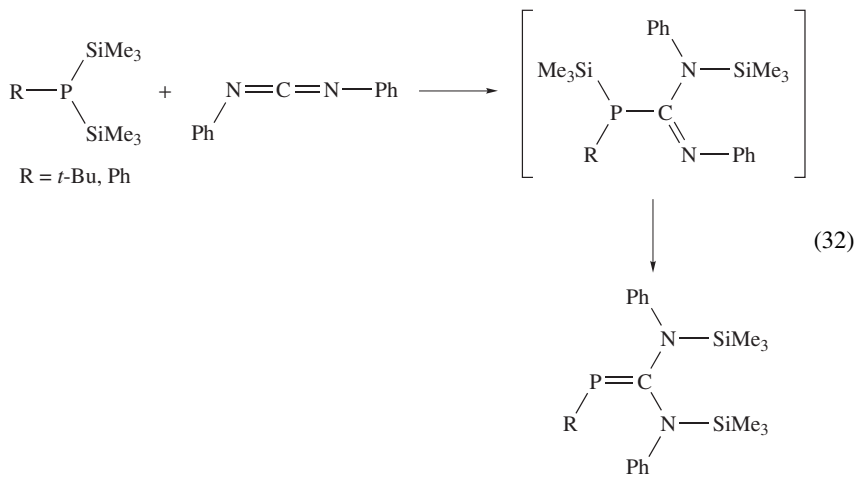
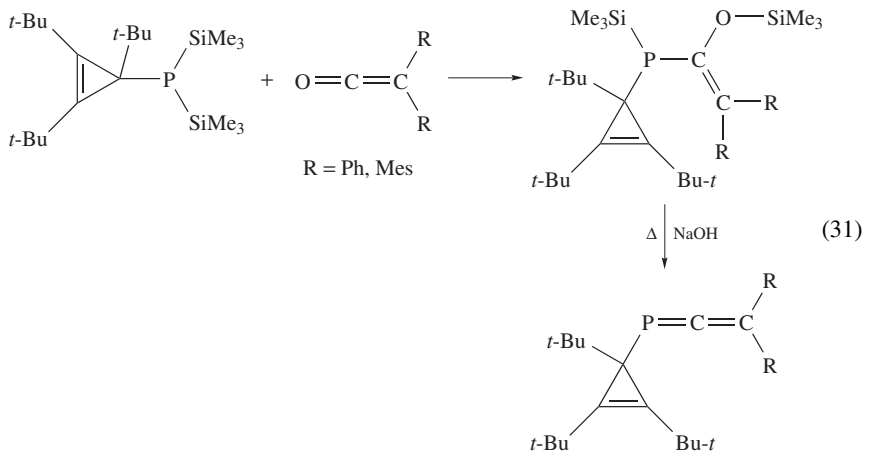
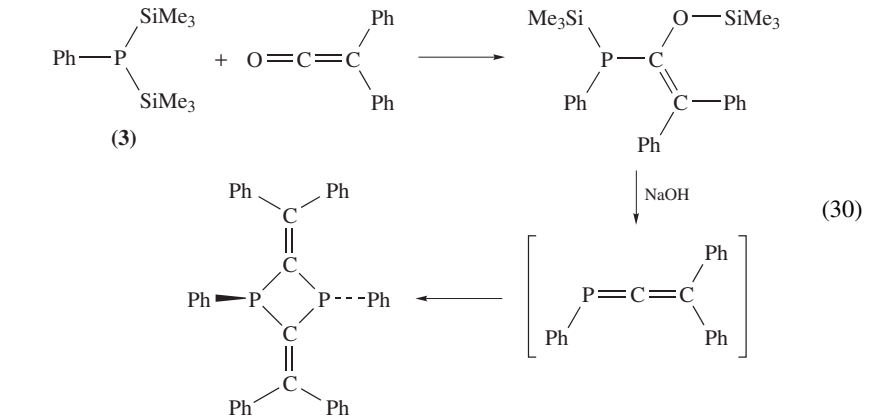


As mentioned in Section II.A (equation 7), 1,3-diphosphabuta-1,3-diene and 1,2,4-triphosphabuta-1,3-diene were prepared by the reaction of $\text{Mes}^*\text{P}=\text{C}(\text{OSiMe}_3)-\text{P}(\text{SiMe}_3)_2$ ²²⁻²⁴. Intermediary formation of 1,2,3-triphosphabuta-1,3-diene ($-\text{P}=\text{P}=\text{P}=\text{C}<$) was assumed in the reaction given in equation 21³⁹.

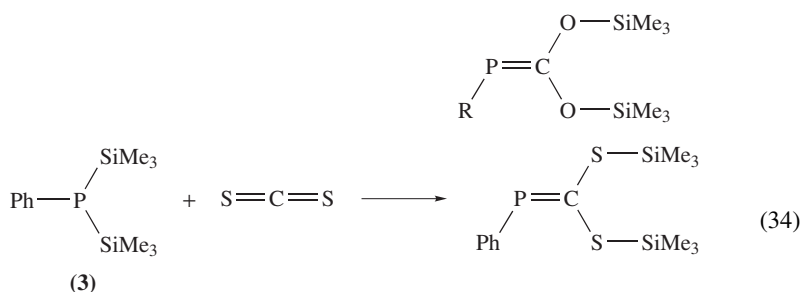
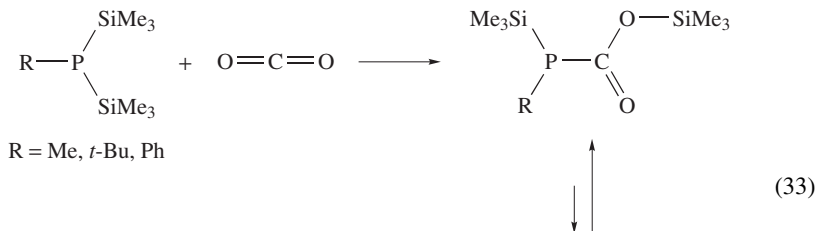


Reaction of $t\text{-BuC}(\text{O})\text{P}(\text{SiMe}_3)_2$ with phosgene gave 1,3-diphosphacyclobutene derivative probably via 1,3-diphosphabuta-1,3-diene (equation 22)³⁷. In this reaction, phosphaketene ($t\text{-BuC}(\text{O})\text{P}=\text{C}=\text{O}$) is also a plausible intermediate leading to the 1,3-diphosphabuta-1,3-diene derivative. In fact, intermediary formation of phosphallenes has been assumed in some reactions of disilylphosphines with phosgene and its analogs of the $\text{X}=\text{CCl}_2$ type, as follows. Reaction of **2** with phosgene led to generation of t -butylphosphaketene (stable below -60°C) (equation 23, cf. equation 68)^{40,41}, while disilylphosphine **3** reacted with phosgene to yield the tetraphosphabicyclo[2.2.0]hexane derivative (equation 24)⁴². Reaction of **3** with $\text{R}=\text{N}=\text{CCl}_2$ gave either tetraphosphahexadiene or 1,3-diphosphetane (equation 25)⁴³.

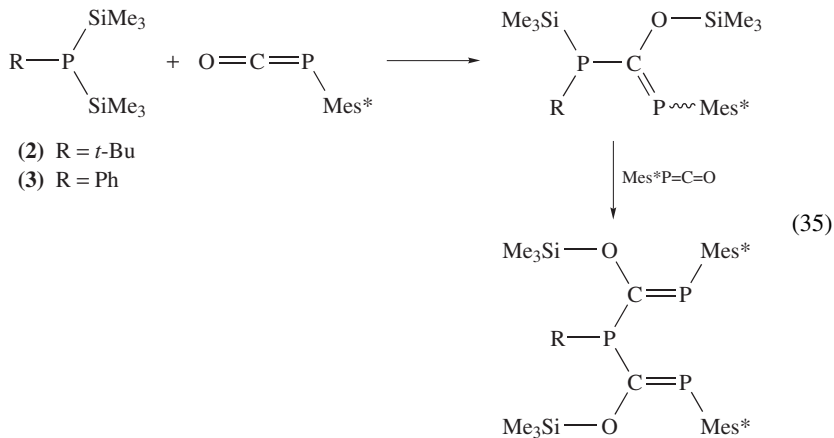


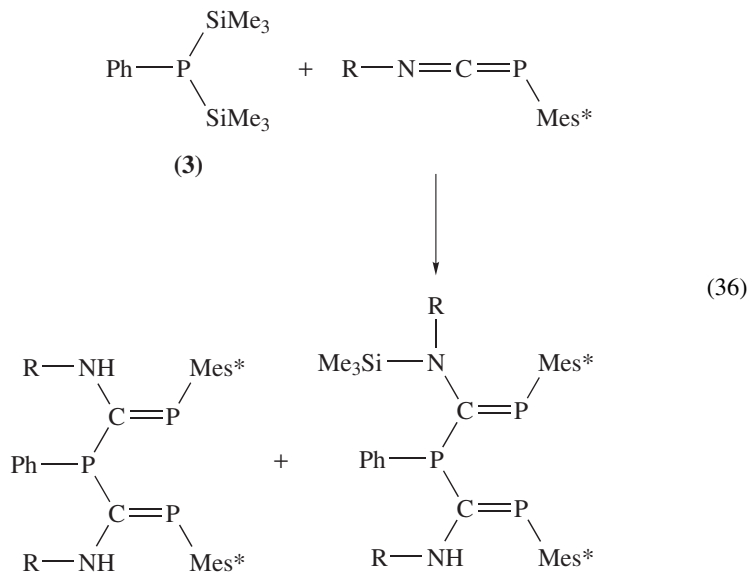


Reaction of bis(trimethylsilyl)phosphines with carbon dioxide afforded adducts and addition–silatropy products instead of phosphaketene or 1,3-diphosphaallene ($R-P=C=P-R'$) (equation 33, compare with equations 72 and 91)⁵². Similarly, reaction of **3** with carbon disulfide resulted in the addition–silatropy product (equation 34, cf. equations 73 and 94)⁵³. Successful preparations of phosphoallenes utilizing alkali metal silylphosphides bearing bulky substituents are described in Section V.

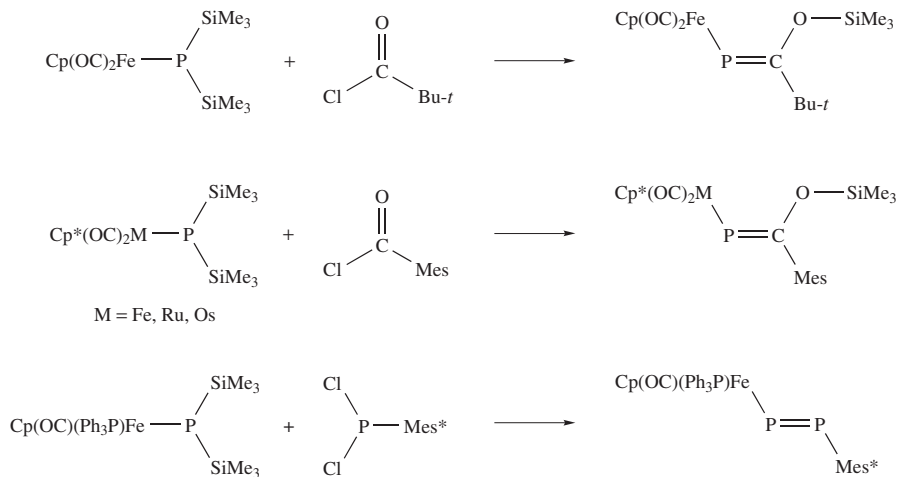


When bis(trimethylsilyl)phosphines were allowed to react with $\text{Mes}^*\text{P}=\text{C}=\text{O}$ (see Section III), 1 : 1 adducts and 1 : 2 adducts were obtained (equation 35, cf. equation 93)²³. Reaction of **3** with kinetically stabilized $\text{Mes}^*\text{P}=\text{C}=\text{NR}$ (see Section V) in polar solvents afforded products derived from 1 : 2 addition (equation 36)⁵⁴.

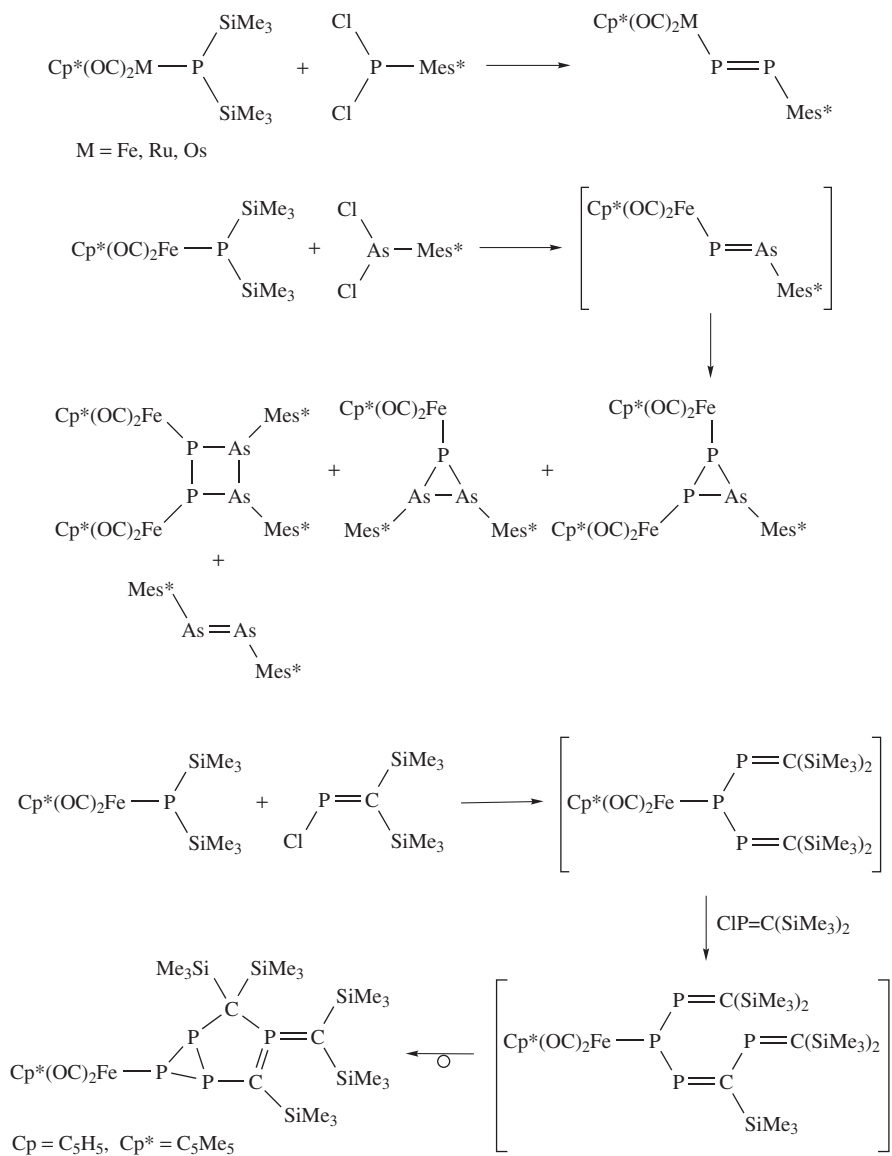




Transition metal-substituted disilylphosphines were prepared and studied by Weber and coworkers (Scheme 5)⁵⁵⁻⁵⁸. Iron, ruthenium or osmium substituted phosphathenes, diphosphenes and phospharsines were introduced from the disilylphosphine.



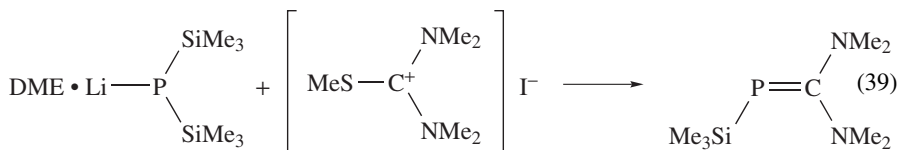
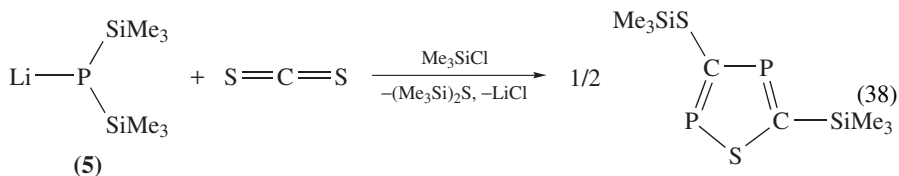
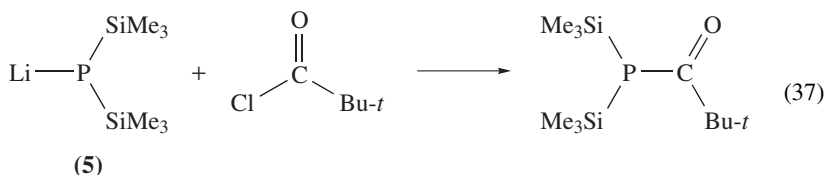
SCHEME 5



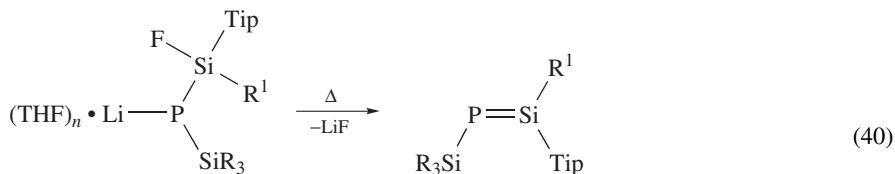
SCHEME 5. (continued)

2. Metal bis(trimethylsilyl)phosphides and related compounds

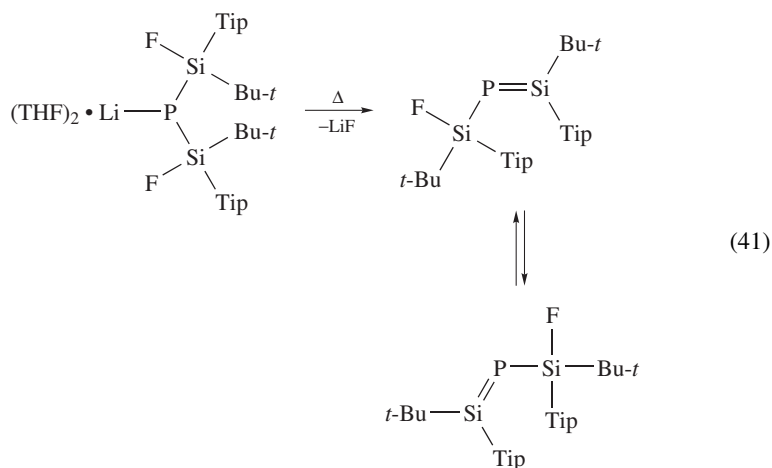
Reactions of lithium bis(trimethylsilyl)phosphide (**5**) have recently been reviewed¹¹. Some reports have been published concerning the structure of **5**⁵⁹. Compound **5** was used in the preparation of phosphathenes and phosphathynes (equation 37 and Scheme 4)^{28,31}. Reaction of **5** with benzophenone led to the observation of a signal probably due to $\text{Me}_3\text{SiP}=\text{CPh}_2$ ³¹. Treatment of **5** with carbon disulfide and then chlorotrimethylsilane afforded a thiadiphosphole derivative (equation 38)⁶⁰. Reaction of $\text{LiP}(\text{SiMe}_3)_2 \cdot \text{DME}$ with a thiuronium iodide formed a phosphathene (equation 39)⁶¹.



Recent studies have revealed that bulky lithium disilylphosphides $\text{R}_3\text{SiP}(\text{Li})-\text{Si}(\text{F})(\text{R}^1)-\text{Tip}$ (Tip = 2,4,6-triisopropylphenyl), generated from $\text{R}_3\text{SiP}(\text{H})-\text{Si}(\text{F})(\text{R}^1)\text{Tip}$ ⁶², lead to trialkylsilyl-substituted phosphasilene $\text{R}_3\text{SiP}=\text{Si}(\text{R}^1)\text{Tip}$ (equation 40)⁶³ and the structure of $i\text{-Pr}_3\text{SiP}=\text{Si}(t\text{-Bu})\text{Tip}$ was analyzed by X-ray crystallography⁶⁴. Phosphasilene $\text{Tip}(t\text{-Bu})(\text{F})\text{Si}-\text{P}=\text{Si}(t\text{-Bu})\text{Tip}$ was also prepared and 1,3-sigmatropic fluorine migration was observed (equation 41)⁶⁵.



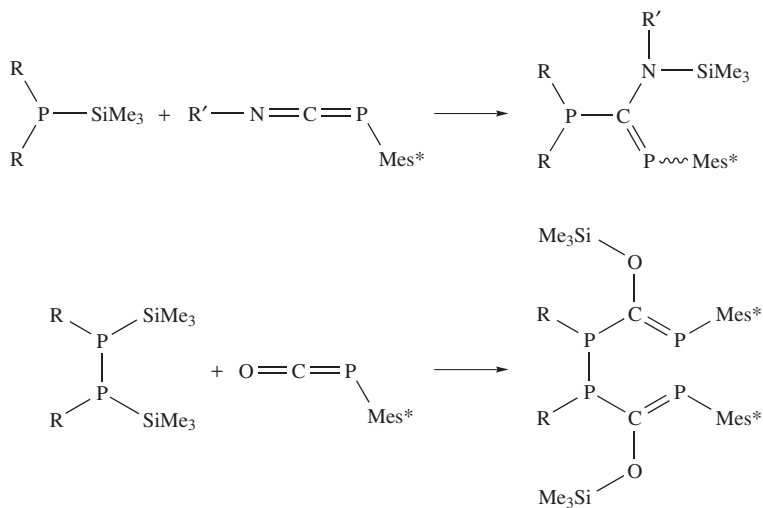
$\text{R}_3\text{Si} = \text{Me}_3\text{Si}, i\text{-Pr}_3\text{Si}, \text{Ph}_3\text{Si}, t\text{-BuMe}_2\text{Si}, \text{etc.}, \text{R}^1 = \text{Tip}, t\text{-Bu}$
 $\text{Tip} = 2,4,6\text{-}(i\text{-Pr})_3\text{C}_6\text{H}_2$



C. Monosilylphosphines and Alkali Metal Monosilylphosphides

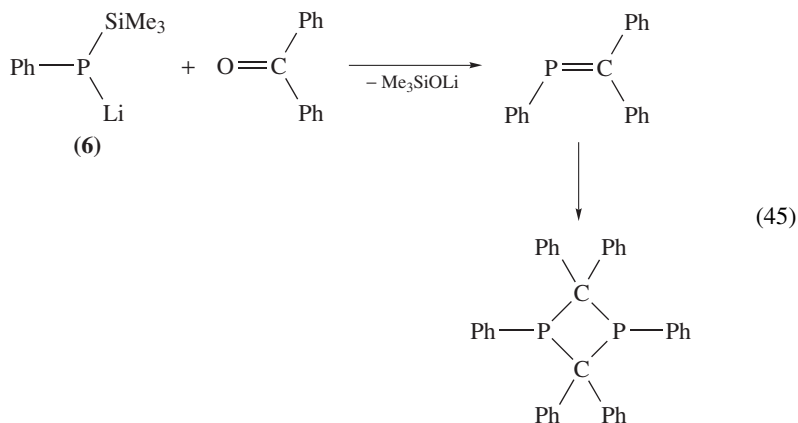
1. Mono(trialkylsilyl)phosphine

Preparations and reactions of some mono(trialkylsilyl)phosphines, which derived from bis(trialkylsilyl)phosphines, were described in Sections II.A and II.B. Other preparative methods of mono(trialkylsilyl)phosphines are described in Reference 10. Reactions of some mono(trialkylsilyl)phosphines with hexachloroethane or phosgene lead to chloro-phosphines (equation 42)⁶⁶. It should be noted that treatment of bis(trialkylsilyl)phosphines

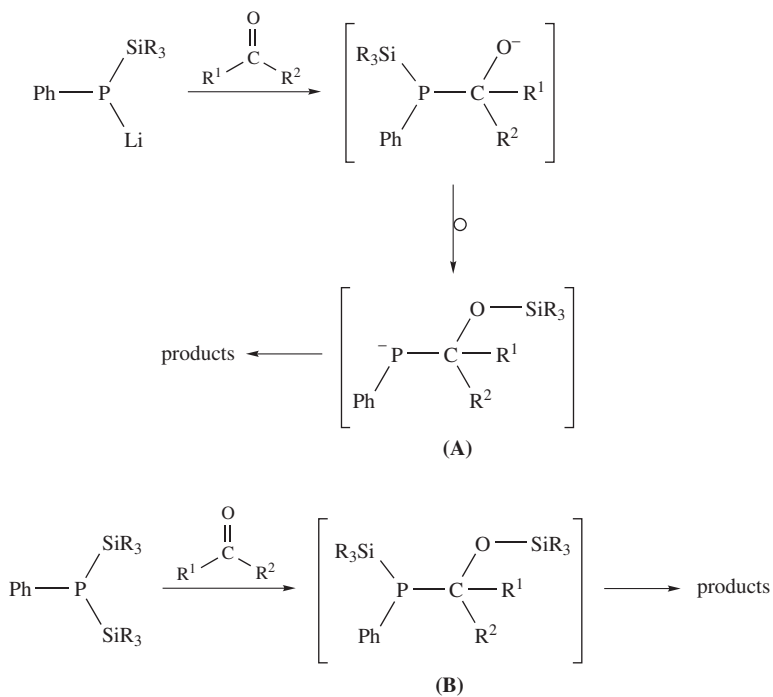


SCHEME 6

Lithium mesityl(trimethylsilyl)phosphide was also used to introduce $\text{MesP}=\text{C}(\text{H})\text{NMe}_2$, by reaction with *N,N*-dimethylformamide³¹. In the present chapter, we call reactions of this type the *phospha*-Peterson reactions.



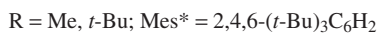
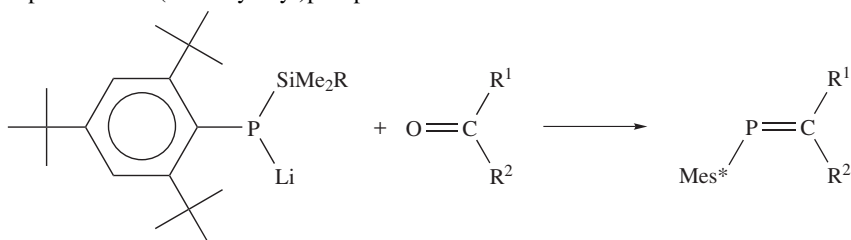
The lithium phosphide $\text{RP}(\text{SiMe}_3)\text{Li}$ has a stronger nucleophilic character than does $\text{RP}(\text{SiMe}_3)_2$. Moreover, in the silatropy reaction, in Scheme 7 the intermediate **A** is rather



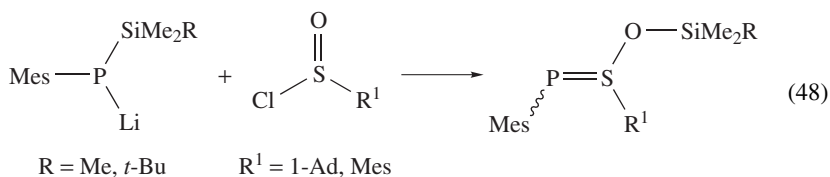
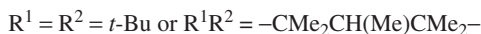
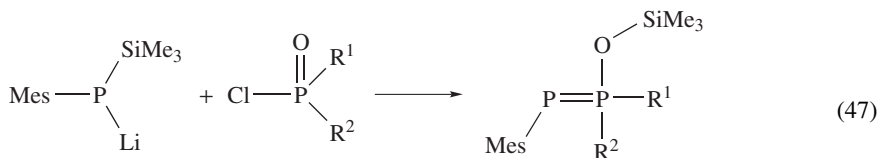
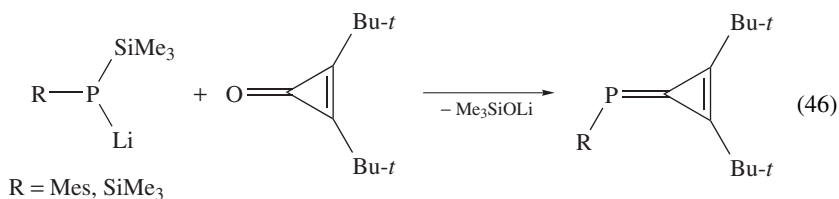
SCHEME 7

unstable, causing facile elimination of silyloxy group, while an intermediate **B** is rather stable and can often be isolated. In fact, it was reported that it took several months for the conversion of **3** to $\text{PhP}=\text{CPh}_2$ (equation 12), to be completed while **6** afforded $\text{PhP}=\text{CPh}_2$ within 10 min³¹.

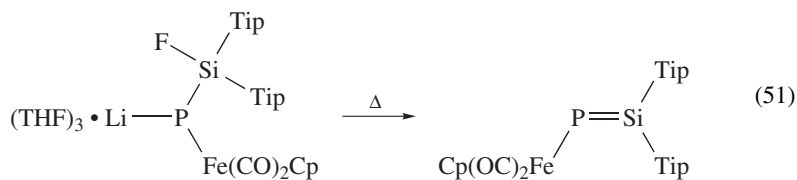
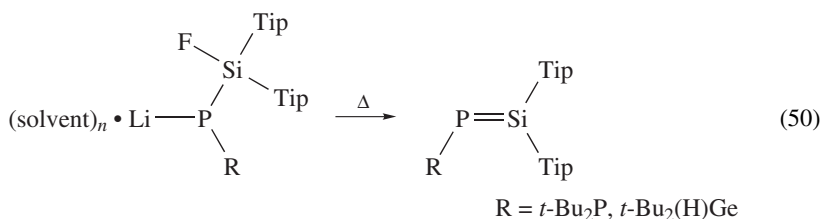
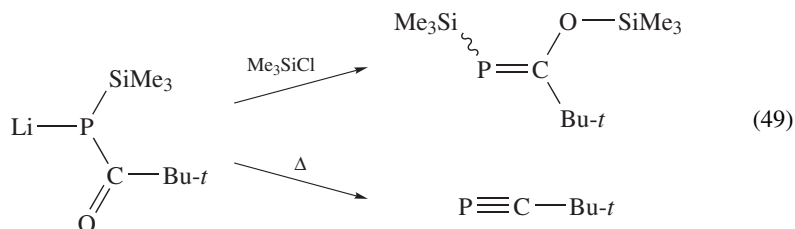
Thus, *phospha*-Peterson reactions with silylphosphides bearing an extremely bulky 2,4,6-tri-*t*-butylphenyl (Mes^*) group seem to be promising from a synthetic point of view, not only because of its efficiency, but also due to a wider range of synthetic applications (Scheme 8). Actually, many successful synthetic applications of $\text{Mes}^*\text{P}(\text{Li})\text{SiR}_3$ have been reported (see Section V), and in some cases it turned out that less bulky silylphosphides are also useful for introducing multiple bonds containing phosphorus atom(s). For example, phosphatriafulvenes were prepared from silylphosphides as shown in equation 46⁶⁹. Similarly, phosphoranylidene phosphines (equation 47) and sulfuranylidene phosphines (equation 48) were prepared from less bulky mesityl(trialkylsilyl) phosphides or bis(trimethylsilyl)phosphide⁷⁰.



SCHEME 8



Acyl(trimethylsilyl)phosphide, another example of mono(trimethylsilyl)phosphide, was converted to phosphoethene or phosphoethyne (equation 49)¹⁹. By a similar method mentioned in Section II.B.2, phosphino- or germyl-substituted phosphasilenes were prepared starting from RP(H)-Si(F)Tip_2 via RP(Li)-Si(F)Tip_2 (equation 50)⁶³. Furthermore, a metallophosphasilene was generated as shown in equation 51⁷¹.

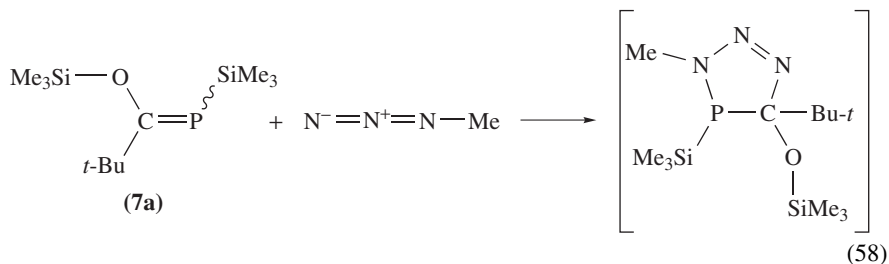
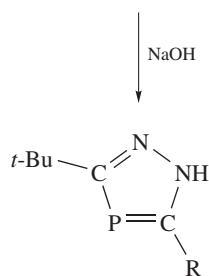
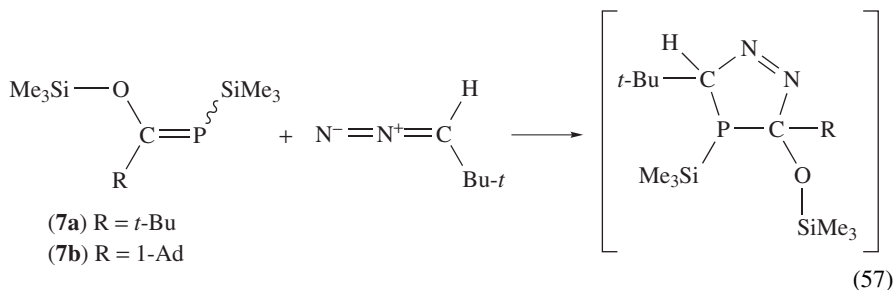


D. Monosilylphosphoethenes

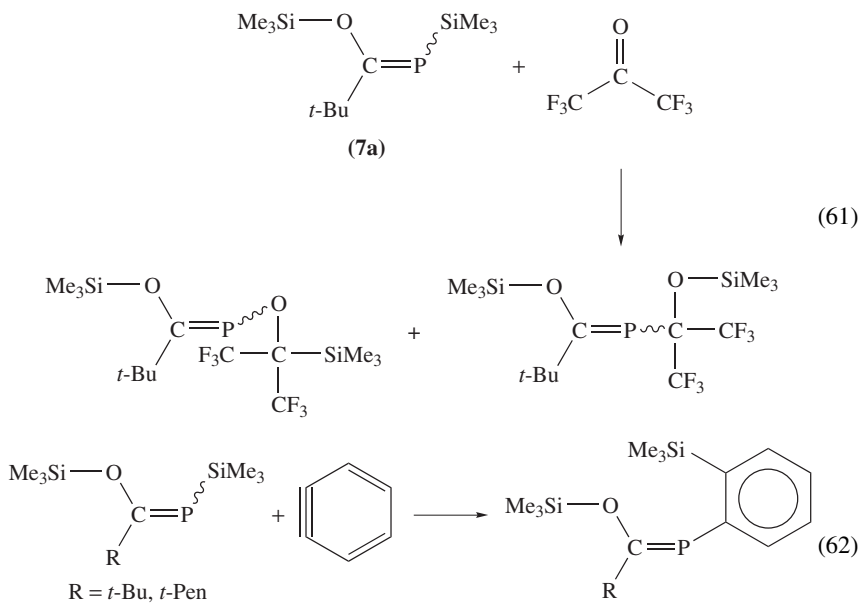
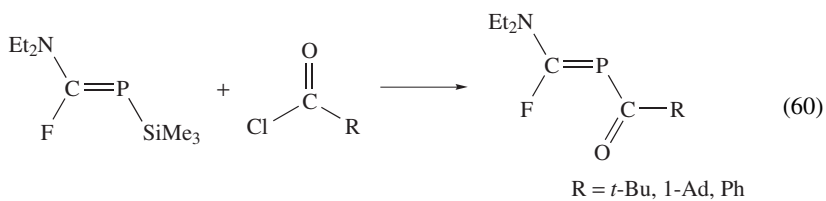
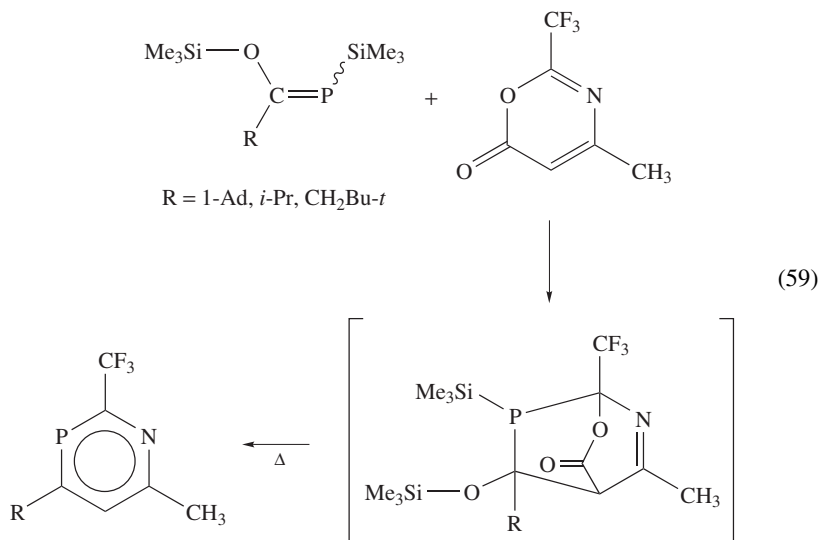
1-Trimethylsilyl-2-trimethylsilyloxy-1-phosphoethenes $\text{Me}_3\text{SiP}=\text{C}(\text{OSiMe}_3)\text{R}$ (**7**) are known to form phosphoethynes by treatment of a base (Scheme 4). In addition, they afford some phosphoethenes in various manners. Some monosilylphosphoethenes were used for preparation of phospho-1,3-butadienes. Reaction of $\text{Me}_3\text{SiP}=\text{C}(\text{OSiMe}_3)\text{-Bu-}t$ (**7a**) with hexachloroethane gave $\text{ClP}=\text{C}(\text{OSiMe}_3)\text{Bu-}t$, which then coupled with the precursor **7a** to give 2,3-diphosphobuta-1,3-diene (equation 52)³⁷. Addition of **7a** to phosphaketene $\text{Mes}^*\text{P}=\text{C}=\text{O}$ gave 1,3-diphosphobuta-1,3-diene (equation 53)²². Addition-silylropy reaction of $\text{Me}_3\text{SiP}=\text{C}(\text{NR}_2)_2$ (**8**) with trimethylsilylketene gave a 2-phosphobuta-1,3-diene (equation 54)⁷². Compound **8** also reacted with $\text{ClP}=\text{C}(\text{SiMe}_3)_2$ to give a 2,3-diphosphobuta-1,3-diene (equation 55)⁷³.

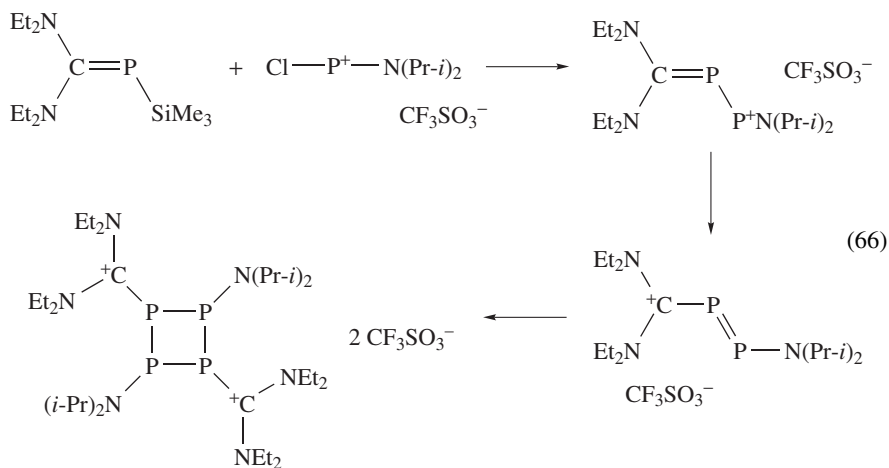
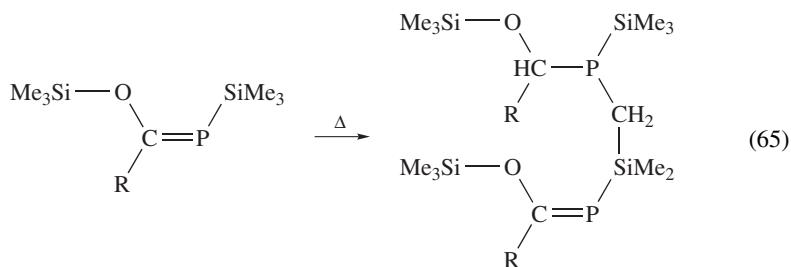
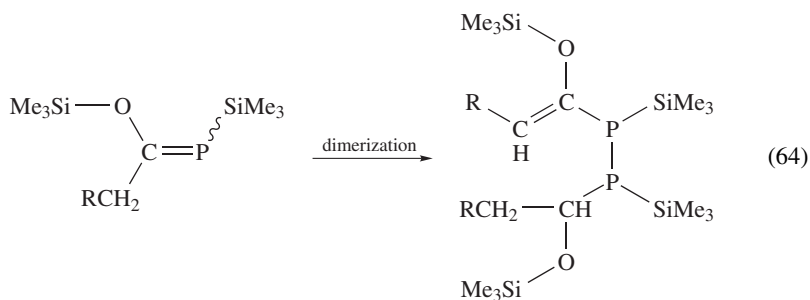
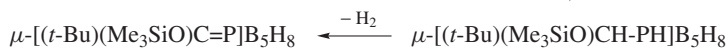
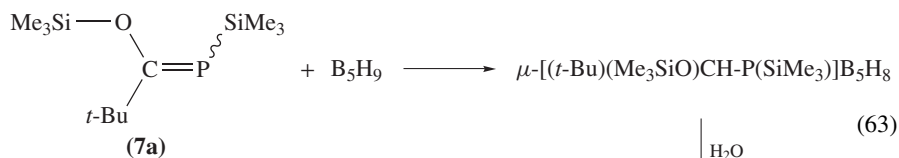
Phosphorus-containing heterocycles were also generated by the use of **7**. Reaction of **7a** or $\text{Me}_3\text{SiP}=\text{C}(\text{OSiMe}_3)\text{Ad}$ (**7b**; Ad = 1-adamantyl) with mesityl nitrile oxide gave the corresponding 1,2,4-oxaazaphosphole via [3 + 2] cycloaddition reaction, followed by elimination reaction (equation 56)^{74,75}.

Similarly, **7a** or **7b** reacted with diazoalkanes to give 1,2,4-diazaphospholes, after base-catalyzed elimination reactions of hexamethyldisiloxane (equation 57)^{74,75}. A triazaphosphole was not obtained in the reaction of **7a** with methyl azide (equation 58)⁷⁵. Diels–Alder reactions of **7** with 1,3-oxazin-6-one, followed by elimination reactions of hexamethyldisiloxane and carbon dioxide, afforded 1-aza-3-phosphabenzene (equation 59)⁷⁶. Other reactions of silylphosphaethenes are shown in equations 60–66^{77–83}.

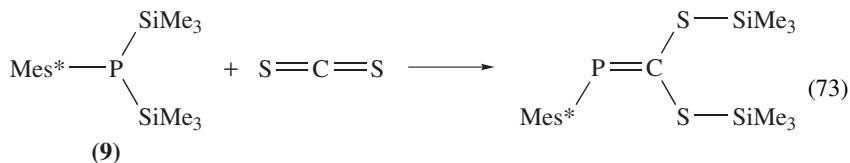
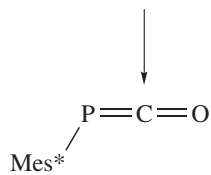
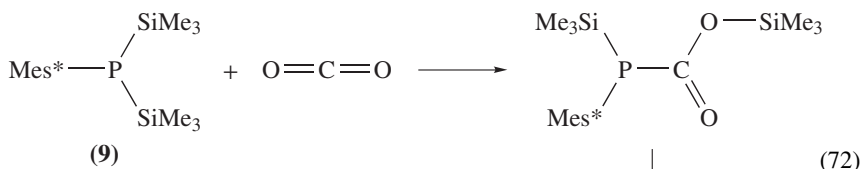
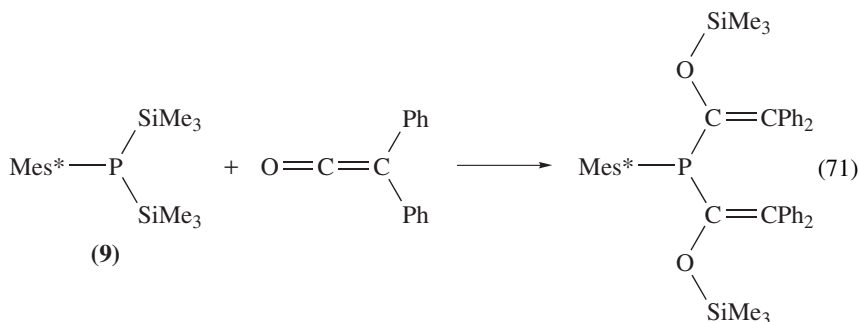


fragmentation



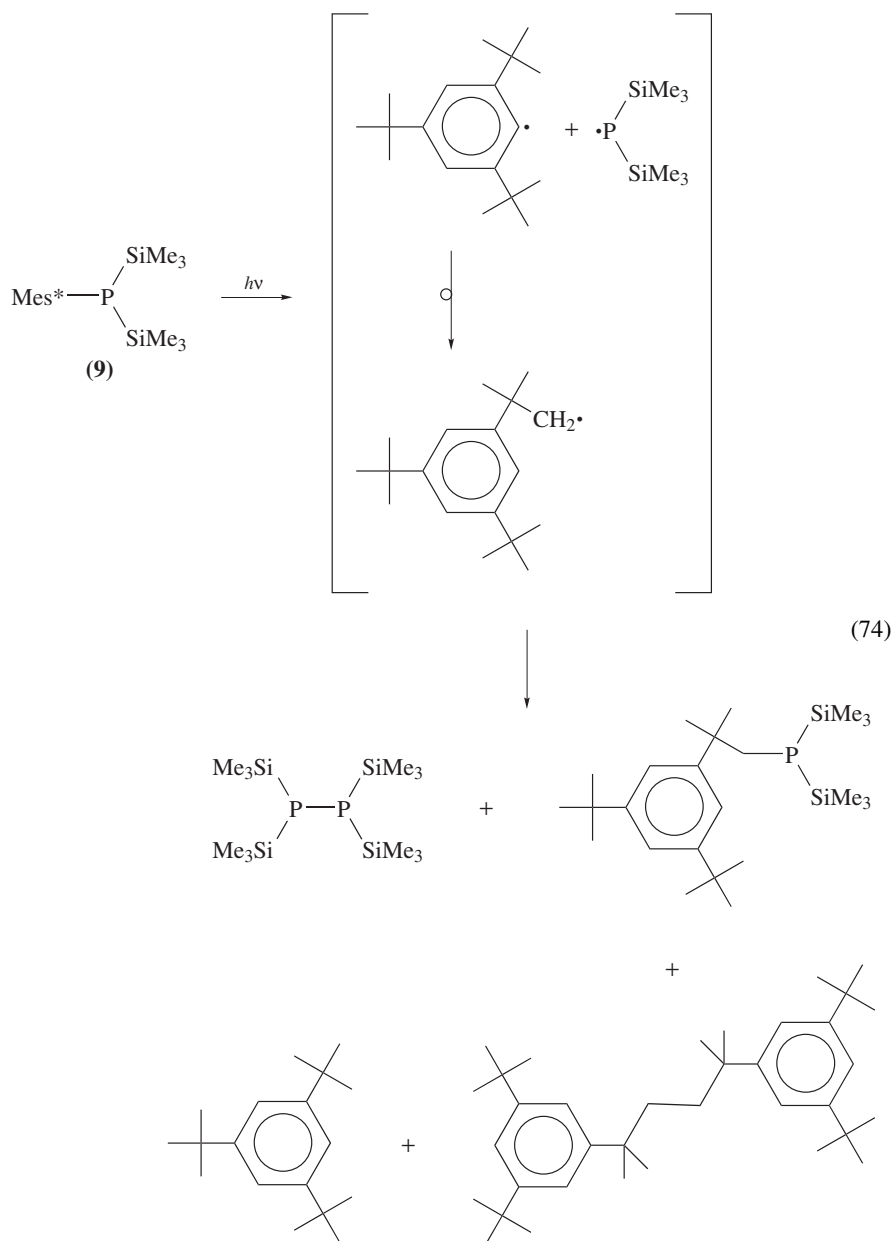


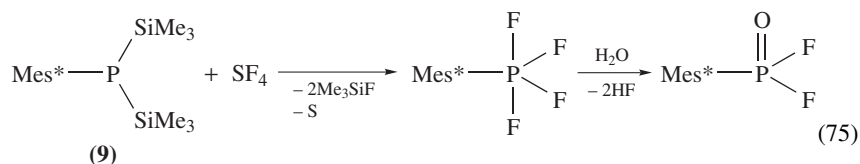
In the reaction of **9** with diphenylketene, the major product was a 1 : 2 adduct (equation 71, cf. equation 88)⁴⁹. Phosphaketene was formed in the reaction of **9** with carbon dioxide (equation 72); however, 1,3-diphosphaallene was not obtained under these conditions⁵². Reaction of **9** with carbon disulfide gave the addition–silatropy product $\text{Mes}^*\text{P}=\text{C}(\text{SSiMe}_3)_2$ (equation 73)⁸⁵ but neither $\text{Mes}^*\text{P}=\text{C}=\text{S}$ nor $\text{Mes}^*\text{P}=\text{C}=\text{PMes}^*$ was obtained.



Therefore, the addition–silatropy–elimination reaction of $\text{RP}(\text{SiR}'_3)_2$ (elimination of hexaalkyldisiloxane) is not a suitable method for the preparation of 1-phosphaallenes and 1,3-diphosphaallenes, probably because spontaneous elimination of hexamethyldisiloxane from an intermediate $\text{R}(\text{Me}_3\text{Si})\text{P}-\text{C}(\text{OSiMe}_3)=\text{X}$ is slower than the second addition reaction or the silatropy reaction. On the other hand, the reaction of alkali metal silylphosphides seems to be promising for the introduction of phosphorus–carbon double bonds and is exemplified in Section V.

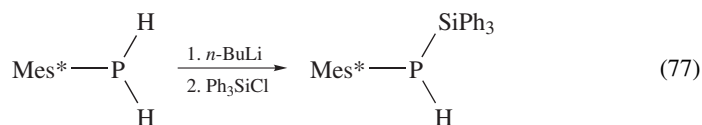
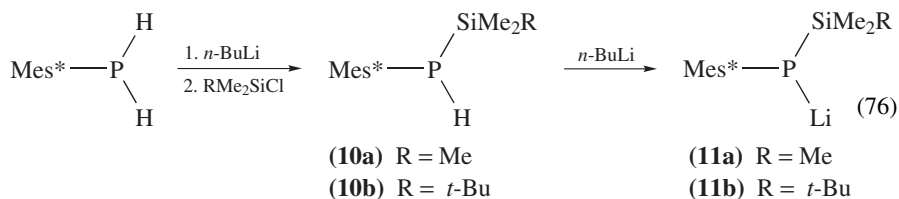
Irradiation of **9** led to homolytic cleavage of the $\text{P}-\text{Mes}^*$ bond (equation 74)⁸⁷. When **9** was treated with SF_4 , Mes^*-PF_4 was formed (equation 75)⁸⁸.



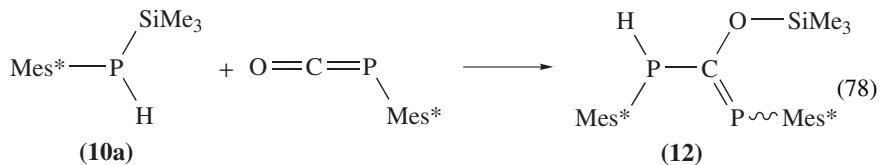


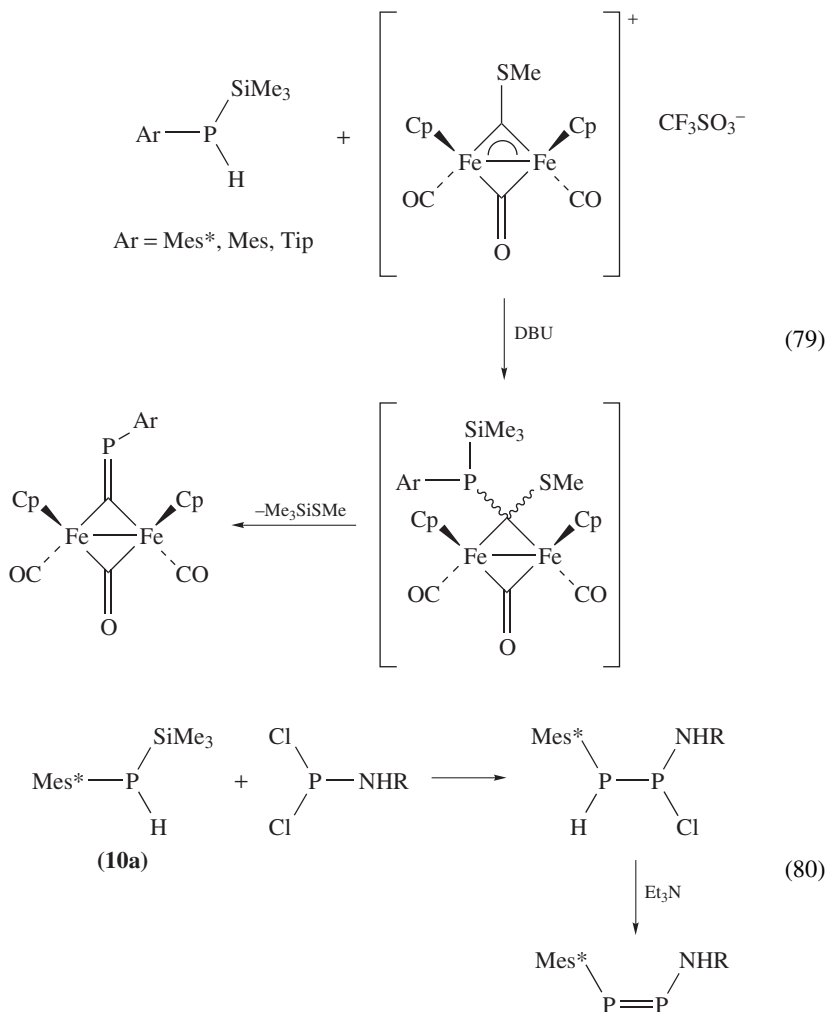
IV. MONOSILYL(2,4,6-TRI-*t*-BUTYLPHENYL)PHOSPHINES

(2,4,6-Tri-*t*-butylphenyl)(trimethylsilyl)phosphine (**10a**) and its *t*-butyldimethylsilyl analog (**10b**) were prepared from (2,4,6-tri-*t*-butylphenyl)phosphine³³ (equation 76)³. Treatment of the silylphosphines **10a** or **10b** with *n*-butyllithium led to the formation of silylphosphides **11a** and **11b**³, which were utilized for the reactions shown in Section V. (2,4,6-Tri-*t*-butylphenyl)(triphenylsilyl)phosphine and related compounds were also prepared starting from Mes*PH₂ (equation 77) and their structures were analyzed^{27,89}.



Reaction of **10a** with Mes*P=C=O afforded the adduct **12** (equation 78)⁹⁰. It should be noted that compounds of the Mes*P=C(OSiR₃)PHMes* type were converted to Mes*P=C=PMes* by addition of alkylolithiums^{90,91}. Isophosphaethyne complexes were prepared using **10a** as well as the related silylphosphines (equation 79)⁹². Stable *cis*-diphosphene was prepared from **10a** and a dichloroaminophosphine, and its structure was analyzed by X-ray crystallography (equation 80)⁹³.





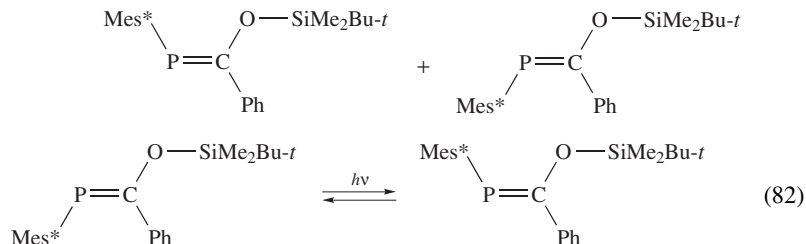
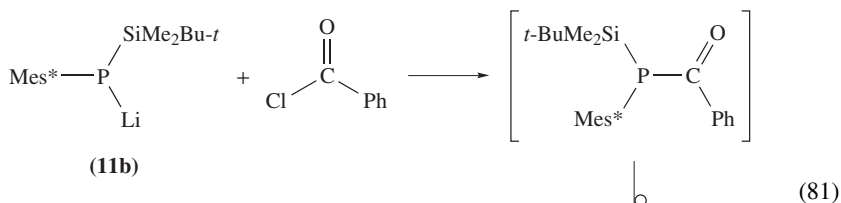
V. ALKALI METAL MONOSILYL(2,4,6-TRI-*t*-BUTYLPHENYL) PHOSPHIDES

A. Preparation of Phosphaethenes

1. Reaction with acyl chlorides

Lithium *t*-butyldimethylsilyl(2,4,6-tri-*t*-butylphenyl)phosphide (**11b**) was allowed to react with benzoyl chloride to give (*E*)- and (*Z*)-Mes*P=C(OSiMe₂Bu-*t*)Ph (equation 81)³. The *E*- and *Z* derivatives were separated and the configuration of (*Z*)-Mes*P=C(OSiMe₂Bu-*t*)Ph was unambiguously determined by the X-ray crystal structure analysis⁹⁴. Irradiation of (*E*)-Mes*P=C(OSiMe₂Bu-*t*)Ph in benzene resulted in

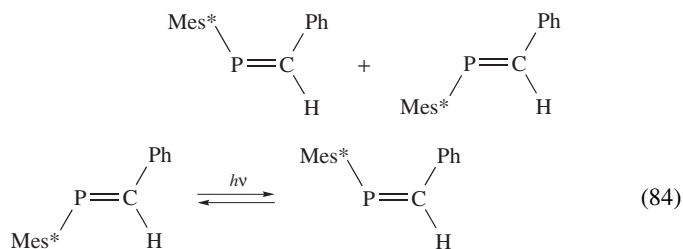
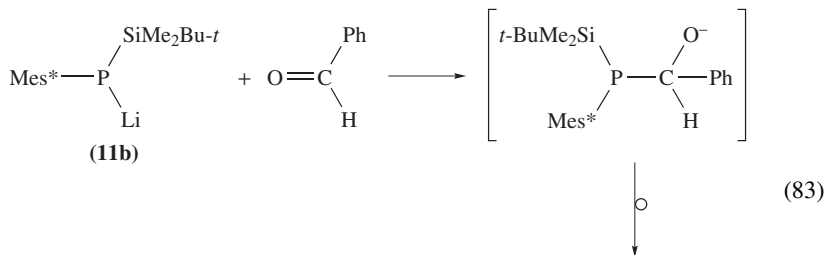
isomerization of the *E* to the *Z* isomer (equation 82)³.



2. Reaction with aldehydes

A similar reaction of silylphosphide **11b** with benzaldehyde followed by chromatographic separation gave (*E*)- and (*Z*)-Mes*P=CHPh (equation 83)⁹⁵. The major product was assigned the *E*-configuration first on the basis of the spectroscopic data⁹⁵ and later by an X-ray crystallographic determination⁹⁶⁻⁹⁸.

It should be noted that (*Z*)-Mes*P=CHPh was not obtained when the reaction was performed in the dark. Thus, (*Z*)-Mes*P=CHPh seems to have been formed from (*E*)-Mes*P=CHPh via photoisomerization. In fact, irradiation of pure (*E*)- or (*Z*)-Mes*P=CHPh led to an equilibrium mixture of the (*E*)- and (*Z*)-isomers (equation 84)⁹⁵.



Various phosphoethenes prepared by the reactions of **11a** and **11b** with aldehydes are shown in Chart 1: *m*-Bromophenyl-substituted phosphoethene was prepared by the *phospha-Peterson* reaction⁹⁹. 2-Pyridyl- or 2-furyl-substituted (*E*)- and (*Z*)-phosphoethenes were prepared by the use of **11b**¹⁰⁰. Compounds bearing several phosphorus–carbon double bonds have been prepared and their transition metal complexes were studied^{101–106}. Azulenyphosphoethenes were also prepared^{107,108}.

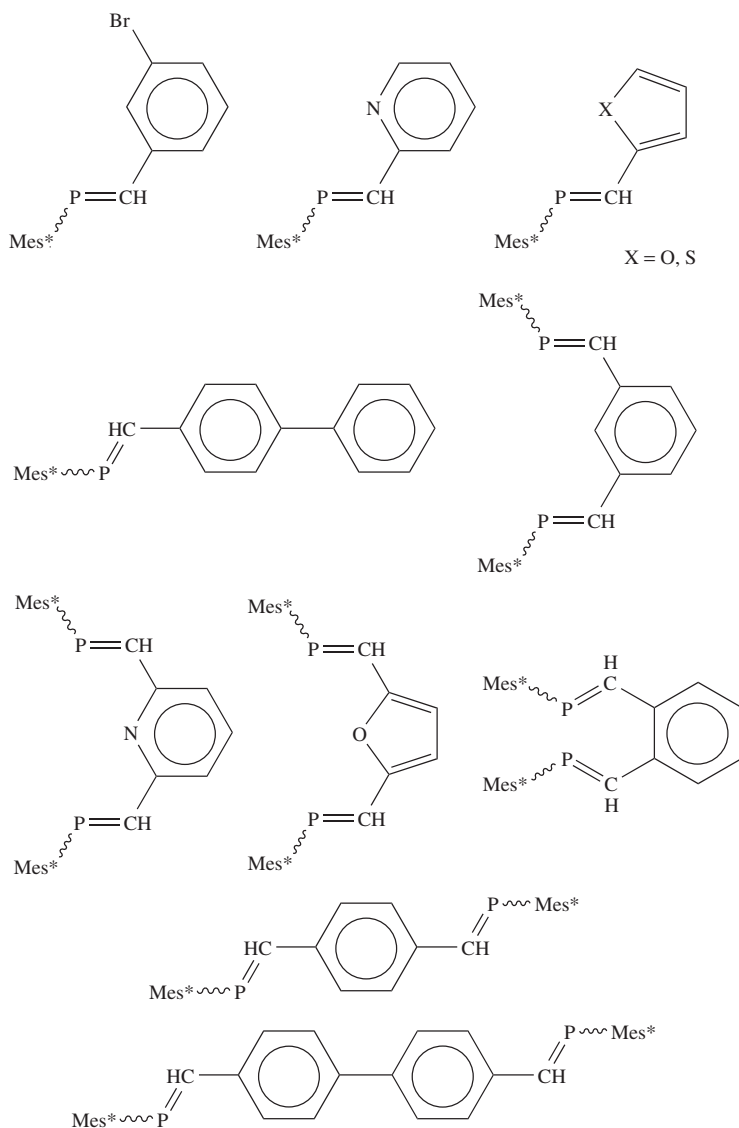


CHART 1

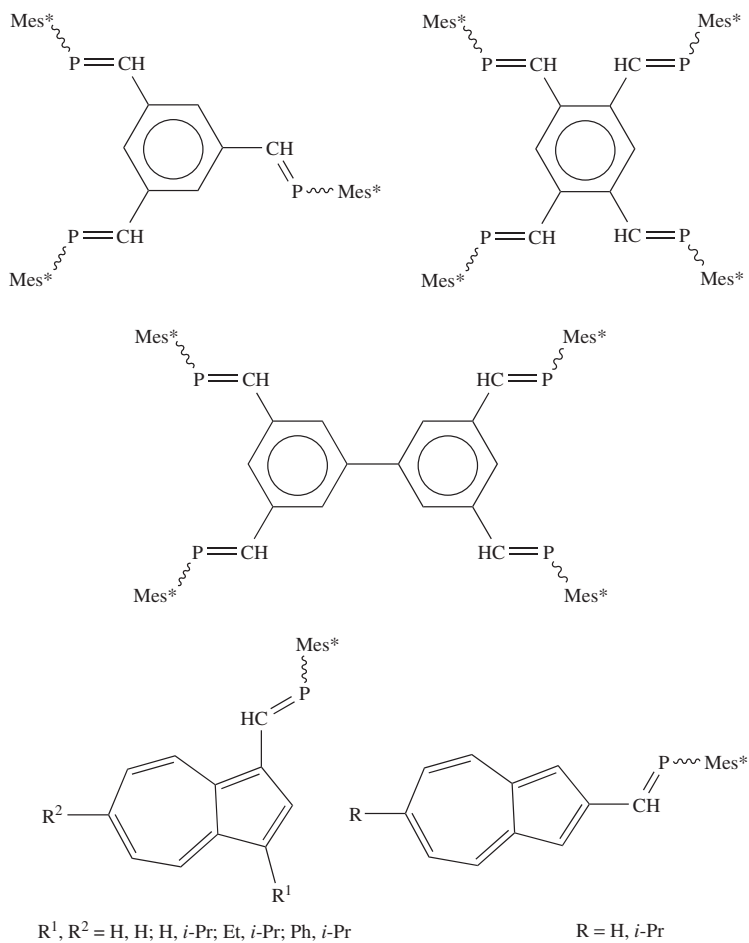
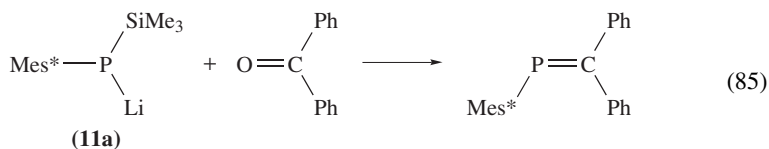


CHART 1. (continued)

3. Reaction with ketones and metal carbonyls

Diphenylphosphaethene $\text{Mes}^*\text{P}=\text{CPh}_2$ was obtained by the use of the sterically less bulky trimethylsilylphosphide **11a** rather than **11b** (equation 85)⁹⁷. Phosphaethenes, shown in Chart 2, which were also prepared by the use of **11a** utilizing the *phospha*-Peterson reaction, are $\text{Mes}^*\text{P}=\text{C}(\text{C}_6\text{H}_4\text{Bu-}i\text{)Ph}$ ¹⁰², fluorenylidene phosphine¹⁰⁹, dibenzocycloheptynylidene phosphine¹¹⁰ and phosphinidenequadricyclane^{111,112}.



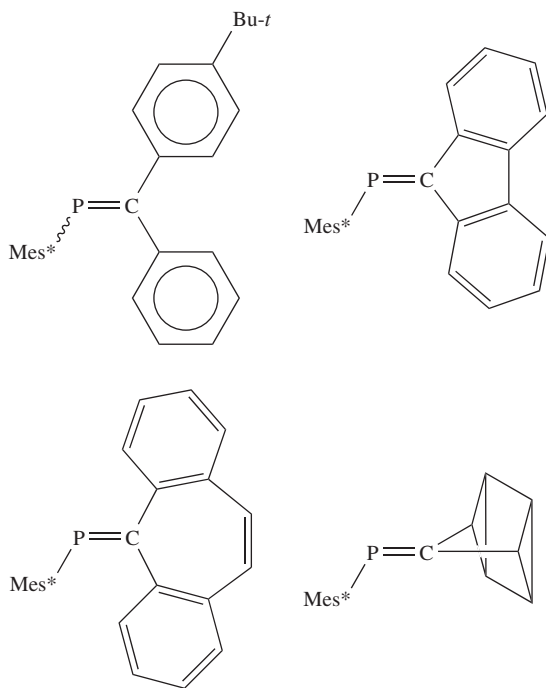
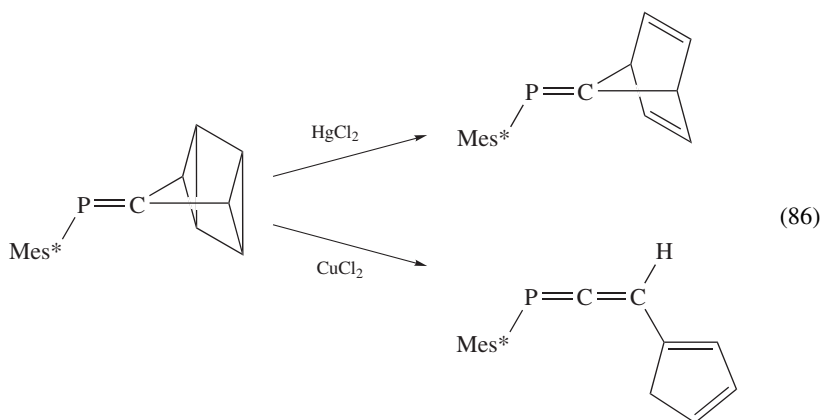
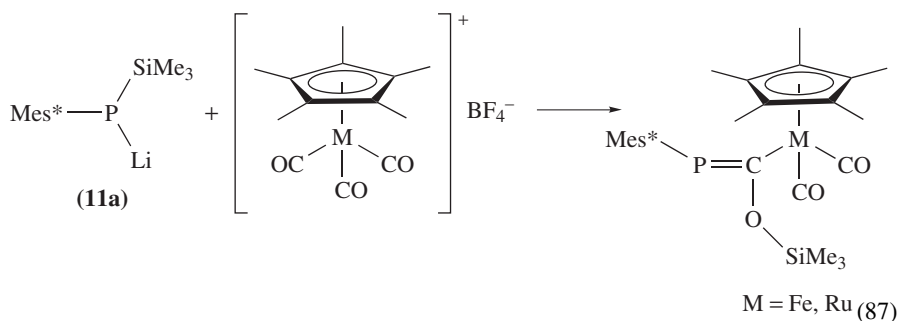


CHART 2

The phosphinidenequadracyclane was converted to phosphinidenenorbornadiene by treatment with HgCl_2 , while its treatment with CuCl_2 led to a phosphallene derivative (equation 86)^{111,112}. Weber and coworkers have prepared phosphalkenyl metal complexes by reaction of the metal carbonyl complexes with the silyl phosphide **11a** (equation 87)¹¹³.

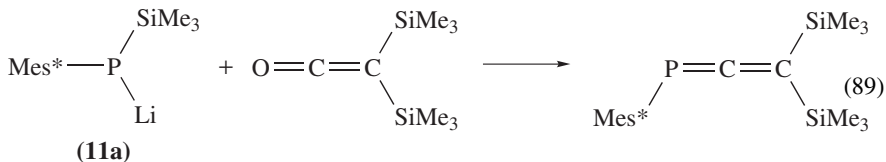
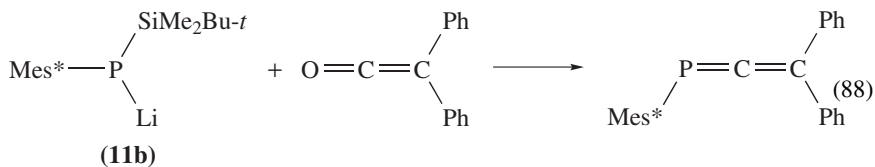


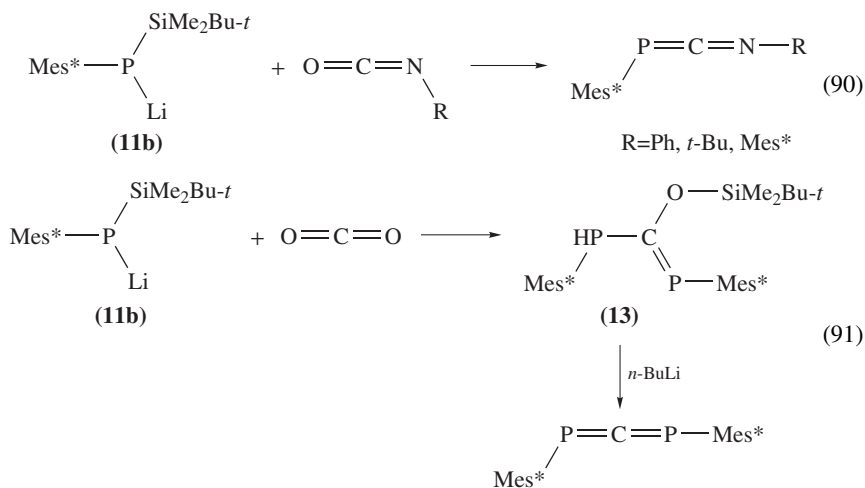


B. Preparation of Phosphaallenes

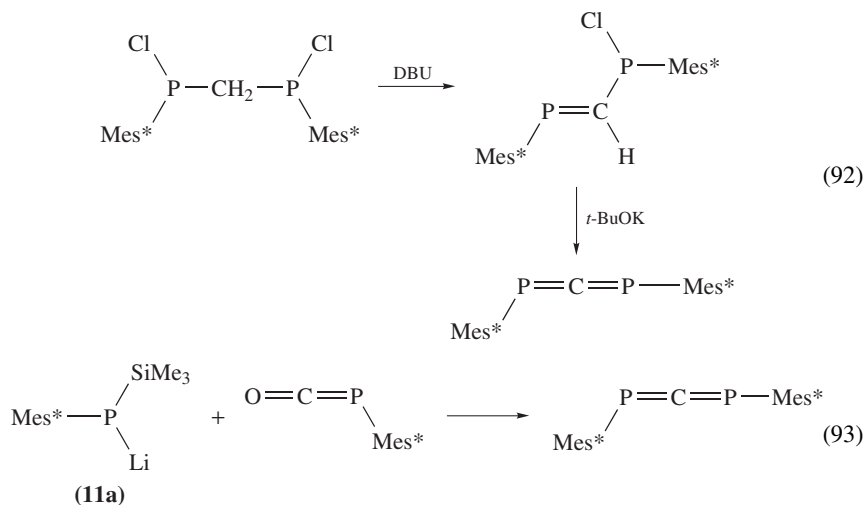
Lithium silylphosphide **11b** was allowed to react with diphenylketene to give the phosphaallene $\text{Mes}^*\text{P}=\text{C}=\text{CPh}_2$ for the first time (equation 88)¹¹⁴ and its crystal structure was analyzed. A bis(trimethylsilyl) derivative was also prepared in a similar way from **11a** by Märkl and Kreitmeier (equation 89)¹¹⁵. Similarly, the reaction of the silylphosphide **11b** with phenyl isocyanate afforded $\text{Mes}^*\text{P}=\text{C}=\text{NPh}$ (equation 90)¹¹⁴ whose crystal structure was reported¹¹⁶. Aza-phosphaallenes $\text{Mes}^*\text{P}=\text{C}=\text{NR}$ (R = *t*-Bu, Mes*) were also prepared in a similar way¹¹⁷.

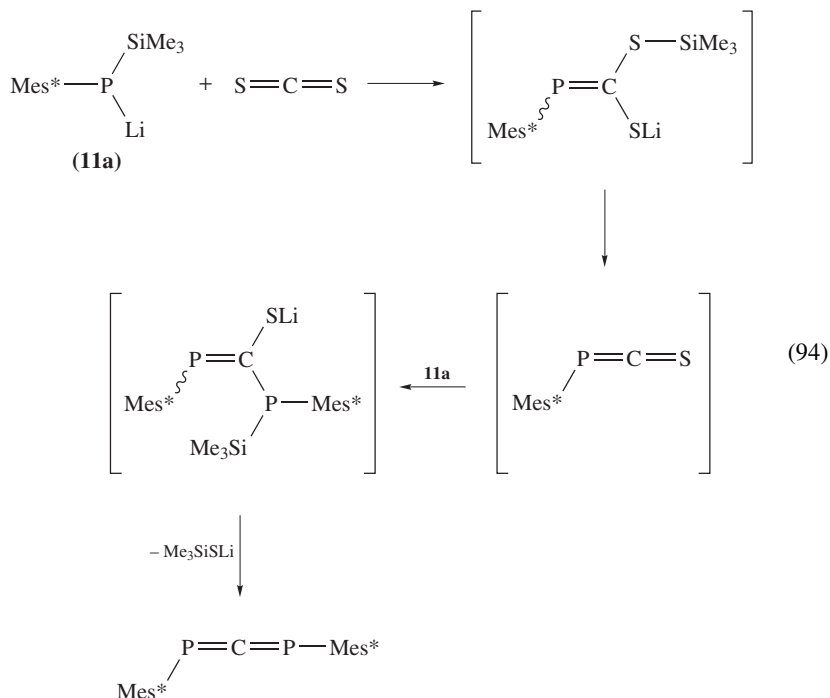
The expected preparation of $\text{Mes}^*\text{P}=\text{C}=\text{O}$ or $\text{Mes}^*\text{P}=\text{C}=\text{PMes}^*$ in a single step from the reaction of silylphosphide **11b** with carbon dioxide resulted in the isolation of phosphino(silyloxy)phosphaethene **13** (equation 91)⁹¹. Proton abstraction from **13** with one equivalent of *n*-butyllithium in ether at room temperature caused elimination of silyl oxide and resulted in the formation of the first stable diphosphaallene $\text{Mes}^*\text{P}=\text{C}=\text{PMes}^*$ ⁹¹.





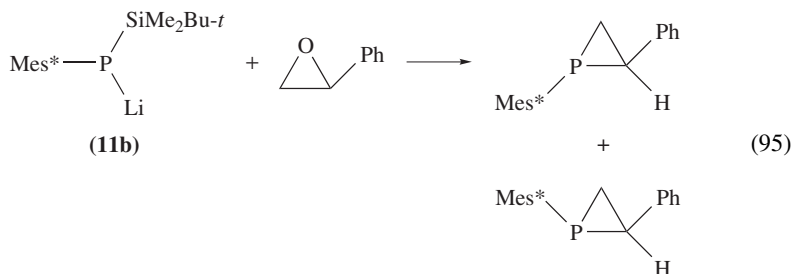
X-ray structure analysis of the 1,3-diphosphaallene was carried out by Karsch and coworkers¹¹⁸, who prepared the diphosphaallene according to equation 92¹¹⁹. The diphosphaallene was also prepared independently by Appel and coworkers by reaction of silylphosphide **11a** and phosphaketene $\text{Mes}^*\text{P}=\text{C}=\text{O}$ (equation 93)⁹⁰. Appel and Knoll mentioned the reaction of the silylphosphide **11a** with carbon disulfide^{8a} and an intermediary formation of phosphathioketene $\text{Mes}^*\text{P}=\text{C}=\text{S}$ was postulated in this reaction (equation 94).



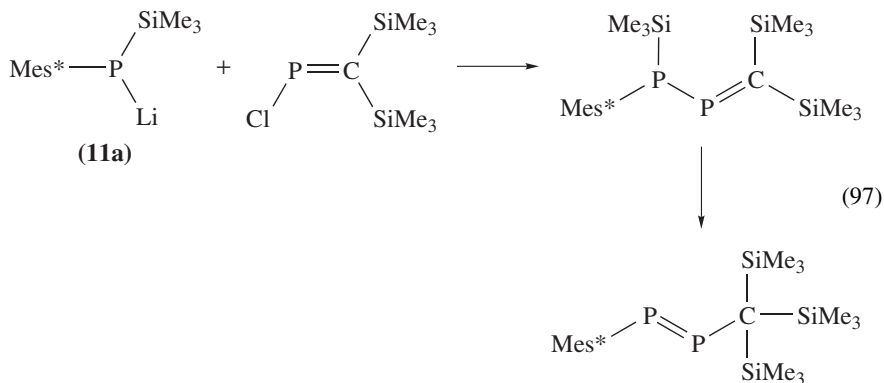
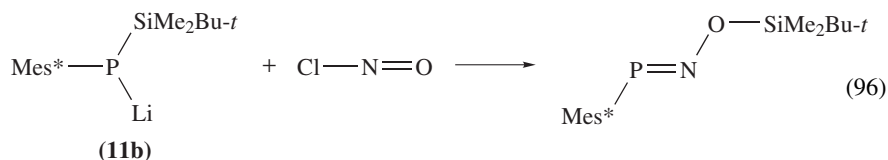


C. Other Synthetic Applications of Silylphosphides

The bulky silylphosphide **11b** was allowed to react with styrene oxide to give the corresponding *trans*- and *cis*-phosphiranes (equation 95)¹²⁰.

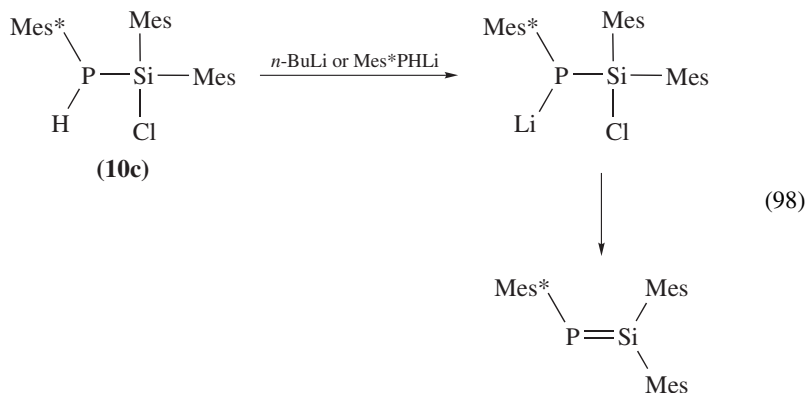


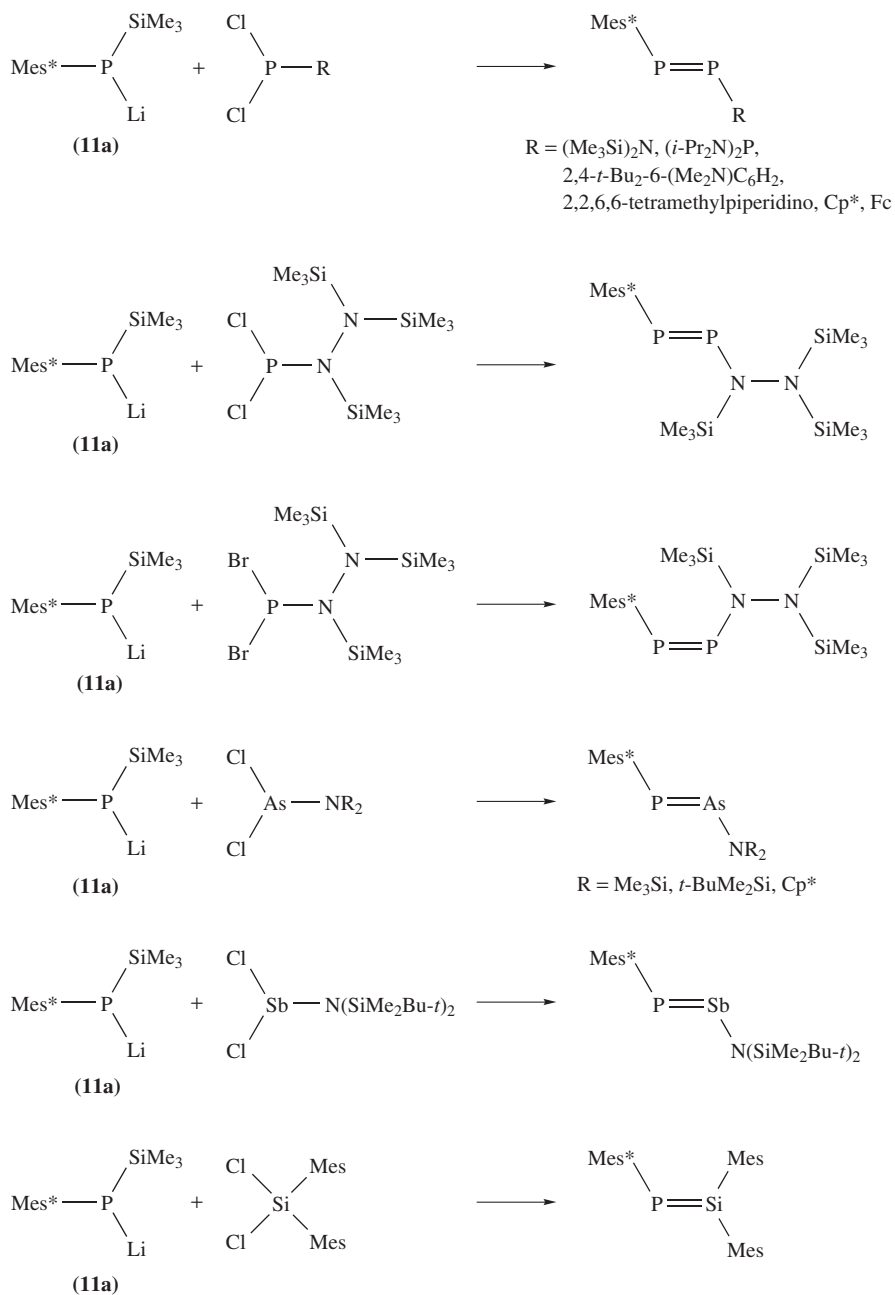
Zurmühlen and Regitz prepared silyloxyiminophosphine by the condensation–silytropy method in the reaction of the silylphosphide **11b** with nitrosyl chloride (equation 96)⁷⁰. The condensation–silytropy method has also been utilized for the introduction of P^{III}=P^{III} bonds. Romanenko and coworkers prepared diphosphene via phosphathene (equation 97), in a reaction where one of the trimethylsilyl groups migrated onto the carbon atom¹²¹.



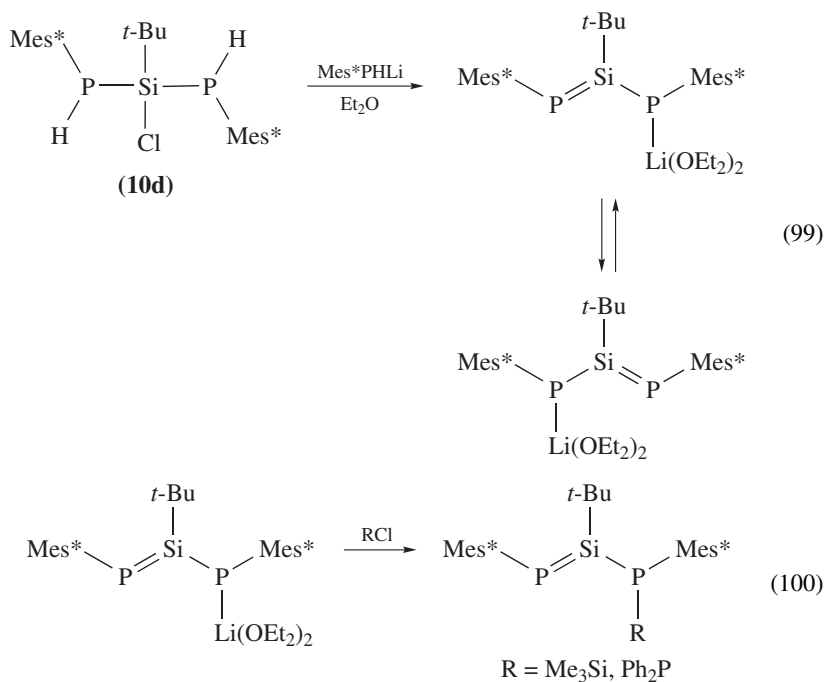
The condensation method has also been applied to the preparation of the 'diphosphene analogs' via the silylphosphides. Diphosphenes¹²²⁻¹²⁷, phospharsenes^{124,128}, phosphasibene¹²⁸ and phosphasilene¹²⁹ were formed in the reaction of the silylphosphide **11a** with the corresponding *gem*-dihalo compounds as shown in Scheme 9.

Reaction of the sterically hindered (chlorodimesitylsilyl)(2,4,6-tri-*t*-butylphenyl) phosphine (**10c**) with butyllithium led to the observation of phosphasilene for the first time via lithium silylphosphide (equation 98)¹³⁰. Some phosphasilenes were formed in analogous methods^{131,132}. A 1,3-diphospha-2-silaallylic lithium was also prepared from (chlorosilyl)phosphine **10d** (equation 99)¹³³. The etherate complex was then converted to phosphasilenes (equation 100) and the structure of $\text{Mes}^*\text{P}=\text{Si}(t\text{-Bu})\text{P}(\text{PPh}_2)\text{Mes}^*$ was analyzed¹³⁴ by Niecke and coworkers.

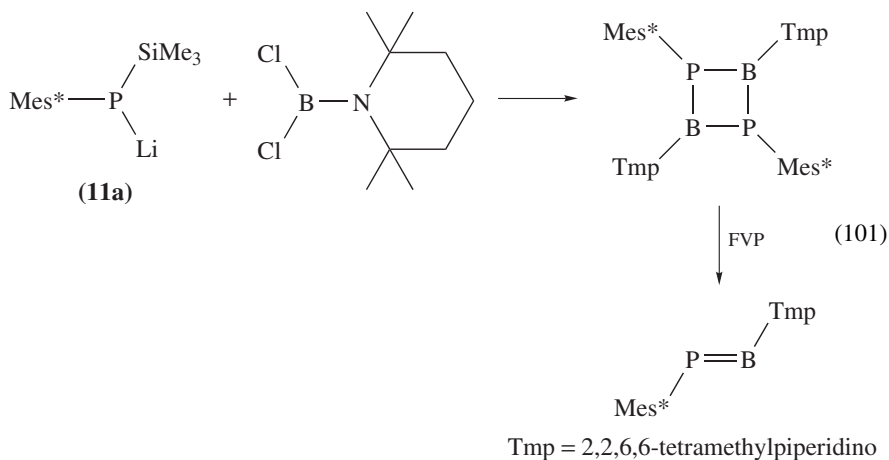


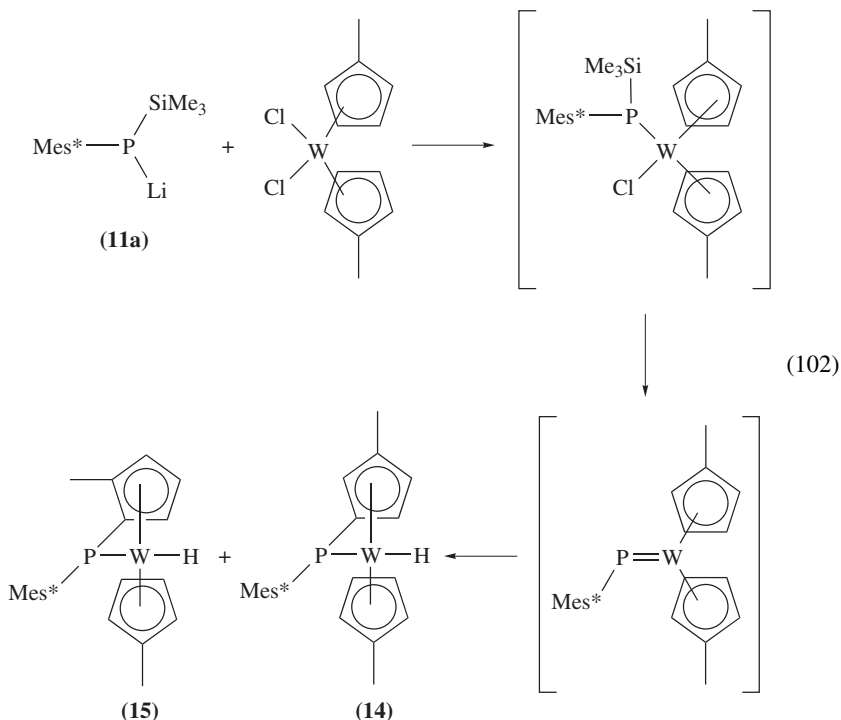


SCHEME 9



Cowley and coworkers have reported two other reactions. One is the reaction of the silylphosphide **11a** with dichloroborane, which afforded the diphosphadiborane, resulting in the formation of the phosphaborene by flash-vacuum pyrolysis (equation 101)¹³⁵. The other is the reaction of the silylphosphide **11a** with $(\eta^5\text{-C}_5\text{H}_4\text{Me})_2\text{WCl}_2$, which gave compounds **14** and **15** (equation 102)¹³⁶. A phosphinidene tungsten complex was assumed to be a reactive intermediate.

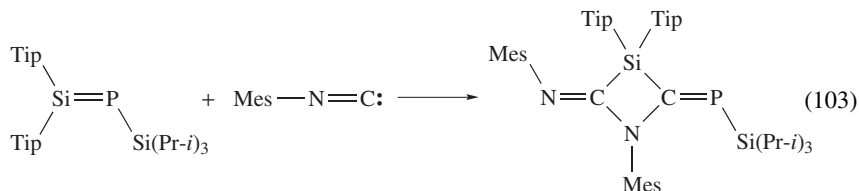


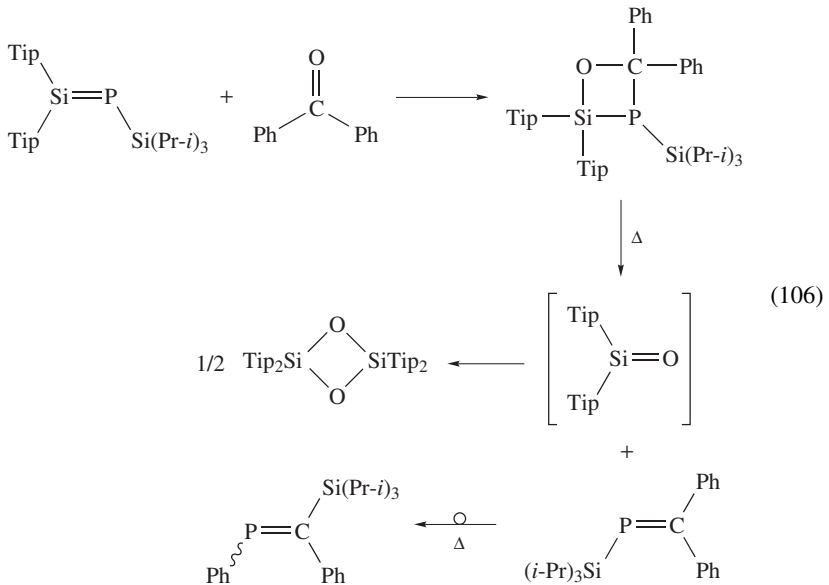
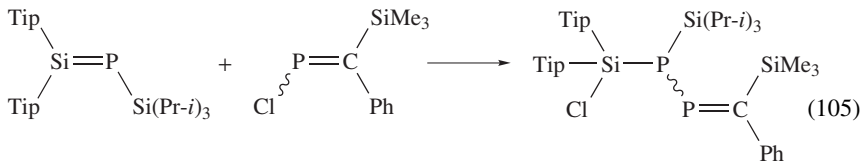
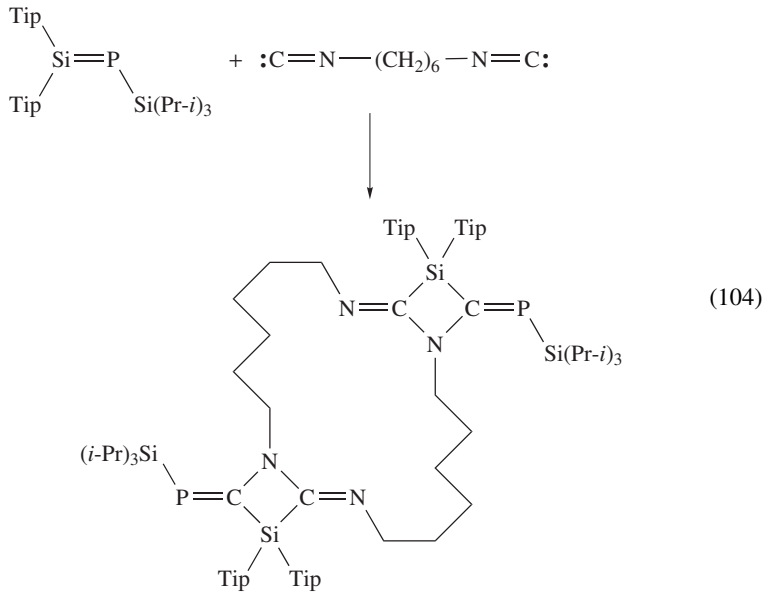


VI. PHOSPHASILENES

Preparations of phosphasilenes have been mentioned in Sections II and V. Driess recently reviewed the synthesis and properties of phosphasilenes¹³⁷. In most of the reported reactions^{63,130,132,137} of phosphasilenes, cleavage of phosphorus–silicon double bonds occur to give compounds with a P–Si single bond, reflecting the high reactivity of the –P=Si< bond; thus they lie beyond the scope of this Chapter.

However, some reactions of phosphasilenes led to another type of double bonded phosphorus compounds. Reaction of *i*-Pr₃SiP=SiTip₂ with mesityl isocyanide gave a 1 : 2 addition-migration product (equation 103)¹³⁸. In a similar manner, reaction with 1,6-diisocyanohexane led to a 2 : 2 addition-migration product (equation 104)¹³⁸. Reaction of the phosphasilene with ClP=C(SiMe₃)Ph resulted in the addition reaction instead of condensation reaction (equation 105)¹³⁷. The phosphasilene reacted with benzophenone to give phosphathene and dioxadisiletane via a [2 + 2] adduct (equation 106)^{63b}.





VII. REFERENCES

1. M. Yoshifuji, I. Shima, N. Inamoto, K. Hirotsu and T. Higuchi, *J. Am. Chem. Soc.*, **103**, 4587 (1981); M. Yoshifuji, I. Shima, N. Inamoto, K. Hirotsu and T. Higuchi, *J. Am. Chem. Soc.*, **104**, 6167 (1982). For reviews see: M. Yoshifuji, in *Multiple Bonds and Low Coordination in Phosphorus Chemistry* (Eds. M. Regitz and O. J. Scherer), Georg Thieme Verlag, Stuttgart, 1990, p. 321; L. Weber, *Chem. Rev.*, **92**, 1839 (1992).
2. R. West, M. J. Fink and J. Michl, *Science*, **214**, 1343 (1981).
3. M. Yoshifuji, K. Toyota, K. Shibayama and N. Inamoto, *Chem. Lett.*, 1653 (1983).
4. R. Appel and W. Paulen, *Angew. Chem., Int. Ed. Engl.*, **22**, 785 (1983).
5. Th. C. Klebach, R. Lourens and F. Bickelhaupt, *J. Am. Chem. Soc.*, **100**, 4886 (1978).
6. D. J. Peterson, *J. Org. Chem.*, **33**, 780 (1968); A. G. Brook, *Acc. Chem. Res.*, **7**, 77 (1974).
7. M. Regitz and O. J. Scherer (Eds.), *Multiple Bonds and Low Coordination in Phosphorus Chemistry*, Georg Thieme Verlag, Stuttgart, 1990.
8. (a) R. Appel and F. Knoll, *Adv. Inorg. Chem.*, **33**, 259 (1989).
(b) L. N. Markovski and V. D. Romanenko, *Tetrahedron*, **45**, 6019 (1989).
(c) R. Appel, F. Knoll and I. Ruppert, *Angew. Chem., Int. Ed. Engl.*, **20**, 731 (1981).
9. G. Becker, *Z. Anorg. Allg. Chem.*, **423**, 242 (1976).
10. D. A. Armitage, in *The chemistry of organic silicon compounds* (Eds. S. Patai and Z. Rappoport), Wiley, Chichester, 1989, p. 1363.
11. G. Fritz and P. Scheer, *Chem. Rev.*, **100**, 3341 (2000).
12. K. B. Dillon, F. Mathey and J. F. Nixon, *Phosphorus: The Carbon Copy*, Wiley, Chichester, 1998.
13. G. W. Parshall and R. V. Lindsey, *J. Am. Chem. Soc.*, **81**, 6273 (1959); A. J. Leffler and E. G. Teach, *J. Am. Chem. Soc.*, **82**, 2710 (1960); G. Becker and W. Hölderich, *Chem. Ber.*, **108**, 2484 (1975); E. Niecke and H. Westermann, *Synthesis*, 330 (1988).
14. G. Märkl, F. Lieb and A. Merz, *Angew. Chem., Int. Ed. Engl.*, **6**, 458 (1967).
15. G. Märkl and G. Dorfmeister, *Tetrahedron Lett.*, **28**, 1093 (1987).
16. G. Märkl and S. Pflaum, *Tetrahedron Lett.*, **27**, 4415 (1986); G. Märkl and G. Dorfmeister, *Tetrahedron Lett.*, **27**, 4419 (1986).
17. For a review see Chapter 8 in Reference 12.
18. G. Becker, *Z. Anorg. Allg. Chem.*, **430**, 66 (1977); R. Appel, C. Casser, F. Knoch and B. Niemann, *Chem. Ber.*, **119**, 2915 (1986).
19. G. Becker, G. Gresser and W. Uhl, *Z. Naturforsch., B*, **36**, 16 (1981). For a review see Chapter 4 in Reference 12.
20. G. Märkl and H. Sejpka, *Tetrahedron Lett.*, **27**, 171 (1986).
21. R. Appel and M. Poppe, *Angew. Chem., Int. Ed. Engl.*, **28**, 53 (1989).
22. R. Appel, P. Fölling, W. Schuhn and F. Knoch, *Tetrahedron Lett.*, **27**, 1661 (1986).
23. R. Appel, P. Fölling, B. Josten, W. Schuhn, H. V. Wenzel and F. Knoch, *Z. Anorg. Allg. Chem.*, **556**, 7 (1988).
24. R. Appel, B. Niemann, W. Schuhn and F. Knoch, *Angew. Chem., Int. Ed. Engl.*, **25**, 932 (1986).
25. A. Schmidpeter, S. Lochschmidt and A. Willhalm, *Angew. Chem., Int. Ed. Engl.*, **22**, 545 (1983).
26. C. N. Smit, Th. A. van der Knaap and F. Bickelhaupt, *Tetrahedron Lett.*, **24**, 2031 (1983).
27. M. A. Petrie and P. P. Power, *J. Chem. Soc., Dalton Trans.*, 1737 (1993).
28. G. Becker, O. Mundt, M. Rössler and E. Schneider, *Z. Anorg. Allg. Chem.*, **443**, 42 (1978).
29. G. Fritz and W. Hölderich, *Z. Anorg. Allg. Chem.*, **422**, 104 (1976).
30. R. Appel, J. Hünerbein and F. Knoch, *Angew. Chem., Int. Ed. Engl.*, **22**, 61 (1983).
31. G. Becker, W. Uhl and H.-J. Wessely, *Z. Anorg. Allg. Chem.*, **479**, 41 (1981).
32. J. Escudié, C. Couret, J. D. Andriamizaka and J. Satgé, *J. Organomet. Chem.*, **228**, C76 (1982).
33. M. Yoshifuji, K. Shibayama, N. Inamoto, T. Matsushita and K. Nishimoto, *J. Am. Chem. Soc.*, **105**, 2495 (1983).
34. C. Couret, J. Satgé, J. D. Andriamizaka and J. Escudié, *J. Organomet. Chem.*, **157**, C35 (1978).
35. C. Couret, J. D. Andriamizaka, J. Escudié and J. Satgé, *J. Organomet. Chem.*, **208**, C3 (1981).
36. R. Appel, F. Knoch and H. Kunze, *Chem. Ber.*, **117**, 3151 (1984).
37. R. Appel, V. Barth and F. Knoch, *Chem. Ber.*, **116**, 938 (1983).
38. R. Appel, U. Kündgen and F. Knoch, *Chem. Ber.*, **118**, 1352 (1985).

39. R. Appel, B. Niemann and M. Nieger, *Angew. Chem., Int. Ed. Engl.*, **27**, 957 (1988).
40. R. Appel and W. Paulen, *Tetrahedron Lett.*, **24**, 2639 (1983).
41. R. Appel and W. Paulen, *Chem. Ber.*, **116**, 109 (1983).
42. R. Appel, V. Barth and M. Halstenberg, *Chem. Ber.*, **115**, 1617 (1982).
43. R. Appel and B. Laubach, *Tetrahedron Lett.*, **21**, 2497 (1980); R. Appel, F. Knoch, B. Laubach and R. Sievers, *Chem. Ber.*, **116**, 1873 (1983).
44. K. Itoh, M. Fukui and Y. Ishii, *J. Chem. Soc., C*, 2002 (1969).
45. G. Becker and O. Mundt, *Z. Anorg. Allg. Chem.*, **459**, 87 (1979).
46. O. I. Kolodiaznyi, *Tetrahedron Lett.*, **23**, 4933 (1982).
47. T. Wegmann, M. Hafner and M. Regitz, *Chem. Ber.*, **126**, 2525 (1993).
48. O. I. Kolodiaznyi and V. P. Kukhar, *Zh. Obshch. Khim.*, **51**, 2189 (1981); *Chem. Abstr.*, **96**, 20167v (1982).
49. R. Appel, V. Winkhaus and F. Knoch, *Chem. Ber.*, **119**, 2466 (1986).
50. M. Hafner, T. Wegmann and M. Regitz, *Synthesis*, 1247 (1993).
51. K. Issleib, H. Schmidt and H. Meyer, *J. Organomet. Chem.*, **192**, 33 (1980).
52. R. Appel, B. Laubach and M. Siray, *Tetrahedron Lett.*, **25**, 4447 (1984).
53. G. Becker, G. Gresser and W. Uhl, *Z. Anorg. Allg. Chem.*, **463**, 144 (1980).
54. R. Appel and C. Behnke, *Z. Anorg. Allg. Chem.*, **555**, 23 (1987).
55. L. Weber, K. Reizig, R. Boese and M. Polk, *Angew. Chem., Int. Ed. Engl.*, **24**, 604 (1985); L. Weber, K. Reizig, M. Frebel, R. Boese and M. Polk, *J. Organomet. Chem.*, **306**, 105 (1986); L. Weber, K. Reizig and M. Frebel, *Chem. Ber.*, **119**, 1857 (1986); L. Weber and D. Bungardt, *J. Organomet. Chem.*, **311**, 269 (1986).
56. L. Weber, K. Reizig, D. Bungardt and R. Boese, *Organometallics*, **6**, 110 (1987); L. Weber, H. Schumann and R. Boese, *Chem. Ber.*, **123**, 1779 (1990).
57. L. Weber, D. Bungardt, U. Sonnenberg and R. Boese, *Angew. Chem., Int. Ed. Engl.*, **27**, 1537 (1988); L. Weber and U. Sonnenberg, *Chem. Ber.*, **122**, 1809 (1989).
58. L. Weber, R. Kirchhoff, H.-G. Stammler and B. Neumann, *J. Chem. Soc., Chem. Commun.*, 819 (1992).
59. G. Becker, H.-M. Hartmann and W. Schwarz, *Z. Anorg. Allg. Chem.*, **577**, 9 (1989); E. Hey, P. B. Hitchcock, M. F. Lappert and A. K. Rai, *J. Organomet. Chem.*, **325**, 1 (1987); E. Hey-Hawkins and E. Sattler, *J. Chem. Soc., Chem. Commun.*, 775 (1992).
60. R. Appel and R. Moors, *Angew. Chem., Int. Ed. Engl.*, **25**, 567 (1986).
61. L. Weber and O. Kaminski, *Synthesis*, 158 (1995).
62. M. Driess, H. Pritzkow and M. Reisgys, *Chem. Ber.*, **124**, 1931 (1991).
63. (a) M. Driess, *Angew. Chem., Int. Ed. Engl.*, **30**, 1022 (1991).
(b) M. Driess, H. Pritzkow, S. Rell and U. Winkler, *Organometallics*, **15**, 1845 (1996).
64. M. Driess, S. Rell and H. Pritzkow, *J. Chem. Soc., Chem. Commun.*, 253 (1995).
65. M. Driess, S. Rell, H. Pritzkow and R. Janoschek, *Angew. Chem., Int. Ed. Engl.*, **36**, 1326 (1997).
66. For example, see References 23 and 24.
67. R. Appel, C. Porz and F. Knoch, *Chem. Ber.*, **119**, 2748 (1986).
68. R. Streubel, E. Niecke and P. Paetzold, *Chem. Ber.*, **124**, 765 (1991).
69. E. P. O. Fuchs, H. Heydt, M. Regitz, W. W. Schoeller and T. Busch, *Tetrahedron Lett.*, **30**, 5111 (1989). See also, T. van der Does and F. Bickelhaupt, *Phosphorus and Sulfur*, **30**, 515 (1987).
70. F. Zurmühlen and M. Regitz, *Angew. Chem., Int. Ed. Engl.*, **26**, 83 (1987); F. Zurmühlen and M. Regitz, *New J. Chem.*, **13**, 335 (1989).
71. M. Driess, H. Pritzkow and U. Winkler, *J. Organomet. Chem.*, **529**, 313 (1997).
72. L. N. Markovski, V. D. Romanenko and T. V. Pidvarko, *Zh. Obshch. Khim.*, **53**, 1672 (1983); *Chem. Abstr.*, **99**, 195100g (1983).
73. V. D. Romanenko, T. V. Sarina, L. S. Kachkovskaya, L. K. Polyachenko and L. N. Markovski, All Union Conference on the Chemistry of Organophosphorus Compounds, Kazan, 1985.
74. T. Allspach, M. Regitz, G. Becker and W. Becker, *Synthesis*, 31 (1986).
75. F. Zurmühlen, W. Rösch and M. Regitz, *Z. Naturforsch., B*, **40**, 1077 (1985).
76. H. Souady, Dissertation, University of Bonn, Germany (1989).
77. J. Grobe, D. Le Van, J. Winnemöller, A. H. Maulitz, B. Krebs and M. Läge, *Z. Anorg. Allg. Chem.*, **626**, 1141 (2000).

78. C. Müller, R. Bartsch, A. Fischer, P. G. Jones and R. Schmutzler, *Chem. Ber.*, **128**, 499 (1995).
79. B. Breit and M. Regitz, *Chem. Ber.*, **126**, 1945 (1993).
80. R. W. Miller, K. J. Donaghy and J. T. Spencer, *Organometallics*, **10**, 1161 (1991).
81. M. Slny and M. Regitz, *Synthesis*, 1262 (1994).
82. B. Breit and M. Regitz, *Synthesis*, 285 (1993).
83. M. Sanchez, V. D. Romanenko, M.-R. Mazières, A. Gudima and L. N. Markovski, *Tetrahedron Lett.*, **32**, 2775 (1991).
84. A. H. Cowley, M. Pakulski and N. C. Norman, *Polyhedron*, **6**, 915 (1987).
85. R. Appel, P. Fölling, L. Krieger, M. Siray and F. Knoch, *Angew. Chem., Int. Ed. Engl.*, **23**, 970 (1984).
86. R. Appel, F. Knoch and H. Kunze, *Angew. Chem., Int. Ed. Engl.*, **22**, 1004 (1983).
87. M. Yoshifuji, K. Shimura and K. Toyota, *Bull. Chem. Soc. Jpn.*, **67**, 1980 (1994).
88. R. Appel and L. Krieger, *J. Fluorine Chem.*, **26**, 445 (1984).
89. M. A. Petrie, K. Ruhlandt-Senge and P. P. Power, *Inorg. Chem.*, **31**, 4038 (1992).
90. R. Appel, P. Fölling, B. Josten, M. Siray, V. Winkhaus and F. Knoch, *Angew. Chem., Int. Ed. Engl.*, **23**, 619 (1984).
91. M. Yoshifuji, K. Toyota and N. Inamoto, *J. Chem. Soc., Chem. Commun.*, 689 (1984).
92. L. Weber, I. Schumann, T. Schmidt, H.-G. Stämmeler and B. Neumann, *Z. Anorg. Allg. Chem.*, **619**, 1759 (1993).
93. E. Niecke, B. Kramer and M. Nieger, *Angew. Chem., Int. Ed. Engl.*, **28**, 215 (1989).
94. M. Yoshifuji, K. Toyota, N. Inamoto, K. Hirotsu, T. Higuchi and S. Nagase, *Phosphorus and Sulfur*, **25**, 237 (1985).
95. M. Yoshifuji, K. Toyota and N. Inamoto, *Tetrahedron Lett.*, **26**, 1727 (1985).
96. M. Yoshifuji, K. Toyota, N. Inamoto, K. Hirotsu and T. Higuchi, *Tetrahedron Lett.*, **26**, 6443 (1985).
97. M. Yoshifuji, K. Toyota, I. Matsuda, T. Niitsu, N. Inamoto, K. Hirotsu and T. Higuchi, *Tetrahedron*, **44**, 1363 (1988).
98. R. Appel, J. Menzel, F. Knoch and P. Volz, *Z. Anorg. Allg. Chem.*, **534**, 100 (1986).
99. M. van der Sluis, V. Beverwijk, A. Termaten, F. Bickelhaupt, H. Kooijman and A. L. Spek, *Organometallics*, **18**, 1402 (1999).
100. A. Jouaiti, M. Geoffroy and G. Bernardinelli, *Tetrahedron Lett.*, **33**, 5071 (1992); M. van der Sluis, V. Beverwijk, A. Termaten, E. Gavrilova, F. Bickelhaupt, H. Kooijman, N. Veldman and A. L. Spek, *Organometallics*, **16**, 1144 (1997); A. Jouaiti, A. Al Badri, M. Geoffroy and G. Bernardinelli, *J. Organomet. Chem.*, **529**, 143 (1997).
101. A. Jouaiti, M. Geoffroy, G. Terron and G. Bernardinelli, *J. Chem. Soc., Chem. Commun.*, 155 (1992).
102. H. Kawanami, K. Toyota and M. Yoshifuji, *Chem. Lett.*, 533 (1996).
103. H. Kawanami, K. Toyota and M. Yoshifuji, *J. Organomet. Chem.*, **535**, 1 (1997).
104. A. Jouaiti, M. Geoffroy and G. Bernardinelli, *Tetrahedron Lett.*, **34**, 3413 (1993).
105. A. Jouaiti, M. Geoffroy and G. Bernardinelli, *J. Chem. Soc., Chem. Commun.*, 437 (1996).
106. A. Al Badri, A. Jouaiti and M. Geoffroy, *Magn. Reson. Chem.*, **37**, 735 (1999).
107. M. Yasunami, T. Ueno, M. Yoshifuji, A. Okamoto and K. Hirotsu, *Chem. Lett.*, 1971 (1992).
108. T. Ueno, M. Yasunami and M. Yoshifuji, *Bull. Chem. Soc. Jpn.*, **67**, 1922 (1994).
109. G. Märkl and K. M. Raab, *Tetrahedron Lett.*, **30**, 1077 (1989).
110. M. Yoshifuji, H. Takahashi, K. Shimura, K. Toyota, K. Hirotsu and K. Okada, *Heteroatom Chem.*, **8**, 375 (1997).
111. T. van der Does and F. Bickelhaupt, *Phosphorus and Sulfur*, **49/50**, 281 (1990).
112. S. J. Goede, L. de Vries and F. Bickelhaupt, *Bull. Soc. Chim. Fr.*, **130**, 185 (1993).
113. L. Weber, K. Reizig and G. Meine, *Z. Naturforsch., B*, **40**, 1698 (1985).
114. M. Yoshifuji, K. Toyota, K. Shibayama and N. Inamoto, *Tetrahedron Lett.*, **25**, 1809 (1984).
115. G. Märkl and P. Kreitmeier, *Angew. Chem., Int. Ed. Engl.*, **27**, 1360 (1988).
116. M. Yoshifuji, T. Niitsu, K. Toyota, N. Inamoto, K. Hirotsu, Y. Odagaki, T. Higuchi and S. Nagase, *Polyhedron*, **7**, 2213 (1988).
117. T. Niitsu, N. Inamoto, K. Toyota and M. Yoshifuji, *Bull. Chem. Soc. Jpn.*, **63**, 2736 (1990).
118. H. H. Karsch, H.-U. Reisacher and G. Müller, *Angew. Chem., Int. Ed. Engl.*, **23**, 618 (1984).
119. H. H. Karsch, F. H. Köhler and H.-U. Reisacher, *Tetrahedron Lett.*, **25**, 3687 (1984).
120. M. Yoshifuji, K. Toyota and N. Inamoto, *Chem. Lett.*, 441 (1985).

121. (a) A. V. Ruban, L. K. Polyachenko, V. D. Romanenko and L. N. Markovski, *Zh. Obshch. Khim.*, **55**, 1190 (1985); *Chem. Abstr.*, **104**, 88677a (1986).
(b) V. D. Romanenko, A. V. Ruban, S. V. Iksanova, L. K. Polyachenko and L. N. Markovski, *Phosphorus and Sulfur*, **22**, 365 (1985).
122. L. N. Markovski, V. D. Romanenko, E. O. Klebanski and S. V. Iksanova, *Zh. Obshch. Khim.*, **55**, 1867 (1985); *Chem. Abstr.*, **105**, 24355g (1986).
123. T. Busch, W. W. Schoeller, E. Niecke, M. Nieger and H. Westermann, *Inorg. Chem.*, **28**, 4334 (1989).
124. P. Jutzi and U. Meyer, *J. Organomet. Chem.*, **326**, C6 (1987).
125. R. Pietschnig and E. Niecke, *Organometallics*, **15**, 891 (1996).
126. E. Niecke, O. Altmeyer and M. Nieger, *Angew. Chem., Int. Ed. Engl.*, **30**, 1136 (1991).
127. M. Yoshifuji, M. Hirano, S. Sangu and K. Toyota, *Science Reports Tohoku Univ., Ser. 1*, **75**, 1 (1992).
128. V. D. Romanenko, E. O. Klebanski and L. N. Markovski, *Zh. Obshch. Khim.*, **55**, 2141 (1985); *Chem. Abstr.*, **105**, 42969q (1986).
129. V. D. Romanenko, A. V. Ruban, A. B. Drapailo and L. N. Markovski, *Zh. Obshch. Khim.*, **55**, 2793 (1985); *Chem. Abstr.*, **105**, 191243a (1986).
130. C. N. Smit, F. M. Lock and F. Bickelhaupt, *Tetrahedron Lett.*, **25**, 3011 (1984).
131. C. N. Smit and F. Bickelhaupt, *Organometallics*, **6**, 1156 (1987); C. N. Smit and F. Bickelhaupt, *Organometallics*, **7**, 246 (1988).
132. Y. van den Winkel, H. M. M. Bastiaans and F. Bickelhaupt, *J. Organomet. Chem.*, **405**, 183 (1991).
133. E. Niecke, E. Klein and M. Nieger, *Angew. Chem., Int. Ed. Engl.*, **28**, 751 (1989); D. Lange, E. Klein, H. Bender, E. Niecke, M. Nieger, R. Pietschnig, W. W. Schoeller and H. Ranaivonjatovo, *Organometallics*, **17**, 2425 (1998).
134. H. R. G. Bender, E. Niecke and M. Nieger, *J. Am. Chem. Soc.*, **115**, 3314 (1993).
135. A. M. Arif, J. E. Boggs, A. H. Cowley, J.-G. Lee, M. Pakulski and J. M. Power, *J. Am. Chem. Soc.*, **108**, 6083 (1986).
136. A. M. Arif, A. H. Cowley, C. M. Nunn and M. Pakulski, *J. Chem. Soc., Chem. Commun.*, 994 (1987).
137. M. Driess, *Adv. Organomet. Chem.*, **39**, 193 (1996).
138. M. Driess and H. Pritzkow, *J. Chem. Soc., Chem. Commun.*, 1585 (1993).

CHAPTER 9

Polysilanes: Conformations, chromotropism and conductivity

ROBERT WEST

*Organosilicon Research Center, Department of Chemistry, University of Wisconsin,
Madison, WI 53706, USA*
Fax: 1-608-262-6143; email: west@chem.wisc.edu

I. INTRODUCTION	541
II. CONFORMATIONS AND ELECTRONIC STRUCTURE	542
III. CHROMOTROPISM	543
A. Thermochromism	543
1. Thermochromism of polysilanes in solution	543
2. Thermochromism of polysilanes as solids	547
B. Solvatochromism	554
C. Ionochromism	556
D. Other Chromotropic Behavior	558
IV. ELECTRICAL CONDUCTIVITY	559
V. ACKNOWLEDGMENTS	561
VI. REFERENCES AND NOTES	561

I. INTRODUCTION

Polysilanes, with their unbroken chains of catenated silicon atoms, are the prototypical σ -conjugated polymers. They can be regarded as one-dimensional analogs to elemental silicon, on which, of course, nearly all of modern electronics is based. Delocalization of the σ electrons in the Si–Si bonds gives the polysilanes unique optoelectronic properties. Indeed, their photophysical behavior is not approached by any other materials, save for the less stable and more costly polygermanes and polystannanes. These remarkable properties of the polysilanes have led to intense interest, and to numerous proposed high-tech applications. But the great promise of polysilanes as materials has yet to be realized. Their only commercial use, at present, is as precursors to silicon carbide ceramics, an application which takes no advantage of their electronic properties.

Polysilanes were comprehensively reviewed in 1986¹, in 1989² and again in 1994³. Detailed information about several aspects of polysilane chemistry has recently appeared

in a book, *Silicon-Based Polymers: The Science and Technology of their Synthesis and Applications*⁴. Pertinent chapters include those on synthesis of polysilanes⁵⁻⁸, polysilane electronic structure and spectroscopy⁹, optoelectronic properties and device applications¹⁰ and thermal and phase behavior of polysilanes¹¹.

It seems unnecessary to cover in detail those aspects of polysilane chemistry which is treated authoritatively in Reference 4. Instead, the coverage here will be selective, concentrating on developments since 1994, especially those which have changed our thinking about the nature of polysilanes, their structures, chemical bonding, molecular conformations and semiconductivity. Recent investigations, both theoretical and experimental, are leading to a much different view of polysilane structures and conformations than was current even five years ago. In solution, and especially as solids, it now appears that conformations of polysilanes are distinctly more complicated than was formerly thought.

In this chapter, the first section will deal with the complex question of conformations of polysilanes. This will be followed by sections on the chromotropism of polysilanes, beginning with their UV thermochromism. Despite intensive study this phenomenon is still not well understood, and is the subject of important recent findings. Solvatochromism, ionochromism and other types of chromotropic behavior of polysilanes will then be considered. A final brief section will deal with the electrical conductivity of polysilanes, a topic which has not previously been reviewed.

II. CONFORMATIONS AND ELECTRONIC STRUCTURE

The delocalized Si-Si σ electrons in polysilanes give rise to σ - σ^* electronic excitations in the near-UV region, with energies depending strongly on the chain conformation. Theoretical calculations¹² as well as experimental observations^{3,9} show that the lowest excitation energy is associated with the fully-extended, all-*anti* conformation ($\omega = 180^\circ$), which produces maximum sigma conjugation. Twisting of the chain away from the 180° dihedral angle leads to successively higher σ - σ^* energies, shifting the absorption to shorter wavelength.

The preferred torsional angles ω for alkane hydrocarbons are 180° (*anti*, A) and $\pm 60^\circ$ (*gauche*, G). These rotational minima, well known from textbooks, are however far from generally valid. When the substituent atoms are somewhat larger, relative to those of the main chain, repulsion interactions between substituents on 1, 3 atoms of the main chain become significant. The result is that the A conformation becomes a transition state between two minima at $\omega = \pm \sim 165^\circ$, now termed *transoid* (T)^{9,13}. Similarly, interaction between substituents on 1,4 atoms causes a splitting of the *gauche* rotations into four minima, with $\omega = \pm \sim 55^\circ$ (G) and $\pm \sim 90^\circ$ (*ortho*, O). This is the situation found by calculations also for the Me(Me₂Si)_nMe oligomers¹⁴. The O conformations were first observed in the cyclic silane, (Me₂Si)₁₆¹⁵, and have recently been observed directly for Si₄Cl₁₀¹⁶.

Calculations on the oligomer Me₃SiSiEt₂SiEt₂SiMe₃ show that for longer-chain substituents, additional interactions may arise, leading to two new minima near $\pm 150^\circ$ (*deviant*, D) and $\pm 40^\circ$ (*cisoid*, C)¹⁷. *Cisoid* rotational minima have not been observed, but several polysilanes are known to adopt *deviant* conformations. Well-known examples are (*n*-pentyl₂Si)_n¹⁸ and (*n*-butyl₂Si)_n¹⁹, both of which exist in a 7/3 helical arrangement in the solid state, with $\omega = \sim 154^\circ$. Figure 1 shows a generalized representation of the potential energy as a function of conformation, for polysilanes and similar polymers.

Until recently, a common tendency has been to account for the behavior of polysilanes in terms of *anti* (often called *trans*) and *gauche* states, following the pattern familiar from hydrocarbons. From the discussion above it follows that the exact A conformation

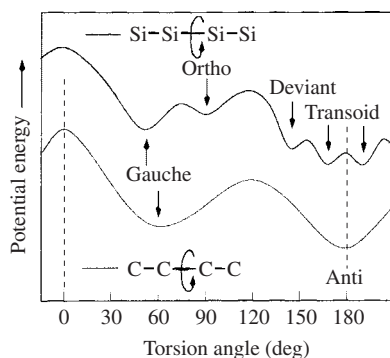


FIGURE 1. Qualitative curves of potential energy vs. torsion angle for hydrocarbons and for polysilanes. (The predicted but as yet unobserved *cisoid* form at $\pm 40^\circ$ is not shown.)

should be disfavored, and indeed this seems now to be true. In the solid state, however, crystal packing forces may favor the A conformation. This may be the case for poly(*n*-hexylsilane)²⁰ and perhaps for other polysilanes with long *n*-alkyl side chains²¹.

III. CHROMOTROPISM

Because the conformation of the polysilane chain may change with environmental factors such as temperature, solvent, pressure etc., many of these polymers are chromotropic⁹. The effects of changes in temperature, leading to thermochromism, have been the most thoroughly investigated.

A. Thermochromism

1. Thermochromism of polysilanes in solution

For many polysilanes in solution, a reversible shift of the $\sigma\text{-}\sigma^*$ absorption band to lower energy is observed when the temperature is decreased. Four types of behavior are known:

1. When the alkyl substituent groups are quite dissimilar, the absorption band shifts gradually to longer wavelength as the temperature is decreased. This is the case for (*n*-HexSiMe)_{*n*}, illustrated in Figure 2a.

2. For alkyl groups which are more nearly similar, the absorption band first shifts gradually, and then narrows and shifts more strongly to lower energy. This intermediate behavior is shown for (*n*-PrSiHex-*n*)_{*n*} in Figure 2b.

3. When the alkyl substituents are identical or nearly so, an abrupt thermochromism is observed. The short-wavelength band, typically near 315 nm, disappears and simultaneously a new, narrow absorption grows in at about 355 nm. This behavior is illustrated in Figure 2c for (*n*-Hex₂Si)_{*n*}. The change may take place over only a small temperature range of a few degrees. Near the transition temperature, two different forms of the polymer must exist in equilibrium.

4. When the substituent groups are large, aryl or branched alkyl, normally no bathochromic shift takes place. This is observed for (*n*-alkylSiPh)_{*n*} polymers, diarylpolysilanes and (*c*-HexSiMe)_{*n*}. In some cases a slight hypsochromic shift is observed as the temperature is decreased, perhaps due to thermal contraction of the polymer molecules.

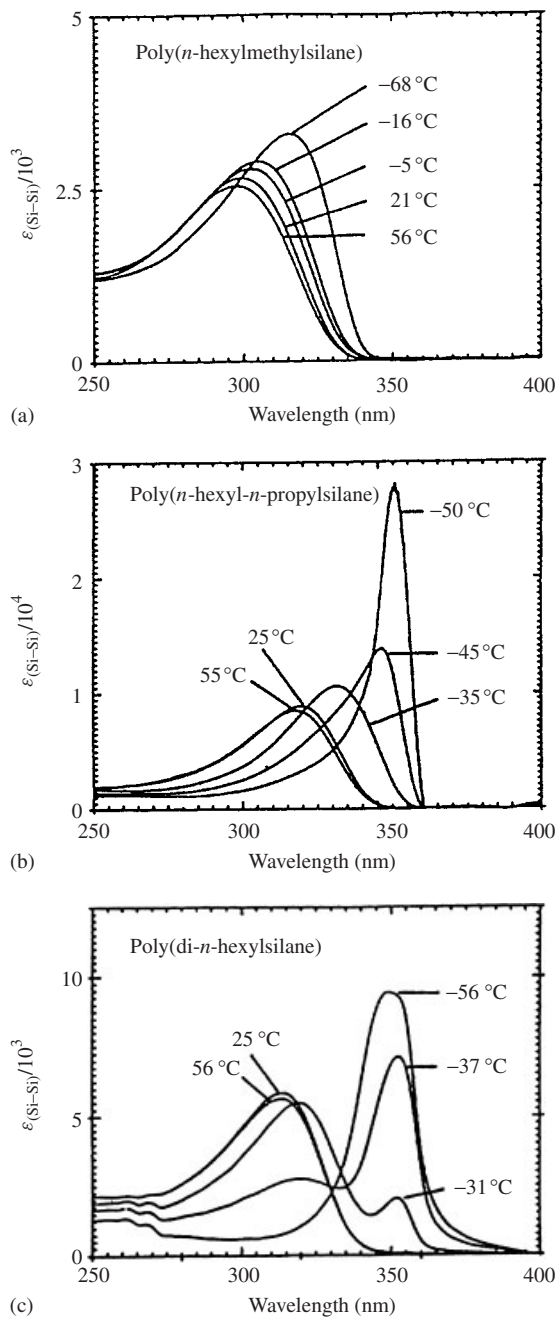
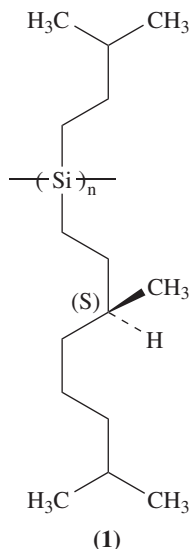


FIGURE 2. Thermochromic behavior of some polysilanes in hexane solution: (a) (*n*-HexSiMe)_{*n*}; (b) (*n*-PrSiHex_{*n*})_{*n*}; (c) [(*n*-Hex)₂Si]_{*n*}. Reprinted with permission from Reference 23. Copyright 1999 American Chemical Society

The thermochromism of polysilanes was described by Schweitzer in terms of a disorder–order transition, driven by polarization interaction between the polymer molecules and the solvent²². According to this model the behavior is determined by a coupling parameter V_D/ϵ , where V_D is the contribution of the polysilane backbone to the polymer–solvent dispersion interaction, per site, when the polymer is in the fully extended *anti* form, and ϵ is the mean free energy of defect formation. The defects are kinks in the chain, which interfere with delocalization. The greater solvation energy of the extended form is the driving force for the thermochromic transition. The model can account for all three types of thermochromic behavior in solution. For smaller values of V_D/ϵ a gradual shift of the transition energy is predicted (Type 1 behavior), but when V_D/ϵ reaches a critical value of 0.37 an abrupt transformation to the *anti* form should take place (Type 3 behavior). Intermediate values lead to the mixed, Type 2 behavior.

Recently, however, Sanji and coworkers have pointed out that the thermochromic change and increase in absorption intensity is too abrupt to be the result of a Boltzmann distribution between *anti* and twisted units along the polymer chain²³. They proposed instead that the transition is an interconversion between two well-ordered states: a tightly-coiled helix, and ‘all-*anti*’.



Important evidence concerning the nature of polysilanes in solution has been published recently by Fujiki and others at NTT laboratories^{24–26}. Studies by these workers have shown that polysilanes containing chiral sidechain substituents exhibit circular dichroism bands corresponding to their UV absorption, and are therefore helical in solution²⁴. Moreover, for both dialkyl and diarylpolysilanes, thermally driven reversal of the helical screw sense has been demonstrated in selected cases. Thus, poly[(*S*)-3,7-dimethyloctyl-3-methylbutylsilane], **1**, undergoes a helical reversal at -20°C in isoctane²⁵. At the transition temperature, the sign of the CD band (Cotton effect) changes from positive to negative (Figure 3). Similarly, the diarylpolysilane copolymer **2** was shown by CD spectroscopy to undergo a thermal inversion of helical screw sense at a transition temperature of -10°C ²⁶. The effect is quite specific; copolymers of the same type with larger fractions

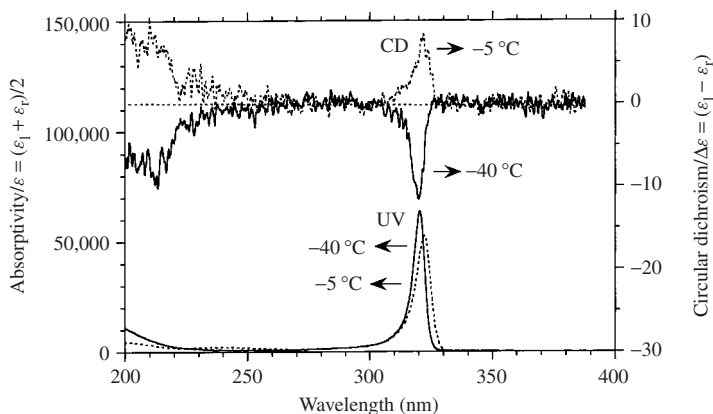
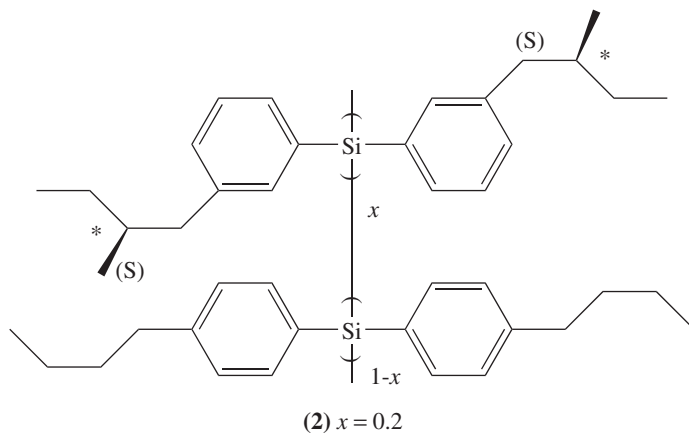


FIGURE 3. CD curve for polymer **1**, showing reversal of the sign of the Cotton effect at -20°C , indicating a reversal of the helical screw sense. Reprinted with permission from Reference 25. Copyright 2000 American Chemical Society



of the chiral substituent groups showed only negative Cotton effects at all temperatures, and so do not reverse their helicity.

In a related study Toyoda and Fujiki showed that the UV absorption and emission spectra of $(\text{PhSiMe})_n$ are essentially identical to those of the copolymer, $(\text{PhSiMe})_{0.95n} [\text{PhSi}-\text{CH}_2\text{C}^*(\text{H})(\text{CH}_3)\text{CH}_2\text{CH}_3]_{0.05n}$. The latter is demonstrably helical in solution, from its CD spectrum. The implication is that $(\text{PhSiMe})_n$, previously described in terms of rigid *anti*-planar segments broken by *gauche* kinks, is actually helical in solution also²⁷. In fact, evidence which is accumulating suggests that nearly all polysilanes adopt helical conformations in solution.

In the light of these new findings, an interpretation of the thermochromic behavior of polysilanes in solution can be offered. In Type 1 behavior, gradual ordering of the polysilane chain into a strongly-twisted helical form takes place as the temperature is lowered. The absorption wavelength of *ca* 315 nm is close to that of the known all-D helices in

some solid polysilanes^{18,19}. Probably the average torsional angle in the solution form is similar, i.e. *deviant*, with ω ca 150°. Increasing the temperature leads to gradual breakdown of the helical arrangement into a more random coil, consistent with the broadening and blue-shift of the absorption band.

In Type 3 behavior, the (mainly) *deviant* helices present at high temperature undergo abrupt transformation to a helical form with a smaller twist angle. This form, with λ_{\max} ca 355 nm, has greater sigma conjugation than the *deviant* helical form, but less than all-*anti* which should absorb near 375 nm. A reasonable model is a helix with *transoid* rotational angles, ca 165°. Transformation from one helical form to another is consistent with the fact that the radius of gyration does not change greatly upon going through the transition²⁸.

2. Thermochromism of polysilanes as solids

The solid polysilanes are far more complicated than polysilane solutions. Frequently, many different phases can be identified for a single polymer, and the transformations between them may be slow, so that the polysilane conformation and spectroscopic behavior often depends on the thermal history of the sample. The compensating fact is that some additional techniques for studying polysilanes become available in the solid phase, including differential scanning calorimetry (DSC), and especially X-ray scattering. Nevertheless, the conformations and structures of polysilanes as solids are poorly understood.

At high temperatures many polysilanes are amorphous. At intermediate temperatures, polysilanes often adopt a hexagonal, columnar mesophase (hcm) arrangement, easily identified by its characteristic, simple X-ray pattern²⁹. With decreasing temperature, if the side chains are similar in length, crystallization is commonly observed. An important observation is that the excitation energies for the amorphous, hcm and all-D phases, the latter being known for $(n\text{-Pen}_2\text{Si})_n$ ¹⁸ and $(n\text{-Bu}_2\text{Si})_n$ ¹⁹, are all quite similar, falling between 305 and 320 nm. This is also close to the value for polysilanes in solution above the transition temperature. It follows that the sigma conjugation must be about equal for these forms, and therefore that the average torsional angles are probably also similar. This suggests that in all these polysilane phases, the rotational conformations are mostly *deviant*, with ω ca 150°, well-ordered in the crystalline structures, but decreasingly ordered in solution, in the hcm and in the amorphous phase.

The structures and phase behavior of individual polysilanes will now be considered, beginning with the simplest example, $(\text{Me}_2\text{Si})_n$. Theoretical calculations for this polymer suggest that the most stable conformation is *transoid*, with ω ca 165°³⁰. X-ray patterns, however, indicate that it adopts an *anti* conformation^{31,32}, probably favored by crystal packing effects. At 160 °C the lattice of $(\text{Me}_2\text{Si})_n$ transforms from monoclinic into hexagonal, but without changing the main chain conformation; a disordering transition to an unknown phase then takes place at 220 °C³².

$(\text{Et}_2\text{Si})_n$ and $(n\text{-Pr}_2\text{Si})_n$ are also reported to have all-A arrangements^{33,34}, mainly from wide-angle X-ray scattering measurements. Consistent with this assignment, these polymers, as well as $(\text{Me}_2\text{Si})_n$, show mutual exclusion of infrared and Raman bands, indicating a centrosymmetric unit cell^{35,36}. Disordering transitions take place near 126 °C for $(\text{Et}_2\text{Si})_n$ and 235 °C for $(n\text{-Pr}_2\text{Si})_n$, in the latter case to a probable nematic liquid crystalline form³⁶.

These three crystalline polysilanes have UV absorption bands at relatively short wavelength, 340 nm for $(\text{Me}_2\text{Si})_n$, 352 for $(\text{Et}_2\text{Si})_n$, 355 for $(n\text{-Pr}_2\text{Si})_n$. These values seem low for a fully-extended polymer chain. The structural assignments as *anti* must therefore be regarded as somewhat doubtful, and indeed Lovinger and coworkers mentioned that small deviations for the planar extended structure may be present in $(\text{Et}_2\text{Si})_n$ and $(n\text{-Pr}_2\text{Si})_n$ ³³.

Turning to the next higher homologs, $(n\text{-Bu}_2\text{Si})_n$ and $(n\text{-Pen}_2\text{Si})_n$, as noted earlier the room temperature conformation for both polymers is *deviani*^{18,19,37}. These two polymers crystallize in a 7/3 helical arrangement, with torsional angles *ca* 154°, and have UV absorption bands at 315 nm. The all-A conformation must, however, lie close in energy to all-D. Application of pressure transforms both polymers to *anti*³⁸, with a corresponding bathochromic shift of the UV absorption band. These polymers are therefore *piezochromic*. For $(n\text{-Pen}_2\text{Si})_n$, cooling to -15°C also transforms the polymer to the all-A state³⁹; upon heating, the all-A structure converts back to all-D at 35 °C. Both polymers undergo a first-order transition to the hcm form, near 85 °C for $(n\text{-Bu}_2\text{Si})_n$ and 56 °C for $(n\text{-Pen}_2\text{Si})_n$. Since the hcm form also has λ_{max} near 315 nm, little thermochromism is observed at this transition, although the absorption bands are broader in the hcm than in the all-D forms.

The next polymer in the dialkyl series is the very well-studied $(n\text{-Hex}_2\text{Si})_n$. Extensive investigations have shown that this polymer adopts an *anti* crystalline form at room temperature, which transforms to hcm near 43 °C^{2,3}. Strong thermochromism is observed, as the all-A band at 375 nm is replaced by the hcm absorption at 315. Numerous papers describe $(n\text{-Hex}_2\text{Si})_n$ in terms only of these two states, but it is slowly becoming apparent that the actual situation is more complex. Studies of the deuterium NMR of deuteriated samples suggest that there is some amorphous polymer mixed into both the crystalline and hcm phases⁴⁰. Also, Kyotani and coworkers have shown that the UV maximum can appear at 357, 370 or 375 nm, depending on how films of the polymer are dried⁴¹. Recently, $(n\text{-Hex}_2\text{Si})_n$ was shown to absorb at 350, 365 or 377 nm, depending on the thermal history of the sample⁴². Various explanations for the multiple absorption bands are discussed elsewhere⁹.

The seven-carbon polysilane $(n\text{-Hep}_2\text{Si})_n$ has not been carefully studied but is reported also to adopt the *anti* form at room temperature. For the next member of the series, $(n\text{-Oct}_2\text{Si})_n$, two low-temperature forms were originally described, all-A and a form with λ_{max} near 350 nm⁴³. The latter was attributed to a TG₊TG₋ structure, with alternating handedness for the *gauche* turns, claimed to exist for all the di-*n*-alkylpolysilanes with linear sidechains from C₈ to C₁₄.

The original suggestion of the TG₊TG₋ arrangement came from an X-ray study of the polysilane $[(n\text{-C}_{14}\text{H}_{29})_2\text{Si}]_n$, showing a Si–Si repeat length of 708 nm. This corresponds to repeat at every fourth atom along the chain. The TG₊TG₋ structure was then assigned, based on semiempirical MO calculations that predicted a relatively low energy for this conformation⁴⁴. This conformational assignment has been repeated several times in reviews^{2,3}, but now seems unlikely to be correct. A TG₊TG₋ arrangement would severely break up the sigma conjugation, and should give a UV absorption at less than 300 nm, whereas the polysilanes assigned this structure absorb near 350 nm. This wavelength suggests conjugation greater than in all-D, but less than in the A conformation. More likely conformations with four-atom repeats include AT₊AT₋, AD₊AD₋, T₊D₊T₋D₋, T₊T₋D₊D₋ and similar variations.

Investigations within the past few years suggest that multiple conformations may exist for many polysilanes. An early, carefully-studied example is $(n\text{-BuSiHex-}n)_n$, which exists in the hexagonal columnar mesophase at room temperature⁴⁵. This polymer exhibits a broad, asymmetric absorption band centered at $\lambda_{\text{max}} = 321$ nm, typical for the hcm. As shown in Figure 4a, slow cooling of a film of this polymer from 300 to 250 K results only in a narrowing of the band, with intensity being lost from the short-wavelength side, and a slight shift to 323 nm. This is consistent with slight straightening of the disordered polymer molecules, increasing the average Si–Si–Si–Si torsional angle and hence the sigma conjugation. When the sample was then slowly cooled from 250 to 248 K and

maintained at the lower temperature, a new absorption band grew in at 339 nm, with loss of intensity from the long-wavelength part of the hcm absorption band (Figure 4b). The 339 nm phase evidently grows in at the expense of the more conjugated molecules of the hcm phase.

However, if the polymer film at 250 K is cooled *rapidly* to 245 K, no band at 339 is observed. Instead, as seen from Figure 4c, the absorption band narrows, becomes symmetrical and shifts to higher energy. The new narrow absorption band at 316 nm is assigned to the well-known, all-D conformation, represented in the 7/3 helical arrangement of polysilanes like $(n\text{-Bu}_2\text{Si})_n$. Next, additional slow cooling to 240 K led to the formation

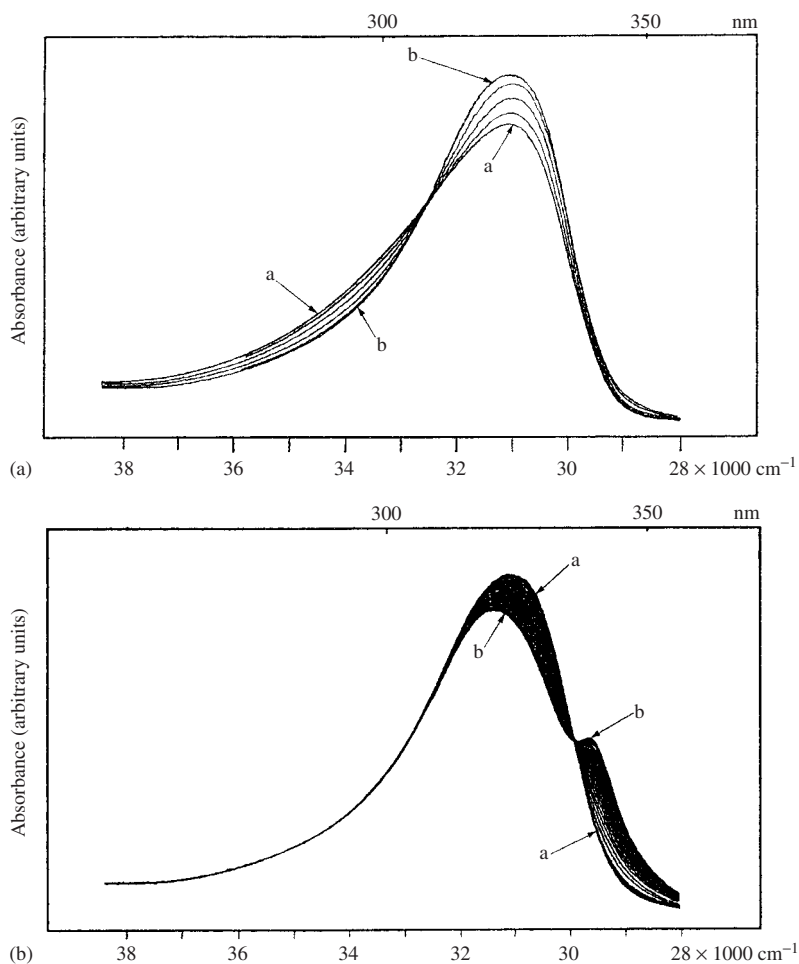


FIGURE 4. UV spectra for $(n\text{-BuSiHex-}n)_n$: (A) slow cooling from 300 (a) to 150 K (b); (B) sample maintained at 248 K (a) initial spectrum (b) after 18 h; (C) sample cooled from 250 (a) to 245 K (b); (D) cooled slowly from 240 (a) to 225 K (b). Reprinted with permission from Reference 45. Copyright 1996 American Chemical Society

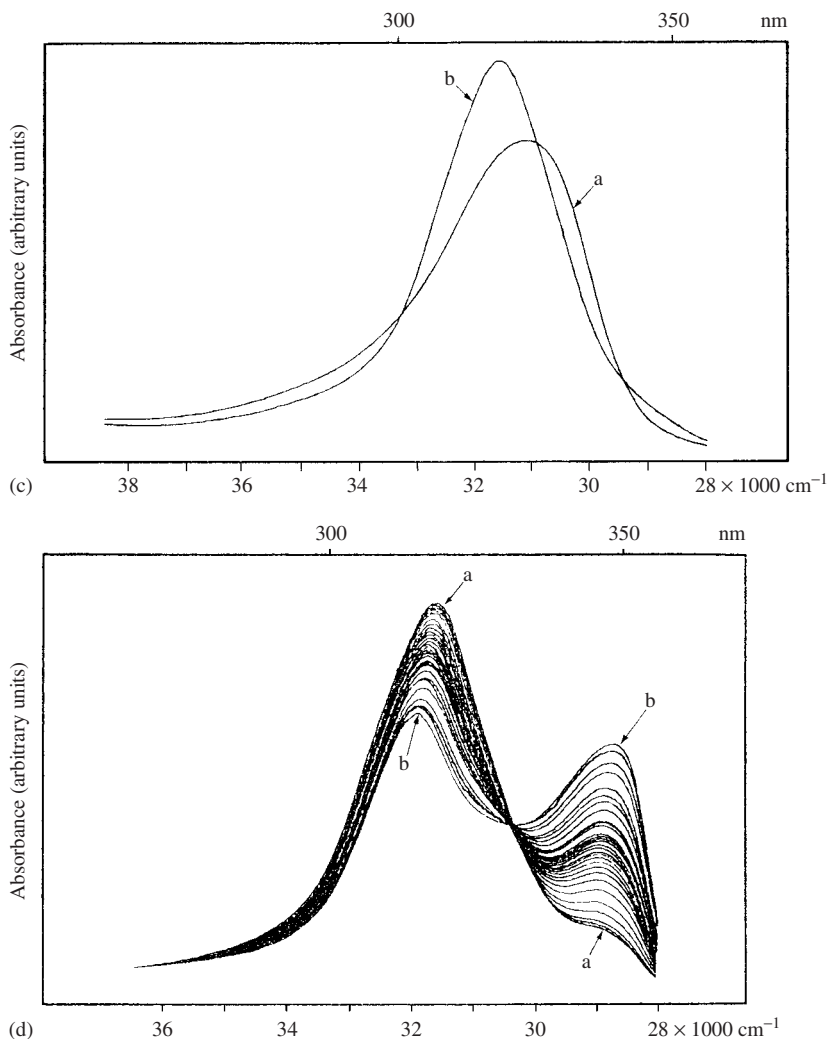


FIGURE 4. (continued)

of a new absorption band at 349 nm, with loss of intensity from the all-D band. Slow cooling to 225 K led to gradual increase in the intensity of the 349 nm band with weakening of the all-D absorption (Figure 4d).

Thus for $(n\text{-BuSin-Hex})_n$, in addition to the hcm and helical all-D phase, two phases of unknown conformation are seen, absorbing at 339 and 349 nm. The latter was originally assigned to an all-*anti* conformation, but both forms are probably helical containing some array of D, T and A conformations. It is important to note that these changes were only observed upon slow, equilibrium cooling; more rapid temperature change obscured these phase changes⁴⁵.

Quite recent investigations have employed, not slow cooling, but rapid quenching of polysilanes followed by slow warming. This can result in a bewildering array of new conformational states. We will consider first di-*n*-decylpolysilane, $(n\text{-Dec}_2\text{Si})_n$ ⁴⁶. At 70 °C this polymer adopts a hexagonal columnar mesophase with $\lambda_{\text{max}} = 316$ nm, giving the typical hcm X-ray pattern shown in Figure 5a (i). Rapid chilling to -30 °C within 1 min produces a new phase with some crystallinity in the sidechains, as shown by the X-ray diagram in the figure. The absorption maximum shifts to 350 nm (Figure 5b). Warming by only 5 °C to -25 °C gives a third phase, with curious long-range ordering, as shown by the low angle peaks in the X-ray pattern. Simultaneously, a new UV absorption band appears at *ca* 380 nm. Next, at -5 °C, long-range order is lost and additional sidechain crystallization is evident (Figure 5a); the principal absorption bands are now at *ca* 360 and 375 nm. Warming to 20 °C yields yet another phase, with λ_{max} *ca* 370 nm, and new long-range order. Isosbestic points were observed for these transformations in the UV spectrum, as illustrated for this last change in Figure 5b, showing that these changes are clear phase transitions. During the warming from -30 to +20 °C, an absorption band at 315 gradually grows back in, perhaps due to a gradually increasing amount of amorphous

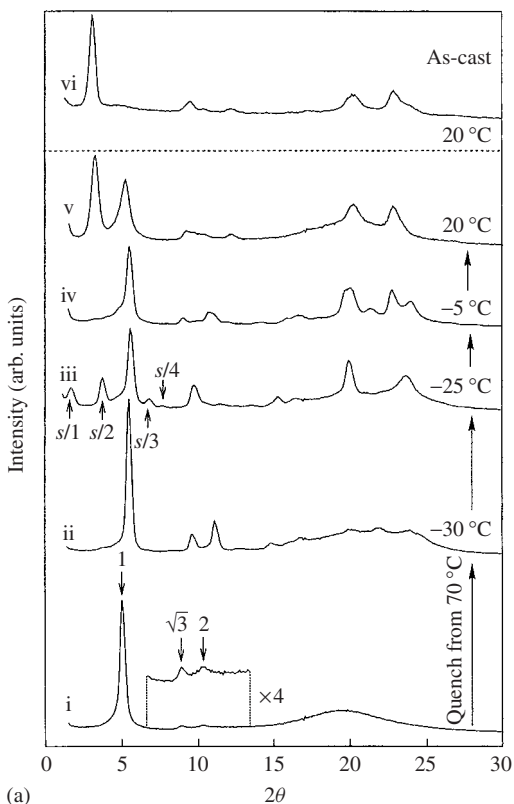


FIGURE 5. (a) X-ray scattering patterns and (b) UV spectra for $[(n\text{-Dec})_2\text{Si}]_n$, showing effects upon quenching followed by warming: (i) hexagonal columnar mesophase at +70 °C; (ii) crystalline phase formed upon quenching to -30 °C; (iii, iv, v) successive new phases formed upon slow warming of b; (vi) film cast from THF solution at 25 °C

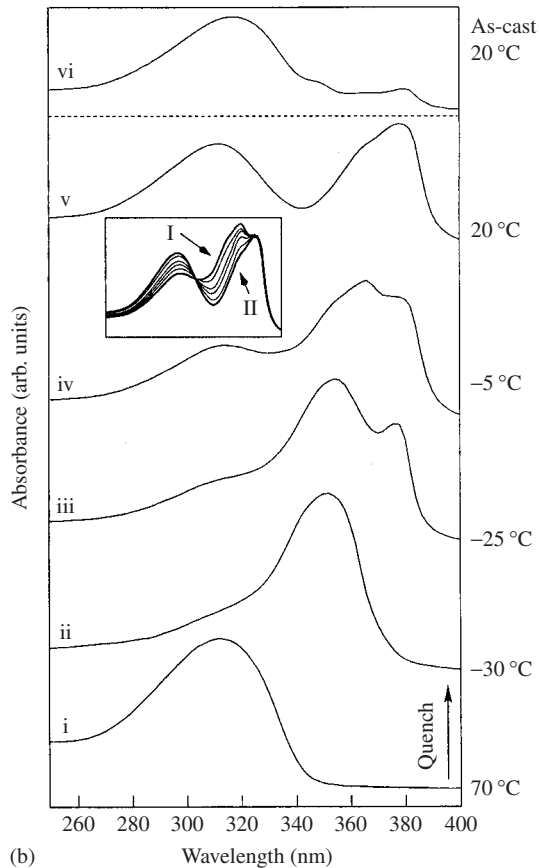


FIGURE 5. (continued)

fraction in the polymer. Finally, the polymer cast from solution at 20 °C has a structure different from any of the phases described, although resembling in some respects the +20 °C phase.

Thus at least five, and perhaps six, different phases can be obtained for $(n\text{-Dec}_2\text{Si})_n$. Four of these have absorption bands in the 350–380 nm region. These unknown structures again probably contain mixtures of A, T and D torsional angles. Tentative attempts to sort out the solid state structures for this polymer are given in a recent paper⁴⁶.

The situation is equally complicated for $(n\text{-Oct}_2\text{Si})_n$. This polymer also has the hcm structure at 70 °C; chilling to –25 °C produces a partially crystalline phase with λ_{max} at 350 and 365 nm (Figures 6a and 6b). The result upon warming to 10 °C is truly astonishing. A *new mesophase* is generated, with an X-ray pattern very like that for the high-temperature hcm, but a totally different UV absorption, at 365 nm! The formation of two different hcm phases seems to be unique. The hexagonal packing of disordered molecules must be present in both, but the average chain conformation must be very different, being much more open and extended in the 10 °C form⁴⁶.

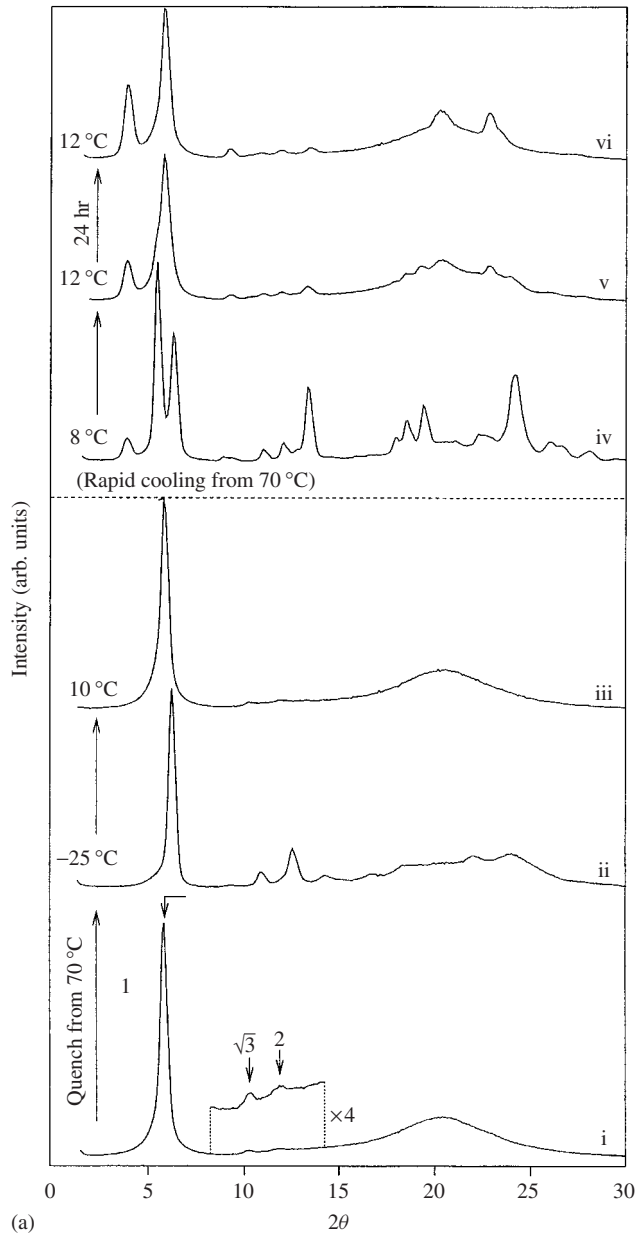


FIGURE 6. (a) X-ray patterns and (b) UV spectra for $[(n\text{-Oct})_2\text{Si}]_n$: (i) hexagonal columnar mesophase at 70°C ; (ii) crystalline phase formed upon quenching to -25°C ; (iii) *new mesophase* obtained upon warming to 10°C ; (iv) crystalline phase formed upon rapid cooling of hcm to 8°C ; (v) new phase obtained upon warming to 12°C ; (vi) change in e after 24 h. Reprinted with permission from Reference 46. Copyright 2000 American Chemical Society

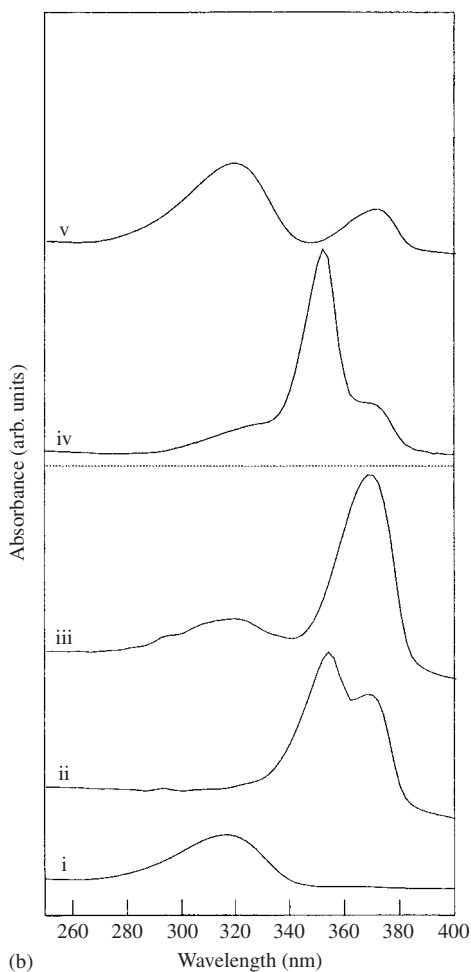


FIGURE 6. (continued)

As shown at the top of Figures 6a and 6b, a yet different, and also complex, pattern of transformations is observed if the $(\text{Oct}_2\text{Si})_n$ is chilled only to 8°C , instead of -25°C , and then gradually warmed.

It now seems evident that the solid state conformations of polysilanes are much more complicated and perplexing than had been thought. Determination of the actual conformations and solid state structures of polysilane polymers is likely to occupy chemists for many years.

B. Solvatochromism

The dependence of electronic absorption on the solvent, solvatochromism, is not generally found for polysilanes. In $(n\text{-Hex}_2\text{Si})_n$, for example, the UV absorption is almost

unaffected even by large changes of solvent polarity⁴⁷. The nature of the solvent may, however, affect the transition temperature between the short- and long-wavelength forms in solution⁴⁸.

Polysilanes bearing polar side groups do exhibit solvent dependence of the UV absorption. The best-studied examples are polysilanes with oxygen atoms in one or both sidechains⁴⁹. In these polymers the UV absorption shifts to longer wavelength as the solvent polarity increases; an example is shown in Figure 7. Interaction of the polar solvent with the oxygen atoms in the sidechains may serve to straighten the polysilane chain somewhat, resulting in increased conjugation. Similar solvatochromism has also been observed for di-*p*-alkoxyphenylpolysilanes⁵⁰.

In some cases, addition of a small amount of a polar compound to a polysilane solution can produce dramatic solvatochromic transitions⁴⁹. As shown in Figure 8, addition of $(\text{CF}_3)_2\text{CHOH}$ to a solution of $\{[n\text{-PrO}(\text{CH}_2)_4]_2\text{Si}\}_n$ in chloroform leads to the sudden disappearance of the absorption band at 325 nm, which is replaced by a band at 348 nm. The critical concentration of $(\text{CF}_3)_2\text{CHOH}$ which will bring about this change is between 4 and 5%. This alcohol is a powerful hydrogen bond donor, which may bind strongly to the oxygen atoms of the sidechains. The curious feature is that this change is abrupt. For the same polymer in benzene a similar sudden transformation also takes place, at a critical concentration of 2.5%. In THF no sudden change is observed, probably because the oxygen of the THF competes favorably for hydrogen bonding from the alcohol protons. This poorly understood phenomenon clearly deserves additional study.

Polysilanes with several oxygen atoms in the sidechains may become water-soluble. This is the case for $[\text{MeSi}(\text{CH}_2)_3\text{O}(\text{CH}_2\text{CH}_2\text{O})_3\text{CH}_3]_n$ studied by Cleij and coworkers⁵¹. In THF solution, this polysilane shows normal Type 1 behavior, with the absorption band shifting gradually from 305 to 317 nm as the temperature is lowered from +20 to -60°C . In water, the absorption occurs at 281 nm at 20°C . Probably the higher energy of the transition in water results because the polymer becomes more coiled, perhaps forming a micelle-like structure with the oxyethylene groups extending into the water and the less polar $\text{MeSi}(\text{CH}_2)_3$ portion at the center. Between 46 and 70°C , aqueous solutions of this polymer undergo phase separation (a lower critical solution temperature

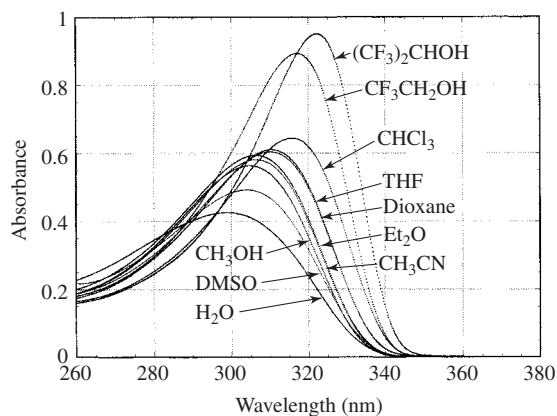


FIGURE 7. UV spectra for $[\text{MeSi}(\text{CH}_2)_3(\text{OCH}_2\text{CH}_2)_3\text{OCH}_3]_n$ in various solvents, showing solvatochromism

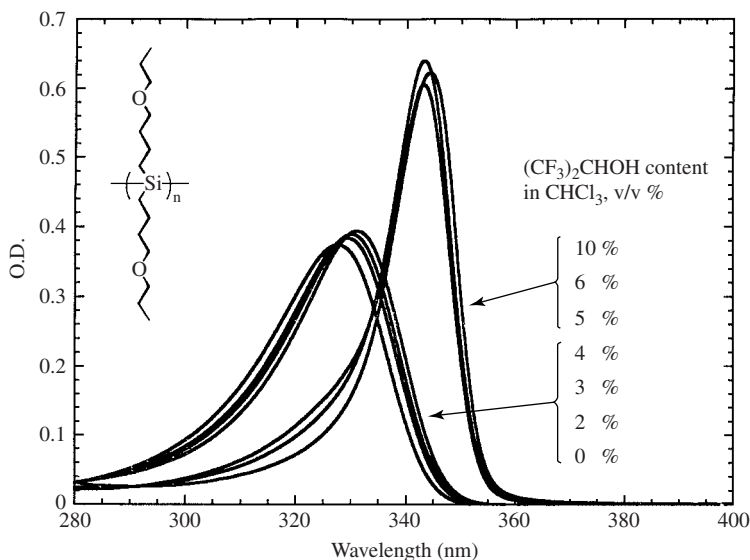


FIGURE 8. UV spectra for $[(n - PrOCH_2CH_2CH_2CH_2)_2Si]_n$ in $CHCl_3$ upon addition of $(CF_3)_2CHOH$, showing the abrupt solvatochromic shift. Reprinted with permission from Reference 49. Copyright 1997 American Chemical Society

phenomenon). The UV absorption shifts bathochromically, to 320 nm, consistent with a straightening of the polymer after phase separation. This polymer also shows some ionochromic behavior.

C. Ionochromism

Dependence of the electronic absorption on the presence of ionic compounds, termed ionochromism, has been observed for some oxygen-containing polysilanes in the solid state⁵². The ionic (usually lithium) salts are added to a solution of the polymer before casting it into a thin film. The nature of this behavior depends greatly on the exact polysilane structure. $[n-OctSi(CH_2)_4OCH_2CH_2OC_2H_5]_n$ exhibits a thermochromic transition in the solid state from 320 to 354 nm, at a temperature of $-32^\circ C$. Addition of lithium trifluoromethanesulfonate progressively inhibits this transformation; when the lithium salt concentration reaches 50 mol% no thermochromism at all is observed. Perhaps this results because lithium ion complexation by the oxygen atoms constrains the polymer into a tight helical form. This inhibition of thermochromism by ions can be termed *negative ionochromism*. The polysilanes $[MeSi(CH_2)_3O(CH_2CH_2O)_nCH_3]_m$ behave similarly⁵³. These polymers show a gradual bathochromic shift as the temperature is decreased, which is inhibited by lithium perchlorate. At a Li : Si ratio of 1 : 1, no bathochromic shift is seen. At still higher lithium content, 4 : 1, with decreasing temperature an unprecedented and unexplained blue shift is observed, from about 300 to 288 nm.

An opposite type of behavior, *positive ionochromism*, is shown by the polymer $\{[C_2H_5OCH_2CH_2O(CH_2)_5]_2Si\}_n$ ⁵². In this case, as shown in Figure 9, addition of lithium triflate to a thin film of the polymer promotes a bathochromic shift, increasing the midpoint temperature of the thermochromic transition from -45 to $+50^\circ C$! Probably in this example the lithium ions, complexed to the ethylene oxide units, lock the polymer

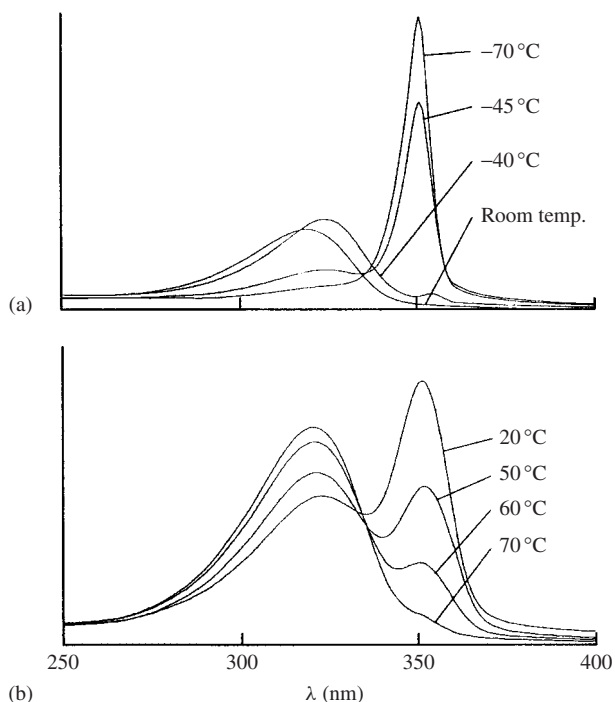


FIGURE 9. UV spectra for a thin film of $\{[C_2H_5OCH_2CH_2O(CH_2)_5]_2Si\}_n$: (a) neat; (b) with addition of 75 mol% $LiSO_3CF_3$, showing a strong positive ionochromic effect

into a more extended conformation, even at relatively high temperature. The effect is, however, reversible by water vapor or THF. Exposure of the polymer to the vapors of either substance reverses the ionochromic effect and returns the polymer to its native state. Evidently this is due to a competition by the basic molecules for the lithium ions, removing them from the polysilane chain and allowing the polymer to relax into its normal, more tightly coiled form. When the THF or water vapor is removed in vacuum, the long-wavelength absorption is regenerated. This polymer thus serves as a UV sensor for basic substances.

The generality of these positive and negative ionochromic effects has not been explored; further studies are needed.

In a recent communication, the first report has appeared on ionochromism of a polysilane in solution⁵⁴. The polymer $\{[C_2H_5OCH_2CH_2O(CH_2)_5]_2Si\}_n$ was investigated in dibutyl ether solvent. Large molar ratios of Li : Si were needed to observe the effect. As shown in Figure 10, upon addition of lithium trifluoromethanesulfonate at a Li : Si ratio of 200, a slight bathochromic shift was observed. Little further change was seen as the ratio was increased to 800, but when the ratio was increased to 1000 an abrupt bathochromic shift was observed, from 325 to 350 nm. This polymer thus exhibits positive ionochromism in dibutyl ether solution. The same effect is also seen in the fluorescence spectrum, which also shifts bathochromically upon addition of the lithium salt. The generality of this phenomenon is unknown; the one other polyoxygenated polysilane studied showed no such ionochromism in solution.

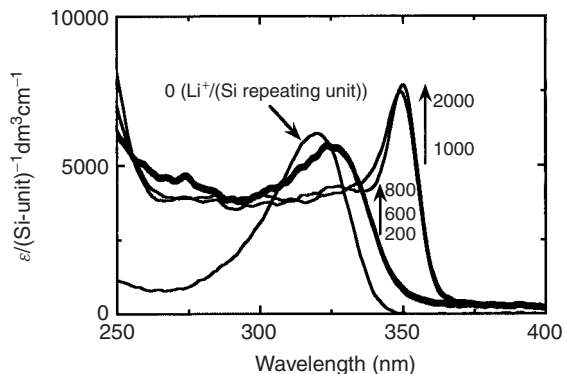


FIGURE 10. UV spectra for $\{[C_2H_5OCH_2CH_2O(CH_2)_5]_2Si\}_n$ in dibutyl ether at $23^\circ C$, showing ionochromic effect in solution. Numbers indicate the molar ratio of $LiSO_3CF_3:Si$. Reprinted with permission from Reference 54. Copyright 2000 American Chemical Society

Clearly the surface of this entire area has hardly been scratched, and much remains to be done in the future.

D. Other Chromotropic Behavior

The conformations and electronic absorption of many polysilanes can be altered by other stimuli as well. The structural transformation of $(n-Bu_2Si)_n$ and $(n-Pen_2Si)_n$ from helical all-D to A structures when subjected to high pressure, *piezochromism*, was described above. Many other polysilanes may also undergo piezochromic behavior, and a thorough study of this phenomenon in polysilanes seems warranted.

Mechanical stretching of the polymer chains, by drawing or rubbing, can also lead to chromotropic effects. An example is $(n-Pen_2Si)_n$, in the normal room temperature all-*deviant* form, which upon drawing converts to the all-*anti* arrangement⁵⁵. A recent report describes the orientation-induced chromism of $(n-HexSiMe)_n$ ⁵⁶. This polymer normally is amorphous at room temperature, with an absorption maximum at 300 nm. Thick films (408 nm) of the polymer, cast onto oriented poly(tetrafluoroethylene), showed absorption at this wavelength, but thin films on the same substrate absorbed mainly at 338, indicating more ordering of the polymer. Similar ordering was produced by drawing of the films.

Surface-mediated chromism of polysilanes in Langmuir–Blodgett films has been carefully investigated by Yoshida and coworkers⁵⁷.

In a few cases, polysilanes are chromotropic in the presence of an electric field (*electrochromism*). This was first shown for the copolymer $(CF_3CH_2CH_2SiMe)_n-co-(n-PrSiMe)_m$, $n : m = 45 : 55$ ⁵⁸. In an electric field of $10^8 V m^{-1}$ the electronic absorption band for this polymer intensified by 50% and shifted from 294 to 299 nm. The changes are reversible when the field is removed. This is apparently the first example of electric field dependence of the absorption for any polymer, unaccompanied by electrochemical oxidation or reduction. The structural change accompanying this chromotropism is not understood. Other polysilanes with polar side groups may also show electrochromic behavior, but have not yet been studied.

Electric fields also affect the orientation of polysilane molecules in solution. Interestingly, the mode of alignment is quite sensitive to the polymer structure. $(PhSiMe)_n$ aligns

perpendicular to the electric field, while (*c*-HexSiMe)_n aligns parallel to the field⁵⁹. No other polysilanes have yet been investigated.

Magnetic fields also can influence the electronic absorption of polysilanes⁶⁰. The intensity of the absorption band for a toluene solution of [MeSiCH₂(CH₂CH₂O)₄CH₃]_n increases by about 5% in a 5 T magnetic field; the effect is reversible when the field is removed. The change was attributed to alignment of the sidechains perpendicular to the field. For (PhSiMe)_n, no change was observed at 5 T, but in a 12 T field the absorption intensity increased by *ca* 15%. Removal of the field led to a rebound effect, with the absorption intensity decreasing to *ca* 2/3 of its original value. These effects probably reflect the large diamagnetic anisotropy of the phenyl rings.

IV. ELECTRICAL CONDUCTIVITY

Pristine polysilanes are electrical insulators, with conductivities well below 10⁻¹⁰ S cm⁻¹. Addition of oxidizing agents, however, can remove electrons from the delocalized, high energy HOMOs, generating vacancies (holes) which can move quite freely along the polysilane chain. Doping with oxidants thus converts polysilanes to one-dimensional semiconductors. This was reported in the 1981 paper which first described the sigma-delocalization in polysilane polymers⁶¹.

The early experiments were done with 'polysilastyrene', the copolymer (Me₂Si)_n(PhSiMe)_m. Addition of SbF₅ or AsF₅ vapor as the oxidant produced conductivities of *ca* 10⁻⁴ to 10⁻³ S cm⁻¹. Later papers from various laboratories reported similar conductivities upon SbF₅ doping for (PhSiMe)_n, (Et₂Si)_n, (EtSiMe)_n⁶², (*n*-Bu₂Si)_n⁶³ and several polysilane copolymers⁶⁴. Copolymers of disilanyl groups with unsaturated organic moieties also become conducting when doped with SbF₅, examples including (R₂SiR₂Si-C≡C)_n⁶² (R₂SiR₂Si-C₆H₄)_n⁶³ and (R₂SiR₂Si-CH=CH-C≡C)_n⁶⁵.

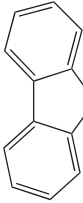
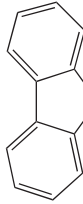
This entire area has been elucidated and put on a firm basis in a series of recent papers by the group from Shin-Etsu Chemical Co.⁶⁶⁻⁶⁸. These workers showed that doping with SbF₅ gave similar conductivities, 10⁻⁴ to 10⁻³ S cm⁻¹, for all polysilanes, regardless of the nature of the substituent groups. This strongly suggests that degradation of the polysilanes is taking place, and this was confirmed by detection of volatile Si-F compounds in the vapor phase above the doped polymers. Evidently the oxidative degradation produces a residue of unknown structure, which is semiconducting⁶⁶.

Doping with iodine, on the other hand, gave lower conductivities (*ca* 10⁻⁶ to 10⁻⁸ S cm⁻¹, see Table 1), but which could be correlated with the ionization potentials of the polymers (lower ionization potentials giving higher conductivity). This is consistent with simple electron transfer from the polysilane to the iodine, with formation of delocalized holes along the polysilane chain.

These workers also showed that polysilanes with nitrogen atoms in the sidechains produced much higher semiconductivity, up to 10⁻² S cm⁻¹ (Table 1)⁶⁷. The mechanism is believed to involve oxidation at the nitrogen atoms with formation of I₃⁻, followed by delocalization of the positive charges from the nitrogen atoms to the polysilane chain.

To show that the polysilane chain is actually involved in the conduction, a carbazolyl-containing polysiloxane was studied, along with the corresponding polysilane. The polysiloxane gave, with I₂, a conductivity of 3.5 × 10⁻⁶ S cm⁻¹, attributed to electron hopping from oxidized nitrogen sites. The conductivity of the polysilane was 1 × 10⁻³ S cm⁻¹, almost 3 orders of magnitude larger, indicating that the Si-Si chain participates directly in the conductivity⁶⁶. A series of copolymers containing carbazolylpropyl(methyl)silicon and phenylmethylsilicon units was also studied; the

TABLE 1. Conductivities of polysilanes (S cm^{-1}) doped with iodine or FeCl_3^a

Sidechains		IP (eV)	Dopant	
			I_2	FeCl_3
<i>n</i> -Bu	<i>n</i> -Bu	5.83	4×10^{-8}	2×10^{-10}
PhCH ₂	PhCH ₂	5.78	9×10^{-7}	8×10^{-7}
<i>n</i> -Oct	<i>n</i> -Oct	5.73	4×10^{-7}	1×10^{-7}
Ph	Me	5.42	1×10^{-6}	6×10^{-6}
$\text{Me}_2\text{NC}_6\text{H}_4\text{-}p$	Me	5.01	1×10^{-3}	4×10^{-4}
$\text{Me}_2\text{NC}_6\text{H}_4(\text{CH}_2)_3$	Me	5.56	1×10^{-2}	7×10^{-6}
	Me	5.65	1×10^{-3}	2×10^{-5}
	Me^b		3.5×10^{-6}	etc.

^aData from Reference 66.

^bPolysiloxane polymer.

conductivity increased regularly with the content of the nitrogen-containing groups, from $1 \times 10^{-6} \text{ S cm}^{-1}$ for pure $(\text{PhSiMe})_n$ to $1.3 \times 10^{-3} \text{ S cm}^{-1}$ for the carbazoylpropyl-SiMe homopolymer⁶⁸.

Simple admixture of arylamines to polysilanes also serves to increase the conductivity upon iodine doping. Addition of 30 wt% of *N,N,N',N'*-tetrakis(3-methylphenyl)-1,3-diaminobenzene to $(\text{PhSiMe})_n$ increased the conductivity of this polymer to $3 \times 10^{-4} \text{ S cm}^{-1}$.

The Shin-Etsu group also studied doping of polysilanes with FeCl_3 vapor. Some results are given in Table 1. FeCl_3 produces relatively higher conductivity in polysilanes containing aromatic substituents. This was explained by charge transfer of electrons from the aromatic π system to FeCl_3 , followed by delocalization of the holes onto the polysilane chain, leading to the conductivity.

Network polysilanes with three-dimensional structure, $[\text{MeSi}(\text{OMe})_x(\text{R})_y]_n$, also become semiconducting when doped with iodine⁶⁹. The highest values, *ca* $10^{-3} \text{ S cm}^{-1}$, were again obtained with nitrogen-containing groups, $\text{R} = (\text{Alkyl})_2\text{NC}_6\text{H}_4$. An interesting study using both network and linear polysilanes showed that the conductivity upon treatment with iodine can be controlled by photooxidation. Exposure to UV light in air converts the Si-Si bonds to Si-O-Si, making the surface nonconducting. Thus by a photolithographic process, it is possible to generate a conducting pattern on a polysilane film⁷⁰.

Nitrogen-containing or amine-doped polysilanes also show excellent properties as hole transport materials, in electrophotographic or printing processes, described fully elsewhere¹⁰.

V. ACKNOWLEDGEMENTS

Research on polysilanes at the University of Wisconsin has been supported by grants from the National Science Foundation, and by the sponsors of the Organosilicon Research Center. Prof. Josef Michl contributed greatly to the model described in Section II. I thank Prof. Kunio Oka and Prof. Michael Winokur for permission to include unpublished data.

VI. REFERENCES AND NOTES

1. R. West, *J. Organometal. Chem.*, **300**, 327 (1986).
2. R. D. Miller and J. Michl, *Chem. Rev.*, **89**, 1359 (1989).
3. R. West, 'Organopolysilanes', in *Comprehensive Organometallic Chemistry II*, Volume 2, (Ed. A. G. Davies) Pergamon, Oxford, 1994, pp. 77–110.
4. J. Chojnowski, R. G. Jones and W. Ando (Eds.), *Silicon-Based Polymers: The Science and Technology of their Synthesis and Applications*, Kluwer Academic, Dordrecht, 2000.
5. R. G. Jones and S. Holder, 'Synthesis of polysilanes by the Wurtz reductive coupling reaction', in Reference 4, pp. 353–374.
6. H. Sakurai and M. Yoshida, 'Synthesis of polysilanes by new synthetic procedures: Ring opening polymerizations and the polymerization of masked disilenes', in Reference 4, pp. 375–400.
7. G. M. Gray and J. Y. Corey, 'Synthesis of polysilanes by new synthetic procedures: Catalytic dehydro-polymerization of hydrosilanes', in Reference 4, pp. 401–418.
8. M. Tanaka and Y. Hatanaka, 'Hydrosilylation and silylation in organosilicon polymer synthesis', in Reference 4, pp. 439–450.
9. J. Michl and R. West, 'Electronics, spectroscopy and photochemistry of polysilanes', in Reference 4, pp. 499–530.
10. N. Matsumoto, H. Suzuki and H. Miyazaki, 'Electronic/optical properties and device applications of polysilanes', in Reference 4, pp. 531–552.
11. S. Demoustier-Champagne and J. Devaux, 'Thermal properties and phase behavior of polysilanes', in Reference 4, pp. 553–574.
12. H. S. Plitt, J. W. Downing, M. K. Raymond, V. Balaji and J. Michl, *J. Chem. Soc., Faraday Trans.*, **90**, 1653 (1994).
13. *Anti* will be used to describe only torsional angles within a few degrees of 180°. Deviations from exact A conformations are known for several polymers, for example poly(tetrafluoroethylene), which has two crystalline forms best described as all-T; see J. J. Weeks, E. S. Clark and R. K. Eby, *Polymer*, **22**, 1480 (1981).
14. H. Teramae and J. Michl, *Mol. Cryst. Liq. Cryst.*, **256**, 149 (1994).
15. F. Shafiee, K. J. Haller and R. West, *J. Am. Chem. Soc.*, **108**, 5478 (1986).
16. R. Zink, T. F. Magnera and J. Michl, *J. Phys. Chem. A*, **104**, 3829 (2000).
17. H. A. Fogarty, C. H. Ottoson and J. Michl, *J. Mol. Struct. (Theochem)*, **526**, 243 (2000).
18. R. D. Miller, B. L. Farmer, W. Fleming, R. Sooriyakumaran and J. F. Rabolt, *J. Am. Chem. Soc.*, **109**, 2509 (1987).
19. F. C. Schilling, A. J. Lovinger, J. M. Zeigler, D. D. Davis and F. A. Bovey, *Macromolecules*, **22**, 3022 (1989).
20. (a) H. Kuzmany, J. F. Rabolt, B. L. Farmer and R. D. Miller, *J. Chem. Phys.*, **85**, 7413 (1986).
(b) S. Furukawa, *Thin Solid Films*, **331**, 222 (1998).
(c) Recent unpublished studies by M. Winokur indicate, however, that the torsional angles in [(n-Hex)₂Si]_n may not be exactly 180°.
21. E. A. Karikari, A. J. Greso, B. L. Farmer, R. D. Miller and J. F. Rabolt, *Macromolecules*, **26**, 3937 (1993).
22. K. S. Schweitzer, *J. Chem. Phys.*, **85**, 1156, 1176 (1986).
23. T. Sanji, K. Sakamoto, H. Sakurai and K. Ono, *Macromolecules*, **32**, 3788 (1999).
24. M. Fujiki, *J. Am. Chem. Soc.*, **118**, 7424 (1996).

25. M. Fujiki, *J. Am. Chem. Soc.*, **122**, 3336 (2000).
26. J. R. Koe, M. Fujiki, M. Motonaga and H. Nakashima, *Chem. Commun.*, 389 (2000).
27. S. Toyoda and M. Fujiki, *Chem. Lett.*, 699 (1999).
28. P. Shukla, P. M. Cotts, R. D. Miller, T. P. Russell, B. A. Smith, G. M. Waalraaf, M. Baier and P. Thiyagarajan, *Macromolecules*, **24**, 5606 (1991).
29. T. Asuke and R. West, *J. Inorg. Organomet. Polym.*, **4**, 45 (1994).
30. (a) S. Patnaik and B. L. Farmer, *Polymer*, **33**, 5121 (1992).
(b) B. Champagne, E. A. Perpete and J. M. Andre, *J. Mol. Struct., (Theochem)*, **391**, 67 (1997).
31. A. J. Lovinger, D. D. Davis, F. C. Schilling, F. J. Padden, Jr., F. A. Bovey and J. M. Zeigler, *Macromolecules*, **24**, 132 (1991).
32. S. Furukawa and K. Takeuchi, *Solid State Commun.*, **87**, 931 (1993).
33. A. J. Lovinger, D. D. Davis, F. C. Schilling, F. A. Bovey and J. M. Zeigler, *Polym. Commun.*, **30**, 357 (1989).
34. S. Takeuchi, M. Mizoguchi, M. Shimana and M. Tamura, *J. Phys.: Condens. Matter*, **5**, L461 (1993).
35. L. A. Leites, T. S. Yadritseva, S. S. Bukalov, T. M. Frunze, B. A. Antipova and V. V Dement'ev, *Polym. Sci.*, **34**, 980 (1992); L. A. Leites, S. S. Bukalov, T.S. Yadritseva, B. A. Antipova, T. M. Frunze and V. V Dement'ev, *Macromolecules*, **25**, 2991 (1992).
36. L. A. Leites, S. S. Bukalov, T. A. Yadritseva, R. Menescal and R. West, *Macromolecules*, **27**, 5885 (1994).
37. S. Furukawa, K. Takeuchi and M. Shimana, *J. Phys: Condens. Matter*, **6**, 11007 (1994).
38. K. Song, R. D. Miller, G. M. Waalraaf and J. F. Rabolt, *Macromolecules*, **24**, 4084 (1991).
39. E. E. Karikari, B. L. Farmer, C. L. Hoffman and J. F. Rabolt, *Macromolecules*, **27**, 7185 (1994).
40. C. Mueller, C. Schmidt and H. Frey, *Macromolecules*, **29**, 3320 (1996).
41. H. Kyotani, M. Shimomura, M. Miyazaki and K. Ueno, *Polymer*, **36**, 915 (1996).
42. L. A. Leites, S. S. Bukalov and R. West, unpublished observations.
43. E. E. Karikari, A. J. Greso, B. L. Farmer, R. D. Miller and J. F. Rabolt, *Macromolecules*, **26**, 3937 (1993).
44. B. L. Farmer, *Bull. Am. Phys. Soc.*, **33**, 657 (1988).
45. S. S. Bukalov, L. A. Leites, R. West and T. Asuke, *Macromolecules*, **29**, 907 (1996). This publication employed the older *anti-gauche* formalism, but here the data will be interpreted using the newer conformational model.
46. W. Chunwachirasiri, R. West and M. Winokur, *Macromolecules*, **33**, 9720 (2000).
47. K. Oka and R. West, unpublished studies.
48. For examples see Table 2 in Reference 9.
49. K. Oka, N. Fujiue, T. Dohmaru, C.- H. Yuan and R. West, *J. Am. Chem. Soc.*, **119**, 4074 (1997).
50. R. D. Miller and R. Sooriyakumaran, *Macromolecules*, **21**, 3122 (1988).
51. T. J. Cleij, L. W. Jennessens and S. G. J. M. Kluijtmans, *Adv. Mater.*, **9**, 961 (1997).
52. C.- H. Yuan and R. West, *Chem. Commun.*, 1825 (1997).
53. K. Oka, N. Fujiue, S. Nakanishi, T. Takata, T. Dohmaru, C.- H. Yuan and R. West, *Chem. Lett.*, 253 (1997).
54. S. Toyoda, M. Fujiki, C.- H. Yuan and R. West, *Macromolecules*, **33**, 1503 (2000).
55. M. Moller, H. Frey and S. Sheiko, *Colloid Polym. Sci.*, **271**, 554 (1993).
56. A. Kaito, H. Kyotani, D. Hajiheidari, N. Tanigaki and M. Shimomura, *Polymer*, **40**, 5857 (1999).
57. M. Yoshida, T. Seki, F. Nakanishi, K. Sakamoto and H. Sakurai, *Chem. Commun.*, 1381 (1996); M. Yoshida, F. Nakanishi, T. Seki, K. Sakamoto and H. Sakurai, *Macromolecules*, **30**, 1860 (1997).
58. M. Fujino, T. Hisaki and N. Matsumoto, *Macromolecules*, **28**, 5017 (1995).
59. T. Nakayama, M. Miyamoto, S. Akita, T. Dohmaru and R. West, *Jpn. J. Appl. Phys.*, Part 2, **34**, L57 (1995).
60. T. Nakamura, H. Nakagawa, K. Oka, H. Naito, I. Mogi, K. Watanabe and T. Dohmaru, *Solid State Commun.*, **106**, 447 (1998).
61. R. West, L. D. David, P. I. Djurovich, K. L. Stearley, K. S. V. Srinivasan and H. Yu, *J. Am. Chem.Soc.*, **103**, 7352 (1981).

62. M. Ishikawa, T. Hatano, Y. Hasegawa, T. Horio, A. Kunai, A. Miyai, T. Ishida, T. Tsukihara, T. Yamanaka, T. Koike and J. Shioya, *Organometallics*, **11**, 1604 (1992).
63. T. Hayashi, Y. Uchimaru, N. P. Reddy and M. Tanaka, *Chem. Lett.*, 647 (1992).
64. C. A. vanWalree, T. J. Dleij, L. W. Jenneskens, E. J. Vliestra, G. P. venderLaan, M. P. deHaas and E. T. G. Lutz, *Macromolecules*, **29**, 7362 (1996).
65. J. Ohshita, A. Matsuguchi, K. Fumiori, R. F. Hong, M. Ishikawa, T. Yamanaka, T. Koike and J. Shioya, *Macromolecules*, **25**, 2134 (1992).
66. M. Fukushima, Y. Hamada, E. Tabei, M. Aramata, S. Mori and Y. Yamamoto, *Synth. Metals*, **94**, 299 (1998).
67. M. Fukushima, E. Tabei, M. Aramata, Y. Hamada, S. Mori and Y. Yamamoto, *Synth. Metals*, **96**, 239 (1998).
68. E. Tabei, M. Fukushima and S. Mori, *Synth. Metals*, **73**, 113 (1995).
69. T. Kobayashi, K. Hatayama, S. Suzuki, M. Abe, H. Watanabe, M. Kijima and H. Shirakawa, *Organometallics*, **17**, 1646 (1998).
70. K. Kabeta, S. Wakamatsu, S. Sugi and T. Imai, *Synth. Metals*, **82**, 210 (1996).

CHAPTER 10

Nanostructured hybrid organic–inorganic solids from molecules to materials

BRUNO BOURY and ROBERT J. P. CORRIU

Laboratoire de Chimie Moléculaire et Organisation du Solide, UMR 5637, Université de Montpellier II, CC007, Place E. Bataillon, 34095 Montpellier cedex, France
Fax: 33-467-143-888; e-mail: boury@crit.univ-montp2.fr

I. INTRODUCTION	566
II. NANOCOMPOSITES VERSUS NANOSTRUCTURED HYBRID MATERIALS	570
A. Nanocomposite Hybrid. An [Organic Host + SiO ₂ or R'SiO _{1.5} Matrix] Association	570
B. Nanostructured Hybrid Material Monocomponent with One Si–C Bond—Organo-silsesquioxanes R'(SiO _{1.5})	572
C. Nanostructured Hybrid Material Monocomponent with At Least Two Si–C Bonds—Organo-polysilsesquioxanes R'(SiO _{1.5}) _n (n ≥ 2)	575
III. SYNTHESIS OF NANOSTRUCTURED ORGANO-POLYSILSESQUIOXANES R'(SiO _{1.5}) _n (n ≥ 2). SOME ASPECTS OF PRECURSORS AND GEL CHEMISTRY	578
A. The Family of R'(SiX ₃) _n (n ≥ 2) Precursors	578
B. Synthesis of the Precursors R'(Si(OR) ₃) _n (n ≥ 2)	578
C. Particular Aspects of the Chemistry during the Sol-gel Polycondensation of R'(Si(OR) ₃) _n (n ≥ 2)	589
IV. KINETIC CONTROL OF THE SOLID'S CHARACTERISTICS OF NANOSTRUCTURED ORGANO-POLYSILSESQUIOXANES R'(SiO _{1.5}) _n (n ≥ 2)	593
A. Polycondensation and Integrity of the Organic Group	593
B. Texture/Kinetic Parameters of the Sol-gel Process	595
C. Effect of the Nature of the Organic Group on the Texture of the Xerogels R'(SiO _{1.5}) _n (n ≥ 2)	600
D. Characteristics of the Surface of Xerogels	600

V. ORGANIZATION AND SHORT-RANGE ORDER IN NANOSTRUCTURED ORGANO-POLYSILSESQUIOXANES $R'(SiO_{1.5})_n$ ($n \geq 2$) . . .	602
A. Chemical Evidence of a Short-range Order	603
B. Characterization of a Short-range Order	603
C. Optical Evidences for an Anisotropic Organization in the Xerogels	604
VI. CHEMISTRY INSIDE THE ARCHITECTURE OF THE HYBRID NANOSTRUCTURED ORGANO-POLYSILSESQUIOXANES $R'(SiO_{1.5})_n$ ($n \geq 2$)	608
A. Chemical Stability	609
B. Inter-activity between the Organic Groups	610
C. Reactivity/Structure Relationship	611
D. Xerogels with Catalytic Properties	614
E. Miscellaneous	619
VII. NANOSTRUCTURED ORGANO-POLYSILSESQUIOXANES $R'(SiO_{1.5})_n$ ($n \geq 2$) AS PRECURSORS FOR POROUS MATERIALS	620
A. Direct Thermal Oxidative Elimination of the Organic Groups	621
B. Non-oxidative Thermal Elimination of the Organic Groups	621
C. Elimination of the Organic Groups by Chemical Treatment	622
VIII. SHAPING OF NANOSTRUCTURED ORGANO-POLYSILSESQUIOXANES $R'(SiO_{1.5})_n$ ($n \geq 2$)	629
A. Monoliths, Aerogels and Thin Films	629
B. Mesoporous Hybrids (MCM Systems)	629
IX. SOME PHYSICAL PROPERTIES OF NANOSTRUCTURED ORGANO-POLYSILSESQUIOXANES $R'(SiO_{1.5})_n$ ($n \geq 2$)	631
A. Thermal Properties	631
B. Electrochemical Properties	631
C. Optical Properties	632
D. Mechanical Properties	634
X. GENERAL SUMMARY	634
XI. REFERENCES	635

I. INTRODUCTION

The phrase 'Chimie Douce' was introduced recently in Materials Science^{1,2}. This method of obtaining solids by inorganic polymerization corresponds to a breakthrough in the general access to materials, since it opens the field of materials science to molecular chemistry (organic, organometallic and inorganic chemistry).

The methodology used in the classical solid state approach is based on the thermodynamic evolution of the reaction. Whatever the experimental conditions, success is based on the self-arrangement of the system leading to stable (or metastable) materials. This approach to the preparation of a material includes high temperature methodologies resulting in crystals or ceramics, and also other technical tools working at low temperatures such as the access to crystalline aggregates, the preparation of polyanions from solutions or the hydrothermal route to zeolites.

The solid materials obtained by these methods are always governed by the general thermodynamic laws represented by the phase diagrams. In contrast, the methodologies included in the phrase 'Chimie Douce' involve kinetic control of the solid synthesis when non-reversible reactions are used. Therefore, solids prepared by this route are not the most

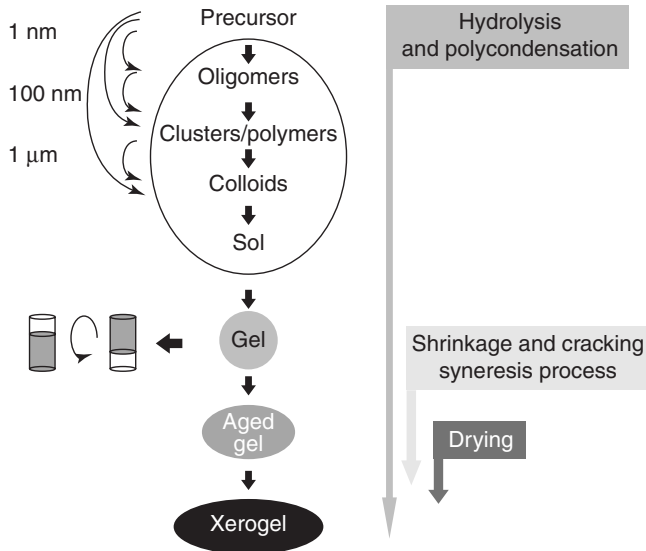
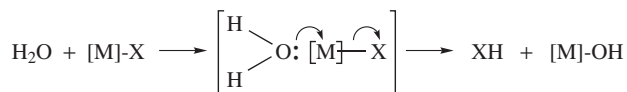


FIGURE 1. General overview of the transformations occurring during the sol-gel process

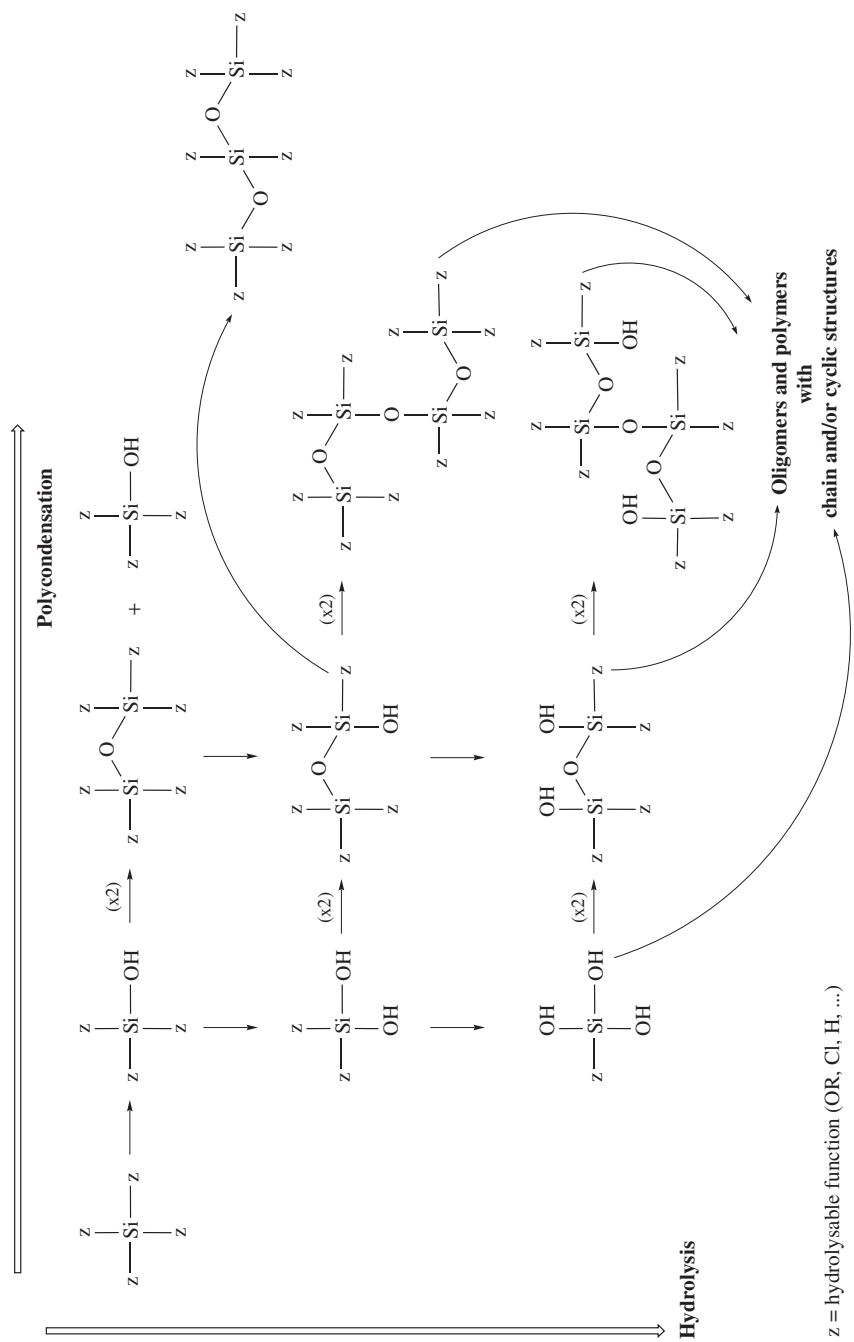
thermodynamically stable, but they are the result of a multi-parameter chemistry based on the mechanistic control of the chemical reactions.

One usual methodology of ‘Chimie Douce’ is the sol-gel process which corresponds to an inorganic polymerization. The different steps involved in this process are depicted schematically in Figure 1 where the term syneresis relates to the spontaneous shrinkage exhibited by some gels, due to bond formation or attraction between particles which induce contraction of the network and expulsion of liquid from the gel. This method is based on the reactivity towards hydrolysis of metal alkoxide bonds, but other leaving groups can be used ($M-X$, $X=OR$, NR_2 , H , Cl etc.); see Scheme 1. Since this process corresponds to an inorganic polymerization, it is directly connected to macromolecular chemistry. Simultaneously, it is controlled by the kinetics of the different chemical transformations occurring around the metal centre via the nucleophilic substitution processes depicted in Scheme 2.

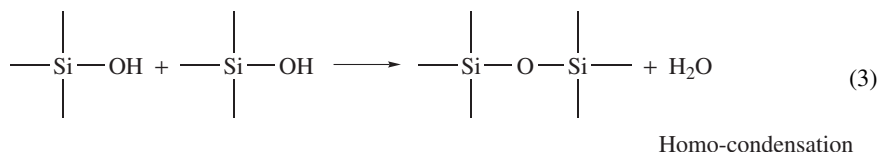
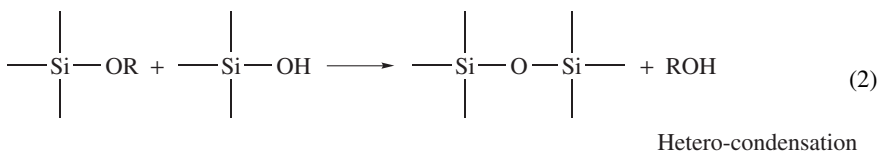
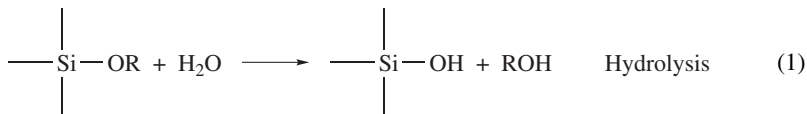


SCHEME 1

Water acts as a nucleophile and displaces the OR leaving group from silicon; the most common case is the synthesis of silica by hydrolytic polycondensation of tetraalkoxysilanes as shown in equations 1, 2 and 3. The condensation leading to $Si-O-Si$ bonds apparently occurs by hydrolysis, hetero-condensation and homo-condensation^{3,4}. Interest in silicon is also based on the fact that very useful and common materials like silicates



and silicones can be prepared by hydrolysis of functionalized organosilicon compounds.



It is possible to recognize some basic transformations corresponding to Scheme 2 as the first steps of the process. It is readily evident that the overall transformation is highly complex: first, because of the tetra-functionality of the monomer; second, due to the possibility of redistribution reactions between the different species, and finally, because very different structures such as chains, rings and clusters can be formed. Although it is possible to have a global overview of the formation of the highly cross-linked solid, the precise pathways remain difficult to detail⁴. Branching and cross-linking result in the formation of a network large enough for the gel transition to occur; it consists of a polymeric solid phase interpenetrated with a solvent phase. Upon ageing, shrinkage is observed and is connected to the non-reversible chemical transformations that increase the cross-linking level of the Si–O–Si framework. Finally, elimination of solvent and volatile compounds leads to a solid, generally as a powder, which is termed xerogel.

In materials science these types of gels are described as unstable solids whose evolution is irreversible. Therefore, each modification of the sol-gel processing parameters may result in a dramatic modification of the characteristics of the final material⁴. It was suggested in the case of silica that even the size of the container may exhibit some influence⁵. Therefore, the reproducibility of the experiments is a prerequisite which is difficult to achieve in the present case. On the other hand, because of this high sensitivity towards the experimental conditions, it is possible to achieve very different textures by simple modifications of the kinetic parameters (temperature, concentration, solvent, catalyst, nature of leaving group, etc.). The predictability of the solid's texture is still a challenge, but it is important to point out that the very flexible sol-gel process methodology allows the preparation of films and fibres by coating and spinning, and also of matrices with the possibility of inclusions of other reagents.

Thus the sol-gel methodology is an alternative to classical thermodynamic routes for the synthesis of solids. It is also evident that the preparation of the solids through 'Chimie Douce' bridges molecular chemistry and solid state chemistry. This chapter will be focused on material prepared by the sol-gel process, where an organic part is associated with a silica or siloxane Si–O–Si network. Two types of organic–inorganic hybrid materials can be prepared by the sol-gel process and are completely different: the *nanocomposites* and the *nanostructured* hybrid materials^{6–9}.

As illustrated in Figure 2, nanostructured materials correspond to monocomponent hybrid organic–inorganic solids elaborated from a molecular precursor used as a building block and designed to permit hydrolytic polycondensation in the presence of the organic unit. On the other hand, nanocomposites are the result of the polycondensation of an inorganic Si–O–Si matrix in the presence of an organic molecule acting as a host.

The preparation of monocomponent hybrid materials is determined by the chemistry of the building block. To prepare them, the first condition is the presence of hydrolysable-function groups in the building block in order to form the oxide matrix by hydrolytic polycondensation. The trialkoxysilyl groups $-\text{Si}(\text{OR})_3$ ($\text{R}=\text{Et}$, Me , $i\text{-Pr}$) is the most commonly used among possible ($-\text{SiX}_3$) groups.

The second condition is the existence of non-hydrolysable and non-oxidizable covalent bonds between the organic unit and the oxide network. Silicon chemistry provides one of the best solutions to this problem since the Si–C bond is generally a stable link in the conditions used for the sol-gel process (some rare exceptions will be discussed below). Moreover, the Si–C bond is generally highly resistant to hydrolysis and oxidation. Finally, the organosilicon chemistry has been widely developed, providing many chemical ways to introduce silicon containing groups into an organic molecule for the synthesis of molecular building blocks.

We will briefly present the general features concerning the nanocomposite materials and polysilsesquioxanes. We will then focus on the nanostructured materials, their preparation and specific properties, which differ profoundly from the nanocomposites.

II. NANOCOMPOSITES VERSUS NANOSTRUCTURED HYBRID MATERIALS

A. Nanocomposite Hybrid. An [Organic Host + SiO_2 or $\text{R}'\text{SiO}_{1.5}$ Matrix] Association

The formation of a nanocomposite is one of the most direct ways to achieve the preparation of hybrid materials, since it is done by adding a host compound to the polymerizing mixture (water/solvent silica source) [TMOS (=tetramethylorthosilicate), TEOS (=tetraethylorthosilicate)]^{10–13}. Figure 3 is a schematic description of how organic, organometallic and bioorganic molecules as well as polymers, cells or inorganic salts can be trapped in the entanglements of the inorganic silica network^{6,14–16}. The use of silica as a matrix is advantageous, due to its chemical and thermal stability but also due to other SiO_2 properties like transparency, porosity, adaptability of the surface polarity, casting ability etc. Although most of these systems appear homogeneous at the macro ($>1\ \mu\text{m}$) or meso (10 nm–1 μm) scale level, they correspond to a multi-component system with a micro-domain ($<10\ \text{nm}$) composed either of the pure SiO_2 matrix or the pure host compound which can be separated using classical separation techniques (washing with an organic solvent, for instance).

Much research in this field is mainly directed towards applications, especially those in analytical chemistry (bio-, chemo-, photo- or electrochemical sensors etc.). Another goal is the preparation of active materials with photochromic, thermochromic, luminescent or electrooptical properties. Modification of the micro-polarity of the matrix surface can be obtained by using $\text{CH}_3\text{Si}(\text{OR})_3$ ^{17–20} or $\text{C}_6\text{H}_5\text{Si}(\text{OR})_3$ ²¹ instead of TMOS or TEOS for the matrix, or by adding a surfactant²². In more fundamental studies, luminescent probes are currently used to follow the formation of the matrix, at different stages of its evolution [with ruthenium complexes²³, 1,12-bis(1-pyrenyl)dodecane²⁴, or hemicyanine molecules²⁵]. Recent research has been directed towards the association of the silica matrix with other oxides (Al_2O_3 ²⁶, ZrO_2 ²⁷, B_2O_3 ²⁸, TiO_2 ²⁹) or the addition of several doping agents.

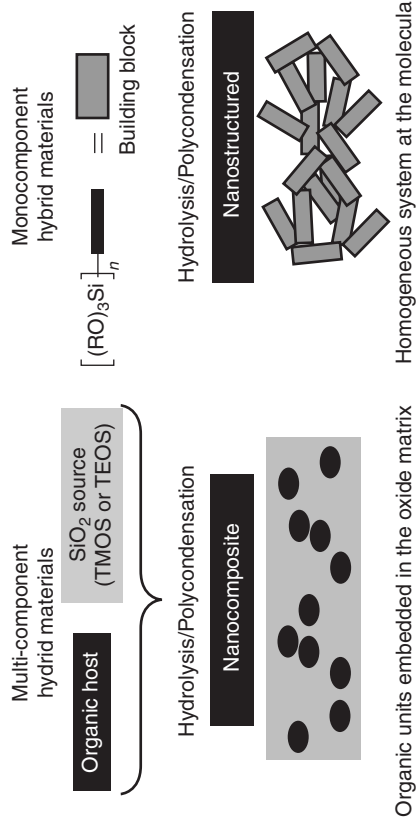


FIGURE 2. The different pathways to nanocomposite and nanostructured materials (TMOS-tetramethylorthosilicate, TEOS-tetraethylorthosilicate)

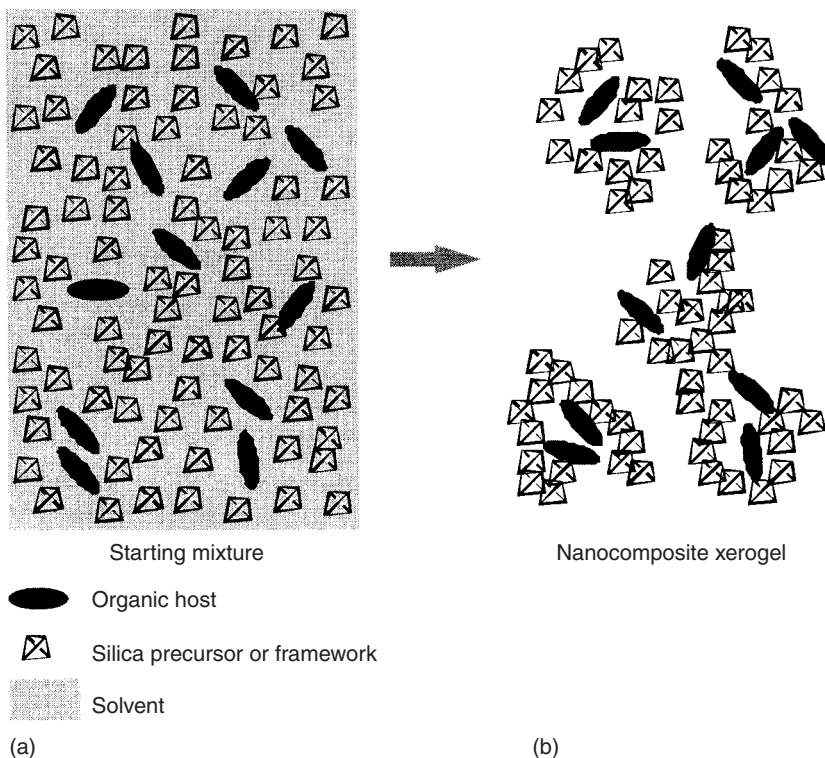


FIGURE 3. The sol-gel approach to the preparation of nanocomposite materials : (a) starting mixture and (b) after gelation and drying

B. Nanostructured Hybrid Material Monocomponent with One Si–C Bond – Organo-silsesquioxanes $R'SiO_{1.5}$

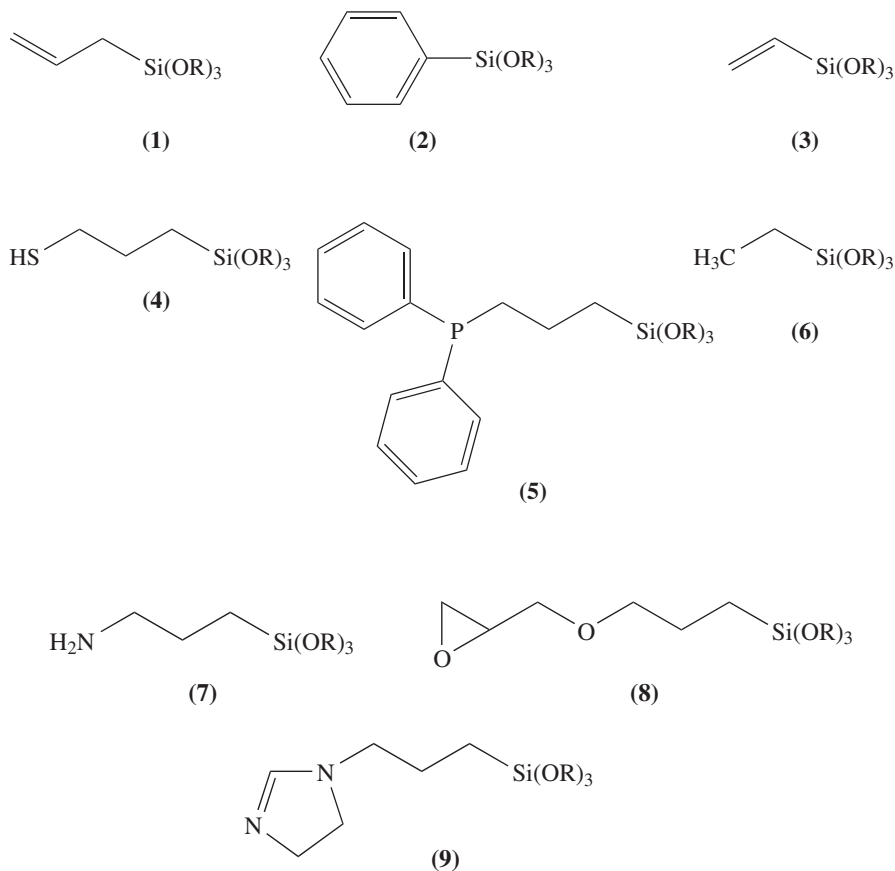
The development of organosilicon chemistry has resulted in the possibility to synthesize a large family of $R'Si(OR)_3$ precursors. The R' group can be chosen with very different architectures and functions and with a high stability of the Si–C link.

Matrix surface modifiers and organically modified mesoporous silica. For instance, methyltrialkoxysilane $CH_3Si(OR)_3$ or phenyltrialkoxysilane $(C_6H_5Si(OR)_3)$ are combined with TMOS or TEOS in order to modify the polarity of the matrix's surface for the preparation of the nanocomposites mentioned above.

Concerning mesoporous silica, they can be prepared by surfactant-assisted micellization of a mixture of solvent, silica precursor and water^{30–35}. Material with hexagonal close-packed arrangements of single-size channel with tunable diameters (2–10 nm) are obtained after eliminating the surfactant^{30,36–38}. This MCM (Mobile Composition of Matter) is generally siliceous materials but can be grafted with organic graft by chemical part treatment.

Recently, modification of the surface of such MCM type solids was obtained by adding to the initial mixture of surfactant/water/(silica source) a $R'Si(OR)_3$ compound chosen

from compounds **1–9** (**1**⁴⁰, **2**⁴⁰, **3**^{32,39}, **4**⁴¹, **5**⁴⁰, **6**^{32,41,42}, **7**^{32,41}, **8**^{43,44}, **9**⁴¹). Adding a $R'Si(OR)_3$ compound to the mixture (or using it as a pure compound) allows the micellization and polycondensation/hydrolysis processes. After drying and elimination of the surfactant, a mesoporous material is obtained as depicted in Figure 4. Generally, the organic group is described as robustly bounded to the silicate structure, with a distribution at the surface of the wall which appears to be more uniform in nature than those obtained by post-treatment of mesoporous silica^{32,39}.



Cage compounds. Another important use of $RSi(OMe)_3$ compounds is in the preparation of compounds with nice cage architecture as depicted in Figure 5 is well-known now, but it is still attractive since it offers access to well-defined building units for hybrid materials. The most recent developments in this field concern the preparation of silsesquioxanes with liquid crystal properties,⁴⁵ silsesquioxanes as building blocks of a three-dimensional structure^{46–49} and silsesquioxanes that mimic zeolite structures with an incompletely condensed structure (open cage) or with incorporation of other metals.

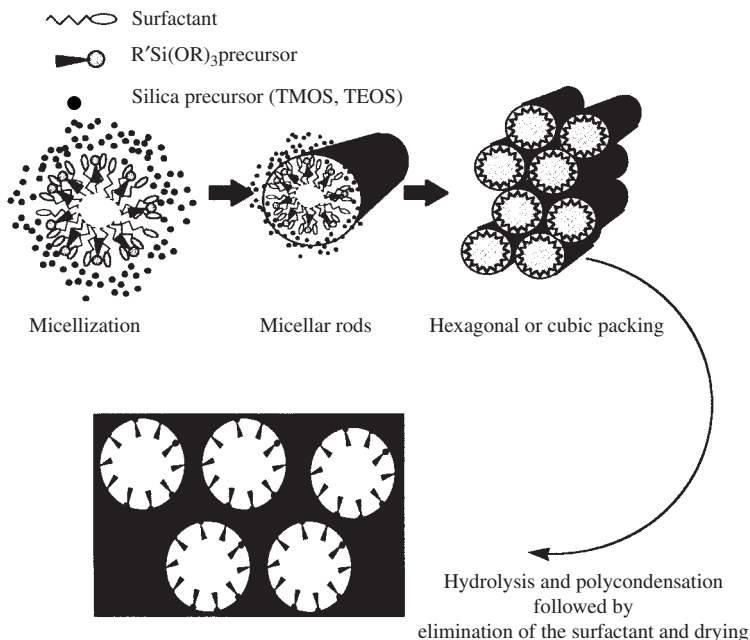


FIGURE 4. Schematic pathway of the elaboration of mesoporous organically modified silica by surfactant templating and micelle formation

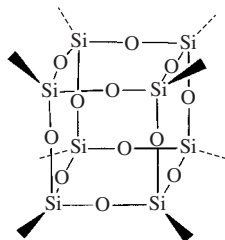


FIGURE 5. Cage structure for silsesquioxane T_8

ORMOSILs. $RSi(OR')_3$ structures can also be used to prepare covalent-extended solids. They are usually known as ORMOSILs (organically modified silicates) or ORMOCER (organically modified ceramics) and they are part of the nanostructured solid family. The formation of glassy solids is mainly dependent on both the nature of the R' group and the hydrolysis/polycondensation conditions^{7,50–52}. In contrast to the nanocomposites, all these solids always appear as a homogeneous single phase at the micro- or the macroscopic scale. The organic and inorganic moieties cannot be separated by the analytical techniques, since all the atoms are covalently bonded. Due to the existing possibility of introducing a very different and reactive R' group, many applications are currently being developed, some of them already available on the market place for

insulation, sealing and coating⁵³. Examples taken from the recent literature describe them for potential applications as metasilicon-oxycarbide ceramic precursors^{54–56}, supports for catalyst^{57–60}, photochromic^{61,62}, photoluminescent⁶³ and optical materials⁶⁴, thin film materials with mechanical^{65–67}, thermomechanical^{68–72}, photopatternable^{73,74}, and low dielectric properties^{75,76}.

Interpenetrated framework and structure. A more fundamental aspect of these materials arises from their structure when in the starting precursor, for example **10**, a sol-gel polymerizable function $-\text{Si}(\text{OR})_3$ and an R' free-radical polymerizable group (methyl methacryl, vinyl, allyl or epoxy groups) are combined. In this case, the formation of the solid can follow two different pathways: (a) hydrolysis of the SiOMe bonds followed by free-radical polymerization of the unsaturated group in the solid state (**10A**) or (b) polymerization of the unsaturated function followed by hydrolysis of the SiOMe bond in the solid state (**10B**); see Scheme 3. In both cases, materials finally form a monocomponent system, however with different homogeneity and short-to-medium range organization that make **10A** and **10B** different from this point of view. Similarly, for dichlorovinylsilane (**11**) the elaboration of the solid can be achieved following the two routes described in Scheme 4. Here, the hydrolysis of the Si–Cl bonds can be performed either after or before hydrosilylation between the Si–H and Si–vinyl bonds⁷⁷, materials **11A** and **11B** are completely different in their texture and composition. As a consequence, their pyrolytic decomposition into oxycarbide is different in the early stage.

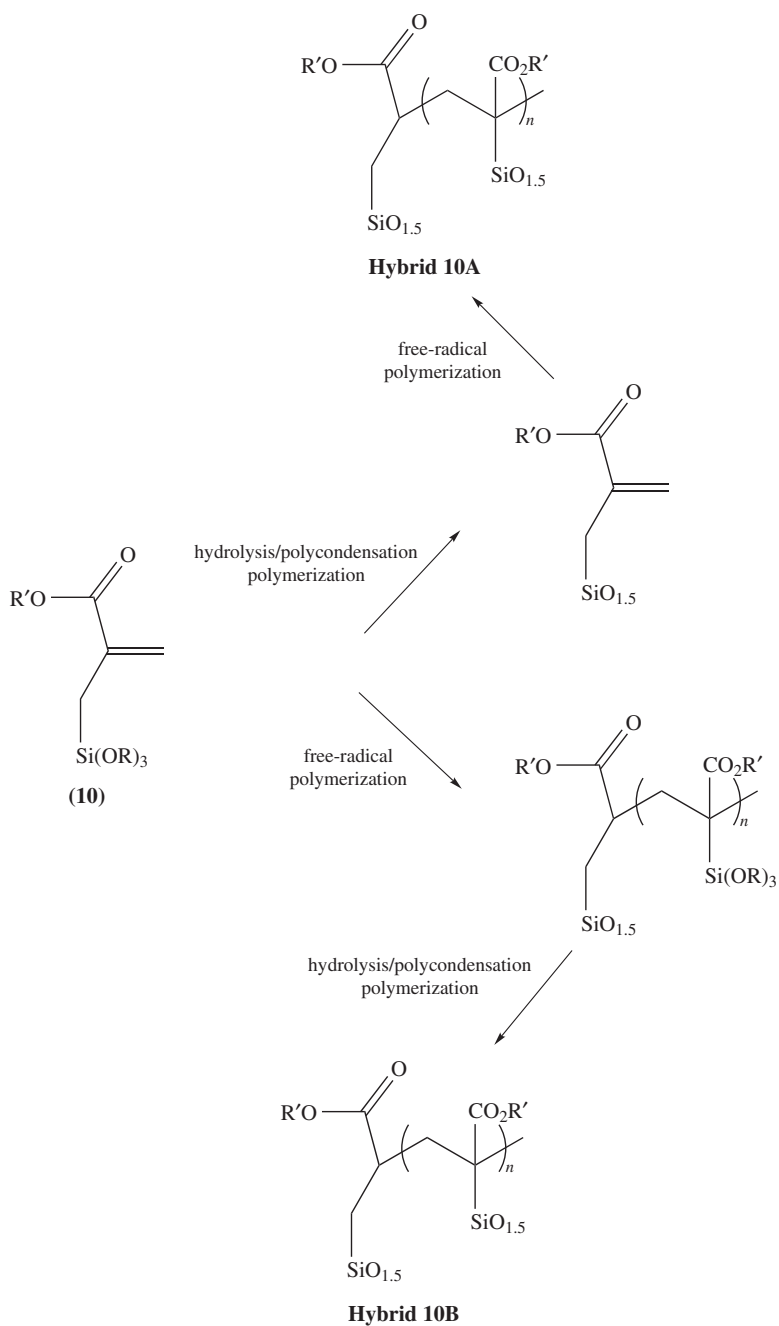
The effect of binding the organic group to the silica network can provide a higher chemical and physical stability compared to a nanocomposite. However, the formation of micro-domains cannot be excluded and this phenomenon is certainly enhanced by increasing the hydrophobicity and the steric hindrance of the organic groups. As a result, the organic part of the precursor is mainly located at the surface of the resulting solid, as demonstrated by the detection of specific organic fragments by TOF SIMS (time of flight secondary ion mass spectroscopy). Some examples are given in Table 1^{78,79}.

This fact is corroborated by the chemical reactivity of these materials: R groups located at the surface are chemically accessible and highly reactive. For example, complexation of phenyl groups of a $\text{C}_6\text{H}_5\text{SiO}_{1.5}$ xerogel by $\text{Cr}(\text{CO})_3$ in phenyl/silsesquioxanes is easy⁸⁰ and $\text{HSiO}_{1.5}$ can be transformed to siliconoxynitride by reaction in a flow of NH_3 ⁸¹.

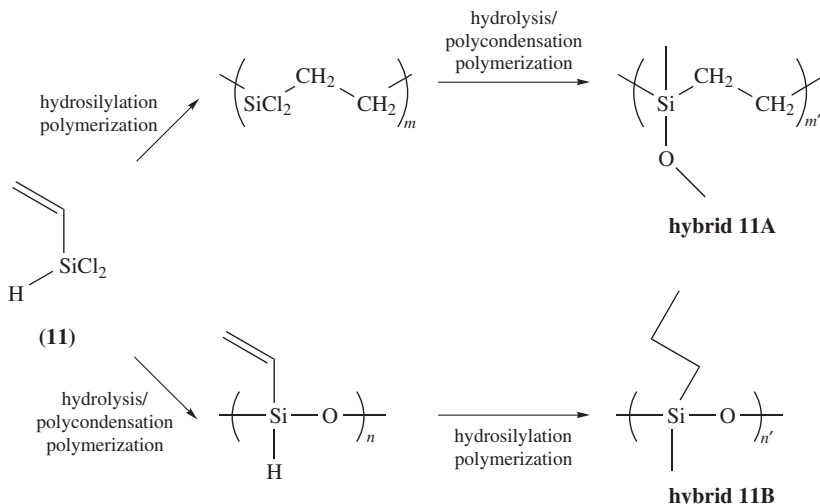
Another limitation of the silsesquioxane approach is evident when a non-linear optic NLO dye is used as the R' group. For these chromophores, relaxation is dependent on the rigidity of the matrix. Their anchoring to one $-\text{SiO}_{1.5}$ unit was found to be insufficient to achieve a highly cross-linked Si–O–Si network around the NLO chromophore and its relaxation could not be restricted. As a consequence, the order that is initially induced in the material by an electrical field pooling effect is lost upon ageing^{82,83}.

C. Nanostructured Hybrid Material Monocomponent with At Least Two Si–C Bonds – Organo-polysilsesquioxanes $\text{R}'(\text{SiO}_{1.5})_n$ ($n \geq 2$)

Precursors with at least two $-\text{SiX}_3$ groups have been developed in the last 10 years. Their general formula $\text{R}'(\text{SiX}_3)_n$ ($n \geq 2$) can present different architectures depending on n , their location on the molecule and the presence of a spacer between the $-\text{SiX}_3$ group and the central part. A higher homogeneous distribution of the organic fragments in the solid was expected due to the possibility of forming a monophasic material^{8,9,84–87}. It is important to emphasize that there is no example of such a precursor being unable to achieve the formation of a solid; in other words, there are efficient building blocks



SCHEME 3



SCHEME 4

TABLE 1. Ions detected by TOF SIMS analysis of different nanostructured hybrid xerogels

Hybrid xerogel	<i>m/z</i> of Ions detected by TOF SIMS analysis
CH ₃ SiO _{1.5}	15 CH ₃ ⁺ , 43 CH ₃ Si ⁺
ICH ₂ CH ₂ CH ₂ SiO _{1.5}	127 I ⁺ , 141 ICH ₂ ⁺ , 155 (ICH ₂ –CH ₂) ⁺
H ₂ NCH ₂ CH ₂ CH ₂ SiO _{1.5}	30 (CH ₂ =NH ₂) ⁺ , 44 H ₂ N–CH ₂ –CH ₂ ⁺
[1-(NMe ₂ –(SiO _{1.5}))]C ₆ H ₄	58 (CH ₂ =NMe ₂) ⁺ , 134 (C ₆ H ₁₂ N) ⁺
C ₆ H ₅ NHCH ₂ CH ₂ CH ₂ SiO _{1.5}	106 (CH ₂ =NHC ₆ H ₅) ⁺ , 77 (C ₆ H ₅) ⁺
(C ₆ H ₅) ₂ PCH ₂ CH ₂ SiO _{1.5}	109 C ₆ H ₅ PH ⁺ , 123 (C ₆ H ₅ PCH ₃) ⁺
	183 C ₁₂ H ₈ P ⁺ , 185 (C ₆ H ₅) ₂ P ⁺
Fe[η ⁵ –(C ₅ H ₄)SiO _{1.5}][η ⁵ –(C ₅ H ₅)]	56 Fe ⁺ , 121 FeC ₅ H ₅ ⁺ , 65 C ₅ H ₅ ⁺
Fe[η ⁵ –(C ₅ H ₃)SiO _{1.5} (CH ₂ NMe ₂)] [η ⁵ –(C ₅ H ₅)]	56 Fe ⁺ , 58 (CH ₂ =NMe ₂) ⁺
	121 (FeC ₅ H ₅) ⁺

for the preparation of solid materials by a sol-gel process. Moreover, in almost every case, the integrity of the organic group is preserved and remains unchanged in the final xerogels.

The required criteria are the existence of both non-hydrolysable non-oxidizable Si–C bonds and at least two Si–O–Si building units such as –Si(OR)₃ groups. However, other possibilities are the use of R'(SiR¹X₂)_n (*n* ≥ 2) systems⁸⁸ or even R'(SiR¹R²X)_n (*n* ≥ 2), or to co-condense the precursor with other polymer precursors like TMOS or TEOS, R¹R²Si(OR)₂ or R'Si(OR)₃. We will briefly consider them here, since they were reviewed recently⁸⁹. However, comparison of these systems with (RO)₃Si–R'–Si(OR)₃ is certainly pertinent and fruitful, since substitution of the Si–X function by an alkyl group increases the hydrophobic property of the material and should reduce cross-linking of the material. For instance, the materials described by Lindner and coworkers⁸⁹ exhibit swelling properties with organic solvents. This behaviour closely resemble that of cross-linked or

high molecular weight linear organic polymers. This is never observed with the hybrid nanostructured materials prepared from $R'(SiX_3)_n$ ($n \geq 2$) precursors.

III. SYNTHESIS OF NANOSTRUCTURED ORGANO-POLYSILSESQUOXANES $R'(SiO_{1.5})_n$ ($n \geq 2$). SOME ASPECTS OF PRECURSORS AND GEL CHEMISTRY

A. The Family of $R'(SiX_3)_n$ ($n \geq 2$) Precursors

Compounds **12–38** in Chart 1 (**12**⁹⁰, **13**^{91–93}, **14**^{92,94,95}, **15**⁹⁶, **16**^{97–99}, **17**^{93–95}, **18**^{100,101}, **19**^{93–95}, **20**^{102,103}, **21**^{80,104–106}, **22**¹⁰⁷, **23**¹⁰⁷, **24**¹⁰⁸, **25**^{109,110}, **26**¹¹¹, **27**¹¹², **28**¹¹³, **29**¹¹⁴, **30**¹¹⁵, **31**¹¹⁶, **32**^{117,118}, **33**¹¹⁹, **34**^{83,120}, **35**¹²¹, **36**^{122,123}, **37**¹²⁴, **38**^{121–123,125,126}) correspond to *almost* all the precursors (or family of precursors) that have been reported at the present time. Only the central organic group is drawn and each free end is attached to a $-SiX_3$ group. It appears evident that many kinds of organic groups with very different structures and functions can be used, and we will see below how the nature of the organic part has an influence on the chemical, physical and textural parameters of the resulting hybrid material.

Once they are hydrolysed and polycondensed, the corresponding xerogels with the corresponding formula $R'(SiO_{1.5})_n$ ($n \geq 2$) are obtained. Two important comments must be kept in mind concerning the writing of this formula. First, it corresponds to a polymeric material and represents the fact that each silicon atom is linked to another one by a Si–O–Si linkage. Second, this corresponds to 100% condensation of the Si–OMe group, but this ideal situation is never observed (see Section IV). This formula is used in the subsequent text for convenience and because the precise level of condensation is rarely measured.

Also, in the rest of the text the same number will be used for the precursor and its corresponding xerogels for convenience. *It must be kept in mind that different xerogels can be prepared from the same precursor, depending on the sol-gel processing parameters. For example, a precursor can lead to xerogels with very different porosity, organization or level of condensation.*

B. Synthesis of the Precursors $R'(Si(OR)_3)_n$ ($n \geq 2$)

The synthesis of the precursors involves both organic and organosilicon chemistry. Silylation of organic molecules with a $-SiMe_3$ group is well-known and it may be achieved by classical methodologies¹²⁷. In contrast, the introduction of a $-Si(OR)_3$ group is much more difficult to achieve due to the reactivity of Si–OR moieties towards nucleophiles. We will see below how developments in organosilicon chemistry provide different chemical tools to introduce silicon-containing groups. Trialkoxysilyl groups $-Si(OR)_3$ (R=Et, Me, *i*-Pr) are the most commonly used polymerizable groups; however, $-SiCl_3$ ^{105,106} and $-SiH_3$ ^{128,129} can also lead to the Si–O–Si network.

The hydrosilylation/methanolysis reaction sequence. One of the most convenient methods is to use a sequence of hydrosilylation/methanolysis reactions as shown in equation 4 for the formation of **39**. This direct synthetic pathway was reported in cases of the alkyl family of precursors **12**⁹⁰. This sequence is also used for the preparation of dendrimers and arborols^{121,123}. Alternatively, hydrosilylation with $HSi(OEt)_3$ can be performed advantageously in the case of dendrimers^{125,126} but it is of more interest in the case of carbonate precursors **26**¹¹¹. Indeed, hydrosilylation of double bonds can be achieved selectively in the presence of a carbonyl group with hexachloroplatinic acid or a rhenium catalyst¹³⁰.

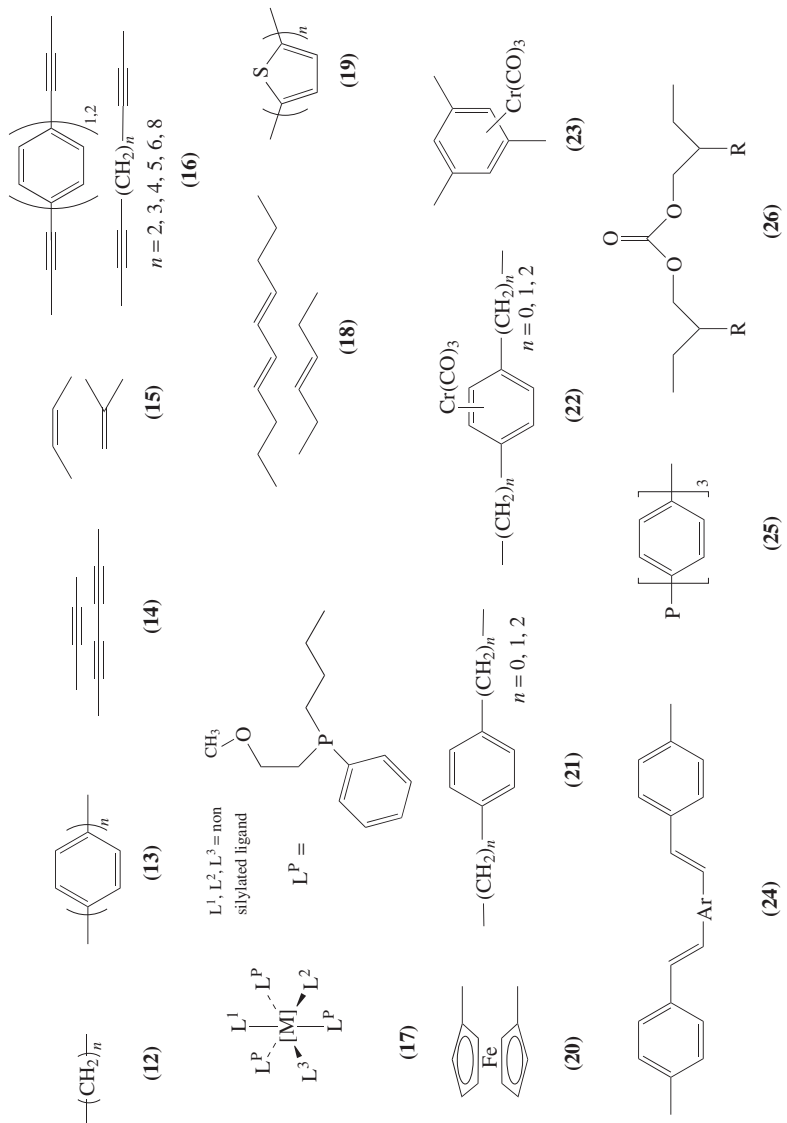
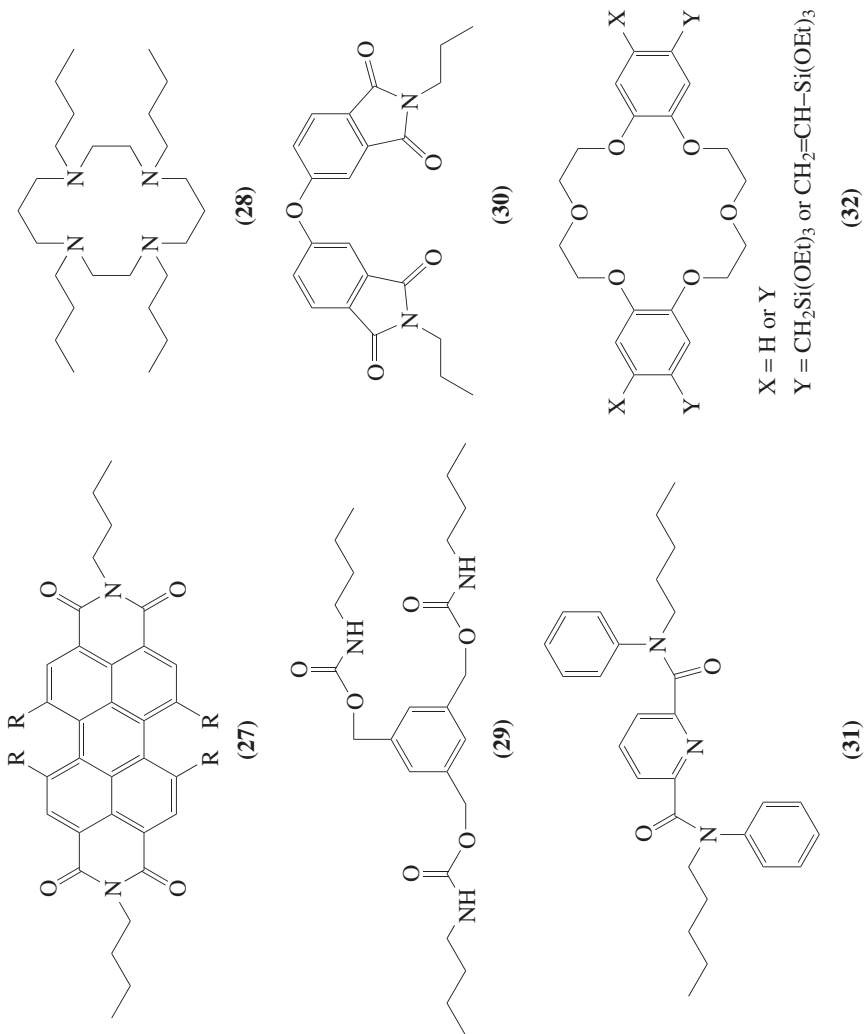


CHART 1



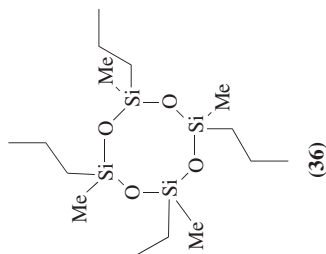
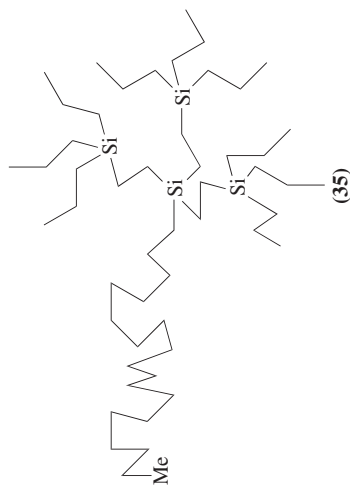
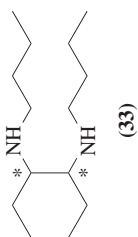
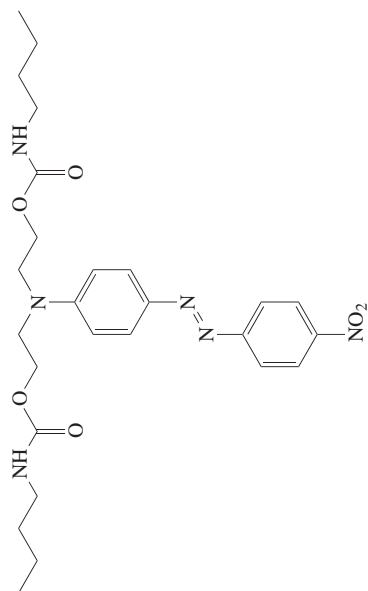


CHART 1. (continued)

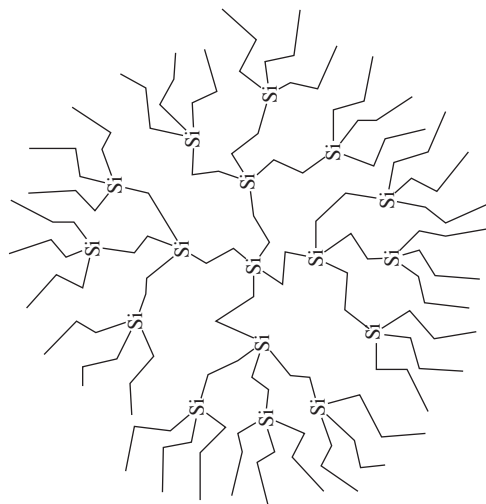
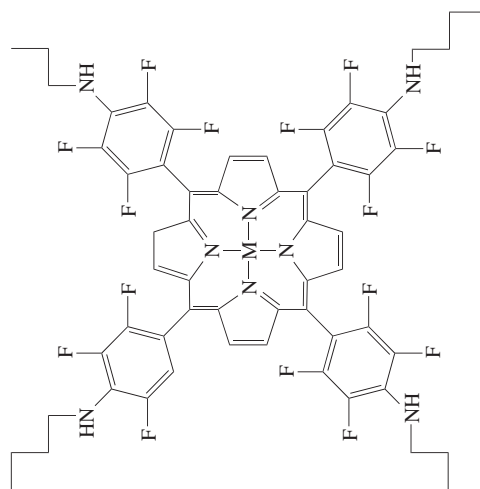
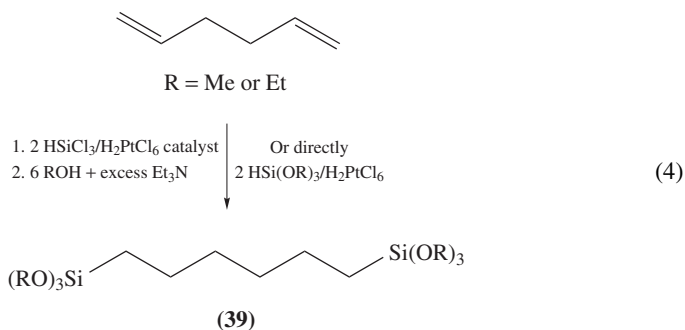
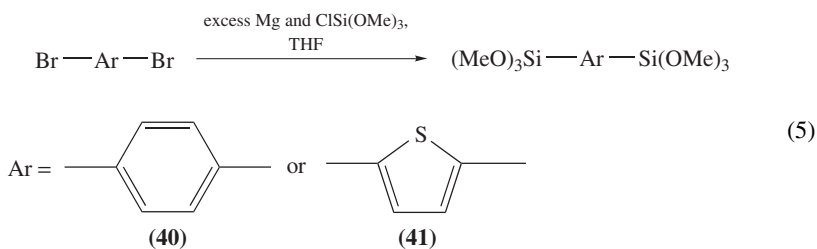


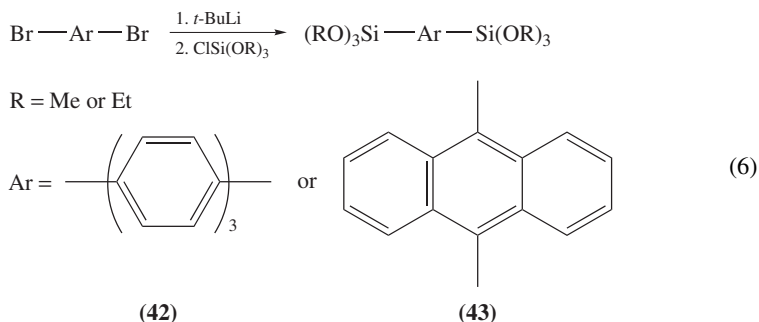
CHART 1. List of the R' organic or organometallic groups used in $R'(\text{SiX}_3)_n$ ($n \geq 2$) precursors. Each end in the structure is attached to an SiX_3 group



Calas–Dunogues reaction with a Grignard reagent. For precursor **40** carrying a substituted phenyl group or **41** carrying a substituted thiophene ring^{92,93}, replacement of the bromines in 1,4-dibromobenzene and 2,5-dibromothiophene by Si(OMe)_3 groups is achieved by a Calas–Dunogues reaction (equation 5)¹³¹.

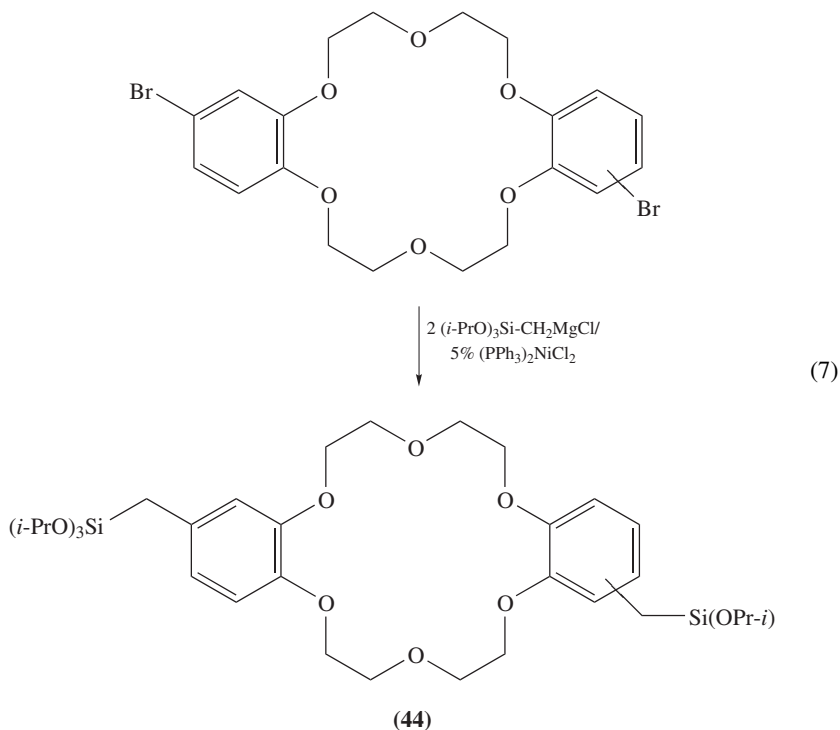


In using the halogenated organic group, an alternative is to form the lithiated compound, followed by silylation with chlorotrialkoxysilane. This was used in particular for the 1,1''' terphenyl precursor **42**, or the precursor with 9,10-anthryl group **43**. The expected compounds are obtained in good yields (equation 6)⁹².

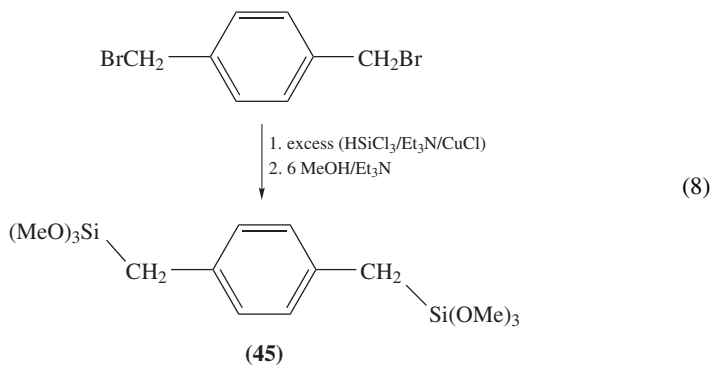


Grignard reagents such as $\text{ClMgCH}_2\text{Si(OPr-}i\text{)}_3$ ¹³² or $\text{BrMgC}_6\text{H}_4\text{Si(OPr-}i\text{)}_3$ ¹³³ are particularly interesting synthetic tools that present the general reactivity of a R-MgX function. Reaction of $4\text{-BrMg(C}_6\text{H}_4\text{)Si(OPr-}i\text{)}_3$ ¹³³ with PCl_3 was particularly efficient for the synthesis of the family of phosphine precursors **25**, which is not obtained in a straightforward reaction by other means¹⁰⁹. The reagent $\text{ClMgCH}_2\text{Si(OPr-}i\text{)}_3$ was also

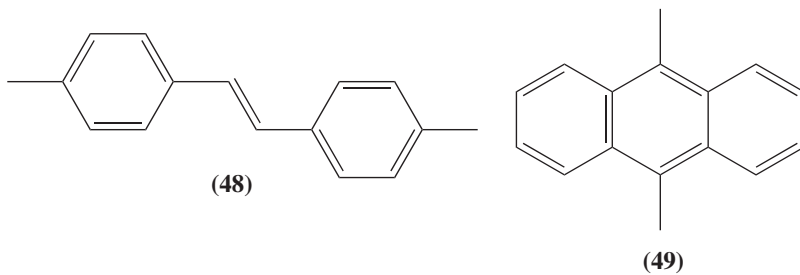
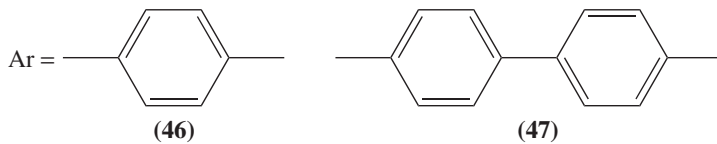
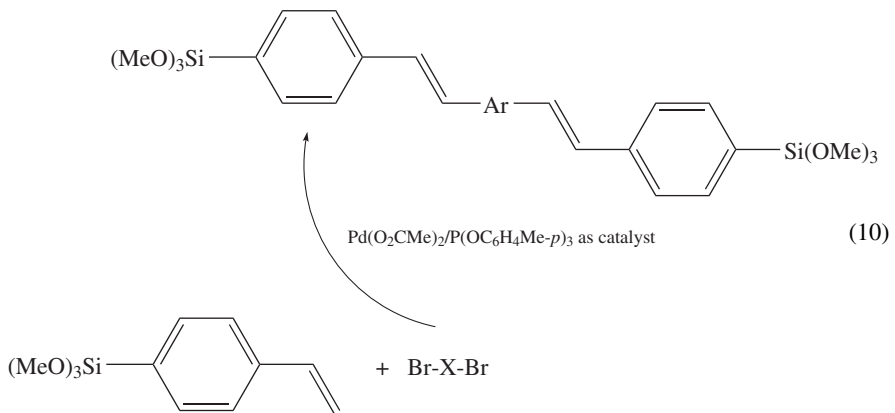
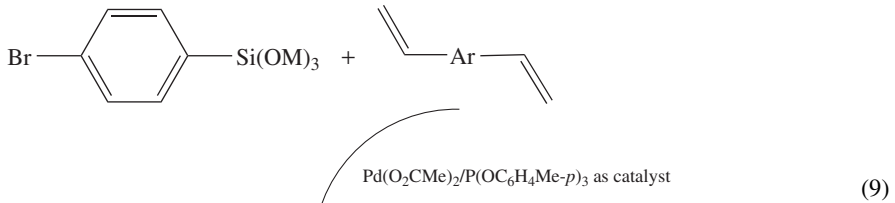
useful for the synthesis of the family of precursors **18** (by condensation on the 1,6-dibromoalkyl-2,6-diene)¹⁰⁰, or for the synthesis of the crown-ether precursor **44** according to equation 7^{117,118}.



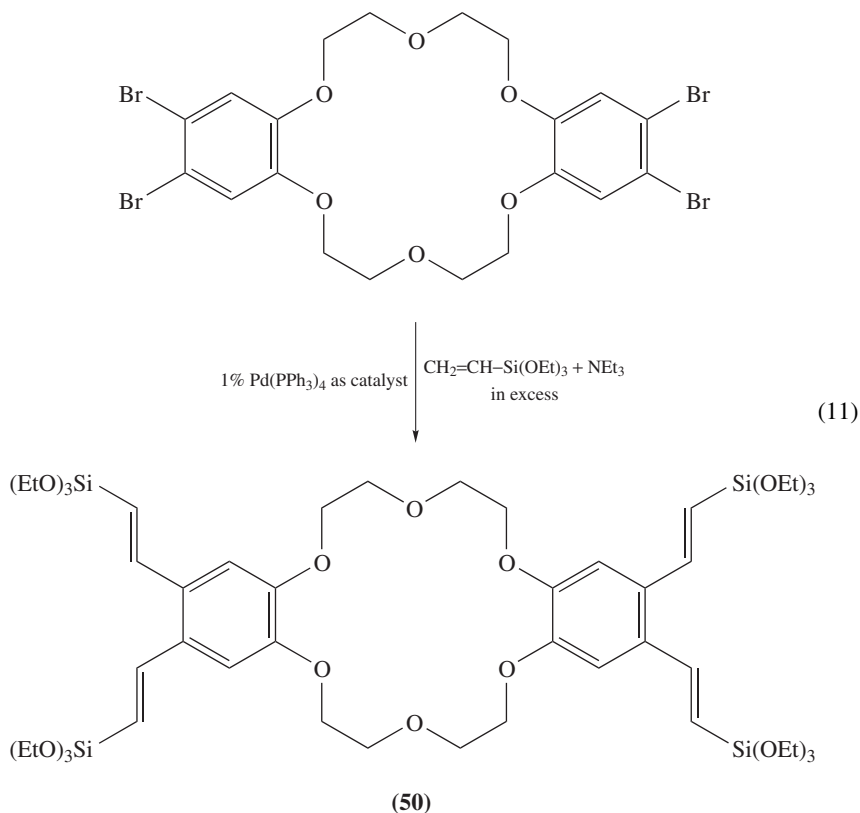
Benkeser reaction. Another general route is the Benkeser reaction, which allows efficient preparation of precursors with an allylic group. Via this reaction the benzylic precursor **45**¹³⁴ is also prepared by silylation and methanolysis of the Si-Cl bond (equation 8)^{93,100}.



The Heck-type reaction. The Heck reaction¹³⁵ (or some modified procedure of it) is certainly one of the most powerful tools used in the preparation of precursors with acetylenic and vinylic subunits. For instance, in the case of precursors **46–49** the synthesis is conveniently achieved by a cross-coupling reaction in the presence of palladium complexes as catalyst. Two pathways are possible, as represented by equations 9 and 10¹⁰⁸.

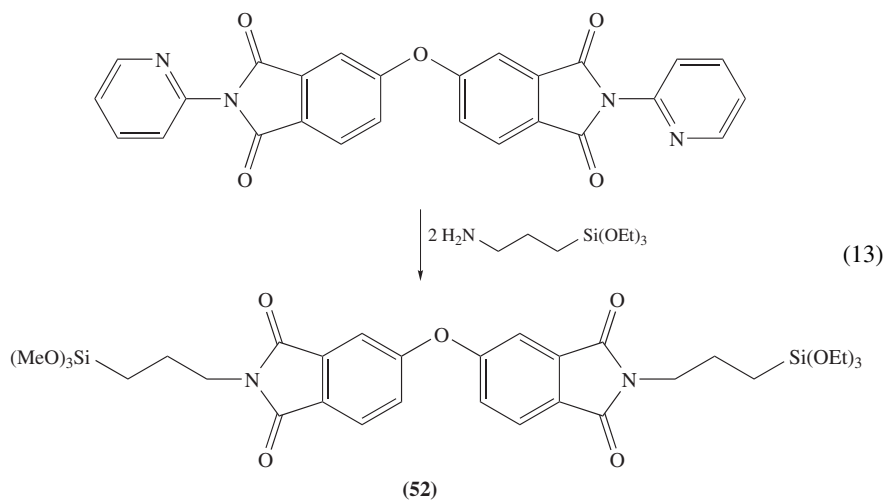
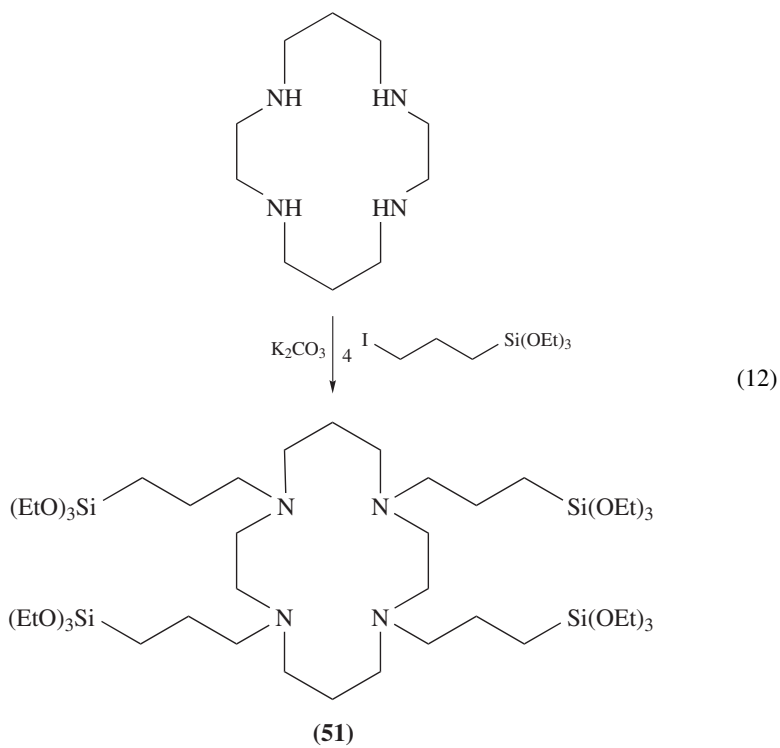


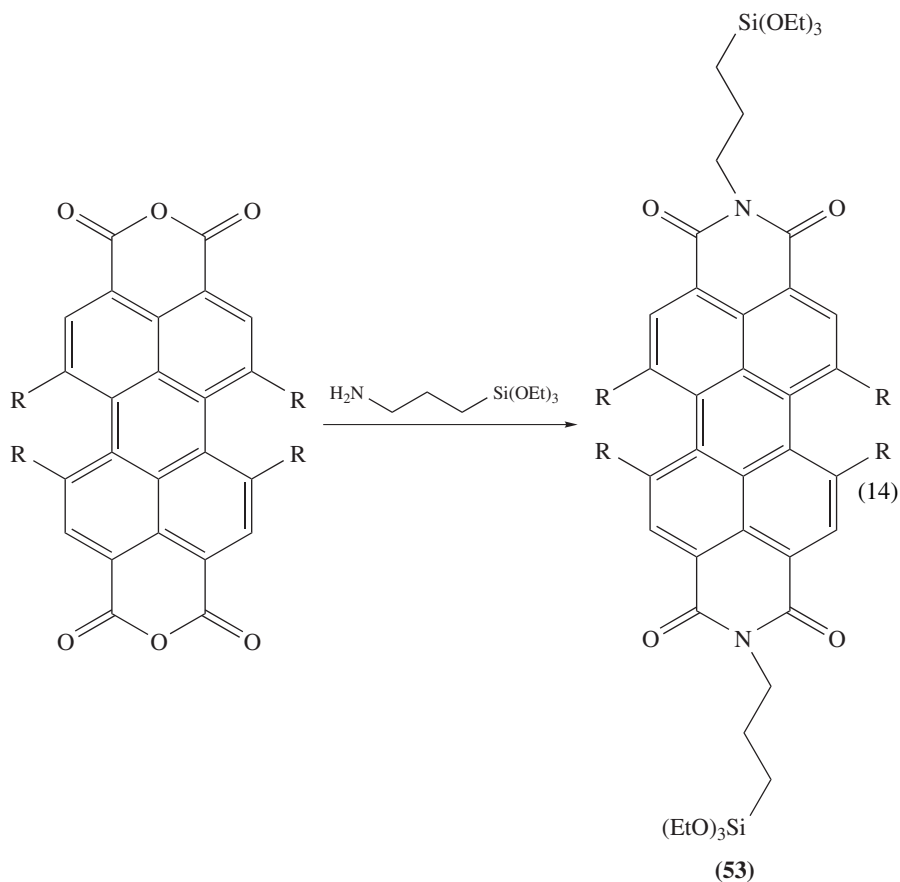
The same reaction was also used in the case of crown-ether precursors. For example, the synthesis of precursor **50** (equation 11) is achieved in high yield¹¹⁷. The same precursor with two silylated arms instead of four was also synthesized by the same route.



Alkyl-functionalized derivatives. Reagents with general formula $X-R'-Si(OR)_3$ are of very wide interest due to the possible use of different X groups such as NH_2 , I or $N=C=O$. Thus, for preparing cyclam precursors **51**, use of the iodo derivative of alkyl(trimethoxysilyl) or alkyl(triethoxysilyl) groups allows one to graft the appropriate $-Si(OR)_3$ -containing group on the nitrogen atom of the starting cyclam molecule (equation 12)¹¹³. In the same way, it is possible to react the $O=C=N-R'-Si(OR)_3$ derivatives with an amine or alcohol function to give urethanes which serve as precursors for hybrid materials.

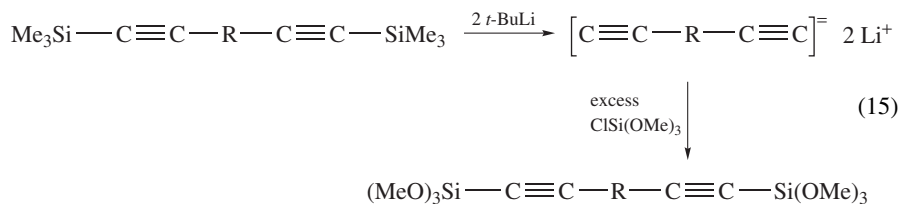
Reagents like $NH_2-R'-Si(OR)_3$ are useful for the synthesis of functional precursors with an imido group. This is possibly achieved by reacting the alkyl(trialkoxysilyl)amine with at least three types of substrates; (1) with a suitable carboxylic acid chloride^{114,116,120}, (2) by transimidation of bisimides, e.g. in the preparation of **52** according to equation 13¹¹⁵, and (3) by the imidization of an anhydride as in the preparation of **53** (equation 14)¹¹².

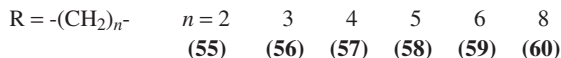
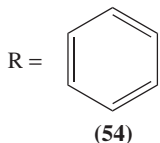




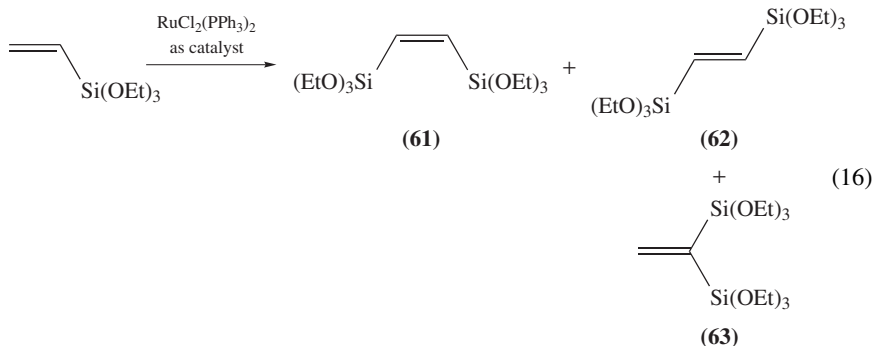
R = H, Ph, *p*-OC₆H₄OC₆H₁₃, *p*-OC₆H₄OC₄H₉

Miscellaneous reactions. For ethynyl-containing precursors like **54–60**, an efficient synthesis is the treatment of the dilithium (or disodium) acetylide intermediates with chlorotrialkoxysilane as a silylating reagent (equation 15). The reaction leads to moderate to high yields and is an alternative to the Heck reaction^{93,98,99}.



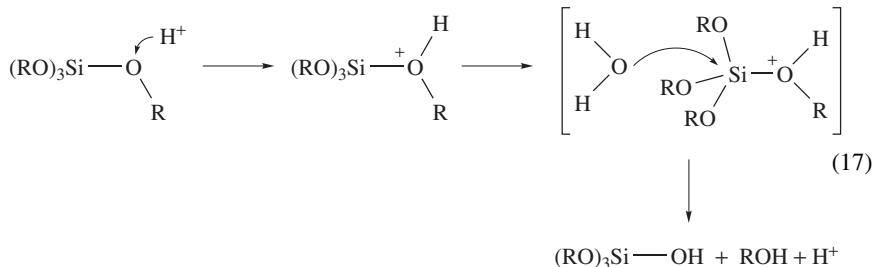


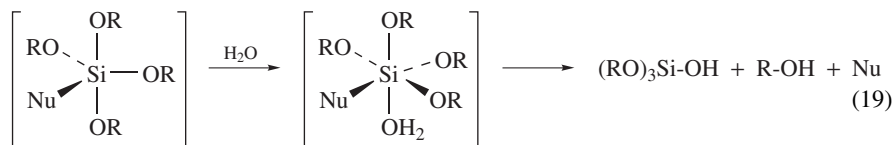
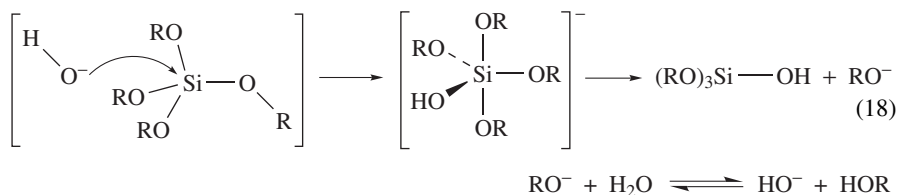
By reacting triethoxyvinylsilane with itself in the presence of a ruthenium catalyst, vinylic precursors **61–63** are obtained (equation 16)⁹⁶.



C. Particular Aspects of the Chemistry during the Sol-gel Polycondensation of $R'(\text{Si}(\text{OR})_3)_n$ ($n \geq 2$)

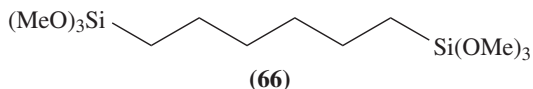
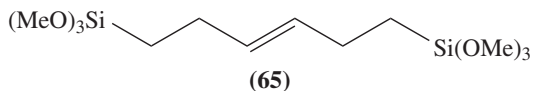
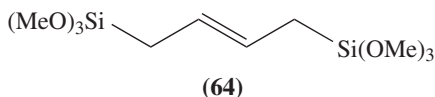
Hydrolysis of tetraalkoxysilane (TMOS or TEOS) is generally performed in the presence of a catalyst which can be an acid, a base or a nucleophile. This is also the case for the hydrolysis of $R'\text{Si}(\text{OR})_3$ ⁵⁰. In the case of TMOS and TEOS, the acid catalysis is due to the reversible protonation of the alkoxy group which converts it to a better leaving group. However, the nucleophilic attack of the oxygen atom of water is still a key step (equation 17). In the case of basic catalysis, nucleophilic attack of the OH^- anion at the silicon centre leads to a penta-coordinated intermediate, followed by the elimination of the RO^- group (equation 18). For nucleophilic catalysis (promoted by F^- , HMPA, imidazole, *N,N*-dimethylaminopyridine as well as OH^-) the formation of a penta-coordinated species (equation 19) increases the reactivity of the silicon atom towards the nucleophilic attack of water that leads to an hexa-coordinated intermediate, which finally leads to the product of hydrolysis or condensation.





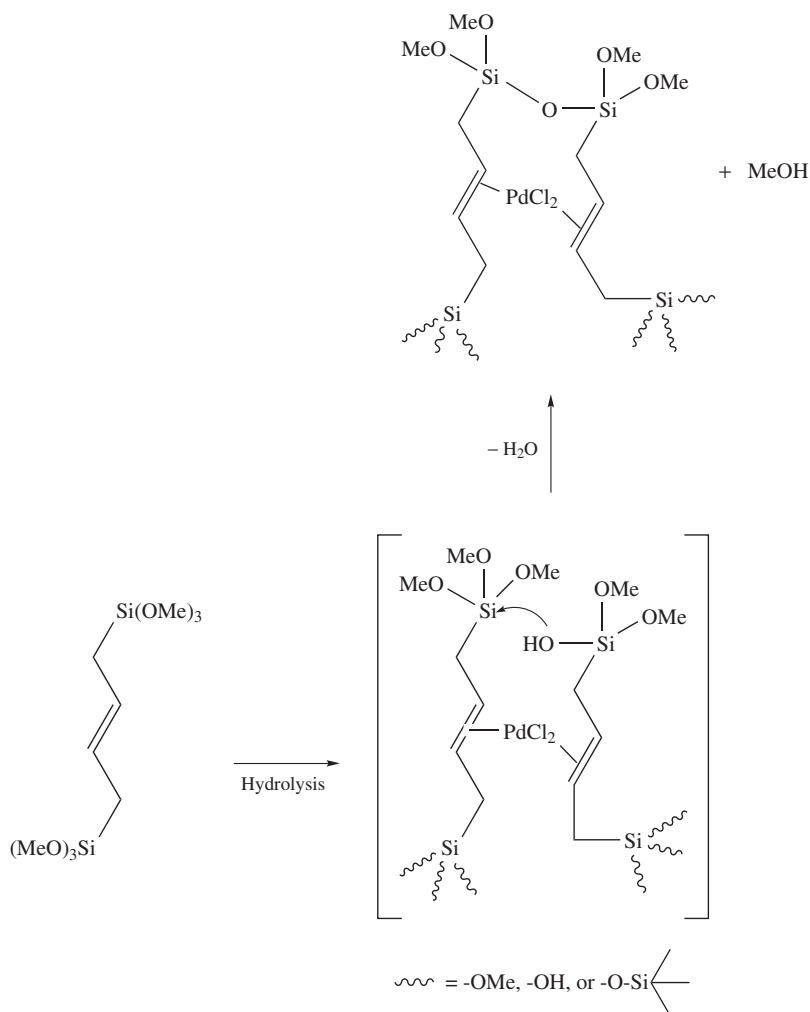
It is not in the scope of this chapter to focus on the mechanism of this reaction, which is reviewed extensively in the literature^{127,136}. However, it must be pointed out that these routes are well known in organosilicon chemistry. Moreover, the final material's texture is highly dependent on the experimental conditions and therefore on the chemistry at the molecular level^{4,8}. This suggests a strong kinetic control in the preparation of the solid; however, the precise relation between the chemical processes and the texture remains difficult to precisely define and this is certainly also the case for the hybrid material presented in Section IV.

When looking at the chemical reactions involved in the sol-gel polycondensation/hydrolysis of $(\text{MeO})_3\text{Si}-\text{R}-\text{Si}(\text{OMe})_3$, it can be assumed that the mechanisms proposed for the catalytic hydrolysis of TEOS and TMOS are still pertinent. However, there are variations in the rate and activation energies due to electronic and steric influences of the organic group. For example, precursors with α,ω -bis(ethynyl)alkyl groups **54–60** are highly reactive and their gelation occurs in a few minutes without any catalyst^{98,99}. In contrast, all the other precursors exhibit a much lower reactivity, and a catalyst is always necessary to obtain the gelation within hours or days.



Another example is the template-assisted hydrolysis/polycondensation of precursors with a C=C bond in the unit that can be bonded to a metal centre like precursors **64** and **65**^{93,101}. The templating effect of palladium(II) compounds was readily demonstrated by the gelation time which is 100 times smaller for **64** when the Pd(II) compound is present. In contrast, the presence of the same palladium(II) compound has no effect on

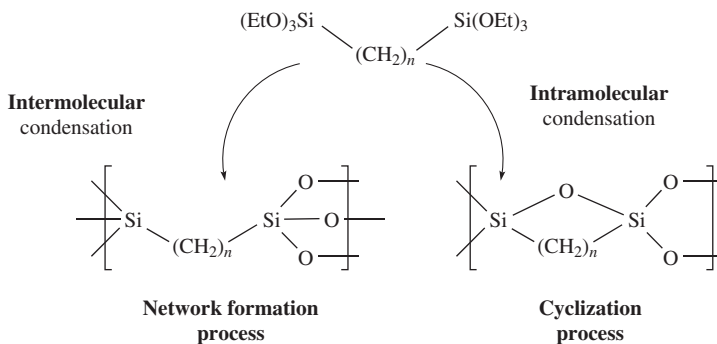
the gelation of **66**. In addition, 80–100% of the palladium(II) was trapped in the hybrid xerogel obtained from an unsaturated precursor, while only a few percent remained in the xerogel of the saturated precursor **66**. The molecular association between palladium(II) and the double bonds is well known¹³⁷ and its presence in the xerogel is also demonstrated by the absence of catalytic activity in a hydrogenation reaction. Formation of an η^2 -olefin complex during the sol-gel process is assumed as depicted in Scheme 5.



SCHEME 5

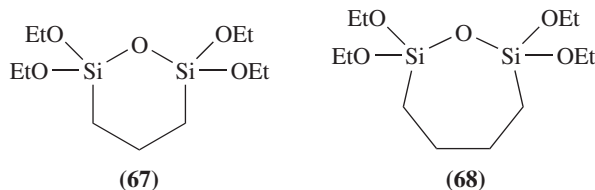
An important aspect of the relationship between the precursor's structure and the chemical process is evident when considering the possibility of having either an intra- or an inter-molecular polycondensation as depicted in Scheme 6. These phenomena have at

least two important implications. First, in contrast to the inter-molecular polycondensation, cyclization does not directly assist the elaboration of the three-dimensional network of the gel. Second, the structures of the units in the gel and in the final xerogel are completely different.



SCHEME 6

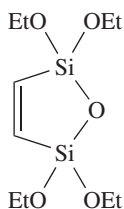
Of course, this competition with the intra-molecular polycondensation can only exist if the structure of the precursor permits it, as is the case for α,ω -bis(trialkoxysilyl)alkylenes where the flexibility of the chain allows the cyclization phenomenon. This was found to be particularly important for $n = 3$ and 4 and for gel prepared in acidic conditions. Compounds **67** and **68** were isolated and characterized^{138,139}.



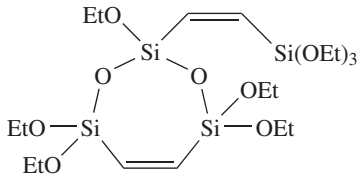
On the contrary, the cyclization phenomenon is limited either when n is $<3-4$ or $>3-4$, or by using basic conditions. The condensation-cyclization phenomenon is exhibited by a downfield shift of the ^{29}Si NMR signals compared to that of the starting precursor (consistent with a Baeyer strain effect) and is different from an upfield shift observed for an acyclic condensation. Among other data, the longer gelation time observed for $(\text{EtO})_3\text{Si}(\text{CH}_2)_n\text{Si}(\text{OEt})_3$ ($n = 3, 4$) in acidic conditions than under basic conditions is consistent with the cyclization phenomenon that prevents the formation of the three-dimensional Si-O-Si network. Interestingly, the isolated compounds **67** and **68** can also be used as precursors. The formation of a solid by their polycondensation in basic conditions may involve ring opening, providing evidence for the possible reversibility of the formation of the Si-O-Si unit in these cases.

A similar phenomenon was also studied when comparing the gelation process of bis(trimethoxysilyl)ethene precursors **61-63**¹⁴⁰. As a consequence of the different precursors' structure, cyclization of **61** and **63** apparently leads to the respective cyclic compound **69, 70** and **71** while no cyclization is observed for **62** having the *trans* geometry. Here again acidic conditions were found to promote the cyclization phenomenon while basic

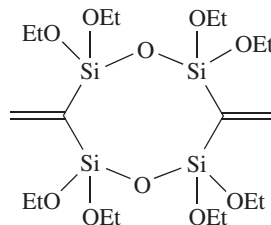
conditions favoured the intermolecular process. The kinetics of the cyclization appear as an important parameter that not only influences the gelation time but also affects the final structure of the xerogel, since the resulting cyclic or open structure is part of the final material's architecture¹⁴¹.



(69)



(70)



(71)

Finally, it should be mentioned that such intramolecular polycondensation is certainly an important phenomenon when a crowded structure forces the $-\text{Si}(\text{OR})_3$ groups to be close to each other. This is particularly the case for dendrimer precursors^{121,125} or related star gel precursors^{142,143} due to the proximity of the hydrolysable functions.

All these results clearly demonstrate the effect of the geometrical differences of the organic groups in the precursors. This is a parameter that can influence the chemical processes, modifying the kinetics or introducing particular phenomena like templating or cyclization. At the end of the process, the characteristic of the xerogel demonstrates the effect of these parameters. However, it is difficult to precisely interpret and quantify this effect due to the complexity of the mechanisms involved in the sol-gel process. Moreover, other parameters such as the solvent and the temperature can modify the texture and structure of the final xerogel (see Sections IV and V).

IV. KINETIC CONTROL OF THE SOLID'S CHARACTERISTICS OF NANOSTRUCTURED ORGANO-POLYSILSESQUIOXANES $\text{R}'(\text{SiO}_{1.5})_n$ ($n \geq 2$)

The characterization of a solid must be considered at different levels. The first one is the sum of its textural characteristics which corresponds to the classical identification of the solid in terms of its granulometry, specific surface area, pore volume, porosity and density.

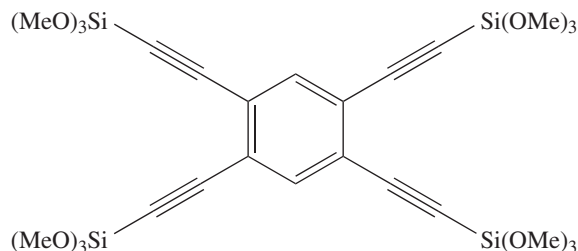
A second type of characterization can be made at the molecular level. The presence of the organic groups is taken into account as well as their distribution in the solid, with a possible organization of building molecular units at a short or a long range. In addition, the architecture of the inorganic framework has to be described by its degree of cross-linking that is connected to the level of polycondensation of the $\text{Si}-\text{O}-\text{Si}$ framework.

Finally, the description of the solid's surface is important since it is in contact with the other compounds of the media. Therefore, the information about the surface must be combined with the description of the material at the molecular and textural levels in order to represent its catalytic activity, complexation properties, molecular sieving effect etc.

A. Polycondensation and Integrity of the Organic Group

The molecular structure of the hybrid xerogel is generally investigated by NMR techniques like ^{13}C and ^{29}Si cross-polarization magic-angle spinning (CP-MAS NMR). In almost all studies, ^{13}C NMR spectroscopy is used to characterize the xerogel obtained

after ageing and drying. The first purpose is to reveal the presence of the residual Si—OR functions left after the hydrolysis/polycondensation. However, interest in this analysis is also to point out the conservation or loss of the Si—C bond, which is particularly important since the presence of this bond is one of the key parameters for these materials. In addition, it is generally possible to control the integrity of the organic group itself after sol-gel processing. For example, the complete hydrolysis of the Si—C_{s/p} bond by chemical treatment of the xerogel with precursor **72** was demonstrated by ¹³C NMR spectroscopy, which revealed a C≡C—Si signal at 89 ppm before chemical treatment and a C≡C—H signal at 81 ppm after the treatment, and by ²⁹Si NMR spectroscopy, which revealed the presence of Tⁿ groups (cf. Table 2) before treatment and the presence of only Qⁿ groups after treatment, although it was not possible to remove the organic groups from the solid⁸.



The ²⁹Si CP-MAS NMR spectroscopy is another useful technique because it could be used for investigating the degree of condensation^{144–147}. With the increased extent of the condensation, Si—OR bonds (R=H or Me, Et) are replaced by Si—O—Si bonds. The ²⁹Si signal is shifted towards high field (it should be noted that the variation of the chemical shift between the Si—OMe bond and the Si—OH bond is too small to be detected due to the broadness of the solid state NMR signals). Depending on the number of hydrolysed and polycondensed Si—OR groups, the Tⁿ units are identified (for nomenclature, see Table 2). Thus, increasing T³ corresponds to an increasing level of condensation and cross-linking while, on the contrary, increasing number of the T⁰ unit corresponds to a low degree of polycondensation and cross-linking.

In all cases a 100% level of condensation (i.e. only a T³ signal) was never achieved, regardless of the organic group used. Instead, the signals corresponding to T¹, T², T³ (and in some cases T⁰) units are always present, although with various relative intensities. Concerning the quantitative aspect of this measure, it must be pointed out that the peak

TABLE 2. Nomenclature for the different silicon species depending on the level of condensation

T ⁰	T ¹	T ²	T ³

R=H, CH₃, CH₂CH₃, etc.

intensity may not accurately represent its population in the sample and the information is mainly qualitative¹⁴⁸. Indeed, in the CP sequence the intensity of the signal is closely dependent on both the distance to and the number of hydrogen atoms in the silicon atom's environment.

Quantitative measurement can only be obtained by determining the contact time (time of energy transfer from the proton to the silicon) and the relaxation time that allows all the signal intensity to be recovered for all the types of silicon atoms. This was done in only very few cases, mainly for xerogels prepared from precursors **40**, **45** and *p*-(MeO)₃Si(CH₂)₂(C₆H₄)(CH₂)₂Si(OMe)₃ (**73**)^{192,149}. In these cases, quite similar results (with variation of 5–10%) were obtained by quantitative measurement of the intensity of the signals and a classical CP MAS sequence. This was attributed to the presence of hydrogen atoms in the close environment of the silicon atom due to the proton-rich organic group attached to it. On the other hand, when a hydrogen-free carbon atom is linked to the silicon as for xerogels **54**, the T³ signal's intensity is significantly lowered by CP MAS ²⁹Si NMR spectroscopy, whereas its relative intensity is increased by more than 50% with an appropriate sequence¹⁵⁰.

In almost all studies, the authors have tried to modify the degree of polycondensation by changing the intensity of at least one kinetic parameter, generally the catalyst. For instance, for xerogel **73** it was found that acidic conditions gave a lower degree of polycondensation than by base-catalysed conditions⁹². For arylene xerogels **73** it is clear from Figure 6 that (*n*-Bu)₄NF in THF as a solvent leads to a much higher degree of polycondensation than NH₄F in the same solvent^{107,149,151}. In addition, for the same catalyst, changing the solvent also has a strong effect, leading to either an increase or a decrease in the level of condensation.

Quantitative determinations of the degree of polycondensation in systematic studies have demonstrated that kinetic parameters such as the temperature have little effect on the level of polycondensation in xerogels **40** and **73**, and the solvent has a more important effect^{149,151,152}. Variations of 5 to 20% are observed like those presented in Table 3. From these data and those shown in Table 4, it is evident that the degree of polycondensation and the textural properties of the xerogels are generally not related for these precursors. A variation of ±5% of the degree of polycondensation is measured while the specific surface area is increased 10 fold.

B. Texture/Kinetic Parameters of the Sol-gel Process

The texture of materials obtained by the sol-gel process is highly dependent on the experimental conditions, as already demonstrated in the case of many mineral oxides^{3,4,153,154}. Along with the gelation time, the specific surface area, the porosity, the pore volume and the granulometry change with all the sol-gel processing parameters such as temperature, solvent, catalyst and concentration of the reagents (and possibly pressure). Nevertheless, it is not possible at present to correlate the different studies on these hybrid materials since very different experimental conditions are used by different authors.

Temperature of the sol-gel processing. Only in cases of the xerogels **40**, **73** and **74** has a systematic study demonstrated how much the texture is temperature-dependent. From data in Table 4, an increase in the temperature of the perforation of the gel leads to a decrease in microporosity, an increase in mesoporosity and an increase in specific surface area¹⁵⁵. It also appears that the texture of the material is not directly correlated to the degree of polycondensation (see Table 3)^{151,152}. The same effect was also found for the xerogel P(C₆H₄SiO_{1.5})₃ (30 m² g⁻¹ at 20 °C and 340 m² g⁻¹ at 60 °C)¹⁰⁹.

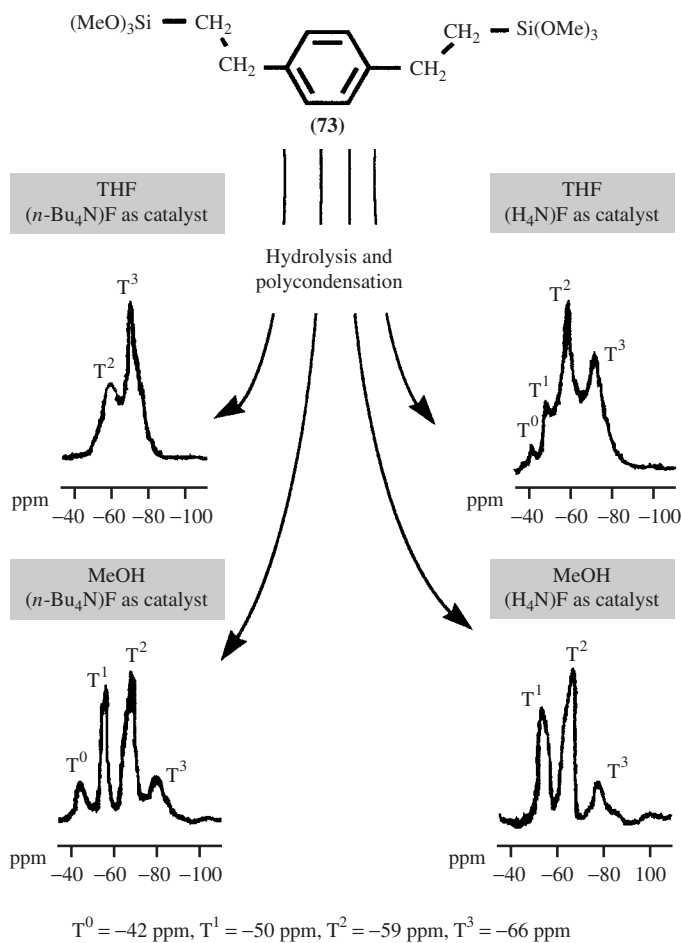


FIGURE 6. CP MAS ^{29}Si solid state NMR spectrum showing the different level of condensation of xerogels $p\text{-O}_{1.5}\text{SiCH}_2\text{CH}_2\text{C}_6\text{H}_4\text{CH}_2\text{CH}_2\text{SiO}_{1.5}$ prepared in different experimental conditions

Nature of the solvent. For xerogels prepared from precursor **54**, a high specific surface area with microporosity is obtained when prepared in methanol while non-porous material is obtained when prepared in THF^{97,98}. This was also demonstrated in the case of xerogels of **40** and **73** of bis-silylated precursors and in the case of xerogels **73t** of a tri-silylated precursor (Table 5)^{149,152,155}.

Nature of the catalyst and its concentration. In the case of hydrolysis/polycondensation of **40** and **73**, the effect of the nature and concentration of the catalyst was investigated by using one of the following catalysts: TBAF, HCl, NaOH, DMAP or NMI. Changing the catalyst modifies both the specific surface area and the relative percentages of micro- and mesopores (Table 6)^{149,152,155}.

TABLE 3. Comparison of the level of condensation of xerogels **40** and **73**

Xerogel	Temperature (°C)	Level of condensation (%)
<i>p</i> -O _{1.5} Si(C ₆ H ₄)SiO _{1.5} (40)		
THF/TBAF	−20	71
THF/TBAF	0	69
THF/TBAF	+20	67
THF/TBAF	+55	74
THF/TBAF	+110	76
MeOH/TBAF	−20	59
MeOH/TBAF	+20	66
MeOH/TBAF	+55	70
MeOH/TBAF	+110	70
<i>p</i> -O _{1.5} Si(CH ₂) ₂ (C ₆ H ₄)(CH ₂) ₂ SiO _{1.5} (73)		
THF/TBAF	−20	82
THF/TBAF	+20	87
THF/TBAF	+55	80
THF/TBAF	+110	81

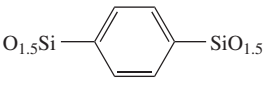
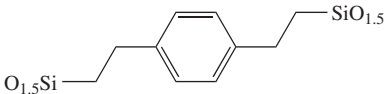
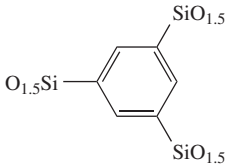
TABLE 4. Textural characteristics of xerogels prepared at different temperature

Xerogel	Specific surface area (m ² g ^{−1})	Micropores (%)	Mesopore size (Å)
<i>p</i> -O _{1.5} Si(C ₆ H ₄)SiO _{1.5} ^{a,b} (40)			
−20 °C	420	50	20–120
+20 °C	550	60	35
+55 °C	940	30	20–50
+110 °C	890	10	20–120
<i>p</i> -O _{1.5} Si(CH ₂) ₂ (C ₆ H ₄)(CH ₂) ₂ SiO _{1.5} ^{a,b} (73)			
−20 °C	<10	50	
+20 °C	565	25	20–120
+55 °C	700	5	40
+110 °C	780	0	100
O _{1.5} Si(CH ₂) ₂ (CH–CH) ₂ (CH ₂) ₂ SiO _{1.5} ^{b,c} 74			
−20 °C	250	20	20–50
+20 °C	665	10	20–60
+55 °C	870	5	35–60
+110 °C	910	0	35 + 55 + 80

^aSolvent: MeOH.^bCatalyst: tetrabutylammonium fluoride (TBAF) (1% molar).^cSolvent: THF.

Nature of the leaving group. A great influence of the catalyst is also observed when using hydrogen as the leaving group [i.e. by using −SiH₃ instead of −Si(OMe)₃ precursor]. Hydrolysis/polycondensation of **75** and **76** catalysed by TBAF gives xerogels with higher specific surface areas than those prepared with chloro(triphenylphosphine)

TABLE 5. Textural characteristics of xerogels prepared in different solvents^a

Xerogel		Specific surface area (m ² g ⁻¹)	Micropores (%)	Mesopore size (Å)
 (40)	THF	1300	10	20–120
	MeOH	550	60	35
 (73)	THF	565	25	20–120
	MeOH	<10	—	—
 (73t)	THF	760	10	20–110
	MeOH	770	10	20–120

^aCatalyst: (*t*-Bu)₄NF (1% molar).

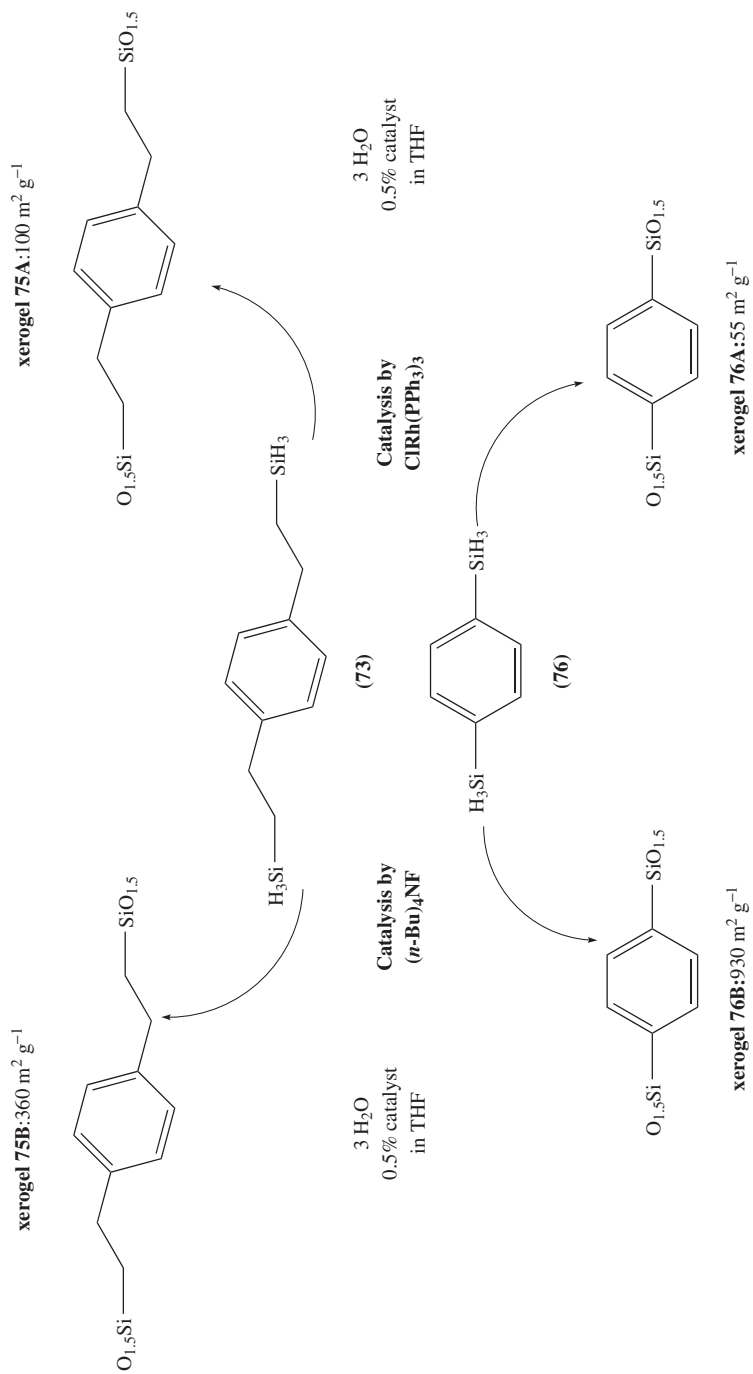
TABLE 6. Textural characteristics of xerogels prepared with different catalyst^a

xerogel		Specific surface area (m ² g ⁻¹)	Micropores (%)	Mesopore size (Å)
<p><i>p</i>-O_{1.5}Si(C₆H₄)SiO_{1.5} (40)</p>	TBAF	1300	10	20–120
	HCl	540	80	20–120
	NaOH	530	75	20–120
	NMI	<10	—	—
	DMAP	680	65	20–70
	<p><i>p</i>-O_{1.5}Si(CH₂)₂(C₆H₄)(CH₂)₂SiO_{1.5} (73)</p>	TBAF	565	25
HCl		<10	—	—
NaOH		<10	—	—
DMAP		<10	—	—
NMI		<10	—	—

^asolvent: THF, 20 °C, molar ratio precursor/catalyst is 1% catalyst: tetrabutylammonium fluoride (TBAF), hydrochloric acid (HCl), sodium hydroxide (NaOH), dimethylaminopyridine (DMAP) and *N*-methylimidazole (NMI).

rhodium(I) as catalyst; the higher the catalyst concentration, the higher the porosity as depicted in Scheme 7¹²⁸.

Replacing the –Si(OR)₃ groups by a –SiCl₃ group is another example. In the cases of arylene precursors like **40** or **43**, trialkoxysilyl precursors generally lead to highly porous xerogels⁹² while those prepared with trichlorosilyl groups are non-porous in most cases¹⁰⁵.



SCHEME 7

This was also illustrated by comparing a series of (trialkoxysilylmethyl)arenes prepared with the precursors with different Si-OR functions (R=Me, Et, *i*-Pr and *n*-Bu)¹⁰⁶.

C. Effect of the Nature of the Organic Group on the Texture of the Xerogels R'(SiO_{1.5})_n (n ≥ 2)

A close look at each of these models indicates that the nature of the organic group is certainly a key parameter for these nanostructured organo-polysilsesquioxanes. As a frequent trend, hybrid xerogels are mostly microporous materials with a high specific surface area (>500 m² g⁻¹) when the R' group is a rigid one as exemplified by the different families of precursors -(C₆H₄)_n- (**13**) (n = 1-3)⁹², -C≡C- (**14**)^{95,156,157}, -C≡C(C₆H₄)C≡C-⁹⁵ and -C≡C(CH₂)_nC≡C- (n = 2) (**16**)⁹⁹. In contrast, non-porous materials are obtained with a flexible long alkyl chain as in the precursor family **12** -(CH₂)_n- (n = 0-8)^{90,158} and the α,ω-bisethynyl alkyl precursors (n = 4-8) in family **16**⁹⁹. This was also observed for the dibenzo-crown ether family **32**^{117,118}, the cyclam family **28**¹¹³ and the bisimide family **30**¹¹⁵. Precursors of the arborol family **35** also belong to this group due to the presence of the octadecyl chain¹²¹. In some cases the precursor **38** of the dendrimer family also produces non-porous materials^{123,125,126}. Such effects might result from the flexibility of these groups that can aggregate and compact more closely, especially during the drying step. Another interesting example is the great difference introduced by modifying a part of the organic group by complexation. While the free cyclam precursor **51** can give either porous xerogels (with specific surface area around 370 m² g⁻¹) or non-porous xerogels, the copper- or cobalt-complexed cyclam precursors give a non-porous material (Scheme 8).

D. Characteristics of the Surface of Xerogels

The nature and structure of the surface of the xerogel are important characteristics with consequences which determine its chemical reactivity and stability.

Hydrophobicity/hydrophilicity balance. One of the simplest analyses currently used is the determination of the hydrophilic property of the solid's surface. This is approximated by measuring the mass increase when the xerogel is placed in a closed vessel with a controlled humidity level¹⁵⁹. When correlated with the extent of the specific surface area, the weight gain is a good indication of the presence of hydrophilic functions such as Si-OH groups at the surface of the solid (for a pure silica prepared by the sol-gel process the weight gain is around 20 to 40%, depending on the sol-gel processing parameters). On the other hand, a low weight gain may indicate a hydrophobic surface resulting from the presence of hydrophobic organic groups.

Surface analysis by mass spectroscopy. The TOF-SIMS (Time of Flight-Secondary Ion Mass Spectroscopy) allows analysis of the surface of the xerogels (Table 7)^{78,79}. In this technique, the fragments that are pulled out by ion impact sputtering are representative of the surface of the solid. Thus, when solids silsesquioxanes R'-SiO_{1.5} are analysed, only fragments of the R groups are observed, indicating that they are mainly located at the surface⁷⁸. With bis-silylated systems, the fragments corresponding to the organic unit are not detected in every case⁷⁹, which clearly illustrates that organization of the organic groups at the surface of the solid can differ in each case. The TOF-SIMS of xerogel **40** and the xerogel of **20** do not exhibit any fragments corresponding to the organic units, suggesting that they are not accessible to the ion beam and are located in the core of the

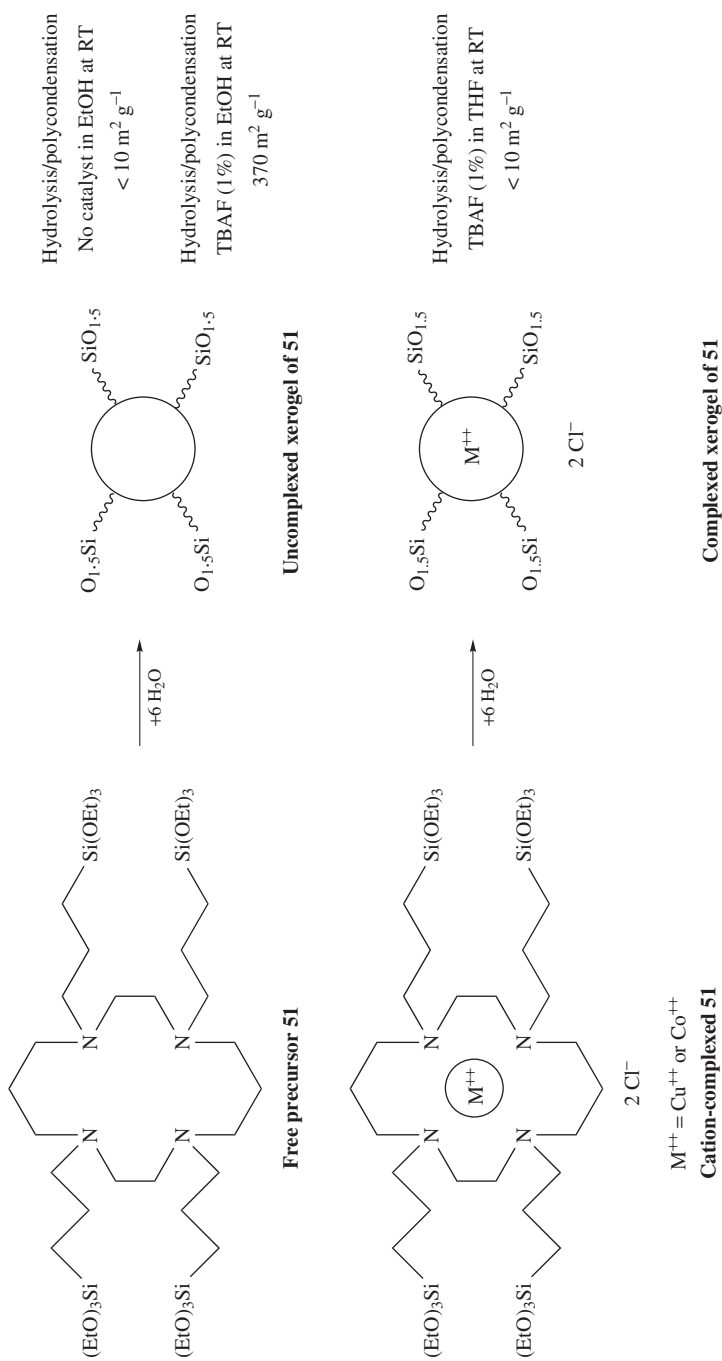


TABLE 7. Correlation between hydrophobicity data and TOF-SIMS analysis for xerogels **40**, **73** and **20**

Xerogel	Ion detected by TOF-SIMS	
$p\text{-O}_{1.5}\text{SiC}_6\text{H}_4\text{SiO}_{1.5}$ (40)	45 (SiOH) ⁺ 59 (SiOCH ₃) ⁺	hydrophilic xerogel
$p\text{-O}_{1.5}\text{SiCH}_2\text{CH}_2\text{C}_6\text{H}_4\text{CH}_2\text{CH}_2\text{SiO}_{1.5}$ (73)	77 (C ₆ H ₅) ⁺ 91 (C ₇ H ₇) ⁺	hydrophobic xerogel
O _{1.5} Si-Ferrocene-SiO _{1.5} (20)	45 (SiOH) ⁺	hydrophilic xerogel

solid. On the other hand, TOF-SIMS analysis of xerogels **73** give completely different results: ions of organic fragments are the only ones observed in this case. Moreover, these results corroborate the fact that **40** is a hydrophilic solid with a high specific surface area (550 m² g⁻¹) while, in contrast, **73** is a hydrophobic resin with a very low specific surface area⁷⁸. Additionally, it will be seen that **40** and **73** present different chemical reactivity towards chromium carbonyl in Section VI.B.

Surface analysis by X-ray scattering (USAXS and SAXS). Small-angle scattering from arylene xerogels was used to evaluate the surface roughness of xerogels of **40** and its analogues. Solids prepared under acidic and basic conditions were found to be identical and a fractal-like surface is assumed¹⁶⁰. A similar result was observed in the case of xerogels of **54–60** by looking in the Porod's region at the intensity vs scattering vector q . A power law between $q^{-2.5}$ and q^{-3} correctly represents the intensity behaviour between 5×10^{-3} and $1 \times 10^{-1} \text{ \AA}^{-1}$. Hence a fractal or bushy behaviour was suggested^{98,99,161}.

In concluding this part, three main points emerge from the summary of these results. *First, the difficulty in achieving the preparation of these solids in a reproducible way can be solved only if a precision in the experimental parameters similar to that employed for physical or analytical chemistry measurements is used.* This is a clear demonstration of the second point, which states that the textural parameters of the materials (porosity, specific surface area and surface composition) are under kinetic control. Temperature, solvent, catalyst, water/precursor ratio and concentration of reagents are the main parameters which, beside the nature of the organic subunit R', control the texture of the final material. The third point is the difficulty in rationalizing the effect of these parameters due to the numerous mechanisms involved in the sol-gel process and their interconnections. However, it must be kept in mind that all these parameters are also powerful tools that can be very useful for the development of further applications, because they allow one to tune the texture of the materials.

V. ORGANIZATION AND SHORT-RANGE ORDER IN NANOSTRUCTURED ORGANO-POLYSILSESQUIOXANES R'(SiO_{1.5})_n (n ≥ 2)

The siliceous materials prepared by the sol-gel process are generally amorphous, and crystallization is obtained only after thermal curing⁴, this is also the case for polysilsesquioxanes R'SiO_{1.5}. The possibility of having a polyhedral or ladder structure as elements of the material's architecture is generally accepted (see Section II.C and References 50 and 84). However, a short- or long-range order organization is apparently absent and the R' groups are located at the surface of the framework. For

organo-polysilsesquioxanes xerogels like $O_{1.5}SiR'SiO_{1.5}$ a different situation is expected due to the presence of several anchoring $SiO_{1.5}$ groups, generally in a symmetric position. Indeed, we will see below that the case of bis and polysilylated precursors is completely different from that of the $R'SiO_{1.5}$ xerogel and there is increasing evidence of the presence of an organization at the molecular level.

A. Chemical Evidence of a Short-range Order

The first experimental observation that suggested the idea of a short-range order in these materials was the possibility to achieve polymerization in solid state between the organic groups. This was achieved in the case of xerogel $2,5-O_{1.5}Si(C_4H_2S)_nSiO_{1.5}$ ($n = 1$ and 3) from precursor family **18**, for which the electrochemical and chemical induced polymerization of thiophene units was obtained⁹⁴, or with a $O_{1.5}SiC\equiv CC\equiv CSiO_{1.5}$ xerogel of precursor **77** whose acetylenic units are polymerized by thermal treatment at $200^\circ C$ under argon (for the chemical aspect, see Section VI.B)⁹⁵. These chemical transformations between fixed organic units in the solid suggest a short-range order in the solid. Indeed, the organic groups have to be close enough to react with each other. Moreover, the mechanism proposed for the coupling of thiophene units (i.e. coupling of two radical cation species) implies a precise geometry in the transition state. Therefore, a similar and close organization has to be present in the solid xerogel of **18** in order to achieve the chemical transformation. The same is true in the case of the xerogel of **77** in which the cross-linking of C_4 units occurs at rather low temperature by a 1,4 addition.

B. Characterization of a Short-range Order

When looking at the X-ray diffraction of xerogels of the general formula $O_{1.5}SiR'SiO_{1.5}$, the absence of any sharp Bragg signal is an obvious sign of the absence of a crystal organization generally analysed by this technique. However, in some cases, the presence of broad signals is indicative of a possible short-range order. These signals, which are always additional to the signal at $q = 3.5$ to 3.7 \AA^{-1} attributed to the Si–O–Si contribution, are listed in Table 8.

TABLE 8. Signals observed for X-ray analysis of nanostructured hybrid xerogels^a

Xerogels (corresponding precursor)	q (\AA^{-1})
$O_{1.5}SiC\equiv CC\equiv CSiO_{1.5}$ ⁹³ (77)	8.1
$p-O_{1.5}SiC\equiv CC_6H_4C\equiv CSiO_{1.5}$ ¹⁶² (54)	5.7–12.5
$p-O_{1.5}SiC\equiv C(C_6H_4)_2C\equiv CSiO_{1.5}$ ¹⁶³ (78)	4.8–7.8–15.7
$p-O_{1.5}Si(C_6H_4)SiO_{1.5}$ ⁹³ (40)	7.6–15.7
$p-O_{1.5}Si(C_6H_4)_2SiO_{1.5}$ ¹⁶³ (79)	5.2–15.7
$p-O_{1.5}Si(C_6H_4)_3SiO_{1.5}$ ¹⁶⁰ (42)	15
$p-O_{1.5}Si(CH_2)_2C_6H_4(CH_2)_2SiO_{1.5}$ ¹⁶³ (73)	5.2–8.9

^aDistances are calculated according to a Bragg assumption.

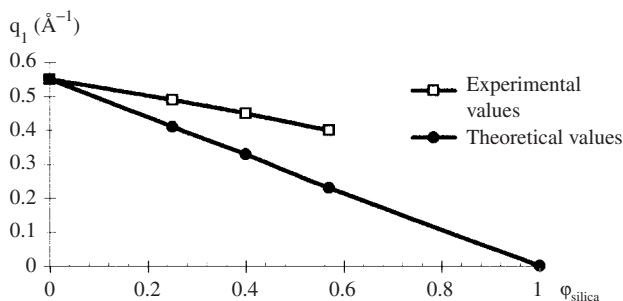


FIGURE 7. Variations of q_1 values with ϕ silica

These peaks are too large to be interpreted in terms of crystalline periodicity over a long range. However, a short-range order in the hybrid xerogel can be considered and is possibly favoured by the presence of the rigid organic unit. For the xerogel of **54** the distance associated with the first peak at $q_1 = 0.55 \text{ \AA}^{-1}$ corresponds to $d = 2\pi/q = 11.4 \text{ \AA}$ (assuming a Bragg law), a value close to the Si...Si distance in the organic spacer as determined by simple molecular simulation ($d_{\text{Si}_1 \cdots \text{Si}_2} : 11.45 \text{ \AA}$)¹⁶². A similar close correspondence is observed with signals in the xerogels **40**⁹³, **78**¹⁶³ and **42**¹⁶⁰.

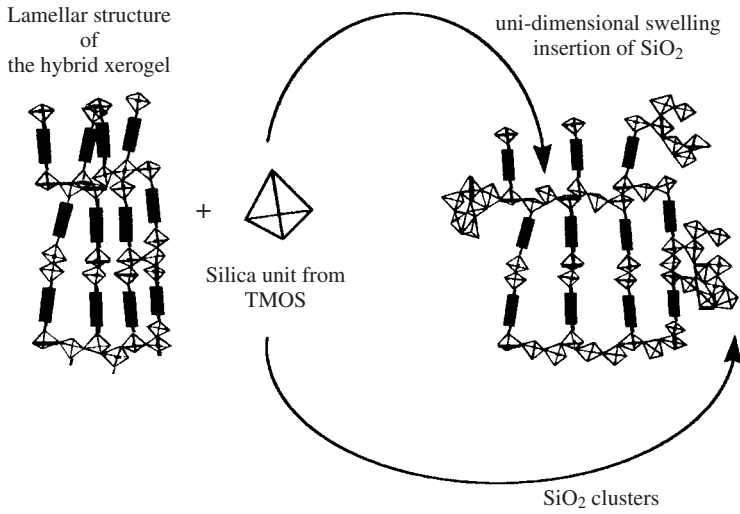
For the xerogel of **54** these peaks are always present, and their position is unchanged regardless of the texture of the solid or of the kinetic parameters (solvent, catalyst, concentration) used in the hydrolysis/polycondensation step. However, co-polymerization with various amounts of TMOS was found useful for the investigation of the structure of these materials.

The fluctuations in the position and the intensity of the peaks resulting from the co-polymerisation suggest a lamellar structure of the hybrid material¹⁶². A uni-dimensional swelling of this lamellar structure was deduced from Figure 7 by correlating the position of the q_1 signal with the volume fraction of silica (ϕ silica) which is deduced from the amount of TMOS. Comparing the experimental swelling law to the theoretical law of a pure uni-dimensional swelling supports the hypothesis that the TMOS does not polycondense as a separate material but is partially inserted in the hybrid xerogel architecture, as illustrated by Scheme 9. A similar lamellar structure was also proposed in the case of the xerogel of **40** and **42** on the basis of computer-aided calculations and the degree of polycondensation of the materials (determined by elemental analysis and ²⁹Si NMR data)¹⁶⁴. All these observations are in agreement with the chemical behaviour described above and agree with an organization at the nanometric scale.

C. Optical Evidence for an Anisotropic Organization in the Xerogels

A convincing demonstration of the anisotropic organization of these hybrid xerogels is their birefringence when observed in polarized light. This analysis is usually performed on liquid crystal compounds in order to determine their mesoscopic anisotropic organization.

From a general point of view, the presence of such short-range order in these hybrid materials is related to the organization of the molecular unit. An isotropic organization corresponds to an orientation of the molecular units in all the directions of the space as presented in Figure 8. In contrast, an anisotropic organization would imply an orientation along a preferential direction.



SCHEME 9

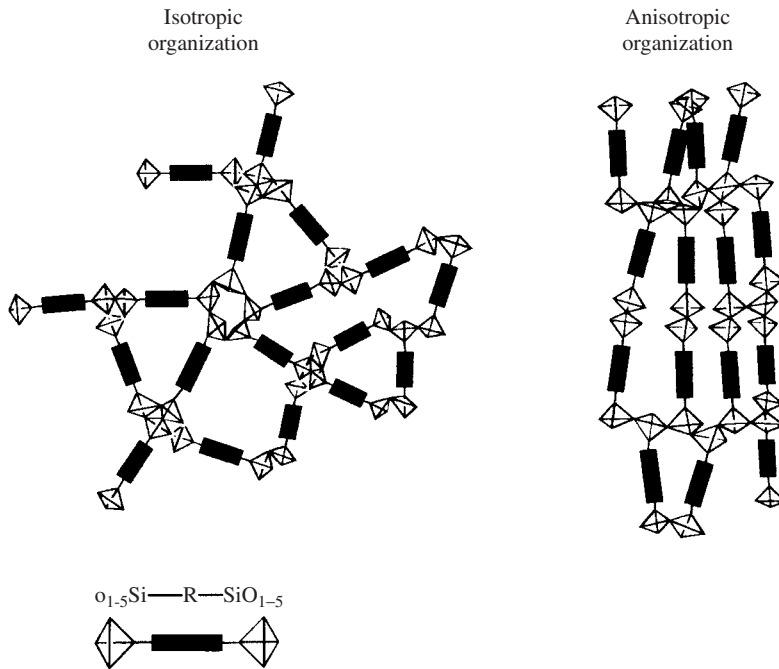
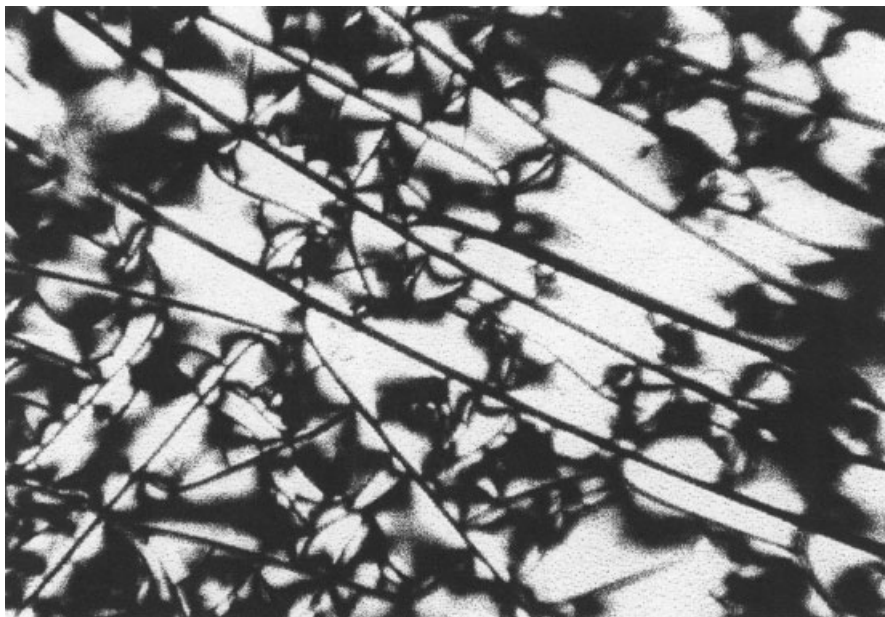


FIGURE 8. Schematic representation of isotropic and anisotropic organization of nanostructured hybrid xerogels

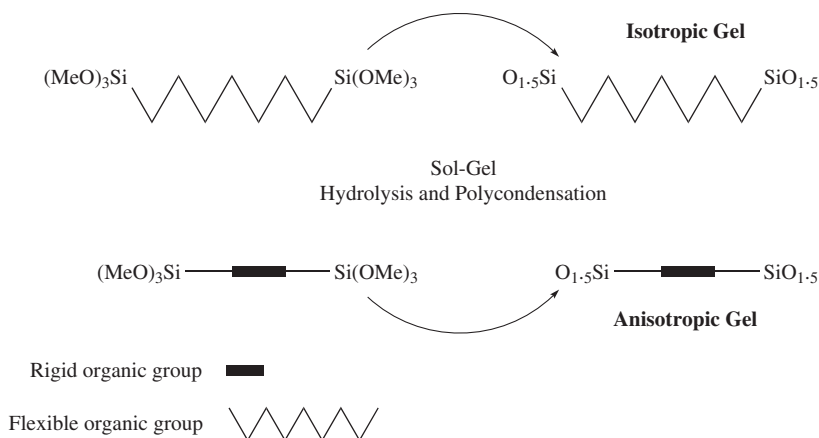


PICTURE 1. Birefringent $p\text{-O}_{1.5}\text{SiC}_6\text{H}_4\text{SiO}_{1.5}$ xerogel observed by microscopy in polarized light

It was found that gelation of precursor **54** results in the formation of a birefringent xerogel with the expected characteristics as illustrated by Picture 1¹⁶⁵. Moreover, an original experimental procedure has permitted the xerogel's formation history to be followed and four successive states are observed: precursor, sol, gel, aged and partially dried gel (not precisely the xerogel). In this case, while sol and gel are both isotropic medium, birefringence is observed only in the final step during the ageing of the solid when cracks are formed.

It was found that the nature of the organic group is one of the key parameters. The presence of a rigid aromatic group [xerogels like $p\text{-O}_{1.5}\text{Si}(\text{C}_6\text{H}_4)_n\text{SiO}_{1.5}$ ($n = 1, 2$ and 3) or $2,5\text{-O}_{1.5}\text{Si}(\text{C}_4\text{H}_2\text{S})_n\text{SiO}_{1.5}$ ($n = 1$ and 3)] appears necessary in order to achieve such anisotropic organization, because an isotropic organization is always obtained when using a flexible alkyl group [xerogels $\text{O}_{1.5}\text{Si}(\text{CH}_2)_n\text{SiO}_{1.5}$, $n = 2, 6, 12$] (Scheme 10)¹⁶⁶.

The value of the birefringence ranges from 1×10^{-3} – 9×10^{-3} in the case of the xerogels of **19** and **54** with rigid organic groups. This range of values is high enough to consider that it results from the organization of the material at a molecular level. These results demonstrate for the first time the possibility of an anisotropic organization in silica-based hybrid xerogels prepared by the sol-gel process. It is important to note that the precursors have no mesogenic properties and are not thermotropic liquid compounds in which the liquid crystal organization varies with the temperature. Moreover, no comparison can be drawn between classical smectic or nematic phases and these xerogels. The organization of the first ones is maintained by weak interactions between the mesogenic units, while the organization of materials described here is fixed by a covalent



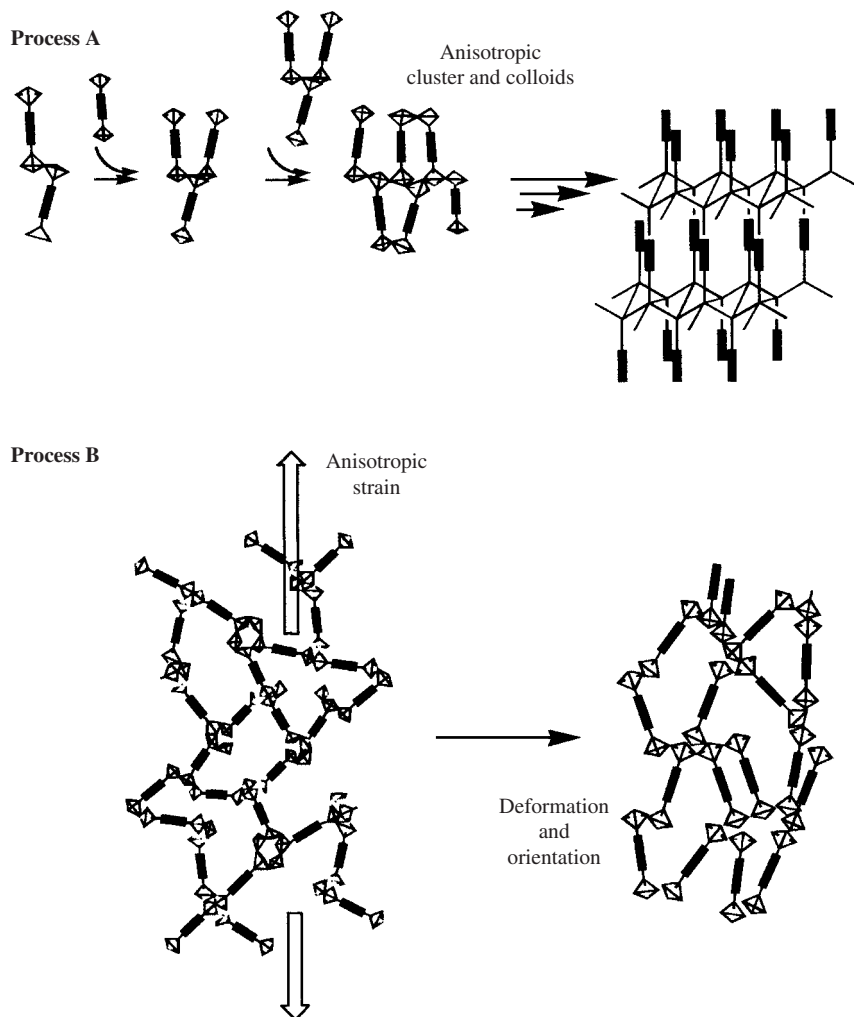
SCHEME 10

Si–O–Si network which is the outcome of the chemical transformations that result from the hydrolysis/polycondensation at each silicon (no T^0 units are observed by ^{29}Si NMR spectroscopy).

The short-range scale organization (nanometric order) observed by X-ray and evidenced by the birefringence property is connected together and observed only in the case of a rigid precursor. A possible explanation for the first phenomenon is the formation of a nanometric order during the polycondensation step. It is known that the Si–O–Si bonds can be formed without breaking weak interactions. For instance, mesoporous silica is obtained by polycondensation in micellar medium whose organization is controlled by weak forces³⁸. In the case of the xerogels discussed here, during the polycondensation step the steric interaction between the rigid units of the precursor could force them to arrange themselves between each other, for example according to process A in Scheme 11.

This order could also be the result of a more complex process occurring during the ageing of the material. A general explanation could be that, after the gel formation, the polymers and aggregates undergo a reorganization involving chemical reactions (Si–O–Si bond breaking or redistribution) which permit one to increase the order in the material. From this point of view the formation of cracks certainly enhances the organization of the material. During the ageing and drying steps, cracking of the gel produces anisotropic stress that can orient the molecular units in the material (Process B in Scheme 11). This mechanical orientation is possible since the level of condensation could be rather low in the freshly formed gel and, in addition, the Si–O–Si bond angle deformation is low in energy¹⁶⁷. This is also supported by the orientation of the optical axis along the crack edges¹⁶⁵.

Altogether, these results demonstrate that the organization of such materials must be investigated with a vision other than the usual one, which considers all the solids prepared by the sol-gel process as amorphous (with the exception of MCM and related materials). A further step will be to enhance and control such organization by chemical and physical means.



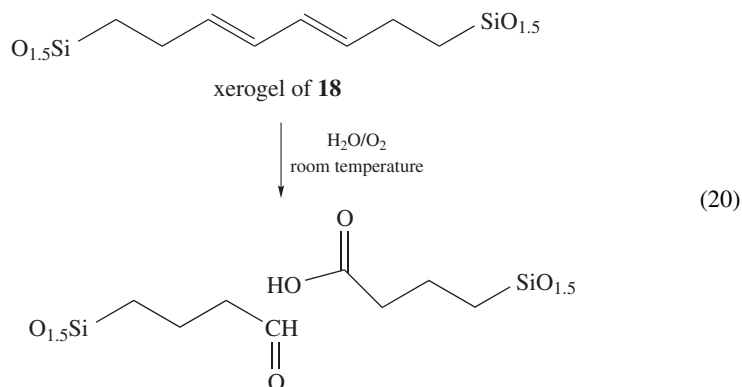
SCHEME 11

VI. CHEMISTRY INSIDE THE ARCHITECTURE OF THE HYBRID NANOSTRUCTURED ORGANO-POLYSILSESQUIOXANES $R'(SiO_{1.5})_n$ ($n \geq 2$)

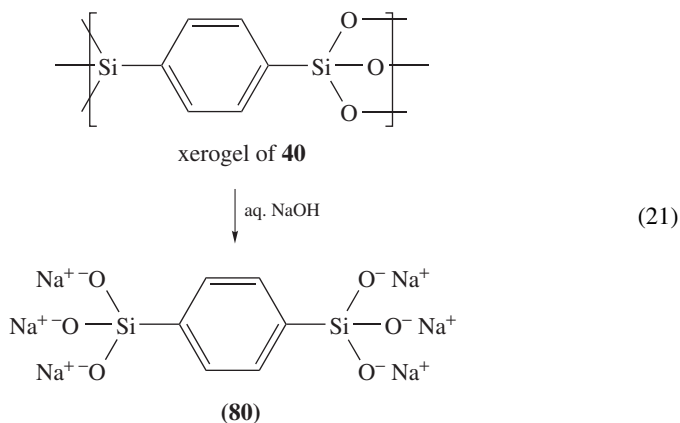
Potentially useful organic and supramolecular functions are introduced into the hybrid xerogels $R'(SiO_{1.5})_n$ via the R' organic group. In this way, the resulting material acquires a precise chemical reactivity that can have a potential application in a sensor system, for example. Moreover, the reactivity of the organic group in these solids can be used as a tool for understanding the specific reactivity in such materials. This reactivity can be either similar or different from that observed in solution. We will therefore present some results that demonstrate simultaneously the chemical transformation of the hybrid xerogels and the structure/reactivity relationship in the solids.

A. Chemical Stability

The xerogels are generally considered as stable materials, but care should be taken due to the particular reactivity that some of them may exhibit. Nevertheless, the textural, physical and chemical stability of these xerogels is very good when they are stored under conditions excluding the presence of air and humidity. However, when stored in an open atmosphere both chemical and textural modifications must be envisaged due to oxidation and hydrolytic processes. Thus, an unexpected reactivity was reported in the case of the xerogel of precursor **18**. For this solid, a total oxidation of the allylic moieties to acid and aldehyde molecules is observed. This requires the simultaneous presence of oxygen and water and corresponds approximately to the process shown in equation 20. Although the reasons for such high reactivity remain unknown, it is interesting to point out that neither the precursor nor the organic part alone exhibit such an oxidability¹⁰⁰, and it is clear that incorporation of the organic group in the solid framework is required. This result demonstrates that the reactivity of the organic part can differ from that of the corresponding organic compound in solution.

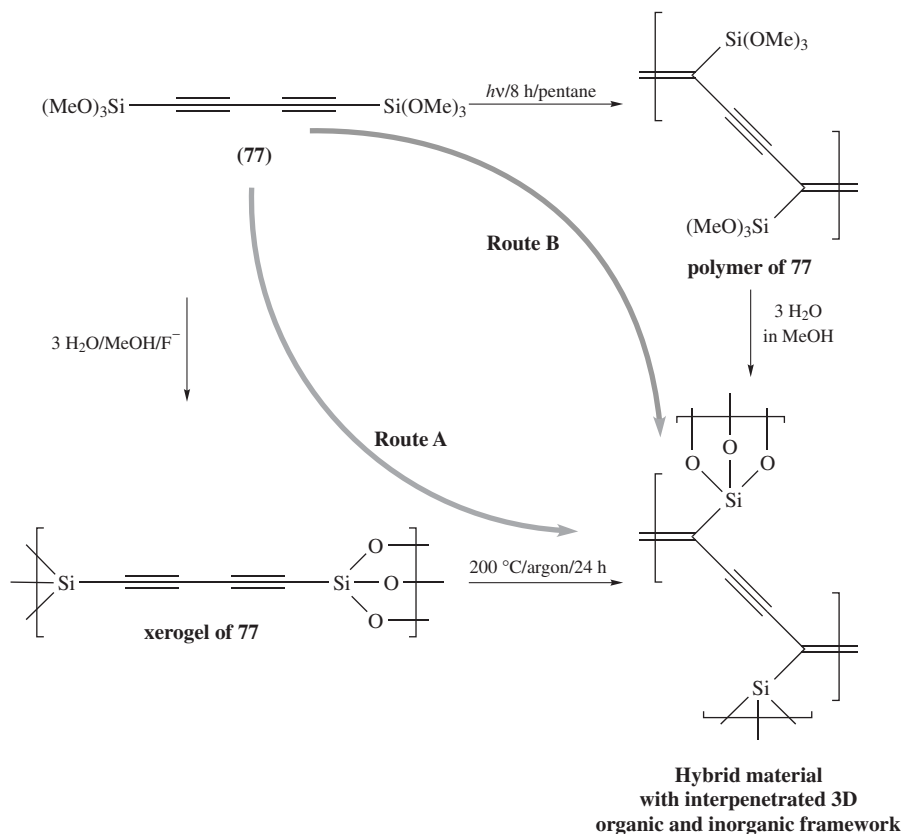


The chemical stability of the Si–O–Si network is high under acidic conditions but is very low when in contact with a basic solution³. Therefore, treatment of the xerogel of **40** with aqueous sodium hydroxide leads to a complete dissolution and to the formation of the bis-trisilanolate **80** (equation 21)¹⁶⁸.



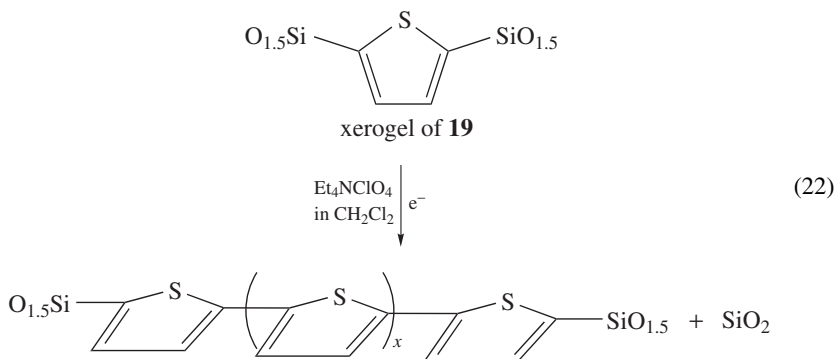
B. Inter-activity between the Organic Groups

One of the chemical transformations used to investigate the solid's structure is the inter-activity between the organic groups of the $O_{1.5}SiR'SiO_{1.5}$ molecular units. The thermal polymerization of diynes has been reported to occur topochemically through 1,4 addition leading to enyne formation^{169,170}. This reaction requires parallel $-C\equiv C-C\equiv C-$ units¹⁷¹. For a xerogel of **77** prepared from 1,4-bis(trimethoxysilyl)buta-1,3-diyne [¹³C NMR: $\delta = 79.4$ and 87.8 ($C\equiv C-C\equiv C$), IR: $\nu_{\max} = 2202$ and 2091 cm^{-1}], heating at $200^\circ C$ under argon results in the formation of enynes as described in Scheme 12. The associated cross-linking is detected by the spectral changes (¹³C NMR: $\delta = 133$, IR: $\nu_{\max} = 2169$ cm^{-1}) and a ²⁹Si signal at $\delta = -74$ ⁹⁵. Moreover, very close materials displaying the same spectroscopic features can be prepared either by gelation before cross-linking (route A) or by irradiation-induced cross-linking before gelation (route B). The cross-linking reaction starts at low temperatures, and the thermal differential analysis (TDA) curve between $100^\circ C$ and $450^\circ C$ exhibits a maximum at *ca* $250^\circ C$. This low temperature is indicative of a favourable arrangement of the diyne moieties and suggests the presence of a short-range order in the nanostructured material (cf Section V.A).



SCHEME 12

Similarly, the polymerization of thiophene units in the xerogel of precursor family **19** was observed (equation 22). Polythiophenes are well-known to be formed by electropolymerization^{172,173}, and silylated thiophenes have been shown to be very efficient precursors for this polymerization¹⁷⁴. For gels of thiophene-containing precursors, ¹³C and ²⁹Si CP MAS NMR spectra show that the structure of the precursor remains intact in the solid without cleavage of the Si-thiophene bond. Both an electrochemical oxidation of gels deposited as films on electrodes and a chemical oxidation using FeCl₃ as the oxidizing agent lead to rapid polymerization of the thiophene units in the solid (equation 22)⁹⁴. The polythiophene formed in situ by oxidation cannot be separated from the solid, since it is bound to silica by a SiO_{1.5} at each end of the chain. It was identified by Raman resonance spectroscopy and visible absorption⁹⁴. Thus, the fast polymerization occurring in the gel, where the mobility of thiophene units is highly restricted, suggests strongly the presence of a short- to medium-range organization within the solid. This conclusion is reinforced when the mechanism of polymerization is taken into account, since the oxidative electropolymerization involves the coupling of two radical cations^{94,175,176}.

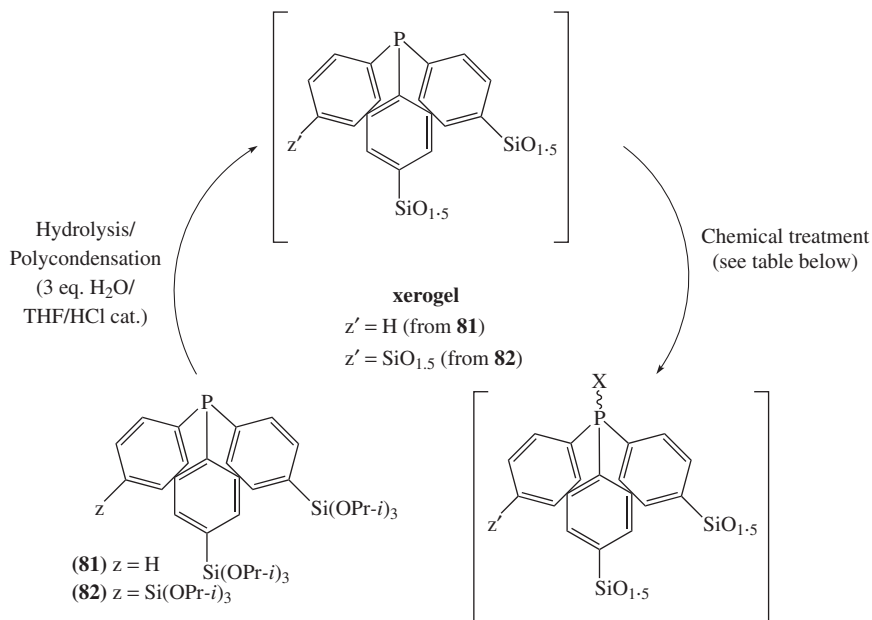


C. Reactivity/Structure Relationship

The most efficient way of looking at the structure/reactivity relationship is to compare the reactivity of a well-known organic group when it is either free in solution or is a part of a hybrid xerogel. In the latter case, the reaction is performed in a heterogeneous solid/liquid medium. Therefore, all reactivity changes could possibly be due to special structures and arrangements in the solid's architecture and it must be kept in mind that mobility of the reactive centres in the solid is highly restricted. As we will see, four parameters must be considered: (a) the flexibility in the material's architecture, (b) the location of the reactive centre at either the surface of the solid or within the solid, (c) the material's texture and (d) the possible juxtaposition of the molecular units.

This reactivity/structure relationship is exemplified by the chemical transformation of phosphino centres of a hybrid xerogel. Such materials can be prepared with precursors like (OC)₅WP[(C₆H₄)Si(OPr-*i*)₃]₃, Cl₂Pt[P(C₆H₄)Si(OPr-*i*)₃]₂ or Cl₂Pd[P(C₆H₄)Si(OPr-*i*)₃]₂. The structure and function of the organic group is not altered by the hydrolysis/polycondensation as demonstrated by ³¹P CP MAS NMR¹⁰⁹. Also, a free phosphino group can be introduced in xerogels by using precursors of (C₆H₅)P(C₆H₄SiO_{1.5}-*P*) (**81**) or P(C₆H₄SiO_{1.5}-*P*)₃ xerogel (**82**). Their chemical transformation is achieved quantitatively using a non-crowded reagent like H₂O₂, S₈, or CH₃I (Scheme 13)¹¹⁰. However, complexation with THF/W(CO)₅ was not achieved

completely in every case. For example, ^{31}P NMR spectroscopy indicates a degree of complexation of 80% for **81** and only 5% for **82**.

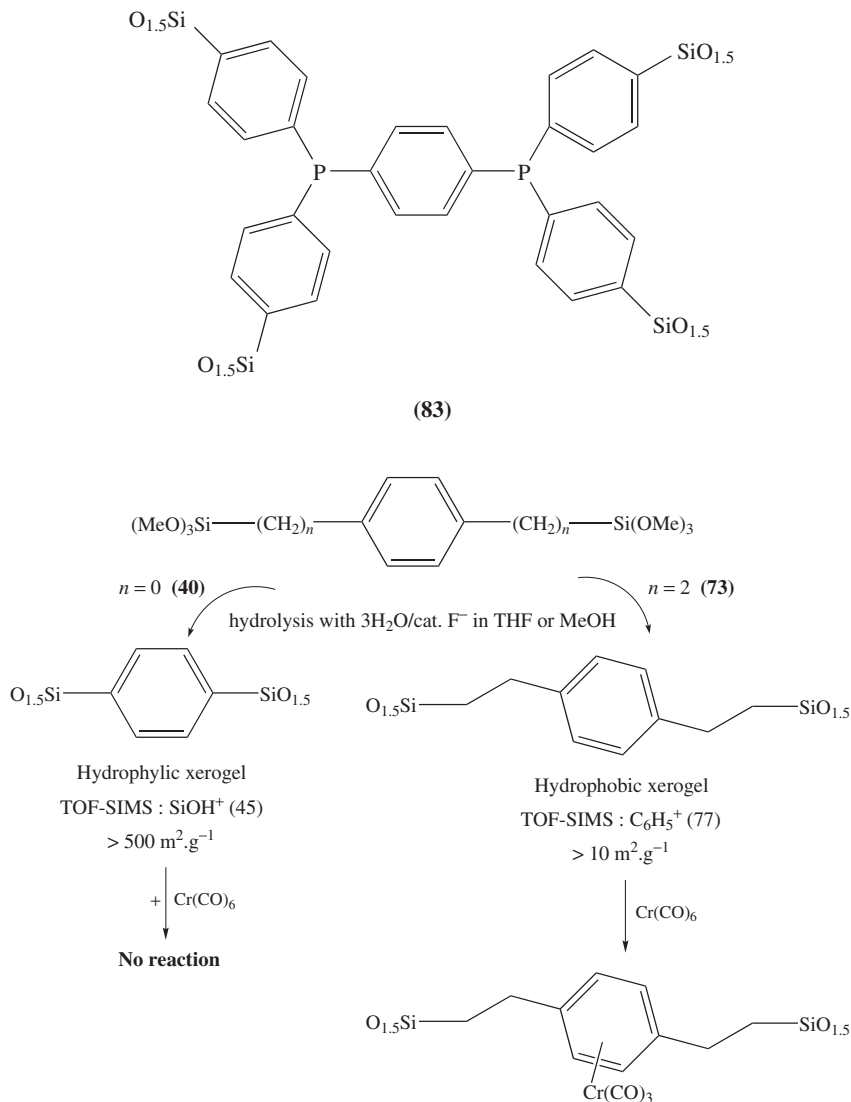


Chemical treatment with	H_2O_2	S_8	CH_3I	$\text{C}_6\text{H}_5\text{CH}_2\text{Br}$	THF-BH_3	$\text{THF-W}(\text{CO})_5$
type of P-X function formed after chemical treatment.	$\text{P}=\text{O}$	$\text{P}=\text{S}$	$^+\text{P-Me}$	$^+\text{P-CH}_2\text{C}_6\text{H}_5$	P-BH_3	$\text{P-W}(\text{CO})_5$
Yield (%) of transformed 81	quant.	quant.	quant.	quant.	90%	quant.
Yield (%) of transformed 82	quant.	quant.	quant.	85%	80%	5%

SCHEME 13

The accessibility of the reactive centre in such a heterogeneous reaction medium is the central question. Obviously, a high specific surface area is advantageous, especially when the reactive sites are located at the surface of the solid, but it is not the dominant factor. The degree of 'flexibility' of the material is apparently another key factor that can govern the diffusion of solvents and reagent molecules (see Section VI.D)^{89,177,178}. In this last case, the flexibility of the Si–O–Si network can be controlled via the degree of condensation in relation to the number of anchoring groups, and xerogels like **81** allow better access to the phosphorus centre than in **82**. Such an assumption is confirmed when considering the lower reactivity exhibited by another phosphino-containing xerogel **83**,

where the phosphino group is sterically hindered and the density of cross-linking of the Si–O–Si network is higher¹⁷⁹.



SCHEME 14

The complexation reaction is another useful reaction for such investigation. Aromatic organosilanes are known to easily form tricarbonyl(η^6 -organosilylarene)chromium(0) complexes upon reaction with $\text{Cr}(\text{CO})_6$ or $(\text{MeCN})_3\text{Cr}(\text{CO})_3$ ¹⁸⁰. The complexation of the aryl groups of the hybrid xerogel of precursors **40** and **73** has been used for comparing their reactivity, as depicted in Scheme 14. Under similar experimental sol-gel conditions,

these precursors with close structures lead to completely different solids. Xerogel **40** is a hydrophilic solid with a high specific surface area ($550 \text{ m}^2 \text{ g}^{-1}$) for which the SIMS analysis exhibits only SiOH fragments^{80,107,155}. Interestingly, this xerogel does not react with $\text{Cr}(\text{CO})_6$, showing that the organic groups are not accessible in the solid. In contrast, the xerogel of **73** is a hydrophobic resin with a very low specific surface area. The mass fragments corresponding to the phenyl and benzyl units are detected by TOF-SIMS and the Si–OH peak is not detectable⁷⁹. The reaction of this xerogel with $\text{Cr}(\text{CO})_6$ takes place in good yield, leading to a new material in which most of the aromatic groups are complexed by $\text{Cr}(\text{CO})_3$. This easy complexation confirms the accessibility of the aromatic units in this case.

The binding of an alkali metal cation to a crown ether is another reaction involving a supramolecular concept^{181–183}. It allows a comparison of the binding property of a crown ether either in solution or when included in a hybrid xerogel. Therefore, with precursor **84** either free crown ether xerogels (route B, xerogel **84B**) or cation-bound (route A, xerogel **84A**) were prepared. Once the xerogel is formed, its cation binding or cation release properties are investigated as summarized in Scheme 15¹¹⁸.

At the same time, the possibility of preparing a cation-binding xerogel is exemplified by route A and xerogel **84A**. This example demonstrates that during the sol-gel process the conformation of the crown ether around the cation is not distorted and is capable of keeping the cation bonded.

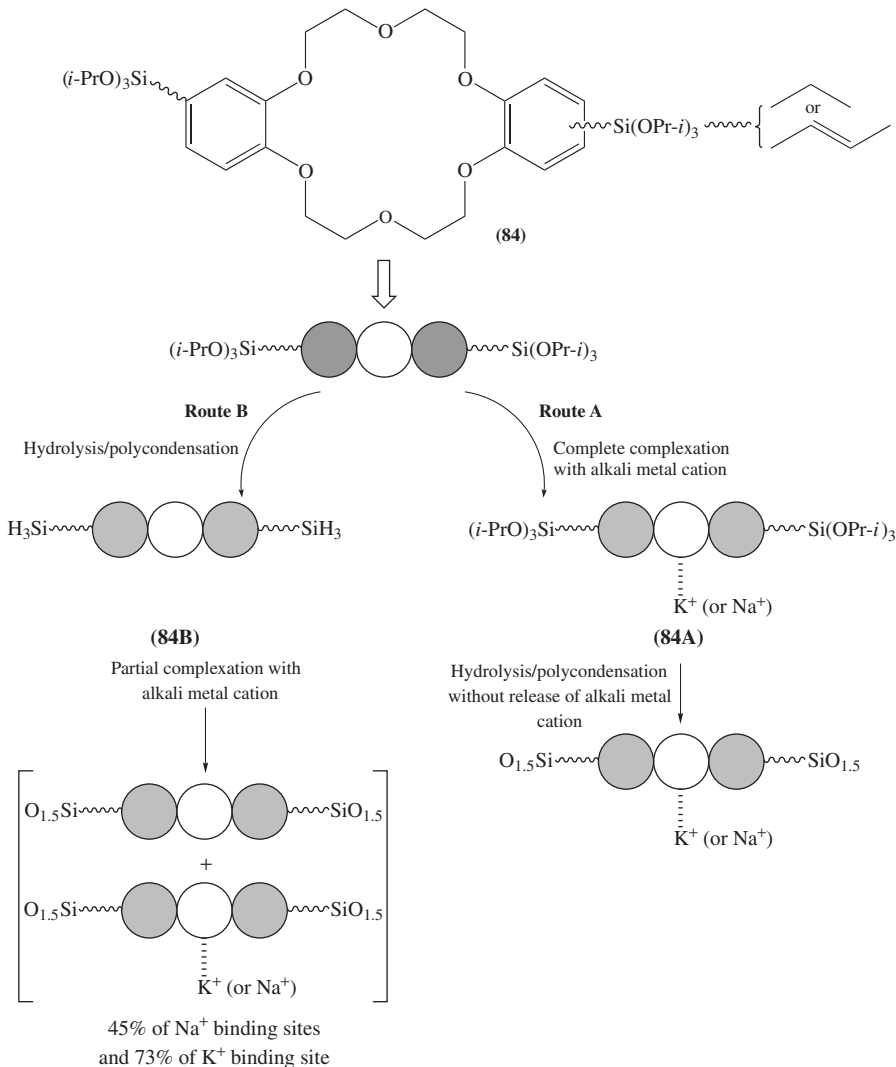
However, the same type of material is not accessible by route B because the reactivity of the crown ether units in xerogel **84B** is clearly modified when incorporated in the solid¹¹⁸. The decrease in the binding property of the crown ether is certainly due to locking of the crown ether in various conformations which are incapable of complexation in the xerogel's architecture. This is consistent with the fact that increasing the anchoring of the crown ether group to the polysiloxane network results in a lowering of its binding property. This effect is increased by a high degree of polycondensation of the material and/or the rigidity of the organic group. This last type of situation corresponds to precursor **85** having 4 anchoring sites (Scheme 16)¹¹⁷. The binding ability of the xerogel of **85** is very low and a major part of the binding sites are unavailable for binding.

The same type of reactivity/structure relationship might be present in xerogels with a cyclam group, as exemplified by the preparation of cyclame containing the xerogel of **51** (Scheme 8). So far, only the synthesis of the free or cation-bonded (Cu^{++} and Co^{++}) xerogels has been reported, although with different textural properties¹¹³. However, this material is able to strongly chelate metal cations, which could remain accessible to chemical reagents. The possibility of having a M–M interaction when a Cu-bond precursor is hydrolysed was observed. On the other hand, this interaction was not observed when a free cyclam precursor is polycondensed and then further react with copper nitrate.

D. Xerogels with Catalytic Properties

Hybrid materials are attractive for the preparation of heterogeneous catalysts, due to the advantage of the tunability of the organic group that can be used and the nature of the inorganic network. Interestingly, the anchoring of the catalytic centre can be obtained either on the silica network or on the organic units. Although they are not systematically studied, three main parameters should be kept in mind in order to achieve an efficient design of the catalyst's environment: the porosity of the hybrid xerogel, its chemical and thermal stability and the nature of both the organic group and the inorganic network.

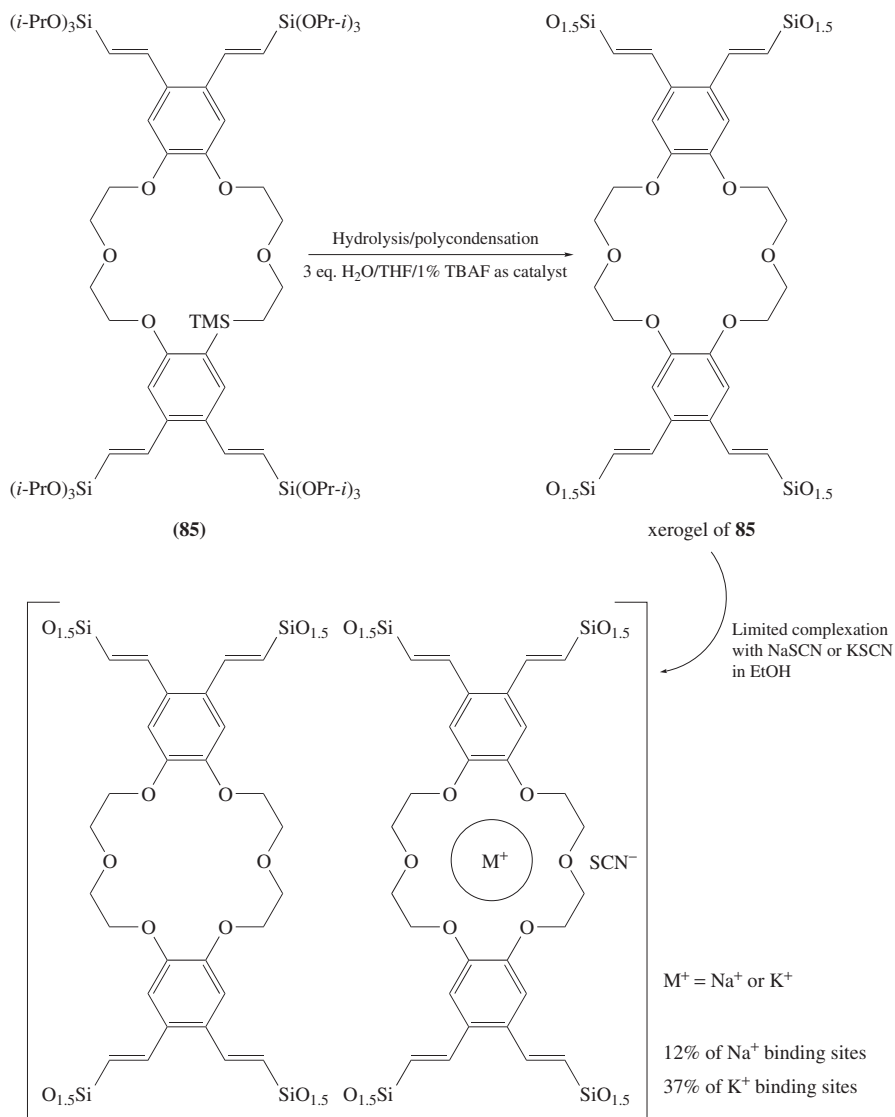
One example of a catalyst anchoring onto the hybrid xerogel's framework is the chemical modification of a dendrimer xerogel¹²⁶. In the starting dendrimer xerogel, the high specific surface area ($>1000 \text{ m}^2 \text{ g}^{-1}$) is combined with a good hydrothermal stability (up



SCHEME 15

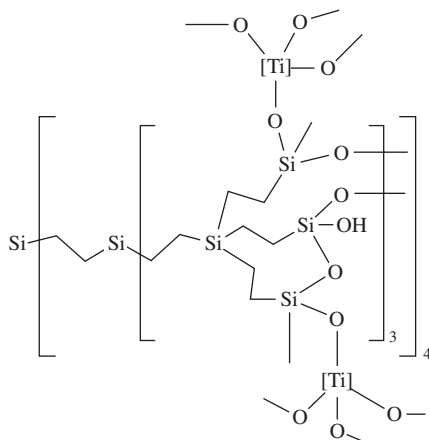
to *ca* 100 °C) and the presence of isolated Si–OH groups. Thus their transformation by treatment with $\text{Ti}(\text{OPr-}i)_4$ or $\text{Ti}[\text{OSi}(\text{OBu-}i)_3]_4$ for 48 hours in refluxing toluene lead to the grafting of titanium centres as demonstrated by elemental analysis, a possible structure being **86**. The resulting material presents an interesting catalytic activity in the epoxidation of cyclohexene.

Here, the catalytic sites are grafted by reaction with residual Si–OH groups of the material. However, another possible approach is by complexation of a transition metal atom using an organic ligand attached to the xerogel. This was used for the preparation of

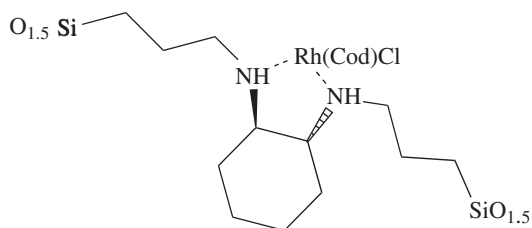


SCHEME 16

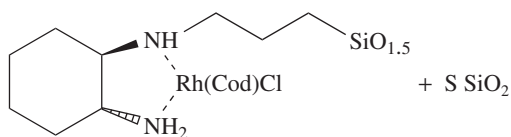
a rhodium-supported catalyst by using a hybrid xerogel with a chiral organic group like the (*R,R*)-*trans*-1,2-diaminocyclohexane unit. The proposed structures correspond to **87** and **88** if co-polycondensation is performed with a silica precursor like TMOS. An efficient catalyst for the asymmetric reduction of aromatic ketones is obtained, this heterogeneous



(86)



(87)

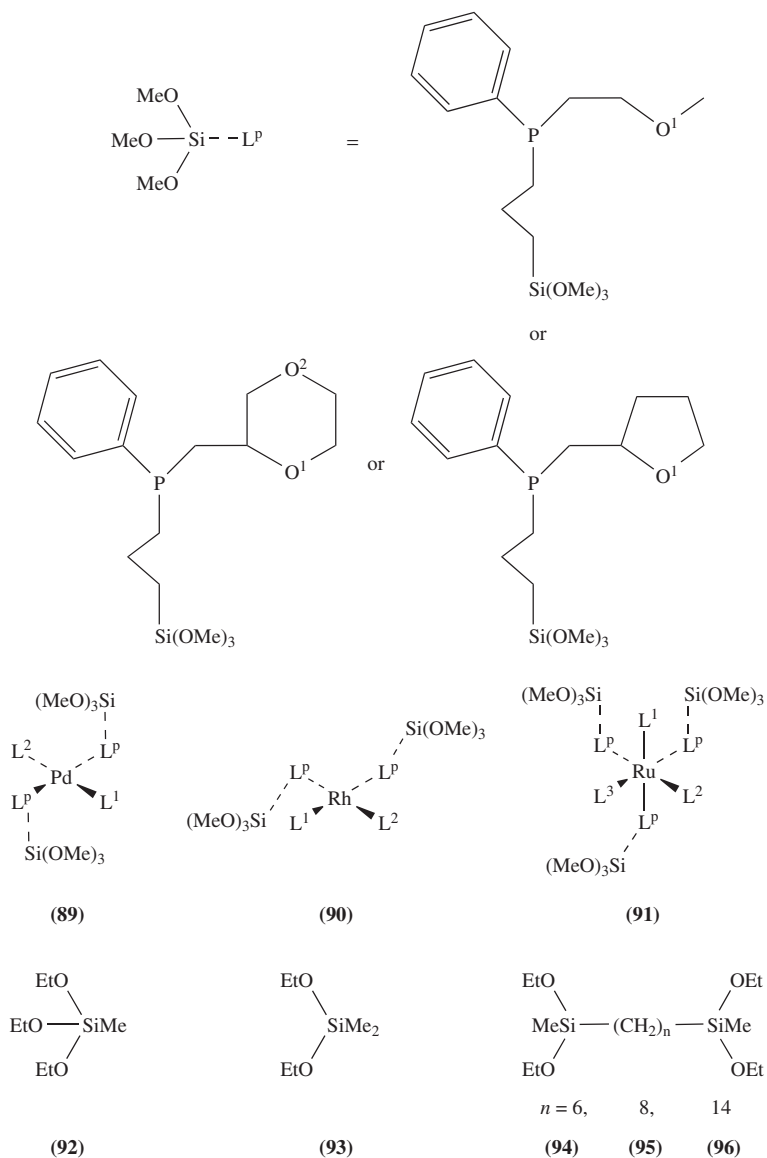


(88)

catalyst gives higher ee values than a homogeneous catalysis with the related soluble compound^{57,119}.

Hybrid nanostructured xerogels with catalytic activity were also prepared by hydrolysis/polycondensation of organometallic precursors containing palladium **89**¹⁸⁴, rhodium **90**^{177,185,186} and ruthenium **91**^{178,187,188} as transition metal centres. These families of precursors is presented in Scheme 17. Xerogels are obtained where the integrity of the transition metal complexes is preserved. However, some specific sol-gel processing parameters must be used in order to avoid decomposition of water-sensitive precursors like **90** or **89** [having a coordinating solvent like pyridine or acetonitrile, and $\text{Bu}_2\text{Sn}(\text{OAc})_2$ as catalyst of the hydrolysis and polycondensation of the precursor].

In the starting precursors and in the xerogel, one out of the L^1 , L^2 or L^3 ligands is the oxygen atom O^1 of the silylated ligand, and therefore they are chelated complexes. For



SCHEME 17

the ruthenium-containing xerogel of **91**, ligand exchange processes are demonstrated by ^{31}P NMR spectroscopy at various temperatures. These analyses demonstrate the mobility in and around the catalytic species¹⁷⁸.

The polycondensation is generally performed in the presence of a 'network modifier' which is chosen among precursors of silica (TEOS, Q^n sub-units), of silsesquioxanes

(**92**) $[R'Si(OR)_3, T^n \text{ sub-units}]$ or siloxanes (**93**) $[R'_2Si(OR)_2, D^n \text{ sub-units}]$ or organopolysilsesquioxanes (**94–96**) $[(RO)_2R''SiR'SiR''(OR)_2, D^n R'D^n \text{ sub-units}]$. By this approach, modulation of the reactivity of the organometallic complex is obtained since the nature of the modifier and the modifier/precursor ratio of this network modulate (a) the level of condensation, (b) the polarity of the inorganic network and (c) the concentration of metal centres. Nevertheless, due to the difference in reactivity, the precursor ratio in the starting mixture is not always the same as that after hydrolysis and polycondensation^{177,186}. These network modifiers also change the mobility of the different units in the material architecture [Si–O–Si network, $Si(CH_2)_nL$ spacer and [M] coordination sphere]. As expected, the mobility is increased in the order $Q^n < T^n < D^n R'D^n < D^n$, which corresponds in CP MAS spectroscopy to a narrowing of the linewidths, a lowering of the spin–lattice relaxation times T_{1X} ($X=^{13}C, ^{29}Si, ^{31}P$) and an increase of the cross-polarization time T_{XH} ^{89,177,178,188}. In the case of rhodium-containing xerogel of **90** this was also observed by 2D NMR spectroscopy^{189,190}. Increasing mobility also increases the possibility of chemical exchange of the ether-phosphine ligands in the coordination sphere and can be studied as for ruthenium complexes in the xerogels of **91**¹⁷⁸.

It must be emphasized that, in contrast to most of the hybrid xerogels presented above, the increasing flexibility of the matrix network enables a swelling phenomenon of the xerogels in different solvents. Consequently, mobility and accessibility of the ether-phosphine ligand can lead to an exchange process with other ligands such as the reagent or another ether-phosphine group at a higher rate in the swollen gels than in the dry xerogels.

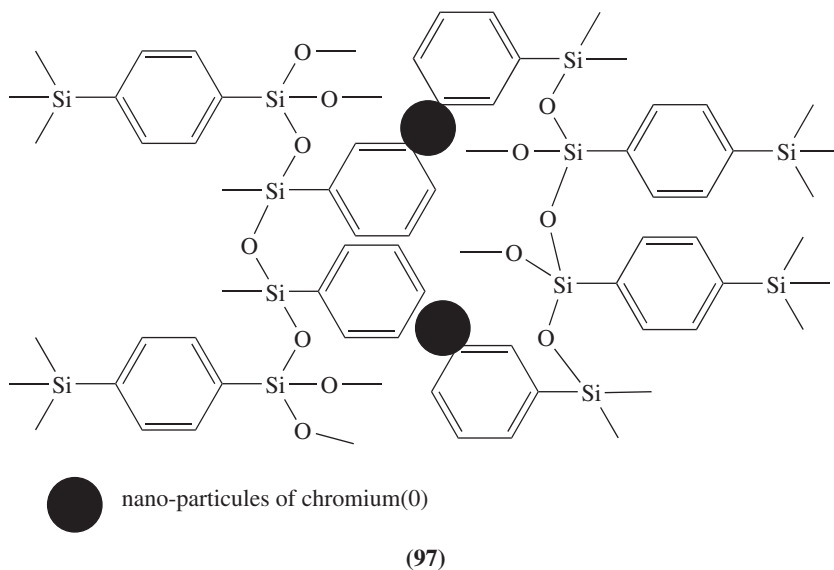
Catalytic activity was demonstrated for the non-porous palladium-containing xerogels prepared from precursor **89**. The solid/gas hydrogenation reaction of 1-hexyne is achieved with a high turnover frequency ($1.15 \text{ mol}_{\text{sub}} \text{ mol}_{\text{cat}}^{-1} \text{ s}^{-1}$) and leaching of the metal is lower than 1%. Nevertheless, for xerogels prepared with increasing proportions of TEOS, increased specific surface areas are observed (up to $250 \text{ m}^2 \text{ g}^{-1}$) but it is accompanied by a decrease in the selectivity of the reaction¹⁹¹.

In the case of a heterogeneous reaction with a rhodium-containing xerogel swollen in various solvents, hydrogenation of tolan under mild conditions results in high selectivity towards formation of *cis*-stilbene¹⁸⁶. The catalytic activity of the co-xerogel of **90** with **94** was found to be higher than that of the pure xerogel of **89**. Similar results are also observed in the case of rhodium-catalysed hydroformylation of 1-hexene⁸⁹. The polarity of the solvent is one of the key parameters, since it defines its ability both to swell the gel and to dissolve the reagents. Optimal swelling of the stationary phase (the hybrid xerogel) must be achieved in order to have reactive centres unaffected by the Si–O–Si matrix. From this point of view the use of **94** as network modifiers represents the best compromise between swollen and cross-linking ability, both properties being required to efficiently achieve chemical transformations at the interphase.

E. Miscellaneous

Organo-polysilsesquioxanes have been used as a matrix for the formation and growth of transition metal clusters for preparing a nanocomposite with a hybrid xerogel as matrix^{192–194}. The possibility of achieving the growth of cadmium sulphide particles (CdS) in the porous texture of a hybrid xerogel of **40** has been demonstrated. Although it is obvious that a high specific surface area is required to achieve the formation of nanoparticles, the effect of the organic group of the matrix on this process is important but not yet clearly understood.

By an approach similar to that described in Scheme 14, nano-sized chromium clusters embedded in a porous hybrid xerogel were obtained. Co-condensation by a sol-gel process of 1,4-bis(triethoxysilyl)benzen (**40**) and tricarbonyl(triethoxysilylbenzene)chromium(0) in a 100/2 molar ratio gives a high specific surface area ($>1000 \text{ m}^2 \text{ g}^{-1}$) hybrid xerogel with a catalytic concentration of chromium¹⁹⁵. By mild thermal decomposition at 120°C , dispersion of nano-clusters of chromium (10–100 Å) throughout the material is obtained without modification of the porosity, a simplified structure being **97**. The hybrid matrix was recognized as the main factor in this process due to the possible formation of bis(η^6 -arene)chromium as intermediate.



VII. NANOSTRUCTURED ORGANO-POLYSILSESQUIOXANES R'(SiO_{1.5})_n (n ≥ 2) AS PRECURSORS FOR POROUS MATERIALS

In the present section we comment further on the chemical modifications of these materials when the R group is chosen for the preparation of micro- and mesoporous silicas. From a general point of view, the control of the porosity of silica via organic molecular templating is an attractive topic connected to molecular recognition, catalysis, chemical sensing and selective adsorption, etc. Many attempts have been made to control the pore size distribution in sol-gel derived silica^{30,196}.

For mesoporous silica (pore $\text{\AA} > 20$), successful results were obtained by the synthesis of the MCM family of silicates and aluminosilicates (of Section II.B). Their preparation is achieved by liquid crystal templating and micellar phases (hexagonal MCM-41, cubic MCM-48, lamellar MCM-50)^{36,37} and further developments are currently reviewed³⁸.

For the preparation of silica with microporosity ($\text{\AA} < 20$) a possible approach is the elimination of the organic component of a silsesquioxane $\text{RSiO}_{1.5}$. In this case, the organic groups serve as templates and their elimination results in the formation of the pores³⁰.

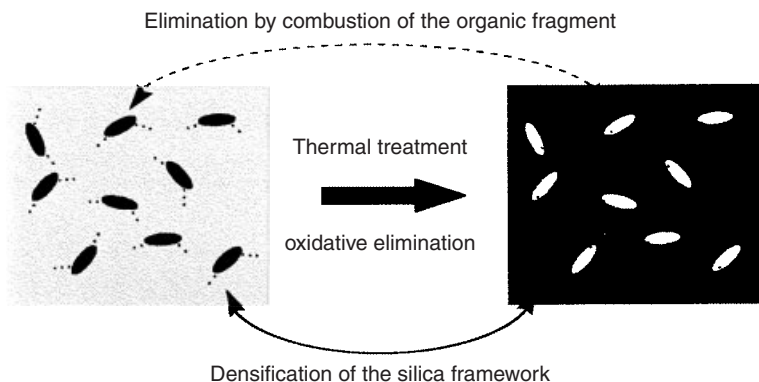


FIGURE 9. Schematic representation of the molecular imprint approach by sacrificial elimination of an organic fragment from a hybrid organic–inorganic material

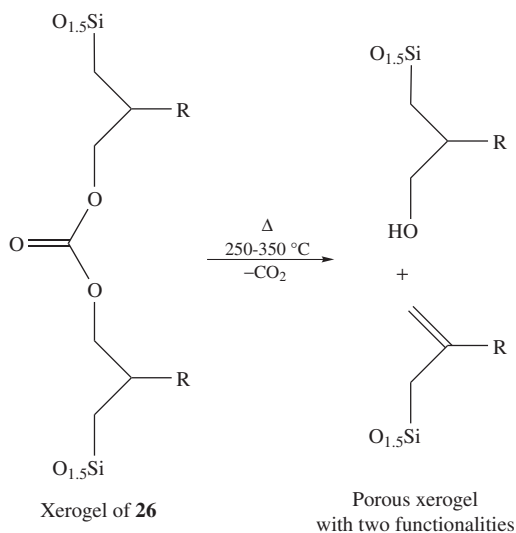
However, two main difficulties must be overcome in order to achieve an efficient and reliable system. The first is to find methods for building up a stable molecular environment around the molecule (or the group of molecules). The second is to find a highly selective method which permits elimination of the molecular units without any modification of the solid framework¹⁹⁷.

A. Direct Thermal Oxidative Elimination of the Organic Groups

Different types of organo-polysilsesquioxane models have been tested in order to prepare microporous silicas by direct thermal oxidative elimination of the organic groups (phenyl, ethynyl, alkyl) as depicted schematically in Figure 9. The basic idea of this approach is to obtain an organic–inorganic solid from which the organic group is removed by combustion in air while the inorganic part remains unchanged. In this way, the formation of a porosity closely related to the size and shape of the organic group is expected. The interest of this approach is the uniform distribution of the template in the silica matrix. In some cases, the thermal oxidative treatment was performed via plasma oxidation¹⁵⁷. However, the thermal treatment (>500 °C in dry air) is generally too drastic and the molecular imprint is erased due to the collapse of the Si–O–Si network and sintering of the residual silica. In some cases an approximate relation between the size of the organic unit and the size of the pore is achieved¹⁹⁸. The presence of micro, meso and macro voids distributed in the starting hybrid xerogel is also a limitation, because they are added to the voids created by the elimination of the organic part and they modify its shape and size.

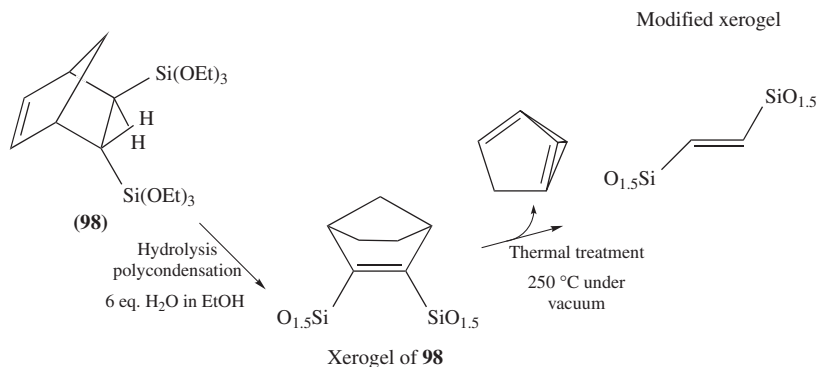
B. Non-oxidative Thermal Elimination of the Organic Groups

More recently, models were developed to achieve the elimination of the template under milder conditions. The first relies on the preparation of a dialkyl carbonate system by polycondensation/hydrolysis of the corresponding precursor family **26**. Thermal treatment of a non-porous xerogel of **26** at 250–350 °C results in the simultaneous elimination of CO₂ and hybrid materials with residual hydroxyalkyl and olefinic functions according to Scheme 18. It is interesting to note that this approach also allows the preparation of materials which cannot be prepared by other routes, such as direct polycondensation of the corresponding allyl and hydroxyalkyl precursors.



SCHEME 18

In the same way, formation of porosity simultaneously with functional modification was tried with the xerogel of **98** containing a *trans*-5,6-bis(triethoxysilyl)norborn-2-ene group. Treatment of **98** at 250 °C leads to a partial elimination of cyclopentadiene (Scheme 19) as confirmed by elemental and spectroscopic data. However, sintering of the material decreases the porosity and specific surface area in the resulting hybrid¹⁹⁹.



SCHEME 19

C. Elimination of the Organic Groups by Chemical Treatment

To avoid the stress due to the high temperature required for the thermal oxidation, different chemical routes were tried.

In a reported example the precursor **29** reacted with an excess of TMOS (TMOS/precursor = 150) to achieve molecular imprinting in silica. A chemical

treatment with trimethylsilyl iodide removes the organic groups in the form of 1,3,5-tris(iodomethyl)benzen and CO_2 . A silica with the templated pore and $-\text{CH}_2\text{CH}_2\text{CH}_2\text{CH}_2\text{NH}_2$ moiety grafted at the surface is obtained¹¹⁴.

Another route was based on the lability of the $\text{Si}-\text{C}_{s/p}$ bond under mild hydrolytic conditions²⁰⁰. It enables (a) to achieve a non-sacrificial route with recovery of the organic component, (b) to compare the oxidation and the chemical treatment and (c) to observe the effect of the molecular architecture defined by the precursor units.

Selective and quantitative cleavage of the $\text{Si}-\text{C}_{s/p}$ bond in xerogel of **54** is achieved with a mixture of water, methanol and NH_4F as a catalyst^{8,97,98,201}. The catalytic cleavage of the $\text{Si}-\text{C}_{s/p}$ bond involves a nucleophilic activation by F^- ^{202,203}. As summarized in Scheme 20, the transformation of the xerogel of **54** lead to silica **54c**, as is also the case for the xerogel of **54** and TMOS. In all cases, material **54c** is stable as attested by the persistence of the same porosity and composition of **54ct** obtained after a thermal curing of **54c** at 600°C . On the other hand, the textural parameters of silica **54c** are completely different from those of **54t** obtained by direct thermal treatment.

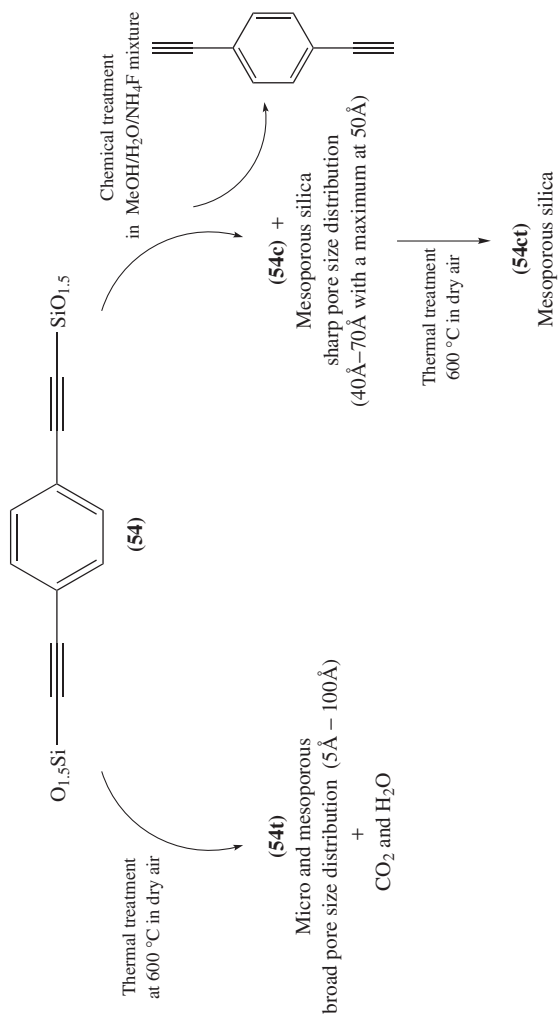
This difference is also supported by Small-angle X-ray scattering (SAXS) data; for **54c** and **54ct** Porod's law is observed [$a q^{-4}$ slope for the linear correlation between $\ln(q \cdot i)$ versus q^2], corresponding to a clear-cut density between the solid silica and the void. For **54t** a completely different feature is observed: a power law $q^{-3.2}$ suggests the possibility of a fractal surface or bushy behaviour. These data correspond to pores in **54c** and **54ct** as elongated cylinders, their size diameters being approximately $42 \text{ \AA} \pm 2$ and an average thickness of solid between two voids of around $32 \text{ \AA} \pm 2$. It is not surprising that slightly different values are obtained by SAXS and porosimetry measurements since the presence of closed porosity cannot be detected by porosimetry. The same type of results is obtained with hybrid xerogels **72** and **99–101** with different rigid aromatic organic groups⁸.

When α,ω -bisethynylalkyl precursors **55–60** are used, the extent of the $\text{Si}-\text{C}_{s/p}$ bond hydrolysis depends on the chain length (Table 9) and the distribution is not as narrow as in the previous cases of **54c** and **54ct**⁹⁹. This is probably the result of a decrease in the accessibility of the reagent due to steric hindrance and hydrophoby of the alkyl group. When elimination is complete ($n = 2$) voids are best described as elongated cylinders with a radius of $27\text{--}30 \text{ \AA}$. On the contrary, direct thermal treatment leads in all cases to a wide pore size distribution ($<15 \text{ \AA}$ to 80 \AA).

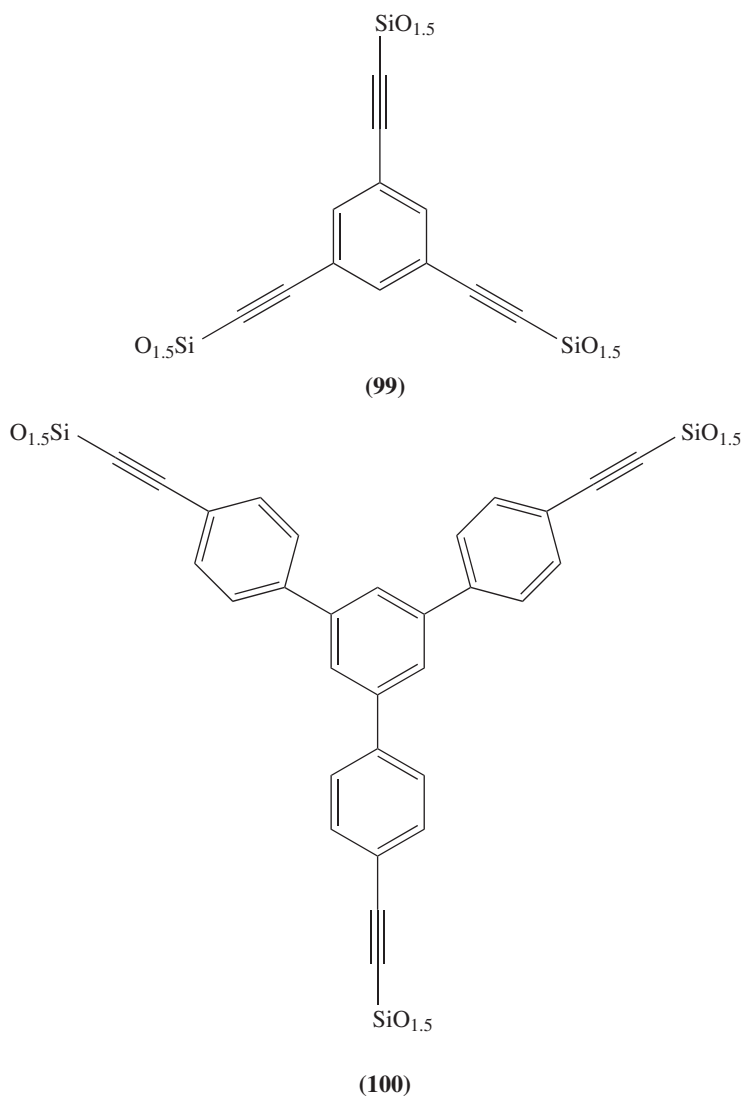
Recently, the generation of microporosity in hybrid xerogels by this route was achieved by co-polycondensation of two precursors **54** and **79** with similar size and geometry, followed by a selective removal of one of the organic spacers²⁰⁴. Elimination of 1,4-bis(ethynyl)benzene from the mixed hybrid xerogels was achieved by a chemical treatment as described in Scheme 21. The resulting hybrid materials exhibit a high specific surface area where the biphenyl groups of precursor **79** remain and act as pillars. The surface of the material is highly hydrophobic. A high level of micropores is formed, their size being very close to the size of the removed organic group (pore size: $4 < \emptyset < 20 \text{ \AA}$, $\text{Si} \cdots \text{Si}$ distance 11.5 \AA).

These results lead to the following interpretation: (1) the thermal oxidative elimination always leads to microporous silica, whatever the nature of the molecular precursor; (2) narrow pore size distributions result from chemical treatment of xerogels with rigid precursors; (3) there is always some discrepancy between the size of the pores and the size of the organic moiety, the pores always being larger.

A possible explanation of points (2) and (3) is the presence of a short-range organization in the starting xerogel leading to the elimination of several stacked organic units during the chemical treatment (see Section V). A reorganization of the silica network can also



SCHEME 20



occur during the chemical treatment. This is supported by the strong influence of the experimental conditions, as demonstrated by chemical treatment of the hybrid xerogel of **54** in different solvents, at different acid concentrations and with different catalysts (Table 10)¹⁶¹.

The classical dissolution/precipitation process could explain this phenomenon. However, under the experimental conditions used, the F⁻ catalysed redistribution process is an alternative process. It is initiated by the coordination of F⁻ at silicon, inducing a catalytic

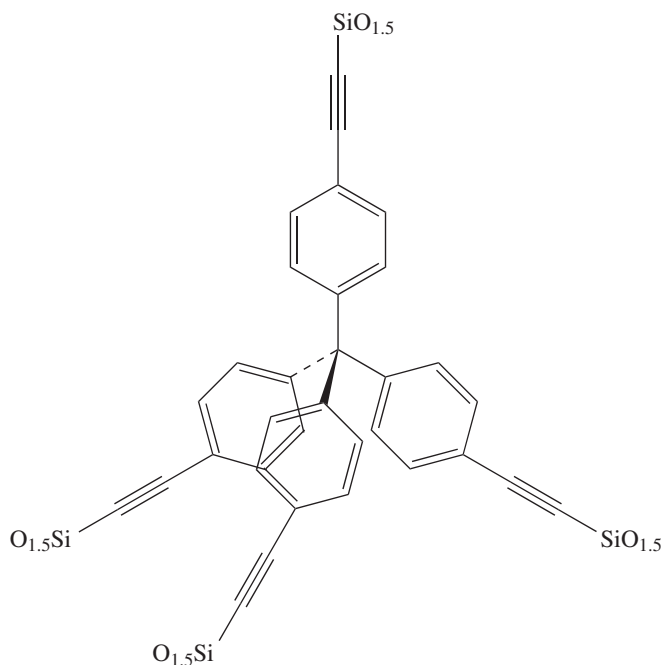
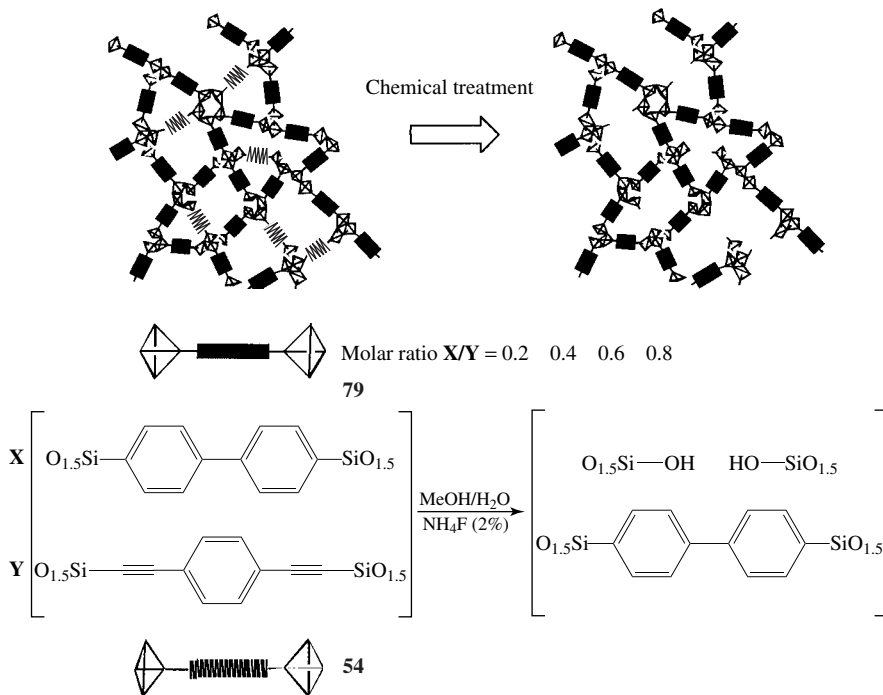


TABLE 9. Efficiency of the chemical treatment related to the nature of the organic group $C\equiv C(CH_2)_n C\equiv C$

Hybrid xerogel $O_{1.5}Si \equiv (CH_2)_n \equiv SiO_{1.5}$	% Organic groups eliminated by chemical treatment	Average pore radius (Å)
$n = 2$ (55)	100	27
$n = 3$ (56)	100	50
$n = 4$ (57)	90	70
$n = 5$ (58)	40	38
$n = 6$ (59)	15	62
$n = 8$ (60)	<5	

redistribution of the oxygen atoms around silicon, as described in Scheme 22^{202,203}. In addition, the nucleophilic activation induced by the F^- can also lead to other kinds of reactions at silicon such as condensation of the silanol (equation 18 and 19) and substitution. The F^- effect on the restructuring of silica for preparing zeolites is currently being investigated^{205,206}. It must also be emphasized that, because the molar volume of the organic part is high in these hybrid materials, their elimination leads to a very thin and fragile Si–O–Si network which is easily accessible to water and catalysts.

Mixex xerogel of **54** and **79**

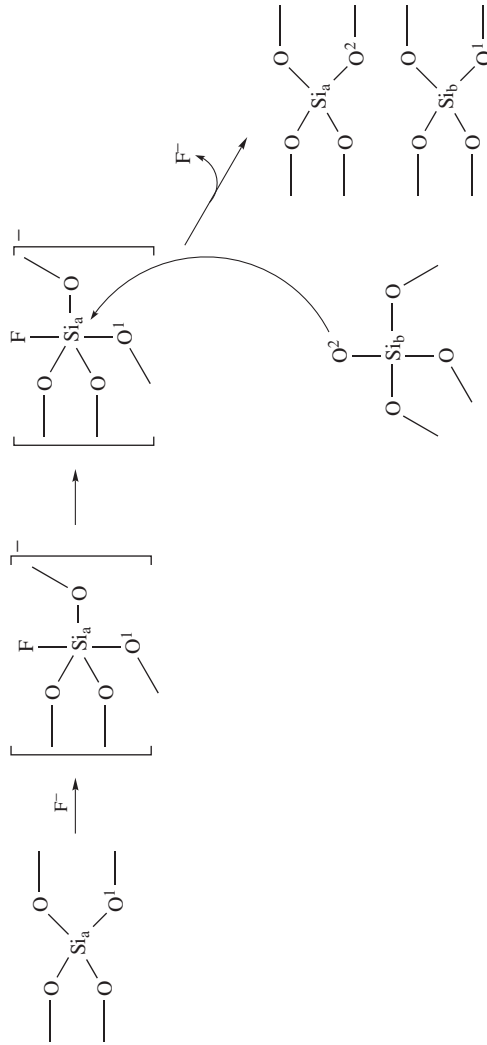
SCHEME 21

TABLE 10. Variation of silica porosity depending on the experimental parameter of the chemical treatment

	Starting xerogel (54)	THF H ₂ O NH ₄	EtOH H ₂ O NH ₄ F	MeOH H ₂ O NBu ₄ F	MeOH H ₂ O NH ₄ F/pH=4	MeOH H ₂ O NH ₄ F/pH=7	MeOH H ₂ O NH ₄ F
Density ^a	1.38	1.55	2.04	2.09	2.04	2.06	2.08
Specific surface area ^b	<10	255	590	180	300	260	655
Average pore radius ^c	—	40	30	65	50	50	50

^ag cm⁻³, ^bm² g⁻¹, ^cin Å.

In conclusion, as mentioned above, the use of silica for molecular imprinting is not straightforward, even if silica is often considered as a chemically stable material. There are at least three main problems: the building of a strong and chemically resistant framework around the template, the reproducibility of the elaboration of the solid and the quantitative elimination of the organic group by mild and selective chemical treatment. However, these results open up interesting perspectives for the rearrangement of silica networks and the chemically-induced textural transformation of solids.



SCHEME 22

VIII. SHAPING OF NANOSTRUCTURED ORGANO-POLYSILSESQUIOXANES $R'(SiO_{1.5})_n$ ($n \geq 2$)

Depending on the procedure, materials with different shapes can be obtained but xerogels are generally obtained as powders since, either at the syneresis or at the drying step, fragmentation of the gel is not prevented. In the following part we describe attempts to control the shape of the material at the macroscopic level (formation of films or monoliths) or at the mesoscopic level (formation of mesoporous hybrid xerogels).

A. Monoliths, Aerogels and Thin Films

During the ageing and mainly drying of the gel, shrinkage and cracking are generally observed, just like for gels prepared with TEOS or TMOS. Slow air drying of the gel or quick processing drying (crush and dry at 100 °C under vacuum) gives the xerogels with more or less the same porosity²⁰⁷. Control of such a process is generally difficult to achieve, but dimethylformamide was used successfully and the rate of evaporation of the solvent is reduced in this case. For xerogel of **40**, monoliths can be obtained⁹¹. Another approach to control the drying process is the preparation of thin films; this was found useful in reducing the specific surface area^{208–210}.

Materials with high specific surface area can be obtained by using supercritical drying with carbon dioxide. Such supercritical drying is most common in sol-gel chemistry²¹¹. Similarly to TEOS or TMOS aerogels, preparation of aerogels of **79** is possible and leads to materials with specific surface area as high as 1880 m² g⁻¹ (20–500 Å Ø pore)^{212,213}.

B. Mesoporous Hybrids (MCM Systems)




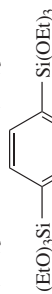
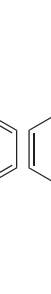
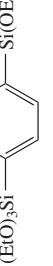
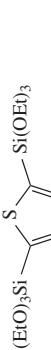
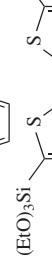
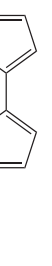


Recently, various authors have been attracted by the possibility to use (RO)₃Si-R'-Si(OR)₃ precursors for the preparation of mesoporous material. The compounds used are listed in Table 11.

The aim is to obtain a hybrid material with a well-defined mesoporosity, a homogeneous distribution of organic and inorganic parts within the framework and a reactive centre. This was inspired by the discovery of the ordered mesoporous silicates with well-defined porosity^{36,37} and the possibility to introduce organic groups on the surface of the mineral oxides (see Figure 4 in Section II.B)^{31,39,214}.

The procedure is similar to that used for the formation of micellar hexagonal phases which is applied in preparing mesoporous oxides. Here, the precursor is mixed with water, a surfactant and a catalyst (NaOH or HCl). The Si–C bond is generally preserved from cleavage, except in the case of basic conditions or with products having a sensitive Si–C_{s/p} bond.

The precursors are used as the only building blocks of the material, but a surfactant is obviously required in order to achieve the formation of the intermediate micellar structure. For TEOS/RSi(OMe)₃ mixture a poorly ordered mixture is obtained, especially with high RSi(OMe)₃ percentages²¹⁹. In contrast, with pure (MeO)₃SiCH₂CH₂Si(OMe)₃ as a precursor, a well-defined hexagonal micellar packing can be achieved. The presence of two Si(OR)₃ groups is certainly advantageous for the formation of the micelle's organization. However, the nature of the organic group can also play a central role due to its hydrophobic character. In such a sophisticated system numerous parameters must be taken into account especially the nature of the precursor and the surfactant. The latter can be chosen from a group of very different structures such as octadecyltrimethylammonium chloride, cetyltrimethylammonium bromide or cetylpyridinium bromide.

TABLE 11. Periodically ordered mesoporous nanostructured organo-polysilsesquioxane

Precursor	Ref.	Surfactant	Specific surface area (m ² g ⁻¹)	Pore size ϕ (Å)
	215	CH ₃ (CH ₂) ₁₇ N ⁺ (CH ₃) ₃ Cl ⁻	750 to 1100 ^a	27–31 ^a
	216	CH ₃ (CH ₂) ₁₅ N ⁺ (CH ₃) ₃ Br ⁻	1134	42 ^a
	216	CH ₃ (CH ₂) ₁₅ N ⁺ (CH ₃) ₃ Br ⁻	1210 ^a	42 ^a
	217	[C ₅ H ₅ N ⁺ -(CH ₂) ₁₅ -CH ₃]	1365	20
	210	CH ₃ (CH ₂) ₁₅ N ⁺ (CH ₃) ₃ Br ⁻ C ₁₆ H ₃₃ (OCH ₂ CH ₂) ₁₀ -OH Na ⁺ (C ₁₂ H ₂₅ OSO ₃) ⁻	18 25	— —
	217	[C ₅ H ₅ N ⁺ -(CH ₂) ₁₅ -CH ₃]		
	217	[C ₅ H ₅ N ⁺ -(CH ₂) ₁₅ -CH ₃] CH ₃ (CH ₂) ₁₅ N ⁺ (CH ₃) ₃ Br ⁻	no mesoporous solid	Si-C cleavage
	217	[C ₅ H ₅ N ⁺ -(CH ₂) ₁₅ -CH ₃] CH ₃ (CH ₂) ₁₅ N ⁺ (CH ₃) ₃ Br ⁻	no mesoporous solid	Si-C cleavage
	210	C ₁₆ H ₃₃ (OCH ₂ CH ₂) ₁₀ -OH	—	—
	210	C ₁₆ H ₃₃ (OCH ₂ CH ₂) ₁₀ -OH	—	—
	218	Na ⁺ (C ₁₂ H ₂₅ OSO ₃) ⁻	bulk density 0.2 g cm ⁻³	lamellar structure

^aDetermined by XRD and TEM analysis.

Thick and hydrophobic walls are present in these materials and, in the case of the CH=CH units, a bromination can be achieved without modification of the pore structure. Such a result reveals the accessibility of the organic group. However, its distribution either at the surface of the solid or in the framework of the walls is not yet clearly demonstrated. The reactivity is of limited interest for this demonstration, but microscopic pictures are more convincing.

Recently, preparation of well-ordered periodic meso-structured hybrid materials was reported with $(\text{MeO})_3\text{Si-R-Si}(\text{OMe})_3$ (R = alkylene, phenylene and 2-butylene) precursors²¹⁰. Using an evaporation-induced self-assembly, thin films with a mesoporous organization can be prepared, and their physical properties (thickness, dielectric constant, modulus and hardness) are closely dependent on the nature of the R group.

There is certainly still much work to do in order to understand and predict the behaviour of such sophisticated [precursor/water/surfactant /catalyst] systems. However, it must be pointed out that they represent one of the most attractive and interesting developments for hybrid material chemistry. Moreover, one may expect that it will be possible to modulate the structure of the mesoporous hybrid, having different functions located at either the surface of the pore or inside the framework of the walls.

IX. SOME PHYSICAL PROPERTIES OF NANOSTRUCTURED ORGANO-POLYSILSESQUIOXANES $\text{R}'(\text{SiO}_{1.5})_n$ ($n \geq 2$)

A. Thermal Properties

Studies of the thermal stability in dry air are frequent for xerogels belonging to the families of precursors **12**, **13**, **14** and **16**, since this property is connected to the preparation of porous silica via oxidative elimination of the organic group (Section VII.A). Generally, two weight losses are observed between 50 °C and 1000 °C. The first, occurring between 50 °C and 250 °C which amounts to 5% loss, corresponds to the elimination of traces of solvent and water, the latest one arising from the condensation of residual silanols. At a higher temperature, degradation of the organic groups by an oxidative process leads to weight losses which are proportional to the molecular weight. This is generally observed between 400 °C and 500 °C for xerogels with an arylene group⁹² or α,ω -bis(ethynyl)alkenes and arylenes^{98,99}. This oxidation temperature is rather high. However, there are only limited data on the chemical process occurring during this transformation which could be compared to that performed with $\text{R}'\text{SiO}_{1.5}$ materials³⁰.

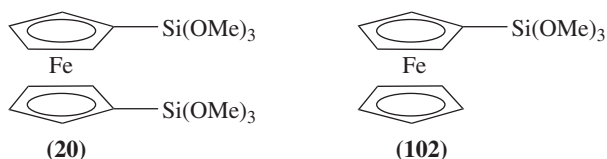
In a few cases, the thermal treatment was performed as a pyrolysis at inert atmosphere, and a very small weight loss was observed for xerogels like **77**⁹⁵, **54** and **78**¹⁵⁰, due to the possible high cross-linking of these materials⁸.

Some $\text{R}'(\text{Si}(\text{OR})_3)_n$ ($n \geq 2$) precursors were also developed for preparing thermo-resistant materials. Thin-film xerogels of the bisimide precursor family **30** are non-porous. Their thermal stability is high, and their decomposition temperature range is 500–520 °C under nitrogen, which is higher than that for the analogous linear polyimides¹¹⁵.

B. Electrochemical Properties

So far, the xerogels with a ferrocene group are the only ones that allow a study of their electrochemical properties. From this point of view, the behaviour of the organometallic unit can be taken as a reference²²⁰, and compared with the xerogel prepared from precursors **20** and **102**¹⁰². When the bis-silylated precursor **20** is co-condensed with a silica precursor (TMOS), the charge transfer of the resulting xerogel follows a law with a fractional exponent. Simultaneously, a complete and reversible oxidation of Fe(II) into

Fe(III) is observed and revealed by Mössbauer spectroscopy. This unique behaviour is indicative of a particular substructure in the gel where ferrocene units are mainly located at the surface of the material. A completely different situation is observed for the bisilylated xerogel obtained from **102** for which a Cottrellian charge transfer is observed and it exhibits a classical reversible voltammogram: the peak current scales linearly with the square root of scan rate. Moreover, it is impossible to achieve a complete Fe(II)/Fe(III) oxidation although the process is still reversible. Such behaviour demonstrates that some of the ferrocenyl units are not accessible and do not participate in the electrochemical process¹⁰³.



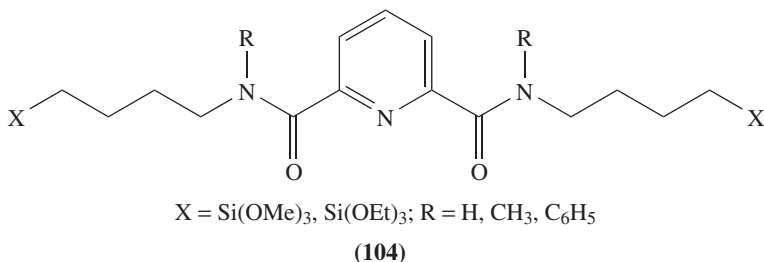
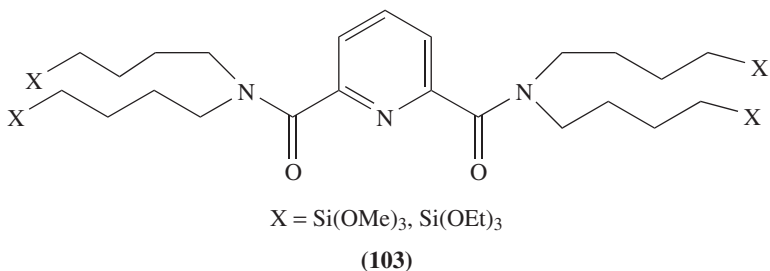
C. Optical Properties

Introduction of optically active molecules into glass is currently under investigation due to the potential application for waveguides, NLO and lasers. Most of the time, a nanocomposite is prepared due to the greater synthetic flexibility and economic advantages of this approach. However, leaching of the dye is often a major drawback which can be overcome by anchoring the organic dye to the silica network. In addition, grafting of the chromophore increases the rigidity of the system and reduces the porosity and both phenomena improve the optical properties^{221,222}. In order to further increase the stability of these systems, to avoid the leaching and micro-segregation phenomena and to enhance the optical properties of the materials, precursors of nanostructured materials have been developed.

In this way, fluorescent transparent xerogels were prepared with terphenyl (**42**) and 9,10-anthryl (**43**) precursors⁹². 1,4-Phenylene-vinylene compounds are another type of chromophore known for their photoluminescent properties which are preserved in the xerogel prepared by hydrolysis/polycondensation of precursors **46–49**. The presence of the chromophore unit is detected from the fluorescent spectra that differ from those of the pure precursors. These differences cannot be directly interpreted in terms of π -stacking effects or molecular deformations. Interestingly, tuning of the optical property can also be achieved by changing the structure of the organic fragment¹⁰⁸.

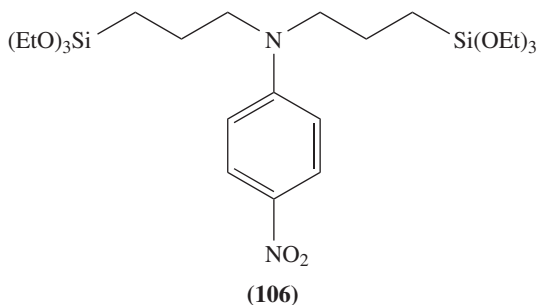
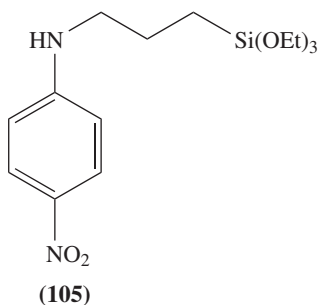
In order to prepare luminescent hybrid xerogels, compounds such as **103** and **104** belonging to the family of precursors **31** have been synthesized. The organic part, a dipicolinic acid derivative, is a chelating group for lanthanides ions. Indeed, hydrolysis/polycondensation in the presence of europium(III) or gadolinium(III) nitrate lead to hybrid xerogels where most of the ligands are bonded to the metal centres^{116,223}. In this system, the organic chelating groups are efficient sensitizers for the luminescence of Eu^{3+} and Gd^{3+} and the silica network does not notably affect the optical characteristics of the organic part. Therefore, the so-called antenna effect (a ligand-to-metal energy transfer process²²⁴) and the luminescent properties of the hybrids are close to those observed in the corresponding organic complexes.

Precursor family **27** with a perylene sub-unit were prepared due to their fluorescent properties and their photostability. Grafting of the perylene unit with $-(\text{CH}_2)_3\text{Si(OR)}_3$ arms (Section III.B) allows their solubility to be increased and thus to prepare materials



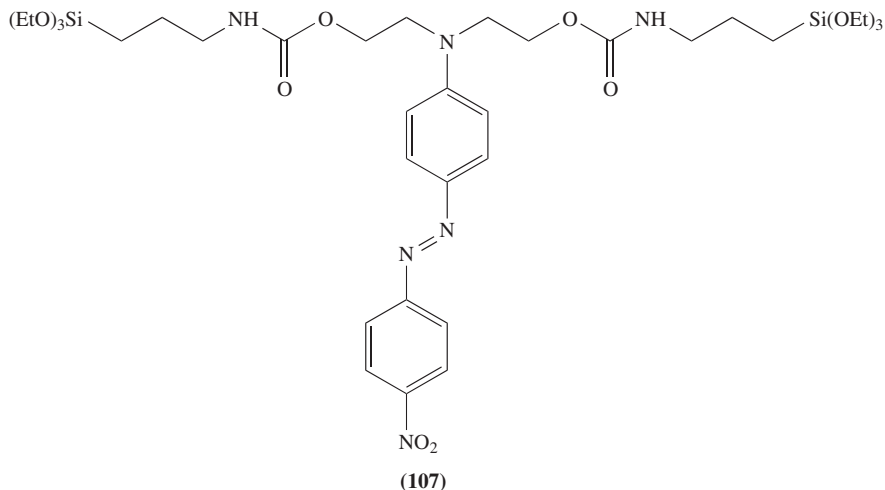
with a dye concentration higher than that available for [silica/perylene] nanocomposites¹¹². Co-condensation with silica or silsesquioxane precursors leads to the preparation of electroluminescent devices, which were further improved by incorporation of charge transport materials (triphenylamine as a hole and 1,3,4-oxadiazole as electron-conducting component) that reduce the necessary amount of dye²²⁵.

Preparation of xerogel with NLO properties was investigated using precursor **105** and **106**. While **105** must be co-condensed with a silica precursor in order to achieve the formation of a solid, only **106** leads to a xerogel. In this case, where the chromophore is attached by two anchoring sites, curing of thin films in the presence of a strong electric field promotes the orientation of the molecule and leads to a NLO property as high as those of lithium niobate^{90,222,226}.



Another type of organic dye was introduced through co-condensation of TMOS and precursor **107**. For a thin film (4.2 μm thick), a very high second-harmonic generation signal was obtained ($d_{33} = 150 \text{ pm V}^{-1}$, $\lambda = 1.34 \mu\text{m}$). Interestingly, this study demonstrates the importance of the processing parameters used for the elaboration of the material

(ageing of the sol, precursor/TMOS ratio) and points out the improvement of the NLO properties by thermal curing^{83,120,227}.



D. Mechanical Properties

Mechanical properties of the gels and xerogels of organo-polysilsesquioxanes have not been the subject of much investigation, but some data exist for hybrid gels and xerogels with a dendrimeric core **38**^{122,123,143}. In these cases stress-strain studies have shown a completely elastic behaviour. From this point of view their behaviour lies in between that of a conventional glass and that of highly cross-linked rubbers. Similar behaviour was observed for bisimide xerogels prepared from precursor family **30**. Their hardness ranges between that of nylon-6 and SiO₂¹¹⁵.

X. GENERAL SUMMARY

The research fields that deal with the hybrid organic-inorganic materials are very broad because they bridge material sciences and molecular chemistry. The great adaptability of the inorganic hydrolytic sol-gel process permits building up of new solids with properties designed at the molecular level. The examples described in this chapter are just the beginning of a long story. The potential for new materials relies on the combined properties of both the organic and inorganic units and also on the possibility to control the texture of the material. Altogether, they provide the tools with which to prepare a large number of materials and design new devices.

These perspectives are enhanced by using templates, as already observed in the case of the so-called mesoporous materials. First attempts are already showing the possibility of including organic units in the 'walls' of the materials. It is also important to note that, at the present time, silica is the most popular material that can be prepared by the sol-gel process. The chemistry that we have presented here will certainly expand this range of materials and combine it with other oxides or mixed oxides. Beside these suggestions which are more or less obvious in the context of the chemistry of this kind of materials, other directions will be also of interest for the preparation of new materials.

XI. REFERENCES

1. J. Livage, *Chem. Scr.*, **28**, 9 (1988).
2. J. Rouxel, *Chem. Scr.*, **28**, 33 (1988).
3. J.-P. Jolivet, *De la solution à l'oxyde*, InterÉditions, Paris, 1994.
4. C. J. Brinker and G. W. Scherer, *Sol-Gel Science*, Academic Press, Boston, 1990.
5. E. Anglaret, A. Hasmy and R. Jullien, *Phys. Rev. Lett.*, **75**, 4059 (1995).
6. J. Livage, C. Sanchez and F. Babonneau, in *Chemistry of Advanced Materials: An Overview* (Eds. L. V. Interrante and M. J. Hampden-Smith), VCH, New York, 1998.
7. P. Judenstein and C. Sanchez, *J. Mater. Chem.*, **6**, 511 (1996).
8. R. J. P. Corriu, *Angew. Chem., Int. Ed. Engl.*, **39**, 1376 (2000).
9. R. J. P. Corriu and D. Leclercq, *Angew. Chem., Int. Ed. Engl.*, **35**, 4001 (1996).
10. D. Avnir, L. C. Klein, D. Levy, U. Schubert and A. B. Wojcik, in *The Chemistry of Organic Silicon Compounds*, Vol. 2 (Eds. Z. Rappoport and Y. Apeloig), Wiley, Chichester, 1998, pp. 2317–2362.
11. C. Sanchez and F. Ribot, *New J. Chem.*, **18**, Special issue, 1007 (1994).
12. J. P. Boilot, F. Chaput, J. Biteau, A. V. Veretlemarinier, J. P. Galaup, D. Riehl and Y. Levy, *Ann. Phys.*, **20**, 727 (1995).
13. M. M. Collinson, *Mikrochim. Acta*, **129**, 149 (1998).
14. J. E. Mark and C. Y. - C. Lee (Eds.) *Hybrid Organic-Inorganic Composites*, ACS, Washington, 1995.
15. B. K. Coltrain, C. Sanchez, D. W. Schaefer and G. L. Wilkes (Eds.), *Better Ceramics Through Chemistry VII. Organic/Inorganic Hybrid Materials*, Materials Research Society, Pittsburg, 1996.
16. R. M. Laine, C. Sanchez, C. Brinker and E. Ganel's (Eds.) *Organic/Inorganic Hybrid Materials*, Materials Research Society, Pittsburg, 1998.
17. A. Lobnik and O. S. Wolfbeis, *Analyst*, **123**, 2247 (1998).
18. M. T. Murtagh, H. C. Kwon, M. R. Shahriari, M. Krihak and D. E. Ackley, *J. Mater. Res.*, **13**, 3326 (1998).
19. M. T. Murtagh, M. R. Shahriari and M. Krihak, *Chem. Mater.*, **10**, 3862 (1998).
20. C. Rottman, G. S. Grader, Y. Dehazan and D. Avnir, *Langmuir*, **12**, 5505 (1996).
21. K. Kitaoka, N. Matsuo, J. Si, T. Mitsuyu and K. Hirao, *Jap. J. Appl. Phys., Part 2 Lett.*, **38**, L1029 (1999).
22. C. Rottman, G. Grader, Y. De Hazan, S. Melchior and D. Avnir, *J. Am. Chem. Soc.*, **121**, 8533 (1999).
23. Y. Kotani, A. Matsuda, M. Tatsumisago, T. Minami and M. A. Haga, *J. Mater. Chem.*, **9**, 3041 (1999).
24. L. M. Ilharco and J. M. G. Martinho, *Langmuir*, **15**, 7490 (1999).
25. L. Y. Liu, L. Xu, Z. J. Hou, Z. L. Xu, J. Chen, W. C. Wang and F. M. Li, *Phys. Lett. A*, **262**, 206 (1999).
26. T. Ishiwaki, H. Inoue and A. Makishima, *J. Non-Cryst. Solids*, **203**, 43 (1996).
27. A. Martucci, P. Innocenzi, J. Fick and J. D. Mackenzie, *J. Non-Cryst. Solids*, **244**, 55 (1999).
28. Y. Zhang and M. Q. Wang, *Mater. Sci. Eng. B, Solid State Mater. Adv. Tech.*, **49**, 205 (1997).
29. L. L. Hu and Z. H. Jiang, *Opt. Commun.*, **148**, 275 (1998).
30. N. K. Raman, M. T. Anderson and C. J. Brinker, *Chem. Mater.*, **8**, 1682 (1996).
31. M. H. Lim and A. Stein, *Chem. Mater.*, **11**, 3285 (1999).
32. D. J. Macquarrie, D. B. Jackson, J. E. G. Mdoe and J. H. Clark, *New J. Chem.*, **23**, 539 (1999).
33. D. Hagrman, D. J. Warren, R. C. Haushalter, C. Seip, C. J. O'Connor, R. S. J. Rarig, K. M. Johnson, R. L. J. LaDuca and J. Zubieta, *Chem. Mater.*, **12**, 188 (2000).
34. M. J. MacLachlan, T. Asefa and G. A. Ozin, *Chem. Eur. J.*, **6**, 2507 (2000).
35. T. Asefa, C. Yoshina-Ishii, M. J. MacLachlan and G. A. Ozin, *J. Mater. Chem.*, **10**, 1751 (2000).
36. C. T. Kresge, M. E. Leonowicz, W. J. Roth, J. C. Vartuli and J. S. Beck, *Nature*, **359**, 710 (1992).
37. J. S. Beck, J. C. Vartuli, W. J. Roth, M. E. Leonowicz, C. T. Kresge, K. D. Schmitt, T. Chu, W. D. H. Olson, E. W. Sheppard, S. B. McCullen, J. B. Higgins and J. L. Schlenker, *J. Am. Chem. Soc.*, **114**, 10834 (1992).

38. A. Corma, *Chem. Rev.*, **97**, 2373 (1997).
39. M. H. Lim, C. F. Blandford and A. Stein, *J. Am. Chem. Soc.*, **119**, 4090 (1997).
40. F. Babonneau, L. Leite and S. Fontlupt, *J. Mater. Chem.*, **9**, 175 (1999).
41. C. E. Fowler, S. L. Burkett and S. Mann, *Chem. Commun.*, 1769 (1997).
42. D. J. Macquarrie, *Chem. Commun.*, 1961 (1996).
43. R. J. P. Corriu, C. Hoarau, A. Mehdi and C. Reyé, *Chem. Commun.*, 71 (2000).
44. R. J. P. Corriu, A. Mehdi and C. Reyé, *C. R. Acad. Sci. Paris*, **2**, *Série II c*, 35 (1999).
45. G. H. Mehl and I. M. Saez, *Appl. Organomet. Chem.*, **13**, 261 (1999).
46. R. Laine, *Appl. Organomet. Chem.*, **13**, 211 (1999).
47. R. Duchateau, U. Cremer, R. J. Harmsen, S. I. Mohamad, H. C. L. Abbenhuis, R. A. van Santen, A. Meetsma, S. K. H. Thiele, M. F. H. van Tol and M. Kranenburg, *Organometallics*, **18**, 5447 (1999).
48. C. Marcolli and G. Calzaferri, *Appl. Organomet. Chem.*, **13**, 213 (1999).
49. R. Murugavel, A. Voigt, G. M. Walawalkar and H. W. Roesky, *Chem. Rev.*, **96**, 2205 (1996).
50. R. H. Baney, M. Itoh, A. Sakakibara and T. Suzuki, *Chem. Rev.*, **95**, 1410 (1995).
51. F. Ribot and C. Sanchez, *Commun. Inorg. Chem.*, **20**, 327 (1999).
52. U. Schubert, N. Hüsing and A. Lorenz, *Chem. Mater.*, **7**, 2010 (1995).
53. B. Arkles, *Chemtech*, **12**, 7 (1999).
54. D. R. Bujalski, S. Grigoras, W. L. N. Lee, G. M. Wieber and G. A. Zank, *J. Mater. Chem.*, **8**, 1427 (1998).
55. T. M. Chaudhry, H. Ho, L. T. Drzal, M. Harris and R. M. Laine, *Mater. Sci. Eng. A, Struct. Mater. Prop. Microstruct. Process.*, **195**, 237 (1995).
56. F. I. Hurwitz, P. Heimann, S. C. Farmer and D. M. Hembree, *J. Mater. Sci.*, **28**, 6622 (1993).
57. J. J. E. Moreau and M. Wong Chi Man, *Coord. Chem. Rev.*, **178**, 1073 (1998).
58. D. Brunel, *Microporous Mesoporous Mater.*, **27**, 329 (1999).
59. D. Brunel, N. Bellocq, P. Sutra, A. Cauvel, M. Lasperas, P. Moreau, F. Di Renzo, A. Galarneau and F. Fajula, *Coord. Chem. Rev.*, **10**, 2951 (1998).
60. K. Moller and T. Bein, *Chem. Mater.*, **10**, 2951 (1998).
61. H. Nakashima and M. Irie, *Macromol. Rapid Commun.*, **18**, 625 (1997).
62. H. Nakashima and M. Irie, *Macromol. Chem. Phys.*, **200**, 683 (1999).
63. C. Ossadnik, S. Veprek, H. C. Marsmann and E. Rikowski, *Monatsh. Chem.*, **130**, 55 (1999).
64. P. Xie and R. B. Zhang, *Polym. Adv. Technol.*, **8**, 649 (1997).
65. W. C. Chen and C. T. Yen, *J. Polym. Res.*, **6**, 197 (1999).
66. W. C. Chen, S. C. Lin, B. T. Dai and M. S. Tsai, *J. Electrochem. Soc.*, **146**, 3004 (1999).
67. A. T. Kohl, R. Mimna, R. Shick, L. Rhodes, Z. L. Wang and P. A. Kohl, *Electrochem. Solid-State Lett.*, **2**, 77 (1999).
68. J. L. Hedrick, H. J. Cha, R. D. Miller, D. Y. Yoon, H. R. Brown, S. Srinivasan, R. Di Pietro, R. F. Cook, J. P. Hummel, D. P. Klaus, E. G. Liniger and E. E. Simonyi, *Macromolecules*, **30**, 8512 (1997).
69. H. C. Liou and J. Pretzer, *Thin Solid Films*, **335**, 186 (1998).
70. P. T. Liu, T. C. Chang, S. M. Sze, F. M. Pan, Y. J. Mei, W. F. Wu, M. S. Tsai, B. T. Dai, C. Y. Chang, F. Y. Shih and H. D. Huang, *Thin Solid Films*, **332**, 345 (1998).
71. J. H. Zhao, I. Malik, T. Ryan, E. T. Ogawa, P. S. Ho, W. Y. Shih, A. J. McKerrow and K. J. Taylor, *Appl. Phys. Lett.*, **74**, 944 (1999).
72. Y. K. Siew, G. Sarkar, X. Hu, J. Hui, A. See and C. T. Chua, *J. Electrochem. Soc.*, **147**, 335 (2000).
73. B. R. Harkness, K. Takeuchi and M. Tachikawa, *Macromolecules*, **31**, 4798 (1998).
74. B. R. Harkness, K. Takeuchi and M. Tachikawa, *Polym. Adv. Technol.*, **10**, 669 (1999).
75. M. J. Loboda, C. M. Grove and R. F. Schneider, *J. Electrochem. Soc.*, **145**, 2861 (1998).
76. N. Yamada and T. Takahashi, *J. Electrochem. Soc.*, **147**, 1477 (2000).
77. V. Belot, R. J. P. Corriu, D. Leclercq, P. H. Mutin and A. Vioux, *J. Non-Cryst. Solids*, **176**, 33 (1994).
78. G. Cerveau, R. J. P. Corriu, J. Dabosi, J. L. Aubagnac, R. Combarieu and Y. de Puydt, *J. Mater. Chem.*, **8**, 1761 (1998).
79. G. Cerveau, R. J. P. Corriu, R. Combarieu, J. Dabosi and C. Lepeytre, *Rapid Commun. Mass Spectrom.*, **13**, 2183 (1999).
80. G. Cerveau, R. J. P. Corriu and C. Lepeytre, *J. Mater. Chem.*, **5**, 793 (1995).

81. V. Belot, R. J. P. Corriu, D. Leclercq, M. Pauthe, J. Phalippou and A. Vioux, *J. Non-Cryst. Solids*, **125**, 187 (1990).
82. C. Sanchez and B. Lebeau, *Pure Appl. Opt.*, **5**, 689 (1996).
83. B. Lebeau, J. Maquet, C. Sanchez, E. Toussaere, R. Hierle and J. Zyss, *J. Mater. Chem.*, **4**, 1855 (1994).
84. D. A. Loy and K. J. Shea, *Chem. Rev.*, **95**, 1431 (1995).
85. R. J. P. Corriu, *Polyhedron*, **17**, 925 (1998).
86. R. J. P. Corriu, *C. R. Acad. Sci. Paris*, **2, Série II c**, 83 (1998).
87. G. Cerveau and R. J. P. Corriu, *Coord. Chem. Rev.*, **180**, 1051 (1998).
88. D. A. Loy, G. M. Jamison, B. M. Baugher, S. A. Myers, R. A. Assink and K. J. Shea, *Chem. Mater.*, **8**, 656 (1996).
89. E. Lindner, T. Scheller, F. Auer and H. A. Mayer, *Angew. Chem., Int. Ed. Engl.*, **38**, 2154 (1999).
90. H. W. Oviatt, K. J. Shea and J. H. Small, *Chem. Mater.*, **5**, 943 (1993).
91. K. J. Shea, D. A. Loy and O. W. Webster, *Chem. Mater.*, **1**, 572 (1989).
92. K. J. Shea, D. A. Loy and O. W. Webster, *J. Am. Chem. Soc.*, **114**, 6700 (1992).
93. R. J. P. Corriu, J. J. E. Moreau, P. Thépot and M. Wong Chi Man, *Chem. Mater.*, **4**, 1217 (1992).
94. R. J. P. Corriu, J. J. E. Moreau, P. Thépot, M. Wong Chi Man, C. Chorro, J. P. Lèreporte and J. L. Sauvajol, *Chem. Mater.*, **6**, 640 (1994).
95. R. J. P. Corriu, J. J. E. Moreau, P. Thépot and M. Wong Chi Man, *Chem. Mater.*, **8**, 100 (1996).
96. D. A. Loy, J. P. Carpenter, S. A. Yamanaka, M. D. McClain, J. Greaves, S. Hobson and K. J. Shea, *Chem. Mater.*, **10**, 4129 (1998).
97. P. Chevalier, R. J. P. Corriu, J. J. E. Moreau and M. Wong Chi Man, *J. Sol-gel Sci. Technol.*, **8**, 603 (1997).
98. P. Chevalier, R. J. P. Corriu, P. Delord, J. J. E. Moreau and M. Wong Chi Man, *New J. Chem.*, **22**, 423 (1998).
99. B. Boury, P. Chevalier, R. J. P. Corriu, P. Delord, J. J. E. Moreau and M. Wong Chi Man, *Chem. Mater.*, **11**, 281 (1999).
100. G. Cerveau, R. J. P. Corriu and B. Dabien, *J. Mater. Chem.*, **10**, 1113 (2000).
101. R. J. P. Corriu, J. J. E. Moreau, P. Thépot and M. Wong Chi Man, *Chem. Mater.*, **4**, 1217 (1992).
102. P. Audebert, P. Calas, G. Cerveau, R. J. P. Corriu and N. Costas, *Electroanal. Chem.*, **372**, 275 (1994).
103. G. Cerveau, R. J. P. Corriu and N. Costas, *J. Non-Cryst. Solids*, **163**, 226 (1993).
104. R. J. P. Corriu, J. J. E. Moreau, P. Thépot and M. Wong Chi Man, *J. Mater. Chem.*, **4**, 987 (1994).
105. P. J. Barri, S. W. Carr, D. Li Ou and A. C. Sullivan, *Chem. Mater.*, **7**, 265 (1995).
106. S. W. Carr, M. Motavelli, D. Li Ou and A. C. Sullivan, *J. Mater. Chem.*, **7**, 265 (1995).
107. G. Cerveau, R. J. P. Corriu and C. Lepeytre, *Chem. Mater.*, **9**, 2561 (1997).
108. R. J. P. Corriu, P. Hesemann and G. Lanneau, *Chem. Commun.*, 1845 (1996).
109. J.-P. Bezombes, C. Chuit, R. J. P. Corriu and C. Reyé, *J. Mater. Chem.*, **8**, 1749 (1998).
110. J.-P. Bezombes, C. Chuit, R. J. P. Corriu and C. Reyé, *J. Mater. Chem.*, **9**, 1727 (1999).
111. D. A. Loy, J. V. Beach, B. M. Baugher, R. A. Assink, K. J. Shea, J. Tran and J. H. Small, *Chem. Mater.*, **11**, 3333 (1999).
112. M. Schneider and K. Mullen, *Chem. Mater.*, **12**, 352 (2000).
113. G. Dubois, R. J. P. Corriu, C. Reyé, S. Brandès, F. Denat and R. Guillard, *Chem. Commun.*, 2283 (1999).
114. A. Katz and M. E. Davis, *Nature*, **403**, 286 (2000).
115. S. Hobson and K. J. Shea, *Chem. Mater.*, **9**, 616 (1997).
116. A.-C. Franville, D. Zambon and R. Mahiou, *Chem. Mater.*, **12**, 428 (2000).
117. G. Dubois, C. Reyé, R. J. P. Corriu and C. Chuit, *J. Mater. Chem.*, **10**, 1091 (2000).
118. G. Dubois, C. Reyé, R. J. P. Corriu and C. Chuit, *Chem. Commun.*, 723 (1999).
119. A. Adima, J. J. E. Moreau and M. Wong Chi Man, *J. Mater. Chem.*, **7**, 2331 (1997).
120. B. Lebeau, S. Brasselet, J. Zyss and C. Sanchez, *Chem. Mater.*, **9**, 1012 (1997).
121. B. Boury, R. J. P. Corriu and R. Nunez, *Chem. Mater.*, **10**, 1795 (1998).

122. M. J. Michalczyk and K. G. Sharp, in *Tailor-Made Silicon-Oxygen Compounds 1* (Eds. R. J. P. Corriu and P. Jutzi), Vieweg, Germany, Wiesbaden, 1996, p. 295
123. K. G. Sharp, *Adv. Mater.*, **10**, 1243 (1998).
124. P. Battioni, E. Cardin, M. Louloudi, B. Schöllhorn, G. A. Spyroulias, D. Mansuy and T. G. Traylor, *Chem. Commun.*, 2037 (1996).
125. J. W. Kriesel and T. D. Tilley, *Chem. Mater.*, **11**, 1190 (1999).
126. J. W. Kriesel and T. D. Tilley, *Chem. Mater.*, **12**, 1171 (2000).
127. C. Eaborn, *Organosilicon Compounds*, Butterworths, London, 1960.
128. G. Cerveau, R. J. P. Corriu and C. Lepeyre, *J. Organomet. Chem.*, **548**, 99 (1997).
129. R. J. P. Corriu, J. J. E. Moreau and M. Wong Chi Man, *J. Sol-gel Sci. Technol.*, **2**, 87 (1994).
130. H. Wolter, W. Glaubbitt and K. Rose, *Mater. Res. Soc. Symp. Proc.*, **271**, 719 (1992).
131. R. Calas and J. Dunogues, *J. Organomet. Chem. Rev.*, **2**, 277 (1976).
132. D. J. Brondani, R. J. P. Corriu, S. El Ayoubi, J. J. E. Moreau and M. Wong Chi Man, *Tetrahedron Lett.*, **34**, 2111 (1993).
133. D. J. Brondani, R. J. P. Corriu, S. El Ayoubi, J. J. E. Moreau and M. Wong Chi Man, *J. Organomet. Chem.*, **451**, C1 (1993).
134. R. A. Benkeser, J. M. Gaul and W. E. Smith, *J. Am. Chem. Soc.*, **91**, 3666 (1969).
135. R. F. Heck, *Org. React.*, **27**, 345 (1982).
136. E. Colvin, *Silicon in Organic Chemistry*, Butterworths, London, 1981.
137. R. J. P. Corriu, N. Escudie and C. Guérin, *J. Organomet. Chem.*, **271**, C7 (1984).
138. D. A. Loy, J. P. Carpenter, S. A. Myers, R. A. Assink, J. H. Small, J. Greaves and K. J. Shea, *J. Am. Chem. Soc.*, **118**, 8501 (1996).
139. D. A. Loy, J. P. Carpenter, S. A. Myers, R. A. Assink, J. H. Small, J. Greaves and K. J. Shea, in *Material Research Symposium Proceeding. Better Ceramics Through Chemistry VII: Organic/Inorganic Hybrid Materials 435* (Eds K. B. Coltain, C. Sanchez, D. W. Schaefer and L. G. Wilkes), Materials Research Society, Pittsburg, 1996, p. 33.
140. D. A. Loy, J. P. Carpenter, A. S. Yamanaka, M. D. McClain, J. Greaves, S. Hobson and K. J. Shea, *Chem. Mater.*, **10**, 4129 (1998).
141. D. A. Loy, J. P. Carpenter, T. D. Alam, R. Shaltout, P. K. Dorthout, J. Greaves, J. H. Small and K. J. Shea, *J. Am. Chem. Soc.*, **121**, 5413 (1999).
142. M. J. Michalczyk, W. J. Simonsick Jr. and K. G. Sharp, *J. Organomet. Chem.*, **521**, 261 (1996).
143. M. J. Michalczyk and K. G. Sharp, *J. Sol-gel Sci. Technol.*, **8**, 541 (1997).
144. R. H. Glaser, G. L. Wilkes and C. E. Bronnimann, *J. Non-Cryst. Solids*, **113**, 73 (1989).
145. H. Marsmann, in *NMR Basic Principles and Progress 17* (Eds. P. Diehl, E. Fluck and R. Kosfeld), Springer-Verlag, Berlin, 1981, p. 65.
146. G. Engelhardt and D. Michel, *High-resolution NMR of Silicates and Zeolites*, Wiley, Chichester, 1987.
147. C. A. Fyfe, G. C. Gobbi, G. J. Kennedy, C. T. De Schutter, W. J. Murphy, R. S. Ozubko and D. A. Slack, *Chem. Lett.*, **2**, 163 (1984).
148. W. G. Klemperer, V. V. Mainz and D. M. Millar, in *Better Ceramics Through Chemistry II. Material Research Symposium Proceedings. 73* (Eds. C. J. Brinker, D. E. Clark and D. R. Ulrich), Materials Research Society, Pittsburg, 1986, p. 15.
149. G. Cerveau, R. J. P. Corriu, C. Lepeyre and H. P. Mutin, *J. Mater. Chem.*, **8**, 2707 (1998).
150. B. Boury, R. J. P. Corriu and V. Le Strat, to appear.
151. G. Cerveau, R. J. P. Corriu and E. Framery, *Chem. Comm.*, 2081 (1999).
152. G. Cerveau, R. J. P. Corriu and E. Framery, *J. Mater. Chem.*, **10**, 1617 (2000).
153. J. Livage, M. Henry and C. Sanchez, *Prog. Solid State Chem.*, **18**, 259 (1988).
154. L. L. Hench and J. K. West, *Chem. Rev.*, **90**, 33 (1990).
155. G. Cerveau, R. J. P. Corriu and C. Lepeyre, *J. Mater. Chem.*, **9**, 1149 (1999).
156. D. A. Loy, R. J. Buss, R. A. Assink, K. J. Shea and H. Oviatt, in *Better Ceramics Through Chemistry VI 346* (Eds. A. K. Cheetham, C. J. Brinker, L. M. Mecartney and C. Sanchez), Materials Research Society, Pittsburgh, 1994, p. 825.
157. D. A. Loy, R. J. Buss, R. A. Assink, K. J. Shea and H. Oviatt, *Polym. Prepr., Am. Chem. Soc., Div. Polym. Chem.*, **34**, 244 (1993).
158. G. M. Jamison, D. A. Loy, R. A. Assink and K. J. Shea, in *Better Ceramics Through Chemistry VI 346* (Eds. A. K. Cheetham, C. J. Brinker, L. M. Mecartney and C. Sanchez), Materials Research Society, Pittsburgh, 1994, p. 487.

159. U. d. S. Rhône Poulenc IOM (Technical procedure).
160. D. W. Schaefer, G. B. Beaucauge, D. A. Loy, T. A. Ulibarri, E. Black, K. J. Shea and R. J. Buss, in *Material Research Symposium Proceeding. Better Ceramics Through Chemistry VII: Organic/Inorganic Hybrid Materials 435* (Eds K. B. Coltain, C. Sanchez, D. W. Schaefer and L. G. Wilkes), Materials Research Society, Pittsburg, 1996, p. 301.
161. B. Boury, R. J. P. Corriu, P. Delord and V. Le Strat, *New J. Chem.*, **23**, 531 (1999).
162. B. Boury, R. J. P. Corriu, P. Delord and V. Le Strat, *J. Non-Cryst. Solids*, **265**, 41 (2000).
163. V. Le Strat, *Thèse de l'Université de Montpellier II*, France (2000).
164. J. L. Faulon, D. A. Loy, G. A. Carlson and K. J. Shea, *Comput. Mater. Sci.*, **3**, 334 (1995).
165. B. Boury, R. J. P. Corriu, P. Delord, M. Nobili and V. Le Strat, *Angew. Chem., Int. Ed. Engl.*, **38**, 3172 (1999).
166. F. Ben, B. Boury, R. J. P. Corriu and V. Le Strat, *Chem. Mater.*, **12**, 3249 (2000).
167. J. Sauer, P. Ugliengo, E. Garrone and V. R. Saunders, *Chem. Rev.*, **94**, 2095 (1994).
168. B. Boury, F. Carre, R. J. P. Corriu and R. Nunez, *Chem. Commun.*, 2309 (1998).
169. R. P. Corriu, P. Gerbier, C. Guérin, B. Henner and R. Fourcade, *J. Organomet. Chem.*, **449**, 111 (1993).
170. R. P. Corriu, P. Gerbier, C. Guérin, B. Henner, A. Jean and H. Mutin, *Organometallics*, **11**, 2507 (1992).
171. V. Enkelman, *Adv. Polym. Sci.*, **63**, 91 (1984).
172. F. Granier, *Angew. Chem., Int. Ed. Engl.*, **28**, 513 (1989).
173. F. Roncali, *Chem. Rev.*, **92**, 711 (1992).
174. J. L. Sauvajol, J. P. Lère-Porte and J. J. E. Moreau, Chap. 14 in *Handbook of Organic Conductive Molecules and Polymers*, Vol. 2 (Ed. H. S. Nalwa), Wiley, New York, 1997, p. 625.
175. R. J. P. Corriu, J. J. E. Moreau, P. Thépot, C. Chorro, J. P. Lèreporte, J. L. Sauvajol and M. Wong Chi Man, *Synth. Met.*, **62**, 233 (1994).
176. M. Bouachrine, J. P. Lère-Porte, J. J. E. Moreau and M. Wong Chi Man, *J. Mater. Chem.*, **5**, 797 (1995).
177. E. Lindner, T. Schneller, H. A. Mayer, H. Bertagnolli, T. S. Ertel and W. Hörner, *Chem. Mater.*, **9**, 1524 (1997).
178. E. Lindner, M. Kemmler, T. Schneller and H. A. Mayer, *Inorg. Chem.*, **34**, 5489 (1995).
179. J.-P. Bezombes, C. Chuit, R. J. P. Corriu and C. Reyé, *Can. J. Chem.*, **78**, 1519 (2000).
180. M. Moran, I. Cuadrado, M. C. Pascual and C. M. Casado, *Organometallics*, **11**, 1210 (1992).
181. J. C. Pedersen, *J. Am. Chem. Soc.*, **89**, 7017 (1967).
182. J. M. Lehn, *Science*, **227**, 849 (1985).
183. I. O. Sutherland, *Chem. Soc. Rev.*, **15**, 63 (1986).
184. E. Lindner, A. Bader, E. Glaser, B. Pfeleiderer, W. Schumann and E. Bayer, *J. Organomet. Chem.*, **255**, 45 (1988).
185. E. Lindner, Q. Wang, H. A. Mayer, R. Fawzi and M. Steimann, *Organometallics*, **12**, 1865 (1993).
186. E. Lindner, T. Schneller, F. Auer, P. Wegner and A. H. Mayer, *Chem. Eur. J.*, **3**, 1833 (1997).
187. E. Lindner, M. Kemmler, A. H. Mayer and P. Weger, *Chem. Ber.*, **125**, 2385 (1992).
188. E. Lindner, M. Kemmler, A. H. Mayer and P. Weger, *J. Am. Chem. Soc.*, **116**, 348 (1994).
189. E. Lindner, A. Jäger, T. Schneller and A. H. Mayer, *Chem. Mater.*, **9**, 81 (1997).
190. E. Lindner, R. Schreiber, M. Kemmler, T. Schneller and A. H. Mayer, *Chem. Mater.*, **7**, 951 (1995).
191. E. Lindner, R. Schreiber, T. Schneller, P. Weger, A. H. Mayer, W. Göpel and C. Ziegler, *Inorg. Chem.*, **25**, 514 (1996).
192. K. M. Choi and K. J. Shea, *J. Phys. Chem. B*, **98**, 3207 (1994).
193. K. M. Choi and K. J. Shea, *Chem. Mater.*, **5**, 1067 (1993).
194. K. M. Choi and K. J. Shea, *J. Phys. Chem. B*, **99**, 4720 (1995).
195. K. M. Choi and K. J. Shea, *J. Am. Chem. Soc.*, **116**, 9052 (1994).
196. C. J. Brinker, R. Sehgal, S. L. Hietal, R. Despande, M. M. Smith, D. Loy and C. S. Ashley, *J. Membrane Sci.*, **94**, 85 (1994).
197. W. F. Maier, private communication.
198. D. A. Loy, R. J. Buss, K. J. Shea and H. Oviatt, in *Material Research Symposium Proceedings. Better Ceramics Through Chemistry VI: Organic/Inorganic Hybrid Materials 346* (Eds. A. K. Cheatham, C. J. Brinker, M. L. Mecartney and C. Sanchez), Materials Research Society, Pittsburg, 1994, p. 825.

199. M. D. McClain, D. A. Loy and S. Pabrakar, in *Material Research Symposium Proceedings. Better Ceramics Through Chemistry VII: Organic/Inorganic Hybrid Materials 435* (Eds. K. B. Coltain, C. Sanchez, D. W. Schaefer and L. G. Wilkes), Materials Research Society, Pittsburgh, 1996, p. 277.
200. K. C. Frisch and R. B. Young, *J. Am. Chem. Soc.*, **74**, 4853 (1952).
201. P. Chevalier *Thèse de l'Université de Montpellier II*, France (1995).
202. A. Bassindale and P. G. Taylor, in *The Chemistry of Organosilicon Compounds*, Vol. 1 (Eds. S. Patai and Z. Rappoport), Wiley, Chichester, 1989, p. 839.
203. C. Chuit, R. J. P. Corriu, C. Reyé and C. Young, *Chem. Rev.*, **93**, 1371 (1993).
204. B. Boury, R. J. P. Corriu and V. Le Strat, *Chem. Mater.*, **11**, 2796 (1999).
205. J. L. Guth, H. Kessler, J. M. Higel, J. M. Lamblin, J. Patarin, A. Sieve, J. M. Chezeau and R. Wey, in *Zeolite Synthesis 398* (Eds. J. Occelli and D. Robson), ACS, Washington, 1989, p. 176.
206. H. Kessler, J. Patarin and C. Schott-Darie, in *Studies in Surface Science and Catalysis, Advanced Zeolite Science and Applications 85* (Eds. J. C. Jansen, M. Stöcker, H. G. Karge and J. Weitkamp), Elsevier, Amsterdam, 1994, p. 75.
207. J. H. Small, K. J. Shea and D. A. Loy, *J. Non-Cryst. Solids*, **160**, 234 (1993).
208. C. J. Brinker, in *Current opinion in solid state and material science*, 1(6), p. 798 (1996).
209. N. K. Raman and C. J. Brinker, *J. Membrane Sci.*, **105**, 203 (1995).
210. Y. Lu, H. Fan, N. Doke, D. Loy, R. A. Assink, D. A. LaVan and C. J. Brinker, *J. Am. Chem. Soc.*, **122**, 5258 (2000).
211. N. Hüsing and U. Schubert, *Angew. Chem., Int. Ed. Engl.*, **37**, 22 (1998).
212. D. A. Loy, E. M. Russick, S. A. Yamanaka, B. M. Baugher and K. J. Shea, *Chem. Mater.*, **9**, 2264 (1997).
213. D. A. Loy, K. J. Shea and E. Russick, in *Material Research Symposium Proceeding 271. Better Ceramics Through Chemistry V* (Eds. M.J. Hampden-Smith, W.G. Klemperer and C.J. Brinker), Materials Research Society, Pittsburgh, 1992, p. 699.
214. L. Mercier and T. Pinnavaia, *Chem. Mater.*, **12**, 188 (2000).
215. S. Inagaki, S. Guan, Y. Fukushima, T. Ohsuna and O. Terasaki, *J. Am. Chem. Soc.*, **121**, 9611 (1999).
216. B. J. Melde, B. T. Holland, C. F. Blandford and A. Stein, *Chem. Mater.*, **11**, 3302 (1999).
217. C. Yoshina-Ishii, T. Asefa, N. Coombs, M. MacLachlan and A. Ozin, *Chem. Commun. Material Research Symposium Proceeding*, 2539 (1999).
218. Y. Guo and A. R. Guadalupe, *Chem. Commun.*, 315 (1999).
219. M. E. Lim, C. F. Blandford and A. Stein, *Chem. Mater.*, **10**, 467 (1998).
220. W. E. Watts, *Organomet, Chem. Rev.*, **2**, 231 (1967).
221. E. Toussaere, J. Zyss, P. Griesmar and C. Sanchez, *Nonlinear Optics*, **1**, 349 (1991).
222. Z. Yang, C. B. Xu, L. R. Dalton, S. Kalluri, W. H. Steier and J. H. Bechtel, *Chem. Mater.*, **6**, 1899 (1994).
223. A. C. Franville, D. Zambon, R. Mahiou, S. Chou, Y. Troin and J. C. Cousseins, *J. All. Comp.*, **275**, 831 (1998).
224. G. A. Crosby, R. E. Whan and R. E. Alire, *J. Chem. Phys.*, **34**, 743 (1961).
225. M. Schneider, J. Hagen, D. Haarer and K. Müllen, *Adv. Mater.*, **12**, 351 (2000).
226. S. Rubinsztajn, M. Zeldin and W. K. Fife, *Macromolecules*, **24**, 2682 (1991).
227. B. Lebeau, C. Sanchez, S. Brasselet, J. Zyss, G. Froc and M. Dumont, *New J. Chem.*, **20**, 13 (1996).

CHAPTER 11

Polysiloles and related silole-containing polymers

SHIGEHIRO YAMAGUCHI AND KOHEI TAMAO

Institute for Chemical Research, Kyoto University, Uji, Kyoto 611-0011, Japan
Fax: 81-774-38-3186; e-mail: tamao@scl.kyoto-u.ac.jp

I. INTRODUCTION	641
II. ELECTRONIC STRUCTURE OF SILOLE	642
III. SYNTHETIC ROUTES TO SILOLE MONOMERS	645
IV. POLY(2,5-SILOLE)S	648
A. Polydiethynylsilanes (PDES)	648
B. Oligo(2,5-silole)s	651
C. Poly(2,5-silole)s	652
V. SILOLE-BASED π -CONJUGATED OLIGOMERS AND POLYMERS	654
A. 2,5-Diarylsilole Derivatives: Structure–Properties Correlation	654
1. Effects of 2,5-diaryl groups	657
2. Effects of 3,4-substituents	657
3. Effects of 1,1-substituents	661
4. Effects of Group 14 metals	661
B. Silole–Arene Copolymers	662
C. Fused Silole Ring Systems	673
VI. POLY(1,1-SILOLE)S AND SILOLE-CONTAINING POLYSILANES	675
VII. OTHER SILOLE-CONTAINING POLYMERS	683
VIII. APPLICATION TO ORGANIC ELECTROLUMINESCENT DEVICES	686
IX. CONCLUSION	690
X. REFERENCES	690

I. INTRODUCTION

Silole (silacyclopentadiene) is a silicon-containing five-membered cyclic diene, that is, a silicon analog of cyclopentadiene. Since the first synthesis of a silole, 1,1,2,3,4,5-hexaphenylsilole, by Bray and Hübel in 1959¹, the chemistry of siloles has been

extensively studied with respect to their syntheses, reactivities, properties, coordination abilities to transition metals, and aromaticity of their anionic or cationic species². In particular, the last two subjects have continued to attract much attention until now from a viewpoint of the comparison with those of cyclopentadiene^{3,4}. Recently, a new aspect has been added to silole chemistry, namely the application of the silole ring as a new building unit in material science, especially for π -conjugated polymers^{5,6}. In 1989, Barton and coworkers reported the attempted synthesis of poly(2,5-silole)s as new π -conjugated polymers^{7,8}. Since this report, growing attention has been paid to this field, which involves not only the synthesis and the study of their fundamental properties, but also their application as optoelectronic materials, such as organic electroluminescent devices. The chemistry of siloles has been well reviewed in the literature², so this chapter will focus on recent efforts devoted to silole-based oligomeric and polymeric materials.

II. ELECTRONIC STRUCTURE OF SILOLE

A notable feature of the silole ring is its high electron-accepting properties, that is, its low-lying LUMO level. This is suggested by several experimental studies. Barton and coworkers⁹ and Sakurai and coworkers¹⁰ have reported the ready photodimerization of 3,4-unsubstituted siloles. More directly, Atwell and his coworkers¹¹ and O'Brien and Breeden¹² independently reported that 2,5-diphenylsilole derivatives are easily reduced by alkali metals to form the corresponding di-anions or tetra-anions. Several theoretical studies on the silole ring have so far been conducted^{4e,f,g,13}. According to our calculations, silole has quite a different electronic structure from that of cyclopentadiene¹⁴. *Ab initio* calculations at the HF/6-31G(d) level of theory show that, while the Highest Occupied Molecular Orbital (HOMO) of the parent silole is about 0.4 eV lower than that of the parent cyclopentadiene, the Lowest Unoccupied Molecular Orbital (LUMO) level of the silole is more than 1.2 eV lower in comparison with that of cyclopentadiene, as shown in Figure 1. This difference in the LUMO energies is rationalized as due to the unique orbital interaction in the silole ring, as shown in Figure 2. Thus, the LUMO of silole consists of the mixing of the σ^* orbital of two exocyclic σ bonds on the silicon atom with the π^* orbital of the butadiene moiety, i.e. $\sigma^*-\pi^*$ conjugation. This orbital interaction is effective because of the fixed orthogonal arrangement of the plane involving the two exocyclic σ (Si-C) bonds on the silicon and the plane of the butadiene moiety and by the energetically comparable σ^* and π^* orbitals. In the case of cyclopentadiene, the $\sigma^*-\pi^*$ conjugation in the LUMO is almost negligible because of the significantly higher energy of the corresponding exocyclic σ^* orbital. The shape of the LUMO of silole is shown in Figure 3, together with that of cyclopentadiene for comparison.

The high electron-accepting properties of silole are further conspicuous by comparison with those of other heteroarenes^{6b,15,16}. Figure 4 compares calculated HOMO and LUMO levels of silole with those of representative heteroarenes such as pyrrole, furan, thiophene and pyridine, all of which are common monomer units of conventional π -conjugated polymers¹⁵. Silole has the lowest LUMO energy level among them, as well as a relatively high-lying HOMO level. This unique electronic structure of silole may reflect on the properties of its homo-polymer, poly(2,5-silole). Recently, Salzner and coworkers have carried out DFT calculations on a series of polyheterocycles **1**, including the parent polyborole, polycyclopentadiene, polysilole [poly(2,5-silole)], polypyrrole, polyphosphole, polythiophene, polyselenophene and polytellurophene¹⁷. The calculations showed that poly(2,5-silole) has the second lowest bandgap E_g (1.39 eV) among these polymers, while the lowest bandgap polymer is polyborole (0.12 eV) (Table 1). Details on poly(2,5-silole)s are described in Section IV.

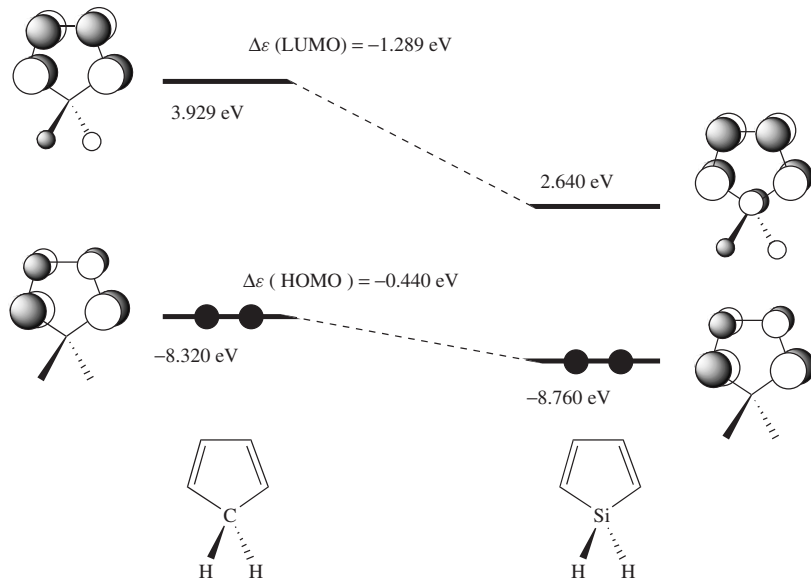


FIGURE 1. Relative energy levels of the HOMO and LUMO for silole and cyclopentadiene, based on HF/6-31G(d) calculations. Reproduced by permission of the Chemical Society of Japan from Reference 14

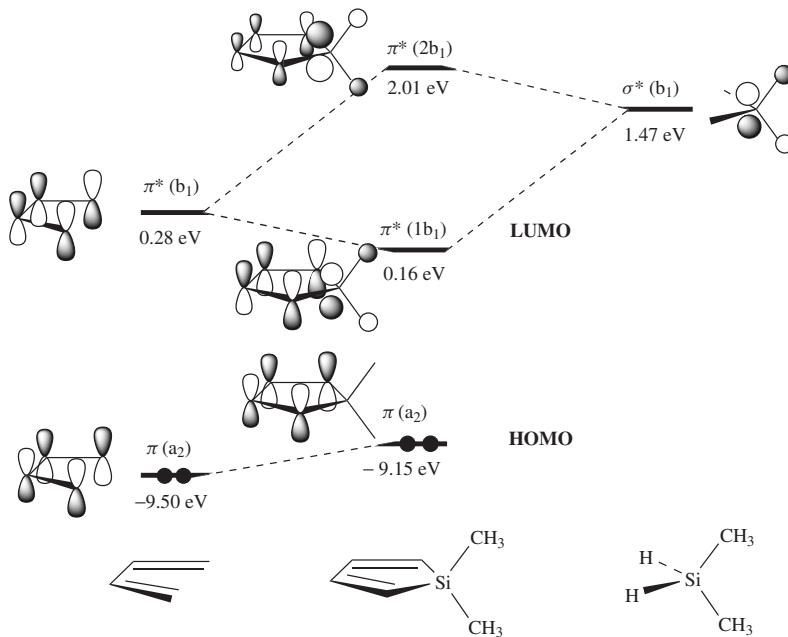


FIGURE 2. Orbital correlation diagram for 1,1-dimethylsilole, based on PM3 calculations. Reproduced by permission of the Royal Society of Chemistry from Reference 6b

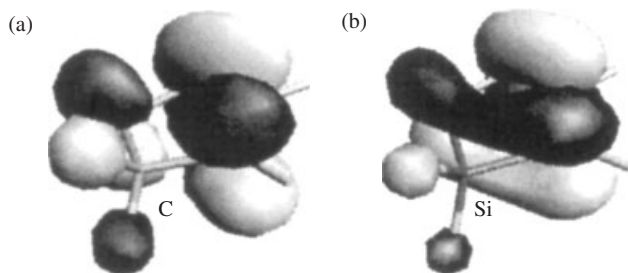


FIGURE 3. The LUMO of cyclopentadiene (a) and silole (b). Reproduced by permission of the Chemical Society of Japan from Reference 14

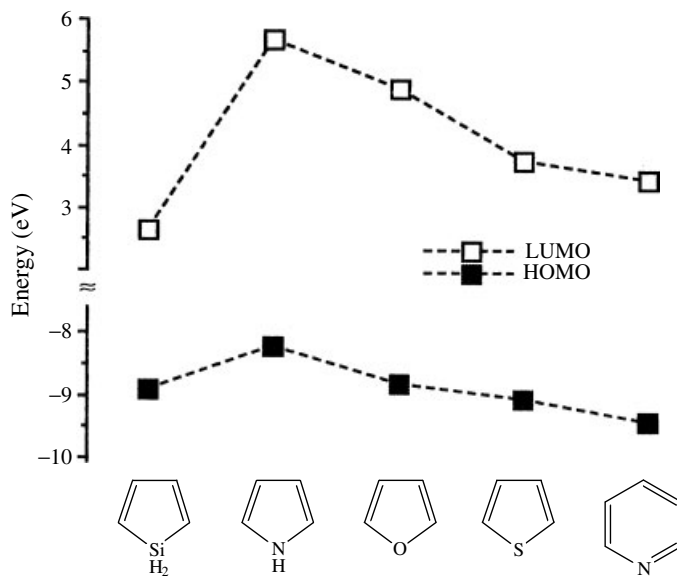


FIGURE 4. Calculated HOMO and LUMO energies of silole and other heteroarenes based on HF/6-31G(d) calculations

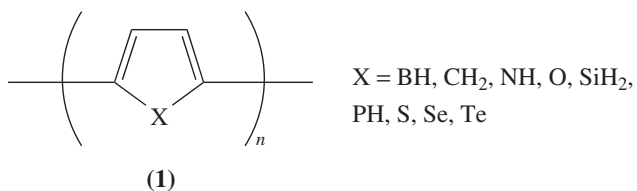


TABLE 1. Electronic structures of a series of polyheterocycles **1** based on DFT calculations^a

X	IP (eV)	EA (eV)	E_g (eV)
BH	4.95	4.83	0.12
CH ₂	4.61	2.97	1.58
NH	4.77	1.61	3.16
O	5.31	2.63	2.67
SiH ₂	5.14	3.75	1.39
PH	5.23	3.73	1.49
S	5.50	3.20	2.30
Se	5.64	3.58	2.06
Te	5.52	3.63	1.87

^aData from Reference 17.

III. SYNTHETIC ROUTES TO SILOLE MONOMERS

The functionalization of the silole ring is essential for the use of silole as a building unit of polymeric materials. However, the traditional synthetic methodologies for functionalized siloles have been quite limited². In principle, the methodologies for the construction of the silole ring from acetylene moieties may be classified into two types of reactions as shown in Figure 5. Route A involves the formation of bonds *a* and *b* to construct the silole ring, while route B can be described as a cyclization accompanied by the synchronous bond formation of bonds *c* and *d*. Recent progress for both synthetic routes is surveyed below. The reader is referred to Reference 2 for the traditional syntheses of 2,5-diphenylsilole derivatives.

A typical example of route A is the reaction of dilithiobutadiene derivatives **2** with dihalosilanes or their equivalents (Scheme 1)^{2a}. The reaction of diphenylacetylene with Li metal¹⁸ followed by treatment with dihalosilanes is a classical synthesis of tetraphenylsilole derivatives **3**^{1,19}. The 1,4-dihalobutadiene **5** derivatives are alternative precursors for dilithiobutadienes²⁰. The halogenolysis of titana- or zirconacyclopentadienes **4** affords 2,3-dialkyl and 2,3-unsubstituted 1,4-dihalobutadienes **5**, which can be converted to the corresponding 3,4-dialkyl and 3,4-unsubstituted siloles **3** via halogen–lithium exchange reactions^{21–25}. 2,5-Diaryltellurophenes **6** can also be transformed into 3,4-unsubstituted 2,5-diarylsiloles based on the tellurium–lithium exchange reactions with *n*-BuLi or *t*-BuLi²⁶.

The transition metal catalyzed or mediated cyclizations of alkynes are also classified into this category. The Ni complex catalyzed reaction of alkynes with

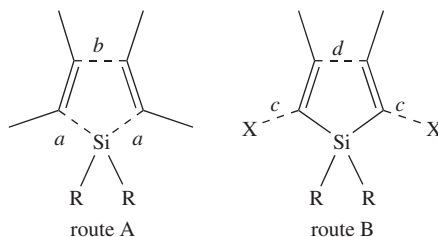
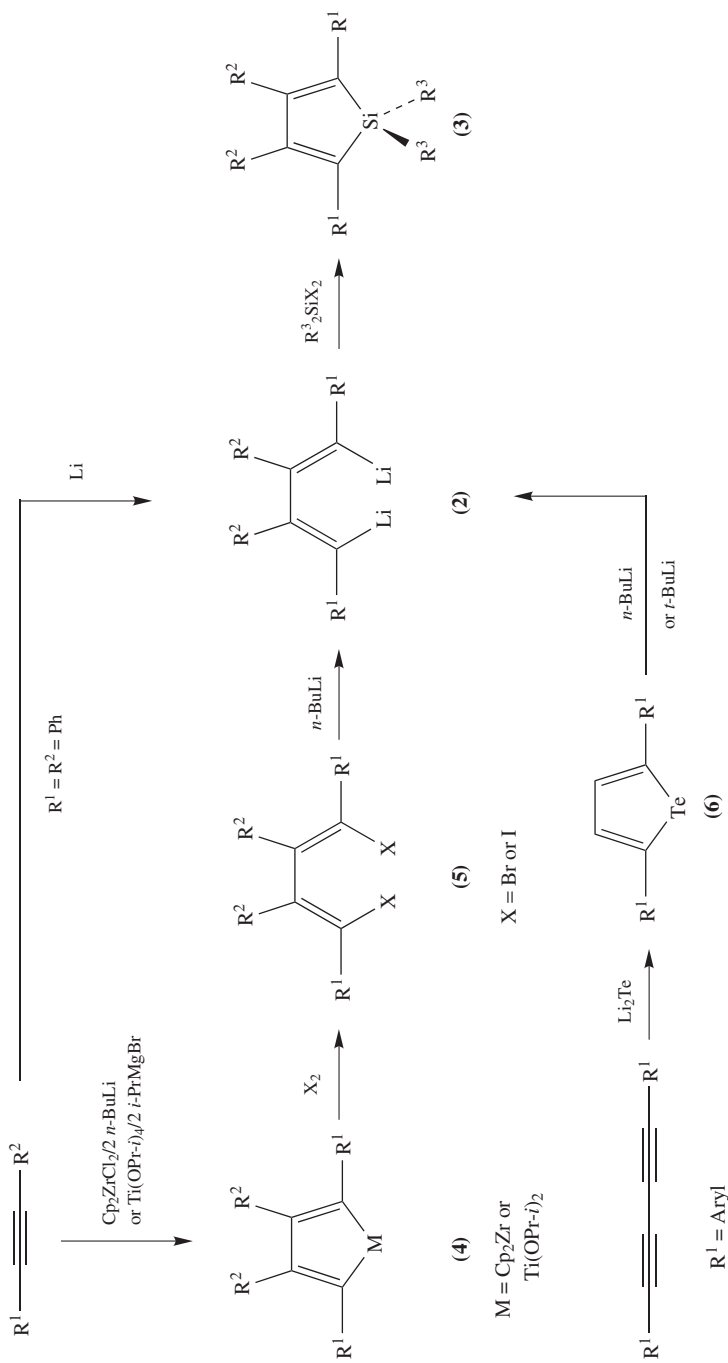
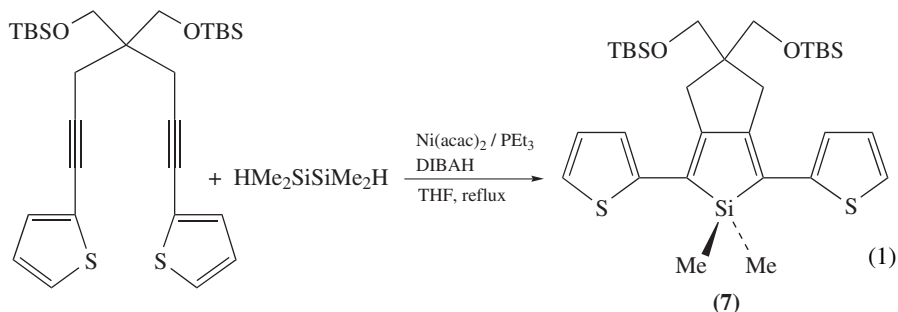


FIGURE 5. Classification of silole synthesis



SCHEME 1

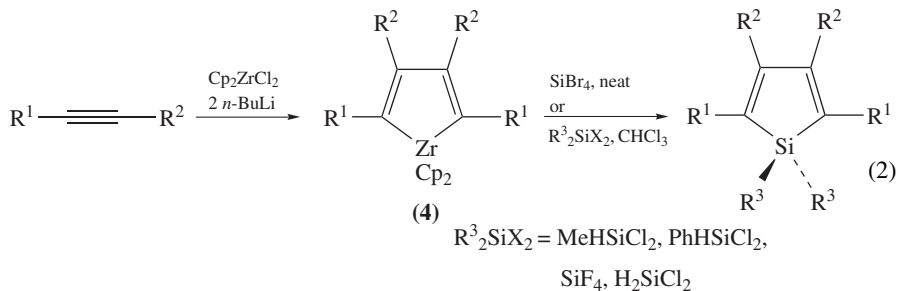
hydrodisilanes to give a silole was originally reported by Kumada and coworkers²⁷. This reaction has been applied to the intramolecular version for the synthesis of 2,5-dithienylsilole **7** (equation 1)²⁸, which has further been used as a monomer unit for a series of silole–thiophene copolymers (see Section V.B). Fagan and coworkers reported a new route to silole, that is, the formation of zirconacyclopentadiene **4** from two alkynes followed by the direct transmetalation with reactive SiBr_4 , although the yield of this procedure was moderate²⁹. This reaction has recently been improved by the use of less sterically hindered halosilanes in chloroform (equation 2)³⁰.



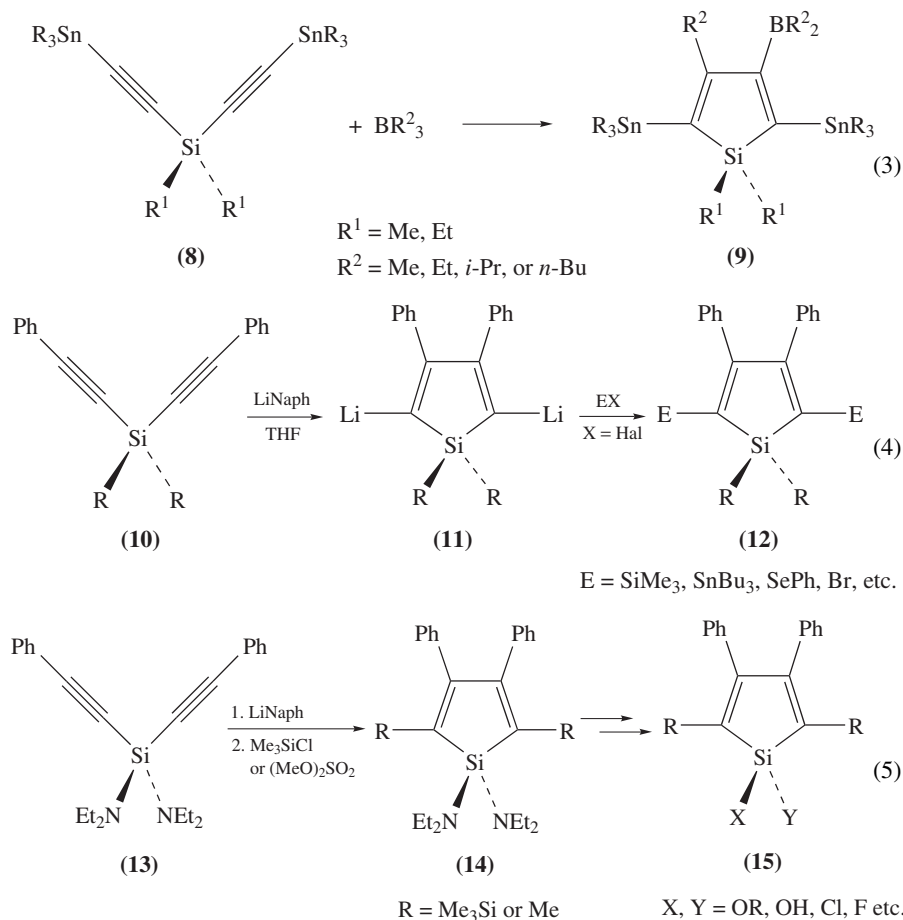
TBS = tert-butyldimethylsilyl

acac = acetylacetonato

DIBAH = diisobutylaluminum hydride (*i*-Bu₂AlH)



While some of the reactions mentioned above can be used for the synthesis of 1,1-difunctionalized siloles³⁰, none of them can afford 2,5-difunctionalized siloles. 2,5-Difunctionalized siloles can be directly prepared only by route B. Wrackmeyer has reported that a reaction of bis(stannyethynyl)silanes **8** with BR_3 ($\text{R} = \text{Me}, \text{Et}, i\text{-Pr},$ and $n\text{-Bu}$) affords 2,5-distannyl-3-borylsiloles **9** (equation 3)³¹. We have recently reported a general synthesis of 2,5-difunctionalized siloles by the intramolecular reductive cyclization of diethynylsilanes (equation 4)³². Thus, the reaction of bis(phenylethynyl)silanes **10** with lithium naphthalenide affords 2,5-dilithiosiloles **11**, which can be further transformed into a variety of 2,5-difunctionalized siloles **12**. In addition, starting from bis(phenylethynyl)diaminosilanes **13**, various 1,1-difunctionalized siloles **15** are also accessible through 1,1-diaminosiloles **14** (equation 5)³³. With these functionalized siloles in hand, various silole-based σ - and π -conjugated compounds have been prepared as described below.



IV. POLY(2,5-SILOLE)S

A. Polydiethynylsilanes (PDES)

Poly(2,5-silole)s, silole-2,5-linked homo-polymers, may be a center of target molecules among the silole-based π -conjugated systems. The polysilole is recognized as a silicon-substituted polyacetylene, in which the labile *trans-cisoid-trans-transoid* polyacetylene backbone is fixed by the silicon bridges (Figure 6)³⁴. As mentioned above, in 1989, Barton and coworkers reported the attempted synthesis of poly(2,5-silole) by Mo- or W-complex catalyzed or thermal polymerization of diethynylsilane **16**, which produced a deep red or violet polymer (Scheme 2)^{7,8,35}. Although the resulting polymer, polydiethynylsilane (PDES), was later characterized spectroscopically to have a methylenesilacyclobutene skeleton **17** instead of the silole ring⁸, this report has prompted a number of theoretical studies on the poly(2,5-silole)s^{34–38}. The early theoretical studies were concerned with the ground state structures of poly(2,5-silole)s from the viewpoint of theoretical characterization of the PDES, where three possible isomers, namely an aromatic-like

form, a quinoid-like form and a four-membered-ring form, were considered (Figure 7). It was suggested that the aromatic-like form is more stable than the four-membered structure by about $15/\text{kcal mol}^{-1}$ per ring³⁴, and among the five-membered structures the quinoid-like form is more stable than the aromatic-like form^{34,35c,36,38}. Some unique properties of the poly(2,5-silole)s (aromatic-like form) have been suggested, such as

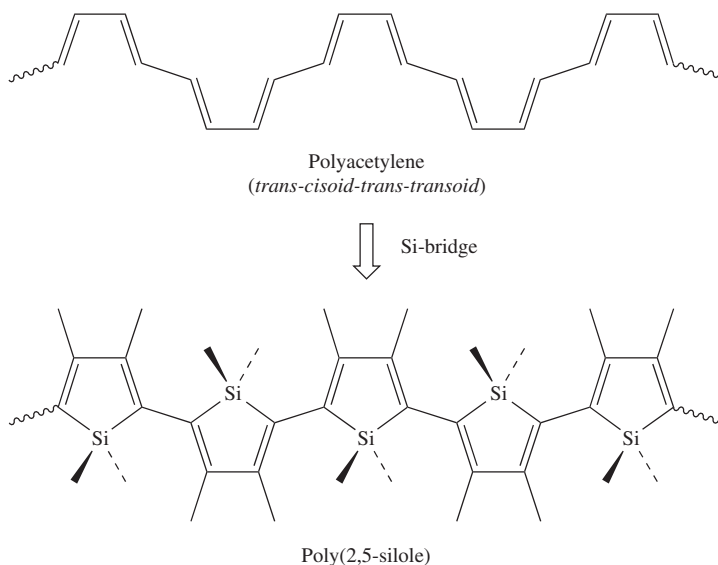


FIGURE 6. Structural similarity between polyacetylene and poly(2,5-silole)s. Reproduced by permission of the Royal Society of Chemistry from Reference 6b

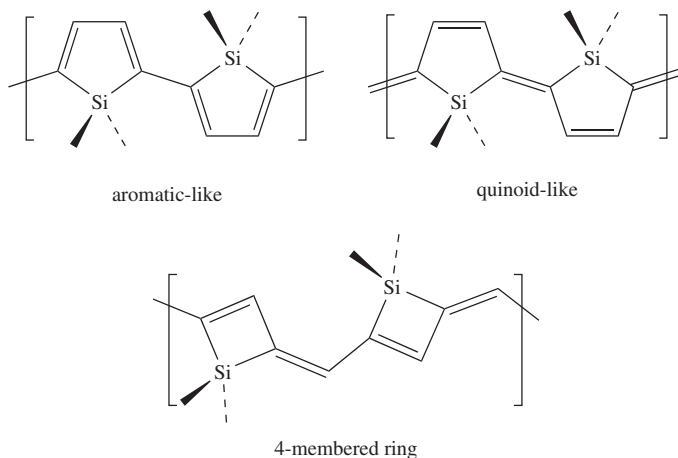
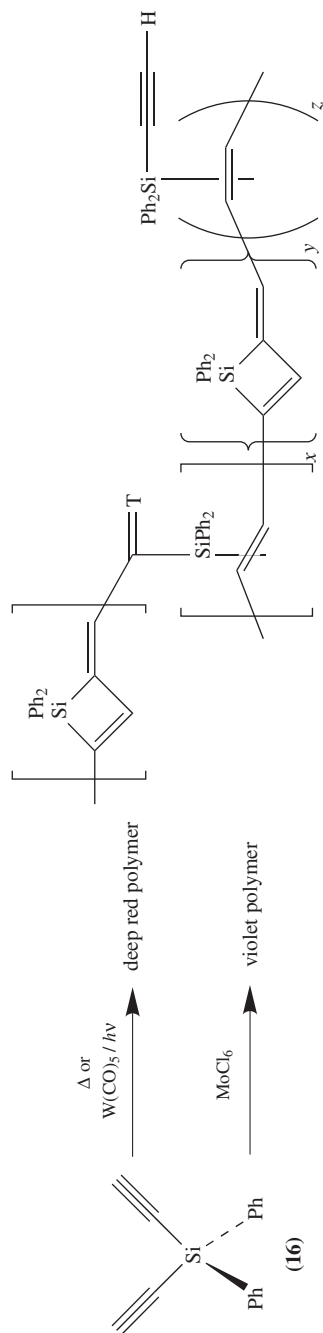


FIGURE 7. Three possible forms of polydiethynylsilanes (PDES)

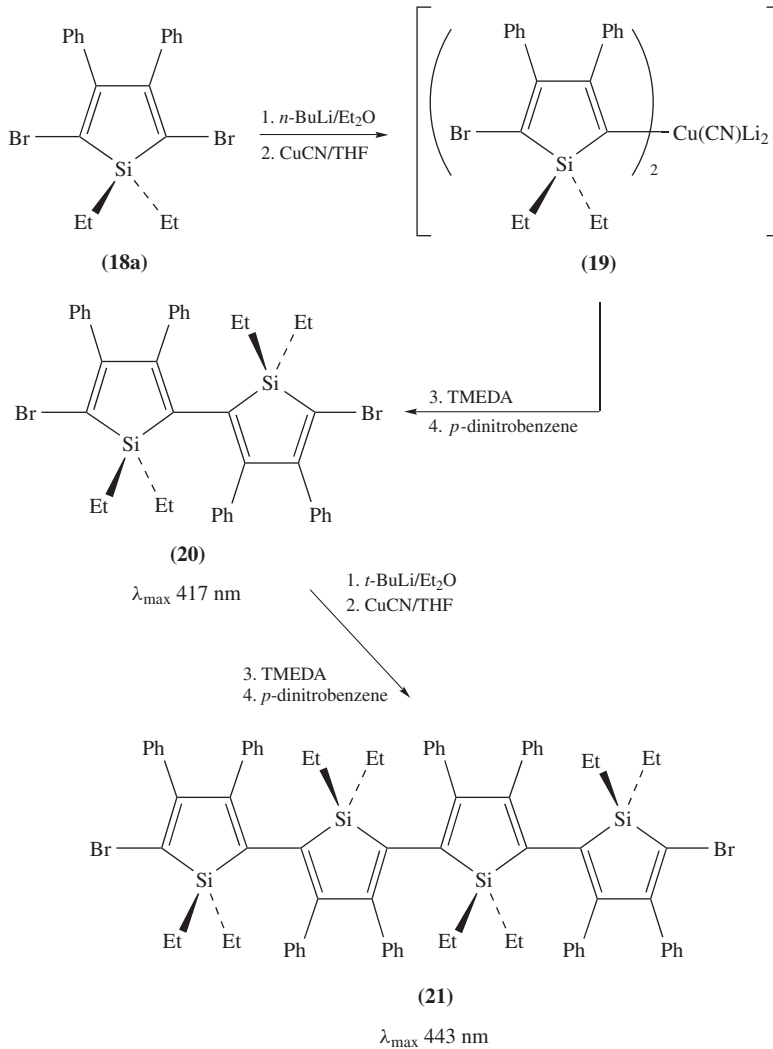


SCHEME 2

low bandgaps (1.1–1.4 eV)^{17,34,38}, large third-order optical nonlinearity^{35c,37} and thermochromic behavior³⁶.

B. Oligo(2,5-silole)s

Using 2,5-dibromosilole **18** obtained in equation 4, a series of oligo(2,5-silole)s as models of poly(2,5-silole)s have been prepared as shown in Scheme 3³². Thus, monolithiation



TMEDA = *N,N,N',N'*-tetramethylethylenediamine

SCHEME 3

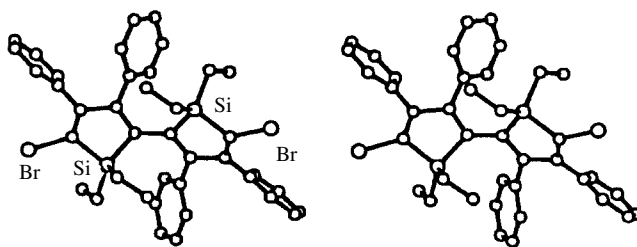
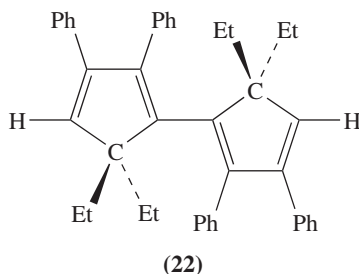


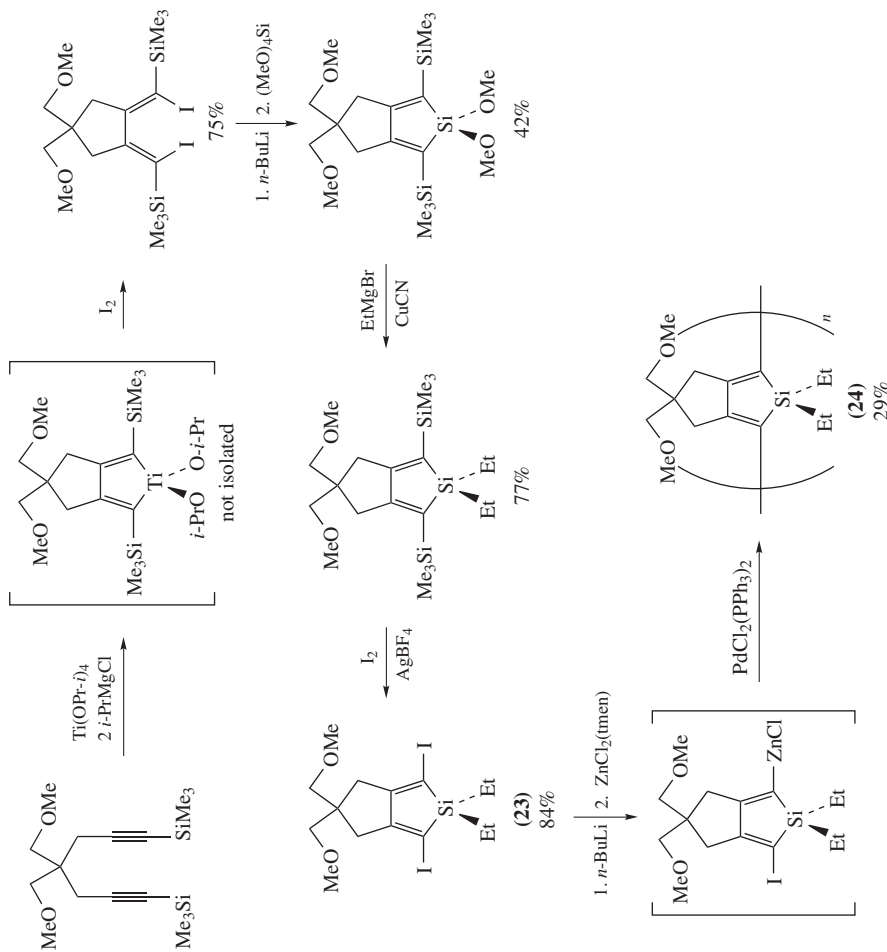
FIGURE 8. Stereoview of the crystal structure of 2,5'-dibromo-2,2'-bisilole **20**. Reproduced by permission from Reference 32. Copyright 1994 American Chemical Society

of **18a** followed by the oxidative coupling³⁹ through so-called higher-order cuprate **19** gave dibromo-terminated bisilole **20**. The repetitive operation successfully produced the quatersilole **21**. X-ray crystallography of the dimer revealed its highly twisted structure having a dihedral angle between two silole planes of 64° , as shown in Figure 8. Nevertheless, the dimer **20** has a considerably long absorption maximum (λ_{max} 417 nm) in the UV-visible absorption spectrum, which is more than 70 nm longer than that of the carbon analog **22** (λ_{max} 340 nm)⁴⁰. The tetramer **21** absorbs only 26 nm longer (443 nm) than that of the dimer **20**, probably due to the severe steric congestion causing the highly twisted structure of the quatersilole skeleton.



C. Poly(2,5-silole)s

All attempts to synthesize poly(2,5-silole)s by the coupling reactions of 3,4-diphenyl-substituted 2,5-difunctionalized siloles **12** have failed, probably due to the severe steric congestion⁴¹. However, recently, poly(2,5-silole) **24** consisting of sterically less-hindered silole rings has actually been synthesized⁴². The outline of the synthesis is shown in Scheme 4. The key step is the halodesilylation reaction of 2,5-disilylsilole⁴¹ to give the crucial precursor, 2,5-diiodosilole **23**, which contains less bulky alkylene bridge at the 3,4-positions than the 3,4-diphenyl analog. The selective monolithiation of **23** followed by the transmetalation with $\text{ZnCl}_2(\text{tmen})$ ($\text{tmen} = N,N,N',N'$ -tetramethylethylenediamine) and the Pd^0 -catalyzed cross-coupling reaction gave **24**, whose average molecular weight (M_n) determined by the MALDI-TOF mass spectrometry technique was about 3,700 ($n \approx 13$). Although the molecular weight is still low and a detailed investigation on the properties of polymer **24** has not yet been conducted, the UV-visible absorption spectra has been determined. The poly(2,5-silole) **24** has its absorption maximum at 482 nm at 293 K, which red-shifts up to 543 nm upon cooling to 153 K (Figure 9). The much longer



SCHEME 4

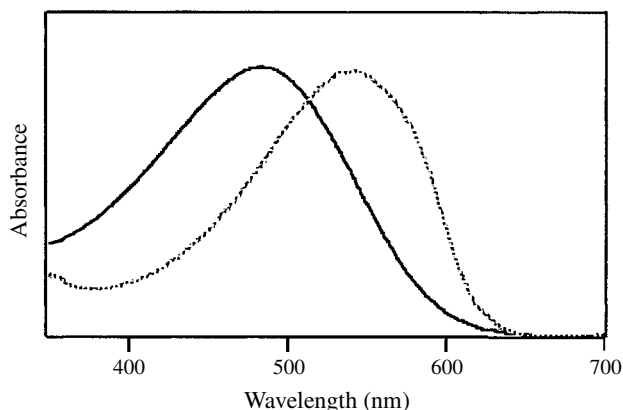


FIGURE 9. UV-visible absorption spectra of poly(2,5-silole) **24** in 2-methyltetrahydrofuran: at 293 K, solid line; at 153 K, dashed line. Reproduced by permission from Reference 42. Copyright 1999 American Chemical Society

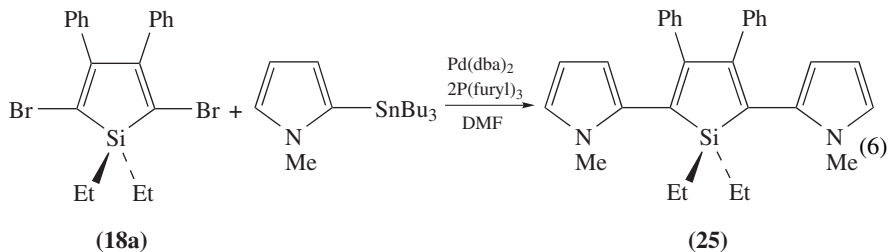
absorption maximum in comparison with those of the oligo(2,5-silole)s **20** and **21** suggests that π -conjugation is substantially extended along the polysilole backbone.

V. SILOLE-BASED π -CONJUGATED OLIGOMERS AND POLYMERS

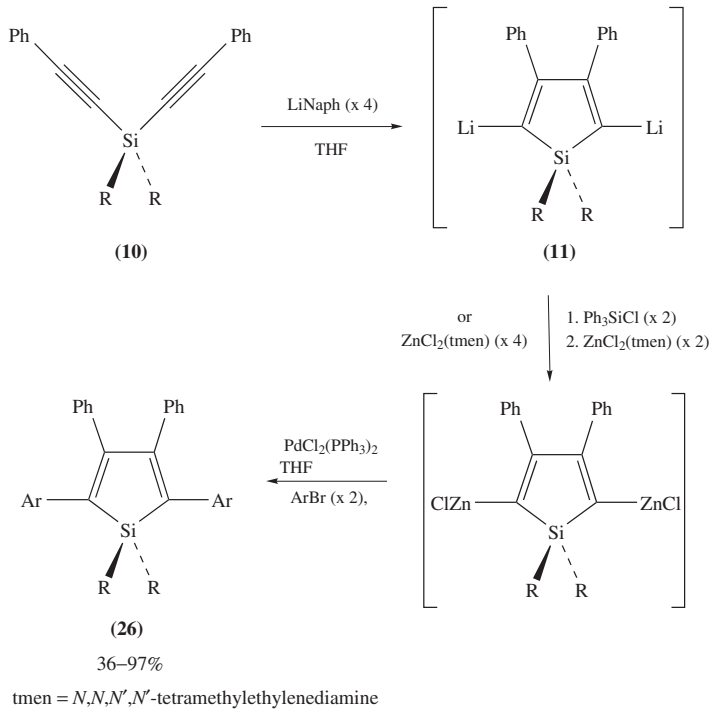
A. 2,5-Diarylsilole Derivatives: Structure–Properties Correlation

This section is concerned with the structure–properties relationships of 2,5-diarylsiloles and related compounds, including the substituent effects of 2,5-aryl groups, 3,4-substituents and 1,1-substituents on the silole rings. This fundamental study provides valuable information for the molecular design of new silole materials applicable to organic electronic devices.

A variety of 2,5-diarylsiloles have been prepared by the methods shown in Scheme 1 and equation 1 (Section III), and by the Pd⁰-catalyzed cross-coupling reactions between 2,5-dihalosiloles **18** with metalated arenes, as represented by the synthesis of 2,5-di(pyrrolyl) silole **25** (equation 6)^{15,32}, or, alternatively, between 2,5-dimetalated siloles and various aryl halides, as shown in Scheme 5^{16,43}. Advantageously, the last procedure can be carried out in one pot starting from bis(phenylethynyl)silane **10** to give a series of 3,4-diphenyl-2,5-diarylsiloles **26** in reasonable yields, thus providing a most versatile general method, although the phenyl groups at the 3,4-positions are essential for this reaction. The 2,5-diarylsiloles **26** prepared by this method are listed in Figure 10⁴³.



dba = dibenzylideneacetone



SCHEME 5

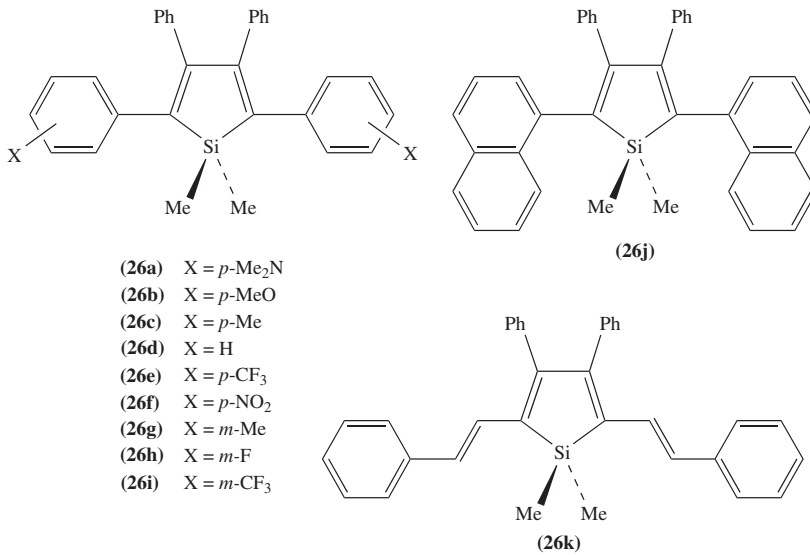


FIGURE 10. 2,5-Diaryl-3,4-diphenylsiloles **26** prepared according to Scheme 5⁴³. Reproduced by permission of Wiley-VCH from Reference 43

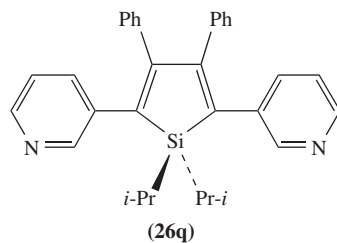
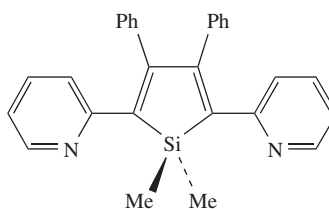
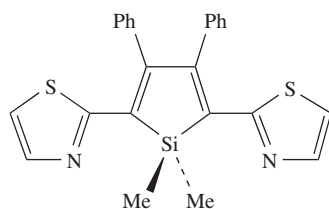
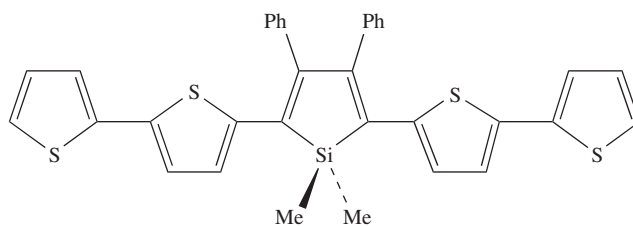
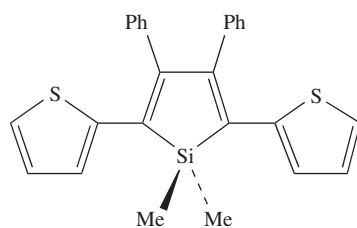
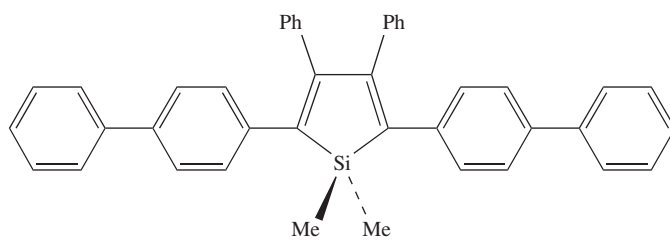


FIGURE 10. (continued)

1. Effects of 2,5-diaryl groups⁴³

Photophysical and electrochemical properties of a series of 3,4-diphenyl-2,5-diarylsiloles **26** are summarized in Table 2⁴³. Since the photophysics of 2,3,4,5-tetraphenylsiloles has been well reviewed in Reference 2, the discussion herein is focused on the substituent effects of aryl groups at the 2,5-positions. In a series of 2,5-bis(mono-substituted phenyl)silole derivatives **26a–26i**, the substituents on the phenyl groups at the 2,5-positions significantly affect their photophysical properties. The λ_{\max} of the absorption and emission spectra vary by about 60 nm in the range of 358–423 nm and 466–529 nm, respectively. Their redox potentials also depend on the substituents on the phenyl groups (Table 2). The differences between the NMe₂ derivative **26a** and the NO₂ derivative **26f** exceed more than 1 V in both $E_{\text{pa}1}$ and $E_{\text{pc}1}$. These results suggest that the HOMO and LUMO levels of the 2,5-diarylsiloles can be readily controlled over a wide range by modification of the 2,5-diaryl groups. Notably, the $E_{\text{pa}1}$ and $E_{\text{pc}1}$ values of **26a–26i** show a good linear relationship with the σ^+ and σ^- values^[20] of the substituents, respectively, as shown in Figure 11. In addition, the emission maximum wavenumbers ν_{em} exhibit a linear relationship against the values of $\Delta E (= E_{\text{pa}1} - E_{\text{pc}1})$, as shown in Figure 12. These relationships afford equation 7, which represents a relationship between the emission wavenumbers and the σ^+ and σ^- values of the substituents. On the basis of this equation, the emission maxima of new 2,5-bis(mono-substituted phenyl)siloles may be predictable with reasonable accuracy.

$$\nu_{\text{em}}(\text{cm}^{-1}) \times 10^{-4} = 2.12 + 0.134\sigma^+ - 0.169\sigma^- \quad (7)$$

The properties of 2,5-diarylsiloles are also highly dependent on the kind of aryl groups. Among 2,5-diarylsiloles having extended π -conjugated groups **26j–26l**, coplanarity of the π -conjugated moiety plays an important role. While bulky aryl-substituted siloles such as **26j** and **26l** show moderate bathochromic shifts of absorption and emission maxima in comparison with the prototype diphenyl derivative **26d**, styryl derivative **26k** exhibits more than 50–70 nm bathochromic shifts, suggesting an effective extension of the π -conjugation by the styryl groups. In a series of siloles with heteroaryls at the 2,5-positions, the nature of π -electronic structures can be widely modified by the heteroaryl groups keeping their absorption and emission maxima almost unchanged. Thus, in spite of the almost identical absorption maxima of thiazolyl- (**26o**, λ_{\max} 413 nm), thienyl- (**26m**, λ_{\max} 418 nm) and pyrrolyl-substituted siloles (**25**, λ_{\max} 406 nm), there are big differences in both $E_{\text{pa}1}$ and $E_{\text{pc}1}$ among these compounds which reach 0.6 V between **26o** and **25**, as shown in Figure 13. Thus, **26o** is characteristic of a low-lying LUMO, while **25** has a high-lying HOMO. These results demonstrate that the appropriate choice of the heteroaryl groups enables us to control the electronic structures, in particular, the HOMO and LUMO levels of the silole π -electron systems over a wide range while maintaining their emission wavelengths.

2. Effects of 3,4-substituents

In contrast to the significant effect of 2,5-substituents, the substituent effects of 3,4-groups are relatively small and may be useful for the secondary fine-tuning of the absorption and emission maxima^{6b,26}. In Table 3, a series of 2,5-dithienylsiloles having various 3,4-substituents are listed with their maximum wavelengths in UV-visible absorption and fluorescence spectra. Comparing 3,4-diphenylsilole **26m** or bicyclic 3,4-dialkylsilole **27**⁴⁴ with the 3,4-unsubstituted silole **28**²⁶, the phenyl and alkyl substitution induce red and blue shift, respectively, in both the absorption and fluorescence spectra. It

TABLE 2. Photophysical and electrochemical data for 2,5-diarylsiloles^{4,3}

Compound	2,5-Aryl groups		Absorption ^d		Fluorescence ^a		Cyclic voltammetry ^b	
	λ_{\max} (nm)	(log ϵ)	λ_{\max} (nm) ^c	Φ_f^d	$E_{\text{pa}1}, E_{\text{pa}2}$ (V) ^e	$E_{\text{pc}1}, E_{\text{pc}2}$ (V) ^e		
26a	423	4.33	529	$2.51 \times 10^{-3}f$	+0.11 ^{g,h}	-2.43		
26b	379	4.11	493	2.40×10^{-3}	+0.66,+0.92	-2.30		
26c	367	4.11	475	1.96×10^{-3}	+0.94,+1.08	-2.36		
26d	359	3.97	467	1.43×10^{-3}	+1.02,+1.17	-2.27		
26e	358	4.02	469	8.78×10^{-4}	+1.18	-1.93,-2.25		
26f	399	4.35	522	2.66×10^{-3}	+1.28	-1.44 ^{g,i} , -2.32		
26g	364	3.78	471 (484)	2.78×10^{-3}	+1.12	-2.30		
26h	358	4.00	466	4.38×10^{-4}	+1.24	-2.15,-2.56		
26i	358	3.99	468	1.09×10^{-3}	+1.30	-2.09,-2.52		
26j	340	3.96	435	4.71×10^{-4}	+1.10,+1.20	-2.36,-2.61		
26k	435	4.04	527	$4.70 \times 10^{-2}f$	+0.64	-2.02 ^{g,j} , -2.25		
26l	381	4.32	497	5.13×10^{-3}	+0.99	-2.16		
26m	418	4.28	515 (525)	1.41×10^{-3}	+0.64	-2.21,-2.57		
26n	476	4.38	556 (604)	$3.90 \times 10^{-3}f$	+0.55 ^{g,k}	-2.04,-2.19		
26o	413	4.33	504	1.02×10^{-3}	+0.97	-1.89,-2.14		
26p	370	4.17	468 (487)	7.57×10^{-4}	+1.00	-2.10,-2.51		
26q	354	3.96	466 (470)	2.56×10^{-3}	+1.22	-2.27,-2.59		
25'	406	3.93			+0.40,+0.79	-2.50		

^aIn CHCl₃.^bDetermined under the following conditions: Sample, 1 mM; *n*-Bu₄NClO₄ (0.1 M) in CH₃CN. All redox processes were irreversible unless otherwise stated.^cEmission maximum wavelengths of the vacuum vapor-deposited thin film (50 nm thickness) are given in parentheses.^dDetermined with reference to quinine sulfate, unless otherwise stated.^evs. Ag/Ag⁺.^fDetermined with reference to fluorescein.^gReversible redox process.^h $E_{1/2} = +0.07$ V. ⁱ $E_{1/2} = -1.37$ V. ^j $E_{1/2} = -1.98$ V. ^k $E_{1/2} = +0.47$ V.^lReference 15.

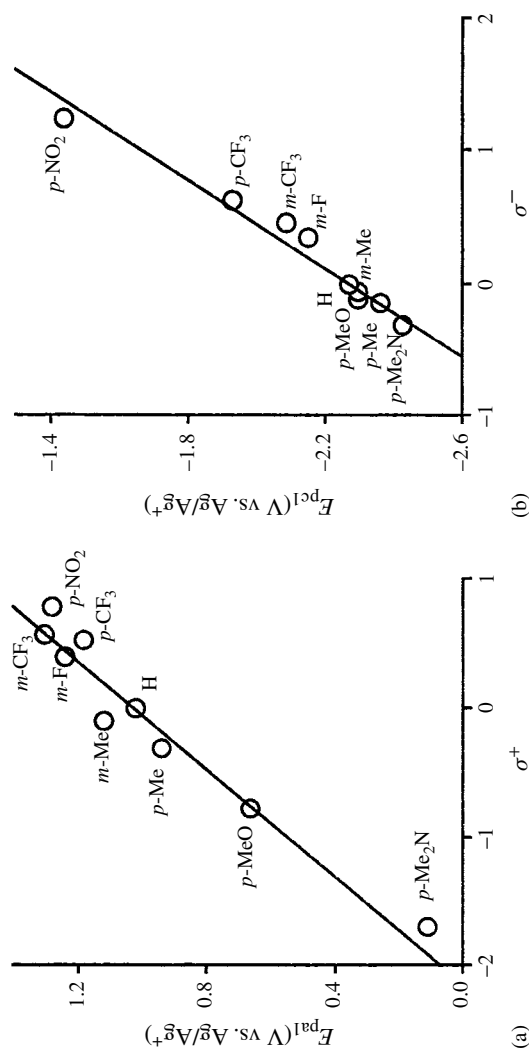


FIGURE 11. Plots of (a) oxidation potentials vs. the σ^+ values of the substituents on the 2,5-diphenyl groups of **26** and (b) reduction potentials vs. the σ^- values of the substituents on the 2,5-diphenyl groups of **26**. Reproduced by permission of Wiley-VCH from Reference 43

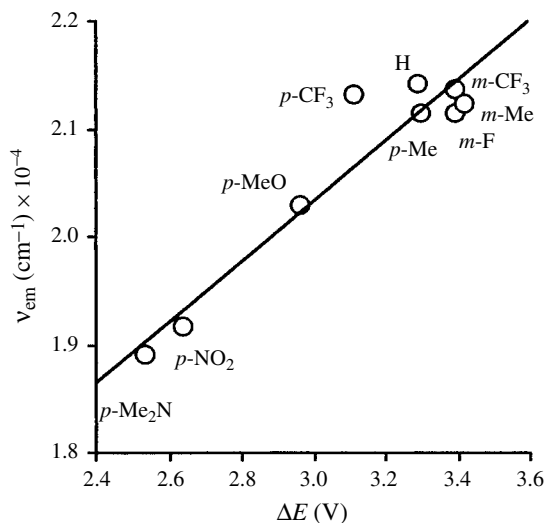


FIGURE 12. Plot of emission wavenumbers of **26** vs. $\Delta E (= E_{\text{pa}1} - E_{\text{pc}1})$ values

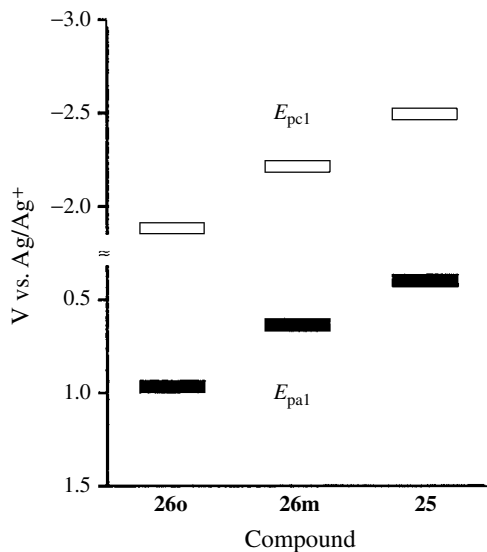
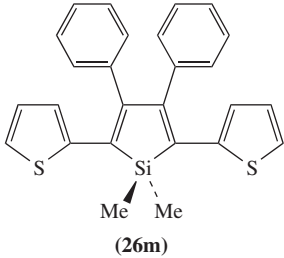
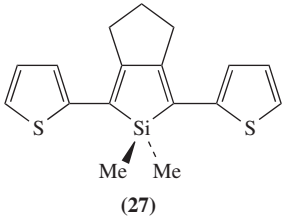
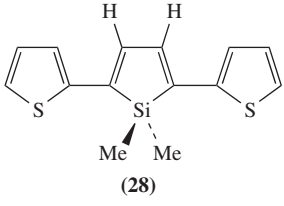


FIGURE 13. The first oxidation potentials ($E_{\text{pa}1}$) and the first reduction potentials ($E_{\text{pc}1}$) for 2,5-diarylsiloles. Reproduced by permission of Wiley-VCH from Reference 43

TABLE 3. Effects of 3,4-substituents on the optical properties of 2,5-dithienylsiloles^{6b}

	UV-vis ^a	Fluorescence ^a
	λ_{\max} (nm) (log ϵ)	λ_{\max} (nm) ($\Phi_f \times 10^2$) ^b
 <p>(26m)</p>	418 (4.28)	515 (0.14)
 <p>(27)</p>	409 (4.38)	492 (5.44)
 <p>(28)</p>	415 (4.22)	505 (3.90)

^aIn chloroform.^bQuantum yields relative to quinine sulfate (0.55).

is also noted that the phenyl groups on the 3,4-positions reduce the quantum yield of the fluorescence significantly.

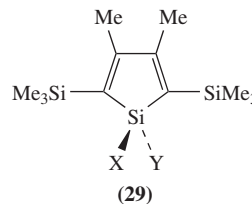
3. Effects of 1,1-substituents

In comparison with the effects of the 2,5-aryl groups and 3,4-substituents, the effects of the 1,1-substituents on the optical properties are rather small, as shown in Table 4^{22b}. In a series of 2,5-disilylsiloles **29** having various groups (i.e. *i*-Pr, Ph, OMe, OH, F) on the ring silicon atom, the absorption maxima become longer as the 1,1-substituents become more electronegative, although the changes are moderate.

4. Effects of Group 14 metals

Considering the peculiar contribution of the central silicon atom to the π -electronic structure of silole derivatives through $\sigma^*-\pi^*$ conjugation, other Group 14 metalloles are also of interest. To elucidate the effects of the central Group 14 elements, we have prepared a series of 2,5-dithienyl-substituted Group 14 metalloles, cyclopentadiene **30**, siloles **26m** and **27**, germole **31** and stannole **32**, and compared their photophysical

TABLE 4. Effect of 1,1-substituents on UV-visible absorption spectra for 2,5-disilylsiloles **29** in chloroform^{22b}

 (29)	λ_{\max} (nm) (log ϵ)
	X = Y = H
X = Y = <i>i</i> -Pr	308 (3.73)
X = Y = Ph	314 (3.73)
X = Y = OMe	315 (3.69)
X = F, Y = OH	316 (3.66)
X = Y = F	318 (3.56)

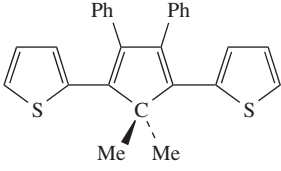
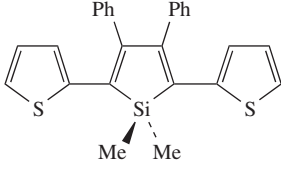
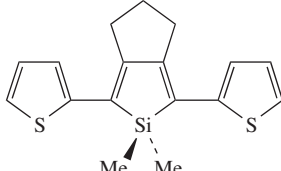
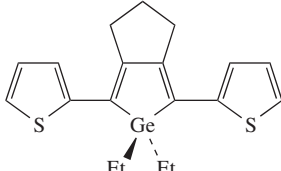
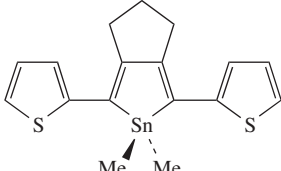
data, as summarized in Table 5⁴⁴. While there is a significant difference between the cyclopentadiene and silole derivatives, other metalloles from silole to stannole show comparable absorption maxima and emission wavelengths. A similar tendency is observed for a series of 2,3,4,5-tetraphenyl-substituted silole, germole and stannole^{2a}. Theoretical calculations have revealed that the Group 14 metalloles from silole to stannole have comparable electronic structures and the central Group 14 elements Si, Ge, and Sn affect the LUMO energy levels to almost the same extent through the $\sigma^*-\pi^*$ conjugation⁴⁴.

B. Silole–Arene Copolymers

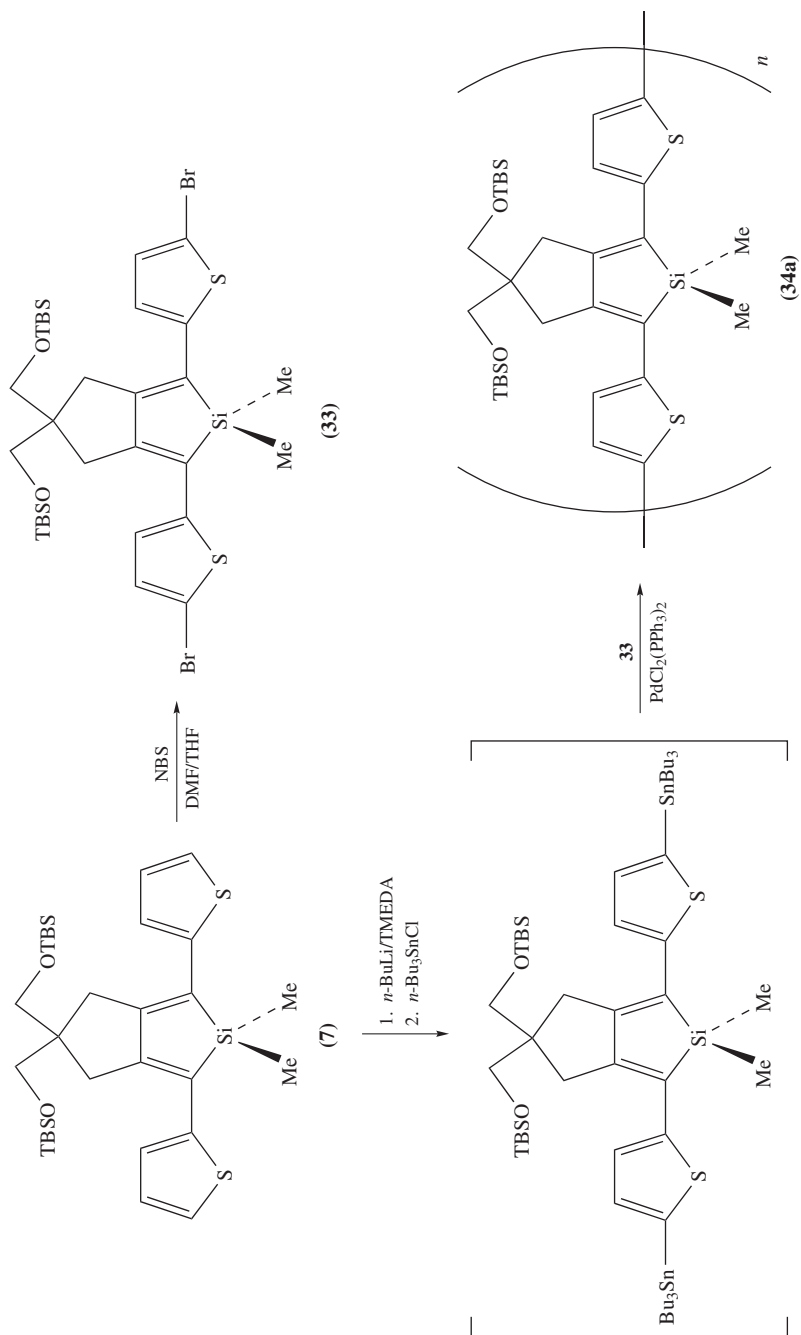
Several types of silole–arene copolymers have been reported in the literature. A representative is the silole–thiophene copolymers. Theoretical calculations on the silole–thiophene alternating copolymers have suggested that they have lower bandgaps (*ca* 1.55 eV) than those of polythiophenes (*ca* 2.3 eV, based on the same level calculations)^{38c,f}. Using 2,5-dithienylsilole derivative **7** as a monomer unit, a series of silole–thiophene copolymers **34** with varied silole:thiophene ratio from 1 : 2 to 1 : 4 have been prepared based on the Stille coupling reactions²⁸. For example, compound **7** has been transformed into the distannylated derivative which, without isolation, has been reacted with dibromide **33** in the presence of Pd complex to give the silole–thiophene 1 : 2 copolymer **34a**, as shown in Scheme 6. The copolymers **34** actually have their absorption maxima at considerably long wavelengths in the UV-visible absorption spectra. The THF solution of **34a** is ink-blue and its absorption maximum exceeds 600 nm. The absorption maximum shifts to longer wavelengths as the silole content increases, while the electrical conductivity becomes larger (**34c**, 2.4 S cm⁻¹) as the thiophene content increases (Table 6)^{28b}.

Silole–arene 1 : 1 alternating copolymers were hardly-accessible compounds until recently. Only the silole 1 : 1 alternating cooligomers **36** had been prepared by the Ni⁰-catalyzed cyclization of thienylene–heptadiyne cooligomers **35** with hydrodisilanes (equations 8 and 9)^{28b} before a new general route to silole–arene 1 : 1 alternating copolymers was developed in 1999 based on the Suzuki–Miyaura coupling using 2,5-silole-diboronic acids **37** as key precursors. The diboronic acids **37** have been obtained by the reaction of 2,5-dilithiosiloles **11** with (Et₂N)₂BCl followed by hydrolysis (Scheme 7)⁴⁵. The Pd⁰-catalyzed cross-coupling of the diboronic acid **37** with 2,5-bis(bromoaryl)siloles gave a series of silole–arene 1 : 1 copolymers containing benzene (**38**), pyridine (**39**), thiophene (**40**) and thiazole (**41**) as the arene unit^{45,46}. Among them, silole–thiophene and silole–thiazole 1 : 1 copolymers, **40** and **41**, show considerably long absorption maxima around 620–690 nm at 298 K. Notably, the λ_{\max} of the copolymer **40** is >100 nm longer than that of butadiene–thiophene copolymer **42** (λ_{\max} 538 nm)⁴⁷,

TABLE 5. UV-vis absorption and fluorescence spectral data for 2,5-dithienyl metalloles⁴⁴

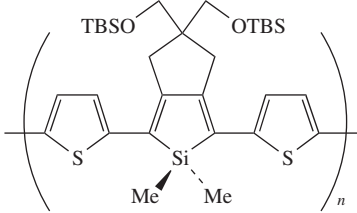
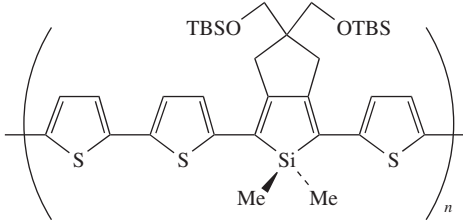
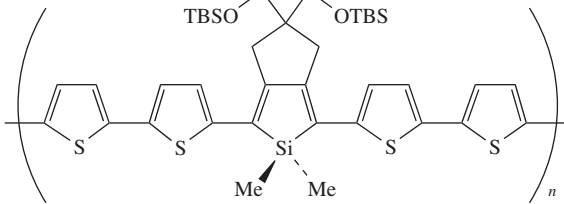
Compound	UV-vis ^a	Fluorescence ^a
	λ_{\max} (nm) (log ϵ)	λ_{\max} (nm) ($\Phi_f \times 10^2$) ^b
 <p>(30)</p>	368 (4.10)	461 (0.996)
 <p>(26m)</p>	418 (4.28)	515 (0.141)
 <p>(27)</p>	409 (4.38)	492 (5.44)
 <p>(31)</p>	405 (4.37) 428 (4.24)	479 (8.72)
 <p>(32)</p>	406 (4.36) 430 (4.24)	479 (0.495)

^aIn chloroform.^bRelative quantum yields to quinine sulfate (0.55).



SCHEME 6

TABLE 6. UV-vis absorption spectral data and electrical conductivities for silole–thiophene copolymers^{28b}

Compound ^a	λ_{max} (nm) ($\log \epsilon$) ^b	conductivity (S cm ⁻¹) ^c
 <p>34a ($n \approx 24$)</p>	576 (4.49) ^d 618 (4.44) ^d	0.13
 <p>34b ($n \approx 27$)</p>	546 (4.51) ^d	0.10
 <p>34c ($n \approx 41$)</p>	549 (4.70) ^d	2.4

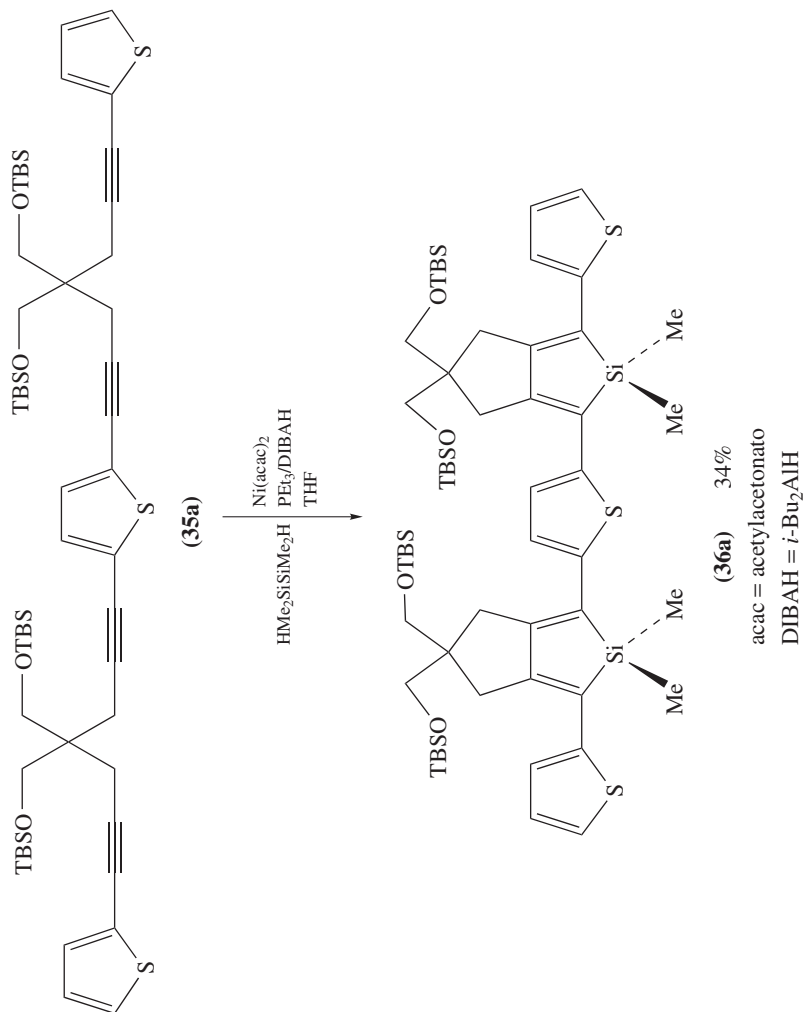
^aTBS = *tert*-butyldimethylsilyl.

^bIn chloroform.

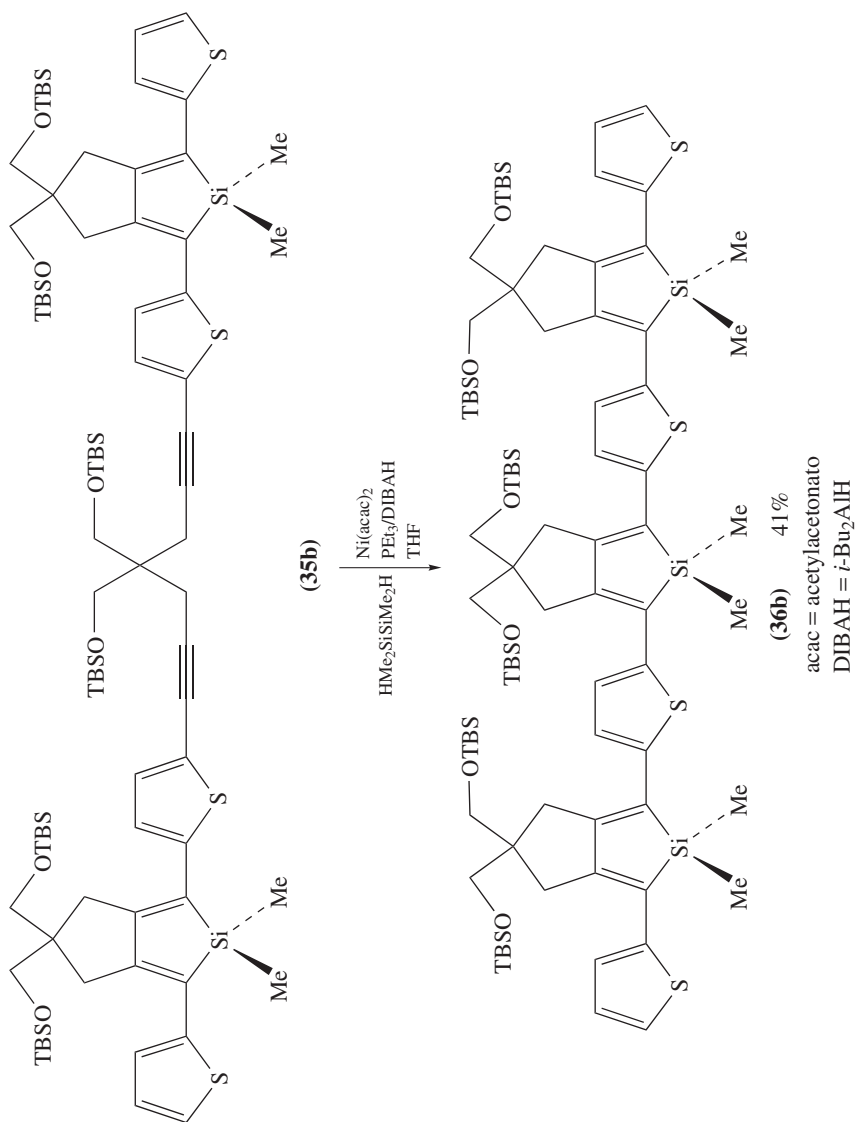
^cUpon doping with iodine vapor. Determined on thin films of polymers cast on glass substrate by the use of the four-probe technique.

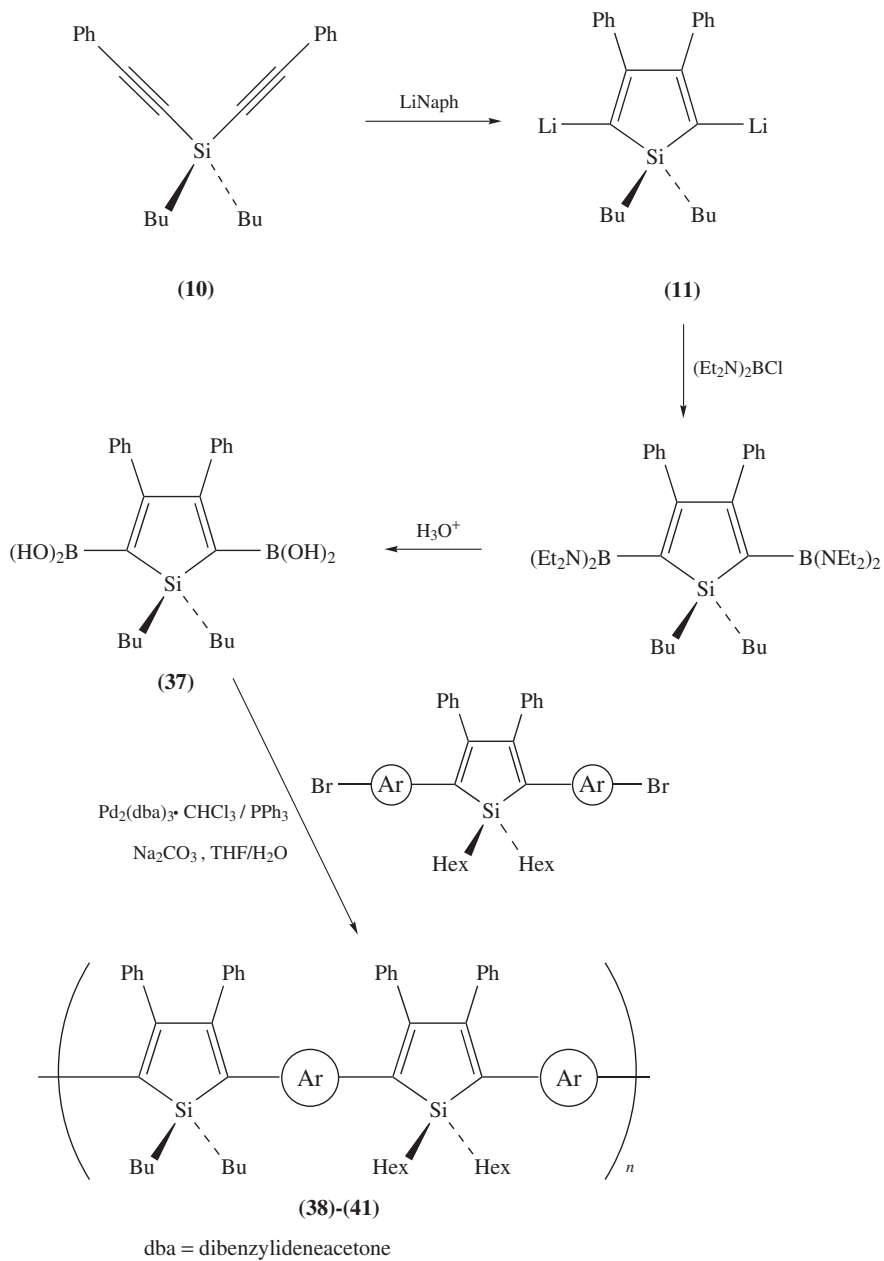
^dPer monomer unit.

suggesting a significant contribution of the silicon atoms to the π -conjugation of the polymer backbone. The bandgap of **40** determined from the λ_{0-0} bandedge is 1.55 eV, which is significantly small for a neutral, linear π -conjugated polymer consisting of 5-membered heteroarenes and well coincides with the theoretically predicted value^{38f}. A comparison of this value with those of the previously prepared silole–thiophene copolymers **34a–c** shows a good linear correlation between the silole–thiophene ratios and the bandgaps, as shown in Figure 14⁴⁵. This may suggest a further possibility of achieving lower bandgaps by increasing the silole content.

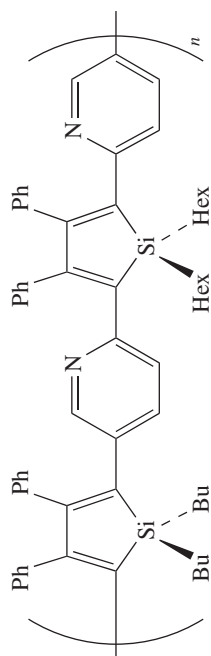


(8)

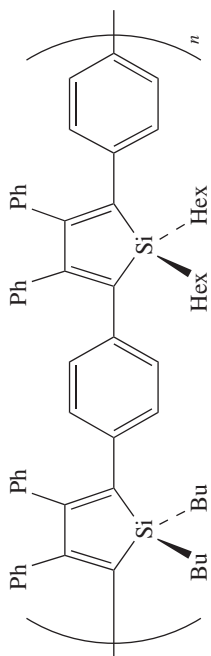




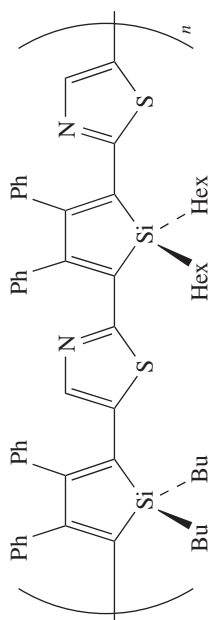
SCHEME 7



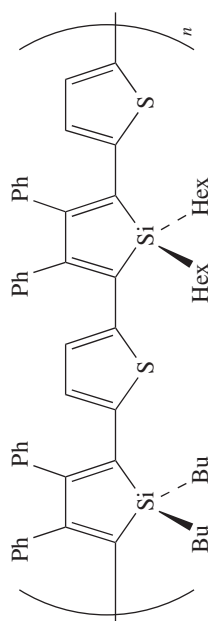
(39)

 λ_{max} 448 nm

(38)

 λ_{max} 402 nm

(41)

 λ_{max} 620, 664 nm

(40)

 λ_{max} 648, 685(sh) nm

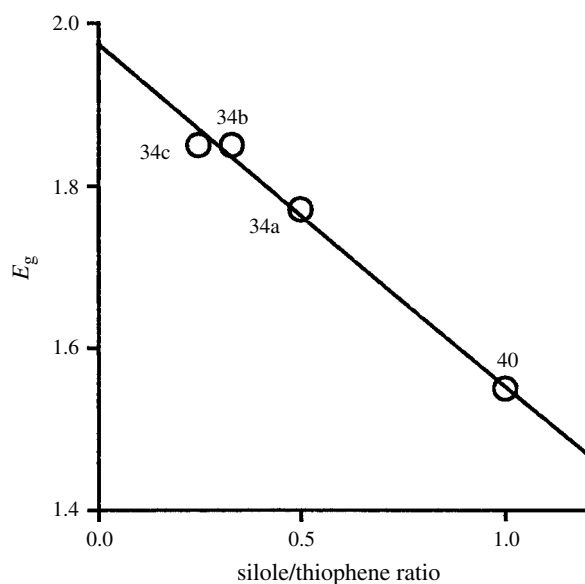
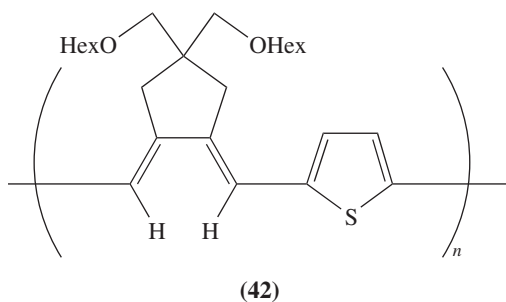
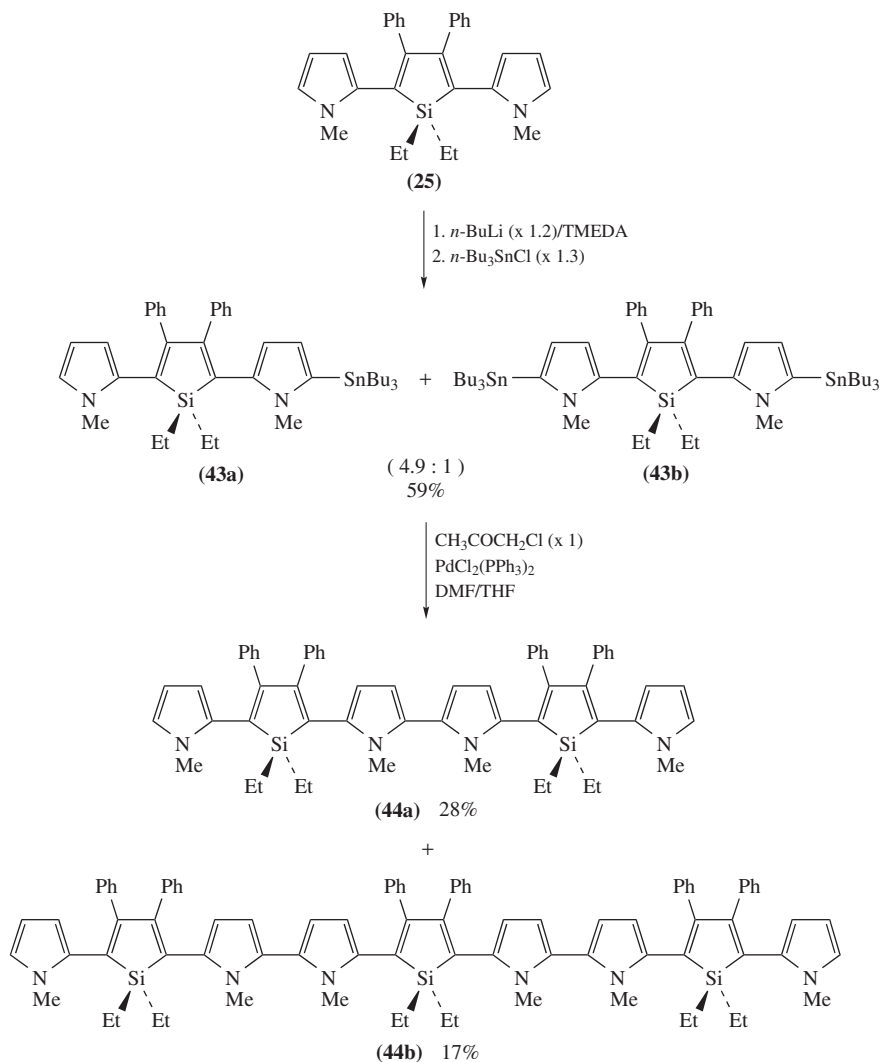


FIGURE 14. Plot of the bandgaps (E_g) determined from absorption edge versus silole/thiophene ratios for a series of silole–thiophene copolymers. Reproduced by permission of Wiley-VCH from Reference 45

π -Conjugated systems consisting of the electron-accepting silole with electron-donating pyrrole have also been reported. The synthesis of 2,5-dipyrrolylsilole **25** is shown in equation 6. The more extended cooligomers **44** with silole–pyrrole 1 : 2 ratio have been synthesized up to the 9-rings system using Pd⁰-catalyzed oxidative coupling of the stannylated precursor **43** (Scheme 8)^{15,48}. In contrast to the coplanar conformation of three rings in 2,5-dithienylsilole **26r**, 2,5-dipyrrolylsilole **25** has a highly twisted conformation of the three rings (torsion angle, 51.7 and 55.7°) due to steric repulsion, as shown in Figure 15. Nevertheless, the absorption maximum of 2,5-dipyrrolylsilole **25** is >100 nm longer than that of *N,N',N''*-trimethylterpyrrole (λ_{\max} , 271 nm)⁴⁹, suggesting that the combination of silole and pyrrole affords a unique electronic structure, although the extended cooligomers **44a** (λ_{\max} , 436 nm) and **44b** (λ_{\max} , 447 nm) have their absorption maxima only comparable to **25** due to the severe steric congestion along the main chain. According to theoretical



TMEDA = *N,N,N',N'*-tetramethylethylenediamine

SCHEME 8. Reproduced by permission of the Royal Society of Chemistry from Reference 15

calculations^{38g,50}, a coplanar silole–pyrrole alternating copolymer would have a bandgap of 1.68 eV^{38g}.

Silole–diethynylarene copolymers **45** have also been synthesized by the coupling reaction of **18b** with distannylated diethynylarenes (equation 10)^{51,52}. These polymers have their absorption at considerably long wavelengths. For instance, thiophene-containing polymer **45a** has the longest absorption maximum [λ_{\max} 576, 605(sh) nm]⁵² among the poly(ethynyleneareylene) type polymers reported to date⁵³.

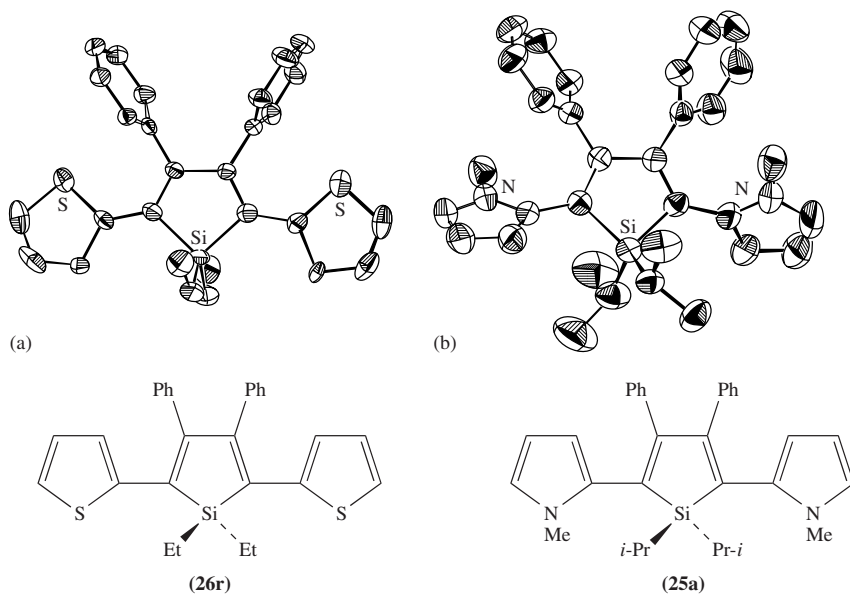
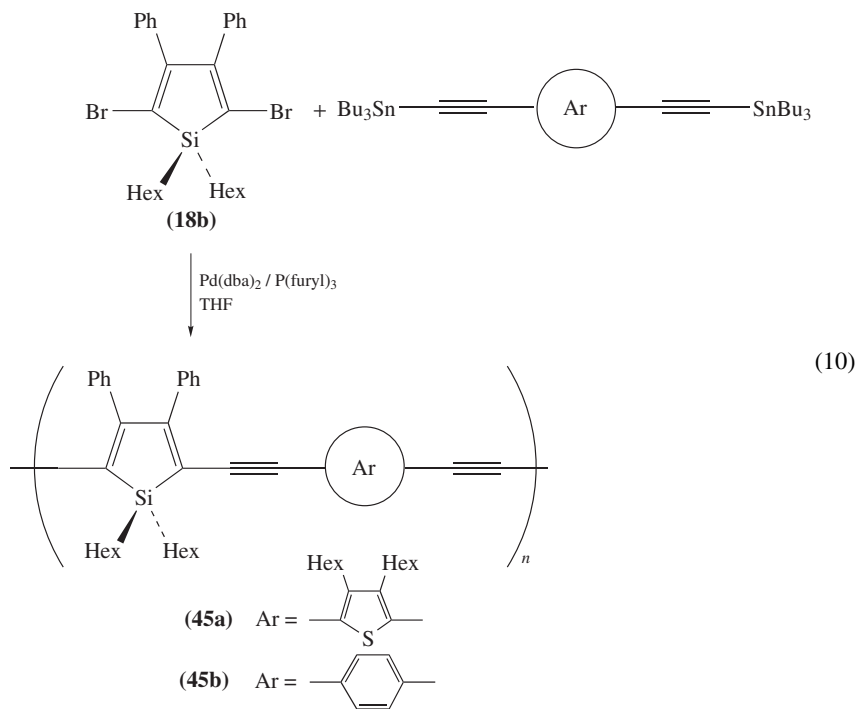
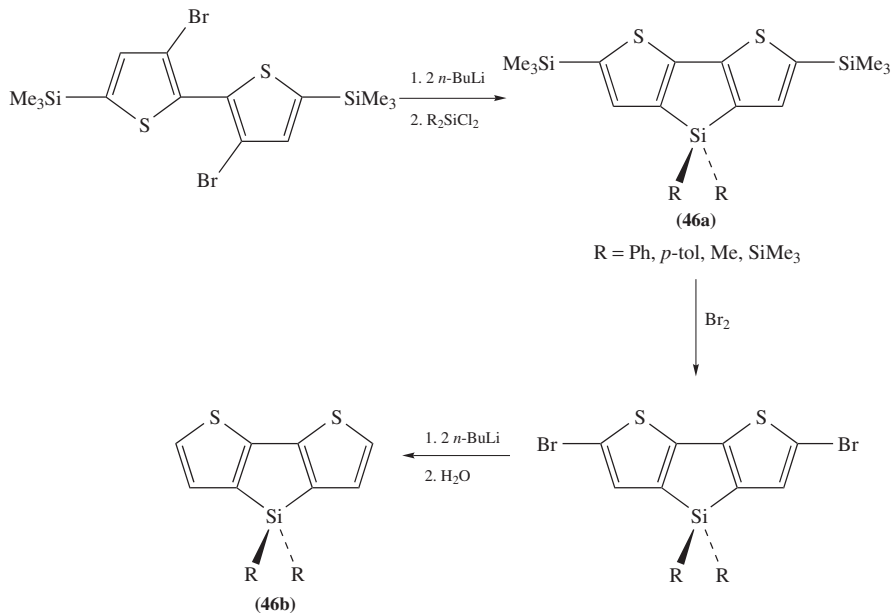


FIGURE 15. X-ray crystal structures of (a) 2,5-dithienylsilole **26r**⁴⁶ and (b) 2,5-dipyrrolylsilole **25a**¹⁵. Reproduced by permission of the Royal Society of Chemistry from Reference 15

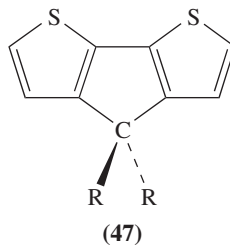


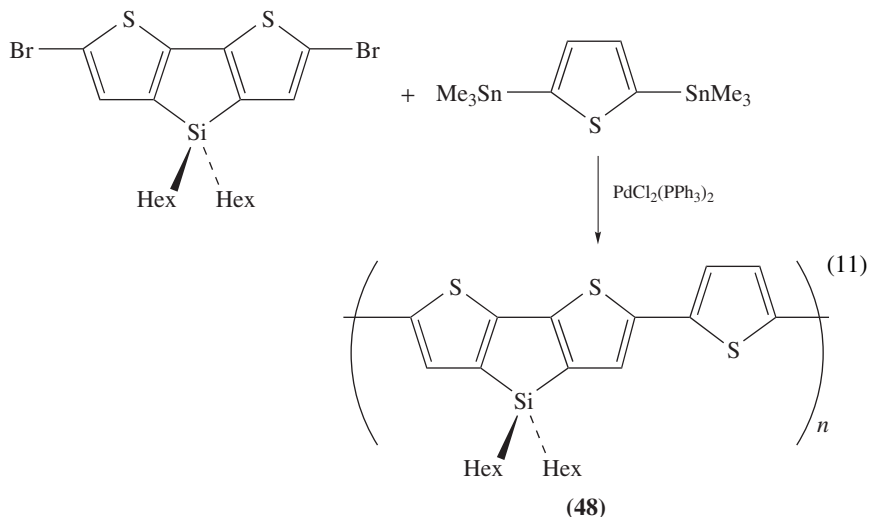
C. Fused Silole Ring Systems

Some new silole-based fused ring systems have been reported. Ohshita and coworkers⁵⁴ and Barton and coworkers⁵¹ have reported independently the synthesis of dithienosiloles **46**. Dithienosiloles can be prepared by the dilithiation of 3,3'-dibromo-2,2'-bithiophene followed by treatment with dichlorosilanes or equivalents (Scheme 9). Theoretical calculations show that dithienosilole has a lower LUMO level than that of the carbon analog **47**, due to the $\sigma^*-\pi^*$ conjugation as seen in the parent silole^{54b}. This is responsible for the longer λ_{max} (356 nm) of **46b** (R = Ph) than that (323 nm) of the carbon analog **47** (R = H)⁵⁵. Dithienosilole–thiophene alternating copolymer **48** has been prepared by the Stille coupling reaction of dibromodithienosilole with distannylthiophene (equation 11)⁵¹. The polymer has long λ_{max} (556 nm in THF solution and 582 nm as a film) and high conductivity (400 S cm^{-1}) upon I_2 doping.

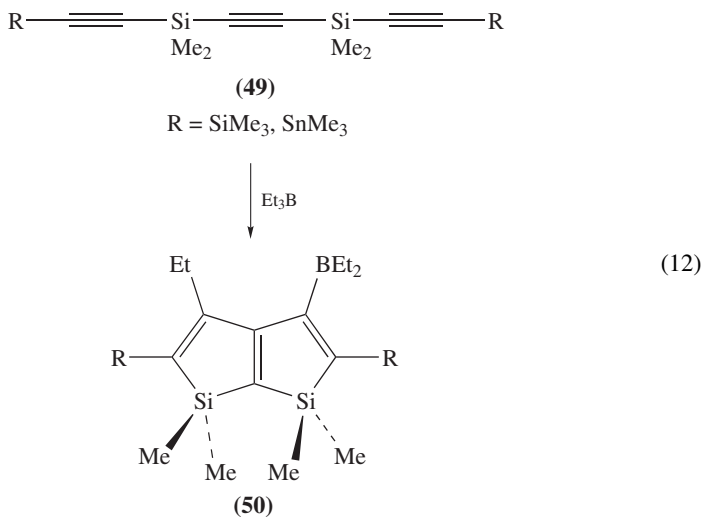


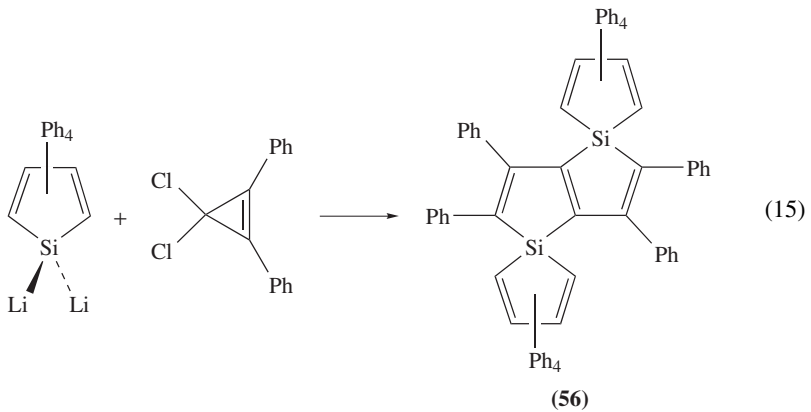
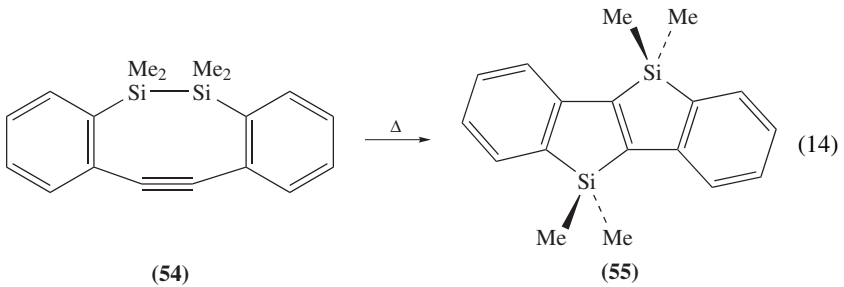
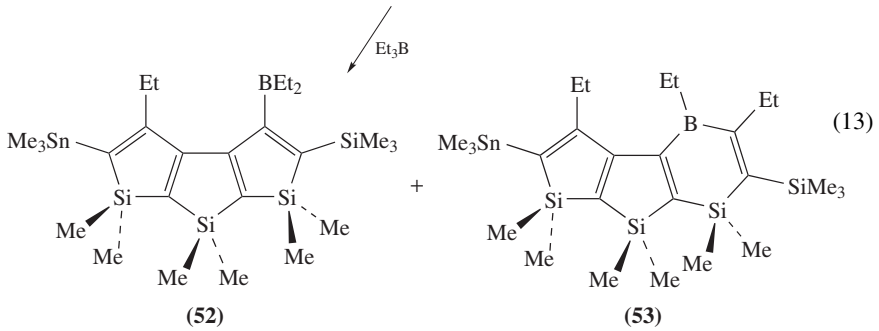
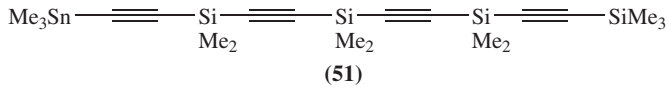
SCHEME 9





Recently, Wrackmeyer and coworkers have reported an interesting synthesis of a new silole-fused system⁵⁶. The reaction of silicon-tethered triyne **49** with BEt_3 affords disilapentalene **50** (equation 12). Starting from tetrayne **51**, a mixture of tricyclic compounds **52** and **53** has also been obtained (equation 13). These reactions are an extended version of equation 2 (Section III). Similar silole-fused ring systems have also been synthesized by Barton and coworkers. The thermal cyclization of **54** produces fluorescent disilapentalene derivative **55** (equation 14)⁵⁷. Quite recently, West and coworkers have reported the reaction of 1,1-dilithiosilole with 1,1-dichlorocyclopropene to give disilaspiropentalene **56** (equation 15)⁵⁸. These compounds are potent monomer units for new π -conjugated polymers, although their photophysical and electrochemical properties have not yet been reported.





VI. POLY(1,1-SILOLE)S AND SILOLE-CONTAINING POLYSILANES

Considering the $\sigma^*-\pi^*$ conjugation in the LUMO of silole, polymers containing silole-1, 1-diyl units are of interest as new entries of polysilanes. Poly(1,1-silole)s are expected to have a high electron affinity due to a specific orbital interaction between the σ^* orbital delocalized over the polysilane main chain and the π^* orbital localized on every silole ring (Figure 16)⁵⁹. Semiempirical calculations actually suggested its low-lying LUMO level (Figure 17)⁶⁰.

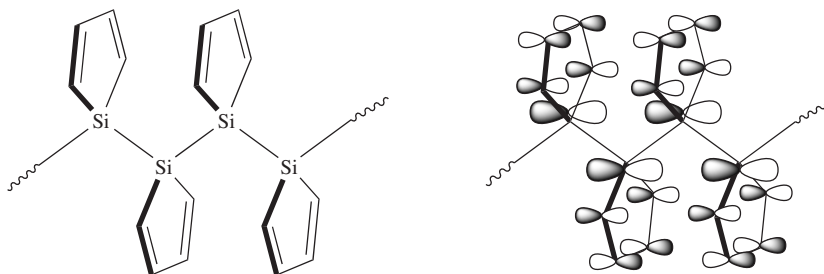


FIGURE 16. Schematic drawings of poly(1,1-silole) and $\sigma^* - \pi^*$ conjugation in the LUMO. Reprinted by permission from Reference 59. Copyright 1997 American Chemical Society

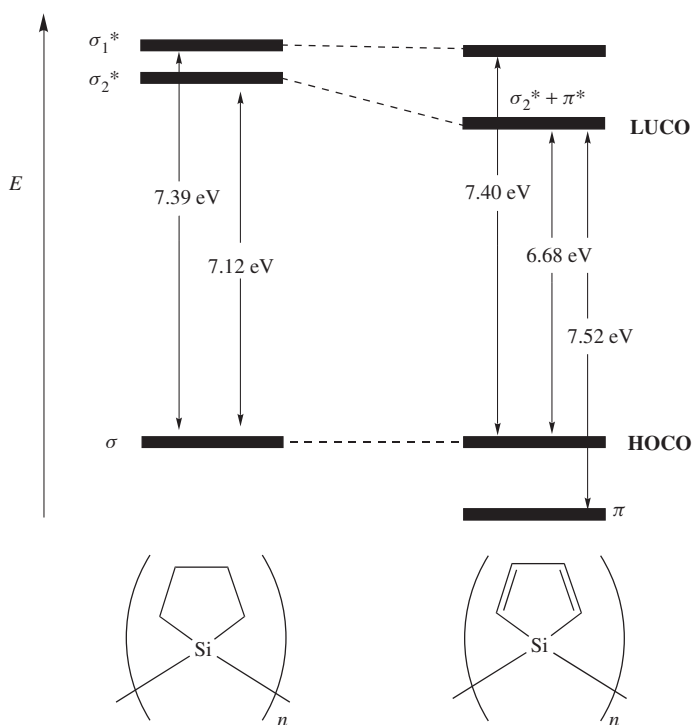
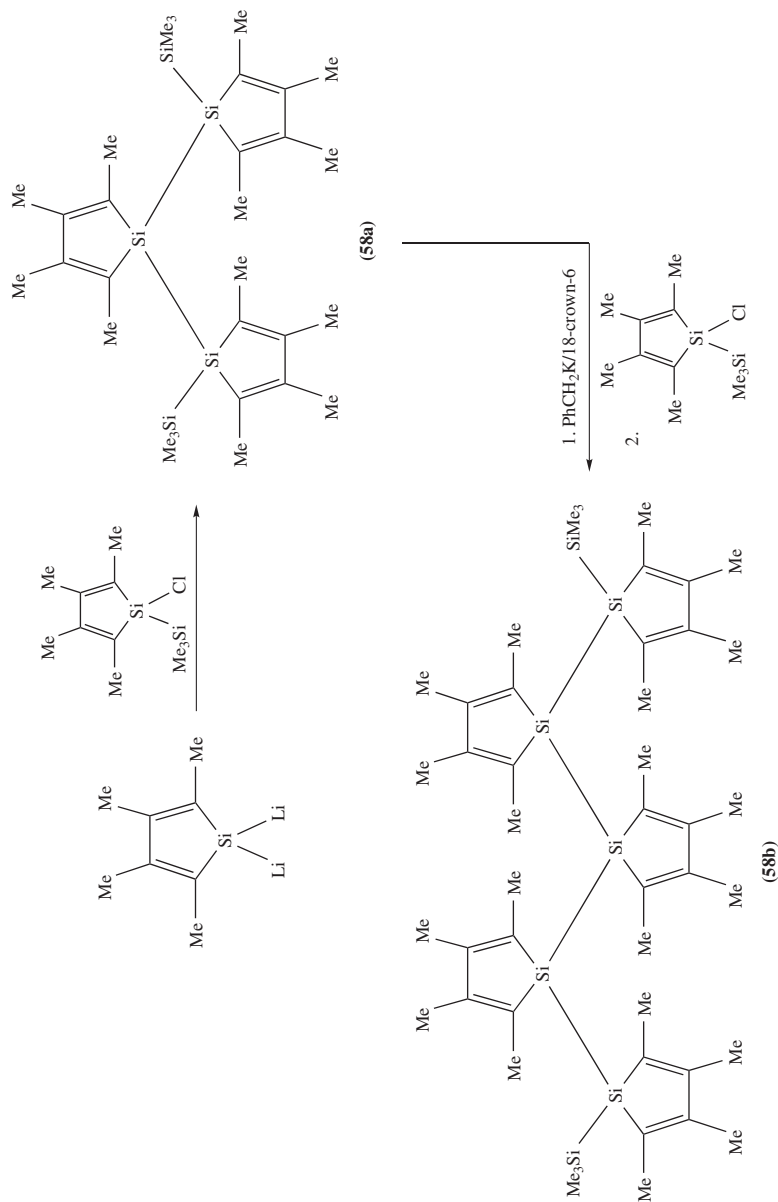


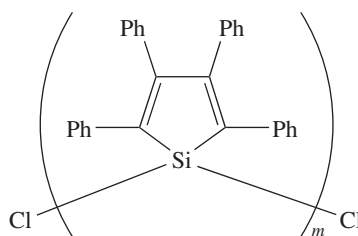
FIGURE 17. Schematic band level diagram for poly(1,1-silole) and its saturated analog⁶⁰

Experimentally, a few series of oligo(1,1-silole)s have been prepared as models of poly(1,1-silole)s and their structures and photophysical properties have been studied in detail^{59,61,62}. We have prepared a series of oligo(1,1-silole)s **57** having 3,4-diphenyl-2,5-dimethylsilole as a monomer unit. The stoichiometrically controlled reduction of 1,1-dichlorosilole with sodium followed by treatment with 1-methyl-1-chlorosilole affords tersilole **57a** and quater-silole **57b**, as shown in Scheme 10⁵⁹. Kira and coworkers have reported the synthesis of



SCHEME 11

2,3,4,5-tetramethylsilole-based oligo(1,1-silole)s **58** up to the pentamer based on the reaction of the corresponding silole anions with 1-silyl-1-chlorosilole (Scheme 11)⁶¹. West and coworkers have also reported the partial reduction of 1,1-dichloro-2,3,4,5-tetraphenylsilole to form the corresponding bisilole **59a** and tersilole **59b**⁶². The structures of these oligo(1,1-silole)s are interesting. The geometries of the oligosilane skeletons of these oligo(1,1-silole)s are greatly dependent on the bulkiness of the substituents on the silole rings (Figure 18). While the bulkiest tetraphenyl-substituted **59b** has an *all-gauche* structure with respect to the silicon linkage, 3,4-diphenyl-2,5-dimethylsilole-based tersilole **57a** has a *gauche-anti* structure, and the tetramethylsilole-based one **58a** has an *all-trans* structure of the oligosilane skeleton. The photophysical properties of oligo(1,1-silole)s are also dependent on the substituents on the siloles. While in a series of **57** the absorption bands shift to longer wavelengths as the chain length becomes longer⁵⁹, the series of the tetramethyl-substituted oligosiloles **58** have their bands assigned to the charge-transfer transitions from oligosilane σ -HOMO to diene π^* -LUMO (σ - π^* transition) at almost identical wavelengths, around 280 nm, irrespective of the oligosilane chain lengths⁶¹.



(**59a**) $m = 2$

(**59b**) $m = 3$

Quite recently, West and coworkers⁶² and our group⁶³ independently have succeeded in the synthesis of poly(1,1-silole)s **60** and **61**, respectively, by Wurtz-type coupling of the corresponding 1,1-dichlorosiloles (Scheme 12). During the synthesis of **61**, cyclic hexamer **62** is also produced. Although the degrees of polymerization of both polymers **60** and **61** are still as low as about 13–15, the key factor to obtain high molecular weight polymers must be the stoichiometry of the alkali metal relative to the dichlorosilole. This is apparent from the fact that complete degradation of the poly(1,1-silole) **61** occurs with excess lithium, giving 1,1-dilithiosilole as sole product⁶³. This may be ascribed to the expected low-lying LUMO level of the poly(1,1-silole)s and high stability of the resulting silole dianion⁴. In the UV-visible absorption spectra, the polymer **61** has λ_{max} which is 30–40 nm longer than that of oligo(1,1-silole) **57**. While the 2,5-dimethylsilole-based polymer **61** has a weak fluorescence around 460 nm, the 2,5-diphenylsilole-based one **60** has an intense fluorescence around 520 nm and there have been attempts to apply this polymer to an organic electroluminescence device (see Section VIII)^{62b}.

Other related polymers, poly(dibenzosilole) **63**⁶⁴ and silole-incorporated polysilane **64**⁶⁵, have been prepared by the metal-catalyzed dehydrogenative coupling of 1,1-dihydrodibenzosilole (equation 16) and by the anionic ring-opening polymerization shown in Scheme 13, respectively. It should be noted that the latter reaction proceeds by a living polymerization process via intermediate **65a**, which is in equilibrium with a stable allyl anionic species **65b**. Recently, this reaction has been applied to the synthesis of germole analog **66**⁶⁶. In the fluorescence spectra of polymer **64**, when excited at 323 nm (which corresponds to the excitation of the polysilane skeleton), a fluorescence band is observed

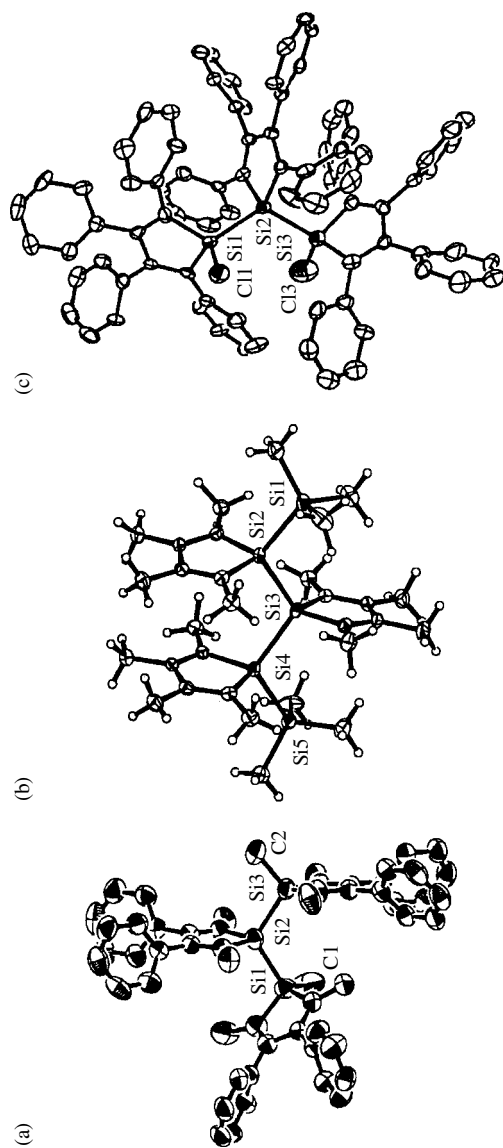
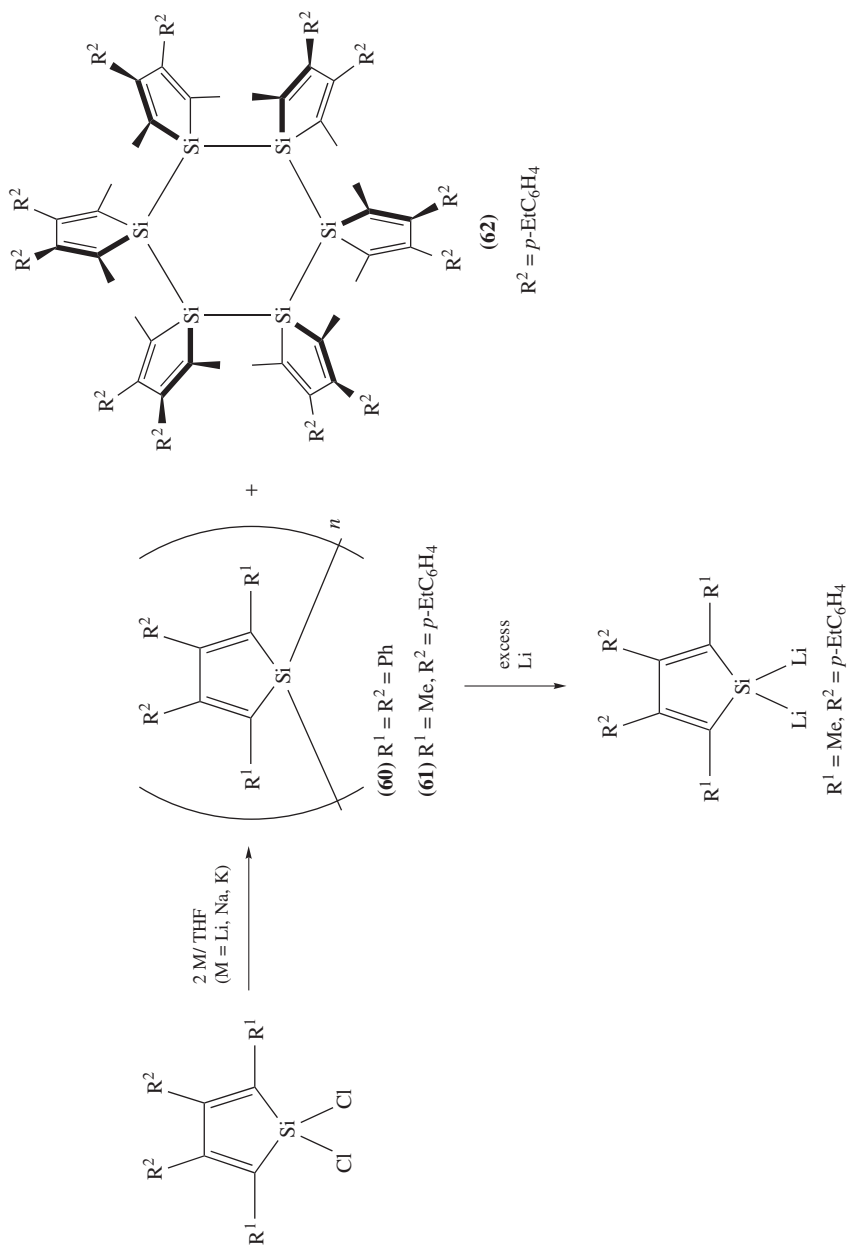
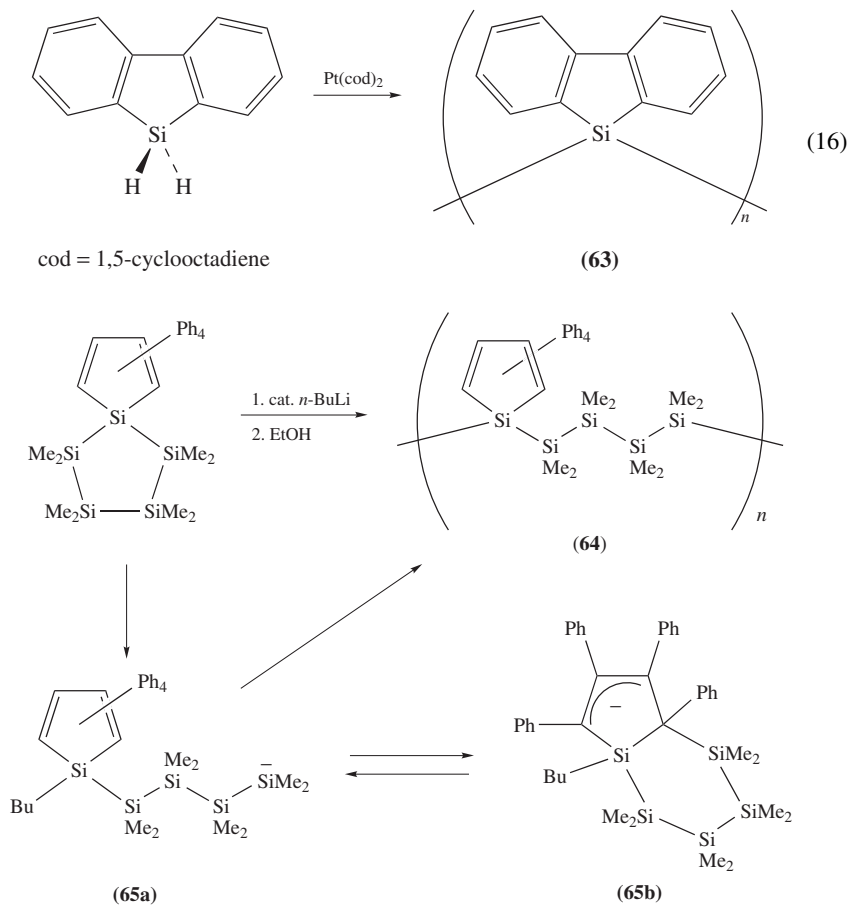


FIGURE 18. Crystal structures of ter(1,1-silole)s: (a) **57a**, reproduced by permission from Reference 59. Copyright 1997 American Chemical Society; (b) **58a**, reproduced by permission of the Chemical Society of Japan from Reference 61; (c) **59b**, reproduced by permission from Reference 62. Copyright 1999 American Chemical Society

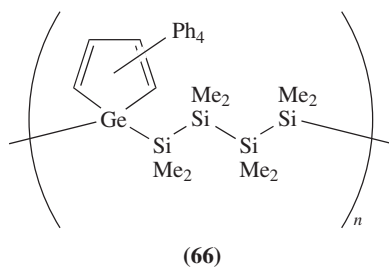


SCHEME 12

at 520 nm, which is assignable to emission from the tetraphenylsilole skeleton. This suggests the occurrence of extensive energy transfer from the polysilane skeleton to the silole skeleton. Notably, the quantum yield of fluorescence of **64** (4.1×10^{-2}) is about 10 times greater than that of the parent hexaphenylsilole (4.5×10^{-3})⁶⁷.

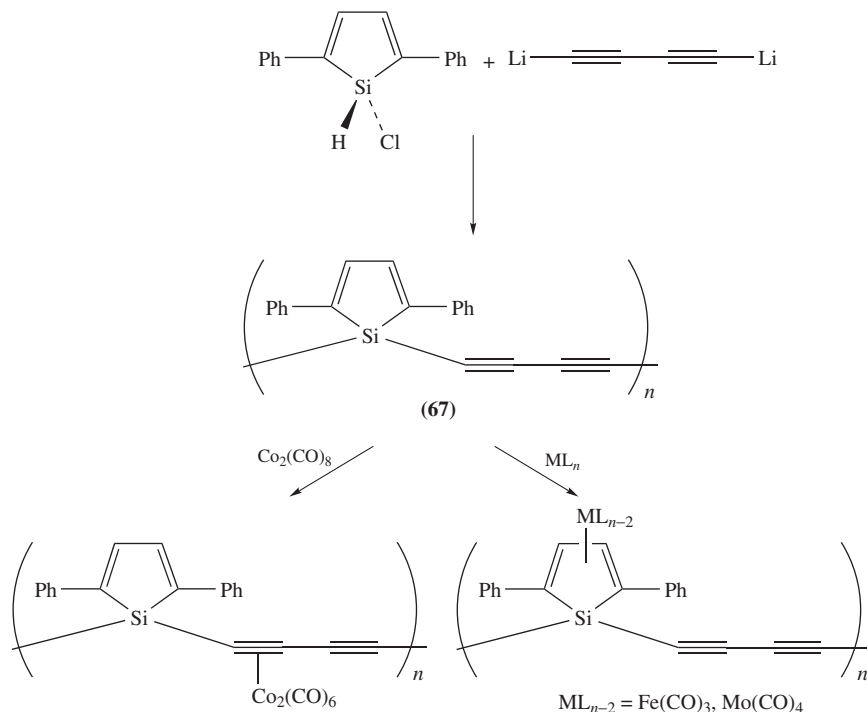


SCHEME 13



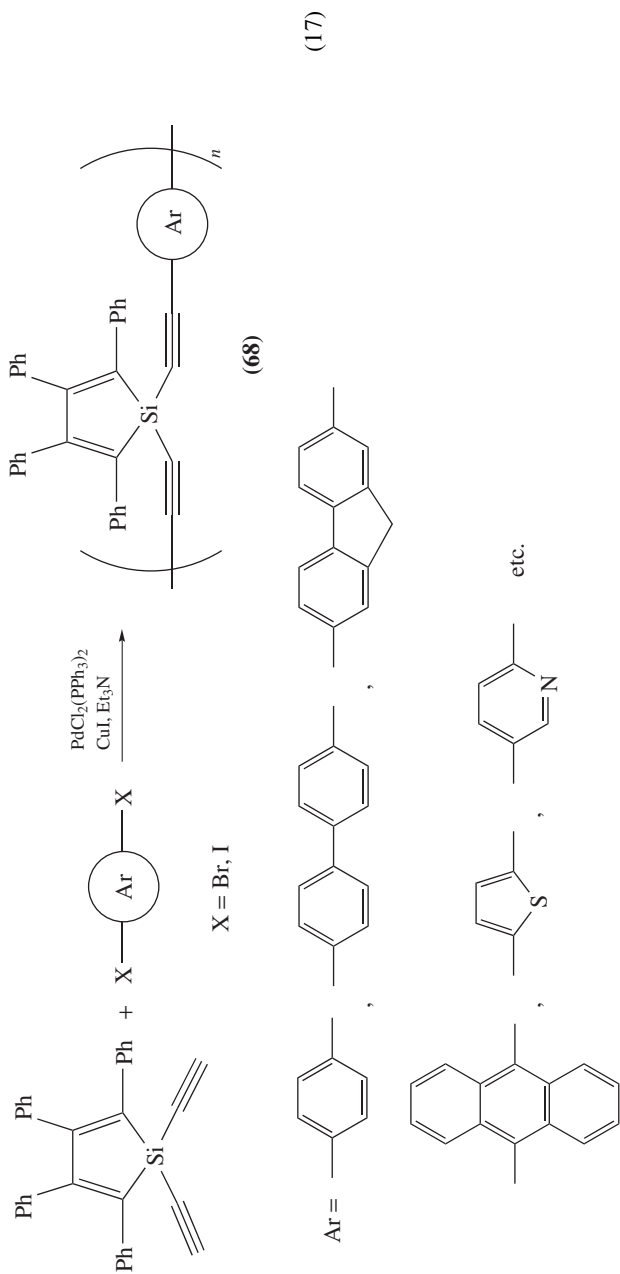
VII. OTHER SILOLE-CONTAINING POLYMERS

Several other types of silole-containing polymers have been reported. Corriu and coworkers have reported the synthesis of polymers consisting of the silole-1,1-diyl unit and π -conjugated moieties as potent conducting materials or precursors for transition-metal-containing ceramics. The reaction of 1-hydro-1-chlorosilole with dithiodiacetylene affords polymer **67**, as shown in Scheme 14⁶⁸. This polymer can be modified by the complexation of triple bonds with $\text{Co}_2(\text{CO})_6$ moieties, or alternatively by the η^4 -complexation of silole rings with $\text{Fe}(\text{CO})_3$ and $\text{Mo}(\text{CO})_4$ moieties^{68b}. The Pd/Cu-catalyzed cross-coupling of 1,1-diethynylsilole with dihaloarenes gave a series of polymers **68** containing the tetraphenylsilole unit and various arene units (equation 17)⁶⁹. Modification of the polymer by η^4 -complexation with $\text{Fe}(\text{CO})_3$ is achievable also in the case of **68**.

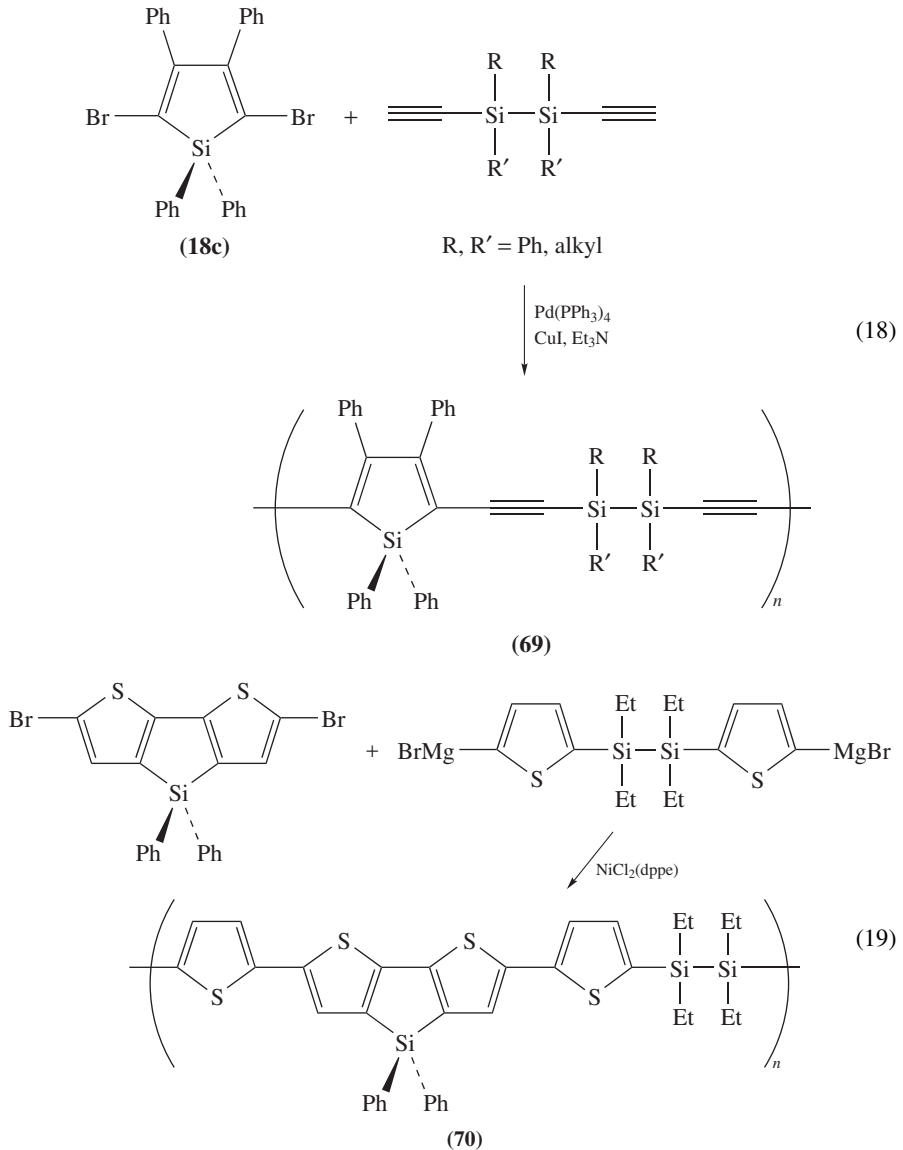


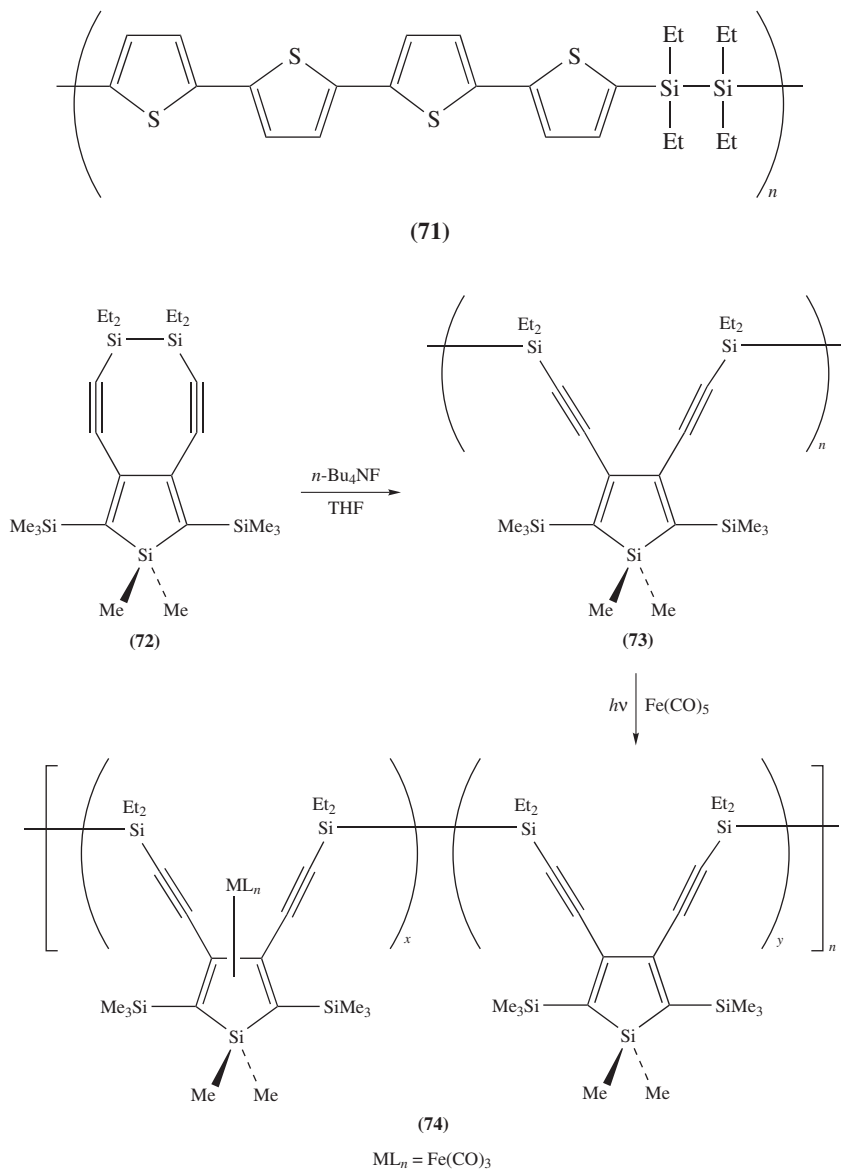
SCHEME 14

Ishikawa and coworkers have prepared copolymers of silole π -conjugated units and disilanylene units as new σ - π conjugated polymers⁷⁰. Polymer **69** has been prepared by the coupling reaction of 2,5-dibromosilole **18c** with 1,2-diethynylsilanes (equation 18)⁷¹. Dithienosilole-containing polymer **70** has also been prepared by the Ni^0 -catalyzed cross-coupling reaction (equation 19)^{54a}. The polymer has λ_{max} (448 nm), which is about 30 nm longer than the corresponding quaterthiophene-disilanylene copolymer **71** (λ_{max} , 415 nm)⁷², clearly indicating the significant contribution of the silicon atoms in the dithienylsilole skeleton. The polymer shows a moderate conductivity ($7.0 \times 10^{-3} \text{ S cm}^{-1}$)



upon doping with FeCl_3 . These researchers have also reported the synthesis of polymer **73** containing the silole-3,4-diyl unit by the ring-opening anionic polymerization of **72** with $n\text{-Bu}_4\text{NF}$, as shown in Scheme 15⁷². The reaction of this polymer with $\text{Fe}(\text{CO})_5$ under irradiation affords a partially $\text{Fe}(\text{CO})_3$ -coordinated polymer **74**^{73b}.





SCHEME 15

VIII. APPLICATION TO ORGANIC ELECTROLUMINESCENT DEVICES

Since the breakthrough made by Tang and VanSlyke, who introduced the thin multilayer cell configuration⁷⁴, the organic electroluminescent (EL) device represents one of the most promising technologies for display materials⁷⁵. Considerable effort has been devoted to

the development of new materials for organic EL devices. One of the current interests in this field is the development of efficient electron-transporting (ET) materials^{76,77}. In this respect, the silole ring is of great interest as a core unit of ET materials due to its high electron affinity. Several types of silole-based π -electron systems have so far been applied to organic EL devices.

We have examined a series of 2,5-diarylsiloles as ET materials and found that 2,5-di(2-pyridyl)silole **26p** has a significantly high performance¹⁶. The device having ITO (indium tin oxide)/TPD/Alq/**26p**/Mg:Ag configuration (Figure 19) emits a greenish yellow light from the Alq layer. The threshold driving voltage is about 3 V and the luminous efficiency to gain 100 cd m^{-2} is 1.9 lm W^{-1} . Figure 20 shows a comparison of the luminance (L)–applied voltage (V) characteristics between the devices with

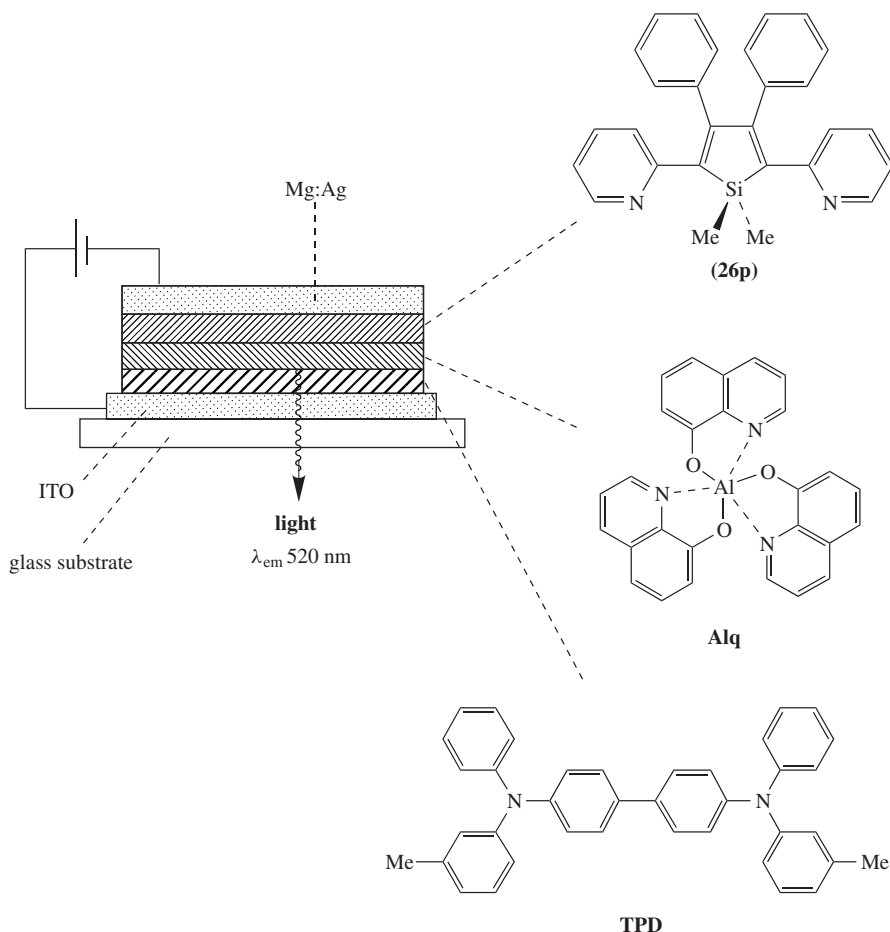


FIGURE 19. A schematic drawing of an organic EL device using **26p**, Alq and TPD as electron-transporting, emissive and hole-transporting materials, respectively. Reproduced by permission of the Royal Society of Chemistry from Reference 6b

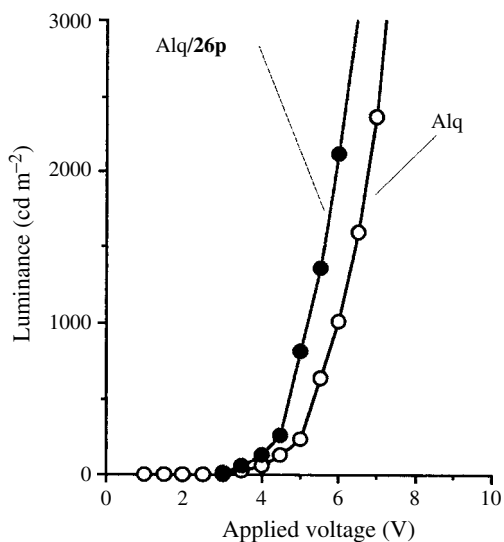
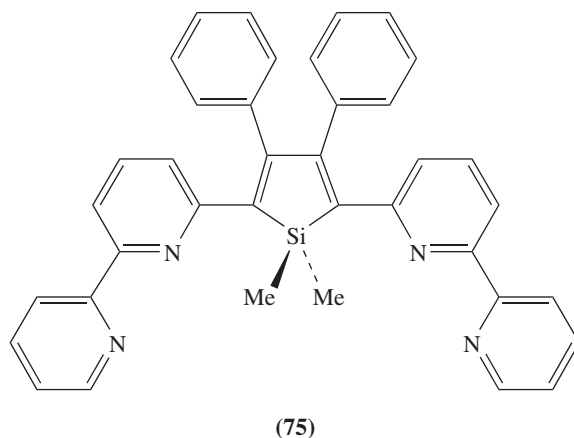


FIGURE 20. Comparison of luminance–voltage (L – V) characteristics between the devices with ITO/TPD/Alq/**26p**/Mg:Ag (solid circle) and with ITO/TPD/Alq/Mg:Ag (open circle)

ITO/TPD/Alq/**26p**/Mg:Ag configuration and with ITO/TPD/Alq/Mg:Ag configuration, and demonstrates that the performance of **26p** as an ET material exceeds that of Alq, one of the best ET materials reported so far. Quite recently, the structure of **26p** has been further optimized and its derivative **75** has been found to have an even higher ET performance and also a higher stability of the vacuum-deposited thin film⁷⁸.



2,5-Diarylsiloles can also be applied as emissive materials¹⁶. The wavelengths of their luminescence are widely tunable from greenish-blue to orange colors by changing the 2,5-aryl groups. Typical examples are shown in Figure 21 (see Section V.A.1). These

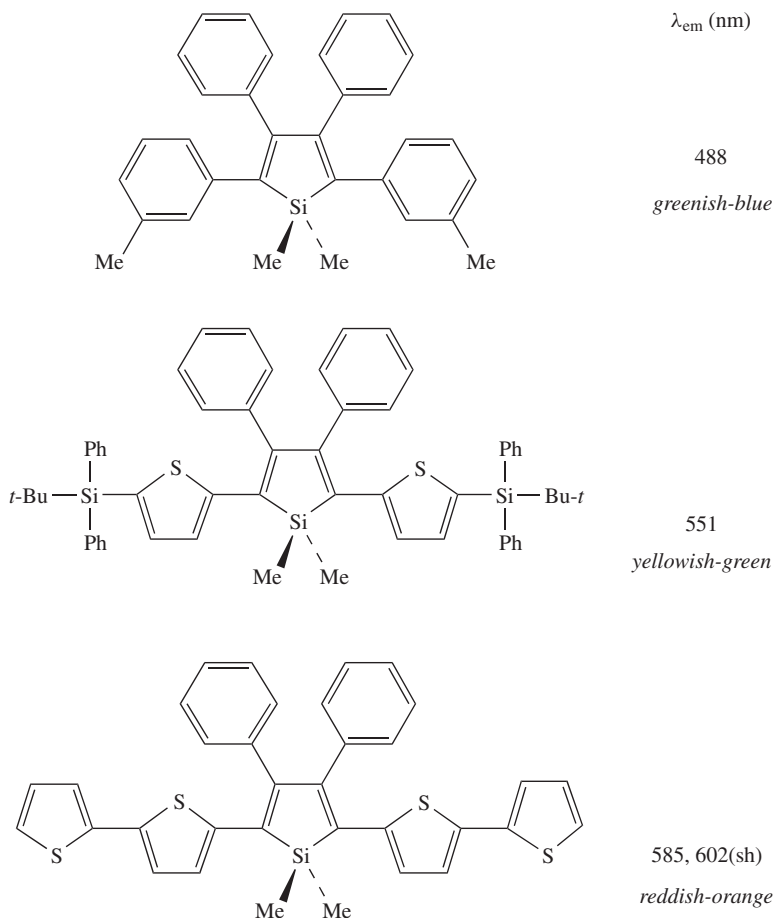
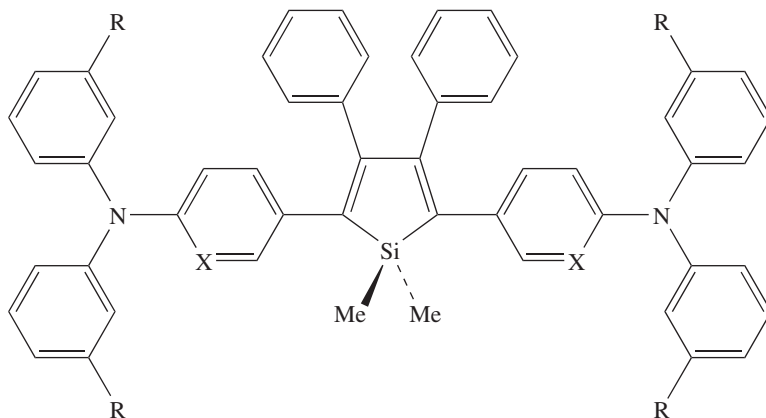


FIGURE 21. Emission wavelengths of organic EL devices using 2,5-diarylsiloles as emissive electron-transporting materials: Cell configuration; ITO/TPD/2,5-diarylsilole/Mg:Ag. Reproduced by permission of the Royal Society of Chemistry from Reference 6b

results suggest an easy access to various colors of light; e.g. blue to red colors required for application to full-color displays, only by modification of the 2,5-aryl groups on the silole ring. Advantageously, this structural modification could be readily achieved by the one-pot synthesis mentioned above (Scheme 5, see Section V.A).

As an example of the structural modification, diphenylamino-substituted 2,5-diarylsiloles **76** have been prepared for single-layer EL devices⁷⁹. The diphenylamino groups significantly contribute to the electronic structures of the 2,5-diarylsilole skeletons and increase their HOMO levels, providing the hole-transporting properties to the electron-transporting silole compounds. Actually, the single-layer device with ITO/silole **76**/Mg:Ag configuration emits a greenish-yellow light with relatively high luminous efficiency (**76a**, 0.058 lm W⁻¹; **76b**, 0.26 lm W⁻¹, to obtain 50 cd m⁻²) as the single-layer EL devices.



(76a) X = CH, R = Me

(76b) X = N, R = H

Besides the 2,5-diarylsiloles, dithienosilole derivatives have been applied to organic EL devices⁸⁰. The device with the ITO/TPD/Alq/**46a** (R = Ph)/Mg:Ag configuration has current density–applied voltage characteristics comparable to that of the ITO/TPD/Alq/Mg:Ag device, although its maximum luminance is moderate. This suggests the ET abilities of **46a** to be comparable to that of Alq, which should be due also to the low LUMO level of the dithienosilole skeleton⁵⁴. Poly(1,1-silole) **60** has also been applied to organic EL devices⁶². The single-layer device with the ITO/**60**/Mg:Ag configuration emits a green light (520 nm) with an external quantum efficiency of *ca* $3 \times 10^{-2}\%$, which is relatively high for a polysilane-based EL device^{62b}. The unique electronic structure of the tetraphenylsilole skeleton might be responsible for this result.

IX. CONCLUSION

The utilization of silole as a key building unit of σ - and π -conjugated systems is a new aspect of silole chemistry. The most notable feature is that the silole is not an aromatic system like heteroarenes such as thiophene and pyrrole, but a cyclic diene bridged by a silicon atom. Due to the $\sigma^*-\pi^*$ conjugation in the ring, silole has a unique electronic structure characterized by having the lowest level of LUMO among some representative traditional heteroarenes. As a consequence, the silole-based oligomeric and polymeric compounds indeed have unique properties, making themselves very promising for application to optoelectronics such as organic EL devices. It should be noted that this chemistry is based on the recent development of several new synthetic methods for silole derivatives: A variety of functionalized siloles are now available based on the new synthesis represented by the intramolecular reductive cyclization of bis(phenylethynyl)silanes. Various kinds of 2,5-diarylsiloles including 3,4-diphenyl-, 3,4-dialkyl- and 3,4-unsubstituted 2,5-diarylsiloles can also be readily prepared. Furthermore, new silole ring systems such as dithienosilole and disilapentalene derivatives have recently been introduced to this chemistry. We are now at the stage where silole compounds with complex structures can be tailor-made for specific application, so further progress in this chemistry based on precise molecular design would provide new attractive silicon-containing conjugated systems.

X. REFERENCES

1. (a) E. H. Braye and W. Hübel, *Chem. Ind. (London)*, 1250 (1959).
(b) E. H. Braye, W. Hübel and I. Caplier, *J. Am. Chem. Soc.*, **83**, 4406 (1961).
2. (a) J. Dubac, A. Laporterie and G. Manuel, *Chem. Rev.*, **90**, 215 (1990).
(b) E. Colomer, R. J. P. Corriu and M. Lheureux, *Chem. Rev.*, **90**, 265 (1990).
(c) J. Hermanns and B. Schmidt, *J. Chem. Soc., Perkin Trans. 1*, 2209 (1998).
(d) J. Dubac, C. Guerin and P. Meunier, in *The Chemistry of Organic Silicon Compounds* (Eds. Z. Rappoport and Y. Apeloig), Vol. 2, Chap. 34, Wiley, Chichester, 1998.
3. W. P. Freeman, T. D. Tilley and A. L. Rheingold, *J. Am. Chem. Soc.*, **116**, 8428 (1994) and references cited therein.
4. (a) W.-C. Joo, J.-H. Hong, S.-B. Choi, H.-E. Son and C. H. Kim, *J. Organomet. Chem.*, **391**, 27 (1990).
(b) J.-H. Hong and P. Boudjouk, *J. Am. Chem. Soc.*, **115**, 5883 (1993).
(c) J.-H. Hong, P. Boudjouk and S. Castellino, *Organometallics*, **13**, 3387 (1994).
(d) S.-B. Choi, P. Boudjouk and P. Wei, *J. Am. Chem. Soc.*, **120**, 5814 (1998).
(e) B. Goldfuss and P. v. R. Schleyer, *Organometallics*, **14**, 1553 (1995).
(f) B. Goldfuss, P. v. R. Schleyer and F. Hampel, *Organometallics*, **15**, 1755 (1996).
(g) B. Goldfuss and P. v. R. Schleyer, *Organometallics*, **16**, 1543 (1997).
(h) R. West, H. Sohn, U. Bankwitz, C. Joseph, Y. Apeloig and T. Mueller, *J. Am. Chem. Soc.*, **117**, 11608 (1995).
(i) H. Sohn, D. R. Powell, R. West, J.-W. Hong and W.-C. Joo, *Organometallics*, **16**, 2770 (1997).
(j) W. P. Freeman, T. D. Tilley, G. P. A. Yap and A. L. Rheingold, *Angew. Chem., Int. Ed. Engl.*, **35**, 882 (1996).
(k) W. P. Freeman, T. D. Tilley, L. M. Liable-Sands and A. L. Rheingold, *J. Am. Chem. Soc.*, **118**, 10457 (1996).
(l) T. Wakahara and W. Ando, *Chem. Lett.*, 1179 (1997).
5. S. Yamaguchi and K. Tamao, in *Silicon-containing Polymers: The Science and Technology of their Synthesis and Applications* (Eds. R. G. Jones, W. Ando and J. Chojnowski), Kluwer Science, New York (2000).
6. (a) K. Tamao, S. Yamaguchi, M. Uchida, T. Izumizawa and K. Furukawa, in *Organosilicon Chemistry IV. From Molecules to Materials* (Eds. N. Auner and J. Weis), Wiley-VCH Verlag GmbH, Weinheim (2000) pp. 245–251.
(b) S. Yamaguchi and K. Tamao, *J. Chem. Soc., Dalton Trans. (Perspective)*, 3693 (1998).
(c) K. Tamao and S. Yamaguchi, *Pure Appl. Chem.*, **68**, 139 (1996).
7. J. Shinar, S. Ijadi-Maghsoodi, Q.-X. Ni, Y. Pang and T. J. Barton, *Synth. Met.*, **28**, C593 (1989).
8. T. J. Barton, S. Ijadi-Maghsoodi and Y. Pang, *Macromolecules*, **24**, 1257 (1991).
9. T. J. Barton and A. J. Nelson, *Tetrahedron Lett.*, 5037 (1969).
10. (a) Y. Nakadaira and H. Sakurai, *Tetrahedron Lett.*, 1183 (1971).
(b) H. Sakurai, A. Nakamura and Y. Nakadaira, *Organometallics*, **2**, 1814 (1983).
11. E. G. Janzen, J. B. Pickett and W. H. Atwell, *J. Organomet. Chem.*, **10**, P6 (1967).
12. D. H. O'Brien and D. L. Breeden, *J. Am. Chem. Soc.*, **103**, 3237 (1981).
13. Calculations on silole rings:
(a) V. Niessen, W. P. Kraemer and L. S. Cederbaum, *Chem. Phys.*, **11**, 385 (1975).
(b) M. S. Gordon, P. Boudjouk and F. Anwari, *J. Am. Chem. Soc.*, **105**, 4972 (1983).
(c) C. Guimon, G. Pfister-Guillouzo, J. Dubac, A. Laporterie, G. Manuel and H. Ploughmane, *Organometallics*, **4**, 636 (1985).
(d) J. R. Damewood, *J. Org. Chem.*, **51**, 5028 (1986).
(e) V. N. Khabashesku, S. E. Balaji, V. Boganov, O. M. Nefedov and J. Michl, *J. Am. Chem. Soc.*, **116**, 320 (1994).
(f) A. Hinchliffe and H. J. Soscún M., *J. Mol. Struct. (Theochem)*, **331**, 109 (1995).
See also References 4e–h.
14. S. Yamaguchi and K. Tamao, *Bull. Chem. Soc. Jpn.*, **69**, 2327 (1996).
15. K. Tamao, S. Ohno and S. Yamaguchi, *Chem. Commun.*, 1873 (1996).
16. K. Tamao, M. Uchida, T. Izumizawa, K. Furukawa and S. Yamaguchi, *J. Am. Chem. Soc.*, **118**, 11974 (1996).
17. U. Salzner, J. B. Lagowski, P. G. Pickup and R. A. Poirier, *Synth. Met.*, **96**, 177 (1998).

18. L. I. Smith and H. H. Hoehn, *J. Am. Chem. Soc.*, **63**, 1184 (1941).
19. (a) F. C. Leavitt, T. A. Manuel and F. Johnson, *J. Am. Chem. Soc.*, **81**, 3163 (1959).
(b) F. C. Leavitt, T. A. Manuel, F. Johnson, L. U. Matternas and D. S. Lehman, *J. Am. Chem. Soc.*, **82**, 5099 (1960).
(c) K. Ruhlmann, *Z. Chem.*, **5**, 354 (1965).
(d) M. D. Curtis, *J. Am. Chem. Soc.*, **89**, 4241 (1967).
20. W. H. Atwell, D. R. Weyenberg and H. Gilman, *J. Org. Chem.*, **32**, 885 (1967).
21. Preparation of 1,4-diiodobutadiene by the halogenolysis of zirconacyclopentadienes:
(a) E. Negishi, F. E. Cederbaum and T. Takahashi, *Tetrahedron Lett.*, **27**, 2829 (1986).
(b) E. Negishi, S. J. Holmes, J. M. Tour, J. A. Miller, F. E. Cederbaum, D. R. Swanson and T. Takahashi, *J. Am. Chem. Soc.*, **111**, 3336 (1989).
(c) S. L. Buchwald and R. B. Nielson, *J. Am. Chem. Soc.*, **111**, 2870 (1989).
See also Reference 23.
22. (a) U. Bankwitz, H. Sohn, D. R. Powell and R. West, *J. Organomet. Chem.*, **499**, C7 (1995).
(b) S. Yamaguchi, R.-Z. Jin and K. Tamao, *J. Organomet. Chem.*, **559**, 73 (1998).
See also Reference 4k.
23. (a) C. Xi, S. Huo, T. H. Afifi, R. Hara and T. Takahashi, *Tetrahedron Lett.*, **38**, 4099 (1997).
(b) H. Ubayama, Z. Xi and T. Takahashi, *Chem. Lett.*, 517 (1998).
24. Formation of titanacyclopentadiene using the Ti(OPr-*i*)₄/2(*i*-PrMgBr) system:
(a) H. Urabe, T. Hata and F. Sato, *Tetrahedron Lett.*, **36**, 4261 (1995).
(b) H. Urabe and F. Sato, *J. Org. Chem.*, **61**, 6756 (1996).
Iodination of titanacyclopentadiene:
(c) J. E. Hill, G. Balaich, P. E. Fanwick and I. P. Rothwell, *Organometallics*, **12**, 2911 (1993).
25. S. Yamaguchi, R.-Z. Jin, K. Tamao and F. Sato, *J. Org. Chem.*, **63**, 10060 (1998).
26. M. Katkevics, S. Yamaguchi, A. Toshimitsu and K. Tamao, *Organometallics*, **17**, 5796 (1998).
27. H. Okinoshima, K. Yamamoto and M. Kumada, *J. Am. Chem. Soc.*, **94**, 9263 (1972).
28. (a) K. Tamao, S. Yamaguchi, M. Shiozaki, Y. Nakagawa and Y. Ito, *J. Am. Chem. Soc.*, **114**, 5867 (1992).
(b) K. Tamao, S. Yamaguchi, Y. Ito, Y. Matsuzaki, T. Yamabe, M. Fukushima and S. Mori, *Macromolecules*, **28**, 8668 (1995).
29. (a) P. J. Fagan and W. A. Nugent, *J. Am. Chem. Soc.*, **110**, 2310 (1988).
(b) P. J. Fagan, W. A. Nugent and J. C. Calabrese, *J. Am. Chem. Soc.*, **116**, 1880 (1994).
30. K. Kanno and M. Kira, *Chem. Lett.*, 1127 (1999).
31. (a) B. Wrackmeyer, *J. Chem. Soc., Chem. Commun.*, 397 (1986).
(b) B. Wrackmeyer, *J. Organomet. Chem.*, **310**, 151 (1986).
(c) R. Köster, G. Seidel, J. Süß and B. Wrackmeyer, *Chem. Ber.*, **126**, 1107 (1993).
(d) B. Wrackmeyer, G. Kehr and J. Süß, *Chem. Ber.*, **126**, 2221 (1993).
32. K. Tamao, S. Yamaguchi and M. Shiro, *J. Am. Chem. Soc.*, **116**, 11715 (1994).
33. S. Yamaguchi, R.-Z. Jin, K. Tamao and M. Shiro, *Organometallics*, **16**, 2230 (1997).
34. (a) G. Frapper and M. Kertész, *Organometallics*, **11**, 3178 (1992).
(b) G. Frapper and M. Kertész, *Synth. Met.*, **55–57**, 4255 (1993).
(c) J. Kürti, P. R. Surján, M. Kertész and G. Frapper, *Synth. Met.*, **55–57**, 4338 (1993).
35. (a) K. S. Wong, S. G. Han, Z. V. Vardeny, J. Shinar, Y. Pang, S. Ijadi-Maghsoodi, T. J. Barton, S. Grigoras and B. Parbhoo, *Appl. Phys. Lett.*, **58**, 1695 (1991).
(b) X. Wei, S. G. Han, K. S. Wong, B. C. Hess, L. X. Zheng, Z. V. Vardeny, Q.-X. Ni, J. Shinar, Y. Pang, S. Ijadi-Maghsoodi, T. J. Barton and S. Grigoras, *Synth. Met.*, **41–43**, 1583 (1991).
(c) S. Grigoras, G. C. Lie, T. J. Barton, S. Ijadi-Maghsoodi, Y. Pang, J. Shinar, Z. V. Vardeny, K. S. Wong and S. G. Han, *Synth. Met.*, **49–50**, 293 (1992).
(d) M. Liess, S. Jeglinski, P. A. Lane and Z. V. Vardeny, *Synth. Met.*, **84**, 891 (1997).
(e) M. Liess, S. Jeglinski, Z. V. Vardeny, M. Ozaki, K. Yoshino, Y. Ding and T. Barton, *Phys. Rev. B*, **56**, 15712 (1997).
36. (a) Y. Yamaguchi and J. Shioya, *Mol. Eng.*, **2**, 339 (1993).
(b) Y. Yamaguchi, *Mol. Eng.*, **3**, 311 (1994).
(c) Y. Yamaguchi and T. Yamabe, *Int. J. Quantum Chem.*, **57**, 73 (1996).

37. (a) Y. Matsuzaki, M. Nakano, K. Yamaguchi, K. Tanaka and T. Yamabe, *Synth. Met.*, **71**, 1737 (1995).
(b) Y. Matsuzaki, M. Nakano, K. Yamaguchi, K. Tanaka and T. Yamabe, *Chem. Phys. Lett.*, **263**, 119 (1996).
38. (a) S. Y. Hong and D. S. Marynick, *Macromolecules*, **28**, 4991 (1995).
(b) S. Y. Hong, S. J. Kwon and S. C. Kim, *J. Chem. Phys.*, **103**, 1871 (1995).
(c) S. Y. Hong, *Bull. Korean Chem. Soc.*, **16**, 845 (1995).
(d) S. Y. Hong, S. J. Kwon, S. C. Kim and D. S. Marynick, *Synth. Met.*, **69**, 701 (1995).
(e) S. Y. Hong, S. J. Kwon and S. C. Kim, *J. Chem. Phys.*, **104**, 1140 (1996).
(f) S. Y. Hong and J. M. Song, *Synth. Met.*, **85**, 1113 (1997).
(g) S. Y. Hong and J. M. Song, *Chem. Mater.*, **9**, 297 (1997).
39. B. H. Lipshutz, K. Siegmann, E. Garcia and F. Kayser, *J. Am. Chem. Soc.*, **115**, 9276 (1993).
40. S. Yamaguchi and K. Tamao, *Tetrahedron Lett.*, **37**, 2983 (1996).
41. S. Yamaguchi, R.-Z. Jin, S. Ohno and K. Tamao, *Organometallics*, **17**, 5133 (1998).
42. S. Yamaguchi, R.-Z. Jin, Y. Itami, T. Goto and K. Tamao, *J. Am. Chem. Soc.*, **121**, 10420 (1999).
43. S. Yamaguchi, T. Endo and K. Tamao, *Chem. Eur. J.*, **6**, 1684 (2000).
44. S. Yamaguchi, Y. Itami and K. Tamao, *Organometallics*, **17**, 4910 (1998).
45. S. Yamaguchi, T. Goto and K. Tamao, *Angew. Chem., Int. Ed.*, **39**, 1695 (2000).
46. S. Yamaguchi, T. Goto and K. Tamao, manuscript in preparation.
47. B. L. Lucht and T. D. Tilley, *Chem. Commun.*, 1645 (1998).
48. S. Yamaguchi, S. Ohno and K. Tamao, *Synlett*, 1199 (1997).
49. T. Kauffmann and L. Hexy, *Chem. Ber.*, **114**, 3674 (1981).
50. A. K. Bakhashi and P. Rattan, *J. Mol. Struct. (Theochem)*, **430**, 269 (1998).
51. W. Chen, S. Ijadi-Maghsoodi and T. J. Barton, *Polym. Prepr.*, **38**, 189 (1997).
52. S. Yamaguchi, K. Iimura and K. Tamao, *Chem. Lett.*, 89 (1998).
53. U. H. F. Bunz, *Chem. Rev.*, **100**, 1605 (2000).
54. (a) J. Ohshita, M. Nodono, T. Watanabe, Y. Ueno, A. Kunai, Y. Harima, K. Yamashita and M. Ishikawa, *J. Organomet. Chem.*, **553**, 487 (1998).
(b) J. Ohshita, M. Nodono, H. Kai, T. Watanabe, A. Kunai, K. Komaguchi, M. Shiotani, A. Adachi, K. Okita, Y. Harima, K. Yamashita and M. Ishikawa, *Organometallics*, **18**, 1453 (1999).
55. A. Kraak, A. K. Wiersma, P. Jordens and H. Wynberg, *Tetrahedron*, **24**, 3381 (1968).
56. (a) B. Wrackmeyer, G. Kehr, J. Stüb and E. Molla, *J. Organomet. Chem.*, **562**, 207 (1998).
(b) B. Wrackmeyer, G. Kehr, J. Stüb and E. Molla, *J. Organomet. Chem.*, **577**, 82 (1999).
57. M. Serby, S. Ijadi-Maghsoodi and T. J. Barton, *XXXIIIth Symposium on Organosilicon Chemistry*, Abstract No. PA-35, April 6–8, 2000, Saginaw, Michigan, USA.
58. I. Tulokhonova, T. C. Stringfellow, D. Powell, S. Ivanov and R. West, *XXXIIIth Symposium on Organosilicon Chemistry*, Abstract No. PA-12, April 6–8, 2000, Saginaw, Michigan, USA.
59. S. Yamaguchi, R.-Z. Jin, K. Tamao and M. Shiro, *Organometallics*, **16**, 2486 (1997).
60. Y. Yamaguchi, *Synth. Met.*, **82**, 149 (1996).
61. K. Kanno, M. Ichinohe, C. Kabuto and M. Kira, *Chem. Lett.*, 99 (1998).
62. (a) H. Sohn, R. Huddleston, D. R. Powell, R. West, K. Oka and X. Yonghua, *J. Am. Chem. Soc.*, **121**, 2935 (1999).
(b) Y. Xu, T. Fujino, H. Naito, T. Dohmaru, K. Oka, H. Sohn and R. West, *Jpn. J. Appl. Phys.*, **38**, 6915 (1999).
63. S. Yamaguchi, R.-Z. Jin and K. Tamao, *J. Am. Chem. Soc.*, **121**, 2937 (1999).
64. B. P. S. Chauhan, T. Shimizu and M. Tanaka, *Chem. Lett.*, 785 (1997).
65. T. Sanji, T. Sakai, C. Kabuto and H. Sakurai, *J. Am. Chem. Soc.*, **120**, 4552 (1998).
66. T. Sanji, M. Funaya and H. Sakurai, *Chem. Lett.*, 547 (1999).
67. H. Hennig, K. H. Heckner, A. A. Pavlov, M. Kuzmin and G. Kuzmin, *Ber. Bunsenges. Phys. Chem.*, **84**, 1122 (1980).
68. (a) J. L. Bréfort, R. J. P. Corriu, P. Gerbier, C. Guérin, B. J. L. Henner, A. Jean, T. Kuhlmann, F. Garnier and A. Yassar, *Organometallics*, **11**, 2500 (1992).
(b) R. J. P. Corriu, N. Devylder, C. Guérin, B. Henner and A. Jean, *Organometallics*, **13**, 3194 (1994).

69. (a) R. J. P. Corriu, W. E. Douglas, Z.-X. Yang, F. Garnier and A. Yassar, *J. Organomet. Chem.*, **417**, C50 (1991).
(b) R. J. P. Corriu, W. E. Douglas and Z.-X. Yang, *J. Organomet. Chem.*, **456**, 35 (1993).
70. M. Ishikawa and J. Ohshita, in *Handbook of Organic Conductive Molecules and Polymers: Vol. 2. Conductive Polymers: Synthesis and Electrical Properties* (Ed. H. S. Nalwa), Chap. 15, Wiley, Chichester, 1997.
71. J. Ohshita, N. Mimura, H. Arase, M. Nodono, A. Kunai, K. Komaguchi and M. Shiotani, *Macromolecules*, **31**, 7985 (1998).
72. A. Kunai, T. Ueda, K. Horata, E. Toyoda, J. Ohshita, M. Ishikawa and K. Tanaka, *Organometallics*, **15**, 2000 (1996).
73. (a) E. Toyoda, A. Kunai and M. Ishikawa, *Organometallics*, **14**, 1089 (1995).
(b) J. Ohshita, T. Hamaguchi, E. Toyoda, A. Kunai, K. Komaguchi, M. Shiotani, M. Ishikawa and A. Naka, *Organometallics*, **18**, 1717 (1999).
74. (a) C. W. Tang and S. A. VanSlyke, *Appl. Phys. Lett.*, **51**, 913 (1987).
(b) C. W. Tang, S. A. VanSlyke and C. H. Chen, *J. Appl. Phys.*, **65**, 3610 (1989).
75. (a) A. Kraft, A. C. Grimsdale and A. B. Holmes, *Angew. Chem., Int. Ed. Engl.*, **37**, 402 (1998).
(b) R. H. Friend, R. W. Gymer, A. B. Holmes, J. H. Burroughes, R. N. Marks, C. Taliani, D. D. C. Bradley, D. A. Dos Santos, J. L. Brédas, M. Lögdlund and W. R. Salaneck, *Nature*, **397**, 121 (1999).
76. (a) M. Strukelj, F. Papadimitrakopoulos, T. M. Miller and L. J. Rothberg, *Science*, **267**, 1969 (1995).
(b) M. Strukelj, T. M. Miller, F. Papadimitrakopoulos and S. Son, *J. Am. Chem. Soc.*, **117**, 11976 (1995).
77. H. E. Katz, A. J. Lovinger, J. Johnson, C. Kloc, T. Siegrist, W. Li, Y.-Y. Lin and A. Dodabalapur, *Nature*, **404**, 478 (2000).
78. M. Uchida, T. Izumizawa, T. Nakano, S. Yamaguchi, K. Tamao and K. Furukawa, *Chem. Lett.*, in press.
79. S. Yamaguchi, T. Endo, M. Uchida, T. Izumizawa, K. Furukawa and K. Tamao, submitted for publication.
80. A. Adachi, J. Ohshita, A. Kunai, J. Kido and K. Okita, *Chem. Lett.*, 1233 (1998). See also Reference 54b.

CHAPTER 12

Polysilanols

PAUL D. LICKISS

*Department of Chemistry, Imperial College of Science, Technology and Medicine,
London SW7 2AY, England
Fax: +44 0207 594 5804; e-mail: p.lickiss@ic.ac.uk*

I. INTRODUCTION	696
II. SYNTHESIS OF POLYSILANOLS	696
A. General Points	696
B. From Halosilanes, Alkoxysilanes, Esters etc.	697
1. Hydrolysis of halosilanes	697
a. Fluorosilanes	697
b. Chlorosilanes	697
c. Bromosilanes	701
d. Iodosilanes	702
2. Hydrolysis of the Si–O function	702
a. Alkoxy and siloxy silanes	702
b. Silyl carboxylates, perchlorates, sulphates and cyanates and related species	705
C. From Si–H Compounds	707
1. Oxidation	707
2. Hydrolysis	708
D. Hydrolysis of Si–N Functions	709
E. Hydrolysis of Si–C Bonds	710
F. Miscellaneous Preparative Methods	710
III. REACTIONS OF POLYSILANOLS	714
A. Introduction	714
B. The Acidity and Basicity of the Silanol Group	714
C. Silica Surfaces and Coupling Agents	715
D. Sol-Gel Processes	716
E. Siloxane Formation	716
F. Metal and Metalloid Derivatives of Silanols	717
1. Derivatives of siloxanediols	717
2. Derivatives of siloxanetriols	719

3. Derivatives of silanediols	721
4. Derivatives of silanetriols	722
IV. STRUCTURAL STUDIES OF SILANOLS	724
A. Introduction	724
B. Calculations of the Structures of Silanols	724
C. Compounds Containing Two Si—OH Groups	724
1. Disiloxanes	724
2. Other siloxanes	727
3. Oligosilanediols	727
4. Other compounds containing two Si—OH groups	728
D. Compounds Containing Three Si—OH Groups	729
E. Compounds Containing Four Si—OH Groups	729
F. Compounds Containing an Si(OH) ₂ Group, Silanediols	730
G. Compounds Containing Two Si(OH) ₂ Groups	733
H. Compounds Containing an Si(OH) ₃ Group, Silanetriols	733
V. CONCLUSIONS	736
VI. ACKNOWLEDGEMENTS	736
VII. REFERENCES	736

I. INTRODUCTION

Polysilanols are, for the purposes of the following discussion, defined as compounds containing more than one SiOH group, one or more Si(OH)₂ groups, one or more Si(OH)₃ groups or a combination of these functions. Compounds containing a single SiOH group will be referred to for comparative purposes. A more detailed description of the synthesis and the structures of many silanols can be found in Reference 1. The discussion will also generally be confined to organosilanols in which there is at least one carbon centred group attached to silicon. This will thus exclude a detailed description of silica surfaces, silicates, the environmental importance of low levels of dissolved silicic acid Si(OH)₄ in the aquatic environment, and sol gel processes for preparing glasses and similar materials. The chemistry of polysilanols is extensive and is of particular importance in the silicone polymer industry and sol gel processing. Thus, only a brief overview of common reaction types, together with leading references is given in Section III. A comprehensive review of silanols including polysilanols appeared in 1995¹ and so, although early work will be described in this Chapter, the discussion will concentrate on work published since then.

II. SYNTHESIS OF POLYSILANOLS

A. General Points

There are a variety of synthetic routes available to polysilanols, most of which are also used for the synthesis of simple monosilanols which have been reviewed in detail elsewhere¹. The most often encountered reaction of simple silanols is self-condensation to give siloxanes, and this is even more rapid for polysilanols most of which are sensitive towards acids and bases and towards heat. Polysilanols are often not isolated but instead are formed as reactive intermediates in processes ultimately designed to give rise to Si-O-Si containing materials. If the isolation of a polysilanol is required, then there are several important considerations to be borne in mind:

1. The use of dilute solutions will reduce the likelihood of bimolecular silanol condensation reactions occurring.
2. Syntheses that involve the formation of either an acid or a base byproduct should be avoided unless they can be neutralized as they are formed.

3. Syntheses involving high temperatures should be avoided.
4. The three previous requirements may be relaxed to some degree if there are bulky groups such as *t*-Bu present as they hinder the formation of siloxanes.

B. From Halosilanes, Alkoxysilanes, Esters etc

Polysilanol is often prepared, as are simple R_3SiOH species, by the hydrolysis of a compound containing an Si–X bond where X is an electronegative atom such as a halogen, O, S, N or P. The silicones industry is largely based on the hydrolysis of chlorosilanes, while the formation of silicas is often achieved by hydrolysis of alkoxysilanes.

A table of physical constants for over 40 silanols is available² together with tabulated data on synthetic routes to a range of silanols^{3,4}.

1. Hydrolysis of halosilanes

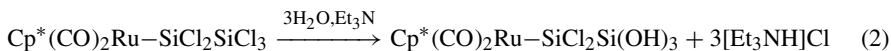
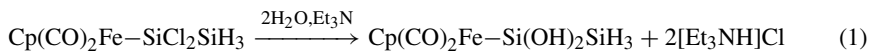
a. Fluorosilanes. Fluorosilanes are rarely used as precursors to polysilanol as they are often more inconvenient to prepare compared to the readily available chlorosilanes, and the hydrolysis may release HF. The hydrolysis of silyl fluorides requires alkaline conditions; thus $(i\text{-Pr})_2SiF_2$, $(t\text{-Bu})_2SiF_2$ and *o*-tolyl₂SiF₂ react with aqueous ethanolic sodium or potassium hydroxide solutions to give the corresponding silanols $R_2Si(OH)_2$ ($R = i\text{-Pr}$, *t*-Bu or *o*-tolyl) in 50 to 80% yields⁵. Hydrolysis of $(i\text{-Pr})_2SiF_2$ using H_2O/KOH /dioxane also gives $(i\text{-Pr})_2Si(OH)_2$ in 50% yield⁵, lower than that obtained from the corresponding dibromide (see Section II.B.1.c below). The hydrolysis of $(t\text{-Bu})_2SiF_2$ gives a mixture of $(t\text{-Bu})_2Si(OH)_2$ and $(t\text{-Bu})_2SiFOH$ ⁶. The steric protection provided by the bulky *t*-butyl groups in $(t\text{-Bu})_2Si(OH)_2$ means that it is reluctant to undergo condensation reactions, and it can be distilled at 210 °C without decomposition or treated with concentrated H_2SO_4 at 110 °C without siloxane formation⁷. This diol does, however, undergo condensation to give the disiloxane in the presence of *p*-MeC₆H₄SO₃H in boiling heptane⁸.

b. Chlorosilanes. Chlorosilanes are often used as starting materials for polysilanol synthesis because of their ready availability and convenient reactivity. If precautions are taken to remove or neutralize the HCl formed on hydrolysis, e.g. by adding a base such as pyridine to the reaction mixture (to give a precipitate of pyridinium hydrochloride) or by adding NaOH or KOH to the solution to maintain neutrality, then silanols (rather than siloxanes) may often be isolated³. In this way $PhSi(OH)_3$ [but not $MeSi(OH)_3$ from $MeSiCl_3$] may be obtained from $PhSiCl_3$ in the presence of aniline⁹.

Although simple hydrolysis of Me_2SiCl_2 affords cyclic and linear siloxanes, if the HCl formed is neutralized then low molecular weight silanols may be isolated. By varying the conditions (temperature, time etc.) the hydrolysis of Me_2SiCl_2 in a $(NH_4)_2CO_3/H_2O$ system can give $Me_2Si(OH)_2$, $(HOMe_2Si)_2O$ or a mixture of oligosiloxanes $HO(SiMe_2O)_nH$ ($n = 3-5$), which can be separated by fractional distillation¹⁰. Similarly, variations in the conditions allow the hydrolysis of Ph_2SiCl_2 in $(NH_4)_2CO_3/H_2O/Et_2O$ to give $Ph_2Si(OH)_2$ or a mixture of $HO(SiPh_2O)_nH$ ($n = 2$ or 3)¹⁰. Diarylsilanedioles ($XC_6H_4)_2Si(OH)_2$ ($X = H, p\text{-F}$ or *p*-Cl) have been prepared as needle-like crystals similarly by hydrolysis of the corresponding chlorosilanes using $(NH_4)HCO_3/H_2O/Et_2O$ at 0 °C¹¹. Hydrolysis of Et_2SiCl_2 with aqueous NaOH gives $Et_2Si(OH)_2$ in good yield¹² and rapid hydrolysis with stirring of Cl_nSi in dioxane does allow $Cl_nSi(OH)_{3-n}$ ($n = 1, 2$ or 3) species to be observed in solution by ²⁹Si NMR spectroscopy before the formation of Si–O–Si linkages occurs¹³. The use of aniline to remove HCl from hydrolytic reaction mixtures has

become more popular in recent years. Thus, treatment of EtRSiCl_2 (where $\text{R} = p\text{-tolyl}$, $4\text{-MeOC}_6\text{H}_4$, $\text{PhCH}=\text{CH}$ or $\text{PhCH}=\text{CPh}$) using $\text{H}_2\text{O}/\text{PhNH}_2/\text{Et}_2\text{O}$ at 0°C affords the corresponding silanediols in good yields¹⁴. This method has also been used successfully to prepare *trans*-1,3-dihydroxy-1,3-dimethyl-1,3-disilacyclobutane from the corresponding dichloride, although the yield in this case is relatively low¹⁵.

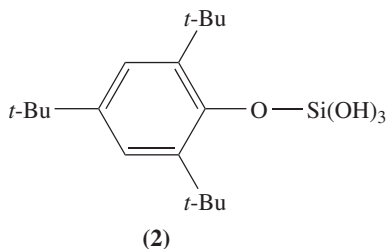
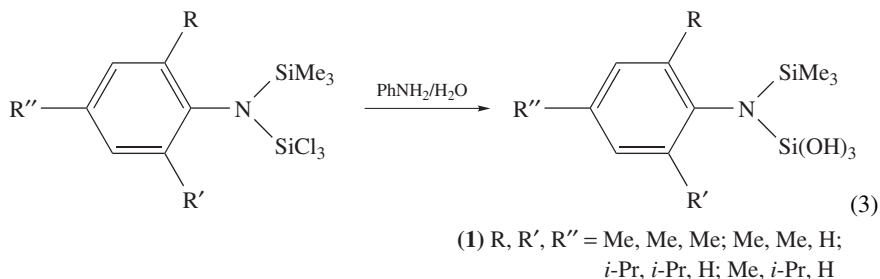
Steric hindrance by a metal cluster may help to prevent condensation of polysilanols. For example, the silanols $\text{Me}_n(\text{OH})_{3-n}\text{SiCCO}_3(\text{CO})_9$ ($n = 0$ or 1) are formed by hydrolysis of the corresponding chlorides in the absence of a base in benzene solution under reflux, conditions that would normally be expected to cause condensation to occur (particularly in the case of the triol)^{16,17}. Even concentrated H_2SO_4 in Et_2O does not bring about siloxane formation¹⁷. Compounds such as $\text{Cp}(\text{CO})_2\text{FeSiMe}(\text{OH})_2$ and $\text{Cp}^*(\text{CO})_2\text{FeSi}(\text{OH})_3$ may be obtained from the corresponding chlorides by hydrolysis using $\text{H}_2\text{O}/\text{Et}_3\text{N}$ ¹⁸. These polysilanols are also remarkably stable towards heat, base or acid, the stability being attributed to the electron-donating nature of the iron fragment which lowers the acidity of the silanol groups, as well as steric effects¹⁸. A related osmium complex, $(\text{CO})(\text{PPh}_3)_2\text{OsCl}[\text{Si}(\text{OH})_3]$, has been prepared in good yield by hydrolysis of $(\text{CO})(\text{PPh}_3)_2\text{OsCl}(\text{SiCl}_3)$ in $\text{NaOH}/\text{H}_2\text{O}/\text{THF}$ ¹⁹. The steric and electronic effects of a transition metal substituent at silicon are shown even more clearly in equations 1 and 2. For equation 1 the analogous $\text{Cp}^*(\text{CO})_2\text{FeSiCl}_2\text{SiH}_3$ does not undergo hydrolysis, presumably due to increased steric effects and greater electron-releasing character by the $\text{Cp}^*(\text{CO})_2\text{Fe}$ substituent reducing nucleophilic attack at Si. In equation 2 the lower electrophilic character for a silicon α to the metal is shown in that nucleophilic attack is so reduced that hydrolysis can be achieved selectively at only the β -silicon to give a stable silanetriol. The stability of these triols has also been attributed to a 'transition metal effect'²⁰.



The steric bulk of the C_5Me_5 group attached to silicon is not sufficient to prevent condensation reactions of $\text{C}_5\text{Me}_5\text{Si}(\text{OH})_3$ from occurring relatively easily. The triol can be prepared in 87% yield by hydrolysis of the corresponding trichloride using $\text{H}_2\text{O}/\text{PhNH}_2/\text{Et}_2\text{O}$ at 0°C . It decomposes slowly at room temperature in the solid state but can be stored without decomposing below 0°C or in dilute solution²¹. The closely related, more bulky silanetriol, $[\text{C}_5\text{H}_4(\text{SiMe}_3)]\text{Si}(\text{OH})_3$, can also be prepared in this way and is much more stable, surviving heating both as a solid and in solution²². A bis-cyclopentadienyl substituted silanediol $[(\eta - \text{C}_5\text{H}_4)\text{Fe}(\eta - \text{C}_5\text{H}_5)]_2\text{Si}(\text{OH})_2$ has also been prepared in 90% yield by hydrolysis of the corresponding dichloride in $\text{Et}_2\text{O}/\text{H}_2\text{O}/\text{Et}_3\text{N}$ ²³. Similarly, hydrolysis of (9-methylfluoren-9-yl)trichlorosilane with $\text{H}_2\text{O}/\text{PhNH}_2/\text{Et}_2\text{O}$ at 0°C gives a 90% yield of the corresponding triol²⁴. The disiloxanediol, $[\text{C}_5\text{H}_4(\text{OH})\text{MeSi}]_2\text{O}$, is obtained by hydrolysis of the analogous chloride obtained by hydrosilylation of dicyclopentadiene with MeCl_2SiH catalysed by H_2PtCl_6 ²⁵. Treatment of the bulky trichlorosilane $(\text{Me}_3\text{Si})_2\text{CHSiCl}_3$ with moist liquid ammonia affords the unusual six-membered ring species $[(\text{Me}_3\text{Si})_2\text{CHSi}(\text{OH})(\text{NH})]_3$ containing both SiOH and Si-N fragments. Protolysis of the Si-N bonds is presumably hindered by the bulky substituents²⁶.

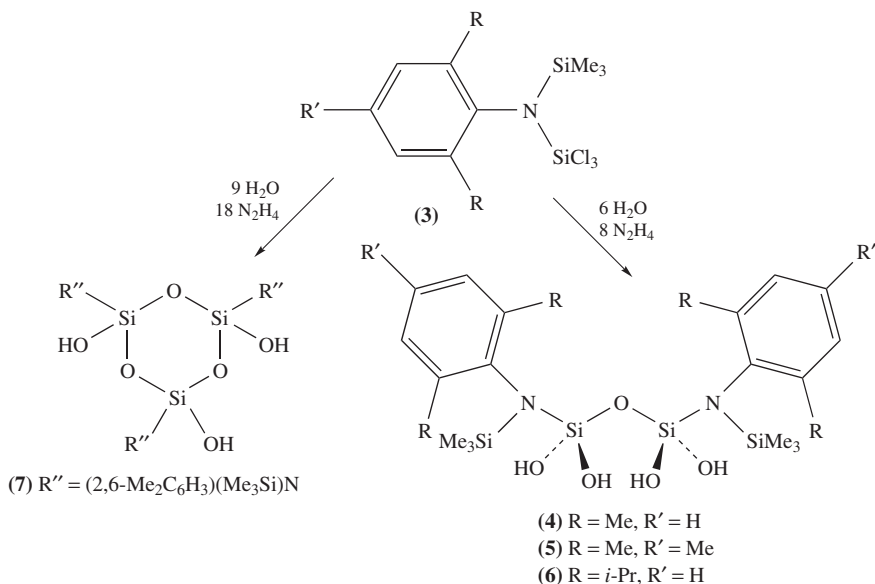
Novel silanetriols containing a nitrogen substituent at silicon can be prepared by hydrolysis if the substituents are large enough to prevent hydrolysis of the Si-N bonds present. This has been elegantly demonstrated by Roesky and coworkers²⁷⁻³⁰ who have shown that the stable silanetriols **1** can be prepared in 70–88% yields according to equation 3.

Such compounds are useful precursors to polyhedral metallasiloxanes (see Section III) which still contain a potentially hydrolysable Si–N bond^{31–33}. The same method has also been used to prepare a silanetriol, **2**, in 77% yield, which bears an alkoxy substituent, which, of course would normally be susceptible to hydrolysis. However, here, even the very bulky aryl group present is not sufficient to give a product as stable as those containing the bulky nitrogen centred substituents and it readily undergoes cleavage to give 2,4,6-*(t*-Bu)₃C₆H₂OH in solution³¹. A similar synthetic route can also be used to prepare stable silanediols containing an Si–N bond. Thus, hydrolysis of RN(SiMe₃)(SiMeCl₂) [where R = 2, 6-Me₂C₆H₃, 2,6-*(i*-Pr)₂C₆H₃ or 2,4,6-Me₃C₆H₂] with Et₂O/H₂O/PhNH₂ affords RN(SiMe₃)[SiMe(OH)₂] in good yield³⁴.



The use of a mixture of water and hydrazine in Et₂O for the hydrolysis of sterically hindered aminotrichlorosilanes **3** affords the tetrahydroxydisiloxanes **4–6** in near-quantitative yields. The hydrazine in these reactions is acting both as an HCl acceptor and as a dehydrating agent. Simple dehydration of silanetriol 2,6-Me₂C₆H₃N(SiMe₃)Si(OH)₃ with hydrazine alone gives the expected disiloxane **4**, and hydrolysis of the tetrachlorosiloxane [2,6-*(i*-Pr)₂C₆H₃N(SiMe₃)SiCl₂]₂O gives **6** (without cleavage of the Si–N bonds) using the conventional H₂O/PhNH₂ route. Changing the H₂O/hydrazine ratio may give rise to other products and **3** (R = Me, R' = H) gives a cyclotrisiloxane triol **7** as shown in Scheme 1³⁵.

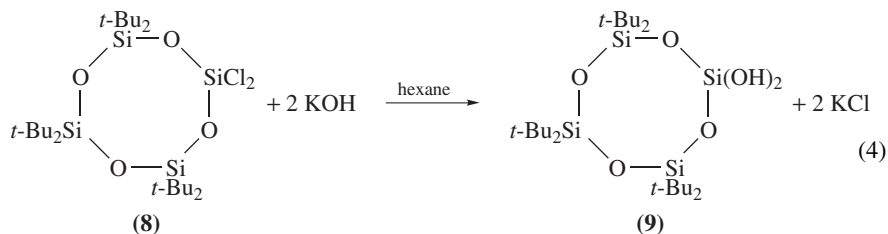
The very large bulk of the (Me₃Si)₃C group causes solvolytic reactions of chlorides to be severely inhibited. The trichloride (Me₃Si)₃CSiCl₃ is stable towards boiling MeOH or aqueous EtOH even in the presence of silver nitrate³⁶. Use of more forcing conditions such as refluxing 2 M NaOMe/MeOH leads to fragmentation rather than simple substitution reactions³⁷. The analogous silicon centred chlorosilane (Me₃Si)₃SiSiCl₃ in which there are longer bonds around the central atom does react 'normally'. Thus, hydrolysis with aniline/H₂O/Et₂O gives (Me₃Si)₃SiSi(OH)₃ in 45 minutes at room temperature. This triol is also unusually thermally stable, only decomposing at its melting point of 210–213 °C³⁸.



SCHEME 1

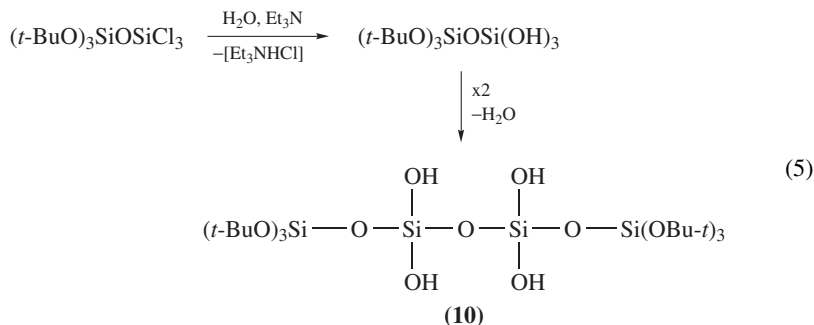
Hydrolysis of trichlorosilanes containing long chain ethers as substituents, MeO(CH₂CH₂O)_n(CH₂)₃SiCl₃ (*n* = 1, 2, 3, 6 or 7), gives the analogous silanetriols, which even in the absence of HCl acceptors are remarkably stable in aqueous solution. This stability has been attributed to intramolecular hydrogen bonding to the ether oxygens³⁹. Long chain alkyl substituted silanols (H₂₉C₁₄)_nSi(OH)_{4-n} (*n* = 1 or 2) are also available by hydrolysis of the corresponding chlorosilanes using aqueous NaHCO₃ at -10 °C, but these species do not condense readily to give siloxanes in the usual way⁴⁰. Hydrolysis of the α,ω-dichloro-oligosilanes Cl(SiPh₂)_nCl (*n* = 4 or 7) affords the corresponding α,ω-dihydroxyoligosilanes^{41,42}.

The Si-Cl bonds in the cyclic dichlorosiloxane **8** react with KOH without causing cleavage of the siloxane bonds in the ring, and so direct substitution gives a 63% yield of **9** (equation 4)⁴³.



The reaction pathway for the hydrolysis of (*t*-BuO)₂SiCl₂ depends greatly on the conditions and on the chlorosilane:water ratio used. Use of a large excess of water (in pyridine/Et₂O) allows (*t*-BuO)₂Si(OH)₂ to be isolated but a chlorosilane:water ratio of 2:1 surprisingly gives (*t*-BuO)₂ClSiOSi(OH)(OBu-*t*)₂ (containing both an

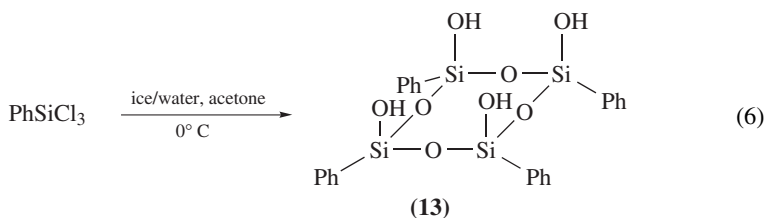
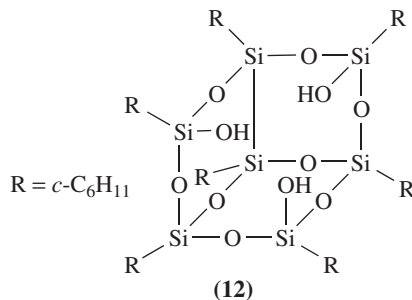
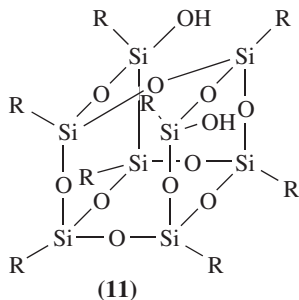
Si-Cl and an SiOH group) and the symmetrical disiloxane $[(t\text{-BuO})_2\text{ClSi}]_2\text{O}$, while a 1:8 ratio gives disiloxane $[(t\text{-BuO})_2(\text{OH})\text{Si}]_2\text{O}$. The hydrolysis of a mixture of $(t\text{-BuO})_2\text{Si}(\text{OH})_2$ and $[(t\text{-BuO})_2\text{ClSi}]_2\text{O}$ gives the trisiloxane $\text{HO}[\text{Si}(\text{OBu-}t)_2\text{O}]_3\text{H}$. These silanols all give the cyclic trisiloxane $[(t\text{-BuO})_2\text{SiO}]_3$ on heating in solution⁴⁴. The hydrolysis of $(t\text{-BuO})_n\text{SiCl}_{4-n}$ (where $n = 1$ or 2) has also been carried out using a water/pyridine/petroleum ether mixture to give the corresponding $(t\text{-BuO})_n\text{Si}(\text{OH})_{4-n}$ compounds⁴⁵. More recent work using Et_3N in place of pyridine has, however, shown that the composition of the product from hydrolysis of the trichloride is actually an unusual disiloxane product, **10**, from condensation of the initially formed triol (equation 5)⁴⁶.



Hydrolysis of RSiCl_3 ($\text{R} = \text{cyclo-C}_6\text{H}_{11}$) in $\text{H}_2\text{O}/\text{acetone}$ over a period of at least several months affords a mixture of siloxanes, including the incompletely condensed silsesquioxanes **11** and **12** which can be separated by fractional crystallization^{47,48}. Hydrolysis of RSiCl_3 ($\text{R} = i\text{-Pr}$ or $t\text{-Bu}$) with 1.5 equivalents of water gives good yields of $[\text{RSiO}_{1.5}]_4$ ⁴⁹. More recent work on the hydrolysis of $i\text{-PrSiCl}_3$ has shown that a 22% yield of the analogous tetrahydroxycyclotetrasiloxane can be formed but that a better yield, 46%, can be obtained if the disiloxane $(i\text{-PrCl}_2\text{Si})_2\text{O}$ is hydrolysed^{50,51}. Hydrolysis of PhSiCl_3 using NaHCO_3 in $\text{Et}_2\text{O}/\text{H}_2\text{O}$ at 0°C has recently been reported to give a good yield of $\text{PhSi}(\text{OH})_3$ ⁵² but hydrolysis using $\text{H}_2\text{O}/\text{acetone}$ at $0\text{--}5^\circ\text{C}$ over 18 h affords a 40% yield of the unusual tetrasilanol **13** (equation 6). This is an incompletely condensed silsesquioxane and can be seen as half of a silsesquioxane cube, which it does indeed form in attempts to reduce it to the cyclohexyl derivative with $\text{H}_2/\text{Pd}/\text{C}$ ⁵³. The careful hydrolysis of $t\text{-BuSiCl}_3$ in $\text{Et}_2\text{O}/\text{H}_2\text{O}/\text{aniline}$ affords $t\text{-BuSi}(\text{OH})_3$ as a stable crystalline solid in 94% yield⁵⁴ while hydrolysis using $\text{H}_2\text{O}/\text{MeOH}/\text{KOH}$ gives $[t\text{-Bu}(\text{OH})_2\text{Si}]_2\text{O}$ ⁵⁵. This is a clear demonstration of how sensitive silanols, even with bulky substituents, are towards condensation reactions if strong bases are present. Hydrolysis of $t\text{-BuSiCl}_3$ in the presence of the polyoxometallate anion $[\gamma\text{-PW}_{10}\text{O}_{36}]$ gives a 60% yield of the yellow crystalline species $[(\gamma\text{-PW}_{10}\text{O}_{36})(t\text{-BuSiOH})_2]^{3-}$ in which there is an intramolecular hydrogen bond between the two silanol groups⁵⁶. The tetrahydroxydisiloxane $[\text{OsCl}(\text{CO})(\text{PPh}_3)_2\text{Si}(\text{OH})_2]_2\text{O}$ is produced in less than 10% yield by the direct hydrolysis of $\text{Os}(\text{SiCl}_3)\text{Cl}(\text{CO})(\text{PPh}_3)_2$ but in 70% yield from the reaction between $\text{Os}(\text{SiCl}_3)\text{Cl}(\text{CO})(\text{PPh}_3)_2$ and $\text{Os}[\text{Si}(\text{OH})_3]\text{Cl}(\text{CO})(\text{PPh}_3)_2$ in moist CH_2Cl_2 ¹⁹.

c. Bromosilanes. Silyl bromides are rarely used as precursors to polysilanols but they react analogously to chlorosilanes, and again special care must be taken to ensure that the strongly acidic HBr formed as a byproduct is not allowed to cause siloxane formation (or cleavage of Si-aryl bonds). Hydrolysis of $(i\text{-Pr})_2\text{SiBr}_2$ with aqueous ammonia gives

$(i\text{-Pr})_2\text{Si}(\text{OH})_2$ in 90% yield, which is much better than the 50% obtained by hydrolysis of $(i\text{-Pr})_2\text{SiF}_2$ (see Section II.B.1.a above)⁵. Hydrolysis of $(\text{BrMe}_2\text{Si})_3\text{CH}$ with 0.5 M aqueous NaOH in Et_2O at 0°C gives the trisilanol $(\text{HOME}_2\text{Si})_3\text{CH}$ ⁵⁷.



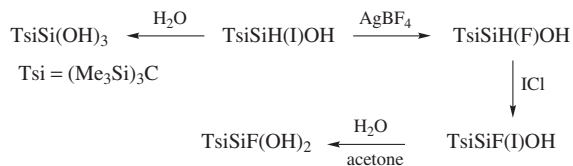
The $(\text{Me}_3\text{Si})_3\text{C}$ group provides such a large degree of steric hindrance that the tribromide $(\text{Me}_3\text{Si})_3\text{CSiBr}_3$ can be recovered after 72 h reflux in 1/1 v/v $\text{H}_2\text{O}/\text{EtOH}$ ⁵⁸. A small decrease in steric hindrance in tetrasilylmethanes increases reactivity greatly and $(\text{HMe}_2\text{Si})_2\text{C}(\text{SiMe}_2\text{Br})_2$ reacts rapidly at room temperature in THF containing 5 vol% H_2O to give $(\text{HMe}_2\text{Si})_2\text{C}(\text{SiMe}_2\text{OH})_2$ ⁵⁹. Solvolysis of $(\text{Me}_3\text{Si})_2\text{C}(\text{SiMe}_2\text{Br})(\text{SiMe}_2\text{OSO}_2\text{CF}_3)$ in 20% H_2O in acetone also gives $(\text{Me}_3\text{Si})_2\text{C}(\text{SiMe}_2\text{OH})_2$ after both bromide and triflate hydrolysis⁶⁰.

d. Iodosilanes. Generally speaking, the hydrolysis of iodosilanes is very rapid and gives the strongly acidic HI as a byproduct.

The silanol $(\text{Me}_3\text{Si})_3\text{CSiH}_2\text{OH}$ reacts with iodine to give the remarkably stable iodohydroxysilane $(\text{Me}_3\text{Si})_3\text{CSiHIOH}$, the steric hindrance provided by the $(\text{Me}_3\text{Si})_3\text{C}$ group preventing bimolecular reactions between the normally incompatible OH and I groups. Scheme 2 outlines how a silanediol and a silanetriol containing the $(\text{Me}_3\text{Si})_3\text{C}$ group have been prepared; all these compounds contain potentially highly reactive functional groups which are stabilized by the bulky substituent^{58,61}. Hydrolysis of $(\text{Me}_3\text{Si})_3\text{CSiPh}(\text{I})\text{OH}$ using $\text{H}_2\text{O}/\text{DMSO}$ affords the related diol $(\text{Me}_3\text{Si})_3\text{CSiPh}(\text{OH})_2$ ⁶². [For the preparation of $(\text{HOME}_2\text{Si})_4\text{C}$ from $(\text{IME}_2\text{Si})_4\text{C}$, see Section II.B.2.b below.] The presence of bulky substituents in $((t\text{-Bu})_2\text{Si})_2$ does not prevent rapid hydrolysis and the formation of the 1,2-disilanediol $((t\text{-Bu})_2\text{HOSi})_2$ ⁶³. The hydrolysis of $\text{SiL}_4\cdot 2\text{bipy}$ (bipy = bipyridine) affords, after an aqueous work-up, the six-coordinate $[\textit{cis}\text{-}(\text{bipy})_2\text{Si}(\text{OH})_2]^{2+} + 2[\text{I}]^- \cdot 2\text{H}_2\text{O}$ ⁶⁴.

2. Hydrolysis of the Si–O function

a. Alkoxy and siloxy silanes. The hydrolysis of alkoxy silanes has been the subject of a considerable amount of research because of their use as coupling agents, in sol gel



SCHEME 2

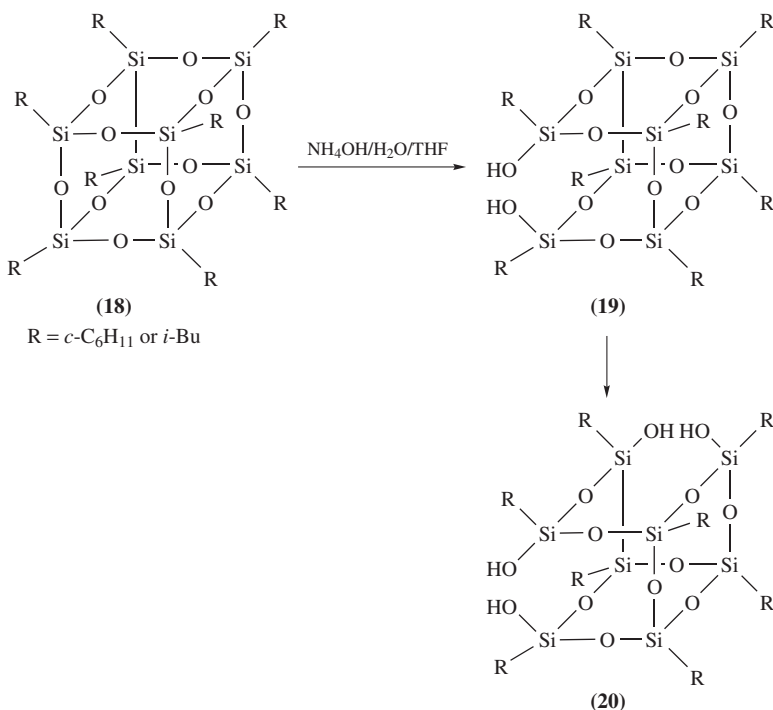
processes, in silicone manufacture and in the treatment of surfaces. The details of the mechanisms of such reactions are complicated and have been the subject of several reviews (see, for example, References 65–79) and they will not be covered further here. The hydrolysis of alkoxyxilanes is slowest at about pH 7; changes in pH away from this to either higher or lower pH increase the rate of hydrolysis (for example, at pH 4 hydrolysis is *ca* 1000 times faster than at pH 7). For a discussion of the relative stabilities of simple methylsilanols in aqueous solution, see References 77–79. The hydrolysis of an alkoxyxilane provides one way of preparing sensitive silanols containing small substituents. For example, careful hydrolysis of $\text{Me}_2\text{Si}(\text{OEt})_2$ gives crystalline $\text{Me}_2\text{Si}(\text{OH})_2$, which is very sensitive towards both acids and bases and undergoes condensation reactions in contact with acid-washed glass⁸⁰. This type of synthesis has also been used to prepare other highly sensitive silanediols containing halogenated methyl groups from dimethoxyxilanes⁸¹. The success of these preparations depends on the formation of an alcohol as a byproduct, rather than a mineral acid which would be formed if an analogous halosilane were hydrolysed. The hydrolysis of Si–S bonds also occurs readily but is not commonly used as a synthetic method for the preparation of polysilanols.

Various arylsilanols, e.g. *p*- or *m*-(HOR_2Si)₂C₆H₄ (R = Me or Ph) and 4,4'-bis(hydroxydimethylsilyl)-biphenyl-ether, have been prepared by hydrolysis of the corresponding ethoxyxilanes in a MeOH/EtOH/H₂O/NaOH reaction medium. It was found that it was difficult to remove solvent of crystallization from some of these compounds, but stoichiometric complexes between silanol and solvent do not seem to be formed⁸² as they are in the case of some other silanols (see Section III). Hydrolysis of *p*-(EtOMe_2Si)₂C₆H₄ with NaOH/H₂O/MeOH gives 85% of *p*-(HOMe_2Si)₂C₆H₄⁸³, and a similar method has also been used to prepare the analogous 4,4'-bis(hydroxydimethylsilyl)biphenyl^{84,85}. Arylsilanetriols $\text{XC}_6\text{H}_4\text{Si}(\text{OH})_3$ (X = *p*-NMe₂, *p*-OMe, *p*-Me, *m*-OMe, *m*-Cl, *m*-CF₃ etc.) have been prepared by hydrolysis of the corresponding X-C₆H₄Si(OMe)₃ compounds in an H₂O/MeOH mixture; again the formation of an alcohol, MeOH, rather than a hydrogen halide is beneficial in the synthesis of such sensitive triols⁸⁶. Silylperoxide derivatives are much less common than alkoxyxilanes but they do hydrolyse to give silanols in a similar way. For example, SiTPP(OOEt)₂ (TPP = 5,10,15,20-tetraphenylporphyrin) reacts with a mixture of H₂O and PPh₃ to give SiTPP(OH)₂, EtOH and P(O)Ph₃⁸⁷.

Although siloxanes are usually prepared by the condensation reactions of silanols, it is also possible for the reverse to occur. Detailed studies using ¹⁴C labelled materials have shown that metabolism of the cyclic siloxane (Me₂SiO)₄ in rats leads to Me₂Si(OH)₂ and MeSi(OH)₃ as the major products with smaller amounts of the siloxyxilanol [(HO)Me₂Si]₂O, [(HO)Me₂SiO]₂SiMe₂, HOMe₂SiOSiMe(OH)₂, [(HO)₂MeSi]₂O and (HO)₃SiOSiMe(OH)₂ being formed⁸⁸. This type of siloxane cleavage is not a useful synthetic route; these highly sensitive silanols were derivatized to give stable Me₃Si derivatives before characterization by HPLC and GC-MS methods.

The hydrolysis of PhSi(OMe)₃ would normally be expected to afford a polymeric mixture of siloxanes, but if it is carried out in the presence of a nanocage formed from

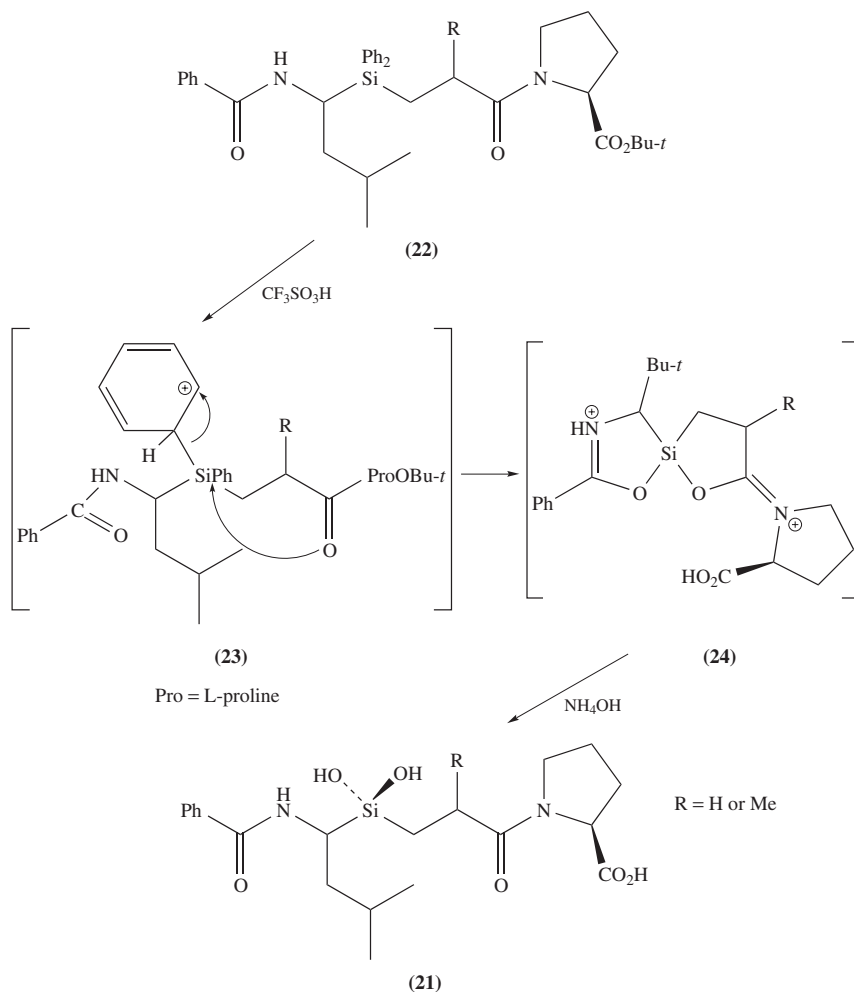
cleavage of a second siloxane linkage (Scheme 4)⁹². Unusual monosodium salts of ethyl- or phenyl-silanetriol $\text{RSi}(\text{OH})_2\text{ONa} \cdot 1.37\text{H}_2\text{O}$ ($\text{R} = \text{Et}$ or Ph) are reported to be obtained by treating the siloxane polymers obtained from the simple hydrolysis of RSiCl_3 with 20% aqueous NaOH/EtOH ⁹³. Relatively few silanols have been isolated from the cleavage of siloxanes as the conditions required to carry out such reactions are likely to cause further reactions of any silanols formed.



SCHEME 4

The silanediol **21** has been prepared for use as a potential protease inhibitor by treatment of arylsilane **22** with $\text{CF}_3\text{SO}_3\text{H}$. This is a convenient method for the preparation of silyl triflates (which are readily hydrolysable, see below) but in this case it is thought that the amide carbonyl intercepts the protonated species **23** (loss of the *t*-Bu ester group also occurring) to give the spirocyclic silyl ether **24**, which is then hydrolysed to give the diol, (Scheme 5)⁹⁴.

b. Silyl carboxylates, perchlorates, sulphates and cyanates and related species. The preparation of α,ω -diols may be achieved by the hydrolysis under various conditions (the best being use of CaCO_3 to neutralize AcOH) of α,ω -acetoxy compounds. Thus $\text{AcO}(\text{SiRR}'\text{O})_n\text{Ac}[\text{Ac} = \text{CH}_3\text{C}(=\text{O})]$ compounds where $\text{R} = \text{R}' = \text{Me}$ ($n = 2-6$) or $\text{R} = \text{Me}$, $\text{R}' = \text{CF}_3\text{CH}_2\text{CH}_2$ ($n = 2-4$) give $\text{HO}(\text{SiRR}'\text{O})_n\text{H}$ species in good yields⁹⁵. The hydrolysis of $\text{Cl}_2\text{C}_6\text{H}_3\text{Si}(\text{OAc})_3$ and $[\text{Cl}_2\text{C}_6\text{H}_3\text{Si}(\text{OAc})_2]_2\text{O}$ in $\text{H}_2\text{O}/\text{Et}_2\text{O}$ with no base present gives $\text{Cl}_2\text{C}_6\text{H}_3\text{Si}(\text{OH})_3$ in 15–20% yield and $[\text{Cl}_2\text{C}_6\text{H}_3\text{Si}(\text{OH})_2]_2\text{O}$, respectively. The addition of base to neutralize the acid formed in these hydrolyses would



SCHEME 5

no doubt give increased yields⁹⁶. The hydrolysis of Me(1-naphthyl)Si(OAc)₂ with aqueous NaOH solution affords the diol Me(1-naphthyl)Si(OH)₂ in about 50% yield⁹⁷. The novel formylsilanes R₂Si(OOCH)₂ (R = Et or Ph) and *p*-C₆H₄(Me₂SiOOCH)₂ all hydrolyse readily in moist air to give the corresponding silanols, which then undergo the expected condensation reactions⁹⁸.

As would be expected for such a good leaving group, silyl triflates hydrolyse very readily, even in crowded molecules⁹⁹. A tetrasiloxanediol, HOMe(*t*-Bu)SiO(SiMePhO)₂ SiMe(*t*-Bu)OH has been prepared by hydrolysis of the corresponding bis-triflate with a H₂O/Et₃N mixture¹⁰⁰. As in the case of triflates, silyl perchlorates are very readily hydrolysed even in severely sterically congested systems^{101,102}, but this method does not seem to have been used for the preparation of polysilanols.

The silyl sulphate group is also readily hydrolysed, but this method is rarely used as the sulphates themselves would often be prepared from species that would also act as good hydrolytic precursors to silanols and the formation of H_2SO_4 on hydrolysis promotes condensation reactions. Ring opening polymerization of cyclic oligosiloxanes may be effected by sulphuric acid to give sulphates which are then hydrolysed, silanol condensation reactions then giving rise to polysiloxanes. An unusual example of sulphate hydrolysis in a sterically hindered molecule is the synthesis of $(\text{Me}_3\text{Si})_2\text{C}(\text{SiMe}_2\text{OH})_2$ from $(\text{Me}_3\text{Si})_3\text{CSiMe}_2\text{OMe}$ using H_2SO_4 ¹⁰³. This is thought to occur via anchimeric assistance by the OMe group to loss of a methyl group as methane followed by the methoxy group being lost as methanol to give the bis-hydrogen sulphate $(\text{Me}_3\text{Si})_2\text{C}(\text{SiMe}_2\text{OSO}_3\text{H})_2$, which undergoes rapid hydrolysis to give the disilanol.

The Si—OCN group is rare, but the cyanate group has been found to be particularly readily hydrolysed from silicon and in sterically hindered compounds it has a leaving group ability similar to triflate and somewhat greater than iodide^{104,105}. The preparation of $(\text{HOME}_2\text{Si})_4\text{C}$ can be achieved by treatment of $(\text{IME}_2\text{Si})_4\text{C}$ with AgOCN in moist ether¹⁰⁶. This presumably occurs via hydrolysis of the initially formed tetracyanate as the iodide itself is inert in moist ether.

C. From Si—H Compounds

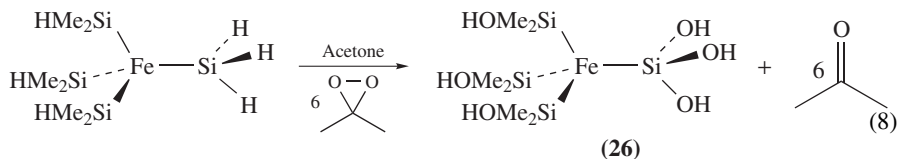
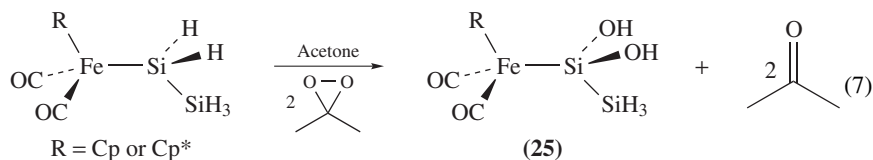
1. Oxidation

Simple silanes may be oxidized using perbenzoic acid¹⁰⁷ but this method does not seem to have been used widely for the preparation of polysilanols. The oxidation of sterically hindered silanes by KMnO_4 has been carried out in the presence of ultrasound, which helps to break down the KMnO_4 in an organic solvent and aids solubility. For example, the hindered silane $(\text{Me}_3\text{Si})_3\text{CSiH}_3$ is readily oxidized in THF to give a good yield of $(\text{Me}_3\text{Si})_3\text{CSi}(\text{OH})_3$ ¹⁰⁸.

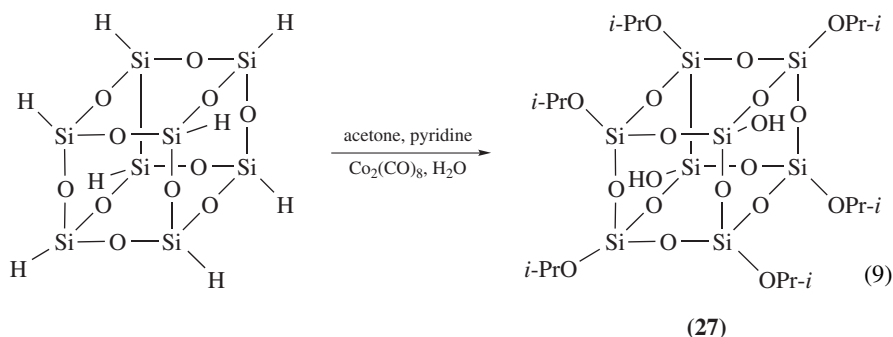
Compounds containing Si—H bonds are rapidly oxidized by ozone in solution at low temperature to give good yields of silanols, which may be isolated if the substituents on silicon are large enough to prevent rapid condensation to the corresponding siloxane^{109,110}, and ozonolysis of the highly sterically hindered silane $(t\text{-Bu})_3\text{SiH}$ gave $(t\text{-Bu})_3\text{SiOH}$ as the only detectable product¹¹¹. The oxidation of Si—H groups by ozone has been reviewed¹¹² as has the chemistry of organosilicon peroxides¹¹³, which will not be covered in this discussion.

A more recent method for the formation of silanols that has found particular application to the synthesis of potentially reactive polysilanols is the insertion of oxygen, derived from highly reactive dioxiranes, into an Si—H bond. The dioxirane can also be used to oxidize Si—H bonds in good yields within the coordination sphere of a transition metal such as iron¹¹⁴, tungsten or molybdenum. For example, $\text{Cp}^*(\text{CO})_2(\text{PMe}_3)\text{WSiRH}_2$ may be oxidized to $\text{Cp}^*(\text{CO})_2(\text{PMe}_3)\text{WSiR}(\text{OH})_2$ ($\text{R} = \text{Me}$ or OH) and $\text{Cp}(\text{CO})_2(\text{PMe}_3)\text{MoSiH}_3$ affords $\text{Cp}(\text{CO})_2(\text{PMe}_3)\text{MoSi}(\text{OH})_3$ ^{18,115,116}. The activation of Si α to a metal towards electrophilic attack is illustrated in equation 7, where the reaction of two equivalents of dimethyldioxirane with the SiH_2SiH_3 grouping gives a product, **25**, in which only the SiH_2 group has reacted. Unfortunately, further reaction with excess dimethyldioxirane leads to decomposition rather than formation of a pentahydroxy species²⁰. This extremely mild method of introducing oxygen, in which the only byproduct is acetone, is suitable for synthesis of species which are particularly sensitive to acids and bases. For example, the hexahydroxy compound **26** is readily formed (equation 8) in 95% yield¹¹⁷. The dioxirane route is also applicable to highly sterically hindered compounds and $\text{TsiSi}(\text{OH})_3$ [where $\text{Tsi} = (\text{Me}_3\text{Si})_3\text{C}$] can be prepared in one step from TsiSiH_3 in near-quantitative

yield much more easily than the hydrolysis route outlined in Scheme 2¹¹⁸. Treatment of $(\text{PhMe}_2\text{Si})_3\text{CSiH}_2\text{OH}$ with two equivalents of dimethyldioxirane gives a related triol, $(\text{PhMe}_2\text{Si})_3\text{CSi}(\text{OH})_3$ ⁵⁸.



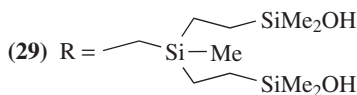
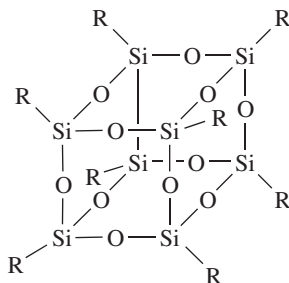
The reaction between the silsesquioxane $\text{H}_8\text{Si}_8\text{O}_{12}$ and acetone in the presence of $\text{Co}_2(\text{CO})_8$, and pyridine gives, after a six-week period for crystallization, a 35% yield of **27** (equation 9). This presumably occurs via initial formation of the octa-substituted $(i\text{-PrO})_8\text{Si}_8\text{O}_{12}$ followed by partial hydrolysis of just two of the substituents to give the diol **27**, which should be of use in the synthesis of polymeric silsesquioxanes¹¹⁹.



2. Hydrolysis

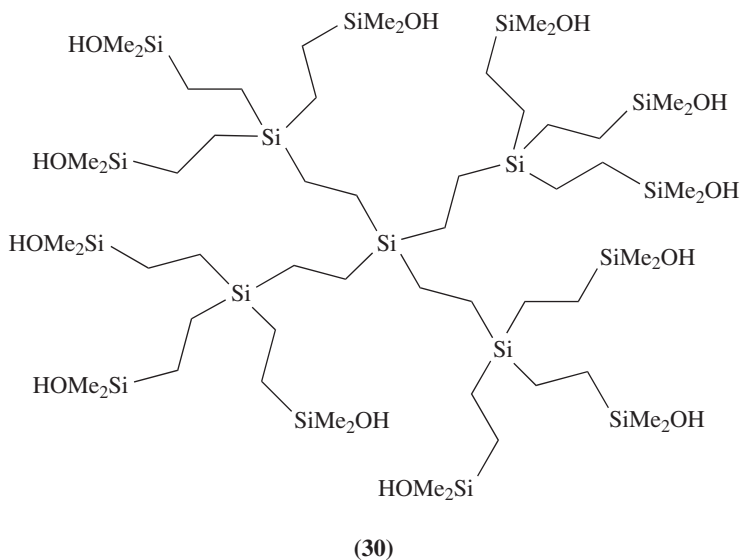
Organosilanes appear to react slowly (if at all) with water alone, but in the presence of acids or bases (e.g. alkali metal hydroxides) reactions to give a silanol and H_2 are rapid, with bases being particularly powerful catalysts. The evolution of H_2 may be used as both a qualitative and quantitative test for Si–H bonds, and the mechanism of the acid and the base hydrolysis has been discussed in detail^{120,121}. This synthetic method is rare for the preparation of silanols that are to be isolated, since both acids and bases catalyse the condensation of silanols to siloxanes and, therefore, only compounds containing large substituents are conveniently made in this way. However, the solvolysis of PhMeSiH_2 using NaOEt/EtOH followed by $\text{NaOH}/\text{MeOH}/\text{H}_2\text{O}$ affords silanediol $\text{PhMeSi}(\text{OH})_2$ and $p\text{-(HMe}_2\text{Si)}_2\text{C}_6\text{H}_4$ gives diol $p\text{-(HOME}_2\text{Si)}_2\text{C}_6\text{H}_4$ ^{122–125}.

Excellent yields of silanols may be obtained by transition metal catalysed reactions between Si–H compounds and a buffered aqueous solution of NaOH. Palladium, ruthenium, platinum or rhodium on either charcoal or alumina as a support catalyse the hydrolysis of *p*-(HMe₂Si)₂C₆H₄ and (HMe₂Si)₂O, at room temperature or slightly above, the two palladium catalysts giving the best results¹²⁶. The reactive silanediol MePhSi(OH)₂, which is difficult to make by hydrolysis of MePhSiCl₂, can be prepared in 90% yield by hydrolytic dehydrogenation of MePhSiH₂ using Pd/C¹⁴. A comparison has been made in the synthesis of silanol terminated carbosilane dendrimers such as MeSi(CH₂CH₂SiMe₂OH)₃, [HOMe₂SiCH₂CH₂Si(Me)O]₄, **28**, **29** and **30**, between the hydrolysis of Si–Cl and Si–H groups as the final step. First generation species are available cleanly via Si–Cl hydrolysis, but for larger compounds this method leads to impure products and hydrolysis of Si–H groups catalysed by Pd/C in dioxane and a buffer solution (containing NaH₂PO₄, H₂O and NaOH) gives better results. For example, Si(CH₂CH₂SiMe₂OH)₄ is prepared in 64 and 91% yields respectively by the Si–Cl and Si–H methods¹²⁷. The conversion of hydrosilanes to silanols is also catalysed by [Ph₃PCuH]₆, but this method does not seem to have been applied to polysilanols¹²⁸.



D. Hydrolysis of Si–N Functions

Compounds containing an Si–N bond are usually susceptible to hydrolysis and, in the same way that hydrolysis of a compound giving an acid requires a base to be present for neutralization, if the reaction yields a basic byproduct, such as NH₃ in the hydrolysis of (Me₃Si)₂NH, then dilute aqueous HCl may be used for the hydrolysis, thus neutralizing the base as it forms¹²⁹. It has also been found possible preferentially to remove by hydrolysis in cold water the NH₂ groups but not the *tert*-alkoxy groups in ((*t*-Bu)₂O)₂Si(NH₂)₂ to give ((*t*-Bu)O)₂Si(OH)₂¹³⁰. Hydrolysis of the sterically hindered diazoacetates (*t*-Bu)₂(NCX)SiC(N₂)CO₂Et (where X = O or S) using acetone/H₂O and a catalytic amount of HCl over a period of several days at room temperature gives (*t*-Bu)₂Si(OH)₂ in 15% (X = O) and 12% (X = S) yields¹³¹.



E. Hydrolysis of Si–C Bonds

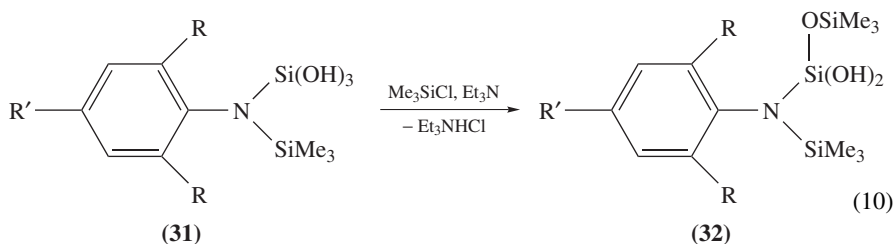
In compounds containing a carbon centred substituent that can act as a relatively good leaving group, the cleavage of an Si–C bond may lead to silanol formation. Thus, base catalysed hydrolysis of $\text{Cl}_3\text{SiCH}_2\text{--CH=CH}_2$ affords propene and presumably Si(OH)_4 (which would condense to give silica) as all four groups undergo hydrolysis¹³². A similar reaction occurs if chloroalkyl substituents are present, an E2-type elimination occurring in the case of the presence of a $\beta\text{-Cl}$. Thus, basic hydrolysis of $\text{Me}_2(\text{CH}_2\text{Cl})\text{SiCl}$ and $\text{Me}(\text{CHCl}_2)\text{SiCl}_2$ affords $\text{Me}_2\text{Si(OH)}_2$ and MeSi(OH)_3 , respectively, while only neutral water is required to hydrolyse $\text{Cl}_3\text{CSiCl}_3$ to Si(OH)_4 ^{133–135}. This type of cleavage is, however, unlikely to be of synthetic use because of the very specific requirements for the nature of the substituents and the presence of acids and bases in the reaction sequence.

The steric bulk of the C_6Cl_5 groups protects $(\text{C}_6\text{Cl}_5)_2\text{SiCl}_2$ from rapid hydrolysis by atmospheric moisture, but, as C_6Cl_5^- is a good leaving group, the compound hydrolyses rapidly in solution to give $\text{C}_6\text{Cl}_5\text{H}$ [and presumably Si(OH)_4] and not the expected diol $(\text{C}_6\text{Cl}_5)_2\text{Si(OH)}_2$ ¹³⁶. The diol can, however, be prepared by treatment of $(\text{C}_6\text{Cl}_5)_2\text{SiCl}_2$ with moist ether for 20 min followed by immediate removal of the volatiles under vacuum¹³⁷. Hydrolysis of $(\text{C}_6\text{Cl}_5)_n\text{Ph}_{3-n}\text{SiCl}$ ($n = 1$ or 2) under basic conditions (THF/ $\text{H}_2\text{O}/\text{NaOH}$) also leads to Si–C bond cleavage and formation of $\text{C}_6\text{Cl}_5\text{H}$ ¹³⁸. Under acidic conditions (THF/ 1 N HCl) only hydrolysis of the Si–Cl group occurs, giving the silanols $(\text{C}_6\text{Cl}_5)_n\text{Ph}_{3-n}\text{SiOH}$ ¹³⁸.

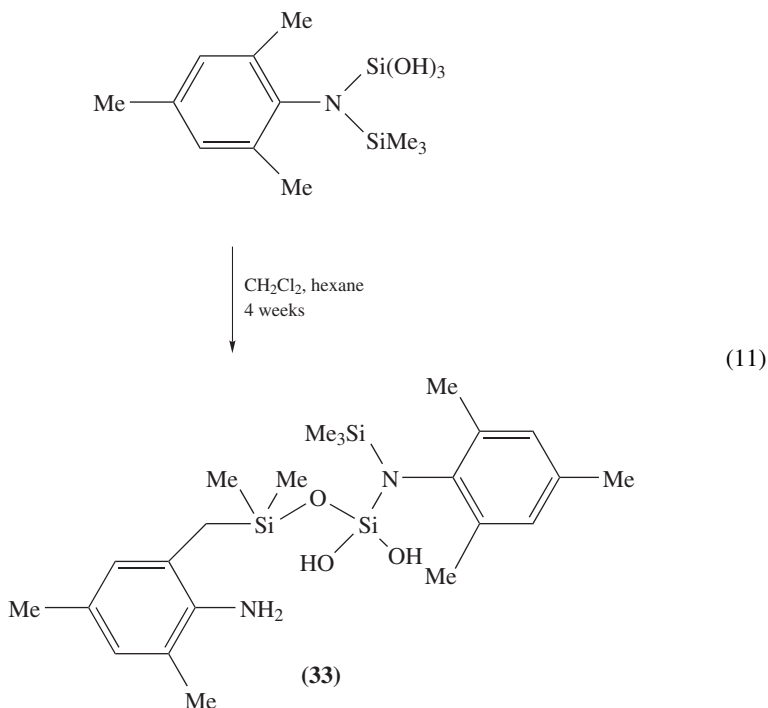
F. Miscellaneous Preparative Methods

Although rarely used as a preparative method, it is possible to derivatize a silanetriol selectively to give a silanediol. Thus, the reaction of triols **31** with Me_3SiCl affords sils **32** in 75–88% yields (equation 10) but further silylation to give the simple monosilanol does not occur. Surprisingly, diol **33**, containing an NH_2 group as well as an Si(OH)_2 group, was formed (equation 11) if the mesityl derivative was stored

in CH_2Cl_2 /hexane or in toluene solution for four weeks. The mechanism by which this occurs is unknown¹³⁹. Derivatization using a transition metal complex is also possible, the reaction between $[(2,6-(i\text{-Pr})_2\text{C}_6\text{H}_3)\text{NSiMe}_3]\text{Si}(\text{OH})_3$ with Cp_2TiCl_2 in a 1 : 1 ratio giving $[(2,6-(i\text{-Pr})_2\text{C}_6\text{H}_3)\text{NSiMe}_3]\text{Si}(\text{OH})_2(\text{TiCp}_2\text{Cl})$ ¹⁴⁰. Similarly, it is possible to silylate the silsesquioxane $[(c\text{-C}_6\text{H}_{11})_7\text{Si}_7\text{O}_9(\text{OH})_3]$, **12**, to give the disilanols $[(c\text{-C}_6\text{H}_{11})_7\text{Si}_7\text{O}_9(\text{OH})_2\text{SiMe}_2\text{R}]$ (R = Me or Ph)¹⁴¹.

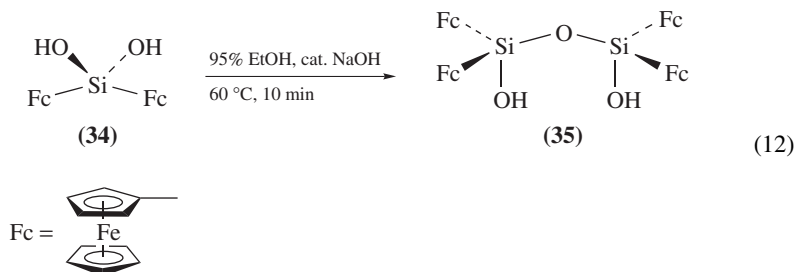


R = R' = Me
 R = Me, R' = H
 R = *i*-Pr, R' = H

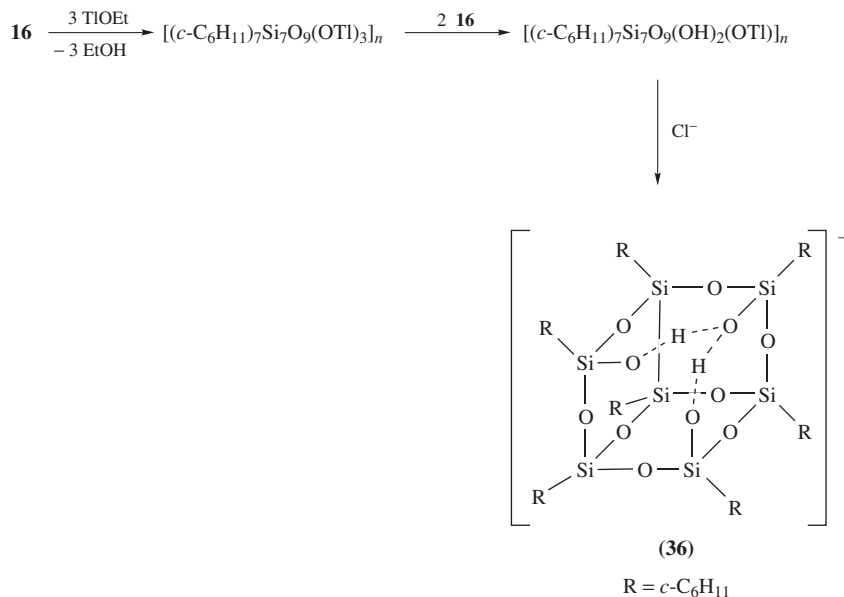


It is often difficult to control the condensation reactions of silanediols so that only a single reaction occurs to give the disiloxanediol, but the sterically hindered ferrocenyl substituted diol **34** can be condensed to give **35** in good yield (equation 12). If **35** is subject to similar conditions but for 2 h at reflux temperature, then further condensation reactions

occur to give a cyclic siloxane¹⁴². The bulky diol $(t\text{-Bu})_2\text{Si}(\text{OH})_2$ also condenses when treated with Cl_4Sn to give, after crystallization of the product from CH_2Cl_2 , the sterically hindered disiloxanediol $(\text{HO}(t\text{-Bu})_2\text{Si})_2\text{O}$ co-crystallized together with $[\text{Cl}_3\text{Sn}(\mu\text{-OH})]_2$ and the precursor, $(t\text{-Bu})_2\text{Si}(\text{OH})_2$ ¹⁴³.



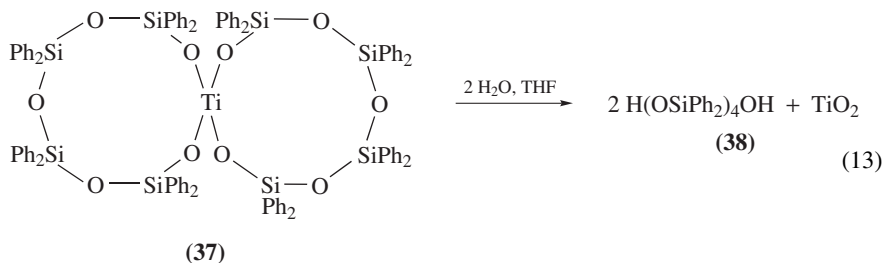
The triol **16** can be deprotonated according to Scheme 6. The initial step involves metallation and this is followed by a coproportionation on addition of two further equivalents of **16**. Finally, addition of an ammonium or phosphonium salt gives **36**. The stability of the ion has implications for the surface chemistry of silica where similar multiply hydrogen bonded anion sites are likely to be more acidic than isolated silanol groups¹⁴⁴. The related cubic polyanion $[\text{Si}_8\text{O}_{18}(\text{OH})_2]^{6-}$ can be prepared directly from aqueous solutions of silica and a quaternary ammonium hydroxide derivative such as $[\text{NPhMe}_3]\text{OH}$ ^{145,146}.



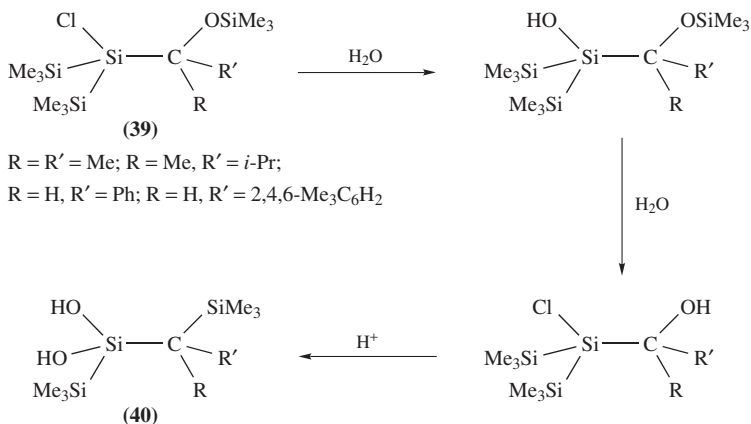
SCHEME 6

Metal siloxides can often be prepared using silanols as precursors, but it is also possible to hydrolyse a siloxide to give a silanol as shown for the spirotitanasiloxane **37**,

which gives the tetrasiloxanediol **38** in 86% yield, (equation 13)¹⁴⁷. The well known triol (*c*-C₆H₁₁)₇Si₇O₉(OH)₃, usually prepared by hydrolysis of *c*-C₆H₁₁SiCl₃, has also been prepared by hydrolysis of the lithium derivative (*c*-C₆H₁₁)₇Si₇O₉(OLi)₃, but this is of little practical use as the trilithio species is itself prepared by metallation of the triol¹⁴⁸.



Although the details of the mechanism are unclear, the final step in the acid hydrolysis of chlorosilanes **39** is an isomerization involving a 1,2-OH/Me₃Si exchange to give a range of diols **40**, (Scheme 7)¹⁴⁹.



SCHEME 7

A final, apparently unique method to form a silanediol is an oxidation of the novel divalent silicon species (η^5 -C₅Me₅)₂Si with moist pyridine-*N*-oxide to give (η^1 -C₅Me₅)₂-Si(OH)₂¹⁵⁰.

Although a wide range of synthetic routes are described above, by far the most common are those involving hydrolysis of halosilanes (particularly chlorosilanes) and of alkoxy-silanes. Use of the dimethyldioxirane method is increasing in popularity and its high yield together with acetone as the only byproduct should mean that it becomes the method of choice for the small-scale preparations of sensitive silanols. Unfortunately, it is not a convenient method for large-scale use. It can also be seen from the discussion above that small variations in reaction conditions can lead to very different products being formed, particularly if condensation reactions are not severely restricted by bulky substituents. Thus, great care should be exercised when choosing a synthetic route to polysilanols bearing small or medium-sized substituents.

III. REACTIONS OF POLYSILANOLS

A. Introduction

The chemistry of polysilanol is dominated by two main types of reaction. The most industrially important reactions are condensation reactions involving the reaction of an SiOH group with either another silanol group or, for example, an Si-Cl group to give an Si-O-Si linkage. A second general type of reaction, and one of increasing interest, involves the replacement of the relatively acidic SiOH proton by a metal or metalloid fragment (M) so as to give a Si-O-M linkage. This reactivity is related to the acidity of the silanol group and so an overview of silanol acidity (and basicity) is given below before details of reactions are described. Only a brief outline of polysilanol chemistry is given here as this is a vast area of research that has been described extensively elsewhere, references to reviews and books are given to provide further reading.

B. The Acidity and Basicity of the Silanol Group

The acidity of silanol groups on surfaces and in aqueous solutions of polysilanol has been studied extensively because of the application of polysilanol in a wide range of industrial situations. Recent computational work in this area can be found in References 3 and 151. Silanol acidity (along with the unusually short and strong bonds between Si and electronegative elements, and the low barrier to linearization of Si-O-Si linkages) has been the subject of considerable discussion most of which concentrates on the nature of the bonding between Si and electronegative atoms. Theories used to account for the anomalies found in Si-X species centre on $d\pi-p\pi$ interactions, σ^* interactions with Si and the ionic nature of such bonds. For a comparison of the various theories, see Reference 152. Despite the controversy over bonding, the high acidity and reactivity of silanol compared to alcohols has been studied for over 50 years¹⁵³. A detailed discussion of the acidities of monosilanol can be found in Reference 1. The change, $\Delta\nu$, in the O-H stretching frequency on formation of a hydrogen bond between a silanol group and a suitable base or acid has been used to estimate the hydrogen bond strength and relative acidity or basicity¹⁵⁴. The value of $\Delta\nu$ is often nearly twice as large for silanol as for analogous carbinol, which is indicative of a stronger hydrogen bonding interaction¹⁵⁵. For example, the change of O-H stretch on going from free OH to an H-bonded adduct with acetone for Ph_3SiOH and Ph_3COH is 226 and 120 cm^{-1} , respectively¹⁵⁶. This type of IR spectroscopic study also shows that the order of relative acidities is arylsilanol > alkylsilanol > arylcarbinol > alkylcarbinol¹⁵⁵. Most of the IR studies on hydrogen bonded adducts of silanol have been carried out with monosilanol such as Ph_3SiOH , but some data for both silanediols and for siloxanediols are available¹. The O-H stretching frequencies in silanetriols $\text{XC}_6\text{H}_4\text{Si}(\text{OH})_3$ compounds (X = *p*- NMe_2 , *p*-OMe, *p*-Me, *m*-OMe, *m*-Cl, *m*- CF_3 etc.) correlate well with Hammett σ constants, the frequency on coordination with DMSO being given by $\nu = 3285.5 - 31.91\sigma$ ($r = 0.996$)⁸⁶. The general lack of data is presumably due to the relative instability of polysilanol and the condensation reactions promoted by the addition of acids or bases to species lacking bulky substituents.

Nuclear magnetic resonance spectroscopy has also been used to probe the chemistry of the SiOH group. A linear correlation has been found between the ^{29}Si NMR chemical shift of SiOH groups and the donor strength of the solvent, with strong donors such as HMPA causing a larger upfield shift than weaker donors¹⁵⁷. Silanol group acidity has also been shown to correlate well with the ^1H chemical shift, $\delta^{158-160}$, in the presence of DMSO, but this seems to hold well only for closely related series of compounds¹⁵⁹. For the triols

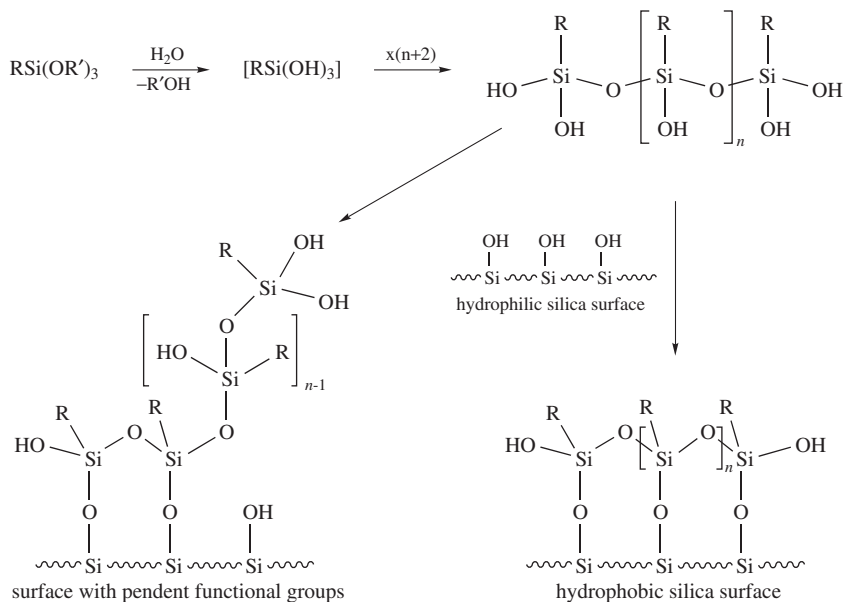
$\text{XC}_6\text{H}_4\text{Si}(\text{OH})_3$ ($X = p\text{-NMe}_2, p\text{-OMe}, p\text{-Me}, m\text{-OMe}, m\text{-Cl}, m\text{-CF}_3$ etc.) an excellent correlation between δ, OH and the Hammett σ constant was found for various bases, for example $\delta = 6.73 + 0.773\sigma$ for HMPA solutions. The $\text{p}K_{\text{a}}$ for $\text{Ph}_2\text{Si}(\text{OH})_2$ in DMSO has been estimated to be 12.08 using the equation $\text{p}K_{\text{a}} = 8.9 + 1.06\tau\text{OH}$ ($\tau\text{OH} =$ chemical shift of OH proton in ppm)¹⁶¹. A correlation is also observed on plotting δ_{OH} (ppm), against ν_{OH} (cm^{-1})⁸⁶. IR and ^{29}Si NMR data for a variety of bulky silanetriols have been tabulated¹⁶². Further studies of this type will no doubt be carried out as the chemistry of compounds, such as incompletely condensed silsesquioxanes, acting as models for silica surfaces and silanetriols, continues to expand.

Infra-red spectra of silanols in the presence of acidic species show the silanol oxygen atoms to be nearly as basic as those in alcohols; the change in stretching frequency, $\Delta\nu$ (of the $\text{SiO}-\text{H}$), on hydrogen bond formation with phenol, is 169, 326, 268 and 190 cm^{-1} respectively for $(\text{PhCH}_2)_2\text{Si}(\text{OH})_2, (m\text{-tolyl})_2\text{Si}(\text{OH})_2, (\text{HOMe}_2\text{Si})_2\text{O}$ and $(\text{HOPh}_2\text{Si})_2\text{O}$ ^{10,163}. Calculations of proton affinities and basicities of free silanols and hydrogen bonded silanols reveal that the silanol oxygen is significantly more basic if the proton is acting as a hydrogen bond donor than if no hydrogen bonding is present¹⁶⁴. The potential of silanols to form strong hydrogen bonds is manifested not only in solution, but also in the solid state where such interactions tend to dominate the crystal packing (see Section IV).

C. Silica Surfaces and Coupling Agents

The silanol groups on a surface of, for example, silica may react with a variety of compounds to give surface modified materials in which useful chemical functions are tethered to the surface by covalent bonding or the hydrophilic surface has been passivated to some extent by a hydrophobic layer. This type of surface modification can be useful not only for the exclusion of water, but also in promoting adhesion and for supporting reactive species on an inert substrate. The reagents used for surface modification may be simple $\text{R}_{3-n}\text{SiCl}_n$ ($n = 0, 1$ or $2, \text{R} =$ alkyl or aryl) compounds which can be used to form a hydrophobic layer or more sophisticated alkoxy-silanes $(\text{RO})_3\text{SiR}'$ ($\text{R} = \text{Me}$ or Et), where R' can be a larger organic fragment containing functional groups such as amine, epoxide, ester or vinyl. These functional groups can then be used to carry out further chemistry after attachment to the surface. The silane coupling reaction of alkoxy-silanes relies on hydrolysis, usually of a trimethoxy-silane derivative, to give a polysilanol which can then react with itself to form a larger polysilanol unit, and with a surface hydroxy group with the elimination of water to form a strong siloxane linkage. This is outlined in Scheme 8 and is actually a very complicated process dependent on factors such as the amount of water present, the organic substituents and the nature of the surface. The uses of silane coupling agents have been described at length elsewhere and they will not be discussed further in this article^{65,165,166}. The reactions of surface $\text{Si}-\text{OH}$ groups are outside the scope of this review but can be found in Reference 167.

A new approach to the investigation of silica surface SiOH groups in recent years has involved the use of small polyhedral silsesquioxanes, such as those shown in Scheme 3 and **36**, as molecular models for the surface. Thus, various species may be attached to the molecular silsesquioxane to give a product that is relatively easy to handle and which can be analysed by a range of traditional spectroscopic techniques as well as single-crystal X-ray crystallography. The preparation and structures of silsesquioxanes used in this type of work are described in Sections II and IV, respectively, and a more detailed description of the chemistry of silsesquioxanes is given in References 92, 168 and 169 and work cited therein. Recent work has shown that controlled condensation (using dicyclohexylcarbodiimide as a dehydrating agent) of polysilanols such as $[\text{c}-\text{C}_6\text{H}_{11}\text{Si}(\text{OH})_2]_2\text{O}$, which can



SCHEME 8

be isolated, can be used for the synthesis of silsesquioxanes rather than the one-pot synthesis from simple chlorosilane precursors¹⁷⁰. This type of synthesis may give access to new ladder and cage silsesquioxanes as well as improved synthesis of known compounds.

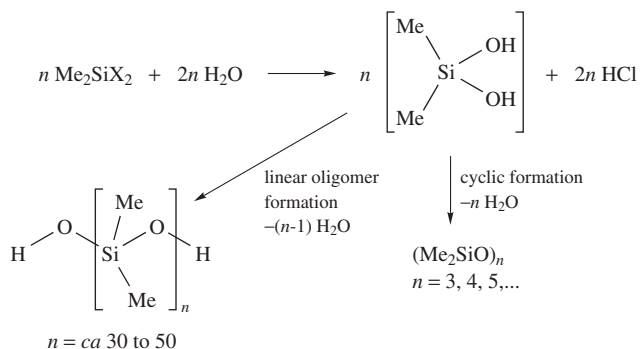
D. Sol-Gel Processes

Sol-gel processes leading to the formation of silicas and glasses have been widely investigated⁷³ because of their industrial importance, but as these processes usually involve the hydrolysis of alkoxy silanes (see, for example, Reference 74) such as $(\text{EtO})_4\text{Si}$, i.e. compounds containing no Si-C bonds, they will not be discussed in detail here. Reactive polysilanols such as $(\text{EtO})_{4-n}\text{Si(OH)}_n$ ($n = 1-4$) are formed by hydrolysis of the alkoxy silane which then undergo acid or base catalysed condensation reactions to give species containing Si-O-Si linkages that build up to form three-dimensional materials; for reviews of this field see References 66-68, 74, 75, 171 and 172. An emerging field which also relies on the polycondensation reactions of polysilanols retaining some organic substituent is that of the production of organically modified silicas or ceramics. These materials comprise networks of silicate units crosslinked by organic fragments such as alkyl chains or aryl groups. Again this will not be discussed in detail here, but see References 173-179 for further reading.

E. Siloxane Formation

The formation of compounds (polysiloxanes or silicones) containing Si-O-Si linkages is an important industrial process, a fundamental step of which is the hydrolytic polycondensation of monomeric silicon containing precursors (usually chlorosilanes). The details of siloxane polymer formation will not be dealt with here but can be found in

more specialized References 66–72. The primary reactions involving polysilanol are outlined in Scheme 9 for the hydrolysis of Me_2SiCl_2 using an excess of water. The rates of the various reactions leading to the product mixture of small cyclic siloxanes and linear α,ω -dihydroxysiloxanes are dependent on pH. The homocondensation reaction, $2\text{SiOH} \rightarrow \text{Si}-\text{O}-\text{Si} + \text{H}_2\text{O}$, is favoured by acidic conditions but heterocondensation, $\text{SiOH} + \text{SiCl} \rightarrow \text{Si}-\text{O}-\text{Si} + \text{HCl}$, is favoured by a basic environment particularly if nucleophiles such as *N,N*-dimethylaminopyridine are present⁶⁹. If the concentration of water is low in the hydrolysis, then chlorosilanol are more likely to be formed as intermediates¹⁸⁰.



SCHEME 9

The mechanisms of the condensation reactions of polysilanol have been the subject of numerous reports (for reviews, see References 181 and 182) and are catalysed by acids and by bases. A simple outline of the mechanisms is given in Scheme 10. The hydrolysis of RSiCl_3 species where R is small and no precautions are taken to remove HCl as it is formed leads to the formation of ladder and branched polymers via $\text{RSi}(\text{OH})_3$ or chlorosilanol. The presence of larger groups or the avoidance of acidic or basic conditions allows the intermediate silanol to be formed as outlined in Section II.

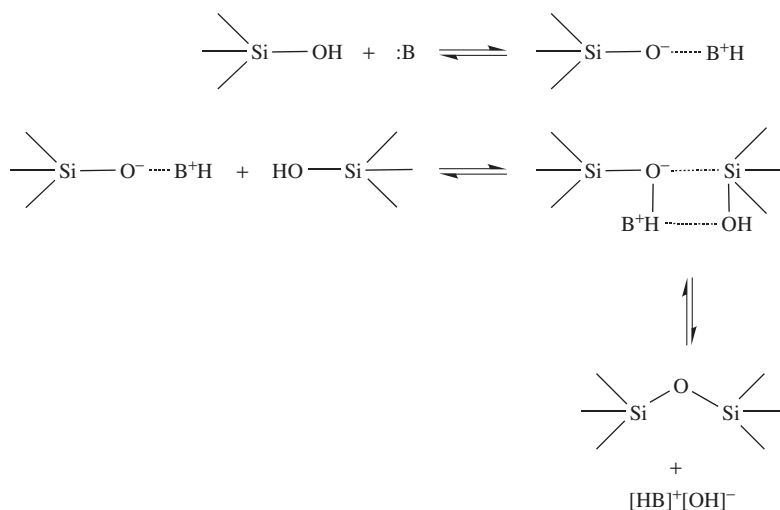
F. Metal and Metalloid Derivatives of Silanols

Metal and metalloid derivatives of silanol, also called metallasiloxanes, have been studied extensively for many years. Early work has been comprehensively reviewed¹⁸³ and the discussion below will concentrate on work carried out in the last five to ten years. Again, this is now a very large area of research and representative examples of reactions rather than a thorough survey will be provided.

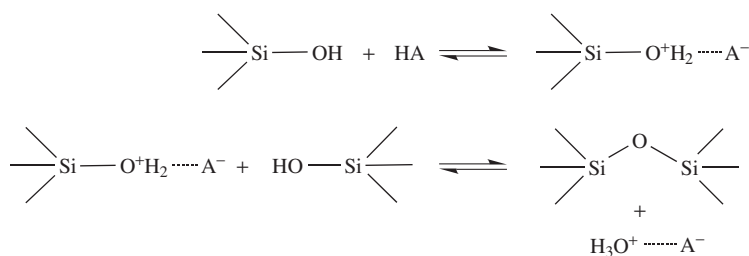
1. Derivatives of siloxanediols

The preparation and structures of siloxanediol derivatives has been reviewed^{29,184} but some representative examples of reactions are given below. Two general methods have been used to make metal siloxides from silanol: one involves the direct reaction of a silanol with the metal derivative, usually an amide, alkoxide, halide or alkyl (to give amine, alcohol, HX or alkane byproducts respectively), while the second involves the preparation of a simple alkali metal derivative which can then be used as a siloxide transfer reagent for further synthesis. Only the direct route will be considered here. Two of the most useful siloxide transfer species, $(\text{MOPh}_2\text{Si})_2\text{O}$ ($\text{M} = \text{Li}$ or Na), are

(a) Base catalysis



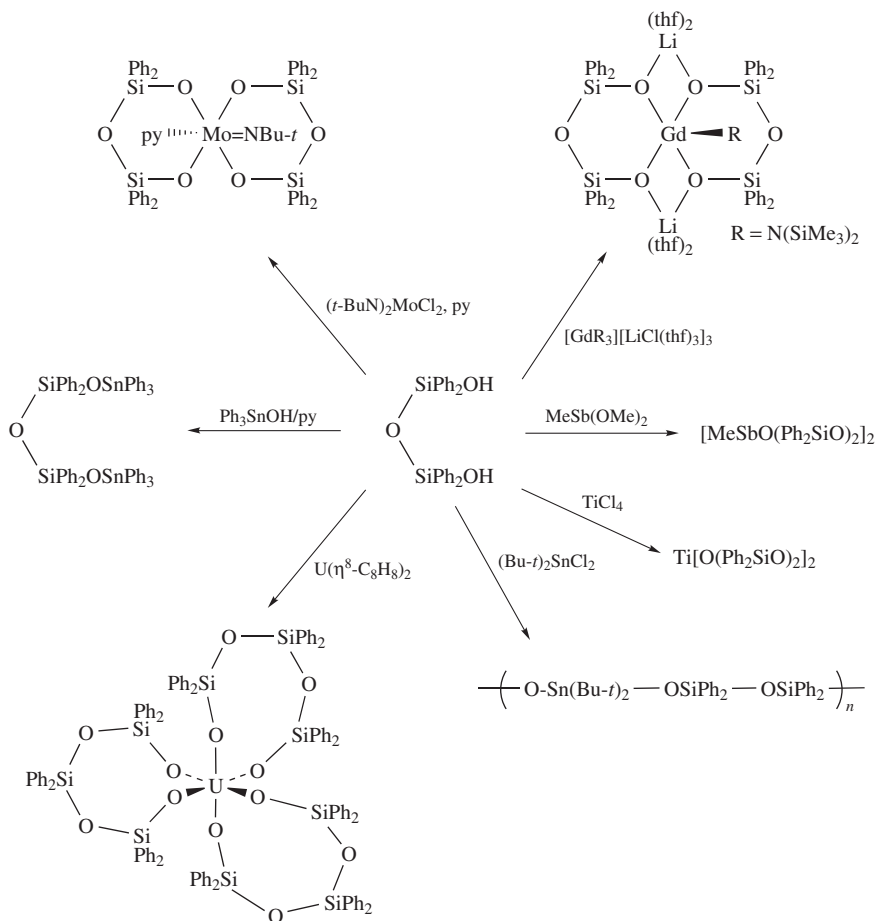
(b) Acid catalysis



SCHEME 10

prepared by reaction of $(\text{HOPh}_2\text{Si})_2\text{O}$ with BuLi ^{185–187} or sodium metal¹⁸⁸, respectively, in the presence of a base such as pyridine. Reactions of disiloxane precursors with metal reagents sometimes, however, give products containing trisiloxane groups. For example, treatment of $(\text{HOPh}_2\text{Si})_2\text{O}$ with $\text{KOBu-}t$ affords $[\text{K}\{\text{O}(\text{Ph}_2\text{SiO})_2\text{SiPh}_2\text{OH}\}]_2$, which is also a rare example of a monometallated α,ω -siloxanediol¹⁸⁹. Further examples of reactions of $(\text{HOPh}_2\text{Si})_2\text{O}$ with a range of metal precursors containing Sn ^{190,191}, Ti ^{192,193}, Sb ¹⁹⁴, Mo ¹⁹⁵, Gd ¹⁹⁶ and U ¹⁹⁶ are given in Scheme 11. The more bulky disiloxane $(\text{HO}(t\text{-Bu})_2\text{Si})_2\text{O}$ has been less widely used but reacts with Re_2O_7 to give $[\text{O}(t\text{-Bu})_2\text{SiOREO}_3]_2$, which has a chain structure with siloxanediolate bridges¹⁹⁷. Tri- and tetra-siloxanediols $\text{HO}(\text{Ph}_2\text{SiO})_n\text{H}$ ($n = 3$ or 4), although more difficult to prepare than the disiloxane analogue, have also been used to prepare a series of borasiloxanes by reaction of the silanol with $\text{B}(\text{OH})_3$ and a diol such as 2,3-dimethyl-2,3-butanediol¹⁹⁸.

There has been significantly less work carried out involving silsesquioxanes containing two SiOH groups compared with those containing three such groups and reactions are generally slower. This is presumably due to the lower acidity of the species containing only two silanol functions. Two silsesquioxane cages can be attached to a four-coordinate metal

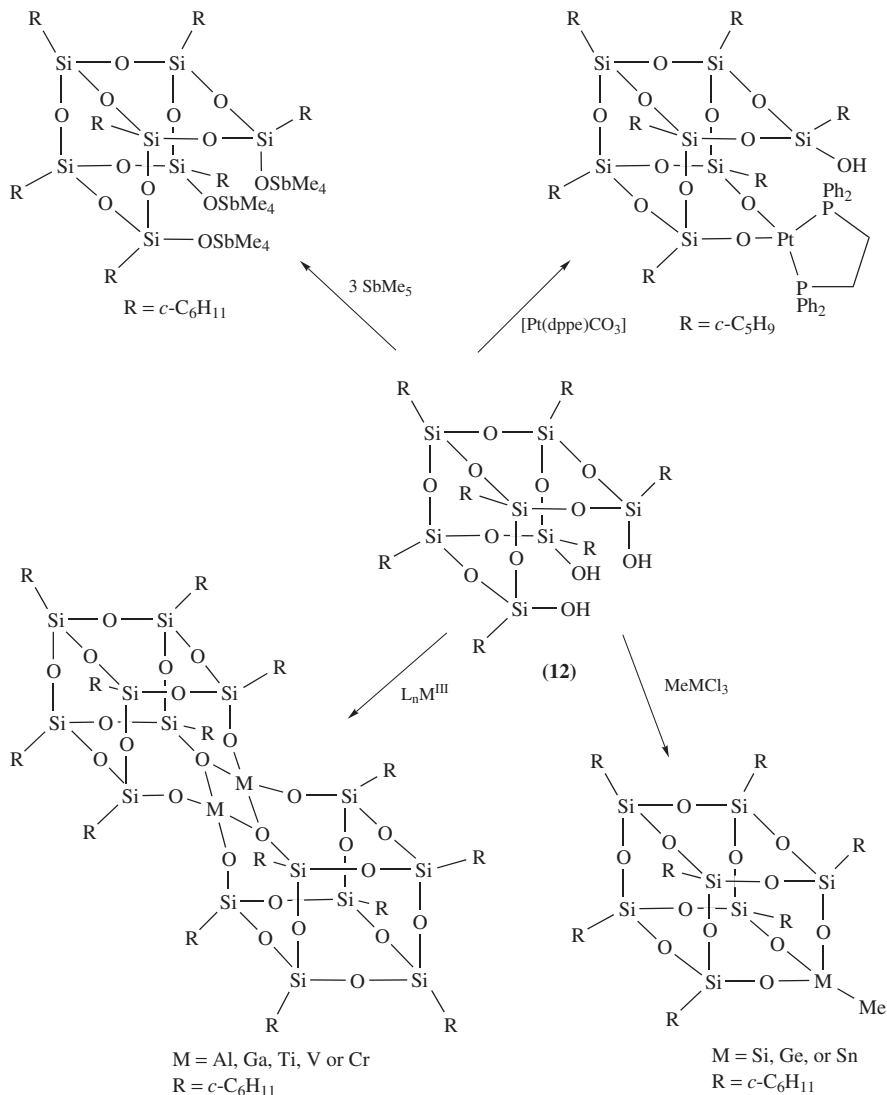


SCHEME 11

centre such as Ti^{199} , **41**, while unusual examples of late transition metal silsesquioxane complexes, **42**, can be prepared according to Scheme 12²⁰⁰.

2. Derivatives of siloxanetriols

The work of Feher and coworkers in the last fifteen years has given an increased understanding of the chemistry of silica surface silanol groups by preparing silsesquioxanes that may act as molecular mimics for surface reactions (see, for example, References 201–203). The most important of these species are the incompletely condensed species **12** ($\text{R} = c\text{-C}_5\text{H}_9$, $c\text{-C}_6\text{H}_{11}$ and $c\text{-C}_7\text{H}_{13}$), $\text{R}_7\text{Si}_7\text{O}_9(\text{OH})_3$, containing three silanol groups. The improvement of these compounds as models for silica surfaces over more conventional R_3SiOH species is due to several factors: that they have three SiOH groups thought to have a geometry similar to those found on the surface of β -cristobalite and of β -tridymite; that the cage nature of the silsesquioxane constrains the geometry of the

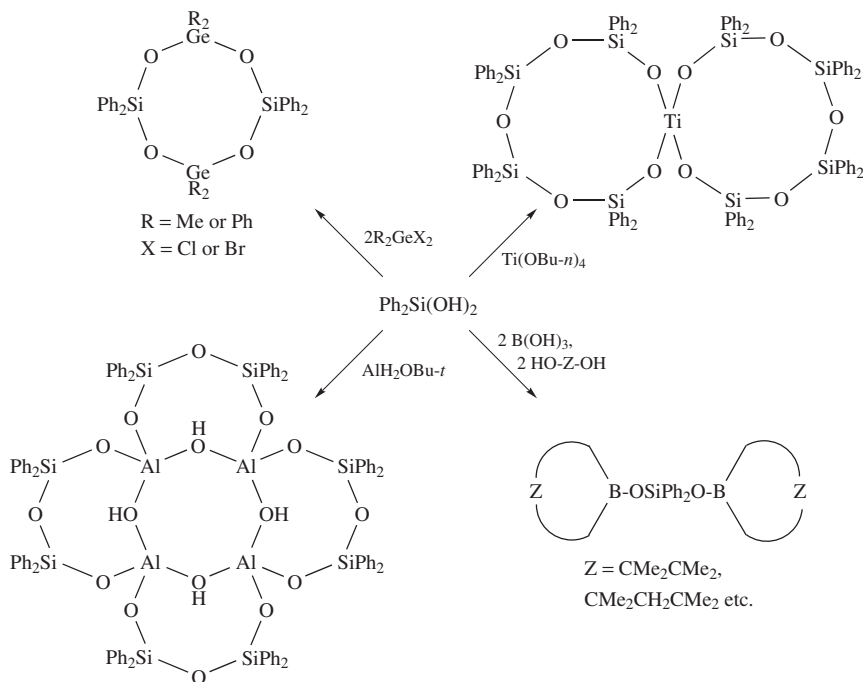


SCHEME 13

3. Derivatives of silanediols

The reactions of $\text{R}_2\text{Si}(\text{OH})_2$ compounds with metal and metalloids derivatives have been reviewed^{29,184} and follow some of the same general trends as the reaction for disilanols and trisilanols described above. Synthetic routes often employ the reaction between the silanediol and a metal amide, chloride etc. and cyclic products are often formed. Only two diols, $\text{Ph}_2\text{Si}(\text{OH})_2$ and $(t\text{-Bu})_2\text{Si}(\text{OH})_2$, have been used extensively, their chemistry often being ruled by the relative ease of oligomerization of the phenyl analogue compared to the

more bulky *t*-butyl compound. Thus, compounds derived from $\text{Ph}_2\text{Si}(\text{OH})_2$ often contain a short α,ω -siloxanediolate chain, while $(t\text{-Bu})_2\text{Si}(\text{OH})_2$ usually gives compounds containing the simple $[(t\text{-Bu})_2\text{SiO}_2]^{2-}$ unit [see, however, the formation of $(\text{HO}(t\text{-Bu})_2\text{Si})_2\text{O}$ in the reaction with SnCl_4 ¹⁴³]. Representative examples of the various types of compound formed from $\text{Ph}_2\text{Si}(\text{OH})_2$ are given in Scheme 14 for B¹⁹⁸, Al²⁰⁹, Ti^{210,211} and Ge^{212,213}. Examples of the reactions of $(t\text{-Bu})_2\text{Si}(\text{OH})_2$ are given in Scheme 15 for Ti²¹⁴, Nb^{197,215}, W^{197,215} and Te²¹⁶.



4. Derivatives of silanetriols

The chemistry of compounds derived from silanetriols has been studied increasingly widely in recent years as they have been used to model, and to act as precursors to, metal-doped silicate materials. Several reviews in this area have appeared^{27–30} and only an outline of the known chemistry is described here. The stability of a silanetriol towards self-condensation reactions is important if it is to be useful as a precursor to a range of materials, and this has meant that only compounds $\text{RSi}(\text{OH})_3$ containing a bulky substituent R have been widely studied. The most popular precursors have been $t\text{-BuSi}(\text{OH})_3$ and a range of unusual N-substituted compounds $\text{R}(\text{Me}_3\text{Si})\text{NSi}(\text{OH})_3$ where $\text{R} = 2,4,6\text{-Me}_3\text{C}_6\text{H}_2$, $2,6\text{-Me}_2\text{C}_6\text{H}_3$, $2,6\text{-}(i\text{-Pr})_2\text{C}_6\text{H}_3$ and $2,6\text{-Me}(i\text{-Pr})\text{C}_6\text{H}_3$ ^{27–30}. The arrangement of three OH groups around a tetrahedral centre (which is not generally available to carbon compounds) means that silanetriols are well suited for the preparation of polyhedral metal-lasiloxanes rather than simple monomeric or cyclic species. Some representative reactions

of RSi(OH)_3 species are given in Scheme 16 for $\text{Ti}^{31,140}$, Ta^{217} and Re^{54} . Detailed infrared and ^{29}Si NMR spectroscopic¹⁶² as well as many X-ray crystallographic studies^{27–30} have been carried out on these metallasiloxanes.

IV. STRUCTURAL STUDIES OF SILANOLS

A. Introduction

This section describes structural studies carried out by computational methods or by X-ray diffraction techniques and will concentrate on how the molecular structures are influenced by hydrogen bonding to the SiOH groups. A detailed discussion of bond lengths and angles will not be given but can be found in Reference 1. A variety of well defined hydrogen bonded adducts of silanols with organic molecules or water are included in the appropriate silanol section rather than being grouped together.

Relatively few of the structures determined by X-ray crystallography are of sufficient quality for meaningful discussion of the precise geometry of the hydrogen bonding interactions present and so $\text{O}\cdots\text{O}$, $\text{O}\cdots\text{N}$, $\text{O}\cdots\text{F}$, or $\text{O}\cdots\pi$ -system distances are commonly used as a basis for the discussion. In the structures drawn below, OH hydrogen atoms are usually omitted, hydrogen bonds are denoted by dashed lines and the molecular backbone joining two or more OH groups within a molecule is often denoted by a curved line. Compounds are arranged in order of increasing numbers of SiOH groups present.

B. Calculations of the Structures of Silanols

Computational studies of polysilanols have not concentrated on compounds containing organic substituents but rather on those compounds of more interest to the mineralogist such as $\text{H}_n\text{Si(OH)}_{4-n}$ ($n = 0, 1$ and 2) and $[(\text{HO})_3\text{Si}]_2\text{O}$. The most stable conformations of $\text{H}_2\text{Si(OH)}_2$ ^{218,219} and of HSi(OH)_3 ^{220,221} (neither of which has been isolated) are calculated to have *gauche* arrangements which are interpreted in terms of a strong anomeric effect^{218–220}. Silicic acid, Si(OH)_4 , which is ubiquitous in aqueous solution in the environment, has been the subject of several computational investigations²²⁰. The lowest energy geometry is of S_4 (hydrogen staggered) symmetry^{219,221} with an Si–O bond length of 1.629 Å and O–Si–O angles of 115.8 and 106.4°²²². Details of the OH groups in $(\text{HO})_3\text{SiCN}$ and $(\text{HO})_3\text{SiNC}$ were not reported in a computational study of these compounds²²³. Disilicic acid, $[(\text{HO})_3\text{Si}]_2\text{O}$, has been studied in some detail by *ab initio* and density functional methods^{151,224–227}. A fully optimized structure at the Becke3LYP6-311G(2d,p) level of theory with no restrictions placed on the positions of the atoms gave a structure containing two intramolecular SiOH \cdots OH hydrogen bonds with the Si–O(bridging) bond length being 1.636 Å and the Si–O–Si angle 126.8°²²⁷.

Most Si–OH bond lengths fall in the range 1.64 ± 0.03 Å^{228,229}, i.e. somewhat shorter than might be expected from the corrected sum of the covalent radii for O and Si. The strength and shortness of the Si–O bond has been attributed to its high polarity^{221,226,230}. Tabulated data for the structures of many silanols and polysilanols can be found in Reference 1.

C. Compounds Containing Two Si–OH Groups

1. Disiloxanes

A range of simple disiloxanes, $(\text{HOR}_2\text{Si})_2\text{O}$ (where R = Me, Et, *n*-Pr, *i*-Pr, *c*-C₅H₉ or Ph), $[(\text{HO})(3\text{-thienyl})\text{MeSi}]_2\text{O}$ and the cyclic species 1,3-dihydroxy-1,3-dimethyl-1,3-disila-2-oxacyclohexane have all been structurally investigated. The hydrogen bonding in

these disiloxanes varies as shown in Figure 1 but is usually based on a double chain structure as shown in Figure 1 a–d, and which is also a feature of many of the other structures described below. The arrangement shown in Figure 1a is adopted by the Me^{231,232}, Et²³³, *n*-Pr²³⁴ and Ph derivatives^{235,236}. The arrangement in Figure 1b is adopted by the *i*-Pr²³⁷ and *c*-C₅H₉²³⁸ compounds and arrangement Figure 1c by the thienyl compound²³⁹. A more complicated sheet structure is adopted by 1,3-dihydroxy-1,3-dimethyl-1,3-disila-2-oxacyclohexane^{1,240}. Unusual thermotropic mesophases are formed by the Et, *n*-Pr and *n*-Bu derivatives^{232,241–243}. These are thought to arise from columns of hydrogen bonded molecules with hydrophobic exteriors that are relatively flexible when compared to the Me and Ph compounds (which do not exhibit liquid crystalline phases)²³². Molecular mechanics calculations suggest that such structures are also present in [R₂(HO)Si]₂CH₂ compounds (R = Et or Pr) and in (*i*-Bu)₂Si(OH)₂ which also exhibits mesogenic behaviour²⁴⁴. An IR spectroscopic study of (HOME₂Si)₂O found that there was no intramolecular hydrogen bonding present, as was shown by X-ray crystallography²⁴⁵. The disiloxanediol (HO(*t*-Bu)₂Si)₂O co-crystallizes with (*t*-Bu)₂Si(OH)₂ and [Cl₃Sn(μ-OH)]₂, however the (HO(*t*-Bu)₂Si)₂O molecules do not hydrogen bond to each other but link columns of (*t*-Bu)₂Si(OH)₂•[Cl₃Sn(μ-OH)]₂ units via SiOH⋯(μ-OH) hydrogen bonds¹⁴³.

The ferrocenyl derivative (HOFc₂Si)₂O (Fc = ferrocenyl) has a slightly different structure to other (HOR₂Si)₂O siloxanes. Hydrogen bonded double chains are also present but in this case only three out of four protons are involved in hydrogen bonds to give a structure shown in Figure 1d¹⁴². Disiloxane (HOFc₂Si)₂O also co-crystallizes with the cyclotrisiloxane (Fc₂SiO)₃ together with CH₂Cl₂ and 3-methylpentane in the lattice. In this case the disiloxane shows no OH⋯OH hydrogen bonding but only OH⋯Cl (with O⋯Cl distance of 2.727 and 3.279 Å) interactions where the CH₂Cl₂ molecules bridge between siloxane molecules to give a helical chain¹⁴².

The siloxanes (HOPh₂Si)₂O and HO(SiPh₂O)₃H form hydrogen bonded adducts with a variety of organic compounds (as does Ph₃SiOH, see Reference 1). Structurally characterized adducts with (HOPh₂Si)₂O include [(HOPh₂Si)₂O]•3pyridazine which forms discrete units with both OH⋯OH (2.71 Å) and OH⋯N (2.75 Å) hydrogen bonds²⁴⁶, (HOPh₂Si)₂O•hexamethylenetetramine²⁴⁷ which comprises simple chains of alternating siloxanediol and amine molecules, [(HOPh₂Si)₂O]₂•pyridazine²⁴⁷ which forms chains of

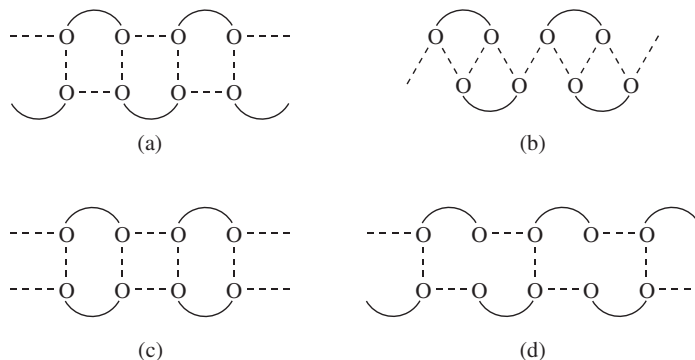
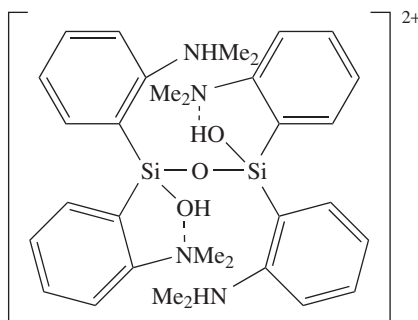
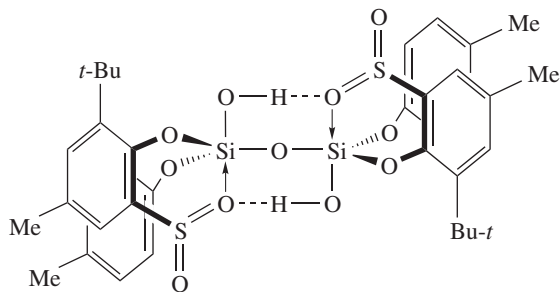


FIGURE 1. Hydrogen bonded chain structures in simple siloxanediols. Curves represent Si–O–Si backbone, dashed lines show hydrogen bonding

rings in which dimeric units of the type shown in Figure 1c are connected to their neighbours by the pyrazine molecules, $(\text{HOPh}_2\text{Si})_2\text{O}\cdot\text{pyridine}^{247}$, $(\text{HOPh}_2\text{Si})_2\text{O}\cdot\text{pyrimidine}^{247}$, $[(\text{HOPh}_2\text{Si})_2\text{O}]_2\cdot 2\text{Et}_2\text{NH}^{248}$ and $(\text{HOPh}_2\text{Si})_2\text{O}\cdot\text{dioxane}^{248}$. The trisiloxane forms adducts $[\text{HO}(\text{SiPh}_2\text{O})_3\text{H}]_4\cdot\text{pyrazine}^{247}$ in which units of the type shown in Figure 1b are linked by pyrazine molecules, and $[\text{HO}(\text{SiPh}_2\text{O})_3\text{H}]_2\cdot 3\text{pyridine}^{247}$. No hydrogen bonding in the bulky siloxane $[(2,6\text{-Et}_2\text{C}_6\text{H}_3)(2,6\text{-Et}_2\text{-4-}t\text{-BuC}_6\text{H}_2)(\text{OH})\text{Si}]_2\text{O}$ was described in the initial report of the structure²⁴⁹, but a more recent examination¹ has shown that the structure contains discrete pairs of disiloxane molecules which are connected via hydrogen bonding to a pair of ethanol molecules from the solvent used for crystallization rather than being directly hydrogen bonded to each other. A salt, $(\text{HOPh}_2\text{Si})_2\text{O}\cdot\text{C}_5\text{H}_5\text{N}\cdot\text{HCl}$, forms a structure in which the Cl^- hydrogen bonds to the pyridinium proton and both silanol groups²⁵⁰.



(43)



(44)

The disiloxanediols **43**²⁵¹ and **44**²⁵² contain only intramolecular hydrogen bonds with an $\text{O}\cdots\text{N}$ distance of 2.644 Å in **43** and an $\text{O}\cdots\text{O}$ distance of 2.899 Å in **44**. These disiloxane diols thus differ from the others in that discrete molecules with no significant intermolecular interactions are formed. They are also both unusual in that the $\text{Si}-\text{O}-\text{Si}$ linkage in each is linear. In **44**, the structure is distorted away from tetrahedral at the Si atoms towards a trigonal bipyramidal geometry by an additional coordination to a sulfoxide oxygen.

2. Other siloxanes

The solid state structures of the trisiloxanes, $\text{HO}(\text{SiPh}_2\text{O})_3\text{H}$ ²⁵³ and $(\text{HO}(t\text{-Bu})_2\text{SiO})_2\text{SiMe}_2$ ²⁵⁴, contain hydrogen bonded dimers. The phenyl compound contains both intra- and inter-molecular hydrogen bonds with $\text{O}\cdots\text{O}$ distances of 2.74 Å and 2.72 Å, respectively, while in the butyl compound there seems to be no intramolecular hydrogen bonding but rather a pair of intermolecular hydrogen bonds. The tetrasiloxane $\text{HO}(\text{SiPh}_2\text{O})_4\text{H}$ has a very surprising structure in which there seem to be no $\text{OH}\cdots\text{O}$ hydrogen bonds present but only a weak $\text{OH}\cdots\pi$ interaction¹⁴⁷.

The cyclic tetrasiloxane *cis*-1,5-dihydroxy-1,5-dimethyl-3,3,7,7-tetraphenylcyclotetrasiloxane has a structure based on intermolecular hydrogen bonding which joins the molecules into chains rather than intramolecular interactions. The hydrogen bonded network is similar in arrangement to that shown above in Figure 1b where both OH groups from one molecule in the chain interact with a single OH group on the opposite side of the double chain²⁵⁵.

The crystal structures of both the *cis* and the *trans* isomers of 2,8-dihydroxy-2,4,4,6,6,8,10,10,12,12-decamethylcyclohexasiloxane have very different hydrogen bonded structures. The *cis* isomer contains an intramolecular hydrogen bond and two further intermolecular hydrogen bonds link the molecules into cyclic dimers. The *trans* isomer forms intermolecular hydrogen bonds to give tetrameric units, which are further hydrogen bonded to form infinite sheets²⁵⁶.

The structures of $[(c\text{-C}_6\text{H}_{11})_7\text{Si}_7\text{O}_9(\text{OH})_2\text{OSiMe}_2\text{R}](\text{R} = \text{Me or Ph})$ are thought to be similar and to comprise hydrogen bonded dimers with intra- and inter-molecular hydrogen bonding, although the SiMe_3 derivative is disordered^{141,257}. The cyclopentyl analogue $[(c\text{-C}_5\text{H}_9)_7\text{Si}_7\text{O}_9(\text{OH})_2\text{OSiMe}_3]$ has, however, been reported to be monomeric²⁰⁰. The related siloxane **11** has also been investigated by X-ray crystallography, but disorder problems have prevented a detailed structural analysis²⁵⁸. Two strong intramolecular hydrogen bonds are present in the $[(n\text{-Bu})_4\text{N}]^+$ salt of anion **36** as depicted in Scheme 6¹⁴⁴. Hydrogen bonding between OH groups appears to be absent in the solid state structure of **9** as they point towards *i*-Pr groups on adjacent molecules rather than towards each other¹¹⁹.

3. Oligosilanedioles

The OH groups in $(\text{HO}(t\text{-Bu})_2\text{Si})_2$ point in opposite directions and intramolecular hydrogen bonds are not possible. Intermolecular interactions are, however, present to give a chain structure⁶³. The less bulky disilane $(\text{HOMe}_2\text{Si})_2$ has a more complicated structure (shown in Figure 2) that does not seem to be adopted by any other simple disilanols. Opposing pairs of molecules are not joined directly together but are bridged by four other SiOH groups to give an overall layer structure²⁵⁹.

The structure of the tetrasilanediol $\text{HO}(\text{SiPh}_2)_4\text{OH}$ has been determined twice with similar but not identical results. One report⁴¹ describes a structure with a single intramolecular hydrogen bond causing a cyclic arrangement and also suggests that intermolecular hydrogen bonding is prevented by the bulk of the phenyl groups. A second report⁴² describes a similar intramolecular interaction but also describes an intermolecular hydrogen bond linking the molecules into pairs. Molecules of the heptasilane $\text{HO}(\text{SiPh}_2)_7\text{OH}$ are also linked by intermolecular hydrogen bonds to give infinite chains. In this oligosilane there is also an intramolecular interaction between an OH group and the π -system of aryl rings⁴². The conformation in solution of disilanols $\text{HO}(\text{SiPh}_2)_n\text{OH}$ ($n = 4, 5$ or 7) has been investigated by IR spectroscopy²⁶⁰. The intramolecular π -interaction in the heptasilane is indicated in CCl_4 by a relatively narrow band at 3605 cm^{-1} ; similar bands are seen

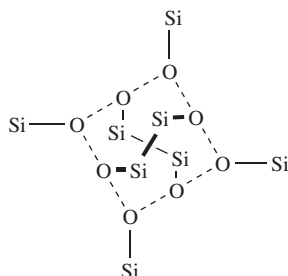


FIGURE 2. Schematic depiction of the hydrogen bonding network in $(\text{HOME}_2\text{Si})_2$. Dashed lines represent hydrogen bonds, Me groups are omitted

for $\text{HO}(\text{SiPh}_2)_4\text{OH}$ and for $\text{HO}(\text{SiPh}_2)_5\text{OH}$. The pentasilane also exhibits a second band at 3405 cm^{-1} attributable to intramolecular $\text{OH}\cdots\text{OH}$ hydrogen bonding [3415 cm^{-1} in $\text{HO}(\text{SiPh}_2)_4\text{OH}$] and a third band at about 3660 cm^{-1} attributable to free $\text{O}-\text{H}$ stretching.

As can be seen from the discussion above, the relatively low basicity of silyl ether and siloxane oxygen atoms tends to mean that, although they are often plentiful in a lattice, they do not participate in hydrogen bonding in the solid state. An exception to this is found for 1,4-dihydroxydecamethylcyclohexasilane which co-crystallizes with a hexasilanorbornane derivative to give a 1 : 2 hydrogen bonded adduct held together only by $\text{OH}\cdots\text{O}$ interactions ($\text{O}\cdots\text{O}$ distance 2.782 \AA) between silanol and siloxane groups²⁶¹. Although this type of interaction is very rare, there are examples of silanol to siloxane hydrogen bonds for monosilanols^{106,262}.

4. Other compounds containing two $\text{Si}-\text{OH}$ groups

A wide variety of compounds containing two SiR_2OH groups, which are often separated by a fairly symmetrical spacer group, have been structurally characterized and do not fall into the general categories described above. Some have the double chain hydrogen bonded structures as shown in Figure 1 while others have completely different structural types. No hydrogen bonding in the cyclic silazane 1,3-bis(diphenylhydroxysilyl)-2,2-dimethyl-4,4-diphenylcyclo-disilazane, $\text{Ph}_2\text{Si}(\text{Ph}_2\text{HOSiN}(\text{Me}_2\text{Si})\text{N}(\text{SiPh}_2\text{OH}))$, was reported in the original publication²⁶³, but a more recent study¹ of the X-ray data reveals that although there do not appear to be any $\text{OH}\cdots\text{OH}$ or $\text{OH}\cdots\pi$ interactions there is a short, 2.393 \AA , *ortho*- $\text{CH}\cdots\text{OH}$ distance indicating a probable $\text{CH}\cdots\text{OH}$ interaction. A second relatively short distance, 2.580 \AA , between the other *ortho*- CH and the second OH group is also indicative of a weak interaction. This appears to be the only silanol exhibiting such interactions and it is not clear why it does not participate in $\text{OH}\cdots\text{OH}$ or $\text{OH}\cdots\pi$ interactions. The structure of 1,7-bis[hydroxy(dimethyl)silylmethyl]-*m*-carborane²⁶⁴ is of the double chain type shown in Figure 1c.

The sterically hindered diorganozinc compound $[(\text{Me}_3\text{Si})_2(\text{HOME}_2\text{Si})\text{C}]_2\text{Zn}$ is very unusual in that such compounds are usually highly reactive towards protic species; steric protection by the Me_3Si substituents presumably prevents reaction at the $\text{C}-\text{Zn}$ bonds. The compound forms cyclic dimers via both intra- and inter-molecular hydrogen bonds²⁶⁵. A related disilanol, $(\text{Me}_3\text{Si})_2\text{C}(\text{SiMe}_2\text{OH})_2$, also shows alternating intra- and inter-molecular hydrogen bonds, but in this case chains are formed rather than discrete dimers²⁶⁶. Unit cell data for $(\text{HOME}_2\text{Si})_2\text{CH}_2$ have been reported but further details are unavailable²⁶⁷.

The intermolecular hydrogen bonding in *p*-(HOMe₂Si)₂C₆H₄ is more complicated than in the other disilanols described above and it has three crystallographically independent molecules in the unit cell. Two of these are joined by hydrogen bonds to form chains and the third cross-links the chains to give a three-dimensional network^{1,268}. The *meta* isomer *m*-(HOMe₂Si)₂C₆H₄ has a different hydrogen bonded arrangement in which dimeric units are linked to form chains [as in [(HO)(3-thienyl)MeSi]₂O described above] with further cooperative C—H⋯π interactions also being present⁸⁵. The biphenyl derivative 4,4'-bis(dimethylhydroxysilyl)biphenyl has a structure based on hydrogen bonded enantiomeric helices which are cross-linked via C—H⋯π interactions to give a three-dimensional network⁸⁵. A helical arrangement of hydrogen bonded molecules is also found in *trans*-1,3-dihydroxy-1,3-dimethyl-1,3-disilacyclobutane in which adjacent planar four-membered rings lie orthogonal to each other¹⁵.

A variety of transition metal complexes have been prepared in which some of the silanol groups present in a polysilanol precursor are retained in the product. No systematic approach to metal complexes containing SiOH groups seems to have been made and their structures follow no trends other than that the silanol groups are usually involved in hydrogen bonding with each other or are directly coordinated to a metal centre. Such structures will not be considered in any detail but include [(RN(SiMe₃)SiO₃)₂{RN(SiMe₃)SiO₂(OH)}₂(Mg.THF)₅](R = 2,6-(*i*-Pr)₂C₆H₃)²⁶⁹, [Zr{η⁵-C₅H₄SiMe₂(μ-OH)}(μ-Cl)Cl₂]₂²⁷⁰, W₂(NHMe₂)₂[O₂Si(OBu-*t*)₂][OSi(OH)(OBu-*t*)₂]₂²⁷¹, [(γ-PW₁₀O₃₆)(*t*-BuSiOH)₂]₃₋₅₆, and [RSi(OH)(OZr Cp₂)O]₂[R = (2,6-(*i*-Pr)₂C₆H₃)NSiMe₃]¹⁴⁰. A rare example of a monometallated α,ω-siloxane diol, [K{O(Ph₂SiO)₂SiPh₂OH}]₂, has also been isolated and has a dimeric structure containing two SiOH groups¹⁸⁹.

D. Compounds Containing Three Si—OH Groups

Several of the incompletely condensed polyhedral oligosilsesquioxanes prepared by Feher's group have been studied by X-ray crystallography, but such compounds often seem to give crystals that diffract poorly. The cyclohexyl derivative [(*c*-C₆H₁₁)₇Si₇O₉(OH)₃], **16**, crystallizes as discrete hydrogen bonded dimers which are thought to have intermolecular hydrogen bonding with O⋯O distances of 2.63–2.64 Å⁴⁸. Diffraction data for the related [(*i*-Bu)₇Si₇O₉(OH)₃] compound are good enough to confirm the identity of the silanol but not of sufficient quality to show any hydrogen bonding present⁹². Poorly diffracting crystals of **17** (R' = vinyl) do, however, give data consistent with a dimeric structure similar to that in **16**⁹¹. The monocyclic trisilanol [(Me₃Si)₂CHSi(OH)(NH)]₃ adopts a *cis, cis* arrangement and also has a simple dimeric structure. The only hydrogen bonding present is OH⋯OH; the NH groups point between the bulky hydrophobic (Me₃Si)₂CH substituents and are not involved²⁶.

E. Compounds Containing Four Si—OH Groups

Compounds containing four SiOH groups are relatively rarely isolated because they tend to undergo condensation reactions readily. Several have, however, been structurally characterized and show very different structures. The tetrasilanol (HOSiMe₂)₄C has a three-dimensional hydrogen bonded network with four independent molecules in the unit cell. Each molecule has two intramolecular hydrogen bonds and is joined by further hydrogen bonding to form sheets, one type of which is shown in Figure 3. The two different types of sheet formed (each using only two of the different molecules in the cell) are linked together by more hydrogen bonds to give an overall three-dimensional network²⁷². The

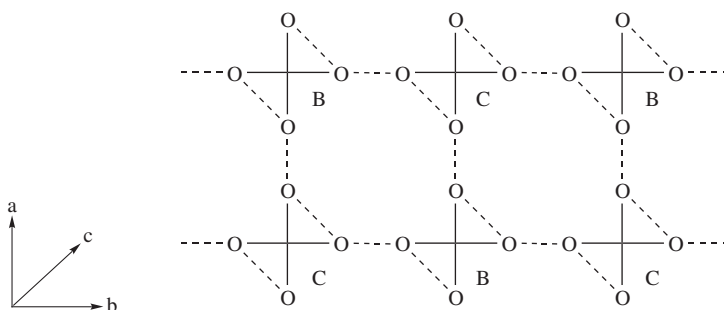


FIGURE 3. A representation of the hydrogen bonding in $(\text{HOME}_2\text{Si})_4\text{C}$ in the (001) plane containing two of the four types of molecules

structure of 1,1,5,5-tetrakis(hydroxydimethylsiloxy)-3,3,7,7-tetraphenylcyclotetrasiloxane is based on tetrameric units of hydrogen bonded molecules that are further linked by hydrogen bonds to give sheets which are independent from their neighbours rather than building up a three-dimensional network²⁷³.

A detailed structure of the incompletely condensed silsesquioxane **15** ($\text{R} = 2\text{-norbornyl}$) is unknown, but the X-ray data available suggests that the silanol groups point towards each other and that there are both intra- and inter-molecular hydrogen bonds present²⁷⁴. Simple cyclic tetrasilanol $[\text{R}(\text{OH})\text{SiO}]_4$ are rare but the structures of two have been determined recently. The phenyl derivative $[\text{Ph}(\text{OH})\text{SiO}]_4$ crystallizes from a $\text{Et}_2\text{O}/\text{C}_6\text{H}_6$ mixture to give a hydrogen bonded dimeric structure with further hydrogen bonding to two Et_2O molecules so that discrete units are formed⁵³. The isopropyl derivative $[i\text{-Pr}(\text{OH})\text{SiO}]_4$ crystallizes from $\text{C}_6\text{H}_6/\text{C}_6\text{H}_{14}/\text{H}_2\text{O}$ to give a complicated structure comprising hydrogen bonded pairs of silanols, which are linked via hydrogen bonding to water molecules so as to give a unit containing four silanol molecules and four water molecules⁵¹. Co-crystallization of $[i\text{-Pr}(\text{OH})\text{SiO}]_4$ with $(i\text{-Pr})_2\text{Si}(\text{OH})_2$ gives an unusual co-crystal of the two silanols in a 6:4 ratio, respectively, which form an infinite hydrogen bonded tube together²⁷⁵. Although the detailed structure of the hydrogen bonding in the first generation dendrimer $\text{Si}(\text{CH}_2\text{CH}_2\text{SiMe}_2\text{OH})_4$ has not been reported, it appears to contain channels of strongly hydrophilic hydrogen bonded OH groups separated by hydrophobic regions containing the alkyl groups¹²⁷.

F. Compounds Containing an $\text{Si}(\text{OH})_2$ Group, Silanediols

The presence of only two organic substituents that can hinder bimolecular condensation reactions of $\text{R}_2\text{Si}(\text{OH})_2$ compounds means that isolation of silanediols is more difficult than that of silanols. Not only does the bulk of the substituents play an important role in determining the stability of silanediols, but their size often determines the hydrogen bonding present. Infinite networks of hydrogen bonds are formed in silanediols with small substituents, while larger substituents often give rise to chains and very sterically demanding groups lead to the formation of simple tetramers or dimers.

The simple diols $\text{Et}_2\text{Si}(\text{OH})_2$ ²⁷⁶ and $(\text{CH}_2=\text{CH})_2\text{Si}(\text{OH})_2$ ²⁷⁷ have both been shown to form similar sheet structures (in contrast to early reports^{267,278,279}). The structure of $\text{Et}_2\text{Si}(\text{OH})_2$ is built up of sheets in which the Et groups sit on either side of a central core of hydrogen bonded OH groups. This general arrangement, in which there are strongly hydrophobic arrangements of organic substituents separated by strongly hydrophilic layers

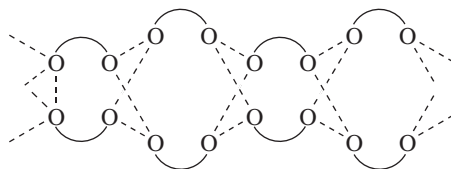
or chains of hydrogen bonded OH groups, is what would be expected, and is a common feature of polysilanol structures.

The aryl substituted diol $\text{Ph}_2\text{Si}(\text{OH})_2$ has been the subject of two structure determinations^{280,281}. The unit cell contains six crystallographically independent molecules which form a chair-shaped hydrogen bonded ring of six oxygens (one from each of the different molecules) with alternating short, medium and long $\text{O}\cdots\text{O}$ distances (2.670, 2.688 and 2.698 Å). Further hydrogen bonding above and below the six-membered ring links the hexameric groups so as to form a column in which all the OH groups are on the inside and the Ph groups point away from the column and prevent hydrogen bonding between different columns.

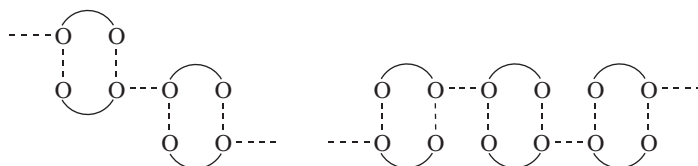
The simple diols $\text{R}_2\text{Si}(\text{OH})_2$ ($\text{R} = i\text{-Pr}$, $t\text{-Bu}$, $c\text{-C}_6\text{H}_{11}$ and $o\text{-tolyl}$) and 3,4-diphenyl-2,5-bis(trimethylsilyl)dihydroxysilole form two slightly different types of hydrogen bonded chains. The structures of the $i\text{-Pr}$ ²⁸², $t\text{-Bu}$ ^{6,254} and $c\text{-C}_6\text{H}_{11}$ ²⁶⁶ and the silole derivative²⁸³ are very similar to each other and comprise ladder chains of the general type shown in Figure 1c in which pairs of molecules are linked and then further hydrogen bonds link the dimers to form infinite chains. The related germanium diol $t\text{-BuGe}(\text{OH})_2$ forms similar ladder chains²⁸⁴. In the $t\text{-Bu}$ derivative, the chair-shaped Si_2O_4 rings of each dimer are inverted with respect to their neighbours but in the $i\text{-Pr}$ and $c\text{-C}_6\text{H}_{11}$ derivatives the Si_2O_4 rings are related simply by unit translation to their neighbours. (The isopropyl derivative $(i\text{-Pr})_2\text{Si}(\text{OH})_2$ also forms a co-crystal with $[i\text{-Pr}(\text{OH})\text{SiO}]_4$ ²⁷⁵.) The bulky nitrogen substituted compound 2,4,6- $\text{Me}_3\text{C}_6\text{H}_2\text{N}(\text{SiMe}_3)[\text{SiMe}(\text{OH})_2]$ has a similar ladder chain structure, but in this case the cyclic hydrogen bonded units are nearly planar³⁴. The structure of $(o\text{-tolyl})_2\text{Si}(\text{OH})_2$ also comprises chains of molecules; however, in this case opposing pairs of molecules are not linked together but interact with the neighbours of the molecule opposite as shown in **45**²⁸⁵. The diol $t\text{-BuPhSi}(\text{OH})_2$ has a structure similar to $(o\text{-tolyl})_2\text{Si}(\text{OH})_2$ rather than that of the related di-*tert*-butyl or the diphenyl analogues²⁸⁶. Some of the interest in $\text{R}_2\text{Si}(\text{OH})_2$ compounds derives from the fact that $(i\text{-Bu})_2\text{Si}(\text{OH})_2$ forms a discotic liquid crystalline phase^{287,288}. It usually crystallizes as fine fibres and a crystallographic determination of the structure of $(i\text{-Bu})_2\text{Si}(\text{OH})_2$ has, so far, not been possible. The discotic phase of $(i\text{-Bu})_2\text{Si}(\text{OH})_2$ has been proposed²⁸⁸ to be due to breaking of the inter-dimer hydrogen bonds in a structure of type shown in Figure 1c to give dimeric 'discs' of molecules at the transition between crystal and mesophase. The bulky diol $(\text{Me}_3\text{Si})(\text{Me}_3\text{SiCMe}_2)\text{Si}(\text{OH})_2$ also forms chains of hydrogen bonded dimers of molecules¹⁴⁹, but in this case only a single hydrogen bond connects the dimers in each direction and the dimers point in opposite directions, **46**. Bis(ferrocenyl)silanediol has a similar structure²³, but here the dimers, **47**, do not point in opposite directions. The iron complex $\text{Cp}(\text{CO})_2\text{FeSi}(\text{Pr-}i)(\text{OH})_2$ has a structure comprising helical ladder chains²⁸⁹.

The presence of very bulky substituents on silicon prevents extended hydrogen bonded networks from being formed in silanediols. Instead, discrete hexamers, tetramers or dimers are formed. The unusual fluorosilanediol $\text{TsiSiF}(\text{OH})_2$ (for its preparation, see Scheme 2) has a solid state structure comprising $[\text{TsiSiF}(\text{OH})_2]_6 \cdot 2\text{H}_2\text{O}$ hydrogen bonded hexamers^{1,58}. Each hexamer has the water molecules sited between two sets of three silanediol molecules. Hydrogen bonding occurs between the water molecules and the silanol groups and further $\text{OH}\cdots\text{OH}$ and $\text{OH}\cdots\text{F}$ hydrogen bonding occurs within each group of three silanediol molecules. The closely related silanediol $\text{TsiSi}(\text{OH})_2\text{O}_2\text{CCF}_3$ forms tetrameric units based on $\text{OH}\cdots\text{OH}$ and $\text{OH}\cdots\text{C}=\text{O}$ interactions with no inclusion of solvent molecules and no hydrogen bonding apparent to the fluorine atoms present²⁹⁰.

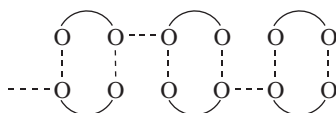
The structures of two silanediols, $(\eta^1\text{-C}_5\text{Me}_5)_2\text{Si}(\text{OH})_2$ ¹⁵⁰ and $[(2,4,6\text{-Me}_3\text{C}_6\text{H}_2)(\text{Me}_3\text{Si})\text{N}](\text{Me}_3\text{SiO})\text{Si}(\text{OH})_2$ ¹³⁹, **48**, provide an interesting progression away from the



(45)

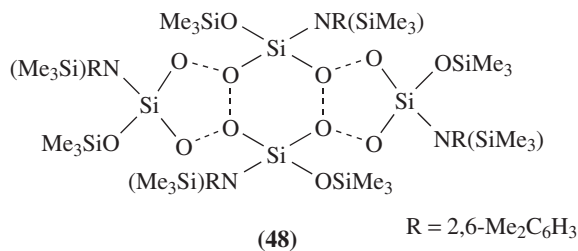


(46)



(47)

chain structures shown in Figure 1 and, by **45**, **46** and **47**, towards discrete hydrogen bonded units. Each structure comprises discrete tetrameric units in which pairs of molecules are hydrogen bonded together, but instead of these being linked into chains they are capped by single molecules at either side. Steric hindrance presumably prevents further hydrogen bonding between tetramers.



The very bulky diol $(\text{Me}_3\text{Si})_3\text{CSiPh}(\text{OH})_2$ ⁶² and the molybdenum complexes $\text{Cp}^*(\text{CO})_2(\text{Me}_3\text{P})\text{MoSiMe}(\text{OH})_2$ ¹¹⁶ and $\text{Cp}^*(\text{O})_2\text{MoOSiR}(\text{OH})\text{OSiR}(\text{OH})_2$ [R = 2,6-(*i*-Pr)₂C₆H₃(Me₃Si)N]²⁹¹ have even more restricted hydrogen bonding and comprise simple dimers only; further hydrogen bonding between dimers is presumably prevented by steric effects. The first example of a hydrido-silanediol 2,6-Me₂C₆H₃SiH(OH)₂ to be structurally characterized has also been determined to have a dimeric structure in the solid state. Two OH...OH hydrogen bonds form a nearly planar eight-membered cyclic arrangement (O-Si-O-H)₂ and there are further OH...π intramolecular interactions; again, all intermolecular hydrogen bonding interactions are prevented by the steric bulk of the aryl substituents²⁹².

The six-coordinate [cis-(bipyridyl)₂Si(OH)₂]²⁺ + 2[I]⁻ · 2H₂O forms a simple structure in which each of the SiOH groups is hydrogen bonded solely to a water molecule⁶⁴. Although not strictly comparable to the four-coordinate organosilanols described above, this molecule is included as it is a rare example of a silanediol that does not form intermolecular hydrogen bonds to itself. The solid state structure of a second six-coordinate diol (5,10,15,20-tetraphenylporphinato)Si(OH)₂ has been determined but details of any hydrogen bonding present were not reported⁸⁷. The structure of **33** contains

no intermolecular hydrogen bonding, but a single intramolecular $\text{OH} \cdots \text{NH}_2$ interaction gives a nine-membered cyclic structure¹³⁹.

G. Compounds Containing Two $\text{Si}(\text{OH})_2$ Groups

Relatively few compounds containing two $\text{Si}(\text{OH})_2$ groups have been isolated because of their instability towards condensation reactions. In $[t\text{-Bu}(\text{HO})_2\text{Si}]_2\text{O}$, the $\text{Si}-\text{O}-\text{Si}$ angle is linear and intermolecular hydrogen bonding gives chains of molecules which are further connected to give sheets. The *tert*-Bu groups alternate above and below the central core of hydrogen bonded OH groups, thus preventing interactions between different sheets of molecules⁵⁵. The tetrahydroxydisiloxane $[\text{OsCl}(\text{CO})(\text{PPh}_3)_2\text{Si}(\text{OH})_2]_2\text{O}$ has an $\text{Si}-\text{O}-\text{Si}$ angle, $137.9(7)^\circ$, in the more usual range, but there seem to be no intermolecular hydrogen bonds present, only a weak intramolecular $\text{OH} \cdots \text{Cl}$ interaction, and possibly an additional $\text{OH} \cdots \pi$ interaction¹⁹. The disiloxane **4** forms a hydrogen bonded trimeric cage as shown in Figure 4 and has average $\text{Si}-\text{O}-\text{Si}$ angles of $141.9(2)^\circ$ ³⁵. The highly hindered aluminosiloxane $[(2,6 - (i\text{-Pr})_2\text{C}_6\text{H}_3)\text{SiO}(\text{OH})_2]_2\text{Al}(\text{SiMe}_3)_3$ also has the SiOH groups in a *cis* arrangement, but the detail of the hydrogen bonding has not been reported³³. A further tetrahydroxydisiloxane, **10**, contains, unusually, two intramolecular hydrogen bonds between the silanol OH groups and a silyl ether oxygen of the $\text{Si}-(\text{O}i\text{-Bu})_3$ grouping. The molecules are further linked by intermolecular hydrogen bonds to form an infinite chain structure⁴⁶ as shown in Figure 5.

The cyclic bis-silanediol 1,1,5,5-tetraphenyl-3,3,7,7-tetrahydroxycyclotetrasiloxane forms hydrogen bonded dimeric units, similar to those in Figure 1c, which are also connected to two pyridine molecules²⁹³. These units are then hydrogen bonded together to form two types of independent infinite chains. Despite the fact that free hydrogen bonding sites are still available, there is no joining of the chains so as to form sheets as in $[t\text{-Bu}(\text{OH})_2\text{Si}]_2\text{O}$; this is presumably prevented by the steric requirements of the Ph substituents.

H. Compounds Containing an $\text{Si}(\text{OH})_3$ Group, Silanetriols

There has been a surge of interest in the chemistry of silanetriols in the last five years and a variety of different structure types have now been identified for them. These

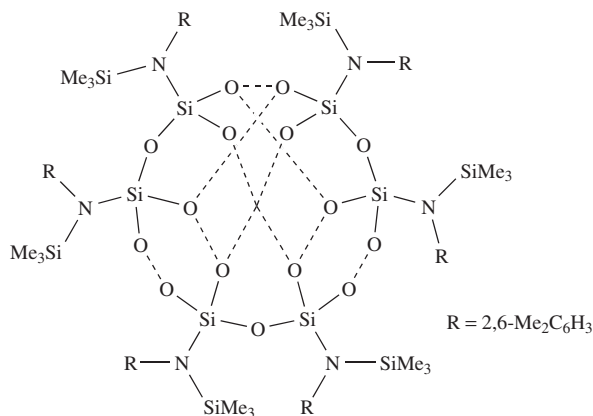


FIGURE 4. The hydrogen bonded cage formed by $\{[2,6\text{-Me}_2\text{C}_6\text{H}_3(\text{Me}_3\text{Si})\text{N}](\text{HO})_2\text{Si}\}_2\text{O}$

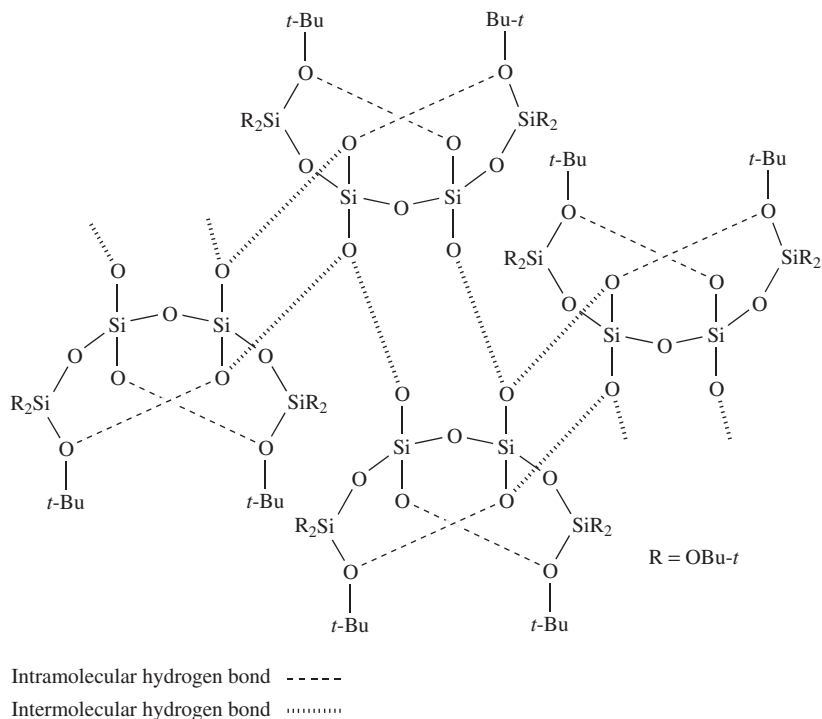


FIGURE 5. The hydrogen bonded network formed by $\{[t\text{-BuO}]_3\text{SiO}\}(\text{HO})_2\text{Si}_2\text{O}$

structures fall into several general types: discrete cages, double sheets and columns or tubes. Surprisingly, the metal substituted triol $\text{Os}[\text{Si}(\text{OH})_3]\text{Cl}(\text{CO})(\text{PPh}_3)_2$ shows no intermolecular hydrogen bonding, but it does have an intramolecular $\text{OH} \cdots \text{C}_{\text{aromatic}}$ distance of 3.17 Å and a band in the IR spectrum at 3616 cm^{-1} which suggest that there is an $\text{OH} \cdots \pi$ interaction¹⁹.

Several silanetriols containing a very bulky fourth substituent at silicon form discrete cage structures, extended networks of hydrogen bonds presumably being prevented by steric hindrance. Perhaps the bulkiest triol, $(\text{PhMe}_2\text{Si})_3\text{CSi}(\text{OH})_3$, has a tetrameric cage structure formed via $\text{OH} \cdots \text{OH}$ hydrogen bonds. Some of the potential hydrogen bonding sites are not used in this arrangement but there are several $\text{O} \cdots \text{C}_{\text{aromatic}}$ distances of less than 3.3 Å, indicative of $\text{OH} \cdots \pi$ interactions^{1,58}. The nitrogen substituted triol $(2,6\text{-}(i\text{-Pr})_2\text{C}_6\text{H}_3)\text{N}(\text{SiMe}_2\text{Pr-}i)\text{Si}(\text{OH})_3$ contains both intra- and inter-molecular hydrogen bonds and also has a structure based on tetrameric units³³.

The related silanetriols, $(\text{Me}_3\text{Si})_3\text{CSi}(\text{OH})_3$ and $(\text{Me}_3\text{Si})_3\text{SiSi}(\text{OH})_3$, have very similar structures to each other, comprising extensively hydrogen bonded hexameric cages^{38,294}. Every cage has a triangular arrangement of oxygen atoms at each end, each of which is surrounded by a six-membered ring of oxygen atoms. These two bowl-shaped units are joined by further hydrogen bonding to give five-membered rings of oxygens around the middle of the cage. The cage in $(\text{Me}_3\text{Si})_3\text{CSi}(\text{OH})_3$ is slightly shorter and wider than the silicon analogue, the distance between the triangular end faces being 6.7 and

7.2 Å, respectively. Finally, the cobalt cluster complex, $\text{Co}_3(\text{CO})_9\text{CSi}(\text{OH})_3$, forms an oval octameric cage, also extensively hydrogen bonded¹⁶.

The first silanetriol to be structurally characterized was *c*- $\text{C}_6\text{H}_{11}\text{Si}(\text{OH})_3$, which has a double sheet structure. This comprises two layers of molecules joined in a head-to-head manner so as to give a strongly hydrophilic layer containing all of the OH groups in the centre, which is surrounded by highly hydrophobic outer regions that prevent further interactions between different double sheets²⁹⁵. The structure of *t*- $\text{BuSi}(\text{OH})_3$ contains molecules that are joined by hydrogen bonds into double sheets with alternating *t*-Bu groups above and below the sheet which again prevent further hydrogen bonding⁵⁴. The pentamethylcyclopentadienyl derivative $\text{Cp}^*\text{Si}(\text{OH})_3$ crystallizes as a hemihydrate and forms a structure related to that of *t*- $\text{BuSi}(\text{OH})_3$, in that double sheets are formed in which alternating Cp^* groups are above and below the plane formed by the SiOH groups and the water molecules²¹ (Figure 6). The monohydrate (9-Me-9-fluoren-9-yl) $\text{Si}(\text{OH})_3 \cdot \text{H}_2\text{O}$ has a similar double sheet structure to that in $\text{Cp}^*\text{Si}(\text{OH})_3 \cdot 0.5\text{H}_2\text{O}$, but contains additional hydrogen bonding between water molecules²⁴.

Tubular or columnar hydrogen bonded structures are adopted by several silanetriols. The first example of this type of structure was found in (2,4,6- $\text{Me}_3\text{C}_6\text{H}_2$) $\text{N}(\text{SiMe}_3)\text{Si}(\text{OH})_3$ ³², which forms tubes containing a hydrophobic interior and hydrophobic exterior built by hydrogen bonding between four individual columns of triol molecules. Intramolecular hydrogen bonds are also present. A similar arrangement, but without the intramolecular hydrogen bonding, is found in $[\text{C}_5\text{H}_4(\text{SiMe}_3)]\text{Si}(\text{OH})_3$ ²². As well as forming the hydrate described above, (9-Me-9-fluoren-9-yl) $\text{Si}(\text{OH})_3$ forms two other hydrogen bonded adducts, (9-Me-9-fluoren-9-yl) $\text{Si}(\text{OH})_3 \cdot \text{EtOH} \cdot \text{H}_2\text{O}$ and (9-Me-9-fluoren-9-yl) $\text{Si}(\text{OH})_3 \cdot 2\text{MeOH}$, both of which form tubular structures²⁴. The adduct with water and ethanol comprises hydrogen bonded pairs of silanol molecules, which are joined by the solvent molecules to form the tube. In contrast, the methanol adduct contains no silanol-to-silanol hydrogen bonding.

The first compound, 1,4-bis(trihydroxysilyl)benzene, to be structurally characterized, containing two $\text{Si}(\text{OH})_3$ units, has been investigated by Rietveld analysis²⁹⁶. It has a complicated hydrogen bonded structure based on a double sheet layer reminiscent of *c*- $\text{C}_6\text{H}_{11}\text{Si}(\text{OH})_3$ and *t*- $\text{BuSi}(\text{OH})_3$, but in this case there is no hydrophobic region of the molecule at the opposite end to the $\text{Si}(\text{OH})_3$ group as here both ends of the molecule are hydrophilic trisilanol functions. Thus, the bilayers are joined to their neighbours by further hydrogen bonding to form a three-dimensional network.

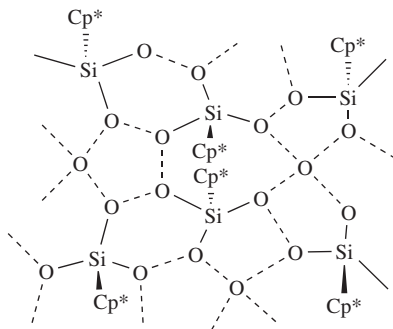


FIGURE 6. Part of the hydrogen bonded sheet structure of $[\text{Cp}^*\text{Si}(\text{OH})_3] \cdot 0.5\text{H}_2\text{O}$

The structures found for the silanetriols follow the same general trends seen earlier for compounds containing SiOH or Si(OH)₂ groups. Most of the structures of polysilanols are based around a strongly hydrogen bonded hydrophilic region which is surrounded by hydrophobic alkyl, aryl groups etc. so as to form extended sheets, tubes or three-dimensional networks. Larger substituents tend to reduce the extent of hydrogen bonding so that discrete units such as tetramers can be formed and, in limiting cases, no intermolecular hydrogen bonding is observed. A more detailed description of polysilanol structures can be found in Reference 1.

V. CONCLUSIONS

The study of polysilanols continues to thrive and to expand as more uses for them are found. The traditional notion that they are unstable species which spontaneously condense to give siloxanes has been replaced by an understanding of better ways to prepare and isolate them, together with the knowledge that the presence of large substituents will allow many novel structures to be stabilized. Very few of the polysilanols so far prepared contain a mixture of SiOH, Si(OH)₂ or Si(OH)₃ groups together in the same molecule [(HOMe₂Si)₃CSi(OH)₃ being a notable example], but such compounds are clearly available synthetically and they are likely to form novel structures and be useful new precursors to metal siloxides. The increasing interest in metal siloxide chemistry is particularly encouraging and the synthesis of tailor-made silanols designed as precursors to particular sized or shaped clusters or three-dimensional networks should provide an ongoing challenge for organosilicon chemists.

VI. ACKNOWLEDGEMENTS

The author wishes to thank Professor C. Eaborn for many interesting discussions about silanol chemistry and Dr. A. J. P. White for his assistance in the preparation of this article.

VII. REFERENCES

1. P. D. Lickiss, *Adv. Inorg. Chem.*, **42**, 147 (1995).
2. C. Eaborn, *Organosilicon Compounds*, Butterworths, London, 1960, pp. 276–277.
3. Reference 2, pp. 233–235.
4. C. H. Van Dyke, in *The Bond to Halogens and Halogenoids* (Ed. A. G. MacDiarmid), Marcel Dekker, New York, 1972, p. 167.
5. C. Eaborn, *J. Chem. Soc.*, 2840 (1952).
6. N. H. Buttrus, C. Eaborn, P. B. Hitchcock and A. K. Saxena, *J. Organomet. Chem.*, **284**, 291 (1985).
7. L. H. Sommer and L. J. Tyler, *J. Am. Chem. Soc.*, **76**, 1030 (1954).
8. M. Weidenbruch, H. Pesel and D. V. Hieu, *Z. Naturforsch.*, **35B**, 31 (1980).
9. T. Takiguchi, *J. Am. Chem. Soc.*, **81**, 2359 (1959).
10. G. I. Harris, *J. Chem. Soc.*, 5978 (1963).
11. G. Schott and W. D. Sprung, *Z. Anorg. Allg. Chem.*, **333**, 76 (1964).
12. P. D. George, L. H. Sommer and F. C. Whitmore, *J. Am. Chem. Soc.*, **75**, 1585 (1953).
13. R. Lehnert, in *Organosilicon Chemistry, From Molecules to Materials* (Eds. N. Auner and J. Weis), VCH, Weinheim, 1994, p. 71.
14. K. Hirabayashi, A. Mori, J. Kawashima, M. Sugaro, Y. Nishihara and T. Hiyama, *J. Org. Chem.*, **65**, 5342 (2000).
15. K. A. Lyssenko, T. V. Astapova, M. Yu. Antipin and N. N. Makarova, *Mendeleev Commun.*, 87 (1998).
16. U. Ritter, N. Winkhofer, H.-G. Schmidt and H. W. Roesky, *Angew. Chem., Int. Ed. Engl.*, **35**, 524 (1996).
17. D. Seyferth and C. L. Nivert, *J. Am. Chem. Soc.*, **99**, 5209 (1977).

18. W. Malisch, S. Schmitzer, G. Kaupp, K. Hindahl, H. Käß and U. Wachtler, in *Organosilicon Chemistry, From Molecules to Materials* (Eds. N. Auner and J. Weis), VCH, Weinheim, 1994, p. 185.
19. C. E. F. Rickard, W. R. Roper, D. M. Salter and L. J. Wright, *J. Am. Chem. Soc.*, **114**, 9682 (1992).
20. W. Malisch, H. Jehle, S. Möller, C. Saha-Möller and W. Adam, *Eur. J. Inorg. Chem.*, 1585 (1998).
21. P. Jutzi, G. Strassburger, M. Schneider, H.-G. Stammer and B. Neumann, *Organometallics*, **15**, 2842 (1996).
22. P. Jutzi, M. Schneider, H.-G. Stammer and B. Neumann, *Organometallics*, **16**, 5377 (1997).
23. M. J. MacLachlan, M. Ginzburg, J. Zheng, O. Knöll, A. J. Lough and I. Manners, *New J. Chem.*, 1409 (1998).
24. M. Schneider, B. Neumann, H.-G. Stammer and P. Jutzi, *Monatsh. Chem.*, **130**, 33 (1999).
25. T. V. Chogovadze, A. I. Nogaideli, L. M. Khananashvili, L. I. Nakaidze, V. S. Tskhovrebashvili, A. I. Gusev and D. U. Nesterov, *Proc. Acad. Sci. USSR*, **246**, 281 (1979); *Chem. Abstr.*, **91**, 123311p (1979).
26. C. Ackerhans, B. Räge, P. Müller, H. W. Roesky and I. Usón, *Eur. J. Inorg. Chem.*, 827 (2000).
27. M. G. Walawalkar, R. Murugavel and H. W. Roesky, in *Tailor-Made Silicon Oxygen Compounds* (Eds. R. Corriu and P. Jutzi), Vieweg, Braunschweig Weisbaden, 1996, p. 61.
28. R. Murugavel, V. Chandrasekhar and H. W. Roesky, *Acc. Chem. Res.*, **29**, 183 (1996).
29. R. Murugavel, A. Voigt, M. G. Walawalkar and H. W. Roesky, *Chem. Rev.*, **96**, 2205 (1996).
30. R. Murugavel, M. Bhattacharjee and H. W. Roesky, *Appl. Organomet. Chem.*, **13**, 227 (1999).
31. N. Winkhofer, A. Voigt, H. Dorn, H. W. Roesky, A. Steiner, D. Stalke and A. Reller, *Angew. Chem., Int. Ed. Engl.*, **33**, 1352 (1994).
32. R. Murugavel, V. Chandrasekhar, A. Voigt, H. W. Roesky, H.-G. Schmidt and M. Noltemeyer, *Organometallics*, **14**, 5298 (1995).
33. A. Klemp, H. Hatop, H. W. Roesky, H.-G. Schmidt and M. Noltemeyer, *Inorg. Chem.*, **38**, 5832 (1999).
34. V. Chandrasekhar, S. Nagendran and R. J. Butcher, *Organometallics*, **18**, 4488 (1999).
35. R. Murugavel, P. Böttcher, A. Voigt, M. G. Walawalkar, H. W. Roesky, E. Parisini, M. Teichert and M. Noltemeyer, *J. Chem. Soc., Chem. Commun.*, 2417 (1996).
36. C. Eaborn, D. A. R. Happer, K. D. Safa and D. R. M. Walton, *J. Organomet. Chem.*, **157**, C50 (1978).
37. C. Eaborn, D. A. R. Happer and K. D. Safa, *J. Organomet. Chem.*, **191**, 355 (1980).
38. S. S. Al-Juaid, N. H. Buttrus, R. I. Damja, Y. Derouiche, C. Eaborn, P. B. Hitchcock and P. D. Lickiss, *J. Organomet. Chem.*, **371**, 287 (1989).
39. J. D. Birchall, J. G. Carey and A. J. Howard, *Nature*, **266**, 154 (1977).
40. A. M. A. Aisa, D. Krätzer and H. Richter, *Pharmazie*, **53**, 751 (1998).
41. L. Párkányi, H. Stüger and E. Hengge, *J. Organomet. Chem.*, **333**, 187 (1987).
42. Y. E. Ovchinnikov, V. E. Shklover, Yu. T. Struchkov, V. V. Dement'ev, T. M. Frunze and B. A. Antipova, *J. Organomet. Chem.*, **335**, 157 (1987).
43. D. Schmidt-Bäse and U. Klingebiel, *Z. Naturforsch.*, **44B**, 395 (1989).
44. G. Schott and H. U. Kibbel, *Z. Anorg. Allg. Chem.*, **311**, 53 (1961).
45. Y. Abe and I. Kijima, *Bull. Chem. Soc. Jpn.*, **42**, 1118, (1969).
46. R. Rulkens, M. P. Coles and T. D. Tilley, *J. Chem. Soc., Dalton Trans.*, 627 (2000).
47. J. F. Brown Jr. and L. H. Vogt Jr., *J. Am. Chem. Soc.*, **87**, 4313 (1965).
48. F. J. Feher, D. A. Newman and J. F. Walzer, *J. Am. Chem. Soc.*, **111**, 1741 (1989).
49. E. Wiberg and W. Simmler, *Z. Anorg. Allg. Chem.*, **282**, 330 (1955).
50. M. Unno, A. Suto, K. Takada and H. Matsumoto, *Bull. Chem. Soc. Jpn.*, **73**, 215 (2000).
51. M. Unno, K. Takada and H. Matsumoto, *Chem. Lett.*, 489 (1998).
52. K. Hirabayashi, A. Mori, J. Kawashima, M. Sugaro, Y. Nishihara and T. Hiyama, *J. Org. Chem.*, **65**, 5342 (2000).
53. F. J. Feher, J. J. Schwab, D. Soulivong and J. W. Ziller, *Main Group Chem.*, **2**, 123 (1997).
54. N. Winkhofer, H. W. Roesky, M. Noltemeyer and W. T. Robinson, *Angew. Chem., Int. Ed. Engl.*, **31**, 599 (1992).
55. P. D. Lickiss, S. A. Litster, A. D. Redhouse and C. A. Wisener, *J. Chem. Soc., Chem. Commun.*, 173 (1991).

56. A. Mazeaud, Y. Dromzee and R. Thouvenout, *Inorg. Chem.*, **39**, 4735 (2000).
57. C. Eaborn, P. B. Hitchcock and P. D. Lickiss, *J. Organomet. Chem.*, **252**, 281 (1983).
58. S. M. Whittaker, PhD thesis, University of Salford, 1993.
59. C. Eaborn and P. D. Lickiss, *J. Organomet. Chem.*, **294**, 305 (1985).
60. C. Eaborn and D. E. Reed, *J. Chem. Soc., Perkin Trans. 2*, 1687 (1985).
61. R. I. Damja and C. Eaborn, *J. Organomet. Chem.*, **290**, 267 (1985).
62. Z. H. Aiube, N. H. Buttrus, C. Eaborn, P. B. Hitchcock and J. A. Zora, *J. Organomet. Chem.*, **292**, 177 (1985).
63. R. West and E. K. Pham, *J. Organomet. Chem.*, **403**, 43 (1991).
64. G. Sawitzki, H. G. v. Schnering, D. Kummer and T. Seshadri, *Chem. Ber.*, **111**, 3705 (1978).
65. K. L. Mittal (Ed.), *Silanes and Other Coupling Agents*, VSP, Utrecht, 1992; E. P. Pluddeman, *Silane Coupling Agents*, Plenum Press, New York, 1st edn., 1982; 2nd edn., 1990.
66. J. J. Lebrun and H. Porte, in *Comprehensive Polymer Science* (Eds. G. Allen and J. C. Bevington), Vol. 5, Pergamon, Oxford, 1989, p. 593.
67. F. O. Stark, J. R. Falender and A. P. Wright, in *Comprehensive Organometallic Chemistry*, (Eds. G. Wilkinson, F. G. A. Stone and E. W. Abel), Pergamon, Oxford, 1982; S. J. Clarson and J. A. Semlyen (Eds.), *Siloxane Polymers*, Ellis Horwood-PTR Prentice-Hall, Englewood Cliffs, NJ, 1993.
68. J. M. Zeigler and F. W. G. Fearon (Eds.), *Silicon Based Polymer Science*, American Chemical Society, Washington, DC, 1990.
69. S. Rubinsztajn, M. Cypryk and J. Chojnowski, *J. Organomet. Chem.*, **367**, 27 (1989).
70. M. Guibergia-Pierron and G. Sauvet, *Eur. Polym. J.*, **28**, 29 (1992).
71. G. Helary and G. Sauvet, *Eur. Polym. J.*, **28**, 37 (1992).
72. K. Kazmierski, J. Chojnowski and J. McVie, *Eur. Polym. J.*, **30**, 515 (1994).
73. See, for example, the 'Proceedings of the Fourth, Fifth, and Sixth International Workshops on Glasses and Ceramics From Gels', published in *J. Non-Cryst. Solids*, **100** (1988); **121** (1990); and **147/148** (1992).
74. J. Chojnowski, M. Cypryk, K. Kazmierski and K. Rózga, *J. Non-Cryst. Solids*, **125**, 40 (1990).
75. L. L. Hench and J. K. West, *Chem. Rev.*, **90**, 33 (1990); and numerous articles in M. J. Hampden-Smith, W. G. Klemperer and C. J. Brinker (Eds.), *Better Ceramics Through Chemistry V*, Vol. 271, Materials Research Society, Pittsburgh, 1992.
76. K. A. Smith, *J. Org. Chem.*, **51**, 3827 (1986).
77. F. D. Osterholz and E. R. Pohl, *J. Adhes. Sci. Tech.*, **6**, 127 (1992).
78. D. J. Oostendorp, G. L. Bertrand and J. O. Stoffer, *J. Adhes. Sci. Tech.*, **6**, 171 (1992).
79. B. Arkles, J. R. Steinmetz, J. Zazyczny and P. Mehta, *J. Adhes. Sci. Tech.*, **6**, 193 (1992).
80. J. F. Hyde, *J. Am. Chem. Soc.*, **75**, 2166 (1953).
81. J. Chojnowski and S. Chrzczonowicz, *Bull. Acad. Pol. Sci. Chem. Ser.*, **13**, 143 (1965); *Chem. Abstr.*, **63**, 9789d (1965).
82. L. W. Breed and R. L. Elliott, *J. Organomet. Chem.*, **9**, 188 (1967).
83. W. R. Sorenson and T. W. Campbell, *Preparative Methods of Polymer Chemistry*, 2nd edn., Wiley, New York, 1968, p. 187.
84. W. J. Patterson, S. P. McManus and C. U. Pittman, *J. Polym. Sci. Polym. Chem.*, **12**, 837 (1974).
85. D. M. L. Goodgame, P. D. Lickiss, S. Menzer and D. J. Williams, *J. Organomet. Chem.*, **593–594**, 161 (2000).
86. Z. Michalska and Z. Lasocki, *Bull. Acad. Pol. Sci. Ser. Chem.*, **19**, 757 (1971); *Chem. Abstr.*, **76**, 139817j (1972).
87. J.-Y. Zheng, K. Konishi and T. Aida, *Chem. Lett.*, 453 (1998).
88. S. Varaprath, K. L. Salyers, K. P. Plotzke and S. Nanavati, *Drug Metab. Disp.*, **27**, 1267 (1999).
89. M. Yoshizawa, T. Kusukawa, M. Fujita and K. Yamaguchi, *J. Am. Chem. Soc.*, **122**, 6311 (2000).
90. F. J. Feher, R. Terroba and R.-Z. Jin, *J. Chem. Soc., Chem. Commun.*, 2513 (1999).
91. F. J. Feher, R. Terroba and J. W. Ziller, *J. Chem. Soc., Chem. Commun.*, 2153 (1999).
92. F. J. Feher, R. Terroba and J. W. Ziller, *J. Chem. Soc., Chem. Commun.*, 2309 (1999).
93. K. A. Andrianov and A. A. Zhdanov, *Proc. Acad. Sci. USSR*, **114**, 597 (1957); *Chem. Abstr.*, **52**, 3675a (1958).

94. S. McN. Sieburth, T. Nittoli, A. M. Mutathi and L. Guo, *Angew. Chem., Int. Ed. Engl.*, **37**, 812 (1998).
95. M. G. Voronkov, N. G. Sviridova and S. N. Borisov, *J. Gen. Chem. USSR*, **39**, 1959 (1969); *Chem. Abstr.*, **72**, 3192q (1970).
96. K. A. Andrianov, A. A. Zhdanov and E. F. Morgunova, *J. Gen. Chem. USSR*, **27**, 173 (1957); *Chem. Abstr.*, **51**, 12845f (1957).
97. M. F. Shostakovskiy and Kh. I. Kondratyev, *Bull. Acad. Sci. USSR*, 985 (1956); *Chem. Abstr.*, **51**, 4983b (1957).
98. A. Jansen, H. Görls and S. Pitter, *Organometallics*, **19**, 135 (2000).
99. G. A. Ayoko and C. Eaborn, *J. Chem. Soc. Perkin Trans. 2*, 1047 (1987).
100. W. Uhlig, *Z. Anorg. Allg. Chem.*, **618**, 144 (1992).
101. S. S. Dua and C. Eaborn, *J. Organomet. Chem.*, **204**, 21 (1981).
102. C. Eaborn and F. M. S. Mahmoud, *J. Chem. Soc., Perkin Trans. 2*, 1309 (1981).
103. C. Eaborn, P. D. Lickiss and A. D. Taylor, *J. Organomet. Chem.*, **340**, 283 (1988).
104. C. Eaborn, Y. Y. El-Kaddar and P. D. Lickiss, *Inorg. Chim. Acta*, **198–200**, 337 (1992).
105. C. Eaborn, Y. Y. El-Kaddar and P. D. Lickiss, *J. Chem. Soc., Chem. Commun.*, 1450 (1983).
106. C. Eaborn, P. B. Hitchcock and P. D. Lickiss, *J. Organometal. Chem.*, **264**, 119 (1984).
107. Y. Nagai, K. Honda and T. Migita, *J. Organomet. Chem.*, **8**, 372 (1967).
108. P. D. Lickiss and R. Lucas, *J. Organomet. Chem.*, **521**, 229 (1995).
109. R. J. Ouellette and D. L. Marks, *J. Organomet. Chem.*, **11**, 407 (1968).
110. L. Spialter, L. Pazdernik, S. Bernstein, W. A. Swansiger, G. R. Buell and M. E. Freeburger, *J. Am. Chem. Soc.*, **93**, 5682 (1971).
111. E. M. Dexheimer and L. Spialter, *J. Organomet. Chem.*, **102**, 21 (1975).
112. Yu. A. Aleksandrov and B. I. Tarunin, *Russ. Chem. Rev.*, **46**, 905 (1977); *Chem. Abstr.*, **88**, 5648u (1978).
113. Yu. A. Alexandrov, *J. Organomet. Chem.*, **238**, 1 (1982).
114. W. Adam, U. Azzena, F. Prechtel, K. Hindahl and W. Malisch, *Chem. Ber.*, **125**, 1409 (1992).
115. W. Malisch, R. Lankat, S. Schmitzer and J. Reising, *Inorg. Chem.*, **34**, 5701 (1995).
116. W. Malisch, R. Lankat, O. Fey, J. Reising and S. Schmitzer, *J. Chem. Soc., Chem. Commun.*, 1917 (1995).
117. C. A. Morrison, D. W. H. Rankin, E. E. Robertson, P. D. Lickiss and P. C. Masangane, *J. Chem. Soc., Dalton Trans.*, 2293 (1999).
118. P. C. Masangane, PhD. Thesis, Imperial College, London, 1999.
119. M. A. Said, H. W. Roesky, C. Rennekamp, M. Andruh, H.-G. Schmidt and M. Noltemeyer, *Angew. Chem., Int. Ed. Engl.*, **38**, 661 (1999).
120. Reference 2, p. 200.
121. E. Wiberg and E. Amberger, *Hydrides of the Elements of Main Groups I–IV*, Elsevier, Amsterdam, 1971, p. 526.
122. C. U. Pittman Jr., W. J. Patterson and S. P. McManus, *J. Polym. Sci.*, **13**, 39 (1975).
123. W. J. Patterson, S. P. McManus and C. U. Pittman Jr., *Macromol. Synth.*, **6**, 99 (1977).
124. R. L. Merker and M. J. Scott, *J. Polym. Sci. A2*, 15 (1964).
125. C. U. Pittman Jr., W. J. Patterson and S. P. McManus, *J. Polym. Sci., Polym. Chem.*, **14**, 1715 (1976).
126. G. H. Barnes Jr. and N. E. Daughenbaugh, *J. Org. Chem.*, **31**, 885 (1966).
127. P. I. Coupar, P.-A. Jaffrès and R. E. Morris, *J. Chem. Soc., Dalton Trans.*, 2183 (1999).
128. U. Schubert and C. Lorenz, *Inorg. Chem.*, **36**, 1258 (1997).
129. R. O. Sauer, *J. Am. Chem. Soc.*, **66**, 1707 (1944).
130. C. S. Miner Jr., L. A. Bryan, R. P. Holysz Jr. and G. W. Pedlow Jr., *Ind. Eng. Chem.*, **39**, 1368 (1947).
131. G. Maas and S. Bender, *Synthesis*, 1175 (1999).
132. D. L. Bailey and A. N. Pines, *Ind. Eng. Chem.*, **46**, 2363 (1954).
133. L. H. Sommer, G. M. Goldberg, E. Dorfman and F. C. Whitmore, *J. Am. Chem. Soc.*, **68**, 1083 (1946).
134. L. H. Sommer and G. A. Baughman, *J. Am. Chem. Soc.*, **83**, 3346 (1961).
135. W. Zimmermann, *Chem. Ber.*, **87**, 887 (1954).
136. F. W. G. Fearon and H. Gilman, *J. Organomet. Chem.*, **6**, 577 (1966).
137. J. Carilla, L. Fajará, L. Juliá, J. Riera, J. Lloveras, N. Verdager and I. Fita, *J. Organomet. Chem.*, **423**, 163 (1992).

138. P. J. Morris, F. W. G. Fearon and H. Gilman, *J. Organomet. Chem.*, **9**, 427 (1967).
139. R. Murugavel, A. Voigt, V. Chandrasekhar, H. W. Roesky, H. G. Schmidt and M. Noltemeyer, *Chem. Ber.*, **129**, 391 (1996).
140. A. Voigt, R. Murugavel, H. W. Roesky and H.-G. Schmidt, *J. Mol. Struct.*, **436–437**, 49 (1997).
141. F. J. Feher and D. A. Newman, *J. Am. Chem. Soc.*, **112**, 1931 (1990).
142. M. J. MacLachlan, J. Zheng, A. J. Lough, I. Manners, C. Mordas, R. LeSeur, W. E. Geiger, L. M. Liable-Sands and A. L. Rheingold, *Organometallics*, **18**, 1337 (1999).
143. A. Mazzah, A. Haudi-Mazzah, M. Noltemeyer and H. W. Roesky, *Z. Anorg. Allg. Chem.*, **604**, 93 (1991).
144. F. J. Feher, S. H. Phillips and J. W. Ziller, *J. Chem. Soc., Chem. Commun.*, 829 (1997).
145. M. Wiebecke, J. Emmer and J. Felsche, *Microporous Mater.*, **4**, 149 (1995).
146. R. K. Harris, J. A. K. Howard, A. Samadi-Maybodi and J. Wen Yao, *J. Solid State Chem.*, **120**, 231 (1995).
147. J. Beckmann, K. Jurkschat, D. Müller, S. Rabe and M. Schürmann, *Organometallics*, **18**, 2326 (1999).
148. J. Annand, H. C. Aspinall and A. Steiner, *Inorg. Chem.*, **38**, 3941 (1999).
149. F. Luderer, H. Reinke and H. Oehme, *Z. Anorg. Allg. Chem.*, **624**, 1519 (1998).
150. S. S. Al-Juaid, C. Eaborn, P. B. Hitchcock, P. D. Lickiss, A. Möhrke and P. Jutz, *J. Organomet. Chem.*, **384**, 33 (1990).
151. J. A. Tossell and N. Sahai, *Geochim. Cosmochim. Acta*, **64**, 4097 (2000).
152. M. A. Brook, *Silicon in Organic, Organometallic and Polymer Chemistry*, Wiley-Interscience, New York, 2000, pp. 29–35.
153. L. H. Sommer, E. W. Pietrusza and F. C. Whitmore, *J. Am. Chem. Soc.*, **68**, 2282 (1946).
154. R. M. Badger and S. H. Bauer, *J. Chem. Phys.*, **5**, 839 (1937).
155. R. West and R. H. Baney, *J. Am. Chem. Soc.*, **81**, 6145 (1959).
156. U. B. Mioc, Lj. J. Bogunovic, S. V. Ribnikar and M. D. Dragojevic, *J. Mol. Struct.*, **177**, 379 (1988).
157. E. A. Williams, J. D. Cargioli and R. W. Larochelle, *J. Organomet. Chem.*, **108**, 153 (1976).
158. J. F. Hampton, C. W. Lacefield and J. F. Hyde, *Inorg. Chem.*, **4**, 1659 (1965).
159. A. G. Brook and K. H. Pannell, *J. Organomet. Chem.*, **8**, 179 (1967).
160. G. J. Peddle, R. J. Woznow and S. G. McGeachin, *J. Organomet. Chem.*, **17**, 331 (1969).
161. A. P. Kreshkov, V. F. Andrianov and V. A. Drozdov, *Russ. J. Phys. Chem.*, **46**, 1605 (1972); *Chem. Abstr.*, **78**, 146953v (1973).
162. A. Voigt, R. Murugavel, U. Ritter and H. W. Roesky, *J. Organomet. Chem.*, **521**, 279 (1996).
163. A. W. Jarvie, A. Holt and J. Thompson, *J. Organomet. Chem.*, **11**, 623 (1968).
164. M. Cypryk, *J. Organomet. Chem.*, **545–546**, 483 (1997).
165. Reference 152, pp. 324–331.
166. H. R. Kricheldorf, in *Silicon in Polymer Synthesis* (Ed. H. R. Kricheldorf), Springer, Berlin, 1996 p. 404; D. E. Leydon (Ed.), *Silanes, Surfaces and Interfaces*, Gordon and Breach, Amsterdam, 1986.
167. R. K. Iler, *The Chemistry of Silica: Solubility, Polymerization., Colloid and Surface Properties, and Biochemistry*, Wiley, New York, 1979; H. Bergna (Ed.), *The Colloid Chemistry of Silica*, American Chemical Society (ACS Adv. Chem. Ser., no. 234), Washington, DC, 1994; E. F. Vansant, P. Van Der Voort and K. C. Vrancken, in *Studies in Surface Science and Catalysis* (Eds. B. Delmon and J. T. Yates), Vol. **93**, Elsevier, Amsterdam, 1995.
168. R. H. Baney, M. Itoh, A. Sakakibara and T. Suzuki, *Chem. Ber.*, **95**, 1409 (1995).
169. G. Cerveau and R. J. P. Corriu, *Coord. Chem. Rev.*, **178–180**, 1051 (1998).
170. M. Unno, S. Bahri Alias, M. Arai, K. Takada, R. Tanaka and H. Matsumoto, *Appl. Organomet. Chem.*, **13**, 303 (1999).
171. B. Arkles, in *Kirk-Othmer Encyclopedia of Chemical Technology*, 4th edition, (Eds. J. I. Kroschwitz and M. Howe-Grant), Vol. 22, Wiley Interscience, New York, 1997, p. 69.
172. D. Avnir, L. C. Klein, D. Levy, Y. Schubert and A. B. Wojcik, in *The Chemistry of Organic Silicon Compounds* (Eds. Z. Rappoport and Y. Apeloig), Vol. 2, Wiley, Chichester, 1998, p. 2317.
173. G. L. Wilkes, H.-H. Huang and R. H. Glaser, in *Silicon-based Polymer Science: A Comprehensive Resource* (Eds. J. M. Zeigler and F. W. G. Fearon), American Chemical Society (ACS Adv. Chem. Ser., no. 224), Washington, DC, 1990, p. 207.

174. M. A. Mauritz and J. T. Payne, *J. Membrane Sci.*, **168**, 39 (2000).
175. M. J. Adeogun and J. N. Hay, *Chem. Mater.*, 767 (2000).
176. B. Boury and R. J. P. Corriu, *Adv. Mater.*, **12**, 989 (2000).
177. D. A. Loy and K. J. Shea, *Chem. Rev.*, **95**, 1431 (1995).
178. G. Cerveau, R. J. P. Corriu and E. Framery, *J. Chem. Soc., Chem. Commun.*, 2081 (1999).
179. R. J. P. Corriu, *Angew. Chem., Int. Ed. Engl.*, **39**, 1376 (2000).
180. O. Graalman and U. Klingebiel, *J. Organomet. Chem.*, **275**, C1 (1984).
181. V. M. Kopylov, L. M. Khananahvili, O. V. Shkol'nik and A. G. Ivanov, *Vysokomolekulyarnye Soedineniya, Ser. A*, **37**, 565 (1995); *Engl. Transl.: Polymer Sci., Ser. A*, **37**, 242 (1995); *Chem. Abstr.*, **123**, 144671a (1995).
182. P. V. Ivanov, *Vysokomolekulyarnye Soedineniya, Ser. A*, **37**, 417 (1995); *Engl. Transl.: Polymer Sci., Ser. A*, **37**, 266 (1995); *Chem. Abstr.*, **123**, 144672b (1995).
183. M. G. Voronkov, E. A. Maletina and V. K. Roman, *Heterosiloxanes Volume 1: Derivatives of Non-Biogenic Elements*, Harwood Academic Publishers, Reading, UK, 1988.
184. L. King and A. C. Sullivan, *Coord. Chem. Rev.*, **189**, 19 (1999).
185. M. B. Hursthouse, M. Motevalli, M. Sanganee and A. C. Sullivan, *J. Organomet. Chem.*, **381**, 293 (1990).
186. M. Motevalli, D. Shah and A. C. Sullivan, *J. Chem. Soc., Dalton Trans.*, 2849 (1993).
187. M. Motevalli, D. Shah and A. C. Sullivan, *J. Organomet. Chem.*, **513**, 239 (1996).
188. I. Abrahams, M. Lazell, M. Motevalli, S. A. A. Shah and A. C. Sullivan, *J. Organomet. Chem.*, **553**, 23 (1998).
189. B. Laermann, M. Lazell, M. Motevalli and A. C. Sullivan, *J. Chem. Soc., Dalton Trans.*, 1263 (1997).
190. J. Brisdon, M. F. Mahon, K. C. Molloy and P. J. Schofield, *J. Organomet. Chem.*, **465**, 145 (1994).
191. J. Beckmann, K. Jurkschat, D. Schollmeyer and M. Schürmann, *J. Organomet. Chem.*, **543**, 229 (1997).
192. K. A. Andrianov, N. A. Kurasheva and L. I. Kuteinikova, *Zh. Obshch. Khim.*, **46**, 1533 (1976); *Chem. Abstr.*, **85**, 177526g (1976).
193. D. Hoebbel, M. Nacken, H. Schmidt, V. Huch and M. Veith, *J. Mater. Chem.*, **8**, 171 (1998).
194. M. Wieber, M. Schröpf and U. Simonis, *Phosphorous Sulfur Silicon*, **104**, 215 (1995).
195. L. King, M. Motevalli and A. C. Sullivan, *J. Chem. Soc., Chem. Commun.*, 1357 (2000).
196. V. Lorenz, A. Fischer, K. Jacob, W. Bruser, T. Gelbrich, P. G. Jones and F. T. Edelman, *J. Chem. Soc., Chem. Commun.*, 2217 (1998).
197. H.-G. Gosink, H. W. Roesky, H.-G. Schmidt, M. Noltemeyer, E. Irmer and R. H. Irmer, *Organometallics*, **13**, 3420 (1994).
198. B. J. O'Leary, T. R. Spalding and G. Ferguson, *Polyhedron*, **18**, 3135 (1999).
199. M. Crocker, R. H. M. Herold and A. G. Orpen, *J. Chem. Soc., Chem. Commun.*, 2411 (1997).
200. H. C. L. Abbenhuis, A. D. Burrows, H. Kooijman, M. Lutz, M. T. Palmer, R. A. van Santen and A. L. Spek, *J. Chem. Soc., Chem. Commun.*, 2627 (1998).
201. H. C. L. Abbenhuis, *Chem., A Eur. J.*, **6**, 25 (2000).
202. R. Duchateau, R. A. van Santen and G. P. A. Yap, *Organometallics*, **19**, 809 (2000).
203. S. Krijen, R. J. Harmsen, H. C. L. Abbenhuis, J. H. C. van Hooff and R. A. van Santen, *J. Chem. Soc., Chem. Commun.*, 501 (1999).
204. F. J. Feher and T. A. Budzichowski, *Polyhedron*, **14**, 3239 (1995).
205. S. Shambayati, J. F. Blake, S. G. Wierschke, W. L. Jorgenson and S. L. Schrieber, *J. Am. Chem. Soc.*, **112**, 697 (1990).
206. F. J. Feher, T. A. Budzichowski, K. Rahimian and J. W. Ziller, *J. Am. Chem. Soc.*, **114**, 3859 (1992).
207. F. J. Feher, S. L. Gonzales and J. W. Ziller, *Inorg. Chem.*, **27**, 3440 (1988).
208. F. J. Feher and J. F. Walzer, *Inorg. Chem.*, **29**, 1604 (1990).
209. M. Veith, M. Jarczyk and V. Huch, *Angew. Chem., Int. Ed. Engl.*, **36**, 117 (1997).
210. V. A. Zeitler and C. A. Brown, *J. Am. Chem. Soc.*, **79**, 4618 (1957).
211. M. B. Hursthouse and M. A. Hussain, *Polyhedron*, **3**, 95 (1984).
212. H. Puff, M. P. Böckmann, T. R. Kök and W. Schuh, *J. Organomet. Chem.*, **268**, 197 (1984).
213. H. Puff, T. R. Kök, P. Nuroth and W. Schuh, *J. Organomet. Chem.*, **281**, 141 (1985).
214. F.-Q. Liu, I. Usón and H. W. Roesky, *J. Chem. Soc., Dalton Trans.*, 2453 (1995).

215. H.-G. Gosink, H. W. Roesky, M. Noltemeyer, H.-G. Schmidt, C. Freire-Erdbrügger and G. M. Sheldrick, *Chem. Ber.*, **126**, 279 (1993).
216. H. W. Roesky, A. Mazzah, D. Hesse and M. Noltemeyer, *Chem. Ber.*, **124**, 519 (1991).
217. A. I. Gouzyr, H. Wessel, C. E. Barnes, H. W. Roesky, M. Teichert and I. Usón, *Inorg. Chem.*, **36**, 3392 (1997).
218. I. Hargittai and H. M. Seip, *Acta Chem. Scand.*, **A30**, 153 (1976).
219. Y. Apeloig and A. Stanger, *J. Organomet. Chem.*, **346**, 305 (1988).
220. Y. Apeloig, in *The Chemistry of Organic Silicon Compounds* (Eds. S. Patai and Z. Rappoport), Part 1, Wiley, Chichester, 1989, p. 79.
221. A. E. Reed, C. Schade, P. v. R. Schleyer, P. V. Kamath, and J. Chandrasekhar, *J. Chem. Soc., Chem. Commun.*, 67 (1988).
222. A. C. Hess, P. F. McMillan and M. O'Keeffe, *J. Phys. Chem.*, **91**, 1395 (1987).
223. W. R. Hertler, D. A. Dixon, E. W. Matthews, F. Davidson and F. G. Kitson, *J. Am. Chem. Soc.*, **109**, 6532 (1987).
224. G. V. Gibbs, *Am. Mineral.*, **67**, 421 (1982).
225. S. E. Johnson, J. A. Deiters, R. O. Day and R. R. Holmes, *J. Am. Chem. Soc.*, **111**, 3250 (1989).
226. M. O'Keeffe, B. Domengès and G. V. Gibbs, *J. Phys. Chem.*, **89**, 2304 (1985).
227. G. V. Gibbs and M. B. Boisen, in *The Chemistry of Organic Silicon Compounds* (Eds. Z. Rappoport and Y. Apeloig), Vol. 2, Part 1, Wiley, Chichester, 1998, pp. 103–118.
228. W. S. Sheldrick, in *The Chemistry of Organic Silicon Compounds* (Eds. S. Patai and Z. Rappoport), Part 1, Wiley, Chichester, 1989, p. 277.
229. M. Kaftory, M. Kapon and M. Botoshansky, in *The Chemistry of Organic Silicon Compounds* (Eds. Z. Rappoport and Y. Apeloig), Vol. 2, Part 1, Wiley, Chichester, 1998, pp. 181–265.
230. B. T. Luke, J. A. Pople, M.-B. Krogh-Jespersen, Y. Apeloig, J. Chandrasekhar and P. v. R. Schleyer, *J. Am. Chem. Soc.*, **108**, 260 (1986).
231. P. D. Lickiss, A. D. Redhouse, R. J. Thompson, W. A. Stanczyk and K. Rózga, *J. Organomet. Chem.*, **453**, 13 (1993).
232. A. P. Polishchuk, T. V. Timofeeva, N. N. Makarova, M. Yu. Antipin and Yu. T. Struchkov, *Liq. Cryst.*, **9**, 433 (1991).
233. A. P. Polishchuk, M. Yu. Antipin, T. V. Timofeeva, N. N. Makarova, N. A. Golovina and Yu. T. Struchkov, *Sov. Phys. Cryst.*, **36**, 50 (1991); *Chem. Abstr.*, **114**, 218655m (1991).
234. A. P. Polishchuk, N. N. Makarova, M. Yu. Antipin, T. V. Timofeeva, M. A. Kravers and Yu. T. Struchkov, *Sov. Phys. Cryst.*, **35**, 258 (1990); *Chem. Abstr.*, **113**, 32311 (1990).
235. M. A. Hossain and M. B. Hursthouse, *J. Cryst. Spectrosc. Res.*, **18**, 227 (1988).
236. V. E. Shklover, Yu. T. Struchkov, I. V. Karpova, V. A. Odinet, and A. A. Zhdanov, *Zh. Strukt. Khim. (Engl. Transl.)*, **26**, 251 (1985); *Chem. Abstr.*, **104**, 509098 (1986).
237. W. Clegg, *Acta Crystallogr.*, **C39**, 901 (1983).
238. P. D. Lickiss, R. Drake and D. J. Williams, unpublished results.
239. L. M. Khananashvili, Ts. N. Vardosanidze, G. Z. Griunova, V. E. Shklover, Yu. T. Struchkov, E. G. Markarashvili and M. Sh. Tsutsunava, *Izv. Akad. Nauk Gruz. SSR, Ser. Khim.*, **10**, 262 (1984); *Chem. Abstr.*, **103**, 87950b (1985).
240. Yu. E. Ovchinnikov, I. A. Zamaev, Yu. T. Struchkov, T. V. Astapova and A. A. Zhdanov, *Organomet. Chem. USSR*, **2**, 452 (1989); *Chem. Abstr.*, **112**, 46056g (1990).
241. A. P. Polishchuk, T. V. Timofeeva, M. Yu. Antipin, N. N. Makarova, N. A. Golovina, Yu. T. Struchkov and O. D. Lavrentovich, *Organomet. Chem. USSR*, **4**, 77 (1991); *Chem. Abstr.*, **114**, 218706d (1991).
242. N. N. Makarova, N. N. Kuz'min, Yu. K. Godovskii and E. V. Matukhina, *Proc. Acad. Sci. USSR*, **300**, 151 (1988); *Chem. Abstr.*, **109**, 120233u (1988).
243. A. P. Polishchuk, N. N. Makarova, T. V. Timofeeva, M. Yu. Antipin, O. D. Lavrentovich, N. A. Golovina, G. A. Puchkovskaya, Yu. T. Struchkov and Yu. K. Godovskii, *Sov. Phys. Crystallogr.*, **35**, 261 (1990); *Chem. Abstr.*, **113**, 32358 (1990).
244. K. Yu. Suponitskii, T. V. Timofeeva and Yu. T. Struchkov., *Russ. Chem. Bull.*, **44**, 1643 (1995); *Chem. Abstr.*, **124**, 289640v (1996).
245. S. Dobros, E. Mátrai and E. Castéllucci, *J. Mol. Struct.*, **43**, 141 (1978).
246. K. A. Ruud, J. S. Sepeda, F. A. Tibbals and D. C. Hrnčir, *J. Chem. Soc., Chem. Commun.*, 629 (1991).

247. B. O'Leary, T. R. Spalding, G. Ferguson and C. Glidewell, *Acta Crystallogr.*, **B56**, 273 (2000).
248. L. D. Cother, PhD Thesis, Imperial College, London, 1998.
249. W. Ando, M. Kako, T. Akasaka and S. Nagase, *Organometallics*, **12**, 1514 (1993).
250. M. A. Hossain, M. T. Rahman, G. Rasul, M. B. Hursthouse and B. Hussain, *Acta Crystallogr.*, **C44**, 1318 (1988).
251. N. Auner, R. Probst, C.-R. Heikenwälder, E. Herdtweck, S. Gamper and G. Müller, *Z. Naturforsch.*, **48B**, 1625 (1993).
252. A. Chandrasekaran, R. O. Day and R. R. Holmes, *Organometallics*, **15**, 3189 (1996).
253. H. Behbehani, B. J. Brisdon, M. F. Mahon, K. C. Molloy, and M. Mazhar, *J. Organomet. Chem.*, **463**, 41 (1993).
254. O. Graalmann, U. Klingebiel, W. Clegg, M. Haase and G. M. Sheldrick, *Chem. Ber.*, **117**, 2988 (1984).
255. V. E. Shklover, I. L. Dubchak, Yu. T. Struchkov, V. P. Mileshekovich, G. A. Nikolaev and Yu. V. Tsiganov, *J. Struct. Chem.*, **22**, 225 (1981); *Chem. Abstr.*, **95**, 81098z (1981).
256. N. G. Furmanova, V. I. Andrianov and N. N. Makarova, *J. Struct. Chem.*, **28**, 256 (1987); *Chem. Abstr.*, **107**, 166091h (1987).
257. See footnote 13 in Reference 141.
258. See footnote 13 in Reference 48.
259. M. Prasse, H. Reinke, C. Wendler and H. Kelling, *J. Organomet. Chem.*, **577**, 342 (1999).
260. L. A. Leites, T. S. Yadritseva, V. V. Dement'ev, B. A. Antipova, T. M. Frunze and A. A. Zhdanov, *Organomet. Chem. USSR*, **2**, 537 (1989); *Chem. Abstr.*, **117**, 198506s (1990).
261. A. Spielberger, P. Gspaltl, H. Siegl, E. Hengge and K. Gruber, *J. Organomet. Chem.*, **499**, 241 (1995).
262. A. I. Gusev, M. G. Los', Yu. M. Varezhkin, M. M. Morgunova and D. Ya. Zhinkin, *J. Struct. Chem. (Engl. Transl.)*, **17**, 329 (1976); *Chem. Abstr.*, **85**, 115029p (1976).
263. B. Chen, Z. Xie and J. Wang, *Jiegou Huaxue (J. Struct. Chem.)*, **3**, 113 (1984); *Chem. Abstr.*, **103**, 62901y (1985).
264. A. I. Yanovskii, I. L. Dubchak, V. E. Shklover, Yu. T. Struchkov, V. N. Kalinin, B. A. Izmailov, V. D. Myakushev and L. I. Zakharin, *J. Struct. Chem.*, **23**, 728 (1982); *Chem. Abstr.*, **98**, 126202j (1983).
265. F. I. Aigbirhio, S. S. Al-Juaid, C. Eaborn, A. Habtemariam, P. B. Hitchcock and J. D. Smith, *J. Organomet. Chem.*, **405**, 149 (1991).
266. N. H. Buttrus, C. Eaborn, P. B. Hitchcock, P. D. Lickiss and A. D. Taylor, *J. Organomet. Chem.*, **309**, 25 (1986).
267. M. Kakudo, N. Kasai and T. Watase, *J. Chem. Phys.*, **21**, 1894 (1953).
268. L. E. Alexander, M. G. Northolt and R. Engmann, *J. Phys. Chem.*, **71**, 4298 (1967).
269. A. Klemp, H. W. Roesky, H.-G. Schmidt, H. S. Park and M. Noltemeyer, *Organometallics*, **17**, 5225 (1998).
270. S. Ciruelos, T. Cuenca, R. Gómez, P. Gómez-Sal, A. Manzanero and P. Royo, *Polyhedron*, **17**, 1055 (1998).
271. K. Su and T. D. Tilley, *Chem. Mater.*, **9**, 588 (1997).
272. S. S. Al-Juaid, C. Eaborn, P. B. Hitchcock and P. D. Lickiss, *J. Organomet. Chem.*, **353**, 297 (1988).
273. I. L. Dubchak, V. E. Shklover, Yu. T. Struchkov, E. S. Khyнку and A. A. Zhdanov, *J. Struct. Chem.*, **22**, 770 (1981); *Chem. Abstr.*, **96**, 52385f (1982).
274. T. W. Hambley, T. Maschmeyer and A. F. Masters, *Appl. Organomet. Chem.*, **6**, 253 (1992).
275. M. Unno, K. Takada and H. Matsumoto, *Chem. Lett.*, 242 (2000).
276. P. E. Tomlins, J. E. Lydon, D. Akrigg and B. Sheldrick, *Acta Crystallogr.*, **C41**, 941 (1985).
277. N. Kasai and M. Kakudo, *Bull. Chem. Soc. Jpn.*, **27**, 605 (1954).
278. *Technol. Repts. Osaka Univ.*, **2**, 247 (1952); *Chem. Abstr.*, **47**, 10309e (1953).
279. M. Kakudo and T. Watase, *J. Chem. Phys.*, **21**, 167 (1953).
280. J. K. Fawcett, N. Camerman and A. Camerman, *Can. J. Chem.*, **55**, 3631 (1977).
281. L. Párkányi and G. Bocelli, *Cryst. Struct. Commun.*, **7**, 335 (1978).
282. N. H. Buttrus, C. Eaborn, P. B. Hitchcock and P. D. Lickiss, *J. Organomet. Chem.*, **302**, 159 (1986).
283. S. Yamaguchi, R.-Z. Jin and K. Tamao, *Organometallics*, **16**, 2230 (1997).
284. H. Puff, S. Franken, W. Schuh and W. Schwab, *J. Organomet. Chem.*, **254**, 33 (1983).

285. S. S. Al-Juaid, C. Eaborn, P. B. Hitchcock and P. D. Lickiss, *J. Organomet. Chem.*, **362**, 17 (1989).
286. H. Kaur, P. D. Lickiss and A. D. Redhouse, unpublished results.
287. C. Eaborn and N. H. Hartshorne, *J. Chem. Soc.*, 549 (1955).
288. J. E. Bunning, J. E. Lydon, C. Eaborn, P. M. Jackson, J. W. Goodby and G. W. Gray, *J. Chem. Soc., Faraday Trans. 1*, **78**, 713 (1982).
289. H. Käb, W. Ries, M. Veith and W. Malisch, abstract for poster 3.25, IXth International Symposium on Organosilicon Chemistry, Edinburgh, July 1990.
290. S. S. Al-Juaid, C. Eaborn and P. B. Hitchcock, *J. Organomet. Chem.*, **423**, 5 (1992).
291. R. Siefken, M. Teichert, D. Chakraborty and H. W. Roesky, *Organometallics*, **18**, 2321 (1999).
292. R. S. Simons, K. J. Galat, B. J. Rapp, C. A. Tessier and W. J. Youngs, *Organometallics*, **19**, 5799 (2000).
293. V. E. Shklover, I. L. Dubchak, Yu. T. Struchkov, E. S. Khyunku and A. A. Zhdanov, *J. Struct. Chem.*, **22**, 229 (1981); *Chem. Abstr.*, **95**, 97896u (1981).
294. N. H. Buttrus, R. I. Damja, C. Eaborn, P. B. Hitchcock and P. D. Lickiss, *J. Chem. Soc., Chem. Commun.*, 1385 (1985).
295. H. Ishida, J. L. Koenig and K. C. Gardner, *J. Chem. Phys.*, **77**, 5748 (1982).
296. G. Cerveau, R. J. P. Corriu, B. Dabiens and J. Le Bideau, *Angew. Chem., Int. Ed. Engl.*, **39**, 4533 (2000).

CHAPTER 13

Silicon-based dendrimers and hyperbranched polymers

DAVID Y. SON

Department of Chemistry, P.O. Box 750314, Southern Methodist University, Dallas, Texas 75275-0314; e-mail: dson@mail.smu.edu

I. INTRODUCTION	745
II. SILICON-BASED DENDRIMERS	746
A. Carbosilane Dendrimers	747
1. Synthesis and characterization	747
2. Functionalization	757
a. Core functionalization	757
b. Exterior functionalization	760
B. Carbosiloxane Dendrimers	771
C. Carbosilazane Dendrimers	776
D. Silane Dendrimers	779
E. Siloxane Dendrimers	782
III. SILICON-BASED HYPERBRANCHED POLYMERS	784
A. Hyperbranched Poly(carbosilanes)	785
1. Hyperbranched poly(carbosilanes) prepared via nucleophilic substitution reactions	785
2. Hyperbranched poly(carbosilanes) prepared via hydrosilylation reactions	787
B. Hyperbranched Poly(carbosiloxanes)	791
C. Hyperbranched Poly(carbosilazanes)	796
D. Hyperbranched Poly(siloxanes)	797
IV. CONCLUDING REMARKS	798
V. REFERENCES	798

I. INTRODUCTION

The syntheses and applications of dendrimers and hyperbranched polymers have attracted considerable scientific interest in recent years. These highly branched polymers possess

many properties that are significantly different from those of linear analogs, especially in areas such as solubility, melt viscosity and host–guest behavior. Although often mentioned together, dendrimers and hyperbranched polymers do possess distinct differences. While dendrimers are symmetrical in shape and monodisperse as a result of their stepwise controlled syntheses, hyperbranched polymers are randomly branched and polydisperse due to the usual one-pot uncontrolled syntheses employed. This difference in branching and structure results in the properties of hyperbranched polymers being intermediate to those of linear polymers and the perfectly branched dendrimers. From a time and labor standpoint, the one-pot synthetic procedure gives hyperbranched polymers a significant advantage over dendrimers. However, dendrimers are still preferable for applications requiring precise structures and molecular weight. For additional information concerning general aspects of dendrimers and hyperbranched polymers, the reader is referred to any of numerous recent review articles^{1–14}.

Silicon-based dendrimers and hyperbranched polymers represent a rapidly growing subset of all known functional dendrimers and hyperbranched polymers. Much of this interest is a natural outgrowth of the longstanding application of linear silicon-containing polymers in materials science¹⁵. In addition, the existence of many clean and high-yielding reactions in organosilicon chemistry and the general robustness and characterizability of organosilicon compounds make the study of these materials attractive from a research point of view.

In this review, complete coverage of the syntheses and applications of silicon-based dendrimers and hyperbranched polymers will be provided. For organizational purposes, dendrimers and hyperbranched polymers will be reviewed in separate sections, and each section will be further divided according to polymer class. For this review, the various classes will be defined according to the branch backbone substituents as follows:

silane: contains only silicon atoms,

siloxane: contains only silicon and oxygen atoms,

carbosilane: contains silicon atoms in addition to carbon atoms or carbon-containing moieties,

carbosiloxane: contains silicon and oxygen atoms in addition to carbon atoms or carbon-containing moieties,

carbosilazane: contains silicon and nitrogen atoms in addition to carbon atoms or carbon-containing moieties.

Exterior functional groups and core groups are excluded when making classifications for these materials.

This review encompasses several earlier reviews^{16–22} on the subject, and additionally provides coverage of more recent publications up through the early part of the year 2000.

II. SILICON-BASED DENDRIMERS

This section describes synthetic approaches to the various classes of organosilicon dendrimers. Applications of these materials will also be discussed. In this review, specific dendrimers will be labeled #G-X, where # is equivalent to the number of layers (or generations, G) around the core, and X represents the endgroups bound to each silicon atom in the outermost layer. This labeling system does not take into account the core or the branching of the dendrimer. Since carbosilane dendrimers are by far the most well-studied of the silicon-based dendrimers, they will be discussed first.

A. Carbosilane Dendrimers

1. Synthesis and characterization

The general synthetic scheme for carbosilane dendrimers was first delineated in the early 1990s by the groups of Roovers^{23,24}, van der Made^{25,26} and Seyferth²⁷. In a typical scheme, these dendrimers are prepared in a divergent process via alternating hydrosilylation and nucleophilic substitution steps starting from a multi-vinylated or -allylated core molecule. The Pt-catalyzed hydrosilylation steps involve chlorosilanes, and the reagents involved in the nucleophilic substitution steps are typically Grignard or organolithium compounds. The nucleophilic reagents determine the spacer length between silicon atom branch points, while the choice of chlorosilane in the hydrosilylation step determines the branching degree of the dendrimers. For example, the use of trichlorosilane introduces three new branch points for every double bond that is hydrosilylated. Addition of layers to the dendrimers cannot continue indefinitely; the gradual development of severe surface congestion eventually makes further growth impossible.

In their reported synthesis, Roovers and coworkers^{23,24} used tetravinylsilane as a core, methylchlorosilane as the hydrosilylating reagent and vinylmagnesium bromide as the nucleophilic reagent (spacer length = 2) to create dendrimers up to the fourth generation. After purification of each layer by chromatography, **1G-MeVi₂** (Vi = vinyl) was obtained in 55% yield, **2G-MeVi₂** was obtained in 48% yield, **3G-MeVi₂** was obtained in 41% yield and **4G-MeVi₂** was obtained in 26% yield (Scheme 1). Dendrimers **1G-MeVi₂** and **2G-MeVi₂** were oils while dendrimers **3G-MeVi₂** and **4G-MeVi₂** were obtained as viscous liquids. The excellent solubilities of these dendrimers in common solvents enabled facile characterization by a number of methods including ¹H and ¹³C NMR spectroscopy, vapor pressure osmometry and laser light scattering measurements, all of which confirmed the structures and molecular weights of the various dendrimers.

In an initial communication, van der Made and coworkers²⁵ utilized tetraallylsilane as a core, trichlorosilane as the hydrosilylating reagent and allylmagnesium bromide (spacer length = 3) as the nucleophilic reagent to synthesize dendrimers up to the fifth generation (**5G-All₃**, All = allyl, Figure 1). After chromatographic purification, all five allyl-terminated generations were reportedly obtained in near quantitative yield. Generations 1 and 2 were obtained as clear, colorless liquids, generation 3 was a wax-like solid, and generations 4 and 5 were obtained as white solids. These dendrimers were also found to be quite soluble in a wide range of solvents including hexane, diethyl ether, chloroform, acetonitrile, ethyl acetate and DMF. Besides ¹H NMR data, no other spectroscopic data were reported. In a later report, Van der Made and coworkers²⁶ discussed the possible ramifications of changing the core, the number of branches and the spacer length between branch points in carbosilane dendrimers. They also presented data that related the maximum generation attainable to the spacer length between branch points. As might be expected, increasing the spacer length increased the maximum generation that could be synthesized. No additional characterization data were reported.

Shortly after these reports, Seyferth and coworkers²⁷ published the synthesis of a series of carbosilane dendrimers utilizing tetravinylsilane as the core, trichlorosilane as the hydrosilylating reagent and vinylmagnesium bromide as the nucleophilic reagent. Each of the intermediate chloro-terminated dendrimers was functionalized by treatment with lithium aluminum hydride (LAH) which converted all the terminal SiCl groups to SiH functionalities. After chromatographic purification, **1G-H₃**, **2G-H₃**, **3G-H₃** and **4G-H₃** (Figure 2) were obtained in 84, 90, 27 and 50% yields, respectively. For the synthesis of the higher generations, increasingly stringent conditions were required for completion of

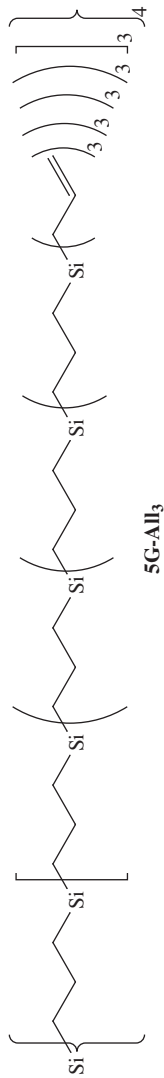


FIGURE 1. Fifth-generation allyl-terminated carbosilane dendrimer²⁵

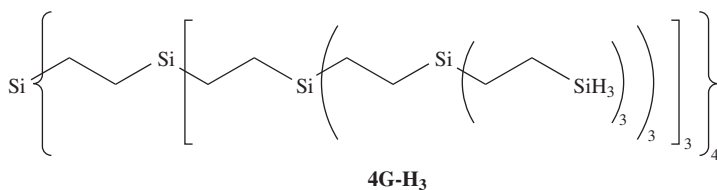


FIGURE 2. Fourth-generation H-terminated carbosilane dendrimer²⁷

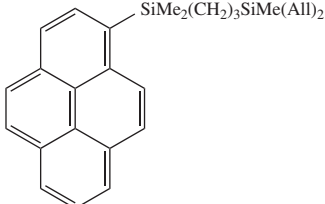
reaction. Dendrimer characterization methods included IR, ¹H, ¹³C and ²⁹Si NMR spectroscopy, and vapor pressure osmometry. The H-terminated dendrimers were found to be stable to air and moisture, although the higher generations slowly underwent crosslinking reactions. Dendrimer **2G-H₃** proved to be a crystalline solid on purification, and a molecular structure was obtained by an X-ray diffraction study. As part of this investigation, thermal stability of the hydrogen-terminated dendrimers was found to increase with increasing generation number.

Once the basic synthetic methodology for carbosilane dendrimers was established by these early reports, many variations of carbosilane dendrimers were synthesized and described in the literature. A primary modification has been the use of different core molecules. Syntheses involving different core molecules are summarized in Table 1. Core molecules containing SiH groups were first reacted with a chlorovinylsilane in a hydrosilylation reaction in order to provide reactive sites for a nucleophilic substitution step. Note also that in some cases, the final dendrimers are terminated with groups different from the nucleophilic reagent.

Although the repetitive hydrosilylation/nucleophilic substitution stepwise scheme is the most common method for the synthesis of carbosilane dendrimers, it is certainly not the only method available. Nakayama and coworkers⁵³ synthesized a small first generation dendrimer consisting of alternating silyl and thiophene units using a deprotonation/nucleophilic substitution sequence (Scheme 2). The final dendrimer, **1G-Thi₃**, was obtained in 19% yield after purification by column chromatography and HPLC, and crystallized to form inclusion complexes with CCl₄, CH₂Cl₂, benzene and acetone. Silylacetylene dendrimers were synthesized recently by a novel procedure outlined in Scheme 3⁵⁴. The first and second generations were obtained in 48 and 18% yields, respectively. The molecular structure of the first generation dendrimer was obtained by X-ray diffraction studies. Carbosilane dendrimers can also be prepared via a *convergent* approach. Van Leeuwen and coworkers⁴⁸ first prepared dendritic carbosilane wedges and then attached them to a triamide core (Scheme 4). Dendrimers **1G-All₃** through **3G-All₃** were obtained in 40–60% yields after column chromatography. An additional report from this group described a different convergent synthesis⁵⁵ in which lithiated carbosilane dendritic wedges were attached to a bis(diphenylphosphino)ferrocene core (Scheme 5).


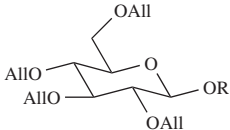
Like their linear analogs, carbosilane dendrimers are reasonably stable to air and moisture and may be handled freely in the open environment. Under ambient conditions, carbosilane dendrimers range in appearance from oils to solids depending mainly on the generation number and the terminal groups on the exterior. Carbosilane dendrimers possess excellent solubilities in common organic solvents, a common general characteristic of dendrimers that makes additional characterization quite straightforward. As expected, however, the hydrophobicity of the carbosilane dendrimer skeleton leads to complete immiscibility in water.

TABLE 1^a.

Core	Hydrosilylating reagent	Nucleophilic reagent	Largest dendrimer attained (yield)	Reference
	HSiMeCl ₂	AllMgCl	5G-(All)₂Me (80-85%)	28
MeSi(All) ₃	HSiMeCl ₂	AllMgBr	5G-(All)₂Me (N/A)	29
MePhSi(All) ₂	HSiMeCl ₂	AllMgBr	5G-(All)₂Me (N/A)	30
MePhSi(All) ₂	HSiCl ₃	AllMgBr	4G-(All)₃ (32%) or 4G-H₃ (65%)	31
Cl ₃ SiCH ₂ CH ₂ SiCl ₃	HSiMeCl ₂	AllMgBr	3G-(All)₂Me (>70%)	32
-[(All) ₂ SiCH ₂ CH ₂ CH ₂] _n -	HSiCl ₃	AllMgBr	3G-(All)₃ (72%)	33
cyc-[SiMe(Vi)O] ₄	HSiMeCl ₂	AllMgBr	3G-R₂Me R = C≡CPh, <i>p</i> -OC ₆ H ₄ Br, All (70-71%)	34
cyc-[SiMe(Vi)O] ₄	various	AllMgBr	2G-(C≡CPh)Me₂ (70%), or 2G- (<i>p</i>-OC₆H₄Br)Me₂ (71%)	35
cyc-[SiMe(Vi)O] ₄	HSiMeCl ₂	AllMgBr	4G-(All)₂Me (71%)	36
MeSi[OSiMe(All) ₂] ₃	HSiMeCl ₂	AllMgCl	7G-(All)₂Me (75%)	37
-[(All) ₂ SiCH ₂ CH ₂ CH ₂] _n -	HSiMeCl ₂	various aryl nucleophiles	1G-(aryl)₂Me (100%)	38
Si(C≡CPh) ₄	HSiMeCl ₂ HSiMe ₂ Cl	PhC≡CLi	4G-(C≡CPh)Me₂ (N/A)	39
Si ₈ Vi ₈ O ₁₂	various	ViMgBr	various (21-100%)	40
Cl ₃ SiCH ₂ CH ₂ SiCl ₃	HSiMeCl ₂ and HSiMe ₂ Cl	AllMgBr	4G-Me₂(R) , R = H, C≡CPh, C ₆ H ₄ C ₆ H ₄ OH- <i>p</i> (78-83%)	41
Si[OAll] ₄	HSiMeCl ₂	AllMgBr	2G-(OAll)₂Me (N/A)	42

(continued overleaf)

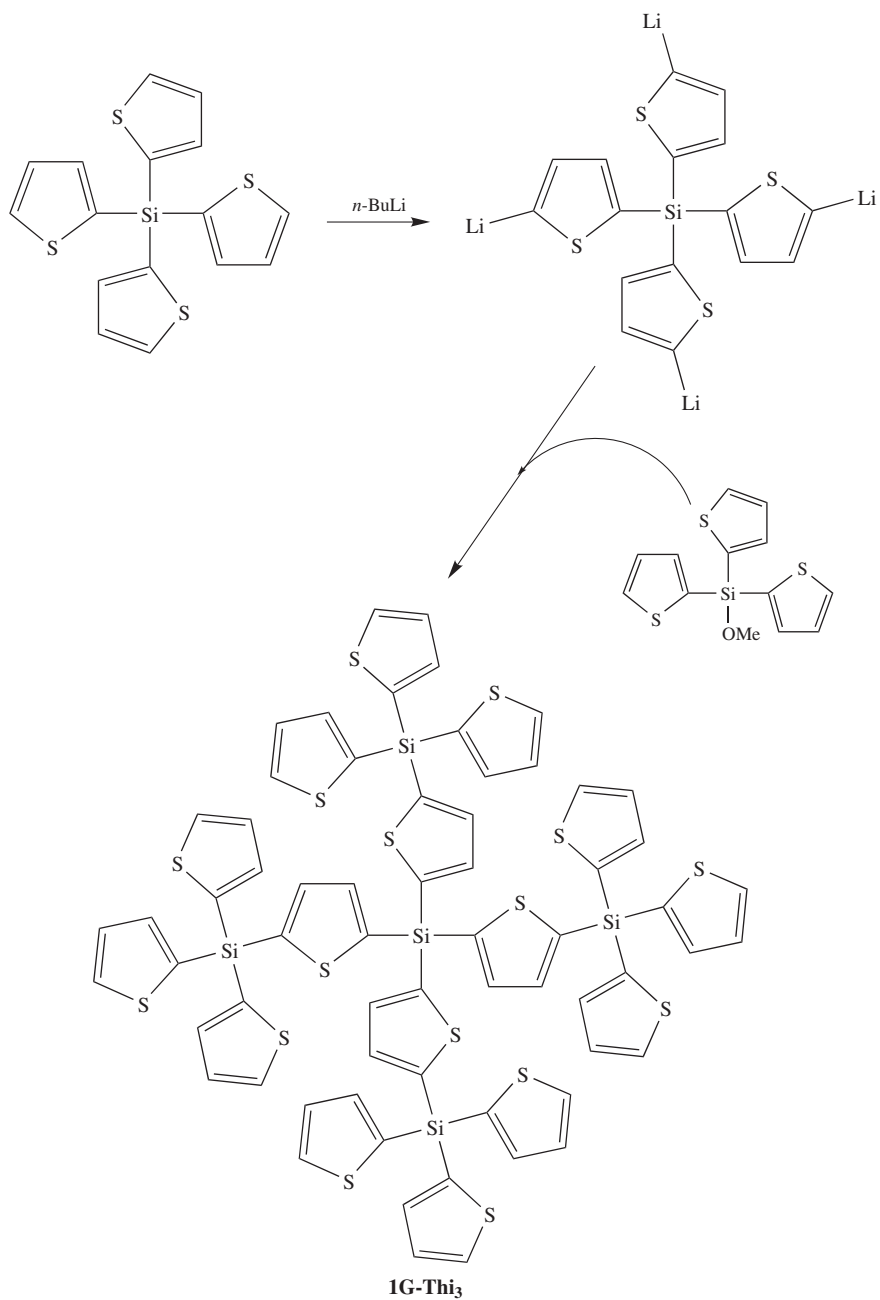
TABLE 1^a. (Continued)

Core	Hydrosilylating reagent	Nucleophilic reagent	Largest dendrimer attained (yield)	Reference
PhSiVi ₃	HSiCl ₃	ViMgCl	2G-(OMe)₃ (93%)	43
CH ₃ (CH ₂) ₁₆ CH ₂ SiVi ₃	HSiCl ₃	ViMgCl	2G-(OMe)₃ (93%)	43
cyc-[SiMe(H)O] ₄	HSiMeCl ₂ HSiMe ₂ Cl	AllMgBr, FcLi	3G-FcMe₂ (28%)	44
[NMe ₄][Si ₈ O ₂₀]•69H ₂ O	HSiCl ₃	ViMgBr	2G-Vi₃ (78%)	45
Si ₈ Vi ₈ O ₁₂	HSiMeCl ₂	ViMgBr	1G-Me(mesogen)₂^b (54%)	46
Si ₈ Vi ₈ O ₁₂	HSiMeCl ₂ HSiMe ₂ Cl	ViMgBr	2G-(OH)Me₂ (96%), or 2G-(H)Me₂ (40%)	47
BrCH ₂ CH ₂ CH ₂ Si(All) ₃	HSiCl ₃	AllMgBr	2G-(All)₃ (quantitative)	48
	HSiMeCl ₂	FcLi	1G-Fc₂Me (45%)	49
MeO(CH ₂ CH ₂ O) _n (CH ₂) ₃ Si(All) ₃	HSiCl ₃	AllMgCl	2G-(All)₃ (50%)	50
	HSiMeCl ₂	AllMgBr	1G-(All)₂Me (36–52%)	51
Me ₃ SiO(SiMeHO) _n SiMe ₃	HSiMeCl ₂	AllMgBr	2G-(All)₂Me (N/A)	52
Me ₃ SiO(SiMeHO) _n SiMe ₃	HSiMeCl ₂	PhC≡CLi	2G-(C≡CPh)₂Me (N/A)	52

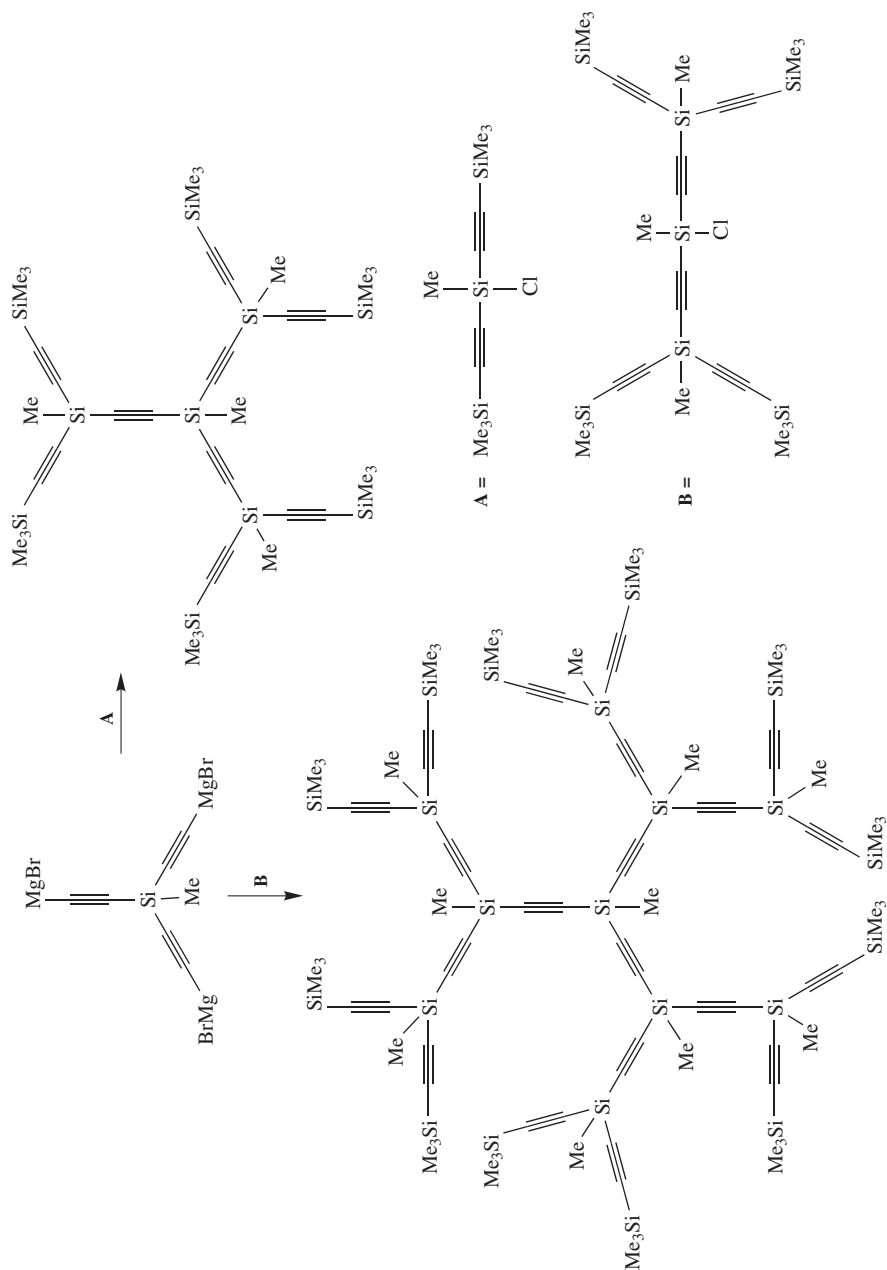
^a All = allyl, Vi = vinyl, Fc = ferrocenyl.

^b mesogen = (CH₂)₂SiMe₂OSiMe₂(CH₂)₁₁OC₆H₄C₆H₄CN-*p*.

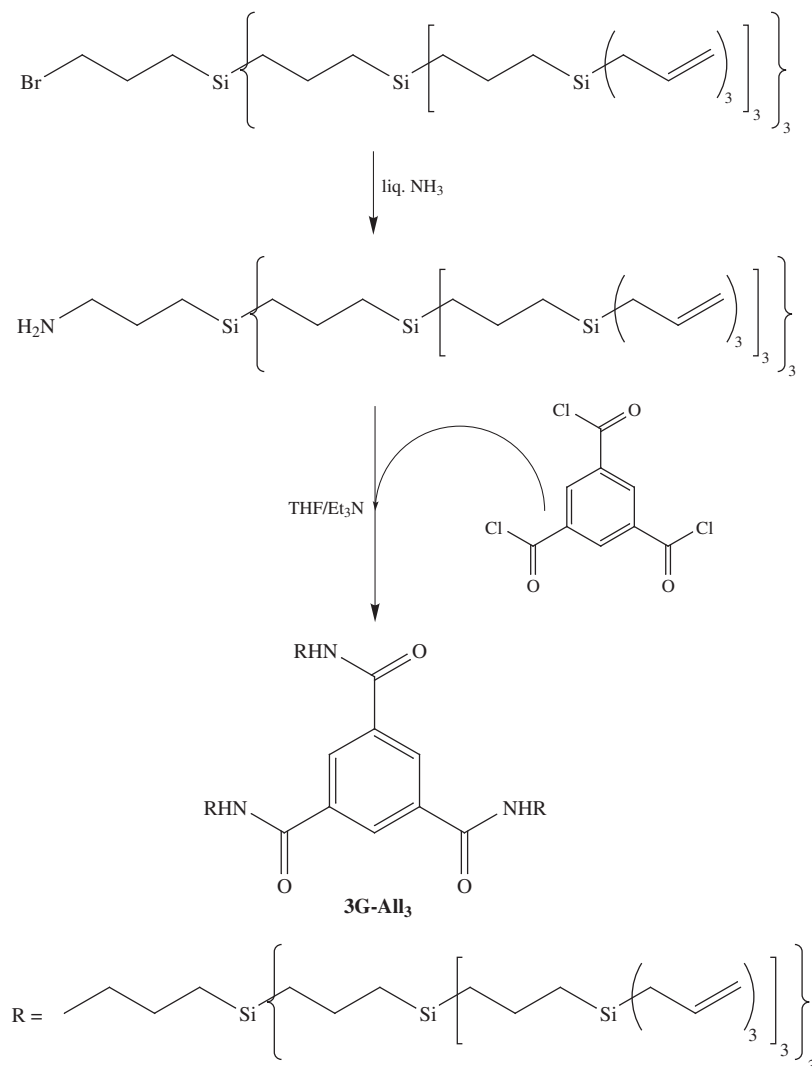
In most cases, structural characterization of carbosilane dendrimers is accomplished by multinuclear one-dimensional NMR spectroscopy (¹H, ¹³C and ²⁹Si). However, as larger dendrimers are characterized standard spectroscopic methods become less useful due to the overlap of signals. This problem has been elegantly circumvented as described in a recent paper by Tessier, Rinaldi and coworkers⁵⁶. In this paper the researchers described the use of ¹H/¹³C/²⁹Si triple resonance, 3D and pulse field gradient NMR techniques to



SCHEME 2

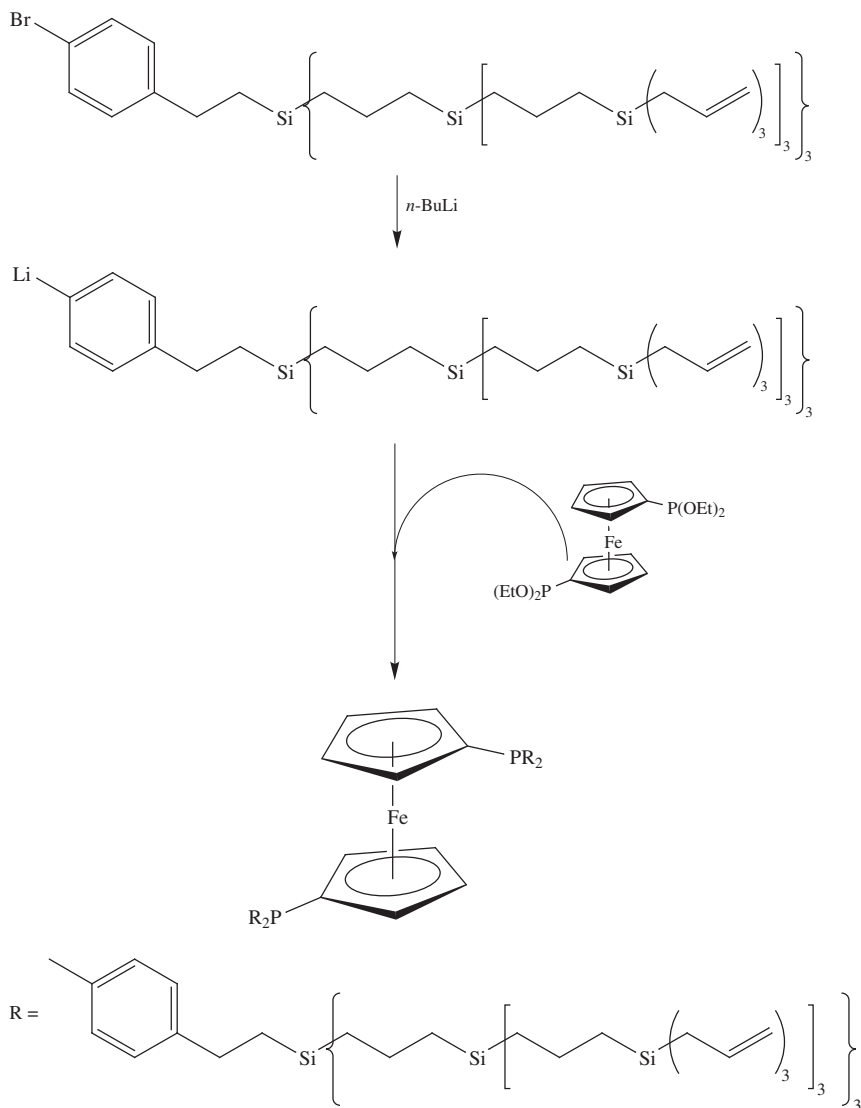


SCHEME 3



SCHEME 4

resolve and unequivocally assign the resonances found in the ^1H , ^{13}C and ^{29}Si NMR spectra of first and second generation carbosilane dendrimers. This technique, which does not rely on isotopic enrichment, may prove to be an invaluable tool for the careful characterization of any silicon-based dendrimer system. Structural characterization of carbosilane dendrimers can also be accomplished using single-crystal X-ray diffraction techniques. However, due to the low crystallinity and high degrees of thermal motion in carbosilane dendrimers, this technique is limited to smaller dendrimers or dendrimers containing stiff moieties^{27,40,54,57,58}.



SCHEME 5

Molecular weight determination of carbosilane dendrimers is best accomplished with electrospray or MALDI-TOF mass spectroscopy, but is also possible with vapor pressure osmometry measurements. In many cases, MALDI-TOF data is sufficiently accurate to indicate slight structural imperfections in dendrimers due to incomplete reactions. Gel permeation chromatography is generally not an effective means of measuring molecular weights of carbosilane dendrimers due to the substantial differences in hydrodynamic volume between spherical dendrimers and linear polystyrene standards.

Thermal properties of carbosilane dendrimers have also been described. A recent report examined T_g and other temperature-related behavior in a series of dendrimers up to the seventh generation (Figure 3)³⁷. For the third generation, a T_g of -95°C was observed, while a T_g of approximately -86°C was observed for the fourth through seventh generations. These researchers also investigated flow temperatures and viscoelastic behavior of the dendrimers.

Many dendrimers are capable of host–guest interactions⁵⁹, much of which depends on the size of the cavities within the dendrimer and the density of the outer functional groups. These parameters in carbosilane dendrimers were examined using molecular force-field calculations⁶⁰. In this study, various hypothetical carbosilane dendritic structures were examined which varied in terms of branching, spacer lengths and generation. The cavity sizes were consistent with all of these variables, with lower branching and increased spacer lengths leading to larger average cavity sizes. Density of the outer functional groups was determined by calculating accessibility to the cavities. For generations possessing dense outer shells, a threshold radius for accessibility was determined which was found to correspond with predetermined cavity size dimensions. This relationship does not hold for generations without densely packed outer shells, which possess an open structure.

2. Functionalization

An increasing emphasis has been placed on the functionalization of known carbosilane dendrimer systems. Functionalization can impart specific properties to the dendrimers or, in some cases, aid in the elucidation of dendrimer structure. Functionalization of carbosilane dendrimers can occur at the core or at the periphery.

a. Core functionalization. As can be seen in Table 1, many different moieties have been described as cores for carbosilane dendrimers. In most cases, the reports served as examples of the extent to which the general synthetic procedure could be applied. However, certain cores were utilized for specific purposes.

Specific core selection is illustrated in the convergent syntheses of van Leeuwen and coworkers described in the previous section⁴⁸. In the synthesis described in Scheme 4, the 1,3,5-benzene triamide core was employed in order to examine the effect of carbosilane size on host–guest interactions via hydrogen bonding with the core. In this case, host–guest interactions were observed with all substrates and generation sizes. The core-functionalized dendrimers described in Scheme 5 served as ligands for Pd complexation. The resulting dendrimer-bound palladium complexes were catalytically active in allylic alkylations. The reaction rate decreased when higher generation dendrimers were used, and product selectivity was also found to depend on dendrimer size⁵⁵.

Krasovskii and coworkers utilized both a divergent²⁸ and convergent⁶¹ approach to synthesize dendrimers containing a pyrene core moiety (e.g. Figure 4). From fluorescence excitation spectra, the researchers were able to unambiguously determine that the pyrenyl fragments were situated at the center of the dendrimers and unexposed at the surface²⁸. Furthermore, fluorescence quenching experiments indicated that for the largest dendrimer, diffusion of small quenching reagents was impeded by the steric hindrance of the exterior branching.

Kim and coworkers observed the formation of micelles in aqueous solutions by synthesizing a amphiphilic linear-dendritic diblock copolymer based on poly(ethylene oxide) (PEO) (Figure 5)^{50,62}. In this case, the PEO can be considered as the core upon which the dendrimer was synthesized via a divergent process. In an aqueous phase, the hydrophilic

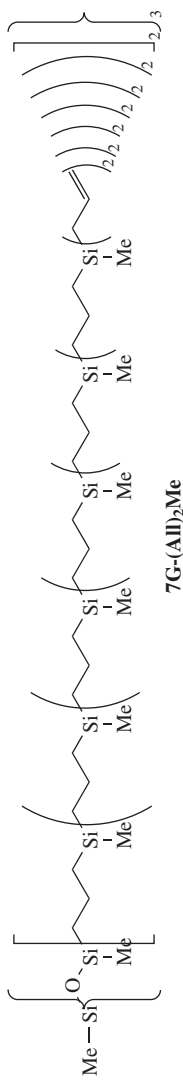
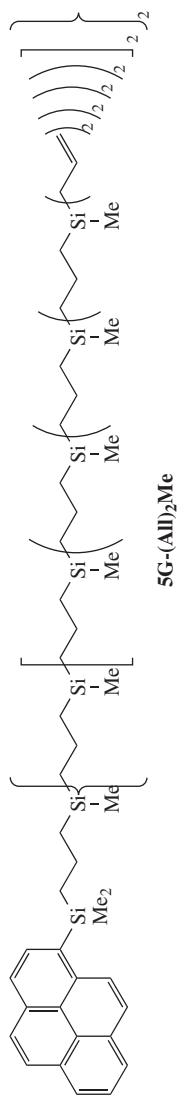
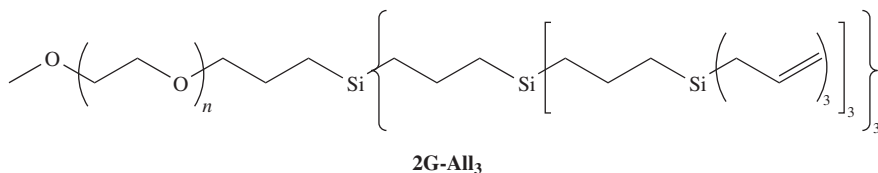
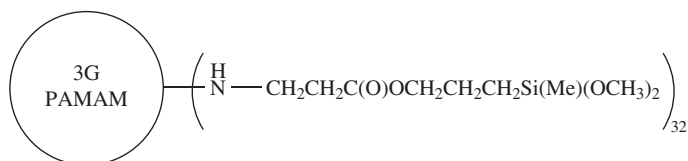


FIGURE 3. Seventh-generation allyl-terminated carborasilane dendrimer³⁷

FIGURE 4. Carbosilane dendrimer with a pyrene core²⁸

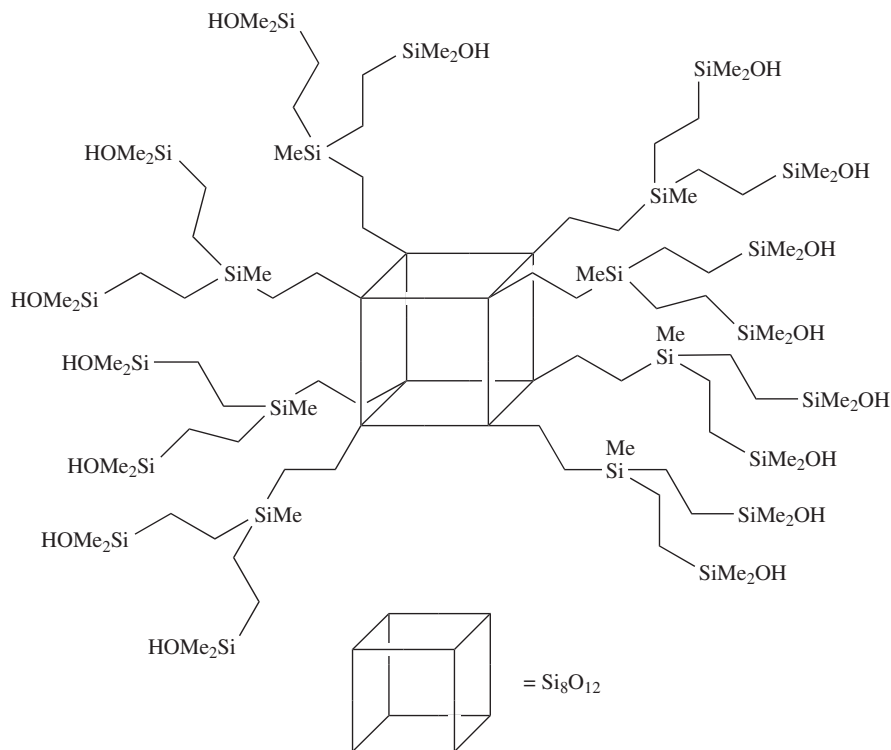
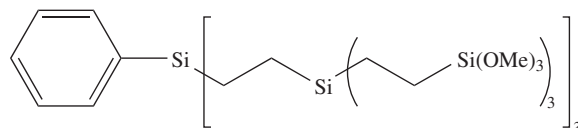
FIGURE 5. A PEO/carbosilane dendrimer block copolymer⁵⁰FIGURE 6. Schematic of a copoly(amidoamine-organosilicon) dendrimer⁶³

PEO formed a surface while the hydrophobic carbosilane dendritic block was incorporated into the micelle core. Micellar characteristics were determined using fluorescence techniques and dynamic light scattering. Copolymers with a third-generation dendritic block could not be dispersed in water.

Other examples of dendrimers that can be placed into the core-functionalized category are the copoly(amidoamine-organosilicon) (PAMAMOS) dendrimers. These dendrimers essentially possess poly(amidoamine) (PAMAM) dendrimers as cores and are functionalized on the surface with layers of silyl moieties (e.g. Figure 6)^{63–65}. The PAMAM cores give the dendrimers a hydrophilic interior while the organosilicon exterior imparts hydrophobic character. The surface properties and water solubility of the dendrimers can be tailored according to the degree and type of exterior silicon functionalization and also the PAMAM generation size^{66,67}. Furthermore, these PAMAMOS dendrimers can be crosslinked into films and coatings that have the capability of absorbing and complexing various metal cations from solution^{68–72}. The metal cations can then be reduced to the zero-valent metal particles within the dendrimers, resulting in the formation of what can be considered a metal-dendrimer ‘nanocomposite’.

b. Exterior functionalization. The vast majority of carbosilane dendrimer functionalization has been performed on the dendrimer exterior. This is due to the greater likelihood of the functionalization affecting properties since the exterior is in greater contact with the outside environment. Furthermore, exterior functionalization is quite simple due to the usual presence of reactive groups such as unsaturation or SiCl linkages.

The simplest type of externally functionalized carbosilane dendrimer is the replacement of the exterior SiCl groups with SiR groups, where R is a relatively small and simple moiety. One of the earliest examples of this type of functionalization was described in the initial carbosilane synthesis report of Seyferth and coworkers²⁷ in which the chlorine-terminated generations were treated with LAH to convert the SiCl linkages to SiH (Figure 2). The SiH terminated dendrimers were found to undergo thermal and metal-catalyzed crosslinking reactions. Phenyl-terminated carbosilane dendrimers were prepared by Friedmann and coworkers⁵⁸ and were found to form inclusion compounds when recrystallized with a suitable solvent, as determined by X-ray diffraction.

FIGURE 7. Silanol-terminated carbosilane dendrimer with a silsesquioxane core⁴⁷FIGURE 8. Methoxy-terminated carbosilane dendrimer precursor to sol-gel materials⁴³

Morris and coworkers prepared new silanol-terminated carbosilane dendrimers based on silsesquioxane cores (Figure 7)⁴⁷ in order to mimic silica surfaces for metal attachment. These dendrimers were prepared by treating the SiH-terminated dendrimers with Pd/C catalyst in a water/dioxane mixture. Corriu and coworkers treated SiCl-terminated carbosilane dendrimers with methanol to obtain SiOMe-termination (e.g. Figure 8)⁴³. Polycondensation via a sol-gel process yielded various hybrid materials. Porosity was found to depend on the core and gelation conditions, and no gels were obtained from first generation dendrimers. In another detailed study, polycondensation was also used to prepare xerogels of varying surface area from different alkoxy-terminated carbosilane dendrimers⁷³. Catalysts based on these xerogels were found to be more active than silica-derived catalysts when used for the epoxidation of cyclohexene. In another report, small

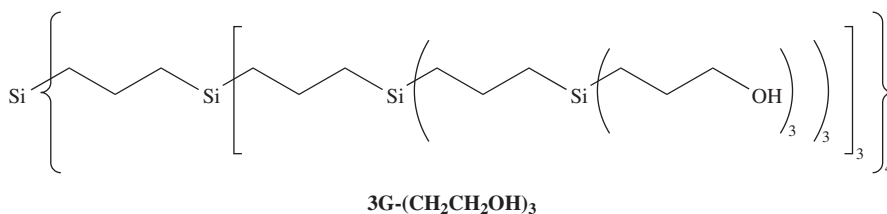
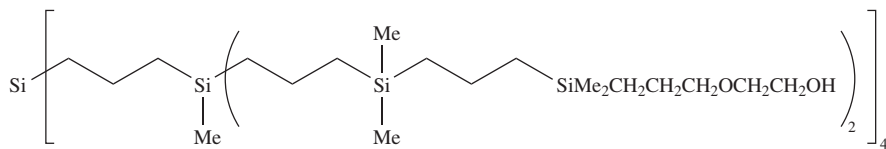
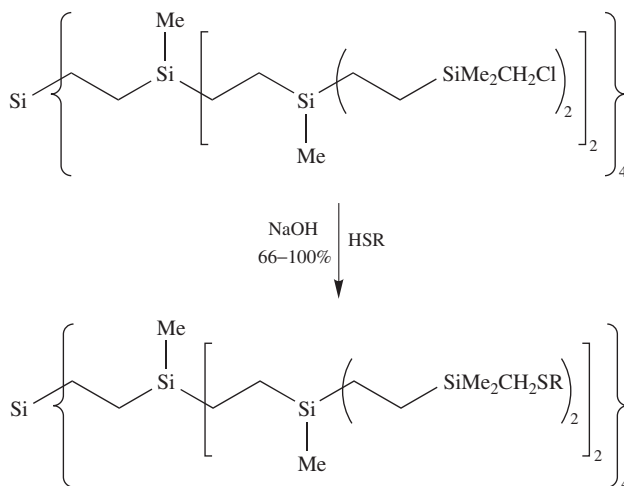


FIGURE 9. Third-generation hydroxy-terminated carbosilane dendrimer⁷⁵

SiOEt-terminated carbosilane dendrimers were prepared and characterized using potassium ionization of desorbed species mass spectrometry⁷⁴. Preliminary investigations into the sol-gel chemistry of these dendrimers were also carried out.

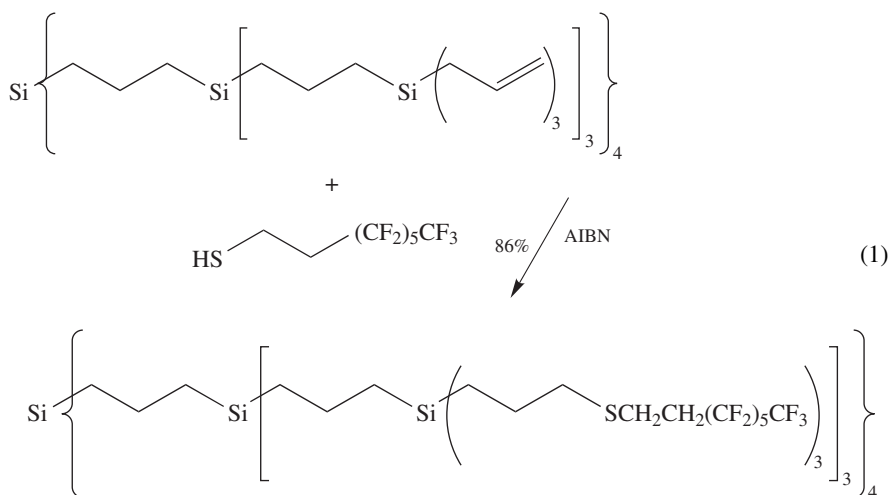
Another common exterior functionalization is the attachment of polar groups in order to affect properties such as solubility, surface energy, glass transition temperature, amphiphilicity and guest-transporting behavior. Frey and coworkers employed a hydroboration/oxidation sequence on allyl-terminated dendrimers to synthesize dendritic polyols up to the third generation (Figure 9)^{75,76}. Characterization with MALDI-TOF mass spectroscopy revealed the presence of structural impurities resulting from incomplete reactions. These polyols were found to be soluble in alcohols and pyridine but not in water. It was further noted that the third generation dendritic polyol possessed a significantly higher T_g than the corresponding allyl-terminated dendrimer, a phenomenon possibly related to hydrogen bonding or the exclusion of the hydroxyl units from the dendrimer core. Kim and coworkers reported a similar synthesis of dendritic polyols several years later (e.g. Figure 10)⁷⁷. Getmanova reported the synthesis of a third generation alcohol-terminated carbosilane (Figure 11) by the deprotection of the corresponding trimethylsiloxy-terminated carbosilane^{78,79}. IR spectroscopic data indicated a significant dependence of hydrogen-bonding on temperature and concentration. Further investigations with this dendrimer focused on surface properties and methods for these characterizations. It was determined that the dendrimer formed a monolayer at the air/water interface^{80,81}. Seyferth and coworkers⁸² utilized nucleophilic substitution reactions to derivatize the exteriors of carbosilane dendrimers with alcohol, dimethylamino and sodium sulfonate groups (Scheme 6). The alcohol- and dimethylamino-terminated dendrimers were soluble in organic solvents but insoluble in water. Dendrimers with sodium sulfonate or protonated dimethylamino terminal groups proved to be completely soluble in water. The sodium sulfonate-terminated dendrimer exhibited micelle-like behavior in enhancing the solubilities of toluene, ethylbenzene and propylbenzene in water.

Stühn, Frey and coworkers^{83–85} synthesized perfluorohexyl (C_6F_{13})-terminated carbosilane dendrimers up to the third generation via the free radical addition of a fluorinated mercaptan to an allyl-terminated dendrimer (equation 1). Whereas the first generation dendrimer exhibited the formation of a mesophase, the second and third generations did not but instead formed a hexagonally ordered array of columns⁸³. Segmental dynamics⁸⁴ and dielectric relaxation⁸⁵ in these dendrimers were also investigated. Externally fluorinated carbosilane dendrimers were also prepared by Shreeve and coworkers via the hydrosilylation of SiH-terminated dendrimers with fluorinated allyl ethers⁸⁶. Atmospheric pressure chemical ionization mass spectrometry and small-angle X-ray light scattering data corresponded well with expected values.

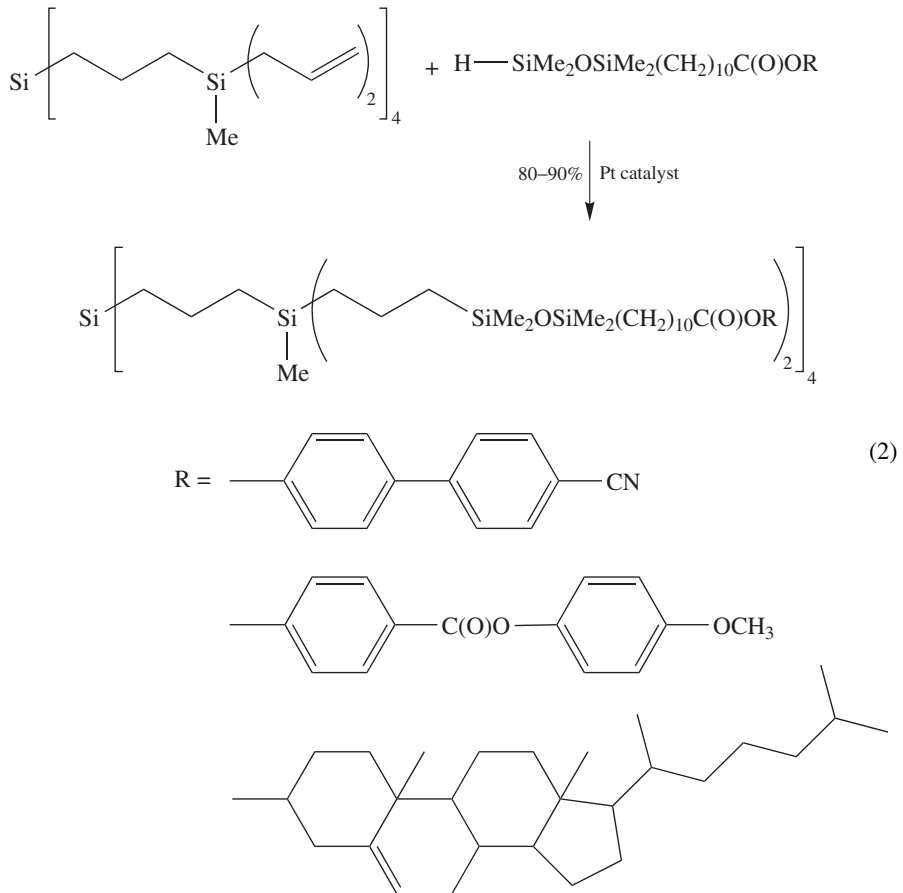
FIGURE 11. Hydroxy-ether terminated carbosilane dendrimer⁷⁸

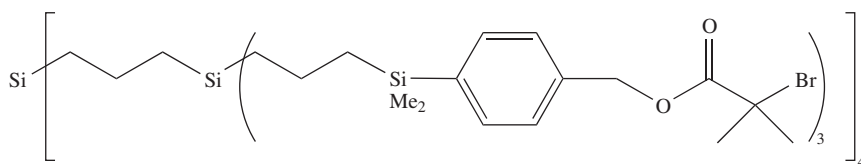
R = CH₂CH₂NMe₂, CH₂CH₂CH₂SO₃Na, CH₂CH₂OH (for reaction with first generation dendrimer)

SCHEME 6



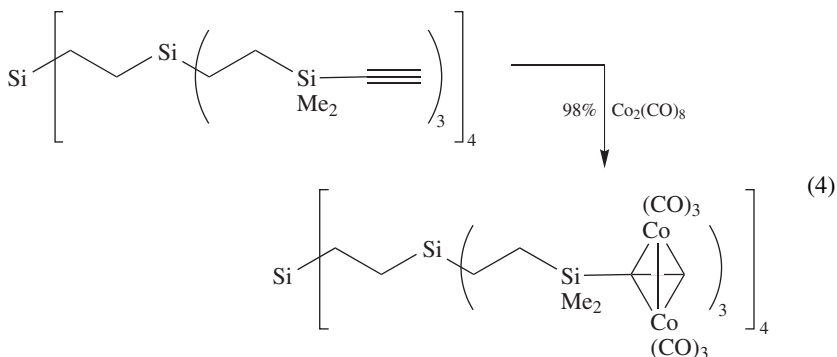
Carbosilane dendrimers substituted with mesogenic groups at the exterior exhibit liquid crystalline behavior. Shibaev and coworkers attached cyanobiphenyl, methoxyphenyl benzoate and cholesteryl mesogens to the dendrimer periphery via hydrosilylation (equation 2)⁸⁷ and observed different smectic mesophases in all cases. Frey and coworkers also attached cyanobiphenyl⁸⁸ mesogens to the dendrimer periphery. This dendrimer, prepared by reaction of a second generation dendritic polyol with an acyl chloride (equation 3), gave rise to a broad smectic A phase from 17 °C to 130 °C. Later studies demonstrated that increasing the spacer unit length between the mesogens and the dendrimer facilitated the development of layered structures⁸⁹. Frey and coworkers also synthesized cholesteryl-substituted dendrimers⁷⁶ that were found to form mono- or multilayers when deposited from solution onto mica⁹⁰. Variables affecting layer formation and topology included dendrimer solution concentration and post-deposition thermal annealing. Soon after these initial reports, similar mesogen-substituted carbosilane dendrimers were synthesized by Terunuma^{91,92} and Goodby^{46,93}, and found to possess comparable liquid crystalline properties. Terunuma and coworkers also successfully attached chiral mesogenic units to the periphery⁹⁴.

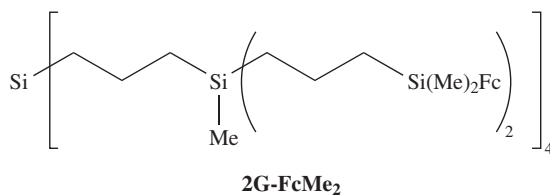
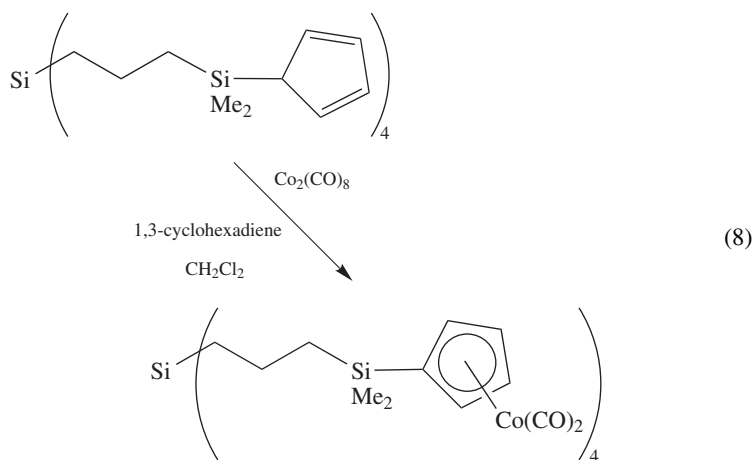
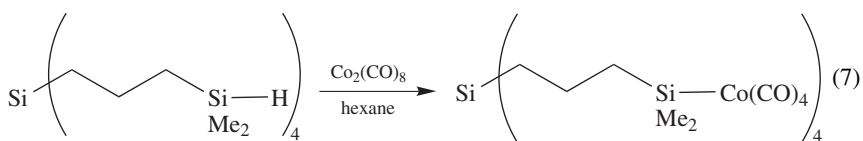
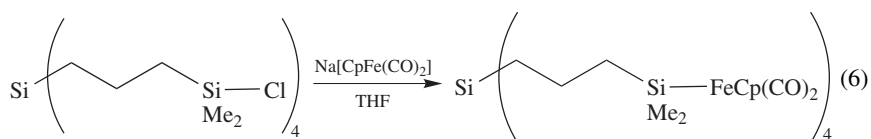
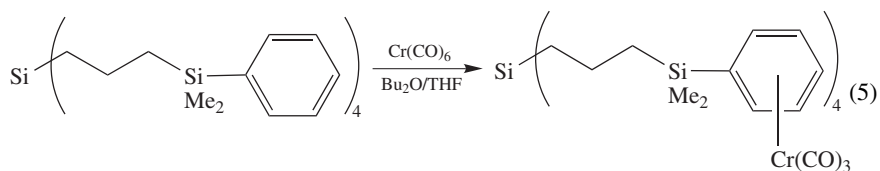


FIGURE 12. Dendritic initiator for methyl methacrylate polymerization¹⁰¹

Star poly(methylmethacrylates) were synthesized via atom transfer polymerization using a small carbosilane dendrimer functionalized with a tertiary bromide moiety as an initiator core (Figure 12)^{100,101}. A convergent approach to star polymers with a carbosilane dendrimer core was described in a report by Allgaier and coworkers¹⁰², in which living poly(butadienyl-lithium) arms were coupled with various SiCl-terminated carbosilane dendrimers. Utilizing smaller dendrimers with lower functionality was found to yield nearly ideal results in terms of substitution and polydispersity.

Perhaps the most common type of exterior functionalization has been the attachment of transition metals to carbosilane dendrimers. This is typically accomplished by first attaching ligands to the exterior followed by binding of the transition metal. An early example is the binding of cobalt to the exterior of carbosilane dendrimers via terminal ethynyl groups, reported by Seyferth and coworkers (equation 4)¹⁰³. Later reports by Kim and Jung utilized terminal phenylethynyl groups as the binding moiety for cobalt^{104,105}. Cuadrado and coworkers utilized phenyl-terminated carbosilane dendrimers for the attachment of chromium moieties to the exterior (equation 5)¹⁰⁶ and also reported synthetic approaches for the attachment of iron (equation 6) and cobalt (equations 7 and 8) to the exteriors of first generation carbosilane dendrimers¹⁰⁷. These researchers have performed extensive studies^{44,49,108–112} on carbosilanes functionalized with exterior ferrocene units (e.g. Figure 13) with particular regard toward electronic properties. The ferrocenyl groups usually are noninteracting in terms of redox properties; however, significant interaction exists between two ferrocenyl units bound to the same silicon atom¹¹⁰. Tilley and coworkers⁵⁷ have utilized benzyl-terminated carbosilane dendrimers to bind ruthenium centers (equation 9). A first generation dendrimer was characterized by single-crystal X-ray diffraction and the entire series of dendrimers was characterized by electrospray ionization mass spectrometry. Carbosilane dendrimers terminated with iron/gold clusters have also been reported by Rossell and coworkers (e.g. Figure 14)^{113,114}.



FIGURE 13. Ferrocene-terminated carbosilane dendrimer¹⁰⁸

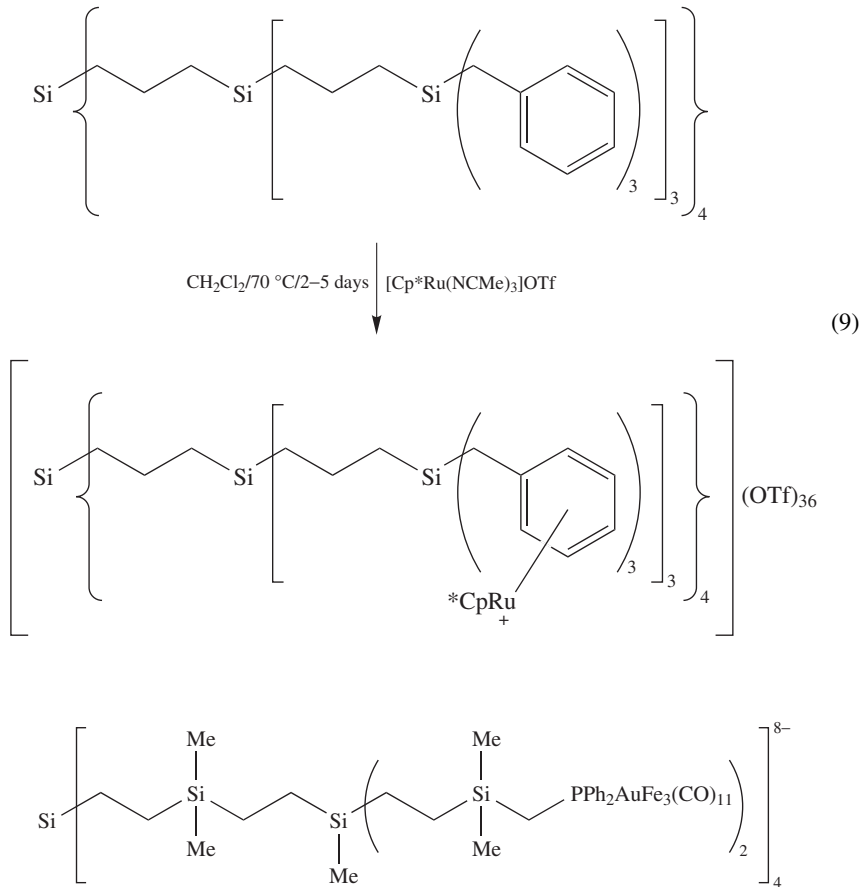
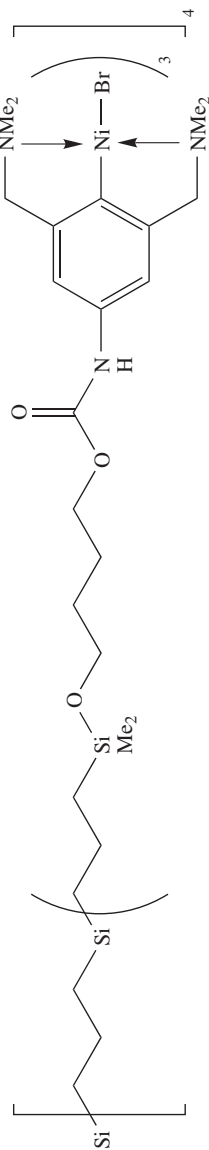
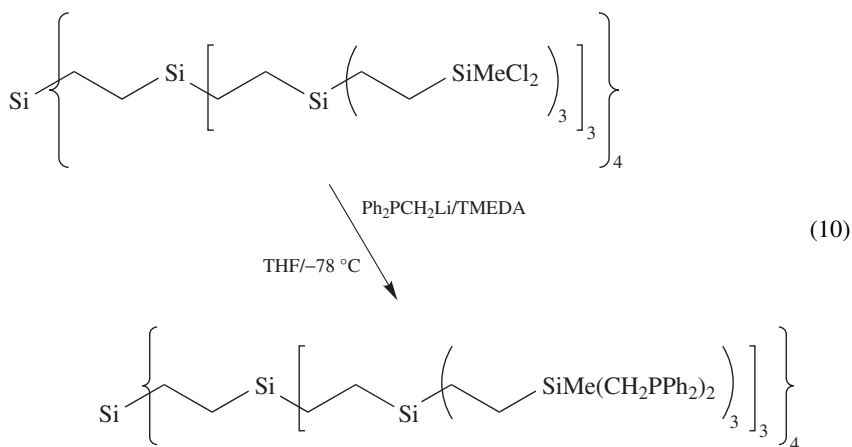


FIGURE 14. Carbosilane dendrimers terminated with iron/gold clusters¹¹⁴

A particular driving force for the attachment of transition metals to carbosilane dendrimers has been the preparation of dendrimer-bound catalysts. Such catalysts would be soluble, but would also be relatively easy to separate from reaction mixtures by ultrafiltration techniques due to their size and globular geometry. Much of this research has been the result of an early report by van Koten and coworkers in which they described the synthesis of carbosilane dendrimers terminated with arylnickel complexes (Figure 15)^{115,116}. As catalysts for the Kharasch addition of haloalkanes to double bonds, these dendrimer-bound complexes were found to be just slightly less active than an analogous monomeric catalytic complex. Since the initial report, this group has attached palladium^{117–119} to the dendrimer periphery and demonstrated significant catalytic activity in certain cases¹¹⁸. Other reports from this group have explored the catalytic mechanism^{120,121} and various synthetic approaches^{122–125} to metal-terminated carbosilane dendrimers. A preliminary

FIGURE 15. Catalytically active carbosilane dendrimers terminated with arylnickel complexes.¹¹⁵

communication also reported the application of a functionalized carbosilane dendrimer as a soluble support for the zinc-mediated synthesis of β -lactams¹²⁶. Besides van Koten's group, it appears that van Leeuwen and coworkers are the only other researchers to report the application of carbosilane dendrimers as catalysts^{55,127}. As mentioned earlier, they synthesized a core-functionalized dendrimer that was active in palladium-catalyzed allylic alkylations⁵⁵. In a related report, carbosilane dendrimers with *exterior* palladium functionalization were described using the dendrimer shown in equation 10 as a ligand¹²⁷. These complexes were found to be quite active for the allylic alkylation reaction of allyl trifluoroacetate and sodium diethyl methylmalonate. Catalytic activity was not found to decrease with increasing generation size. Application of the catalyst in a continuous process utilizing a membrane reactor resulted in an unexpected loss of catalytic activity after fifteen reactor volumes had been pumped through the reactor. This loss in activity was ascribed to catalyst decomposition and not to removal of the dendrimer complex.



B. Carbosiloxane Dendrimers

The earliest example of a dendritic carbosiloxane was reported in 1992 by Kakimoto and coworkers¹²⁸, who employed a convergent synthesis. A typical step in the synthesis is illustrated in equation 11. Using similar steps, the first through fourth generation dendrimers were obtained in 80, 48, 41 and 17% yields, respectively, after purification by distillation or column chromatography. The T_g values of the dendrimers increased from approximately -60°C for the first generation dendrimer to approximately -38°C for the fourth generation.

In 1997, Ignat'eva and coworkers¹²⁹ developed what they termed a 'universal scheme' for the synthesis of organosilicon dendrimers. In this scheme, divergent and convergent approaches were combined. Small dendrimers were prepared in a divergent process, and in a convergent process, dendritic wedges were joined to these dendritic cores. This approach was utilized to synthesize dendritic carbosiloxanes up to the third generation (Scheme 8).

Kim and Kwon reported the divergent synthesis of a dendritic carbosiloxane from a cyclic siloxane tetramer core¹³⁰ using the standard carbosilane dendrimer synthetic approach. Allyl alcohol was employed as the nucleophilic reagent and trichlorosilane

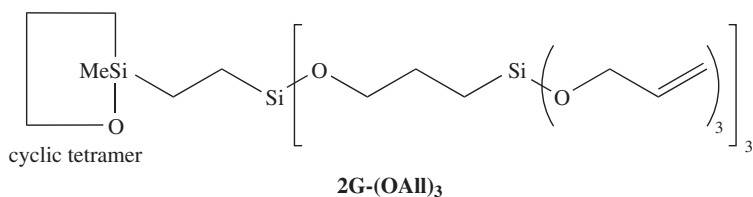
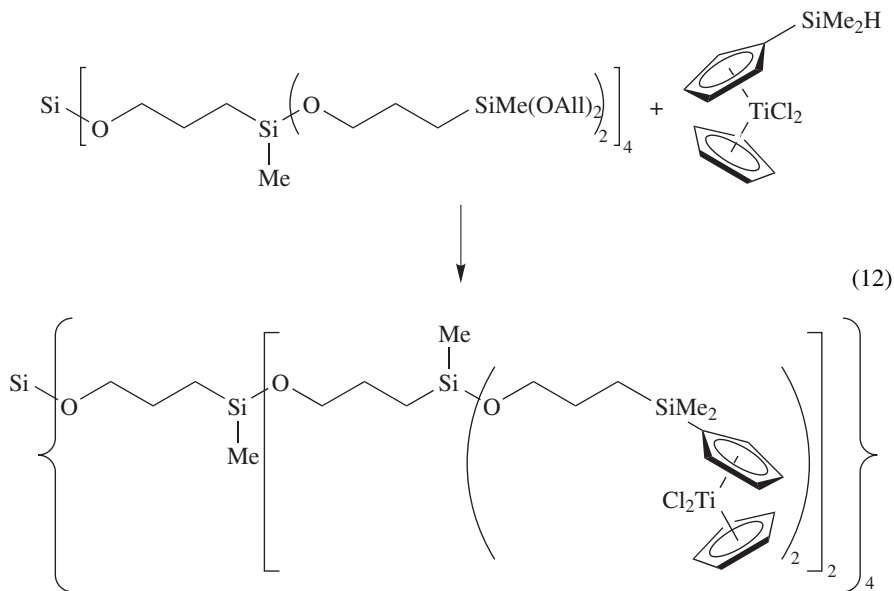
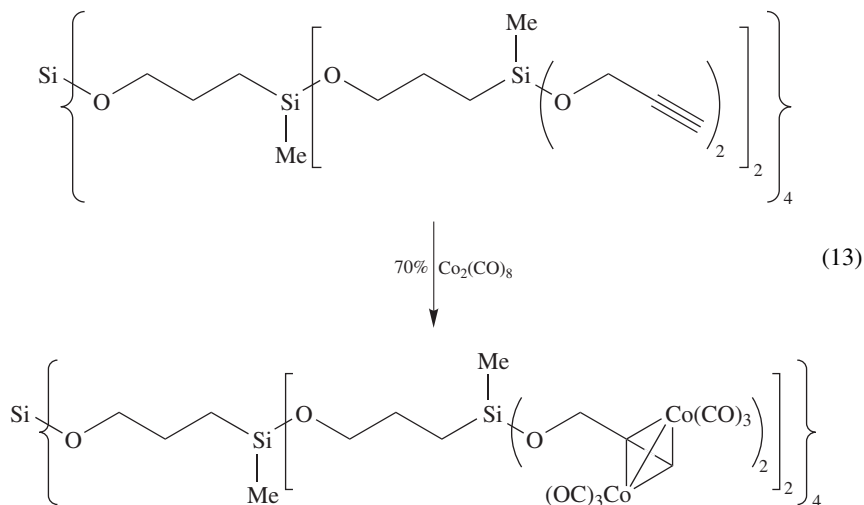


FIGURE 16. Allyloxy-terminated carbosiloxane dendrimer¹³⁰

as the hydrosilylating reagent. A second generation dendrimer was the largest obtained (Figure 16). The dendrimers were characterized with MALDI-TOF mass spectroscopy. Later papers from this group described the use of propargyl alcohol as the nucleophilic reagent¹³¹ and various other cores and hydrosilylating agents to prepare similar carbosiloxane dendrimers¹³². Combining these approaches with lithium phenylacetylide as a nucleophilic agent led to the formation of 'double-layered' carbosiloxane dendrimers (e.g. Figure 17)¹³³.

The utilization of allyl alcohol as the nucleophilic reagent to prepare dendritic carbosiloxanes was also reported by Lang and Brüning^{134,135}. Using a second generation allyl-terminated carbosiloxane dendrimer, they were able to attach titanium moieties via a simple hydrosilylation reaction (equation 12)¹³⁴. Lang and coworkers were also successful in binding cobalt moieties to ethynyl-terminated carbosiloxane dendrimers (e.g. equation 13)^{136,137}.





Certain characterization studies performed on carbosilane dendrimers (as described previously) were also carried out with carbosiloxane dendrimers. Vitukhnovsky and coworkers^{138,139} described fluorescent properties of carbosiloxane dendrimers (Figure 18) synthesized via a convergent approach with a pyrene moiety as the core⁶¹. The researchers demonstrated excimer formation using a variety of techniques. Sheiko and coworkers^{81,140} found that a SiMe₃-terminated dendritic carbosiloxane (Figure 19) did not form a monolayer but instead retracted into a thicker film at the air–water interface.

C. Carbosilazane Dendrimers

Carbosilazane dendrimers have been described only recently, with the first report by Son and Hu^{141,142}. In their synthesis, tris(vinyltrimethylsilyl)amine was utilized as the core and the dendrimer was built up with alternating hydrosilylation and nucleophilic substitution steps, using chlorodimethylsilane as the hydrosilylating agent and lithium bis(vinyltrimethylsilyl)amide as nucleophilic agent (Scheme 9). Dendrimers up to the second generation were obtained in yields over 87%. The third generation could not be obtained with this synthetic approach. These carbosilazane dendrimers were characterized by NMR spectroscopy, vapor pressure osmometry and MALDI-TOF mass spectroscopy which confirmed the molecular weights of the products. The dendrimers were found to be stable to neutral aqueous solutions and anhydrous protic acid solutions, but decomposed rapidly on exposure to aqueous protic acid solutions.

Shortly thereafter, Veith and coworkers reported the synthesis of the same dendrimers, but they were able to synthesize dendrimers up to the fourth generation¹⁴³. The larger dendrimers were obtained by the use of potassium bis(vinyltrimethylsilyl)amide as nucleophilic reagent, which is more reactive than the lithium analog. The fourth generation vinyl-terminated dendrimer was obtained in 74% yield. Methyl and phenyl groups were also used as terminal groups.

Other dendrimers that can be placed into this category are the dendritic silatrane wedges reported by Kemmitt and Henderson¹⁴⁴ based on the building block **1**. The dendrimers were synthesized up to the third generation and characterized using NMR spectroscopy and electrospray mass spectroscopy.

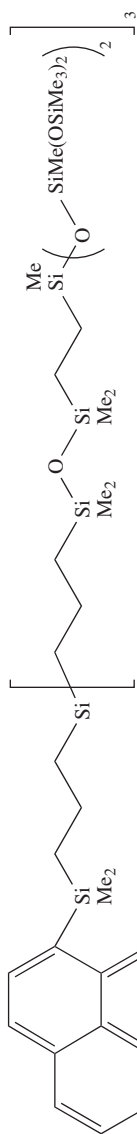
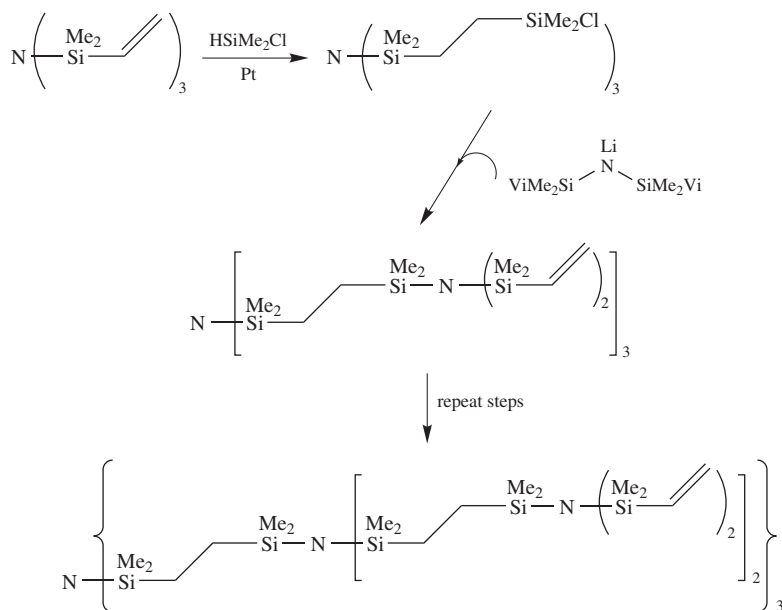
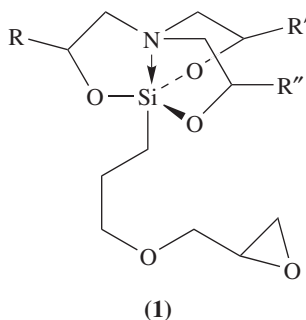


FIGURE 18. Carbosiloxane dendrimer with a pyrene core^{138,139}



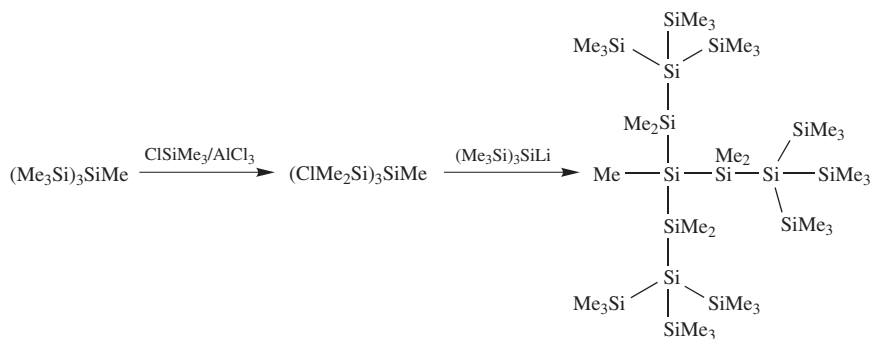
SCHEME 9



D. Silane Dendrimers

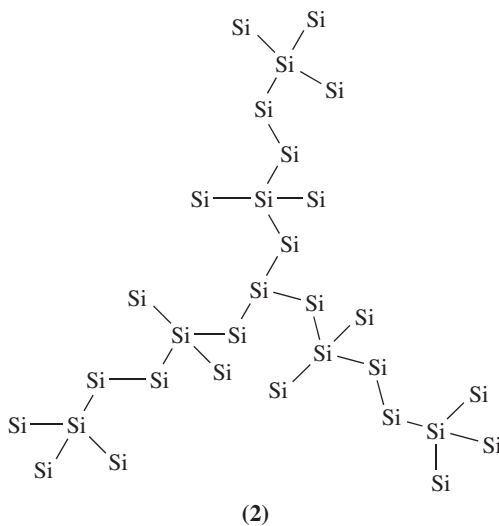
In 1995, the first syntheses of polysilane dendrimers were reported independently by Lambert, Sekiguchi, Suzuki and their coworkers. These reports will be discussed separately.

The synthesis described by Lambert and coworkers¹⁴⁵ is outlined in Scheme 10. The final step afforded the first generation dendrimer in 85% yield after recrystallization. The structure of the dendrimer was confirmed by mass spectroscopy, NMR spectroscopy and X-ray crystallography, which indicated significant steric interaction between the three dendritic wedges. There exist twenty-seven pathways with seven silicon atoms within the dendrimer, but none of these pathways corresponds to an all-*anti* configuration which is optimal for electron delocalization. In spite of this, the maximum absorbance in the UV spectrum is red-shifted with respect to linear heptasilane and very similar to that of linear

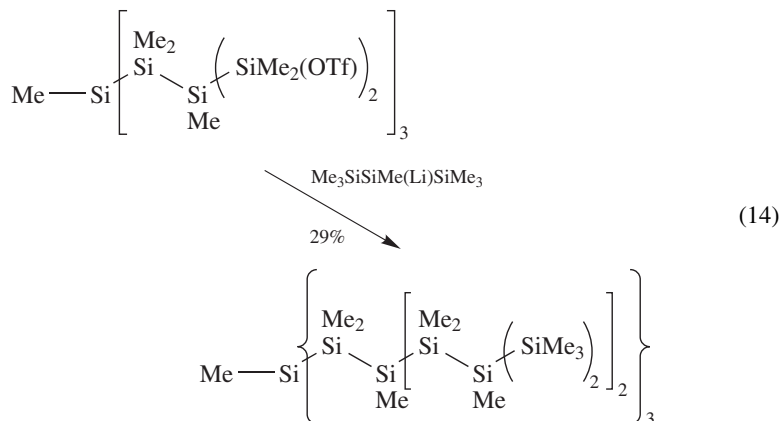


SCHEME 10

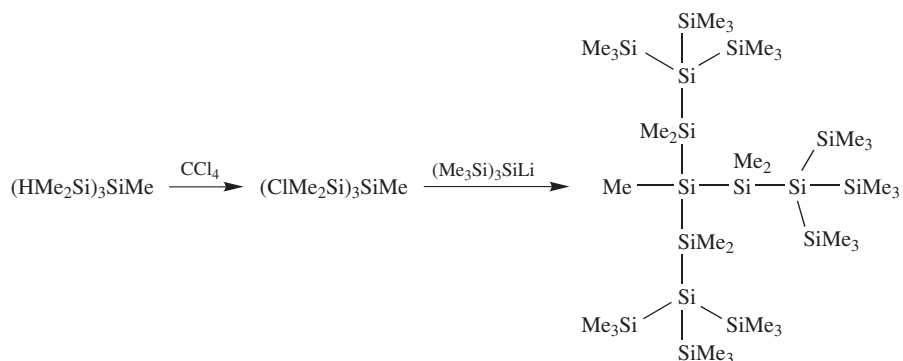
octasilane. Furthermore, the extinction coefficient is approximately one order of magnitude greater than those of linear polysilanes of six to eight silicon atoms. In later papers, these researchers described the synthesis and characterization of other first generation silane dendrimers with varying spacer lengths and branching¹⁴⁶ and also described the practical use of 2D ²⁹Si NMR techniques in elucidating the structure of dendritic silanes¹⁴⁷ (the use of standard 1D ²⁹Si NMR spectroscopy to characterize dendritic silanes was briefly described by another research group¹⁴⁸). In a more recent paper, Lambert and Wu reported the convergent synthesis of a larger dendritic silane that possessed 13 silicon atoms in its longest chain (**2**, skeleton structure)¹⁴⁹. Despite the fact that none of the Si₁₃ pathways is in the all-*anti* configuration, the UV absorbances of the dendrimer corresponded closely to those observed for linear Si₁₂, but with a significantly stronger absorption. The structure of the dendrimer was confirmed by X-ray crystallography.



Sekiguchi, Sakurai and coworkers utilized a stepwise approach to synthesize a second generation silane dendrimer in which the longest chain consisted of 11 silicon atoms (the final step is shown in equation 14)¹⁵⁰. The dendrimer was characterized by NMR spectroscopy, mass spectroscopy, UV spectroscopy and X-ray diffraction. The researchers did not compare the UV data to an analogous linear polysilane, but did observe that the absorbance maximum for the second generation dendrimer was red-shifted compared to the first generation, and also that the absorption was significantly more intense for the larger dendrimer.

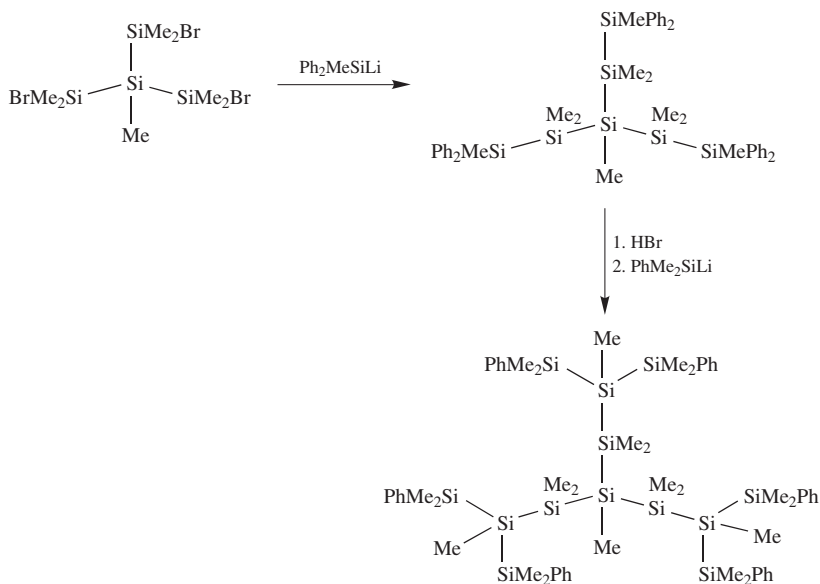


Later in the same year, Suzuki and coworkers¹⁵¹ reported the synthesis of the identical dendrimer described in Lambert's initial report¹⁴⁵, although via a slightly different synthetic pathway (Scheme 11). The dendrimer was characterized with NMR spectroscopy, X-ray diffraction and UV spectroscopy. Interestingly, these researchers reported¹⁵¹ a maximum absorbance at a slightly higher energy than that reported by Lambert with a significantly lower extinction coefficient (reported per silicon atom).



SCHEME 11

After these initial reports appeared, Marschner and Hengge¹⁵² reported the synthesis of a series of first generation dendrimers via another stepwise approach (Scheme 12). ¹³C and ²⁹Si NMR characterization data were included in this report.



SCHEME 12

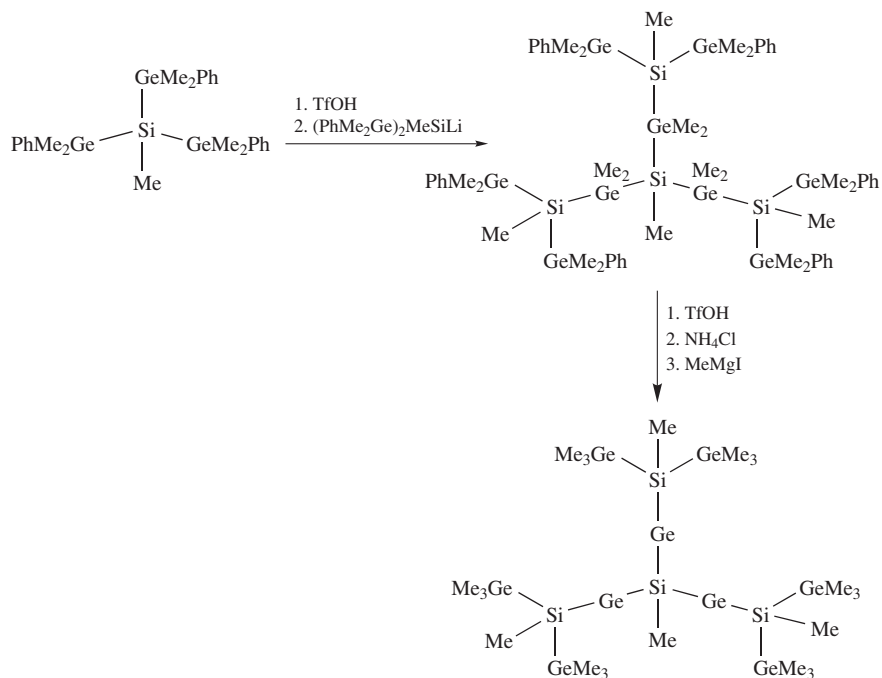
Although strictly speaking not a dendritic silane, a hybrid dendrimer synthesized by Sekiguchi and Nanjo¹⁵³ merits mention here. Utilizing a stepwise approach similar to those already described, a first generation dendrimer consisting of alternating germanium and silicon atoms was prepared (Scheme 13). The structure of this novel dendrimer was confirmed by an X-ray diffraction study, and UV data were reported.

E. Siloxane Dendrimers

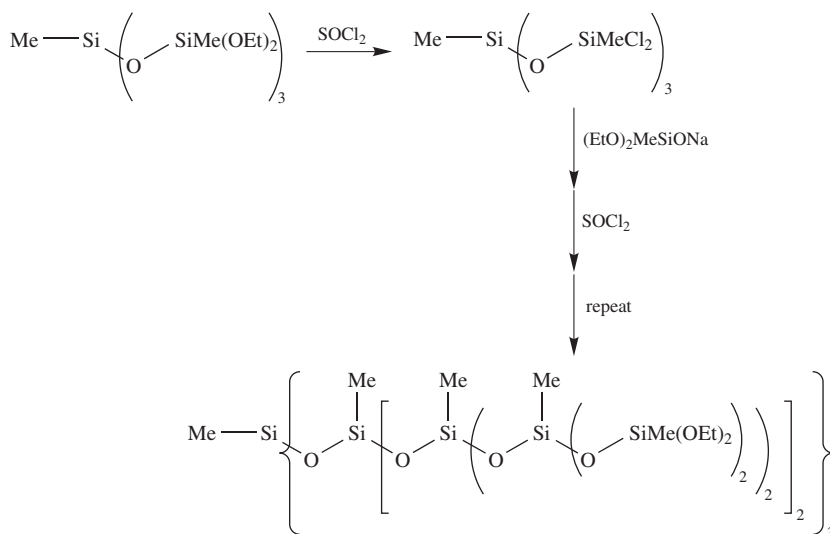
The first dendrimers of this type were reported by Rebrov and coworkers in 1989¹⁵⁴. Reaction of MeSiCl_3 with $(\text{EtO})_2\text{MeSiONa}$ followed by reaction with SOCl_2 gave the SiCl -terminated first generation. Repetition of the $(\text{EtO})_2\text{MeSiONa}$ and SOCl_2 sequences led to formation of siloxane dendrimers up to the fourth generation (Scheme 14).

Masamune and coworkers reported a divergent stepwise synthesis of siloxane dendrimers as shown in Scheme 15¹⁵⁵. The third generation dendrimer was the largest obtained. Characterization techniques included ¹H, ¹³C and ²⁹Si NMR spectroscopy, mass spectroscopy and size-exclusion chromatography.

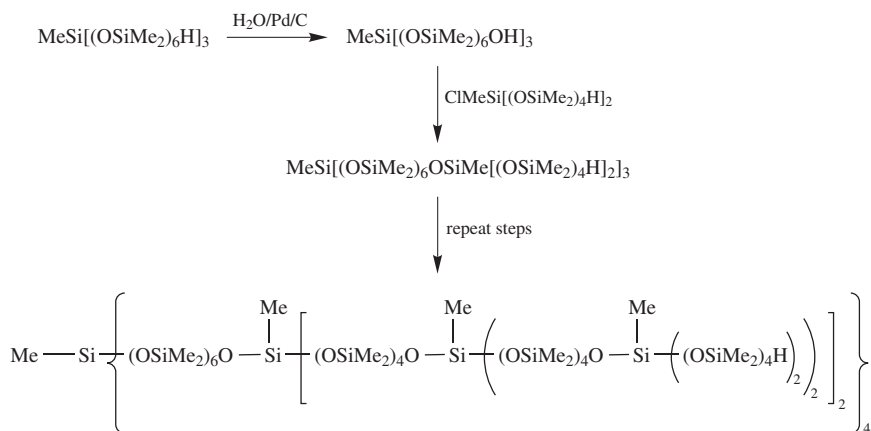
Another stepwise approach to siloxane dendrimers was described by Morikawa and coworkers¹⁵⁶ and is outlined in Scheme 16. Using the key building block, **A**, the researchers were able to construct dendrimers up to the third generation in 32% yield after purification. The dendrimers were characterized with NMR spectroscopy and intrinsic viscosity measurements, which indicated globular geometries.



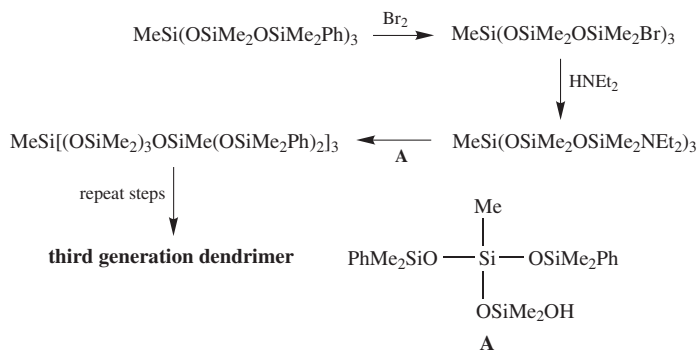
SCHEME 13



SCHEME 14



SCHEME 15

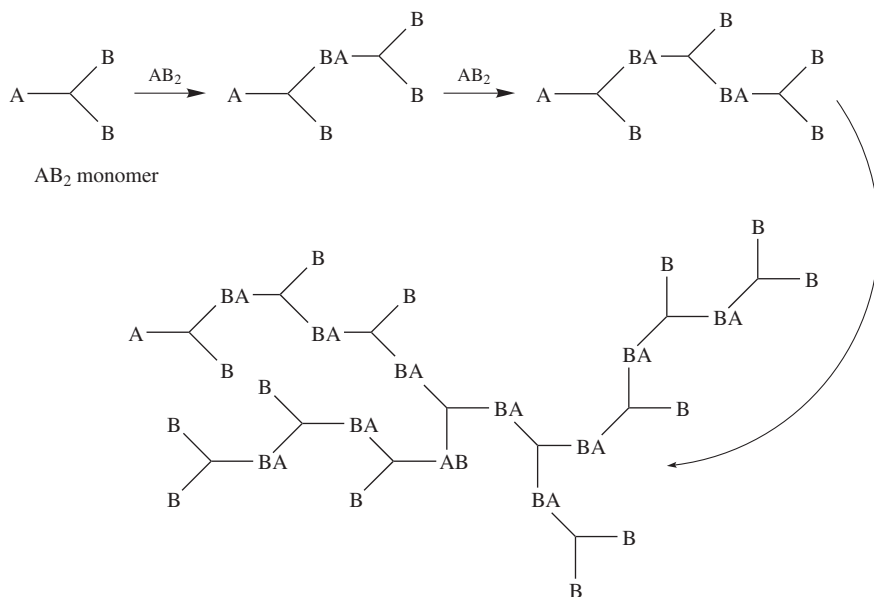


SCHEME 16

III. SILICON-BASED HYPERBRANCHED POLYMERS

Although not as monodisperse and symmetrically branched as dendrimers, hyperbranched polymers are attracting increased attention because they are relatively easy to synthesize. A typical one-pot hyperbranched polymer synthesis begins with an AB_n monomer where $n \geq 2$ and A and B are functional groups that can react with each other to form a new linkage. A general hyperbranched polymerization for an AB_2 monomer is illustrated in Scheme 17. It should be apparent that as the polymerization progresses, the branching becomes increasingly random in nature. Intramolecular cyclization is also a problem that can hinder polymer growth. A significant feature of the polymerization is that a considerable number of B groups will remain unreacted in the hyperbranched polymer. These B groups can be exploited for further chemical modification of the polymers. It should also be noted that the degree of branching in hyperbranched polymers is intermediate to that of dendrimers (which are perfectly and completely branched) and linear polymers (which are not branched).

As in dendrimer synthesis, organosilicon chemistry gives the synthetic chemist many tools with which to make new hyperbranched polymers. The existence of clean,



SCHEME 17

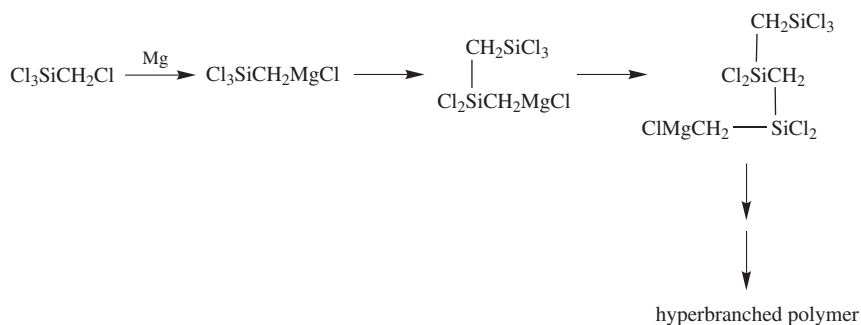
high-yielding reactions makes it relatively easy to make monomers with a variety of functional groups that are subsequently incorporated into the polymer. The increasing number of synthetic reports attests to this fact. Currently, hyperbranched poly(carbosilanes), poly(carbosiloxanes) and poly(siloxanes) are known. The synthesis and characterization of each polymer class will be discussed separately below.

A. Hyperbranched Poly(carbosilanes)

An examination of all papers describing the synthesis of hyperbranched poly(carbosilanes) reveals that only two reactions have been used in the polymerization step: nucleophilic substitution and hydrosilylation.

1. Hyperbranched poly(carbosilanes) prepared via nucleophilic substitution reactions

The first hyperbranched organosilicon polymer of any type was reported by Interrante and Whitmarsh in 1991¹⁵⁷. Treatment of chloromethyltrichlorosilane with magnesium converted the monomer to the Grignard reagent, which then reacted indiscriminately with SiCl linkages in the reaction mixture (Scheme 18). The hyperbranched chlorinated polymer was then reduced with lithium aluminum hydride (LAH) to yield a hyperbranched 'hydridopolycarbosilane' in 40% overall yield after an aqueous workup. This hydridopolycarbosilane, a viscous oil, has proved to be an excellent precursor to silicon carbide due to a 1:1 Si:C ratio in the polymer and also the presence of numerous crosslinkable SiH groups¹⁵⁸. Modification of the hydridopolycarbosilane could also be achieved^{159,160} by first converting some of the SiH groups to SiBr groups using Br₂. Reaction of the brominated polymer with Grignard or organolithium reagents resulted in new substituted polymers that were fully characterized. Polymers substituted with allyl groups could be



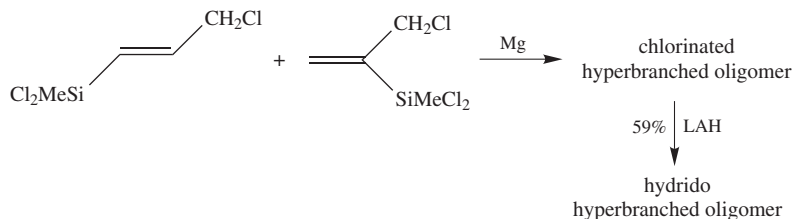
SCHEME 18

further modified by hydrosilylation with various monohydridotrialkylsilanes. The ethoxy-derivative of the original hyperbranched chlorinated polymer was also investigated as a precursor to silicon oxycarbide¹⁶¹. After sol-gel processing of the ethoxy polymer, the dried gel was pyrolyzed. In comparison to a gel derived from a linear precursor, the hyperbranched gel maintained a higher overall surface area at 1000 °C but was less stable toward weight loss at temperatures above 1000 °C. Microstructural differences were also noted.

Neckers and coworkers reported a similar polymerization using (chloromethyl)dichloromethylsilane as a starting material (equation 15)¹⁶². Oligomers were obtained in addition to cyclic trimers and tetramers. In the presence of a platinum catalyst and tetravinylsilane, the oligomer crosslinked when irradiated to form a hard, porous material that could be pyrolyzed to a silicon carbide char containing excess carbon. A later report described other platinum photo- and thermal catalysts that could be used in this crosslinking reaction¹⁶³.

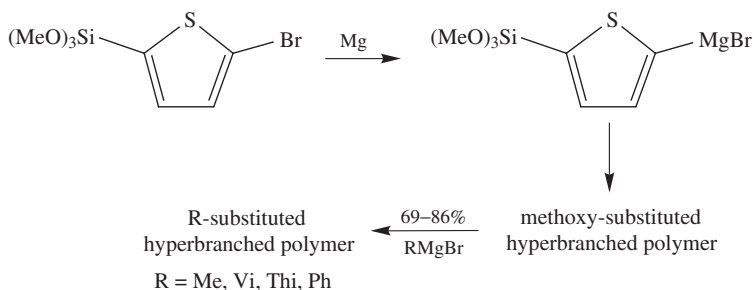


Son and coworkers utilized a mixture of AB₂ alkenyl chlorosilanes in another polymerization of this type (Scheme 19)¹⁶⁴. Due to the high reactivity of the monomers, it was necessary to add the monomer to the reaction mixture at a slow rate. The resulting LAH-reduced oily product could best be characterized as oligomeric, with an average molecular weight of 670 as determined by vapor pressure osmometry. The oligomer rapidly crosslinked in the presence of a platinum catalyst to form an infusible solid. Heating this solid to 975 °C in nitrogen resulted in a 31% weight loss.



SCHEME 19

Son and coworkers also utilized nucleophilic substitution to synthesize a series of hyperbranched poly(2,5-silylthiophenes)¹⁶⁵. The monomer, 2-bromo-5-trimethoxysilylthiophene, was converted to the corresponding AB₃ Grignard reagent and allowed to polymerize overnight (Scheme 20). Rather than perform a tedious isolation of the moisture-sensitive methoxy-substituted hyperbranched polymer, the researchers modified the polymer in solution by adding various Grignard reagents directly to the mixture. The resulting moisture-stable polymers were isolated by a simple aqueous workup. The degree of branching was determined by ¹H NMR spectroscopy, according to the method suggested by Frey and coworkers¹⁶⁶, and found to correspond closely to theoretical values. UV-visible spectroscopic studies indicated that the polymers absorbed at wavelengths similar to linear poly(silylthiophenes), thus indicating that the hyperbranched structure had little effect on $\sigma-\pi$ electron delocalization.

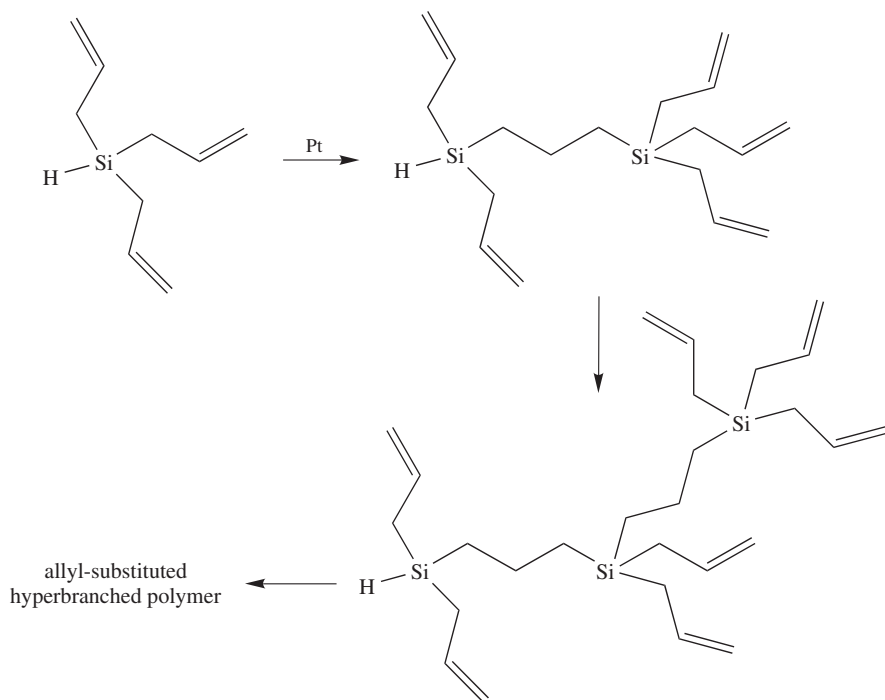


SCHEME 20

2. Hyperbranched poly(carbosilanes) prepared via hydrosilylation reactions

The first hyperbranched polymers of this type were reported in 1993 by Muzafarov and coworkers¹⁶⁷, who used methylvinylsilane, methyldiallylsilane, triallylsilane and methyldivinylsilane as monomers. A typical polymerization procedure involving triallylsilane is illustrated in Scheme 21. After addition of platinum catalyst, polymerization was complete within several hours at 85 °C with quantitative conversion to yield clear, viscous liquids. It was found that polymer molecular mass decreased as the monomer concentration decreased or as the platinum catalyst concentration increased. The researchers also found that molecular mass could not be increased by adding monomer to the polymerization reaction; they concluded that growth of hyperbranched polymer was limited by kinetic factors. They did suggest that increased molecular mass could be achieved by increasing the reaction temperature, utilizing more active catalysts, or by adding layers to the polymers manually as in dendrimer synthesis. The hyperbranched polymers of this study were found to be effective modifiers of composite polymer blends. For example, adding 1 to 2 wt% of hyperbranched allyl carbosilane polymer to siloxane rubber blends resulted in a 20% increase in tensile strength and a twofold increase in tear strength.

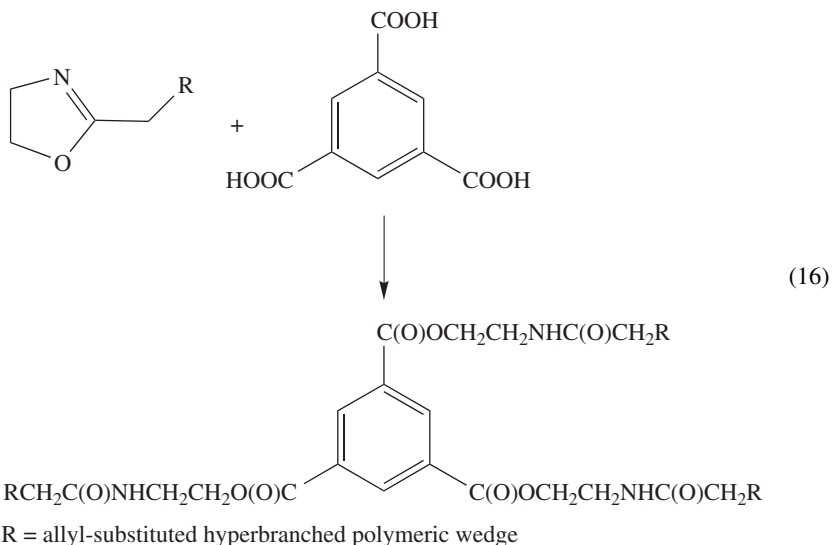
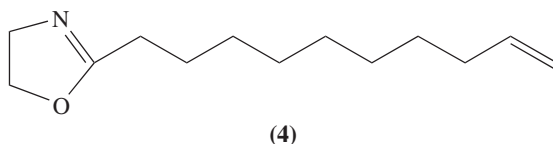
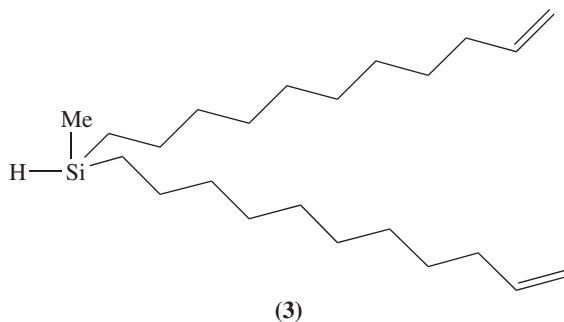
A more careful study of the polymerization conditions was described by this group in collaboration with Drohmann and Möller^{168,169}. In addition to the monomers previously polymerized, methyldiundecenylsilane (**3**) was synthesized in order to examine the effects of spacer length on polymerization. In general, it was found that methyldiundecenylsilane led to polymers of higher molecular weight. As observed previously, dilution of the monomer resulted in polymers of lower molecular weight accompanied by the formation



SCHEME 21

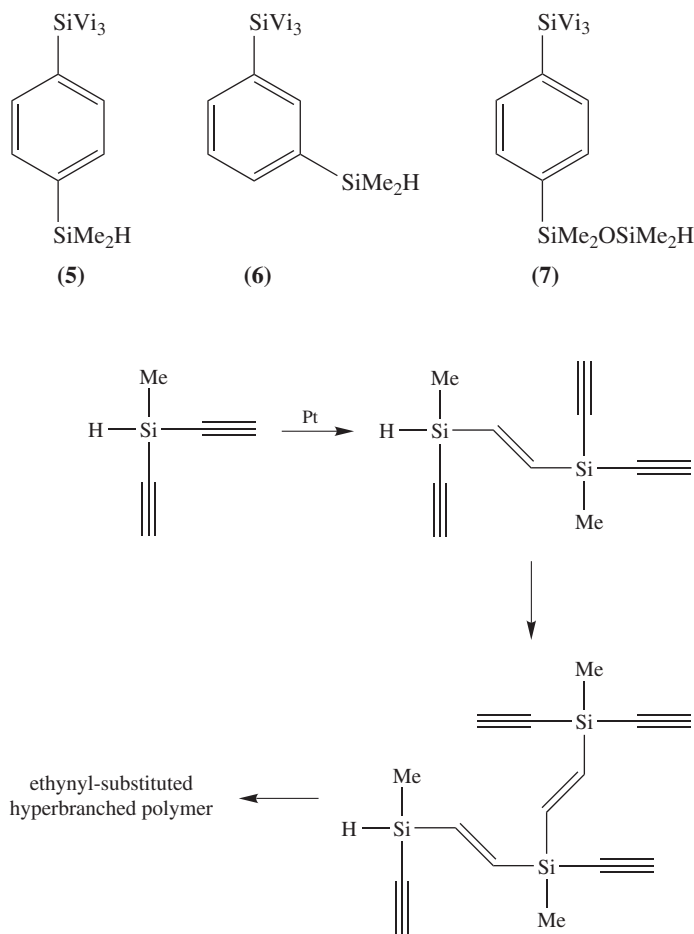
of small cyclic compounds. This study also confirmed that addition of monomer to the polymerization mixture was ineffective in increasing polymer molecular weight for the polymerization of the divinyl and diallyl silanes. However, with methyldiundecenylsilane, it was demonstrated that the polymer molecular weight unequivocally increased after six sequential additions of new monomer. This difference was attributed to decreased steric interactions and the increased flexibility of methyldiundecenylsilane in comparison to the shorter chain monomers.

Frey and coworkers also reported the synthesis of hyperbranched polymer from triallylsilane, but also performed a polymerization in the presence of 2-(10-decen-1-yl)-1,3-oxazoline (**4**) in order to control molecular weight¹⁷⁰. The polymer from triallylsilane alone was characterized by GPC and ²⁹Si NMR spectroscopy, the latter allowing calculation of degree of branching. Polymerization of triallylsilane with 2-(10-decen-1-yl)-1,3-oxazoline proceeded slowly but did decrease the polydispersity and the degree of polymerization. The oxazoline-functionalized hyperbranched poly(carbosilane) could be attached to a trimesic acid core in a convergent fashion (equation 16), or cationically homopolymerized or copolymerized with phenyloxazoline¹⁷¹. The trimesic core-functionalized polymers were later shown to aggregate into stacked columns over several hundreds of nanometers in length¹⁷². This aggregation, attributed to hydrogen bonding, was examined using WAXS, AFM and IR spectroscopy.



Son and coworkers also reported the syntheses of hyperbranched poly(carbosilanes) via hydrosilylation. In one report, they prepared a series of AB₃ carbosilylene monomers (**5**, **6** and **7**)¹⁷³ which polymerized cleanly and rapidly to form soluble hyperbranched polymers in high yields. The polymers, ranging in appearance from sticky solids to oils, were characterized by NMR spectroscopy, thermogravimetric analysis, differential scanning calorimetry and vapor pressure osmometry. The polymers possessed subambient *T_g*

values and excellent thermal stability in nitrogen. Copolymers of intermediate properties could be synthesized by polymerizing mixtures of the monomers. Degrees of branching in the polymers, as determined by ^{29}Si NMR spectroscopy, were close to theoretical values. A more recent report described the synthesis of hyperbranched poly(carbosilane) from methyldiethynylsilane (Scheme 22)¹⁷⁴. After a three-hour reaction period, the air- and moisture-stable polymer was isolated as a clear, sticky solid after precipitation from hexane. The polymer exhibited excellent thermal stability in nitrogen, losing only 13% mass on heating to 1300 °C. The remaining ethynyl groups in the polymer provide crosslinking sites and sites for transition metal attachment. The degree of branching in this polymer was close to the theoretical value.



SCHEME 22

Additional studies have focused on the structure, modification and characterization of hyperbranched poly(carbosilanes) synthesized via hydrosilylation. The structure of the hyperbranched polymer derived from methyldiallylsilane was examined using small-angle

X-ray scattering and molecular modeling¹⁷⁵. Among the primary findings was that in solution, the hyperbranched polymer (1) was considerably more dense compared to Gaussian coils of similar molecular weight, (2) was less dense than dendrimers of similar molecular weight and (3) was capable of retaining its shape.

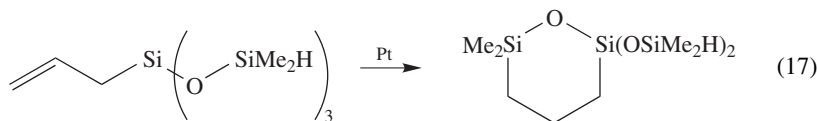
Frey and Lach reported a method for the enhancement of degree of branching in hyperbranched poly(carbosilanes)¹⁷⁶. Using the polymer obtained previously from the polymerization of triallylsilane in the presence of 2-(10-decen-1-yl)-1,3-oxazoline (4), they hydrosilylated the remaining allyl groups with trichlorosilane to convert the end groups to branch units. Subsequent reaction with allylmagnesium bromide gave a new hyperbranched poly(carbosilane) with dramatically enhanced degree of branching (Scheme 23). The hydrosilylation step did not proceed to completion, which was attributed to the existence of particularly well-shielded allyl groups in the interiors of the hyperbranched polymer molecules.

Möller and coworkers modified the hyperbranched polymer derived from methylallylsilane by attaching methacrylate groups to the unreacted allyl groups (Scheme 24)¹⁷⁷. Various weight percentages of this functionalized hyperbranched poly(carbosilane) were copolymerized with methacrylate monomers to form homogeneous copolymers. Initial observations indicated that degradation of the copolymer by alcoholysis of the SiO linkages created small functional pores within the polymer body.

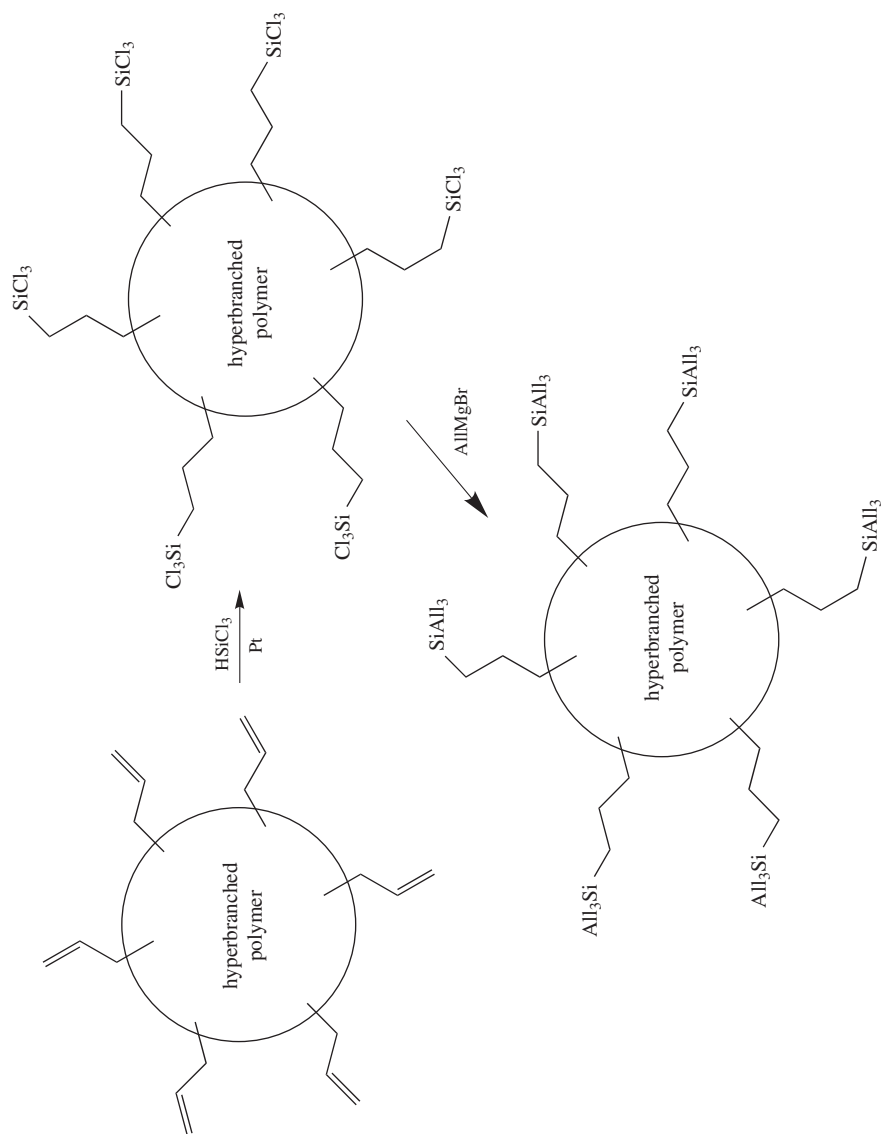
Getmanova and coworkers attached polar groups to the periphery of the hyperbranched poly(carbosilane) obtained from the polymerization of methylallylsilane (Scheme 25)⁷⁸. This modified hyperbranched polymer possessed certain properties, such as zero shear viscosity, T_g and surface tension, that were similar to comparably modified carbosilane dendrimers⁸¹.

B. Hyperbranched Poly(carbosiloxanes)

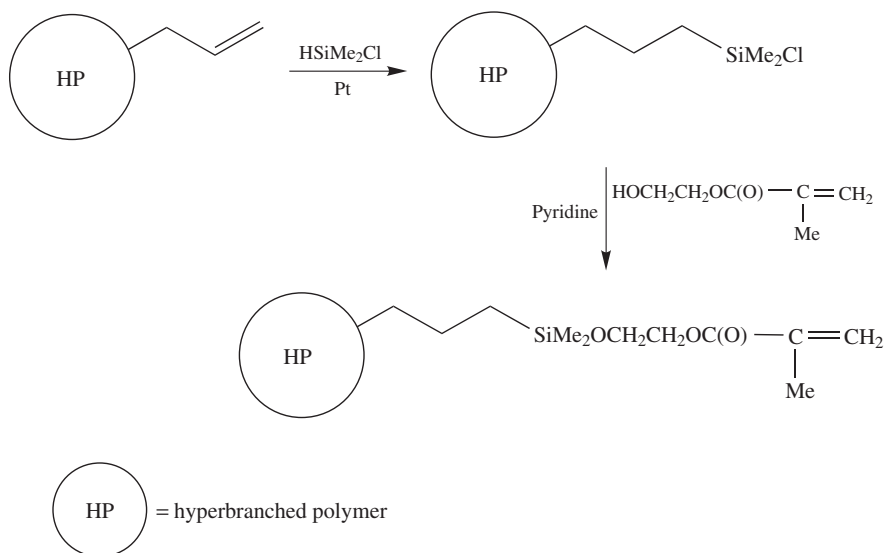
The first synthesis of hyperbranched poly(carbosiloxanes) was reported in 1991 by Mathias and Carothers¹⁷⁸. The polymer was prepared via hydrosilylation reactions of the AB₃ siloxy monomer **8**. Size exclusion chromatography indicated a narrow peak corresponding to a molecular weight of 19,000 (referenced to polystyrene). The polymer slowly became insoluble due to SiH crosslinking reactions, which could be avoided by the hydrosilylation reaction of the SiH groups with various substrates¹⁷⁹. In a later paper, the researchers reported that intramolecular cyclization of the monomer to a six-membered ring was a significant side-reaction of the polymerization (equation 17)¹⁸⁰, which was also confirmed independently by Rubinsztajn¹⁸¹. Intramolecular cyclization could be avoided by utilizing longer spacer groups between the SiH and the double bond groups in the monomer¹⁶.



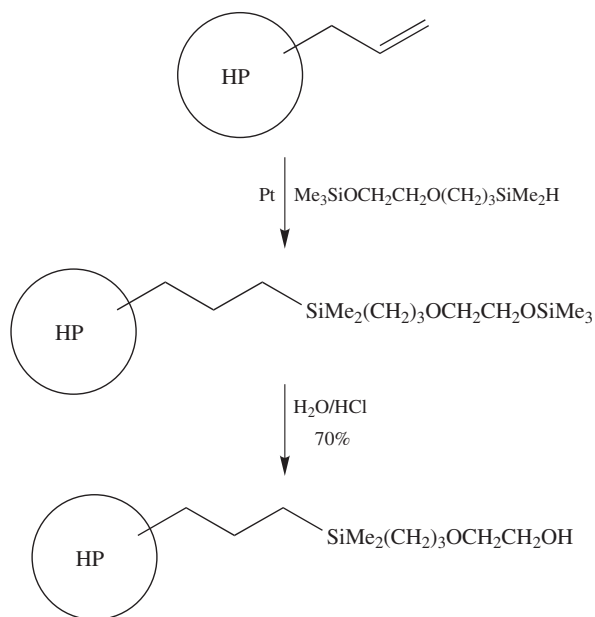
In 1994, Rubinsztajn reported the hyperbranched hydrosilylation polymerization of the AB₃ carbosiloxane monomers **9** and **10**¹⁸¹. Since intramolecular cyclization of these monomers would lead to more highly strained five-membered rings, it was expected that intermolecular reaction would be preferred. This was indeed the case, and molecular weights were highest when polymerizations were performed in bulk. Furthermore, slow addition of monomer resulted in polymers of much higher molecular weight. Functionalization of the polymers could be performed via hydrosilylation reactions, although these



SCHEME 23

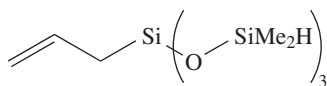


SCHEME 24

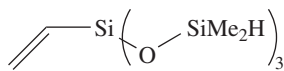


SCHEME 25

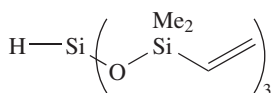
reactions did not go entirely to completion. The T_g values of the original and functionalized hyperbranched polymers ranged from -100 to -58°C . In a later paper, the same group reported the polymerization of the AB_3 aryl-containing monomer **11**¹⁸². Size exclusion chromatography indicated a molecular weight of 9800, and the T_g of the polymer was determined to be -58°C . Modifications of the polymer could be performed by hydrosilylation with various olefins. The monomer could also be copolymerized with styrene via a free-radical process to yield linear polymers. The SiH groups of the copolymer could be further modified through hydrosilylation with olefins.



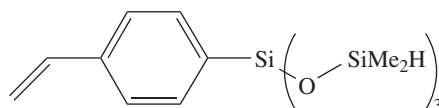
(8)



(9)

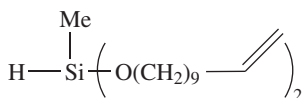


(10)

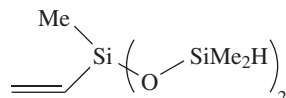


(11)

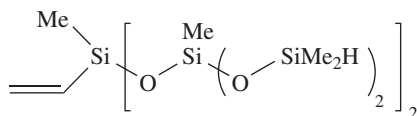
Degradable hyperbranched poly(carbosiloxanes) were reported by Möller and coworkers, who synthesized and polymerized an AB_2 monomer (**12**)¹⁸³. Platinum-catalyzed hydrosilylation in hexane led to the formation of a soluble polymer. Degradation could be induced by stirring the polymer with methanol under reflux conditions or by stirring with aqueous acid solutions. Mixing this hyperbranched polymer with methacrylate monomers followed by photopolymerization resulted in the formation of a blend in which the hyperbranched polymer was not covalently bonded to the poly(methacrylate) resin¹⁷⁷. Phase separation in the blend was observed with aggregation of the hyperbranched polymer molecules, presumably due to incompatibility of the hyperbranched polymer functional groups with the resin material.



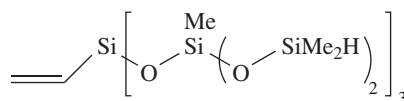
(12)



(13)



(14)

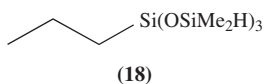
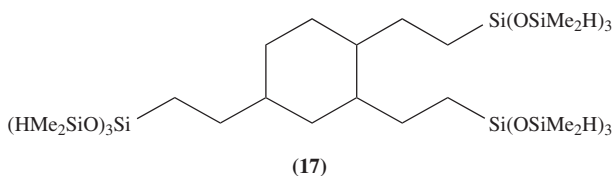
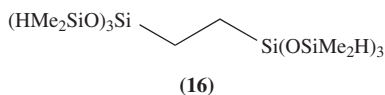


(15)

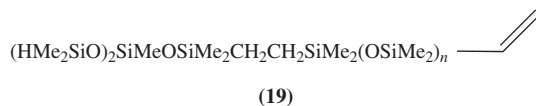
Fréchet and coworkers reported the hydrosilylation polymerization of the AB_2 and AB_3 carbosilyloxy monomers **13**, **14** and **15**^{184–187}. After polymerization in bulk, soluble polymers were obtained in 55–69% yields. Molecular weight analysis revealed the

formation of some small molecules, presumably cyclics resulting from intramolecular cyclization. Overall polymer M_w values were in the range 5000–9000. Modification of the polymers could be achieved by hydrosilylation reactions of the unreacted SiH groups with various olefins and aldehydes. The T_g values of the original polymers were below -100°C , but could be adjusted by choice of endcapping modification reagent^{184,185}. In later studies^{186,187}, it was found that the slow addition of monomer to the polymerization mixture increased the molecular weight and polydispersity of the hyperbranched polymer, with the final weight dependent on the total amount of monomer added. Slow addition of monomer to previously formed B_n cores also resulted in hyperbranched polymers of controllable molecular weight.

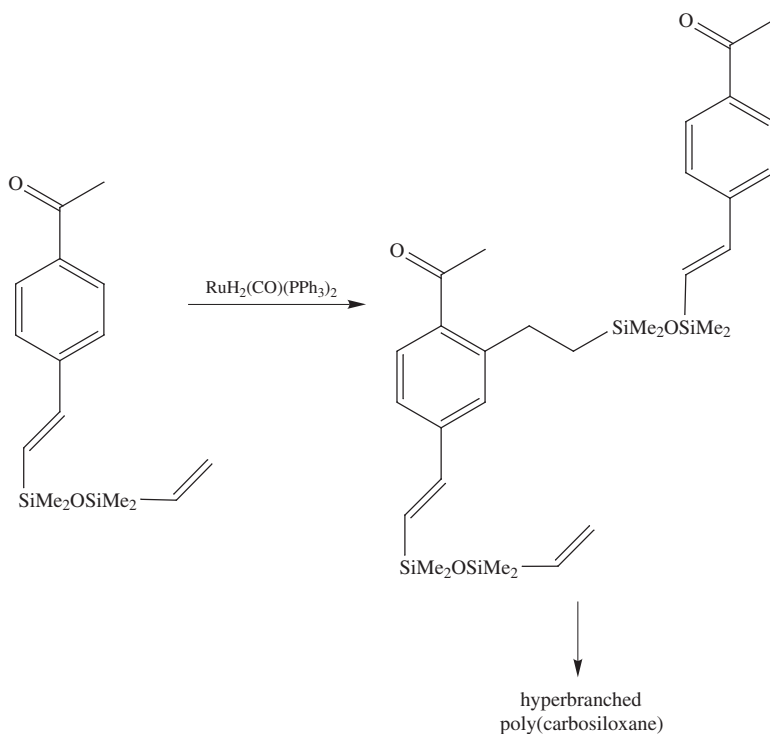
Herzig and Deubzer also reported the slow monomer addition process in the formation of hyperbranched poly(carbosiloxanes)¹⁸⁸. In this report, they added vinyltris(dimethylsiloxy)silane (**9**) (previously reported by Rubinsztajn¹⁸¹) to various cores (**16**, **17** and **18**). A dependence of polymer molecular weight on overall amount of monomer added was established by viscosity measurements. In addition, the formation of small cyclic compounds was reported and quantified.



Vasilenko and coworkers reported the hydrosilylation polymerization of AB_2 monomers containing extremely long spacers between the SiH and vinyl groups (**19**)¹⁸⁹. For the monomer with $n = 10$, polymers of 15,000–30,000 molecular weight were obtained in neat polymerizations. In solution, the monomer apparently cyclized intramolecularly. In the monomers with $n = 50$ or 100, crosslinked polymers were obtained in neat polymerizations, but soluble polymers were obtained in solution polymerizations.



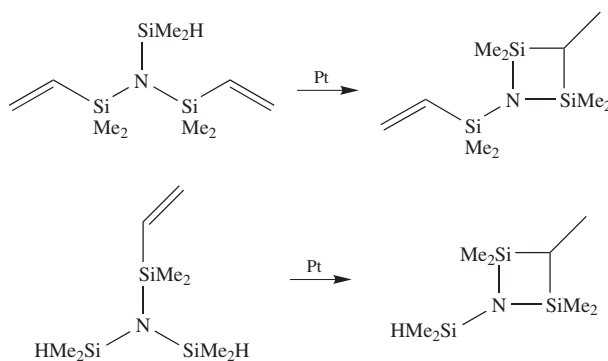
Hydrosilylation is not the only reaction available for the preparation of hyperbranched poly(carbosiloxanes). In a recent report, Weber and Londergan described the preparation of hyperbranched poly(carbosiloxanes) by ruthenium-catalyzed addition of ortho C–H bonds across terminal double bonds (Scheme 26)¹⁹⁰. Depending on reaction conditions, soluble or insoluble polymers could be obtained. NMR endgroup molecular weight analysis of the soluble polymer gave a value of 12,200. The structure of the polymer was established with ^1H , ^{13}C and ^{29}Si NMR analysis.



SCHEME 26

C. Hyperbranched Poly(carbosilazanes)

Thus far, no successful syntheses of hyperbranched poly(carbosilazanes) have been reported. An attempt to prepare polymers of this type by hydrosilylation led to the formation of intramolecularly cyclized products in nearly quantitative yields (Scheme 27)¹⁹¹.



SCHEME 27

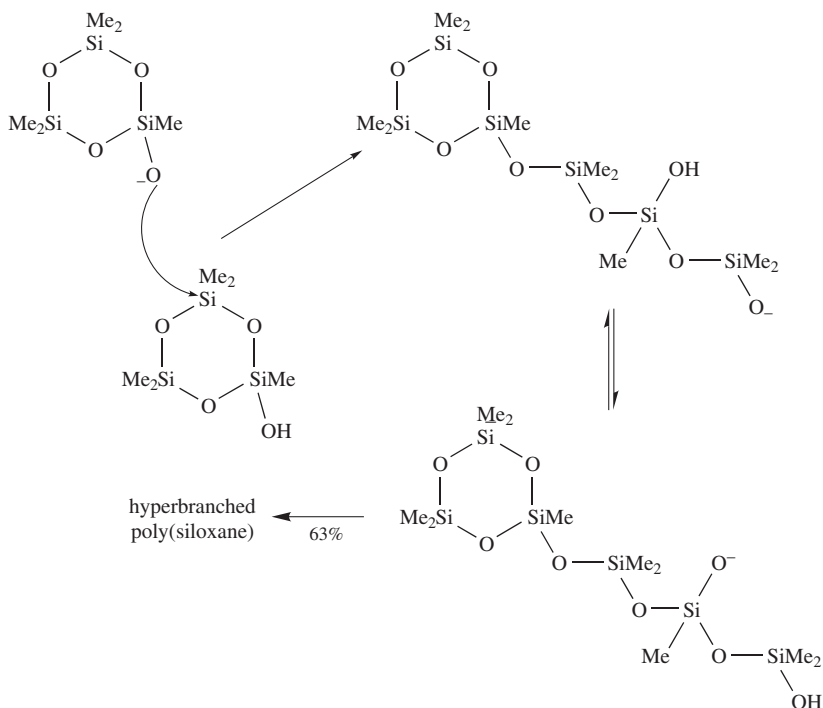
D. Hyperbranched Poly(siloxanes)

In 1999, Muzafarov and coworkers published a preliminary report describing the synthesis of a hyperbranched poly(siloxane) from triethoxysilanol via a rapid, ammonia-catalyzed condensation process (Scheme 28)¹⁹². The authors acknowledged the potential difficulties of this process (e.g. head–head condensation leading to crosslinked products) but presented ²⁹Si NMR data to support their conclusion that hyperbranched polymer was formed. The fact that no gel formation was observed also suggested that the polymerization proceeded as expected. The polymer, a transparent, yellow liquid, was characterized with NMR and IR spectroscopy, and GPC.



SCHEME 28

More recently, Weber and Paulasaari reported the synthesis of a hyperbranched poly(siloxane) via the ring-opening of 1-hydroxypentamethylcyclotrisiloxane (e.g. Scheme 29)^{193,194}. After ring-opening attack of the initial silanolate ion, the resulting silanolate ion can undergo reversible proton transfer, thus creating branching sites. ²⁹Si NMR data provided structural evidence and allowed for the calculation of M_n (19 400). GPC and MALLS molecular weight data were also reported.



SCHEME 29

IV. CONCLUDING REMARKS

It is clear that the field of organosilicon dendrimers and hyperbranched polymers is rapidly growing. Although much work has already been performed, there are still areas that require further research. For example, silazane dendrimers and hyperbranched poly(silanes), poly(silazanes) and poly(carbosilazanes) are yet unknown. The syntheses of these materials certainly represent significant challenges for the synthetic chemist. Furthermore, improved preparations of organosilicon hyperbranched polymers need to be developed, particularly in areas of polydispersity and branching control. Successful achievements in this area will enhance the viability of hyperbranched polymers as alternatives to dendrimers. Finally, further investigations are needed in the practical application of organosilicon dendrimers and hyperbranched polymers. Fundamental research is now being done in this area, and successful implementation of these materials in real-world applications will help to ensure a healthy future for the field.

V. REFERENCES

1. J. Issberner, R. Moors and F. Vögtle, *Angew. Chem., Int. Ed. Engl.*, **33**, 2413 (1994).
2. M. N. Bochkarev and M. A. Katkova, *Russ. Chem. Rev.*, **64**, 1035 (1995).
3. B. I. Voit, *Acta Polym.*, **46**, 87 (1995).
4. C. J. Hawker and J. M. J. Fréchet, in *Step-Growth Polymers for High-Performance Materials* (Eds. J. L. Hedrick and J. W. Labadie), American Chemical Society, Washington DC, 1996, p. 133.
5. G. R. Newkome, C. N. Moorefield and F. Vögtle, *Dendritic Molecules—Concepts, Syntheses, Perspectives*, VCH, Weinheim, 1996.
6. E. Malmström and A. Hult, *J. Macromol. Sci., Rev. Macromol. Chem. Phys.*, **C37**, 555 (1997).
7. H.-F. Chow, T. K. Mong, M. F. Nongrum and C.-W. Wan, *Tetrahedron*, **54**, 8543 (1998).
8. Y. H. Kim, *J. Polym. Sci., Pt. A, Polym. Chem.*, **36**, 1685 (1998).
9. O. A. Matthews, A. N. Shipway and J. F. Stoddart, *Prog. Polym. Sci.*, **23**, 1 (1998).
10. A. W. Bosman, H. M. Janssen and E. W. Meijer, *Chem. Rev.*, **99**, 1665 (1999).
11. M. Fischer and F. Vögtle, *Angew. Chem., Int. Ed. Engl.*, **38**, 884 (1999).
12. C. J. Hawker, in *Macromolecular Architectures* (Ed. J. G. Hilborn), Springer-Verlag, Berlin, 1999, p. 113.
13. A. Hult, M. Johansson and E. Malmström, in *Branched Polymers II* (Ed. J. Roovers), Vol. 143, Springer-Verlag, Berlin, 1999, p. 1.
14. J. Roovers and B. Comanita, in *Branched Polymers I* (Ed. J. Roovers), Vol. 142, Springer-Verlag, Berlin, 1999, p. 179.
15. J. M. Zeigler and F. W. G. Fearon, *Silicon-Based Polymer Science*, American Chemical Society, Washington, D.C., 1990.
16. L. J. Mathias and T. W. Carothers, in *Advances in Dendritic Macromolecules* (Ed. G. R. Newkome), Vol. 2, Jai Press Inc., Greenwich, 1995, p. 101.
17. D. Gudat, *Angew. Chem., Int. Ed. Engl.*, **36**, 1951 (1997).
18. H. Frey, C. Lach and K. Lorenz, *Adv. Mater.*, **10**, 279 (1998).
19. J.-P. Majoral and A.-M. Caminade, *Chem. Rev.*, **99**, 845 (1999).
20. C. Schlenk and H. Frey, *Monatsh. Chem.*, **130**, 3 (1999).
21. S. W. Kraska, D. Y. Son and D. Seyferth, in *Silicon-Based Polymers: The Science and Technology of Their Synthesis and Applications* (Eds. J. Chojnowski, R. G. Jones and W. Ando), Chapman & Hall, London, 2000.
22. D. Y. Son, *Main Group Chem. News*, **7**, 16 (2000).
23. J. Roovers, P. M. Toporowski and L.-L. Zhou, *Polym. Prepr.*, **33(1)**, 182 (1992).
24. L.-L. Zhou and J. Roovers, *Macromolecules*, **26**, 963 (1993).
25. A. W. van der Made and P. W. N. M. van Leeuwen, *Chem. Commun.*, 1400 (1992).
26. A. W. van der Made, P. W. N. M. van Leeuwen, J. C. de Wilde and R. A. C. Brandes, *Adv. Mater.*, **5**, 466 (1993).
27. D. Seyferth, D. Y. Son, A. L. Rheingold and R. L. Ostrander, *Organometallics*, **13**, 2682 (1994).

28. V. G. Krasovskii, N. A. Sadovskii, O. B. Gorbatshevich, A. M. Muzafarov, V. D. Myakushev, M. N. Il'ina, I. I. Dubovik, T. V. Strelkova and V. S. Papkov, *Polym. Sci.*, **36**, 589 (1994).
29. C. Kim, E. Park and E. Kang, *J. Korean Chem. Soc.*, **39**, 799 (1995).
30. C. Kim, D.-D. Sung, D.-I. Chung, E. Park and E. Kang, *J. Korean Chem. Soc.*, **39**, 789 (1995).
31. C. Kim, E. Park and E. Kang, *Bull. Korean Chem. Soc.*, **17**, 419 (1996).
32. C. Kim, E. Park and E. Kang, *Bull. Korean Chem. Soc.*, **17**, 592 (1996).
33. C. Kim, E. Park and I. Jung, *J. Korean Chem. Soc.*, **40**, 347 (1996).
34. C. Kim and K. An, *J. Organomet. Chem.*, **547**, 55 (1997).
35. C. Kim and S.-K. Choi, *Main Group Met. Chem.*, **20**, 143 (1997).
36. C. Kim and K. An, *Bull. Korean Chem. Soc.*, **18**, 164 (1997).
37. G. M. Ignat'eva, E. A. Rebrov, V. D. Myakushev, A. M. Muzafarov, M. N. Il'ina, I. I. Dubovik and V. S. Papkov, *Polym. Sci., Ser. A*, **39**, 874 (1997).
38. C. Kim and A. Kwon, *Main Group Met. Chem.*, **21**, 9 (1998).
39. C. Kim and M. Kim, *J. Organomet. Chem.*, **563**, 43 (1998).
40. P.-A. Jaffrès and R. E. Morris, *J. Chem. Soc., Dalton Trans.*, 2767 (1998).
41. C. Kim and Y. Jeong, *Main Group Met. Chem.*, **21**, 593 (1998).
42. K. Brüning and H. Lang, *J. Organomet. Chem.*, **571**, 145 (1998).
43. B. Boury, R. J. P. Corriu and R. Nuñez, *Chem. Mater.*, **10**, 1795 (1998).
44. C. M. Casado, I. Cuadrado, M. Morán, B. Alonso, M. Barranco and J. Losada, *Appl. Organomet. Chem.*, **13**, 245 (1999).
45. E. Müller and F. T. Edelman, *Main Group Met. Chem.*, **22**, 485 (1999).
46. I. M. Saez and J. W. Goodby, *Liq. Cryst.*, **26**, 1101 (1999).
47. P. I. Coupar, P.-A. Jaffrès and R. E. Morris, *J. Chem. Soc., Dalton Trans.*, 2183 (1999).
48. R. van Heerbeek, J. N. H. Reek, P. C. J. Kamer and P. W. N. M. van Leeuwen, *Tetrahedron Lett.*, **40**, 7127 (1999).
49. B. García, C. M. Casado, I. Cuadrado, B. Alonso, M. Morán and J. Losada, *Organometallics*, **18**, 2349 (1999).
50. Y. Chang, Y. C. Kwon, S. C. Lee and C. Kim, *Polym. Prepr.*, **40(2)**, 269 (1999).
51. M. M. K. Boysen and T. K. Lindhorst, *Org. Lett.*, **1**, 1925 (1999).
52. C. Kim and S. Kang, *J. Polym. Sci., Pt. A, Polym. Chem.*, **38**, 724 (2000).
53. J. Nakayama and J.-S. Lin, *Tetrahedron Lett.*, **38**, 6043 (1997).
54. T. Matsuo, K. Uchida and A. Sekiguchi, *Chem. Commun.*, 1799 (1999).
55. G. E. Oosterom, R. J. van Haaren, J. N. H. Reek, P. C. J. Kamer and P. W. N. M. van Leeuwen, *Chem. Commun.*, 1119 (1999).
56. M. Chai, Z. Pi, C. Tessier and P. L. Rinaldi, *J. Am. Chem. Soc.*, **121**, 273 (1999).
57. J. W. Kriesel, S. König, M. A. Frietas, A. G. Marshall, J. A. Leary and T. D. Tilley, *J. Am. Chem. Soc.*, **120**, 12207 (1998).
58. G. Friedmann, Y. Guilbert and J. C. Wittmann, *Eur. Polym. J.*, **35**, 1097 (1999).
59. F. Zeng and S. C. Zimmerman, *Chem. Rev.*, **97**, 1681 (1997).
60. C. Lach, D. Brizzolara and H. Frey, *Macromol. Theory Simul.*, **6**, 371 (1997).
61. V. G. Krasovskii, G. M. Ignat'eva, V. D. Myakushev, N. A. Sadovskii, T. V. Strelkova and A. M. Muzafarov, *Polym. Sci., Ser. A*, **38**, 1070 (1996).
62. Y. Chang, Y. C. Kwon, S. C. Lee and C. Kim, *Macromolecules*, **33**, 4496 (2000).
63. A. M. de Leuze-Jallouli, D. R. Swanson, S. V. Perz, M. J. Owen and P. R. Dvornic, *Polym. Mater. Sci. Eng.*, **77**, 67 (1997).
64. P. R. Dvornic, A. M. de Leuze-Jallouli, M. J. Owen and S. V. Perz, *Polym. Prepr.*, **39(1)**, 473 (1998).
65. P. R. Dvornic, A. M. de Leuze-Jallouli, D. Swanson, M. J. Owen and S. V. Perz, U.S. Patent 5,739,218 (1998).
66. A. M. de Leuze-Jallouli, D. Swanson, P. R. Dvornic, S. V. Perz and M. J. Owen, *Polym. Mater. Sci. Eng.*, **77**, 93 (1997).
67. A. M. De Leuze-Jallouli, P. R. Dvornic, S. V. Perz and M. J. Owen, *Polym. Prepr.*, **39(1)**, 475 (1998).
68. L. Balogh, A. M. de Leuze-Jallouli, P. R. Dvornic, M. J. Owen, S. V. Perz and R. Spindler, U.S. Patent 5,938,934 (1999).
69. P. R. Dvornic, A. de Leuze-Jallouli, M. J. Owen and S. V. Perz, *Polym. Prepr.*, **40(1)**, 408 (1999).

70. P. R. Dvornic, A. M. de Leuze-Jallouli, M. J. Owen, D. A. Dalman, P. Parham, D. Pickelman and S. V. Perz, *Polym. Mater. Sci. Eng.*, **81**, 187 (1999).
71. P. R. Dvornic, A. M. De Leuze-Jallouli, M. J. Owen and S. V. Perz, U.S. Patent 5,902,863 (1999).
72. E. Ruckinstein and W. Yin, *J. Polym. Sci., Pt. A, Polym. Chem.*, **38**, 1443 (2000).
73. J. W. Kriesel and T. D. Tilley, *Chem. Mater.*, **12**, 1171 (2000).
74. M. J. Michalczyk, W. J. Simonsick, Jr. and K. G. Sharp, *J. Organomet. Chem.*, **521**, 261 (1996).
75. K. Lorenz, R. Mülhaupt, H. Frey, U. Rapp and F. J. Mayer-Posner, *Macromolecules*, **28**, 6657 (1995).
76. H. Frey, K. Lorenz, R. Mülhaupt, U. Rapp and F. J. Mayer-Posner, *Macromol. Symp.*, **102**, 19 (1996).
77. C. Kim, S. Son and B. Kim, *J. Organomet. Chem.*, **588**, 1 (1999).
78. E. V. Getmanova, T. B. Chenskaya, O. B. Gorbatsevich, E. A. Rebrov, N. G. Vasilenko and A. M. Muzafarov, *React. Polym.*, **33**, 289 (1997).
79. E. V. Getmanova, E. A. Rebrov, N. G. Vasilenko and A. M. Muzafarov, *Polym. Prepr.*, **39(1)**, 581 (1998).
80. S. S. Sheiko, A. M. Muzafarov, R. G. Winkler, E. V. Getmanova, G. Eckert and P. Reineker, *Langmuir*, **13**, 4172 (1997).
81. S. S. Sheiko, A. I. Buzin, A. M. Muzafarov, E. A. Rebrov and E. V. Getmanova, *Langmuir*, **14**, 7468 (1998).
82. S. W. Kraska and D. Seyferth, *J. Am. Chem. Soc.*, **120**, 3604 (1998).
83. K. Lorenz, H. Frey, B. Stühn and R. Mülhaupt, *Macromolecules*, **30**, 6860 (1997).
84. B. Stark, B. Stühn, H. Frey, C. Lach, K. Lorenz and B. Frick, *Macromolecules*, **31**, 5415 (1998).
85. B. Trahasch, B. Stühn, H. Frey and K. Lorenz, *Macromolecules*, **32**, 1962 (1999).
86. B. A. Omotowa, K. D. Keefer, R. L. Kirchmeier and J. N. M. Shreeve, *J. Am. Chem. Soc.*, **121**, 11130 (1999).
87. S. A. Ponomarenko, E. A. Rebrov, A. Y. Bobrovsky, N. I. Boiko, A. M. Muzafarov and V. P. Shibaev, *Liq. Cryst.*, **21**, 1 (1996).
88. K. Lorenz, D. Hölter, B. Stühn, R. Mülhaupt and H. Frey, *Adv. Mater.*, **8**, 414 (1996).
89. K. Lorenz, D. Hölter, H. Frey and B. Stühn, *Polym. Mater. Sci. Eng.*, **77**, 168 (1997).
90. M. C. Coen, K. Lorenz, J. Kressler, H. Frey and R. Mülhaupt, *Macromolecules*, **29**, 8069 (1996).
91. D. Terunuma, T. Kato, R. Nishio, K. Matsuoka, H. Kuzuhara, Y. Aoki and H. Nohira, *Chem. Lett.*, 59 (1998).
92. D. Terunuma, T. Kato, R. Nishio, Y. Aoki, H. Nohira, K. Matsuoka and H. Kuzuhara, *Bull. Chem. Soc. Jpn.*, **72**, 2129 (1999).
93. G. H. Mehl and J. W. Goodby, *Chem. Commun.*, 13 (1999).
94. D. Terunuma, R. Nishio, Y. Aoki, H. Nohira, K. Matsuoka and H. Kuzuhara, *Chem. Lett.*, 565 (1999).
95. N. G. Vasilenko, E. V. Getmanova, V. D. Myakushev, E. A. Rebrov, M. Möller and A. M. Muzafarov, *Polym. Sci., Ser. A*, **39**, 977 (1997).
96. N. G. Vasilenko, E. A. Rebrov and A. M. Muzafarov, *Polym. Prepr.*, **39(1)**, 479 (1998).
97. N. G. Vasilenko, E. A. Rebrov, A. M. Muzafarov, B. Ebwein, B. Striegel and M. Möller, *Macromol. Chem. Phys.*, **199**, 889 (1998).
98. B. Comanita and J. O. Roovers, *Polym. Mater. Sci. Eng.*, **79**, 271 (1998).
99. B. Comanita, B. Noren and J. Roovers, *Macromolecules*, **32**, 1069 (1999).
100. N. J. Hovestad, J. T. B. H. Jastrzebski, G. van Koten, S. A. F. Bon, C. Waterson and D. M. Haddleton, *Polym. Prepr.*, **40(2)**, 393 (1999).
101. N. J. Hovestad, G. van Koten, S. A. F. Bon and D. M. Haddleton, *Macromolecules*, **33**, 4048 (2000).
102. J. Allgaier, K. Martin, H. J. Räder and K. Müllen, *Macromolecules*, **32**, 3190 (1999).
103. D. Seyferth, T. Kugita, A. L. Rheingold and G. P. A. Yap, *Organometallics*, **14**, 5362 (1995).
104. C. Kim and I. Jung, *Inorg. Chem. Commun.*, **1**, 427 (1998).
105. C. Kim and I. Jung, *J. Organomet. Chem.*, **588**, 9 (1999).
106. F. Lobete, I. Cuadrado, C. M. Casado, B. Alonso, M. Morán and J. Losada, *J. Organomet. Chem.*, **509**, 109 (1996).

107. I. Cuadrado, M. Morán, A. Moya, C. M. Casado, M. Barranco and B. Alonso, *Inorg. Chim. Acta*, **251**, 5 (1996).
108. B. Alonso, I. Cuadrado, M. Morán and J. Losada, *Chem. Commun.*, 2575 (1994).
109. B. Alonso, M. Morán, C. M. Casado, F. Lobete, J. Losada and I. Cuadrado, *Chem. Mater.*, **7**, 1440 (1995).
110. I. Cuadrado, C. M. Casado, B. Alonso, M. Morán, J. Losada and V. Belsky, *J. Am. Chem. Soc.*, **119**, 7613 (1997).
111. C. M. Casado, I. Cuadrado, M. Morán, B. Alonso, B. García, B. González and J. Losada, *Coord. Chem. Rev.*, **185–6**, 53 (1999).
112. I. Cuadrado, M. Moran, C. M. Casado, B. Alonso and J. Losada, *Coord. Chem. Rev.*, **193–195**, 395 (1999).
113. M. Benito, O. Rossell, M. Seco and G. Segalés, *Inorg. Chim. Acta*, **291**, 247 (1999).
114. M. Benito, O. Rossell, M. Seco and G. Segalés, *Organometallics*, **18**, 5191 (1999).
115. J. W. J. Knapen, A. W. van der Made, J. C. de Wilde, P. W. N. M. van Leeuwen, P. Wijkens, D. M. Grove and G. van Koten, *Nature*, **372**, 659 (1994).
116. G. van Koten and J. T. B. H. Jastrzebski, *J. Mol. Catal. A*, **146**, 317 (1999).
117. J. L. Hoare, K. Lorenz, N. J. Hovestad, W. J. J. Smeets, A. L. Spek, A. J. Canty, H. Frey and G. van Koten, *Organometallics*, **16**, 4167 (1997).
118. N. J. Hovestad, E. B. Eggeling, H. J. Heidebüchel, J. T. B. H. Jastrzebski, U. Kragl, W. Keim, D. Vogt and G. van Koten, *Angew. Chem., Int. Ed. Engl.*, **38**, 1655 (1999).
119. N. J. Hovestad, J. L. Hoare, J. T. B. H. Jastrzebski, A. J. Canty, W. J. J. Smeets, A. L. Spek and G. van Koten, *Organometallics*, **18**, 2970 (1999).
120. P. Dani, T. Karlen, R. A. Gossage, W. J. J. Smeets, A. L. Spek and G. van Koten, *J. Am. Chem. Soc.*, **119**, 11317 (1997).
121. A. W. Kleij, R. A. Gossage, J. T. B. H. Jastrzebski, J. Boersman and G. van Koten, *Angew. Chem., Int. Ed. Engl.*, **39**, 176 (2000).
122. R. A. Gossage, E. Muñoz-Martínez and G. van Koten, *Tetrahedron Lett.*, **39**, 2397 (1998).
123. R. A. Gossage, E. Munoz-Martinez, H. Frey, A. Burgath, M. Lutz, A. L. Spek and G. van Koten, *Chem. Eur. J.*, **5**, 2191 (1999).
124. A. W. Kleij, H. Kleijn, J. T. B. H. Jastrzebski, W. J. J. Smeets, A. L. Spek and G. van Koten, *Organometallics*, **18**, 268 (1999).
125. A. W. Kleij, H. Kleijn, J. T. B. H. Jastrzebski, A. L. Spek and G. van Koten, *Organometallics*, **18**, 277 (1999).
126. N. J. Hovestad, J. T. B. H. Jastrzebski and G. van Koten, *Polym. Mater. Sci. Eng.*, **80**, 53 (1999).
127. D. de Groot, E. B. Eggeling, J. C. de Wilde, H. Kooijman, R. J. van Haaren, A. W. van der Made, A. L. Spek, D. Vogt, J. N. H. Reek, P. C. J. Kamer and P. W. N. M. van Leeuwen, *Chem. Commun.*, 1623 (1999).
128. A. Morikawa, M. Kakimoto and Y. Imai, *Macromolecules*, **25**, 3247 (1992).
129. G. M. Ignat'eva, E. A. Rebrov, V. D. Myakushev, T. B. Chenskaya and A. M. Muzafarov, *Polym. Sci., Ser. A*, **39**, 843 (1997).
130. C. Kim and A. Kwon, *Synthesis*, 105 (1998).
131. C. Kim and J. Park, *Synthesis*, 1804 (1999).
132. C. Kim, Y. Jeong and I. Jung, *J. Organomet. Chem.*, **570**, 9 (1998).
133. C. Kim and M. Ryu, *J. Polym. Sci., Pt. A, Polym. Chem.*, **38**, 764 (2000).
134. K. Brüning and H. Lang, *J. Organomet. Chem.*, **575**, 153 (1999).
135. K. Brüning and H. Lang, *Synthesis*, 1931 (1999).
136. K. Brüning and H. Lang, *J. Organomet. Chem.*, **592**, 147 (1999).
137. K. Brüning, B. Lühmann and H. Lang, *Z. Naturforsch.*, **54b**, 751 (1999).
138. A. G. Vitukhnovskiy, M. I. Sluch, V. G. Krasovskii and A. M. Muzafarov, *Synth. Met.*, **91**, 375 (1997).
139. M. I. Sluch, I. G. Scheblykin, O. P. Varnavsky, A. G. Vitukhnovskiy, V. G. Krasovskii, O. B. Gorbatshevich and A. M. Muzafarov, *J. Lumin.*, **76–77**, 246 (1998).
140. S. S. Sheiko, A. I. Buzin, A. M. Muzafarov, E. A. Rebrov and E. G. Getmanova, *Polym. Prepr.*, **39(1)**, 481 (1998).
141. J. Hu and D. Y. Son, *Polym. Prepr.*, **39(1)**, 410 (1998).
142. J. Hu and D. Y. Son, *Macromolecules*, **31**, 8644 (1998).
143. M. Veith, R. Elsässer and R.-P. Krüger, *Organometallics*, **18**, 656 (1999).

144. T. Kemmitt and W. Henderson, *J. Chem. Soc., Perkin Trans. 1*, 729 (1997).
145. J. B. Lambert, J. L. Pflug and C. L. Stern, *Angew. Chem., Int. Ed. Engl.*, **34**, 98 (1995).
146. J. B. Lambert, J. L. Pflug and J. M. Denari, *Organometallics*, **15**, 615 (1996).
147. J. B. Lambert, E. Basso, N. Qing, S. H. Lim and J. L. Pflug, *J. Organomet. Chem.*, **554**, 113 (1998).
148. U. Herzog, C. Notheis, E. Brendler, G. Roewer and B. Thomas, *Fresenius J. Anal. Chem.*, **357**, 503 (1997).
149. J. B. Lambert and H. Wu, *Organometallics*, **17**, 4904 (1998).
150. A. Sekiguchi, M. Nanjo, C. Kabuto and H. Sakurai, *J. Am. Chem. Soc.*, **117**, 4195 (1995).
151. H. Suzuki, Y. Kimata, S. Satoh and A. Kuriyama, *Chem. Lett.*, 293 (1995).
152. C. Marschner and E. Hengge, in *Organosilicon Chemistry III: From Molecules to Materials* (Eds. N. Auner and J. Weis), Wiley-VCH, Weinheim, 1998, p. 333.
153. M. Nanjo and A. Sekiguchi, *Organometallics*, **17**, 492 (1998).
154. E. A. Rebrov, A. M. Muzafarov, V. S. Papkov and A. A. Zhdanov, *Dokl. Akad. Nauk SSSR*, **309**, 376 (1989); *Chem. Abstr.*, 112, 235956m (1990).
155. H. Uchida, Y. Kabe, K. Yoshino, A. Kawamata, T. Tsumuraya and S. Masamune, *J. Am. Chem. Soc.*, **112**, 7077 (1990).
156. A. Morikawa, M. Kakimoto and Y. Imai, *Macromolecules*, **24**, 3469 (1991).
157. C. K. Whitmarsh and L. V. Interrante, *Organometallics*, **10**, 1336 (1991).
158. C. K. Whitmarsh and L. V. Interrante, U.S. Patent 5,153,295 (1992).
159. I. L. Rushkin, Q. Qhen, S. E. Lehman and L. V. Interrante, *Macromolecules*, **30**, 3141 (1997).
160. L. V. Interrante, I. Rushkin and Q. Shen, *Appl. Organomet. Chem.*, **12**, 695 (1998).
161. G. D. Sorarù, Q. Liu, L. V. Interrante and T. Apple, *Chem. Mater.*, **10**, 4047 (1998).
162. B. E. Fry, A. Guo and D. C. Neckers, *J. Organomet. Chem.*, **538**, 151 (1997).
163. A. Guo, B. E. Fry and D. C. Neckers, *Chem. Mater.*, **10**, 531 (1998).
164. J. Yao and D. Y. Son, *J. Polym. Sci., Pt. A, Polym. Chem.*, **37**, 3778 (1999).
165. J. Yao and D. Y. Son, *Organometallics*, **18**, 1736 (1999).
166. D. Hölter, A. Burgath and H. Frey, *Acta Polym.*, **48**, 30 (1997).
167. A. M. Muzafarov, O. B. Gorbatshevich, E. A. Rebrov, G. M. Ignat'eva, T. B. Chenskaya, V. D. Myakushev, A. F. Bulkin and V. S. Papkov, *Polym. Sci.*, **35**, 1575 (1993).
168. C. Drohmann, O. B. Gorbatshevich, A. M. Muzafarov and M. Möller, *Polym. Prepr.*, **39(1)**, 471 (1998).
169. C. Drohmann, M. Möller, O. B. Gorbatshevich and A. M. Muzafarov, *J. Polym. Sci., Pt. A, Polym. Chem.*, **38**, 741 (2000).
170. C. Lach, P. Müller, H. Frey and R. Mülhaupt, *Macromol. Rapid Commun.*, **18**, 253 (1997).
171. C. Lach, R. Hanselmann, H. Frey and R. Mülhaupt, *Macromol. Rapid Commun.*, **19**, 461 (1998).
172. H. Frey, C. Lach, C. Schlenk and T. Pusel, *Polym. Prepr.*, **41(1)**, 568 (2000).
173. K. Yoon and D. Y. Son, *Macromolecules*, **32**, 5210 (1999).
174. R. A. Wong, Y. Xiao and D. Y. Son, *Polym. Prepr.*, **41(1)**, 608 (2000).
175. M. A. Fadeev, A. V. Rebrov, L. A. Ozerina, O. B. Gorbatshevich and A. N. Ozerin, *Polym. Sci., Ser. A*, **41**, 189 (1999).
176. C. Lach and H. Frey, *Macromolecules*, **31**, 2381 (1998).
177. A. M. Muzafarov, E. A. Rebrov, O. B. Gorbatshevich, M. Golly, H. Gankema and M. Möller, *Macromol. Symp.*, **102**, 35 (1996).
178. L. J. Mathias and T. W. Carothers, *J. Am. Chem. Soc.*, **113**, 4043 (1991).
179. L. J. Mathias and T. W. Carothers, *Polym. Prepr.*, **32(3)**, 633 (1991).
180. T. W. Carothers and L. J. Mathias, *Polym. Prepr.*, **34(2)**, 538 (1993).
181. S. Rubinsztajn, *J. Inorg. Organomet. Polym.*, **4**, 61 (1994).
182. S. Rubinsztajn and J. Stein, *J. Inorg. Organomet. Polym.*, **5**, 43 (1995).
183. A. M. Muzafarov, M. Golly and M. Möller, *Macromolecules*, **28**, 8444 (1995).
184. J. F. Miravet and J. M. J. Fréchet, *Polym. Mater. Sci. Eng.*, **77**, 141 (1997).
185. J. F. Miravet and J. M. J. Fréchet, *Macromolecules*, **31**, 3461 (1998).
186. C. Gong, J. Miravet and J. M. J. Fréchet, *J. Polym. Sci., Pt. A, Polym. Chem.*, **37**, 3193 (1999).
187. C. Gong, J. F. Miravet and J. M. J. Fréchet, *Polym. Mater. Sci. Eng.*, **80**, 139 (1999).
188. C. Herzig and B. Deubzer, *Polym. Prepr.*, **39(1)**, 477 (1998).
189. N. G. Vasilenko, E. A. Rebrov, V. D. Myakushev, A. M. Muzafarov, S. E. Cray, T. Okawa and R. Mikami, *Polym. Prepr.*, **39(1)**, 603 (1998).

190. T. M. Londergan and W. P. Weber, *Polym. Bull.*, **40**, 15 (1998).
191. K. Yoon and D. Y. Son, *Org. Lett.*, **1**, 423 (1999).
192. V. V. Kazakova, V. D. Myakushev, T. V. Strelkova and A. M. Muzafarov, *Polym. Sci., Ser. A*, **41**, 283 (1999).
193. J. K. Paulasaari and W. P. Weber, *Polym. Prepr.*, **41(1)**, 159 (2000).
194. J. K. Paulasaari and W. P. Weber, *Macromolecules*, **33**, 2005 (2000).

CHAPTER 14

Biotechnology reveals new routes to synthesis and structural control of silica and polysilsesquioxanes

DANIEL E. MORSE

Marine Biotechnology Center and Department of Molecular, Cellular and Developmental Biology, University of California, Santa Barbara, California 93106, USA.
Fax: 805-893-8062; e-mail: d_morse@lifesci.ucsb.edu

I. INTRODUCTION	806
II. OVERVIEW OF SILICA SYNTHESIS IN THE EXPERIMENTAL SYSTEMS	806
A. Diatoms	806
B. Sponges	807
III. SILICON TRANSPORT	807
IV. SEARCH FOR INTRACELLULAR SILICON CARRIERS OR CONJUGATES	807
V. CONTROL OF POLYCONDENSATION	808
A. Proteins Surrounding Diatom Biosilica	808
B. Polycationic Peptides Occluded in Diatom Biosilica Accelerate Silicic Acid Condensation	809
C. Silicateins: Structure-Directing, Polycondensation-Catalyzing Proteins from Sponge Biosilica	810
D. Catalytic, Structure-Directing Peptides Confirm and Extend these Conclusions	814
E. Protein and Genetic Engineering for Enhanced Control of Structure	817
F. Possible Relationships between Mechanisms in Sponges and Diatoms	817
VI. CONCLUSIONS	817

VII. ACKNOWLEDGMENTS	818
VIII. REFERENCES	818

I. INTRODUCTION

Thousands of species of living organisms produce structures of silica under mild physiological conditions of near-neutral pH and low temperature¹. The diversity of forms, the precision of nanoscale architectural control, the vast global scale and the paradoxically mild conditions of these biological syntheses of silica all demonstrate that biology has evolved novel mechanisms for the control of siloxane polycondensation and structural control that are of great potential interest to silicon chemists and materials scientists^{2,3}. While studies of biosilica synthesis have advanced across a broad front in a number of systems ranging from microalgae to plants and animals, two groups of marine organisms—diatoms and sponges—recently have been found uniquely tractable for analysis with the tools of modern biotechnology. This has proven to be an especially productive level of analysis of the complex mechanisms involved, as the diversity of biosilica structures and their strict genetic inheritance tell us that the keys to biosilicification and its structural control are completely encoded in the DNA². Recent findings of the underlying molecular mechanisms governing silica biosynthesis have led to the development of new structure-directing catalysts and new environmentally benign routes to the synthesis and structural control of silica and organosilicon-based materials at neutral pH and low temperature^{3,4}. Yet more questions remain than have been answered thus far. This chapter reviews recent progress and the limitations that remain in our efforts to understand and harness the mechanisms governing biosilicification.

II. OVERVIEW OF SILICA SYNTHESIS IN THE EXPERIMENTAL SYSTEMS

A. Diatoms

Diatoms are unicellular, photosynthetic microalgae that are abundant in the world's oceans and fresh waters. It is estimated that several tens of thousands of different species exist; sizes typically range from *ca* 5 to 400 μm , and most contain an outer wall of amorphous hydrated silica. These outer walls (named 'frustules') are intricately shaped and fenestrated in species-specific (genetically inherited) patterns^{5,6}. The intricacy of these structures in many cases exceeds our present capability for nanoscale structural control. In this respect, the diatoms resemble another group of armored unicellular microalgae, the coccolithophorids, that produce intricately structured shells of calcium carbonate. The silica wall of each diatom is formed in sections by polycondensation of silicic acid or as-yet unidentified derivatives (see below) within a membrane-enclosed 'silica deposition vesicle'^{1,7,8}. In this vesicle, the silica is coated with specific proteins that act like a coat of varnish to protect the silica from dissolution (see below). The silica is then extruded through the cell membrane and cell wall (lipid- and polysaccharide-based boundary layers, respectively) to the periphery of the cell.

The exquisite structures and diversity of the diatoms' silica walls are so remarkable that these organisms are widely considered Nature's paragons of nanostructural architecture^{2,3,7,8}. Indeed, Parkinson and Gordon have recently suggested the direct use of the diatom biosilica structures in nanotechnology, including applications involving their use as molds and masks for nanoscale casting, etching and lithography, as well as applications in advanced separation media and sensors⁹. While these uses may not be readily practicable, the more lasting contributions of diatoms to nanotechnology will likely involve further resolution of the basic molecular and subcellular mechanisms controlling

the biological synthesis and nanostructures of silicon-based materials, and applications of these findings to the development of new routes to synthesis and structural control of advanced materials and devices^{3,7,10}.

B. Sponges

Sponges are among the simplest multicellular organisms known. These animals, consisting of relatively few differentiated cell types, inhabit both marine and fresh waters, ranging from the abyssal depths to the shoreline. Some species produce defensive spines (called 'spicules') or supporting structures of silica, while others produce similar structures of calcium carbonate. Dimensions of the silica structures range from small spines, needles and stellate 'microscleres' of just a few microns dimension, to axial supporting rods approximately 1 m long and 1 cm in diameter^{11,12}. As in the case of the diatoms, the smaller silica structures are formed within a membrane-enclosed vesicle, while the larger structures are formed within the space enclosed by the cell membranes of multiple, closely appressed cells¹¹⁻¹³.

III. SILICON TRANSPORT

Studies with diatoms have revealed that silicic acid is pumped from the surrounding marine or freshwater environment into the cell against a concentration gradient through specific, outer membrane-associated transporters that were revealed recently by Hildebrand, Volcani and their colleagues¹⁴. Transporters related to those in the outer membrane may also facilitate entry into the membrane-enclosed silica deposition vesicle within the cell¹⁵.

Known mainly from studies of the cloned DNAs that code for these molecules, this family of multiple transporters includes at least one protein that has been shown directly to import Ge (as germanic acid); because this transport is competitively inhibited by silicic acid, the protein can be identified as a true silicon transporter. Its transport of silicic acid into the cell against a strong concentration gradient is dependent on the presence of Na⁺ ion. Apparently like the activity of numerous other ion transporters, the 'co-transport' of silicon is driven by the energy-dependent sodium cation transporter, which in turn is driven by the enzymatic cleavage of the energy-rich adenosine 5'-triphosphate. Dramatic proof that the cloned DNA does in fact code for a silicon transporter was obtained when that DNA was enzymatically copied to make messenger RNA *in vitro*, and this mRNA then injected into frog eggs. The injected mRNA served as the template for the synthesis of new protein molecules that promoted the transport of Ge and Si into the frog cells which previously did not take up these species¹⁴.

The Si transporting proteins (structures of which are deduced from the cloned DNA sequences) are closely related in structure to other, well-characterized ion transporters¹⁴. They contain 12 α -helical transmembrane domains that fold to form a cylindrical channel— assembled like staves of a barrel— through the lipid bilayer membrane of the cell. However, the evidence suggesting an ion-type transporter needs to be resolved with results of recent physiological analyses of the pH-dependence of silicon uptake, suggesting that many diatom species most efficiently take up the unionized, neutral silicic acid¹⁶.

IV. SEARCH FOR INTRACELLULAR SILICON CARRIERS OR CONJUGATES

Details of the intracellular speciation of Si and the mechanisms of its intracellular transport prior to condensation remain uncertain in all of the biological systems studied. Several possible alternatives have been suggested, including association with an intracellular carrier or ionophore¹⁷, covalent complex formation by condensation with alcohols, polyols or

catechols^{18–23}, and/or sequestration within small membrane-enclosed transport vesicles inside the cell^{24,25}. It is apparent that some such mechanism is operative to stabilize intracellular ‘silicic acid’. This conclusion is drawn from the fact that the intracellular pools of hot water-extractable silicic acid in diatoms are much higher than the concentration required for spontaneous condensation, yet something prevents the ectopic polycondensation within the body of the cell (the cytoplasm) until the silicic acid is transported to the silica deposition vesicle. One interesting possibility that offers clues to the control of silicic acid chemistry and reactivity is the *in vitro* formation of conjugates by the condensation of silicic acid and organic moieties. Such complexes could effectively stabilize silicic acid, preventing premature polycondensation in the cytoplasm of silica-forming cells. Kinrade and colleagues recently obtained ²⁹Si NMR spectroscopic evidence for the formation of alkoxide-like complexes by reaction of silicic acid with simple alcohols¹⁸ and biological polyols including simple sugars and oligosaccharides¹⁹. Although formed in aqueous solution at alkaline pH, conditions for condensation with some of the polyols tested approach physiological values of pH. These conjugates might represent more reactive and labile intermediates (and thus, more likely precursors for biosynthetic processes) than the very stable conjugates formed by condensation of silicic acid with catechols²⁰. If the pH within the silica deposition vesicle is more acidic than the surrounding cytoplasm, as has been reported²⁶, this acidity could be sufficient to hydrolyze a labile conjugate and initiate spontaneous condensation of the liberated silicic acid once the conjugate had been delivered to the vesicle. Other alternative possibilities exist, however.

V. CONTROL OF POLYCONDENSATION

Polymer hydroxyl groups have been suggested to play a role in the organization of biosilicification^{21–23,27–29}. Hecky and colleagues²⁷ proposed that protein hydroxyl groups, in a regular array, could facilitate silica synthesis by alignment of silicic acid precursors, either by direct condensation or by hydrogen bonding. Thermodynamic calculations have verified that such a mechanism would be energetically feasible³⁰. Recent results have shown that other polymer functionalities also are involved, and that these play a more dynamic role in biosilicification than first envisioned. These results are discussed below.

A. Proteins Surrounding Diatom Biosilica

Kröger and his colleagues first reported the isolation, cloning and characterization of proteins they called ‘frustulins’ (named for the diatom’s silica wall, or frustule)^{31–34}. Isolated from the cell walls of diatoms, the relationship of these proteins to the dynamic process of silica formation remains uncertain. These proteins were first extracted by EDTA solubilization from the organic cell wall of the diatom and subsequently found to be a family of calcium-binding glycoproteins. Immunolocalization (staining with antibodies specific for frustulins, and visualization by light and electron microscopy) shows the frustulins to be ubiquitously distributed in the outer layer of the cell wall, and overlying the silica-specific HEP-200 protein (see below). This team also described the extraction, cloning and characterization of 3 closely related ‘HEPs’, or HF-extractable proteins^{33,34}. Extraction by anhydrous HF suggested the tight association of members of this novel protein family with the silica, but sensitivity to enzymatic digestion prior to HF extraction showed that these proteins lie outside, not inside, the silica. Evidence suggests that these proteins may coat the silica like a layer of varnish, protecting it against dissolution by the surrounding water. Immunolocalization shows association with only certain specific

silica strips in the diatom wall, with the frustulins providing further shielding of the exterior surface of the HEPs. Strong association between the HEPs and the silica or some other component of the cell wall is indicated by the dependence on HF for release of these proteins. Boiling detergent (SDS), EDTA and sodium perchlorate all fail to extract these proteins, suggesting the possibility of covalent linkage either via the silanols of the silica (as originally proposed by Hecky and his colleagues²⁷; see above) or via glycosidic bonds. Both types of linkage would be hydrolyzed by HF under the conditions employed. Antibodies that recognize the HEPs cannot access their target until the frustulins have first been stripped from the outer layer by extraction with a detergent (SDS) and metal chelator (EDTA), thus demonstrating that the HEPs are normally shielded by the frustulins^{33,34}.

B. Polycationic Peptides Occluded in Diatom Biosilica Accelerate Silicic Acid Condensation

In a recent major breakthrough, Kröger and his colleagues have identified, cloned and characterized a third family of proteins associated with diatom biosilica³⁵. These proteins, named 'silaffins' (for their affinity for silica), are wholly occluded within the biosilica. Three small proteins (molecular weight *ca* 6,7 and 17 kDa) have been resolved. Gene cloning revealed that the silaffins contain multiple repeating, highly cationic peptides with unusual lysine-lysine dipeptides, lysine-arginine-arginine tripeptides and additional lysine residues at highly conserved (regular, repeating) positions. The cationic side chains of the lysine and arginine amino acids are illustrated in Figure 1. Purification and

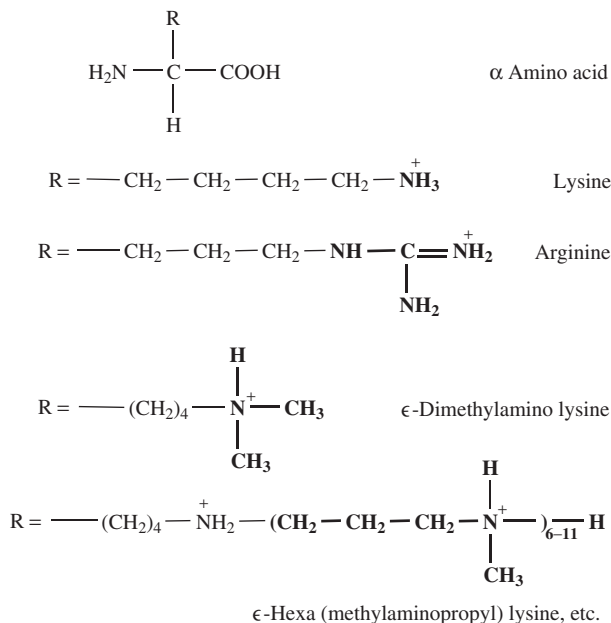


FIGURE 1. The lysine family of cationic amino acids. Structures include the typical α -amino acid found in proteins, and the cationic side-chains of lysine, arginine and the two substituted lysine derivatives recently found in high abundance in the silaffins occluded within the biosilica of a diatom³⁵. The derivatives with multiple methylaminopropyl units were previously unknown in biological systems

biochemical characterization revealed that the dilysine repeats contain highly modified side chains (one of which had never been found previously in any biological system) that further increase the cationic character of these residues (Figure 1). When tested *in vitro*, these unique polycationic proteins (essentially, substituted polyamines) accelerate the polycondensation of metastable silicic acid to form silica nanoparticles.

Within seconds after their addition to dilute silicic acid, the silaffins induce co-precipitation of silica nanospheres³⁵. Rates of formation of the nanoparticles are rapid and constant from pH 5 to pH 7; the precipitates form stoichiometrically with the silaffins, which become occluded within the silica. The nanoparticles produced *in vitro* are comparable in dimension to those that have been observed in the developing biosilica in diatoms^{36,37}, as well as those revealed by differential etching of the biosilica produced by sponges³⁸.

This activity of the silaffins is similar to that of simple amines and polyamines. Mizutani and his colleagues previously demonstrated that amines catalyze the polycondensation of silicic acid in water at neutral pH, with polyamines such as poly(allylamine) and poly(L-lysine) proving most effective³⁹. In these experiments, the polyamines also formed composites with the resulting silica gels. The molar ratios of Si/N were >2.0 ; IR and powder X-ray diffraction showed 'hybridization' between the gels and polyamines mediated by hydrogen bonding. Induced circular dichroism of indigo carmine adsorbed to the hybrid gels (but not on gels formed by acid polymerization) suggested that the hybrid provides a chiral environment. These observations also are related to those of Tanev and Pinnavaia⁴⁰, who reported 'biomimetic templating' of porous lamellar silicas by vesicular surfactant assemblies containing alkyl diamines.

Other than accelerating the formation of spherical nanoparticles of silica from metastable silicic acid solutions, the silaffins appear to have no structure-directing activity. If they are responsible for silica formation in the living diatom, as seems quite likely, control of the higher order architecture of the resulting silica apparently must be determined by the pre-formed shape of the silica deposition vesicle (the envelope within which the silica grows) serving as a complex three-dimensional mold.

C. Silicateins: Structure-Directing, Polycondensation-Catalyzing Proteins from Sponge Biosilica

In studies of the molecular mechanisms of biosilicification in sponges, we discovered a very different class of proteins, and a very different molecular mechanism that simultaneously catalyzes the polycondensation of silicon alkoxides while directing the structure of the resulting silica or silsesquioxane produced^{2,3,41-44}. Taking advantage of a simple marine sponge that produces 75% of its dry weight in the form of macroscopic silica needles (2 mm \times 30 μ m diameter; cf Figure 2), we were able to purify significant quantities of the proteins occluded within the silica. These proteins, which we named 'silicateins' (for silica proteins), self-assemble to form supramolecular axial filaments (2 mm \times 2 μ m diameter) that are wholly occluded within the silica needles⁴¹. The filaments consist of regular, repeating (X-ray diffracting) subassemblies of three very similar subunits (silicateins α , β and γ , present in the approximate ratio 12 : 6 : 1). Peptide sequencing and sequence analysis of the cloned cDNAs that code for these proteins revealed the surprising fact that silicateins α and β are highly homologous to cathepsin L, a member of the well-known super-family of papain-like proteolytic (protein hydrolyzing) enzymes^{41,44}. The silicateins and protease exhibit a striking 77% overall sequence homology (52% identity, and an additional 25% close similarity, when the two sequences are aligned and compared point-for-point). This discovery led to the recognition that the silicateins and the proteases (hydrolases) must have evolved from a shared molecular ancestor^{2,3,41,44}.

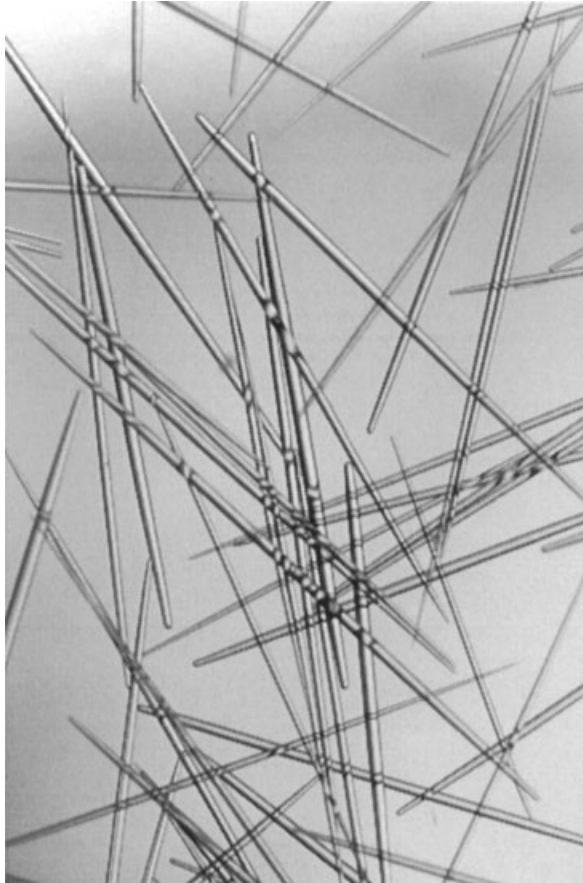


FIGURE 2. Glassy silica needles ($2\text{ mm} \times 30\text{ }\mu\text{m}$) produced in copious amount by a marine sponge. Each needle contains an occluded axial filament comprised of silicateins, enzyme-like proteins that catalyze and spatially direct the polycondensation of silicon alkoxides and silicic acid at neutral pH^{41,42}. Reprinted from Reference 3, copyright (1999), with permission from Elsevier Science

Most significantly, the catalytic ‘active site’ of the protease (hydrolase) is preserved with only minor changes in the silicateins.

As predicted from this finding, we discovered that the purified silicatein filaments catalyze the polycondensation of silica *in vitro* from silicon alkoxides such as TEOS (tetraethylorthosilicate)⁴². The filaments exhibit both a catalytic activity (catalyzing the hydrolysis and subsequent condensation of the monomers at neutral pH, in a reaction that typically requires extremes of pH and heat in the absence of a catalyst), and a ‘scaffolding’ or structure-directing template-like activity, in which they direct the assembly of the polymerized silica to follow the molecular contours of the underlying protein filament. The silicatein filaments also exhibit these two activities with organically substituted silicon alkoxides, catalyzing and spatially directing the polymerization of phenyl- and methyl-silsesquioxanes from the corresponding silicon triethoxides⁴². Structures of the resulting

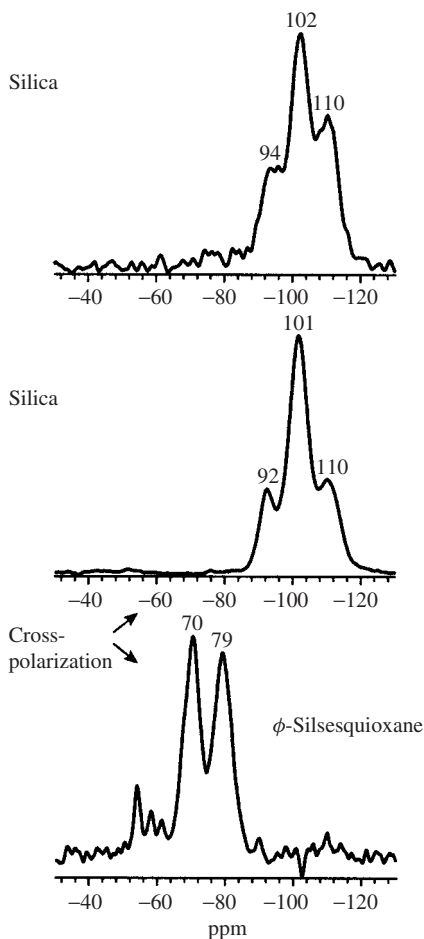


FIGURE 3. ^{29}Si -magic angle spinning NMR of silica and phenylsilsesquioxane products formed by the action of silicatein filaments on tetraethylorthosilicate (TEOS) or phenyltriethoxysilane, respectively. Single-pulse and cross-polarization spectra are shown. Results are discussed in the text. Redrawn from data in Reference 42

silica and silsesquioxanes were confirmed by ^{29}Si -magic angle spinning NMR (Figure 3), which demonstrates the broad Q^2 , Q^3 and Q^4 species typical of biologically produced silica, and the T^1 , T^2 and T^3 species characteristic of the silsesquioxane, respectively. For the Q species Q_2 , Q_3 and Q_4 , denote $\text{Si}(\text{OSi})_2(\text{OH})_2$, $\text{Si}(\text{OSi})_3(\text{OH})$ and $\text{Si}(\text{OSi})_4$ units, respectively. For the T species T_1 , T_2 and T_3 , denote $\text{RSi}(\text{OSi})(\text{OH})_2$, $\text{RSi}(\text{OSi})_2(\text{OH})$ and $\text{RSi}(\text{OSi})_3$ units, respectively, where R is an organic functionality. The catalytic activity is abolished by thermal denaturation, proving that it depends on the intact three-dimensional conformation of the silicatein proteins.

We found that this catalytic activity is also present in the disaggregated silicatein subunit monomers and —most significantly— in the purified and reconstituted silicatein

α and β subunits produced by bacteria from cloned, recombinant DNAs^{42,43,45}. Because the silicateins are highly homologous to cathepsin L—and this homology includes the exact conservation and position of 6 cysteine (–SH side chain) residues that form three intramolecular disulfide crosslinks in the proteases—we can be confident that the homology between the proteins includes the major features of their three-dimensional conformations. Since the structure of the protease is known from X-ray crystallography to the 1.78 Å level of resolution, further energy-minimization corrections to reflect the unique sequences of the silicateins thus provide us with good three-dimensional molecular models of these silica-synthesizing proteins (Figure 4)⁴⁴. Because we find that the structure of the known catalytic active site of the protease is conserved with high fidelity in the silicateins, and because the molecular mechanism of catalysis of the proteases is known in very precise detail, we are able to make very specific predictions concerning the mechanism of action of the silicateins in their catalysis of the rate-limiting hydrolytic step in silicon alkoxide polycondensation (Figure 5)^{2,3,42}. Based on the well-established molecular mechanism of the homologous proteases (which are simply specialized hydrolases), we suggest that the nucleophilic side-chain of the serine residue at position 26 in the peptide chain of silicatein α forms a hydrogen bond with the imidazole nitrogen of the histidine residue at position 165 in the silicatein (Figures 4 and 5), just as they do in the structurally related proteases⁴⁶, acting cooperatively across the active site cleft in the protein to increase the nucleophilicity of the serine-26 hydroxyl oxygen. As a result, nucleophilic attack on the silicon atom would be facilitated (Figure 5). This attack is postulated to form a transitory covalent protein–silicon intermediate, which would be additionally favored by the potential for stabilization as the pentavalent silicon species via a donor bond from the imidazole nitrogen. This intermediate is then subject to hydrolysis (as is the corresponding intermediate known to be formed by the protease), with the resulting generation and release of the reactive silanol, and regeneration of the serine–histidine hydrogen-bonded pair at the active site. This mechanism is suggested to account for the observed catalysis of polycondensation of the silicon ethoxides at neutral pH, in which it is known that hydrolysis to generate the silanol is the rate-limiting step⁴⁷.

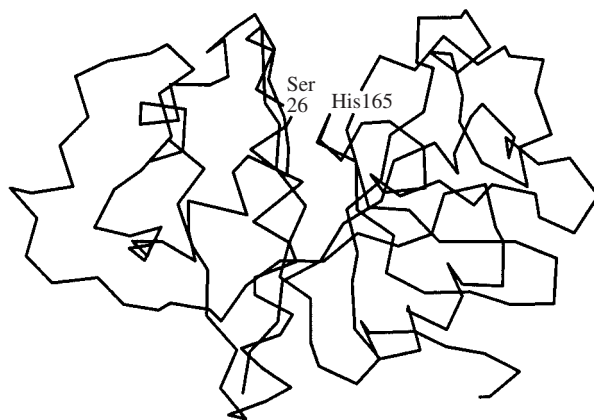


FIGURE 4. Molecular model of the peptide backbone of silicatein α (221 amino acid residues, constrained by three intramolecular disulfide cross-links), determined as described in the text. Locations of the putative catalytically active serine (at position 26) and histidine (at position 165) in juxtaposition on both sides of the active-site (substrate binding) cleft are identified. These features are very similar to those in the homologous protease (hydrolytic enzyme)

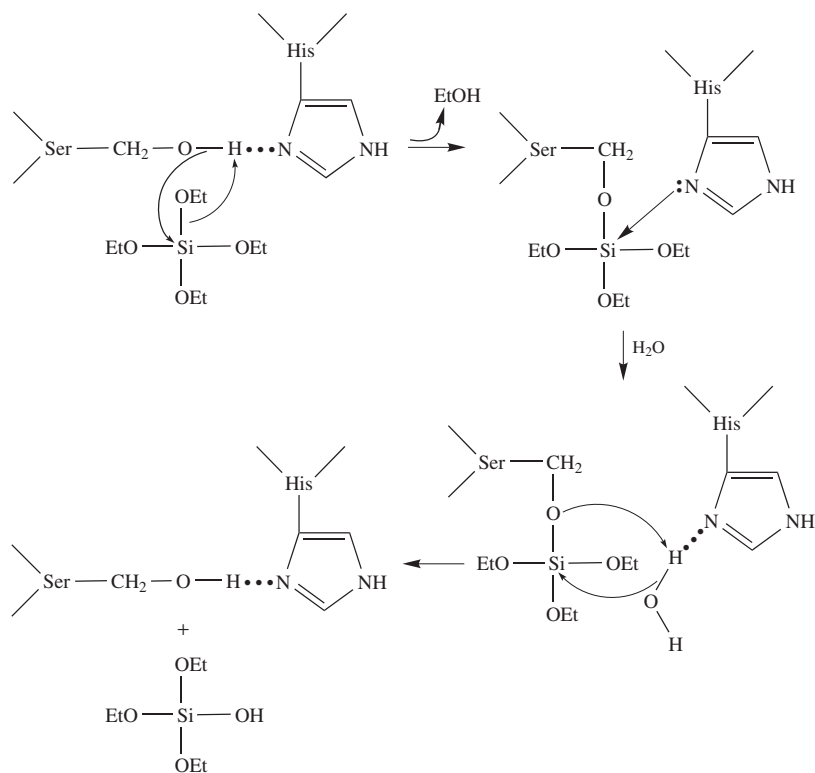


FIGURE 5. Proposed mechanism of catalysis of the rate-limiting step in tetraethylorthosilicate (TEOS) hydrolysis and polycondensation catalyzed by silicatein, as explained in the text⁴² Redrawn with permission from Reference 43

Recently we were able to test and confirm these predictions by site-directed mutagenesis, a genetic engineering method enabling us to replace at will any amino acid in the silicatein protein (Figure 6). Using this approach, we replaced each of the two amino acid residues whose side-chains we predicted to be essential for catalysis in silicatein α with a nonfunctional methyl group⁴³. Both of these replacements significantly inactivated the silicatein, confirming our hypothesis that a specific serine residue (with a hydroxyl side-chain at position 26 in the protein chain) and a specific histidine residue (with an imidazole side-chain at position 165) are essential for catalysis. These results support the hypothesis that the mechanism of action of the silicatein-mediated catalysis of the rate-limiting hydrolysis of the alkoxides is highly analogous to the known mechanism of action of the closely related proteases. This conclusion is further supported by results with synthetic peptides that mimic the activity of the silicateins.

D. Catalytic, Structure-Directing Peptides Confirm and Extend these Conclusions

To further test the conclusions based on the results described above, we synthesized a family of self-assembling diblock copolypeptides that incorporate the features found

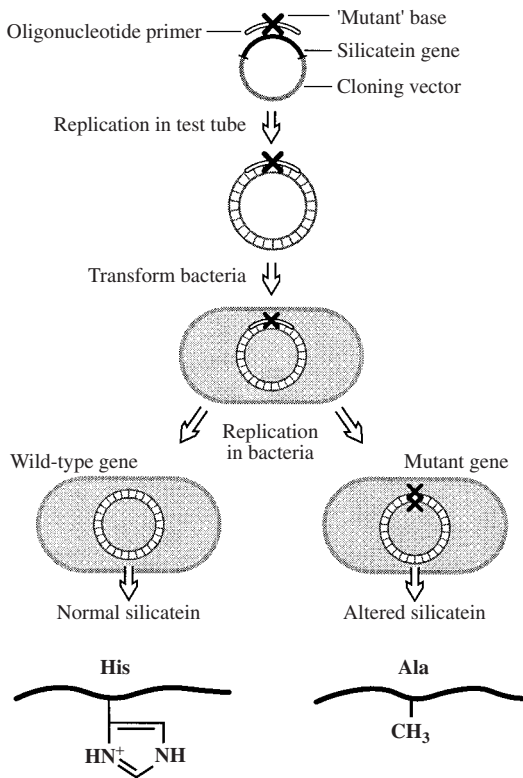


FIGURE 6. Genetic engineering. Method of site-directed mutagenesis used to test and confirm the proposed mechanism of silicon alkoxide polycondensation catalyzed by silicatein α^{43} . The precise sequence of nucleotides in the cloned DNA of the gene coding for the silicatein protein is known, as is the corresponding sequence of amino acids in the protein. To produce a desired substitution of any of the amino acids, a DNA oligonucleotide corresponding to one strand of the silicatein-encoding sequence is chemically synthesized, with an alteration (corresponding to a 'mutation') incorporated at the site that codes for the amino acid to be replaced. The specific alteration is chosen with reference to the genetic code (the correspondence of specific nucleotide triplets to each of the 20 amino acids commonly found in proteins), to direct the replacement of any 'target' amino acid with any other at that position. To incorporate this mutation into the functional gene, the synthetic oligonucleotide is first annealed with the complementary single-stranded recombinant DNA containing the complete silicatein gene in a 'cloning vector' (a small, covalently closed circular mini-chromosome) to form the Watson-Crick double-stranded structure; the remainder of the circular molecule is then replicated *in vitro* (by DNA polymerase) using the oligonucleotide as a 'primer'. This results in the incorporation of the mutation-bearing synthetic oligonucleotide in a faithful copy of one DNA strand of the cloned silicatein gene. The resulting double-stranded hybrid DNA is then introduced into bacterial cells, where strand-separation and replication give rise to two clones of cells: one carries the replicated normal gene and produces the normal silicatein protein; the other carries the replicated mutant gene, and produces silicatein containing the substituted amino acid. Finally, the relative specific activities of the normal and mutationally substituted silicatein proteins are quantitatively compared to evaluate the contributions of each of the targeted amino acids. In this way, it was determined that both the serine residue (Ser) at position 26 and the histidine residue (His) at position 156 are required for efficient catalysis of silicon alkoxide polycondensation, as proposed in Figure 5; when either is substituted by Alanine (Ala), >90% of the catalytic activity is lost⁴³

essential for catalysis by the silicatein active site⁴. Like the silicateins on which they are based, these relatively simple synthetic peptides prove capable of both catalyzing the polycondensation of TEOS at neutral pH and directing the structure of the resulting silica (Figure 7). Using Ni-catalyzed ring-opening polymerization of amino acid *N*-carboxyanhydrides to yield well-defined block copolypeptides with low polydispersity⁴⁸, we synthesized a series of defined diblock and triblock copolypeptides incorporating functionalities suggested by the sequencing, molecular modeling and site-directed mutagenesis results discussed above to be required for the catalysis and templating of polysiloxane synthesis from Si-alkoxides. Analysis of the performance of these peptides⁴ confirms and extends the conclusions of the site-directed mutagenesis analyses, demonstrating that: (1) diblocks containing both nucleophilic side-chains and hydrogen-bonding amine side-chains are more efficient catalysts of TEOS polycondensation at neutral pH than congeners that lack either of these functionalities; (2) catalytic efficiency (measured as the rate of catalyzed polycondensation at neutral pH) increases with the strength of the nucleophile: $-\text{SH} > -\text{Ph}-\text{OH} > -\text{CH}_2\text{OH} > -\text{CONH}_2 > -\text{CH}_3$; and (3) the peptides exhibit unique (peptide structure-specific) structure-directing control over the resulting silica (Figure 7).

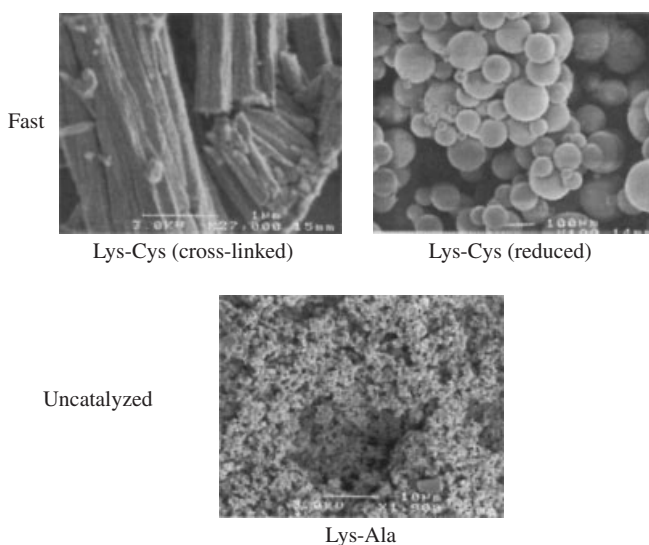


FIGURE 7. Biomimetic, self-assembling block copolypeptides that incorporate the essential requirements identified by site-directed mutagenesis mimic the action of silicatein, catalyzing and structurally directing the polycondensation of TEOS to form the silica structures shown⁴. In the example illustrated, the $-\text{SH}$ side-chains of the cysteine residues in a Lysine₂₀₀-Cysteine₃₀ diblock provide the required nucleophiles, and the ϵ -amino side-chains of the lysine residues provide the required hydrogen-bonding amino groups. The rate of polycondensation is faster, and the structure of the polymerized silica composite is directed by the diblock, in contrast to the reaction with peptides in which either of the required functionalities is absent (e.g. Lysine₂₀₀-Alanine₃₀). When the sulfhydryl side-chains are partially cross-linked via oxidatively formed disulfides, the resulting silica-organic composite has a strikingly uniform, fiber-like microstructure; when no disulfide cross-linking is permitted, the silica-composite forms hard transparent spheres⁴.

E. Protein and Genetic Engineering for Enhanced Control of Structure

We are building on the findings described above, using the tools of biotechnology in conjunction with detailed molecular modeling of the three-dimensional structure of the silicatein molecule, to genetically probe and engineer additional features of the silicatein structure. Our goal is to identify and then modify the determinants responsible for the structural control of the polymerized products, and thereby learn the requirements for structure-directed synthesis of more highly ordered and coherent polysilsesquioxanes for improved optoelectronic performance. The ultimate aim of these studies is to transfer the lessons learned from the modified biological system to the synthesis of improved structure-directing synthetic catalysts.

F. Possible Relationships between Mechanisms in Sponges and Diatoms

The discovery and characterization of the silicateins in sponges and the silaffins in diatoms suggest the possibility that different cellular and molecular mechanisms controlling silica formation may have evolved independently in these phylogenetically distant organisms. Indeed, evidence suggesting that mechanisms of biosilicification may have arisen independently more than once during the course of biological evolution is seen in the fact that numerous green plants (horsetails, grasses, grains, bamboos and even oak leaves) produce microgranular deposits of silica, yet the physical form of these 'phytoliths' (literally, 'plant rocks') bears little resemblance to the exquisitely nanostructured shells and spicules of diatoms and sponges¹. (In a similar manner, the capacity for flight has evolved independently, based on different but related anatomical structures and mechanisms, in insects, reptiles, birds, mammals and fish.)

The more intriguing alternative possibility is that both systems of biosilicification may share elements in common, although all of the similarities may not yet have been found. Polymerization within a shape-defining membrane-enclosed space and the essential roles of the transmembrane transporters are apparently common features of both systems. And recent results demonstrate that the silicateins are also capable of directing the polycondensation of silicic acid as well as of the silicon alkoxides⁴⁹. The identities of the intracellular silicon species, the precise pH and chemical composition within the membrane-enclosed sites of silica synthesis and the proximate precursors for silica synthesis remain virtually unknown in all systems of silica biosynthesis. It might thus be possible, for example, that silicon alkoxides or other conjugates (of sugars, catechols etc.) may be formed within the cells, and that these require hydrolysis by silicatein-like catalysts before silaffin- or silicatein-like elements can accelerate and/or direct polycondensation of the resulting silanols^{2,35}. Identification of the cytoplasmic form of silicic acid and of the proximate precursor to silica in the silica deposition vesicle is required in both systems, to help resolve the sequence of biosynthetic events.

VI. CONCLUSIONS

Recent biotechnological analyses have revealed at least two mechanisms by which nature can control the synthesis and nanofabrication of silica under physiological conditions. These findings have led to the design of synthetic catalysts for the structure-directed synthesis of silica and polysilsesquioxanes at neutral pH and low temperature. Prospects for enhanced structure-directing catalysts based on genetically engineered variants of the biological controllers are under investigation.

VII. ACKNOWLEDGMENTS

I wish to thank my close colleagues, Jennifer Cha, Katsuhiko Shimizu, Yan Zhou, Jixiang Cao, Camille Lawrence, Sean Christiansen, Mark Hildebrand, Galen Stucky, Mark Brzezinski and Brad Chmelka, for allowing me to report the results of our collaborative research; and Forrest Stark, Gordon Fearon, Gregg Zank, Norbert Auner, Mikhail Voronkov, Yolanda del Amo, John Gaul, Markus Merget and Jan Sumerel for stimulating discussions. This work was supported by grants from the U.S. Army Research Office Multidisciplinary University Research Initiative (DAAH04-96-1-0443), the U.S. Office of Naval Research (N00014-93-1-0584), the Materials Research Division of the National Science Foundation (MCB-9202775), the NOAA National Sea Grant College Program, U.S. Department of Commerce, under grant NA36RG0537, Project E/G-2, through the California Sea Grant College System, the MRSEC Program of the National Science Foundation under award No. DMR-96-32716 to the UCSB Materials Research Laboratory, and a generous donation from the Dow Corning Corporation. The U.S. Government is authorized to reproduce and distribute copies for governmental purposes.

VIII. REFERENCES

1. T. L. Simpson and B. E. Volcani, *Silicon and Siliceous Structures in Biological Systems*, Springer-Verlag, New York, 1981.
2. D. E. Morse, in *Organosilicon Chemistry IV: From Molecules to Materials* (Eds. N. Auner and J. Weis), 5, Wiley-VCH, Weinheim, 1999.
3. D. E. Morse, *Trends Biotechnol.*, **17**, 230 (1999).
4. J. N. Cha, G. D. Stucky, D. E. Morse and T. J. Deming, *Nature*, **403**, 289 (2000).
5. G. Hallegraeff, *Plankton: A Microscopic World*, CSIRO/Robert Brown and Assoc., Melbourne, 1988.
6. F. E. Round, R. M. Crawford and D. G. Mann, *The Diatoms: Biology and Morphology of the Genera*, Cambridge University Press, Cambridge, 1990.
7. E. G. Vrieling, T. P. M. Beelen, R. A. van Santen and W. W. C. Gieskes, *J. Biotechnol.*, **70**, 39 (1999).
8. E. G. Vrieling, L. Poort, T. P. M. Beelen and W. W. C. Gieskes, *Eur. J. Phycol.*, **34**, 307 (1999).
9. J. Parkinson and R. Gordon, *Trends Biotechnol.*, **17**, 190 (1999).
10. C. M. Zaremba and G. D. Stucky, *Curr. Opin. Solid State Mater. Sci.*, **1**, 425 (1996).
11. T. L. Simpson, *The Cell Biology of Sponges*, Springer, New York, 1984.
12. C. Levi, J. L. Barton, C. Guillemet, E. Le Bras and P. Lehuede, *J. Mater. Sci. Lett.*, **8**, 337 (1989).
13. G. Imsiecke, R. Steffen, M. Custodio, R. Borojevic and W. E. G. Müller, *In Vitro Cell Dev. Biol.*, **31**, 528 (1995).
14. M. Hildebrand, B. E. Volcani, W. Gassman and J. I. Schroeder, *Nature*, **385**, 688 (1997).
15. M. Hildebrand, K. Dahlin and B. E. Volcani, *Mol. Gen. Genet.*, **260**, 480 (1998).
16. Y. Del Amo and M. Brzezinski, *J. Phycol.*, **35**, 1162 (1999).
17. P. Battacharyya and B. E. Volcani, *Biochem. Biophys. Res. Commun.*, **114**, 365 (1983).
18. S. D. Kinrade, K. J. Maa, A. S. Schach, T. A. Sloan and C. T. G. Knight, *J. Chem. Soc., Dalton Trans.*, 3149 (1999).
19. S. D. Kinrade, J. W. Del Nin, A. S. Schach, T. A. Sloan, K. L. Wilson and C. T. G. Knight, *Science*, **385**, 1542 (1999).
20. D. F. Evans, J. Parr and E. N. Coker, *Polyhedron*, **9**, 813 (1990).
21. C. C. Harrison, *Phytochemistry*, **41**, 37 (1996).
22. C. C. Harrison and N. J. Loton, *J. Chem. Soc., Faraday Trans.*, **91**, 4287 (1995).
23. C. C. Perry and L. J. Yun, *J. Chem. Soc., Faraday Trans.*, **88**, 2915 (1992).
24. J. Pickett-Heaps, A. M. Schmid and L. Edgar, *Prog. Phycol. Res.*, **7**, 1 (1990).
25. R. Gordon and R. W. Drum, *Int. Rev. Cytol.*, **150**, 243 (1994).
26. E. G. Vrieling, W. W. C. Gieskes and T. P. M. Beelen, *J. Phycol.*, **35**, 548 (1999).
27. R. E. Hecky, K. Mopper, P. Kilham and E. T. Degens, *Mar. Biol.*, **19**, 323 (1973).

28. D. M. Swift and A. P. Wheeler, *Phycologia*, **28**, 209 (1992).
29. D. W. Schwab and R. E. Shore, *Nature*, **232**, 501 (1971).
30. K. D. Lobel, J. K. West and L. L. Hench, *Mar. Biol.*, **126**, 353 (1996).
31. N. Kröger, C. Bergsdorf and M. Sumper, *EMBO J.*, **13**, 4676 (1994).
32. N. Kröger, C. Bergsdorf and M. Sumper, *Eur. J. Biochem.*, **239**, 259 (1995).
33. N. Kröger, G. Lehmann, R. Rachel and M. Sumper, *Eur. J. Biochem.*, **250**, 99 (1997).
34. N. Kröger and M. Sumper, *Protistologica*, **149**, 213 (1999).
35. N. Kröger, R. Deutzmann and M. Sumper, *Science*, **286**, 1129 (1999).
36. M. L. Chiappino and B. E. Volcani, *Protoplasma*, **93**, 205 (1977).
37. M. A. Borowitzka and B. E. Volcani, *J. Phycol.*, **14**, 10 (1978).
38. J. N. Cha and D. E. Morse, unpublished observations.
39. T. Mizutani, H. Nagase, N. Fujiwara and H. Ogoshi, *Bull. Chem. Soc. Jpn.*, **71**, 2017 (1998).
40. P. T. Tanev and T. J. Pinnavaia, *Science*, **271**, 1267 (1996).
41. K. Shimizu, J. N. Cha, G. D. Stucky and D. E. Morse, *Proc. Natl. Acad. Sci. U.S.A.*, **95**, 6234 (1998).
42. J. N. Cha, K. Shimizu, Y. Zhou, S. Christiansen, B. F. Chmelka, G. D. Stucky and D. E. Morse, *Proc. Natl. Acad. Sci. U.S.A.*, **96**, 361 (1999).
43. Y. Zhou, K. Shimizu, J. N. Cha, G. D. Stucky and D. E. Morse, *Angew. Chem., Int. Ed. Engl.*, **38**, 779 (1999).
44. K. Shimizu and D. E. Morse, in *Biomineralization of Nano- and Micro-structures* (Ed. E. J. Baeuerlein), Wiley-VCH, New York, 2000, in press.
45. J. Cao and D. E. Morse, manuscript in preparation.
46. G. Dodson and A. Wlodawer, *Trends Biochem. Sci.*, **23**, 347 (1998).
47. R. K. Iler, *The Chemistry of Silica: Solubility, Polymerization, Colloid and Surface Properties, and Biochemistry*, Wiley, New York, 1979.
48. T. J. Deming, *Nature*, **390**, 386 (1997).
49. K. Shimizu and D. E. Morse, manuscript in preparation.

CHAPTER 15

Chemistry on silicon surfaces

CHEOL HO CHOI and MARK S. GORDON

Department of Chemistry, Iowa State University, Ames, Iowa 50011, USA
Fax: 515-294-5204; e-mail: mark@si.fi.ameslab.gov

I. LIST OF ABBREVIATIONS	821
II. INTRODUCTION	822
III. THEORETICAL METHODS AND SURFACE MODELS	823
A. Slab Model	823
B. Cluster Approach	823
C. QM/MM Approach	825
D. Linear Scaling Methods	825
IV. 2 × 1 RECONSTRUCTION OF A CLEAN SILICON SURFACE	825
V. CHEMICAL REACTIONS INVOLVING Si–C BOND FORMATION	827
A. Reactions of Alkynes and Alkenes with the Reconstructed Si(100) Surface	827
B. Reactions of Dienes with a Reconstructed Si(100) Surface	831
C. Reactions of Aromatic Compounds with a Reconstructed Si(100) Surface	833
VI. HYDRATION OF THE RECONSTRUCTED Si(100) SURFACE	834
VII. HYDROGENATION OF THE RECONSTRUCTED Si(100) SURFACE	837
VIII. OXIDATION REACTIONS ON THE Si(100) SURFACE	838
A. Passive Oxidation	838
B. Active Oxidation	841
IX. ETCHING OF Si(100) WITH HALOGEN	844
X. SUMMARY AND OUTLOOK	845
XI. ACKNOWLEDGMENT	846
XII. REFERENCES	846

I. LIST OF ABBREVIATIONS

AES Auger Electron Spectroscopy
ARPES Angle-Resolved Photoemission Spectroscopy

BLYP	Becke exchange and LYP correlation functional
CASSCF	Complete Active Space Self-Consistent Field
CI	Configuration Interaction
CNDO	Complete Neglect Differential Overlap
DFT	Density Functional Theory
ESDIAD	Electron Stimulated Desorption Ion Angular Distributions
FMM	Fast Multipole Method
GGA	Generalized Gradient Approximation
GVB-PP1	Generalized Valence Bond method with one pair of correlated orbitals
HREELS	High Resolution Electron Energy Loss Spectroscopy
IMOMM	Integrated Molecular Orbital/Molecular Mechanics
KMC	Kinetic Monte Carlo
LDA	Local Density Approximation
LEED	Low Energy Electron Diffraction
MCQDPT2	Multi-Configurational Quasi-Degenerate Second-Order Perturbation Theory
MIR-FTIR	Multiple Internal Reflection Fourier Transform Infrared Spectroscopy
MMB	Employed Modulated Molecular Beam
MNDO	Modified Neglect Differential Overlap
MP2	Møller–Plesset Second-Order Perturbation Theory
NEXAFS	Near-Edge X-ray Adsorption Fine Structure
PES	Photoelectron Spectroscopy
QM/MM	Quantum Mechanics and Molecular Mechanics. It is a general acronym for the hybrid method
SCF	Self-Consistent Field
SEXAFS	Surface Extended X-ray Absorption Fine Structure
SIMOMM	Surface Integrated Molecular Orbital/Molecular Mechanics
SREM	Scanning Reflection Electron Microscopy
STM	Scanning Tunneling Microscope [or Microscopy]
STO-3G	Slater Type Orbital using 3 primitive Gaussians
TCSCF	Two Configuration Self-Consistent Field
TDS	Thermal Desorption Study
TOF-SARS	Time-Of-Flight Scattering And Recoiling Spectrometry
TPD	Temperature-Programmed Desorption
TS	Transition State
TZ	Triple Zeta
UHF	Unrestricted Hartree Fock
UPS	Ultraviolet Photoelectron Spectroscopy
XPS	X-ray Photoemission Spectroscopy

II. INTRODUCTION

As the size of electronic devices based on crystalline silicon wafers shrinks, the surface characteristics of semiconductor materials are becoming crucial^{1,2} for the proper functioning of devices. Thus, the understanding and tailoring of interfacial chemistry of silicon surfaces in particular is becoming of great importance. In addition to the traditional modifications of the silicon surface such as etching, doping and film deposition, much attention is being directed to synthetically modified surfaces³ in the pursuit not only of enhanced properties for microelectronics, but other applications including sensors, biologically active surfaces etc. With the help of traditional organic and organometallic chemistry, a wide variety of new chemically modified silicon surfaces can be synthesized which will allow for fine tailoring of surface characteristics for a broad range of applications. By studying to what degree our knowledge of organic chemistry may be applied to silicon

surfaces, insight into the fundamental characteristic features of surface reactions can be gained.

In addition, to gain the control needed to fabricate an organic function into existing semiconductor technologies and ultimately to make new molecule-scale devices, a detailed understanding of the adsorbate surface as well as interfacial chemical reactions and their products at the atomic/molecular level is critical. To accomplish this, both novel experiments and theoretical investigations need to play a significant role in the advance of this emerging field.

This chapter begins with a summary of the theoretical methodologies adapted for surface studies and then proceeds to a consideration of the unique features of clean silicon surfaces. Then, the main focus is directed to the structures and reaction mechanisms of organic molecules on silicon surfaces. Surface chemical reactions involving the Si–C bond, especially reactions with alkynes, alkenes, conjugated dienes and aromatic molecules, are presented in Section V. Hydrogenation, hydration, etching and oxidation reactions are also reviewed in the subsequent sections, although not exhaustively.

III. THEORETICAL METHODS AND SURFACE MODELS

A. Slab Model

Traditional band structure programs that allow one to perform electronic structure calculations of solids have been used to model surfaces^{4–7}. In this approach, one models a real system using the basic repeating unit cell (or slab) with two-dimensional translational symmetry for the surface and then employs periodic boundary conditions. Such a model introduces the reciprocal or k vectors, leading to the k -dependent energy levels of the system. The calculations involve the evaluations of interactions over a certain range of cells (lattice sum). Non-self consistent field (non-SCF) methods such as Hückel theory⁴, and the tight binding method (or Extended Hückel Theory)⁵ were used early on to provide the potential, and this method is still frequently employed. With the advance of methodologies, more sophisticated density functional theory methods have been used in combination with plane-wave basis sets⁶ or with Gaussian basis sets⁷ to expand the wave functions. There are advantages to both approaches. Plane waves appear to be most useful for incorporating periodic boundary conditions, whereas Gaussian expansions are more appropriate for describing the details.

The conjugate gradient⁸ method has most frequently been used to find stable geometries. Recent analytic gradient development⁹ based on the periodic fast multipole method (FMM)¹⁰ may provide more promising methods.

The main advantage of periodic boundary conditions is the elimination of ‘edge effects’ or terminal atom problems that occur in the finite cluster approach. The Hamiltonian in slab calculations is generally limited to density functional theory¹¹, an approach that is not always an appropriate choice.

B. Cluster Approach

The cluster approach suffers from the finite edge effects noted above. On the other hand, this approach can take advantage of well-developed high-level quantum chemical methods, which in some cases is essential for even a qualitative accounting of surface phenomena. In the cluster approach, the choice of a cluster that is representative of a real system is crucial, and not always feasible. Computational considerations limit the size of the cluster model, but the model needs to retain the essential features of the system of interest. Dangling bonds are usually capped with hydrogens¹² or simple capping atoms¹³.

The most common cluster model that has been used for the Si(100)- 2×1 surface is comprised of nine silicon atoms capped with hydrogens, Si_9H_{12} (see Figure 1a)¹². Since this cluster contains only one dimer, it will clearly be inadequate for investigating phenomena for which dimer-dimer interactions are important. Shoemaker and coworkers¹⁴ systematically studied clusters of varying size up to $\text{Si}_{66}\text{H}_{52}$ (Figure 1b) with the GVB-PP1¹⁵ (Generalized Valence Bond-PP1) level of theory, the simplest correct model for a singlet diradical, to investigate the utility of such clusters as prototypes for the study of silicon surfaces. They revealed that surface rearrangement due to dimer bond formation is 'felt' several layers into the bulk, so small clusters, such as Si_9H_{12} , cannot adequately represent bulk behavior.

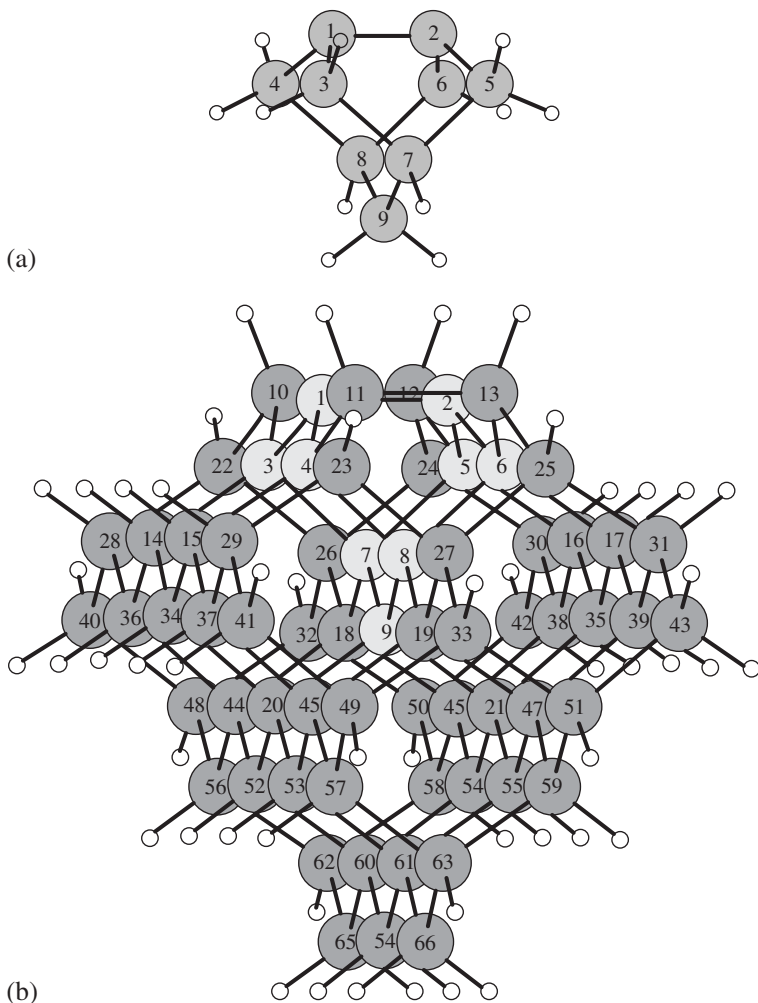


FIGURE 1. (a) Si_9H_{12} , a typical cluster model. (b) $\text{Si}_{66}\text{H}_{52}$ cluster model

C. QM/MM Approach

Hybrid quantum mechanics/molecular mechanics (QM/MM) techniques have gained popularity for modeling large molecular systems. In this approach, one assumes that a large molecular system can be partitioned into a small, chemically active part where a reaction will occur, and a larger, chemically inactive piece. Such methods have gained considerable popularity for the study of solvent effects¹⁶ in which the solute and solvent parts of the system are well separated. More recently, QM/MM methods have been developed across covalent bonds, in order to represent bulky substituents with molecular mechanics¹⁷. A particularly promising approach is the IMOMM (integrated molecular orbital/molecular mechanics) method^{17c}. In an attempt to minimize time-consuming electronic structure computations while maintaining the effect of the 'bulk' in surface chemistry calculations, Shoemaker and coworkers developed the IMOMM method into an embedded cluster approach called SIMOMM¹⁸ (Surface Integrated Molecular Orbital/Molecular Mechanics). In this method, the 'action' region where the actual chemical reaction occurs is treated quantum mechanically, while the spectator region that primarily provides the effect of bulk is treated using molecular mechanics. It has been shown that SIMOMM is especially effective for systems, such as semiconductors, in which the surface reaction is localized¹⁹. An important consideration in such embedded cluster or QM/MM methods is the way in which the transition is made from the QM to the MM region. This is not an issue for solvation, where solute and solvent are well separated, but it is important when the transition is made across a covalent bond. As noted above, the common approaches are to use hydrogens or model atoms as 'place holders' in the link region, and this is the approach used in both IMOMM and SIMOMM. Recently, several groups have developed a more promising approach, based on the use of frozen localized orbitals to represent the link region²⁰ for calculations on large biological species. This approach may also be a viable alternative for embedded cluster surface methods, and is being explored in this laboratory.

D. Linear Scaling Methods

It is, of course, desirable to develop a fully quantum mechanical method for the study of surface science, since such a method is certain to be more generally applicable to a wide range of surface problems, including metallic surfaces. A very promising method is the linear scaling quantum technique²¹, which has the potential to overcome the traditional high-order scaling barrier. Combined with high-level quantum mechanics methods, this new technique may present a very appealing alternative to QM/MM approaches. This technique has the potential to extend our ability to study more realistic surface models.

IV. 2×1 RECONSTRUCTION OF A CLEAN SILICON SURFACE

The most common crystal of silicon has the diamond structure, such that all atoms make four bonds with nearest neighbors in tetrahedral coordination. One of the most well studied and technologically most important silicon surfaces is Si(100). Figure 2(a) illustrates the Si(100) surface in which the topmost layer of the unreconstructed surface possesses silicon atoms (layer 1) bonded only to two silicon atoms (layer 2) yielding two singly occupied orbitals at each surface Si. These are called surface dangling bonds. Since this is an unstable arrangement, the entire surface undergoes reconstructions in order to stabilize the dangling bonds. The commonly accepted reconstruction is 'dimerization' of adjacent surface Si atoms. Schlier and Farnsworth proposed the first model of this kind on the basis of their observation of the (2×1) LEED (Low Energy Electron Diffraction) pattern²².

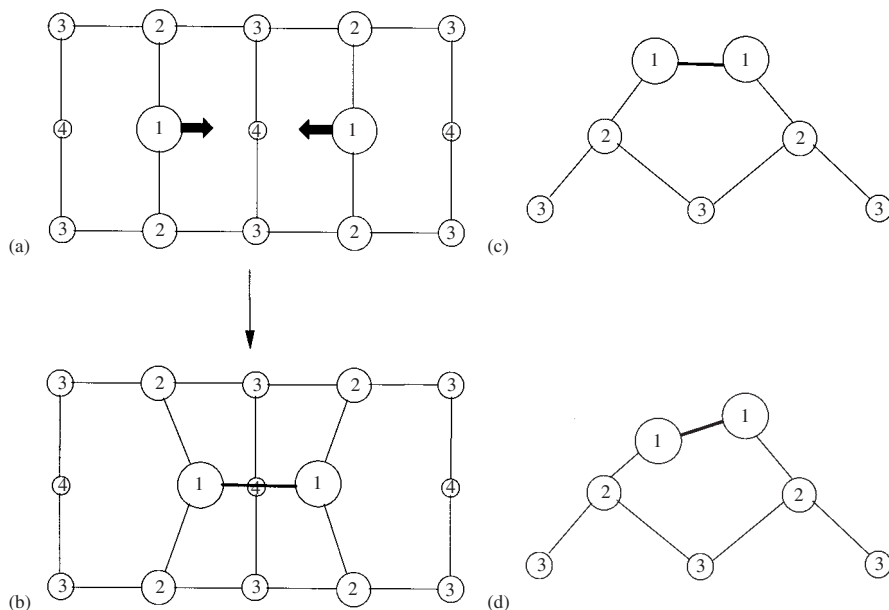


FIGURE 2. (a) Si(100) surface before reconstruction. Topmost layers are represented by the largest circle. (b) Si(100) surface after the 2×1 reconstruction. (c) Symmetric structure of surface dimer. (d) Asymmetric structure of surface dimer

Figure 2(b) shows this (2×1) reconstruction of the surface Si along the (011) direction yielding dimerized silicon atoms.

The question regarding whether the dimer is symmetric (Figure 2c) or buckled (Figure 2d) has been controversial since Levine²³ and Chadi²⁴ proposed that the dimers could be asymmetric. Many experimental²⁵ and theoretical²⁶ papers predict the Si(100) surface to be buckled, while others^{14,27–29} predict symmetric dimers. Data from room-temperature STM suggested that no buckling occurs on terraces, but it occurs on steps and defects^{27a,b,e}. However, more recent STM data showed that large regions of the Si(100) surface consist of buckled dimers far from defect sites^{25e}. The observation of predominantly symmetric dimers at room temperature may be due to rapid flipping of buckled dimers between different buckling directions in defect-free regions. Weakiem and coworkers³⁰ have indeed argued that a static picture of the Si(100) surface is insufficient and that the dynamics as a function of temperature is critical.

Several calculations based on density functional theory, using both the extended slab and cluster approaches, and employing both the local density (LDA) and generalized gradient (GGA) approximations, as well as plane wave basis sets²⁶, predict the surface dimer to be buckled. However, it is important to recognize that because of the distance between the two silicon atoms in a dimer and the weakness of Si–Si π bonding³¹, the dimer pair has significant diradical character. To the extent that this is true, a dimer requires a multi-reference wave function for a proper description.

Redondo and Goddard²⁸ first reported that the lowest energy configuration for a dimer in a small silicon cluster model, Si_9H_{12} , shown in Figure 1a, is the symmetric geometry.

They showed that the dimerized bond should be considered as a singlet diradical. Therefore, a qualitatively correct description of the dimer requires at least a generalized valence bond, GVB-PP1³², or a two configuration self-consistent field (TCSCF)³³ wave function. More recently, Paulus²⁹ performed a more exhaustive multi-reference analysis of silicon clusters and reconfirmed this conclusion.

Shoemaker and coworkers¹⁴ used TCSCF calculations and clusters of increasing size to show that the surface dimer is symmetric with a small buckling frequency on the order of *ca* 190 cm⁻¹, in agreement with the earlier results of Redondo and Goddard²⁸ and Paulus²⁹. More recently, these same authors showed that the addition of dynamic correlation (via second-order perturbation theory) to either single reference or multi-reference wave functions does not alter the conclusion that Si₉H₁₂ is symmetric (unbuckled)³⁴. Preliminary recent calculations, as well as previous ones by Shoemaker and coworkers⁵, suggest that the simplest two-dimer cluster Si₁₅H₁₆ is also symmetric. So, it seems clear at this point that small silicon dimer clusters are symmetric. This does not necessarily mean that there is a dichotomy between theory and experiment. The buckling frequency of 190 cm⁻¹ (130 cm⁻¹ when dynamic correlation is included) is small enough to suggest that any asymmetric attack on the surface, by a substrate or a probe, will be likely to cause buckling. It is also possible that high temperatures will cause buckling. So, the *chemistry* that occurs on the surface may be somewhat independent of the exact structure of Si₉H₁₂, especially since it is calculated at 0 K.

V. CHEMICAL REACTIONS INVOLVING SI-C BOND FORMATION

A. Reactions of Alkynes and Alkenes with the Reconstructed Si(100) Surface

[2_s + 2_s] Cycloadditions (Figure 3a) are formally orbital symmetry forbidden³⁵. Thus, a large reaction barrier is expected along the symmetric reaction pathway. In fact, it is known from carbon solution chemistry that even the low symmetry reaction path has a high reaction barrier, mainly due to unfavorable geometric configurations along the reaction pathway³⁶. The analogous [2 + 2] reactions of disilenes have been found to be extremely slow³⁷, indicating that the same symmetry rule applies in silicon chemistry. However, the rules governing [2 + 2] additions on surfaces may be different, since many instances of formally forbidden reactions have been reported.

Using high-resolution electron energy loss spectroscopy (HREELS) and LEED measurements, Nishijima and coworkers³⁸ showed that both acetylene and ethylene adsorb molecularly on Si(100). Based on the observed C-H stretching frequencies, they concluded that adsorption takes place on top of the Si dimers with an individual acetylene molecule being bonded to a single Si-Si surface dimer through formation of two strong Si-C bonds per dimer site. This 'di-σ bond structure' results from cleavage of two 'π bonds', one each from the alkene and the Si dimer (see Figure 3b). Yates and coworkers³⁹ also showed that unsaturated hydrocarbons including ethylene, propylene and acetylene chemisorb on Si(100)-(2 × 1) surfaces and are able to resist temperatures of up to 600 K. However, there is some disagreement regarding the nature of the C-Si bonds that result from acetylene adsorption. Nishijima and coworkers³⁸ concluded that the carbon atoms are hybridized to 'near sp³' in the observed structure, while subsequent theoretical^{40,41} and experimental^{39c,42} studies suggest sp² hybridization.

Recent experiments by Wolkow⁴³ and by Mezheny and coworkers⁴⁴ yielded another adsorption configuration: an end-bridge structure with an acetylene molecule binding to two adjacent dimers and oriented perpendicular to the dimer rows (Figure 4a); a tetra-coordinated structure with the acetylene binding to the four Si-atoms of two adjacent

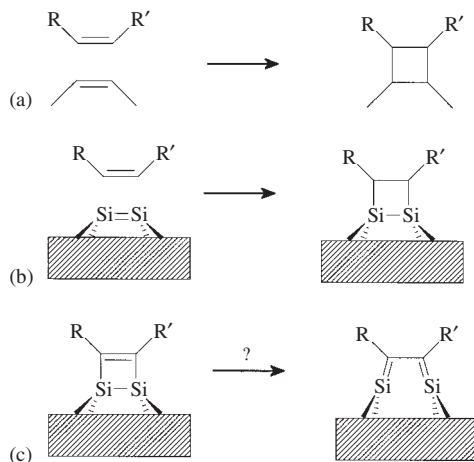


FIGURE 3. (a) Ordinary [2 + 2] cycloaddition reaction. (b) [2 + 2] Surface cycloaddition reaction. (c) Surface electrocyclic reaction

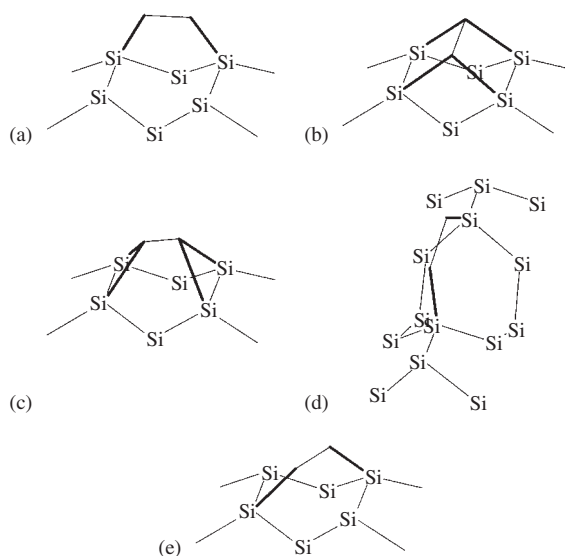


FIGURE 4. Ecliptics represent the surface Si dimer and solid lines represent acetylene: (a) end-bridge, (b) p-bridge, (c) r-bridge, (d) inter-row, (e) cross configurations

surface dimers in a dimer row. Their DFT calculations⁴⁴ also suggest that the p-bridge (Figure 4b) and the r-bridge (Figure 4c) structures are the most probable tetra-coordinated ones. They⁴⁴ also showed that the relative populations of the various configurations change with coverage. These experimental results illustrate that the Si(100)/acetylene surface is far more complex than previously assumed.

Liu and Hoffmann⁴¹ studied the chemisorption mechanism of acetylene on Si(100) using Si₉H₁₂ models at the UHF/STO-3G level of theory (Figure 5). They concluded that the symmetric path is forbidden following the gas-phase symmetry rule. However, they found a low symmetry pathway composed of a π -complex precursor and a biradical intermediate that has a low energy barrier to [2 + 2] cycloaddition products (see Figure 5). The initial intermediate, **I1**, is predicted to be a π -complex that is 0.25 eV lower in energy than the reactants. The initial transition state, **TS1**, is only about 0.007 eV above **I1**. The second intermediate, **I2**, that is 3.61 eV lower in energy than **I1**, now forms one C–Si bond. The second TS, **TS2**, leads to the formation of another C–Si bond yielding [2 + 2] products via a small (0.2 eV) energy barrier relative to **I2**. The final [2 + 2] product is 1.5 eV more stable than **I2**. Despite the relatively low level of theory used in this study, it demonstrates that a non-concerted asymmetric low energy pathway to the [2 + 2] product exists. This low energy pathway may be attributed to the ‘pinned-back’ *cis*-bent C_{2v} geometry forced upon the surface Si dimer that reduces the geometric hindrance in the initial ene-ene approach and makes the Si dimer more reactive than simple disilene. The very flat bucking potential may also facilitate the reaction, since buckling is likely to result in a Si–Si charge separation.

Turning to the sp² vs. sp³ hybridization at carbon issue, acetylene has one C–C π bond left after chemisorption. The remaining Si–Si σ bond and the C–C π bond may undergo a further pericyclic reaction (Figure 3c) releasing four-membered ring strain

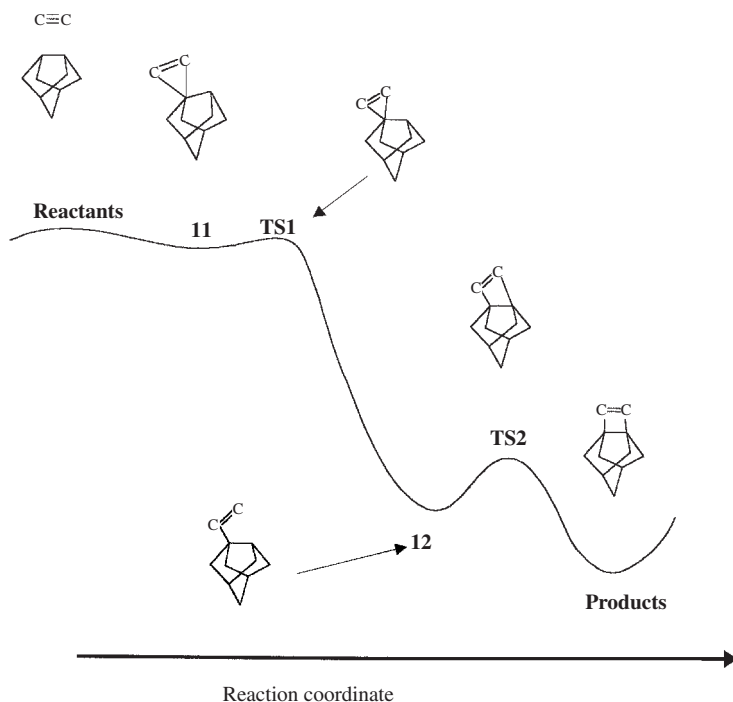


FIGURE 5. Non-concerted, asymmetric [2 + 2] cycloaddition reaction of acetylene on a Si(100)- 2×1 surface. All atoms, except the C atoms, are Si atoms

energy and making two new Si–C *double bonds*. This reaction resembles the electrocyclic ring-opening reaction, in which cyclobutene, on heating, gives 1,3-butadiene. Using Auger spectroscopy and temperature-programmed desorption (TPD), Taylor and coworkers^{39c} proposed that the Si–Si dimer bond is cleaved when the acetylene molecule adsorbs on top of a dimer. The structure with this complete cleavage of the Si–Si dimer bond was subsequently confirmed⁴² by scanning tunneling microscopy (STM) as a major product. However, independent experimental studies concluded that no direct evidence regarding the structure of the Si–Si σ bond has been observed⁴⁵.

Except for the early studies⁴⁶, a majority of the theoretical studies support the unbroken Si–Si dimer structure^{40,41,47}. The most recent slab model DFT study by Sorescu and Jordan⁴⁸ showed that the broken Si–Si dimer structure is about 30 kcal mol⁻¹ less stable than the unbroken structure. A Si₉H₁₂ cluster study of the same system⁴⁹ predicts that the Si–Si cleaved structure is not a minimum on the potential energy surface. Since some of the stationary points on the potential energy surface for the addition of acetylene to Si(100) are likely to have significant diradical character, additional calculations that employ multi-configurational wave functions would be useful in clarifying this point.

Sorescu and Jordan⁴⁸ have performed extensive theoretical studies to explore the recent speculation about tetra-coordinate configurations. Their study included the unbroken and broken Si–Si dimer configurations, end-bridge (Figure 4a), p-bridge (Figure 4b), r-bridge (Figure 4c), inter-row (Figure 4d) and cross configurations (Figure 4e). They showed that the two most stable species are di-coordinated ones: the unbroken Si–Si dimer and end-bridge structures. These two di-coordinated species are predicted to have adsorption energies of 56.5 to 67.6 kcal mol⁻¹, respectively. Of the tetra-coordinate structures, the r-bridge structure is about 19.3 kcal mol⁻¹ more stable than the p-bridge structure. The adsorption energies are 49.2 and 29.9 kcal mol⁻¹, respectively. The barrier for the r-bridge to p-bridge isomerization is about 39 kcal mol⁻¹, making this surface inter-conversion unlikely. However, the barrier for the r-bridge to end-bridge isomerization is only 4.5 kcal mol⁻¹, so the r-bridge may be unimportant. The barrier for isomerization of the p-bridge to one of the dimerized structures shown in Figure 4b is about 19 kcal mol⁻¹. This suggests that the p-bridge structure may be a viable candidate for the tetra-coordinated species observed in STM measurements.

Whether or not the Si–Si dimer σ bond is cleaved, it seems to be the consensus that the majority of the surface product forms two Si–C bonds, an analog of the [2 + 2] product. This is useful, since the orientation of the individual molecules can be controlled, yielding anisotropic physical properties of a chemically modified silicon surface as discussed in recent accounts⁵⁰.

Hamers and coworkers have recently demonstrated that a wide range of complex cyclic olefins react in manner that is similar to acetylene. They showed, in general, that molecules with high symmetry such as cyclopentene⁵¹, 1,5-cyclooctadiene⁵² and 1,3,5,7-cyclooctatetraene⁵³ chemisorb into a unique [2 + 2] geometry. More complex molecules, such as 3-pyrroline⁴⁵ and norbornadiene⁴⁵, form multiple bonding geometries. In these cases, attempts to control the surface product distributions lead to molecular fragmentation rather than surface conversions.

Another important issue related to surface cycloaddition reactions is the stereochemistry of the products. Advances in this area may open new methods for developing new chemical sensors that may be used for complex molecular recognition tasks. In one study, Wolkow and coworkers⁵⁴ showed that a scanning tunneling microscope can be used to determine the absolute chirality of individual molecules of *cis*- and *trans*-2-butene adsorbed on

silicon. Another study⁵⁵ demonstrated that 1*S*(+)-3-carene, a naturally occurring bicyclic alkene belonging to the terpene family, adsorbs enantiospecifically on silicon. That reaction leads to formation of four chiral centers and a chiral surface.

B. Reactions of Dienes with a Reconstructed Si(100) Surface

The surface reactions of dienes with the Si(100)-(2 × 1) surface are of particular interest due to their relation to the [4 + 2] cycloaddition or ‘Diels–Alder’ reaction of carbon chemistry (Figure 6a), in which a conjugated diene reacts with the dienophile silicon surface to form a six-membered ring (Figure 6b). Since unsaturated hydrocarbons such as acetylene, ethylene and propylene can readily react with the Si(100)-(2 × 1) surface yielding [2 + 2] products, the [2 + 2] reaction involving only one π -bond of a diene may compete with the corresponding [4 + 2] reaction in diene chemisorption reactions (Figure 6c).

The [4 + 2] cycloaddition produces a six-membered ring that is less strained than the four-membered ring produced by [2 + 2] cycloaddition. Therefore, [4 + 2] products are expected to be thermodynamically more stable than the [2 + 2] products. In the case of the adsorption of 1,3-cyclohexadiene, Konecny and Doren⁵⁶ predicted, based on DFT calculations, that the [4 + 2] product is more stable than the [2 + 2] product by 15.2 kcal mol⁻¹ and that the reaction barrier to the [4 + 2] product is 0.3 kcal mol⁻¹. They further showed that the predicted vibrational spectra of the Diels–Alder products of 1,3-butadiene and 2,3-dimethyl-1,3-butadiene onto the Si(100)-(2 × 1) surface at room temperature are consistent with the observed spectra and inconsistent with significant formation of [2 + 2] addition product. However, these authors did consider the competing reaction, arguing that if the entire reactions are determined thermodynamically, only [4 + 2] products can exist on the surface. The corresponding experimental results by Bent and coworkers^{57,58} for the adsorption of these two products showed evidence for only the [4 + 2] product. These theoretical and experimental investigations established that the Si dimer of the reconstructed Si(100)-(2 × 1) surface could act as a dienophile in a Diels–Alder cycloaddition fashion, and that the Diels–Alder reaction is facile.

Reinvestigation of the 2,3-dimethyl-1,3-butadiene reaction on the Si(100)-(2 × 1) surface by Hamers and coworkers⁵⁹ supported the observation of a Diels–Alder product

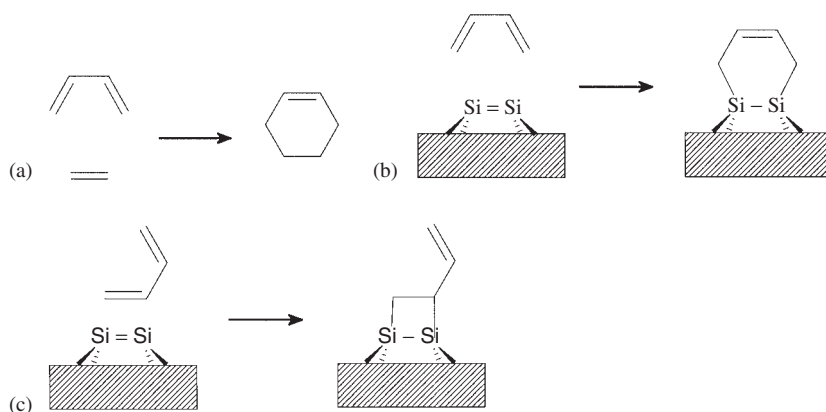


FIGURE 6. (a) Ordinary [4 + 2] cycloaddition reaction. (b) Surface [4 + 2] cycloaddition reaction. (c) Surface [2 + 2] cycloaddition reaction

for 80% of the surface products. However, they noted a minor (20%) [2 + 2] product as well. In the case of 1,3-cyclohexadiene, they observed 55% of the [4 + 2] product, 35% of [2 + 2] product and 10% unknown product, strongly indicating the existence of competition between [4 + 2] and [2 + 2] cycloaddition reactions of the diene on the Si(100) surface. Attempts to convert the product distribution to the thermodynamically more stable product by annealing to higher temperatures failed. Surface annealing leads to C–H bond cleavage rather than to rearrangement of the [2 + 2] product to the [4 + 2] product. They⁵⁹ concluded that the formation of multiple products and the lack of temperature effects indicate that the product distribution is controlled primarily by the kinetics of the adsorption process, not by the thermodynamics.

The primary issue is whether the final products are determined by the initial stage of the surface reactions, or if the initial products are subject to subsequent reactions such as surface isomerization. The question regarding whether and why the [4 + 2] product is exclusively formed ultimately bears on the chemical selectivity of the Si(100)-(2 × 1) surface toward conjugated diene systems. By studying the factors that govern the reactivity of these reactions, one hopes to gain control over these surface reactions to an extent that eventually leads to a technique to tailor the reaction selectivity.

Recently, Choi and Gordon¹⁹ have performed systematic investigations on this intriguing system with the multi-configurational quasi-degenerate second-order perturbation theory (MCQDPT2)⁶⁰ method in combination with CASSCF⁶¹ wave functions, performing potential energy surface searches along the possible reaction paths. In the case of chemisorption of 1,3-cyclohexadiene on the Si(100)-(2 × 1) surface, they showed that both the [2 + 2] and [4 + 2] cycloaddition reactions can occur readily, indicating strong competition between these two reactions at least at the initial stage of the chemisorption. Symmetric [4 + 2] cycloaddition has a negligibly small reaction barrier in agreement with Konecny and Doren's result⁵⁶.

Choi and Gordon¹⁹ showed that the low energy [2 + 2] cycloaddition pathway on the Si(100) surface constituting a nonsymmetric, nonconcerted reaction path exists. There are at least two reaction paths to the [2 + 2] product depending on which Si–C bond forms first. Both transition states have small barriers of about 5 kcal mol⁻¹ suggesting that [2 + 2] cycloaddition is facile.

Most importantly, surface isomerization reactions connecting [4 + 2] and [2 + 2] products turn out to be very unlikely due to a high (>40 kcal mol⁻¹) energy barrier. In the transition state that connects [2 + 2] and [4 + 2] products, one of the Si–C bonds is being broken and another one being made.

This calculation as well as new experiments by Hamers' group⁵⁹ indicate that the final surface reaction products are determined during the initial stage of the surface reactions, and they are not subject to further thermal redistributions or isomerizations among surface products. Using multiple internal reflection Fourier transform IR (MIR-FTIR) spectroscopy, near-edge X-ray absorption fine structure (NEXAFS), Kong and coworkers⁶² confirmed that in the case of 1,3-cyclohexadiene, multiple chemisorption configurations are implicated, consistent with the co-existence of [4 + 2] and [2 + 2] cycloaddition products.

The theoretical investigation also demonstrated that methods based on a multiconfiguration wave function are essential in order to consistently study the entire potential energy surface, since many points on the surface are highly multiconfigurational in nature. The bonding and anti-bonding orbital pair in the active space of the transition state that leads to [2 + 2] product clearly exhibits singlet diradical character¹⁹. Recent theoretical studies⁶³ of 1,3-cyclopentadiene on an Si(100) surface yield similar results, extending the general picture of surface reactions obtained with 1,3-cyclohexadiene.

These recent experimental and theoretical results make it clear that *control of selectivity depends on the kinetics rather than thermodynamics*. It is interesting to speculate how one might improve the [4 + 2] addition selectivity of a Si(100)-(2 × 1) surface toward the diene systems. By replacing hydrogens with other appropriate groups, one may be able to alter the barrier for either the [2 + 2] reaction or the isomerization reaction. The former may control the initial distribution of surface products, while the latter may change the selectivity of the surface by thermal redistribution.

C. Reactions of Aromatic Compounds with a Reconstructed Si(100) Surface

Aromatic molecules have a conjugated π system in common with the conjugated dienes discussed above. Due to their unusual stability, however, they do not undergo many of the reactions typical of alkenes and dienes, except electrophilic substitution reactions that preserve the integrity of the π system. It is interesting, therefore, that benzene appears to rather easily undergo addition reactions on the Si(100) surface, especially since such reactions make new C–Si bonds thereby removing aromatic stability^{64,65}. While adsorption of simple alkenes and dienes on Si(100) is essentially irreversible due to the formation of strong C–Si bonds, benzene has been shown to adsorb reversibly⁶⁴ and even exhibits redistributions of surface products⁶⁵.

Wolkow and coworkers⁶⁵ have performed semiempirical and *ab initio* calculations to determine preferred bonding configurations of benzene on Si(100). As shown in Figure 7, at room temperature benzene bonds to silicon dimers in three configurations: 1,4-single dimer (a), tight bridge (b) and twisted bridge (c). The STM image shows that the 1,4-dimer configuration converts into the tight bridge configuration. The 1,2-single dimer (d) and symmetric bridge configurations (e) are not observed. However, the level of

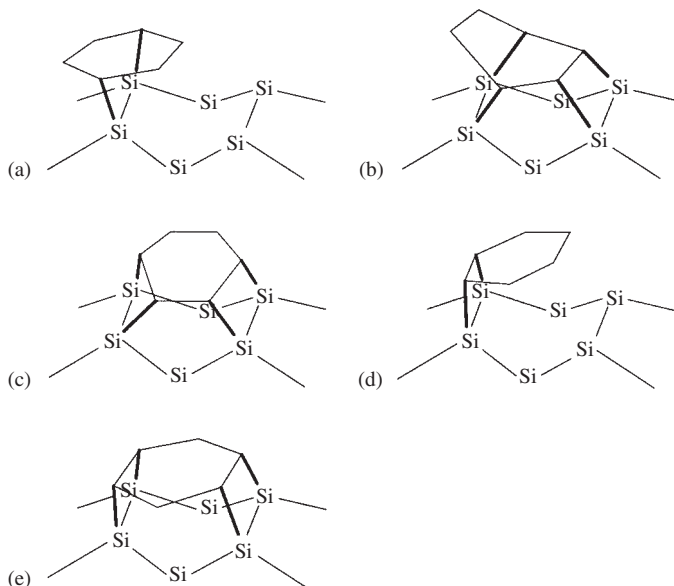


FIGURE 7. Possible surface structures of benzene on an Si(100)-2 × 1 surface. They are 1,4-single dimer (a), tight bridge (b), twisted bridge (c), 1,2-single dimer (d) and symmetric bridge configurations

theory used was not sufficient to conclusively determine relative energetics among plausible structures. Moreover, it may be kinetics, rather than net energetics, that play a major role in determining the product distribution. Therefore, one has to study the relevant potential energy surfaces to fully understand the surface reactions of aromatic systems.

For styrene, Hamers and coworkers showed that adsorption occurs almost exclusively through the vinyl group and not through the aromatic ring⁶⁶. This illustrates that due to the aromatic stability, given a choice, adsorption only occurs through the more reactive vinyl group. In another study with toluene, *para*-xylene, *meta*-xylene and *ortho*-xylene, they⁶⁷ concluded that the differences in relative peak intensity in the FTIR spectrum as compared with benzene point to the possibility that the methyl substituent groups may steer the ring into different ratios of specific bonding geometries.

VI. HYDRATION OF THE RECONSTRUCTED Si(100) SURFACE

It is known that an oxide layer (SiO_2) grows more easily in the presence of water^{68,69}. Therefore, wet oxidation is a preferred choice for the formation of a thick oxide layer. Although there now appears to be a consensus that the water undergoes dissociative adsorption on the Si(100) surface, there has been controversy concerning whether the initial adsorption of water is molecular or dissociative. Molecular adsorption (Figure 8a) leaves one surface Si dangling bond intact, while dissociative adsorption (Figure 8b) saturates the surface dangling bonds. Initial interpretations of ultraviolet photoelectron spectroscopy (UPS) on Si(100)⁷⁰ and Si(111)⁷¹ suggested molecular adsorption, while electron energy loss spectroscopy (EELS)⁷² and surface IR⁷³ studies showed dissociative adsorption on the basis of the Si–H and Si–O–H stretching modes. Later, photoelectron spectroscopy (PES)⁷⁴ reinterpretation of the earlier UPS^{74a} data and other experiments⁷⁵ were all consistent with dissociative adsorption.

At room temperature the sticking coefficient of water on Si(100) is near unity and constant up to saturation⁷⁶. The saturation coverage is reported to be 0.5 monolayer (ML): one OH and H per Si dimer⁷⁷. These observations suggest a small or zero barrier for the adsorption reaction.

Some structural information is available. An ESDIAD experiment^{75a,78} revealed that the O–H bond adsorbed on Si(100) is pointing away from the surface and tilted away from the vertical plane of the dimer bond. TOF-SARS results⁷⁹ showed that one hydrogen is close to the surface, while the other is high above the surface. These were attributed to the hydrogens of Si–OH, respectively, and interpreted in favor of the O–H bond pointing away from the surface. The ESDIAD experiment^{78b} also revealed that the torsional mode about the Si–O bond in Si–OH is of high amplitude, suggesting a nearly free rotation about the Si–O bond.

Early theoretical studies using extended Hückel⁸⁰ or tight binding methods⁸¹ predicted dissociative adsorption, in good agreement with experiment. However, MNDO⁸² results

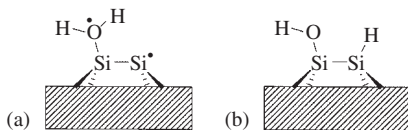


FIGURE 8. (a) Molecular adsorption of H_2O on an Si(100)- 2×1 surface. (b) Dissociative adsorption of H_2O on an Si(100)- 2×1 surface

suggested that the most stable structure is OH bridging between the two atoms of a dimer. A CNDO⁸³ study found the O–H bond to be coplanar with the surface dimer bond. These last two theoretical studies are not consistent with experimental evidence.

Konecny and Doren⁸⁴ detailed the reaction pathway and geometries of the product, the transition state and a molecular precursor state using density functional theory and the Si₉H₁₂ cluster model of the surface (see Figure 9). As a water molecule approaches the surface, it forms a molecular precursor state, **I**, that is about 10 kcal mol⁻¹ below reactants, with no intervening reaction barrier. Recent, MCQDPT2//GVB-PP1 results⁸⁵ on similar and larger clusters predict **I** to lie 5 kcal mol⁻¹ below reactants. BLYP/TZ94P⁸⁴ and GVB-PP1⁸⁵ calculations predict the Si–O distance in **I** to be 2.23 and 1.99 Å, respectively. This rather large difference, consistent with the large difference in stabilization energy, is due to the large decrease in diradical character upon moving from reactants to intermediate. The consequence of this is that a single-reference wave function is much less appropriate at reactants than at **I**, so that a multi-reference wave function is required for a consistent picture of this first step in the mechanism. Since the diradical character is not significant for the rest of the mechanism, single-reference methods are adequate to describe subsequent steps, provided that no bare dimers are present.

The transition state **T** that connects the molecular precursor state, **I**, with product, **P**, is in the process of breaking one O–H bond and forming a Si–H bond. The reaction barrier at **T** relative to **I** is 1–8 kcal mol⁻¹, depending on basis set and level of theory, providing an easy migration of H from O to Si. The final product, **P**, is 45–55 kcal mol⁻¹ more stable than **I**. Cho and coworkers⁸⁶ studied this water adsorption using DFT and a slab model and obtained results that are very similar to those obtained with the cluster models. According to MCQDPT2 results, the net reaction has a small barrier, in contrast with the DFT results. This may be due to the fact that DFT may not be able to adequately

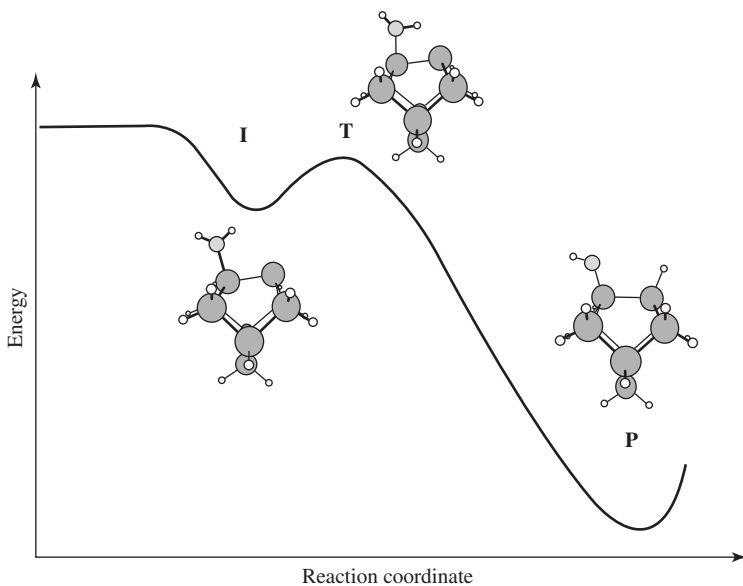


FIGURE 9. Reaction mechanism of dissociative adsorption of H₂O on an Si(100)-2 × 1 surface

describe the bare Si dimer of the reactants. In either case, little or no barrier is predicted for the overall process.

Regarding secondary interactions after the chemisorptions of water, Konecny and Doren⁸⁴ proposed three types of inter-site interactions that increase the tendency of the O–H bond to lie orthogonal to the dimer bond: Either the oxygen lone pair or the hydroxyl hydrogen may interact with an unoccupied adjacent dimer, or two hydroxyls on adjacent dimers may interact as in a weak hydrogen bond.

By combining *ab initio* quantum chemical cluster calculations and IR experiments, Gurevich and coworkers⁸⁷ predicted that the initial surface is actually comprised of arrays of isolated and intra-row coupled dimers. The latter are coupled by a hydrogen bonding interaction between OH groups that reside on the same end of adjacent dimers in a dimer row (see Figure 10a). They further estimated that this inter-dimer bonding increases the stability by *ca* 2 kcal mol⁻¹ relative to the isolated dimer case. Experiment suggests that the hydroxyl-mediated inter-dimer coupling does not extend to the second adjacent dimer, since there was no further shift of the OH stretch frequency as the coverage was increased. Cho and coworkers⁸⁶ also concluded that, while the interaction between water molecules is repulsive, the interaction between dissociated OH species is attractive due to hydrogen bonding.

Large-scale SIMOMM cluster calculations⁸⁵ depicted in Figure 10b also show that hydrogen bonding occurs only between the nearest hydroxyls and does not propagate further. The authors⁸⁵ concluded that due to the long distance between dimer rows, the formation of hydrogen bonds requires one OH group to be tilted forward and the other OH group backward. This pattern makes the extension of hydrogen bonding difficult. A consequence of the coupling is that the Si–Si–O–H torsion potential becomes more rigid in order to direct each H-bonding hydrogen toward its oxygen partner on the neighboring site.

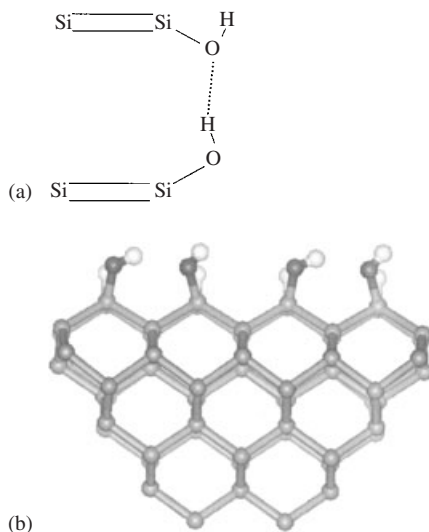


FIGURE 10. (a) Schematic illustration of surface hydrogen bonding between dissociatively adsorbed OH of two surface dimers on an Si(100)-2 × 1 surface. (b) Structure of surface hydrogen bonding between dissociatively adsorbed OH of four surface dimers on an Si(100)-2 × 1 surface

Depending on the surface temperature and water pressure, the adsorbed water undergoes further reactions yielding an oxide film, decomposition of OH into adsorbed O and H or desorption of SiO⁸⁸. Gurevich and coworkers⁸⁷ postulated that the coupling through hydrogen bonding has a significant effect on subsequent oxygen agglomeration, such that single oxygen insertion reactions occur on 'isolated' dimers, whereas the coupled dimers lead to the facile production of the doubly inserted dimers.

VII. HYDROGENATION OF THE RECONSTRUCTED SI(100) SURFACE

In view of the many important applications in semiconductor technology, the interaction of hydrogen with silicon surfaces has been intensively studied. Recombinative H₂ desorption from Si(100)-2 × 1 follows first-order kinetics⁸⁹, unusual when compared with the second-order kinetics observed for H₂ desorption from Si(111)-7 × 7. The measured activation barriers for the desorption of H₂ on Si(100) range from 45 to 66 kcal mol⁻¹^{89,90}.

Several reaction mechanisms have been proposed for the hydration of Si(100)⁹¹. The two most accepted of these are the 'preparing' mechanism and the 'surface defect' mechanism. Figures 11a and 11b illustrate the symmetric and asymmetric approaches in the preparing mechanism. This preparing mechanism is based on experimental⁹² and theoretical⁹³ evidence that hydrogen atoms are initially *prepared* on silicon dimers due to the thermodynamic stability of the preparing configuration by about 20 kcal mol⁻¹. Using a simple statistical mechanical model, D'Evelyn and coworkers⁹⁴ showed that if one assumes the preparing mechanism, desorption follows first-order kinetics. However, many electronic structure calculations with cluster models of the surface have suggested that the activation energy for this mechanism is too high^{93,95}. Using MCSCF and CI levels of theory, Jing and Whitten⁹⁶ found both symmetric and asymmetric transition states. For the symmetric transition state, MCSCF is required to obtain the saddle point. At the CI level, they predicted the activation energies for the symmetric and asymmetric pathways to be 86.3 and 85.0 kcal mol⁻¹, respectively. Due to these large activation energies compared with experiment (45–66 kcal mol⁻¹), Jing and Whitten suggested a multistep desorption mechanism.

Pai and Doren⁹⁷ using DFT and cluster models found only the asymmetric transition state. They predicted the desorption activation energy to be 55 kcal mol⁻¹ using LSD and

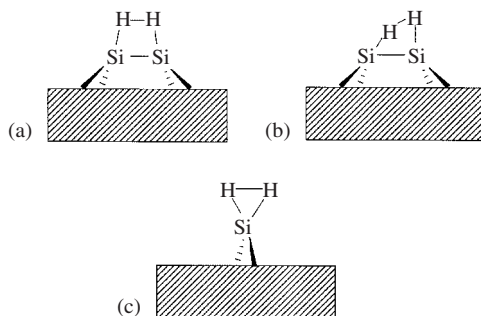


FIGURE 11. Schematic illustration of (a) symmetric transition state of H₂ adsorption on an Si(100)-2 × 1 surface (b) asymmetric transition state of H₂ adsorption on an Si(100)-2 × 1 surface and (c) isolated dihydride on an Si(100)-2 × 1 surface

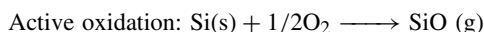
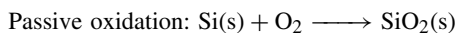
64 kcal mol⁻¹ using BLYP exchange–correlation functional. These values are in good agreement with experimental values of 45–66 kcal mol⁻¹. However, similar calculations with B3LYP predict 77 kcal mol⁻¹^{195a}.

For the surface defect mechanism, using a HF derived kinetic Monte Carlo model, Radeke and Carter⁹⁸ showed that H₂ desorption from Si(100)-2 × 1 via isolated dihydrides (Figure 11c) follows first-order kinetics. They further showed that the concentration of defects on the surface has a profound effect on the desorption rate constant. Recent studies proposed the importance of step sites rather than terraces⁹⁹.

Despite extensive experimental and theoretical studies, it appears that no consensus regarding the mechanism of hydrogen desorption/adsorption reactions exists. Perhaps, better modeling of the systems in combination with accurate *ab initio* methods will help to resolve this long-standing issue.

VIII. OXIDATION REACTIONS ON THE SI(100) SURFACE

Interactions of atomic or molecular oxygen with a silicon surface can lead to either silicon oxide film growth on the silicon surface (passive oxidation) or to etching of the surface (active oxidation)¹⁰⁰. The outcome of such interactions depends primarily on the surface temperature and also on the oxygen pressure. In the low temperature or high pressure regime, one finds passive oxidation. In the high temperature or low pressure regime, one finds active oxidation or etching of the surface by removal of SiO. The two oxidation processes are:



A. Passive Oxidation

Since gate oxide thicknesses of 10 Å or smaller are being grown and will be standard in the near future¹⁰¹, understanding the initial oxidation processes and structures of the SiO₂/Si interface is critical. In crystalline SiO₂, oxygen is in a bridging position between two silicon atoms; each silicon atom in turn is surrounded by four oxygen atoms in a tetrahedral configuration in bulk SiO₂, illustrating that di-coordinated oxygen is the most abundant configuration with silicon.

N₂O is a common source of atomic oxygen, as it dissociates at the surface into O and N₂¹⁰². Many experiments have shown that molecular oxygen (O₂) adsorption on Si(100) is predominantly dissociative¹⁰³. Using silicon clusters containing as many as seven Si atoms and MCSCF wave functions, Batra and coworkers¹⁰⁴ have provided theoretical support that the dissociative adsorption of an oxygen molecule is exothermic by 3 eV. Conflicting results for the initial oxidation of the Si(100) surface have been reported. Most AES and XPS studies¹⁰⁵ report saturation coverage of 1.0 monolayer (ML) for O₂ adsorption at 300 K. Lower coverage was also reported¹⁰⁶. An atomic oxygen beam experiment showed no true saturation for atomic oxygen exposure, but the uptake slowed considerably at a coverage of 2–3 ML^{105a}. Avouris and Lyo¹⁰⁷ concluded that the initial adsorption occurred predominantly at defect sites not at terraces. Many experiments have been devoted to revealing the oxide surface structure. Figure 12 illustrates the possible initial surface configurations of oxygen on the Si(100)-2 × 1 surface that have been proposed.

HREELS¹⁰⁸ and surface extended X-ray adsorption fine structure (SEXAFS)¹⁰⁹ measurements reveal that Si–O–Si complexes exist in the early stage of oxidation. Based on

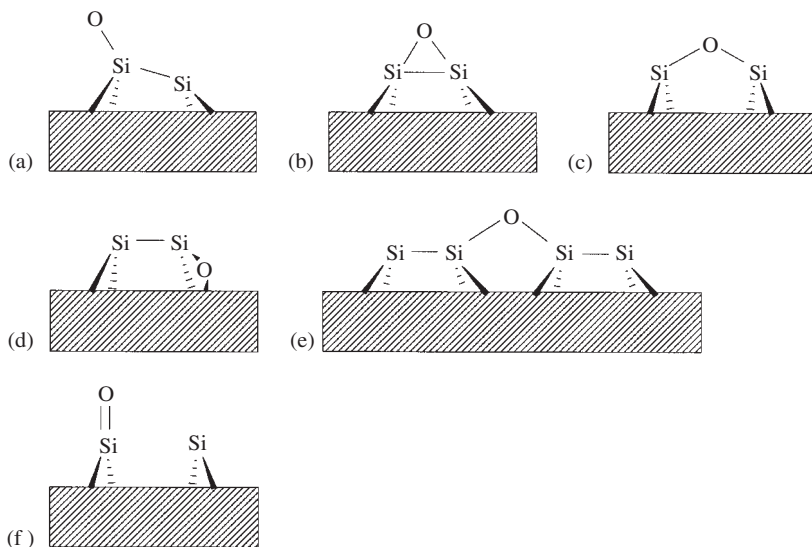


FIGURE 12. Schematic illustrations of (a) on-top, (b) on-dimer, (c) dimer-bridge, (d) backbond, (e) non-dimer bridge and (f) silanone structures on an $\text{Si}(100)\text{-}2 \times 1$ surface

the HREELS experiment, it is inferred that the oxygen atom is inserted into the Si–Si ‘backbond’ (Figure 12d). The SEXAFS experiment suggests that the oxygen atom occupies two different bridge positions, ‘backbond’ and dimer-bridge (Figure 12c). The Si–O bond length is reported to be 1.65 \AA and the Si–O–Si bond angle to be about 120° or 130° . The on-top site (Figure 12a) has also been proposed^{105a,110}. Scanning tunneling microscopy (STM) has been used to study the oxidation. However, the observed features such as position, height and thermal stability are interpreted differently in these experiments. Avouris and Cahill¹¹¹ identified the observed bumps as isolated dimers comprised of Si atoms ejected from the surface, while Kliese and coworkers¹¹² have concluded that they are weakly bound species of oxygen atoms or molecules. In addition, small protrusions appear at the very early stage of the oxidation, most frequently in a bridging position between dimer rows with a height of about 0.2 \AA .

Theoretically, Smith and Wander¹¹³ have investigated the adsorption of atomic oxygen on Si(100) using a $\text{Si}_{18}\text{H}_{24}\text{O}$ cluster model with HF/STO-3G. These authors predicted that atomic oxygen is adsorbed at the dimer bridge sites (Figure 12c). The corresponding Si–O bond lengths lie in the range of $1.635 \pm 0.022 \text{ \AA}$. They further found that the dimer and non-dimer (Figure 12e) bridge sites become equivalent in the high coverage limit, giving rise to a 1×1 pattern. Using a slab model and local density approximation, Miyamoto and Oshiyama have found three stable sites for the adsorption of atomic oxygen¹¹⁴. Of the three, the geometry in which the oxygen atom is inserted into the dimer bond (‘dimer-bridge’, Figure 12c) is more stable than the on-dimer (Figure 12b) and the backbond sites. For molecular oxygen, they found¹¹⁵ that the backbond site is the most stable. On the other hand, using a molecular dynamics method based on the local density approximation, Uchiyama and Tsukada¹¹⁶ predicted that the backbond site is more stable than the dimer-bridge site by 0.12 eV even in the case of

atomic oxygen. Following calculations of STM images¹¹⁷, they showed that, in the filled states (negative applied surface bias voltage), the STM images for the backbond and the dimer-bridge site appear to be very similar and almost indistinguishable. The empty-states images (positive applied surface voltage) showed characteristic features of the oxygen site.

There have been some attempts to understand the reaction mechanisms of the initial oxidation. Hoshino and coworkers¹¹⁸ studied the symmetric mechanism of the direct insertion of molecular oxygen into the dimer bond using silicon cluster models containing two and nine silicon atoms, with the MP2/3-21G method. The activation energy required for this reaction was calculated to be $60.4 \text{ kcal mol}^{-1}$. These authors concluded that the reconstructed dimer is barely oxidized at room temperature and that defect sites may be the cause of the natural oxidation of Si(100). This conclusion supported some experiments¹⁰⁷ but contradicted others¹⁰⁵. Since this symmetric path is formally symmetry forbidden, a low energy asymmetric reaction pathway may exist. Conflicting theoretical results were obtained by Miyamoto and Oshiyama, who predicted using LDA slab models that the dissociative chemisorption of O_2 can occur without any activation barrier at all sites they studied^{114,115}.

Recently, using scanning reflection electron microscopy (SREM), Watanabe and coworkers¹¹⁹ obtained strong evidence that the molecular O_2 oxidation of Si(100) proceeds in a layer-by-layer mode and that the first submonolayer including backbonds is oxidized with almost no activation energy. Kato and coworkers¹²⁰ studied asymmetric pathways using spin-polarized DFT. They found that O_2 does not directly attack the backbond. Rather, the oxidation occurs via metastable chemisorption states along barrierless reaction paths or channels. Figure 13a shows that the oxygen molecule is proposed to initially dissociate onto two different surface dimers yielding the on-dimer structure, **II**. The first transition state, **T1**, connects **II** and **I2**, the on-top structure. The second transition state, **T2**, connects **I2** and the final 'backbond' product. Figure 13b shows another channel in which the oxygen molecule initially binds on one dimer, **I**. After the transition state, **T**, where the O–O is being broken, the final product has a 'backbond' oxygen and an on-top oxygen. They argued that a narrowing reaction channel (reduced reaction probability) yielding a small sticking coefficient with molecular oxygen can be explained by the intersystem crossing (triplet to singlet) that occurs in the middle of the reaction. They estimated the probability of this crossing to be 0.08 and 0.025 for incident kinetic energies of 0.1 and 1.0 eV, respectively.

Choi and coworkers¹²¹ systematically studied the initial O atom oxidations using CASSCF wave functions augmented by MCQDPT2 for dynamic correlation. The SIMOMM method was used in order to study clusters as large as $\text{OSi}_{15}\text{H}_{20}$ (these are the quantum mechanically calculated atoms) imbedded in a $\text{OSi}_{136}\text{H}_{92}$ cluster. It is found that both symmetric and asymmetric approaches of atomic oxygen have no initial reaction barrier. The asymmetric approach initially yields the on-top structure shown in Figure 12a. The backbond structure is obtained by surmounting a low energy transition state. The symmetric approach yields an on-dimer structure (Figure 12b), and only a singlet state is found at this geometry. By breaking the remaining Si–Si bond of the dimer, the dimer-bridge structure (Figure 12c) is obtained. Except for reactants, the singlet surface is lower in energy than the triplet along the entire reaction path. This study shows the detailed reaction mechanisms of both 'backbond' and dimer-bridge structures.

It appears that di-coordinated oxygen configurations such as backbond and dimer-bridge are the most stable forms and play a significant role in the initial growth of silicon oxide film.

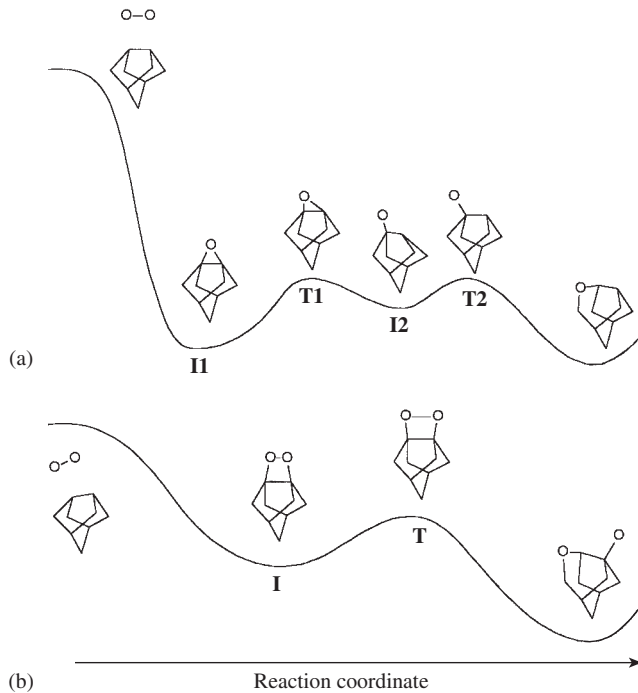


FIGURE 13. Total energy variation along the two possible initial oxidation reactions. All atoms, except the oxygens, are Si atoms

B. Active Oxidation

For typical oxygen pressures, the transition from 'passive' to 'active' oxidation occurs at around 600–750 °C surface temperature. Curves for oxygen uptake vs. time display a transition from a simple Langmuir–Hinshelwood (LH) form for passive oxidation, to a more slowly increasing but sigmoidal form (reflecting autocatalytic aspects to the oxide island formation process) for active oxidation.

Many investigations have been devoted to the elucidation of the reaction mechanisms and the associated energetics of active oxidation of silicon surfaces. Extensive experiments by Engel and coworkers^{100,122} that employed modulated molecular beam (MMB) and thermal desorption studies (TDS) at high temperature suggested either the presence of two distinct adsorbed oxygen species (in addition to stable oxide islands), or two distinct desorption behaviors for isolated vs. aggregated species. More recent experimental studies and detailed modeling have provided further insight into the process. Pelz and coworkers¹²³ performed kinetic Monte Carlo (KMC) simulations on a single species model to reproduce morphological changes during etching observed with STM. Ultimately, they proposed a dual species model which produces an observed decoupling of the etching and nucleation rate¹²⁴.

Figure 14 presents a schematic illustration of a two-species oxidation model. This model assumes the existence of a 'desorption precursor' configuration, shown in Figure 14c,

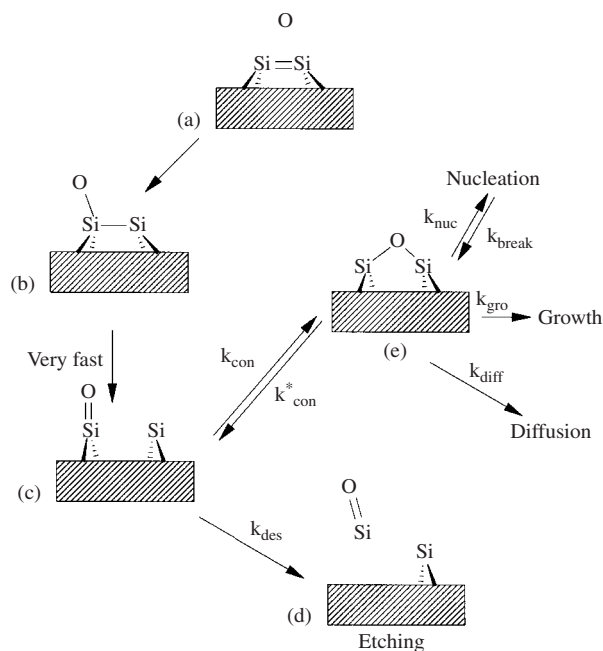


FIGURE 14. Schematic illustrations of passive-active oxidations of an Si(100)- 2×1 surface with silanone intermediates: (a) reactant, (b) on-top, (c) silanone, (d) product and (e) dimer bridge

which may be described as a surface silanone species¹²⁵. This silanone can either desorb from the surface as SiO (at rate k_{des}), or convert (at rate k_{con}) to a bridge or other more stable configuration as in Figure 14e. The latter can, in turn, diffuse across the surface (at rate k_{diff}) and lead to oxide-cluster nucleation (at rate k_{nuc}) or growth (at rate k_{gro}).

Choi and coworkers¹²¹ found that the surface silanone, Figure 12f and Figure 14c, does not appear to exist, at least not when there is a nearby Si atom. One reason is that such a configuration has an unstable diradical Si atom adjacent to the silanone. According to their calculations (summarized in Figure 15), initial symmetric and asymmetric reaction pathways are both barrierless yielding on-top (Figure 15b) and on-dimer (Figure 15e) configurations. The on-top configuration is converted into the backbond configuration (Figure 15c) by surmounting a low energy transition state with a barrier of $4.8 \text{ kcal mol}^{-1}$. The backbond structure eventually leads to etching (Figure 15d) via a complex reaction mechanism with a net barrier of 93 kcal mol^{-1} , similar to experimental values of $79\text{--}88 \text{ kcal mol}^{-1}$ ^{100,122}. They further studied the secondary active oxidation, in which the remaining Si atom of the actively oxidized dimer is oxidized. The most stable structure was found to be an inserted configuration (Figure 16a), similar to the backbond configuration. With a large activation barrier of $39.2 \text{ kcal mol}^{-1}$, the inserted configuration is converted into the silanone structure (Figure 16b). Subsequently, the SiO leaves the surface without a reaction barrier. This channel may be compared with the experimental barrier of 46 kcal mol^{-1} ¹²⁶, showing there may be multiple channels of active oxidation. Recent KMC studies based on these *ab initio* results successfully describe the transition from passive to active oxidation¹²⁷.

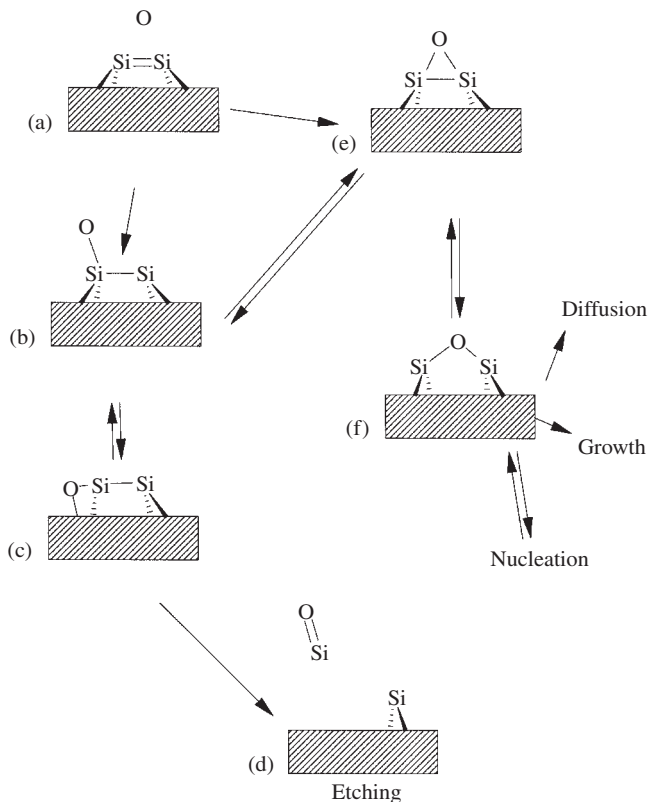


FIGURE 15. Schematic illustrations of passive-active oxidations of an Si(100)-2 × 1 surface without silanone intermediates: (a) reactant, (b) on-top, (c) backbond, (d) product, (e) on-dimer and (f) dimer bridge

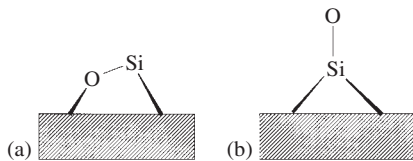


FIGURE 16. Schematic illustrations of (a) inserted and (b) silanone structures on Si(100)-2 × 1 surface

The on-dimer configuration Figure 15e can be converted into either the on-top species, Figure 15b, or the dimer-bridge species, Figure 15f, via transition states with MCQDPT2 barriers of 66.2 and 12.1 kcal mol⁻¹, respectively. The on-top configuration further contributes to the etching process, while the dimer-bridge configuration can be nucleated, grow an oxide film or diffuse to other sites.

According to this study, the backbond and dimer-bridge configurations are responsible for the etching and oxide film growth, respectively. However, at low temperature, the

backbond configuration may be also responsible for film growth. The delicate balance of passive and active oxidation, therefore, to some degree depends on the surface conversions between on-dimer and on-top configurations. More elaborate KMC simulations of this process are underway.

IX. ETCHING OF SI(100) WITH HALOGEN

Halogen etching of silicon surfaces has been extensively studied^{1,128}. Figure 17 shows the proposed surface bonding structures of chlorine on Si(100) that imply dissociative adsorption. The symmetric dimer (Figure 17a) has been suggested by NEXAFS¹²⁹, ARPES¹³⁰ and EELS experiments¹³¹. By combining several experimental techniques, Gao and coworkers¹³² showed that, in addition to the symmetric dimer, there is also a bridging species (Figure 17b). Several theoretical studies¹³³ have also shown that both the symmetric dimer and bridging species are stable, with the symmetric dimer lower in energy. Different interpretations have been given from other NEXAFS¹³⁴ and ESDIAD¹³⁵ studies. In these studies, to account for the surface normal Si–Cl bond direction, the asymmetric dimer (Figure 17c) was suggested as the dominant structure. The possibility of a dichloride species¹³⁶ (Figure 17d) was also proposed to account for another non-perpendicular bond direction.

In contrast to oxygen, which prefers a di-coordinate configuration, halogen seems to prefer single bond configurations similar to hydrogen and water. This preference may prevent the halogen from diffusing into the silicon bulk, prohibiting growth of a halogen film on the surface.

A majority of the studies^{132,136b,137} reported that the thermal etching of Cl occurs exclusively by the desorption of SiCl_2 and SiCl_4 . The former is mainly produced at high temperature (*ca* 900 K) and the latter at low and intermediate temperatures (150–400 K). However, Cl_2 ¹³⁷ and SiCl ¹³⁸ also have been observed. According to the ion-enhanced etching of silicon, Si, SiCl_3 , Si^+ and SiCl^+ desorption species have been also observed¹³⁹. Of these, Si and SiCl were the major products.

To elucidate the reaction mechanisms of SiCl_2 desorption, de Wijs and coworkers¹⁴⁰ performed first principle studies using a local density functional in combination with slab models. The study showed that the two monochlorinated Si atoms (Figure 17a) of a surface dimer can rearrange into a metastable SiCl_2 adsorbed species plus a Cl-free Si atom (Figure 17d, Figure 18a). They suggested that desorption of SiCl_2 occurs via a

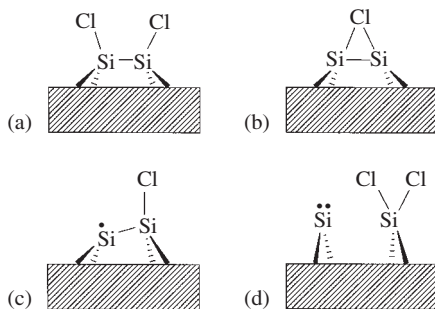


FIGURE 17. Schematic illustrations of (a) symmetric dimer, (b) bridging dimer, (c) asymmetric dimer and (d) dichloride structures on an $\text{Si}(100)\text{-}2 \times 1$ surface

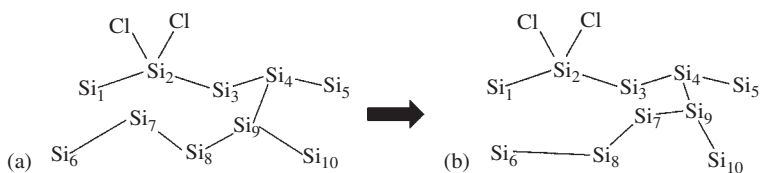


FIGURE 18. Proposed intermediates for the SiCl_2 desorption reactions: (a) Dichloride configuration. (b) The free Si atom migrates and is inserted into a neighbor Si dimer

two-step mechanism. In the first step the adsorbed species SiCl_2 is initially stabilized, since the nearby isolated Si diffuses away and is inserted into the Si–Si bond (Figure 18b). After this, SiCl_2 desorption occurs. The estimated activation energy is *ca* 3.1 eV. This is in reasonable agreement with the experimental value of *ca* 2.4 eV^{137a} and comparable with the fluorine etching energy of 3–3.7 eV¹⁴¹.

Due to the multiple desorption products, the surface mechanism of adsorption and desorption of Cl etching seems to be quite complex. More theoretical studies are expected.

Compared with chlorine, studies of other halogens are rare. Iodine¹⁴², fluorine¹⁴¹ and bromine¹⁴³ have been shown to etch the Si(100) surface. ESDIAD experiments^{75a, 135, 144} indicated that F bonds to the dangling bonds of the dimers, similar to the structure shown in Figure 17a. Using molecular beam techniques, XPS, TPD and LEED, Engstrom and coworkers¹⁴¹ showed that molecular fluorine adsorbs dissociatively, and that the saturation coverage of *ca* 1.5 ML is inconsistent with bonding only to the dangling bonds. Ceyer and coworkers¹⁴⁵ have proposed an F atom abstraction mechanism, where by making one Si–F with a surface dangling bond, the F_2 molecule ejects an F atom that can either desorb or chemisorb elsewhere on the surface.

Theoretically, Wu and Carter¹⁴⁶ showed that the 1.5 ML coverage may be explained by the difluoride species. Molecular dynamics simulations by Carter and Carter¹⁴⁷ suggested a stepwise mechanism which yields two pathways involving Si–F bond formation: (a) F atom abstraction, where one Si–F bond is formed at the expense of the F–F bond while the remaining F atom is ejected from the surface, and (b) dissociative chemisorption, where both F atoms in the incident F_2 molecule form Si–F bonds in a consecutive fashion. They showed that, depending on the conditions, the preferred reaction channel varies.

X. SUMMARY AND OUTLOOK

It is clear that the chemistry that occurs on silicon surfaces, Si(100) in particular, is not a simple extension of solution chemistry. One of the main reasons is the unique semi-rigid surface structure, as exemplified by the ‘pinned back’ *cis*-bent structure accompanying very flat buckling potentials. Consequently, such a unique structure reduces the geometric hindrance along the asymmetric approach of substrates, making the surface quite reactive. Cluster models predict both symmetric and buckled static structures, depending on the level of theory. The highest levels of theory, based on multi-reference wave functions, favor the symmetric structure. The discrepancy with some experiments may be due to the experimental conditions, surface defects or insufficient cluster size used in the theoretical studies. In any event, a static picture of the surface structure is likely to be inadequate.

The existence of low symmetry reaction pathways obviates the importance of symmetry rules. The consequence of this is especially apparent in the reactions of enes and dienes

with the surface, where the formally symmetry forbidden $[2 + 2]$ reaction occurs readily and the overall reaction is kinetically controlled. In the case of reactions with dienes, the surface loses its selectivity for the Diels–Alder product. A unique feature of reactions involving unsaturated hydrocarbons is that more than one Si–C bond are formed, and the integrity of the adsorbate is intact. Furthermore, except for aromatic molecules, surface product inter-conversion is rare.

Surface modification via chemical reactions is currently a very active field due to potential applications in the development of new materials. In addition to the ene and diene systems, other surface reactions including ionic, radical and photochemical reactions with a variety of functional groups are expected to extend the scope of potentially useful surface techniques.

In contrast to the reactions of unsaturated hydrocarbons, hydration, hydrogenation and oxidation by molecular oxygen seem to be dissociative rather than molecular.

In the case of hydration, an asymmetric stepwise low energy pathway to dissociative adsorption is generally accepted. The mechanism initially involves molecular adsorption as a precursor state. A secondary interaction through hydrogen bonding between neighbor dimer OH groups, that seems to affect further surface reactions of adsorbed OH and H, has been illustrated by theoretical and experimental studies.

For hydrogenation, the reaction mechanism is still controversial largely due to discrepancies between theoretical and experimental desorption barriers. Although some alternative mechanisms have been proposed, more studies are needed.

The most stable structures of initial oxidation may be the backbond and dimer bridge structures. Both structures contain di-coordinated oxygen. These two configurations seem to be the initial building blocks of oxide film growth and the key species for surface etching.

Due to the multiple desorption products, the etching of the surface with halogen appears to be quite complex. A multi-step reaction mechanism has been suggested to account for the SiCl_2 desorption species. In the case of fluorine atom adsorption, F atom abstraction and dissociative chemisorption mechanisms have been suggested. In order to account for the complex surface reactions, more studies are needed.

With the help of new experimental techniques (such as STM) and more sophisticated theoretical methodologies, many fascinating surface structures and mechanisms have been revealed with molecular detail. These combined efforts continue to elucidate new interesting features of surface chemistry. Developments of new theoretical techniques will facilitate the analysis of much larger, and therefore more realistic, clusters. Combined with periodic boundary conditions, sophisticated levels of theory, and dynamics and non-equilibrium statistical mechanics techniques, these efforts will advance the convergence of theory and experiment.

XI. ACKNOWLEDGMENT

This work was supported by a grant from the Air Force Office of Scientific Research.

XII. REFERENCES

1. H. N. Waltenburg and J. T. Yates, Jr., *Chem. Rev.*, **95**, 1589 (1995).
2. M. J. Sailor and E. J. Lee, *Adv. Mater.*, **9**, 783 (1997).
3. J. M. Buriak, *J. Chem. Soc., Chem. Commun.*, 1051 (1999).
4. (a) H. C. Longuet-Higgins and L. Salem, *Proc. R. Soc. London, Ser. A*, **251**, 172 (1959).
(b) Y. S. Lee and M. Kertesz, *Int. J. Quantum. Chem., Symp.*, **21**, 163 (1987).
5. (a) R. Hoffmann, *Solid and Surfaces: A Chemist's View of Bonding in Extended Structure*, VCH, New York, 1988.
(b) S. Y. Hong and D. Marynick, *J. Chem. Phys.*, **96**, 5497 (1992).

6. (a) O. H. Nielsen and R. M. Martin, *Phys. Rev. B*, **32**, 3780 (1985).
(b) C. Dal, *Lect. Notes Chem.*, **67**, 155 (1996).
(c) K. Schwarz and P. Blaha, *Lect. Notes Chem.*, **67**, 139 (1996).
(d) G. Kresse and J. Furthmüller, *Phys. Rev. B*, **54**, 11169 (1996).
7. P. J. Feibelman, *Phys. Rev. B*, **44**, 3916 (1991).
8. (a) M. P. Teter, M. C. Payne and D. C. Allan, *Phys. Rev. B*, **40**, 12255 (1989).
(b) D. M. Bylander, L. Kleinman and S. Lee, *Phys. Rev. B*, **42**, 1394 (1990).
9. K. N. Kudin and G. E. Scuseria, *Phys. Rev. B*, **61**, 5141 (2000).
10. (a) K. E. Schmidt and M. A. Lee, *J. Stat. Phys.*, **63**, 1223 (1991).
(b) C. L. Berman and L. Greengard, *J. Math. Phys.*, **35**, 6036 (1994).
(c) C. G. Lambert, T. A. Darden and J. A. Board, *J. Comput. Phys.*, **126**, 274 (1996).
(d) M. Challacombe, C. White and M. Head-Gordon, *J. Chem. Phys.*, **107**, 10131 (1997).
(e) K. N. Kudin and G. E. Scuseria, *Chem. Phys. Lett.*, **283**, 61 (1998).
11. D. J. Singh, *Planewaves, Pseudopotentials and the LAPW Method*, Kluwer Academic, Boston, 1994.
12. P. Nachtigall, K. D. Jordan and K. C. Janda, *J. Chem. Phys.*, **95**, 8652 (1991).
13. A. Redondo and W. A. Goddard III, *J. Vac. Sci. Technol.*, **21**, 344 (1982).
14. J. Shoemaker, L. W. Burggarf and M. S. Gordon, *J. Chem. Phys.*, **112**, 2994 (2000).
15. F. W. Bobrowicz and W. A. Goddard III, Chap. 4 in *Modern Theoretical Chemistry*, Vol. 3 (Ed. H. F. Schaefer III), Plenum press, London (1977).
16. (a) W. L. Jorgensen, J. Chandrasekhar, J. D. Madura, R. W. Impey and M. L. Klein, *J. Chem. Phys.*, **79**, 926 (1983).
(b) P. N. Day, J. H. Jensen, M. S. Gordon, S. P. Webb, W. J. Stevens, M. Krauss, D. Garmer, H. Basch and D. Cohen, *J. Chem. Phys.*, **105**, 1968 (1996).
(c) H. J. C. Berendsen, J. R. Grigera and T. P. Straatsma, *J. Phys. Chem.*, **91**, 6269 (1987).
(d) B. Guillot and Y. Guissani, *J. Chem. Phys.*, **99**, 8075 (1993).
(e) J. Alejandro, D. J. Tildesley and G. A. Chapela, *J. Chem. Phys.*, **102**, 4 (1995).
17. (a) B. Weiner, C. S. Carmer and M. Frenklach, *Phys. Rev. B*, **43**, 1678 (1991).
(b) C. S. Carmer, B. Weiner and M. Frenklach, *J. Chem. Phys.*, **99**, 1356 (1993).
(c) F. Maseras and K. Morokuma, *J. Comput. Chem.*, **16**, 1170 (1995).
18. J. Shoemaker, L. W. Burggarf and M. S. Gordon, *J. Phys. Chem. A*, **103**, 3245 (1999).
19. C. H. Choi and M. S. Gordon, *J. Am. Chem. Soc.*, **121**, 11311 (1999).
20. (a) X. Assfeld and J.-L. Rivail, *Chem. Phys. Lett.*, **263**, 100 (1996).
(b) J. Gao, P. Amara, C. Alhambra and M. J. Field, *J. Phys. Chem. A*, **102**, 4714 (1998).
(c) D. M. Philipp and R. A. Friesner, *J. Comput. Chem.*, **20**, 1468 (1999).
(d) V. Kairys and J. H. Jensen, *J. Phys. Chem. A*, **104**, 6656 (2000).
21. (a) M. Challacombe and E. Schwegler, *J. Chem. Phys.*, **106**, 5526 (1997).
(b) C. A. White, B. G. Johnson, P. M. W. Gill and M. Head-Gordon, *Chem. Phys. Lett.*, **253**, 268 (1996).
(c) T.-S. Lee, D. M. York and W. Yang, *J. Chem. Phys.*, **105**, 2744 (1996).
(d) M. C. Strain, G. E. Scuseria and M. J. Frisch, *Science*, **271**, 51 (1996).
(e) C. H. Choi, J. Ivanic, M. S. Gordon and K. Ruedenberg, *J. Chem. Phys.*, **111**, 8825 (1999).
22. R. E. Schlier and H. E. Farnsworth, *J. Chem. Phys.*, **30**, 917 (1959).
23. J. D. Levine, *Surf. Sci.*, **34**, 90 (1973).
24. D. J. Chadi, *Phys. Rev. Lett.*, **43**, 43 (1979).
25. (a) N. Jedrecy, M. Sauvage-Simkin, R. Pinchaux, J. Massies, N. Greiser and V. H. Etgens, *Surf. Sci.*, **230**, 197 (1990).
(b) D.-S. Lin, T. Miller and T.-C. Chiang, *Phys. Rev. Lett.*, **67**, 2187 (1991).
(c) E. Landemark, C. J. Karlsson, Y.-C. Chao and R. I. G. Uhrberg, *Phys. Rev. Lett.*, **69**, 1588 (1992).
(d) E. Landemark, C. J. Karlsson, Y.-C. Chao and R. I. G. Uhrberg, *Surf. Sci.*, **287/288**, 529 (1993).
(e) R. A. Wolkow, *Phys. Rev. Lett.*, **68**, 2636 (1992).
26. (a) P. C. Weakliem, G. W. Smith and E. A. Carter, *Surf. Sci.*, **232**, L219 (1990).
(b) J. Dabrowski and M. Scheffler, *Appl. Surf. Sci.*, **56-58**, 15 (1992).
(c) N. Roberts and R. J. Needs, *Surf. Sci.*, **236**, 112 (1990).
(d) P. Kruger and J. Pollmann, *Phys. Rev. B*, **47**, 1898 (1993).
(e) J. E. Northrup, *Phys. Rev. B*, **47**, 10032 (1993).

- (f) A. Ramstad, G. Brocks and P. J. Kelly, *Phys. Rev. B*, **51**, 14504 (1995).
(g) C. Yang, S. Y. Lee and H. C. Kang, **107**, 3295 (1997).
(h) R. Konecny and D. J. Doren, *J. Chem. Phys.*, **106**, 2426 (1997).
27. (a) R. M. Tromp, R. J. Hamers and J. E. Demuth, *Phys. Rev. Lett.*, **55**, 1303 (1985).
(b) R. J. Hamers, R. M. Tromp and J. E. Demuth, *Phys. Rev. B*, **34**, 5343 (1986).
(c) R. J. Hamers, P. Avouris and F. Bozso, *Phys. Rev. Lett.*, **59**, 2071 (1987).
(d) R. J. Hamers, P. Avouris and F. Bozso, *J. Vac. Sci. Technol. A*, **6**, 508 (1988).
(e) R. Wiesendanger, D. Burgler, G. Tarrach and H. J. Guntherodt, *Surf. Sci.*, **232**, 1 (1990).
(f) Z. Jing and J. L. Whitten, *Surf. Sci.*, **274**, 106 (1992).
(g) M. Tsuda, T. Hoshino, S. Oikawa and I. Ohdomari, *Phys. Rev. B*, **44**, 11241 (1991).
(h) T. Hoshino, S. Oikawa, M. Tsuda and I. Ohdomari, *Phys. Rev. B*, **44**, 11248 (1991).
(i) T. Hoshino, M. Hata, S. Oikawa and M. Tsuda, *Phys. Rev. B*, **54**, 11331 (1996).
(j) I. P. Batra, *Phys. Rev. B*, **41**, 5048 (1990).
28. A. Redondo and W. A. Goddard III, *J. Vac. Sci. Technol.*, **21**, 344 (1982).
29. B. Paulus, *Surf. Sci.*, **408**, 195 (1998).
30. P. C. Weakiem, G. W. Smith and E. A. Carter, *Surf. Sci. Rep.*, **232**, L219 (1990).
31. M. W. Schmidt, P. Truong and M. S. Gordon, *J. Am. Chem. Soc.*, **109**, 5217 (1987).
32. F. W. Bobrowicz and W. A. Goddard, III, Chap. 4 in *Modern Theoretical Chemistry*, Vol. 3 (Ed. H. F. Schaefer III), Plenum Press, London (1977).
33. M. W. Schmidt and M. S. Gordon, *Annu. Rev. Phys. Chem.*, **49**, 233 (1998).
34. M. S. Gordon, J. Shoemaker and L. W. Burggraf, *J. Chem. Phys.* (in Press).
35. R. B. Woodward and R. Hoffmann, *The Conservation of Orbital Symmetry*, Verlag Chemie, Weinheim, 1970.
36. I. Fleming, *Frontier Orbitals and Organic Chemical Reactions*, Wiley, New York, 1976, p. 90.
37. R. West, *Angew. Chem., Int. Ed. Engl.*, **26**, 1201 (1987); P. J. Domaille, *J. Am. Chem. Soc.*, **106**, 7677 (1984).
38. (a) M. Nishijima and J. Yoshinobu, H. Tsuda and M. Onchi, *Surf. Sci.*, **192**, 383 (1987).
(b) J. Yoshinobu, H. Tsuda, M. Onchi and M. Nishijima, *J. Chem. Phys.*, **87**, 7332 (1987).
39. (a) J. T. Yates, *J. Phys.: Condensed Matter*, **3**, S43 (1991).
(b) M. J. Bozack, P. A. Taylor, W. J. Choyke and J. T. Yates, *Surf. Sci.*, **177**, L933 (1986).
(c) P. A. Taylor, R. M. Wallace, C. C. Cheng, W. H. Weinberg, M. J. Dresser, W. J. Choyke and J. T. J. Yates, *J. Am. Chem. Soc.*, **114**, 6754 (1992).
(d) L. Clemen, R. M. Wallace, P. A. Taylor, M. J. Dresser, W. J. Choyke, W. H. Weinberg and J. T. Yates, *Surf. Sci.*, **268**, 205 (1992).
(e) C. C. Cheng, R. M. Wallace, P. A. Taylor, W. J. Choyke and J. T. Yates, *J. Appl. Phys.*, **67**, 3693 (1990).
(f) C. C. Cheng, W. J. Choyke and J. T. Yates, *Surf. Sci.*, **231**, 289 (1990).
40. Y. Imamura, Y. Morikawa, T. Yamasaki and H. Nakatsuji, *Surf. Sci.*, **341**, L1091 (1995).
41. Q. Liu and R. Hoffmann, *J. Am. Chem. Soc.*, **117**, 4082 (1995).
42. L. Li, C. Tindall, O. Takaoka, Y. Hasegawa and T. Sakurai, *Phys. Rev. B*, **56**, 4648 (1997).
43. R. A. Wolkow, *Annu. Rev. Phys. Chem.*, **50**, 413 (1999).
44. S. Mezheny, L. Lyubintsky, W. J. Choyke, R. A. Wolkow and J. T. Yates, *Phys. Rev. Lett.* (in press).
45. J. Hovis, S. Lee, H. Liu and R. J. Hamers, *J. Vac. Sci. Technol. B*, **15**, 1153 (1997).
46. (a) B. I. Craig and P. V. Smith, *Surf. Sci.*, **276**, 174 (1992).
(b) C. S. Cramer, B. Weiner and M. Frenklach, *J. Chem. Phys.*, **99**, 1356 (1993).
47. (a) A. J. Fisher, P. E. Blochl and G. A. D. Briggs, *Surf. Sci.*, **374**, 298 (1997).
(b) W. Pan, T. Zhu and W. Yang, *J. Chem. Phys.*, **107**, 3981 (1997).
48. D. C. Sorescu and K. D. Jordan, *J. Phys. Chem. A*, **104**, 8259 (2000).
49. R. Konecny and D. J. Doren, *Surf. Sci.*, **417**, 169 (1998).
50. R. J. Hamers, S. K. Coulter, M. D. Ellison, J. S. Hovis, D. F. Padowitz, M. P. Schwartz, C. M. Greenlief and J. N. Russell, Jr., *Acc. Chem. Res.* (in press).
51. R. J. Hamers, J. S. Hovis, S. Lee, H. Liu and J. Shan, *J. Phys. Chem. B*, **101**, 1489 (1997).
52. J. S. Hovis and R. J. Hamers, *J. Phys. Chem. B*, **101**, 9581 (1997).
53. J. S. Hovis and R. J. Hamers, *J. Phys. Chem. B*, **102**, 687 (1998).
54. G. P. Lopinski, D. J. Moffatt, D. D. M. Wayner and R. A. Wolkow, *J. Am. Chem. Soc.*, **122**, 3548 (2000).

55. G. P. Lopinski, D. J. Moffatt, D. D. M. Wayner, M. Z. Zgierski and R. A. Wolkow, *J. Am. Chem. Soc.*, **121**, 4532 (1999).
56. R. Konecny and D. Doren, *J. Am. Chem. Soc.*, **119**, 11098 (1997).
57. A. V. Teplyakov, M. J. Kong and S. F. Bent, *J. Am. Chem. Soc.*, **119**, 11100 (1997).
58. A. V. Teplyakov, M. J. Kong and S. F. Bent, *J. Chem. Phys.*, **108**, 4599 (1998).
59. J. S. Hovis, H. B. Liu and R. J. Hamers, *J. Phys. Chem. B*, **102**, 6873 (1998).
60. (a) H. Nakano, *J. Chem. Phys.*, **99**, 7983 (1993).
(b) H. Nakano, *Chem. Phys. Lett.*, **207**, 372 (1993).
61. (a) K. R. Sunberg and K. Ruedenberg, in *Quantum Science* (Eds. J. L. Calais, O. Goswami, J. Linderberg and Y. Ohrn), Plenum, New York, 1976.
(b) L. M. Cheung, K. R. Sunberg and K. Ruedenberg, *Int. J. Quantum Chem.*, **16**, 1103 (1979).
(c) K. Ruedenberg, M. Schmidt, M. M. Gilbert and S. T. Elbert, *Chem. Phys.*, **71**, 41 (1982).
(d) B. O. Roos, P. Taylor and P. E. Siegbahn, *Chem. Phys.*, **48**, 157 (1980).
(e) M. W. Schmidt and M. S. Gordon, *Annu. Rev. Phys. Chem.*, **49**, 233 (1998).
62. M. J. Kong, A. V. Teplyakov, J. Jagmohan, J. G. Lyubovitsky, C. Mui and S. F. Bent, *J. Phys. Chem. B*, **104**, 3000 (2000).
63. Y. Jung, C. H. Choi and M. S. Gordon, *J. Phys. Chem.* (submitted).
64. Y. Taguchi, M. Fujisawa, T. Takaoka, T. Okasa and M. Nishijima, *J. Chem. Phys.*, **95**, 6870 (1991).
65. (a) G. P. Lopinski, T. M. Fortier, D. J. Moffatt and R. A. Wolkow, *J. Vac. Sci. Technol. A*, **16**, 1937 (1998).
(b) G. P. Lopinski, D. J. Moffatt and R. A. Wolkow, *Chem. Phys. Lett.*, **282**, 305 (1998).
66. M. Schwartz, S. Coulter, J. Hovis and R. J. Hamers, *J. Phys. Chem. B* (submitted).
67. S. K. Coulter, J. S. Hovis, M. D. Ellison and R. J. Hamers, *J. Vac. Sci. Technol. A*, **18**, 1965 (2000).
68. E. A. Irene, *J. Electrochem. Soc.*, **125**, 1708 (1978).
69. P. A. Thiel and T. E. Madey, *Surf. Sci. Rep.*, **1**, 211 (1987).
70. D. Schmeisser, F. J. Himpsel and G. Hollinger, *Phys. Rev. B*, **27**, 7813 (1983).
71. K. Fujiwara, *Surf. Sci.*, **108**, 124 (1981).
72. M. Nishijima, K. Edamoto, Y. Kubota, S. Tanaka and M. Onchi, *J. Chem. Phys.*, **84**, 6458 (1986).
73. Y. J. Chabal and S. B. Christman, *Phys. Rev. B*, **29**, 6974 (1984).
74. (a) E. M. Oellig, R. Butz, H. Wagner and H. Ibach, *Solid State Commun.*, **51**, 7 (1984).
(b) C. U. S. Larsson, A. S. Flodstrom, R. Nyholm, L. Incoccia and F. Senf, *J. Vac. Sci. Technol. A*, **5**, 3321 (1987).
(c) K. Fives, R. McGrath, C. Stephens, I. T. McGovern, R. Cimino, D. S.-L. Law, A. L. Johnson and G. Thornton, *J. Phys.: Condensed Matter*, **1**, SB105 (1989).
75. (a) A. L. Johnson, M. M. Walczak and T. E. Madey, *Langmuir*, **4**, 277 (1988).
(b) Q. Gao, Z. Dohnalek, C. C. Cheng, W. J. Choyke and J. T. Yates, Jr., *Surf. Sci.*, **312**, 261 (1994).
(c) H. Bu and J. W. Rabalais, *Surf. Sci.*, **301**, 285 (1994).
(d) A. T. S. Wee, C. H. A. Huan, P. S. P. Thong and K. L. Tan, *Corros. Sci.*, **36**, 9 (1994).
76. W. Ranke and Y. R. Xing, *Surf. Sci.*, **157**, 339 (1985).
77. (a) E. Schröder-Bergen and W. Ranke, *Surf. Sci.*, **236**, 103 (1990).
(b) M. Chander, Y. Z. Li, J. C. Patrin and J. H. Weaver, *Phys. Rev. B*, **48**, 2493 (1993).
78. (a) C. U. S. Larsson, A. L. Johnson, A. S. Flodstrom and T. E. Madey, *J. Vac. Sci. Technol. A*, **5**, 842 (1987).
(b) Q. Gao, Z. Dohnalek, C. C. Cheng, W. J. Choyke and J. T. Yates, Jr., *Surf. Sci.*, **312**, 261 (1994).
79. H. Bu and J. W. Rabalais, *Surf. Sci.*, **301**, 285 (1994).
80. S. Ciraci and H. Wagner, *Phys. Rev. B*, **27**, 5180 (1983).
81. S. Katircioglu, *Surf. Sci.*, **187**, 569 (1987).
82. (a) N. Russo, M. Toscano, V. Barone and F. Lelj, *Surf. Sci.*, **180**, 599 (1987).
(b) V. Barone, *Surf. Sci.*, **189/190**, 106 (1987).
83. C. K. Ong, *Solid State Commun.*, **72**, 1141 (1989).
84. R. Konecny and D. J. Doren, *J. Chem. Phys.*, **106**, 2426 (1997).
85. Y. Jung and M. S. Gordon, (in preparation).
86. J. Cho, K. S. Kim, S. Lee and M. Kang, *Phys. Rev. B*, **61**, 4503 (2000).

87. A. B. Gurevich, B. B. Stefanov, M. K. Weldon, Y. J. Chabal and K. Raghavachari, *Phys. Rev. B*, **58**, R13434 (1998).
88. (a) X.-L. Zhou, C. R. Flores and J. M. Whilte, *App. Surf. Sci.*, **62**, 223 (1992).
(b) R. K. Schulze and J. F. Evans, *App. Surf. Sci.*, **81**, 449 (1994).
(c) L. Andersohn and U. Köhler, *Surf. Sci.*, **284**, 77 (1993).
89. (a) K. Sinniah, M. G. Sherman, L. B. Lewis, W. H. Weinberg, J. T. Yates, Jr. and K. C. Janda, *Phys. Rev. Lett.*, **62**, 567 (1989).
(b) K. Sinniah, M. G. Sherman, L. B. Lewis, W. H. Weinberg, J. T. Yates, Jr. and K. C. Janda, *J. Chem. Phys.*, **92**, 5700 (1990).
(c) M. L. Wise, B. G. Koehler, P. Gupta, P. A. Coon and S. M. George, *Surf. Sci.*, **258**, 5482 (1991).
(d) U. Höfer, L. Li and T. F. Heinz, *Phys. Rev. B*, **45**, 9485 (1992).
(e) M. C. Flowers, N. B. H. Honathan, Y. Liu and A. Morris, *J. Chem. Phys.*, **99**, 7038 (1993).
90. (a) R. J. Hamers, R. M. Tromp and J. E. Demuth, *Phys. Rev. B*, **34**, 5343 (1986).
(b) G. Schulze and M. Henzler, *Surf. Sci.*, **124**, 336 (1983).
(c) P. Gupta, V. L. Colvin and S. M. George, *Phys. Rev. B*, **37**, 8234 (1988).
(d) M. L. Wise, B. G. Koehler, P. Gupta, P. A. Coon and S. M. George, *Mater. Res. Soc. Symp. Proc.*, **204**, 319 (1991).
91. M. R. Radeke and E. A. Carter, *Phys. Rev. B*, **54**, 11803 (1996).
92. J. J. Boland, *Phys. Rev. Lett.*, **67**, 1539 (1991).
93. (a) P. Nachtigall, K. D. Jordan and K. C. Janda, *J. Chem. Phys.*, **95**, 8652 (1991).
(b) C. J. Wu and E. A. Carter, *Chem. Phys. Lett.*, **185**, 172 (1991).
94. (a) M. P. D'Evelyn, Y. L. Yang and L. F. Sutcu, *J. Chem. Phys.*, **96**, 852 (1992).
(b) Y. L. Yang and M. P. D'Evelyn, *J. Vac. Sci. Technol. A*, **11**, 2200 (1993).
95. (a) P. Nachtigall and K. D. Jordan, *J. Chem. Phys.*, **101**, 2648 (1994).
(b) Z. Jing and J. L. Whitten, *Phys. Rev. B*, **50**, 5506 (1994).
96. Z. Jing and J. L. Whitten, *J. Chem. Phys.*, **102**, 3867 (1995).
97. S. Pai and D. Doren, *J. Chem. Phys.*, **103**, 1232 (1995).
98. M. R. Radeke and E. A. Carter, *Phys. Rev. B*, **55**, 4649 (1997).
99. (a) P. Kratzer, E. Pehlke, M. Scheffler, M. B. Raschke and U. Köfer, *Phys. Rev. Lett.*, **81**, 5596 (1998).
(b) E. Pehlke and P. Kratzer, *Phys. Rev. B*, **59**, 2790 (1999).
100. T. Engel, *Surf. Sci. Rep.*, **18**, 91 (1993).
101. (a) M. S. Krishnan, L. Chang, T. King, J. Bokor and C. Hu, *Tech. Dig.-Int. Electron Devices Meet.*, 241 (1999).
(b) Y. Ma, Y. Ono, L. Stecker, D. R. Evans and S. T. Hsu, *Tech. Dig.-Int. Electron Devices Meet.*, 149 (1999).
102. H. Wormeester, E. G. Keim and A. van Silfhout, *Surf. Sci.*, **271**, 340 (1992).
103. (a) X. M. Zheng and P. V. Smith, *Surf. Sci.*, **232**, 6 (1990).
(b) U. Höfer, P. Mogen and W. Wurth, *Phys. Rev. B*, **40**, 1130 (1989).
(c) P. Gupta, C. H. Mak, P. A. Coon and S. M. George, *Phys. Rev. B*, **40**, 7739 (1989).
(d) B. Schubert, P. Avouris and R. Hoffmann, *J. Chem. Phys.*, **98**, 7593 (1993).
(e) K. Sakamoto, K. Nakatsuji, H. Daimon, T. Yonezawa and S. Suga, *Surf. Sci.*, **306**, 93 (1994).
104. I. P. Batra, P. S. Bagus and K. Hermann, *Phys. Rev. Lett.*, **52**, 384 (1984).
105. (a) J. R. Engstrom, D. J. Bonser and T. Engel, *Surf. Sci.*, **268**, 238 (1992).
(b) J. Westermann, H. Nienhous and W. Mönch, *Surf. Sci.*, **311**, 101 (1994).
(c) K. E. Johnson, P. K. Wu, M. Sander and T. Engel, *Surf. Sci.*, **290**, 213 (1993).
106. H. Yaguchi, K. Fujita, S. Fukatsu, Y. Shiraki, R. Ito, T. Igarashi and T. Hattori, *Surf. Sci.*, **275**, 395 (1992).
107. P. Avouris and I.-W. Lyo, *Appl. Surf. Sci.*, **60/61**, 426 (1992).
108. J. A. Schaefer, F. Stucki, D. J. Frankel, W. Göpel and G. L. Lapeyre, *J. Vac. Sci. Technol. B*, **2**, 359 (1984).
109. L. Incoccia, A. Balerna, S. Cramm, C. Kunz, F. Senf and I. Storzjohann, *Surf. Sci.*, **189/190**, 453 (1987).
110. (a) A. Namiki, K. Tanimoto, T. Nakamura, N. Ohtake and T. Suzaki, *Surf. Sci.*, **222**, 530 (1989).

111. (a) P. Avouris and D. G. Cahill, *Ultramicroscopy*, **42–44**, 838 (1992).
(b) D. G. Cahill and P. Avouris, *Appl. Phys. Lett.*, **60**, 326 (1992).
112. P. Kliese, B. Röttger, D. Badt and H. Neddermeyer, *Ultramicroscopy*, **42–44**, 824 (1992).
113. P. V. Smith and A. Wander, *Surf. Sci.*, **219**, 77 (1989).
114. Y. Miyamoto and A. Oshiyama, *Phys. Rev. B*, **41**, 12680 (1990).
115. Y. Miyamoto and A. Oshiyama, *Phys. Rev. B*, **43**, 9287 (1991).
116. T. Uchiyama and M. Tsukada, *Phys. Rev. B*, **53**, 7917 (1996).
117. T. Uchiyama and M. Tsukada, *Phys. Rev. B*, **55**, 9356 (1997).
118. T. Hoshino, M. Tsuda, S. Oikawa and I. Ohdomari, *Phys. Rev. B*, **50**, 14999 (1994).
119. H. Watanabe, K. Kato, T. Uda, K. Fujita, M. Ichikawa, T. Kawamura and K. Terakura, *Phys. Rev. Lett.*, **80**, 345 (1998).
120. K. Kato, T. Uda and K. Terakura, *Phys. Rev. Lett.*, **80**, 2000 (1998).
121. C. H. Choi, D.-J. Liu, J. W. Evans and M. S. Gordon (in preparation).
122. J. R. Engstrom, D. J. Bonser, M. M. Nelson and T. Engel, *Surf. Sci.*, **256**, 317 (1991).
123. (a) C. Ebner, J. V. Seiple and J. P. Pelz, *Phys. Rev. B*, **52**, 16651 (1996).
(b) J. V. Seiple and J. P. Pelz, *Phys. Rev. Lett.*, **73**, 999 (1994).
124. J. V. Seiple, C. Ebner and J. P. Pelz, *Phys. Rev. B*, **53**, 15432 (1996).
125. R. Ludeke and A. Koma, *Phys. Rev. Lett.*, **34**, 1170 (1975).
126. (a) J. B. Hannon, M. C. Bartelt, N. C. Bartelt and G. L. Kellogg, *Phys. Rev. Lett.*, **81**, 4676 (1998).
(b) M. C. Bartelt, J. B. Hannon, A. K. Schmid, C. R. Stoldt and J. W. Evans, *Colloids and Surfaces A*, **165**, 373 (2000).
127. D.-J. Liu, C. H. Choi, M. S. Gordon and J. W. Evans, *MRS Proc.*, **619** (2000).
128. H. F. Winters and J. W. Coburn, *Surf. Sci. Rep.*, **14**, 161 (1992).
129. G. Thornton, P. L. Wincott, R. McGrath, I. T. McGovern, F. M. Quinn, D. Norman and D. D. Vvedensky, *Surf. Sci.*, **211/212**, 959 (1989).
130. L. S. O. Johansson, R. I. G. Uhrberg, R. Lindsay, P. L. Wincott and G. Thornton, *Phys. Rev. B*, **42**, 9534 (1990).
131. N. Aoto, E. Ikawa and Y. Kurogi, *Surf. Sci.*, **199**, 408 (1988).
132. Q. Gao, C. C. Cheng, P. J. Chen, W. J. Choyke and J. T. Yates, Jr., *J. Chem. Phys.*, **98**, 8308 (1993).
133. (a) B. I. Craig and P. V. Smith, *Surf. Sci.*, **290**, L662 (1993).
(b) L.-Q. Lee and P.-L. Gao, *J. Phys.: Condensed Matter*, **6**, 6169 (1994).
(c) P. Kruger and J. Pollmann, *Phys. Rev. B*, **47**, 10032 (1993).
134. D. Purdie, N. S. Prakash, K. G. Purcell, P. L. Wincott, G. Thornton and D. S.-L. Law, *Phys. Rev. B*, **48**, 2275 (1993).
135. S. L. Bennett, C. L. Greenwood and E. M. Williams, *Surf. Sci.*, **290**, 267 (1993).
136. (a) J. Matsuo, K. Karahashi, A. Sato and S. Hijiyu, *Jpn. J. Appl. Phys.*, **31**, 2025 (1992).
(b) A. Szabó, P. D. Farrall and T. Engel, *Surf. Sci.*, **312**, 284 (1994).
137. (a) R. B. Jackman, H. Ebert and J. S. Foord, *Surf. Sci.*, **176**, 183 (1986).
(b) M. A. Mendicino and E. G. Seebauer, *Appl. Surf. Sci.*, **68**, 285 (1993).
138. K. Karahashi, J. Matsuo and S. M. Gates, *Appl. Surf. Sci.*, **60/61**, 126 (1992).
139. (a) D. J. Oostra, A. Haring, R. P. v. Ingen, A. E. de Vries and G. N. A. v. Veen, *J. Appl. Phys.*, **64**, 315 (1988).
(b) N. Materer, R. S. Goodman and S. R. Leone, *J. Phys. Chem. B*, **104**, 3261 (2000).
140. (a) G. A. de Wijs, A. De Vita and A. Selloni, *Phys. Rev. Lett.*, **78**, 4877 (1997).
(b) G. A. de Wijs, A. De Vita and A. Selloni, *Phys. Rev. B*, **57**, 10021 (1998).
141. J. R. Engstrom, M. M. Nelson and T. Engel, *Surf. Sci.*, **215**, 437 (1989).
142. E. G. Michel, T. Pauly, V. Eteläniemi and O. Materlik, *Surf. Sci.*, **241**, 111 (1991).
143. D. D. Koleske and S. M. Gates, *J. Chem. Phys.*, **99**, 8218 (1993).
144. M. J. Bozack, M. J. Dresser, W. J. Choyke, P. A. Taylor and J. T. Yates, Jr., *Surf. Sci.*, **184**, L332 (1987).
145. Y. L. Li, D. P. Pullman, J. J. Yang, A. A. Tsekouras, D. B. Gosalvez, K. B. Laughlin, Z. Zhang, M. T. Schulberg, D. J. Gladstone, M. McGonigal and S. T. Ceyer, *Phys. Rev. Lett.*, **74**, 2603 (1995).
146. C. J. Wu and E. A. Carter, *Phys. Rev. B*, **45**, 9065 (1992).
147. L. E. Carter and E. A. Carter, *J. Phys. Chem.*, **100**, 873 (1996).

CHAPTER 16

Silyl migrations

MITSUO KIRA AND TAKEAKI IWAMOTO

*Department of Chemistry, Graduate School of Science, Tohoku University, Aoba-ku,
Sendai 980-8578, Japan*

Fax: 81-22-217-6589; e-mail: mkira@si.chem.tohoku.ac.jp

I. INTRODUCTION	854
II. 1,2-SILYL MIGRATIONS	854
A. Mechanistic Aspects	854
1. Dyotropic and related rearrangements	854
2. Cationic 1,2-silyl migrations and related 1,2-migrations	856
3. Anionic 1,2-silyl migrations	864
4. Radical 1,2-silyl migrations	867
5. Miscellaneous	868
B. 1,2-Silyl Migrations in Unsaturated Silicon Compounds	869
1. Silylmethylsilylene–silylsilaethene rearrangements	869
2. Disilanylcarbene–silylsilaethene rearrangements	870
3. Silylsilanone–siloxysilylene rearrangements	872
4. Disilanylsilylene–silyldisilene rearrangements	872
5. Disilanyldisilene–2-silylcyclotrisilane rearrangements	874
C. Synthetic Applications	875
1. Cationic 1,2-silyl migrations from C to C	875
a. [3 + 2] Annulations	875
b. [2 + 1] Annulations	878
c. Intramolecular cyclizations and ring openings	879
d. Miscellaneous	881
2. Anionic 1,2-silyl migrations from C to O	885
a. Preparation of silyl enol ethers	885
b. Cyclizations involving the Brook rearrangement	893
c. Miscellaneous	895
3. Anionic 1,2-silyl migrations from O to C	898
4. Anionic 1,2-silyl migrations between C and N	899
5. Radical 1,2-silyl migrations	901
III. 1,3-SILYL MIGRATIONS	902
A. Mechanistic Aspects	902
1. Migrations across allylic frameworks	902
2. 1,3-Silyl migrations in allylsilanes	904

3.	1,3-Silyl migrations in β -ketosilanes	906
4.	Comparison of the retention transition states for 1,3-silyl migrations in allylsilane and formylmethylsilane	906
5.	Anionic 1,3-silyl migrations across σ frameworks	908
B.	1,3-Silyl Migrations in Unsaturated Silicon Compounds	910
C.	Synthetic Applications	911
IV.	1, <i>n</i> -SILYL MIGRATIONS ($n \geq 4$)	912
A.	1,4-Silyl Migrations	912
1.	1,4-Silyl migration from C to C	912
2.	Anionic 1,4-silyl migrations from C to O	914
3.	Anionic 1,4-silyl migrations from O to C	920
4.	Anionic 1,4-silyl migrations from O to O	926
5.	Anionic 1,4-silyl migrations incorporating N	930
B.	1,5-Silyl Migrations	933
1.	1,5-Silyl migrations between C and O	933
2.	1,5-Silyl migrations from O to N	934
3.	1,5-Silyl migrations from O to O	934
4.	1,5-Silyl migrations from Si to C	936
C.	1,6-Silyl Migrations	937
V.	REFERENCES	938

I. INTRODUCTION

Owing to the high migratory aptitudes of silyl groups compared to carbon groups and hydrogen, a huge number of silyl migrations have been studied so far. However, to the best of our knowledge, there has been no recent review on silyl migrations since 1980, when a review was written by Brook and Bassindale (BB)¹. The review is still of great importance, since almost all types of silyl migrations in common organosilicon compounds have been dealt with extensively. The purpose of our review is to survey the advance in the studies of silyl migrations in the last two decades. Significant advances in this field have been achieved, especially in the following aspects: (i) A number of unique silyl migrations have been disclosed in unsaturated silicon molecules such as silylenes, silaethenes, disilenes etc., which have been generated as reactive intermediates and even isolated as stable molecules. (ii) Detailed microscopic mechanisms for several prototypical silyl migrations have been investigated using high level *ab initio* MO calculations. (iii) During a number of studies of the synthetic application of organosilicon reagents, many novel silyl migrations have been found and applied to the syntheses of useful organic compounds that were difficult to obtain by other methods²⁻¹¹. These three aspects of silyl migrations are the major concern of this review.

A number of interesting photochemical 1,*n*-silyl migrations¹²⁻¹⁴ as well as silyl migrations to transition metal centers¹⁵⁻¹⁹ have not been covered in the present review, since they have been surveyed in excellent review articles.

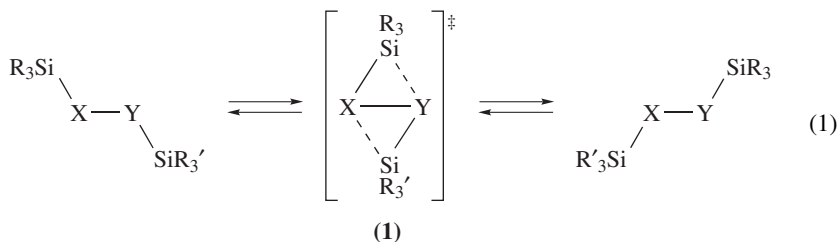
II. 1,2-SILYL MIGRATIONS

A. Mechanistic Aspects

1. Dyotropic and related rearrangements

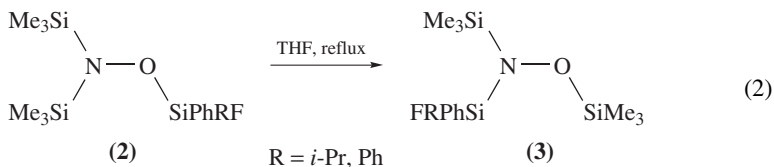
Dyotropic rearrangements are defined as the uncatalyzed concerted rearrangements in which two groups migrate intramolecularly and exchange positions (equation 1). Although

concerted dyotropic rearrangements are thermally forbidden pericyclic $[\sigma_s^2 + \sigma_s^2]$ type reactions according to the Woodward–Hoffmann rules, dyotropic type reactions involving silyl migrations are particularly rapid. A number of dyotropic rearrangements were discussed in BB¹ and a review by Reetz was published in 1977²⁰.

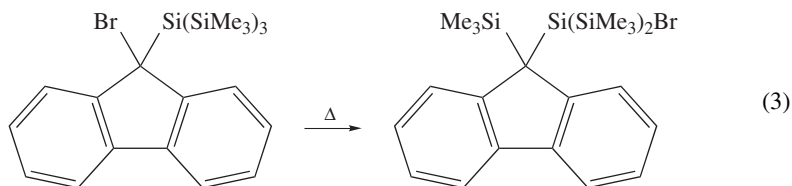


Among a number of dyotropic rearrangements, Nowakowski and West found previously a reversible rearrangement involving positional exchange between the organosilyl groups on oxygen and nitrogen in tris(trialkylsilyl)hydroxylamines²¹. They have suggested that the rearrangement proceeds via a dyotropic transition state **1** (equation 1), where (X, Y=N, O).

Klingebiel and coworkers reported irreversible rearrangement from **2** to **3** (equation 2)^{22,23}. *Ab initio* MO calculations showed that the rearrangement from $(\text{H}_3\text{Si})_2\text{N}-\text{OSiF}_3$ (**4**) to $(\text{H}_3\text{Si})(\text{F}_3\text{Si})\text{N}-\text{OSiH}_3$ (**5**) proceeded in one step via a dyotropic transition state, which was rather symmetric compared with that for the dyotropic rearrangement in $(\text{H}_3\text{Si})_2\text{N}-\text{OSiH}_3$, where the new Si–N bond was nearly formed but the Si–O bond was still longer than regular Si–O bonds. The theoretical calculations showed that **5** was more stable than **4** due to a more efficient contribution of $[\text{F}^- \text{F}_2\text{Si}=\text{NR}^+]$ type resonance structure (negative hyperconjugation) and a more advantageous $n(\text{O})-\sigma^*(\text{SiMe})$ delocalization in **5**.

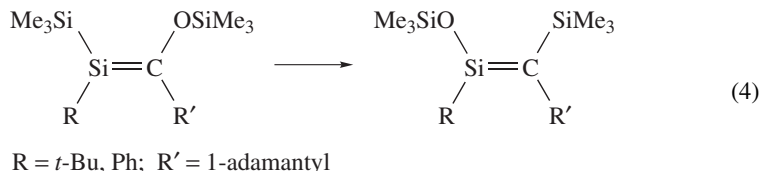


The 1,2-silyl migration shown in equation 3 may also proceed via a dyotropic rearrangement²⁴.

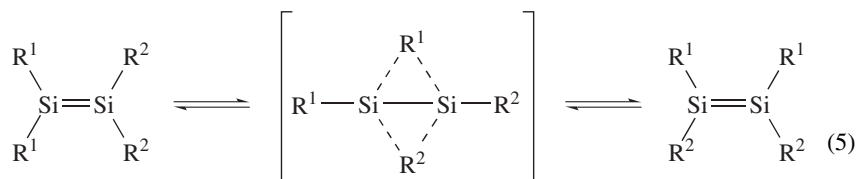


A dyotropic rearrangement was reported for the redistribution of the ligands in transition metal complexes²⁵. Several other dyotropic silyl migrations have been reported^{26–29}.

During a photochemical silene-to-silene rearrangement, Brook and coworkers mentioned the possibility that both the two groups, Me_3Si and Me_3SiO , migrated simultaneously across a $\text{Si}=\text{C}$ double bond (equation 4)³⁰.



Dyotropic type rearrangements were also found in stable disilenes (equation 5)^{31,32}. The rates of these rearrangements were strongly dependent on the substituents. Thus, for the rearrangement in 1,1-dimesityl(2,2-dixylyl)disilenes, 70 days were needed at 298 K to attain equilibrium, while the rearrangement in tetrasilyl disilenes was completed within 10 days at 273 K.

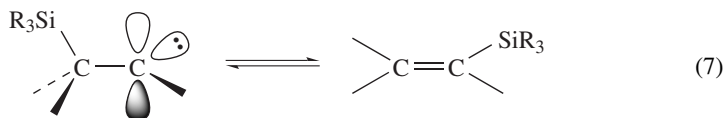
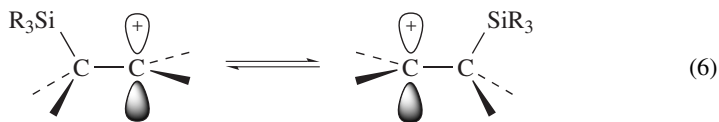


$\text{R}^1 = 2,4,6\text{-trimethylphenyl}$, $\text{R}^2 = 2,6\text{-dimethylphenyl}$

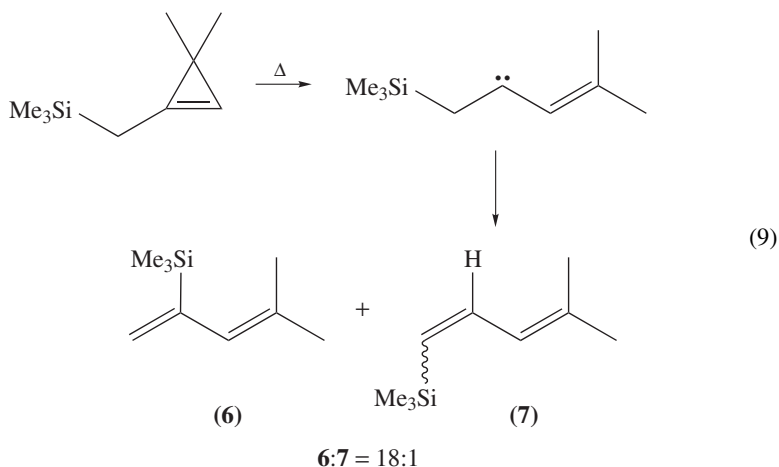
$\text{R}^1 = \text{SiMe}_2(\text{Bu-}i)$, $\text{R}^2 = \text{SiMe}(\text{Pr-}i)_2$

2. Cationic 1,2-silyl migrations and related 1,2-migrations

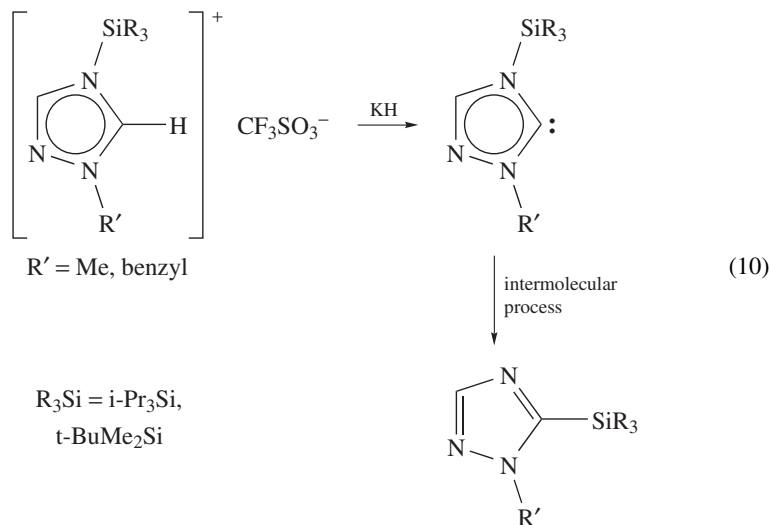
It has been well known that intramolecular migrations of silyl groups to neighboring carbocation centers as well as to neighboring carbenes^{33–35} occur quite easily, because the transition states as well as the electron-deficient reactants are stabilized significantly by hyperconjugation ($\sigma\text{-}\pi$ conjugation) (equations 6 and 7).



Similarly, high migratory aptitudes of silyl groups compared with carbon groups and hydrogen have been observed in the rearrangements from carbenes to olefins. The following are typical examples reported by Baird and coworkers³⁶ (equation 8) and by Walsh and coworkers³⁷ leading to **6** and **7** (equation 9).

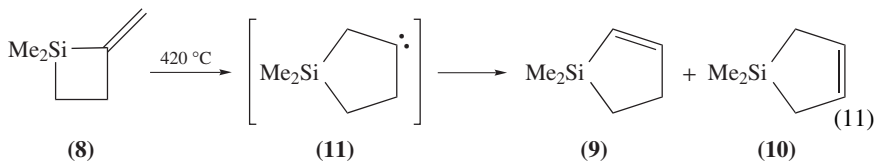


Bertrand and coworkers showed, however, that apparent 1,2-silyl migrations in aromatic carbenes occurred by intermolecular silyl exchange (equation 10)³⁸.

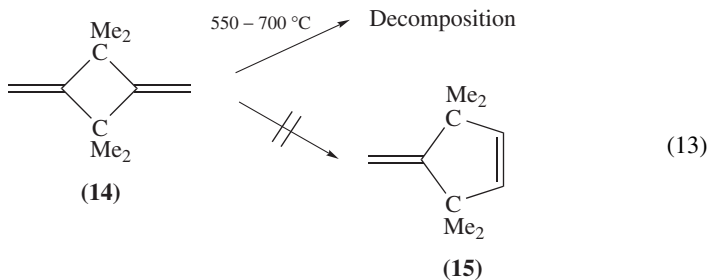
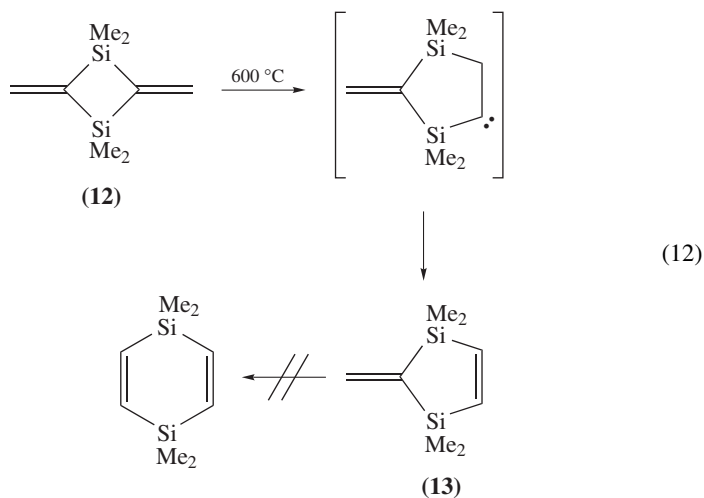


The reverse migrations, i.e. the thermal isomerization of olefins to carbenes, have been well established to occur if the system involves the significantly twisted double bonds. Although no evidence of this isomerization was found for acyclic vinylsilanes, Conlin and coworkers first observed the isomerization of α -methylenesilacyclobutane **8** to a mixture

of 2- and 3-silacyclopentenes **9** and **10** (equation 11)³⁹. The mechanism was believed to involve an initial 1,2-silyl shift to give silylmethylcarbene **11** as an intermediate.



Recently, Barton and coworkers investigated the mechanism of the 1,2-silyl migration in a related system through a combination of experiment and theory⁴⁰. Pyrolysis of **12** at 600 °C cleanly produced a mixture of **12** and methylenedisilacyclopentene **13** (25%) (equation 12). A kinetic study of this reaction was conducted over the temperature range of 520–600 °C in a stirred flow reactor. The Arrhenius parameters for the first order formation of **13** were $\log A = 12.5\text{ s}^{-1}$ and $E_a = 54\text{ kcal mol}^{-1}$. In the pyrolysis of a related all-carbon system **14**, decomposition occurred at 550 °C but no isomerization to the methylene cyclopentene **15** was observed up to 700 °C (equation 13).



Theoretical calculations at the MP2/6-31G(d)//HF/6-31G(d) level for the isomerization of **16** to **17** and of **18** to **19** revealed an interesting feature of the migrations (Figure 1).

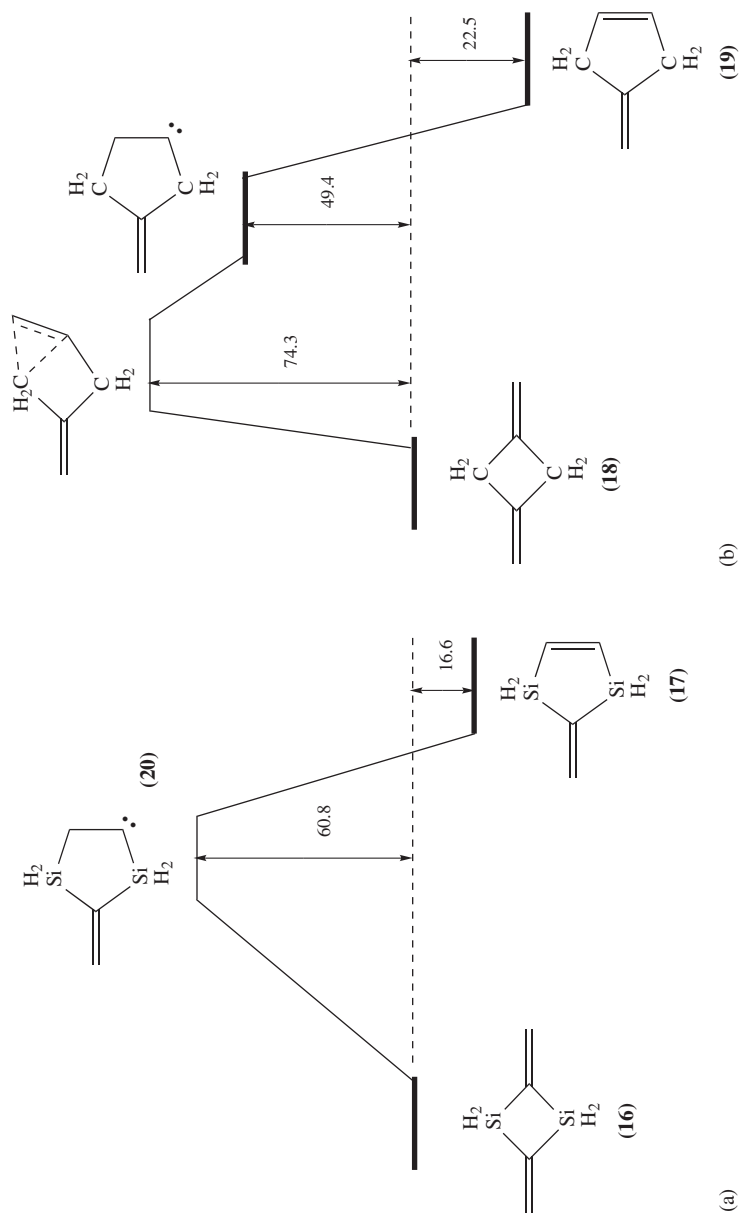
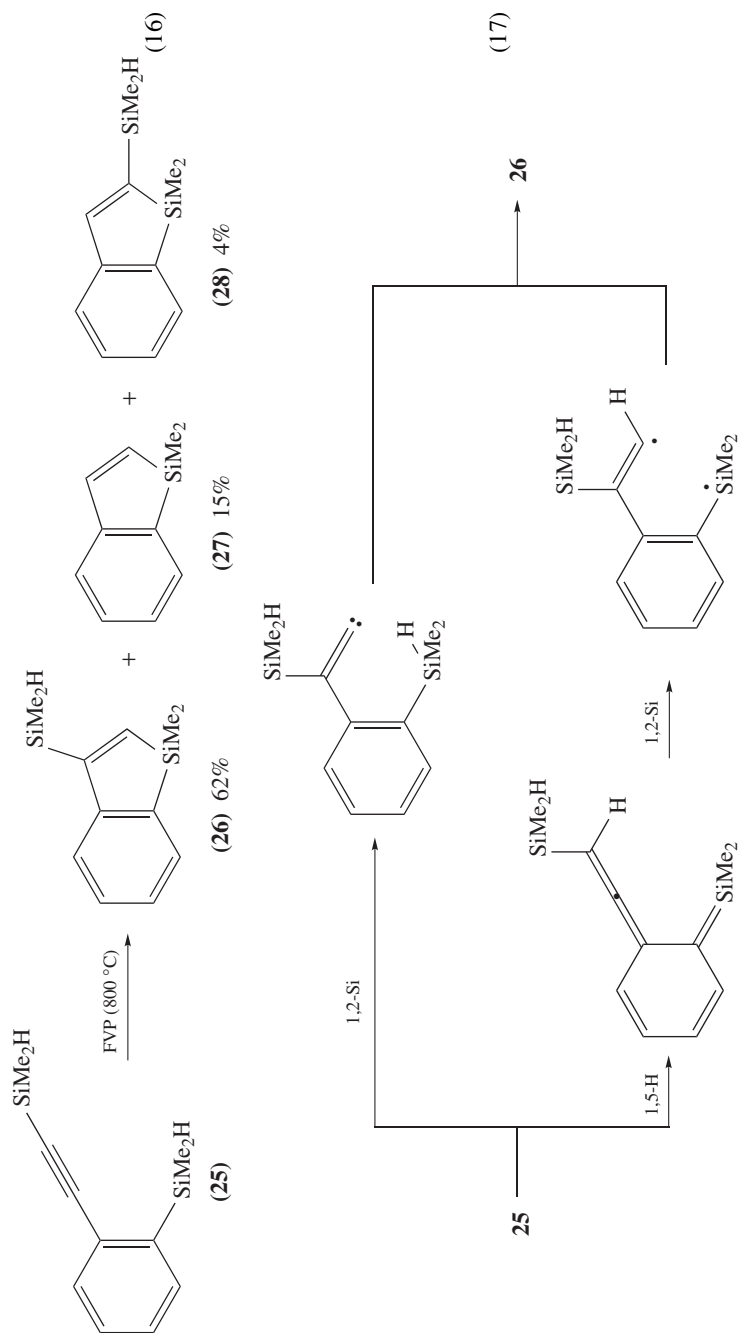
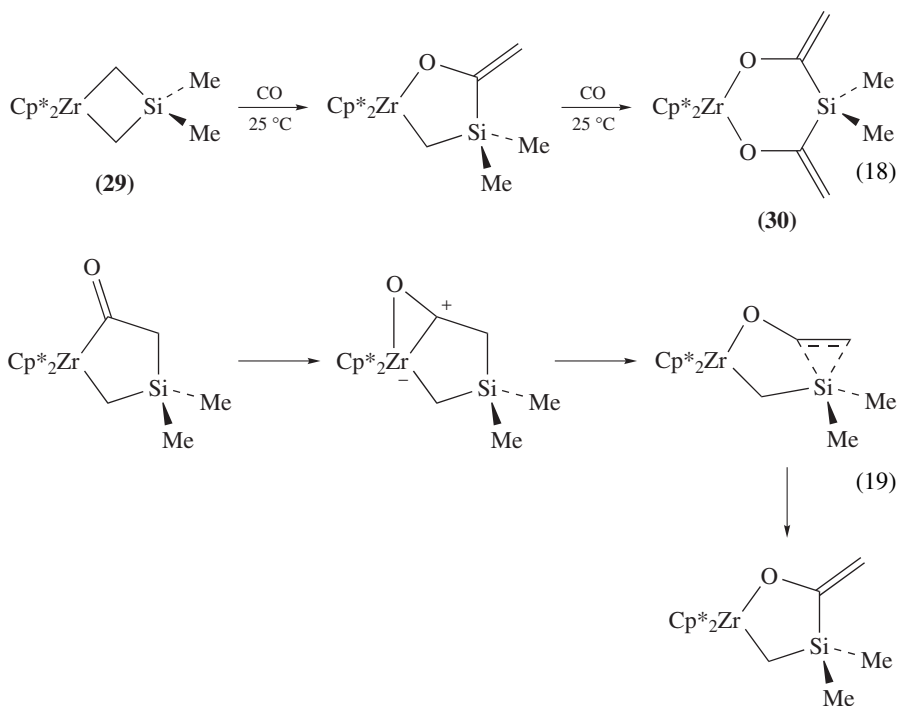


FIGURE 1. Calculated schematic energy surfaces for the isomerization of (a) **16** and (b) **18**. Energies in kcal mol⁻¹ are at MP2/6-31G(d)//HF/6-31G(d) + 0.9 ZPE(HF)

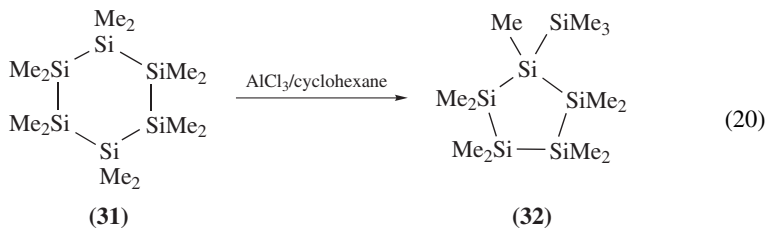


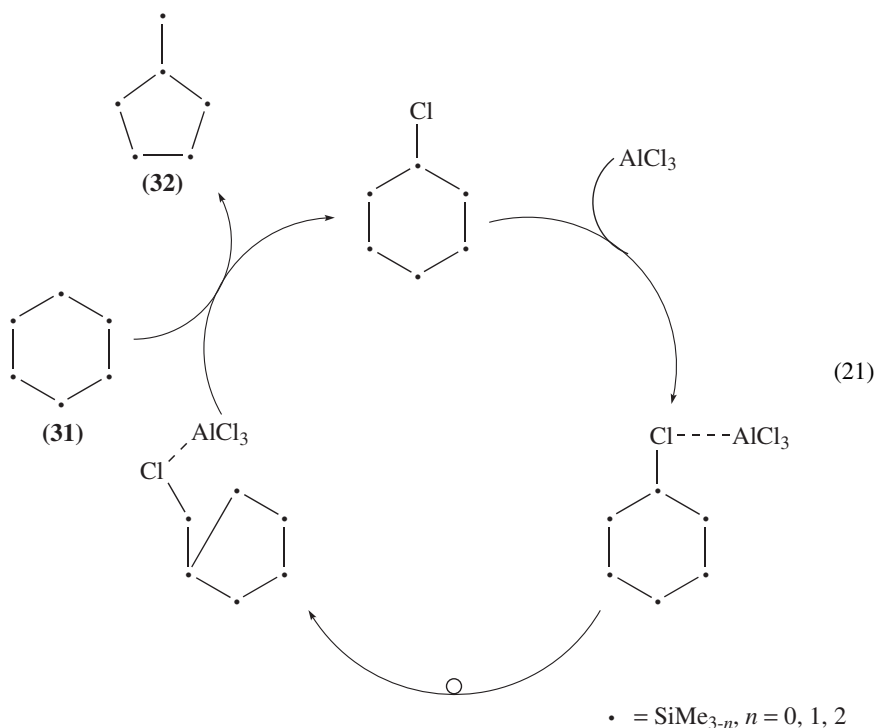
A number of transition metal-induced acetylene–vinylidene rearrangements^{44–54} and a carbene–carbyne rearrangement⁵³ involving 1,2-silyl migration have been reported.

Cationic 1,2-silyl migration was proposed to be involved during the reactions of carbon monoxide and isocyanides with transition metal–carbon bonds (ligand distribution) (equation 18)^{55–65}. Typically, the reaction of 1-sila-3-zirconacyclobutane **29** with carbon monoxide afforded a dioxasilazirconacyclohexane derivative **30**. The reaction was considered to proceed via a CO insertion into a Zr–C bond followed by a 1,2-silyl migration as shown in equation 19⁶⁰. This type of reactions are well-documented in a review of Durfee and Rothwell⁶⁶.

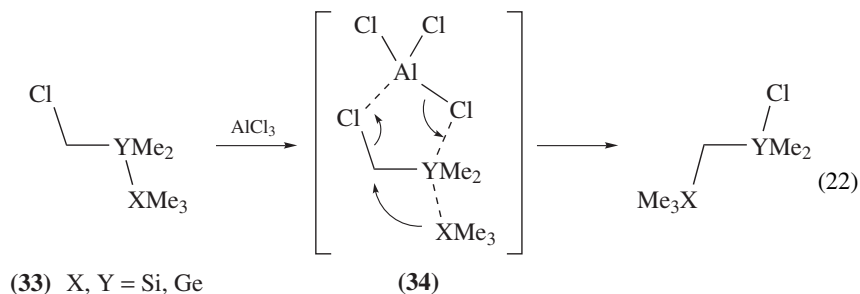


Cationic 1,2-silyl migrations from Si to Si were reported by Ishikawa, Kumada and coworkers⁶⁷ and by Hengge and coworkers⁶⁸ (equation 20). The ring contraction of dodecamethylcyclohexasilane **31** to 1-trimethylsilylnonamethylcyclopentasilane **32** in the presence of AlCl_3 (equation 20) was proposed to proceed via a 1,2-silyl migration to a cationic silicon center as shown in equation 21^{67,69}.

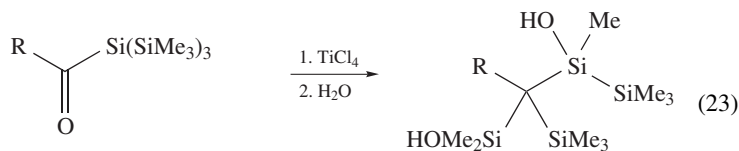




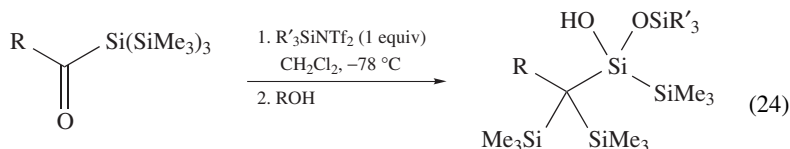
1,2-Silyl migration in chloromethylpentamethyldisilane **33** X=Y=Si has been known to occur thermally or more easily in the presence of aluminum chloride⁷⁰. Similar rearrangements promoted by a Lewis acid were observed in (chloromethyl)pentamethylgermasilanes⁷¹. Presumably, the reaction does not involve a carbenium or a silenium cation as a discrete reactive intermediate but proceeds via the cyclic transition state **34** involving aluminum chloride participation (equation 22).



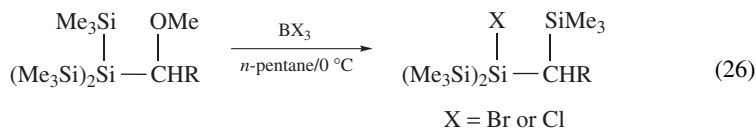
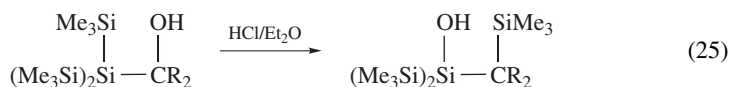
The following reactions are examples of cationic 1,2-silyl migrations from silicon to carbon during the reactions of tris(trialkylsilyl)silyl-substituted ketones^{72,73} (equations 23 and 24), alcohols⁷⁴ (equation 25) and ethers⁷⁵ (equation 26) in the presence of Lewis acids.



R = *t*-Bu, 1-adamantyl, bicyclo[2,2,2] octyl

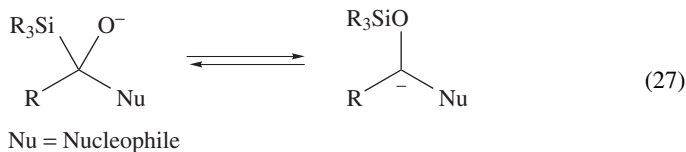


R = Ph, C₆H₄CF₃-*p*, C₆H₄OCH₃-*p*; R' = *t*-BuMe₂Si, Me₃Si

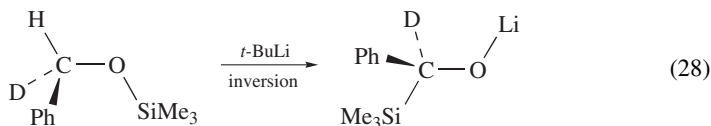


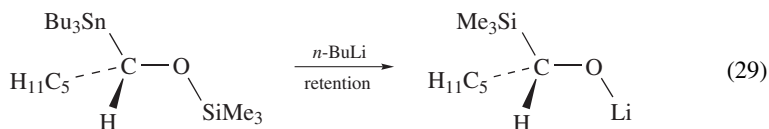
3. Anionic 1,2-silyl migrations

Anionic 1,2-silyl migrations from C to O are well known as the Brook rearrangement. On the other hand, an anionic 1,2-silyl migration similar to the Wittig rearrangement is often called the Wright–West^{76–79} or the reverse Brook rearrangement (equation 27). Much attention has been focused on the mechanisms of typical anionic 1,2-silyl migrations from C to O and their reverse migrations.

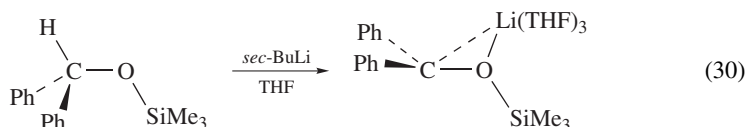


Interestingly, the stereochemical outcomes of these reactions depend on the substituents. With aryl substituents at the carbon atom, an inversion of stereochemistry was observed (equation 28)⁷⁸, while with alkyl groups at the carbon atom, the reverse Brook rearrangement occurs with retention of the stereochemistry (equation 29)⁸⁰.

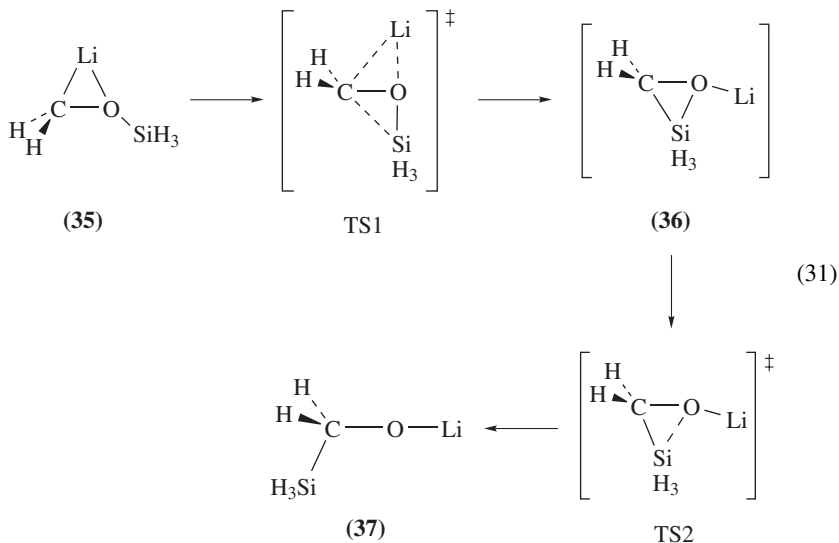


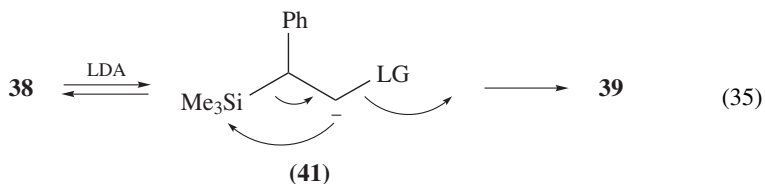


Boche and coworkers have revealed that in the molecular structure of diphenyl(trimethylsiloxy)methylithium · 3THF in the solid state, Li is bound only to the oxygen (O–Li and C–Li distances, 1.49 and 2.80 Å, respectively) and that a slight inversion at the carbanionic carbon takes place (equation 30)⁸¹. On this basis, they rationalized the inversion of stereochemistry in the reverse Brook rearrangement for systems carrying aryl substituents at the carbon atom. The retention of configuration in the reverse Brook rearrangement of alkyl-substituted siloxycarbanions was suggested not to be surprising if the high configurational stability of the carbanion and a front-side attack by the electrophile were taken into account.

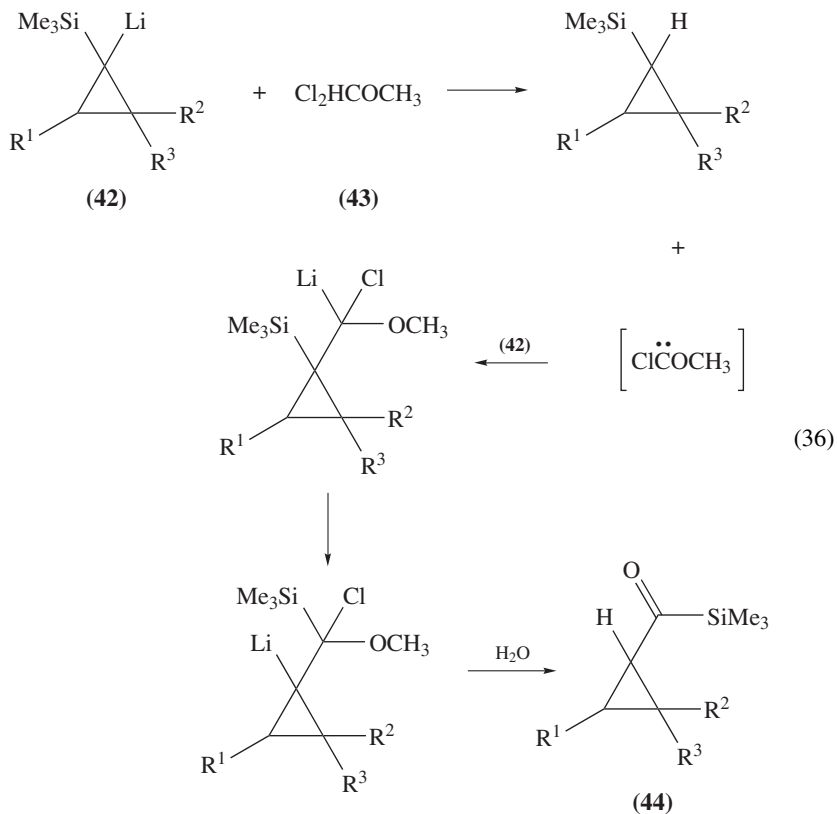


On the other hand, Antoniotti and Tonachini offered a different view on the elementary process in the reverse Brook rearrangement occurring without and with counter cations (equation 31)^{82–84}. In accord with a number of calculations on hydroxymethylithium, the most stable structure of siloxymethylithium **35** resembles a lithium bridged carbenoid, where Li and Si are in an antiperiplanar conformation to each other. During the isomerization of siloxymethylithium **35** (H₃SiOCH₂Li) to silylmethoxylithium **37** (H₃SiCH₂OLi), they found that a pentacoordinate silicon intermediate **36** was formed via the dyotropic type bicyclic transition state (TS1). This nondissociative migration required the inversion of configuration at the carbanionic center. The reason for the stereochemical diversity does not seem to be well understood until now.





Another 1,2-silyl migration from C to C was found during the reaction of an α -silyl cyclopropyllithium **42** with dichloromethyl methyl ether **43** to give the silyl ketone **44** (equation 36)⁸⁷.

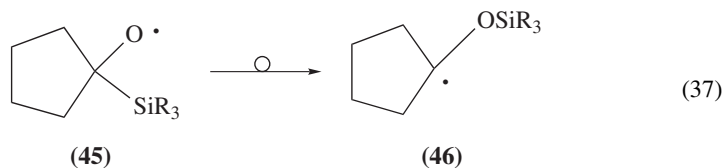


$R^1, R^2, R^3 = \text{H, alkyl, Ph}$

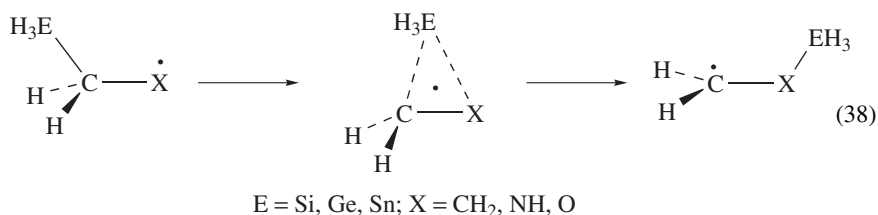
4. Radical 1,2-silyl migrations

In addition to the radical Brook rearrangement from α -silylalkoxy radical **45** to the siloxyalkyl radical **46** shown in equation 37, several 1,2-silyl migrations to a radical

center have been reported^{88–94}.

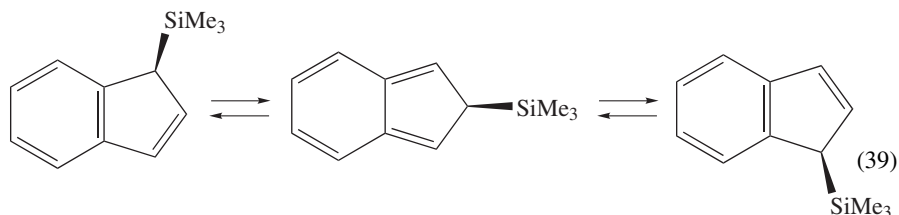


Ab initio MO calculations for the prototypical radical Brook and related rearrangements were carried out⁹⁴. The homolytic 1,2-migrations of silyl, germyl and stannyl groups between C and C, C and N, and C and O were found to proceed via a homolytic substitution involving front-side attack of the radical center on the group-14 atoms (equation 38). It was predicted theoretically that while the homolytic 1,2-silyl migration between carbons was unlikely, the migrations from C to N and from C to O were facile; the calculated activation barriers for the migrations from C to C, from C to O, and from C to N were 23, 12 and 4.8 kcal mol⁻¹, respectively, at the MP2/DZP +ZPE level. The results are in good accord with the experimental data. The migratory aptitude among the group-14 atoms followed the order: Sn > Si > Ge. Somewhat unexpectedly, the stannylmethoxy radical was predicted to rearrange to the stannylloxymethyl radical without a barrier.



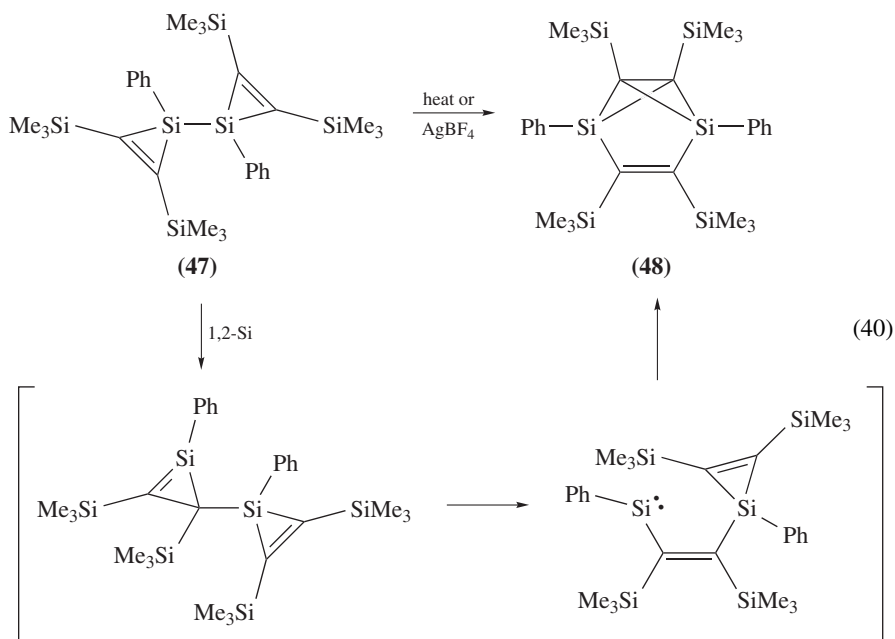
5. Miscellaneous

Facile migration of silyl groups in 5-silylcyclopentadienes is usually referred to as fractional 1,2-silyl rearrangement or 1,5-suprafacial silatropic rearrangement (equation 39). The fundamentals of this migration have been well discussed in BB¹. Several examples of this type of migration have also appeared in recent papers^{95–105}.



A bis(silacyclopropene) **47** was converted to the corresponding disilabenzvalene **48** by heating or by treating **47** with AgBF₄ (equation 40). The following pathway involving a

1,2-migration of a silyl group to the adjacent olefinic carbon was proposed¹⁰².

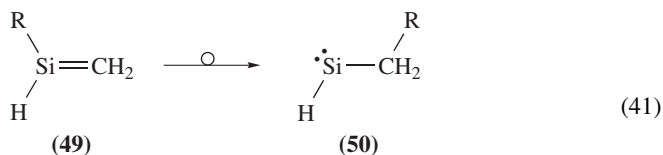


B. 1,2-Silyl Migrations in Unsaturated Silicon Compounds

Much attention has been focused on possible 1,2-silyl migrations in unsaturated silicon compounds like disilenes, silaethenes and silylenes, especially since their stable derivatives had been isolated.

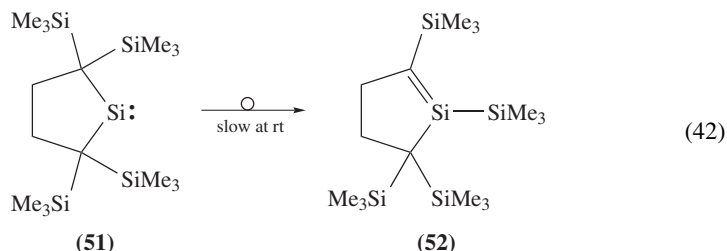
1. Silylmethylsilylene–silylsilaethene rearrangements

The migration of silyl groups from Si to C in silaethene (equation 41) was investigated theoretically¹⁰⁶. The barrier heights were significantly dependent on the migrating group R. They were 42.2, 54.7 and 26.2 kcal mol⁻¹ for the rearrangement of **49** to **50**, for R=H, CH₃ and SiH₃, respectively; for the reverse reactions, the barriers were 43.0, 44.4 and 24.8 kcal mol⁻¹, respectively.



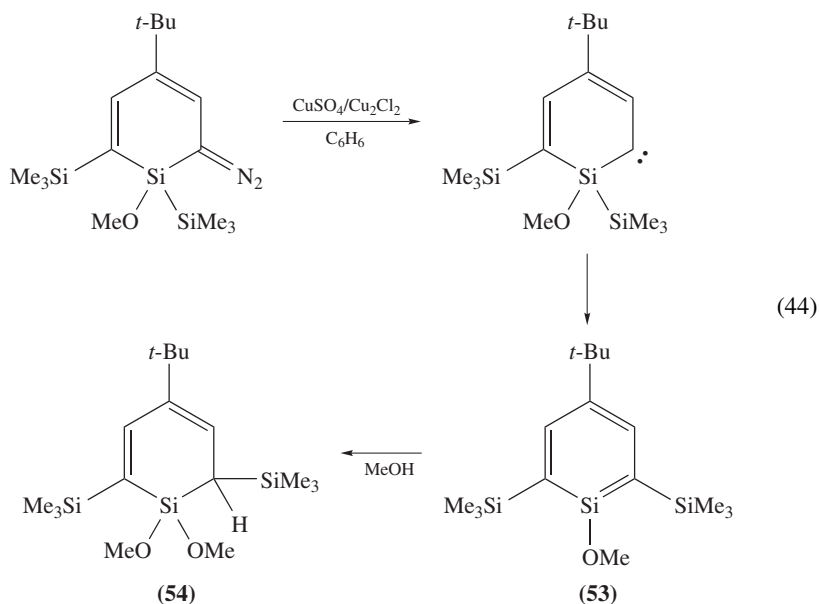
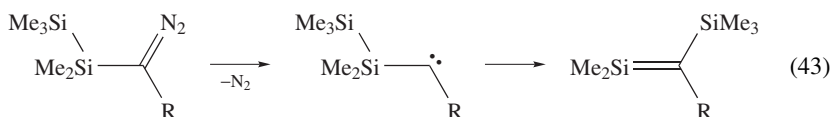
Experimentally, Barton and coworkers reported the migration from silylsilene to silylmethylsilylene, but at very high temperatures^{107–109}. Very recently, Kira and

coworkers found a thermal isomerization of an isolable β -silylsilylene **51** to the corresponding silaethene **52** with the following activation parameters: $\Delta H^\ddagger = 20 \text{ kcal mol}^{-1}$ and $\Delta S^\ddagger = -17 \text{ cal mol}^{-1} \text{ K}^{-1}$ (equation 42). The activation enthalpy was in good accord with the theoretical activation barrier given above¹¹⁰.

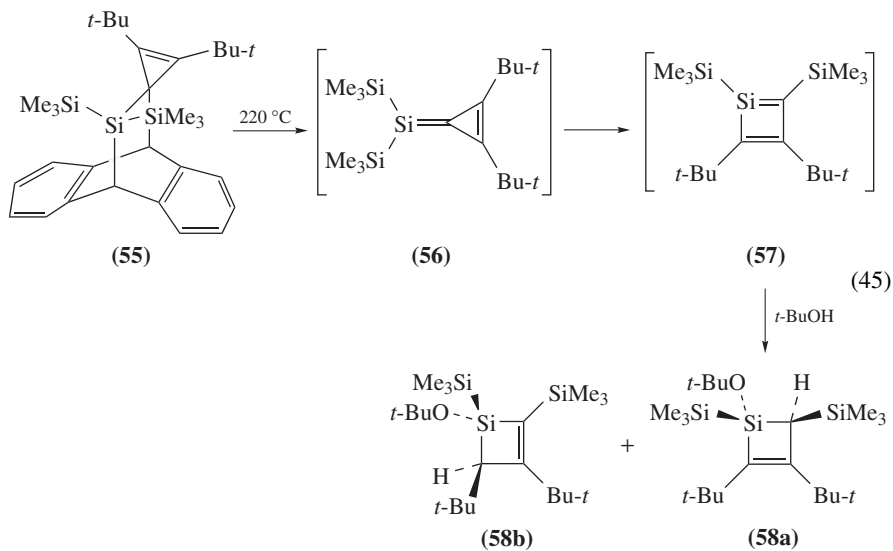


2. Disilanylcarbene–silylsilaethene rearrangements

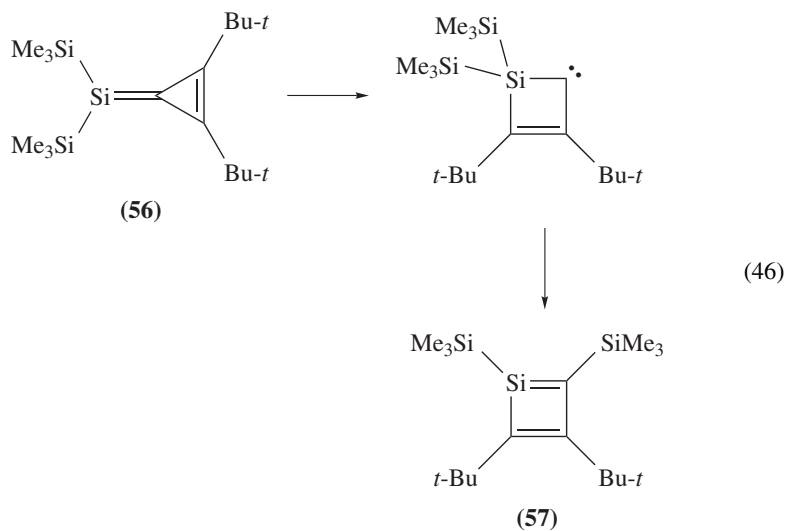
Disilanylcarbene–silylsilaethene rearrangements have been well studied by Ando, Sekiguchi, Maas and their coworkers (equation 43)^{111–119}. Märkl and coworkers used this type of rearrangement for generation of a silabenzene **53**, which was trapped by methanol to give the corresponding adduct **54** (equation 44)¹²⁰.



Thermolysis of an anthracene adduct **55** of a transient 4-silatriafulvene **56** in the presence of *t*-butyl alcohol was found to provide a pair of alcohol adducts (**58a** and **58b**) of a silacyclobutadiene **57** (equation 45)¹²¹.

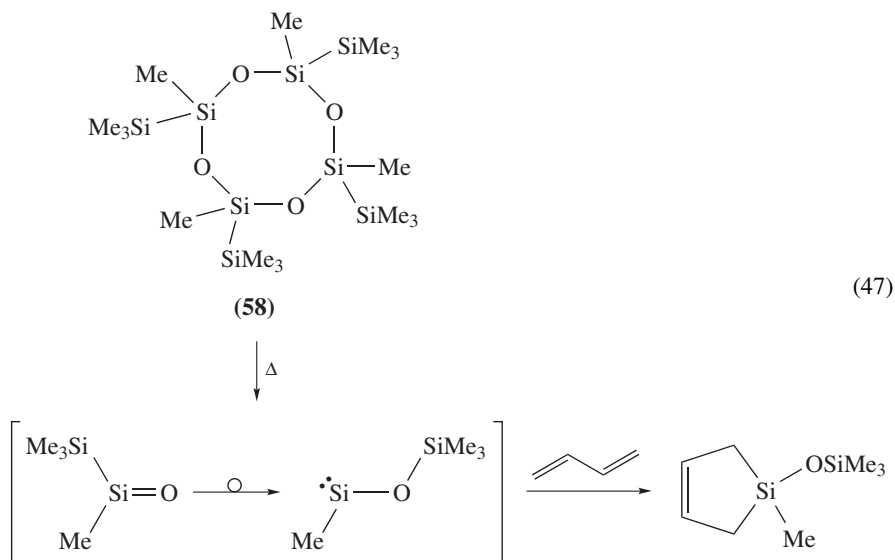


The occurrence of the 1,2-silyl migration from Si to C during the isomerization of the 4-silatriafulvene **56** to the corresponding silacyclobutadiene **57** (equation 46) was supported by theoretical calculations¹²².

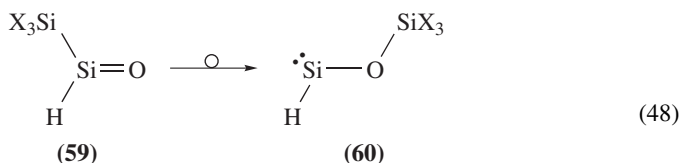


3. Silylsilanone-siloxysilylene rearrangements

Barton and Hussmann suggested that a silylsilanone-to-siloxysilylene rearrangement occurred during the copyrolysis of cyclotetrasiloxane **58** with butadiene to afford the corresponding silacyclopentene (equation 47)¹²³.



Kudo and Nagase calculated at the MP4SDTQ/6-31+G(2d,p)+ZPC level¹²⁴ that in contrast to the parent rearrangement from $\text{H}_2\text{Si}=\text{O}$ to $\text{H}(\text{OH})\text{Si}\cdot$, whose barrier was 61 kcal mol^{-1} ¹²⁵, the isomerization of **59** to **60** was *ca* 18 kcal mol^{-1} exothermic and proceeded via a least-motion pathway of C_s symmetry with a barrier of $22.7 \text{ kcal mol}^{-1}$ (equation 48)¹²⁴. At the same level, the barrier for the corresponding migration of SiF_3 group was $18.4 \text{ kcal mol}^{-1}$. The lowering of the barrier height by electronegative substituents suggested that the substituents stabilized the hypervalent silicon transition state.

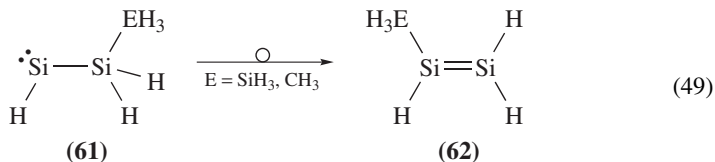


$\text{X} = \text{H}$, $E_a = 22.7 \text{ kcal mol}^{-1}$; $\text{X} = \text{F}$, $E_a = 18.4 \text{ kcal mol}^{-1}$

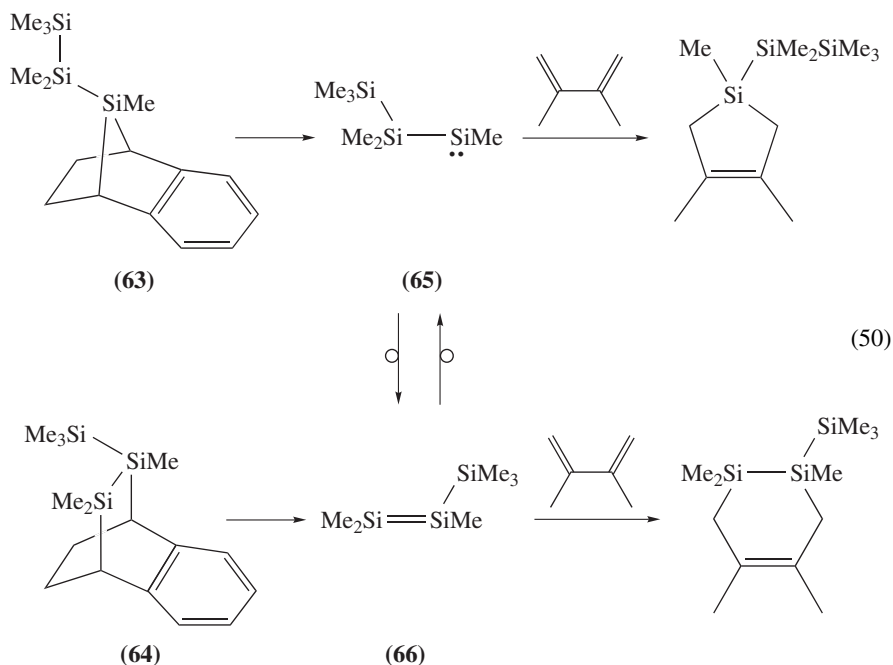
4. Disilanylsilylene-silyldisilene rearrangements

Transition states and barrier heights for the silylsilylene (**61**)–disilene (**62**) isomerization via 1,2-silyl and 1,2-methyl migrations were investigated by *ab initio* MO calculations at the 6-31G* level (equation 49). The 1,2-silyl migration of disilanylsilylene

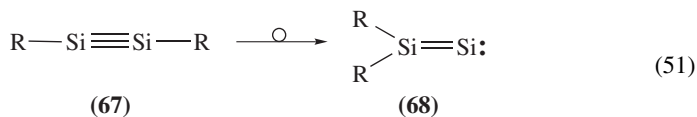
to silyldisilene was much faster than the corresponding 1,2-methyl migration; the calculated barriers were 8.5 and 27.8 kcal mol⁻¹ for the 1,2-silyl and 1,2-methyl migrations, respectively¹²⁶.



Sakurai, Nakadaira and Sakaba observed a facile thermal isomerization from disilanylilylene **65** to silyldisilene **66**¹²⁷ as well as its reverse isomerization¹²⁸ during thermolysis of the corresponding precursors **63** and **64** (equation 50).

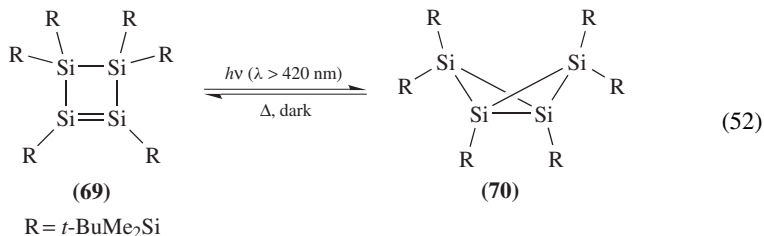


1,2-Silyl migrations from disilynes **67** to disilynylidenes **68** were theoretically predicted to occur (equation 51). When the substituents R were sterically bulky, the disilynylidene form was less stable than the disilyne form¹²⁹.

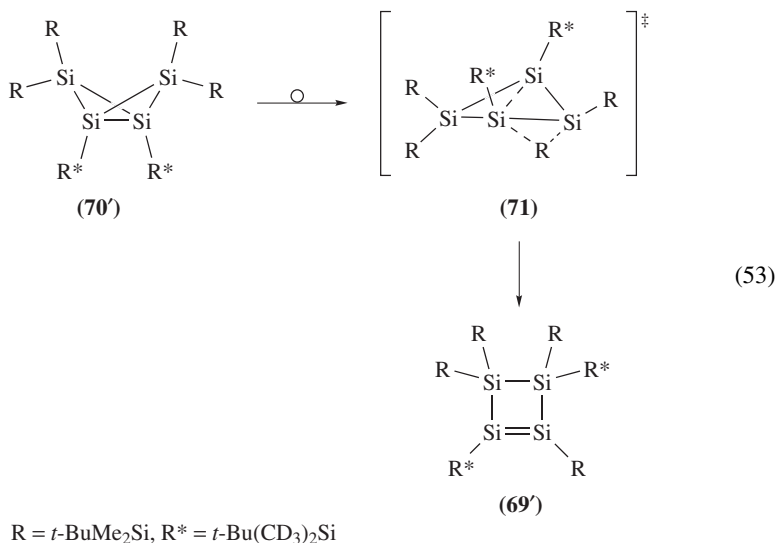


5. Disilanyldisilene-2-silylcyclotrisilane rearrangements

Kira, Iwamoto and Kabuto reported the isolation and characterization of the first stable cyclic disilene, hexakis(*t*-butyldimethylsilyl)tetrasilacyclobutene (**69**, R=*t*-BuMe₂Si), together with its facile photochemical conversion to the corresponding tetrasilabicyclo[1.1.0]butane **70** and its thermal reversion to **69** (equation 52)¹³⁰.

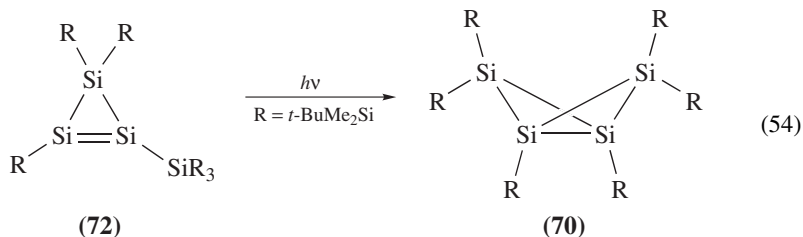


The activation parameters for the thermal isomerization of **70** to **69** were $\Delta H^\ddagger = 16.5 \text{ kcal mol}^{-1}$ and $\Delta S^\ddagger = -20.8 \text{ cal mol}^{-1} \text{ K}^{-1}$. The large negative ΔS^\ddagger value suggested that the transition state structure for the thermal isomerization was significantly restricted, and therefore, any multi-step mechanism involving bond cleavage at the rate-determining step was eliminated. This apparent skeletal isomerization between **69** and **70** was found, however, to involve a facile 1,2-silyl migration by labeling the two *t*-Bu(CH₃)₂Si groups on the bridgehead silicon atoms of **70** (cf **70'**) with two *t*-Bu(CD₃)₂Si groups¹³¹. The thermal isomerization to **69'** may occur through a concerted dyotropic-type rearrangement with transition state **71** (equation 53) or via the intermediary formation of a tetrasilacyclobutane-1,3-diyl diradical, followed by the 1,2-silyl migration to the radical center.

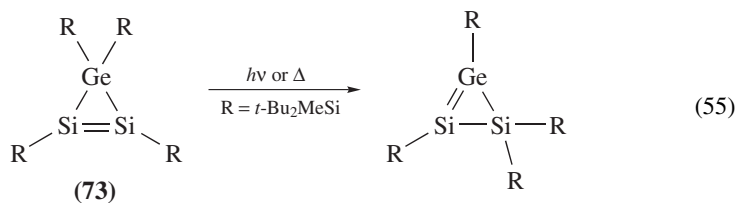


It is well known that the thermal decomposition of a bicyclo[1.1.0]butane gives the corresponding 1,3-butadiene probably via the Woodward–Hoffmann allowed concerted pathway, while photolysis of cyclobutene also provides 1,3-butadiene as a major product. A remarkable difference in the reaction modes between the silicon and carbon analogs of the bicyclo[1.1.0]butane/cyclobutene system would partially be a consequence of the fact that the formation of the silicon analog of a conjugated diene is highly undesirable.

Photochemical 1,2-silyl migration from 1-tris(trialkylsilyl)cyclotrisilene **72** occurred to give the corresponding bicyclo[1.1.0]tetrasilane **70** (equation 54)¹³². During the photochemical and thermal interconversion among the Si₄R₆ isomers **69**, **70** and **72**, the corresponding 1,3-tetrasiladiene derivative was never detected.



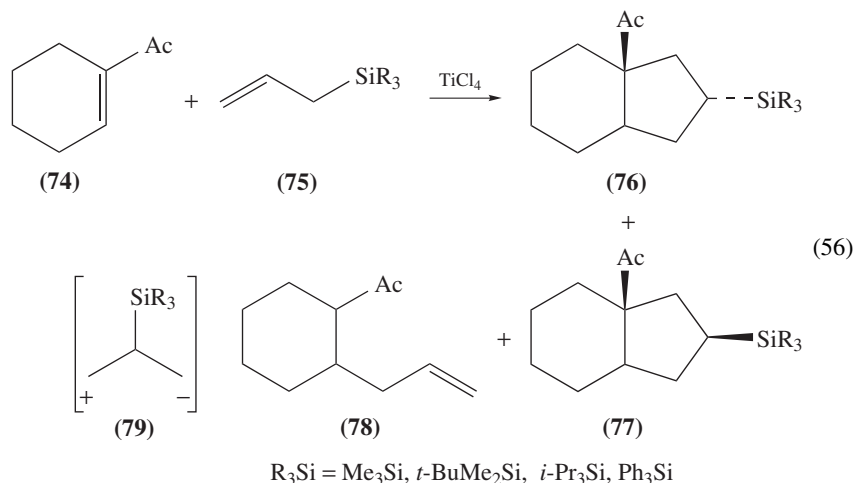
Sekiguchi and coworkers observed the thermal and photochemical 1,2-silyl migrations in persilyl-1-disilagermirene **73** (equation 55)¹³³.



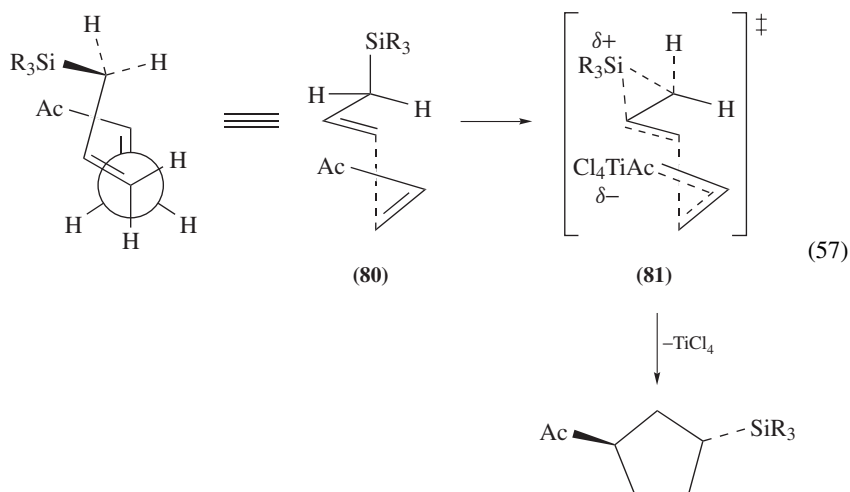
C. Synthetic Applications

1. Cationic 1,2-silyl migrations from C to C

a. [3 + 2] Annulations. Cationic 1,2-silyl migrations from C to C appear in the [3 + 2] annulation of allylsilanes, allenylsilanes and propargylsilanes with various electrophiles^{134–148}. Typically, the [3 + 2] cycloaddition of allyltrimethylsilane **75** to an α,β -unsaturated ketone **74** in the presence of Lewis acids such as TiCl₄ gave cyclopentane derivatives **76** and **77** together with the Sakurai product **78** (equation 56). In this cyclization, allylsilanes served as synthetic equivalents of 2-silyl-1,3-dipoles (**79**). When bulkier alkyl groups were employed, the cycloadducts were obtained in higher yields. The cyclization took place stereoselectively with the preferable formation of **76** to **77**. The regio- and stereoselectivity of the annulation were highly dependent on the substituents in the allylic silanes; the details were summarized in a review of Masse and Panek³.



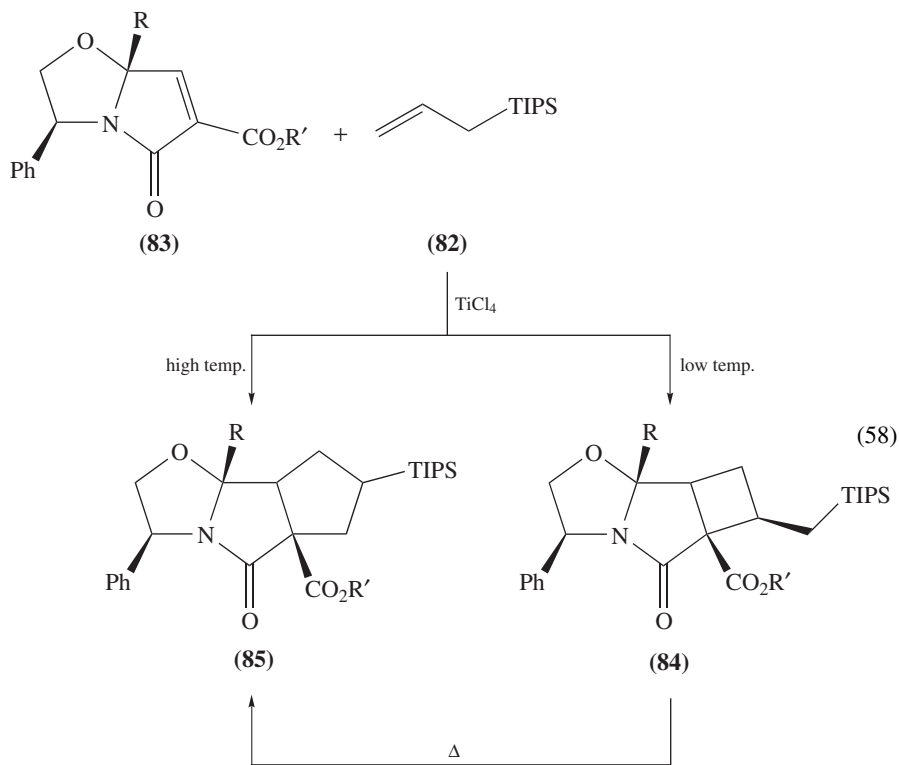
The [3 + 2] reaction of an allylsilane with an enone was proposed to proceed via a regioselective electrophilic substitution (cf **80**) of the enone at C-3 of the allylsilane followed by a cationic 1,2-silyl migration (equation 57). At the *syn*-clinal transition state (**81**), the carbonyl group of the unsaturated ketone was assumed to occupy an *endo* orientation in relation to the allylsilane¹⁴². The transition state was thought to be favorable due to minimization of the charge separation and to possible secondary orbital stabilization.



Similar cyclopentane annulations of allylsilanes with benzotropylium salts^{149,150}, tetracyanoethylene¹⁵¹, benzyl cations¹⁵² and 1,2,4-triazoline-3,5-diones had been reported¹⁵³.

The cationic 1,2-silyl migrations affording [3 + 2] cycloadducts (**85**) were suppressed in the reactions of triisopropylallylsilane **82** with α,β -unsaturated bicyclic lactams **83**

at lower temperatures (equation 58). The reactions afforded only [2 + 2] cycloadducts **84**, which readily underwent ring expansion accompanied by 1,2-silyl migrations in the presence of Lewis acids at room temperature^{137,138}. The product ratio of [2 + 2] to [3 + 2] adducts depended on the electrophiles and the Lewis acid catalysts^{154,155}.

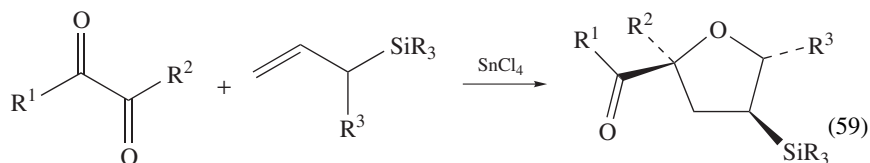


R = Ph, Me

TIPS = (*i*-Pr)₃Si

R' = *t*-Bu, benzyl

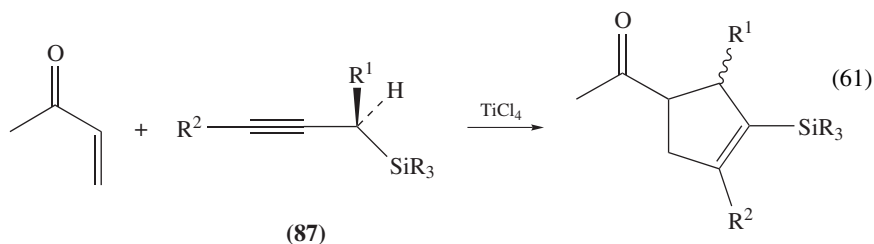
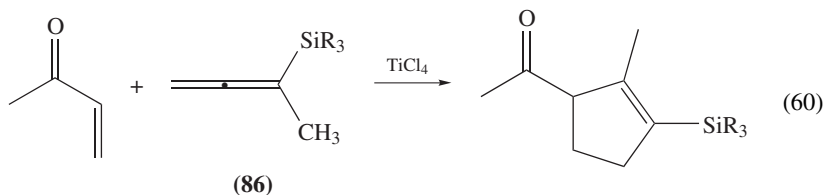
The [3 + 2] stereoselective annulations using allylsilanes were also applied to the syntheses of furans (equation 59)^{156–162} *N*-acylpyrrolidines^{163,164}, a 2-thiabicyclo[2.2.1]hept-5-ene-3-spiro-2'-indan-1'-one¹⁶⁵ and Δ^2 -isoxazoline derivatives^{166,167}.



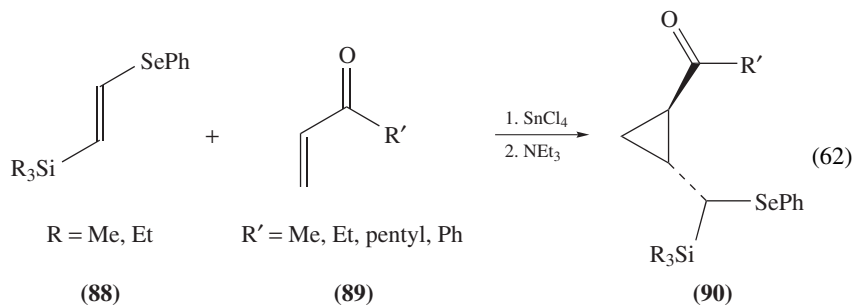
R¹, R² = alkyl, alkoxy; R³ = H, Me

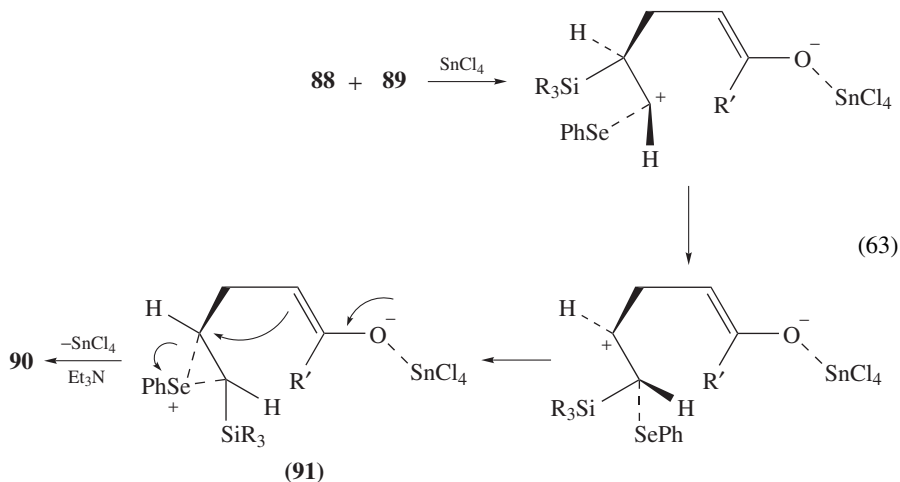
R₃Si = Me₃Si, *t*-BuMe₂Si, *t*-BuPh₂Si

Similar [3 + 2] annulations of allenylsilanes **86** and propargylsilanes **87** with α , β -unsaturated ketones, ketones, *N*-acyliminium ions, nitrosonium ions and tropylium cations giving the corresponding cyclopentenes (cyclohexenes), dihydrofurans, 3-pyrrolines, isoxazoles and azulene derivatives, respectively, have been reported (equations 60 and 61)^{142,154,168–172}.

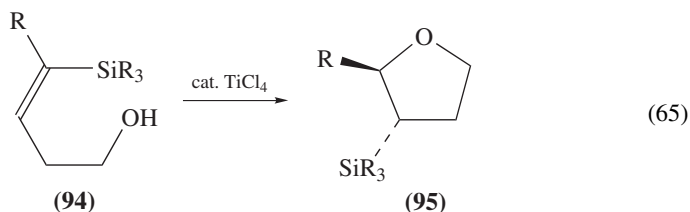
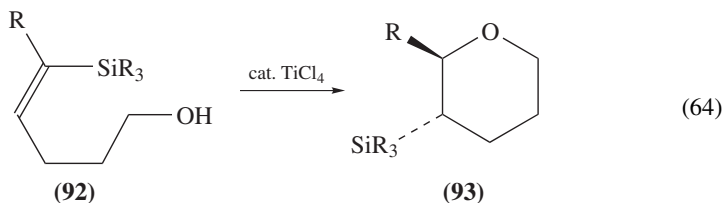


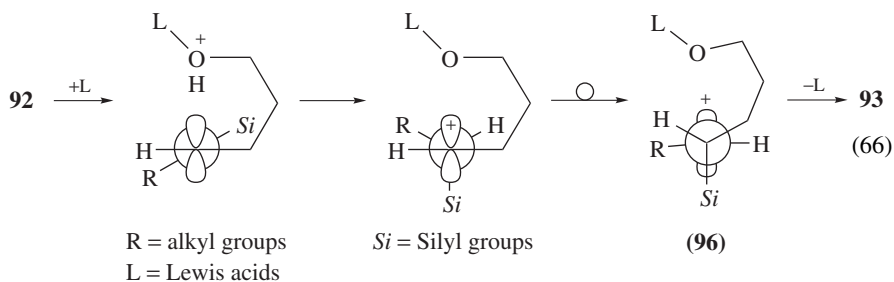
b. [2 + 1] Annulations. The reactions of 1-(phenylseleno)-2-silylethenes **88** with α , β -unsaturated ketones **89** in the presence of a Lewis acid such as SnCl_4 were found by Yamazaki and coworkers to afford unsymmetrically substituted cyclopropane derivatives **90** in a stereoselective manner (equation 62)^{173–175}. The proposed reaction pathway is shown in equation 63. Thus, initial electrophilic addition of a selenosilylethene to the α , β -unsaturated ketone followed by the 1,2-silyl migration gave a zwitterionic enolate intermediate **91** stabilized by selenium bridging. Finally, intramolecular nucleophilic attack of the enolate moiety in **91** on the cationic center at the γ -position provided a cyclopropane derivative **90**. In this [2 + 1] cyclization, the role of the phenylseleno group was essential; a similar reaction of 1-phenylthio-2-silylethene did not give the desired cyclopropanes but a complex mixture. Theoretical calculations of model reactions supported the importance of the selenium group in this cyclopropanation.



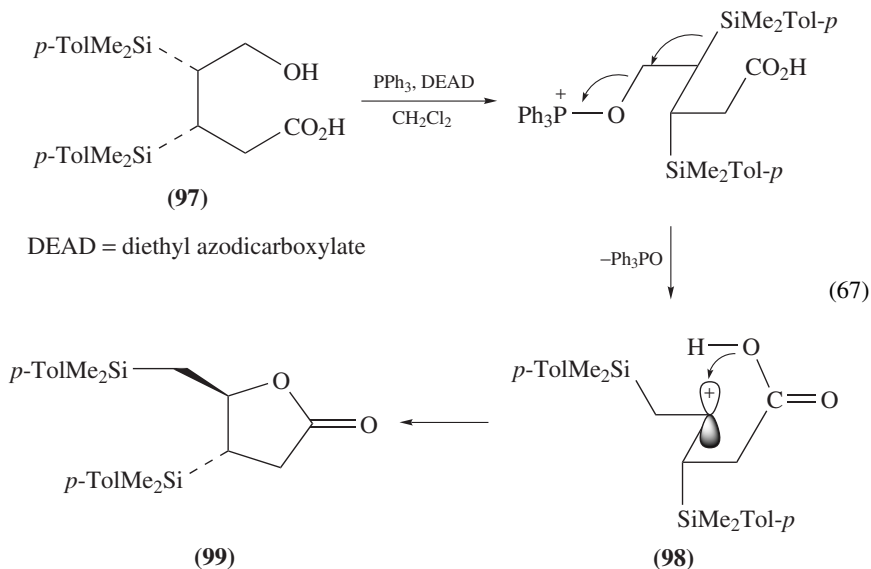


c. Intramolecular cyclizations and ring openings. Cationic 1,2-silyl migrations from C to C have been found in various intramolecular cyclizations. Reactions of 5- and 4-hydroxy-(*Z*)-1-silylalkenes (**92** and **94**) in the presence of TiCl_4 , HCl or acetyl chloride afforded the corresponding tetrahydropyrans **93** and tetrahydrofurans **95**, respectively, in a highly stereoselective manner with *E/Z* ratios of 99/1 for tetrahydropyrans and >96/4 for tetrahydrofurans (equations 64 and 65). The origin of the high stereoselectivity was ascribed to the preferred conformation of the intermediate carbocation **96**, where the β -silyl group should eclipse the neighboring vacant π -type orbital in order to gain maximum stabilization due to the σ - π conjugation as shown in equation 66. When $\text{R} = \text{phenyl}$ in the vinylsilane, a fast desilylation prevented the cyclization, and when $\text{R} = \text{SiMe}_3$, the 1,2-silyl migration did not occur at all¹⁷⁶.

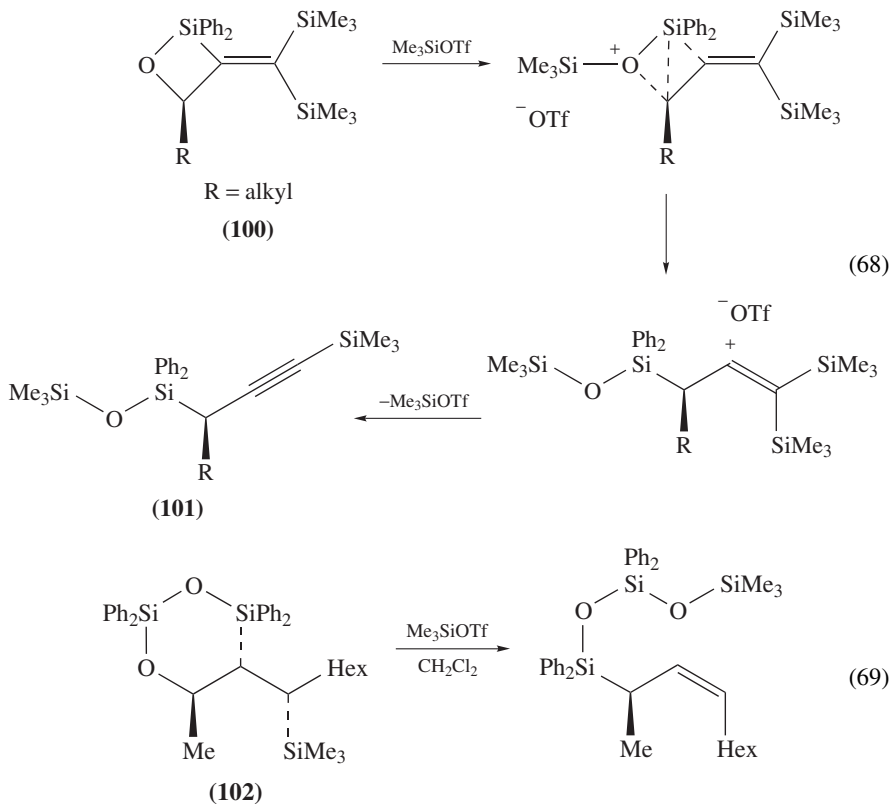




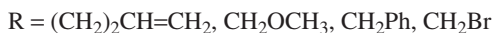
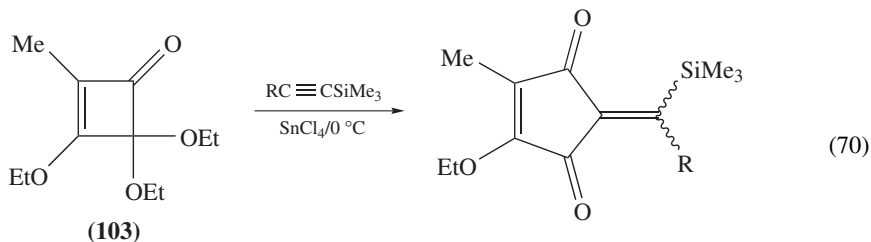
The Mitsunobu reactions of 3,4-disilyl-5-hydroxypentanoic acid derivatives **97** gave the corresponding butyrolactones **99** in a stereospecific manner (equation 67). The two silyl groups in the cationic intermediate **98** were suggested to be arranged in a way enabling to gain the maximum stabilization due to the $\sigma-\pi$ conjugation and to avoid their mutual steric repulsion¹⁷⁷. This intramolecular cyclization was applied to the synthesis of nonactin¹⁷⁸.



When optically active oxasiletanes **100** were treated with trimethylsilyl triflate at -78°C and then at 0°C , the cationic 1,2-silyl migration took place in a concerted and stereospecific manner to give the corresponding propargylic siloxanes **101** (equation 68)¹⁷⁹. The stereochemical outcome suggested that the ring oxygen atom activated by trimethylsilyl triflate triggered a concurrent O–C bond cleavage and 1,2-silyl migration. The reason for the stereospecific *syn* migration was ascribed to the stabilization due to the *syn*-periplanar $\sigma-\pi$ conjugation. Presumably, the two trimethylsilyl groups at the methylenide terminal carbon promote the silyl migration for both a steric and electronic reason. Similar retentive 1,2-silyl migrations were observed in the reactions of disiladioxanes **102** (equation 69).

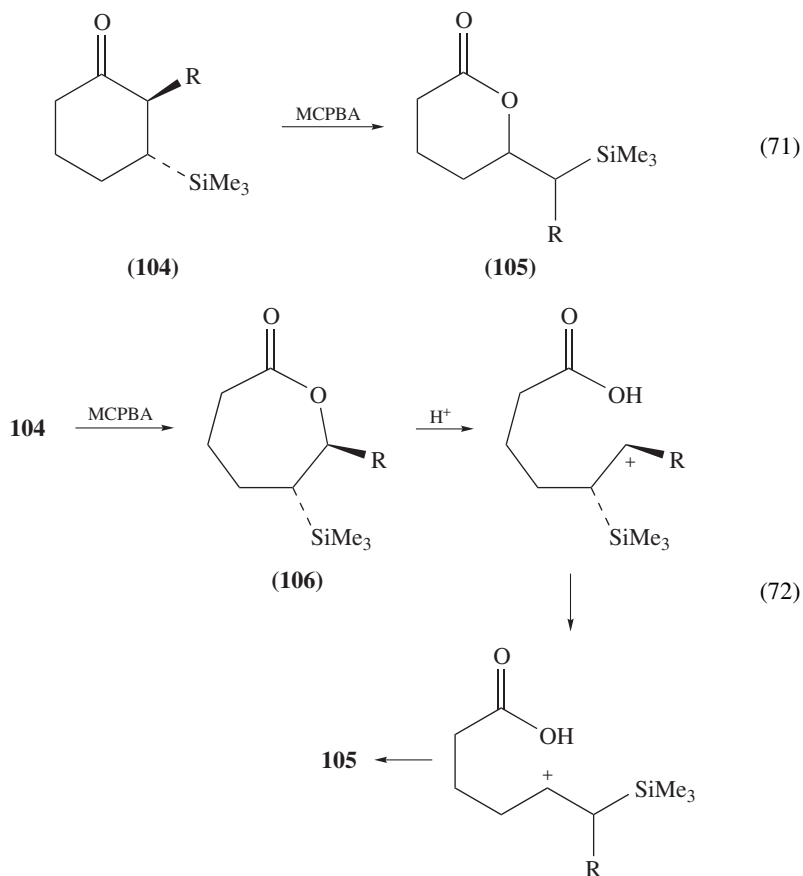


Ring expansion accompanied by 1,2-silyl migration was observed in the reactions of a cyclobutenedione monoacetal **103** with alkynylsilanes (equation 70)¹⁸⁰.

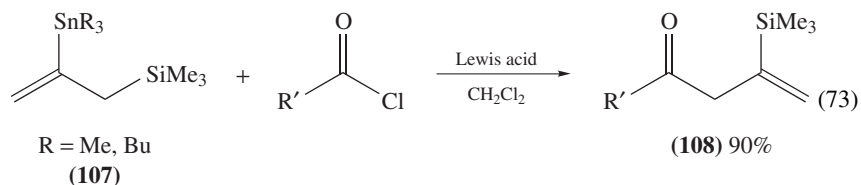


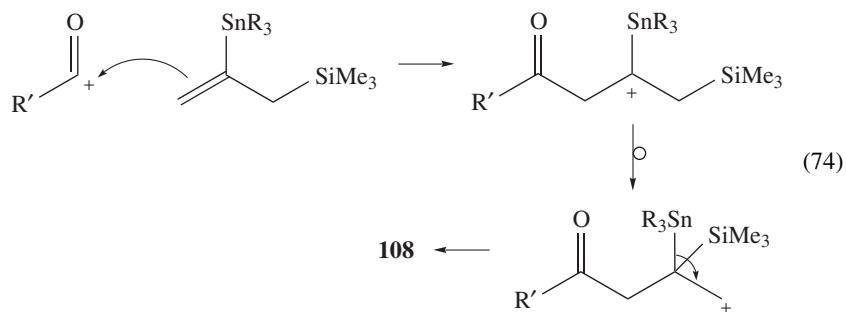
d. Miscellaneous. The Baeyer–Villiger oxidation of β -silylcyclohexanones **104** with MCPBA in the presence of Na₂HPO₄ provided rather unexpectedly the thermally more stable six-membered lactones **105** rather than the normal seven-membered lactones **106** (equation 71)¹⁸¹. The reactions were suggested to involve acid catalyzed ring opening of

the initial seven-membered lactones **106**, followed by a 1,2-silyl migration and then a ring closure (equation 72). This migration was suppressed in a neutral media.

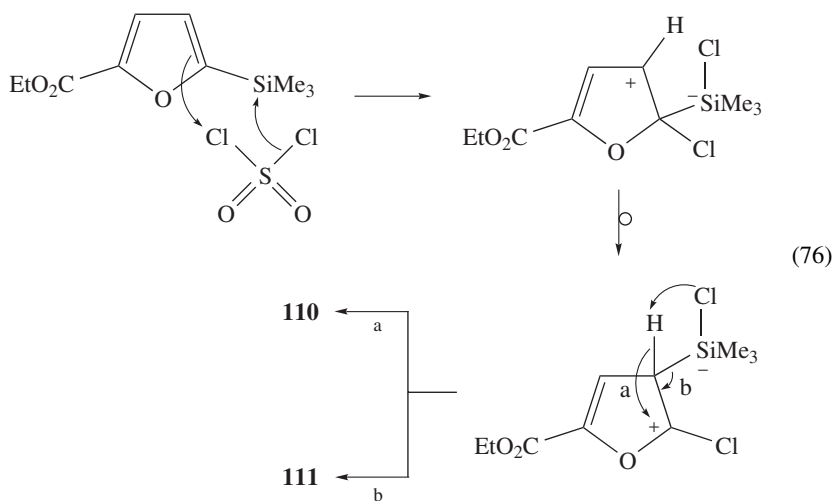
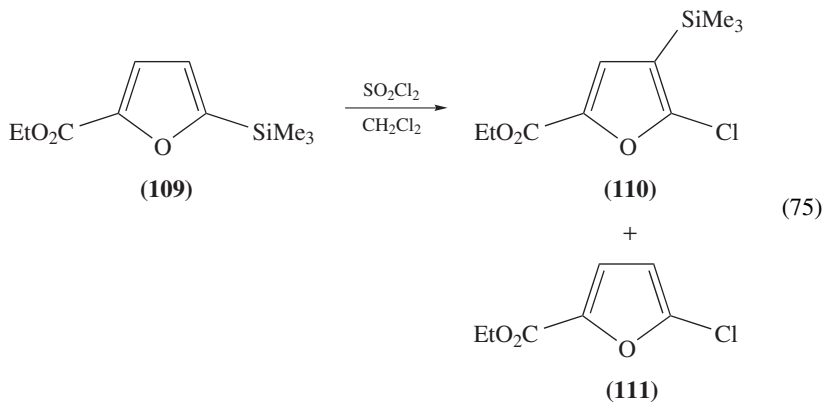


Reactions of 2-stannyl-3-trimethylsilylpropene **107** (R=Me) with a variety of acid chlorides proceeded smoothly in the presence of AlCl_3 at -78°C to give 2-silylallyl ketones **108** in high yields instead of the corresponding 2-stannylallyl ketones (equations 73 and 74). EtAlCl_2 and TiCl_4 worked well as catalysts but SnCl_4 and $\text{BF}_3\cdot\text{OEt}_2$ were not effective even at room temperature¹⁸². Exclusive destannylation over desilylation was also found during the Lewis acid promoted reactions of 1-silyl-3-stannylpropenes with aldehydes¹⁸³.

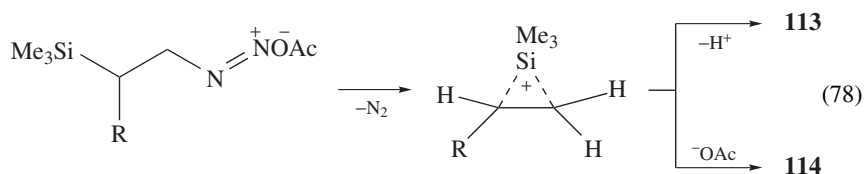
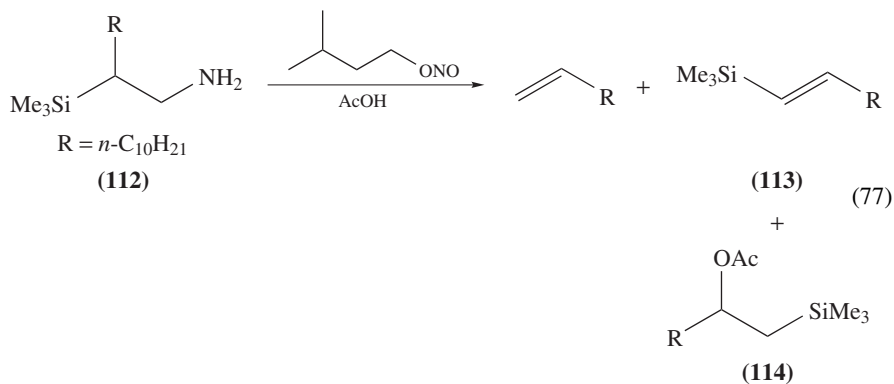




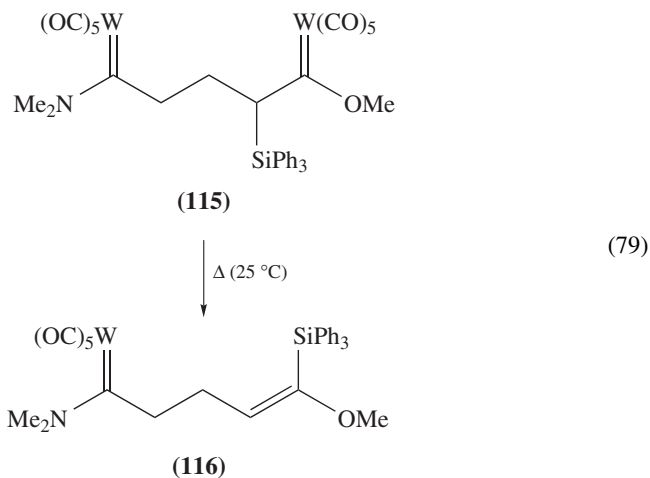
Nakayama and Tanaka found that the chlorination of 2-silylfuran **109** with sulfuryl chloride gave the corresponding 2-chloro-3-silylfuran **110** and 2-chlorofuran **111** as shown in equation 75¹⁸⁴. 1,2-Migration of a pentacoordinate silicate group was assumed to be involved in this reaction (equation 76).

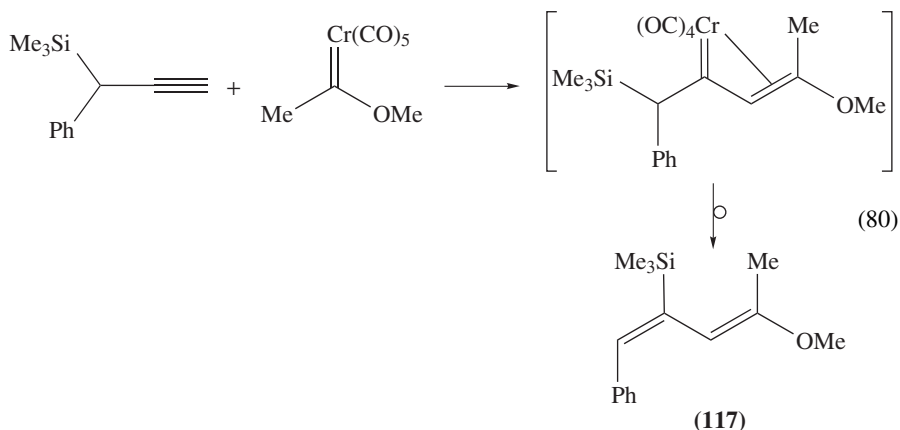


A cationic 1,2-silyl migration was observed during the deaminosilylation through the diazotization of β -aminosilanes **112**, which gave **113** and **114** (equations 77 and 78)¹⁸⁵.



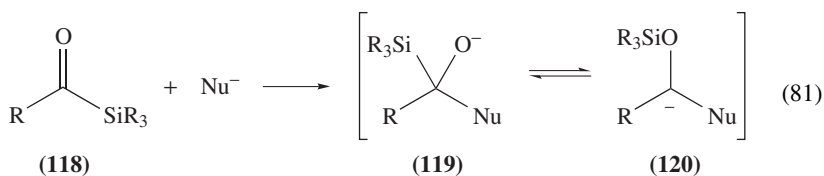
A Fischer carbene complex containing an α -silyl group like **115** underwent a facile 1,2-silyl migration to the corresponding vinylsilane **116** (equation 79)¹⁸⁶. Herndon and Patel applied the reaction to the synthesis of a dienol ether **117** (equation 80)¹⁸⁷.



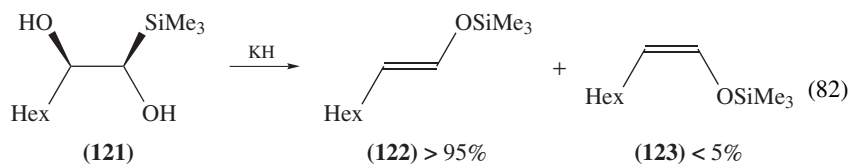


2. Anionic 1,2-silyl migrations from C to O

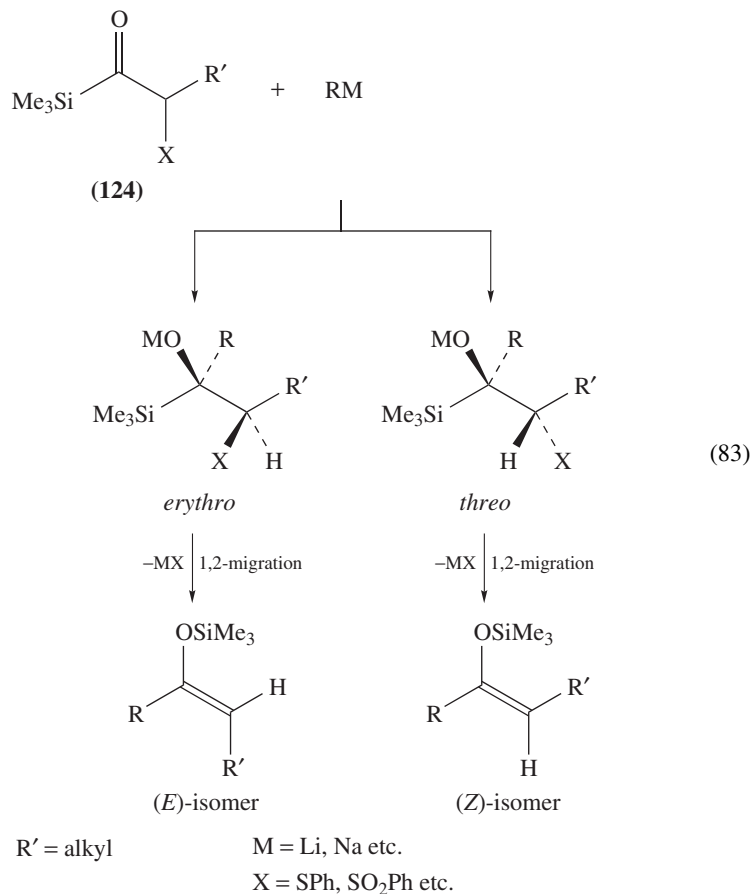
α -Silylalkoxides prepared by the reactions of acylsilanes **118** with nucleophiles or by other methods have attracted considerable attention from the synthetic point of view (equation 81). As demonstrated in Section II.A.3, silylalkoxides **119** undergo a facile Brook rearrangement to attain an equilibrium with the corresponding siloxy carbanions **120**. Although the equilibrium generally favors the alkoxide form unless a substituent on the central carbon is a carbanion stabilizing group such as an aryl group, carbanions **120** serve as key intermediates for subsequent derivatization. A review on the synthetic applications of the Brook rearrangements has been published⁷.



a. Preparation of silyl enol ethers. Hudrlik found that treatment of α,β -dihydroxysilane **121** with KH gave the corresponding silyl enol ethers **122** and **123** with high stereoselectivity (equation 82). This reaction was explained by the Brook rearrangement of the initially formed α -silylalkoxide, followed by a predominant *anti*-elimination of siloxypotassium^{188–189}.



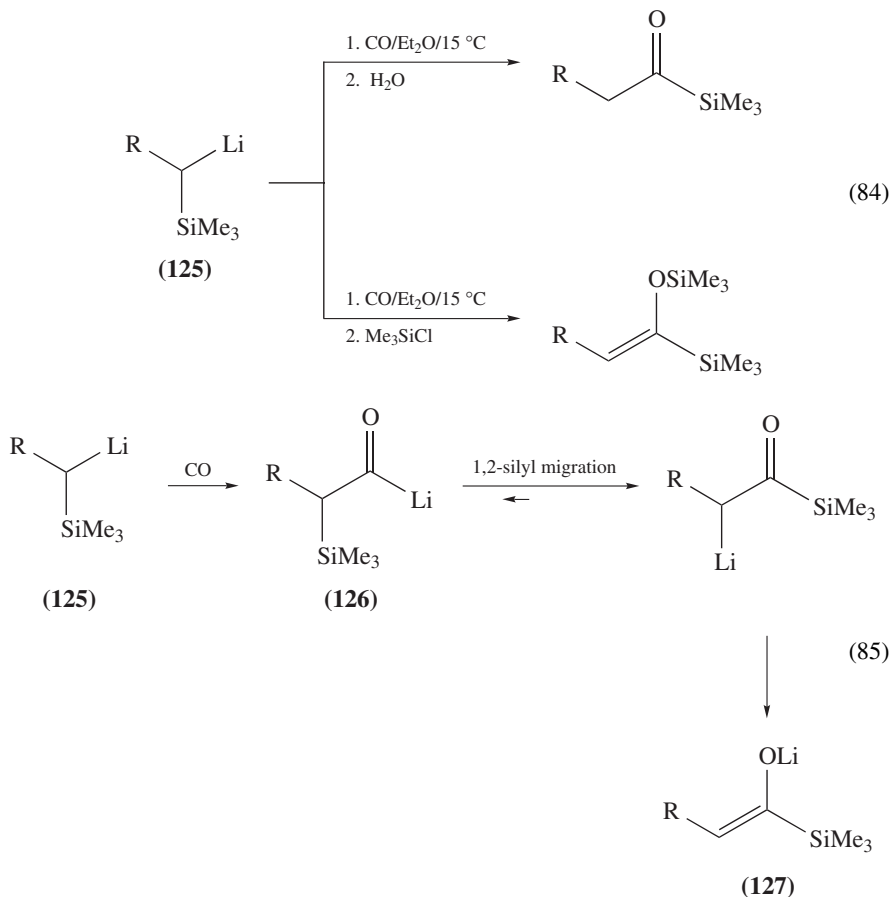
The reactions of acylsilanes with nucleophiles followed by the Brook rearrangement gave silyl enol ethers, silyl allenol ethers and silyl homoenolate derivatives, regio- and stereoselectively, when either the acylsilanes or the nucleophiles contained good leaving groups X, such as SPh, SePh, SO₂Ph and F at the α -position^{190–199}. The addition of a salt of a nucleophile RM to an acylsilane **124** carrying the group X at the α -position occurred in the Felkin–Anh mode, where X was *anti* to the attacking nucleophile R (equation 83). When R' were electron-donating substituents such as alkyl groups, the final elimination was stereospecific, but when the carbanion was stabilized by aryl and alkynyl groups, the elimination process was often nonstereospecific.



The α -silyl- β -X-alkoxides were generated in the reactions of acylsilanes with α -X-substituted nucleophiles^{190,191,193,195} and in the reactions of silyllithiums with ketones substituted by α -X groups^{193,200}.

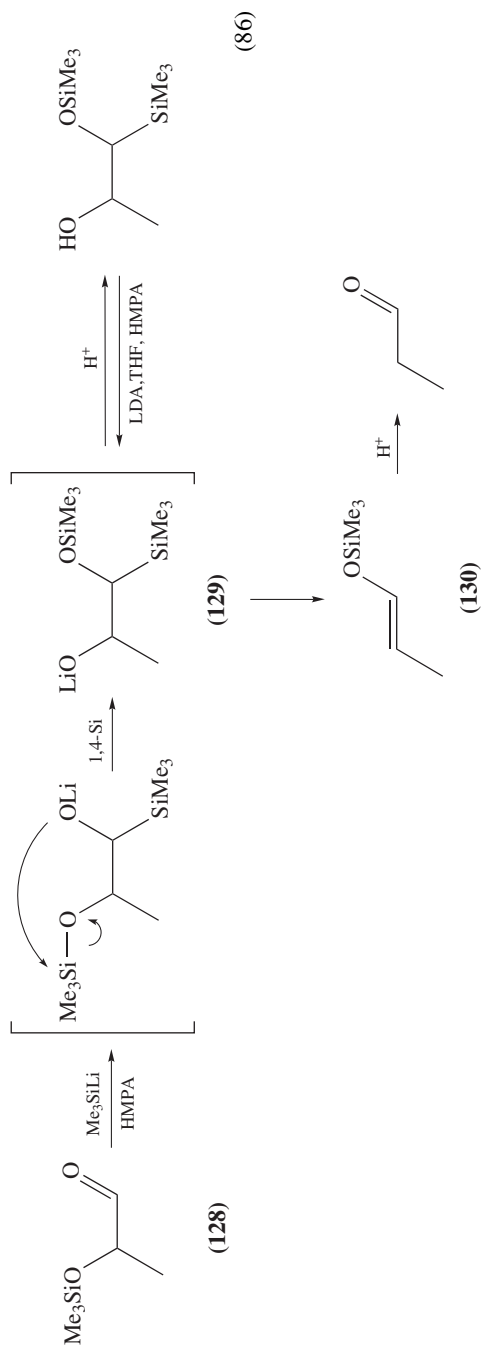
Murai and coworkers reported a simple synthetic method of acylsilane enolates using the reactions of silylmethylolithiums **125** with carbon monoxide (equation 84)²⁰¹. The

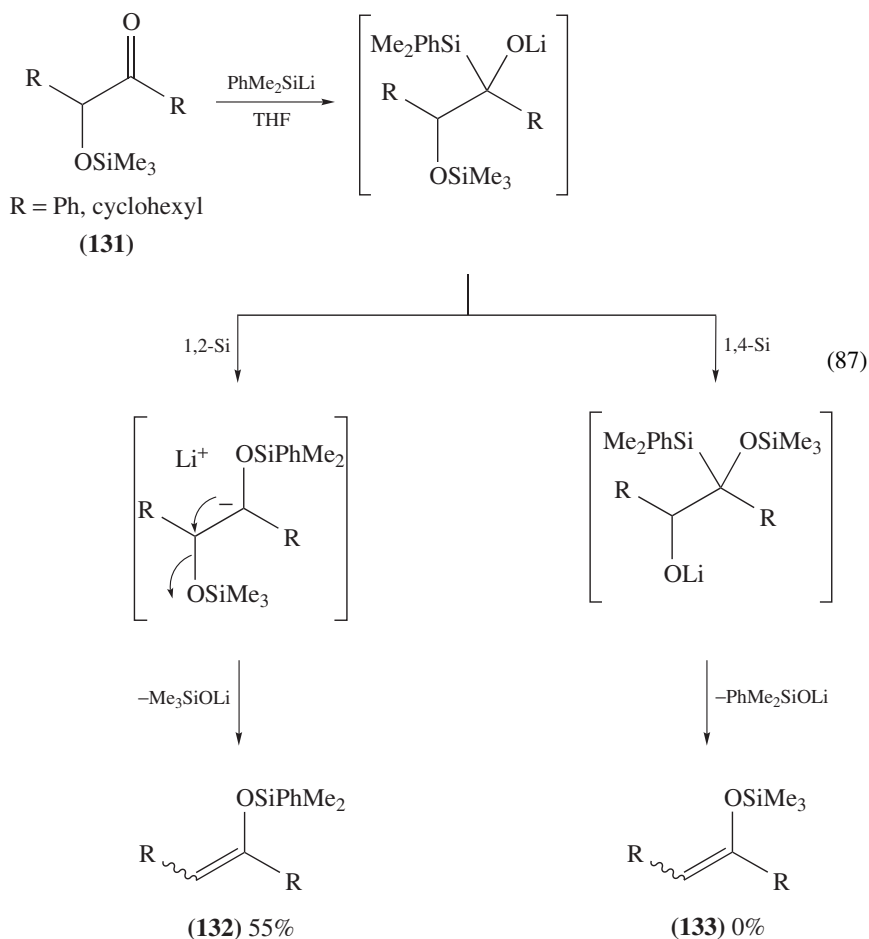
reactions gave initially highly reactive acyllithiums **126**, which underwent an anionic 1,2-silyl migration from C to C, thus affording the more stable lithium enolates **127** (equation 85). Crossover experiments verified the intramolecularity of the silyl migration. The lithium enolates were converted to acylsilanes or their enol silyl ethers by treatment with H₂O or with a trialkylchlorosilane.



Corey and coworkers reported the reactions of α -siloxyketones **128** with trimethylsilyllithiums in the presence of HMPA which gave the corresponding silyl enol ethers **130** (equation 86). The elimination of α -siloxy groups was proposed to occur via the 1,4-silyl migration followed by the Peterson elimination. In accord with this mechanism, the intermediate **129** was trapped by hydrolysis²⁰².

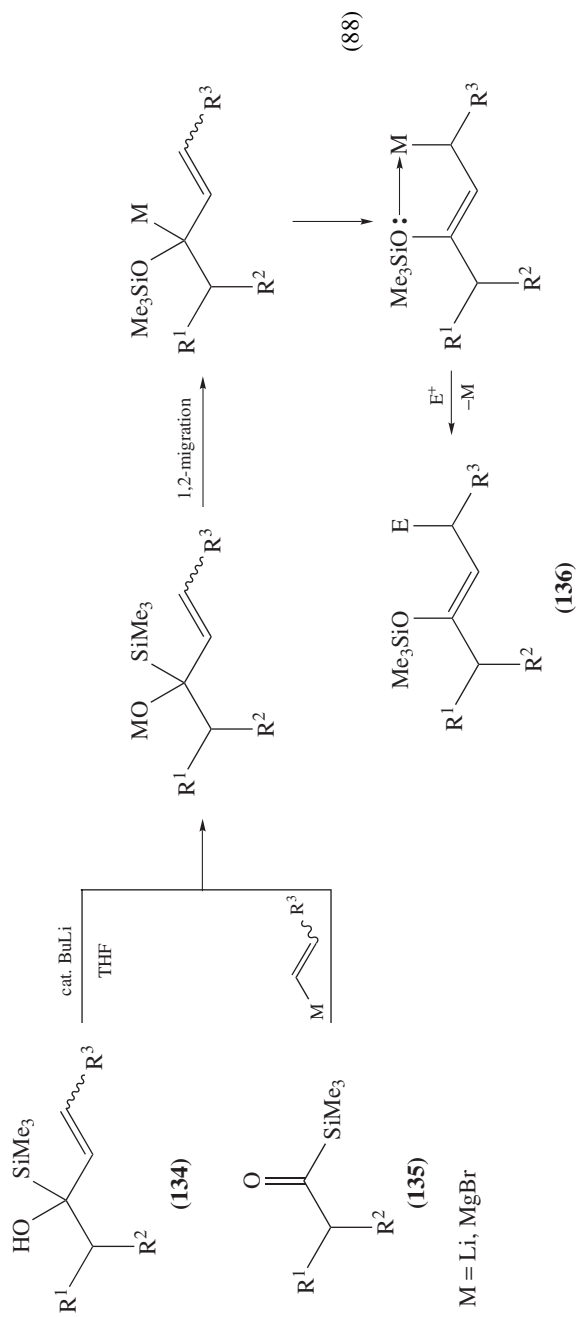
In contrast, Fleming and coworkers proposed another mechanism involving a Brook rearrangement coupled with desilylative β -elimination for similar reactions of α -siloxy ketones **131** with phenyldimethylsilyllithium to give silyl enol ethers **132** (equation 87); no trimethylsilyl enol ether **133** was detected in the reaction mixture²⁰³.

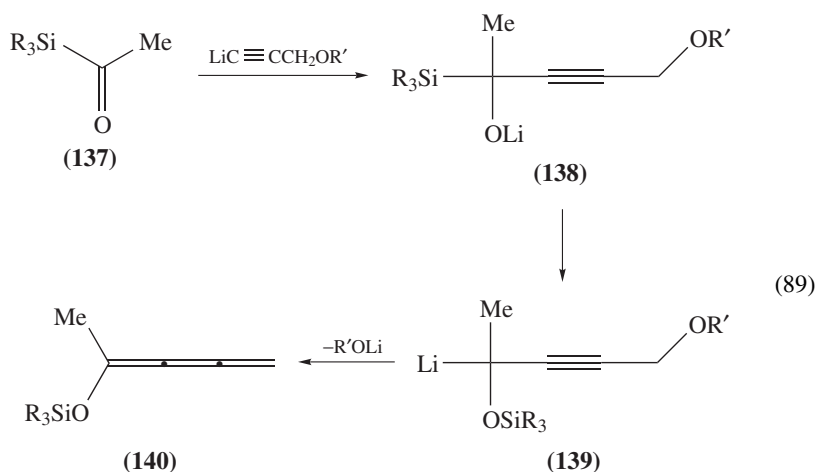




α -Trimethylsilyl(allyl)alkoxides were generated by the reactions of α -silylallyl alcohols **134** with a catalytic amount of bases or by the reactions of acylsilanes **135** with vinyl metal reagents. The stereo- and regioselective Brook rearrangements of the silyl(allyl)alkoxides gave the corresponding metallated (*Z*)-silyl enol ethers **136**, which afforded synthetically useful silyl enol ethers by reactions with various electrophiles E (equation 88)^{200,204–207}.

The reactions of acylsilanes **137** with 3-alkoxy-1-propynyllithium gave the corresponding α -silylated propargylic alkoxides **138**, which led to the 4-siloxy-1,2,3-pentatrienes **140** through a Brook rearrangement and then 1,4-elimination of the alkoxyolithiums **139** (equation 89)^{208,209}. 1,2,3-Pentatriene **140** having a bulky silyl substituent was stable towards neutral aqueous solutions but rapidly polymerized in the presence of oxygen even at low temperatures.

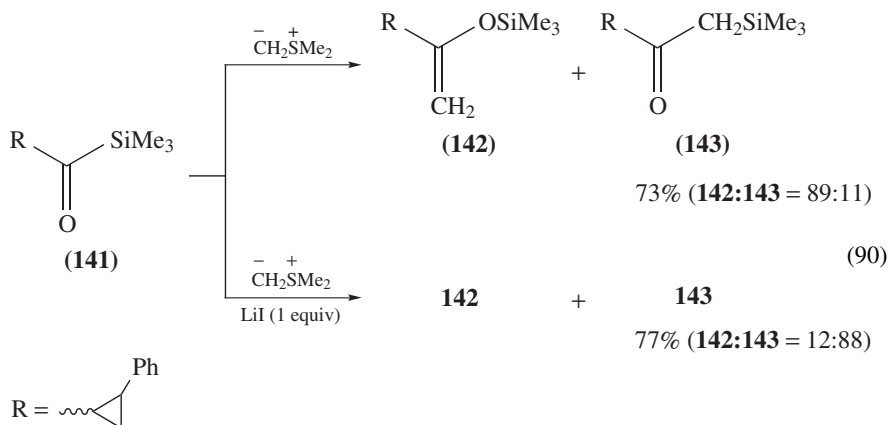


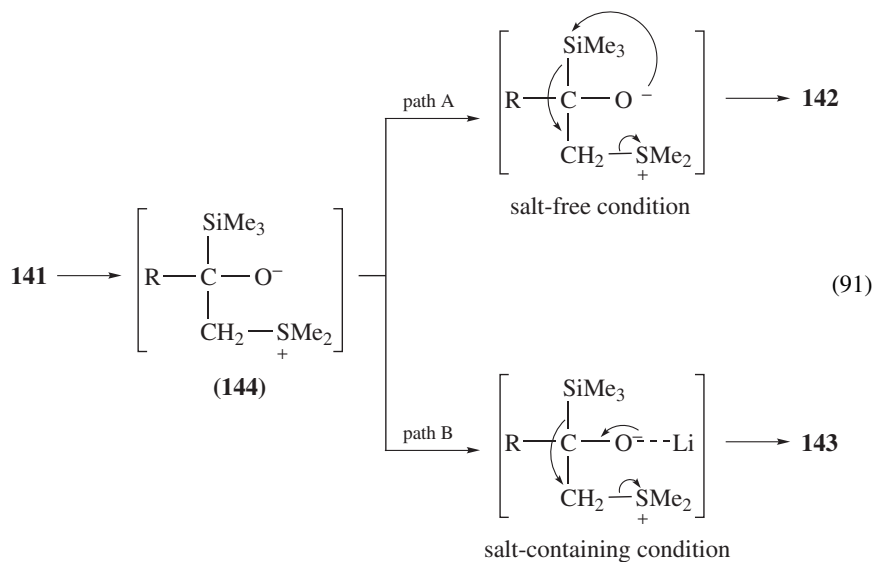


R' = Me, 3-tetrahydropyranyl

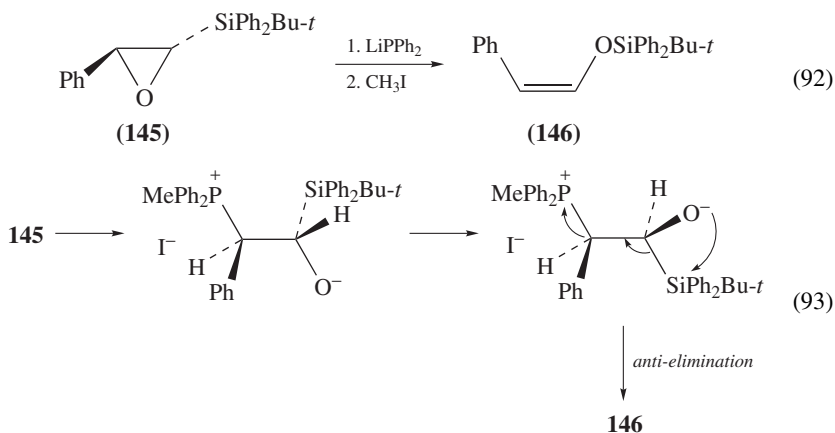
R₃Si = Me₃Si, *t*-Bu(PhCH₂OCH₂)MeSi

The reaction of 2-(phenylcyclopropyl)acylsilane **141** with a sulfur ylide provided a β -silyl ketone together with the corresponding silyl enol ether (equation 90)²¹⁰. In the absence of inorganic salts, silyl enol ether **142** was preferentially formed. In contrast, in the presence of an equivalent of lithium iodide, the β -silyl ketone **143** was obtained as the major product. As shown in equation 91, the reaction was proposed to proceed through the common betain intermediate **144**, which underwent two different silyl migration modes: 1,2-silyl migrations to O (path A) and to C (path B). It was suggested that in the presence of a lithium salt, path A was prevented by the formation of a tight ion pair between the oxyanion and lithium cation.

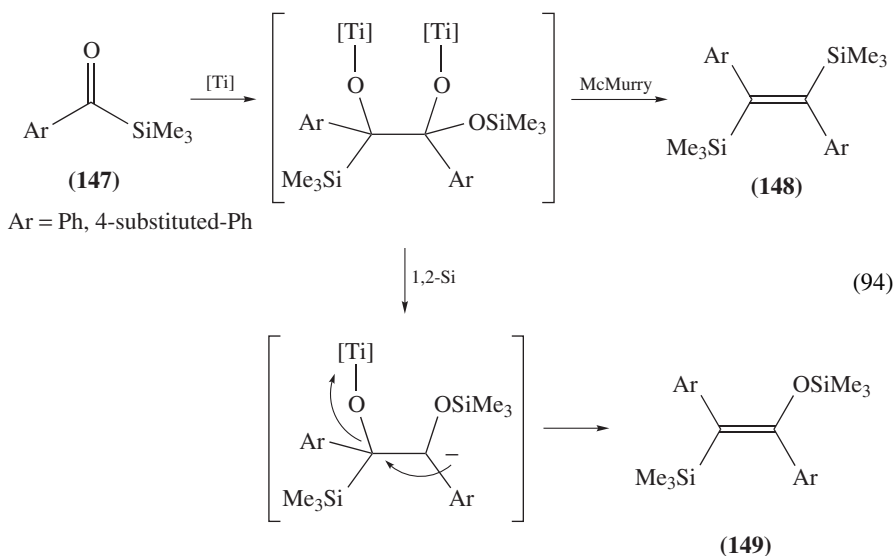




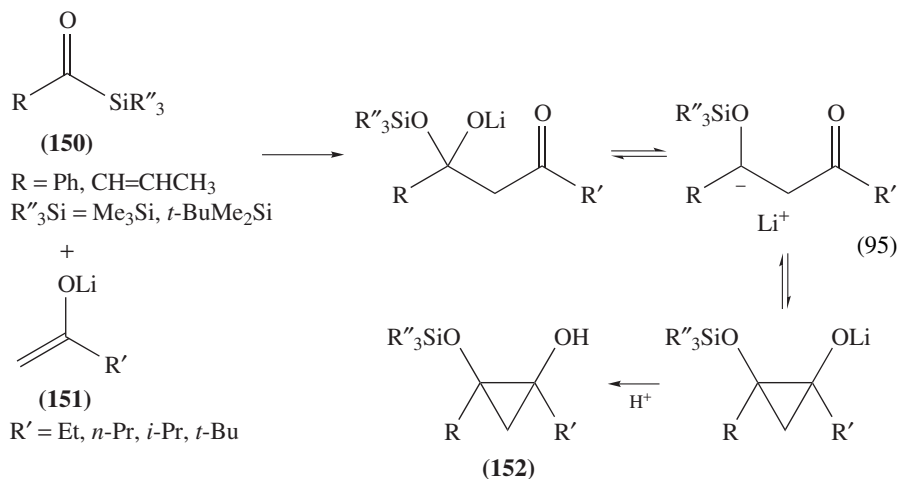
Treating *t*-butyldiphenyl(phenylepoxy)silane **145** with lithium diphenylphosphide and then with methyl iodide provided (*Z*)-silyl enol ether **146**²¹¹ (equation 92). The formation of the *Z*-isomer suggested an *anti* arrangement between the phosphonium and silyl groups at the silyl migration step (equation 93).



Fürstner and coworkers found that the McMurry coupling of aroylsilanes **147** gave silyl enol ethers **149** via the Brook rearrangement in addition to the normal McMurry coupling products **148** (equation 94)²¹². The product ratio **148/149** was dependent on the reaction conditions, especially on the catalyst. The coupling reactions of aliphatic acyltrimethylsilanes were unsuccessful.

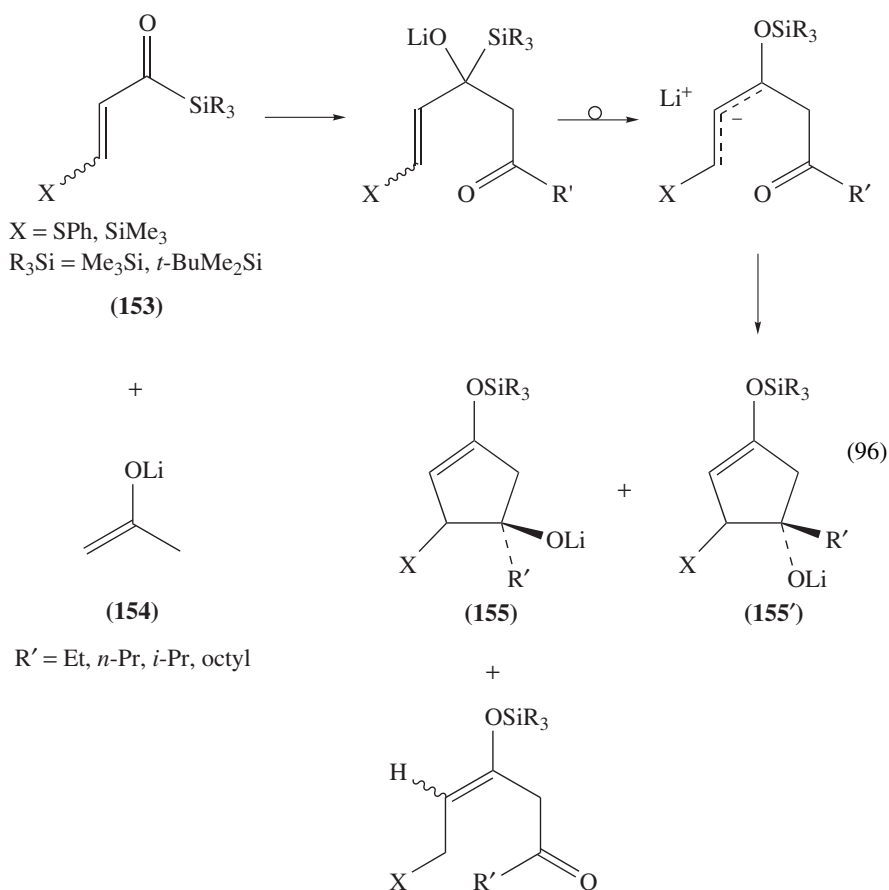


b. Cyclizations involving the Brook rearrangement. The Brook rearrangements were often applied to the syntheses of highly functionalized carbocycles. Reactions of benzoylsilane and crotonylsilane **150** with lithium enolates **151** afforded the cyclopropane diol derivatives **152** (equation 95)²¹³.

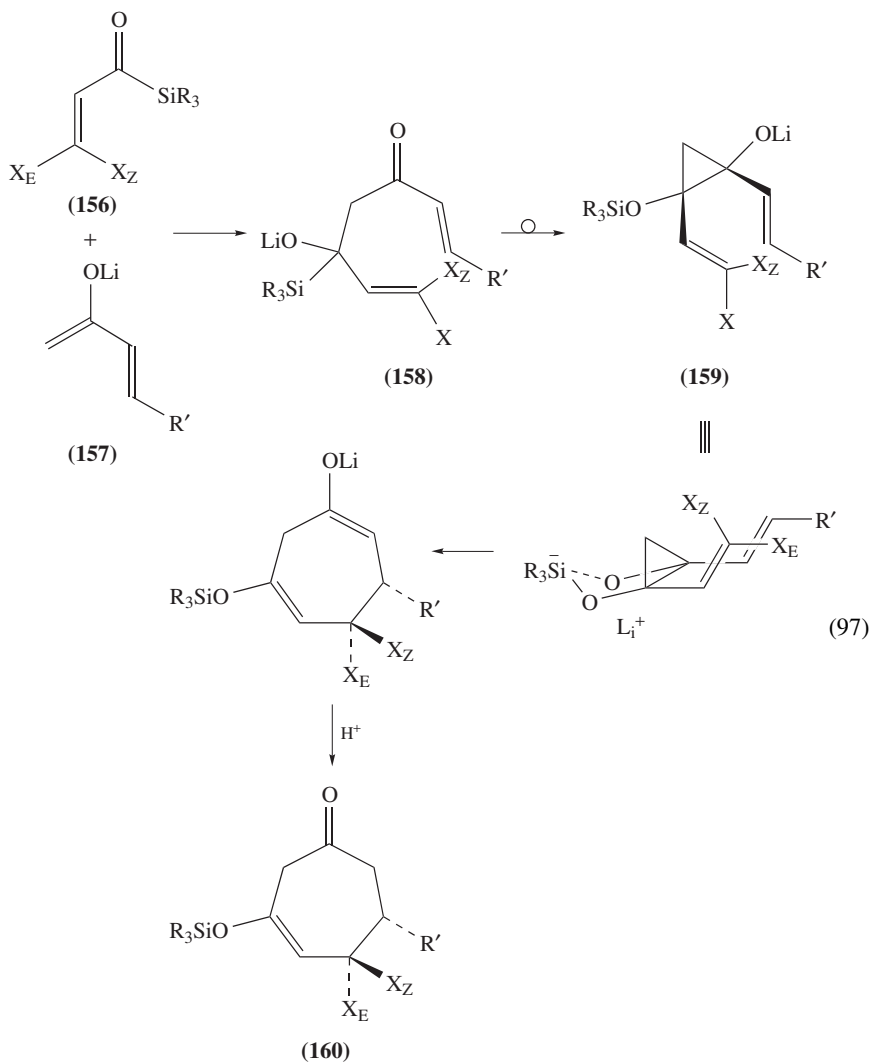


Anionic 1,2-silyl migrations from C to O were applied to the [3 + 2] annulations of β -X-substituted α,β -unsaturated acylsilanes (X=SPh and SiMe₃) **153** with lithium enolates **154**,

which afforded diastereomeric cyclopentenol derivatives **155** and **155'** (equation 96)^{214,215}. The *E/Z* ratio of the cyclopentenols was independent of the initial stereochemistry of the acylsilanes. Although the annulation took place exclusively when X=SPh, an acyclic product was formed competitively when X=SiMe₃²¹⁶. This method was applied to the syntheses of Untenone A²¹⁷, chromomoric acid D-II methyl ester²¹⁴ and an antitumor marine prostanoid clavulones²¹⁸.



Similarly, the [3 + 4] annulation of the *E*- and *Z*-isomers of β -heteroatom-substituted acryloylsilanes **156** with lithium enolates of α,β -unsaturated methyl ketones **157** gave stereospecifically *cis*-5,6- and *trans*-5,6-disubstituted-3-cycloheptenones **160**, respectively (equation 97). The stereospecificity in the annulation was explained by an anionic oxy-Cope rearrangement of the 1,2-divinylcyclopropanediol intermediate **159**, which was generated through the Brook rearrangement of the initial 1,2-adduct **158**^{219–223}.



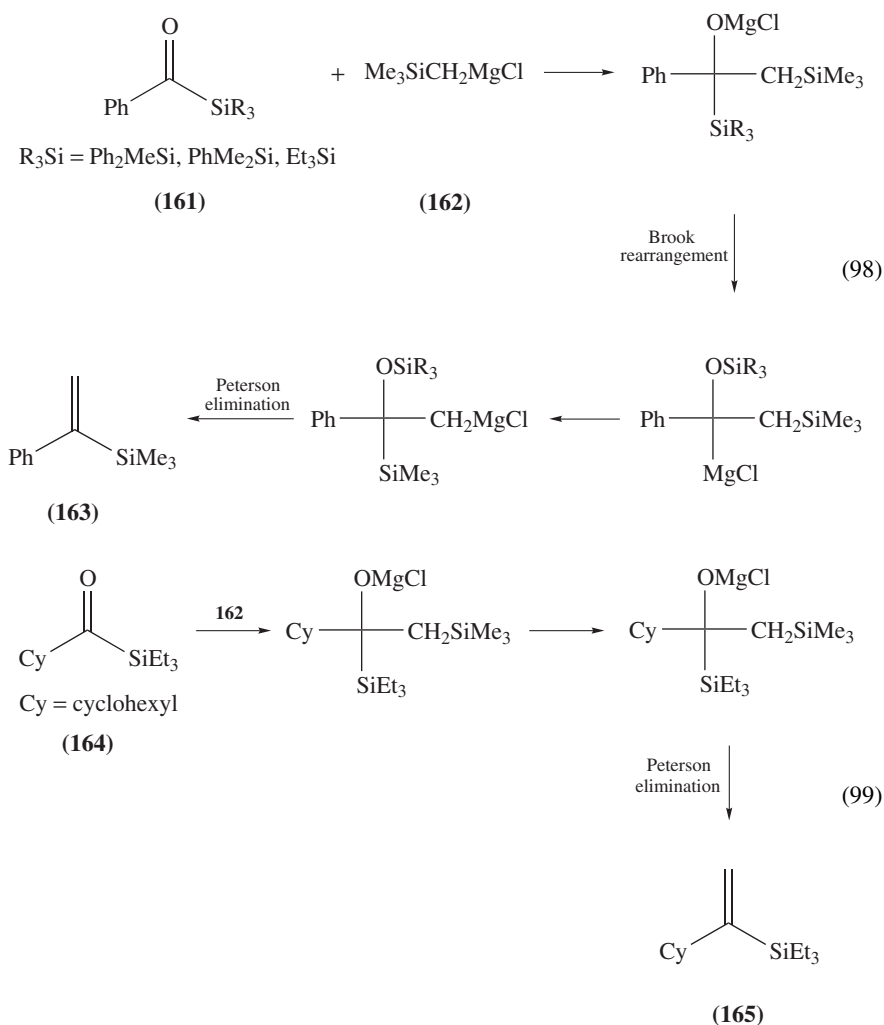
$\text{R}_3\text{Si} = t\text{-BuMe}_2\text{Si}, \text{PhMe}_2\text{Si}; \text{R}' = \text{Et}, \text{Pr}, i\text{-Pr}, \text{octyl}$

$\text{X}_\text{E} = \text{H}, \text{X}_\text{Z} = \text{alkyl}, \text{silyl}, \text{stannyl};$

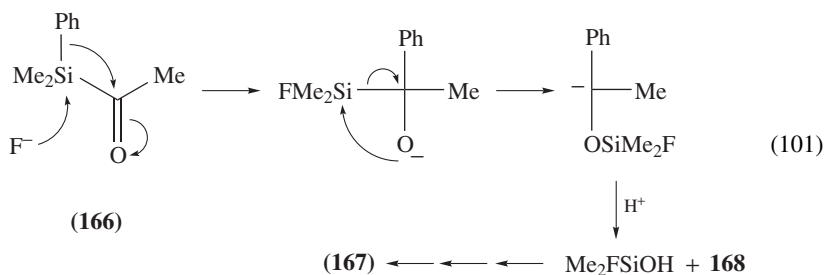
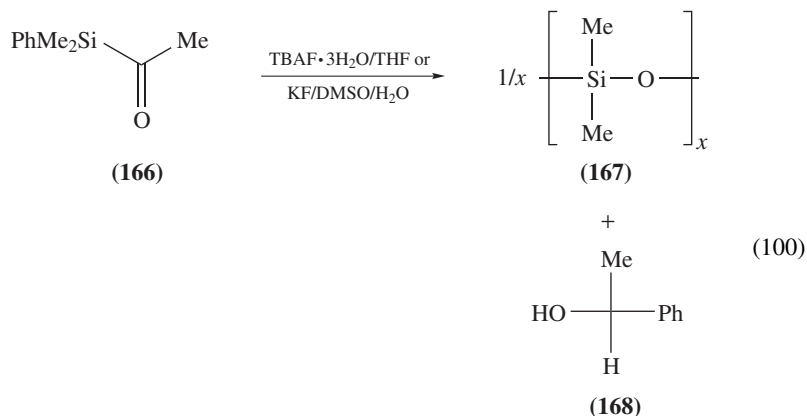
$\text{X}_\text{E} = \text{alkyl}, \text{silyl}, \text{stannyl}, \text{X}_\text{Z} = \text{H}$

c. Miscellaneous. Anionic 1,2-silyl migrations from C to O were observed in the reactions of epoxysilanes with α -sulfonyl carbanions giving allyl silyl ethers²²⁴ and in the stereospecific desilylations of α -hydroxysilanes^{225–227} and β -hydroxysilanes²²⁷.

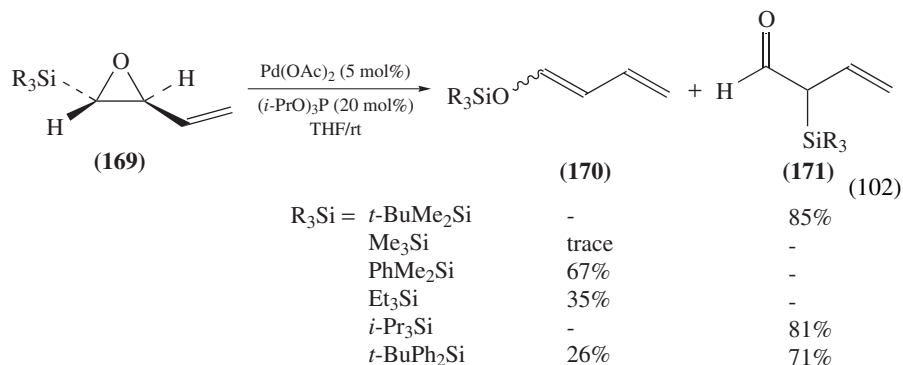
Fürstner and coworkers revealed a competition between the Brook rearrangement and the Peterson olefination. The adducts of aroylsilanes **161** with (trimethylsilyl)methylmagnesium chloride **162** underwent a Brook rearrangement and then a Peterson elimination affording vinylsilane **163** (equation 98). On the other hand, the reaction of cycloalkylcarbonylsilane **164** with **162** gave vinylsilane **165** via the direct Peterson elimination (equation 99)²²⁸.

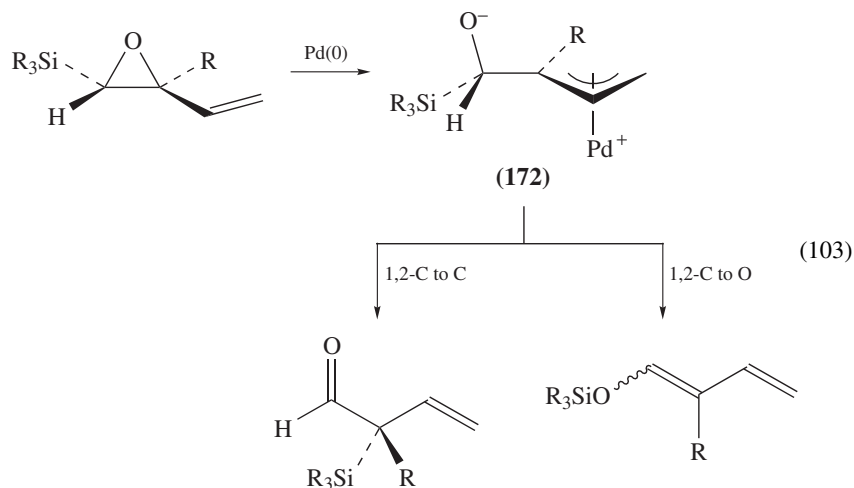


A reaction of acetyldimethylphenylsilane **166** with TBAF·3H₂O in THF or with KF in DMSO/H₂O gave [Me₂SiO]_x (**167**) and 1-phenylethanol **168** quantitatively (equation 100). The reaction was considered to involve a 1,2-phenyl shift followed by a Brook rearrangement (equation 101)²²⁹.

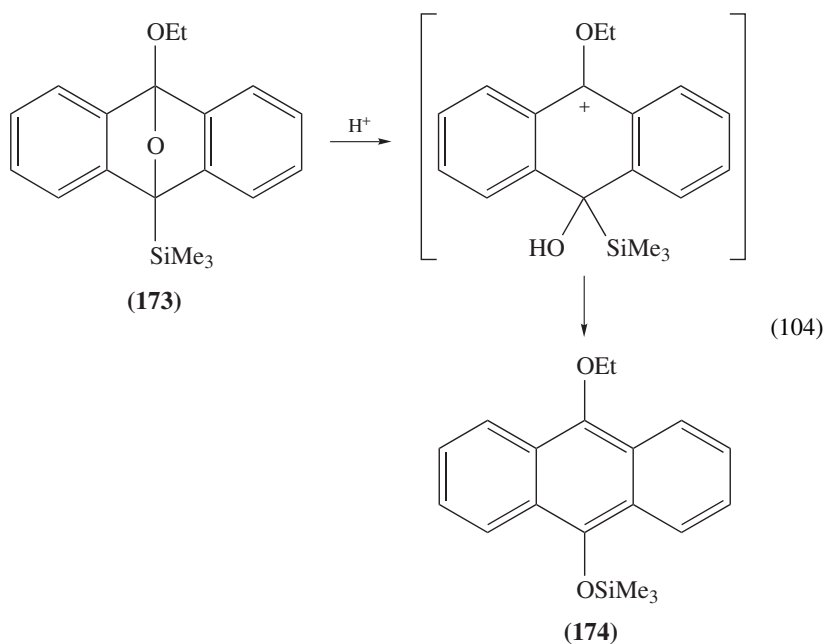


Bideau and coworkers found that vinyloxyasilanes **169** underwent a palladium-catalyzed transformation to give siloxybutadienes **170** and β,γ -unsaturated- α -silyl ketones **171** (equation 102)²³⁰. The product ratio was dependent on the bulkiness of the silyl substituents; β,γ -unsaturated- α -silyl ketones were preferentially obtained when the silyl substituent was bulky. The selectivity was explained by a competition between the Brook rearrangement and the migration from C to C of the intermediate π -allyl palladium complex **172** (equation 103). The product ratio also depended on the ligands on palladium; $\text{P}(\text{OPh})_3$ as an additive induced the highest degree of 1,2-silyl migration from C to C (with a high level of the chirality transfer), while a TMEDA ligand favored the Brook rearrangement.





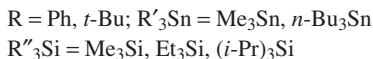
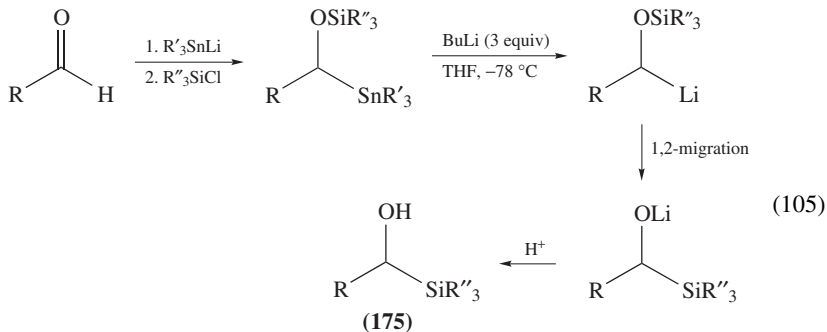
Bridgehead trimethylsilylated ketal **173** underwent an acid-catalyzed rearrangement to 9-alkoxy-10-(trimethylsiloxy)anthracene **174** (equation 104)²³¹.



3. Anionic 1,2-silyl migrations from O to C

The direct synthesis of (α -hydroxyalkyl)trialkylsilane by a nucleophilic addition of a trialkylsilyl anion to an aldehyde or a ketone has not been readily accomplished because of the difficulty in the preparation of trialkylsilyl anions. Tin-mediated reverse Brook

rearrangements were applied alternatively for the syntheses of the α -hydroxyalkylsilanes **175** (equation 105). The reverse Brook rearrangements occurred with retention of configuration at carbon when R=alkyl^{80,93,232}, although an inversion at carbon was preferred when R=aryl. For example, optically active (*S*)-[α -[(trimethylsilyl)oxy]alkyl] trialkylstannane (98% ee) provided 1-(trimethylsilyl)hexanol in 97% ee.

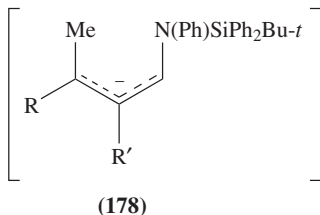
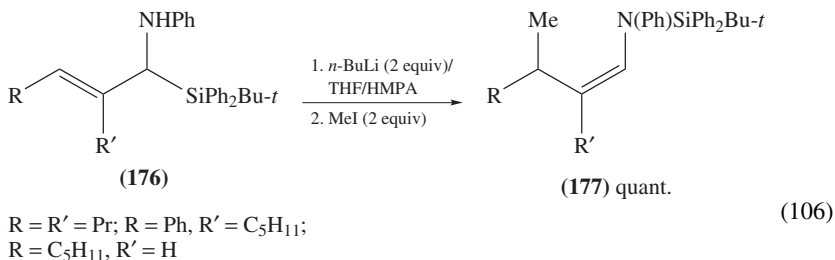


Similarly, β -hydroxyacylsilanes²³³, α,β -unsaturated acylsilanes²³⁴, α -silylallyl alcohols^{235–237}, α,β -bissilylated enals and enols²³⁸, and enol silylesters of acylsilanes²³⁹ were obtained via the reverse Brook rearrangements.

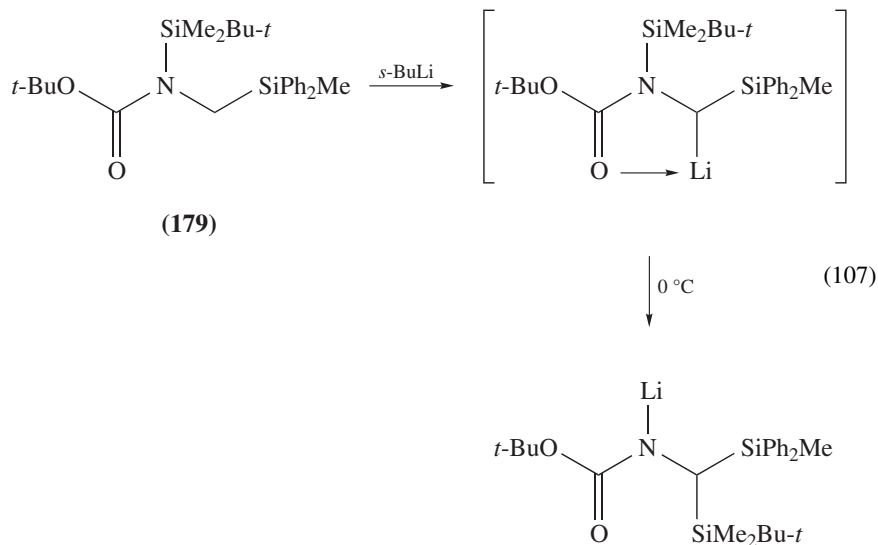
4. Anionic 1,2-silyl migrations between C and N

In contrast to 1,2-migrations between C and O, only a few synthetic applications of 1,2-migrations between C and N have been reported.

The reaction (equation 106) of (α -silylallyl)amines **176** with *n*-BuLi in THF and HMPA followed by quenching the resulting allylic anion **178** by MeI provided the corresponding *N*-silyl(vinyl)amines **177** quantitatively²⁴⁰.

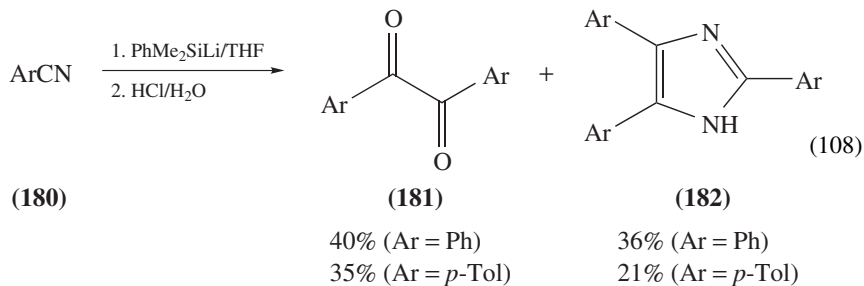


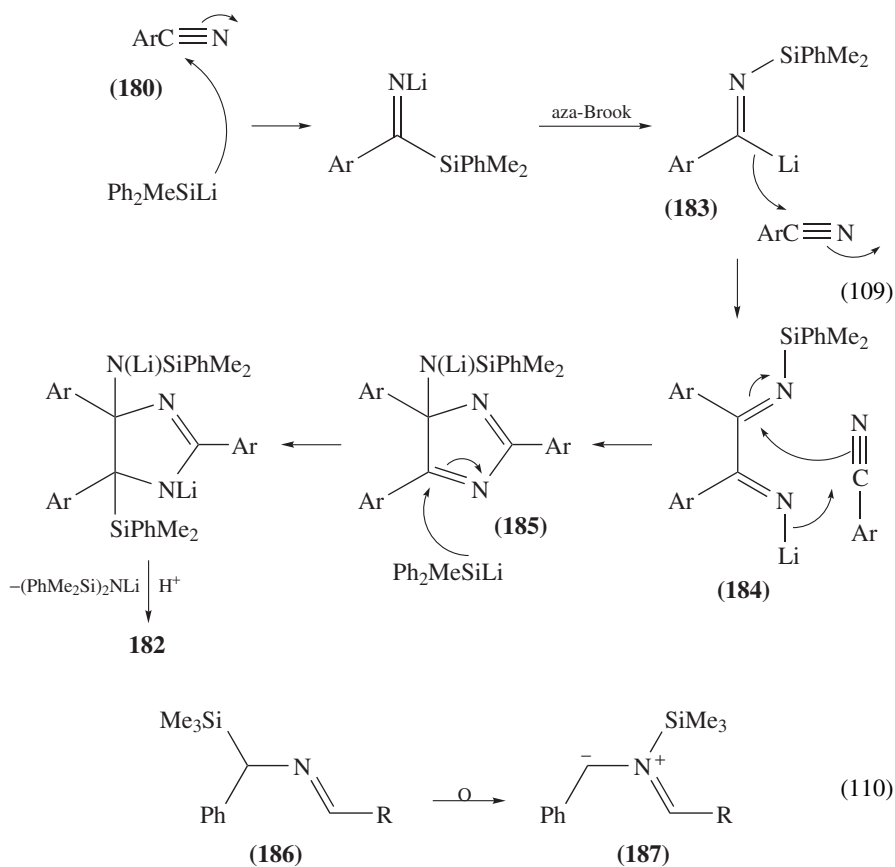
Anionic 1,2-silyl migrations from N to C were found in the reactions of α -silyl amines **179** with *s*-BuLi (equation 107)^{241,242}.



Fleming and coworkers found that the reactions of benzonitriles **180** with phenyldimethylsilyllithium afforded unexpected imidazoles **182** together with the corresponding benzils **181** (equation 108). The whole reaction profile was explained as in equation 109. The nucleophilic attack of the silyllithium on the nitrile carbon followed by the aza-Brook rearrangement gave iminyllithium **183**, which reacted with another molecule of benzonitrile to form an intermediate **184**. Intermediate **184** reacted further with a third molecule of benzonitrile to give an intermediate **185**, and then an aza-Peterson elimination afforded finally imidazole **182**, while **184** was probably hydrolyzed to give partially **181**²⁴³.

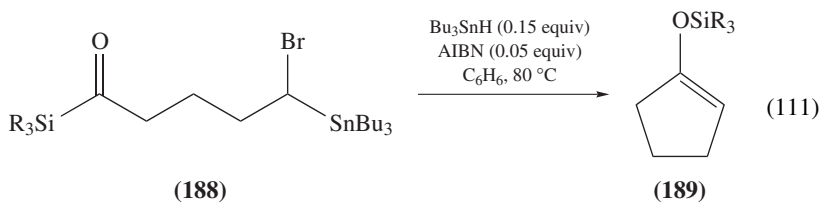
Komatsu and coworkers had found that heating of *N*-(silylmethyl)imines **186** gave diazomethyne ylide **187** via a 1,2-silyl migration (equation 110). This type of migration from C to N was used in the stereoselective synthesis of *cis*-2,3-diarylaziridine²⁴⁴ and pyrroline derivatives²⁴⁵.

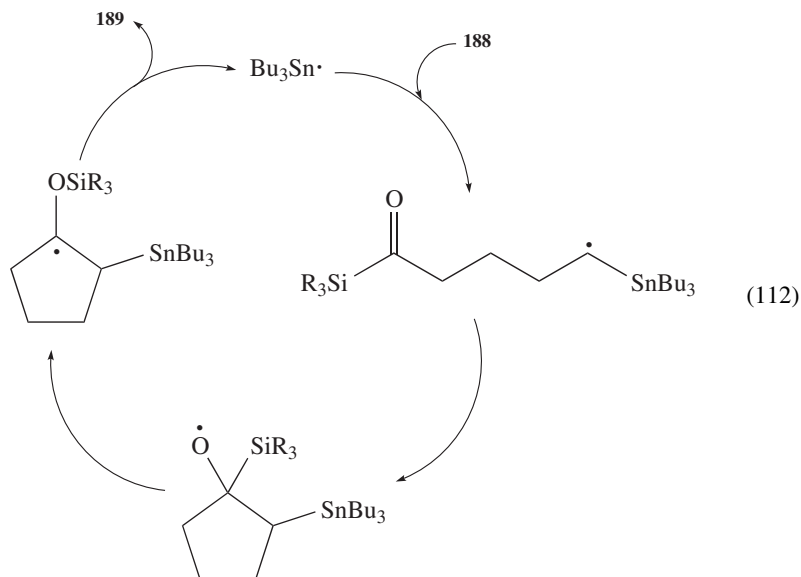




5. Radical 1,2-silyl migrations

Tsai and coworkers^{89,91,246,247} reported the synthesis of cyclic silyl enol ethers and silyl ethers by using a radical cyclization followed by the radical Brook rearrangement (equation 111). The cyclization of 4-bromo-4-stannylbutyl silyl ketones **188** in benzene with a catalytic amount of tributyltin hydride and AIBN gave cyclic silyl enol ethers **189**^{89,91,247}. The whole catalytic cycle proposed is shown in equation 112.



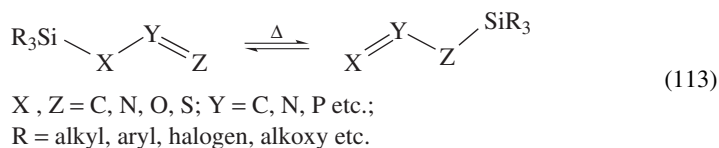


III. 1,3-SILYL MIGRATIONS

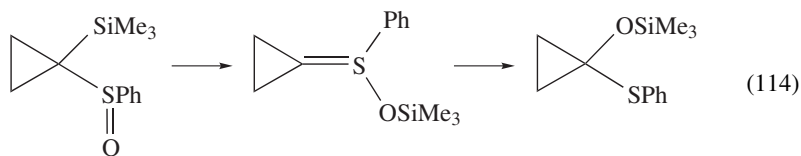
A. Mechanistic Aspects

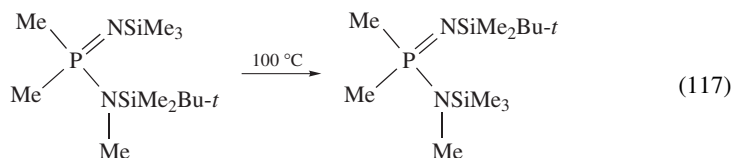
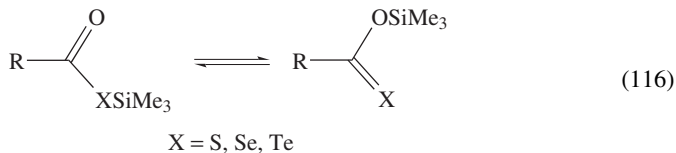
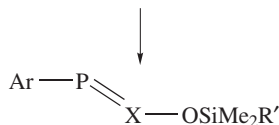
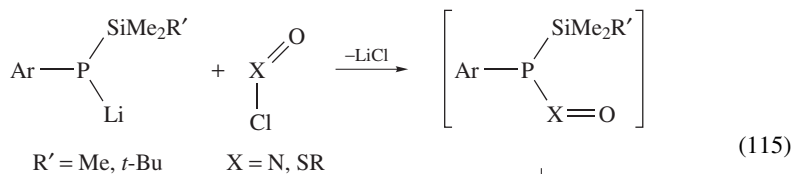
1. Migrations across allylic frameworks

In this category, there have been reported recently a large number of thermal 1,3-silyl migrations between C and C^{248–254}, C and O^{74,255–268}, C and N^{269–275}, C and S²⁷⁶, N and O^{277–283}, N and N^{271,273,274,284–289}, O and O²⁹⁰, P and O^{291–295}, P and N²⁹⁵, As and O²⁹⁴, Te and O²⁹⁰, Si and C (equation 113)²⁹⁶.

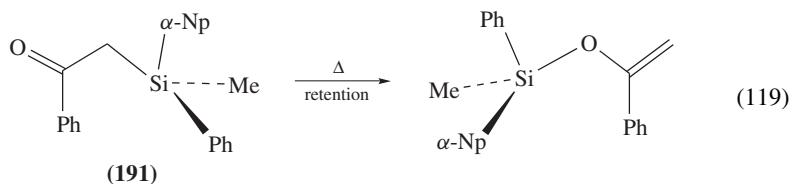
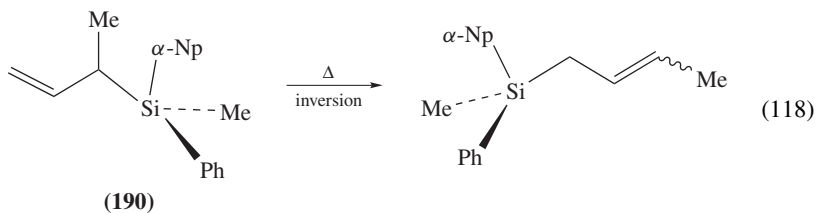


Equations 114–117 illustrate some examples of 1,3-silyl migrations across allylic frameworks that were recently investigated.





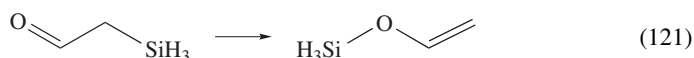
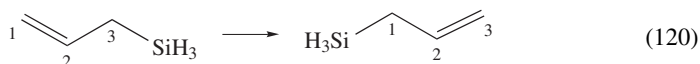
This type of thermal 1,3-silyl migration is mechanistically very interesting, because two typical intramolecular 1,3-silyl migrations in allylsilanes **190** (equation 118) and β -ketosilanes **191** (equation 119) were shown to occur concertedly but with different stereochemistry at the silicon center¹.



The 1,3-silyl migrations from C to C occurred with inversion of configuration at silicon and with a rather high activation enthalpy: for the 1,3-silyl migration of α -methylallyltrimethylsilane studied by Kwart and Slutsky, $\Delta H^\ddagger = 47.7 \text{ kcal mol}^{-1}$ and $\Delta S^\ddagger = -6.2 \text{ cal mol}^{-1} \text{ K}^{-1}$ ²⁹⁷. On the other hand, 1,3-silyl migrations in ketosilanes

occurred with retention of configuration at silicon and with rather lower activation enthalpies; for the migration of trimethylsilylacetone, $\Delta H^\ddagger = 30.1 \text{ kcal mol}^{-1}$ and $\Delta S^\ddagger = -9.8 \text{ cal mol}^{-1} \text{ K}^{-1}$ ²⁹⁸. The former migrations were characterized as fully concerted [1,3] sigmatropic rearrangements, while the latter were characterized as intramolecular nucleophilic substitutions.

Recent *ab initio* MO studies of the prototypical migrations shown in equations 120 and 121 revealed three interesting features^{299,300}: (1) The 1,3-silyl migration in allylsilane can proceed concertedly in both inversion and retention manners at silicon. (2) 1,3-Silyl migration in formylmethylsilane occurs concertedly *without* any hypercoordinate *intermediate* with retention of configuration at silicon. (3) The two concerted 1,3-silyl migrations with retention of stereochemistry described above are mechanistically differentiated by Bader's topological analysis³⁰¹.



2. 1,3-Silyl migrations in allylsilanes

The thermal 1,3-silyl migration in allylic silanes was shown by Kwart and Slutsky to proceed concertedly with inversion of configuration at the migrating silicon^{297,302}. Takahashi and Kira²⁹⁹ and Yamabe and coworkers³⁰⁰ independently investigated in detail the transition structures (TS) and the stereochemistry of 1,3-silyl migration in allylsilane by using *ab initio* molecular orbital theory.

Two transition structures with a retention (**192**, TS_{ret}) and an inversion (**193**, TS_{inv}) configuration (Figure 2) were optimized for 1,3-silyl migration in allylsilane at HF/6-31G*, MP2/6-31G* and DFT/6-31G* levels. The TS_{inv} **193** was found to be a distorted trigonal bipyramid (TBP) around the silicon *with the two allylic carbons at the equatorial positions* different from the TS illustrated by Kwart and Slutsky^{297,302}, while **192** has a distorted square pyramid (SP) structure around silicon. Analysis of the orbital interaction in the transition states showed that the major stabilization of **193** was caused by the MO interaction as predicted by the Woodward–Hoffmann rules, while the major stabilization in **192** was ascribed to the subjacent orbital control. **192** was more stable than **193** at

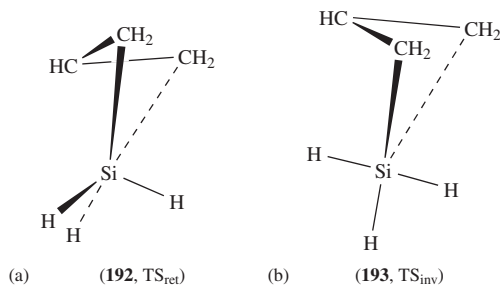
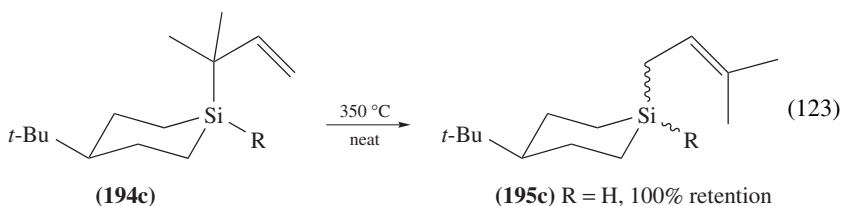
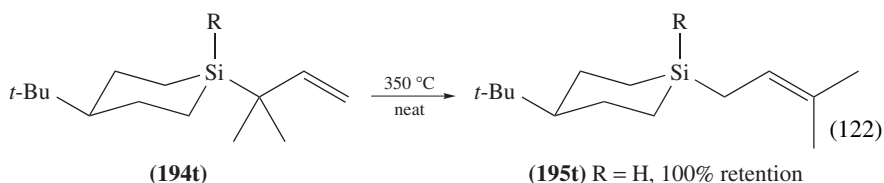


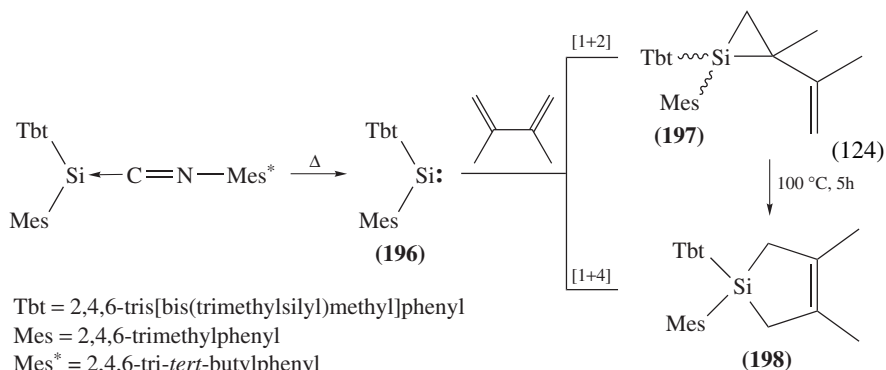
FIGURE 2. Schematic representation of the retention (**192**, TS_{ret}, a) and inversion transition states (**193**, TS_{inv}, b) in the 1,3-silyl migration of $\text{CH}_2=\text{CHCH}_2\text{SiH}_3$

all levels of calculations performed, in contrast to the experimental results by Kwart and Slutsky^{297,302}.

Theoretical calculations of the effects of substituents at silicon on the geometry and energy of the transition structures suggested that both electronic and steric effects accounted for the discrepancy between theory and experiment. Actually, Kira, Zhang and Kabuto found 1,3-silyl migrations in allylic silanes with retention of configuration at the silicon atom³⁰³. Thus, facile 1,3-silyl migrations in 1,1-dimethylallylsilanes **194t** (R=H) and **194c** (R=H) took place at 350 °C to give the corresponding 3,3-dimethylallylsilane derivatives **195t** and **195c**, respectively, in almost quantitative yields, with complete retention of configuration (equations 122 and 123). Interestingly, the stereochemical outcome of the migration varied, depending on the substituents at the silicon atom. Thus, when R=H and Ph in **194**, the 1,3-silyl migrations occurred with complete retention of the stereochemistry, while the stereochemistry of the starting materials were lost to a significant extent when R=4-phenylphenyl and 1-naphthyl.



The reactions of silylenes with 1,3-butadienes affording the corresponding silacyclopentenes have been considered to proceed through an initial [1 + 2] addition to give 2-vinylsilacyclopropanes, followed by the 1,3-silyl migrations^{304,305}. Tokitoh and coworkers obtained convincing evidence for the initial formation of the [1 + 2] adduct **197** during the reaction of the silylene **196** with 2,3-dimethylbutadiene and for the subsequent 1,3-silyl migration giving **198** upon heating (equation 124)³⁰⁶.



3. 1,3-Silyl migrations in β -ketosilanes

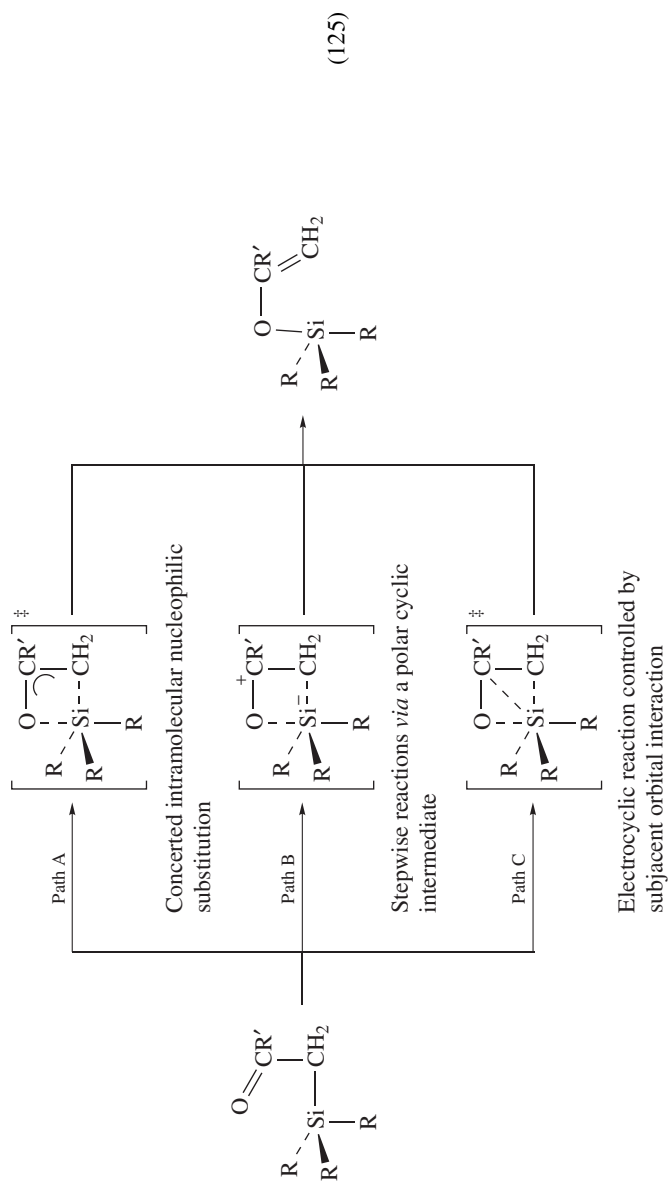
1,3-Silyl migrations in β -ketosilanes, β -silylcarboxylic acids, *N*-silylamides etc. are well known to occur in the presence and absence of catalysts¹. The first uncatalyzed thermal 1,3-silyl migration in silylmethyl ketones giving the corresponding siloxyalkenes was reported by Brook and coworkers in 1967³⁰⁷. However, the mechanisms of the 1,3-migrations were controversial³⁰⁸. Three pathways were taken into consideration. Brook and coworkers proposed a concerted four-center mechanism with synchronous Si–O bond making and Si–C bond breaking (path A in equation 125). The reasoning was the exclusive retention of configuration at silicon in the reaction products and the relatively insensitive substituent and solvent polarity effects on the migration rates³⁰⁹. Though the possibility of a fully associative mechanism involving the formation and pseudorotation of polar pentacoordinate silicon intermediates was addressed (path B in equation 125)³⁰⁹, it was ruled out^{298,308}. On the other hand, Kwart and Barnette³¹⁰ claimed that since the kinetic data reported by Brook and coworkers²⁹⁸ and others³⁰⁸ were accumulated at temperatures close to the isokinetic temperature, the substituent effects might not have meaningful mechanistic information. They concluded that path B in equation 125 was operating, on the basis of the solvent effects on the rates, the kinetic isotope effects³¹⁰ and the different stereochemical outcome between the 1,3-silyl migrations in allylsilanes^{297,302} and in silylmethyl ketones³⁰⁹. Recent theoretical results on the 1,3-silyl migration in allylsilane suggested that the migration in silylmethyl ketones proceeded via a concerted pathway controlled by a subjacent orbital interaction (path C in equation 125).

Two four-centered cyclic transition structures were found theoretically for the 1,3-silyl migration in formylmethylsilane **199** to form siloxyethene **200**, i.e. TS_{ret} and TS_{inv}, which led to retention and inversion products, respectively (equation 126). TS_{ret} and TS_{inv} had distorted SP and TBP structures, respectively, but the degree of distortion from the ideal TBP or SP was much larger than those in allylsilane. Pentacoordinate silicon *intermediates*, as suggested by Kwart and Barnette³¹⁰, were not found, indicative of the concerted nature of the migration. The activation energy for the retention pathway [$E_a(\text{ret}) = 32 \text{ kcal mol}^{-1}$ at MP2/6-311++G(3df,2p)+ZPE] was much lower than that for the inversion pathway [$E_a(\text{inv}) = 61 \text{ kcal mol}^{-1}$]; this clearly showed that the inversion pathway was unable to compete with the retention pathway, being in good accord with the experimental results.

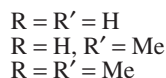
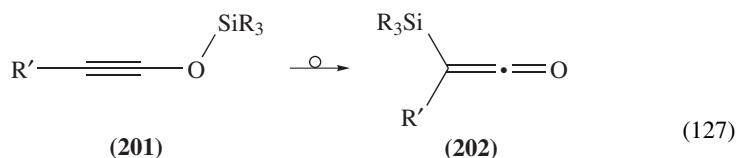
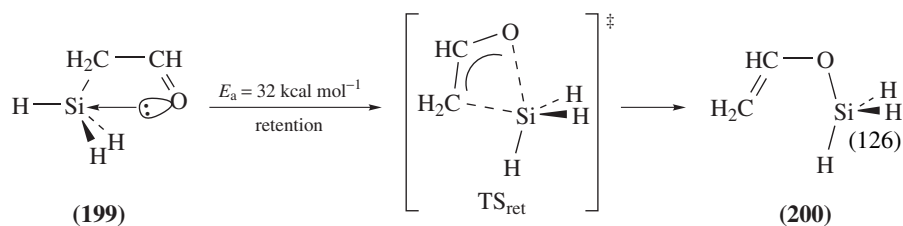
The 1,3-silyl migrations from silyloxyacetylenes **201** to silylketenes **202** were studied theoretically (equation 127)³¹¹.

4. Comparison of the retention transition states for 1,3-silyl migrations in allylsilane and formylmethylsilane

Theoretical calculations of the 1,3-silyl migrations in allylsilane and in formylmethylsilane indicated that both migrations proceeded concertedly via four-membered cyclic transition structures, preferably with retention of configuration at the migrating silicon atom. However, these theoretical results suggested also that the electronic and geometric properties of the retention transition structures in the two reactions were quite different in character, as indicated by the detailed analysis of the geometries, NBO and the Laplacian of the electron density. The retention transition state of 1,3-silyl migration in formylmethylsilane was characterized by significant distortion from an ideal square pyramidal structure around silicon, a relatively flat four-membered ring, a HOMO which

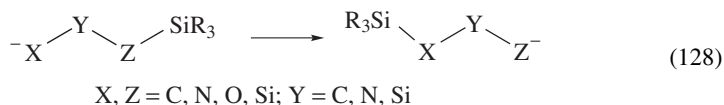


approximates the non-bonding MO of a pentacoordinate silicate and a ring critical point. On the other hand, the corresponding transition state for allylsilane had a near-square pyramidal structure, a seriously bent four-membered ring, a bond critical point between C² and Si and a HOMO which resembled the non-bonding MO of the allyl π system. The activation energy for formylmethylsilane was much lower than that for allylsilane. The 1,3-silyl migration with retention in formylmethylsilane was best described as an *intramolecular nucleophilic substitution at silicon*, while the corresponding migration in allylsilane was described as an *electrocyclic sigmatropic rearrangement controlled by subjacent orbital interactions*.

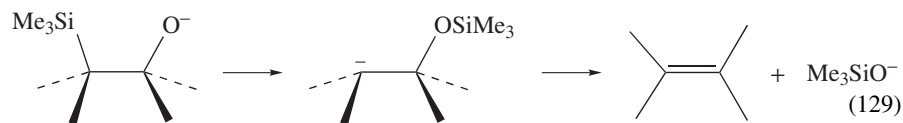


5. Anionic 1,3-silyl migrations across σ frameworks

Anionic 1,3-silyl migrations across σ frameworks with the general formula given in equation 128 are very common and are considered as intramolecular nucleophilic substitutions at silicon^{312–321}.

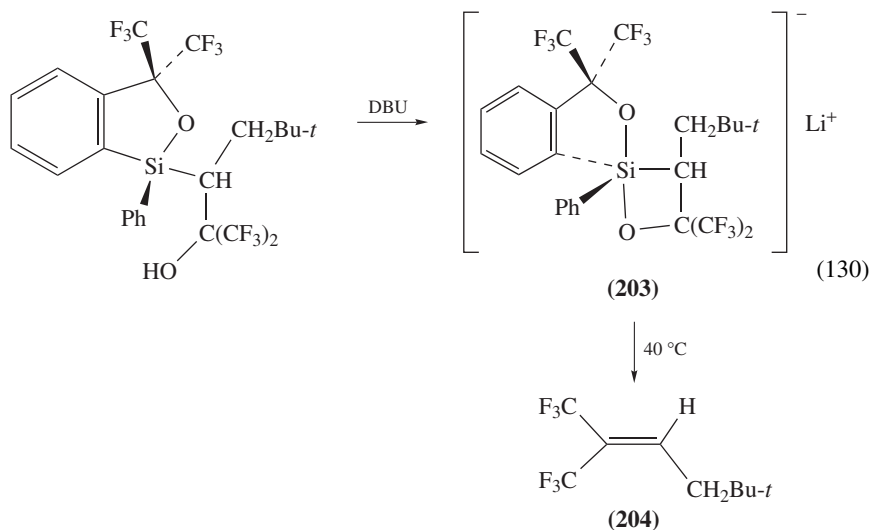


Among such migrations, the Peterson reactions to give olefins have been shown to proceed via intramolecular 1,3-silyl migrations from C to O (equation 129).

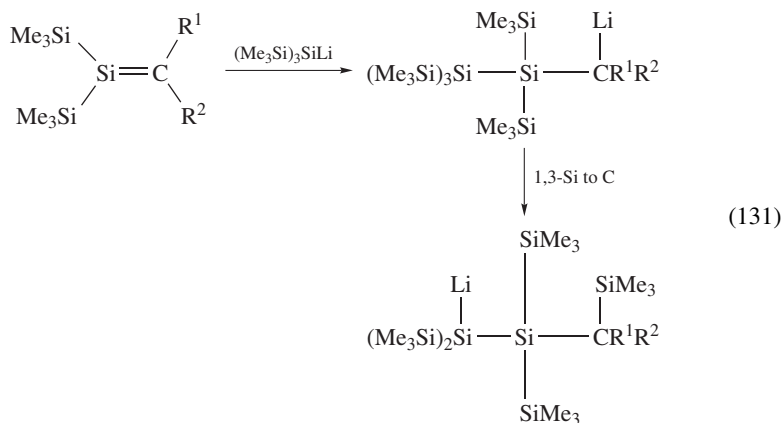


In this connection, it is interesting to note that a pentacoordinate siloxyethane **203** having a Martin ligand was isolated recently as a model for the intermediate of the Peterson

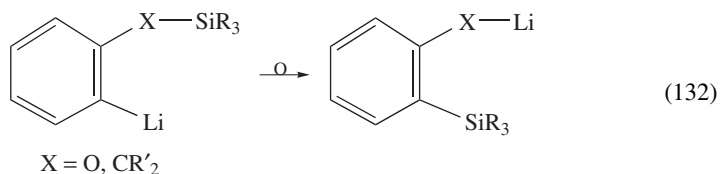
reactions (equation 130)³²²; **203** gave the corresponding alkene **204** upon heating.



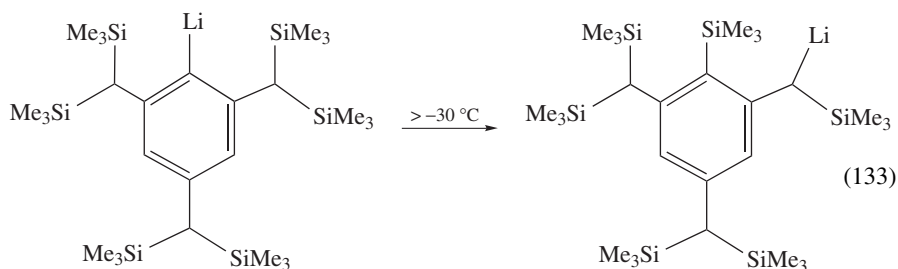
A 1,3-silyl migration from Si to C was reported by Oehme and coworkers (equation 131)³²¹.



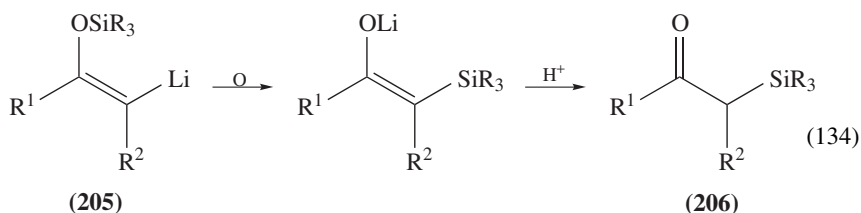
The type of 1,3-migration shown in equation 132 occurred at relatively low temperatures^{312,323–325}.



Rather exceptional examples of the anionic 1,3-silyl migrations from C to C were reported (equation 133)^{312,325}.

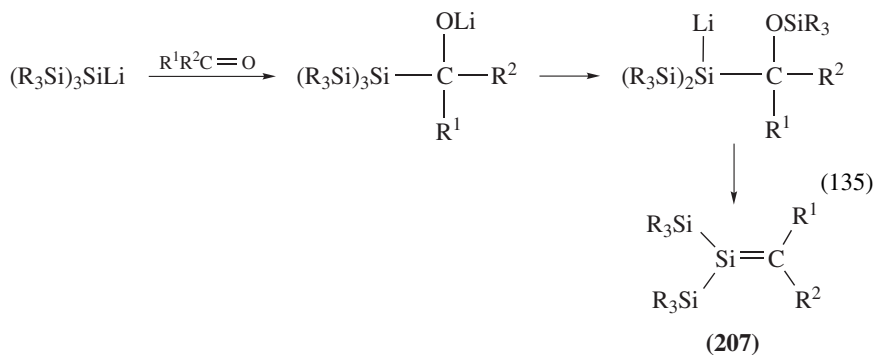


The 1,3-silyl migrations from O to C in lithiated silyl enol ethers **205** afforded α -silylcarbonyl compounds **206** after hydrolysis (equation 134)^{326–330}.



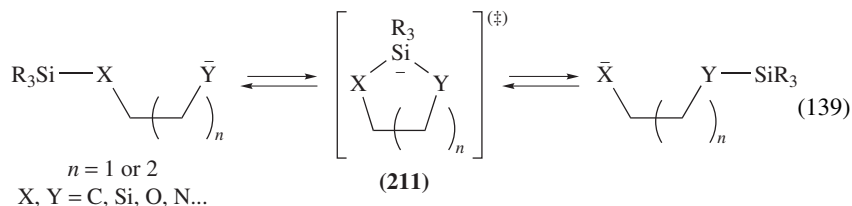
B. 1,3-Silyl Migrations in Unsaturated Silicon Compounds

Recently, Peterson-type reactions have been applied to the syntheses of transient and stable heavy element analogues of alkenes and alkynes. Transient and isolable silaethenes **207**³³¹ were prepared by the sila-Peterson reactions^{121,321,332–340}. Similarly to the original Peterson reactions^{341,342}, the sila-Peterson reactions were found to involve a 1,3-silyl migration from silicon to oxygen (equation 135)³²¹.



IV. 1,*N*-SILYL MIGRATIONS ($n \geq 4$)

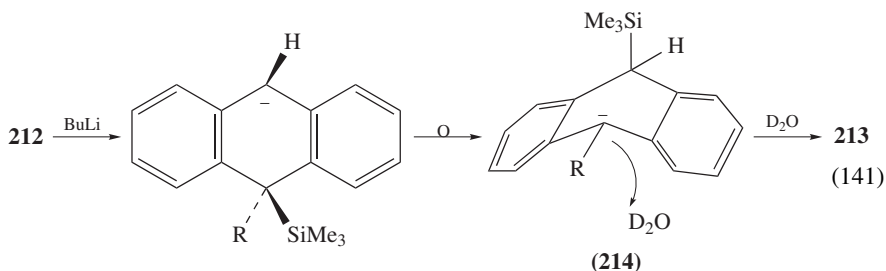
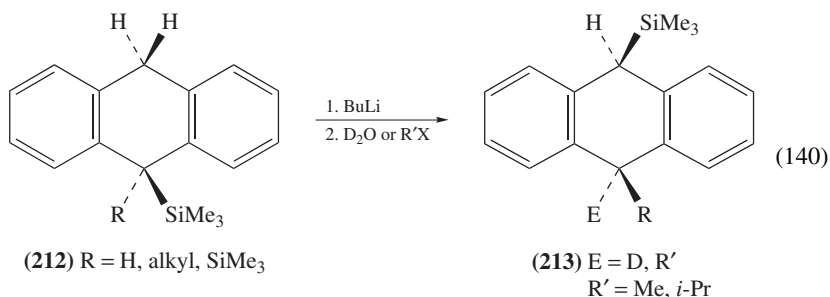
Most of the known 1,4- and 1,5-silyl migrations have been described as involving pentacoordinate silicon intermediates or transition states **211** via a facile nucleophilic attack of an intramolecular nucleophile at silicon (equation 139). Some of these reactions have been also applied to organic syntheses.



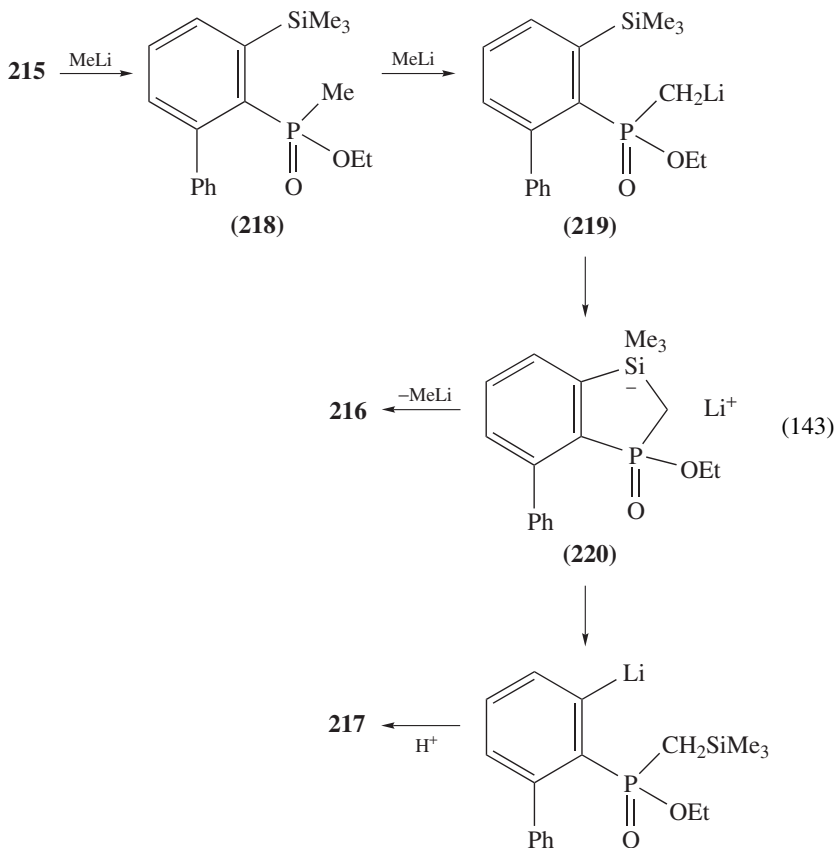
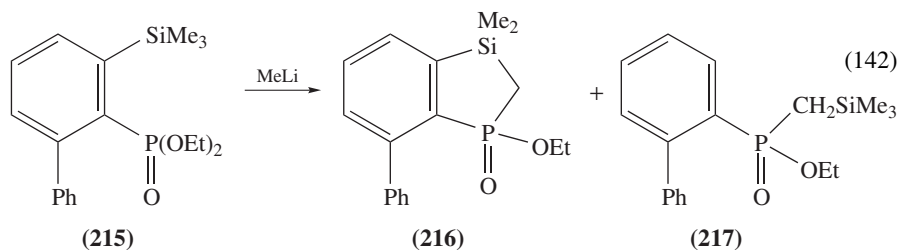
A. 1,4-Silyl Migrations

1. 1,4-Silyl migration from C to C

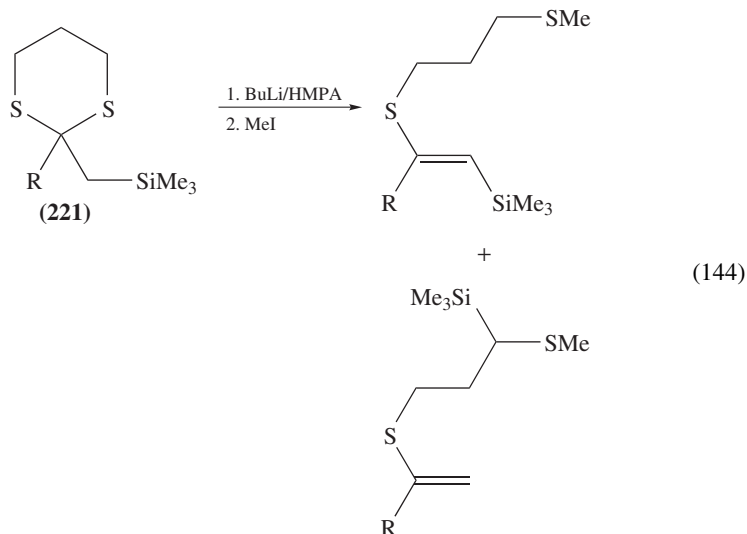
An anionic 1,4-silyl migration from C to C was observed during the lithiation of 9,10-dihydroanthracene (DHA) derivatives (equation 140)^{349–353}. Typically, treatment of DHA **212** (R=SiMe₃) with butyllithium followed by hydrolysis gave only *cis*-9,10-bis(trimethylsilyl)-DHA **213** (R=SiMe₃, E=H) stereospecifically. The crossover and deuterium labeling experiments confirmed the intramolecular and irreversible feature of the 1,4-silyl migration. The formation of *cis*-isomers of **213** suggested that the alkylation and protonation of **214** occurred at the bottom side of the folded DHA ring (equation 141). 1,4-Proton migration occurred competitively to some extent during the lithiation.



The reaction of diethyl 2-(3-trimethylsilyl)biphenylphosphonate **215** with excess methyllithium provided a mixture of **216** and **217** (equation 142). Deuterium labeling studies showed that the key intermediate was a pentacoordinate silicon species **220**, which was formed through the conversion of **215** to **218** and then to **219**. The cleavage of an exocyclic Si–C bond in **220** gave **216**, while a 1,4-silyl migration involving the cleavage of the endocyclic Si–C bond led to **217** (equation 143)³⁵³.

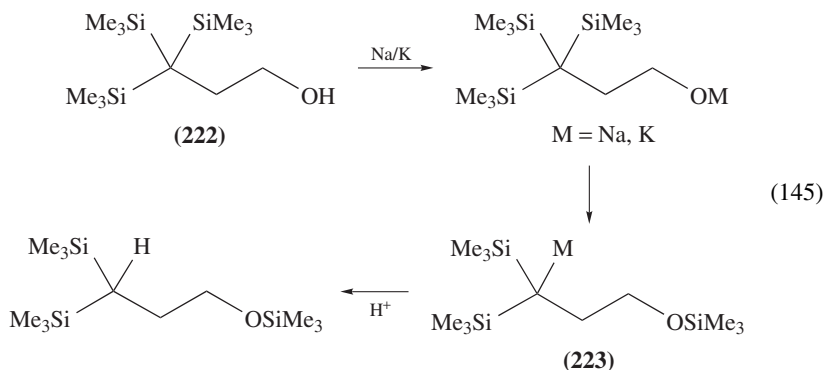


An anionic 1,4-migration from C to C was also observed during the lithiation of 2-trimethylsilyl-1,3-dithiane derivatives **221** (equation 144)³⁵⁴.

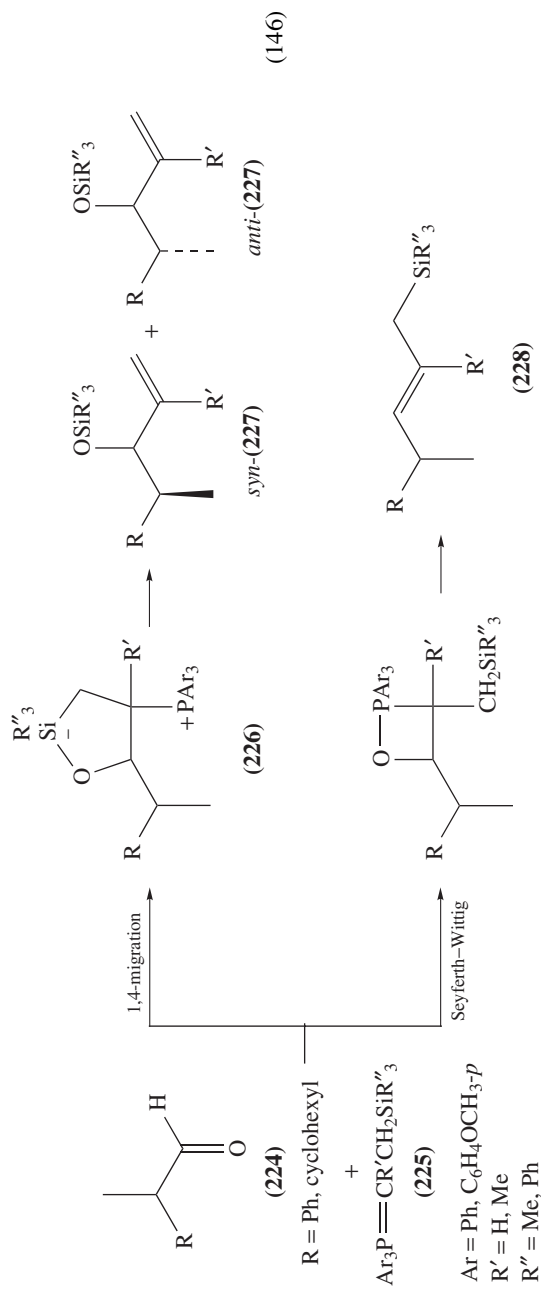


2. Anionic 1,4-silyl migrations from C to O

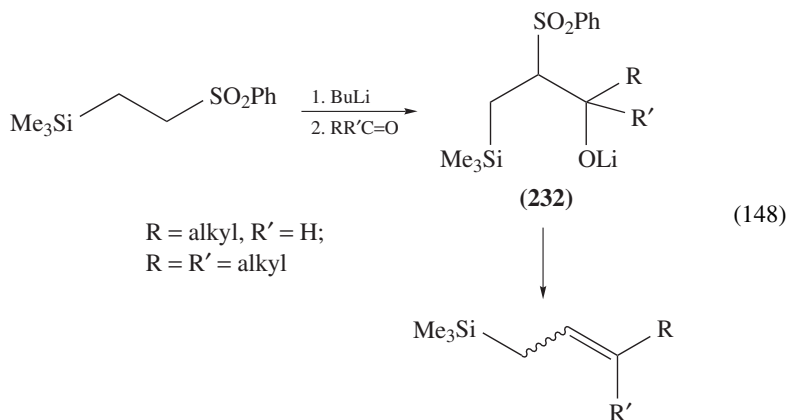
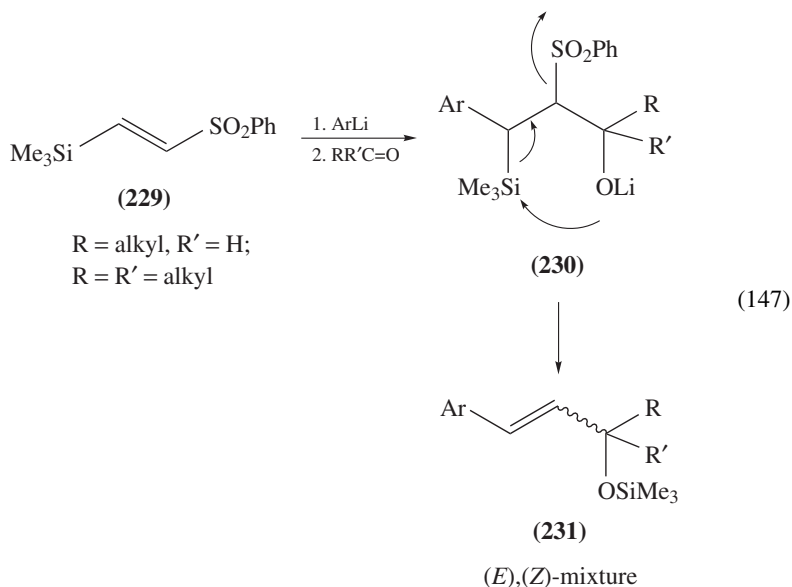
1,4-Silyl migrations from C to O are often termed 1,4-Brook rearrangements. This type of migration was found during the reactions of γ -silyl alcohols **222** with strong bases which give the corresponding γ -silyloxycarbanions **223** (equation 145)^{355,356}.



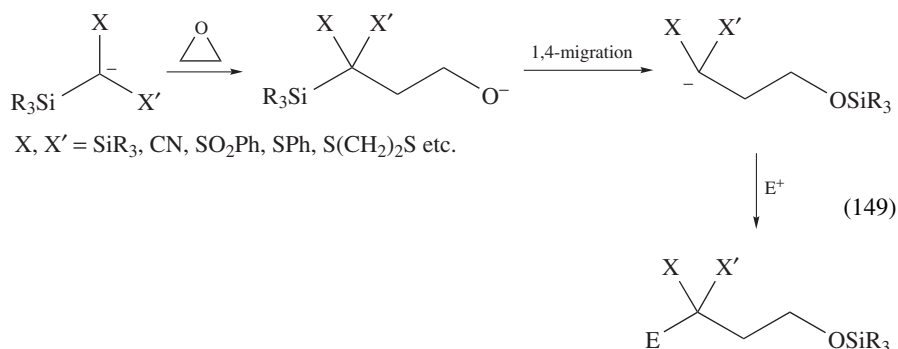
Tokoroyama and coworkers found that the reactions of α -methylaldehydes **224** with 2-(trimethylsilylethylidene)triarylphosphoranes (Seyferth–Wittig reagent³⁵⁷) **225** afforded allyloxysilanes **227** in moderate yields with *syn*-diastereoselectivity together with regular Wittig products **228** (equation 146). Allyloxysilanes **227** were suggested to be formed from the eliminative 1,4-silyl migrations of pentacoordinate silicon intermediates **226**. Electron-donating substituents on the phosphorane phenyl groups and electron-withdrawing groups on the silicon stabilized the intermediates **226** with a consequent increase in the ratio of **227** to **228**^{358,359}.



A 1 : 1 mixture of (*E*)- and (*Z*)-allyloxysilanes **231** was prepared by the reactions of (*E*)-trimethylsilylvinyl sulfone **229** with aryllithiums followed by the addition of aliphatic aldehydes and cyclohexanone (equation 147). An anionic 1,4-silyl migration from C to O in the lithium alkoxide **230** was proposed to be involved. On the other hand, lithium alkoxide **232** lacking an aryl group was stable and gave no rearranged product even at room temperature (equation 148)³⁶⁰.

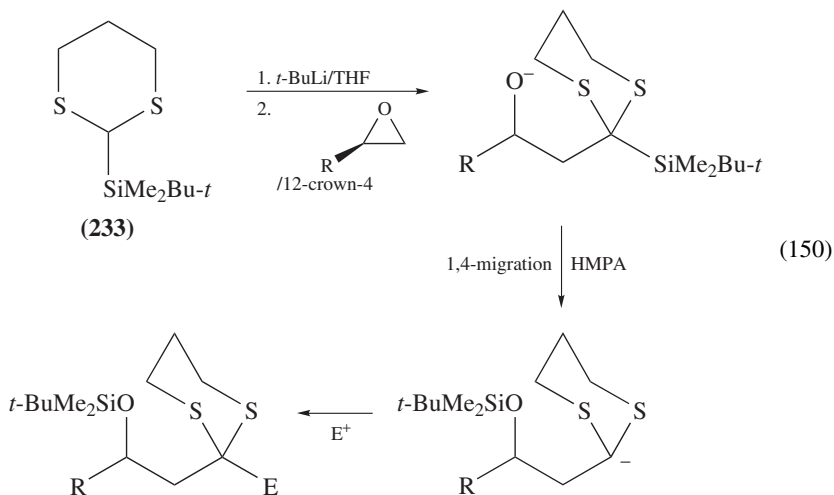


Silyl-substituted carbanions stabilized by heteroatom substituents reacted with epoxides providing the corresponding 3-siloxy carbanions via the anionic 1,4-silyl migrations, which reacted with various electrophiles (equation 149)^{361–370}.

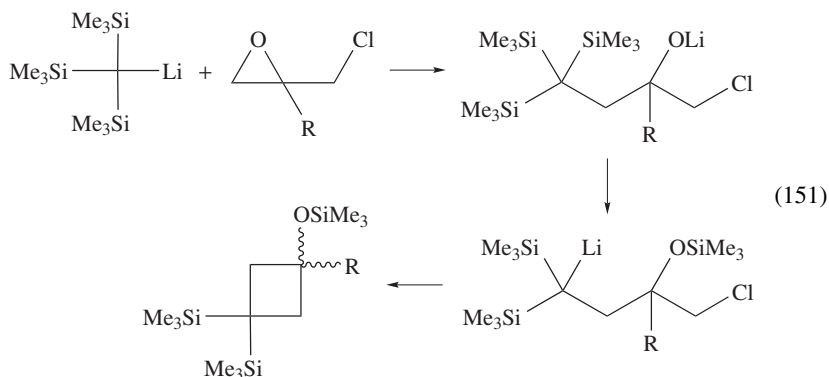


Electrophile (E⁺) = H⁺, aldehyde, oxirane

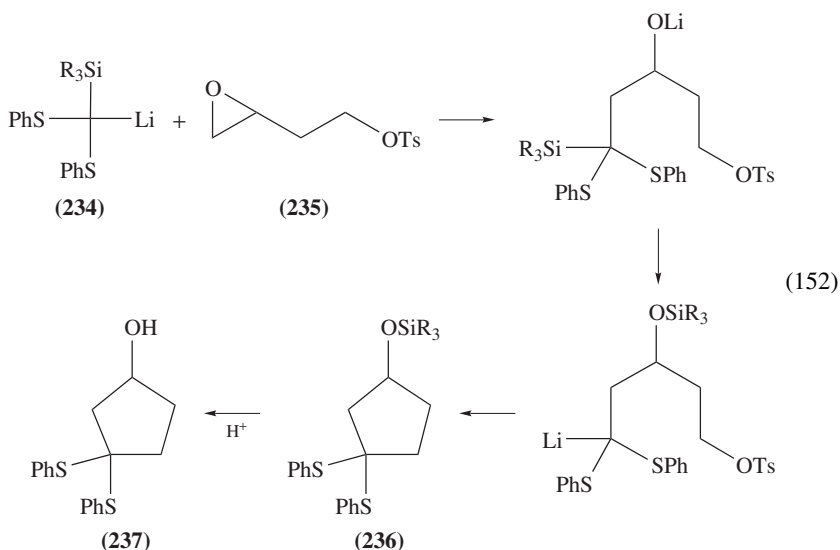
Tietze and coworkers found a symmetrical bisalkylation of a silyl dithiane with 2 equivalents of an epoxide involving 1,4-silyl migrations³⁶⁹. Smith and Boldi applied the method to the unsymmetrical bisalkylation of silyldithiane **233** (equation 150)³⁶⁸.



Takeda and coworkers showed that the reaction of a silylmethyl lithium with a halo-methyloxirane gave the corresponding cyclobutane derivatives via a 1,4-silyl migration of the initial lithium alkoxide followed by an intramolecular nucleophilic substitution of the resulting carbanion (equation 151)³⁷⁰.

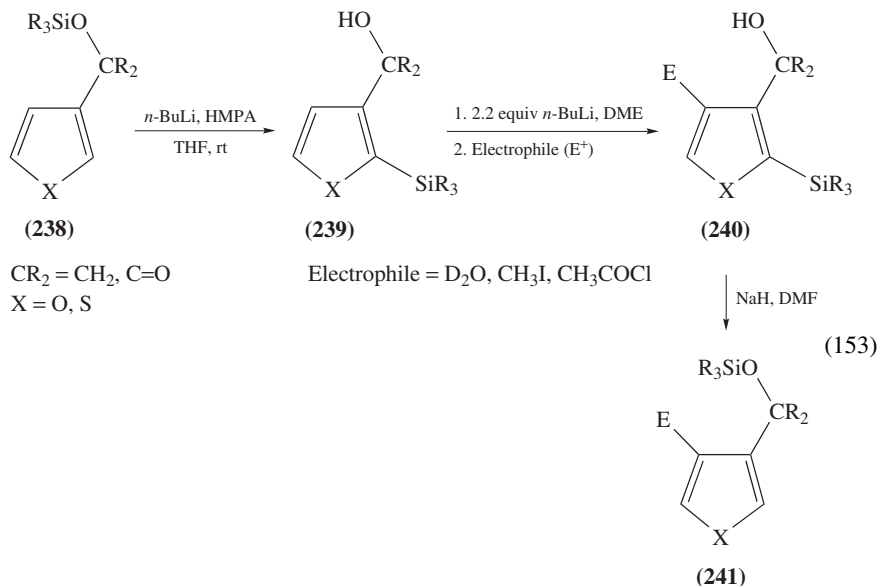


The reactions of silylmethylolithiums **234** with epoxy *p*-toluenesulfonates **235** gave siloxycyclopentanes **236**. These were hydrolyzed to the corresponding cyclopentanol **237** (equation 152)³⁷¹.

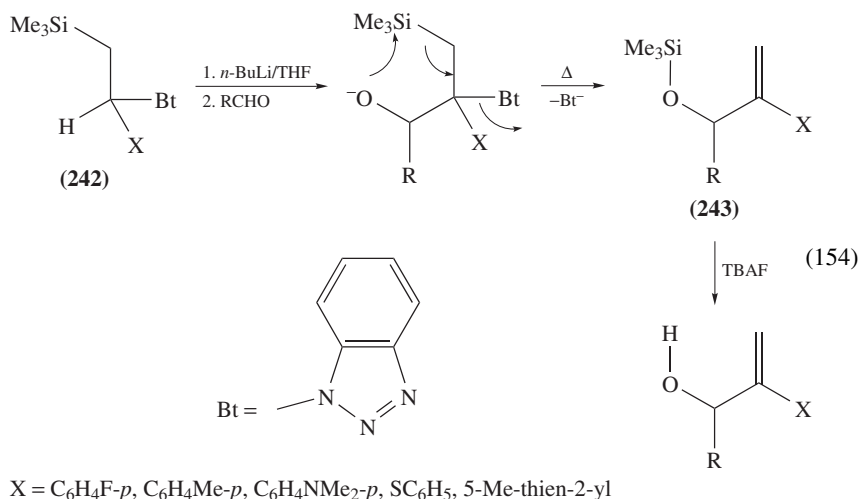


Reversible 1,4-silyl migrations between C and O were effectively applied to the regioselective syntheses of 2,3- and 3,4-disubstituted and 2,3,4-trisubstituted furan and thiophene rings by Key and coworkers^{372–383} and by Danso-Danquah and Scott³⁸⁴. Typically, the reactions of 3-(silyloxymethyl)furans and-thiophenes **238** with *n*-BuLi in HMPA and THF provided 2-silyl-3-(hydroxymethyl)furans and-thiophenes **239** in good to excellent yields (equation 153). Similarly, the reaction of silyl esters of 2-furoic acids (**238**, CR₂ = CO) with a mixture of LDA and HMPA gave the corresponding 2-silyl-3-furoic acids in moderate yields. Regiospecific C-4 lithiations of **239** were performed using 2.2 equiv of BuLi in DME. Quenching the anions with a variety of electrophiles E⁺ provided 2,3,4-trisubstituted furans and thiophenes **240**. Finally, the reactions of **240** with NaH in DMF gave the corresponding 3,4-disubstituted furans and thiophenes **241** in excellent yields via the 1,4-silyl

migration from C to O. This procedure provides a successful route to 3,4-disubstituted furans and thiophenes, which are otherwise difficult to be synthesized.

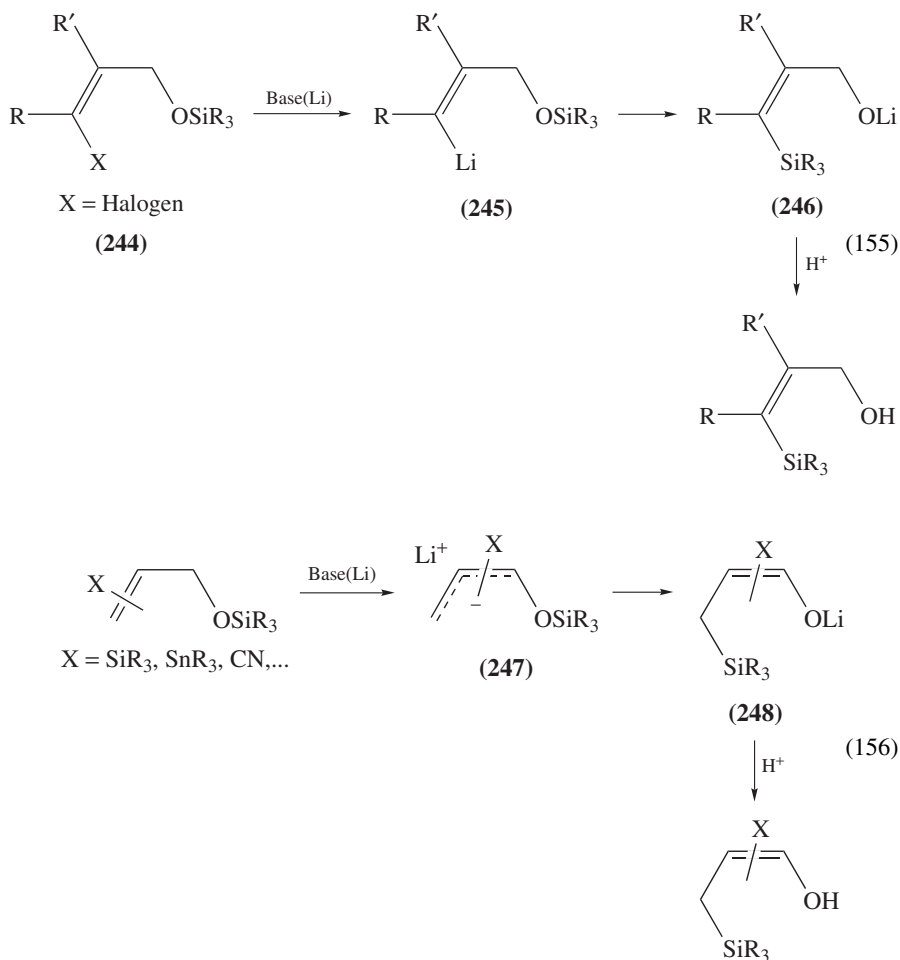


The carbanions derived from (2-(benzotriazol-1-yl)-2-substituted-ethyl)trimethylsilanes having an acidic β -proton **242** reacted with non-enolizable aldehydes to afford the corresponding (1-aryllkenyl)siloxymethanes **243** via the 1,4-silyl migration with the elimination of benzotriazol-1-yl group (equation 154)^{385,386}. Compounds **242** serve as the synthetic equivalents of α -X-substituted alkenyllithiums.



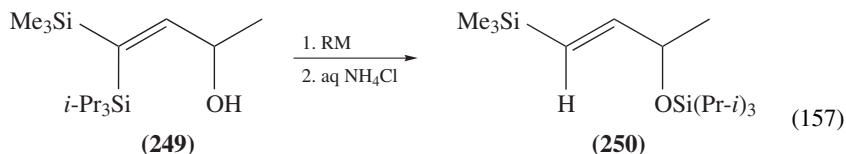
3. Anionic 1,4-silyl migrations from O to C

Anionic 1,4-silyl migrations from O to C were found to occur in the reactions of γ -siloxy carbanions (equations 155 and 156). Typically, γ -siloxyvinylolithiums **245** generated from 3-haloallyl silyl ethers **244** underwent anionic 1,4-silyl migrations to give (Z)-3-silylallyloxyolithiums **246** (equation 155)^{387–389}. Preferential formation of (Z)-isomers was suggested to be a result of intramolecular O–Li complexation in the vinylolithiums. *o*-(α -Siloxyalkyl)phenyllithium^{390,391} and *o*- and *m*-(trialkylsiloxy)benzamide³⁹² underwent the same type of migration. Similar 1,4-migrations in γ -siloxyallyloxyolithiums **247** with anion stabilizing substituents X led to the corresponding vinyloxyanions **248** (equation 156)^{393,394}.



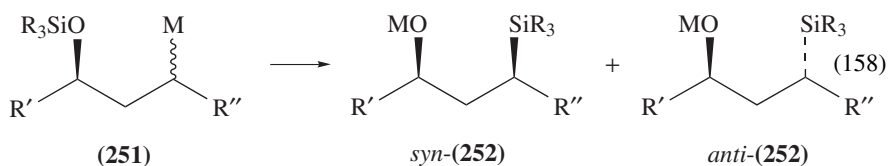
The driving force for this migration was proposed to be the more favorable formation of a covalent O–Li (hard–hard) bond than that of a C–Li (soft–hard) bond^{389,395}.

When softer counter cations such as sodium and potassium ions were used instead of the lithium ion, a reversal of the migration was found. The reaction of **249** in the presence of a catalytic amount of NaH in DMF followed by hydrolysis gave **250** in excellent yield (equation 157), while the reaction of **249** with 0.2 equiv of MeLi in THF did not result in any detectable amount of silyl ether **250** even after a prolonged reaction time.

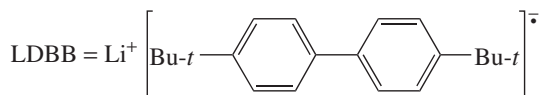
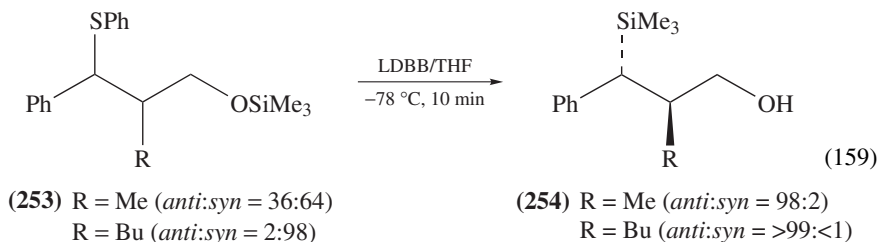


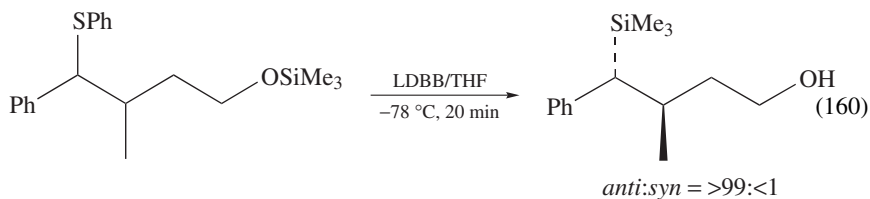
90% (RM = NaH (0.1 equiv)/DMF)
0% (RM = MeLi (0.2 equiv)/THF)

γ -Siloxy carbanions **251** easily underwent a retro 1,4-Brook rearrangement to afford mixtures of *syn*- and *anti*- γ -silyl alkoxides **252** (equation 158). The *syn/anti* ratios of the products were quite dependent on the substituents and the reaction conditions, e.g. for $\text{R}_3\text{Si} = \text{Ph}_3\text{Si}$ and $\text{R}'' = \text{trimethylsilylethynyl}$, *syn/anti* = 19/81 ($\text{R}' = \text{Me}$), 36/64 ($\text{R} = n\text{-Bu}$), 43/57 ($\text{R} = \text{Pr}$) and 87/13 ($\text{R} = t\text{-Bu}$)^{396–408}.

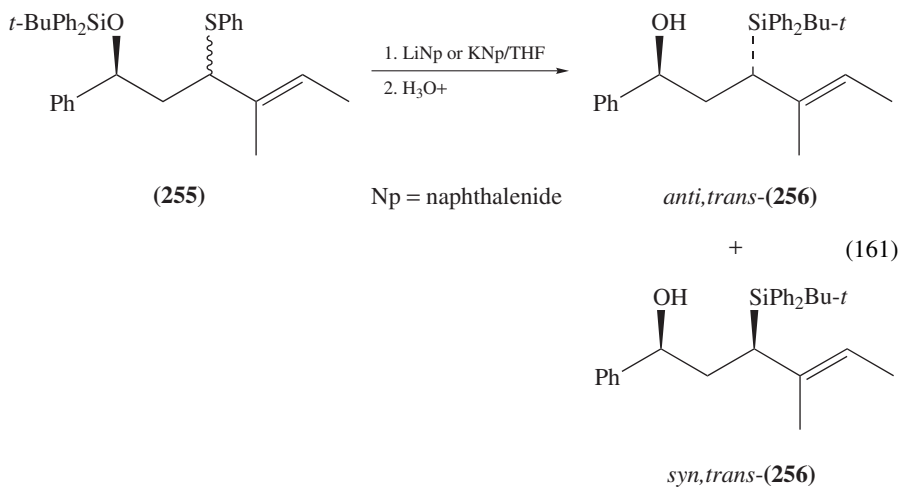


When an appropriate group substituted the carbon next to a carbanionic center, the silyl migration proceeded with high *anti* selectivity^{396–398}. The reactions of silyl ethers **253** with lithium di-*t*-butylbiphenylide (LDBB) afforded the corresponding 3-silylated alkanols **254** with high *anti* selectivity (equation 159). The reactions were applied to the regio- and stereo-defined synthesis of various acyclic and cyclic allylsilanes. Similar high diastereoselectivity was observed in a retro 1,5-Brook rearrangement (equation 160)^{397,399}.

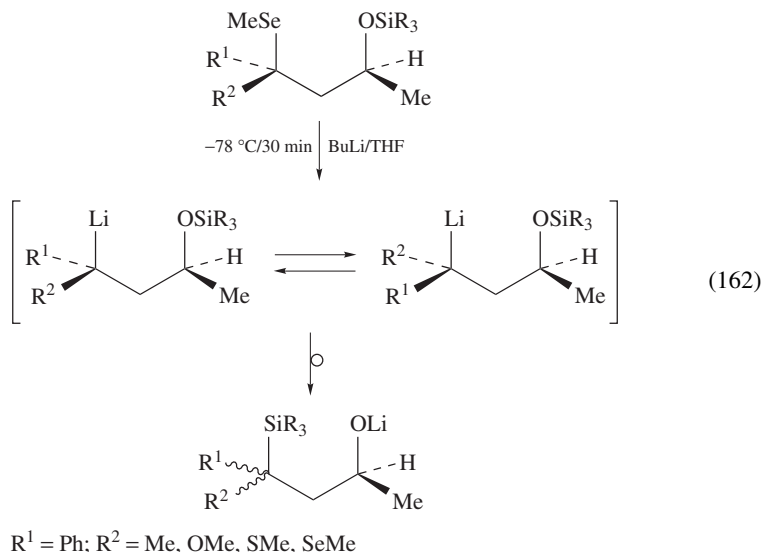




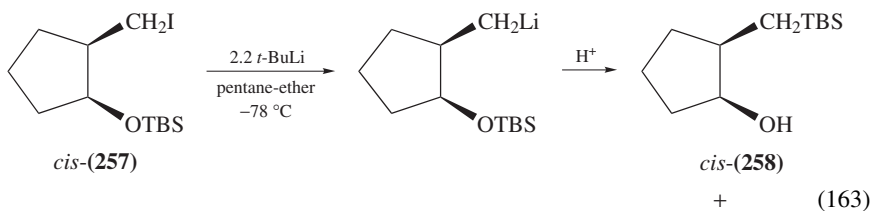
The *syn/anti* selectivity in the retro 1,4-Brook rearrangement was dependent on the counter alkali metal cations of the γ -siloxy carbanions^{400,401}. The reaction of tiglyl phenyl sulfide **255** with lithium naphthalenide gave a tiglyl lithium species, which underwent an irreversible retro 1,4-Brook rearrangement giving a 22 : 78 mixture of the *anti,trans* and the *syn,trans* diastereomers of tiglyl silane **256** after hydrolysis (equation 161). However, the reaction of the same sulfide with potassium naphthalenide provided the same product mixture but with the *anti,trans* to *syn,trans* ratio of 96 : 4⁴⁰⁰.



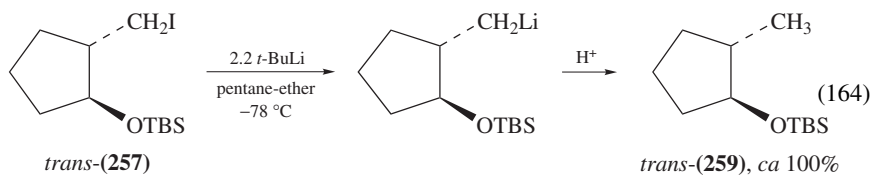
The *syn/anti* selectivity mentioned above was also dependent on the substituents at the migrating silicon atoms^{402–404} and at the carbon atoms connecting the siloxy groups⁴⁰⁵. While very high diastereoselectivities were obtained in the syntheses of crotylsilanes^{403,406} and allylsilanes⁴⁰⁴, retention of configuration at the carbanion center was observed in some cases⁴⁰⁷. The reason for the selectivity of the retro 1,4-Brook rearrangement still remains open. The selectivities, i.e. the configuration at the carbon connected to the migrating silicon, would depend to some extent on whether the precursor γ -siloxy carbanion is configurationally stable or not within the time scale of the retro 1,4-Brook rearrangement. If the carbanion involves configurationally unstable C–Li bonds, epimerization (or enantiomerization) at the Li-bearing stereocenter of the precursor is kinetically possible before the silyl group migrates⁴⁰³. Indeed, during the retro 1,4-Brook rearrangement of a γ -siloxy benzyl anion, epimerization of the benzyl anion took place (equation 162)⁴⁰⁸.



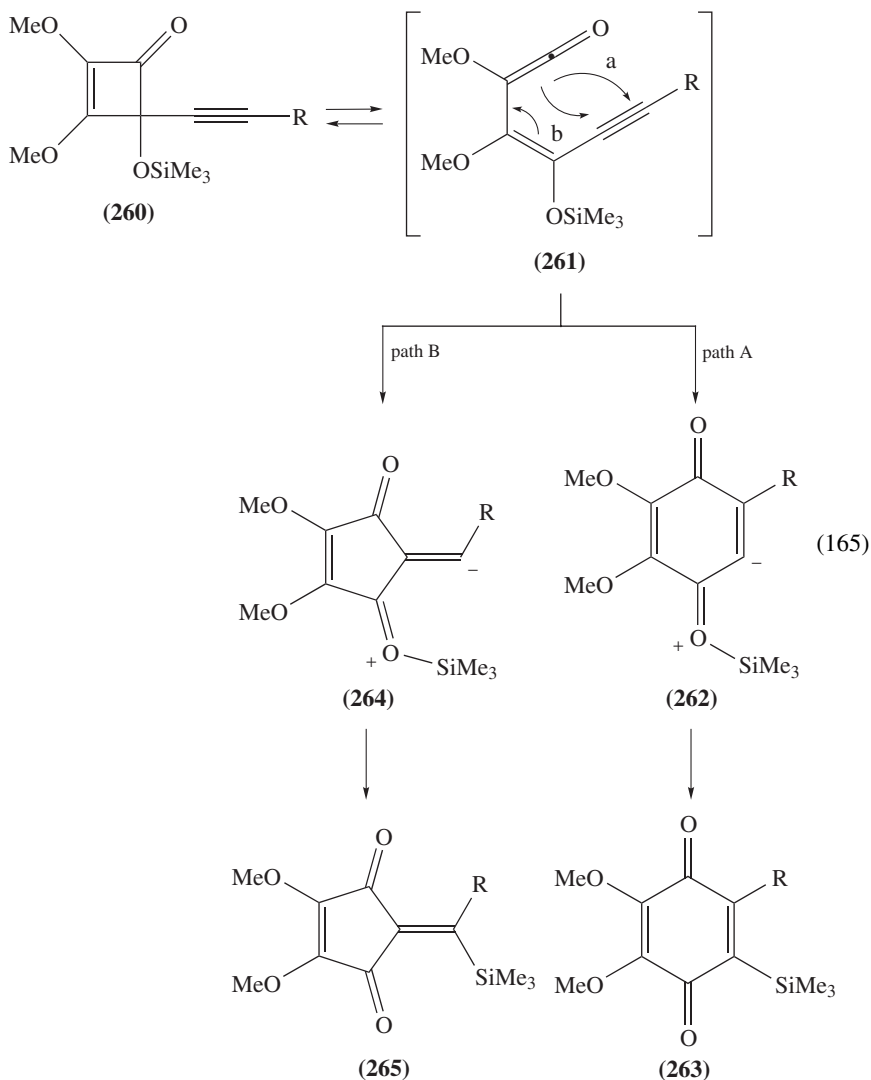
The retro 1,4-Brook rearrangement in cyclic systems was unfavorable when the pertinent siloxy groups were in an *anti* position to the carbanion centers (equations 163 and 164). When a 2 : 1 mixture of *cis*- and *trans*-**257** was treated with *t*-BuLi at $-78\text{ }^\circ\text{C}$ and then warmed, and stood at $+20\text{ }^\circ\text{C}$ for 1 h followed by hydrolysis, *trans*-**257** was completely transformed to *trans*-**259**, while 85% of *cis*-**257** was converted to *cis*-**258**, indicating that the 1,4-silyl migration was confined to *cis*-**257**⁴⁰⁹. In some other cyclic systems, a retro 1,4-Brook rearrangement was observed even in the *anti* isomers⁴¹⁰.

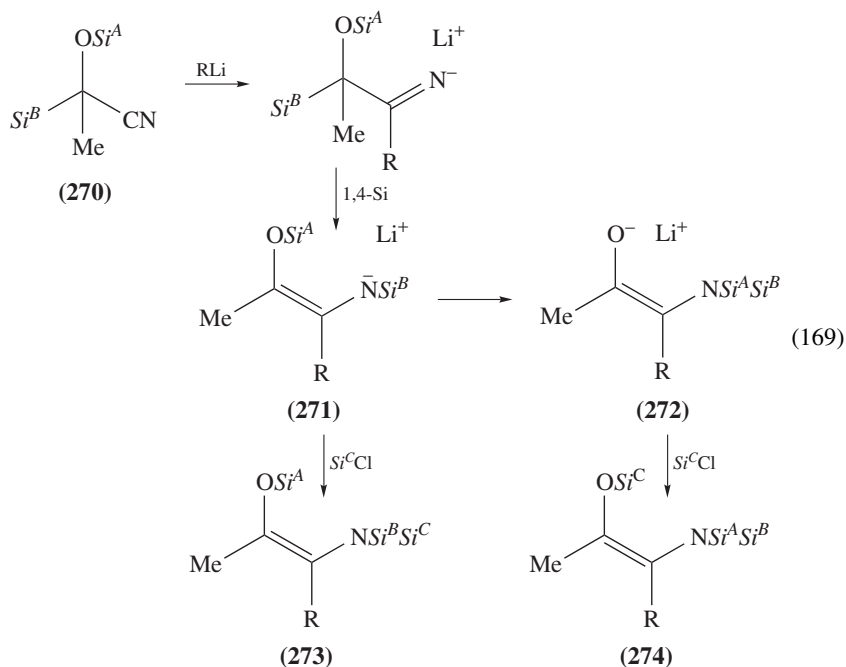


TBS = *t*-BuMe₂Si



(2-Siloxyalkynenyl)ketenes **261** generated by the thermolysis of the corresponding 4-alkynyl-4-siloxy-2-cyclobutenones **260** underwent ring closures to zwitterions **262** and **264**, which provided **263** through the 1,3-silyl migration and **265** through the 1,4-migration, respectively (equation 165). The quinone formation (path A) was favored by electron-donating R groups (Bu, benzyl, $\text{CH}_2\text{OSiMe}_3$), while the formation of cyclopentadienone (path B) was favored by electron-withdrawing R groups (Ph, CO_2Et)⁴¹¹.

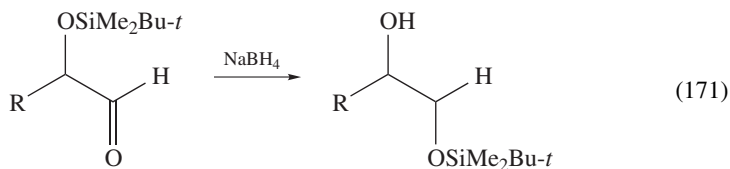
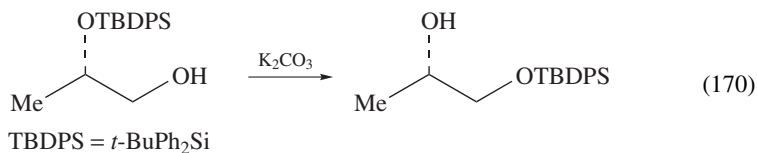


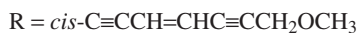
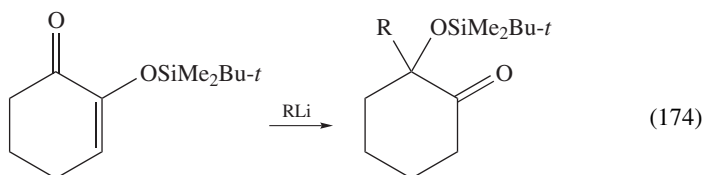
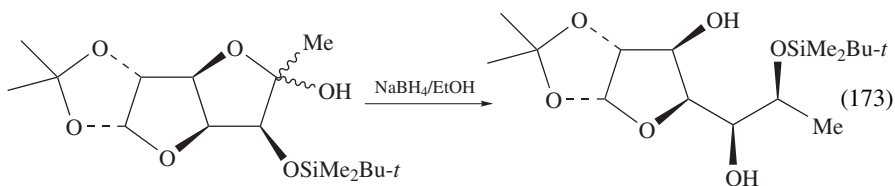
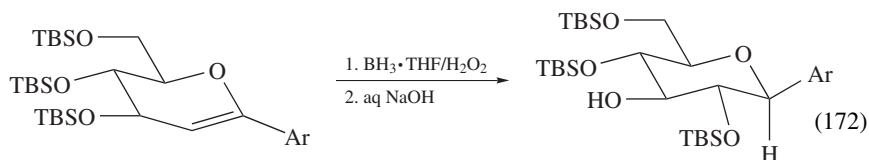


1,4-Silyl migrations from O to C were also found during the synthesis of α -halomethylsilanes⁴¹⁵ and diastereoselective preparations of (*Z*)-vinyl-, epoxy- and cyclopropylsilanes^{389,416}.

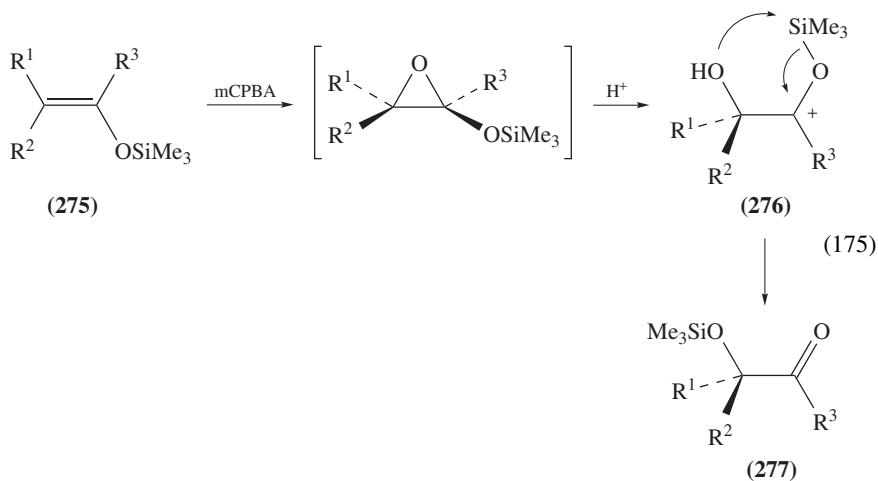
4. Anionic 1,4-silyl migrations from O to O

A number of anionic 1,4-silyl migrations from O to O have been reported: the reaction of mono-silylated diols^{417–420} and polyols^{421–427} (equation 170), the reduction of α -siloxyketones (equation 171)^{428,429}, the hydroboration of C-arylglucals (equation 172)⁴³⁰, the highly stereoselective reduction of silylated lactols (equation 173)^{431,432}, the addition of acetylides to 2-*t*-butyldimethylsilyloxycyclohexenone (equation 174)⁴³³ and the facile exchange of tropolonate ligands on the hexacoordinate organosilicon compounds⁴³⁴.

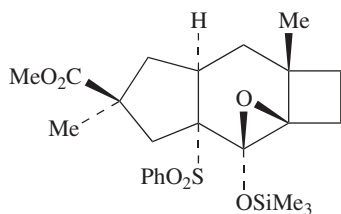




The reaction of silyl enol ether **275** with mCPBA gave α -siloxyketones **277** through oxycarbenocations **276** (equation 175)¹. Paquette and coworkers isolated siloxyepoxide **278** as the initial product in the mCPBA oxidation of a silyl enol ether and determined the structure by X-ray structural analysis⁴³⁵.

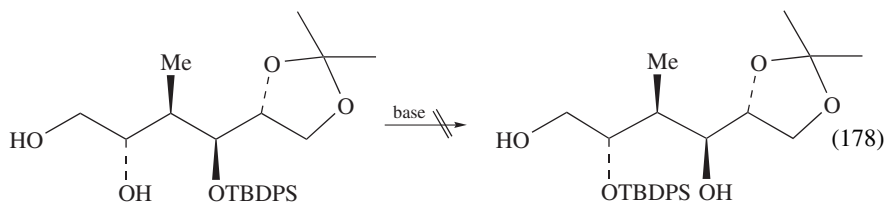
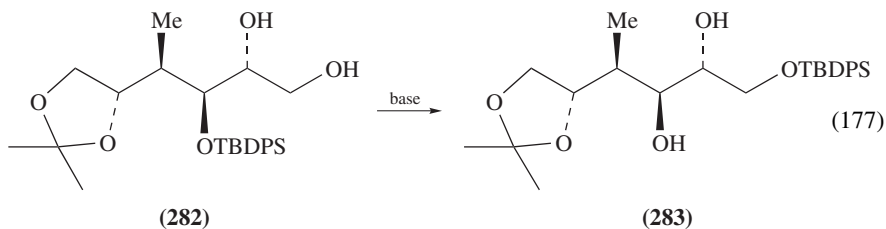
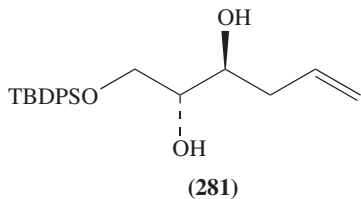
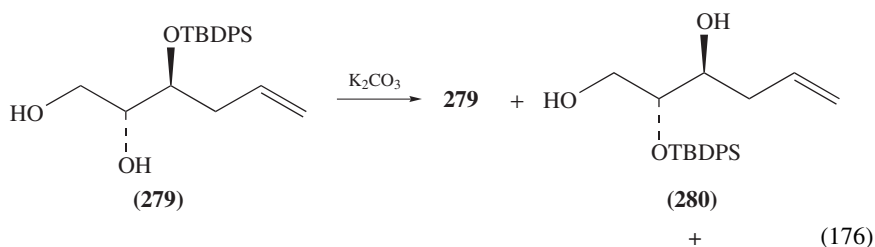


Mulzer and Schöllhorn showed that the reaction of triol monosilyl ether **279** with potassium carbonate gave a 6 : 7 : 87 mixture of **279**, **280** and **281** at equilibrium (equation 176), indicating that the terminal primary position was favored as the location of the *t*-butyldiphenylsilyl (TBDPS) group. Similarly, **282** afforded **283** as a major migration



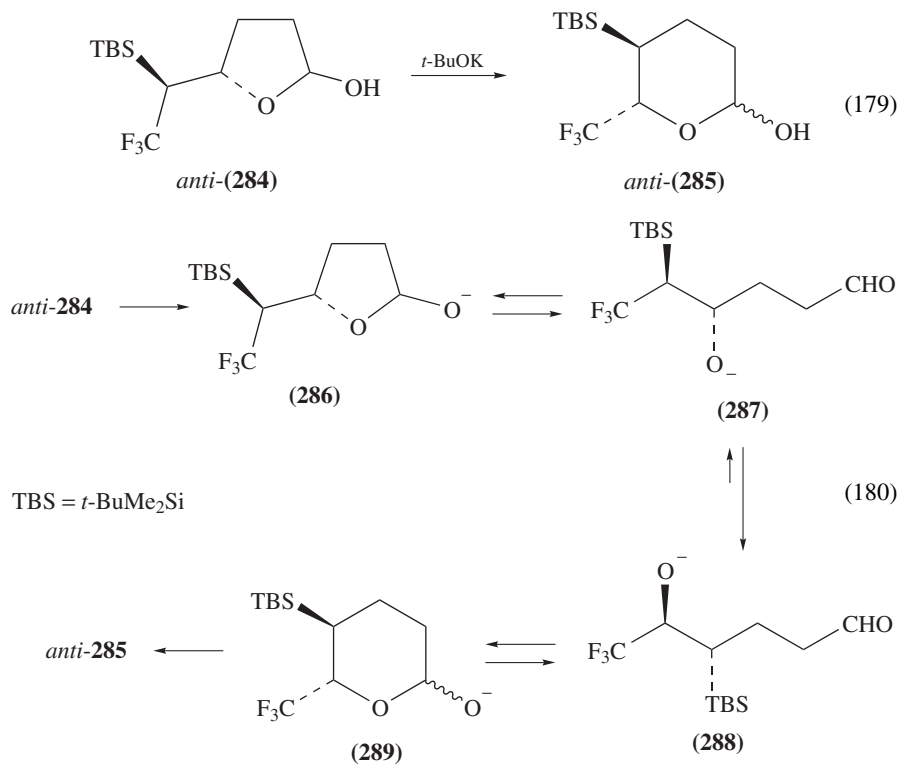
(278)

product (equation 177). In contrast, if there was a methyl branch between the TBDPS-substituted oxygen and an OH group, the migration in the direction of this branch was prevented (equations 178), indicative of the intramolecular nature of the 1,4-migration⁴²¹.

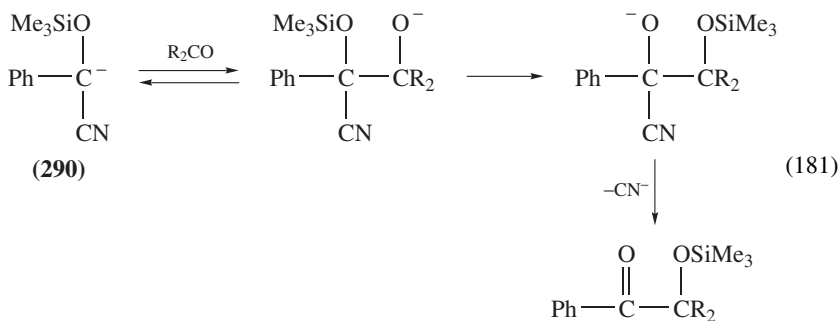


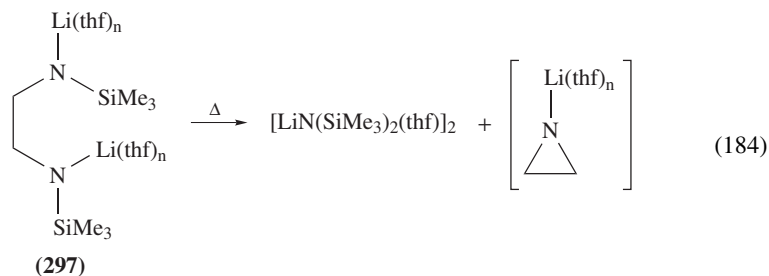
Yamazaki, Kitazume and coworkers developed an expedient route to obtain optically active 6-deoxy-6,6,6-trifluorosugars (*anti*-285) from *anti*-284 via a 1,4-silyl migration

from O to O (equation 179)^{436–439}. In the proposed mechanism, cyclic alkoxide **286** derived from *anti*-**284** is in equilibrium with **287**, **288** and **289** (equation 180), where the driving force for the formation of **289** is electronic stabilization of the oxyanion **288** by the CF₃ group and destabilization of **287** due to the steric repulsion between the TBS and CF₃ groups. The substituent effect of the CF₃ group on the equilibrium of equation **180** was supported by theoretical calculations on model compounds⁴³⁶.

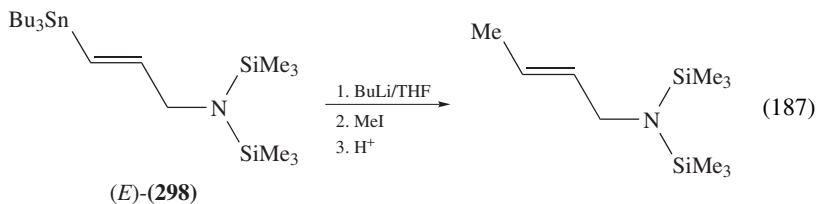
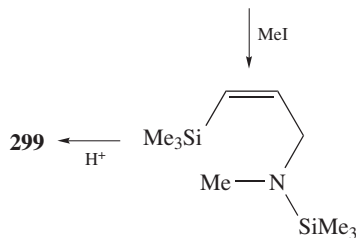
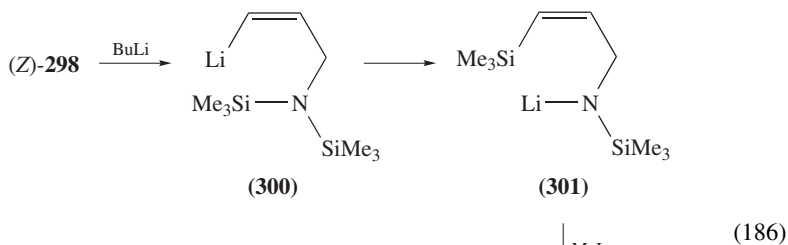
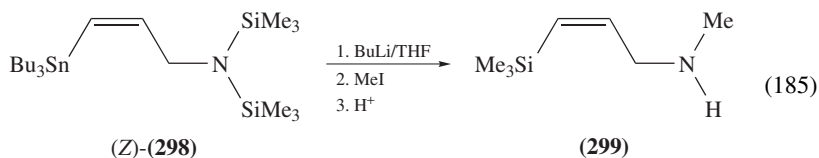


Hünig and coworkers found that carbanion **290** which is derived from *O*-trimethylsilyl-cyanohydrin reacted with carbonyl compounds to afford the corresponding α -siloxyketones through a 1,4-silyl migration (equation 181)^{440–442}.

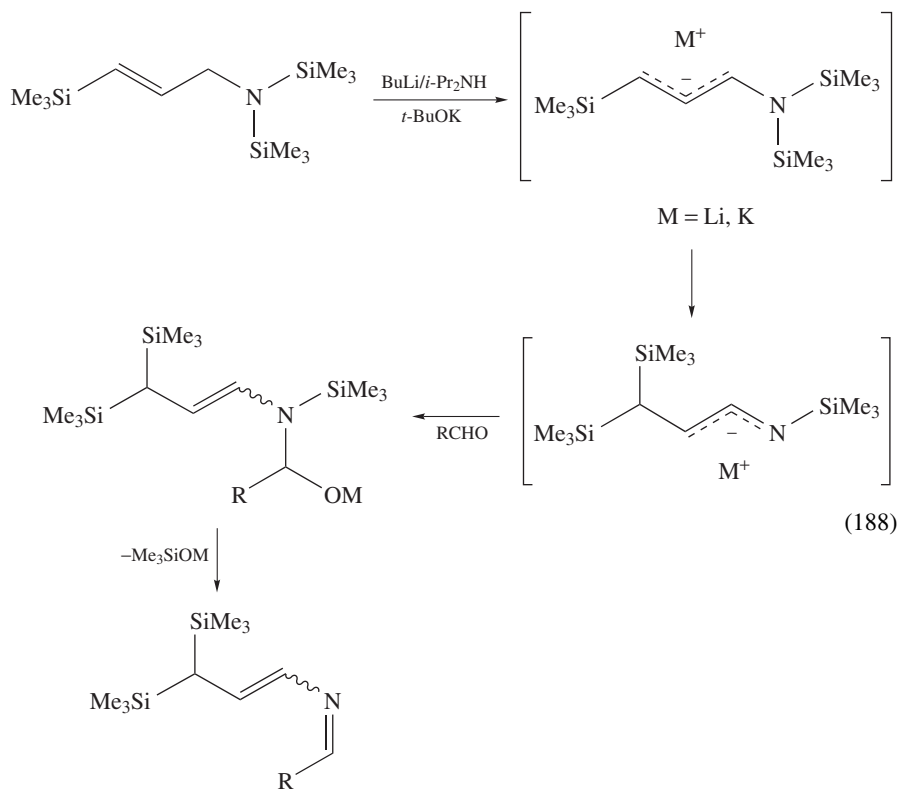




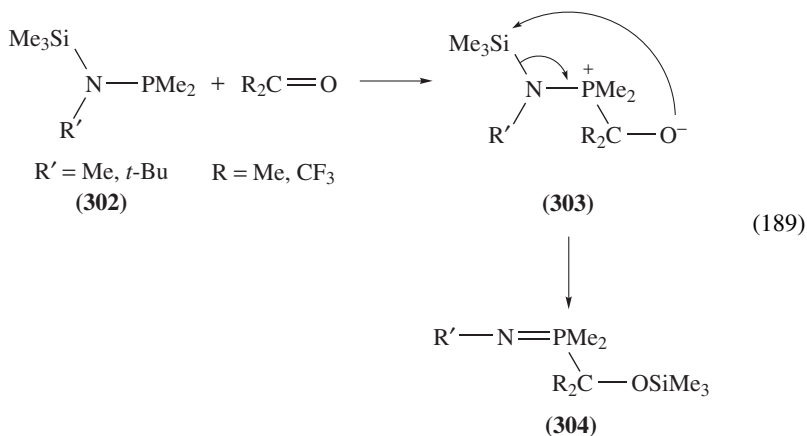
Corriu and coworkers found that the reaction of (*Z*)- γ -*N,N*-bis(trimethylsilyl)amino-1-propenylstannane **298** with butyllithium, followed by quenching with methyl iodide and then hydrolysis, provided 3-methylamino-1-propenylsilane **299** in high yield (equation 185)⁴⁴⁶, suggesting an anionic 1,4-silyl migration from N to C in the (*Z*)-vinylolithium **300** to give **301** (equation 186). The transmetalation of the (*E*)-isomer of **298** gave no silyl migration products (equation 187)⁴⁴⁷.

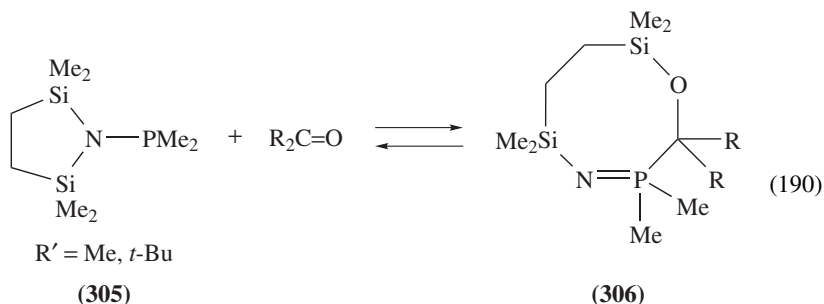


Degl'Innocenti and coworkers showed a similar migration that occurred in an *N*-silylated aminoallyl anion (equation 188)⁴⁴⁸.



Silylaminophosphines **302** reacted smoothly with carbonyl compounds to give *O*-silylphosphinimine **304** via a 1,4-silyl migration from N to O in the initial zwitterionic adduct **303** (equations 189 and 190)^{449,450}. Upon heating, the cyclic phosphinimines **306** in equation 190 decomposed cleanly to the starting materials **305**⁴⁵⁰.





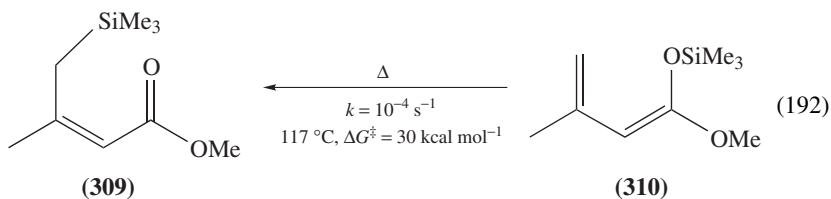
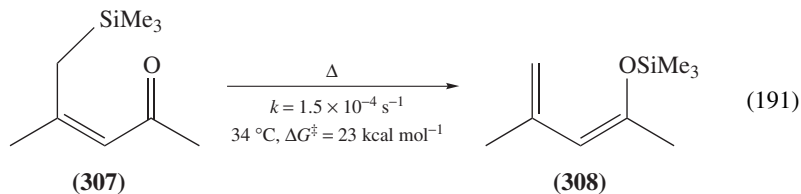
Anionic 1,4-silyl migrations from N to O were also observed in the Dieckman reactions⁴⁵¹ and in debenzoylations⁴⁵².

B. 1,5-Silyl Migrations

1. 1,5-Silyl migrations between C and O

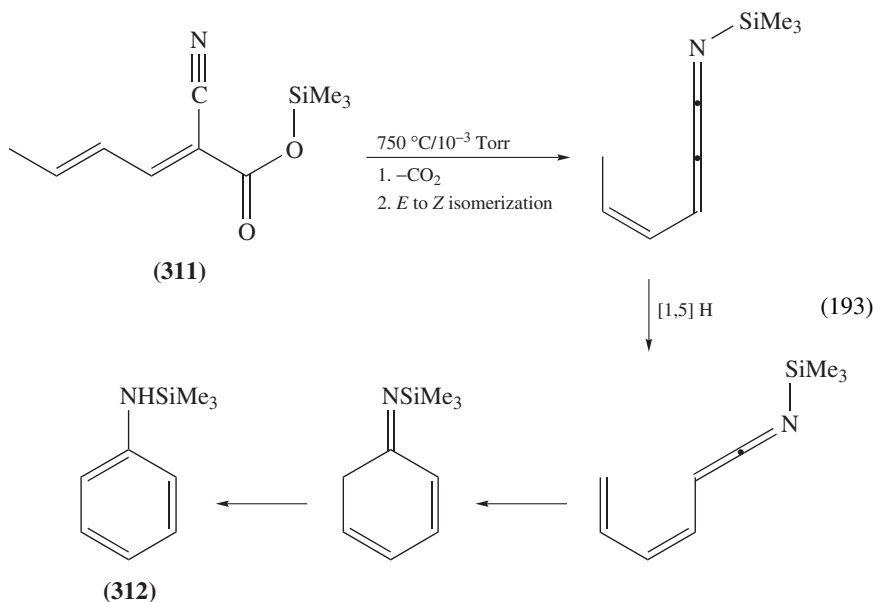
1,5-Silyl migrations between C and O are observed frequently in the thermal rearrangements of γ -silyl- α,β -unsaturated carbonyl compounds to butadienyl silyl ethers^{453,454} and their reverse reactions⁴⁵⁵⁻⁴⁵⁷. The migrations are regarded as the vinylogs of the 1,3-silyl migrations from β -silyl carbonyl compounds to silyl enol ethers.

Casey and coworkers found that the direction of the 1,5-silyl migrations was very dependent on the nature of carbonyl compounds⁴⁵⁸, similarly to the related 1,3-silyl migrations¹. Upon heating at 34 °C, vinyl ketone **307** was readily converted to the corresponding butadienyl silyl ether **308** (equation 191). In contrast, thermolysis of the vinyl ketene silyl acetal **310** at 117 °C gave gradually the corresponding ester **309** (equation 192). *O*-Silyl isomers were favored in the ketone-silyl ether rearrangements, while *C*-silyl isomers were prominent in the ester-ketene silyl acetal rearrangements, as expected from the bond energy difference between Si-O and Si-C bonds and the large delocalization energy in the ester.



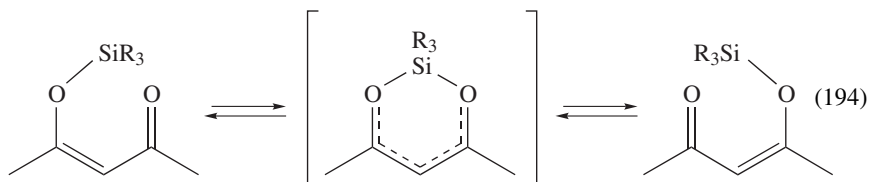
2. 1,5-Silyl migrations from O to N

Flash vacuum pyrolysis of trimethylsilyl (*E,E*)-2-cyanohepta-2,4-dienoate (α -cyanosorbate) **311** gave *N*-trimethylsilylaniline **312** in 53% yield. The reaction proceeded probably through a decarboxylation with 1,4-silyl migration from O to N (equation 193)⁴⁵⁹.

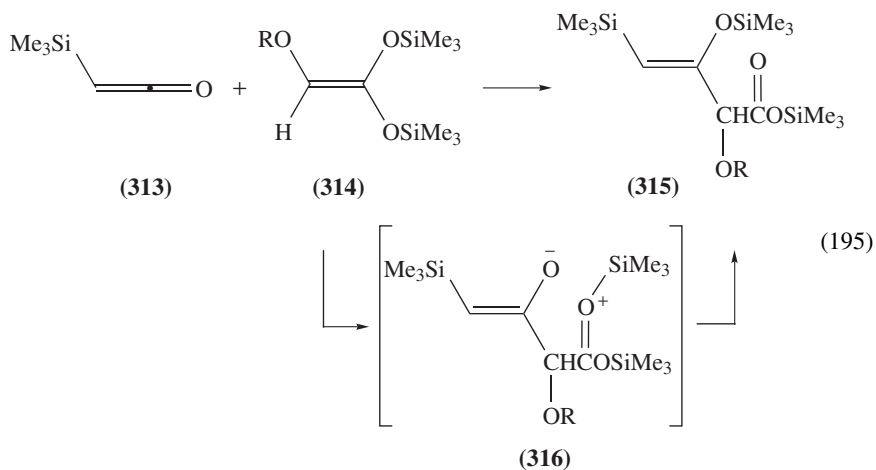


3. 1,5-Silyl migrations from O to O

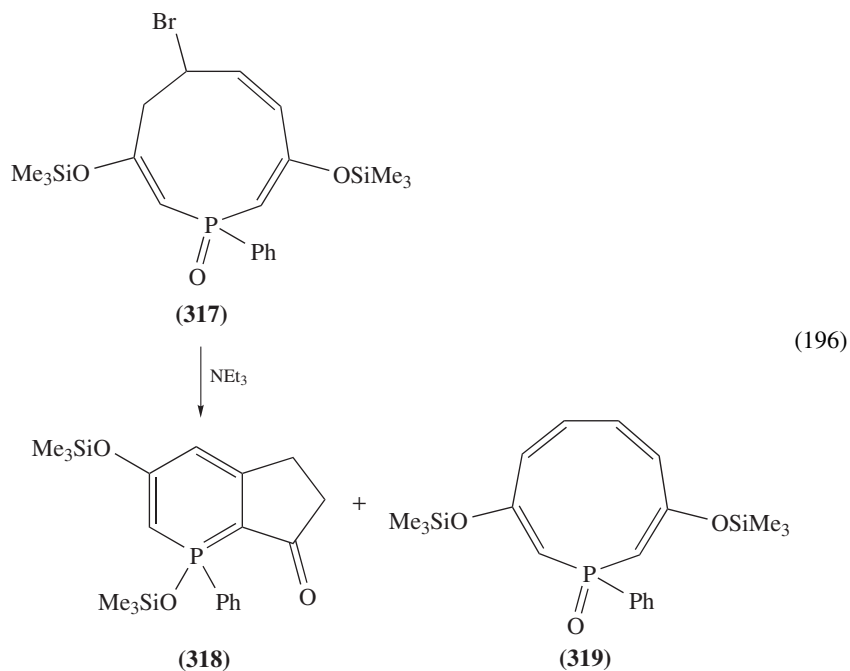
1,5-Silyl migrations between oxygen atoms are often observed in the degenerate rearrangements of silyl diketonates (equation 194). This type of rearrangement has been well documented in the review of BB¹. McClarin and coworkers suggested that the migration process should better be viewed as an internal nucleophilic displacement rather than as a sigmatropic shift⁴⁶⁰.

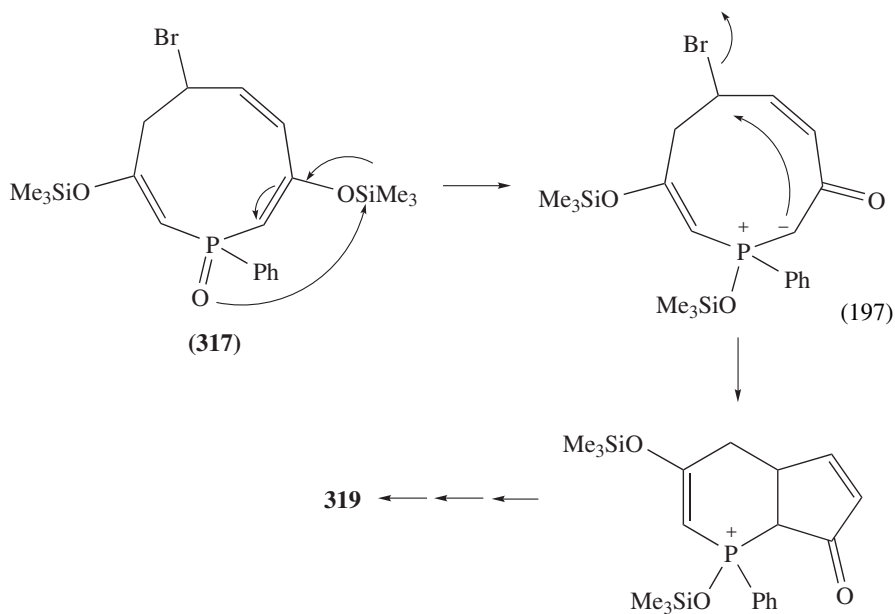


The reactions of the trimethylsilylketene **313** with silyl ketene acetals **314** provided β,γ -unsaturated esters **315** (equation 195) via a 1,5-silyl migration in the intermediate adduct **316**^{461,462}.



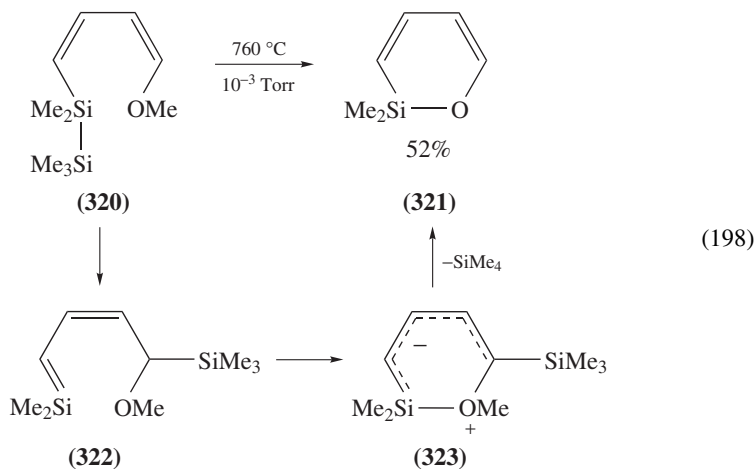
Rao and Quin found that the dehydrobromination of dihydrophosphonin **317** gave bicyclic enone **318** together with the expected product **319** (equation 196). A 1,5-silyl migration was involved as an important step (equation 197)⁴⁶³.





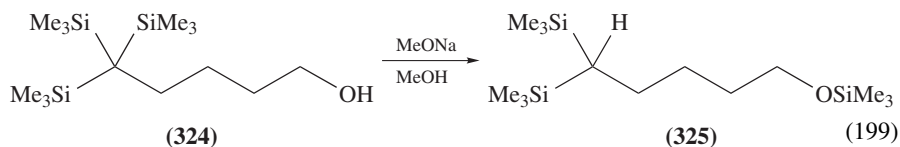
4. 1,5-Silyl migrations from Si to C

Flash vacuum pyrolysis of 1-disilanyl-4-methoxybutadiene **320** afforded silaoxacyclohexadiene **321** in 52% (equation 198). The formation of **321** was rationalized by a 1,5-sigmatropic migration of trimethylsilyl group to generate 1-sila-1,3-pentadiene **322**, followed by the silicon–oxygen bond formation to produce the zwitterion intermediate **323** and then elimination of tetramethylsilane⁴⁶⁴. Similar 1,5-silyl migrations were observed in the pyrolysis of 1-disilanyl-3-methylbutadiene⁴⁶⁵.

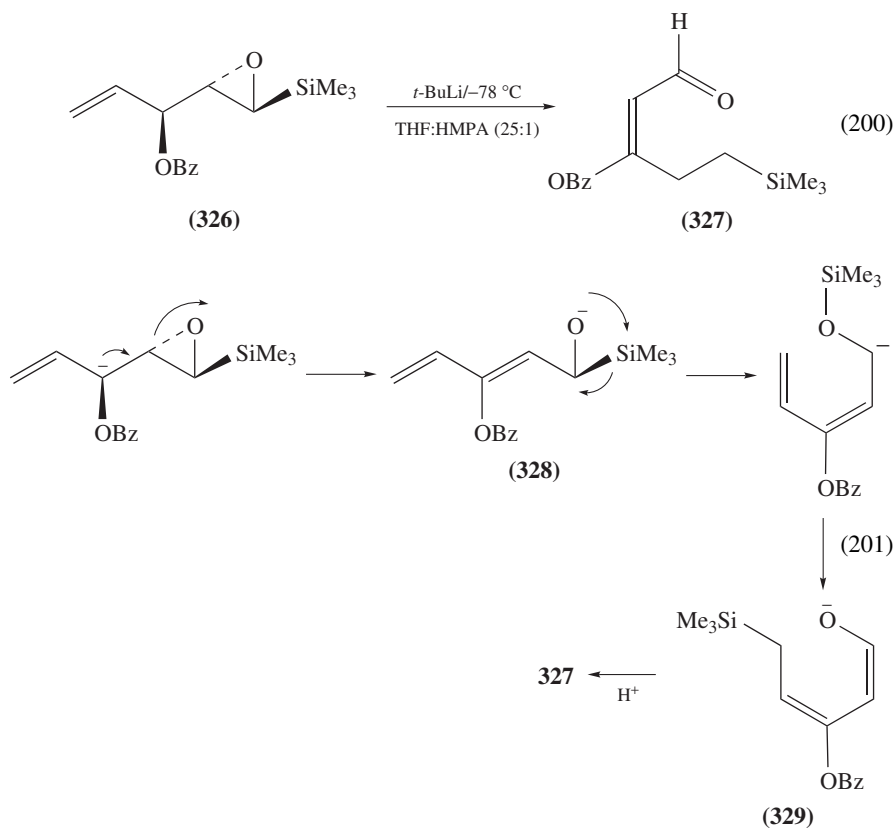


C. 1,6-Silyl Migrations

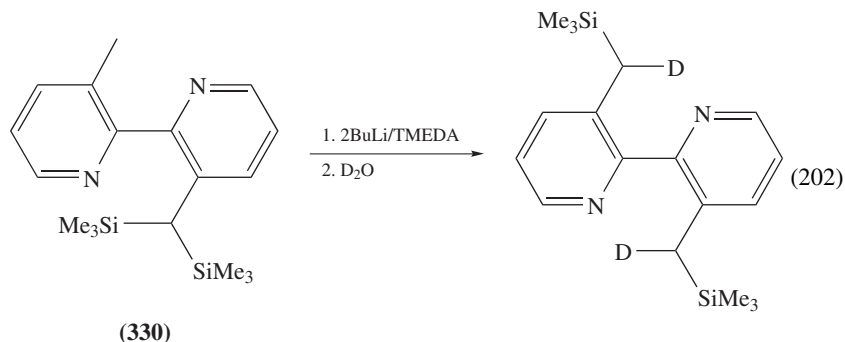
An anionic 1,6-silyl migration from C to O (1,6-Brook rearrangement) was observed during the deprotonation of ϵ -silyl alcohol **324**, which gave the corresponding silyl ether **325** (equation 199)⁴⁶⁶.



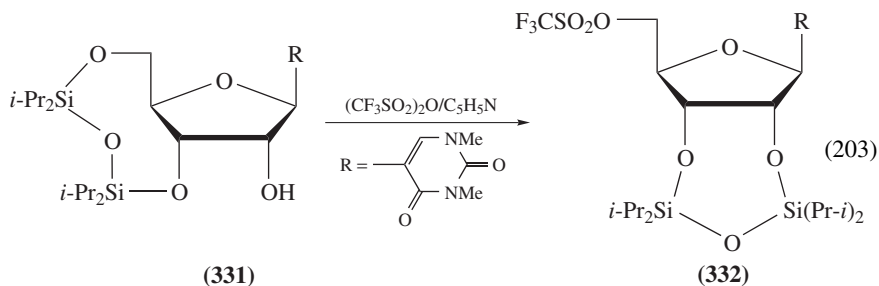
A 1,6-silyl migration from C to O was also observed in the reaction of allylepoxyisilane **326** with *t*-BuLi in a THF/HMPA (25 : 1) mixed solvent at low temperature, which afforded 5-silylpentenal **327** (equation 200). It was proposed that an initial proton abstraction from **326** gave α -silyl alkoxide **328**, which underwent 1,2-silyl and then 1,6-silyl migrations to afford dienolate **329**. Hydrolysis of **329** provided **327** (equation 201). The intramolecular nature of the transformation was suggested because the facile reaction occurred even in very dilute (0.02 mol⁻¹) and low-temperature (-78 °C) conditions⁴⁶⁷.



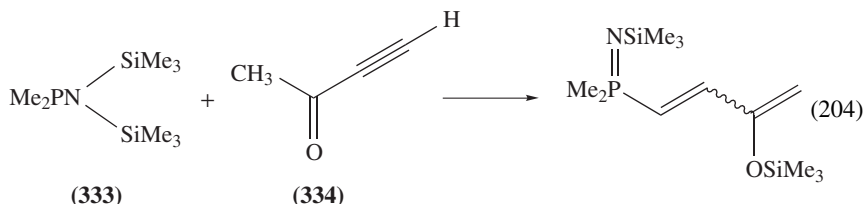
Leung and coworkers found an anionic 1,6-silyl migration from C to C during the metallation of bis(trimethylsilyl)methyl-2,2'-bipyridyl **330** (equation 202). In the proposed mechanism, the less hindered methyl proton is abstracted preferably to give the corresponding carbanion, to which a trimethylsilyl group migrates through a nucleophilic substitution at silicon⁴⁶⁸.



A 1,6-silyl migration from O to O was observed in the reactions of 3',5'-cyclic disiloxanyl ϕ -uridine derivatives **331** with triflic anhydride which give quantitatively the 2',3'-cyclic disiloxanyl ϕ -uridine derivatives **332** (equation 203)^{469,470}.



A 1,6-silyl migration from N to O was postulated in the reaction of *N,N*-bis(trimethylsilyl)aminophosphine **333** with ethynyl methyl ketone **334** (equation 204)⁴⁷¹.



V. REFERENCES

1. A. G. Brook and A. R. Bassindale, Chap. 9 in *Rearrangements in Ground and Excited States*, Vol 2 (Ed. P. de Mayo), Academic Press, New York, 1980, p. 149.
2. J. S. Panek, in *Comprehensive Organic Synthesis* (Ed. B. M. Trost), Pergamon Press, Oxford, 1991.

3. C. E. Masse and J. S. Panek, *Chem. Rev.*, **95**, 1293 (1995).
4. A. Hosomi, *Acc. Chem. Res.*, **21**, 200 (1988).
5. S. Murai, *Kagaku*, **39**, 615 (1984); *Chem. Abstr.*, **102**, 24671 (1984).
6. Y. Kita, *Yakugaku Zasshi*, **106**, 269 (1984); *Chem. Abstr.*, **106**, 32640 (1986).
7. K. Takeda, *Yakugaku Zasshi*, **117**, 368 (1997); *Chem. Abstr.*, **127**, 95107 (1999).
8. I. Kuwajima, *J. Organomet. Chem.*, **285**, 137 (1985).
9. I. Fleming, in *Comprehensive Organic Synthesis* (Ed. B. M. Trost), Pergamon Press, Oxford, 1991.
10. E. W. Colvin, Chap. 5 in *Silicon in Organic Synthesis*, Butterworths, London, 1981, p. 30.
11. C. Rücker, *Chem. Rev.*, **95**, 1009 (1995).
12. A. G. Brook, Chap. 15 in *The Chemistry of Organic Silicon Compounds* (Eds. S. Patai and Z. Rappoport), Wiley, Chichester, 1989, p. 965.
13. M. G. Steinmetz, *Chem. Rev.*, **95**, 1527 (1995).
14. A. Alberti, *Rev. Chem. Intermed.*, **7**, 71 (1986).
15. P. Braunstein, M. Knorr and C. Stern, *Coord. Chem. Rev.*, **178**, 903 (1998).
16. H. K. Sharma and K. H. Pannel, *Chem. Rev.*, **95**, 1351 (1995).
17. T. D. Tilley, Chap. 24 in *The Chemistry of Organic Silicon Compounds* (Eds. S. Patai and Z. Rappoport), Wiley, Chichester, 1989, p. 1415.
18. J. V. Ortiz, Z. Havlas and R. Hoffmann, *Helv. Chim. Acta*, **67**, 1 (1984).
19. H. Ogino and H. Tobita, *Adv. Organomet. Chem.*, **42**, 223 (1998).
20. M. T. Reetz, *Adv. Organomet. Chem.*, **16**, 33 (1977).
21. P. Nowakowski and R. West, *J. Am. Chem. Soc.*, **98**, 5616 (1976).
22. R. Wolfgramm, T. Müller and U. Klingebiel, *Organometallics*, **17**, 3222 (1998).
23. R. Wolfgramm and U. Klingebiel, *Z. Anorg. Allg. Chem.*, **624**, 1031 (1998).
24. U. Schubert and C. Steib, *J. Organomet. Chem.*, **238**, C1 (1982).
25. G. Erker, M. Bendix and R. Petrenz, *Organometallics*, **13**, 456 (1994).
26. T. Albrecht, G. Elter and A. Meller, *Z. Anorg. Allg. Chem.*, **625**, 1453 (1999).
27. M. G. Steinmetz, M. A. Langston, R. T. Mayes and B. S. Udayakumar, *J. Org. Chem.*, **51**, 5051 (1986).
28. H. Schwarz, C. Wesdemiotis and M. T. Reetz, *J. Organomet. Chem.*, **161**, 153 (1978).
29. M. A. Edelman, P. B. Hitchcock, M. F. Lappert, D.-S. Liu and S. Tian, *J. Organomet. Chem.*, **550**, 397 (1998).
30. K. M. Baines, A. G. Brook, R. R. Ford, P. D. Lickiss, A. K. Saxena, W. J. Chatterton, J. F. Sawyer and B. A. Behnam, *Organometallics*, **8**, 693 (1989).
31. M. Kira, S. Ohya, T. Iwamoto, M. Ichinohe and C. Kabuto, *Organometallics*, **19**, 1817 (2000).
32. H. B. Yokelson, D. A. Siegel, A. Millevolte, J. Maxka and R. West, *Organometallics*, **9**, 1005 (1990).
33. X. Creary and Y.-X. Wang, *Tetrahedron Lett.*, **30**, 2493 (1989).
34. X. Creary and Y.-X. Wang, *J. Org. Chem.*, **59**, 1604 (1994).
35. M. Trommer, W. Sander, C.-H. Ottosson and D. Cremer, *Angew. Chem., Int. Ed. Engl.*, **34**, 929 (1995).
36. M. S. Baird, C. M. Dale and J. R. Al Dulayymi, *J. Chem. Soc., Perkin Trans 1*, 1373 (1993).
37. R. Walsh, C. Wolf, S. Unittiedt and A. deMeijere, *J. Chem. Soc., Chem. Commun.*, 422 (1992).
38. S. Solé, H. Gornitzka, O. Guerret and G. Bertrand, *J. Am. Chem. Soc.*, **120**, 9100 (1998).
39. R. T. Conlin, H. B. Huffaker and Y.-W. Kwak, *J. Am. Chem. Soc.*, **107**, 731 (1985).
40. T. J. Barton, J. Lin, S. Ijadi-Maghsoodi, M. D. Power, X. Zhang, Z. Ma, H. Shimizu and M. S. Gordon, *J. Am. Chem. Soc.*, **117**, 11695 (1995).
41. T. J. Barton and B. L. Groh, *J. Am. Chem. Soc.*, **107**, 7221 (1985).
42. T. J. Barton and G. C. Paul, *J. Am. Chem. Soc.*, **109**, 5292 (1987).
43. T. J. Barton and B. L. Groh, *Organometallics*, **4**, 575 (1985).
44. F. Hojo, K. Fujiki and W. Ando, *Organometallics*, **15**, 3606 (1996).
45. H. Sakurai, T. Fujii and K. Sakamoto, *Chem. Lett.*, 339 (1992).
46. P. Braunstein, T. Faure and M. Knorr, *Organometallics*, **18**, 1791 (1999).
47. H. Sakurai, K. Hirma, Y. Nakadaira and C. Kabuto, *J. Am. Chem. Soc.*, **109**, 6880 (1987).
48. D. Schneider and H. Werner, *Angew. Chem., Int. Ed. Engl.*, **30**, 700 (1991).
49. K. Onitsuka, H. Katayama, K. Sonogashira and F. Ozawa, *J. Chem. Soc., Chem. Commun.*, 2267 (1995).
50. T. Matsuo, H. Fure and A. Sekiguchi, *Chem. Lett.*, 1101 (1998).

51. T. Matsuo, A. Sekiguchi, M. Ichinohe, K. Ebata and H. Sakurai, *Organometallics*, **17**, 3143 (1998).
52. T. Matsuo, A. Sekiguchi and H. Sakurai, *Bull. Chem. Soc. Jpn.*, **72**, 1115 (1999).
53. S. R. Allen, M. Green, A. G. Orpen and I. D. Williams, *J. Chem. Soc., Chem. Commun.*, 826 (1982).
54. T. J. Barton and B. L. Groh, *J. Org. Chem.*, **50**, 158 (1985).
55. L. Lee, D. J. Berg, F. W. Einstein and R. J. Batchelor, *Organometallics*, **16**, 1819 (1997).
56. J. M. Manriquez, P. J. Fagan, T. J. Marks, C. S. Day and V. W. Day, *J. Am. Chem. Soc.*, **100**, 7112 (1978).
57. D. C. Sonnenberger, E. A. Mintz and T. J. Marks, *J. Am. Chem. Soc.*, **106**, 3484 (1984).
58. F. J. Berg and J. L. Petersen, *Organometallics*, **12**, 3890 (1993).
59. F. J. Berg and J. L. Petersen, *Organometallics*, **8**, 2461 (1989).
60. J. L. Petersen and J. W. Egan, Jr., *Organometallics*, **6**, 2007 (1987).
61. F. J. Berg and J. L. Petersen, *Organometallics*, **10**, 1599 (1991).
62. L. Kloppenburg and J. L. Petersen, *Polyhedron*, **14**, 69 (1995).
63. J. D. Debad, P. Legzdins, R. J. Batchelor and F. W. B. Einstein, *Organometallics*, **12**, 2094 (1993).
64. M. F. Lappert, C. L. Raston, L. M. Engelhardt and A. H. White, *J. Chem. Soc., Chem. Commun.*, 521 (1985).
65. S. J. Simpson and R. A. Andersen, *J. Am. Chem. Soc.*, **103**, 4063 (1981).
66. L. D. Durfee and I. P. Rothwell, *Chem. Rev.*, **88**, 1059 (1988).
67. M. Ishikawa, M. Watanabe, J. Iyoda, H. Ikeda and M. Kumada, *Organometallics*, **1**, 317 (1982).
68. E. Hengge, P. K. Jenkner, A. Spielberger and P. Gspaltl, *Monatsh. Chem.*, **124**, 1005 (1993).
69. E. Hengge and R. Janoschek, *Chem. Rev.*, **95**, 1495 (1995).
70. M. Kumada and K. Tamao, *Adv. Organomet. Chem.*, **6**, 19 (1968).
71. S. Sharma, N. Caballero, H. Li and K. H. Pannell, *Organometallics*, **18**, 2855 (1999).
72. M. B. Berry, R. J. Griffiths, D. S. Yufit and P. G. Steel, *Chem. Commun.*, 2155 (1998).
73. A. G. Brook, M. Hesse, K. M. Baines, R. Kumarathasan and A. J. Lough, *Organometallics*, **12**, 4259 (1993).
74. K. Sternberg and H. Oehme, *Eur. J. Inorg. Chem.*, 177 (1998).
75. G. Märkl, M. Horn and W. Schlosser, *Tetrahedron Lett.*, **27**, 4019 (1986).
76. A. Wright and R. West, *J. Am. Chem. Soc.*, **96**, 3214 (1974).
77. A. Wright and R. West, *J. Am. Chem. Soc.*, **96**, 3222 (1974).
78. A. Wright and R. West, *J. Am. Chem. Soc.*, **96**, 3227 (1974).
79. R. West, *Adv. Organomet. Chem.*, **16**, 1 (1977).
80. R. J. Linderman and A. Ghannam, *J. Am. Chem. Soc.*, **112**, 2392 (1990).
81. G. Boche, A. Opel, M. Marsch, K. Harms, F. Haller, J. C. W. Lohrenz, C. Thümmeler and W. Koch, *Chem. Ber.*, **125**, 2265 (1992).
82. P. Antoniotti, C. Canepa and G. Tonachini, *J. Org. Chem.*, **59**, 3952 (1994).
83. P. Antoniotti and G. Tonachini, *J. Org. Chem.*, **58**, 3622 (1993).
84. P. Antoniotti and G. Tonachini, *Organometallics*, **18**, 4538 (1999).
85. J. R. Hwu, S.-C. Tsay, N. Wang and G. H. Hakimelahi, *Organometallics*, **13**, 2461 (1994).
86. S. Menichetti, G. Griffiths and C. J. M. Stirling, *J. Chem. Soc., Chem. Commun.*, 54 (1992).
87. T. Nakajima, M. Tanabe, K. Ohno, M. Segi and S. Suga, *Chem. Lett.*, 177 (1986).
88. G. C. Johnson, J. J. Stofko, Jr., T. P. Lockhart, D. W. Brown and R. G. Bergman, *J. Org. Chem.*, **44**, 4215 (1979).
89. Y.-M. Tsai and S.-Y. Chang, *J. Chem. Soc., Chem. Commun.*, 981 (1995).
90. Y.-M. Tsai and C. D. Cherng, *Tetrahedron Lett.*, **32**, 3515 (1991).
91. Y.-M. Tsai, K.-H. Tang and W.-T. Jiaang, *Tetrahedron Lett.*, **34**, 1303 (1993).
92. D. P. Curran, W.-T. Jiaang, M. Palovich and Y.-M. Tsai, *Synlett*, 403 (1993).
93. R. Hoffmann, T. Rückert and R. Brückner, *Tetrahedron Lett.*, **34**, 297 (1993).
94. C. H. Schiesser and M. L. Styles, *J. Chem. Soc., Perkin Trans 2*, 2335 (1997).
95. M. Stradiotto, M. A. Brook and M. J. McGlinchey, *Inorg. Chem. Commun.*, **1**, 105 (1998).
96. J. A. Butcher, Jr. and R. M. Pagni, *J. Am. Chem. Soc.*, **101**, 3997 (1979).
97. S. S. Rigby, H. K. Gupta, N. H. Werstiuk, A. D. Bain and M. J. McGlinchey, *Polyhedron*, **14**, 2787 (1995).
98. C. Glidewell, *J. Organomet. Chem.*, **266**, 25 (1984).

99. L. A. Paquette, P. Charumilind and J. C. Gallucci, *J. Am. Chem. Soc.*, **105**, 7364 (1983).
100. S. S. Rigby, L. Girard, A. D. Bain and M. J. McGlinchey, *Organometallics*, **14**, 3798 (1995).
101. M. Stradiotto, S. S. Rigby, D. W. Hughes, M. A. Brook, A. D. Bain and M. J. McGlinchey, *Organometallics*, **15**, 5645 (1996).
102. W. Ando, T. Shiba, T. Hidaka, K. Morihashi and O. Kikuchi, *J. Am. Chem. Soc.*, **119**, 3629 (1997).
103. C. Roos, G. A. McGibbon and M. A. Brook, *Can. J. Chem.*, **74**, 1470 (1996).
104. H.-J. Wu, C.-H. Yen and C.-T. Chuang, *J. Org. Chem.*, **63**, 5064 (1998).
105. W. Kirmse and F. Söllenhömer, *J. Am. Chem. Soc.*, **111**, 4127 (1989).
106. S. Nagase and T. Kudo, *J. Chem. Soc., Chem. Commun.*, 1392 (1984).
107. T. J. Barton and S. A. Jacobi, *J. Am. Chem. Soc.*, **102**, 7979 (1980).
108. S. A. Burns, G. T. Burns and T. J. Barton, *J. Am. Chem. Soc.*, **104**, 6140 (1982).
109. T. J. Barton, S. A. Burns and G. T. Burns, *Organometallics*, **1**, 210 (1982).
110. M. Kira, S. Ishida, T. Iwamoto and C. Kabuto, *J. Am. Chem. Soc.*, **121**, 9722 (1999).
111. A. Sekiguchi and W. Ando, *Chem. Lett.*, 871 (1983).
112. A. Sekiguchi and W. Ando, *Tetrahedron Lett.*, **24**, 2791 (1983).
113. A. Sekiguchi, T. Sato and W. Ando, *Chem. Lett.*, 1083 (1983).
114. A. Sekiguchi and W. Ando, *Organometallics*, **6**, 1857 (1987).
115. A. Sekiguchi, T. Sato and W. Ando, *Organometallics*, **6**, 2337 (1987).
116. G. Maas and A. Fronda, *J. Organomet. Chem.*, **398**, 229 (1990).
117. A. Fronda and G. Maas, *Angew. Chem., Int. Ed. Engl.*, **28**, 1663 (1989).
118. W. Ando, M. Sugiyama, T. Suzuki, C. Kato, Y. Arakawa and Y. Kabe, *J. Organomet. Chem.*, **499**, 99 (1995).
119. W. Ando, H. Yoshida, K. Kurishima and M. Sugiyama, *J. Am. Chem. Soc.*, **113**, 7790 (1991).
120. G. Märkl, W. Schlosser and W. S. Sheldrick, *Tetrahedron Lett.*, **29**, 467 (1988).
121. K. Sakamoto, J. Ogasawara, H. Sakurai and M. Kira, *J. Am. Chem. Soc.*, **119**, 3405 (1997).
122. T. Veszprémi, M. Takahashi, J. Ogawawara, K. Sakamoto and M. Kira, *J. Am. Chem. Soc.*, **120**, 2408 (1998).
123. T. J. Barton and G. P. Hussmann, *J. Am. Chem. Soc.*, **107**, 7581 (1985).
124. T. Kudo and S. Nagase, *J. Phys. Chem.*, **88**, 2833 (1984).
125. T. Kudo and S. Nagase, *Organometallics*, **6**, 1586 (1987).
126. S. Nagase and T. Kudo, *Organometallics*, **3**, 1320 (1984).
127. H. Sakurai, Y. Nakadaira and H. Sakaba, *Organometallics*, **2**, 1484 (1983).
128. H. Sakurai, H. Sakaba and Y. Nakadaira, *J. Am. Chem. Soc.*, **104**, 6156 (1982).
129. K. Kobayashi and S. Nagase, *Organometallics*, **16**, 2489 (1997).
130. M. Kira, T. Iwamoto and C. Kabuto, *J. Am. Chem. Soc.*, **118**, 10303 (1996).
131. T. Iwamoto and M. Kira, *Chem. Lett.*, 277 (1998).
132. M. Kira and T. Iwamoto, *J. Organomet. Chem.*, **611**, 236 (2000).
133. V. Y. Lee, M. Ichinohe, A. Sekiguchi, N. Tagaki and S. Nagase, *J. Am. Chem. Soc.*, **122**, 9034 (2000).
134. H. J. Knölker, P. G. Jones and J.-B. Pannek, *Synlett*, 427 (1990).
135. J. S. Panek and N. F. Jain, *J. Org. Chem.*, **58**, 2345 (1993).
136. R. L. Danheiser, D. J. Carini, D. M. Fink and A. Basak, *Tetrahedron*, **39**, 935 (1983).
137. G. P. Brengel, C. Rithner and A. I. Meyers, *J. Org. Chem.*, **59**, 5144 (1994).
138. G. P. Brengel and A. I. Meyers, *J. Org. Chem.*, **61**, 3230 (1996).
139. H.-J. Knölker and R. Graf, *Synlett*, 131 (1994).
140. H.-J. Knölker, N. Foitzik, H. Goesmann and R. Graf, *Angew. Chem., Int. Ed. Engl.*, **32**, 1081 (1993).
141. R. L. Danheiser, T. Takahashi, B. Bertók and B. R. Dixon, *Tetrahedron Lett.*, **34**, 3845 (1993).
142. R. L. Danheiser, B. R. Dixon and R.-W. Gleason, *J. Org. Chem.*, **57**, 6094 (1992).
143. B. B. Snider and Q. Zhang, *J. Org. Chem.*, **56**, 4908 (1991).
144. J. Ipaktschi and A. Heydari, *Angew. Chem., Int. Ed. Engl.*, **31**, 313 (1992).
145. H.-J. Knölker, N. Foitzik, R. Graf, J.-B. Pannek and P. G. Jones, *Tetrahedron*, **49**, 9955 (1993).
146. H.-J. Knölker and R. Graf, *Tetrahedron Lett.*, **34**, 4765 (1993).
147. H. Monti, G. Audran, J.-P. Monti and G. Léandri, *Synlett*, 403 (1994).
148. G. M. Choi, S. H. Yeon, J. Jin, B. R. Yoo and I. N. Jung, *Organometallics*, **16**, 5158 (1997).
149. K. Ohkata, K. Ishimaru, Y.-G. Lee and K.-y. Akiba, *Chem. Lett.*, 1725 (1990).

150. Y.-G. Lee, K. Ishimaru, H. Iwasaki, K. Ohkata and K.-y. Akiba, *J. Org. Chem.*, **56**, 2058 (1991).
151. S. Imazu, N. Shimizu and Y. Tsuno, *Chem. Lett.*, 1845 (1990).
152. S. R. Angle and J. P. Boyce, *Tetrahedron Lett.*, **35**, 6461 (1994).
153. S. Ohashi, W. E. Ruch and G. B. Butler, *J. Org. Chem.*, **46**, 614 (1981).
154. R. L. Danheiser, D. J. Carini and C. Kwasigroch, *J. Org. Chem.*, **51**, 3870 (1986).
155. H. Monti, G. Audran, G. Léandri and J.-P. Monti, *Tetrahedron Lett.*, **35**, 3073 (1994).
156. T. Akiyama, T. Yasusa, K. Ishikawa and S. Ozaki, *Tetrahedron Lett.*, **35**, 8401 (1994).
157. T. Akiyama, K. Ishikawa and S. Ozaki, *Chem. Lett.*, 627 (1994).
158. D. Schinzer and G. Panke, *J. Org. Chem.*, **61**, 4496 (1996).
159. J. K. Whitesell, K. Nabora and D. Deyo, *J. Org. Chem.*, **54**, 2258 (1989).
160. J. S. Panek and R. Beresis, *J. Org. Chem.*, **58**, 809 (1993).
161. J. S. Panek and M. Yang, *J. Am. Chem. Soc.*, **113**, 9868 (1991).
162. R. L. Danheiser, E. J. Stoner, H. Koyama, D. S. Yamashita and C. A. Klade, *J. Am. Chem. Soc.*, **111**, 4407 (1989).
163. J. S. Panek and N. F. Jain, *J. Org. Chem.*, **59**, 2674 (1994).
164. A. Stahl, E. Steckhan and M. Nieger, *Tetrahedron Lett.*, **35**, 7371 (1994).
165. J. B. M. Rewinkel, S. Garcia-Granda, P. T. Beurskens, R. Raaijmakers and B. Zwanenburg, *Recl. Trav. Chim. Pays-Bas*, **108**, 61 (1989).
166. J. S. Panek and R. T. Beresis, *J. Am. Chem. Soc.*, **115**, 7898 (1993).
167. R. L. Danheiser and D. A. Becker, *Heterocycles*, **25**, 277 (1987).
168. R. L. Danheiser, D. J. Carini and A. Basak, *J. Am. Chem. Soc.*, **103**, 1604 (1981).
169. R. L. Danheiser, C. A. Kwasigroch and Y.-M. Tsai, *J. Am. Chem. Soc.*, **107**, 7233 (1985).
170. D. A. Becker and R. L. Danheiser, *J. Am. Chem. Soc.*, **111**, 389 (1989).
171. R. L. Danheiser and D. M. Fink, *Tetrahedron Lett.*, **26**, 2513 (1985).
172. J. Pornet, L. Miginiac, K. Jaworski and B. Randrianoelina, *Organometallics*, **4**, 333 (1985).
173. S. Yamazaki, S. Katoh and S. Yamabe, *J. Org. Chem.*, **57**, 4 (1992).
174. S. Yamazaki, M. Tanaka, A. Yamaguchi and S. Yamabe, *J. Am. Chem. Soc.*, **116**, 2356 (1994).
175. S. Yamazaki, M. Tanaka, A. Yamaguchi and S. Yamabe, *J. Am. Chem. Soc.*, **117**, 8297 (1995).
176. K. Miura, T. Hondo, H. Saito, H. Ito and A. Hosomi, *J. Org. Chem.*, **62**, 8292 (1997).
177. I. Fleming and S. K. Ghost, *J. Chem. Soc., Chem. Commun.*, 1777 (1992).
178. I. Fleming and S. K. Ghost, *J. Chem. Soc., Perkin Trans. 1*, 2733 (1998).
179. M. Suginome, A. Takama and Y. Ito, *J. Am. Chem. Soc.*, **120**, 1930 (1998).
180. Y. Yamamoto, M. Noda, M. Ohno and S. Eguchi, *J. Org. Chem.*, **62**, 1292 (1997).
181. P. F. Hudrlik, A. M. Hudrlik, G. Nagendrappa, T. Yimenu, E. T. Zellers and E. Chin, *J. Am. Chem. Soc.*, **102**, 6894 (1980); **104**, 1157 (1982).
182. K.-T. Kang, J. C. Lee and J. S. U. *Tetrahedron Lett.*, **33**, 4953 (1992).
183. Y. Yamamoto, Y. Saito and K. Maruyama, *J. Organomet. Chem.*, **292**, 311 (1985).
184. K. Nakayama and A. Tanaka, *Chem. Pharm. Bull.*, **40**, 1966 (1992).
185. R. Cunico, *J. Org. Chem.*, **55**, 4474 (1990).
186. D. W. Macomber, P. Madhuker and R. D. Rogers, *Organometallics*, **10**, 2121 (1991).
187. J. W. Herndon and P. P. Patel, *J. Org. Chem.*, **61**, 4500 (1996).
188. P. F. Hudrlik, R. H. Schwarz and A. K. Kulkarni, *Tetrahedron Lett.*, **20**, 2233 (1979).
189. P. F. Hudrlik, G. Nagendrappa, A. K. Kulkarni and A. M. Hudrlik, *Tetrahedron Lett.*, **20**, 2237 (1979).
190. H. J. Reich, M. J. Kelly, R. E. Olson and R. C. Holtan, *Tetrahedron*, **39**, 949 (1983).
191. H. J. Reich and M. J. Kelly, *J. Am. Chem. Soc.*, **104**, 1119 (1982).
192. H. J. Reich, E. K. Eisenhart, R. E. Olson and M. J. Kelly, *J. Am. Chem. Soc.*, **108**, 7791 (1986).
193. H. J. Reich, R. C. Holtan and C. Bolm, *J. Am. Chem. Soc.*, **112**, 5609 (1990).
194. B. Dondy and C. Portella, *J. Org. Chem.*, **58**, 6671 (1993).
195. K.-T. Kang, T. M. Sung, K.-R. Lee, J. G. Lee and K. K. Jyung, *Bull. Korean Chem. Soc.*, **14**, 757 (1993).
196. H. J. Reich, J. J. Rusek and R. E. Olson, *J. Am. Chem. Soc.*, **101**, 2225 (1979).
197. H. J. Reich, R. E. Olson and M. C. Clark, *J. Am. Chem. Soc.*, **102**, 1423 (1980).
198. H. J. Reich, M. C. Clark and W. W. Willis, Jr., *J. Org. Chem.*, **47**, 1618 (1982).
199. H. J. Reich, R. C. Holtan and S. L. Borkowsky, *J. Org. Chem.*, **52**, 312 (1987).
200. M. Koreeda and S. Koo, *Tetrahedron Lett.*, **31**, 831 (1990).

201. S. Murai, I. Ryu, J. Iriguchi and N. Sonoda, *J. Am. Chem. Soc.*, **106**, 2440 (1984).
202. E. J. Corey, M. A. Tius and J. Das, *J. Am. Chem. Soc.*, **102**, 1742 (1980).
203. I. Fleming, R. S. Roberts and S. C. Smith, *J. Chem. Soc., Perkin Trans. 1*, 1215 (1998).
204. J. Enda and I. Kuwajima, *J. Am. Chem. Soc.*, **107**, 5495 (1985).
205. I. Kuwajima and M. Kato, *J. Chem. Soc., Chem. Commun.*, 708 (1979).
206. I. Kuwajima, M. Kato and A. Mori, *Tetrahedron Lett.*, **21**, 2745 (1980).
207. M. Kato, A. Mori, H. Oshino, J. Enda, K. Kobayashi and I. Kuwajima, *J. Am. Chem. Soc.*, **106**, 1773 (1984).
208. S. Bienz, V. Enev and P. Huber, *Tetrahedron Lett.*, **35**, 1161 (1994).
209. I. Kuwajima and M. Kato, *Tetrahedron Lett.*, **21**, 623 (1980).
210. T. Nakajima, M. Segi, F. Sugimoto, R. Hioki, S. Yokota and K. Miyashita, *Tetrahedron*, **49**, 8343 (1993).
211. P. Cuadrado and A. M. González-Nogal, *Tetrahedron Lett.*, **38**, 8117 (1997).
212. A. Fürstner, G. Seidel, B. Gabor, C. Kopsiske, C. Krüger and R. Mynott, *Tetrahedron*, **51**, 8875 (1995).
213. K. Takeda, J. Nakatani, H. Nakamura, K. Sako, E. Yoshii and K. Yamaguchi, *Synlett*, 841 (1993).
214. K. Takeda, M. Fujisawa, T. Makino and E. Yoshii, *J. Am. Chem. Soc.*, **115**, 9351 (1993).
215. K. Takeda, Y. Ohtani, E. Ando, K.-i. Fujimoto, E. Yoshii and T. Koizumi, *Chem. Lett.*, 1157 (1998).
216. K. Takeda, H. Ubayama, A. Sano, E. Yoshii and T. Koizumi, *Tetrahedron Lett.*, **39**, 5243 (1998).
217. K. Takeda, I. Nakayama and E. Yoshii, *Synlett*, 178 (1994).
218. K. Takeda, A. Nakajima and E. Yoshii, *Synlett*, 225 (1997).
219. K. Takeda, M. Takeda, A. Nakajima and E. Yoshii, *J. Am. Chem. Soc.*, **117**, 6400 (1995).
220. K. Takeda, A. Nakajima and E. Yoshii, *Synlett*, 753 (1996).
221. K. Takeda, A. Nakajima, M. Takeda and E. Yoshii, *Org. Synth.*, **76**, 199 (1999).
222. K. Takeda and Y. Ohtani, *Org. Lett.*, **1**, 677 (1999).
223. K. Takeda, A. Nakajima, M. Takeda, Y. Okamoto, T. Sato, E. Yoshii, T. Koizumi and M. Shiro, *J. Am. Chem. Soc.*, **120**, 4947 (1998).
224. P. Jankowski, S. Marczyk, M. Masnyk and J. Wicha, *J. Organomet. Chem.*, **403**, 49 (1991).
225. S. R. Wilson, M. S. Hague and R. N. Misra, *J. Org. Chem.*, **47**, 747 (1982).
226. I. Fleming and U. Ghosh, *J. Chem. Soc., Perkin Trans. 1*, 257 (1994).
227. P. F. Hudrlik, A. M. Hudrlik and A. K. Kulkarni, *J. Am. Chem. Soc.*, **104**, 6809 (1982).
228. A. Fürstner, G. Kollegger and H. Weidmann, *J. Organomet. Chem.*, **414**, 295 (1991).
229. H. Zilch and R. Tacke, *J. Organomet. Chem.*, **316**, 243 (1986).
230. F. Le Bideau, F. Gilloir, Y. Nilsson, C. Aubert and M. Malacria, *Tetrahedron*, **52**, 7487 (1996).
231. D. J. Pollart and B. Rickborn, *J. Org. Chem.*, **52**, 792 (1987).
232. R. J. Linderman and A. Ghannam, *J. Org. Chem.*, **53**, 2878 (1988).
233. J.-B. Verlhac, H.-A. Kwon and M. Pereyre, *J. Organomet. Chem.*, **437**, C13 (1992).
234. M. A. Tius and H. Hu, *Tetrahedron Lett.*, **39**, 5937 (1998).
235. D. P. Curran and S. A. Gothe, *Tetrahedron*, **44**, 3945 (1988).
236. R. L. Danheiser, D. M. Fink, K. Okano, Y.-M. Tsai and S. W. Szczepanski, *J. Org. Chem.*, **50**, 5393 (1985).
237. T. Cohen and J. R. Matz, *J. Am. Chem. Soc.*, **102**, 6900 (1980).
238. B. Mergardt, K. Weber, G. Adiwidjaja and E. Schaumann, *Angew. Chem., Int. Ed. Engl.*, **30**, 1687 (1991).
239. T. Inoue, N. Kambe, I. Ryu and N. Sonoda, *J. Org. Chem.*, **59**, 8209 (1994).
240. T. Honda and M. Mori, *J. Org. Chem.*, **61**, 1196 (1996).
241. C. Barberis and N. Voyer, *Tetrahedron Lett.*, **39**, 6807 (1998).
242. S. McN. Sieburth, J. J. Somers, H. K. O'Hare and G. W. Hewitt, *Appl. Organomet. Chem.*, **11**, 337 (1997).
243. I. Fleming, M. Solay and F. Stolwijk, *J. Organomet. Chem.*, **521**, 121 (1996).
244. M. Komatsu, M. Ohno, S. Tsuno and Y. Ohshiro, *Chem. Lett.*, 575 (1990).
245. M. Ohno, M. Komatsu, H. Miyata and Y. Ohshiro, *Tetrahedron Lett.*, **32**, 5813 (1991).
246. D. P. Curran, W. T. Jiaang, M. Palovich and Y.-M. Tsai, *Synlett*, 403 (1993).
247. Y.-M. Tsai and C. O. Cherng, *Tetrahedron Lett.*, **32**, 3515 (1991).

248. Y. Nakadaira, T. Kobayashi and H. Sakurai, *Bull. Chem. Soc. Jpn.*, **59**, 1509 (1986).
249. M. S. Loft, D. A. Widdowson and T. J. Mowlem, *Synlett*, 135 (1992).
250. J.-P. Beteille, M. P. Clarke, I. M. T. Davidson and J. Dubac, *Organometallics*, **8**, 1292 (1989).
251. B. Coleman, N. D. Conrad, M. W. Baum and M. Jones, Jr., *J. Am. Chem. Soc.*, **101**, 7743 (1979).
252. A. Sekiguchi, K. Ebata, Y. Terui and H. Sakurai, *Chem. Lett.*, 1417 (1991).
253. T. J. Barton and G. T. Burns, *Organometallics*, **2**, 1 (1983).
254. K. L. Bobbitt and P. P. Gaspar, *J. Organomet. Chem.*, **499**, 17 (1995).
255. A. Sekiguchi and W. Ando, *Chem. Lett.*, 1385 (1978).
256. H. Shinokubo, K. Oshima and K. Utimoto, *Chem. Lett.*, 461 (1995).
257. M. Bhupathy and T. Cohen, *Tetrahedron Lett.*, **28**, 4793 (1987).
258. E. J. Corey and C. Rücker, *Tetrahedron Lett.*, **25**, 4345 (1984).
259. S. V. Kirpichenko, E. N. Suslova, A. I. Albanov and B. A. Shainyan, *Tetrahedron Lett.*, **40**, 185 (1999).
260. S. Raucher and D. C. Schindele, *Synth. Commun.*, **17**, 637 (1987).
261. G. Maas and R. Brückmann, *J. Org. Chem.*, **50**, 2801 (1985).
262. R. Munschauer and G. Maas, *Angew. Chem., Int. Ed. Engl.*, **30**, 306 (1991).
263. P. Paetzold, S. Neyses and L. Gèret, *Z. Anorg. Allg. Chem.*, **621**, 732 (1995).
264. H.-M. He, P. E. Fanwick, K. Wood and M. Cushman, *J. Org. Chem.*, **60**, 5905 (1995).
265. K. Maruoka, T. Ito, Y. Araki, T. Shirasaka and H. Yamamoto, *Bull. Chem. Soc. Jpn.*, **61**, 2975 (1988).
266. S. Sato, I. Matsuda and Y. Izumi, *Tetrahedron Lett.*, **24**, 3855 (1983).
267. S. Chamberlin and W. D. Wulff, *J. Org. Chem.*, **59**, 3047 (1994).
268. R. Munschauer and G. Maas, *Chem. Ber.*, **125**, 1227 (1992).
269. E. Niecke, J. Böske, B. Krebs and M. Dartmann, *Chem. Ber.*, **118**, 3227 (1985).
270. V. D. Romanenko, L. K. Polyachenko and L. N. Markovskii, *Phosphorus and Sulfur*, **19**, 189 (1984).
271. J. C. Wilburn and R. H. Neilson, *Inorg. Chem.*, **18**, 347 (1979).
272. W. Schnurr and M. Regitz, *Z. Naturforsch., B: Chem. Sci.*, **43b**, 1285 (1988).
273. J. C. Wilburn, P. Wisian-Neilson and R. H. Neilson, *Inorg. Chem.*, **18**, 1429 (1979).
274. Z. M. Xie and R. H. Neilson, *Organometallics*, **2**, 921 (1983).
275. H. L. van Maanen, H. Keijn, J. T. B. H. Jastrzebski and G. van Koten, *Recl. Trav. Chim. Pays-Bas*, **113**, 567 (1994).
276. G. Ossig, A. Meller, C. Brönneke, O. Müller, M. Schäfer and R. Herbst-Irmer, *Organometallics*, **16**, 2116 (1997).
277. C. P. Gerlach and J. Arnold, *Inorg. Chem.*, **35**, 5770 (1996).
278. B. Dejak, Z. Lasocki and H. Jancke, *Bull. Pol. Acad. Sci. Chem.*, **33**, 275 (1985).
279. S. Jonas, M. Westerhausen and G. Simchen, *J. Organomet. Chem.*, **548**, 131 (1997).
280. M. Veith, A. Rammo and M. Hans, *Phosphorus, Sulfur and Silicon*, **93-94**, 197 (1994).
281. K. V. Katti and R. G. Cavell, *Inorg. Chem.*, **28**, 3033 (1989).
282. D. Schmidt-Baese and U. Klingebiel, *J. Organomet. Chem.*, **364**, 313 (1989).
283. W. Adam and X. Wang, *J. Org. Chem.*, **56**, 7244 (1991).
284. W.-K. Wong, C. Sun, T. Jiang, W.-T. Wong, F. Xue and T. C. W. Mak, *J. Chem. Soc., Dalton Trans.*, 693 (1997).
285. P. K. G. Hodgson, R. Katz and G. Zon, *J. Organomet. Chem.*, **117**, C63 (1978).
286. M. Gruber and R. Schmutzler, *Chem. Ber.*, **123**, 289 (1990).
287. M. Veith and A. Rammo, *Z. Anorg. Allg. Chem.*, **623**, 861 (1997).
288. W.-K. Wong, T. Jiang, D. W. J. Kwong and W.-T. Wong, *Polyhedron*, **14**, 1695 (1995).
289. E. W. Colvin, A. K. Beck, B. Bastani, D. Seebach, Y. Kai and J. D. Dunitz, *Helv. Chim. Acta*, **63**, 697 (1980).
290. T. Severengiz and W.-W. du Mont, *J. Chem. Soc., Chem. Commun.*, 820 (1987).
291. F. Zurmühlen and M. Regitz, *New J. Chem.*, **13**, 335 (1989).
292. F. Zurmühlen and M. Regitz, *Angew. Chem., Int. Ed. Engl.*, **26**, 83 (1987).
293. R. Appel and V. Barth, *Tetrahedron Lett.*, **21**, 1923 (1980).
294. G. Becker and G. Gutekunst, *Angew. Chem., Int. Ed. Engl.*, **16**, 463 (1977).
295. E. Fuchs, B. Breit, U. Bergsträßber, J. Hoffmann, H. Heydt and M. Regitz, *Synthesis*, 1099 (1991).
296. T. J. Barton and W. D. Wulff, *J. Organomet. Chem.*, **168**, 23 (1979).

297. H. Kwart and J. Slutsky, *J. Am. Chem. Soc.*, **94**, 2515 (1972).
298. A. G. Brook, D. M. MacRae and A. R. Bassindale, *J. Organomet. Chem.*, **86**, 185 (1975).
299. M. Takahashi and M. Kira, *J. Am. Chem. Soc.*, **119**, 1948 (1997).
300. T. Yamabe, K. Nakamura, Y. Shiota, K. Yoshizawa, S. Kawauchi and M. Ishikawa, *J. Am. Chem. Soc.*, **119**, 807 (1997).
301. R. F. W. Bader, *Atoms in Molecules. A Quantum Theory*, Oxford University Press, Oxford, 1990.
302. J. Slutsky and H. Kwart, *J. Am. Chem. Soc.*, **95**, 8678 (1973).
303. L. C. Zhang, C. Kabuto and M. Kira, *J. Am. Chem. Soc.*, **121**, 2925 (1999).
304. M. P. Clarke and I. M. T. Davidson, *J. Chem. Soc., Chem. Commun.*, 241 (1988).
305. P. P. Gaspar and R. West, in *The Chemistry of Organic Silicon Compounds*, Vol. 2, Part 3 (Eds. Z. Rappoport and Y. Apeloig), Wiley, Chichester, 1998, p. 2463.
306. N. Takeda, N. Tokitoh and R. Okazaki, *Chem. Lett.*, 622 (2000).
307. A. G. Brook, D. M. MacRae and W. W. Limburg, *J. Am. Chem. Soc.*, **89**, 5493 (1967).
308. A. G. Brook, *Acc. Chem. Res.*, **7**, 77 (1974).
309. G. L. Larson and Y. V. Fernandez, *J. Organomet. Chem.*, **86**, 193 (1975).
310. H. Kwart and W. E. Barnette, *J. Am. Chem. Soc.*, **99**, 614 (1977).
311. M. Oblin, F. Fotiadu, M. Rajzmann and J.-M. Pons, *J. Chem. Soc., Perkin Trans. 2*, 1621 (1997).
312. D. K. Anderson, J. M. Curtis and J. A. Sikorski, *Phosphorus, Sulfur and Silicon*, **101**, 291 (1995).
313. A. Maercker and R. Stötzel, *Chem. Ber.*, **120**, 1695 (1987).
314. R. Radinov and E. S. Schnurman, *Tetrahedron Lett.*, **40**, 243 (1999).
315. A. I. Al-Mansour, M. A. M. R. Al-Gurashi, C. Eaborn, F. A. Fattah and P. D. Lickiss, *J. Organomet. Chem.*, **393**, 27 (1990).
316. U. Klingebiel, S. Pohlmann, L. Skoda, C. Lensch and G. M. Sheldrick, *Z. Naturforsch., B.* **40b**, 1023 (1985).
317. H. A. Firgo and W. P. Weber, *Organometallics*, **1**, 649 (1982).
318. R. Damrauer, C. Eaborn, D. A. R. Happer and A. I. Mansour, *J. Chem. Soc., Chem. Commun.*, 348 (1983).
319. A. Padwa, W. H. Dent, A. M. Schoffstall and P. E. Yeske, *J. Org. Chem.*, **54**, 4430 (1989).
320. S. R. Wilson and G. M. Georgiadis, *J. Org. Chem.*, **48**, 4143 (1983).
321. K. Sternberg, H. Reinke and H. Oehme, *Z. Anorg. Allg. Chem.*, **625**, 467 (1999).
322. T. Kawashima, K. Naganuma and R. Okazaki, *Organometallics*, **17**, 367 (1998).
323. E. Nietzschmann, Y. Mrestani and M. Liebau, *Phosphorus, Sulfur and Silicon*, **116**, 65 (1996).
324. Y. Ohba, K. Ito, H. Maeda, H. Ebara, S. Takaki and T. Nagasawa, *Bull. Chem. Soc. Jpn.*, **71**, 2393 (1998).
325. N. Tokitoh, T. Matsumoto, H. Suzuki and R. Okazaki, *Tetrahedron Lett.*, **32**, 2049 (1991).
326. I. Kuwajima and R. Tanaka, *Tetrahedron Lett.*, **22**, 2381 (1981).
327. P. F. Hudrlik, R. R. Roberts, D. Ma and A. M. Hudrlik, *Tetrahedron Lett.*, **38**, 4029 (1997).
328. P. Sampson and D. F. Wiemer, *J. Chem. Soc., Chem. Commun.*, 1746 (1985).
329. M. Obayashi, K. Utimoto and H. Nozaki, *Bull. Chem. Soc. Jpn.*, **52**, 2646 (1979).
330. L. Duhamel, J. Gralak and B. Ngono, *J. Organomet. Chem.*, **464**, C11 (1994).
331. T. Müller, W. Ziche and N. Auner, Chap. 16 in *The Chemistry of Organic Silicon Compounds*, Vol. 2, (Eds. Z. Rappoport and Y. Apeloig), Wiley, Chichester, 1998, p. 857.
332. C. Krempner, H. Reinke and H. Oehme, *Chem. Ber.*, **128**, 143 (1995).
333. D. Hoffmann, H. Reinke and H. Oehme, *J. Organomet. Chem.*, **526**, 185 (1996).
334. F. Luderer, H. Reinke and H. Oehme, *Z. Anorg. Allg. Chem.*, **624**, 1519 (1998).
335. C. Krempner, H. Reinke and H. Oehme, *Chem. Ber.*, **128**, 1083 (1995).
336. C. Wendler and H. Oehme, *Z. Anorg. Allg. Chem.*, **622**, 801 (1996).
337. F. Luderer, H. Reinke and H. Oehme, *J. Organomet. Chem.*, **510**, 181 (1996).
338. Y. Apeloig, M. Bendikov, M. Yuzefovich, M. Nakash and D. Bravo-Zhivotovskii, *J. Am. Chem. Soc.*, **118**, 12228 (1996).
339. D. Bravo-Zhivotovskii, V. Braude, A. Stanger, M. Kapon and Y. Apeloig, *Organometallics*, **11**, 2326 (1992).
340. D. Bravo-Zhivotovskii, I. Zharov, M. Kapon and Y. Apeloig, *J. Chem. Soc., Chem. Commun.*, 1625 (1995).
341. D. J. Ager, *Synthesis*, 384 (1984).

342. G. L. Larson, *Pure Appl. Chem.*, **62**, 2021 (1990).
343. A. G. Brook, S. C. Nyburg, F. Abdesaken, B. Gutekunst, G. Gutekunst, R. K. M. R. Kallury, Y. C. Poon, Y.-M. Chang and W. Wong-Ng, *J. Am. Chem. Soc.*, **104**, 5667 (1982).
344. K. Toyota and M. Yoshifuji, *Rev. Heteroatom Chem.*, **5**, 152 (1991).
345. L. N. Markovski and V. D. Romanenko, *Tetrahedron*, **45**, 6019 (1989).
346. L. Weber, *Adv. Organomet. Chem.*, **41**, 1 (1997).
347. H. Shinokubo, K. Miura, K. Oshima and K. Utimoto, *Tetrahedron Lett.*, **34**, 1951 (1993).
348. H. Shinokubo, K. Miura, K. Oshima and K. Utimoto, *Tetrahedron*, **52**, 503 (1996).
349. R. K. Dhar, D. K. Clawson, F. R. Fronczek and P. W. Rabideau, *J. Org. Chem.*, **57**, 2917 (1992).
350. M. Daney, R. Lapouyade, B. Labrande and H. Bouas-Laurent, *Tetrahedron Lett.*, **21**, 153 (1980).
351. M. Daney, R. Lapouyade and H. Bouas-Laurent, *J. Org. Chem.*, **48**, 5055 (1983).
352. M. Daney, B. Labrande, R. Lapouyade and H. Bouas-Laurent, *J. Organomet. Chem.*, **159**, 385 (1978).
353. E. Vedejs, O. Daugulis, S. T. Diver and D. R. Powell, *J. Org. Chem.*, **63**, 2338 (1998).
354. T. A. Hase and L. Lahtinen, *J. Organomet. Chem.*, **240**, 9 (1982).
355. A. G. Brook and J. J. Chrusciel, *Organometallics*, **3**, 1317 (1984).
356. Y. Kitano, M. Kusakabe, Y. Kobayashi and F. Sato, *Chem. Lett.*, 523 (1986).
357. D. Seyferth, K. R. Wursthorn and R. E. Mammarella, *J. Org. Chem.*, **42**, 3104 (1977).
358. M. Tsukamoto, H. Iio and T. Tokoroyama, *Tetrahedron Lett.*, **26**, 4471 (1985).
359. M. Tsukamoto, H. Iio and T. Tokoroyama, *J. Chem. Soc., Chem. Commun.*, 880 (1986).
360. M. Ochiai, K. Sumi and E. Fujita, *Chem. Pharm. Bull.*, **32**, 3686 (1984).
361. I. Matsuda, S. Murata and Y. Izumi, *Bull. Chem. Soc. Jpn.*, **52**, 2389 (1979).
362. I. Matsuda, S. Murata and Y. Ishii, *J. Chem. Soc., Perkin Trans. 1*, 26 (1979).
363. D. A. Evans, J. M. Takacs and K. M. Hurst, *J. Am. Chem. Soc.*, **101**, 371 (1979).
364. M. Isobe, M. Kitamura and T. Goto, *Tetrahedron Lett.*, **20**, 3465 (1979).
365. M. Isobe, M. Kitamura and T. Goto, *Tetrahedron Lett.*, **21**, 4727 (1980).
366. I. Fleming and C. D. Floyd, *J. Chem. Soc., Perkin Trans. 1*, 969 (1981).
367. R. P. Woodbury and M. W. Rathke, *J. Org. Chem.*, **43**, 1947 (1978).
368. A. B. Smith, III and A. M. Boldi, *J. Am. Chem. Soc.*, **119**, 6925 (1997).
369. L. F. Tietze, H. Geissler, J. A. Gewert and U. Jakobi, *Synlett*, 511 (1994).
370. T. Takeda, S. Naito, K. Ando and T. Fujiwara, *Bull. Chem. Soc. Jpn.*, **56**, 967 (1983).
371. M.-R. Fischer, A. Kirschning, T. Michel and E. Schaumann, *Angew. Chem., Int. Ed. Engl.*, **33**, 217 (1994).
372. B. A. Keay, *Chem. Soc. Rev.*, **28**, 209 (1999).
373. E. J. Bures and B. A. Keay, *Tetrahedron Lett.*, **29**, 1247 (1988).
374. P. G. Spinazzé and B. A. Keay, *Tetrahedron Lett.*, **30**, 1765 (1989).
375. W. A. Christofoli and B. A. Keay, *Tetrahedron Lett.*, **32**, 5881 (1991).
376. B. A. Keay and J.-L. J. Bontront, *Can. J. Chem.*, **69**, 1326 (1991).
377. W. A. Christofoli and B. A. Keay, *Synlett*, 625 (1994).
378. S. P. Maddaford and B. A. Keay, *J. Org. Chem.*, **59**, 6501 (1994).
379. S. P. Maddaford, N. G. Andersen, W. A. Christofoli and B. A. Keay, *J. Am. Chem. Soc.*, **118**, 10766 (1996).
380. S. Yu and B. A. Keay, *J. Chem. Soc., Perkin Trans. 1*, 2600 (1991).
381. E. Bures, P. G. Spinazzé, G. Beese, I. R. Hunt, C. Rogers and B. A. Keay, *J. Org. Chem.*, **62**, 8741 (1997).
382. E. J. Bures and B. A. Keay, *Tetrahedron Lett.*, **28**, 5965 (1987).
383. G. Beese and B. A. Keay, *Synlett*, 33 (1991).
384. R. E. Danso-Danquah, A. I. Scott and D. Becker, *Tetrahedron*, **49**, 8195 (1993).
385. A. R. Katritzky, D. Toader and X. Wang, *J. Org. Chem.*, **63**, 9978 (1998).
386. A. R. Katritzky and D. Toader, *J. Am. Chem. Soc.*, **119**, 9321 (1997).
387. K. D. Kim and P. A. Magriotis, *Tetrahedron Lett.*, **31**, 6137 (1990).
388. K. K. Wang, C. Liu, Y. G. Gu and F. N. Burnett, *J. Org. Chem.*, **56**, 1914 (1991).
389. M. Lautens, P. H. M. Delanghe, J. B. Goh and C. H. Zhang, *J. Org. Chem.*, **60**, 4213 (1995).
390. Y. M. Hijji, P. F. Hudrlik and A. M. Hudrlik, *Chem. Commun.*, 1213 (1998).
391. B. M. Comanita, S. Woo and A. G. Fallis, *Tetrahedron Lett.*, **40**, 5283 (1999).
392. R. J. Billedeau, M. P. Sibi and V. Snieckus, *Tetrahedron Lett.*, **24**, 4515 (1983).

393. S. Hünig and M. Öller, *Chem. Ber.*, **113**, 3803 (1980).
394. T. N. Mitchell and M. Schütze, *Tetrahedron*, **55**, 1285 (1999).
395. K. Yamamoto, T. Kimura and Y. Tomo, *Tetrahedron Lett.*, **26**, 4505 (1985).
396. S. Marumoto and I. Kuwajima, *Chem. Lett.*, 1421 (1992).
397. S. Marumoto and I. Kuwajima, *J. Am. Chem. Soc.*, **115**, 9021 (1993).
398. C. A. A. van Boeckel, S. F. van Aelst and R. Beetz, *Recl. Trav. Chim. Pays-Bas*, **102**, 415 (1983).
399. H.-J. Gais, H. Müller, J. Decker and R. Hainz, *Tetrahedron Lett.*, **36**, 7433 (1995).
400. C. Gibson, T. Buck, M. Noltemeyer and R. Brückner, *Tetrahedron Lett.*, **38**, 2933 (1997).
401. C. Gibson, T. Buck, M. Walker and R. Brückner, *Synlett*, 201 (1998).
402. R. Hoffmann and R. Brückner, *Chem. Ber.*, **125**, 1471 (1992).
403. K. Behres, B. O. Kneisel, M. Noltemeyer and R. Brückner, *Liebigs Ann.*, 385 (1995).
404. E. Winter and R. Brückner, *Synlett*, 1049 (1994).
405. F. Samtleben, M. Noltemeyer and R. Brückner, *Tetrahedron Lett.*, **38**, 3893 (1997).
406. D. Goepfel and R. Brückner, *Tetrahedron Lett.*, **38**, 2937 (1997).
407. R. Hoffmann and R. Brückner, *Chem. Ber.*, **125**, 2731 (1992).
408. J. Bousbaa, F. Ooms and A. Krief, *Tetrahedron Lett.*, **38**, 7625 (1997).
409. X.-L. Jiang and W. F. Bailey, *Organometallics*, **14**, 5704 (1995).
410. C. Rücker, *Tetrahedron Lett.*, **25**, 4349 (1984).
411. J. O. Karlsson, N. V. Nguyen, L. D. Foland and H. W. Moore, *J. Am. Chem. Soc.*, **107**, 3392 (1985).
412. H. Fritz, P. Sutter and C. D. Weis, *J. Org. Chem.*, **51**, 558 (1986).
413. J. Mora and A. Costa, *Tetrahedron Lett.*, **25**, 3493 (1984).
414. R. F. Cunico and C. P. Kuan, *J. Org. Chem.*, **55**, 4634 (1990).
415. J. Clayden and M. Julia, *Synlett*, 103 (1995).
416. M. Lauten, P. H. M. Delanghe, J. B. Goh and C. H. Zhang, *J. Org. Chem.*, **57**, 3270 (1992).
417. S. S. Jones and C. B. Reese, *J. Chem. Soc., Perkin Trans. 1*, 2762 (1979).
418. G. H. Dodd, B. T. Golding and P. V. Ioannow, *J. Chem. Soc., Perkin Trans. 1*, 2273 (1976).
419. J. M. Lassaletta and R. R. Schmidt, *Synlett*, 925 (1995).
420. C. A. A. van Boeckel, S. F. van Aelst and T. Beetz, *Recl. Trav. Chim. Pays-Bas*, **102**, 415 (1983).
421. J. Mulzer and B. Schöllhorn, *Angew. Chem., Int. Ed. Engl.*, **29**, 431 (1990).
422. T. K. M. Shing and Y. Tang, *Tetrahedron*, **46**, 6575 (1990).
423. K. K. Ogilvie, S. L. Beaucage, A. L. Schifman, N. Y. Theriault and K. L. Sadana, *Can. J. Chem.*, **56**, 2768 (1978).
424. W. Köhler and W. Pfeleiderer, *Liebigs Ann. Chem.*, 1855 (1979).
425. U. Peters, W. Bankova and P. Welzel, *Tetrahedron*, **43**, 3803 (1987).
426. J. Jurczak, S. Pikul and K. Ankner, *Pol. J. Chem.*, **61**, 767 (1987).
427. M. Braun and H. Mahler, *Liebigs Ann.*, 29 (1995).
428. J. Mulzer and S. Greifenberg, *Heterocycles*, **40**, 93 (1995).
429. S.-H. Chen and S. J. Danishefsky, *Tetrahedron Lett.*, **31**, 2229 (1990).
430. R. W. Friesen and A. K. Daljeet, *Tetrahedron Lett.*, **31**, 6133 (1990).
431. C. F. Masaguer, Y. Blériot, J. Charlwood, B. G. Winchester and G. W. J. Fleet, *Tetrahedron*, **53**, 15147 (1997).
432. Y. Blériot, C. F. Masaguer, J. Charlwood, B. G. Winchester, A. L. Lane, S. Crook, D. J. Watkin and G. W. J. Fleet, *Tetrahedron*, **53**, 15135 (1997).
433. J. F. Kadow, M. G. Saulnier, M. M. Tun, D. R. Langley and D. M. Vyas, *Tetrahedron Lett.*, **30**, 3499 (1989).
434. M. Kira, L. C. Zhang, C. Kabuto and H. Sakurai, *Chem. Lett.*, 659 (1995).
435. L. A. Paquette, H.-S. Lin and J. C. Gallucci, *Tetrahedron Lett.*, **28**, 1363 (1987).
436. T. Yamazaki, T. Oniki and T. Kitazume, *Tetrahedron*, **52**, 11753 (1996).
437. T. Yamazaki, K. Mizutani and T. Kitazume, *J. Org. Chem.*, **58**, 4346 (1993).
438. T. Yamazaki, K. Mizutani and T. Kitazume, *J. Org. Chem.*, **60**, 6046 (1995).
439. T. Yamazaki, K. Mizutani, M. Takeda and T. Kitazume, *J. Chem. Soc., Chem. Commun.*, 55 (1992).
440. S. Hünig and G. Wehner, *Chem. Ber.*, **112**, 2062 (1979).
441. S. Hünig and C. Marschner, *Chem. Ber.*, **123**, 107 (1990).
442. S. Hünig and G. Wehner, *Synthesis*, 391 (1975).

443. R. E. Koenigkramer and H. Zimmer, *J. Org. Chem.*, **45**, 3994 (1980).
444. M. Well and R. Schmutzler, *Phosphorus, Sulfur and Silicon*, **72**, 189 (1992).
445. H. Mack, G. Frenzen, M. Bendikov and M. S. Eisen, *J. Organomet. Chem.*, **549**, 39 (1997).
446. R. J. P. Corriu, B. Geng and J. J. E. Moreau, *J. Org. Chem.*, **58**, 1443 (1993).
447. R. J. P. Corriu, G. Bolin and J. J. E. Moreau, *Tetrahedron Lett.*, **32**, 4121 (1991).
448. A. Degl'Innocenti, A. Mordini, D. Pinzani, G. Reginato and A. Ricci, *Synlett*, 712 (1991).
449. R. H. Neilson and D. W. Goebel, *J. Chem. Soc., Chem. Commun.*, 769 (1979).
450. D. W. Morton and R. H. Neilson, *Organometallics*, **1**, 289 (1982).
451. J. L. Adams, T.-M. Chen and B. W. Metcalf, *J. Org. Chem.*, **50**, 2730 (1985).
452. S. Katsumura, S. Iwama, T. Matsuda, T. Tani, S. Fujii and K. Ikeda, *Bioorg. Med. Chem. Lett.*, **3**, 2703 (1993).
453. A. S. Kende, P. Hebeisen and R. C. Newbold, *J. Am. Chem. Soc.*, **110**, 3315 (1988).
454. M. C. Pirrung and Y. R. Lee, *Tetrahedron Lett.*, **34**, 8217 (1993).
455. G. Anderson, D. W. Cameron, G. I. Feutrill and R. W. Read, *Tetrahedron Lett.*, **22**, 4347 (1981).
456. P. R. Brook, B. Devadas and P. G. Sammes, *J. Chem. Res., Synop.*, 135 (1982).
457. J. R. Green, M. Majewski, B. I. Alo and V. Snieckus, *Tetrahedron Lett.*, **27**, 535 (1986).
458. C. P. Casey, C. R. Jones and H. Tukada, *J. Org. Chem.*, **46**, 2089 (1981).
459. J. Besida and R. F. C. Brown, *Aust. J. Chem.*, **35**, 1385 (1982).
460. J. A. McClarin, A. Schwartz and T. J. Pinnavaia, *J. Organomet. Chem.*, **188**, 129 (1980).
461. W. T. Brady and K. Saidi, *J. Org. Chem.*, **55**, 4215 (1990).
462. D. A. Evans, J. A. Murry and M. C. Kozlowski, *J. Am. Chem. Soc.*, **118**, 5814 (1996).
463. N. S. Rao and L. D. Quin, *J. Org. Chem.*, **49**, 3157 (1984).
464. G. Hussmann, W. D. Wulff and T. J. Barton, *J. Am. Chem. Soc.*, **105**, 1263 (1983).
465. T. J. Barton, W. D. Wulff and S. A. Burns, *Organometallics*, **2**, 4 (1983).
466. C. Eaborn, M. N. El-Kheli, N. Retta and J. D. Smith, *J. Organomet. Chem.*, **249**, 23 (1983).
467. M. E. Jung and C. J. Nichols, *J. Org. Chem.*, **61**, 9065 (1996).
468. W.-P. Leung, K. S. M. Poon, T. C. W. Mak and Z.-Y. Zhang, *Organometallics*, **15**, 3262 (1996).
469. K. W. Pankiewicz, K. A. Watanabe, H. Takayanagi, T. Itoh and H. Ogura, *J. Heterocycl. Chem.*, **22**, 1703 (1985).
470. C. H. M. Verdegaal, P. L. Jansse, J. F. M. de Rooij and J. H. van Boom, *Tetrahedron Lett.*, **21**, 1571 (1980).
471. C. M. Angelov, D. A. Mazzuca and R. G. Cavell, *Phosphorus, Sulfur and Silicon*, **109-110**, 541 (1996).

CHAPTER 17

Kinetic studies of the reactions of Si=C and Si=Si bonds

TRACY L. MORKIN, THOMAS R. OWENS and WILLIAM J. LEIGH

*Department of Chemistry, McMaster University, 1280 Main Street West, Hamilton,
Ontario, Canada L8S 4M1
Fax: (1) 905 522-2509; e-mail: leigh@mcmaster.ca*

I. INTRODUCTION	950
II. EXPERIMENTAL METHODS	950
III. KINETICS AND MECHANISMS OF THE REACTIONS OF SILENES	951
A. Unimolecular Reactions	951
B. Bimolecular Reactions	954
1. General trends	954
2. Dimerization	959
3. Nucleophilic addition	964
a. Addition of water and alcohols	964
b. Addition of acetic acid	974
c. Addition of aliphatic amines	976
d. Addition of alkoxy silanes	978
4. Ene- and [2 + 2]-addition of ketones, aldehydes and esters	980
5. Ene-, [2 + 2]- and [4 + 2]-cycloaddition of alkenes and dienes	986
6. Other reactions—oxygen, sulphoxides and halocarbons	988
7. Solvent effects on silene reactivity	991
C. Substituent Effects on Silene Reactivity	994
1. Silenes of the type (R)MeSi=CH ₂ and Me ₂ Si=CHR	995
2. 1-Silaallenes	1001
IV. KINETICS AND MECHANISMS OF THE REACTIONS OF DISILENES	1004
A. Unimolecular Reactions	1004
B. Bimolecular Reactions	1006
1. Addition of alcohols and phenols	1007
2. [2 + 4]-, [2 + 2]- and [2 + 1]-Cycloadditions of dienes, carbonyl compounds and oxygen	1017

V. CONCLUSIONS	1020
VI. APPENDIX: NEGATIVE ARRHENIUS ACTIVATION ENERGIES	1021
VII. REFERENCES	1022

I. INTRODUCTION

The study of compounds containing multiple bonds to silicon has been an area of active interest since the mid-1960s, when Gusel'nikov and Flowers reported the first evidence of the possible existence of a silicon-carbon doubly bonded species as a reactive intermediate in the high temperature pyrolysis of a silacyclobutane derivative¹. Hundreds of examples of silenes and disilenes are now known, and their chemistries have been reviewed on a regular basis since the mid-1970s [Silenes: References 2–13; Disilenes: References 7, 8, 11, 14–16]. Many examples of stable silenes and disilenes have been synthesized since the first examples were reported by Brook and West and their coworkers^{17,18}, respectively, and many of the qualitative aspects of the rich reactivities of these compounds are well established. However, a detailed understanding of the mechanisms of their characteristic reactions can only be provided by chemical kinetics, and precious little information of this type existed prior to the early 1990s, particularly in the field of silene chemistry. This is partly because the direct detection and quantitative study of the reactivity of these typically highly reactive, transient species requires the use of fast time-resolved spectroscopic techniques that have only become readily available in recent years.

This chapter reviews the body of literature (to August 2000) that deals specifically with kinetic studies of the reactions of silenes and disilenes and the mechanistic information that has been derived from them. The spectroscopic properties, structures, methods of synthesis and qualitative aspects of the reactivity of silenes and disilenes have been covered comprehensively in the preceding two volumes in this series and elsewhere, and so will not be treated extensively here.

The focus of the section on silene reaction kinetics is mainly on studies of *bimolecular* reactions of *transient* silene derivatives, because little absolute kinetic data exist for the reactions of stable derivatives and there have been few quantitative studies of the kinetics of unimolecular isomerizations such as *E,Z*-isomerization and pericyclic rearrangements, although a number of examples of such reactions are of course well known. In contrast, most of the studies of disilene reaction kinetics that have been reported have employed kinetically stable derivatives, and *E,Z*-isomerization has thus been fairly well characterized. The paucity of absolute rate data for unimolecular isomerizations of *transient* silenes and disilenes is most likely due to the fact that it is comparatively difficult to obtain reliable data of this type for transient species whose bimolecular reactions (including dimerization) are so characteristically rapid, unless the unimolecular process is itself relatively facile. Such instances are rare, at least for transient silenes and disilenes at ambient temperatures.

II. EXPERIMENTAL METHODS

Since the bulk of the data to be discussed below have been obtained using the technique of laser flash photolysis, it is appropriate to begin with a brief description of the experiment and the way in which absolute rate constants are extracted from the data it provides.

The laser flash photolysis technique relies on the use of a pulsed UV laser for the rapid synthesis of the reactive intermediate of interest by photochemical decomposition of a suitable stable precursor, and (most commonly) fast time-resolved UV/VIS spectrophotometry to detect the species and monitor its decay¹⁹. The absorbance-time profile so

obtained is then analysed to extract the kinetic parameters governing the transient's decay under the particular experimental conditions employed. The analysis is simplest and most precise when the transient decays with first- or pseudo-first-order kinetics; in this situation, the transient absorbance varies with time according to equation 1, where $(\Delta OD)_t$ is the transient absorbance at time t after the laser pulse, $(\Delta OD)_0$ is the absorbance at the peak of the laser pulse and k_{obs} is the pseudo-first-order rate constant for decay. Most laser photolysis systems available today employ lasers with 5–25 ns pulse widths, sufficient power to enable the generation of transient species at initial concentrations in the range of 10^{-4} – 10^{-6} M, and the ability to monitor their decay with nanosecond time resolution. However, it should be remembered that so long as the decay follows pseudo-first-order kinetics, the actual concentration of the transient need not be known in order to extract the absolute rate constant for reaction of the species. This is fortunate, because the determination of extinction coefficients for transient, photochemically-produced species is a rather involved procedure, and the values obtained have sizeable errors associated with them²⁰.

$$(\Delta OD)_t = (\Delta OD)_0 \exp(-k_{\text{obs}}t) \quad (1)$$

In terms of chemical significance, k_{obs} is the sum of the rate constants for all first- and pseudo-first-order reactions that the transient undergoes under the particular conditions of the experiment (equation 2)—unimolecular reaction (k_{uni}) and reaction of the transient with other species, such as one or more impurities (I_t) in the system of unknown concentration (e.g. oxygen or water) or something that is intentionally added ('Q') at a known concentration. For most silenes and disilenes, unimolecular reactions are relatively slow at ambient temperatures, and k_{obs} is thus comprised predominantly of pseudo-first-order terms reflecting bimolecular reaction with other substrates. When great care is taken to exclude oxygen and water from the solvent and in the absence of intentionally added co-reactants, the decay of most silenes takes on a second-order component due to dimerization. Unless there is specific interest in determining rate constants for dimerization or for a true unimolecular reaction of a silene or disilene, completely ridding the solution of reactive impurities is not essential.

$$k_{\text{obs}} = k_{\text{uni}} + \Sigma k_I[I] + k_Q[Q] \sim \Sigma k_I[I] + k_Q[Q] \quad (2)$$

The determination of the bimolecular rate constant for reaction of the transient with an intentionally added reagent Q is determined by measuring k_{obs} for several solutions of known concentration in Q. For a 'simple' bimolecular reaction (i.e. one which is first order in the transient and first order in Q), a plot of k_{obs} vs. [Q] according to equation 3, where k_0 is the pseudo-first-order rate constant for decay in the absence of Q ($=\Sigma k_I[I]$ in equation 2), is linear with slope equal to k_Q .

$$k_{\text{obs}} = k_0 + k_Q[Q] \quad (3)$$

III. KINETICS AND MECHANISMS OF THE REACTIONS OF SILENES

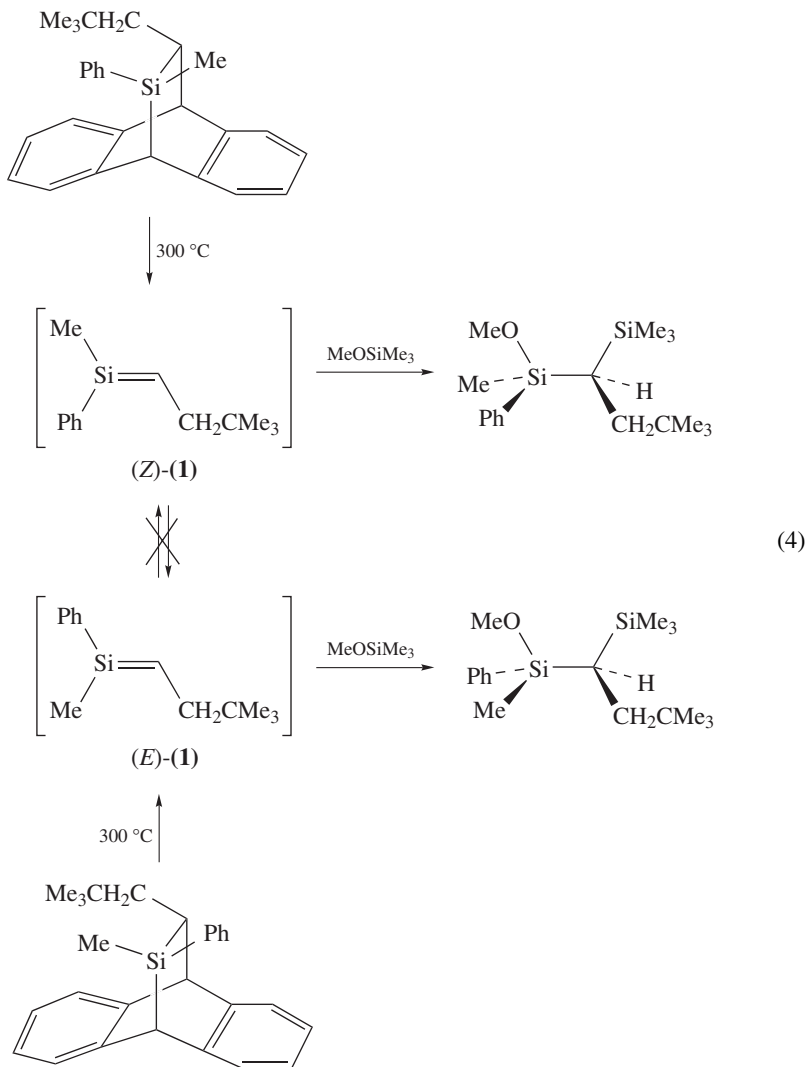
A. Unimolecular Reactions

As mentioned earlier, few absolute kinetic data exist for unimolecular reactions of silenes, largely because most of the known silene rearrangements occur under high temperature pyrolytic conditions and are difficult to measure directly^{8,10,12}.

Geometric isomerization is normally quite slow except at exceedingly high temperatures, as a result of the fairly substantial strength of the Si=C bond (*ca* 160 kJ mol⁻¹)*^{21,22}. For

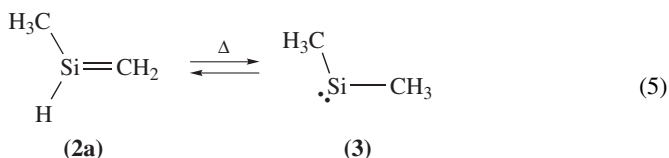
* 1 kJ mol⁻¹ = 0.239 kcal mol⁻¹.

example, (*E*)- and (*Z*)-1-methyl-1-phenyl-2-neopentylsilene (**1**) are known to be 'configurationally stable' up to *ca* 300 °C, on the basis that they can be trapped stereospecifically with methoxytrimethylsilane upon generation by thermolysis of the corresponding anthracene adducts (equation 4)²³. Interconversion of the two isomers occurs competitively with alkoxylation only at temperatures in excess of 400 °C²³.

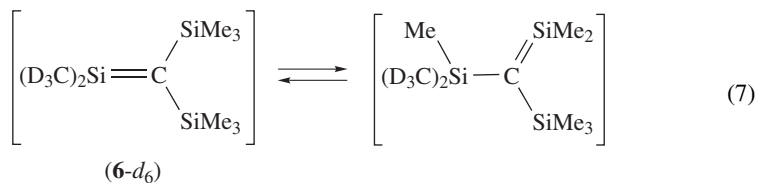
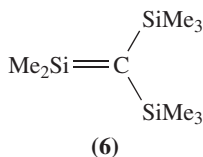
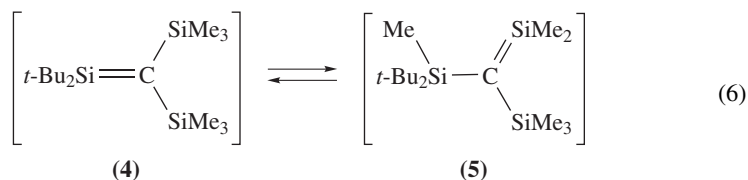


Arrhenius parameters for the reversible interconversion of 1-methylsilene ($\text{MeHSi}=\text{CH}_2$, **2a**) and dimethylsilylene (**3**) via 1,2-H shift, an example of the well-known silene-to-silylene isomerization (equation 5), have been reported by two groups^{24,25}. The earlier values of Davidson and Scampton [$E_a = 166 \text{ kJ mol}^{-1}$ and $\log(A/\text{s}^{-1}) \sim 13.5$ in both

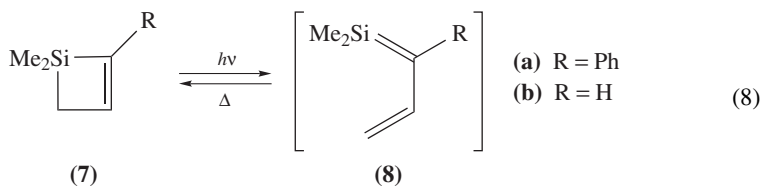
directions²⁴] are in better agreement with the theoretical estimate of $E_a = 172 \text{ kJ mol}^{-1}$.²⁶



Relatively few absolute rate constants have been reported for the silene rearrangements that are known to occur at or near room temperature, such as the interconversion of 1,1-*tert*-butyl-2,2-bis(trimethylsilyl)silene (**4**) and its kinetically stable isomer **5** via 1,3-methyl migration (equation 6)^{27–29}. The analogous migration in the simpler dimethyl derivative of this type (**6**) occurs with a half-life $\tau_{1/2} \sim 30 \text{ min}$ at 120°C , as measured by monitoring the scrambling of the $-\text{CD}_3$ groups in **6-d**₆ (equation 7)³⁰.



Conlin and coworkers reported a rate constant for the thermal electrocyclic ring closure of the transient 1,3-(1-sila)butadiene derivative **8a** in cyclohexane at 25°C , $k = (1.19 \pm 0.06) \times 10^5 \text{ s}^{-1}$.³¹ The rate constant corresponds to the inverse of the lifetime of the silene in the dry solvent, as measured by laser flash photolysis of the isomeric silacyclobutene derivative **7a**, the stable product of the thermal ring closure reaction (equation 8). An Arrhenius activation energy of $E_a \text{ ca } 38 \text{ kJ mol}^{-1}$ was estimated from the single rate constant, assuming a pre-exponential factor of 10^{12} s^{-1} .



A similar first-order decay rate constant was later reported for silene **8b** in deoxygenated isooctane solution, $k_{\text{decay}} = (1.5 \pm 0.1) \times 10^5 \text{ s}^{-1}$ at 23°C ³². Arrhenius parameters for decay of the silene were determined to be $E_a = 2.0 \pm 0.8 \text{ kJ mol}^{-1}$ and $\log(A/\text{s}^{-1}) = 5.7 \pm 0.2$ from rate constants obtained over the $20\text{--}60^\circ\text{C}$ temperature range. These values are unreasonable for a unimolecular isomerization reaction, and it was proposed that the first-order decay rate constant measured under these conditions likely contains a pseudo-first-order component due to reaction of the silene with trace hydroxylic impurities in the solvent. Reaction with such species was verified in the case of methanol addition to be sufficiently fast (*vide infra*) that an impurity concentration of only 10^{-4} M would be required in order to produce a silene lifetime on the order of $5 \mu\text{s}$, as was found for both **8b** and **8a**. It was further found that the Arrhenius activation energy for reaction of MeOH with **8b** is *negative* (*vide infra*); thus the value of E_a *ca* 2.0 kJ mol^{-1} found for the unimolecular decay of **8b** is very likely a composite of a larger positive activation energy for thermal electrocyclic ring closure and a negative activation energy for impurity quenching, assuming that water or a solvent-derived alcohol is the most likely culprit.

This exemplifies one of the inherent problems with rate measurements for unimolecular processes in solution-phase laser flash photolysis experiments, that was alluded to in the previous section — *ruling out* pseudo-first-order contributions to an observed lifetime due to impurity quenching. Such problems usually cannot be discounted on the basis of product analyses from steady-state photolysis experiments using higher bulk substrate concentrations, as was suggested in the original work on **8a**³¹. It has thus been concluded that the absolute rate constants for thermal electrocyclic ring closure of **8a,b** are very likely to be less than 10^5 s^{-1} in hydrocarbon solvents at 25°C ³²; they are probably not lower than *ca* 10^4 s^{-1} , however. The determination of more accurate values will require further, more detailed study of these compounds under better-controlled experimental conditions.

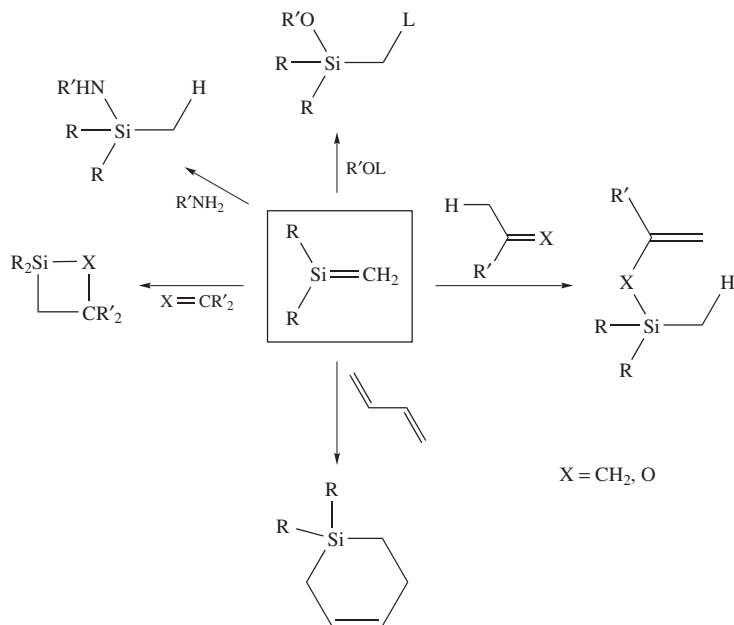
B. Bimolecular Reactions

Many of the common bimolecular trapping reactions of transient silenes have been investigated using time-resolved spectroscopic methods. Our discussion will begin with an overview of the trends in absolute and relative reactivities that are exhibited by a few representative silenes toward various trapping reagents. The following sections will deal with the information that these data and those for other derivatives provide on the mechanisms of silene trapping reactions, a discussion of the general effects of solvent on silene reactivity, and finally, the contribution that such data have made to our present understanding of the effects of substituents on the kinetic stability of the Si=C bond.

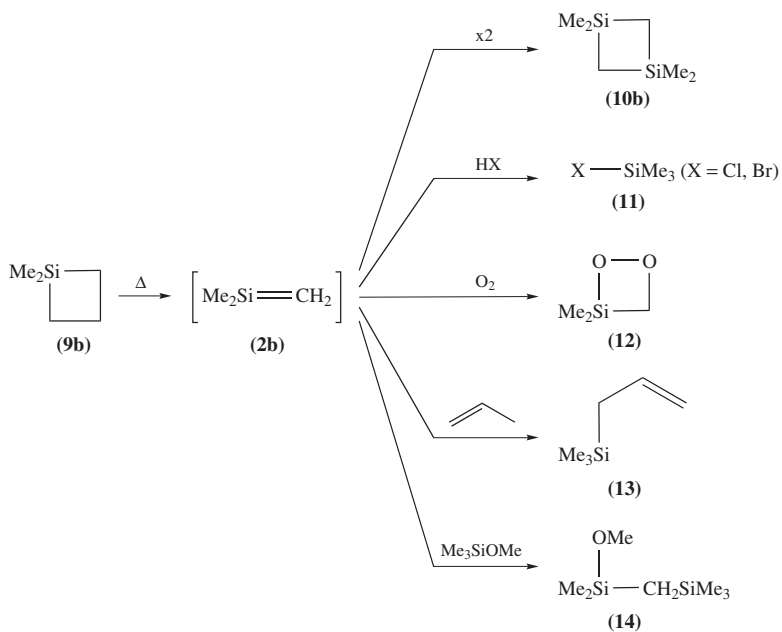
1. General trends

Over the past ten years, absolute rate data have been reported on the kinetics of several bimolecular silene reactions in solution, including both head-to-tail and head-to-head dimerization; the [1,2]-addition reactions of nucleophilic reagents such as water, aliphatic alcohols, alkoxy silanes, carboxylic acids and amines; and the ene-addition, [2 + 2]-cycloaddition and/or [4 + 2]-cycloaddition of ketones, aldehydes, esters, alkenes, dienes and oxygen. The normal outcomes of these reactions are summarized in Scheme 1.

Prior to the late 1980s, the only absolute kinetic data that had been reported for bimolecular reactions of transient silenes were the gas-phase values of Gusel'nikov, Nametkin and coworkers on the dimerization of 1,1-dimethylsilene (**2b**), produced by thermal cycloreversion of 1,1-dimethylsilacyclobutane (**9b**)³³, and those of Davidson and Wood³⁴, who studied the competitive trapping of **2b** with hydrogen halides, oxygen, methoxytrimethylsilane and propene to yield the products **11–14** (Scheme 2). Rate constants and Arrhenius



SCHEME 1



SCHEME 2

TABLE 1. Absolute rate constants and Arrhenius activation energies for the addition of various reagents to 1,1-dimethylsilene (**2b**) in the gas phase (relative to $k_{\text{dim}} = 5.9 \times 10^{-15} \text{ cm}^3 \text{ s}^{-1}$)^a

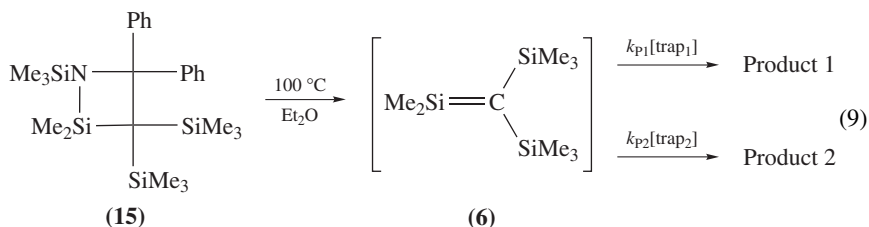
Quencher	$\log (A/M^{-1} \text{ s}^{-1})$	E_a (kJ mol ⁻¹)	k^{800K} ($10^{-15} \text{ cm}^3 \text{ s}^{-1}$)
Me ₃ SiOMe	5.3 ± 0.2	6.3 ± 2.2	0.128
HCl	7.5 ± 0.5	10 ± 7	11.6
O ₂	7.6 ± 0.3	15 ± 5	6.98
HBr	7.4 ± 0.5	36 ± 7	0.0018
C ₃ H ₆	5.2 ± 0.6	35 ± 4	0.0014

^aData from Reference 34.

parameters were calculated from the relative yields of the individual trapping products with respect to that of the head-to-tail dimer (**10b**) over the 500–540 °C temperature range, using the values of the rate constant and Arrhenius parameters for dimerization reported by Gusel'nikov, Nametkin and coworkers: $k_{\text{dim}} = 5.9 \times 10^{-15} \text{ cm}^3 \text{ s}^{-1}$ and $E_a = 0 \text{ kJ mol}^{-1}$ ³³. The trapping reaction with methanol was also attempted, but proved to be too fast for the low pressure pyrolysis (LPP) technique employed.

The rate constants and Arrhenius parameters reported by Davidson and Wood are listed in Table 1. Unfortunately, these values are meaningful only in a relative sense, since the dimerization rate constant on which their calculation was based is now known to be incorrect (*vide infra*)^{22,35}.

The only solution-phase data that existed were the relative rate data of Wiberg, for the competitive reaction of various trapping reagents with the transient silene **6** (equation 9)^{6,36}. Silene **6** was produced by thermolysis of the silazetidine **15** in ether solution at 100 °C in the presence of two competing trapping reagents present in known concentrations, and relative rates were determined from the relative yields of the two resulting products. Competition kinetic data and product studies have been reported by Wiberg and coworkers for an impressively extensive range of silene trapping reagents, and the work has been summarized in a 1987 paper from this group³⁶. Table 2 lists the relative rate data from this publication; it should be noted that the statistical correction factors that were originally applied to the values for some of the reagents have been removed in the present tabulation, since our purpose is to show the trends in relative *total* reactivity of these reagents.



Absolute rate constants have recently been measured for some of these reactions in hexane solution³⁷, using laser flash photolysis methods to generate **6** by photodecomposition of diazo compound **16** (equation 10)^{38,39}. These are likely to be significantly greater than they would be in ether solution (see Section III.B.6), but their relative magnitudes are in good agreement with Wiberg's estimates. The absolute rate constants for the two silene traps that have been studied so far (MeOH and *t*-BuOH) are collected along with

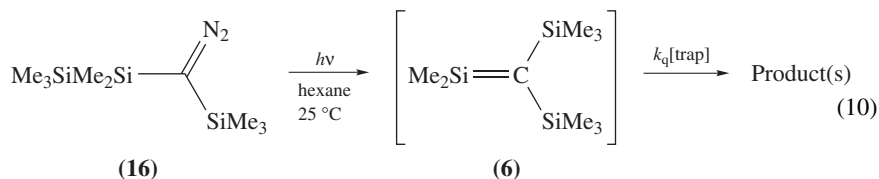
TABLE 2. Relative and absolute rate constants for reactions of silene **6** with various reagents in solution

Reagent	k_{rel}^a [$k_{\text{q}}/10^9 \text{ M}^{-1} \text{ s}^{-1}$] ^b	Type of reaction
MeOH	10,500 [14 ± 1]	1,2-addition
EtOH	6,500	1,2-addition
<i>i</i> -PrOH	5,000	1,2-addition
<i>t</i> -BuOH	3,400 [7.3 ± 0.4]	1,2-addition
<i>n</i> -C ₅ H ₁₁ OH	850	1,2-addition
<i>c</i> -C ₆ H ₁₁ OH	380	1,2-addition
PhOH	105	1,2-addition
PhSH	140	1,2-addition
CH ₃ CO ₂ H (AcOH)	8,500	
Ph ₂ C=O	2,340	[2+2]-cycloaddition
Me ₂ C=O	420	ene-addition
<i>i</i> -PrNH ₂	11,500	1,2-addition
<i>t</i> -BuNH ₂	5,500	1,2-addition
PhNH ₂	235	1,2-addition
Ph ₂ C=NH	7,000	1,2-addition
<i>t</i> -BuN ₃	115	[2+3]-cycloaddition
isoprene	2.9	[2+4]:ene:[2+2] = 4.6:1.5:0.32
2,3-dimethyl-1,3-butadiene (DMB)	4.6	[2+4]:ene = 3.7:0.95
<i>trans</i> -piperylene	1.5	[2+4]-cycloaddition
cyclopentadiene	2.9	[2+4]-cycloaddition
1,3-butadiene	1	[2+4]-cycloaddition
<i>cis</i> -piperylene	<i>ca</i> 0.0075	[2+2]-cycloaddition
propene	1.45	ene-addition
isobutene	2.3	ene-addition
<i>cis</i> -2-butene	0.42	ene-addition
<i>trans</i> -2-butene	0.31	ene-addition

^aIn ether solution at 100 °C. Data from Reference 36.

^bIn hexane solution at 25 °C. Data from Reference 37.

Wiberg's relative rate data in Table 2.



1,1-Diphenylsilene (**19a**), produced by photolysis of 1,1-diphenyl- or 1,1,2-triphenylsilacyclobutane (**17a** and **18**, respectively; equation 11), has been particularly well studied, and absolute rate constants have been reported for a wide variety of silene trapping reactions in various solvents at room temperature (see Table 3)^{40–46}. Not all of these have been accompanied by product studies, unfortunately. A number of other transient silenes have been characterized as well with solution-phase kinetic data for a range of bimolecular silene trapping reactions, though much less extensively than **19a**. These include the cyclic 1,3,5-(1-sila)hexatriene derivatives **21a–c** (formed by photolysis

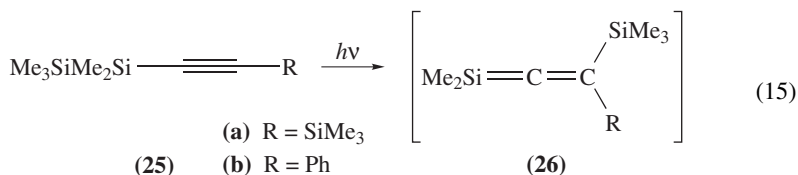
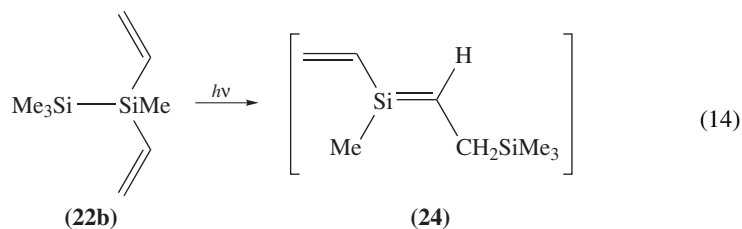
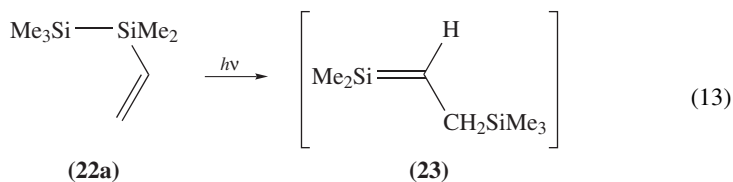
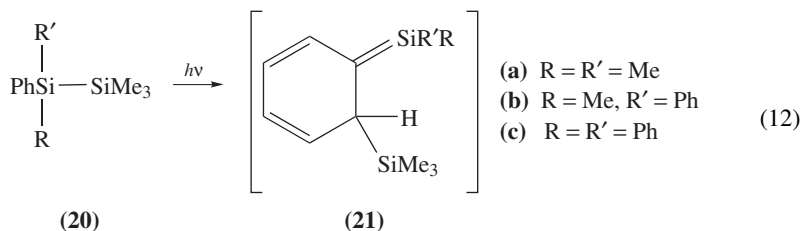
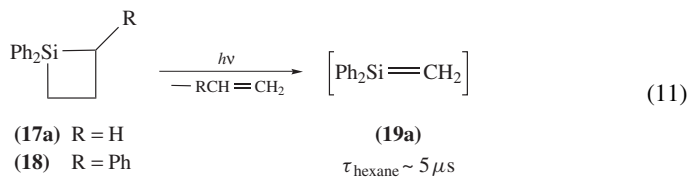
TABLE 3. Absolute rate constants for reaction of 1,1-diphenylsilene with various trapping agents in acetonitrile, hexane or isooctane solution at 23–25 °C

Reagent	k_q ($10^8 \text{ M}^{-1} \text{ s}^{-1}$)	Solvent	Reference
Ph ₂ Si = CH ₂	110 ± 30	hexane	46
MeOH	15 ± 1	MeCN	45
	19 ± 1	hexane	
EtOH	10 ± 1	MeCN	45
H ₂ O	7.6 ± 0.9	MeCN	45
<i>i</i> -PrOH	7.2 ± 0.5	MeCN	45
<i>t</i> -BuOH	4.1 ± 0.2	MeCN	45
	4.0 ± 0.7	hexane	
CF ₃ CH ₂ OH	14 ± 1	MeCN	56
(F ₃ C) ₂ CHOH	12 ± 1	MeCN	56
AcOH	12 ± 2	MeCN	45
	31 ± 3	hexane	
CF ₃ COOH	9.6 ± 0.2	MeCN	56
<i>n</i> -BuNH ₂	53 ± 1	MeCN	43
	97 ± 1	hexane	
<i>t</i> -BuNH ₂	6.9 ± 0.2	hexane	43
Et ₂ NH	17 ± 1	MeCN	56
Me ₃ SiOMe	0.86 ± 0.06	MeCN	57
	0.21 ± 0.1	hexane	
Me ₂ C = O	1.8 ± 0.1	MeCN	41
	3.8 ± 0.2	isooctane	
Me(<i>t</i> -Bu)C=O	2.3 ± 0.1	MeCN	42
	4.0 ± 0.2	isooctane	
Me(F ₃ C)C = O	0.16 ± 0.01	isooctane	42
Cyclopentanone	5.1 ± 0.2	MeCN	42
	11.7 ± 0.8	isooctane	
H(<i>t</i> -Bu)C=O	2.9 ± 0.3	hexane	44
ethyl acetate	0.073 ± 0.004	MeCN	42
	0.088 ± 0.002	isooctane	
DMB ^a	0.037 ± 0.002	isooctane	42
<i>trans</i> -piperylene	0.14 ± 0.02	isooctane	56
Cyclohexene	≤ 0.0001	isooctane	
methylenecyclopentane	0.7 ± 0.1	isooctane	56
methyl vinyl ketone	16 ± 2	isooctane	56
methyl acrylate	0.33 ± 0.02	isooctane	56
dicyclopropyl ketone	0.017 ± 0.002	isooctane	56
cyclopropyl methyl ketone	12.3 ± 0.8	isooctane	56
O ₂	< 0.05	isooctane	42

^a2,3-Dimethyl-1,3-butadiene.

of the corresponding phenyldisilanes **20a–c**; equation 12)^{47–52}, the trimethylsilylmethyl-substituted 1,1-dimethylsilene **23** and 2-methyl-1,3-(2-sila)butadiene **24** (formed by photolysis of the vinyldisilanes **22a,b**; equations 13 and 14)⁵³ and the 1-silaallene derivatives **26a,b** (formed by photolysis of the alkynyldisilanes **25a,b**; equation 15)^{54,55}. Representative data for reactive quenching of four of these compounds in hexane and/or acetonitrile solution at 23 °C are collected in Table 4.

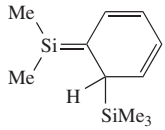
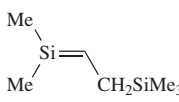
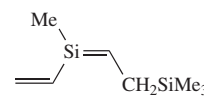
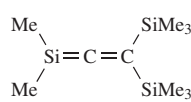
In general, the data confirm the general trends in relative reactivity established earlier for **6** by Wiberg and coworkers^{6,36}.



2. Dimerization

In the absence of anything else to react with, silenes dimerize in either head-to-tail or head-to-head fashion depending on the identity of the substituents at silicon and carbon, and their effect on the natural ($\delta^+\text{Si}=\text{C}\delta^-$) polarity of the silenic double bond. The head-to-tail regiochemistry leading to the formation of the corresponding 1,3-disilacyclobutane is most common, while head-to-head dimerization leading to either the corresponding

TABLE 4. Absolute rate constants for reaction of 1,3,5-(1-sila)hexatriene **21a**⁵¹, 2-trimethylsilyl-methyl-1,1-dimethylsilene (**23**)⁵³, 1,3-(2-sila)butadiene **24**⁵³ and 1-silaallene **26a**⁵⁵ in hexane or acetonitrile solution at 23–25 °C

Quencher	$k_q(10^7 \text{ M}^{-1} \text{ s}^{-1})$			
				
	21a ^{48, 51}	23 ⁵³	24 ⁵³	26a ⁵⁵
MeOH	30 ± 8 ^a 23 ± 7 ^{a,b}	15 ± 2 1.7 ± 0.2 ^b	8.3 ± 1.0	0.17 ± 0.01
<i>t</i> -BuOH	3.7 ± 0.8 ^{a,b}	10 ± 2 0.38 ± 0.06 ^b	4.2 ± 0.5	<i>ca</i> 0.002
AcOH	29 ± 1 ^b	73 ± 7 ^b	—	9.8 ± 0.6
acetone	90 ± 3 ^b	1.9 ± 0.2 0.60 ± 0.08 ^b	0.20 ± 0.02	0.178 ± 0.005
cyclohexene	0.12 ± 0.02 ^b	0.0040 ± 0.0015	0.006 ± 0.003	—
DMB ^d	12.8 ± 0.3 ^b	0.32 ± 0.06	~ 0.5	≤ 0.004 ^c
O ₂	85 ± 8 ^b	2.6 ± 0.3	~ 0.5	11 ± 2

^aMixed first and second order in ROH.

^bSolvent = acetonitrile.

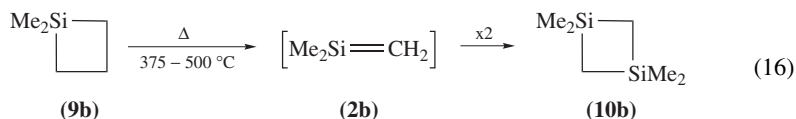
^cQuenching by 1,3-octadiene.

^d2,3-Dimethyl-1,3-butadiene.

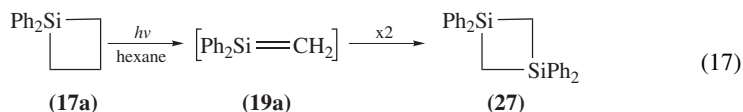
1,2-disilacyclobutane and/or linear ene-dimer (when the silenic carbon is alkyl-substituted) is observed in silenes bearing substituents that reduce Si=C bond polarity, as suggested by theoretical calculations⁵⁸. Only four systems have been characterized with absolute rate data, but all three modes of dimerization are represented.

Gusel'nikov, Nametkin and coworkers employed a gas-phase flow pyrolysis technique to measure absolute rate constants for the head-to-tail dimerization of 1,1-dimethylsilene (**2b**) at 25, 150 and 300 °C (equation 16)³³. The same value ($k_{\text{dim}} = 6.6 \times 10^{-15} \text{ cm}^3 \text{ s}^{-1}$, corresponding to a solution-phase value of $3.55 \times 10^6 \text{ M}^{-1} \text{ s}^{-1}$) was obtained at all three temperatures, leading to an Arrhenius activation energy of $E_a = 0 \pm 4 \text{ kJ mol}^{-1}$. The implied pre-exponential factor of $\log(A/\text{cm}^3 \text{ s}^{-1}) = -14.18$ was later shown to be incompatible with the thermochemistry of the system²², and Potzinger and coworkers determined a value of $k_{\text{dim}} = (3.3 \pm 0.8) \times 10^{-11} \text{ cm}^3 \text{ s}^{-1}$ at *ca* 298 K by laser flash photolysis techniques³⁵. This corresponds to a solution-phase value of *ca* $2 \times 10^{10} \text{ M}^{-1} \text{ s}^{-1}$, which makes much better sense considering the values that have been reported for the dimerization of other transient silenes in solution (*vide infra*); further corroboration comes from a recent determination of the absolute rate constant for dimerization of 1-methylsilene (**2a**) in the gas phase, $k_{\text{dim}} = (2.4 \pm 0.5) \times 10^{-11} \text{ cm}^3 \text{ s}^{-1}$ (presumably at *ca* 300 K)⁵⁹. Previous studies by Potzinger and coworkers on the photolysis of tetramethylsilane led to the conclusion that the dimerization of **2b** proceeds with a negligible activation energy⁶⁰, in agreement with the conclusions of Gusel'nikov, Nametkin and coworkers³³. Activation parameters for the dimerization of **2b** have still not been determined directly, however. It would be of great interest to do so, both because they are of fundamental interest and so

that the data of Davidson and Wood (Table 1)³⁴ might be re-evaluated.



Head-to-tail dimerization of 1,1-diphenylsilene (**19a**), produced by laser flash photolysis of 1,1-diphenylsilacyclobutane (**17a**), yields the 1,3-disilacyclobutane **27**^{61,62} with a rate constant $k_{\text{dim}} = (1.3 \pm 0.3) \times 10^{10} \text{ M}^{-1} \text{ s}^{-1}$ in hexane solution at 25 °C (equation 17)⁴⁶. This value is within a factor of two of the diffusional rate constant in hexane at this temperature, indicating that dimerization of this silene is faster than reaction with even the most potent of nucleophilic trapping reagents (see Table 3). More recently, the temperature dependence of the rate constant for dimerization of **19a** has been studied⁶³. The results of these experiments are shown in Figure 1, and lead to Arrhenius activation parameters of $E_a = -4 \pm 2 \text{ kJ mol}^{-1}$ and $\log(A/\text{M}^{-1} \text{ s}^{-1}) = 9.2 \pm 0.4$.



The Brook silene **28**, produced photochemically as shown in equation 18, dimerizes to yield a mixture of the 1,2-disilacyclobutane **29** and the acyclic ene-dimer **30**⁶⁴, the common mode of dimerization for the large majority of 1,1-bis(trialkylsilyl)silenes that have been studied to date¹². Conlin and coworkers determined the absolute rate constant for dimerization of **28** in cyclohexane solution, $k_{\text{dim}} = 1.3 \times 10^7 \text{ M}^{-1} \text{ s}^{-1}$ at 23 °C⁶⁵. Arrhenius activation parameters for the reaction were determined over the 0–60 °C temperature range. The values obtained, $E_a = 0.9 \pm 0.4 \text{ kJ mol}^{-1}$ and $\log(A/\text{M}^{-1} \text{ s}^{-1}) = 7 \pm 1$, are consistent with the stepwise mechanism for head-to-head dimerization originally proposed by Baines and Brook (equation 19)⁶⁴, provided that the rate of reversion of the

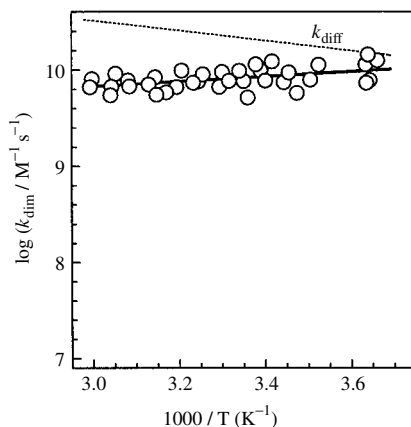
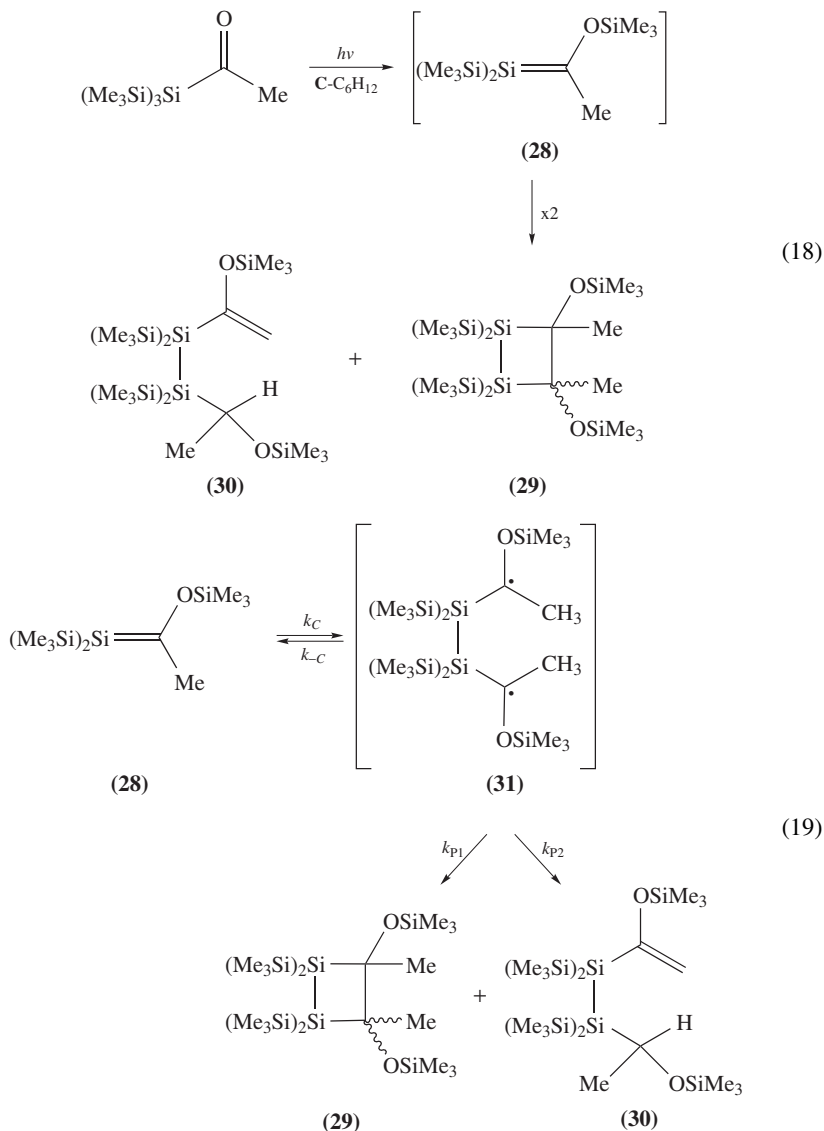


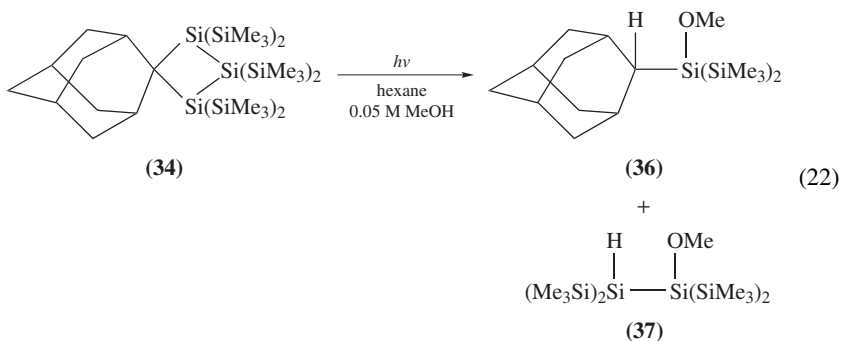
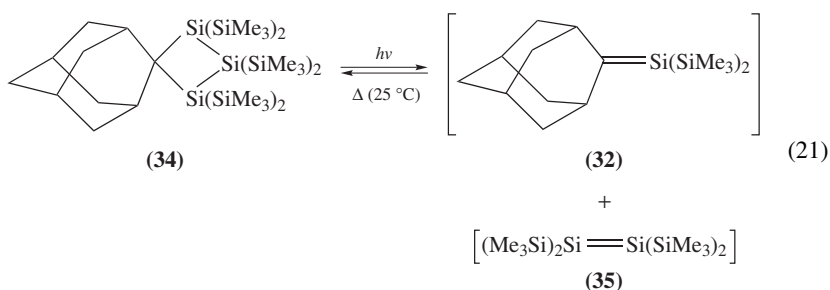
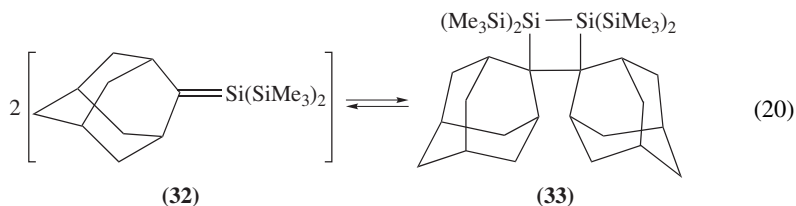
FIGURE 1. Arrhenius plot for the dimerization of 1,1-diphenylsilene (**19a**) in hexane solution. T.L. Morkin and W.J. Leigh, submitted for publication in *Organometallics*. Copyright 2001 American Chemical Society

1,4-biradical intermediate (**31**) to silene (k_{-C}) is similar to the sum of those for the product forming steps ($k_{P1} + k_{P2}$) and the latter rates are predominantly entropy-controlled⁴⁴.



An upper limit of $k_{\text{dim}} \leq 10^5 \text{ M}^{-1} \text{ s}^{-1}$ has recently been estimated for the rate of dimerization of the sterically hindered silene, 1,1-bis(trimethylsilyl)-2-(2-adamantylidene)silene (**32**)⁶⁶. Originally synthesized by a ground state route, **32** is known to dimerize in head-to-head fashion to yield the 1,2-disilacyclobutane **33** (equation 20)⁶⁷. The silene was generated and detected in hexane solution at 25 °C along with the tetrasilyl-substituted

disilene **35**⁶⁸ by laser flash photolysis of trisilacyclobutane **34** (equation 21)⁶⁶. Both species have lifetimes on the order of a few milliseconds under these conditions, and appear to decay with (different) mixed pseudo-first- and second-order kinetics, suggesting that both react predominantly by dimerization. Product studies show that the photolysis of **34** is surprisingly inefficient, however, and that none of the silene dimer is formed in detectable amounts. This suggests that the main pathway for decay of both silene **32** and disilene **35** under these conditions is by [2 + 2]-cycloaddition to re-form **34** (equation 21), a reaction which has only a single precedent in the literature⁶⁹. Indeed, addition of just 0.05 M MeOH to the solution results in a pronounced shortening of the lifetime of **35** (due to reaction with the alcohol), a remarkable *lengthening* of the lifetime of the silene **32** (τ ca 32 ms) and a substantial increase in the quantum yield for disappearance of **34** due to formation of the silene and disilene trapping products **36** and **37**, respectively (equation 22). The upper limit of $10^5 \text{ M}^{-1} \text{ s}^{-1}$ for the rate constant for dimerization of **32** was calculated on the basis of the estimated lifetime of the silene in the presence of 0.05 M MeOH, an estimated upper limit for the yield of the dimer produced and an assumed extinction coefficient of ϵ ca $15,000 \text{ M}^{-1} \text{ cm}^{-1}$ at the UV absorption maximum of the silene, based on the value reported for an isolable homologue⁷⁰.



Additional kinetic work needs to be done in order to establish the mechanism for the head-to-tail dimerization of silenes.

The dimerization of the parent molecule ($\text{H}_2\text{Si}=\text{CH}_2$) has been examined theoretically by several groups, and the results of these studies are summarized in Scheme 3.

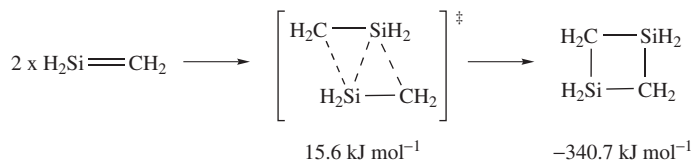
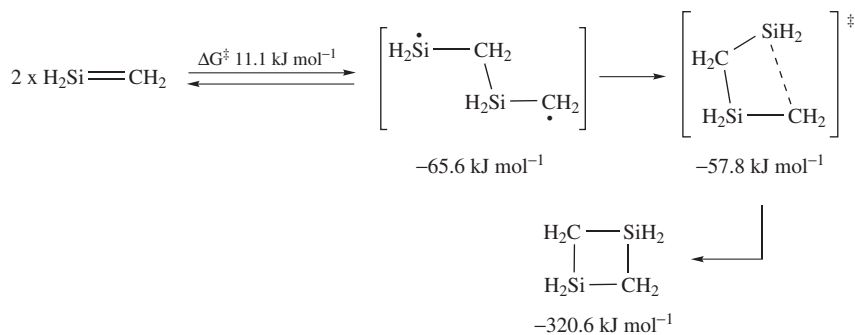
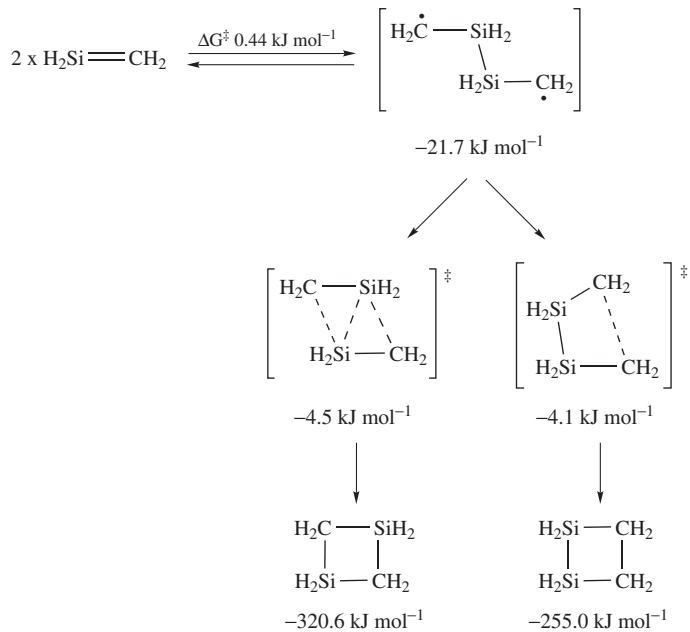
Based on the results of coupled cluster calculations at the CCSD (DZ + d) level of theory, Schaefer and coworkers suggested that the process occurs via a concerted [$\pi 2s + \pi 2s$] mechanism, through a C_{2h} -symmetric transition state that is 15.6 kJ mol^{-1} higher in (free) energy than the reactants (Scheme 3)⁷¹.

Bernardi and Robb and their coworkers have published two separate studies at different levels of theory, and both led to different mechanistic conclusions than those of Schaefer and coworkers. In the first study^{72,73}, CAS-SCF calculations with geometries optimized at either the DZ + d or 3-21 G* levels of theory predicted the reaction to proceed via the initial irreversible formation of an *anti* $\bullet\text{Si}-\text{C}-\text{Si}-\text{C}\bullet$ 1,4-biradical intermediate, which was calculated to lie *ca* 65 kJ mol^{-1} lower in energy than the reactants. Bond rotation and coupling of the biradical to the product is predicted to proceed with an activation barrier of 11.1 kJ mol^{-1} . This mechanism was later revised by these authors on the basis of higher level (CASPT2/6-311 G* // CAS-SCF/6-31 G*) calculations⁷⁴, which revealed a lower energy pathway for reaction, i.e. initial formation of the *anti* $\bullet\text{C}-\text{Si}-\text{Si}-\text{C}\bullet$ 1,4-biradical via an essentially barrierless pathway, followed by concerted [1,2]-migration to 1,3-disilacyclobutane through a barrier of 17 kJ mol^{-1} . The calculated energy of the $\bullet\text{C}-\text{Si}-\text{Si}-\text{C}\bullet$ biradical relative to reactants (-21 kJ mol^{-1}) is such that its formation is predicted to be reversible. It is noteworthy that the calculated transition state for formation of the final product from the biradical is very similar to that for the concerted mechanism proposed by Schaefer and coworkers in their earlier calculations. Most interestingly, the results of these calculations suggest that head-to-head and head-to-tail dimerization of silenes involves the same 1,4-biradical intermediate, whose ultimate fate (coupling to the head-to-head dimer vs. 1,2-migration + coupling to the head-to-tail dimer; see Scheme 3) is controlled by electronic factors of the substituents at silicon and carbon. The fact that near-zero or negative Arrhenius activation energies have been observed for all of the silene dimerizations that have so far been studied experimentally is consistent with this mechanism, although it does not demand it. Negative activation energies are also possible for strongly exothermic concerted reactions⁷⁵, and so the mechanism for head-to-tail dimerization cannot be considered as conclusively established on the basis of the experimental work done to date.

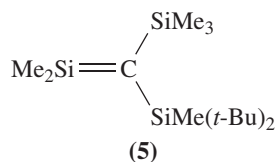
3. Nucleophilic addition

a. Addition of water and alcohols. The [1,2]-addition of alcohols is the most widely studied and mechanistically best understood reaction of the Si=C bond, and both product and transient kinetic studies have contributed greatly to the development of our current level of understanding of the reaction. This reaction is the prototype for the addition of all nucleophiles to silenes, or at least all that have been studied to date, as well as the formal ene-addition reactions of acetone and acetic acid, and thus will be discussed in some detail.

Wiberg determined the relative rates of addition of various alcohols and amines to silene **6**, the results of which have been summarized above in Table 2⁶. The fastest rates of addition were observed with aliphatic alcohols and amines, leading to the hypothesis that the first step of the reaction involves complexation of the neutral nucleophile at silicon, followed by proton transfer to the silenic carbon. Subsequent reports of the X-ray crystal

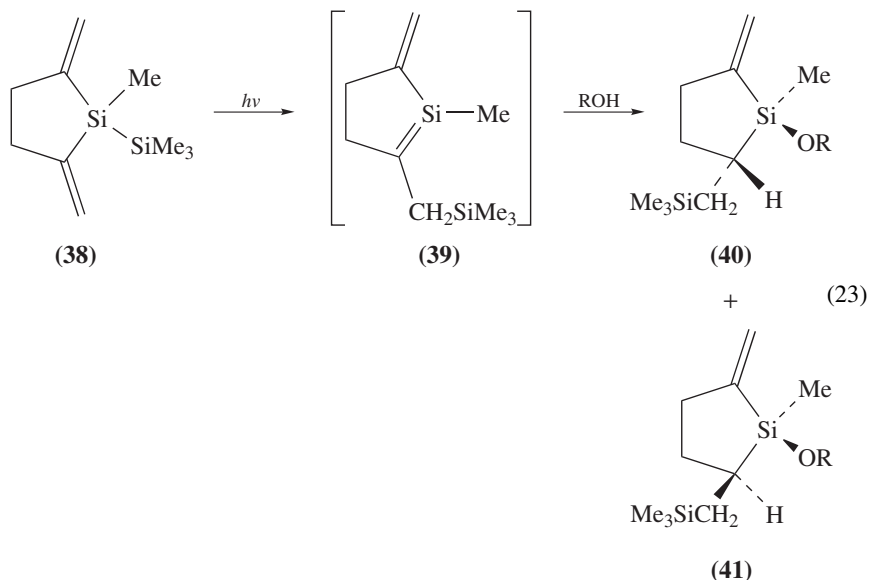
1. Concerted mechanism for $\text{H}_2\text{Si}=\text{CH}_2$ dimerization (Reference 68)2. $\cdot\text{Si-C-Si-C}\cdot$ biradical mechanism for $\text{H}_2\text{Si}=\text{CH}_2$ dimerization (Reference 72–74)3. $\cdot\text{C-Si-Si-C}\cdot$ biradical mechanism for $\text{H}_2\text{Si}=\text{CH}_2$ dimerization (Reference 74)

SCHEME 3



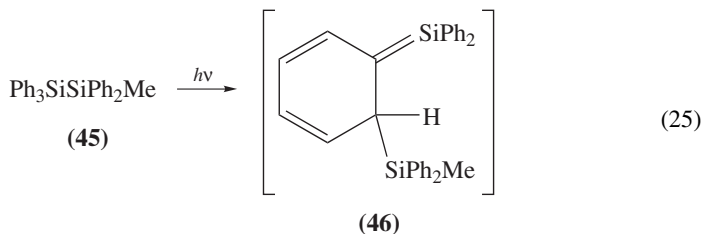
structures of the complexes of the stable silene **5** with THF⁷⁶ and trimethylamine⁷⁷, as well as theoretical calculations⁷⁸, lent further support to this hypothesis.

Wiberg's mechanism was further elaborated on by Kira and coworkers, who found that the stereochemistry of addition of various aliphatic alcohols to the transient cyclic silene **39** (formed photolytically from the vinyldisilane **38**; equation 23) varies with the alcohol *and its concentration*⁷⁹. This concentration dependence demands the involvement of an intermediate, such as Wiberg's σ -complex, which collapses to product by competing uni- and bimolecular proton transfer, the latter requiring a second molecule of alcohol. Intramolecular proton transfer is the favoured pathway at lower alcohol concentrations and yields the *syn*-alkoxysilane **40**, while intermolecular proton transfer, involving a second molecule of alcohol, is the favoured pathway at higher concentrations and yields the *anti*-isomer **41**. This mechanism provides a satisfying explanation for the results of earlier studies of the stereochemistry of alcohol addition to silenes, which appeared to conflict with one another^{80,81}.



A more pronounced effect of this type occurs in the addition of MeOH to the transient (1-sila)hexatriene **21a**, the product of photochemical [1,3]-trimethylsilyl migration in pentamethylphenyldisilane (**20a**; equation 12)^{82,83}. Photolysis of **20a** in the presence of methanol in acetonitrile solution leads to the formation of three regioisomeric addition

21a, for example, $k_{\text{ROH}}/k_{2\text{ROH}} \sim 0.05$ for $\text{ROH} = \text{MeOH}$ ⁴⁸ and $k_{\text{ROH}}/k_{2\text{ROH}} \sim 0.4$ for $\text{ROH} = t\text{-BuOH}$ ⁵¹.



$$k_{\text{decay}} = k_0 + k_{\text{ROH}}[\text{ROH}] + k_{2\text{ROH}}[\text{ROH}]^2 \quad (26)$$

This is precisely the behaviour predicted by the Kira mechanism, provided that the formation of the silene–ROH complex is reversible and the proton transfer steps are rate-limiting. The complete mechanism is shown in Scheme 4, while equation 27 gives the predicted expression for the pseudo-first-order rate constant for decay of the silene, derived assuming the steady-state approximation for the silene–alcohol complex. Equation 27 reduces to the quadratic expression in $[\text{ROH}]$ of equation 28 when $k_{-C} \gg (k_H + k_H'[\text{ROH}])$, i.e. under the conditions of the equilibrium assumption for the complex. In practice, it is difficult to distinguish between the two situations given by equations 27 and 28. The experimentally determined second- and third-order rate constants k_{ROH} and $k_{2\text{ROH}}$ are defined in equations 29 and 30, respectively, in terms of the mechanism of Scheme 4 and using the

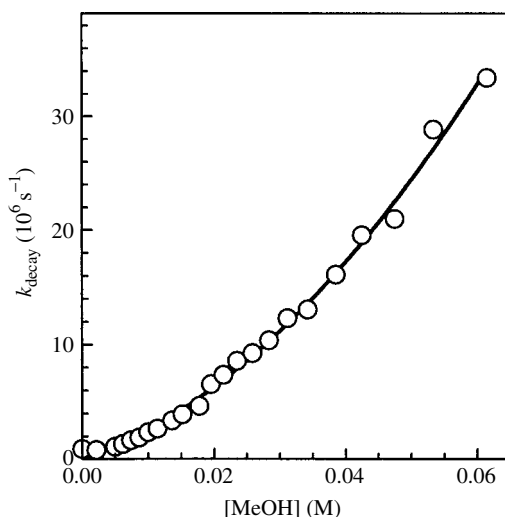
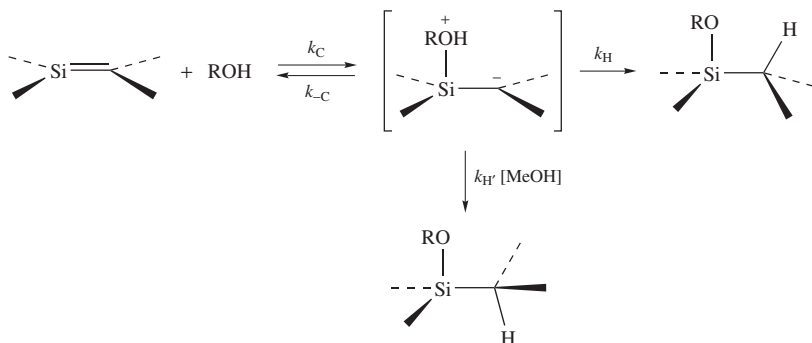


FIGURE 2. Stern–Volmer plot of the pseudo-first-order rate constant for decay of silene **21a** versus MeOH concentration in deoxygenated acetonitrile solution at 24 °C. Reproduced with permission from Reference 48. Copyright 1994 American Chemical Society



SCHEME 4

equilibrium assumption for the intermediate silene–alcohol complex.

$$k_{\text{decay}} = k_0 + k_C \frac{k_H + k'_H [\text{ROH}]}{k_{-C} + k_H + k_{H'} [\text{ROH}]} [\text{ROH}] \quad (27)$$

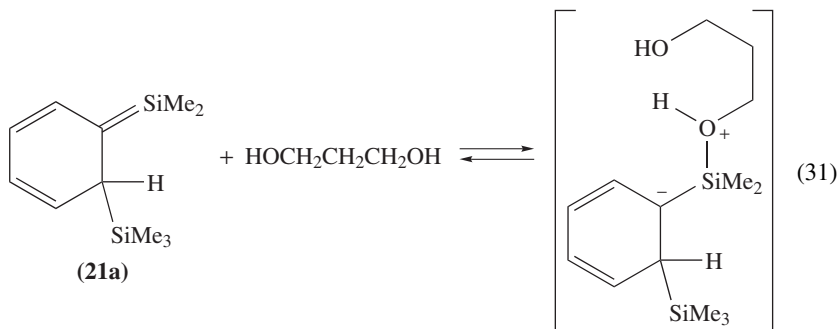
$$k_{\text{decay}} = k_0 + (k_C/k_{-C})k_H[\text{ROH}] + (k_C/k_{-C})k'_H[\text{ROH}]^2 \quad (28)$$

$$k_{\text{ROH}} = (k_C/k_{-C})k_H \quad (29)$$

$$k_{2\text{ROH}} = (k_C/k_{-C})k'_H \quad (30)$$

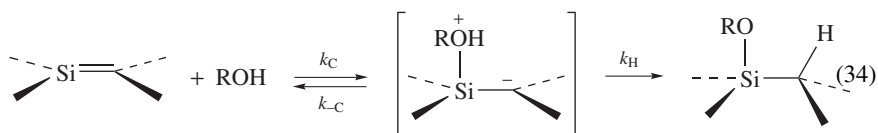
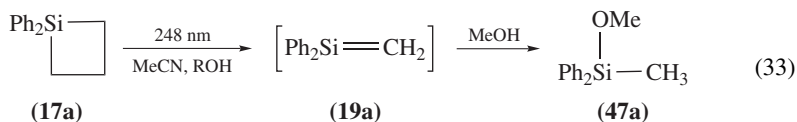
Several additional observations provide further support for the mechanism of Scheme 4. The first-order term in ROH (k_{ROH}) was found to exhibit a primary deuterium kinetic isotope effect on the order of $k_{\text{H}}/k_{\text{D}} = 1.7$ and 1.9 for $\text{H}_2\text{O}/\text{D}_2\text{O}$ and MeOH/MeOD addition, respectively, consistent with proton transfer being the rate-limiting step in the mechanism⁵¹. Furthermore, the silene decay rate constant (k_{decay}) was found to obey a linear dependence on $[\text{ROH}]$ for addition of 2,2,2-trifluoroethanol (TFE) and acetic acid (AcOH), whose greater acidity and lower nucleophilicity would be expected to result in a change in rate-determining step from proton transfer to complexation⁵¹. Accordingly, the rate constants for quenching by AcOH and AcOD are identical, consistent with $k_{\text{ROH}} \sim k_C$ in these two cases. Furthermore, the overall second-order rate constant for quenching of **21a** by TFE in acetonitrile solution was found to be a factor of about 12 slower than that by AcOH under the same conditions [$k_{\text{TFE}} = (2.36 \pm 0.04) \times 10^7 \text{ M}^{-1} \text{ s}^{-1}$ at 23 °C]⁵¹, consistent with the relative nucleophilicities of the two reagents⁸⁵. Finally, a linear dependence of k_{decay} on $[\text{ROH}]$ was also found for quenching by 1,3-propanediol, whose second hydroxyl group provides a catalytic site that enables both the direct and catalyzed proton-transfer processes within the complex to occur intramolecularly (equation 31)⁴⁸. In contrast, quenching by ethylene glycol followed a quadratic dependence on $[\text{ROH}]$, as with methanol and *tert*-butanol, indicating that intramolecular catalysis is less effective in this case than with the 1,3-diol. This is most consistent with a deprotonation/protonation mechanism (i.e. general base catalysis) for the catalytic proton transfer pathway; in the case of 1,3-propanediol, deprotonation by the remote hydroxyl group occurs via a six-membered transition state, while it must involve a less favourable five-membered transition state in the case of ethylene glycol. Additional evidence for the base catalysis mechanism is provided by the fact that the second-order rate constant for reaction of silene **21c** with MeOH is larger in THF solution than in MeCN⁴⁸. This was attributed to the

addition of a pseudo-first-order pathway for proton transfer involving the solvent, which can be expressed quantitatively as shown in equation 32. This will be discussed in detail in Section III.B.6.



$$k_{\text{ROH}} = (k_{\text{C}}/k_{-\text{C}})(k_{\text{H}} + k_{\text{THF}}[\text{THF}]) \quad (32)$$

Methanol quenching of more reactive silenes such as 1,1-diphenylsilene (**19a**) leads to the corresponding alkoxy silane (**47a** from **19a**) by simple 1,2-addition (equation 33), and follows a linear dependence on methanol concentration over the range of alcohol concentrations for which lifetime data can be measured. The linear concentration dependence is expected when $k_{\text{H}} \gg k_{\text{H}}'[\text{ROH}]$ in the mechanism of Scheme 4. When this is the case, the mechanism reduces to that shown in equation 34, while the expression for k_{decay} given by equation 27 reduces to that of equation 35, i.e. k_{ROH} is given by the product of the rate constant for complexation (k_{C}) and the fraction of complexes that proceed to the final product(s) by intramolecular proton transfer [$k_{\text{H}}/(k_{\text{H}} + k_{-\text{C}})$, equation 36]. Competitive trapping experiments with different aliphatic alcohols suggest that the catalytic proton transfer pathway still operates in the reaction of **19a** with MeOH, but only at much higher bulk alcohol concentrations than can be probed by nanosecond laser flash photolysis⁴⁵. As with **21a-c**, small primary deuterium kinetic isotope effects (on the order of 1.3–1.5) are observed for quenching of **19a** by MeOH(D), EtOH(D), *iso*-PrOH(D) and *tert*-BuOH(D), but not for AcOH(D).

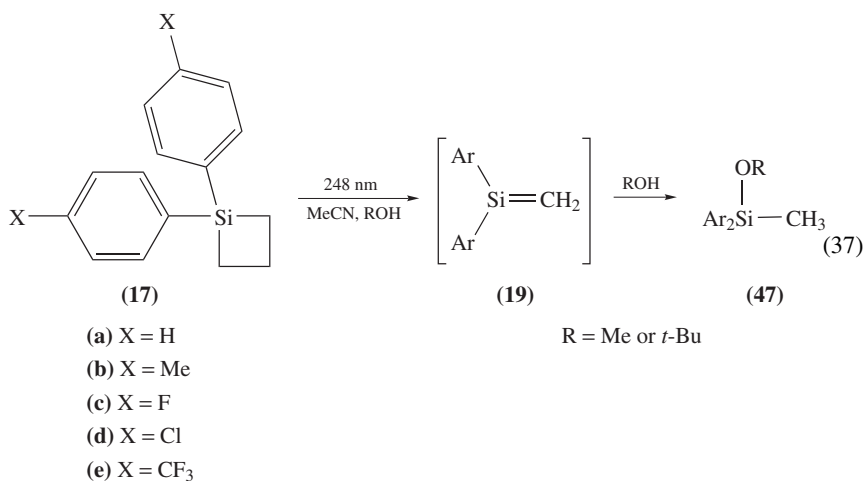


$$k_{\text{decay}} = k_0 + k_{\text{C}} \frac{k_{\text{H}}}{k_{-\text{C}} + k_{\text{H}}} [\text{ROH}] \quad (35)$$

$$k_{\text{ROH}} = k_{\text{C}} [k_{\text{H}} / (k_{\text{H}} + k_{-\text{C}})] \quad (36)$$

The trends in the absolute rate constants for addition of MeOH(D) and *tert*-BuOH to the series of *para*-substituted 1,1-diarylsilenes **19a-e** in acetonitrile solution (equation 37

and Table 5) indicate that inductive electron-withdrawing groups at the *para*-position of the phenyl rings increase overall reactivity at 23 °C compared to the parent compound **19a**, providing additional evidence for a mechanism in which nucleophilic attack at silicon precedes protonation at carbon⁴⁰. As is shown in Figure 3, the rate constants correlate with the Hammett substituent constants σ_p^{86} according to equation 38, leading to Hammett ρ -values of +0.31 and +0.55 for the addition of MeOH and *t*-BuOH, respectively⁴⁰. The difference in ρ -values is small, presumably because the overall rate constants for both alcohols are so large. However, the effect is slightly greater for the less reactive alcohol, as would be expected.



$$\log(k_X/\text{M}^{-1} \text{s}^{-1}) = \log(k_H/\text{M}^{-1} \text{s}^{-1}) + \rho \sum \sigma_p^X \quad (38)$$

TABLE 5. Absolute rate constants for addition of aliphatic alcohols to 1,1-diarylsilenes (XC_6H_4)₂Si = CH₂ (**19a–e**) in acetonitrile solution at 23 °C^{40,89}.

19 (X)	ROH	$k_{\text{ROH}}(10^9 \text{ M}^{-1} \text{ s}^{-1})$	$k_{\text{H}}/k_{\text{D}}$	Reference
a (H)	H ₂ O	0.76	1.4 ± 0.2	45
	MeOH	1.5 ± 0.1	1.4 ± 0.2	89, 45
	EtOH	1.0 ± 0.1	1.0 ± 0.1	45
	<i>i</i> -PrOH	0.72 ± 0.05	<i>a</i>	45
	<i>t</i> -BuOH	0.41 ± 0.02	2.2 ± 0.3	45
b (4-Me)	MeOH	1.12 ± 0.06	1.9 ± 0.1	40
	<i>t</i> -BuOH	0.130 ± 0.006	1.9 ± 0.2	40
c (4-F)	MeOH	1.89 ± 0.08	<i>a</i>	40
	<i>t</i> -BuOH	0.33 ± 0.02	<i>a</i>	40
d (4-Cl)	MeOH	2.13 ± 0.10	<i>a</i>	40
	<i>t</i> -BuOH	0.39 ± 0.02	<i>a</i>	40
e (4-CF ₃)	MeOH	2.99 ± 0.16	1.0 ± 0.1	40
	<i>t</i> -BuOH	0.75 ± 0.04	1.7 ± 0.2	40

^aNot determined.

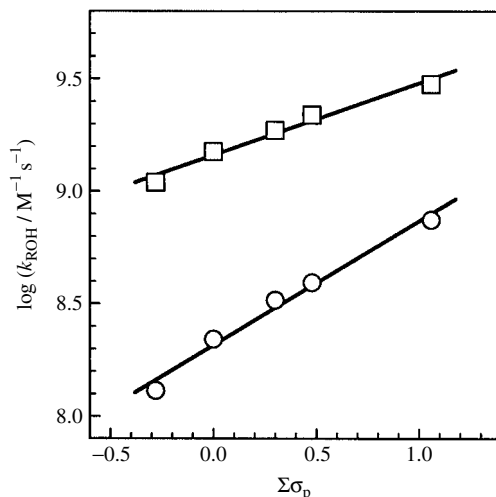


FIGURE 3. Hammett plots for the reactions of MeOH (□) and *t*-BuOH (○) with 1,1-diarylsilenes **19a–e** in acetonitrile solution at 23 °C. Reproduced with permission from Reference 40. Copyright 1997 National Research Council of Canada

To a first approximation, these reaction constants (ρ) can be viewed as the sum of those of the individual complexation and proton transfer steps. The ρ -value for the proton transfer step should be small because the process involves charge neutralization within the zwitterionic complex. Thus, the positive overall ρ -values can be interpreted as reflecting mainly the effects of substituents on the initial complexation step of the reaction, i.e. the ratio k_C/k_{-C} increases with increasing electron-withdrawing power of the aryl substituents attached to silicon. This has obvious analogies to Michael addition reactions in organic chemistry, and indeed, the addition of various nucleophiles to substituted β -nitrostyrenes exhibit Hammett ρ -values in the range of +0.2–+1, depending on the nucleophile and the solvent^{87,88}.

The increase in k_{MeOH} with increasing substituent electron-withdrawing power throughout this series of silenes is accompanied by a corresponding decrease in the k_H/k_D values for reaction of MeOH(D) (see Table 5). This can be explained in terms of variations in the relative magnitudes of the rate constants for reversion of the complex to reactants (k_{-C}) and collapse to product (k_H), since the isotope effect on k_C should be a secondary one and hence be close to unity. The overall isotope effect is predicted to be a maximum in the limit of $k_{-C} \gg k_H$ (i.e. fully reversible complex formation) and to be reduced in magnitude as k_{-C} decreases and/or k_H increases. Only a secondary isotope effect should be obtained in the limit of $k_H \gg k_{-C}$, where complex formation is fully rate-determining. The data are consistent with an increase in the ratio $k_H/(k_{-C} + k_H)$ with increasing substituent electron-withdrawing power, a trend which also manifests itself in the temperature dependences of the absolute rate constants for reaction of MeOH with **19a** and **19e**^{40,89}. The positive sign of the Hammett ρ -value indicates that the variation in $k_H/(k_{-C} + k_H)$ throughout the series is most likely due largely to a retarding effect on k_{-C} with increasing electron-withdrawing power of the aryl substituents attached to silicon.

Still more evidence for the stepwise mechanism of equation 34 has been obtained from a study of the temperature dependences of the rates of addition of MeOH and MeOD to **19a–e**^{40,89}, the results of which are summarized in Figure 4 in the form of Arrhenius

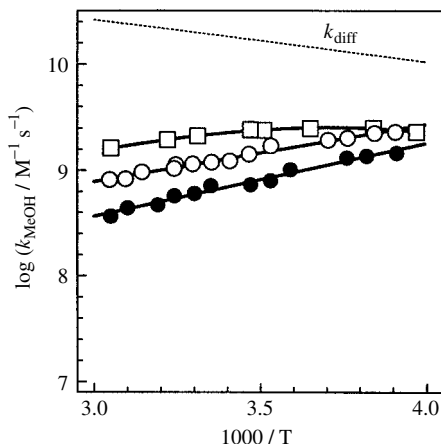


FIGURE 4. Arrhenius plots for the reaction of 1,1-diarylsilenes **19a** (○) and **19e** (□) with MeOH and **19a** with MeOD (●) in acetonitrile solution. Reproduced with permission from Reference 40. Copyright 1997 National Research Council of Canada

plots for reaction of **19a** and **19e** with MeOH and of **19a** with MeOD in acetonitrile solution. As is explained in detail in Appendix 1, the overall rates of reactions proceeding via mechanisms of this type very commonly exhibit a *negative* temperature dependence (i.e. the rate decreases with increasing temperature), particularly in the cases of highly exergonic reactions such as these. Indeed, the reaction of **19a** with MeOH proceeds with an Arrhenius activation energy of $E_a = -10.3 \pm 1.2 \text{ kJ mol}^{-1}$ ⁸⁹. On its own, this does not demand a reaction mechanism of the type shown in equation 34, since strongly exergonic *concerted* reactions can also proceed with negative activation energies^{75,90}. However, the result that addition of MeOD exhibits an even more strongly negative $E_a (= -13.1 \pm 1.2 \text{ kJ mol}^{-1})$ ⁴⁰ is compatible only with the non-concerted pathway.

The negative E_a results from the fact that the complex partitioning ratio ($k_H/[k_H + k_{-C}]$) in equation 35) decreases with increasing temperature, and does so more precipitously than k_C increases (see Appendix 1). The inverse temperature dependence of the partitioning ratio is caused by the fact that the two reaction channels available to the intermediate complex have relatively low enthalpies of activation, and entropies of activation that vary with temperature in opposing fashion. In fact, a negative E_a is obtained only over the temperature range where $k_H/[k_H + k_{-C}] < 0.5$; $E_a = 0$ at the temperature where $k_H = k_{-C}$ and it is positive over the range where $k_H/[k_H + k_{-C}] > 0.5$. Thus, a mechanism of this type is predicted to give rise to a bell-shaped Arrhenius plot provided that the observed temperature range is large enough to span both sides of the point where $k_H = k_{-C}$. In the high temperature limit where $k_{-C} \gg k_H$, the overall rate constant for reaction is given by $k_{\text{ROH}} = (k_C/k_{-C})k_H$, while $k_{\text{ROH}} = k_C$ in the low temperature limit where $k_H \gg k_{-C}$.

The plot for **19e** shows precisely this behaviour, exhibiting an apparent negative activation energy at temperatures above *ca* 13 °C and distinct curvature over the -20 to 13 °C temperature range as the rate of product formation (k_H) approaches and then surpasses that of reversion of the complex to reactants (k_{-C}). The turnover point where $k_H = k_{-C}$ occurs at a temperature of *ca* -6 °C. Since at this point $k_{\text{ROH}} = 1/2k_C$, it is possible to calculate a value of k_C for the reaction of this silene with MeOH at this particular temperature. The value obtained, $k_C \sim 5 \times 10^9 \text{ M}^{-1} \text{ s}^{-1}$, is roughly a factor of three

less than the diffusional rate constant in MeCN at this temperature, calculated using the modified Debye equation ($k_{\text{diff}} = 8RT/3000\eta$) and published viscosities⁹¹: k_{diff} (at -6°C) = $1.4 \times 10^{10} \text{ M}^{-1} \text{ s}^{-1}$.

The temperature dependencies of the rates of methanol addition to **19a** and **19e** show an important difference that can ultimately be linked to the higher electrophilicity of **19e** compared to **19a**: over the same temperature range, the activation energy observed for **19e** is less negative (or more positive) than that observed for **19a**. For example, $E_a = -7.8 \pm 0.8 \text{ kJ mol}^{-1}$ for **19e** at the high end of the temperature range examined ($>13^\circ\text{C}$), while $E_a = -10.3 \pm 1.2 \text{ kJ mol}^{-1}$ for the less reactive derivative **19a**. This must result from the complex partitioning ratio $k_{\text{H}}/(k_{\text{H}} + k_{-\text{C}})$ for **19e** being greater than that for **19a** at any particular temperature. As will be seen in subsequent sections, this same behaviour shows up in the temperature dependence of the absolute rate constants for reaction of other reagents with these two compounds, and provides valuable clues as to their reaction mechanisms.

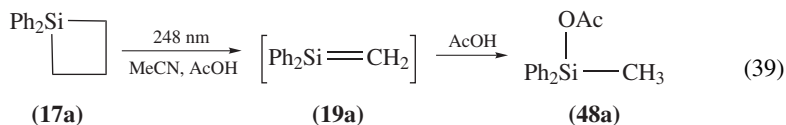
The rate constants for addition of aliphatic alcohols and water to **19a** decrease in the order $\text{MeOH} > \text{EtOH} > \text{H}_2\text{O} \sim i\text{-PrOH} > t\text{-BuOH}$ in acetonitrile at 23°C ⁴⁵, due to a combination of steric effects, nucleophilicity and acidity, all of which can be expected to affect the magnitudes of the individual rate constants involved in the mechanism for the reaction. The Arrhenius activation energy for addition of *t*-BuOH to this silene, $E_a = -1.7 \pm 0.4 \text{ kJ mol}^{-1}$ ⁸⁹, is closer to zero than that for MeOH addition, suggesting that the intracomplex product partitioning ratio is closer to 0.5 than is the case for the more reactive alcohol over the temperature range examined. It thus follows that the factor of *ca* 10 lower reactivity of *t*-BuOH compared to MeOH is mainly due to a reduction in the rate constant (k_{C}) for initial complexation of the alcohol with the silene.

While the rate constant and general kinetic behaviour exhibited by the reaction of 2,2,2-trifluoroethanol (TFE) with **21a** fit consistently with its lower nucleophilicity and higher acidity compared to other aliphatic alcohols, it is unusually reactive toward **19a** [$k_{\text{TFE}} = (1.4 \pm 0.1) \times 10^9 \text{ M}^{-1} \text{ s}^{-1}$ in acetonitrile at 23°C]⁹². Even more surprising is the fact that 1,1,1,3,3,3-hexafluoroisopropanol (HFIP) exhibits similar reactivity to TFE under the same conditions (see Table 3). The reactions of both alcohols with **19a** in acetonitrile solution are more complex than those of non-fluorinated alcohols, however, as they give rise to a second product in addition to the alkoxy silanes expected from simple 1,2-addition across the $\text{Si}=\text{C}$ bond⁴⁵. This intriguing behaviour has unfortunately not been fully sorted out, but GC/MS evidence indicates that the product arises from a reaction of the silene with both the acetonitrile solvent and the alcohol⁹².

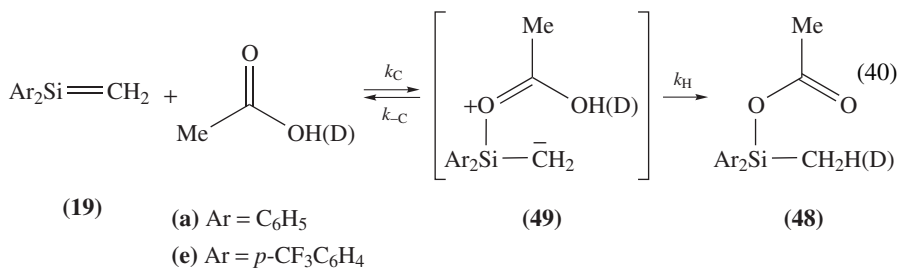
Absolute rate constants for reaction of MeOH with a wide variety of other transient silenes have also been reported, but with the main goal of quantitatively defining the effects of substituents on the kinetic and/or thermodynamic stability of the $\text{Si}=\text{C}$ bond in various structural situations. These data are discussed in Section III.C of this chapter.

b. Addition of acetic acid. Carboxylic acids have been used much less frequently than alcohols for trapping reactive silenes in product-oriented studies, presumably because the product(s) tend to be more labile and difficult to isolate than the corresponding alkoxy silanes from alcohol trapping. However, the quenching of transient silenes by acetic acid has proven to be an extremely valuable tool in kinetic studies for sorting out the various details of the mechanism for alcohol addition, as was discussed above^{40,51,54,55,89}. The product of the reaction is the corresponding carboxy silane (e.g. **48a**), formed by formal 1,2-addition across the $\text{Si}=\text{C}$ bond, as is illustrated in equation 39 for the trapping of **19a** by acetic acid⁴⁰. In all cases that have been studied, the absolute rate constant for silene quenching by acetic acid in hydrocarbon, MeCN or THF solution is similar to or within

a factor of 10 *greater* than that of MeOH quenching, depending on the silene and the solvent.



The reaction is generally not subject to a detectable deuterium isotope effect and, in the case of the (1-sila)hexatrienes (**21a–c**), the reaction is strictly first order in acetic acid. This is consistent with a mechanism analogous to that of equation 34 for alcohol addition, where the substantially higher acidity of the trapping agent renders $k_{\text{H}} \gg k_{\text{C}}$ and makes the initial formation of the complex (k_{C}) the rate-determining step for reaction. In this case, however, the site of initial attack is most likely to be at the carbonyl oxygen, with proton transfer occurring from the hydroxylic oxygen to carbon in the complex (**49**; equation 40) via a six-membered transition state. With k_{H} being so fast, the $k_{\text{H}}/k_{\text{D}}$ value obtained from the ratio of the rate constants for quenching by AcOH and AcOD is expected to be very close to unity, and indeed, that is generally the case. However, other mechanistic possibilities are also consistent with the isotope effect data and the linear dependence on $[\text{AcOH}]$, such as a concerted mechanism or a stepwise pathway initiated by protonation at carbon; neither of these would be expected to show a substantial isotope effect, given that the rate constants are normally within an order of magnitude of the diffusional limit. Substituent and temperature effect studies have been reported which address these possibilities⁴⁰.



The absolute rate constants for reaction of **19a–e** with AcOH in acetonitrile solution at 23 °C (Table 6) vary only slightly with aryl substituent, spanning a range of $k_{\text{AcOH}} = (1.41 \pm 0.05) \times 10^9 \text{ M}^{-1} \text{ s}^{-1}$ ($k_{\text{H}}/k_{\text{D}} = 1.2 \pm 0.2$) for the least reactive silene in the series (**19b**) to $k_{\text{AcOH}} = (2.3 \pm 0.4) \times 10^9 \text{ M}^{-1} \text{ s}^{-1}$ ($k_{\text{H}}/k_{\text{D}} = 1.1 \pm 0.1$) for the most reactive (**19e**). A Hammett plot for the five compounds affords a reaction constant $\rho = +0.17$ ⁴⁰. The variation in the rate constants throughout the series, though smaller than those observed for MeOH and *t*-BuOH, rules out the mechanism involving initial protonation followed by rapid reaction of the resulting silicenium ion with acetate. A comparison of the temperature dependence of the rate constants for addition of AcOH to the 1,1-diarylsilenes **19a** and **19e** allows a distinction to be made between the two remaining mechanistic possibilities.

Figure 5 shows the Arrhenius plots obtained for reactive quenching of **19a** and **19e** by AcOH in acetonitrile solution over the -20 to 50 °C temperature range⁴⁰. The activation energies are positive in both cases, as would be predicted to be the case for any of the three possible mechanisms. However, only the mechanism of equation 34 is consistent with the

TABLE 6. Absolute rate constants and deuterium kinetic isotope effects for reaction of 1,1-diarylsilenes (XC_6H_4)₂Si=CH₂ (**19a–e**) with acetic acid (AcOH) in acetonitrile solution at 23 °C (in units of $10^9 \text{ M}^{-1} \text{ s}^{-1}$)^a

19a (X = H)	19b (X = 4-CH ₃)	19c (X = 4-F)	19d (X = 4-Cl)	19e (X = 4-CF ₃)
1.5 ± 0.2 ($k_{\text{H}}/k_{\text{D}} = 1.1$)	1.41 ± 0.05 ($k_{\text{H}}/k_{\text{D}} = 1.2$)	1.8 ± 0.2	2.0 ± 0.2	2.3 ± 0.4 ($k_{\text{H}}/k_{\text{D}} = 1.1$)

^aData from Reference 40.

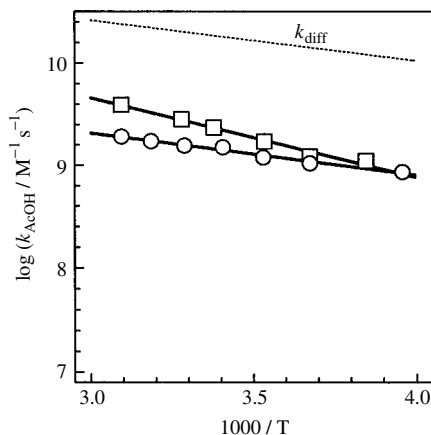
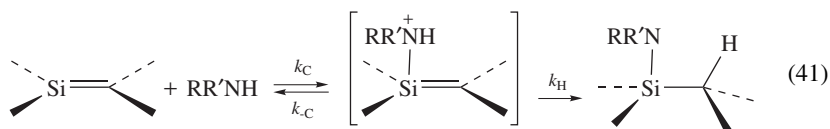


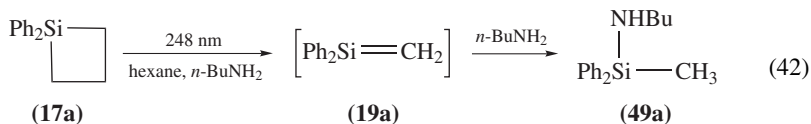
FIGURE 5. Arrhenius plots for the reaction of 1,1-diarylsilenes **19a** (○) and **19e** (□) with acetic acid in acetonitrile solution. Reproduced with permission from Reference 40. Copyright 1997 National Research Council of Canada

fact that the larger E_a is obtained for the *more reactive* of the two silenes (**19e**). This would be the result expected if at any given temperature, the complex partitioning ratio $k_{\text{H}}/(k_{\text{H}} + k_{-\text{C}})$ is greater for the more electrophilic silene **19e**, as was shown to be the case in the preceding section for MeOH addition. The closer this ratio is to unity, the more closely the observed Arrhenius parameters for reaction reflect those of the complexation step of the reaction.

c. Addition of aliphatic amines. Primary and secondary amines react with silenes by 1,2-addition to yield the corresponding aminosilanes^{6,93,94}. Wiberg's relative rate data (Table 2) show that for silene **6**, reaction with primary aliphatic amines (RNH_2) is generally about a factor of two faster than reaction with the alcohol of analogous structure (ROH). This and the subsequent successful isolation and crystal structure determination of the complex of **5** (the stable analogue of **6**) with trimethylamine⁷⁷ provide strong support for his proposal that the reaction proceeds by a similar mechanism to that for alcohol addition, as depicted in equation 41⁶.



This trend in relative rates is magnified in the case of 1,1-diphenylsilene (**19a**), which reacts with *n*-butylamine with an absolute rate constant $k_{n\text{-BuNH}_2} = (9.7 \pm 0.4) \times 10^9 \text{ M}^{-1} \text{ s}^{-1}$ in hexane solution at 23 °C⁴⁴. This should be compared to the rate constant for reaction of **19a** with methanol under the same conditions, $k_{\text{MeOH}} = (1.9 \pm 0.2) \times 10^9 \text{ M}^{-1} \text{ s}^{-1}$. Compared to **19a**, a slight rate acceleration is observed for reaction of **19e**, $k_{n\text{-BuNH}_2} = (1.36 \pm 0.08) \times 10^{10} \text{ M}^{-1} \text{ s}^{-1}$, as expected⁴³. Product studies verify that the expected aminosilane **49a** is the sole product of the reaction (equation 42).



A recent study of the temperature dependence of the rates of addition of *n*-BuNH₂ to **19a** and **19e** in hexane and acetonitrile solution lends further support to the mechanism of equation 41⁴³. The Arrhenius plots for reaction of the two silenes in hexane are shown in Figure 6. Both show the curvature that this mechanism predicts should occur when k_{H} and $k_{-\text{C}}$ are of similar magnitudes to one another, and as was observed in the Arrhenius plots for reaction of the two silenes with MeOH and AcOH. The relative placement of the plots along the T^{-1} axis is consistent with the ratio $k_{\text{H}}/(k_{\text{H}} + k_{-\text{C}})$ being larger for the more reactive silene (**19e**) at any single temperature within the range studied. In this case, both compounds show the predicted turnover in the temperature dependence that occurs when the rates of complex dissociation and collapse to product are equal. This point occurs at temperatures of *ca* 0 °C and *ca* 40 °C for **19a** and **19e**, respectively. The calculated values of k_{C} for the two silenes at these temperatures, $k_{\text{C}} \sim 3 \times 10^{10} \text{ M}^{-1} \text{ s}^{-1}$ for **19e** (at *ca* 40 °C) and $k_{\text{C}} \sim 2 \times 10^{10} \text{ M}^{-1} \text{ s}^{-1}$ for **19a** (at 0 °C), are both roughly equal to the diffusional rate constants in hexane at the same temperature: k_{diff} (at 40 °C) = $2.6 \times 10^{10} \text{ M}^{-1} \text{ s}^{-1}$ and k_{diff} (at 0 °C) = $1.4 \times 10^{10} \text{ M}^{-1} \text{ s}^{-1}$. This analysis indicates that complexation of *n*-BuNH₂ with both silenes occurs at the diffusion-controlled rate in

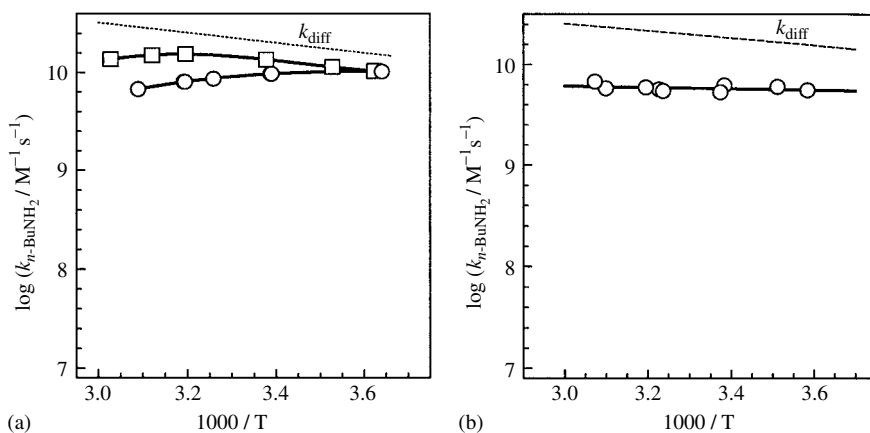
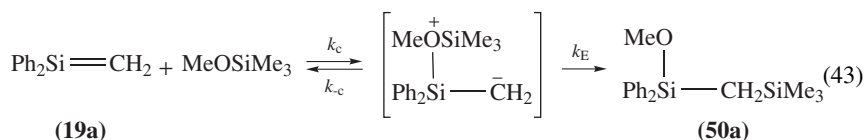


FIGURE 6. Arrhenius plots for the reaction of 1,1-diarylsilenes **19a** (○) and **19e** (□) with *n*-butylamine in (a) hexane and (b) acetonitrile solution

hexane solution, and that the higher overall reactivity of **19e** compared to **19a** is entirely due to the fact that the **19e**-amine complex proceeds to product more efficiently than that formed from **19a** [i.e. the complex partitioning ratio $k_H/(k_H + k_{-C})$ is again larger for the more reactive silene **19e** at any particular temperature within the range studied]. This is most likely due mainly to a difference in k_{-C} for the two silenes, with the value for the more electrophilic derivative **19e** being the smaller of the two. This conclusion could presumably be verified by an examination of the complexation equilibria of the two silenes with a tertiary amine.

d. Addition of alkoxy silanes. The last silene trapping reaction to be considered in this section is that of addition of alkoxy silanes (RO-SiR₃). To a first approximation, this reaction can be expected to be formally related to alcohol additions, except that the electrophilic component of the addend is a silyl group rather than a proton (equation 43). The reaction is known to take place with clean *syn*-stereospecificity, at least in the few examples for which the stereochemistry of the reaction has been studied in detail^{23,95,96}.



The absolute rate constants for addition of methoxytrimethylsilane (MeOTMS) to 1,1-diphenylsilene (**19a**) in hexane and acetonitrile solution (Table 3), which yields alkoxy silane **50a** as the sole product (equation 43), are roughly two orders of magnitude slower than those for addition of methanol under the same conditions⁵⁷. This difference is magnified to a factor of more than 1000 in the case of the less reactive (1-sila)hexatriene derivative **21a**, where only an upper limit of $k_{\text{MeOTMS}} < 10^5 \text{ M}^{-1} \text{ s}^{-1}$ could be established from the pseudo-first-order rate of decay of the silene in acetonitrile containing 0.6 M MeOTMS⁴⁷.

The rates of addition of MeOTMS to the series of substituted 1,1-diphenylsilenes **19a-e** in hexane at 23 °C (Table 7) correlate with Hammett substituent constants (Figure 7), affording a reaction constant $\rho = +1.2 \pm 0.3$ ⁵⁷. Thus, the rates are more sensitive to substituent than those for alcohol and acetic acid addition, but the trends with substituent electronic character are the same. Both the Hammett ρ -value observed for **19a-e** and the stereochemical evidence established by other workers are consistent with a stepwise mechanism analogous to that of alcohol addition (equation 43). The 100-fold reduction in rate compared to alcohol addition is most reasonably expected to be largely due to a slower rate of transfer of the electrophilic group (-SiMe₃, relative to -H) within the initially-formed complex, since this involves cleavage of a relatively strong Si-O bond.

Again, verification of the stepwise mechanism follows from the observed temperature dependences of the rate constants for reaction of **19a** and **19e** with this reagent (Figure 8)⁵⁷. Both show good linearity over the temperature range studied, and the

TABLE 7. Absolute rate constants (in units of $10^7 \text{ M}^{-1} \text{ s}^{-1}$) for reaction of 1,1-diarylsilenes (XC₆H₄)₂Si=CH₂ (**19a-e**) with methoxytrimethylsilane (MeOTMS) in hexane solution at 25 °C^a

19a (X = H)	19b (X = 4-CH ₃)	19c (X = 4-F)	19d (X = 4-Cl)	19e (X = 4-CF ₃)
1.9 ± 0.2	0.60 ± 0.05	2.4 ± 0.2	3.0 ± 0.2	12.0 ± 0.9

^aData from Reference 57.

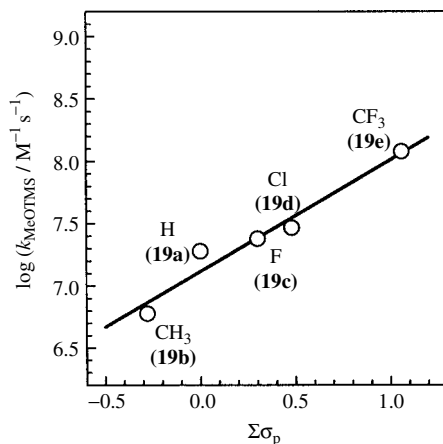


FIGURE 7. Hammett plot for the reactions of MeOTMS with 1,1-diarylsilenes **19a–e** in hexane solution at 25 °C. Reproduced with permission from Reference 57. Copyright 2001 American Chemical Society

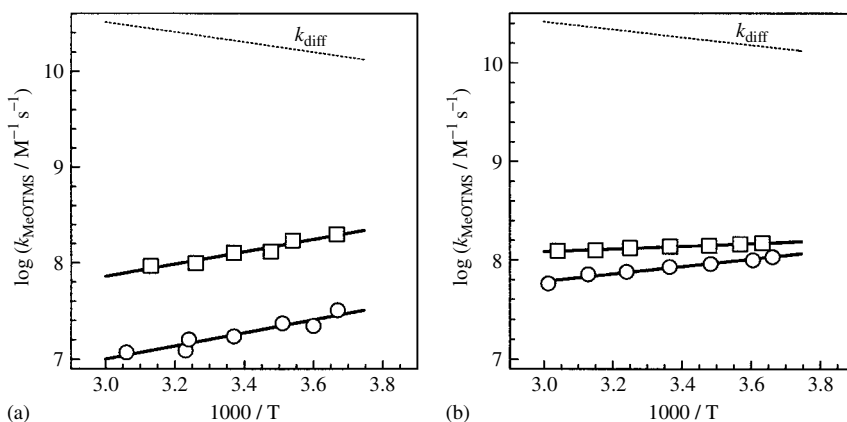


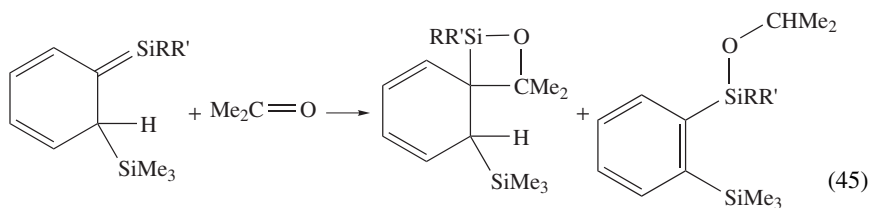
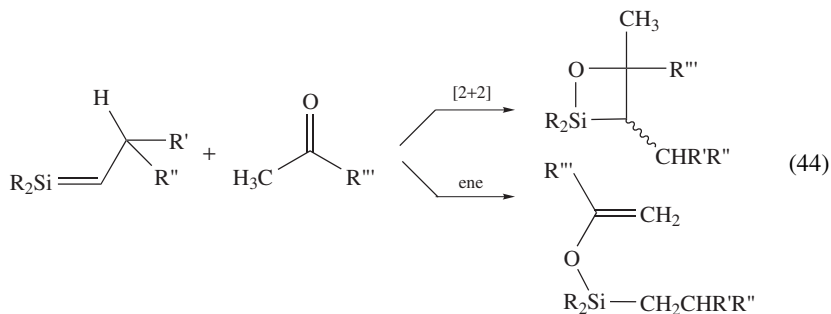
FIGURE 8. Arrhenius plots for the reaction of 1,1-diarylsilenes **19a** (○) and **19e** (□) with methoxytrimethylsilane in (a) hexane and (b) acetonitrile solution. Reproduced with permission from Reference 57. Copyright 2001 American Chemical Society

data in hexane solution (Figure 8a) yield nearly identical, strongly negative Arrhenius activation energies on the order of $E_a \sim -12 \text{ kJ mol}^{-1}$. This is consistent with the expectation that intracomplex electrophile transfer should be much slower in this case than in alcohol, carboxylic acid or amine addition. The fact that nearly identical E_a values are observed suggests that the observable temperature range lies well within the regime where $k_{-C} \gg k_E$ for both silenes. Differences in E_a analogous to those found for MeOH show up in acetonitrile solution (Figure 8b), however, showing that in this solvent, the same differences in the relative magnitudes of k_{-C} and k_E hold for MeOTMS addition as with MeOH, *n*-BuNH₂ and AcOH addition (where $k_E \equiv k_H$).

Methoxytrimethylsilane addition to 1,1-dimethylsilene (**2b**) was studied in the gas phase over the 450–550 °C temperature range by Davidson and Wood, who reported $E_a = +6.3 \pm 2.2 \text{ kJ mol}^{-1}$ and $\log(A/M^{-1} \text{ s}^{-1}) = 5.3 \pm 0.2$ (see Table 1)³⁴. While the rate constants were calculated based on the erroneous rate constants of Gusel'nikov, Nametkin and coworkers for the gas-phase dimerization of **2b** (*vide supra*)³³, this should not affect the activation energy obtained so long as the activation energy for dimerization is truly close to zero. As mentioned earlier, there is indirect evidence from other experiments that this is so⁶⁰. However, silene **2b** exhibits similar overall reactivity toward MeOH addition as **19a** under the same conditions, a similarity which extends to the sign and magnitude of the Arrhenius activation energies for reaction of the two silenes^{89,97} (*vide infra*). We thus find it difficult to rationalize the positive value of E_a reported by Davidson and Wood for the addition of MeOTMS to **2b** in the gas phase.

4. Ene- and [2 + 2]-addition of ketones, aldehydes and esters

The reactions of silenes with aldehydes and ketones is another area whose synthetic aspects have been particularly well-studied^{4,6,7,10,12}. The favoured reaction pathways for reaction are generally ene-addition (in the case of enolizable ketones and aldehydes) to yield silyl enol ethers and [2 + 2]-cycloaddition to yield 1,2-siloxetanes (equation 44), but other products can also arise in special cases. For example, the reaction of aryldisilane-derived (1-sila)hexatrienes (e.g. **21a–c**) with acetone yields mixtures of 1,2-siloxetanes (**51a–c**) and ene-adducts (**52a–c**) in which the carbonyl compound rather than the silene has played the role of the enophile (equation 45)^{47,50,52,98,99}. Also, [4 + 2]-cycloadducts are frequently obtained from reaction of silenes with α,β -unsaturated- or aryl ketones, where the silene acts as a dienophile in a formal Diels–Alder reaction^{6,29,100–102}.



(21)

(51)

(52)

(a) R = R' = Me

21%

41%

(b) R = Me; R' = Ph

28%

54%

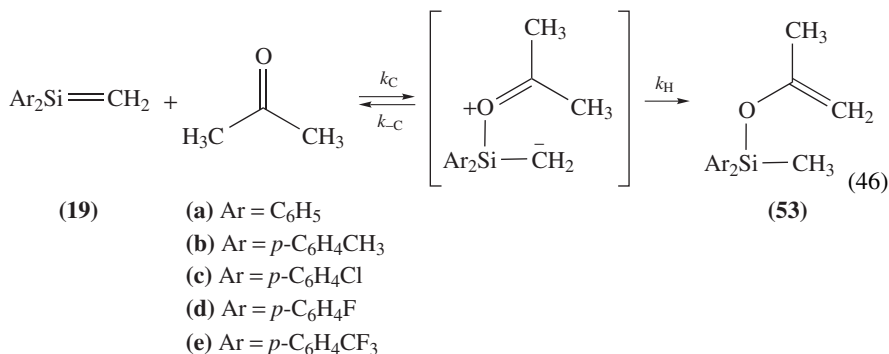
(c) R = R' = Ph

69%

33%

Early mechanistic suggestions notwithstanding⁴², there is now excellent evidence to suggest that the ene-addition reaction of silenes with enolizable carbonyl compounds is initiated by Lewis acid–base complexation, in an analogous way to the nucleophilic addition reactions discussed in the previous section⁴¹. Indeed, it seems reasonable to expect that complexation is the initial step in all the reactions of carbonyl compounds with silenes, with the final outcome being controlled by the propensity of the complex to react in whatever particular ways are possible with a given silene and carbonyl compound¹⁰³.

The absolute rate constants for ene-addition of acetone to the substituted 1,1-diphenylsilenes **19a–e** at 23 °C (affording the silyl enol ethers **53**; equation 46) correlate with Hammett substituent parameters, leading to ρ -values of +1.5 and +1.1 in hexane and acetonitrile solution, respectively⁴¹. Table 8 lists the absolute rate constants reported for the reactions in isooctane solution, along with k_H/k_D values calculated as the ratio of the rate constants for reaction of acetone and acetone-*d*₆. In acetonitrile the kinetic isotope effects range in magnitude from $k_H/k_D = 3.1$ (i.e. 1.21 per deuterium) for the least reactive member of the series (**19b**) to $k_H/k_D = 1.3$ (i.e. 1.04 per deuterium) for the most reactive (**19e**)⁴¹. Arrhenius plots for the reactions of **19a** and **19e** with acetone in the two solvents are shown in Figure 9, and were analysed in terms of the mechanism of equation 46.



Again, the same general trends as were found for MeOH, AcOH, *n*-BuNH₂ and MeOTMS are observed in the temperature dependences for reaction of the two silenes, **19a** and **19e**, with acetone. In both solvents, the differences are consistent with the efficiency of product formation from the intermediate complex, being greater for **19e** than for **19a**. Interestingly, the curvature observed in the temperature dependence for silene **19e** in hexane solution indicates a turnover temperature of *ca* –15 °C, and the calculated complexation rate constant at this temperature, $k_C \sim 1.5 \times 10^{10} \text{ M}^{-1} \text{ s}^{-1}$, is identical to the diffusional rate constant within experimental error ($k_{\text{diff}} = 1.3 \times 10^{10} \text{ M}^{-1} \text{ s}^{-1}$).

It is instructive to compare the results obtained for these two compounds with the analogous data for AcOH addition, to the extent that the latter can be viewed formally

TABLE 8. Absolute rate constants and deuterium kinetic isotope effects for reaction of 1,1-diarylsilenes (XC₆H₄)₂Si=CH₂ (**19a–e**) with acetone in isooctane solution at 23 °C (in units of 10⁹ M⁻¹ s⁻¹)^a

19a (X = H)	19b (X = 4-CH ₃)	19c (X = 4-F)	19d (X = 4-Cl)	19e (X = 4-CF ₃)
0.38 ± 0.02 ($k_H/k_D = 2.1$)	0.17 ± 0.01 ($k_H/k_D = 1.7$)	1.29 ± 0.09 ($k_H/k_D = 1.8$)	2.04 ± 0.02 ($k_H/k_D = 1.7$)	3.52 ± 0.04 ($k_H/k_D = 1.4$)

^aData from Reference 41.

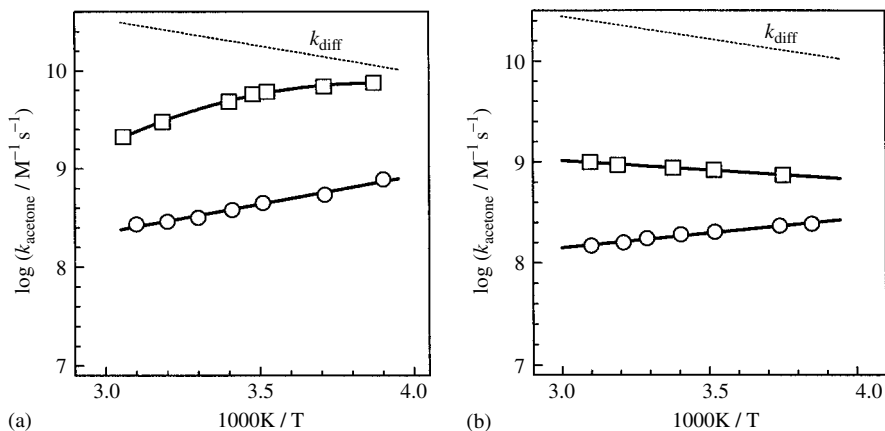


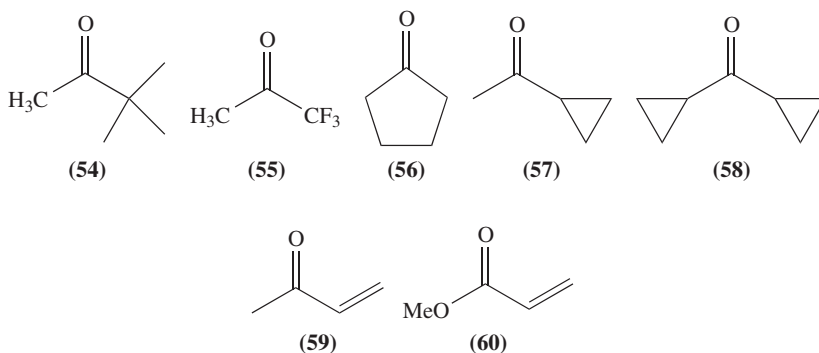
FIGURE 9. Arrhenius plots for the reaction of 1,1-diarylsilenes **19a** (○) and **19e** (□) with acetone in (a) hexane and (b) acetonitrile solution. Reproduced with permission from Reference 41. Copyright 1998 American Chemical Society

as an ene-addition, in which hydrogen is transferred from oxygen rather than carbon. The differences are consistent with the silene–AcOH complexes proceeding to product with considerably greater efficiency than those involved in acetone addition, as would clearly be expected considering the much higher proton acidity of the carboxylic acid compared to the ketone. For a given silene, this difference results in a substantially more positive apparent activation energy for reaction of the acid than for the ketone under similar conditions. For example, the reactions of **19e** with acetone and acetic acid in acetonitrile solution exhibit Arrhenius activation energies of $E_a = +3.5 \pm 0.2 \text{ kJ mol}^{-1}$ and $E_a = +14.5 \pm 1.0 \text{ kJ mol}^{-1}$, respectively.

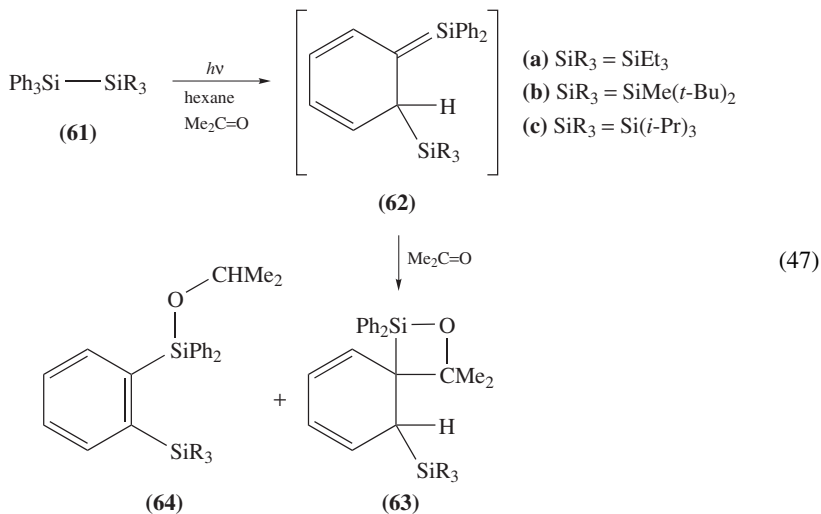
A similar comparison to the temperature dependences for addition of MeOH to these two silenes in acetonitrile leads to the surprising conclusion that the intracomplex product partitioning ratio $k_{\text{H}}/(k_{\text{H}} + k_{-\text{C}})$ is apparently *greater* for acetone addition than for methanol addition, in contrast to what might be expected based on the relative proton acidities of the two reagents. One possible explanation for this is that the entropic contribution to k_{H} is likely to be considerably more pronounced in the case of MeOH addition, where proton transfer within the complex must proceed via a 4-centre transition state rather than the 6-centre transition state involved in the acetone reaction; furthermore, there are six transferable hydrogens in acetone compared to only one in MeOH. Inspection of the Arrhenius plots in Figures 9b and 4 suggest that the product partitioning ratio appears to vary more precipitously with temperature in the case of MeOH than with acetone, which is consistent with this explanation. The Arrhenius data also indicate that both k_{C} and the complex partitioning ratio increase with substituent electron-withdrawing power in the case of acetone addition. In contrast, in the case of methanol addition the data suggest that k_{C} is relatively insensitive to substituents.

Absolute rate constants for quenching of **19a** have been reported for other ketones besides acetone, although product studies were not carried out⁴². These data are included in Table 3. The rate constant for quenching by pinacolone [**54**; $k_{\text{q}} = (4.0 \pm 0.2) \times 10^8 \text{ M}^{-1} \text{ s}^{-1}$] is similar to that by acetone under similar conditions, as would be expected for ene-addition by the mechanism of equation 46. The factor of *ca* 20 reduction in the rate constant for quenching by 1,1,1-trifluoroacetone [**55**; $k_{\text{q}} = (1.6 \pm 0.1) \times 10^7 \text{ M}^{-1} \text{ s}^{-1}$]

compared to acetone is consistent with the presumably lower Lewis basicity of the fluorinated ketone, which would be expected to reduce the rate of the initial complexation step of reaction. Cyclopentanone [**56**; $k = (1.2 \pm 0.1) \times 10^9 \text{ M}^{-1} \text{ s}^{-1}$]⁴² and cyclopropyl methyl ketone [**57**; $k = (1.2 \pm 0.1) \times 10^9 \text{ M}^{-1} \text{ s}^{-1}$]⁵⁶ most likely react by ene-addition, a pathway that is effectively retarded by the absence of enolizable hydrogens in the case of dicyclopropyl ketone [**58**; $k = (1.7 \pm 0.2) \times 10^6 \text{ M}^{-1} \text{ s}^{-1}$]⁵⁶. Methyl vinyl ketone [**59**; $k = (1.6 \pm 0.2) \times 10^9 \text{ M}^{-1} \text{ s}^{-1}$] and methyl acrylate [**60**; $k = (3.3 \pm 0.2) \times 10^7 \text{ M}^{-1} \text{ s}^{-1}$] most likely react by [2 + 2]- and/or [2 + 4]-cycloaddition to the Si=C bond in **19**^{100,101}.



The kinetics of acetone addition have also been studied for several aryldisilane-derived (1-sila)hexatrienes, including **21a-c**^{47,51}, **46**⁵¹ and **62** (from photolysis of **61**; equation 47), where the reaction follows a different course than that of simpler silenes such as **19**⁵². In these cases, the reaction proceeds via two competing pathways, formal [2 + 2]-cycloaddition and ene-addition. Unlike the case with the simpler silenes, however, the ketone rather than the silene acts as the enophile in the reaction, presumably because this alternative has the formation of an aromatic ring as an added driving force.

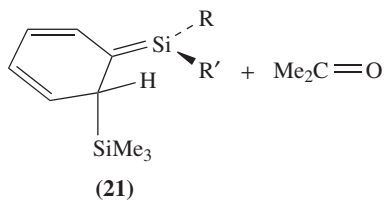


Accordingly, the (1-sila)hexatrienes **21c**, **62a–c** and **46**, generated by photolysis of the corresponding arylidisilanes **20c**, **61a–c** and **45**, respectively, afford mixtures of the corresponding 1,2-siloxetane (**63**) and *iso*-propoxysilane (**64**). The yield of siloxetane increases at the expense of that of alkoxyisilane with increasing steric bulk of the $-\text{SiR}_3$ group. The siloxetanes are the major products in all five cases, unlike the situation with **21a,b**, which both yield mixtures favouring the alkoxyisilane. Photolysis of **61c** in the presence of acetone under the same conditions (-78°C or 25°C) led to an intractable mixture of products which contained only small amounts of the corresponding siloxetane and alkoxyisilane, and the relative yield of siloxetane:alkoxyisilane is considered to be a lower limit in this case. This was ascribed to secondary decomposition owing to the formation of triplet-derived^{47,50,104} silyl free radicals, which compete particularly effectively with the formation of (1-sila)hexatriene from the lowest excited singlet state in highly hindered arylidisilanes¹⁰⁴.

The variation in the relative yields of siloxetane and alkoxyisilane with substituent (either the $-\text{SiR}'\text{R}_2$ group⁵² or those attached to the silenic silicon atom⁴⁷) was explained in terms of conformational factors associated with an initially-formed biradical/zwitterion intermediate in the reaction. On the basis of the kinetic results discussed above for the addition of acetone to **19a–e**, we can now identify this intermediate as the zwitterionic complex of the carbonyl compound with the silene (equation 48). The hydrogen transfer required for collapse of the complex to alkoxyisilane would be expected to proceed via a transition state in which the allylic C–H bond in the cyclohexadienyl ring overlaps well with the cyclohexadienyl π -system, thus providing maximal aromatic stabilization (equation 48). Such a conformation contains the $-\text{SiR}'\text{R}_2$ substituent in a pseudo-equatorial arrangement where steric buttressing with the adjacent Si=C bond will be significant, particularly when the silenic silicon atom bears two phenyl substituents. Such conformational factors would not be expected to be important in coupling to form the siloxetane product. Thus, the relative yield of siloxetane is dramatically higher from **21c** than from **21a,b**, and increases further as the $-\text{SiMe}_3$ substituent in **21c** is replaced with successively bulkier trialkylsilyl groups.

Absolute rate constants and relative product yields for the reaction of **21c**, **62a–c** and **46** with acetone in hexane are listed in Table 9. There is a slight increase in rate constant as the steric bulk of the $-\text{SiR}_3$ group increases throughout the series, which was tentatively attributed to the effects of sterically-induced distortions in the Si=C bond in the molecules as a result of the $-\text{SiR}'\text{R}_2$ substituents. The variation in rate constant is not really very well understood, however.

Absolute rate constants have also been reported for quenching of 1,1-diphenylsilene (**19a**) and the silatriene **21a** by ethyl acetate (AcOEt)^{42,51}, and while product studies have never been completed, it seems reasonable to speculate that the ester should react in an analogous fashion to acetone. The rate constants are in both cases substantially slower than those for reactive quenching by the ketone under similar conditions. For example, values of $k_{\text{AcOEt}} = (7.3 \pm 0.4) \times 10^6 \text{ M}^{-1} \text{ s}^{-1}$ and $(3.3 \pm 0.3) \times 10^6 \text{ M}^{-1} \text{ s}^{-1}$ have been reported for quenching of **19a**⁴² and **21a**⁵¹, respectively, in acetonitrile solution at $21\text{--}23^\circ\text{C}$. These should be compared to those for acetone quenching, $k_{\text{acetone}} = (1.8 \pm 0.1) \times 10^8 \text{ M}^{-1} \text{ s}^{-1}$ for **19a**⁴¹ and $(9.0 \pm 0.3) \times 10^8 \text{ M}^{-1} \text{ s}^{-1}$ for **21a**⁵¹ under the same conditions. To the extent that the ester is expected to be a stronger Lewis base than the ketone, it seems unlikely that the reduced reactivity toward AcOEt might be due to effects on the complexation step of the reaction. A slower rate constant for intracomplex proton transfer in the (possible) ene-addition to **19a** might be expected owing to the lower proton acidity of AcOEt relative to acetone, but this cannot explain the reduced overall reactivity in the case of **21a**, where α -proton transfer from the ester to the silenic carbon presumably does not occur.



- (a) R = R' = Me
 (b) R = Ph; R' = Me
 (c) R = R' = Ph

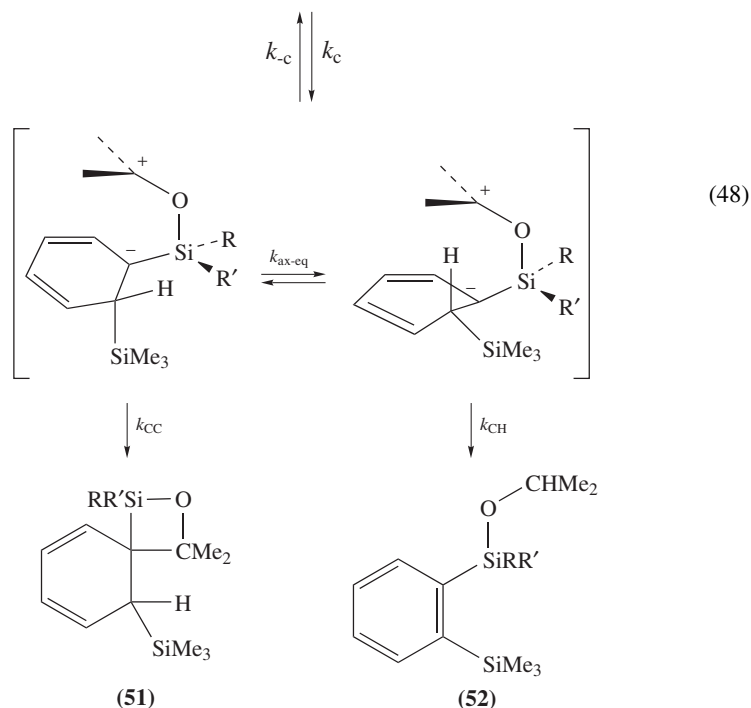
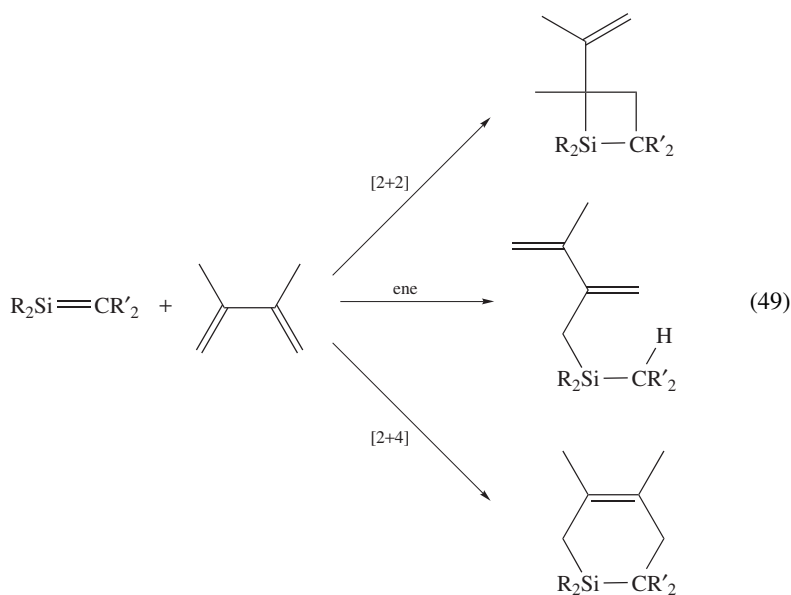


TABLE 9. Absolute rate constants and relative product yields for reaction of acetone with silenes **21c**, **62a-c** and **46** in deoxygenated hexane solution at 22 °C^{47,52,105}

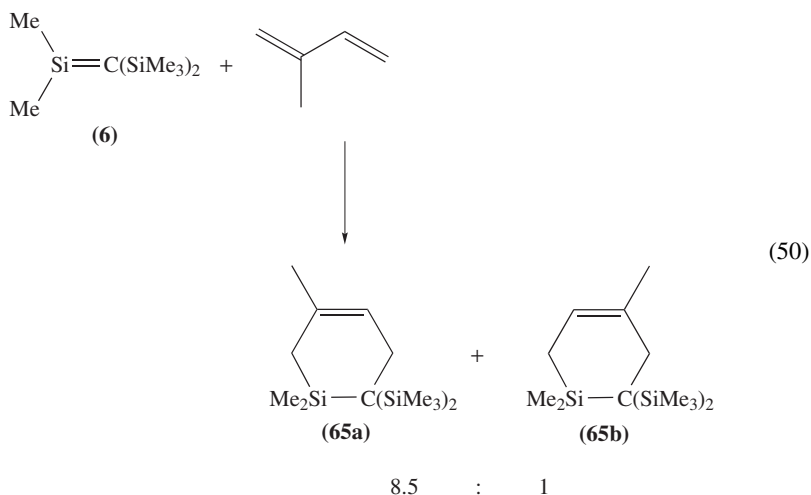
Silene	-SiR ₃	$k_{\text{acetone}} (10^8 \text{ M}^{-1} \text{ s}^{-1})$	51 : 52
21c	-SiMe ₃	6.0 ± 0.2	2.7 ± 0.2
62a	-SiEt ₃	6.2 ± 0.3	4.7 ± 0.6
62b	-SiMe ₂ Bu- <i>t</i>	8.7 ± 0.2	6.4 ± 0.4
62c	-Si(<i>i</i> -Pr) ₃	9.2 ± 0.3	≥ 1.6
46	-SiPh ₂ Me	7.6 ± 0.3	7.1 ± 0.5

5. Ene-, [2 + 2]- and [4 + 2]-cycloaddition of alkenes and dienes

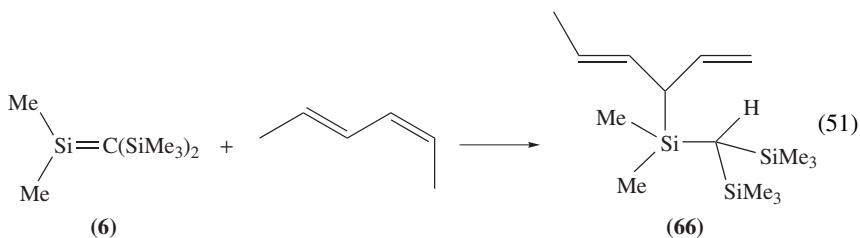
Although the reactions of silenes with alkenes and dienes have been widely investigated in product-oriented studies, absolute rate constants have been reported in only a relatively small number of cases. One practical reason for this is that the reactions are generally quite slow, and hence one needs to measure silene decay rates in the presence of reasonably high concentrations of added alkene or diene in order to observe quenching at all. It is often impossible to work with such high concentrations simply because most silene precursors that have been studied to date require excitation in the 248 nm or 266 nm range, where dienes also absorb. Nevertheless, enough data have been reported to give a sense of the reactivity of dienes and alkenes relative to nucleophilic silene trapping reagents. Reaction with alkenes generally proceeds via ene-addition or [2 + 2]-cycloaddition, and in the case of conjugated dienes via [2 + 4]-cycloaddition as well (equation 49)^{8,10,12}.



Wiberg and coworkers published relative rate constants and the products of reaction of silene **6** with a number of alkenes and dienes in ether solution at 100 °C^{6,106–108}. These data are listed in Table 2 along with an indication of the type of product formed in each case. As is the norm in Diels–Alder additions by more conventional dienophiles, the rate of [2 + 4]-cycloaddition of **6** to dienes increases with sequential methyl substitution in the 2- and 3-positions of the diene, as is illustrated by the data for 2,3-dimethyl-1,3-butadiene (DMB), isoprene and 1,3-butadiene. The well-known effects of methyl substitution at the 1- and 4-positions of the diene in conventional Diels–Alder chemistry are also reflected with **6** as the dienophile. For example, *trans*-1,3-pentadiene reacts significantly faster than the *cis*-isomer, an effect that has been attributed to steric destabilization of the transition state for [2 + 4]-cycloaddition. In fact, the reaction of *cis*-1,3-pentadiene with **6** yields silacyclobutane adducts, while the *trans*-diene reacts by [2 + 4]-cycloaddition¹⁰⁸. No detectable reaction occurs with 2,5-dimethyl-2,4-hexadiene. The reaction of **6** with isoprene occurs regioselectively to yield adducts **65a** and **65b** in the ratio **65a** : **65b** = 8.5 (equation 50)^{106,107}.

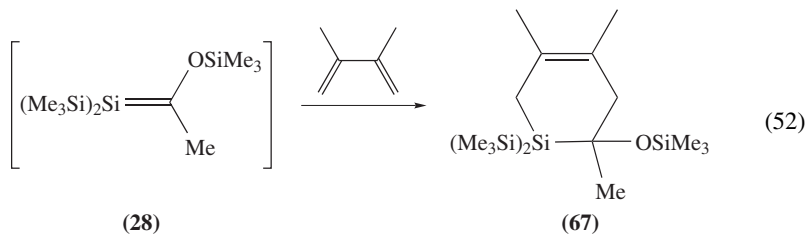


Ene-additions of alkenes and dienes to silene **6** are considerably slower than [2 + 4]-cycloadditions. *cis*-Substitution in the ene component of the reaction causes a small acceleration in rate relative to *trans*-substitution, as illustrated in Table 2 by the relative rate constants for reaction of **6** with *cis*- and *trans*-2-butene. Reaction with *cis*, *trans*-2,4-hexadiene produces only a single adduct (**66**; equation 51), corresponding to selective ene-reaction with the *cis*-methyl group in the diene.



Absolute rate constants or upper limits have been reported for reaction of 1,1-diphenylsilene (**19a**) with the conjugated dienes DMB [$k_q = (3.7 \pm 0.2) \times 10^6 \text{ M}^{-1} \text{ s}^{-1}$]⁴² and *trans*-1,3-pentadiene [$k_q = (8.1 \pm 0.2) \times 10^6 \text{ M}^{-1} \text{ s}^{-1}$]⁵⁶, and the alkenes methylenecyclopentane [$k_q = (6.8 \pm 0.8) \times 10^7 \text{ M}^{-1} \text{ s}^{-1}$]⁵⁶ and cyclohexene ($k_q < 10^4 \text{ M}^{-1} \text{ s}^{-1}$), all in isooctane solution¹⁰⁹. None of the products of these reactions has been identified, unfortunately. Similar values have been reported for the reaction of DMB with the C-substituted 1,1-dimethylsilene **23** [$k_q = (3.2 \pm 0.6) \times 10^6 \text{ M}^{-1} \text{ s}^{-1}$] and the related 1,3-(2-sila)butadiene derivative **24** [$k_q = (5 \pm 2) \times 10^6 \text{ M}^{-1} \text{ s}^{-1}$]⁵³. Again, product studies were not carried out, but it was shown that **23** reacts with 1,3-butadiene to yield a mixture of at least seven products, of which four were tentatively identified as [2 + 2]-cycloadducts and two others as [2 + 4]-cycloadducts. Thus, the [2 + 2]-reaction can be concluded to proceed via a stepwise, biradical pathway, as has been proposed previously by other workers. Quenching of **23** and **24** by cyclohexene proceeds with rate constants on the order of $4 \times 10^4 \text{ M}^{-1} \text{ s}^{-1}$ or less in isooctane solution at 23 °C⁵³. Finally, Conlin and coworkers reported a value of $k_{\text{DMB}} = 0.23 \text{ M}^{-1} \text{ s}^{-1}$ for reaction of

DMB with the Brook silene **28**, which yields the Diels–Alder adduct **67** as the major product (equation 52)⁶⁵.



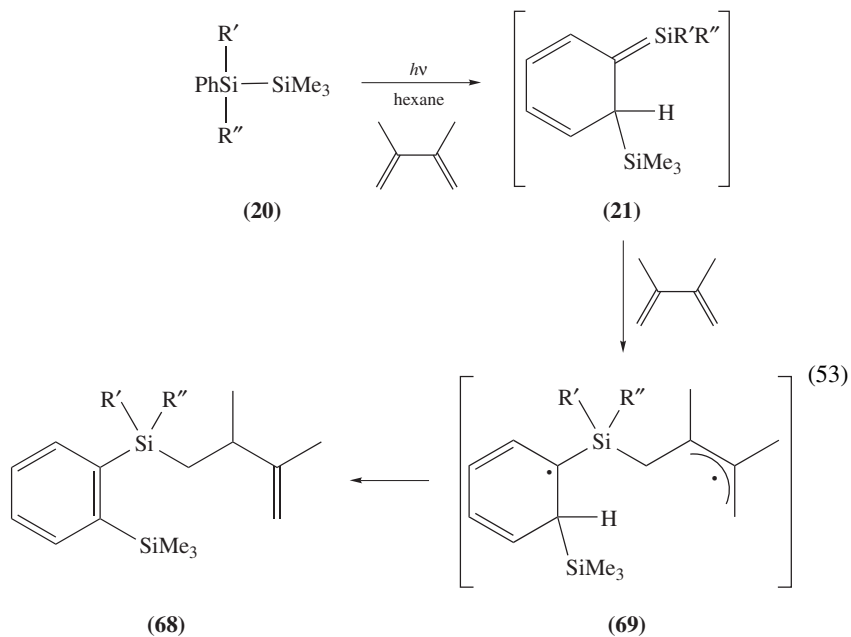
Aryldisilane-derived 1,3,5-(1-sila)hexatrienes react with both alkenes and dienes by exclusive ene-addition, where the silene plays the role of the ene component (due to the presence of the labile cyclohexadienyl hydrogen) and the alkene or diene serves as an enophile^{47,82,99,110}. For example, reaction of the silatrienes **21a–c** with DMB produces the ene-adducts **68** (equation 53)^{47,110}. A second, unidentified adduct is formed along with **68c** in the reaction with **21c**; this and other evidence⁴⁹ suggests that the reaction proceeds via the initial formation of the 1,4-biradical intermediate **69**. Absolute rate constants for reaction of **21a–c** with DMB decrease with increasing phenyl substitution on the silenic silicon, from a value of $k_{\text{DMB}} = (1.28 \pm 0.03) \times 10^8 \text{ M}^{-1} \text{ s}^{-1}$ for **21a** to $k_{\text{DMB}} = (3.0 \pm 0.1) \times 10^7 \text{ M}^{-1} \text{ s}^{-1}$ for **21c** in isooctane solution at 21 °C⁴⁷. The significantly greater reactivity of these silenes toward DMB compared to 1,1-diphenylsilene (**19a**) is noteworthy, in view of the fact that **21a–c** and **19a** exhibit comparable reactivities toward nucleophiles such as MeOH and acetone (*vide supra*). The enhanced reactivity of **21a–c** toward dienes is believed to be the result of the radical-stabilizing ability of the cyclohexadienyl substituent, which specifically promotes reactions that proceed through radical or biradical intermediates. Other examples of this unique reactivity of silenes of this type are described in the next section.

6. Other reactions – oxygen, sulphoxides and halocarbons

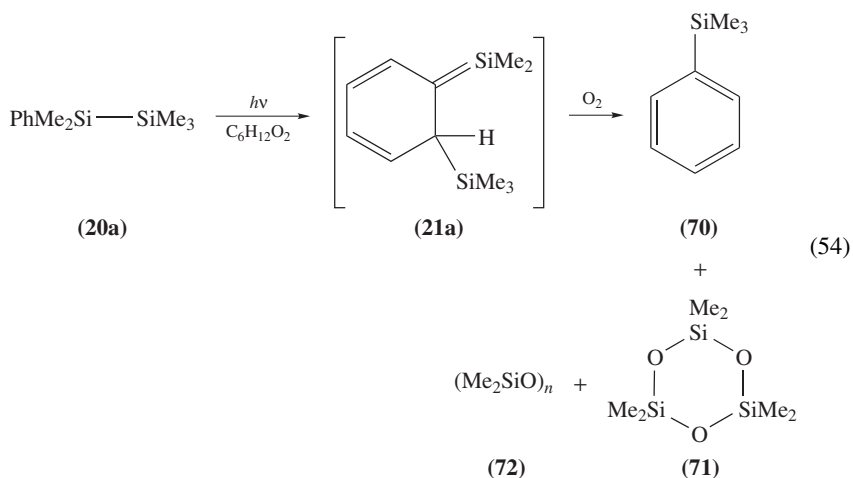
Unlike the cases of methanol and acetone addition, the reactivity of transient silenes toward oxygen varies widely with silene structure. For example, no difference in the *ca* 15 μs lifetime of **19a** in nitrogen-saturated isooctane solution is observed upon saturating the solution with oxygen⁴², which allows an upper limit of $k_{\text{O}_2} \leq 5 \times 10^5 \text{ M}^{-1} \text{ s}^{-1}$ to be estimated for the absolute rate constant for reaction of this silene with oxygen in hydrocarbon solvents. Silenes with $-\text{CH}_2\text{R}$ substituents attached to carbon exhibit somewhat higher reactivity; for example, **23** and **24** are quenched by O_2 with rate constants of $(2.6 \pm 0.3) \times 10^7 \text{ M}^{-1} \text{ s}^{-1}$ and *ca* $5 \times 10^6 \text{ M}^{-1} \text{ s}^{-1}$, respectively, in hexane at 23 °C⁵³. The hindered 1,1-bis(trimethylsilyl)silene **32** is quenched by oxygen with a rate constant of $k_{\text{O}_2} \sim 2 \times 10^5 \text{ M}^{-1} \text{ s}^{-1}$ in hexane at 25 °C⁶⁶, similar to the value $k_{\text{O}_2} = (7.3 \pm 1.5) \times 10^5 \text{ M}^{-1} \text{ s}^{-1}$ reported for silene **28**⁶⁵.

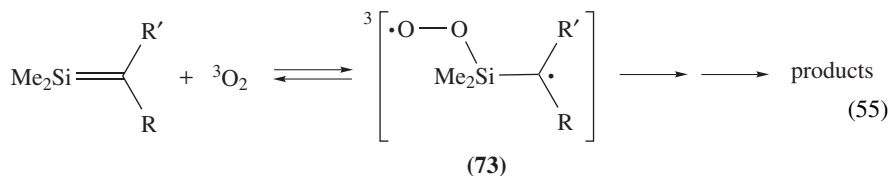
Derivatives in which the silenic silicon atom is at the terminus of a higher conjugated system exhibit significantly higher reactivity toward oxygen than other silenes. This is evident from the rate constants for oxygen quenching of the 1,3-(1-sila)butadiene derivative **8b** [$k_{\text{O}_2} = (3.0 \pm 0.9) \times 10^8 \text{ M}^{-1} \text{ s}^{-1}$]³² and the 1,3,5-(1-sila)hexatriene derivative **21a** [$k_{\text{O}_2} = (6.9 \pm 0.4) \times 10^8 \text{ M}^{-1} \text{ s}^{-1}$]⁴⁷ in hydrocarbon solvents at 23 °C. The products of the reaction of **21a** with O_2 are trimethylphenylsilane (**70**) and dimethylsilanone oligomers

71 and **72** (equation 54). These trends in rate suggest that the first step in the addition of oxygen to all of these silenes is the formation of a triplet 1,4-biradical intermediate (**73**) as shown in equation 55. The overall rate constant for reaction is determined primarily by the rate of this first step, consistent with the generalization that k_{O_2} increases with the radical-stabilizing ability of the $-R$ and $-R'$ substituents at the silenic carbon.

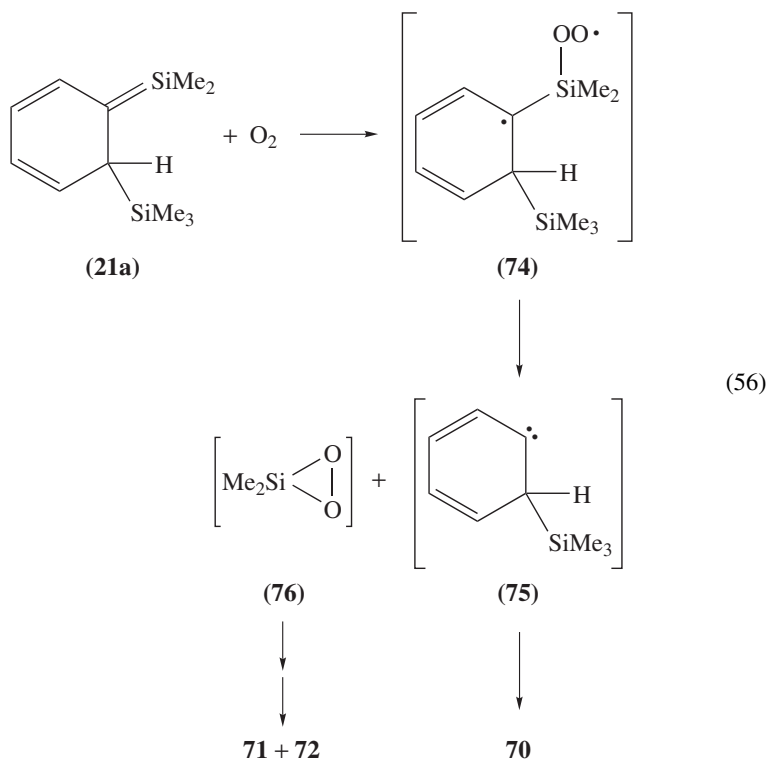


- (a) $R = R' = \text{Me}$
 (b) $R = \text{Me}, R' = \text{Ph}$
 (c) $R = R' = \text{Ph}$



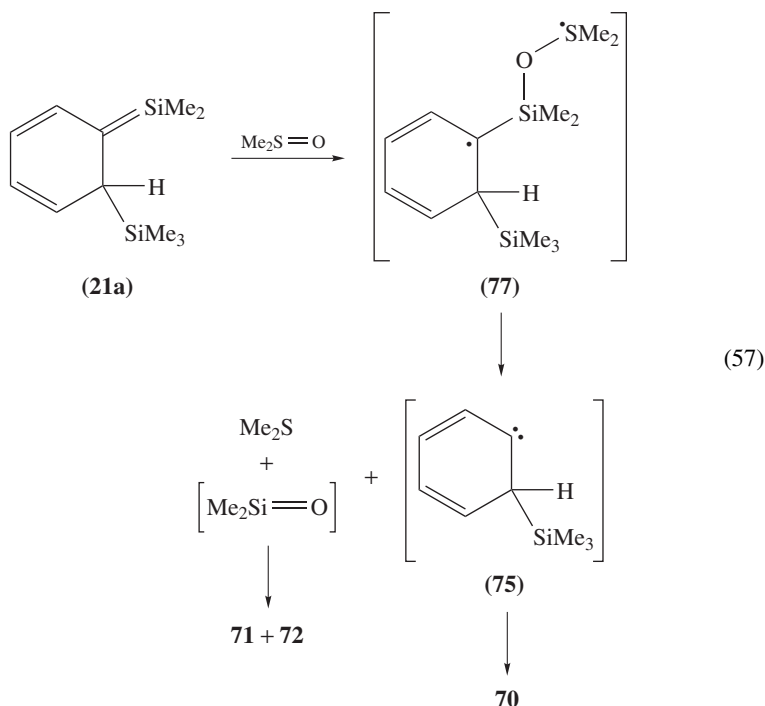


The formation of **70** in the case of **21a** was proposed to proceed via collapse of triplet biradical **74** to carbene **75** followed by [1,2]-SiMe₃ migration (equation 56), for which there is now good evidence to suggest it should proceed faster than the alternative [1,2]-H migration¹¹¹. The dimethylsilanone-derived products were proposed to be formed upon thermal decomposition of the other proposed product of the biradical, dimethyldioxasilirane (**76**), which had earlier been identified spectroscopically at low temperatures¹¹².



The same products are also formed in the photolysis of **21a** in dioxane in the presence of dimethyl sulphoxide (equation 57)^{113,114}, and the fact that silatriene **21a** is quenched rapidly by dimethyl sulphoxide in the same solvent [$k = (3.0 \pm 0.2) \times 10^9 \text{ M}^{-1} \text{ s}^{-1}$] indicates that the reaction involves the intermediacy of the silene⁴⁷. Reaction of the sulphoxide with **21a** presumably involves an intermediate, such as (singlet) **77** (equation 57), that

collapses to the same carbene as that involved in the reaction of **21a** with O₂.



Reaction with carbon tetrachloride is another example of the unique reactivity exhibited by 1,3,5-(1-sila)hexatrienes compared to simpler silene derivatives. The halocarbon quenches **21a** in isoctane solution with a rate constant $k_{\text{CCl}_4} = (4.4 \pm 0.1) \times 10^8 \text{ M}^{-1} \text{ s}^{-1}$ ⁴⁷, and proceeds about 50% faster in the more polar solvent acetonitrile. Based on the fact that quenching by chloroform is at least 100 times slower than by CCl₄, an electron transfer mechanism has been suggested⁴⁹. The specific products of the reaction have not been identified, however, because the analysis is complicated by the fact that CCl₄ also interacts directly with the excited singlet state of the disilene precursor, leading to exceedingly complex product mixtures⁴⁷. Simpler silenes such as **19a** generally show no evidence of reactivity toward carbon tetrachloride or chloroform.

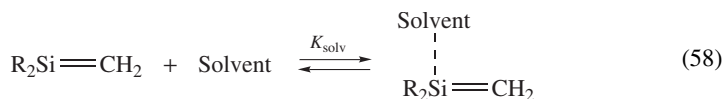
7. Solvent effects on silene reactivity

Most of the kinetic studies described in the preceding sections have been carried out in both hydrocarbon and acetonitrile solvents. In general, the overall rate constant for reaction is slightly slower in the more polar solvent, regardless of the structures of either the silene or the trapping reagent, or the nature of the initially-formed intermediates in the reaction. This has been suggested to be due to solvation effects on the free silene, since the nitrile solvent would be expected to form weak Lewis acid–base complexes with the Si=C bond⁴⁵. Indeed, products tentatively ascribed on the basis of GC/MS evidence to MeCN-addition products have been observed to be formed in some cases (such as **19a** and **21a**) under certain conditions^{48,92}.

The retarding effects of solvent complexation on the absolute rate constants for **19a** and **21a** are even greater in THF solution, where the presence of solvent–silene complexes are clearly detectable by transient UV absorption spectroscopy^{45,48}. Table 10 provides a comparison of the absolute rate constants for reaction of **19a** with various reagents in hydrocarbon, MeCN and THF solution. While the differences are small, the rate constants for reaction of these two silenes with almost all the nucleophilic reagents that have been studied to date vary with the relative basicities of the three solvents rather than their bulk polarities. Thus, pure solvent polarity effects on the rates appear to be rather small. This could either be because the effect on *both* the initial complexation event and the transition state for collapse of the complex to product(s) is small, or the effect on one is opposite to that of the other. The exception to this generalization is the addition of methoxytrimethylsilane to **19a,e**, which proceeds slightly faster in MeCN than in hexane⁵⁷.

The temperature dependences for reaction of these reagents with **19a** show systematic differences in hydrocarbon and MeCN solution (*vide supra*), with the Arrhenius activation energies consistently being more positive in MeCN solution than in hexane over the same temperature range. In the language used earlier to discuss the effects of variations in the relative magnitudes of k_C , k_{-C} and k_H on the form of the Arrhenius dependences observed for these reactions (Sections III.B.2 and II.B.3), these systematic differences are consistent with k_C being smaller and $k_H/(k_{-C} + k_H)$ being larger in the more polar solvent at any particular temperature throughout the range studied. However, it can readily be shown that the differences may in fact originate mainly from solvent complexation effects.

Equation 58 defines the equilibrium between free silene and its Lewis acid–base complex with a nucleophilic solvent. Since the complexed form of the silene can clearly be expected to be relatively unreactive toward nucleophiles compared to the free silene, then the result will be a reduction in the overall rate constant for reaction with a nucleophilic reagent (Nu-H) in a complexing solvent relative to a non-complexing one like hexane. This rate reduction is described quantitatively in equation 59.



$$k_{\text{Nu-H}} = \frac{1}{(1 + K_{\text{solv}})} \cdot k_C \cdot \frac{k_H}{k_{-C} + k_H} \quad (59)$$

TABLE 10. Absolute rate constants (in units of $10^9 \text{ M}^{-1} \text{ s}^{-1}$) for reaction of **19a** with various reagents in hydrocarbon, MeCN and THF solution at 23–25 °C

Reagent / Solvent	Hexane	MeCN	THF
MeOH ^a	1.9 ± 0.2	1.5 ± 0.1	0.31 ± 0.03
<i>t</i> -BuOH ^a	0.40 ± 0.07	0.41 ± 0.02	0.024 ± 0.002
AcOH ^a	3.1 ± 0.3	1.23 ± 0.07	0.33 ± 0.02
<i>n</i> -BuNH ₂ ^b	9.7 ± 0.1	5.3 ± 0.1	0.39 ± 0.01
MeOTMS ^c	0.021 ± 0.01	0.086 ± 0.006	0.017 ± 0.002
Acetone ^d	0.38 ± 0.02 ^e	1.8 ± 0.1	0.059 ± 0.009

^aData from Reference 45.

^bData from Reference 43 and 115.

^cData from Reference 57 and 115.

^dData from Reference 41 and 115.

^eIsooctane solution.

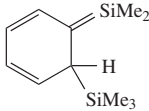
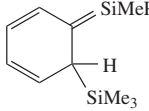
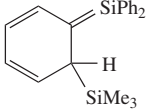
The equilibrium constant for solvent complexation (K_{solv}) decreases with increasing temperature, and thus tends to increase the overall value of $k_{\text{Nu-H}}$ as the temperature is raised. The effect of temperature on K_{solv} is apparent from the transient UV absorption spectra of **19a** in THF at +1.5 °C and 5 °C¹¹⁵; the high temperature spectrum is similar to that of the silene in hexane solution, while the low temperature spectrum is broadened and red-shifted due to the presence of solvent complexes in higher relative concentration. The net result of superimposing the temperature dependence for solvent complexation on that for reaction of the free silene with the nucleophile will be a *more positive* apparent E_a for reaction in a complexing solvent than in a non-complexing one. Indeed, this is exactly what is observed in all of the cases discussed in the preceding section.

Arrhenius studies have recently been carried out for the reactions of several of these reagents with **19a** in THF solution, and *positive* Arrhenius activation energies are observed in every case¹¹⁵. The positive E_a values in THF solution can be explained as being due to the superposition of the intrinsic temperature dependence of the reaction on the temperature dependence of the complexation equilibrium between the silene and the solvent. The latter is such that the concentration of free silene increases with increasing temperature, and hence has the effect of increasing the overall rate of reaction compared to what it would be in a non-complexing solvent. The net result is a higher (more positive) activation energy for reaction in complexing relative to non-complexing solvents.

Solvent complexation can have intriguing effects on the *relative* reactivities of different silenes in ether solvents. For example, the absolute rate constant for reaction of MeOTMS with silene **19e** in THF solution is significantly *slower* than that for reaction with **19a** under identical conditions¹¹⁵, a complete inversion of the relative reactivities of these two silenes compared to what they are in hexane or MeCN solution! The effect in these cases is probably due to the fact that complexation of the solvent with the more electrophilic silene (**19e**) is substantially stronger (i.e. K_{solv} is much larger) than with **19a**. Perhaps the most astonishing manifestation of this effect is Auner and coworkers' recent report of the ¹H, ¹³C and ²⁹Si spectra of silene, 1-methylsilene (**2a**) and 1,1-dimethylsilene (**2b**) in dimethyl ether-*d*₆ solution at low temperatures, where complexation with the solvent suppresses dimerization of these normally highly reactive species¹¹⁶. It would appear that the higher the intrinsic electrophilicity of a particular silene is, the more it is stabilized in complexing solvents such as ether or THF. Indeed, silene **6** (the most potently electrophilic silene that has been studied to date; *vide infra*) is almost four orders of magnitude less reactive toward alcohols in THF solution than in hexane at 25 °C³⁷.

THF can also have an accelerating effect on reactivity, in cases where the weakly basic solvent can get directly involved in the reaction via a catalytic pathway and complexation with the free silene is weak. Such an effect has been observed for the reaction of alcohols with the aryldisilane-derived 1,3,5-(1-sila)hexatriene derivatives **21a-c**, as shown by the second-order rate constants for reaction of the three silenes by MeOH and TFE in isoctane, MeCN and THF solution (Table 11; note that the third-order rate constants for reaction of **21a-c** with MeOH have been omitted)⁴⁸. Table 11 also includes data for the reactions with acetone in the same three solvents, as an example of a reaction which has no catalytic component⁴⁷. The rate constants for all three reactions decrease in the order: isoctane > MeCN > THF for **21a**, which complexes relatively strongly with the ether solvent, as demonstrated by the distinctive red shift in its UV absorption spectrum in THF ($\lambda_{\text{max}} = 460$ nm) compared to isoctane and MeCN ($\lambda_{\text{max}} = 425$ nm)⁴⁸. Compound **21b** exhibits a *ca* 10 nm shift of its absorption band in THF solution while none is detectable in the case of **21c**, indicating that the equilibrium constant for THF complexation within this series of silenes decreases with increasing phenyl substitution at

TABLE 11. Second-order rate constants (in units of $10^8 \text{ M}^{-1} \text{ s}^{-1}$) for reaction of (1-sila)hexatrienes **21a–c** with acetone, methanol (MeOH) and 2,2,2-trifluoroethanol (TFE) in isooctane (OCT), acetonitrile (MeCN) and tetrahydrofuran (THF) solution at 23°C ^{47,48}

Reagent	Solvent	 (21a)	 (21b)	 (21c)
Acetone	OCT	45.0 ± 0.6	15.8 ± 0.6	5.42 ± 0.05
	MeCN	7.7 ± 0.2	3.1 ± 0.2	1.5 ± 0.1
	THF	2.46 ± 0.05	1.62 ± 0.02	1.22 ± 0.03
MeOH	OCT	3.0 ± 0.8	1.8 ± 0.5	1.1 ± 0.4
	MeCN	2.3 ± 0.7	0.60 ± 0.25	0.17 ± 0.1
	THF	1.2 ± 0.1	0.95 ± 0.05	0.7 ± 0.1
TFE	OCT	2.3 ± 0.6	—	—
	MeCN	0.236 ± 0.004	0.056 ± 0.001	0.017 ± 0.001
	THF	0.168 ± 0.003	0.063 ± 0.002	0.051 ± 0.003

silicon. So do the rate constants for reaction with the three reagents, an effect which is largest in isooctane solution and smallest in THF. Most significantly, the second-order rate constant for MeOH and TFE quenching of **21c** (k_{MeOH}) is *faster* in THF than in MeCN solution. It was proposed that this unique rate enhancement for **21c** in THF is due to catalysis of the proton transfer step by the solvent, which adds a second pseudo-first-order pathway for product formation in addition to the intracomplex pathway, i.e. the expression for k_{MeOH} (equation 29) expands to that of equation 32, where k_{THF} is the second-order rate constant for catalytic proton transfer by the solvent. Since this can only occur by initial deprotonation of the complex, the result provides evidence that the intercomplex proton transfer pathway described by k'_{H} (Scheme 4) most likely occurs by a deprotonation/protonation sequence (i.e. general base catalysis) rather than by the general acid catalysis pathway originally suggested by Kira and coworkers⁷⁹.

C. Substituent Effects on Silene Reactivity

Several examples were discussed earlier of the use of substituent effects for the elucidation of the mechanisms of silene reactions with nucleophilic reagents. For example, the trends in the rate constants for reaction of the series of 1,1-diarylsilenes **19a–e** with alcohols, acetic acid, amines, methoxytrimethylsilane and acetone all indicate that inductive electron-withdrawing substituents at silicon enhance the reactivity of the Si=C bond, and are consistent with a common reaction mechanism in which reaction is initiated by the formation of an intermediate complex between the silene and the nucleophile.

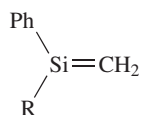
The effects of substituting a phenyl group for –H or –Me at the silicon end of the Si=C bond has different effects on the rates of silene reactions depending on the substituents present at carbon. For example, the 1,3,5-(1-sila)hexatriene derivatives **21a–c** exhibit a significant decrease in reactivity toward methanol and acetone with increasing phenyl substitution (Table 11). This too is consistent with the stepwise mechanisms proposed for

TABLE 12. Absolute rate constants for reaction of 1-methyl- and 1-phenyl-substituted silenes ($RR'Si=CH_2$) with MeOH and acetone in hexane or isooctane solution at 23–25 °C

R,R'	$k_{MeOH}(10^9 M^{-1} s^{-1})$	$k_{acetone}(10^9 M^{-1} s^{-1})$
Me, H (2a) ^a	4.41 ± 0.14	—
Me, Me (2b) ^a	4.9 ± 0.2	—
Ph, H (78) ^b	3.1 ± 0.1	0.22 ± 0.02
Ph, Me (2f) ^b	3.2 ± 0.2	0.33 ± 0.02
Ph, Ph (19a) ^b	1.9 ± 0.2	0.38 ± 0.02

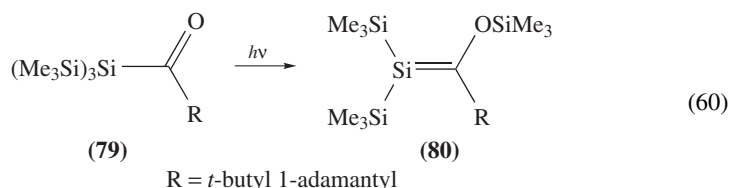
^aData from Reference 117.^bMethanol data from Reference 118; acetone data from Reference 41.

these reactions, and has been explained in terms of steric effects on the initial complexation step. On the other hand, phenyl substitution has a much smaller effect on reaction rate in the case of silenes of the type $RR'Si=CH_2$, as is illustrated in Table 12 for 1-methyl- (**2a**), 1,1-dimethyl- (**2b**), 1-phenyl- (**78**), 1-methyl-1-phenyl- (**2f**) and 1,1-diphenylsilene (**19a**)^{41,117,118}.

**(78)** R = H**(2f)** R = Me

1. Silenes of the type $(R)MeSi=CH_2$ and $Me_2Si=CHR$

Considerable insight into the broader question of how the kinetic and thermodynamic stability of the Si=C bond is affected by substituents at silicon and carbon was obtained in the late 1970s, when Brook and coworkers reported the isolation and characterization of the first stable silene derivatives (**80**), prepared by photolysis of the corresponding acylpolysilanes (**79**) as shown in equation 60¹⁷. The unique stability of these compounds is clearly due to steric stabilization effects to some extent, but it was suggested that the siloxy substituent at carbon also reduces the reactivity of these silenes toward dimerization as a result of resonance effects on the degree of positive charge character at silicon.

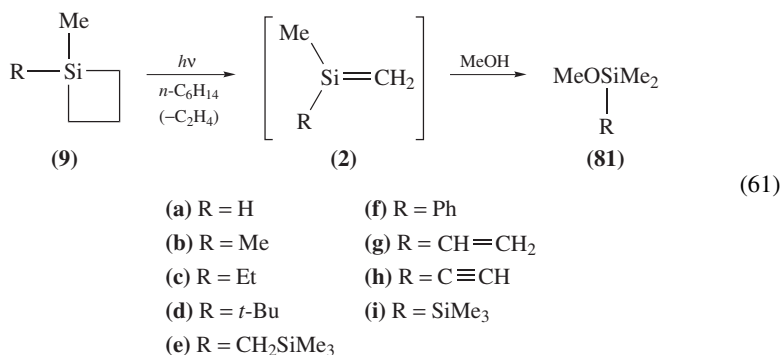


A few years later, Apeloig and Karni reported *ab initio* calculations of the structure, frontier molecular orbital energies and Mulliken charge distributions in a series of substituted silenes of structure $RHSi=CH_2$ and $H_2Si=CHR$, which indicated that *all four* of the substituents in the Brook silenes contribute to the reduction in Si=C bond polarity that was suggested to give rise to their unusual stability⁵⁸. Their systematic study led to the conclusion that Si=C bond polarity is reduced by the presence of σ -donor/ π -acceptor

substituents at silicon and σ -acceptor/ π -donor substituents at carbon, and is increased when they are placed the other way around. Since the former is precisely the substitution pattern possessed by the Brook silenes, they suggested that bond polarity factors played a dominant role in determining the kinetic stability of the Si=C bond. Therefore, of particular significance is Wiberg's subsequent report of the isolation and X-ray structure determination of **5**^{17,27}, the di-*tert*-butylmethyl analogue of the silene derivative (**6**) for which his extensive relative rate data had been reported earlier in this review. If Si=C bond polarity really is the main factor that determines silene reactivity, then the stability of **5** must be almost completely due to steric effects, opposing the strong degree of substituent-induced kinetic destabilization that is suggested by the results of Apeloig and Karni.

Kinetic studies have recently been reported in an effort to assess systematically the effects of substituents at silicon and carbon on silene reactivity, and put the earlier theoretical work on a firm experimental basis^{111,117}. Absolute rate constants for addition of methanol served as the diagnostic indicator of silene reactivity in these studies, since methanol addition is mechanistically the best understood reaction of transient silenes (*vide infra*) and can be studied under the widest possible range of conditions in photochemical experiments. Both studies were carried out in hydrocarbon solution at 23 °C, so as to provide a standard set of experimental conditions for the analysis and to minimize the effects of solvation on Si=C reactivity.

A homologous series of nine simple silenes of the type R(Me)Si=CH₂ (**2a-i**) were generated and studied by laser flash photolysis of the corresponding silacyclobutane (**9**) precursors, as shown in equation 61^{97,117}. Most of these compounds have no UV absorption above *ca* 220 nm and thus require the use of a 193-nm laser for photoexcitation, while the phenylated derivative **2f** was excited at 248 nm¹¹⁸. Laser flash photolysis of these precursors led in each case to a transient absorbing in the 255–350 nm range, that could be definitively assigned to the corresponding silene on the basis of its UV spectrum, characteristically high reactivity toward aliphatic alcohols and the results of steady-state product studies. The latter demonstrate that all the silacyclobutanes in the series undergo photocycloreversion to the corresponding silene and ethylene, cleanly and with reasonable efficiency, as evidenced by the formation of the corresponding methoxysilane **81** in high chemical yield when photolysis is carried out in the presence of methanol.



The photolysis of α -silyldiazomethanes (**82**) and α -silylketenes (**83**) was chosen as the main synthetic methodology for the generation of a homologous series of 1,1-dimethylsilenes bearing substituents at carbon (**85**; equation 62)^{37,111}, on the basis of the results of previous studies of the photochemistry of α -silyldiazomethanes. It had been

shown that compounds of this type undergo efficient nitrogen photoextrusion to yield the corresponding α -silyl carbenes (**84**), which rearrange to silenes via [1,2]-migration of a substituent from silicon to carbon^{39,119–121}. Photolysis of **82** and **83** in the presence of MeOH hence yields the corresponding methoxysilanes **86** exclusively. Three other silenes (**2b**, **23** and **7**), generated from silacyclobutane (equation 61), vinyldisilane (equation 13) or silacyclobutene (equation 8) precursors, respectively, complete the series. Wiberg's silene **6** (from photolysis of **16** or silylketene **87**) was not included in the original study¹¹¹, but has recently been added to the series³⁷.

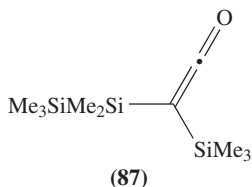
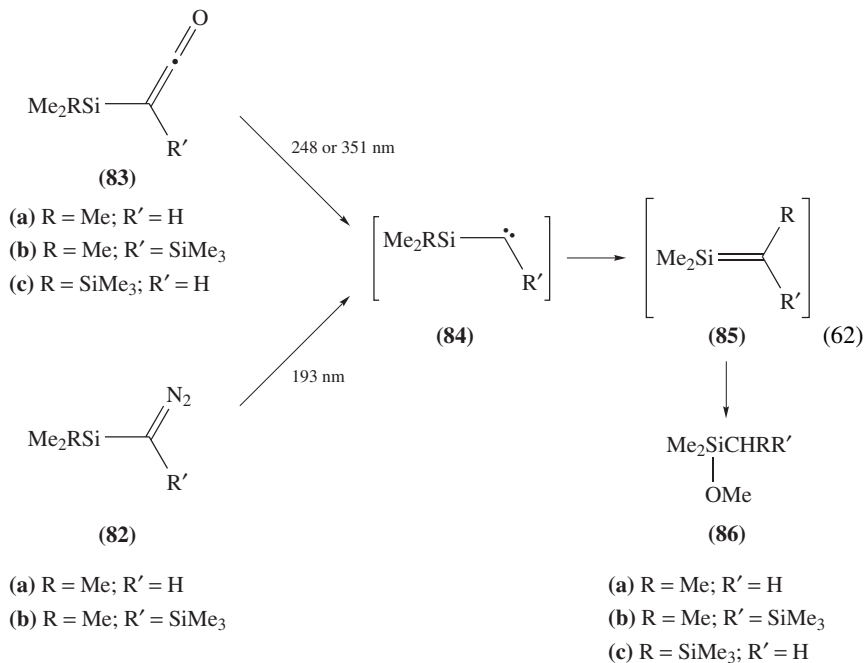
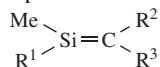
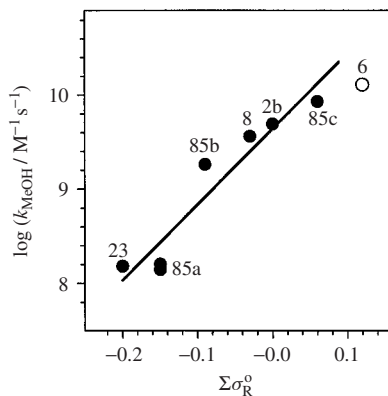


Table 13 lists the UV absorption maxima and absolute rate constants for reaction of the two series of silenes in hexane or isooctane solution at 23 °C. The reactivities vary by more than two orders of magnitude throughout the series, depending on the substituents at the silenic silicon and carbon atoms.

The absolute rate constants for reaction of the carbon-substituted silenes **2b**, **6**, **7**, **23** and **85a–c** are plotted against the resonance substituent parameter $\Sigma\sigma_{\text{R}}^{\text{q}}$ ⁸⁶ in Figure 10. The data appear to correlate reasonably well, if one assumes that the curvature in the plot results from the fact that k_{MeOH} for the more reactive derivatives in the series approaches

TABLE 13. Absolute rate constants for reaction of $R^1(\text{Me})\text{Si}=\text{CH}_2$ and $\text{Me}_2\text{Si}=\text{CR}^2\text{R}^3$ with methanol in hexane at 23 °C and UV absorption maxima

#	R ¹	R ²	R ³	λ _{max} (nm)	k _{MeOH} (10 ⁹ M ⁻¹ s ⁻¹)	Reference
2a	H	H	H	265	4.41 ± 0.14	117
2b	Me	H	H	255	4.9 ± 0.2	97
2c	Et	H	H	255	4.2 ± 0.5	117
2d	<i>t</i> -Bu	H	H	260	3.7 ± 0.1	117
2e	CH ₂ SiMe ₃	H	H	260	1.86 ± 0.09	117
2f	Ph	H	H	315	3.2 ± 0.2	118
2g	CH=CH ₂	H	H	305	1.75 ± 0.10	117
2h	C≡CH	H	H	290	10.0 ± 0.1	117
2i	SiMe ₃	H	H	285	0.18 ± 0.01	117
2j	C≡CPh	H	H	320	5 ± 2	118
8a	Me	H	CH=CH ₂	312	3.6 ± 0.1	32
23a	Me	H	CH ₂ SiMe ₃	270, 300	0.15 ± 0.02	53
85a	Me	H	Me	260, 283	0.14 ± 0.4	111
85c	Me	H	SiMe ₃	270	8.5 ± 0.6	111
85b	Me	Me	SiMe ₃	280	1.8 ± 0.1	111
6	Me	SiMe ₃	SiMe ₃	260	13 ± 2	37

FIGURE 10. Plot of $\log(k_{\text{MeOH}}/\text{M}^{-1}\text{s}^{-1})$ vs. $\Sigma\sigma_{\text{R}}^{\circ}$ for the reaction of carbon-substituted 1,1-dimethylsilenes (**2b**, **6**, **8**, **23** and **85a–c**) in hexane solution at 23 °C. Compound **6** is excluded from the correlation. Reproduced with permission from Reference 111. Copyright 1999 American Chemical Society

the rate of diffusion in hexane at this temperature. This indicates that substituents at carbon affect silene reactivity toward nucleophilic addition mainly through resonance effects. Inductive and steric effects are relatively unimportant, at least for this particular type of reaction. The original analysis did not include the data point for Wiberg's silene (**6**), and involved only a linear least-squares fit of the data for the other six silenes to equation 63. This afforded a reaction constant $\rho_{\text{R}} = +8.0 \pm 2.2$ ($r^2 = 0.909$), and the indication that π -electron donor substituents at carbon strongly stabilize the Si=C bond

toward reaction with nucleophiles. Again, this is precisely what theory predicts⁵⁸, and is fully consistent with the remarkable kinetic stability of the Brook silenes.

$$\log(k_{\text{MeOH}}/M^{-1}s^{-1}) = \log(k_{\text{MeOH}}^{2b}) + \rho_R \sigma_R^0 \quad (63)$$

The more recently acquired data for Wiberg's silene (**6**) verifies the prediction that the Si=C bond in this compound ought to be significantly polarized and hence intrinsically quite reactive toward nucleophiles. In fact, **6** bears the distinction of being the most potentially electrophilic silene that has yet been studied, and it can be concluded that the stability of the analogue **5** toward dimerization is solely due to steric stabilization afforded by the $-\text{SiMe}(t\text{-Bu})_2$ substituent³⁷.

In contrast, the rate constants for methanol addition to the series of silicon-substituted silenes **2a-i** (Table 13) do not vary in a straightforward way with either inductive (σ_I) or resonance (σ_R^0) substituent parameters associated with the R substituent. However, a multi-parameter fit of the data to equation 64, in which E_s is the steric substituent parameter of Unger and Hansch¹²² and ρ_I , ρ_R and ρ_s are the related standard reaction constants describing the individual effects of inductive, resonance and steric effects on the rate (and are the variables in the analysis), led to an excellent least-squares fit of the data ($r^2 = 0.965$). This afforded the coefficients $\rho_R = -3.6 \pm 1.2$, $\rho_I = 3.1 \pm 1.0$ and $\rho_s = 0.21 \pm 0.08$, where the quoted errors represent the 95% confidence limits of the analysis. Figure 11 shows a plot of the data against the function obtained from the least-squares fit (equation 65).

$$\log(k_{\text{MeOH}}/M^{-1}s^{-1}) = \log(k_{\text{MeOH}}^{2a}) + \rho_I \sigma_I + \rho_R \sigma_R^0 + \rho_s E_s \quad (64)$$

$$\log(k_{\text{MeOH}}/M^{-1}s^{-1}) = \log(k_{\text{MeOH}}^{2a}) + (3.1 \pm 1.0)\sigma_I + (-3.6 \pm 1.2)\sigma_R^0 + (0.21 \pm 0.08)E_s \quad (65)$$

The negative ρ_R and positive ρ_I values obtained from the analysis suggest that the reactivity of the Si=C bond in 1-methylsilene (**2a**), the base compound in the analysis, is enhanced by substitution of the silicon hydrogen with resonance electron donors or

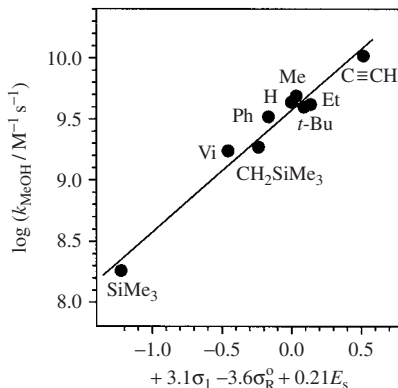


FIGURE 11. Plot of $\log(k_{\text{MeOH}}/M^{-1}s^{-1})$ vs. the three-parameter substituent constant function $[(3.1 \pm 1.0)\sigma_I + (-3.6 \pm 1.2)\sigma_R^0 + (0.21 \pm 0.08)E_s]$ for the reaction of silicon-substituted 1-methylsilenes (**2a-i**) in hexane solution at 23 °C. Reproduced with permission from Reference 117. Copyright 1998 American Chemical Society

inductive electron acceptors, in agreement with the theoretical conclusions of Apeloig and Karni⁵⁸. The relatively small, positive E_s value indicates that reactivity is also moderately sensitive to the steric bulk of the substituents at silicon, as would be expected given that nucleophilic attack at this site is the first step in the reaction.

As noted above, diffusional effects are expected to truncate the reactivity of those derivatives exhibiting absolute rate constants above $k_{\text{MeOH}} \sim 5 \times 10^9 \text{ M}^{-1} \text{ s}^{-1}$. The linear free-energy correlations for both the C- and Si-substituted silenes are improved considerably when the limiting effects of diffusion are explicitly accounted for, using the expression given in equation 66 and a value of $k_{\text{diff}} = 2.4 \times 10^{10} \text{ M}^{-1} \text{ s}^{-1}$ for the diffusional rate constant in hexane at 25 °C¹²³. The coefficients obtained from analysis of the two sets of corrected data as described above change only slightly, however, to $\rho_{\text{R}} = +8.1 \pm 1.6$ ($r^2 = 0.937$) for the C-substituted silenes (now including the data point for **6**), and $\rho_{\text{R}} = -3.7 \pm 0.8$, $\rho_{\text{I}} = 3.5 \pm 0.7$ and $\rho_{\text{S}} = 0.23 \pm 0.06$ ($r^2 = 0.977$). These correlations are shown in Figure 12.

$$k_{\text{MeOH}}^{\text{corr}} = k_{\text{diff}} k_{\text{MeOH}} / (k_{\text{diff}} - k_{\text{MeOH}}) \quad (66)$$

Arrhenius activation energies for MeOH addition were determined for several of the silenes in this series and were found to be negative in every case, with a clear trend toward larger negative values as overall reactivity decreases (Table 14)^{97,117}. The trend suggests that the rate deceleration effected by σ -donor/ π -acceptor substituents at silicon is due to a combination of a decrease in both the rate constant for complexation and the partitioning of the complex between product and starting materials, i.e. both k_{C} and $k_{\text{H}}/(k_{\text{H}} + k_{-\text{C}})$ decrease as overall reactivity decreases throughout the series.

All of the silenes discussed above and in Section III.B.3.a appear to react with MeOH by the stepwise mechanism shown in Scheme 4, as judged by the fact that negative Arrhenius activation energies have been observed in every example whose temperature dependence has been studied⁴⁴. Those derivatives for which k_{MeOH} is on the order of $10^9 \text{ M}^{-1} \text{ s}^{-1}$ or higher exhibit linear dependences of k_{decay} on MeOH concentration (i.e. $k_{\text{H}} \gg k'_{\text{H}} [\text{MeOH}]$) over the range of alcohol concentrations for which data are obtainable

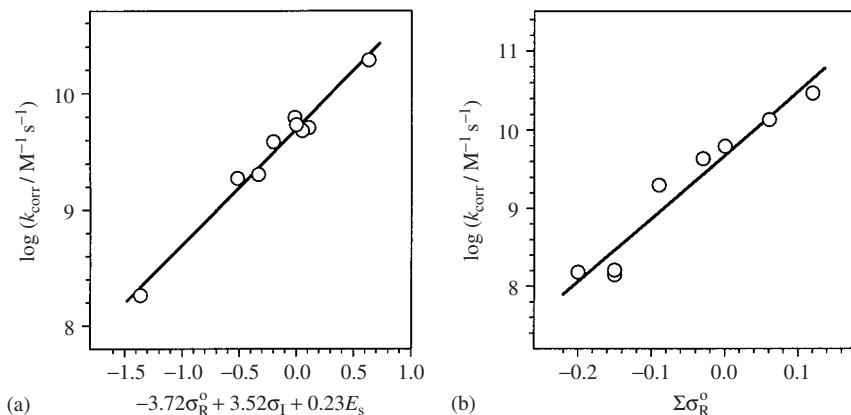


FIGURE 12. Plots of the corrected rates of reaction of (a) silicon-substituted silenes and (b) carbon-substituted silenes vs. substituent parameter functions, accounting for diffusion effects on the overall rate constants

TABLE 14. Arrhenius parameters for reaction of representative methylsilenes with MeOH in hexane or isooctane solution^a

$\begin{array}{c} \text{Me} \\ \diagdown \\ \text{Si}=\text{CH}_2 \\ \diagup \\ \text{R} \end{array}$	E_a (kJ mol ⁻¹)	$\log(A/M^{-1} \text{ s}^{-1})$
H (2a)	-7.8 ± 1.2	8.3 ± 0.3
Me (2b)	-10.7 ± 1.2	7.7 ± 0.3
CH ₂ SiMe ₃ (2e)	-8.2 ± 2.0	7.8 ± 0.6
CH=CH ₂ (2g)	-9.8 ± 0.4	7.5 ± 0.3
C≡CH (2h)	-3.3 ± 0.4	9.3 ± 0.2
SiMe ₃ (2i)	-14.8 ± 2.4 q	5.5 ± 0.5

^aData from Reference 117.

by nanosecond laser flash photolysis methods. As overall reactivity is reduced into the $10^8 \text{ M}^{-1} \text{ s}^{-1}$ range, the kinetic plots generally assume some degree of non-linearity⁴⁸, consistent with the bimolecular (general base catalysed) proton transfer pathway for collapse of the intermediate complex taking on increased importance. This is presumably due to a reduction in the magnitude of k_H as overall reactivity decreases, which comparison of the Arrhenius activation energies for reaction of MeOH with **2a–f** indicate to indeed be the case¹¹⁷.

Recent computational studies by Apeloig and coworkers suggest that the mechanism for alcohol addition to silenes changes to a concerted one in silenes of the type $(R_3Si)_2Si=CR_2$ ¹²⁴. The structure–reactivity correlations discussed above suggest that the reactivity of such silenes toward nucleophilic addition should be significantly lower than that of any of the transient silenes for which kinetic data currently exist, but somewhat higher than that which might be predicted for the Brook silene **28**. The absolute rate constant for reaction of the currently unknown silene $(Me_3Si)_2Si=CMe_2$ with MeOH is predicted to be on the order of $k_{MeOH} = 10^4 - 10^5 \text{ M}^{-1} \text{ s}^{-1}$ in hexane, by extrapolation of the published rate constants for reaction of MeOH with $Me_2Si=CH_2$ (**2b**; $k_{MeOH} \sim 5 \times 10^9 \text{ M}^{-1} \text{ s}^{-1}$)⁹⁷, $(Me_3Si)(Me)Si=CH_2$ (**2i**; $k_{MeOH} \sim 2 \times 10^8 \text{ M}^{-1} \text{ s}^{-1}$)¹¹⁷ and $Me_2Si=CHMe$ (**85a**; $k_{MeOH} \sim 2 \times 10^8 \text{ M}^{-1} \text{ s}^{-1}$)¹¹¹. The study of the kinetics of alcohol addition to transient silenes whose reactivity is so low will be challenging, but clearly well worth the effort. There is still much to learn of the kinetics and mechanisms of the reactions of the Si=C bond in different structural situations.

2. 1-Silaallenes

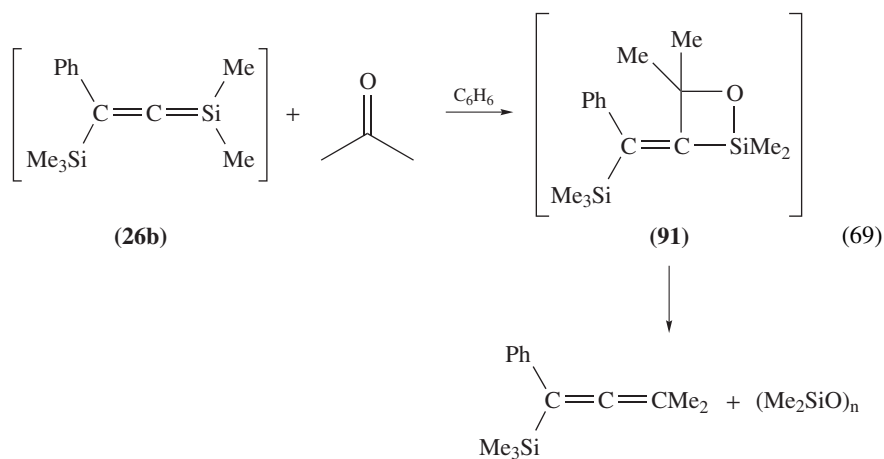
While our understanding of the reactivity of silenes is now fairly well developed, analogues in which the Si=C bond forms part of a cumulated polyene structure—1-silaallene ($H_2Si=C=CH_2$) being the simplest homologue—have only recently begun to receive detailed attention. Several stable derivatives containing sterically-stabilizing aryl groups at silicon have been synthesized and isolated¹², and the chemistry of several transient derivatives, produced as minor products from the photolysis of alkynyldisilanes, was studied several years ago by Ishikawa and coworkers^{125–130}. The transient 1-silaallenes are known to react in a manner typical of silenes: they react with methanol by 1,2-addition and undergo head-to-tail dimerization in the absence of added trapping reagents.

Only two studies have been reported on the quantitative aspects of 1-silaallene reactivity^{54,55}. The two compounds (**26a** and **26b**) were generated and detected by laser flash photolysis of the corresponding alkynyldisilane derivatives **25a** and **25b**, respectively

in hexane at the concentrations necessary for the kinetic analyses. In the case of AcOH quenching, this resulted in negative curvature in plots of k_{decay} vs. [AcOH], indicating that only the monomeric form of the carboxylic acid is reactive toward addition to the silaallenes. Indeed, plots of the decay rates vs. the concentration of monomeric [AcOH] at each of the bulk concentrations employed (calculated using the known monomer–dimer equilibrium constant for AcOH in hexane¹³¹) were linear in both cases, and afforded rate constants of $ca\ 10^8$ and $ca\ 5 \times 10^9\ \text{M}^{-1}\ \text{s}^{-1}$ for **26a** and **26b**, respectively.

Positive curvature was observed in plots of k_{decay} vs. [ROH] for the more reactive of the two silaallenes (**26b**) in the presence of MeOH and *t*-BuOH, and the data fit acceptably to the quadratic expression in [ROH] of equation 26⁵⁴. This suggests that the reaction with ROH proceeds by the dual proton-transfer mechanism characteristic of simpler silene analogues (Scheme 4). The second-order rate constants for the component of reaction involving a single molecule of alcohol are about two orders of magnitude slower than those for addition to 1,1-dimethylsilene (**2b**), which was attributed to a combination of steric protection of the central carbon toward protonation and a reduction in Si=C bond polarity owing to hyperconjugative electron donation by the trimethylsilyl substituent at C3 of the 1-silaallene moiety. One would expect both of these effects to be accentuated in the bis-trimethylsilyl derivative **26a** and, indeed, reaction of both alcohols with this compound is substantially slower than with **26b**. The kinetics of ROH addition to **26a** appeared to be more complex than the mechanism of Scheme 4 allows, however⁵⁵.

Similar differences in reactivity were observed toward acetone, and quenching plots according to equation 3 showed excellent linearity. The product studies of Ishikawa and coworkers indicate that the reaction of **26b** with the ketone proceeds by [2 + 2]-cycloaddition to yield **91**, which decomposes under the experimental conditions employed (equation 69).



The two silaallenes **26a** and **26b** exhibit lifetimes in air-saturated hexane solution of $ca\ 2.5\ \mu\text{s}$ and $ca\ 10\ \mu\text{s}$, respectively. Saturation of the solutions with oxygen leads to shortening of the lifetime in both cases, and allows estimates of $k_{\text{O}_2} \sim 1.1 \times 10^8$ and $\sim 1.5 \times 10^7\ \text{M}^{-1}\ \text{s}^{-1}$ for the rate constants for oxygen quenching of **26a** and **26b**, respectively. Interestingly, silaallene **26a** appears to be somewhat more reactive than **26b** toward O_2 .

TABLE 16. Rate constants and Arrhenius parameters for thermal *E,Z*-isomerization of disilenes **92–95**^a

Compound	Temperatures (°C)	$k_{Z \rightarrow E}^{T-\text{low}}$ (s ⁻¹)	E_a (kJ mol ⁻¹)	Log (A/s ⁻¹)	$K^{T-\text{low}}$	Reference
92a	69.5–85.0	4.6×10^{-5}	130 ± 15	15.7	54	135
92a ^b	71.5	1.1×10^{-4}	—	—	24	135
93	52.6–74.9	1.6×10^{-5}	121 ± 3	14.2	31	136
94	42.5–65.8	4.7×10^{-5}	106 ± 9	13.2	17	135
95a	64–87	1.35×10^{-5}	113 ± 3	12.2	1.29	133
95b	69–92	1.53×10^{-5}	113 ± 2	12.4	1.26	133

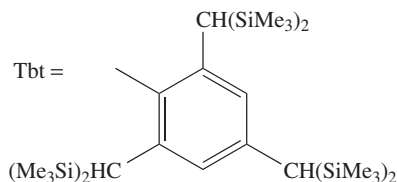
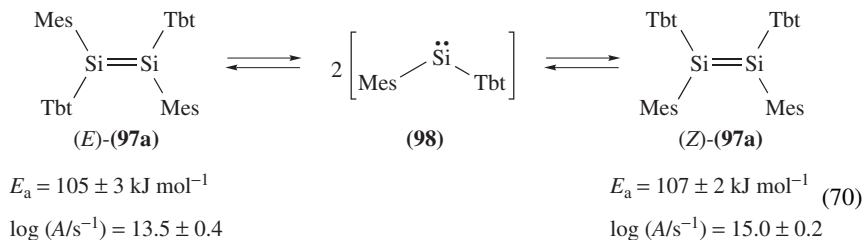
^aIn C₆D₆ solution, except where otherwise noted.

^bIn THF – *d*₈ solution.

pure) isomers. *E,Z*-Isomerization of all of these compounds proceeds relatively slowly at room temperature, and kinetic measurements were generally carried out at temperatures over the 40–90 °C range. Table 16 lists Arrhenius activation parameters obtained from analysis of the reported kinetic data for isomerization of the (*Z*)-isomers, along with the rate constants for reaction and the *E,Z*-equilibrium constants at the lowest temperature studied for each compound.

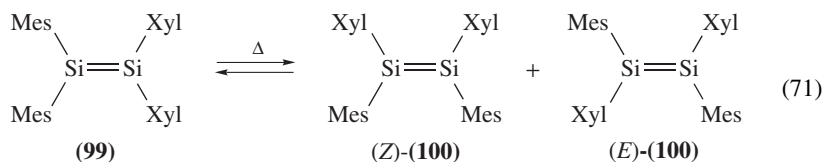
Geometrical isomerization in these compounds is thought to proceed via rotation about the Si=Si bond, and the enthalpies of activation are considered to reflect the Si=Si π -bond energy. These vary over the range 101–125 kJ mol⁻¹ in these compounds, in good agreement with various calculated estimates of the π -bond strength in disilene itself (90–115 kJ mol⁻¹)^{137–139}. They are also significantly smaller than those that have been reported for similarly substituted alkene derivatives^{140,141}.

The evidence that *E,Z*-isomerization of **92–95** proceeds by Si=Si bond rotation and not a mechanism involving silylene intermediates, produced by cleavage of the Si=Si bond followed by recombination, rests upon the fact that no trapping products consistent with the intermediacy of the corresponding diarylsilylenes could be detected upon heating the disilenes in the presence of known silylene traps such as methanol, triethylsilane or 2,3-dimethyl-1,3-butadiene. In fact, one tetraaryldisilene has been shown to isomerize by this mechanism, the 1,2-dimesityl-1,2-bis(2,4,6-tris[bis(trimethylsilyl)methyl]phenyl) derivatives (*E*)- and (*Z*)-**97a** (equation 70)^{142,143}. Arrhenius parameters for the thermal dissociation of (*E*)- and (*Z*)-**97a** to diarylsilylene **98** are listed in equation 70.



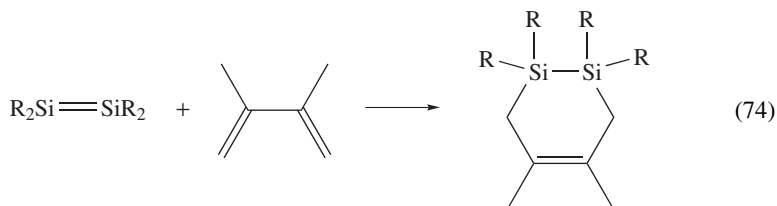
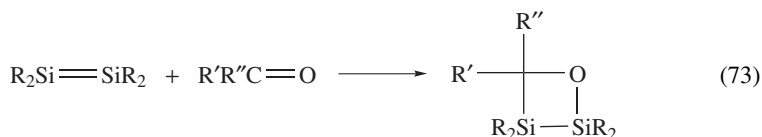
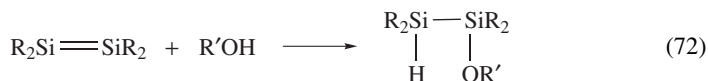
In the case of the tetrasilyldisilene **96**, *E,Z*-isomerization is rapid even at 0 °C, and dynamic NMR experiments were employed to estimate a value of $\Delta G^\ddagger \sim 62 \text{ kJ mol}^{-1}$ for the interconversion of (*E*)- and (*Z*)-**96** at 30 °C¹³⁴. The considerably lower barrier to *E,Z*-isomerization of this compound compared to **92–95** was ascribed to hyperconjugative stabilization of the perpendicular transition state by the trialkylsilyl substituents^{134,144}.

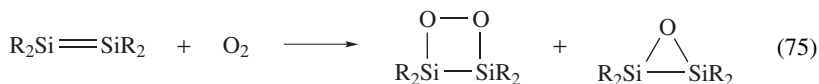
Some tetraaryldisilenes have been found to undergo a novel intramolecular exchange of aryl groups across the Si=Si bond, that competes with *E,Z*-isomerization^{145–147}. Kinetic studies have been reported in one case, for the interconversion of **99** and a mixture of (*E*)- and (*Z*)-**100** (equation 71, Xyl = 2, 6-dimethylphenyl). The activation parameters were $\Delta H^\ddagger = 62 \pm 8 \text{ kJ mol}^{-1}$ and $\Delta S^\ddagger = -148 \pm 16 \text{ J mol}^{-1} \text{ K}^{-1}$ for the conversion of **99** to **100**, and $\Delta H^\ddagger = 57 \pm 8 \text{ kJ mol}^{-1}$ and $\Delta S^\ddagger = -152 \pm 16 \text{ J mol}^{-1} \text{ K}^{-1}$ for the reverse¹⁴⁶. The reaction was shown to be intramolecular and stereoselective, and although the identity of the initially formed isomer of **100** from isomerization of **99** could not be rigorously established, NMR evidence suggested that it is most likely the (*E*)-isomer. On the basis of these observations and the large negative entropy of activation, a concerted dyotropic mechanism involving a bicyclobutane-like transition state was proposed.



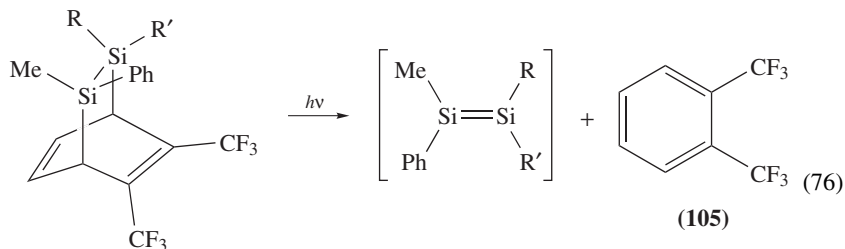
B. Bimolecular Reactions

Absolute kinetic data have been reported for four of the characteristic bimolecular reactions of disilenes: 1,2-addition of alcohols and phenols (equation 72), [2 + 2]-cycloaddition of ketones (equation 73), [2 + 4]-cycloaddition of aliphatic dienes (equation 74) and oxidation with molecular oxygen (equation 75). As with silenes, the addition of alcohols has been studied in greatest detail.





Only four transient disilenes have been studied to date by fast time-resolved spectroscopic techniques: 1,1,2-trimethyl-2-phenyldisilene (**103**), (*E*)- and (*Z*)-1,2-dimethyl-1,2-diphenyldisilene (**104**) and tetrakis(trimethylsilyl)disilene (**35**). The first three compounds were generated by photolysis of the 7,8-disilabicyclo[2.2.2]octa-2,5-diene derivatives **101** and **102** (equation 76)¹⁴⁸ while **35** was generated, together with **106**, by photolysis of the 1,2-disilacyclobutane derivative **33** (equation 77)⁶⁸.



(**101**) R = R' = Me

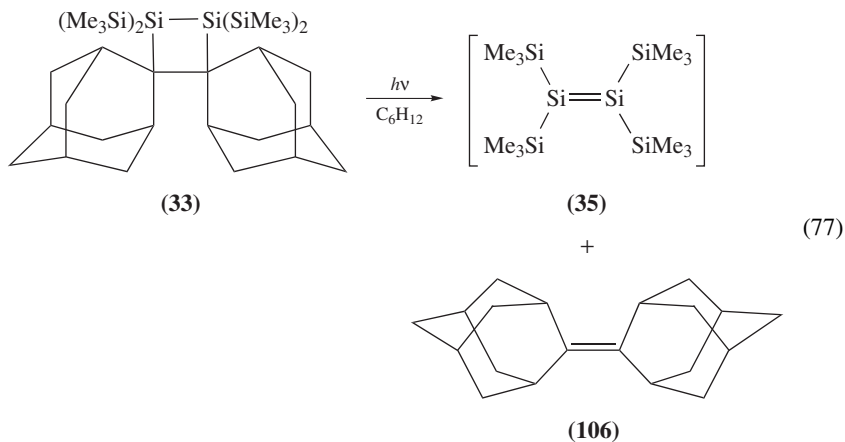
(*E*)-(**102**) R = Ph, R' = Me

(*Z*)-(**102**) R = Me, R' = Ph

(**103**) R = R' = Me

(*E*)-(**104**) R = Ph, R' = Me

(*Z*)-(**104**) R = Me, R' = Ph



1. Addition of alcohols and phenols

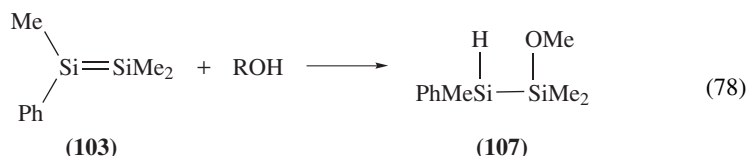
Absolute rate constants have been reported for the reaction of aliphatic alcohols with the transient disilenes **103**, **104** and **35** in hydrocarbon solvents and are collected in Table 17^{68,148}. In all cases, linear dependences of k_{decay} on alcohol concentration were observed, indicative of a mechanism that is first order in alcohol over the range of concentrations examined. Product studies carried out with **103** (equation 78) indicate that the reaction is highly regioselective, with the alkoxy group affixing itself to the less hindered

TABLE 17. Absolute rate constants for reaction of transient disilenes **103**, **104** and **35** with aliphatic alcohols in methylcyclohexane or isooctane solution at 20–23 °C

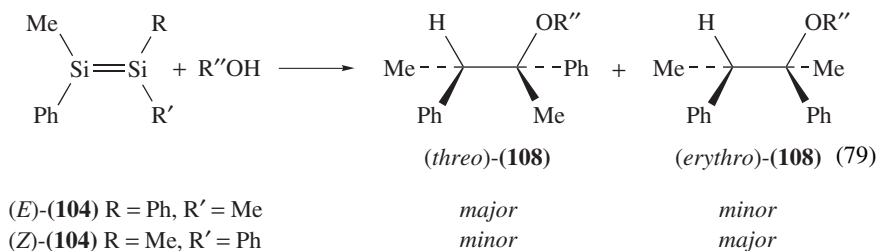
ROH	$k_{\text{MeOH}} (10^8 \text{ M}^{-1} \text{ s}^{-1})$			
	103	(<i>E</i>)- 104	(<i>Z</i>)- 104	35
MeOH ^a	—	—	—	0.003 ± 0.001
EtOH ^b	1.9	1.7	1.9	—
EtOD ^b	1.8	1.7	1.7	—
<i>i</i> -PrOH ^b	1.3	1.2	1.2	—
<i>t</i> -BuOH ^b	0.16	0.09	0.11	—

^aIn methylcyclohexane, 20 °C. See Reference 148.^bIn isooctane, 23 °C. See Reference 68.

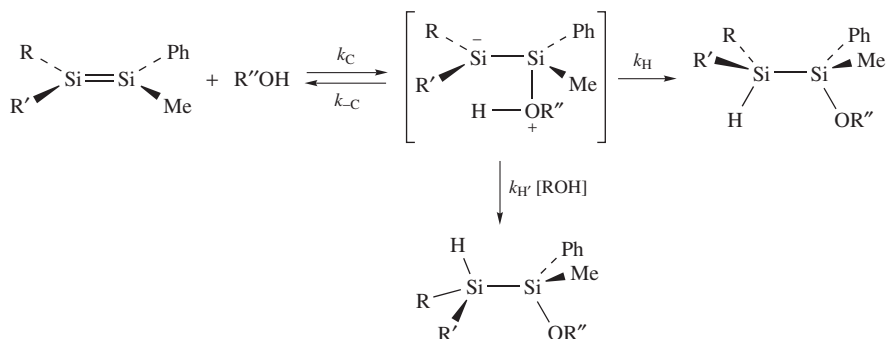
site in the starting disilene to yield alkoxydisilane **107**¹⁴⁸.



Reaction of (*E*)- and (*Z*)-**104** with methanol affords mixtures of the diastereomeric alkoxydisilanes (*threo*)- and (*erythro*)-**108** (equation 79). The diastereoselectivity of the reaction varies with ROH concentration, to a degree that depends on the identity of the alcohol¹⁴⁸. The variation is particularly pronounced with ethanol as addend; for both isomers of **104**, the degree of *syn* stereoselectivity decreases from *ca* 92% at [EtOH] = 0.85 M to *ca* 50% at [EtOH] = 5.65 M. With isopropanol on the other hand, *syn*-stereoselectivity reduces from >99% at [*i*-PrOH] = 1.31 M to *ca* 90% at [*i*-PrOH] = 4.33 M. On the basis of these observations and the fact that $k_{\text{H}}/k_{\text{D}} \sim 1$ for the addition of EtOH(D), the reaction was proposed to occur by a stepwise mechanism similar to that discussed earlier for nucleophilic additions to silenes; reaction is initiated by Lewis acid–base complexation, followed by fast proton transfer by competing intra- (leading to the *syn*-adduct) and intermolecular (leading to the *anti*-adduct) routes. We have formulated the mechanism (Scheme 5) to include reversibility in the initial complexation step. In this case, the negligible deuterium kinetic isotope effect will result so long as the intramolecular proton transfer step is faster than reversion of the complex to starting materials.



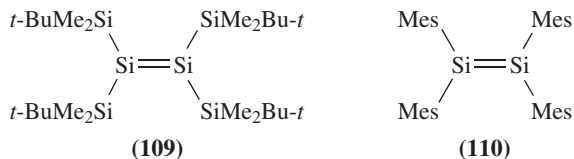
Different regiochemistry is evidently associated with the addition of alcohols to alkoxy- and dialkylamino-substituted disilenes¹¹. In these cases, addition of ROH occurs so as to



SCHEME 5

place the -OR group at the hetero-substituted silicon, the site that would be predicted to be the one of higher positive charge density in the starting disilene. The regioselectivity increases with less nucleophilic, more acidic alcohols such as 1,1,1,3,3,3-hexafluoro-2-propanol (HFIP), suggesting that the reaction might be initiated by full or partial protonation of the $\text{Si}=\text{Si}$ bond in such cases. Full details of these systems unfortunately have not yet been reported.

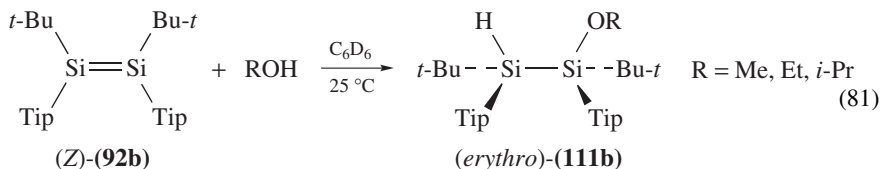
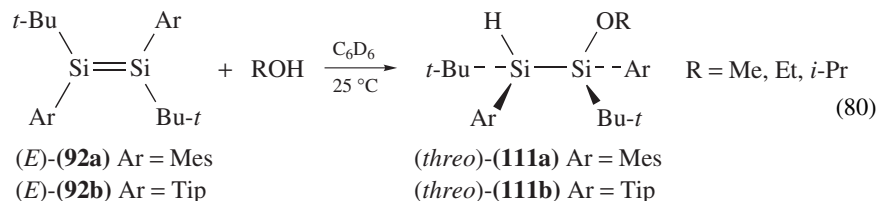
Trialkylsilyl substitution on the $\text{Si}=\text{Si}$ bond, as in disilene **35**, results in a substantial decrease in reactivity toward addition of alcohols relative to **103–104**⁶⁸. Product studies have been carried out for the addition of water and methanol to the tetrakis(*tert*-butyldimethylsilyl) homologue **109**, and show that the reaction proceeds to yield the expected 1,2-addition product¹⁴⁹. The stabilizing effect of trialkylsilyl substituents on simple disilenes was predicted earlier by Karni and Apeloig on the basis of *ab initio* theoretical calculations¹⁵⁰.



Most of the work done so far on the mechanism of alcohol additions to disilenes has been carried out with the kinetically stabilized derivatives (*E*)-**92a**^{151–153}, (*E*)- and (*Z*)-**92b**¹⁵² and tetramesityldisilene (**110**)^{151,153,154}. These compounds react with alcohols some 10^9 – 10^{12} times more slowly than do the transient disilenes **103** and **104** and, as was shown specifically for **110**, the rates vary more dramatically as a function of alcohol structure¹⁵³.

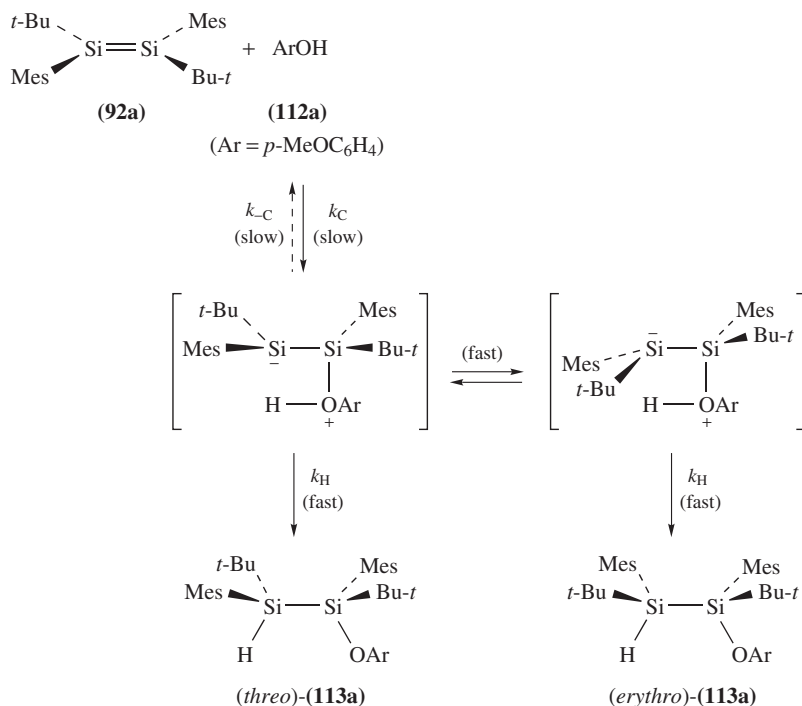
Addition of MeOH, EtOH and *i*-PrOH to (*E*)-**92a,b** and (*Z*)-**92b** in C_6D_6 solution at 25°C yields the *syn*-addition products *threo*-**111a,b** with $>99\%$ stereoselectivity (equations 80 and 81)¹⁵². The stereoselectivity was reduced somewhat in THF solution, where addition of EtOH to (*E*)-**92a** produced *threo*- and *erythro*-**111a** in a ratio of 96 : 4 at 25°C and in a 3 : 1 ratio at reflux temperature¹⁵². In an earlier study, the same group reported obtaining a 1 : 1 ratio of *syn*- and *anti*-addition products from reaction of (*E*)-**92a** with water, MeOH and EtOH in refluxing THF solution¹⁵¹. All of these reactions were carried out in the presence of *ca* 10^{-4} M alcohol. The results were explained in terms

of the mechanism of Scheme 5, with the formation of *erythro*-**111a** in THF attributed to a more effective competition between inter- and intramolecular H-transfer as a result of a solvent polarity effect on the lifetime of the intermediate complex. The possibility that the formation of the *anti*-addition product results from trapping of (*Z*)-**92a** [produced by thermal *E,Z*-isomerization of (*E*)-**92a**] was not specifically considered, though it can be ruled out on the basis of the fact that the reported reaction times are considerably shorter than those required for significant *E,Z*-isomerization to occur, given the rate constant listed in Table 16 for this process¹³⁵.



Apelöig and Nakash obtained a 9 : 1 ratio of *syn*- and *anti*-addition products (*threo*- and *erythro*-**113a**, respectively, Scheme 6) from the addition of *para*-methoxyphenol (**112a**) to (*E*)-**92a** in refluxing C₆D₆ solution, and reported an absolute rate constant of $k = 2.33 \times 10^{-3} \text{ M}^{-1} \text{ s}^{-1}$ for the reaction at 75 °C¹⁵⁵. The product distribution was found not to vary with phenol concentration over the range 0.006–0.9 M. In contrast, the same products were obtained in a 1:4 ratio, again independent of phenol concentration, when the reaction was carried out in refluxing THF¹⁵⁵. A mechanism was proposed (Scheme 6) in which both the *syn*- and *anti*-addition products arise from intramolecular H-transfer within an initially formed zwitterionic complex, which can undergo rotation about the Si–Si bond in competition with intramolecular H-transfer. Thus, the *syn*-product results from H-transfer within the complex in its initially formed geometry, while the *anti*-product results from H-transfer after Si–Si bond rotation to the more stable conformer of the zwitterion (Scheme 6). The increased yield of the *anti*-product in THF was ascribed to an increased lifetime of the complex in the more polar solvent, which would allow more complete conformational equilibration in the zwitterionic intermediate. The possibility that the *anti*-product results from a trivial mechanism involving prior *E,Z*-isomerization to the potentially more reactive (*Z*)-isomer can be excluded on the basis of the rate constants (see above and Table 11), and the fact that the product ratio is independent of phenol concentration over a considerable range. The initial complexation step must of course be formally reversible, and we have drawn it as such in Scheme 6. However, there is as yet no evidence to suggest that the reverse step is fast enough (relative to H-transfer and rotational equilibration) to provide the catalytic pathway for *E,Z*-isomerization that it implies there should be.

This mechanism provides a viable alternative to the mechanism proposed earlier by Sekiguchi and coworkers to explain the concentration-dependent product ratios obtained from reaction of (*E*)- and (*Z*)-**104** with EtOH and *i*-PrOH (Scheme 5)¹⁴⁸, particularly in the absence of kinetic data to provide concrete support for the overall third-order



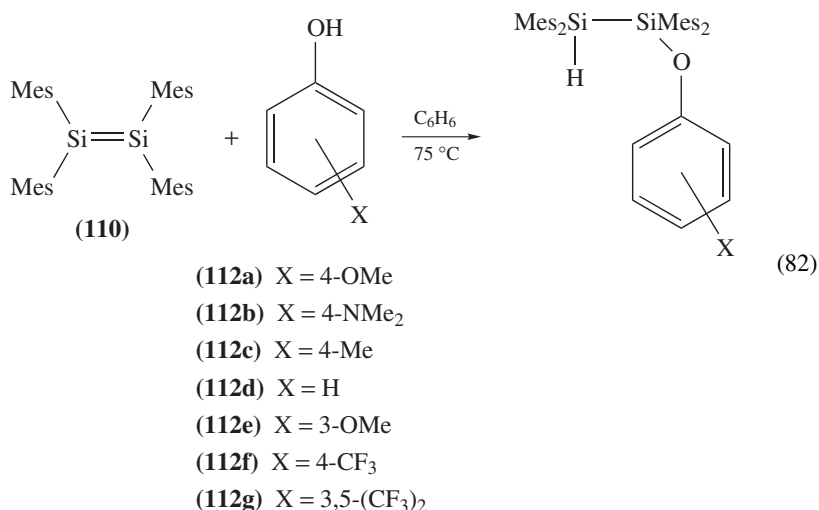
SCHEME 6

addition pathway. By the Apeloig/Nakash mechanism, the decreased stereoselectivity in the addition of ROH to **104** with an increase in alcohol concentration would be attributed to a solvent polarity effect on the rotational equilibration of the zwitterionic complex.

Excellent evidence thus exists, from both kinetic and product studies, for an addition mechanism in which reaction is initiated by nucleophilic attack at silicon, followed by transfer of the hydroxylic proton to the other disilenic silicon. This contrasts the results of early *ab initio* (RHF/6-31G*) theoretical calculations by Nagase and coworkers on the addition of water to $\text{H}_2\text{Si}=\text{SiH}_2$, which predicted the reaction to occur via a concerted pathway involving a cyclic, four-centred transition state⁷⁸. The stepwise nucleophilic mechanism appears to hold for the addition of aliphatic alcohols to disilenes which possess relatively non-polar Si=Si bonds, because either they are symmetrically substituted or they bear electronically neutral substituents. The regiochemistry associated with alcohol additions to alkoxy- and dialkylamino-substituted disilenes (*vide supra*) suggests that in the case of relatively polar disilenes, the mechanism changes to one in which proton transfer precedes nucleophilic attack. One might also expect this mechanism to operate in the reaction of non-polar disilenes with alcohols of relatively low nucleophilicity and high acidity. Evidence that this is indeed the case has recently been reported^{153,154}.

Apeloig and Nakash have reported absolute rate constants for the addition of seven *meta*- and *para*-substituted phenols (**112a–g**) to tetramesityldisilene (**110**) in benzene at 75 °C (equation 82)¹⁵⁴, as well as deuterium kinetic isotope effects¹⁵⁴ and Arrhenius

parameters¹⁵³ for addition of the *para*-methoxy (**112a**) and *para*-trifluoromethyl (**112g**) derivatives. The data are listed in Table 18. Tetramesityldisilene (**110**) is roughly half as reactive as (*E*)-**92a** toward *para*-methoxyphenol (**112a**) in benzene at 75 °C^{154,155}.



A Hammett plot of the rate data according to equation 83, where k_X is the absolute rate constant for reaction of the X-substituted phenol and k_H is that for reaction of the parent phenol (Figure 13), shows clear evidence for different addition mechanisms depending on whether the phenol is substituted with electron-donating or electron-withdrawing substituents.

$$\log(k_X/M^{-1}\text{s}^{-1}) = \log(k_H/M^{-1}\text{s}^{-1}) + \rho\sigma_X \quad (83)$$

The negative Hammett ρ -value observed for addition of electron donor-substituted phenols ($\rho = -1.77$) suggests that for these compounds, the reaction proceeds by a mechanism in which positive charge develops at the phenolic oxygen in the transition state for the rate-determining step. This is consistent with the stepwise nucleophilic addition mechanism proposed for the addition of non-acidic aliphatic alcohols to non-polar disilenes (Scheme 5), which is shown again in simpler form in equation 84. The reaction

TABLE 18. Absolute rate constants, deuterium kinetic isotope effects and Arrhenius parameters for addition of substituted phenols (**112a–g**) to tetramesityldisilene (**110**) in benzene solution at 75 °C^{153,154}

Phenol	k_{ArOH} ($10^{-4} \text{ M}^{-1} \text{ s}^{-1}$)	$k_{\text{H}}/k_{\text{D}}$	E_a (kJ mol ⁻¹)	$\log(A/M^{-1} \text{ s}^{-1})$
112a (X = 4-OMe)	13.9 ± 0.3	0.71	56 ± 1	5.6 ± 0.2
112b (X = 4-NMe ₂)	60.8 ± 0.7	—	—	—
112c (X = 4-Me)	5.9 ± 0.2	—	—	—
112d (X = H)	4.0 ± 0.1	—	—	—
112e (X = 3-OMe)	5.7 ± 0.2	—	—	—
112f (X = 4-CF ₃)	23.2 ± 0.4	5.3	40 ± 1	3.4 ± 0.1
112g (X = 3,5-(CF ₃) ₂)	141 ± 8	—	—	—

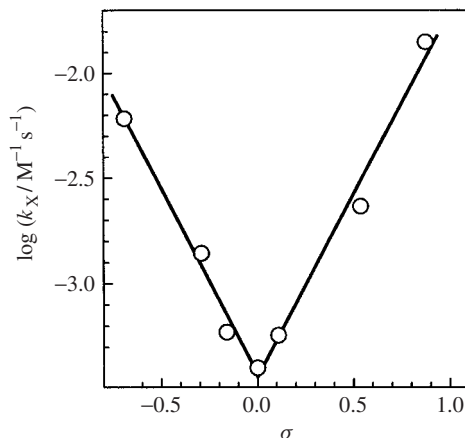
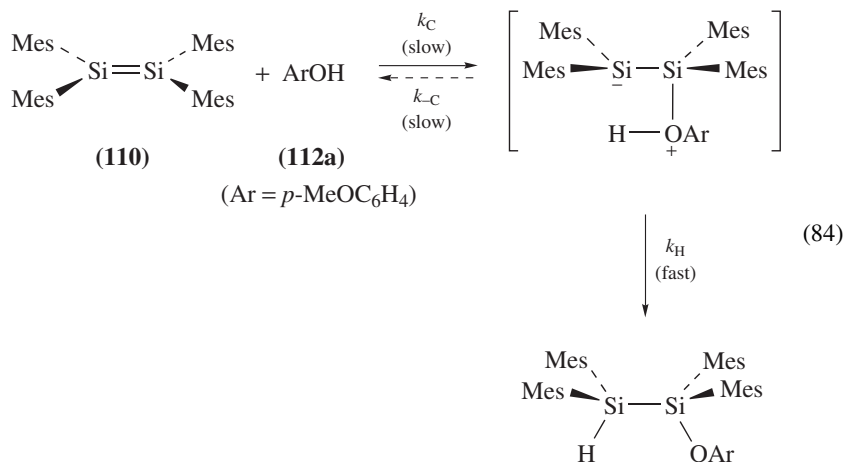
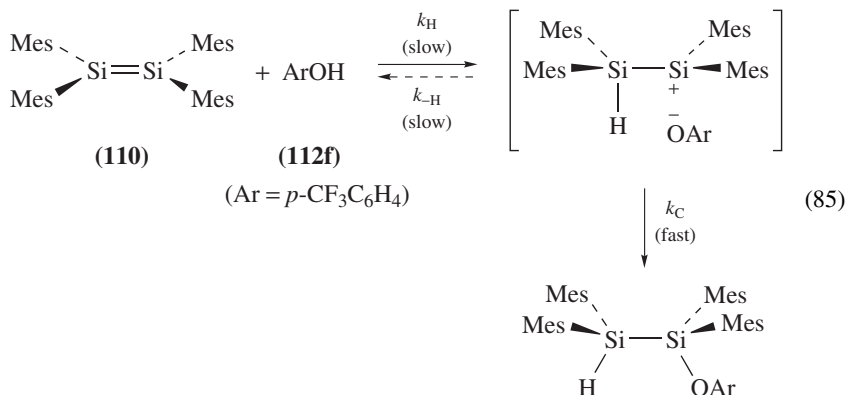


FIGURE 13. Hammett plot for the reactions of tetramesityldisilene with substituted phenols in benzene at 75 °C. Reproduced with permission from Reference 154. Copyright 1996 American Chemical Society

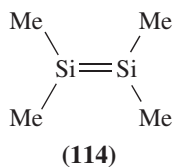
with **112a** exhibits an inverse secondary deuterium kinetic isotope effect of $k_H/k_D = 0.71$, which is also nicely consistent with the mechanism of equation 84¹⁵⁶.



In contrast, reaction of electron acceptor-substituted phenols exhibits $\rho = +1.72$, indicating the development of *negative* charge at the phenolic oxygen in the rate-determining step for reaction of relatively acidic, weakly nucleophilic phenols with **110**, and the addition of **112f** exhibits a large primary deuterium kinetic isotope effect of $k_H/k_D = 5.3$. This is consistent with the electrophilic addition mechanism of equation 85, in which full or partial protonation at silicon precedes nucleophilic attack.



The additions of both **112a** and **112f** to **110** exhibit positive activation energies and large negative entropies of activation ($E_a = 56 \pm 1 \text{ kJ mol}^{-1}$ and $\Delta S^\ddagger = -143 \pm 2 \text{ J mol}^{-1} \text{ K}^{-1}$ for **112a**; $E_a = 40 \pm 1 \text{ kJ mol}^{-1}$ and $\Delta S^\ddagger = -186 \pm 3 \text{ J mol}^{-1} \text{ K}^{-1}$ for **112f**), consistent with the proposed mechanisms in both cases. The larger negative value of ΔS^\ddagger exhibited by the reaction of **112f** was interpreted as indicative of a more ordered, compact transition state in the electrophilic addition pathway (equation 85) compared to the nucleophilic mechanism (equation 84). Both the large negative activation entropy and large primary deuterium kinetic isotope effect are also consistent with a concerted addition mechanism, however. Thus *ab initio* (MP3/6-31G*//HF/6-31G*) theoretical calculations were carried out on the addition of CH_3OH and CF_3OH to tetramethyldisilene (**114**) in order to investigate the mechanisms further¹⁵³.



The calculations indicate that the addition of both alcohols to **114** is more than 250 kJ mol^{-1} exergonic, and verify that the mechanism for addition of CH_3OH is much different than that for the more acidic, less nucleophilic alcohol CF_3OH . The calculations for addition of CH_3OH (Figure 14a) agree completely with the nucleophilic mechanism of equation 84; the reaction proceeds via initial, rate-determining association of the alcohol with the disilene to form a zwitterionic complex, followed by proton transfer via a transition state which is lower in free energy than that for the initial complexation step. The addition of CF_3OH (Figure 14b), on the other hand, was found to be concerted, with the alcohol involved both as a nucleophile and as an electrophile, and proton transfer to silicon being well advanced in the transition state. Coincidentally, the calculated entropies of activation and deuterium kinetic isotope effects for addition of the two alcohols to **114** agree very well with the experimental values obtained for the addition of **112a,f** to **110**, lending further credence to the calculations and their relevance to the experiments.

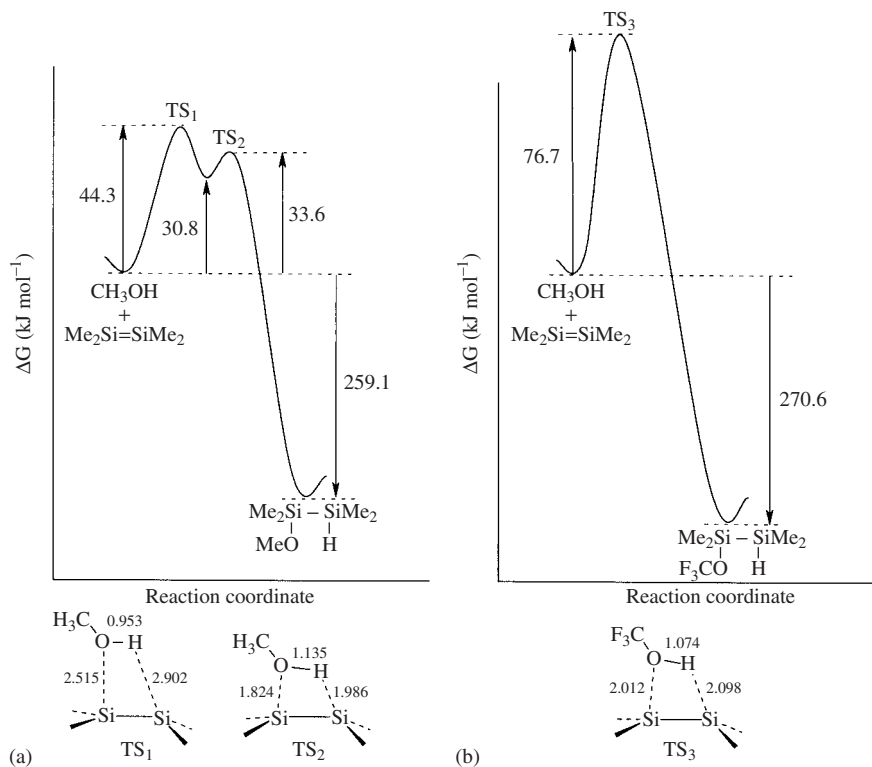


FIGURE 14. Calculated (MP3/6-31G*/HF-6-31G*) reaction coordinate diagrams for the addition of (a) CH_3OH and (b) CF_3OH to $\text{Me}_2\text{Si}=\text{SiMe}_2$ (**114**)

The statement was made earlier that tetramesityldisilene (**110**) is 10^9 – 10^{12} times less reactive toward aliphatic alcohols than the transient disilenes **103** and **104** investigated previously by Sekiguchi and coworkers¹⁴⁸. This statement is derived from the results of a study of the competitive trapping of **110** by EtOH, *i*-PrOH and *t*-BuOH relative to **112a** in benzene at 25 °C¹⁵³. The results established the order of reactivity: EtOH (77) > *i*-PrOH (7) > **112a**(1) \gg *t*-BuOH (≤ 0.02), where the relative rates are indicated in parentheses. A rate constant of $ca\ 4 \times 10^{-5}\ \text{M}^{-1}\ \text{s}^{-1}$ at 25 °C can be extrapolated from the reported Arrhenius data for **112a**, allowing an estimate of $k_{\text{EtOH}} \sim 3 \times 10^{-3}\ \text{M}^{-1}\ \text{s}^{-1}$ to be made for the rate constant for reaction of EtOH with **110** in benzene at 25 °C. Inspection of Table 17 indicates that this is almost 10^{11} times slower than the rate of reaction of **103** and **104** with EtOH in hexane solution at the same temperature. While the rates of reaction of **103** and **104** vary by only a factor of about ten throughout the series EtOH \sim *i*-PrOH > *t*-BuOH, those for reaction of **110** vary by at least 4000. This gives an excellent quantitative indication of the degree of steric stabilization afforded to the Si=Si bond in **110** by the mesityl substituents¹⁵³.

It will be of considerable interest to carry out detailed kinetic studies of the addition of aliphatic alcohols and phenols to transient disilenes, for comparison to the results discussed above for tetramesityldisilene **110**. Preliminary experiments have been carried out on the addition of methanol to the transient tetrakis(trialkylsilyl)disilene **35**¹⁵⁷. It will be recalled that this disilene has been shown to react with MeOH in isooctane solution by a mechanism that is overall first order in MeOH over the 0–0.5 M concentration range, and characterized by a rate constant $k_{\text{MeOH}} = (3 \pm 1) \times 10^5 \text{ M}^{-1} \text{ s}^{-1}$ (Table 17)⁶⁸. Additional studies of the reactive quenching of the disilene by MeOH have now been carried out in MeOH/THF and MeOD/THF of various compositions as a function of temperature¹⁵⁷. For example, Figure 15 shows plots of k_{decay} vs. $1/T$ for the decay of the disilene in 85% MeOH(D)/THF over the 10–50 °C temperature range. At 25 °C, the decay rate of the disilene is more than 10^4 times faster in 85% MeOH/THF ($k_{\text{decay}} = 1.8 \times 10^7 \text{ s}^{-1}$) than in neat THF solution ($k_{\text{decay}} < 600 \text{ s}^{-1}$), from which it can be concluded that the only significant decay pathway for the disilene under these conditions is reaction with the alcohol. At all temperatures studied, the decay rate of the disilene is significantly slower in MeOD/THF solution than in MeOH/THF, leading to calculated kinetic isotope effects ranging from $k_{\text{H}}/k_{\text{D}} \sim 2.7$ at 50 °C to $k_{\text{H}}/k_{\text{D}} \sim 4.0$ at 10 °C. Interestingly, the Arrhenius activation energies are *negative* in both cases, indicating that the transition state for the rate-determining step is lower in enthalpy than the starting materials under these conditions. The Arrhenius parameters for decay in 85% MeOH/THF are $E_{\text{a}} = -20 \pm 1 \text{ kJ mol}^{-1}$ and $\log (A/\text{s}^{-1}) = 3.6 \pm 0.3$; correcting the latter for the methanol concentration leads to an estimated activation entropy of $\Delta S^{\ddagger} \sim -200 \text{ J mol}^{-1} \text{ K}^{-1}$ at 25 °C. While much additional work will be necessary to sort out the undoubtedly complex role that solvation plays on the observed reaction kinetics under these conditions, the results suggest that proton transfer is involved in the rate-determining step for reaction, and are hence most consistent with an electrophilic addition pathway. Discriminating between a concerted or stepwise electrophilic mechanism is not yet possible, and will require kinetic data for reaction in dilute THF solution

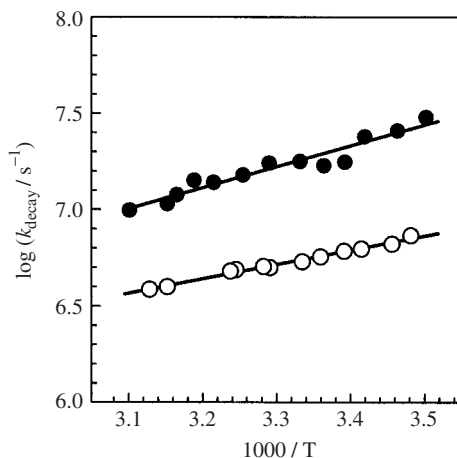


FIGURE 15. Arrhenius plots for the decay of tetrakis(trimethylsilyl)disilene (**35**) in 85% MeOH/THF (●) and 85% MeOD/THF (○)

TABLE 19. Absolute rate constants (in units of $10^8 \text{ M}^{-1} \text{ s}^{-1}$) for reaction of **103**, **104** and **35** with 2,3-dimethyl-1,3-butadiene, oxygen and aliphatic ketones in hexane solution at 22–25 °C

Reagent/Disilene	$k_{\text{MeOH}} (10^8 \text{ M}^{-1} \text{ s}^{-1})$			
	103 ^a	(<i>E</i>)- 104 ^a	(<i>Z</i>)- 104 ^a	35 ^b
2,3-dimethyl-1,3-butadiene	0.43	0.40	0.56	0.00040 ± 0.00002
O ₂ ^c	10	8	8	0.011 ± 0.001
acetone	5.8	2.6	2.2	—
acetone- <i>d</i> ₆	5.7	2.5	2.0	—
3-pentanone	3.6	1.2	1.0	—
2,4-dimethyl-3-pentanone	1.6	1.3	1.2	—

^aReference 158.^bReference 68.^cEstimated from the lifetimes in air-saturated hexane ($[\text{O}_2] \sim 0.003\text{M}$).

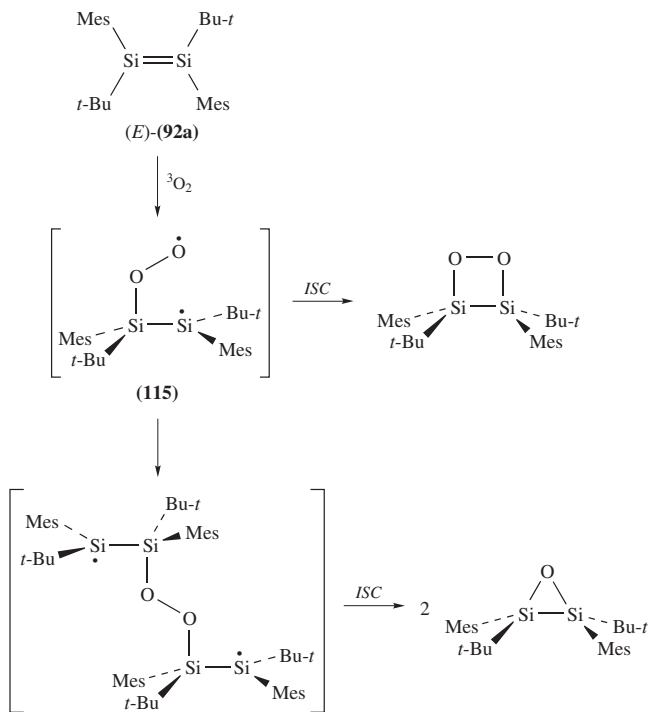
as well as other polar solvents with a lower propensity for non-productive complexation with the disilene.

2. [2 + 4]-, [2 + 2]- and [2 + 1]-Cycloadditions of dienes, carbonyl compounds and oxygen

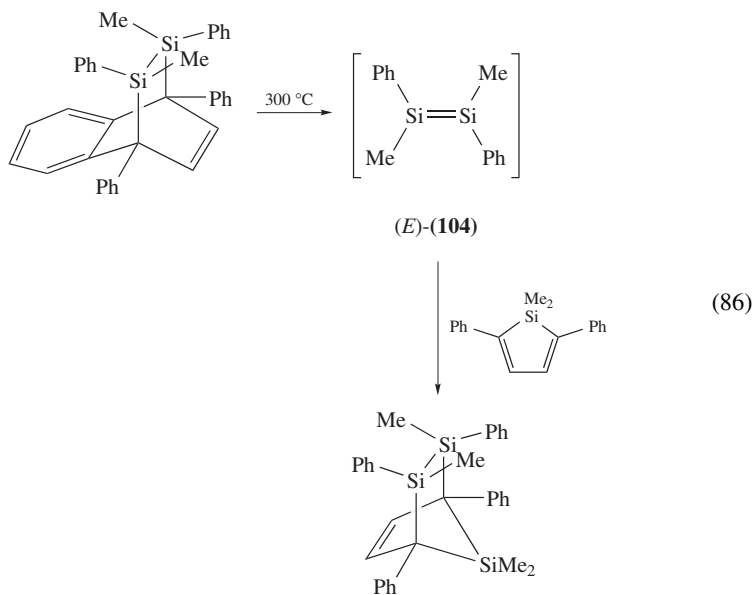
Kinetic data for other characteristic bimolecular reactions of disilenes are much more limited than is the case with alcohol and phenol additions, and hence contribute little to the understanding that product studies have already provided in regards to reaction mechanisms. The only absolute kinetic data known at the present time, for reaction of disilenes **103**, **104** and **35** with 2,3-dimethyl-1,3-butadiene, oxygen and a few symmetric *n*-alkanones in hydrocarbon solution at room temperature, are listed in Table 19. Unfortunately, none of these reactions has been specifically characterized with product studies, as far as we know. The data indicate that the reactivity of relatively non-polar disilenes toward these reagents decreases in the order $k_{\text{O}_2} > k_{\text{R}_2\text{C}=\text{O}} \sim k_{\text{EtOH}} > k_{\text{diene}}$.

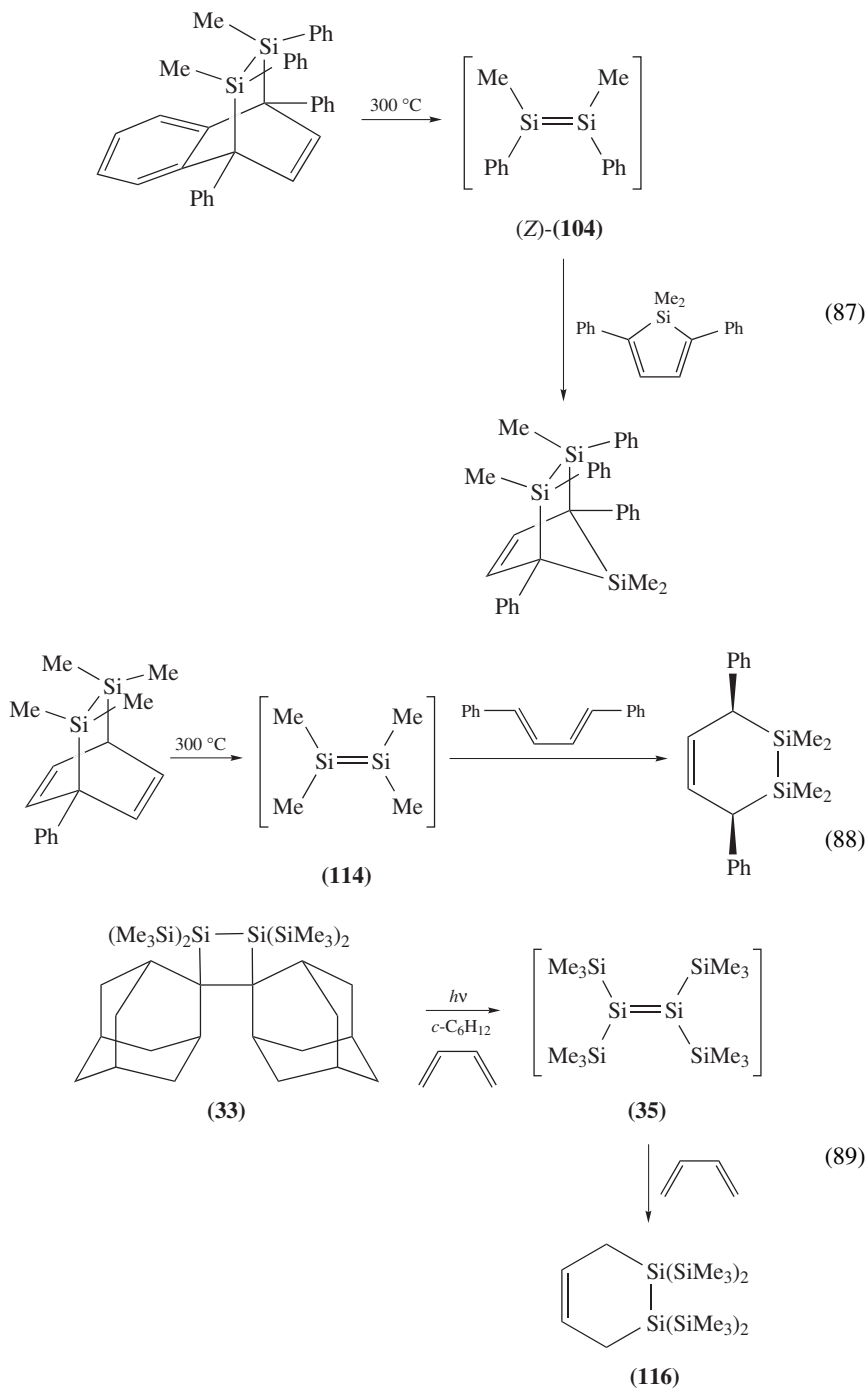
Oxidation of kinetically stabilized disilenes by atmospheric O₂ proceeds stereospecifically to form 1,2-cyclodisiloxanes and minor amounts of the corresponding 1,2-disilaoxiranes¹⁶. *Ab initio* (UHF/6-31G*) calculations on the oxidation of the parent disilene suggests that the first step in the reaction is the unactivated formation of the triplet biradical **115**¹⁵⁹, in which *trans-gauche* intersystem crossing and closure to the 1,2-cyclodisiloxane is rapid compared to rotation about the Si–Si bond. 1,2-Disiloxirane formation has been proposed to involve trapping of the initially-formed biradical by a second molecule of disilene, followed by collapse of the resulting 1,6-biradical to yield two molecules of the disiloxirane. These processes are illustrated in Scheme 7 (where ISC = intersystem crossing), using the oxidation of (*E*)-**92a** as an example¹⁶⁰.

Stable disilenes generally do not undergo Diels–Alder cycloaddition with conjugated dienes¹⁶, but the reaction is well known in the cases of more reactive disilene derivatives⁸. The stereochemistry of the reaction has not been widely studied, but isolated examples such as those shown in equations 86–88 show that the reaction proceeds with retention of the original stereochemistry of both the diene (equation 88)¹⁶¹ and the disilene (equations 86 and 87)¹⁶². Reaction of tetrakis(trimethylsilyl)disilene (**35**) with 1,3-butadiene in solution yields the expected Diels–Alder adduct **116** (equation 89)⁶⁸.



SCHEME 7





exploration of how silene chemistry might be exploited for the development of useful applications.

VI. APPENDIX. NEGATIVE ARRHENIUS ACTIVATION ENERGIES

A reaction proceeding by a mechanism of the general type shown in equation 34 will exhibit a negative Arrhenius activation energy if the free energy of activation for the product-forming step (proton transfer in the case of methanol addition to the Si=C bonds) is dominated by the entropic term, so that the enthalpy of the transition state is lower than that of the reactants (see Figure A1). In addition, the first step must be reversible, i.e. reversion of the intermediate to reactants (k_{-C}) must be faster than its collapse to product (k_H). If the opposite is true, then the first step is clearly the rate-determining step for reaction and the overall activation energy will be positive, of a value equal to or greater than that of diffusion (E_a^{diff}). Provided that a large enough temperature range can be spanned experimentally, the Arrhenius plot for a situation of this type should be bell-shaped, because the two reaction pathways available to the intermediate complex have opposing entropic requirements (i.e. $\Delta S_{-C}^\ddagger > 0$ and $\Delta S_H^\ddagger < 0$) and the magnitudes of k_H and k_{-C} will thus vary in opposing fashion as the temperature is changed. The predicted form of the temperature dependence over a very broad range in temperature is illustrated in Figure A2. At the high temperature extreme, $k_{-C} \gg k_H$, and the overall rate will increase with decreasing temperature, while at the low temperature extreme, the opposite is true and the rate will increase with increasing temperature. The apex in the bell-shaped plot of $\log k$ vs. $1/T$ (i.e. the point where $E_a = 0$) occurs at the particular temperature where $k_{-C} = k_H$.

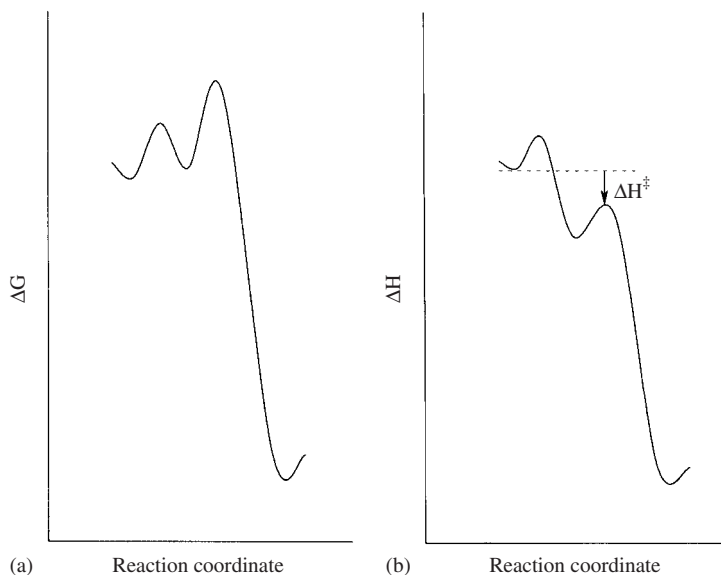


FIGURE A1. Reaction coordinate diagrams for a strongly exergonic stepwise reaction mechanism of the type shown in equation 34, illustrating the origin of a negative energy of activation: (a) ΔG vs. reaction coordinate, (b) ΔH vs. reaction coordinate

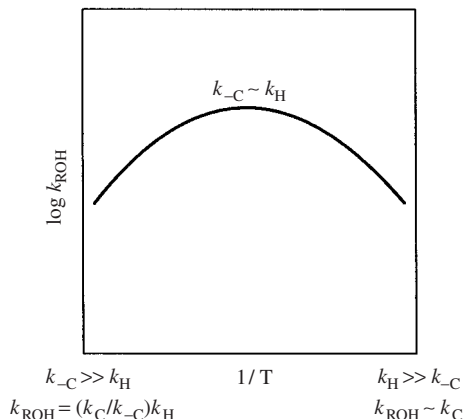


FIGURE A2. Bell-shaped Arrhenius plot expected for the mechanism of equation 34, over a wide range in temperature

Since one normally samples only a relatively small range in temperature, the Arrhenius behaviour observed can vary widely depending on the actual chemical situation and hence where the idealized curve of Figure A2 lies in relation to the experimentally observable window. The curve moves up or down on the $\log k$ axis as the rate of the initial complexation step described by k_C increases or decreases, and from left to right on the T^{-1} axis as the mean value of the complex partitioning ratio ($k_E/[k_E + k_{-C}]$, as defined by the identity of the trapping agent being examined) increases. This could be caused by fundamental changes in either k_E or k_{-C} from one reagent to another. If the possibility exists for a competing non-productive complexation process (e.g. with the solvent), then this results in an apparent shift of the curve to the left; the stronger such complexation is, the greater the shift. The overall degree of curvature is dependent on how precipitously the partitioning ratio varies with temperature; the greater the variation in this ratio, the greater the curvature. In the limit where it does not vary at all, then a positive Arrhenius activation energy would be obtained.

An isotopic change in the E-group that is transferred in the product-forming step will result in an overall isotope effect on the observed rate of reaction, the magnitude of which increases as the partitioning ratio decreases. Thus, a reaction mechanism of this type is characterized by an isotope effect that increases with increasing temperature.

VII. REFERENCES

1. L. E. Gusel'nikov and M. C. Flowers, *J. Chem. Soc., Chem. Commun.*, 864 (1967).
2. L. E. Gusel'nikov, N. S. Nametkin and V. M. Vdovin, *Acc. Chem. Res.*, **8**, 18 (1975).
3. L. E. Gusel'nikov and N. S. Nametkin, *Chem. Rev.*, **79**, 529 (1979).
4. A. G. Brook and K. M. Baines, *Adv. Organomet. Chem.*, **25**, 1 (1986).
5. B. Coleman and M. Jones, *Rev. Chem. Intermed.*, **4**, 297 (1981).
6. N. Wiberg, *J. Organomet. Chem.*, **273**, 141 (1984).
7. G. Raabe and J. Michl, *Chem. Rev.*, **85**, 419 (1985).
8. G. Raabe and J. Michl, in *The Chemistry of Organic Silicon Compounds* (Eds. S. Patai and Z. Rappoport), Chap. 16, Wiley, New York, 1989.
9. N. Auner, *J. Prakt. Chem.*, **337**, 79 (1995).
10. A. G. Brook and M. A. Brook, *Adv. Organomet. Chem.*, **39**, 71 (1996).

11. H. Sakurai, in *The Chemistry of Organic Silicon Compounds* (Eds. Z. Rappoport and Y. Apeloig), Vol. 2, Chap. 15, Wiley, Chichester, 1998.
12. T. Muller, W. Ziche and N. Auner, in *The Chemistry of Organic Silicon Compounds* (Eds. Z. Rappoport and Y. Apeloig), Vol. 2, Chap. 16, Wiley, Chichester, 1998.
13. T.L. Morkin and W.J. Leigh, *Acc. Chem. Res.*, in press.
14. R. West, *Angew. Chem., Int. Ed. Engl.*, **26**, 1201 (1987).
15. M. Weidenbruch, *Coord. Chem. Rev.*, **130**, 275 (1994).
16. R. Okazaki and R. West, *Adv. Organomet. Chem.*, **39**, 231 (1996).
17. (a) A. G. Brook, J. W. Harris, J. Lennon and M. El Sheikh, *J. Am. Chem. Soc.*, **101**, 83 (1979).
(b) A. G. Brook, S. C. Nyburg, F. Abdesaken, B. Gutekunst, G. Gutekunst, R. K. M. R. Kallury, Y. C. Poon, Y.-M. Chan and W. Wong-Ng, *J. Am. Chem. Soc.*, **104**, 5667 (1982).
18. R. West, M. Fink and J. Michl, *Science*, **214**, 1343 (1981).
19. L. M. Hadel, in *Handbook of Organic Photochemistry* (Ed. J. C. Scaiano), Vol. 1, Chap. 11, CRC Press, Boca Raton, 1989.
20. I. Carmichael and G. L. Hug, *Appl. Spectrosc.*, **41**, 1033 (1987).
21. R. Walsh, *Acc. Chem. Res.*, **14**, 246 (1981).
22. R. Walsh, *J. Phys. Chem.*, **90**, 389 (1986).
23. P. R. Jones and M. E. Lee, *J. Am. Chem. Soc.*, **105**, 6725 (1983).
24. I. M. T. Davidson and R. J. Scampton, *J. Organomet. Chem.*, **271**, 249 (1984).
25. R. T. Conlin and Y.-W. Kwak, *J. Am. Chem. Soc.*, **108**, 834 (1986).
26. S. Nagase and T. Kudo, *J. Chem. Soc., Chem. Commun.*, 141 (1984).
27. N. Wiberg and G. Wagner, *Chem. Ber.*, **119**, 1467 (1986).
28. N. Wiberg and G. Wagner, *Chem. Ber.*, **119**, 1455 (1986).
29. N. Wiberg, H.-S. Hwang-Park, H.-W. Lerner and S. Dick, *Chem. Ber.*, **129**, 471 (1996).
30. N. Wiberg and H. Kopf, *Chem. Ber.*, **120**, 653 (1987).
31. R. T. Conlin, S. Zhang, M. Namavari, K. L. Bobbitt and M.J. Fink, *Organometallics*, **8**, 571 (1989).
32. C. Kerst, M. Byloos and W. J. Leigh, *Can. J. Chem.*, **75**, 975 (1997).
33. L. E. Gusel'nikov, K. S. Konobeyevsky, V. M. Vdovin and N. S. Nametkin, *Dokl. Akad. Nauk SSSR*, **235**, 1086 (1977); *Chem. Abstr.*, **87**, 167111v (1977).
34. I. M. T. Davidson and I. T. Wood, *J. Chem. Soc., Chem. Commun.*, 550 (1982).
35. Th. Brix, N. L. Arthur and P. Potzinger, *J. Phys. Chem.*, **93**, 8193 (1989).
36. N. Wiberg, G. Preiner, G. Wagner and H. Kopf, *Z. Naturforsch. [B]*, **42B**, 1062 (1987).
37. T. L. Morkin, W. J. Leigh and T. T. Tidwell, to appear.
38. A. Sekiguchi and W. Ando, *Organometallics*, **6**, 1857 (1987).
39. A. Sekiguchi and W. Ando, *Chem. Lett.*, 2025 (1986).
40. C. J. Bradaric and W.J. Leigh, *Can. J. Chem.*, **75**, 1393 (1997).
41. C. J. Bradaric and W. J. Leigh, *Organometallics*, **17**, 645 (1998).
42. W. J. Leigh, C. J. Bradaric and G. W. Sluggett, *J. Am. Chem. Soc.*, **115**, 5332 (1993).
43. W. J. Leigh, C. Harrington, X. Li and N. P. Toltl, to appear.
44. W. J. Leigh, *Pure Appl. Chem.*, **71**, 453 (1999).
45. W. J. Leigh, C. J. Bradaric, C. Kerst and J. H. Banisch, *Organometallics*, **15**, 2246 (1996).
46. N. P. Toltl, M. J. Stradiotto, T. L. Morkin and W. J. Leigh, *Organometallics*, **18**, 5643 (1999).
47. W. J. Leigh and G. W. Sluggett, *Organometallics*, **13**, 269 (1994).
48. W. J. Leigh and G. W. Sluggett, *J. Am. Chem. Soc.*, **116**, 10468 (1994).
49. W. J. Leigh, N. P. Toltl, P. Apodeca, M. Castruita and K. H. Pannell, *Organometallics*, **19**, 3232 (2000).
50. W. J. Leigh and G. W. Sluggett, *J. Am. Chem. Soc.*, **115**, 7531 (1993).
51. G. W. Sluggett and W. J. Leigh, *J. Am. Chem. Soc.*, **114**, 1195 (1992).
52. N. P. Toltl and W. J. Leigh, *Organometallics*, **15**, 2554 (1996).
53. W. J. Leigh, C. J. Bradaric, G. W. Sluggett, P. Venneri, R. T. Conlin, M. S. K. Dhurjati and M. B. Ezhova, *J. Organomet. Chem.*, **561**, 19 (1998).
54. C. Kerst, R. Ruffolo and W. J. Leigh, *Organometallics*, **75**, 5804 (1997).
55. C. Kerst, C. W. Rogers, R. Ruffolo and W. J. Leigh, *J. Am. Chem. Soc.*, **119**, 466 (1997).
56. J. H. Banisch and W. J. Leigh, unpublished results.
57. W. J. Leigh, T. L. Morkin, C. J. Bradaric and X. Li, *Organometallics*, **20**, 932 (2000).
58. Y. Apeloig and M. Karni, *J. Am. Chem. Soc.*, **106**, 6676 (1984).

59. R. K. Vatsa, A. Kumar, P. D. Naik, H. P. Upadhyaya, U. B. Pavanaja, R. D. Saini, J. P. Mittal and J. Pola, *Chem. Phys. Lett.*, **255**, 129 (1996).
60. E. Bastian, P. Potzinger, A. Ritter, H.-P. Schuchmann, C. von Sonntag and G. Weddle, *Ber. Bunsenges. Phys. Chem.*, **84**, 56 (1980).
61. N. Auner and J. Grobe, *J. Organomet. Chem.*, **197**, 147 (1980).
62. P. Jutzi and P. Langer, *J. Organomet. Chem.*, **202**, 401 (1980).
63. T. L. Morkin and W. J. Leigh, to appear.
64. K. M. Baines and A. G. Brook, *Organometallics*, **6**, 692 (1987).
65. S. Zhang, R. T. Conlin, P. F. McGarry and J. C. Scaiano, *Organometallics*, **11**, 2317 (1992).
66. W. J. Leigh, T. Owens, M. Bendikov, D. Bravo-Zhivotovskii and Y. Apeloig, to appear.
67. D. Bravo-Zhivotovskii, V. Braude, A. Stanger, M. Kapon and Y. Apeloig, *Organometallics*, **11**, 2326 (1992).
68. Y. Apeloig, D. Bravo-Zhivotovskii, I. Zharov, V. Panov, W. J. Leigh and G. W. Sluggett, *J. Am. Chem. Soc.*, **120**, 1398 (1998).
69. D. Bravo-Zhivotovskii, Y. Apeloig, Y. Ovchinnikov, V. Igonin and Y. T. Struchkov, *J. Organomet. Chem.*, **446**, 123 (1993).
70. D. Bravo-Zhivotovskii and Y. Apeloig, unpublished results.
71. E. T. Seidl, R. S. Grev and H. F. Schaefer, III, *J. Am. Chem. Soc.*, **114**, 3643 (1992).
72. F. Bernardi, A. Bottoni, M. Olivucci, M. A. Robb and A. Venturini, *J. Am. Chem. Soc.*, **115**, 3322 (1993).
73. F. Bernardi, A. Bottoni, M. Olivucci, A. Venturini and M. A. Robb, *J. Chem. Soc., Faraday Trans.*, **90**, 1617 (1994).
74. A. Venturini, F. Bernardi, M. Olivucci, M.A. Robb and A. Rossi, *J. Am. Chem. Soc.*, **120**, 1912 (1998).
75. K. N. Houk, N. G. Rondan and J. Mareda, *Tetrahedron*, **41**, 1555 (1985).
76. N. Wiberg, G. Wagner, G. Muller and J. Riede, *J. Organomet. Chem.*, **271**, 381 (1984).
77. N. Wiberg, K. S. Joo and K. Polborn, *Chem. Ber.*, **126**, 67 (1993).
78. S. Nagase, T. Kudo and K. Ito, in *Applied Quantum Chemistry* (Eds. V. H. Smith Jr., H. F. Schaefer and K. Morokuma), D. Reidel, Dordrecht, 1986.
79. M. Kira, T. Maruyama and H. Sakurai, *J. Am. Chem. Soc.*, **113**, 3986 (1991).
80. A. G. Brook, K. D. Safa, P. D. Lickiss and K. M. Baines, *J. Am. Chem. Soc.*, **107**, 4338 (1985).
81. P. R. Jones and T. F. Bates, *J. Am. Chem. Soc.*, **109**, 913 (1987).
82. M. Ishikawa, T. Fuchikami and M. Kumada, *J. Organomet. Chem.*, **118**, 139 (1976).
83. M. Ishikawa, T. Fuchikami and M. Kumada, *J. Organomet. Chem.*, **118**, 155 (1976).
84. M. G. Steinmetz, B. S. Udayakumar and M. S. Gordon, *Organometallics*, **8**, 530 (1989).
85. F. L. Schadt, T. W. Bentley and P. v. R. Schleyer, *J. Am. Chem. Soc.*, **98**, 7667 (1976).
86. D. D. M. Wayner, in *CRC Handbook of Organic Photochemistry* (Ed. J. C. Scaiano), Vol. 2, Chap. 21, CRC Press, Boca Raton, 1989.
87. C. F. Bernasconi, R. A. Renfrow and P. R. Tia, *J. Am. Chem. Soc.*, **108**, 4541 (1986).
88. Z. Gross and S. Hoz, *J. Am. Chem. Soc.*, **110**, 7489 (1988).
89. C. J. Bradaric and W. J. Leigh, *J. Am. Chem. Soc.*, **118**, 8971 (1996).
90. M. Patz, H. Mayr, J. Bartl and S. Steenken, *Angew. Chem., Int. Ed. Engl.*, **34**, 490 (1995).
91. *CRC Handbook of Chemistry and Physics*, CRC Press, Boca Raton, 75th Edn., 1995, pp. 6-241.
92. C. J. Bradaric, C. Kerst and W. J. Leigh, unpublished results.
93. R. D. Bush, C. M. Golino, G. D. Homer and L. H. Sommer, *J. Organomet. Chem.*, **80**, 37 (1974).
94. A. G. Brook and Z. Yu, *Organometallics*, **19**, 1859 (2000).
95. A. H. B. Cheng, P. R. Jones, M. E. Lee and P. Roussi, *Organometallics*, **4**, 581 (1985).
96. P. R. Jones, T. F. Bates, A. F. Cowley and A. M. Arif, *J. Am. Chem. Soc.*, **108**, 3122 (1986).
97. C. Kerst, R. Boukherroub and W. J. Leigh, *J. Photochem. Photobiol. A: Chem.*, **110**, 243 (1997).
98. M. Ishikawa, T. Fuchikami and M. Kumada, *J. Organomet. Chem.*, **133**, 19 (1977).
99. M. Ishikawa and H. Sakamoto, *J. Organomet. Chem.*, **414**, 1 (1991).
100. A. G. Brook, S. S. Hu, A. K. Saxena and A. J. Lough, *Organometallics*, **10**, 2758 (1991).
101. A. G. Brook, S. S. Hu, W. J. Chatterton and A. J. Lough, *Organometallics*, **10**, 2752 (1991).
102. A. G. Brook, R. Kumarathasan and W. Chatterton, *Organometallics*, **12**, 4085 (1993).

103. N. Wiberg and M. Link, *Chem. Ber.*, **128**, 1231 (1995).
104. G. W. Sluggett and W. J. Leigh, *Organometallics*, **11**, 3731 (1992).
105. G. W. Sluggett and W. J. Leigh, *Organometallics*, **13**, 1005 (1994).
106. N. Wiberg, S. Wagner and G. Fischer, *Chem. Ber.*, **124**, 1981 (1991).
107. N. Wiberg, K. Schurz and G. Fischer, *Chem. Ber.*, **119**, 3498 (1986).
108. N. Wiberg, G. Fischer and K. Schurz, *Chem. Ber.*, **120**, 1605 (1987).
109. C. J. Bradaric, Ph.D. Thesis, McMaster University (1998).
110. M. Ishikawa, T. Fuchikami and M. Kumada, *J. Organomet. Chem.*, **162**, 223 (1978).
111. W. J. Leigh, C. Kerst, R. Boukherroub, T. L. Morkin, S. Jenkins, K. Sung and T. T. Tidwell, *J. Am. Chem. Soc.*, **121**, 4744 (1999).
112. A. Patyk, W. Sander, J. Gauss and D. Cremer, *Angew. Chem., Int. Ed. Engl.*, **28**, 898 (1989).
113. H. Okinoshima and W. P. Weber, *J. Organomet. Chem.*, **149**, 279 (1978).
114. H. S. D. Soysa and W. P. Weber, *J. Organomet. Chem.*, **173**, 269 (1979).
115. W. J. Leigh and X. Li, to appear.
116. N. Auner, J. Grobe, T. Muller and H. W. Rathmann, *Organometallics*, **19**, 3476 (2000).
117. W. J. Leigh, R. Boukherroub and C. Kerst, *J. Am. Chem. Soc.*, **120**, 9504 (1998).
118. W. J. Leigh, R. Boukherroub, C. J. Bradaric, C. C. Cserti and J. M. Schmeisser, *Can. J. Chem.*, **77**, 1136 (1999).
119. O. L. Chapman, C.-C. Chang, J. Kolc, M. E. Jung, J. A. Lowe, T. J. Barton and M. L. Turney, *J. Am. Chem. Soc.*, **98**, 7844 (1976).
120. M. R. Chedekel, M. Skoglund, R. L. Kreeger and H. Shechter, *J. Am. Chem. Soc.*, **98**, 7846 (1976).
121. R. N. Haszeldine, D. L. Scott and A. E. Tipping, *J. Chem. Soc., Perkin Trans. 1*, 1440 (1974).
122. S. H. Unger and C. Hansch, *Prog. Phys. Org. Chem.*, **12**, 91 (1976).
123. J. H. Espenson, *Chemical Kinetics and Reaction Mechanisms*, 2nd ed., McGraw-Hill, New York, 1995.
124. M. Bendikov, S. Quadt, O. Rabin, T. Moshny and Y. Apeloig, The 12th International Symposium on Organosilicon Chemistry, Sendai, Japan, 1999, p. 207.
125. M. Ishikawa, T. Fuchikami, M. Kumada, T. Higuchi and S. Miyamoto, *J. Am. Chem. Soc.*, **101**, 1348 (1979).
126. M. Ishikawa, D. Kovar, T. Fuchikami, K. Nishimura, M. Kumada, T. Higuchi and S. Miyamoto, *J. Am. Chem. Soc.*, **103**, 2324 (1981).
127. M. Ishikawa, T. Fuchikami and M. Kumada, *J. Am. Chem. Soc.*, **99**, 245 (1977).
128. M. Ishikawa, K. Nishimura, H. Sugisawa and M. Kumada, *J. Organomet. Chem.*, **194**, 147 (1980).
129. M. Ishikawa, H. Sugisawa, T. Fuchikami, M. Kumada, T. Yamabe, H. Kawakami, K. Fukui, Y. Ueki and H. Shizuka *J. Am. Chem. Soc.*, **104**, 2872 (1982).
130. M. Ishikawa, S. Matsuzawa, H. Sugisawa, F. Yano, S. Kamitori and T. Higuchi, *J. Am. Chem. Soc.*, **107**, 7706 (1985).
131. Y. Fujii, H. Yamada and M. Mizuta, *J. Phys. Chem.*, **92**, 6768 (1988).
132. R. West, *Science*, **225**, 1109 (1984).
133. S. A. Batcheller, T. Tsumuraya, O. Tempkin, W. M. Davis and S. Masamune, *J. Am. Chem. Soc.*, **112**, 9394 (1990).
134. M. Kira, S. Ohya, T. Iwamoto, M. Ichinohe and C. Kabuto, *Organometallics*, **19**, 1817 (2000).
135. M. J. Michalczyk, R. West and J. Michl, *Organometallics*, **4**, 826 (1985).
136. B. D. Shepherd, D. R. Powell and R. West, *Organometallics*, **8**, 2664 (1989).
137. G. Olbrich, P. Potzinger, B. Reimann and R. Walsh, *Organometallics*, **3**, 1267 (1984).
138. M. W. Schmidt, P. N. Truong and M. S. Gordon, *J. Am. Chem. Soc.*, **109**, 5217 (1987).
139. H. Jacobsen and T. Ziegler, *J. Am. Chem. Soc.*, **116**, 3667 (1994).
140. J. Saltiel and J. L. Charlton, in *Rearrangements in Ground and Excited States*, Vol. III (Ed. P. De Mayo), Academic Press, New York, 1980.
141. W. J. Leigh and D. R. Arnold, *Can. J. Chem.*, **59**, 609 (1981).
142. N. Tokitoh, H. Suzuki, R. Okazaki and K. Ogawa, *J. Am. Chem. Soc.*, **115**, 10428 (1993).
143. H. Suzuki, N. Tokitoh and R. Okazaki, *Bull. Chem. Soc. Jpn.*, **68**, 2471 (1995).
144. H. Sakurai, H. Tobita, M. Kira and Y. Nakadaira, *Angew. Chem., Int. Ed. Engl.*, **19**, 620 (1980).
145. R. S. Archibald, Y. van den Winkel, D. R. Powell and R. West, *J. Organomet. Chem.*, **446**, 67 (1993).

146. H. B. Yokelson, D. A. Siegel, A. J. Millevolte, J. Maxka and R. West, *Organometallics*, **9**, 1005 (1990).
147. H. B. Yokelson, J. Maxka, D. A. Siegel and R. West, *J. Am. Chem. Soc.*, **108**, 4239 (1986).
148. A. Sekiguchi, I. Maruki and H. Sakurai, *J. Am. Chem. Soc.*, **115**, 11460 (1993).
149. T. Iwamoto, H. Sakurai and M. Kira, *Bull. Chem. Soc. Jpn.*, **71**, 2741 (1998).
150. M. Karni and Y. Apeloig, *J. Am. Chem. Soc.*, **112**, 8589 (1990).
151. D. J. De Young, M. Fink and R. West, *Main Group Metal Chemistry*, **10**, 19 (1987).
152. J. Budaraju, D. R. Powell and R. West, *Main Group Metal Chemistry*, **19**, 531 (1996).
153. Y. Apeloig and M. Nakash, *Organometallics*, **17**, 2307 (1998).
154. Y. Apeloig and M. Nakash, *J. Am. Chem. Soc.*, **118**, 9798 (1996).
155. Y. Apeloig and M. Nakash, *Organometallics*, **17**, 1260 (1998).
156. O. Matsson and K. C. Westaway, *Adv. Phys. Org. Chem.*, **31**, 143 (1998).
157. W. J. Leigh, T. Owens, M. Bendikov, D. Bravo-Zhivotovskii and Y. Apeloig, to appear.
158. A. Sekiguchi, I. Maruki and H. Sakurai, unpublished results.
159. K. McKillop, R. West, T. Clark and H. Hofmann, *Z. Naturforsch.* [b], **49b**, 1737 (1994).
160. K. McKillop, G. R. Gillette, D. R. Powell and R. West, *J. Am. Chem. Soc.*, **114**, 5203 (1992).
161. D. N. Roark and G. J. D. Peddle, *J. Am. Chem. Soc.*, **94**, 5837 (1972).
162. H. Sakurai, Y. Nakadaira and T. Kobayashi, *J. Am. Chem. Soc.*, **101**, 487 (1979).
163. C. E. Dixon, D. W. Hughes and K. M. Baines, *J. Am. Chem. Soc.*, **120**, 11049 (1998).

CHAPTER 18

Ion–molecule reactions of silicon cations

SIMONETTA FORNARINI

*Dipartimento di Studi di Chimica e Tecnologia delle Sostanze Biologicamente Attive,
Università di Roma “La Sapienza”, P.le A. Moro 5, I-00185 Roma, Italy;
e-mail: simonetta.fornarini@uniroma1.it*

I. INTRODUCTION	1028
II. REACTIONS OF THE SILICON ION, $\text{Si}^{+(\bullet)}$	1028
A. Reactions with Simple Inorganic Molecules	1028
B. Reactions with Simple Organic Molecules	1030
III. REACTIONS OF HYDROGEN-CONTAINING SILACATIONS, $\text{Si}_x\text{H}_y^{+(\bullet)}$	1033
A. Reactions with Simple Inorganic Compounds	1033
B. Reactions with Hydrocarbons	1034
IV. REACTIONS OF HALOGEN-CONTAINING SILACATIONS	1035
V. REACTIONS OF O- AND S-SUBSTITUTED SILACATIONS	1038
VI. REACTIONS OF $\text{Si}_x\text{H}_y^{+\bullet}$ IONS	1040
A. Ion Chemistry in Me_4X ($\text{X} = \text{Si}, \text{Ge}, \text{Sn}$)	1040
B. Ion–Molecule Reactions of $\text{R}_{3-x}\text{SiH}_x^+$ as Probes of Ion Structures and Interconversion Pathways	1041
C. R_3Si^+ : Reactions with n-Bases	1043
D. R_3Si^+ : Reactions with Aromatic Compounds	1044
E. R_3Si^+ : Reactions with Alkenes and Alkynes	1047
F. Reactions of SiC_6H_7^+ and Related Ions	1049
G. Reactions of Organosilane Radical Cations	1051
VII. REACTIONS OF TRANSITION METAL-CONTAINING SILACATIONS	1051
VIII. ACKNOWLEDGMENTS	1053
IX. REFERENCES	1053

I. INTRODUCTION

The study of ion–molecule reactions is a branch of gas phase ion chemistry that is attracting increasing interest as the various kinds of techniques that are eminently suited for it are gaining increasing development and diffusion. A few instrumental methods that may be cited include flow tube techniques¹, ion cyclotron resonance (ICR) spectrometry^{2,3}, ion trap techniques⁴ and a high pressure (up to *ca* 1 atm) radiolytic approach⁵.

The quest towards the understanding of the bimolecular reactivity of positively charged silicon ions is sustained by several reasons besides its intrinsic fundamental interest. One reason is that reactive processes in ionized gaseous mixtures containing silanes are relevant to the design and control of CVD procedures in semiconductor technology. A second one is attached to the role of ionic processes in the growth of silicon-bearing ions and molecules in interstellar and circumstellar environments. A third reason regards a longstanding issue in silicon chemistry in condensed phases, namely the attainment and characterization of stable tricoordinate silicon-centered ions. This goal has been achieved only recently with the first believable example of triarylsilicenium ion, Mes_3Si^+ (Mes = mesityl)⁶. Such species are instead easily obtained in gaseous environments from the EI ionization or ion–molecule reactions of inorganic silanes and organosilicon compounds. The gas phase study of their thermodynamic and kinetic features therefore represents an especially valuable reference for condensed phase studies. The elusive character of tricoordinate silicon-centered ions in condensed phases stands in contrast with the acknowledged existence and mechanistic role of the analogous carbenium ions, an observation that provides a leit-motiv underlining many investigations on silicon cations and a major spur towards the understanding of their reactivity in the gas phase. A further point of interest attached to the investigation of the bimolecular reactivity of selected ionic species lies in the potential of reaction kinetics and product studies to give information on the structure of the reagent ion. Specific ion–molecule reactions can be quite selective probes of ion structure and may in fact be used as a powerful tool to obtain information about the existence of isomeric species and their relative abundancies in an ion population and the evaluation of their interconversion pathways^{7,8}.

We will highlight, whenever appropriate, which of the cited premises provides the basis of the cited work. The literature coverage is focussed on, but not restricted to, the years 1990–99. The reader is also referred to the chapter on the ion chemistry of gaseous silicon-containing species that appeared in a previous volume of this series⁹. Care was taken to avoid superposition of cited references, though an exception was made when presenting results that were thought to deserve a somewhat more extensive discussion in the present context of ion–molecule reactivity.

II. REACTIONS OF THE SILICON ION, $\text{Si}^{+\bullet}$

The reactions of atomic silicon cations with a large variety of neutral molecules have been reported and summarized in reviews focussed on the kinetic, energetic and the mechanistic study of these reactions by selected-ion flow tube (SIFT)¹⁰ and guided ion beam techniques¹¹.

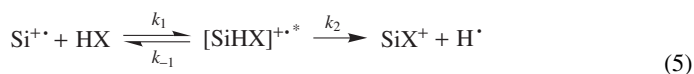
A. Reactions with Simple Inorganic Molecules

These reactions usually proceed by incorporation of Si into the product ions by way of long-lived intermediate complexes which allow a rearrangement of the existing bonds and the formation of new bonds. The reactions of ground state $\text{Si}^{+\bullet}(^2\text{P})$ with HCl, H_2O , H_2S and NH_3 have been studied as a function of the ion-neutral center of mass kinetic

energy (KE_{CM}) in a selected-ion flow drift tube (SIFDT) apparatus¹². At near thermal energies the reactions are described by equations 1–4.



These highly efficient reactions are characterized by rate coefficients in the range of 10^{-10} – 10^{-9} $cm^3 s^{-1}$, showing a pronounced negative energy dependence that is accounted for by a model reaction pathway proceeding via the formation of a long-lived complex (equation 5). Reactions 1–4 are only moderately exothermic and the standard entropy changes are negative due to the formation of atomic hydrogen. It is plausible that the dissociation of the intermediate complex back to the reactants (k_{-1}) becomes therefore increasingly favored with respect to dissociation into products (k_2) as KE_{CM} , namely the temperature, increases. In other words the increase of k_{-1} with KE_{CM} is more pronounced than that of k_2 , thus accounting for the resulting decrease of the overall rate constant as KE_{CM} increases.



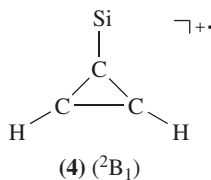
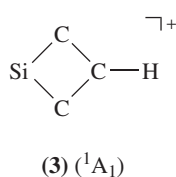
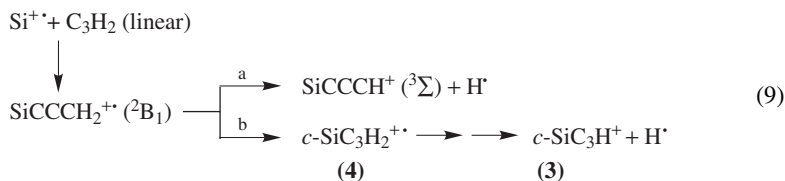
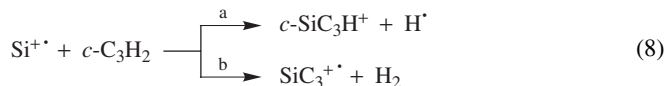
The formation of two possible isomers as the products of reaction 2 is exothermic; both $SiSH^+$ and $HSiS^+$ may therefore be formed. At high KE_{CM} an endothermic channel leading to SiH^+ (+SH) becomes dominant with regard to reaction 2. Among the two possible products of reaction 3, $SiOH^+$ and $HSiO^+$, only the first one, more stable by >58 $kcal mol^{-1}$, can be formed within the explored KE_{CM} range¹³. The SIFDT rate data for reaction 3 at near thermal energy are in good agreement with SIFT experiments at room temperature¹⁴, showing that at thermal energy the rate coefficient is only 1/4 of the capture rate coefficient. The energy profile of the reaction has been examined by *ab initio* MO calculations, showing the existence of a stable $[SiOH_2]^+$ adduct ion whose dissociation into products is allowed by the initial energy of the reactants¹⁵. The energy profile of the $Si^{++} + H_2O$ reaction has been recently compared with the reaction profile of the analogous $C^{++} + H_2O$ reaction¹⁶. A major difference lies in the relative stability of H_2SiO^{++} , 43.5 $kcal mol^{-1}$ higher in energy with respect to *trans*- $HSiOH^{++}$, the most stable structure on the $[H_2SiO]^{++}$ potential energy surface (PES). Whereas H_2SiO^{++} is not accessible from the $Si^{++} + H_2O$ reaction, due to the existence of high energy transition states, H_2CO^{++} is the most stable isomer on the $[H_2CO]^{++}$ PES¹⁷, showing HCO^+ as the favored dissociation product. The $Si^{++} + NH_3$ reaction (equation 4) has been studied at room temperature by the SIFT technique^{18,19} and shown to lead to $SiNH_2^+$, the most stable isomer among $[H_2SiN]^+$ ions^{20,21}. The potential role of $SiNH_2^+$ in interstellar silicon chemistry as a precursor of silicon–nitrogen products has stimulated a theoretical study on its spectral properties to allow its identification²². The calculated energy profile of reaction 4 bears a close relationship to that of the $Si^{++} + H_2O$ reaction^{23,24}. The primary $SiNH_3^{++}$ adduct ion, favored by 95 $kcal mol^{-1}$ relative to $Si^{++} + NH_3$, may dissociate

and transition states lying in energy above reactants. The third one implies insertion of $\text{Si}^{+\bullet}$ into a C–H bond giving the $\text{HSiCCH}^{+\bullet}$ isomer which may release the hydrogen atom bound to Si in a barrierless process.

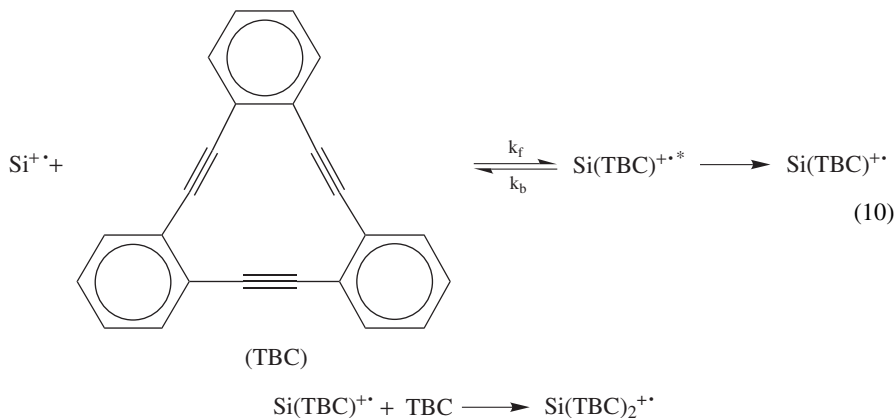
The $\text{Si}^{+\bullet}({}^2\text{P})$ reaction with ethylene has been studied by SIFDT as a function of He pressure and $\text{KE}_{\text{CM}}^{32}$. Two product ions are formed, $[\text{SiC}_2\text{H}_4]^{+\bullet}$ and $[\text{SiC}_2\text{H}_3]^+$, according to a reaction scheme similar to equation 7, holding at low values of KE_{CM} . For $\text{KE}_{\text{CM}} > 0.1$ eV the pressure dependence of the product distribution suggests that the excited intermediate collision complex, $[\text{SiC}_2\text{H}_4]^{+\bullet*}$, may evolve by an additional pathway, namely dissociation to $[\text{SiC}_2\text{H}_3]^+$ upon activation by collisions with He. Also on the $[\text{SiC}_2\text{H}_4]^{+\bullet}$ PES the global minimum is found to be a three-membered cyclic structure, $\text{SiC}_2\text{H}_4^{+\bullet}({}^2\text{B}_2)$, the product of a symmetry-allowed addition of $\text{Si}^{+\bullet}({}^2\text{P})$ to ethylene³¹.

The reaction of $\text{Si}^{+\bullet}({}^2\text{P})$ with benzene leading to $[\text{SiC}_6\text{H}_6]^{+\bullet}$ in a SIFDT apparatus has been described as occurring via distinct long-lived complexes²⁶. With increasing KE_{CM} , a channel forming $[\text{SiC}_6\text{H}_5]^+$ ions becomes dominant, according to a reactivity pattern that closely parallels the $\text{Si}^{+\bullet}({}^2\text{P})$ reactions with ethylene and acetylene. The reactivity of the $[\text{SiC}_6\text{H}_6]^{+\bullet}$ adduct formed at thermal energy under SIFT conditions has been discussed in terms of a π -complex structure between $\text{Si}^{+\bullet}$ and the aromatic ring^{9,33}.

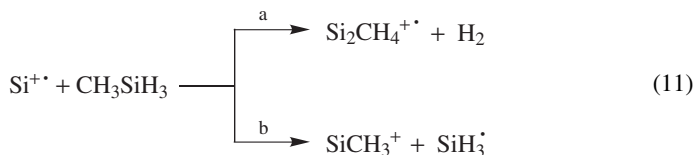
Two C_3H_2 isomers, cyclic and linear, are present in the interstellar medium and their reaction with $\text{Si}^{+\bullet}$ has been examined in a theoretical study³⁴. Barrier-free processes have been found that may ultimately contribute to the formation of SiC_3 in the interstellar medium. Multiple pathways are allowed to the exothermic reaction (equation 8a) of $\text{Si}^{+\bullet}$ with cyclopropenylidene to form cyclic SiC_3H^+ (**3**). All of them involve attachment of $\text{Si}^{+\bullet}$ giving a species (**4**) that isomerizes into a four-membered ring skeleton. Loss of atomic hydrogen may occur directly or following further isomerizations by 1,2-H shift. The formation of $\text{SiC}_3^{+\bullet}$, (equation 8b), only slightly exothermic, is found to involve a small barrier protruding above the energy level of the reactants. The calculated energy profiles of the $\text{Si}^{+\bullet}$ reaction with vinylidene carbene are sensitive to the computational method used. The most likely routes to the exothermic formation of SiC_3H^+ may involve either a direct H elimination leading to a triplet linear isomer (equation 9a) or an isomerization to **4** leading finally to $c\text{-SiC}_3\text{H}^+$ (**3**) (equation 9b).



The formation of charged adducts between $\text{Si}^{+\bullet}$ and ligands such as the macrocyclic molecule tribenzocyclotriene (TBC) is allowed even in the low pressure FT-ICR ion trap by radiative stabilization³⁵. Among several atomic metal cations, $\text{Si}^{+\bullet}$ shows a fast rate of formation of both monomer and dimer complexes (equation 10), ascribed to electronic reasons³⁶.



The reactions of $\text{Si}^{+\bullet}$ with methylsilane, CH_3SiH_3 , and silaethylene, $\text{CH}_2=\text{SiH}_2$, have been examined by *ab initio* quantum chemical studies and discussed in relation to experimental studies. Several possible isomers are predicted on the $[\text{Si}_2\text{CH}_4]^{+\bullet}$ and $[\text{Si}_2\text{CH}_6]^{+\bullet}$ potential energy surfaces, arising from initial complex formation followed by insertion of $\text{Si}^{+\bullet}$ into Si–H, C–H, and Si–C bonds^{37,38}. The $\text{Si}^{+\bullet}$ reaction with methylsilane leads to $[\text{Si}_2\text{CH}_4]^{+\bullet}$ as the major ionic product at thermal energy (equation 11a). A minor pathway yields $[\text{SiCH}_3]^+$ ions (equation 11b). An addition–elimination pathway formally analogous to reaction 11a is shared also by the $\text{Si}^{+\bullet}$ reaction with silaethylene.



The low energy collisions of $\text{Si}^{+\bullet}$ with perfluorohexane have been studied in the search for analogies with the ion–surface reactions at fluorinated alkane monolayer surfaces. A fluorine atom abstraction product was observed, SiF^+ , in analogy to the corresponding ion/surface reaction, though its abundance was relatively low with respect to fluorocarbon fragment ions³⁹.

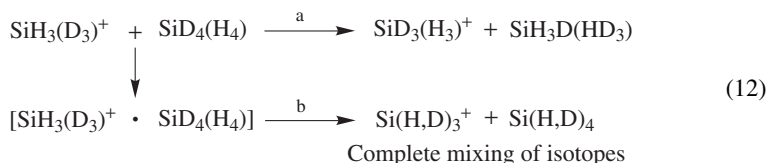
Reactions of $\text{Si}^{+\bullet}$ with simple oxygen-containing organic molecules that have been the focus of experimental studies have also been examined computationally⁴⁰ and related to the analogous reactions by $\text{C}^{+\bullet}$. Insertion of $\text{Si}^{+\bullet}$ into the C–O bonds of formaldehyde and methanol is found to lead to the most stable products, a result that is accounted for by the stabilization afforded by silyl substitution at the oxygen atom.

III. REACTIONS OF HYDROGEN-CONTAINING SILACATIONS, $\text{Si}_x\text{H}_y^{+\bullet}$

Depending on the number of hydrogen atoms, $\text{Si}_x\text{H}_y^{+\bullet}$ species will be either radical cations, $\text{Si}_x\text{H}_y^{+\bullet}$ (y an even number), or even-electron ions, Si_xH_y^+ (y an odd number).

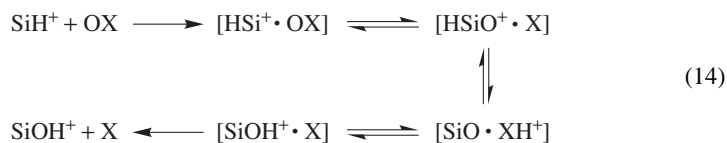
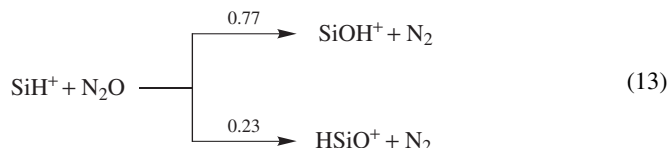
A. Reactions with Simple Inorganic Compounds

EI ionization and ensuing fragmentation of SiH_4 yields $\text{SiH}_y^{+\bullet}$ ions which undergo clustering reactions with neutral SiH_4 . A hydride exchange reaction between SiH_3^+ and SiH_4 has been observed occurring via competing pathways (equation 12)⁴¹. A long-range hydride stripping reaction (equation 12a) is reported to take place at a rate greater than the collision rate and not to involve H/D scrambling, at variance with an alternative pathway via the formation of an intermediate collision complex, whereby complete H/D mixing is expected (equation 12b).



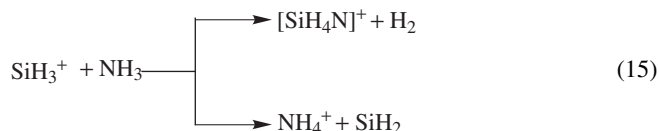
The formation of ion–molecule complexes, $[\text{SiH}_3^+ \cdot (\text{SiH}_4)_n]$ with $n = 1, 2$, has been indeed observed in a pulsed electron beam high-pressure mass spectrometric study which suggests 35 kcal mol^{-1} as the lower limit for the dissociation energy of $[\text{SiH}_3^+ \cdot (\text{SiH}_4)]$ ⁴². The SiH_3^+ clusters with H_2 , $[\text{SiH}_3^+ \cdot (\text{H}_2)_n]$ with $n = 1, 2$, were found to be bound by 14.2 and $4.8 \text{ kcal mol}^{-1}$, respectively.

A potential O-atom donor molecule, N_2O , has been allowed to react with SiH^+ to probe the formation of HSiO^+ , a higher energy isomer of SiOH^+ . The expectations were fulfilled (equation 13)⁴³, as tested by reaction with a base capable of deprotonating HSiO^+ but not SiOH^+ . The formal O-atom insertion product, SiOH^+ , was ascribed to a proton ‘shuttle’ mechanism which is dominant when OX is SO_2 and CO_2 (equation 14). In fact, with these two neutrals the formation of HSiO^+ and X as bare species is somewhat endothermic and the proton transfer process within the ion-neutral complex, driven by the stability of SiOH^+ , is allowed by the proton affinity (PA) of X which is intermediate between those of the Si and O sites of SiO . On the other hand, when O_2 is used as the neutral reagent this pathway is not accessible and HSiO_2^+ is the only observed product ion.



Two isomeric species appear to be formed in the CI of SiH₄ in the presence of CO, SiH₃OC⁺ and SiH₃CO⁺, although the latter is predicted to be more stable by 15 kcal mol⁻¹. The transition state allowing interconversion of the two isomers is calculated to be energetically close to the SiH₃⁺-CO bond cleavage, whereas a high energy barrier separates the methoxysilicon cation, CH₃OSi⁺, representing the global minimum on the [SiCH₃O]⁺ PES^{44,45}.

The reaction of NH₃ with SiH_y^{+(*)} (*y* = 1–3) ions, which may be studied in SiH₄/NH₃ or MeSiH₃/NH₃ mixtures^{9,46,47}, occurs predominantly by an addition–elimination pathway involving loss of H₂ as well as H^{*} in the case of SiH₂⁺. The addition–elimination and the competing proton transfer pathways of the SiH₃⁺ reaction (equation 15) have been studied theoretically and found to be obviously favored with respect to an endothermic hydrogen abstraction and charge or H⁻ transfer processes⁴⁸. The H₂SiNH₂⁺ isomer is predicted to be more stable than HSiNH₃⁺ by over 10 kcal mol⁻¹.

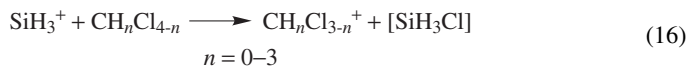


The rate constants for the reactions of SiH_y^{+(*)} (*y* = 0–3) ions with PH₃ in a PH₃/CH₃SiH₃ mixture have been reported⁴⁹. Just as in the NH₃ reaction, an addition–elimination route by loss of H₂ is the dominant pathway^{9,49}, the only exception being SiH₂⁺, which shows also products of hydrogen atom and proton transfer.

Ion–molecule reactions in SiH₄/GeH₄ mixtures have been studied for their relevance to the radiolytic deposition of thin films of potential interest in photovoltaic technology, where formation of ions containing mutually bonded silicon and germanium atoms is considered promising. To this end the SiH_y^{+(*)} (*y* = 0–2) reaction with GeH₄ is fairly efficient, whereas SiH₃⁺ reacts only by hydride transfer⁵⁰. Ions containing C, besides Si and Ge, may be grown from the MeGeH₃ reaction with Si_xH_y^{+(*)} (*x* = 1, 2; *y* = 2, 4, 5) in MeGeH₃/SiH₄ mixtures⁵¹.

B. Reactions with Hydrocarbons

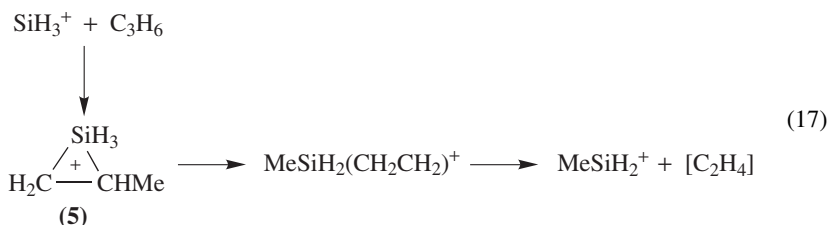
Lim and Lampe have studied the reaction of SiH₃⁺ with chloromethanes⁵². The kinetic energy of the reactant ion was varied in the 1.0–10.0 eV range. By far the predominant process is the direct abstraction of Cl⁻ (equation 16). The reaction involves no hydrogen atom scrambling and is probably driven by the high silicon–halogen bond energy. Products of collisionally induced dissociation, SiH⁺ and SiH₂⁺, are also formed. The rate of the CH₃Cl reaction is comparatively low, a result that has been ascribed to the estimated endothermicity of the Cl⁻ abstraction process. However, the kinetic energy dependence of the cross sections for Cl⁻ abstraction shows the features of an exothermic process in all cases.



Recent studies have reported on the ion–molecule reaction sequences taking place in mixtures of SiH₄ with various hydrocarbons (C₂H₂, C₂H₄, C₂H₆, C₃H₆, C₃H₈), whose major focus is the growth of ions of increasing size potentially playing a role in plasma and

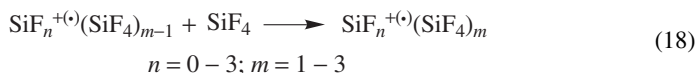
deposition processes⁵³. In particular, major reaction pathways of $\text{SiH}_y^{+(\bullet)}$ ($y = 1-3$) lead to product ions involving elimination of H^\bullet or H_2 , SiC_2H_n^+ ($n = 1, 3$ from the ethyne reaction or $n = 6, 7$ from ethane). Only SiH_3^+ reacts with propane, giving a H^- -transfer product, whereas $\text{SiH}_y^{+(\bullet)}$ ($y = 1-3$) ions react with propene by addition–elimination processes involving loss of hydrocarbon fragments. In the above-mentioned gaseous mixtures, also Si_2H_n^+ and Si_3H_5^+ ions from the self-condensation of the primary ions of silane play a role in the growth of ions containing several Si and C atoms. The formation of adduct ions stabilized against dissociation is only rarely observed in these ion trap mass spectrometric studies, a notable exception being SiC_2H_7^+ from the SiH_3^+ reaction with C_2H_4 , an ion which may have the structure of a cyclic, silyl-bridged $\text{H}_3\text{SiC}_2\text{H}_4^+$ species⁵⁴.

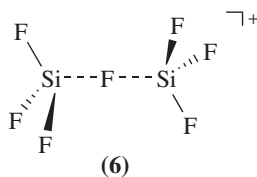
The SiH_3^+ reaction with propene yielding SiCH_5^+ ions (equation 17) conforms to a general H/Me exchange reaction which has been studied by FT-ICR using specific isotopic labelling⁵⁵. The H/Me exchange reaction, which is common to the series of ions $\text{SiH}_x(\text{Me})_{3-x}^+$ ($x = 0-3$), is suggested to proceed via a protonated silacyclopropane intermediate (**5**) and to involve H and Me migration processes activated by the energy released in the silicenium ion–alkene interaction. Isobutene may deliver up to two methylene groups.



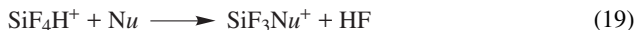
IV. REACTIONS OF HALOGEN-CONTAINING SILICATIONS

$\text{SiF}_n^{+(\bullet)}$ ions ($n = 1-3$) are observed as fragment ions when SiF_4 is ionized by EI or by a charge transfer reagent. The clustering equilibria in SiF_4 (equation 18) have been studied using a pulsed electron beam mass spectrometer in association with *ab initio* calculations⁵⁶. The binding energies of $\text{SiF}_n^{+(\bullet)}(\text{SiF}_4)$ increase with n (0–3), in parallel with the increasing electrophilic character of the $\text{SiF}_n^{+(\bullet)}$ ions. Thus, whereas the calculated bond energy of 13 kcal mol^{-1} for $\text{Si}^{+(\bullet)}(\text{SiF}_4)$ is indicative of an electrostatic interaction, the value for $\text{SiF}_3^+(\text{SiF}_4)$ is estimated experimentally to be $\geq 35 \text{ kcal mol}^{-1}$. Theoretical results predict a bond energy of 38 kcal mol^{-1} for the $\text{SiF}_3^+(\text{SiF}_4)$ cluster and a symmetrical D_{3d} geometry (**6**) with a F atom bridging two SiF_3 groups. A striking difference with the low bond energy of $\text{CF}_3^+(\text{CF}_4)$ of only $6.6 \text{ kcal mol}^{-1}$ is ascribed to the low electrophilicity of CF_3^+ , stabilized by hyperconjugation between the $2p\pi(\text{C})$ and $2p\pi(\text{F})$ orbitals. It is instead recognized that the extent of mixing of $3p\pi(\text{Si})$ and $2p\pi(\text{F})$ orbitals is only minor. In fact, π -donating α -substituents, such as F, are stabilizing in silicenium ions and in silications in general, but less so than in their carbon analogues⁵⁷.

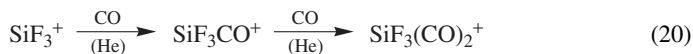




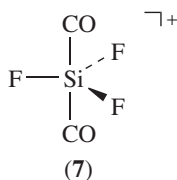
The proton transfer reactions between protonated SiF_4 and reference bases (N_2 , Xe) have been studied in a SIFT apparatus to provide an updated proton affinity value⁵⁸ of $117.7 \text{ kcal mol}^{-1}$. *Ab initio* calculations give a comparable PA value and predict a geometry for SiF_4H^+ showing the features of a nearly planar SiF_3^+ solvated by a HF molecule, $\text{F}_3\text{Si}^+ \cdots \text{FH}$. Therefore, it is not surprising that SiF_4H^+ ions may react by nucleophilic substitution (equation 19, where Nu is a nucleophile). The reaction with CO_2 yields $\text{SiF}_3^+(\text{CO}_2)$ ions, which have been found to react with benzene by a carbonylation process, consistent with their expected structure of $\text{F}_3\text{Si}-\text{OCO}^+$ adducts⁵⁹. Ligand displacement is by far the preferred pathway with unsaturated hydrocarbons such as C_2H_2 , C_2H_4 , C_3H_6 , whereas alkanes are unreactive.



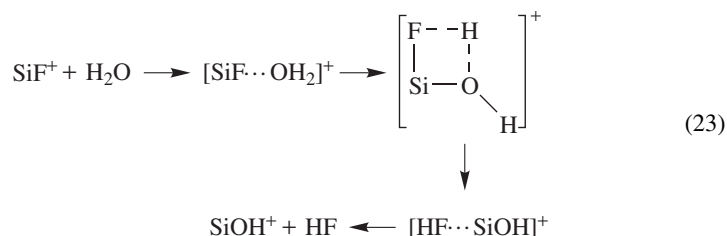
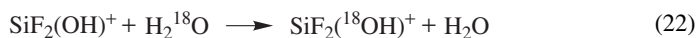
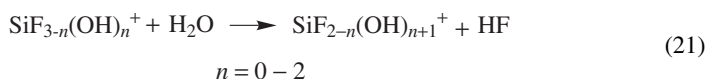
The addition of SiF_3^+ to CO in He buffer gas yields the two isomers SiF_3CO^+ and SiF_3OC^+ in approximately 0.85 : 0.15 ratio according to CID experiments⁶⁰. This relative abundance may be in part the outcome of collision dynamics due to ion-dipole interactions. However, interconversion of the two isomers is possible before collisional stabilization because the activation energy for the isomerization lies below the energy level of the separated reactants. According to *ab initio* calculations, SiF_3CO^+ is lower in energy by $17.8 \text{ kcal mol}^{-1}$ with respect to SiF_3OC^+ and the potential energy profile is very similar to the one calculated for $[\text{SiCH}_3\text{O}]^+$ at the same level of theory. A comparison with the carbon analogue, CH_3CO^+ , shows a relatively small perturbation of the planar geometries of the $\text{SiH}_3^+/\text{SiF}_3^+$ moieties in $\text{SiH}_3\text{CO}^+/\text{SiF}_3\text{CO}^+$. Such finding is assigned to the weaker overlap between orbitals of Si and C than that existing between atoms (C and C) of the same period. The addition of CO may proceed further and lead to $\text{SiF}_3(\text{CO})_2^+$ ions (equation 20), which have been assayed by multicollision CID⁶¹. Evidence is found for the presence of at least three isomers with different dissociation thresholds. The pentacoordinate ion (7) is calculated to be the most stable isomer, a noticeable example of pentacoordinate Si^+ . The dissociation energy for the loss of the first CO molecule is $19.7 \text{ kcal mol}^{-1}$ at 0 K, which may be compared with the $\text{SiF}_3^+ - \text{CO}$ dissociation energy⁶⁰ of $42.5 \text{ kcal mol}^{-1}$. In a similar way also SiF_2^{2+} ions undergo stepwise addition of two CO molecules⁶¹. The oxygen-bound isomer, SiF_2OC^+ , is predicted to be $15.7 \text{ kcal mol}^{-1}$ higher in energy with respect to SiF_2CO^+ . The CID spectrum suggests the formation of both of these isomers, whereas only one isomer of $\text{SiF}_2(\text{CO})_2^{2+}$ may be present. SiF^+ was found to be unreactive with CO.



The binding of the CO ligand to SiF_3^+ is peculiar in that the adduct ion cannot undergo any simple elimination reaction other than the back dissociation of CO. At variance with



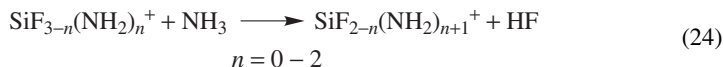
this straightforward behavior, ligands such as H_2O or NH_3 are able to initiate a reaction sequence with SiF_3^+ involving the stepwise addition and elimination of HF. The high thermodynamic stability of HF provides an important driving force for these reactions involving the fission of the strong Si-F bond. The reactivity of $\text{SiF}_{3-n}(\text{OH})_n^+$ ($n = 0-2$) in the stepwise sequence (equation 21) decreases as n increases. However, the reactivity differences are close to cancel if a competing ligand exchange reaction (equation 22 for $n = 1$) is taken into account by using ^{18}O -labelled water as the neutral reagent in a FT-ICR cell⁶². The terminal ion in reaction 21, $\text{Si}(\text{OH})_3^+$, undergoes addition of up to two water molecules at the higher pressures of a SIFT study⁶³, which investigated also the reactions of SiF^+ and $\text{SiF}_2^{+\bullet}$ with H_2O . According to *ab initio* calculations the energy profiles of the HF elimination following the reaction of SiF^+ , $\text{SiF}_2^{+\bullet}$ and $\text{SiF}_{3-n}(\text{OH})_n^+$ ($n = 0-2$) with H_2O show common features. All of them are exothermic, the exothermicity of the $\text{SiF}_{3-n}(\text{OH})_n^+$ reaction decreasing with increasing n , and proceed by way of ion/neutral complexes separated by a transition state for H-transfer, as exemplified by equation 23 for the SiF^+ reaction.



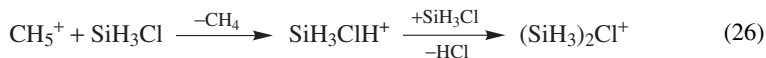
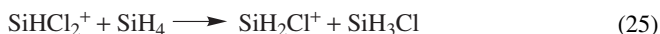
The major pathway of the SiF_3^+ reaction with simple alcohols (ROH , $\text{R} = \text{Me}$, Et) releases R^+ , confirming the ‘Lewis superacid’ character of SiF_3^+ and its ability to generate highly unstable carbocations by interaction with the n electrons of ROH ^{64,65}. A competitive process in the MeOH reaction yields CH_2OH^+ , suggested to arise by a common oxonium intermediate.

The SiF_3^+ reaction with NH_3 initiates a sequence of addition-elimination reactions analogous to the H_2O reaction (equation 24)⁶⁶. Molecular orbital investigations show a similar energy profile with minima corresponding to reactant and product ion-neutral complexes, $[\text{SiF}_{3-n}(\text{NH}_2)_n]^+ \cdot \text{NH}_3$ and $[\text{SiF}_{2-n}(\text{NH}_2)_{n+1}]^+ \cdot \text{HF}$ with the former complex being considerably more stable than the latter. The NH_3 addition reactions followed by HF elimination are predicted to be exothermic for $n = 0, 1$ but endothermic when $n = 2$.

Accordingly, $\text{SiF}(\text{NH}_2)_2^+$ is unreactive with NH_3 in a helium buffer gas whereas the reactivity observed in a FT-ICR cell is assigned to a suprathreshold energy content of the reactant ions formed in a low pressure environment^{65,66}. Rather, under SIFT conditions $\text{SiF}(\text{NH}_2)_2^+$ ions are prone to add up to two NH_3 molecules yielding ultimately $\text{SiF}(\text{NH}_2)_2(\text{NH}_3)_2^+$. This ion was found by theory to have a preferred tetrahedral geometry at Si with the second NH_3 molecule linked by a H-bond to the first one covalently bound to Si. The reaction of SiF_3^+ with MeNH_2 yields both CH_3^+ (resembling the MeOH reaction) and $\text{SiF}_2\text{NHCH}_3^+$ (in analogy to the NH_3 reaction)⁶⁵.



The gas phase ion chemistry in chlorosilanes and in binary mixtures of chlorosilanes or silane/chlorosilane was investigated in order to obtain information both on the thermochemistry and on the reactivity of chlorosilyl ions, $\text{SiH}_n\text{Cl}_{3-n}^+$ ($n = 0-2$)^{67,68}. The Cl^- affinities lie within a range of 1.2 kcal mol⁻¹, to be compared with a span of around 30 kcal mol⁻¹ for the Cl^- affinities of the chloromethyl ions. A similarly narrow range is obtained for the H^- affinities. Besides formal Cl^- and H^- transfer processes, disproportionation reactions take place where a partitioning of atoms occurs as in equation 25. These reactions are suggested to involve chloronium ion intermediates, which are formed by interaction of the vacant orbital on Si in the silicenium ion with the lone pair electrons on the Cl atom of the chlorosilane. Dimethylhalonium ions are well characterized intermediates both in the gas phase and in superacid solution. A first example of disilylchloronium ion, $(\text{SiH}_3)_2\text{Cl}^+$, has been obtained in the gas phase from a reaction sequence parallel to the one known to lead to $(\text{CH}_3)_2\text{Cl}^+$ (equation 26)⁶⁸, where protonation of SiH_3Cl by the strong Brönsted acid CH_5^+ is followed by nucleophilic displacement of HCl by a second SiH_3Cl molecule.

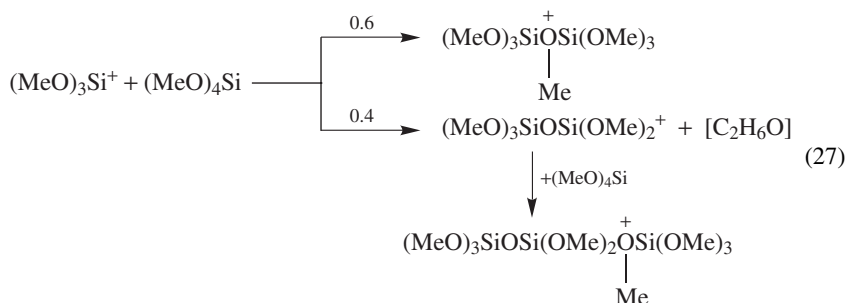


V. REACTIONS OF O- AND S-SUBSTITUTED SILACATIONS

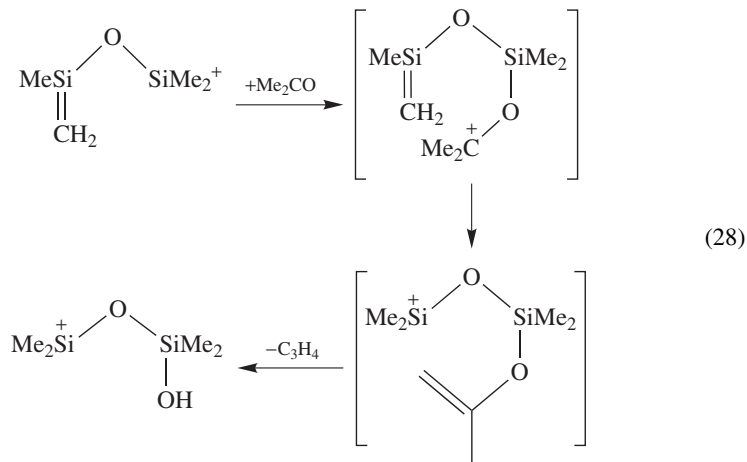
SiOH^+ and SiSH^+ are two simple ions of interest in interstellar chemistry as the conjugate acids of SiO and SiS. The PA values of these two small molecules have been determined in a SIFT study based on a kinetic bracketing procedure, namely on the dependence of the rate of proton transfer reactions from SiOH^+ and SiSH^+ to reference bases on the PA of the base⁶⁹. SiOH^+ and SiSH^+ were obtained by reactions 2 and 3 and SiSH^+ may be converted into SiOH^+ by reaction with water. A similar reaction mechanism may be responsible for the formation of SiOCH_3^+ from the reaction of SiOH^+ with methanol¹⁴. Whereas insertion and adduct formation are common reactions of SiOH^+ , SiSH^+ was found to react by proton transfer as the only reaction channel with the selected bases. The derived proton affinities at 295 K are 189.3 ± 2.6 kcal mol⁻¹ for SiO and 170.3 ± 2.0 kcal mol⁻¹ for SiS. Oxygen and sulfur are the favored protonation sites, at variance with the carbon analogues CO and CS, as confirmed by

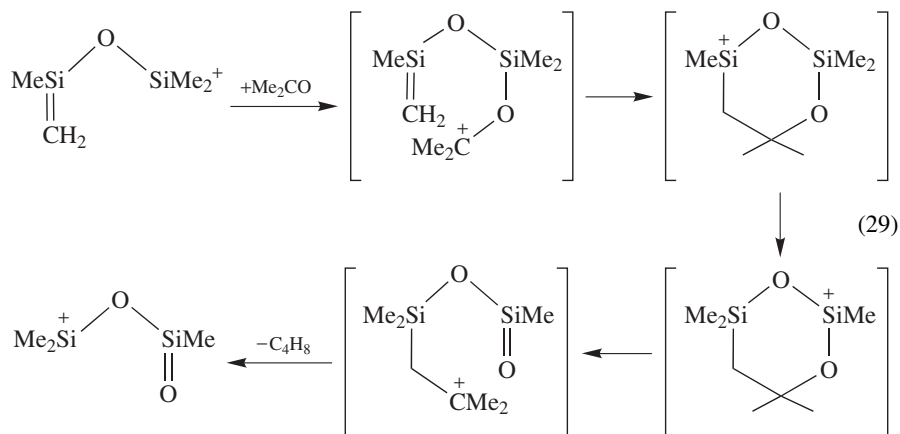
ab initio calculations^{13,69}. *Ab initio* calculations have also been recently reported for $\text{Si}(\text{XH})_3^+$, $\text{HSi}(\text{XH})_2^+$ and $\text{H}_2\text{Si}(\text{XH})^+$ ions ($\text{X} = \text{O}, \text{S}, \text{Se}, \text{Te}$), where the $\text{X} \rightarrow \text{Si}$ $p(\pi)$ donation and the thermodynamic stabilization was found to increase in the order $\text{O} < \text{S} < \text{Se} < \text{Te}$ ⁷⁰.

The ion chemistry of tetraalkoxysilanes is relevant to plasma processes. FT-ICR studies have shown a drive towards the growth of $-\text{Si}-\text{O}-\text{Si}-$ units⁷¹. For example, the reaction of $\text{Si}(\text{OMe})_3^+$, the major fragment ion from the EI ionization of $(\text{MeO})_4\text{Si}$, leads to an adduct ion and to an addition–elimination product which undergoes further addition of $(\text{MeO})_4\text{Si}$ (equation 27)^{71b,72}.



The EI ionization of $(\text{Me}_3\text{Si})_2\text{O}$ yields two major fragment ions, $\text{Me}_3\text{SiOSiMe}_2^+$ and $\text{CH}_2=\text{Si}(\text{Me})\text{OSiMe}_2^+$, whose reactions with water and acetone have been studied by FT-ICR⁷³. Whereas $\text{Me}_3\text{SiOSiMe}_2^+$ yields a stable adduct with acetone, $\text{CH}_2=\text{Si}(\text{Me})\text{OSiMe}_2^+$ reacts by addition–elimination mechanisms as illustrated in equations 28 and 29, on the basis of experiments with isotopically labelled acetone. It is noteworthy that the 1,3-methyl transfer from silicon to silicon, a step in sequence 29, appears to be a facile feature at variance with the chemistry of the carbon analogues^{73b}.





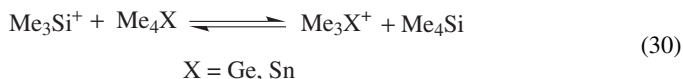
SiOH^+ , SiOCH_3^+ , and Si(OH)_3^+ and their hydrates were observed in the ionic flame chemistry of methane–oxygen mixtures doped with Me_3SiH , thus showing the existence of ions that were the topic of fundamental studies in real systems such as flames⁷⁴. In this environment the presence of SiO , by far the dominant gaseous silicon species, plays a role in the ion chemistry. For example, the likely source of SiOCH_3^+ ions, which are known to be formed by the above-mentioned reaction of SiOH^+ with methanol, is due to a methyl cation transfer from CH_3CO^+ , a major ion present in the flame, to SiO . The silicon ion chemistry in flames is dominated as usual by the strong drive towards Si-O bond formation and by the tendency of Si to become tetracoordinate. Only few carbonaceous ions have been observed, e.g. SiC_2H_3^+ and SiC_3H_5^+ .

VI. REACTIONS OF $\text{SiC}_x\text{H}_y^{+(\bullet)}$ IONS

Depending on the number of hydrogen atoms, $\text{SiC}_x\text{H}_y^{+(\bullet)}$ species will be either radical cations, $\text{SiC}_x\text{H}_y^{+\bullet}$ (y an even number), or even-electron ions, SiC_xH_y^+ (y an odd number).

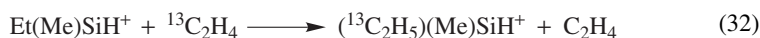
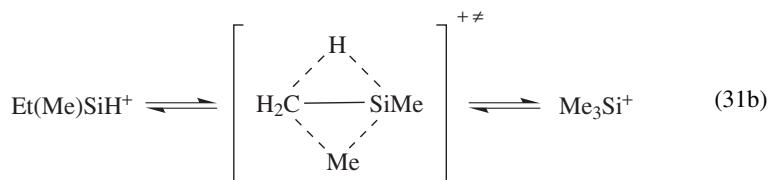
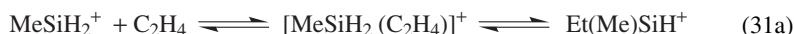
A. Ion Chemistry in Me_4X ($\text{X} = \text{Si}, \text{Ge}, \text{Sn}$)

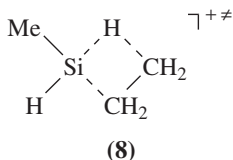
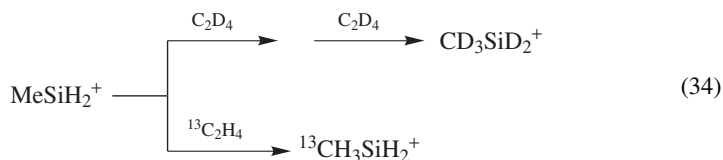
The EI or CI ionization of tetramethylsilane (TMS) is used as a source of Me_3Si^+ ions⁷⁵. The ion chemistry of TMS, also relevant to the plasma processes for the production of silicon carbide films⁷⁶, shows that MeSiH_2^+ and MeSi^+ ions, formed by dissociative ionization of TMS besides the dominant Me_3Si^+ species, react with TMS to form Me_3Si^+ . In a high pressure (0.2 Torr) ion source, Me_3Si^+ ions associate with TMS to yield Me_7Si_2^+ . The reaction of Me_3Si^+ with Me_4X ($\text{X} = \text{Ge}, \text{Sn}$) occurs by a formal Me^- transfer process according to equation 30⁷⁷.



B. Ion–Molecule Reactions of $R_{3-x}SiH_x^+$ as Probes of Ion Structures and Interconversion Pathways

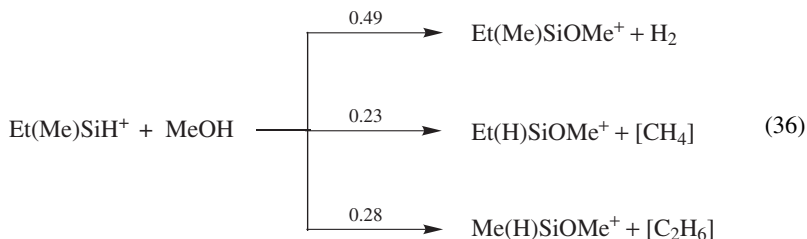
Reactivity studies using isotopically labelled reagents in combination with CAD mass spectrometry have provided diagnostic methods to distinguish between isomeric forms. A general type of rearrangement effecting the interconversion of $RSiMe_2^+$ and $R(H)SiEt^+$ has been suggested to involve a concerted 1,2-hydrogen/1,2-methyl migration^{9,78}, although attempts at locating such a transition state have so far been unsuccessful⁷⁹. The stepwise sequence described in equation 31 accounts for both the CAD behavior of isomeric Me_3Si^+ and $Et(Me)SiH^+$ ions and the exchange reactions of $MeSiH_2^+$ with labelled ethylene. Reaction 31a describes an overall process of olefin insertion/ β -hydrogen migration that is ubiquitous for transition metal systems (transition state **8**). The reversibility of equation 31a accounts for the H/D exchange of the silyl hydrogens of $MeSiH_2^+$ with C_2D_4 . The same kind of process explains also the displacement of unlabelled ethylene with ethylene- $^{13}C_2$ by $Et(Me)SiH^+$ ions (equation 32) and the exclusively single H/D exchange of Me_2SiH^+ with C_2D_4 (equation 33). Remarkably, however, also the methyl group of $MeSiH_2^+$ is involved in an exchange with C_2D_4 and ethylene- $^{13}C_2$ (equation 34), which is ascribed to the overall reversible mechanism depicted in equation 31a,b. CAD results suggest that Me_3Si^+ (the lowest energy isomer) and $Et(Me)SiH^+$ ions interconvert upon multiple low-energy collisions. The potential energy surface for ethylene elimination from Me_3Si^+ and $Et(Me)SiH^+$ has been characterized by *ab initio* computations^{78–80} and used to discuss the translational energy distribution of the fragments of the unimolecular dissociation⁷⁹. Me_3Si^+ and $Et(Me)SiH^+$ do not equilibrate prior to dissociation at variance with Me_2SiH^+ and $EtSiH_2^+$ which show the same translational energy distribution and product ratios⁷⁹. The isomerization of $EtSiH_2^+$ to the more stable isomer, Me_2SiH^+ , has been probed by reaction with C_2D_4 . The reaction of $EtSiH_2^+$ leads to seven H/D exchanges, by a similar process to the one described by equation 32, whereas Me_2SiH^+ exchanges only a single hydrogen (equation 33)⁸¹. The detailed mechanism by which these reactions take place has been analyzed by *ab initio* calculations⁸². The existence of a significant barrier for the isomerization of $EtSiH_2^+$ to Me_2SiH^+ , which is slow unless activated by collisions, has been confirmed by calculations, showing, however, that the barrier lies below the energy level of SiH_3^+ and C_2H_4 , the products of the lowest energy dissociation pathway^{82,83}. Also in this case the calculations predict that the isomerization of $EtSiH_2^+$ to Me_2SiH^+ occurs in a stepwise manner rather than by synchronous 1,2-hydrogen/1,2-methyl migration⁷⁸.





Tritiated Et_2SiH^+ ions have been obtained by the β -decay of tritiated diethylsilane, $\text{Et}_2\text{SiT}^{84}$, exploiting a nucleogenic method for the generation of cations^{85–87}. Ion–molecule reactions with gaseous benzene have been used to gain information about their unimolecular reactions. The vibrational excess energy typical of the nucleogenic formation process⁸⁷ of Et_2SiH^+ allows its dissociation by loss of ethylene, a process that is less energy-demanding than the rearrangement to the more stable Me_2SiEt^+ isomer. A fraction of the so-formed EtSiH_2^+ ions is sufficiently excited to isomerize to Me_2SiH^+ , as testified by the neutral products obtained by addition to benzene.

Specific ion–molecule reactions with methanol and isotopically labelled ethylene have been used as probes of the ion structures resulting from rearrangement of incipient α -silyl-substituted carbenium ions^{9,88}. In fact, these neutral reagents are known to discriminate among isomeric silicenium ions. For example, nascent $\text{Me}_2\text{Si}(\text{H})\text{CH}_2^+$ ions formed by the $\text{CH}_5^+/\text{C}_2\text{H}_5^+$ reaction with $\text{Me}_2\text{Si}(\text{H})\text{CH}_2\text{Cl}$ in an FT-ICR cell undergo competitive 1,2-H and 1,2-Me migration yielding Me_3Si^+ and $\text{Et}(\text{Me})\text{SiH}^+$, respectively. These two isomers react with methanol by different addition–elimination pathways, besides a minor addition process, as described by equations 35 and 36. Alternatively, Me_3Si^+ is inert towards labelled ethylene, whereas $\text{Et}(\text{Me})\text{SiH}^+$ reacts with ethylene-¹³ C_2 according to equation 32. Reactions 35 and 36 presumably involve an intermediate oxonium ion that may either be stabilized or undergo the listed fragmentation processes and describe the general behaviour of alkyl- and phenyl-substituted silicenium ions in their reaction with methanol. The reactivity pattern that was obtained from the nascent α -silyl-substituted carbenium ions that were considered in this study suggested the following relative migratory aptitude: phenyl > hydrogen \gg methyl.



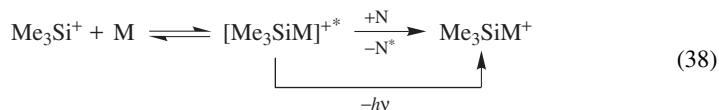
The reaction with methanol has also been used to characterize the ionic species from the protonation of vinyltrimethylsilane in radiolytic experiments⁵ at atmospheric pressure. In this pressure range the intermediate oxonium ions are stable against dissociation and are deprotonated to yield methyl ethers whose structure is indicative of the ionic precursor. Thus, the formation of $\text{Me}_2\text{CHSiMe}_2\text{OMe}$ suggests protonation at the β -carbon of the vinyl group of $\text{CH}_2=\text{CHSiMe}_3$, followed by 1,2-Me migration on the so-formed α -silylcarbenium ion, whereas $\text{MeOCH}_2\text{CH}_2\text{SiMe}_3$ is suggested to derive from the MeOH reaction with the β -silylcarbenium ion, $\text{Me}_3\text{SiCH}_2\text{CH}_2^+$ or its bridged isomer⁸⁹.

C. R_3Si^+ : Reactions with n-Bases

In the previous section the reaction of $\text{R}_{3-x}\text{SiH}_x^+$ ions, such as Me_3Si^+ and $\text{Et}(\text{Me})\text{SiH}^+$, with methanol was reported to give addition and addition/elimination products in the low-pressure gas phase environment typical of FT-ICR experiments (10^{-7} – 10^{-8}). A third reaction pathway appears when using highly basic neutral reagents which are able to abstract a proton from the reagent silicenium ion. Equation 37 shows the proton transfer process that is observed as an efficient reaction when Me_3Si^+ reacts with amines with $\text{PA} \geq 228 \text{ kcal mol}^{-1}$. The point of major interest in this reaction is the neutral silene formed, $\text{Me}_2\text{Si}=\text{CH}_2$, for which a PA value of $228 \pm 2 \text{ kcal mol}^{-1}$ has been obtained from ICR bracketing experiments based on the kinetics of deprotonation of its conjugate acid, Me_3Si^+ , by bases of varying PA⁹⁰. The PA values experimentally obtained for $\text{Me}_2\text{Si}=\text{CH}_2$ and fluoro-substituted analogues have been used in thermochemical cycles to calculate the strength of the $\text{Si}=\text{C}$ π bond.



At the intermediate pressures (0.1–5 Torr) typical of CI-MS, Me_3Si^+ ions have been found to give Me_3SiM^+ as major product with various n-bases M, such as alcohols, ethers, ketones, amines and halogenoalkanes^{75,91–93}. This feature together with the formation of structurally informative fragment ions makes Me_3Si^+ a valuable reagent ion in CI-MS^{91,92}. Whereas Me_3SiM^+ ions may be formed by a termolecular process under typical CI conditions where the primarily excited adduct ion can dissipate its excess energy by unreactive collisions with the bulk gas (N) at relatively high pressure, at the low ICR pressures the association mechanism is by radiative emission (equation 38)⁹⁴. Accordingly, the association efficiency was found to increase with the bond dissociation energy and with an increasing number of degrees of freedom of the adduct ion⁹⁵.



The formation of Me_3Si^+ adducts with polyfunctional molecules raises the question of which is the site of addition. CAD mass spectra of the Me_3Si^+ adducts with monosubstituted aromatic compounds suggest that silylation occurs predominantly at the heteroatom of PhOH , PhNO_2 , PhCN and PhCOMe ⁹⁶. Similarly, the high affinity of silicon for oxygen directs the attack of Me_3Si^+ at the nitro groups of 2,4,6-trinitrotoluene and 1,3,5-trinitro-1,3,5-triazacyclohexane yielding adducts and fragment ions that are an easily recognizable feature for these common explosives⁹⁷. The difference in stability of the Me_3Si^+ adducts with *cis*- and *trans*-1,2- and -1,4-cyclohexanediols and -cyclopentane-diols, which arises

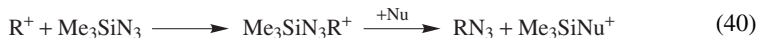
from the formation of intramolecular hydrogen bonding, has a direct influence on an ensuing dehydration process^{9,98}.

In high pressure mass spectrometry (HPMS: 0.1–5 Torr), association reactions have been studied under conditions where an equilibrium is attained, allowing thermodynamic data to be obtained⁷⁵. For example, the association reactions of R_3Si^+ ($R = Me, Et$) with H_2O have been studied^{99,100}. The $Me_3SiOH_2^+$ adduct shows the same reactivity behavior as protonated trimethylsilanol, in particular with regard to the deprotonation reaction by bases of varying PA. By this bracketing technique the PA value of Me_3SiOH has been determined to be $194 \text{ kcal mol}^{-1}$, about the same value as the one known for Me_3COH ¹⁰¹. A dominant reaction pathway of $Me_3SiOH_2^+$ and related silyloxonium ions is Me_3Si^+ transfer to nucleophiles, whenever the process is thermodynamically allowed. For example, a major Me_3Si^+ transfer process is undergone by disilyloxonium ions, such as $(Me_3Si)_2OH^+$ and $(Me_3Si)_2O(CT_3)^+$, that were obtained by mild protonation of $(Me_3Si)_2O$ by Me_3C^+ in HPMS or by the $(Me_3Si)_2O$ reaction with CT_3^+ ions formed by β -decay of tritium in CT_4 , respectively^{102,103}.

Me_3Si^+ forms stable complexes with a variety of O- and N-bases. Me_3Si^+ association reactions (equation 38) and Me_3Si^+ transfer equilibria (equation 39, where M and N are n-bases) have been characterized thermodynamically by HPMS studies which provided Me_3Si^+ cation affinity (TMSA) scales, namely $-\Delta H^\circ$ of equation 38, for classes of compounds such as oxygen bases and amines^{104,105}. The TMSA values were found to correlate linearly with the PA values of the bases within compounds of the same series. The kinetics for the association of Me_3Si^+ to amines have been determined in a flowing afterglow apparatus at 1 Torr. The rate constants decrease as the number of alkyl groups on nitrogen increases, a trend that goes in the opposite direction to that expected on the basis of relative PA values, which is ascribed to steric effects. With a highly basic amine such as Et_3N , proton transfer competes with the formation of the adduct¹⁰⁶. The gas phase basicities of an extensive series of *m*, *p*-substituted acetophenones towards Me_3Si^+ ($-\Delta G^\circ$ of equation 38) have been the topic of an ICR study, suggesting that the positive charge is formed on the benzylic carbon by Me_3Si^+ bound to the O atom of the carbonyl group, in the same manner as the protonation¹⁰⁷. A linear correlation with the corresponding proton basicities shows a slope of unity, indicating a similar response to the ring substituents in both systems. A detailed analysis of the substituent effects points to a somewhat weaker resonance stabilization by π -donors in the Me_3Si^+ adduct with respect to the protonated species.



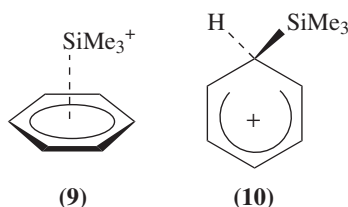
The remarkable ease of Me_3Si^+ transfer, which has gained the Me_3Si^+ ion the term 'super proton'¹⁰⁸, has been exploited in the use of trimethylsilyl azide, Me_3SiN_3 , as a nucleophile to probe gaseous carbenium ions. Nucleophilic attack by the azide end followed by Me_3Si^+ transfer yields neutral products that may be used to characterize the R^+ ion of interest (equation 40, where Nu is a nucleophile)¹⁰⁹.



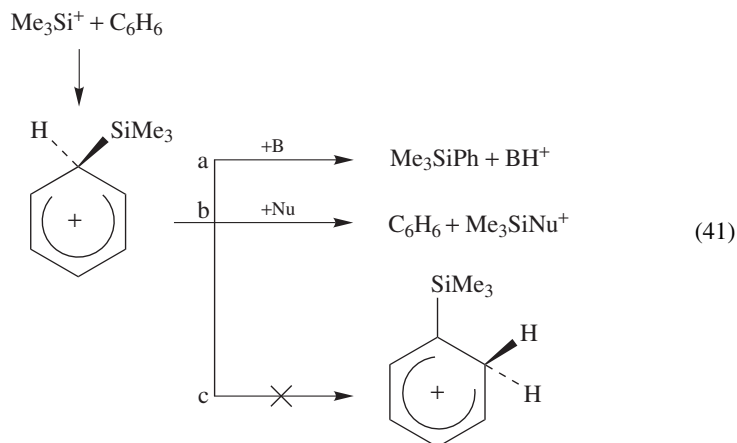
D. R_3Si^+ : Reactions with Aromatic Compounds

Me_3Si^+ yields adduct ions with simple aromatic compounds at pressures in the range 2–5 Torr and Me_3Si^+ transfer equilibria are readily established (equation 39: M, N = benzene, toluene, *o*-, *m*-, *p*-xylene, mesitylene)^{75,110–112}. Me_3Si^+ is also readily

transferred from the aromatic adduct to various oxygen bases and amines. For example, benzene is displaced from the $[\text{benzene} \cdot \text{SiMe}_3]^+$ adduct by H_2O , which led to the conjecture that the Me_3Si^+ adduct with aromatic compounds possessed the structure of a π -complex (9). In fact, in early investigations even moderately strong bases were found to remove the Me_3Si^+ ion rather than the proton, as expected if the $[\text{aromatic} \cdot \text{SiMe}_3]^+$ adduct resembled a σ -complex species (10).

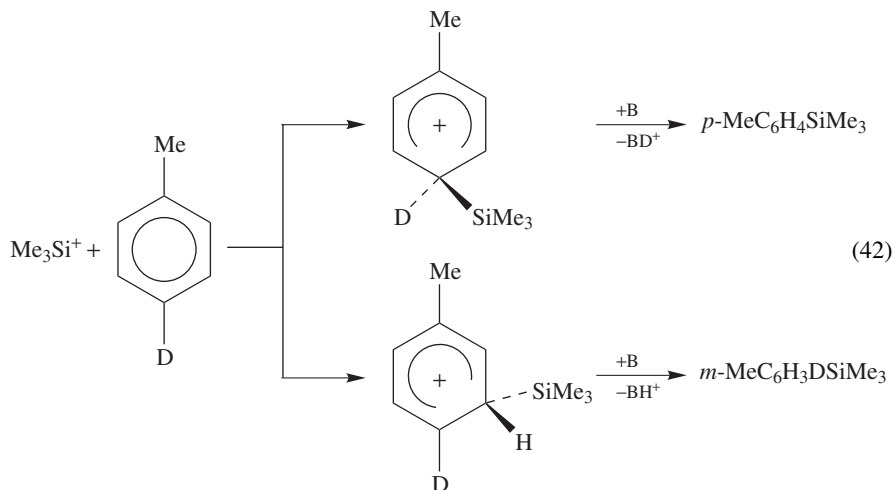


The deprotonation of $[\text{aromatic} \cdot \text{SiMe}_3]^+$ adducts was finally achieved by using strong, sterically encumbered nitrogen bases, such as Et_3N ^{113–117}. Firm evidence for the intermediacy of a σ -complex, finally undergoing deprotonation, was obtained from radiolytic experiments, leading to the neutral silylated products of the aromatic substitution reaction. The detailed mechanism of this reaction (equation 41, drawn for benzene as the aromatic substrate) must, however, take into account the competitive pathways of the σ -complex, which can be either deprotonated or desilylated, depending on the features of the base. Only strong nitrogen bases perform the deprotonation, yielding the silylated product, whereas oxygen bases, even when endowed with an amino functionality and a high basicity (e.g. $\text{Me}_2\text{NCH}_2\text{CH}_2\text{OH}$), remove preferably the silyl group, a reaction driven by the high affinity of oxygen nucleophiles for silicon. Noteworthy is the fact that the σ -complex intermediate is susceptible to the competitive desilylation/deprotonation processes because of the presence of both H and Me_3Si on the tetrahedral carbon. In other words, the σ -complex does not isomerize by 1,2-hydrogen shift (equation 41c), as reported for alkylated arenium ions, to give an isomer which may only undergo deprotonation.



This behavior reflects the high basicity of the silylated carbon and, in fact, protonation of phenylsilane and aryltrimethylsilanes yields the *ipso*-protonated species as the

thermodynamically favored product, as shown both by theory^{118–120} and by experiment. For example, the trimethylsilylation of *p*-MeC₆H₄D shows loss of D in the *p*-trimethylsilyltoluene product and complete retention in the *m*-isomer (equation 42)¹²¹.



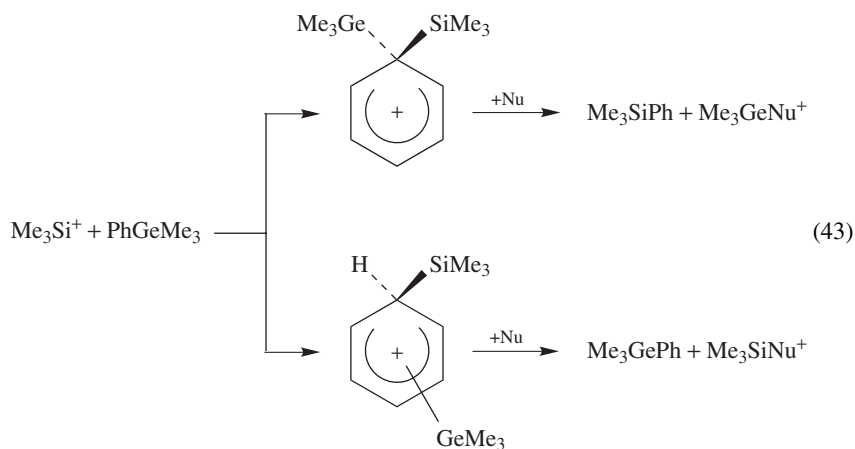
In the framework of equation 41, it may be observed that the desilylation of the intermediate arenium ion competes with the deprotonation process, so that a H/D kinetic isotope effect (KIE) is expected to arise when the Me₃Si⁺ transfer competes with either H⁺ or D⁺ transfer. Indeed, kinetic isotope effects for the formation of silylated products arising from the different rates of H⁺ vs D⁺ transfer have been reported from the reaction of selectively D-labelled toluene and 1,2-diphenylethane or from mixtures of unlabelled and labelled substrates (Table 1)^{121–123}. The kinetic isotope effects listed in Table 1 are the ones reported when the base used is Et₃N. The use of bases of different strength to effect the H⁺ or D⁺ transfer should have an influence on the observed kinetic isotope effect. The role of the base on the values of the KIE was indeed verified in the competitive silylation of CH₃C₆H₅/CD₃C₆D₅ mixtures¹²².

TABLE 1. Kinetic isotope effects in aromatic silylation

Substrate(s)	Products	k_H/k_D	Reference
		1.5	121
$\begin{cases} \text{CH}_3\text{C}_6\text{H}_5 \\ \text{CD}_3\text{C}_6\text{D}_5 \end{cases}$	$\begin{cases} \text{CH}_3\text{C}_6\text{H}_4\text{SiMe}_3 \\ \text{CD}_3\text{C}_6\text{D}_4\text{SiMe}_3 \end{cases}$	1.3	122
$\begin{cases} (\text{C}_6\text{H}_5\text{CH}_2)_2 \\ (\text{C}_6\text{D}_5\text{CH}_2)_2 \end{cases}$	$\begin{cases} \text{C}_6\text{H}_5(\text{CH}_2)_2\text{C}_6\text{H}_4\text{SiMe}_3 \\ \text{C}_6\text{D}_5(\text{CH}_2)_2\text{C}_6\text{D}_4\text{SiMe}_3 \end{cases}$	1.4	123
$\text{C}_6\text{H}_5(\text{CH}_2)_2\text{C}_6\text{D}_5$	$\begin{cases} \text{C}_6\text{D}_5(\text{CH}_2)_2\text{C}_6\text{H}_4\text{SiMe}_3 \\ \text{C}_6\text{H}_5(\text{CH}_2)_2\text{C}_6\text{D}_4\text{SiMe}_3 \end{cases}$	1.5	123

In comparison with Me_3C^+ , Me_3Si^+ behaves as a similarly mild electrophile. However, the considerably more negative ΔS° values for the association of Me_3C^+ with simple aromatic compounds¹¹¹ is indicative of its greater steric encumbrance compared to the Me_3Si group. The lesser steric demand of Me_3Si , which allows, for example, for the formation of trimethylsilylation products of *p*-xylene, is probably due to the longer Si–C bond distance^{113,124}.

The remarkable tendency of the trimethylsilyl group to cleave heterolytically from **10** by transfer to oxygen nucleophiles is responsible for the requirement of an appropriate base to achieve an aromatic silylation reaction. Such a requisite, which holds also for silylation reactions run in solution¹²⁵, may be overcome by placing a substituent on the aromatic substrate with more pronounced leaving ability than the Me_3Si group itself. To this end the Me_3Ge group proved to be a successful choice and the silylation of Me_3GePh was achieved by nucleophilic displacement of Me_3Ge^+ in the absence of any nitrogen base (equation 43)¹²⁶.



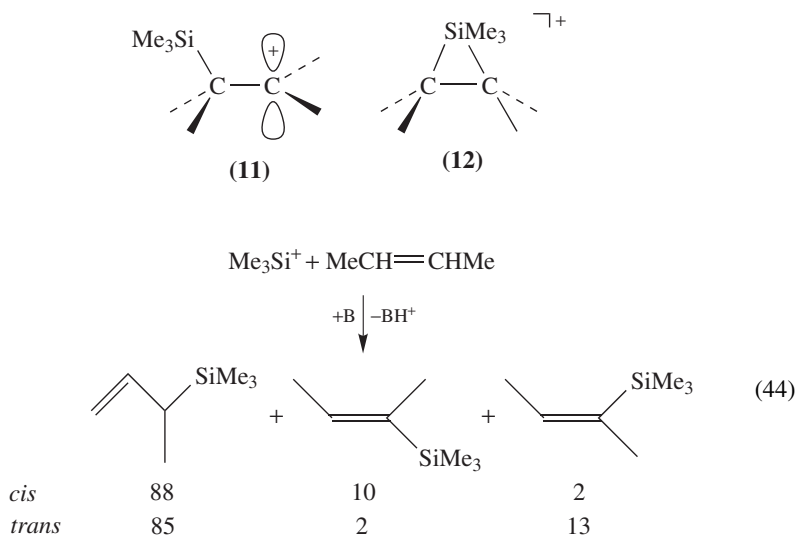
Polycyclic aromatic hydrocarbons such as octamethylbiphenylene and dodecamethylbinaphthylene are also found to react with Me_3Si^+ in CI/MS, giving abundant adduct ions which on CID dissociate by loss of Me_3Si , retaining the charge on the aromatic moiety¹²⁷.

The silylation of simple heteroaromatic compounds by gaseous Me_3Si^+ ions presents the question of which sites, either the ring carbons or the heteroatom, are involved in the electrophilic attack. The product pattern from radiolytic studies has shown that the β -carbons of pyrrole and *N*-methylpyrrole, the α -carbon of thiophene and the oxygen atom of furan are preferentially attacked. This positional selectivity, directed at the positions of highest negative charge, suggests a major role of electrostatic interactions within the ion–molecule encounter¹²⁸.

E. R_3Si^+ : Reactions with Alkenes and Alkynes

The silylation of alkenes by Me_3Si^+ ions has been studied by various approaches, also in view of the considerable interest attached to the ionic products which can benefit from the operation of the so-called β -silyl effect¹²⁹. The Me_3Si^+ reaction with C_2H_4 in a stream of He at 1 Torr leads to $\text{C}_5\text{H}_{13}\text{Si}^+$ adducts, showing the same reactivity as the

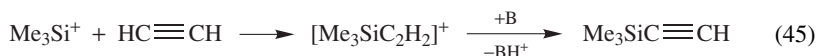
$C_5H_{13}Si^+$ ions from the protonation of $Me_3SiCH=CH_2$. In particular, both species display a Me_3Si^+ transfer reaction towards benzene and methanol¹³⁰. If $C_5D_4H_9Si^+$ ions were obtained from the reaction of C_2D_4 with Me_3Si^+ , the ensuing Me_3Si^+ transfer reaction involved neat cleavage of C_2D_4 as the leaving group, showing that no hydrogen scrambling occurred within the ion. All gained evidence is in favor of a $[Me_3SiC_2H_4]^+$ adduct that may correspond either to an open **(11)** or a silicon-bridged **(12)** structure. In fact, a model ion of a possible third isomer that could be conceivably formed, $Me_2SiCHMe_2^+$, was found to react exclusively by addition with methanol. The $p-\sigma_{CSi}$ hyperconjugation confers on $[Me_3SiC_2H_4]^+$ a stabilization energy of *ca* 40 kcal mol⁻¹ with respect to an unsubstituted ethyl cation. The effect has been confirmed in a later study of the association reactions of Me_3Si^+ with a variety of alkenes in HPMS¹³¹. The association equilibria as a function of temperature allowed the determination of the thermodynamic parameters ΔH° and ΔS° . However, an insight into the features of the adduct ion was provided only by a radiolytic study of the trimethylsilylation of alkenes at atmospheric pressure. In fact, the neutral silylated products were found to retain the stereochemistry of the reactant alkene to a large extent (equation 44)¹³². The conclusion was drawn that either a cyclic species **(12)** was involved, or else in the event of an open β -silylated intermediate **(11)** the $p-\sigma_{CSi}$ hyperconjugation is exerted to the point of preventing free rotation of the formerly C=C double bond.



An ICR study of the TMSA of substituted styrenes has shown a linear correlation with the corresponding PA values¹³³. The analysis of the correlation parameters suggests that there is no effective π -delocalization of positive charge into the aryl π -system, at variance with the behavior of α -phenylethyl cation, an ordinary benzylic carbocation. On this basis, it is suggested that the $[Me_3Si \cdot \text{styrene}]^+$ adduct is either a bridged species **(12)** or endures a strong $p-\sigma_{CSi}$ electronic interaction **(11)**.

The association of Me_3Si^+ with alkynes is complicated by gas phase polymerization in HPMS and only few representative alkynes could be studied¹³⁴. Comparatively, ΔH° and $-\Delta S^\circ$ are larger for the alkenes with respect to the alkynes and the derived β -silicon effect is considerably smaller for vinyl cations. This conclusion is in some disagreement

with the substantial stabilization energies for α - (30 kcal mol⁻¹) and β -Me₃Si-substitution (44 kcal mol⁻¹) in the vinyl cation relative to hydrogen obtained from the appearance energies for metastable peaks for loss of I^{*} from the ionized iodo-derivatives¹³⁵. At variance with HPMS conditions which do not allow an association equilibrium of Me₃Si⁺ with C₂H₂ to be established, a radiolytic study at atmospheric pressure showed the formation of silylated products from various simple alkynes and allene¹³². The typical reaction of C₂H₂ (equation 45) shows that indeed a covalently bound [Me₃Si•C₂H₂]⁺ adduct is formed, which can be deprotonated to give the neutral silylated alkyne. In the alkyne reactions, no stereochemical features aid in elucidating the structure of the adduct, which may be cyclic or open, possibly with a geometrical distortion towards β -silyl hyperconjugation¹³⁶. However, any rearrangement of [Me₃Si•C₂H₂]⁺ into a conceivably more stable silaallyl cation¹³⁷ [Me₂SiCH=CHMe⁺ or Me₂SiC(Me)=CH₂⁺] may be excluded in the high pressure environment.

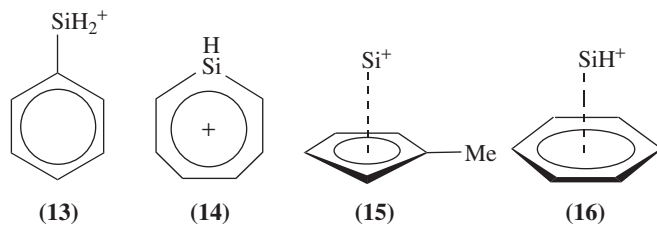


F. Reactions of SiC₆H₇⁺ and Related Ions

The study of the bimolecular reactivity of SiC₆H₇⁺ and related ions from the EI ionization of PhSiH₃ has been a valuable tool in recognizing and characterizing isomeric structures^{137–140}. SiC₆H₇⁺ ions from the EI ionization of PhSiH₃ have been found to consist of at least two isomers, a reactive (equation 46) and an unreactive component with respect to an addition–elimination process with the precursor itself¹³⁷.

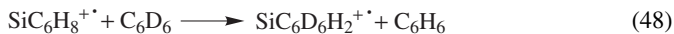
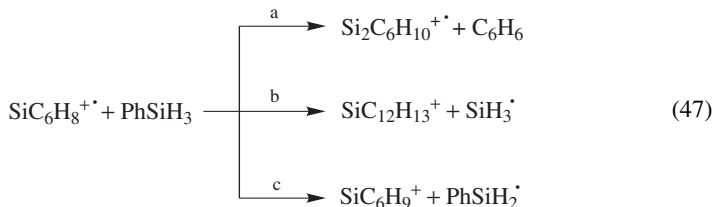


Alternatively, the reactive isomer could be formed by hydride abstraction from PhSiH₃ by ionic reagents such as CH₂F⁺, C₇H₇⁺, and CF₃⁺. In analogy to the well-known carbon analogues, namely the C₇H₇⁺ isomers corresponding to the benzyl cation and the more stable tropylium ion, phenylsilyl cation **13** was suggested to be the reactive species and silacycloheptatrienyl cation **14** to be the inert component. The reactive isomer was found to engage in a hydride transfer equilibrium with 2-methylbutane, which allowed one to establish a H⁻ affinity value of 230 kcal mol⁻¹ for the phenylsilyl cation. Theoretical calculations by Nicolaides and Radom provided quantitative agreement with the experimental H⁻ affinity of the phenylsilyl cation, which was found to lie lower in energy with respect to silacycloheptatrienyl cation, quite in contrast with the carbon analogues¹⁴¹. Moreover, among the examined SiC₆H₇⁺ isomers the energetically favored one is neither **13** nor **14** but (η^5 -methylcyclopentadienyl)-silylium cation (**15**), which is therefore suggested as a likely candidate for the unreactive species. A high degree of bond reorganization is required for the formation of **15** from ionized PhSiH₃, though. The structure of the unreactive SiC₆H₇⁺ isomer has been reexamined in a recent experimental and theoretical study¹⁴⁰. Whereas thermal ‘unreactive’ SiC₆H₇⁺ ions do not react with benzene-d₆¹³⁹, vibrationally excited ions were found to undergo SiH⁺ transfer to C₆D₆, indicating a distinct SiH⁺ unit which may undergo displacement. Furthermore, the same unreactive species submitted to low energy CID give SiH⁺ and SiC₆H₅⁺ as dissociation products. These combined pieces of evidence led to the suggestion that ‘unreactive’ SiC₆H₇⁺ may in fact correspond to η^6 -C₆H₆•SiH⁺ (**16**), an isomer close in energy to silacycloheptatrienyl cation^{140,141}. A pathway for its formation has been proposed by



computations to proceed by 1,2-H-migration from Si to C in ionized PhSiH₃, leading first to C₆H₆SiH₂⁺, followed by loss of a hydrogen atom from silicon.

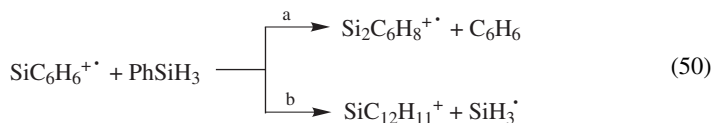
The formation of two SiC₆H₈⁺ isomers from the EI ionization of PhSiH₃ is inferred from their reactivity within PhSiH₃/benzene-d₆ mixtures^{139–140}. The transfer of a SiH₂⁺ unit that is implied in equation 47a is also observed when ionized PhSiH₃ reacts with benzene-d₆ (equation 48) to yield an ion, C₆D₆SiH₂⁺, that is in turn able to transfer SiH₂⁺ to neutral PhSiH₃ (equation 49). Noteworthy is that a reaction of C₆D₆SiH₂⁺ corresponding to equation 47b is not observed. Moreover, whereas the SiC₆H₈⁺ ion population from EI ionization of PhSiH₃ may undergo SiH₂⁺ transfer with benzene, SiC₆H₈⁺ ions formed by photoionization do not. The latter ions are expected to retain the structure of the molecular ion, since any intramolecular rearrangement should be allowed only to those vibrationally hot ions formed by EI ionization. Reaction 47b was assigned to these unrearranged PhSiH₃⁺ species, which are otherwise unreactive with benzene¹⁴⁰. A third reaction pathway of SiC₆H₈⁺ ions is proton transfer to neutral PhSiH₃ (equation 47c).



(PhSiH₃)₂ dimers were photoionized and photoexcited in a study aimed at comparing the bimolecular reaction of ionized PhSiH₃ with neutral PhSiH₃ with the intracuster reaction¹⁴². The absorption in the near-IR region corresponding to a charge resonance transition of the dimer cation does activate the formation of SiC₁₂H₁₃⁺ and Si₂C₆H₁₀⁺⁺ besides the monomer ion SiC₆H₈⁺. The two product ions are the same as those obtained from the bimolecular reaction (equation 47a,b) and their different relative yields can be traced to the fact that their formation is ascribed to two distinct SiC₆H₈⁺ isomers¹³⁹.

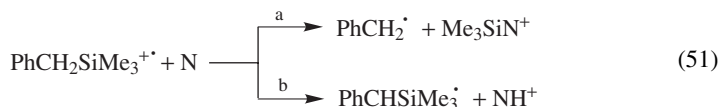
The ion–molecule chemistry of SiC₆H₆⁺ ions from the EI ionization and fragmentation of phenylsilane shows the existence of three isomers¹³⁹, which have been characterized theoretically¹⁴³. Only part of the SiC₆H₆⁺ ions react with PhSiH₃ according to equation 50a,b. The unreactive isomer has been assigned a seven-member ring structure. A clue to the identification of the other two isomers comes from the observed reactivity in PhSiH₃/benzene-d₆ mixtures, as reported for SiC₆H₈⁺ ions. In fact, the SiC₆H₆⁺

reaction with C_6D_6 yields $SiC_6D_6^{+\bullet}$ ions, which react further with $PhSiH_3$ by a second formal $Si^{+\bullet}$ transfer process (equation 50a). $SiC_6D_6^{+\bullet}$ ions are otherwise unreactive with respect to equation 50b. Therefore, the $SiC_6H_6^{+\bullet}$ ions that react according to equation 50a have a different structure from those reacting according to equation 50b. The gathered evidence favors a $C_6H_6-Si^{+\bullet}$ complex structure³³ for the ions undergoing $Si^{+\bullet}$ transfer (50a) whereas a $C_6H_5-SiH^{+\bullet}$ structure is proposed for the ions leading to $SiC_{12}H_{11}^{+\bullet}$ (50b). The product ions of reaction 50b have been suggested to correspond to Ph_2SiH^+ .



G. Reactions of Organosilane Radical Cations

The bimolecular reactivity of ionized organosilanes has received little attention in the gas phase, where the major focus has been on the unimolecular decomposition or rearrangement processes of these species. This situation is quite in contrast with several studies performed in condensed phases on the mechanistic and synthetic aspects of the reactivity of organosilane radical cations. A notable exception is the characterization of $SiC_6H_8^{+\bullet}$ isomers via their ion–molecule gas phase chemistry reported in the previous section. Recently, the bimolecular reactivity of organosilane radical cations of the general formula $RSiMe_3^{+\bullet}$ towards oxygen and nitrogen bases has been examined¹⁴⁴. The two major processes involve either Me_3Si^+ or H^+ transfer to the neutral (N), as exemplified by the reaction of the benzyltrimethylsilane radical cation (equation 51a and 51b, respectively). The onset for Me_3Si^+ transfer is close to its thermochemical threshold, which is accounted for by the negligible activation barriers involved in thermoneutral Me_3Si^+ transfer between n-bases, as is well established for the corresponding H^+ transfer process. In addition to H^+ and Me_3Si^+ transfer, ionized $Ph(CH_2)_2SiMe_3$ displays a homolytic bond cleavage process not shown by the lower homologue (equation 52). The reason lies in the high stability of the $PhCHCH_2SiMe_3^+$ product ion where the positively charged benzylic carbon gains additional stabilization by the β -silyl group.

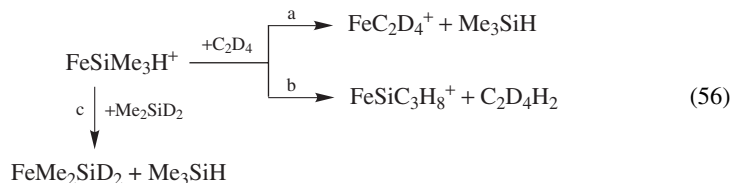


Ions containing a Si–C double bond can be generated in the gas phase via dissociative ionization of silacyclobutane derivatives. The silene radical cation $[Me_2Si=CH_2]^{+\bullet}$ has been obtained by EI ionization of 1,1-dimethyl-1-silacyclobutane¹⁴⁵. The reactions with ethylene-d₄ and propene are suggested to occur by way of a [2 + 2] cycloaddition, leading to a cyclic four-membered intermediate.

VII. REACTIONS OF TRANSITION METAL-CONTAINING SILACATIONS

Gas phase ion chemistry has provided the means for obtaining labile intermediates that are thought to play a relevant role in solution chemistry. An example is given by cationic iron–silene and iron–silylene complexes that have been studied as model systems in

$[\text{Fe} \cdot \text{silane}]^+$ complexes have been formed by the reaction of FeCO^+ with silanes of the general formula $\text{Me}_x\text{SiH}_{4-x}$ ($x = 0-4$) by CO displacement¹⁴⁸. Ligand displacement reactions of $[\text{Fe} \cdot \text{silane}]^+$ with $\text{Me}_x\text{SiH}_{4-x}$ enabled an order of relative silane binding energies to be derived. Similarly, $[\text{Fe} \cdot \text{silane}]^+$ ions undergo a major ligand displacement process with ethylene or with silanes (equation 56a and 56c). It is noteworthy that no evidence for any H/D exchange process was obtained in the reaction with ethylene-d₄ or with deuteriated silanes (equation 56), suggesting the $[\text{Fe} \cdot \text{silane}]^+$ complex to resemble a Fe^+ /silane adduct rather than an insertion species (e.g. $[\text{Me}_3\text{SiH} \cdot \text{Fe}^+]$ vs $\text{HFe}(\text{SiMe}_3)^+$ for Me_3SiH as exemplary silane). Regarding the structure of the $[\text{Fe} \cdot \text{silane}]^+$ complexes, the activation of ethane loss in reaction 56b is consistent with Fe^+ interacting with a Si–H bond, forming ion **22**.



VIII. ACKNOWLEDGMENTS

The author is grateful to Prof. F. Cacace for his helpful comments and to Dr. A. Di Marzio for his kind assistance.

IX. REFERENCES

1. S. T. Graul and R. R. Squires, *Mass Spectrom. Rev.*, **7**, 263 (1988).
2. A. G. Marshall, *Mass Spectrom. Rev.*, **17**, 1 (1998).
3. A. G. Marshall, *Acc. Chem. Res.*, **18**, 316 (1985).
4. J. F. J. Todd, *Mass Spectrom. Rev.*, **10**, 3 (1991).
5. F. Cacace, *Acc. Chem. Res.*, **21**, 215 (1988).
6. (a) J. B. Lambert and Y. Zhao, *Angew. Chem., Int. Ed. Engl.*, **36**, 400 (1997).
(b) P. v. R. Schleyer, *Science*, **275**, 39 (1997).
(c) C. A. Reed, *Acc. Chem. Res.*, **31**, 325 (1998).
7. (a) M. J. McEwan, in *Advances in Gas Phase Ion Chemistry* (Eds. N. G. Adams and L. M. Babcock), Vol. 1, JAI Press, Greenwich, Conn., 1992, pp. 1–42.
(b) N. G. Adams and N. D. Fisher, in *Advances in Gas Phase Ion Chemistry* (Eds. N. G. Adams and L. M. Babcock), Vol. 3, JAI Press, Greenwich, Conn., 1998, pp. 81–123.
8. H.-H. Bükér, H.-F. Grützmacher, M. E. Crestoni and A. Ricci, *Int. J. Mass Spectrom. Ion Processes*, **160**, 167 (1997).
9. N. Goldberg and H. Schwarz, in *The Chemistry of Organic Silicon Compounds* (Eds. Z. Rappoport and Y. Apeloig), Chap. 18, Wiley, Chichester, 1998, pp. 1105–1142.
10. (a) D. K. Bohme, *Int. J. Mass Spectrom. Ion Processes*, **100**, 719 (1990).
(b) D. K. Bohme, in *Advances in Gas Phase Ion Chemistry* (Eds. N. G. Adams and L. M. Babcock), Vol. 1, JAI Press, Greenwich, Conn., 1992, pp. 225–270.
11. P. B. Armentrout, in *Advances in Gas Phase Ion Chemistry* (Eds. N. G. Adams and L. M. Babcock), Vol. 1, JAI Press, Greenwich, Conn., 1992, pp. 83–119.
12. J. Glosik, P. Zakouril and W. Lindinger, *J. Chem. Phys.*, **103**, 6490 (1995).
13. R. Srinivas, D. Sulzle, W. Koch, C. H. DePuy and H. Schwarz, *J. Am. Chem. Soc.*, **113**, 5970 (1991).
14. S. Wlodek, A. Fox and D. K. Bohme, *J. Am. Chem. Soc.*, **109**, 6663 (1987).
15. J. Hrusak, D. K. Bohme, S. Wlodek and H. Schwarz, *J. Phys. Chem.*, **96**, 5355 (1992).
16. A. I. Gonzalez, D. C. Clary and M. Yanez, *Theor. Chem. Acc.*, **98**, 33 (1997).

17. N. L. Ma, B. J. Smith, J. A. Pople and L. Radom, *J. Am. Chem. Soc.*, **113**, 7903 (1991).
18. S. Wlodek, C. F. Rodriguez, M. H. Lien, A. C. Hopkinson and D. K. Bohme, *Chem. Phys. Lett.*, **143**, 385 (1988).
19. S. Wlodek and D. K. Bohme, *J. Am. Chem. Soc.*, **110**, 2396 (1988).
20. J. R. Flores and J. Largo-Cabrerizo, *J. Mol. Struct. (THEOCHEM)*, **183**, 17 (1989).
21. N. Goldberg, M. Hiraqi, J. Hrusak and H. Schwarz, *J. Phys. Chem.*, **97**, 10687 (1993).
22. O. Parisel, M. Hanus and Y. Ellinger, *J. Phys. Chem.*, **100**, 2926 (1996).
23. S. Ye and S. Dai, *J. Mol. Struct. (THEOCHEM)*, **236**, 259 (1991).
24. J. R. Flores, P. Redondo and S. Azpeleta, *Chem. Phys. Lett.*, **240**, 193 (1995).
25. J. Hrusak, D. Schröder, H. Schwarz and S. Iwata, *Bull. Chem. Soc. Jpn.*, **70**, 777 (1997).
26. J. Glosik, P. Zakouril, V. Skalsky and W. Lindinger, *Int. J. Mass Spectrom. Ion Processes*, **149/150**, 499 (1995).
27. E. Herbst, T. J. Millar, S. Wlodek and D. K. Bohme, *Astron. Astrophys.*, **222**, 205 (1989).
28. R. Srinivas, D. Sülzle and H. Schwartz, *Chem. Phys. Lett.*, **175**, 575 (1990).
29. J. R. Flores, A. Largo-Cabrerizo and J. Largo-Cabrerizo, *J. Mol. Struct. (THEOCHEM)*, **148**, 33 (1986).
30. A. Largo and C. Barrientos, *J. Phys. Chem.*, **98**, 3978 (1994).
31. A. E. Ketvirtis, D. K. Bohme and A. C. Hopkinson, *J. Mol. Struct. (THEOCHEM)*, **313**, 1 (1994).
32. J. Glosik, P. Zakouril and W. Lindinger, *Int. J. Mass Spectrom. Ion Processes*, **145**, 155 (1995).
33. D. K. Bohme, S. Wlodek and H. Wincel, *J. Am. Chem. Soc.*, **113**, 6396 (1991).
34. P. Redondo, A. Saguillo, C. Barrientos and A. Largo, *J. Phys. Chem. A*, **103**, 3310 (1999).
35. R. C. Dunbar, *Mass Spectrom. Rev.*, **11**, 309 (1992).
36. R. C. Dunbar, G. T. Uechi, D. Solooki, C. A. Tessier, W. Youngs and B. Asamoto, *J. Am. Chem. Soc.*, **115**, 12477 (1993).
37. K. A. Nguyen, M. S. Gordon and K. Raghavachari, *J. Phys. Chem.*, **98**, 6704 (1994).
38. J. Moc, K. A. Nguyen and M. S. Gordon, *Organometallics*, **15**, 5391 (1996).
39. J. S. Patrick, T. Pradeep, H. Luo, S. Ma and R. G. Cooks, *J. Am. Soc. Mass Spectrom.*, **9**, 1158 (1998).
40. A. Luna, O. Mò and M. Yanez, *J. Mol. Struct. (THEOCHEM)*, **310**, 135 (1994).
41. W. D. Reents, Jr. and M. L. Mandich, *J. Chem. Phys.*, **93**, 3270 (1990).
42. K. Hiraoka, J. Katsuragawa and A. Minamitsu, *Chem. Phys. Lett.*, **267**, 580 (1997).
43. A. Fox and D. K. Bohme, *Chem. Phys. Lett.*, **187**, 541 (1991).
44. W. Koch and M. C. Holthausen, *Int. J. Mass Spectrom. Ion Processes*, **127**, 183 (1993).
45. M. C. Holthausen, D. Schröder, W. Zummack, W. Koch and H. Schwarz, *J. Chem. Soc., Perkin Trans. 2*, 2389 (1996).
46. I. Haller, *J. Phys. Chem.*, **94**, 4135 (1990).
47. L. Operti, R. Rabezzana, G. A. Vaglio and P. Volpe, *J. Organomet. Chem.*, **509**, 151 (1996).
48. A. Tachibana, S. Kawachi, N. Yoshida, T. Yamabe and K. Fukui, *J. Mol. Struct.*, **300**, 501 (1993).
49. G. Cetini, L. Operti, R. Rabezzana, G. A. Vaglio and P. Volpe, *J. Organomet. Chem.*, **519**, 169 (1996).
50. L. Operti, M. Splendore, G. A. Vaglio, A. M. Franklin and J. F. J. Todd, *Int. J. Mass Spectrom. Ion Processes*, **136**, 25 (1994).
51. M. Castiglioni, L. Operti, R. Rabezzana, G. A. Vaglio and P. Volpe, *Int. J. Mass Spectrom.*, **179/180**, 277 (1998).
52. K. P. Lim and F. W. Lampe, *Int. J. Mass Spectrom. Ion Processes*, **92**, 53 (1989).
53. (a) P. Antoniotti, C. Canepa, L. Operti, R. Rabezzana, G. Tonachini and G. A. Vaglio, *J. Organomet. Chem.*, **589**, 150 (1999).
(b) P. Antoniotti, C. Canepa, L. Operti, R. Rabezzana, G. Tonachini and G. A. Vaglio, *J. Phys. Chem. A*, **103**, 10945 (1999).
(c) P. Antoniotti, L. Operti, R. Rabezzana, G. A. Vaglio and P. Volpe, *Int. J. Mass Spectrom.*, **190/191**, 243 (1999).
54. (a) Y. Apeloig, M. Karni, A. Stanger, H. Schwarz, T. Drewello and G. Czekay, *J. Chem. Soc., Chem. Commun.*, 989 (1987).
(b) S. G. Wierschke, J. Chandrasekhar and W. L. Jorgensen, *J. Am. Chem. Soc.*, **107**, 1496 (1985).

55. K. A. Reuter and D. B. Jacobson, *Organometallics*, **8**, 1126 (1989).
56. K. Hiraoka, M. Nasu, A. Minamitsu, A. Shimizu, D. Oomori and S. Yamabe, *J. Phys. Chem. A*, **103**, 568 (1999).
57. A. C. Hopkinson and M. H. Lien, *Can. J. Chem.*, **67**, 991 (1989).
58. Y. Ling, R. K. Milburn, A. C. Hopkinson and D. K. Bohme, *J. Am. Soc. Mass Spectrom.*, **10**, 848 (1999).
59. P. Cecchi, M. E. Crestoni, F. Grandinetti and V. Vinciguerra, *Angew. Chem., Int. Ed. Engl.*, **35**, 2522 (1996).
60. A. E. Ketvirtis, V. I. Baranov, D. K. Bohme and A. C. Hopkinson, *Int. J. Mass Spectrom. Ion Processes*, **153**, 161 (1996).
61. A. E. Ketvirtis, V. I. Baranov, A. C. Hopkinson and D. K. Bohme, *J. Phys. Chem. A*, **101**, 7258 (1997).
62. M. E. Crestoni and M. Speranza, *Int. J. Mass Spectrom. Ion Processes*, **130**, 143 (1994).
63. A. E. Ketvirtis, V. I. Baranov, A. C. Hopkinson and D. K. Bohme, *J. Phys. Chem. A*, **102**, 1162 (1998).
64. F. Grandinetti, G. Occhiucci, M. E. Crestoni, S. Fornarini and M. Speranza, *Int. J. Mass Spectrom. Ion Processes*, **127**, 123 (1993).
65. F. Grandinetti, G. Occhiucci, O. Ursini, G. de Petris and M. Speranza, *Int. J. Mass Spectrom. Ion Processes*, **124**, 21 (1993).
66. A. E. Ketvirtis, V. I. Baranov, Y. Ling, A. C. Hopkinson and D. K. Bohme, *Int. J. Mass Spectrom.*, **185/186/187**, 381 (1999).
67. S. Murthy and J. L. Beauchamp, *J. Phys. Chem.*, **96**, 1247 (1992).
68. S. Murthy and J. L. Beauchamp, *J. Phys. Chem.*, **99**, 9118 (1995).
69. A. Fox, S. Wlodek, A. C. Hopkinson, M. H. Lien, M. Sylvain, C. Rodriguez and D. K. Bohme, *J. Phys. Chem.*, **93**, 1549 (1989).
70. C. M. Marchand, U. Pidun, G. Frenking and H. Grützmacher, *J. Am. Chem. Soc.*, **119**, 11078 (1997).
71. (a) M. L. P. da Silva and J. M. Riveros, *Int. J. Mass Spectrom. Ion Processes*, **165/166**, 83 (1997).
(b) J. Holtgrave, K. Riehl, D. Abner and P. D. Haaland, *Chem. Phys. Lett.*, **215**, 548 (1993).
72. M. L. P. da Silva and J. M. Riveros, *J. Mass Spectrom.*, **30**, 733 (1995).
73. (a) D. Leblanc, H. E. Audier and J. P. Denhez, *C. R. Acad. Sci. Paris, Ser. II*, **1**, 195 (1998).
(b) D. Leblanc, H. E. Audier and J. P. Denhez, *J. Mass Spectrom.*, **34**, 969 (1999).
74. J. H. Horton and J. M. Goodings, *Can. J. Chem.*, **70**, 1069 (1992).
75. J. A. Stone, *Mass Spectrom. Rev.*, **16**, 25 (1997).
76. S. McGinnis, K. Riehl and P. D. Haaland, *Chem. Phys. Lett.*, **232**, 99 (1995).
77. A. C. M. Wojtyniak, X. Li and J. A. Stone, *Can. J. Chem.*, **65**, 2849 (1987).
78. R. Bakhtiar, C. M. Holzngel and D. B. Jacobson, *Organometallics*, **12**, 880 (1993).
79. B. B. Willard and S. T. Graul, *J. Phys. Chem. A*, **102**, 6942 (1998).
80. I. S. Ignatyev and T. Sundius, *Organometallics*, **17**, 2819 (1998).
81. R. Bakhtiar, C. M. Holzngel and D. B. Jacobson, *Organometallics*, **12**, 621 (1993).
82. A. E. Ketvirtis, D. K. Bohme and A. C. Hopkinson, *Organometallics*, **14**, 347 (1995).
83. I. S. Ignatyev and T. Sundius, *Organometallics*, **15**, 5674 (1996).
84. T. A. Kochina, D. A. Vrazhnov and I. S. Ignatyev, *J. Organomet. Chem.*, **586**, 241 (1999).
85. F. Cacace, *Adv. Phys. Org. Chem.*, **8**, 79 (1970).
86. V. D. Nefedov, T. A. Kochina and E. N. Sinotova, *Russ. Chem. Rev.*, **55**, 426 (1986).
87. M. Speranza, *Chem. Rev.*, **93**, 2933 (1993).
88. R. Bakhtiar, C. M. Holzngel and D. B. Jacobson, *J. Am. Chem. Soc.*, **114**, 3227 (1992).
89. G. Angelini, Y. Keheyian, G. Laguzzi and G. Lilla, *Tetrahedron Lett.*, **29**, 4159 (1988).
90. C. E. Allison and T. B. McMahon, *J. Am. Chem. Soc.*, **112**, 1672 (1990).
91. D. Clemens and B. Munson, *Org. Mass Spectrom.*, **20**, 368 (1985).
92. (a) R. Orlando, D. P. Ridge and B. Munson, *Org. Mass Spectrom.*, **23**, 527 (1988).
(b) R. Orlando, F. Strobels, D. P. Ridge and B. Munson, *Org. Mass Spectrom.*, **22**, 597 (1987).
93. O. S. Chizhov, V. I. Kadentsev and A. A. Stomakhin, *Org. Mass Spectrom.*, **26**, 757 (1991).
94. (a) R. C. Dunbar, *Int. J. Mass Spectrom. Ion Processes*, **100**, 423 (1990).
(b) R. C. Dunbar, *Mass Spectrom. Rev.* **11**, 309 (1992).
(c) R. C. Dunbar, in *Unimolecular and Bimolecular Ion-Molecule Reaction Dynamics* (Eds. C.-Y. Ng, T. Baer and I. Powis), Chap. 5, Wiley, Chichester, 1994, pp. 279–335.

95. Y. Lin, D. P. Ridge and B. Munson, *Org. Mass Spectrom.*, **26**, 550 (1991).
96. R. Srinivas, A. Rama Devi and G. K. Viswanadha Rao, *Rapid Commun. Mass Spectrom.*, **10**, 12 (1996).
97. K. C. Crellin, M. Widmer and J. L. Beauchamp, *Anal. Chem.*, **69**, 1092 (1997).
98. V. I. Kadentsev, N. G. Kolotyrkina, A. A. Stomakhin and O. S. Chizhov, *Russ. Chem. Bull.*, **45**, 1921 (1996).
99. J. A. Stone, A. C. M. Wojtyniak and W. Wytenburg, *Can. J. Chem.*, **64**, 575 (1986).
100. X. Li and J. A. Stone, *Can. J. Chem.*, **66**, 1288 (1988).
101. R. Orlando, C. Allgood and B. Munson, *Int. J. Mass Spectrom. Ion Processes*, **92**, 93 (1989).
102. X. Li and J. A. Stone, *Can. J. Chem.*, **65**, 2454 (1987).
103. I. S. Ignatyev and T. A. Kochina, *J. Mol. Struct. (THEOCHEM)*, **236**, 249 (1991).
104. A. C. M. Wojtyniak and J. A. Stone, *Int. J. Mass Spectrom. Ion Processes*, **74**, 59 (1986).
105. X. Li and J. A. Stone, *Int. J. Mass Spectrom. Ion Processes*, **101**, 149 (1990).
106. Q.-F. Chen and J. A. Stone, *Int. J. Mass Spectrom. Ion Processes*, **165/166**, 195 (1997).
107. M. Mishima, C. H. Kang, M. Fujio and Y. Tsuno, *Chem. Lett.*, 493 (1992).
108. I. Fleming, *Chem. Soc. Rev.*, **10**, 83 (1981).
109. M. Aschi, M. Attinà and A. Ricci, *Int. J. Mass Spectrom. Ion Processes*, **139**, 59 (1994).
110. A. C. M. Wojtyniak and J. A. Stone, *Int. J. Mass Spectrom. Ion Processes*, **74**, 59 (1986).
111. J. M. Stone and J. A. Stone, *Int. J. Mass Spectrom. Ion Processes*, **109**, 247 (1991).
112. X. Li and J. A. Stone, *Can. J. Chem.*, **70**, 2070 (1992).
113. S. Fornarini, *J. Org. Chem.*, **53**, 1314 (1988).
114. F. Cacace, M. E. Crestoni, S. Fornarini and R. Gabrielli, *Int. J. Mass Spectrom. Ion Processes*, **84**, 17 (1988).
115. F. Cacace, M. Attinà and S. Fornarini, *Angew. Chem., Int. Ed. Engl.*, **34**, 654 (1995).
116. S. Fornarini and M. E. Crestoni, *Acc. Chem. Res.*, **31**, 827 (1998).
117. S. Fornarini, *Mass Spectrom. Rev.*, **15**, 365 (1996).
118. F. Cacace, M. E. Crestoni, G. de Petris, S. Fornarini and F. Grandinetti, *Can. J. Chem.*, **66**, 3099 (1988).
119. C. Maerker, J. Kapp and P. v. R. Schleyer, in *Organosilicon Chemistry II* (Eds. N. Auner and J. Weis), VCH, Weinheim, 1996, pp. 329–359.
120. P. v. R. Schleyer, P. Buzek, T. Müller, Y. Apeloig and H.-U. Siehl, *Angew. Chem., Int. Ed. Engl.*, **32**, 1471 (1993).
121. F. Cacace, M. E. Crestoni and S. Fornarini, *J. Am. Chem. Soc.*, **114**, 6776 (1992).
122. M. E. Crestoni and S. Fornarini, *Angew. Chem., Int. Ed. Engl.*, **33**, 1094 (1994).
123. M. E. Crestoni, S. Fornarini and D. Kuck, *J. Phys. Chem.*, **99**, 3144 (1995).
124. V. I. Kadentsev, N. G. Kolotyrkina, A. A. Stomakhin and O. S. Chizhov, *Russ. Chem. Bull.*, **44**, 1698 (1995).
125. J. A. Olah, T. Bach and G. K. S. Prakash, *J. Org. Chem.*, **54**, 3770 (1989).
126. B. Chiavarino, M. E. Crestoni and S. Fornarini, *Organometallics*, **14**, 2624 (1995).
127. K. K. Laali, *J. Chem. Soc., Perkin Trans. 2*, 1873 (1993).
128. M. E. Crestoni, S. Fornarini and M. Speranza, *J. Am. Chem. Soc.*, **112**, 6929 (1990).
129. H.-U. Siehl and T. Müller, in *The Chemistry of Organic Silicon Compounds* (Eds. Z. Rappoport and Y. Apeloig), Chap. 12, Wiley, Chichester, 1998, pp. 595–701.
130. D. Hajdasz and R. Squires, *J. Chem. Soc., Chem. Commun.*, 1212 (1988).
131. X. Li and J. A. Stone, *J. Am. Chem. Soc.*, **111**, 5586 (1989).
132. B. Chiavarino, M. E. Crestoni and S. Fornarini, *J. Am. Chem. Soc.*, **120**, 1523 (1998).
133. M. Mishima, C. H. Kang, M. Fujio and Y. Tsuno, *Chem. Lett.*, 2439 (1992).
134. W. Zhang, J. A. Stone, M. A. Brook and G. A. McGibbon, *J. Am. Chem. Soc.*, **118**, 5764 (1996).
135. G. A. McGibbon, M. A. Brook and J. K. Terlouw, *J. Chem. Soc., Chem. Commun.*, 360 (1992).
136. H.-U. Siehl, *Pure Appl. Chem.*, **67**, 769 (1995).
137. A. E. Ketvirtis, D. K. Bohme and A. C. Hopkinson, *J. Phys. Chem.*, **98**, 13225 (1994).
138. S. Murthy, Y. Nagano and J. L. Beauchamp, *J. Am. Chem. Soc.*, **114**, 3573 (1992).
139. Y. Nagano, S. Murthy and J. L. Beauchamp, *J. Am. Chem. Soc.*, **115**, 10805 (1993).
140. R. L. Jarek and S. K. Shin, *J. Am. Chem. Soc.*, **119**, 6376 (1997).
141. A. Nicolaidis and L. Radom, *J. Am. Chem. Soc.*, **118**, 10561 (1996).
142. H. Ishikawa, J. Hashimoto and N. Mikami, *J. Phys. Chem. A*, **101**, 9257 (1997).

143. R. Srinivas, J. Hrusak, D. Sülzle, D. K. Bohme and H. Schwarz, *J. Am. Chem. Soc.*, **114**, 2802 (1992).
144. B. Chiavarino, M. E. Crestoni and S. Fornarini, *Organometallics*, **19**, 844 (2000).
145. T. Takeuchi, R. H. Fokkens, L. J. de Koning and N. M. M. Nibbering, *Adv. Mass Spectrom.*, **14**, 748 (1998).
146. D. B. Jacobson and R. Bakhtiar, *J. Am. Chem. Soc.*, **115**, 10830 (1993).
147. R. Bakhtiar, C. M. Holznagel and D. B. Jacobson, *J. Am. Chem. Soc.*, **115**, 345 (1993).
148. R. Bakhtiar and D. B. Jacobson, *Organometallics*, **12**, 2876 (1993).

Author Index

This author index is designed to enable the reader to locate an author's name and work with the aid of the reference numbers appearing in the text. The page numbers are printed in normal type in ascending numerical order, followed by the reference numbers in parentheses. The numbers in italic refer to the pages on which the references are actually listed.

- Aagaard, G. 265(198), 334
Abbenhuis, H. C. L. 239(59), 331, 573(47),
636, 719(200, 201, 203), 720, 727(200), 741
Abdesaken, F. 5, 6, 63(12a), 147, 284, 290,
292(261), 336, 913(343), 948, 952, 997,
998(17b), 1025
Abe, H. 349(26), 388
Abe, M. 560(69), 563
Abe, Y. 701(45), 737
Abid, M. A. R. 240(62), 331
Abner, D. 1041(71b), 1057
Abrahams, I. 718(188), 741
Abrahams, P. 259(177), 334
Achiba, Y. 166, 169, 174(5), 217
Ackerhans, C. 698, 729(26), 737
Ackley, D. E. 570(18), 635
Adachi, A. 673(54b), 690(54b, 80), 693, 694
Adam, W. 698(20), 707(20, 114), 737, 739,
904(283), 946
Adams, B. R. 51(225b), 154, 277(236, 239),
295(236), 335
Adams, D. R. 393, 395, 400(22b), 424
Adams, J. L. 935(451), 950
Adams, N. G. 1030(7b), 1055
Adeogun, M. J. 716(175), 741
Adima, A. 578, 616(119), 637
Adiwidjaja, G. 901(238), 945
Aelst, S. F. van 923(398), 928(420), 949
Aerts, P. J. C. 13, 15(82), 150
Afiti, T. H. 645(23a), 692
Ager, D. J. 912(341), 947
Ahlrichs, R. 12(76), 150, 168(22), 218
Aida, T. 703(87), 738
Aigbirhio, F. I. 728(265), 743
Aisa, A. M. A. 700(40), 737
Aiube, Z. H. 702, 732(62), 738
Aizpurua, J. M. 248, 311, 313(121),
332
Akasaka, T. 352, 354(39), 388, 404(93), 426,
726(249), 743
Akiba, K.-y. 878(149, 150), 943, 944
Akita, S. 559(59), 562
Akiyama, T. 879(156, 157), 944
Akrigg, D. 730(276), 743
Aksnes, D. W. 315, 322(346), 337
Alam, T. D. 593(141), 638
Alam, T. M. 248, 249(124), 333
Al Badri, A. 525(100, 106), 538
Albanov, A. I. 904(259), 946
Albert, K. 470(4), 486
Alberti, A. 368(83b), 386(128), 389, 390,
856(14), 941
Albinate, A. 397(55b), 425
Albrecht, K. 192(58), 220
Albrecht, T. 857(26), 941
Albright, T. A. 108(388), 159
Alcaide, B. 367(78), 389
Aldbbagh, E. 119(438), 161
Al Dulayymi, J. R. 858(36), 941
Alejandre, J. 825(16e), 847
Aleksandrov, Yu. A. 707(112, 113), 739
Alexander, L. E. 729(268), 743
Alexander, U. N. 127(455b), 161
Alexseyev, A. B. 92(361b), 158
Al-Gurashi, M. A. M. R. 910(315), 947
Alhambra, C. 825(20b), 847
Ali, S. 307(315), 337
Ali, Z. 316, 318, 319(351), 338
Alire, R. E. 632(224), 640

- Al-Juaid, S. S. 699(38), 713(150), 728(265),
729(272), 731(150, 285, 290), 734(38), 737,
740, 743, 744
- Alla, M. 282, 296–298(253), 336
- Allan, D. C. 823(8a), 847
- Allen, L. C. 7(36), 64, 68, 69(267), 148, 155,
398(61), 425
- Allen, S. R. 864(53), 942
- Allen, T. L. 94(365), 158
- Allen, W. D. 110(397), 159
- Allerhand, A. 325(404), 339
- Allgaier, J. 767(102), 800
- Allgood, C. 1046(101), 1058
- Allinger, N. L. 5, 12(25a), 148
- Allison, C. E. 1045(90), 1057
- Allred, A. L. 7(35a, 35b), 11, 45(35a), 148
- Allspach, T. 514, 516(74), 537
- Al-Mansour, A. I. 910(315), 947
- Almond, M. J. 16(117), 151
- Alo, B. I. 935(457), 950
- Alonso, A. 360(57), 388
- Alonso, B. 752(44, 49), 767(44, 49,
106–112), 768(108), 799–801
- Alonso, J. A. 38(178), 152
- Al-Rubaiey, N. 124(447), 125(447, 452a,
452b), 161
- Alt, H. 180, 181, 192, 208(40), 219
- Altmeyer, O. 531(126), 539
- Alvarez-Builla, J. 368(80), 389
- Al-Zahrani, M. M. 110, 112(405), 159
- Amara, P. 825(20b), 847
- Amberger, E. 708(121), 739
- Amlöf, J. 14, 15, 25, 29(104), 151
- An, K. 751(34, 36), 799
- Andersen, N. G. 920(379), 948
- Andersen, N. R. 265(198), 334
- Andersen, R. A. 864(65), 942
- Andersohn, L. 837(88c), 850
- Anderson, D. K. 910–912(312), 947
- Anderson, D. W. W. 320(385), 338
- Anderson, G. 935(455), 950
- Anderson, M. T. 572, 620, 631(30), 635
- Ando, E. 896(215), 945
- Ando, K. 919(370), 948
- Ando, W. 44(208a, 208b), 48, 49(219), (382a),
153, 159, 268, 269(208), 335, 352(36–38),
353(37, 38), 388, 404(93), 409(115), 426,
427, 542(4), 561, 642, 679(41), 691,
726(249), 743, 864(44), 870, 871(102),
872(111–115, 118, 119), 904(255), 941,
943, 946, 958(38, 39), 999(39), 1025
- Andre, J. M. 547(30b), 562
- Andrés, J. L. 119(438), 161
- Andrews, L. 78(308), 79(314e, 314f, 315a),
156, 157
- Andrey, O. 366(74), 389
- Andriamizaka, J. D. 499(32, 34, 35), 536
- Andrianov, K. A. 705(93), 706(96), 718(192),
738, 739, 741
- Andrianov, V. F. 715(161), 740
- Andrianov, V. I. 727(256), 743
- Andruh, M. 708, 727(119), 739
- Andzelm, J. 12(77), 150
- Andzelm, J. W. 12(70a), 149
- Anet, F. A. L. 325(408), 339
- Angelini, G. 1045(89), 1057
- Angelov, C. M. 940(471), 950
- Anglaret, E. 569(5), 635
- Angle, S. R. 878(152), 944
- Ankner, K. 928(426), 949
- Annand, J. 713, 720(148), 740
- Antic, D. 199(65b), 220
- Antipin, M. Yu. 698(15), 725(232–234, 241,
243), 729(15), 736, 742
- Antipova, B. A. 547(35), 562, 700(42),
727(42, 260), 737, 743
- Antonioti, P. 867(82–84), 868(82), 942,
1037(53a–c), 1056
- Anwari, F. 124, 125(446), 161, 642(13b), 691
- Aoki, M. 102–104(378), 159
- Aoki, Y. 765(91, 92, 94), 800
- Aoto, N. 844(131), 852
- Apeloig, Y. 5(1b, 7, 9, 28a, 29), 6(1b, 9), 7(7),
21(9), 22, 23(54), 36(7), 41(1b), 50(223),
63(7, 9), 64(7, 258, 263), 67(274), 69(263),
70(263, 274, 285a), 71(274), 74(7, 293),
78(285a, 306, 311a, 311b), 89, 90(339a),
91(7, 258, 339a, 339b, 340, 341), 92(362),
93(364), 94(7, 340), 95(258, 340), 96(341),
98(362), 101, 103(28a), 105(340),
107(386a), 108(28a, 386b), 110(7),
112(28a), 114, 115(28a, 420c, 425),
116(293), 117, 118(425), 128(7), 132,
133(470a), 138(29), 141(496), 147–149,
154–160, 162, 163, 192(58, 59), 220,
365(72), 389, 392(7), 393(24a, 24b, 26, 27),
394(26–28), 397(28, 54, 55a), 398(24a, 27,
28), 399(28, 64), 400(64), 424, 425, 445,
446(88), 467, 473(27, 28), 487, 642,
679(4h), 691, 724(219, 220, 230), 742,
912(338–340), 947, 962(58), 964(66–68),
965, 967(69, 70), 990(66), 997, 1001,
1002(58), 1003(124), 1009, 1010(68),
1011(68, 150, 153, 154), 1012(155),
1013(153, 154), 1014(153–155), 1015(154),
1016, 1017(153), 1018(68, 157), 1019,
1022(68), 1025–1028, 1037(54a),
1048(120), 1056, 1058
- Apodeca, P. 960, 993(49), 1025
- Appel, A. 58(239g), 154
- Appel, R. 492(4, 8a, 8c), 495(18, 21–24),
498(8a, 8c, 30), 500(36–38), 501(22–24,
37, 39–43), 504(49), 506(23, 52, 54),
509(60), 510(66), 511(54, 67), 514(22, 37),
519(4, 36, 85, 86), 520(49, 52, 85, 88),

- 522(90), 524(98), 528(90), 529(8a, 90),
536–538, 904(293), 946
- Apple, T. 786(161), 802
- Ara, M. 352, 354(39), 388
- Arad, C. 169, 186, 187(24), 218
- Arad, D. 11(59g), 141(496), 149, 163
- Arai, J. 325, 326(413), 339
- Arai, M. 716(170), 740
- Arakawa, Y. 872(118), 943
- Araki, Y. 904(265), 946
- Aramata, M. 559(66, 67), 560(66), 563
- Arase, H. 683(71), 694
- Archibald, R. S. 395(37, 42), 397, 420(42),
425, 1008(145), 1027
- Archibong, E. F. 141(495), 163
- Arduengo, A. J. III 114(418a–c), 115,
116(428), 160, 161, 202(77, 78), 203(77),
220, 221
- Arif, A. M. 533(135, 136), 539, 980(96), 1026
- Arkles, B. 575(53), 636, 703(79), 716(171),
738, 740
- Armentrout, P. B. 1030, 1032(11), 1055
- Armitage, D. A. 430(7), 465, 494, 510(10),
536
- Armstrong, D. R. 108, 109(393), 159
- Arnold, C. C. 217(98), 221
- Arnold, D. R. 1007(141), 1027
- Arnold, J. 904(277), 946
- Arpe, H.-J. 167(18), 218
- Arrington, C. A. 200, 201(68), 220
- Arshadi, M. 136, 137(478), 162
- Arthur, N. L. 348(23), 388, 958, 962(35), 1025
- Asamoto, B. 1034(36), 1056
- Aschi, M. 1046(109), 1058
- Asefa, T. 572(34, 35), 595(34), 630(217), 635,
640
- Ashe, A. J. III 178, 179(36), 219
- Ashley, C. S. 620(196), 639
- Aslam, M. 208, 210, 211(90), 221
- Aspinall, H. C. 713, 720(148), 740
- Assfeld, X. 825(20a), 847
- Assink, R. A. 316(353), 338, 577(88),
578(111), 592(138, 139), 600(156–158),
621(157), 629–631(210), 637, 638, 640
- Astapov, B. 293(291), 336
- Astapova, T. V. 698(15), 725(240), 729(15),
736, 742
- Asuke, T. 547(29), 548, 550(45), 562
- Atashroo, T. 13–15, 17(89a, 89b), 150
- Attinà, M. 1046(109), 1047(115), 1058
- Atwell, W. H. 642(11), 645(20), 691, 692
- Atwood, J. L. 434(37), 466
- Aubagnac, J. L. 575, 600, 602(78), 636
- Aubert, C. 899(230), 945
- Audebert, P. 578, 631(102), 637
- Audier, H. E. 1041(73a, 73b), 1057
- Audran, G. 877(147), 879(155), 943, 944
- Auer, F. 577, 612(89), 617(186), 619(89, 186),
637, 639
- Auer, H. 418, 419, 421(140), 427
- Auner, N. 430(10), 465, 484(122), 489,
726(251), 743, 912(331), 947, 952(9, 12),
953(12), 963(12, 61), 982, 988(12),
995(116), 1003(12), 1024–1027
- Avnir, D. 570(10, 20, 22), 635, 716(172), 740
- Avouris, P. 826(27c, 27d), 838(103d, 107),
839(111a, 111b), 840(107), 848, 851, 852
- Aygen, S. 191–193(55), 220
- Aylett, B. J. 433(24), 439(51), 465, 466
- Ayoko, G. A. 706(99), 739
- Azpeleta, S. 1031(24), 1056
- Azzena, U. 707(114), 739
- Babinec, P. 20(135), 151
- Babonneau, F. 478(69), 488, 569, 570(6),
572(40), 635, 636
- Baboul, A. G. 82(326a), 157
- Bach, R. D. 119(438), 161
- Bach, T. 1049(125), 1058
- Bacon, M. 227, 231(18, 19), 330
- Bada, A. 379(105), 390
- Bader, A. 617(184), 639
- Bader, R. F. W. 14(96a, 97a, 97b, 98, 99),
42(202), 56(99), 150, 153, 906(301), 947
- Badger, R. M. 714(154), 740
- Badt, D. 839(112), 852
- Baerends, E. J. 9(48a, 49), 13(84), 149, 150
- Baggett, J. E. 119(434a), 161
- Baguley, P. A. 381(112), 390
- Bagus, P. S. 838(104), 851
- Bahlmann, E. K. F. 320, 322(381), 324(395),
398), 338, 339
- Bahri Alias, S. 716(170), 740
- Baier, M. 547(28), 562
- Bailey, D. L. 710(132), 739
- Bailey, W. F. 925(409), 949
- Bailleaux, S. 79(314a), 156
- Bain, A. D. 870(97, 100, 101), 942, 943
- Baines, K. M. 5, 6(11a, 11f), 41, 43(11f),
63(11a, 11f), 74, 75(301), 147, 156,
199(65a), 220, 402(70), 408(70, 111), 426,
427, 858(30), 865(73), 941, 942, 952(4),
963(64), 968(80), 982(4), 1022(163), 1024,
1026, 1028
- Baird, M. S. 858(36), 941
- Baker, A. D. 166, 167(2, 3), 169(3), 172,
191(2), 217
- Baker, C. 166, 167, 172, 191(2), 217
- Baker, E. B. 261(189), 334
- Bakhashi, A. K. 671(50), 693
- Bakhtiar, R. 1043(78, 81), 1044(88),
1054(146, 147), 1055(148), 1057, 1059
- Balaich, G. 645(24c), 692
- Balaji, S. E. 642(13e), 691

- Balaji, V. 47(212c), 64(257c), 153, 155,
 192(58), 220, 542(12), 561
 Balakhchi, G. K. 208, 213(87), 221
 Balasubramanian, K. 5, 8, 9(30c), 13(86, 93a,
 93b), 16(114, 124a, 124b), 19, 29(114),
 92(124a, 361c), 110(396, 400, 405, 407,
 408), 112(396, 405, 407, 408), 128(114),
 148, 150, 151, 158–160
 Balch, A. L. 249(134), 333
 Baldrige, K. K. 5(27c), 101, 102, 104(380),
 148, 159
 Balduzzi, S. 368(84a, 84b), 389
 Baldwin, L. C. 349(24), 388
 Baldwin, N. J. 253, 320(142), 333
 Balerna, A. 838(109), 851
 Balkir, A. 484(127), 489
 Ball, J. L. 87, 89(338a), 157
 Ballestri, M. 377(100), 382(121a, 121b),
 385(126, 127), 386(128), 389, 390
 Bally, T. 48, 49(220), 153, 393, 395(19), 424
 Balogh, L. 760(68), 799
 Bammel, B. P. 240, 326(68), 331
 Bancroft, G. M. 199(65a), 220
 Baney, R. H. 574, 589(50), 636, 714(155),
 715(168), 740
 Banisch, J. H. 959(45), 960(45, 56), 972, 973,
 976(45), 985, 989(56), 994(45), 1025
 Bankmann, M. 168(20), 191–193(55), 218,
 220
 Bankova, W. 928(425), 949
 Bankwitz, U. 107(386a), 159, 472(26),
 473(28), 487, 642(4h), 645(22a), 679(4h),
 691, 692
 Baradirán, Z. 13, 14(87a, 87b), 150
 Barandiarán, Z. 15, 17(103), 150
 Baranov, V. I. 1038(60, 61), 1039(63, 66),
 1040(66), 1057
 Barbe, B. 243(88), 248, 311, 313(121), 332
 Barberis, C. 902(241), 945
 Barbosa, F. 347(21a), 388
 Bargon, J. 249(130), 251, 252(131), 333
 Bari, L. D. 315, 316, 318(344), 337
 Barlow, S. E. 95(366a), 158
 Barnes, C. E. 724(217), 742
 Barnes, G. H. Jr. 709(126), 739
 Barnette, W. E. 908(310), 947
 Barone, V. 834(82a, 82b), 850
 Barranco, M. 752(44), 767(44, 107), 799, 801
 Barrau, J. 5, 6, 51, 63(16), 147
 Barri, P. J. 578, 600(105), 637
 Barrientos, C. 1032(30), 1033(34), 1056
 Barta, I. 208(85), 221
 Bartelt, M. C. 842(126a, 126b), 852
 Bartelt, N. C. 842(126a), 852
 Barth, V. 500(37), 501(37, 42), 514(37), 536,
 537, 904(293), 946
 Barthelat, J.-C. 67, 75(277), 110(398), 156,
 159
 Barthelat, J.-P. 68, 75, 77(281), 156
 Bartholdi, E. 328(415), 339
 Bartholmei, S. 445(86), 467
 Bartl, J. 975(90), 1026
 Bartlett, R. A. 433(25), 465
 Bartlett, R. J. 12(66), 149
 Bartmess, J. E. 16(121), 125(449), 151, 161
 Barton, D. H. R. 381(113), 390
 Barton, J. L. 807(12), 818
 Barton, M. 648(35e), 692
 Barton, T. J. 642(7–9), 648(7, 8, 35a–c), 649,
 651(35c), 671, 673(51), 674(57), 691–693,
 860(40), 862(41–43), 864(54),
 871(107–109), 874(123), 904(253, 296),
 938(464, 465), 941–943, 946, 950,
 999(119), 1027
 Bartsch, R. 516(78), 538
 Baryshok, V. P. . 239(58), 331
 Basak, A. 877(136), 880(168), 943, 944
 Basch, H. 6(34), 7(34, 45), 11(45), 13(34), 20,
 21(45, 136), 22, 23(45), 24(45, 136), 25,
 26(45), 58, 59(242), 132, 134, 135(471),
 136(471, 476), 137(45, 471), 141(490), 148,
 149, 151, 154, 162, 163, 825(16b), 847
 Bassindale, A. 623, 626(202), 640
 Bassindale, A. R. 236(53), 318(364, 365), 331,
 338, 483(110, 113), 488, 856, 857, 905(1),
 906, 908(298), 929, 935(1), 940, 947
 Basso, E. 274, 275(223), 335, 780(147), 802
 Bastani, B. 904(289), 946
 Bastiaans, H. M. M. 531, 534(132), 539
 Bastian, E. 962, 982(60), 1026
 Bastide, J. 178, 179(36), 219
 Batcheller, S. A. 5, 6, 48, 49, 64, 67(19), 147,
 392, 393(4), 395(44), 401(4), 424, 425,
 1006, 1007(133), 1027
 Batchelor, R. J. 864(55, 63), 942
 Bates, T. F. 968(81), 980(96), 1026
 Batey, R. A. 381(117), 390
 Batich, C. 178, 179(36), 219
 Batra, I. P. 826(27j), 838(104), 848, 851
 Bats, J. W. 213(95), 221
 Batta, Gy. 261(187), 334
 Battacharyya, P. 807(17), 818
 Battioni, P. 578(124), 638
 Baudler, M. 208(86), 221
 Baudrillard, V. 244, 259, 312(93), 332
 Bauer, G. 286(268), 336
 Bauer, H. 277(237), 335
 Bauer, S. H. 714(154), 740
 Baugher, B. M. 577(88), 578(111), 629(212),
 637, 640
 Baughman, G. A. 710(134), 739
 Baukov, Yu. I. 239(54–56), 331
 Baum, C. 431(15), 465
 Baum, M. W. 904, 913(251), 946
 Baumann, W. 434(42), 466
 Baumeister, U. 480(84), 488

- Baur, R. 187, 190(53), 220
 Bauschlicher, C. W. Jr. 18, 118(128b), 151
 Bax, A. 242, 245(81), 257(158), 258(161),
 261, 263(194, 195), 265(200), 269(211),
 273(220, 221), 274(225, 227), 275(229),
 281(220), 304(301, 302), 332–335, 337
 Baxter, J. L. 31(158b), 152
 Bayer, E. 617(184), 639
 Beach, J. V. 578(111), 637
 Beagly, B. 31(159), 152
 Bear, Y. 166(13), 218
 Beattie, I. R. 483(117), 488
 Beatty, A. M. 397(55b), 425
 Beaucage, G. B. 602, 604(160), 638
 Beaucage, S. L. 928(423), 949
 Beauchamp, J. L. 1040(67, 68), 1045(97),
 1051(138, 139), 1052(139), 1057, 1058
 Becerra, R. 118(430), 119(434b, 434c, 435,
 436), 120(435, 436), 122(436), 125(452a),
 127(454a, 454b, 455a), 161
 Becherer, R. 168(22), 218
 Bechtel, J. H. 632, 633(222), 640
 Beck, A. K. 904(289), 946
 Beck, J. S. 572, 620, 629(36, 37), 635
 Becke, A. 16(122), 151
 Becke, A. D. 12(72a, 72b), 16(72b), 149
 Becker, A. 113(413a, 413b), 160
 Becker, C. 434(31), 465
 Becker, D. 920(384), 948
 Becker, D. A. 879(167), 880(170), 944
 Becker, G. 178, 180(38), 219, 492(9), 494(13),
 495(18, 19), 498(28, 31), 503(45), 506(53),
 509(28, 31, 59), 511–513(31), 514(19, 74),
 516(74), 536, 537, 904(294), 946
 Becker, W. 514, 516(74), 537
 Beckmann, J. 713(147), 718(191), 727(147),
 740, 741
 Beelen, T. P. M. 806(7, 8), 807(7), 808(26),
 818
 Beese, G. 920(381, 383), 948
 Beetz, R. 923(398), 949
 Beetz, T. 928(420), 949
 Begemann, C. 80(317), 157
 Behbehani, H. 727(253), 743
 Behm, J. 114, 115(422), 160
 Behn, J. 202(79), 221
 Behnam, B. A. 858(30), 941
 Behnke, C. 506, 511(54), 537
 Behrens, U. 312(327), 337
 Behres, K. 923, 924(403), 949
 Bein, T. 575(60), 636
 BelBruno, J. J. 92(361a), 158
 Bell, A. T. 316(359), 338
 Bellama, J. M. 225, 226, 311(9), 330
 Bellamy, F. 381(116), 390
 Bellina, F. 312(326), 337
 Bellocq, N. 575(59), 636
 Belot, V. 575(77, 81), 636
 Belsky, V. 767(110), 801
 Belyakov, A. V. 114(420a), 160
 Belyakow, A. V. 202(80), 221
 Belzner, J. 259(175), 292(287, 288), 334, 336,
 408(113), 409(113, 117), 410(119), 427,
 484(123, 124), 489
 Ben, F. 606(166), 639
 Benavides-Garcia, M. 110, 112(407, 408), 160
 Bendall, M. R. 245(99, 101), 246(99, 101,
 106, 107), 332
 Bender, C. F. 18, 118(128b), 151
 Bender, H. 531(133), 539
 Bender, H. R. G. 531(134), 539
 Bender, S. 709(131), 739
 Bendikov, M. 912(338), 932(445), 947, 950,
 964, 990(66), 1003(124), 1018(157),
 1026–1028
 Bendix, M. 857(25), 941
 Benesi, A. 132(469), 162
 Benfield, R. E. 324(396), 339
 Benito, M. 767(113, 114), 769(114), 801
 Benkeser, R. A. 474(30, 31), 487, 584(134),
 638
 Benn, R. 282(251), 336
 Bennett, M. A. 10, 11, 14, 33(53), 149
 Bennett, S. L. 844, 845(135), 852
 Benson, S. W. 71(287), 156
 Bent, H. A. 34(161), 152
 Bent, S. F. 831(57, 58), 832(62), 849
 Bentham, J. E. 320(385), 338
 Bentley, T. W. 971(85), 1026
 Berbst-Irmer, R. 410(119), 427
 Beresis, R. 879(160), 944
 Beresis, R. T. 879(166), 944
 Berg, D. J. 864(55), 942
 Berg, F. J. 864(58, 59, 61), 942
 Berger, S. 230(30), 241, 257(30, 72), 261,
 268(192), 298(296), 300, 301(297),
 322(392), 327(30), 330, 331, 334, 336, 338
 Berggren, E. 316, 318(350), 338
 Bergman, R. G. 870(88), 942
 Bergmark, T. 166(13), 218
 Bergna, H. 715(167), 740
 Bergner, A. 13(92a), 15, 17, 139(106), 150,
 151
 Bergsdorf, C. 808(31, 32), 819
 Bergsträßer, U. 904(295), 946
 Berkowitz, J. 16(116, 120), 151, 201(73), 220
 Berman, C. L. 823(10b), 847
 Bermel, W. 241, 257(73), 331
 Bernardelli, G. 525(101, 104, 105), 538
 Bernardi, F. 966(72–74), 1026
 Bernardinelli, G. 525(100), 538
 Bernasconi, C. F. 974(87), 1026
 Berndsen, H. J. C. 825(16c), 847
 Bernstein, H. J. 229(22), 330
 Bernstein, S. 707(110), 739
 Berry, D. H. 402(77), 426

- Berry, M. B. 865(72), 942
 Bertagnolli, H. 612, 617, 619(177), 639
 Bertók, B. 877(141), 943
 Bertrand, G. 859(38), 941
 Bertrand, G. L. 703(78), 738
 Bertrand, R. D. 255(147), 256(147, 148, 150–152), 333
 Beruda, H. 432(20), 465
 Besida, J. 936(459), 950
 Beteille, J. H. P. 904(250), 946
 Betsuyaku, T. 344, 345(11a), 387
 Beurskens, P. T. 879(165), 944
 Beverwijk, V. 525(99, 100), 538
 Bezombes, J.-P. 578(109, 110), 583, 595(109), 611(109, 110), 613(179), 637, 639
 Bhattacharjee, M. 698, 722, 724(30), 737
 Bhattacharjee, M. 433(26), 465
 Bhupathy, M. 904(257), 946
 Bibal, C. 64(259), 155
 Bickelhaupt, F. 492(5), 496, 499(26), 513(69), 525(99, 100), 526, 527(111, 112), 531(130–132), 534(130, 132), 536–539
 Bickelhaupt, F. M. 11, 24, 128, 138, 139(57), 149, 343(9), 387
 Bickerstaff, R. D. 54, 56(234), 154
 Bienz, S. 312(323, 324), 314(323), 337, 891(208), 945
 Bieri, G. 166(7), 217
 Bigelow, R. W. 28(149), 152
 Bildsøe, H. 245(97), 248(116), 282(249), 311(97), 332, 335
 Billedeau, R. J. 922(392), 948
 Binkley, J. S. 12(65, 74b, 75), 16(111, 119), 92, 96(357), 118(111), 149–151, 158
 Binnewies, M. 168(22), 218
 Binning, R. C. Jr. 16(115), 151
 Birchall, J. D. 700(39), 737
 Birgele, I. 265(197), 334
 Birkhofer, L. 481(100), 488
 Birot, M. 243(87), 332, 471(12), 486
 Bissinger, P. 484(122), 489
 Bissky, G. 483(107), 488
 Biteau, J. 570(12), 635
 Black, E. 602, 604(160), 638
 Blaha, P. 823(6c), 847
 Blake, J. F. 720(205), 741
 Blakeman, P. 114(421c), 160
 Blandford, C. F. 572, 573(39), 629(39, 219), 630(216), 636, 640
 Blank, E. 72(289), 156
 Bläser, D. 114(419, 421a, 421b), 160
 Blayden, H. E. 483(116), 488
 Blechta, V. 236(52), 247(109), 251(134, 136–138), 254(138), 259(109), 262, 263, 265(196), 304, 305(304), 306(136), 307(316), 308(138), 323(393), 331–334, 337, 338
 Blechtz, V. 255, 325(144), 333
 Blériot, Y. 928(431, 432), 949
 Bliefert, C. 234(48), 331
 Blinka, T. A. 248(117), 332
 Blitz, M. A. 119(434a), 161
 Blochl, P. E. 830(47a), 849
 Block, E. 208, 210, 211(90), 221
 Blom, R. 197(64), 220
 Blount, J. F. 48, 49(220), 153, 393, 395(19), 424
 Blümel, J. 484(122), 489
 Blumenkopf, T. A. 481(99), 488
 Board, J. A. 823(10c), 847
 Boatz, J. A. 5(27c), 48–50(217), 126, 127(453), 148, 153, 161, 405(100), 426
 Boaz, J. A. 74(298), 156
 Bobbitt, K. L. 904(254), 946, 955, 956(31), 1025
 Bobrovsky, A. Y. 765(87), 800
 Bobrowicz, F. W. 824(15), 827(32), 847, 848
 Bocelli, G. 731(281), 743
 Boche, G. 867(81), 942
 Bochkarev, M. N. 746(2), 798
 Bock, C. W. 62(246a, 246b), 154
 Bock, H. 64(257d), 114(422), 115(422, 428), 116(428), 155, 160, 161, 166(1, 8–12), 167(11, 15–19), 168(11, 12, 16, 20–22), 169(9–12, 15, 16, 23–25), 170(10), 172(9–11, 15, 16, 25, 26), 173(9, 26), 174(1, 9, 10, 15, 16, 26, 29), 175(1, 8–10, 15, 16, 29–31), 176(26, 29), 178(1, 10, 15, 16, 31, 37, 38), 179(15, 37), 180(8, 9, 15, 16, 31, 38–40), 181(9, 15, 16, 25, 40, 41, 44, 45), 182(41), 184(15, 16, 25), 185(15, 16, 25, 46), 186(9, 15, 16, 24, 48, 49), 187(24, 48, 50, 53), 190(10, 48, 50, 53, 54), 191(9–11, 16, 25, 48, 49, 55), 192(11, 12, 16, 21, 23, 40, 55, 57, 61, 62), 193(55), 195(10, 16, 63), 197(15, 16, 63), 199(10, 15, 16, 25, 50, 57), 201(10), 202(61, 74, 77, 79), 203(77, 81), 205, 206(81), 208(10, 15, 16, 40, 88, 89), 209(88), 210(10, 15, 25, 50, 88, 89), 211(88, 89, 93), 212(10, 15, 88, 89), 213(95), 214(9, 10, 16, 61, 96), 216(10, 15, 16, 96), 217(15, 100), 217–221
 Böckmann, M. P. 722(212), 741
 Bode, K. 439(53, 57, 58), 466
 Bodenhausen, G. 248(115), 259(176), 268(209), 332, 334, 335
 Boeckel, C. A. A. van 923(398), 928(420), 949
 Boehme, C. 81, 114, 115, 117–119(323), 157
 Boelens, R. 266, 271(206), 335
 Boersman, J. 769(121), 801
 Boese, R. 108(390c), 114(419, 421a, 421b), 159, 160, 440(61a), 441(61a, 64), 442(64), 450, 451, 465(99), 466, 467, 507(55–57), 537
 Boganov, S. 79(315b), 157

- Boganov, S. E. 47(212c), 81, 82(320), 118(430), 119, 120(435), 127(455a), 153, 157, 161
- Boganov, V. 642(13e), 691
- Boger, D. L. 405(101), 426
- Bogey, M. 79(314a, 314b), 96(370a, 370b, 372), 156, 158, 421(145), 428
- Bogge, H. 78(307), 156
- Boggs, J. E. 533(135), 539
- Bogunovic, Lj.J. 714(156), 740
- Böhler, B. 300, 302, 320(298), 336
- Bohme, D. K. 79(314c), 157, 1030(10a, 10b), 1031(14, 15, 18, 19), 1032(10a, 10b, 14, 27, 31), 1033(31, 33), 1035(43), 1038(58, 60, 61), 1039(63, 66), 1040(14, 66, 69), 1041(69), 1043(82), 1051(137), 1052(143), 1055–1059
- Böhme, U. 478(69), 488
- Boiko, N. I. 765(87), 800
- Boilot, P. 570(12), 635
- Boisen, M. B. 724(227), 742
- Boisen, M. B. Jr. 35(163), 152
- Bokor, J. 838(101a), 851
- Boland, J. J. 837(92), 851
- Boldi, A. M. 919(368), 948
- Bolin, G. 933(447), 950
- Bolm, C. 888(193), 944
- Bolte, M. 483(115), 488
- Bolton, E. E. 38(174c), 152
- Bolton, P. H. 245(105), 332
- Bolvin, H. 96(370a, 370b), 158, 421(145), 428
- Bon, S. A. F. 767(100, 101), 800
- Bonazzola, L. 199, 200(66), 220
- Bonderson, E. K. 69(283), 156
- Bonjoch, J. 374(96), 389
- Bonjock, J. 367(79), 389
- Bonser, D. J. 838–840(105a), 841, 842(122), 851, 852
- Bontront, J.-L. J. 920(376), 948
- Boom, J. H. van 940(470), 950
- Boomsgaarden, S. 418, 419, 421(142), 427
- Boone, A. J. 91, 94, 97, 98(355), 158
- Borden, W. T. 74(294), 156
- Borisov, S. N. 705(95), 739
- Borkowsky, S. L. 888(199), 944
- Bornais, J. 230(29), 330
- Borojevic, R. 807(13), 818
- Borowitzka, M. A. 810(37), 819
- Borrmann, H. 187, 190(51b), 220
- Borthwick, I. 349(24), 388
- Borzatta, V. 351(32), 388
- Böske, J. 904(269), 946
- Bosman, A. W. 746(10), 798
- Bossart, M. 350(28, 29b), 388
- Botoshansky, M. 396, 397(49a), 425, 724(229), 742
- Botschwina, P. 343(10a, 10b), 387
- Böttcher, B. 434(36), 466
- Böttcher, P. 699, 733(35), 737
- Bottoni, A. 354, 356(42), 360(42, 56), 388, 966(72, 73), 1026
- Bouachrine, M. 611(176), 639
- Bouas-Laurent, H. 914(350–352), 948
- Boudjouk, P. 482(103), 483(120), 488, 489, 642(4b–d, 13b), 679(4b–d), 691
- Boukherroub, R. 382(121a), 390, 982(97), 992(111), 997(117, 118), 998(97, 111, 117, 118), 999(111), 1000(111, 117, 118), 1001(117), 1002(97, 117), 1003(117), 1026, 1027
- Bouquet, P. 381(116), 390
- Boury, B. 578(99, 121), 588, 590(99), 593(121), 595(150), 602(99, 161), 604(162), 606(165, 166), 607(165), 609(168), 623(99, 204), 625(161), 631(99, 150), 637–640, 716(176), 741, 752, 761(43), 799
- Bousbaa, J. 923, 924(408), 949
- Bovey, F. A. 542(19), 547(19, 31, 33), 548(19), 561, 562
- Boyce, J. P. 878(152), 944
- Boyd, P. D. W. 132(469), 162
- Boysen, M. M. K. 752(51), 799
- Bozack, M. J. 827(39b), 845(144), 849, 853
- Bozso, F. 826(27c, 27d), 848
- Bradaric, C. J. 959(40–42, 45), 960(40–42, 45, 53, 57), 962(53), 972(45), 973(40, 45, 89), 974, 975(40, 89), 976(40, 45, 89, 92), 977, 978(40), 980(57, 109), 981(57), 982(89), 983, 984(41, 42), 985(42), 986(41, 42), 989(42, 53, 109), 993(92), 994(41, 45, 57), 997(41, 118), 998(118), 1000(53, 118), 1025–1027
- Braddock-Wilking, J. 397(55b), 425
- Bradley, D. D. C. 686(75b), 694
- Brady, W. T. 936(461), 950
- Brandes, R. A. C. 747(26), 798
- Brandès, S. 578, 586, 600, 614(113), 637
- Brasselet, S. 578, 586(120), 634(120, 227), 637, 640
- Bratovanov, S. 312(323, 324), 314(323), 337
- Braude, V. 912(339), 947, 964(67), 1026
- Brauman, J. I. 139, 140(486b), 162
- Braun, M. 928(427), 949
- Braun, S. 230, 241, 257, 327(30), 330
- Braunschweig, H. 114(424), 160
- Braunstein, P. 856(15), 864(46), 941
- Bravo-Zhivotovskii, D. 912(338–340), 947, 964(66–68), 965, 967(69, 70), 990(66), 1009–1011(68), 1018(68, 157), 1019, 1022(68), 1026, 1028
- Braye, E. H. 641, 645(1a, 1b), 691
- Brédas, J. L. 686(75b), 694
- Breed, L. W. 444(81), 467, 703(82), 738
- Breeden, D. L. 642(12), 691
- Bréfort, J. L. 683(68a), 693
- Breidung, J. 29(154), 152

- Breit, B. 516(79, 82), 538, 904(295), 946
 Bremer, M. 24–26, 29(139), 151
 Brendler, E. 288(273, 277), 289(277), 336, 474(40), 478(71), 479(75), 483(71), 487, 488, 780(148), 802
 Breneman, W. C. 470(3), 486
 Brengel, G. P. 877, 879(137, 138), 943
 Breuer, O. 191–193(55), 220
 Breunig, H. J. 207(83), 221
 Brevard, C. 225(11), 251(139), 330, 333
 Brewer, S. D. 442(65), 466
 Brey, W. S. 244(92), 332
 Brežný, R. 282, 296, 297(254), 336
 Briggs, G. A. D. 830(47a), 849
 Briguet, A. 315(330, 332), 316(355), 337, 338
 Brinckman, F. E. 240(63–65), 331
 Brinker, C. J. 567, 569(4), 570(16), 572(30), 590, 602(4), 620(30), 629(208–210), 630(210), 631(30, 210), 635, 640
 Brinker, J. 620(196), 639
 Brisdon, B. J. 727(253), 743
 Brisdon, J. 718(190), 741
 Brisson, J.-R. 269, 270(212), 335
 Brix, Th. 958, 962(35), 1025
 Brizzolara, D. 757(60), 799
 Brocks, G. 826(26f), 848
 Brondani, D. J. 583(132, 133), 638
 Brönnecke, C. 445, 446(87), 467
 Brönnecke, C. 904(276), 946
 Bronnimann, C. E. 594(144), 638
 Brook, A. G. 5, 6, 63(11a, 11b, 12a–c), 147, 284, 290, 292(261), 336, 392(14, 15), 424, 714(159), 740, 856(1, 12), 857(1), 858(30), 865(73), 905(1), 906(298), 908(298, 307, 308), 913(343), 916(355), 929, 935(1), 940–942, 947, 948, 952(4, 10, 17a, 17b), 953(10), 963(64), 968(80), 978(94), 982(4, 10, 100–102), 985(100, 101), 988(10), 997, 998(17a, 17b), 1024–1026
 Brook, M. A. 5, 6(10, 11b), 43(10), 63(10, 11b), 147, 213, 216(94), 221, 368(84a, 84b), 389, 714(152), 715(165), 740, 870(95, 101, 103), 942, 943, 952, 953, 982, 988(10), 1024, 1050(134), 1051(135), 1058
 Brook, P. R. 935(456), 950
 Brooks, W. 245, 246(101), 332
 Brooks, W. M. 246(107), 332
 Brough, A. R. 320(383), 338
 Brown, C. A. 722(210), 741
 Brown, D. W. 870(88), 942
 Brown, H. R. 575(68), 636
 Brown, J. F. Jr. 701(47), 737
 Brown, R. F. C. 936(459), 950
 Brownstein, S. 230(29), 330
 Brückmann, R. 904(261), 946
 Brückner, R. 870, 901(93), 923, 924(400–407), 942, 949
 Brundle, C. R. 166, 167(2, 3), 169(3), 172, 191(2), 217
 Brunel, D. 575(58, 59), 636
 Brunet, F. 247(110, 112), 248(123), 282, 293(256–258), 332, 336
 Brüning, K. 751(42), 774(134–137), 799, 801
 Bruser, W. 718(196), 741
 Bruzard, S. 240(60), 331
 Bryan, L. A. 709(130), 739
 Brzezinski, M. 807(16), 818
 Bu, H. 834(75c, 79), 850
 Büchner, K. D. 195, 197(63), 220
 Buchwald, S. L. 645(21c), 692
 Buck, T. 923, 924(400, 401), 949
 Budaraju, J. 1011(152), 1028
 Buddrus, J. 277(237), 335
 Budzichowski, T. A. 720(204, 206), 741
 Buell, G. R. 707(110), 739
 Buenker, R. J. 92(361b), 158, 192(56), 220
 Buffy, J. J. 399, 400(64), 425, 432(17), 465, 475(51, 52), 487
 Bühl, M. 62, 75(245), 154
 Buhro, W. E. 113(411b), 160
 Bujalski, D. R. 575(54), 636
 Bukalov, S. 394, 397–399(28), 424
 Bukalov, S. S. 195, 197(63), 220, 547(35, 36), 548(42, 45), 550(45), 562
 Büker, H.-H. 1030(8), 1055
 Bulkalov, S. 67, 70, 71(274), 155
 Bulkin, A. F. 787(167), 802
 Bundgaard, T. 242(82), 332
 Bungardt, D. 507(55–57), 537
 Bunker, P. R. 112(404a, 404b), 159
 Bunning, J. E. 731(288), 744
 Bunte, E.-A. 321(389), 338
 Bunz, U. H. F. 671(53), 693
 Burczyk, K. 479(81), 488
 Burdett, J. K. 108(388), 159
 Bures, E. J. 920(373, 381, 382), 948
 Burford, N. D. 108, 109(389), 159
 Burgath, A. 769(123), 787(166), 801, 802
 Bürger, H. 479(81), 488
 Burggarf, L. W. 824(14), 825(18), 826, 827(14), 847
 Burggraf, L. W. 827(34), 848
 Burgler, D. 826(27e), 848
 Burgos, C. 368(80), 389
 Buriak, J. M. 822(3), 846
 Burke, L. P. 319(366), 338
 Burkett, S. L. 572(41), 636
 Burnett, F. N. 922(388), 948
 Burns, G. T. 871(108, 109), 904(253), 943, 946
 Burns, S. A. 871(108, 109), 938(465), 943, 950
 Burroughes, J. H. 686(75b), 694
 Burrows, A. D. 719, 720, 727(200), 741
 Burum, D. P. 245, 247(104), 332

- Busch, K. 478(69), 488
 Busch, R. 483(118), 488
 Busch, T. 513(69), 531(123), 537, 539
 Bush, R. D. 978(93), 1026
 Buss, R. J. 600(156, 157), 602, 604(160),
 621(157, 198), 638, 639
 Butcher, J. A. Jr. 870(96), 942
 Butcher, R. J. 699, 731(34), 737
 Butler, G. B. 878(153), 944
 Buttrus, N. H. 697(6), 699(38), 702(62),
 728(266), 731(6, 266, 282), 732(62),
 734(38, 294), 736–738, 743, 744
 Butz, R. 834(74a), 850
 Buzek, P. 132, 133(470a), 162, 1048(120),
 1058
 Buzin, A. I. 762(81), 776(81, 140), 778,
 791(81), 800, 801
 Bylander, D. M. 823(8b), 847
 Byloos, M. 83(331), 157, 956, 990, 1000(32),
 1025
 Bytheway, I. 93(363h), 158
 Byun, K. S. 96(368), 158

 Caballero, N. 865(71), 942
 Cabane, B. 247(110), 248(123), 282, 293(258),
 332, 336
 Cabrita, E. J. 322(392), 338
 Cacace, F. 1030(5), 1044(85), 1045(5),
 1047(114, 115), 1048(118, 121), 1055,
 1057, 1058
 Cahill, D. G. 839(111a, 111b), 852
 Cai, Y. 382(118), 390
 Calabrese, J. 473(28), 487
 Calabrese, J. C. 412(124), 427, 647(29b), 692
 Calas, P. 578, 631(102), 637
 Calas, R. 583(131), 638
 Callaghan, O. 377(102), 389
 Calzaferrri, G. 573(48), 636
 Camerman, A. 731(280), 743
 Camerman, N. 731(280), 743
 Cameron, D. W. 935(455), 950
 Caminade, A.-M. 746(19), 798
 Campana, C. F. 397, 398(50), 425
 Campbell, T. W. 703(83), 738
 Campbell-Ferguson, H. J. 483(114), 488
 Canepa, C. 867, 868(82), 942, 1037(53a, 53b),
 1056
 Canet, D. 316(349), 338
 Canty, A. J. 769(117, 119), 801
 Cao, J. 813(45), 819
 Caplier, I. 641, 645(1b), 691
 Cardin, E. 578(124), 638
 Carey, J. G. 700(39), 737
 Cargioli, J. D. 227(15), 231(40, 41), 233,
 234(41), 283, 285, 286, 288, 289, 291(259),
 315, 318(334, 347), 324(397), 326(15, 334,
 347), 330, 331, 336, 337, 339, 714(157), 740
 Carilla, J. 710(137), 739
 Carini, D. J. 877(136), 879(154), 880(154,
 168), 943, 944
 Carlson, G. A. 604(164), 639
 Carmer, C. S. 825(17a, 17b), 847
 Carmichael, I. 953(20), 1025
 Carneiro, J. W. de M. 141(491), 163
 Carothers, T. W. 746(16), 791(178–180), 798,
 802
 Carpenter, I. W. 125(452a), 161
 Carpenter, J. P. 578, 589(96), 592(138–140),
 593(141), 637, 638
 Carpita, A. 312(326), 337
 Carr, R. W. 17(127), 151
 Carr, S. W. 578, 600(105, 106), 637
 Carre, F. 609(168), 639
 Carroll, M. T. 37(170), 54, 56(231, 232),
 57(232), 145(170), 152, 154
 Carroll, P. J. 402(77), 426
 Carrozza, P. 351(32), 388
 Carter, E. A. 826(26a, 30), 837(91, 93b),
 838(98), 845(146, 147), 848, 851, 853
 Carter, L. E. 845(147), 853
 Casado, C. M. 613(180), 639, 752(44, 49),
 767(44, 49, 106, 107, 109–112), 799–801
 Casey, C. P. 935(458), 950
 Casser, C. 495(18), 536
 Castellino, S. 642, 679(4c), 691
 Castéllucci, E. 725(245), 742
 Castiglioni, M. 1036(51), 1056
 Castruita, M. 960, 993(49), 1025
 Catalina, F. 360(57), 388
 Cauvel, A. 575(59), 636
 Cavalieri, J. D. 399(63, 64), 400(64), 425
 Cavell, R. G. 904(281), 940(471), 946, 950
 Cavezza, A. 374(94), 389
 Cecchi, P. 1038(59), 1057
 Cederbaum, F. E. 645(21a, 21b), 692
 Cederbaum, L. S. 642(13a), 691
 Čermák, J. 234(48), 236(49, 50), 238(49),
 251(136, 137), 306(136), 331, 333
 Černý, M. 236, 258(51), 331
 Cerveau, G. 575(78–80, 87), 578(80, 100,
 102, 103, 107, 128), 584(100), 595(107,
 149, 151, 152, 155), 596(149, 152, 155),
 598(128), 600(78, 79), 602(78), 609(100),
 614(79, 80, 107, 155), 631(102), 632(103),
 636–638, 715(169), 716(178), 735(296),
 740, 741, 744
 Cetini, G. 1036(49), 1056
 Ceyer, S. T. 845(145), 853
 Cha, H. J. 575(68), 636
 Cha, J. N. 806(4), 810(38, 41–43), 811(41,
 42), 812(42), 813–815(42, 43), 816(4), 818,
 819
 Chabal, Y. J. 834(73), 836, 837(87), 850
 Chadi, D. J. 826(24), 848
 Chai, M. 266, 301(205), 303(205, 300), 334,
 336, 752(56), 799

- Chakraborty, D. 732(291), 744
 Challacombe, M. 823(10d), 825(21a), 847
 Chamberlin, S. 904(267), 946
 Champagne, B. 547(30b), 562
 Chan, S. I. 230(32), 330
 Chan, Y.-M. 952, 997, 998(17b), 1025
 Chander, M. 834(77b), 850
 Chandler, G. S. 12(74a), 150
 Chandrasekaran, A. 726(252), 743
 Chandrasekhar, J. 11, 35(59f), 74, 116(293),
 120, 122, 123(442), 149, 156, 161, 724(221),
 230, 742, 825(16a), 847, 1037(54b), 1056
 Chandrasekhar, V. 698(28), 699(32, 34),
 711(139), 722, 724(28), 731(34, 139),
 733(139), 735(32), 737, 740
 Chang, C.-C. 999(119), 1027
 Chang, C. Y. 575(70), 636
 Chang, J. 38(178), 152
 Chang, L. 838(101a), 851
 Chang, N.-Y. 96(369a), 158
 Chang, S.-Y. 870, 903(89), 942
 Chang, T. C. 575(70), 636
 Chang, Y. 752(50), 757(50, 62), 760(50), 799
 Chang, Y.-M. 5, 6, 63(12c), 147, 913(343),
 948
 Chao, Y.-C. 826(25c, 25d), 848
 Chapela, G. A. 825(16e), 847
 Chapleur, Y. 381(116), 390
 Chapman, O. L. 999(119), 1027
 Chaput, F. 570(12), 635
 Charlton, J. L. 1007(140), 1027
 Charlwood, J. 928(431, 432), 949
 Charumilind, P. 870(99), 943
 Chase, M. W. Jr. 31(156), 152
 Chatgililoglu, C. 5, 138(29), 148, 341(1),
 342(1-4), 345(1), 346(4, 15, 16, 19),
 351(32), 357(4, 46), 358(46), 359(1-4),
 361(1), 362(2, 3, 67), 363(4), 364(2-4, 69,
 70), 366(75, 76), 367(77), 368(82, 83b),
 377(100), 381(114, 115), 382(119, 120,
 121a, 121b), 383(19), 385(126, 127),
 386(128), 387-390
 Chatt, J. 48(221b), 154, 405(95), 426
 Chatterton, W. J. 858(30), 941, 982(101, 102),
 985(101), 1026
 Chaubon, M. A. 5, 6, 105(24e), 148
 Chaubon-Deredempt, M.-A. 83-85(337), 157
 Chaudhry, S. C. 483(119), 485(133), 489
 Chaudhry, T. M. 575(55), 636
 Chaudret, B. 251(140), 333
 Chauhan, B. P. S. 679(64), 693
 Chedekel, M. R. 999(120), 1027
 Chen, B. 486(136), 489, 728(263), 743
 Chen, C. H. 686(74b), 694
 Chen, H. 115, 116(428), 161, 202, 203(77),
 220
 Chen, J. 570(25), 635
 Chen, P. J. 844(132), 852
 Chen, Q.-F. 1046(106), 1058
 Chen, S. 347, 348(21b), 388
 Chen, S.-H. 928(429), 949
 Chen, T. 397(55b), 425
 Chen, T.-M. 935(451), 950
 Chen, W. 671, 673(51), 693
 Chen, W.-C. 69, 70(282), 156, 575(65, 66),
 636
 Chen, Y. L. 477(64), 487
 Chenards, B. I. 181, 182(43), 219
 Cheng, A. H. B. 980(95), 1026
 Cheng, C. C. 827(39c, 39e, 39f), 830(39c),
 834(75b, 78b), 844(132), 849, 850, 852
 Chenskaya, T. B. 762, 764(78), 771(129),
 787(167), 791(78), 800-802
 Cherng, C. D. 870(90), 942
 Cherng, C. O. 903(247), 945
 Chernyshev, E. A. 471(8), 486
 Cheung, L. M. 832(61b), 849
 Chevalier, P. 578(97-99), 588, 590(98, 99),
 596(97, 98), 602(98, 99), 623(97-99, 201),
 631(98, 99), 637, 640
 Chey, J. H. 402(77), 426
 Chezeau, J. M. 626(205), 640
 Chiang, M. Y. 113(411b), 160
 Chiang, T.-C. 826(25b), 848
 Chiappino, M. L. 810(36), 819
 Chiavarino, B. 1049(126), 1050(132),
 1053(144), 1058, 1059
 Chin, E. 883(181), 944
 Chingas, G. C. 255(147), 256(147, 148),
 150-153, 333
 Chizhov, O. S. 1045(93), 1046(98),
 1049(124), 1057, 1058
 Chmelka, B. F. 810-815(42), 819
 Cho, H. 16(120), 151
 Cho, J. 835, 836(86), 850
 Chogovadze, T. V. 698(25), 737
 Choi, C. H. 825(19, 21e), 832(19, 63),
 840(121), 842(121, 127), 847, 849, 852
 Choi, G. M. 877(148), 943
 Choi, K. M. 619(192-194), 620(195), 639
 Choi, S.-B. 642, 679(4a, 4d), 691
 Choi, S.-K. 751(35), 799
 Chojnowski, J. 542(4), 561, 703(69, 72, 74,
 81), 716(74), 717(69, 72), 738
 Chorro, C. 578, 603(94), 611(94, 175), 637,
 639
 Chou, S. 632(223), 640
 Chow, H.-F. 746(7), 798
 Choyke, W. J. 827(39b-f, 44), 828(44),
 830(39c), 834(75b, 78b), 844(132),
 845(144), 849, 850, 852, 853
 Christiansen, P. A. 13-15(88a, 88b, 89a, 89b),
 16(124b), 17(88a, 88b, 89a, 89b), 150, 151
 Christiansen, S. 810-815(42), 819
 Christman, S. B. 834(73), 850
 Christofoli, P. G. 920(375, 377, 379), 948

- Chrostowska-Senio, A. 206(82a, 82b),
 207(82a), 221
 Chrusciel, J. 477(67), 488
 Chrusciel, J. J. 916(355), 948
 Chrzczonowicz, S. 703(81), 738
 Chu, J. O. 118(433), 161
 Chu, S.-Y. 19(131), 69, 70(282), 81, 82(319a,
 319b), 91, 94, 95(356), 115, 116(427),
 120(131, 427, 440, 441), 122(131, 440),
 123(440), 124(440, 441, 445), 125,
 126(445), 151, 156–158, 161
 Chu, T. 572, 620, 629(37), 635
 Chua, C. T. 575(72), 636
 Chuang, C.-T. 870(104), 943
 Chuit, C. 578(109, 110, 117, 118), 583(109),
 584(117, 118), 586(117), 595(109),
 600(117, 118), 611(109, 110), 613(179),
 614(117, 118), 623, 626(203), 637, 639, 640
 Chung, D.-I. 751(30), 799
 Chung, G. 127(456), 161
 Chunwachirasiri, W. 551, 552(46), 562
 Chvalovský, V. 234(48), 236(51), 255(144),
 258(51, 165), 260(165), 325(144), 331, 333,
 334
 Cimino, R. 834(74c), 850
 Ciraci, S. 834(80), 850
 Ciro, S. M. 132, 133, 136(468b), 162
 Ciruelos, S. 729(270), 743
 Clabo, D. A. Jr. 61(244a), 154
 Clague, A. D. H. 324(394), 338
 Claridge, T. D. W. 257, 266, 323(159), 333
 Clark, D. T. 178, 179(36), 219
 Clark, E. S. 542(13), 561
 Clark, J. H. 572, 573(32), 635
 Clark, K. B. 382(120), 390
 Clark, M. C. 888(197, 198), 944
 Clark, T. 5(25a), 11(59g), 12(25a), 148, 149,
 1019(159), 1028
 Clarke, M. P. 471(10), 486, 904(250),
 907(304), 946, 947
 Clarke, T. 38(174b), 152
 Clary, D. C. 1031(16), 1055
 Clawson, D. K. 914(349), 948
 Clayden, J. 928(415), 949
 Clegg, W. 181, 182(42), 219, 443(73–75, 79),
 466, 467, 725(237), 727, 731(254), 742, 743
 Cleij, T. J. 555(51), 562
 Clemen, L. 827(39d), 849
 Clemens, D. 1045(91), 1057
 Clouthier, D. J. 95(366e, 367), 158
 Clowes, R. T. 266(204), 334
 Coburn, J. W. 844(128), 852
 Coen, M. C. 765(90), 800
 Coffin, J. M. 78(309), 156
 Cohen, D. 825(16b), 847
 Cohen, S. M. 230(25), 330
 Cohen, T. 901(237), 904(257), 945, 946
 Coker, E. N. 808(20), 818
 Colbey, U. T. 178, 179(36), 219
 Cole, S. J. 357(48), 388
 Colegrove, B. T. 91, 94, 96, 97(344),
 98(373b), 158, 421(146), 422(153), 428
 Coleman, B. 904, 913(251), 946, 952(5), 1024
 Coles, M. P. 701, 733(46), 737
 Collier, W. 67, 71, 73(278b), 156
 Collins, S. 395(34), 415(132), 425, 427
 Collinson, M. M. 570(13), 635
 Colomer, E. 642, 645(2b), 691
 Coltrain, B. K. 570(15), 635
 Colvin, E. 590(136), 638
 Colvin, E. W. 856(10), 904(289), 941, 946
 Colvin, V. L. 837(90c), 851
 Comanita, B. 746(14), 766(98, 99), 798, 800
 Comanita, B. M. 922(391), 948
 Combarieu, R. 575, 600(78, 79), 602(78),
 614(79), 636
 Comerlato, N. M. 404(92), 413(127, 128),
 414(128), 426, 427
 Conlin, R. T. 860(39), 941, 954(25), 955,
 956(31), 960, 962(53), 963(65), 989(53),
 990(65), 1000(53), 1025, 1026
 Conrad, N. D. 904, 913(251), 946
 Constantieux, T. 248, 311, 313(121), 332
 Constantine, S. P. 108, 109(391), 159
 Contini, S. 267(207), 335
 Cook, R. F. 575(68), 636
 Cooke, J. E. 408(111), 427
 Cooks, R. G. 1034(39), 1056
 Coolidge, M. B. 74(294), 156
 Coombs, N. 630(217), 640
 Coon, P. A. 837(89c, 90d), 838(103c), 851
 Cooper, D. L. 11(60), 18(128a), 36(60),
 93(364), 149, 151, 158
 Copley, B. C. 315(340), 337
 Cordonnier, M. 96(370b, 371), 158
 Corey, E. J. 472(24), 487, 889(202), 904(258),
 945, 946
 Corey, J. Y. 5, 7, 63(3), 147, 542(7), 561
 Corma, A. 572, 607, 620(38), 635
 Corriu, R. J. P. 484(121), 489, 569(8, 9),
 572(43, 44), 575(8, 9, 77–81, 85–87),
 578(80, 93–95, 97–104, 107–110, 113,
 117, 118, 121, 128, 129), 583(93, 109, 132,
 133), 584(93, 100, 117, 118), 585(108),
 586(113, 117), 588(93, 98, 99), 590(8, 93,
 98, 99, 101), 591(137), 593(121), 594(8),
 595(107, 109, 149–152, 155), 596(97, 98,
 149, 152, 155), 598(128), 600(78, 79, 95,
 113, 117, 118), 602(78, 98, 99, 161),
 603(94, 95), 604(93, 162), 606(165, 166),
 607(165), 609(100, 168), 610(95, 169, 170),
 611(94, 109, 110, 175), 613(179), 614(79,
 80, 107, 113, 117, 118, 155), 623(8, 97–99,
 203, 204), 625(161), 626(203), 631(8, 95,
 98, 99, 102, 150), 632(103, 108), 635–640,
 642, 645(2b), 683(68a, 68b, 69a, 69b), 691,

- 693, 715(169), 716(176, 178, 179),
735(296), 740, 741, 744, 752, 761(43), 799,
933(446, 447), 950
- Costa, A. 927(413), 949
- Costantino, C. 364(69), 389
- Costas, N. 578(102, 103), 631(102), 632(103),
637
- Cother, L. D. 726(248), 743
- Cotton, F. A. 93(363c), 113(410), 158, 160
- Cotts, P. M. 547(28), 562
- Coulter, S. 834(66, 67), 850
- Coulter, S. K. 830(50), 849
- Coupar, P. I. 709, 730(127), 739, 752,
761(47), 799
- Couret, C. 5, 6(20, 24d), 63(20), 64(259), 67,
83(20), 105(24d), 147, 148, 155, 499(32, 34,
35), 536
- Cousseins, J. C. 632(223), 640
- Cowan, R. D. 13(83a), 150
- Cowley, A. F. 980(96), 1026
- Cowley, A. H. 5, 6(17), 93(363c), 147, 158,
249(129), 291(278), 333, 336, 519(84),
533(135, 136), 538, 539
- Cox, H. 108, 109(391), 159
- Coyle, T. D. 240(63–65), 261(190), 331, 334
- Cradock, S. 64(257b), 155, 192(56), 220
- Craig, B. I. 830(46a), 844(133a), 849, 852
- Craig, R. A. 245(96), 332
- Cramer, C. S. 830(46b), 849
- Cramm, S. 838(109), 851
- Crawford, R. M. 806(6), 818
- Cray, S. E. 795(189), 802
- Creary, X. 858(33, 34), 941
- Crellin, K. C. 1045(97), 1058
- Cremer, D. 10(52), 41(189), 42(52, 198–200,
202), 43, 48–50(52), 128(459d), 132(470b),
133(459d, 470b), 134(459d), 136(459d,
477), 137(477), 149, 153, 162, 405(99), 426,
858(35), 941, 992(112), 1027
- Cremer, E. 10, 42, 43, 48–50(52), 149,
405(99), 426
- Cremer, U. 573(47), 636
- Crestoni, M. E. 1030(8), 1038(59), 1039(62,
64), 1047(114, 116), 1048(118, 121–123),
1049(126, 128), 1050(132), 1053(144),
1055, 1057–1059
- Crich, D. 362(63), 388
- Crocker, M. 719(199), 741
- Crohmann, C. 787(168, 169), 802
- Cromack, K. R. 346(18), 387
- Cronauer, D. C. 324(401), 339
- Crook, S. 928(432), 949
- Crosby, G. A. 632(224), 640
- Csaszar, A. G. 96(370b), 158
- Cserti, C. C. 997, 998, 1000(118), 1027
- Csonka, G. 208(85), 221
- Cuadrado, I. 613(180), 639, 752(44, 49),
767(44, 49, 106–112), 768(108), 799–801
- Cuadrado, P. 894(211), 945
- Cuenca, T. 729(270), 743
- Cundari, T. R. 102, 103(376b), 159
- Cunico, R. 886(185), 944
- Cunico, R. F. 927(414), 949
- Cunningham, T. P. 11, 36(60), 149
- Curran, D. P. 362(61b, 64–66), 377(103),
384(125), 385(126, 127), 386(128),
388–390, 870(92), 901(235), 903(246), 942,
945
- Curtis, J. M. 910–912(312), 947
- Curtis, L. A. 14(101), 150
- Curtis, M. D. 645(19d), 692
- Curtiss, L. A. 16(109, 115, 118, 123b),
81(318), 138(483c), 139(483c, 485),
140(485), 151, 157, 162
- Curzon, E. H. 311, 320(319), 337
- Cushman, M. 904(264), 946
- Custodio, M. 807(13), 818
- Cypryk, M. 477(67), 488, 703(69, 74),
715(164), 716(74), 717(69), 738, 740
- Czekay, G. 1037(54a), 1056
- Dabien, B. 578, 584, 609(100), 637
- Dabiens, B. 735(296), 744
- Dabisch, T. 54(229c), 154
- Dabosi, J. 575, 600(78, 79), 602(78), 614(79),
636
- Dabrowski, J. 826(26b), 848
- Dahlin, K. 807(15), 818
- Dai, B. T. 575(66, 70), 636
- Dai, D. 110, 112(405), 159
- Dai, S. 1031(23), 1056
- Daimon, H. 838(103e), 851
- Dakternieks, D. 343(8a, 8b), 358(51), 359(8a,
8b, 51), 360(8a, 8b), 387, 388
- Dal, C. 823(6b), 847
- Dale, C. M. 858(36), 941
- Daljeet, A. K. 928(430), 949
- Dalling, D. K. 230(27), 330
- Dalman, D. A. 760(70), 800
- Dalton, L. R. 632, 633(222), 640
- Damewood, J. R. 642(13d), 691
- Damja, R. I. 699(38), 702(61), 734(38, 294),
737, 738, 744
- Dammel, R. 64(257d), 155, 166, 168, 169(12),
180, 181(40), 191(55), 192(12, 40, 55, 57,
62), 193(55), 199(57), 208(40), 218–220
- Damrauer, R. 95(366a), 158, 479(82), 488,
910(318), 947
- Daney, M. 914(350–352), 948
- Danheiser, R. L. 877(136, 141, 142),
878(142), 879(154, 162, 167), 880(142, 154,
168–171), 901(236), 943–945
- Dani, P. 769(120), 801
- Danishefsky, S. J. 928(429), 949
- Danovich, D. 93(364), 158
- Danso-Danquah, R. E. 920(384), 948

- Daprich, S. 96(368), 158
 Daran, J.-C. 251(140), 333
 D'Arco, P. 35(163), 152
 Darden, T. A. 823(10c), 847
 Da Roit, G. 351(32), 388
 Dartmann, M. 904(269), 946
 Das, J. 889(202), 945
 Das, K. K. 16, 19, 29, 128(114), 151
 Dat, Y. 206(82b), 221
 Dathe, C. 480(88), 488
 Daudel, R. 166(7), 217
 Daughenbaugh, N. E. 709(126), 739
 Daugulis, O. 914, 915(353), 948
 Davalli, S. 267(207), 335
 Davaux, J. 542(11), 561
 David, D. E. 199(65b), 220
 David, L. D. 559(61), 562
 Davidson, E. R. 199(69), 220
 Davidson, F. 724(223), 742
 Davidson, I. M. T. 19, 122(130b), 151,
 904(250), 907(304), 946, 947, 954, 955(24),
 956, 958, 963, 982(34), 1025
 Davidson, J. 63(252a), 155
 Davidson, M. G. 108, 109(393), 159
 Davidson, P. J. 63(252c), 155
 Davis, A. L. 266(204), 334
 Davis, D. D. 542(19), 547(19, 31, 33),
 548(19), 561, 562
 Davis, D. G. 257(158), 333
 Davis, M. E. 578, 586, 623(114), 637
 Davis, W. M. 195, 197(63), 220, 395(44), 425,
 1006, 1007(133), 1027
 Davoust, D. 244, 259, 312(93), 332
 Day, C. S. 864(56), 942
 Day, P. 166(6), 217
 Day, P. N. 825(16b), 847
 Day, R. O. 724(225), 726(252), 742, 743
 Day, V. W. 864(56), 942
 Debad, J. D. 864(63), 942
 Debaerdemaeker, T. 483(119), 489
 DeBellis, A. D. 319(366), 338
 Decker, J. 923(399), 949
 Decker, R. 471(16), 486
 Degens, E. T. 808(27), 818
 Degl'Innocenti, A. 933(448), 950
 deHaas, M. P. 559(64), 563
 De Hazan, Y. 570(20, 22), 635
 Dehnert, U. 484(123), 489
 Deiters, J. A. 724(225), 742
 Dejak, B. 904(278), 946
 De Jéso, B. 248, 250(125), 311(125, 321),
 333, 337
 Del Amo, Y. 807(16), 818
 Delanghe, P. H. M. 922(389), 928(389, 416),
 948, 949
 Delcroix, B. 79(314b), 156
 DeLeeuw, B. J. 91, 94(346, 347, 353), 96(346,
 347), 158
 Déléris, G. 243(87, 88), 332, 471(12), 486
 Delmau, J. 315(330, 332), 337
 Del Nin, J. W. 808(19), 818
 Delord, P. 578, 588, 590(98, 99), 596(98),
 602(98, 99, 161), 604(162), 623(98, 99),
 625(161), 631(98, 99), 637, 639
 Delouvrié, B. 368(81), 389
 Delpech, F. 251(140), 333
 Demaison, J. 29(154), 152
 deMeijere, A. 858(37), 941
 De Menezes, S. C. 329(417, 418), 339
 Dement'ev, V. V. 547(35), 562, 700(42),
 727(42, 260), 737, 743
 Deming, T. J. 816(48), 819
 Demoustier-Champagne, S. 542(11), 561
 Demuth, J. E. 826(27a, 27b), 837(90a), 848,
 851
 Demuyneck, C. 96(370a, 370b, 372), 158,
 421(145), 428
 Demuynek, C. 79(314a), 156
 Denari, J. M. 780(146), 802
 Denat, F. 578, 586, 600, 614(113), 637
 Denhez, J. P. 1041(73a, 73b), 1057
 Denisov, E. T. 361(59), 388
 Denk, K. M. 202, 203(77), 220
 Denk, M. 114(420a-d, 422), 115(420b-d,
 422, 428), 116(428), 160, 161, 202(79, 80),
 221
 Dent, W. H. 910(319), 947
 Depmeier, W. 485(133), 489
 DePuy, C. H. 95(366a), 158, 1031, 1041(13),
 1055
 Dereppe, J.-M. 324(399, 400), 339
 Derouiche, Y. 699, 734(38), 737
 D'Errico, J. J. 479(72), 488
 De Santis, M. 312(326), 337
 De Schutter, C. T. 594(147), 638
 Desclaux, J. P. 5(31), 7(40), 14, 15(31), 148
 Deshpande, R. 316(353), 338
 DeSimone, R. E. 230(35), 331
 Despande, R. 620(196), 639
 Desper, J. M. 395, 397, 420(42), 425
 Destombes, J. 79(314a), 156
 Destombes, J.-L. 96(370a, 370b, 372), 158,
 421(145), 428
 Desvaux, H. 282, 293(256, 257), 336
 Detty, M. R. 481(91), 488
 Deubzer, B. 795(188), 802
 Deutsch, P. P. 249(130), 333
 Deutzmann, R. 809, 810, 817(35), 819
 Devadas, B. 935(456), 950
 D'Evelyn, M. P. 837(94a, 94b), 851
 De Vita, A. 844(140a, 140b), 852
 Devylder, N. 683(68b), 693
 Dewar, M. J. S. 13(78a, 79-81), 42(197),
 48(221a), 59, 60(197), 150, 153, 154,
 405(94), 426
 Dexheimer, E. M. 707(111), 739

- Deyo, D. 879(159), 944
 De Young, D. J. 259(175), 292(288), 334, 336,
 401(67, 68), 403, 404(78), 408(67, 112,
 113), 409(113), 411(67), 419(78), 425–427,
 1011(151), 1028
 Dhar, R. K. 914(349), 948
 Dhurjati, M. S. K. 960, 962, 989, 1000(53),
 1025
 Diaba, F. 374(96), 389
 Dianxun, W. 208, 213(87), 221
 Dias, H. V. R. 202(78), 221
 Diau, E. W. -G. 217(99), 221
 Dick, S. 955, 982(29), 1025
 Dielkus, S. 439(54), 445, 448(93), 450, 451,
 459, 465(100), 466, 467
 Dill, J. D. 43(205a), 153
 Dillon, K. B. 494(12, 17), 495, 514(19), 536
 Ding, W. F. -X. 352(33), 388
 Ding, Y. 648(35e), 692
 Di Pietro, R. 575(68), 636
 Dippel, K. 438(46), 444(84), 458(103),
 459(84, 104), 460(84, 105, 106, 108, 109),
 462(103, 105), 463(105, 106, 108, 109),
 466, 467
 Di Renzo, F. 575(59), 636
 Distefano, G. 207(83), 221
 Diver, S. T. 914, 915(353), 948
 Dixon, B. R. 877(141, 142), 878, 880(142),
 943
 Dixon, C. E. 402(70), 408(70, 111), 426, 427,
 1022(163), 1028
 Dixon, D. A. 79(314d), 115, 116(428), 138,
 139(483a), 157, 161, 162, 202(77, 78),
 203(77), 220, 221, 724(223), 742
 Djurovich, P. I. 559(61), 562
 Dleij, T. J. 559(64), 563
 Do, J. Y. 144(500), 163
 Dobbs, K. D. 67, 71, 73(278a), 156
 Dobros, S. 725(245), 742
 Dobson, C. M. 320(383), 338
 Dodabalapur, A. 687(77), 694
 Dodd, G. H. 928(418), 949
 Doddrell, D. M. 245(99, 101), 246(99, 101,
 106, 107), 332
 Dodson, G. 813(46), 819
 Does, T. van der 513(69), 526, 527(111), 537,
 538
 Dohmaru, T. 555(49), 556(53), 559(59, 60),
 562, 676, 679, 680, 690(62b), 693
 Dohnalek, Z. 834(75b, 78b), 850
 Doke, N. 629–631(210), 640
 Dolbier, W. R. 43(205b), 153
 Dolbier, W. R. Jr. 346(17), 387
 Dolg, M. 10, 11(53), 13(91, 92a, 92b), 14(53),
 15, 17(106), 33(53), 139(106), 149–151,
 192, 202, 214(61), 220
 Domengès, B. 724(226), 742
 Donaghy, K. J. 516(80), 538
 Donaldson, B. R. 230(34), 331
 Doncaster, A. D. 16(117), 151
 Dondy, B. 888(194), 944
 Donogues, J. 248, 311, 313(121), 332
 Doren, D. 831, 832(56), 837(97), 849, 851
 Doren, D. J. 826(26h), 830(49), 835, 836(84),
 848–850
 Dorfman, E. 710(133), 739
 Dorfmeister, G. 494(15, 16), 536
 Dorn, H. 699, 724(31), 737
 Dörr, J. 191–193(55), 220
 Dort, P. C. van 380(111), 390
 Dorthout, P. K. 593(141), 638
 Dos Santos, D. A. 686(75b), 694
 Douglas, W. E. 683(69a, 69b), 693
 Downing, J. W. 542(12), 561
 Doyle, M. P. 474(29), 487
 Dragojevic, M. D. 714(156), 740
 Drake, J. E. 481(95), 488
 Drake, R. 725(238), 742
 Drapailo, A. B. 531(129), 539
 Dreeskamp, H. 284(263), 336
 Dresser, M. J. 827(39c, 39d), 830(39c),
 845(144), 849, 853
 Drewello, T. 1037(54a), 1056
 Driess, M. 5, 6(11e, 22), 48–50(22), 63(11e),
 81, 82(324), 112(22), 113(22, 324), 115(22),
 147, 157, 413(126, 127), 427, 509(62, 63a,
 63b, 64, 65), 514(71), 534(63a, 63b, 137,
 138), 537, 539
 Dromzee, Y. 701, 729(56), 738
 Drost, C. 439(54, 58), 466
 Drozdov, V. A. 715(161), 740
 Drum, R. W. 808(25), 818
 Drzal, L. T. 575(55), 636
 Dua, S. S. 706(101), 739
 Dubac, J. 46(210a, 210b), 153, 642(2a, 2d,
 13c), 645(2a, 2d), 662(2a), 691, 904(250),
 946
 Dubchak, I. L. 727(255), 728(264), 730(273),
 733(293), 743, 744
 Dubois, G. 578(113, 117, 118), 584(117, 118),
 586(113, 117), 600, 614(113, 117, 118), 637
 Dubovik, I. I. 751, 757(28, 37), 758(37),
 759(28), 799
 Duchamp, J. C. 399(63, 64), 400(64), 425
 Duchateau, R. 573(47), 636, 719(202), 741
 Duer, M. J. 108, 109(393), 159
 Duhamel, L. 912(330), 947
 Duke, B. J. 94, 98(358), 158
 Dumont, M. 634(227), 640
 Dunbar, R. C. 1034(35, 36), 1045(94a–c),
 1056, 1057
 Duncanson, L. A. 48(221b), 154, 405(95), 426
 Dunitz, J. D. 904(289), 946
 Dunkel, R. 277(231, 232), 335
 Dunoguès, J. 243(88), 332, 471(12), 486,
 583(131), 638

- Duplan, J.-C. 315(330, 332), 337
 Durfee, L. D. 864(66), 942
 Dvornic, P. R. 760(63–71), 799, 800
 Dyall, K. G. 5, 6(32), 13(32, 94), 15(32),
 17–19(126), 148, 150, 151
 Dykema, K. J. 82(326b), 120, 122, 123(442),
 157, 161
 Dzarnoski, J. 17(127), 151
- Eaborn, C. 240(61), 331, 433(23), 465, 578,
 590(127), 638, 697(2, 3, 5, 6), 699(36–38),
 702(57, 59–62), 706(99, 101, 102),
 707(103–106), 708(120), 713(150), 714(3),
 728(106, 265, 266), 729(272), 731(6, 150,
 266, 282, 285, 287, 288, 290), 732(62),
 734(38, 294), 736–740, 743, 744, 910(315,
 318), 939(466), 947, 950
 Early, C. W. 58–60, 62(241), 154
 Ebara, H. 911(324), 947
 Ebata, K. 395, 397, 399(39a), 425, 864(51),
 904(252), 942, 946
 Ebert, H. 844(137a), 852
 Ebner, C. 841(123a, 124), 852
 Ebsworth, E. A. V. 483(114), 488
 Ebwein, B. 766(97), 800
 Eby, R. K. 542(13), 561
 Eckert, G. 762(80), 800
 Edamoto, K. 834(72), 850
 Edelman, M. A. 857(29), 941
 Edelmann, F. T. 718(196), 741, 752(45), 799
 Edgar, L. 808(24), 818
 Edgell, R. G. 166(6), 217
 Edlund, U. 136, 137(478), 162
 Egan, J. W. Jr. 864(60), 942
 Egenolf, H. 96(371), 158
 Egert, E. 450, 452, 453(95), 467
 Eggeling, E. B. 769(118), 771(127), 801
 Egorov, M. P. 118(430), 119, 120(435),
 127(455a), 161
 Eguchi, S. 883(180), 944
 Ehrlich, H. 470(6), 486
 Eibl, M. 294(292), 336, 476(57), 487
 Eich, G. V. 259(176), 334
 Eichler, B. E. 75(303), 87, 89(338b–d), 98,
 100, 101(303), 156, 157
 Eichler, E. 269, 270(212), 335
 Einstein, F. W. 864(55), 942
 Einstein, F. W. B. 864(63), 942
 Eisen, M. S. 932(445), 950
 Eisenberg, R. 249(130), 333
 Eisenhart, E. K. 888(192), 944
 Eisenschmid, T. C. 249(130), 333
 El Ayoubi, S. 583(132, 133), 638
 Elbert, S. T. 832(61c), 849
 El-Kaddar, Y. Y. 707(104, 105), 739
 El-Kheli, M. N. 939(466), 950
 Ellinger, Y. 1031(22), 1056
 Elliott, R. L. 703(82), 738
- Ellis, G. B. 139, 140(486a), 162
 Ellis, P. D. 277(234), 335
 Ellison, G. B. 140(488), 163, 419(143), 427
 Ellison, M. D. 830(50), 834(67), 849, 850
 Elsässer, R. 776(143), 801
 Elschenbroich, C. 5(8), 147
 El Sheikh, M. 5, 6, 63(12b), 147, 952, 997,
 998(17a), 1025
 Elter, G. 857(26), 941
 Emmer, J. 712(145), 740
 Emsley, J. W. 224(1), 330
 Enda, J. 891(204, 207), 945
 Endo, T. 654, 655, 657, 659, 660(43), 689(79),
 693, 694
 Enev, V. 891(208), 945
 Enevoldsen, T. 16(108), 151
 Engel, T. 838(100, 105a, 105c), 839(105a),
 840(105a, 105c), 841, 842(100, 122),
 844(136b), 845(141), 851, 852
 Engelhardt, G. 236, 258(51), 318(362, 363),
 331, 338, 594(146), 638
 Engelhardt, L. M. 864(64), 942
 Engels, B. 478(70), 488
 Englekling, P. C. 139, 140(486a), 162
 Engmann, R. 729(268), 743
 Engstrom, J. R. 838–840(105a), 841,
 842(122), 845(141), 851, 852
 Enkelman, V. 610(171), 639
 EnBlin, W. 172, 173(26), 174(26, 29), 175(29),
 176(26, 29), 178, 180(38), 218, 219
 Enzelberger, M. M. 113(411c), 160
 Erbeia, A. 316(355), 338
 Ericsson, A. 315, 318, 319(342), 337
 Eriyama, Y. 393, 395(20), 424
 Erker, G. 857(25), 941
 Ermler, W. C. 13–15, 17(88b, 89a, 89b), 150
 Ernst, M. 241, 257(73), 292(284), 331, 336
 Ernst, R. R. 241(73), 244(94), 245(104),
 247(104, 113), 255(146), 257(73), 259(176),
 281(244, 247), 282(255), 292(281, 282),
 328(415), 331–336, 339
 Ertel, T. S. 612, 617, 619(177), 639
 Escalante, S. 28–31, 110, 112, 113(153), 152
 Escolano, C. 367(79), 374(96), 389
 Escudíé, J. 5, 6(16, 20, 24d, 24e), 51(16),
 63(16, 20), 67, 83(20), 105(24d, 24e), 147,
 148, 499(32, 34, 35), 536
 Escudie, N. 591(137), 638
 Espenson, J. H. 1002(123), 1027
 Eswarakrishnan, V. 208, 210, 211(90), 221
 Eteläniemi, V. 845(142), 853
 Etgens, V. H. 826(25a), 848
 Ethridge, E. 67, 71, 73(278b), 156
 Evans, D. A. 919(363), 936(462), 948, 950
 Evans, D. F. 808(20), 818
 Evans, D. R. 838(101b), 851
 Evans, J. F. 837(88b), 850

- Evans, J. W. 840(121), 842(121, 126b, 127), 852
 Evans, N. A. 258, 320(166), 334
 Evans, P. A. 376(97, 98, 99a, 99b), 389
 Evans, P. J. 324(396), 339
 Evans, S. 166(6), 217
 Evanseck, J. D. 117(429b), 161
 Evanson, K. M. 112(404a), 159
 Evilia, R. F. 240, 326(68), 331
 Ezhova, M. B. 960, 962, 989, 1000(53), 1025
- Fabry, L. 64(257c), 155, 192(58), 220
 Fäcke, T. 261, 268(192), 298(296), 334, 336
 Fadeev, M. A. 791(175), 802
 Faegri, K. 9, 17, 18, 32(48b), 149
 Faegri, K.Jr. 5, 6, 13(32), 14(104), 15(32, 104), 25, 29(104), 148, 151
 Fagan, P. J. 647(29a, 29b), 692, 864(56), 942
 Fajari, L. 710(137), 739
 Fajula, F. 575(59), 636
 Falender, J. R. 703, 716, 717(67), 738
 Fallis, A. G. 922(391), 948
 Fan, H. 629–631(210), 640
 Fanta, A. D. 259(175), 292(287, 288), 334, 336, 408(113), 409(113, 117), 413(126, 127), 427
 Fanwick, P. E. 645(24c), 692, 904(264), 946
 Farmer, B. L. 542(18), 543(20a, 21), 547(18, 30a), 548(18, 39, 43, 44), 561, 562
 Farmer, S. C. 575(56), 636
 Farnsworth, H. E. 825(22), 848
 Farrall, P. D. 844(136b), 852
 Farrar, T. C. 240(63, 65), 283, 285, 286, 288, 289, 291(259), 331, 336
 Fässler, J. 312(324), 337
 Fässler, T. F. 66(273), 73(292), 75(273), 93(292), 155, 156
 Fattah, F. A. 910(315), 947
 Fau, S. 132, 134(467), 135(467, 474), 162
 Faulon, J. L. 604(164), 639
 Faure, T. 864(46), 941
 Faustov, V. I. 118(430), 119, 120(435), 161
 Fawcett, J. K. 731(280), 743
 Fawzi, R. 617(185), 639
 Fearon, F. W. G. 703(68), 710(136, 138), 716, 717(68), 738–740, 746(15), 798
 Feeney, J. 224(1), 330
 Feher, F. 172–174, 176(26), 218
 Feher, F. J. 701(48, 53), 704(90, 91), 705(92), 711(141), 712(144), 715(92), 720(141, 204, 206–208), 727(141, 144, 257, 258), 729(48, 91, 92), 730(53), 737, 738, 740, 741, 743
 Fehlnr, T. P. 192(60), 220
 Feibelman, P. J. 823(7), 847
 Feller, D. 138, 139(483a), 162
 Felsche, J. 712(145), 740
 Feng, X. 93(363c), 158
 Fenical, W. 282(252), 336
 Fensterbank, L. 368(81), 389
 Ferguson, G. 718, 722(198), 725, 726(247), 741, 743
 Ferman, J. 47, 48(214), 153
 Fernandez, Y. V. 908(309), 947
 Ferreira, L. 481(98), 488
 Ferreri, C. 342(3), 346(19), 359, 362(3), 364(3, 69), 367(77), 377(100), 381(114, 115), 382(121a), 383(19), 385(127), 387, 389, 390
 Ferrige, A. G. 328(416), 339
 Fessner, W.-D. 370(86a, 86b), 389
 Feutrill, G. I. 935(455), 950
 Fey, O. 707, 732(116), 739
 Fick, J. 570(27), 635
 Field, M. J. 825(20b), 847
 Fife, W. K. 633(226), 640
 Filippou, A. C. 64(261c), 155
 Finger, C. M. M. 58, 61, 62(238), 154, 417, 423(139), 427
 Fink, D. M. 877(136), 880(171), 901(236), 943–945
 Fink, J. 63(251), 155
 Fink, M. 952(18), 1011(150), 1025, 1028
 Fink, M. J. 349(24), 388, 392(1), 395(1, 32), 397(32), 399(62), 401(67, 68), 408(67), 411(67, 120), 412(123), 424–427, 492(2), 536, 955, 956(31), 1025
 Fink, W. 442(66), 444(80), 466, 467
 Fink, W. H. 94(365), 158
 Firgo, H. A. 910(317), 947
 Firman, T. K. 412, 413(125), 427
 Fischer, A. 516(78), 538, 718(196), 741
 Fischer, F. 192(62), 220
 Fischer, G. 988(106–108), 1027
 Fischer, M. 746(11), 798
 Fischer, M.-R. 920(371), 948
 Fisel, C. R. 423(155), 428
 Fisher, A. J. 830(47a), 849
 Fisher, N. D. 1030(7b), 1055
 Fita, I. 710(137), 739
 Fitch, J. W. 318(364), 338
 Fives, K. 834(74c), 850
 Fjeldberg, T. 63, 67(253–255), 68, 70(254), 113(413a), 155, 160, 397(56), 425
 Fleet, G. W. J. 928(431, 432), 949
 Fleischer, H. 271, 319(214), 335
 Fleming, I. 827(36), 848, 856(9), 882(177, 178), 889(203), 897(226), 902(243), 919(366), 941, 944, 945, 948, 1046(108), 1058
 Fleming, W. 542, 547, 548(18), 561
 Flintjter, B. 187(52b), 220, 402, 406(72), 407, 408(109), 426
 Flodstrom, A. S. 834(74b, 78a), 850
 Flores, C. R. 837(88a), 850
 Flores, J. R. 1031(20, 24), 1032(29), 1056
 Flowers, M. C. 837(89e), 851, 952(1), 1024

- Floyd, C. D. 919(366), 948
 Fogarty, H. A. 542(17), 561
 Foitzik, N. 877(140, 145), 943
 Fokkens, R. H. 1053(145), 1059
 Foland, L. D. 926(411), 949
 Foley, K. M. 474(30), 487
 Fölling, P. 495, 501(22, 23), 506(23), 510(66), 514(22), 519, 520(85), 522, 528, 529(90), 536–538
 Fontlupt, S. 572(40), 636
 Foord, J. S. 844(137a), 852
 Ford, R. R. 858(30), 941
 Fornarini, S. 1039(64), 1047(113–117), 1048(118, 121–123), 1049(113, 126, 128), 1050(132), 1053(144), 1057–1059
 Fortier, T. M. 833(65a), 850
 Fossum, E. 477(67), 488
 Foster, M. P. 277(232), 335
 Fotiadu, F. 908(311), 947
 Fourcade, R. 610(169), 639
 Fowler, C. E. 572(41), 636
 Fox, A. 1031, 1032(14), 1035(43), 1040(14, 69), 1041(69), 1055–1057
 Framery, E. 595(151, 152), 596(152), 638, 716(178), 741
 Francisco, J. S. 5(27d), 148
 Frankel, D. J. 838(108), 851
 Franken, S. 731(284), 743
 Franklin, A. M. 1036(50), 1056
 Franville, A.-C. 578, 586(116), 632(116, 223), 637, 640
 Frapper, G. 648, 649, 651(34a–c), 692
 Frebel, M. 507(55), 537
 Fréchet, J. M. J. 746(4), 794, 795(184–187), 798, 802
 Freeburger, M. 707(110), 739
 Freeman, R. 240(70), 245, 247(98), 257(154, 157), 261, 262(193), 273(220–222), 274(222, 227), 275(229), 277(233), 281(220), 331–335
 Freeman, W. P. 642(3, 4j, 4k), 679(4j, 4k), 691
 Freire-Erdbrügger, C. 722(215), 742
 Freitag, D. 271(215), 335
 Freitag, S. 437(45), 466
 Frenkiel, T. 257(154, 157), 274(227), 277(233), 333, 335
 Frenkiel, T. A. 273(221), 335
 Frenking, G. 28, 29, 31, 32(152), 81(323), 91(346, 350), 92(350), 94(346, 350), 95(350), 96(346), 112(403), 114, 115, 117–119(323), 132(467), 134(467, 472, 473), 135(467, 473, 474), 140(473), 152, 157–159, 162, 1041(70), 1057
 Frenklach, M. 825(17a, 17b), 830(46b), 847, 849
 Frenzel, A. 431(14), 432(17), 450(98), 465, 467
 Frenzen, G. 932(445), 950
 Freund, R. 172–174, 176(26), 218
 Frey, H. 548(40), 558(55), 562, 746(18, 20), 757(60), 762(75, 76, 83–85), 765(76, 88–90), 769(117, 123), 787(166), 788(170–172), 791(176), 798–802
 Frey, H. M. 119(434a–c, 436), 120, 122(436), 125(452b), 127(454a), 161
 Frey, R. D. 199(69), 220
 Frick, B. 762(84), 800
 Friedheim, J. 13(78a), 150
 Friedman, J. M. 31(159), 152
 Friedmann, G. 755, 760(58), 799
 Friedrich, O. 108(392), 159
 Friend, R. H. 686(75b), 694
 Friesen, R. W. 928(430), 949
 Friesner, R. A. 825(20c), 847
 Frietas, M. A. 755, 767(57), 799
 Frisch, K. C. 623(200), 640
 Frisch, M. J. 12(61–63, 73, 75), 16(111, 119), 96(368), 118(111), 149–151, 158, 825(21d), 847
 Fritz, G. 471(14), 486, 494(11), 498(29), 509(11), 536
 Fritz, H. 927(412), 949
 Froc, G. 634(227), 640
 Fronczek, F. R. 914(349), 948
 Fronda, A. 872(116, 117), 943
 Fronzoni, G. 291(279), 336
 Frunze, T. M. 547(35), 562, 700(42), 727(42, 260), 737, 743
 Fry, B. E. 786(162, 163), 802
 Fry, C. 399, 400(64), 425
 Fuchikami, T. 968(82, 83), 969(83), 982(98), 990(82, 110), 1003(125–127, 129), 1026, 1027
 Fuchkami, T. 475(45), 487
 Fuchs, E. 904(295), 946
 Fuchs, E. P. O. 513(69), 537
 Fuchs, P. L. 380(111), 390
 Fuhrer, H. 319(366), 338
 Fujii, S. 935(452), 950
 Fujii, T. 864(45), 941
 Fujii, Y. 1005(131), 1027
 Fujiki, K. 864(44), 941
 Fujiki, M. 545(24–26), 546(25, 27), 557(54), 561, 562
 Fujimoto, K.-i. 896(215), 945
 Fujino, M. 58(239c, 239d), 154, 558(58), 562
 Fujino, T. 676, 679, 680, 690(62b), 693
 Fujio, M. 1046(107), 1050(133), 1058
 Fujisawa, M. 833(64), 850, 896(214), 945
 Fujita, E. 918(360), 948
 Fujita, K. 838(106), 840(119), 851, 852
 Fujita, M. 48, 49(219), 153, 704(89), 738
 Fujitsuka, M. 352, 354(39), 388
 Fujiue, N. 555(49), 556(53), 562
 Fujiwara, K. 834(71), 850

- Fujiwara, N. 810(39), 819
 Fujiwara, T. 919(370), 948
 Fukatsu, S. 838(106), 851
 Fukava, N. 395, 397, 412(36), 425
 Fukaya, N. 101(375), 106, 137(375, 385c), 159
 Fukui, K. 1003(129), 1027, 1036(48), 1056
 Fukui, M. 503(44), 537
 Fukushima, M. 559(66–68), 560(66, 68), 563, 647, 662, 665(28b), 692
 Fukushima, Y. 630(215), 640
 Fumiori, K. 559(65), 563
 Funaya, M. 679(66), 693
 Fure, H. 864(50), 941
 Furmanova, N. G. 727(256), 743
 Fürstner, A. 894(212), 898(228), 945
 Furthmüller, J. 823(6d), 847
 Furukawa, K. 46(211a), 58(239c, 239d), 153, 154, 642, 654, 687(16), 688(16, 78), 689(79), 691, 694
 Furukawa, S. 543(20b), 547(32), 548(37), 561, 562
 Fyfe, C. A. 255(145), 333, 594(147), 638
- Gabor, B. 894(212), 945
 Gabrielli, R. 1047(114), 1058
 Gade, L. H. 434(31, 32), 465
 Gais, H.-J. 923(399), 949
 Gal, J.-F. 139, 140(486c), 162
 Galarneau, A. 575(59), 636
 Galasso, V. 291(279), 336
 Galat, K. J. 732(292), 744
 Galaup, J. P. 570(12), 635
 Galbraith, J. M. 72(289), 91(352), 156, 158
 Gale, D. J. 251(132), 258, 320(132, 166), 333, 334
 Gallego-Planas, N. 57(237a, 237b), 154
 Gallucci, J. C. 870(99), 929(435), 943, 949
 Gamper, S. 726(251), 743
 Gankema, H. 791, 794(177), 802
 Gannelis, E. 570(16), 635
 Gano, D. R. 16, 118(111), 151
 Gao, J. 11(59a), 149, 825(20b), 847
 Gao, P.-L. 844(133b), 852
 Gao, Q. 834(75b, 78b), 844(132), 850, 852
 Garber, L. T. 376(99a), 389
 Garbow, J. R. 265(199), 334
 García, B. 752(49), 767(49, 111), 799, 801
 Garcia, E. 652(39), 693
 García de Viedma, A. 368(80), 389
 Garcia-Granda, S. 879(165), 944
 Gardner, K. C. 735(295), 744
 Gardy, G. 13(78a), 150
 Garmer, D. 825(16b), 847
 Garnier, F. 683(68a, 69a), 693
 Garrat, J. 18(128a), 151
 Garrone, E. 607(167), 639
- Garroway, A. N. 255(147), 256(147, 148, 150–153), 333
 Gaspar, P. P. 397(55b), 414(129), 425, 427, 904(254), 907(305), 946, 947
 Gassman, W. 807(14), 818
 Gasteiger, J. 5, 12(25a), 148
 Gates, S. M. 845(143), 853
 Gaul, J. M. 584(134), 638
 Gauss, J. 10(52), 41(189), 42(52, 200), 43, 48–50(52), 149, 153, 405(99), 426, 992(112), 1027
 Gavrilova, E. 525(100), 538
 Gebhardt, F. 483(115), 488
 Gehrhus, B. 114(423, 424), 160
 Gehrhus, B. 114(415a, 415b, 421a–c), 160
 Geiger, W. E. 712, 725(142), 740
 Geissler, H. 919(369), 948
 Gelbrich, T. 718(196), 741
 Gelius, U. 166(13), 218
 Geng, B. 933(446), 950
 Geoffroy, M. 525(100, 101, 104–106), 538
 George, P. D. 697(12), 736
 George, S. M. 837(89c), 838(103c), 851
 Georgiadis, G. M. 910(320), 947
 Gerbier, P. 610(169, 170), 639, 683(68a), 693
 Gérard, L. 904(263), 946
 Gerlach, C. P. 904(277), 946
 Gerrat, J. 11, 36(60), 149
 Gerson, F. 203, 205, 206(81), 221
 Gerstein, B. C. 256(149), 333
 Gerstmann, S. 307(310), 337
 Gescheidt, G. 347(21a), 388
 Getmanova, E. G. 776(140), 801
 Getmanova, E. V. 762(78–81), 764(78), 766(95), 776, 778(81), 791(78, 81), 800
 Gewert, J. A. 919(369), 948
 Ghannam, A. 866(80), 901(80, 232), 942, 945
 Ghosh, U. 897(226), 945
 Ghost, S. K. 882(177, 178), 944
 Gibbs, G. V. 35(163), 152, 724(224, 226, 227), 742
 Gibby, M. G. 241(75), 331
 Gibson, C. 923, 924(400, 401), 949
 Giese, B. 362(62, 64), 368(82, 83a), 388, 389
 Gieskes, W. W. C. 806(7, 8), 807(7), 808(26), 818
 Gilbert, M. M. 832(61c), 849
 Gilette, G. R. 421(151), 428
 Gill, P. M. W. 12(73), 16(123a), 149, 151, 825(21b), 847
 Gillette, G. R. 277, 278(238), 295(238, 294), 335, 336, 403, 404(79, 82, 85), 409, 410(116), 411(121), 419(79), 426, 427, 1019(160), 1028
 Gilliam, W. F. 471(18), 486
 Gilloir, F. 899(230), 945
 Gilman, H. 477(61), 487, 645(20), 692, 710(136, 138), 739, 740

- Gimarc, B. M. 102, 104(377a), 159
 Gimisis, T. 342, 359, 362(3), 364(3, 69, 70),
 366(75, 76), 382(121a), 387, 389, 390
 Ginsburg, D. 54(228a), 154
 Ginzburg, M. 698, 731(23), 737
 Girard, L. 870(100), 943
 Gladstone, D. J. 845(145), 853
 Gladysz, J. A. 243, 326(86), 332
 Glaser, E. 617(184), 639
 Glaser, R. H. 594(144), 638, 716(173), 740
 Glatthaar, J. 64(257a), 155
 Glaubitt, W. 578(130), 638
 Glavincevskii, B. M. 481(95), 488
 Gleason, R. W. 877, 878, 880(142), 943
 Gleiter, R. 197(64), 202(76), 208(86), 220, 221
 Glendening, E. D. 14(102a, 102b), 150
 Glidewell, C. 725, 726(247), 743, 870(98), 942
 Gliński, R. J. 79(314d), 157
 Glosik, J. 1031(12), 1032(26), 1033(26, 32),
 1055, 1056
 Glukhovtsev, M. 105, 106(383), 159
 Glukhovtsev, M. N. 103, 108(381a), 159
 Gluth, M. 431(14), 439(57), 465, 466
 Gobbi, A. 112(403), 134(472, 473), 135,
 140(473), 159, 162
 Gobbi, G. C. 594(147), 638
 Göbel, I. 169, 186, 187(24), 218
 Goddard, W. A. III 823(13), 824(15), 826(28),
 827(28, 32), 847, 848
 Godovskii, Yu. K. 725(242, 243), 742
 Goebel, D. W. 934(449), 950
 Goede, S. J. 526, 527(112), 538
 Goel, S. C. 113(411b), 160
 Goepfel, D. 923, 924(406), 949
 Goerge, S. M. 837(90c, 90d), 851
 Goerlich, J. R. 114(418c), 160
 Goemann, H. 877(140), 943
 Goh, J. B. 922(389), 928(389, 416), 948, 949
 Goldberg, D. E. 63(252b), 155, 397(56), 425
 Goldberg, G. M. 710(133), 739
 Goldberg, N. 93(363i), 132(466), 158, 162,
 1030(9), 1031(21), 1032, 1033, 1035, 1036,
 1043, 1044, 1046(9), 1055, 1056
 Goldfuss, B. 47, 106(213), 153, 642,
 679(4e–g), 691
 Golding, B. T. 928(418), 949
 Gole, J. L. 79(314d), 157
 Golino, C. M. 978(93), 1026
 Golly, M. 791(177), 794(177, 183), 802
 Golovina, N. A. 725(233, 241, 243), 742
 Gómez, F. J. 379(109), 390
 Gómez, R. 729(270), 743
 Gómez-Sal, P. 729(270), 743
 Gong, C. 794, 795(186, 187), 802
 Gonzales, S. L. 720(207), 741
 Gonzalez, A. I. 1031(16), 1055
 González, B. 767(111), 801
 González-Nogal, A. M. 894(211), 945
 Goodby, J. W. 731(288), 744, 752(46),
 765(46, 93), 799, 800
 Goodgame, D. M. L. 703, 729(85), 738
 Goodings, J. M. 1042(74), 1057
 Goodman, R. S. 844(139b), 852
 Göpel, W. 619(191), 639, 838(108), 851
 Gorbacevich, O. B. 791, 794(177), 802
 Gorbatshevich, O. B. 751, 757, 759(28), 762,
 764(78), 776, 777(139), 787(167–169),
 791(78, 175), 799–802
 Gordon, M. S. 5(27a, 27c, 27d), 16(111),
 37(170), 48–50(217), 54, 56(231, 232),
 57(232), 66, 67(272), 69(283), 71(272),
 72(290), 73(272), 74(295, 298), 82(326b),
 101(376a), 102(376a, 376b), 103(376b),
 104(376a), 110, 112(401), 118(111, 432a),
 119(434b, 436), 120, 122(436, 439, 442),
 123(442), 124(446), 125(446, 450, 452a),
 126(453), 127(453, 456), 145(170), 148,
 151–157, 159, 161, 397(59), 405(100), 425,
 426, 642(13b), 691, 824(14), 825(16b, 18,
 19, 21e), 826(14, 31), 827(14, 33, 34),
 832(19, 61e, 63), 835, 836(85), 840(121),
 842(121, 127), 847–850, 852, 860(40), 941,
 969(84), 1007(138), 1026, 1027, 1034(37,
 38), 1056
 Gordon, R. 806(9), 808(25), 818
 Görls, H. 706(98), 739
 Gornitzka, H. 64(259), 155, 859(38), 941
 Gosalvez, D. B. 845(145), 853
 Gosink, H.-G. 718(197), 722(197, 215), 741,
 742
 Gossage, R. A. 769(120–123), 801
 Gothe, S. A. 901(235), 945
 Goto, M. 40(188b), 54(230), 79(313a), 153,
 154, 156, 393(21), 395(21, 36, 46), 397,
 412(36, 46), 424, 425
 Goto, S. 58(239e), 154
 Goto, T. 652, 654(42), 662(45, 46), 665, 670,
 672(45), 693, 919(364, 365), 948
 Gottardo, C. 368(84a, 84b), 389
 Gouron, V. 248(119), 332
 Gouzyr, A. I. 724(217), 742
 Graalman, O. 181, 182(42), 219, 717(180),
 727, 731(254), 741, 743
 Grabandt, O. 202, 216(75), 220
 Grader, G. 570(22), 635
 Grader, G. S. 570(20), 635
 Grady, G. L. 13(79–81), 150
 Graf, R. 877(139, 140, 145, 146), 943
 Gräfenstein, J. 128, 133, 134, 136(459d), 162
 Gralak, J. 912(330), 947
 Grandinetti, F. 1038(59), 1039(64, 65),
 1040(65), 1048(118), 1057, 1058
 Granger, P. 225(11), 229(24), 271, 272,
 306(216), 330, 335
 Granier, F. 611(172), 639

- Grant, D. M. 230(27), 240(71), 277(231, 232), 330, 331, 335, 399(62), 425
 Grant, I. P. 9(47), 149
 Graul, S. T. 1030(1), 1043(79), 1055, 1057
 Graveron-Demilly, D. 315(330), 337
 Gray, G. M. 542(7), 561
 Gray, G. W. 731(288), 744
 Greaves, J. 578, 589(96), 592(138–140), 593(141), 637, 638
 Green, J. C. 114(420d, 421c), 115(420d, 428), 116(428), 160, 161, 207(84), 221
 Green, J. C. C. 202, 203(77), 220
 Green, J. R. 935(457), 950
 Green, M. 864(53), 942
 Greenberg, A. 43(205a, 205b), 153
 Greene, J. P. 16(120), 151
 Greengard, L. 823(10b), 847
 Greenlief, C. M. 830(50), 849
 Greenwood, C. L. 844, 845(135), 852
 Gregory, K. 434(29), 465
 Greifenberg, S. 928(428), 949
 Greiser, N. 826(25a), 848
 Grelier, S. 248, 311, 313(121), 332
 Gresio, A. J. 543(21), 548(43), 561, 562
 Gresser, G. 495(19), 506(53), 514(19), 536, 537
 Grev, R. S. 5(26), 19(130a), 39–42(182), 43(182, 204), 44(26, 204), 48(218), 49(204, 218), 51, 57(218), 64, 67, 69, 70(26), 74(26, 295, 296, 301), 75(296, 301), 81(296), 91(26, 345, 347, 353, 354), 94(347, 353, 354), 95(354), 96(345, 347), 98(373a), 118(130a), 125, 126(204), 138(26), 148, 151–153, 156, 158, 393(25), 404(89), 405(98), 421(147), 424, 426, 428, 966, 967(71), 1026
 Grev, S. 93(363e), 158
 Griesinger, C. 241, 257(73), 261(188), 269(210), 282(252), 311(188), 331, 334–336
 Griesmar, P. 632(221), 640
 Griffey, R. H. 261, 263(194, 195), 334
 Griffin, D. C. 13(83a), 150
 Griffiths, G. 868(86), 942
 Griffiths, R. J. 865(72), 942
 Grigera, J. R. 825(16c), 847
 Grignon-Dubois, M. 243(89–91), 244(90), 261(89), 312(325), 332, 337
 Grigoras, S. 575(54), 636, 648(35a–c), 649, 651(35c), 692
 Griller, D. 382(120), 390
 Grimsdale, A. C. 686(75a), 694
 Griunova, G. V. 725(239), 742
 Grobe, J. 516(77), 537, 963(61), 995(116), 1026, 1027
 Grogger, C. 293(289), 336
 Groh, B. L. 862(41, 43), 864(54), 941, 942
 Grohmann, A. 484(122), 489
 Gronert, S. 95(366a), 158
 Groot, D.de 771(127), 801
 Gropen, O. 13(85), 150
 Großkopf, D. 438(47), 445, 448(92, 93), 449(92), 466, 467
 Gross, G. 64(257c), 155, 192(58), 220
 Gross, Z. 974(88), 1026
 Grove, C. M. 575(75), 636
 Grove, D. M. 769, 770(115), 801
 Groves, G. W. 320(383), 338
 Gruber, K. 476(58), 487, 728(261), 743
 Gruber, M. 904(286), 946
 Grunenberg, J. 93(363i), 158
 Grtning, R. J. 434(37), 466
 Grützmaker, H. 5, 6, 48–50(22), 66(273), 73(292), 75(273), 93(292), 112, 113, 115(22), 132, 134(467), 135(467, 474), 147, 155, 156, 162, 1041(70), 1057
 Grützmaker, H.-F. 1030(8), 1055
 Grutzner, J. B. 474(30), 487
 Grybat, A. 394(43, 47), 395(35, 43), 397(35, 43, 47), 416(135), 418, 419, 421(142), 425, 427
 Gspaltl, P. 476(58), 487, 728(261), 743, 864(68), 942
 Gu, J. 93(363e), 158
 Gu, Y. G. 922(388), 948
 Guadalupe, A. R. 630(218), 640
 Guan, S. 630(215), 640
 Gudat, D. 746(17), 798
 Gudima, A. 516(83), 538
 Guera, M. 382(120), 390
 Guérin, C. 46(210b), 153, 591(137), 602, 604(160), 610(170), 638, 639, 642, 645(2d), 683(68a, 68b), 691, 693
 Guéron, M. 306(305), 337
 Guerra, M. 342(5), 344, 345(12a–c), 387
 Guerret, O. 859(38), 941
 Guerrini, A. 351(32), 382(119, 120), 388, 390
 Guest, M. F. 192(56), 220
 Guibergia-Pierron, M. 703, 717(70), 738
 Guillard, R. 578, 586, 600, 614(113), 637
 Guilbert, Y. 755, 760(58), 799
 Guillemet, C. 807(12), 818
 Guillemin, J.-C. 79(314b), 156
 Guillot, B. 825(16d), 847
 Guimon, C. 642(13c), 691
 Guissani, Y. 825(16d), 847
 Günther, H. 229, 257(23), 300, 302(298), 320(298, 388), 330, 336, 338
 Guntherodt, H. J. 826(27e), 848
 Günzl, A. 271(215), 335
 Guo, A. 786(162, 163), 802
 Guo, L. 705(94), 739
 Guo, Y. 630(218), 640
 Gupta, H. K. 870(97), 942
 Gupta, P. 837(89c, 90c, 90d), 838(103c), 851
 Gurevich, A. B. 836, 837(87), 850

- Gusel'nikov, L. E. 952(1–3), 956, 958, 962, 982(33), 1024, 1025
- Gusev, A. I. 698(25), 728(262), 737, 743
- Gutekunst, B. 5, 6, 63(12a), 147, 913(343), 948, 952, 997, 998(17b), 1025
- Gutekunst, G. 5, 6, 63(12a), 147, 904(294), 913(343), 946, 948, 952, 997, 998(17b), 1025
- Gutenkunst, G. 284, 290, 292(261), 336
- Guth, J. L. 626(205), 640
- Gutmann, V. 231(42, 43), 232(42), 331
- Gutowsky, H. S. 319(369), 338
- Gymer, R. W. 686(75b), 694
- Haaf, M. 5, 6(23b), 67, 70, 71(274), 113, 114, 117(23b), 148, 155, 394, 397–399(28), 424
- Haake, M. 251, 252(131), 333
- Haaland, A. 63, 67(253–255), 68, 70(254), 113(413a), 114(420a), 155, 160, 202(80), 221, 397(56), 425
- Haaland, P. D. 1041(71b), 1042(76), 1057
- Haaren, R. J. van 750(55), 771(55, 127), 799, 801
- Haarer, D. 633(225), 640
- Haase, D. 402, 406(72), 426
- Haase, M. 181, 182(42), 219, 727, 731(254), 743
- Habber, K. 18, 118(128b), 151
- Haber, C. P. 442(65), 466
- Habtemariam, A. 728(265), 743
- Haddleton, D. M. 767(100, 101), 800
- Hadel, L. M. 952(19), 1025
- Hafner, M. 503(47), 504(50), 537
- Haga, M. A. 570(23), 635
- Hagen, J. 633(225), 640
- Hagman, D. 572(33), 635
- Hague, M. S. 897(225), 945
- Hahn, E. L. 241, 255, 256(74), 307(308), 331, 337
- Hahn, F. E. 114(419), 160
- Haiduc, I. 430(3), 442(67), 465, 466
- Haile, T. 397(55b), 425
- Haines, A. H. 251(132), 258, 320(132, 167), 322, 325(167), 333, 334
- Hainz, R. 923(399), 949
- Hajdasz, D. 1050(130), 1058
- Hajitheidari, D. 558(56), 562
- Hakimelahi, G. H. 868(85), 942
- Halim, S. H. A. 239(57), 331
- Hallegraeff, G. 806(5), 818
- Haller, F. 867(81), 942
- Haller, I. 1036(46), 1056
- Haller, K. J. 395, 397(32), 403(78), 404(78, 88), 411(120), 412(123), 419(78), 421(152), 424, 426–428, 542(15), 561
- Halstenberg, M. 501(42), 537
- Hamada, M. 373(93a, 93b), 389
- Hamada, Y. 559(66, 67), 560(66), 563
- Hamaguchi, T. 685(73b), 694
- Hambley, T. W. 730(274), 743
- Hamers, R. J. 826(27a–d), 830(45, 50–53), 831, 832(59), 834(66, 67), 837(90a), 848–851
- Hamilton, T. P. 78(309), 156
- Hamnett, A. 166(6), 217
- Hampel, F. 24–26, 29(139), 151, 642, 679(4f), 691
- Hampel, G. 315(333), 337
- Hampton, J. F. 714(158), 740
- Hamrin, K. 166(13), 218
- Han, I. S. 471(15), 486
- Han, S. G. 648(35a–c), 649, 651(35c), 692
- Handa, M. 232, 233(44), 331
- Handwerker, H. 484(122), 489
- Hänel, P. 180(40), 181(40, 43), 182(43), 192, 208(40), 219
- Haney, B. P. 377(103), 389
- Hannon, J. B. 842(126a, 126b), 852
- Hans, M. 904(280), 946
- Hansch, C. 1001(122), 1027
- Hansen, R. S. 241(78), 332
- Hanson, J. 409(114), 427
- Hanus, M. 1031(22), 1056
- Hanusa, T. P. 108(390d), 159
- Hanzawa, Y. 48, 49(220), 153, 393, 395(19), 424
- Happer, D. A. R. 699(36, 37), 737, 910(318), 947
- Hara, R. 645(23a), 692
- Harada, J. 395, 397, 412(46), 425
- Hargittai, I. 78(308, 309), 156, 724(218), 742
- Hargittai, M. 77(305), 156
- Hargreve, T. L. 79(315b), 157
- Harima, Y. 673(54a, 54b), 683(54a), 690(54a, 54b), 693
- Haring, A. 844(139a), 852
- Harket, M. 248, 250(125), 311(125, 321), 333, 337
- Harkness, B. R. 575(73, 74), 636
- Harlow, R. L. 114(418a, 418b), 160, 202(78), 221
- Harmony, M. D. 419(143), 427
- Harms, K. 867(81), 942
- Harmsen, R. J. 573(47), 636, 719(203), 741
- Harper, W. W. 95(366e), 158
- Harria, R. K. 311, 320(319), 337
- Harrington, C. 959, 960, 979, 994(43), 1025
- Harris, D. H. 63(252b, 252c), 155, 430, 434(2), 465
- Harris, G. I. 697, 715(10), 736
- Harris, J. W. 5, 6, 63(12b), 147, 952, 997, 998(17a), 1025
- Harris, M. 575(55), 636
- Harris, R. K. 225(6, 7, 10), 230(10, 28), 231(39), 245(96), 251(132), 258(132, 167), 283(28), 315(28, 335–338, 345), 316(358),

- 318(28, 335–338, 361), 320(132, 167, 370, 371, 373, 374, 379, 381), 322(167, 381), 324(395, 398), 325(167), 326(39), 328(415, 416), 330–334, 337–339, 712(146), 740
- Harrison, C. C. 808(21, 22), 818
- Harrison, P. G. 31(158a, 160), 152
- Hartmann, H.-M. 509(59), 537
- Hartmann, S. R. 241, 255, 256(74), 331
- Hartshorne, N. H. 731(287), 744
- Hase, T. A. 916(354), 948
- Hasegawa, M. 371(88), 389
- Hasegawa, Y. 559(62), 563, 827, 830(42), 849
- Hashimoto, H. 344, 345(11c), 387
- Hashimoto, J. 1052(142), 1058
- Hashimoto, M. 277, 279, 285, 290, 293(240), 335
- Hasmy, A. 569(5), 635
- Hassler, K. 273(219), 275, 284(230), 285(230, 264), 286(268), 287(269, 270, 272), 288(274, 276), 289(219, 275), 291(264), 292(230, 269, 270, 274, 284–286), 293(230), 294(219), 335, 336, 475(43, 44, 53), 476(55), 477(60, 66, 68), 479(80), 480(84), 482(102), 487, 488
- Haszeldine, R. N. 999(121), 1027
- Hata, M. 826(27i), 848
- Hata, T. 645(24a), 692
- Hatanaka, Y. 542(8), 561
- Hatano, T. 559(62), 563
- Hatayama, K. 560(69), 563
- Hatop, H. 699, 733, 734(33), 737
- Hattori, T. 838(106), 851
- Haubrich, S. T. 64(261b), 155
- Haudi-Mazzah, A. 712, 722, 725(143), 740
- Haushalter, R. C. 572(33), 635
- Havlas, Z. 136(480), 162, 169(24), 186(24, 49), 187(24), 191(49), 213(95), 218, 219, 221, 856(18), 941
- Hawker, C. J. 746(4, 12), 798
- Hawkins, B. L. 261, 263(194, 195), 334
- Hay, J. N. 716(175), 741
- Hay, P. J. 13, 15, 17(90a–c), 150
- Hayase, S. 475(52), 487
- Hayashi, R. 114(420a, 420c), 115(420c), 160, 202(80), 221
- Hayashi, R. K. 402(75), 426
- Hayashi, T. 559(63), 563
- Hays, M. L. 108(390d), 159
- He, H.-M. 904(264), 946
- Head-Gordon, M. 12(61–63, 69), 149, 823(10d), 825(21b), 847
- Healy, E. F. 13(78a, 79), 150
- Heath, G. A. 10, 11, 14, 33(53), 149
- Hebeisen, P. 935(453), 950
- Heck, R. F. 585(135), 638
- Heckner, K. H. 682(67), 693
- Hecky, R. E. 808(27), 818
- Heden, P. F. 166(13), 218
- Hedman, J. 166(13), 218
- Hedrick, L. 575(68), 636
- Heeg, M. J. 108(390b), 159, 374(94), 389
- Heerbeek, R. van 750, 752, 757(48), 799
- Hehre, W. J. 5, 12(25c), 67, 71, 73(278a), 148, 156
- Heidbüchel, H. J. 769(118), 801
- Heikenwälder, C.-R. 726(251), 743
- Heilbronner, E. 166(7), 175(31), 178(31, 36), 179(36), 180(31), 217, 219
- Heimann, P. 575(56), 636
- Hein, T. A. 15, 17–19, 118, 122(105), 151
- Heine, A. 284(262), 336, 404(91), 426
- Heinemann, C. 81, 114, 115, 118(322), 157
- Heinicke, J. 114(421a–c), 160, 287, 292(271), 336, 474(39), 487
- Heinz, T. F. 837(89d), 851
- Helary, G. 703, 717(71), 738
- Helmer, B. J. 245(102), 248(117), 332
- Hembree, D. M. 575(56), 636
- Hemme, I. 5, 6, 63(11d), 147, 430(9), 434(40), 435, 436(9, 40), 437(45), 440, 441(9), 445, 446(88), 465–467
- Hemmings, R. T. 481(95), 488
- Hench, L. L. 595(154), 638, 703, 716(75), 738, 808(30), 819
- Hendan, B. J. 274, 276(226), 335
- Henderson, H. E. 481(95), 488
- Henderson, W. 776(144), 802
- Henge, E. 864(68, 69), 942
- Hengge, E. 40(188a), 153, 273(218), 275(218, 230), 277(218), 283(260), 284(230), 285(218, 230), 286, 291(267), 292(230, 260), 293(230), 294(292), 335, 336, 475(48–50), 476(54, 56–58), 480(85, 87), 481(94), 487, 488, 700, 727(41), 728(261), 737, 743, 782(152), 802
- Henkel, G. 82, 83, 87(327a), 157, 414(130), 427
- Henner, B. 610(169, 170), 639
- Henner, B. J. L. 683(68a, 68b), 693
- Hennig, H. 682(67), 693
- Henriksson, U. 315(329), 337
- Henry, D. J. 343(8a, 8b), 358(51), 359(8a, 8b, 51), 360(8a, 8b), 387, 388
- Henry, M. 595(153), 638
- Hensen, K. 271, 319(214), 335, 483(108, 109, 115, 118), 488
- Hensler, D. 40, 41(185), 153
- Henzler, M. 837(90b), 851
- Herberhold, M. 260(183), 307(310), 334, 337
- Herbert, I. R. 324(394), 338
- Herbst, E. 1032(27), 1056
- Herbst-Irmer, R. 431(14, 15), 434(27, 38, 40, 41), 435(40), 436(40, 41), 439(50, 54, 57), 445(87, 89, 93), 446(87, 89), 447(89), 448(93), 450(98, 100), 451, 459, 465(100), 465–467, 904(276), 946

- Herdewijn, P. 251(137, 138), 254, 308(138), 333
 Herdtweck, E. 484(122), 489, 726(251), 743
 Herek, J. L. 217(99), 221
 Hermann, K. 838(104), 851
 Hermanns, J. 642, 645(2c), 691
 Herndon, J. W. 886(187), 944
 Herold, R. H. M. 719(199), 741
 Herrmann, H.-F. 169, 186, 187(24), 218
 Herrmann, U. 224(2), 330
 Herrmann, W. A. 81(322), 114(322, 417, 422), 115(322, 422, 428), 116(428), 118(322), 157, 160, 161, 202(77, 79), 203(77), 220, 221
 Hertkorn, N. 271(215), 335
 Hertler, W. R. 724(223), 742
 Herzberg, G. 5(33), 148
 Herzig, C. 795(188), 802
 Herzog, S. 485(132), 489
 Herzog, U. 286(265, 266), 287(266), 288(266, 273), 336, 474(35, 41, 42), 478(71), 479(73–77), 481(93), 482(104), 483(71), 487, 488, 780(148), 802
 Hesemann, P. 578, 585, 632(108), 637
 Hess, A. C. 724(222), 742
 Hess, B. A. 9(50a, 50b), 13(50b), 149
 Hess, B. C. 648(35b), 692
 Hess, M. 315(341), 337
 Hesse, D. 722(216), 742
 Hesse, K. 470(6), 486
 Hesse, M. 181, 182(42), 219, 865(73), 942
 Hetflejš, J. 236(52), 331
 Hewitt, G. W. 902(242), 945
 Hexy, L. 670(49), 693
 Hey, E. 509(59), 537
 Heydari, A. 877(144), 943
 Heyde, W. 277(237), 335
 Heydt, H. 513(69), 537, 904(295), 946
 Hey-Hawkins, E. 509(59), 537
 Hibbs, D. 377(102), 389
 Hiberty, P. 72(289), 156
 Hiberty, P. C. 11, 24(55), 149
 Hidaka, T. 870, 871(102), 943
 Hieinemann, C. 114(425, 426), 115, 117, 118(425), 160, 161
 Hierholzer, B. 180(40), 181(40, 45), 192, 208(40), 219
 Hierle, R. 575, 578, 634(83), 637
 Hietal, S. L. 620(196), 639
 Hieu, D. V. 697(8), 736
 Higel, J. M. 626(205), 640
 Higgins, J. B. 572, 620, 629(37), 635
 Higuchi, K. 58(239b, 239e), 154
 Higuchi, T. 404(90), 426, 492(1), 523(94), 524(96, 97), 528(116), 536, 538, 1003(125, 126, 130), 1027
 Hijjaya, S. 844(138), 852
 Hijjiya, S. 844(136a), 852
 Hijji, Y. M. 922(390), 948
 Hildebrand, M. 807(14, 15), 818
 Hildebrandt, H. 478(70), 488
 Hill, H. D. W. 240(70), 331
 Hill, J. E. 645(24c), 692
 Himpfel, F. J. 834(70), 850
 Hinchliffe, A. 642(13f), 691
 Hindahl, K. 698(18), 707(18, 114), 737, 739
 Hintze, J. 174(28), 218
 Hioki, R. 893(210), 945
 Hirabayashi, K. 698(14), 701(52), 709(14), 736, 737
 Hirabayashi, T. 191–193(55), 220
 Hiram, K. 864(47), 941
 Hirano, M. 531(127), 539
 Hirano, R. 113(414c), 160
 Hirao, K. 570(21), 635
 Hiraoka, K. 1035(42), 1037(56), 1056, 1057
 Hiraqi, M. 1031(21), 1056
 Hirayama, M. 325, 326(413), 339
 Hirota, K. 470(7), 486
 Hirotsu, K. 404(90), 426, 492(1), 523(94), 524(96, 97), 525(107), 526(110), 528(116), 536, 538
 Hirsch, H. 92(361b), 158
 Hirsch, J. 259(173), 334
 Hisaki, T. 558(58), 562
 Hitchcock, P. B. 63, 67, 68, 70(254), 108, 109(391), 114(415a, 415b, 421b, 423, 424), 155, 159, 160, 240(61), 331, 397(56), 425, 509(59), 537, 697(6), 699(38), 702(57, 62), 707(106), 713(150), 728(106, 265, 266), 729(272), 731(6, 150, 266, 282, 285, 290), 732(62), 734(38, 294), 736–740, 743, 744, 857(29), 941
 Hiyama, T. 698(14), 701(52), 709(14), 736, 737
 Hluchy, H. 443(72), 466
 Ho, H. 575(55), 636
 Ho, P. S. 575(71), 636
 Hoarau, C. 572(43), 636
 Hoare, J. L. 769(117, 119), 801
 Hobson, S. 578(96, 115), 586(115), 589(96), 592(140), 600, 631, 634(115), 637, 638
 Hochmuth, W. 58(239g), 154
 Hodgson, P. K. G. 904(285), 946
 Hoebbel, D. 718(193), 741
 Hoehn, H. H. 645(18), 691
 Hofer, O. 325(412), 339
 Höfer, U. 837(89d), 838(103b), 851
 Hoffman, C. L. 548(39), 562
 Hoffman, D. M. 423(155), 428
 Hoffmann, D. 912(333), 947
 Hoffmann, J. 904(295), 946
 Hoffmann, R. 124(448a, 448b), 161, 176(33), 219, 405(97), 423(155), 426, 428, 823(5a), 827(5a, 35, 41), 829, 830(41), 838(103d),

- 847–849, 851, 856(18), 870, 901(93), 923,
924(402, 407), 941, 942, 949
- Hoffmann, U. 197(64), 220
- Hofmann, H. 1019(159), 1028
- Hofmann, M. 432(18), 465
- Hohlneicher, G. 40, 41(185), 153
- Hojo, F. 864(44), 941
- Holder, S. 542(5), 561
- Holder, S. J. 324(396), 339
- Hölderich, W. 494(13), 498(29), 536
- Holland, B. T. 630(216), 640
- Hollinger, G. 834(70), 850
- Holloway, M. K. 13(81), 150
- Holmes, A. B. 686(75a, 75b), 694
- Holmes, J. L. 16(121), 125(449), 151, 161
- Holmes, R. R. 724(225), 726(252), 742, 743
- Holmes, S. J. 645(21b), 692
- Holt, A. 715(163), 740
- Holt, E. M. 31(158b), 152
- Holtan, R. C. 888(190, 193, 199), 944
- Hölter, D. 765(88, 89), 787(166), 800, 802
- Holtgrave, J. 1041(71b), 1057
- Holthausen, M. C. 12(70c), 149, 397(55a),
425, 1036(44, 45), 1056
- Holtman, U. 78(307), 156
- Holysz, R. P. Jr. 709(130), 739
- Holz, H. 471(16), 486
- Holznagel, C. M. 1043(78, 81), 1044(88),
1054(147), 1057, 1059
- Homer, G. D. 978(93), 1026
- Homer, J. 230(31), 241(76), 249(126–128),
255(127), 330, 332, 333
- Hommeltoft, S. I. 249(130), 333
- Hommes, N. v. E. 102, 103(379), 159
- Honathan, N. B. H. 837(89e), 851
- Honda, K. 707(107), 739
- Honda, T. 901(240), 945
- Hondo, T. 386(129), 390, 881(176), 944
- Hong, J.-H. 642, 679(4a–c), 691
- Hong, J.-W. 642, 679(4i), 691
- Hong, R. F. 559(65), 563
- Hong, S. Y. 648, 649(38a–g), 662(38c, 38f),
665(38c), 671(38g), 693, 823, 827(5b), 847
- Hooff, J. H. C. van 719(203), 741
- Hop, C. E. C. A. 345, 346(14), 387
- Hopkinson, A. C. 140(489a), 163, 1031(18),
1032, 1033(31), 1037(57), 1038(58, 60, 61),
1039(63, 66), 1040(66, 69), 1041(69),
1043(82), 1051(137), 1056–1058
- Hoppe, D. 312(327), 337
- Höppner, M. 471, 475(11), 486
- Horata, K. 683, 685(72), 694
- Horchler, K. 260(178, 181), 334
- Horchler von Locquenghien, K. 251(141), 333
- Horio, T. 559(62), 563
- Horn, H. 12(76), 150
- Horn, M. 343(10a), 387, 865(75), 942
- Horner, D. A. 43, 44, 49, 125, 126(204), 153
- Hörner, W. 612, 617, 619(177), 639
- Horton, J. H. 1042(74), 1057
- Horvat, S. M. 142, 144(498b), 163, 357(44),
388
- Hoshino, T. 826(27g–i), 840(118), 848, 852
- Hoshino, Y. 58(239b), 154
- Hosomi, A. 386(129), 390, 856(4), 881(176),
941, 944
- Hossain, M. A. 725(235), 726(250), 742, 743
- Hostutler, D. A. 95(367), 158
- Hotop, H. 7(43a), 149
- Hou, Z. J. 570(25), 635
- Houk, K. N. 11(59g), 117(429b), 128(457),
149, 161, 162, 966, 975(75), 1026
- Hovestad, N. J. 767(100, 101), 769(117–119),
771(126), 800, 801
- Hovis, J. 830(45), 834(66, 67), 849, 850
- Hovis, J. S. 830(50–53), 831, 832(59), 849
- Howard, A. J. 700(39), 737
- Howard, J. A. K. 712(146), 740
- Howarth, O. W. 311, 320(319), 337
- Hoz, S. 136(476), 141(490), 162, 163,
974(88), 1026
- Hoz, T. 7, 11, 20–26(45), 136(476), 137(45),
141(490), 149, 162, 163
- Hrncir, D. C. 725(246), 742
- Hrusak, J. 1031(15, 21), 1032(25), 1052(143),
1055, 1056, 1059
- Hsiao, Y.-L. 383(123), 390
- Hsu, S. T. 838(101b), 851
- Hu, C. 838(101a), 851
- Hu, C.-H. 141, 142(497), 163
- Hu, H. 901(234), 945
- Hu, J. 776(141, 142), 801
- Hu, L. L. 570(29), 635
- Hu, S. S. 982, 985(100, 101), 1026
- Hu, X. 575(72), 636
- Huan, C. H. 834(75d), 850
- Huang, H. D. 575(70), 636
- Huang, H.-H. 716(173), 740
- Huang, J. Q. 25(142), 26(143), 29(142), 151,
152
- Huang, L.-M. 259, 277(169), 334
- Hübel, W. 641, 645(1a, 1b), 691
- Huber, G. 431(12, 13, 16), 437(44), 465, 466
- Huber, K. P. 5(33), 148
- Huber, P. 891(208), 945
- Hübner, M. 484(123), 489
- Huch, V. 437(43), 466, 718(193), 722(209),
741
- Huddleston, R. 676, 679, 680, 690(62a), 693
- Hudlicky, T. 379(109), 390
- Hudrlík, A. M. 883(181), 887(189), 897(227),
912(327), 922(390), 944, 945, 947, 948
- Hudrlík, P. F. 883(181), 887(188), 888(199),
897(227), 912(327), 922(390), 944, 945,
947, 948
- Huffaker, H. B. 860(39), 941

- Huffmann, J. C. 132, 133, 136(468a), 162
Hug, G. L. 953(20), 1025
Hughes, D. W. 870(101), 943, 1022(163), 1028
Huheey, J. E. 10(51), 30, 31(155), 149, 152
Hui, J. 575(72), 636
Hull, W. E. 261, 311(186), 320(371), 334, 338
Hülser, P. 213, 216(94), 221
Hult, A. 746(6, 13), 798
Hummel, J. P. 575(68), 636
Hünterbein, J. 498(30), 536
Hünig, S. 922(393), 931(440–442), 949
Hunt, I. R. 920(381), 948
Hunter, B. K. 226, 240(13), 330
Huo, S. 645(23a), 692
Hurd, R. E. 266, 271(206), 335
Hurley, M. M. 13–15, 17(88b), 150
Hurst, K. M. 919(363), 948
Hursthouse, M. B. 377(102), 389, 718(185), 722(211), 725(235), 726(250), 741–743
Hurwitz, I. 575(56), 636
Hüsing, N. 574(52), 629(211), 636, 640
Hussain, B. 726(250), 743
Hussain, M. A. 722(211), 741
Hussmann, G. 938(464), 950
Hussmann, G. P. 874(123), 943
Huzinaga, S. 12(77), 13, 14(87a), 150
Hwang-Park, H.-S. 955, 982(29), 1025
Hwu, J. R. 868(85), 942
Hyde, J. F. 703(80), 714(158), 738, 740
Hyla-Krispin, I. 197(64), 220
Ialongo, G. 366(75), 389
Ibach, H. 834(74a), 850
Ichihohé, M. 101, 106, 137(375), 159
Ichikawa, M. 840(119), 852
Ichinohe, M. 72(288), 83(329), 106(385b, 385c), 113(414b), 137(385b, 385c), 156, 157, 159, 160, 344, 345(11c), 387, 395, 397, 399(39b), 418, 419(141), 425, 427, 676, 679, 680(61), 693, 858(31), 864(51), 877(133), 941–943, 1006, 1008(134), 1027
Igarashi, T. 838(106), 851
Ignat'eva, G. M. 751(37), 757(37, 61), 758(37), 771(129), 776(61), 787(167), 799, 801, 802
Ignatovich, L. 113(414b), 160
Ignatyev, I. S. 1043(80, 83), 1044(84), 1046(103), 1057, 1058
Igonin, V. 965, 967(69), 1026
Ihara, M. 377(101), 389
Ihmels, H. 410(119), 427, 484(123), 489
Iimura, K. 671(52), 693
Iio, H. 916(358, 359), 948
Ijadi-Maghssoodi, S. 642(7, 8), 648(7, 8, 35a–c), 649, 651(35c), 671, 673(51), 674(57), 691–693, 860(40), 941
Ikawa, E. 844(131), 852
Ikeda, H. 470(2), 486, 864(67), 942
Ikeda, K. 935(452), 950
Ikeda, M. 373(93a, 93b), 389
Ikegami, F. 373(93b), 389
Iksanova, S. V. 530(121b), 531(122), 539
Ikura, M. 269(211), 335
Iler, R. K. 715(167), 740, 813(47), 819
Ilharco, L. M. 570(24), 635
Il'ina, M. N. 751, 757(28, 37), 758(37), 759(28), 799
Illas, F. 39–41, 49(181), 152
Iloughmane, H. 642(13c), 691
Imai, T. 560(70), 563
Imai, Y. 771(128), 782(156), 801, 802
Imamura, Y. 827, 830(40), 849
Imazu, S. 878(151), 944
Imhof, R. 199(65b), 220
Impey, R. W. 825(16a), 847
Imsiecke, G. 807(13), 818
Inagaki, S. 630(215), 640
Inamoto, N. 492(1, 3), 499(33), 522(3, 33, 91), 523(3, 94), 524(3, 95–97), 528(91, 114, 116), 530(120), 536, 538
Inamoto, T. 528(117), 538
Incoccia, L. 834(74b), 838(109), 850, 851
Ingen, R. P. v. 844(139a), 852
Ingri, N. 320, 324(372), 338
Innocenzi, P. 570(27), 635
Inoue, H. 570(26), 635
Inoue, S. 477(61), 487
Inoue, T. 901(239), 945
Interrante, L. V. 785(157–160), 786(161), 802
Ioannow, P. V. 928(418), 949
Ipaktschi, J. 877(144), 943
Ireland, C. M. 277(232), 335
Irene, E. A. 834(68), 850
Irie, M. 575(61, 62), 636
Iriguchi, J. 888(201), 945
Irmer, E. 718, 722(197), 741
Irmer, R. H. 718, 722(197), 741
Ishibashi, H. 373(93a, 93b), 389
Ishibitsu, K. 283, 285, 286, 288, 289, 291(259), 336
Ishida, H. 735(295), 744
Ishida, S. 113(414a, 414b), 160, 872(110), 943
Ishida, T. 559(62), 563
Ishida, Y. 106, 137(385c), 159
Ishidawa, M. 990(110), 1027
Ishido, Y. 364(71), 389
Ishigure, K. 346(18), 387
Ishiguro, M. 392(9, 10), 424
Ishii, Y. 503(44), 537, 919(362), 948
Ishikawa, H. 1052(142), 1058
Ishikawa, K. 879(156, 157), 944
Ishikawa, M. 83(330a, 333), 84–86(333), 157, 201(72), 220, 392(8–10, 12), 404(90), 424, 426, 475(45), 487, 559(62, 65), 563, 673(54a, 54b), 683(54a, 70), 685(73a, 73b),

- 690(54a, 54b), 693, 694, 864(67), 906(300), 942, 947, 968(82, 83), 969(83), 982(98, 99), 990(82, 99), 1003(125–130), 1026, 1027
- Ishimaru, K. 878(149, 150), 943, 944
- Ishiwaki, T. 570(26), 635
- Ishkawa, M. 683, 685(72), 694
- Isobe, M. 919(364, 365), 948
- Israel, G. 315(333), 337
- Issberner, J. 746(1), 798
- Issleib, K. 486(134), 489, 504(51), 537
- Itami, Y. 47(215), 153, 652, 654(42), 657, 662, 663(44), 693
- Ito, H. 881(176), 944
- Ito, K. 911(324), 947, 968, 1013(78), 1026
- Ito, O. 352, 354(39), 388
- Ito, R. 838(106), 851
- Ito, T. 904(265), 946
- Ito, Y. 47(216), 153, 349(25), 388, 474(36–38), 487, 647, 662(28a, 28b), 665(28b), 692, 882(179), 944
- Itoh, K. 503(44), 537
- Itoh, M. 574, 589(50), 636, 715(168), 740
- Itoh, T. 940(469), 950
- Ivanic, J. 825(21e), 847
- Ivanov, A. G. 717(181), 741
- Ivanov, P. V. 717(182), 741
- Ivanov, S. 674(58), 693
- Iwama, S. 935(452), 950
- Iwamoto, T. 72(288), 113(414a, 414b), 156, 160, 399, 400(64), 401, 402(69), 417(136–138), 418(137), 419(136, 137), 420(69, 137), 425–427, 858(31), 872(110), 876(130, 131), 877(132), 941, 943, 1006, 1008(134), 1011(149), 1027, 1028
- Iwasaki, H. 878(150), 944
- Iwata, S. 166, 169, 174(5), 217, 1032(25), 1056
- Iyoda, J. 404(90), 426, 864(67), 942
- Izmailov, B. A. 728(264), 743
- Izuha, M. 95(366d), 158
- Izumi, Y. 904(266), 919(361), 946, 948
- Izumizawa, T. 46(211a), 153, 642, 654, 687(16), 688(16, 78), 689(79), 691, 694
- Jackman, R. B. 844(137a), 852
- Jackson, D. B. 572, 573(32), 635
- Jackson, P. M. 731(288), 744
- Jacob, K. 718(196), 741
- Jacobi, S. A. 871(107), 943
- Jacobsen, H. 64, 66–69, 72, 73(268), 155, 397(60), 425, 1007(139), 1027
- Jacobson, D. B. 1037(55), 1043(78, 81), 1044(88), 1054(146, 147), 1055(148), 1057, 1059
- Jaculi, D. 191–193(55), 220
- Jaffrès, P.-A. 709, 730(127), 739, 751(40), 752(47), 755(40), 761(47), 799
- Jäger, A. 619(189), 639
- Jäger, C. 439(58), 466
- Jagmohan, J. 832(62), 849
- Jain, N. F. 877(135), 879(163), 943, 944
- Jäkle, F. 271(215), 335
- Jakobi, U. 919(369), 948
- Jakobsen, H. J. 241(78, 79), 242(80, 82, 83), 243(80), 244(92), 245(97), 248(116, 118), 282(249, 250), 311(97), 332, 335
- Jakoubková, M. 233, 235(46), 331
- Jameson, A. K. 230(25, 26, 36), 330, 331
- Jameson, C. J. 230(25, 26, 36), 330, 331
- Jamison, G. M. 577(88), 600(158), 637, 638
- Jancke, H. 236(51), 258(51, 168), 259(168), 318(362, 363), 331, 334, 338, 904(278), 946
- Janda, K. C. 823, 824(12), 837(89a, 89b, 93a), 847, 850, 851
- Jang, D. O. 381(113), 390
- Janiak, C. 108(390b), 159
- Jankowski, P. 897(224), 945
- Janoscheck, R. 216(97), 221
- Janoschek, R. 35, 36(164), 52(226a), 54(226a, 229a), 81, 82(324), 102(377b), 113(324), 152, 154, 157, 159, 509(65), 537, 864(69), 942
- Jansen, A. 706(98), 739
- Jansen, C. L. 12(67), 149
- Jansse, P. L. 940(470), 950
- Janssen, H. M. 746(10), 798
- Janzen, A. F. 480(89), 488
- Janzen, E. G. 642(11), 691
- Jaramillo, L. M. 370(87), 389
- Jaramillo-Gómez, L. M. 379(106, 109), 390
- Jarczyk, M. 722(209), 741
- Jarek, R. L. 1051, 1052(140), 1058
- Jarvie, A. W. 714(153), 740
- Jaschke, B. 434(27), 445–447(89), 450, 452, 457–460(102), 465, 467
- Jasien, P. G. 6, 7, 13(34), 148
- Jasinski, J. M. 118(433), 161
- Jastrzebski, J. T. B. H. 767(100), 769(116, 118, 119, 121, 124, 125), 771(126), 800, 801, 904(275), 946
- Jaszberenyi, J.Cs. 381(113), 390
- Jaworski, K. 880(172), 944
- Jean, A. 610(170), 639, 683(68a, 68b), 693
- Jedrecy, N. 826(25a), 848
- Jeglinski, S. 648(35d, 35e), 692
- Jehle, H. 698, 707(20), 737
- Jemmis, E. D. 39, 40, 44(183), 45(183, 209a, 209b), 46(183, 209b), 59, 61(243), 62, 63(247), 105, 106(209a), 108(387), 131(209a), 153–155, 159
- Jenkins, S. 992, 998–1000(111), 1027
- Jenkner, P. K. 294(292), 336, 480(85), 488, 864(68), 942
- Jenneskens, L. W. 555(51), 559(64), 562, 563
- Jensen, F. S. 12(25b), 148
- Jensen, H. J. A. 16(108), 151

- Jensen, J. H. 825(16b, 20d), 847
 Jensen, K. F. 17(127), 151
 Jensen, P. 112(404b), 159
 Jeong, Y. 751(41), 774(132), 799, 801
 Jeske, J. 474(32), 487
 Jiaang, W.-T. 870(91, 92), 903(91, 246), 942, 945
 Jiang, T. 904(284, 288), 946
 Jiang, X.-K. 352(33), 388
 Jiang, X.-L. 925(409), 949
 Jiang, Z. H. 570(29), 635
 Jiao, H. 102(379), 103(379, 381b), 159
 Jimenez-Vazquez, H. A. 132(464b), 162
 Jin, J. 877(148), 943
 Jin, R.-Z. 645(22b, 25), 647(33), 652(41, 42), 654(42), 661, 662(22b), 675, 676(59), 679(59, 63), 692, 693, 704(90), 731(283), 738, 743
 Jing, Z. 826(27f), 837(95b, 96), 848, 851
 Joanteguy, S. 206(82a, 82b), 207(82a), 221
 Jockisch, A. 431(12), 437(44), 465, 466
 Johannesen, R. B. 240(63–65), 261(190), 331, 334
 Johannson, G. 166(13), 218
 Johansson, L. S. O. 844(130), 852
 Johansson, M. 746(13), 798
 John, A. 169, 186, 187(24), 218
 John, B. 266, 271(206), 335
 John, B. K. 320(387), 338
 Johnels, D. 136, 137(478), 162
 Johnson, A. L. 834(74c, 75a, 78a), 845(75a), 850
 Johnson, B. G. 12(73), 16(123a), 149, 151, 825(21b), 847
 Johnson, C. S. Jr. 322, 323(391), 338
 Johnson, D. L. 243, 326(86), 332
 Johnson, F. 645(19a, 19b), 692
 Johnson, G. C. 870(88), 942
 Johnson, J. 687(77), 694
 Johnson, K. E. 838, 840(105c), 851
 Johnson, K. M. 572(33), 635
 Johnson, L. F. 316(354), 338
 Johnson, S. E. 724(225), 742
 Johnson, S. G. 403, 404, 412(84), 426
 Jolivet, J.-P. 567(3), 635
 Jonas, S. 904(279), 946
 Jonas, V. 28, 29, 31, 32(152), 152
 Jones, C. R. 935(458), 950
 Jones, J. 320(370), 338
 Jones, M. 952(5), 1024
 Jones, M.Jr. 904, 913(251), 946
 Jones, N. L. 115, 116(428), 161
 Jones, P. G. 287, 292(271), 336, 474(32, 34), 487, 516(78), 538, 718(196), 741, 877(134, 145), 943
 Jones, P. R. 954(23), 968(81), 980(23, 95, 96), 1025, 1026
 Jones, R. 415(132, 133), 427
 Jones, R. G. 324(396), 339, 542(4, 5), 561
 Jones, S. S. 928(417), 949
 Jones, T. B. 166(7), 217
 Jónsson, H. 16(113), 151
 Joo, K. S. 968, 978(77), 1026
 Joo, W.-C. 642, 679(4a, 4i), 691
 Jordan, K. D. 16(113), 151, 823, 824(12), 830(48), 837(93a, 95a), 847, 849, 851
 Jordens, P. 673(55), 693
 Jorgensen, W. L. 825(16a), 847, 1037(54b), 1056
 Jorgenson, W. L. 720(205), 741
 Joseph, C. 642, 679(4h), 691
 Josten, B. 495, 501, 506(23), 510(66), 522, 528, 529(90), 536–538
 Jouaiti, A. 525(100, 101, 104–106), 538
 Jouany, C. 83, 84(335–337), 85(335, 337), 86(335, 336), 87, 88(336), 157
 Journet, M. 371(89), 389
 Jousseau, B. 248(119), 311(320), 332, 337
 Judenstein, P. 569, 574(7), 635
 Juliá, L. 710(137), 739
 Julia, M. 928(415), 949
 Juliano, P. C. 315, 318, 326(334, 347), 337
 Julien, R. 569(5), 635
 Jung, I. 751(33), 767(104, 105), 774(132), 799–801
 Jung, I. N. 83(330b), 157, 471(15), 486, 877(148), 943
 Jung, M. E. 481(97, 99), 488, 939(467), 950, 999(119), 1027
 Jung, Y. 835, 836(85), 850
 Junge, K. 434(42), 466
 Junker, H.-D. 370(86a, 86b), 389
 Jurczak, J. 928(426), 949
 Jurkschat, K. 713(147), 718(191), 727(147), 740, 741
 Jursic, B. S. 91, 94, 96(351a, 351b), 158
 Jutzi, P. 63(250), 64(262), 78(307), 91–93(262), 108(389, 390a), 109(389), 113(413b, 413c), 114(416a), 155, 156, 159, 160, 197(64), 220, 321(389), 338, 472(25), 487, 531(124), 539, 698(21, 22, 24), 713, 731(150), 735(21, 22, 24), 737, 740, 963(62), 1026
 Jyung, K. K. 888(195), 944
 Käb, H. 698, 707(18), 731(289), 737, 744
 Kabe, Y. 44(208a, 208b), 54(230), (382a), 153, 154, 159, 268, 269(208), 277, 279, 285, 290, 293(240), 335, 409(115), 415(132, 133), 427, 782(155), 802, 872(118), 943
 Kabeta, K. 409(114), 427, 560(70), 563
 Kabuto, C. 58(239a, 239f, 239h), 72(288), 106(385a), 113(414a–c), 137(385a), 154, 156, 159, 160, 295(295), 336, 395, 397, 399(39a), 417(136, 137), 418(137), 419(136, 137), 420(137), 425, 427, 676(61),

- 679(61, 65), 680(61), 693, 781(150), 802, 858(31), 864(47), 872(110), 876(130), 907(303), 928(434), 941, 943, 947, 949, 1006, 1008(134), 1027
- Kachkovskaya, L. S. 514(73), 537
- Kaczmarczyk, A. 484(126), 489
- Kadentsev, V. I. 1045(93), 1046(98), 1049(124), 1057, 1058
- Kadow, J. F. 928(433), 949
- Kaftory, M. 396, 397(49a), 425, 724(229), 742
- Kagramanov, N. D. 78(308), 156
- Kai, H. 673, 690(54b), 693
- Kai, Y. 904(289), 946
- Kaim, W. 169, 172(25), 175(30), 181(25, 44), 184(25), 185(25, 46), 191, 199, 210(25), 218, 219
- Kairys, V. 825(20d), 847
- Kaito, A. 558(56), 562
- Kakareka, J. P. 47, 48(214), 153
- Kakimoto, M. 771(128), 782(156), 801, 802
- Kako, M. 351(30), 352, 354(39), 388, 404(93), 426, 726(249), 743
- Kakudo, M. 728(267), 730(277, 279), 743
- Kakui, T. 479(79), 488
- Kalchauer, W. 476(56), 487
- Kalcher, J. 52, 54(226a), 154
- Kalikhman, I. 36(166), 152, 319(367, 368), 338
- Kalinin, V. N. 728(264), 743
- Kalinowski, H.-O. 230, 241, 257, 327(30), 330
- Kalluri, S. 632, 633(222), 640
- Kallury, R. K. 5, 6, 63(12a), 147
- Kallury, R. K. M. R. 913(343), 948, 952, 997, 998(17b), 1025
- Kamatani, H. 58(239f), 154
- Kamath, P. V. 724(221), 742
- Kambe, N. 379(105), 390, 901(239), 945
- Kamer, P. C. J. 750(48, 55), 752, 757(48), 771(55, 127), 799, 801
- Kaminski, O. 509(61), 537
- Kamitori, S. 1003(130), 1027
- Kamiya, K. 351(31), 388
- Kanabus-Kaminska, J. 382(120), 390
- Kang, C. H. 1046(107), 1050(133), 1058
- Kang, E. 751(29–32), 799
- Kang, H. C. 826(26g), 848
- Kang, K.-T. 884(182), 888(195), 944
- Kang, M. 835, 836(86), 850
- Kang, S. 752(52), 799
- Kang, S.-Y. 83–86(333), 157
- Kania, L. 128, 132, 136(458), 162
- Kanne, D. 108(390a), 159, 197(64), 220
- Kanner, B. 479(82), 488
- Kanno, K. 647(30), 676, 679, 680(61), 692, 693
- Kanter, F. J. J. de 483(105, 106), 488
- Kanyha, P. J. 244(92), 332
- Kapon, M. 396, 397(49a), 425, 724(229), 742, 912(339, 340), 947, 964(67), 1026
- Kapp, J. 5(4), 25, 29(142), 38, 39(177), 45(209a), 50, 51, 64, 66–68, 73, 77(224), 79, 80(224, 316), 81(316), 105, 106(209a), 112(406), 128(4, 316, 461), 129(461), 131(209a), 132–134(4), 139(461), 147, 151–154, 157, 159, 162, 1048(119), 1058
- Kaptein, R. 266, 271(206), 335
- Kapur, G. S. 322(392), 338
- Kapuy, E. 94, 96–98(360), 158
- Karadakov, P. B. 11, 36(60), 149
- Karahashi, K. 844(136a, 138), 852
- Karikari, E. A. 543(21), 561
- Karikari, E. E. 548(39, 43), 562
- Karl, A. 472(25), 487
- Karlen, T. 769(120), 801
- Karlsson, C. J. 826(25c, 25d), 848
- Karlsson, J. O. 926(411), 949
- Karna, S. P. 345(13), 387
- Karni, M. 5(28a), 64(258, 263), 69, 70(263), 74(293), 78(311b), 91(258, 340, 341), 92(362), 93(364), 94(340), 95(258, 340), 96(341), 98(362), 101, 103(28a), 105(340), 108, 112(28a), 114, 115(28a, 420c), 116(293), 148, 155–158, 160, 192(59), 220, 393, 398(24a), 424, 962, 997, 1001, 1002(58), 1011(150), 1025, 1028, 1037(54a), 1056
- Karpova, I. V. 725(236), 742
- Karsch, H. H. 529(118, 119), 538
- Karsmann, H. 396(52), 425
- Kasai, N. 728(267), 730(277), 743
- Kasal, A. 233(46), 234(48), 235(46), 236, 238(49), 331
- Kastel, A. 138(484), 162
- Kataoka, M. 232, 233(44), 331
- Katayama, H. 864(49), 941
- Katircioglu, S. 834(81), 850
- Katkevics, M. 645, 657(26), 692
- Katkova, M. A. 746(2), 798
- Kato, C. 872(118), 943
- Kato, K. 840(119, 120), 852
- Kato, M. 395, 397, 412(36), 425, 891(205), 206, 209, 945
- Kato, T. 765(91, 92), 800
- Katoh, S. 880(173), 944
- Katritzky, A. R. 921(385, 386), 948
- Katsumata, A. 377(101), 389
- Katsumata, S. 166, 169, 174(5), 217
- Katsumura, S. 935(452), 950
- Katuragawa, J. 1035(42), 1056
- Katti, K. V. 904(281), 946
- Katz, A. 578, 586, 623(114), 637
- Katz, H. E. 687(77), 694
- Katz, R. 904(285), 946
- Katzenbeisser, U. 287(272), 292(285), 336, 475(53), 476(57), 482(102), 487, 488

- Kauffmann, T. 670(49), 693
 Kaufmann, E. 38(174b), 152
 Kaup, M. 26, 27(144), 152
 Kaupp, G. 698, 707(18), 737
 Kaupp, M. 7, 10, 11, 14, 23(44), 24–26(139),
 29(44, 139), 31(44, 157), 32(44), 33(44,
 157), 34, 35, 51(44), 149, 151, 152
 Kaur, H. 731(286), 744
 Kawachi, A. 474(36, 38), 487
 Kawahara, Y. 382(122b), 390
 Kawakami, H. 1003(129), 1027
 Kawamata, A. 782(155), 802
 Kawamura, T. 840(119), 852
 Kawanami, H. 525(103), 530(120), 538
 Kawase, T. 54(230), 154, 393, 395(20), 424
 Kawashima, E. 364(71), 389
 Kawashima, J. 698(14), 701(52), 709(14), 736,
 737
 Kawashima, T. 911(322), 947
 Kawachi, S. 906(300), 947, 1036(48), 1056
 Kay, L. E. 269(211), 335
 Kayser, C. 293(289), 336
 Kayser, F. 652(39), 693
 Kazakova, V. V. 797(192), 803
 Kazi, G. H. 240(62), 331
 Kazmierski, K. 703(72, 74), 716(74), 717(72),
 738
 Keay, B. A. 920(372–383), 948
 Keefer, K. D. 762(86), 800
 Keeler, J. 257(154), 266(204), 333, 334
 Keheyang, Y. 1045(89), 1057
 Kehr, G. 259(171, 172), 260(180, 182),
 264(171, 172), 266(180), 293, 294(290),
 307(314, 315), 334, 336, 337, 647(31d),
 674(56a, 56b), 692, 693
 Keijn, H. 904(275), 946
 Keijzer, A. H. J. F. de 483(105, 106), 488
 Keim, E. G. 838(102), 851
 Keim, W. 769(118), 801
 Keiter, E. A. 30, 31(155), 152
 Keiter, R. L. 30, 31(155), 152
 Keith, T. A. 14, 56(99), 150
 Keller, P. J. 278(241), 335
 Kelling, H. 471, 475(11), 486, 727(259), 743
 Kellog, G. L. 842(126a), 852
 Kelly, M. J. 888(190–192), 944
 Kelly, P. J. 826(26f), 848
 Kemmitt, T. 776(144), 802
 Kemmler, M. 612(178), 617(178, 187, 188),
 618(178), 619(178, 188, 190), 639
 Kempe, R. 434(42), 466
 Kempssell, S. P. 273(220), 275(229), 281(220),
 335
 Kende, A. S. 935(453), 950
 Kennedy, G. J. 594(147), 638
 Kennedy, J. D. 225(6), 330
 Kerst, C. 83(331), 157, 271(217), 335,
 348(23), 388, 956(32), 959(45), 960(45, 54,
 55), 962(55), 972, 973(45), 976(45, 54, 55,
 92), 982(97), 990(32), 992(111), 993(92),
 994(45), 997(117), 998(97, 111, 117),
 999(111), 1000(32, 111, 117), 1001(117),
 1002(97, 117), 1003(54, 55, 117), 1004,
 1005(54, 55), 1025–1027
 Kertész, M. 648, 649, 651(34a–c), 692,
 823(4b), 846
 Kerzina, Z. A. 79(314g), 157
 Kessler, H. 261, 311(188), 334, 626(205, 206),
 640
 Kettrup, A. 271(215), 335
 Ketvirtis, A. E. 1032, 1033(31), 1038(60, 61),
 1039(63, 66), 1040(66), 1043(82),
 1051(137), 1056–1058
 Khabashesku, V. N. 47(212c), 79(314g, 315b),
 81, 82(320), 153, 157, 642(13e), 691
 Khananashvili, L. M. 698(25), 717(181),
 725(239), 737, 741, 742
 Khanzada, A. W. K. 240(62), 331
 Khyнку, E. S. 730(273), 733(293), 743, 744
 Kibbel, H. U. 701(44), 737
 Kido, J. 690(80), 694
 Kijima, I. 701(45), 737
 Kijima, M. 560(69), 563
 Kikuchi, O. 870, 871(102), 943
 Kilcast, D. 178, 179(36), 219
 Kilham, P. 808(27), 818
 Kilian, W. 479(81), 488
 Kim, B. 762, 763(77), 800
 Kim, B.-K. 483(120), 489
 Kim, C. 751(29–36, 38, 39, 41), 752(50, 52),
 757(50, 62), 760(50), 762, 763(77),
 767(104, 105), 771(130), 774(130–133),
 775(133), 799–801
 Kim, C. H. 642, 679(4a), 691
 Kim, K. D. 922(387), 948
 Kim, K. S. 835, 836(86), 850
 Kim, M. 751(39), 799
 Kim, S. 144(500), 163
 Kim, S. C. 648, 649(38b, 38d, 38e), 693
 Kim, S.-J. 141(493), 163
 Kim, Y. H. 746(8), 798
 Kim, Z. H. 217(99), 221
 Kimata, Y. 781(151), 802
 Kimber, B. J. 230(28), 231(39), 242, 243(80),
 283(28), 315(28, 335, 336, 338, 345),
 318(28, 335, 336, 338, 361), 326(39),
 330–332, 337, 338
 Kimpenhaus, W. 277(237), 335
 Kimtys, L. 315, 322(346), 337
 Kimura, K. 166, 169, 174(5), 217
 Kimura, T. 922(395), 949
 Kindermann, M. 114(421c), 160, 287,
 292(271), 336
 King, B. T. 136(480), 162
 King, K. D. 127(455b), 161
 King, L. 717(184), 718(195), 721(184), 741

- King, T. 838(101a), 851
 King, T. J. 31(158a), 152
 Kingebiel, U. 443(69–78), 466, 467
 Kinoshita, I. 54(235a, 235b), 58(239j, 239k), 154
 Kinrade, S. D. 320(382, 384), 321(384), 338, 808(18, 19), 818
 Kipping, F. S. 63(248a–d), 155
 Kiprof, P. 484(122), 489
 Kira, M. 70(285a–c), 72(288), 78(285a–c), 113(414a–c), 136, 137(479b), 156, 160, 162, 175(30), 185(46), 199(71), 218–220, 392(16), 393(17, 23, 27), 394(27), 395, 397(39a), 398(27), 399(39a, 64), 400(64), 401, 402(69), 417(136–138), 418(137), 419(136, 137), 420(69, 137), 424–427, 647(30), 676, 679, 680(61), 692, 693, 858(31), 872(110), 873(121, 122), 876(130, 131), 877(132), 906(299), 907(303), 912(121), 928(434), 941, 943, 947, 949, 968, 969, 996(79), 1006(134), 1008(134, 144), 1011(149), 1026–1028
 Kira, T. 344, 345(11c), 387
 Kiran, B. 39, 40, 44–46(183), 153
 Kirchhoff, R. 507(58), 537
 Kirchmeier, R. L. 762(86), 800
 Kirkpatrick, R. J. 320(376–378, 380), 338
 Kirmaier, L. 407(110), 427
 Kirmse, W. 870(105), 943
 Kirpichenko, S. V. 904(259), 946
 Kirsch, P. 483(107), 488
 Kirschning, A. 920(371), 948
 Kirss, R. U. 249(130), 333
 Kiruchi, O. 200(67), 220
 Kirwan, J. N. 357(48), 388
 Kishikawa, K. 89(338e), 157
 Kita, Y. 856(6), 941
 Kitamura, M. 919(364, 365), 948
 Kitano, Y. 916(356), 948
 Kitaoka, K. 570(21), 635
 Kitazume, T. 931(436–439), 949
 Kitson, F. G. 724(223), 742
 Kizil, M. 377(102), 389
 Klade, C. A. 879(162), 944
 Klapötke, T. M. 5, 8, 9(30b), 148
 Klaus, D. P. 575(68), 636
 Klaus, U. 260(184), 334
 Klebach, Th.C. 492(5), 536
 Klebanski, E. O. 531(122, 128), 539
 Klebe, G. 483(109), 488
 Kleij, A. W. 769(121, 124, 125), 801
 Kleijn, H. 769(124, 125), 801
 Klein, E. 531(133), 539
 Klein, L. C. 570(10), 635, 716(172), 740
 Klein, M. L. 825(16a), 847
 Kleinman, L. 823(8b), 847
 Klemp, A. 699(33), 729(269), 733, 734(33), 737, 743
 Klemperer, W. G. 595(148), 638
 Klessinger, M. 292(283), 336
 Kliebisch, U. 443(77), 450, 452, 453(95), 467
 Kliese, P. 839(112), 852
 Kline, M. 114(418a, 418b), 160, 202(78), 221
 Klingan, F.-H. 202(79), 221
 Klingan, F.-R. 114, 115(422), 160
 Klingebiel, U. 5, 6, 63(11d), 147, 181, 182(42), 219, 430(4, 5, 8, 9), 431(14, 15), 434(8, 27, 38, 40, 41), 435(9, 40), 436(9, 40, 41), 437(45), 438(8, 46–48), 439(50, 53, 54, 57–60), 440(8, 9, 60, 61a), 441(8, 9, 61a, 62–64), 442(64), 443(4, 8), 444(82–84), 445(85–89, 91–93), 446(85, 87–89), 447(89), 448(91–94), 449(92), 450(95–102), 451(96, 99, 100), 452(95, 102), 453(95–97), 454(97), 455(96, 97), 456(96), 457(102), 458(102, 103), 459(84, 100–102, 104), 460(84, 102, 105–109), 462(103, 105), 463(105–110), 464(111), 465(99, 100), 465–467, 700(43), 717(180), 727, 731(254), 737, 741, 743, 857(22, 23), 904(282), 910(316), 941, 946, 947
 Klinkhammer, K. W. 63(256b), 66(273), 70(286), 75(273), 93(363d), 113, 114(286), 155, 156, 158, 396(53), 425
 Klintschar, G. 288(276), 336
 Kłobutowski, M. 12(77), 150
 Kloc, C. 687(77), 694
 Kloos, S. D. 483(120), 489
 Klooster, W. T. 47, 48(214), 153, 397(55b), 425
 Kloppenburg, L. 864(62), 942
 Kloster, W. T. 202(78), 221
 Kloster-Jensen, E. 166(7), 217
 Kluijtmans, S. G. J. M. 555(51), 562
 Klumpp, G. W. 483(105, 106), 488
 Knaap, Th.A. van der 496, 499(26), 536
 Knaben, J. W. J. 769, 770(115), 801
 Kneisel, B. O. 410(119), 427, 923, 924(403), 949
 Knight, C. T. G. 316(358), 320(370, 371), 373–378, 380, 384, 321(384), 338, 808(18, 19), 818
 Knight, L. B. 200, 201(68), 220
 Knizek, J. 418, 419, 421(140), 427
 Knoch, F. 495(18, 22–24), 498(30), 500(36–38), 501(22–24, 37, 43), 506(23), 514(22, 37), 519(36, 85, 86), 520(85), 522(90), 524(98), 528, 529(90), 536–538
 Knock, F. 504(49), 510(66), 511(67), 520(49), 537
 Knölker, H.-J. 877(134, 139, 140, 145, 146), 943
 Knoll, F. 492, 498, 529(8a), 536
 Knöll, O. 698, 731(23), 737
 Knorr, M. 856(15), 864(46), 941

- Kobayashi, K. 41, 42(191, 196), 43(191), 58, 60, 62(191, 196), 91, 92(342, 343a, 343b), 93(343a), 94(342, 343a), 96, 97(343a), 98(342, 343a, 343b), 102, 104, 105(196), 153, 157, 352, 354(39), 370(85), 388, 389, 422(154), 428, 875(129), 891(207), 943, 945
- Kobayashi, T. 560(69), 563, 904(248), 946, 1019(162), 1028
- Kobayashi, Y. 916(356), 948
- Koch, W. 12(70c), 149, 397(55a), 425, 867(81), 942, 1031(13), 1036(44, 45), 1041(13), 1055, 1056
- Köcher, C. 114(417), 160
- Kochi, J. K. 20(134), 151
- Kochina, T. A. 1044(84, 86), 1046(103), 1057, 1058
- Köck, M. 282(252), 336
- Koe, J. R. 475(51, 52), 487, 545(26), 562
- Koehler, B. G. 837(89c, 90d), 851
- Koenig, J. L. 735(295), 744
- Koenigkramer, R. E. 932(443), 950
- Koetzle, T. F. 397(55b), 425
- Köfer, U. 838(99a), 851
- Kohl, A. T. 575(67), 636
- Kohl, P. A. 575(67), 636
- Köhler, F. H. 529(119), 538
- Köhler, H. 96(369b), 158, 421(144), 427
- Kohler, H.-J. 64(270a, 270b), 155
- Köhler, U. 837(88c), 850
- Köhler, W. 928(424), 949
- Koike, T. 559(62, 65), 563
- Koizumi, T. 896(215, 216, 223), 945
- Kök, T. R. 722(212, 213), 741
- Kolc, J. 999(119), 1027
- Koleske, D. D. 845(143), 853
- Köll, W. 292(284), 336, 476(55), 487
- Kolleger, G. M. 288(276), 336
- Kollegger, G. 288, 292(274), 336, 479(80), 488, 898(228), 945
- Kollman, P. A. 5, 12(25a), 148
- Kolodiazhnyi, O. I. 503(46), 504(48), 537
- Kolomeitsev, A. 483(107), 488
- Kolotyrkina, G. 1049(124), 1058
- Kolotyrkina, N. G. 1046(98), 1058
- Koma, A. 842(125), 852
- Komaguchi, K. 201(72), 220, 673(54b), 683(71), 685(73b), 690(54b), 693, 694
- Komáromi, I. 96(368), 158
- Komatsu, M. 379(105, 107, 110), 390, 902(244, 245), 945
- Kon, I. 344, 345(11c), 387
- Kondratyev, Kh.I. 706(97), 739
- Konecny, R. 405(97), 426, 826(26h), 830(49), 831, 832(56), 835, 836(84), 848–850
- Kong, M. J. 831(57, 58), 832(62), 849
- König, S. 755, 767(57), 799
- Koning, L. J. de 1053(145), 1059
- Konishi, K. 703(87), 738
- Konobeyevsky, K. S. 956, 958, 962, 982(33), 1025
- Koo, S. 888, 891(200), 944
- Kooijman, H. 525(99, 100), 538, 719, 720, 727(200), 741, 771(127), 801
- Kopelevich, M. 325(408), 339
- Kopf, H. 955(30), 958, 959(36), 1025
- Kopiske, C. 894(212), 945
- Kopping, B. 368(82), 389
- Kopylov, V. M. 717(181), 741
- Koreeda, M. 888, 891(200), 944
- Korkin, A. 105, 106(383), 159
- Korkin, A. A. 45, 105, 106, 131(209a), 153
- Kos, A. J. 11(59g), 149
- Koseki, S. 5(27c), 110, 112(401), 148, 159
- Kosfeld, R. 240(67), 315(341), 316(67), 331, 337
- Koshi, M. 351(31), 388
- Koshihara, S. 393(17), 424
- Kosse, P. 437(43), 466
- Kost, D. 11(56), 36(166), 66, 72, 79(56), 149, 152, 319(367, 368), 338
- Köster, H. 484(127), 485(129, 130), 489
- Köster, R. 260, 266(179, 180), 271(213), 293, 294(290), 307, 308(213), 325(411), 334–336, 339, 647(31c), 692
- Kotani, Y. 570(23), 635
- Koten, G. van 767(100, 101), 769(115–125), 770(115), 771(126), 800, 801, 904(275), 946
- Kottke, T. 319(368), 338, 443(78), 458(103), 459(104), 460(105), 462(103, 105), 463(105), 467
- Kovar, D. 475(48, 50), 487, 1003(126), 1027
- Kövér, K. E. 261(187), 334
- Kowalewski, J. 315(328, 329, 342, 344), 316(344, 350–352, 354, 357), 317(357), 318(342, 344, 350–352), 319(342, 351), 329(417, 418), 337–339
- Koyama, H. 879(162), 944
- Kozłowski, M. C. 936(462), 950
- Kozmiński, W. 312(323, 324), 314(323), 337
- Kraak, A. 673(55), 693
- Kraemer, W. P. 642(13a), 691
- Kraft, A. 686(75a), 694
- Kragl, U. 769(118), 801
- Krahé, E. 234(48), 331
- Kraka, E. 42(198, 199, 202), 128, 133, 134(459d), 136(459d, 477), 137(477), 153, 162
- Kramarova, E. P. 239(54), 331
- Kramer, B. 522(93), 538
- Krämer, E. 481(100), 488
- Krampe, C. 443(74), 466
- Kranenburg, M. 573(47), 636
- Krasovskii, V. G. 751(28), 757(28, 61), 759(28), 776(61, 138, 139), 777(138, 139), 799, 801
- Kratky, C. 40(188a), 153

- Kratt, A. 347(21a), 388
 Krätzer, D. 700(40), 737
 Kratzer, P. 838(99a, 99b), 851
 Krause, R. 240(67), 315(341), 316(67), 331, 337
 Krauss, M. 6, 7, 13(34), 58, 59(242), 148, 154, 825(16b), 847
 Kravers, M. A. 725(234), 742
 Krebs, B. 516(77), 537, 904(269), 946
 Krebs, F. 485(132), 489
 Krechkov, A. P. 715(161), 740
 Kreeger, R. L. 999(120), 1027
 Kreitmeier, P. 528(115), 538
 Kremer, M. 192(61), 202(61, 74), 214(61), 220
 Krempner, C. 912(332, 335), 947
 Krennrich, G. 202(76), 220
 Krenzel, V. 186, 191(49), 219
 Kresge, C. T. 572, 620, 629(36, 37), 635
 Kresse, G. 823(6d), 847
 Kressler, J. 765(90), 800
 Kreuzburg, C. 240, 316(67), 331
 Kricheldorf, H. R. 715(166), 740
 Krief, A. 923, 924(408), 949
 Krieger, L. 519(85), 520(85, 88), 538
 Kriesel, J. W. 755(57), 761(73), 767(57), 799, 800
 Kriesel, W. 578(125, 126), 593(125), 600(125, 126), 614(126), 638
 Krihak, M. 570(18, 19), 635
 Krijen, S. 719(203), 741
 Krishnan, M. S. 838(101a), 851
 Krishnan, R. 12(64, 65, 74b), 149, 150
 Krivonos, S. 319(368), 338
 Krivtsun, V. M. 19(129), 151
 Kröger, N. 808(31–34), 809(33–35), 810, 817(35), 819
 Krogh-Jespersen, K. 64, 70(264), 74(299), 155, 156
 Krogh-Jespersen, M.-B. 22, 23(54), 74, 116(293), 149, 156
 Krogh-Jespersen, M.-B. 724(230), 742
 Kroke, E. 402(71, 74), 404(74), 405(71), 406(106), 407(74), 426
 Kroth, H.-J. 113(411a), 160
 Krotto, H. W. 192(56), 220
 Krska, S. W. 746(21), 762(82), 798, 800
 Krüger, C. 197(64), 220, 293, 294(290), 336, 894(212), 945
 Krüger, C. J. 108(390a), 159
 Kruger, P. 826(26d), 844(133c), 848, 852
 Krüger, R.-P. 776(143), 801
 Krynitz, U. 203, 205, 206(81), 221
 Kuan, C. P. 927(414), 949
 Kuang, B. 486(136), 489
 Kubota, T. 342(6), 387
 Kubota, Y. 834(72), 850
 Küchle, W. 13(92a, 92b), 150
 Kuck, D. 1048(123), 1058
 Kudelko, P. 200, 201(68), 220
 Kudin, K. N. 79(314g, 315b), 81, 82(320), 157, 823(9, 10e), 847
 Kudo, H. 38(175), 152
 Kudo, T. 19, 20(132, 133), 41(190, 194, 196), 42(190, 196), 52(226b, 227), 53(194, 227), 54(190, 194, 226b, 227, 229b, 233), 56, 57(233, 236), 58(190, 196), 59(190), 60(190, 196), 62(196), 67(275, 276), 68(275), 75(275, 276), 82(325), 102(196, 378), 103(378), 104(196, 378), 105(196), 151, 153–155, 157, 159, 871(106), 874(124, 125), 875(126), 943, 955(26), 968, 1013(78), 1025, 1026
 Kugita, T. 767(103), 800
 Kuhlmann, B. 136, 137(479a, 481), 162
 Kuhlmann, K. F. 240(71), 331
 Kuhlmann, T. 683(68a), 693
 Kuhn, D. R. 13(80), 150
 Kühnel, E. 187, 190(51b), 220
 Kukhar, V. P. 504(48), 537
 Kulicke, K. J. 368(83a), 389
 Kulkarni, A. K. 887(188), 888(199), 897(227), 944, 945
 Kumada, M. 392(8–10, 12), 404(90), 424, 426, 475(45, 46), 479(79), 487, 488, 647(27), 692, 864(67), 865(70), 942, 968(82, 83), 969(83), 982(98), 990(82, 110), 1003(125–129), 1026, 1027
 Kumar, A. 962(59), 1025
 Kumarathasan, R. 865(73), 942, 982(102), 1026
 Kumashiro, K. K. 202(78), 221
 Kummer, D. 239(57), 331, 483(119), 484(127), 485(129–131, 133), 486(135), 489, 702, 732(64), 738
 Kunai, A. 83(330a), 157, 559(62), 563, 673(54a, 54b), 683(54a, 71), 685(73a, 73b), 690(54a, 54b, 80), 693, 694
 Kündgen, U. 500(38), 536
 Kunz, C. 838(109), 851
 Kunze, H. 500(36), 519(36, 86), 536, 538
 Kupče.É. 251(135, 141), 253(143), 260(185), 266(201–203), 270(201, 203), 271(201, 203, 213, 216), 272(216), 293(291), 302, 304(135), 306(143, 216), 307(135, 213), 308(213, 317), 311(318), 325(405–407, 409, 410), 333–337, 339
 Kurasheva, N. A. 718(192), 741
 Kurihara, A. 371(88), 379(110), 389, 390
 Kurishima, K. 872(119), 943
 Kuritsin, Y. A. 19(129), 151
 Kuriyama, A. 781(151), 802
 Kuroda, M. 277, 279, 285, 290, 293(240), 335
 Kurogi, Y. 844(131), 852
 Kuroyanagi, J. 377(101), 389
 Kurreck, H. 181(45), 219
 Kürti, J. 648, 649, 651(34c), 692

- Kusakabe, M. 916(356), *948*
 Kusukawa, K. 352, 353(38), 388
 Kusakawa, T. 268, 269(208), 335, 352(36, 37), 353(37), 388, 704(89), *738*
 Kuteinikova, L. I. 718(192), *741*
 Kutzelnigg, W. 5, 7, 10, 11, 33, 63, 92(6), *147*
 Kuwajima, I. 856(8), 891(204–207, 209), 912(326), 923(396, 397), *941, 945, 947, 949*
 Kuzmany, H. 543(20a), *561*
 Kuzmin, G. 682(67), *693*
 Kuzmin, M. 682(67), *693*
 Kuz'min, N. N. 725(242), *742*
 Kuzuhara, H. 765(91, 92, 94), *800*
 Kvičalová, M. 233, 235(46), 251(136–138), 254(138), 255(144), 258, 260(165), 306(136), 308(138), 325(144), *331, 333, 334*
 Kwak, Y.-W. 860(39), *941, 954(25), 1025*
 Kwart, H. 905(297), 906, 907(297, 302), 908(297, 302, 310), *947*
 Kwasigroch, C. 879, 880(154), *944*
 Kwasigroch, C. A. 880(169), *944*
 Kwon, A. 751(38), 771, 774(130), *799, 801*
 Kwon, H. 248(120), *332*
 Kwon, H.-A. 901(233), *945*
 Kwon, H. C. 570(18), *635*
 Kwon, S. J. 648, 649(38b, 38d, 38e), *693*
 Kwon, Y. C. 752(50), 757(50, 62), 760(50), *799*
 Kwong, D. W. J. 904(288), *946*
 Kyotani, H. 548(41), 558(56), *562*
 Kypčė, E. 307, 308(306, 307), 309, 310(306), *337*
 Kyushin, K. 58(239e), *154*
 Kyushin, S. 342(6), 344, 345(11a–c), *387*
- Laali, K. K. 1049(127), *1058*
 Laarhoven, L. J. J. 364(68), *389*
 Labanowski, J. K. 12(70a), *149*
 Labrande, B. 914(350, 352), *948*
 Laceyfield, C. W. 714(158), *740*
 Lach, C. 746(18), 757(60), 762(84), 788(170–172), 791(176), *798–800, 802*
 Lacôte, E. 368(81), *389*
 LaDuca, R. L. J. 572(33), *635*
 Laermann, B. 718, 729(189), *741*
 Läge, M. 516(77), *537*
 Lagowski, J. B. 642, 645, 651(17), *691*
 Laguerre, M. 243(89–91), 244(90), 261(89), 312(325), *332, 337*
 Laguzzi, G. 1045(89), *1057*
 Lahtinen, L. 916(354), *948*
 Laidig, W. D. 38(174c), *152*
 Laine, R. 573(46), *636*
 Laine, R. M. 570(16), 575(55), *635, 636*
 LaJohn, L. A. 13–15, 17(89a), *150*
 Lambert, C. G. 823(10c), *847*
 Lambert, J. 292(283), *336*
 Lambert, J. B. 128(458, 459a, 459c), 132(458, 468a, 468b), 133(459a, 459c, 468a, 468b), 134(459c), 136(458, 459a, 459c, 468a, 468b, 479a, 481), 137(479a, 481), *162, 274, 275(223), 280, 281(243), 335, 348(22), 388, 779(145), 780(146, 147, 149), 781(145), 802, 1030(6a), 1055*
 Lamblin, J. M. 626(205), *640*
 Lampe, F. W. 1036(52), *1056*
 Landemark, E. 826(25c, 25d), *848*
 Lane, A. L. 928(432), *949*
 Lane, P. A. 648(35d), *692*
 Lang, H. 751(42), 774(134–137), *799, 801*
 Lange, C. A. de 202, 216(75), *220*
 Lange, D. 531(133), *539*
 Lange, L. 114(416b), *160*
 Langer, P. 963(62), *1026*
 Langhoff, S. R. 112(404a), *159*
 Langley, D. R. 928(433), *949*
 Langston, M. A. 857(27), *941*
 Lankat, R. 707(115, 116), 732(116), *739*
 Lanneau, C. 578, 585, 632(108), *637*
 Lapeyre, G. L. 838(108), *851*
 Laporterie, A. 46(210a), *153, 642(2a, 13c), 645, 662(2a), 691*
 Lapouyade, R. 914(350–352), *948*
 Lappert, M. F. 5, 6(23a), 63(252a–c, 253–255), 67(253–255), 68, 70(254), 113(23a, 412, 413a), 114(415a, 415b, 421a–c, 423, 424), 117(23a), *148, 155, 160, 397(56), 425, 430(2), 434(2, 35), 465, 466, 509(59), 537, 857(29), 864(64), 941, 942*
 Largo, A. 1032(30), 1033(34), *1056*
 Largo-Cabrerizo, A. 1032(29), *1056*
 Largo-Cabrerizo, J. 1031(20), 1032(29), *1056*
 Larin, M. F. 261(191), *334*
 LaRochelle, R. W. 231(40, 41), 233, 234(41), 324(397), *331, 339, 714(157), 740*
 Larson, G. L. 908(309), 912(342), *947, 948*
 Larsson, C. U. S. 834(74b, 78a), *850*
 Larsson, K. M. 315(328, 329), *337*
 Lartigue, J.-C. 248(119, 125), 250(125), 311(125, 320, 321), *332, 333, 337*
 Lasocki, Z. 703, 714, 715(86), *738, 904(278), 946*
 Lasperas, M. 575(59), *636*
 Lassaletta, J. M. 928(419), *949*
 Laszlo, P. 227(16, 17), *330*
 Lau, W. 20(134), *151*
 Laubach, B. 501(43), 506, 520(52), *537*
 Laube, T. 132(465b), *162*
 Laude, D. A. Jr. 324(403), *339*
 Laue, E. D. 266(204), *334*
 Laughlin, K. B. 845(145), *853*
 Laurent, S. 374(94), *389*
 Lauten, M. 928(416), *949*
 Lautens, M. 922, 928(389), *948*
 Lauterbur, P. C. 240(69), *331*

- LaVan, D. A. 629–631(210), 640
 Lavrentovich, O. D. 725(241, 243), 742
 Law, D. S. -L. 834(74c), 844(134), 850, 852
 Lawler, R. G. 249(130), 333
 Lawless, G. A. 108, 109(391), 159
 Lawrance, W. D. 127(455b), 161
 Lawrence, F. T. 19, 122(130b), 151
 Lazell, M. 718(188, 189), 729(189), 741
 Lazzarini, E. 384(125), 390
 Léandri, G. 877(147), 879(155), 943, 944
 Leary, J. A. 755, 767(57), 799
 Leavitt, F. C. 645(19a, 19b), 692
 Lebeau, B. 575(82, 83), 578(83, 120),
 586(120), 634(83, 120, 227), 637, 640
 Le Bideau, F. 899(230), 945
 Le Bideau, J. 735(296), 744
 Leblanc, D. 1041(73a, 73b), 1057
 Le Bras, E. 807(12), 818
 Lebrun, J. J. 703, 716, 717(66), 738
 Lechner-Knoblauch, U. 180(40), 181(40, 41,
 43), 182(41, 43), 192, 208(40), 219
 Leclercq, D. 569(9), 575(9, 77, 81), 635, 636
 Lee, C. 202(78), 221
 Lee, C. J. 257(156), 333
 Lee, C. Y. -C. 570(14), 635
 Lee, E. 366(73), 389
 Lee, E. J. 822(2), 846
 Lee, J. C. 884(182), 944
 Lee, J.-G. 533(135), 539, 888(195), 944
 Lee, J.-S. 5, 6, 63(12c), 147
 Lee, K.-R. 888(195), 944
 Lee, L. 864(55), 942
 Lee, L.-Q. 844(133b), 852
 Lee, M. A. 823(10a), 847
 Lee, M. E. 83(330b), 157, 954(23), 980(23,
 95), 1025, 1026
 Lee, S. 823(8b), 830(45, 51), 835, 836(86),
 847, 849, 850
 Lee, S. C. 752(50), 757(50, 62), 760(50), 799
 Lee, S. Y. 826(26g), 848
 Lee, T. J. 15, 17–19(105), 108(394), 118,
 122(105), 151, 159
 Lee, T.-S. 825(21c), 847
 Lee, V. Y. 39, 58(180), 83(329), 101, 106,
 137(375),(382b), 152, 157, 159, 877(133),
 943
 Lee, W. L. N. 575(54), 636
 Lee, Y.-G. 878(149, 150), 943, 944
 Lee, Y. R. 935(454), 950
 Lee, Y. S. 823(4b), 846
 Leeuwen, P. W. N. M. 750, 771(55), 799
 Leeuwen, P. W. N. M. van 747(25, 26),
 749(25), 750, 752, 757(48), 769, 770(115),
 771(127), 798, 799, 801
 Lefèvre, V. 206(82b), 221
 Leffler, A. J. 494(13), 536
 Léger, J.-M. 248, 311, 313(121), 332
 Legzdins, P. 864(63), 942
 Lehman, D. S. 645(19b), 692
 Lehman, S. E. 785(159), 802
 Lehmann, G. 808, 809(33), 819
 Lehn, M. 614(181), 639
 Lehnert, R. 471, 475(11), 486, 697(13),
 736
 Lehuède, P. 807(12), 818
 Lei, D. 397(55b), 425
 Leigh, W. J. 83(331), 157, 271(217), 335,
 952(13), 956(32), 958(37), 959(37, 40–46),
 960(40–57), 962(51, 53, 55), 963(46, 63),
 964(44, 66, 68), 969(48, 51), 970(51),
 971(48, 51), 972(45), 973(40, 45, 89), 974,
 975(40, 89), 976(40, 45, 51, 54, 55, 89, 92),
 977, 978(40), 979(43, 44), 980(47, 57),
 981(57), 982(47, 50, 52, 89, 97), 983,
 984(41, 42), 985(42, 47, 51, 52, 56),
 986(41, 42, 47, 50–52, 104), 987(47, 52,
 105), 989(42, 53, 56), 990(32, 47, 66),
 992(47, 111), 993(47–49, 92), 994(41, 43,
 45, 48, 57, 115), 995(37, 47, 48, 115),
 996(47, 48), 997(41, 117, 118), 998(37, 97,
 111, 117, 118), 999(37, 111), 1000(32, 37,
 53, 111, 117, 118), 1001(37, 117), 1002(44,
 97, 117), 1003(48, 54, 55, 117), 1004,
 1005(54, 55), 1007(141), 1009–1011(68),
 1018(68, 157), 1019, 1022(68), 1025–1028
 Lein, I. 348(23), 388
 Leis, C. 484(122), 489
 Leite, L. 572(40), 636
 Leites, L. A. 195, 197(63), 220, 547(35, 36),
 548(42, 45), 550(45), 562, 727(260),
 743
 Lelj, F. 834(82a), 850
 Lemairé, B. 315, 318(337), 337
 Lempka, H. J. 173, 174(27), 218
 Lendvay, G. 73(291), 156
 Lennon, J. 952, 997, 998(17a), 1025
 Lennon, R. 114(420a), 160, 202(80), 221
 Lensch, C. 910(316), 947
 Leone, S. R. 844(139b), 852
 Leonowicz, M. E. 572, 620, 629(36, 37), 635
 Lepeyre, C. 575(79, 80), 578(80, 107, 128),
 595(107, 149, 155), 596(149, 155),
 598(128), 600(79), 614(79, 80, 107, 155),
 636–638
 Lère-Porte, J. P. 578, 603(94), 611(94),
 174–176), 637, 639
 Lerner, H.-W. 58(239i), 154, 955, 982(29),
 1025
 Lernnon, J. 5, 6, 63(12b), 147
 Lesch, A. 402(73), 405(104), 406(107),
 407(107, 108), 426
 LeSeur, R. 712, 725(142), 740
 Le Strat, V. 595(150), 602(161), 604(162,
 163), 606(166), 623(204), 625(161),
 631(150), 638–640

- Leszczyński, J. 20(135), 25(142), 26(143),
 29(142), 45(209a), 91, 94, 97, 98(355), 105,
 106, 131(209a), 141(495), 151–153, 158,
 163
 Leue, C. 113(413c), 160
 Leung, W.-P. 940(468), 950
 Leuze-Jallouli, A. M. de 760(63–71), 799, 800
 Le Van, D. 516(77), 537
 Levi, C. 807(12), 818
 Levin, R. D. 16(121), 125(449), 151, 161
 Levine, J. D. 826(23), 848
 Levitt, M. H. 257(157), 259(176), 274(227),
 281(244, 245, 247), 333–335
 Levy, D. 570(10), 635, 716(172), 740
 Levy, G. C. 226(14), 227(14, 15), 315(14,
 334, 347), 316(349, 354), 318(14, 334,
 347), 326(15, 334, 347), 330, 337, 338
 Levy, Y. 570(12), 635
 Lewis, L. B. 837(89a, 89b), 850, 851
 Lheureux, M. 642, 645(2b), 691
 Li, D. 277(232), 335
 Li, F. M. 570(25), 635
 Li, G. 70, 75, 77(284a, 284b), 99(284a),
 100(284b), 156
 Li, H. 95(367), 158, 865(71), 942
 Li, L. 827, 830(42), 837(89d), 849, 851
 Li, Q. 70, 75, 77(284a, 284b), 99(284a),
 100(284b), 156
 Li, S. 243, 326(86), 332
 Li, W. 687(77), 694
 Li, X. 959(43), 960(43, 57), 979(43), 980,
 981(57), 994(43, 57, 115), 995(115), 1025,
 1027, 1042(77), 1046(100, 102, 105, 112),
 1050(131), 1057, 1058
 Li, X.-W. 93(363e), 158
 Li, Y. L. 845(145), 853
 Li, Y. Z. 834(77b), 850
 Liable-Sands, L. M. 642, 679(4k), 691, 712,
 725(142), 740
 Liang, C. 64, 68, 69(267), 155, 398(61), 425
 Liao, H.-Y. 91, 94, 95(356), 158
 Lias, S. G. 16(121), 125(449), 151, 161
 Lickiss, P. D. 5, 112, 128, 132, 133(28c), 148,
 480(83), 488, 696(1), 699(38), 701(55),
 702(57, 59), 703(85), 707(103–106, 108,
 117), 713(150), 714, 724(1), 725(1, 231,
 238), 726(1), 728(1, 106, 266), 729(1, 85,
 272), 731(1, 150, 266, 282, 285, 286),
 733(55), 734(1, 38, 294), 736(1), 736–740,
 742–744, 858(30), 910(315), 941, 947,
 968(80), 1026
 Lie, G. C. 648, 649, 651(35c), 692
 Lieb, F. 494(14), 536
 Liebau, M. 911(323), 947
 Lieberman, H.-P. 92(361b), 158
 Lieberman, J. F. 16(121), 43(205a, 205b),
 50(222), 125(449), 151, 153, 154, 161
 Lien, M. H. 140(489a), 163, 1031(18),
 1037(57), 1040, 1041(69), 1056, 1057
 Liepinš, E. 265(197), 293(291), 325(407), 334,
 336, 339
 Liepinsh, E. 258(163), 334
 Lieske, H. 470(6), 486
 Liess, M. 648(35d, 35e), 692
 Lilla, G. 1045(89), 1057
 Lim, K. M. 144(500), 163
 Lim, K. P. 1036(52), 1056
 Lim, M. E. 629(219), 640
 Lim, M. H. 572(31, 39), 573(39), 629(31, 39),
 635, 636
 Lim, S. H. 274, 275(223), 335, 780(147), 802
 Limburg, W. W. 908(307), 947
 Lin, C.-L. 81, 82(319a, 319b), 157
 Lin, D.-S. 826(25b), 848
 Lin, H.-S. 929(435), 949
 Lin, J. 860(40), 941
 Lin, J.-S. 750(53), 799
 Lin, S. C. 575(66), 636
 Lin, Y. 1045(95), 1058
 Lin, Y.-Y. 687(77), 694
 Lin, Z. 93(363h), 158
 Linde, S.Aa. 241(79), 242(80, 83), 243(80),
 332
 Linderman, R. J. 866(80), 901(80, 232), 942,
 945
 Lindhorst, T. K. 752(51), 799
 Lindinger, W. 1031(12), 1032(26), 1033(26,
 32), 1055, 1056
 Lindner, E. 577(89), 612(89, 177, 178),
 617(177, 178, 184–188), 618(178), 619(89,
 177, 178, 186, 188–191), 637, 639
 Linton, J. C. 328(416), 339
 Lindsay, R. 844(130), 852
 Lindsey, R. V. 494(13), 536
 Lineberger, W. C. 7(43a, 43b), 139,
 140(486a), 149, 162
 Ling, Y. 1038(58), 1039, 1040(66), 1057
 Liniger, E. G. 575(68), 636
 Link, M. 983(103), 1026
 Li Ou, D. 578, 600(105, 106), 637
 Liou, H. C. 575(69), 636
 Lippmaa, E. 233, 236(47), 282(253, 254), 296,
 297(47, 253, 254), 298(253), 315(331),
 318(362), 331, 336–338
 Lipshutz, B. H. 652(39), 693
 Liptaj, T. 304(303), 337
 Lischka, H. 64(270a, 270b), 96(369b), 155,
 158, 421(144), 427
 Litster, S. A. 701, 733(55), 737
 Littmann, D. 64(257c), 155, 192(58), 220
 Liu, C. 393(17), 424, 922(388), 948
 Liu, D.-J. 840(121), 842(121, 127), 852
 Liu, D.-S. 857(29), 941
 Liu, F. 347, 348(21b), 388
 Liu, F.-Q. 722(214), 741

- Liu, H. 830(45, 51), 849
 Liu, H. B. 831, 832(59), 849
 Liu, H. W. 402, 408(70), 426
 Liu, L. Y. 570(25), 635
 Liu, P. T. 575(70), 636
 Liu, Q. 786(161), 802, 827, 829, 830(41), 849
 Liu, X. 348(22), 388
 Liu, Y. 837(89e), 851
 Liu, Z. 199(65a), 220
 Livage, J. 566(1), 569, 570(6), 595(153), 635, 638
 Live, D. 304(301), 337
 Live, D. H. 230(32), 330
 Lloveras, J. 710(137), 739
 Lobel, K. D. 808(30), 819
 Lobete, F. 767(106, 109), 800, 801
 Lobnik, A. 570(17), 635
 Loboda, M. J. 575(75), 636
 Lobreyer, T. 24, 25(140), 151, 470(6), 486
 Lochschmidt, S. 496(25), 536
 Lock, F. M. 531, 534(130), 539
 Locke, J. A. M. 324(396), 339
 Lockhart, T. P. 870(88), 942
 Loft, M. S. 904(249), 946
 Lögdlund, M. 686(75b), 694
 Lohrenz, J. C. W. 867(81), 942
 Lohse, C. 132(465b), 162
 Londergan, T. M. 795(190), 803
 Longuet-Higgins, H. C. 823(4a), 846
 Loosli, H. R. 261, 311(188), 334
 Lopez, R. 128, 141(462), 162
 Lopinski, G. P. 830(54), 831(55), 833(65a, 65b), 849, 850
 Lorenz, A. 574(52), 636
 Lorenz, C. 709(128), 739
 Lorenz, K. 746(18), 762(75, 76, 83–85), 765(76, 88–90), 769(117), 798, 800, 801
 Lorenz, V. 718(196), 741
 Lork, E. 483(107), 488
 Los, M.G. 728(262), 743
 Losada, J. 752(44, 49), 767(44, 49, 106, 108–112), 768(108), 799–801
 Loton, N. J. 808(22), 818
 Lough, A. J. 698(23), 712, 725(142), 731(23), 737, 740, 865(73), 942, 982, 985(100, 101), 1026
 Louloudi, M. 578(124), 638
 Lourens, R. 492(5), 536
 Loustau Cazalet, C. 381(116), 390
 Lovinger, A. J. 542(19), 547(19, 31, 33), 548(19), 561, 562, 687(77), 694
 Lowe, J. A. 999(119), 1027
 Loy, D. 620(196), 629–631(210), 639, 640
 Loy, D. A. 575(84), 577(88), 578(91, 92, 96, 111), 583(92), 589(96), 592(138–140), 593(141), 595, 598(92), 600(92, 156–158), 602(160), 604(160, 164), 621(157, 198), 622(199), 629(91, 207, 212, 213), 631, 632(92), 637–640, 716(177), 741
 Lozano, A. E. 360(57), 388
 Lu, Y. 629–631(210), 640
 Lubitz, W. 181(45), 219
 Lucarini, M. 346(16, 19), 351(32), 367(77), 377(100), 381(114), 382(119), 383(19), 387–390
 Lucas, D. J. 16(109), 81(318), 151, 157
 Lucas, R. 480(83), 488, 707(108), 739
 Lucchini, V. 351(32), 388
 Lucht, B. L. 662(47), 693
 Ludeke, R. 842(125), 852
 Luderer, F. 713, 731(149), 740, 912(334, 337), 947
 Lühmann, B. 774(137), 801
 Luisa Izquiedro, M. 368(80), 389
 Luke, B. T. 16(119), 22, 23(54), 74, 116(293), 141(496), 149, 151, 156, 163, 724(230), 742
 Lukevics, E. 258(163), 265(197), 266(202), 293(291), 307, 308(307), 325(405–407), 334, 336, 337, 339
 Luna, A. 1034(40), 1056
 Lunazzi, L. 248, 311, 313(121), 332
 Luo, H. 1034(39), 1056
 Luo, J. 208, 210, 211(90), 221
 Luo, Y. 347, 348(21b), 388
 Lutsyl, D. S. 346(15), 387
 Lutz, E. T. G. 559(64), 563
 Lutz, F. 293, 294(290), 336
 Lutz, M. 719, 720, 727(200), 741, 769(123), 801
 Lux, P. 247(110, 112), 282, 293(256–258), 332, 336
 Lydon, J. E. 730(276), 731(288), 743, 744
 Lyo, I.-W. 838, 840(107), 851
 Lyssenko, K. A. 698, 729(15), 736
 Lyster, M. A. 481(97), 488
 Lyubnetsky, L. 827, 828(44), 849
 Lyubovitsky, J. G. 832(62), 849
 Ma, B. 117(429a), 161
 Ma, D. 912(327), 947
 Ma, N. L. 1031(17), 1056
 Ma, S. 1034(39), 1056
 Ma, Y. 838(101b), 851
 Ma, Z. 860(40), 941
 Maa, K. J. 808(18), 818
 Maanen, H. L. van 904(275), 946
 Maas, G. 709(131), 739, 872(116, 117), 904(261, 262, 268), 943, 946
 Macae, D. M. 906, 908(298), 947
 Macciantelli, D. 386(128), 390
 Maciel, G. E. 227(15, 18, 19), 231(18, 19, 37), 326(15), 330, 331
 Mack, H. 932(445), 950
 MacKay, D. B. 381(117), 390
 Mackay, K. M. 36, 40, 48, 49(167), 152

- Mackenzie, J. D. 570(27), 635
 MacLachlan, M. 630(217), 640
 MacLachlan, M. J. 572(34, 35), 595(34), 635, 698(23), 712, 725(142), 731(23), 737, 740
 Macomber, D. W. 886(186), 944
 Macquarrie, D. J. 572(32, 42), 573(32), 635, 636
 MacRae, D. M. 908(307), 947
 Maddaford, S. P. 920(378, 379), 948
 Made, A. W. van der 747(25, 26), 749(25), 769, 770(115), 798, 801
 Made, P. W. N. M. van der 771(127), 801
 Madey, T. E. 834(69, 75a, 78a), 845(75a), 850
 Madhuker, P. 886(186), 944
 Madsen, J. C. 248(116), 332
 Madura, J. D. 825(16a), 847
 Maeda, H. 911(324), 947
 Maeda, Y. 352, 354(39), 388
 Maercker, A. 910(313), 947
 Maerker, C. 5(4, 28b), 112(28b), 128(4, 28b), 132(4, 28b, 465a), 133(4, 28b), 134(4), 137(28b), 147, 148, 162, 1048(119), 1058
 Magers, D. H. 91, 94, 97, 98(355), 158
 Mägi, M. 318(362), 338
 Magnera, T. F. 542(16), 561
 Magnusson, E. 11(59c, 59d), 140(489b), 149, 163
 Magriotis, P. A. 922(387), 948
 Mahiou, R. 578, 586(116), 632(116, 223), 637, 640
 Mahler, H. 928(427), 949
 Mahmoud, F. M. S. 706(102), 739
 Mahon, M. F. 718(190), 727(253), 741, 743
 Mahr, N. 434(32), 465
 Maier, G. 64(257a), 96(371), 155, 158, 168(21), 169(23), 178, 179(37), 181, 182(43), 192(21, 23), 218, 219, 347(21a), 388
 Maier, J. P. 166(7), 178, 179(36), 217, 219
 Maier, W. F. 621(197), 639
 Mains, G. J. 62(246a, 246b), 154
 Mainz, V. V. 595(148), 638
 Maisel, H. E. 307(309, 314), 337
 Maître, P. 37(171), 152
 Majewski, M. 935(457), 950
 Majoral, J.-P. 746(19), 798
 Mak, C. H. 838(103c), 851
 Mak, T. C. W. 904(284), 940(468), 946, 950
 Makarova, N. N. 698(15), 725(232–234, 241–243), 727(256), 729(15), 736, 742, 743
 Maker, P. D. 62(246b), 154
 Makino, T. 896(214), 945
 Makishima, A. 570(26), 635
 Maksic, Z. B. 43(203), 153
 Malacria, M. 362(61a), 368(81), 371(89), 388, 389, 899(230), 945
 Mäler, L. 315, 316, 318(344), 337
 Maletina, E. A. 717(183), 741
 Malik, I. 575(71), 636
 Malisch, W. 481(92), 488, 698(18, 20), 707(18, 20, 114–116), 731(289), 732(116), 737, 739, 744
 Malkin, V. G. 102, 103(379), 159
 Malkina, O. 102, 103(379), 159
 Mallard, W. G. 16(121), 125(449), 151, 161
 Malmström, E. 746(6, 13), 798
 Malrieu, J.-P. 68(279, 280), 83(332), 92(280), 156, 157, 265a, 265b 64, 68(266), 155, 397(57), 425
 Maltsev, A. K. 78(308), 156
 Mammarella, R. E. 916(357), 948
 Manangan, T. 376(97), 389
 Manatt, S. L. 249(129), 333
 Mandich, M. L. 1035(41), 1056
 Mangette, J. E. 403(80, 81, 83), 404(81), 412(80, 83, 124, 125), 413(125), 426, 427
 Manmaru, K. 79(313c), 156
 Mann, D. G. 806(6), 818
 Mann, S. 572(41), 636
 Manne, R. 166(13), 218
 Manners, I. 698(23), 712, 725(142), 731(23), 737, 740
 Manning, J. 132(469), 162
 Manriquez, J. M. 864(56), 942
 Mansour, A. I. 910(318), 947
 Mansuy, D. 578(124), 638
 Mantey, S. 287, 292(271), 336, 474(39), 487
 Manuel, G. 46(210a), 153, 382(121a), 390, 642(2a, 13c), 645, 662(2a), 691
 Manuel, T. A. 645(19a, 19b), 692
 Manzanero, A. 729(270), 743
 Maple, S. R. 325(404), 339
 Maquet, J. 575, 578, 634(83), 637
 Marat, K. 320, 321(384), 338
 Marat, R. K. 480(89), 488
 Maraus, M. S. 480(86), 488
 March, J. 415(131), 427
 Marchand, C. M. 132, 134(467), 135(467, 474), 162, 1041(70), 1057
 Marchesi, E. 346(16), 387
 Marchioro, C. 267(207), 335
 Marco-Contelles, J. 372(90), 389
 Marcolli, C. 573(48), 636
 Marcus, L. 438(47), 460, 463(109), 466, 467
 Marczak, S. 897(224), 945
 Mareci, T. H. 261, 262(193), 273(222), 274(222, 225), 277(233), 334, 335
 Mareda, J. 966, 975(75), 1026
 Margrave, J. L. 81, 82(320), 157
 Margulès, L. 29(154), 152
 Mariam, Y. H. 259(177), 334
 Mark, J. E. 570(14), 635
 Markarashvili, E. G. 725(239), 742
 Märkl, G. 494(14–16), 495(20), 526(109), 528(115), 536, 538, 865(75), 872(120), 942, 943

- Markovski, L. H. 514(73), 537
 Markovski, L. N. 492, 498(8b), 514(72), 516(83), 530(121a, 121b), 531(122, 128, 129), 536–539, 913(345), 948
 Markovskii, L. N. 904(270), 946
 Marks, D. L. 707(109), 739
 Marks, R. N. 686(75b), 694
 Marks, T. J. 864(56, 57), 942
 Maroshina, M. Y. 208, 211(91), 221
 Marsch, M. 867(81), 942
 Marschner, C. 293(289), 336, 782(152), 802, 931(441), 949
 Marsden, C. 36–39(165), 152
 Marshall, A. G. 755, 767(57), 799, 1030(2, 3), 1055
 Marshall, W. J. 114(418c), 160
 Marsmann, H. 63(256a, 256b), 114(416c), 155, 160, 224(2), 225(4, 8), 228(8), 330, 393, 395, 400(22a), 402(71, 74), 404(74), 405(71, 96, 103), 407(74, 110), 411, 412(96), 416(135), 418, 419, 421(142), 424, 426, 427, 472, 481, 482(21), 487, 594(145), 638
 Marsmann, H. C. 274, 276(226), 283, 292(260), 315, 318(343), 335–337, 474(34), 487, 575(63), 636
 Martens, J. 402, 406(72), 426
 Martin, G. E. 257(160), 333
 Martin, H.-P. 478(69), 488
 Martin, J. 370(87), 389
 Martin, J. M. L. 101, 102, 104(380), 159
 Martin, K. 767(102), 800
 Martin, R. L. 13(83b), 150
 Martin, R. M. 823(6a), 847
 Martinez-Barrasa, V. 368(80), 389
 Martín-Franco, J. 379(106), 390
 Martinho, J. M. G. 570(24), 635
 Martinho-Simoes, J. A. 382(120), 390
 Martucci, A. 570(27), 635
 Maruki, I. 1009, 1010, 1012, 1017(148), 1019, 1022(158), 1028
 Marumoto, S. 923(396, 397), 949
 Maruoka, K. 904(265), 946
 Maruyama, K. 884(183), 944
 Maruyama, T. 395, 397, 399(39a), 425, 968, 969, 996(79), 1026
 Marynick, D. 823, 827(5b), 847
 Marynick, D. S. 648, 649(38a, 38d), 693
 Marzilli, L. G. 265(200), 334
 Masaguer, C. F. 928(431, 432), 949
 Masaki, N. 37(172, 173), 152
 Masamune, A. 5, 6, 48, 49, 64, 67(19), 147
 Masamune, S. 48, 49(220), 54(230), 153, 154, 277, 279, 285, 290, 293(240), 335, 392(4), 393(4, 19, 20), 395(19, 20, 33, 34, 44), 397(33), 401(4), 403, 404(86), 405(102), 415(132, 133), 424–427, 782(155), 802, 1006, 1007(133), 1027
 Masangane, P. C. 707(117), 708(118), 739
 Maschmeyer, T. 730(274), 743
 Maseras, F. 825(17c), 847
 Masnyk, M. 897(224), 945
 Mason, B. P. 119(434b, 434c, 436), 120, 122(436), 125(452b), 127(454a), 161
 Mason, S. A. 397(55b), 425
 Masse, C. E. 856, 877(3), 941
 Massies, J. 826(25a), 848
 Masters, A. F. 730(274), 743
 Masumune, S. 5, 6(18), 147
 Materer, N. 844(139b), 852
 Materlik, O. 845(142), 853
 Matern, E. 471(14), 486
 Mathey, F. 494(12, 17), 495, 514(19), 536
 Mathias, L. J. 746(16), 791(178–180), 798, 802
 Mathieu, S. 83–85(337), 157
 Mathur, R. 132(469), 162
 Mátrai, E. 725(245), 742
 Matsson, O. 1015(156), 1028
 Matsubayashi, S. 384(124), 390
 Matsuda, A. 349(26), 388, 570(23), 635
 Matsuda, I. 524(97), 538, 904(266), 919(361, 362), 946, 948
 Matsuda, T. 935(452), 950
 Matsuguchi, A. 559(65), 563
 Matsui, H. 351(31), 388
 Matsui, K. 373(93a), 389, 404(90), 426
 Matsui, Y. 347(20), 387
 Matsumoto, A. 349(25), 388
 Matsumoto, H. 40(188b), 58(239b), 153, 154, 176–178(32), 219, 342(6), 344, 345(11a–c), 387, 701(50, 51), 716(170), 730, 731(275), 737, 740, 743
 Matsumoto, M. 58(239c–e), 154
 Matsumoto, N. 28(150), 152, 542(10), 558(58), 561(10), 561, 562
 Matsumoto, T. 79(313b, 313c), 156, 911, 912(325), 947
 Matsunaga, N. 110, 112(401), 159
 Matsunaga, N. 101(376a), 102(376a, 376b), 103(376b), 104(376a), 159
 Matsuno, T. 418, 419(141), 427
 Matsuo, J. 844(136a, 138), 852
 Matsuo, T. 750, 755(54), 799, 864(50–52), 941, 942
 Matsuoka, K. 765(91, 92, 94), 800
 Matsuoka, N. 570(21), 635
 Matsushita, T. 499, 522(33), 536
 Matsuzaki, Y. 647(28b), 648, 651(37a, 37b), 662, 665(28b), 692
 Matsuzawa, S. 1003(130), 1027
 Mattern, G. 485(133), 489
 Matternas, L. U. 645(19b), 692
 Matthews, E. W. 724(223), 742
 Matthews, O. A. 746(9), 798
 Matukhina, E. V. 725(242), 742

- Matyjaszewski, K. 477(64), 487
 Matyjaszewski, K. 477(67), 488
 Matz, J. R. 901(237), 945
 Maudsley, A. A. 255(146), 333
 Maulitz, A. H. 516(77), 537
 Mauritz, M. A. 716(174), 741
 Maxka, J. 78(306), 156, 259(169, 170, 174),
 277(169, 238, 239), 278, 295(238),
 319(170), 334, 335, 395(38), 409, 410(116),
 425, 427, 858(32), 941, 1008(146, 147),
 1027
 Maxka, M. 393(24b), 424
 Mayer, A. H. 617(186–188), 619(186,
 188–191), 639
 Mayer, H. A. 577(89), 612(89, 177, 178),
 617(177, 178, 185), 618(178), 619(89, 177,
 178), 637, 639
 Mayer, P. M. 139, 140(486c), 162
 Mayer-Posner, F. J. 762(75, 76), 765(76), 800
 Mayes, R. T. 857(27), 941
 Mayne, C. L. 277(231, 232), 335
 Mayr, H. 975(90), 1026
 Mazeaud, A. 701, 729(56), 738
 Mazhar, M. 484(121), 489, 727(253), 743
 Mazières, M.-R. 516(83), 538
 Mazières, S. 64(259), 155
 Mazzah, A. 712(143), 722(143, 216),
 725(143), 740, 742
 Mazzuca, D. A. 940(471), 950
 McAloon, K. 31(159), 152
 McCall, D. W. 319(369), 338
 McClain, M. D. 578, 589(96), 592(140),
 622(199), 637–639
 McClarin, J. A. 936(460), 950
 McClung, R. E. D. 281(246, 248), 320(387),
 335, 338
 McCormick, A. V. 316(359), 338
 McCullen, S. B. 572, 620, 629(37), 635
 McEwan, M. J. 1030(7a), 1055
 McFarlane, W. 225(6), 231(38), 330, 331
 McGarry, P. F. 352(34), 388, 963, 990(65),
 1026
 McGeachin, S. G. 714(160), 740
 McGibbon, G. A. 870(103), 943, 1050(134),
 1051(135), 1058
 McGinnis, S. 1042(76), 1057
 McGlinchey, M. J. 870(95, 97, 100, 101), 942,
 943
 McGonigal, M. 845(145), 853
 McGovern, I. T. 834(74c), 844(129), 850, 852
 McGrath, R. 834(74c), 844(129), 850, 852
 McKee, M. L. 62, 63(247), 155
 McKellar, A. R. W. 112(404a), 159
 McKerrow, A. J. 575(71), 636
 McKillop, K. 1019(159, 160), 1028
 McKillop, K. L. 411(121), 427
 McLean, A. D. 12(74a), 110, 112(396), 150,
 159
 McMahon, C. 125(452b), 161
 McMahon, T. B. 1045(90), 1057
 McManus, S. P. 703(84), 708(122, 123, 125),
 738, 739
 McMillan, P. F. 724(222), 742
 McVie, J. 703, 717(72), 738
 Mdoe, J. E. G. 572, 573(32), 635
 Medinger, K. S. 43(205b), 153
 Meetsma, A. 573(47), 636
 Mehdi, A. 572(43, 44), 636
 Mehl, G. H. 573(45), 636, 765(93), 800
 Mehta, P. 703(79), 738
 Mei, Y. J. 575(70), 636
 Meier, H. 319(366), 338
 Meijer, E. W. 746(10), 798
 Meine, G. 527(113), 538
 Melchior, S. 570(22), 635
 Melde, B. J. 630(216), 640
 Meller, A. 443(69–72), 466, 857(26),
 904(276), 941, 946
 Menandez, M. I. 128, 141(462), 162
 Mendicino, M. A. 844(137b), 852
 Menescal, R. 547(36), 562
 Menichetti, S. 868(86), 942
 Menzel, J. 524(98), 538
 Menzer, S. 703, 729(85), 738
 Mercier, L. 629(214), 640
 Mergardt, B. 901(238), 945
 Merker, R. L. 708(124), 739
 Merz, A. 494(14), 536
 Merz, K. M. 13(80), 150
 Métail, V. 206(82a, 82b), 207(82a), 221
 Metcalf, B. W. 935(451), 950
 Metcalfe, K. 320, 322(381), 324(395), 338
 Metz, B. 26, 27(144), 152
 Metzler, N. 114(420a, 420d), 115(420d), 160,
 202(77, 80), 203(77), 220, 221, 439(55), 466
 Metzler, R. 256(149), 333
 Meudt, A. 96(371), 158
 Meunier, P. 46(210b), 153, 642, 645(2d), 691
 Meuret, J. 169(24), 186(24, 48), 187(24, 48,
 50, 53), 190(48, 50, 53, 54), 191(48),
 199(50), 203, 205, 206(81), 208(88, 89),
 209(88), 210(50, 88, 89), 211, 212(88, 89),
 213(95), 218–221
 Meyer, B. 114(416b), 160
 Meyer, E. 315, 318(343), 337
 Meyer, H. 504(51), 537
 Meyer, U. 531(124), 539
 Meyers, A. I. 877, 879(137, 138), 943
 Mezheny, S. 827, 828(44), 849
 Michalczyk, M. J. 395(32, 40), 397(32),
 399(40), 412(123), 424, 425, 427, 578(122),
 593(142, 143), 634(122, 143), 637, 638,
 762(74), 800, 1006, 1007, 1012(135), 1027
 Michalska, Z. 703, 714, 715(86), 738
 Michaut, J. P. 199, 200(66), 220
 Michel, D. 594(146), 638

- Michel, E. G. 845(142), 853
 Michel, T. 920(371), 948
 Michl, J. 5, 6, 43(14), 47(212c), 63(14, 251), 64(257c), 81, 82(320), 128(460), 136(460, 480), 147, 153, 155, 157, 162, 192(58), 199(65b), 220, 392(1, 3), 395(1, 32, 40), 397(32), 399(40, 62), 401(3, 67, 68), 408(67), 411(67, 120), 412(123), 421(150), 424–428, 492(2), 536, 542(9, 12, 14, 16, 17), 543, 548(9), 555(48), 561, 562, 642(13e), 691, 952(7, 8, 18), 953(8), 982(7), 988(8), 1006(7, 8, 135), 1007, 1012(135), 1022(8), 1024, 1025, 1027
 Mieda, A. 470(2), 486
 Miehlich, B. 15, 19, 33(107), 151
 Miginiac, L. 880(172), 944
 Migita, T. 707(107), 739
 Mihm, G. 169, 192(23), 218
 Mikami, N. 1052(142), 1058
 Mikami, R. 795(189), 802
 Milburn, R. K. 1038(58), 1057
 Mileshevich, V. P. 727(255), 743
 Milius, W. 260(182), 307(310, 311), 334, 337
 Millar, D. M. 595(148), 638
 Millar, T. J. 1032(27), 1056
 Miller, A. E. S. 7(43b), 149
 Miller, J. A. 645(21b), 692
 Miller, J. H. 78(308), 156
 Miller, R. D. 541(2), 542(18), 543(20a, 21), 547(18, 28), 548(2, 18, 38, 43), 555(50), 561, 562, 575(68), 636
 Miller, R. W. 516(80), 538
 Miller, T. 826(25b), 848
 Miller, T. M. 7(43b), 149, 687(76a, 76b), 694
 Millevolte, A. 858(32), 941
 Millevolte, A. J. 51(225b), 154, 259(174), 277(236), 295(236, 294), 334–336, 393(22b), 395(22b, 38), 400(22b), 403(82, 84), 404(82, 84, 88), 412(84), 424–426, 1008(146), 1027
 Mimna, R. 575(67), 636
 Mimura, N. 683(71), 694
 Minakata, S. 379(107), 390
 Minami, T. 570(23), 635
 Minamitsu, A. 1035(42), 1037(56), 1056, 1057
 Minemura, M. 40(188b), 153
 Miner, C. S. Jr. 709(130), 739
 Mineva, T. 110, 112(402), 159
 Mingotaud, A.-F. 240(60), 331
 Minkin, I. V. 103, 108(381a), 159
 Mintz, E. A. 864(57), 942
 Mintzer, J. 167(19), 191–193(55), 218, 220
 Mioc, U. B. 714(156), 740
 Miracle, G. E. 87, 89(338a, 338b), 157
 Miravet, J. F. 794, 795(184–187), 802
 Mironov, B. F. 471(8), 486
 Mishima, M. 1046(107), 1050(133), 1058
 Mislow, K. 24–26, 29(139), 151
 Misra, R. N. 897(225), 945
 Mitchell, T. D. 315, 318, 326(334, 347), 337
 Mitchell, T. N. 922(394), 949
 Mitsuyu, T. 570(21), 635
 Mittal, J. P. 962(59), 1025
 Mittal, K. L. 703, 715(65), 738
 Mitter, F. K. 259, 319(170), 334
 Mitzel, N. W. 11(59b), 149, 432(18–22), 465
 Miura, K. 386(129), 390, 881(176), 913(347, 348), 944, 948
 Miyahara, M. 364(71), 389
 Miyai, A. 559(62), 563
 Miyamoto, M. 559(59), 562
 Miyamoto, S. 1003(125, 126), 1027
 Miyamoto, Y. 839, 840(114, 115), 852
 Miyashita, K. 893(210), 945
 Miyata, H. 902(245), 945
 Miyazaki, H. 542, 561(10), 561
 Miyazaki, M. 548(41), 562
 Miyazawa, T. 392(16), 393(17), 424
 Mizoguchi, M. 547(34), 562
 Mizuta, H. 382(122b), 390
 Mizuta, M. 1005(131), 1027
 Mizutani, K. 931(437–439), 949
 Mizutani, T. 810(39), 819
 Mò, O. 1034(40), 1056
 Mo, Y. 11(59a), 149
 Moc, J. 36(168), 37(168, 169a, 169b), 138, 139, 144–146(168), 152, 1034(38), 1056
 Mochida, K. 138(482), 162
 Modarelli, D. A. 117(429c), 161
 Moffat, H. K. 17(127), 151
 Moffatt, D. J. 830(54), 831(55), 833(65a, 65b), 849, 850
 Mogen, P. 838(103b), 851
 Mogi, I. 559(60), 562
 Mohamed, M. 368(84a, 84b), 389
 Mohamud, S. I. 573(47), 636
 Mohmand, S. 191–193(55), 220
 Möhrke, A. 713, 731(150), 740
 Molla, E. 259, 264(171, 172), 334, 674(56a, 56b), 693
 Moller, K. 575(60), 636
 Möller, M. 558(55), 562, 766(95, 97), 787(168, 169), 791(177), 794(177, 183), 800, 802
 Möller, S. 698, 707(20), 737
 Molloy, K. C. 718(190), 727(253), 741, 743
 Molnar, Z. 312(324), 337
 Mönch, W. 838, 840(105b), 851
 Moncrieff, D. 108, 109(393), 159
 Mong, T. K. 746(7), 798
 Moniz, W. B. 255(147), 256(147, 148, 150–152), 333
 Mont, W.-W. du 113(411a), 114(416b), 160, 474(32–34), 487, 904(290), 946
 Montii, H. 877(147), 879(155), 943, 944
 Monti, J.-P. 877(147), 879(155), 943, 944

- Moore, C. E. 7(41, 42a–c), 11, 39(41), 148
 Moore, H. W. 926(411), 949
 Moorefield, C. N. 746(5), 798
 Moors, R. 509(60), 537, 746(1), 798
 Mootz, D. 434(36), 445, 448(91), 466, 467
 Mooyman, R. 202, 216(75), 220
 Mopper, K. 808(27), 818
 Mora, J. 927(413), 949
 Morán, M. 613(180), 639, 752(44, 49),
 767(44, 49, 106–112), 768(108), 799–801
 Mordas, C. 712, 725(142), 740
 Mordini, A. 933(448), 950
 Moreau, J. J. E. 575(57), 578(93–95, 97–99,
 101, 104, 119, 129), 583(93, 132, 133),
 584(93), 588(93, 98, 99), 590(93, 98, 99,
 101), 596(97, 98), 600(95), 602(98, 99),
 603(94, 95), 604(93), 610(95), 611(94,
 174–176), 616(57, 119), 623(97–99),
 631(95, 98, 99), 636–639, 933(446, 447),
 950
 Moreau, P. 575(59), 636
 Moreno-Fuquen, R. 379(106), 390
 Morgon, N. H. 138–140(483d), 162
 Morgunova, E. F. 706(96), 739
 Morgunova, M. M. 728(262), 743
 Mori, A. 698(14), 701(52), 709(14), 736, 737,
 891(206, 207), 945
 Mori, M. 901(240), 945
 Mori, S. 559(66–68), 560(66, 68), 563, 647,
 662, 665(28b), 692
 Morihashi, K. 200(67), 220, 870, 871(102),
 943
 Morikawa, A. 771(128), 782(156), 801, 802
 Morikawa, Y. 827, 830(40), 849
 Morin, F. G. 230(27), 330
 Morita, T. 481(96), 488
 Mork, R. V. 64(261b), 155
 Morkin, T. L. 952(13), 958(37), 959(37, 46),
 960(46, 57), 963(46, 63), 980, 981(57),
 992(111), 994(57), 995(37), 998–1000(37,
 111), 1001(37), 1025–1027
 Morokuma, K. 96(368), 158, 825(17c), 847
 Morris, A. 837(89e), 851
 Morris, G. A. 245(98, 100), 247(98),
 248(122), 261, 262(193), 316(356, 357),
 317(357), 332, 334, 338
 Morris, P. J. 710(138), 740
 Morris, R. E. 709, 730(127), 739, 751(40),
 752(47), 755(40), 761(47), 799
 Morrison, C. A. 707(117), 739
 Morrow, R. J. 245(96), 332
 Morse, D. E. 806(2–4), 807(3), 810(2, 3,
 41–44), 811(41, 42), 812(42), 813(2, 3,
 42–45), 814, 815(42, 43), 816(4), 817(2,
 49), 818, 819
 Morton, D. W. 934(450), 950
 Moshny, T. 1003(124), 1027
 Moss, R. A. 123(444b), 161
 Mossman, A. B. 481(97), 488
 Motavelli, M. 578, 600(106), 637
 Motevalle, M. 718(195), 741
 Motevalli, M. 718(185–189), 729(189), 741
 Motherwell, W. B. 362(63), 388
 Motonaga, M. 545(26), 562
 Mouse, D. E. 810(38), 819
 Movchun, V. 483(107), 488
 Mowlem, T. J. 904(249), 946
 Moya, A. 767(107), 801
 Mrestani, Y. 911(323), 947
 Mueller, C. 548(40), 562
 Mueller, T. 642, 679(4h), 691
 Muhandiram, D. R. 281(248), 335
 Mui, C. 832(62), 849
 Mulder, P. 364(68), 389
 Mühlhaupt, R. 762(75, 76, 83), 765(76, 88, 90),
 788(170, 171), 800, 802
 Mulin, J. L. 47, 48(214), 153
 Müllen, K. 578, 586(112), 633(112, 225), 637,
 640, 767(102), 800
 Muller, A. 78(307), 156
 Müller, C. 516(78), 538
 Müller, D. 713, 727(147), 740
 Müller, E. 478(69), 488, 752(45), 799
 Müller, G. 440, 441(61b), 466, 529(118), 538,
 726(251), 743, 968(76), 1026
 Müller, H. 191–193(55), 220, 923(399), 949
 Müller, L. 255(146), 333, 474(33, 34), 487
 Müller, L. P. 474(32, 33), 487
 Müller, O. 904(276), 946
 Müller, P. 434, 464(28), 465, 484(123), 489,
 698, 729(26), 737, 788(170), 802
 Müller, R. 480(88), 488
 Müller, T. 67(274), 70(274, 285a), 71(274),
 78(285a, 311a, 311b), 83(328a, 328b), 84,
 86–88(328b), 107(386a), 108(386b), 114,
 115, 117, 118(425), 128(459c), 132(470a),
 133(459c, 470a), 134, 136(459c), 155–157,
 159, 160, 162, 393(26, 27), 394(26–28),
 397(28), 398(27, 28), 399(28, 64), 400(64),
 415(134), 424, 425, 427, 430(10), 432(17),
 445, 446(88), 465, 467, 473(27, 28),
 483(108), 487, 488, 857(22), 912(331), 941,
 947, 952, 953, 963, 982, 988(12), 995(116),
 1003(12), 1025, 1027, 1048(120),
 1049(129), 1058
 Müller, W. E. G. 807(13), 818
 Mulliken, R. S. 63(249b), 155
 Mulvey, R. E. 434(34), 466
 Mulzer, J. 928(421, 428), 930(421), 949
 Mundt, O. 498(28), 503(45), 509(28), 536, 537
 Muñoz-Martínez, E. 769(122, 123), 801
 Munschauer, R. 904(262, 268), 946
 Munson, B. 1045(91, 92a, 92b, 95),
 1046(101), 1057, 1058
 Muragavel, R. 699, 735(32), 737
 Murai, S. 856(5), 888(201), 941, 945

- Murakami, S. 48, 49(220), 153, 393(19), 395(19, 33, 34), 397(33), 403, 404(86), 405(102), 424–426
- Murakami, Y. 351(31), 388
- Murata, S. 919(361, 362), 948
- Murphy, J. A. 377(102), 389
- Murphy, P. D. 256(149), 333
- Murphy, W. J. 594(147), 638
- Murrel, J. N. 192(56), 220
- Murry, J. A. 936(462), 950
- Murtagh, M. T. 570(18, 19), 635
- Murthy, S. 1040(67, 68), 1051(138, 139), 1052(139), 1057, 1058
- Murugavel, R. 232(45), 331, 433(26), 465, 573(49), 636, 698(27–30), 699(35), 711(139, 140), 715(162), 717, 720, 721(29), 722(27–30), 724(27–30, 140, 162), 729(140), 731(139), 733(35, 139), 737, 740
- Musker, W. K. 227(18), 231(18, 37), 330, 331
- Mutathi, A. M. 705(94), 739
- Mutin, H. 610(170), 639
- Mutin, H. P. 595, 596(149), 638
- Mutin, P. H. 575(77), 636
- Muzafarov, A. M. 751(28, 37), 757(28, 37, 61), 758(37), 759(28), 762(78–81), 764(78), 765(87), 766(95–97), 771(129), 776(61, 81, 138–140), 777(138, 139), 778(81), 782(154), 787(167–169), 791(78, 81, 177), 794(177, 183), 795(189), 797(192), 799–803
- Myakushev, V. D. 728(264), 743, 751(28, 37), 757(28, 37, 61), 758(37), 759(28), 766(95), 771(129), 776(61), 787(167), 795(189), 797(192), 799–803
- Myers, S. A. 577(88), 592(138, 139), 637, 638
- Mynott, R. 894(212), 945
- Nabora, K. 879(159), 944
- Nachtigall, P. 16(113), 151, 823, 824(12), 837(93a, 95a), 847, 851
- Nacken, M. 718(193), 741
- Nagahara, K. 379(105, 110), 390
- Nagai, Y. 58(239b), 154, 393(21), 395(21, 36), 397, 412(36), 424, 425, 707(107), 739
- Nagano, Y. 1051(138, 139), 1052(139), 1058
- Naganuma, K. 911(322), 947
- Nagasawa, T. 911(324), 947
- Nagase, H. 810(39), 819
- Nagase, S. 5, 8, 10(5), 19, 20(132, 133), 39(184), 40(184, 187), 41(5, 184, 187, 190–196), 42(184, 190–193, 195, 196), 43(191, 192, 195), 44(5, 184), 46(184), 52(184, 187, 226b, 227), 53(194, 227), 54(184, 187, 190, 193, 194, 226b, 227, 229b, 233), 55(184), 56, 57(184, 233, 236), 58(184, 190, 191, 193, 195, 196, 240), 59(184, 190, 193), 60(190–193, 195, 196), 61(244b), 62(191, 192, 195, 196), 63(240), 67(275, 276), 68(275), 75(275, 276), 79(313a), 82(325), 91(342, 343a, 343b), 92(5, 342, 343a, 343b), 93(343a, 363g), 94(342, 343a), 96, 97(343a), 98(342, 343a, 343b), 101(184, 192), 102(184, 196, 378), 103(378), 104(196, 378), 105(196, 240), 106, 137(385a), 147, 151, 153–159, 320(386), 338, 352, 354(39), 388, 404(93), 422(154), 426, 428, 523(94), 528(116), 538, 726(249), 743, 871(106), 874(124, 125), 875(126, 129), 877(133), 943, 955(26), 968, 1013(78), 1025, 1026
- Nagashima, M. 41–43, 58, 60, 62(191), 153
- Naga Srinivas, G. 39, 40, 44–46(183), 153
- Nagendran, S. 699, 731(34), 737
- Nagendrappa, G. 883(181), 887(189), 944
- Nagi, Y. 40(188b), 153
- Nagy, A. 207(84), 221
- Naik, P. D. 962(59), 1025
- Naito, H. 559(60), 562, 676, 679, 680, 690(62b), 693
- Naito, S. 919(370), 948
- Naka, A. 83–86(333), 157, 685(73b), 694
- Nakadaira, Y. 351(30), 352, 354(39), 388, 642(10a, 10b), 691, 875(127, 128), 904(248), 943, 946, 1008(144), 1019(162), 1027, 1028
- Nakagawa, H. 559(60), 562
- Nakagawa, K. 392(9, 10), 424
- Nakagawa, T. 386(129), 390
- Nakagawa, Y. 47(216), 153, 474(38), 487, 647, 662(28a), 692
- Nakaidze, L. I. 698(25), 737
- Nakajima, A. 896(218–221, 223), 945
- Nakajima, K. 393, 395(21), 424
- Nakajima, T. 869(87), 893(210), 942, 945
- Nakajo, E. 474(37), 487
- Nakamura, A. 642(10b), 691
- Nakamura, H. 895(213), 945
- Nakamura, K. 37(172, 173), 152, 906(300), 947
- Nakamura, M. 119, 120, 122(437), 161
- Nakamura, T. 559(60), 562, 839(110), 851
- Nakanishi, F. 558(57), 562
- Nakanishi, S. 556(53), 562
- Nakano, H. 832(60a, 60b), 849
- Nakano, M. 40(187), 41(187, 190), 42(190), 52(187), 54(187, 190), 58–60(190), 61(244b), 153, 154, 648, 651(37a, 37b), 692
- Nakano, T. 688(78), 694
- Nakash, M. 365(72), 389, 392(7), 424, 912(338), 947, 1011(153, 154), 1012(155), 1013(153, 154), 1014(153–155), 1015(154), 1016, 1017(153), 1028
- Nakashima, H. 545(26), 562, 575(61, 62), 636
- Nakashima, T. T. 281(246, 248), 320(387), 335, 338
- Nakatani, J. 895(213), 945

- Nakatsuji, H. 827, 830(40), 849
 Nakatsuji, K. 838(103e), 851
 Nakayama, I. 896(217), 945
 Nakayama, J. 750(53), 799
 Nakayama, K. 885(184), 944
 Nakayama, T. 559(59), 562
 Nakazawa, H. 199(71), 220
 Nakdaira, Y. 864(47), 941
 Namavari, M. 955, 956(31), 1025
 Nametkin, N. S. 952(2, 3), 956, 958, 962, 982(33), 1024, 1025
 Nami, C. (382a), 159
 Namiki, A. 839(110a), 851
 Nanavati, S. 703(88), 738
 Nanjo, M. 295(295), 336, 781(150), 782(153), 802
 Nanz, D. 312(323, 324), 314(323), 337
 Naoi, Y. 58(239b), 154
 Narang, S. C. 483(112), 488
 Nardin, R. 258(164), 334
 Nasu, M. 1037(56), 1057
 Näther, C. 169(24), 186, 187(24, 48), 190, 191(48), 203, 205, 206(81), 218, 219, 221
 Natsuhash, Y. 79(313c), 156
 Natterer, J. 251, 252(131), 333
 Natterstad, J. J. 227, 326(15), 330
 Nauroth, P. 722(213), 741
 Neckers, D. C. 786(162, 163), 802
 Neddermeyer, H. 839(112), 852
 Needs, R. J. 826(26c), 848
 Nefedov, O. M. 47(212c), 79(314g, 315b), 81, 82(320), 118(430), 119, 120(435), 127(455a), 153, 157, 161, 642(13e), 691
 Nefedov, V. D. 1044(86), 1057
 Negishi, E. 645(21a, 21b), 692
 Negrebetsky, V. V. 239(54), 331
 Neilson, R. H. 904(273, 274), 934(449, 450), 946, 950
 Neison, R. H. 904(271), 946
 Nelson, A. J. 642(9), 691
 Nelson, M. M. 841, 842(122), 845(141), 852
 Nenner, A.-M. 320, 324(372), 338
 Nesterov, D. U. 698(25), 737
 Neugebauer, P. 445, 446(87, 89), 447(89), 467
 Neuhaus, D. 317, 318(360), 338
 Neumann, B. 113(413b, 413c), 114(416a), 160, 507(58), 522(92), 537, 538, 698, 735(21, 22, 24), 737
 Neumann, D. U. 64(261c), 155
 Neumark, D. M. 217(98), 221
 Newbold, R. C. 935(453), 950
 Newcomb, M. 342, 346, 357, 359, 363, 364(4), 387
 Newkome, G. R. 746(5), 798
 Newman, C. G. 17(127), 151
 Newman, D. A. 701(48), 711, 720(141), 727(141, 257, 258), 729(48), 737, 740, 743
 Newmark, R. A. 315(340), 337
 Neyses, S. 904(263), 946
 Ngono, B. 912(330), 947
 Nguyen, K. A. 54, 56(231, 232), 57(232), 154, 1034(37, 38), 1056
 Nguyen, M. T. 91, 94, 95(349), 125(451), 158, 161
 Nguyen, N. V. 926(411), 949
 Nguyen, V. Q. 345, 346(14), 387
 Nguyen-Dang, T. T. 14(97a, 97b), 150
 Ni, Q.-X. 642(7), 648(7, 35b), 691, 692
 Nibbering, N. M. M. 1053(145), 1059
 Nichols, C. J. 939(467), 950
 Nick, S. 169, 186, 187(24), 218
 Nicklass, A. 25(141), 151
 Nicolaidis, A. 1051(141), 1058
 Niecke, E. 494(13), 511(68), 522(93), 531(123, 125, 126, 133, 134), 536–539, 904(269), 946
 Niedermayer, W. 396, 397(48), 425
 Nieger, M. 501(39), 522(93), 531(123, 126, 133, 134), 537–539, 879(164), 944
 Nielsen, N. C. 248(116), 274, 280(228), 282(249), 332, 335
 Nielsen, O. H. 823(6a), 847
 Nielson, R. B. 645(21c), 692
 Niemann, B. 495(18, 24), 501(24, 39), 510(66), 536, 537
 Nieminen, M. O. J. 324(402), 339
 Nienhous, H. 838, 840(105b), 851
 Niesmann, J. 440(61a), 441(61a, 63), 466
 Niessen, V. 642(13a), 691
 Nietzsche, E. 911(323), 947
 Nieuwpoort, W. C. 13, 15(82), 150
 Niitsu, T. 524(97), 528(116, 117), 538
 Niki, H. 62(246b), 154
 Nikolaev, G. A. 727(255), 743
 Nillevolte, A. J. 395, 397, 420(42), 425
 Nilsson, T. 316, 318(352), 338
 Nilsson, Y. 899(230), 945
 Nimlos, M. R. 140(488), 163
 Nishida, K. 347(20), 387
 Nishihara, Y. 698(14), 701(52), 709(14), 736, 737
 Nishijima, M. 827(38a, 38b), 833(64), 834(72), 848, 850
 Nishimoto, K. 499, 522(33), 536
 Nishimura, K. 1003(126, 128), 1027
 Nishio, R. 765(91, 92, 94), 800
 Nishiyama, K. 382(122a, 122b), 390
 Nittoli, T. 705(94), 739
 Nitzsche, S. 471(17), 486
 Niu, C.-H. 304(301), 337
 Nivert, C. L. 698(17), 736
 Nixon, J. F. 494(12, 17), 495, 514(19), 536
 Noble, P. N. 16(117), 151
 Noda, M. 883(180), 944
 Nodono, M. 673(54a, 54b), 683(54a, 71), 690(54a, 54b), 693, 694

- Nogaideli, A. I. 698(25), 737
 Nohira, H. 765(91, 92, 94), 800
 Noiret, N. 311(320), 337
 Noltemeyer, M. 434(38), 438(47, 48), 439(50, 57–59), 440(61a), 441(61a, 62, 63), 443(78), 444(83), 445(85, 88, 91), 446(85, 88), 448(91), 450(97, 101, 102), 452(102), 453–455(97), 457, 458(102), 459(101, 102), 460(102), 463(110), 466, 467, 699(32, 33, 35), 701(54), 708(119), 711(139), 712(143), 718(197), 722(143, 197, 215, 216), 724(54), 725(143), 727(119), 729(269), 731(139), 733(33, 35, 139), 734(33), 735(32, 54), 737, 739–743, 923, 924(400, 403, 405), 949
 Noltemeyer, N. 434, 436(41), 466
 Nondek, L. 255, 325(144), 333
 Nongrum, M. F. 746(7), 798
 Noren, B. 766(99), 800
 Norman, D. 844(129), 852
 Norman, N. C. 5, 6(17), 147, 519(84), 538
 Nornung, V. 178, 179(36), 219
 Northolt, M. G. 729(268), 743
 Northrup, J. E. 826(26e), 848
 Nöth, H. 58(239g, 239i), 154, 181, 182(43), 219, 418, 419, 421(140), 427, 439(55, 56), 466
 Notheis, C. 288, 289(277), 336, 780(148), 802
 Nowakowski, P. 857(21), 941
 Nozaki, H. 912(329), 947
 Nugent, W. A. 647(29a, 29b), 692
 Nuñez, R. 578, 593(121), 609(168), 637, 639, 752, 761(43), 799
 Nunn, C. M. 533(136), 539
 Nyburg, S. C. 5, 6, 63(12c), 147, 913(343), 948, 952, 997, 998(17b), 1025
 Nyholm, R. 834(74b), 850
 Nynlaszi, L. 208, 211(92), 221
 Nyulaszi, L. 208(85), 221

 Oba, M. 382(122a, 122b), 390
 Obata, T. 344, 345(11c), 387
 Obayashi, M. 912(329), 947
 Oberhammer, H. 11(59b), 24, 25(140), 149, 151, 445, 446(87), 467
 Oblin, M. 908(311), 947
 O'Brien, D. H. 642(12), 691
 Occhiucci, G. 1039(64, 65), 1040(65), 1057
 Ochiai, M. 918(360), 948
 O'Connor, C. J. 572(33), 635
 O'Connor, M. J. 311, 320(319), 337
 Odagaki, Y. 528(116), 538
 Oddershede, J. 16(108), 151
 Odinets, V. A. 725(236), 742
 Oehme, H. 284(262), 336, 713, 731(149), 740, 865, 904(74), 910, 911(321), 912(321, 332–337), 942, 947
 Oellig, E. M. 834(74a), 850
 Ogasawara, J. 873(121, 122), 912(121), 943
 Ogawa, A. 371(88), 389
 Ogawa, E. T. 575(71), 636
 Ogawa, K. 395(45, 46), 397, 412(46), 425, 1007(142), 1027
 Ogilvie, J. F. 64(257b), 155, 192(56), 220
 Ogilvie, K. K. 928(423), 949
 Ogino, H. 856(19), 941
 Ogliaro, F. 93(364), 158
 Ogoshi, H. 810(39), 819
 Ogura, J. H. van 940(469), 950
 Ogura, S. 379(107), 390
 O'Hare, H. K. 902(242), 945
 Ohashi, S. 878(153), 944
 Ohba, Y. 911(324), 947
 Ohdimari, I. 826(27g, 27h), 848
 Ohdomari, I. 840(118), 852
 Ohgaki, H. 44(208a, 208b), 153
 Ohi, F. 392(9, 10), 424
 Ohkata, K. 878(149, 150), 943, 944
 Ohkubo, K. 352(36), 388
 Öhman, L.-O. 320, 324(372), 338
 Ohno, K. 869(87), 942
 Ohno, M. 883(180), 902(244, 245), 944, 945
 Ohno, S. 642(15), 652(41), 654, 658(15), 670(15, 48), 672(15), 691, 693
 Ohshiro, Y. 902(244, 245), 945
 Ohshita, J. 559(65), 563, 673(54a, 54b), 683(54a, 70–72), 685(72, 73b), 690(54a, 54b, 80), 693, 694
 Ohsuna, T. 630(215), 640
 Ohtake, N. 839(110), 851
 Ohtani, Y. 896(215, 222), 945
 Ohya, S. 72(288), 156, 858(31), 941, 1006, 1008(134), 1027
 Oikawa, S. 826(27g–i), 840(118), 848, 852
 Oka, K. 555(47, 49), 556(53), 559(60), 562, 676, 679, 680, 690(62a, 62b), 693
 Okada, K. 54(230), 154, 526(110), 538
 Okamoto, A. 525(107), 538
 Okamoto, M. 37(173), 152, 471(13), 472(19), 486
 Okamoto, Y. 481(96), 488, 896(223), 945
 Okano, K. 901(236), 945
 Okano, T. 483(113), 488
 Okasa, T. 833(64), 850
 Okawa, T. 795(189), 802
 Okazaki, R. 5, 6(11c, 23b), 63(11c), 79(312, 313a–e), 89(338e), 113, 114, 117(23b), 147, 148, 156, 157, 295(293), 320(386), 336, 338, 392(6), 395(45, 46), 396(6), 397(46), 399, 401(6), 412(6, 46), 414(6), 424, 425, 479(78), 488, 907(306), 911(322, 325), 912(325), 947, 952, 1006(16), 1007(142, 143), 1019, 1022(16), 1025, 1027
 O'Keeffe, M. 724(222, 226), 742
 Okinoshima, H. 647(27), 692, 992(113), 1027
 Okita, K. 673(54b), 690(54b, 80), 693, 694
 Olah, G. A. 132(464a), 162, 483(112), 488

- Olah, J. A. 1049(125), 1058
 Olbrich, G. 64(271), 118(432b), 155, 161, 1007(137), 1027
 Oldfield, E. 320(376–378, 380), 338
 O'Leary, B. 94, 98(358), 158, 725, 726(247), 743
 O'Leary, B. J. 718, 722(198), 741
 O'leary, P. 94, 98(358), 158
 Olivucci, M. 966(72–74), 1026
 Öller, M. 922(393), 949
 Olmstead, M. M. 64(261a, 261b), 78(310), 94(359), 155, 156, 158, 433(25), 465
 Olson, R. E. 888(190, 192, 196, 197), 944
 Olson, W. D. H. 572, 620, 629(37), 635
 Olsson, L. 132, 133(470b), 136, 137(477), 162
 Olthoff, S. 410(118), 427
 Omotowa, B. A. 762(86), 800
 Onchi, M. 827(38a, 38b), 834(72), 848, 850
 O'Neal, H. E. 17(127), 151, 358(52), 388
 Ong, C. K. 835(83), 850
 Oniki, T. 931(436), 949
 Onitsuka, K. 864(49), 941
 Ono, K. 544, 545(23), 561
 Ono, Y. 471(13), 472(19), 486, 838(101b), 851
 Onodera, S. 471(13), 472(19), 486
 Oomori, D. 1037(56), 1057
 Ooms, F. 923, 924(408), 949
 Oostendorp, D. J. 703(78), 738
 Oosterom, G. E. 750, 771(55), 799
 Oostra, D. J. 844(139a), 852
 Opel, A. 867(81), 942
 Operti, L. 1036(47, 49–51), 1037(53a–c), 1056
 Oprea, A. 287, 292(271), 336
 Orchard, A. F. 166(6), 217
 Ordnung, I. 307(313), 337
 Oritz, J. V. 140(487), 163
 Orlando, R. 1045(92a, 92b), 1046(101), 1057, 1058
 Orpen, A. G. 719(199), 741, 864(53), 942
 Ortiz, J. V. 856(18), 941
 Osaki, S. 879(156, 157), 944
 Osawa, H. 185(46), 219
 Oshima, K. 904(256), 913(347, 348), 946, 948
 Oshino, H. 891(207), 945
 Oshita, J. 201(72), 220
 Oshiyama, A. 839, 840(114, 115), 852
 Osinga, V. P. 483(105), 488
 Ossadnik, C. 575(63), 636
 Ossig, G. 904(276), 946
 Ostah, N. A. 19, 122(130b), 151
 Osterholz, F. D. 703(77), 738
 Ostrander, R. L. 747, 750, 755, 760(27), 798
 Oswald, M. 343(10a, 10b), 387
 Oswald, R. 343(10a), 387
 Otimoto, K. 913(347, 348), 948
 Otting, G. 280(242), 335
 Ottoson, C. H. 542(17), 561
 Ottosson, C.-H. 858(35), 941
 Ouellette, R. J. 707(109), 739
 Ovchinnikov, Y. E. 700, 727(42), 737
 Ovchinnikov, Yu. E. 725(240), 742
 Ovchinnikov, Y. 965, 967(69), 1026
 Oviatt, H. 600(156, 157), 621(157, 198), 638, 639
 Oviatt, H. W. 578, 600, 633(90), 637
 Owen, M. J. 760(63–71), 799, 800
 Owen, N. L. 277(232), 335
 Owens, T. 964, 990(66), 1018(157), 1026, 1028
 Oyamada, T. 136, 137(479b), 162
 Ozaki, M. 648(35e), 692
 Ozawa, F. 864(49), 941
 Ozerin, A. N. 791(175), 802
 Ozerina, L. A. 791(175), 802
 Ozin, A. 630(217), 640
 Ozin, G. A. 483(117), 488, 572(34, 35), 595(34), 635
 Ozubko, R. S. 594(147), 638
 Pabrakar, S. 622(199), 639
 Pachler, K. G. R. 241(77), 242(84, 85), 244(95), 332
 Pacios, L. F. 13–15, 17(88a, 88b), 150
 Padden, F. J. Jr. 547(31), 562
 Padowitz, D. F. 830(50), 849
 Padwa, A. 910(319), 947
 Paetzold, P. 511(68), 537, 904(263), 946
 Page, M. 483(120), 489
 Pagni, R. M. 870(96), 942
 Pai, S. 837(97), 851
 Pai, Y.-M. 315(348), 338
 Pak, C. 74, 96(297), 156
 Pakulski, M. 519(84), 533(135, 136), 538, 539
 Palágyi, Z. 94, 96–98(360), 158
 Palfreyman, S. A. 241(76), 249(128), 332, 333
 Palmer, L. 316(354), 338
 Palmer, M. T. 719, 720, 727(200), 741
 Palomo, C. 248, 311, 313(121), 332
 Palovich, M. 870(92), 903(246), 942, 945
 Pan, F. M. 575(70), 636
 Pan, W. 830(47b), 849
 Pan, Y. 393, 395, 400(22a), 424
 Panek, J. S. 856(2, 3), 877(3, 135), 879(160), 161, 163, 166, 940, 941, 943, 944
 Pang, Y. 642(7, 8), 648(7, 8, 35a–c), 649, 651(35c), 691, 692
 Panke, G. 879(158), 944
 Pankiewicz, K. W. 940(469), 950
 Pannek, J.-B. 877(134, 145), 943
 Pannel, K. H. 856(16), 941
 Pannell, K. H. 318(364, 365), 338, 714(159), 740, 865(71), 942, 960, 993(49), 1025
 Panov, V. 964, 1009–1011, 1018, 1019, 1022(68), 1026
 Papadimitrakopoulos, F. 687(76a, 76b), 694

- Pape, T. 431(15), 434(27), 445–447(89), 465, 467
- Papkov, V. S. 751, 757(28, 37), 758(37), 759(28), 782(154), 787(167), 799, 802
- Paquette, L. 38, 62(179), 152
- Paquette, L. A. 374(95), 379(108), 389, 390, 870(99), 929(435), 943, 949
- Parbhoo, B. 247(111), 324(399, 400), 332, 339, 648(35a), 692
- Pardi, A. 136(480), 162
- Parella, T. 300(299), 327(414), 336, 339
- Parham, P. 760(70), 800
- Parisel, O. 1031(22), 1056
- Parisini, E. 699, 733(35), 737
- Park, C. M. 366(73), 389
- Park, E. 751(29–33), 799
- Park, H. S. 729(269), 743
- Park, J. 774(131), 801
- Párkányi, L. 700, 727(41), 731(281), 737, 743
- Parkinson, J. 320(379), 338, 806(9), 818
- Parr, J. 808(20), 818
- Parr, R. G. 12(70b), 149
- Parshall, G. W. 494(13), 536
- Partridge, H. 5, 6, 13, 15(32), 148
- Pascual, M. C. 613(180), 639
- Pasinszki, T. 208(85), 221
- Passmore, T. R. 173, 174(27), 218
- Past, J. 233, 236(47), 282(253, 254), 296, 297(47, 253, 254), 298(253), 331, 336
- Pastor, S. D. 319(366), 338
- Patai, S. 5, 6, 41(1a, 2), 63(2), 147
- Patarin, J. 626(205, 206), 640
- Patel, P. P. 886(187), 944
- Patnaik, S. 547(30a), 562
- Patrick, J. S. 1034(39), 1056
- Patrin, J. C. 834(77b), 850
- Patro, B. 377(102), 389
- Pattenden, G. 378(104), 389
- Patterson, W. J. 703(84), 708(122, 123, 125), 738, 739
- Patyk, A. 992(112), 1027
- Patz, M. 975(90), 1026
- Pätzold, U. 479(73, 74), 488
- Pauer, F. 434(30), 458(103), 459(104), 460(105), 462(103, 105), 463(105), 465, 467
- Paul, G. C. 862(42), 941
- Paul, M. 432(19), 465
- Paulasaari, J. K. 797(193, 194), 803
- Paulen, W. 492(4), 501(40, 41), 519(4), 536, 537
- Pauling, L. 7(37), 148
- Paulus, B. 826, 827(29), 848
- Pauly, T. 845(142), 853
- Paunz, R. 114, 115(420c), 160
- Pauthe, M. 575(81), 636
- Pavanaja, U. B. 962(59), 1025
- Pavlov, A. A. 682(67), 693
- Pawson, D. 320(370), 338
- Payne, J. T. 716(174), 741
- Payne, M. C. 823(8a), 847
- Pazdernik, L. 707(110), 739
- Peat, I. R. 316(349), 338
- Peddle, G. J. 714(160), 740
- Peddle, G. J. D. 1019(161), 1028
- Pedersen, J. C. 614(181), 639
- Pedlow, G. W. Jr. 709(130), 739
- Pedrielli, P. 367(77), 389
- Pedulli, G. F. 346(16, 19), 351(32), 367(77), 383(19), 387–389
- Peel, J. B. 208, 213(87), 221
- Pegg, D. T. 245(99, 101), 246(99, 101, 106, 107), 332
- Pehk, T. 282, 296, 297(254), 336
- Pehlke, E. 838(99a, 99b), 851
- Peinado, C. 360(57), 388
- Péllissier, M. 37(171), 152
- Pellmann, A. 393, 395, 400(22a), 405, 411, 412(96), 424, 426
- Pelnař, J. 258, 260(165), 262, 263, 265(196), 334
- Pelz, J. P. 841(123a, 123b, 124), 852
- Perdue, E. M. 271(215), 335
- Pereyre, M. 248(120), 332, 901(233), 945
- Perpete, E. A. 547(30b), 562
- Perry, C. C. 808(23), 818
- Perry, M. C. 241(76), 249(126–128), 255(127), 332, 333
- Perz, S. V. 760(63–71), 799, 800
- Pesel, H. 697(8), 736
- Pestunovich, V. A. 239(55, 56, 58), 261(191), 331, 334
- Peters, K. 114(416c), 160, 187(51a, 52a, 52b), 190(51a), 220, 400(65), 402(73), 405(104), 406(106, 107), 407(107, 108, 110), 410(118), 425–427
- Peters, U. 928(425), 949
- Petersen, J. L. 864(58–62), 942
- Peterson, D. J. 492(6), 536
- Peterson, K. A. 138, 139(483a), 162
- Petit, N. 311(320), 337
- Petráková, E. 323(393), 338
- Petráková, E. 258(165), 259(173), 260(165), 334
- Pétraud, M. 243(88, 89), 248(119, 121, 125), 250(125), 261(89), 311(121, 125, 320, 321), 313(121), 332, 333, 337
- Petrenz, R. 857(25), 941
- Petrie, M. A. 496(27), 522(27, 89), 536, 538
- Petris, G.de 1039, 1040(65), 1048(118), 1057, 1058
- Petrov, A. D. 471(8), 486
- Peyerimhoff, S. D. 192(56), 220
- Pfeifer, K.-H. 208(86), 221
- Pfisterer, G. 284(263), 336
- Pfister-Guillouzo, G. 206(82a, 82b), 207(82a), 221, 642(13c), 691

- Pflaum, S. 494(16), 536
 Pfeleiderer, B. 617(184), 639
 Pfeleiderer, W. 928(424), 949
 Pflug, J. L. 274, 275(223), 335, 348(22), 388, 779(145), 780(146, 147), 781(145), 802
 Phalippou, J. 575(81), 636
 Pham, E. K. 402(76), 426, 702, 727(63), 738
 Philip, R. C. 31(158a), 152
 Philipp, D. M. 825(20c), 847
 Philippopoulos, A. I. 64(261c), 155
 Philipsborn, W. von 246, 247(108), 248(114), 332
 Phillips, S. H. 712, 727(144), 740
 Phung, N. 370(86a), 389
 Pi, Z. 266, 301(205), 303(205, 300), 334, 336, 752(56), 799
 Piana, H. 403(87), 426
 Pianet, I. 243, 261(89), 332
 Piantini, U. 282(255), 336
 Picard, J.-P. 5, 6, 63(12c), 147, 248(121), 311(121, 322), 313(121), 332, 337
 Pickel, P. 483(108, 109), 488
 Pickelman, D. 760(70), 800
 Pickett, J. B. 642(11), 691
 Pickett-Heaps, J. 808(24), 818
 Pickup, P. G. 642, 645, 651(17), 691
 Pidun, U. 1041(70), 1057
 Pidvarko, T. V. 514(72), 537
 Piel, H. 405(104), 426
 Pieper, U. 443(78), 467
 Pietrusza, E. W. 714(153), 740
 Pietschnig, R. 531(125, 133), 539
 Pikul, S. 928(426), 949
 Pillot, J.-P. 243(88), 332
 Pinchaux, R. 826(25a), 848
 Pines, A. 241(75), 257(156), 265(199), 331, 333, 334
 Pines, A. N. 710(132), 739
 Pinnavaia, T. 629(214), 640
 Pinnavaia, T. J. 810(40), 819, 936(460), 950
 Pinzani, D. 933(448), 950
 Pirrung, M. C. 935(454), 950
 Pitter, S. 706(98), 739
 Pittman, C. U. 703(84), 738
 Pittman, C. U. Jr. 67, 71, 73(278b), 156, 708(122, 123, 125), 739
 Pitzer, K. 92(361c), 158
 Pitzer, K. S. 16(124a, 124b), 63(249a), 92(124a), 151, 155
 Plateau, P. 306(305), 337
 Platz, M. S. 117(429c), 161
 Plavac, N. 284, 290, 292(261), 336
 Ple, G. 244, 259, 312(93), 332
 Plitt, H. S. 542(12), 561
 Plotzke, K. P. 703(88), 738
 Podkorytov, I. S. 277(235), 335
 Pohl, E. R. 703(77), 738
 Pohl, S. 393, 395(22a), 400(22a, 66), 402(71, 72, 74), 404(74), 405(71, 96), 406(66, 72), 407(66, 74, 109), 408(109), 411, 412(96), 424–426
 Pohlmann, S. 910(316), 947
 Poirier, M. 484(121), 489
 Poirier, R. A. 642, 645, 651(17), 691
 Pola, J. 236, 258(51), 331, 962(59), 1025
 Polborn, K. 58, 61, 62(238), 154, 396, 397(48), 417(139), 418, 419, 421(140), 423(139), 425, 427, 968, 978(77), 1026
 Polishchuk, A. P. 725(232–234, 241, 243), 742
 Polk, M. 507(55), 537
 Pollart, D. J. 900(231), 945
 Pollmann, J. 826(26d), 844(133c), 848, 852
 Polyachenko, L. K. 514(73), 530(121a, 121b), 537, 539, 904(270), 946
 Ponikvar, W. 58(239i), 154
 Ponomarenko, S. A. 765(87), 800
 Ponomarenko, V. A. 471(8), 486
 Pons, J.-M. 908(311), 947
 Poon, K. S. M. 940(468), 950
 Poon, Y. C. 5, 6, 63(12c), 147, 913(343), 948, 952, 997, 998(17b), 1025
 Poort, L. 806(8), 818
 Popelier, P. 14(96b, 99), 56(99), 150
 Pople, J. A. 5(25c), 12(25c, 61–65, 69, 73, 74b, 75), 16(109, 118, 119, 123a, 123b), 22, 23(54), 38(174b), 74(293), 81(318), 116(293), 138(483c), 139(483c, 485), 140(485), 141(496), 148–152, 156, 157, 162, 163, 229(22), 330, 724(230), 742, 1031(17), 1056
 Popowski, E. 434(42), 437(43), 466
 Poppe, M. 495(21), 536
 Pernet, J. 880(172), 944
 Porte, H. 703, 716, 717(66), 738
 Portella, C. 888(194), 944
 Porter, N. A. 362(64), 388
 Portius, P. 64(261c), 155
 Porz, C. 511(67), 537
 Porzel, A. 258, 259(168), 334
 Pöschl, U. 273, 289, 294(219), 335, 477(66, 68), 487, 488
 Potts, A. W. 166(6), 173, 174(27), 217, 218
 Potzinger, P. 348(23), 388, 958(35), 962(35, 60), 982(60), 1007(137), 1025–1027
 Pouységu, L. 248, 250, 311(125), 333
 Powell, D. 674(58), 693
 Powell, D. R. 51(225a), 87, 89(338a–d), 108(386b), 154, 157, 159, 259(170), 292(287), 319(170), 334, 336, 395(37, 41), 397(41), 403(79–81, 83, 84), 404(79, 81, 84, 92), 409(114, 117), 411(121), 412(80, 83, 84, 122, 124, 125), 413(125–128), 414(128), 419(79), 51), 425–427, 432(17), 434, 435(39), 465, 466, 472(26), 475(51,

- 52), 487, 642(4i), 645(22a), 676(62a), 679(4i, 62a), 680, 690(62a), 691–693, 914, 915(353), 948, 1006, 1007(136), 1008(145), 1011(152), 1019(160), 1027, 1028
- Power, J. M. 533(135), 539
- Power, M. D. 860(40), 941
- Power, P. P. 5, 6(24a, 24c), 64(24a, 260, 261a, 261b), 66, 69(24a), 75(303), 78(310), 79(24a, 24c), 92(260), 93(24a, 24c), 94(359, 365), 98(260, 303), 100, 101(303), 105(24a, 24c), 148, 155, 156, 158, 396, 397(49b), 425, 433(25), 434(30, 35), 465, 466, 496(27), 522(27, 89), 536, 538
- Power, W. P. 202(78), 221
- Powers, J. M. 13–15, 17(89b), 150
- Pradeep, T. 1034(39), 1056
- Prakash, G. K. S. 1049(125), 1058
- Prakash, N. S. 844(134), 852
- Prasad, B. V. 45, 46(209b), 153
- Prasse, M. 727(259), 743
- Pratt, W. E. 419(143), 427
- Prechtel, F. 707(114), 739
- Preiner, G. 958, 959(36), 1025
- Pretzer, J. 575(69), 636
- Preuss, H. 13(91, 92a, 92b), 150
- Preuss, H.-W. 192, 202, 214(61), 220
- Preuss, R. 192(56), 220
- Prewitt, C. T. 7(39a, 39b), 148
- Price, W. C. 173, 174(27), 218
- Pritzkow, H. 81, 82, 113(324), 157, 509(62, 63b, 64, 65), 514(71), 534(63b, 138), 537, 539
- Probst, R. 484(122), 489, 726(251), 743
- Pross, A. 123(444a, 444b), 161
- Provera, S. 267(207), 335
- Prystansky, R. E. 346(15), 387
- Pu, L. 64(260, 261a, 261b), 78(310), 92, 98(260), 155, 156
- Puchkovskaya, G. A. 725(243), 742
- Puentes, M. J. 358(52), 388
- Puff, H. 722(212, 213), 731(284), 741, 743
- Pugh, G. 372(91, 92a), 389
- Pugmire, R. J. 277(231, 232), 335
- Pulay, P. 78(309), 156
- Pulkkinen, E. 324(402), 339
- Pullman, D. P. 845(145), 853
- Pullmann, B. 166(7), 217
- Purcell, K. G. 844(134), 852
- Purdie, D. 844(134), 852
- Purvis, G. D. 12(66), 149
- Pusel, T. 788(172), 802
- Puskar, J. 233, 236(47), 282(253, 254), 296, 297(47, 253, 254), 298(253), 315(331), 331, 336, 337
- Puydt, Y.de 575, 600, 602(78), 636
- Pyper, N. C. 9(47), 149
- Pyykkö, P. 5(30a, 31), 8, 9, 13(30a), 14, 15(31), 25(30a), 148
- Qhen, Q. 785(159), 802
- Qing, N. 274, 275(223), 335, 780(147), 802
- Qu, Z. 486(136), 489
- Quadt, S. 1003(124), 1027
- Quattrucci, J. 47, 48(214), 153
- Quin, L. D. 937(463), 950
- Quinn, F. M. 844(129), 852
- Quirante, J. 367(79), 374(96), 389
- Raab, K. M. 526(109), 538
- Raabe, G. 5, 6, 43, 63(14), 147, 392, 401(3), 424, 952(7, 8), 953(8), 982(7), 988(8), 1006(7, 8), 1022(8), 1024
- Raaijmakers, R. 879(165), 944
- Rabalais, J. W. 166, 167(4), 217, 834(75c, 79), 850
- Raban, M. 319(367), 338
- Rabbezzana, R. 192(59), 220
- Rabe, S. 713, 727(147), 740
- Rabezzana, R. 64, 91, 95(258), 155, 1036(47, 49, 51), 1037(53a–c), 1056
- Rabideau, P. W. 914(349), 948
- Rabin, O. 1003(124), 1027
- Rablen, P. R. 14(95), 150
- Rabolt, J. F. 542(18), 543(20a, 21), 547(18), 548(18, 38, 39, 43), 561, 562
- Rachel, R. 808, 809(33), 819
- Radeke, M. R. 837(91), 838(98), 851
- Räder, H. J. 767(102), 800
- Radinov, R. 910(314), 947
- Radke, C. J. 316(359), 338
- Radnic, M. 43(203), 153
- Radom, L. 5, 12(25c), 139, 140(486c), 148, 162, 1031(17), 1051(141), 1056, 1058
- Radzio-Andzelm, E. 12(77), 150
- Radziszewski, J. G. 64(257c), 155, 192(58), 220
- Raghavachari, K. 12(69), 16(110a, 110b, 123b), 120, 122, 123(442), 138(483c), 139(483c, 485), 140(485), 149, 151, 161, 162, 836, 837(87), 850, 1034(37), 1056
- Rahimian, K. 720(206), 741
- Rahkamaa, E. 324(402), 339
- Rahman, M. T. 726(250), 743
- Rai, A. K. 509(59), 537
- Raimondi, M. 11(60), 18(128a), 36(60), 149, 151
- Rajzmann, M. 908(311), 947
- Räke, B. 434, 464(28), 465, 698, 729(26), 737
- Rakebrandt, H.-J. 438(48), 444(83), 445(91), 448(91, 94), 450(97, 101), 453–455(97), 459(101), 463(110), 466, 467
- Rama Devi, A. 1045(96), 1058
- Raman, N. K. 572, 620(30), 629(209), 631(30), 635, 640
- Raml, W. 283, 292(260), 336
- Rammo, A. 445, 447, 458(90), 467, 904(280, 287), 946

- Ramsey, B. G. 166, 175, 180(8), 217
 Ramstad, A. 826(26f), 848
 Ranaivonjatovo, H. 5, 6(20, 24d, 24e), 63, 67, 83(20), 105(24d, 24e), 147, 148, 531(133), 539
 Rance, M. 257(155), 333
 Randrianoelina, B. 880(172), 944
 Ranke, W. 834(76, 77a), 850
 Rankers, R. 482(101), 488
 Rankin, D. W. H. 320(385), 338, 432(18), 465, 707(117), 739
 Rao, N. S. 937(463), 950
 Rao, R. C. 258, 320, 322, 325(167), 334
 Rapp, B. J. 732(292), 744
 Rapp, U. 762(75, 76), 765(76), 800
 Rappoport, Z. 5, 6(1b, 2, 9), 21(9), 41(1b, 2), 63(2, 9), 147
 Rarig, R. S. J. 572(33), 635
 Raschke, M. B. 838(99a), 851
 Rasika Dias, H. V. 114(418b), 160
 Rassolov, V. 138, 139(483c), 162
 Raston, C. L. 864(64), 942
 Rasul, G. 726(250), 743
 Ratajczak, H. 37(169a, 169b), 152
 Rath, N. P. 397(55b), 425
 Rathke, M. W. 919(367), 948
 Rathmann, H. W. 995(116), 1027
 Ratier, M. 248(119, 125), 250(125), 311(125, 320, 321), 332, 333, 337
 Rattan, P. 671(50), 693
 Raucher, S. 904(260), 946
 Rauk, A. 24, 112(138), 151
 Rauschenbach, A. 169, 186, 187(24), 218
 Rauscher, D. J. 113(411b), 160
 Raymond, M. K. 542(12), 561
 Raynes, W. T. 240(66), 331
 Raza, G. H. 267(207), 335
 Read, R. W. 935(455), 950
 Reber, G. 440, 441(61b), 466
 Rebrov, A. V. 791(175), 802
 Rebrov, E. A. 751, 757, 758(37), 762(78, 79, 81), 764(78), 765(87), 766(95–97), 771(129), 776(81, 140), 778(81), 782(154), 787(167), 791(78, 81, 177), 794(177), 795(189), 799–802
 Reddy, N. P. 559(63), 563
 Redfern, P. C. 138, 139(483c), 162
 Redhouse, A. D. 701(55), 725(231), 731(286), 733(55), 737, 742, 744
 Redondo, A. 823(13), 826, 827(28), 847, 848
 Redondo, P. 1031(24), 1033(34), 1056
 Reed, A. E. 11(58, 59e, 59f), 14(100a, 100b, 101), 35(59f, 162, 164), 36(58, 164), 149, 150, 152, 724(221), 742
 Reed, C. A. 5, 112, 128(28d), 132(28d, 469), 133(28d), 148, 162, 1030(6c), 1055
 Reed, D. E. 702(60), 738
 Reed, K. J. 139, 140(486b), 162
 Reed, R. W. 132(469), 162
 Reek, J. N. H. 750(48, 55), 752, 757(48), 771(55, 127), 799, 801
 Reents, W. D. Jr. 1035(41), 1056
 Rees, W. S. 195, 197(63), 220
 Reese, C. B. 928(417), 949
 Reetz, M. T. 28, 29, 31, 32(152), 152, 857(20, 28), 941
 Reeves, L. W. 226, 240(13), 330
 Reffy, J. 208(85, 92), 211(92), 221
 Reginato, G. 933(448), 950
 Regitz, M. 208(86), 221, 492, 494(7), 503(47), 504(50), 513(69, 70), 514(74, 75), 516(74, 75, 79, 81, 82), 530(70), 536–538, 904(272, 291, 292, 295), 946
 Reich, H. J. 888(190–193, 196–199), 944
 Reichel, F. 136, 137(477), 162
 Reidel, D. 166(7), 217
 Reif, B. 282(252), 336
 Reimann, B. 1007(137), 1027
 Reineker, P. 762(80), 800
 Reinke, H. 713(149), 727(259), 731(149), 740, 743, 910, 911(321), 912(321, 332–335, 337), 947
 Reinstra-Kiracofe, J. C. 81, 82(321a, 321b), 157
 Reisacher, H.-U. 529(118, 119), 538
 Reisenauer, H. 96(371), 158
 Reisenauer, H. P. 347(21a), 388
 Reisgys, M. 509(62), 537
 Reising, J. 707(115, 116), 732(116), 739
 Reiter, B. 475(44, 53), 487
 Reizig, K. 507(55, 56), 527(113), 537, 538
 Rell, S. 81, 82, 113(324), 157, 509(63b, 64, 65), 534(63b), 537
 Reller, A. 699, 724(31), 737
 Remko, M. 50, 51, 64, 66–68, 73, 77(224), 79, 80(224, 316), 81, 128(316), 154, 157
 Renaud, P. 362(67), 366(74), 389
 Renfrow, R. A. 974(87), 1026
 Rennekamp, C. 708, 727(119), 739
 Reřicha,Ř. 251, 254, 308(138), 333
 Restrepo-Sánchez, N. E. 379(109), 390
 Retta, N. 939(466), 950
 Reuter, K. A. 1037(55), 1057
 Rewinkel, J. B. M. 879(165), 944
 Reyé, C. 572(43, 44), 578(109, 110, 113, 117, 118), 583(109), 584(117, 118), 586(113, 117), 595(109), 600(113, 117, 118), 611(109, 110), 613(179), 614(113, 117, 118), 623, 626(203), 636, 637, 639, 640
 Reynolds, W. F. 5, 6, 63(12c), 147
 Rheingold, A. L. 642(3, 4j, 4k), 679(4j, 4k), 691, 712, 725(142), 740, 747, 750, 755, 760(27), 767(103), 798, 800
 Rheinhold, H. 486(134), 489
 Rhodes, L. 575(67), 636
 Ribnikar, S. V. 714(156), 740

- Ribot, F. 570(11), 574(51), 635, 636
 Ricci, A. 933(448), 950, 1030(8), 1046(109),
 1055, 1058
 Ricci, J. 47, 48(214), 153
 Rice, J. E. 108(394), 159
 Richard, J. A. 31(158a), 152
 Richards, C. A. Jr. 91, 94, 96(346), 158
 Richardson, I. G. 320(383), 338
 Richardson, N. A. 81, 82(321a, 321b), 157
 Richter, H. 700(40), 737
 Richter, R. 478(69, 71), 483(71), 488
 Rickard, C. E. F. 698, 701, 733, 734(19), 737
 Rickborn, B. 900(231), 945
 Ridge, D. P. 1045(92a, 92b, 95), 1057, 1058
 Riede, J. 432(19, 22), 465, 968(76), 1026
 Riedel, R. 450, 451(99), 464(111), 465(99),
 467
 Riehl, D. 570(12), 635
 Riehl, K. 1041(71b), 1042(76), 1057
 Rienstra-Kiracofe, J. C. 74, 96(297), 156
 Riera, J. 710(137), 739
 Ries, W. 731(289), 744
 Rigby, J. H. 374(94), 389
 Rigby, S. S. 870(97, 100, 101), 942, 943
 Rihs, G. 319(366), 338
 Rikowski, E. 575(63), 636
 Rinaldi, P. L. 253(142), 266, 301(205),
 303(205, 300), 320(142), 333, 334, 336,
 752(56), 799
 Ring, M. A. 17(127), 151, 358(52), 388
 Rio, E.del 128, 141(462), 162
 Ripoll, J. L. 206(82a, 82b), 207(82a), 221
 Rist, G. 319(366), 338
 Rithner, C. 877, 879(137), 943
 Ritter, A. 962, 982(60), 1026
 Ritter, U. 232(45), 331, 698(16), 715,
 724(162), 735(16), 736, 740
 Rittmeyer, P. 181, 182(43), 219
 Rivail, J.-L. 825(20a), 847
 Riveros, J. M. 138–140(483d), 162, 1041(71a,
 72), 1057
 Rivière, P. 68(279), 138(484), 156, 162
 Riviere-Baudet, M. 138(484), 162
 Roark, D. N. 1019(161), 1028
 Robb, M. A. 966(72–74), 1026
 Roberts, B. P. 357(47–49), 358(47, 50),
 381(49), 382(118), 388, 390
 Roberts, N. 826(26c), 848
 Roberts, R. R. 912(327), 947
 Roberts, R. S. 889(203), 945
 Robertson, E. E. 707(117), 739
 Robinson, G. H. 93(363a, 363b, 363e, 363f),
 158
 Robinson, W. T. 701, 724, 735(54), 737
 Rochow, E. G. 471(18), 472, 481, 482(20),
 486, 487
 Rochow, E. J. 7, 11, 45(35a), 148
 Rockliffe, J. W. 320, 322(381), 338
 Rodebaugh, R. K. 319(366), 338
 Rodríguez-Fernández, M. 372(90), 389
 Rodríguez-Vicente, A. 367(78), 389
 Rodriguez, C. 1040, 1041(69), 1057
 Rodriguez, C. F. 1031(18), 1056
 Roesky, H. W. 232(45), 331, 433(26), 434,
 464(28), 465, 573(49), 636, 698(16,
 26–30), 699(31–33, 35), 701(54),
 708(119), 711(139, 140), 712(143),
 715(162), 717(29), 718(197), 720, 721(29),
 722(27–30, 143, 197, 214–216),
 724(27–31, 54, 140, 162, 217), 725(143),
 727(119), 729(26, 140, 269), 731(139),
 732(291), 733(33, 35, 139), 734(33),
 735(16, 32, 54), 736, 737, 739–744
 Roewer, G. 286(265, 266), 287(266), 288(266,
 273), 336, 474(40–42), 478(69, 71),
 479(73–77), 481(93), 482(104), 483(71),
 487, 488, 780(148), 802
 Rogers, C. 920(381), 948
 Rogers, C. W. 271(217), 335, 960, 962, 976,
 1003–1005(55), 1025
 Rogers, R. D. 434(37), 466, 886(186), 944
 Rohde, C. 11(59g), 149
 Rohonczy, J. 327(414), 339
 Romagnoli, A. 364(69), 389
 Roman, V. K. 717(183), 741
 Romanenko, V. D. 492, 498(8b), 514(72, 73),
 516(83), 530(121a, 121b), 531(122, 128,
 129), 536–539, 904(270), 913(345), 946,
 948
 Romeo, R. 364(69), 389
 Roncali, F. 611(173), 639
 Roncin, J. 199, 200(66), 220
 Rondan, N. G. 11(59g), 149, 966, 975(75),
 1026
 Rooij, J. F. M. de 940(470), 950
 Roos, B. O. 832(61d), 849
 Roos, C. 870(103), 943
 Roovers, J. 746(14), 747(23, 24), 798
 Roovers, J. O. 766(98, 99), 800
 Roper, W. R. 698, 701, 733, 734(19), 737
 Rosch, W. 514, 516(75), 537
 Rösenthaler, G.-V. 483(107), 488
 Rose, A. 9(47), 149
 Rose, K. 578(130), 638
 Roseman, J. D. 376(98, 99a, 99b), 389
 Rosenberg, R. E. 352(35), 388
 Rosental, E. 141(490), 163
 Rosmus, P. 169(23), 178, 179(37), 180,
 181(40), 191(55), 192(23, 40, 55), 193(55),
 208(40), 218–220
 Ross, R. B. 13–15, 17(88b, 89a, 89b), 150
 Rossell, O. 767(113, 114), 769(114), 801
 Rossi, A. 966(74), 1026
 Rossi, R. 312(326), 337
 Rössler, M. 498, 509(28), 536
 Roth, B. 191–193(55), 220

- Roth, R. 181, 182(43), 219
 Roth, W. J. 572, 620, 629(36, 37), 635
 Rothberg, L. J. 687(76a), 694
 Röthlisberger, U. 38(176), 152
 Rothwell, I. P. 645(24c), 692, 864(66), 942
 Röttger, B. 839(112), 852
 Rottman, C. 570(20, 22), 635
 Round, F. E. 806(6), 818
 Roussi, P. 980(95), 1026
 Rouxel, J. 566(2), 635
 Royo, G. 484(121), 489
 Royo, P. 729(270), 743
 Rozenski, J. 251, 254, 308(138), 333
 Rózga, K. 703, 716(74), 725(231), 738, 742
 Rozhenko, A. 108(392), 159
 Ruban, A. V. 530(121a, 121b), 531(129), 539
 Ruben, D. J. 268(209), 335
 Rubinsztajn, S. 633(226), 640, 703, 717(69),
 738, 791(181), 794(182), 795(181), 802
 Rubio, J. 39–41, 49(181), 152
 Ruch, W. E. 878(153), 944
 Rucker, C. 856(11), 904(258), 925(410), 941,
 946, 949
 Rückert, T. 870, 901(93), 942
 Ruckinstein, E. 760(72), 800
 Rudolph, S. 434(38), 466
 Rudzinski, J. M. 37(169a, 169b), 152
 Ruedenberg, K. 825(21e), 832(61, 61b, 61c),
 847, 849
 Ruff, O. 470(4), 486
 Ruffolo, R. 271(217), 335, 960(54, 55),
 962(55), 976, 1003–1005(54, 55), 1025
 Ruhlandt-Senge, K. 433(25), 465, 522(89), 538
 Ruhlmann, K. 645(19c), 692
 Rulkens, R. 701, 733(46), 737
 Ruppert, I. 492, 498(8c), 536
 Ruppert, K. 169(24), 186(24, 48), 187(24, 48),
 50, 53), 190(48, 50, 53, 54), 191(48), 199,
 210(50), 218–220
 Rusanov, E. 483(107), 488
 Ruscic, B. 16(120), 151
 Ruscic, R. 16(116), 151
 Rusek, J. J. 888(196), 944
 Rushkin, I. L. 785(159, 160), 802
 Russel, C. A. 108, 109(393), 159
 Russell, J. N. Jr. 830(50), 849
 Russell, T. P. 547(28), 562
 Russick, E. M. 629(212, 213), 640
 Russo, N. 110, 112(402), 159, 834(82a), 850
 Russow, J. 167(19), 218
 Ruta, M. 227, 326(15), 330
 Ruthe, F. 474(34), 487
 Ruud, K. A. 725(246), 742
 Ruwisch, L. 434(38), 466
 Ryan, T. 575(71), 636
 Ryu, I. 362(61b), 371(88), 379(105, 107, 110),
 388–390, 888(201), 901(239), 945
 Ryu, M. 774, 775(133), 801
 Saak, W. 63(256a, 256b), 82, 83, 87(327a,
 327b), 155, 157, 393(22a), 394(29, 30, 43),
 395(22a, 43), 396(52, 53), 397(43),
 400(22a), 402(71, 74), 404(74), 405(71, 96),
 407(74, 109), 408(109), 411, 412(96),
 414(130), 416(135), 418, 419, 421(142),
 424–427
 Šabata, S. 236(52), 331
 Sabo-Etienne, S. 251(140), 333
 Sachdev, H. 439(55, 56), 466
 Sadana, K. L. 928(423), 949
 Sadovskii, N. A. 751(28), 757(28, 61),
 759(28), 776(61), 799
 Saebø, S. 67, 71, 73(278b), 156
 Saez, I. M. 573(45), 636, 752, 765(46), 799
 Safa, K. D. 699(36, 37), 737, 968(80), 1026
 Sagan, B. L. 230(33), 331
 Saguiillo, A. 1033(34), 1056
 Sahai, N. 714, 724(151), 740
 Saha-Möller, C. 698, 707(20), 737
 Said, M. A. 708, 727(119), 739
 Saidi, K. 936(461), 950
 Sailot, M. J. 822(2), 846
 Saini, R. D. 962(59), 1025
 Saint Roch, B. 110(398), 159
 Saito, H. 386(129), 390, 881(176), 944
 Saito, M. 79(313c–e), 156
 Saito, S. 95(366d), 158
 Saito, T. 266, 301, 303(205), 334
 Saito, Y. 884(183), 944
 Saka, Y. 12(77), 150
 Sakaba, H. 875(127, 128), 943
 Sakai, S. 44(207), 83, 86(334), 119, 120,
 122(437), 124–126(207), 153, 157, 161
 Sakai, T. 679(65, 66), 693
 Sakakibara, A. 409(115), 427, 574, 589(50),
 636, 715(168), 740
 Sakamoto, H. 83(330a), 157, 982, 990(99),
 1026
 Sakamoto, K. 70, 78(285a–c), 156, 393(23),
 424, 544, 545(23), 558(57), 561, 562,
 838(103e), 851, 864(45), 873(121, 122),
 912(121), 941, 943
 Sakata, K. 470(7), 486
 Sakurai, H. 5, 6, 39(21), 58(239a, 239f, 239h),
 70, 78(285c), 106(385a), 113(414b, 414c),
 136(479b), 137(385a, 479b), 147, 154, 156,
 159, 160, 162, 180, 181(40), 185(46),
 192(40), 199(71), 202(76), 208(40), 219,
 220, 295(295), 336, 344, 345(11a–c), 387,
 392(7, 11), 393(17), 395, 397, 399(39a),
 401, 402, 420(69), 424–426, 475(46, 47),
 481(96), 487, 488, 542(6), 544, 545(23),
 558(57), 561, 562, 642(10a, 10b), 679(65,
 66), 691, 693, 781(150), 802, 864(45, 47,
 51, 52), 873(121), 875(127, 128), 904(248,
 252), 912(121), 928(434), 941–943, 946,
 949, 952(11), 968, 969, 996(79), 1006(11),

- 1008(144), 1009(148), 1010(11, 148),
1011(149), 1012, 1017(148), 1019(158,
162), 1022(158), 1025–1028
- Sakurai, T. 827, 830(42), 849
- Sakurai, Y. 362(60), 388
- Salahub, D. R. 110(399), 159
- Salaneck, W. R. 686(75b), 694
- Salem, L. 823(4a), 846
- Salter, D. M. 698, 701, 733, 734(19), 737
- Saltiel, J. 1007(140), 1027
- Saluvere, T. 315(331), 337
- Salyers, K. L. 703(88), 738
- Salzer, A. 5(8), 147
- Salzner, U. 138, 139(483b), 162, 642, 645,
651(17), 691
- Samadi-Maybodi, A. 320(379), 338, 712(146),
740
- Sammes, P. G. 935(456), 950
- Sammleben, F. 923, 924(405), 949
- Sampson, P. 912(328), 947
- Samreth, S. 381(116), 390
- Sanchez, C. 569(6, 7), 570(6, 11, 15, 16),
574(7, 51), 575(82, 83), 578(83, 120),
586(120), 595(153), 632(221), 634(83, 120,
227), 635–638, 640
- Sanchez, M. 516(83), 538
- Sander, M. 838, 840(105c), 851
- Sander, W. 858(35), 941, 992(112), 1027
- Sanganee, M. 718(185), 741
- Sanger, A. R. 434(35), 466
- Sangu, S. 531(127), 539
- Sanji, T. 544, 545(23), 561, 679(65), 693
- Sano, A. 208, 210, 211(90), 221, 896(216),
945
- Santen, R. A. van 239(59), 331, 573(47), 636,
719(200, 202, 203), 720, 727(200), 741,
806, 807(7), 818
- Sarina, T. V. 514(73), 537
- Sarkar, S. K. 242, 245(81), 332
- Sarker, G. 575(72), 636
- Sasaki, K. 201(72), 220
- Sasaki, Y. 232, 233(44), 331
- Satgé, J. 5, 6(16, 20, 24e), 51(16), 63(16, 20),
67(20, 277), 75(277), 83(20), 105(24e),
110(398), 147, 148, 156, 159, 499(32, 34,
35), 536
- Sato, A. 844(136a), 852
- Sato, F. 370(85), 389, 645(24a, 24b, 25), 692,
916(356), 948
- Sato, S. 37(172, 173), 152, 904(266), 946
- Sato, T. 373(93a, 93b), 389, 872(113, 115),
896(223), 943, 945
- Satoh, S. 781(151), 802
- Sattler, E. 509(59), 537
- Sattler, M. 269(210), 335
- Saue, T. 16(108), 151
- Sauer, J. 607(167), 639
- Sauer, R. O. 709(129), 739
- Sauires, R. R. 1030(1), 1055
- Saulnier, M. G. 928(433), 949
- Saunders, M. 132(464b), 162
- Saunders, V. R. 607(167), 639
- Sauvage-Simkin, M. 826(25a), 848
- Sauvajol, J. L. 578, 603(94), 611(94, 174,
175), 637, 639
- Sauvet, G. 703, 717(70, 71), 738
- Sawitzki, G. 485(128), 489, 702, 732(64), 738
- Sawyer, J. F. 858(30), 941
- Sax, A. 118(432b), 161
- Sax, A. F. 40(186), 52, 54(226a), 102(377b),
153, 154, 159
- Saxena, A. K. 697, 731(6), 736, 858(30), 941,
982, 985(100), 1026
- Say, B. J. 324(398), 339
- Saykally, R. J. 112(404a), 159
- Scaiano, J. C. 352(34), 388, 963, 990(65),
1026
- Scampton, R. J. 954, 955(24), 1025
- Scanlan, I. 178, 179(36), 219
- Schach, A. S. 808(18, 19), 818
- Schade, C. 11, 35(59f), 149, 724(221), 742
- Schadt, F. L. 971(85), 1026
- Schaefer, D. W. 570(15), 602, 604(160), 635,
638
- Schaefer, H. F. III 5(25a), 12(25a, 67, 68),
18(128b), 19(130a), 25, 29(142), 38(174c),
39–42(182), 43(182, 204), 44(204),
48(218), 49(204, 218), 51, 57(218),
61(244a, 244c), 70(284a, 284b),
74(295–297, 300, 301), 75(284a, 284b, 296,
301), 77(284a, 284b), 81(296, 321a, 321b),
82(321a, 321b), 91(344–347, 352, 353),
93(363e, 363f), 94(344, 346, 347, 353, 358,
360), 95(366c), 96(297, 344–347, 360),
97(344, 360), 98(358, 360, 373a, 373b),
99(284a), 100(284b), 110(395b, 397),
117(429a), 118(128b, 130a), 125, 126(204),
141(492–494, 497), 142(494, 497), 148,
149, 151–154, 156–159, 161, 163, 404(89),
405(98), 421(146, 147), 422(153), 426, 428,
966, 967(71), 1026
- Schaefer, J. A. 838(108), 851
- Schäfer, A. 12(76), 114(416c), 150, 160,
187(52a), 220, 394(29, 30), 400(65, 66),
405(103), 406(66, 105), 407(66), 424–426,
482(101), 488
- Schäfer, H. 82, 83, 87(327b), 157
- Schäfer, M. 434–436(40), 439(57, 60),
440(60), 441, 442(64), 445, 446(87),
450(98), 466, 467, 904(276), 946
- Schäfer, W. M. 202(76), 220
- Schaible, S. 450, 451(99), 464(111), 465(99),
467
- Schakel, M. 483(105, 106), 488
- Schär, D. 484(124), 489
- Schaumann, E. 901(238), 920(371), 945, 948

- Schaumburg, K. 265(198), 334
 Scheblykin, I. G. 776, 777(139), 801
 Scheer, P. 494, 509(11), 536
 Scheffler, M. 826(26b), 838(99a), 848, 851
 Scheiner, A. C. 74(295), 156
 Scheller, T. 577, 612, 619(89), 637
 Schenker, K. V. 246, 247(108), 248(114), 332
 Schenzel, K. 287, 292(269, 270), 336, 475(43), 480(84), 487, 488
 Scherer, G. W. 567, 569, 590, 602(4), 635
 Scherer, O. J. 492, 494(7), 536
 Scherer, W. 114, 115(422), 160, 202(79), 221
 Schick, A. 347(21a), 388
 Schier, A. 431(13, 16), 432(20–22), 465
 Schiesser, C. H. 142(498a, 498b), 143(498a), 144(498b, 499), 145(499), 163, 343(7a, 7b, 8a, 8b), 349, 352(27), 354, 356(40, 41, 43), 357(41, 44, 45), 358(51), 359(8a, 8b, 51, 54), 360(8a, 8b), 387, 388, 870(94), 942
 Schiffman, A. L. 928(423), 949
 Schilling, B. E. R. 63, 67(253–255), 68, 70(254), 113(413a), 155, 160, 397(56), 425
 Schilling, F. C. 542(19), 547(19, 31, 33), 548(19), 561, 562
 Schimpf, R. 251(139), 333
 Schindele, D. C. 904(260), 946
 Schinzer, D. 879(158), 944
 Schlaefke, J. 114(416c), 160
 Schlag, E. W. 166, 217(14), 218
 Schlegel, B. H. 118, 123, 124(431), 161
 Schlegel, H. B. 5(27d), 12(65), 16(112), 82(326a), 119(438), 123(443), 148, 149, 151, 157, 161
 Schlenk, C. 746(20), 788(172), 798, 802
 Schlenker, J. L. 572, 620, 629(37), 635
 Schleucher, J. 269(210), 335
 Schleyer, P. v. R. 5(4, 25a, 25c, 28b), 7, 10(44), 11(44, 56–58, 59e–g), 12(25a, 25c), 14, 23(44), 24(57, 139), 25(139, 142), 26(139, 143), 29(44, 139, 142), 31(44, 157), 32(44), 33(44, 157), 34(44), 35(44, 59f, 162, 164), 36(58, 164), 38(174a–c, 177), 39(177), 42(201), 45(209a), 47(213), 50(224), 51(44, 224), 52(226a), 54(226a, 229a), 62(245), 64(224), 66(56, 224), 67, 68(224), 72(56), 73(224), 74(293), 75(245), 77(224), 79(56, 224, 316), 80(224, 316), 81(316), 93(363e), 102(379), 103(379, 381b), 105(209a, 383), 106(209a, 213, 383), 108(387), 112(28b, 406), 116(293), 128(4, 28b, 57, 316, 459b, 461), 129(461), 131(209a), 132(4, 28b, 465a, 470a), 133(4, 28b, 459b, 470a), 134(4), 136(459b), 137(28b), 138(57, 483b), 139(57, 461, 483b), 141(491–494, 496), 142(494), 147–149, 151–154, 156–159, 162, 163, 343(9), 387, 432(18), 434(29), 465, 642, 679(4e–g), 691, 724(221, 230), 742, 971(85), 1026, 1030(6b), 1048(119, 120), 1055, 1058
 Schlier, R. E. 825(22), 848
 Schlosser, W. 865(75), 872(120), 942, 943
 Schmedake, T. A. 5, 6(23b), 67, 70, 71(274), 113, 114, 117(23b), 148, 155, 394, 397–399(28), 424
 Schmeisser, D. 834(70), 850
 Schmeisser, J. M. 997, 998, 1000(118), 1027
 Schmid, A. K. 842(126b), 852
 Schmid, A. M. 808(24), 818
 Schmid-Base, D. 438(46), 466
 Schmidbaur, H. 202(74), 220, 431(11–13, 16), 432(18–22), 437(44), 465, 466
 Schmidpeter, A. 496(25), 536
 Schmidt, B. 642, 645(2c), 691
 Schmidt, C. 548(40), 562
 Schmidt, D. 450, 452, 453(95), 467
 Schmidt, H. 114(416a), 160, 504(51), 537, 718(193), 741
 Schmidt, H.-G. 441(62), 466, 698(16), 699(32, 33), 708(119), 711(139, 140), 718(197), 722(197, 215), 724(140), 727(119), 729(140, 269), 731(139), 733(33, 139), 734(33), 735(16, 32), 736, 737, 739–743
 Schmidt, K. D. 572, 620, 629(37), 635
 Schmidt, M. 439(56), 466, 832(61c, 61e), 849
 Schmidt, M. W. 72(290), 93(363g), 102, 103(376b), 156, 158, 159, 826(31), 827(33), 848, 1007(138), 1027
 Schmidt, R. R. 928(419), 949
 Schmidt, T. 522(92), 538
 Schmidt-Bäse, D. 434, 436(41), 441(62), 445, 446(85), 460, 463(109), 466, 467, 700(43), 737, 904(282), 946
 Schmidtt, K. E. 823(10a), 847
 Schmitz, R. F. 483(106), 488
 Schmitzer, S. 698(18), 707(18, 115, 116), 732(116), 737, 739
 Schmörlzer, H. 481(94), 488
 Schmutzler, R. 516(78), 538, 904(286), 932(444), 946, 950
 Schneider, D. 864(48), 941
 Schneider, E. 498, 509(28), 536
 Schneider, H. 315(333), 337
 Schneider, M. 578, 586(112), 633(112, 225), 637, 640, 698, 735(21, 22, 24), 737
 Schneider, R. F. 575(75), 636
 Schneider, W. 23, 29(137), 151
 Schneider, W. G. 229(22), 330
 Schneller, T. 612(177, 178), 617(177, 178, 186), 618(178), 619(177, 178, 186, 189–191), 639
 Schnering, H. G. von 114(416c), 160, 187(52a, 52b), 220, 400(65), 402(73), 405(104), 406(106, 107), 407(107, 110), 410(118), 425–427, 485(128), 489, 702, 732(64), 738
 Schnurman, E. S. 910(314), 947

- Schnurr, W. 904(272), 946
 Schödel, H. 190(54), 220
 Schoeller, W. W. 54(229c), 80(317), 91(348), 154, 157, 158, 513(69), 531(123, 133), 537, 539
 Schoffstall, A. M. 910(319), 947
 Schofield, P. J. 718(190), 741
 Scholl, R. 227, 231(18), 330
 Schöllhorn, B. 578(124), 638, 928, 930(421), 949
 Schollmeyer, D. 718(191), 741
 Scholz, G. 208(86), 221
 Schott, G. 697(11), 701(44), 736, 737
 Schott-Daric, C. 626(206), 640
 Schraml, J. 225, 226(9), 227(21), 233(46, 47), 234(48), 235(46), 236(47, 49–52), 238(49), 245, 246(103), 247(109), 251(21, 133, 134, 136–138), 253(21), 254(138), 255(144), 258(51, 161, 165), 259(109, 173), 260(165), 261(191), 262, 263, 265(196), 282(253, 254), 296, 297(47, 253, 254), 298(253), 304, 305(304), 306(136), 307(316), 308(138), 311(9), 323(393), 325(144), 330–334, 336–338
 Schrank, F. 273(218), 275(218, 230), 277(218), 284(230), 285(218, 230, 264), 291(264), 292, 293(230), 335, 336, 476(56), 487
 Schreiber, R. 619(190, 191), 639
 Schreiner, P. R. 5, 12(25a), 25(142), 26(143), 29(142), 128, 129, 139(461), 141(492–494), 142(494), 148, 151, 152, 162, 163
 Schrieber, S. L. 720(205), 741
 Schröder, D. 64, 91, 95(258), 155, 192(59), 220, 1032(25), 1036(45), 1056
 Schröder-Bergen, E. 834(77a), 850
 Schroeder, J. I. 807(14), 818
 Schroll, R. L. 231(37), 331
 Schröpf, M. 718(194), 741
 Schubert, B. 838(103d), 851
 Schubert, U. 403(87), 426, 570(10), 574(52), 629(211), 635, 636, 640, 709(128), 739, 857(24), 941
 Schubert, Y. 716(172), 740
 Schuchmann, H.-P. 962, 982(60), 1026
 Schuck, R. 277(233), 335
 Schuh, H. 431(11), 465
 Schuh, W. 722(212, 213), 731(284), 741, 743
 Schuhn, W. 495, 501(22–24), 506(23), 510(66), 514(22), 536, 537
 Schulberg, M. T. 845(145), 853
 Schultz, A. 5, 8, 9(30b), 148
 Schultz, G. 78(308), 156
 Schültze, M. 922(394), 949
 Schultze, R. K. 837(88b), 850
 Schulze, G. 837(90b), 851
 Schumacher, E. 38(176), 152
 Schumann, H. 507(56), 537
 Schumann, I. 522(92), 538
 Schumann, W. 617(184), 639
 Schumb, W. C. 481(90), 488
 Schürmann, M. 713(147), 718(191), 727(147), 740, 741
 Schurz, K. 187, 190(51b), 220, 440, 441(61b), 466, 988(107, 108), 1027
 Schuster, H. 187, 190(51a), 220, 475(49), 487
 Schuster, H.-G. 40(188a), 153
 Schwab, D. W. 808(29), 819
 Schwab, J. J. 701, 730(53), 737
 Schwab, W. 731(284), 743
 Schwalbe, H. 269(210), 335
 Schwartz, A. 936(460), 950
 Schwartz, M. 834(66), 850
 Schwartz, M. P. 830(50), 849
 Schwarz, H. 64(258), 79(314c), 91(258), 95(258, 366b), 114, 115, 117, 118(425), 132(466), 155, 157, 158, 160, 162, 192(59), 220, 857(28), 941, 1030(9), 1031(13, 15, 21), 1032(9, 25, 28), 1033, 1035(9), 1036(9, 45), 1037(54a), 1041(13), 1043, 1044, 1046(9), 1052(143), 1055, 1056, 1059
 Schwarz, J. C. P. 230(34), 331
 Schwarz, K. 823(6c), 847
 Schwarz, M. 16(116), 151
 Schwarz, R. H. 887(188), 944
 Schwarz, W. 70(286), 113(286, 411c), 114(286), 156, 160, 434(33), 466, 509(59), 537
 Schwarz, W. H. E. 9(46, 48a, 49), 29, 33(46), 149
 Schwarze, B. 307(311–313), 337
 Schwegler, E. 825(21a), 847
 Schweitzer, K. S. 545(22), 561
 Schwenk, H. 439(56), 466
 Schwerdtfeger, P. 9(48a, 48b), 10, 11, 14(53), 15(107), 17, 18(48b), 19(107), 32(48b), 33(53, 107), 149, 151
 Schmidt-Amelunxen, M. 58(239g), 154
 Scott, A. I. 920(384), 948
 Scott, D. L. 999(121), 1027
 Scott, M. J. 38(178), 152, 708(124), 739
 Scuseria, G. E. 12(67, 68), 74(295), 149, 156, 823(9, 10e), 825(21d), 847
 Seaby, J. M. 231(38), 331
 Sears, T. J. 112(404a), 159
 Sebal, A. 251(141), 333
 Sechadri, T. 486(135), 489
 Seco, M. 767(113, 114), 769(114), 801
 Seconi, G. 382(120), 390
 See, A. 575(72), 636
 Seebach, D. 904(289), 946
 Seebauer, E. G. 844(137b), 852
 Seeger, R. 12(74b), 150
 Segalés, G. 767(113, 114), 769(114), 801
 Segi, M. 869(87), 893(210), 942, 945
 Sehgal, R. 620(196), 639

- Seidel, G. 260, 266(179, 180), 271(213), 293, 294(290), 307, 308(213), 334–336, 647(31c), 692, 894(212), 945
- Seidl, E. T. 966, 967(71), 1026
- Seidl, H. 180, 181, 192, 208(40), 219
- Seijo, L. 13, 14(87a, 87b), 15, 17(103), 150
- Seip, C. 572(33), 635
- Seip, H. M. 724(218), 742
- Seip, R. 63, 67(253), 155
- Seipel, G. 325(411), 339
- Seiple, J. V. 841(123a, 123b, 124), 852
- Seitz, D. E. 481(98), 488
- Seitz, W. 169, 186, 192, 208(40), 218
- Sejpká, H. 495(20), 536
- Sekacis, I. 258(163), 334
- Seki, S. 346(18), 347(20), 387
- Seki, T. 558(57), 562
- Sekiguchi, A. 5, 6(21), 39(21, 180), 48, 49(219), 58(180, 239a, 239f, 239h, 240), 63(240), 83(329), 98(374), 101(375), 105(240), 106, 137(375, 385a–c), (382b), 147, 152–154, 157–159, 295(295), 336, 395, 397, 399(39b), 418, 419(141), 421(150–152), 425, 427, 428, 750, 755(54), 781(150), 782(153), 799, 802, 864(50–52), 872(111–115), 877(133), 904(252, 255), 941–943, 946, 958(38, 39), 999(39), 1009, 1010, 1012, 1017(148), 1019, 1022(158), 1025, 1028
- Selloni, A. 844(140a, 140b), 852
- Selmani, A. 110(399), 159
- Senf, F. 834(74b), 838(109), 850, 851
- Senge, M. O. 64(261a), 155
- Sengupta, D. 91, 94, 95(349), 125(451), 158, 161
- Sepeda, J. S. 725(246), 742
- Serby, M. 674(57), 693
- Servis, K. L. 243(86), 315(348), 326(86), 332, 338
- Seshadri, K. S. 324(401), 339
- Seshadri, T. 485(131), 489, 702, 732(64), 738
- Seth, M. 9, 17, 18, 32(48b), 149
- Severengiz, T. 904(290), 946
- Seyfert, D. 195, 197(63), 220
- Seyferth, D. 698(17), 736, 746(21), 747, 750, 755, 760(27), 762(82), 767(103), 798, 800, 916(357), 948
- Shaffer, S. A. 345, 346(14), 387
- Shafiee, F. 542(15), 561
- Shah, D. 718(186, 187), 741
- Shah, S. A. A. 718(188), 741
- Shahriari, M. R. 570(18, 19), 635
- Shaik, S. 11, 24(55), 72(289), 93(364), 123(443), 149, 156, 158, 161
- Shainyan, B. A. 904(259), 946
- Shaka, A. J. 257(154, 156), 333
- Shaltout, R. 593(141), 638
- Sham, T. K. 199(65a), 220
- Shambayati, S. 720(205), 741
- Shan, J. 830(51), 849
- Shannon, R. D. 7(39a, 39b), 148
- Sharma, H. K. 856(16), 941
- Sharma, S. 865(71), 942
- Sharp, K. G. 283, 285, 286, 288, 289, 291(259), 336, 479(72), 488, 578(122, 123), 593(142, 143), 600(123), 634(122, 123, 143), 637, 638, 762(74), 800
- Shavitt, I. 110(395a), 159
- Shaw, D. 226, 314(12), 330
- Shea, K. J. 575(84), 577(88), 578(90–92, 96, 111, 115), 583(92), 586(115), 589(96), 592(138–140), 593(141), 595, 598(92), 600(90, 92, 115, 156–158), 602(160), 604(160, 164), 619(192–194), 620(195), 621(157, 198), 629(91, 207, 212, 213), 631(92, 115), 632(92), 633(90), 634(115), 637–640, 716(177), 741
- Shechter, H. 999(120), 1027
- Sheiko, S. 558(55), 562
- Sheiko, S. S. 762(80, 81), 776(81, 140), 778, 791(81), 800, 801
- Sheldrick, B. 730(276), 743
- Sheldrick, G. M. 181, 182(42), 219, 284(262), 336, 443(73–75, 79), 445(86), 458(103), 459(104), 460(105), 462(103, 105), 463(105), 466, 467, 722(215), 727, 731(254), 742, 743, 910(316), 947
- Sheldrick, W. S. 186, 187(47), 219, 724(228), 742, 872(120), 943
- Shen, M. 141, 142(497), 163
- Shen, M.-Y. 96(369a), 158
- Shen, Q. 785(160), 802
- Shephard, B. D. 395(41), 397(41, 50), 398(50), 425
- Shepherd, B. D. 1006, 1007(136), 1027
- Sheppard, E. W. 572, 620, 629(37), 635
- Sherman, M. G. 837(89a, 89b), 850, 851
- Sherril, D. 95(366c), 158
- Shiba, T. 870, 871(102), 943
- Shibaev, V. P. 765(87), 800
- Shibata, K. 27(148), 79(313c), 152, 156
- Shibayama, K. 492(3), 499(33), 522(3, 33), 523, 524(3), 528(114), 536, 538
- Shibley, J. L. 402(75), 426
- Shick, R. 575(67), 636
- Shih, F. Y. 575(70), 636
- Shih, W. Y. 575(71), 636
- Shima, I. 492(1), 536
- Shimana, M. 547(34), 548(37), 562
- Shimizu, A. 1037(56), 1057
- Shimizu, H. 860(40), 941
- Shimizu, K. 810(41–44), 811(41, 42), 812(42), 813(42–44), 814, 815(42, 43), 817(49), 819
- Shimizu, N. 878(151), 944
- Shimizu, T. 409(115), 427, 679(64), 693

- Shimokoshi, K. 37(172, 173), 152
 Shimomura, M. 548(41), 558(56), 562
 Shimura, K. 520(87), 526(110), 538
 Shin, S. K. 1051, 1052(140), 1058
 Shinar, J. 642(7), 648(7, 35a–c), 649, 651(35c), 691, 692
 Shing, T. K. M. 928(422), 949
 Shinnai, T. 342(6), 387
 Shinokubo, H. 904(256), 913(347, 348), 946, 948
 Shiota, Y. 906(300), 947
 Shiotani, M. 201(72), 220, 673(54b), 683(71), 685(73b), 690(54b), 693, 694
 Shioya, J. 47(212b), 153, 559(62, 65), 563, 648, 649, 651(36a), 692
 Shiozaki, H. 362(60), 388
 Shiozaki, M. 47(216), 153, 647, 662(28a), 692
 Shipov, A. G. 239(54), 331
 Shipway, A. N. 746(9), 798
 Shiraiishi, K. 28(150, 151), 152
 Shirakawa, H. 560(69), 563
 Shiraki, Y. 838(106), 851
 Shirasaka, T. 904(265), 946
 Shiro, M. 647(32, 33), 651, 652, 654(32), 675, 676, 679(59), 692, 693, 896(223), 945
 Shizuka, H. 1003(129), 1027
 Shklover, V. E. 700(42), 725(236, 239), 727(42, 255), 728(264), 730(273), 733(293), 737, 742–744
 Shkol'nik, O. V. 717(181), 741
 Shoeller, W. W. 108(392), 159
 Shoemaker, J. 824(14), 825(18), 826(14), 827(14, 34), 847, 848
 Shomaly, W. 439(57), 466
 Shore, R. E. 808(29), 819
 Shostakovsky, M. F. 706(97), 739
 Shreeve, J. N. M. 762(86), 800
 Shruchkov, Yu. T. 733(293), 744
 Shtarev, A. B. 346(17), 387
 Shterenberg, B. Z. 239(58), 331
 Shukla, P. 547(28), 562
 Shum, S. P. 319(366), 338
 Shurki, A. 11, 24(55), 149
 Shuto, S. 349(26), 388
 Si, J. 570(21), 635
 Sibi, M. P. 922(392), 948
 Sicilia, E. 110, 112(402), 159
 Sidorkin, V. F. 208, 213(87), 221
 Sieburth, S. McN. 705(94), 739, 902(242), 945
 Siefken, R. 732(291), 744
 Siegbahn, P. E. 832(61d), 849
 Siegbahn, K. 166(13), 218
 Siegel, D. A. 259(174), 334, 395(38), 425, 858(32), 941, 1008(146, 147), 1027
 Siegl, H. 273(219), 288(276), 289, 294(219), 335, 336, 476(58), 477(66), 487, 728(261), 743
 Siegmann, K. 652(39), 693
 Siegrist, T. 687(77), 694
 Siehl, H.-U. 132, 133(470a), 162, 1048(120), 1049(129), 1051(136), 1058
 Sierra, M. A. 367(78), 389
 Sieve, A. 626(205), 640
 Sievers, R. 501(43), 537
 Siew, Y. K. 575(72), 636
 Sigal, N. 89, 90(339a), 91(339a, 339b), 157
 Sikorski, J. A. 910–912(312), 947
 Silberbach, H. 15, 19, 33(107), 151
 Silfhout, A. van 838(102), 851
 Silva, M. L. P. da 1041(71a, 72), 1057
 Simchen, G. 904(279), 946
 Simkin, B. Ya. 103, 108(381a), 159
 Simmler, W. 701(49), 737
 Simon, A. 187, 190(51a, 51b), 220
 Simon, R. A. 479(82), 488
 Simonis, U. 718(194), 741
 Simons, R. S. 64(261b), 78(310), 94(359), 155, 156, 158, 732(292), 744
 Simonsick, W. J. Jr. 593(142), 638, 762(74), 800
 Simonyi, E. E. 575(68), 636
 Simpson, S. J. 864(65), 942
 Simpson, T. L. 806(1), 807(11), 817(1), 818
 Singh, D. J. 823(11), 847
 Sinniah, K. 837(89a, 89b), 850, 851
 Sinotova, E. N. 1044(86), 1057
 Siray, M. 506(52), 519(85), 520(52, 85), 522, 528, 529(90), 537, 538
 Sironi, M. 18(128a), 151
 Sita, L. R. 27(146–148), 54(234, 235a, 235b), 56(234), 58(239j, 239k), 126, 127(453), 152, 154, 161
 Sitzmann, H. 108(390c), 159
 Sjöberg, S. 320, 324(372), 338
 Sjöqvist, L. 201(72), 220
 Skalsky, V. 1032, 1033(26), 1056
 Skancke, A. 43(205b), 153
 Skancke, P. N. 50(222), 154
 Skidmore, M. A. 354, 356(43), 359(54, 55), 388
 Skoda, L. 910(316), 947
 Skoglund, M. 999(120), 1027
 Slack, D. A. 594(147), 638
 Slany, M. 516(81), 538
 Slee, T. S. 42(202), 153
 Sloan, T. A. 808(18, 19), 818
 Sluch, M. I. 776, 777(138, 139), 801
 Sluggett, G. W. 959(42), 960(42, 47, 48, 50, 51, 53), 962(51, 53), 964(68), 969(48, 51), 970(51), 971(48, 51), 976(51), 980(47), 982(47, 50), 983, 984(42), 985(42, 47, 51), 986(42, 47, 50, 51, 104), 987(47, 105), 989(42, 53), 990, 992(47), 993(47, 48), 994(48), 995, 996(47, 48), 1000(53), 1003(48), 1009–1011, 1018, 1019, 1022(68), 1025, 1026

- Sluis, M. van der 525(99, 100), 538
 Slutsky, J. 905(297), 906–908(297, 302), 947
 Small, J. H. 578(90, 111), 592(138, 139),
 593(141), 600(90), 629(207), 633(90), 637,
 638, 640
 Smart, B. A. 354, 356(40, 41), 357(41), 388,
 432(18), 465
 Smart, B. E. 346(17), 387
 Smeets, W. J. J. 239(59), 331, 769(117, 119,
 120, 124), 801
 Smit, C. N. 496, 499(26), 531(130, 131),
 534(130), 536, 539
 Smith, A. 16(113), 151
 Smith, A. B. III 919(368), 948
 Smith, B. A. 547(28), 562
 Smith, B. J. 1031(17), 1056
 Smith, D. M. 316(353), 338
 Smith, E. G. 320, 322(381), 324(395), 338
 Smith, G. W. 826(26a, 30), 848
 Smith, J. D. 240(61), 331, 728(265), 743,
 939(466), 950
 Smith, K. A. 703(76), 738
 Smith, L. I. 645(18), 691
 Smith, M. M. 620(196), 639
 Smith, P. V. 830(46a), 838(103a), 839(113),
 844(133a), 849, 851, 852
 Smith, S. C. 889(203), 945
 Smith, T. C. 95(367), 158
 Smith, W. E. 474(30), 487, 584(134), 638
 Snaith, R. 434(29), 465
 Snegirev, E. P. 19(129), 151
 Snider, B. B. 877(143), 943
 Snieckus, V. 922(392), 935(457), 948, 950
 Snijders, J. G. 9(48a, 49), 13(84), 149, 150
 Snow, J. T. 395, 397(33), 425
 So, S. P. 106(384), 159
 Sogabe, T. 256(149), 333
 Sohn, H. 51(225a), 107(386a), 108(386b), 154,
 159, 472(26), 473(27, 28), 487, 642(4h, 4i),
 645(22a), 676(62a, 62b), 679(4h, 4i, 62a,
 62b), 680, 690(62a, 62b), 691–693
 Sokolikova, O. K. 227(20), 330
 Solay, M. 902(243), 945
 Solé, S. 859(38), 941
 Söllerböhmer, F. 870(105), 943
 Söllradi, H. 286, 291(267), 336
 Söllradl, H. 476(54), 487
 Solooki, D. 1034(36), 1056
 Solouki, B. 114, 115(422), 160, 166(10, 11),
 167(11, 16, 18), 168(11, 16, 21, 22), 169(10,
 11, 16, 23, 24), 170(10), 172(10, 11, 16),
 174, 175(10, 16), 178(10, 16, 37), 179(37),
 180, 181(16, 40), 184, 185(16), 186(16, 24),
 187(24), 190(10), 191(10, 11, 16, 55),
 192(11, 16, 21, 23, 40, 55), 193(55),
 195(10, 16, 63), 197(16, 63), 199(10, 16),
 201(10), 202(79), 208(10, 16, 40), 210,
 212(10), 214, 216(10, 16), 218–221
 Solum, M. S. 230(27), 330
 Somers, J. J. 902(242), 945
 Sommer, L. H. 472(23), 480(86), 487, 488,
 697(7, 12), 710(133, 134), 714(153), 736,
 739, 740, 978(93), 1026
 Son, D. Y. 746(21, 22), 747, 750, 755,
 760(27), 776(141, 142), 786(164), 787(165),
 789(173), 790(174), 796(191), 798,
 801–803
 Son, H. 412(122), 427
 Son, H.-E. 642, 679(4a), 691
 Son, S. 687(76b), 694, 762, 763(77), 800
 Song, J. M. 648, 649(38f, 38g), 662(38f),
 671(38g), 693
 Song, K. 548(38), 562
 Sonnenberg, U. 507(57), 537
 Sonnenberger, D. C. 864(57), 942
 Sonntag, C. von 962, 982(60), 1026
 Sonoda, M. 386(129), 390
 Sonoda, N. 362(61b), 371(88), 379(105, 110),
 388–390, 888(201), 901(239), 945
 Sonogashira, K. 864(49), 941
 Sooritikumaran, R. 542, 547, 548(18), 561
 Sooriyakumaran, R. 482(103), 488, 555(50),
 562
 Sorarù, G. D. 786(161), 802
 Sordo, T. L. 128, 141(462), 162
 Sørensen, O. W. 245(97), 247(113), 248(116,
 118), 259(176), 274(228), 277(233),
 280(228), 281(247), 282(249, 250, 255),
 292(281, 282), 311(97), 332, 334–336
 Sørensen, S. 241(78, 79), 332
 Sørensen, U. B. 282(250), 335
 Sorensen, W. R. 703(83), 738
 Sorescu, D. C. 830(48), 849
 Sosa, C. 118, 123, 124(431), 161
 Sosa, C. P. 128, 133, 134, 136(459d), 162
 Sosćun, H. J. 642(13f), 691
 Souady, H. 516(76), 537
 Soukuporá, L. 323(393), 338
 Soukupová, L. 236(52), 331
 Soulivong, D. 701, 730(53), 737
 Soum, A. 240(60), 331
 Soysa, H. S. D. 992(114), 1027
 Sözerli, S. E. 240(61), 331
 Spada, G. P. 366(76), 389
 Spalding, T. R. 718, 722(198), 725, 726(247),
 741, 743
 Sparks, S. W. 277(234), 335
 Speck, M. 485(129), 489
 Spek, A. L. 239(59), 331, 525(99, 100), 538,
 719, 720, 727(200), 741, 769(117, 119, 120,
 123–125), 771(127), 801
 Spencer, J. T. 516(80), 538
 Speranza, M. 1039(62, 64, 65), 1040(65),
 1044(87), 1057
 Spialter, L. 707(110, 111), 739

- Spielberger, A. 294(292), 336, 476(58), 487, 728(261), 743, 864(68), 942
- Spinazzé, P. G. 920(374, 381), 948
- Spindler, R. 760(68), 799
- Spitznagel, G. W. 11(59g), 149
- Splendore, M. 1036(50), 1056
- Sprung, W. D. 697(11), 736
- Spyroulias, G. A. 578(124), 638
- Squires, R. 1050(130), 1058
- Squires, T. G. 256(149), 333
- Srinivas, G. N. 45(209a), 59, 61(243), 105, 106, 131(209a), 153, 154
- Srinivas, R. 79(314c), 95(366b), 157, 158, 1031(13), 1032(28), 1041(13), 1045(96), 1052(143), 1055, 1056, 1058, 1059
- Srinivasan, K. S. V. 559(61), 562
- Srinivasan, S. 575(68), 636
- Srivastava, R. C. 434(35), 466
- Stahl, A. 879(164), 944
- Stalke, D. 108, 109(393), 159, 284(262), 319(368), 336, 338, 404(91), 426, 437(45), 443(78, 79), 445(86), 458(103), 459(104), 460(105), 462(103, 105), 463(105), 466, 467, 699, 724(31), 737
- Stammler, H.-G. 113(413b, 413c), 114(416a), 160, 507(58), 522(92), 537, 538, 698, 735(21, 22, 24), 737
- Stanczyk, W. A. 725(231), 742
- Stanger, A. 724(219), 742, 912(339), 947, 964(67), 1026, 1037(54a), 1056
- Stanton, J. F. 41(189), 153
- Stark, B. 762(84), 800
- Stark, F. O. 703, 716, 717(67), 738
- Staut, T. 483(113), 488
- Stearley, K. L. 559(61), 562
- Stecker, L. 838(101b), 851
- Steckhan, E. 879(164), 944
- Steel, A. J. 357, 358(47), 388
- Steel, P. G. 865(72), 942
- Steen, H. 350(28, 29a), 388
- Steenken, S. 975(90), 1026
- Stefanov, B. B. 836, 837(87), 850
- Steffen, R. 807(13), 818
- Stegmann, R. 91, 92, 94, 95(350), 158
- Steib, C. 857(24), 941
- Steier, W. H. 632, 633(222), 640
- Steimann, M. 617(185), 639
- Stein, A. 572(31, 39), 573(39), 629(31, 39, 219), 630(216), 635, 636, 640
- Stein, J. 794(182), 802
- Stein, U. 181, 182(43), 208, 210–212(89), 219, 221
- Steinbrenner, U. 15, 17, 139(106), 151
- Steiner, A. 108, 109(393), 159, 699(31), 713, 720(148), 724(31), 737, 740
- Steinmetz, J. R. 703(79), 738
- Steinmetz, M. G. 392(13), 424, 856(13), 857(27), 941, 969(84), 1026
- Stejskal, E. O. 321(390), 338
- Stellberg, P. 108(390c), 159
- Stephens, C. 834(74c), 850
- Stern, C. 856(15), 941
- Stern, C. L. 132, 133, 136(468a), 162, 779, 781(145), 802
- Sternberg, K. 865, 904(74), 910–912(321), 942, 947
- Stevens, W. J. 6, 7, 13(34), 58, 59(242), 148, 154, 825(16b), 847
- Stewart, J. P. 13(78a, 78b, 81), 150
- Stibbs, W. G. 5, 6, 41, 43, 63(11f), 147
- Stirling, C. J. M. 868(86), 942
- Stock, A. 470(5), 486
- Stoddart, J. F. 746(9), 798
- Stoffer, J. O. 703(78), 738
- Stofko, J. J. Jr. 870(88), 942
- Stogner, S. M. 91, 94, 95(354), 158
- Stoldt, C. R. 842(126b), 852
- Stoll, H. 13(91, 92a, 92b), 15, 17(106), 25(141), 26, 27(144), 139(106), 150–152
- Stolwijk, F. 902(243), 945
- Stomakhin, A. A. 1045(93), 1046(98), 1049(124), 1057, 1058
- Stone, J. A. 136(475), 162, 1042(75, 77), 1045(75), 1046(75, 99, 100, 102, 104–106, 110–112), 1049(111), 1050(131, 134), 1057, 1058
- Stone, J. M. 1046, 1049(111), 1058
- Stoner, E. J. 879(162), 944
- Storek, W. 315(339), 337
- Storjohann, I. 838(109), 851
- Stötzel, R. 910(313), 947
- Stourton, C. 108, 109(393), 159
- Stout, T. 236(53), 331
- Straatsma, T. P. 825(16c), 847
- Stradiotto, M. 870(95, 101), 942, 943
- Stradiotto, M. J. 959, 960, 963(46), 1025
- Strain, M. C. 825(21d), 847
- Strassburger, G. 698, 735(21), 737
- Strelkova, Yu. T. 751(28), 725(28, 61), 759(28), 776(61), 797(192), 799, 803
- Streubel, R. 511(68), 537
- Striegel, B. 766(97), 800
- Stringfellow, T. C. 674(58), 693
- Strobel, F. 1045(92b), 1057
- Stroble, S. 67, 71, 73(278b), 156
- Struchkov, Y. T. 965, 967(69), 1026
- Struchkov, Yu. T. 700(42), 725(232–234, 236, 239–241, 243, 244), 727(42, 255), 728(264), 730(273), 737, 742, 743
- Strukelj, M. 687(76a, 76b), 694
- Strümann, M. 63(256a, 256b), 155
- Strutwolf, J. 80(317), 91(348), 157, 158
- Stucki, F. 838(108), 851
- Stucky, G. D. 806(4), 807(10), 810(41–43), 811(41, 42), 812(42), 813–815(42, 43), 816(4), 818, 819

- Studer, A. 350(28, 29a, 29b), 388
 Stüger, H. 216(97), 221, 700, 727(41), 737
 Stühn, B. 762(83–85), 765(88, 89), 800
 Stumpf, T. 271, 319(214), 335
 Stürmann, M. 396(52, 53), 425
 Styles, M. L. 142, 143(498a), 144, 145(499),
 163, 357(45), 388, 870(94), 942
 Su, J. 93(363e), 158
 Su, K. 729(271), 743
 Su, M.-D. 16(112), 19(131), 69, 70(282), 81,
 82(319a, 319b), 91, 94, 95(356), 115,
 116(427), 119(438), 120(131, 427, 440,
 441), 122(131, 440), 123(440), 124(440,
 441, 445), 125, 126(445), 151, 156–158,
 161
 Subramanian, G. 62, 63(247), 155
 Suga, S. 838(103e), 851, 869(87), 942
 Sugaro, M. 698(14), 701(52), 709(14), 736,
 737
 Sugi, S. 560(70), 563
 Sugimoto, F. 893(210), 945
 Sugimoto, I. 349(26), 388
 Suginome, M. 882(179), 944
 Sugisawa, H. 404(90), 426, 1003(128–130),
 1027
 Sugiyama, M. 872(118, 119), 943
 Sulkes, M. 349(24), 388
 Sullivan, A. C. 578, 600(105, 106), 637,
 717(184), 718(185–189, 195), 721(184),
 729(189), 741
 Sülzle, D. 79(314c), 95(366b), 157, 158,
 1031(13), 1032(28), 1041(13), 1052(143),
 1055, 1056, 1059
 Sumi, K. 918(360), 948
 Summers, M. F. 265(200), 334
 Sumper, M. 808(31–34), 809(33–35), 810,
 817(35), 819
 Sun, C. 904(284), 946
 Sunberg, K. R. 832(61a, 61b), 849
 Sundermann, A. 108(392), 159
 Sundermeyer, W. 24, 25(140), 151
 Sundius, T. 1043(80, 83), 1057
 Sung, D.-D. 751(30), 799
 Sung, K. 361(58), 388, 992, 998–1000(111),
 1027
 Sung, T. M. 888(195), 944
 Suponitskii, K. Yu. 725(244), 742
 Surján, P. R. 648, 649, 651(34c), 692
 Su, J. 259, 264(171, 172), 334, 647(31c),
 674(56a, 56b), 692, 693
 Suslova, E. N. 904(259), 946
 Sutcliffe, L. H. 224(1), 330
 Sutcu, L. F. 837(94a), 851
 Sutherland, D. G. J. 199(65a), 220
 Sutherland, O. 614(183), 639
 Suto, A. 701(50), 737
 Sutor, P. A. 283, 285, 286, 288, 289,
 291(259), 336
 Sutra, P. 575(59), 636
 Sutter, P. 927(412), 949
 Sutton, L. E. 7(38), 148
 Suzuki, T. 839(110), 851
 Suzuki, E. 471(13), 472(19), 486
 Suzuki, H. 79(313a, 313c), 156, 320(386), 338,
 395(45, 46), 397, 412(46), 425, 479(78),
 488, 542, 561(10), 561, 781(151), 802, 911,
 912(325), 947, 1007(142, 143), 1027
 Suzuki, S. 560(69), 563
 Suzuki, T. 352, 354(39), 388, 574, 589(50),
 636, 715(168), 740, 872(118), 943
 Sviridova, N. G. 705(95), 739
 Swaddle, T. W. 320(382), 338
 Swansiger, W. A. 707(110), 739
 Swanson, D. R. 645(21b), 692, 760(63, 65,
 66), 799
 Swift, D. M. 808(28), 819
 Sylvain, M. 1040, 1041(69), 1057
 Systemans, A. 206, 207(82a), 221
 Syvitski, R. T. 320, 321(384), 338
 Szabó, A. 844(136b), 852
 Szczepanski, S. W. 901(236), 945
 Sze, S. M. 575(70), 636
 Szepes, L. 207(83, 84), 221
 Tabei, E. 559(66–68), 560(66, 68), 563
 Tachibana, A. 1036(48), 1056
 Tachikawa, M. 575(72, 73), 636
 Tacke, R. 898(229), 945
 Tagaki, N. 877(133), 943
 Tagawa, S. 346(18), 347(20), 387
 Taguchi, Y. 833(64), 850
 Tahai, M. 67, 71, 73(278b), 156
 Takacs, J. M. 919(363), 948
 Takada, K. 701(50, 51), 716(170), 730,
 731(275), 737, 740, 743
 Takagi, N. 91, 92(343a, 343b), 93(343a, 363g),
 94, 96, 97(343a), 98(343a, 343b), 157, 158
 Takahashi, H. 526(110), 538
 Takahashi, M. 70, 78(285a), 156, 393, 394,
 398(27), 424, 873(122), 906(299), 943, 947
 Takahashi, O. 200(67), 220
 Takahashi, T. 575(76), 636, 645(21a, 21b, 23a,
 23b), 692, 877(141), 943
 Takaki, S. 911(324), 947
 Takama, A. 882(179), 944
 Takaoka, O. 827, 830(42), 849
 Takaoka, T. 833(64), 850
 Takasu, K. 377(101), 389
 Takata, T. 556(53), 562
 Takatsuna, K. 40(188b), 153
 Takayama, T. 224, 225(3), 330
 Takayanagi, H. 940(469), 950
 Takeda, K. 28(150, 151), 152, 176–178(32),
 219, 856, 887(7), 895(213), 896(214–223),
 941, 945

- Takeda, M. 896(219, 221, 223), 931(439), 945, 949
 Takeda, N. 320(386), 338, 907(306), 947
 Takeda, T. 919(370), 948
 Takeuchi, K. 393(21), 395(21, 36), 397, 412(36), 424, 425, 547(32), 548(37), 562, 575(73, 74), 636
 Takeuchi, S. 547(34), 562
 Takeuchi, T. 1053(145), 1059
 Takeuchi, Y. 224, 225(3), 330
 Taki, T. 256(149), 333
 Takiguchi, T. 697(9), 736
 Tal, Y. 14(97a), 150
 Taliani, C. 686(75b), 694
 Tamao, K. 46(211a, 211b), 47(212a, 215, 216), 153, 474(36–38), 479(79), 487, 488, 642(5, 6a–c, 14–16), 643(6b, 14), 644(14), 645(22b, 25, 26), 647(32, 33), 649(6b), 651(32), 652(32, 40–42), 654(15, 16, 32, 42, 43), 655(43), 657(6b, 26, 43, 44), 658(15), 659, 660(43), 661(6b, 22b), 662(22b, 44–46), 663(44), 665(45), 670(15, 45, 48), 671(52), 672(15, 45), 675, 676(59), 679(59, 63), 687(6b, 16), 688(16, 78), 689(6b, 79), 691–694, 731(283), 743, 865(70), 942
 Tamso, K. 647, 662(28a, 28b), 665(28b), 692
 Tamura, M. 547(34), 562
 Tan, K. H. 199(65a), 220
 Tan, K. L. 834(75d), 850
 Tan, R. P. 51(225a), 154, 403(79), 404(79, 92), 412(122), 413(127, 128), 414(128), 419(79), 426, 427, 434, 435(39), 466
 Tanabe, K. 45, 46(209b), 153
 Tanabe, M. 869(87), 942
 Tanaka, A. 885(184), 944
 Tanaka, K. 648, 651(37a, 37b), 683, 685(72), 692, 694
 Tanaka, M. 542(8), 559(63), 561, 563, 679(64), 693, 880(174, 175), 944
 Tanaka, R. 716(170), 740, 912(326), 947
 Tanaka, S. 834(72), 850
 Tandura, S. N. 239(58), 331
 Tanev, P. T. 810(40), 819
 Tang, A. 38(174d), 152
 Tang, C. W. 686(74a, 74b), 694
 Tang, K.-H. 870, 903(91), 942
 Tang, Y. 928(422), 949
 Tani, T. 935(452), 950
 Tanigaki, N. 558(56), 562
 Tanimoto, K. 839(110), 851
 Tanner, J. E. 321(390), 338
 Tanovskii, A. I. 728(264), 743
 Tarrach, G. 826(27e), 848
 Tarunin, B. I. 707(112), 739
 Tateiwa, J. 386(129), 390
 Tatewaki, H. 12(77), 150
 Tatsumisago, M. 570(23), 635
 Taylor, A. D. 707(103), 728, 731(266), 739, 743
 Taylor, K. J. 575(71), 636
 Taylor, P. 5, 6, 13, 15(32), 148, 832(61d), 849
 Taylor, P. A. 827(39b–e), 830(39c), 845(144), 849, 853
 Taylor, P. G. 623, 626(202), 640
 Teach, E. G. 494(13), 536
 Tecklenburg, B. 445, 446(85), 467
 Tecklenburg, P. 434, 436(41), 466
 Teichart, M. 732(291), 744
 Teichert, M. 699(35), 724(217), 733(35), 737, 742
 Tempkin, O. 395(44), 425, 1006, 1007(133), 1027
 Teplyakov, A. V. 831(57, 58), 832(62), 849
 Terakura, K. 840(119, 120), 852
 Teramae, H. 176–178(32), 219, 542(14), 561
 Terasaki, O. 630(215), 640
 Terlouw, J. K. 1051(135), 1058
 Termaten, A. 525(99, 100), 538
 Terroba, R. 704(90, 91), 705, 715(92), 729(91, 92), 738
 Terron, G. 525(101), 538
 Terry, K. W. 27(148), 152
 Terui, Y. 904(252), 946
 Terunuma, D. 765(91, 92, 94), 800
 Tessier, C. 266, 301(205), 303(205, 300), 334, 336, 752(56), 799
 Tessier, C. A. 402(75), 426, 732(292), 744, 1034(36), 1056
 Teter, M. P. 823(8a), 847
 Theil, W. 29(154), 152
 Thépot, P. 578(93–95, 101, 104), 583, 584, 588(93), 590(93, 101), 600(95), 603(94, 95), 604(93), 610(95), 611(94, 175), 631(95), 637, 639
 Theriault, N. Y. 928(423), 949
 Thewalt, U. 483(119), 489
 Thiel, P. A. 834(69), 850
 Thiel, W. 13(78c, 78d), 15, 17–19(105), 23, 29(137), 81(322), 114(322, 426), 115(322), 118(105, 322), 122(105), 150, 151, 157, 161
 Thiele, S. K. H. 573(47), 636
 Thies, B. S. 98(373a), 158
 Thilo, T. 54(229c), 154
 Thiyagajan, P. 547(28), 562
 Thogersen, H. 274, 280(228), 335
 Thom, K. L. 406(105), 426
 Thomas, B. 288, 289(277), 336, 780(148), 802
 Thomas, J. R. 94, 98(358), 158
 Thomas, K. M. 63(252b, 254), 67, 68, 70(254), 155, 397(56), 425
 Thompson, J. 715(163), 740
 Thompson, R. J. 725(231), 742
 Thong, P. S. P. 834(75d), 850
 Thorne, A. J. 63, 67(253–255), 68, 70(254), 113(413a), 155, 160, 397(56), 425

- Thornton, G. 834(74c), 844(129, 130, 134), 850, 852
 Thouvenout, R. 701, 729(56), 738
 Thümmeler, C. 867(81), 942
 Tia, P. R. 974(87), 1026
 Tian, S. 857(29), 941
 Tibbals, F. A. 725(246), 742
 Tidwell, T. T. 361(58), 388, 958, 959(37), 992(111), 995(37), 998–1000(37, 111), 1001(37), 1025, 1027
 Tietze, L. F. 919(369), 948
 Tildesley, D. J. 825(16e), 847
 Tilley, T. D. 578(125, 126), 593(125), 600(125, 126), 614(126), 638, 642(3, 4j, 4k), 662(47), 679(4j, 4k), 691, 693, 701(46), 729(271), 733(46), 737, 743, 755(57), 761(73), 767(57), 798, 800, 856(17), 941
 Timofeeva, T. V. 725(232–234, 241, 243, 244), 742
 Timokhin, V. I. 346(15), 377(100), 382(121b), 387, 389, 390
 Tindall, C. 827, 830(42), 849
 Tipping, A. E. 999(121), 1027
 Tius, M. A. 889(202), 901(234), 945
 Toader, D. 921(385, 386), 948
 Tobita, H. 395, 397(33), 403, 404(86), 405(102), 425, 426, 856(19), 941, 1008(144), 1027
 Todd, J. F. J. 1030(4), 1036(50), 1055, 1056
 Togo, H. 384(124), 390
 Tokitoh, N. 5, 6(23b, 24b), 79(24b, 312, 313a–e), 89(338e), 105(24b), 113, 114, 117(23b), 148, 156, 157, 320(386), 338, 395(45, 46), 397, 412(46), 425, 479(78), 488, 907(306), 911, 912(325), 947, 1007(142, 143), 1027
 Tokoroyama, T. 916(358, 359), 948
 Tol, M. F. H. van 573(47), 636
 Toldt, N. P. 959(43, 46), 960(43, 46, 49, 52), 963(46), 979(43), 982, 985–987(52), 993(49), 994(43), 1025
 Tominaga, K. 475(47), 487
 Tomlins, P. E. 730(276), 743
 Tomo, Y. 922(395), 949
 Tomoda, S. 395, 397, 412(46), 425
 Tomsons, P. 265(197), 334
 Tonachini, G. 867(82–84), 868(82), 942, 1037(53a, 53b), 1056
 Toporowski, P. M. 747(23), 798
 Torchia, D. A. 269(211), 335
 Törnroos, K. W. 316, 318(352), 338
 Torres, A. M. 281(246, 248), 335
 Toscano, M. 110, 112(402), 159, 834(82a), 850
 Tshida, H. 48, 49(219), 153
 Toshimitsu, A. 645, 657(26), 692
 Tossell, J. A. 714, 724(151), 740
 Tour, J. M. 645(21b), 692
 Toussaere, E. 575, 578(83), 632(221), 634(83), 637, 640
 Toyoda, E. 683(72), 685(72, 73a, 73b), 694
 Toyoda, S. 546(27), 557(54), 562
 Toyota, K. 492(3), 520(87), 522(3, 91), 523(3, 94), 524(3, 95–97), 525(102, 103), 526(110), 528(91, 114, 116, 117), 530(120), 531(127), 536, 538, 539
 Trachtman, M. 62(246a, 246b), 154
 Tracy, H. J. 47, 48(214), 153
 Trahasch, B. 762(85), 800
 Tran, J. 578(111), 637
 Tran, T.-A. 354, 356(40), 388
 Traylor, T. G. 578(124), 638
 Tremmel, J. 78(308), 156
 Tretner, C. 477(63, 65), 487
 Trifunac, A. D. 346(18), 387
 Trinquier, G. 27, 28(145), 64(265a, 265b, 266, 269), 67(277), 68(265a, 265b, 266, 269, 279–281), 70(265a), 74(269), 75(269, 277, 281, 302), 77(269, 281, 302), 83(332, 335–337), 84(335–337), 85(335, 337), 86(335, 336), 87, 88(336), 92(280), 110(398), 119–121(145), 129(145, 463), 130(463), 131(269, 463), 152, 155–157, 159, 162, 397(57, 58), 425
 Tröbs, V. 260(183), 334
 Troin, Y. 632(223), 640
 Trommer, K. 474(40–42), 487
 Trommer, M. 858(35), 941
 Tromp, R. M. 826(27a, 27b), 837(90a), 848, 851
 Trough, T. N. 120, 122(439), 161
 Trucks, G. W. 139, 140(485), 162
 Truong, P. 826(31), 848
 Truong, P. N. 72(290), 156, 1007(138), 1027
 Truong, T. 82(326b), 157
 Truong, T. N. 69(283), 156
 Tsai, M. S. 575(66, 70), 636
 Tsai, Y.-M. 870(89–92), 880(169), 901(236), 903(89, 91, 246, 247), 942, 944, 945
 Tsay, S.-C. 868(85), 942
 Tschudin, R. 269(211), 335
 Tse, W. C. 136, 137(481), 162
 Tsekouras, A. A. 845(145), 853
 Tsiganov, V. I. 727(255), 743
 Tskhovrebashvili, V. S. 698(25), 737
 Tsuda, H. 827(38a, 38b), 848
 Tsuda, M. 826(27g–i), 840(118), 848, 852
 Tsuji, S. 347(20), 387
 Tsukada, M. 839(116), 840(117), 852
 Tsukamoto, M. 106, 137(385b), 159, 916(358, 359), 948
 Tsukihara, T. 559(62), 563
 Tsumuraya, T. S. 6, 48, 49, 64, 67(19), 147, 392, 393(4), 395(44), 401(4), 424, 425, 782(155), 802, 1006, 1007(133), 1027
 Tsunashima, M. 470(2), 486

- Tsuno, S. 902(244), 945
 Tsuno, Y. 878(151), 944, 1046(107),
 1050(133), 1058
 Tsunoi, S. 371(88), 389
 Tsutsui, S. 70, 78(285a–c), 156, 393(23), 424
 Tsutsunava, M.Sh. 725(239), 742
 Tsuzuki, S. 45, 46(209b), 153
 Tubbesing, U. 80(317), 157
 Tukada, H. 935(458), 950
 Tulokhonova, I. 674(58), 693
 Tun, M. M. 928(433), 949
 Turecek, F. 345, 346(14), 387
 Turner, D. L. 274(224), 335
 Turner, D. W. 166, 167, 172, 191(2), 192(60),
 217, 220
 Turney, M. L. 999(119), 1027
 Twamley, B. 64(260, 261b), 92, 98(260), 155
 Tyagi, M. S. 110(409), 160
 Tyler, L. J. 472(23), 487, 697(7), 736
 Tzschach, A. 477(62), 487
- Ubayama, H. 645(23b), 692, 896(216), 945
 Uchida, H. 782(155), 802
 Uchida, K. 750, 755(54), 799
 Uchida, M. 46(211a), 153, 642(6a, 16), 654,
 687(16), 688(16, 78), 689(79), 691, 694
 Uchida, S. 364(71), 389
 Uchimaru, Y. 559(63), 563
 Uchiyama, T. 839(116), 840(117), 852
 Uda, T. 840(119, 120), 852
 Udayakumar, B. S. 857(27), 941, 969(84),
 1026
 Uechi, G. T. 1034(36), 1056
 Ueda, T. 683, 685(72), 694
 Ueki, Y. 1003(129), 1027
 Ueno, K. 548(41), 562
 Ueno, T. 525(107, 108), 538
 Ueno, Y. 673, 683, 690(54a), 693
 Ugliengo, P. 607(167), 639
 Uhl, W. 495(19), 498(31), 506(53), 509,
 511–513(31), 514(19), 536, 537
 Uhlig, F. 224(2), 330
 Uhlig, W. 476(59), 477(62, 63, 65), 487,
 706(100), 739
 Uhrberg, R. I. G. 826(25c, 25d), 844(130),
 848, 852
 Uhrin, D. 269, 270(212), 304(303), 335, 337
 Uhrínová, S. 269, 270(212), 335
 Ulibarri, T. A. 602, 604(160), 638
 Umeyama, H. 351(31), 388
 Underiner, G. E. 434, 435(39), 466
 Unger, S. H. 1001(122), 1027
 Unitiesd, S. 858(37), 941
 Unno, M. 701(50, 51), 716(170), 730,
 731(275), 737, 740, 743
 Upadhyaya, H. P. 962(59), 1025
 Urabe, H. 370(85), 389, 645(24a, 24b), 692
- Urban, J. 26(143), 152
 Urry, G. 484(125, 126), 489
 Ursini, O. 1039, 1040(65), 1057
 Usón, I. 434, 464(28), 465, 484(123), 489,
 698(26), 722(214), 724(217), 729(26), 737,
 741, 742
 Usui, S. 374(95), 379(108), 389, 390
 Utimoto, K. 904(256), 912(329), 946, 947
 Uzan, O. 101, 102, 104(380), 159
- Vacek, G. 25(142), 26(143), 29(142), 151, 152
 Vaglio, G. A. 1036(47, 49–51), 1037(53a–c),
 1056
 Van der Kant, C. M. 402, 408(70), 426
 Van Der Voort, P. 715(167), 740
 Van Dyke, C. H. 697(4), 736
 Vanquickborne, L. G. 91, 94, 95(349), 158
 Vansant, E. F. 715(167), 740
 VanSlyke, S. A. 686(74a, 74b), 694
 vanWalree, C. A. 559(64), 563
 Van Zijl, P. C. M. 260, 271(206), 335
 Varaprath, S. 703(88), 738
 Vardeny, Z. V. 648(35a–e), 649, 651(35c),
 692
 Vardosanidze, Ts. N. 725(239), 742
 Varezhkin, Yu. M. 728(262), 743
 Vargas, R. 28–31, 110, 112, 113(153), 152
 Varnavsky, O. P. 776, 777(139), 801
 Vartuli, J. C. 572, 620, 629(36, 37), 635
 Vasella, T. 350(29b), 388
 Vasilenko, N. G. 762(78, 79), 764(78),
 766(95–97), 791(78), 795(189), 800, 802
 Vater, N. 443(73, 76, 77), 466, 467
 Vatsa, R. K. 962(59), 1025
 Vaupel, T. 169, 186, 187(24), 218
 Vdovin, V. M. 952(2), 956, 958, 962, 982(33),
 1024, 1025
 Vecchi, D. 346, 383(19), 385(126), 387, 390
 Vedejs, E. 914, 915(353), 948
 Veen, G. N. A. v. 844(139a), 852
 Veith, M. 430(6), 437(43), 438(49), 445, 447,
 458(90), 465–467, 718(193), 722(209),
 731(289), 741, 744, 776(143), 801, 904(280,
 287), 946
 Vela, A. 28–31, 110, 112, 113(153), 152
 Veldman, N. 525(100), 538
 venderLaan, G. P. 559(64), 563
 Venkateswarlu, A. 472(24), 487
 Venneri, P. 960, 962, 989, 1000(53), 1025
 Venturini, A. 377(100), 389, 966(72–74),
 1026
 Veprek, S. 575(63), 636
 Verdaguer, N. 710(137), 739
 Verdegaal, C. H. M. 940(470), 950
 Veretlemarinier, A. V. 570(12), 635
 Verlhac, J.-B. 248(120), 332, 901(233), 945
 Verne, H. P. 114(420a), 160, 202(80), 221
 Vernooijs, P. 202, 216(75), 220

- Vestin, R. 315, 318, 319(342), 337
 Veszprèmi, T. 5(27b), 114(421c), 148, 160, 208(85, 92), 211(92), 221, 873(122), 943
 Villar, F. 366(74), 389
 Vincendon, M. 258(164), 334
 Vinciguerra, V. 1038(59), 1057
 Vining, W. J. 47, 48(214), 153
 Vioux, A. 575(77, 81), 636
 Virlet, J. 247(110, 112), 282, 293(256–258), 332, 336
 Vishnu Kamath, P. 11, 35(59f), 149
 Visscher, L. 13, 15(82), 150
 Visser, O. 13, 15(82), 150
 Vissler, L. 16(108), 151
 Viswanadha Rao, G. K. 1045(96), 1058
 Vitukhnovsky, A. G. 776, 777(138, 139), 801
 Vlasova, N. N. 208, 211(91), 221
 Vliestra, E. J. 559(64), 563
 Vogele, K. E. 278(241), 335
 Vogt, D. 769(118), 771(127), 801
 Vogt, L. H. Jr. 701(47), 737
 Vögtle, F. 746(1, 5, 11), 798
 Voigt, A. 232(45), 331, 573(49), 636, 698(29), 699(31, 32, 35), 711(139, 140), 715(162), 717, 720–722(29), 724(29, 31, 140, 162), 729(140), 731(139), 733(35, 139), 735(32), 737, 740
 Voit, B. I. 746(3), 798
 Voityuk, A. A. 13(78c, 78d), 150
 Volcani, B. E. 806(1), 807(14, 15, 17), 810(36, 37), 817(1), 818, 819
 Vollbrecht, S. 474(33), 487
 Volpe, P. 1036(47, 49, 51), 1037(53c), 1056
 Voltaron, F. 37(171), 152
 Volz, P. 524(98), 538
 Vorhoeve, R. J. H. 471(9), 486
 Voronkov, M. G. 208, 211(91), 221, 239(55, 56, 58), 331, 705(95), 717(183), 739, 741
 Vorstenbosch, M. L. W. 239(59), 331
 Voyer, N. 902(241), 945
 Vrancken, K. C. 715(167), 740
 Vrazhnov, D. A. 1044(84), 1057
 Vrieling, E. G. 806(7, 8), 807(7), 808(26), 818
 Vries, A. E. de 844(139a), 852
 Vries, L. de 526, 527(112), 538
 Vuister, G. W. 266, 271(206), 335
 Vvedensky, D. D. 844(129), 852
 Vyas, D. M. 928(433), 949
- Waalraaf, G. M. 547(28), 548(38), 562
 Wachtler, U. 698, 707(18), 737
 Waddel, K. W. 95(366e), 158
 Wadell, S. T. 352(35), 388
 Wadt, W. R. 13, 15, 17(90a–c), 150
 Wagner, G. 955(27, 28), 958, 959(36), 968(76), 998(27), 1025, 1026
 Wagner, H. 834(74a, 80), 850
 Wagner, M. 114(420a, 420d, 422), 115(420d, 422, 428), 116(428), 160, 161, 202(77, 79, 80), 203(77), 220, 221
 Wagner, R. 241, 257(72), 261, 268(192), 298(296), 331, 334, 336
 Wagner, S. 988(106), 1027
 Wakahara, T. 352, 354(39), 388, 642, 679(41), 691
 Wakamatsu, S. 470(7), 486, 560(70), 563
 Wakaumi, M. 232, 233(44), 331
 Walawalkar, G. M. 573(49), 636
 Walawalkar, M. G. 699, 733(35), 737
 Walawalker, M. G. 698(27, 29), 717, 720, 721(29), 722, 724(27, 29), 737
 Walczak, M. M. 834, 845(75a), 850
 Waldhör, S. 480(87), 488
 Walker, M. 923, 924(401), 949
 Wallace, R. M. 827(39c–e), 830(39c), 849
 Wallace, S. 47, 48(214), 153
 Walmsley, J. A. 230(33), 331
 Walsh, R. 16(117), 17(125), 118(430), 119(434a–c, 435, 436), 120(435, 436), 122(436), 124(447), 125(447, 452a, 452b), 127(454a, 454b, 455a), 151, 161, 470(1), 486, 858(37), 941, 953(21, 22), 958, 962(22), 1007(137), 1025, 1027
 Waltenburg, H. N. 822, 844(1), 846
 Walter, S. 430, 434, 438, 440, 441(8), 443(8, 78), 465, 467
 Walters, A. 79(314a, 314b), 156
 Walther, B. W. 20(134), 151, 199, 203(70), 220
 Walton, D. R. M. 699(36), 737
 Walton, J. C. 381(112), 390
 Walzer, J. F. 701(48), 720(208), 727(258), 729(48), 737, 741, 743
 Wan, C.-W. 746(7), 798
 Wander, A. 839(113), 852
 Wang, J. 728(263), 743
 Wang, K. K. 922(388), 948
 Wang, M. Q. 570(28), 635
 Wang, N. 868(85), 942
 Wang, P. G. 370(87), 389
 Wang, Q. 617(185), 639
 Wang, S. G. 9, 29, 33(46), 149
 Wang, W. C. 570(25), 635
 Wang, X. 904(283), 921(385), 946, 948
 Wang, Y.-X. 858(33, 34), 941
 Wang, Z. 38(174d), 152
 Wang, Z. L. 575(67), 636
 Wannagat, U. 430, 434(1), 439(52), 442(68), 465, 466
 Warren, D. J. 572(33), 635
 Watanabe, H. 393(21), 395(21, 36), 397, 412(36), 424, 425, 560(69), 563, 840(119), 852
 Watanabe, K. 83(330a), 157, 559(60), 562
 Watanabe, K. A. 940(469), 950

- Watanabe, M. 864(67), 942
 Watanabe, T. 475(46, 47), 487, 673(54a, 54b),
 683(54a), 690(54a, 54b), 693
 Watase, T. 728(267), 730(279), 743
 Waterson, C. 767(100), 800
 Watkin, D. J. 928(432), 949
 Watts, W. E. 631(220), 640
 Waugh, J. S. 241(75), 331
 Waymouth, R. 383(123), 390
 Wayner, D. D. M. 364(68), 389, 830(54),
 831(55), 849, 973, 999(86), 1026
 Weakiem, P. C. 826(30), 848
 Weakliem, P. C. 826(26a), 848
 Weatt, D. T. 483(120), 489
 Weaver, J. H. 834(77b), 850
 Webb, S. P. 825(16b), 847
 Weber, K. 901(238), 945
 Weber, L. 492(1), 507(55–58), 509(61),
 522(92), 527(113), 536–538, 913(346), 948
 Weber, W. P. 315(348), 338, 483(111), 488,
 795(190), 797(193, 194), 803, 910(317),
 947, 992(113, 114), 1027
 Webster, M. 483(116), 488
 Webster, O. W. 578(91, 92), 583, 595, 598,
 600(92), 629(91), 631, 632(92), 637
 Weddle, G. 962, 982(60), 1026
 Wedig, U. 13(91), 150
 Wee, A. T. S. 834(75d), 850
 Weeks, J. J. 542(13), 561
 Weger, P. 617(186–188), 619(186, 188, 191),
 639
 Wegmann, T. 503(47), 504(50), 537
 Wehner, G. 931(440, 442), 949
 Wei, P. 642, 679(4d), 691
 Wei, X. 648(35b), 692
 Weidenbruch, M. 5, 6(24f), 43(206), 63(256a,
 256b), 82, 83, 87(327a, 327b), 105,
 113(24f), 114(416c), 148, 153, 155, 157,
 160, 187(52a, 52b), 220, 275, 284, 285,
 292, 293(230), 335, 392(5), 393(18, 22a),
 394(29–31, 43, 47), 395(22a, 35, 43),
 396(52, 53), 397(35, 43, 47), 400(22a, 65,
 66), 401(5), 402(71–74), 404(74), 405(71,
 96, 103, 104), 406(66, 72, 105–107),
 407(66, 74, 107–110), 408(109), 410(118),
 411, 412(96), 414(130), 416(135), 418, 419,
 421(142), 424–427, 482(101), 488, 697(8),
 736, 952, 1006(15), 1025
 Weidmann, H. 898(228), 945
 Weigelt, J. 280(242), 335
 Weinberg, W. H. 827(39c, 39d), 830(39c),
 837(89a, 89b), 849–851
 Weiner, B. 825(17a, 17b), 830(46b), 847, 849
 Weinhold, F. 14(100a, 100b, 101, 102a, 102b),
 150
 Weinreb, S. M. 405(101), 426
 Weinstock, R. B. 14(100a), 150
 Weis, C. D. 927(412), 949
 Weitekamp, D. P. 265(199), 334
 Weldon, M. K. 836, 837(87), 850
 Well, M. 932(444), 950
 Wells, A. F. 77(304), 156
 Wendler, C. 727(259), 743, 912(336), 947
 Wendolowski, J. J. 419(143), 427
 Wentrup, C. 192(62), 220
 Wen Yao, J. 712(146), 740
 Wenzel, H. V. 495, 501, 506(23), 510(66),
 536, 537
 Wenzel, U. 445, 448(91), 467
 Werme, L. O. 166(13), 218
 Werner, E. 444(84), 450, 451(96, 99, 100),
 453, 455, 456(96), 459(84, 100), 460(84,
 107), 463(107), 464(111), 465(99, 100), 467
 Werner, H. 864(48), 941
 Werstiuk, N. H. 213, 216(94), 221, 870(97),
 942
 Wesdemiotis, C. 857(28), 941
 Wesemann, L. 195, 197(63), 220
 Wesener, J. R. 320(388), 338
 Wessel, H. 724(217), 742
 Wessels, P. L. 241(77), 242(84, 85), 332
 Wessely, H.-J. 498, 509, 511–513(31), 536
 West, C. T. 474(29), 487
 West, J. K. 595(154), 638, 703, 716(75), 738,
 808(30), 819
 West, R. 5, 6(11c, 13, 23b), 43(13), 51(225a,
 225b), 63(11c, 251), 67, 70, 71(274), 87,
 89(338a–d), 98(374), 107(386a), 108(386b),
 113(23b), 114(23b, 420a–c), 115(420b,
 420c, 428), 116(428), 117(23b), 147, 148,
 154, 155, 157–161, 175(30), 178(35),
 202(77, 80), 203(77), 218–221, 245(102),
 248(117), 259(169, 170, 174, 175), 277(169),
 236, 238, 239), 278(238), 292(287, 288),
 295(236, 238, 293, 294), 319(170), 332,
 334–336, 392(1, 2, 6), 393(22b), 394(28),
 395(1, 22b, 32, 37, 38, 40–42), 396(6),
 397(28, 32, 41, 42, 50), 398(28, 50), 399(2,
 6, 28, 40, 62–64), 400(22b, 64), 401(2, 6,
 67, 68), 402(75, 76), 403(78–85), 404(78,
 79, 81, 82, 84, 85, 88, 92), 408(67, 112,
 113), 409(113, 114, 116, 117), 410(116),
 411(67, 120, 121), 412(6, 80, 83, 84,
 122–125), 413(125–128), 414(6, 128, 129),
 419(78, 79), 420(42), 421(150–152), (51),
 424–428, 432(17), 434, 435(39), 465, 466,
 472(26), 473(27, 28), 474(35), 475(51, 52),
 487, 492(2), 536, 541(1, 3), 542(3, 9, 15),
 543(9), 547(29, 36), 548(3, 9, 42, 45),
 550(45), 551, 552(46), 555(47–49), 556(52,
 53), 557(54), 559(59, 61), 561, 562, 642(4h,
 4i), 645(22a), 674(58), 676(62a, 62b),
 679(4h, 4i, 62a, 62b), 680, 690(62a, 62b),
 691–693, 702(63), 714(155), 727(63), 738,
 740, 827(37), 848, 857(21), 858(32),
 866(76–79), 907(305), 941, 942, 947,

- 952(14, 16, 18), 1006(14, 16, 132, 135, 136), 1007(135, 136), 1008(145–147), 1011(151, 152), 1012(135), 1019(16, 159, 160), 1022(16), 1025, 1027, 1028
 Westaway, K. C. 1015(156), 1028
 Westerhausen, M. 113(411c), 160, 434(33), 466, 904(279), 946
 Westermann, H. 494(13), 531(123), 536, 539
 Westermann, J. 838, 840(105b), 851
 Wettinger, D. 260(182), 334
 Wettling, T. 208(86), 221
 Wey, R. 626(205), 640
 Weyenberg, D. R. 645(20), 692
 Wezenbeek, E. M. van 9(49), 149
 Whan, R. E. 632(224), 640
 Whangbo, M.-H. 108(388), 159
 Wheeler, A. P. 808(28), 819
 Whilte, J. M. 837(88a), 850
 Whipple, E. B. 227, 326(15), 330
 White, A. H. 864(64), 942
 White, C. 823(10d), 847
 White, C. A. 825(21b), 847
 White, W. D. 249(129), 291(278), 333, 336
 Whitehead, M. A. 57(237a, 237b), 154
 Whitesell, J. K. 879(159), 944
 Whitmarsh, C. K. 785(157, 158), 802
 Whitmore, F. C. 480(86), 488, 697(12), 710(133), 714(153), 736, 739, 740
 Whittaker, S. M. 702, 708, 731, 734(58), 738
 Whitten, J. L. 826(27f), 837(95b, 96), 848, 851
 Wiberg, E. 701(49), 737
 Wiberg, K. B. 14(95), 54(228b), 150, 154, 352(35), 388, 419(143), 427
 Wiberg, N. 5, 6(15), 58(238, 239g, 239i), 61, 62(238), 147, 154, 187, 190(51a, 51b), 220, 396, 397(48), 417(139), 418, 419, 421(140), 423(139, 156), 425, 427, 428, 440, 441(61b), 466, 952(6), 955(27–30), 958(6, 36), 959(36), 960, 966(6), 968(76, 77), 978(6, 77), 982(6, 29), 983(103), 988(6, 106–108), 998(27), 1024–1027
 Wibert, E. 708(121), 739
 Wicha, J. 897(224), 945
 Widdowson, D. A. 904(249), 946
 Widmer, M. 1045(97), 1058
 Wiebcke, M. 712(145), 740
 Wieber, G. M. 575(54), 636
 Wieber, M. 718(194), 741
 Wiedenau, P. 378(104), 389
 Wielzel, P. 928(425), 949
 Wiemer, D. F. 912(328), 947
 Wierschke, S. G. 720(205), 741, 1037(54b), 1056
 Wiersema, A. K. 673(55), 693
 Wiesendanger, R. 826(27e), 848
 Wijkens, P. 769, 770(115), 801
 Wijs, G. A. de 844(140a, 140b), 852
 Wilburn, J. C. 904(271, 273), 946
 Wild, L. M. 142(498a, 498b), 143(498a), 144(498b), 163, 349, 352(27), 388
 Wilde, J. C. de 747(26), 769, 770(115), 771(127), 798, 801
 Wilhelm, K. 292(283), 336
 Wilkes, G. L. 570(15), 594(144), 635, 638, 716(173), 740
 Wilkins, C. L. 324(403), 339
 Wilkinson, G. 113(410), 160
 Willard, B. B. 1043(79), 1057
 Willhalm, A. 496(25), 536
 Williams, D. 199, 203(70), 220
 Williams, D. J. 395, 397(33), 403, 404(86), 415(132, 133), 425–427, 703(85), 725(238), 729(85), 738, 742
 Williams, E. A. 225(5), 231(40, 41), 233, 234(41), 283, 285, 286, 288, 289, 291(259), 324(397), 330, 331, 336, 339, 714(157), 740
 Williams, E. M. 844, 845(135), 852
 Williams, F. 20(134), 151
 Williams, G. A. 319(369), 338
 Williams, I. D. 864(53), 942
 Williamson, M. P. 317, 318(360), 338
 Willis, C. R. 357(48), 388
 Willis, W. W. Jr. 888(198), 944
 Willms, S. 82, 83, 87(327a), 157, 394, 397(47), 414(130), 416(135), 425, 427
 Wilson, K. L. 808(19), 818
 Wilson, S. R. 897(225), 910(320), 945, 947
 Wilson, Z. 67, 71, 73(278b), 156
 Wimperis, S. 248(115), 332
 Wincel, H. 1033(33), 1056
 Winchester, B. G. 928(431, 432), 949
 Winchester, W. R. 397(55b), 425
 Wincott, P. L. 844(129, 130, 134), 852
 Wind, M. (51), 425
 Windus, T. L. 37(170), 66, 67, 71, 73(272), 145(170), 152, 155, 397(59), 425
 Winiski, M. 200, 201(68), 220
 Winkel, Y. van den 395(37, 42), 397, 420(42), 425, 531, 534(132), 539, 1008(145), 1027
 Winkhaus, V. 504, 520(49), 522, 528, 529(90), 537, 538
 Winkhofer, N. 698(16), 699(31), 701(54), 724(31, 54), 735(16, 54), 736, 737
 Winkler, R. G. 762(80), 800
 Winkler, U. 81, 82, 113(324), 157, 509(63b), 514(71), 534(63b), 537
 Winnemöller, J. 516(77), 537
 Winokur, M. 543(20c), 551, 552(46), 561, 562
 Winter, E. 923, 924(404), 949
 Winters, H. F. 844(128), 852
 Wise, M. L. 837(89c, 90d), 851
 Wisener, C. A. 701, 733(55), 737
 Wisian-Neilson, P. 904(273), 946
 Withers, J. D. 230(27), 330
 Withnall, R. 79(314e, 314f, 315a), 157
 Witte-Abel, H. 439(57, 59, 60), 440(60), 466

- Wittel, K. 214, 216(96), 221
 Wittenbecher, L. 114(419), 160
 Wittmann, J. 167(18, 19), 191–193(55), 218, 220
 Wittmann, J. C. 755, 760(58), 799
 Wlodawer, A. 813(46), 819
 Wlodek, S. 1031(14, 15, 18, 19), 1032(14, 27), 1033(33), 1040(14, 69), 1041(69), 1055–1057
 Wobst, M. 315(333), 337
 Wojcik, A. B. 570(10), 635, 716(172), 740
 Wojtyniak, A. C. M. 1042(77), 1046(99, 104, 110), 1057, 1058
 Wolf, C. 858(37), 941
 Wolf, H.-P. 191–193(55), 220
 Wolf, H. P. 180, 181, 192, 208(40), 219
 Wolfbeis, O. S. 570(17), 635
 Wolfe, S. 123(443), 161
 Wolff, C. 312(327), 337
 Wolfram, R. 857(22, 23), 941
 Wolk, J. L. 141(490), 163
 Wolkow, R. A. 826(25e), 827(43, 44), 828(44), 830(54), 831(55), 833(65a, 65b), 848–850
 Wolter, H. 578(130), 638
 Wong, K. S. 648(35a–c), 649, 651(35c), 692
 Wong, R. A. 790(174), 802
 Wong, W.-K. 904(284, 288), 946
 Wong, W.-T. 904(284, 288), 946
 Wong Chi Man, M. 575(57), 578(93–95, 97–99, 101, 104, 119, 129), 583(93, 132, 133), 584(93), 588(93, 98, 99), 590(93, 98, 99, 101), 596(97, 98), 600(95), 602(98, 99), 603(94, 95), 604(93), 610(95), 611(94, 175, 176), 616(57, 119), 623(97–99), 631(95, 98, 99), 636–639
 Wong-Ng, W. 913(343), 948, 952, 997, 998(17b), 1025
 Woo, S. 922(391), 948
 Wood, I. T. 956, 958, 963, 982(34), 1025
 Wood, K. 904(264), 946
 Woodbury, R. P. 919(367), 948
 Woodward, R. B. 124(448a), 161, 827(35), 848
 Wormeester, H. 838(102), 851
 Woznow, R. J. 714(160), 740
 Wrackmeyer, B. 251(135, 141), 253(143), 259(171, 172), 260(178–185), 264(171, 172), 266(179, 180, 201–203), 270(201, 203), 271(201, 203, 213, 216), 272(216), 292(280), 293, 294(290), 302, 304(135), 306(143, 216), 307(135, 213, 306), 309–315), 308(213, 306, 317), 309, 310(306), 311(318), 325(410, 411), 333–337, 339, 647(31a–d), 674(56a, 56b), 692, 693
 Wright, A. 866(76–78), 942
 Wright, A. P. 703, 716, 717(67), 738
 Wright, D. S. 108, 109(393), 159
 Wright, L. J. 698, 701, 733, 734(19), 737
 Wu, C. J. 837(93b), 845(146), 851, 853
 Wu, H. 136, 137(481), 162, 280, 281(243), 335, 348(22), 388, 780(149), 802
 Wu, H.-J. 870(104), 943
 Wu, P. K. 838, 840(105c), 851
 Wu, S. 347, 348(21b), 388
 Wu, W. F. 575(70), 636
 Wuerthwein, E. V. 38(174b), 152
 Wulff, W. D. 904(267, 296), 938(464, 465), 946, 950
 Wursthorn, K. R. 916(357), 948
 Wurth, W. 838(103b), 851
 Wustrack, R. 284(262), 336
 Wynberg, H. 673(55), 693
 Wytenburg, W. 1046(99), 1058
 Wytenburg, W. J. 136(475), 162
 Xi, C. 645(23a), 692
 Xi, Z. 645(23b) 692
 Xiao, Y. 790(174), 802
 Xie, P. 575(64), 636
 Xie, Y. 70, 75, 77(284a, 284b), 93(363e, 363f), 99(284a), 100(284b), 156, 158
 Xie, Z. 132(469), 162, 728(263), 743
 Xie, Z. M. 904(274), 946
 Xing, Y. R. 834(76), 850
 Xiong, J. Z. 199(65a), 220
 Xu, C. B. 632, 633(222), 640
 Xu, J. 384(125), 390
 Xu, L. 570(25), 635
 Xu, W. 70, 75, 77(284a, 284b), 99(284a), 100(284b), 156
 Xu, Y. 676, 679, 680, 690(62b), 693
 Xu, Z. L. 570(25), 635
 Xue, F. 904(284), 946
 Yadritseva, T. S. 547(35, 36), 562, 727(260), 743
 Yaguchi, H. 838(106), 851
 Yamabe, S. 880(173–175), 944, 1037(56), 1057
 Yamabe, T. 83–86(333), 157, 647(28b), 648(36c, 37a, 37b), 649(36c), 651(36c, 37a, 37b), 662, 665(28b), 692, 906(300), 947, 1003(129), 1027, 1036(48), 1056
 Yamada, H. 1005(131), 1027
 Yamada, N. 575(76), 636
 Yamada, R. 382(122b), 390
 Yamaguchi, A. 880(174, 175), 944
 Yamaguchi, K. 648, 651(37a, 37b), 692, 704(89), 738, 895(213), 945
 Yamaguchi, S. 46(211a), 47(212a, 212b, 215, 216), 153, 395, 397, 399(39b), 425, 642(5, 6a–c, 14–16), 643(6b, 14), 644(14), 645(22b, 25, 26), 647(28a, 28b, 32, 33),

- 649(6b), 651(32), 652(32, 40–42), 654(15, 16, 32, 42, 43), 655(43), 657(6b, 26, 43, 44), 658(15), 659, 660(43), 661(6b, 22b), 662(22b, 28a, 28b, 44–46), 663(44), 665(28b, 45), 670(15, 45, 48), 671(52), 672(15, 45), 675, 676(59), 679(59, 63), 687(6b, 16), 688(16, 78), 689(6b, 79), 691–694, 731(283), 743
- Yamaguchi, Y. 91, 94, 96(346), 158, 648, 649, 651(36a–c), 675, 676(60), 692, 693
- Yamamoto, H. 904(265), 946
- Yamamoto, K. 647(27), 692, 922(395), 949
- Yamamoto, S. 95(366d), 158
- Yamamoto, Y. 472(19), 486, 559(66, 67), 560(66), 563, 883(180), 884(183), 944
- Yamanaka, A. S. 592(140), 638
- Yamanaka, S. A. 629(212), 640
- Yamanaka, T. 559(62, 65), 563
- Yamanaker, S. A. 578, 589(96), 637
- Yamasaki, T. 827, 830(40), 849
- Yamashita, D. S. 879(162), 944
- Yamashita, K. 673(54a, 54b), 683(54a), 690(54a, 54b), 693
- Yamashita, O. 54(230), 154
- Yamashita, T. 373(93a, 93b), 389
- Yamazaki, H. 106, 137(385a), 159, 379(105), 390
- Yamazaki, O. 384(124), 390
- Yamazaki, S. 880(173–175), 944
- Yamazaki, T. 166, 169, 174(5), 217, 931(436–439), 949
- Yanez, M. 1031(16), 1034(40), 1055, 1056
- Yang, C. 826(26g), 848
- Yang, J. J. 845(145), 853
- Yang, M. 879(161), 944
- Yang, W. 825(21c), 830(47b), 847, 849
- Yang, Y. L. 837(94a, 94b), 851
- Yang, Z. 632, 633(222), 640
- Yang, Z.-X. 683(69a, 69b), 693
- Yano, F. 1003(130), 1027
- Yao, J. 786(164), 787(165), 802
- Yap, G. P. A. 642, 679(4j), 691, 719(202), 741, 767(103), 800
- Yassar, A. 683(68a, 69a), 693
- Yasunami, M. 525(107, 108), 538
- Yasusa, T. 879(155), 944
- Yatabe, T. 58(239a, 239f), 154
- Yates, B. F. 61(244a, 244c), 154
- Yates, J. T. 827(39a–f, 44), 828(44), 830(39c), 849
- Yates, J. T. Jr. 822(1), 834(75b, 78b), 837(89a, 89b), 844(1, 132), 845(144), 846, 850–853
- Yauchibara, R. 113(414c), 160
- Ye, S. 1031(23), 1056
- Yen, C.-H. 870(104), 943
- Yen, C. T. 575(65), 636
- Yencha, A. J. 208, 210, 211(90), 221
- Yeon, S. H. 471(15), 486, 877(148), 943
- Yeretzian, C. 38(176), 152
- Yeske, P. E. 910(319), 947
- Yimenu, T. 883(181), 944
- Yin, W. 760(72), 800
- Yokelson, H. B. 51(225b), 154, 259(174), 277(236), 295(236, 294), 334–336, 393(22b), 395(22b, 38), 400(22b), 403(82), 404(82, 88), 424–426, 858(32), 941, 1008(146, 147), 1027
- Yokota, S. 893(210), 945
- Yokoyama, M. 362(60), 384(124), 388, 390
- Yonezawa, T. 838(103e), 851
- Yonghua, X. 676, 679, 680, 690(62a), 693
- Yoo, B. R. 83(330b), 157, 471(15), 486, 877(148), 943
- Yoon, D. Y. 575(68), 636
- Yoon, K. 789(173), 796(191), 802, 803
- York, D. M. 825(21c), 847
- Yoshida, H. 872(119), 943
- Yoshida, M. 542(6), 558(57), 561, 562
- Yoshida, N. 1036(48), 1056
- Yoshida, S. 481(96), 488
- Yoshida, Y. 347(20), 387
- Yoshifujii, M. 492(1, 3), 499(33), 520(87), 522(3, 33, 91), 523(3, 94), 524(3, 95–97), 525(102, 103, 107, 108), 526(110), 528(91, 114, 116, 117), 530(120), 531(127), 536, 538, 539, 913(344), 948
- Yoshii, E. 895(213), 896(214–221, 223), 945
- Yoshina-Ishii, C. 572(35), 630(217), 635, 640
- Yoshino, K. 648(35e), 692, 782(155), 802
- Yoshinobu, J. 827(38a, 38b), 848
- Yoshizawa, K. 83–86(333), 157, 906(300), 947
- Yoshizawa, M. 704(89), 738
- Young, C. 623, 626(203), 640
- Young, D. C. 5, 12(25d), 148, 324(401), 339
- Young, R. B. 623(200), 640
- Young, R. C. 481(90), 488
- Young, W. 12(70b), 149
- Youngs, W. 1034(36), 1056
- Youngs, W. J. 732(292), 744
- Yoyota, K. 913(344), 948
- Yu, C.-H. 96(369a), 158
- Yu, H. 559(61), 562
- Yu, S. 920(380), 948
- Yu, Z. 978(94), 1026
- Yuan, C.-H. 555(49), 556(52, 53), 557(54), 562
- Yufit, D. S. 865(72), 942
- Yun, J. S. 366(73), 389
- Yun, L. J. 808(23), 818
- Yung, Y. 832(63), 849
- Yuzefovich, M. 912(338), 947
- Zaborovskiy, A. B. 346(15), 387
- Zahirovic, S. 343(7a, 7b), 387
- Zahouily, M. 371(89), 389

- Zak, Z. 439(58), 463(110), 466, 467
 Zakharin, L. I. 728(264), 743
 Zakouril, P. 1031(12), 1032(26), 1033(26, 32), 1055, 1056
 Zamaev, I. A. 725(240), 742
 Zambon, D. 578, 586(116), 632(116, 223), 637, 640
 Zamboni, M. 366(75), 389
 Zanathy, L. 207(83, 84), 221
 Zanim, A. 474(33), 487
 Zank, G. A. 575(54), 636
 Zarbock, J. 261, 311(188), 334
 Zaremba, C. M. 807(10), 818
 Zavitsas, A. A. 357(46), 358(46, 53), 377(100), 388, 389
 Zazyczny, J. 703(79), 738
 Zehnder, M. 368(82), 389
 Zeidler, L. 470(5), 486
 Zeigler, J. M. 542(19), 547(19, 31, 33), 548(19), 561, 562, 703, 716, 717(68), 738, 746(15), 798
 Zeitler, V. A. 722(210), 741
 Zektzer, A. S. 257(160), 333
 Zeldin, M. 633(226), 640
 Zellers, E. T. 883(181), 944
 Zemlyanskij, N. N. 227(20), 330
 Zeng, F. 757(59), 799
 Zengerly, T. 483(108, 109), 488
 Zewail, A. H. 217(99), 221
 Zgierski, M. Z. 831(55), 849
 Zhang, C. H. 922(389), 928(389, 416), 948, 949
 Zhang, L. C. 907(303), 928(434), 947, 949
 Zhang, Q. 486(136), 489, 877(143), 943
 Zhang, R. B. 575(64), 636
 Zhang, S. 128(458), 132(458, 468a, 468b), 133(468a, 468b), 136(458, 468a, 468b), 162, 955, 956(31), 963, 990(65), 1025, 1026
 Zhang, W. 372(91, 92a, 92b), 389, 1050(134), 1058
 Zhang, X. 860(40), 941
 Zhang, Y. 11(59a), 149, 570(28), 635
 Zhang, Y.-H. 352(33), 388
 Zhang, Z. 845(145), 853
 Zhang, Z.-Y. 940(468), 950
 Zhao, J. H. 575(71), 636
 Zhao, M. 102, 104(377a), 159
 Zhao, Y. 128, 133(459a, 459c), 134(459c), 136(459a, 459c, 481), 137(481), 162, 1030(6a), 1055
 Zharov, I. 128(460), 136(460, 480), 162, 912(340), 947, 964, 1009–1011, 1018, 1019, 1022(68), 1026
 Zhdanov, A. A. 705(93), 706(96), 725(236, 240), 727(260), 730(273), 733(293), 738, 739, 742–744, 782(154), 802
 Zheng, J. 698(23), 712, 725(142), 731(23), 737, 740
 Zheng, J.-Y. 703(87), 738
 Zheng, L. X. 648(35b), 692
 Zheng, X. 38(174d), 152
 Zheng, Z. M. 838(103a), 851
 Zhinkin, D. Ya. 728(262), 743
 Zhou, H. 260(178), 292(280), 307(309, 314, 315), 334, 336, 337
 Zhou, L.-L. 747(23, 24), 798
 Zhou, X.-L. 837(88a), 850
 Zhou, Y. 810(42, 43), 811, 812(42), 813–815(42, 43), 819
 Zhu, T. 830(47b), 849
 Ziche, W. 430(10), 465, 912(331), 947, 952, 953, 963, 982, 988, 1003(12), 1025
 Zicmane, I. 325(407), 339
 Ziegler, C. 619(191), 639
 Ziegler, T. 11(57), 12(71), 13(84), 24(57, 138), 64, 66–69, 72, 73(268), 112(138), 128, 138, 139(57), 149–151, 155, 343(9), 387, 397(60), 425, 1007(139), 1027
 Zigler, S. 98(374), 158
 Zigler, S. S. 421(150, 152), 428
 Zilch, H. 898(229), 945
 Ziller, J. W. 701(53), 704(91), 705(92), 712(144), 715(92), 720(206, 207), 727(144), 729(91, 92), 730(53), 737, 738, 740, 741
 Zilm, K. W. 202(78), 221, 399(62–64), 400(64), 425
 Zimmer, H. 932(443), 950
 Zimmer, M. 438(49), 466
 Zimmerman, S. C. 757(59), 799
 Zimmermann, W. 710(135), 739
 Zink, R. 542(16), 561
 Zinnius, A. 434(36), 466
 Zipin, H. S. 402(77), 426
 Zon, G. 904(285), 946
 Zora, J. A. 702, 732(62), 738
 Zubieta, J. 572(33), 635
 Zuckerman, J. 31(158b), 152
 Zuckerman, J. J. 108(390b), 159
 Zummack, W. 64, 91, 95(258), 155, 1036(45), 1056
 Zunnack, W. 192(59), 220
 Zurmühlen, F. 513(70), 514, 516(75), 530(70), 537, 904(291, 292), 946
 Zwanenburg, B. 879(165), 944
 Zybilla, C. 484(122), 489
 Zyss, J. 575(83), 578(83, 120), 586(120), 632(221), 634(83, 120, 227), 637, 640

Subject Index

- Ab initio* calculations, for molecules containing Group 14 elements 12
- Absolute scale, in shielding theory 230
- Acetyl bromide, as brominating agent 481
- Acetyl chloride, as chlorinating agent 474, 475
- Acetylenes — *see* Silylacetylenes, Silyloxyacetylenes
- Acidity,
of carbinol groups 714
of silanol groups 714, 715
- Acrylates, reactions with silenes 985
- Acryloylsilanes, [3+4]annulations of 896, 897
- Activation parameters, for thermal isomerizations 872, 876
- Active coupling-pattern tilting (ACT) 312
- Acyl anion equivalents, reactions with carbonyls 932
- Acylpyrrolidines, synthesis of 879
- Acylsilane enolates, synthesis of 888, 889
- Acylsilanes — *see also* β -Hydroxyacylsilanes
enol silyl esters of 901
reactions of 898, 899
with lithium enolates 895, 896
with nucleophiles 888
with organometallics 891–894
with sulphur ylides 893
synthesis of 889
 α,β -unsaturated 901
- Acyl(trialkylsilyl)phosphides, in synthesis of phospho-ethenes/-ethynes 514
- Acyl(trialkylsilyl)phosphines, in synthesis of phosphoethenes 492, 493, 511
- Addition–elimination method 492, 493
- Addition–silatropy–elimination method 520
- Addition–silatropy method 492, 494, 514, 515
- ADRF experiments 256
- Aerogels 629
- Aldehydes, reactions with silenes 982
- Alkenes — *see also* Phosphaethenes, Silaethenes, Siloxyethenes, Silylalkenes
reactions with silenes 988–990
- Alkoxy silanes — *see also* Tetraalkoxy silanes
as coupling agents 702, 715
hydrolysis of 702–704
in silicone manufacture 703
in sol-gel processes 702, 703
reactions with hydrofluoric acid 480
- 3-Alkylamino-1-propenylsilanes, synthesis of 933
- Alkynyldisilanes, photolysis of 960, 961, 1003, 1004
- Alkynylsilanes — *see also*
Bis(phenylethynyl)silanes,
Bis(stannyethynyl)silanes
reactions of 883
4-Alkynyl-4-siloxy-2-cyclobutenones 926
- Allen electronegativity 7
- Allenes — *see also* Metallaallenes,
Phosphaallenes
heavy analogs of, theoretical studies of 87–91
synthesis of 368
- Allenylsilanes, [3+2]annulations of 877, 880
- Allred–Rochow electronegativity 7
- Allylation, radical 384–387
- Allylepoxy silanes, reactions of 939
- Allyloxysilanes, synthesis of 918
 π -Allylpalladium complexes 899, 900
- Allylsilanes — *see also* Allylepoxy silanes,
Allyloxysilanes
[3+2]annulations of 877–879
rearrangement of 905–908, 910
- Allyl silyl ethers — *see also* 3-Haloallyl silyl ethers
synthesis of 897
- ALTADENA 250, 252
- Aluminium chloride, as Lewis acid catalyst 475–477
- Aluminosiloxanes, structure of 733
- Amines — *see also* Silylamines
reactions with halosilanes 430, 431
- Aminoallyl anions, *N*-silylated 933, 934
- Aminophosphines — *see* Silylaminophosphines

- Aminosilanes — *see also* Silylamines
 geometry of 434
 synthesis of 430–433, 978, 979
 β -Aminosilanes, diazotization of 886
 Anchimeric assistance 707
 Animals, in studies of biosilica synthesis 806
 Anions,
 pentacoordinated 144–146
 tricoordinated 138–141
 Anisotropic organization, in xerogels 604–608
 Annulations, cyclopentane 878
 [2+1]Annulations, of
 1-(phenylseleno)-2-silylethenes 880, 881
 [3+2]Annulations,
 of acylsilanes 895, 896
 of allenylsilanes 877, 880
 of allylsilanes 877–879
 of propargylsilanes 877, 880
 regio-/stereo-selectivity of 877
 [3+4]Annulations, of acryloylsilanes 896,
 897
 Anomeric effect, in polysilanol 724
 Antenna effect 632
 Anthracenes — *see* 9,10-Dihydroanthracenes
 Aromaticity,
 of germabenzenes 103
 of silabenzenes 103, 104
 sigma 42
 Aromatic stabilization energies 102
 Aroylsilanes, reactions of,
 with coupling reagents 894, 895
 with lithium enolates 895–897
 with (trimethylsilyl)Grignard reagents 897
 ARPES (Angle-Resolved Photoemission
 Spectroscopy) 844
 ARRF experiments 256
 Arrhenius activation energies, negative 1023,
 1024
 Arrhenius parameters,
 for disilene isomerization 1006, 1007
 for reactions of disilenes,
 with alcohols 1018
 with phenols 1013, 1014
 for reactions of silenes,
 with acetic acid 977, 978
 with alcohols 974–976, 1002, 1003
 with alkoxy silanes 981
 with amines 979
 with carbonyls 983, 984
 for silene dimerization 958, 963
 for silene isomerization 954–956
 for solvent effects on silene reactivity 994,
 995
 Aryldisilanol, formation of 703
 C-Arylglucals, hydroboration of 928, 929
 Aryl group transfer, silicon-to-carbon 350, 351
 Arylsilanetriols, formation of 703
 Atomic radii, of Group 14 elements 7
 Atoms-in-molecules procedure 14
 Azadiphosphiridines, synthesis of 511
 Azadisilacyclopropanes, synthesis of 403, 404
 Azaphosphaallenes, synthesis of 503, 50, 528
 Azaphosphabenzenes, synthesis of 494, 516
 Azaphosphaboriridines, synthesis of 511
 Azaphosphenes, reactions of 511
 Azaphospholes — *see also*
 1,2,4-Diazaphospholes,
 1,2,4-Oxaazaphospholes, Triazaphospholes
 synthesis of 494
 Azetidinone enolates, 1,4-silyl migration in
 927
 Aziridines, synthesis of 902
 Azulenes, synthesis of 880
 Azulenylphosphaethenes, synthesis of 525
 Bader's topological analysis 906
 Baeyer–Villiger oxidation 883, 884
 Bandgaps,
 in poly(2,5-silole)s 651
 in silole–thiophene copolymers 662, 665,
 670
 Basis sets 13, 14
 Benkeser reaction 474, 584
 Bent bonds 42, 43
 Bent's rule 34
 Benzofurans, synthesis of 932
 Benzonitriles, reactions of 902
 Benzotropylium salts, reactions of 878
 Benzyl cations, reactions of 878
 Bicyclo[1.1.0]tetrasilanes, synthesis of 877
 BINEPTR 251
 Biosilicification 805–817
 control of polycondensation in 808–817
 environmentally benign routes to 806
 structure-directing catalysts for 806
 Bipyridyls — *see also*
 Bis(silyl)methyl-2,2'-bipyridyls
 adducts with silicon halides 483, 484
 Biradical intermediates, in reactions of
 silatrienes with dienes 990
 BIRD 259, 265, 266
 Ψ -BIRD HMQC 266, 303
 Ψ -BIRD HSQC 270, 271
 Bisiloles 652
 synthesis of 679
 Bis(phenylethynyl)silanes, in silole synthesis
 647, 648
 Bis(silacyclopropene)s, rearrangement of 870,
 871
N,N-Bis(silyl)aminophosphines, reactions of
 940
N,N-Bis(silyl)amino-1-propenylstannanes,
 reactions of 933
 α,β -Bissilylated enals, synthesis of 901
 α,β -Bissilylated enols, synthesis of 901
N,N-Bis(silyl)ethylenediamines 932, 933

- Bis(silyl)methyl-2,2'-bipyridyls, metallation of 940
- Bis(stanny lethynyl)silanes, in silole synthesis 647, 648
- Bis(trialkylsilyl)phosphides 513
in synthesis of multiply-bonded phosphorus compounds 509, 510
- Bis(trialkylsilyl)phosphines 510
in synthesis of multiply-bonded phosphorus compounds 496–508
- 1,4-Bis(trimethylsilyl)dihydronaphthalenes, reactions of 481, 482
- Bis(trimethylsilyl)(triphenylsilyl)phosphine, structure of 496
- Boltzmann distribution 545
- Bond order method 73
- Boranes — *see* Dichloroboranes, Iminoboranes, Metallaboranes
- Borasiloxanes 718
- Boratanes — *see* Diphosphadiboratanes
- Bromosilanes 480
hydrolysis of 701, 702
physical properties of 482
synthesis of 481, 482
- Brook rearrangement 866, 897–900
aza- 902
cyclizations involving 895–897
in synthesis,
of 4-siloxy-1,2,3-pentatrienes 891, 893
of silyl enol ethers 887–894
radical 869, 870, 903
reverse 866, 867, 900, 901
- 1,4-Brook rearrangement 916–921, 923
retro- 925
- 1,5-Brook rearrangement, retro- 923, 924
- 1,6-Brook rearrangement 939
- Brook silenes,
dimerization of 963
reactions with dienes 990
- Buckminsterfullerenes, radical reactions of 352–355
- Butadienes — *see* 1,3-Butadienes,
Cyclobutadienes, 1,4-Dihalobutadienes,
Dilithiobutadienes, 1-Disilanylbutadienes,
Metallabutadienes, Phosphabuta-1,3-dienes,
Siloxybutadienes
1,3-Butadienes,
heavy analogs of, theoretical studies of 82–87
reactions with silenes 988, 989
- Butadienyl silyl ethers, synthesis of 935
- t*-Butylphosphaketene, synthesis of 501, 502
- Butyrolactones, synthesis of 882
- Cage compounds 573, 574
- Calas–Dunogues reaction 583, 584
- Carbanions,
3-siloxy 919
 γ -siloxy, rearrangement of 922–926
silyl-substituted, reactions of 919
- Carbenes — *see also* α -Ketocarbenes,
Metallavinylidenecarbene,
Silylmethylcarbene
as intermediates in reaction of silenes with oxygen 992
rearrangement of 858, 859
- Carbon π -systems, Si-substituted 178–180
- Carbosilane dendrimers 709, 747–771
alcohol-terminated 762, 764
alkoxy-terminated 761, 762
attachment of transition metals to 767–771
characterization of 750, 752, 755–757
functionalization of,
core 757, 759, 760
exterior 760–771
hydroxy-terminated 762, 763
mesogen-terminated 765
NMR spectra of 752, 755
perfluorohexyl-terminated 762, 764
SiH-terminated 760
silanol-terminated 761
synthesis of 747–755
- Carbosilanes, synthesis of 471
- Carbosilazane dendrimers 776, 779
- Carbosiloxane dendrimers 771–778
allyloxy-terminated 774
attachment of transition metals to 774, 776
double-layered 774, 775
- Carr–Purcell–Meiboom–Gill (CPMG) train,
for measurement of spin–spin relaxation times 314
- Catalysts,
for asymmetric reduction 616
for biosilicification 806
for cross-coupling reactions 654, 655
for dehydrogenative coupling 679
for disproportionation reactions 478
for hydrogenation 479
for oxidative coupling 670
for 1,2-silyl migrations 865
heterogeneous 614
Lewis acid 475–477
xerogels as 614–619
- Catechols 808
- Cations,
pentacoordinated 141, 142
tricoordinated 128–138
- C–C bond formation,
intermolecular 370, 371
intramolecular 371–380
- Chalcogenatetrasilacyclopentenes,
electron spectra of 419
molecular structure of 419
synthesis of 418, 419

- Charge-shift bonds 24
- Chlorohydrogendisilanes, synthesis of 476
- Chlorophosphines, synthesis of 510, 511
- Chlorosilanes — *see also* Ethylchlorosilanes, Methylchlorosilanes, Phenylchlorosilanes, Triorganochlorosilanes
 hydrogenation of 479
 hydrolysis of 697–701
 acid 713
- (Chlorosilyl)phosphines, reactions of 531, 533
- Chloro(trimethylsilyl)phosphines, reactions of 511
- Cloning vectors 815
- Cog wheel dynamics 185
- COLOC 261, 311
- Condensation–silatropy–elimination method 495
- Condensation–silatropy method 492, 494, 495, 530
- Configuration, in 1,3-silyl migrations,
 inversion of 905, 906
 of transition states 906
 retention of 906, 907
- Configuration interaction (CI) method 12
- Conjugation,
 sigma, in polysilanes 542, 547, 548
 σ – π 858, 881, 882
syn-periplanar 882
 σ^* – π^*
 in 2,5-diarylmatalloles 662
 in dithienosiloles 673
 in poly(1,1-silole)s 675, 676
 in silole 642
- Cope rearrangement, oxy- 896
- Copolypeptides 814, 816
 biomimetic 816
- COSY 258
 ^1H – ^{29}Si 259
- Cotton effect 545, 546
- Coupled-cluster (CC) method 12
- Coupling agents 702, 715
- Coupling constants,
 determination of 311–314
 ^{29}Si – ^{29}Si 283–295
 in disilanes 284, 286
 in oligosilanes 288, 289
 in tetrasilanes 288, 289
 in trisilanes 286, 287
 long-range 293
- β -Cristobalite 719
- Cross-coupling reactions, palladium-catalysed 654, 655
- Crossover experiments 889
- Cross-polarization experiments 241
 AJCP 256
 JCP 255–257
 refocussed 256
- Crotonoylsilanes, reactions of 895
- Crotylsilanes, synthesis of 924
- Crown ethers, as hybrid precursors 584, 586, 614
- Crystal packing forces, in polysilanes 543
- Cubanes — *see* Metallacubanes
- 2-Cyanohepta-2,4-dienoates, pyrolysis of 936
- Cyanohydrins — *see* Silacyanohydrins
- α -Cyanosorbate 936
- Cyclams 586, 614
- Cyclization,
 intramolecular 881, 882
 involving Brook rearrangement 895–897
 radical 903
- [2+1]Cycloaddition reactions, of disilenes 403
- [2+2]Cycloaddition reactions,
 of disilenes 402, 405–410, 1022
 of silenes,
 with alkenes and dienes 988–990
 with carbonyls 982–987
- [2+3]Cycloaddition reactions, of disilenes 403, 409, 410
- [2+4]Cycloaddition reactions,
 of disilenes 405, 406, 409
 with dienes 402, 407, 1019, 1021
 of silenes, with dienes 988–990
- Cyclobutadienes — *see* Silacyclobutadienes
- Cyclobutanes — *see also*
 Metallabicyclobutanes, Silacyclobutanes
 synthesis of 919
- Cyclobutenediones, reactions of 883
- Cyclobutenes — *see* Diphosphacyclobutenes, Silacyclobutenes
- Cyclobutenones — *see*
 4-Alkynyl-4-siloxy-2-cyclobutenones
- Cyclodisilanes,
 geometrical parameters of 445–447
 reactions of 447–449
 structure of 728
 synthesis of 436, 445
- Cyclodisiloxanes, synthesis of 411, 412, 1019, 1020
- Cyclohexadienes — *see*
 Silaoxacyclohexadienes
- Cyclohexanes — *see*
 Tetraphosphabicyclo[2.2.0]hexanes
- Cyclohexanones — *see* β -Silylcyclohexanones
- Cyclohexasilanes — *see also*
 Dichlorodecamethylcyclohexasilanes,
 Dodecamethylcyclohexasilane
 ring contraction of 864
- Cyclohexasilane skeleton, synthesis of 476
- Cyclohexasiloxanes, structure of 727
- Cyclohexenes,
 epoxidation of 615
 reactions with silenes 989
- Cyclohexenones — *see* Siloxycyclohexenones

- Cyclopentadienes — *see* Dicyclopentadiene,
Silacyclopentadienes,
5-Silylcyclopentadienes,
Titanacyclopentadienes,
Zirconacyclopentadienes
- Cyclopentadienones, synthesis of 926
- Cyclopentadienyl anions — *see*
Metallacyclopentadienyl anions
- Cyclopentanes — *see also*
Methylenecyclopentanes, Silacyclopentanes,
Siloxycyclopentanes
formation of 877
- Cyclopentanols, synthesis of 920
- Cyclopentanones, reactions with silenes 985
- Cyclopentenes — *see also* Silacyclopentenes
synthesis of 880
- Cyclopentenols, synthesis of 896
- Cyclopropanes — *see also* Silacyclopropanes
formation of 880
- Cyclopropenes — *see* Metallacyclopropenes
- Cyclopropenium cations — *see*
Metallacyclopropenium cations
- Cyclopropylsilanes, synthesis of 928
- Cyclosilanes — *see* Perchlorocyclosilanes
- Cyclosilatetrazenes, synthesis of 432
- Cyclosilazanes,
as precursors for silicon-based ceramics
464, 465
cage 463, 464
interconversions of 444, 453–457, 460–463
synthesis of 442, 443
- Cyclotetrasilazanes,
reactions of 458–460
synthesis of 458
- Cyclotetrasilenes,
electron spectra of 419, 420
molecular structure of 419
reactions of 420, 421
synthesis of 417, 418
- Cyclotetrasiloxanes 874 — *see also*
Octamethylcyclotetrasiloxanes
- Cyclotrisilazanes,
reactions of 450–452
synthesis of 449
- Cyclotrisilenes — *see also*
1-Tris(trialkylsilyl)cyclotrisilenes
electron spectra of 419, 420
molecular structure of 419
reactions of 420
synthesis of 418
- DANTE 304
- Deaminosilylation 886
- Debenzoylation 935
- Decamethyl-7-oxa-hexasilanorbornane 476
- Decarboxylation 936
- Dehalogenation 364–366
- Dehydrogenation 709
- Dehydrogenative coupling, metal-catalysed
679
- Dendrimers 578, 614, 634
silicon-based 746–784
carbosilane 709, 747–771
carbosilazane 776, 779
carbosiloxane 771–778
silane 779–783
siloxane 782–784
structure of 730
- Density functional theory (DFT) 12
- 6-Deoxy-6,6,6-trifluorosugars, synthesis of
930, 931
- DEPT 241, 245, 246, 253, 261, 320
- DEPT–INADEQUATE 277
- Desilylation 884 — *see also* Halodesilylation,
Protodesilylation
- Destannylation 884
- Deuterium labelling studies, of 1,4-silyl
migrations 914, 915
- Dewar-benzenes — *see*
Metalla-Dewar-benzenes
- Dewar–Chatt–Duncanson model 405
- Diaminodisilyldisilenes 67
- Diaminophosphaethenes, synthesis of 504,
505
- 1,1-Diaminosiloles 647, 648
- Diarylsilanediods, formation of 697
- 2,5-Diarylsiloles,
as emissive materials 688, 689
effects of 2,5-aryl groups on 654, 657–660
effects of 1,1-substituents on 661, 662
effects of 3,4-substituents on 657, 661
synthesis of 654–656
- Diastereoselectivity, in 1,4-silyl migrations 916
- Diatoms, in studies of biosilica synthesis
806–810
- 1,2,4-Diazaphospholes, synthesis of 516
- Diazoacetates, hydrolysis of 709
- Diazomethanes — *see* α -Silyldiazomethanes
- Diazomethyne ylides, formation of 902, 903
- Dibenzocycloheptylidene phosphine,
synthesis of 526, 527
- 2,5-Dibromosiloles, coupling reactions of 683
- Dichloroboranes, reactions of 533
- Dichlorodecamethylcyclohexasilanes 476
- α,ω -Dichlorooligosilanes, hydrolysis of 700
- α,ω -Dichloropermethylogosilanes 477, 478
- 1,1-Dichloro-1-silacyclopentane 483
- 1,1-Dichlorosiloles, reduction of 676, 677
- Dichlorotetramethyldisilanes,
disproportionation of 478
- Dicyclopentadiene, hydrosilylation of 698
- Dieckman reaction 935
- Diels–Alder reactions 831
of disilenes 1019, 1021
of silenes 982, 988–990

- Dienes — *see also* Butadienes, Hexadienes, Pentadienes, 1,3-Tetrasiladienes
cycloaddition reactions of,
 with disilenes 402, 407, 1019, 1021
 with silenes 982, 988–990
ene reactions of 988, 989
- Dienol ethers, synthesis of 886
- Differential scanning calorimetry 547
- Diffusional effects, on silene reactivity 1002
- Difluorodigermene 100, 101
- Difluorodisilyne 98
- Difluorosilylidene 98
- Digermabutadienes, structural/conformational aspects of 83–85
- 1,4-Dihalobutadienes, in silole synthesis 645, 646
- 9,10-Dihydroanthracenes, lithiation of 914
- Dihydrofurans, synthesis of 880
- Dihydronaphthalenes — *see*
 1,4-Bis(trimethylsilyl)dihydronaphthalenes
- Dihydrophosphonin 937
- α,ω -Dihydroxyoligosilanes, formation of 700
- α,β -Dihydroxysilanes, reactions of 887
- 2,5-Diiodosiloles, in poly(2,5-silole) synthesis 652, 653
- Dilithiobutadienes, in silole synthesis 645, 646
- 1,1-Dilithiosiloles, synthesis of 679
- 2,5-Dilithiosiloles 647, 648
- 1,1-Dimesityl(2,2-dixylyl)disilenes,
 rearrangement of 858
- Dimetaletanes — *see*
 1,3-Dioxa-2,4-dimetaletanes
- Dimetallabutadienes, structural/conformational aspects of 83–85
- Dimetallacyclobutenes 86
- p-N,N*-Dimethylaminopyridine, as nucleophile 483
- 1,1-(Dimethylsilyl)(trimethylsilyl)ketene,
 decomposition of 862
- Diols — *see also* Silanediols, Siloxanediols
 monosilylated, reactions of 928
- α,ω -Diols, synthesis of 705
- 1,3-Dioxa-2,4-dimetaletanes 50, 51
- Dioxiranes, reactions of 707, 708
- Diphenylketene, reactions of 504, 505
- 1,1-Diphenylsilenes,
 dimerization of 963
 reactions of, rate constants for 959, 960,
 972–981, 983, 984, 986, 989
- Diphosphaallenes, synthesis of 520, 528, 529
- 1,3-Diphosphabuta-1,3-dienes,
 as reaction intermediates 501
 synthesis of 495, 497, 501
- 1,4-Diphosphabuta-1,3-dienes, as reaction intermediates 500
- 2,3-Diphosphabuta-1,3-dienes, synthesis of 495, 500, 501
- 1,3-Diphosphacyclobutenes, synthesis of 501, 502
- 3,4-Diphosphacyclobutenes, synthesis of 500
- Diphosphadiboratanes 533
- 1,3-Diphospha-2-silaallylic lithium 531, 533
- Diphosphenes 494
 synthesis of 492, 496, 499, 522, 523,
 530–532
 transition metal-substituted, synthesis of
 507, 508
- 1,3-Diphosphetanes, synthesis of 501,
 503–505
- Diphosphiridines — *see* Azadiphosphiridines
- DIPSI-2 257
- 2,5-Di(2-pyridyl)siloles, as ET materials 687,
 688
- 2,5-Dipyrrolylsiloles,
 synthesis of 654, 670
 X-ray structure of 672
- Dirac equation 13
- Dirac–Hartree–Fock (DHF) codes 13
- Discotic liquid crystalline phase, in silanediols 731
- Disilabenzenes, aromaticity of 104
- Disilabenzvalenes, synthesis of 870, 871
- Disilabutadienes, structural/conformational aspects of 83–85
- 1,3-Disilacyclobutadienes 95
- 1,2-Disilacyclobutanes, photolysis of 1009
- Disilacyclopentenes — *see*
 Methylenedisilacyclopentene
- Disilacyclopropanes 404 — *see also*
 Azadisilacyclopropanes
- 1,2-Disiladodecaboranes, PE spectra of
 195–197
- Disilanes — *see also* Alkynyldisilanes,
 Chlorohydrogendisilanes,
 Hexachlorodisilanes,
 Hexakis(trimethylsilyl)disilane,
 Hexamethyldisilane, Hydrodisilanes,
 Methylchlorodisilanes, Phenylidisilanes,
 Vinylidisilanes
 NMR coupling constants for 284, 286
 PE spectra of 172, 173
- Disilanol — *see also* Aryldisilanol
 formation of 707, 711
 hydrogen bonding in 729
- 1-Disilanylbutadienes, pyrolysis of 938
- Disilanylene copolymers 683
- Disilanyl ketones, rearrangement of 913
- Disilaoxiranes 403, 412
- Disilapentalenes 674
- Disilavinylidene anion 96
- Disilazanes — *see* Cyclodisilazanes
- Disilenes — *see also* Diaminodisilyldisilenes,
 1,1-Dimesityl(2,2-dixylyl)disilenes,
 Tetraaryldisilenes,

- Tetrakis(trialkylsilyl)disilenes,
Tetramesityldisilene, Tetrasilyldisilenes
1,2-addition reactions of 401, 402
 with alcohols 1008–1013, 1016–1018
 with phenols 1008, 1013–1016
bimolecular reactions of, kinetics of
 1008–1022
cycloaddition reactions of 401–410
 [2+1] 402–405
 [2+2] 402, 405–410, 1022
 [2+3] 403, 409, 410
 [2+4] 402, 405–407, 409, 1008, 1019,
 1021
 with acid chlorides 1022
 with aldehydes 1022
 with dienes 1008, 1019–1021
 with esters 1022
 with ketones 1008, 1019, 1022
electron spectra of 399
isomerization of 1006, 1007
molecular structure of 396–398
NMR spectra of 1006
 solid-state 399, 400
oxidation of,
 with atmospheric oxygen 411, 412, 1008,
 1019, 1020
 with epoxides 412, 413
 with white phosphorus 413
 with yellow arsenic 414
pyramidalization at Si 396–398
rearrangement of 858, 871, 874–876
stabilizing effect of trialkylsilyl substituents
 on 1011
synthesis of 392–396, 492
 by dimerization of silylenes 394
 by photolysis of cyclotrisilanes 393, 400,
 401
 by photolysis of siliranes 392, 393
 by photolysis of trisilanes 392, 393
 by reduction of 1,2-dihalodisilanes 396
 $\pi-\pi^*$ transitions in 83
unimolecular reactions of, kinetics of
 1006–1008
Disilylenidenes 875
Disilicic acid 724
Disiloxanediols 711, 712
 formation of 698
Disiloxanes — *see also* Cyclodisiloxanes,
 Hexamethyldisiloxanes,
 Tetrahydroxydisiloxanes
 formation of 699, 701
 structure of 724–726
Disiloxanyl ϕ -uridines, cyclic 940
Disiloxetanes, synthesis of 1022
3,4-Disilyl-5-hydroxypentanoic acids, reactions
 of 882
Disilylmethanes, synthesis of 471
Disilylphosphides, in synthesis of
 multiply-bonded phosphorus compounds
 509, 510
Disilylphosphines — *see also*
 Disilyl(2,4,6-tri-*t*-butylphenyl)phosphines
 in synthesis of multiply-bonded phosphorus
 compounds 496–508
 transition metal-substituted, in synthesis of
 phosphaethenes 507
2,5-Disilylsiloles,
 effects of 1,1-substituents on 661, 662
 in poly(2,5-silole) synthesis 652, 653
Disilyl(2,4,6-tri-*t*-butylphenyl)phosphines, in
 synthesis of multiply-bonded phosphorus
 compounds 519–522
Disilynes 93, 94 — *see also* Difluorodisilyne
 rearrangement of 875
 structure of 421–423
 transient species 421–423
Disproportionation reactions 478
Dissolution/reprecipitation 625
Distannanes 26, 27
2,5-Distannyl-3-borylsiloles, synthesis of 647,
 648
Dithienosiloles,
 in organic EL devices 690
 synthesis of 673, 674
Dithienosilole–thiophene copolymers 673, 674
2,5-Dithienylmetallobes, effects of Group 14
 metals on 661–663
2,5-Dithienylsiloles 662, 670
 effects of 3,4-substituents on 657, 661
 synthesis of 647
 X-ray structure of 672
Dithioxophosphoranes, synthesis of 519
Divalent state stabilization energy (DSSE) 17
DNA, role in biosilicification 806, 807, 815
Dodecahedranes — *see* Metalladodecahedranes
Dodecamethylcyclohexasilane, stepwise
 cleavage of Si–Si bonds in 477
DOSY 257, 321–323
Double-INEPT constant-time phase-sensitive
 sequence 269
DQF COSY 255, 258, 282, 283, 303

EELS (Electron Energy Loss Spectroscopy)
 834, 844
Effective core potentials 13, 14
Electrical conductivity,
 of dithienosilole–thiophene copolymers 673
 of polysilanes 559–561
 of silole-containing polymers 683, 685
 of silole–thiophene copolymers 662, 665
Electrochromism, in polysilanes 558, 559
Electroluminescent (EL) devices 633, 686, 687
Electron affinities, of Group 14 elements 7

- Electronegativities 7
 and bonding 11
 correlation with coupling constants 285, 291
- Electron localization functions (ELF) 73
- Electron proton resonance (EPR) spectroscopy, of silyl radicals 344–348
- Electron-transporting (ET) materials 687
- Electrophilic substitution reactions, of silanes 477
- Elimination reactions, E2-type, in hydrolysis of Si–C bonds 710
- anti*-Elimination reactions 887
- 1,4-Elimination reactions 891, 893
- β -Elimination reactions, desilylative 889
- Enals, α,β -bissilylated 901
- Enantiomerization 924
- Ene reactions, of silenes,
 with alkenes and dienes 988–990
 with carbonyls 982–987
- Enolates, zwitterionic 880, 881
- Enols, α,β -bissilylated 901
- Epimerization 924, 927
- Epoxyxilanes — *see also* Allylepoxyxilanes, Phenylepoxyxilanes, Vinylepoxyxilanes
 reactions of 897
 synthesis of 928
- ESDIAD (Electron Stimulated Desorption Ion Angular Distributions) 834,844,845
- Ethylchlorosilanes 472
- Ethylenediamines — *see*
N,N-Bis(silyl)ethylenediamines,
 Tetramethylethylenediamines
- Felkin–Anh mode 888
- Fischer carbene complexes 886
- Flow tube techniques 1030
- Fluorenylidene phosphine, synthesis of 526, 527
- Fluorescence spectroscopy, of
 2,5-diarylmatalloles 657, 658, 661, 663
- Fluorosilanes — *see also* Organofluorosilanes
 hydrolysis of 697
- Fluorosilicates 480
- Force constants, correlation with coupling constants 292
- Formylmethylsilane, rearrangement of 906, 908, 910
- Frustules 806
- Frustulins 808
- Fulvenes — *see* Phosphatrafulvenes,
 4-Silatrafulvenes
- Furans — *see also* Benzofurans,
 Dihydrofurans, 2-Silylfurans,
 Tetrahydrofurans
 synthesis of 879, 920, 921
- Furoic acids — *see* 2-Silyl-3-furoic acids
- Genetic engineering 814, 815
- Geometrical imprint domain 311
 1-Germaallenes 87, 89
- Germabenzenes — *see* Hexagermabenzene
- Germabutadienes — *see also*
 Digermabutadienes, Tetragermabutadienes
 theoretical aspects of 82–87
- Germenes — *see* Phosphagermenes
- Germiranes 43, 44
- Germirenes — *see* Persilyl-1-disilagermirenes
- Germoles, synthesis of 679, 682
- Germylenes 110
- Germylsilanes, synthesis of 474
- Glucals — *see* C-Arylglucals
- Grignard reagents, reactions of 583, 584
 with SiF₄ 479, 480
- Gyromagnetic ratios 225
- HaHa match 256
- 3-Haloallyl silyl ethers 922
- Halodesilylation 652, 653
- Halogen abstraction reactions 352
- Halogen–lithium exchange reactions 645
- α -Halomethylsilanes, synthesis of 928
- Halosilanes — *see also* Bromosilanes,
 Chlorosilanes, Fluorosilanes, Iodosilanes,
 Trihalosilanes
 hydrolysis of 697–702, 713
 Lewis base adducts of 482–486
 reactions with amines 430, 431
 synthesis of 470–482
- Hammert plots,
 for addition of acetic acid to silenes 977
 for addition of alkoxyxilanes to silenes 980, 982
 for addition of phenols to disilenes 1014, 1015
- Hammert ρ values, for addition of alcohols to silenes 973, 974
- Hartmann–Hahn condition 241
- Hartree–Fock (HF) method 12
- Heck reaction 585, 586, 588
- HEED 303, 307–311
- HEED-DEPT 307
- HEED filter 260
- HEED-HETCOR 307–309
- HEED-INEPT 307, 308
- HETCOR 259, 298–300
- Heterophosphabenzenes, synthesis of 494
- Heterophospholes, synthesis of 494
- Hexachlorodisilane, Lewis base adducts of 484
- Hexacoordinated compounds, theoretical aspects of 36, 38
- Hexadienes — *see also*
 Tetraphosphahexadienes
 reactions with silenes 988, 989
- Hexadienoates — *see*
 2-Cyanohepta-2,4-dienoates

- 1,1,1,3,3,3-Hexafluoroisopropanol, reactions with silenes 976
- Hexagermabenzene, aromaticity of 103
- Hexakis(trimethylsilyl)disilane, PE spectrum of 199, 200
- Hexaleadprismane 104
- Hexamethyldisilane, as secondary reference in ^{29}Si NMR 228
- Hexamethyldisiloxane, as secondary reference in ^{29}Si NMR 228 reactions of 481
- Hexanols — *see* 1-Silylhexanols
- Hexasilabenzene, aromaticity of 103, 104
- Hexasilanes — *see* Cyclohexasilanes
- Hexasiloxanes — *see* Cyclohexasiloxanes
- Hexatrienes — *see* (1-Sila)hexatrienes
- Hexenes — *see also* Cyclohexenes hydroformylation of 619
- HMBC 267, 268
- HMPA, as nucleophile 483
- HMPT, as catalyst for disproportionation reactions 478
- HMQC 261–268, 298–300
- ge-HMQC 267
- Homolytic substitution, at carbon 352 at halogen 356 at silicon 351
- HREELS (High Resolution Electron Energy Loss Spectroscopy) 827, 838, 839
- HSQC 268, 298–300
- $^1\text{H-X}$ COSY 259
- Hybridization 9–11
- Hybrid precursors 570, 572–589
- Hydrazines, lithium derivatives of 439, 440
- Hydroboration, of *C*-arylglucals 928, 929
- Hydrodisilanes, in silole synthesis 645, 647
- Hydrofluoric acid, as fluorinating agent 480
- Hydrogen abstraction reactions 357–360, 362–364
- Hydrogen bonding, in disilanols 729 in oligosilanedioles 727, 728 in silanetriols 700, 734–736 in siloxanes 725–727 in tetrahydroxydisiloxanes 733 in tetrasilanols 729, 730
- Hydrogen bromide, as brominating agent 481
- Hydrolases 810, 811
- Hydrophobicity/hydrophilicity, of xerogel surfaces 600, 602, 623
- Hydrosilanes, hydrolysis of 709
- Hydrosilylation 368, 369, 474 in synthesis of hyperbranched poly(carbosilane)s 787–793 in synthesis of hyperbranched poly(carbosiloxane)s 791, 794, 795
- Hydrosilylation/methanolysis reaction 578
- β -Hydroxyacylsilanes, synthesis of 901
- α -Hydroxyalkylsilanes, synthesis of 900, 901
- Hydroxysilanes, desilylation of 897
- Hydroxysilylalkenes, reactions of 881
- Hydroxysilylenes 874
- Hyperbranched polymers, silicon-based 784–797 poly(carbosilane)s 785–793 poly(carbosilazane)s 796 poly(carbosiloxane)s 791, 794–796 poly(siloxane)s 797
- Hyperconjugation 858, 862 negative 857
- Hypercoordinate compounds 24 as intermediates 906
- ICR (Ion Cyclotron Resonance) spectrometry 1030
- Imidazoles — *see* *N*-Methylimidazole
- Imidazole-silylene, PE spectrum of 202, 203
- Imines — *see* *N*-(Silylmethyl)imines
- Iminoboranes, reactions of 511
- Iminophosphines — *see* Siloxyiminophosphines
- Iminosilanes 440 reactions of 441, 442
- Iminylolithiums, formation of 902, 903
- INADEQUATE 255, 258, 273–282, 311 heteronuclear 297 *J*-resolved 275
- INADEQUATE CR 280
- Indirect detection probe 261
- INDOR 261
- INEPT 241, 245–248, 250–255, 268, 269, 303–311, 316, 320, 323, 324
- INEPT DQF COSY 282
- INEPT+HE 307
- INEPT–HMQC 300
- INEPT–INADEQUATE 274, 277, 279
- Inert s-pair effect 10
- Infrared spectroscopy, of disilanols 727, 728 of silanols 715
- INSIPID 278
- Iodosilanes 480–482 hydrolysis of 702
- Iodotrimethylsilanes, synthesis of 481
- Ionic radii, of Group 14 elements 7
- Ionization energies, of Group 14 elements 7
- Ionization potentials, of polysilanes 559
- Ionochromism, in polysilanes 556–558
- Ion structures, of silicon cations 1043–1045
- Ion trap techniques 1030
- Isomerization, geometric, of silenes 953 silene–silylene 954, 955 thermal *E,Z*, of disilenes 1006–1008

- Isophosphaethyne complexes 522
Isoprene, reactions with silenes 988, 989
Isotopic substitution 258
Isotropic organization, in xerogels 604–607
Isoxazoles, synthesis of 880
 ²-Isoxazolines, synthesis of 879
- JR-INEPT 305
- Ketenes — *see*
 1,1-(Dimethylsilyl)(trimethylsilyl)ketene,
 Diphenylketene, Phosphaketenes,
 (2-Siloxyalkynenyl)ketenes, Silylketenes,
 Thioketenes
- α -Ketocarbenes 862
- Ketones,
 heavy analogs of, theoretical studies of
 79–82
 reactions with silenes 982–987
- β -Ketosilanes, rearrangement of 905, 908,
 909
- Kinetic isotope effects, deuterium,
 for reactions of disilenes with phenols 1013,
 1014
 for reactions of silenes with acetic acid
 978
 for reactions of silenes with alcohols 972
 for reactions of silenes with carbonyls 983
- Kinetic stabilization 491
- Kira mechanism, for addition of alcohols to
 transient silenes 969, 970
- KMC (Kinetic Monte Carlo) simulations 841,
 842, 844
- Lactols, silylated, reduction of 928, 929
- Lactones — *see also* Butyrolactones
 synthesis of 883, 884
- Langmuir–Blodgett films 558
- Laser flash photolysis 952, 953
- LC NMR 324
- LEED (Low Energy Electron Diffraction) 825,
 827, 845
- Lewis base adducts, of silicon halides
 482–486
- Ligands,
 distribution of 864
 redistribution of 857
- Lithium aluminium hydride, as hydrogenating
 agent 479
- Lithium carbenoids 913
- Lithium fluoride, as fluorinating agent 480
- Lithium silylamides 434, 435
- Lysine amino acids, in studies of biosilica
 synthesis 809, 810
- Macrocyclization 379
- Magnetic susceptibility 227, 229
- MALDI-TOF mass spectrometry 652
 of carbosilane dendrimers 756
- Marine organisms, in studies of biosilica
 synthesis 806, 807
- Martin ligand 910
- Matrices, micropolarity of 570, 572
- MCM (Mobile Composition of Matter) 572,
 573, 620, 629, 631
- McMurray coupling 894
- Mesoporosity 595, 596
- Mesoporous hybrids 629, 631
- Mesoporous materials 573, 574
- Metallaallenes — *see also* 1-Germaallenes,
 1-Silaallenes
 theoretical aspects of 87–91
- Metallaallyl cations 135
- Metalla-aromatic compounds 101–109
- Metallabenzenes — *see also* Germabenzenes,
 Silabenzenes
 theoretical aspects of 101–105
- Metallabenzvalenes 104 — *see also*
 Silabenzvalenes
- Metallabicyclobutanes 87
- Metallaboranes 62, 63 — *see also*
 1,2-Disiladodecaboranes
- Metallabutadienes — *see also*
 Germabutadienes, Silabutadienes
 theoretical aspects of 82–87
- Metallacubanes, structural aspects of 58–60,
 62
- Metallacyclobutanes — *see*
 Tetrasilabicyclo[1.1.0]butanes
- Metallacyclopentadienyl anions 106–108
- Metallacyclopropenes 127 — *see also*
 3-Silacyclopropenes
- Metallacyclopropenium cations 105, 106
- Metalla-Dewar-benzenes 104
- Metalladiyls 110
- Metalladodecahedranes, structural aspects of
 58, 59
- Metallanes — *see also* Germanes, Silanes,
 Stannanes
 bond dissociation energies 16, 17
 of monosubstituted 21–24, 26, 27
 of multiply-substituted 30, 31
 charged species 19, 20
 cyclic 38–63
 bicyclic 52–54
 monocyclic 38–51
 polycyclic 52–57
 polyhedral compounds 58–63
 ethane analogs 24–27
 bridged structures of 27
 geometries 14, 15
 of monosubstituted 23–26
 of multiply-substituted 28–32, 35, 36
 hypercoordinated systems 36–38
 ionization potentials 14, 15

- monosubstituted 20–28
- multiply-substituted 28–36
- nuclear spin–spin couplings 14–16
- rotational barriers, of monosubstituted
 - 24–26
- stability 17–19
 - of multiply-substituted 32–35
- Metallapagodanes 58
- Metallaprismanes — *see also*
 - Hexaleadprismane
 - stability of 104
 - structural aspects of 58–60, 62
- [1.1.1]Metallapropellanes — *see also*
 - Pentastanna[1.1.1]propellane
 - structural aspects of 54–57
- Metallasiloxanes 717
- NMR spectra of 724
 - synthesis of 722–724
- Metallasilsesquioxanes 720
- Metallatetrahedranes — *see also*
 - Silatetrahedranes
 - structural aspects of 58–62
- Metallavinylidene carbene 94, 95
- Metallenes 63–78 — *see also* Germenes, Silenes, Stannenes
 - double-bond strength in 69–73
 - isomers of 74–78
 - stability of,
 - relative to bridged isomers 75–78
 - relative to metallylenes 74, 75
 - structure of 64–69
- Metalliranes — *see also* Germiranes, Plumbiranes
 - theoretical aspects of 43, 44
- Metalloenes 108, 109
- Metalloles — *see also* 2,5-Dithienylmetalloles, Germales, Siloles
 - theoretical aspects of 46–48
- Metallophosphasilenes, synthesis of 514
- Metallylenes 110–128 — *see also* Germylenes, Silylenes
 - as isomers of heavy ketones 80–82
 - as isomers of metallenes 74, 75
 - reactions of,
 - addition 124–128
 - 1,2-hydrogen shift 116–118
 - insertion 118–124
 - stable 113–116
- Metallynes — *see also* Silynes
 - bond nature of 91–94
 - potential energy surfaces for 94–101
 - structure of 91–94
- Methylchlorodisilanes 471 — *see also*
 - Dichlorotetramethyldisilanes,
 - Tetrachlorodimethyldisilanes
- Methylchlorooligosilanes, hydrogenation of 479
- Methylchlorosilanes 469 — *see also*
 - Trimethylchlorosilanes
 - disproportionation of 478
 - synthesis of 471
- Methylenecyclopentane, reactions with silenes 989
- Methylenedisilacyclopentene 860
- α -Methylenedisilacyclobutane, isomerization of 859, 860
- N*-Methylimidazole,
 - as catalyst,
 - for disproportionation reactions 478
 - for hydrogenation 479
 - as nucleophile 483
- 1,3-Methyl migration, in silenes 955
- Micellar packing 629
- Micelle formation 574
- Microalgae, in biosilicification 806
- Microporosity 595, 596, 623
- Migratory aptitudes 870
- MIR-FTIR (Multiple Internal Reflection Fourier Transform IR) spectroscopy 832
- Mitsunobu reaction 882
- MLEV-16/17 257
- MMB (Modulated Molecular Beam) studies 841
- Molecular imprinting 621, 622, 627
- Molecular modelling 817
- Molecular states, of silicon compounds 169–172
- Monosilylphosphaethenes, in synthesis of multiply-bonded phosphorus compounds 514–518
- Monosilylphosphines — *see also*
 - Monosilyl(2,4,6-tri-*t*-butylphenyl)phosphine
 - in synthesis of multiply-bonded phosphorus compounds 510, 511
- Monosilyl(2,4,6-tri-*t*-butylphenyl)phosphides, in synthesis of multiply-bonded phosphorus compounds 523–534
- Monosilyl(2,4,6-tri-*t*-butylphenyl)phosphine, in synthesis of multiply-bonded phosphorus compounds 522, 523
- Mono(trialkylsilyl)phosphides, in synthesis of multiply-bonded phosphorus compounds 511–514
- Mutagenesis 814, 815
- Nanocomposite hybrids 569–572
- Nanoparticles, formation of 619, 620
- Nanostructured hybrid materials 569, 572–578
- Nanotechnology 806
- Naphthalenes — *see* Dihydronephthalenes
- Natural bond order (NBO) analysis 14
- Network modifiers 619
- NEXAFS (Near-Edge X-ray Absorption Fine Structure) 832, 844
- Nitriles — *see* Benzonitriles

- Nitroxides, deoxygenation of 368
 NLO properties 632, 633
 NOESY 317
 Norbornadienes — *see*
 Phosphinidenenorbornadiene
 Nuclear magnetic resonance (NMR)
 spectroscopy,
¹³C 593, 594
 CP-MAS 593–595
 multinuclear one-dimensional, of
 carbosilane dendrimers 752, 755
 of disilenes 399, 400, 1006
 of hybrid xerogels 593–595
 of metallasiloxanes 724
 of silanols 697, 714, 715
²⁹Si — *see* ²⁹Si NMR
 Nuclear Overhauser effect (NOE) 316–319
 dynamic 315, 316
 Nucleophilic attack, intramolecular 868, 869
 Nucleophilic substitution reactions,
 in synthesis of hyperbranched
 poly(carbosilane)s 785–787
 intramolecular, at silicon 910
 Nucleus independent chemical shift (NICS)
 103
- Octachlorotrisilane, Lewis base adducts of 485
 Octamethylcyclotetrasiloxane, as secondary
 reference in ²⁹Si NMR 228
 Oligosaccharides, reactions with silicic acid
 808
 Oligosilanedioles, structure of 727, 728
 Oligosilanes — *see also*
 α,ω -Dichlorooligosilanes,
 α,ω -Dihydroxyoligosilanes,
 Methylchlorooligosilanes
 NMR coupling constants for 288, 289
 photochemistry of 349
 reactions of 474, 475
 Oligo(1,1-silole)s 676, 677
 Oligo(2,5-silole)s 651, 652
 Oligosiloxanes, formation of 697
 Oligosilsesquioxanes, structure of 729
 Optical nonlinearity, third-order, in
 poly(2,5-silole)s 651
 Orbital control, subjacent 906
 Orbital interactions 906
 in silole ring 642, 643
 subjacent 908, 910
 Orbitals, d, role of 11
 Orbital stabilization, secondary 878
 Organofluorosilanes, synthesis of 479, 480
 Organopolysilsesquioxanes,
 as hybrid precursors 575–578
 synthesis of 578–589
 nanostructured 593–602
 anisotropic organization in 604–608
 as precursors for porous materials
 620–628
 chemical stability of 609
 interactivity between chemical groups in
 610, 611
 physical properties of 631–634
 reactivity–structure relationship of
 611–614
 shaping of 629–631
 short-range order in 602–604, 610, 611
 Organosilane radical cations, reactions of 1053
 Organosilicon cations, matrix isolation of
 199–201
 Organosilsesquioxanes 572–575
 ORMOCERs (organically modified ceramics)
 574
 ORMOSILs (organically modified silicates)
 574, 575
 1,2,4-Oxaazaphospholes, synthesis of 514, 515
 Oxasiletanes, reactions of 882
 Oxidative coupling, palladium-catalysed 670
 Oxiranes — *see* Disilaoxiranes
- Pagodanes — *see* Metallapagodanes
 PAMAMOS dendrimers 760
 PASADENA 245, 249, 252
 Pauling electronegativity 7
 PENDANT 245, 249, 255
 Pentacoordinated compounds, structure of 36,
 37
 Pentadienes — *see also* Cyclopentadienes,
 1-Sila-1,3-pentadienes
 reactions with silenes 988, 989
 Pentalenes — *see* Disilapentalenes
 Pentanals — *see* 5-Silylpentanal
 Pentastanna[1.1.1]propellane 54
 Peptides, structure-directing 814–816
 Perchlorocyclosilanes, synthesis of 475
 Pericyclic reactions 857
 Persilyl-1-disilagermirenes 877
 Peterson elimination 889, 898, 910–913
 aza- 902
 modified 913
 phospho- 512, 513, 525, 526
 sila- 912
 1,10-Phenanthroline, as Lewis base 484
 Phenylchlorosilanes, synthesis of 471
 Phenyldisilanes, photolysis of 960, 961
 Phenylepoxyxilanes, reactions of 894
 1-(Phenylseleno)-2-silylethenes,
 [2+1]annulations of 880, 881
 1,2-Phenyl shifts 898, 899
 Phenylsilyl cation, reactions of 1051, 1052
 1-(Phenylthio)-2-silylethenes, reactions of 880
 Phosgene, reactions of 501
 Phosphaallenes — *see also* Azaphosphaallenes
 synthesis of 503, 504, 520, 527–530
 2-Phosphaallyl cation 496

- Phosphaarsenes, synthesis of 531, 532
Phosphaarsines, transition metal-substituted, synthesis of 507, 508
Phosphabenzenes — *see also*
Azaphosphabenzenes,
Heterophosphabenzenes
synthesis of 494, 495
Phosphaborenes, synthesis of 533
Phosphaboriridines — *see*
Azaphosphaboriridines
Phosphabuta-1,3-dienes — *see also*
Diphosphabuta-1,3-dienes,
Triphosphabuta-1,3-dienes
synthesis of 500, 514, 515, 519
Phosphacumulenes 494
Phosphaethenes 494 — *see also*
Azulenylphosphaethenes,
Diaminophosphaethenes,
Monosilylphosphaethenes,
Phosphino(silyloxy)phosphaethenes
as reaction intermediates 503, 504
synthesis of 511, 512, 514
addition–elimination method for 492, 493
addition–silatropy method for 492, 494
condensation method for 492, 493
condensation–silatropy method for 492,
494, 495
1,2-elimination method for 492, 493
from bis(trialkylsilyl)phosphides 509
from bis(trialkylsilyl)phosphines 498, 499
from silylphosphides 523–528
1,3-silyl migration method for 492, 493
transition metal-substituted, synthesis of 507
Phosphaethynes 494
synthesis of 514
addition–elimination–silatropy method
for 495, 496
condensation–silatropy–elimination
method for 495
from bis(trialkylsilyl)phosphides 509
Phosphagermenes, synthesis of 499
Phosphaketenes 511 — *see also*
t-Butylphosphaketene
as reaction intermediates 501
reactions of 495, 497, 529
synthesis of 520
Phosphapolyenes 494
Phosphasilenes — *see also*
Metallophosphasilenes
reactions of 534, 535
synthesis of 509, 510, 514, 531–534
Phosphastannenes, synthesis of 499
Phosphastilbenes, synthesis of 531, 532
Phosphathioketenes,
formation of 529, 530
synthesis of 519
Phosphatriafulvenes, synthesis of
513
Phosphenes — *see* Azaphosphenes,
Diphosphenes
Phosphetanes — *see* 1,3-Diphosphetanes
Phosphides — *see* Silylphosphides
Phosphines — *see* Aminophosphines,
Chlorophosphines, Fluorenylidene phosphine,
Iminophosphines,
Phosphoranylidene phosphines,
Siloxylphosphines, Silylphosphines,
Sulphuranylidene phosphines
Phosphinidenebornadiene, synthesis of 527
Phosphinidenequadracyclane, synthesis of 526,
527
Phosphinidene tungsten complexes 533, 534
Phosphinimines — *see* *O*-Silylphosphinimines
Phosphinines, synthesis of 494, 495
Phosphino groups, in xerogels 611
Phosphino(silyloxy)phosphaethenes 528,
529
Phosphiranes, synthesis of 530
Phospholes — *see* Azaphospholes,
Heterophospholes, Thiadiphospholes
Phosphonates — *see*
1-Siloxy-1-phenylmethane phosphonates,
2-(3-Silyl)biphenyl phosphonates
Phosphonins — *see* Dihydrophosphonins
Phosphoranes — *see* Dithioxophosphoranes,
2-(Silylethylidene)triaryl phosphoranes
Phosphoranylidene phosphines, synthesis of
513
Phosphorus tribromide, as brominating agent
481
Photoelectron spectroscopy (PES) 165–217,
834
and bonding in silicon-containing molecules
172–195
of organosilicon compounds,
containing Group 13 elements 195–197
containing Group 14 elements 197–202
containing Group 15 elements 202–208
containing Group 16 elements 208–213
containing Group 17 elements 214–216
vertical ionization fingerprints from
167–172
Photoisomerization 524
Phytoliths 817
Piezochromism, in polysilanes 548, 558
Pinacolone, reactions with silenes 984, 985
Plants, in studies of biosilica synthesis 806
Plumbiranes 44
Polarization interactions, in thermochromism 545
Polyamines, in studies of biosilica synthesis
810
Poly(carbosilane)s, hyperbranched 785–793
Poly(carbosilazane)s, hyperbranched 796
Poly(carbosiloxane)s, hyperbranched 791,
794–796

- Polycondensation 589–593
 hydrolytic 716, 717
 inter-/intra-molecular 592
- Poly(dibenzosilole), synthesis of 679, 682
- Polydiethynylsilanes (PDES) 648–651
- Poly(ethynylenearylene)-type polymers 671
- Polyhedral compounds 38
 cage 58–62
 metallaboranes 62, 63
- Polyheterocycles, electronic structure of 642, 645
- Polymerization,
 inorganic 567
 ring-opening,
 anionic 679, 685
 of cyclic oligosilanes 707
 topochemical 610, 611
- Polymers, silole-containing,
 as conducting materials 683
 as precursors for transition metal-containing ceramics 683
- Polyols,
 biological, reactions of 808
 monosilylated, reactions of 928
- Polyoxometallate anions 701
- Polysilanes — *see also* Poly(carbosilane),
 Polydiethynylsilanes
 as reducing agents 383, 384
 conformation of 542, 543
 electrical conductivity of 559–561
 electronic structure of 542, 543
 fragmentation of 348
 ionization potentials of 559
 ionochromism in 556–558
 γ -irradiation of 346
 mesophase in 547, 548, 551, 552
 PE spectra of 175–178
 phase transitions in 551
 piezochromism in 548, 558
 quenching of 551
 radical cations of, charge delocalization in 174–178
 sigma conjugation in 542, 547, 548
 sigma delocalization in 559
 silole-containing 675–682
 solvatochromism in 554–556
 thermochromism of 542
 as solids 547–554
 in solution 543–547
- Polysilanolols 696
 acidity/basicity of silanol groups in 714, 715
 anomeric effect in 724
 reactions of 714–724
 condensation 716, 717
 structure of 724–736
 synthesis of 696–713
 by hydrolysis of halosilanes 697–702
 by hydrolysis of Si–C bonds 710
 by hydrolysis of Si–H compounds 708, 709
 by hydrolysis of Si–N function 709, 710
 by hydrolysis of Si–O function 702–707
 by oxidation of Si–H compounds 707, 708
- Poly(silole)s — *see* Poly(dibenzosilole)
- Poly(1,1-silole)s 675–682
 in organic EL devices 690
- Poly(2,5-silole)s 648–654
 structural comparison with polyacetylene 648, 649
 synthesis of 652, 653
- Poly(siloxane)s — *see also*
 Poly(carbosiloxane)s
 hyperbranched 797
- Polysilsesquioxanes 811, 812 — *see also*
 Organopolysilsesquioxanes
- Polythiophenes, formation of 611
- Population transfer experiments 241
- Potassium fluoride, as fluorinating agent 479
- Prismanes — *see* Metallaprismanes
- Propargylsilanes, [3+2]annulations of 877, 880
- Propellanes — *see* [1.1.1]Metallapropellanes
- Propenes — *see* Cyclopropenes, Silylpropenes
- Propynyllithiums, reactions of 891, 893
- Proteases, active site of 811, 813
- Proteins, surrounding diatom biosilica 808, 809
- Protodesilylation 477
- Proton affinities 1035, 1040, 1045, 1046
- Pyrans — *see* Tetrahydropyrans
- Pyridines — *see also*
p-*N,N*-Dimethylaminopyridine
 adducts with silicon halides 483
- Pyrrolidines — *see* Acylpyrrolidines
- Pyrrolines, synthesis of 880, 902
- Quadricyclanes — *see*
 Phosphinidenequadricyclane
- Quatersiloles 652
 synthesis of 676, 677
- Radial orbital extensions 8, 9
- Radical addition reactions 360–362, 379, 380
- Radical chain reactions 362–387
- Radical cyclization 371–380
- Radical reactions, consecutive 369–380
- Radicals,
 pentacoordinated 142–144
 tricoordinated 138
- Radiolytic techniques 1030
- Reaction cascades 377–379

- Reaction kinetics,
of disilene reactions 1006–1022
of ion–molecule reactions of silicon cations 1030
of silene reactions 953–1005
- Rearrangements,
acetylene–vinylidene 864
carbene–carbyne 864
carbene–ketene, reverse 862
disilanylcarbene–silylsilaethene 872, 873
disilanyldisilene–2-silylcyclotrisilane 876, 877
disilanylsilylene–silyldisilene 874, 875
dyotropic 856–858, 867, 876
ester–ketene silyl acetal 935
ketone–silyl ether 935
sigmatropic 910, 936, 938
silatropic 870
silene–silene 858
silylmethylsilylene–silylsilaethene 871, 872
silylsilanone–siloxysilylene 874
- Reduction, asymmetric, catalysis of 616
- Relativistic effects 9, 10
- Relativistic methods 13
- Relaxation reagents 323, 326
- Relaxation times,
in the rotating frame 314
spin–lattice 226, 240, 314–317
spin–spin 226, 314, 315
- Resonance substituent parameters,
for carbon-substituted silenes 999, 1000
for silicon-substituted silenes 1000, 1001
- Retro-Wolff rearrangement 862
- Rietveld analysis 735
- Ring closure, electrocyclic, of
1,3-(1-sila)butadienes 955
- Ring compounds, theoretical aspects of,
for four-membered 38–44
for three-membered 38–46
- Ring expansion 879, 883
- Ring opening 881–883
- RNA, role in biosilicification 807
- Satellite spectrum 274
- Selective polarization inversion (SPI) 241
- Selective polarization transfer (SPT) 241–245, 303–305
- Selenoesters,
radical cyclization of 376
reduction of 367, 368
- Self-diffusion, NMR measurement of 315
- SEMINA 282
- Sensors 570
- SEXAFS (Surface Extended X-ray Absorption Fine Structure) 838, 839
- Seyferth–Wittig reagent 916
- Shift reagents 258, 325
- ²⁹Si,
isotopic enrichment of 225, 226, 319–321
natural abundance of 225
relaxation times of 226, 240
- Sigmatropic rearrangements 936, 938
electrocyclic 910
- Signal winnowing 261
- 1-Silaallenes 87, 89
reactions of, rate constants for 962
reactivity of, substituent effects on 1003–1005
- Silaamidides 435, 436
- Silabenzenes — *see also* Disilabenzenes, Hexasilabenzene, Tetrasilabenzenes, Trisilabenzenes
formation of 872
PE spectra of 178, 179
theoretical aspects of 101–105
- Silabenzvalenes — *see* Disilabenzvalenes
- Silabutadienes — *see also* Disilabutadienes
theoretical aspects of 82–87
(1-Sila)butadienes, reactions with oxygen 990
(2-Sila)butadienes, reactions of, rate constants for 962, 989
- Silacations,
halogen-containing, reactions of 1037–1040
hydrogen-containing,
clusters with hydrogen 1035
reactions of 1035–1037
- O- and S-substituted 1040–1042
transition metal-containing, reactions of 1053–1055
- Silacyclobutadienes 873 — *see also* 1,3-Disilacyclobutadienes
- Silacyclobutanes — *see also* 1,2-Disilacyclobutanes, α -Methylenesilacyclobutane, 1-Sila-3-zirconacyclobutane
cycloreversion of 956, 957
photolysis of 959, 961, 998, 999
- Silacyclobutenes — *see also* Tetrasilacyclobutenes
photolysis of 999
- Silacycloheptatrienyl cation, reactions of 1051, 1052
- Silacyclopentadienes — *see also* Siloles
synthesis of 472
- Silacyclopentanes — *see* 1,1-Dichloro-1-silacyclopentane
- Silacyclopentenes — *see also* Disilacyclopentenes, Tetrasilacyclopentenes
formation of 874
1-Silacyclopent-3-enes 471
- Silacyclopropanes — *see* Disilacyclopropanes
- Silacyclopropenes — *see also* Bis(silacyclopropene)s
formation of 1004

- Silaethenes,
 rearrangement of 871–873
 synthesis of 912, 913
- Silaffins 809, 810
- (1-Sila)hexatrienes, reactions of,
 rate constants for 962, 996
 with acetic acid 977
 with alcohols 968, 969
 with alkenes and dienes 990
 with carbonyls 982, 985, 986
 with oxygen 990
- Silane dendrimers 779–783
- Silanedioles — *see also* Diarylsilanedioles,
 Oligosilanedioles
 formation of 698, 699, 702, 703, 705,
 708–710, 713
 metal derivatives of 721, 722
 molybdenum complexes of 732
 reactions of 711
 structure of 730–733
- Silanes — *see also* Acryloylsilanes,
 Acylsilanes, Alkoxysilanes,
 3-Alkylamino-1-propenylsilanes,
 Alkynylsilanes, Allenylsilanes, Allylsilanes,
 Aminosilanes, Aroylsilanes, Carbosilanes,
 Crotonylsilanes, Crotylsilanes,
 Cyclopropylsilanes, Cyclosilanes,
 α,β -Dihydroxysilanes, Disilanes,
 Epoxy silanes, Formylmethylsilane,
 Germylsilanes, α -Halomethylsilanes,
 Halosilanes, Hydrosilanes,
 α -Hydroxyalkylsilanes, Hydroxysilanes,
 Iminosilanes, β -Ketosilanes, Oligosilanes,
 Polysilanes, Propargylsilanes,
 Stannylsilanes, Tetramethylsilane,
 Tetrasilanes, Tigylsilanes, Triorganosilanes,
 Trisilanes, Tris(trimethylsilyl)silane,
 Vinylsilanes
 hydrolysis of 708, 709
 ozonolysis of 707
- Silanethiones 862
- Silanetriols 715 — *see also* Arylsilanetriols
 formation of 698–700, 702
 metal derivatives of 722–724
 reactions of 710
 structure of 733–736
- Silanimines — *see* Trimethylsilanimine
- Silanolates 609
- Silanols — *see also* Disilanols, Tetrasilanols
 IR spectra of 715
 metalloid derivatives of 717–724
 NMR spectra of 697, 715
- Silanones 862
 rearrangement of 874
- Silaneborbanes — *see*
 Decamethyl-7-oxa-hexasilanorbornane
- Silanthzenes 382
- Silaoxacyclohexadienes 938
- 1-Sila-1,3-pentadienes 938
- Silatetrazenes — *see* Cyclosilatetrazenes
- 4-Silatriafulvenes 873
- Silatrienes, reactions with dienes 990
- Silatropy 492–494, 511–513
- Silazanes — *see* Cyclosilazanes, Disilazanes,
 Poly(carbosilazane)s, Tetrasilazanes,
 Trisilazanes
- 1-Sila-3-zirconacyclobutane, reactions of 864
- Silenes — *see also* Brook silenes, Disilenes,
 Phosphasilenes, Silylsilenes, Tetrasilenes,
 Trisilenes
 bimolecular reactions of, kinetics of
 956–1005
 [2+2]cycloaddition reactions of,
 with alkenes 988
 with carbonyls 982, 985
 [2+4]cycloaddition reactions with dienes
 988–990
 dimerization of 956–958, 961–966
- Arrhenius parameters for 958, 963
 head-to-head 963
 head-to-tail 962, 963
 theory of 966
- ene reactions of,
 with alkenes and dienes 988–990
 with carbonyls 982–987
- isomerization of 954–956
- nucleophilic addition reactions of,
 with acetic acid 976–978
 with alkoxy silanes 980–982
 with amines 978–980
 with water/alcohols 966–976, 1002, 1003
- oxidation of 990–992
- quenching reactions with DMSO and CCl₄
 992, 993
- reactivity of,
 solvent effects on 993–996
 substituent effects on 996–1005
- rearrangement of 858
- resonance substituent parameters for
 999–1001
- trapping reactions of 956–961
 rate constants for 958–960
- unimolecular reactions of, kinetics of
 953–956
- Silenylidenes — *see* Disilenylidenes
- Siletanes — *see* Oxasiletanes
- Silica,
 biosynthesis of 815–817
 redistribution of oxygen atoms in 625, 626,
 628
- Silica deposition vesicle 808
- Silica surfaces 715, 716
- Silicate groups, pentacoordinate, migration of
 885

- Silicateins 810–817
 catalytic activity of 811–813
 template-like activity of 811
- Silicates — *see* Fluorosilicates
- Silicenium ions 128
 reactions of 1042–1045
 with alkenes 1049, 1050
 with alkynes 1050, 1051
 with aromatic compounds 1046–1049
 with n-bases 1045, 1046
- Silicic acid 724, 808
 polycondensation of 809–811, 817
- Silicocene, PE spectrum of 197–199
- Silicon,
 effective nuclear potential of, compared to carbon 172–174
 intracellular speciation of 807, 808
 pentacoordinate, in intermediates 908, 914, 916
- Silicon alkoxides, polycondensation of 810–817
- Silicon cations — *see also* Organosilane radical cations, Silacations, Silicenium ions, Silicon ion
 ion–molecule reactions of 1029–1055
- Silicon compounds,
 bonding in 172–195
 molecular states of 169–172
 schematic time-scale for 170
 one-electron oxidation of 180–186
 sterically overcrowded 186–191
- Silicones, manufacture of 703, 717
- Silicon halides,
 Lewis base adducts of 482–486
 PE spectra of 214–216
 synthesis of 470–482
- Silicon hydrides, radical reactions of 362–387
- Silicon intermediates, kinetically unstable 191, 192
- Silicon ion, reactions of,
 with simple inorganic molecules 1030–1032
 with simple organic molecules 1032–1034
- Silicon surfaces 822, 823, 845, 846 — *see also* Si(100) surface
 theoretical models for,
 cluster model 823, 824
 linear scaling methods 825
 QM/MM approach 825
 slab model 823
- Silicon tetrabromide 481
- Silicon tetrachloride 469
 synthesis of 470
- Silicon tetrafluoride, reactions with Grignard reagents 479, 480
- Silicon transporters 807
- Silole 641, 642
 electronic structure of 642–645
- Silole–arene copolymers 662, 664–672
 synthesis of 662, 666–669
- Silole–benzene copolymers 662, 669
- Silole dianions 679
- 2,5-Silole-diboronic acids, in synthesis of silole–arene copolymers 662, 668
- Silole–diethynylarene copolymers, synthesis of 671, 672
- Silole monomers, synthesis of 645–648
- Silole–pyridine copolymers 662, 669
- Silole–pyrrole cooligomers 670, 671
- Silole–pyrrole copolymers 671
- Siloles — *see also* Bisiloles,
 1,1-Diaminosiloles, 2,5-Diarylsiloles,
 2,5-Dibromosiloles, 1,1-Dichlorosiloles,
 2,5-Diiodosiloles, Dilithiosiloles,
 2,5-Di(2-pyridyl)siloles,
 2,5-Dipyrrolylsiloles, 2,5-Disilylsiloles,
 2,5-Distannyl-3-borylsiloles, Dithienosiloles,
 Oligosiloles, Quatersiloles, Tersiloles
 synthesis of 645–648
 theoretical aspects of 46, 47
- Silole–thiazole copolymers 662, 669
- Silole–thiophene copolymers 647, 662–670
- Siloxane dendrimers 782–784
- Siloxanediols — *see also* Disiloxanediols,
 Tetrasiloxanediols
 metal derivatives of 717–719
- Siloxanes — *see also* Aluminosiloxanes,
 Borasiloxanes, Disiloxanes, Hexasiloxanes,
 Metallasiloxanes, Oligosiloxanes,
 Tetrasiloxanes, Trisiloxanes
 formation of 716, 717
 hydrogen bonding in 725–727
 oxygen lone-pair ionization of 208–210
 propargylic, synthesis of 882
- Siloxanetriols, metal derivatives of 719–721
- Siloxetanes — *see* Disiloxetanes
- (α -Siloxyalkyl)phenyllithiums 922
- Siloxyl radicals 869
- (2-Siloxylalkynenyl)ketenes, ring closure of 926
- γ -Siloxylallyllithiums 922
- β -Siloxy-*N,N*-bissilylamines 927
- Siloxybutadienes, formation of 899
- Siloxycarbanions 887
 rearrangement of 867
- γ -Siloxycarbanions 916
- Siloxycyclohexenones, reactions of 928, 929
- Siloxycyclopentanes 920
- Siloxycythenes, synthesis of 908, 910
- α -Siloxyketones,
 reactions of 889–891
 reduction of 928
 synthesis of 929, 931
- Siloxymethyl lithium 867
- 1-(Siloxy)-1-phenylmethanephosphonates 932
- Siloxylphosphines, reactions of 932

- γ -Siloxyvinylolithiums 922
 Siloxyvinyl phosphine oxides, synthesis of 932
 Silsesquioxanes 715, 716, 810–812 — *see also*
 Metallasilsesquioxanes,
 Oligosilsesquioxanes,
 Organosilsesquioxanes, Polysilsesquioxanes
 formation of 701, 704
 metal derivatives of 718–721
 reactions of 708
 silylation of 711
 structure of 730
 Silthianes, sulphur lone-pair ionization of
 210–213
 Silylacetylenes — *see also*
 Trimethylsilylacetylenes
 PE spectra of 178–180
 γ -Silyl alcohols, reactions of 916
 Silylalkenes — *see also* Hydroxysilylalkenes,
 Silylethenes, Vinylsilanes
 reactions of 880, 881
 Silylalkoxides — *see also*
 α -Silyl(allyl)alkoxides
 rearrangement of 887
 synthesis of 888
 γ -Silylalkoxides 923
 α -Silylalkoxy radicals 869
 Silyl allenol ethers, synthesis of 888
 α -Silylallyl alcohols,
 reactions of 891, 892
 synthesis of 901
 α -Silyl(allyl)alkoxides, synthesis of 891, 892
 (α -Silylallyl)amines, reactions of 901
 2-Silylallyl ketones, synthesis of 884, 885
N-Silylamides, rearrangement of 908
 Silylamines — *see also* Aminosilanes,
 β -Siloxy-*N,N*-bissilylamines,
 N-Silyl(vinyl)amines
 lithium derivatives of 434–439
 α -Silylamines, reactions of 902
 Silylaminophosphines — *see also*
 N,N-Bis(silyl)aminophosphines
 reactions of 934
N-Silylanilines 936
 Silylation agents 483
 2-(3-Silyl)biphenylphosphonates, reactions of
 915
 γ -Silyl carbonyl compounds, α,β -unsaturated,
 rearrangement of 935
 Silylcarboxylates, hydrolysis of 705, 706
 β -Silylcarboxylic acids,
 rearrangement of 908
 synthesis of 927
 Silylcyanohydrins 931
 reactions of 927
 β -Silylcyclohexanones, oxidation of 883, 884
 5-Silylcyclopentadienes, rearrangement of 870
 α -Silylcyclopropyllithium, reactions of 869
 α -Silyldiazomethanes, photolysis of 998, 999
 (Silyl)dihalomethylolithiums, reactions of
 913
 Silyl diketonates, rearrangement of 936
 2-Silyl-1,3-dipoles 877
 Silyl dithianes, bisalkylation of 919
 Silylenes 110 — *see also* Hydroxysilylenes,
 Silylsilylenes
 as reaction intermediates 478
 reactions of 907
 rearrangement of 871, 872, 874
 singlet ground state of 397
 Silyl enol ethers,
 reactions of 929
 rearrangement of 912
 synthesis of 887–895, 982, 983
 Silyl esters, reactions of 920
 Silylethenes — *see*
 1-(Phenylseleno)-2-silylethenes,
 1-(Phenylthio)-2-silylethenes
 Silyl ethers — *see also* Allyl silyl ethers,
 Butadienyl silyl ethers, Silyl allenol ethers,
 Silyl enol ethers, Triol monosilyl ethers
 reactions of 923
 synthesis of 923
 2-(Silylethylidene)triarylphosphoranes,
 reactions of 916, 917
 2-Silylfurans, reactions of 885
 2-Silyl-3-furoic acids, synthesis of 920
 1-Silylhexanols, synthesis of 901
 Silyl homoenolates, synthesis of 888
 Silylidenes 96 — *see also* Difluorosilylidene
 Silylium cations 128
 Silyl ketals, rearrangement of 900
 Silyl ketene acetals, reactions of 936
 Silylketenes,
 reactions of 936
 synthesis of 908, 910
 α -Silylketenes, photolysis of 998, 999
 Silyl ketones, formation of 869
 α -Silyl ketones,
 synthesis of 912
 β,γ -unsaturated, formation of 899
 β -Silyl ketones, formation of 893
 α -Silyl ketoximes 927
 Silyllithiums, reactions of 888–891, 902
 Silylmethoxylithium 867
 Silylmethylcarbene 860
N-(Silylmethyl)imines, reactions of 902, 903
 Silylmethyl ketones, rearrangement of 908
O-Silyl methyl ketoximes 927
 Silylmethylolithiums, reactions of 919, 920
 Silyl migrations, nondissociative 867
 1,2-Silyl migrations 856–904
 anionic 866–869
 β -elimination–1,2-addition pathway for
 868
 synthetic applications of 887–903

- catalysed 865
cationic 858–866
 synthetic applications of 877–887
fractional 870
in unsaturated silicon compounds 871–877
radical 869, 870
 synthetic applications of 903, 904
 theoretical calculations for 860–862, 873
- 1,3-Silyl migrations,
 anionic 910–912
 configuration in 905–907
 in unsaturated silicon compounds 912
 mechanistic aspects of 904–912
 photochemical 913
 solvent effects on 913
 synthetic applications of 913
 thermal 905
- 1,4-Silyl migrations 914–935
 anionic 916–935
 diastereoselectivity in 916
- 1,5-Silyl migrations 935–938
- 1,6-Silyl migrations 939, 940
- Silyloxyacetylenes, rearrangement of 908, 910
- Silyloxyiminophosphines, synthesis of 530, 531
- 5-Silylpentanal 939
- Silyl perchlorates, hydrolysis of 705, 706
- Silylperoxide derivatives, hydrolysis of 703
- Silylphosphides — *see*
 Acyl(trialkylsilyl)phosphides,
 Bis(trialkylsilyl)phosphides,
 Disilylphosphides, Monosilyl(2,4,6-tri-*t*-butylphenyl)phosphides,
 Mono(trialkylsilyl)phosphides
- Silylphosphines — *see*
 Acyl(trialkylsilyl)phosphines,
 Bis(trialkylsilyl)phosphines,
 Bis(trimethylsilyl)(triphenylsilyl)phosphine,
 (Chlorosilyl)phosphines,
 Chloro(trimethylsilyl)phosphines,
 Disilylphosphines, Monosilylphosphines,
 Trisilylphosphines
- O*-Silylphosphinimines, synthesis of 934
- Silylpropenes — *see* 1-Silyl-3-stannylpropenes, 2-Stannyl-3-trimethylsilylpropenes
- Silyl radicals 341–387
 chemical properties of 345–362
 theoretical studies 354, 356–362
 EPR spectra of 344–348
 rearrangement of 350–352
 structure of 342–345
- Silylsilenes, rearrangement of 871
- β -Silylsilylenes, rearrangement of 872
- 1-Silyl-3-stannylpropenes, reactions of 884
- Silyl sulphates, hydrolysis of 705, 707
- Silyl triflates 477
 hydrolysis of 706
 reactions of 480
- N*-Silyl(vinyl)amines, synthesis of 901
- Silylvinyl sulphones, reactions of 918
- Silynes — *see also* Disilynes
 theoretical aspects of 91–95
- SIMMOM (Surface Integrated Molecular Orbital/Molecular Mechanics) method 825,836,840
- Si–N bond formation 430, 431
- Singlet–triplet energy splitting 110–112
- ²⁹Si NMR 399, 400, 593–595, 697, 714, 715, 724, 1006
 accuracy and precision in 328, 329
 acquisition time in 327
 digital resolution in 328
 J-resolved 311–314
 LC 324
 line assignments and connectivity in 257–311
 measuring frequency in 326, 327
 quantitative measurements of 323–325
 referencing in 226–230, 328
 external 227, 229
 internal 228
 secondary 227, 228, 230
 universal 229, 230
 relaxation times of 314–316
 selective decoupling in 303
 selective detection in 303, 306–311
 selective excitation in 303–306
 selective isotopic substitution in 319–321
 sensitivity enhancements for 240–257
 solvent effects on 230–240
 ultrahigh resolution 325
- Si–S bonds, hydrolysis of 703
- Si(100) surface,
 halogen etching of 844, 845
 hydration of 834–837
 hydrogenation of 837, 838
 oxidation of,
 active 841–844
 passive 838–841
 reactions of,
 with alkenes 827–831
 with alkynes 827–831
 with aromatic compounds 833, 834
 with dienes 831–833
 2x1 reconstruction of 825–827
- Sol-gel process 567, 569, 589–593, 702, 703, 716
 catalytic effects on 596
 reproducibility of 569
 solvent effects on 596
 temperature effects on 595
- Solid materials, texture of 595–600
 kinetic control of 602

- Solid synthesis,
 cyclization in 592, 593
 heterocondensation in 567, 569
 homocondensation in 567, 569
 hydrolysis in 567, 569
 kinetic control of 566, 590, 593–602
 short-range organization in 575, 602–608
- Solvatochromism, in polysilanes 554–556
- Solvent-accessible surfaces 234, 238
- Solvent complexation 994, 995
 temperature effects on 995
- Solvent effects,
 on silene reactivity 993–996
 on 1,3-silyl migrations 913
 on ^{29}Si NMR 230–240
 on sol-gel processes 596
- Solvents,
 donor numbers of 231, 232
 hydrogen bonding in 232, 233
- Spicules 807
- SPINEPTR 253, 303, 304
- Spin-orbit coupling 11
- Sponges, in studies of biosilica synthesis 806,
 807, 810–814, 817
- SREM (Scanning Reflection Electron
 Microscopy) 840
- Stannanes — *see*
N,N-Bis(silyl)amino-1-propenylstannanes,
 Distannanes, Triorganostannanes
- Stannenes — *see* Phosphastannenes
- 2-Stannylallyl ketones 884
- Stannylsilanes, synthesis of 474
- 2-Stannyl-3-trimethylsilylpropenes, reactions
 of 884, 885
- Star polymers 766, 767
- Stereochemistry, inversion of, in anionic
 1,2-silyl migrations 866
- Steric hindrance,
 due to tris(trimethylsilyl) group 699, 702
 in silanediol tetramers 732
- Steric protection 491
 by trimethylsilyl substituents 728
- Stern–Volmer plots 970
- Stilbenes — *see* Phosphastilbenes
- Stille coupling 662, 673
- STM (Scanning Tunnelling Microscopy) 833,
 840, 846
- Strain, in ring systems 41–43
- Sugars, reactions with silicic acid 808
- Sulphuranylidene phosphines, synthesis of 513
- Supersilyl substituents, π -interactions of 190,
 191
- Suzuki–Miyaura coupling 662
- TDS (Thermal Desorption Studies) 841
- Tellurium–lithium exchange reactions 645,
 646
- Tellurophenes, in silole synthesis 645, 646
- Templates, in formation of porous silicas
 620–622
- Templating effects, in solid synthesis 590, 591,
 593
- Tersiloles, synthesis of 676, 677, 679
- Tetraalkoxysilanes, hydrolysis of 589
- Tetraaryldisilenes,
 intramolecular exchange of aryl groups in
 1008
 thermodynamic stability of *E,Z*-isomers
 1006
- Tetrachlorodimethyldisilanes 478
- Tetracyanoethylene, reactions of 878
- Tetraethyl orthosilicate (TEOS) 811
- Tetragermabutadienes 82, 83, 87
- Tetrahedranes — *see* Metallatetrahedranes
- Tetrahydrofurans, synthesis of 881
- Tetrahydropyrans, synthesis of 881
- Tetrahydroxydisiloxanes,
 structure of 733
 synthesis of 699
- Tetrakis(trialkylsilyl)disilenes, addition of
 alcohols, kinetics of 1018
- Tetrakis(trimethylsilyl)methane, as secondary
 reference in ^{29}Si NMR 227
- Tetramesityldisilene, addition of phenols,
 kinetics of 1013–1016
- Tetrametallabutadienes — *see also*
 Tetrasilabutadienes
 theoretical aspects of 82, 83, 87, 88
- Tetramethylethylenediamine, as Lewis base
 483
- Tetramethylsilane (TMS), as reference in ^{29}Si
 NMR 226, 227
- Tetraphosphabicyclo[2.2.0]hexanes, synthesis
 of 501, 502
- Tetraphosphahexadiene, synthesis of 501, 503
- Tetrasilabenzenes 104
- Tetrasilabicyclo[1.1.0]butanes 876, 877
- Tetrasilabutadienes,
 electron spectra of 415
 molecular structure of 414, 415
 reactions of 405, 416, 419, 420
 synthesis of 414
 theoretical aspects of 82, 83, 87
- Tetrasilacyclobutenes, rearrangement of 876,
 877
- Tetrasilacyclopentenes — *see*
 Chalcogenatetrasilacyclopentenes
- 1,3-Tetrasiladienes 877
- Tetrasilanes 417, 418, 423 — *see also*
 Bicyclo[1.1.0]tetrasilanes
 NMR coupling constants for 288, 289
- Tetrasilanols,
 formation of 701
 structure of 729, 730
 synthesis of 704

- Tetrasilatetrahedrane 61
Tetrasilazanes — *see* Cyclotetrasilazanes
Tetrasilenes — *see* Cyclotetrasilenes
Tetrasiloxanediols, metal derivatives of 718
Tetrasiloxanes — *see also* Cyclotetrasiloxanes
 structure of 727
Tetrasilyldisilenes,
 dyotropic rearrangement of 858
 E,Z-isomerization in 1008
Tetrasilylmethanes 702
Tetrazenes — *see* Silatetrazenes
Thermochroism, of polysilanes 542
 as solids 547–554
 in solution 543–547
Thermochromic behaviour, in poly(2,5-silole)s
 651
Thermotropic mesophases 725
Thiabicyclo[2.2.1]heptenespiroindanones,
 synthesis of 879
Thiadiphospholes, synthesis of 509
Thioketenes — *see* Phosphathioketenes
Thiophenes — *see also* Polythiophenes
 synthesis of 920, 921
Thiophosgene, reactions of 519
Tiglylsilanes 924
Titanacyclopentadienes, in silole synthesis
 645, 646
TOF-SARS (Time-Of-Flight Scattering And
 Recoiling Spectrometry) 834
TOF-SIMS (Time-Of-Flight Secondary Ion
 Mass Spectrometry) 575, 600, 602
TPD (Temperature Programmed Desorption)
 845
Transannular cyclization 378
Transition states, *syn-clinal* 878
Transition temperatures, in thermochroism 543
Transmetallation 647
Trialkoxysilyl groups 578
(Trialkylsiloxy)benzamides 922
Triazaphospholes, synthesis of 516
1,2,4-Triazoline-3,5-diones, reactions of 878
2,4,6-Tri-*t*-butylphenyl group, as substituent
 491, 492
(2,4,6-Tri-*t*-butylphenyl)phosphonous
 dichloride, reactions of 496
(2,4,6-Tri-*t*-
 butylphenyl)(trimethylsilyl)phosphines, in
 synthesis of multiply-bonded phosphorus
 compounds 519–522
 β -Tridymite 719
Trienes — *see* Silatrienes
Triflic acid, in functionalization of silanes 477
1,1,1-Trifluoroacetone, reactions with silenes
 984, 985
2,2,2-Trifluoroethanol, reactions with silenes
 976
Trigermacyclopropenium cations 106
Trihalosilanes 469
 hydrolysis of 700
 reactions of 470, 471, 473
 synthesis of 470, 481
Trihalosilylphosphanes, synthesis of 474
Trimethylchlorosilane 471
Trimethylsilanimine, PE spectrum of 206, 207
Trimethylsilylacetylenes 862
1-Trimethylsilylethanes 868
2-Trimethylsilylethylenes 868
Trimethylsilyl-*p*-phenylenediamines, PE
 spectra of 203, 205, 206
Triol monosilyl ethers, reactions of 929, 930
Triols — *see also* Silanetriols, Siloxanetriols
 condensation of 704
Triorganochlorosilanes, synthesis of 474
Triorganosilanes, synthesis of 473
Triorganostannanes, Lewis base-assisted
 hydrogenation with 479
Triphosphabuta-1,3-dienes, synthesis of 495,
 501
Triple resonance experiments 296–303
Trisilabenzenes 104
Trisilanes — *see also* Octachlorotrisilane
 NMR coupling constants for 286, 287
Trisilazanes — *see* Cyclotrisilazanes
Trisilenes — *see* Cyclotrisilenes
Trisiloxanes,
 formation of 701
 structure of 727
Trisilylphosphines, in synthesis of
 multiply-bonded phosphorus compounds
 494–496
1-Tris(trialkylsilyl)cyclotrisilenes,
 rearrangement of 877
Tris(trialkylsilyl)hydroxylamines 857
Tris(trialkylsilyl)silyl-substituted ketones,
 reactions of 865, 866
Tris(trimethylsilyl) group, steric hindrance due
 to 699, 702
Tris(trimethylsilyl)methylamine radical cation,
 cog wheel dynamics of 185
Tris(trimethylsilyl)silane 362, 364–380
 as reducing agent 364–369
 consecutive radical reactions of 369–380
Tropolonate ligands 928
Tropylium salts — *see* Benzotropylium salts

Ultrasound 707
Ultraviolet absorption maxima, for
 carbon-substituted silenes 999, 1000
 β,γ -Unsaturated esters 936, 937
UV-visible absorption spectroscopy,
 of bisiloles 652
 of 2,5-diarylsiloles 657, 658, 661
 of 2,5-disilylsiloles 661, 662
 of 2,5-dithienylmetalloses 661–663
 of poly(1,1-silole)s 679

- UV-visible (*continued*)
of poly(2,5-silole)s 652, 654
of silole–thiophene copolymers 662, 665
- Valence bond (VB) method 72, 93
- Van der Waals bonding, intramolecular 187–190
- Vinylidene silanes, photolysis of 960, 961, 999
- Vinylepoxy silanes, reactions of 899
- Vinylidene anions — *see* Disilavinylidene anion
- Vinyl ketene silyl acetals 935
- Vinylsilanes — *see also* Silylalkenes
synthesis of 886, 928
- WALTZ-16/17 257
- Wiberg bond index 73
- Wittig reaction 866, 916, 917
- Woodward–Hoffmann rules 857, 877, 906
- Wright–West rearrangement 866
- Wurtz-type coupling 679
- Xerogels 567, 572, 577
anisotropic organization in 604–608
as films 629
as monoliths 629
as precursors for porous materials 620–628
birefringent 606, 607
bisimide 634
catalytic properties of 614–619
cation-binding 614
characterization of 593–595
chemical stability of 609
complexes of 611–614
cracking of 607
crown ether 614
dendrimer 614, 634
electrochemical oxidation of 611
electrochemical properties of 631, 632
ferrocenyl 631, 632
fluorescent 632
interactivity between the organic groups in 610, 611
lamellar structure of 604
luminescent 632
mechanical properties of 634
optical properties of 632–634
precursors of 578–589
reactivity of 611–614
shaping of 629–631
short-range order in 603, 604, 610, 611, 623
surface of 600–602
swollen 619
texture of 595–600
thermal properties of 631
thermal treatment of 621, 622
X-ray diffraction of 603
- XPS (X-ray Photoemission Spectroscopy) 845
- X-ray scattering 547
in xerogel surface analysis 602
- XVI sequence 271
- Ylides, diazomethyne 902, 903
- Zinc fluoride, as fluorinating agent 479, 480
- Zirconacyclopentadienes, in silole synthesis 645–647
- Zwitterion intermediates 880, 881, 938

Contents of Volume 1

1	Historical overview and comparison of silicon with carbon J. Y. Corey	1
2	Theoretical aspects of organosilicon compounds Y. Apeloig	57
3	Structural chemistry of organic silicon compounds W. S. Sheldrick	227
4	Dynamic stereochemistry at silicon R. J. P. Corriu, C. Guerin and J. J. E. Moreau	305
5	Thermochemistry R. Walsh	371
6	Analysis of organosilicon compounds T. R. C. Crompton	393
7	Positive and negative ion chemistry of silicon-containing molecules in the gas phase H. Schwarz	445
8	NMR spectroscopy of organosilicon compounds E. A. Williams	511
9	Photoelectron spectra of silicon compounds H. Bock and B. Solouki	555
10	General synthetic pathways to organosilicon compounds L. Birkofer and O. Stuhl	655
11	Recent synthetic applications of organosilanes G. L. Larson	763
12	Acidity, basicity and complex formation of organosilicon compounds A. R. Bassindale and P. G. Taylor	809
13	Reaction mechanisms of nucleophilic attack at silicon A. R. Bassindale and P. G. Taylor	839

Contents of Volume 1

14	Activating and directive effects of silicon A. R. Bassindale and P. G. Taylor	893
15	The photochemistry of organosilicon compounds A. G. Brook	965
16	Trivalent silyl ions J. B. Lambert and W. J. Schulz, Jr.	1007
17	Multiple bonds to silicon G. Raabe and J. Michl	1015
18	Bioorganosilicon chemistry R. Tacke and H. Linoh	1143
19	Polysilanes R. West	1207
20	Hypervalent silicon compounds R. J. P. Corriu and J. C. Young	1241
21	Siloxane polymers and copolymers T. C. Kendrick, B. Parbhoo and J. W. White	1289
22	Organosilicon derivatives of phosphorus, arsenic, antimony and bismuth D. A. ('Fred') Armitage	1363
23	Chemistry of compounds with silicon–sulphur silicon–selenium and silicon–tellurium D. A. ('Fred') Armitage	1395
24	Transition-metal silyl derivatives T. D. Tilley	1415
25	The hydrosilylation reaction I. Ojima	1479
	Author index	1527
	Subject index	1639

Contents of Volume 2

1	Theoretical aspects and quantum mechanical calculations of silaaromatic compounds Yitzhak Apeloig and Miriam Karni	1
2	A molecular modeling of the bonded interactions of crystalline silica G. V. Gibbs and M. B. Boisen	103
3	Polyhedral silicon compounds Akira Sekiguchi and Shigeru Nagase	119
4	Thermochemistry Rosa Becerra and Robin Walsh	153
5	The structural chemistry of organosilicon compounds Menahem Kaftory, Moshe Kapon and Mark Botoshansky	181
6	²⁹ Si NMR spectroscopy of organosilicon compounds Yoshito Takeuchi and Toshio Takayama	267
7	Activating and directive effects of silicon Alan R. Bassindale, Simon J. Glynn and Peter G. Taylor	355
8	Steric effects of silyl groups Jih Ru Hwu, Shwu-Chen Tsay and Buh-Luen Cheng	431
9	Reaction mechanisms of nucleophilic attack at silicon Alan R. Bassindale, Simon J. Glynn and Peter G. Taylor	495
10	Silicenium ions: Quantum chemical computations Christoph Maerker and Paul von Ragué Schleyer	513
11	Silicenium ions — experimental aspects Paul D. Lickiss	557
12	Silyl-substituted carbocations Hans-Ullrich Siehl and Thomas Müller	595
13	Silicon-substituted carbenes Gerhard Maas	703

Contents of Volume 2

14	Alkaline and alkaline earth silyl compounds – preparation and structure Johannes Belzner and Uwe Dehnert	779
15	Mechanism and structures in alcohol addition reactions of disilenes and silenes Hideki Sakurai	827
16	Silicon–carbon and silicon–nitrogen multiply bonded compounds Thomas Müller, Wolfgang Ziche and Norbert Auner	857
17	Recent advances in the chemistry of silicon–heteroatom multiple bonds Norihiro Tokitoh and Renji Okazaki	1063
18	Gas-phase ion chemistry of silicon-containing molecules Norman Goldberg and Helmut Schwarz	1105
19	Matrix isolation studies of silicon compounds Günther Maier, Andreas Meudt, Jörg Jung and Harald Pacl	1143
20	Electrochemistry of organosilicon compounds Toshio Fuchigami	1187
21	The photochemistry of organosilicon compounds A. G. Brook	1233
22	Mechanistic aspects of the photochemistry of organosilicon compounds Mitsuo Kira and Takashi Miyazawa	1311
23	Hypervalent silicon compounds Daniel Kost and Inna Kalikhman	1339
24	Silatranes and their tricyclic analogs Vadim Pestunovich, Svetlana Kirpichenko and Mikhail Voronkov	1447
25	Tris(trimethylsilyl)silane in organic synthesis C. Chatgililoglu, C. Ferreri and T. Gimisis	1539
26	Recent advances in the direct process Larry N. Lewis	1581
27	Acyl silanes Philip C. Bulman Page, Michael J. McKenzie, Sukhbinder S. Klair and Stephen Rosenthal	1599
28	Recent synthetic applications of organosilicon reagents Ernest W. Colvin	1667
29	Recent advances in the hydrosilylation and related reactions Iwao Ojima, Zhaoyang Li and Jiawang Zhu	1687

Contents of Volume 2

30	Synthetic applications of allylsilanes and vinylsilanes Tien-Yau Luh and Shih-Tzung Liu	1793
31	Chemistry of compounds with silicon-sulphur, silicon-selenium and silicon-tellurium bonds D. A. ('Fred') Armitage	1869
32	Cyclic polychalcogenide compounds with silicon Nami Choi and Wataru Ando	1895
33	Organosilicon derivatives of fullerenes Wataru Ando and Takahiro Kusukawa	1929
34	Group 14 metalloles, ionic species and coordination compounds Jacques Dubac, Christian Guérin and Philippe Meunier	1961
35	Transition-metal silyl complexes Moris S. Eisen	2037
36	Cyclopentadienyl silicon compounds Peter Jutzi	2129
37	Recent advances in the chemistry of cyclopolysilanes Edwin Henge and Harald Stüger	2177
38	Recent advances in the chemistry of siloxane polymers and copolymers Robert Drake, Iain MacKinnon and Richard Taylor	2217
39	Si-containing ceramic precursors R. M. Laine and A. Sellinger	2245
40	Organo-silica sol-gel materials David Avnir, Lisa C. Klein, David Levy, Ulrich Schubert and Anna B. Wojcik	2317
41	Chirality in bioorganosilicon chemistry Reinhold Tacke and Stephan A. Wagner	2363
42	Highly reactive small-ring monosilacycles and medium-ring oligosilacycles Wataru Ando and Yoshio Kabe	2401
43	Silylenes Peter P. Gaspar and Robert West	2463
	Author index	2569
	Subject index	2721